Proceedings of the 36th ASMS Conference on Mass Spectrometry and Allied Topics

June 5 - 10, 1988
San Francisco, California

THE 36th ASMS CONFERENCE ON MASS SPECTROMETRY AND ALLIED TOPICS
June 5-10, 1988

TABLE OF CONTENTS

INTRODUCTION iv

ASMS BOARD OF DIRECTORS v

ASMS COMMITTEES v

CORPORATE MEMBERS vi

ASMS INTEREST GROUPS viii

LISTING OF EXTENDED ABSTRACTS ix

Monday Morning
- Symposium: Elemental and Isotopic Analysis by Mass Spectrometry 1
- Ion Molecule Reactions. Chemical and Atmospheric Ionization 11
- Environmental Mass Spectrometry 29
- Cluster Ions. Ion Activation. Biomedical Mass Spectrometry 49

Monday Afternoon
- Symposium: Mass Spectrometry and Complex Lipids 198
- Isotopic and Elemental Analysis 202
- Symposium: Cluster Ion Mass Spectrometry 224
- Environmental. Fuels and Geoscience. SIMS and Surface Analysis 230

Tuesday Morning
- Plenary Lecture 363
- Symposium: Mass Education 365
- Cluster Ions. Ion Activation 367
- Lipid Biochemistry 385
- Peptides. Polymers. Nucleic Acids. Isotopic, Inorganic and Elemental 405

Tuesday Afternoon
- Symposium: Measurement of Peptides 549
- Reaction Mechanisms I 557
- Symposium: Environmental Fate of Organo-Chlorine Cmpds. in the Atmosphere 575
- Ion Traps and FT-ICR. Ion Molecule Reactions. Chem. and Atmospheric Inztn 586

Wednesday
- Plenary Lecture 727
- Symposium: Applications of Continuous-Flow FAB 729
- Reaction Mechanisms II 741
- Ionization Methods 763
- Instrumentation. Lipids. Environmental Applications of LC/MS 783

Thursday Morning
Oligosaccharides, Nucleic Acids, and General Biochemistry 921
Symposium: Crossing the Solution-Vacuum Barrier 939
Instrumentation 948
Pharmacology and Drugs. LC/MS Applications 970

Thursday Afternoon
Ion Traps and FT-ICR 1106
Symposium: The Drug Industry in Japan 1130
Peptides 1136
Ionization Methods. LC/MS Instrumentation and Techniques. Oligosaccharides 1156

Friday Morning
Plenary Lecture 1299
Symposium: Ion Trapping - Methods and Applications 1302
Liquid Introduction Mass Spectrometry 1308
A Mass Spectral Potpourri 1326

INDEX OF AUTHORS 1427

MINUTES OF THE ASMS BUSINESS MEETING 1440

MEMORIAL PAGE 1443

Terms to Use in Your Research Presentation 1444

COMMITTEE, INTEREST GROUP AND WORKSHOP REPORTS
Academic Laboratory Managers Interest Group 1445
Biomedical Interest Group 1446
Analysis of Drugs and Drug Metabolites by Tandem MS 1447
Education Committee 1448
Ethics in the Workplace 1449
Environmental Interest Group 1450
New Ionization Techniques for Environmental MS 1451
Fundamentals Interest Group 1452
Making Metal Ions 1453
History of Mass Spectrometry Interest Group 1455
Instrumentation and Ion Physics Interest Group 1457
Isotope Ratio Interest Group 1458
Isotope Ratio Mass Spectrometry - A look to the Future 1459
Measurement and Standards Committee 1460
Quantitative Analysis of Peptides 1462
Solids and Surface Analysis Interest Group 1464
Use of Mass Spectrometry in Space 1466
Young Mass Spectrometrists Interest Group 1468

1988 ASMS MEMBERS AND CONFERENCE ATTENDEES 1469

INTRODUCTION

By action of the ASMS Board of Directors, this official record of the annual meeting will henceforth be known as the Proceedings instead of the more informal term "bound volume". Thus, the 1988 designation is Proceedings of the 36th ASMS Conference on Mass Spectrometry and Allied Topics.

The extended abstracts that comprise the bulk of the Proceedings provide a valuable and timely view of the most current research in this very dynamic field. A large number (more than 90 %) of those presenting papers and posters at the conference contribute extended abstracts to the Proceedings. Also included in the Proceedings are workshop and interest group reports and a directory of names, addresses, and telephone numbers of members and conference attendees.

The efforts of Judith A. Watson and her staff of Professional Association Management, Inc. in compiling the Proceedings and arranging for timely printing and distribution in a cost effective manner are gratefully acknowledged. The work presented here also reflects the hard work and creativity of the Vice-President for Programs, Ronald A. Hites, in arranging the technical program.

The Proceedings find a greater audience each year and form a valuable asset to the members of the Society. No doubt there are ways it could be improved, and suggestions or comments directed toward making this a more useful resource are appreciated.

Willard W. Harrison
Editor and Member-at-Large
ASMS Board of Directors

CITATION NOTICE

This volume contains the extended abstracts of papers presented at the 36th ASMS Conference on Mass Spectrometry and Allied Topics. The material is not copyrighted and appearance of material in this volume does not jeopardize the author's right to publish the information in scientific journals.

Reference to individual abstracts contained in this volume should be cited as follows:

Author(s); title; Proceedings of the 36th ASMS Conference on Mass Spectrometry and Allied Topics, San Francisco, California, June 5-10, 1988.

BOARD OF DIRECTORS

President	Gerry G. Meisels 1223 Old Father Hall Univeristy of Nebraska Lincoln, NE 68588
Vice President for Programs	Ronald A. Hites SPEA 410H Indiana University Bloomington, IN 47405
Vice President for Arrangements	Gary L. Glish Oak Ridge National Laboratory Analytical Chemistry Division Oak Ridge, TN 37831
Secretary	Susan T. Weintraub University of Texas Health Science Center San Antonio, TX 78284
Treasurer	Kelsey D. Cook Department of Chemistry University of Tennessee Knoxville, TN 37996
Member-at-Large (Publications)	Willard W. Harrison Department of Chemistry University of Virginia Charlottesville, VA 22901
Member-at-Large Education	Christie G. Enke Department of Chemistry Michigan State University East Lansing, MI 48824
Member-at-Large (Measurements and Standards)	Paul C. Goodley Hewlett-Packard Co. 1601 California Avenue Palo Alto, CA 94304
Past President	R. Graham Cooks Department of Chemistry Purdue University West Lafayette, IN 47907

SOCIETY OFFICE

Post Office Box 1508
East Lansing, MI 48826-1508

Courier address
750 Audubon Road
East Lansing, MI 48823

ASMS COMMITTEES

Nominating	P. Jane Gale, Chair Lazlo Tokes Klaus Biemann James A. McCloskey Marvin Vestal
Education	Harry S. Hertz, Chair Paul C. Goodley Ann G. Goetz Alfred Yergey
Measurements and Standards	Henry M. Fales, Chair Ronald Grigsby William Budde Douglas Cameron
Asilomar Conference	Lazlo Tokes Arnold Falick J. Ronald Hass Ronald A. Hites Gary L. Glish

1988 CORPORATE MEMBERS

ARTHUR D LITTLE
15 ACORN PARK
CAMBRIDGE MA 02138
PHONE: 617/864-5770

BIO-ION
PO BOX 15045
UPPSALA S-75215
PHONE: 018-104440

CAMBRIDGE ISOTOPE LABS
20 COMMERCE WAY
WOBURN MA 01801
PHONE: 617/938-0067

DETECTOR TECHNOLOGY INC
PO BOX K-300
BROOKFIELD MA 01506
PHONE: 617/867-5411

EXTREL
250 ALPHA DRIVE
PITTSBURGH PA 15238
PHONE: 412/782-3884

GALILEO ELECTRO-OPTICS
GALILEO PARK
STURBRIDGE MA 01566
PHONE: 617/347-9191

HEYDEN & SON LTD
SPECTRUM HOUSE
LONDON NW4 2JQ
PHONE:

IONSPEC
ONE LONGSTREET
IRVINE CA 92720
PHONE: 714/857-0793

JEOL LTD USA
11 DEARBORN ROAD
PEABODY MA 01960
PHONE: 617/535-5900

KRATOS ANALYTICAL
535 E CRESCENT AVE
RAMSEY NJ 07446
PHONE: 201/825-7500

M-SCAN LTD
SILWOOD PARK
BERKSHIRE SL5 7PZ
PHONE: 302 453 8151

MERCK SHARP & DOHME
PO BOX 899
QUEBEC H9R 4P7
PHONE: 514/695-7920

BALZERS
8 SAGAMORE PK RD
HUDSON NH 03051-4914
PHONE: 603/889-6888

BRUKER INSTRUMENTS
MANNING PARK
BILLERICA MA 01821
PHONE: 617/667-9580

COLORADO GROUP
6385 W 52ND AVENUE #5
ARVADA CO 80002
PHONE: 303/420-7700

ELSEVIER SCIENCE PUBLISHERS
PO BOX 330
AMSTERDAM 1000AH
PHONE:

FINNIGAN MAT
355 RIVER OAKS PKWY
SAN JOSE CA 95134-1991
PHONE: 408/433-4800

HEWLETT-PACKARD
1601 CALIFORNIA AVE
PALO ALTO CA 94304
PHONE: 415/857-6090

INFICON LEYBOLD-HERAEUS
6500 FLY ROAD
E SYRACUSE NY 13057
PHONE: 315/437-0377

ISOTEC INC
3858 BENNER ROAD
MIAMISBURG OH 45842
PHONE: 513/859-1808

KM ELECTRONICS
123 INTERSTATE DRIVE
WEST SPRINGFIELD MA 01089
PHONE: 413/781-1350

LINDEN-CHROMASSPEC
PO BOX 3451
PRINCETON NJ 08542
PHONE: 609 452 1451

MEASUREMENT & ANALYSIS SYSTEMS
1155 ZION ROAD
BELLEFONTE PA 16823
PHONE: 814/535-0600

NATIONAL BUREAU OF STANDARDS

GAITHERSBURG MD 20899
PHONE:

1988 CORPORATE MEMBERS

NERMAG
15701 WEST HARDY
HOUSTON TX 77060
PHONE: 713/847-0811

ONEIDA RESEARCH
ONE HALSEY ROAD
WHITESBORO NY 13492
PHONE: 315/736-3050

PHRASOR SCIENTIFIC
1536 HIGHLAND AVE
DUARTE CA 91010
PHONE: 213/357-3201

R M JORDAN CO
990 GOLDEN GATE TERR
GRASS VALLEY CA 95945
PHONE: 916 272 4580

SCIENTIFIC GLASS ENGIN
2007 KRAMER LANE
AUSTIN TX 78758
PHONE: 512/837-7190

SHIMADZU SCIENTIFIC INSTR
7102 RIVERWOOD DR
COLUMBIA MD 21046
PHONE: 301/997-1227

SPECTROSPIN AG
INDUSTRIESTRASSE 26
CH-8117 FAELLANDEN
PHONE: 01/825 48 55

TMS ANAL SERVICES
6376 MORENCI TRAIL
INDIANAPOLIS IN 46268
PHONE: 317/291-5697

TRACER TECHNOLOGIES
20 ASSEMBLY SQ DRIVE
SOMMERVILLE MA 02145
PHONE:

VACUMETRICS
2261 PALMA DRIVE
VENTURA CA 93003-5789
PHONE: 805/644-7461

VG INSTRUMENTS INC
32 COMMERCE CTR
DANVERS MA 01923
PHONE: 617/777-8034

NICOLET INSTRUMENT CORP
POST OFFICE BOX 4508
MADISON WI 53711
PHONE: 608/271-3333

PERNICKA CORPORATION
112 RACQUETTE DR
FORT COLLINS CO 80524
PHONE: 303/224 0220

R J BRUNFELDT CO
PO BOX 2066
BARTLESVILLE OK 74005
PHONE: 918/336-4467

RUSKA INSTRUMENT CORPORATION
PO BOX 742688
HOUSTON TX 77274
PHONE:

SCIEX INC
55 GLENCAMERON RD
THORNHILL ONTARIO L3T 1P2
PHONE: 416/881-4646

SHRADER ANALYTICAL LAB
3814 VINEWOOD
DETROIT MI 48208
PHONE: 313/894-4440

TEKNIVENT CORPORATION
11684 LILBURN PK DR
ST LOUIS MO 63146
PHONE: 314/994-0500

TOFTEC
PO BOX 12877
GAINESVILLE FL 32604
PHONE: 904/472-2668

UTI INSTRUMENTS CO
497 S HILLVIEW DR
MILPITAS CA 95035-2008
PHONE: 408 945 1955

VESTEC CORP
9299 KIRBY DRIVE
HOUSTON TX 77054
PHONE: 713/796-9677

WATERS CHROMATOGRAPHY
34 MAPLE STREET
MILFORD MA 01757
PHONE: 617/478-2000

ASMS INTEREST GROUPS

The following is a brief decription of the role of each interest group as provided by their coordinators.

Academic Laboratory Managers, *Richard W. Kondrat*
The problems encountered by those responsible for academic service mass spectrometry facilities.

Biomedical Applications, *Richard M. Caprioli*
Mass spectrometric relevance to biological and medical systems, including areas such as enzymology, macromolecular sequencing, metabolic screening, natural products, etc.

Computer Applications, *Jon D. Onstot*
Enhancement of the science of mass spectrometry by exploitation of computer technology either through electronic data acquisition, data processing, artificial intelligence or other technologies.

Environmental Applications, *Michelle V. Buchanan*
The development and application of mass spectrometry and related techniques to the qualitative and quantitative analysis of chemicals in environmental systems.

Fundamentals, *Keith R. Jennings*
The chemistry of gas phase ions including structural, spectroscopic, thermodynamic and kinetic properties and their influence on other areas of mass spectrometry.

History of Mass Spectrometry, *Robert W. Kiser*

Instrumentation and Ion Physics, *Scott A. McLuckey*
Techniques for forming, transporting, analyzing, and detecting charged particles with the goal of improving mass spectrometry as a research tool.

Isotope Ratio Measurements, *Philip H. Hemberger*
The application and development of isotope ratio mass spectrometry in all areas of science, including but not limited to archeology, atmospheric science, geology, medicinal chemistry, and nuclear science.

Physical Organic Mass Spectrometry, *John L. Holmes*
The physiochemical processes taking place among organic ions in the gas phase.

Pharmacology, *James Vrbanac*
The structural and quantitative analysis of drugs and their metabolites, and of endogenous bioactive compounds and their metabolites.

Solids, Surface Analysis and Inorganic Materials, *Peter J. Todd*
The application of mass spectrometry to the study of solid-state materials and processes, including the determination of the elemental and chemical composition and structure of bulk solids or solid surfaces and the characterization of atomic and molecular adsorbates.

Young Mass Spectrometrists, *Mark M. Ross*
The support and advancement of mass spectrometrists in the early stages of their careers.

Presented at the 36th ASMS Conference on Mass Spectrometry and Allied Topics
June 5-10, 1988, San Francisco, CA

Symposium: Elemental and Isotopic Analysis by Mass Spectrometry.

ELEMENTAL AND ISOTOPIC ANALYSIS BY SECONDARY ION MASS SPECTROMETRY 1
*MAGEE, C W

NONRESONANT MULTIPHOTON IONIZATION FOR SENSITIVE ELEMENTAL ANALYSIS 3
*BECKER, C H AND PALLIX, J B

SOLIDS ELEMENTAL ANALYSIS BY GLOW DISCHARGE MASS SPECTROMETRY 5
*HARRISON, W W

THE DEVELOPMENT OF HIGH PRECISION MASS SPECTROMETRY 7
*BARNES, I L

ADVANCES IN THERMAL IONIZATION MASS SPECTROMETRY 9
*PAPANASTASSIOU, D A

Ion Molecule Reactions. Chemical and Atmospheric Ionization.

LIGAND SUBSTITUTION REACTION OF 17 ELECTRON METAL CARBONYL RADICAL ANIONS IN GAS PHASE 11
*PAN, Y AND RIDGE, D P

A FTMS STUDY OF METAL-CATALYZED OLIGOMER FORMATION IN THE GAS PHASE 13
*BJARNASON, A AND TAYLOR, J W

EXPERIMENTAL EVIDENCE FOR THE FORMATION OF H*3 BY H+5/e DISSOCIATIVE RECOMBINATION 15
MIDERSKI, C A AND *GELLENE, G I

KINETIC ENERGY RELEASE DISTRIBUTIONS IN THE DISSOCIATION OF ION-DIPOLE COMPLEXES 17
*BASS, L M,ROEHL, C AND BOWERS, M T

A MASS SPECTROMETRIC AND AB INITIO CALCULATION STUDY OF THE POTENTIAL ENERGY SURFACE FOR REACTIONS OF CARBENE-LIKE CATIONS 19
*FISHER, J J AND MCMAHON, T B

AN INVESTIGATION OF THE GAS PHASE BASE CATALYZED ALDOL REACTION: COLLISION INDUCED DISSOCIATION OF -HYDROXY-CARBONYL NEGATIVE IONS 21
*HAYES, R N,GRESE, R P AND GROSS, M L

GAS-PHASE ELECTROPHILIC SUBSTITUTION REACTIONS OF ORGANOSILANES 23
HAJDASZ, D J AND *SQUIRES, R R

TEMPERATURE DEPENDENCE OF API SENSITIVITY 25
IKONOMOU, M,KEBARLE, P AND *SUNNER, J

ON THE REACTIVITY OF NO+ TO LOCATE CC DOUBLE BONDS IN ALIPHATIC COMPOUNDS USING A QUADRUPOLE TRIPLE ANALYZER INSTRUMENT 27
*EINHORN, J,ROLONDO, C AND MALOSSE, C

Environmental Mass Spectrometry

QUANTITATIVE DETERMINATION OF SELECTED COMPOUNDS IN CIGARETTE MAINSTREAM SMOKE USING MULTI-DIMENSIONAL GAS CHROMATOGRAPHY AND SELECTED-ION-MONITORING MASS SPECTROMETRY 29
*WHITE, E L,UHRIG, M S,GORDON, B M,NANNI, E J,BORGERDING, M F AND HICKS, R D

ANALYSIS OF ETHYL DIMETHYLPHOSPHORAMIDOCYANIDATE (TABUN) BY CAPILLARY COLUMN GAS CHROMATOGRAPHY-MASS SPECTROMETRY 30
*D'AGOSTINO, P A,PROVOST, L R AND LOOYE, K M

HPLC/MS AND HPLC/MS/MS ANALYSIS OF WASTE SAMPLES FOR ORGANOPHOSPHOROUS PESTICIDES 32
*BETOWSKI, L D AND JONES, T L

ON-COLUMN GC/MS OF NON-IONIC DYES 34
*ROSEN, R T,ROVIN, L H,HARTMAN, T G,OXENFORD, J,HO, C T AND ROSEN, J D

THE APPLICATION OF A HIGH RESOLUTION MASS SPECTROMETRIC METHOD FOR MEASURING 2,3,7,8-TCDD IN HUMAN ADIPOSE TISSUE AND SERUM 36
*PATTERSON, D G,ALEXANDER, L R,TURNER, W E,NEEDHAM, L L,ANDREWS, J S, PIRKLE, J L AND SAMPSON, E J

DETECTION OF POLYCHLORINATED TERPHENYLS BY GAS CHROMATOGRAPHY-MASS SPECTROMETRY WITH NEGATIVE CHEMICAL IONIZATION 38
*GREAVES, J AND HALE, R

LASER DESORPTION MASS SPECTROMETRY OF HIGH MOLECULAR WEIGHT PAH FROM HYDROCARBON SOOTS 39
*SO, H Y AND WILKINS, C L

CAD ANALYSIS OF METHYL PAH: FUSED-RING TROPYLIUM ION FORMATION AND FRAGMENTATION 41
*STANDLEY, L J AND HITES, R A

THE ANALYSIS OF ORGANIC COMPOUNDS IN DRINKING WATERS BY MASS SPECTROMETRY: SOME REMAINING PROBLEMS 43
*JAMES, H A,GIBSON, T M AND HAMMOND, I

VOLATILE ORGANIC ANALYZER FOR SPACECRAFT AIR QUIALITY MONITORING 45
*GALEN, T J AND PIERSON, D L

TRACE ANALYSIS FOR ORGANICS IN AIR USING AN ATMOSPHERIC SAMPLING GLOW DISCHARGE IONIZATION SOURCE 47
GRANT, B C,*ASANO, K G,GLISH, G L AND MCLUCKEY, S A

Cluster Ions. Ion Activation. Biomedical Mass Spectrometry

MIXED CLUSTER ION FORMATION BETWEEN SMALL MOLECULES AND H2SO4 49
*SHARP, T R

LARGE CARBON CLUSTER FORMATION BY LASER ABLATION OF POLYIMIDE 51
*CREASY, W R AND BRENNA, J T

LITHIUM AND SODIUM CLUSTERS EMITTED FROM LIQUID METAL ION SOURCE 53
SAITO, Y,MINAMI, K,ISHIDA, T,INOUE, M,NISHIGAKI, S AND *NODA, T

FORMATION, FRAGMENTATION, AND REACTIONS OF TRANSITION-METAL/OXYGEN CLUSTERS 55
*YU, W AND FREAS, R B

HCN REACTIONS REVEAL NEW CARBON CLUSTER ION ISOMERS 57
*PARENT, D C AND MCELVANY, S W

A STUDY OF THE MASS SPECTRA OF COBALT(II) SALTS OF ORGANIC ACIDS 59
SUN, Z L,DONG, Z W,LIN, C H AND *CAO, Z M

SIGNIFICANCE OF CLUSTER IONS IN THE GENERATION OF FAST ATOM BOMBARDMENT MASS SPECTRA 61
*PERREAULT, H AND BERTRAND, M J

MEASUREMENTS OF ION DISSOCIATION IN A REFLECTING TIME-OF-FLIGHT MASS SPECTROMETER 63
*MAYER, F,ENS, W,SCHUELER, B,STANDING, K G,TANG, X AND WESTMORE, J B

TANDEM MASS SPECTROMETRIC ANALYSIS OF THE FIRST PERFLUORINATED CRYPTAND: 4,7,13,21, 24-HEXAOXA-1,10-BIAZABICYCLO[8.8.8]HEXACOSANE 65
*MALEKNIA, S,CLARK, W D AND LAGOW, R J

REACTIVE AND DISSOCIATIVE COLLISIONS AT A METAL SURFACE IN A TANDEM TIME-OF-FLIGHT INSTRUMENT 67
*SCHEY, K L,COOKS, R G,KRAFT, A,GRIX, R AND WOLLNIK, H

FRAGMENTATION OF THE [M-H]- IONS OF SOME SULFOXIDES AND SULFONES 69
*CHOWDHURY, S AND HARRISON, A G

ISOMER IDENTIFICATION BY METASTABLE DECAY RATES OF LASER PRODUCED IONS 71
*KINSEL, G R AND JOHNSTON, M V

A NEW METHOD OF SURFACE INDUCED DISSOCIATION FOR MASS SPECTROMETRY 73
*ABERTH, W

APPEARANCE POTENTIAL MEASURMEMENTS ON SULFURIC ACID VAPOR 75
SNOW, K B AND *THOMAS, T F

CID OF ISOTOPICALLY LABELLED SURFACTANTS 77
*TUINMAN, A AND COOK, K

ION KINETICS IN THE ACCELERATION REGION 79
*MARCH, R E,HUGHES, R J,KOYANAGI, G K AND MCMAHON, A W

DYNAMICS OF COLLISION-INDUCED DISSOCIATION OF ACETONE IONS 81
*SHUKLA, A,SOHLBERG, K AND FUTRELL, J H

ENERGY UPTAKE IN COLLISIONAL ACTIVATION 83
*GIBLIN, D E AND GROSS, M L

PHOTODISSOCIATION OF 2-METHYL-1-PENTEN-3-YNE 85
*FAULK, J AND DUNBAR, R C

CHOPPED-LASER TWO-PHOTON PHOTODISSOCIATION MEASUREMENT OF COLLISIONAL RELAXATION IN EXCITED BENZENE IONS 87
*AHMED, M S AND DUNBAR, R C

INTERNAL ENERGY DISTRIBUTIONS DETERMINED FOR COLLISIONALLY SCATTERED Fe(CO)5 IONS USING ANGLE RESOLVED TECHNIQUES 89
*HORNING, S R,VINCENTI, M AND COOKS, R G

LASER INDUCED PHOTODISSOCIATION OF C5H5+ IONS DERIVED FROM DIFFERENT NEUTRALS 91
*MOINI, M,OZTURK, F AND EYLER, J R

HIGH RESOLUTION LASER-ION BEAM PHOTODISSOCIATION STUDIES OF THE CLUSTER FRAGMENTS OF IRON CARBONYLS 93
*TECKLENBURG, R E AND RUSSELL, D H

STUDIES OF THE ACTIVATION AND DISSOCIATION OF DANSYL AND DINITROPHENYL DERIVATIZED PEPTIDES 95
*TECKLENBURG, R E AND RUSSELL, D H

LASER-ION BEAM PHOTODISSOCIATION UTILIZING A BIASED ACTIVATION CELL 97
SELLERS-HANN, L,*TECKLENBURG, R E AND RUSSELL, D H

COLLISION-INDUCED DISSOCIATION REACTIONS OF DOUBLY-CHARGED MOLECULAR IONS OF POLYCYCLIC AROMATIC HYDROCARBONS 99
*BOYD, R K,JAMIESON, W D AND SIM, P G

THE DISSOCIATION DYNAMICS OF ION-DIPOLE COMPLEXES: HCL LOSS FROM ETHYL CHLORIDE 101
*MORROW, J C,BAER, T AND SHAO, J D

SOLID FAB MS AND FAB MS/MS FOR THE GENERATION AND STUDY OF SOME UNUSUAL SPECIES 103
*CALDWELL, K,DAVOLI, E AND GROSS, M L

A GEOMETRIC MODEL FOR SIMULATING THE SHAPES OF ION KINETIC ENERGY RELEASE SIGNALS 105
*KOYANAGI, G K AND MARCH, R E

DIRECTIONAL PROPERTIES IN PHOTODISSOCIATION STUDIED IN A LASER-TOF-MS SYSTEM 107
*MARCUS, P,PLATZNER, I,BAR, I AND ROSENWAKS, S

REACTION-INDUCED MASS DISCRIMINATION IN XQQ INSTRUMENTS: ABSOLUTE CROSS SECTIONS FOR N+2* + SF6 -- N2 + SF+X (X=1-5) 109
*MARTINEZ, R I AND GANGULI, B

A COMPARISON OF DAUGHTER ION SPECTRA OBTAINED USING HYBRID AND 4-SECTOR TANDEM MASS SPECTROMETERS 111
*GASKELL, S J,REILLY, M H,CARR, S A,ROBERTS, G D AND VICKERS, R

THE EFFECT OF CHEMICAL IONIZATION ON COLLISION INDUCED FRAGMENTATION IN THE THERMOSPRAY SOURCE 113
*BENCSATH, F A

THE MS/MS OF DOUBLY CHARGED IONS 115
BARBER, M,*BELL, D J,MORRIS, M,TETLER, L W,WOODS, M,MONAGHAN, J J AND MORDEN, W E

COLLISIONAL ACTIVATION SPECTRA OF BISBENZYLISOQUINOLINE ALKALOIDS 117
MADHUSUDANAN, K P,*DAS, P R AND PRAMANIK, B N

FAB-MS-MS OF PEPTIDES: UNAMBIGUOUS RECOGNITION OF SEQUENCE PEAKS IN THE CAD SPECTRA 119
*DAS, B C,DE MAACK, F AND DEVANT, G

INFLUENCE OF REAGENT GAS PROTON AFFINITY ON COLLISIONALLY-ACTIVATED *DECOMPOSITIONS OF ISOMERIC PROTONATED MORPHINANES* 121
*CHARLES, B,COLE, R,BRUNETON, J AND TABET, J C

INFLUENCE OF CATIONIZING ALKALI METALS ON THE STABILITY OF FAB DESORBED PYRIMIDINE DERIVATIVES 123
COLE, R B,*TABET, J C AND BLAIS, J C

IMFRARED MULITPHOTON DISSOCIATION OF SMALL PEPTIDES FORMED BY LASER DESORPTION 125
*WATSON, C H AND EYLER, J R

COLLISIONALLY-ACTIVATED DISSOCIATION (CAD) STUDIES IN THE OPTIMIZATION OF MS/MS FOR THE TRACE DETERMINATION OF PROSTAGLANDINS 127
*GILLESPIE, T A AND YOST, R A

FRAGMENTATION AND SEQUENCING OF PEPTIDES INVESTIGATED BY MULTIPHOTON IONIZATION MASS SPECTROMETRY 129
*GROTEMEYER, J,BEAVIS, R C,LINDNER, J AND SCHLAG, E W

MS-MS IN A FOUR-SECTOR MASS SPECTROMETER: PARAMETERS AFFECTING THE MS-II LINKED SCAN 131
*TOMER, K B AND VERMA, S

COMPARISON OF THE COLLISIONAL ACTIVATION DECOMPOSITION SPECTRA OF PEPTIDES CONTAINING BACKBONE MODIFICATIONS 133
*DETERDING, L J,TOMER, K B AND SPATOLA, A F

COLLISIONAL ACTIVATION TANDEM MASS SPECTROMETRY OF LITHIUM-CATIONIZED PEPTIDES 135
*GRESE, R P AND GROSS, M L

TANDEM MASS SPECTROMETRIC ANALYSES OF PEPTIDES USING HIGH AND LOW COLLISION ENERGIES ON A HYBRID INSTRUMENT 137
*REILLY, M H AND GASKELL, S J

FAB MASS SPECTRA AND CAD SPECTRA OF GLYCEROL AND AMINO ACIDS WITH SEVERAL METAL CHLORIDES 139
*ISA, K AND TERAI, Y

TANDEM MASS SPECTROMETRY INVESTIGATIONS ON LICHEN'S METABOLITES 141
*TSOUPRAS, G,ALLEMAND, P AND TABACCHI, R

FABMS AND FAB MS/MS INVESTIGATIONS OF TECHNETIUM AND RHENIUM COMPLEXES 143
*COSTELLO, C E,ZENG, C-H,DEVRIES, N H,O'CONNELL, L A,PEARLSTEIN, R M, DAVISON, A AND JONES, A G

TANDEM MASS SPECTROMETRY OF NUCLEIC ACID HYDROLYSATES 145
*NELSON, C C AND MCCLOSKEY, J A

THE EFFECT OF TARGET GAS TYPE AND PRESSURE ON DAUGHTER ION SPECTRA OF PEPTIDES USING A TANDEM DOUBLE-FOCUSING MASS SPECTROMETER 147
*CURTIS, J M,RONG, L S,MILBERG, R M AND RINEHART, K L

EI AND COLLISIONAL ACTIVATION MASS SPECTROMETRY OF BHT AND CERTAIN ALTERATION PRODUCTS 149
*BRUMLEY, W C

APPLICATIONS OF CONTINUOUS FLOW FAB MASS SPECTROMETRY FOR THE STUDY OF DRUG METABOLISM 151
*SCHROEDER, E,SCHUBERT, R AND JACOBS, P

ACCUMULATION OF FURANCARBOXYLIC ACIDS AND INDOXYL SULFATE IN UREMIC SERUM AS INHIBITORS OF DRUG-BINDING 153
*NIWA, T,TAKEDA, N,YOSHIZUMI, H AND TATEMATSU, A

EFFECT OF EXTENDED USE OF SINGLE ANABOLIC STEROIDS ON URINARY STEROID EXCRETION AND METABOLISM 155
HARRISON, L M,MARTIN, D,GOTLIN, R W AND *FENNESSEY, P V

NEGATIVE ION ISOTOPE DILUTION GC/MS ASSAY FOR PUTRESCINE IN BIOLOGIGAL FLUIDS 157
*NORWOOD, D L AND MILLINGTON, D S

STUDY ON MASS SPECTRA OF NEW SESQUITERPENE 159
*PU, Q-L,LINXING, H AND ZHANG, J

INVESTIGATION OF NONCOVALENT INTERACTIONS BY FAB-MASS SPECTROMETRY 161
*MICHAUD, D P,BRENNAN, T F AND VOUROS, P

REACTION MASS SPECTROMETRY - AN APPROACH TO STEREOCHEMICAL ANALYSIS OF ORGANIC COMPOUNDS 163
*CHEN, Y-Z,LI, H,YANG, H-J AND HUA, S

REACTION OF CYANIDE AND FORMALDEHYDE WITH NEUROTRANSMITTER AMINES: FORMATION OF NEW COMPOUNDS FROM CIGARETTE SMOKE 165
*DURDEN, D A,DAVIS, B A,YU, P H AND BOULTON, A A

A MICROMETHOD FOR THE DERIVATIZATION OF ORGANIC COMPOUNDS USING REAGENT VAPOR 167
*VATH, J E AND BIEMANN, K

INVESTIGATION OF THE TEMPERATURE DEPENDENCE IN THE MASS SPECTRUM OF HYDROXAMIC ACIDS 169
*STRINGHAM, K R AND WOOD, K V

SYNTHESIS AND ANALYTIC UTILITY OF DEUTERIUM LABELED 3-NITROBENZYLALCOHOL 171
REDDY, A M,SCHRAM, K H AND *MYKYTYN, V

IDENTIFICATION OF THE SEX ATTRACTANT PHEROMONE IN THE RED-SIDED GARTER SNAKE BY GC/MS AND GC/MS/MS OR "CAN A SEX-STARVED CANADIAN GARTER SNAKE FIND HAPPINESS WITH A PAPER TOWEL IN AUSTIN, TEXAS" 173
*CHINN, J W,HOLLY, E,MASON, R T AND CREWS, D

APPLICATION OF GC/MS IN MONITORING THE ISOLATION AND PURIFICATION OF AN IMMUNO-REACTIVE PATHOGENIC FUNGAL PRODUCT 175
*CHINN, J W,KRUSE, D AND COLE, G T

MASS SPECTROMETRY AS A TOOL FOR THE STUDY OF CHEMICAL REACTIVITY OF PAH RADICAL CATIONS WITH CELLULAR NUCLEOPHILES 177
*DAVOLI, E,CERNY, R L,CHIARELLI, M P AND GROSS, M L

LSIMS INVESTIGATION OF MAGNETIC RESONANCE IMAGING (MRI) CONTRAST AGENTS: [Gd-EDTA]-, [Gd-CDTA]-, [Gd-HEDTA]-, AND [Gd-DTPA]2- 179
*GRANT, J L,WHITE, D L,BRASCH, R C,BETHEL, P W AND BURLINGAME, A L

LIQUID-IONIZATION MASS SPECTROMETRY OF BIOORGANIC COMPOUNDS ABIOTICALLY SYNTHESIZED FROM SIMULATED PRIMITIVE EARTH ATMOSPHERES 181
*KOBAYASHI, K,KANEKO, T AND TSUCHIYA, M

SURFACE-ACTIVE REAGENTS FOR INCREASED SPUTTERED ION YIELDS IN BIOMOLECULAR ANALYSIS 183
*BROWN, S M AND BUSCH, K L

RAPID ANALYSIS OF BIOMOLECULES USING LASER VAPORIZATION, MULTIPHOTON IONISATION AND TIME-OF-FLIGHT MASS DETECTION 185
*FREY, R,HOLLE, A,KAMINSKI, H,WEISS, G,FRANZEN, J AND KOCH, D

DETECTION OF TETRAHYDROISOQUINOLINE IN PARKINSONIAN AND NORMAL HUMAN BRAINS AS AN ENDOGENOUS AMINE BY USE OF GC/MS 187
*NIWA, T,TAKEDA, N,SASAOKA, T,KANEDA, N,HASHIZUME, Y,TATEMATSU, A AND NAGATSU, T

FAST ATOM BOMBARDMENT OF PYOCHELIN COMPLEXES OF IRON AND ZINC: BEHAVIOR OF FE(III) IN FAB MS 189
*BEIER, R C AND STIPANOVIC, R D

APPLICATION OF MS/MS TO THE ANALYSIS OF BIOLOGICAL MIXTURES 191
BARBER, M,BELL, D J,MORRIS, M,*TETLER, L W,WOODS, M,BYCROFT, B W, MONAGHAN, J J,MORDEN, W E AND GREEN, B N

CONSTANT NEUTRAL LOSS SPECTRA OF PEPTIDES 193
*DEPAUW, E,NASAR, K AND *FACCHETTI, S

MASS SPECTROMETRY AND HERBAL MEDICINE 195
*LIANG, X-T

SCANNING TLC/SIMS 196
*NAKAGAWA, Y AND IWATANI, K

Symposium: Mass Spectrometry and Complex Lipids.

FAST ATOM BOMBARDMENT MASS SPECTROMETRY OF GLYCOSPHINGOLIPIDS 198
*SWEELEY, C C,GAGE, D,BECKER, H AND LADISCH, S

IMMUNOAFFINITY PURIFICATION-GAS CHROMATOGRAPHY-MASS SPECTROMETRIC ANALYSIS OF PROSTAGLANDINS AND THROMBOXANES 200
*KNAPP, D R AND VRBANAC, J J

Isotopic and Elemental Analysis.

THE IMPORTANCE OF HIGH SENSITIVITY IN THE MEASUREMENT OF VERY LOW ABUNDANCE ISOTOPES USING THERMAL IONISATION MASS SPECTROMETRY 202
*TURNER, P J,CANTLE, J E AND BARRETT, P

ISOTOPE RATIO MEASUREMENTS BY TOTAL SAMPLE VOLATILIZATION AND SIGNAL INTEGRATION UTILIZING A MULTICOLLECTOR SYSTEM 204
*CALLIS, E L AND ABERNATHEY, R M

TOTAL EVAPORATION/INTEGRATION WITH MIXED MULTI-COLLECTION MODES: NEW EFFECTIVE APPROACHES FOR THERMAL IONIZATION MS 206
*WAGNER, G,TUTTAS, D,POESTHORST, D,ROMKOWSKI, M,FRANZINI, S AND KOCH, L

NEUTRON ACTIVATION AND MASS SPECTROMETRIC MEASUREMENT OF 129I 208
STREBIN, R S,BRAUER, F P,KAYE, J H,RAPIDS, M S AND *STOFFELS, J J

RESONANCE IONIZATION MASS SPECTROMETRY OF PROMETHIUM 210
*SMITH, D H,SHAW, R W AND YOUNG, J P

FOURIER TRANSFORM MASS SPECTROMETRY FOR ELEMENTAL ISOTOPE RATIO DETERMINATION AND QUANTITATIVE ANALYSIS 212
*BRENNA, J T AND CREASY, W R

STUDIES OF SPUTTERING IN GLOW DISCHARGE MASS SPECTROMETRY 214
*BARSHICK, C M AND HARRISON, W W

COLLISION-INDUCED DISSOCIATION OF MOLECULAR IONS IN GLOW DISCHARGE MASS SPECTROMETRY (CID-GDMS) 216
*KING, F L AND HARRISON, W W

ION ASSOCIATION BY TIME-OF-FLIGHT MASS SPECTROMETRY 218
*HUANG, L Q,CONZEMIUS, R J,JUNK, G A AND HOUK, R S

SUPERCONDUCTOR ANALYSIS BY GDMS 220
CLARK, J,*KIRBY, D J AND SANDERSON, N E

ENHANCEMENT OF SPARK SOURCE MASS SPECTROGRAPHIC DATA USING STATISTICAL CLUSTER ANALYSIS 222
WILSON, C R,*JACOBS, M L AND HUTCHINSON, R M

Symposium: Cluster Ion Mass Spectrometry.

MASS SPECTROMETRIC PROBES OF METAL CLUSTER DISTRIBUTIONS AND METASTABLE ION DECAY 224
PARKS, E K,LIU, K,COLE, S K AND *RILEY, S J

GUIDED ION BEAM STUDIES OF TRANSITION METAL CLUSTER ION CHEMISTRY 226
LOH, S K,LI, L,HALES, D H AND *ARMENTROUT, P B

STRUCTURE AND REACTIVITY OF CLUSTER IONS 228
*BARONAVSKI, A P

Environmental. Fuels and Geoscience. SIMS and Surface Analysis.

HRGC/HRMS ANALYSIS OF BROMINATED/CHLORINATED ANALOGS OF TCDD AND TCDF IN MUNICIPAL INCINERATOR FLY ASH 230
*TONG, H Y AND GROSS, M L

DEVELOPMENT AND APPLICATION OF A THREE-PHASE COUPLED CAPILLARY GC COLUMN FOR GC-MS ISOMER-SPECIFIC DETERMINATION OF BOTH 2,3,7,8-TCDD AND 2,3,7,8-TCDF IN ENVIRONMENTAL SAMPLES 232
*HARDEN, L A,TIERNAN, T O,SOLCH, J G AND GARRETT, J H

INVESTIGATION OF ANOMOLOUS DIOXIN SIGNALS IN DIOXIN ANALYSIS 234
*HILKER, D R,DING, W H,ALDOUS, K M AND CONNOR, S

METABOLISM OF 2,3,7,8-TCDD 236
*MCREYNOLDS, J H AND OLSON, J R

OPTIMIZATION OF MS/MS PARAMETERS FOR THE DETERMINATION OF CHLORINATED DIBENZO-P-DIOXINS AND DIBENZOFURANS IN ENVIRONMENTAL SAMPLES 238
SCHELLENBERG, D H,BOBBIE, B A,*REINER, E J AND TAGUCHI, V Y

ACCURATE MASS DETERMINATIONS OF POLYCHLORINATED DIBENZOTHIOPHENES IN SOIL FROM A CAPACITOR PLANT'S INCINERATION SITE 240
*PETERMAN, P H,LEBO, J A AND MAJOR, H J

A NEGATIVE CHEMICAL IONIZATION GC/MS METHOD FOR THE DETERMINATION OF CHLORINATED PARAFFINS IN ENVIRONMENTAL MATRICES 242
STEELE, D H,*SACK, T M,MOODY, L A,MURRAY, T M AND BREEN, J J

ANALYSIS OF NITRO PAH METABOLITES AND THEIR DNA ADDUCTS USING ELECTROPHORIC DERIVATIZATIONS, NCI-GC-MS AND FAB-MS 244
*ANNAN, R,BAKTHAVACHALAM, J,GIESE, R AND VOUROS, P

CHARACTERIZATION OF POLYCHLORINATED BIPHENYL PYROLYSIS MIXTURES 246
*ALLEY, C C,GROCE, D F AND PATTERSON, D G

ANALYSIS OF SELECTED HERBICIDES AND THEIR METABOLITES IN RIVER WATER SAMPLES BY CHEMICAL IONIZATION TANDEM MASS SPECTROMETRY 248
*ROSTAD, C E,PEREIRA, W E AND LEIKER, T J

CONFIRMATION OF FENVALERATE IN ENVIRONMENTAL SAMPLES BY NEGATIVE ION CHEMICAL IONIZATION MS/MS 250
*STAFFORD, C J AND SWINEFORD, D M

USE OF MASS SPECTROMETRY IN ENVIRONMENTAL HEALTH EMERGENCIES: LABORATORY INVESTIGATION OF A POISONING IN SIERRA LEONE 252
*HILL, R H,ALLEY, C A,ASHLEY, D L,CLINE, R E,HEAD, S L,NEEDHAM, L L AND ETZEL, R A

APPLICATION OF GC/MS/MS IN THE ANALYSIS OF NITROSAMINES IN FOOD AND FOOD RELATED PRODUCTS 254
*WEBER, D,SEN, N P AND LAU, B P-Y

DEVELOPMENT AND IMPLEMENTATION OF A GC/MS METHOD FOR SIMULTANEOUS DETERMINATION OF SOME FORTY BIOACCUMULATING COMPOUNDS IN FISH 256
*SOLCH, J G,GARRETT, J H,WAGEL, D J,HARDEN, L A,HANES, M,VANNESS, G F AND TIERNAN, T O

THERMAL DECOMPOSITION OF A SERIES OF 2-CHLOROETHYL ALKYL AND ARYL SULFIDES 258
*ROHRBAUGH, D K,YANG, Y-C AND WARD, J R

CHARACTERIZATION OF REACTION PRODUCTS OF CHLORINE DIOXIDE AND FATTY ACIDS OF WHEAT FLOUR USING MASS SPECTROMETRY 260
*HEIKES, D L

ANALYSIS OF AMBIENT AIR SAMPLES UTILIZING AN AIR TOXICS INTERFACE SYSTEM BY MEGABORE CAPILLARY GC/MS/DS 262
*PORCH, R L,BURSEY, J T,DAYTON, D P,MCALLISTER, R A,RICE, J AND WAGONER, D E

MODIFICATION OF A GC/MS SYSTEM TO INCREASE THE LINEARITY OF RESPONSE FOR COMPOUNDS ANALYZED BY EPA METHOD 625 264
*GRINDSTAFF, O G,SLAGLE, R E,VANCE, J C AND TERNES, T N

DETEMINATION OF ORGANIC COMPOUNDS IN DRINKING WATER USING LIQUID-SOLID EXTRACTION, CAPILLARY COLUMN GAS CHROMATOGRAPHY, AND HIGH SENSITIVITY FULL MASS RANGE MASS SPECTROMETRY 266
*BEHYMER, T D,EICHELBERGER, J W AND BUDDE, W L

ANALYSIS OF ORGANIC POLLUTANTS IN AIR AND WATER BY CAPILLARY COLUMN GC/MS 268
*QIAO, S-J,WU, R-M AND GE, N-C

ENVIRONMENTAL CHAMBER/MS TECHNIQUES FOR CONSUMER PRODUCT EMISSIONS 270
*BAYER, C W AND BLACK, M S

COMPARATIVE DISTRIBUTION OF HYDROCARBONS IN AIRBORNE PARTICLES COLLECTED BY SIZE FRACTIONATION 272
*INFANTE, R,CARRASQUILLO, A AND SANTIAGO, N

APPLICATION OF MULTIFUNCTIONAL DERIVATIVE TO THE DETERMINATION OF NITRO-PAH's IN ENVIRONMENTAL SAMPLES BY GAS CHROMATOGRAPHY/MASS SPECTROMETRY 274
*DEAN, T A,POOLE, C F AND AULD, J

A COMPARISON OF GAS, LIQUID AND SUPERCRITICAL FLUID CHROMATOGRAPHIES IN COMBINATION WITH MASS SPECTROMETRY FOR DETERMINATION OF POLYCYCLIC AROMATIC COMPOUNDS IN ENVIRONMENTAL SAMPLES 276
*JAMIESON, W D,ELSON, C M,QUILLIAM, M A AND SIM, P G

ELECTRON IMPACT MASS SPECTRA OF POLYCYCLIC AROMATIC HYDROCARBONS: A REFERENCE COLLECTION 278
*SHARP, T R,LEE, H,FERGUSON, A,MARSH, K N AND HARVEY, R G

DETERMINATION OF TRANSIENT BIODEGRADATION INTERMEDIATES OF LINEAR ALKYLBENZENESULFONATES (LAS) BY NCI/GC/MS 280
*TREHY, M L,GLEDHILL, W E AND ORTH, R G

THE EFFECT OF SURFACE ACTIVITY ON QUANTITATION OF LINEAR ALKYLBENZENE SULFONATES BY FAST ATOM BOMBARDMENT MASS SPECTROMETRY 282
WERNERY, J D,BRAIN, D K AND *PEAKE, D A

ANALYSIS OF SULFONATED AZO DYES USING FAB AND CONTINUOUS FLOW FAB/MS 284
*MILLER, D L AND PETERSON-WRIGHT, L J

COMPARISON OF DYNAMIC AND EQUILIBRIUM HEAD-SPACE SAMPLING OF EPA VOLATILE ORGANIC COMPOUNDS WITH ION TRAP DETECTION 286
*PATKIN, A J

SUMMARY OF RESULTS FROM THE GC/MS ANALYSIS OF A WASTE BIODEGRADATION STUDY 288
*HUGHES, B M,MCKENZIE, D E,BIANCHINI-AKBEG, M A,ADAMS, W J,SIMPSON, B J, LEE, J M AND KIMERLE, R A

US EPA NATIONAL DIOXIN STUDY: RESULTS AND CONCLUSIONS FROM PHASE I INTRODUCTION OF PHASE II 290
*KUEHL, D W,BUTTERWORTH, B C,BAHNICK, D AND HANSON, R L

ISOTOPE DILUTION MASS SPECTROMETRY IN THE ANALYSIS OF ENVIRONMENTAL SAMPLES. A COMPARISON OF EPA METHODS 1624/1625 AND 624/625 292
*SHEPHERD, M C,SCHRYNEMEECKERS, P J,HAYES, D A,MERTENS, S K AND SHORE, F L

GC/MS ANALYSIS OF BSTFA DERIVATIZED POLAR COMPONENTS OF DIESEL PARTICULATE MATTER (NBS SRM-1650) EXTRACT 294
*WENCLAWIAK, B,JENSEN, T E AND RICHERT, J F O

GC/MS ANALYSIS OF HYDROPHOBIC ORGANIC CONTAMINANTS IN CATFISH FROM THE MISSISSIPPI RIVER 296
*LEIKER, T J,PEREIRA, W E AND ROSTAD, C E

HYDROCARBONS OF EVOLUTIONARY SIGNIFICANCE IN HOT SPRING MICROBIAL MATS 298
*SHIEA, J,WARD, D M AND BRASSELL, S

STRUCTURAL ANALYSIS OF PORPHYRINS: ANALYSIS OF IN VITRO PREPARED PORPHYRINOGENS USING AN ION TRAP MASS SPECTROMETER 300
*VAN BERKEL, G J,GLISH, G L AND MCLUCKEY, S A

MECHANISM OF PORPHYRIN HYDROGENATION AND DECOMPOSITION IN A CHEMICAL IONIZATION SOURCE 302
*VAN BERKEL, G J,GLISH, G L AND MCLUCKEY, S A

ANALYSIS OF THE NICKEL AND VANADYL GEOPORPHYRINS FROM NEW ALBANY BITUMEN BY ELECTRON IONIZATION AND AMMONIA CHEMICAL IONIZATION TANDEM MASS SPECTROMETRY 304
*BEATO, B D,YOST, R A,QUIRKE, J M E,CONCHA, M A,FILBY, R H,MERCER, G E AND VAN BERKEL, G J

A CALCULATING METHOD OF PETROPORPHYRIN STRUCTURE ISOMERS COMPOSITION BY TANDEM MASS SPECTROMETRY 306
*XU, L

THE DETERMINATION OF FREE ALCOHOLS IN ZINC DIALKYL DITHIOPHOSPHATES BY MASS SPECTROMETRY/MASS SPECTROMETRY 308
*NERO, V P

MASS SPECTROMETRIC ANALYSIS OF SEDIMENTS FROM AGED JET FUELS 310
*STURM, G P,GRIGSBY, R D,GREEN, J B AND BRINKMAN, D W

THE CHARACTERIZATION OF FUNCTIONAL FLUIDS BY HIGH TEMPERATURE CAPILLARY GAS CHROMATOGRAPHY/MASS SPECTROMETRY 312
*WANG, T H

A MOLECULAR BEAM MASS SPECTROMETRIC INVESTIGATION OF THE COMBUSTION OF SINGLE COAL PARTICLES 314
*GREENE, F T,O'DONNELL, J E AND ROBAUGH, D

CHARACTERIZATION OF COKE MATERIALS FORMED ON ZEOLITE CATALYSTS: APPLICATIONS OF THERMAL CHROMATOGRAPHY-MASS SPECTROMETRY 316
RICHARDSON, B R,*SHARP, T R AND HAW, J F

DERIVATIZATION IN COMBINATION WITH LMS AND SIMS FOR ANALYSIS OF OXIDIZED COAL SURFACES 318
*JENSEN, N J,SHARKEY, A G,VISWANADHAM, S K,LINEMAN, D AND HERCULES, D M

PROCESSING OF HIGH RESOLUTION MASS SPECTRAL DATA RECORDED FROM THE PROBE MICRODISTILLATION OF COMPLEX MIXTURES 320
*GRIGSBY, R D

HYDROCARBON TYPE ANALYSIS BY NITRIC OXIDE CHEMICAL IONIZATION GC/MS 322
*PETERSEN, H A,DZIDIC, I AND HART, H V

MASS SPECTROMETRIC CHARACTERIZATION OF A POTENTIAL SHALE OIL-BASED CO-PROCESSING SOLVENT 324
*WOOD, K V,NARAYAN, R,STRINGHAM, K R AND HUANG, S L

HYDROCARBON TYPE ANALYSIS BY GC/MS 326
*HSU, C S,ACZEL, T,ASHE, T R AND FEDORA, J W

PETROCHEMICAL HYDROCARBON COMPOUND TYPES ANALYSIS BY QUARDUPOLE MASS SPECTROMETER 328
*ASHE, T R

ANALYSIS AND DEACTIVATION MONITORING OF CATALYST IN THE WILSONVILLE PROCESS BY LOW VOLTAGE PY/MS AND MULTIVARIATE ANALYSIS 329
*TAGHIZADEH, K,DAVIS, B H AND MEUZELAAR, H L C

STUDY OF NITROGEN CONTAINING COMPOUNDS IN FLUID CATALYTICALLY CRACKED OILS BY NH3 CHEMICAL IONIZATION GC/MS AND MS/MS TECHNIQUES 331
*DAVIS, D V,CARDIN, D B AND SCHERZER, J

APPLICATION OF GAS CHROMATOGRAPHY/MASS SPECTROMETRY TO THE STUDY OF BIOSOLUBILIZED COAL 333
*CAMPBELL, J A AND BEAN, R M

APPLICATION OF CHROMATOGRAPHY/SECONDARY ION MASS SPECTROMETRY TO FUELS-RELATED MATERIALS: ANALYSIS OF POLYNUCLEAR AROMATIC HYDROCARBONS AND BIOMARKERS 335
*DEAN, L K L,BUSCH, K L AND VAN BERKEL, G J

RADIAL VELOCITY DISTRIBUTIONS OF LARGE SECONDARY MOLECULAR IONS 337
*ENS, W,SUNDQVIST, B U R,HAKANSSON, P,HEDIN, A AND JONNSON, G

SPUTTERING FROM THE GLASSY STATE AND PRESERVATION OF SPATIAL RESOLUTION IN CHROMATOGRAPHY/SIMS 339
*DOHERTY, S J AND BUSCH, K L

DEVELOPMENT OF A CCD DETECTOR FOR SIMS IMAGING 341
*TURNER, L K,MANTUS, D S,LING, Y C AND MORRISON, G H

MOLECULAR COMPOSITIONAL MAPPING BY SECONDARY ION MASS SPECTROMETRY 343
*GILLEN, G AND SIMONS, D S

STATIC SIMS ANALYSIS OF NITROGEN CONTAINING HETEROCYCLIC AROMATIC COMPOUNDS 345
*MAHAFFY, P R,HARPOLD, D N AND NIEMANN, H B

APPLICATION OF A SIMS/TSQ SPECTROMETER FOR ORGANIC SURFACE ANALYSIS IN THE ELECTRONICS INDUSTRY 347
*BENTZ, B L AND GALE, P J

CHARACTERIZATION OF MULTILAYER THIN FILMS BY LASER-INDUCED THERMAL DESORPTION MASS SPECTROMETRY 349
*LAND, D P,TAI, T-L,LINDQUIST, J M,HEMMINGER, J C AND MCIVER, R T

SIMS ION IMAGING OF ORGANIC MOLECULES ON SURFACES 351
*ODOM, R W AND NIEMEYER, I

TIME-OF-FLIGHT MASS SPECTROMETRY: A NEW INSTRUMENT FOR SURFACE CHEMICAL ANALYSIS WITH SUB-MICRON SPATIAL RESOLUTION 353
WAUGH, A R,KINGHAM, D R,RICHARDSON, C H AND *WOLSTENHOLME, J

THE POSSIBLE RELATION OF SIMS ION YIELDS FROM Ni3Mn(100) TO SURFACE ORDERING 355
VINEBERG, K A AND *DAWSON, P H

INDUSTRIAL APPLICATIONS OF FOURIER TRANSFORM MASS SPECTROMETRY (FTMS) 357
BLEASE, T G,*SCRIVENS, J H AND WEIL, D

METHOD FOR AVOIDING INSTRUMENT RELATED ARTIFACTS IN TRIPLE QUADRUPOLE MASS SPECTRA - A STEP TOWARDS MS/MS CAD DATABASE 359
*KETKAR, S N AND FITE, W L

PULSED HIGH PRESSURE LIQUID INJECTION OF SMALL PEPTIDES INTO TIME OF FLIGHT MASS SPECTROMETRY 361
*LUBMAN, D M AND PANG, H M

PLENARY LECTURE: TIME-OF-FLIGHT MASS SPECTROMETRY: MEETING CHROMATOGRAPHY'S CHALLENGE 363
*ENKE, C G

Symposium: Mass Education.

MASS SPECTROMETRIC APPROACHES TO THE ANALYSIS OF BIOPOLYMERS 365
*MCEWEN, C N

Cluster Ions. Ion Activation.

SECONDARY MASS SPECTRA FROM IMPACTS OF ENERGETIC WATER CLUSTER IONS 367
*BEUHLER, R J AND FRIEDMAN, L

UNIMOLECULAR FRAGMENTATION OF LARGE ARGON ION CLUSTERS 369
*LETHBRIDGE, P G AND STACE, A J

CROSSED BEAM STUDY OF THE COLLISION INDUCED DISSOCIATION OF METHANE ION 371
HOWARD, S,QIAN, K,BIGGERSTAFF, J,SHUKLA, A AND *FUTRELL, J

SEQUENTIAL SOLVATION OF ATOMIC TRANSITION METAL IONS 373
MARINELLI, P J AND *SQUIRES, R R

ISOMER CHARACTERIZATION VIA NEUTRALIZATION-REIONIZATION MASS SPECTROMETRY (NRMS) 375
*WESDEMIOTIS, C,FENG, R,ZHANG, M-Y,MARCHETTI, M AND MCLAFFERTY, F W

ON THE INTERMEDIACY OF ION-MOLECULE COMPLEXES IN UNIMOLECULAR DECOMPOSITIONS OF POSITIVE IONS 377
*MORTON, T H

LOW ENERGY DECOMPOSITIONS OF SOME CLOSED-SHELL IONS: NEW INSIGHTS ON CHARGE-REMOTE FRAGMENTATIONS 379
*ADAMS, J AND GROSS, M L

REMOTE SITE FRAGMENTATION BY LOW-ENERGY COLLISIONAL ACTIVATION 381
*WYSOCKI, V H,ROSS, M M AND COOKS, R G

CHARACTERIZATION OF THE DISSOCIATION OF PROTONATED CYCLIC KETONES USING HIGH AND LOW ENERGY ACTIVATION 383
*BRODBELT-LUSTIG, J S AND COOKS, R G

Lipid Biochemistry.

ANALYSIS OF CERAMIDE & GLYCOLIPID DERIVATIVES BY HIGH PERFORMANCE TANDEM MASS SPECTROMETRY 385
*COSTELLO, C E,DOMON, B AND VATH, J E

FOLATE AND VITAMIN B6 BIOAVAILABILITY STUDIES WITH HUMAN SUBJECTS USING STABLE ISOTOPE LABELLING AND ELECTRON CAPTURE GCMS 387
*TOTH, J P,TRUMBO, P R AND GREGORY, J F

NEGATIVE ION FAB ANALYSIS OF FATTY ACIDS IN INSECT WAXES: CUTICULAR WAX OF THE HONEY BEE 389
*WARNER, C D,HAYES, R N AND GROSS, M L

DIRECT ANALYSIS OF BILE ACIDS USING CHROMATOGRAPHY/SECONDARY ION MASS SPECTROMETRY 391
*DUNPHY, J C AND BUSCH, K L

NEGATIVE ION CHEMICAL IONISATION-COLLISIONAL ACTIVATION OF FATTY ACIDS: IMPROVED SENSITIVITY AND STRUCTURAL INFORMATION 393
*HAYES, R N,CERNY, R L AND GROSS, M L

COMBINED LC-MS ANALYSIS OF NEUTRAL LIPIDS, GLYCOLIPIDS AND PHOSPHOLIPIDS IN TOTAL LIPID EXTRACTS 395
*EVANS, J E,EVANS, B A AND MCCLUER, R H

MASS SPECTROMETRICAL IDENTIFICATION OF TRIMETHYLSILYLATED AND N-METHYLATED STANOZOLOL AND IT'S METABOLITES 397
*SCHANZER, W,OPFERMANN, G AND DONIKE, M

TRIPLE QUADRUPOLE, FAB AND EXPERT SYSTEM FOR THE ANALYSIS OF ACYLCARNITINES 399
*HOFFMAN, E DE,LIBERT, R AND VANHOOF, F

GENERATION OF FATTY ACID METHYL ESTER PROFILES BY DIRECT CURIE-POINT PYROLYSIS GC/MS OF WHOLE CELL SAMPLES 401
*MEUZELAAR, H L C AND DWORZANSKI, J

CURIE-POINT DESORPTION, SHORT COLUMN GC/MS OF LARGE POLAR MOLECULES 403
*MCCLENNEN, W H,RICHARDS, J M AND MEUZELAAR, H L C

Peptides. Polymers. Nucleic Acids. Isotopic, Inorganic and Elemental.

INTEGRATION OF MICROSEQUENCING, MASS SPECTROMETRY, AND TANDEM MASS SPECTROMETRY FOR MAXIMUM EFFICIENCY IN PEPTIDE SEQUENCING 405
*STULTS, J T,HENZEL, W J AND CHAKEL, J A

STYRENE OXIDE ALKYLATION OF HUMAN SERUM ALBUMIN DETERMINED BY FAST ATOM BOMBARDMENT MASS SPECTROMETRY 407
*VAN BREEMEN, R B AND CREECH, J

FAST ATOM BOMBARDMENT MASS SPECTROMETRY STUDIES OF HUMAN RECOMBINANT GRANULOCYTE-MACROPHAGE COLONY-STIMULATING FACTOR 409
*PRAMANIK, B N,NAGABHUSHAN, T L,LABDON, J E,REICHERT, P AND TROTTA, P P

MAPPING OF COLICIN Ia BY HPLC AND MS/MS 411
*FALICK, A M,MEL, S,STROUD, R M AND BURLINGAME, A L

ULTRA-HIGH SENSITIVITY MEASUREMENT OF PEPTIDES AND PROTEINS WITH keV AND MeV ION BOMBARDMENT 413
*KATTA, V,GRACE, L I,CHAUDHARY, T AND CHAIT, B T

COVALENT AND NON-COVALENT BINDING 415
*CHEN, L,MURPHY, C,COTTER, R J,FRANKEL, A D,OSAWA, Y AND POHL, L R

SYNTHESIS OF A DEUTERATED ANALOG OF LEU-ENKEPHALIN FOR FAB QUANTITATIVE ANALYSIS 417
*BENFENATI, E,CHEN, S,FANELLI, R AND ICARDI, G

CHARACTERIZATION OF BIOTECHNOLOGY PRODUCTS - AMINO ACID ANALYSIS OF PEPTIDES BY LC/MS 419
CHEN, T M AND *COUTANT, J E

FAB MASS SPECTROMETRIC INVESTIGATION OF PROTEASE-MEDIATED HYDROLYSIS WITHIN THE DISULFIDE-LINKED CORE OF ATRIAL NATRIURETIC FACTOR 421
*ACKERMANN, B L,CHEN, T M,COUTANT, J E AND BERMAN, J M

CHARACTERIZATION OF GUINEA PIG PANCREATIC HORMONES BY MASS SPECTROMETRY 423
*ALAI, M,COTTER, R J,ANDREWS, P C AND STEINER, D F

STRUCTURAL FINGERPRINTING OF ASN-LINKED CARBOHYDRATES AT SPECIFIC ATTACHMENT SITES IN GLYCOPROTEINS BY MASS SPECTROMETRY 425
*CARR, S A,ROBERTS, G D,JUREWICZ, A AND FREDERICK, B

STRUCTURAL ANALYSIS OF INTERLEUKIN-1 AND INTERLEUKIN-1 BY MASS SPECTROMETRY 427
*ROBERTS, G D,CARR, S A,MEYERS, C A,JOHANSON, K O,MILES, L M AND GREEN, B N

COMPLEMENTARY APPROACHES TO COMPUTER-ASSISTED SEQUENCING OF PEPTIDES FROM FAB-MS AND MS/MS DATA 429
ALEXANDER, A J,ANDERSON, G,BOYD, R K,*THIBAULT, P AND BERTRAND, M

DIGIT PRINTING OF PROTEIN VARIANTS 431
*HAYASHI, A,WADA, Y,MATSUO, T,KATAKUSE, I AND MATSUDA, H

ANALYSIS OF PHENYLALANINE LIBERATED UPON HYDROLYSIS OF THERAPEUTIC PEPTIDES USING CAPILLARY COLUMN GAS CHROMATOGRAPHY/NEGATIVE CHEMICAL IONIZATION MASS SPECTROMETRY 433
*LIBERATO, D J,FUKUDA, E K AND GARLAND, W A

MORPHINANS IN MAMMALS 435
*FAULL, K R,FEISTNER, G J AND WEITZ, C J

CHARACTERIZATION OF SYNTHETIC ADHESIVE DECAPEPTIDES BY FAB-MS AND HPLC-MS 437
GABRIEL, M K,HINDENLANG, D M,*SEDGWICK, R D,SWERDLOFF, M D AND WILLIAMS, J I

STRUCTURAL CHARACTERIZATION OF TWO FORMS OF CELLULAR RETINOL BINDING PROTEIN TYPE II USING A COMBINATION OF FAB AND EI MASS SPECTROMETRY AND EDMAN CHEMISTRY 439
*SCHAEFER, W H,ONG, D E,KAKKAD, B AND BLAIR, I A

QUANTITATION OF HIGH MOLECULAR WEIGHT NEUROPEPTIDES BY THERMOSPRAY HPLC/MS 441
*VOYKSNER, R D,PACK, T AND WILLIAMS, F

PYROLYTIC AND THERMAL DESORPTION STUDIES OF SYNTHETIC POLYMERS 443
*TAYLER, P J,PRICE, D,MILNES, G J,SCRIVENS, J H AND BLEASE, T G

PD-MS AND FAB-MS IN THE SEARCH FOR NEUROPEPTIDES 445
*FEISTNER, G J,ROEPSTORFF, P,HORUP, P,FAULL, K F,EVANS, C J AND BAROFSKY, D

THERMOSPRAY MASS SPECTROMETRY OF METHIONINE ENKEPHALIN 447
*MARTIN, L L AND GREER, J F

IMPORTANT FACTORS IN THE FAB/MS ANALYSIS OF LARGER PEPTIDES 449
*PETERSON, G S,ELLIOTT, J,ROBERTS, W J,WILLIAMS, K AND MCMURRAY, W J

APPLICATIONS OF PLASMA DESORPTION MASS SPECTROMETRY 450
*LACEY, M P,KEOUGH, T,LUCAS, D S,GRANT, R A AND SULLIVAN, J F

THE STUDY OF ACETAMINOPHEN CONJUGATE FORMATION BY OXIDATIVE ELECTROCHEMISTRY AND THERMOSPRAY MASS SPECTROMETRY 452
*GETEK, T A AND KORFMACHER, W A

TRIPLE QUADRUPOLE MASS SPECTROMETRY WITH MIXED MODE SCANNING FOR THE RECOGNITION AND CHARACTERIZATION OF GLUTATHIONE CONJUGATES 454
*GOULD, V,HAROLDSEN, P AND GASKELL, S

THERMOSPRAY LC/MS DETECTION OF GLUTATHIONE- AND GLUTATHIONE-DERIVED CONJUGATES IN BILE AND URINE OF MICE TREATED WITH 3-HYDROXYACETANILIDE, A NONHEPATOXIC REGIOIOSOMER OF ACETAMINOPHEN 456
*RASHED, M S,MYERS, T G AND NELSON, S D

APPLICATIONS OF TANDEM MASS SPECTROMETRY TO THE CHARACTERIZATION OF DERIVATIZED GLUTATHIONE CONJUGATES 458
*PEARSON, P G,HOWALD, W N,THREADGILL, M D AND BAILLIE, T A

SCREENING FOR MERCAPTURATE CONJUGATES OF XENOBIOTIC SUBSTANCES IN URINE USING NEGATIVE IONIZATION AND NEUTRAL LOSS SCANNING 460
*JONES, A D,WINTER, C K,SEGALL, H J AND BUONARATI, M H

FD AND MS/MS STUDIES OF HIGH MASS POLYMERS 462
*MOORE, C AND BARTON, E C

ELECTRON IMPACT IONIZATION MASS SPECTRA OF POLYSTYRENE OLIGOMERS BY THERMABEAM LC/MS 464
*JONES, G G,MCCOY, R W,PAULS, R E AND WILLOUGHBY, R C

ASSESSMENT OF RESIDUAL VOLATILES IN PHENOLIC NOZZLE COMPOSITES OF THE SPACE SHUTTLE SOLID ROCKET BOOSTER 466
*MONCUR, J G,PINOLI, P C,KAWASAKI, E H,ELY, T L AND HOLST III, W P

MONITORING POLYESTER POLYMERIZATIONS BY K+IDS WITH MASS SPECTROMETRIC DETECTION 468
GRADY, M C AND *SIMONSICK, W J

OLIGOMER ANALYSIS BY POTASSIUM IONIZATION OF DESORBED SPECIES WITH MASS SPECTROMETRIC DETECTION 470
*SIMONSICK, W J AND VOLPE, T P

APPLICATION OF APCI MASS SPECTROMETRIC DETECTION TO PROBLEMS IN MASS TRANSFER 472
*HALLIDAY, J

QUANTITATIVE ANALYSIS OF REACTIVE DECOMPOSITION PRODUCTS USING THERMALLY LABILE SALTS 474
*MORELLI, J J,GRAYSON, M A AND WOLF, C J

LOW-TEMPERATURE THERMAL AGING OF POLY(PHENYLENE SULFIDE) [PPS] 476
*GRAYSON, M A,SMITH, E G AND ROBINSON, M J

FRAGMENTATION OF POLYSILOXANES UNDER ELECTRON IMPACT: DIFFERENCES FOR OLIGOMERIC SERIES 478
*GALE, P J AND BENTZ, B L

ORGANIC POLYMER ANALYSIS BY LASER IONIZATION MASS SPECTROMETRY (LIMS) 480
*RADICATI DI BROZOLO, F AND ODOM, R W

NEGATIVE ION FAB MASS SPECTROMETRY OF PROCYANIDIN OLIGOMERS 482
KARCHESY, J J,FOO, L Y,ARBOGAST, B AND *BAROFSKY, D F

CHARACTERIZATION OF EPOXY DERIVED OLIGOMERS BY FAST ATOM BOMBARDMENT MASS SPECTROMETRY 484
*KYRANOS, J N,VOUROS, P,HAGNAUER, G AND ZUKAS, W

METHYLATION STUDIES OF PROTEIN AND NUCLEIC ACIDS 486
*STILLWELL, W G,GAN, L-S,WISHNOK, J S,XU, H-X AND TANNENBAUM, S

TIME-OF-FLIGHT SECONDARY ION MASS SPECTROMETRY OF PROTECTED ISOMERIC TRINUCLEOTIDES 488
*LAFORTUNE, E,ENS, W,STANDING, K G,WESTMORE, J B,DAMHA, M J AND OGILVIE, K K

MASS SPECTROMETRIC AND CHROMATOGRAPHIC PROPERTIES OF RING-PENTAFLUORO-BENZYLATED NUCLEOBASES USED IN THE TRACE DETECTION OF ALKYL DNA ADDUCTS 490
*KRESBACH, G M,ANNAN, R S,SAHA, M G,GIESE, R W AND VOUROS, P

ISOLATION AND CHARACTERIZATION OF TWO NEW NUCLEOSIDES FROM HUMAN URINE 492
*CHHEDA, G B,TWOREK, H A,BHARGAVA, A K,ANTKOWIAK, J G,DUTTA, S P AND PATRZYC, H B

CHARACTERIZATION OF 2'-O-METHYLINOSINE AND OTHER 2'-O-METHYLNUCLEOSIDES IN HUMAN URINE BY GC-MS 494
*DUTTA, S P,TWOREK, H A,BHARGAVA, A K,PATRZYC, H B AND CHHEDA, G B

STRUCTURAL STUDIES OF DNA COVALENT ADDUCTS OF A BENZENE METABOLITE BY LIQUID SECONDARY ION MASS SPECTROMETRY AND HIGH RESOLUTION ELECTRON-IMPACT MASS SPECTROMETRY 496
*KAUR, S,PONGRACZ, K,BODELL, W AND BURLINGAME, A L

LOW NANOGRAM DETECTION OF NUCLEOTIDES USING FAB/LIQUID SIMS 498
*WENG, Q,HAMMARGREN, W M,SCHRAM, K H,BORYSKO, C,WOTRING, L AND TOWNSEND, L B

INVESTIGATION OF THE FRAGMENTATION PATTERNS OF THE TMS DERIVATIVES OF 2', 3', AND 5'-DEOXYNUCLEOSIDES 500
*REIMER, M,MCCLURE, T D AND SCHRAM, K H

ANALYSIS OF PRODUCTS FROM THE REACTION OF THE TRIETHYL LEAD CATION WITH A HEXANUCLEOTIDE 502
*LINSCHEID, M AND RUSTLER, E M

ANALYSIS OF 5-METHYL-DEOXYCYTIDINE IN DNA BY GCMS 504
*LINSCHEID, M AND RANDT, C

MAGNESIUM METABOLISM IN HUMANS: QUANTITATION OF STABLE ISOTOPES BY FABMS 506
*LIU, Y M,SMITH, D L,NEAL, P AND LEMONS, J

EQUILIBRATION OF CALCIUM ISOTOPIC TRACER IN INFANT FORMULA 508
*VIEIRA, N E AND YERGEY, A L

TRACE-METALS ANALYSIS BY GAS CHROMATOGRAPHY-MASS SPECTROMETRY EMPLOYING VOLATILE CHELATES 510
*AGGARWAL, S K,KINTER, M,HEROLD, D A,WILLS, M R AND SAVORY, J

COPPER ISOTOPE RATIO MEASUREMENT BY LOW TEMPERATURE THERMO-IONIZATION 512
*FUJII, Y,HOSOE, M AND OKAMOTO, M

MEASUREMENTS OF BORON ISOTOEPS BY NEGATIVE ION THERMAL IONISATION MASS SPECTROMETRY 514
*TURNER, P J,CANTLE, J E,BARRETT, P AND PALACZ, Z

QUANTITATIVE GAS ANALYSIS BY MASS SPECTROMETRY AT THE PART-PER-TRILLION LEVEL: THE HELIUM-3 CONTENT OF ATMOSPHERIC AIR 516
*DAVIDSON, T A AND EMERSON, D E

CORRECTION OF INTERFERENCES IN THE DETERMINATION OF OXYGEN-18 CONTENT IN ORGANIC MATERIALS 518
*AISSA, M AND HATCH, G E

SIMULTANEOUS DETECTION OF MULTIPLE ISOTOPES BY GATED PULSE COUNTING IN RESONANCE IONIZATION TIME-OF-FLIGHT MASS SPECTROMETRY 520
*GREEN, L W AND SOPCHYSHYN, F C

MODIFICATION OF JMS D-300 TO THE MASS SPECTROMETER FOR PRECISE ISOTOPIC ANALYSIS 522
TORIGOYE, N,NISHIMURA, H AND *SHIMA, M

SIMULTANEOUS DETERMINATION OF TRACE LEVELS OF GROUP IIIA AND VA HYDRIDES IN SILANE BY SIM GC/MS 524
*MCGUIRE, J M

CHARACTERIZATION OF NICKEL COMPLEXES BY FAST ATOM BOMBARDMENT MASS SPECTROMETRY 526
ROCZKO, A,*VISWANADHAM, S K,SHARKEY, A G AND HERCULES, D M

A STUDY OF FABMS OF 2-ETHYLHEXYL PHOSPHONIC ACID MONO-2-ETHYLYHEXYL ESTER AND ITS COPPER SALT 528
YUAN, M,*LIU, S,ZHU, Y AND LI, X

FAB-DESORPTION-MULTIPHOTON IONIZATION MASS SPECTROMETRY 530
LINDNER, J,BEAVIS, R C,*GROTEMEYER, J AND SCHLAG, E W

URANIUM CONCENTRATION IN FOSSILS 532
*OKANO, J AND UYEDA, C

EVALUATION OF FAST ATOM BOMBARDMENT MASS SPECTROMETRY FOR THE STUDY OF CEMENTITIOUS STABILIZED WASTES 534
*HEADLEY, J V,BROOKS, P W AND HANNAK, P

ANALYSIS OF AIR AND MOISTURE SENSITIVE ORGANOMETALLIC COMPOUNDS USING AN ARGON STREAMING INTRODUCTION SYSTEM 536
*MALLIS, L M,TING, C,HAMMER, M S AND MESSERLE, L

CHARACTERIZATION OF AIR-SENSITIVE METALLOPHOPHYRINS BY FABMS 538
*TOLUN, E AND LEARY, J A

DESIGN AND CHARACTERIZATION OF A RADIO FREQUENCY (RF) POWERED GLOW DISCHARGE SOURCE FOR SOLIDS MASS SPECTROMETRY 540
*MARCUS, R K,DUCKWORTH, D AND KOLAR, W

ATMOSPHERIC PRESSURE PLASMA MASS SPECTROMETRY - CONSIDER THE SOURCE 542
*SATZGER, R D

CARBON AND OXYGEN ISOTOPE GEOCHEMISTRY OF AMMONIA BECCARIL IN CHINA SEAS AND ITS GEOLOGICAL IMPLICATION 543
*ZHE, H,LUNG, W AND PING, K Y

MASS SPECTROMETRIC STUDIES OF AIR/MOISTURE SENSITIVE COMPOUNDS BY CF-FAB 545
BARBER, M,BELL, D J,*MORRIS, M,TETLER, L W,WOODS, M,GOTT, G A,MACRORY, P P AND MCAULIFFE, C A

ANALYSIS OF SYNTHETIC AND NATURAL POLYMERS USING PYROLYSIS SHORT COLUMN GC/MS 547
*RICHARDS, J M,MCCLENNEN, W H,BUNGER, J A AND MEUZELAAR, H L C

Symposium: Measurement of Peptides.

PEPTIDE ANALYSES USING CONTINUOUS FLOW FABMS 549
*CAPRIOLI, R M

PEPTIDE QUANTIFICATION BY MASS SPECTROMETRY 551
*DESIDERIO, D M,DASS, C AND KUSMIERZ, J

OLIGOPEPTIDE ANALYSIS BY FT-MS 553
*SHABANOWITZ, J,GRIFFIN, P R,ZHU, N Z,YATES, J R AND HUNT, D F

PROGRESS IN THE MASS SPECTROMETRIC ANALYSIS OF PEPTIDES AND PROTEINS AT THE PICOMOLE LEVEL 555
*GIBSON, B W

Reaction Mechanisms I.

THE MCLAFFERTY REARRANGEMENT IN THE UNIMOLECULAR DISSOCIATION OF FORMATE ESTERS 557
*ZHA, Q,HAYES, R N,NISHIMURA, T,GROSS, M L AND MEISELS, G G

THE INVOLVEMENT OF RING HYDROGENS IN THE REACTION C6H5NH2+ -- C5H6+ + HNC 559
*ZIMMERMAN, J A AND O'MALLEY, R M

THE APPLICATION OF BUTYL NITRITE CI AND LINKED SCANS TO THE STUDY OF ISOTOPE EFFECTS ON THE FRAGMENTATION OF DEPROTONATED ALCOHOLS 561
IBRAHIM, S,WILSON, J M AND *MOORE, C

THE EFFECT OF STRONG ANHARMONIC POTENTIAL ON UNIMOLECULAR DISSOCIATION DYNAMICS: THE ENERGY SELECTED N-BUTANOL AND I-BUTANOL IONS 563
*SHAO, J-D,BAER, T AND LEWIS, D K

STEREOCHEMICAL CONTROL OF CID REACTIONS OF PERACETYLATED HEXOSES AND AMINO-HEXOSES 565
*GUEVREMONT, R AND WRIGHT, J L C

GC/MS IDENTIFICATION OF THE MACROCYCLES 567
*DUBAY, G R,CHANG, V AND PORTER, N A

ELECTRON IONIZATION-INDUCED FRAGMENTATION OF , -UNSATURATED ESTERS: A STUDY OF THE META AND PARA DERIVATIVES OF ETHYL -FLUOROCINNAMATE 569
*DASS, C,ROBINSON, C N,PFLUG, J L AND DESIDERIO, D M

MECHANISM OF FRAGMENTATION OF DIQUATERNARY AMMONIUM SALTS BY FAST ATOM BOMBARDMENT 571
*CHENG, M T

BORATE IONS IN THE GAS PHASE. FAST-ATOM BOMBARDMENT OF CONDENSED-PHASE BORATES 573
*DOYLE, R J

Symposium: Environmental Fate of Organo-Chlorine Compounds in the Atmosphere.

CHLOROFLUOROCARBONS IN THE ENVIRONMENT: A REVIEW 575
*MOLINA, M J

ATMOSPHERIC TRANSPORT OF PESTICIDES BY FOG 577
*MAJEWSKI, M S,GLOTFELTY, D W AND SEIBER, J N

DIOXINS AND FURANS IN THE AMBIENT ATMOSPHERE: A BASELINE STUDY 579
*HITES, R A

DETERMINATION OF THE PHOTOINDUCED LOSS RATE OF LOW VAPOR PRESSURE ORGANOCHLORINE COMPOUNDS 582
*ORTH, R G

PEAK EXPOSURES AND DISSIPATION RATE MEASUREMENTS OF HALOGENATED VOLATILE ORGANIC COMPOUNDS IN INDOOR AIR 584
*PLEIL, J D,MCCLENNY, W A AND OLIVER, K D

Ion Traps and FT-ICR. Ion Molecule Reactions. Chemical and Atmospheric Ionization.

EXACT MASS ERRORS IN FOURIER TRANSFORM MASS SPECTROMETRY: EXPERIMENTAL EVIDENCE FOR INDIRECT COULOMBIC MECHANISMS 586
*YANG, S S AND REMPEL, D L

NEW AND IMPROVED MASS CALIBRATION LAW FOR FT/ICR MASS SPECTROMETRY 588
WANG, M AND *MARSHALL, A G

EXTENSION OF LOWER MASS LIMIT IN DIRECT-MODE FT/ICR MASS SPECTROMETRY BY MEANS OF ALTERNATED DELAY SAMPLING 590
*VERDUN, F R,RICCA, T L AND MARSHALL, A G

UPPER MASS AND ENERGY LIMITS IN FT/ICR MASS SPECTROMETRY: DESIGN AND TESTING OF NEW ION TRAPS 592
GROSSHANS, P B,WANG, M,RICCA, T L,LEDFORD, E B AND *MARSHALL, A G

HARTLEY TRANSFORM ION CYCLOTRON RESONANCE MASS SPECTROMETRY 594
WILLIAMS, C P AND *MARSHALL, A G

HIGH-RESOLUTION MULTIPLE ION SIMULTANEOUS MONITORING BY MEANS OF MULTIPLE FOLDOVER FT/ICR MASS SPECTROMETRY 596
WANG, M AND *MARSHALL, A G

RESOLUTION IMPROVEMENT IN FTMS BY HARMONIC DETECTION 598
*PAN, Y,RIDGE, D P AND ROCKWOOD, A L

IMPROVED MASS RESOLUTION IN FTICR BY DATA-FILLING 600
*WATSON, C H AND EYLER, J R

TWO DIMENSIONAL FTMS 602
RAPIN, J,WALSER, M-E AND *GAUMANN, T

AN ION TRAJECTORY MODEL FOR FOURIER TRANSFORM ION CYCLOTRON RESONANCE MASS SPECTROMETRY 604
*HEARN, B A,WATSON, C H,BAYKUT, G AND EYLER, J R

STUDIES OF ION MOTION IN AN ICR CELL BY DUAL CELL FTMS 606
*HONOVICH, J P AND MARKEY, S P

IMPROVEMENT OF THE ELECTRIC FIELD IN FT-ICR TRAPPED ION CELL 608
*NAITO, Y AND INOUE, M

HIGH PRESSURE ION SOURCE FOURIER TRANSFORM ION CYCLOTRON RESONANCE SPECTROMETRY 610
*KOFEL, P AND MCMAHON, T B

THE IMPLICATIONS OF ION INJECTION FROM AN EXTERNAL ION SOURCE ON THE DYNAMICS OF TRAPPING AND DETECTION IN FT-ICR 612
*HANSON, C D,KERLEY, E L AND RUSSELL, D H

FOURIER TRANSFORM ION CYCLOTRON RESONANCE MASS SPECTROMETRY OF METAL IONS GENERATED BY LASER DESORPTION IN AN EXTERNAL SOURCE 614
*WELLER, R R,GHADERI, S,VORBURGER, O AND FREISER, B S

FAST ATOM BOMBARDMENT COMBINED WITH FOURIER TRANSFORM MASS SPECTROMETRY 616
*GROSSMANN, P,CARAVATTI, P,ALLEMANN, M AND KELLERHALS, H P

HIGH RESOLUTION MULTIPURPOSE SOLID SAMPLE PROBE FOR FIELD DESORPTION ION CYCLOTRON RESONANCE SPECTROMETRY 618
PEZSA, I,KNOLL, H,*WANCZEK, K P AND LINDEN, H B

DIRECT DETERMINATION OF SURFACTANTS ON TEXTILES BY LASER DESORPTION FOURIER TRANSFORM MASS SPECTROMETRY 620
*CHIARELLI, M P,PEAKE, D A AND GROSS, M L

STRATEGY FOR SEQUENCING LINEAR OLIGOPEPTIDES USING LASER DESORPTION FOURIER-TRANSFORM MASS SPECTROMETRY AND COLLISION-ACTIVATED DISSOCIATION 622
*YANG, L C AND WILKINS, C L

STORED WAVEFORM INVERSE FOURIER TRANSFORM EXCITATION: ANALYTICAL APPLICATIONS FOR FOURIER TRANSFORM MASS SPECTROMETRY 624
*CODY, R B,GOODMAN, S D,HEIN, R E AND WEIL, D A

LASER MICROPROBE FOURIER TRANSFORM MASS SPECTROMETRY: INSTRUMENTATION AND APPLICATIONS 626
PELLETIER, M,KRIER, G,TOLLITTE, F,MULLER, J F,*WEIL, D AND JOHNSTON, M

THE APPLICATION OF NOVEL ION TRAP SCAN MODES FOR HIGH-SENSITIVITY GC/MS 628
*TUCKER, D B,HAMEISTER, C H,BRADSHAW, S C,HOEKMAN, D J AND WEBER-GRABAU, M

CHARACTERIZATION OF TANDEM MASS SPECTROMETRY IN THE QUADRUPOLE ION TRAP 630
*JOHNSON, J V AND YOST, R A

COMPUTER SIMULATION OF ION TRAJECTORIES IN A QUADRUPOLE ION TRAP MASS SPECTROMETER 632
*PEDDER, R E AND YOST, R A

QUANTITATIVE EVALUATION OF ION INJECTION INTO A QUADRUPOLE ION TRAP 634
*SCHWARTZ, J C,COOKS, R G,WEBER-GRABAU, M AND KELLEY, P E

COUPLING OF AN ATMOSPHERE SAMPLING ION SOURCE WITH AN ION TRAP MASS SPECTROMETER 636
*ASANO, K G,GLISH, G L AND MCLUCKEY, S A

NON-CHROMATOGRAPHIC APPLICATIONS OF ION TRAP MASS SPECTROMETRY 638
*HEMBERGER, P H AND SPALL, W D

ANALYSIS OF PORPHYRINS USING AN ION TRAP MASS SPECTROMETER 639
*VAN BERKEL, G J,GLISH, G L AND MCLUCKEY, S A

RAPID MICROORGANISM CHARACTERIZATION WITH PYROLYSIS, SHORT-COLUMN GC-ION TRAP MASS SPECTROMETRY 641
*SNYDER, A P,MCCLENNEN, W H AND MEUZELAAR, H L C

ANALYSIS OF FRAGRANCE MATERIALS USING AUTOMATIC GAIN CONTROL CHEMICAL IONIZATION ON THE ION TRAP DETECTOR 643
*KELLER, P R,HARVEY, G J AND FOLTZ, D J

TRACE ANALYSIS OF ORGANIC COMPOUNDS IN AQUEOUS SOLUTIONS USING A MEMBRANE PROBE AND AN ION TRAP DETECTOR 645
*LISTER, A K AND COOKS, R G

REMEASUREMENT AND DETECTION OF HIGH MASS IONS IN FOURIER TRANSFORM MASS SPECTROMETRY 647
*WILLIAMS, E R,WANG, B H,LOO, J A,HENRY, K D AND MCLAFFERTY, F W

CROSSED-BEAM STUDIES OF ENERGY TRANSFER IN LOW ENERGY ION-MOLECULE COLLISIONS 649
HOWARD, S,SHUKLA, A,BIRKINSHAW, K,WANG, J AND *FUTRELL, J

THE KINETIC ENERGY DEPENDENCES OF THE RATE CONSTANTS FOR THE REACTIONS OF O WITH CH4N2O, AND SO2 AT SEVERAL TEMPERATURES 651
*VIGGIANO, A A,MORRIS, R A,PAULSON, J F AND DALE, F

RATE CONSTANTS FOR ION-MOLECULE REACTIONS OF ATMOSPHERIC SULFUR COMPOUNDS 653
*THOMAS, T F,VIGGIANO, A A,DALE, F AND PAULSON, J F

USING THE METHOD OF EQUIVALENT CORES FOR ESTIMATING CATION HEATS OF FORMATION -- COMPARISON WITH AB INITIO RESULTS 655
*STAMS, D A,MORTON, T H,THOMAS, T D,MACLAREN, D C AND JI, D

THERMOCHEMISTRY AND GAS-PHASE ION/MOLECULE REACTIONS OF BOROHYDRIDE IONS 657
WORKMAN, D B AND *SQUIRES, R R

TEMPERATURE AND METHYL H3/D3 ISOTOPE EFFECTS ON THE ENTHALPY AND ENTROPY CHANGES OF METHYLATED ACETONE ONTO ACETONE AND DIMETHYL ETHER 659
*SZULEJKO, J E AND MCMAHON, T B

GAS-PHASE ACIDITIES FROM ENDOTHERMIC REACTIONS 661
*GRAUL, S AND SQUIRES, R R

-BOND STRENGTHS IN FLUORO-METHYL SILAETHYLENES 663
*ALLISON, C E AND MCMAHON, T B

STRUCTURAL FACTORS THAT EFFECT THE EXTENT OF DEUTERIUM EXCHANGE WHEN USING ND3 AS A CI REAGENT GAS 665
*KILLMER, L

THE BICYCLOBUTYL ANION: AN ALKYL CARBANION 667
CHOU, P AND *KASS, S

THE DETECTION OF NEUTRAL PRODUCTS OF CHEMICAL IONIZATION REACTIONS 669
*ALLGOOD, C AND MUNSON, B

THE REACTION OF THE BUTADIENE RADICAL CATION AND METHYL VINLY KETONE: A GAS PHASE ANALOGOUE OF A [4+2] CYCLOADDITION 671
*CASTLE, L W AND GROSS, M L

GAS PHASE ION CHEMISTRY OF BENZENE RADICAL CATION AND CYCLIC ETHERS 673
*WARNER, C D,HOLMAN, R W AND GROSS, M L

GAS PHASE SYNTHESIS OF DODECAHEDRENE AND DETERMINATION OF ITS DOUBLE BOND STRAIN ENERGY 675
*KIPLINGER, J P,MARSHALL, A G,KOBAYASHI, T AND PAQUETTE, L A

SITE OF PROTONATION OF FUNCTIONALIZED CARBONYL COMPOUNDS 677
*SHALER, T A AND MORTON, T H

FOURIER TRANSFORM MASS SPECTROMETRIC GENERATION AND STUDIES OF CARBOTHEOXY RADICAL ANION, EtOCOCH- 679
*CHOWDHURY, A K AND WILKINS, C L

ION/MOLEUCLE REACTIONS OF C5H3+ AND C7H7+ IN THE GAS PHASE 681
*OZTURK, F AND EYLER, J R

ION-MOLECULE REACTIONS OF ISOMERIC TERPENE DERIVATIVES UNDER POSITIVE AMMONIA CI: A STUDY OF STEREOCHEMICAL EFFECTS 683
*COLE, R B AND TABET, J C

ENERGY DEPOSITION VIA COLLISIONALLY INDUCED DISSOCIATION IN A HYBRID MASS SPECTROMETER 685
BLEASE, T G,*SCRIVENS, J H AND SCHRODER, E

A COMPARISON OF THEORETICAL AND EXPERIMENTAL RELATIVE SENSITIVITIES IN GAS CHROMATOGRAPHY/CHEMICAL IONIZATION MASS SPECTROMETRY 687
*ORLANDO, R AND MUNSON, B

ION MOLECULE REACTIONS OBSERVED FOR NITRO AROMATIC COMPOUNDS IN NEGATIVE ION FAST ATOM BOMBARDMENT MASS SPECTROMETRY 689
BALASANMUGAM, K,MILLER, J M AND *SMITH, R W

EFFECT OF COLLISION GAS PRESSURE AND ENERGY ON THE MASS SPECTRA OF SOME TRICHOTHECENES OBTAINED BY REACTIVE COLLISIONS WITH AMMONIA 691
*KOSTIAINEN, R

GOLD CHEMICAL IONIZATION MASS SPECTRA OF ALKANES AND ALKENES USING LASER DESORPTION FOURIER TRANSFORM MASS SPECTROMETRY 693
*CHOWDHURY, A K AND WILKINS, C L

METHYLENE CHLORIDE - A USEFUL REAGENT FOR POSITIVE ION CI/MS OF ALCOHOLS, ALDEHYDES AND KETONES 695
RAMJIT, H G AND *POWERS, R E

REACTIVITY AND COLLISIONAL DEEXCITATION OF ELECTRONICALLY EXCITED METAL IONS 697
*STROBEL, F AND RIDGE, D P

GAS-PHASE REACTIONS OF BIS(CYCLOPENTADIENYL)METHYL-ZIRCONIUM(1+) WITH UNSATURATED HYDROCARBONS 699
*CHRIST, JR, C S,EYLER, J R AND RICHARDSON, D E

AN FTMS STUDY OF THE GAS-PHASE CHEMISTRY OF THE METAL DIMER ScFe+ 701
*LECH, L M AND FREISER, B S

BIMOLECULAR REACTIONS OF DOUBLY CHARGED METAL IONS IN THE GAS PHASE 703
MACMAHON, T J,BUCKNER, S W,HUANG, Y AND *FREISER, B S

CLUSTERING REACTIONS AND THERMOCHEMISTRY OF LASER OBLATED METAL IONS 705
*BOUCHARD, F,HEPBURN, J W AND MCMAHON, T B

TRANSITION METAL CATION MEDIATED CARBON-CARBON BOND FORMATION IN A MULTIQUADRUPOLE MS/MS/MS INSTRUMENT 707
BEAUGRAND, C,MESTDAGH, H AND *ROLANDO, C

EXPERIMENTAL AND THEORETICAL INVESTIGATIONS INTO CHAINLENGTH EFFECTS IN THE CHEMISTRY OF TRANSITION METAL IONS WITH ORGANIC MOLECULES 709
*ALLISON, J,HANKINSON, D J,MILLER, C,HOOPER, E AND TSARBOPOULOS, A

THE GAS PHASE CHEMISTRY OF NICKEL AND NICKEL-CONTAINING IONS WITH AROMATIC COMPOUNDS 711
*STEPNOWSKI, R AND ALLISON, J

TIME-RESOLVED METASTABLE FRAGMENTATIONS OF METHYL ACETATE IONS 713
*ARAKAWA, R

USE OF A VG 70-4SE TANDEM 4-SECTOR SPECTROMETER IN STRUCTURAL STUDIES 715
*MILBERG, R M,CURTIS, J M,RONG, L S,RINEHART, K L,BATEMAN, R H,GREEN, B N AND LEE, G W T

AN EXPERIMENTAL INVESTIGATION OF FACTORS AFFECTING THE EFFICIENCY OF COLLISION-INDUCED DISSOCIATIONS OF PROTONATED PEPTIDE IONS 717
ALEXANDER, A J AND *THIBAULT, P

A NEW TOTALLY AUTOMATED HYBRID MS/MS SYSTEM 719
CLENCH, M R,OWEN, R,PARR, V C AND *WOOD, D

STRUCTURAL STUDIES OF OLIGOMERIC AND POLYMERIC AROMATIC SYSTEMS BY TANDEM MASS SPECTROMETRY 721
BLEASE, T G,*SCRIVENS, J H,MORDEN, W E AND MONAGHAN, J J

REMOTE CHARGE SITE DECOMPOSITIONS MODELED BY MOLECULAR ORBITAL CALCULATIONS 723
*SIEGEL, M M AND COLTHUP, N B

PLENARY LECTURE: MASS SPECTROMETRY AND STRUCTURAL BIOLOGY: AN EXCITING SYMBIOSIS 727
*BURLINGAME, A L

Symposium: Applications of Continuous-Flow FAB.

CONTINUOUS-FLOW FABMS - AN OVERVIEW 729
*CAPRIOLI, R M

QUANTITATION OF NEUROPEPTIDES BY HPLC/CONTINUOUS-FLOW FABMS 731
*JARDINE, I

CONTINUOUS FLOW FAST ATOM BOMBARDMENT MASS SPECTROMETRY OF PEPTIDE AND PEPTIDE DIGESTS 733
*JENNINGS, K R,HUTCHINSON, D W AND WOOLFITT, A R

ANALYSES OF PERMETHYL-OLIGOSACCHARIDES BY CONTINUOUS FLOW FAB MS AND BY COUPLING LC-MS WITH CONTINUOUS FLOW FAB AS INTERFACE 735
*FOURNET, B,LEROY, Y,RICART, G AND MONTREUIL, J

TANDEM MASS SPECTROMETRY OF BIOMOLECULES BY USING CONTINUOUS FLOW FAB 737
*CERNY, R L,HAYES, R N AND GROSS, M L

QUANTITATIVE ANALYSIS OF POLAR COMPOUNDS BY CONTINUOUS FLOW FAB 739
*MARKEY, S P,WANG, T C-L,SHIH, M,BONI, R,DUNCAN, M AND YANG, S-C

Reaction Mechanisms II.

AN RRKM EXPLORATION OF WHETHER THE MCLAFFERTY REARRANGEMENT OF IONIZED N-BUTANAL IS STEPWISE OR CONCERTED 741
*GRIFFIN, L L AND MCADOO, D J

COMPETING REACTIONS OF THE ACETONE CATION-RADICAL; RRKM-QET CALCULATIONS ON AN ab initio POTENTIAL ENERGY SURFACE 743
*LIFSHITZ, C,LOUAGE, F,HEINRICH, N AND SCHWARZ, H

THE UNIMOLECULAR DISSOCIATION MECHANISM OF METHYLNITRITE 745
ZHA, Q,HAYES, R N,GROSS, M L AND *MEISELS, G G

SELECTIVITY IN THE REACTIONS OF ANIONS WITH DIMETHYLDISULFIDE 747
*GRABOWSKI, J J AND ZHANG, L

ION-MOLECULE REACTIONS OF ETHYL VINYL ETHER WITH VARIOUS OXYGEN-CONTAINING CATIONS IN A TRIPLE QUADRUPOLE MASS SPECTROMETER AND A QUADRUPOLE ION TRAP 749
*KENTTAMAA, H I AND COOKS, R G

THE STRUCTURE OF IONIZED n-PROPANOL PRECEDING THE LOSS OF WATER 751
*ZHA, Q,NISHIMURA, T AND MEISELS, G G

MEDIUM RESOLUTION ATMOSPHERIC PRESSURE IONIZATION MASS SPECTROMETRY OF TOLUENE'S PHOTOOXIDATION PRODUCTS 753
*GRANGE, A H,O'BRIEN, R J AND BAROFSKY, D F

FAST ATOM BOMBARDMENT MASS SPECTROMETRY AS A PROBE FOR THE ANALYSIS OF SHORT LIVED REACTION INTERMEDIATES 755
*MALLIS, L M AND SCOTT, W J

CLUSTER IONS AS A PROBE FOR BIMOLECULAR SUBSTITUTION REACTIONS UNDER SIMS CONDITIONS -CHOLINES- 757
*OHASHI, M,IINO, T AND TANI, T

MASS SPECTROMETRIC MEASUREMENT OF ISOTOPIC OXYGEN ABUNDANCES OCCURRING WITHIN TRANSIENT PRODUCTS GENERATED FROM HOT 18O(3P) ATOM REACTIONS WITH FORMALDEHYDE 759
*FERRIERI, R A AND WOLF, A P

CALCULATED STRUCTURES FOR SMALL COPPER- AND SILVER-CONTAINING IONS: COMPARISON WITH RESULTS FROM MS/MS EXPERIMENTS 761
*FLURER, R A AND BUSCH, K L

Ionization Methods.

PLASMA DESORPTION MASS SPECTROMETRY OF SUCROSE POLYESTERS 763
KEOUGH, T,LACEY, M,*SANDERS, R AND GARDNER, D

COMPARISON OF FAST ATOM BOMBARDMENT MASS SPECTRA WITH CHEMICAL IONIZATION MASS SPECTRA USING GLYCEROL AS A REAGENT GAS 765
*DUFFIN, K L AND BUSCH, K L

GAS-PHASE ION-MOLECULE AND SURFACE-CATALYZED OXIDATION REACTIONS OF POLYCYCLIC AROMATIC HYDROCARBONS UNDER NEGATIVE ION CHEMICAL IONIZATION CONDITIONS 767
*BUCHANAN, M V AND STEMMLER, E A

ISOMERIC DIFFERENTIATION OF PAH, METHYL-PAH AND AMINO-PAH USING SURFACE-CATALYZED OXIDATION REACTIONS 769
*STEMMLER, E A AND BUCHANAN, M V

ELECTROSPRAY IONIZATION OF SOME POLYPEPTIDES AND SMALL PROTEINS 771
MENG, C K,MANN, M AND *FENN, J B

PHOTO-ASSISTED FRAGMENTATION SPECTROSCOPY BY NEUTRALIZATION-REIONIZATION MASS SPECTROSCOPY 773
SELGREN, S F AND *GELLENE, G I

LASER IONIZATION SPECTROSCOPY OF AMINO ACIDS AND PEPTIDES USING SUPERSONIC JET INJECTION INTO A TIME-OF-FLIGHT MASS SPECTROMETER 775
*LUBMAN, D M AND LI, L

SEQUENCE SPECIFIC FRAGMENTATION OF DERIVITIZED DIPEPTIDES USING RESONANCE ENHANCED MULTIPHOTON IONIZATION 777
*SEGAR, K R AND JOHNSTON, M V

GENERATION OF Li+ BEAM DURING FABMS AND ITS APPLICATIONS TO LITHIATION OF NEUTRAL MOLECULES 779
*LEARY, J A AND TOLUN, E

NONLINEAR SECONDARY ION YIELD ENHANCEMENT WITH FAST PRIMARY INCIDENT MOLECULAR IONS 781
*SALEHPOUR, M,FISHEL, D AND HUNT, J

Instrumentation. Lipids. Environmental Applications of LC/MS.

A ROBOTIC BASED SAMPLE PREPARATION AND INTRODUCTION SYSTEM FOR AUTOMATED EI AND CI PROBE ANALYSIS 783
*SMITH, D C,GOULD, V,HAMMOND, M J AND TODD, D E

A NEW DEVICE FOR PYROLYSIS MASS SPECTROMETRY OF BIOLOGICAL MATERIALS 785
*LAGNA, W M

DEVELOPMENT OF A SELECTIVE SECONDARY ION ENHANCER FOR SIMS 787
INOUE, M,SUGIYAMA, Y,NISHIGAKI, S AND *NODA, T

AN AUTOMATED REDUCED-PRESSURE INTERFACE DEVICE FOR THE HEWLETT-PACKARD MASS SELECTIVE DETECTOR 789
*LANGVARDT, P W AND BARTELS, M J

DYNAMIC FAB WITH A DIP GUN 791
*PEREL, J AND MAHONEY, J F

DESIGN AND CHARACTERIZATION OF A CONTINUOUS FLOW FAB PROBE AND AN ION SOURCE MODIFIED FOR DYNAMIC SAMPLE INTRODUCTION 793
*BAUER, M R AND YANCEY, M F

THERMOELECTRICALLY COOLED SAMPLE PROBE FOR FABMS (LSIMS) 795
*MARTIN, S A,HILL, J A AND BIEMANN, K

STUDIES WITH FAB PROBE TIPS 797
*SIEGEL, M M,TSAO, R AND BOULAY, W

MINIATURIZED SOLID-STATE EI/FI ION SOURCE 799
*YOUNG, S AND COGGIOLA, M J

A GAS TRAP FOR GC/MS HEADSPACE ANALYSIS 801
*WANG, J-S AND ROSENBERG, I E

CONCEPTS AND APPLICATIONS OF SHORT OPEN TUBULAR COLUMNS IN GAS CHROMATOGRAPHY/MASS SPECTROMETRY 803
*HAIL, M E AND YOST, R A

CAPILLARY GC/MS FOR THE DETECTION OF ORGANIC FIREARMS DISCHARGE RESIDUE 805
*FETTEROLF, D D AND KOONS, R D

CAPILLARY SUPER CRITICAL FLUID CHROMATOGRAPHY NEGATIVE ION CI MASS SPECTROMETRY 807
*ROACH, J A G,ANDRZEJEWSKI, D AND SPHON, J A

DESIGN AND PERFORMANCE OF A CONTINUOUS FLOW PROBE HPLC INTERFACE FOR A LIQUID SIMS TIME OF FLIGHT MASS SPECTROMETER 809
*CHEN, K-H,MARCUS, P AND COTTER, R J

ION CONFINEMENT IN THE RF-ONLY QUADRUPOLE COLLISION CELL OF TANDEM QUADRUPOLE MASS SPECTROMETERS: ACCESS TO THERMODYNAMIC EQUILIBRIUM AND ION REJECTION 811
*BEAUGRAND, C,DEVANT, G,JAOUEN, D,MESTDAGH, H AND ROLANDO, C

CHARACTERIZATION OF MULTIPOLE FRAGMENTATION CHAMBERS USING COMPUTER SIMULATIONS OF ION TRAJECTORIES 813
*DELBERT, S-S AND ENKE, C G

LONGITUDINAL FIELD FAULTS IN QUADRUPOLE MASS FILTERS 815
*DAWSON, P H

ISOBARIC DOUBLET ION SEPARATION ON QUADRUPOLAR SINGLE AND TANDEM MASS SPECTROMETRS 817
*DE MAACK, F,DEVANT, G,LEPETIT, G AND ROLANDO, C

IMPROVED PERFORMANCE FROM A HYBRID MASS SPECTROMETER 819
MONAGHAN, J J AND *WRIGHT, B

A COMPARISON OF THE USE OF LOW AND HIGH ENERGY COLLISIONS FOR THE ANALYSIS OF OLIGOPEPTIDES BY TANDEM MASS SPECTROMETRY 821
BARBER, M,BELL, D,MORRIS, M,TETLER, L,*CLENCH, M,OWEN, R,PARR, V,WEIR, O AND WOOD, D

SCAN MODES FOR HYBRID MASS SPECTROMETERS 823
*GLISH, G L AND MCLUCKEY, S A

KINETIC ENERGY RELEASE EFFECTS ON RESOLUTION IN MS/MS 825
*GLISH, G L AND MCLUCKEY, S A

A GRAND SCALE MASS SPECTROMETER "GEMMY" AT OSAKA UNIVERSITY 827
*MATSUO, T,SAKURAI, T,MORRIS, M,KATAKUSE, I,MATSUDA, H,AZUMA, M,KAMMEI, Y AND KUBOTA, E

CALIBRATION AND OPTIMIZATION OF AN EBQQ SYSTEM FOR QUANTITATIVE ANALYSIS - A NOVEL APPROACH 829
*FARROW, P E,YELLE, L M AND DUDEK, G

OPERATION OF A HYBRID TANDEM MASS SPECTROMETER OF BEqQ CONFIGURATION IN UNLINKED SCAN MODES; THEORY AND APPLICATIONS 831
ALEXANDER, A J,BOYD, R K,*GUEVREMONT, R AND THIBAULT, P

A MODEL FOR MASS-INDEPENDENT SPACE AND ENERGY FOCUSING IN TIME-OF-FLIGHT MASS SPECTROMETRY USING DYNAMIC POST-SOURCE ACCELERATION 833
*YEFCHAK, G E,HOLLAND, J F AND ENKE, C G

INSTRUMENTATION FOR MASS SPECTROMETRY/COINCIDENT FRAGMENT DETECTION 835
*GOERINGER, D E,MCLUCKEY, S A AND BERTRAM, L K

A DIRECT COMPARISON OF TWO-, THREE-, AND FOUR-SECTOR MASS SPECTROMETERS FOR MEASURING CID SPECTRA OF PEPTIDES 837
*STULTS, J T AND CHAKEL, J A

A FOUR SECTOR MASS SPECTROMETER FOR NEUTRALIZATION-REIONIZATION (NR) STUDIES 839
FENG, R,*ZHANG, M-Y,WESDEMIOTIS, C,BALDWIN, M A,DRINKWATER, D E,LEYH, B AND MCLAFFERTY, F W

DESIGN AND PERFORMANCE OF A NEW REVERSE GEOMETRY MASS SPECTROMETER WITH HIGH SENSITIVITY AND HIGH ION TRANSMISSION 841
*KUNIHIRO, F,ISHIHARA, M,KAMMEI, Y,KUBOTA, E,ITAGAKI, Y,MUSSELMAN, B D AND HIGUCHI, T

IMPROVEMENT IN HIGH MASS ION DETECTION OF A TANDEM QUADRUPOLE MASS SPECTROMETER USING A HIGH VOLTAGE POST-ACCELERATION DETECTOR 843
*SCHOEN, A E AND SYKA, J E P

IMPROVING DETECTION SENSITIVITY FOR HIGH MASS IONS 845
*MAHONEY, J F,PEREL, J,LEE, T D AND LEGESSE, K

AN IMPROVED 252-Cf PLASMA DESORPTION MASS SPECTROMETRIC SYSTEM FOR LARGE BIOMOLECULES 847
*MUDGETT, P D,HILL, J C AND MACFARLANE, R D

USE OF A MICROCHANNEL ARRAY DETECTOR IN A FOUR-SECTOR TANDEM MASS SPECTROMETER 849
*HILL, J A,MARTIN, S A AND BIEMANN, K

MIXTURE ANALYSIS BY PY-APCI TIME-RESOLVED MS AND MS/MS 851
*SNYDER, A P AND WINDIG, W

AN ION-OPTICAL BENCH FOR TESTING ION SOURCE LENSES 853
*STOFFELS, J J AND ELLS, D R

GAS ANSLYSIS OF LOW-PRESSURE MERCURY-ARGON DISCHARGE 855
*PANG, E AND EICH, A

A SINGLE COLLECTOR MAGNETIC MASS SPECTROMETER FOR RESPIRATORY APPLICATIONS 857
UNGARELLI, R,LEHR, J L AND *MARSHALL, D J

A MAGNETIC FIELD SELECTOR (MFS) FOR A VG 7070F DOUBLE FOCUSSING MASS SPECTROMETER TO ENABLE MULTIPLE PROGRAM HIGH RESOLUTION SELECTED ION MONITORING 859
*DURDEN, D A

THE USE OF CYCLIC NITROBENZAL ACETAL DERIVATIVES IN NEGATIVE ION MASS SPECTROMETRY OF LONG CHAIN 1,2 AND 1,3 DIOLS 861
*MALLET, A I,RENDELL, N B AND MINNIKIN, D E

QUANTITATIVE DETERMINATION OF FUNGAL STEROLS BY GC-MS-SIM AND ITS APPLICATION TO THE CHEMOTAXONOMY OF DERMATOPHYTES 863
*MALLET, A I AND HOWELL, S A

HOW PURE IS PURE? THE CERTIFICATION OF SRM 911b CHOLESTEROL 865
*WELCH, M J,COHEN, A AND WHITE, E

QUANTITATION OF PLATELET ACTIVATING FACTOR BY FAB/MS/MS 867
*BUSH, E D,STEVENS, D L AND MILLER, D L

MASS SPECTROMETRIC DETERMINATION OF PLATELET-ACTIVATING FACTOR FROM HUMAN SUBJECTS 869
*SATOUCHI, K,ODA, M AND SAITO, K

MASS SPECTROMETRY ANALYSIS OF PLATELET ACTIVATING FACTOR (PAF) IN MOUSE URINE 871
*BENFENATI, E,BETTAZZOLI, L,DAVOLI, E,GAVINELLI, M,MACCONI, D AND NORIS, M

QUANTITATIVE ANALYSIS OF LYSOPHOSPHATIDYLSERINE (LPS) BY FAB-MS 873
*BENFENATI, E,BETTAZZOLI, L,CHEN, S,DE BELLIS, G,FANELLI, R AND PEGE, G

CHARACTERIZATION OF UNSATURATED EPOXY FATTY ACIDS BY MASS SPECTROMETRY VIA PICOLINYL ESTERS 875
*BALAZY, M AND NIES, A S

STRUCTURAL ELUCIDATION OF CAROTENOID PIGMENTS BY FAB-CAD MS/MS 877
*GAGE, D A,ROCK, C,ZEEVAART, J A D AND WATSON, J T

QUANTITATIVE ANALYSIS OF PLATELET ACTIVATING FACTOR BY TANDEM MASS SPECTROMETRY 879
*HAROLDSEN, P E AND GASKELL, S J

A COMPARISON OF PROSTAGLANDIN LEVELS IN HUMAN AND RHESUS MONKEY CEREBROSPINAL FLUID 881
*YERGEY, J A,SALEM, N,KARANIAN, J W,LINNOILA, M AND HEYES, M P

QUANTIFICATION OF 12S-HYDROXYEICOSATETRAENOIC ACID RELEASE FROM HUMAN PLATELETS BY NEGATIVE ION MASS SPECTROMETRY 883
*YAMASHITA, K,CAPDEVILA, J AND BLAIR, I A

AN APPLICATION OF FAB-MS; STRUCTURAL CHARACTERIZATION OF A SINGLE LIPID-A ANALOG RESPONSIBLE FOR HUMAN PLATELET ACTIVATION 885
*REINHOLD, V N,HER, G R,GRABAREK, J AND HAWIGER, J

IMPROVEMENTS IN STRUCTURAL DETAIL FOR GLYCOSPHINGOLIPID SAMPLES USING CO2 & CO2/CH3OH MIXTURES AS A DCI REAGENT GAS 887
*HER, G R AND REINHOLD, V N

MEASUREMENT OF URINARY ARACHIDONIC ACID METABOLITES (AAMs): IMMUNOAFFINITY PURIFICATION WITH GC/MS, GC/MS/MS AND DCI/MS/MS 889
*GILLESPIE, T A,VRBANAC, J J,KNAPP, D R,HAIL, M E AND YOST, R A

COMPARATIVE GC/MS TECHNIQUES FOR THE IDENTIFICATION OF FATTY ACIDS AND ALCOHOLS FROM HUMAN CERUMEN 891
*HARVEY, D J

DETERMINATION OF THE PHOSPHOCHOLINE MOLECULAR SPECIES WHICH ARE DIRECT PRECURSORS OF PLATELET ACTIVATING FACTOR 893
*CLAY, K L AND JOHNSON, C A

ANAYLSIS FOR LEUKOTRIENE B4 IN HUMAN SERUM BY GC-MS 895
*HUGHES, H,MITCHELL, J R AND GASKELL, S J

ANALYSIS OF LTB4 AND 20-HYDROXY-LTB4 IN WHOLE BLOOD CHALLENGED WITH ZYMOSAN 897
*ZIRROLLI, J A,FRADIN, A,MACLOUF, J AND MURPHY, R C

EI, CI LC/MS THROUGH FRIT VAPORIZATION SYSTEM 899
MATSUURA, K,OTSUKA, K,KOBAYASHI, T,KUBOTA, E,*ITAGAKI, Y,MUSSELMAN, B D AND HIGUCHI, T

CAPILLARY ZONE ELECTROPHORESIS/MASS SPECTROMETRY OF ORGANIC DYES 901
*COVEY, T,LEE, E AND HENION, J

ANALYSIS OF SULFONATED AZO DYES USING SELECTED ION MONITORING AND THEMOSPRAY LIQUID CHROMATOGRAPHY/MASS SPECTROMETRY 903
*MCLEAN, M A,FLORY, D A,VESTAL, M L AND FREAS, R B

IDENTIFICATION OF SELCTED CARBONYL COMPOUNDS IN TOBACCO SMOKE BY LIQUID CHROMATOGRAPHY/MASS SPECTROMETRY (LC/MS) 905
*CHUNG, H L,BORGERDING, M F AND DUNN, R S

DLI- AND OTLC-MS ANALYSIS OF METRIBUZIN AND ITS METABOLITES 906
*ESCOFFIER, B,PARKER, C E,DEWIT, J S M,MESTER, T C AND TOMER, K B

POSITIVE- AND NEGATIVE-ION MASS SPECTROMETRY OF ALDICARB AND ITS DERIVATIVES BY PARTICLE BEAM HPLC/MS 908
*LYNN, B C,MARBURY, G D,TUSCHALL, J R,WILLOUGHBY, R C AND KANTOR, E J

A COMPARISON BETWEEN POSITIVE AND NEGATIVE ION MODES IN THERMOSPRAY LC-MS FOR THE DETERMINATION OF CHLOROPHENOLS AND HERBICIDES 910
*BARCELO, D

THE ROLE OF MASS SPECTROMETRY COMBINED WITH REVERSED PHASE HPLC IN THE IDENTIFICATION OF AN UNUSUAL SHELLFISH TOXIN 912
BOYD, R K,HOGGE, L R,*JAMIESON, W D,MCLAREN, J W,QUILLIAM, M A,SIM, P G, THIBAULT, P AND WRIGHT, J L C

RESIDUE ANALYSIS OF FOSAMINE AMMONIUM IN SOIL BY LIQUID CHROMATOGRAPHY/ MASS SPECTROMETRY 914
*SHALABY, L M AND EBLE, J E

A COMPARATIVE EVALUATION OF LIQUID CHROMATOGRAPHY/THERMOSPRAY/MASS SPECTROMETRY AND IMMUNOCHEMICALASSAY FOR PARAQUAT AND MONOQUAT 916
*JONES, T L,BETOWSKI, L D AND VAN EMON, J M

SURFACE ANALYSIS WITH A TIME-OF-FLIGHT MASS SPECTROMETER WITH CHARGE COMPENSATION FOR SECONDARY IONS AND POSTIONIZED SPUTTERED NEUTRALS 918
NIEHUIS, E,HAGENHOFF, B,KEMPWERTH, G,VAN LEYEN, D AND *BENNINGHOVEN, A

ANALYSIS OF DRUGS OF ABUSE BY MAGIC LC/MS 920
*APFFEL, A

Oligosaccharides, Nucleic Acids, and General Biochemistry.

LSIMS OF INTACT OLIGOSACCHARIDES: COMPARISON OF SENSITIVITY AND SPECTRAL QUALITY AMONG SELECTED DERIVATIVES 921
JIANG, K,*POULTER, L,KARRER, R AND BURLINGAME, A L

CHARACTERIZATION OF COMPLEX OLIGOSACCHARIDES FROM HEPATITIS B SURFACE ANTIGEN BY LIQUID SECONDARY ION MASS SPECTROMETRY 923
*GILLECE-CASTRO, B L,BURLINGAME, A L AND PETERSON, D L

LSIMS ANALYSIS OF HIGH MANNOSE AND COMPLEX SIALYLATED OLIGOSACCHARIDES ISOLATED FROM LOW LEVELS OF GLYCOPROTEIN: APPLICATION TO ACID GLYCOPROTEIN AND NICOTINIC ACETYLCHOLINE RECEPTOR 925
*POULTER, L AND BURLINGAME, A L

IDENTIFICATION OF 5'-DEOXYXANTHOSINE IN HUMAN URINE 927
*MCCLURE, T D,SCHRAM, K H,NAKANO, K AND YASAKA, T

MASS SPECTRAL CHARACTERIZATION OF ACRYLONITRILE OXIDE DNA ADDUCTS. ALKYLATION AT N-3 OF CYTOSINE RESULTS IN HYDROLYTIC DEAMINATION TO A URACIL ADDUCT 929
*SOLOMON, J J,DECKER, K,MUKAI, F AND SEGAL, A

FAB-MS/MS AS A SCREENING METHOD FOR DETECTING TRACE AMOUNT OF BIOMOLECULES IN HPLC FRACTIONS 931
*DIETRICH, A M,GUENAT, C R,TOMER, K B AND BALL, L M

TANDEM MASS SPECTROMETRY OF ANTIVIRAL OLIGODEOXYNUCLEOTIDE CARBAMATE ANALOGS 933
*LARAMEE, J A,ARBOGAST, B,STIRCHAK, G,WELLER, D AND DEINZER, M L

MASS SPECTROMETRIC APPROACHES TO THE CONFIRMATION OF MADURAMICIN IN CHICKEN FAT 935
*STOUT, S J,WILSON, L A,KLEINER, A I,DACUNHA, A R AND FRANCL, T J

INFLUENCE OF DIET ON THE OXIDATION OF FATTY ACIDS IN HUMANS USING ISOTOPE RATIO MASS SPECTROMETRY 937
*FRENCH, M A,KIELO, E,PHARAZYN, S,THOMSON, A B R,WANG, L,RAJOTTE, R AND CLANDININ, M T

Symposium: Crossing the Solution-Vacuum Barrier.

THE ROLE OF SOLVENT CHEMISTRY IN DESORPTION IONIZATION MASS SPECTROMETRY 939
*COOK, K D

ELECTROSPRAY IONIZATION PHENOMENA AND THE INTERFACE OF CAPILLARY ZONE ELECTROPHORESIS AND MASS SPECTROMETRY 941
*SMITH, R D,BARINAGA, C J AND UDSETH, H R

MAGIC-LC/MS: A VERSATILE SAMPLE INTRODUCTION PATH FOR MASS SPECTROMETRY 943
*BROWNER, R F,KIRK, J D,HARRIS, W E AND PERKINS, D D

MECHANISM OF FAB SPECTRA FORMATION TEMPERATURE DEPENDENCE 944
*SUNNER, J,KEBARLE, P AND MORALES, A

MASS TRANSPORT IN LIQUID SIMS 946
*TODD, P J

Instrumentation.

APPLICATIONS OF ELECTROPHORESIS COUPLED WITH SECONDARY ION MASS SPECTROMETRY 948
*STANLEY, M S AND BUSCH, K L

CAPILLARY ZONE ELECTROPHORESIS/CONTINUOUS FLOW FAB MS 950
*MINARD, R D,LONG, E,CURRY, P AND EWING, A

COMPLETE MS/MS DATA FIELD ACQUISITION ON THE CHROMATOGRAPHIC TIME SCALE BY TIME-RESOLVED ION MOMENTUM SPECTROMETRY (TRIMS) WITH TIME ARRAY DETECTION (TAD) 952
*ECKENRODE, B A,WATSON, J T,HOLLAND, J F AND ENKE, C G

AN IMPROVED INTERFACE FOR CAPILLARY ZONE ELECTROPHORESIS-MASS SPECTROMETRY 954
*SMITH, R D,LOO, J A,BARINAGA, C J AND UDSETH, H R

PARTICLE-INDUCED DESORPTION MASS SPECTROMETRY: PRODUCTION, IDENTIFICATION, AND USE OF INCIDENT MEV MOLECULAR IONS 956
*HUNT, J E,RUTHENBERG, A E,SALEHPOUR, M AND FISHEL, D L

A NEW UHV INSTRUMENT FOR ION/SURFACE COLLISIONS 958
LAUE, H-J,AMY, J W,WINGER, B AND *COOKS, R G

QUADRATURE FT/ICR MASS SPECTROMETRY 960
*VERDUN, F R,MULLEN, S L,RICCA, T L AND MARSHALL, A G

ICR-TOF. TIME OF FLIGHT MEASUREMENT OF PHOTOFRAGMENT ENERGIES IN THE ICR ION TRAP 962
*DUNBAR, R C AND WEDDLE, G H

THE EXTERNAL ION SOURCE FOR HIGH MAGNETIC FIELD ICR SPECTROMETRY - EXPERIMENT AND THEORY 964
KOFEL, P,PEZSA, I,KNOLL, H,BAMBERG, M AND *WANCZEK, K P

NEW FTMS METHOD FOR TRAPPING IONS THAT ARE INJECTED FROM AN EXTERNAL ION SOURCE INTO AN ICR CELL 966
*LEBRILLA, C B,AMSTER, I J AND MCIVER, R T

DESORPTION IONIZATION AND ION INJECTION INTO A QUADRUPOLE ION TRAP MASS SPECTROMETER 968
*LOURIS, J N,KAISER, R E AND COOKS, R G

Pharmacology and Drugs. LC/MS Applications.

STEREOCHEMICAL INVERSION OF HALOXFOP IN THE FISCHER 344 RAT 970
*BARTELS, M J AND SMITH, F A

LY186641 METABOLISM IN HUMANS: DETERMINATION OF URINE AND PLASMA METABOLITE STRUCTURES BY THERMOSPRAY LC/MS AND FAST ATOM BOMBARDMENT MS 972
*DHAHIR, P H,HAMILTON, M,BARTON, R D,SATTERLEE, W G AND BREAU, A

CHARACTERIZATION OF RAT BILIARY METABOLITES OF DALTROBAN (BM 13,505/ SK&F 96148) BY FAST ATOM BOMBARDMENT AND THERMOSPRAY LIQUID CHROMATOGRAPHY/ MASS SPECTROMETRY 974
*DULIK, D,GAGNON, R,DAVIS, M,KUO, G AND KAO, J

CHARACTERIZATION OF CONJUGATED BENZAZEPINE METABOLITES IN FEMALE DOGS 976
*DAVIS, M R AND STRAUB, K M

STRUCTURE DETERMINATION OF A54145A. A PEPTOLIPID CONTAINING NON-MAMMALIAN AMINO ACIDS 978
CHANCE, R E,FUKUDA, D S,GILLIAM, J M,HUNT, A H,MYNDERSE, J S AND *OCCOLOWITZ, J L

THERMOSPRAY LC/MS ANALYSIS OF METABOLITES OF THE CANDIDATE 8-AMINOQUINOLINE ANTILEISHMANIAL DRUG WR 6026 GENERATED IN THE ISOLATED PERFUSED RAT LIVER MODEL (IPRL) 980
*ASHMORE, R W,SHIPLEY, L A,COLEMAN, M D,BREWER, T G AND THEOHARIDES, A D

GC/MS CONFIRMATION OF SULFAMETHAZINE AND SULFISOXAZOLE IN MILK 982
*VAN LANGENHOVE, A AND ZOMER, E

EXAMINATION OF THE MASS SPECTRA OF AMINOGLYCOSIDE ANTIBIOTICS BY THERMOSPRAY MASS SPECTROMETRY AND FAB MASS SPECTROMETRY 984
*GETEK, T A,KORFMACHER, W A AND FREEMAN, J P

CAPILLARY GAS CHROMATOGRAPHY-REACTION INTERFACE/MASS SPECTROMETRY. A HIGHLY SELECTIVE METHOD FOR THE DETECTION OF 13C AND 15N LABELLED DRUGS AND THEIR METABOLITES 986
*CHACE, D H AND ABRAMSON, F P

QUANTIFYING THE METABOLIC PATTERN OF PRAZIQUANTEL IN THE MOUSE USING MS/MS 988
ALI, M H,FETTEROLF, D,*ABRAMSON, F P AND COHN, V H

IDENTIFICATION, FRAGMENTATION, AND TANDEM MASS SPECTROMETRY OF PENICILLINS 990
*SUWANRUMPHA, S AND FREAS, R B

DETERMINATION OF DIETHYLSTILBESTROL AND DIENESTROL IN CHICKEN BY GC AND SELECTED ION MONITORING 992
*YINGHUA, Y AND LI, L

IDENTIFICATION OF PRODUCTS OF CO-SYNTHESIZED IN THE PRODUCTION OF THIENYLCYCLOHEXYLPIPERDINE (TCP) 994
*JONES, L A,LEE, M K AND HANEY, C A

DIRECT ANALYSIS OF BODY FLUIDS FOR IONIC DRUGS BY LC/MS AND LC/LC/MS 996
*COVEY, T,MAYLIN, G,ECKERLIN, R,LEE, E,HENION, J AND EDLUND, P O

STUDIES OF ANABOLIC STEROIDS BY THERMABEAM LC/MS 998
*DILTS, M J,SHEEHAN, E W AND WILLOUGHBY, R C

ON-LINE ANALYSIS OF DRUGS IN LIVE ANIMALS USING CF-FAB AND MICRODIALYSIS 1000
*LIN, S-N AND CAPRIOLI, R M

A SOLID PHASE EXTRACTION METHOD FOR GC/MS ANALYSIS OF COCAINE AND ITS MAJOR METABOLITES IN URINE 1002
*ESPINOSA-LENIZ, R,HILPERT, L R,WELCH, M J AND WHITE, E

STUDIES ON LASTING CONTRACEPTIVE BY MASS SPECTRA METHOD 1004
*YANG, K Q

QUANTIFICATION OF PHYSOSTIGMINE IN PLASMA BY CAPILLARY COLUMN CHROMATOGRAPHY USING ISOBUTANE CHEMICAL IONIZATION MASS SPECTROMETRY 1006
*JAKUBOWSKI, E M,SMITH, J R,MUSSER, S M AND CALLERY, P S

MASS FRAGMENTATION OF ISOQUINOLONES - AN UTILITY TO CHARACTERIZE THALICTRUM ALKALOIDS 1008
GALAL, A M,ALY, Y,SCHIFF, P L,WONG, L K AND *FU, E W

IDENTIFICATION OF SOME DECOMPOSITION PRODUCTS OF DELTA-9-TETRAHYDRO-CANNABINOL BY GC/MS 1010
*HARVEY, D J AND BROWN, N K

QUANTIFICATION OF PYRIDOSTIGMINE IN PLASMA BY PACKED CAPILLARY HPLC/FAB-MS/MS 1012
*BAUER, M R AND YANCEY, M F

MASS SPECTRAL ANALYSIS AND FRAGMENTATION OF SECOND GENERATION ACE-INHIBITORS CONTAINING PHOSPHINIC AND PHOSPHORUS ACIDS 1014
*BOLGAR, M S,DIDONATO, G C,GEDAMKE, R,MCCORMICK, T J,UNGER, S E AND WARRACK, B M

QUANTITATION BY GC/NICI-MS OF TWO ANTI-HYPERCHOLESTEROLEMIC DRUGS IN PLASMA AFTER SOLID PHASE EXTRACTION 1016
*WANG-IVERSON, D,IVASHKIV, E,FUNKE, P T,ARNOLD, M E,JEMAL, M AND COHEN, A I

MASS SPECTRAL STUDIES OF CHOLESTEROL-LOWERING AGENTS 1018
*WARRACK, B M,BOLGAR, M S,DIDONATO, G C AND UNGER, S E

FAB-MS OF NOVEL FLUOROGENIC IONOPHORES 1020
*HINDENLANG, D M,LUCAS, M E,MASILAMANI, D AND SEDGWICK, R D

HRGC-MS MEASUREMENT OF PLASMA NICOTINE LEVELS AFTER SMOKING CIGARETTES OR CHEWING NICOTINE GUMS 1022
*DAVOLI, E,MARIANI, G,BENFENATI, E AND FANELLI, R

PRELIMINARY STUDIES ON THIOTEPA-DNA ADDUCTS USING THERMOSPRAY LC/MS 1024
*MUSSER, S M,CALLERY, P S AND PAN, S-S

SIMULTANEOUS QUANTITAION OF CARBAMAZEPINE, CARBAMAZEPINE-10,11-EPOXIDE, AND CARBAMAZEPINE-10,11-DIOL IN PLASMA BY GAS CHROMATOGRAPHY/MASS SPECTROMETRY 1026
*ALKALAY, D,MIOTTO, J AND GAUDRY, D

QUANTITATION OF THE SELECTIVE DOPAMINE AGONIST CGS 15873A IN PLASMA BY GAS CHROMATOGRAPHY/MASS SPECTROMETRY 1028
*CARLSEN, S,ALKALAY, D,GAUDRY, D AND MIOTTO, J

DETERMINATION OF ARECOLINE IN HUMAN PLASMA BY SELECTED ION MONITORING GC/MS 1029
*HAYES, M J,KHEMANI, L,BAX, M AND ALKALAY, D

DECHLORINATION REACTIONS IN FAB MASS SPECTROMETRY OF PHENOTHIAZINE RELATED DRUGS 1031
*EDOM, R W,BROOKS, P W AND MCKAY, G

QUANTITATION OF DIDEOXYCYTIDINE IN HUMAN PLASMA BY GC-MS 1033
RUBIO, F R,CREWS, T,GARLAND, W A AND *FUKUDA, E K

APPLICATION OF DICYANDIAMIDE AS A MATRIX ADDITIVE IN FAST ATOM BOMBARDMENT MASS SPECTROMETRY 1035
*MASUCCI, J A,CALDWELL, G W AND REITZ, A B

LIQUID SIMS OF METALLOPORPHYRINS WITH A STRONG AFFINITY TO TUMOR TISSUE 1037
*SUZUKI, M,TAKEDA, N,HARADA, K I,TATEMATSU, A,SAKATA, I AND NAKAJIMA, S

UTILITY OF LC-MS FOR THE ANALYSIS OF CHLORAMPHENICOL AND SEVERAL OF ITS ANALOGUES 1039
*KORFMACHER, W A,GETEK, T A,HANSEN, E B,CERNIGLIA, C E,ABOU-KHALIL, S AND YUNIS, A A

THERMOSPRAY (TSP) FRAGMENTATIONS OF AMIDINOUREAS AND LC/MS METHOD FOR QUANTIFICATION OF LIDAMIDINE AND ITS N-DESMETHYL METABOLITE 1041
*TANG, S Y

THE USE OF THERMOSPRAY LC/MS/MS FOR THE CLASS IDENTIFICATION AND STRUCTURAL VERIFICATION OF PHYTOESTROGENS IN SOY PROTEIN PREPARATIONS 1043
*BARBUCH, R J,COUTANT, J E,SETCHELL, K D R AND WELCH, M B

THERMOSPRAY LC/MS AND GC/MS ANALYSIS OF OXYGENATED METABOLITES OF POLYUNSATURATED FATTY ACIDS 1045
*KIM, H-Y AND SALEM, N

INVESTIGATION OF FLAVONE-8-ACETIC ACID METABOLITES BY THERMOSPRAY MASS SPECTROMETRY 1047
*CROWLEY, J R,HOOD, R J AND CHABOT, G

ANALYSIS OF URINARY ORGANIC ACIDS BY LC-MS AND LC-MS/MS 1049
MILLS, G,WALKER, V,*CLENCH, M R,OWEN, R,PARR, V C,WEIR, O AND WOOD, D

APPLICATION OF THERMOSPRAY LIQUID CHROMATOGRAPHY-MASS SPECTROMETRY TO THE ANALYSIS OF BILE ACIDS 1051
*VESTAL, C H AND SETCHELL, K D R

THERMOSPRAY LC/MS STUDIES WITH INOSITOL PHOSPHATES 1053
*HSU, F F,GOLDMAN, H D AND SHERMAN, W R

DEVELOPMENT OF A QUANTITATIVE LCMS ASSAY FOR THE DETERMINATION OF GR 43175 BASE IN PLASMA 1055
*OXFORD, J AND LANT, M S

PH-RELATED CHANGES IN RELATIVE ION INTENSITIES OF FRAGMENTS OF LY170680 DURING LC/MS ANALYSES 1057
*BREAU, A P AND GOODWIN, R M

DEVELOPING ANALYTICAL METHODS FOR DETERMINATION AND CONFIRMATION OF -LACTAM ANTIBIOTICS IN MILK AND TISSUE USING HPLC/UV, AND HPLC/MS 1059
*VOYKSNER, R D AND RAYMER, J

ANALYSIS OF NEUROMUSCULAR BLOCKING AGENTS BY MOVING BELT LC/MS 1061
*BAKER, T R,MICHAUD, D P,VOUROS, P AND MARTYN, J A A

THERMOSPRAY LC-MS OF SELECTED METABOLITES AND DEGRADATION PRODUCTS OF MUSTARD 1063
*JAKUBOWSKI, E M AND MUNAVALLI, S

APPLICATION OF QUANTITATIVE THERMOSPRAY LC/MS TO PULSE DOSE PHARMACOKINETIC STUDIES OF CARBAMAZEPINE IN HUMANS 1065
MOOR, M J,LEVY, R H,RASHED, M S AND *HOWALD, W N

THERMOSPRAY LC/MS - A VERSATILE TECHNIQUE FOR DETERMINATION OF DRUGS IN PLASMA 1067
*LINDBERG, C AND PAULSON, J

MAGIC-LC/MS ANALYSIS OF ALKALOIDS 1069
*HARRIS, W E AND BROWNER, R F

THERMOSPRAY LC/MS OF PYRROLIZIDINE ALKALOIDS AND METABOLITES 1071
*PARKER, C E,VERMA, S,TOMER, K B,REED, R L,KEDZIERSKI, B AND BUHLER, D R

ANALYSIS OF ACYLCARNITINE BY HPLC AND LC/MS 1073
SHINKA, T,MIZUNO, T AND *MATSUMOTO, I

STUDY ON THE DECOMPOSITION OF QUARTERNARY AMMONIUM SALTS BY THERMOSPRAY LC/MS 1075
*VICCHIO, D AND YERGEY, A L

THERMOSPRAY LC/MS OF -CARBOXYAMIDO AMINO ACIDS AND PEPTIDES 1077
*TRESTON, A M,YERGEY, A L,CUTTITTA, F AND MULSHINE, J L

IDENTIFICATION OF PHENYLTHIOCARBAMYL AMINO ACIDS BY THERMOSPRAY LC/MS FOR AMINO ACID COMPOSITION ANALYSIS OF PROTIENS AND PEPTIDES 1079
PRAMANIK, B C,MOOMAW, C R,COHEN, S A AND *SLAUGHTER, C A

REACTION MONITORING USING MICROBORE AND FRONTAL LIQUID CHROMATOGRAPHY WITH CF-FAB 1081
*MOORE, W T,DAGUE, B,MARTIN, M AND CAPRIOLI, R M

ANALYSES OF HIGH MOLECULAR WEIGHT POLAR COMPOUNDS BY THERMOSPRAY MASS SPECTROMETRY 1083
*JONES, D S,KROLIK, S T AND BATEMAN, R H

ON-LINE CAPILLARY ZONE ELECTROPHORESIS/ION SPRAY TANDEM MASS SPECTROMETRY OF SMALL PEPTIDES 1085
*LEE, E D,HENION, J AND COVEY, T

QUANTITATION OF ENDOGENOUS SUBSTANCE P BY COMBINED MICRO-LC/DYNAMIC FAB/MS 1087
*LISEK, C A,AIMONE, L D,YAKSH, T L AND JARDINE, I

MIXTURE ANALYSIS BY COMBINED CAPILLARY COLUMN LIQUID CHROMATOGRAPHY-DYNAMIC FAB MASS SPECTROMETRY 1089
BATEMAN, R H AND JONES, D S

THERMOSPRAY LC MS/MS STUDIES ON THE ANTIANXIETY DRUG BUSPIRONE AND ITS METABOLITES 1091
*GARTEIZ, D,JAJOO, H K,MAYOL, R F AND BLAIR, I A

RAPID ANALYSIS OF IFOSFAMIDE IN HUMAN PLASMA BY THERMOSPRAY-LC/MS/MS 1092
*GARTEIZ, D A,NEWMAN, R A AND ANDERSON, M D

DETERMINATION OF DIANABOL AND ITS METABOLITES BY COUPLED COLUMN LC TANDEM MASS SPECTROMETRY 1095
EDLUND, P O AND *HENION, J

THERMOSPRAY LC/MS OF THE LL-F28249 MACROCYCLIC LACTONES 1097
*KENION, G B,CARTER, G T AND BORDERS, D B

THERMOSPRAY LC/MS OF LL-F42248 ALPHA 1099
*KENION, G B,CARTER, G T AND BORDERS, D B

MASS SPECTRAL INVESTIGATIONS OF BORON NEUTRON CAPTURE THERAPY (BNCT) AGENTS 1101
*MILLER, D L AND PETERSON-WRIGHT, L J

SIMULTANEOUS IDENTIFICATION AND QUANTITATION OF MORPHINE AND CODEINE IN URINE BY GAS CHROMATOGRAPHY/MASS SPECTROMETRY 1103
*LIN, W-N,CHU, J-W AND FOREBACK, C C

ANALYSIS OF PIPECOLIC ACID IN PEROXISOMAL DISEASES BY GCMS WITH SELECTED ION MONITORING 1104
*LIN, Y Y

Ion Traps and FT-ICR.

ADVANCES IN MS/MS ANALYSIS WITH THE ION TRAP MASS SPECTROMETER 1106
*WEBER-GRABAU, M,KELLEY, P E,BRADSHAW, S C AND HOEKMAN, D J

NEGATIVE CHEMICAL IONIZATION AND MS/MS OF NEGATIVE IONS IN AN ION TRAP MASS SPECTROMETER 1108
*MCLUCKEY, S A,ASANO, K G AND GLISH, G L

COMPARISON OF CHARGE EXCHANGE AND ELECTRON IONIZATION IN QUADRUPOLE ION TRAP AND TRIPLE QUADRUPOLE MASS SPECTROMETERS 1110
*BERBERICH, D W,HAIL, M E AND YOST, R A

MSn EXPERIMENTS WITH AN ION TRAP MASS SPECTROMETER 1112
*GLISH, G L,VAN BERKEL, G J,ASANO, K G AND MCLUCKEY, S A

ION TRAP MS-MS ASSAYS OF BIOLOGICAL EXTRACTS WITH AN RF/DC SCAN FUNCTION 1114
*STRIFE, R J

SIMULTANEOUS MS-II MEASUREMENTS USING HADAMARD TRANSFORM-FOURIER TRANSFORM MASS SPECTROMETRY 1116
*LOH, S Y,WILLIAMS, E R,MCLAFFERTY, F W AND CODY, R B

FOURIER TRANSFORM TANDEM MASS SPECTROMETRY FOR THE QUALITATIVE ANALYSIS OF COMPLEX MIXTURES 1118
*WISE, M B AND BUCHANAN, M V

IR LASER DESORPTION FOURIER TRANSFORM ION CYCLOTRON RESONANCE MASS SPECTROMETRY OF NUCLEOSIDES AND NUCLEOTIDES 1120
WILLIAMS, J L,MAYERNIK, J A,CONNER, M K,WELLER, R R AND *GIAM, C S

LASER IONIZATION FOURIER TRANSFORM MASS SPECTROMETRY FOR THE DIFFERENTIATION OF METHYL GUANOSINE ISOMERS 1122
*HETTICH, R L

SYSTEM FOR LASER MICROPROBE FOURIER TRANSFORM MASS SPECTROMETRY 1124
*BRENNA, J T,CREASY, W R,MCBAIN, W AND SORIA, C

APPLICATIONS OF LASER MICRO-PROBE USING FOURIER TRANSFORM MASS SPECTROMETRY 1126
*GHADERI, S

Symposium: The Drug Industry in Japan.

PRIMARY STRUCTURE OF PAIM I, -AMYLASE INHIBITOR FROM STREPTOMYCES CORCHORUSHII USING THE COMBINATION OF EDMAN DEGRADATION AND FAST ATOM BOMBARDMENT MASS SPECTROMETRY 1130
*HIRAYAMA, K

STRUCTURE ELUCIDATION OF MERREMOSIDES BY LIQUID SECONDARY ION MASS SPECTROMETRY 1132
*NAKAGAWA, Y,IKENISHI, Y,UCHIDA, M AND KITAGAWA, I

SEX AND AGE DEPENDENT SULFOCONJUGATION AND IDENTIFICATION OF N-SULFONATE WITH NEGATIVE SECONDARY ION MASS SPECTROMETRY 1134
*IWASAKI, K,FUJIOKA, M AND NOGUCHI, H

Peptides.

AMINO ACID MIXTURE ANALYSIS BY LASER DESORPTION FOURIER TRANSFORM MASS SPECTROMETRY 1136
*CHIARELLI, M P,DAVOLI, E AND GROSS, M L

ON-LINE ENZYMATIC HYDROLYSIS - THERMOSPRAY HPLC/MS DETERMINATION OF ENDORPHINS 1138
*VOYKSNER, R D,PACK, T,SWAISGOOD, H AND CHEN, D

DETERMINATION OF CHYMOTRYPTIC PEPTIDES OF LYSOZYME BY FAB/MS 1140
HO, C T,WU, V,GOVINDARAJAN, S,HARTMAN, T G,ROSEN, R T AND *ROSEN, J D

MS/MS METHODS FOR PEPTIDE SEQUENCING SUCCESS AND FAILURE 1142
*TAYLOR, L C E AND POULTER, L

CHARACTERIZATION OF E. COLI EXPRESSED HUMAN INTERLEUKIN-3 BY HIGH PERFORMANCE TANDEM MASS SPECTROMETRY 1144
*SCOBLE, H A,BOLOGNA, M L AND FOSTER, W B

STRUCTURAL CHARACTERIZATION OF THE IMMUNOACTIVE ENZYMATIC DEGRADATION PRODUCTS OF THE C3 COMPLEMENT PROTEIN BY FAB AND PLASMA DESORPTION-MS 1146
SCHNEIDER, K,MANZ, I,GERARDI, R,BITTER-SUERMANN, D AND *PRZYBYLSKI, M

A COMPREHENSIVE SUMMARY OF THE FRAGMENTATION OF PEPTIDE IONS UNDER CID CONDITIONS AND THEIR IMPLICATION FOR PEPTIDE SEQUENCING 1148
JOHNSON, R S,MARTIN, S A,VATH, J E AND *BIEMANN, K

CHARACTERIZATION OF INPURITIES IN SYNTHETIC PEPTIDES BY FAB MASS SPECTROMETRY 1150
*MATHEWS, W R,HAROLDSEN, P E AND GASKELL, S J

FAST ATOM BOMBARDMENT MASS SPECTROMETRY OF RECOMBINANT HUMAN -2 INTERFERON 1152
NAGABHUSHAN, T L,*LABDON, J E,PRAMANIK, B,TSARBOPOULOS, A,DAS, P, REICHERT, P,HASSELL, T C,BARTNER, P L AND TROTTA, P P

INACTIVATION OF DOPAMINE -HYDROZYLASE BY P-CRESOL: CHARACTERIZATION OF COVALENTLY MODIFIED ACTIVE SITE PEPTIDES BY MS AND TANDEM MS 1154
*CARR, S A,DEWOLF, W E,MENTZER, M,ROBERTS, G D AND KRUSE, L I

Ionization Methods. LC/MS Instrumentation and Techniques. Oligosaccharides.

RECENT DEVELOPMENTS IN HIGH MASS IONIZATION AND DETECTION SYSTEMS 1156
*ASHCROFT, A E,COLES, A D,EVANS, S,MILTON, D J AND WRIGHT, B

LIQUID SIMS OF SYNTHETIC PEPTIDES 1158
*KENNY, P T M,XU, W H,TACHIBANA, K AND NAOKI, H

FAST ATOM BOMBARDMENT, THERMOSPRAY AND DESORPTION CHEMICAL IONIZATION MASS SPECTROMETRY OF DIHYDROPYRIDINE PYRIDINIUM SALT-TYPE REDOX SYSTEMS 1160
*PROKAI, L,HSU, B-H AND BODOR, N

COMPARISON OF LSIMS (FAB) AND DCI MASS SPECTRA OF COBALTCARBONYL COMPLEXES OF PROSTAGLANDIN ANALOGUES 1162
*CHAN, K,SPILKIN, A,CARPIO, H,MENDEZ, J AND STRAUB, K

BEHAVIOR OF FATTY ACID MIXTURES IN VARIOUS FAST ATOM BOMBARDMENT MATRICES 1164
*CALDWELL, K,HAYES, R N AND GROSS, M L

MATRIX EFFECTS AND ION FORMATION IN FAST ATOM BOMBARDMENT MASS SPECTROMETRY OF CYCLIC DITHIO-DIAZA COMPOUNDS 1166
*HSU, B H

QUANTITATIVE FAB: IS WHAT YOU SEE WHAT YOU'VE GOT? 1168
*HUNT, S L AND LYON, P A

THE BEHAVIOR OF MIXTURES OF PHOSPHOLIPIDS IN THE FAB MATRIX 1170
*HELLER, D N,COTTER, R J,MURPHY, C M,UY, O M AND FENSELAU, C C

3-NITROBENZYL ALCOHOL - A VERSATILE MATRIX COMPOUND FOR FAB/MS 1172
*SWEETMAN, B J AND BLAIR, I A

OBSERVATION OF SURFACTANT CLUSTERS BY LIQUID SIMS 1174
*DORWIN, E L AND BETHEL, P W

ENHANCEMENT OF PEPTIDE IONIZATION IN FAST ATOM BOMBARDMENT MASS SPECTROMETRY USING A NITROCELLULOSE MATRIX 1176
*VAN BREEMEN, R B AND LE, J C

CHARACTERIZATION OF TETRAKIS(BENZAMIDINATO)DIRHODIUM(II) BY FIELD DESORPTION AND FAST ATOM BOMBARDMENT MASS SPECTROMETRY 1178
*LE, J C AND VAN BREEMEN, R B

FORMATION OF MOLECULAR IONS OF SUBSTITUTED GROUP VIB TRANSITION METAL CARBONYLS BY NEGATIVE ION FAST ATOM BOMBARDMENT MASS SPECTROMETRY 1180
VAN BREEMEN, R B,*MARTIN, L B AND SCHREINER, A F

VARIATIONS IN ANALYTE/MATRIX ION ABUNDANCES IN HIGH-PRESSURE FAST-ATOM BOMBARDMENT MASS SPECTROMETRY 1182
ROSS, M M AND *CALLAHAN, J H

THE INFLUENCE OF SURFACE EXCESS CONCENTRATION IN FAB-MS OF PEPTIDES 1184
*ALLMAIER, G M

AN INVESTIGATION OF TETRABUTYLAMMONIUM SALTS UNDER +/- FABMS 1186
*KEMPFF, M B AND HOOD, R J

MOLECULAR ION ENHANCEMENT OF NATURAL PRODUCTS USING SALTS IN FAB MATRICES 1188
*DAS, P R,PRAMANIK, B N AND BARTNER, P L

GLUTATHIONE AND NITROCELLULOSE: SOME OBSERVATIONS OF THE DEPENDENCE OF PEAK WIDTHS AND INTENSITIES IN PDMS SPECTRA UPON pH AND pI 1190
*SILLY, L,COTTER, R J AND FENSELAU, C C

COMPARISON OF FAB AND Cf-252-PD MASS SPECTROMETRY FOR THE ANALYSIS OF POLAR PESTICIDE METABOLITES 1192
*ALLMAIER, G M,SCHMID, E R AND ROEPSTORFF, P

ENHANCED PERFORMANCE OF A VOLCANO-FI SOURCE IN PULSED MODE 1194
YOUNG, S AND *COGGIOLA, M J

ELECTROHYDRODYNAMIC MASS SPECTROMETRY OF PEPTIDES 1196
*LEE, T D,LEGESSE, K,MAHONEY, J F AND PEREL, J

RECENT DEVELOPMENTS IN ELECTROCHEMICALLY ASSISTED FAB MS 1198
*BARTMESS, J AND PHILLIPS, L R

SOLID MATRICES: A METHOD OF IMPROVING INFRARED NEUTRAL MOLECULE DESORPTION 1199
BEAVIS, R C,LINDNER, J,*GROTEMEYER, J AND SCHLAG, E W

RESONANCE ENHANCED MULTIPHOTON IONIZATION OF NUCLEOSIDES AND OLIGONUCLEOTIDES 1201
*LUBMAN, D M AND LI, L

ANALYSIS OF ORGANIC SOLIDS BY COMBINED ION BEAM BOMBARDMENT AND SINGLE-PHOTON IONIZATION 1203
*PALLIX, J B AND BECKER, C H

INITIAL KINETIC ENERGY OF LARGE MOLECULES DESORBED BY 252Cf FISSION FRAGMENTS 1205
*JACOBS, D AND MACFARLANE, R D

PARENT MASS INFORMATION FROM SEQUENCES OF PEAKS FOR MULTIPLY CHARGED IONS 1207
*MANN, M,MENG, C K AND FENN, J B

SPUTTERING YIELDS FROM GLYCEROL BOMBARDED WITH IONS FROM A FOCUSED LIQUID METAL ION COLUMN 1209
*JIANG, L F,BAROFSKY, E AND BAROFSKY, D F

ALKALINE EARTH SALTS AS CATIONIZATION AGENTS IN LASER DESORPTION FOURIER TRANSFORM ION CYCLOTRON RESONANCE MASS SPECTROMETRY 1211
*BRACKEN, D E AND NIZOLEK, T J

WHAT HEATING RATES AND FINAL TEMPERATURES ARE REQUIRED FOR DESORPTION OF THERMALLY LABILE MOLECULES? INSIGHTS FROM THE DESROPTION/IONIZATION TECHNIQUE, K+IDS (K+ IONIZATION OF DESORBED SPECIES) 1213
*LIGHT, K J,KASSEL, D B AND ALLISON, J

EFFECTS OF ION PAIRING ON DESORPTION IONIZATION SAMPLING EFFICIENCIES 1215
*REYNOLDS, J D AND COOK, K D

AUTONEUTRALIZED SF6- FOR FAST NEUTRAL BEAM FT/ICR MASS SPECTROMETRY 1217
SHAMO, R E,DELMORE, J E,APPELHANS, A D,DAHL, D A AND *MARSHALL, A G

NEW CHEMICAL IONIZATION SOURCE FOR MASS SPECTROMETRY: USE OF LITHIUM ION ATTACHMENT TO MOLECULE 1219
*FUJII, T,OGURA, M AND JIMBA, H

TUNING AND CALIBRATION IN THERMOSPRAY MASS SPECTROMETRY 1221
*GREER, J F AND MARTIN, L L

OPTIMIZATION OF THERMOSPRAY VAPORIZER AND ION SOURCE 1223
VESTAL, C H,WILKES, J G,FERGUSSON, G J AND *VESTAL, M L

THE DEPENDENCE OF ION FORMATION ON THERMOSPRAY PLUME CHARACTERISTICS 1225
*LEE, M S AND YOST, R A

EFFECTS OF REPELLER GEOMETRIES ON THERMOSPRAY MASS SPECTRA 1227
*FINK, S W,FLORY, D A AND FREAS, R B

ENHANCED DETECTION OF SULFONATED AZO DYES USING THERMOSPRAY MASS SPECTROMETRY 1229
*MCLEAN, M A,FLORY, D A,VESTAL, M L AND FREAS, R B

METHODS TO PRODUCE LESS ACTIVE PROBE SURFACES TO MINIMIZE THE ADSORPTION AND CATALYSIS OF THERMOSPRAY PROBES 1231
*SMITH, P C AND YERGEY, A L

ALTERNATIVE IONIZATION PATHS FOR MAGIC-LC/MS 1233
*KIRK, J D AND BROWNER, R F

ON-LINE HPLC-MS WITH A CONTINUOUS-FLOW FAB INTERFACE 1235
*MCDOWALL, M A,GOULD, V,DOURDEVILLE, T,SLAUGHTER, C AND PRAMANIK, B

ACCURATE MASS MEASUREMENT IN CONTINUOUS FLOW FAST ATOM BOMBARDMENT QUADRUPOLE MASS SPECTROMETRY 1237
*MCDOWALL, M A AND ROBOZ, J

STUDIES WITH CONTINUOUS FLOW FAB LC/MS 1239
*PLEASANCE, S,VERGES, F M,RAMSEY, E D AND GAMES, D E

LC/MS WITH ATMOSPHERIC PRESSURE IONIZATION USING THE NERMAG R3010 TRIPLE QUADRUPOLE MASS SPECTROMETER 1241
*BRUINS, A P AND DEVANT, G

MASS SPECTROMETRY AS AN ONLINE ANALYSIS TECHNIQUE FOR COUNTER CURRENT CHROMATOGRAPHY 1243
*PANNELL, L K,ZHANG, T Y,CHOU, F E AND ITO, Y

PRELIMINARY STUDIES WITH AN ION CHROMATOGRAPHY MASS SPECTROMETERY SYSTEM 1245
*AL-OMAIR, A S AND TODD, J F J

DEVELOPMENT OF A THERMOSPRAY INTERFACE FOR FTICR MASS SPECTROMETRY 1247
*MILLEN, W G,MEEK, J T,THOMSON, M L,STOCKTON, G W AND WAYNE, R S

NEW DESIGN OF A SPLITTER FOR FRIT-FAB LC/MS AND BATCH LIQUID INLET SYSTEM 1249
KOBAYASHI, T,MATSUURA, K,OTSUKA, K,*KUBOTA, E,ITAGAKI, Y,MUSSELMAN, B D AND HIGUCHI, T

A DIRECT LIQUID INLET FOR TIME-OF-FLIGHT MASS SPECTROMETRY USING RESONANCED ENHANCED MULTIPHOTON IONIZATION/FRAGMENTATION 1251
*KINSEL, G R,SEGAR, K R AND JOHNSTON, M V

THERMOSPRAY AND NEGATIVE IONS. PURE ELECTRON CAPTURE PROCESS BY DISCHARGE IONIZATION 1252
*DE MAACK, F,DEVANT, G AND LESIEUR, M

OTLC/MS-COMPARISON OF QUADRUPOLE, ION TRAP AND MAGNETIC SECTOR INSTRUMENTS 1254
*MCGOWN, S R,MOSELEY, M A,DEWIT, J S M,TOMER, K B AND JORGENSON, J W

DEUTERIUM EXCHANGE AND ACTIVE HYDROGEN DETERMINATION IN MULTICOMPONENT ANALYSIS BY COMBINED LIQUID CHROMATOGRAPHY/THERMOSPRAY MASS SPECTROMETRY 1256
*EDMONDS, C G,POMERANTZ, S C,HSU, F F AND MCCLOSKEY, J A

HYDROGEN-DEUTERIUM EXCHANGE STUDIES UTILIZING THERMOSPRAY MASS SPECTROMETRY 1258
*SIEGEL, M M

SFC/MS ANALYSIS OF BIOLOGICAL SAMPLES WITH ELECTRON IONIZATION 1260
*HENION, J,LEE, E AND MCLAUGHLIN, L

APPLICATIONS OF SFC-MS TO TOXINS AND COMPOUNDS OF BIOLOGICAL INTEREST 1262
*UDSETH, H R,KALINOSKI, H T AND SMITH, R D

SUPERCRITICAL FLUID CHROMATOGRAPHY-MASS SPECTROMETRY (SFC/MS) USING A SIMPLE CAPILLARY-DIRECT INTERFACE 1264
*HAWTHORNE, S B AND MILLER, D J

INTRODUCTION OF AN SFC-CIMS INTERFACE: APPLICATION TO CARBOHYDRATES AND GLYCOCOCONJUGATES 1266
*SHEELEY, D M,KUEI, J C H,HER, G R AND REINHOLD, V N

STUDIES WITH PACKED AND CAPILLARY COLUMN SFC/MS 1268
*MYLCHREEST, I C AND GAMES, D E

THE IDENTIFICTATION OF INDOLE ALKOLOIDS USING SUPERCRITICALFLUID CHROMATOGRAPHY 1270
BALSEVICH, J,BERRY, A J,GAMES, D E,*HOGGE, L R AND MYLCHREEST, I C

PDMS OF 1-PROTEASE INHIBITOR GLYCOPEPTIDES 1272
*ALAI, M,TOWNSEND, R,HARDY, M,LEE, Y C AND FENSELAU, C

ANALYSIS OF BIOLOGICALLY-IMPORTANT OLIGOSACCHARIDES BY LC-MS 1274
*LAPPIN, G,GOULD, V AND ROGERS, M

POLYSACCHARIDE STRUCTURAL STUDIES USING LASER DESORPTION/FOURIER TRANSFORM MASS SPECTROMETRY 1275
*COATES, M L AND WILKINS, C L

NOVEL O-LINKED OLIGOSACCHARIDES ISOLATED FROM HUMAN GASTROINTESTINAL MUCINS 1277
*LAWSON, A M,HOUNSELL, E F,WILSON, S B,CASHMORE, G,STOLL, M AND FEIZI, T

EFFECTS OF CHEMICAL DERIVATIZATION OF OLIGOSACCHARIDES ON FRAGMENTATION IN LASER DESORPTION, PLASMA DESORPTION AND FAST ATOM BOMBARDMENT MASS SPECTROMETRY 1279
BEAN, M F,*MARTIN, W B,RALEY, T J,MURPHY, C M,COTTER, R J AND FENSELAU, C

FRAGMENTATION OF LIPOPOLYSACCHARIDE ANCHORS IN PLASMA DESORPTION MASS SPECTRA: THE LIPID A STRUCTURES FROM E COLI, R SPHAEROIDES, AND B ABORTUS 1281
*WANG, R,CHEN, L,COTTER, R J,QURESHI, N AND TAKAYAMA, K

CARBOHYDRATE ANALYSIS OF THE PRE-S(2) REGION OF HEPATITIS B SURFACE ANTIGEN 1283
*HEMLING, M E,CARR, S A,CAPIAU, C AND PETRE, J

FAB MS/MS FOR ANALYSIS OF A COMPLEX MIXTURE OF LIPO-OLIGOPEPTIDES FROM NOCARDIA RUBRA CELL WALL SKELETON 1285
*FUJIOKA, M,SENTOH, F,KODA, S AND MORIMOTO, Y

CHARACTERIZATION OF AN ACIDIC EXOPOLYSACCHARIDE ISOLATED FROM AN R. MELIOTI MUTANT 1287
*HER, G R,CHAN, S Y,REINHOLD, V N AND WALKER, G

PDMS ANALYSIS OF PEPTIDES, OLIGOSACCHARIDES AND GLYCOPEPTIDES 1289
*SCANLAN, G,BENSON, L,TSARBOPOULOS, A AND JARDINE, I

FAST ATOM BOMBARDMENT MASS SPECTROMETRY OF HEPARIN-DERIVED, HIGHLY SULFATED OLIGOSACCHARIDES 1291
*MALLIS, L M,WANG, H M AND LINHARDT, R J

ENHANCED SEPARATION AND LSIMS FRAGMENTATION OF CHEMICAL DERIVATIVES OF OLIGOSACCHARIDES CONTAINING 2-KETO-3-DEOXY OCTONIC ACID (KDO) 1293
*JOHN, C AND GIBSON, B W

APPLICATIONS AND FURTHER DEVELOPMENTS OF LIQUID CHROMATOGRAPHY-FAST ATOM BOMBARDMENT-MASS SPECTROMETRY (LC-FAB-MS) USING A CONTINUOUS FLOW FAB PROBE 1295
*ASHCROFT, A E AND HEROD, A A

SECONDARY ION MASS SPECTROMETRY OF SOLUTE PARTICLE BEAMS BY THERMABEAM LC/MS 1297
*WILLOUGHBY, R C,BUCHNER, J D AND SHEEHA, E W

PLENARY LECTURE: THE FUTURE OF MASS SPECTROMETRY: PART I 1299
COOKS, R G

Symposium: Ion Trapping - Methods and Applications.

ANALYTICAL CAPABILITIES AND APPLICATIONS OF FT/ICR MASS SPECTROMETRY 1302
*MARSHALL, A G

ENERGY- AND TIME-RESOLVED MEASUREMENTS IN MASS SPECTROMETRY 1304
*LIFSHITZ, C

RF QUADRUPOLE ION TRAPS - PAST, PRESENT AND FUTURE (?) 1306
*TODD, J F J

Liquid Introduction Mass Spectrometry.

COMPARISON OF THERMAL ASSISTED AND PHNEUMATIC ASSISTED NEBULIZATION FOR ELECTROSPRAY LC/MS 1308
*LEE, E D,HENION, J AND COVEY, J

EVALUATION AND OPTIMIZATION OF CONTINUOUS FLOW FAST ATOM BOMBARDMENT INTERFACES BETWEEN OPEN TUBULAR LIQUID CHROMATOGRAPHY AND MASS SPECTROMETRY 1310
*MOSELEY, M A,DEWIT, J S M,DETERDING, L J,TOMER, K B AND JORGENSON, J W

MS/MS AND CF-FAB FOR THE ANALYSIS OF DRUGS 1312
*SEIFERT, W E,LIN, S-N,MOORE, W T,CAPRIOLI, R M,STORY, M AND BRADFORD, D

CONTINUOUS-FLOW FAB LC/MS ANALYSIS OF ACYL-CoA COMPOUNDS USING MICROBORE HPLC COLUMNS 1314
*MILLINGTON, D S AND NORWOOD, D L

ON LINE MONITORING OF NONVOLATILE PRODUCTS OF BIOCATALYTIC REACTIONS BY MASS SPECTROMETRIC DETECTION 1316
*BRUINS, A P AND PRAS, N

IMPROVEMENTS IN A MAGIC LC/MS INTERFACE 1318
*APFFEL, A AND NORDMAN, R

CHARGE EXCHANGE REACTIONS WITH WATER IN THE DETECTION OF PERFLUOROCARBONS BY THERMOSPRAY LIQUID CHROMATOGRAPHY/MASS SPECTROMETRY 1319
*HUANG, S K,MCLOUGHLIN, M AND KLEIN, D H

ANALYSIS OF MIDDLE MASS PEPTIDES BY THERMOSPRAY LC/MS AND LC/MS/MS 1321
LEWIS, S AND *RUDEWICZ, P

FUNDAMENTAL STUDIES OF SOLUTION-PHASE AND GAS-PHASE REACTIONS IN ELECTROCHEMISTRY/THERMOSPRAY/TANDEM MASS SPECTROMETRY 1323
*VOLK, K J,BRAJTER-TOTH, A AND YOST, R A

A FUNDAMENTAL STUDY OF SUPERCRITICAL FLUID MASS SPECTROMETRY 1325
*OLESIK, S V AND PEKAY, L A

A Mass Spectral Potpourri.

ON-LINE (PYROLYSIS) AND OFF-LINE MICROSCALE DEGRADATION COMBINED WITH GC-MS AND FAB-MS: A USEFUL TOOL FOR STRUCTURE ELUCIDATION OF COMPLEX ORGANIC MOLECULES 1326
*VANGAEVER, F

CHARACTERISTICS OF MULTIPOLE COLLISION CELLS 1328
*SYKA, J E P,COTTRELL, J S AND SZABO, I

OBTAINING STRUCTURE INFORMATION OF PERFLUOROCARBONS FROM MASS SPECTRA: EFFECT OF TEMPERATURE, ELECTRON ENERGY, COLLISION GAS, AND HIGH ENERGY COLLISIONAL ACTIVATION 1330
*HUANG, S K

COLLISIONAL ACTIVATION WITH THE DUAL CELL FOURIER TRANSFORM MASS SPECTROMETER: RECENT RESULTS 1332
*CODY, R B AND WEIL, D A

CHEMICAL IONIZATION AS A POSTIONIZATION METHOD FOR LASER-DESORBED NEUTRALS 1334
*AMSTER, I J,LAND, D P,HEMMINGER, J C AND MCIVER, R T

BUTYLBENZENE RADICAL CATION THERMOCHEMISTRY FROM PEPICO EXPERIMENT USING SYNCHROTRON RADIATION; COMPARISON WITH ION ENERGY MEASUREMENT IN LOW ENERGY CAD 1336
DUTUIT, O,BAER, T,JAOUEN, D AND *ROLANDO, C

HIGH RESOLUTION LDI-FT-ICR MASS SPECTROMETRY OF UNDERIVATIZED OLIGOSACCHARIDES OBTAINED FROM BIOPOLYMERS 1338
COMISAROW, M B,DUTTON, G G S,*LAM, Z,WEIL, D A AND BJARNASON, A

MASS SPECTROMETRIC ANALYSIS OF SYNTHETIC PEPTIDES 1340
*CHAIT, B T

TAGA6000E QA/QC ANALYSIS PROCEDURES USED AND THE ASSOCIATED DATA GATHERED DURING FOUR, TWO WEEK BLOCKS OF INDOOR AIR ANALYSES AT THE LOVE CANAL EMERGENCY DECLARATION AREA 1342
PRITCHETT, T H,*MICKUNAS, D AND BERNICK, M

Metabolism and Toxicology. Computational Aspects.

OPTIMIZATION OF THE GCMS METHODOLOGY TO MONITOR MULTIPLE LABELED ANALOGS OF ARGININE AND ORNITHINE 1344
*VAN LANGENHOVE, A,MARKS, L M,LIN, V K,HOERR, R A AND YOUNG, V R

QUALITATIVE AND QUANTITATIVE ANALYSIS OF ACYLCARNITINES IN HUMAN PLASMA AND TISSUES BY FAB-MS 1346
INOUE, F,*GALE, D AND MILLINGTON, D S

IDENTIFICATION AND QUANTITATION OF URINARY ADIPIC ACID METABOLITES BY GC/MS 1348
*JIN, S-J AND TSERNG, K-Y

A GC/MS INVESTIGATION OF IN VITRO METABOLITES OF CANNABICHROMENE AND CANNABIGEROL IN SEVERAL SPECIES 1350
*HARVEY, D J AND BROWN, N K

METABOLISM STUDY OF ETHYLCYCLOHEXANE IN MALE FISCHER 344 RATS 1352
*YU, K O,ROBERTS, J,SERVE, M P AND MCDONALD, G A

IDENTIFICATION OF THE URINARY ARGININOSUCCINIC ACID IN ADULT CITRULLINEMIA BY FAB MS/MS 1354
*MATSUMOTO, M,INOUE, Y,OHKURA, T,ISA, K AND MATSUMOTO, I

ASSESSMENT OF HEXOSE MONOPHOSPHATE SHUNT ACTIVITY IN NEOPLASTIC CELLS 1356
*KRICK, T P,MITCHELL, S,ROSS, B D AND GARWOOD, M

SIMULTANEOUS QUANTITATION OF GEPIRONE AND 1-PP IN HUMAN PLASMA BY CAPILLARY GAS CHROMATOGRAPHY-MASS SPECTROMETRY 1358
*SCIACCA, M A,SHEA, J P,DUNCAN, G F,FAULKNER III, H C,FARMEN, R H AND PITTMAN, K A

METABOLIC PROFILING OF VALPROIC ACID IN PATIENTS USING NEGATIVE ION CHEMICAL IONIZATION GCMS 1360
ABBOTT, F S,*KASSAHUN, K,BURTON, R AND FARRELL, K

HIGH VOLTAGE AND MAGNETIC SCANNING FOR MIXTURE AND TYPE ANALYSIS USING A PERSONAL COMPUTER 1394
*WITTSTRUCK, T A AND ESKEW, T J

A NEW METHOD FOR ACCURATE MASS MEASUREMENT OF POSITIVE AMMONIA CHEMICAL IONIZATION MASS SPECTRA 1396
*HADDON, W F,MILLINGTON, D S,ENGLAND, R E,ELLIGER, C A AND MANNERS, G D

COMPUTER PROGRAMS FOR THE INTERPRETATION OF CID MASS SPECTRA OBTAINED FROM PEPTIDES OF UNKNOWN SEQUENCE 1398
*JOHNSON, R S AND BIEMANN, K

COMPUTER AIDED PEPTIDE SEQUENCING (CAPS) BY FAB MASS SPECTROMETRY 1400
ISHIKAWA, K AND *NIWA, Y

COMPUTER IDENTIFICATION OF BACTERIA VIA MS WITH CI 1402
*CONWAY, D C,LOPEZ, H AND QUARLES, J M

TOF-SIMS DATA SYSTEM 1404
*WYATT, J R,COLTON, R J AND HUES, S M

USE OF AN HP-1000 GC/MS DATA REDUCTION ENVIRONMENT AND LOTUS/1-2-3 FOR THE RAPID EVALUATION OF LOW-LEVEL PCB ANALYSIS DATA 1406
*MCKENZIE, D E AND HUGHES, B M

NETWORKING MASS SPECTROMETER DATA SYSTEMS 1408
*JOHNSON, R,JACKSON, J,HEWITT, J AND TAYLOR, L

UTILITY PROGRAMS FOR FACILITATING CONTRACT LABORATORY PROGRAM DATA PACKAGE PREPARATION 1409
*HWANG, E Y AND WINGENDER, R J

OPTIMIZATION OF GC/MS DATA ANALYSIS USING HEWLETT PACKARD MACRO PROGRAM ENHANCEMENTS 1411
CODY, J T AND *MARCOVICH, D T

DEVELOPMENT OF NOVEL ON-LINE TECHNIQUES FOR GC/MS AUTOMATION IN ENVIRONMENTAL LABORATORIES 1413
*PRILL, G E AND HEADLEY, J V

A STRUCTURED MACRO LANGUAGE FOR CONTROLLING GC/MS DATA REDUCTIONS 1415
*COLBY, B N,RYAN, P W,D'ARCY, P H AND BUTTLER, I

THE PC AS A VIABLE ALTERNATIVE TERMINAL FOR THE INCOS DATA SYSTEM 1417
*BENOIT, F M

THE USE OF PC-COMPATIBLE COMPUTERS TO PULL AND FURTHER REDUCE DATA FROM A SCIEX TAGA 6000E MASS SPECTROMETER/MASS SPECTROMETER 1419
*LOY, G,BOTTOMLEY, S AND PRITCHETT, T H

AN IMPROVED VERSION OF THE NBS/EPA/MSDC MASS SPECTRAL DATA BASE WITH SEARCH AND DISPLAY SOFTWARE FOR AN MS-DOS PERSONAL COMPUTER 1421
STEIN, S E,LIAS, S G,*BUDDE, W L,TERWILLIGER, D T AND BEHBEHANI, A L

DEVELOPMENT OF A PROPOSED NATIONAL REFERENCE SET OF ELECTRON IMPACT GC/MS RELATIVE RESPONSE FACTORS FOR THE U.S. ENVIRONMENTAL PROTECTION AGENCY'S CONTRACT LABORATORY PROGRAM 1423
*SAUTER, A D,DOWNS, J J,ISAACSON, P,BOTTRELL, D,YOUNGMAN, D,FISK, J, DEMPSEY, C AND CARASEA, A

AN ELECTRONIC MASS SPECTRAL DATA BOOK 1425
*MAEDA, K AND ROKUSHA, H

Presented at the 36th ASMS Conference on Mass Spectrometry and Allied Topics
June 5-10, 1988, San Francisco, CA

ELEMENTAL AND ISOTOPIC ANALYSIS BY SECONDARY ION MASS SPECTROMETRY

Charles W. Magee
Evans East, Inc.
666 Plainsboro Road, Suite 1236
Plainsboro, New Jersey 08536

Secondary ion mass spectrometry has been used for elemental and isotopic analysis for over 20 years. Yet, contrary to what one might expect, the technique is not a mature one by almost any measure one would like to make. Instrumentation is still evolving. The theory of ion production is still not understood. Most importantly, however, as the materials research community develops new technologies and continues to shrink the dimensions of current technology, SIMS analysts and instrument developers are forced to push the technique to its limits in order to provide answers to questions which continue to get more difficult. The current state of SIMS as applied to elemental and isotopic analysis will be reviewed, with emphasis on the following areas:

Bulk elemental detection limits
Bulk elemental precision and accuracy
Depth profiling detection limits
Depth profiling precision and accuracy
Depth resolution
X Y Spatial resolution

A central theme common to all these topics will become apparent, and that is the fact that elemental and isotopic analysis by secondary ion mass spectrometry is a science of numbers. It is not and "observational" technique where questions can be answered by the presence or absence of a peak(s) in a mass spectrum. Rather, one must measure elemental concentra-tions or isotopic ratios with great precision and accuracy, at very low concentrations and often with very good depth resolution. These are the challenges which continue to make SIMS such an interesting field.

Bulk Detection Limits

SIMS is not often thought of as a bulk analysis technique because of its unparalleled sensitivity as a depth profiling tool for thin films. This same high sensitivity can be further exploited in a bulk analysis mode where one is not limited by the amount of sample which may be consumed in order to make a measurement. This has been demonstrated recently [1] by using SIMS for the ultra trace detection of uranium and thorium in aluminum used in integrated circuit manufacturing. These elements have been measured (not just detected) at the 0.02 part per billion level, or 20 parts per trillion, or approximately 10^{-20} moles of U and Th detected per measurement point. This is a truly impressive analysis.

Bulk Precision and Accuracy

SIMS, when used for bulk analysis, is also capable of very impressive performance in terms of precision and accuracy. Again, the inherent high sensitivity of the technique makes it possible to obtain high countrates for even trace impurities thus making it possible to obtain high precision analyses. The technique has been used for detection of oxygen in single crystal silicon at the 10 ppm level with precisions and accuracies considerably better than +/ 10% [2].

Depth Profiling Detection Limits

As stated above, SIMS is best known as a depth profiling technique, and as such, it is capable of obtaining exceptionally low detection limits for elements in thin films while maintaining depth resolutions of better than 500 Angstroms. SIMS has been shown by at least one laboratory [3] to be capable of routine detection of trace impurities in III-V materials at the mid 10^{13} atom/cc range, with demonstrated detection limits of some elements down to 10^{12} atoms/cc, or 0.02 ppb atomic. At this level of performance, one is detecting the presence of only several hundred atoms within the analyzed volume of the sample.

Depth Profiling Precision and Accuracy

Not only must one be able to obtain high sensitivity in SIMS depth profiling, but the analyses must be precise and accurate. One particularly exacting requirement for such analyses is in the determination of the total dose of ions which are implanted into semiconductors in integrated circuit fabrication. SIMS has been shown [4] to be able to measure doses of the order of 10^{15} atoms/cm^2 (equivalent to approximately one monolayer of atoms) with precisions and accuracies of better than 2%. This is approaching the accuracy obtainable with more conventional techniques such as electron probe microanalysis, but the concentrations of elements being measured using SIMS are several orders of magnitude lower than those detectable by the electron probe.

Depth Resolution

As stated in the preamble of this work, materials researchers are continuing to develop fabrication technologies which push the state of SIMS to its limits. This is especially true in IC processing where the trend is to smaller and smaller dimensions, not only across the surface of the chip, but also in depth. SIMS is now being called on to measure accurately changes in elemental concentrations over depths of as little as several tens of Angstroms. An example of such an analysis is the determination of in-depth profiles of dopants which are implanted into semiconductors to exceedingly shallow depths, typically less than 100 Angstroms. It has been shown that SIMS can determine such profiles (arsenic implanted into silicon, for example) with depth resolutions of better than 15 Angstroms [5]. But in the future, we will be called upon to analyze even thinner layers as the use of strained layer superlattices becomes more widespread. In that technology, layers are grown which are only several atoms thick. This will certainly provide a formidable challenge to the SIMS analyst in the coming years.

X - Y Spatial Resolution

SIMS has also advanced to an unprecedented level in the area of spatial resolution across the sample surface, and in the area of image processing. Mass resolved elemental images can now be obtained with resolutions of better than 200 Angstroms [6]. This is approaching the lateral extent of an individual collision cascade induced in a sample by the primary ion. This level of achievement is one of the few examples in analytical chemistry where instrumentation has approached ultimate limit of a measurement imposed by the physics of the measurement itself; the analytical chemist's version of the Heisenberg Uncertainty Principle.

However, not only can we obtain very high resolution ion images of surfaces using SIMS, but we have advanced in our use of the image data. Hardware and computer techniques have been developed [7] which enable the analyst to keep track of the total number of secondary ions detected in each pixel of and image, and to store a succession of images in memory such that one can reconstruct the entire three-dimensional concentration distribution of one or several elements within a given analyzed volume. And in keeping with the theme of quantitative analyses, these 3-D data can be converted into quantitative depth profiles, line scans and x - y maps which are quantitative in concentration.

---

1. J.C. Huneke, S.P. Smith, and R.J. Blattner, CHARLES EVANS AND ASSOCIATES, (personal communication)
2. R.J. Bleiler, R.S. Hockett, P. Chu, and E. Strathman, Materials Research Society Symp. Proc. Vol. 59, MRS 1986.
3. A.M. Huber and G. Morillot, SIMS V, Springer Series in Chemical Physics Vol. 44, 353, Springer-Verlag, Berlin, (1986).
4. C.W. Magee and K.G. Amberiadis, ibid, 279.
5. C.W. Magee (unpublished).
6. R. Levi-Setti, G. Crow, and Y.L. Wang, Springer Series in Chemical Physics Vol. 44, 132, Springer-Verlag, Berlin, (1986).
7. These techniques developed by CHARLES EVANS AND ASSOCIATES.

Presented at the 36th ASMS Conference on Mass Spectrometry and Allied Topics
June 5-10, 1988, San Francisco, CA

Nonresonant Multiphoton Ionization for Sensitive Elemental Analysis

C. H. Becker and J. B. Pallix
Chemical Physics Laboratory
SRI International
Menlo Park, California 94025

High detection efficiency and quantitation are necessary for measurements of small amounts of solid sample requiring high spatial resolution. When examining non-uniform materials, especially interfacial regions, matrix effects associated with SIMS make this technique unreliable. Because most sputtered atoms and molecules are neutral in charge, detection of the sputtered neutral fraction by nonselective postionization is a much more stable and reliable approach. A high sensitivity like SIMS enjoys is desirable because high dynamic range measurements can be made with high lateral and depth spatial resolutions. For general (nonselective) analysis, to date only the surface analysis by laser ionization (SALI) method[1,2] has a high efficiency comparable to but more uniform than SIMS (useful yield $\sim 10^{-3}$). For comparison, overall system useful yields are lower by 4-5 orders of magnitude using other nonselective postionization approaches (electron impact and RF low pressure plasma).

The SALI method uses nonselective photoionization of desorbed atoms and molecules by an untuned laser source followed by reflecting time-of-flight mass spectrometry (TOF-MS). For elemental analysis, nonresonant multiphoton ionization (MPI) by a very intense, pulsed, focused, UV laser beam is used. This nonlinear photoionization typically requires laser beam intensities $>10^9$ W/cm^2 for efficient and uniform ionization due to saturation. The intensity required to reach saturation depends to a large extent on the number of photons required, especially for small numbers of photons (say 1-4). Most species can be efficiently ionized by 2 photons with wavelengths such as 193, 248, and 266 nm. Just a few atoms require more than 2 photons at 193 nm (6.42 eV/photon), and are generally not efficiently ionized with common lasers. Common lasers for ionization are a single-cavity excimer or frequency-quadrupoled Nd:YAG laser. More powerful lasers such as chirped-pulse amplified solid-state lasers[3] could routinely saturate even He photoionization.

Material removal is usually by ion beam sputtering though electron-stimulated, laser-induced, and thermal desorptions are used in some instances. Ion beam sputtering is a very convenient spatially resolved surface probe.

An example of a sputter depth profile through an interface is shown in Fig. 1. The sample was a 2000 Å thick polycrystalline Si sample on a thin SiO_2 layer on crystalline Si implanted with 10^{15} F atoms/cm^2 at 93 keV. The mobility of F under annealing conditions was the processing issue highlighted in this work. But in Fig. 1, the F depth distributions are shown of unannealed samples where a smooth F distribution is expected. A comparison is made of SALI and a SIMS profile, the latter taken on a Cameca instrument. The SIMS data shows the common influence of matrix effects at an interface. Using a standard excimer laser focused to about 10^{10} W/cm^2 the atomic F ionization efficiency at 193 nm (3 photons to ionize) is low, but the neutral sputtered diatomic molecule SiF still provides a sensitive and useful monitor of the F concentration.

Another study involved thin anodic oxide layer growth on alloys for corrosion prevention. For the dilute alloys based on Ni (6% of Al, Ti, or Mo), an enhancement effect in the amount of dilute metal incorporated into the oxide is seen to be in the order Mo>Ti>Al in agreement with the prediction of a theory of solute segregation which says the dominating effect is the difference in valency between the solute metal and the base metal vacancy. Furthermore, the compensating depletion of this minor alloy component is clearly seen; these data will determine diffusion coefficients for the solute metals in the base metal. Though O atoms are not efficiently detected, note the direct O atom signal marks the oxide layer. Note also the H detection. The nonzero H signal at longer sputter times is from H_2 gas phase background.

The authors thank Peter Wright and Mordehai Ben-Haim for providing the F/Si and Ni alloy samples, respectively.

References

1. C. H. Becker and K. T. Gillen, Anal. Chem. 56, 1671 (1984).
2. J. B. Pallix, C. H. Becker, and N. Newman, Bulletin Mat. Res. Soc., Vol XII, No. 6 (1987), p. 52.
3. D. Strickland, P. Maine, M. Bouvier, S. Williamson, and G. Mourou, in Ultrafast Phenomena V. G. R. Fleming and A. E. Sigmond, eds. (Springer-Verlag, Berlin, 1986), p. 38.

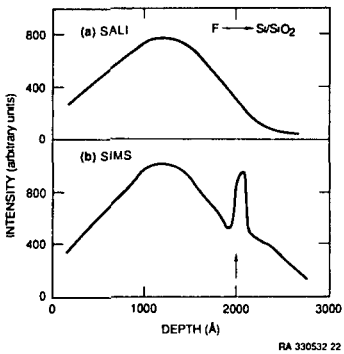

Fig 1. Relative concentrations as a function of depth (depth profiles) of F implanted into Si on SiO_2 measured by (a) SALI with Ar^+ sputtering and 248 nm photoionization, and by (b) positive ion SIMS with O_2^+ sputtering. The arrow marks the Si/SiO_2 interface. A smooth distribution of F through the interface is expected.

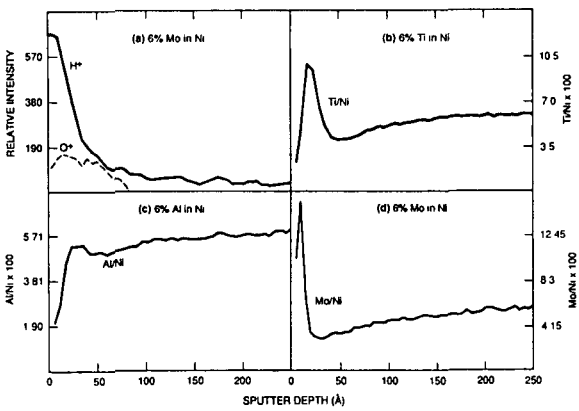

Fig 2. Depth profiles of anodic oxides grown on Ni. Part (a) shows the relative variations in O and H in the oxide layer grown on the alloy 6% Mo in Ni. Part (b), (c), and (d) shows the ratios of three different 6% solutes (Ti, Al, and Mo, respectively) to the base metal Ni through the oxide region into the metal.

Presented at the 36th ASMS Conference on Mass Spectrometry and Allied Topics
June 5-10, 1988, San Francisco, CA

SOLIDS ELEMENTAL ANALYSIS BY GLOW DISCHARGE MASS SPECTROMETRY: W. W. Harrison, Department of Chemistry, University of Virginia, Charlottesville, VA 22901.

Introduction

Glow discharge mass spectrometry (GDMS) is a technique generating increasing interest (1) in elemental analysis circles. A key factor is its ability to perform direct analysis of solids, obviating the need to carry out tedious, time consuming, and at times incomplete dissolutions. GDMS has several analytical advantages that make it increasingly attractive: low to sub-ppb detection limits; relatively uniform elemental response (3X); minimal matrix effects; isotopic information; simple spectra; rapid qualitative and quantitative results. Figure 1 shows a simplified drawing of a glow discharge ion source.

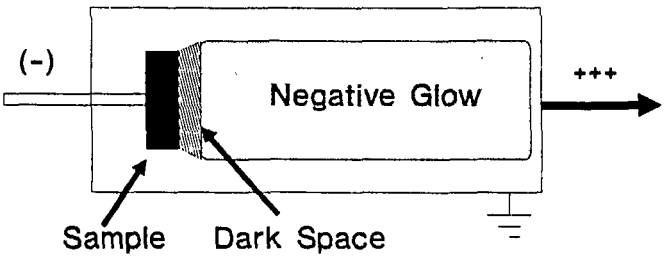

Figure 1. Representation of a glow discharge ion source.

Gas discharges have been studied for many years by both optical and mass spectrometry. Emphasis has been on gaining better insight into the species formed, the reactions they undergo, and other fundamental aspects of discharges. Only more recently, however, has attention turned to analytical details and the role of sputtered species (the analytical sample) in these rich and efficient plasma interactions. As this area becomes more fully developed, GDMS will operate from a better foundation so that theory enhances practice.

GDMS Instrumentation

The glow discharge source lends itself to various types of mass analysis apparatus. Quadrupole units have found the greatest application in research, although the only present commercial instrument is a magnetic sector type (2). The latter approach provides sufficient mass resolution to separate many spectral interferences, but certainly not all. Quadrupole based instruments have a significant price advantage and are easily interfaced to the glow discharge; the analyst must, however, be alert to potential unresolved interferences at high sensitivity conditions. New approaches are being studied in which collision induced dissociation (CID) is used to break up polyatomic ions in a glow discharge effluent, thus permitting in principle the broader use of quadrupole analyzers.

Relevance of GDMS in Elemental Analysis

The major use of GDMS has been in the elemental analysis of metals and alloys, in many cases replacing spark source mass spectrometry as the technique of choice. Metal samples require little or no pretreatment, other than cutting to fit the sample holder. The glow discharge serves to perform a final cleaning of the surface in the initial sputter process. Nonconducting samples must be mixed with a conducting matrix and compacted into a form suitable for source mounting. Selection of matrix is important; the material must be of high purity, have good compacting characteristics, and contribute minimal background. The opportunity exists to select chemically reactive matrices, such as getters, that can produce favorable plasma conditions for complex samples. Earth materials are particularly difficult given their strong bond energies and built-in oxygen environment, but the glow discharge has been effective in breaking down such samples into atomic components.

The nature of glow discharge sputtering suggests the possibility of surface analysis, applications of which have been reported. The low energy ions in a glow discharge do not penetrate far into the surface, minimizing atomic mixing. However, sharp transitions between films can be broadened by redeposition effects. RF discharges, operating at lower pressures than do DC discharges, may be useful in reducing these redeposition problems. In addition to thin film analysis, similar methodology can be applied to the residue analysis of solutions dried onto a conducting support. Some utility can be realized for small solution samples, particularly considering the concentration effect produced by the evaporation step.

At present, the more rapid spread of GDMS is limited by the high cost of commercial instrumentation. The availability of less expensive alternatives could make it much more accessible to a wide variety of laboratories where it would seem logically to have potential application.

References

1. W.W. Harrison and B.L. Bentz, Prog. Analyt. Spectros. 11, 55 (1988).
2. N. Sanderson, E. Hall, J. Clark, P. Charlambous, and D. Hall, Mikrochim Acta, I, 275 (1987).

Presented at the 36th ASMS Conference on Mass Spectrometry and Allied Topics
June 5-10, 1988, San Francisco, CA

The Development of High Precision Mass Spectrometry

I. Lynus Barnes
National Bureau of Standards
Center for Analytical Chemistry
A-23 Physics Building
Gaithersburg, MD 20899

The search for high precision in mass spectrometric measurements has been fundamental since the invention of the instrument even though it was most difficult to obtain in the early spectrometers. Most of them used photographic plates as detectors, small "furnaces" as sources for solids and stabilized power supplies were still to be discovered. Aston, for example, analyzed a number of elements[1] and with improved versions of his instrument measured both concentration and composition of a number of different elements. High precision only as a relative term was obtained from the blackening of the photographic plates.

The invention (or discovery) of the electrometer tube in the 1930s however meant that truly high precision measurements were possible, but the most important development came in 1940 with the construction by A.O. Nier of the first successful sector mass spectrometer[2] This meant that instruments with lighter magnets (with the corresponding lower power requirements) but with adequate resolution and sensitivity could be used for isotopic measurements. During the following few years many sector mass spectrometers were constructed for measurements of the enrichment of uranium isotopes in separation facilities and for controlling the process stream in the gas diffusion plant[3]. As a natural part of this, many improvements were made in the instruments and in the associated electrical and electronic circuitry. Of developments during this period that were important to later general use, the author counts the development of the "gaussmeter", early "electrometer amplifiers", and the refinement of the electron impact ion source (discovered earlier by Bleakney[4]) as of particular interest. Because of the use of these instruments for the measurements of small isotopic differences, high precision became an important concept.

With the end of the War there was renewed interest in the use of mass spectrometers in solving problems in physics, chemistry and geology, many new instruments were constructed and commercial instruments became available with the result that vast amounts of very high quality data became available. A few examples of this are the work done by Wasserburg and his colleagues on the returned Lunar samples[5] and on many other materials, that done by Tatsumoto and co-workers[6] also on the returned Lunar materials, the work on the redetermination of the atomic weights of the elements done at the National Bureau of Standards[7] and that done by Lugmair and co-workers[8] on the development of the Nd-Sm dating system. Limited space forces the omission of many, many others with significant contributions to the very high precision data obtained within the past decade.

Although steady improvement continues on these spectrometers, recent advances in high precision mass spectrometry have come with the development of a new group of instruments based on multiple collection of several (3 or more) beams at the same time. These are the result of work published many years ago by Cross[9] that showed that if ion beams were allowed to enter a magnetic field at an angle (selected) other than normal increased dispersion resulted. While this increased dispersion permitted the use of multiple collectors with the advantageous of time, an at least equal benefit is that focussing in the "Z" direction is achieved and greatly improved ion beam throughput results. Several commercial instruments are now available and data is becoming available to demonstrate that the predicted improvements are obtained. In fact, precision obtained indicate that the limit of error in many analyses come from the inability to prepare samples sufficiently well in the laboratory and research effort in the chemical manipulation will be required before further advances will be realized.

References:

1. Aston, F.W., 1919, A positive ray spectrograph, Phil. Mag., v.38, 707-714.

2. Nier, A.O., 1940, A mass spectrometer for routine isotope abundance measurements, Rev. Sci. Instrum., v.11, 212-216.

3. Nier, A.O., Pickard, T.A., Leland, W.T., Taylor, T.I., Stevens, C.M., Drukey, D.L. and Goertzel, G., 1948, Recording mass spectrometer for process analysis, Anal. Chem., v. 20, 188-192.

4. Bleakney, W., 1932, The ionization potential of molecular hydrogen, Phys. Rev., v. 40, 496-501.

5. Piepgras, D.J. and G.J. Wasserburg, 1982, Isotopic composition of neodymium in waters from the Drake Passage, Science, v. 217, 207-214.

6. Nakamura, N., Tatsumoto, M., Nunes, P.D., Unruh, D.M., Schwab, A.P., and Wildeman, T.R., 1976, 4.4 b.y.-old Clast in Boulder 7, Apollo 17, Proc. Lun. Sci. Conf. 7, v. 2, 2309.

7. Machlan, L.A., Gramlich, J.W., Powell, L.J. and Lambert, G.M., 1986, Absolute isotopic abundance ratio and atomic weight of a reference sample of gallium, J. Res. N.B.S., v. 91, 323-331.

8. Lugmair, G.W., Scheinin, N.B., and Marti, K., 1975, Sm-Nd age and history of Apollo 17 basalt 75075, Proc. Lun. Sci. Conf. 6th., v. 2, 1419-1429.

9. Cross, W.G., 1951, Two-directional focusing of charged particles with a sector-shaped uniform magnetic field., Rev. Sci. Instrum., v. 22, 717-722.

Presented at the 36th ASMS Conference on Mass Spectrometry and Allied Topics
June 5-10, 1988, San Francisco, CA

ADVANCES IN THERMAL IONIZATION MASS SPECTROMETRY

D. A. Papanastassiou, Division of Geological and Planetary Sciences, California Institute of Technology, Mail Code 170-25, Pasadena, CA 91125.

During the last decade it has been possible to demonstrate that thermal ionization mass spectrometry can yield high sensitivity and high precision isotopic analyses. The major advances for high precision have involved improvements in the duty cycle for the measurement of isotopic ratios and in the ionization efficiency for a substantial number of elements. Improvements in the duty cycle were provided by a new generation of mass spectrometers which included: a) the ability to control precisely the magnetic field (2ppm under static conditions); b) the ability to step the magnetic field at a fast rate (2kgauss/sec slewing rate; 0.3sec lock-in time; 10ppm reproducibility under these dynamic conditions); c) fast response electrometers, coupled with digitization of the ion beam measurement (Wasserburg, Papanastassiou, Nenow, and Bauman, 1968). These improvements can, for the last ten years be found also in commercially available mass spectrometers. In addition, recent advances include the introduction of multiple Faraday cup detectors for the simultaneous measurement of ion beams. The use of these systems on relatively low dispersion instruments has resulted in delicate, low mechanical tolerance collector assemblies which depend on continued manufacturer support and development. With care, high precision data can be obtained by the use of simultaneous ion beam detector systems. The obvious advantages are increased duty cycle (by the inverse of the number of isotopes that are measured) and less dependence on the ion beam stability in the source. The disadvantages include the need for calibration of multiple electrometer systems, and the need to ascertain that the ion transmission and detection are independent of the source parameters and beam shape, at the level of the quoted precision. More experience with multiple collector systems is required before these issues can be resolved. Care will be required to establish that reproducibility ("external precision") is consistent with error estimates from individual analyses ("internal precision"). It is also important to consider that a substantial improvement in multiple collector systems can be obtained by their introduction to higher dispersion instruments.

For improvement in sensitivity for thermal ionization sources, extensive work has been devoted to improvements in ionization efficiency for various elements. Since ionization efficiency ($f_N = N^+/N^o$) is an exponential function of the ionization potential, the filament work function, and the temperature, substantial improvements have been possible. Specific cases include: a) f_{Mg} up to 10%, using as an emitter colloidal SiO_2 (Si-gel; typically obtained by hydrolysis of $SiCl_4$) and phosphoric acid; b) f_{Cr} of about 10^{-3}, using Si-gel and boric acid; c) f_{Pb} of 15% using Si-gel and phosphoric acid; d) NdO^+/Nd of up to 50%, with a slight increase of the oxygen partial pressure in the filament region, without adverse effects in mass resolution; f_{NdO^+} on a single filament assembly is at least a factor of 100 higher than f_{Nd^+} from a double filament source assembly; e) f_{TiO^+} of 0.01%; TiO^+ is typically a factor of 20 more efficiently ionized than Ti^+; control of the oxygen isotopic composition in TiO^+ is critical and requires the use of a slurry of fine grained Ta_2O_5 on Ta filaments which themselves have been oxidized at a partial pressure of oxygen of 0.2 torr; f) for U and Th ionization efficiencies of 0.5% and 0.1%, respectively, are obtained by the loading of these elements in a colloidal graphite matrix, which enhances the formation of U^+ and Th^+ at high filament temperatures. This list provides an indication of substantial improvements, sometimes by many orders of magnitude (e. g., 10^5 for Mg) which have been possible by a careful consideration of matrix effects and of the species that are emitted from a heated filament in a vacuum. An important and general observation has also been that the ionization efficiency is not a linear function of the amount of an element loaded on a source filament. For example, f_{NdO^+} of 2% to 4% and of 25% to 50% are obtained for amounts of 5 x 10^{-8}g and 5 x 10^{-10}g of Nd, respectively, loaded on a filament. Similarly, Edwards, Chen, and Wasserburg (1986) have documented a precipitous drop of ionization efficiency for Th, from a high value of 0.1%, as the amount of Th loaded on the filament was increased. This has important implications for the measurement of ^{230}Th and for the use of the U-series for dating, based on disequilibrium effects.

The improvement in ionization efficiency appears to have had as an important and beneficial side-effect a substantial reduction in the range of instrumental isotope fractionation. This is important for elements with only two isotopes (e. g., Rb, Tl, Ag) and for elements with only three isotopes (e. g., Mg) for which a double spike technique is not possible, in the absence of longlived radioactive isotopes (e. g., the case of U using a double tracer enriched in $^{233,236}U$). The observed narrow range of instrumental isotope fractionation is most probably attributable to the depletion of the emitter (e.

g., Si-gel) well before the element of interest on the filament has been depleted. The measurement of intrinsic isotope fractionation has been important for the investigation of substantial kinetic isotope fractionation effects in refractory inclusions in primitive meteorites. These effects are attributed to kinetic isotope fractionation during condensation and/or evaporation in the early solar nebula.

It has also been established that it is possible to obtain isotope data for a variety of major and trace elements on micro-samples without the need of chemical separation of the element of interest, e.g., Mg, Ca, Cr, Rb, Sr. This technique has been labelled the direct loading technique (Lee, Papanastassiou, and Wasserburg, 1977). It has permitted isotopic analyses with a substantial reduction in the amount of laboratory introduced contamination; these types of analyses have also taken advantage of the sharp increase in ionization efficiency for micro-samples. Applications of these techniques can be found in the literature. Examples include a) analyses of interplanetary dust particles, less than 10 micrometers in size, as well as deep sea spherules of extraterrestrial origin; b) the study of correlated isotopic anomalies in meteorites which resulted in the identification of exotic components from specific nucleosynthetic processes; c) Rb-Sr and Sm-Nd studies of microtektites and the identification of the characteristics and mean age of the impact source materials; d) the study by mass spectrometry of U and Th for the purpose of disequilibrium series dating of corals with a sensitivity a factor of 10^4 better than obtained by alpha counting.

It is now possible to consider the types of problems worthy of investigation without the common restriction on sensitivity based on the limitation of terrestrial contamination and of ionization efficiency. It is now possible to consider also a much greater overlap between thermal ionization mass spectrometry and other complementary techniques, e.g., resonance photon ionization, nonresonance photoionization, and ionization by ion sputtering.

References

R. Lawrence Edwards, J. H. Chen, and G. J. Wassergurg (1986) ^{238}U-^{234}U-^{230}Th-^{232}Th systematics and the precise measurement of time over the past 500,000 years. Earth Planet. Sci. Letters, 81, 175-192.

T. Lee, D. A. Papanastassiou, and G. J. Wasserburg (1977) Mg and Ca isotopic study of individual microscopic crystals from the Allende meteorite by the direct loading technique. Geochim. Cosmochim. Acta, 41, 1473-1485.

G. J. Wasserburg, D. A. Papanastassiou, E. V. Nenow and C. A. Bauman (1968) A programmable magnetic field mass spectrometer with on-line data processing. Rev. Sci. Instum., 40, 288-295.

Presented at the 36th ASMS Conference on Mass Spectrometry and Allied Topics
June 5-10, 1988, San Francisco, CA

LIGAND SUBSTITUTION REACTION OF 17 ELECTRON METAL CARBONYL RADICAL ANIONS IN THE GAS PHASE

Y. Pan, D. P. Ridge

Department of Chemistry and Center for Catalytic Science and Technology, Univ. of Delaware, Newark, DE 19716

Ligand substitution reactions of the 17 electron species, $Cr(CO)_5^-$, $Fe(CO)_4^-$, and $Ni(CO)_3^-$, with activated olefins and aromatic compounds have been examined. 17 electron species are usually less reactive than corresponding 16 and 15 electron species because of their lower electron deficiency. However the 17e species do react with various ligands with activated double bonds. The reaction rates measured indicate that the reactions are sometimes highly efficient. The number of carbonyls replaced in each metal-ligand reaction varies from one to three. It is found that ligands with low electron affinity, for example 2,3-cyclohexene-1-one and succinic anhydride, tend to be less reactive or not reactive at all. By contrast ligands with high electron affinity, for example p-quinone and maleic anhydride, are very reactive. The correlation of electron affinity and reactivity suggests that the reaction involves incipient electron transfer between ligand compounds and metal carbonyls.

To measure the reaction rates the metal carbonyl was admitted to the source of a Nicolet FTMS 2000 through the batch inlet and the anion formed by electron attachment. The ligand was admitted through the batch inlet or on the probe. The ligand pressure was deduced from a positive ion mass spectrum. The sum of the peak intensities in the spectrum was taken to be proportional to the product of the pressure and the ionization cross section of the ligand. The ionization cross sections were taken from a formula given by Bartmess. The absolute pressure scale was determined by using reactions of known rate constants.

The results of the rate constant measurements for a large set of ligands and the three seventeen electron metal carbonyl anions are summarized in Fig. 1. As outlined above the reaction rate increases dramatically with electron affinity of the ligand. Note also that $Ni(CO)_3^-$ is substantially more reactive than the other ions. This corresponds with the lower electron affinity of $Ni(CO)_3$ (1.08 eV) relative to that of $Fe(CO)_4$ (2.4 eV). The behaviour of $Cr(CO)_5^-$ suggests that $Cr(CO)_5$ has an electron affinity between 1.08 eV and 2.4 eV. These correlations with electron affinity substantiate the postulated electron transfer mechanism for the ligand substitution.

Another observation supports the electron transfer mechanism. Two products are observed for reaction of bromonitrobenzene with $Cr(CO)_5^-$: ligand substitution (rate constant = k_1) and $Cr(CO)_5Br^-$ (rate constant = k_2). It is found that for the ortho compound $k_2/k_1 = 0.5$, while for the para compound $k_2/k_1 = 0.1$. This is consistent with the electrochemistry of the two isomers which shows that on reduction the ortho compound readily loses Br^- ($k = 110s^{-1}$) while the para compound does not ($k = .004s^{-1}$).

This suggests that the metal carbonyl radical anion behaves towards the bromobenzenes much as an electrode. It transfers an electron. The resulting anion then attaches itself to the metal.

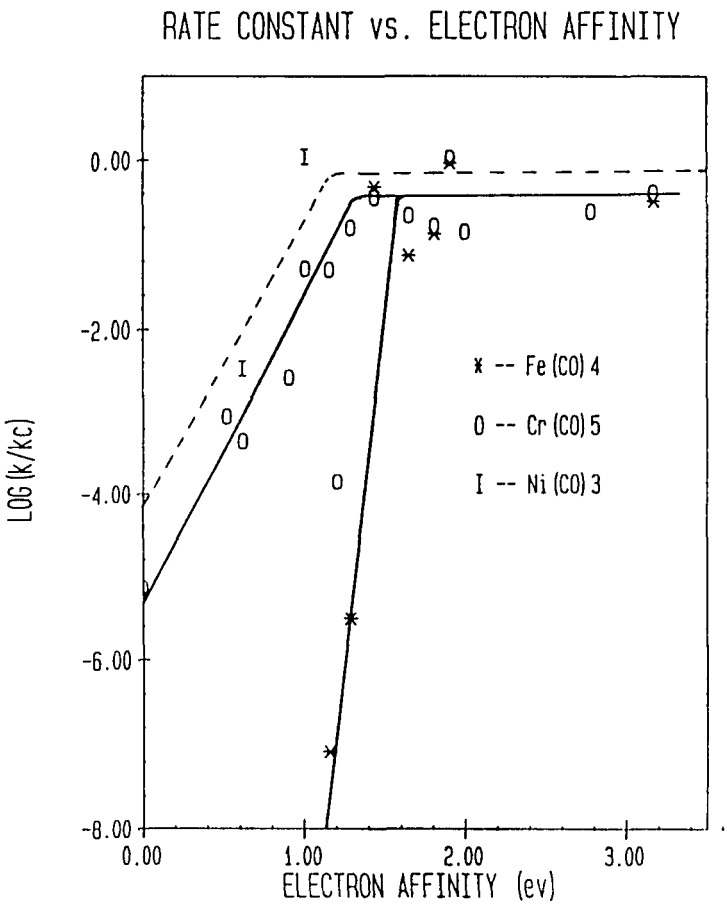

Figure 1.

Presented at the 36th ASMS Conference on Mass Spectrometry and Allied Topics
June 5-10, 1988, San Francisco, CA

AN FTMS STUDY OF METAL-CATALYZED OLIGOMER FORMATION IN THE GAS PHASE.

Asgeir Bjarhason
Science Institute, University of Iceland, Dunhaga 3, 107 Reykjavik, Iceland.
James W. Taylor
University of Wisconsin-Madison, Madison, WI 53705.

INTRODUCTION

Polymerization via metal catalyzed synthesis is a well known technique. The details of the mechanisms are in many cases understood to a lesser extent. Polyphenylenes and related compounds have received considerable interest in recent years due to their unique electrical conductive properties. Various synthetic routes have been investigated for the production of polymers with specific properties, and Brown and coworkers[1)] have developed a technique to analyze the products using laser desorption in a FTMS. A decade ago, Dietz et al.[2)] reported a study of the reactions of iron ions with phenyl halides in the gas phase using an ion cyclotron resonance spectrometer. Several interesting reaction products were observed, including $Fe(C_6H_4)_n^+$ (n=1-3). Instrumental advances have allowed us to probe these reactions in more detail, and we wish to report a number of additional reactions for these systems, including the direct observation of iron-catalyzed phenylene oligomer formation.

EXPERIMENTAL

A Nicolet FTMS-2000 Fourier transform mass spectrometer equipped with a 3.0 T superconducting magnet was used for these experiments. Iron ions were generated using the laser ionization technique developed by Freiser and coworkers[3)], using here a stainless steel target on the direct insertion probe and a pulsed CO_2 laser. Iron(I) ions were isolated using double ejection pulses, stored in the cell, and allowed to react with the sample during a delay event, which was varied from 0.003 to 25.6 seconds. All reaction paths were established using double resonance techniques.

RESULTS AND DISCUSSION

Dietz et al.[2)] report the following reaction for fluorobenzene, chlorobenzene, and bromobenzene:

$$Fe^+ + C_6H_5X \text{ --------> } Fe(C_6H_4)^+ + HX \qquad (1)$$

In the case of chlorobenzene, two more steps of dehydrohalogenation were observed to form $Fe(C_{12}H_8)^+$ and $Fe(C_{18}H_{12})^+$. Iodobenzene, however, was found to react differently.

We have observed a number of additional steps of

dehydrohalogenation. Fluorobenzene was found to yield $Fe(C_6H_4)_n^+$ with n=1,2, chlorobenzene with n=1-7, and bromobenzene with n=1-6. Chlorobenzene was the most reactive of the three. These reactions all proceed according to:

$$Fe(C_6H_4)_n^+ + C_6H_5X \text{ -----> } Fe(C_6H_4)_{n+1}^+ + HX \qquad (2)$$

Another reaction channel competes with (2) for certain values of n:

$$Fe(C_6H_4)_n^+ + C_6H_5X \text{ -----> } (C_6H_4)_n^+ + Fe(C_6H_5X) \qquad (3)$$

The phenylene oligomers are observed for fluorobenzene with n=2 and, in the case of chlorobenzene and bromobenzene, for n=2-4. To the best of our knowledge, these are the first direct observations of metal-catalyzed oligomer formation in the gas phase.

Iron ions also react to form molecular ion clusters of the type $Fe(C_6H_5X)_n^+$, which are observed for fluorobenzene (n=1,2), chlorobenzene (n=1), and bromobenzene (n=1,2). Ions of the form $Fe(C_6H_5X)(C_6H_4)_n^+$ were also detected for fluorobenzene (n=1,2) and chlorobenzene (n=2-6). No ions of this type were observed for bromobenzene or iodobenzene.

At longest reaction times the dominant ions become $(C_6H_4)_3^+$ and $Fe(C_6H_4)_5^+$, suggesting that they have the most stable configuration.

The results presented here were obtained with instrument access provided through the courtesy of the Nicolet Instrument Corporation, which is gratefully acknowledged. Studies are continuing using other transition metal ions and a wider variety of arenes to gain a more complete understanding of these processes.

LITERATURE CITED

1) C.E.Brown, P.Kovacic, C.A.Wilkie, R.B.Cody, Jr. and J.A.Kinsinger *J.Polym.Sci. Polym. Lett. Ed.*, **1985,** *23*, 453
2) T.G.Dietz, D.S.Chatellier and D.P.Ridge,*J.Am.Chem.Soc.*,**1978,***100*,4905
3) a) R.C.Burnier, T.C.Carlin, W.D.Reents, R.B.Cody, Jr., R.K.Lengel and B.S.Freiser, *J.Am.Chem.Soc.*,**1979**, *101*, 7127
b) B.S. Freiser, *Talanta,* **1985**,*32*, 697

Presented at the 36th ASMS Conference on Mass Spectrometry and Allied Topics
June 5-10, 1988, San Francisco, CA

Experimental Evidence for the Formation of H_3^* by H_5^*/e^- Dissociative Recombination

C. A. Miderski and Gregory I. Gellene
Department of Chemistry
University of Notre Dame
Notre Dame, IN 46556

In the early 1980's, Herzberg and co-workers observed and analyzed several electronic emission band systems of H_3^* in hydrogen discharges. In that work the localization of the spectra to the hollow cathode region and its enhancement with low discharge temperature suggested a role for hydrogen cluster ion/e^- dissociative recombination in the formation of H_3^*. This hypothesis was investigated by determining the effect of discharge temperature and hydrogen density on the intensity of H_3^* emission and comparing the results with the predictions of a kinetic model (Fig. 1) which incorporates known rates for relevant diffusional, clustering, and recombination processes.

The 6025 Å band ($3s^2A'_1 \rightarrow 2p^2A''_2$) of H_3 was monitored optically with nine lines being observed giving the relative population for seven individual upper state rotational levels (Fig. 2) which collectively provides a measure of the efficiency of production of H_3^* in the discharge (points plotted in Fig. 3). Comparing these results with those of the kinetic model it is found that the observed discharge pressure and temperature dependence on H_3^* spectral intensity can be adequately accounted for (curve in Fig. 3) if the reaction sequence:

$$H_5^+ + e^- \rightarrow H_5^{**} \rightarrow H_3^* + H_2 + KE \rightarrow h\nu \qquad (1)$$

is assumed to be the primary process leading to H_3^* in the discharge.

In the context of this mechanism, the kinetic energy released in the unimolecular dissociation of H_5^{**} would be expected to give rise to spectral line broadening. The analysis of the observed spectral line shape was simplified by assuming that the dissociative kinetic energy release gives rise to an isotropic single valued velocity distribution which combines with the original thermalized H_5^+ velocity distribution. The normalized emission line intensity contour, G, as a function of wave number shift $\tilde{\nu}$ is then given by:

$$G(\tilde{\nu}) = (a/4b)\ [\mathrm{erf}(a\tilde{\nu}+b) - \mathrm{erf}(a\tilde{\nu}-b)] \qquad (2)$$

where $a = (Mc^2/2kT)^{1/2}/\nu_o$ and $b = (m_2E_D/m_1kT)^{1/2}$. ν_o is the wave number of the line center, M is the total mass (m_1+m_2), m_1 is the mass of the observed fragment, and E_D is the dissociation energy. An optimized fit of Eq. (2) convolved with a gaussian instrumental line shape function to the $R_0(0)$ line (Fig. 4) resulted in a value of $E_D = 0.7 \pm 0.1$ eV. With this result conservation of energy consideration applied to reaction 1 indicates that the initial products of recombination are either $H_3^*(3s^2A'_1) + H_2(v=1)$ or $H_3^*(4p^2E'$ or $4p^2A''_2) + H_2(v=0)$.

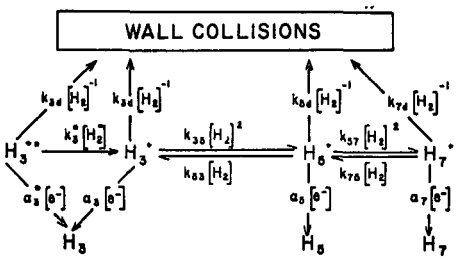

Fig. 1. Reaction scheme employed in the kinetic modeling of the hydrogen discharge.

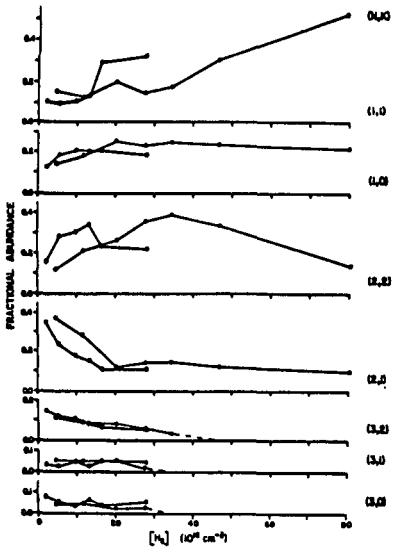

Fig. 2. Relative population of the observed rotational levels of the $3s^2A_1'$ Rydberg state of H_3 as a function of discharge temperature and density. Open and closed circles correspond to discharge bath temperatures of 195 K and 77 K respectively. The rotational levels are denoted by (N,K) where N and K are the rotational quantum numbers of a symmetric top.

Fig. 3. Relative total population observed for the $3s^2A_1'$ Rydberg state of H_3 (plotted points in a) and relative optical intensity of the undispersed cathode glow between 4000 A and 8000 A (plotted points in b) as a function of discharge temperature and density. The curves in (a) represent the results of the kinetic calculations for the relative production of H_5^{**} scaled as described in the text. In both plots, open and closed circles corresponded to discharge bath temperatures of 195 K and 77 K respectively.

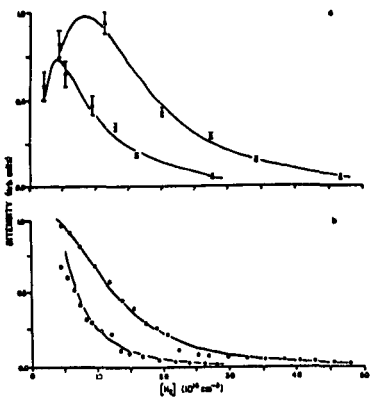

Fig. 4. Photodensitometer trace (solid curve) of the $R_0(0)$ line of the 6025 A band of H_3 obtained at a hollow cathode pressure and bath temperature of 0.5 Torr and 77 K respectively. The dotted curve represents an optimized fit of Eq. 2 to the observed lineshape as described in the text.

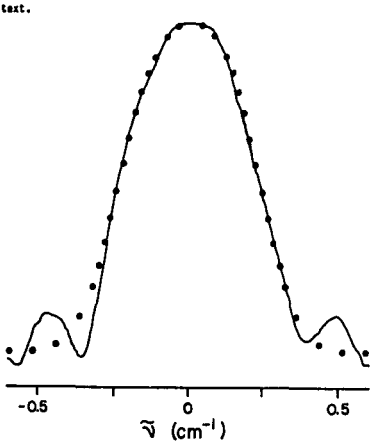

Presented at the 36th ASMS Conference on Mass Spectrometry and Allied Topics
June 5-10, 1988, San Francisco, CA

KINETIC ENERGY RELEASE DISTRIBUTIONS IN THE DISSOCIATION OF ION-DIPOLE COMPLEXES

Lewis M. Bass
Millersville University, Millersville, PA 17551

Coleen Roehl and Michael T. Bowers
University of California, Santa Barbara, CA 93106

We have undertaken a study aimed at determining the effect of the charge-dipole interaction on the kinetic energy release distribution (KERD) produced in the dissociation of ion-dipolar molecule complexes. Two systems were chosen for initial experiments: (1) cis- and trans- difluoroethylene, and (2) meta- and para- difluorobenzene. In each case, one isomer has a non-zero permanent dipole moment while the other isomer is nonpolar. Other parameters, such as reduced mass, polarizability, and internal vibrational modes are essentially the same for the two isomers. Hence, differences in the KERD's can be attributed entirely to the difference in dipole moments between the two isomers.

Measurements were carried out using a ZAB-2F mass spectrometer. The reaction sequences are as follows:

$$AH^+ + A \longrightarrow (A_2H^+)^* \quad (1A)$$

$$(A_2H^+)^* \longrightarrow AH^+ + A \quad (1B)$$

A = cis- or trans- difluoroethylene,

and

$$B^+ + B \longrightarrow (B_2{}^+)^* \quad (2A)$$

$$(B_2{}^+)^* \longrightarrow B^+ + B \quad (2B)$$

B = meta- or para- difluorobenzene.

In each case, the excited ion-molecule complex is formed in the ion source and then mass-selected through the magnetic sector. Fragment ions (AH^+ in reaction 1B or B^+ in reaction 2B) produced in the second field-free region are energy-analyzed by scanning the voltage on the electric sector. The plot of ion intensity vs. electric sector voltage is then analyzed to determine the KERD.

Results are shown in Figures 1 and 2 below. In both cases the KERD is shifted to lower values for the polar isomer. This is consistent with the

general predictions of statistical phase space theory [see L. M. Bass and M. T. Bowers, J. Chem. Phys., 86, 2611 (1987)], although detailed calculations on these systems have not yet been completed.

ACKNOWLEDGMENTS

We wish to acknowledge support for this project under National Science Foundation grant NSF# CHE85-12711. One of us (LMB) also acknowledges support through the Petroleum Research Fund grant PRF# 16955-GB6, and through a Faculty Professional Development Grant from the Pennsylvania State System of Higher Education.

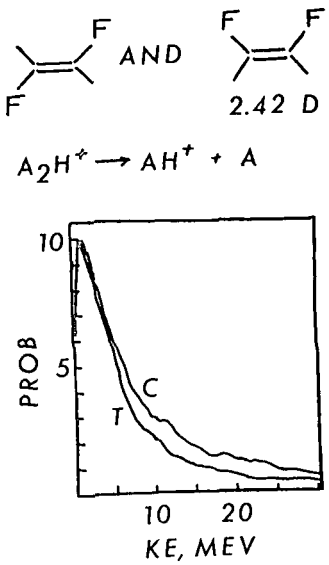

Figure 1. KERD's for difluoroethylene systems. C = cis, T = trans.

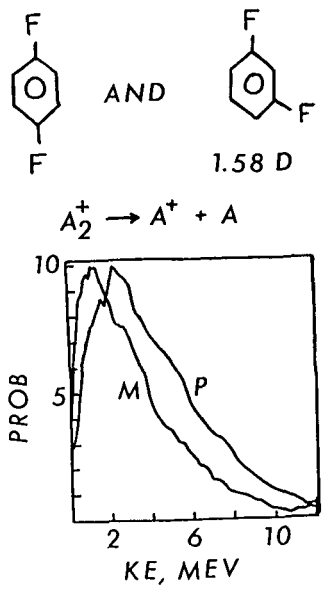

Figure 2. KERD's for difluorobenzene systems. M = meta, P = para.

Presented at the 36th ASMS Conference on Mass Spectrometry and Allied Topics
June 5-10, 1988, San Francisco, CA

A MASS SPECTROMETRIC AND *AB INITIO* CALCULATION STUDY OF THE POTENTIAL ENERGY SURFACE FOR REACTIONS OF CARBENE-LIKE CATIONS

J.J. Fisher and T.B. McMahon

Department of Chemistry and Guelph-Waterloo Centre
for Graduate Work in Chemistry
University of Waterloo
Waterloo, Ontario, N2L 3G1
CANADA

The potential energy surface for the reaction of difluoronitrenium ion (NF_2^+) with methane (CH_4) has been explored experimentally using ion cyclotron resonance spectroscopy (ICR), high pressure mass spectrometer (HPMS) and CID/MIKES technquies, as well as an extensive *ab initio* calculation study. Preliminary high pressure mass spectrometric (HPMS) studies of NF_3 and CH_4 showed that the major product ion formed was an ion of m/z 28. It was concluded that the only feasible structure of m/z 28 was $HCNH^+$. Examination of mixtures of various compositions established that NF_2^+ is by far the most probable source of m/z 28 species and that a single step reaction must occur with CH_4 in which a C-N bond is formed and at least one new N-H bond is made.

NF_2^+ is isoelectronic and isolobal with difluorocarbene and it is therefore tempting to propose that the first step in the formation of $HCNH^+$ may be the result of the insertion of NF_2^+ into the carbon-hydrogen bond of methane. It has been proposed that NF_2^+ can insert into C-H bonds by a direct (3-centered transition state) insertion mechanism or abstraction-recombination mechanism (Figure 1.) analogous to that of neutral carbenes. The *ab initio* calculations yield a transition structure which resembles a $[NF_2H + CH_3^+]$ ion molecule complex. Since a stable minimum and/or saddle point was not located for this complex, the abstraction-recombination mechanism for the insertion of NF_2^+ into C-H bond of methane is the preferred mechanism. This process leaves the newly formed $CH_3NF_2H^+$ with a significicant extent of internal excitation which can then promote unimolecular decomposition of this ion. Figure 2 shows the probable subsequent steps in the production of $HCNH^+$. The protonated N,N-difluoromethylamine eliminates an HF to yield protonated N,N-difluoromethylenimine which also subsequently eliminates HF to give the final product, $HCNH^+$, protonated HCN.

ICR double resonance experiments also established that NF_3H^+ reacts with CH_4 to produce m/z 28. In devising a reaction mechanism for NF_3H^+ and CH_4, two possible structures of NF_3H^+ must be considered; one involving protonation of NF_3 on the nitrogen site and the second involving protonation on a fluorine site. ICR and CID/MIKES experiments as well as *ab initio* calculations support protonation of NF_3 on the fluorine site. There CH_4 reacting with NF_3H^+ undergoes a nucleophilic displacement forming a $[NF_2 \cdots CH_4]^+$ ion molecule complex. This complex then forms a protonated N,N-difluoromethylamine intermediate which undergoes sequential loss of two HF.

Presented at the 36th ASMS Conference on Mass Spectrometry and Allied Topics
June 5-10, 1988, San Francisco, CA

Figure 1

Proposed Mechanisms for Insertion of NF_2^+ into C-H Bond of Methane

MECHANISM A

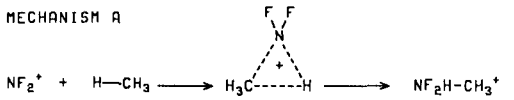

MECHANISM B

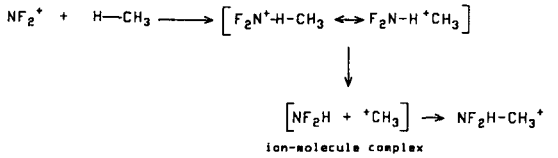

Figure 2

Mechanism for the Production of $HCNH^+$

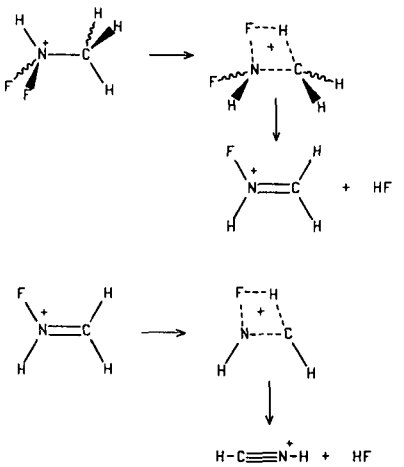

Presented at the 36th ASMS Conference on Mass Spectrometry and Allied Topics
June 5-10, 1988, San Francisco, CA

AN INVESTIGATION OF THE GAS PHASE BASE-INITIATED ALDOL REACTION: COLLISION INDUCED DISSOCIATIONS OF β-HYDROXY-CARBONYL NEGATIVE IONS.

R.N. Hayes, R.P. Grese, and M.L. Gross, Midwest Center for Mass Spectrometry, Dept. of Chemistry, University of Nebraska, Lincoln, NE 68588.

The aldol condensation is an important class of organic reactions. The generally accepted mechanism for the base-catalyzed aldol reaction in the condensed phase invokes the intermediacy of an β-hydroxy-carbonyl species (Scheme 1).[1] In contrast, gas-phase aldol condensations are not well understood; in particular, the structures of stable adducts so formed have not been fully characterized.

We have employed tandem mass spectrometry (MS/MS) techniques to isolate and characterize representative adducts produced by reactions between simple enolate anions with carbonyl compounds in a chemical ionization source. Enolate negative ions were easily produced by deprotonation of alkyl carbonyl compounds by using MeO- [produced by dissociative secondary electron capture of methyl nitrite[2]]. Adducts from subsequent reactions of the enolate anions with neutral aldehyde or ketone were mass selected by using the first stage of the tandem mass spectrometer, and then collisionally activated (CA) by collision with He gas. The CA mass spectra of these adducts were compared with those of appropriate deprotonated β-hydroxy-carbonyl model compounds. The structures of the condensation products were then assigned on the basis of these comparisons.

In common with the model compounds, the gas-phase adducts upon collisional activation decompose by elimination of neutral aldehyde (ketone), H·, CH_4 and H_2O (see Figures 1A and 1B); kinetic energy releases for each loss are nearly identical for adduct and model compound. The eliminations of H·, CH_4 and H_2O are representative of a species of tetrahedral geometry (Equations 1-3).

A comparison of the CA mass spectra indicate that there are, however, differences in the relative abundances of ions corresponding to loss of neutral aldehyde (ketone) between adduct and model compound. These differences are rationalized in terms of at least three adducts being formed; viz, an ion-dipole complex, a proton-bound dimer and a species of tetrahedral geometry. A hypothetical reaction coordinate diagram for a reaction between acetaldehyde enolate ion and acetaldehyde (Figure 2) shows all three possible species as stable intermediates. The energy barrier between the ion-dipole complex and the proton-bound dimer is more likely entropic in nature rather than enthalpic because of the losses of rotational and vibrational degrees of freedom as the ion-dipole complex evolves into the proton-bound dimer. The energy barriers for the losses of H_2O and CH_4 through the tetrahedral species are unknown but can be expected to be of higher energy than reactants because of the absence of these losses in the metastable spectra.

The charge reversal (positive ion) spectra[3] of the adducts and model compounds are also very similar; thus indicating a high probability that a fraction of the original negatively charged species each had a common structure. However, little evidence of the more loosely bound species (i.e., ion-dipole and proton-bound dimer) can be obtained from the charge reversal mass spectra. One reason that the cross section for charge stripping of

these loosely bound species is appreciably lower than that of the tetrahedral adducts is that the favored process for the ion-dipole and hydrogen-bonded complexes is to revert to starting materials; that is, these species never survive a charge stripping collision.

The conclusion then, is that adducts of tetrahedral geometry are formed in base-initiated gas phase aldol condensations. These adducts undergo fragmentation in a characteristic and novel manner upon collisional activation. However, a significantly higher proportion of at least two more species of adduct are formed; namely, an ion-dipole complex and a proton-bound dimer.

References

1. H.O. House, Modern Synthetic Reactions, 2nd Edn, pp. 629-733. Benjamin/Cummings Pub. Co., Menlo Park, CA (1972).

2. K. Jaeger and A. Henglein, Z. Naturforsch. Teil A, 22, 700 (1967).

3. I. Howe, J.H. Bowie, J.E. Szulekjo and J.H. Beynon, Int. J. Mass Spectrom. Ion Phys., 34, 99 (1980).

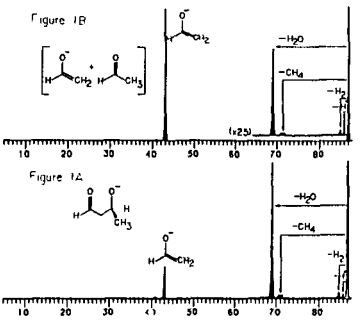

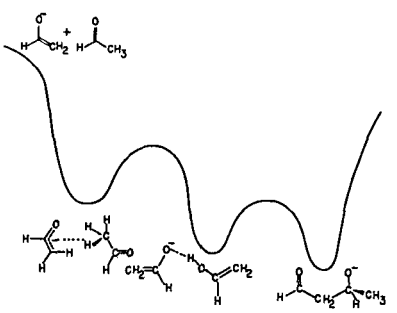

Figure 2

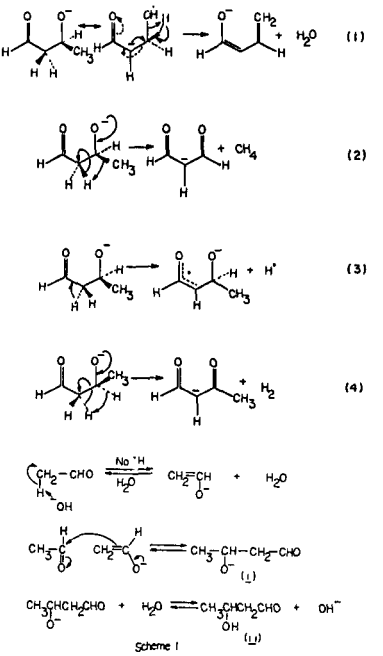

Presented at the 36th ASMS Conference on Mass Spectrometry and Allied Topics
June 5-10, 1988, San Francisco, CA

GAS-PHASE ELECTROPHILIC SUBSTITUTION REACTIONS OF ORGANOSILANES

David J. Hajdasz and Robert R. Squires
Department of Chemistry, Purdue University, West Lafayette, IN 47907

Electrophilic substitution represents an important class of organic reaction commonly used in synthesis.[1] The wide availability of trimethylsilyl-substituted organic compounds and the desirable characteristics of the Me_3Si^+ ion as a cationic "leaving group" make organosilanes excellent substrates for studies of bimolecular electrophilic substitution reactions in the gas phase (eq 1). We have undertaken a

(1) $$R^+ + X\text{-}SiMe_3 \longrightarrow RX + Me_3Si^+$$

$$X = Me,\ Cl,\ Ph,\ CH_2CH,\ CH_2CHCH_2$$

program of study of this type of reaction with use of a flowing afterglow-triple quadrupole instrument. Electrophilic cations are chosen such that protolytic cleavage of the substrate which would also produce Me_3Si^+ as a product (eq 2) is endothermic.[2]

(2) $$RH^+ + X\text{-}SiMe_3 \longrightarrow R + HX + Me_3Si^+$$

A wide range of reactivity is found that depends on the nature of the attacking electrophile and the type of reactive site in $X\text{-}SiMe_3$. The tertiary butyl cation does not react with Me_4Si at room temperature in the 0.4 torr helium flow reactor, despite the mild exothermicity computed for methyl anion transfer. Reaction does occur in the triple quadrupole (Q2) when the Me_3C^+ reactant ion is translationally excited; the observed kinetic energy dependence of the rate is typical of an exothermic reaction (eq 3). Acetyl cation reacts with Me_4Si in the flow reactor (P = 0 4 torr)

(3) $$Me_3C^+(KE) + Me_4Si \xrightarrow{\Delta H = -2\ kcal/mol} Me_4C + Me_3Si^+$$

exclusively by addition, and reacts by (exothermic) methyl anion transfer in Q2 (eq 4). The stabilized adduct undergoes CID by loss of both

(4) $$CH_3CO^+ + Me_4Si \longrightarrow (CH_3)_2CO + Me_3Si^+$$

$(CH_3CO^+ + Me_4Si)$ and $((CH_3)_2CO + Me_3Si^+)$, while an authentic $Me_3Si^+/(CH_3)_2CO$ adduct fragments to produce <u>only</u> Me_3Si^+. Thus, the CH_3CO^+/Me_4Si adduct represents a mixture of structures <u>A</u> and <u>B</u>.

$$[CH_3CO^+ \cdot \cdot Me_4Si] \qquad\qquad [(CH_3)_2\overset{+}{C}O\text{-}SiMe_3]$$

<u>A</u> <u>B</u>

Thermoneutral, symmetric exchange reactions in which the electrophile is $Me_3^{29}Si^+$ or $Me_2(CH_2D)Si^+$ (= $Me_3^*Si^+$) have been examined in order to obtain information about the shapes of the potential energy profiles for electrophilic substitution reactions. Bimolecular Me_3Si-group exchange does not occur in reactions of $Me_3^*Si^+$ with $X\text{-}SiMe_3$ where X = CH_3, Ph, Cl, vinyl, allyl. However, each of the stabilized $Me_3^*Si^+/X\text{-}SiMe_3$ adducts

formed in the flow tube undergoes CID to produce equal amounts of $Me_3^*Si^+$ and Me_3Si^+ daughter ions (eq 5). Thus, the Me_3Si^+ groups become equivalent

(5)

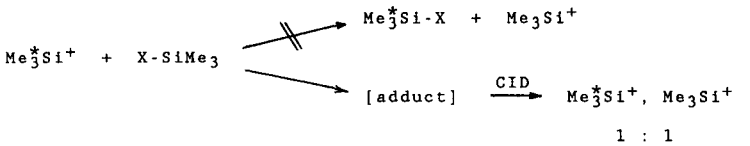

in the long-lived adducts, or as a result of collisional activation. The mechanistic implications of these results are discussed in terms of double- or triple-minimum potential energy profiles for Me_3Si^+ exchange.

1. Bamford, C. H.; Tipper, C.F.H., Eds, "Electrophilic Substitution at a Saturated Carbon Atom:, Elsevier: Amsterdam, 1973.

2. Wojtyniak, A.C.M.; Stone, J. A. Int. J. Mass Spec. Ion Proc. 1986, 74, 59.

Presented at the 36th ASMS Conference on Mass Spectrometry and Allied Topics
June 5-10, 1988, San Francisco, CA

TEMPERATURE DEPENDENCE OF API SENSITIVITY

Ikonomou, M., Kebarle, P., Department of Chemistry
University of Alberta, Edmonton, AB; Canada T6G 2G2.
Sunner, J., Department of Chemistry
Montana State University, Bozeman, MT 59717.

In ambient air Atmospheric Pressure Ionization (API) Mass Spectrometry, analyte molecules (B) are ionized by proton hydrates,

$$H_3O^+(H_2O)_n + B = BH^+(H_2O)_b + (n+1-b)\ H_2O \qquad (1)$$

With API many compounds in air can be detected at sub-ppb levels. Previously, we found that a combination of thermo-dynamic and kinetic factors determines the relative sensitivities for analytes in ambient air API (1). Thus, the sensitivities for compounds belonging to the "T-group", Figure 1, are thermodynamically controlled, i.e. determined by the equilibrium constants, $K_{eq}(1)$ for reaction 1. These compounds are mostly oxygen bases with gas-phase basicities (GB) < ca. 200 kcal/mol, and the sensitivities tend to increase with increasing GB. A second group of compounds, the "K-group" shows high and uniform sensitivities that do not vary with GB, Figure 1. These sensitivities are kinetically controlled and determined by the nearly Langevin rate of reaction 1 for these mostly nitrogen bases with GB > ca. 200 kcal/mol. The compounds belonging to the third group, the "L-group", have much lower sensitivities than expected from their GB's alone. The ion intensities for these mostly carbon and sulfur bases are thermodynamically controlled, i.e. determined by $K_{eq}(1)$. However, the equilibrium is pushed very far to the left because of very weak gas-phase solvation interactions of these BH^+ ions with water molecules. By varying the conditions in the API source, for example the water pressure or ion residence time, specific compounds may change from thermodynamic control to kinetic control or vice versa.

In the present work, the sensitivities for a range of analytes were studied as a function of ion source temperature from 30°C to 400°C. The experimental arrangement is shown in Figure 2. The most noteworthy finding is that the sensitivities of the sulfur and carbon bases in group L, that are very low at 30°C, increase by many orders of magnitude as the temperature is increased, Figure 3. These large temperature effects can be explained as follows: For the sulfur and carbon bases, the equilibrium constant, $K_{eq}(1)$ is small due to the very unfavorable hydration of the BH^+-ions relative to the hydronium ion, H_3O^+. At high temperature, the extent of hydration is low, however. This results in an increase in $K_{eq}(1)$ and thus an increase in sensitivity.

The equilibrium constant for reaction 1 can be calculated from the GB of B and from the thermodynamic data for the step-wise gas-phase solvation of H_3O^+ and BH^+, respectively. Thus, when the solvation data is available, the temperature dependence of the sensitivity of a thermodynamically controlled analyte B can be calculated. Such calculations show good agreement with experimental sensitivities. The calculations also reveal that all analytes with GB>210 kcal/mol should have high, kinetically controlled sensitivities at 25°C and at a water pressure of a few torr.

1) Sunner, J., Nicol, G., P.Kebarle, Anal.Chem., in print.
2) Sunner, J., Ikonomou, M., Kebarle, P., Anal. Chem., in print.

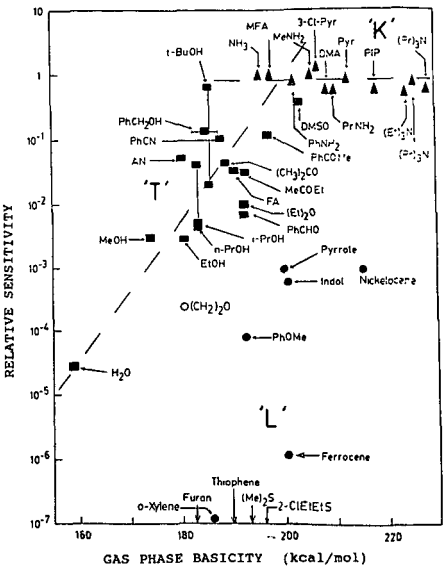

Figure 1. Relative sensitivities of analytes at ≈ 25°C vs analyte gas-phase basicity, G.B.
High sensitivity group K analytes;
Group T, thermodynamic control;
Group L, low sensitivity, thermodynamic control.

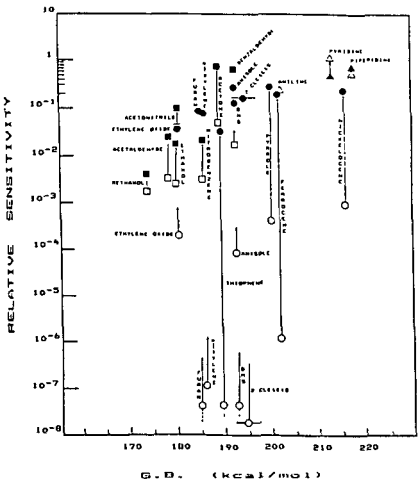

Figure 3. Relative sensitivities of analytes as a function of analyte GB; Open symbols at 25°C; Full symbols maximum sensitivity at high temperature; group K, group T; group L.

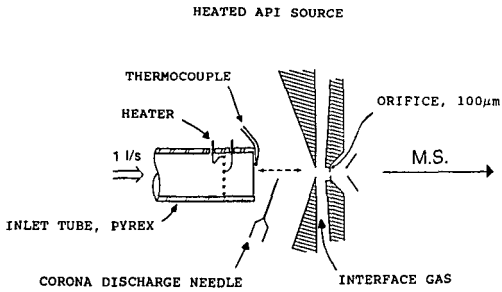

Figure 2. Schematic diagram of heated TAGA 6000E API source.

Presented at the 36th ASMS Conference on Mass Spectrometry and Allied Topics
June 5-10, 1988, San Francisco, CA

On the Reactivity of NO^+ to Locate CC Double Bonds in Long Chain Aliphatic Compounds Using a Multiquadrupole Triple Analyzer Instrument

Jacques Einhorn (1), Christian Rolando (2) and Christian Malosse (1)
(1) INRA-CNRS
Laboratoire des Médiateurs Chimiques
Magny-les-Hameaux, 78470 St-Rémy-Les-Chevreuse, France

(2) Ecole Normale Supérieure
UA1110, Laboratoire de l'Activation Moléculaire
24 rue Lhomond, 75231 Paris cedex 05, France

It has been shown recently that the characteristic odd-mass fragment ions observed (1) in the CI-NO^+ mass spectra of long chain mono-unsaturated alcohols, acetates and aldehydes can also be formed for alkenes and alkenoic acid esters in certain conditions (2). For the latter compounds, these acylium type ions might then, in principle, be used for structural assignment together with ions of other origins (3,4).

In order to optimize the production of the acylium ions, we have investigated the role of various experimental factors. The observed strong influence of the sample pressure as well as that of the reagent gas (5) might explain the origin of the acylium ions as follows:

$$R_1CH{=}CHR_2 \xrightarrow[\text{or } N_2O_2^+]{NO^+} (R_1CH{=}CHR_2)^+ \xrightarrow{NO^{\cdot}} R_1CO^+ \text{ and/or } R_2CO^+$$

R_1, R_2 = alkyl

According to this hypothesis, the diagnostic products would result from an adduct ion $(M+NO)^+$ after a secondary ion-molecule reaction. The purpose of the present study is to verify this assumption using a multiquadrupole triple analyzer instrument (6) which allows: (i) a primary reaction to be performed in the first collision cell after selection of the cation NO^+ or its dimer $N_2O_2^+$ by the first analyzer. (ii) Selection of the adduct ion by the second analyzer, (iii) a secondary ion-molecule reaction in the second collision cell between the adduct ion and neutral NO·.

Another strategy consists of introducing the alkene with or without NO· in the first collision cell and studying the structure of any of the produced ions by CAD (Ar used as collision gas in the second collision cell). In this case, conventional spectra may be recorded by maintaining the second analyzer transparent.

Ion confinement can also be achieved in either RF-only collision cell using the entrance and exit lenses as electrostatic mirrors (7) to examine the influence of residence time(s).

According to our experiments (Table 1), the only way to produce an acylium ion was to select NO^+ (of various origins) as reactive species from the reagent plasma and allow it to react with both the sample (E-4-nonene) and NO· in the same collision cell (Figure 1, cf. ion at m/z 85). Any attempt to generate an acylium ion through introduction of the alkene alone, even with ion confinement, failed, generating only alkyl ions (cf. CAD or typical profile in the conventional spectrum).

On the other hand, the adduct ion formed using $N_2O_2^+$ is only responsible for the formation of alkyl ions or NO-containing ions (i.e. m/z 114, see Figure 2).

All these results suggest the diagnostic acylium ion(s) produced from alkenes under CI-NO^+ conditions, to originate from an excited adduct ion after stabilization to the required energy by neutral NO·. Further studies are necessary to define the nature (collisional or reactive) of this interaction.

Acknowledgement:
R.G. Cooks (Purdue University, W. Lafayette, IN) is greatly acknowledged for fruitful discussions.

References:
1. C. Malosse and J. Einhorn, Adv. Mass Spectrom., 1369 (1986).
2. H. Budzikiewicz, B. Schneider, E. Busker, W. Boland and W. Francke, Org. Mass Spectrom., 22, 458 (1987).
3. H. Budzikiewicz and E. Busker, Tetrahedron, 36, 255 (1980).
4. A. Brauner, H. Budzikiewicz and W. Francke, Org. Mass Spectrom., 20, 578 (1985).
5. J. Einhorn and C. Malosse, submitted.
6. C. Beaugrand, G. Devant, D. Jaouen and C. Rolando, Int. J. Mass Spectrom. Ion Proc., in press.

7. C. Beaugrand, G. Devant, D. Jaouen, H. Meetdagh and C. Rolando, Spectros. Int. J., 5, 265 (1987).

Table 1. Reactions performed on E-4-nonene (S) in the multiquadrupole triple analyzer instrument.

A_1, A_2, A_3 = analyzer 1, 2 or 3; C_1, C_2 = collision cell 1 or 2; ion confinement in (ms).

	A_1	C_1	A_2	C_2	A_3	Results
i-$C_5H_{11}ONO$	NO^+	S	/	/	scan	alkyls
	"	S (10 ms)	/	/	"	alkyls
	"	S, NO	/	/	"	acylium/adduct
	$N_2O_2^+$	S	/	/	"	adduct
	"	S, NO	/	/	"	no acylium
	"	S	$(M+NO)^+$	NO (5 ms)	"	alkyls
	"	"	"	NO/O_2	"	"
	"	"	"	Ar	"	"
N_2O	NO^+	S	/	/	"	alkyls
	"	S, NO	/	/	"	acylium/adduct
	"	S, NO	$(M+NO)^+$	Ar	"	alkyls
NO	NO^+	S	m/z 85 or 71	Ar	"	alkyls

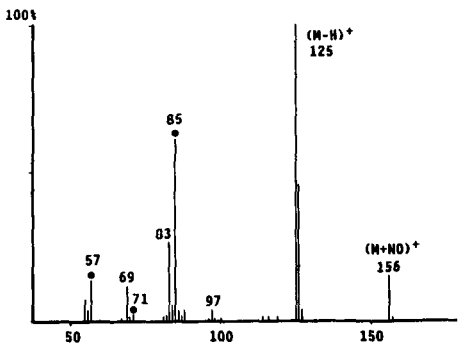

Figure 1. Pattern obtained for ions m/z 57, 71 and 85 by reaction of NO^+ with alkene and NO· in the same collision cell (m/z 85 = acylium ion).

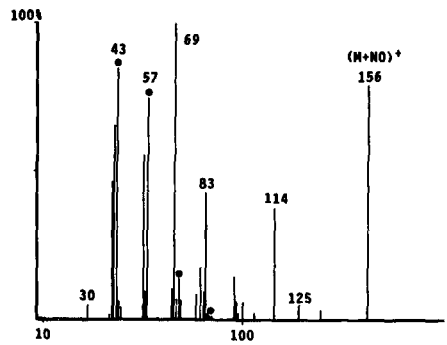

Figure 2. Pattern obtained for ions m/z 43, 57, 71 and 85 in a two-step reaction sequence (profile of alkyl ions only).

Presented at the 36th ASMS Conference on Mass Spectrometry and Allied Topics
June 5-10, 1988, San Francisco, CA

QUANTITATIVE DETERMINATION OF SELECTED COMPOUNDS IN CIGARETTE MAINSTREAM SMOKE USING MULTI-DIMENSIONAL GAS CHROMATOGRAPHY AND SELECTED-ION-MONITORING MASS SPECTROMETRY.

Earl L. White, Mary S. Uhrig, Bert Gordon, Ed J. Nanni, Jr.
Mike F. Borgerding and Richard D. Hicks

R. J. Reynolds Tobacco Company
Bowman Gray Technical Center
Winston-Salem, NC 27102

An automated multidimensional gas chromatographic (MDGC) technique has been developed and optimized for use as an analytical tool for complex mixture analyses. This system utilizes the precolumn of the MDGC system to effectively replace the chemical fractionations employed in more classical sample preparation schemes. MDGC systems interfaced to a mass spectrometer and to a matrix isolation/Fourier Transform-infrared spectrometer were used to identify components of a flue-cured tobacco essential oil sample.[1] Eight (8) compounds from a Kentucky 1R4F reference cigarette smoke condensate were selected for determination by selected-ion-monitoring mass spectrometry to confirm the validity of MDGC as a quantitative tool in complex mixture analyses.

Four (4) electrostatically precipitated smoke condensates from 100 cigarettes were each reconstituted in 60 ml of 2-propanol containing 2 esters (C_8 and C_{14}) used as internal standards (IS) and a second set of samples reconstituted in 60 ml of 2-propanol containing 5 deuterium-labeled compounds. A 5 ul aliquot of each sample was injected onto a precolumn using cool on-column injection. At pre-selected times, the eluant of the first column was transferred (heartcut) to a second (analytical) column via a multidimensional capillary switching device (SGE) modified for use in two separate standard chromatograph ovens.

A series of solutions containing authentic compounds of interest was prepared and subjected to identical analyses as the samples to obtain standard dilution curves. Analysis of the compounds of interest, pyridine, acetamide, acrylamide, phenol, o-, m-, p-cresol, and quinoline was accomplished using two heartcuts and two of the three IS selected for injection volume and heartcut-corrections in analyses similar to the essential oil analyses. Three heartcuts were made in the portion of this study employing deuterium-labeled internal standards. The result of this study showed that the MDGC technique developed could be used for quantitative analyses. The precision of the technique using esters as internal standards was determined by injecting a single sample eight (8) times and determining the mean $\pm$ std. dev. for each compound. These values were 1.96 $\pm$ 0.08, 11.30 $\pm$ 0.09, 2.27 $\pm$ 0.09, 12.22 $\pm$ 0.19, 3.29 $\pm$ 0.08, 6.92 $\pm$ 0.10, 0.99 $\pm$ 0.05 and 0.30 $\pm$ 0.01 for pyridine, acetamide, acrylamide, phenol, o-cresol, p-cresol, m-cresol and quinoline, respectively. Mean values $\pm$ std. dev. for a different sample injected seven (7) times using deuterium-labeled internal standards were 2.27 $\pm$ 0.04, 5.56 $\pm$ 0.08, 1.43 $\pm$ 0.12, 7.71 $\pm$ 0.03, 2.51 $\pm$ 0.24, 5.48 $\pm$ 0.15, 2.16 $\pm$ 0.11 and 0.23 $\pm$ 0.01 for pyridine, acetamide, acrylamide, phenol, o-cresol, p-cresol, m-cresol and quinoline, respectively. These results showed that the precision of the technique using methyl esters as internal standards was comparable to that using deuterium-labeled compounds as internal standards.

1. B. M. Gordon, M. S. Uhrig, M. F. Borgerding, H. L. Chung, W. M. Coleman, III, J. F. Elder, Jr., J. A. Giles, D. S. Moore, C. E. Rix, and E. L. White, J. Chromatogr. Sci., **26**, 174-180, (1988).

Presented at the 36th ASMS Conference on Mass Spectrometry and Allied Topics
June 5-10, 1988, San Francisco, CA

ANALYSIS OF ETHYL DIMETHYLPHOSPHORAMIDOCYANIDATE (TABUN) BY CAPILLARY COLUMN GAS CHROMATOGRAPHY-MASS SPECTROMETRY, Paul A. D'Agostino, Lionel R. Provost and Karen M. Looye, Defence Research Establishment Suffield, Ralston, Alberta, Canada, TOJ 2NO.

The alleged use of the nerve agent ethyl dimethylphosphoramidocyanidate (tabun) in the Iran-Iraq war emphasizes the need for specific detection and identification procedures for the verification of this and other chemical warfare agents (1). Gas chromatographic-mass spectrometric (GC-MS) techniques have been used extensively for the analysis of organophosphorus compounds. Electron impact (EI) ionization of organophosphorus compounds provides valuable structural information, but the presence of little or no molecular ion data often hinders the identification of unknowns. Chemical ionization (CI) has been used with increasing frequency to provide the molecular ion information necessary for the identification of these organophosphorus compounds (2-4).

Previous GC-MS analysis of tabun samples by several laboratories has resulted in the detection of several tabun related impurities including diethyl dimethylphosphoramidate, ethyl isopropyl dimethylphosphoramidate, triethyl phosphate, ethyl tetramethylphosphorodiamidate, tetramethylphosphorodiamidic cyanide and two pyrophosphates (3, 5, 6). Recent analysis of a munitions grade tabun sample by our laboratory indicated the presence of all of the above compounds and a number of other impurities. The primary objective of this GC-MS study was the identification of these unknown sample components, as this information may aid future chemical event verification.

Capillary column GC-MS analyses were performed with a VG 70/70E mass spectrometer equipped with a Varian 3700 gas chromatograph under the following conditions: (GC column: 15 m x 0.32 mm ID J+W DBWAX or DB-1701; Temperature program: 50°C (2 min) 10°/min 230°C (DBWAX) or 280°C (DB-1701) (5 min); Injector: cold on-column at 50°C; EI: 200°C, 100 µA; 70 eV; 2 x 10^{-6} torr; Ammonia CI: 120-140°C; 500 µA; 50 eV; 5-6 x 10^{-5} torr; Scan rate and function: 500 to 35 u, 1 sec/decade).

Figure 1 illustrates a typical capillary column GC-MS total-ion-current chromatogram for about 1 µg of munitions grade tabun. Tabun and nineteen sample components, listed in Table I, were identified (or tentatively identified) based on the acquired mass spectral data. Figures 2 to 4 illustrate the EI, NH_3-CI and ND_3-CI mass spectra acquired for tabun, the isopropyl analogue of tabun, isopropyl dimethylphosphoramidocyanidate and diisopropyl ethyl phosphate. Characteristic fragmentation ions, and in some cases molecular ions, were obtained for these and the other organophosphorus sample components during EI operation. Complementary pseudo-molecular $(M+X)^+$ and/or $(M+NX_4)^+$ (where X=H during NH_3-CI and X=D during ND_3-CI) ions, along with a limited number of CI fragmentation ions, were observed for all the tabun related impurities. ND_3-CI data was also valuable for the identification of previously unreported compounds such as diisopropyl ethyl phosphate, since the CI fragmentation ions contained active hydrogens which underwent isotopic exchange (H/D ex.) with deuterium during CI analysis. Successive losses of C_3H_6 from the pseudo-molecular ions, illustrated below, suggested this was a compound with two isopropoxy substituents (Figure 4).

NH$_3$-CI:	$(M+H)^+$	$\xrightarrow{-C_3H_6}$	m/z 169	$\xrightarrow{-C_3H_6}$	m/z 127
	$(M+NH_4)^+$		m/z 186		m/z 144
ND$_3$-CI:	$(M+D)^+$	$\xrightarrow{-C_3H_6}$	m/z 171	$\xrightarrow{-C_3H_6}$	m/z 130
	$(M+ND_4)^+$	H/D ex.	m/z 191	H/D ex.	m/z 150

Interpretation of the EI, NH_3-CI and ND_3-CI data enabled the identification of nineteen tabun related impurities, including twelve new monophosphorus and pyrophosphate compounds previously unreported or unassociated with tabun. Application of the methodology and reported findings is anticipated since characteristic sample components may provide analysts with sample origin, synthetic method or munitions type information.

References

1. Chemical and Engineering News 62 (14), 4, 1984.
2. S. Sass and T.L. Fisher, Org. Mass Spectrom., 14, 257, 1979.
3. P.A. D'Agostino, A.S. Hansen, P.A. Lockwood and L.R. Provost, J. Chromatogr., 347, 257, 1985.
4. P.A. D'Agostino, L.R. Provost and J. Visentini, J. Chromatogr., 402, 221, 1987.
5. "Report of the Specialists Appointed by the Secretary General to Investigate Allegations by the Islamic Republic of Iran concerning the use of Chemical Weapons". Report S/16433, United Nations, New York, March 26, 1984.
6. G. Andersson, NBC Defence and Technology International, 62, April 1986.

Presented at the 36th ASMS Conference on Mass Spectrometry and Allied Topics
June 5-10, 1988, San Francisco, CA

GC-MS (DBWAX) CHROMATOGRAM OF TABUN

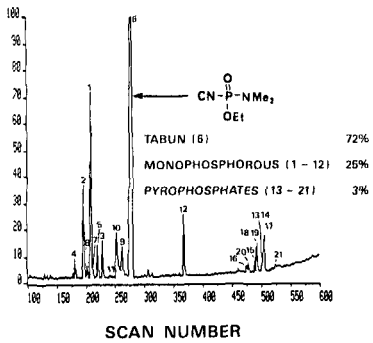

Fig.1

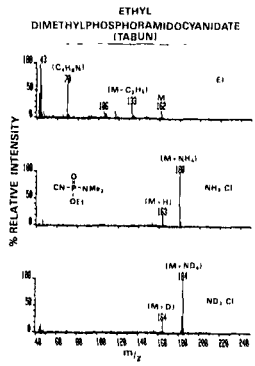

Fig.2

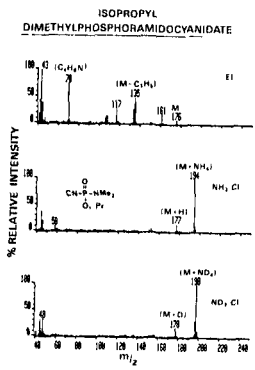

Fig.3

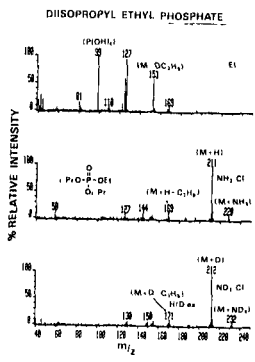

Fig.4

Table I. COMPOUNDS IDENTIFIED IN TABUN SAMPLE

PEAK NO.[a]	MOL. WT.	COMPOUND IDENTIFIED
1[c]	181	Diethyl dimethylphosphoramidate
2[c]	195	Ethyl isopropyl dimethylphosphoramidate
3[c]	182	Triethyl phosphate
4	209	Diisopropyl dimethylphosphoramidate[b]
5	196	Diethyl isopropyl phosphate[b]
6	162	Ethyl dimethylphosphoramidocyanidate (Tabun)
7	210	Diisopropyl ethyl phosphate[b]
8	224	Triisopropyl phosphate
9	176	Isopropyl dimethylphosphoramidocyanidate[b]
10[c]	180	Ethyl tetramethylphosphorodiamidate
11	194	Isopropyl tetramethylphosphordiamidate[b]
12[c]	161	Tetramethylphosphorodiamidic cyanide
13	290	Bis(diethyl phosphoric) anhydride
14, 19	288	Bis(ethyl dimethylphosphoramidic) anhydride
15	304	Diethyl phosphoric ethyl isopropyl phosphoric anhydride[b]
16	318	Diethyl phosphoric diisopropyl phosphoric anhydride (or isomer)[b]
17	289	Diethyl phosphoric ethyl dimethylphosphoramidic anhydride[b]
18	303	Diethyl phosphoric isopropyl dimethylphosphoramidic anhydride (or isomer)[b]
20	317	Diisopropyl phosphoric ethyl dimethylphosphoramidic anhydride (or isomer)[b]
21	287	Ethyl dimethylphosphoramidic tetramethylphosphorodiamidic anhydride

a Refer to Figure 1; Retention order (1 – 21) for DB-1701

b Tentative identification based on interpretation of acquired EI and CI mass spectral data

c Compounds previously identified as tabun impurities (References 3, 5 and 6)

Presented at the 36th ASMS Conference on Mass Spectrometry and Allied Topics
June 5-10, 1988, San Francisco, CA

HPLC/MS AND HPLC/MS/MS ANALYSIS OF WASTE SAMPLES FOR ORGANOPHOSPHORUS PESTICIDES

L.D. Betowski and T.L. Jones, U.S.
Environmental Protection Agency, Las Vegas,
Nevada 89193-3478

INTRODUCTION

The U.S. Environmental Protection Agency recently conducted a single laboratory validation of SW-846 Method 8140, Organophosphorus Pesticide Parameters[1]. This procedure is a gas chromatographic method for the analysis of organophosphorus pesticides in water, soil, and hazardous waste. In addition to the presentation of data on precision and accuracy, the validation report provided findings on analytical difficulties encountered with specific organophosphorus pesticides. The purpose of this present work is to investigate the use of high performance liquid chromatography/mass spectrometry (HPLC/MS) and HPLC/MS/MS for the analysis of problem compounds.

EXPERIMENTAL

A Finnigan TSQ®45 was operated with a Vestec Thermospray LC/MS interface and a Spectra-Physics SP8700XR pump to generate the HPLC/MS and HPLC/MS/MS data. An Isco LC-5000 syringe pump was used o deliver a ostcolumn flow of ammonium acetate. A 10cm x 2mm ODS Hypersil 5um PN-Special analytical column from Keystone Scientific was the chromatographic element.

The CAD experiments were conducted at a collision energy of 20eV with argon at a pressure of 1 mTorr.

RESULTS AND DISCUSSION

Ten organophosphorus pesticides were chosen to be studied by HPLC/MS because of their poor recoveries under Method 8140. Thermospray ionization generated mainly the protonated molecule at $(M + 1)^+$ and the ammoniated adduct ion at $(M + 18)^+$ in the single quadrupole mass spectra of these compounds. Methyl parathion showed a 30 amu loss from these ions which can be attributed to either a loss of NO_2 or the reduction to the corresponding amine. Trichlorfon and, to a lesser extent, naled show evidence of degradation to dichlorvos. Merphos showed a large contamination of merphos oxide which eluted 2.5 minutes before the merphos peak.

While most of the ion current remains in the protonated molecules and adduct ions upon thermospray introduction, CAD daughter ion spectra show ions characteristic of the structure of the molecule or class of compound. For example, the organophosphates show a significant m/z 127 ion while for the phosphorothionates and the phosphorodithioates, the O,O-dimethyl compounds show a strong m/z 125 ion. These are also characteristic ions formed under electron impact mass spectrometry conditions[2].

The CAD daughter ion spectra were useful in identifying the organophorphorus pesticides in soil samples. For example, one large and one smaller peak at m/z 275 eluted in the retention window for disulfoton (molecular weight, 274). Only by subjecting the m/z 275 ions to the CAD process were we able to identify the smaller peak as disulfoton.

The limits of detection for these organophosphorus pesticides ranged from 200pg injected in the full scan mode for naled to 30ng for methyl parathion. Precision results from triplicate injections on standards for these compounds gave a grand mean of 7.1%.

Four soil samples that were known by GC/MS to contain organophosphorus pesticides were chosen for analysis by LC/MS. The results from these analysis along with the amounts from GC/MS are listed on Table 1. Qualitatively, the results show good agreement. Only in sample 1 is there some doubt about the presence of compounds. The same compounds were detected by both techniques in the rest of the samples. In some cases the results are quantitatively very close as for phorate and methyl parathion in sample 2 and disulfoton in sample 3. The amounts calculated for dimethoate and phorate are higher under LC/MS analysis for all occurrences of these compounds. Since these compounds have shown difficulties under GC analysis, it is possible that some of these compounds were degraded or irreversibly bonded on the GC.

1. V. Taylor, D.M. Hickey, and P.J. Marsden. U.S. EPA Report 600/4-87/009; Environmental Protection Agency: Las Vegas, NV, 1987.

2. S. Safe and O. Hutzinger. "Mass Spectrometry of Pesticides and Pollutants"; CRC Press Inc.: Boca Ratan, FL. p.193, 1973.

TABLE 1. CONCENTRATION OF ORGANOPHOSPHORUS PESTICIDES FOUND IN ENVIRONMENTAL SAMPLES

	Compound	Quant. Ion	Amount Calculated (mg/kg) LC/MS	Amount Calculated (mg/kg) GC/MS	LC/MS LODc (mg/kg)	GC/MS LOQd (mg/kg)
Sample 1	Disulfoton	275	4.41	0.750Ja	0.24	1.3
	Methyl Parathion	231	NDb	1.10 Ja	7.1	2.0
	Phorate	261	4.80	NDb	0.47	1.3
Sample 2	Dimethoate	230	1740	144	0.82	9.4
	Phorate	261	66.9	54.3	0.82	3.4
	Disulfoton	89	26.8	4.85	0.41	3.4
	Methyl Parathion	281	28,500	28,700	12	5.4
Sample 3	Disulfoton	275	98.8	110	0.79	9.3
	Phorate	261	44.7	19.0	1.6	9.3
Sample 4	Disulfoton	89	45.0	130	0.51	2.5
	Methyl Parathion	281	115	150	15	4.5

a value indicates detected but under Limit quantitation (LOQ).
b indicates not detected.
c Limit of detection
d Limit of quantitation

Presented at the 36th ASMS Conference on Mass Spectrometry and Allied Topics
June 5-10, 1988, San Francisco, CA

ON-COLUMN CAPILLARY GC/MS OF NON-IONIC DYES, **Robert T. Rosen**[1], Lise H. Royin[2], Thomas G. Hartman[1], Linda B. Clark[2], Jeffrey Oxenford[3], Chi-Tang Ho[2] and Joseph D. Rosen[2]. Center for Advanced Food Technology[1] and Food Science Department[2], Cook College, New Jersey Agricultural Experiment Station, Rutgers University, New Brunswick, New Jersey 08903, and New Jersey Department of Environmental Protection[3], Trenton, New Jersey 08625.

Dyes derived from coal tar and from synthetic sources are important because some of them are known mutagens. Examples include aminobiphenyl and naphthylamine which have been identified as bladder carcinogens.

On-column capillary GC/MS has, for the first time, been used to determine the presence of non-ionic dyes in plant waste streams. This includes those compounds containing an azo functionality. Previous methodology[1,2] has required LC/MS accompanied by MS/MS to identify these species.

On-column capillary GC/MS using electron ionization is a technique whose simplicity makes analysis applicable to any environmental laboratory, even when using automatic injectors. Using an on-column injector of our own design[3] EI spectra were obtained for a series of compounds including Disperse Orange 3 (MW 242), Solvent Red 3 (MW 292), Pigment Red 3 (MW 307), Solvent Red 23 (MW 352), and Sudan Red 7B (MW 379). Although hundreds of azo dyes are utilized by the dye industry, this analysis was limited by the lack of their commercial availability.

Samples from an industrial dye facility were screened using on-column capillary GC/MS. While most of the compounds identified were precursors such as substituted anilines and nitrogen heterocycles, several dyes were identified. These include methoxynitroaminobiphenyl and its azo analog, as well as two analogs also containing an acid moiety. An isolated fraction containing these four species was active in the Ames test. The Spectra and Structures of the two major dyes are shown below.

References

1. R. D. Voyksner Anal. Chem. 57, 2600 (1985).
2. L. D. Betowski and J. M. Ballard Anal. Chem. 56, 2604,(1985).
3. T. G. Hartman, R. T. Rosen, C.-T. Ho and J. D. Rosen LC-GC 5, 834 (1987).

This project was supported by the New Jersey Department of Environmental Protection, Department of Science and Research, and the NJ Agricultural Experiment Station. Publication #J-10542-1-88. Also acknowledged is CAFT, an initiative of the New Jersey Commission on Science and Technology.

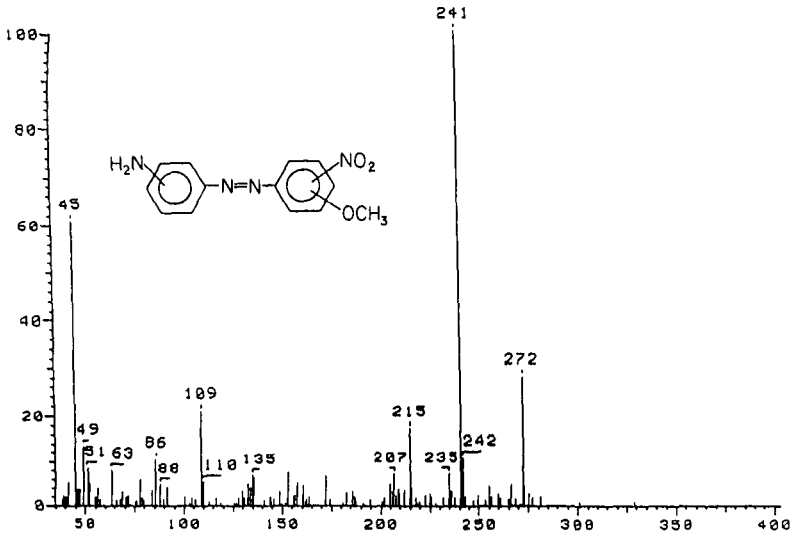

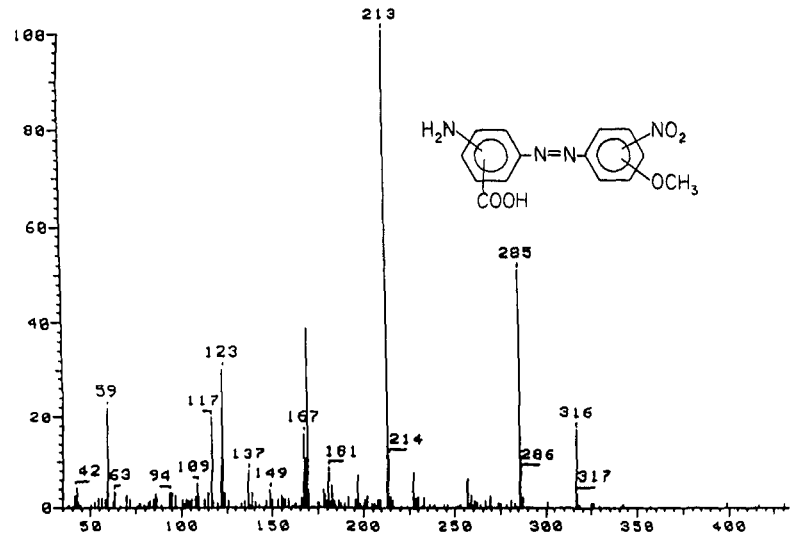

EI SPECTRA WITH TWO POSSIBLE STUCTURES

OBTAINED BY ON-COLUMN GC-MS

Presented at the 36th ASMS Conference on Mass Spectrometry and Allied Topics
June 5-10, 1988, San Francisco, CA

THE APPLICATION OF A HIGH RESOLUTION MASS SPECTROMETRIC METHOD FOR MEASURING 2,3,7,8-TCDD IN HUMAN ADIPOSE TISSUE AND SERUM: THE VIETNAM VETERAN AGENT ORANGE AND RANCH HAND VALIDATION STUDIES; 2,3,7,8-TCDD HUMAN HALF-LIFE STUDY; MISSOURI RESIDENTS CASE/CONTROL STUDY; AND OCCUPATIONALLY EXPOSED WORKERS.

D.G. Patterson, Jr., L.R. Alexander, W.E. Turner, L.L. Needham, J.S. Andrews, Jr., J.L. Pirkle, and E.J. Sampson

Division of Environmental Health Laboratory Sciences, Center for Environmental Health and Injury Control, Centers for Disease Control, Public Health Service, U.S. Department of Health and Human Services, Atlanta, GA 30333

Introduction

Intense public health interest continues to focus on the polychlorinated dibenzo p-dioxins and related compounds. Humans are exposed to many of these compounds from such sources as municipal incinerators and automobile exhausts; other sources, such as the manufacture and use of compounds for which 2,4,5 trichlorophenol is a synthetic intermediate, give rise primarily to 2,3,7,8-TCDD. A number of recent studies have shown that the level of 2,3,7,8-TCDD in the adipose tissue of individuals from several industrialized countries is about 6-7 parts per-trillion. Over the past two years we have analyzed more than 2,000 adipose tissue and serum sample and over 800 quality control samples in five different studies.

The Vietnam Veteran Agent Orange Validation Study

Purpose of the Study: To determine whether military records can be used to identify veterans likely to have been exposed to Herbicide Agent Orange.

Indirect Exposure Measures: 1) "Hits": Weighted number of days within 2 km of an Agent Orange spray, within 6 days after the spray; 2) Slow decay: Weighted number of days within 2 km of a previous Agent Orange Spray; 3) the same scores for sprays with agent unknown; 4) the number of days in 5 heavily sprayed areas; and 5) Two self-reported measures of exposure.

Summary of Results: 1) No association between current serum TCDD levels and any indirect measure of exposure; and 2) Serum TCDD distribution in these Vietnam veterans is the same as in unexposed veterans (see Table 1 and Figure 1).

Table 1. TCDD Levels by Place of Service

Place of Service	Mean I s.d. (ppt)
Non-Vietnam (n = 97)	4.1 ± 2.3
Vietnam (n = 646)	4.2 ± 2.6

Figure 1. TCDD Distribution in Vietnam and Non-Vietnam Ground Troop Veterans

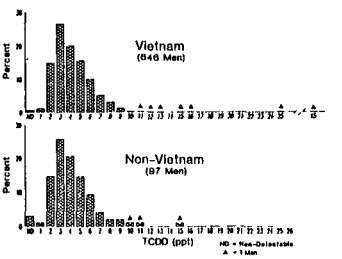

Ranch Hand Vietnam Veterans Pilot Study

Purpose of the Study: To assess the validity of the study design and exposure index for evaluating the possible exposure of Ranch Hand veterans to Agent Orange.

Summary of Results: 39% of Ranch Hand Veterans had TCDD < 20 ppt, while 98% of the comparisons had TCDD < 20 ppt (see Table 2 and Figure 2).

Table 2. Current TCDD Levels by Group (ppt)

2378-TCDD	Ranch Hand (n = 147)	Comparison (n = 49)
Mean	49.4	5.2
Median	26.5	4.7
Range	3.2-313	2.0-21.3

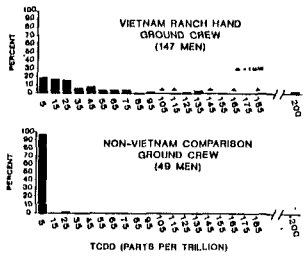

Figure 2. TCDD Distribution in Vietnam and Non-Vietnam Ground Crew Veterans

Conclusions: 1) Some Ranch Hand Veterans have had unusual TCDD exposure; 2) Since 39% of exposed group had TCDD < 20 ppt, an actual body burden measurement is necessary.

2,3,7,8-TCDD Half-Life in Humans

Purpose of the study: To better estimate the half-life of 2,3,7,8-TCDD in humans.

Summary of Results: The half-life of 2,3,7,8-TCDD in serum has been measured in 36 Air Force Vietnam veterans of Operation Ranch Hand. From serum samples taken in 1982 and 1987, the median half life of 2,3,7,8-TCDD in these Ranch Hand veterans was found to be 7.1 years (95% confidence internal about the median of 5.8 to 9.6 years). Levels of 2,3,7,8-TCDD in the 1982 serum samples ranged from 16.9 to 423 ppt.

Missouri Residents Case/Control Study

Purpose of the study: To compare 2,3,7,8-TCDD levels in persons from Missouri with exposure to waste oils and Missouri residents with no known exposure.

Summary of Results: 1) Participants from each of the four exposed groups (TCP production; horse arena riding; residential; waste hauling) had adipose tissue TCDD levels that exceeded 20.2 ppt, the highest level measured in persons with no known exposure (see Table 3 and Figures 3 and 4); 2) Twenty-two (43%) of the 51 exposed participants had TCDD levels of 20.2 ppt or less.

Conclusion: An objective measure of adipose tissue 2,3,7,8-TCDD makes it possible to minimize misclassification when studying the association of TCDD exposure and health effects.

Table 3. Adipose Tissue Levels (Whole-Weight Basis) in ppt in 51 Exposed Participants, Missouri 1986.

Exposure Status	n	Range	Mean	s.d.	Median
TCP Production	9	41.9-750	245	287	122
Horse Arena	16	5.0-577	145	202	24.1
Residential	16	5.2-59.1	26.8	18.9	19.5
Waste Handling	10	3.7-25.8	12.4	8.3	9.0

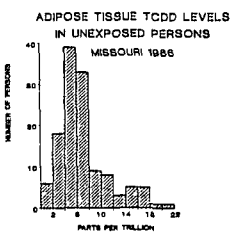

Figure 3.
Adipose Tissue TCDD Levels in Unexposed Persons

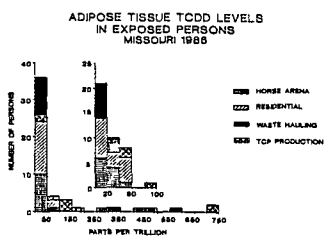

Figure 4.
Adipose Tissue TCDD Levels in Exposed Persons

Presented at the 36th ASMS Conference on Mass Spectrometry and Allied Topics
June 5-10, 1988, San Francisco, CA

Detection of polychlorinated terphenyls by gas chromatography mass spectrometry with negative chemical ionisation

J. Greaves and R. C. Hale
Virginia Institute of Marine Science
College of William and Mary
Gloucester Point, Virginia 23062

Polychlorinated terphenyls (PCT) are a group of compounds that were recommended as alternatives to polychlorinated biphenyls (PCB) for certain industrial applications. Although not used to the same extent as PCB, production was of the order of 10% that of PCB. PCT have been used in a wide variety of applications which included: waxes for investment casting, printers ink, sealants, adhesives, resins and lubricants. PCT manufactured in the United States were marketed as components of the Aroclor 25, 44, 50, 54 and 60 series, with the 54 series being the only formulation consisting purely of PCT. The 25, 44 and 60 series were mixtures of PCT and PCB and the 50 series formulations were unpurified versions of the 54 series. The two major members of the 54 series were 5432 and 5460, where the 32 and 60 in the nomenclature designated the percentage chlorine by weight. There have been few reports published on the analysis of these compounds, due in part to their relatively high molecular weight, the large number of isomers making chromatographic separation difficult, and the fact that U.S. manufacture ceased in 1972. PCT are, however, both highly persistent and toxic and, in addition, since the toxicity of this type of compound is related to isomeric structure and degree of chlorination, a more detailed study of them may be important. The first stages of this research are reported here.

Late eluting peaks detected on a GC with a Hall detector were identified as PCT using an Extrel ELQ 400-2 GC-MS with negative chemical ionisation. Methane was the moderator gas. The spectra obtained were typical of chlorinated hydrocarbons when negative chemical ionisation is used and showed $[M]^-$, $[M + O - Cl]^-$, $[M - Cl]^-$ ions and sequential losses of chlorine. The extent of fragmentation was positively correlated with increasing degree of chlorination. Aroclor 5432 consisted of terphenyl substituted with 2-5 chlorine atoms. In Aroclor 5460 the predominant congeners contained from 7-10 chlorine atoms, though as many as 12 chlorine atoms were seen. A 25 m fused silica GC column, coated with SE-54, was used. The column was run directly to the ionisation volume of the MS. The Aroclor 5432 and 5460 components eluted before and after decachlorobiphenyl, respectively. Some minor overlap between Aroclor 5432 and highly chlorinated PCB formulations (eg. Aroclor 1254), was observed.

Freeze-dried sediment samples, dry weight approximately 70 g, were soxhlet extracted with dichloromethane and cleaned up by gel permeation and Florisil chromatography. Decachlorobiphenyl was used as the internal standard. The sediment samples were obtained near effluent outfalls at a wide variety of sites, including ship repair and building facilities, military installations and research centers. Both mass spectral and GC peak patterns matched those obtained for standard mixtures, confirming the presence of PCT. Mass spectra and GC peak patterns matched those obtained for both Aroclor 5432 and 5460. Concentrations detected were in the 0.6 to 30 ppm range, based on response factors calculated for the Aroclors against decachlorobiphenyl. In certain samples the PCT concentration exceeded that for PCB. Initial work has been carried out to examine biota from these sites and there is some preliminary evidence that selective accumulation of the lower chlorinated PCT may be occurring.

Presented at the 36th ASMS Conference on Mass Spectrometry and Allied Topics
June 5-10, 1988, San Francisco, CA

LASER DESORPTION FOURIER TRANSFORM MASS SPECTROMETRY OF HYDROCARBON SOOT

Hun Young So and Charles L. Wilkins
Department of Chemistry
University of California, Riverside
Riverside, CA 92521

Laser desorption Fourier Transform mass spectrometry (LD/FT/MS) (1) is applied to characterize molecular weight distribution of benzene soot. Soot is chosen as an example of a complicated sample matrix. It is well known that soot contains a variety of polycyclic aromatic hydrocarbons (PAH) and large size spherical carbonaceous material. Most of PAH analysis of environmental samples have been limited to lower molecular weight PAH, due to their low volatility and lack of standard materials (2). The LD technique is used to investigate the distribution of higher molecular weight (>400 amu) PAH in soot. The spherical structure of soot was discussed in relation to the carbon clusters (3). We investigated soot as a possible source of carbon clusters.

A Nicolet FT-2000 equipped with an autoprobe and a CO_2 laser was used in this experiment. Soot was collected directly on the stainless steel probe tip. A typical LD/FT/MS spectrum of benzene soot is shown in Fig. 1. The empirical formulas of high intensity peaks are assigned by comparing with spectra given by deuterated benzene soot (Fig. 2b). Most of the high intensity peaks of each peak groups are characterized as PAH. It is interesting to observe that PAH with even numbers of carbons (lettered in Fig 2) show higher intensities than those with odd numbers of carbons (numbered in Fig. 2). Detection of PAH with higher molecular weight than the previously reported is shown in Fig. 1. Similar distributions of PAH are also observed with soot from other hydrocarbon fuels.

A series of peaks 24 amu apart are observed in the high mass region of the LD/FT/MS spectrum of benzene soot , and are appeared to be carbon clusters. In a spectrum acquired with 131K data points, carbon clusters with up to 120 carbons could be detected with reasonable resolution, in addition to PAH components.

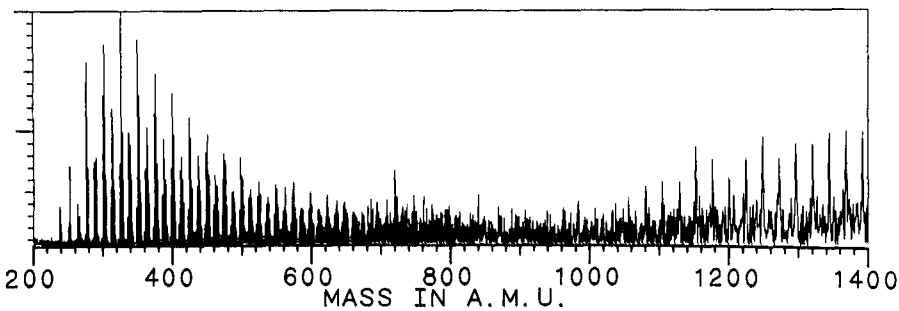

Fig. 1 LD/FT/MS spectrum of benzene soot, 50 time domain signals were coadded, band width-2.6 MHz, data points-131K

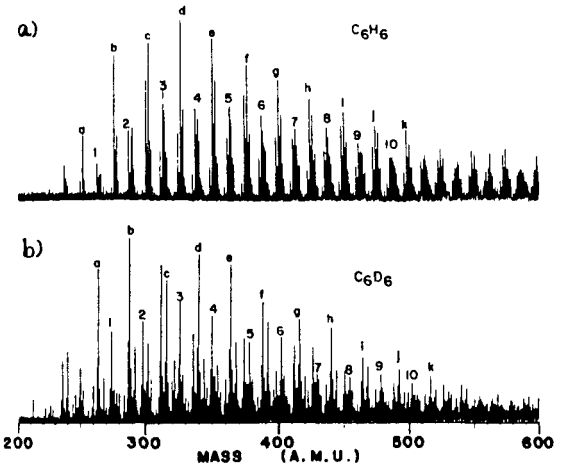

Fig 2. Comparison of the two spectra to assign empirical formulas of the peaks.

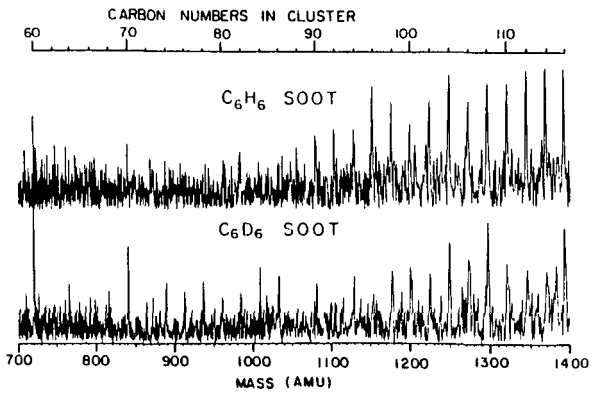

Fig 3. Carbon clusters observed in LD/FT/MS of soot samples.

References

1. L. M. Nuwaysir and C. L. Wilkins, *Anal Chem.* **1988**, *60*, 279

2. A. Bjorseth, and T. Ramdahl (Ed.) "Handbook of Polycyclic Aromatic Hydrocarbons," Vol. II, Marcel Dekker, New York, 1985

3. Q. L. Zhang, S. C. O'Bnen, J. R. Heath, Y. Liu, R. F. Curl, H. W. Kroto, and R.E. Smalley, *J. Phys. Chem.* **1986**, *90*, 525

Presented at the 36th ASMS Conference on Mass Spectrometry and Allied Topics
June 5-10, 1988, San Francisco, CA

CAD Analysis of Methyl PAH: Fused-ring Tropylium Ion Formation and Fragmentation:

Laurel L. Standley and Ronald A. Hites; School of Public and Environmental Affairs and Department of Chemistry, Indiana University, Bloomington, IN, 47405.

The formation of tropylium ions by the rearrangement of alkyl benzenes is well documented in mass spectrometric studies[1]. The most likely mechanism for the formation of these ions is through a cyclopropyl intermediate as shown below[2,3]. Early research also demonstrated that the carbons in the tropylium ion are scrambled[4]. An equilibrium between the benzylium and tropylium ions through the cyclopropyl intermediate was considered to be the mechanism for carbon atom scrambling[2,3]. The question arises as to whether alkyl polycyclic aromatic hydrocarbons (PAH) also rearrange to form a tropylium-type ion. They might form and scramble by the same mechanism:

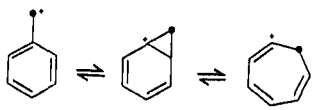

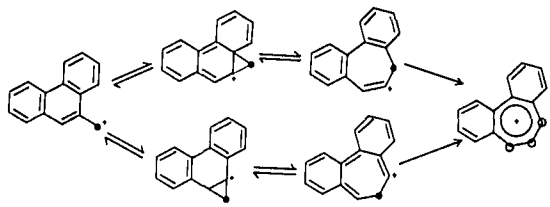

Note the large $(M-1)^+$ ion (m/z 191) in the mass spectrum of 9-methyl phenanthrene shown in Figure 1. The structure of this ion parallels the $(M-1)^+$ ion in methyl benzene, which corresponds to the tropylium ion rearrangement product. In this study, we demonstrate the formation of fused-ring tropylium ions from methyl phenanthrenes and anthracenes. Four possible fused-ring tropylium structures can be formed from these compounds, depending on whether the methyl group is on the center or terminal ring.

The fragmentation patterns of the methyl phenanthrenes and anthracenes were studied using MS/MS on a VG 30-250 triple quadrupole instrument. The major fragmentation route, after loss of a hydrogen to form the $(M-1)^+$ (m/z 191) ion, was a sequential loss of several neutral acetylene molecules (see Figure 2). A minor amount of CH_3 was also lost from the m/z 191 ion forming an ion which subsequently lost an acetylene group. However, the predominant fragment formed from the m/z 191 ion was the m/z 165 ion. This is the fragmentation which proved most useful as an indicator of structure as will be discussed below. No statistically significant differences were found between the methyl phenanthrene and anthracene isomers in the MS/MS results with respect to either the fragmentation pathway or the intensity of fragments formed.

To prove whether the structures of these m/z 191 ions were in the form of fused-ring tropylium ions, we studied labeled compounds. We synthesized ^{13}C-labeled methyl phenanthrenes and anthracenes and then monitored the loss of that label during fragmentation of the m/z 192 (the labeled ion equivalent to m/z 191) ion to the m/z 165 and 166 fragment ions. Two mechanisms can affect the loss of the label (see Figure 3): (a) whether or not the methyl carbon scrambles after incorporation into the tropylium ring; and (b) from where in the structure the acetylene group is lost.

The C_2H_2 group could either be lost from the seven membered tropylium ring (losses 1 and 2 as shown in Figure 3) and/or from either of the six membered rings (losses 3 through 8 as shown in Figure 3). In order to determine which loss would be more likely, if either, we calculated the heats of formation of the various structures using the semi-empirical model MNDO. The heats of formation give a relative measure of the stability of structures, i.e.- the more stable a structure the lower its heat of formation. Two of the fused-ring tropylium structures and the possible fragmentation products are shown in Figure 4. The calculated heats of formation in kcal/mole are listed below the structures. In the first example, the structure with the tropylium ring in the center of the molecule (formed from 9-methyl anthracene) could fragment by losing the acetylene molecule either from the six membered ring or from the seven membered ring to form structures with heats of formation of 280 and 240 kcal/mole, respectively. The structure resulting from fragmentation of the seven-membered ring is clearly more stable, as reflected in its heat of formation being 40 kcal/mole less than that of the other fragmentation product; it is thus more likely to form. Fragmentation products of the fused-ring tropylium ion formed from 1, 2, 3, or 4-methyl phenanthrene can be compared in a similar fashion. Again note that the product resulting from the loss of the acetylene molecule from the seven-membered

ring is more stable than the product forming from a loss from the six-membered ring, this time by 11 kcal/mole.

Thus far our results have documented that fragmentation of these $(M-1)^+$ ions occurs predominantly by losing an acetylene molecule from the seven-membered ring. Whether or not the labeled carbon scrambles in the structure, as has been shown to occur in the tropylium ion, will also affect whether or not it will be lost upon fragmentation. Based on the mechanism proposed earlier (i.e.- the cyclopropyl intermediate), the methyl carbon should be scrambled in the tropylium ring only. Experimental results for the methyl phenanthrenes support the two predictions discussed above (i.e.- loss of the acetylene molecule from and scrambling in the seven-membered ring only). The methyl anthracenes, however, did not match the theoretical predictions as well as the phenanthrenes. The only mechanism which explained the results was an equilibrium between the two fused-ring anthracene tropylium ions (i.e. - one with the tropylium ring in the center of the three rings and the other in the terminal position). We calculated the heats of formation (as described earlier) for the most likely transition states to see if an equilibrium between the two ions would be energetically feasible. There was no additional energy barrier beyond those necessary to form and equilibrate the fused-ring tropylium ions in the first place. The phenanthrene ions may not equilibrate to the extent of the anthracene ions due to a rate limiting step or a high energy intermediate which we have not yet considered. Formation of the benzylium ion with no rearrangement to the fused-ring tropylium ion was ruled out with these results.

1. Rylander, P.N.; Meyerson, S.; Grubb, H.M. (1957). J. Amer. Chem. Soc. 79, 842-846.
2. Cone, C.; Dewar, M.J.S.; Landman, D. (1977). J. Amer. Chem. Soc. 99, 372-376.
3. Grotemeyer, J.; Grutzmacher, H-Fr. (1982). in: Current Topics in Mass Spectrometry and Chemical Kinetics. Beynon, J.H.; McGlashan, M.L. (eds.), Heydon, London, pp. 29-59.
4. Siegel, A. (1974). J. Amer. Chem. Soc. 96, 1251-1252.

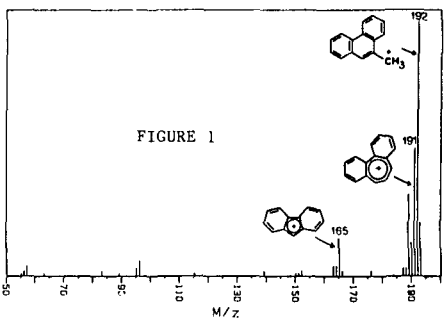

FIGURE 1

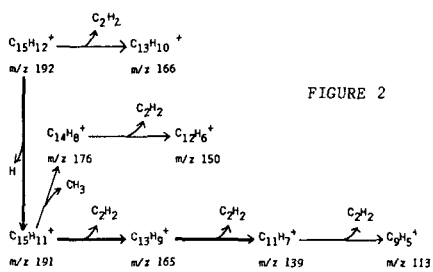

FIGURE 2

FIGURE 3

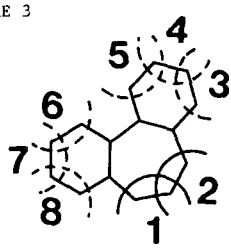

FIGURE 4

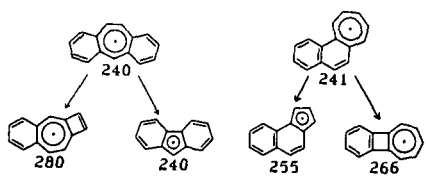

Presented at the 36th ASMS Conference on Mass Spectrometry and Allied Topics
June 5-10, 1988, San Francisco, CA

THE ANALYSIS OF ORGANIC COMPOUNDS IN DRINKING WATERS BY MASS SPECTROMETRY: SOME REMAINING PROBLEMS

H A James, T M Gibson and I Hammond, Water Research Centre, Medmenham Laboratory, PO Box 16 Marlow, Bucks SL7 2HD, UK

Mass spectrometry has been applied to the identification and quantification of organic compounds in drinking waters for over 20 years. Examination of published data indicates that there are some areas in which MS has yet to be totally successful and where effort needs to be directed. Experience in our laboratory over the last fifteen years suggests that three such areas are the identification of unknowns detected by GCMS, the identification of non-volatile compounds (ie compounds not amenable to analysis by GCMS), and quantification.

We find that unknowns (compounds not immediately identifiable by comparison with reference data or by manual interpretation) are regularly detected during general-survey GCMS examination of extracts from drinking waters. It has been noted (1) that due to the effort and expense arising from the application of non-routine MS and other techniques, it is not practical to attempt to identify most of these unknowns. However, in certain instances, eg when a sample is being analysed because of customer complaints, there may be an urgent requirement to identify an unknown. The identification of 2-t-butyl-5-methyl-p-benzoquinone is one such instance. We found that this compound was responsible for a "graphitic" taste in some drinking waters. Its electron impact spectrum, which as far as is known is not present in any reference collections is shown in Figure 1.

It is difficult to form a scientifically credible view of the correct reaction following the detection of an unknown in a sample of water examined during routine monitoring activities. Even if identification is possible, because of insufficient toxicological data, the implications of the findings are usually not clear. Frequently unknown spectra are added to a library of unknowns, but this is only of value if some positive action is taken in the event of regular and frequent detection of a particular unknown.

A related problem which has recently been noted (2), concerns mis-identification. This is particularly likely to occur when automated spectral interpretation techniques are employed, and the only remedy appears to be expert scrutiny of results.

The identification of non-volatile compounds (ie compounds not amenable to analysis by GCMS) is an area which seems to be developing very slowly at present. There are many possible reasons for this.

We have found that a target compound approach has been more productive than a general-survey approach for non-volatiles. Compound classes successfully analysed at WRc in drinking waters using off-line LC - "soft-ionisation" MS include epoxy resin components (3), surfactants and pharmaceuticals (4). Initial experience with thermospray LCMS suggests that, as for LC combined with FD or FAB, its main utility at present lies in its use in a target compound mode, as the spectra produced from some compounds can be difficult to predict.

Quantification, even following well documented methodology, is often not an easy task (5). We have found, along with others, that for general survey analysis, the use of deuterated internal standards can assist in the provision of preliminary quantitative information (6), which is often useful in deciding whether further (better) quantification is necessary. Normally, this latter data would be

produced using selected ion monitoring, which is a widely used and fairly routine technique. However, we encountered problems with the quantification of 3-chloro-4-(dichloromethyl)-5-hydroxy -2(3H)-furanone, a potent mutagen which may be present in some drinking waters (7). Its analysis as the methyl ether had been previously described (8), but we found that initially the response on GCMS was non-linear. Following the inclusion of a combined oxygen/water trap in the carrier gas line (rather than just an oxygen trap) it gave a linear response, which improved the detection limit.

Some of the problems mentioned above, particularly those related to GCMS, will undoubtedly be alleviated by improvements and advances in instrumentation (eg the more widespread availability and use of triple quadrupole mass spectrometers). However, at present it appears unlikely that there will be similar progress in the identification of non-volatiles, unless many more laboratories show an interest in this type of work.

References

1. Bursey, J T. EPA Project Summary EPA-600/54-84-072 (1984).

2. Swallow, K C , Shifrin, N S and Doherty, P J. Environ Sci Technol 22, 136-142 (1988).

3. Watts, C D, James, H A, Gibson, T M and Steel, C P. Environ Tech Letts 4, 59-64 (1983).

4. Crathorne, B, Fielding, M, Steel, C P and Watts, C D. Environ Sci Technol 18, 797-802 (1984)

5. Stanko, G H, Fortini, P E. Haz Waste Haz Materials 2, 67-97 (1985).

6. James, H A, Fielding, M, Gibson, T M and Steel, C P. Adv in Mass Spectrometry, 8B, 1429-1435 (1980).

7. Horth, H, Fielding, M, James, H A, Thomas, M J, Gibson, T and Wilcox, P. (In press) Water Chlorination: Environmental Impact and Health Effects, Vol 6, Eds R J Jolley et al

8. Hemming, J, Holmbom, B, Reunanen, M and Kronberg, L. Chemosphere 15, 549-556 (1986).

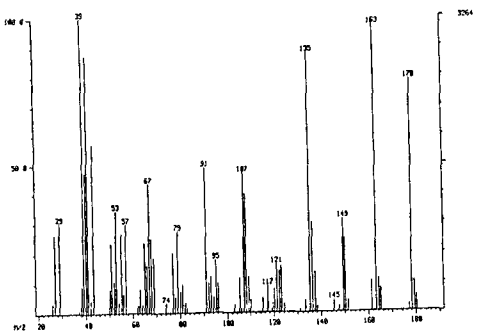

Figure 1. Electron impact mass spectrum of 2-t-butyl-5-methyl-p-benzoquinone

Presented at the 36th ASMS Conference on Mass Spectrometry and Allied Topics
June 5-10, 1988, San Francisco, CA

A VOLATILE ORGANIC ANALYZER FOR SPACECRAFT AIR QUALITY MONITORING

*Theodore J. Galen, Duane L. Pierson, Biomedical Laboratories,
NASA Johnson Space Center, *KRUG International, Houston, TX 77058

In manned space exploration, maintaining the quality of the air which the astronauts breathe in the spacecraft is extremely critical. Sources of air contaminants can include materials offgassing, utility chemicals, thermal degradation, inflight scientific experiments, and human metabolites. Analogous to the Environmental Protection Agency's air quality standards here on Earth, NASA has established spacecraft maximum allowable concentration limits for many volatile compounds. The environmental control and life support system on board the spacecraft is equipped with various technologies (e.g. scrubbers containing lithium hydroxide and charcoal and active catalytic processes) to remove contaminants such as carbon dioxide, carbon monoxide, and volatile organics. The environmental control system maintains a constant level of oxygen, supplementing the oxygen consumed by respiration; it is a partially closed-loop system supplying only make-up oxygen and nitrogen and removing only selected contaminants. In the Space Shuttle Program, the operational efficiency of the system has been assessed by collecting samples during each mission and performing postflight analysis for trace-level contaminants using gas chromatography/mass spectrometry. For long-term shuttle missions, planetary missions, or missions on board the permanently manned space station, monitoring the levels of potentially harmful volatile compounds in the spacecraft atmosphere in flight, on a real-time basis will be essential.

To verify that the air in the spacecraft is safe and that the purification system is operating effectively, particularly on long-term missions, a Volatile Organic Analyzer system is being developed in the Toxicology Laboratory of the Biomedical Laboratories Branch at the Johnson Space Center in Houston. The Volatile Organic Analyzer is being developed to unequivocally identify all the known potentially harmful volatile compounds and to quantitatively determine that these compounds are not exceeding the predetermined maximum allowable limits. In addition, this system will be used to characterize volatile organics which have not been previously identified in the spacecraft atmosphere. The following is a list of the primary design considerations: the system must be space-flight compatible with respect to size, weight, and power requirements; it must be capable of withstanding the launch- and boost-vibration profile; it must be able to function in microgravity; and it must be as fully automated as possible, providing ease of operation and requiring minimum crew/operator time.

The Volatile Organic Analyzer prototype system is composed of a combination of four subsystems: a sample inlet, a gas chromatograph, a mass detector, and a computer. The sample inlet subsystem contains a sampling pump and solenoid valve, a series of Tenax traps to concentrate the volatile organics, and a 10-port micro switching valve. The gas chromatograph subsystem utilizes a temperature-programmable oven containing a state-of-the-art fused-silica capillary column. A commercially available ion trap detector functions as the mass analyzer. The computer subsystem operates using a standard lap-top IBM-compatible computer.

The sample inlet and gas chromatograph subsystems are only available commercially as large standard laboratory equipment. After extensive evaluation and modification of various candidate technologies, a flight-prototype of these subsystems has been developed. In designing the gas chromatograph subsystem, significant reductions were made in the size, weight, and power required to operate the subsystem. The gas chromatograph was integrated with an automatic sampling system for preconcentration of the trace-level contaminants present in an air sample. This integration required requiring isolation and precise control of five independent temperature zones: the sample inlet, the two Tenax traps, the micro switching valve, and the analytical column oven. To maximize the analytical performance, the inlet and the gas chromatograph were designed to be compatible with the fused-silica capillary columns. With accurate helium carrier gas control, the analytical column was directly coupled to the ion trap detector without the need for an open/split interface. To control the Volatile Organic Analyzer, integrated software was developed for the lap-top computer. The computer subsystem controls the overall system sequence timing; the sample inlet functions, including the operation of the sample pump and solenoid valve; the position and timing of the 10-port valve driver; and the four thermal zones. The computer also controls and monitors the analytical column temperature in both isothermal and temperature-programming modes. It functions as the operational computer

for the ion trap detector, controlling the temperature and performing data acquisition and analysis.

Over the past year, the major progress in this development effort has been the reduction in the size and weight of the inlet and gas chromatograph subsystems. The operation of these subsystems can be described as follows: in valve position "A," an air sample is drawn into the first Tenax trap by the sampling pump. The solenoid vent valve is closed at this time. The switching valve then rotates to position "B," and the compounds collected on the first Tenax trap are thermally desorbed and transferred to the second and smaller Tenax trap. The switching valve then rotates back to position "A," and the smaller trap is ballistically heated to desorb the organics as a narrow band onto the fused-silica analytical column. Separation of the mixture of organic compounds present in the sample occurs by temperature-programmed capillary gas chromatography. The ion trap is used to detect and identify the compounds as they elute from the analytical column. Finally, the valve rotates to position "B," where both Tenax traps are thermally cleaned and the sample inlet is purged in preparation for the next sample.

The overall system has been operated both with non-polar and polar capillary columns. Typical operational parameters for the ion trap detector are scanning from 35 to 300 AMU at one scan per second with a trap temperature of 150 degrees and a multiplier setting of 1550 volts. Utilizing version 3 software, the trap is run with the AGC on. Checks are performed of the total system background by introducing zero air samples as blanks into the analyzer system. Overall system sensitivity has been measured by sampling a 1 ppm standard of fluorobenzene at various times, ranging from 2 to 20 seconds and equivalent to 12 to 120 pg on column. To test the overall performance of the system, 2 test mixtures composed of 10 and 25 selected volatile organics were blended as standards. The concentration of the the individual components ranged from 70 to 150 ppb or 70 to 150 ng of each compound on column. The analysis of these standards demonstrated that the system could automatically sample an atmosphere, concentrate the organic components, and subsequently separate and identify individual compounds based on their mass fragmentation. In addition, all operations were performed in an automated manner, including sequence timing, temperature and valve control, data acquisition and analysis.

The goal of this NASA development effort has been to maintain or enhance the Volatile Organic Analyzer's analytical performance, while combining the four subsystems into an integrated package. A source has been identified for mechanical and electrical integration of the four subsystems into a single package. This effort will include further significant reductions in total system size and weight and will entail converting the system to spacecraft power sources. To date, engineering drawings have been prepared, and a one- to-one scale model system has been fabricated. Future work on the Volatile Organic Analyzer will include system integration of the mechanical and electronic components into a flight-qualified package. A series of laboratory-verification tests will then be performed, followed by flight- verification evaluations in NASA aircraft and on the shuttle. The system is currently targeted as a primary component of the space station Environmental Health Subsystem. When in operation, the Volatile Organic Analyzer will be a vital instrument in verifying that the air inside a spacecraft is safe for the crewmembers to breathe.

Presented at the 36th ASMS Conference on Mass Spectrometry and Allied Topics
June 5-10, 1988, San Francisco, CA

TRACE ANALYSIS FOR ORGANICS IN AIR USING AN ATMOSPHERIC SAMPLING GLOW DISCHARGE IONIZATION SOURCE

Barry C. Grant, Keiji G. Asano, Gary L. Glish,
and Scott A. McLuckey
Analytical Chemistry Division
Oak Ridge National Laboratory
Oak Ridge, TN

We have developed an ion source for the real-time analysis of trace organics in ambient air.[1] The ion source is based on the establishment of a glow discharge in a region of reduced pressure sustained by air drawn into an interelectrode region. Figure 1 shows a schematic of the ion source attached to a quadrupole mass filter. The discharge is established either by using the plate containing aperture A1 as the cathode and the plate containing the aperture A2 as the anode or by establishing the discharge between the half-plates labelled P1 and P2. A voltage difference of 400 V between the electrodes is sufficient for establishing a stable discharge under the normal pressure conditions of 0.2-0.8 torr.

Features of this ion source include, briefly, a high sampling rate (5 ml/s), short memory, a degree of flexibility in ionization, minimal clustering, simplicity, and ruggedness. A degree of flexibility in ionization in the positive ion mode is afforded via the discharge voltage. The relative abundance of proton hydrates, the major proton transfer reagent ions, is maximized at low discharge voltages whereas at higher discharge voltages (>450 V) reagent ions that undergo charge transfer, such as $O_2^{+\cdot}$, are by far most abundant. Conditions can be established where some clustering of water molecules is observed but this can be avoided by operating at slightly higher discharge voltages. The relative lack of clustering is largely due to the fact that cooling by expansion from one pressure region to the next is minimized by use of relatively large aperture sizes (A1=200 μm, A2=800 μm) and two stages of pressure reduction. A significant advantage of the ion source is its relative simplicity and ruggedness. Since the source relies on no materials that are rapidly oxidized or pitted it can operate for long periods of time without maintenance. We have operated this ion source 24 hours a day for months at a time without maintenance and have noted no noticeable loss in performance.

The ion source was developed for the analysis of trace quantities of explosives in ambient air. These compounds typically contain several NO_2 or NO_3 groups and are therefore readily detected in the negative ion mode. We find that we can detect such species with high electron affinities at the parts per trillion level. For example, Figure 2 shows the response curve obtained for 2,4,6-trinitrotoluene (TNT) by monitoring the molecular anion. The concentration of TNT that enters the ion source at the point where the signal is three times the standard deviation of the noise is about 1 ppt.

Recently we have measured detection limits for members of several other compound classes choosing to monitor one relatively intense ion at or near the molecular weight. For example, in the positive ion mode detection limits have been measured for anthracene ($M^{+\cdot}$, 5 ppb), butanol ((MH^+-H_2O), 1 ppb), propionic acid ($M^{+\cdot}$, 2 ppb), and trichloroethylene ($(M-Cl)^+$, 3

ppt). In the negative ion mode detection limits have been measured for anthracene ($(M+O-H)^-$, 1 ppb), butanol ($(M-H^+)^-$, 10 ppb), and propionic acid ($(M-H^+)^-$, 2 ppb). The detection limit is, of course, a reflection of the performance of the entire system and is determined by, in addition to the performance of the ion source, ion transport through the system, detection efficiency, and background noise. Considering the limitations of the mass spectrometers used to acquire these data, the reported detection limits are deemed to be conservative estimates. Furthermore, in some cases in the positive ion mode, significant chemical noise was present at the mass used to measure the detection limit. In these cases, a lower detection limit should be attainable using MS/MS.

1. S.A. McLuckey, G.L. Glish, K.G. Asano, and B.C. Grant, Anal. Chem., In Press.

Research sponsored by the U.S. Department of Energy, Office of Basic Energy Sciences, under Contract DE-AC05-84OR21400 with Martin Marietta Energy Systems, Inc.

Fig. 1 Schematic diagram of the ASGDI source

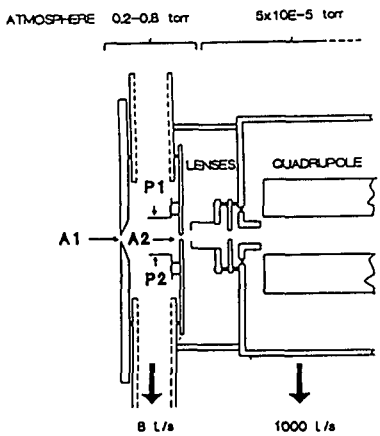

Fig. 2 TNT response curve

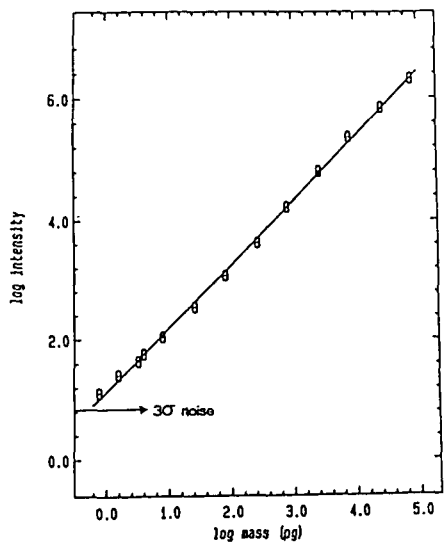

"The submitted manuscript has been authored by a contractor of the U S Government under contract No DE-AC05-84OR21400 Accordingly, the U S Government retains a nonexclusive, royalty-free license to publish or reproduce the published form of this contribution, or allow others to do so, for U S Government purposes."

Presented at the 36th ASMS Conference on Mass Spectrometry and Allied Topics
June 5-10, 1988, San Francisco, CA

MIXED CLUSTER ION FORMATION BETWEEN SMALL MOLECULES AND H_2SO_4 CLUSTERS FORMED WITH WATER

Thomas R. Sharp
Mass Spectrometry Applications Laboratory
Center for Chemical Characterization and Analysis
Department of Chemistry, Texas A&M University, College Station, Texas 77843 U.S.A.

Previous reports [1,2] describe observation of both positively charged and negatively charged cluster ions from concentrated mineral acids -- H_2SO_4 and H_3PO_4 -- produced by fast atom bombardment. In marked contrast to the behavior of H_3PO_4 [3], certain small molecules can be mixed with H_2SO_4, with the resulting mixture yielding mixed cluster ions. The results of further investigations into the nature of these mixed molecule clusters are reported here.

Observation of the FAB mass spectrum of concentrated H_2SO_4 showed the production of cluster ions of the formula $(H_2SO_4)_nH^+$, n=1,2,3..., with n as high as 15 being easily seen. In addition, the small H_2O content of reagent H_2SO_4 contributed to the occurrence of an additional cluster ion series of formula $(H_2SO_4)_nH_3O^+$, n=1,2,3..., with high n clusters being as easily observed, if not moreso, than for $(H_2SO_4)_nH^+$. Figure 1 shows the positive ion FAB spectrum of H_2SO_4 over the mass range m/z 10-300. Upon absorption of H_2O from the atmosphere due to the hydroscopic nature of concentrated H_2SO_4, the intensities of $(H_2SO_4)_nH_3O^+$ increase with respect to $(H_2SO_4)_nH^+$ for a given n.

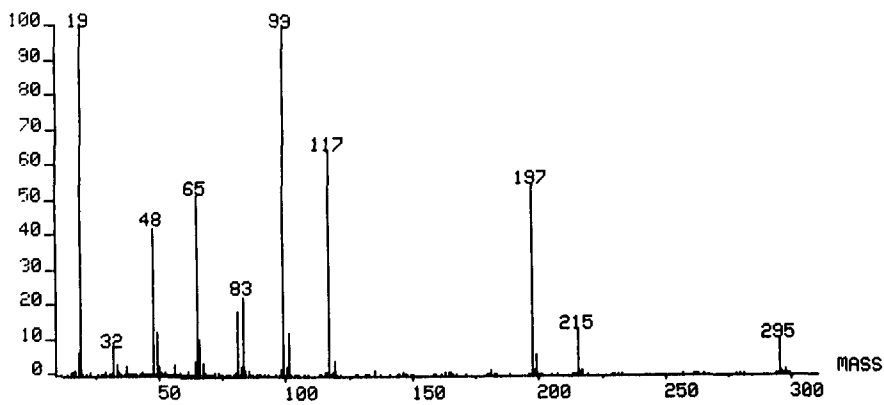

Figure 1: Positive ion FAB mass spectrum of H_2SO_4, illustrating the $(H_2SO_4)_nH^+$ series (m/z 99, 197, 295) and $(H_2SO_4)_nH_3O^+$ series (m/z 117, 215) as well as the fragments of H_2SO_4 below the protonated molecular ion. Note that m/z 19 (H_3O^+) and m/z 99 are off scale.

To investigate the formation of hydrated clusters further, mixtures of H_2SO_4 and H_2O were prepared gravimetrically to give varying mole ratios spanning the range from "100%" H_2SO_4 to 1:11 H_2SO_4:H_2O. Positive ion FAB-MS spectra were recorded on these mixtures to monitor changes in intensity ratios and appearance of new cluster ions. Comments made here pertain to positively charged ions only. The negative ion spectrum of conc. H_2SO_4 consists exclusively of clusters of formula $(H_2SO_4)_nHSO_4^-$, n=0,1,2,3..., regardless of the amount of H_2O added to the acid.

Figure 2 plots the relative intensities of the two cluster ion series as a function of cluster number, showing that no apparent "magic number" phenomena exist in this system. This is consistent with the "amorphous" nature of the liquid droplet from which the cluster ions are being formed, as opposed to the presence of such magic number clusters in the alkali metal halides being attributed to stable crystal lattice arrangements [4]. Comparison of the slopes of the lines in Figure 2 indicates that the $(H_2SO_4)_nH_3O^+$ series is slightly more stable than the $(H_2SO_4)_nH^+$ series. At a given H_2O content, the hydrated clusters are more intense than the protonated clusters, especially above n=3. Cluster series intensities were plotted for all of the different acid:water mixtures. Slopes of the lines stayed remarkably constant for all mixtures. The only noticeable change was that the point where the two lines crossed changed from slightly above n=3 for low H_2O concentrations to slightly below n=3 for high H_2O content. With increasing H_2O concentration, no new cluster ions or series appear. In spite of acid:water mole ratios as high as 1:11, the $(H_2SO_4)_nH^+$ and $(H_2SO_4)_nH_3O^+$ clusters are the only series present.

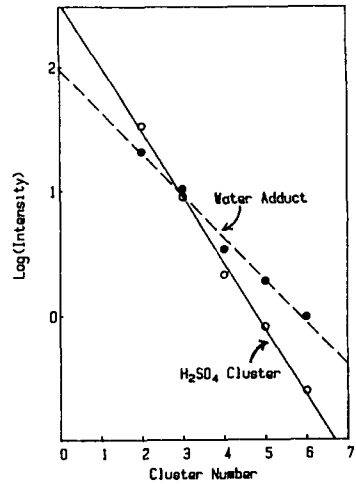

Figure 2: Log relative intensity vs. cluster number for $(H_2SO_4)_nH^+$ and $(H_2SO_4)_nH_3O^+$ cluster ions.

The results of B/E linked scan experiments are summarized in the accompanying table. Fragmentations of H_2SO_4 itself were relatively unaffected, while certain decomposition reactions of the larger clusters could be enhanced by collisional activation.

Parent	Daughter Ions			
m/z	m/z	ion yield - CID	ion yield + CID	fragmentation
99	81	50%	53%	$HSO_3^+ + H_2O$
	65	16%	17%	$HSO_2^+ + H_2O_2$ (?)
	48	8%	10%	$SO^+ + H_2O + OH$ (?)
117	99	75%	75%	$H_2SO_4H^+ + H_2O$
	81	10%	8%	
	65	4%	3%	
	48	2%	2%	
197	117	85%	21%	$H_2SO_4H_3O^+ + SO_3$
	99	15%	63%	$H_2SO_4H^+ + H_2SO_4$
	81	0%	8%	$HSO_3^+ + H_2SO_4 + H_2O$
215	197	77%	41%	$(H_2SO_4)_2H^+ + H_2O$
	117	23%	33%	$H_2SO_4H_3O^+ + H_2SO_4$
	99	0%	20%	$H_2SO_4H^+ + H_2SO_4 + H_2O$

The acid:water observations were made on a VG Analytical 70-E instrument with DS2000 datasystem, operated at +5KV. The linked scan experiments were performed on a VG 70-S with 11/250J datasystem, operated at +8KV. The Ion Tech fast atom gun produced a 6-8 KeV neutral argon beam. Sufficient helium target gas was introduced into an electrically grounded first field-free region collision cell to attenuate the parent ion intensities by appx. 50%. B/E linked scans were performed under datasystem control, after mass calibration against H_2SO_4 [2]. Daughter ion yields are expressed as a percentage of total daughter ion intensity. Funds from NSF Grants CHE-8310031 for the 70-E and CHE-8705697 for the 70-S are gratefully acknowledged.

---

1. Sharp, T.R., Jones, H.K. (1986). **34th. ASMS Meetings,** Cincinnati, OH. Pp. 535-6.
2. Sharp, T.R. (1986). **Org. Mass Spectrom.** 21,793-5.
3. Fietkau, R., Sharp, T.R., Russell, D.H. (1987). **194th. ACS Meetings,** New Orleans, LA.,
4. Campana, J.E. (1987). **Mass Spectrom. Rev.** 6,395-442.

Presented at the 36th ASMS Conference on Mass Spectrometry and Allied Topics
June 5-10, 1988, San Francisco, CA

LARGE CARBON CLUSTER FORMATION BY LASER ABLATION OF POLYIMIDE

William R. Creasy and J. T. Brenna
IBM Corp. (T43), 1701 North St., Endicott, NY 13760

Polyimide (Dupont Kapton®) is an important polymer for electronics packaging applications. We have studied it using a laser microprobe/ Fourier Transform Mass Spectrometer (FTMS) apparatus in order to analytically identify small areas of the polymer. The polymer is ablated and ionized by the 266 nm pulsed laser radiation, and the ions are mass analyzed by FTMS. Laser ablation is found to form a positive ion distribution of high mass carbon cluster ions. A more detailed discussion of the laser ablation, and of the carbon cluster ion distribution, has been submitted for publication.[1]

Laser ablation of polyimide was studied using a laser microprobe/ FTMS system which has been described in detail elsewhere.[2] A Nicolet FTMS/2000 was used for the ion detection, and a Quantel Nd:YAG laser (fourth harmonic at 266 nm) was used for the laser ablation/ionization. The polyimide samples were 15 um films which are chemically identical to Dupont Kapton.

A sample mass spectrum is shown in Figures 1, 2A, and 3A. The single spectrum is divided into three distributions. All three distributions can be observed in the same experiment, but the relative intensities depend strongly on the incident laser power and focussing conditions.

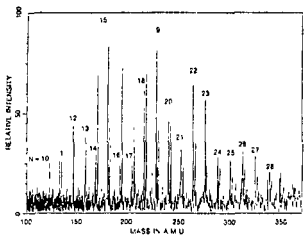

Figure 1 Low Mass Distribution

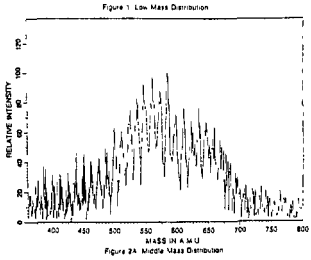

Figure 2A Middle Mass Distribution

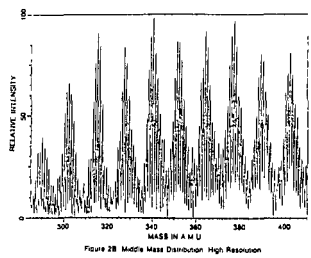

Figure 2B Middle Mass Distribution High Resolution

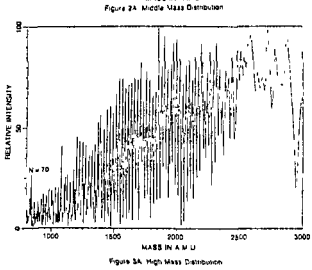

Figure 3A High Mass Distribution

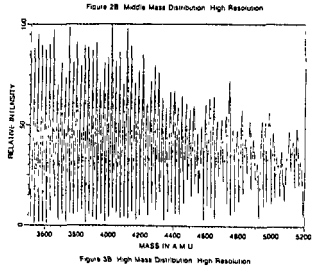

Figure 3B High Mass Distribution High Resolution

At the lowest fluence (approximately 200-500 mJ/cm^2, which is near threshold for positive ion formation), the distribution in Figure 3A has the largest relative intensity by at least a factor of 10. A higher resolution expansion of another spectrum is shown in Figure 3B. All of the ions which are observed correspond to even carbon cluster ions up to mass 5000. For calibration, the distribution was compared to a similar carbon cluster ion distribution formed from laser ablation of graphite with 532 nm radiation. Using the same FTMS conditions, the corresponding peaks of the graphite and polyimide spectra have the same masses, within the resolution of the spectrum.

The middle mass distribution is shown in Figure 2A, and an expanded section is in Figure 2B. This distribution has a peak at nearly every mass unit, and has a periodic oscillation over 12 amu. The maxima of the oscillations corresponds to carbon cluster ions with 6 to 8 H atoms. The low mass distribution in Figure 1 consists of carbon cluster ions with 0, 1, 2, and 3 H atoms. Both of these distributions are only formed with higher than threshold laser fluence on the sample. This observation suggests that photodissociation in the laser generated plasma may be responsible for the formation of the smaller ions.

In order to determine the mechanism of formation of the high mass carbon cluster ions, it is helpful to estimate of the gas phase particle density of the laser generated plasma which is formed during the laser pulse. This can be done[1] by measuring the depth of the crater which is ablated per laser pulse[2]. Previous work in the literature by Srinivasan, Dreyfus, and co-workers[3] provides estimates for the laser plasma temperature, compostion, and bulk expansion velocity. These results can be used to estimate the plasma density, which is about 10^{19} molecules/cm^3, giving a pressure on the order of 10 atm. This estimate is similar to the plasma density found by the same method for the laser ablation of graphite using 532 nm radiation. A density of this magnitude is consistent with the formation of large carbon cluster ions by gas phase condensation reactions. These ions are therefore probably not desorbed directly from the surface for these systems.

The negative ion mass spectrum of polyimide was also measured. Negative ions can be formed at lower laser fluence, and for lower values of etch depth/pulse, than positive ions. At the lowest fluence, the ions CN^-, OCN^-, and C_3N^- are observed. Increasing the fluence slightly produces other ions which can be assigned to structural fragments of polyimide.

Further study of the laser ablation of polymers is in progress. A study is being done to determine the fingerprint spectra of other high molecular weight polymers. It is also interesting to examine the feasibility of depth profiling and surface analysis of polymers by laser ablation, and to analyze the mechanisms of ion formation from laser ablation.

References

1. W. R. Creasy and J. T. Brenna, Chem. Phys., submitted for publication.
2. J. T. Brenna, W. R. Creasy, W. McBain, and C. Soria, Rev. Sci. Instrum., in press; and oral presentation ROD 500, this conference.
3. For example, see E. Sutcliffe and R. Srinivasan, J. Appl. Phys. 60 3315 (1986); R. Srinivasan, B. Braren, and R. W. Dreyfus, J. Appl. Phys. 61 372 (1987); R. W. Dreyfus, R. Kelly, R. E. Walkup, and R. Srinivasan, SPIE Vol. 710-Eximer Lasers and Optics, 46 (1986).

Presented at the 36th ASMS Conference on Mass Spectrometry and Allied Topics
June 5-10, 1988, San Francisco, CA

LITHIUM AND SODIUM CLUSTERS EMITTED FROM LIQUID METAL ION SOURCE

Yahachi Saito,* Kazuaki Minami, Toshiyuki Ishida, Masahiko Inoue, Satoshi Nishigaki and Tamotsu Noda

Department of Electrical and Electronic Engineering, Toyohashi University of Technology, Toyohashi 440, Japan
(*) Department of Applied Physics, Nagoya University, Nagoya 464-01, Japan

Studying metal clusters by mass spectrometric technique has been developing rapidly. For many metals, mass spectra often display ion abundance anomalies where the intensity of a cluster with specific size(magic number) is more abundant than its neighbors. The magic number is related with stability of the clusters. The relative stability of atomic clusters depends strongly on their size. For mass spectra obtained by ionization of neutral cluster beam, the interpretation of the relative ion intensities is followed by a severe problem where the size-dependent ionization cross section and fragmentation play a role. On the other hand, for mass spectra of ions produced by a secondary cluster ion source or liquid metal ion source, it is usually accepted that the ion abundance reflects the relative stability of the ionic clusters under an assumption that they have been born in the ion production process. Therefore, detailed investigations of the "born ionized" clusters are fundamentally important for understanding the electronic and geometric structures of neutral clusters. In the field of atomic cluster studies, alkali metals have attracted considerable attention because of their character as a typical metal. The purpose of the present study is to produce "born ionized" alkali metal clusters by a liquid metal ion source(LMIS), and to investigate the origin of the magic numbers.

The LMIS used in the present experiment is equipped with a closed-type reservoir of source material and with an emitter tip, which are heated by electron bombardment. The detailed structure of the LMIS has been described elsewhere.[1)] Pure metals(99.99 % for Li, 99.5% for Na) were used as the source material. The needle emitters were made of a piece of tungsten wire for Li, and iron for Na. The needle emitters were sharpened to a tip radius of several um by electrochemical etching. The mass distribution of cluster ions was measured with a single focusing magnetic analyzer.

Figures 1 and 2 show relative ion intensities of Li_n^+ and Na_n^+, respectively. For Li, singly charged clusters containing up to 19 atoms were distinctly detected, but multiply charged ones were not observed. Ion intensity as a function of cluster size showed peaks or steps at n = 3, 7, 9, 13 and 19. For Na, on the other hand, singly charged clusters up to 25 atoms were observed, and n = 3, 5, 11, 13, 19 and 21 were found as magic numbers. As for multiply charged clusters, only Na_7^{2+} was identified. In either metal, a sharp decline in the ion signal is observed after n = 19. The odd-

even alternation in the intensity variation is prominently found for Na in a region from n = 5 up to 19, where clusters with an odd number of atoms show higher intensity. This alternation shows a significant contribution of the spin-pairing energy to the total energy of these cluster cations.

The magic numbers observed for singly charged Li and Na clusters are summarized below, together with those predicted from the electronic shell model.[2)]

Li_n^+	3,	7, 9,		13,	19
Na_n^+	3, 5,		11, 13,		19, 21
Shell Model	3,	9,			19, 21, 35

For Li, n = 3, 9 and 19 coincide with the magic numbers predicted from the model, whereas the others(n = 7 and 13) can not be explained. It is interesting that the latter magic numbers(n = 7 and 13) coincide with those derived from sphere packing consideration: a pentagonal bipyramid for 7 atoms, and an icosahedron for 13 atoms. For Na, more serious discrepancy between the observation and the model is found: (1) a predicted magic number n = 9 does not show distinct feature in mass spectra, (2) the model can not explain the observed magic numbers n = 5, 11 and 13. This unsatisfactory agreement indicates the importance of considering geometric structure in predicting stability and other physical properties of metallic clusters.

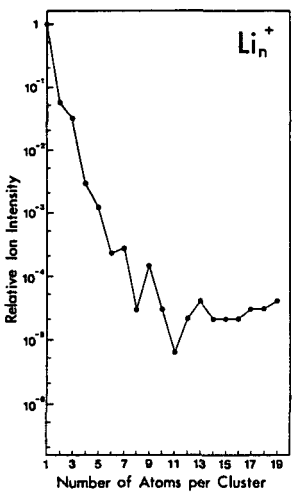

Fig. 1.

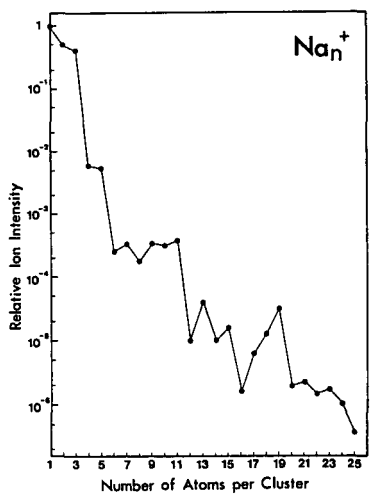

Fig. 2.

References

1) T. Noda et al.: Advances in Mass Spectrometry 1985 (John Wiley & Sons, New York, 1986) part B, p. 1531.

2) W. D. Knight et al.: Phys. Rev. Lett. 52(1984) 2141.

Presented at the 36th ASMS Conference on Mass Spectrometry and Allied Topics
June 5-10, 1988, San Francisco, CA

FORMATION, FRAGMENTATION, AND REACTIONS OF METAL/OXYGEN CLUSTER IONS

WEN YU AND ROYAL B. FREAS
DEPARTMENT OF CHEMISTRY, UNIVERSITY OF HOUSTON, HOUSTON, TX 77204-5641

INTRODUCTION: Transition-metals and their oxides are widely used as catalysts. Metal clusters serve as an useful model for studying catalysis. We have used mass spectrometry to study the structure and reactivity of first-row transition-metal/oxygen cluster ions. Titanium/oxygen and vanadium/oxygen cluster ions have been produced using high-pressure, fast-atom bombardment desorption ionization and collision-induced dissociation. We have used an elementary, pair-potential ionic model to calculate the geometrical structures of titanium/oxygen cluster ions based on observed stoichiometries and fragmentations.

EXPERIMENTAL: Metal/oxygen cluster ions were produced by sputtering metal foils or metal oxides (TiO_2 or V_2O_5) with an energetic (8 KeV) beam of fast Xenon atoms. In the high-pressure fast-atom bombardment (HPFAB) ionization technique[1], a reactant gas (O_2) is added to the ion source at a pressure ranging from 0.1 to 0.5 torr, as measured using a thermocouple gauge. Low kinetic energy (10 to 50 eV) collision-induced dissociation (CID) studies were performed using a VG 70-SEQ (EBQQ) instrument with argon as the collision gas. The pressure of the collision gas was adjusted to reduce the intensity of the main beam by 50-70%. The collision energy ranged from 10 to 50 eV, and was adjusted to optimize fragmentation.

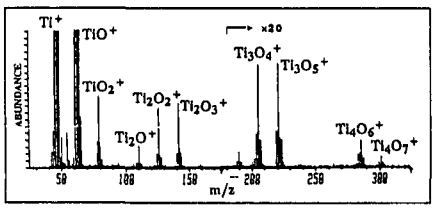

Figure 1. FAB Mass Spectrum of TiO_2

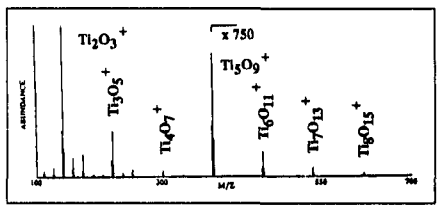

Figure 2. HPFAB Mass Spectrum of Ti Foil and O_2

RESULTS: Two major classes of $[Ti(TiO_2)_x]^+$ and $[TiO(TiO_2)_x]^+$ cluster ions were seen (Figure 1) when sputtering TiO_2 powder and Ti foil in the FAB source. Reactions between titanium/oxygen cluster ions and O_2 were observed in the HPFAB ion source . As the O_2 pressure increased, $[TiO(TiO_2)_x]^+$ (Figure 2) became the dominant type of clusters, while other types of cluster ions decreased in relative intensity.

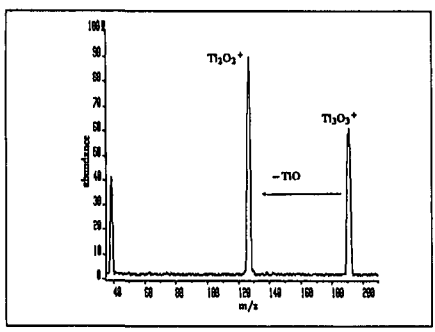

Figure 3. Collision-induced dissociation of $Ti_3O_3^+$

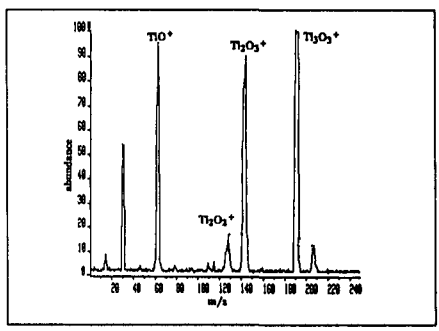

Figure 4. Hyperthermic Reaction of $Ti_3O_3^+$ and O_2

Hyperthermic reactions were studied in the collision cell (RF-only quadrupole) of the EBQQ instrument. Reactant gas (O_2) pressure ranged from $8x10^{-4}$ to $1x10^{-5}$ mbar in the cell housing. The exact pressure in the cell can not yet be determined. The collision energy ranged from 1 to 10 eV. Mass-selected titanium/oxygen cluster ions were injected into the collision cell where they react with O_2. Reactions

were examined as a function of reaction gas pressure and collision energy. Cluster ions with the formula $[TiO(TiO_2)_x]^+$ also were the major products (Figures 3 & 4).

VANADIUM/OXYGEN CLUSTER IONS: Vanadium/oxygen cluster ions have been formed by sputtering V_2O_5 powder. Figure 5 shows the FAB mass spectrum of V_2O_5. Three abundant classes of cluster ions were seen: $[V_2O(VO_2)_x]^+$, $[V(VO_2)_x]^+$, and $[VO(VO_2)_x]^+$.

The relative intensity of $V_nO_m^+$ clusters sputtered from foil were fitted (Figure 6) to the empirical formula of Kloppel and Jegers[2]:

$$I = I_o \cdot \exp[-(K - K_o)^2 / 2r^2]$$

$$K = (2m + 1) / n$$

where I = rel.abundance, K = modified fragment valence, and I_o, K_o, and r are constants.

n	I_o	K_o	r
2	5.900	0.585	0.972
3	0.386	1.576	0.682
4	0.109	1.491	0.589
5	2.00×10^{-2}	1.470	0.610
6	8.45×10^{-3}	1.516	0.470
7	1.21×10^{-3}	1.587	0.458

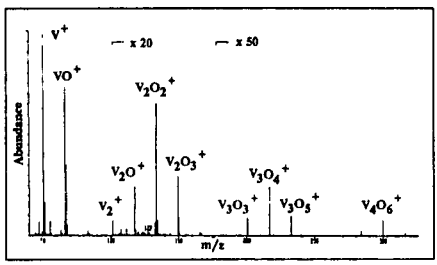

Figure 5. FAB Mass Spectrum of V_2O_5

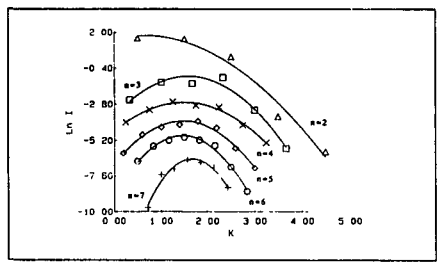

Figure 6. Distribution of vanadium/oxygen cluster ions

CLUSTER STRUCTURES: Titanium/oxygen and vanadium/oxygen cluster ions consisted of multiples of MO_2 units. This contrasts with iron/oxygen and cobalt/oxygen cluster ions, which consist of MO units[3]. The cluster ions were collisionally dissociated to produce fragments indicative of their structure. The observed fragmentations (loss of MO or MO_2) were used to confirm the stoichiometries of the cluster ions.

An elementary pair-potential ionic model[3] was used to calculate structures of metal/oxygen clusters. The observed stoichiometries of the clusters provided the basis for calculating the geometric structures. Calculated structures correlate with observed fragmentations of the metal/oxygen cluster ions. Several low-energy isomeric structures were found for each cluster suggesting that a single "magic" structure for each cluster is not likely.

$$V_T(r) = V_{MO}(r) + V_{MM}(r) + V_{OO}(r)$$

$$V(r) = Q_iQ_j/R_{ij} + A \cdot \exp(R_{ij}/P)$$

R_{ij} = the internuclear distance; Q_M,Q_O are the atomic charges ; A,P are adjustable parameters obtained by requiring them to give the nearest-neighbor distance for the monomer and for the bulk solid.

ACKNOWLEDGEMENTS: The Robert A. Welch Foundation is acknowledged for support of this work. The computer programs that were used to calculate the structures of the clusters were written by Dr. Brett I. Dunlap (Naval Research Laboratory).

Reference:

[1] Royal B. Freas, Mark M. Ross, Joseph E. Campana *J. Am. Chem. Soc.* **1985**, 107, 6195-6201.
[2] K.D. Kloppel, E. Jegers, G. Von Bunan *Int. J. Mass Spectrom. Ion Phys.* **1983**, 49, 11-24
[3] R.B. Freas, B.I. Dunlap, B.A. Waite, J.E. Campana *J. Chem. Phys.* **1987**, 86, 1276-1288.

Presented at the 36th ASMS Conference on Mass Spectrometry and Allied Topics
June 5-10, 1988, San Francisco, CA

HCN REACTIONS REVEAL NEW CARBON CLUSTER ION ISOMERS

Denise C. Parent and Stephen W. McElvany

Chemistry Division/Code 6110
Naval Research Laboratory, Washington, D.C. 20375-5000

In a previous study on the reactivity of positive carbon cluster ions with D_2 and O_2 [Ref. 1] an abrupt decrease in the reaction rate constant between n=9 and 10 was observed. This correlates with theoretical predictions of a change in structure from linear to monocyclic at n=10 [Ref. 2]. (A large decrease in photodissociation cross-section between n=9 and 10 has also been reported [Ref. 3].) The proposed structures for carbon clusters have reactive carbene sites (a pair of nonbonding electrons) at the end of the linear chains, which are missing in the cyclic structures. Thus the clusters with $n < 10$ are expected to be more reactive than the larger clusters. The reactivity studies also revealed that C_7^+ is present as two structural isomers when formed by direct laser vaporization. It was postulated that one isomer is linear (high reactivity) while the other isomer is cyclic (much lower reactivity) [Ref 1].

For the present work, we chose HCN as the neutral reactant so as to compare the reactivity of carbon cluster ions with polar HCN and the nonpolar molecules used previously [Ref. 1]. Also, HCN is an abundant species in the interstellar medium (ISM) and its reactions with other ISM species such as carbon chains are of interest for chemical modelling.

We studied the primary and secondary reactions of C_n^+ ($3 \leq n \leq 20$) with HCN and used collision-induced dissociation (CID) to investigate the structure (bonding) of the product ions. Experiments were performed in a Fourier-transform (ICR) mass spectrometer (FTMS) . The frequency-doubled output of a Nd:YAG laser was focused onto a graphite sample to produce cluster ions by direct laser vaporization. Reaction rate constants were determined by varying the reaction time at a constant HCN pressure.

In agreement with previous results, a large decrease in reactivity between n=9 (linear) and 10 (cyclic) was observed, as shown in Figure 1. A new result is that both the n=8 and 9 clusters, as well as n=7, have two components of differing reactivity with HCN. The parameters characterizing the two component decay are listed below.

n	fraction slow	K_{fast}/K_{slow}
7	0.7	35
8	0.3	300
9	0.2	43

The only products formed by the primary reactions are addition of H, CN or HCN to the cluster ion, as shown in Figure 2 for the linear isomers. (The cyclic isomers' only reaction pathway was radiative association.) No products involving breakup of the cluster are observed and a significant fraction of radiative association occurs. Both observations are in contrast to previous work [Ref. 1], indicating that the HCN reactions are lower energy processes. Most of the product ions formed from linear clusters subsequently react by adding HCN once. No further reactions were observed. This appears to agree with the proposed mechanism, whereby reactions occur at the two carbene sites of the linear cluster ions.

The CID results partially contradict this mechanism. The bonding of HCN to the cluster ions in the primary reaction is covalent (ie. at the carbene site), but the secondary product ions (C_nXHCN^+, X=H, CN or HCN) lose HCN at very low CID excitation energies. This suggests that the bonding does not occur at the second carbene site. Instead, H-bonding to the "X" end of the cluster ion is proposed to be the favored pathway. The cyclic cluster ions also bond only very weakly to HCN, with the exception of C_7^+, which forms a strong (covalent) bond with HCN.

The seven-carbon cluster ion exhibits anomalous behavior in other ways (ie. the decay curve is not a simple biexponential, the primary association product is reactive (for n <> 7 it is not reactive), and the fraction of the "cyclic" form is high). From these observations, we suggest that the cyclic C_7^+ isomerizes to the linear form during the reaction with HCN. Thus the seven-carbon ring appears to be less stable than the eight- or nine-carbon ring, yet it has a relatively high abundance, which we are unable to explain.

Presented at the 36th ASMS Conference on Mass Spectrometry and Allied Topics
June 5-10, 1988, San Francisco, CA

References

1. S.W. McElvany, B.I. Dunlap and A. O'Keefe, J. Chem. Phys. 86 (1987) 715.
2. J. Bernholc and J.C. Phillips, ibid. 85 (1986) 3258.
3. M.E. Geusic, T.J. McIlrath, M.F. Jarrold, L.A. Bloomfield, R.R. Freeman and W.L. Brown, ibid. 84 (1986) 2421.
4. V.G. Anicich, W.T. Huntress, Jr. and M.J. McEwan, J. Phys. Chem. 90 (1986) 2446.

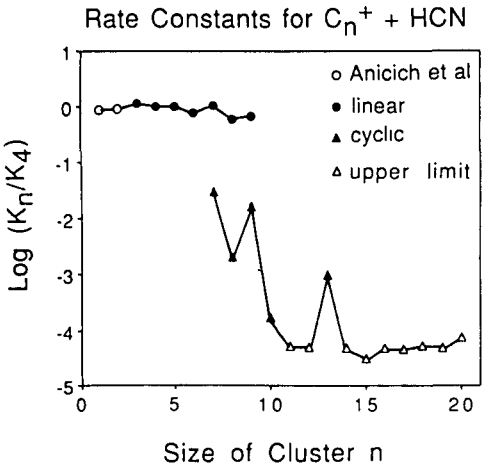

Figure 1. The rate constants for the primary reactions with HCN (normalized to one for n=4) are plotted for the "linear" and "cyclic" forms of the clusters. The values for n=1 and 2 [Ref. 4] are included for completeness, normalized by the n=4 rate constant measured in the same work.

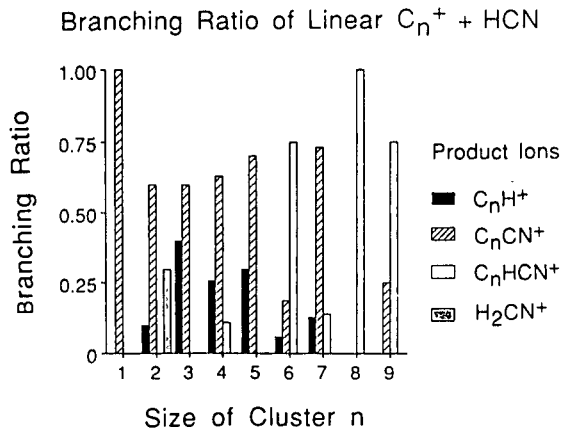

Figure 2. The branching ratios for the primary reactions of the linear carbon cluster ions with HCN are shown. Values for n=1 and 2 were taken from Ref. 4. Note the trend towards association as n increases, and that even n clusters form more association product than the odd n clusters.

Presented at the 36th ASMS Conference on Mass Spectrometry and Allied Topics
June 5-10, 1988, San Francisco, CA

A STUDY OF THE MASS SPECTRA OF COBALT(II) SALTS OF ORGANIC ACIDS

Z. L. Sun, Z. W. Dong, C. H. Lin and Z. M. Cao

Dalian Institute of Technology, Dalian, CHINA

INTRODUCTION

Metal carboxylates have long been known, but their mass spectrometry has not been much investigated until recent fifteen years. Cobalt carboxylates are now widely used in different fields of industries. While the mass spectrometry of only those of lower fatty acids was studied (1-3). In this work the following cobalt salts: acetate, propionate, n-butyrate, isovalerate, n-hexanoate, 2-ethylbutyrate, n-heptanoate, n-octanoate, 2-ethylhexanoate, n-decanoate, n-dodecanoate and n-tetradecanoate are studied. Due to the limitation of our machine, high mass cluster ions in the spectra are neglected.

EXPERIMENTAL

Cobalt acetate was GR chemical purchased from Beijing Chemicals Co., and was used without further purification. The other 11 kinds of carboxylates were synthesized in our laboratory by either fusion or precipitation method (4). The former method was used in preparing salts of C_3-C_8 acids while those of C_9-C_{14} acids were prepared by the latter method. The purity of the prepared salts was checked by elemental analysis, and IR and UV spectra.

All spectra were recorded on a Finnigan MAT 312 mass spectrometer. Isobutane was used as the reacting gas in the CI mode.

RESULTS AND DISCUSSION

EI spectra

It has been shown that EI spectra of neutral cobalt carboxylates do not show molecular ion peak, $[Co(OCOR)_2]^{+\cdot}$, but that of basic salt, $[Co_4O(OCOR)_6]^{+\cdot}$ instead (2). It is supposed that neutral cobalt carboxylate converts, during vaporizing, into its basic form which is more stable in the vapor phase. Just as mentioned in the literature (2), the initial fragmentation involves in the loss of a ligand radical to give $[Co_4O(OCOR)_5]^+$ which further loses a neutral salt molecule forming $[Co_3O(OCOR)_3]^+$. The molecular ion and the above-mentioned two fragment ions form the three most intense peaks in all the spectra of cobalt carboxylates (Table). Due to the ability of Co atom to change oxidation state, the molecular ion can act as an even electron ion. So do the two even electron fragment ions can behave as odd electron ions. Thus two modes of fragmentation of losing radicals and neutral molecules can take place at the same time with the same parent ion. The molecular ion and the two abundant fragment ions all lose anhydride molecule giving fragment ions whose abundance changes with the length of the acid chain (Table). The longer the acid chain of the carboxylate, the less intense the anhydride abstracted ion peak. Three doubly charged ions $[Co_4O(OCOR)_5]^{+2}$, $[Co_4O(OCOR)_4]^{+2}$ and $[Co_4O_2(OCOR)_3]^{+2}$ are observed.

CI (isobutane) spectra

There is only one report in the literature (3) on the CIMS (methane) of cobalt carboxylates. The CI spectrum of cobalt acetate (i-C_4H_{10}) in this paper differs from that reported in the literature in the intensity of the protonated molecular ion. In their work the protonated molecular ion was observed only with 14% relative abundance of the base peak, while in our work the protonated molecular ion is the base peak. This might be due to the fact that in our work isobutane is used as the reacting gas instead of methane which forms a stronger Bronsted acid and leads to more fragmentation of the protonated molecular ions. The three most abundant ions in EI spectra also appear in CI spectra, but with less intensity.

Presented at the 36th ASMS Conference on Mass Spectrometry and Allied Topics
June 5-10, 1988, San Francisco, CA

Negative ion (electron capture) spectra

The negative ion mass spectra of cobalt carboxylates have not been reported previously. Due to the 3d electron configuration of $3d^7$, the neutral molecule, $Co_4O(OCOR)_6$, readily captures a thermal electron to form a stable anion. The negative ion spectra of cobalt carboxylates are unique in that they consist of nearly the molecular ion $[Co_4O(OCOR)_6]^-$, which forms the base peak, and $[Co_4O(OCOR)_6 \pm n14]^-$ peaks on both sides of it, where n is a small whole number.

CONCLUSION

1. Negative ion spectra (electron capture) of cobalt carboxylates have been recorded for the first time. These spectra are unique in that they are dominated by the molecular ion peak, which is the base peak, and peaks of ± n14 amu on either side of the base peak.
2. The phenomenon of ± n14 amu on either side of a peak of high intensity can also be observed in both EI and CI spectra, but not so typical as in negative ion spectra.
3. $[Co_4O(OCOR)_6]^{+\cdot}$, $[Co_4O(OCOR)_5]^+$ and $[Co_3O(OCOR)_3]^+$ form the three most abundant peaks in all EI spectra of the carboxylates. They lose acid anhydride molecule forming fragment ions whose intensities depend on the length of the chain of the acid redical in the salt. The longer the chain of the acid radical, the less abundant the anhydride abstracted fragment peak.
4. The change of valence in Co atom makes it possible to convert an odd electron ion to an even one and vice versa. Thus two sets of fragmentation of losing both radical and neutral molecule from the same parent ion occur.
5. Doubly charged ions are observed.

REFERENCES

1. Marshall, G.L., Org. Mass Spectrom. 18, 168 (1983)
2. Charalambous, U., Inorg. Chem. Acta 14, 53 (1975)
3. DiDonato, G.C. and Bush, K.L., Inorg. Chem. 25, 1551 (1986)
4. Kambe, H., Bull, Chem. Soc. Japan, 34, 1786 (1961)

TABLE. Relative intensities of molecular ion and some fragment ions in EI and CI spectra

Ion		Acid radicals in the carboxylates											
		C2	C3	C4	iC5	C6	iC6*	C7	C8	iC8#	C10	C12	C14
(A)	EI	63.0	61.8	48.8	100	100	100	100	100	92.0	74.6	100	41.7
	CI	30.8	26.2	36.6	40.6	-	-	-	-	-	-	-	-
(B)	EI	97.0	100	97.1	85.3	89.7	91.3	42.7	48.5	100	100	50.1	100
	CI	70.0	32.7	49.3	27.1	-	-	-	-	-	-	-	-
(C)	EI	100	35.9	100	41.3	57.7	22.2	20.0	33.3	58.0	43.1	18.2	56.0
	CI	10.8	4.1	18.3	11.2	-	-	-	-	-	-	-	-
(D)	EI	3.7	1.2	0.9	0.8	w	w	w	w	w	w	w	w
(E)	EI	7.0	4.6	7.1	3.3	2.5	1.4	0.9	w	w	w	w	w
(F)	EI	9.9	4.1	2.7	w	w	w	w	w	w	w	w	w

* 2-ethylbutyrate; # 2-ethylhexanoate; "w" too weak to be observed
(A) $[Co_4O(OCOR)_6]^{+\cdot}$; (B) $[Co_4O(OCOR)_5]^+$; (C) $[Co_3O(OCOR)_3]^+$
(D) $[A-(RCO)_2O]^+$; (E) $[B-(RCO)_2O]^+$; (F) $[C-(RCO)_2O]^+$

Presented at the 36th ASMS Conference on Mass Spectrometry and Allied Topics
June 5-10, 1988, San Francisco, CA

SIGNIFICANCE OF CLUSTER IONS IN THE GENERATION OF FAST ATOM BOMBARDMENT MASS SPECTRA

H. Perreault and M.J. Bertrand
Regional Center for Mass Spectrometry, Department of Chemistry
University of Montreal, P.O. Box 6128, Station A,
Montreal, Quebec, Canada H3C 3J7

In recent years, fast atom bombardment has been widely used as a desorption-ionization technique for the mass spectral analysis of polar and high molecular weight compounds. However, the processes responsible for ionization and generation of the mass spectrum are still not fully understood and several models have been proposed in the literature. Three of the models that have received special attention are:

i) The precursor model: Molecular ions are preformed in solution and directly ejected upon impact of the atom beam.

ii) The gas phase model: Ions are mostly formed by gas phase collisons in a microplasma generated by the atom beam in the selvedge region of the impact.

iii) Charged aerosol droplets: Ions solvated by matrix molecules are desorbed from the solution and these charged droplets further dissociate to yield ions observed in the resulting spectrum.

An important feature of the FAB spectra of polar analytes dissolved in glycerol is the presence of cluster ions composed of molecules of the matrix G_nH^+, of the analyte M_mH^+ or both $G_nM_mH^+$. These clusters can be observed in figure 1a that shows the FAB spectrum of the dipeptide glycylphenylalanine obtained in glycerol. In order to investigate the origin of these clusters, experiments in the present work were conducted in the gas phase using CI and in solution using FAB. In the gas phase experiments, the dipeptide was vaporized in a chemical ionization source using a direct insertion probe and glycerol was used as a reagent gas in order to simulate the gas phase reactions that may occur in FAB. In the solution experiments using FAB, the concentration of the dipeptide glycylglycine was varied in glycerol and the internal energy of the mixted clusters $(MG\pm H)^{\pm}$ and $(MG_2\pm H)^{\pm}$ was monitored by measuring the ratios of ion intensities $(M\pm H)/(MG\pm H)$ and $(MG\pm H)/(MG_2\pm H)$ in the unimolecular MIKE spectrum of the corresponding species.

The spectrum of the dipeptide obtained under conditions of chemical ionization is shown in figure 1b and even though dimers are observed at m/z 185 (G_2H^+), 315 (MGH^+) and 445 (M_2H^+), polymolecular clusters of higher masses are absent and could not be observed under the range of temperatures and pressures used in these experiments. Another difference that is observed when comparing the CI and FAB spectra resides in the loss from the MH^+ of water (m/z 205) which is present in CI and absent in FAB, indicating that the two processes may be different. Other results obtained in the solution experiment show a clear dependance of the internal energies of the $(MG_2\pm H)$ and $(MG\pm H)$ ions on concentration. As the concentration is increased the $MG\pm H/MG_2\pm H$ and $M\pm H/MG\pm H$ ratios measured in the unimolecular MIKE spectrum of the corresponding ions increase accordingly, indicating a dependance of the internal energy of the clusters with concentration. This phenomena which is hard to explain by the gas phase model, but in agreement with the desorption of charged aerosol droplets, seems to indicate that the latter would be responsible for the generation of the cluster ions observed in FAB.

Since the results obtained indicate that the ejection of charged droplets might play an important role in the generation of a FAB spectrum, the unimolecular and collison activated spectra of G_nH^+, M_mH^+ and $G_nM_mH^+$ clusters were recorded to verify that ions observed in

the FAB spectrum could be rationalized by the decomposition of clusters of different sizes and different internal energies. Figures 2a and 2b show the unimolecular and CA spectra of the MG_3H^+ cluster of glycyl-phenylalanine at m/z 499. It can be observed that relatively low energy clusters decompose mainly by loss of glycerol and water and that hot clusters decompose by loosing one, two or several molecules of glycerol and can also generate fragments of the peptide.

The results presented can be used to rationalize the ions observed in a FAB spectrum of a polar analyte in glycerol in terms of fragmentation of analyte and matrix molecules around the point of impact, with the desorption of clusters of different sizes and internal energies as the distance from impact increases. The fragments produced on impact and the decomposition products of the clusters are in agreement with the ions observed in the spectrum. This rationalization is also consistent with the intensities of parent-molecular ions of labile compounds that are observed in FAB since the MH^+ ions are stabilized by the evaporating of matrix molecules from the clusters.

FIGURE 1

A) FAB SPECTRUM OF GLYCYL-PHENYLALANINE /GLYCEROL 0.5 M, XENON 7 kV

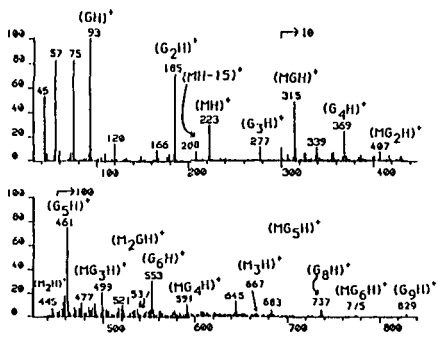

B) CI SPECTRUM OF GLYCYL-PHENYLALANINE REAGENT GAS: GLYCEROL

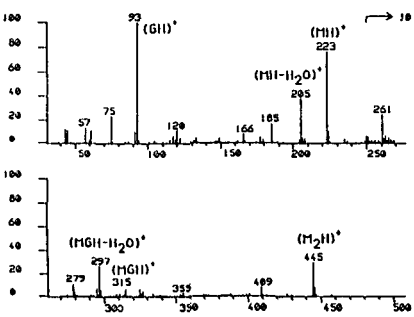

FIGURE 2

A) UNIMOLECULAR DISSOCIATION M.I.K.E. SPECTRUM OF GLY-PHE $(MG_3H)^+$ CLUSTER ION

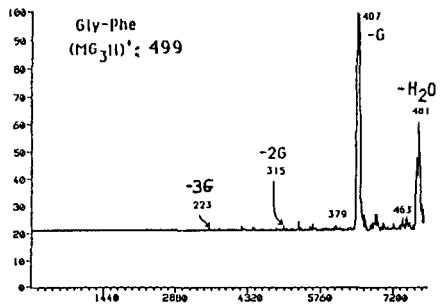

B) C.A.D. M.I.K.E. SPECTRUM OF GLY-PHE $(MG_3H)^+$ CLUSTER ION

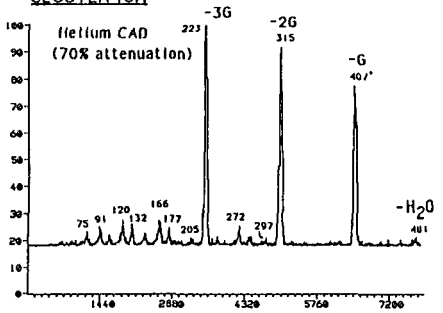

Presented at the 36th ASMS Conference on Mass Spectrometry and Allied Topics
June 5-10, 1988, San Francisco, CA

Measurement of the Ion Dissociation in a Reflecting Time-of-Flight Mass Spectrometer

Franz J. Mayer, W, Ens, B. Schueler, K. G. Standing, X. Tang and J.B. Westmore,
Physics and Chemistry Departments, University of Manitoba, Winnipeg, Canada R3T 2N2

Installation of a single-stage ion mirror in a time-of flight mass spectrometer enables measurements of daughter ion masses from parents that decay in the first leg of the flight path. Measurements of the unimolecular decay of several small peptides with a reflecting TOF spectrometer (Manitoba TOF II) have been reported [1]. Some further progress is described below.

^{18}O-Labelling Studies: The C-terminal of gly-gly-phe was labelled with ~50% incorporation of ^{18}O into the carbonyl group. The resulting $(M+Na)^+$ doublet was partially resolved in the neutral spectrum, so time windows could be chosen to select parent ions with and without ^{18}O. The resulting daughter ion spectra confirmed that $(M+Na)^+$ parent ion decomposed into a B_2+OH+Na daughter, with the addition of OH from the C-terminal group. [1].

Analysis of Metastable Ions from a Mixture of Three Peptides: An equimolar mixture of the peptides gly-gly-phe, leu-enkephalin and met-enkephalin, has been examined. Fig.1 shows the "direct" spectrum, i.e. the normal TOF spectrum observed in detector #1 behind the mirror with the mirror voltage off. Parent and daughter ions as well as neutral fragments are recorded.

With the mirror voltage on, the parent and daughter ions are measured in a second detector #2 at ~177 degrees (fig.2), while the neutral fragments appear in detector #1(fig.3) as before. The TOF of the neutral fragment identifies its parent ion.

Decay of a given parent ion may be examined by selecting the daughter ions correlated with neutral fragments having the correct flight time. The daughter ion spectra of some of the parent ions in the peptide mixture are shown in fig. 4. These spectra are much simpler than the overall reflected spectra, so unambiguous assignments of decay pathways can be made. Thus the technique has advantages similar to those of conventional tandem mass spectrometry.

(1) X. Tang et al, Int. J. Mass Spectrom. Ion Processes, in press; Anal. Chem. , in press; ASMS 1987, p.195.

Fig.1:
Direct Spectrum

Fig.2:
Neutral Spectrum

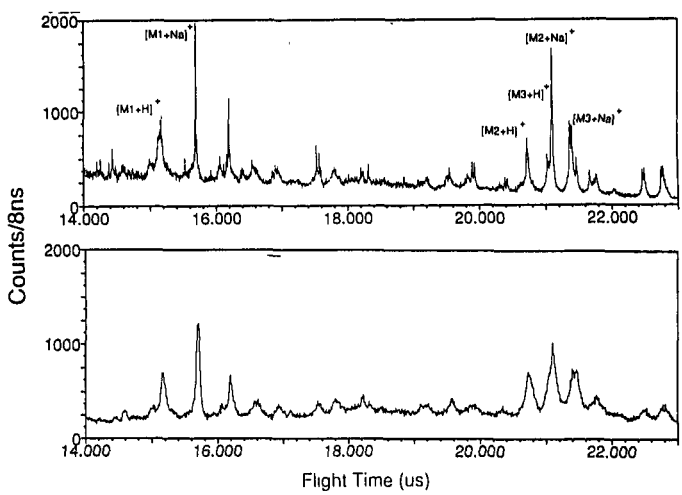

Fig.3

Reflected Spectrum

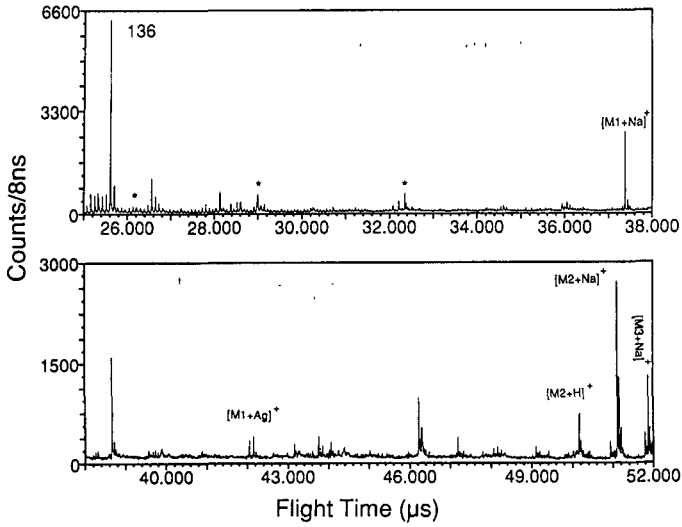

Fig.4 :

DAUGHTER ION SPECTRA

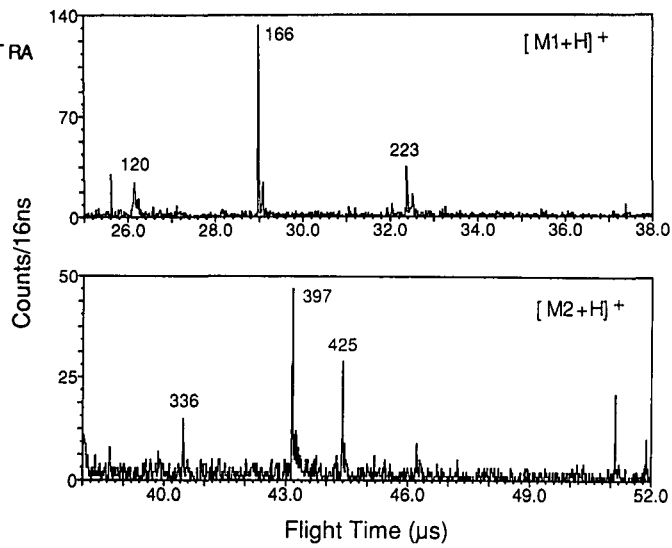

Presented at the 36th ASMS Conference on Mass Spectrometry and Allied Topics
June 5-10, 1988, San Francisco, CA

Tandem Mass Spectrometric Analysis of The First Perfluorinated cryptand: 4,7,13,16,21,24-hexaoxa-1,10-diazabicyclo[8.8.8]hexacosane

S. D. Maleknia, W. D. Clark, and R. J. Lagow, UT of Austin, Austin, TX 78712.

INTRODUCTION: The most important unique properties of perfluorinated compounds are their biological compatibility and high oxgygen carrying capacity. Recently, human clinical trials on Fluosol-DA, a patented emulsion of perfluorodecalin and perfluorotripropylamine, a major component of "artificial blood" have been started (1), and the rapid developement of this technology perpetuates the need for analytical techniques, especially MS, developed specifically to provide identification and limited structural characterization of perfluorinated compounds (2). The chemistry of perfluorinated compounds is as diverse as it is interesting. Presently the only facile route to syntheses of sterically hindered macrocyles is by the LaMar direct fluorination process of hydrocarbon analogues, which has in the past decade successfully introduced new perfluorocyclic and branched molecules (3), and was recently applied to the synthesis of the first perfluorinated cryptand, 1. Perfluorinated compounds differ from their hydrocarbon analogues by the special properties that fluorines confer upon the molecule. Properties which favor MS analysis are high volatility and thermal stability. The high electronegativity of fluorine causes strong inductive effects which significantly alter the stability and lability of chemical bonds, and such perturbations are expected to influence the mass spectral fragmentation pathway. Electron capture negative ion (ECNI) mass spectrometry combined with collision induced dissociation were used to determine the fragmentation characteristics of the title compound.

EXPERIMENTAL: A Finnigan MAT(TSQ-70) triple stage quadrupole was operated in negative chemical ionization mode at source pressure of 1.2 T of methane, and temperature of 80°C. A Varian GC model 3400 equipped with a 15m, BP5 capillary column with 5% methyl phenyl silicone coating was temperature programmed to 220°C at 25°C/min. A solution of 1 in Freon was injected into the column, and the perfluorinated cryptand eluted at 100°C. For CID analyses the sample was coated on a rhenium filament of the direct exposure probe, and further heating was not required. Argon was used as the collision gas at 1.2 mT. All MS/MS tuning parameters were software controlled.

RESULTS & CONCLUSION: A GC/ECNI spectrum of 1, is shown in Figure 1. The base peak is attributed to the molecular ion at M/Z 1024, and reagent gas adduct ions were not observed under any of the investigated CI conditions; this points to the high electron affinity of the title compound. Ions observed at M/Z 986, 908, 792 are attributed to losses of F_2, C_2F_4O, and $C_4F_8O_2$, respectively. Other ions in the spectrum at M/Z 496, 346, and 296 are the result of further ionization in the CI source and are not major features in the CID spectra . The stepwise or concerted multiple extrusion of neutral perfluoro ethylene oxide is observed by the ions at M/Z 908, 792, and 560 in Figures 2 and 3. Further loss of C_2F_4O or C_3F_6N fragments results production of ions at M/Z 428, 444, and 676. CID studies suggest that the cyclic structure of the perfluorinated cryptand is preserved as the fragmentation proceeds. The structural validity of these ring contracted homologs may be tested in future studies by the synthesis of molecules similar to the M/Z 792 ion.

Presented at the 36th ASMS Conference on Mass Spectrometry and Allied Topics
June 5-10, 1988, San Francisco, CA

REFERENCES:

1. R. Weiss, Science News, 1987, 132, 200-202.
2. P. A. Lyon, S. L. Hunt, F. E. Behr, L. D. Winter, R. L Cerny, K. B. Tomer, and M. J. Gross, Anal. Chem., 1987, 59, 2658-2662.
3. H. Huang, and R. J. Lagow, Bull. de la Soc. Ch. de France, 1986, 6, 993-1000.

ACKNOWLEDGEMENTS

We gratefully acknowledge the support of NIH (RR-02520-01), the Air Force Office of Scientific Research (AFOSR-88-0197-0084), the Department of Chemistry of the University of Texas at Austin and Dr. K. R. Pope for helpful discussions..

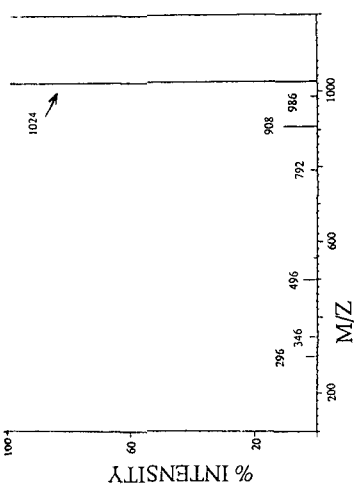

Figure 1: GC/ECNI spectrum of 1

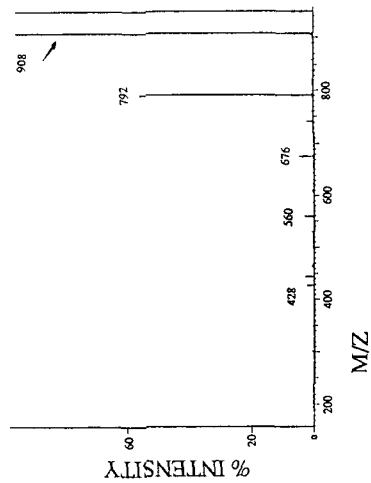

Figure 3: CID spectrum of M/Z 908, at 80 eV collision energy.

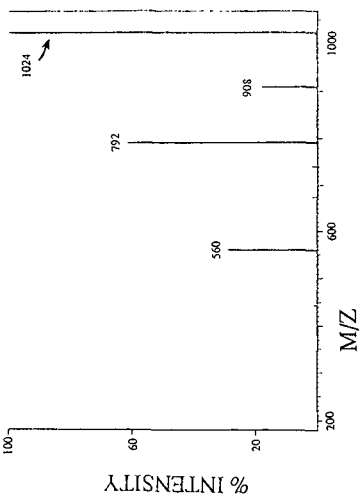

Figure 2: CID spectrum of 1, at 100 eV collision energy.

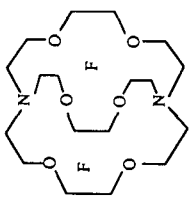

1

Presented at the 36th ASMS Conference on Mass Spectrometry and Allied Topics
June 5-10, 1988, San Francisco, CA

REACTIVE AND DISSOCIATIVE COLLISIONS AT A METAL SURFACE IN A TANDEM TIME-OF-FLIGHT INSTRUMENT

K.L. Schey and R.G. Cooks
Department of Chemistry, Purdue University
West Lafayette, IN 47907

A. Kraft, R. Grix and H. Wollnik
II. Physikalisches Institut, Justus Liebig Universitat
6300 Giessen, FRG

Ion/surface collisions are examined in a tandem time-of-flight (TOF/TOF) mass spectrometer. An earlier TOF/TOF instrument[1] has been modified to improve mass resolution by adding an electrostatic mirror to the second time-of-flight analysis stage (Fig. 1). In addition, improvements in source electronics allow collision energies of up to 750 eV to be achieved, over seven times the capabilities of existing instruments which examine inelastic ion/surface collisions.

The addition of the electrostatic mirror improved the mass resolution by one order of magnitude as seen in the surface induced dissociation (SID) daughter spectra of the phenetole molecular ion at 40 ev collisions (Fig. 2).

Surface induced dissociation of relatively stable molecular ions of polynuclear aromatic hydrocarbons (PAH) show increased fragmentation as the collision energy is increased providing mainly two and three carbon containing fragments at high collision energies. The SID daughter spectra of the anthracene molecular ion at 100 eV and 150 eV (Fig. 3) are indicative of the large amount of internal energy being deposited in inelastic ion/surface collisions. The internal energy deposition characteristics of the surface induced dissociation method are valuable in ion structural analysis of stable ions.

The improved mass resolution reveals the occurence ion/surface reactive collisions whereby one, two, and three carbon groups are abstracted from the surface by incident PAH ions. As seen in Fig. 4, the pyrene molecular ion abstracts one, two, and three carboon groups from the surface. Ion/surface reactions are competitive with SID at collision energies between 50 and 150 eV. and these processes provide information on ion reactivity and on the nature of surface adsorbates.

As the collision energy is raised above 100 eV, efficient sputtering of surface adsorbates is observed to compete with SID. The sputtering spectra (Fig. 5) are similar to the spectra of hydrocarbon background observed in high energy secondary ion mass spectrometry (SIMS), but here occur at relatively low kinetic energies. This low energy sputtering has been observed previously at very low kinetic energy for fluorocarbon ions[2] and is indicative of a different mechanism than momentum transfer operative in SIMS. The sputtering spectra provide information on the nature of surface adsorbates.

In summary. a simple tandem time-of-flight mass spectrometer is capable of examining a variety of ion/surface collision phenomena at larger collision energies and with comparable resolution to existing, more complex, instruments. The ion/surface collision phenomena observed in the TOF/TOF instrument provide valuable information on the nature and reactivity of the parent ions, on the nature of the surface, as well as fundamental information on inelastic ion/surface collisions.

[1] K. Schey, R.G. Cooks, R. Grix and H. Wollnik, Int. J. Mass Spectrom. Ion Processes, 77 (1987) 49.

[2] M. Vincenti and R.G. Cooks, Org. Mass Spectrom., in press.

Presented at the 36th ASMS Conference on Mass Spectrometry and Allied Topics
June 5-10, 1988, San Francisco, CA

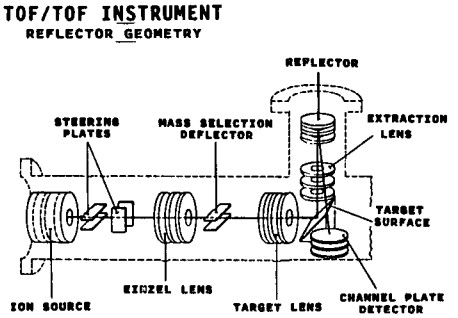

Fig. 1 Schematic of TOF/TOF instrument in reflector geometry.

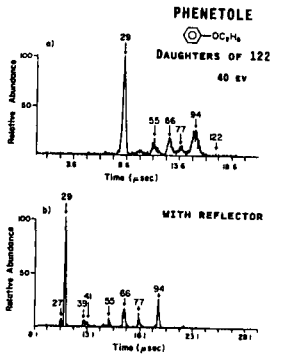

Fig. 2 Improved resolution in SID daughter spectra of Phenetole (m/z 122).

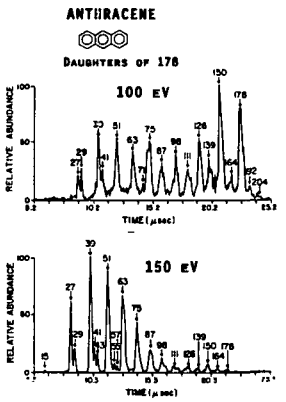

Fig. 3 SID daughter spectra of Anthracene (m/z 178).

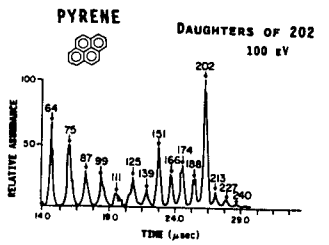

Fig. 4 Ion/surface reactions and SID of Pyrene (m/z 202).

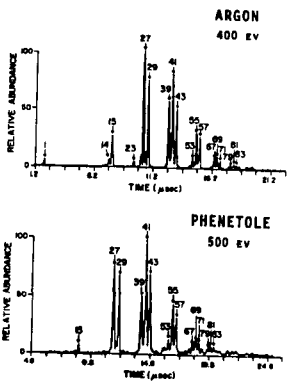

Fig. 5 Low energy sputtering spectra.

Presented at the 36th ASMS Conference on Mass Spectrometry and Allied Topics
June 5-10, 1988, San Francisco, CA

FRAGMENTATION OF SOME DEPROTONATED SULFOXIDES AND SULFONES

S. Chowdhury and A. G. Harrison
Department of Chemistry
University of Toronto
Toronto, Canada M5S 1A1

Fragmentation of enolate ions of the formula $RCOCH_2^-$ is known(1) to proceed through formation of an intermediate ion/dipole complex as shown by Scheme 1.

$$RCOCH_2^- \longrightarrow [R\text{—}CH_2CO]^- \begin{cases} \nearrow R^- + CH_2CO \\ \searrow RH + HCCO^- \end{cases}$$

SCHEME 1

The present work was undertaken, in part, to explore the effect of replacing the carbonyl group by the sulfoxyl (SO) or sulfonyl (SO_2) group on the fragmentation of the ions $RSOCH_2$ and $RSO_2CH_2^-$, analagous to the enolate ions. The $(M - H)^-$ ions were prepared by reaction of $RSOCH_3$ or RSO_2CH_3 with OH^- in a chemical ionization source. High energy (8 keV) and low energy (5—100 eV) collision–induced dissociation mass spectra, as well as unimolecular metastable ion mass spectra, were studied using a hybrid BEQQ mass spectrometer(2).

Although the major metastable ion fragmentation reaction of the $(M - H)^-$ ion of methyl phenyl sulfoxide involves elimination of H_2O, over much of the breakdown graph (Fig. 1) the $C_6H_5^-$ and $HCSO^-$ ions dominate, indicating a fragmentation sequence analagous to enolate ions

$$C_6H_5SOCH_2^- \rightarrow [C_6H_5\text{—}CH_2SO]^- \begin{cases} \nearrow C_6H_5^- + CH_2SO \\ \searrow C_6H_6 + HCSO^- \end{cases}$$

The metastable ion mass spectrum of $CH_3SOCH_2^-$ shows predominate formation of SO^-, obviously requiring rearrangement of the molecular framework. In the breakdown graph (Fig. 2) $HCSO^-$ and H_2CSO^- are the two most important products indicating the reaction channels.

$$CH_3SOCH_2^- \rightarrow [CH_3\text{—}CH_2SO]^- \begin{cases} \nearrow CH_4 + HCSO^- \\ \searrow CH_3 + H_2CSO^- \end{cases}$$

The latter reaction channel is not observed for enolate ions, but the analagous reaction becomes even more important (Fig. 3) for $CH_3SO_2CH_2^-$ where no $HCSO_2^-$ formation is observed

$$CH_3SO_2CH_2^- \rightarrow [CH_3\text{—}CH_2SO_2]^- \begin{cases} \nearrow\!\!\!\times\ CH_4 + HCSO_2^- \\ \searrow CH_3 + H_2C\text{–}SO_2^- \end{cases}$$

The opening of this new reaction channel for deprotonated sulfoxides and sulfones presumably is related to the stability of the radical anions CH_2SO^- and $CH_2SO_2^-$ compared to CH_2CO^-. The electron affinity of CH_2S is 10.7 kcal mol^{-1}(3) and the oxygens bonded to sulphur should increase this electron affinity. The electron affinity of CH_2CO does not appear to have been measured but would be expected to be quite low.

The full paper, to be submitted, will extend the work to a greater variety of compounds, including cyclic sulfones, and will include a comparison of high energy and low energy collisional activation.

Presented at the 36th ASMS Conference on Mass Spectrometry and Allied Topics
June 5-10, 1988, San Francisco, CA

1. C.R. Moylan, J.M. Jasinski and J.I. Brauman, J. Am. Chem. Soc. 107, 934(1985).
2. A.G. Harrison et al. Int. J. Mass Spectrom. Ion Processes, 74, 13 (1986).
3. S. Moran and G.B. Ellison, Int. J. Mass Spectrom. Ion Processes, 80, 83 (1987).

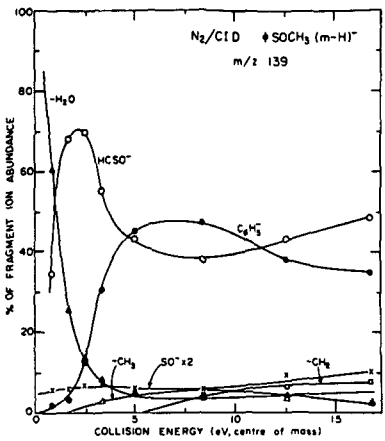

FIGURE 1

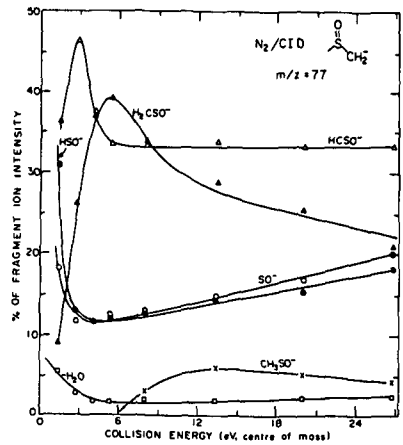

FIGURE 2

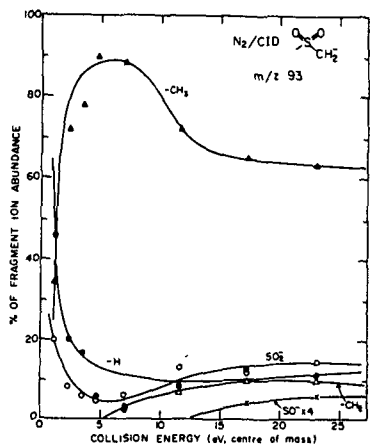

FIGURE 3

Presented at the 36th ASMS Conference on Mass Spectrometry and Allied Topics
June 5-10, 1988, San Francisco, CA

ISOMER IDENTIFICATION BY METASTABLE DECAY RATES OF LASER PRODUCED IONS: G.R. Kinsel and M.V. Johnston; Dept. of Chemistry and Biochemistry, CIRES, University of Colorado, Boulder, CO 80309-0215.

The narrow internal energy (E_{INT}) distributions created during Resonance Enhanced Multiphoton Ionization / Dissociation (REMPI/D) mass spectrometry make this technique uniquely sensitive to small changes in molecular energetics. This unique sensitivity can be exploited to identify isomer configuration from metastable tailing of daughter ion signals. Calculated rates for metastable decompositions also yield information about the fragmentation mechanism for the molecule.

A program has been developed which emulates a mass spectrometer and produces a theoretical mass spectrum across the m/z region of metastable ion production for a given set of rate constants. A simplex routine varies the set of rate constants until a best fit with the experimental mass spectrum is obtained. The program offers several advantages in that it can be applied to spectra with overlapping metastable ion signals, can account for isotopic contributions to metastable ion production, and yields a high level of precision as a result of requiring a fit to both the individual and total decay rates simultaneously. The program was tested by calculating a decay rate for the production of M^+-Cl (m/z 77) in the 271.5 nm REMPI/D mass spectrum of chlorobenzene. An example of the experimental and calculated data is shown in Fig. 1. When the proper set of fitting parameters is chosen the program correctly discriminates against the non-metastable contribution at the daughter ion peak position which arises from a two-photon dissociation of the parent ion. The calculated rate is in good agreement with previously reported values for this process.

The program was used to calculate decay rates for the metastable production of M^+-HCl (m/z 91), M^+-Cl (m/z 90), and M^+-HNC (m/z 100,102) from the three isomers of the chloroanilines at 266 nm. Examples of experimental and calculated spectra are shown in Figs. 2, 3, and 4. Note that regions of the experimental spectra containing non-metastable ion signals have been omitted for clarity. The tabulated results for the calculated rates are shown in Fig. 5. The uncertainties reflect the precision of fits of 5 separate spectra.

The calculated rates show that the o-, m-, and p- isomers can easily be distinguished on the basis of their individual or total decay rates. Evidence of the "ortho" affect resulting in an increase in rate for loss of HCl and a decrease in rate for loss of HNC as substituent positions move together is also observed. An intriguing isomer dependent isotope affect also seems to exist, although this may be an artifact of the assumptions made in applying the calculational program. Interpretation of the rates also supports minimal isomerization of the parent ions prior to dissociation as evidenced by the fact that individual and total rates will never converge simultaneously.

Presented at the 36th ASMS Conference on Mass Spectrometry and Allied Topics
June 5-10, 1988, San Francisco, CA

The narrow E_{INT} created during REMPI/D can be exploited as a tool for isomer identification. Improvements to the experimental setup used here to further refine the E_{INT} (PES, Jet Spectroscopy) and addition of second laser to extend the applicability of the technique to molecules having higher and lower A.E.'s would enhance this method dramatically. Nevertheless, successful isomer distinction with this simple one-color experiment has been demonstrated. REMPI/D with calculation of decay rates from metastable decompositions shows promise as a useful method for isomer identification.

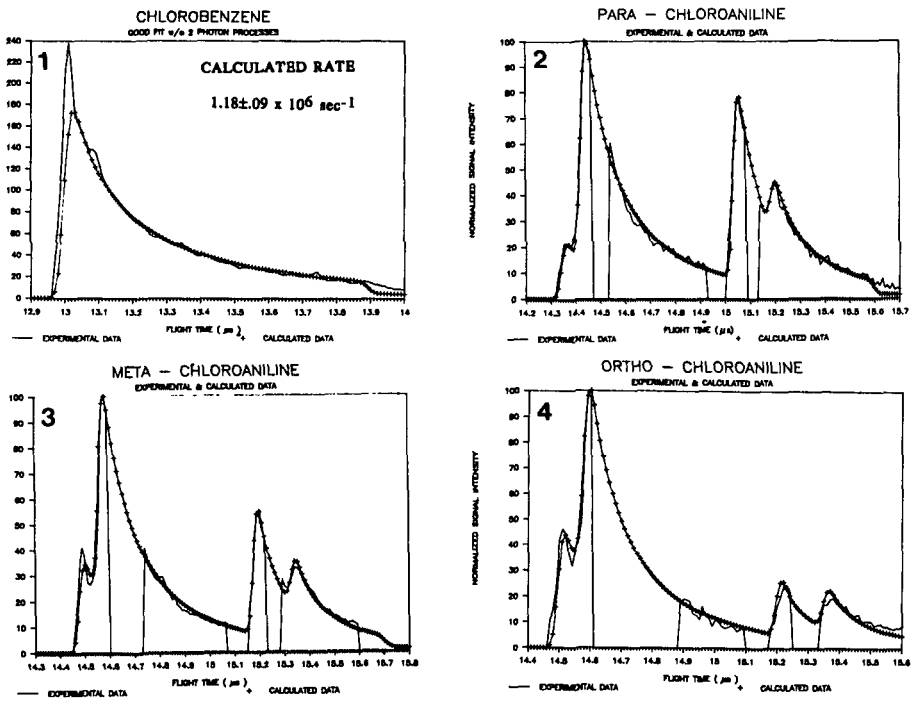

5 **CALCULATED METASTABLE DECAY RATES**

	ORTHO	META	PARA
M/z 91	4.29±.08	2.48± 10	1.36± 12
M/z 92	7.06± 08	5.68± 12	5.37± 15
M/z 100	2 29±.02	3 81±.08	4 62 ±.12
M/z 102	4.26±.13	3.99± 11	3.5±.17
M/z 91 + 92	11.35± 11	8.15± 16	6.73± 20
M/z 100 + 102	6.55±.13	7 80±.14	8.21±.20
Total	17.90±.17	15.95± 21	14.94±.28

All Rates x 10^5 sec $^{-1}$

Presented at the 36th ASMS Conference on Mass Spectrometry and Allied Topics
June 5-10, 1988, San Francisco, CA

Use of a Microchannel Plate for Surface Induced Dissociation (McSID)

William Aberth
Mass Spectrometry Facility
Department of Pharmaceutical Chemistry
University of California, San Francisco, CA 94143-0446

The technique of collision-induced dissociation (CID), as applied to mass spectrometry, typically uses a gas target to fragment mass-selected energetic molecular ions The use of a gas for CID has several drawbacks 1) Large energy spreads occur in the fragment ions resulting in reduced resolution and sensitivity, 2) The efficiency of collisional fragmentation decreases with increasing molecular size due to a reduction in translational energy available for internal energy conversion and a lower primary ion velocity; 3) The introduction of a collision gas raises the background pressure resulting in poorer resolution and transmission of the high mass compounds.

The technique of surface induced dissociation (SID) was introduced to overcome some of these difficulties [1-4] The use of a surface to collisionally fragment molecules does not degrade the instrument vacuum and offers the possibility of large amounts of internal energy conversion for effective high-mass fragmentation. The SID technique typically involves collisions of parent molecules with energies below 300eV on a metallic surface at an incident angle of about 45 degrees Encouraging results have been achieved with this technique, using a variety of instrumental arrangements, for compounds below about 250d [1-4]

A new SID method has been developed which utilizes the channel surfaces of a microchannel plate (McSID) In this arrangement energetic (100-1,000eV) parent ions undergo grazing (1-5 degrees) collisions on a surface of very high surface resistance (about 10^{13} ohms) (see Fig 1) The in-line nature of the McSID geometry should facilitate its adaptation to magnet sector, quadrupole and TOF type instruments. Several surface bounces of each molecular ion passing through the channel are likely since the ratio of channel length to diameter is about 50 The high surface resistance greatly reduces the probability of ion neutralization. The average amount of internal energy absorbed by the parent ion is proportional to its translational energy and to the square of its grazing angle θ (see Fig. 1). By varying these two parameters a broad range of fragmentation quality control is possible A tandem Wien MS [5] was used to demonstrate the McSID technique. The instrument operated at 25keV beam energy for mass separation and is provided with a floatable microchannel plate target to permit lower collision energies. The resolution of Wien MS-1 was set at 500 while that of Wien MS-2 was 80. The microchannel plate contained an array of channels 9.6 microns in diameter and 432 microns long with an open area ratio of 59% The plate was aligned so that the channel axis differed by about 3 degrees from the beam axis. Figure 2 shows a positive McSID spectrum of the peptide leu-enkephlin (Tyr-Gly-Gly-Phe-Leu, 555d) obtained at 250eV collision energy showing good sequence structure. Figure 3 is the McSID spectrum of negative leu-enkephalin obtained at 1,000eV, and yielding complimentary structural information. In all McSID spectra the dominant peak is the parent molecular ion and fragmentation efficiencies are typically 10-20%. Figure 4 shows the McSID spectrum of $(CsI)_{23}Cs^+$ (6113d) showing all $(CsI)_nCs^+$ fragments from n=0 to 23, and demonstrates the high-mass capability of the McSID technique Because of the distinct advantages provided by the McSID techniq;ue it should become an important addition to the MS/MS methodology

Acknowledgment. This work was suppoorted in part by NIH Grant GM 32315

References

1. M. A Mabud, M. J Dekrey and R. G.,Cooks, Int. J. Mass Spectrom. Ion Proc., 67, 285, (1985).

2 M J Dekrey, M. A Mabud, R. G. Cooks and J. E. P. Syka, Int. J Mass Spectrom. Ion Proc., 67, 295, (1985).

3 M E. Bier, J. W Amy, R G. Cooks, J. E P. Syka, P. Ceja and G. Stafford, Int. J Mass Spectrom Ion Proc., 77, 31, (1987).

4. K Shey, R. G. Cooks, R. Grix and H. Wollnick, Int. J. Mass Spectrom. Ion Proc., 77, 49, (1987).

5. W Aberth, Anal. Chem.,58, 1221,(1986).

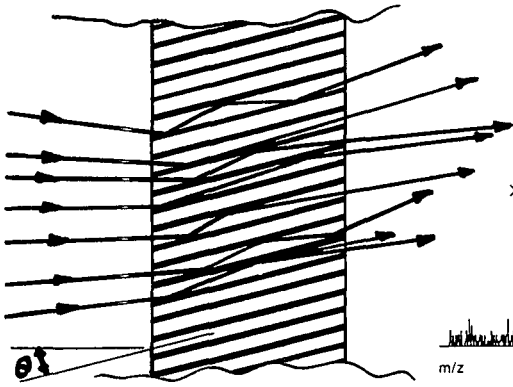

Figure 1. Schematic of collision process showing multiple internal channel collisions.

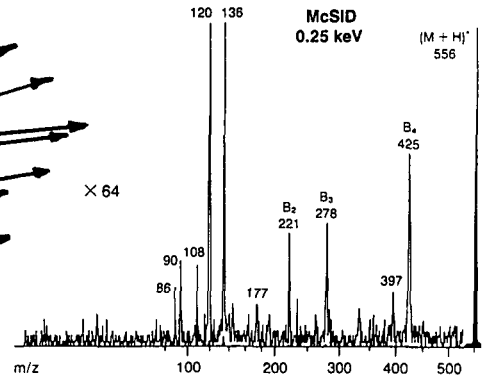

Figure 2. Positive ion McSID spectrum of leu-enkephalin at 250 eV impact.

Figure 3. Negative ion McSID spectrum of leu-enkephalin.

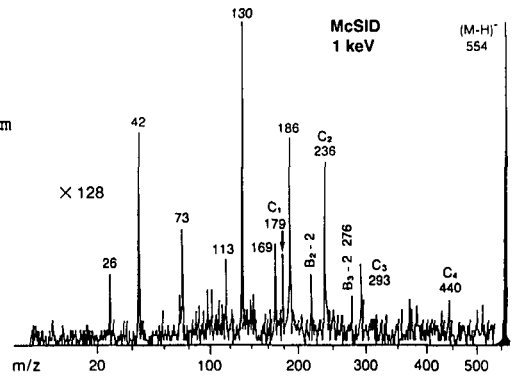

Figure 4. McSID spectrum of $(CsI)_{23}Cs^+$ at 1,000 eV showing all $(CsI)_nCs^+$ fragments from n=0 to 23.

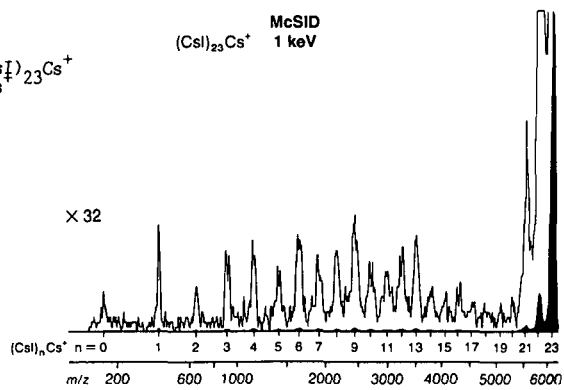

Presented at the 36th ASMS Conference on Mass Spectrometry and Allied Topics
June 5-10, 1988, San Francisco, CA

APPEARANCE POTENTIAL MEASUREMENTS ON SULFURIC ACID VAPOR

K.B. Snow and T.F. Thomas, Dept. of Chemistry, University of Missouri-Kansas City, Kansas City, MO 64110

After a long effort to develop a suitable inlet system, mass spectra of $H_2SO_4(g)$ have been obtained which-for the first time, to our knowledge-show a significant parent peak. Key details include using a helium carrier gas flowing over $H_2SO_4(l)$ at 75°C and exposing the entrained vapor only to quartz, teflon and gold-plated surfaces (including the ion source). A mass spectrum obtained from vapor at the azeotropic composition (∿98.3%, by weight, is shown in Figure 1 for an ion source temperature of 108°C and an electron impact energy of 50ev. The intensity of the $H_2SO_4^+$ peak was found to be strongly dependent on the temperature of the ion source, declining from 28% to 0.79%, relative to the base peak (SO_3^+), as T_{source} was raised from 92 to 152°C. This effect appears to be due to the temperature dependence of the equilibrium constant for

$$H_2SO_4(g) \rightarrow SO_3(g) + H_2O(g).$$

The ionization potential of H_2SO_4 and the appearance potentials of its fragment ions were determined using a previously-described Fox-type RPD ion source,[1,2] modified for computer-controlled data acquisition and using ion-counting in place of analog detection. Ionization efficiency curves for $H_2SO_4^+$, several fragment ions, and one of the gases (Xe) used to calibrate the electron energy scale, are shown in Figure 2. Experimental results for the ions derived from H_2SO_4 are presented in Table II.

Table I. Appearance Potentials from $H_2SO_4(g)$
T_{source} = 108°C

No.	Reaction	A.P.(ev)
1.	$H_2SO_4^+ \rightarrow H_2SO_4^+ + e^-$	12.40 ± .05
2.	$H_2SO_4 \rightarrow H_2O^+ + SO_3 + e^-$	13.2 ± .2
3.	$H_2SO_4 \rightarrow SO_3^+ + H_2O + e^-$	13.8 ± .2
4.	$H_2SO_4 \rightarrow HSO_3^+ + OH + e^-$	13.9 ± .1
5.	$H_2SO_4 \rightarrow SO_2^+ + H_2O_2 + e^-$	16.0 ± .15

In the cases of H_2O^+, SO_3^+, and SO_2^+ it was necessary to subtract a contribution by direct EI ionization of the small amounts of H_2O, SO_3 and SO_2 present in the sample stream from the total ionization efficiency curves obtained. Thus the uncertainties indicated for the results are larger in those cases.

Acknowledgement:

This work was supported by an Air Force Systems Command Contract No. F19628-84-K-0038 and a UMKC Faculty Research Grant.

1) T.J. Eskew, Paper No. S11, 21st ASMS Conference (1973).
2) H.J. Rodriquez, J.C. Chang, and T.F. Thomas, J. Am. Chem. Soc. 98, 2027 (1976).

Presented at the 36th ASMS Conference on Mass Spectrometry and Allied Topics
June 5-10, 1988, San Francisco, CA

Figure 1. Mass Spectrum of H_2SO_4

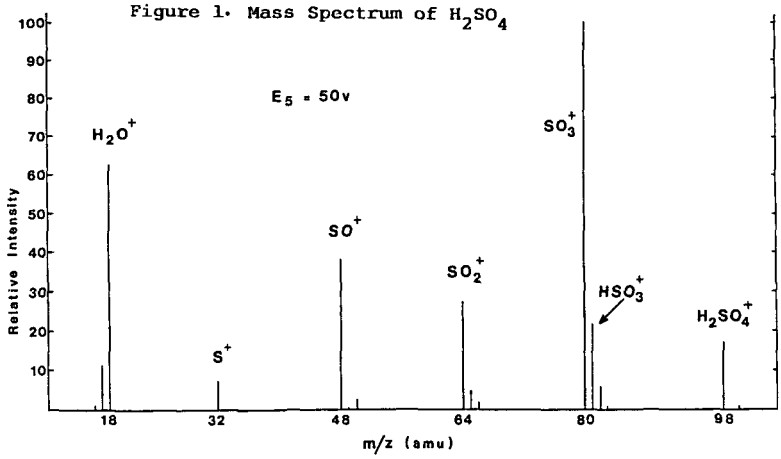

Figure 2. Ionization Efficiency curves

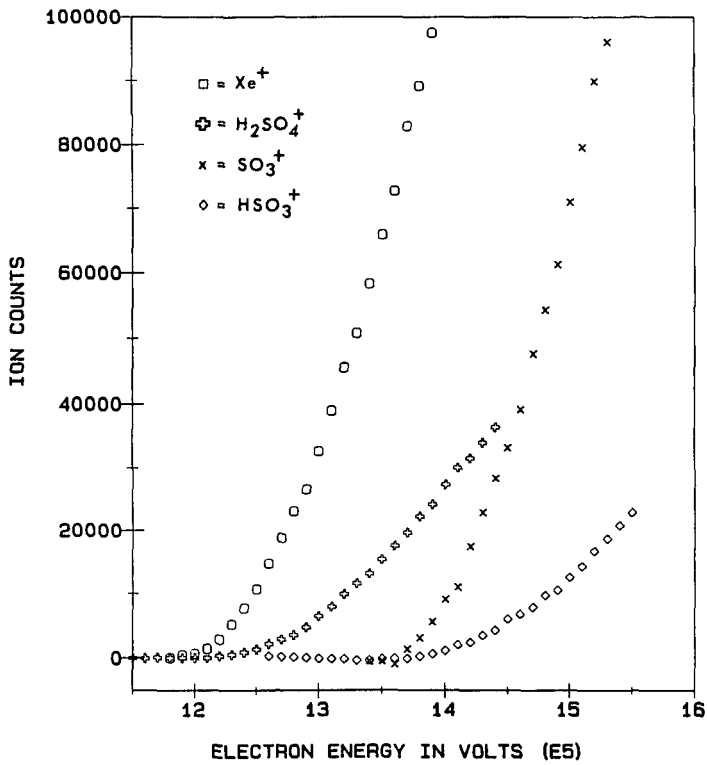

Presented at the 36th ASMS Conference on Mass Spectrometry and Allied Topics
June 5-10, 1988, San Francisco, CA

CID OF ISOTOPICALLY LABELLED SURFACTANTS:

Albert Tuinman and Kelsey Cook
University of Tennessee, Knoxville, TN 37996

Three synthetic surfactants (1-3) were examined by FAB and collision induced decomposition (CID), with the object of determining the extent and positional integrity of their deuterium isotope labelling.

	Structures	El.-Comp.	Cation Mass
1	Br^- $(CH_3)_3N^+(C_{13}H_{26}\text{-}CH_3)$	$C_{17}H_{38}D_{00}NBr$	256
2	Br^- $(CH_3)_3N^+(C_{13}D_{26}\text{-}CD_3)$	$C_{17}H_{09}D_{29}NBr$	285
3	Br^- $(CD_3)_3N^+(C_{13}D_{26}\text{-}CH_3)$	$C_{17}H_{03}D_{35}NBr$	291

The FAB spectrum of 1 at 20000 resolution in the multi-channel acquisition mode over a small mass range (around m/z = 256), demonstrated that the "M-1" peak consisted of one elementary composition only, $C_{16}C^{*}H_{36}N$. No loss of a single H from the ammonium cation could be detected. It follows that all "M-1" ions recorded for 2 and 3 must be caused by incomplete deuterium labelling. Relative abundances of peaks in the cation mass region of 2 and 3 are given in Table 1.

Table 1. Relative Ion Abundances of 2 and 3.

Cmpd.	M-4	M-3	M-2	M-1	M	M+1
2 (M=285)	11.5	3.2	13.6	56.2	100	18.3
3 (M=291)	10.2	3.0	8.9	36.6	100	17.0

From the data in Table 1, the specific isotope incorporation can be calculated at 98.2% for 2 and 98.8% for 3.

Determination of the positions at which deuterium incorporation was incomplete ("mislabelling") was achieved using MS/MS. The experiment requires at least unit resolution of the parent ion (total separation of the mislabelled parent from the isotopically pure parent) as well as unit resolution of the daughters (to quantify the isotope distribution between neutral and ionic daughters).

Neither B/E linked scans or the MIKES experiment meet both of these requirements, and are therefore unsuited to the experiment. Quadrupole

scanning in the hybrid ZAB-EQ does meet the criteria, and this method was employed.

Energy resolved CID spectra of 2 and 3 displayed a maximum of remote site fragmentation intensity with collision energies between 200V and 400V when the collision quadrupole was flushed with Argon to a reading of $2x10^{-5}$ Torr.

Daughter scans of the "isotopically pure" parent ion of 2 (m/z=285.5) displayed i.a. unit resolved singlets at intervals of 14 Dalton, from mass m/z=124 to 268, representing remote site fragmentation.[1] The equivalent ions in the daughter scan of the "mislabelled" parent (m/z=284.5) appeared as doublets differing by one Dalton. The relative intensities within each doublet varied, with the lighter of the two gaining intensity at higher mass. Relative intensities within these daughter pairs closely matched those calculated for random distribution of the errant atom in the mislabelled parent. It is thus indicated that incomplete isotopic labelling of 2 is random, rather than concentrated on any one carbon atom.

Exactly the same situation was found to apply to 3.

[1] J.Adams and M.L.Gross, *J.Amer.Chem.Soc.*,

Presented at the 36th ASMS Conference on Mass Spectrometry and Allied Topics
June 5-10, 1988, San Francisco, CA

Ion Kinetics in the Acceleration Region

Raymond E. March, Richard J. Hughes*,
Gregory K. Koyanagi* and Adam W. McMahon
Department of Chemistry, Trent University
Peterborough, ON, Canada K9J 7B8
*Registered at Queen's University, Kingston, ON, Canada

A method is presented for the investigation of unimolecular reactions which occur during the first 10^{-9} to 10^{-7}s in the acceleration region of a double-focussing mass spectrometer equipped with a standard Nier-type source. This method, which is described as Acceleration Region Kinetics (ARK), has been applied initially to an investigation of unimolecular fragmentation of molecular ions of nitrous oxide, n-butylbenzene and nitrobenzene-d_5. Studies which have been conducted with xenon and with n-butylbenzene have been applied to the determination of ionization cross-section by charge exchange as a function of collision energy and the effects of pressure in the acceleration region on charge transfer.

The position of ion formation in the acceleration region may be determined to within 0.02mm, in favourable cases, due to the relatively high resolving power of the electric sector of the ZAB 2FQ mass spectrometer. The ARK technique is similar to that of Field Ionization Kinetics (FIK) and has the advantage that it may be used with a standard Nier-type source.

Dissociation of ions in a non field-free region was first discussed by Hipple *et al.* [1] who considered the reaction

$$m_1^{x+\bullet} \longrightarrow m_2^{y+}\, m_3^{z+} \tag{1}$$

where unimolecular dissociation occurs as the ion is being accelerated following emergence from the source. This fragmentation occurs when $m_1^{x+\bullet}$ has fallen through a fraction b of the accelerating potential V_o. After fragmentation, the nascent daughter ion , m_2^{y+} , has kinetic a energy of $m_2\, bexV_o/m_1$. It is assumed here that there is zero kinetic energy release; the argument for fragmentation with release of kinetic energy is presented elsewhere [2]. The daughter ion falls through the remaining fraction, $(1-b)$, of the accelerating potential. The apparent mass/charge ratio, m_b^*, at which m_2^+ is transmitted through the magnetic sector is given by

$$m_b^* = \frac{m_2^2}{m_1}\left[\frac{m_2\, xb + m_1\,(1-b)y}{m_2\, y^2}\right] \tag{2}$$

as discussed by Cooks *et al.* [3]. From eqn.(2), the point of fragmentation, b, may be calculated as

$$b = \frac{m_1\, y - m_b^*\, m_1\,/m_2\, y^2}{m_1\, y - m_2\, x} \tag{3}$$

When $b = 0$, m_2^{y+} is formed in the source; when $b = 0$, m_2^{y+} is formed in the 1ST FFR and $m^* = m_2^2\, x/m_1\, y^2$. The voltage required for transmission of the daughter ion is E_b where

$$E_b = \left[\frac{m_2\, bx}{m_1} + y(1-b)\right] E_o \tag{4}$$

Rearrangement of eqn.(4) yields

$$b = \left[\frac{y - E_b/E_o}{y - m_2 x/m_1} \right] \tag{5}$$

Equations (2) and (4) relate the operating conditions for the magnetic sector and ESA, respectively, to the transmission through both sectors of a fragment ion formed at a given point in the acceleration region. Elimination of b gives

$$E_b = m_b^{\cdot} E_o y^2 / m_2 \tag{6}$$

thus for a given value of b, E_b is proportional to $m_b^{\cdot}$ and thus to B^2; therefore, for a specific m_2, a linked scan at constant B^2/E will reveal the metastable decomposition to $m_2^{\cdot +}$ throughout the range of b.

Investigation of unimolecular reactions must be conducted in a pressure regime where collisional processes may be neglected. A study of the dissociation of n-butylbenzene (m/z 134) via scission to form m/z 91 and rearrangement to form m/z 92 as a function of pressure has been conducted. As shown in Figure 1, the scission process is the more sensitive to collisional activation but the intensities due to both processes vary linearly with indiated pressure below 2×10^{-6} mbar.

Figure 1: Intensities of two competing reactions of n-butylbenzene as a function of pressure

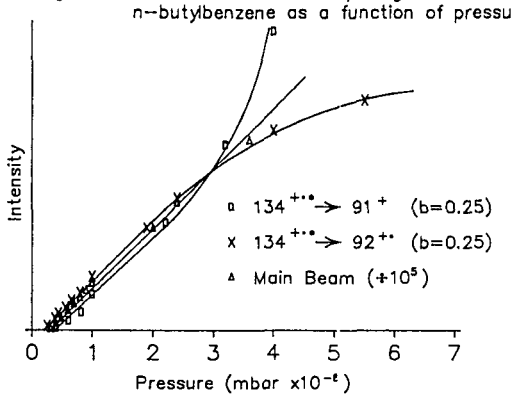

References

1. J.A.Hipple, R.E.Fox and G.U.Condon, Phys. Rev. 69 (1946)347.
2. G.K.Koyanagi, A.W.McMahon and R.E.March, Rapid Commun. Mass. Spectrom., 1 (1987)132.
3. R.G.Cooks, J.H.Beynon, R.M.Caprioli and G.R.Lester, *Metastable Ions*, Elsevier, Amsterdam (1973).
4. G.K.Koyanagi, A.W.McMahon, R.E.March and A.G.Harrison, Int. J. Mass Spectrom. Ion Processes, 83 (1988)245.

Presented at the 36th ASMS Conference on Mass Spectrometry and Allied Topics
June 5-10, 1988, San Francisco, CA

DYNAMICS OF COLLISION-INDUCED DISSOCIATION OF ACETONE IONS

A. Shukla, S. Howard, S. Anderson, and J. Futrell
Department of Chemistry, University of Delaware, Newark, DE 19716.

Interest in the detailed dynamics of collision-induced dissociation (CID) of polyatomic ions has grown since the technique has become well established in organic and analytical mass spectrometry. A recent publication by van der Zande et al. [1] showed that in 5 keV acetone ion CID the fragment ion (CH3CO+) intensity is maximum at non-zero scattering angle. It was suggested that excitation takes place in close collisions with momentum transfer rather than by electronic excitation at such high energies. With these results in mind we initiated a study of CID of acetone ions at low energies where momentum transfer is suggested to be the dominant channel for ion excitation.

Experiments were performed on a tandem hybrid mass spectrometer-supersonic beam instrument which has been described in detail earlier [2]; only sailent features are mentioned here. A high energy (3keV) beam of acetone ions generated by electron impact ionization from a double focussing mass spectrometer was decelerated to the desired final energy via a series of cylindrical and rectangular tube lenses and focussed at the collision region where it collides with a supersonic beam of argon neutrals at right angles. Fragment ions were energy and mass analyzed at a series of angles using a hemispherical energy analyzer and a quadrupole mass filter. Laboratory angular and energy distributions were taken at angles up to 22 deg for the fragment ions. The data were collected on an IBM PC, smoothed and tranformed into Cartesian probabilities. Details of the transformation specific to our instrument configuration are described elsewhere [3].

Scattering contour diagrams for the CID of acetone ion into acetyl ion at 4.5, 14, and 25 eV (laboratory energy) are shown in Figures 1, 2, and 3 respectively. Considerable scattering is observed in these experiments and the intensity maximum in each case is at a non-zero angle. This is consistent with high energy observations [1]. It is therefore obvious that the excitation of acetone ions proceeds via strong collisions with momentum transfer at both low and high energy.

The most interesting new observation in the present study is the evidence for a complex formation (Figure 1) at 4.5 eV laboratory energy (1.9 eV center-of-mass). Besides intensity maximum near the center-of-mass there are intensity maxima suggesting forward-backward scattering in the process. At this energy therefore the colliding acetone ion forms a complex with neutral argon with an appreciable amount of internal excitation which then fragments after a lifetime longer compared to usual collision time. Since almost all the kinetic energy is transferred into internal modes and the dissociation process requires only 0.6 eV it is quite likely that substantial energy is transferred to the neutral CH_3 (internal and translational) and argon (translational only) in the dissociation process.

References:

1. W.J. van der Zande, D.P. de Bruijn, P.G. Kistemaker, and S.A. McLuckey, Int. J. Mass Spectrom. Ion Phys., 67(1985) 161.
2. A.K. Shukla, S.G. Anderson, S.L. Howard, K.W. Sohlberg, and J.H. Futrell, Int. J. Mass Spectrom. Ion Proc., in press.
3. A.K. Shukla, S.G. Anderson, S.L. Howard, and J.H. Futrell, to be submitted.

Presented at the 36th ASMS Conference on Mass Spectrometry and Allied Topics
June 5-10, 1988, San Francisco, CA

$$CH_3COCH_3^{+\cdot} + Ar \longrightarrow CH_3CO^+ + CH_3^{\cdot} + Ar$$

at 25 eV laboratory

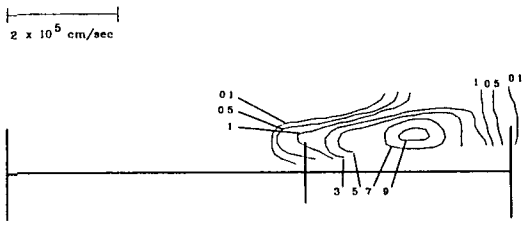

$$CH_3COCH_3^{+\cdot} + Ar \longrightarrow CH_3CO^+ + CH_3^{\cdot} + Ar$$

at 14 eV laboratory

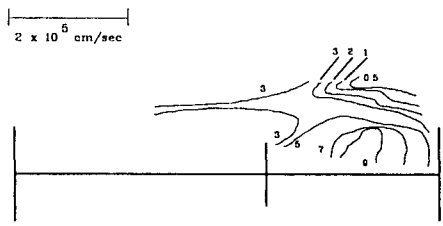

$$CH_3COCH_3^{+\cdot} + Ar \longrightarrow CH_3CO^+ + CH_3^{\cdot} + Ar$$

at 4.5 eV laboratory

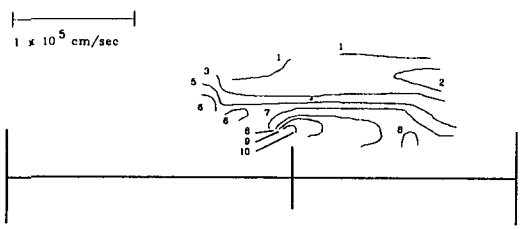

Center of Mass Cartesian velocity probability contour diagram for the collision-induced-dissociation of acetone ions with Ar at the indicated (ion) laborabory kinetic energy. Vertical bars correspond to the velocity vectors for Ar (left) and $CH_3COCH_3^+$ (right) and the center-of-mass location. Contour lines of equal relative intensity are shown, ranging from a high value of 9 to a low value of 0.1.

(a) Diagram for 25 eV (LAB)
(b) Diagram for 14 eV (LAB)
(c) Diagram for 4.5 eV (LAB)

Presented at the 36th ASMS Conference on Mass Spectrometry and Allied Topics
June 5-10, 1988, San Francisco, CA

ENERGY UPTAKE IN COLLISIONAL ACTIVATION

D.E. Giblin and M.L. Gross
Midwest Center for Mass Spectrometry
Dept. of Chemistry, University of Nebraska,
Lincoln, NE 68588-0304.

INTRODUCTION

During collisional activation (CA), some of the translational kinetic energy is converted to internal energy of the incident ion. In recent years, the internal energy required to induce fragmentation has been studied primarily by the appearance energy method in conjunction with low-energy collisions (<100eV) with massive target gases or surfaces[1]. The amount of energy deposited in the internal modes of the incident ion is estimated indirectly. There are several critical assumptions of this approach. First, that the fractional conversion of kinetic energy (T) to internal energy (Q) as a function of available kinetic energy is the same for all ionic species including a well-characterized calibrant. Second, that all internal energy is partitioned to the incident ion in collisions with quite polarizable target gas molecules.

Particularly troublesome has been the difficulty of estimating the internal energy requirements for charge-remote fragmentation by he low-energy approach. Reported energetics for such fragmentations indicate widely different energy requirements for similar ionic species. Also different mechanisms are implied for an apparently homologous set of fragmentations from the same parent ionic species.

To circumvent such problems, a high-energy method which measures the kinetic energy loss due to CA of a parent ionic species as manifest in the kinetic energy shift of a daughter species. The internal energy again is then calculated from the kinetic energy loss by using a basic physical relationship[2]. The energetics of high-energy CA and fragmentation with regard to charge-remote fragmentation has been investigated by using this approach.

EXPERIMENTAL PROCEDURE

This study of the energy requirements of CA was performed on a Kratos MS-50TA. CA took place in the 2nd collision cell located between MS-I and MS-II. The potential of the 2nd ESA (MS-II) was controlled by a custom MID which produced a centered sweep of preset width (ppm) of that potential and also performed a precision, programmable division of that potential. Sweeps over parent and daughter masses thus have the same proportional width in ppm about the central energy (mass). Signals were collected and averaged by a Nicolet 1170 signal averager. Data was then transferred to a Data General Nova 4X computer for smoothing, peak centroiding by fitting to Gaussian peaks, and the calculation of the kinetic energy loss and internal energy uptake.

In practice, the parent ionic mass, m_1, is selected by MS-I. The daughter ionic mass, m_2, is selected by setting the voltage divider in the MID to the exact ratio of m_2/m_1. The 2nd beta slits are closed down until the peak shape of m_1 in energy space becomes Gaussian (~0.005"). Scans are collected over m_1 and m_2 by the Nicolet signal averager. From the displacement of the centroid of m_2 from its unshifted position is derived a proportional kinetic energy displacement, ΔW. The kinetic energy loss of the parent species which fragment to the selected daughter species is given by: $\Delta T = T\Delta W$. The internal energy gain, Q, is then calculated using an approximation derived from the basic relationship[2]:

$$Q = \Delta T[1-0.25(m_1/m_T)(\Delta T/T)] = Q_a+(m_1/m_T)T \sin^2(\theta_s/2)$$

where Q_a is the actual internal energy uptake, m_T is the mass of the target gas, and θ_s is the scattering angle of m_1 by collision. In practice, θ_s is usually considered to be negligible.

RESULTS AND DISCUSSION

To check the consistency of this high-energy approach, the internal energy gain was determined for several fragmentations by both CA and metastable decomposition. (The latter should give Q=0.) It was found necessary to improve the high-vacuum pumping efficiency on the MS-50TA to

eliminate the residual CA. After the modifications were made, values of Q=0 were found for the chosen fragmentations. A particularly striking example was the loss of NO· from the anion formed by electron attachment to 1-nitro-2-naphthol. This fragmentation had a Q=7.9eV for 30% He CA (by beam reduction). The large value of Q=7.9eV probably reflects a large kinetic shift for this fragmentation. (Most fragmentations we have studied have Q=1.0 to 5.0eV except for charge-remote fragmentations for which Q>12eV). The certainty of kinetic shifts means that the values obtained for Q by this method are therefore upper limits to the energetic requirements for CA. In addition, the information from peak broadening due to kinetic energy release upon fragmentation is preserved in at least some cases, as in the previous example.

The energy gain requirements of CA for charge-remote decompositions of some fatty acid anions were studied at 8kV. The energy gain, Q, was determined for the losses of CH_4, C_2H_6, C_3H_8, C_4H_{10}, and C_6H_{14} from palmitate, oleate, elaidate, and linoleate and for the loss of $C_{11}H_{20}$ from linoleate and $C_{11}H_{22}$ from oleate and elaidate. The values of Q appear to be the same within statistical variation with no apparent function related parent or loss. The average values for Q are 12.7, 13.3, 12.5, and 12.8eV for palmitate, oleate, elaidate, and linoleate, respectively. Such results are consistent with the same mechanism for the homologous series of fragmentations. In addition, the energy widths of the peaks corresponding to these losses are all about 60eV which indicate that scattering due to CA dominates over kinetic energy release as the primary cause of peak broadening for this class of fragmentations.

A further study of the energetics of CA leading to charge-remote fragmentation was conducted on the putative alkane losses from dodecyl sulfate anion as a function of incident ion kinetic energy. The energy gain was determined for the losses of CH_4, C_2H_6, C_3H_8, C_4H_{10}, C_6H_{14}, and C_7H_{16} at an incident ion kinetic energy of 8 and 4kV and for the losses of methane through butane at 2kV. Again, no significant variation of Q as a function of loss was found. However, a significant variation in the average values of Q as a function of kinetic energy was discovered. The average values of Q are 13.9, 16.3, and 20eV for kinetic energies of 8, 4, and 2kV, respectively. The corresponding available energies are 119, 59, and 30eV, respectively. Likely, the increasing Q values reflect increased scattering at lower kinetic energies associated with the production of that population of parent ions that undergo the alkane-loss fragmentations. If scattering is assumed negligible for the 8kV parent ions, then the increases in Q correspond to mean scattering angles of .12 and .19° for 4 and 2kV parent ions, respectively. Thus the mean Q=13.9eV associated with the 8kV parent ions probably has a scattering component and is therefore an upper limit. Since the envelope of the intensities of the alkane-loss series is unchanged with respect to this range of kinetic energies the result constitutes an additional piece of evidence along with similar Q values at a given kinetic energy for a common mechanism. As in the previous example, the energy widths of the peaks at a given kinetic energy are the same which indicates the dominance of scattering over kinetic energy release as the primary cause of peak broadening. Finally, the much lesser fragmentation probabilities at 2kV and the Q value that approaches the maximum available energy indicate that double-collision processes may be important at this kinetic energy.

REFERENCES

[1]V.H. Wysocki, M.E. Bier, and R.G. Cooks, 35th Annual Conference ASMS, Denver, 223 (1987).

[2]G.M. Neumann, M.M.Sheil, and P.J. Derrick, Z. Naturforsch., 39a, 584 (1984).

Presented at the 36th ASMS Conference on Mass Spectrometry and Allied Topics
June 5-10, 1988, San Francisco, CA

PHOTODISSOCIATION OF 2-METHYL-1-PENTN-3-YNE CATION.

J. Faulk and R.C. Dunbar; Chemistry Dept., Case Western Reserve University
Cleveland, Ohio 44106.

OBJECTIVES

The objectives of this study were to compare the changes in geometry that accompany the electronic transitions in the phtodissociation and photoelectron experiments, to compare the resolution of a photoelectron spectrum with that available from a photodissociation spectrum and to determine if the two spectra agree as expected from the known electronic transitions.

INTRODUCTION

The high resolution photodissociation spectrum of gas phase 2-methyl-1-penten-3-yne cation was measured from 600nm to 540nm. The photodissociation at 5 Ar ion laser lines (514.5, 501, 497, 488 and 476nm) was also measured

EXPERIMENTAL

The ions were trapped in an icr spectrometer with capacitance bridge detection. The light source was a dye laser pumped with the 514.5nm line of an Ar ion laser The dissociation products were determined using an Ion Spec FTICR spectrometer.

RESULTS

Hydrogen loss is the primary photoprocess:

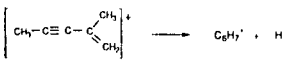

The photodissociation data points are compared in figure 1 with the He I photoelectron spectrum (solid black line) taken from reference 1 The energy scale is adjusted so that the photoelectron band of the ground state ion appears at 0eV on the left hand side of the figure The π electronic transitions appear above the corresponding photoelectron bands The red line drawn through the photodissociation data points is not fitted to the data points but is only intended to guide the eye

DISCUSSION

Vibrational fine structure:

It is suggested that the vibrational progression shown in figure 2 (with a peak spacing of 1310cm^{-1}; 0 16eV) is due to a stretching mode involving the double bond and probably the central single bond (ref 1).The shoulders on the lower energy photoelectron peak indicate underlying vibrational fine structure with a spacing on the order of 230cm^{-1}. We are not able to assign this frequency to a vibrational mode at this time.

Comparison of spectra:

The photodissociation spectrum is shifted by about 250cm-1 to the high energy side of the photoelectron peak. This is probably due to a difference in the Franck-Condon factors for the two spectra Since the electronic transitions that occur in the photoelectron and photodissociation experiments are different it is not unreasonable to expect them to be accompanied by different changes in the equilibrium geometry and therefore to have different Franck-Condon factors

The small amount of photodissociation occuring in the hot band region (to the low energy side of the photoelectron peak) is probably due to dissociation of vibrationally excited electronic ground state ions At 370K (a reasonable temperature for ions in our instrument) the occupation of the v=1 level of a 250cm-1 vibrational mode is about 35% of the v=0 level Ions with this much internal energy can reasonably be expected to give a significant 1,0 peak

CONCLUSIONS

It appears that the electronic transitions occuring in the photodissociation and photoelectron experiments are accompanied by significantly different changes in cation equilibrium geometry

The vibrational fine structure in the photoelectron spectrum is resolved in the photodissociation spectrum, however hot band absorption and rotational broadening broaden the photodissociation peaks

When compared as in figure 1(where the ground state neutral to ground state ion transition energy is set equal to zero) the two spectra are in good agreement.

FIGURE 1

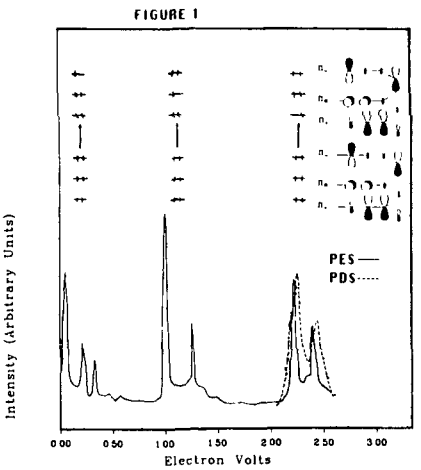

Figure 2

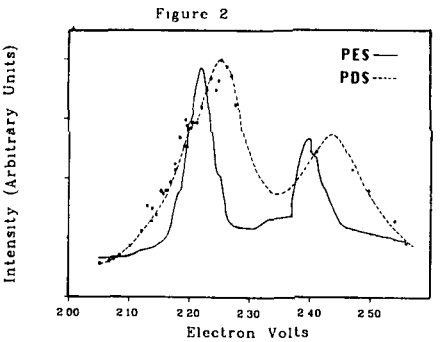

Reference.
G Mouvier etal, J Elect. Spec. Rel. Phenom. 1979, 16, 147

Presented at the 36th ASMS Conference on Mass Spectrometry and Allied Topics
June 5-10, 1988, San Francisco, CA

Chopped-Laser Two-photon Photodissociation Measurement of Collisional Relaxation in Benzene Ion

Mohammed S. Ahmed and R C Dunbar
Case Western Reserve Univertsity, Cleveland, OH 44106

INTRODUCTION

One of the principal motivations of the present study was to compare the quenching of benzene ion with that of bromobenzene ions, which we have reported in detail[1]. Collisional quenching of bromobenzene ion showed several trends A number of small closed-shell molecules and saturated hydrocarbons had quenching efficiencies which correlated in a very regular way with the quenching molecule and its number of internal degrees of freedom. A number of quenchers with open-shell or unsaturated electronic structures had quenching efficiencies substantially enhanced above this normal rate. This enhanced quenching probably reflects some specific chemical interaction between the bromobenzene ion and the odd electrons or the p electrons of the unsaturated quench molecule. It was speculated that this interaction might involve the lone-pair electrons of the bromine atom of bromobenzene. To clarify this possibility, it seemed interesting to measure the quenching effiency of some of the same neutral molecules with benzene ion: any dramatic difference in the pattern of quenching effiencies could be attributed to effects specific to the presence or absence of the bromine substituent.

TECHNIQUE

The sequential two-photon absorption model is given by the kinetic scheme:

$$C_6H_6^{+\cdot} \xrightarrow{\sigma_1 I} C_6H_6^{+\cdot *} \xrightarrow{\sigma_2 I} C_6H_5^{+} + H \qquad K_cP + K_r$$

$$1/D = \frac{K_cP + K_r}{I^2\sigma_1\sigma_2 t} + \frac{\sigma_1 + \sigma_2}{I^2\sigma_1\sigma_2 t} \quad . \quad . \quad (1)$$

where, D is the dissociation defined by $-\ln\left(\frac{S_{on}}{S_{off}}\right)$, S_{on} and S_{off} are the signal intensities at light on and light off conditions repectively P is the pressure of quench gas

EXPERIMENTAL

The chopped-laser two photon technique in the ICR spectrometer has been described in previous reports[2]. In this study, using the pulsed ICR spectrometer with bridge detection, benzene ions were formed by electron impact with an electron beam pulse of 10-200 ms duration at a nominal electron energy of 11-12 eV. Ions were trapped and irradiated for 3 s Illumination at 488 nm was with the Coherent Radiation I -12 argon ion laser.. The data were analyzed by the usual procedure of fitting to a numerical simulation of the dissociation kinetics, to find the actual relaxation rate at the given pressure.

RESULTS

Table I displays the results for the quench gases used. The number of collisions , Z required for quenching of the photo-excited ion is defined as(K_{orb}/ K_q), where K_{orb} and K_q are the orbiting rate constant and observed collisional quenching rate constant respectively. Z is the inverse of the collisional efficiency for quenching In order to make comparisons among different systems, it is convenient to reduce the observed quenching rates to a calculated energy lost on the first collision[2]. This is readily calculated assuming that collisional energy loss is exponential. This assumption gives the expression

$$\Delta E = E_{\emptyset}(\,(1-(E_T/E_o)^{1/Z})$$

where $E_{\emptyset}$ is the photon energy, E_T is the one-photon threshold energy and E_o is the internal energy above one-photon threshold. These values are compared for benzene and bromobenzene in the last columns of Table II

Presented at the 36th ASMS Conference on Mass Spectrometry and Allied Topics
June 5-10, 1988, San Francisco, CA

TABLE 1

BENZENE ION COLLISIONAL QUENCHING

NEUTRAL	QUENCHING RATE CONSTANT	ORBITING RATE[a] CONSTANT	COLLISION NUMBER, Z
C_6H_6	12.0	12 1	1 0
OCS	2.1	10.7	5 0
SF_6	1 4	6.8	5 0
CO_2	72	7 2	10
C_2H_6	62	10.6	17
CH_4	43	10 4	24
N_2	18	7 2	41
HE	057	5 4	95

a 10^{-10} CM^3 $MOLECULE^{-1}$ S^{-1}

TABLE II

COMPARISON BETWEEN BENZENE AND BROMOBENZENE

NEUTRAL	ΔE(1ST COLL) CM^{-1} $C_6H_6^+$	$C_6H_5Br^+$
HE	110	250
N_2	250	650
CH_4	430	1140
C_2H_6	610	1860
CO_2	1020	2400
SF_6	2000	--
COS	2000	4500
C_6H_6	8400	--

CONCLUSIONS

1 The quenching efficiency for benzene ion follows the expected trends, increases with increasing size and complexity of the neutral partners.

2 The quenching efficiency for bromobenzene ion is 2.5 times higher than that for benzene ion

3 The quenching efficiency for bromobenzene ion could be a result of the dipole moment or the extended lone-pair electrons of the bromine atom, or the longer duration of collisions in the heavier system or some combination of these factors.

4. The presence of bromine atom appears not to have a specific effect on quenching by a particular gas

5. The chopped-laser two-photon technique is an excellent method in measuring the efficiency of even inefficient quench gas

REFERENCES

1 M.S Ahmed and R C. Dunbar, J Am Chem. Soc, 109, 3215(1987)

2. R. C. Dunbar, B Asamoto, J H. Chen, and H Y. So, J. Chem. Phys, 86, 2081(1987).

Presented at the 36th ASMS Conference on Mass Spectrometry and Allied Topics
June 5-10, 1988, San Francisco, CA

Internal Energy Distributions Determined For Scattered $Fe(CO)_5^+$ Ions Using Angle Resolved Techniques

S.R. Horning, R.G. Cooks
Department of Chemistry
Purdue University
West Lafayette IN 47904 USA

M. Vincenti
Istituto Guido Donegani
Via Fauser 4, 28100 Novara, Italy.

Internal energy distributions for polyatomic ions collected through scattering angles increasing from 0 - 2.5°, following high energy (keV) collision activation, afford explicit confirmation that the average internal energy ($\Delta\epsilon$) of the excited ion increases with the scattering angle. In addition, the $P(\epsilon)$ curves show a marked dependence on the collision energy (E) and the angle (θ) through which the scattered ions are collected, the data suggesting that ions which are scattered through small angles in high energy collisions are excited through vibrational, as well as through electronic, excitation channels.

Angle resolved experiments were performed on a Finnigan MAT 8200 mass spectrometer. Argon was introduced into the first field-free region of the instrument and the daughter ions were recorded through a linked (B/E) scan of the sector fields. The scattering angle was varied by electrical deflection of the ion beam in the x-z plane as it left the ion source before entering the collision region (1,2). Effects due to multiple collisions were examined by performing the experiments over a wide range of sample and collision gas pressures. No changes which could be attributed to multiple collisions could be detected. In addition contributions to scattering through isotropic kinetic energy release (3) were shown to be small by measuring kinetic energy releases for the contributing reactions.

Internal energy distributions are approximated using known activation energies for each successive decarbonylation process, in conjunction with fragment ion abundances observed in the angle resolved daughter ion spectra (4). Several $P(\epsilon)$ curves obtained at laboratory scattering angles increasing from 0°to 2.5° at 3 keV collision energy are shown in Fig. 1. These curves establish that the average energy deposited during collisional activation increases as the scattering angle is raised. Similar data were obtained at collision energies of 2.25 and 1.5 keV. A plot of the reduced parameter (θE), see Fig. 2, demonstrates that the average energy of the activated ion ($\bar{\epsilon}$) increases approximately linearly with θ, in parallel with earlier studies at much lower collision energies (5).

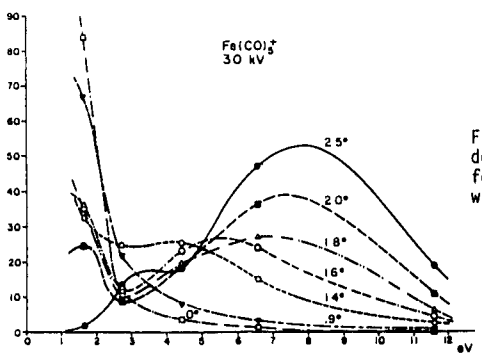

Figure 1. Internal energy distributions determined at several scattering angles for $Fe(CO)_5^+$ upon activation by collision with argon at 3 keV.

Further insight into the nature of these highly structured $P(\epsilon)$ curves for scattered ions can be made by considering the internal energy distributions associated with other methods of activation (see Fig. 3). Under electron impact (EI) conditions, where strict Franck-Condon factors control the formation and internal energy of the ionic species, the region between 2 and 5 eV ion internal energy remains unpopulated. This is in contrast to the distributions found in Fig. 1, and suggests that a mechanism besides electronic excitation may be contributing to the formation of these excited ions. A possible contributor is vibrational excitation or an oblique transition process as proposed by Russek (6). Evidence for participation of vibrational excitation in small angle keV collisions is found in the following observations. First, excitation of $Fe(CO)_5^+$ at a solid surface in the SID experiment, presumably a vibrational process, readily populates the region between 2 and 5 eV in the $P(\epsilon)$ curve (Fig. 2). Second, at low collision energies, where vibrational modes predominate, a linear relationship between the internal energy deposited ($\Delta\epsilon$) during the collision and reduced parameter ($E\theta$) is found (5), resembling the data shown in Fig. 2. These results support the role of both electronic and vibrational excitation processes in keV collisions leading to laboratory scattering angles of a few degrees.

These data hold the promise that with more precise definition of the scattering angle it should be possible to acquire a much more detailed description of the mechanism of collision activated dissociation. It is of interest to note that both $W(CO)_6^+$ and $Cr(CO)_6^+$ show similar structured internal energy distributions with strong angular dependence.

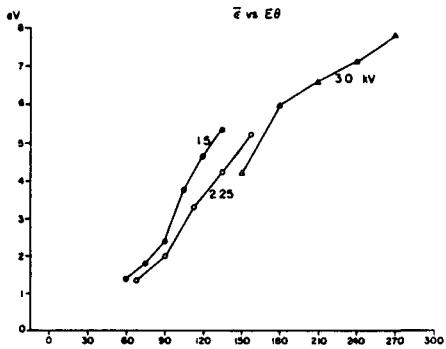

Figure 2. Plot of average $Fe(CO)_5^+$ internal energy ($\bar{\epsilon}$) vs. the reduced parameter ($E\theta$).

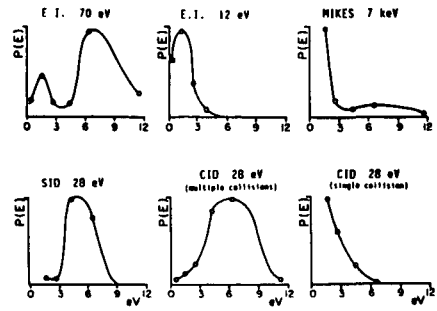

Figure 3. Internal energy distributions for $Fe(CO)_5^+$ activated by various methods.

References

1. S. Verma, J.D. Ciupek, R.G. Cooks, A.E. Schoen, P. Dobberstein Int. J. Mass Spectrom. Ion Processes 1983, 52, 311.
2. R.S. Mason, M.J. Farncombe, K.R. Jennings, R.G. Cooks Int. J. Mass Spectrom. Ion Processes 1982, 43, 327.
3. P.J. Todd, R.J. Warmack, E.H. McBay Int. J. Mass Spectrom. Ion Processes 1983, 50, 299.
4. V.H. Wysocki, H.I. Kenttamaa, R.G. Cooks, Int. J. Mass Spectrom. Ion Processes 1987, 75, 181.
5. Z. Herman, J.H. Futrell, B. Friedrich, Int. J. Mass Spectrom. Ion Processes 1984, 58, 181.
6. N. Anderson, M. Vedder, A. Russek, E. Pollack, Phys Rev. A 1980, 21, 782.

Presented at the 36th ASMS Conference on Mass Spectrometry and Allied Topics
June 5-10, 1988, San Francisco, CA

LASER INDUCED PHOTOFRAGMENTATION OF C5H5+ IONS DERIVED FROM DIFFERENT PRECURSORS

Mehdi Moini
Department of Pharmacology, The George Washington University, Washington DC
Feza Ozturk and John R. Eyler
Department of Chemistry, University of Florida, Gainesville FL

In order to identify different isomeric forms of the $C_5H_5^+$ ion, laser induced photodissociation (PD) of $C_5H_5^+$ ions derived from five different precursors was studied. Photodissociation thresholds, photofragmentation pathways and reactivities of the photofragment ions were then used as a probe of the $C_5H_5^+$ isomeric forms. Reactions of $C_5H_5^+$ produced from these five precursors with diacetylene have also been compared to the PD study of $C_5H_5^+$.

Fourier transform ion cyclotron resonance mass spectrometry (Nicolet FT/MS-1000) was utilized for these studies in conjunction with a pulsed Nd:YAG pumped dye laser (Quantel International). Two different magnets and laser beam configurations were used. The first was a superconducting magnet with a magnetic field of 3 Tesla (Figure 1). The second was an electromagnet which was operated at 1 Tesla (Figure 2).

Photodissociation and reactivity of photofragment ions of $C_5H_5^+$ derived from dicyclopentadiene, norbornadiene, cycloheptatriene, 1-penten-3-yne, and cyclopentadiene were studied according to:

$$\text{precursor} + e \rightarrow C_5H_5^+ + \text{neutral(s)} + 2e \quad (1)$$

$$C_5H_5^+ + h\nu \rightarrow C_3H_3^+ + (C_2H_2) \quad (2)$$

$$\text{precursor} + C_3H_3^+ \rightarrow \text{product(s)} \quad (3)$$

The results of PD of $C_5H_5^+$ at a wavelength of 355 nm show that $C_5H_5^+$ ions produced from dicyclopentadiene, 1-penten-3-yne, norbornadiene, and cycloheptatriene dissociate according to Reaction (2). Within the range of the laser pulse energy used and the signal to noise ratio obtained in these experiments no photodissociation were observed for $C_5H_5^+$ ions produced from cyclopentadiene. $C_3H_3^+$ ions produced in Reaction (2) were >90% reactive for norbornadiene, cycloheptatriene, and dicyclopentadiene while only 50% reactive for 1-pentene-3-yne. The spectra showing the photodissociation of $C_5H_5^+$ ions derived from cycloheptatriene and the reactivity of the photofragment ion ($C_3H_3^+$) are given in Figure 3.

The main reaction of $C_5H_5^+$ produced following charge transfer chemical ionization of a mixture of diacetylene and a precursor compound was:

$$C_5H_5^+ + C_4H_2 \longrightarrow C_9H_7^+ \quad (4)$$

A minor reaction

$$C_5H_5^+ + C_4H_2 \longrightarrow C_7H_5^+ + (C_2H_2) \quad (5)$$

was also observed for all precursors <u>except for cyclopentadiene</u>.

To compare the behavior of ions produced from cycloheptatriene and norbornadiene precursors, relative abundances as a function of electron energy were obtained. Based on the higher relative intensity of $C_5H_6^+$ for norbornadiene, there exists the possibility of formation of $C_5H_5^+$ ions from the $C_5H_6^+$ channel too. In fact, $C_5H_5^+$ ions formed from cycloheptatriene in the energy range of 12-50 eV show similar behavior in reactivity, i.e., the percent of unreactive $C_5H_5^+$ remains constant at 5% while in the norbornadiene case, the amount of unreactive ions increases to 20%,

indicating that $C_5H_5^+$ formed from the $C_5H_6^+$ channel has a higher percent of unreactive isomer.

The results of photodissociation of $C_5H_5^+$ ions using 6 different wavelengths (532 nm, 460 nm, 420 nm, 365 nm, 355 nm, and 266 nm) indicate that the dissociation energy of Reaction (2) is in the range of 420 - 365 nm (2.8 - 3.4 eV). This is in agreement with the calculated energy of dissociation based on thermochemical information. A schematic potential energy surface for the $C_5H_5^+$ system is shown in Figure 4.

$C_5H_5^+$ produced from different precursors exhibit two populations, reactive isomers and unreactive isomers. Photodissociation and chemistry of $C_5H_5^+$ and its photofragment, $C_3H_3^+$, implies that at least two different isomers of $C_5H_5^+$ exist within the pool of the "reactive isomers". Heat of formation of one isomer is estimated to be 255 kcal/mol with the activation energy for dissociation of about 3.4 eV. This isomer also reacts with diacethylene according to Reaction (5). The heat of formation of the other isomer is less than 255 kcal/mol and does not react according to Reaction (5). There may exist a third isomeric form of $C_5H_5^+$ which dissociates according to Reaction (2), but it produces a photofragment, $C_3H_3^+$, with different percentages of the reactive and unreactive isomers.

Figure 1

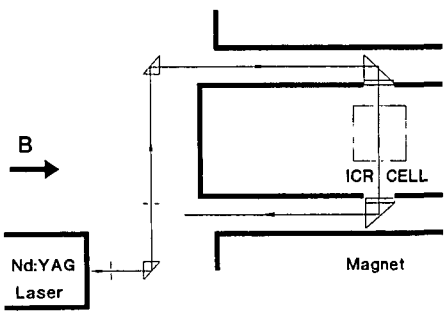

Figure 2

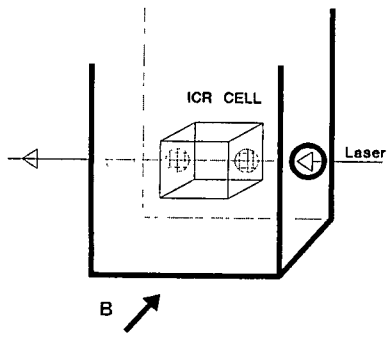

Figure 3

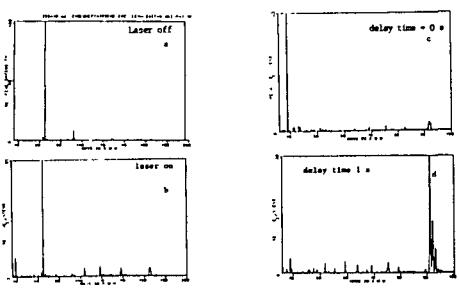

Figure 4

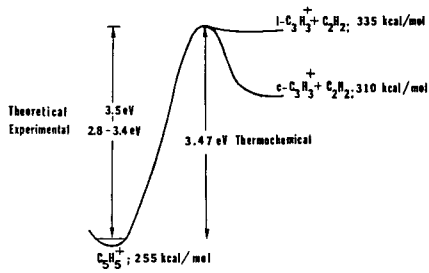

Presented at the 36th ASMS Conference on Mass Spectrometry and Allied Topics
June 5-10, 1988, San Francisco, CA

HIGH RESOLUTION LASER-ION BEAM PHOTODISSOCIATION STUDIES OF IONIC CLUSTER FRAGMENTS OF IRON CARBONYLS.

R.E. Tecklenburg, Jr., and D.H. Russell

Texas A & M University
Department of Chemistry
College Station, Texas 77843

The chemical and physical properties of ionic transition-metal species, e.g., monatomic bare and ligated metals, as well as dimer, trimer, and small metal clusters, have been the subject of intense research over the past decade.[a,b] There have been numerous recent studies that demonstrate the change in chemical reactivities as a function of cluster size and the dependence of the chemical reactions on the electron environment.[c,d] Recent studies also clearly indicate the existence of long-lived electronic states of metal ions and the importance of these species on chemical reactivities.[e,f] These studies demonstrate the need for additional information on the physical properties of transition-metal species, and how such properties influence the chemical reactivities of these species.

Previous work from this laboratory described various aspects of the production of ionic cluster fragments by ion-molecule reactions within an ICR cell.[g] A specific outgrowth of this work is the structure-reactivity relationships of ionic cluster fragments as a function of cluster size and metal-to-ligand ratios (M/L). The reactivities of some clusters were much less than expected based purely on M/L ratio considerations. Photodissociation is potentially useful for characterization of ionic cluster fragments, specifically metal-metal and metal-ligand binding energies, as a function of M/L ratios.[h] Thus, photodissociation provides an additional method for understanding the structure/reactivity relationships of ionic cluster fragments.

The results from laser-ion beam photodissociation studies of ionic cluster fragments of iron carbonyls are presented. Ionic cluster fragments of the type $Fe_x(CO)_y^+$ (x=1-3; y=0-6) are mass resolved by high resolution (R= 7500) prior to photodissociation in the third field-free region of an EBE tandem mass spectrometer. The ions studied are formed by the direct 70 eV electron impact of $Fe_3(CO)_{12}$. Relative photodissociation cross-sections and upper and lower limits to the bond dissociation energies for both Fe-CO and Fe-Fe bonds are reported.

Table I compares the average metal-ligand and metal-metal bond dissociation energies for the various $Fe_x(CO)_y^+$ ions (x=1-3; y=0-6). The metal-metal bond for Fe_3^+ is estimated to be <27.8 kcal/mol. The Fe_2^+ ion does not photodissociate over the wavelength range (458-514.5 nm), placing the lower limit for the bond dissociation energy

---

a Armentrout, P. B.; Beauchamp, J. L. *J. Am. Chem. Soc.* 1981, *103*, 6628.
b Jarrold, M. F.; Misev, L.; Bowers, M. T. *J. Phys. Chem.* 1984, *88*, 3928.
c Elkind, J. L.; Weiss, F. D.; Alford, J. M.; Laaksonen, R. T.; Smalley, R. E. J. Chem. Phys. in press.
d Freas, R. B.; Ridge, D. P. *J. Am. Chem. Soc.* 1984, *106*, 825.
e Reents, Jr., W. D.; Strobel, F.; Freas, R. B., III; Wronka, J.; Ridge, D. P. *J. Phys. Chem.* 1985, *89*, 5666.
f Elkind, J. L.; Armentrout, P. B. *J. Am. Chem. Soc.* 1986, *108*, 2765.
g Anderson Fredeen, D. J.; Russell, D. H. *J. Am. Chem. Soc.* 1985, *107*, 3762.
h Tecklenburg, Jr., R. E.; Russell, D. H. *J. Am. Chem. Soc.* 1987, *109*, 7654.

at <62.4 kcal/mol. These metal-metal bond energies determined are in agreement with those reported by Smalley.[i] Binding energies in the range 19.5-58.6 kcal/mol are found for metal-ligand bonds. In general, the metal-ligand bond energies for the $Fe_x(CO)_y^+$ species follow the same general trend as observed for $Mn_x(CO)_y^+$ and $Co_x(CO)_y^+$ systems also studied in this laboratory. That is, low metal-ligand bond energies of *ca.* 20 kcal/mol for small x/y ratios, and metal-ligand bond energies which increase to as much as 58 kcal/mol for $x/y \geq 1$. Note from Table I that the $Fe_3(CO)_4^+$ ion has as surprisingly large bond dissociation energy for the loss of one carbonyl ligand. The stability of the $Fe_3(CO)_4^+$ ion relative to other $Fe_3(CO)_y^+$ ions is supported by complimentary information derived from the high resolution collision-induced dissociation (CID) data of the same ions. For example, Figure 1 contains the CID spectra for the $Fe_3(CO)_{10}^+$ ion. Note the unusually large CID signal corresponding to the production of the $Fe_3(CO)_4^+$ daughter ion. Collision-induced dissociation of other $Fe_3(CO)_y^+$ ions (y=5-12) also reveal anonymously large $Fe_3(CO)_4^+$ daughter ion intensities suggesting the $Fe_3(CO)_4^+$ ion has an uncommon stability. This stability may be rationalized in terms of a different type of iron metal center-to-ligand bonding. For example, the carbonyl ligands in the $Fe_3(CO)_4^+$ ion may bind to the metal center through both the carbon and oxygen end of the carbonyl ligands (e.g., four electron donating ligands rather than two electron donating terminal and/or bridging ligands), thus increasing the Fe-CO binding energies.

Table XII. Bond dissociation energies measured from the crossed laser-ion beam photodissociation thresholds for $Fe_3(CO)_y^+$ ions.

TRANSITION	THRESHOLD		THRESHOLD ENERGY • BONDS BROKEN
	(nm)	(kcal/mole)	(kcal/mole)
$Fe_3(CO)_4^+ \longrightarrow Fe_3(CO)_3^+$	502	56.9	56.9
$Fe_3^+ \longrightarrow Fe_2^+$	>514.5	<55.6	<27.8[a]
$Fe_3^+ \longrightarrow Fe_2^+$	>514.5	<55.6	<55.6[b]
$Fe_3^+ \longrightarrow Fe^+$	<458	>62.4	>62.4
$Fe_3(CO)_3^+ \longrightarrow Fe_3(CO)^+$	488	58.6	19.5
$Fe_3(CO)_3^+ \longrightarrow Fe_3^+$	488	58.6	39.3
$Fe_3(CO)^+ \longrightarrow Fe_3^+$	488	58.6	58.6

[a] Triangular arrangement of three iron atoms assumed in the bond energy calculation.

[b] Linear arrangement of three iron atoms assumed in the bond energy calculation.

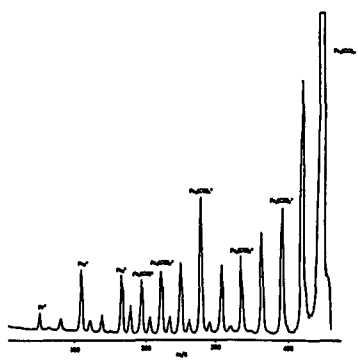

Figure 13. The $Fe_3(CO)_{10}^+$ ion activated by 8 keV high energy collisions with helium target gas. Note the large signal intensity for production of the $Fe_3(CO)_4^+$ daughter ion.

[i] Brucat, P. J.; Zheng, L. S.; Pettiette, C. L.; Yang, S.; Smalley, R. E. *J. Chem. Phys.* 1986, *84*, 3078.

Presented at the 36th ASMS Conference on Mass Spectrometry and Allied Topics
June 5-10, 1988, San Francisco, CA

STUDIES OF THE ACTIVATION AND DISSOCIATION OF DANSYL AND DINITROPHENYL DERIVATIZED PEPTIDES

R.E. Tecklenburg, Jr., and D.H. Russell

Texas A & M University
Department of Chemistry
College Station, Texas 77843

Tandem mass spectrometry has become an important analytical tool for identification and structural characterization of complex molecules. The use of tandem mass spectrometry in conjunction with fast atom bombardment (FAB) ionization[a] has many advantages for structural characterization of large biomolecules (m/z=1,000-2,000 amu), especially problems related to sensitivity and sample purification.[b,c] The intrinsic advantages for the combined use of FAB and tandem mass spectrometry is that the molecular ion, e.g., $[M+H]^+$, $[M-H]^-$, etc., of a thermally labile, polar molecule can be formed, and the mass-selected $[M+H]^+$ or $[M-H]^-$ ion can be subjected to collision-induced dissociation (CID). Structural information for the $[M-H]^+$ or $[M-H]^-$ ion can then be inferred from the collision-induced dissociation spectrum. However, the factors that control and influence the dissociation of large molecular weight species are not easily probed by CID. For example, the ion internal energy distributions and energy transfer accompanying CID of high molecular weight species are ill-defined and not well understood. Photodissociation offers an alternative to CID for the study of ion activation/dissociation, and the determination of ion structures.[d,e] Although photodissociation may develop as a method for structurally characterizing complex molecules,[f] our studies are designed to understand the underlying factors that influence dissociation.

The results of the laser-ion beam photodissociation studies for a series of derivatized amino acids and di- and tri-peptides are presented herein. The protonated molecular peptide ions are formed by fast-atom bombardment and photodissociated in the third field-free region of a EBE tandem mass spectrometer. Photoexcitation is performed using the visible (514.5 nm - 458 nm) and ultraviolet (385 nm - 333 nm) lines of a CW argon ion laser. Because peptides do not absorb at the visible and uv lines of the argon-ion laser, suitable chromophores (either the dansyl (uv chromophore) or dinitrophenyl group (uv and visible chromophore)) are attached to the N-terminus of the peptide. The times required for ions to undergo photodissociation are measured in the present study using a biased activation cell.[g]

---

[a] Barber, M.; Bordoli, R. S.; Elliott, G. J.; Sedgwick, R. D.; Tyler, A. N. *Anal. Chem.* 1982, *54*, 645A.

[b] Biemann, K.; Martin, S. A. *Mass Spectrom. Rev.* 1987, *6*, 1.

[c] Jensen, N. J.; Gross, M. L. *Mass Spectrom. Rev.* 1987, *7*, 1.

[d] Fukuda, E. K.; Campana, J. E. *Anal. Chem.* 1985, *57*, 949.

[e] Beynon, J. H.; Brenton, A. G.; Harris, F. M. *Int. J. Mass Spectrom. Ion Phys.* 1982, *45*, 5.

[f] Hunt, D. F.; Shabanowitz, J.; Yates, III, J. R. *J. Chem. Soc., Chem. Commun.* 1987, 548.

[g] Tecklenburg, Jr., R. E., Sellers Hann, M. L.; Russell, D. H. submitted to International Journal Mass Spectrometry and Ion Processes.

Presented at the 36th ASMS Conference on Mass Spectrometry and Allied Topics
June 5-10, 1988, San Francisco, CA

The relative photofragment ion yields and rates of photodissociation for individual reaction channels are reported for the DNP amino acids in Table I. The column labeled prompt (%) lists the percentage of the incident ions that undergo prompt dissociation following photoexcitation (dissociate entirely within the activation cell). The results of these studies can be generalized in the following manner: i) photoexcitation of the dinitrophenyl group by a visible photon results in cleavages within the peptide chain, with little cleavage within the chromophore (e.g. loss of DNP, NO_2, or NO); ii) photoexcitation of the dinitrophenyl group with uv radiation results in both cleavages within the chromophore as well as cleavages within the peptide chain, (but loss of NO, or NO_2 dominant the photofragment ion spectrum); and iii) the percentage of ions that undergo prompt photodissociation decreases in going from uv to visible wavelengths and as the mass of the incident ion increases. These results are rationalized by an "energy selective"[h] model for the dissociation of large ionic systems.

Table XVI. Photodissociation kinetic data, normalized metastable, CID, and photofragment ion yields for the $[M+H]^+$ ions of DNP amino acids.

	PHOTODISSOCIATION						CID		H^+	
	Visible			UV						
Channel	R.I.(%)	I/Σ I.(%)	Prompt.(%)	R.I.(%)	I/Σ I.(%)	Prompt.(%)	R.I.(%)	I/Σ I.(%)	R.I.(%)	I/Σ I.(%)
DNP-GLYCINE										
-NO_2	-	-	-	63	26	90	69	18	46	27
-CH_2CO_2H	-	-	-	35	24	75	-	-	-	-
-CO_2H	31	24	60	100	41	80	25	6	9	3
-OH	100	76	25	31	9	50	100	26	100	39
DNP-ALANINE										
-NO_2	-	-	-	26	11	75	92	30	71	39
$DNPNH_2^+$	-	-	-	38	16	70	8	2	-	-
-CO_2H-CH_3	67	29	35	100	42	60	71	16	3	3
-CO_2H	63	28	30	31	32	70	34	7	4	3
-CH_3	100	43	43	32	9	90	100	22	100	53
DNP-β-ALANINE										
-CH_2CO_2H	100	51	35	100	73	60	100	34	100	37
-OH	93	49	65	33	23	73	81	27	66	37
DNP-VALINE										
-NO_2	-	-	-	100	27	70	22	5	-	-
-CO_2H-CH_3	18	8	30	36	16	50	13	17	-	-
-CO_2H	40	17	35	72	30	55	100	23	68	47
-CH_3	100	43	35	73	30	65	-	-	-	-
-OH	76	32	40	65	17	65	96	22	100	53
DNP-LEUCINE										
-NO_2	-	-	-	80	33	35	13	3	-	-
$DNPA^+$	-	-	-	13	6	30	11	2	-	-
-CO_2H-CH_3	60	26	30	27	11	35	73	16	-	-
-CO_2H	100	43	30	100	41	40	98	22	54	45
-CH_3	71	31	30	33	9	30	-	-	-	-
DNP-ISOLEUCINE										
-NO_2	-	-	-	100	36	30	18	4	-	-
$DNPNH_2^+$	-	-	-	29	10	45	19	3	-	-
-$CH_2CH_3CH_3$	96	33	25	54	22	40	-	-	-	-
-CO_2H-CH_3	30	17	25	68	17	35	66	15	-	-
-CO_2H	100	33	25	42	11	45	100	22	100	53
-CH_3	36	18	30	53	14	45	-	-	-	-
DNP-METHIONINE										
-NO_2	100	29	25	100	61	40	10	2	-	-
-NO	23	9	45	42	26	55	-	-	-	-
$DNPNH_2^+$	41	12	0	-	-	-	14	3	-	-
R^+	79	33	0	-	-	-	72	17	-	-
-R	36	16	25	21	13	30	14	3	-	-
$RCHOH_2^+$	37	11	30	-	-	-	10	3	-	-
DNP-PHENYLALANINE										
-NO_2	-	-	-	100	30	45	19	2	-	-
-NO_2-OH	-	-	-	34	7	35	33	6	-	-
-$DNPNH_2$	33	15	30	49	13	40	-	-	-	-
$DNPNHCH_2^+$	-	-	-	30	9	30	80	8	-	-
R^+	18	6	25	34	7	35	93	15	-	-
-R	-	-	-	34	11	35	60	7	-	-
-R-OH	26	11	30	-	-	-	-	-	-	-
-CO_2H	49	25	30	-	-	-	100	12	100	34
-OH	100	44	25	72	31	40	67	8	-	-
DNP-TRYPTOPHANE										
-NO_2-OH	-	-	-	27	17	45	-	-	-	-
-$DNPNH_2$	100	71	25	100	63	30	100	46	100	66
R^+	41	29	30	23	18	45	40	42	10	7

h Chen, J. H.; Dunbar, R. C. *Int. J. Mass Spectrom. Ion Proc.* **1986**, *72*, 115.

Presented at the 36th ASMS Conference on Mass Spectrometry and Allied Topics
June 5-10, 1988, San Francisco, CA

Laser-Ion Beam Photodissociation Utilizing A Biased Activation Cell

L. Sellers-Hann, R. E. Tecklenburg, and D. H. Russell

Texas A&M University
Department of Chemistry
College Station, TX 77843

Although the sensitivity and dynamic range of photodissociation measurements performed on an ion-beam apparatus are much better than for ion cyclotron resonance, photofragment ion yields are low and long data acquisition times are required. The laser-ion beam photodissociation experiment is complicated by the presence of background signals from metastable and/or collision-induced dissociation reactions. In order to study a photodissociation process free from metastable and/or collision-induced dissociation background, the photon source must be modulated by a mechanical chopper and the photofragment ion signal is monitored in phase with the laser modulation. In cases where the photofragment ion signals are weak and the background signal is large, long data acquisition times are necessary to achieve adequate signal-to-noise ratios (i.e. >10). An objective of this paper is to show a method that can help reduce the background signal associated with metastable background.

The laser-ion beam photodissociation experiment has been modified to utilize a biased activation cell (Fig. 1) for signal-to-noise enhancements. The biased activation cell acts as a symmetrical einsel lens and decelerates the ions as they enter the cell and then accelerates them as they exit the cell. The net effect is a change in the kinetic energy of the ions that dissociate with in the activation cell , thus product ions formed in the activation cell are separated from ions which dissociate in the field-free region. For example, ions which undergo photodissociation within the biased activation cell (B^*) have a kinetic energy defined by $[(m_2/m_1)V + (1-(m_2/m_1))V']$,[1] while ions dissociating outside the cell (A^*) have a kinetic energy defined by $[(m_2/m_1)V]$, where V is the main beam accelerating voltage, and V' the biased cell voltage. The principle advantage of the biased activation cell for photodissociation studies is the separation of the metastable ion dissociation signal (noise) from the photodissociation signal. This gives an overall reduction in the metastable ion signal by *ca.* a factor of 20.

Signal-to-noise enhancements are most realized for transition metal compounds as they dissociate promptly (<≈50 ns). As an example, a S/N enhancement from 2.3 to 44 is achieved for the photofragment ion yields for cleavage of the Mn-Mn bond of $Mn_2(CO)_{10}^+$ and data collection times are reduced from 6.7 minutes to 1.7 minutes for this system using the biased activation cell. This example shows that the poor signal-to-noise ratios for the photofragment ion signal obtained without biasing the activation cell is a result of the metastable background rather than instrument noise. The utility of the biased activation cell technique is the increased sensitivity for weak photofragment ion signals. Thus, improvements in peak heights/peak areas measurements (used in the calculation of photodissociation cross-sections) as well as photodissociation threshold measurements (used to determine bond dissociation energies) can be obtained.

The biased activation cell also provides a means of distinguishing between ions that dissociate promptly (within the biased activation cell) and those which are longer lived (dissociate outside the biased activation cell). This allows for the measurement of the fraction of prompt/slow photofragmenting ions thus, providing dissociation rates to be estimated. For example, photodissociation rates of $>5.6\times10^6\ s^{-1}$ and $5.6\text{-}0.29\times10^6\ s^{-1}$ can be specified for a 500 amu ion (V=8 kV, V'≈1 kV) photodissociating within the activation cell (length=1.9 cm) and between the exit of the activation cell and entrance to the second electrostatic analyzer (length=19.4 cm), respectively. Slow dissociation reactions occur most often for hydrocarbons that have excited states lying close to the dissociation threshold or for ions that undergo isomerization prior to dissociation. An example of such an ion is the 1,3-butadiene ion that has its first excited state *ca.* 0.1 eV below the dissociation threshold for loss of the methyl radical and this ion shows both prompt (64%) and slow (36%) dissociation.

Presented at the 36th ASMS Conference on Mass Spectrometry and Allied Topics
June 5-10, 1988, San Francisco, CA

It is interesting to compare the ratio of prompt to slow photodissociation reactions (Table I). For example, trans,trans-2,4-hexadiene, cis,trans-2,4-hexadiene, and cis,cis-2,4-hexadiene ions photodissociate to form $C_5H_7^+$ and $C_4H_6^{+\cdot}$. For the $C_6H_{10}^{+\cdot}$ isomers the prompt/slow photodissociation ratios give an indication for isomer differentiation. For example the trans,trans-2,4-hexadiene prompt/slow ratios ($C_5H_7^+$, 51/49; and $C_4H_6^{+\cdot}$, 79/21) differ significantly from the cis,trans-2,4-hexadiene ($C_5H_7^+$, >95/<5; and $C_4H_6^{+\cdot}$, 65/35), and cis,cis-2,4-hexadiene ($C_5H_7^+$, >95/<5; and $C_4H_6^{+\cdot}$, 69/31). In an earlier paper these $C_6H_{10}^+$ isomers were differentiated on the basis of kinetic energy release data for the photofragment ions.[2] The isomer dependent kinetic energy release values were interpreted in terms of the photoexcited trans,trans-2,4-hexadiene ions undergoing a slow rearrangement reaction prior to dissociation. The prompt/slow photodissociation ratio data for the $C_6H_{10}^{+\cdot}$ isomers is also consistent with the previous explanation.

The biased activation cell has utility for the laser-ion beam photodissociation experiment especially in the area of signal-to-noise enhancement. The signal-to-noise enhancement is realized most for those ions that dissociate promptly. Also, the kinetics data for photodissociation may be of considerable interest from a fundamental point-of-view and may have analytical utility as well.

---

[1] Morgan, R. P.; Beynon, J. H; Bateman, R. H.; Green, B. N. *Int J. Mass Spectrom. Ion Phys.* 1978, *28*, 171.

[2] Krailler, R. E.; Russell, D. H. *Anal Chem* 1985, *57*, 1211.

BIASED ACTIVATION CELL

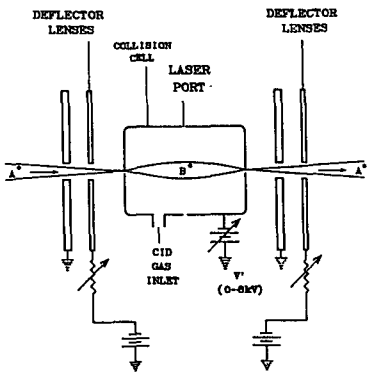

Table I: Relative percent of "prompt" and "slow" photodissociation fragments for the 2,4-hexadiene isomers.

Molecule	Transition	Relative Percent Photodissociation Prompt	Slow
trans,trans-2,4-hexadiene	82 --> 54	79	21
	82 --> 67	51	49
cis,trans-2,4-hexadiene	82 --> 54	>95	<5
	82 --> 67	65	35
cis,cis-2,4-hexadiene	82 --> 54	>95	<5
	82 --> 67	69	31

Presented at the 36th ASMS Conference on Mass Spectrometry and Allied Topics
June 5-10, 1988, San Francisco, CA

COLLISION-INDUCED DISSOCIATION REACTIONS OF DOUBLY-CHARGED IONS OF POLYCYCLIC AROMATIC HYDROCARBONS#

R.K. Boyd, W.D. Jamieson and P.G. Sim

Atlantic Research Laboratory
National Research Council of Canada
1411 Oxford St., Halifax, Nova Scotia, CANADA B3H 3Z1.

In a largely unsuccessful attempt to achieve isomer distinction for PAHs via tandem mass spectrometry of their molecular dications, a striking difference was noted between these spectra for "large" and "small" PAHs. Small PAH dications undergo charge separation reactions and (for collisionally activated spectra) electron capture (both dissociative and non-dissociative). Large PAH dications, however, preferentially expel small neutral molecules such as C_2H_2, C_4H_2 and, at higher collision energies, even free radicals such as $CH_3\cdot$ and $C_2H_5\cdot$. These trends are illustrated by Fig. 1, which compares MIKE spectra for benzo[b]fluoranthene as a typical large PAH and for furan as a small PAH (benzene is not suitable for this comparison since the $C_6H_6^{2+}$ ion is dominated by the $C_3H_3^+$ fragment ion).

These trends have been studied using a tandem hybrid instrument of BEqQ configuration (VG Analytical ZAB-EQ) at both high collision energies MIKES and in the range 50 - 400 eV (qQ). Though this work will be reported separately, the following trends can be summarized here:

(a) The dominant unimolecular reaction of dications of large PAHs is expulsion of neutral acetylene; this reaction is the most sensitive to isomeric structural differences.
(b) Below about m/z 70 the fragment spectra are essentially identical for all large PAHs studied (anthracene, phenanthrene and larger); this suggests some common intermediate(s) in the fragmentation pathways (see Pachuta et al., J. Am Chem. Soc. 110, 657 (1988), for similar discussion of the monocations) leading to the ion series $C_nH_m^{2+}$ for m = 2, 4, 6 and n even.
(c) The qualitative difference between large and small PAHs can be rationalized in terms of different means of avoiding anti-aromaticity (4n pi-electrons, see Moran et al., Org. Mass Spectrom. 16, 92 (1981)) in the dications. Small PAHs, e.g. benzene, form aromatic cyclopropenium structures amenable to charge separation reactions (Lammertsmaa et al., J. Am. Chem. Soc. 105, 1049 (1983)). Larger aromatic systems can form diradical dication structures (McLafferty et al., Chem. Commun. 533 (1967)) from which radical site initiated reactions (including radical loss) can occur.
(d) The monoradical fragment dications observed in this work all contain odd numbers of carbon atoms, in agreement with previous work on ion-source reactions (2E mass spectra, Ast et al., Org. Mass Spectrom. 6, 749 (1972)); it seems likely that a similar interpretation applies here.

Although necessarily speculative these mechanistic proposals can rationalize the present observations. A more complete account will be published elsewhere.

NRCC No. 29013

Presented at the 36th ASMS Conference on Mass Spectrometry and Allied Topics
June 5-10, 1988, San Francisco, CA

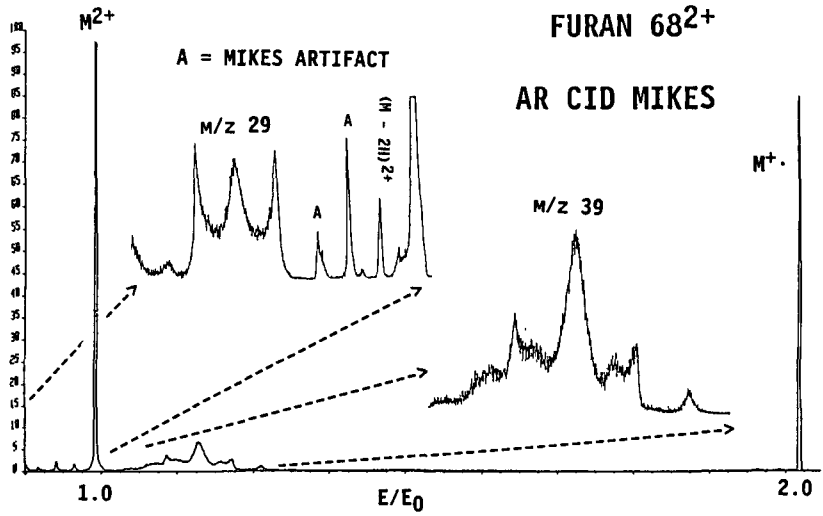

FIGURE 1

BENZO [B] FLUORANTHENE 252^{2+}

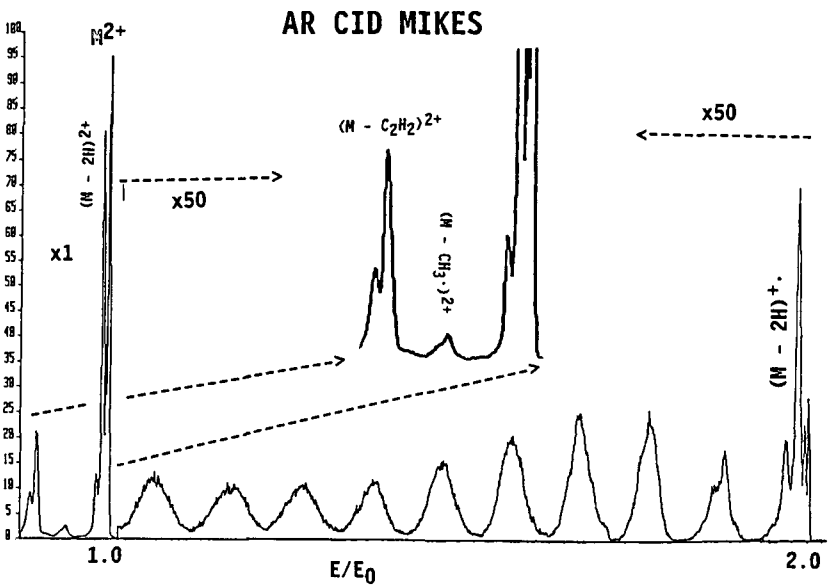

Presented at the 36th ASMS Conference on Mass Spectrometry and Allied Topics
June 5-10, 1988, San Francisco, CA

THE DISSOCIATION DYNAMICS OF ION-DIPOLE COMPLEXES: HCL LOSS FROM ETHYL CHLORIDE

J.C.Morrow, Tomas Baer, and Jian-Dong Shao

Department of Chemistry
University of North Carolina, Chapel Hill, N.C. 27599-3290

The dissociation rates of energy selected ethyl chloride ions are known from the measurements made by Tsai, Werner, and Baer (1) using the technique of photoelectron photoion coincidence (PEPICO). The present experimental investigation of CH_3CH_2Cl and CD_3CH_2Cl has shown that the activation energy for the loss of DCl from the deuterated parent ion is 0.13 eV higher than the activation energy for the non-deuterated ion. This difference, which is three times the shift arising from the difference in the zero point energies, is probably a result of the H atom transfer in a tunneling mechanism. Thus the tunneling is inhibited in the case of the deuterated compound. The dissociation rates, which are measured as a function of the ion internal energy, have two components, with the slower component in the 10^6 sec^{-1} range near the dissociation threshold. This rate is orders of magnitude less than that expected on the basis of the statistical theory (Rice-Marcus/quasiequilibrium theory).

The dissociation mechanism has been investigated by ab initio calculations at the MP2/6-31G* level. These results show that the ethyl chloride ion rearranges to a more stable ion-dipole complex configuration which is 0.27 eV (when zero point energies are used) more stable than the dissociation products HCl and $C_2H_4^{+\cdot}$. It is thus more stable than the ethyl chloride ion itself by about 0.19 eV. Calculations also show that the ethyl chloride molecule experiences a considerable change in geometry upon ionization. As discussed previously (2) for the case of the n-propanol ion dissociation, the dissociation from the ion-dipole complex is slow because of the long range interaction potential between the ion and the dipole.

This work was supported by the National Science Foundation, the Pittsburgh Supercomputing Center, and the Computation Center of the Technical University of Berlin.

References

(1) B. P. Tsai, A. S. Werner, and T. Baer, J. Chem. Phys. 63, 4384 (1975)

(2) J.-D. Shao, T. Baer, J. C. Morrow, and M. L. Fraser-Monteiro, J. Chem. Phys. 87, 5242 (1987)

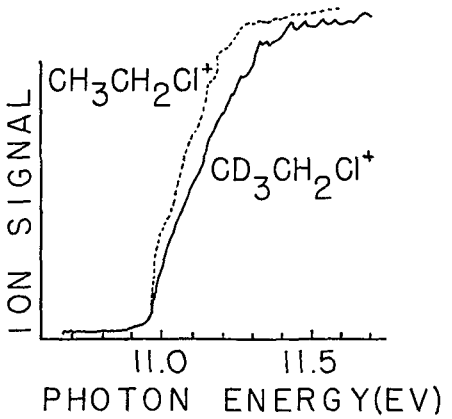
ION SIGNAL
$CH_3CH_2Cl^+$
$CD_3CH_2Cl^+$
11.0
11.5
PHOTON ENERGY(EV)

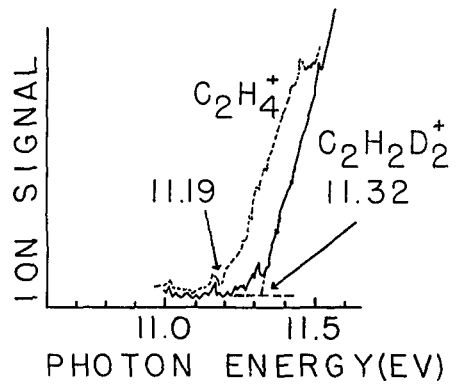
ION SIGNAL
$C_2H_4^+$
$C_2H_2D_2^+$
11.19
11.32
11.0
11.5
PHOTON ENERGY(EV)

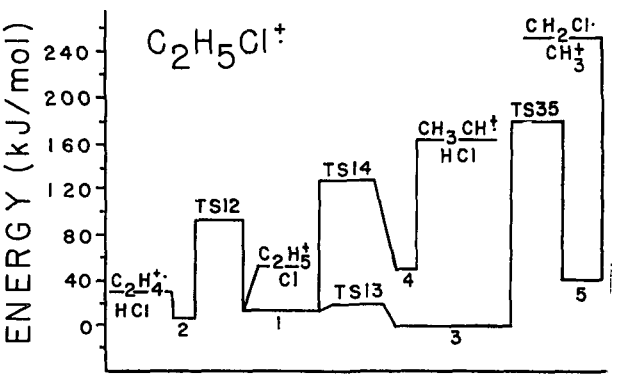
ENERGY (kJ/mol)
240
200
160
120
80
40
0
$C_2H_5Cl^+$
$C_2H_4^{+\cdot}$
HCl
2
TS12
$C_2H_5^+$
Cl
1
TS14
TS13
4
3
CH_3CH^+
HCl
TS35
$CH_2Cl\cdot$
CH_3^+
5

Presented at the 36th ASMS Conference on Mass Spectrometry and Allied Topics
June 5-10, 1988, San Francisco, CA

SOLID FAB MS AND FAB MS/MS FOR THE GENERATION AND STUDY OF SOME UNUSUAL SPECIES

K. Caldwell[2], E. Davoli[1], and M.L. Gross[2].

(1) "Mario Negri" Pharmacological Research Institute, Via Eritrea 62, Milano, Italy; (2) Midwest Center for Mass Spectrometry, Dept. of Chemistry, University of Nebraska, Lincoln, NE 68588.

Fast Atom Bombardment (FAB) is a technique generally used for the desorption of large organic molecules. A liquid matrix is used in order to, at least in part, prevent the extensive radiolytic damage produced by the atom beam. To study extremely nonvolatile inorganic species we have used matrixless FAB conditions and MS/MS along with high resolution peak matching. Under these conditions (solid FAB) it is also possible to detect, isolate, and study ions that are normally suppressed or that readily react with the matrix.

Spectroscopic studies of extremely nonvolatile materials are generally done by heating the sample to obtain a sufficient vapor pressure. Mass spectrometry may be performed with subsequent ionization of these neutrals. However, for metal alloys composed of metals with differing vapor pressures, as well as for salts, practical difficulties exist for obtaining gas phase ions. Under solid FAB conditions we have observed the species listed in Table 1.

Experiments were carried out on a Kratos Triple Analyzer. The instrument is equipped with an Ion Tech FAB gun operated normally at 6 kV with a discharge current of 6 mA. The MS/MS spectra are MIKES CAD spectra obtained scanning ESA 2. The pressure in the collision cell was raised until the main beam was suppressed by 30%. The target gas was Helium.

Aqueous solutions of alkali halides are deposited on the probe tip and dried in vacuo. Generally low resolution is sufficient in MS1 to produce a clear, interference free spectra. All spectra are MIKES spectra and parent ions are collisionally activated since these species do not decay metastably. For certain species, such as F^+, it is necessary to remove completely the water of hydration in an oven in order to have a sufficiently intense ion. Less than a milligram of salt on the probe will produce a steady current for several hours.

The CAD spectra (Fig. 1 and 2) of these molecular radical ions confirms their compositions. The high precision of the ESA scans allows measurements of the products with a precision sufficient to show a logarithmic trend (Fig. 3). It is shown that solid FAB offers a means for producing ions of unusual species from refractory precursors. FAB MS/MS can be used to characterize and study these ions. CAD MIKES spectra, as well as energetic measurements, provide information on the mechanism of the dissociation. Experiments are currently under way.

Presented at the 36th ASMS Conference on Mass Spectrometry and Allied Topics
June 5-10, 1988, San Francisco, CA

X^+	M^-
$MX^{+\cdot}$	$MX^{-\cdot}$
M^+	X^-
$M^{\prime}M^{+\cdot}$	$X^{\prime}X^{-\cdot}$
$M^{*}M^{+\cdot}$	$X^{*}X^{-\cdot}$

Table 1. Ions formed under solid FAB conditions.
M = Alkali metal
X = Halogen
* indicates a different isotope
' indicates a different metal or halogen

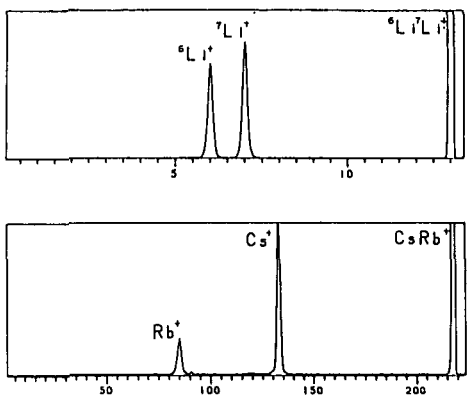

Fig.1 Example of CAD spectra of A) homo and B)heteronuclear molecular diatomic alkali metal radical cation.

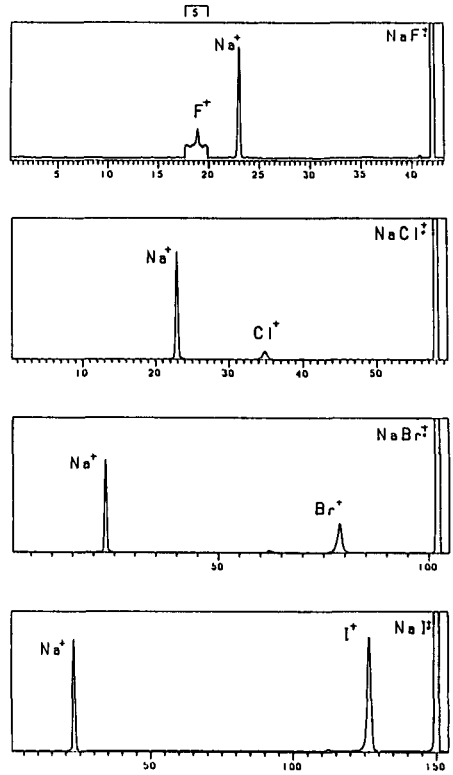

Fig.2. CAD spectra of the $NaX^{+\cdot}$ series.

ln[M+/X+] vs. THE DIFFERENCE IN THE IONIZATION POTENTIALS OF THE METAL MINUS THE HALOGEN

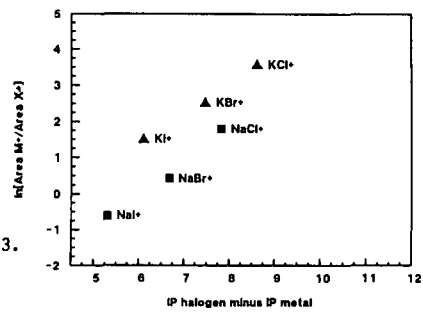

Fig. 3.

Presented at the 36th ASMS Conference on Mass Spectrometry and Allied Topics
June 5-10, 1988, San Francisco, CA

A GEOMETRIC MODEL FOR THE DECONVOLUTION OF ION KINETIC ENERGY SIGNALS

G.K. Koyanagi† and R.E. March, Trent University, Peterborough, ON, Canada, K9J 7B8
† Registered at Queen's University, Kingston, ON, Canada, K7L 3N6

Much kinetic and energetic data have been extracted from generalized examinations of the shape of Mass-analysed Ion Kinetic Energy (MIKE) signals. There exist several approximate formulae to determine the mean kinetic energy, <T>, released in a unimolecular fragmentation reaction from a measure of the width of the MIKE signal [1]. The deconvolution of MIKE signals to the associated Kinetic Energy Release Distribution (KERD) is a more complex process which can yield more descriptive kinetic and energetic data.

In 1974 Terwilliger *et al.* [2] produced an excellent model for describing the trajectory of ions through the electric sector of a reversed geometry mass spectrometer. In the above work several extensions were discussed which could increase the accuracy of the geometric model and extend the applicability of the deconvolution process. Recently, Rumpf and Derrick [3] have examined some of the extensions discussed by Terwilliger *et al.* and have produced an improved model. Since the deconvolution process is iterative; where the KERD is slowly refined to reproduce the experimentally observed peak shape, minimized computational time is paramount. Rumpf and Derrick reduced computational time by utilizing an approximated 'basis set' description of variables intermediate in the calculation. Also, the model by Rumpf and Derrick accounted for fragmentation reactions occurring before the intermediate slit in the second field free region, a necessary extension to the original model by Terwilliger *et al.*

A major failure of the original model by Terwilliger *et al.* was the prediction that the peak should be symmetric about the mean electric sector potential. The model produced by Rumpf and Derrick predicts that the high energy side of a dish-topped peak is slightly more intense than the low energy side. Rumpf and Derrick attributed this to decompositions occurring within the electric sector.

In the model presented, briefly here and in detail in reference [4], the major extensions consider: (i) fragmentations occurring along the entire length of the 2ndFFR, (ii) the difference in ion beam intensity before and after the intermediate slit, and (iii) the slight difference in angular acceptance between forward scattered and backward scattered product ions. In addition, several mathematical approximations have been introduced which speed, greatly, the computation of a theoretical peak shape. In all cases the accuracy of each approximation was found to be better than 1 part in 10^6.

To calculate contributions to the MIKE signal for fragmentation reactions occurring before the intermediate slit of the 2ndFFR, the angular acceptance, (in the x-y plane) of the intermediate slit must be considered simultaneosly with the angular acceptance of the electric sector collector slit. Figure 1 is a schematic representation of the determination of $\Delta\varsigma$, the angular acceptance of the intermediate slit, here u_2 is the velocity of the product ion relative to the centre-of-mass and v_1, the initial velocity of the reactant ion. In Figure 1 the magnitude of v_1 has been reduced to accentuate the difference in angular acceptance for forward and backward projected fragment ions. It should be noted that the model presented here also correctly predicts that the high energy horn of a dished peak is of greater intensity than the low energy horn, based solely on the difference in angular acceptance at the intermediate slit.

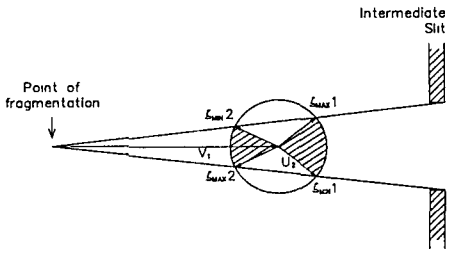

Figure 1. Schematic representation for the determination of $\Delta\varsigma$. The magnitude of v_1 has been reduced to accentuate the difference in $\Delta\varsigma$ between forward and backward fragmentations.

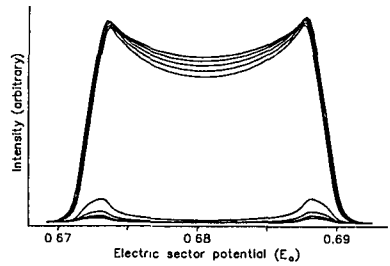

Figure 2. Plots of intermediate peak shapes for the nine selected points of fragmentation along the second field free region.

Logically, from Figure 1, there will also exist a difference in angular acceptance between forward and backward fragmentations in the z-direction, which also contributes to the asymmetry of the MIKE signal. All three models discussed here do not account for this as it would increase the computational time required by at least ten-fold. Fortunately, however, owing to the typically large height of z-direction restrictions to the ion beam the relative difference in angular acceptance is small, and therefore adds little to the asymmetry of the MIKE peak.

In practice it was found that a numerical integration of nine theoretical peak shapes calculated along the length of the 2ndFFR gave satisfactory results. Increasing the numerical integration to fifteen points along the 2ndFFR gave similar results and almost doubled the computational time required. In Figure 2 are presented plots of the intensity profiles of nine typical intermediately calculated peak shapes, the ordering is from magnet exit to electric sector enterance in ascending intensity. In the numerical integration of the intermediate peaks along the 2ndFFR a weighting factor must be applied to peaks originating before the intermediate slit to account for the removal of ions from the main beam at the intermediate slit.

Also, the algorithm allows for the expression of the KERD as either a step function in T, or as a polynomial function of T. If the KERD can be described sufficiently well by a polynomial the calculation time can be reduced by up to half.

References

1. J.L. Holmes and J.K. Terlouw, Organic Mass Spectrom., **15**(1980)383–396.
2. D.T. Terwilliger, J.F. Elder Jr., J.H. Beynon and R.G. Cooks, Int. J. Mass Spectrom. Ion Physics, **16**,(1975)225–242.
3. B.A. Rumpf and P.J. Derrick, Int. J. Mass Spectrom. Ion Processes, **82**(1988)239–257.
4. G.K. Koyanagi M.Sc. Thesis, Department of Chemistry, Queen's University, Kingston, ON, Canada. (1988).

Presented at the 36th ASMS Conference on Mass Spectrometry and Allied Topics
June 5-10, 1988, San Francisco, CA

Directional Properties in Photodissociation Studied in a Laser TOF-MS System

P.Marcus, I.Platzner, N.R.C.Negev, Div. of Chemistry,
I.Bar & S.Rosenwaks;Dept. of Physics, Ben-Gurion Univ. of the Negev,
Beer-Sheva Israel.

Introduction: Any initial velocity and spatial distribution of ions in a time of flight mass spectrometer source will be reflected in the ion peak profile, unless a compensation method like "time delay"[1] or "reflectron technique" [2,3] is used. These profile changes can be monitored if a recording system of sufficiently high time resolution is used. The photofragment spectroscopy with mass spectrometric detection has the advantage of not being restricted to small photofragments with accurately known spectroscopic properties, as laser induced fluorescence (LIF) requires, and hence such studies have aroused a growing interest[4]. In view of the recent application of TOF-MS in this field, experiments have mainly been involved in verifying and complementing the results obtained thus far by the LIF method[5-9].
NO produced following the photodissociation of tert-Butylnitrite (TBN) by a pulsed polarized laser at 266, 355 and 532 nm in a time-of-flight mass spectrometer[10,11] showed an anisotropic spatial velocity distribution. The dynamics of the photodissociation process and, in particular, its directional properties are discussed in view of these experimental results.
Experimental: The laser beam was focused into the center of the mass spectrometer ionization cell by a 20 cm focal length, plano-convex quartz lens. The laser energy varied between 5-85, 1-19, and 0.15-6.5 mJ, for 532, 355 and 266 nm, respectively. Mass spectra of TBN were obtained at 266, 355 and 532 nm as a function of sample pressure and laser power at two perpendicular laser polarization directions, one parallel and one perpendicular to the ions' flight direction (hereafter referred to as parallel and perpendicular polarization, respectively). For more details see Ref.10&11.
Results and discussion: A splitting of the NO fragment ion peak profile depending on the polarization direction of the laser beam was observed . The split peak has a trough coinciding with the apex of the NO ion peak originating from pure NO. At 532 nm and 266 nm with parallel laser polarization the peak is split, while at 355 nm the same effects are observed with perpendicular laser polarization (see figs.1&2). The kinetic energy of the NO fragment formed in the laser source was evaluated by comparing the pure NO and the fragment NO kinetic energy obtained for the same laser flux (10^{10} W/cm^2) at 532nm, 355nm, and 266nm. From energy balance calculations we conclude that at 532nm , the fragmentation takes place as a result of a two photon resonant absorption process, although one photon is enough to cause dissociation (~1.7eV[12]). The NO fragment peak profile dependence on the laser polarization direction is attributed to the vector correlation between the transition dipole moment of TBN and the NO fragment velocity direction. It indicates, that the CONO skeleton of the excited TBN is planar, and its life time is shorter than the rotation period. At both 532 and 266 nm the transition dipole moment is parallel to the CONO skeleton, while at 355 nm the transition dipole moment is perpendicular to the CONO skeleton. These findings are similar to the results obtained for methylnitrite in the same wavelength region[6,9] and also correspond to the LIF results[13,14] obtained in our laboratory at 250, 351.8 and 363.5 nm.

Conclusion: Using a TOF-MS in conjunction with a laser, vector correlation measurements and kinetic energy balance are relatively easy to perform. The results provide information about the excited parent molecule symmetry properties and its lifetime and about the mechanism by which it fragments.

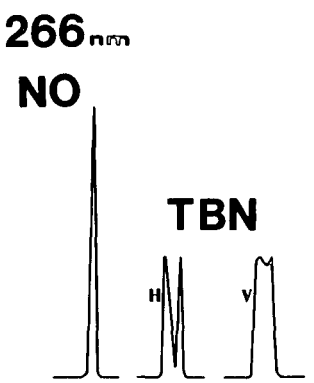

Fig. 1

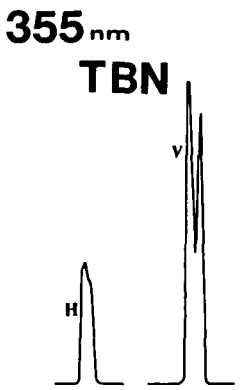

Fig. 2

m/e=30 ion peak profiles in high resolution spectra of NO gas and TBN, Fig. 1 at 266nm and Fig. 2 at 355nm.
"H" & "V" design the two perpendicular laser field polarization directions.

REFERENCES

1 W.C. Wiley and I. H. McLaren, Rev. Sci. Instr., **26** (1955) 1150.
2 B.A. Mamyrin, V.I. Karataev, D.V. Shmikk and V.A. Zagulin, Sov. Phys. JETP., **37** (1973) 45.
3 E.W. Schlag and H.J. Neusser, Acc. Chem. Resch.,**16** (1983) 355.
4 H.J. Neusser, Int. J. Mass Spectrom. and Ion Proc.,**79** (1987) 141.
5 B.A. Keller, P. Felder and J.R. Huber, Chem. Phys. Lett.,**124** (1986) 135.
6 B.A. Keller, P. Felder and J.R. Huber, J. Phys. Chem.,**91** (1987) 1114.
7 G.E. Hall, N. Sivakumar, R. Ogorzalek, G. Chawla, H.-P. Haerri, P.L. Houston, I. Burak and J.W. Hepburn, Faraday Discuss. Chem. Soc.,**82** (1986) 13.
8 R. Ogorzalek, G.E. Hall, H.-P. Haerri and P.L. Houston, J. Phys. Chem., **92** (1988) 5.
9 G. Inoue, M. Kawasaki, H. Sato, T. Kikuch, S. Kabayashi and T.J. Arikawa, Chem. Phys., **87** (1987) 5722.
10 P. Marcus, I. Platzner, I. Bar and S. Rosenwaks, Int. J. MS and Ion Phys., **82** (1988) 319.
11 P. Marcus, I. Platzner, I. Bar and S. Rosenwaks, J. Chem. Phys, in preparation .
12 L. Batt and R.T. Milne, Intern. J. Chem. Kinet.,**8** (1976) 59.
13 R. Lavi, D. Schwartz-Lavi, I. Bar and S. Rosenwaks, J. Phys. Chem., **91** (1987) 5398.
14 D. Schwartz-Lavi and S. Rosenwaks, J. Chem. Phys. 1988, in press.

Presented at the 36th ASMS Conference on Mass Spectrometry and Allied Topics
June 5-10, 1988, San Francisco, CA

REACTION-INDUCED MASS DISCRIMINATION IN XQQ INSTRUMENTS: Absolute Cross Sections for $N_2^+ + SF_6 \rightarrow N_2 + SF_x^+$ (x=1-5)

Richard I. Martinez
Center for Chemical Physics
National Bureau of Standards
Gaithersburg, MD 20899

and

B. Ganguli
Department of Chemistry
Georgetown University
Washington, DC 20057

ABSTRACT

Dynamically-correct branching ratios can be measured in a XQQ tandem mass spectrometer (MS/MS) under single-collision conditions when the key MS/MS parameters are properly selected to correct for reaction-induced mass discrimination within the rf-only quadrupole mass filter (Q2). The energy dependence of the cross section, $\sigma(E)$, for the reaction $N_2^+ + SF_6 \rightarrow N_2 + SF_x^+$ (x=1-5) was measured in the NBS triple quadrupole (QQQ) tandem mass spectrometer. Identical $\sigma(E)$ were measured from both the rate of reactant ion decay and the rate of product ion formation. Therefore, these σ values are substantially free from kinetic interferences (i.e., no back reactions, no impurity reactions, no scattering losses, minimal fringing fields, no mass discrimination, well-defined gas target, etc.). Moreover, there is probably no significant systematic error in our measurements of the absolute σ values for $N_2^+ + SF_6 \rightarrow N_2 + SF_x^+$ (x=1-5) because the σ values we measured with this same technique for $Ne^+ + Ne \rightarrow Ne + Ne^+$, $Ar^+ + Ar \rightarrow Ar + Ar^+$, and $Ar^+ + N_2 \rightarrow Ar + N_2^+$ agreed well with literature values obtained with several well-established techniques.

INTRODUCTION

XQQ instruments (QQQ, BEQQ hybrid, etc.) are complex ion-optical devices.[1-7] Instrument parameters affect the observed ion distribution. Therefore, the observed ion abundances may not accurately reflect the molecular dynamics of a reaction occurring within Q2. That is, instrument-dependent spectra will be observed [8].

To develop an instrument-independent MS/MS database (library) for XQQ instruments one must obtain an undistorted (dynamically-correct) representation of any reaction studied within such instruments [8]. The prerequisites for obtaining dynamically-correct branching ratios within XQQ instruments have been detailed elsewhere [8].

Of special concern is the reaction-induced "mass discrimination" which is intrinsic to XQQ instruments [8]. When reaction occurs within Q2, the mass changes from that of the reactant (projectile) ion, m_{react}, to that of the product ion, m_{prod}. Any ion will follow an unstable trajectory when its Mathieu parameter q exceeds 0.908 (the stable-trajectory limit) [4]. Thus, when CAD experiments are carried out in XQQ instruments, low-mass daughters are not detected when $m_{prod} < m_{react} \cdot q_{react}/0.908$ within Q2. However, $q_{prod} < q_{react}$ when $m_{prod} > m_{react}$. Then, product ions will always follow stable trajectories within the Q2Q3 structure (so long as $q_{react} < 0.908$).

In this study of the dissociative charge-transfer reaction $N_2^+ + SF_6 \rightarrow N_2 + SF_x^+$ (x=1-5) we assess the complex interplay among the key MS/MS parameters [8] under optimum dynamical conditions (i.e., when $m_{prod} > m_{react}$). Note that SF_6^+ product ion is never observed; it always predissociates to SF_5^+.

EXPERIMENTAL

All experiments were carried out in the NBS QQQ instrument.[9] Briefly, the instrument consists of (i) a standard electron impact ionizer, (ii) three standard quadrupole rod assemblies (Q1, Q2, Q3) operated in phase at 1.2 MHz and mounted in tandem on a special multipurpose track, and (iii) a continuous-dynode electron multiplier which incorporates a conversion dynode. Q2 is surrounded by a collision chamber enclosure.

Reaction cross sections σ were derived by using equations (1)-(3), etc. with reference to the following reaction sequence.

$$A^+ + B \rightarrow C^+ + S \qquad [\alpha\sigma]$$
$$\rightarrow D^+ + T \qquad [\beta\sigma]$$
$$\text{etc.}$$

$$\text{Ln } Y \equiv \text{Ln } \{[A^+]_o/[A^+]\} = \sigma[B]L \quad (1)$$

and

$$\text{Ln } W_\alpha \equiv \text{Ln } \{\alpha[A^+]_o/(\alpha[A^+]_o - [C^+])\} = \sigma[B]L \quad (2)$$
$$\text{Ln } W_\beta \equiv \text{Ln } \{\beta[A^+]_o/(\beta[A^+]_o - [D^+])\} = \sigma[B]L \quad (3)$$

etc.

Presented at the 36th ASMS Conference on Mass Spectrometry and Allied Topics
June 5-10, 1988, San Francisco, CA

Equations (1)-(3) are applicable under pseudo-first order $\{[B]_o >> [A^+]_o\}$, single-collision conditions for a reaction zone of length L wherein the number density of the target gas is [B] and the "target thickness" is [B]L. Here σ $(=\alpha\sigma+\beta\sigma+...)$ is the total cross section for the A^++B interaction, and the sum of the branching ratios $\alpha+\beta+...$ is equal to 1. Also, A^+, B, α, β, γ, δ, and ϵ correspond, respectively, to N_2^+, SF_6, SF_5^+, SF_4^+, SF_3^+, SF_2^+, and SF^+.

N_2^+ ions were generated by 70 eV electron impact, and the N_2^+ projectiles were selected by Q1. The collision energy E_{coll} was selected by setting the Q2 pole bias = $E_{50\%} - E_{coll}$. $E_{50\%}$ corresponds to the Q2 potential required to stop 50% of the projectile ions entering Q2.

RESULTS

Plots of Ln Y vs. P [based on equation (1)] and of Ln W_{α}, etc. vs. P [based on equations (2), (3), etc.] were linear. Table 1. summarizes the branching ratios ($\alpha-\epsilon$) and the σ at E_{cm}= 4.3 and 34 eV. For comparison, the table includes the characteristic branching ratios $\alpha-\epsilon$ observed during the electron ionization of SF_6 with 70 eV electrons.

Table 1. Branching Ratios ($\alpha-\epsilon$)

		Branching Ratio Value		
Product	Symbol	at E_{cm}= 34 eV	at E_{cm}= 4.3 eV	Electron Ionization E_e= 70 eV
SF_5^+	α	0.89±0.08	1.01±0.08	0.68
SF_4^+	β	0.007±0.0006	0.01	0.06
SF_3^+	γ	0.04±0.004	0.02	0.18
SF_2^+	δ	0.005±0.0004	<0.002	0.036
SF^+	ϵ	<0.0006	--	0.051
$\alpha+\beta+\gamma+\delta+\epsilon$	$\longrightarrow$	0.94±0.08	1.04±0.08	1.0
σ	$\longrightarrow$	56 Å^2 (±10%)	61 Å^2 (±10%)	

DISCUSSION

The results show that $\alpha+\beta+\gamma+\delta+\epsilon$ = 1.0. That is, there is no mass discrimination. Under all conditions $\Sigma[SF_x^+] = [N_2^+]_o - [N_2^+]$. Therefore, when $m_{prod} > m_{react}$, careful control of the key MS/MS parameters makes it possible to account properly for reaction-induced mass discrimination within Q2 over a four-fold change in mass (SF_5^+/N_2^+).

CONCLUSIONS

The observation of the SF_x^+ (x=1-4) product ions under single-collision conditions suggests that a large fraction of the center-of-mass kinetic energy of some ($\lesssim$10%) of the N_2^++SF_6 interactions is efficiently converted to internal excitation of the SF_6^+.

Dynamically-correct branching ratios can be measured under single-collision conditions when the key MS/MS parameters [8] are properly selected to compensate for reaction-induced mass discrimination.

REFERENCES

1. P.H. Dawson, Quadrupole Mass Spectrometry and its Applications, Elsevier, Amsterdam, 1976.
2. P.H. Dawson, Adv. Electronics Electron Phys. 53, 153 (1980).
3. P.H. Dawson, Int. J. Mass Spectrom. Ion Phys. 20, 237 (1976).
4. P.H. Dawson and J.E. Fulford, Int. J. Mass Spectrom. Ion Phys. 42, 195 (1982).
5. P.H. Dawson, J.B. French, J.A. Buckley, D.J. Douglas, and D. Simmons, Org. Mass Spectrom. 17, 205 (1982).
6. P.H. Dawson, J.B. French, J.A. Buckley, D.J. Douglas, and D. Simmons, Org. Mass Spectrom. 17, 212 (1982).
7. B. Shushan, D.J. Douglas, W.R. Davidson, and S. Nacson, Int. J. Mass Spectrom. Ion Phys. 46, 71 (1983).
8. R.I. Martinez, Rapid Commun. Mass Spectrom., 2, 8 (1988).
9. R.I. Martinez, Rev. Sci. Instrum., 58, 1702 (1987).

Presented at the 36th ASMS Conference on Mass Spectrometry and Allied Topics
June 5-10, 1988, San Francisco, CA

A COMPARISON OF DAUGHTER ION SPECTRA OBTAINED USING HYBRID AND 4-SECTOR TANDEM MASS SPECTROMETERS.

Simon J. Gaskell and Marc H. Reilly, Center for Experimental Therapeutics, Baylor College of Medicine, Houston, Texas 77030

Steven A. Carr, Mark Bean and Richard Vickers, Mass Spectrometry Facility, Smith Kline and French Laboratories, King of Prussia, Pennsylvania 19406.

The theoretical relative advantages of tandem mass spectrometers of hybrid sector/quadrupole (specifically BEqQ)and 4-sector (BEEB) design may be summarized as follows: (i) The hybrid design provides greater facility for the performance of parent and neutral loss, as well as daughter, scans; (ii) The advantages of the 4-sector design lie in the double-focusing of daughter ions, with expected benefits with respect to both transmission and resolution, particularly at higher masses.

The principal tandem MS operating modes for the two instruments are distinct. Collisionally-activated decomposition (CAD) usually occurs in an RF-only quadrupole (q) in the BEqQ instrument and in a collision cell in the third field-free region in the BEEB instrument. Experimental conditions for CAD differ in the following respects: (a) collision energy (laboratory frame-of-reference) - KeV for the BEEB instrument, eV for BEqQ; (b) multiplicity of collisions - generally higher in the quadrupole collision region; (c) residence time in the decomposition region: longer for the BEqQ instrument. The analytical implications of these differences are poorly understood. We have therefore compared data for a series of peptides and oligosaccharides obtained by tandem MS using hybrid and 4-sector instruments.

Analyses were performed on VG ZAB SEQ (BEqQ) and ZAB 4SE (BEEB) instruments. Ionization was by xenon atom and cesium ion bombardment on the BEqQ and BEEB instruments, respectively. For both instruments, parent ion resolution was unit. Daughter ion resolution was set to 1000 for the BEEB instrument and generally 1-2u (though poorer for analytes with M_r > 2000) for the BEqQ instrument.

The conclusions may be summarized as follows: (1) For lower molecular weight analytes (M_r < 1000), daughter ion spectra were obtained from both instruments which included excellent structural information. The spectra obtained for the pentapeptide, methionine-enkephalin, for example, were similar from the two instruments. Daughter ion spectra for maltopentaose MH^+ ions are shown in Figure 1. (2) For the peptides in this study with M_r > 1000, determinations of complete sequence were more readily made from spectra obtained on the BEEB instrument. Thus, for Substance P (Figure 2), the predominance of the A and D ion series facilitated the "reading" of the sequence. The daughter ion spectrum obtained using the BEqQ instrument included C- and N-terminal ions, together with "internal" fragments, which provided confirmatory evidence for structure. The daughter ion spectrum recorded on the 4-sector instrument for ACTH (18-39) was clearly superior to that obtained on the hybrid. (3) The yield of daughter ions from low mass (M_r < 1000) analytes appeared to be superior with the hybrid instrument; this advantage was not apparent at higher masses. A rigorous quantitative comparison, however, is complicated by the several factors influencing transmission of the parent ion through the quadrupole collision region. A detailed investigation of this aspect of the comparative study is the subject of continuing research.

Presented at the 36th ASMS Conference on Mass Spectrometry and Allied Topics
June 5-10, 1988, San Francisco, CA

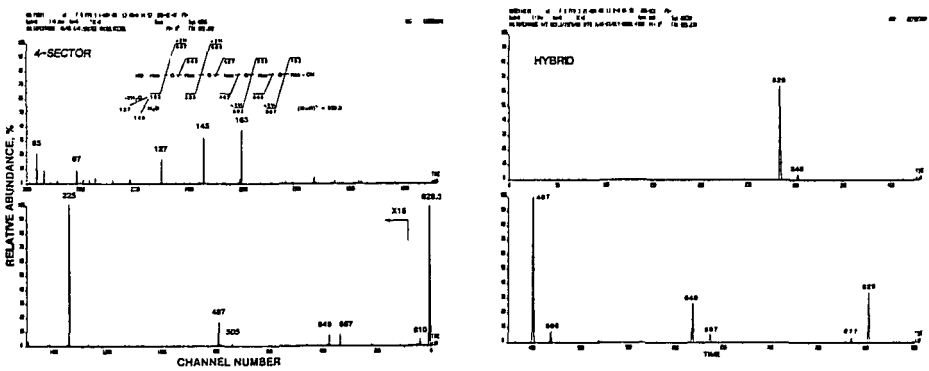

Figure 1. Daughter ion spectra for the MH^+ ion of maltopentaose, obtained using the 4-sector (left) and hybrid (right) instruments.

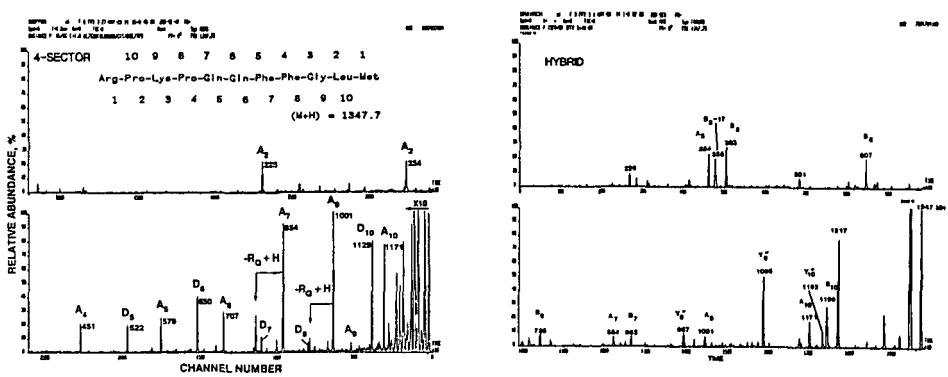

Figure 2. Daughter ion spectra for the MH^+ ion of Substance P, obtained using the 4-sector (left) and hybrid (right) instruments.

Presented at the 36th ASMS Conference on Mass Spectrometry and Allied Topics
June 5-10, 1988, San Francisco, CA

THE EFFECT OF CHEMICAL IONIZATION ON COLLISION-INDUCED FRAGMENTATION IN THE THERMOSPRAY SOURCE.

F. Aladar Bencsath
University of South Alabama, College of Medicine
Department of Biochemistry, Mobile, Alabama 36688

Lewis, Smith and Veares found [1] that a positively biased electrode placed downstream from the ion exit hole influenced remarkably the thermospray spectra. Beside meaningful intensity enhancement, they observed definite qualitative changes in the spectral pattern that occurred at higher electrode potentials. Using an electrode with proper shape and in proper position in the source, we were able to confirm their results as reported recently [2], and we also could provide evidences that all those changes observed were the results of collisionally activated reactions with useful analytical information.

The addition of the Chemical Ionization (=CI) to the Thermospray (=TS) process in form of external electron beam [3] or internal glow discharge [4] opened a wider field of applications for this valuable LC/MS interface. It is desirable, therefore, to explore the retarder's influence on the CI spectra and assess its analytical use under CI conditions in the TS source.

Experiments.

As in our earlier studies, a modified Vestal-type TS source and interface was used with a BIOSPECT quadrupole mass spectrometer. We studied the spectra obtained with pure methanol as LC solvent under CI conditions, compaired the TS and CI spectra of ammonium acetate solution in 95% methanol / 5% water, and we also recorded CI spectra of several solutes (oligopeptides, organic acids, nucleosides) observing in all experiments the effect of the retarder potential between 0 and 500 V. Negative spectra with negatively biased retarder electrode were also studied.

Results.

1. Interesting changes appear in the pure methanol spectra as the retarding potential increases. At zero volt, the protonated methanol dominates; at 100 V, the cluster ions are the chief charge carriers indicating a collision induced addition

$$MeOH + MeOH \rightarrow (MeOH)\,H \text{ and}$$
$$(MeOH)\,H + MeOH \rightarrow (MeOH)\,H\ .$$

The further increase of the retarding potential (i.e., the collision energy) results in the decrease of the trimer's (200 V) then the dimer's (250 V) intensity with the consecutive rise of the protonated methanol m/z 33 and the daughters CH OCH H m/z 47, CH O m/z 31 and CH m/z 15.

2. The retarding field in the source has a stronger effect under CI conditions than under TS conditions as the comparative experiments with ammonium acetate/methanol/water solvent showed. The fragmentation is more extensive in CI mode; the CI spectra obtained at 200 V exhibited a pattern that was observable in the TS spectra only above 300 V. As for the ionization efficiency, the TIC in the CI spectra was larger by one order of magnitude than it was in the corresponding TS spectra. The useful range of retarder potential, however, proved to be narrower in CI mode by about 150-200 V; its upper limit was determined by the onset of electric breakdown in the source. This limit appeared to be 500 V in TS mode.

3. Negative spectra obtained with negatively biased retarder electrode exhibited analogous changes upon the increase of the retarding potential, both in TS and CI mode. The symmetrical behaviour of the + and - charges indicates that mainly ion retardation and collision induced decomposition processes are responsible for the retarder-caused spectral changes.
4. Ions in solute spectra undergo the same changes that was described for the solvent ions: intensity enhancement at moderate retarder potentials, fragmentation and intesity enhancement at higher potencials. These changes are well demonstrated on the positive and negative spectra of homovanillic acid in CI mode, at 0 V and 250 V. At 0 V, only the ammoniated molecular ion at m/z 200 appears in the positive, and the de-protonated molecular anion at m/z 181 appears in the negative spectra. At 250 V, both spectra exhibit several intense ions, each of them can be associated with a well defined fragment structure.

Conclusion.

The retarder electrode in the TS source if properly shaped, positioned and biased, reproducibly increases the total ion current and induces, also reproducibly, collisionally activated decompositions both in TS and in CI mode. This simple electrode thus promises to become a useful analytical tool.

References.

1. Lewis, I.A.S.; Smith, D.C.; Veares, M. 32nd ASMS, San Antonio, TX, 1984.
2. Bencsath, F.A.; Field, F.H. 34th ASMS, Cincinnati, OH, 1986; and Anal Chem. 60. Jul.1. 1988.
3. Vestal, M.L.; Ferguson, G.J. Anal Chem. 51, 2373, 1985.
4. Vestal, C.R.; Garteiz, D.A.; Smit, R.; Blakeley, C.R. 33rd ASMS, San Diego, CA, 1985.

Presented at the 36th ASMS Conference on Mass Spectrometry and Allied Topics
June 5-10, 1988, San Francisco, CA

MASS SPECTRA OF DOUBLY CHARGED IONS

M.Barber, D.J.Bell, M.R.Morris, L.W.Tetler, M.D.Woods, UMIST, PO Box 88, Manchester M60 1QD, UK.
J.J.Monaghan, W.E.Morden, ICI C&P Group, Runcorn Heath, Cheshire.

Previously reported studies of peptides have concentrated on the generation of the singly charged pseudo-molecular ion, such as $(M+H)^+$. An alternative approach to the study of high mass samples is to consider the multiply charged ions and the resulting fragments. Indeed, it has been observed that the mass spectra of small proteins (r.m.m. 10-25000 daltons) contain multiply charged molecular ion species of considerable intensity, with the doubly charged ion often being the most intense ion in the spectrum representative of the molecular mass (1)

Spectra consisting of ions originating from a doubly charged parent can be acquired using a hybrid or triple quadrupole mass spectrometer with selection of the doubly charged ion in MS1 and MS2, i.e. the quadrupole analyser, scanned in the normal way as it is not energy focusing.

Results of the study of ions in sector instruments show that the instrument should be set up with the parent ion at H and E and scanned with B/E constant from 2H and 2E downwards. To scan in this way, assuming the singly charged species is within the mass range of the instrument, the instrument is operated at half the full accelerating voltage to enable 2E to set on the ESA.

Although intense multiply charged ions are usually observed with peptides of r.m.m. greater than 5000 daltons it was considered more appropriate to initially study smaller compounds as the resulting spectra are less complex and fragmentation pathways are more readily determined.

Doubly protonated Gramicidin S was studied by B/E scans, from 2E downwards, on a two sector instrument. The observation of sequence ions of greater m/z ratio than the parent illustrate that the instrument is being scanned in the correct fashion and that the doubly charged ions are fragmenting in the first field free region to form singly charged ions.

Sequence ions found in the singly charged spectra were also observed in the spectra, but some of these were of reduced intensity. Overall, the prominent sequence ions observed above the parent ion m/z value are different to those observed from the singly charged parent due to the loss charged rather than neutral residues. Only the ions above the parent ion m\z were considered as this sample, being symmetrical, can produce an ion at m/z=571 corresponding to $(M/2+H)^+$ and hence the ions below this may originate from the singly charged species. To avoid the interference of the singly charged ion the $(^{13}C_1.M+2H)^{2+}$ isotope was studied. The instrument used was a hybrid of BEQQ geometry allowing the CID spectra of $(M+2H)^{2+}$ and its ^{13}C isotope to be compared. The spectrum from the monoisotopic species (fig. 1) was

quite similar to that from the B/E scan focusing on m/z=571, although an additional ion was detected at m/z=441 which corresponds to $(M+2H-PheLeu)^{2+}$. In comparison the $^{13}C_1$ doubly charged parent produced noticeably fewer ions of m/z less than 571 suggesting that daughters of the singly charged parent did contribute to the previous spectra. Sequence ions were observed both above and below the parent m/z value with the expected 1 a.m.u shift of singly charged daughters compared with the daughters of the monoisotopic parent. It was also observed that the ion at m/z=441 shifted by only 0.5 a.m.u. when the the $^{13}C_1$ parent was selected. Another doubly charged daughter was observed in the spectrum corresponding to $(M+2H-Phe)^{2+}$.

The CID spectrum of doubly protonated Angiotensin I, obtained on the hybrid instrument, produced sequence ions both above and below the parent ion. (fig. 2) It is interesting to note that complimentary ions are observed in the spectrum i.e. those that produce the molecular mass when combined.

In order to confirm the proposed fragmentation the mono- and di-methyl esters of Angiotensin were studied. The daughter ion spectrum of the mono-methyl ester is a combination of the diacid and dimethyl ester spectrum indicating that esterification occurs at both acid sites as both methylated and non-methylated fragments are observed.

Daughter ion spectra of doubly charged ions provided structural information often in excess of that provided by the spectra of singly charged ions as a doubly charged ion can form two singly charged daughters and, additionally, doubly charged daughters may be collected. The fragmentation observed for the peptides studied is generally similar to the fragmentation of singly protonated ions although the fact that both fragments remain charged affects the intensity of some sequence ions.

This successful study of multiply charged ions presents the possibility that such ions generated from high mass samples bombarded with liquid metal ions may be analysed using extended mass range tandem mass spectrometers.

References
1 M.Barber and B.N.Green, Rapid Communications in Mass Spectrometry, 1, 80 (1987)

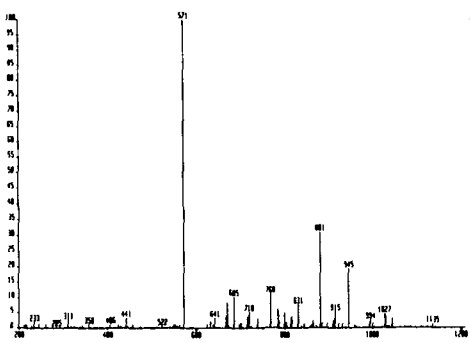

Fig. 1 The CID spectrum of Gramicidin S $(M+2H)^{2+}$.

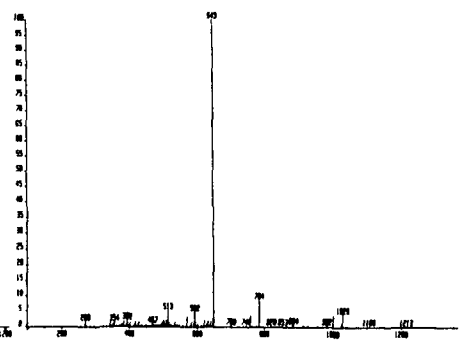

Fig. 2 The CID spectrum of Angiotensin I $(M+2H)^{2+}$.

Presented at the 36th ASMS Conference on Mass Spectrometry and Allied Topics
June 5-10, 1988, San Francisco, CA

COLLISIONAL ACTIVATION SPECTRA OF BISBENZYLISOQUINOLINE ALKALOIDS

K.P. Madhusudanan+, P.R. Das and B.N. Pramanik
Schering-Plough Corporation, Bloomfield, N.J. 07003.
Sudha Jain and D.S. Bhakuni
Central Drug Research Institute, Lucknow 226001, India.

Bisbenzylisoquinoline alkaloids are characterized by the number and type of linkages between the two benzylisoquinoline moieties and the nature of the substituents. Mass spectrometry has been one of the analytical tools successfully used for the structure elucidation of bisbenzylisoquinoline alkaloids (1). Recently, there has been a report of the evaluation of FAB/MS and FAB/MS/MS for the structure elucidation of a few of these alkaloids (2). The results indicate that FAB/MS is a less useful technique than EIMS for the structural studies of bisbenzylisoquinolines containing two ether linkages. However, the EI spectra of these alkaloids are often complicated by the presence of very abundant doubly charged ions (1,3). It was therefore decided to investigate the collisional activation (CA) spectra of the $[M]^+$ of a few bisbenzylisoquinolines having 1-3 ether linkages and/or a C-C linkage. The results of this investigation are described here.

The bisbenzylisoquinolines studied have been isolated from natural sources (4). The collisionally activated mass analyzed ion kinetic energy spectra (CA MIKES) were recorded on a VG-ZAB-SE instrument using a VG 11-250 data system. The ion source conditions were : electron energy, 70 eV and temperature, 200°C. Helium was used as the collision gas . The pressure of helium in the collision cell was adjusted so that there was a 70-80% suppression of the main beam. Samples were introduced through the direct inlet system and heated to 200°C.

The compounds studied and the collision induced fragmentation of their molecular ions are indicated in Figure 1-6. The bisisoquinoline ions $[BIQ]^+$, arising out of double benzylic cleavage give rise to the most intense peak in the CA MIKE spectra of these compounds. Loss of Me and OMe are the other two fragmentation pathways observed. $[M-Me]^+$ ion is more abundant (>50%) in compounds having no 1,4-dioxine bridge (compounds 1-5) than in bisbenzylisoquinolines with 1,4-dioxine bridge (compounds 6-16).
The bisbenzylisoquinolines 1-5 are further characterized by the presence of ions corresponding to loss of isoquinoline and benzyl moieties. Because of the proximal benzyl group only C(8)-O ether linkage is cleaved, followed by rupture of C(1')-C(α') bond resulting in [M-IQ]+ ions. This cleavage is not observed in bisbenzylisoquinolines having 1,4-dioxine bridge. For the formation of $[M\text{-benzyl}]^+$ ion, cleavage occurs at either side of the diaryl ether oxygen leading to either $[M\text{-benzyl}_1]^+$ or $[M\text{-benzyl}_2]^+$ ions.

References:
(1) J. Baldas, I.R.C. Bick, T. Ibuka, R.S. Kapil and Q.N. Porter, J. Chem. Soc. Perkin I, 592 (1972).
(2) J.A. Masucci, G.W. Caldwell, W.H. Wu, R.K. Isensee and J.R.B. Slayback, 35th. ASMS Conference on Mass Spectrometry and Allied Topics, May 24-29, 1987, Denver, Colorado.
(3) P. Bel and A. Mandelbaum, Org. Mass Spectrom., 15, 568 (1980).
(4) K.P. Guha and B. Mukherjee, J. Nat. Prod. (Lloydia), 42, 1 (1979).

+ Present Address: Central Drug Research Institute, Lucknow, India.

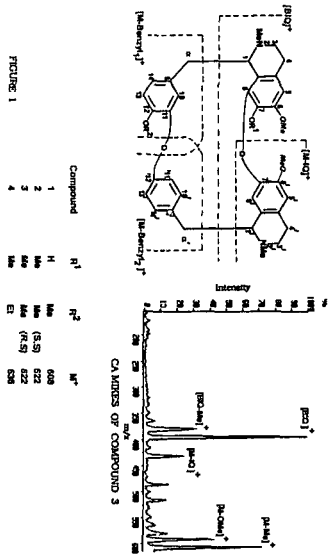

Compound	R^1	R^2	$M^{+\cdot}$
1	H	Me	608
2	Me	Me	622
3	Me	Me	622
4	Me	Me	622
		(S,S)	622
		(R,S)	622
	Et		636

FIGURE 1

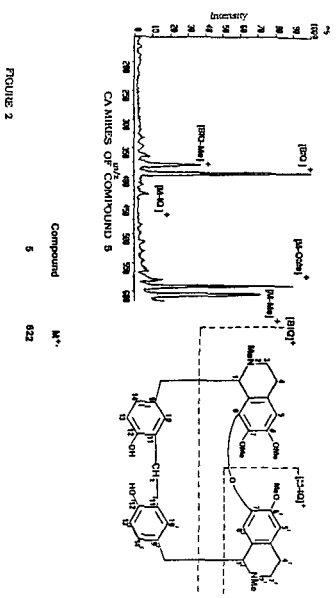

Compound	$M^{+\cdot}$
5	622

FIGURE 2

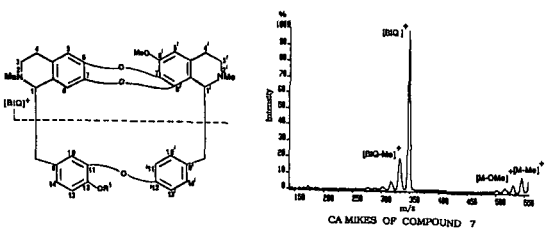

Compound	R^1	M^+
6	Me	576
7	H	562
8	Et	590

FIGURE 3

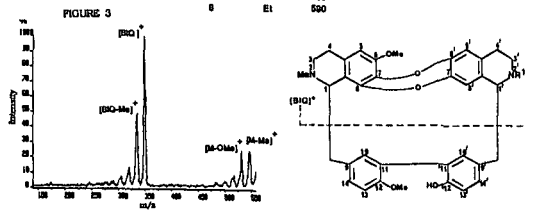

Compound	R^1	$M^{+\cdot}$
14	H	562
15	Me	576 (R,S)
16	Me	576 (R,S)

FIGURE 4

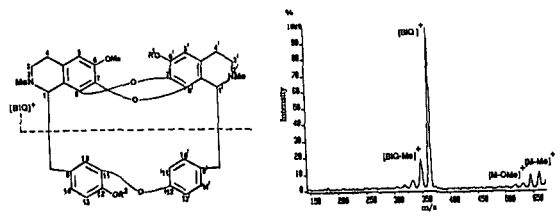

Compound	R^1	R^2	$M^{+\cdot}$
9	Me	Me	606
10	H	H	578
11	Et	Et	634

FIGURE 5

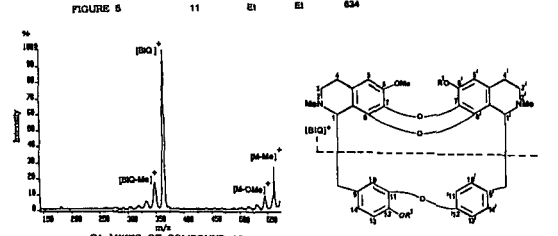

Compound	R^1	$M^{+\cdot}$
12	H	578
13	Me	606

FIGURE 6

Presented at the 36th ASMS Conference on Mass Spectrometry and Allied Topics
June 5-10, 1988, San Francisco, CA

FAB-MS-MS OF PEPTIDES : UNAMBIGUOUS RECOGNITION OF SEQUENCE PEAKS IN THE CAD SPECTRA.

Bhupesh C. DAS
Institut de Chimie des Substances Naturelles, CNRS
91190 Gif-sur-Yvette, France.

Frédéric de Maack, Gérard Devant
S.N. NERMAG 49 quai du Halage, 92500 Rueil, France

Recent reports from several laboratories have suggested that FAB-MS in combination with MS-MS can provide the amino acid sequences of peptides (R.S. Johnson et al., Anal. Chem. 1987, 59, 2621-2625 and references cited therein). In contrast to the normal FAB spectra, the Collision Activated Decomposition (CAD) mass spectra of peptides often exhibit extensive series of peaks due to different types of fragment ions. However, recognition of the sequence determining peaks in these spectra can be a difficult task particularly when one is confronted with a completely unknown peptide.
The problem can be clearly appreciated from the FAB-MS/MS spectrum of the underivatized pentapeptide H-TYR-GLY-GLY-PHE-LEU-OH presented in Figure 1.

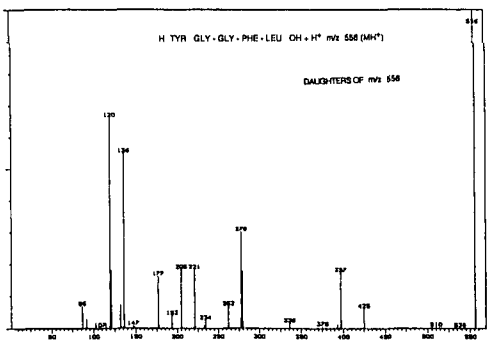

Figure 1

Our objective was to explore simple means for unambiguous recognition of sequence determining peaks. For this purpose, we investigated the FAB-MS/MS spectra of peptides whose amino terminals were acetylated (CH_3CO/CD_3CO) with an equimolecular mixture of acetic anhydride and deuterated acetic anhydride, a reaction which can be easily performed with sub nanomolar quantities.

When only one acetyl group is introduced, the protonated molecular ions in the FAB spectra appeared as two peaks of equal intensity separated by 3 amu, representing the acetylated CH_3CO and trideutero acetylated CD_3CO- species.

Thus, after N-acetylation of the above pentapeptide with the mixture of anhydrides, the protonated molecules in the FAB spectrum appeared at m/z 598 and 601. Comparison of the CAD spectra (Figures 2 and 3) produced selectively from each of these two parent ion species readily differentiated the N-terminal sequence peaks which are shifted 3 amu higher in the deuterated acetyl-bearing fragments. Also, all other fragment ions could be assigned with certainty as a result of this study with deuterium label.

FAB/MS/MS of CH_3CO-TYR-GLY-GLY-PHE-LEU-OH
DAUGHTERS of MH^+ 598

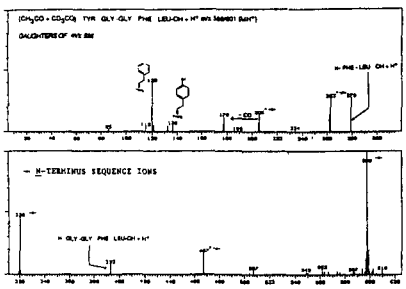

Figure 2

FAB/MS/MS of CD_3CO-TYR-GLY-GLY-PHE-LEU-OH
DAUGHTERS of MH^+ 601

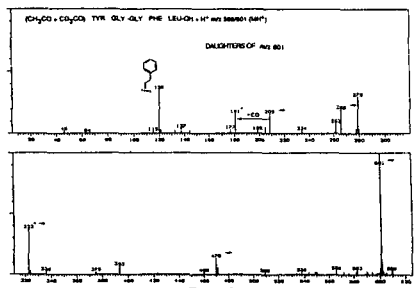

Figure 3

Experiments conducted with several other peptides of both synthetic and natural origin gave similar results. It is expected that this simple methodology, when applied to unknown peptides, should provide unambiguous sequence information. Further work is in progress to extend this method to poly-functionnalized amino acid containing peptides.

Presented at the 36th ASMS Conference on Mass Spectrometry and Allied Topics
June 5-10, 1988, San Francisco, CA

INFLUENCE OF REAGENT GAS PROTON AFFINITY ON COLLISIONALLY-ACTIVATED DECOMPOSITIONS OF ISOMERIC PROTONATED MORPHINANS

B. CHARLES[1], R.B. COLE[2], J. BRUNETON[1] and J.C. TABET[2]*

[1]UER des Sciences Medicales et Pharmaceutiques, ANGERS, FRANCE

[2]Laboratoire de Chimie Organique Structurale, UA 455, Université Pierre et Marie CURIE, Place Jussieu, PARIS Cedex 05, FRANCE

The possibility to differentiate isomeric and stereoisomeric compounds using MS/MS techniques is now well documented. Often, CAD spectra are not dependent upon the mode of protonated molecule preparation in the ion source because the initial internal energy of source ions is low in comparison to the excitation energy transferred during the collision process (case of keV collisions, lab. frame of reference). In this report, we use a triple quadrupole (Nermag R30-10) to investigate some unusual behavior observed in the decompositions of protonated isomeric morphinans characterized by a ketone group in one of two positions on the C-ring, and either cis or trans B/C ring junction stereochemistry:

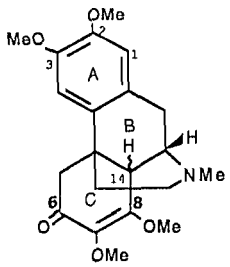

1c $H_{14\,eq}$

1t $H_{14\,ax}$

B/C ring junction

cis

trans

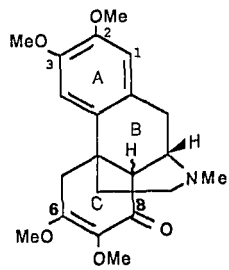

2c $H_{14\,eq}$

2t $H_{14\,ax}$

B/C ring junction

cis

trans

CAD spectra of CI/NH_3 generated MH^+ ions (Fig. 2) are characterized by an unusual "silhouette" as primarily low mass daughter ions predominate for the four isomers. Among these lower mass daughters, even mass nitrogen-containing ions are detected in high yields. The abundance ratios of m/z 44 : m/z 58 immonium or aziridinium species are almost identical for both cis and trans isomers, thus stereochemical effects are not linked to their forma-

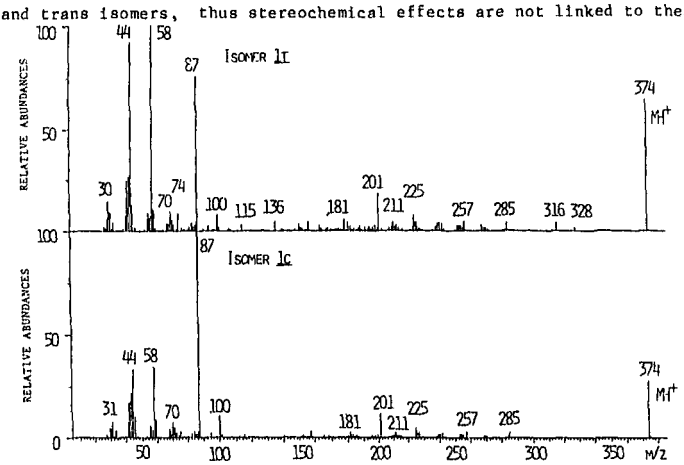

Figure 2

tion. Furthermore, the relative abundances of these ions remain constant even when the collision energy is varied from 10 to 80 eV (laboratory frame of reference). This constancy may indicate that these even-mass ions are produced as a result of the decomposition of a common intermediate ion (D-ring open) formed prior to CAD in the ion source (or in flight). This resultant intermediate ion, common to both cis and trans configurations, could decompose via competitive pathways to yield the even-mass daughter ion fragments, plus highly conjugated (stable) neutrals. To activate opening of the D-ring, attachment of the ionizing proton must be localized to one of two nucleophilic sites: either the $-NCH_3$ group (favored) or the keto-enonic system of the C-ring.

In sharp contrast to the results above, when switching CI reagent gas from NH_3 to CH_4, CAD spectra of MH^+ ions (Fig. 3) obtained using identical collision conditions present mainly higher mass daughter ions (above m/z 200); the low mass nitrogen-containing ions are detected in far lower abundances. The distinct behavior of each of the two reactive plasma systems towards the analyte morphinans can be explained by two interralated phenomona: (i) the average internal energy of MH^+ ions prepared by CI/CH_4 is very much higher than that of MH^+ ions prepared by CI/NH_4^+, and (ii) in contrast to the latter conditions where mainly the $N-CH_3$ group was protonated, for the CI/CH_4 system significant protonation takes place at other nucleophilic sites (i.e., methoxy and carbonyl groups, and the aromatic ring). The losses of low mass neutrals (species having relatively low proton affinities, e.g., $H_2C=O$, H_3C-OH, $H_3C-O-CH_3$) yielding daughter ions at m/z 344, 342, 328, respectively, and m/z 310 (by consecutive losses of two CH_3OH molecules), are consequently favored over formation of low-mass nitrogen containing ions.

The finding that reagent gas (protonating agent) composition exerts a tremendous effect upon the profile of daughter ions observed in the CAD spectrum of protonated molecules of a given isomer is attributed to a higher regioselectivity of protonation for the NH_3 reagent gas which possesses a higher proton affinity than methane. Relative to the methane reagent, ammonia plasma protons may thus be transferred to a smaller number of sites, and product molecules protonated at a given site contain lower internal energies, hence, possess more limited possibilities for internal proton transfer prior to collisional activation.

Figure 3

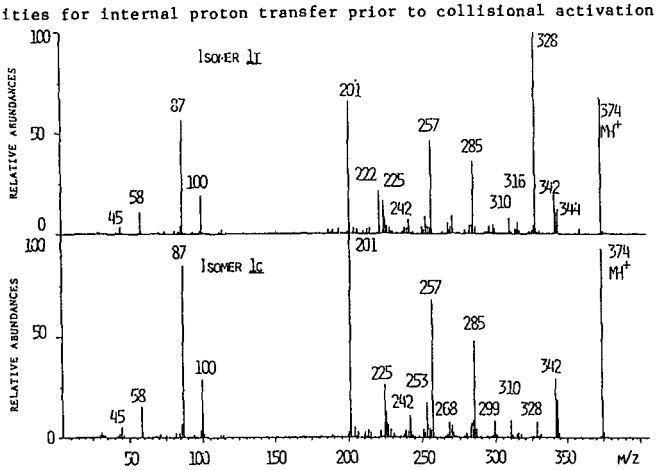

Presented at the 36th ASMS Conference on Mass Spectrometry and Allied Topics
June 5-10, 1988, San Francisco, CA

INFLUENCE OF CATIONIZING ALKALI METALS ON THE STABILITY OF FAB DESORBED PYRIMIDINE DERIVATIVES

Richard B. Cole and Jean-Claude Tabet
Laboratoire de Chimie Organique Structurale, UA 455,
Université Pierre et Marie Curie (Paris VI), 4 Place Jussieu, 75230 Paris Cedex 05, FRANCE

Jean-Claude Blais
Laboratoire de Physique et Chimie Biomoléculaire, CNRS, UA 198, Institut Curie and
Université Pierre et Marie Curie, 11 Rue Pierre et Marie Curie, 75231 Paris Cedex 05, FRANCE

The presence of alkali cations is known to affect the distribution of organic molecular adducts desorbed from surfaces undergoing particle bombardment in secondary ion mass spectrometric analysis. Using various pyrimidines (e.g. 4(2'-hydroxyphenyl)-5-methyl-2-hydrazinopyrimidine, Fig. 2a) as model compounds for studying the cationization phenomenon, we have investigated the stability of alkali metal adduct molecules (i.e., MH^+, $(M+Li)^+$, $(M+Na)^+$) as a function of cation size. Such cationized molecules were desorbed from a thioglycerol matrix using 8 keV Ar bombardment; decompositions were monitored using a Triple Quadrupole (Nermag R30-10) under conditions of collisional activation (CAD), as well as in the metastable mode. Metastable decompositions are generally more sensitive probes of ion internal energy than high pressure CAD's because subtle differences in the intensities of daughter ions arising from low-energy decompositions may be lost if a huge excess of internal energy is acquired by the molecule (i.e., CAD).

MH^+ ions were observed to undergo metastable decompositions via competitive pathways (Fig. 1a) resulting in the losses of neutrals at 16 amu (postulated to be a rearrangement loss of CH_4) and 17 amu (NH_3), plus consecutive losses of 27 amu (HCN) or 28 amu following NH_3 loss (verified by constant daughter scans). In contrast, $(M+Li)^+$ ions exhibited metastable decomposition solely via loss of 16 amu neutrals (Fig. 1b). Incorporation of a second

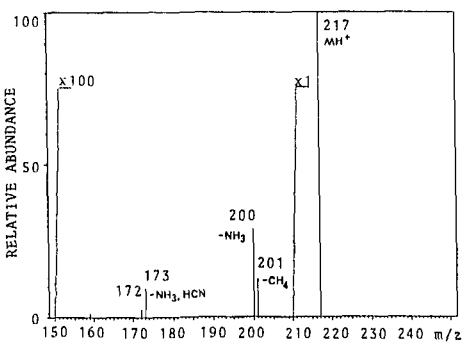

Figure 1A

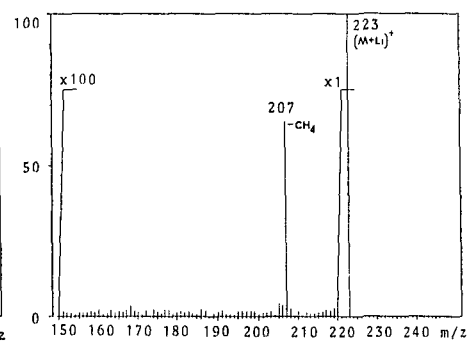

Figure 1B

lithium atom into the pyrimidine structure by Li^+/H^+ substitution, however, blocked even this process. With an even larger cation, Na^+, metastable decompositions of $(M+Na)^+$ ions were also suppressed entirely. These results indicate an augmented stability of molecular ion adducts with increasing cation size, and number of incorporated metal atoms. Thermodynamic and kinetic factors involved in this stabilization may include processes such as increased ground state stability of the precursor adduct ion, increased decompositional activation barriers, and/or reduced internal energy of the cation-molecule complex.

Li^+ adduct molecules thus decompose by a single metastable process (loss of 16 amu), whereas protonated molecules decompose by competitive pathways (e.g., losses of 16 or 17 amu). Under CAD conditions, however, the 17 amu loss from the $(M+Li)^+$ adduct appears. Collisional activation also promotes loss of 17 amu (relative to 16 amu) for MH^+ molecules. The loss of 17 amu must then be regarded as a process requiring a relatively higher internal energy content. An internal energy vs. log k(E) scheme describing the competition between these two processes which conforms to the classic Wahrhaftig diagram is offered in Fig. 2b.

In comparing relative intensities of MH^+ metastable daughter ion peaks over the course of FAB sputtering, the 17 amu loss was observed to increase relative to the 16 amu loss, with disappearance of the matrix. In combination with the scheme below, this finding supports the contention that evaporation of the matrix results in a slight increase in the internal energy of desorbed molecules.

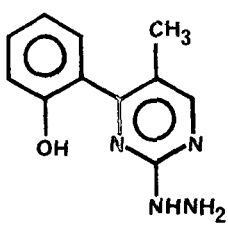

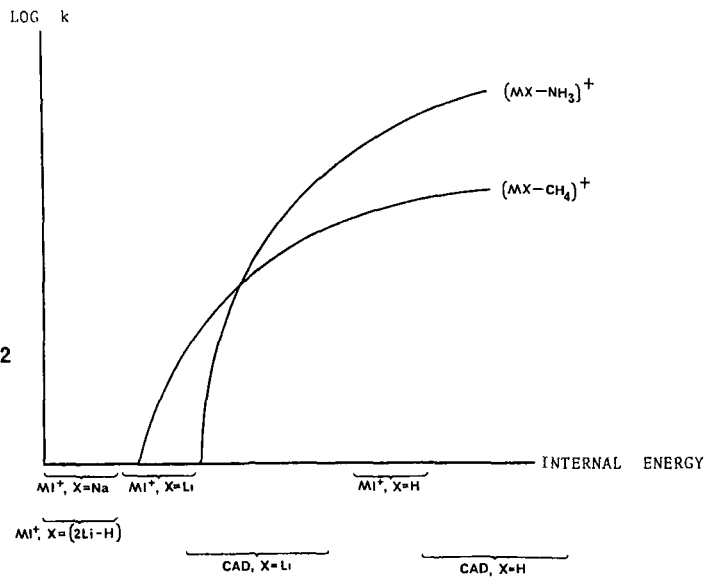

SCHEMATIC REPRESENTATION

Figure 2A

Figure 2B

Presented at the 36th ASMS Conference on Mass Spectrometry and Allied Topics
June 5-10, 1988, San Francisco, CA

INFRARED MULTIPHOTON DISSOCIATION OF SMALL PEPTIDE IONS FORMED BY LASER DESORPTION

Clifford H. Watson and John R. Eyler
Department of Chemistry, University of Florida
Gainesville, FL 32611

Pseudo-molecular ions ($M+H^+$, $M+Na^+$, $M+K^+$, and $M-H^-$) of selected peptides were formed by laser desorption with a pulsed carbon dioxide laser. The desorbed ions were trapped within the analyzer cell of a Fourier Transform Ion Cyclotron Resonance (FTICR) mass spectrometer where they could be irradiated by the output from a grating-tuned continuous wave (cw) carbon dioxide laser. Fragment ions potentially useful for elucidation of peptide sequence were observed after irradiation for 0.5 to 5 s with the cw laser.

Irradiation of the ions was facilitated by replacing the rear trap plate of the analyzer cell with one containing a 1.5 cm hole covered by a fine stainless steel mesh. The normal laser desorption optics (as supplied by the manufacturer) were used to obtain the ions in the gas phase, and light from the cw laser irradiated the ions by passing through a salt window mounted on the hollow solids probe as illustrated in Figure 1. The estimated power density from the cw laser inside the FTICR cell was about 4.3 to 17.1 Watts/cm^2. The peptides were mixed with methanol and deposited on a hollow solids probe with a micropipette, allowed to dry, then inserted into the FTICR vacuum chamber and evacuated to ca. 2×10^{-8} torr.

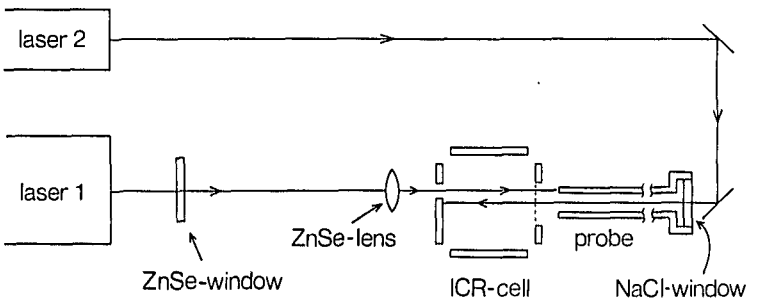

Figure 1.
Light from a pulsed CO_2 laser (1) is used to desorb the peptide sample.

The negative ion laser desorption mass spectrum often contained much less chemical noise than the positive ion spectrum, greatly simplifying interpretation. Typically, only the pseudo-parent ion $(M-H)^-$ or $(M-OH)^-$ was observed in the negative ion laser desorption mass spectra. For example, the parent ion $(M-H)^-$ of L-arginyl-L-lysine dissociated upon irradiation with cw laser producing the Lys^- ion (see Table 1).

The positive ion spectrum, on the other hand, was often complicated by the excessive amounts of Na^+, K^+, and contaminant hydrocarbon ions. For most peptides studied to date, the positive ion mass spectrum was often dominated by the presence of $(M+K)^+$ which fragmented upon irradiation to yield K^+. However, exceptions to this behavior were found. *Protonated L-arginyl-L-phenylalaninyl-L-alanine produced structurally useful fragment ions* upon irradiation. The fragment ions produced by this peptide are listed in Table 1.

Doping with a 4:1 mole ratio of LiCl to peptide resulted in the production of the $(M+2Li-H)^+$ ion which was more stable than the $(M+K)^+$ cation. The photodissocation pathways of two peptides with Li attachment are listed in Table 1. For example, the dipeptide L-arginyl-L-phenylalanine dissociates to produce the $(Phe+2Li)^+$ ion as the major fragmentation pathway. *Thus, with lithium cation attachment the pathway of lowest activation energy is cleavage of the* peptide rather than loss of the alkali cation.

All of the peptides that were observed to photodissociate contained an arginine unit, and no photodissociation was observed when arginine was absent. For example, the dipeptides Trp-Gly and Pro-Phe did not photodissociate under identical conditions to the compounds listed in Table 1. The presence of more than one fragmentation pathway for several of the peptide ions *suggests that vibrational energy is completely randomized throughout the ion prior to* dissociation.

Table 1

Infrared Multiphoton Dissociation of Peptide Ions

Peptide	Ion Studied	Fragment Observed
Arg-Glu	$(M-H)^-$	Arg^- (A_1)
		Phe^- (X_1)
Arg-Lys	$(M-H)^-$	Lys^- (Y_1)
	$(M+2Li)^+$	$(Lys+2Li)^+$ (Y_1)
		$(Arg+2Li)^+$ (A_1)
	$(M+K+Li)^+$	$(Lys+K+Li)^+$ (Y_1)
Arg-Phe	$(M-H)^-$	Phe^- (Y_1)
	$(M+2Li)^+$	$(Phe+2Li)^+$ (Y_1)
		$(Arg+2Li)^+$ (A_1)
Arg-Trp	$(M-H)^-$	Trp^- (Y_1)
		Arg^- (B_1)
Arg-Phe-Ala	$(M-H)^-$	$Phe\text{-}Ala^-$ (X_2)
		Phe^- (B_2Y_2)
	$(M+H)^+$	$Arg\text{-}Phe^+$ (B_2)
		Arg^+ (B_1)
Leu-Tyr-Met-Arg-Phe-Ala	$(M+H)^+$	$Leu\text{-}Tyr^-$ (B_2)
		Leu^- (B_1)
		$Leu\text{-}Tyr\text{-}Met^-$ (C_3)
		$Phe\text{-}Ala^-$ (Z_2)

The major fragmentation pathway is listed first when more than one dissociation pathway was observed.

Presented at the 36th ASMS Conference on Mass Spectrometry and Allied Topics
June 5-10, 1988, San Francisco, CA

COLLISIONALLY-ACTIVATED DISSOCIATION (CAD) STUDIES IN THE OPTIMIZATION OF MS/MS FOR THE TRACE DETERMINATION OF PROSTAGLANDINS

Todd A. Gillespie and Richard A. Yost
Department of Chemistry, University of Florida, Gainesville, FL 32611

The pentafluorobenzyl (PFB) ester trimethyl silyl (TMS) derivative or the methoxime (MO)-PFB-TMS derivative used in electron-capture negative chemical ionization (EC-NCI) are the most sensitive and specific means for the trace determination of prostaglandins (PGs). Although these studies were first initiated to optimize the MS/MS conditions for trace determination of PGs, some rather intriguing discoveries were made concerning the CAD fragmentation behavior of derivatized PGs.

For example, it was discovered that the carboxylate anion $(M-PFB)^-$ formed from electron-capture negative chemical ionization (EC-NCI) of $PGF_{2\alpha}$-PFB-TMS showed little fragmentation under typical (collision gas pressure < 2.0 mTorr N_2 and collision energy < 30 eV) CAD conditions. In contrast, the daughter spectra of the carboxylate anion of PGE_2-MO-PFB-TMS produced many intense fragments under the same conditions. The fragmentation efficiency (E_f) of the PGs (Figure 1) may be compared by examining the differences in fragmentation behavior of their respective carboxylate anions. Various PGs were then studied to determine the reason the two derivatized PGs, which are similar in structure (Figure 2), behave differently during CAD experiments. The E_f of PGD_2 and $DHKF_{2\alpha}$ provided no useful information to explain the differences in fragmentation behavior.

It was first believed that the additional TMS group on $PGF_{2\alpha}$-PFB-TMS would add to the ion's stability during CAD experiments. In order to test this hypothesis, the $PGF_{2\alpha}$-PFB and PGE_2-PFB derivatives were examined. A conventional solids probe was used to introduce the derivatized PGs, since with only PFB derivatization the PGs were no longer amenable to GC. The E_f data from this study is shown in Figure 3. The fragmentation behavior of the $PGF_{2\alpha}$- and PGE_2-PFB derivatives are similar to those found with the fully derivatized PGs (Figure 1). The $PGF_{2\alpha}$-PFB derivative appears to be more stable than the PFB-TMS derivative at collision gas pressures > 2.0 mTorr N_2. This suggests the additional TMS group found on $PGF_{2\alpha}$-PFB-TMS has little or no effect on the observed differences in the fragmentation behavior of $PGF_{2\alpha}$ and PGE_2.

The original purpose of the efficiency studies was to optimize the MS/MS conditions for trace analysis of PGs by GC/MS/MS. General information can be obtained from the overall efficiency (E_O) graph of the MO-PFB-TMS derivatives in Figure 4. The graph shows that $PGF_{2\alpha}$ and $DHKF_{2\alpha}$ exhibit low E_O which will lead to difficulties when performing selected-reaction monitoring (SRM) experiments. A pressure resolved breakdown curve for selected fragment ions of $PGF_{2\alpha}$ is shown in Figure 5. This type of information is useful in determining the optimum conditions for obtaining qualitative daughter spectra. The parent-to-daughter selected reaction (Figure 6) with the highest collection efficiency should be selected to yield the highest sensitivity for SRM determination of trace PGs. Similar curves can be obtained for all PGs for both energy and pressure. Table 1 lists the optimum conditions which should be used to obtain qualitative daughter spectra, as well as conditions for SRM analysis for $PGF_{2\alpha}$ and PGE_2.

In summary, the difference in the MS/MS fragmentation behavior between $PGF2_\alpha$ (-OH) and PGE_2 (=O) appears to be due to the difference in functional groups. We have hypothesized that the 3-D conformation of the PG anion permits interaction of the carboxylate group with the -OH groups. The additional -OH group on $PGF_{2\alpha}$ and $DHKF_{2\alpha}$ could account for the added stability of the PG anions. PGE_2 and PGD_2 are less stable due to the =O group. Thus, lower collision pressure and energy is required to fragment the 3-D conformation of the PGE_2 and PGD_2 anion. The above studies demonstrate the utility of efficiency curves in the optimization of MS/MS conditions for trace determinations.

Presented at the 36th ASMS Conference on Mass Spectrometry and Allied Topics
June 5-10, 1988, San Francisco, CA

Figure 1: (MO)-PFB-TMS Derivatives

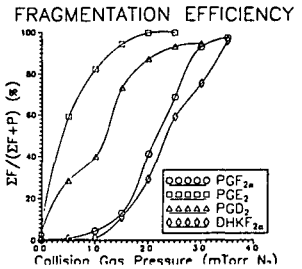

Figure 3: PFB-Only Derivatives

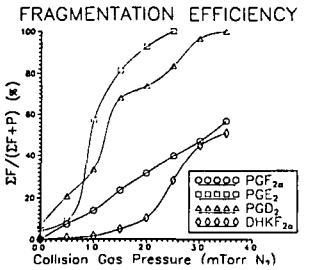

Figure 2: Prostaglandins $F_{2\alpha}$ and E_2

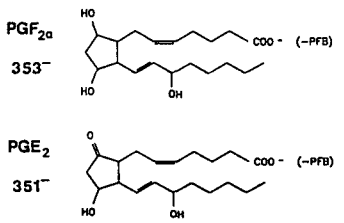

Figure 4: (MO)-PFB-TMS Derivatives

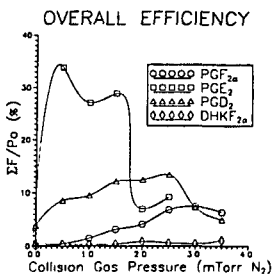

Figure 5: Optimization of $PGF_{2\alpha}$-PFB-TMS

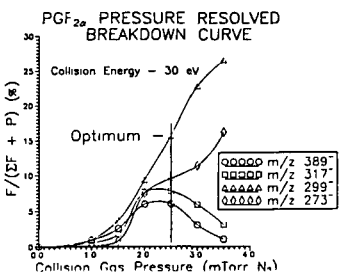

Figure 6: Optimization of $PGF_{2\alpha}$-PFB-TMS for SRM

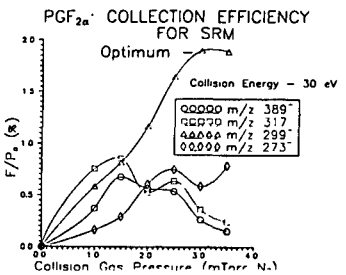

Table 1: Optimum Conditions for $PGF_{2\alpha}$ & PGE_2

Qualitative Daughter Spectra

Optimum Pressure : $PGF_{2\alpha}$ - 2.5 mTorr N_2
PGE_2 - 0.5 mTorr N_2

Optimum Energy : $PGF_{2\alpha}$ - 30 eV
PGE_2 - 25 eV

Quantitative SRM

Selected Reaction: $PGF_{2\alpha}$ $569^- \rightarrow 299^-$
PGE_2 $524^- \rightarrow 268^-$

Optimum Pressure : $PGF_{2\alpha}$ - 3.0 mTorr N_2
PGE_2 - 1.5 mTorr N_2

Optimum Energy : $PGF_{2\alpha}$ - 30 eV
PGE_2 - 30 eV

Presented at the 36th ASMS Conference on Mass Spectrometry and Allied Topics
June 5-10, 1988, San Francisco, CA

FRAGMENTATION AND SEQUENCING OF PEPTIDES INVESTIGATED BY MULTIPHOTON IONIZATION MASS SPECTROMETRY.

J. Grotemeyer, R.C. Beavis, J. Lindner, C. Köster, E.W. Schlag

Institut für Physikalische und Theoretische Chemie, TU München
Lichtenbergstr. 4, D-8046 Garching, Germany.

Investigations of peptides by well established mass spectrometric methods, such as electron impact, are often disturbed by several features. First, the intensities of sequence ions as well as the stability of the molecular ion usually decrease considerably with increase in the number of amino acid residues, because sequence ions of higher order decompose to those of lower order. This fact is due to the broad energy distribution in the ions by the ionization procedure. Secondly, other ions beside sequence ions are also formed from the peptide molecular ion. These additional fragmentations occur by reactions in the functional groups of the peptide chain.

It has been demonstrated [1] that multiphoton ionization (MUPI) with its intrinsic features, the real soft ionization and the tuneable fragmentation, allow to overcome these shortcomings of conventional methods. The soft ionization at laser powers between 10^5 and 10^6 W/cm^2 produces mainly the molecular ion. By increasing the laser intensity to roughly 10^7 W/cm^2 fragmentation reactions beside the formation of the molecular ion occur.

Figure 1 displays the EI mass spectrum and the metastable ion decomposition (MIKE) spectrum from the molecular ion as well as the soft and hard MUPI mass spectra of the protected tripeptide BzO-Val-Leu-Asp-(O-Bz)$_2$. A comparison of the mass spectra show that the MIKE and the partial hard MUPI mass spectrum show some similarities in their fragmentation behaviour. In both cases mostly sequence specific fragment ions of the A- and B-type are formed, while the EI mass spectrum shows a extense fragmentation especially in the low mass region. This behaviour can be understood by the fact of the broad energy distribution in EI contrary to MUPI. While electron ionization yield in energy distribution of 5-15 eV, MUPI has a typical distribution of a few 100 meV.

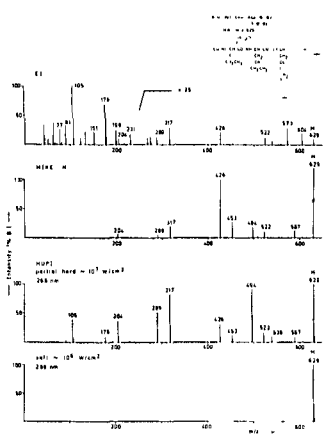

Fig.1 EI, MIKE, MUPI (hard) and MUPI MUPI (soft) mass spectrum of the protected Tripeptide Val-Leu-Asp.

The preferred formation of the A- and B-ions can be explained comparing quantum mechanical calculations and MUPI investigations of phenylalanyl-glycine. It could be shown that the formation of the N-terminal sequence ions is energetically favored over other cleavage reactions. The calculation predicts that these reactions should have transition energies close to the three photon level of the multiphoton absorption. The results of the calculations fits very close to the experimental findings. Because of the different energy distributions in the ionization methods MUPI mass spectra display only fragments which have appearence energies very close to or lower than the total energy accumulated in the molecule. Therefore a direct comparison of EI and MUPI mass spectra is often difficult.

A further example of the possibilities of MUPI in peptide investigations is shown in figure 2. Here the partial hard ionization mass spectrum of substance P is shown.

Clearly the complete series of fragment ions containing the N-terminal end of the peptide chain can be identified. This series starts with the formation of the A_9, B_9 ion and goes down to the formation of even the A_1, B_1 ion. But also some fragmentations containing the C-terminal end are observed. These ions yield in the signals at masses 465, 612 and 868. These ions are of type Y'. Note also the high intensity of the fragment ions close to the aromatic residues.

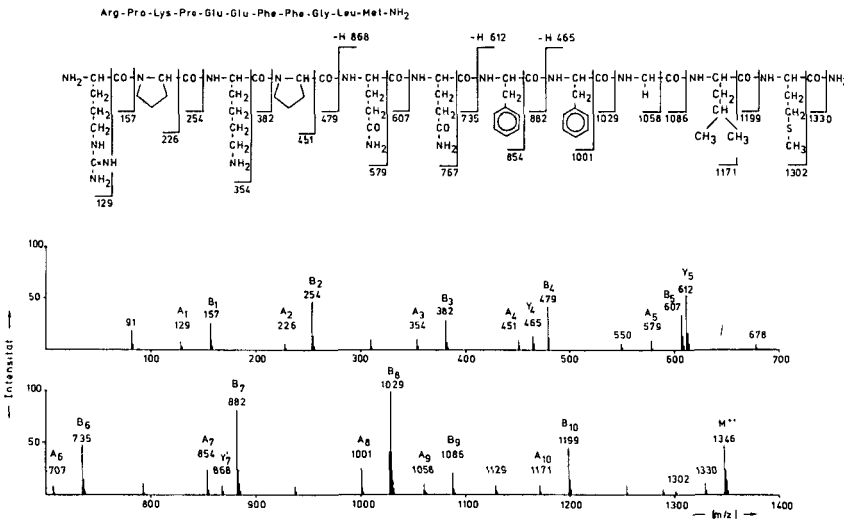

Fig.2 MUPI mass spectrum of substance P.

The table below shows a comparison of peptide investigations by various ionization methods. As can be seen, MUPI gives an intermediate number of fragment ions that is well sufficient to deduce the structure of any peptide.

Ionization Method	Typical Sequence Ions
Electron Ionization (metastable Ions)	$(A_n)^+$, $(B_n)^+$
Multiphoton Ionization	$(A_n)^+$, $(B_n)^+$, $(Y'_n)^+$
Fast Atom Bombardment	$(A_n)^+$, $(B_n)^+$, $(C_n)^+$ $(Y_n)^+$, $(Z_n)^+$

ACKNOWLEDGEMENTS.

The authors would like to thank dem Bundesministerium für Forschung und Technologie, der Deutschen Forschungsgemeinschaft and Bruker-Franzen Analytik (Bremen) for supporting this work. R.C.B. was supported by a NATO PDF Reseach Grant.

REFERENCES.

[1] J. Grotemeyer, E.W. Schlag; Angewan.Chem. 100, 461 (1988).

Presented at the 36th ASMS Conference on Mass Spectrometry and Allied Topics
June 5-10, 1988, San Francisco, CA

MS-MS IN A FOUR SECTOR MASS SPECTROMETER: PARAMETERS AFFECTING THE MS-II LINKED SCAN

K.B. Tomer and S. Verma

Laboratory of Molecular Biophysics, National Institute of Environmental Health Sciences, P.O. Box 12233, Research Triangle Park, NC 27709

FAB in conjunction with MS-MS is rapidly becoming the method of choice for the structure determination of peptides and other biomolecules. The major advantages of MS-MS are that components of mixtures can be analyzed without prior separation and, with collisional-activation, fragments are produced that give the complete sequence of many biopolymers. Several groups have pointed out that with increasing mass of the parent ion, daughter ions produced by high energy collisional activation undergo peak broadening and exhibit an increasing kinetic energy loss, E. In an MS-MS instrument in which MS-II is an electrostatic analyzer, these phenomena translate into broad peaks whose apparent mass has shifted significantly.

The B/E ratio of the daughter ions is proportional to $(E- E)^{-1/2}$ where E is the energy loss experienced by the parent ion during collisional excitation. E varies from ~5 eV for a small molecule (<200 amu) to 40 eV for a peptide of molecular mass 1500 (1). When E is negligible, the B/E ratio for daughter ions is identical to that of the parent. However, for large E, the B/E ratio of daughter ions is higher than that of the parent. Table 1 shows the effect of E on the B/E ratio of fragments by defining a daughter ion mass that should have the same B/E ratio as the parent.

Increasingly four sector tandem instruments have come into use for MS-MS studies in which the daughter ions are analyzed via a linked (B/E) scan of MS-II. In the B/E scan based on negligible E and an exponential scan law for B_2 there are no mass shifts observed since the daughter ions that have significant E are not passed to the detector. Thus the effects of E are "hidden".

The experimental results reported here are the outcome of a study aimed at investigating the effect of energy loss on the relative abundances of daughter ions observed during a B/E linked scan. The experiments were performed on a VG ZAB-4F of BEEB geometry. CA spectra were recorded at the 3rd and 4th sector. The collisional excitation conditions were varied by changing the nature of the target gas (eg. He vs Xe) and the pressure of the target gas. Unimolecular dissociation spectra at the 3rd sector were compared to corresponding CAD spectra to determine the energy loss E. Data were acquired by either scanning MS-II manually across the desired mass window or by computer generated scans of MS-II after calibration of MS-II by using the second source located between MS-I and MS-II immediately before the 3rd collision cell.

The results of our experiments are presented in Table 2 and Figures 1-3. One thus concludes:

i) conditions used to obtain optimum fragmentation may not correspond to single collision experiments.

ii) a single scan law may not be possible for a substance and/or the scan laws may differ for different compounds depending on whether a given fragment occurs under single collision or multiple collision conditions.

iii) a scan law generated for He may not yield good data for Xe.

iv) Although the position of the peaks do not change at the 4th sector, the relative abundances may be significantly affected due to energy loss.

References

1. a) M.L. Gross et al. in "Mass Spect. Anal. Large Molecules", C.J. McNeal, Ed., p.171, J. Wiley and Sons, Chichester, 1986 and references therein. b) G.M. Neumann et al., Naturforsch. 39a, 584 (1984).

Presented at the 36th ASMS Conference on Mass Spectrometry and Allied Topics
June 5-10, 1988, San Francisco, CA

TABLE 1. APPARENT DAUGHTER ION MASS VS. ΔE IN AN 8000 eV COLLISIONAL ACTIVATION

m_p \ ΔE	0	5	10	20	50
100.0	50.0	49.97	49.94	49.88	49.69
500 0	250.0	249 84	249.69	249.38	248.44
1000.0	500.0	499.69	499.38	498.75	496.88
2000.0	1000.0	999.38	998.75	997.50	993.75

FIGURE 1. EFFECT OF ENERGY LOSS ON THE RA IS DEMONSTRATED BY COMPARING THE PEAK PROFILE OF 1951 --> 912.335 a) WITH He b) WITH Xe

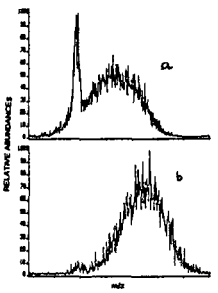

Xe AS COLLISION GAS HAS BEEN SUGGESTED AS A WAY TO DECREASE ΔE FOR HIGH MASS IONS (1). IF THE B/E SCAN IS SET WITH HELIUM AS TARGET GAS, SEVERE DISTORTIONS IN THE SPECTRUM CAN BE INTRODUCED BY USING Xe.

TABLE 2. ΔE VARIES WITH COLLISION GAS PRESSURE AND FRAGMENT ION
CAD OF 1431.95; CsI CLUSTER ION; He TARGET GAS.

m_d in amu \ ΔE in eV at	$10^{-5.8}$ mbar 50% BEAM ATTENUATION	$10^{-5.0}$ mbar "OPTIMUM FRAGMENTATION CONDITIONS"
1172.145	38.48	53 63
912.335	32.83	57.85
652.525	59.20	95.04
372.712	*not measurable*	59 91

FIGURE 2. CAD SPECTRA OF SUBSTANCE P RECORDED *AT 4TH SECTOR IN A B/E LINKED SCAN* USING a) He AND b) Xe AS TARGET GAS.

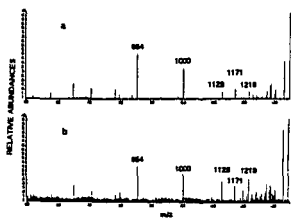

RELATIVE ABUNDANCES IN THE CA SPECTRA OF SUBSTANCE P WITH (a) He AND (b) Xe AS THE TARGET GAS. NORMALIZED TO THE ABUNDANCES OF FRAGMENT ION OF M/Z 854 5

M/Z	He	Xe
854	100	100
1000	65	79
1129	15	60
1171	22	46
1218	18	67

FIGURE 3. CAD SPECTRA OF CsI M/Z 1951.95 CLUSTER ION RECORDED IN a) B/E LINKED SCAN IS COMPARED TO ITS b) E-SCAN. XENON WAS THE COLLISION GAS EMPLOYED.

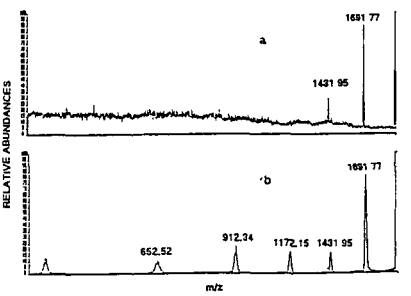

Presented at the 36th ASMS Conference on Mass Spectrometry and Allied Topics
June 5-10, 1988, San Francisco, CA

COMPARISON OF THE COLLISIONAL ACTIVATION DECOMPOSITION SPECTRA OF PEPTIDES CONTAINING BACKBONE MODIFICATIONS

L. J. Deterding[1], K. B. Tomer[1], and A. F. Spatola[2]

[1]Laboratory of Molecular Biophysics, N.I.E.H.S.,
P.O. Box 12233, Research Triangle Park, NC 27709

[2]Department of Chemistry
University of Louisville, Louisville, KY 40292

Fast atom bombardment (FAB) in conjunction with tandem mass spectrometry (MS/MS) has become a useful approach for the determination and confirmation of the structures of peptides. Upon collisional activation (CA), peptides readily decompose into fragment ions. These fragment ions can be assigned structures which usually are the result of cleavages of the backbone and/or side chain cleavages of the amino acids. Therefore, collisionally activated decomposition (CAD) is very useful for the structural elucidation and amino acid sequencing of peptides.

Recently, Spatola et al. (1) have shown that variations in the backbone elements in peptides have assisted in determining the functional role of the normal -CONH- peptide linkage. These variations include the replacement of -CONH- bonds with such groups as thiomethylene ether (CH_2S), thiomethylene sulfoxide (CH_2SO), thioamide (CSNH), and methylene amine (CH_2NH) moieties. Among the benefits of such modifications can be: 1) enhanced receptor selectivity; 2) increased resistance to enzymatic degradation; and 3) altered solubility properties. The CAD spectra of these backbone modified peptides are compared in order to determine the effect of the modification on the daughter ion spectra.

Upon collisional activation, the $(M+H)^+$ ions of straight-chain and cyclic peptides, which have been modified by substitution of a [CH_2NH] moiety for a [CONH] group in the backbone chain, fragment to give typical amino acid sequence ions (Fig. 1). However, internal fragment ions are also observed which are the result of a cleavage alpha to the substituted methylene group (Fragment F).

Substitution of a [CSNH] group into the backbone chain of peptides does not seem to have a large effect on the fragmentation of the peptide (Fig. 2). Cleavages around the thioamide are of relatively low abundance if present at all. Amino acid sequence fragmentations are observed and are of relatively high abundance.

In comparing the CAD spectra of straight chain peptides which have been modified by thiomethylene ether vs thiomethylene sulfoxide moieties (Fig. 3), the presence of the [CH_2SO] group leads to much more abundant N-terminal fragment ions than does the presence of the [CH_2S] group. The major difference observed in the CAD spectra is the relative abundance of fragmentations resulting from cleavages alpha to the thiopeptide linkages (Fragments B_3 and C_3). For the [CH_2SO] modified peptide of Tyr-Ala-Gly-Phe-Leu, the B_3 and C_3 fragment ions are relatively abundant (i.e. approximately 72% and 95%, respectively), whereas, with the [CH_2S] substitution, these same fragment ions are of relatively low abundance (i.e. <5%). In addition, it should be noted that these modified peptides tend to decompose into C-terminal fragment ions whereas the unmodified peptides tend to fragment into N-terminal ions.

The MS/MS spectra of cyclic peptides containing thioether/sulfoxide linkages have also been compared (Fig. 4). The C-terminal ions of X_4 and Y_4 are major fragmentations observed in the CAD spectra of these modified peptides. However, both the [CH_2S] and [CH_2SO] substituted peptide of Tyr-c(Lys-Gly-Phe-Leu) fragments to give the ion of m/z 420, which corresponds to the loss of $-CH_2CH_2SCH(CHC_6H_5)CO$ and $-CH_2CH_2SOCH(CHC_6H_5)CO$, respectively, from the $(M+H)^+$ ions.

Presented at the 36th ASMS Conference on Mass Spectrometry and Allied Topics
June 5-10, 1988, San Francisco, CA

Upon collisional activation, peptides containing modifications in the backbone chain undergo amino acid sequence fragmentations and side-chain fragmentations. Straight-chain peptides containing [CH_2S] and [CH_2SO] groups decompose to give daughter ions indicating the presence of a sulfur in the backbone chain. However, the presence of a [CSNH] group has little effect on the fragmentation of the peptide. In comparison, the backbone modified peptides tend to give relatively more abundant C-terminal fragment ions than the normal unmodified peptides. However, the daughter ion spectra vary with the presence of the amide bond replacement. Therefore, useful structural information may be obtained. In addition, these peptide backbone modifications have been recognized as having the potential for yielding structures with biological selectivity and increased resistance to enzymatic degradation.

References
1. A. F. Spatola, H. Saneii, J. V. Edwards, A. L. Bettag, M. K. Anwer, P. Rowell, B. Browne, R. Lahti, and P. Von Boigtlander, Life Sciences, 38, 1243-1249.

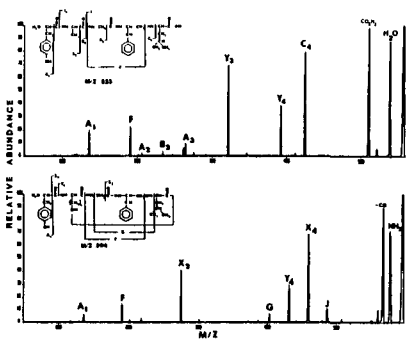

Figure 1

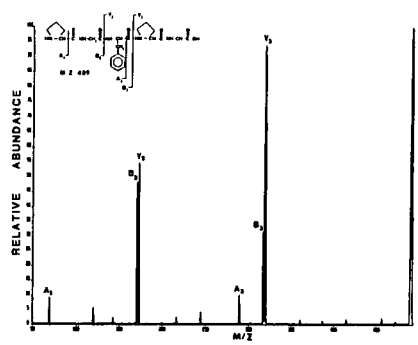

Figure 2

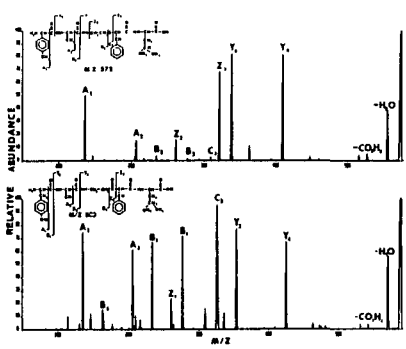

Figure 3

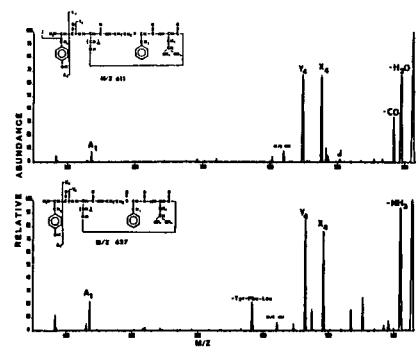

Figure 4

Presented at the 36th ASMS Conference on Mass Spectrometry and Allied Topics
June 5-10, 1988, San Francisco, CA

COLLISIONAL ACTIVATION TANDEM MASS SPECTROMETRY OF LITHIUM-CATIONIZED PEPTIDES

R.P. Grese and M.L. Gross
Midwest Center for Mass Spectrometry
Dept. of Chem., U. of Nebraska, Lincoln, NE 68588-0304.

Complexes of metal ions and peptides can be produced in the gas phase by FAB and the site of interaction determined by using collisional activation (CA) and tandem mass spectrometry (MS/MS). This methodology gives complementary information to CA of protonated peptides and may be useful in understanding interactions of peptides and biologically important metals.

Generally, monovalent metal ions interact with the C-terminus of a peptide in the gas phase. Both the metastable and CA decompositions of [peptide + Li]$^+$ ions produce an abundant fragment ion by loss of the C-terminal amino acid residue. The [M + Li]$^+$ ion of HisLeuGlyLeuAlaArg (Figure 1a) fragments upon CA to give an abundant ion of m/z 516 formed by loss of an arginine residue. Also in the spectrum are sequence ions which provide complementary information to that from the CA mass spectrum of the protonated species (Figure 1b). We have observed that this process occurs for sixty peptides, from tri- to nonapeptides, for all common amino acids at the C-terminus, and for N-terminally blocked peptides. The structural utility of the method is clearly seen -- the C-terminus is rapidly verified.

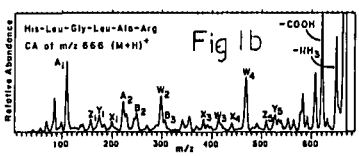

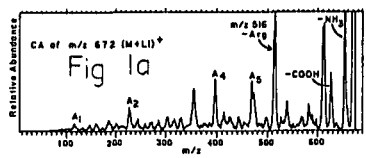

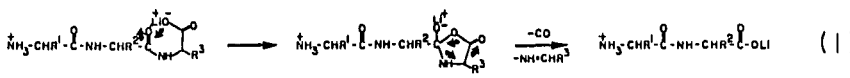

(1)

Recently, Renner and Spiteller[1] suggested, with little experimental support, a mechanism (Equation 1) for the C-terminus elimination. We report three substantial pieces of experimental evidence that the process occurs as per Equation 1: (1) The fragment ion, a smaller peptide, decomposes in manner identical to a metal-peptide complex. This is illustrated in the MS/MS/MS spectrum of the m/z 449 ion from CA of leu-enkephalin (Figure 2). (2) CA of ^{18}O and ^{15}N labelled peptides give neutral losses consisent with the losses of CO and an imine. (3) CA of [M + Li]$^+$ ions of various model compounds (Table 1) reveal that a free C-terminal and a carbonyl on the amino acid next to the C-terminus are necessary for this fragmentation.

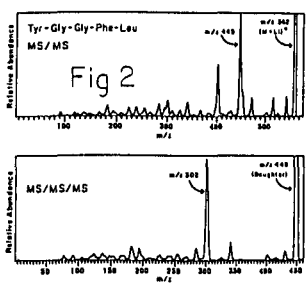

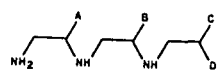

Table 1 "Glycine-Glycine-Glycine" Model Compounds

Compounds	A	B	C	D	Loss of C-terminus from (M + Li)+
I	O	O	O	OH	Yes
II	NH_2	NH_2	NH_2	OH	No
III	NH_2	NH_2	O	OH	No
IV	O	NH_2	O	OH	No
V	O	O	NH_2	CH_3	No
VI	O	O	O	OCH_3	No
VII	O	O	O	NH_2	No

1 Renner, D.; Spiteller, G. Biomed. Mass Spectrom. **1988**, 15, 75-77.

The loss of the C-terminus has also been observed for peptides complexed with Na^+, Ag^+, and Cu^+, but not with K^+. Presumably the K^+-peptide interaction is weaker and is released upon CA. Elimination of the C-terminus also occurs upon IR laser desorption of cationized-peptide in a Fourier transform mass spectrometer (Figure 3) suggesting that this process is thermally allowed. The use of laser desorption-FTMS is attractive because with multiple resonance techniques it may be possible to sequence small peptides by sequentially eliminating the C-terminus.

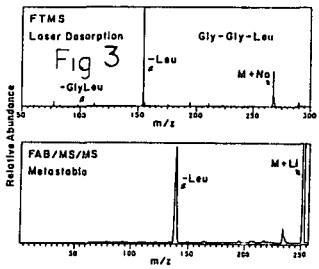

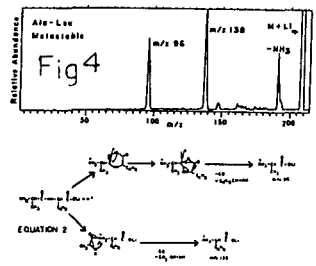

Loss of the C-terminus residue occurs also with $[M + Li]^+$ of dipeptides; however, the most abundant fragment ion in the metastable (and CA) mass spectrum is $[Y + H + Li]^+$ (Figure 4). Preliminary MS/MS/MS and deuterium labelling experiments are consistent with the proposed mechanism (Equation 2).

The decomposition of metal-cationized peptides containing histidyl residues are exceptions to the general fragmentation described above. The most abundant fragment ion is cleavage at the histidyl residue indicating that the Li^+ preferentially chelates to the imidazole nitrogens of histidine (see Figure 5 for proposed structure). This underscores the potential of this research for establishing solution analogies because histidine has been shown to be a prinicipal binding site for transition metals in metalloproteins.

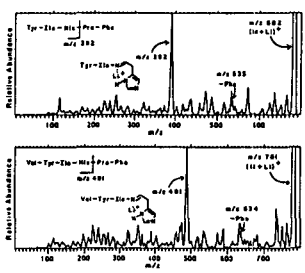

Fig 5

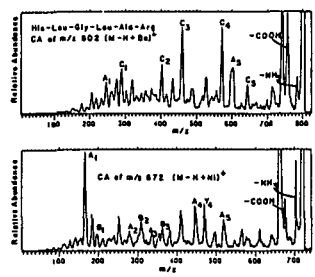

Fig 6

One area of future research will be the study of the intrinsic reactivities of divalent metal ions with peptides in the gas phase. Divalent transition metal ions are important biologically in many metalloenzyme systems. Comparison of the CA mass spectra of the $[M - H + Ba]^+$ and $[M - H + Ni]^+$ ions of HisLeuGlyLeuAlaArg (Figures 6 a and b) point to differences in the gas phase reactivities of these two metal ions with the same peptide which may be useful in understanding the reactivities is solution.

Acknowledgement. We are grateful to Dr. R.L. Cerny for helpful discussions during the course of this research.

Presented at the 36th ASMS Conference on Mass Spectrometry and Allied Topics
June 5-10, 1988, San Francisco, CA

TANDEM MASS SPECTROMETRIC ANALYSIS OF PEPTIDES ON A HYBRID INSTRUMENT.

Marc H. Reilly and Simon J. Gaskell, Center for Experimental Therapeutics, Baylor College of Medicine, Houston, Texas 77030

Tandem MS with collisionally activated decomposition (CAD) of peptide $[M+H]^+$ ions can provide improved mixture analysis capabilities and increased structural information. Though comparisons between multiple analyzer configurations for tandem MS may be made on the basis of mass range and ultimate resolution capabilities, these appear not to be the critical issues at present. Decreasing parent ion yield during FAB and decreasing conversion to daughter ions both occur as the mass of the analyte increases, generally limiting to 3-4000 the mass range currently accessible in tandem MS experiments and dictating that analyses be operated at close to maximum transmission, corresponding to low resolution of both parents and daughters. More important considerations in the comparison of instrument configurations are the conditions under which decompositions of selected parent ions are allowed or induced to occur. These conditions are markedly different when decompositions occur in a quadrupole region (as in the triple quadrupole or hybrid configurations) and in a field-free region of a multi-sector instrument. Thus, for the example of hybrid instruments (combining double focusing and quadrupole components) parent ions are selected using the double-focusing section and decelerated to kinetic energies of (usually) <100eV before introduction into the RF-only quadrupole collision region. Collision energies (in the laboratory frame-of-reference) are therefore <100eV and, importantly, residence times in the decomposition region are of the order of milliseconds. The collimating properties of the RF-only quadrupole facilitate the use of heavy collision gases (increasing the center-of-mass collision energy) at pressures favoring multiple collisions, conditions which might otherwise lead to excessive scattering losses. There is a growing body of data derived from FAB/tandem MS of peptides on four sector instruments and some data obtained using a triple quadrupole. Analytical data for peptides obtained with hybrid sector/quadrupole instruments are few.

We have analyzed a number of peptides in the 1000-1500 mass range using a hybrid instrument of BEqQ design (VG ZAB SEQ). Sample introduction used a conventional FAB probe with the liquid matrix thioglycerol/2,2'-dithiodiethanol (1/1). The primary FAB beam was xenon atoms. Argon was the collision gas. As an example, we present data for the decapeptide Substance P, fragment 2-11 (Pro-Lys-Pro-Glu-Glu-Phe-Phe-Gly-Leu-Met $[NH_2]$). Figure 1a shows the daughter ion spectrum of MH^+ ions, m/z 1191. Very clear fragmentation information is apparent but interpretation is ambiguous without consideration of complementary data obtained by CAD of MH^+ ions of the terminal N-acetyl derivative. These data are shown in Figure 1b. Mass shifts of 42u, observed for a number of the major fragments, are consistent with assignments as B-series ions (Figure 1). Daughters with m/z 966 and 949 are not shifted and are assigned Y_8'' and Z_8 structures. They are the only prominent representatives of C-terminal ions in the spectrum. A further series of ions is attributed to $(B_nY_8)'_{n-2}$ structures. The prominence of these fragments is similar to that of the B-series. The ion of m/z 226 in the spectrum of the underivatized peptide is shown by N-acetylation to have a dual origin. A pair of ions of m/z 226 and 268 are observed in the spectrum of the derivatized peptide (Figure 1b), attributable to B_2 and $(B_4Y_8)'_2$ fragments (which are isobaric for the native peptide).

(a) Daughters of m/z 1191

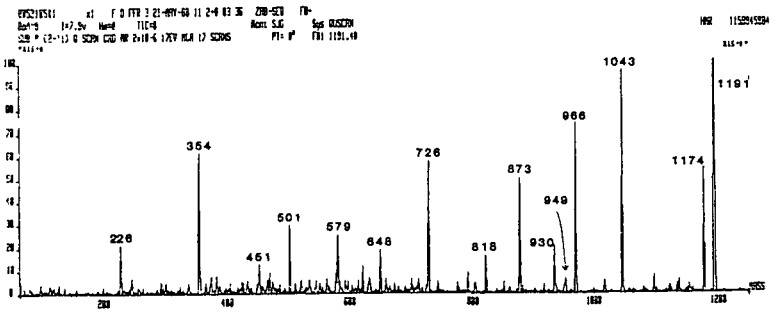

(b) N-acetyl derivative : daughters of m/z 1233

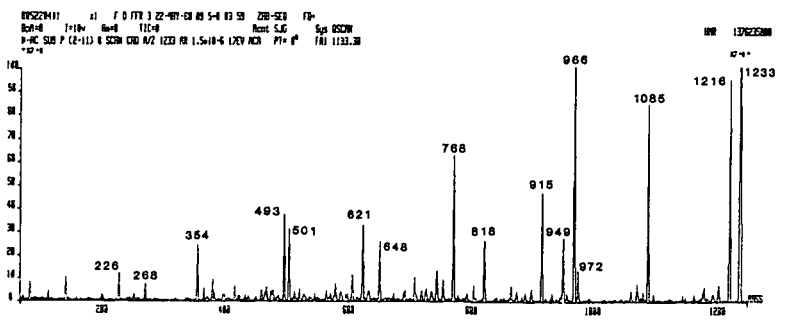

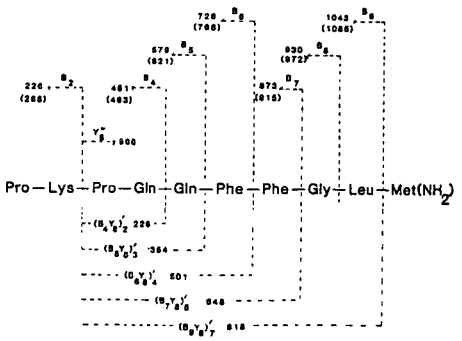

Fig. 1. CAD of MH^+ ions derived from Substance P, fragment 2-11 (m/z 1191) and the N-acetyl derivative (m/z 1233). The pressure of argon collision gas was calculated to be 0.3 mtorr in the collision region. The collision energy was 17eV.

Presented at the 36th ASMS Conference on Mass Spectrometry and Allied Topics
June 5-10, 1988, San Francisco, CA

FAB MASS SPECTRA AND CAD SPECTRA OF GLYCEROL AND AMINO ACIDS WITH SEVERAL CHLORIDES.

Kimio ISA and Yasuhiko TERAI
Department of Chemistry, Faculty of Education, Fului University;
Bunkyo 3-9-1, Fukui-shi, 910, JAPAN

I.

The relation between metal ion (alkali or alkaline earth metals) with amino acid is an important problem in biophysics. Soft ionization methods makes easily to get the cationized ions of biomolecular substances, especially amino acids, peptides and sugars. Relation between alkali ion affinity and ionic radius ratio in the case of glycerol (G) by means of fast atom bombardment tandem mass spectrometry (FABTMS) has been already published (1). This report explains the relation between the alklai and alkaline earth metals (Li,Na, K, Rb, Cs and Mg, Ca) with L-α-amino acids by FABTMS.

II.

Collisionally activated decomposition (CAD) and metastable ion (MI) decomposition spectra of the pre-selected ions which are seperated by a high resolution mass spectrometer (JEOL DX303, EBE type), operating an ion accelerating voltage of 3 kV and a mass resolution of approximately 1000 (10 % valley definition) are studied by a tandem mass spectrometer (2). Post acceleration high sensitive detector (conversion dynode) was set up to increase the sensitivity. The gases for the fast atom gun and collision are both Ar. The energy of this fast Ar atom beam was 6 keV and tube current was 20 mA. The pressure of collision gas was increased until the precursor ion signal was reduced to about 1/3 of it soriginal value and CAD spectrum was obtained by a scan of the second electric sector analyzer. The mass spectra were processed with a JEOL DA-5000 data system. Commercial Glycerol, alklai halide(AX), alkaline earth halide (BX_2) and 20 L-α-amino acids are used with no further purification.

III.

1) FABMS spectra of mixtures of amino acids, glycerol and AX showed that typical four ions, $(M+H)^+$, $(M+A)^+$, $(M+G+H)^+$, and $(M+G+A)^+$ were identified. In the case of using only glycerol, $(M+A)^+$ is dominantly appeared, but in the case of the mixture of amino acids and glycerol, $(M+H)^+$ was the dominant peak. Therefore, alkali halide as additive to sample of FABMS did not help to increase the signal.

2) Affinity of various metal ions (Li to Cs) with amino acids with alkyl side chain, Gly (R=H), Ala (R=CH_3), Val (R=C_3H_7), Leu (R=C_4H_9), Ile (R=C_4H_9), and glycerol was studied. The CAD spectra of precursor ion , $(M+G+A)^+$ was measured, and the results were listed below (where M=

amino acid, A=alkali metal),

Gly	all A	M<G
Ala	Li, Na, K, Rb,	M<G
	Cs	M>G
Val, Leu	Li, Na, K,	M<G
	Rb, Cs	M>G
Ile	Li,Na,	M<G
	K, Rb, Cs	M>G.

3) The fragment ion A^+ from the CAD spectra of $(M+A)^+$ decreases with alkyl side chain's length was considered to be complex in three dimension.
4) The mixtures of the glycerol, 20 amino acids, and three chlorides, Mg, Ca, and Al were measured by FABMS. Six characteristic ions, $(M+Mg-H)^+$, $(M+MgCl)^+$, $(M+Ca-H)^+$, $(M+CaCl)^+$, $(M+Al-2H)^+$, $(M+AlCl_2)^+$, were identified (where M=glycerol and amino acids). The CAD spectra from $(M+Mg-H)^+$, $(M+Ca-H)^+$, $(M+Al-2H)^+$, showed the typical dehydration ($-H_2O$, -18) and the intensities of these ions decrease in order of Al, Ca, Mg. The ionic radii of these ions reflects the intensity of dehydration has already been established (2 or 3). But the disorder of Ca and Mg was not been understood until now.
5) Almost all amino acids can combine the $(Ca-H)^+$ easily, but $(M+AlCl_2)^+$ ion can not be obtained in almost all amino acids except Glu and Trp.
6) The precursor ion $(M+A)^+$ and $(M+B-H)^+$ were measured and discused in the form of gaseous structures, where M represents Gly, Ala, Val, Leu, and Ile. The alklai ion, A^+, was placed between two oxygens of carboxylate and the alklaine earth metal ion, B^{2+}, was placed between nitrogen of amide and oxygen of carboxylate.
7) The precursor ion, $(M+BX)^+$ was mainly decomposed to $(M+B-H)^+$ with elimination of HCl.

This work was partly supported by the Grant-in-Aid for Scientific Research (6254032) from the Ministry of Education , Science and Culture.

1) K.Isa, H.Kido, Y.Takeuchi, and H.Konishi, Proc. IInd Japan-China Joint Symposium on Mass Spectrometry, Sep 15-18 (Osaka), 157-160 1987.
2) K.Isa, T.Kinoshita, H.Kido, R.Nakata, and K.Mizuta, Nippon Kagaku Kaishi, 1657 (1986).
3) K.Isa, Y.Terai, Noppon Kagaku Kaishi, 572-577 (1988).

Presented at the 36th ASMS Conference on Mass Spectrometry and Allied Topics
June 5-10, 1988, San Francisco, CA

TANDEM MASS SPECTROMETRY INVESTIGATIONS ON LICHEN'S METABOLITES

P. Allemand, G. Tsoupras and R. Tabacchi

Institute of Chemistry, University of Neuchâtel,
Av. de Bellevaux 51, CH-2007 Neuchâtel, Switzerland

INTRODUCTION

Lichens are organisms of very slow growth. In spite of being widely distributed, for certain species it is difficult, if not impossible, to obtain sufficient quantities of material to carry out an investigation on their composition by classical methods (i.e. extraction, isolation and identification). We have undertaken a study to assertain whether direct analysis of lichens by MS-MS offers a rapid and sure alternative.
The presence of a few compounds in large quantities and many others in small, even trace quantities, in lichens means that any method of direct analysis is difficult.
Depsides and depsidones are the most abundant metabolites in lichens. In spite of their chemical structure, depsides rarely show a molecular peak and consequently are difficult to identify by mass spectrometry.
We investigated first a series of typical compound: Atranorine (1), Chroratranorine (2) and Methyl-barbatate (3). Using different ionisation methods and CAD spectra of molecular, quasimolecular, isotopic and fragment ions.

(1) R = CHO R' = H R" = H

(2) R = CHO R' = H R" = Cl

(3) R = CH_3 R' = CH_3 R" = H

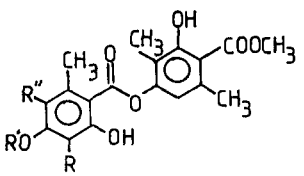

RESULTS

Under E.I. conditions depsides gave a number of small fragments of large intensity and very weak parent ions which were lost in the spectral noise. Under positive CI conditions quasimolecular ions were observed but the CAD spectra gave no useful fragmentation information. In our study negative CI gave the best results. These results have been used in the direct study of very small quantities of crude samples of *Pseudevernia Furfuracea* and *Lobaria Pulmonaria*.

NCI/MS STUDY OF ATRANORIN AND SOME OTHER DEPSIDES

When a depside is analysed by NCI/MS, two ions are formed : $M^{-\cdot}$ and $(M-H)^-$. An MS-MS study of these two ions shows that their fragments give ions containing either the A or the S ring. m/z 373 gives two fragments (m/z 195 and 177) from S and A rings respectively. m/z 374 has two possible origins, $M^{-\cdot}$ or $(M-H)^-$-^{13}C. Four fragments are observed from this peak, m/z 177, 195 and m/z 178, 196 which correspond either to the same fragments containing ^{13}C, or to $S^{-\cdot}$ and $A^{-\cdot}$ (cf scheme).

NCI/MS with thermalyse electrons (CH_4) gives only $M^{-\cdot}$ and leads mainly to m/z 178. A new ion (m/z 552 is formed by combination of an atranorin molecule with an S unit. This spectrum confirms that the other peaks in NCI-NH_3/CAD-spectra are due mainly to the fragmentation of $(M-H)^-$-^{13}C.

The fragmentation pathways of Cl-atranorin are similar to those of atranorin. However, ionization by loss of a hydroxyl proton is favoured by their greater lability. Consequently, in this case m/z 408 is principaly due to $(M-H)^-$-^{13}C. The spectrum of the daughter ions confirm this through the relative intensities of the ions compared with the one of the spectrum of daughter ions on m/z 374 from atranorin.

Daughter ions of m/z 407 (^{35}Cl-atranorin) compared to daughter ions of m/z 409 (^{37}Cl-atranorin) confirm that m/z 195 corresponds to cycle A and m/z 211 (m/z 213) to cycle S.

Comparison of the MS-MS spectra of atranorin and methyl-barbatate gives useful information. Both compounds have the same molecular weight, but substitution of ring S is different.
The substituents in methyl-barbatate are less electrophilic than those of atranorin. Thus, fragmentation of $M^{-\cdot}$ (m/z 374 / CH_4) leads mainly to m/z 195.
In the collision spectrum of m/z 373 ($(M-H)^-$ / CH_4), no fragment from ring S is observed, because there is only one hydroxyl on this ring. For fragmentation, two are necessary, one for ionization $(M-H)^-$, and the other for the fragmentation transfer mechanism.

DIRECT NCI/MS-MS STUDY OF *LICHENS*

NCI/MS-MS has been used to characterise compounds directly from lichens without prior extraction.
Pseudevernia Furfuracea has been investigated in our laboratories in a previous study. Several compounds have been isolated and identified. Through direct NCI/MS-MS on a piece of lichen we were able to identify five of these metabolites.

The NCI/MS-MS spectra obtained directly from the lichen *Lobaria Pulmonaria* and those from the isolated compounds show that this technique gives results reproducible enough to allow the comparison of data from different sources.
The peak at m/z 368 in the spectrum of 8'O-methyl stitic acid obtained directly for the lichen is probably due to the presence of a compound of the same molecular weight or a compound which gives a fragment at m/z 400. This illustrates one of the problems encountered in using MS-MS when substances have common ions.

CONCLUSION

Our results show that direct study of lichens by negative CI/MS-MS is rapid and can be carried out on very small samples. The obtention of meaningfull results is dependent on many factors, above all the composition of the mixture under study. The thermal instability and low volatility of the depsides and depsidones are the major problems. Use of chromatographic methods (TLC and HPLC) in parallel with MS-MS can be a very powerfull tool for investigations on lichens.

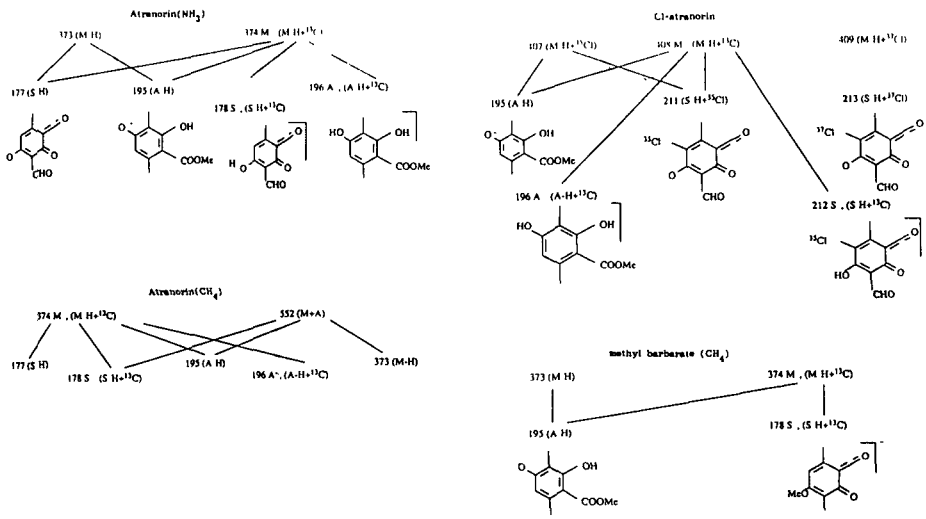

Presented at the 36th ASMS Conference on Mass Spectrometry and Allied Topics
June 5-10, 1988, San Francisco, CA

FABMS AND FAB MS/MS INVESTIGATIONS OF TECHNETIUM AND RHENIUM COMPLEXES

C. E. Costello[1], C-H. Zeng[1], N. H. de Vries[1], L. A. O'Connell[1], R. M. Pearlstein[1], A. Davison[1] and A. G. Jones[2]

[1]Dept. of Chemistry, Mass. Inst. of Technology, Cambridge, MA 02139 and [2]Dept. of Radiology, Harvard Medical School, Boston, MA 02115

Technetium-based radioimaging agents are very important for clinical diagnosis. A thorough understanding of the structure and chemistry of Tc complexes is essential for rational design and efficient synthesis of new agents targeted to specific organs or tissues. Fragmentation pathways of technetium and rhenium complexes have been explored by recording the metastable (MS/MS) and collision induced decomposition (CID MS/MS) spectra of molecular ions, cluster ions and fragment ions that appear in the fast atom bombardment mass spectra (FABMS) of three series of related compounds. This information should provide insight into the effects that variations in the ligands, the metal core and the oxidation state of the metal have upon ion structure and chemistry. The three series for which data are reported are chloro(1,2-dioxolato)oxo-(1,10-phenanthroline)technetium(V) complexes, sterically hindered arene thiolates of the general structure $Tc(III)(SAr)_3L_2$, and hexakis aryl isonitrile technetium(I) cations.

FABMS and MS/MS spectra of the three classes of technetium complexes, obtained with or without the use of a collision gas, exhibit quite unique and informative characteristics. The mass spectral behavior of these complexes seems to be an accurate reflection of the changes in properties that accompany modifications of ligand, oxidation states and the metal core itself. Because the MS/MS spectra are free of matrix-related ions, they are simpler to interpret than the FABMS spectra. The MS/MS spectra are useful to clarify the many fragmentation pathways because they permit observation of products originating from individual species.

Chloro(1,2-dioxolato)oxo-(1,10-phenanthroline)technetium(V) complexes have proven to be a useful source of the TcO^{3+} core for ligand exchange reactions. $TcOCl_3$(phen) reacts with olefins to produce *cis*-diols. The fragmentation pattern shown below was deduced on the basis of MS/MS spectra obtained for six members of the series, chosen as representative of the structural variations among more than ten 1,10-phenanthroline analogs and many more analogs containing other aromatic ligands for which two-sector spectra had been recorded. Facile chlorine loss is always observed, but there is a minor pathway which retains the chlorine atom while the ethanedioxolate ligand is lost. Fragmentation may occur within the ethanedioxolate ligand or it may be lost completely. Only after loss of the other ligands is bond-breaking within the phenanthroline ligand observed, and then it may be fragmented or stripped away entirely to leave Tc(I).

Complexes of technetium with sterically hindered arene thioxolates, $Tc(III)(SAr)_3(L)_2$, can exchange their ligands without disturbing the $Tc(SAr)_3$ core. The MS/MS spectra of common ions, obtained with or without the presence of collision gas, derived from complexes that vary in the axial ligand, are indistinguishable, suggesting the formation of identical intermediates. The spectra obtained from analogs that contain Re instead of Tc show quite different fragmentation patterns that reflect the difference in the oxidation potentials of the two metals. Like the first group of compounds, the Tc arene thioxolates form dimers in their FAB mass spectra. However, while the CID MS/MS spectrum of $(2M-Cl)^+$ Tc(V)dioxolato species indicates that the dimer most readily collapses back to the monomer, the $(2M-L_n)^+$ ions of the $Tc(III)(SAr)_3L_2$ complex form a variety of product ions by sequential loss of ligands but with retention of both Tc atoms.

Presented at the 36th ASMS Conference on Mass Spectrometry and Allied Topics
June 5-10, 1988, San Francisco, CA

The hexakis Tc(I) alkyl isonitrile cations generally produce FABMS and MS/MS spectra that are characterized by multiple alkyl or alkene losses to form $Tc(CN[H])_n(CNR)_{6-n}$ species. The spectrum of the hexakis aryl isonitrile cation is quite simple, dominated by CNAr losses. Upon CID, the doubly-charged ion is formed from the singly-charged ion by two routes, apparently equally probable: loss of a second electron and loss of a proton. CID of the doubly charged cation leads predominantly to $(M-CNAr_n)^{++}$ species; the few singly-charged ions formed show loss of Ar and/or CNAr. The substitution of aryl for alkyl groups affects both the spectra and the chemistry of these complexes.

Acknowledgement

These studies are supported by the NIH Division of Research Resources and by the Department of Energy.

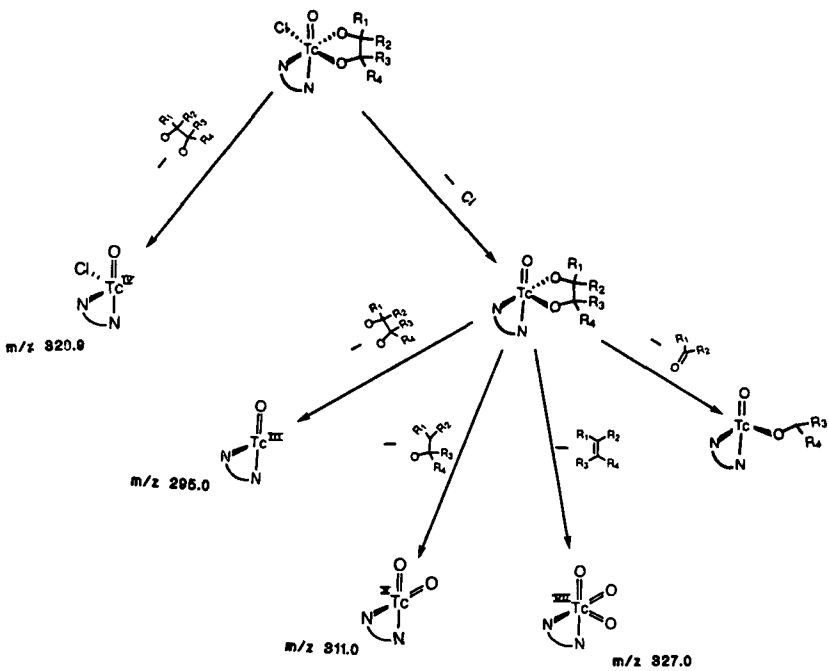

Fig. 1. Fragmentation pattern of chloro(1,2-dioxolato)oxo-(1,10-phenanthroline)technetium(V) complexes.

Presented at the 36th ASMS Conference on Mass Spectrometry and Allied Topics
June 5-10, 1988, San Francisco, CA

TANDEM MASS SPECTROMETRY OF NUCLEIC ACID HYDROLYSATES

C.C. Nelson and J.A. McCloskey.
Department of Medicinal Chemistry, University of Utah, Salt Lake City, Utah 84112

The combination of FAB and tandem mass spectrometry has been shown to provide useful structural information about nucleosides and nucleotides[1,2]. Modified nucleosides, such as nucleoside antibiotics and constituents of nucleic acids, frequently occur as minor components in complex biological mixtures and are often difficult to isolate and characterize[3]. The present study demonstrates the utility of tandem mass spectrometry with FAB ionization as a method for identification and structure analysis of minor component modified nucleosides in enzymatic digests of transfer ribonucleic acid (tRNA) without prior sample purification.

Experiments were carried out on a VG 70 - SEQ mass spectrometer (EBQQ geometry). A series of low-energy collision-induced dissociation (CID) reactions of the molecular ions (MH^+) were first examined for two model nucleosides 2'-O-methylcytidine (Cm) and threonyladenosine (t^6A), which are sugar modified and base modified nucleosides, respectively. Relative fragment ion intensities were determined as a function of incident ion (MH^+) translational energy and pressure in the rf-only quadrupole using helium, argon, krypton, and xenon collision gases. Optimum energies and MH^+ transmissions for the model nucleosides were then used for tRNA hydrolysate mixtures assuming general applicability to other modified nucleosides.

For low-energy collisions of the model nucleosides, Ar and Kr collision gases provided more efficient fragmentation of MH^+ within the rf-only quadrupole than He or Xe. This was determined by comparing relative fragment ion intensities and collision losses after normalization of MH^+. Kr yielded more total fragment ion current, however, compared to Ar when the transmission through the entire QQ system was determined at the same transmission of MH^+ through the rf-only quadrupole. It is possible that collision losses outside the rf-only quadrupole are greater for Ar than Kr at the 20% transmission used. Subsequent low-energy CID of tRNA hydrolysates were therefore analyzed using Kr as collision gas.

Full scan CID daughter spectra were acquired on preselected parent ions (MH^+) of nucleosides from E. coli tRNA - Phe and E. coli B tRNA - Tyr. The collision gas pressure used corresponded to an MH^+ transmission of approximately 20% as determined at 50 eV energy through the rf only quadrupole. Daughter scans and neutral loss spectra were acquired on hydrolysates corresponding to 5 μg of tRNA. Daughter ion spectra taken on about 70 ng of the highly modified nucleosides queuosine (Q) (fig. 1) and methylthioisopentenyladenosine (ms^2i^6A) (fig. 2) from tRNA - Tyr were acquired directly in the crude hydrolysate mixture. Structurally informative fragment ions were obtained as indicated by intense protonated base (BH_2^+) ions as well as characteristic side chain fragment ions m/z 295, 312 and 182, 194, 314 for Q and ms^2i^6A, respectively.

The presence of minor component nucleosides in complex mixtures such as enzymatic digests are not always evident from primary FAB mass spectra (fig. 3) because of varying ionization efficiencies and / or matrix effects. However, with a suitably designed neutral loss scan, such as loss of 132 amu

(ribose) to produce BH_2^+ ions, the majority of nucleoside molecular ions can by rapidly identified in 1 - 5 μg of crude tRNA hydrolysate (10 - 100 ng of individual nucleosides) (fig. 4). Subsequently, daughter ion spectra of these molecular ions can provide significant leads toward structural characterization for known nucleosides or unknown nucleosides of undetermined modification.

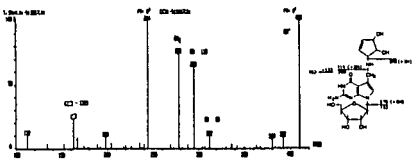

Fig. 1 Daughter ion spectrum of queuosine nucleoside (~ 70 ng). 20 eV energy (lab frame). Krypton collision gas.

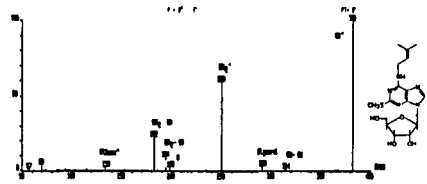

Fig. 2 Daughter ion spectrum of ms^2i^6A nucleoside (~70 ng). 25 eV energy (lab frame). Krypton collision gas.

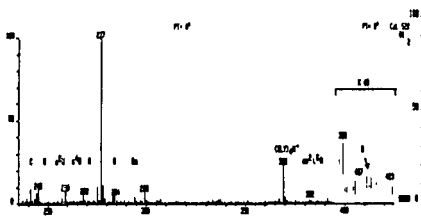

Fig. 3 Primary FAB spectrum of enzymatic digest of 5 μg of tRNA -Tyr.

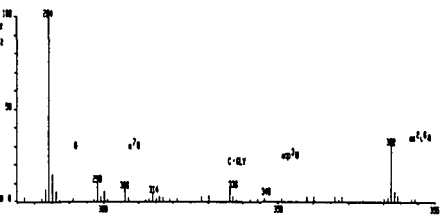

Fig. 4 Neutral loss scan for 132 (ribose). Enzymatic digest of 5 μg of tRNA-Phe. 10 eV energy (lab frame). Krypton collision gas.

This work was supported by NIH grant # GM 21584

1. F. W. Crow, K. B. Tomer, M. L. Gross, J. A. McCloskey, and D. E. Bergstrom *Anal. Biochem.*, **139**, 243 (1984).
2. D. L. Slowikowski and K. H. Schram *Nucleosides and Nucleotides*, **4**, 309 (1985).
3. J. A. McCloskey in *Mass Spectrometry in Biomedical Research*, (Ed. S. Gaskell) Wiley: Chichester, 1986, pp.75-95

Presented at the 36th ASMS Conference on Mass Spectrometry and Allied Topics
June 5-10, 1988, San Francisco, CA

THE EFFECT OF COLLISION GAS AND GAS MIXTURES ON DAUGHTER ION SPECTRA OF PEPTIDES USING A TANDEM DOUBLE-FOCUSING MASS SPECTROMETER

J.M.Curtis, L.S.Rong, R.M.Milberg, and K.L.Rinehart
School of Chemical Sciences, Univ. of Illinois, Urbana, IL 61801

Introduction

A new tandem double-focusing mass spectrometer of EB-EB geometry (VG Analytical 70-4SE) has recently been installed in our laboratory. One of the principal uses of the machine is to run MS/MS spectra of peptide ions produced by FAB. Since typical sample sizes are in the 0.2-10 microgramme range, it is essential that the optimum conditions for the production of structurally significant daughter ions are known prior to analysis. The aim of this study is to identify collision regimes which give daughter ions in high intensity throughout their possible mass range, and hence to provide the best possible sequence information.

Results and Discussion For Peptides of Mass 500-1500 Daltons

Previous studies [1] on the CID of peptide ions demonstrated the existence of an optimum collision gas pressure (the pressure giving the maximum abundance of fragment ions) which corresponds to a beam attenuation of 60-70% and is mass dependent. In order to investigate this, a test compound, the undecapeptide physalaemin (MH+ = 1265.59) was selected and the intensity of four fragment ions were recorded for different beam attenuations using H_2, He, N_2, Ar, and Xe collision gases (Figure 1). In general, light target gases (H_2, He) produce abundant high mass fragments at all pressures but less abundant low mass fragments except at high pressures. In contrast, the heavy target gases (Xe, Ar, N_2) produce low mass fragments in the greatest intensity corresponding to a greater conversion of translational energy into internal energy.

The optimum spectrum is defined here as one in which fragment ions are observed in good intensity throughout their possible mass range. This corresponds to a beam attenuation of 70% for the heavy target gases which is below that giving the maximum total daughter ion current. For light target gases the optimum beam attenuation is 90%.

A more detailed comparison of spectra produced using either heavy or light collision gases reveals that some fragment ions may be weak or missing in either case. An excellent compromise is to use as collision gas a mixture of a light gas with a heavy gas e.g., using a 1:1 mixture of H_2 and Xe, all the fragment ions are observed with good intensity at high and low masses.

CID of Peptides of Mass >1500 Daltons

The above results for physalaemin appear to apply well for parent ions of mass 500-1500 daltons. At higher masses, parent ions are produced in lower intensity by FAB so it becomes essential to maximize the intensity of daughter ions. A study of the effect of collision gas on the spectra of peptides in the 1500-2500 dalton range showed that light target gases become very much less efficient than heavy ones (Ar and Xe) at inducing fragmentation, and that some fragments (especially low mass) are completely absent from their spectra. Hence only heavy target gases are useful for this mass range.

Peptide ions of mass >2500 daltons readily undergo unimolecular decomposition, but the daughter ion spectra are usually missing important ions for structure determination. However, even moderate pressures of collision gas tend to drastically reduce the daughter ion currents. Thus, only low beam attenuations (<30%) using a heavy target gas can be used.

[1] G.M.Neumann and P.J.Derrick,Org.Mass Spectrom.,19,165,(1984).

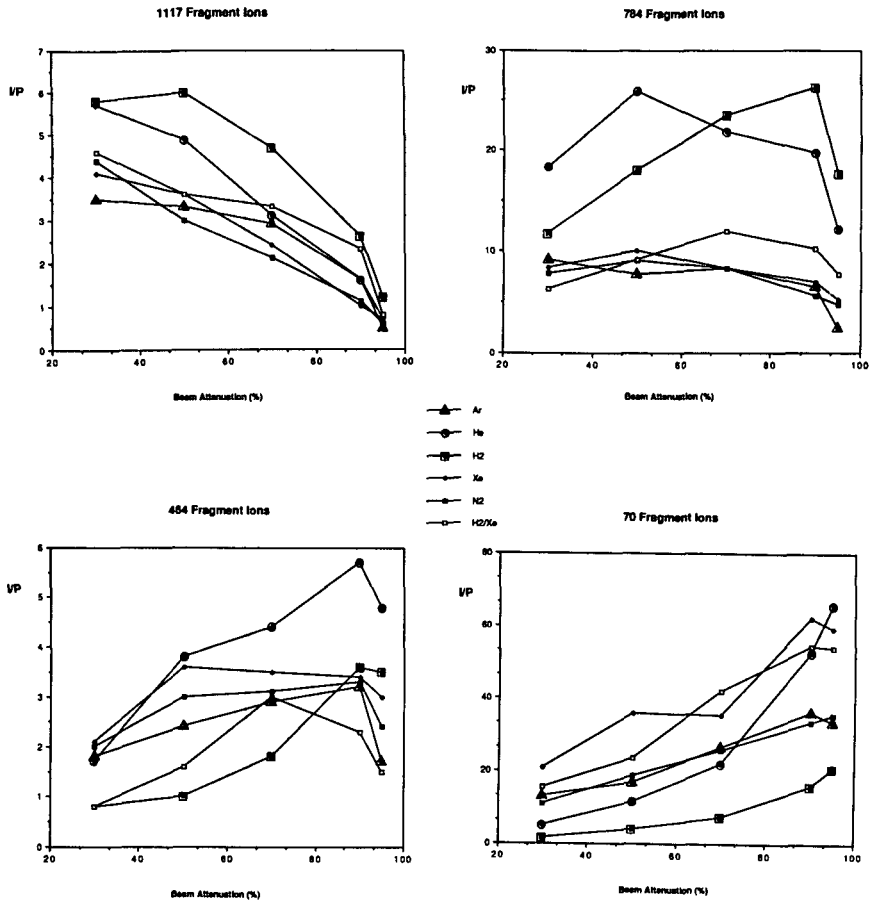

Figure 1. The Effect of Collision Gas Pressure on the Intensities (I x 10^{-4}) of Four Fragment Ions of Physalaemin, Relative to the Parent Ion Intensity (P). The Collision Cell was Floated to Half the Accelerating Voltage (ie. 4kV).

Acknowledgement: This work was supported by NIH grant GM27029

Presented at the 36th ASMS Conference on Mass Spectrometry and Allied Topics
June 5-10, 1988, San Francisco, CA

EI AND COLLISIONAL ACTIVATION MASS SPECTROMETRY OF BHT AND CERTAIN ALTERATION PRODUCTS:

William C. Brumley; U.S. Environmental Protection Agency,
EMSL-LV, Las Vegas, NV 89193-3478

BHT (2,6-di-t-butyl-4-methylpheonol) is a widely used antioxidant that has applications in food, cosmetics, medicines, and feeds. This paper describes the EI mass spectra of BHT and many of its alteration products. The alteration products arise from the study of BHT in a food simulating solvent of water/ethanol and in the pyrolysis study of hydroperoxy BHT. Hydroperoxy BHT is a plausible intermediate in the antioxidant role of BHT. The EI mass spectra are studied using accurate mass measurements and collisional activation of selected ions on a triple quadrupole instrument at -10eV energy. Compounds characterized include BHT (RMM=220) and BHT derived hydroperoxy (RMM=252), quinone (RMM=220), aldehyde (RMM=234), alcohol (RMM=236), acid (RMM=250), epoxide (RMM=252), dimer (RMM=438), ethyl ether (RMM=264), and butyl derivatives (RMM=276).

Fragmentation involves pure hydrocarbon losses and losses including oxygen, as revealed by high resolution MS. The elemental compositions of selected fragment ions are given in the EI spectra of Fig. 1. For example in the spectrum of BHT it is of interest to note that $(M-31)^+$ results from loss of $CH_3\cdot$ and CH_4. The ion corresponding to $(M-59)^+$ is also the result of pure hydrocarbon losses. Ions represented as $(M-57)^+$ and $(M-75)^+$ each consist of two different elemental compositions.

The CA spectra of the $(M-CH_3\cdot)^+$ ion of BHT and similar compounds exhibit an abundant ion at m/z 57 correlated with the presence of the second tert butyl group in the molecule. This provides a convenient tool for examining whether alterations have occurred at the tert-butyl moieties.

Distinguishing between the benzoid and cyclohexadienone structure is apparent in the CA spectra of the $(M-15)^+$ ions. The cyclohexadiene and quinone structures exhibit specific framentations with rearrangement. The CA mass spectrum of m/z 219 afforded by some of the compounds provides a fingerprint to verify this moiety in various alteration products; an ethyl ether and butyl derivative attached at the 4-methyl position are examples. (Fig. 2)

Two cases for the application of CA spectra to analogous structures are obvious. In one, different compounds fragment to the same ion structure. For example, m/z 161 of BHT, the ethyl ether derivative and the butyl derivative are probably the same; m/z 219 of Fig. 2 is also illustrated and is the same or similar for other compounds fragmenting at this position. The fragmentations leading to these ions involve the site of structural difference. In the second case, different compounds show parallel fragmentations but the ions are separated by a constant mass difference (e.g., 14 u); fragmentations resulting in these ions do not involve the site of structural difference.

Figure 1. EI mass spectrum of BHT.

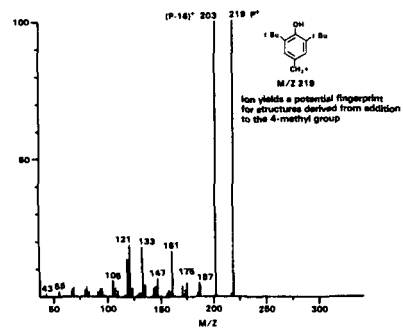

Figure 2. CA mass spectrum of m/z 219 from the ethyl ether derivative.

These studies provide a basis for the identification of many alteration products of BHT, the correlation of structure to the spectra, and the recognition of common ion structures as an aid to structure elucidation.

Presented at the 36th ASMS Conference on Mass Spectrometry and Allied Topics
June 5-10, 1988, San Francisco, CA

APPLICATIONS OF CONTINUOUS FLOW FAB MASS SPECTROMETRY FOR THE STUDY OF DRUG METABOLISM

Ralf Schubert*, **Ernst Schroeder***, Peter Jacobs**

*Finnigan MAT GmbH, Barkhausenstraße 2, D-2800 Bremen, FRG
**Organon Int. B.V., Scientific Development Group, Oss, The Netherlands

Introduction

Since its introduction in 1986 (1), continuous flow FAB (CFF) has been applied to various mass spectrometric problems. In this paper, we report on a new CFF development that we have used for quantitative determination of vecuronium bromide (figure 1) in plasma.
Vecuronium bromide is a clinically effective non-depolarizing neuromuscular blocking agent that has a wide margin of cardiovascular safety (2-4). Published assay methods have not been sensitive enough to monitor vecuronium in all clinical situations (5). Sensitivity could be improved using CFF.

Results

The conventional FAB mass spectrum of vecuronium bromide is shown in figures 2 and 3. The detection limit with FAB is 10 ng. The ion at m/z 553 is from the glycerol matrix. On the other hand, the CFF mass spectrum (figure 4) shows a signal-to-noise ratio that is 50 times higher than seen in the conventional FAB spectrum.
This increase in detection limit, along with improved reproducibility (figure 5), makes CFF better suited for the assay of vecuronium bromide in plasma than conventional FAB. With CFF, the linear response of the drug is approximately 3 orders of magnitude (figure 6).
Sensitivity can be enhanced further by multiple ion detection (MID) of selected ions. We have used an internal standard with stable isotopes for quantitative measurements (figure 7, Table 1), specifically, vecuronium bromide with a CD_3-group at the quaternary nitrogen (figure 1).

Experimental

All measurements were performed on a Finnigan MAT 90 sector-field mass spectrometer. BioProbe™ was used for introduction and ionization of the samples. The eluent was a solution of 20 % glycerol in water, and the samples were injected through a loop.
MID experiments used m/z 553, from the glycerol background, as a lock mass, with electrostatic peak jumping. Resolution was set at 2 000 (10 % valley definition). Sample preparation has been described in detail elsewhere (5).

Conclusion

Continuous flow FAB is a sensitive ionization method for the identification and quantification of vecuronium bromide in plasma. Concentrations in the low picogram range can be detected and quantified. Matrix effects from the plasma have been observed and need further investigation. The on-line coupling of LC, with CFF as the LC/MS interface, may be a solution for this problem.

References

(1) R.M. Caprioli, F. Fan, and J.S. Cottrell, Anal. Chem. **58**, 2949 (1986).
(2) N.N. Durant, I.G. Marshall, D.S. Savage, D.J. Nelson, T. Sleigh, and I.C. Carlyle, J. Pharm. Pharmacol. **31**, 831 (1979).
(3) L.H.D.J. Booij, R.P. Edwards, Y.J. Sohn, and R.D. Miller, Anaesth. Analg. **59**, 26 (1980).
(4) R.J. Marshall, J.C. McGrath, R.D. Miller, J.R. Docherty, and J.C. Lamar, Br.J. Anaesth. **52**, 218 (1980).
(5) J.E. Paanakker, J.M.S.L. Thio, H.M. van den Wildenberg, and F.M. Kaspersen, J. Chromatogr. **421**, 327 (1987).

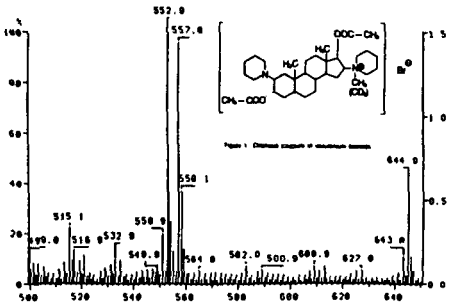

Figure 2: Conventional FAB mass spectrum of 100 ng of vecuronium bromide.

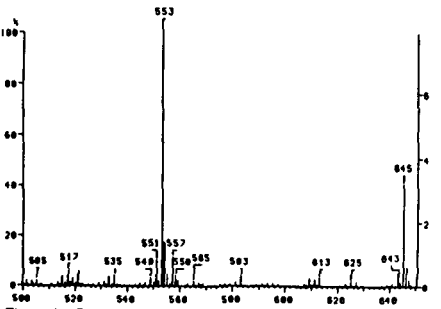

Figure 3: Conventional FAB mass spectrum of 10 ng of vecuronium bromide.

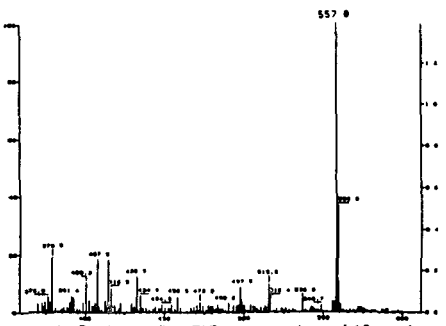

Figure 4: Continuous flow FAB mass spectrum of 1.6 ng of vecuronium bromide.

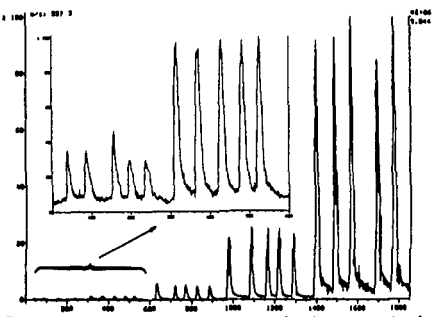

Figure 5: Loop injection chromatogram of various amounts of vecuronium bromide; scan mode.

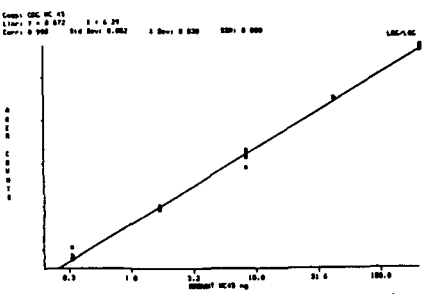

Figure 6: Response curve of various amounts of vecuronium bromide (320 pg, 1.6 ng, 8 ng, 40 ng and 200 ng); mass range scanned was 350—600 u.

Presented at the 36th ASMS Conference on Mass Spectrometry and Allied Topics
June 5-10, 1988, San Francisco, CA

ACCUMULATION OF FURANCARBOXYLIC ACIDS AND INDOXYL SULFATE IN UREMIC SERUM AS INHIBITORS OF DRUG-BINDING

T. Niwa, N. Takeda*, H. Yoshizumi*, A. Tatematsu*

Nagoya University Branch Hospital, Nagoya 461, Japan
*Meijyo University, Nagoya 468, Japan

Introduction The albumin binding of many drugs and endogenous metabolites is well known to be reduced in uremic serum. The reduction of albumin binding of drugs is considered to be due to the accumulation of endogenous protein-bound metabolites in uremic serum. To detect the protein-bound metabolites accumulated in uremic serum, we analyzed the organic acid fraction extracted from isopropanol-deproteinized uremic serum using GC/MS, and also analized the protein-bound metabolites in uremic serum using HPLC (1,2).

Experimental Serum samples were obtained from uremic patients before and after hemodialysis, and healthy subjects. For GC/MS analysis, serum was deproteinized with isopropanol. After centrifugation the supernate was collected. After evaporation the extract was dissolved with water. To extract the organic acids, the solution was acidified to pH 1 with HCl, saturated with NaCl, and extracted three times with ethyl acetate. The organic phase was collected after centrifugation, dehydrated over anhydrous sodium salfate and evaporated with a nitrogen stream. The extract was methylated with diazomethane. After evaporation with a nitrogen stream, the sample was dissolved with methanol/ethyl acetate, and then analyzed by GC/MS.

For quantitation of 3-carboxy-4-methyl-5-propyl-2-furanpropionic acid, serum was deproteinized by boiling at 100 °C for 5 min, and centrifuged to remove protein. The supernate filtered through a filter was subjected to ODS-HPLC with an eluate of acetonitrile/water/trifluoroacetic acid (40/60/0.08, by vol).

For quantitation of indoxyl sulfate, serum was filtered through a filter and then subjected to internal-surface reversed-phase (ISRP) HPLC with an eluate of 0.2M acetic acid/triethylamine (pH 7)-isopropanol-tetrahydrofuran (84/10/6). The identification of indoxyl sulfate was carried out using liquid secondary ion mass spectrometry (SIMS).

Results and Discussion Figure 1 shows the EI mass spectra of 3-carboxy-4-methyl-5-ethyl-2-furanpropionic acid (a), 3-carboxy-5-propyl-2-furanpropionic acid (b), 3-carboxy-4-methyl-5-propyl-2-furanpropionic acid (c), 3-carboxy-4-methyl-5-pentyl-2-furanpropionic acid (d), which were detected in the organic acid fraction from uremic serum. Mass chromatography revealed that the serum levels of the furancarboxylic acids were increased in the chronic hemodialysis patients, and that the acids were not detected in the uemic serum ultrafiltrate. Scince the furancarboxylic acids were strongly albumin-bound, the acids could not be removed from blood by hemodialysis.

3-Carboxy-4-methyl-5-propyl-2-furanpropionic acid was also quantitated by HPLC. Serum levels of the acid showed significant but weak correlation with serum levels of urea and duration on hemodialysis.

Indoxyl sulfate was detected and quantitated in uremic serum by ISRP-HPLC. Identification of indoxyl sulfate was performed only by use of liquid SIMS. Serum level of indoxyl sulfate was markedly increased in chronic hemodialysis patients, and its removal by hemodialysis was not enough due to its binding to serum albumin.

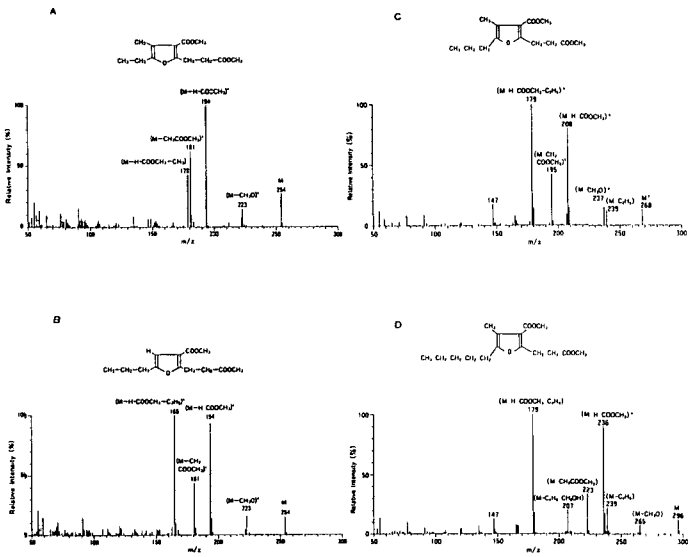

Figure 1 EI mass spectra of 3-carboxy-4-methyl-5-ethyl-2-furanpropionic acid dimethyl ester (a), 3-carboxy-5-propyl-2-furanpropionic acid dimethyl ester (b), 3-carboxy-4-methyl-5-propyl-2-furanpropionic acid dimethyl ester (c), 3-carboxy-4-methyl-5-pentyl-2-furanpropionic acid dimethyl ester(d).

Equilibrium dialysis demonstrated that 3-carboxy -4-methyl-5-propyl-2-furanpropionic acid, 3-carboxy-4-methyl-5-pentyl-2-furanpropionic acid, and indoxyl sulfate inhibited the binding of salicylate to albumin.

The urinary excretion of the furancarboxylic acis and indoxyl sulfate seems to be performed by renal tubular secretory function in healthy subjects. Since the conventional hemodialysis method cannot remove the protein-bound metabolites, a novel hemodialysis method which can remove these strongly protein-bound metabolites, should be developed to prevent possible complications of uremic patients on long-term hemodialysis due to accumulation of the furancarboxylic acids and indoxyl sulfate.

References

1. N. Takeda, T. Niwa, A. Tatematsu, and M. Suzuki, Clin. Chem., 33 (1987) 682.
2. T. Niwa, N. Takeda, K. Maeda, M. Shibata, and A. Tatematsu, Clin. Chim. Acta, 173 (1988) 127.

Presented at the 36th ASMS Conference on Mass Spectrometry and Allied Topics
June 5-10, 1988, San Francisco, CA

EFFECT OF EXTENDED USE OF SINGLE ANABOLIC STEROIDS ON URINARY STEROID EXCRETION AND METABOLISM,

LM Harrison, D Martin, RW Gotlin, PV Fennessey,
University of Colorado Health Sciences Center, Denver, CO 80262 USA

The use of anabolic steroids in athletes who compete in strength and body fitness events is widespread. In the past, research has centered on those endocrine effects that are associated with reproductive organs and regulation. As a results of this research anabolic steroids have been shown to: reduce endogenous serum testosterone production; lead to testicular hypoplasia after long term use; and to inhibit gonadotrophin release. Desirable effects such as weight gain, increased muscle mass and strength increase have been more difficult to demonstrate (1). In spite of the lack of solid data, anabolic steroids are used solely for these desired results. Known effects, such as testicular hypoplasia, are circumvented by taking the steroids in high doses for a limited period of time (4-6 weeks) and then remaining steroid free for an equal or longer period of time.

In our initial study, where athletes were taking multiple steroids (stacking) in order to be able to attain very high levels of anabolic agents, we found a reduction in endogenous adrenal steroid production (2). Because of the mixture of steroid being used there was a question about whether this was a general effect of anabolic steroids, a result of the combined high doses, or caused by one or two of the steroids being used.

Male body builders were asked to collect 24h urine samples at each of the following intervals: 1) at least 3 weeks subsequent to any prior steroid use; 2) after using a single anabolic steroid (nandrolone decanoate, methandrostenolone, oxandrolone or oxymetholone) at dosages >25 mg/d for at least three weeks; 3) following at least 3 weeks recovery after last using the anabolic steroid. The volume of each sample was measured and recorded and an aliquot was frozen at -70C until analysis.

Samples were processed using a standard technique (3) and the concentration (mg/24h) of each steroid was determined.

For the evaluation of adrenal function, we compared the concentration of androsterone (A), etiocholanolone (E), tetrahydrocortisone (THE), tetrahydrocortisol (THF), and allo-tetrahydrocortisol (aTHF) before, during and after a steroid cycle. These compounds were selected because together they make up the bulk of the urinary steroids. For all subjects where the five test compounds were in the normal range at the beginning of the test (before sample), we found suppression of adrenal output while they were taking anabolics. Some patients had abnormally low levels of some or all of the test compounds in their before sample. In this group, the effect on adrenal output was difficult to assess. All four of the anabolic agents studied showed apparent reduction in adrenal function indicating that this may be a general effect of anabolic steroids.

Metabolism in man is often times completely different from the animal models that have been used to study these compounds. Of the four compounds in this study oxandrolone was the only compound excreted in the urine without major metabolism. The other three compounds underwent substantiated biotransformation before excretion. A further interesting observation was that, regardless of the agent used, only 10-20% of the anabolic agent (2-5 mg) were excreted each day.

References

1) Haupt, H.A. and Rovere, G.: Anabolic Steroids: A review of the literature, Am. J. Sports Medicine 12:469-484, 1984.

2) Fennessey, P.V., Gotlin, R.W. and Harrison, L.M.: Anabolic steroids in body builders: Use, metabolic disposition and physiological effects, J. of Pharmaceutical and Biomedical Analysis, accepted 1987.

3) Pike, A.W., et al.: Semi-micro quantitative analysis of complex urinary steroid mixtures in healthy and diseased states, J. Chrom. 306:39-50, 1984.

Presented at the 36th ASMS Conference on Mass Spectrometry and Allied Topics
June 5-10, 1988, San Francisco, CA

NEGATIVE ION CI ISOTOPE DILUTION GC/MS ASSAY FOR PUTRESCINE IN BIOLOGICAL FLUIDS

Daniel L. Norwood and David S. Millington
Duke University Medical Center, Division of Pediatric Genetics and Metabolism, Box 3028, Durham, NC 27710

Putrescine (1,4-butanediamine) is a low molecular weight polyamine produced during cell growth and proliferation. Increased levels of putrescine in biological fluids and tissues are associated with increased rates of cell division, as occurs during the the proliferation of malignant tumors. For example, elevated levels of putrescine in cerebrospinal fluid (CSF) correlate with active medulloblastoma, a malignant brain tumor that affects young children. The objective of this research was to develop a definitive assay for putrescine, based on electron-capture NICI isotope-dilution GC/MS, applicable to CSF, urine and other biological fluids. Two different derivatives of putrescine were evaluated.

Methods

The bis-pentafluorobenzyl (PFB) imine derivative of putrescine was prepared using pentafluorobenzaldehyde according to the method of Avery and Junk (J. Chromatogr. Biomed. Appl. 420:379-384, 1987). The bis-pentafluoropropionyl (PFP) amide derivative was prepared with pentafluoropropionic anhydride according to the method of Rattenburg, et al. (Clin. Chim. Acta 95:61-67, 1979).

Aliquots of normal urine (1 mL) were spiked with putrescine and the internal standard, $^{15}N_2$-putrescine, at the nmol/mL level. In-situ derivatization and recovery were accomplished by Avery and Junk's procedure. Normal CSF (1 mL) was treated in a similar manner.

Analyses were performed on a TRIO-2 quadrupole mass spectrometer (VG Masslab) operated in NCI mode with argon as buffer gas. Separations were performed on a non-polar fused-silica capillary column (DB-1, 30m).

Results

The electron-capture NCI spectra of the PFP (amide) and PFB (imine) derivatives of putrescine are shown in Figures 1 and 2 respectively. The amide shows less fragmentation and therefore potentially better sensitivity than the imine. However, the PFB derivative is prepared in aqueous solution, i.e. directly in the urine or CSF and recovered by solid-phase extraction, whereas the PFP derivative is formed after recovery of the putrescine by an ion-exchange procedure. In our hands, the former procedure was more efficient and successful.

The results of a standard addition experiment in which putrescine was added to normal urine at levels of 10-400 nmol/mL and the internal standard was added at 100 nmol/mL are shown in Figure 3. Selected-ion monitoring was carried out on the molecular anions (m/z 444, 446) of the corrresponding imine derivatives. Excellent sensitivity and linearity were observed at these concentrations.

The endogenous putrescine was also easily detected in unhydrolyzed normal CSF (extract of 1 mL) by SIM after formation and extraction of the PFB derivative, indicating the potential of the method for application to the diagnosis and management of patients with medulloblastoma.

Presented at the 36th ASMS Conference on Mass Spectrometry and Allied Topics
June 5-10, 1988, San Francisco, CA

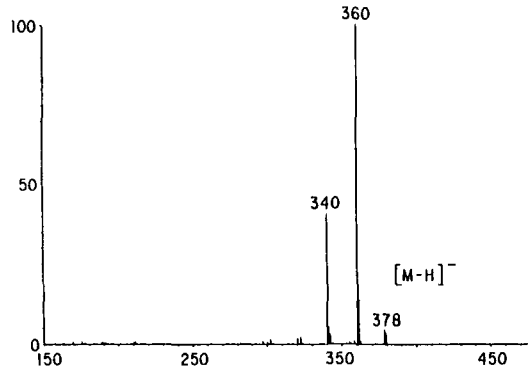

Figure 1. NCI spectrum of putrescine PFP amide.

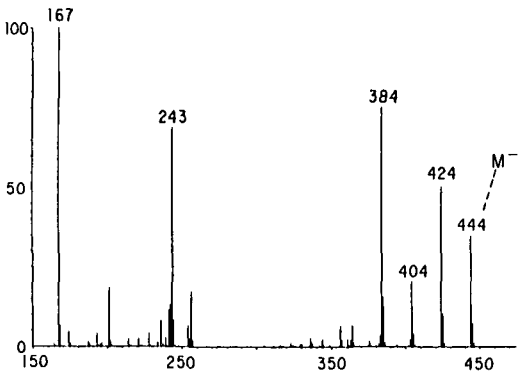

Figure 2. NCI spectrum of putrescine PFB imine.

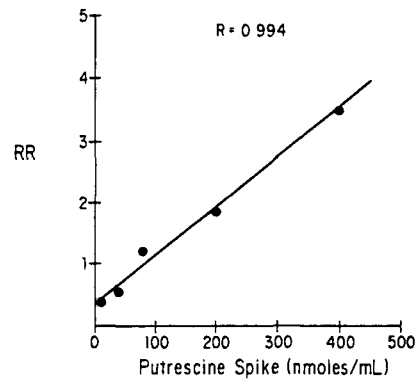

Figure 3. Standard addition of putrescine and $^{15}N_2$ - putrescine to normal urine.

Study on Mass Spectra of New Sesquiterpene

Quan-Long Pu*[1], Linxing He[2] and Ju Zhang[2]

[1]Guangxi Institute of Traditional, Medical and Pharmaceutical Sciences, Nanning, P.R. China (present address: NIDDK, NIH, Bethesda, MD 20892).
[2]Nanjing Institute of Wild Plants, Nanjing, P.R. China

AIM: The plant species Aristalochia versicolar S.M. Hwang has been used as a traditional Chinese medicine in the cure of problems including sore throat/laryngitis, angina and breast abscesses. As part of an investigation of the compounds present in such species which may account for their activities, we isolated two new sesquiterpene lactones with structures different from any previously reported. The structures of these compounds were obtained by a combination of mass spectrometry, NMR and IR techniques and were subsequently confirmed by X-ray crystal diffraction methods.

ISOLATION: The dried powder of the plant root was extracted with hot ethanol three times. After evaporating to dryness, the residue was extracted with petroleum ether, shaken with water and the aqueous portion extracted with ethyl acetate. The ethyl acetate was concentrated and chromatographed on a silica column. The first lactone eluted with petroleum ether/ ethyl acetate (8:2) and the second one with petroleum ether/ethyl acetate (5:5). The following paper describes the mass spectral fragmentation of the compounds.

INSTRUMENTATION: All mass spectra were recorded on a MAT-311A mass spectrometer connected to a MAT-200 data system located at the Guangxi Institute of Traditional, Medical and Pharmaceutical Sciences. The EI source was operated at 70ev with an accelerating voltage of 3kv. Samples were desorbed from the solids probe at approximately 120°C.

VERSICOLACTONE C: This compound crystallized to give a compound with a melting point of 181-182°C and a high resolution measured formula of $C_{15}H_{22}O_4$. On the basis of its mass spectra, NMR and IR spectra, it was assigned the structure in Figure 1.

Figure 1.

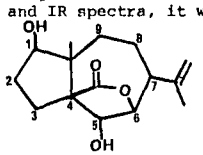

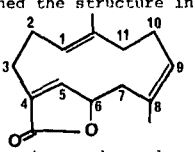

Figure 2.

High resolution measurements were made on the major peaks and metastable ion peaks were mapped using a computer B^2/E scanning function.

The skeleton has three possible modes of fragmentation:

A: Ring A fragmentation: The ion m/z 223 ($C_{13}H_{19}O_3$) results from bond cleavage as shown in Figure 3. This fragmentation is characteristic of this new sesquiterpene lactone structure in that the loss of C_2H_3O is observed instead of the more usual C_3H_6O.

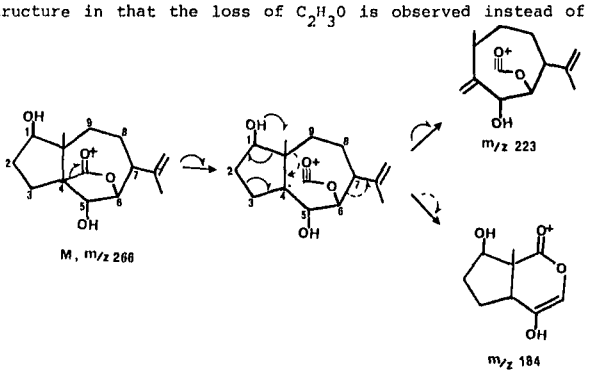

Presented at the 36th ASMS Conference on Mass Spectrometry and Allied Topics
June 5-10, 1988, San Francisco, CA

B: Ring B fragmentation: The ion at m/z 184 ($C_9H_{12}O_4$) results from cleavage at bonds C(9)-C(10) and C(6)-C(7).

C: Figure 4 shows the fragmentations observed following cleavage of the lactone ring. It results in the formation of intense ions at m/z 95, 109, 151, 191, etc. as in A, and these fragmentations are again characteristic of this sesquiterpene skeleton and are absent in the mass spectra of the more common azulene-lactone structures.

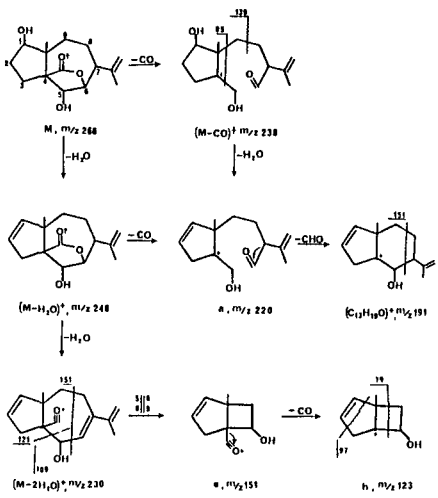

Figure 4

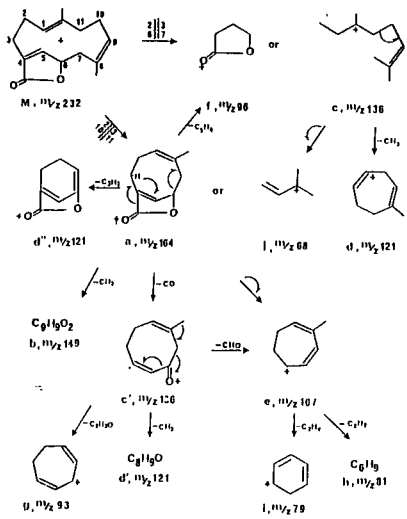

Figure 5

Versicolactone M: This compound had a melting point of 132-134°C and a molecular formula of $C_{15}H_{20}O_2$. Its structure is shown in Figure 2.

High resolution mass measurements were made on the major ions and the metastable ion transition recorded.

Fragmentations at the C(2)-C(3), C(6)-C(7) and C(10)-C(11) bonds are predominant. The intense ions at m/Z 164 ($C_{10}H_{12}O_2$) and m/z 68 (C_5H_8) indicate that the two double bonds in the twelve membered ring are located at C(8) and C(12). Another strong ion at m/z 96 ($C_5H_4O_2$) confirms that there are no other functional groups in the lactone ring. A weak ion and m/z 217 ($C_{14}H_{17}O_2$) was found to fragment to the m/z 81 (C_6H_9) and this allowed the placement of the two methyl groups at C(8) and C(12). Figure 5 shows the fragmentation pathways determined.

SUMMARY: The mass spectra of these two sesquiterpene lactones are consistent with the structures which have since been confirmed by X-ray crystallography. Investigations into the biological effects of these compounds is continuing.

Presented at the 36th ASMS Conference on Mass Spectrometry and Allied Topics
June 5-10, 1988, San Francisco, CA

INVESTIGATION OF NONCOVALENT INTERACTIONS BY FAB-MASS SPECTROMETRY

Dennis P. Michaud, Thomas F. Brennan and Paul Vouros
Barnett Institute of Chemical Analysis and
Department of Chemistry, Northeastern University,
Boston, MA 02115

Noncovalent interactions involving ligands, receptors, and enzymes are extremely important in biological systems. A number of methods are available for studying these interactions but until recently there has been no mass spectrometric technique capable of addressing the problem. The introduction of FAB methodology has renewed interest in the mass spectrometry of larger biological molecules.

Information about noncovalent interactions can be obtained by analyzing the formation of clusters. Cluster ion formation involving the matrix is a prominent feature in FAB mass spectra, but analyte-analyte clusters have also been detected. Since FAB/MS has been used successfully by many (1,2,3) for the study of liquid phase chemistry, the examination of analyte-analyte clusters should yield information about the association of biomolecules in solution.

Molecular association is evidenced by the formation of peaks above the molecular ion peak of the monomeric species in the mass spectrum. For solutions containing more than one component, complexes due to mixed-association as well as self-association are observed. When a mixture of kyotorphin (MW=337) and leu-enkephalin (MW=555) is examined by FAB, a protonated complex at m/z 893 (337+555+1) is observed along with the protonated dimer of kyotorphin at m/z 675 (Figure 1). Examination of a possible structure of the kyotorphin/leu-enkephalin complex reveals that such a structure can be stabilized by several hydrogen bonds, an electrostatic attraction , and a pi-stacking interaction. Kyotorphin also forms a mixed-associated complex with phe-enkephalin at m/z 926 (337+588+1). When a ternary mixture of kyotorphin (MW=337), leu-enkephalin (MW=555) and TRH (MW=362) was examined by FAB, all possible binary mixtures were present but apparently greater preference was observed for the complex between TRH and leu-enkephalin.

Recently it was reported (4) that the gas phase basicity rather than the solution phase basicity is what determines which protonated species is preferentially expressed. In order to distinguish the formation of complexes in FAB as solution or vapor phase phenomena, we utilized a probe tip that was divided horizontally by a paraffin barrier. If two different analytes of sufficient concentration are placed on opposite sides of the barrier, then the formation of a complex of the two analytes would suggest that the complex is formed in the vapor phase. Figure 2 shows a mixture of arginine (A) and leu-enkephalin (L) placed on both sides of the paraffin barrier. The mixed-associated as well as the self-associated complexes are observed. When arginine (A) is placed on one side of the barrier and leu-enkephalin (L) on the other the resulting spectrum (Figure 3) is similar to that in Figure 2 except that the ion of the mixed complex is absent. This suggests that the formation of complexes of biomolecules in FAB is a solution phenomenon.

We are continuing our investigation of structural and solution effects on the complex formation of biomolecules in FAB.

REFERENCES:

1. R.M. Caprioli, Anal. Chem., 55, 2387 (1984).
2. R.A.W. Johnstone, I.A.S. Lewis, and M.E. Rose, Tetrahedron, 39, 1597 (1983).
3. R.M. Caprioli and L. Smith, Anal. Chem., 58, 1080 (1986).
4. J. Sunner, A. Morales, and P. Kebarle, Anal. Chem. 59,1378 (1987).

Figure 1.

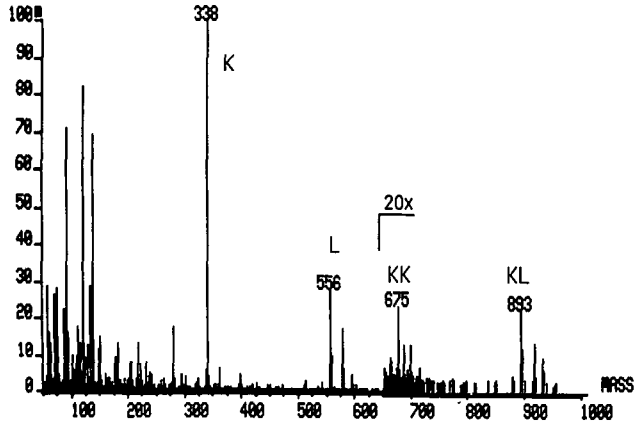

Figure 2.

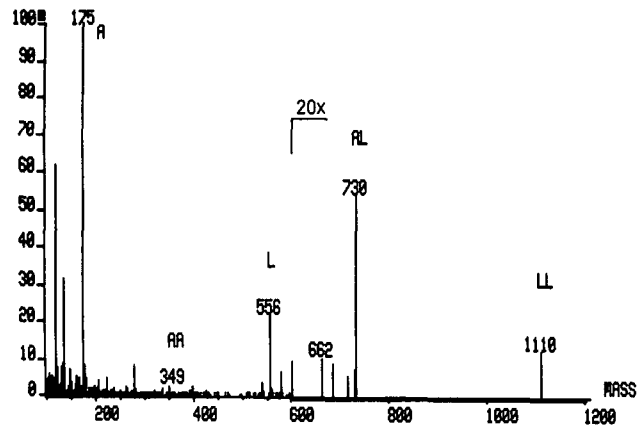

Figure 3.

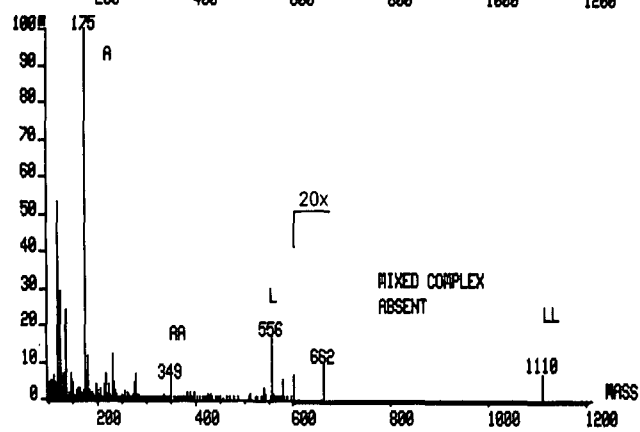

Presented at the 36th ASMS Conference on Mass Spectrometry and Allied Topics
June 5-10, 1988, San Francisco, CA

Reaction of Mass Spectrometry

—— An Approach to Stereochemical Analysis of Organic Compounds

Yao-Zu Chen Suming Hua Honng Li Houjun Yang
(Chemistry Department, Lanzhou University, Lanzhou, China)

Reaction mass spectrometry (RMS) is a technique in which a stereospecific reagent is introduced into the ion source (EI, CI or FAB), where the reagent may react as ions or molecule with the sample molecule to form some characteristic ions. From the relative abundances of these characteristic ions, the stereochemical information about the sample molecule may be obtained. The work done along this line in our lab in recent years are summarized in Table 1. The experimental results showed that the RMS proved to be a promising tool for differentiation of diastereoisomers and conformers, detection of chirality and determination of absolute configuration of some organic compounds.

In continuing our work on RMS for stereochemical analysis, the negative ion fast atom bombardment mass spectra (NIFAB-MS) of mono-, disaccharides and glycosides with phenylboronic acid(PBA) as reagent have been studied. In the ion source, PBA react stereoselectively with cis-vicinal Hydroxyl groups to form characteristic ions $(M_s+M_r - H - 2H_2O)^-$ and $(M_s+2\ M_r - H - 4H_2O)^-$, from relative abundances of which the stereoisomers of saccharides and glycosides can be definitely distinguished. The structures of these characteristic ions have been elucidated by means of MS/MS technique.

Table 1 in situ Reactions of Stereospecific Reagents

Reagent	Ionization	Information
Trimethylborate	DCI	diastereoisomerism of saccharides
l-Amyl alcohol	CI, in beam	chirality of amino acids
Me_3SiNEt_2	EI, CI	conformation of steroidols
D- & L-Mandelic acid D- & L-Methylbutyric acid D- & L-Phenylethylamine	CI	detection of enantiomers of amino acids
R- & S-Phenylbutyric anhydride	CI	determination of absolute configuration of alkaloids, etc.
Phenyl boronic acid	NIFAB	differentiation of epimers of saccharides and glycosides

Table 2 NIFAB-RMS of Mono-saccharides with PBA as Reagent

Saccharides	B/A X 1oo
D-Glucose	70
D-Galactose	20
D-Mannose	35
D-Fructose	10
L-Rhamnose	0

A : relative abundance of $(M_s+M_r-H-2H_2O)^-$
B : relative abundance of $(M_s+2M_r-H-4H_2O)^-$

Table 3 NIFAB-RMS of Di-saccharides with PBA as Reagent

Saccharide	A	B	C
	$(M-H)^-$	$(M-H)^-$	$(M-H)^-$
Cellobiose	1.50	0.72	0
Sucrose	0.22	0.44	0
Lactose	1.47	4.67	1.67
Maltose	1.85	0.50	0.70
Trehalose	0.80	1.25	1.75

A : relative abundance of m/z 265
B ; relative abundance of $(M_s+M_r-H-2H_2O)^-$
C : relative abundance of $(M_s+2M_r-H-4H_2O)^-$

References

1. M.E.Rose et al.,Biomed.Mass Spectrom.,10(9),512(1983).
2. Suming Hua,Yao-Zu Chen et al.,Org.Mass Spectrom.,20,719(1985); 21,7(1986).
3. Hong Li,Yao-Zu Chen et al.,ibid,21,7(1986).
4. Hong Li,Yao-Zu Chen et al.,Bull.Sci.,919(1987).
5. Yao-Zu Chen et al.,Biomed.Environ.Mass Spectrm.,14,9(1987).

Presented at the 36th ASMS Conference on Mass Spectrometry and Allied Topics
June 5-10, 1988, San Francisco, CA

Reaction of Cyanide and Formaldehyde with Neurotransmitter Amines: Formation of New Compounds from Cigarette Smoke

D.A. Durden, B.A. Davis, P.H. Yu and A.A. Boulton
Neuropsychiatric Research Unit, University of Saskatchewan, Saskatoon, Saskatchewan, Canada S7N 0W0.

Introduction

When aqueous solutions of cigarette smoke are mixed with solutions of biogenic neurotransmitter amines or when smoke is passed over rat lung tissue slices, the concentrations of the neurotransmitters are reduced and new compounds appear (1). Initial experiments with phenylethylamine lead to the identification of N-cyanomethyl-phenylethylamine (2).Although cigarette smoke contains a large number of reactive combustion products it appears that the new compounds are formed by reaction with a mixture of cyanide and formaldehyde in a manner similar to that proposed by Winstead et al(3).

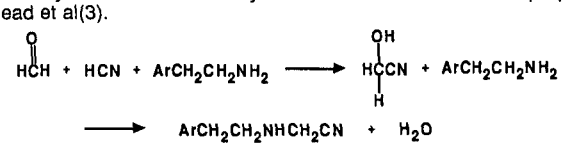

With 5-hydroxytryptamine the major organically extractable product was not N-cyanomethyl-5-hydroxytryptamine but 2-cyanomethyl-6-hydroxy-1,2,3,4-tetrahydro-beta-carboline Thus the indolylalkylamines, histamines and some of the ring substituted phenylethylamines may be expected to undergo cyclization with additional formaldehyde via the Pictet-Spengler reaction.

We wished to investigate the products of the following putative neurotransmitter amines: phenylethylamine (PE), p-tyramine (pTA), m-tyramine (mTA), p-octopamine (pOct), m-octopamine (mOct), dopamine (DA), noradrenaline (NA), 3-methoxytyramine (3-MT), 3,4-dimethoxyphenyl-ethylamine (DMPEA), tryptamine (T), 5-hydroxy-tryptamine (5-HT) and histamine with mixtures of cyanide and formaldehyde and to develop derivatives suitable for their detection in physiological fluids and tissues.

Methods

A solution of 37% formaldehyde (1.5 eq), sodium cyanide (1.0 eq) and sodium bisulphite (1.5 eq) was added to the amine free base or hydrochloride salt in 2 to 5 ml water (3). After one hour the products were extracted with ether and examined by GC-MS. Pentafluoropropionyl derivatives were made with pentafluoropropionic anhydride (1-2 mg product + 50 µl PFPA reacted at 80c, 1h) and t-butyldimethylsilyl (TBDS) derivatives using N-Methyl-N-(t-butyldimethylsilyl)-trifluoroacetamide (MTBSTFA, 80C,1h with 50µl acetonitrile or dimethylformamide solvent). The derivatives were analysed by GC-MS using capillary columns: DB-1, 1.5 µm, 30m x 0.5 mm id , and BP-5, 1.0 µm, 60m x 0.32 mm id, at low resolution using a VG 7070F mass spectrometer.

Results and Discussion

When reacted with approximately equal amounts of formaldehyde and cyanide phenylethylamine and p-tyramine, as predicted, produce simple cyanomethylamine products that have been confirmed by spectra of several derivatives.

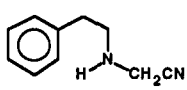

N-cyanomethylphenylethylamine

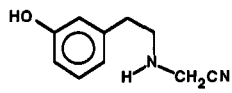

N-cyanomethyl-p-tyramine

It appears that p-Oct, however, cyclises to form 2-cyanomethyl-4,7-dihydroxy-tetra-hydroisoquinoline. The meta substituted phenylethylamines: m-tyramine, dopamine, noradrenaline and dimethoxyphenylethyl-amine all produce several products mainly substituted tetrahydroisoquinolines (THIQs)

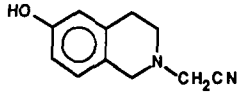

2-cyanomethyl-6-hydroxy-1,2,3,4-tetrahydroisoquinoline

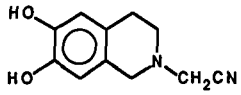

2-cyanomethyl-6,7-dihydroxy-1,2,3,4-tetrahydroisoquinoline

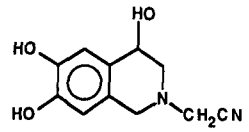

2-cyanomethyl-4,6,7-trihydroxy-1,2,3,4-THIQ

This is followed by the cyanomethyl derivative of the amine and in some cases by the tetrahydroisoquinoline. The indolylethylamines, tryptamine and 5-hydroxytryptamine similarly react to form primarily the 2-cyanomethyl-beta-carbolines followed by the N-cyanomethyl amines and the beta carbolines.Truptamine produced

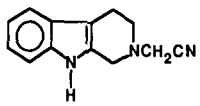

2-cyanomethyl-1,2,3,4-tetrahydro-beta-carboline

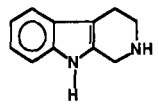

1,2,3,4-tetrahydro-beta-carboline

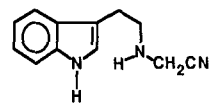

N-cyanomethyl-tryptamine

Although a large number of products were predicted for histamine the major product was 6-cyanomethyl-4,5,6,7-tetrahydro-aza-benzimidazole with a small amount of the unsubstituted alkaloid 4,5,6,7-tetrahydro-aza-benzimidazole also observed.

PFPA and MTBSTFA both react with the cyanomethyl products to give derivatives suitable for GC-MS. PFPA appears to cause additional reactions and may indicate the presence of compounds that were not in the original product mixture. For example PFPA produced about 6 derivatives from the products of a m-tyramine/ HCHO/ KCN mixture wheras there were only 3 TBDS derivatives. When PFPA was reacted with purified N-cyanomethyl-phenylethylamine the PFP derivative of tetrahydroisoquinoline was found wheras with MTBSTFA only the TBDS derivative of N-cyanomethylphenylethylamine was observed. Thus it appears that PFPA will cause cyclization of the cyanomethyl group (with loss of the cyanide) in a manner similar to the Pictet-Spengler cyclization of formaldehyde Schiff bases. This has important implications for the identification of THIQ in tissues as almost all of the published reports used PFPA or one of its analogs and the THIQ could be formed from the Schiff base itself

Many of the alkaloid products are similar to compounds known to have physiological activity. For example the THIQs and THBCs are similar to methylated alkaloids associated with alcohol addiction and may contribute to the addictive properties of smoking and some appear to have enzyme inhibiting properties(1), and will be investigated further.

Conclusion

The major products of reaction of formaldehyde and cyanide in aqueous solution are the cyanomethyl derivatives of the amines in the case of the simple phenylalkylamines and the cyanomethyl derivatives of the tetrahydroisoquinolines (THIQs) and beta carbolines (THBCs) in the case of the meta substituted phenylethylamines and indolylethylamines. Derivatization with PFPA is not suitable due to the possibility of formation of unwanted cyclized derivatives. The use of the TBDS derivative or other mild reagent appears to be more approprate.

References

1. P.H. Yu, D.A. Durden, B.A.Davis and A.A. Boulton, (1988), Biochem. Pharmacol. (In Press).
2. D.A. Durden, B.A. Davis, P.H. Yu and A.A. Boulton, (1988), in The Trace Amines: Their Comparative Neurobiology and Clinical Significance. (Eds A.A.Boulton, A.V Juorio and R.G.H. Downer), Humana Press New Jersey.
3. M.B. Winstead, C.A. Ciccarelli and H.S. Winchell, (1978), J. Pharm. Exp. Therap., 205, 751.

Presented at the 36th ASMS Conference on Mass Spectrometry and Allied Topics
June 5-10, 1988, San Francisco, CA

A Micromethod For The Derivatization Of Organic Compounds Using Reagent Vapor

J.E. Vath and K. Biemann
Department of Chemistry
MIT, Cambridge, MA 02139

Many analytical measurements require an organic compound to be converted into a derivative. In mass spectrometry this is commonly done either to make a compound more volatile for introduction into a GCMS, to enhance sensitivity or to change the fragmentation to obtain more structural information. Often the need to react sample becomes a problem when there is only a very small amount of material available. Because it is hard to perform reactions with solvent volumes less than 50 µl, one is forced to use a very large excess of reagent when reacting less than a microgram. In this case impurities in reagents and multistep reactions make the situation difficult. Another consideration is how one is going to introduce the small amount of derivative into the mass spectrometer.

We have, therefore, extended a technique that was presented last year to analyze peptide derivatives by GCMS[1] to one that is useful for a broader range of reactions that are applied to mass spectrometry. The strategy is one where the sample, present as a solid, is exposed to an environment of reagent vapor in a form which is well suited for both GC and FAB MS. The sample is deposited by placing 1-2 µl of a sample solution into a capillary which contains an indentation to hold the sample in place (Fig. 1, top). The tube is then placed in a vacuum causing the solvent to evaporate leaving the sample as a thin band of solid on the inner wall of the tube (Fig. 1, bottom). The tube is then placed into a reaction vessel which contains 200 µl of the proper reagent or reagent mixture in a vertical side arm well (Fig. 2). After cooling the well the vessel is briefly evacuated to remove air, sealed and heated in an oven to the required temperature for a period of time. After that, the reagent well is cooled again and excess reagent and volatile products are removed by evacuation at room temperature. The tube is then removed for transfer into the instrument or into another reaction vessel for a subsequent reaction step. For GCMS the sample is placed directly into a solid sample GC injector[2]. For FAB the derivative is washed out of the tube directly onto the FAB probe with a 2 µl plug of matrix in a suitable solvent, manipulated by a micrometer controlled piston attached to the sample tube by a short piece of rubber tubing.

Examples of some applications we have found for the technique are: 1) the derivatization of peptides at their C-terminus using an ammonium ethyl ester derivative[3] for FAB analysis, 2) hydroboration and silylation of unsaturated fatty acids for double bond location using GCMS, 3) reduction and hydroboration of ceramides and cerebrosides to increase sensivity and structural information in their FABMS and CID spectra respectively. The reaction sequence in the latter example is detailed with reaction conditions in Scheme I. The dramatic increase in sensitivity can be noted by comparison of Figs. 3 and 4. Fig. 3 is the spectrum of 1 µg of underivatized palmitoyl-sphingosine while that in Fig. 4 was obtained with 10 ng of the derivatized material directly from the sample tube.

Our experience with this technique has led us to believe that it has many useful applications. The most imporatant aspects of the method are its ability to convert a very small sample into a derivative which is not contaminated from large amounts of solvent or reagent, the minimization of losses due to sample handling and contact with large surfaces and the ability to tranfer the entire product to the instrument for measurement.

References

1) Vath, J.E., Biemann, K. Proceedings of the 35th Annual Conference on Mass Spectrometry and Allied Topics, 1987, 570.
2) Caplan, P.J., Cronin, D.A. *J. Chromatogr.* 1983, 267, 19.
3) Bennet, B.D., Day, R.A. Proceedings of the 35th Annual Conference on Mass Spectrometry and Allied Topics, 1987, 568.

Presented at the 36th ASMS Conference on Mass Spectrometry and Allied Topics
June 5-10, 1988, San Francisco, CA

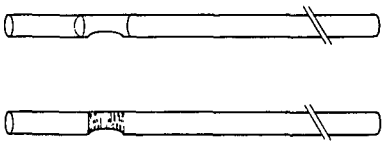

Figure 1 Deposition of sample. Top: 1-3 µl of solution is placed into the sample tube; bottom: deposit after evaporation of the solvent.

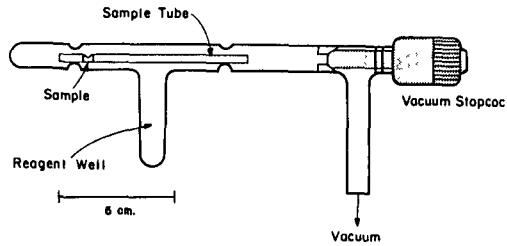

Figure 2 Diagram of the reaction vessel.

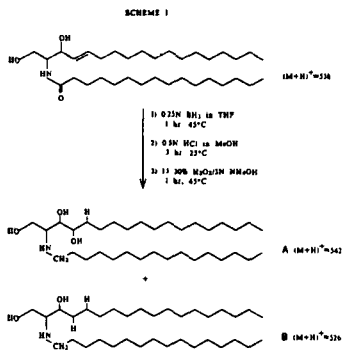

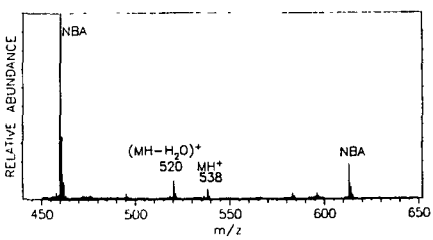

Figure 3 m/z 450 to 650 region of the FAB spectra of 1 µg of palmitoyl-sphingosine. The sample was applied to the probe as 0.5 µl of a 2 µg/µl solution in m-nitrobenzyl alcohol. The peaks labeled NBA are due to the matrix.

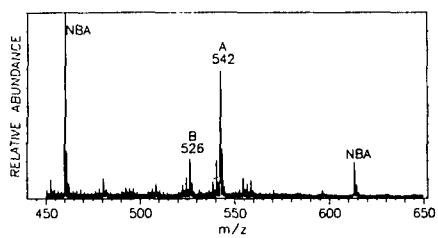

Figure 4 m/z 450 to 650 region of the FAB spectra of 10 ng of derivatized palmitoyl-sphingosine. The sample was washed from the tube onto the probe tip with 2 µl of a 25% solution of m-nitro-benzyl alcohol in methanol. The peaks labeled NBA are due to the matrix. A and B correspond to the structures in Scheme I.

One of the authors (J.V.) wishes to thank the ASMS for the generous travel stipend.

Presented at the 36th ASMS Conference on Mass Spectrometry and Allied Topics
June 5-10, 1988, San Francisco, CA

INVESTIGATION OF THE TEMPERATURE DEPENDENCE IN THE MASS SPECTRUM OF HYDROXAMIC ACIDS.

Kelly R. Stringham, Phil C. Lyons, Ralph L. Nicholson, and Karl V. Wood; Department of Biochemistry, Department of Botany and Plant Pathology, and Campus-Wide Mass Spectrometry Center, Purdue University, West Lafayette, IN 47907.

Cyclic hydroxamic acids found in plant tissues are believed to have a role in disease and insect resistance.[1] 2-(2,4-dihydroxy-7-methoxy-2H-1,4-benzoxazin-3(4H)-one)β-D-glucopyranoside (DIMBOA-glc) is the major hydroxamic acid in corn and wheat with the demethoxy analog (DIBOA-glc) being a minor component. Both glucosides may be enzymatically converted *in vivo* to the corresponding aglycones DIMBOA and DIBOA, respectively. The reported electron impact mass spectra of DIMBOA and DIBOA showed molecular ions whereas the highest mass peak observed for the glucosides was $(M-O)^{+\cdot}$.[2] Low abundance ions were observed for the loss of O, $OH^{\cdot}$, and H_2O in the aglycones with the base peak corresponding to the loss of CO from the $M-H_2O$ ion.

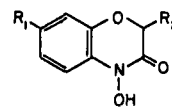

DIMBOA-glc:	$R_1 = OCH_3$	R_2 = O-glucosyl
DIMBOA:	$R_1 = OCH_3$	$R_2 = OH$
DIBOA-glc:	$R_1 = H$	R_2 = O-glucosyl
DIBOA:	$R_1 = H$	$R_2 = OH$

The loss of O from N-oxides is a known thermal decomposition[3] that at sufficiently high ion source temperatures, can direct the majority of the ion abundance of the EI spectra. Hydroxamic acids form N-oxides in the gas phase by keto-enol tautomerization and so can readily lose O. The loss of H_2O from many compounds is also a known thermal decomposition that can dominate the mass spectrum. Since DIMBOA and DIBOA lose both O and H_2O their EI spectra would be expected to be a combination of these two competing thermal decompositions along with unimolecular fragmentation. In this study, DIMBOA was analyzed at various ion source temperatures to evaluate the effect of temperature on the two decompositions, and EI/MS/MS daughter spectra were utilized to ascertain the origin of the major fragment ions.

The daughter spectrum of the molecular ion of DIMBOA, m/z 211, differs from the EI spectrum of DIMBOA (Figure 1). Not only is the base peak different in the two spectra but the fragment ions $(M-O)^{+\cdot}$ and $(M-H_2O)^{+\cdot}$ are absent in the daughter spectrum. This demonstrates that these ions, unlike $(M-OH)^+$, are due to thermal decomposition and not unimolecular fragmentation. The daughter spectra of the thermal decomposition products, $(M-O)^{+\cdot}$ and $(M-H_2O)^{+\cdot}$, were also obtained (Figure 2). They differ from each other and from that of $M^{+\cdot}$, indicating the existence of a different fragmentation scheme for each of the three ions. The ions which dominate the EI spectrum of DIMBOA, however, are associated with the daughter spectra of the $(M-O)^{+\cdot}$ and $(M-H_2O)^{+\cdot}$ ions, demonstrating the effect of thermal decomposition on the observed EI spectrum.

The ion source temperature was varied from 150°C to 350°C to investigate the effect of temperature on the relative abundances of the thermal decomposition products $(M-O)^{+\cdot}$ and $(M-H_2O)^{+\cdot}$. Since a change in either of the thermal decompositions would affect both of the ratios to the molecular ion, *i.e.*, $(M-O)^{+\cdot}/M^{+\cdot}$ and $(M-H_2O)^{+\cdot}/M^{+\cdot}$, by reducing the abundance of the molecular ion, these ratios could not be used to assess the effect of temperature on the individual decompositions. The range of m/z 190-215 amu was scanned and ratios of $(M-O)^{+\cdot}$, $(M-OH)^+$, and $(M-H_2O)^{+\cdot}$ to the total ion count (essentially m/z 193, 194, 195, 211, and their ^{13}C isotopes) were plotted as a function of increasing source temperature (Figure 3). Both

the $(M-O)^{+\cdot}$ and $(M-H_2O)^{+\cdot}$ ratios increased while the $(M-OH)^+$ ratio decreased slightly. The increase in relative abundances of $(M-O)^{+\cdot}$, a 60% increase, and $(M-H_2O)^{+\cdot}$, a 120% increase, demonstrates the degree to which these thermal decompositions are affected by ion source temperature.

From these results and the EI/MS/MS results, it can be concluded that the major part of the EI spectra of DIMBOA and probably DIBOA results from thermal decomposition and not unimolecular fragmentation from the molecular ion. Even at fairly low ion source temperatures these decompositions dominate the spectrum.

In DIMBOA-glc and DIBOA-glc the hydroxyl group responsible for the loss of H_2O in the aglycones is replaced by a glucosyl group. The EI mass spectrum of DIMBOA-glc matches the daughter spectrum of the $(M-O)^{+\cdot}$ ion of DIMBOA except for small peaks at m/z 357 $(M-O)^{+\cdot}$, m/z 178, and m/z 179. Thus, despite the absence of the thermal loss of H_2O, thermal decomposition dominates the EI mass spectra of these glycosylated compounds also, and to a degree that a molecular ion is not obtained.

Acknowledgement. The authors acknowledge R. G. Cooks for the use of the MS/MS.

References:

1. Stoessl, A. Secondary Plant Metabolites in Preinfectional and Postinfectional Resistance. Bailey, J. A. and B. J. Deverall, Eds.; Academic, New York, 1983; Chapter 3, 71-122.
2. Lyons, P. L., J. P. Hipskind, K. V. Wood, and R. L. Nicholson, J. Agric. Food Chem. 1988, 36, 57-60.
3. Duffield, A. M. and O. Buchardt. Acta Chemica Scandinavica, 1972, 26, 2423-2426.

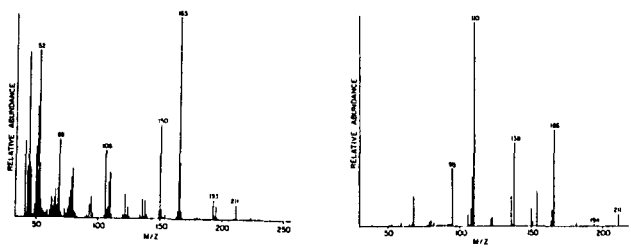

Figure 1. EI spectrum of DIMBOA (left) and daughter ion spectrum of molecular ion (m/z 211) of DIMBOA (right).

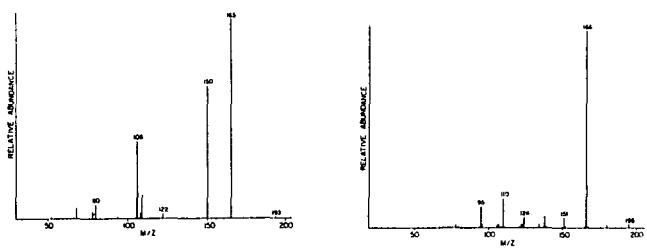

Figure 2. Daughter spectra of $M-H_2O$ (left) and M-O (right) of DIMBOA

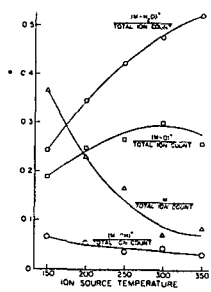

Figure 3.

Presented at the 36th ASMS Conference on Mass Spectrometry and Allied Topics
June 5-10, 1988, San Francisco, CA

SYNTHESIS AND ANALYTIC UTILITY OF DEUTERIUM LABELED 3-NITROBENZYLALCOHOL

Victoria V. Mykytyn, A. Mahendar Reddy and Karl H. Schram
Department of Pharmaceutical Sciences
College of Pharmacy
University of Arizona
Tucson, AZ 85721

There are various organic liquids available for use as matricies in Fast Atom Bombardment (FAB) mass spectrometry. Criteria for determining the utility of these liquids as matrix compounds for FAB include 1) the ability to solubilize compounds of interest 2) minimal background contribution to sample spectrum and the absence of high mass ions 3) a suitable viscosity and boiling point to permit convenient handeling 4) and the absence of any chemical reaction with the compound of interest. A widely used sample matrix for FABMS is glycerol. However, a significant disadvantage of glycerol is that it has been found to participate in redox reactions of some sample molecules prior to particle bombardment. This concern is exemplified by Callahan and co-workers who used proton nuclear magnetic resonance to quantitatively confirm the reduction of m-phenylenebis (trimethylammonium iodide) in a solution with glycerol as observed by electrohydrodynamic mass spectrometry.[1] As a result, other organic liquids were evaluated for their usefulness as FAB matricies.[2] For example, Meili and Seihl found that o-nitrophenyloctylether (NPOE) was useful as a matrix for corrin- and porphyrin type esters.[3] Another alternative matrix to glycerol is m-nitrobenzylalcohol (m-NBA). Barber et al,[4] have sucessfully used m-NBA to obtain FAB mass spectra from a variety of compounds, including cholesterol and chlorophyll which have previously been difficult to run by FAB using gylcerol.

A particular advantage of glycerol, however, is the utility of [hydroxy-$^2H_3$]glycerol-^2H_2O in establishing the number of active hydrogens in molecules with complex structures.[5] In determining the overall structure of an unknown molecule, its exact active hydrogen content is useful in identifying and determining the structure and arrangement of structural subunits and/or functional groups. The number of active hydrogens in a molecule can be determined from the magnitude of the mass shift of the M+H/M+^{2}H ion following hydrogen-deuterium exchange and correction for the contribution of natural heavy isotopes.[6,7]

We have expanded the analytical utility of m-NBA by preparing [hydroxy-^{2}H]m-NBA (^{2}H-NBA) which was used to establish the active hydrogen content of the anti-tumor agents **Mitomycin-C, Tetrocarcin-A, Tricyclonucleoside, Streptonigrin,** and **Mitoxantrone.** Deuterated m-NBA was prepared by vigorously shaking a 1:1 mixture of m-NBA and D_2O, allowing the bilayers of the mixture to separate, removing the aqueous layer, and repeating this procedure two additional times with a final ratio of m-NBA to D_2O of 1:3. Anti-tumor agents were labeled by preparing solutions in deuterated m-NBA at a concentration of 1ug per 1ul. In some cases, a solvent was used to increase sample solubility in m-NBA. The following precautions were taken in order to avoid re-exchange of deuterium by absorbed moisture: 1) Prior to the application of samples to the FAB probe tip, the tip was rinsed with deuterated water and bombarded with argon atoms 2) 1ul of each sample solution was transfered to the tip of the probe using a 10ul glass syringe that had been previously rinsed with deuterated water 3) The probe was then transfered quickly to the vacuum lock of the instrument. Positive ion FAB mass spectra were acquired using a Varian MAT 311A instrument equiped with an SS 300 data system. Magnetic scanning was done at an accelerating potential of 3kV. An Ion Tech saddle field gun producing a neutral argon beam at a potential of 9 kV was used for ion desorption. The ion source temperature was maintained at 30°C. Resolution was 1000.

Presented at the 36th ASMS Conference on Mass Spectrometry and Allied Topics
June 5-10, 1988, San Francisco, CA

The results of the hydrogen-deuterium exchange experiments (using deuterated and undeuterated m-NBA) to determine the active hydrogen content of five anti-tumor agents are sumarized as follows:

NAME	M.W. UNLBD	# ACT. H	M.W. RELATED IONS FROM H_2-^2H EXC[1] $(M+^2H-3)^+$	$(M+^2H-2)^+$	$(M+^2H-1)^+$	$(M+^2H)^+$	SOLUB (^{2}HNBA)	COSOLVENT
MITOMYCIN-C	334	5	338(22)	339(47)	340(79)	341(100)	NO	D_2O
TETROCARCIN-A (Na salt)	1335	5	1338(62)	1339(96)	1340(98)	1341(100)	YES	MeOD[2]
TCN[3]	320	5	324(36)	325(72)	326(52)	327(100)	YES	MeOD
STREPTONIGRIN	506	6	511(40)	512(55)	513(97)	514(100)	NO	D_2O
MITOXANTRONE	444	8	451(54)	452(92)	453(98)	454(100)	YES	MeOD

1 M/Z (relative intensity). Isotopic clusters normalized to the most intense peak in the cluster
2 Deuterated methanol.
3 Tricyclonucleoside.

In general, m-NBA proves to be a valuable alternative to the conventional glycerol matrix. Both polar and non-polar compounds can be solubilized in m-NBA with the addition of cosolvents such as water or methanol. The selection of a particular cosolvent depends on the exact nature of the compounds under investigation. Specifically, combinations of deuterated m-NBA/D_2O or deuterated m-NBA/MeOD are shown to be acceptable matrices for the FAB MS analysis of selected anti-tumor agents in hydrogen-deuterium experiments. From such experiments, the exact number of active hydrogens in complex molecules can be easily determined. Deuterated m-NBA is easy to prepare, offers minimal background interference by exhibiting low mass ions that are relatively few in number, and does not appear to react chemically with sample compounds.

Acknowledgement: This reasearch is supported by NIH under Grant No. CA42309.

1. J.H. Callahan, K. Hool, J.D. Reynolds and K.D. Cook, Anal. Chem., 60, (1988) 714.

2. J. Meili and J. Seibl, Inter. J. of Mass Spectrom. and Ion Physics, 46, (1983) 367.

3. Meili and J. Seibl, Org. Mass Spectrom., 19, (1984) 581.

4. M. Barber, D. Bell, M. Eckersley, M. Morris and L. Telter, Rapid Comm. in Mass Spectrom., No. 1, Vol. 2, (1988) 18.

5. S.K. Sethi, D.L. Smith and J.A. McCloskey, Biochem. Biophys. Res. Commun., 112, (1983) 126.

6. S. Verma, S.C. Pomerantz, S.K. Sethi and J.A. McCloskey, Anal. Chem., 58, (1986) 2898.

7. H. Budzikiewicz, C. Djerassi and D.H. Williams, Structural Elucidation of Natural Products by Mass Spectrometry, Vol. 1, Holden-Day, San Francisco, 1964, Chap. 2.

Presented at the 36th ASMS Conference on Mass Spectrometry and Allied Topics
June 5-10, 1988, San Francisco, CA

IDENTIFICATION OF THE SEX ATTRACTANT PHEROMONE IN THE RED-SIDED GARTER SNAKE BY GC/MS AND GC/MS/MS or "CAN A SEX-STARVED CANADIAN GARTER SNAKE FIND HAPPINESS WITH A PAPER TOWEL IN AUSTIN, TEXAS?"

J. W. Chinn, Jr.*, E. Holly*, R. T. Mason† and D. Crews†
Departments of Chemistry* and Zoology†
The University of Texas at Austin, Austin, Texas 78712

The red-sided garter snake, *Thamnophis sirtalis parietalis*, breeds in large aggregations (mating balls) consisting of hundreds of individuals. The females produce a sex attractant pheromone which serves to elicit courtship behavior from conspecific males during the spring breeding season. The pheromone is expressed along the dorsal surface of the female's body, but unlike nearly all insect pheromones, which are volatile, this pheromone is nonvolatile at ambient temperatures found in the field (southern Manitoba, Canada). Males detect and begin to court sexually active females when rapid tongue-flicks deliver the pheromone from the female's dorsal surface to the male's vomeronasal system. We have found that the pheromone is soluble in nonpolar solvents, since hexane washes of the female's back will elicit stereotyped courtship behavior from sexually active males when the solution is applied to moist paper towels. In contrast, garter snake males express on their skin surface a pheromone which will mask the female sex attractant pheromone, thereby inhibiting courtship behavior.

Hexane washes of dead snakes were first filtered and then fractionated on a Cellite column with hexane/ethylacetate, incrementing in 5% steps from 100% hexane to 100% ethylacetate. Each fraction was subjected to both analytical thin-layer chromatography (TLC) [hexane : diethylether : ethylacetate = 125 : 5 : 3] and capillary column [12m BP1 (0.1u film)] GC/MS [Finnigan MAT 4023/4500; 70 eV ionization; 150°C source setting; 250° C injector temp.; 60°C(1min) to 290°C(@10°/min)] and correlated against field behavior trials.

Only one fraction of the female skin lipids (fraction 5) elicited any courtship behavior. That fraction produced a single spot via TLC but at least 12 peaks with GC/MS [**Figure 1A**], encompassing three homologous series of compounds (two major, one minor). Based on the E.I. and C.I. (methane, 0.4mm) spectra [shown for one pair of peaks in **Figure 2**], the compounds were initially determined to be sets of unsaturated wax esters, having chain lengths varying from 26 to 36 carbons. However, high field NMR studies on the mixture and MS studies on synthetic standards proved this incorrect and indicated that the compounds were long chain saturated and unsaturated methyl ketones. Analysis of the male fraction 5 showed the dramatic absence of the major unsaturated series found in the female fraction 5 [**Figure 1B**]. Peaks in **Figure 1** are labeled by the chain length of the hydrocarbon side chain.

It is suggested by the E.I. spectrum of **C31'** that the double bond is located between carbons 5 and 6 (read from the carbonyl). MS/MS studies were thus conducted using a Finnigan MAT TSQ-70 on the protonated molecular ion of **C31'** to verify the double bond site. However, no additional information resulted from the C.I.D. experiments, even though the collision energy was varied from 0 to 200 eV.

With regard to the male inhibitory pheromone, analysis of the other male skin lipid fractions revealed that fraction 2 contained one major component, identified as squalene by the NBS library. Coinjection of an authentic standard with the male fraction 2 confirmed the

identity of this peak as squalene. In field trials squalene was found to inhibit courtship, but only half as well as whole male skin lipid.

We conclude, therefore, that the sex attractiveness pheromone produced by the female is a series of unsaturated methyl ketones ranging from **C29'** to **C35'**. The male red-sided garter snake recognizes this fingerprint pattern is different from the pattern borne by other males. We also conclude that squalene is one of the chemicals produced by the male which inhibits courtship behavior, but it is not the only one.

Figure 1.

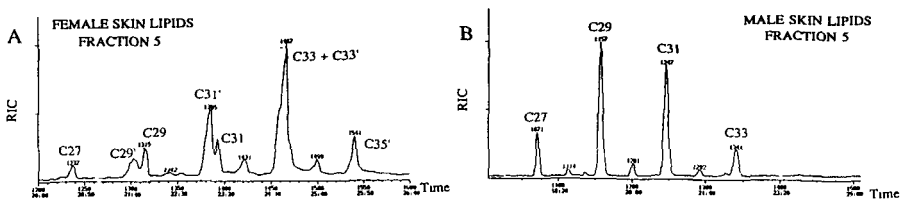

Figure 2.

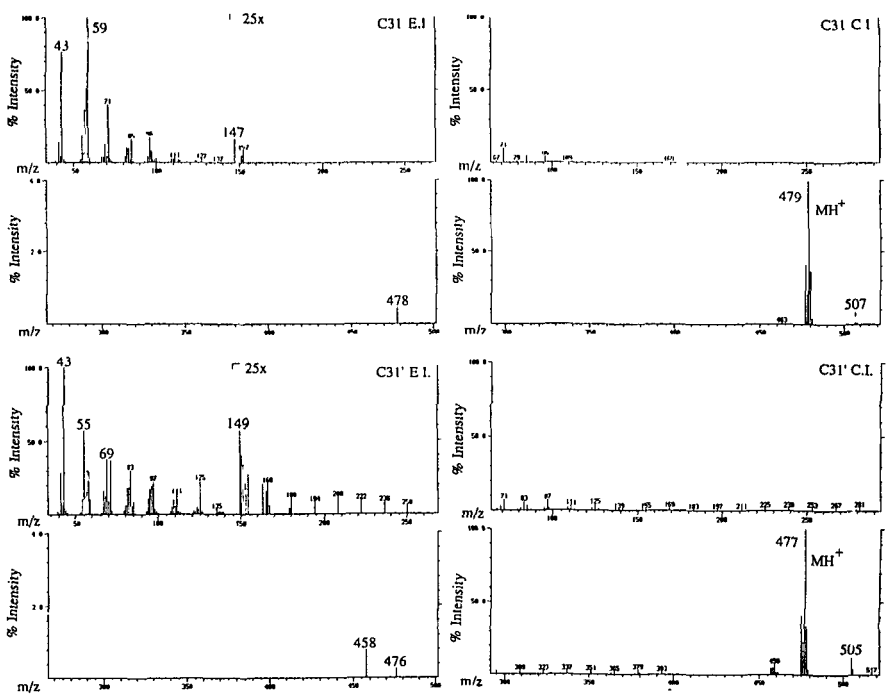

Presented at the 36th ASMS Conference on Mass Spectrometry and Allied Topics
June 5-10, 1988, San Francisco, CA

APPLICATION OF GC/MS IN MONITORING THE ISOLATION AND PURIFICATION OF AN IMMUNOREACTIVE PATHOGENIC FUNGAL PRODUCT.

J.W. Chinn, Jr.*, D. Kruse† and G.T. Cole†
Departments of Chemistry* and Botany†
The University of Texas at Austin, Austin, Texas 78713.

Our earlier investigations have suggested that 3-*O*-methylmannose (3-*O*-MM) is unique to *Coccidioides* among the fungal respiratory pathogens. This methylated sugar has been identified in several immunoreactive wall fractions of *C. immitis*, including an alkali-soluble, water-soluble (ASWS) extract of the conidial wall. The purpose of this study was to determine whether 3-*O*-MM represents the reactive epitope of the diagnostic tube precipitin (TP) antigen of this pathogen.

Crude mycelial culture filtrates of *C. immitis* contain 3-*O*-MM but only in easily detected amounts after 10-20 days growth, at which stage the cells have begun to autolyse. The ASWS fractions of the conidial wall, which contains relatively abundant amounts of 3-*O*-MM, has been shown to consist of three antigenic components, identified by SDS-PAGE as 66kD, 31kD and 19kD polypeptides. One of these fractions has been shown to be the immunoreactive component responsible for human tube precipitin (TP) antibody reactivity, An important reagent used for immunodiagnosis of this respiratory disease. It seemed likely that a correlation may exist between the immunoreactivity of at least one of these components and the presence of 3-*O*-MM.

In this study, we have reexamined the antigenic, carbohydrate, and protein composition of ASWS wall extracts of *C. immitis*. After dialysis, the ASWS product fractionated by solid phase immunoadsorption (SPIA) using a monoclonal antibody to the 66kD component. The unbound fraction of the ASWS extract was further purified by Con A-Sepharose 4B affinity chromatography which binds a 31kD component. The Con A bound fraction was shown to be reactive with human anti-*Coccidioides* tube precipitin (TP) antibody in the standardized immunodiffusion (ID) assay and was further fractionated by HPLC. The 66kD component showed no IDTP reactivity but did contain 3-*O*-MM as shown by gas chromatography/mass spectrometry (GC/MS) using a synthetic methylated sugar standard, while the 31kD component showed only a trace of 3-*O*-MM. The same Con A bound fraction (31kD glycoprotein) was also isolated from the 3-day mycelial culture filtrate, shown to be reactive in the IDTP assay, but lacked 3-*O*-MM, as did the 66kD component isolated form mycelial culture filtrate. Figure 1 summarizes our isolation and analytical procedure.

GC/MS comparison of xylose and 3-*O*-MM standard revealed two peaks for each, with the second peak (in terms of retention time) of xylose overlapping with the first peak of 3-*O*-MM. Since all of the glycoproteins isolated contained xylose, confirmation of the presence of 3-*O*-MM depended upon the use of mass spectrometry to distinguish the two sugars in the chromatograms. Figure 2 shows the mass spectra of xylose and 3-*O*-MM.

We conclude that the methylated mannose-containing poly-saccharide appears to be a structural component of the cell wall of *Coccidioides*. The polysaccharide can be extracted from the walls using 1N NaOH. This same polysaccharide is released naturally from cell walls during autolysis in stationary phase cultures. However, the immunoreactive 66kD, 31kD and 19kD glycoproteins can be isolated from filtrates of logarithmic phase cultures in the absence of 3-*O*-MM. The methylated polysaccharide is not responsible for the specific immunoreactivity demonstrated by the three glycoproteins examined in this study. Instead, we suggest that this unusual polysaccharide mediates natural release of immunoreactive components from the cell wall of *C. immitis* both *in vitro* and *in vivo*.

Presented at the 36th ASMS Conference on Mass Spectrometry and Allied Topics
June 5-10, 1988, San Francisco, CA

Figure 1. ISOLATION/ANALYTICAL PROCEDURE

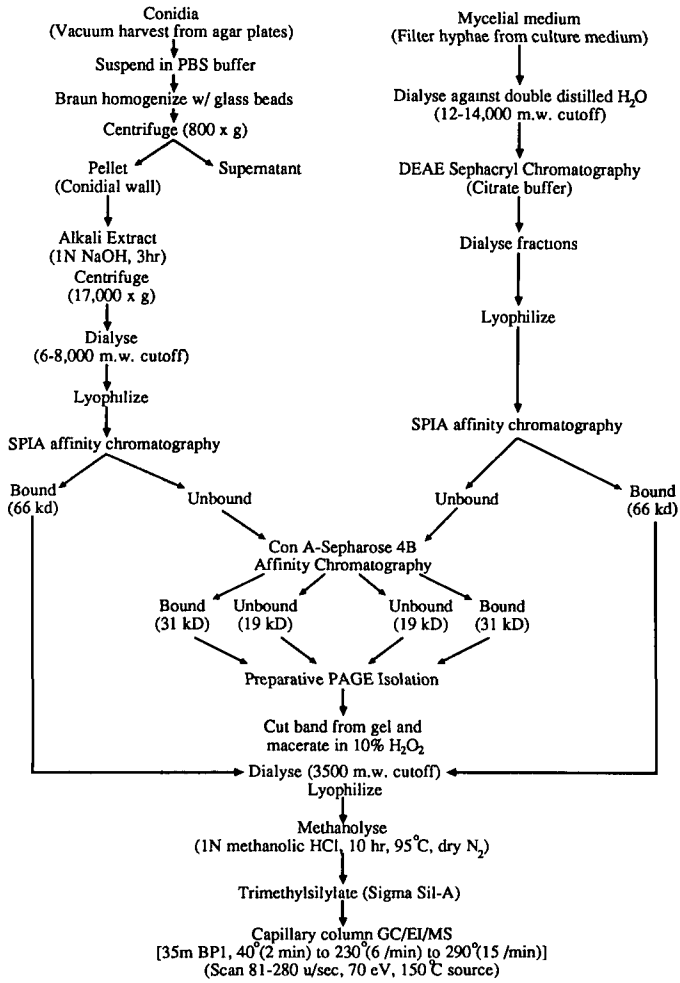

Figure 2.

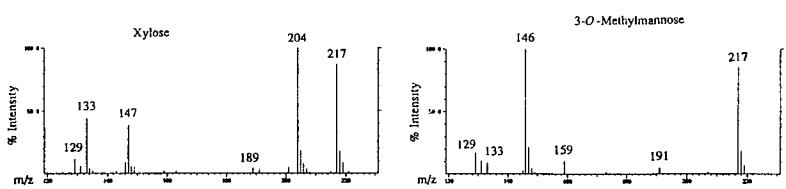

Presented at the 36th ASMS Conference on Mass Spectrometry and Allied Topics
June 5-10, 1988, San Francisco, CA

MASS SPECTROMETRY AS A TOOL FOR THE STUDY OF CHEMICAL REACTIVITY OF PAH RADICAL CATIONS WITH CELLULAR NUCLEOPHILES

E. Davoli[1], R.L. Cerny[2], M.P. Chiarelli[2], and M.L. Gross[2].

(1) "Mario Negri" Pharmacological Research Institute, Via Eritrea 62, Milano, Italy. (2) Midwest Center for Mass Spectrometry, Dept. of Chemistry, University of Nebraska, Lincoln, NE 68588.

The first step in the carcinogenicity of the stable polynuclear aromatic hydrocarbons (PAHs) is their activation to chemically reactive metabolites. The formation of active arene oxides by the oxigenase enzymes, that occurs principally on the microsomes of the endoplasmic reticulum, is generally accepted. More recently a different pathway in the activation of the PAHs has been proposed. It involves a one-electron oxidation, catalized by peroxidases enzymes, to an active radical cation. There is evidence now for a covalent binding of benzo[a]pyrene (BP) to DNA via a one-electron oxidation during in vitro studies[1]. Chemical reactivity of BP radical cation toward nucleic acids has been proven in solution. The BP radical cation is generally induced electrochemically, by UV irradiation or by one-electron oxidants such as I_2.

We have evidences for their reactivity with nucleophiles in the gas phase: benzene, anthracene and BP readily react with pyridine in a CI source to give a covalently bound adduct (Fig. 1). On the basis of these results the mechanism in Fig. 2 is proposed.

Most of the biochemically important nucleophiles (nucleosides, nucleotides, peptides, etc.) are nonvolatile, therefore research was focussed on 3 different instrumental approaches for studying nonvolatile nucleophiles and/or nonvolatile radical cation sources: FAB, LD FTMS and high pressure FAB.

FAB gave no adducts even if PAH and nucleophiles+H are desorbed together on the same matrix. The presence of the $PAH^{+\cdot}$ and the nucleophile+H^+ indicate that, although both are codesorbed, they do not react together in the FAB selvedge.

LD FTMS: thermal desorption of guanosine (1064 nm laser) and ionization of PAH with a 8 eV electron beam seems to give an adduct formation. When anthracene and pyridine are studied, it seems that the adduct formation is enhanced at high electron energies (35-70 eV).

High pressure FAB: we developed a gas tight FAB source (Fig. 3) in order to increase the number of collisions and/or the collision stabilization of the eventually formed products. The high pressure capabilities have been tested with isobutane (measuring the ratio of *m/z* 57 over 43). Results indicate that the source is even suitable for chemical ionization. However, even at these pressures, no adduct was detected.

Interestingly, the system anthracene/imidazole, which has been shown to be a facile reaction in the CI source, under these conditions forms an ion dipole product, easily identified in the MS/MS spectra by the low energy spread of the peaks.

These results and the FT MS experiments, seem to indicate that the excess internal energy is insufficient to affect covalent bonding.

Future developments might consider the design of a high pressure FAB source with a filament option to raise the internal energies of the reagents.

[1] Rogan, E., Cavalieri, E., Tibbels, S., Cremonesi, P., Warner, C., Nagel, D., Tomer, K., Cerny, R. and Gross M., J. Am. Chem. Soc., In press.

[2] Mahoney, J.F., Perel, J. and Forrester, A.T. Appl. Phys. Lett. 38, 320 (1981).

Presented at the 36th ASMS Conference on Mass Spectrometry and Allied Topics
June 5-10, 1988, San Francisco, CA

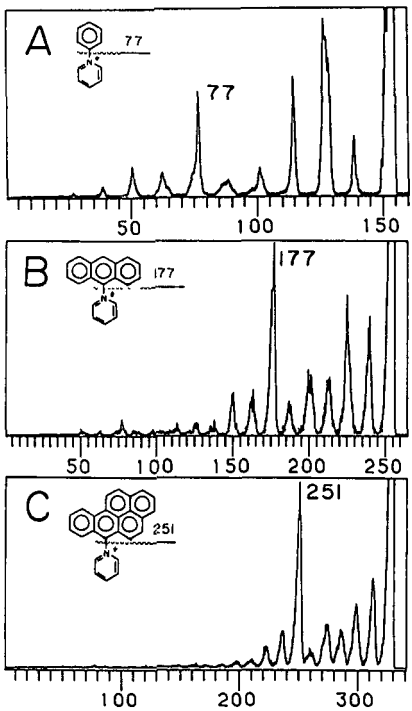

Fig.1. CAD spectra of adducts formed in the CI source between pyridine and:
A) benzene B) anthracene
C) benz[a]pyrene

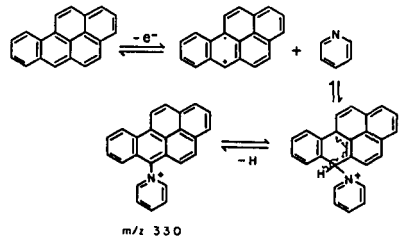

Fig.2. The mechanism proposed.

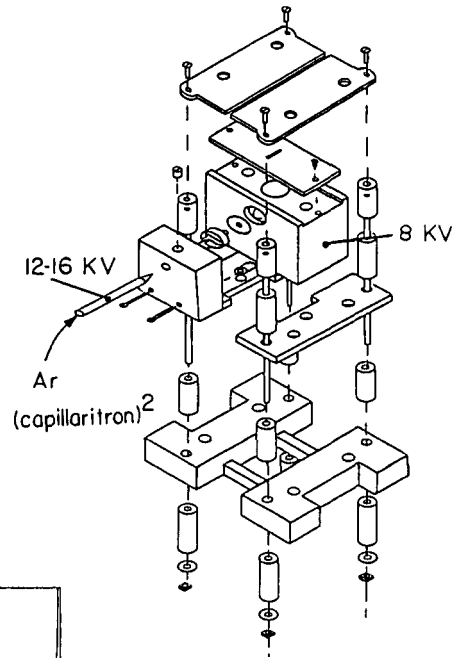

Fig.3. The high pressure FAB source developed for this study

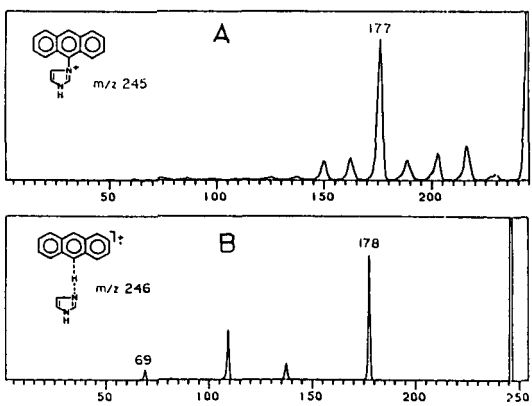

Fig.4. Adducts formed between imidazole and anthracene:
A) CI source
B) High pressure FAB source

Presented at the 36th ASMS Conference on Mass Spectrometry and Allied Topics
June 5-10, 1988, San Francisco, CA

LSIMS INVESTIGATION OF MAGNETIC RESONANCE IMAGING (MRI) CONTRAST AGENTS: [Gd-EDTA], [Gd-CDTA], [Gd-HEDTA], and [Gd-DTPA].

James L. Grant, D.L. White, and Robert C. Brasch
Contrast Media Laboratory, University of California
San Francisco, CA, 94143

P.W. Bethel and A.L. Burlingame
Mass Spectrometry Facility, University of California
San Francisco, CA, 94143

Introduction

The development of Magnetic Resonance Imaging (MRI) as a clinical modality has brought about the need for new, biocompatible drugs, which are used to enhance the image contrast between normal and diseased tissue.[1] Relaxation rates of in vivo water can be affected by stable complexes containing paramagnetic metals, with Gd-complexes being especially effective as image enhancers.[2,3] [Gd-DTPA] is the only contrast agent presently being considered in clinical trials.[4] To improve the efficacy of these monomeric contrast agents, considerable research effort is underway to synthesize a large variety of $[Gd\text{-}DTPA]_n$ (n = 1-50) macromolecular contrast agents (2000-90000 daltons) which would increase the number of [Gd-DTPA] units per dose of agent as well as influence the extracellular or intravascular distribution of the agents due to increasing molecular size.[5],

Methods

All Gd-complexes were prepared from commercially available complexing ligands (Aldrich) and Gd_2O_3 (Aldrich) by methods described in the literature.[2] Mass spectra were obtained with a Kratos MS-50S Double Focusing Mass Spectrometer equiped with post-acceleration detection and a Cs^+ ion LSIMS ion source designed in this laboratory.[6] The Cs^+ primary beam energy was approximately 8 keV. A scan rate of 300 s/decade was used, and the resulting spectra were recorded on a Gould ES-1000 electrostatic recorder. The LSIMS matrix was glycerol/diethanolamine in negative mode.

Results and Discussion

LSIMS has proven to be an effective mass spectral technique in obtaining information concerning the identity and purity of these nonvolatile, highly charged monomeric contrast agents: [Gd-EDTA], [Gd-CDTA], [Gd-HEDTA], and [Gd-DTPA]. Dimers (MW 800-1100 daltons) of monomeric contrast agents were also observed in all LSIMS spectra. LSIMS spectra of the starting complexing ligands EDTA, CDTA, HEDTA, and DTPA were also obtained (See Ref. 7 for molecular structures of all complexing ligands), and all spectra correspond to calculated isotope distribution patterns (Fig. 1).

All complexes are structurally related; therefore, only the synthetic route to the [Gd-DTPA] contrast agent, currently undergoing clincal trials, is shown schematically.

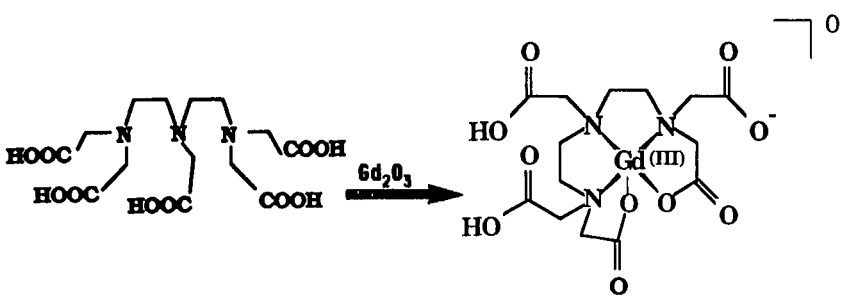

DTPA MW 393

$[Gd\text{-}DTPA]^0$ MW 548

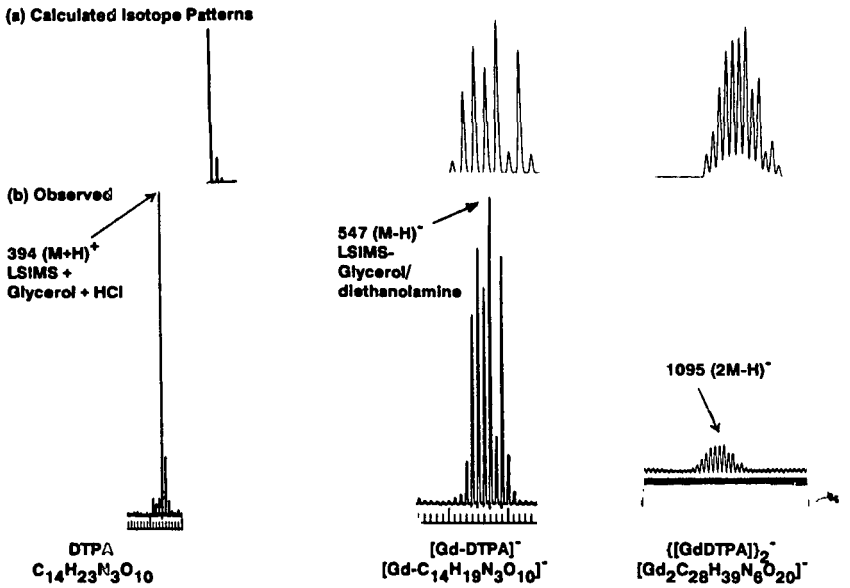

Fig. 1 Calculated (a) and observed (b) mass spectra for complexing ligand DTPA and monomeric [Gd-DTPA] and dimeric $\{[Gd\text{-}DTPA]\}_2$ products (not according to scale).

Works In Progress

Synthetic modification of suitable organic hosts [Cluster contrast agents, e.g.,quinones (1), porphyrins, or Starburst oligomers[8] (2)] permit the covalent attachment of the [Gd-DTPA] moiety at multiple sites on these molecules to produce a large range of $[Gd\text{-}DTPA]_n$-macromolecular contrast agents.

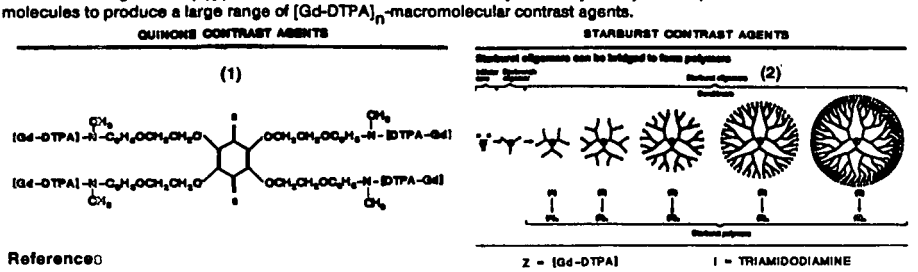

References

(1) R.B. Lauffer, Chem. Rev., 1987, 87, 901-927.
(2) D.H. Carr, J. Brown, G.M. Bydder, H-J. Weinmann, U. Speck, D.J. Thomas, and I.R. Young, The Lancet, March 3, 1984, 484-486.
(3) U. Schmiedl, M.M. Moseley, M.D. Ogan, W. M. Chew, and R.C. Brasch, Radiation Medicine, Vol. 5, No. 1 January-February 1987, 1-5.
(4) Book of Abstracts: Society of Magnetic Resonance In Medicine, 5th Annual Meeting, August 19-22, 1986, Volumes 1-4.
(5) D.D. Stark and W.G. Bradley, Jr. (Editors), Magnetic Resonance Imaging, The C.V. Mosby Company, St. Louis, 1988.
(6) A.M. Falick, G.H. Wang, and F.C. Walls, Anal. Chem., 1986, 58, 1308-1311.
(7) C.C. Bryden and C.N. Reilley, Anal. Chem. 1982, 54, 610-615.
(8) D.A. Tomalia et al., Macromolecules, 1986, 19(9), 2466-2468.

Presented at the 36th ASMS Conference on Mass Spectrometry and Allied Topics
June 5-10, 1988, San Francisco, CA

Liquid-Ionization Mass Spectorometry of Bioorganic Compounds Abiotically Synthesized from Simulated Primitive Earth Atmosphers

Kensei Kobayashi, Takeo Kaneko and Masahiko Tsuchiya
Department of Physical Chemistry, Faculty of Engineering
Yokohama National University, Hodogaya-ku, Yokohama 240, Japan

Numerous studies have been reported on abiotic syntheses of compounds of biological importance such as amino acids from simulated primitive earth atmospheres since 1950's. From the mixtures of methane, ammonia (or nitrogen) and water , various amino acids and nucleic acid bases have been reported to be synthesized with such energy sources as spark discharges (1,2). They have been analyzed mainly by chromatography and EI mass spectrometry. The products of abiotic syntheses have, however, so many kinds of components that it is very difficult to detect and to identify trace amount of compounds in them.

Liquid ionization (LI) mass spectrometry is a promising technique to analyze compounds of low volatility in aqueous solution only with simple pretreatments (3). We performed proton irradiation of mixtures of carbon monoxide (or methane), nitrogen and water, simulating an action of cosmic rays, and analyzed the products by LI-MS, and compared the results with those by conventional techniques.

Forty mL of water with some kinds of ions and nitrogen gas mixed with carbon monoxide or methane were introduced into a 420mL Pyrex glass tube (Fig.1). The gas mixture was irradiated with high energy protons (4.0 MeV, 0.8-1.0 μA) generated by a Van de Graaff accelerator at room temperature. After 2.5-5.0 hours' irradiation, the resulting aqueous solution was filtered through membrane filter and concentrated. It was separated into several fractions (reffered as "AA", "NB" and "SG") by adsorption technique with charcoal-celite and/or a cation-exchange resin (Bio-rad AG-50) as shown in Fig. 2. Each fraction was analyzed by LI-MS (JEOL JMS-QH100 with the LI source). Mass spectra were scanned over the range of m/z= 10-400 in 1 second. The scan was repeated 100 times in 5 minutes, while heater current was linearly increased from 0 to 0.75 A. It was also analyzed by ion-exchange chromatography (Irica Automated Amino Acid Analyzer Model A-5500), gas chromatography (Shimadzu Model GC-9A) and gas chromatography combined with mass spectrometry (GC/MS; Shimadzu Model GCMS-QP1000).

An LI mass spectrum of "AA" fraction of the product after 5 hour's irradiation of methane, nitrogen and water is shown in Fig. 3. Peaks at m/z= 76 + 14n (n=0, 1,2,..) were observed to indicate such aliphatic amino acids as glycine (MW=75), alanines (MW=89), aminobutylic acids (MW=103) and so on. Among them, the peak at m/z=118 is predominent. Amino acids in the same fraction were determined by ion-exchange chromatography, and the results are summarized in Table 1. Glycine was the most abundant amino acid product, followed by alanine. The yield of amino acids with 5 carbons (such as valine; MW=117) was far less than that of glycine. Under the present conditions, aliphatic amino acids with higher molecular weights are detected more sensitively than those with lower molecular weights because of their proton affinity. The higher molecular weight an amino acid has, the more isomers there are. They are the reasons why the peak of m/z=118 was higher than m/z=76 or 90.

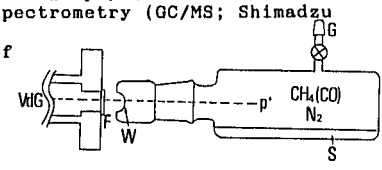

Fig.1. Proton irradiation apparatus. VdG: Van de Graaff accelerator; F: Havar foil; W: concave end window; p^+: proton; G: gas inlet; S: water.

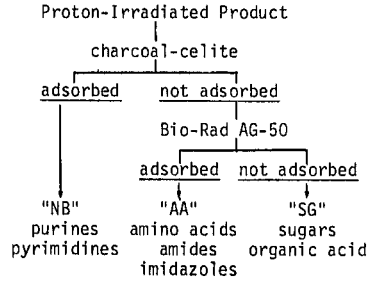

Fig.2. Fractionation of Proton-Irradiated Products.

The peak at m/z=69 was often observed in mass spectra of the "AA" fractions, suggesting some cationic compounds of mass 68, which was plausibly $C_3H_4N_2$. The "AA" fraction was fractionated by HPLC. The fraction with the same retention time as imidazole gave a strong peak at m/z=69 in LI mass spectrum, which fact showed imidazole, a component of histidine, is likely to be abiotically synthesized in the present reactions.

LI mass spectra of the "NB" fraction and the "SG" fraction of the proton-irradiated product are shown in Figs. 4 and 5. The "SG" fraction gave peaks at m/z=(99 + 18n), while the "NB" fraction at m/z= (113 +14n). These compounds have not identified yet, but some of them may be the peaks of nucleic acid components; e.g., uracil gives the peak at m/z=113, and deoxyribose at m/z=99 + 18n. Some nucleic acid bases including uracil have been detected by HPLC. Further identification of these compounds by the combination of HPLC and LI-MS is in progress.

Major amino acids in simulated primitive earth atmosphere experiments have been analyzed chromatography and conventional mass spectrometry. Some bioorganic compounds, which had not been detected by conventional methods, were detected by LI-MS technique. LI-MS can be a useful tool to find new pathways in abiotic syntheses.

References

1) Kobayashi, K. and Ponnamperuma, C., Origins Life, 16, 57 (1985).
2) Kobayashi, K., et al., Origins Life, 16, 299 (1986).
3) Tsuchiya, M., et al., Anal.Chem., 58, 695 (1986).

Table 1. Determination of Aliphatic Amino Acids in Proton-Irradiated Product by Ion-Exchange Chromatography.

# of carbon	# of isomers	amino acid	yield (μmol)
2	1	glycine	26
3	2	alanine	5.7
		β-alanine	0.36
4	5	α-aminobutylic acid	0.62
		β-aminobutylic acid	N.D.
		γ-aminobutylic acid	0.03
		α-aminoisobutylic acid	N.D.
		β-aminoisobutylic acid	0.08
5	12	valine	0.051
		norvaline	0.092
6	31	leucine	0.021
		isoleucine	0.009

A mixture of CH_4(5.7 mmol), N_2(5.7 mmol) and water was proton-irradiated for 2.5h. N.D.: not detected by this method.

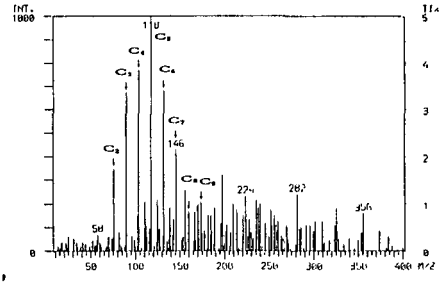

Fig.3. LI mass spectrum of the "AA" fraction (acid-hydrolyzed).
System: CH_4-N_2-H_2O; irradiation: 2.5 hrs.
Heater current: 0.42-0.60 μA.

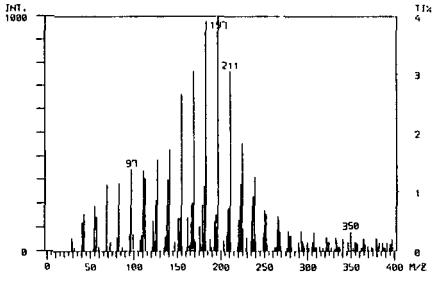

Fig.4. LI mass spectrum of the "NB" fraction.
System: CH_4-N_2-H_2O; irradiation: 2.5 hrs.
heater current: 0.56-0.60 μA.

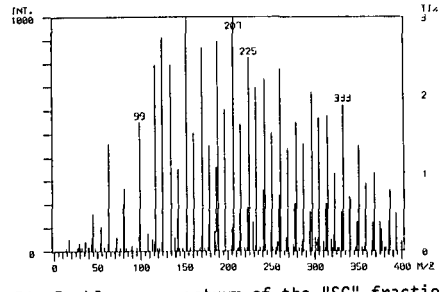

Fig.5. LI mass spectrum of the "SG" fraction (acid-hydrolyzed).
System: CO-N_2-H_2O; irradiation: 5.0 hrs.
Heater current: 0.15-0.38 μA.

Presented at the 36th ASMS Conference on Mass Spectrometry and Allied Topics
June 5-10, 1988, San Francisco, CA

SURFACE-ACTIVE REAGENTS FOR INCREASED SPUTTERED ION YIELDS IN BIOMOLECULAR ANALYSIS. Stephen M. Brown and Kenneth L. Busch, Department of Chemistry, Indiana University, Bloomington, IN 47405.

The development of fast atom bombardment in 1981 greatly increased the number of compounds that could be analyzed by mass spectrometry. This "soft" ionization technique made it possible to analyze involatile, thermally labile biological compounds such as steroids, peptides, and proteins.

The usual procedure in FAB is dissolution of the sample in a suitable matrix, ususally glycerol, followed by bombardment with a 2-7 keV beam of energetic atoms. The ions sputtered from the solution into the gas phase are mass-analyzed to produce the SIMS spectrum. One mechanistic model suggests that ionization takes place in a two-step process, (i) the transfer of the sample from the solution into the gas phase, and (ii) ionization of the sample molecules by various reactions, such as protonation to form $(M+H)^+$ or cationization to form, for example, $(M+Na)^+$. FAB mass spectra usually contain a lower abundance of ions such as $(M+H)^+$ and $(M+Na)^+$ relative to intact cations of ammonium, sulfonium, iodonium and other onium salts that exist in the glycerol solution as preformed ions. Therefore, it is usually advantageous to convert the sample molecules to an ionic form prior to FAB analysis. The desorption/ ionization process then takes place in a single step (the sputtering of a preformed ion). This single-step process can be shown to be much more efficient than the two-step process. Also, if the preformed ionic species is present predominantly at the surface of the liquid matrix, i.e. they are surface-active, these species are almost invariably sputtered with even higher efficiency. Therefore, derivatization of neutral molecules to form surface-active, ionic compounds should increase sensitivity by at least an order of magnitude over that of the neutral molecule.

2-Fluoro-N-substituted-pyridinium salts have been shown to derivatize hydroxyl (1), sulfhydryl (2), and primary amino (3) functionalities. Scheme 1 shows the pathway for the derivatization of cysteine with 2-fluoro-N-methyl pyridinium. Figure 1 is the positive ion FAB mass spectrum of that very compound, derivatized cysteine. Cysteine was chosen as a model compound because it possesses both a primary amino and a sulfhydryl group. Not surprisingly, the derivatized intact cation, m/z 213, and its fragments are very abundant. Also, note the two different functionalities were derivatized, evidenced by the ion at m/z 304. This doubly-derivatized ion exists, however, as a singly-charged species.

This derivatization procedure is not only viable for single amino acids, but also for peptide chains. Figure 2 shows the FAB spectrum for Ala-Gly-Ser-Glu derivatized with 2-fluoro-N-methyl pyridinium. Again, two functionalities are able to be derivatized in this molecule.

Although the reagent used, 2-fluoro-N-methyl-pyridinium, imparts a positive charge on the analyte, it shows only a slight increase in surface-activity. Similar derivatizing agents that are specific for the above mentioned functionalities that impart both a charge and surface-activity to the analyte are being developed in this laboratory. The reagents differ from the commercially available methyl pyridinium in the substituent on the N position. The substituents are an octyl group, and a pentafluorobenzyl group. These three pyridinium compounds exhibit varying degrees of reactivity with the molecules of interest, as well as differing amounts of surface-activity in a number of commonly used SIMS matrices. Figure 3 is the positive-ion FAB mass spectra of an equimolar mixture of the methyl- and pentafluorobenzyl-substituted pyridinium salts in glycerol. Notice that the pentafluorobenzyl pyridinium is preferentially sputtered from the matrix. As expected, preliminary results suggest that the octyl substituted pyridinium will be even more surface-active than both the methyl and pentafluorobenzyl substituted salts.

References

1. Flurer, R., Busch, K. Proc. In. Acad. Sci. 1986, 95, 171.
2. Bald, E. J. Chromatog. 1979, 174, 483-7.
3. Hannah, J., et al. J. Med. Chem. 1982, 25, 457-69.

Presented at the 36th ASMS Conference on Mass Spectrometry and Allied Topics
June 5-10, 1988, San Francisco, CA

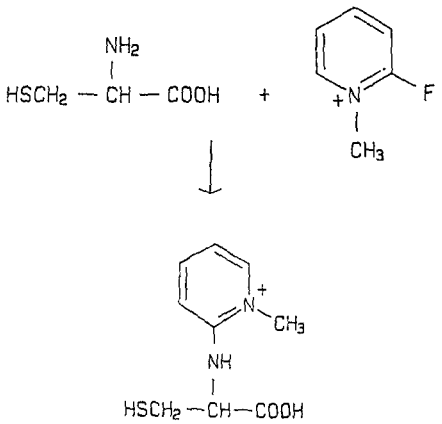

Scheme 1

Cysteine derivatized with Methyl-substituted pyridinium in glycerol

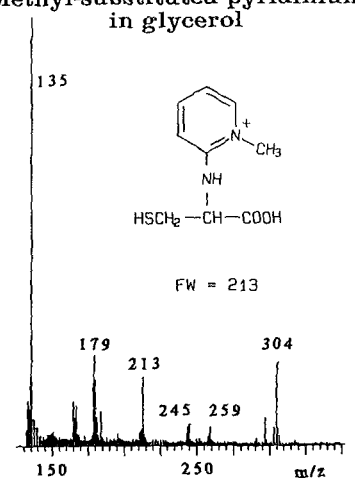

Figure 1

Ala-Gly-Ser-Glu derivatized with methyl-substituted salt in glycerol

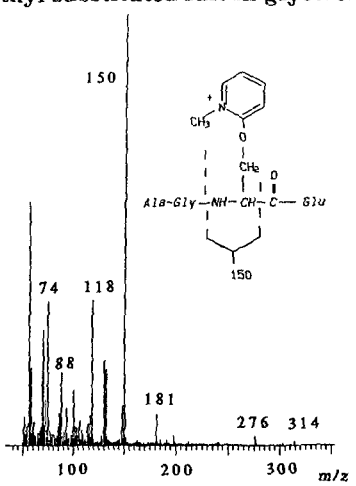

Figure 2

Mixture of two salts in glycerol

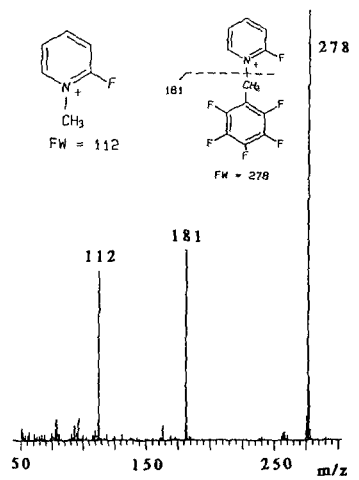

Figure 3

Presented at the 36th ASMS Conference on Mass Spectrometry and Allied Topics
June 5-10, 1988, San Francisco, CA

RAPID ANALYSIS OF BIOMOLECULES USING LASER VAPORIZATION, MULTIPHOTON IONIZATION AND TIME-OF-FLIGHT MASS DETECTION

R.Frey, A.Holle, H.Kaminski, G.Weiss, J.Franzen and D.Koch
Bruker-Franzen Analytik GmbH,
Kattenturmer Heerstr. 122, D-2800 Bremen, FRG

The Bruker TOF 1 Photon Resonance Mass Spectrometer has been used to obtain mass spectra of peptides and other molecules of biological interest. Due to the particular properties of this system the mass spectra of the biomolecules are simple and very easy to interprete.

The system consists of a high resolution time-of-flight mass spectrometer, a new multistage ion source based on resonance-enhanced multiphoton ionization, and an appropriate fast data system (1),(2).
A mass resolution of 10 000 at mass 106 (50 % definition) has been achieved (3) using very short laser pulse duration. Typically, using 5 ns laser pulses a mass resolution of higher than 5 000 holds for the full mass range up to 10 000. This mass range is only limited by the efficiency of the ion detector.

The multistage ion source is characterized by the following steps:

a. desorption of neutral molecules by short IR-laser pulses.
b. cooling of the desorbed molecules and transfer into the ionization region with a cold supersonic jet.
c. resonance-enhanced multiphoton ionization with tunable pulsed laser radiation

This ionization method provides the possibility to control the degree of the fragmentation which simplifies greatly the molecular weight determination and structure analysis. In the soft ionization mode at moderate laser power, almost only molecular ions are produced. This is illustrated by the mass spectrum of the organic salt safranin-O, see fig. 1 upper curve.

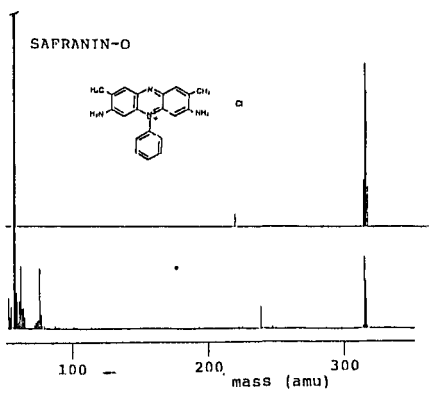

In the hard ionization mode at increased laser power, structure significant fragment masses appear in the spectrum, see fig.1, lower curve. Another example is the spectrum of gramicidin, seen in fig. 2.
In particular these modes of operation represent a unique methode of rapid sequence analysis of peptides (4).

The ability of selective ionization of a single compound of a mixture is another important property of the ion source. This is accomplished

by tuning the laser wavelength to spectral regions where efficient absorption and thus ionization only of this compound occurs. This is illustrated by the spectrum of a methyl-chlorophyllide complex which was taken from a methanol extract of a plant leaf sample.
Further mass spectra are shown covering a broad range of applications: Mass spectra of amoxicillin (see fig. 3), of the steroid testosterone, of clusters of mesoporphyrine dimethyl ester with masses up to 4800 and of the polymer p-polyphenylene.

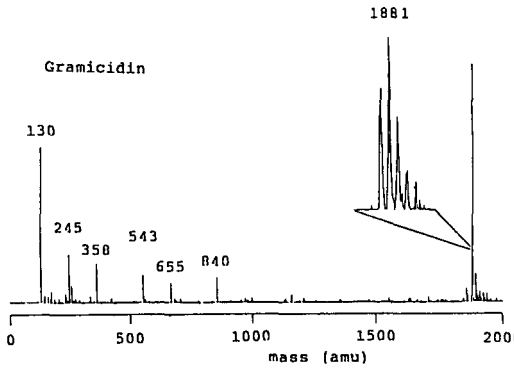

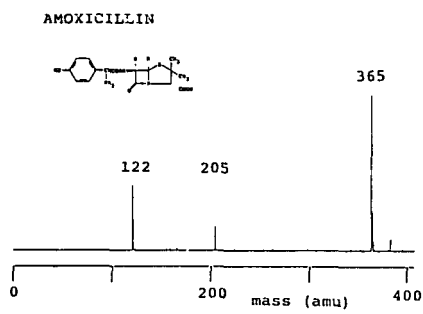

It is important to note that the method described above involves the desorption and ionization as separated steps with respect to time and space. Each step can singly controlled and adjusted to the substance to be analyzed. In particular the resonance-enhanced multiphoton can thus be applied on those large, nonvolatile and thermally labile molecules, for which its unique features are most valuable.

1. R.Frey, G.Weiss, H.Kaminski and E.W.Schlag, Z. Naturforsch. 40a, 1349 (1985)
2. R.Frey, G.Weiss, H.Kaminski, U.Boesl, J.Grotemeyer, K.Walter and E.W.Schlag, Int.J.Mass Spectrom. Ion Proc., submitted
3. K.Walter, U.Boesl and E.W.Schlag, Int.J.Mass Spectrom. Ion Proc. 71, 309 (1986)
4. J.Grotemeyer,U.Boesl, K.Walter and E.W.Schlag, Org. Mass Spectrom. 21,645 (1986)

Financial support from the Bundesministerium fr Forschung und Technologie is gratefully acknowledged.

Presented at the 36th ASMS Conference on Mass Spectrometry and Allied Topics
June 5-10, 1988, San Francisco, CA

DETECTION OF TETRAHYDROISOQUINOLINE IN PARKINSONIAN AND NORMAL HUMAN BRAINS AS AN ENDOGENOUS AMINE BY USE OF GC/MS

T. Niwa, N. Takeda*, T. Sasaoka**, N. Kaneda**,
Y. Hashizume**, A. Tatematsu*, T. Nagatsu**

Nagoya University Branch Hospital, Nagoya 461, Japan,
*Meijyo University, Nagoya 468, Japan,
**Nagoya University School of Medicine, Nagoya 466, Japan

Introduction Since a highly selective, irreversible neurotoxin, 1-methyl-4-phenyl-1,2,3,6-tetrahydropyridine (MPTP) that induces parkinsonian state in humans, monkeys and mice, was discovered, extensive studies on the search for endogenous or exogenous compounds which induce parkinsonism have been elaborated by many researchers. We screened for the neurotoxicity of various compounds structually related to MPTP by assaying the inhibition of tyrosine hydroxylase system in tissue slices of the mouse striatum (1-3). After screening 1,2,3,4-tetrahydroisoquinoline (TIQ) and N-methyl-1,2,3,4-tetrahydroisoquinoline were proposed as candidates for the possible endogenous neurotoxins. We detected TIQ in parkinsonian and normal human brains as an endogenous compound (4). Repeated administration of TIQ to marmosets produced parkinsonian symptoms with reduction in tyrosine hydroxylase, dopamine and total biopterin concentrations in the substantia nigra (5). To determine if subcutaneously administered TIQ can pass through the blood-brain barrier, and if TIQ can be metabolized in the brain and liver, we analyzed the brains and livers of the TIQ-treated marmosets.

Experimental The parkinsonian human brain was obtained from a patient with Parkinson's disease, and a normal human brain was obtained from a patient with stomach cancer. The brain samples were prepared for GC/MS. The brain was homogenized in perchloric acid containing EDTA and ascorbic acid. The supernatant was transfered to a glass test tube, and the pellet was vortexed with perchloric acid containing EDTA and ascorbic acid, and centrifuged again. The combined supernatant was extracted with diethyl ether. The aqueous phase was adjusted to pH 11 with NaOH and extracted twice with dichloromethane. The organic phase was extracted with HCl solution containing EDTA and ascorbic acid. The aqueous phase was dehydrated over anhydrous sodium sulfate and the filtrate evaporated to dryness with nitrogen stream. The residue was derivatized in ethyl acetate/heptafluorobutyric anhydride (HFBA).

Brains and livers were obtained from 2 saline-treated marmosets and 2 TIQ-treated marmosets. TIQ was injected subcutaneously at a dose of 50 mg/kg for 16 days. TIQ concentration was quantitated in the brains and livers of saline-treated marmosets and TIQ-treated marmosets using d3-/d4-TIQ as an internal standard by GC/MS.

Results and Discussion Figure 1a shows the EI mass spectrum of HFB derivatized TIQ. Figure 1b shows EI mass spectrum of a peak in the gas chromatogram of the HFB derivatized extracts from the parkinsonian human brain. Since figure 1b compound showed identical EI mass spectrum and identical retention time on the gas chromatogram with those of TIQ,figure 1b compound was identified as TIQ. TIQ was also detected in the normal human brain. The identification of TIQ in the parkinsonian and normal human brains was also confirmed by using PFP derivatization.

The concentration of TIQ in the brains of TIQ-treated marmosets, 201 and 149 µg/g wet tissue, were highly increased to the same degree as in the livers of the TIQ-treated marmosets, 296 and 142 µg/g wet tissue, respectively. This suggest that TIQ can pass easily through the blood-brain barrier. Any metabolite of TIQ, such as 1,2-dihydroisoquinoline, could not be detected in the brains and livers of TIQ-treated marmosets.

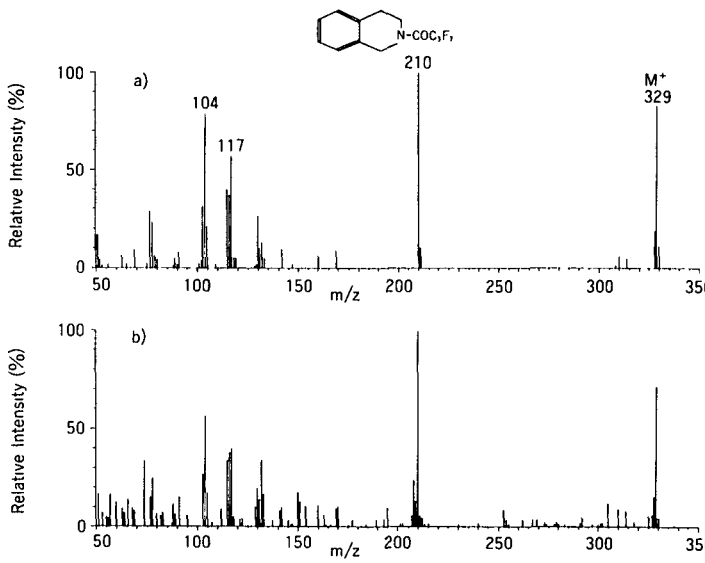

Figure 1 EI mass spectra of the HFB derivative of TIQ (a), and a peak in the gas chromatogram of the HFB derivatized extract from parkinsonian human brain (b).

This suggests that TIQ is not a substrate of monoamine oxidase. TIQ was also detected as an endogenous compound in the brains (0.149 and 0.193 ug/g wet tissues) and livers (0.193 and 0.180 ug /g wet tissue) of saline-treated marmosets at low concentrations.

TIQ injected to marmosets could not be metabolized in the liver and brain, passed easily through the blood-brain barrier, then accumulated in the brain, and produced parkinsonian symptoms with reductions of dopamine and biopterin concentrations, and tyrosine hydroxylase activity. Thus, TIQ may be an important endogenous compound that was demonstrated for the first time to produce an experimental parkinson's disease in monkey.

References

1. Y. Hirata and T. Nagatsu, Brain Res., 397 (1986) 341.
2. Y. Hirata and T. Nagatsu, Shinkei Kagaku, 24 (1985) 169.
3. T. Nagatsu and Y. Hirata, Europ. Neurol., s1-159 (1986) 1.
4. T. Niwa, N. Takeda, N. Kaneda, Y. Hashizume and T. Nagatsu, Biochem. Biophys. Res. Commun., 144 (1987) 1084.
5. T. Nagatsu and M. Yoshida, Neurosci. Lett., 87 (1988) 178.

Presented at the 36th ASMS Conference on Mass Spectrometry and Allied Topics
June 5-10, 1988, San Francisco, CA

FAST ATOM BOMBARDMENT OF PYOCHELIN COMPLEXES OF IRON AND ZINC: BEHAVIOR OF FE(III) IN FAB MS. Ross C. Beier and Robert D. Stipanovic, Veterinary Toxicology and Entomology Research Laboratory and Southern Crops Research Laboratory, ARS, U.S. Department of Agriculture, College Station, TX 77841-5125.

Introduction. Pyochelin (1) is an iron binding compound, which can be isolated from culture media of *Pseudomonas aeruginosa*.[1] *P. aeruginosa* can cause infections which may be fatal in immunocompromised, cystic fibrosis, and burn patients.[2] Pyochelin increases the lethality of virulent bacteria. Eighteen of 21 isolates of *P. cepacia* which produce pyochelin were obtained from patients with severe infections resulting in 11 deaths.[3]

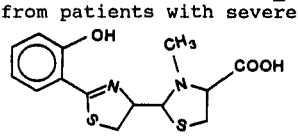

1

Pyochelin also complexes very well with the Zn(II) ion.[4] The ability of pyochelin to complex so well with Fe^{+3} and Zn^{+2} is intriguing.

Objective. The objectives of this study were three-fold: 1) obtain the FAB MS of the suspect zinc pyochelin complex, and verify the presence of zinc and determine the number of pyochelin molecules in the complex, 2) obtain the FAB MS of the iron pyochelin complex, and determine the oxidation state of the iron, if possible, and determine the number of pyochelin molecules in the complex, and 3) study ion formation, in the FAB mode, of various iron compounds using different matrices, to evaluate the oxidation state of iron in these different complexes and matrices.

Instrumentation. The mass spectrometer used for these FAB measurements was a double-focusing VG 70-250 EHF spectrometer. The instrument is equipped with a saddle-field cold cathode ion gun and used stainless steel targets (6 x 1.5mm). Xenon gas was used as the particle source and the ion gun was adjusted to 8 kV and 1 ma current. Each sample (0.1-1 μg solid) and HOAc was added to 1-2 μl of glycerol on the target. Data was recorded by a VG 11-250 data system.

Results and Discussion. The positive ion FAB mass spectrum of ferripyochelin is shown in Fig. 1. The intense parent ion at m/z 379 contains one molecule of pyochelin and one iron plus a proton (i.e., $[322+Fe+H]^+$).

Fig. 2 shows the positive ion FAB mass spectrum of zinc-pyochelin in HOAc. The parent ion and base peak at m/z 387 contains one molecule of pyochelin and one zinc plus a proton (i.e., $[322+Zn+H]^+$).

The positive ion FAB mass spectra of ferric chloride and ferrous chloride are essentially identical. The only observable iron ion species in both spectra is Fe(II). This result was the same in every matrix or condition attempted.

Results in Table 1 show the major ion produced from FAB ionization of ferric chloride, ferric nitrate, and ferric sulfate in glycerol, thioglycerol or the magic bullet matrix was the Fe(II) ion. In fact, no Fe(III) ions were observed in any attempted conditions, with or without acetic acid.

Iron-pyochelin was determined to contain Fe(III) and not Fe(II) by wet chemical methods.[5]

Conclusion. The FAB mass spectra clearly show that both iron and zinc appear to complex with pyochelin in a 1:1 relationship. It has been earlier indicated from NMR studies that pyochelin exists as two species in solution when complexed with zinc.[4]

FAB mass spectrometry can not be used to determine the presence of Fe(III) ions with typical conditions as used in this study. Every Fe(III) compound ionized by FAB gave rise only to Fe(II) ions. Iron-pyochelin was determined to contain Fe(III) and not Fe(II) by wet chemical methods. However, FAB mass spectra indicated that iron-pyochelin contained Fe(II) ions.

Presented at the 36th ASMS Conference on Mass Spectrometry and Allied Topics
June 5-10, 1988, San Francisco, CA

References.
1. CD Cox, KL Rinehart, Jr., ML Moore and JC Cook, Jr., Proc. Natl. Acad. Sci., U.S.A. 78, 4256 (1981).
2. RE Wood, Hosp. Pract. 11(August), 91 (1976).
3. PA Sokol, J. Clin. Micro. 23, 560 (1986).
4. DA Cuppels, RD Stipanovic, A Stoessl and JB Stothers, Can. J. Chem. 65, 2126 (1987).
5. F Feigl and V Anger, in Spot Tests in Inorganic Analysis, P. 263, 271. Elsevier Publishing Company, Inc., New York (1972).

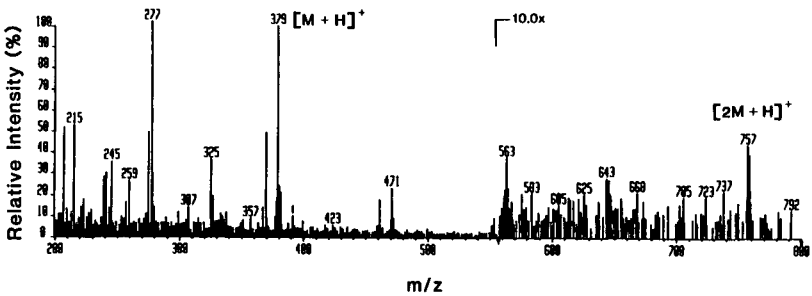

Figure 1. Positive ion FAB mass spectrum of ferripyochelin dissolved in glycerol with HOAc.

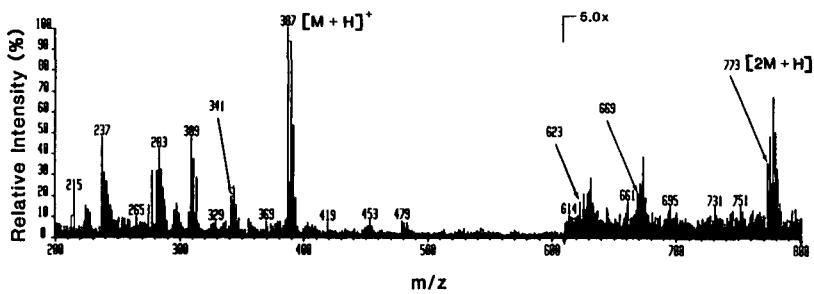

Figure 2. Positive ion FAB mass spectrum of zinc-pyochelin dissolved in glycerol with HOAc.

Table 1. The major ion observed during FAB studies with ferric salts and various matrices. In some cases more than one ion is indicated and given as a percentage of the Base Peak.

	Matrix		
Compound	Glycerol	Thioglycerol	Magic Bullet[1]
Ferric Chloride	$[FeCl+Gly]^+$	$[Fe+TG-H]^+$	$[Fe+MB-H]^+$
		$[FeCl+TG]^+$ 99%	$[FeCl+MB]^+$ 74%
Ferric Nitrate	$[Fe+2Gly-H]^+$	$[Fe+2TG-H]^+$	$[Fe+MB-H]^+$
Ferric Sulfate	$[Fe+2Gly-H]^+$	$[Fe+2TG-H]^+$	$[Fe+2MB-H]^+$
			$[Fe+MB-H]^+$ 99%

[1] Magic Bullet is derived of dithiothreitol and dithioerythritol

Presented at the 36th ASMS Conference on Mass Spectrometry and Allied Topics
June 5-10, 1988, San Francisco, CA

APPLICATION OF MS/MS TO THE ANALYSIS OF BIOLOGICAL MIXTURES

M.Barber, D.J.Bell, M.Morris, L.W.Tetler, M.Woods, UMIST, Sackville St., Manchester, UK. B.W.Bycroft, University of Nottingham, UK. J.J.Monaghan, W E.Morden, ICI C&P Group, Runcorn, UK. B.N.Green, VG Analytical, Manchester, UK.

INTRODUCTION

Many antimicrobial agents produced by bacterial metabolism contain a multiplicity of closely related components.
FABMS often allows identification of the components of such complex mixtures(although one must be aware of suppression effects).We have previously shown [1] that application of MS/MS techniques enables "facile separation" of such mixtures and subsequent structural analysis of the components.

We have applied such techniques to an unknown actinomycin complex [2], the bacitracin complex and nisin [3].

EXPERIMENTAL

Low energy CID was carried out on a VG ZAB-HSQ. High energy CID employed a VG ZAB-4F and a VG 70/70-4SE. MIKES results were obtained on a VG ZAB-SE.

RESULTS AND DISCUSSION

a) Actinomycin (fig.1)
The molecular ion region (fig 2) of a previously unidentified streptomyces strain was shown to exhibit a number of components. Actinomycin D was chosen as the model for fragmentation pathways. Both high and low energy CID were performed, providing complementary information The structures elucidated are shown in table 1. Furthermore, it was found that the cationised species exhibited very different fragmentation patterns.

b) Bacitracin (fig 3)
It was found that the high and low energy CID spectra showed significant differences These differences are energy dependent (fig 4) The significant daughter ions formed at high energy CID are of the W_n type [4], whereas at low energy, the ions are of type Y_n.

Interpretation of the MS/MS spectra for Bacitracin B indicate that each Ile may be replaced by a Val, i.e. there are at least three different, isomeric structures for Bacitracin B.

SUMMARY

(1) A previously unidentified streptomyces strain was characterised employing MS/MS methodology
(2) Ideally, both high and low energy CID spectra are required to enable full structural analysis.
(3) Daughter ion spectra for Bacitracin produced by high energy CID were found to be energy related.

References

1 Barber et al., 35th ASMS Conference on Mass Spectrometry and Allied Topics, Denver, 1987.
2 Barber et al., Talanta, in press.
3. Barber et al , Experientia, 44 (1988) 266.
4. Johnson et al , Anal Chem., 59 (1987) 2621.

Presented at the 36th ASMS Conference on Mass Spectrometry and Allied Topics
June 5-10, 1988, San Francisco, CA

FIG 1

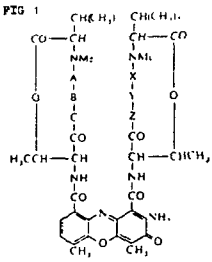

FIG.3

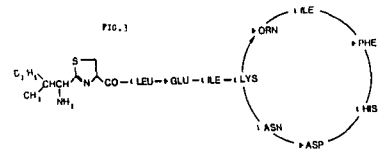

Structure of bacitracin A

FIG.2

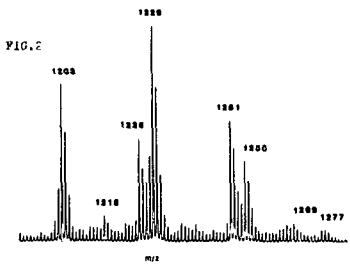

FIG.4

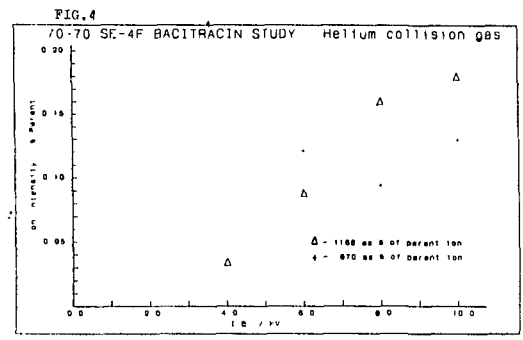

TABLE 1

Actinomycin 'SA' Complex - major components

M_R	Trivial Name	A	B	C	X	Y	Z
1254	Actinomycin D, C_2	Sar	Pro	Val	Sar	Pro	Val
1228	Actinomycin F_9	Sar	Pro	Val	Sar	Sar	Val
1202	Actinomycin F_8	Sar	Sar	Val	Sar	Sar	Val

Actinomycin 'SA' Complex - minor components

M_R	Trivial Name	A	B	C	X	Y	Z
1268	Actinomycin C_2 and/or	Sar	Pro	Val	Sar	Pro	aIle
	Actinomycin iso-C_2	Sar	Pro	aIle	Sar	Pro	Val
1242	Actinomycin F_2	Sar	Pro	Val	Sar	Sar	aIle
1214	-	Sar	Pro	Val	Gly	Sar	Val
1188	-	Sar	Sar	Val	Gly	Sar	Val
1174	-	Gly	Sar	Val	Gly	Sar	Val

Presented at the 36th ASMS Conference on Mass Spectrometry and Allied Topics
June 5-10, 1988, San Francisco, CA

CONSTANT NEUTRAL LOSS SPECTRA OF PEPTIDES

DE PAUW E.*, NASAR K. **, FACCHETTI S. *
* Commission of the European Communities, Joint Research Center, 21020 ISPRA (Varese) ITALY
** Physical Chemistry Department, Liege University, 4000-LIEGE BELGIUM

Secondary ion mass spectrometry of liquids (LSIMS) and fast atom bombardment (FAB) are successfully used for peptide sequencing. However fragmentation patterns are often difficult to interprete in terms of sequence owing to the mixing of both C- and N- terminal specific ions. Daughter ion spectra can help to obtain unambigous information as well as chemical modifications of the sample (matrix doping or derivatization).
In this paper, a strategy is presented, which is designed to monitor specifically C- and N- terminal fragment ions using the so called constant neutral loss scans.

EXPERIMENTAL TECHNIQUE

Peptides are dissolved in glycerol (2 nm/ul) acidified with a slightly surfactant acid.
Two microliters of the solution are deposited on the FAB target and are bombarded by 8 KeV Xe. The spectra are recorded on a VG 70 - 250 SE as well as on a VG 70 - 250 SEQ for comparison.
First field free region linked scans are monitored in the absence of collision gas either as single scans followed by averaging, if needed, or in a *multichannel mode to monitor resolution and peak shape.*
Low mass calibration is performed using a LiCl/glycerol mixture. No difference has been noticed between 1 FFR and 3 FFR spectra.

RESULTS

According to the peptide structure, several specific losses can be foreseen:
a) the loss of H_2O, H_2CO_2 from the carboxylic end
b) the loss of NH_3 from the amino end
c) the loss of CO already detected in normal spectra and occuring from the $B_n \longrightarrow A_n$ transition.

For each peptide, the following set of seven scans is recorded :
a) the normal spectrum
b) the daughter ion spectrum
c) the CNL spectra monitoring the above losses, as well as in addition, the CO_2 scan in negative ion mode.

From this set of spectra, a table including all the major ions is constructed. Structurally significant ions can be identified taking into account rules deduced from the spectra of known peptides.
B_n as well as Y_n ions can be readily identified with the help of the low mass part of the normal spectrum containing iminium ions indicators for the residue composition and after comparison with the daughter ion spectrum.
Two examples of tetrapeptide analysis are given below.
In the first example, the residue composition is known from the iminium ions. The CNL 28 spectrum allows to place GLU and SER in Ct position, GLY being the next suspected one (Fig. 1). The identification of Y" in the CNL 17 spectrum allows full sequence determination, confirmed by the analysis of the normal and daughter ion spectrum.

The same analysis applies in the case of another tetrapeptide analysed as a blind test with the help of VG Manchester Mass Lab. The results were communicated in the following form.

Table 1. Major peaks in the unknown peptide spectra [a,b]

FAB	Daughter ions	CNL 28	CNL 46	CNL 18	CNL 17
427(70)	409(25)	409(15)	427(60)	427(100)	426(82)
217(20)	382(15)	262(13)	318(45)	336(40)	279(55)
197(15)	280(35)	233(17)	223(77)	280(70)	222(60)
181(18)	262(40)	205(100)	178(15)	223(68)	178(50)
120(80)	223(55)	189(13)	166(100)	149(42)	120(100)
91(100)	205(20)	161(12)		121(70)	
	177 *	131(12)			
	166 *	119(15)			
	120 *				

a Peaks originated from the matrix have to be omitted.
b Intensities in brackets (% relative to the base peak).
* Appearing only with collision gas.

The m/3 427 is identified as MH^+. It can lose H_2O and H_2CO_2. The CNL 28 allows to identify the -GLY-PHE CT structure as followed:

427 - 18 = 409 - H_2O
409 - 262 = 147 - Phe
262 - 205 = 57 -GLY

From CNL 18 and 17, M/3 280 and 279 are Y''_3 and Y''_3 candidates. The structure should then be - GLY - GLY - PHE, the last PHE-residue is identified by difference.

CONCLUSIONS

The above results show how the monitoring of neutral losses can help to solve sequencing problems for small peptides. Larger size peptides are currently under study.

For this purpose, an interactive computer program including all the above features has been developed and is actually under testing.

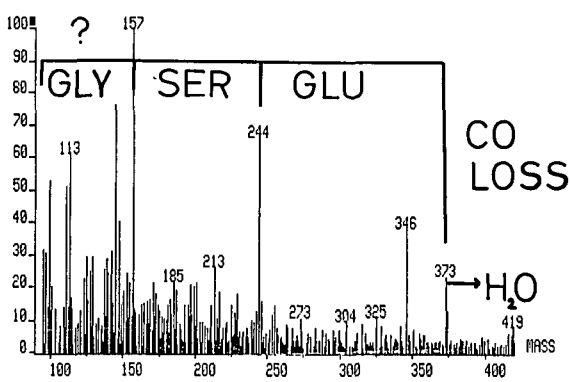

Presented at the 36th ASMS Conference on Mass Spectrometry and Allied Topics
June 5-10, 1988, San Francisco, CA

MASS SPECTROMETRY AND HERBAL MEDICINE

LIANG, XIAO-TIAN

Institute of Materia Medica, Nan-wei Road, Beijing 100050, China

Mass spectrometry is well suited for the examination of minute amounts of isolates from natural sources, e.g., herbal drugs of traditional Chinese medicine. In our institute, we have had occasion to make heavy use of this tool in the course of structural elucidation of these isolates.

In this paper, we will give three examples. The last one is actually a toxin, not exactly belonging to herbal medicine.

The relative disposition of the methylenedioxy grouping and the hydroxy group in 1 was determined by close scrutiny of very weak peaks amidst the background continuum (1). Dehydration of 1 gave the expected mixture of three isomeric alkenes. One of the oxidation products thereof is an acid which can be readily separated from the other two ketones. A closely similar natural product with six methoxy groups (identical oxygenation pattern as 1) was treated in the same manner. Subtle but definitive differences of the two acids in fragment ions involving the cleavage of the biphenyl linkage, all with relative intensities below 1%, were invoked to establish the structure of 1.

Recently a series of triterpenoid glycosides (2) were isolated from Stauntonia chinensis DC, a herb prescribed for analgesic purposes (2). The sequencing of the sugar residues was mainly solved by negative FAB MS, coupled with partial alkaline hydrolysis to remove R^2.

The Ke-shan disease is a serious heart disease in a number of rural districts, with the exact causative factor still not fully known. Deficiency of Se in the diet is now considered by many specialists to be of minor importance only. We have suspected toxin(s) in the food and small amounts of moniliformin (3) were actually detected in the grains of the inflicted areas (2). It is of interest to note that p-toluenesulfonylhydrazone (4) displayed the M+2 peak in the EI mode.

References
1. Y.Y. Chen et al., Scientia Sinica, 19, 276 (1976).
2. X.T. Liang et al., unpublished results.

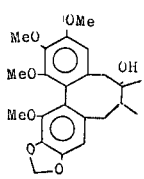

(1)

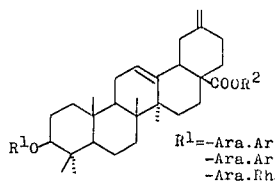

(2)

R^1=-Ara.Ara, R^2=-Glu.Glu.Rha
-Ara.Ara, -Glu.Glu
-Ara.Rha, -Glu.Glu
-Ara.Rha, -Glu.Glu.Rha
-Ara, -Glu.Glu.Rha

(3)

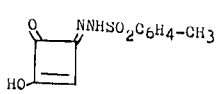

(4)

Presented at the 36th ASMS Conference on Mass Spectrometry and Allied Topics
June 5-10, 1988, San Francisco, CA

SCANNING TLC/SIMS

Yuzo Nakagawa and Kouji Iwatani
Shionogi Research Laboratories
Fukushima-ku, Osaka 553, Japan

The scanning thin-layer chromatography/secondary ion mass spectrometry system (Scanning TLC/SIMS) was newly devised to obtain good separation and good mass spectra of thermally unstable and nonvolatile mixtures [1-4]. The new method was successfully used to analyze drug metabolites and other organic compound mixtures.

EXPERIMENTAL

A sintered glass thin-layer chromatography plate was prepared by heating a mixture of silica gel, fluorescent powder and glass powder on a glass plate which is one of our inventions[3,5,6].

A Hitachi M-68 Mass Spectrometer (equivalent to an M-80 Mass Spectrometer) was used for mass spectrometry measurement. The probe of Scanning TLC/SIMS was designed and constructed by ourselves. A special holder for a thicker plate, such as a glass plate, can be used to retain the plate surface in a suitable position. Driving of the probe is controlled by electric motor.

RESULTS AND DISCUSSION

1. TLC/SIMS (batch process)

The new technique TLC/SIMS enables very simple yet precise measurement of thermally unstable mixture sample [2,3,4].

This technique uses a small strip of TLC plate taken from conventionally developed TLC plate which is TLC aluminum sheet coated with silica gel or our new sintered TLC/MS plate described above, as the primary ion target instead of the usual silver plate. The plate are held by the primary ion target holder of the Liq. SIMS ion source. The sample that collides with the primary ion should be at the same electric voltage as the ionization chamber wall because this electric condition is essential for the ion optics. Chang et al [7] and Iwabuchi et al. [8] also reported the almost same method except the consideration of this electric condition.

Three different target plates, namely a small piece of aluminum sheet, which is the support of the "TLC aluminum sheet silica gel", a small sheet of "TLC aluminum sheet silica gel 60 F_{254}", and a small piece of our sintered glass TLC plate were compared with the usual silver plate as to the sensitivity of the secondary ion. All three targets gave sensitivity of more than 80% sensitivity of that of the silver plate.

The reproducibility and stability of the secondary ion current from the TLC plate gave almost the same results as these from the conventional silver plate, showing that TLC/SIMS can be applied to quantitative analysis using stable isotope labeled internal standard.

No back ground spectra which might interfere with the spectra were found in the mass spectra of TLC/SIMS using silica gel, alumina and cellulose as adsorbent. Reversed phase adsorbent also gave no back ground spectra.

2. Scanning TLC/SIMS

Successive ionization along the chromatogram in TLC/SIMS is very important and was achieved by reconstructing the sample introduction probe, part of the ion source housing and part of the ionization chamber. Movement of the TLC plate, mounted on the TLC/SIMS probe, led to successive collision of the primary ion with the spots to generate secondary ions. The plate drive could be controlled to move at a constant or variable-programmed speed and even to hold at the same position. Schematic diagram of the system is shown in the Fig. 1. Independently of our work, Kushi et al. [9] reported a similar method using the small piece of TLC plate attached to the SIMS target.

A mixture of a new sleep inducer rilmazafone and its metabolites, aminoglycosides in a mixture and many other mixture were also analyzed by Scanning TLC/SIMS, which provided a good chromatogram and mass spectra. A TLC

sintered glass plate also gave good results.

We prepared the reversed phase chromatography plate by processing the normal phase chromatography plate coated on an aluminum sheet, and our sintered TLC plate. Scanning TLC/SIMS of steroids and cephalosporins using reversed phase (RP-8) plate gave good chromatograms with excellent resolutions and mass spectra. In the examples of steroids and cephalosporins, less than 1 ug of sample can give good mass spectra for identification. The spectra from reversed phase TLC plate were more sensitive than those from normal phase TLC plate and, sometimes, from conventional silver plate SIMS. In many drug metabolism experiments, this method was successfully applied.

The limitation of the TLC/SIMS, including batch processing TLC/SIMS, and Scanning TLC/SIMS, are only the cases when the TLC can not separate the mixture and when the conventional SIMS measurement of the pure component sample can not provide the SIMS spectrum. In case sodium ion adducts $[M + Na]^+$ of small amount of sample which can interfere with spectrum analysis, it can be diminished by using our new TLC sintered glass plate.

CONCLUSION

The Scanning TLC/SIMS system can be used to analyze nonvolatile and thermally unstable mixtures in biomedical studies. The chromatograms and mass spectra observed by this system are of excellent quality like those of authentic compounds examined individually observed by the conventional methods. The Scanning TLC/SIMS system is especially excellent for analyzing mixtures of drug metabolites. The handling simplicity and versatility of the systems should make them widely accepted in the biomedical studies, and may even replace GC/MS and LC/MS as powerful tools in life science research.

1. Y. Nakagawa and K. Iwatani, Jpn. Kokai Tokkyo Koho JP61-260149
2. Y. Nakagawa, Proc. Soc. Med. Mass Spectrom. 9, 39 (1984)
3. Y. Nakagawa, Ann. Rpt. Shionogi Res. Labs. 35, 1 (1985)
4. K. Iwatani and Y. Nakagawa, Mass Spectrosc., 34, 189 (1986)
5. Y. Nakagawa, K. Iwatani and T. Kadono, Jpn.Kokai Tokkyo Koho JP60-42653, USP4587020
6. K.Iwatani K. Iwatani and T. Kadono, Mass Spectrosc., 34, 181 (1986)
7. T.T. Chang, J.O. Lay, Jr. and R.F. Francel, Anal. Chem. 56,109(1984)
8. H. Iwabuchi, A. Kitagawa and K. Nakamura, 20th Applied Spectrom. (Tokyo, Nov. 14, 1984)

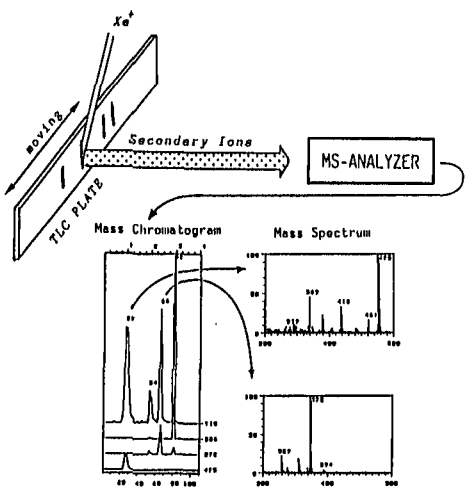

Fig. 1. Scanning TLC/SIMS

Presented at the 36th ASMS Conference on Mass Spectrometry and Allied Topics
June 5-10, 1988, San Francisco, CA

FAST ATOM BOMBARDMENT MASS SPECTROMETRY OF GLYCOSPHINGOLIPIDS

Charles C. Sweeley[1], Douglas A. Gage[1], Heber Becker[2] and Stephen Ladisch[2]

[1]Department of Biochemistry, Michigan State University, East Lansing, Michigan 48824

[2]Department of Pediatrics and Oncology, UCLA School of Medicine, Los Angeles, California 90024

Mass spectral analysis has long been important in the structural elucidation of derivatized glycosphingolipids using trimethylsilylation, acetylation or permethylation to decrease hydrogen bonding and increase volatility. The development of fast atom bombardment (FAB) techniques for the analysis of underivatized polar molecules has enabled small amounts of glycolipids to be studied, opening up a previously difficult area, the study of tumor cell gangliosides.

Two examples are presented. The first involves the use of this technique to characterize (or to distinguish among) several gangliosides isomeric in their oligosaccharide component. In this study negative FAB MS was used to identify the two major components of the total gangliosides shed from highly tumorigenic murine lymphoma cell lines. The purified total gangliosides from these lines when coinjected with poorly tumorigenic lymphoma cells dramatically increase the amount of tumor formation observed (1). The FAB MS spectrum showed one of the two major components was $GD_{1\alpha}$, NeuAc (α2-3) Gal (β1-3) Neu Ac (α2-6) Gal NAc (β1-4) Gal (β1-4) Glc Cer, with fragments clearly distinguishing it from alternative isomers, GD_{1a} and GD_{1b}. The second major component of the shed gangliosides was the monosialo compound GM_{1b}, Neu Ac (α2-3) Gal (β1-3) Gal NAc (β1-4) Gal (β1-4) Glc Cer. Again, several key fragments indicated the terminal position of the sialic acid residue rather than attachment to the internal galactose as in the isomer GM_1. Examination of the molecular ion region of the negative FAB spectra of these two major components $GD_{1\alpha}$ and GM_{1b}, indicates both are quite heterogeneous in their ceramide composition. Note that the ion at m/z 1735 does not represent an unusually large fatty acyl group-containing ceramide, but rather a thioglycerol adduct to the 24 1 fatty acid-containing species at m/z 1627 (figure 1)

The second example concerns the identification of multiple lipid (ceramide) isomers of GM_2 from human neuroblastoma tumor The ceramide composition of GM_2 from tumor cells differs from that of normal human brain GM_2. In the positive FAB CAD MS/MS spectra of gangliosides, fragments containing the sphingosine moeity (W") are observed which allow the entire ceramide composition to be determined by difference from the ceramide ion (Y_0 or Y_0') (2, 3, 4) The W" sphingosine ion is particularly prominent when the ceramide ion (Y_0 or Y_0') is selected as the parent in the MS/MS experiment. It is also possible to directly determine the acyl group in the ceramide by a negative FAB CAD MS/MS experiment (4). Two fatty acyl group containing fragments (S and T) are produced by CAD of the total ceramide fragment (see figure 2).

A combination of positive and negative FAB CAD MS/MS was used to identify a number of the GM_2 components occurring in neuroblastoma tissue.

EXPERIMENTAL

Gangliosides were isolated and purified by diisoproplyl ether/butanol/water partition and gel filtration, followed by normal phase HPLC and either HPTLC (lymphoma cells) or reverse phase HPLC (neuroblastoma and normal brain GM_2).

Approximately one µl of ganglioside solution in MeOH (1-5nmol/µl) was mixed with 2 µl of matrix (thioglycerol or triethanolamine for negative mode, glycerol/thioglycerol (1:1) for positive mode) on the FAB probe tip. Ions were formed by bombardment with a 6 keV beam of Xe atoms in a JEOL HX-110 double focussing mass spectrometer The accelerating voltage was 10 kV and the resolution was 3000. For CAD MS/MS helium was used the collision gas in a cell located in the first field-free region. The helium pressure was adjusted to reduce the abundance of the precursor ion by 75%. A JEOL DA-5000 data system generated linked scans at constant B/E.

REFERENCES

1 Ladisch, S., Kitada, S. and Hays, E.F. (1987) *J. Clin. Invest.* 79, 1879.

2 Hemling, M.E., Yu, R.K., Sedgwick, D. and Rinehart, K.L., Jr., (1984) *Biochemistry* 23, 5706.

3. Ohashi, Y., Iwamori, M., Ogawa, T. and Nagai, Y. (1987) *Biochemistry* 26, 3990.

4. Doman, B. and Costello, C.E. (1988) *Biochemistry* 27, 1534

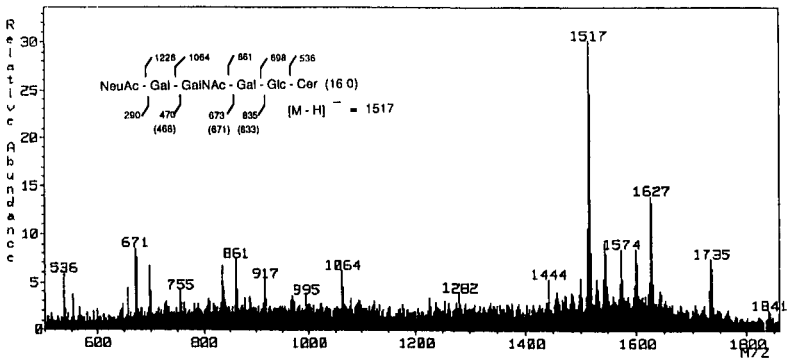

Figure 1. Negative FAB MS of GM_{1b} (thioglycerol matrix) showing diagnostic oligosaccharide fragments and heterogeneity of $[M-H]^-$ region. Ion at m/z 1517 represents ceramide containing d18:1 sphingosine and 16:0 fatty acyl group.

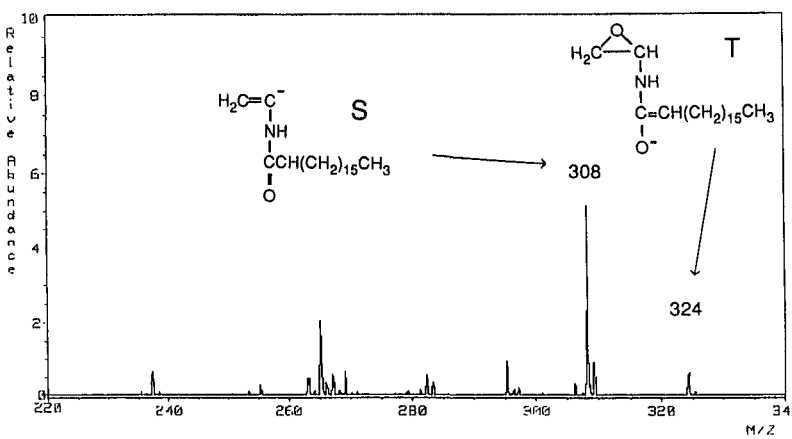

Figure 2. GM_2 Negative FAB CAD MS/MS spectrum of ceramide parent ion at m/z 564. The acylating fatty acid is indicated by fragments labelled S and T (4), in this case C18:0.

Presented at the 36th ASMS Conference on Mass Spectrometry and Allied Topics
June 5-10, 1988, San Francisco, CA

Immunoaffinity Purification - Gas Chromatography - Mass Spectrometric Analysis of Prostaglandins and Thromboxanes

D.R. Knapp and J.J. Vrbanac

Department of Pharmacology, Medical University of South Carolina
Charleston, S.C. 29425

Prostaglandins and thromboxanes play an important role in regulating vascular tone and platelet aggregation and appear to be important in the pathophysiology of cardiovascular diseases and shock. Much of the biological work in this area relies upon radioimmunoassay analyses, but GC-MS is regarded as the benchmark method for analysis of these lipids. Although the application of GC-MS to prostaglandin quantitation dates back nearly 20 years, the methods are still not widely utilized by biological investigators, due partly to the technological barrier of mass spectrometry and partly to the difficulties of sample preparation. We have sought to enable wider utilization of GM-MS methods in this field of biology via simplification of the methodology and utilization of simpler, less expensive GC-MS instrumentation. In efforts to simplify sample preparation we have employed immobilized antibodies to isolate these lipids from biological samples. The first reported application of immunoaffinity extraction in conjunction with mass spectrometric analysis employed a batch extraction of estradiol-17β by antibodies bound to cyanogen bromide activated microcellulose (1). Krause, et al. (2) utilized cyanogen bromide activated Sepharose 4B in a column procedure to extract Iloprost®, a stable prostaglandin analog. We have employed antibodies immobilized on silica gel and on agarose in the GC-MS analysis of thrombaxane B_2 (TXB_2)(3), 6-keto-prostaglandin $F_{1\alpha}$ (6K-$PGF_{1\alpha}$)(4), and prostaglandin E_2 (5). Cross reactivity of the antibodies to TXB_2 and 6K-$PGF_{1\alpha}$ to their respective dinor metabolites has been exploited to quantitate the parent compounds and dinor metabolites in the same procedure (6,7).

The technological barrier to employing a biological tool such as immobilized antibodies should not deter the mass spectrometrist. Numerous books on immunoassay methods (e.g. 8) are available as information sources on antibody production. Most institutions have scientists experienced in antibody production who could give advice, and animal care personnel can provide all aspects of dealing with the antibody producing animals. The essentials of antibody production, immobilization, and application are given below.

Small molecules such as prostaglandins must be conjugated to a larger molecule to elicit an immune response. The prostaglandin carboxyl group can be activated as a mixed anhydride with isobutyl chloroformate to couple to free amino groups on a carrier protein such as bovine serum albumin or keyhole limpet hemocyanin. The resulting conjugated antigen is emulsified with Freund's adjuvant and used to immunize rabbits at monthly intervals. Blood collected from the rabbits a week following immunization is allowed to clot at 4°C to yield antiserum. Antisera must be "titred" to determine the amount of antibody present. This is most simply done by adding radiolabeled analyte to series of dilutious of the serum followed by separation of the free analyte from that bound to the antibodies using dextran coated charcoal. Scintillation counting of the separated forms of the analyte is used to determine the percent bound and therefrom the serum dilution which binds 50% of a standard amount added (the "titre"). A titre of at least 1:1000 is generally needed for production of immobilized antibodies. The antibodies are isolated from the antiserum using an affinity column of commerically available immobilized protein-A. The serum is diluted with buffer and applied to the protein-A column, the column is washed with buffer, and the immunoglobulin G fraction eluted with acetic acid. The eluate is lyophilized and the antibodies coupled to a commercially available N-hydroxysuccinimyl activated carboxy substituted agarose (Affi-Gel 10®). The immobilized antibodies are then packed into columns with 1-2 ml of the gel per column.

Although biological samples can be applied directly to the columns, for prostaglandin analysis, we have found it advantageous to precede the immunoaffinity extraction with an ODS cartridge extraction. After washing, the ODS cartridge is eluted with ethyl acetate, and eluent dried, dissolved in buffer,

and applied to the immunoaffinity column. After washing the column with buffer and water, the analytes are eluted with 95% acetonitrile in water. The extracted prostaglandins are derivatized as the methoxime, pentafluorobenzyl ester, silyl ether derivatives and analyzed by gas chromatography-negative ion chemical ionization spectrometry-selected ion monitoring. Although TMS ethers are most commonly used, we have found the TBDMS ether useful to resolve 6-keto-$PGF_{1\alpha}$ from a commonly encountered interference. The figure below shows a typical urine analysis using this procedure.

The work on prostaglandins and thromboxanes as endogenous signal molecules is now evolving to study of the receptors for these signals. In collaboration with P.V. Halushka who is isolating and purifying thromboxane receptors, we are working toward the application of mass spectrometry to study of the receptor structure. Since the thromboxane receptor is believed to be of the rhodopsin class, we are beginning this work, with S. Martin and R. Crouch, with studies on the rhodopsin receptor model protein bacteriorhodopsin. Using photoaffinity labeled retinal analogs we are seeking to learn about the movements in bacteriorhodopsin associated with signal tranduction and lay the groundwork for the study of the thromboxane receptor as well as other receptors of the thromboxane class.

Supported in part by N.I.H. grants RR 01239 and HL 29566.

References

1. S.J. Gaskell and B.G. Brownsey, Clin. Chem. 29, 677 (1983).
2. W. Krause, U. Jakobs, P.E. Schulze, B. Nieuweboer, and M. Hümpel, Prostaglandins Leukotrienes Med. 17, 167 (1985).
3. H.L. Hubbard, T.D. Eller, D.E. Mais, P.V. Halushka, R.H. Baker, I.A. Blair, J.J. Vrbanac, and D.R. Knapp, Prostaglandins 33, 149 (1987).
4. J.J. Vrbanac, T.D. Eller, and D.R. Knapp, J. Chromatogr. 425, 1 (1988).
5. J.J. Vrbanac, T.D. Eller, C.J. Beischel, W.F. Oehlenschlager, and D.R. Knapp, submitted to Anal. Biochem.
6. J.J. Vrbanac, T.D. Eller, H.L. Hubbard, R.H. Baker, P.V. Halushka, I.A. Blair, and D.R. Knapp, Presented at the 34th Annual Conference on Mass Spectrometry and Allied Topics, June 8-13, 1986, Cincinnati, OH.
7. C. Chiabrando, A. Benigni, A. Piccinelli, C. Carminati, E. Cozzi, G. Remuzzi, and R. Fanelli, Anal. Biochem. 163, 255 (1987).
8. T. Chard, An Introduction to Radioimmunoassay and Related Techniques, Elsevier, New York, 1982.

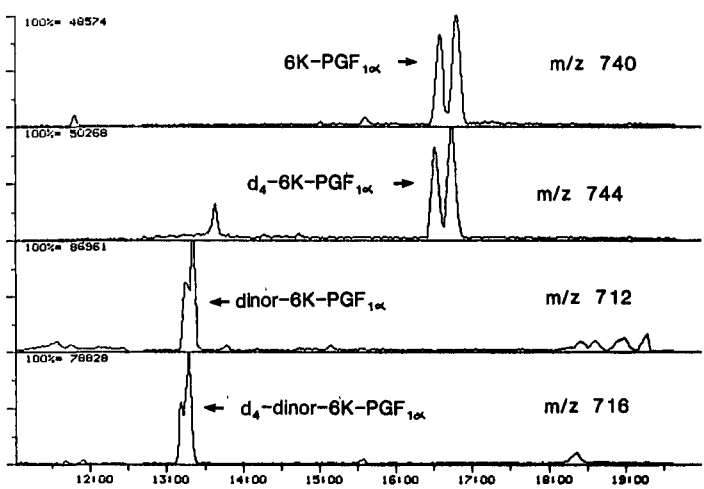

Presented at the 36th ASMS Conference on Mass Spectrometry and Allied Topics
June 5-10, 1988, San Francisco, CA

The Importance of High Abundance Sensitivity in Thermal Ionisation Mass Spectrometry used for the Measurement of very low abundance Isotopes.

P J Turner VG Isotopes, Winsford, UK

It is necessary in some isotope systems to be able to measure as accurately as possible the abundance of certain minor isotopes which may be in close proximity to major components in the system. Examples of this are the measurement of the thorium 230/232 ratio in uranium-thorium disequilibrium studies where the ^{230}Th ion beam is typically a few ppm of the ^{232}Th beam or the measurement of 234/238 and 236/238 ratios in uranium samples. The thorium data is used for dating oceanic processes whilst the uranium data is used for monitoring burn-up history of fuel in the nuclear power industry.

The ability of the mass spectrometer to make these measurements depends not only on the abundance sensitivity of the instrument but also on the dynamic range of the measuring system. The abundance sensitivity of a mass spectrometer is usually defined as the ratio of the height of the tail of the peak at unit mass separation from the peak to the height of the peak itself. In a thermal ionisation isotope mass spectrometer with a 30cm radius analyser magnet the abundance sensitivity will typically be a few ppm.Tailing is symmetric on both high mass and low mass sides of the peak and is found to be directly proportional to analyser residual pressure.

Measurements are conveniently carried out using the NBS U005 or U010 uranium isotope standards and figure 1 shows a scan of the uranium spectrum from 233 to 237.5 with a mass spectrometer abundance sensitivity of approx 2ppm. Measurement was carried out on a Daly Multiplier system operating in analogue mode on a VG354 mass spectrometer.

The main mechanism contributing to tailing is inelastic scattering of ions by collision with residual gas atoms in the analyser, although there may also be a small contribution from scattering processes in the ion source.

The abundance sensitivity may be very substantially improved by adding an electrostatic analyser to the ion optical system in a double focussing configuration. This has been done in the VG54-38 mass spectrometer (fig 3) where the parameters have been chosen such that not only is the system double focussing (in terms of angle and energy) but is also close to stigmatic. The intermediate slit is 0.7mm wide, the final slit is 0.9mm wide which provides a flat topped peak mode of operation at approx 400 resolving power in mass and 240 resolving power in energy.

Transmission in the two-sector instrument is the same as that in the single focussing instrument, and the abundance sensitivity is improved to better than 0.1ppm. With this level of performance low levels of hydrocarbons (mass positive wrt the metal ion) and low

levels of K_6^+ ions (mass negative wrt the metal ion) can be readily detected. This emphasises the importance of clean preparation methods if reliable results are to be obtained.

With the 54-38 mass spectrometer in its basic form it is only possible to analyse one ion beam at any given time so that isotope ratio measurements may only be carried out in the single collector peak hopping mode. There is not enough physical space to transmit more than one ion beam through the electrostatic sector, but it is possible to add additional Faraday collectors at the intermediate focal point. This arrangement is shown in figure 6. Since the dispersion length is only 325mm it is not possible to have collectors operating at unit mass separation at uranium. It is however possible to operate at two unit mass separation so that, for example, the ratio 236/238 may be measured in the static (non-peak-hopping) mode.

With this arrangement it is possible to measure very large dynamic range isotope ratios without the necessity of having an intermediate abundance isotope available. Calibration is carried out by peak switching a beam of appropriate size between the Faraday collector at the intermediate focus and the multiplier collector at the final focal point. The dynamic range of the measuring system in this mode may be in excess of 10 orders of magnitude depending on the value of the measuring resistor which is chosen for the intermediate Faraday collectors.

Results from a direct 236/238 ratio measurement are shown in figure 8. Reproducibility is better than +/- 1% using the analogue system, and better than +/- 0.3% if a pulse counting system is used.

For full multiple collection in the double focussing mode, it is necessary to use a forward geometry Nier-Johnson configuration, and this has now been constructed and designated ISOLAB 54. The dispersion length with this arrangement of components is 540mm, so that the established VG Multicollector system may be used, providing unit mass separation at uranium. This system is shown in figure 9. It is particularly suitable for measuring ratios on ion beams produced from an energetic ion source which may also be temporally unstable. However since the magnetic sector is now the second stage of the mass spectrometer, there is no filtering against scattered particles. The abundance sensitivity follows the same analyser pressure dependency as it does for the single focussing analyser, but an overall substantial improvement is still possible since the electrostatic sector can be used as an additional differential pumping stage between the source and the magnetic analyser.

The final magnetic stage can be operated in the 10^{-10} torr range resulting in an abundance sensitivity better than 0.5ppm. This is shown in figure 10.
It would be possible to add a second 38cm radius filter to this system on the axial collector position to further improve the abundance sensitivity while retaining full multiple collector operation.

Presented at the 36th ASMS Conference on Mass Spectrometry and Allied Topics
June 5-10, 1988, San Francisco, CA

ISOTOPE RATIO MEASUREMENTS BY TOTAL SAMPLE VOLATILIZATION AND SIGNAL INTEGRATION UTILIZING A MULTICOLLECTOR SYSTEM

E. L. Callis and Robert M. Abernathey
Los Alamos National Laboratory
Los Alamos, NM 87545

In thermal ionization mass spectrometry, observed ratios must normally be corrected for fractionation introduced by the evaporation process. Because the composition of the sample remaining on the filament, and hence the observed ratios, is constantly changing throughout the analysis, carefully controlled and reproducible conditions must be applied to both sample and standard to achieve accurate results. Typically, only a small fraction, 10% to 50%, of the sample is volatilized.

It has long been theorized that the effects of fractionation should be virtually eliminated by evaporation of the entire sample while integrating the signal from each isotope over the life of the sample. The availability of commercial multicollector instrumentation now makes this an attractive alternative to conventional techniques.

Experimental: A VG-354 mass spectrometer, equipped with five Faraday collectors and a Daly detector ion-counting system was employed in this work. All analyses were performed using multiple-filament geometry in which sample evaporation and ionization can be controlled independently. The instrument software was modified to perform the analyses in the following manner. While holding the sample filament current at zero, the ionizing filament is brought to operating temperature by monitoring the ^{187}Re intensity. The element peaks are next located and the total beam intensity is set to 10^{-14} A using the ion-counting system. Use of the ion-counting system at this stage, while not essential, minimizes the consumption of sample before initiation of the integration. After the peaks have been located and focusing has been completed, the Daly system is turned off, Faraday amplifier zeroes are measured, and the integration/current ramp is started. Before each 5-second integration period, the sample filament current is incremented in steps of 20 to 100 mA, depending on the present beam intensity. The maximum beam intensity is controlled roughly between 6×10^{-11} and 7×10^{-11} A by suspending the current ramp when the intensity is within these limits. Because all isotopes are collected simultaneously, no attempt is made to obtain a stable beam. The integration/current ramp continues until sample exhaustion ($<10^{-13}$ A intensity). A second set of amplifier zeroes is measured at the end of the analysis.

Results and Discussion: Results obtained on uranium and plutonium standards are shown in Table 1. These data have been corrected only for relative collector efficiencies, which are determined in a separate experiment by cycling a single ion beam, ^{238}U for example, onto each collector in turn. These data indicate that within the uncertainty limits of the standards, "true" or unfractionated ratios are obtained. In addition, the between-run precision using the total integration technique is typically <0.02% RSD, which represents an improvement over all but the most carefully made nonnormalized measurements using conventional techniques.

The amount of sample loaded in these experiments was typically 10 ng plutonium and 100 ng uranium. With 10^{11} Ω input resistors, these sample sizes yield integrated intensities of approximately 10 V-min for plutonium and 50 V-min for uranium. Although much smaller samples can be analyzed, some degradation of the minor isotope measurement should be expected.

The results on uranium and plutonium are very encouraging. However, much work remains in evaluating various effects of the vaporization and ionization processes, especially for elements not so well behaved as uranium and plutonium, to determine the degree to which absolute measurements can be approached by this technique.

Acknowledgment: Work performed under the auspices of the U.S. Department of Energy.

TABLE 1. Results on Uranium and Plutonium Standards

Standard	Element	Ratio	Observed Value	Deviation from Certified
NBS-946	Pu	240/239	0.144945	-0.040%
947	Pu	240/239	0.241236	-0.024%
948	Pu	240/239	0.086352	+0.038%
CRM-128	Pu	242/239	1.00096	+0.029%
NBS-U500	U	235/238	0.99985	+0.015%
U900	U	235/238	10.3785	+0.034%
U100	U	235/238	0.113642	+0.037%
U020	U	235/238	0.020812	+0.010%
U010	U	235/238	0.010144	+0.040%

Presented at the 36th ASMS Conference on Mass Spectrometry and Allied Topics
June 5-10, 1988, San Francisco, CA

Total Evaporation/Integration with Mixed Multicollection Modes: New Effective Approaches for Thermal Ionization MS

Günter Wagner, Dietmar Tuttas, Dirk Poesthorst
Finnigan MAT GmbH, P.O. Box 14 40 62, 2800 Bremen, FRG

Manfred Romkowski, Silvia Franzini, Lothar Koch,
European Institute for Transuranium Elements,
P.O. Box 3240, 7500 Karlsruhe, FRG

The users of thermal ionization mass spectrometry are increasingly concentrating on higher accuracy and, at the same time, on smaller and smaller sample loads. Stringent transportation regulations combined with increasing levels of radioactivity in reprocessed fuels demand that nuclear analysts be able to accurately analyze sub nanoCurie samples of uranium and plutonium (i.e.<10 ng U and <1 ng Pu). Similarly, geochronologists and geochemists now require Pb measurements from single zircon crystals that contain less than 1 ng total lead (1,2) and Sr measurements from small crystalline domains or from fluid inclusions (less than 1 ng of total strontium). Isotope ratios of greater than 150,000 for $^{232}Th/^{230}Th$ and greater than 20,000 for $^{238}U/^{234}U$ need to be accurately measured by simultaneous SEM ion counting/Faraday multiple ion collection to apply the uranium/thorium disequilibrium method for precise measurement of time over the past million of years,

In nuclear applications, simultaneous Faraday cup ion multicollection, combined with flash evaporation of <1 ng Pu or <5 ng U, samples produce accuracies comparable to previous techniques requiring a factor of 100 larger samples. Sample fractionation can be neglected as all ions from a totally consumed sample are integrated simultaneously, Additionally, sample throughput can be drastically increased, as a single sample can be measured in 10 to 12 minutes, to a rate of 5 to 6 per hour.

Ion counting a minor isotope peak simultaneously with Faraday cup measurement of the major isotope(s), further improves the precision that can be obtained with small samples. The ionization efficiency for uranium is about a factor of 10 less than that of plutonium. Thus, ion counting employed on small uranium samples (less than 2 ng) provides the same precision that multiple Faraday ion collection achieves for similar size plutonium samples (Fig. 1 and Fig. 2).

Advances in geochronology and geochemistry have traditionally driven and have been driven by advances in instrumentation. Thermal ionization mass spectrometry, employing simultaneous multiple collection of several ion beams has not only changed the "state-of-the-art" in terms of sample size and data precision. The simultaneous use of SEM (analog detection) or SEM (ion counting) with multiple Faraday collection has dramatically improved the capabilities for precise measurement of extremely large

isotope ratios, even when measured on small samples. Radiogenic lead samples, with $^{206}Pb/^{204}Pb$ ratios ranging from 250 to 30,000, have been accurately measured on samples containing less than 1 ng total Pb and less than 0.1 pg ^{204}Pb (3). Geochronologists employing the uranium/thorium disequilibrium method require the measurement of extreme isotope ratios on small samples. Less than 1 ng of thorium having a $^{232}Th/^{230}Th$ isotope ratio of >150,000 has been measured to better than ± 0.5 % relative, in "mixed multicollection mode" with a SEM (ion counting) registering the minor isotope beam.

MAT 261
SMALL SAMPLE SIZE — NUCLEAR

ION COUNTING *)

1) SIMULTANEOUS: ION COUNTING FOR MINOR ISOTOPE, FARADAY COLLECTION FOR MAJOR ISOTOPE

	SIZE	ISOTOPE	RATIO	INTERNAL PRECISION
8 ng U 005	40 pg	^{235}U	$^{235}U/^{238}U$	± 0.06 %
1.3 ng U 005	6 pg	^{235}U	$^{235}U/^{238}U$	± 0.19 %
0.3 ng U 005	1.5 pg	^{235}U	$^{235}U/^{238}U$	± 0.36 %
0.12 ng U 005	0.6 pg	^{235}U	$^{235}U/^{238}U$	± 0.7 %

2) ION COUNTING ON MAJOR AND MINOR ISOTOPE, WITH PEAKJUMR

1 ng U 010	10 pg	^{235}U	$^{235}U/^{238}U$	± 0.16 %
0.3 ng U 010	3 pg	^{235}U	$^{235}U/^{238}U$	± 0.24 %

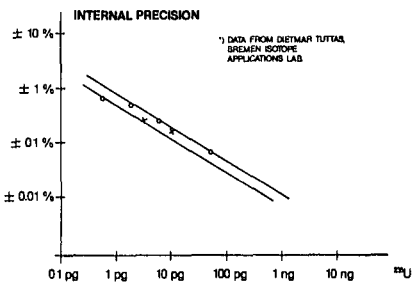

Fig. 1 Ion Counting - Uranium

MAT 261
SMALL SAMPLE SIZE — NUCLEAR

TOTAL EVAPORATION / INTEGRATION WITH STATIC FARADAY MULTICOLLECTION *)

	SIZE	ISOTOPE	RATIO	EXT REPRODUCIBILITY
0.5 ng NBS Pu-947	125 pg	^{240}Pu	$^{240}Pu/^{239}Pu$	± 0.05 %
	8 pg	^{240}Pu	$^{240}Pu/^{239}Pu$	± 0.5 %
1 ng NBS Pu-947	250 pg	^{240}Pu	$^{240}Pu/^{239}Pu$	± 0.02 %
	15 pg	^{240}Pu	$^{240}Pu/^{239}Pu$	± 0.2 %
1 ng NBS Pu-948	115 pg	^{240}Pu	$^{240}Pu/^{239}Pu$	± 0.03 %
	5 pg	^{240}Pu	$^{240}Pu/^{239}Pu$	± 1 %
1 ng NBS Pu-948	80 pg	^{240}Pu	$^{240}Pu/^{239}Pu$	± 0.03 %
	0.3 pg	^{240}Pu	$^{240}Pu/^{239}Pu$	± 4 %

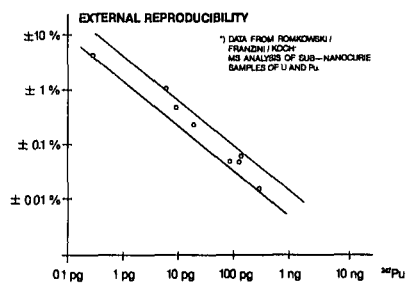

Fig. 2 Faraday Multicollection - Plutonium

(1) Bernd Kober, Whole-grain evaporation for $^{207}Pb/^{206}Pb$ age investigations on single zircons using a double filament thermal ion source, Contrib. Mineral. Petrol. (1986) 93; 482-490

(2) Bernd Kober, Single zircon evaporation coambined with Pb^{+} emitter bedding for $^{207}Pb/^{206}Pb$ age investigations using thermal ion mass spectrometry, and implications to zirconology; Contrib. Mineral. Petrol. (1987) 96; 63-71

(3) J.C. Roddick and W.D. Loveridge, Finnigan MAT Application Report No. 66, 1986.

Presented at the 36th ASMS Conference on Mass Spectrometry and Allied Topics
June 5-10, 1988, San Francisco, CA

NEUTRON ACTIVATION AND MASS SPECTROMETRIC MEASUREMENT OF IODINE-129

R. S. Strebin, Jr., F. P. Brauer, J. H. Kaye,
M. S. Rapids and J. J. Stoffel(s)

Pacific Northwest Laboratory*
Richland, Washington 99352

An integrated procedure has been developed at our laboratory for measure -ment of iodine-129 by neutron activation analysis and mass spectrometry. Work has been completed on procedures for extracting iodine from environmental materials in a form and purity suitable for analysis by both methods. Steps in the sample processing include spiking with iodine-125 for yield and isotope dilution measurements; combustion in oxygen; adsorption on charcoal; iodine separation by either CCl_4 extraction or gas-phase hydrated manganese dioxide separation; and precipitation as silver iodide for filament loading.

Negative surface ionization is used in a triple filament arrangement to produce I^- ions with high efficiency. At an ionizer brightness temperature of 1000 C, stable nanoampere currents of mass analyzed iodine ions are consistently produced from 100-ng samples of silver iodide. The overall sample efficiency averages 1%; that is, 1% of the iodine atoms loaded are measured as I^- ions.

Mass spectrometric analysis is performed with a computer-controlled, three-stage mass spectrometer (see figure), which provides an abundance sensitivity better than 10^{-12} for the measurement of I-129 relative to natural I-127. The spectrometer is equipped with a dual detector system to measure the large isotope ratios encountered in environmental samples. An electron multiplier operated in the pulse-counting mode measures the I-129 signal at the exit of the third stage. A Faraday collector located in the focal plane of the first stage simultaneously determines the I-127 intensity by direct-current measurement. The I-125 spike is measured by the electron multiplier as are adjacent masses used to check for interferences and impurities. The sample solution remaining is processed further for neutron activation analysis.

A variety of reference standards and environmental sample materials have been analyzed in replicate by the integrated procedure. Agreement has been achieved down to the measurement limit of about 10^7 atoms or 2×10^{-15} g of I-129. For neutron activation analysis, this value defines the inherent limit of the measurement method. For mass spectrometry, however, this value defines only the current state-of-the-art. Continued development may extend this limit by one or more orders of magnitude.

---

*Operated for the U.S. Department of Energy by Battelle Memorial Institute.

Presented at the 36th ASMS Conference on Mass Spectrometry and Allied Topics
June 5-10, 1988, San Francisco, CA

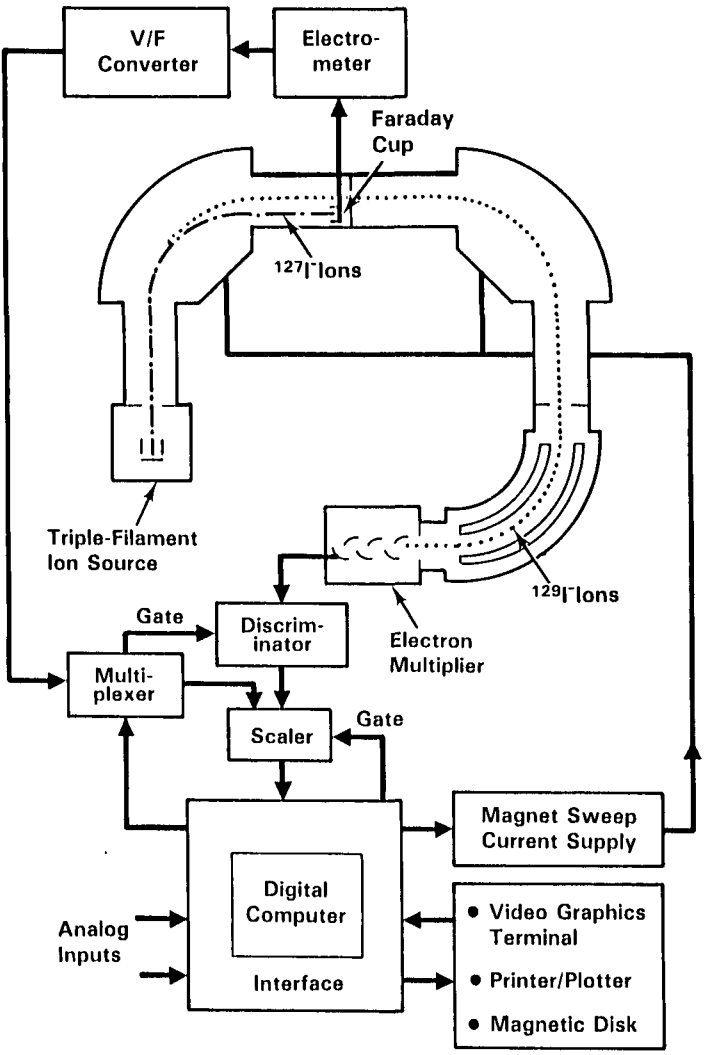

Presented at the 36th ASMS Conference on Mass Spectrometry and Allied Topics
June 5-10, 1988, San Francisco, CA

RESONANCE IONIZATION MASS SPECTROMETRY OF PROMETHIUM

D. H. Smith, R. W. Shaw, and J. P. Young
Analytical Chemistry Division
Oak Ridge National Laboratory
Oak Ridge, TN 37831

Promethium is difficult to analyze mass spectrometrically because of isobaric interferences from neodymium and samarium. This situation arises because promethium, unique among the lanthanides, has no naturally occurring isotopes. It is synthesized in a reactor by neutron capture from samarium starting material. The longest lived promethium isotope is 145, which has a 17.7-year half-life. All of the promethium isotopes whose half-lives are long enough to allow measurement of the properties of the element decay in one of two ways, both of which give rise to isobaric interference. Some decay via beta emission to produce the samarium isotope of the same mass as the promethium. Others decay via electron capture or positron emission to produce the neodymium isotope of the same mass as the original promethium. Efforts to analyze promethium using thermal ionization have failed to achieve adequate separation of the three elements,[1] and it was decided to investigate resonance ionization mass spectrometry (RIMS) for this purpose.

A tunable, flashlamp-pumped dye laser was interfaced to a mass spectrometer comprised of a single magnetic 90-degree sector of 30 cm. radius.[2] Rhodamine 6G dye was used, and pulses with energies of about 2 mJ were produced. The laser was focused so that ion formation occurred at the object focal point of the mass spectrometer's ion source. A neutral plume of atoms was obtained from a heated rhenium filament to which had been added a small chip of charcoal; temperatures of this filament were about 1400 degrees C. The charcoal provided a reducing atmosphere that encouraged evaporation of the analytes as neutral atoms. Much care was expended to achieve maximum overlap of the neutral analyte plume and the ionizing laser beam. Samarium and promethium were loaded onto the charcoal as dilute nitric acid solutions. Optical spectra were obtained by focusing on one isotope and scanning over the range of the dye, using the mass spectrometer as the detector. Each element was ionized by a single-color, three-photon process: successive resonant absorption of two photons of essentially the same wavelength brings the atom close enough to the ionization limit that non-resonant absorption of a third photon causes ionization.

The resonance ionization spectra for a limited region are shown in the figure. Trace A was acquired from a loading of 600 ng of samarium of natural isotopic abundance; the most abundant samarium isotope (152) was monitored. It is extremely unlikely promethium was present as the half-life of 152-Pm is 18 minutes. The lines at 587.55 and 587.8 are among the strongest samarium transitions in the range of R6G dye. Wavelength was calibrated using mercury emission lines; accuracy is better than 0.1 nm. Trace B (shaded) was obtained after adding 100 ng of promethium to the filament and is thus comprised of contributions from both elements. Note the strong doublet at 584.6 and 585.0; these are the strongest promethium transitions within the dye range. Note, too, that both the promethium and samarium transitions are entirely free of interference from contributions from the other element. We measured an elemental selectivity of 1000:1 for Pm/Sm at the 584.6 transition. The actual selectivity is undoubtedly greater as the number quoted is limited by counting statistics.

Earlier work has shown that the nearest neodymium transitions lie 0.7 nm on either side of the 584.6 transition.[3] It will thus be possible to analyze any one of the three elements from any combination of them. The only question that remains unresolved is that of isotopic bias in isotope ratio measurements using resonant three-photon ionization processes. This is an important issue that transcends this particular application.

Presented at the 36th ASMS Conference on Mass Spectrometry and Allied Topics
June 5-10, 1988, San Francisco, CA

Research sponsored by the U. S. Department of Energy, Office of Basic Energy Sciences, under contract DE-AC05-84OR21400 with Martin Marietta Energy Systems, Inc.

REFERENCES

1. R. L. Walker, personal communication.

2. D. L. Donohue, J. P. Young, and D. H. Smith, Int. J. Mass Spectrom. and Ion Phys. 43, 293-297 (1982)

3. D. H. Smith, D. L. Donohue, and J. P. Young, Int. J. Mass Spectrom. and Ion Processes 65 287-297 (1985).

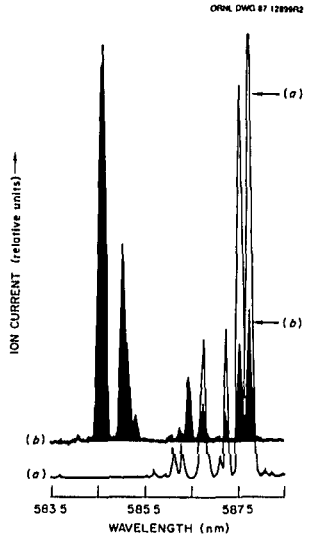

"The submitted manuscript has been authored by a contractor of the U.S. Government under contract No. DE-AC05-84OR21400. Accordingly, the U.S. Government retains a nonexclusive, royalty-free license to publish or reproduce the published form of this contribution, or allow others to do so, for U.S. Government purposes."

Presented at the 36th ASMS Conference on Mass Spectrometry and Allied Topics
June 5-10, 1988, San Francisco, CA

FOURIER TRANSFORM MASS SPECTROMETRY FOR ELEMENTAL ISOTOPE RATIO DETERMINATION AND QUANTITATIVE ANALYSIS

J. T. Brenna and W. R. Creasy
IBM Corporation, D/T43
1701 North Street
Endicott, New York 13760

Quantitative isotopic and elemental analysis is a common goal for microprobe analyses. Though quantitative analysis is routinely achieved by microprobe mass spectrometers based on conventional mass dispersion systems (quad, TOF, magnetic sector), there is a wide variety of specimen types which do not easily lend themselves to quantitative analysis. Often selectivity, in the form of mass resolution or the inability to perform multiple stage MS, is inadequate to remove interferences from the peaks of interest.

FTMS has established itself as capable of selectivity unparalleled by other mass spec techniques. Recently we have assembled a laser microprobe system for FTMS (1). We report here some of our investigations of the instrument's capabilities as a quantitative tool. The goal for this work is to identify optimum analysis conditions and experimental parameters while establishing practical limits for critical figures-of-merit such as precision and accuracy. Our strategy is to work from simplest analysis to most complex systems. These studies serve as a benchmark toward an eventual goal of quantitative molecular microprobe analysis.

All analyses were performed with a Nicolet FTMS-2000 system, with a home built laser microprobe interfaced to the mass spectrometer. The laser was operated at 266 nm, and fluence at the surface is estimated to 10^8 J/cm^2. All analyses, including ultra-high mass resolution studies, were performed in the source cell, with no ion transfer to the analyzer cell.

Repetitive gas phase spectra of $Mo(CO)_6$ and $Cr(CO)_6$ were acquired and analyzed for reproducibility of isotopes ratios in the elemental sections of the spectra. Reproducibility of 1% (rel. std. dev.(RSD)) for Mo and 5% for Cr, representative of major and minor isotopes respectively, were obtained for single EI scans. RSD's of a factor of 8 smaller than these values were obtained for spectra of 200 co-added scans.

The effect of apodization function on RSD's of identical transients was determined. The following functions were evaluated for their effect on RSD's: No apodization, Hanning, Kaiser-Bessel, Kaiser-Bessel 4-term, Blackman-Harris 3-term and 4-term, and Noest-Kort. A series of transients was acquired, apodized by each function, Fourier transformed, and evaluated for RSD. For both major and minor isotopes, the Noest-Kort function provides superior reproducibility to the other functions studied. For minor isotopes, RSD's are smaller by 30%.

We have previously observed fast damping of transients acquired from specimens of polymers analyzed under ablative conditions. This phenomenon has precluded ultra-high mass resolution analysis of these specimens. However, we have been able to generate long-lived transients from Pb wire, and ultra-high mass resolution is demonstrated for laser ablated Pb metal. Transients lasting in excess of 10 s were acquired in the source cell of the instrument. Mass resolution of 4×10^5 was acquired from apodized, Fourier transform transients.

Reproducibility of isotopic and elemental ratios from ablated species was examined with NBS isotopic standards. NBS lead standard yields reproducibility in the 10% range (single shot). NBS microprobe standard glasses yield reproducibility in the 30-40% range for certified major elements. These values are in the range of published values for quantitative analysis of similar specimens by commercial TOF-based laser microprobe mass spectrometers. In addition, the spectra show similarities to published spectra acquired on TOF systems.

References

1) J.T.Brenna, W.R.Creasy, W.McBain, C.Soria, this meeting.

Presented at the 36th ASMS Conference on Mass Spectrometry and Allied Topics
June 5-10, 1988, San Francisco, CA

STUDIES OF SPUTTERING IN GLOW DISCHARGE MASS SPECTROMETRY: C.M. Barshick and W.W. Harrison, University of Virginia, Charlottesville, Va. 22901. USA.

INTRODUCTION

The continued growth of glow discharge mass spectrometry (GDMS) has required a reevaluation of the fundamentals of the glow discharge with regard to the optimization of analytical results. The glow discharge is comprised of a multistep process of sputter-atomization, thermalization, and ionization. While these have been reviewed in some detail, little has been done to characterize the role of sputtering in GDMS. The sputter process is critical, since it is this initial step whereby target atoms are ejected from the cathode surface before being ionized and eventually detected by the mass spectrometer.

While sputter yields are known to vary by a factor of 2-3 across the periodic table, it is still unclear how they vary overall as a function of ion energy, and pressure. In addition, previous investigations have shown that the sputter rate varies with the mass and energy of the bombarding ion, but the exact manner in which it varies is still unclear. The present investigations center on the correlation between sputtering of an atomic population and subsequent detection of an ionic population as a function of (a) the mass and energy of the incident ions and (b) the pressure of the discharge. The results of these investigations are the basis of this paper.

EXPERIMENTAL

The glow discharge mass spectrometer system used for these studies is quadrupole based. The glow discharge ion source takes the form of a 1.0 mm diameter iron coaxial cathode fitted on the end of a direct insertion probe. Ions are sampled from the negative glow region through a 0.5 mm orifice into an einzel lens system that focuses the ion beam into a Bessel-box energy analyzer mounted on the quadrupole mass filter. A DEC-MINC-11/23 microcomputer controls mass scanning and data acquisition, and the ion signal is collected and converted into a form suitable for computer processing by a Princeton Applied Research Model #112 ion counter/processor.

Subsequent net sputter yield data were obtained by sputter weight loss measurements. Samples were weighed on a Sartorius-Werke microanalytical balance, sputtered for one hour and then reweighed. The following expressions were used to calculate the net sputter yield (atoms/ion):

$$Y = 10^5 \, [W/ \, (M \, i^+ \, t)]$$
$$i^+ = i/(1 + \gamma)$$

where W is weight loss in grams, M is atomic weight, i^+ is ion current in amperes, t is sputter time in seconds, i is total current in amperes, and γ is the secondary electron fraction.

RESULTS AND DISCUSSION

Ion energy. The effect of ion energy was studied using an argon discharge run at a constant pressure of 1.0 torr. The voltage was varied to obtain the desired energy of incident ions, as per Davis and Vanderslice (1). Results of net sputter yield vs ion energy are illustrated in Figure 1A. The sharp increase in slope at 50 eV is attributed to a pressure dependent threshold for sputtering, and is similar to results seen in high vacuum ion beam studies. Similarly, Figure 1B is a plot of relative ion signal vs ion energy. The fact that the two curves mimic one another shows that the ion signal detected is directly affected by the sputtered atomic population. The small range of ion energies studied in this investigation is the result of the inability of the instrument to detect ion signals when the incident sputtering energies are below 25 eV, and overheating of the cathode material when the energies are above 100 eV.

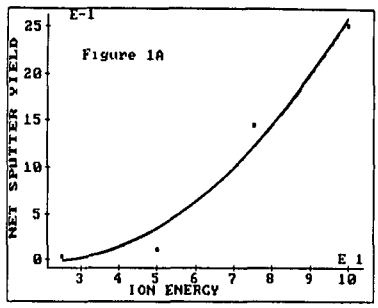

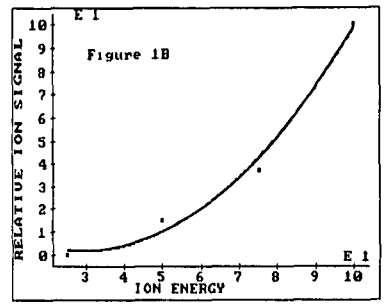

Pressure. The effect of pressure was studied using an argon discharge run at a constant 50 eV ion energy. In this manner, the pressure dependent nature of the threshold energy could be determined. Figure 2A and 2B show the effect of pressure on the net sputter yield and relative ion signals, respectively. The curves increase over the entire range investigated with a threshold at a pressure of 1.0 torr. While larger ion signals appear to be obtainable beyond the range of pressures investigated, limitations in the ability to differentially-pump the ion source preclude operating beyond 1.5 torr.

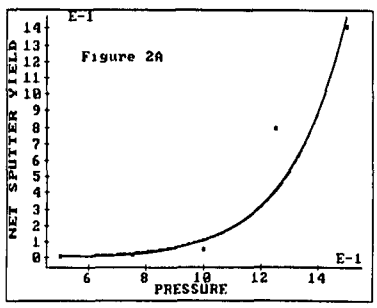

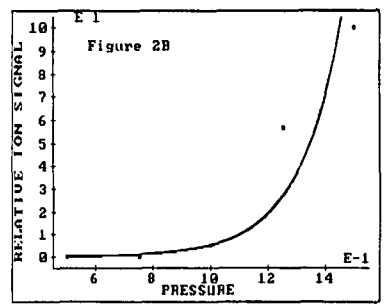

Discharge gas. The effect of varying discharge gas species was studied at a constant pressure of 1.0 torr and bombarding ion energy of 50 eV. Figure 3A and 3B are plots of net sputter yield vs projectile mass, and relative ion signal vs projectile mass, respectively. The data show a maximum at a target-projectile mass ratio of $M_2/M_1 \simeq 1$, a result similar to those observed in ion beam studies.

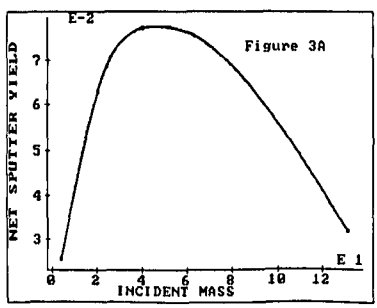

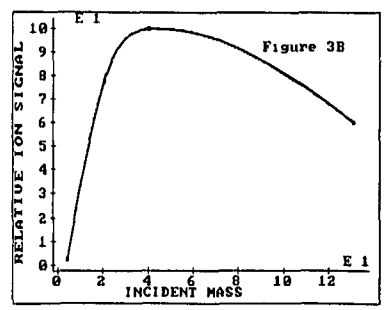

(1) Davis, W.D.; Vanderslice, T.A. Phys. Rev. 1963, 131, 219.

Presented at the 36th ASMS Conference on Mass Spectrometry and Allied Topics
June 5-10, 1988, San Francisco, CA

COLLISION-INDUCED DISSOCIATION OF MOLECULAR IONS IN GLOW DISCHARGE MASS SPECTROMETRY (CID-GDMS).

F. L. King and W. W. Harrison, University of Virginia, Charlottesville, VA 22901.

INTRODUCTION

Glow discharge mass spectrometry (GDMS) is gaining wide acceptance as a viable technique for the direct elemental analysis of solids and is perceived as having certain advantages over competing techniques. The problem of isobaric interferences due to polyatomic ions has evolved as the principle hindrance to quadrupole based GDMS. Common approaches taken in the circumvention of this problem in elemental MS are the utilization of high resolution instrumentation, the selection of alternative isotopes for analysis, and the implementation of an expert data system to correct for the interferences. The latter two solutions are employed with varying degrees of success in inductively coupled plasma mass spectrometry (ICP-MS) utilizing quadrupole mass analyzers exclusively. Recently, this laboratory has undertaken investigations aimed at the elimination of polyatomic interferences, rather than simply their compensation.

A glow discharge ion source was installed on a triple quadrupole mass spectrometer to facilitate the investigation of collision-induced dissociation (CID) for the removal of polyatomic ions from the ion beam prior to mass analysis. Additionally, the application of various tandem mass spectrometry (MS/MS) techniques to GDMS permitted investigations of the isobaric interferences not previously possible. Such investigations are shown to provide results of fundamental as well as analytical interest. The investigations reported on here show the removal of molecular interferences by CID, the identification of ion composition from daughter spectra, and the prediction of interfered m/z from parent spectra.

RESULTS AND DISCUSSION

Analytical Response. A concern in employing CID was the effect on ion transmission efficiency due to increases in scattering in the collision cell at higher pressures. Table I demonstrates the effect of scattering on the sensitivities of selected species as a function of collision cell pressure. One compensating feature is that the noise level is also reduced by the collision cell, so that although the sensitivity worsens by an average factor of 7 at the highest pressure of 2.4 mtorr, the detection limits only suffer by an average factor of 3. The negative influence on sensitivity and detection limit observed in the CID attack on polyatomic interferences has its counterpart in the high resolution approach, in that the cost of increased mass resolution is reduced ion transmission.

CID of Interferences. The main thrust of this study was an examination of the polyatomic ion problem in GDMS. Figure 1 shows spectra acquired for a 1264a steel sample. In Spectrum A an interference due to $^{56}Fe^{40}Ar^{+}$ prevents the analytical use of $^{96}Mo^{+}$. Spectrum B shows the effect of CID indicating that at this level of sensitivity the isobaric interference due to the iron argide is effectively eliminated. Also the contribution of iron dimers is seen to be eliminated. While some of these interferences can be mass resolved with commercial GDMS equipment, metal argides and numerous oxides require higher resolution than is presently available, making the CID approach especially attractive.

TABLE I

CELL PRESSURE milliTorr	Sensitivity (Counts/ppm) ^{100}Mo	^{121}Sb	^{181}Ta	^{186}W	^{208}Pb	Isotope Ratio 96/100*
0.0	704	389	148	231	717	2.5
0.7	514	276	105	199	366	2.0
1.4	306	155	65	126	222	1.8
2.4	106	79	27	58	50	1.7

* The natural ratio for $^{96}Mo/^{100}Mo$ is 1.716

Collision Energy Effect. The effect of collision energy on the dissociation of a potentially interfering species was undertaken to evaluate the correspondence of dissociation threshold with bond energy, and to determine the ability of increased collision energy to increase dissociation. Figure 2 is a plot of Ta^+/TaO^+ as a function of the center-of-mass collision energy. The vertical line drawn on the plot in Figure 2 corresponds to the reported bond energy of TaO^+; this differs from the threshold value by ca. 6 eV. The observed results indicate that species produced in the discharge have appreciable internal energy complicating attempts at bond strength measurement by CID. Figure 2 also demonstrates that once the threshold energy for dissociation is reached the percent dissociation increases rapidly with increasing energy, but the slope of the curve can already be seen to indicate the approach of a maximum for dissociation. It does not appear that this maximum will correspond to 100% dissociation.

Daughter Spectra. A well known molecular ion observed in GDMS is the Ar_2H^+ species at m/z = 81. Utilizing a brass sample the daughter spectrum of m/z = 81 was acquired. The daughter spectrum shows the expected signal at m/z = 41 due to the fragmentation of the Ar_2H^+ yielding ArH^+. An unexpected contribution attributed to CuH_2O^+ at m/z = 81 is identified from the fragment appearing at m/z = 63. This demonstrates the ability to evaluate any m/z for the presence of isobaric interferences and to identify the interfering species.

Parent Spectra. The utilization of parent spectra to identify spectral regions of potential interference were investigated employing a stainless steel cathode. The observed signals correspond to parent ions which upon CID yield fragment ions of m/z = 56. In addition to the expected indication of FeAr at m/z 96 there is also signal at m/z 73 which is attributable to $FeOH^+$. Thus the parent scan was shown to predict interfered mass values in a spectrum.

CONCLUSIONS

These initial investigations into the application of tandem mass spectrometry techniques to trace elemental analysis have yielded promising results. CID is effective in eliminating certain isobaric interferences due to polyatomic ions, enhancing the ability to pursue GDMS with quadrupole-based mass spectrometry systems. The technique is not limited by resolution or the lack of alternative isotopes. The ability to obtain daughter and parent spectra permits the identification of interfered species and the prediction of interferences in the spectrum. Before the full potential of CID GDMS can be assessed, however, additional development and exploration are required.

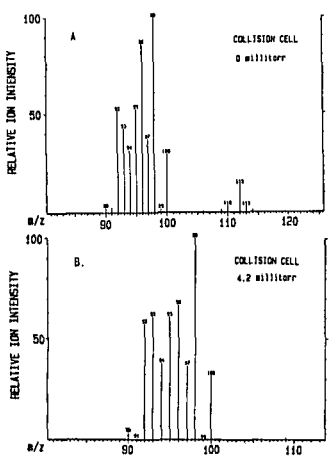

FIGURE 1

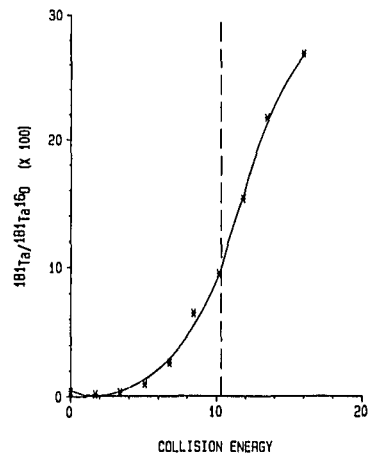

FIGURE 2

Presented at the 36th ASMS Conference on Mass Spectrometry and Allied Topics
June 5-10, 1988, San Francisco, CA

ION ASSOCIATION BY TIME-OF-FLIGHT MASS SPECTROMETRY

L. Q. Huang[a], R. J. Conzemius, G. A Junk and R. S. Houk
Ames Laboratory-U.S. Department of Energy and Department of Chemistry
Iowa State University, Ames, Iowa 50010 (USA)

Time-of-flight (TOF) mass spectra are normally obtained by averaging repetitive mass scans of ions accelerated from a pulsed source. In the present work, individual mass scans from each pulse were tested for probable associations between ions of different m/z, i.e., was the presence of one ion contingent upon the presence of the other in the same scan? The tendency for ions to be associated was evaluated statistically by testing data obtained from solid specimens of cesium iodide and the superconductor, $YBa_2Cu_3O_7$. A low power, short duration laser (300 ps, 10 uJ) was used to produce ions at only a few masses per laser pulse. With few ions produced per pulse, ion associations could be observed which might otherwise be masked when the number of ions per pulse was very high as in most ion sources. A data acquisition system was developed (Fig. 1) to allow convenient recording and study of the information in the individual scans and two classical statistical methods were used to identify associations.

The results of ion association tests for the CsI sample indicate that Cs^+ and $[(CsI)Cs]^+$ are associated. Both statistical treatments for the $YBa_2Cu_3O_7$ sample show association between the pairs Ba^+ and BaO^+, BaO^+ and $BaCuO^+$, BaO^+ and $YBaCuO^+$ (or $Ba_2O_2^+$), and $BaCuO^+$ and $YBaCuO^+$ (or $Ba_2O_2^+$). These associations infer some commonality in their formation by laser desorption (LD).

The preliminary ion association data show promise for providing information about structure and ion formation mechanisms that cannot be obtained from interpretation of conventional (i.e., averaged) LD mass spectra. The instrumentation stores each scan separately from each ionization event so all of the possible associations can be tested in retrospect by simply examining the data already collected; no instrument modification is needed and the experiment need not be repeated. Also, statistical tests could be applied for other criteria such as association and unassociation of three or more ions. Naturally, the general concept of ion association need not be limited to LD or even condensed phase samples. Further experiments with various sample types and operating conditions are warranted to delineate the value of the information provided by ion association.

[a]Present address:
The Connecticut Agricultural Experiment Station
123 Huntington Ave.
P. O. Box 1106
New Haven, CT 06504

Presented at the 36th ASMS Conference on Mass Spectrometry and Allied Topics
June 5-10, 1988, San Francisco, CA

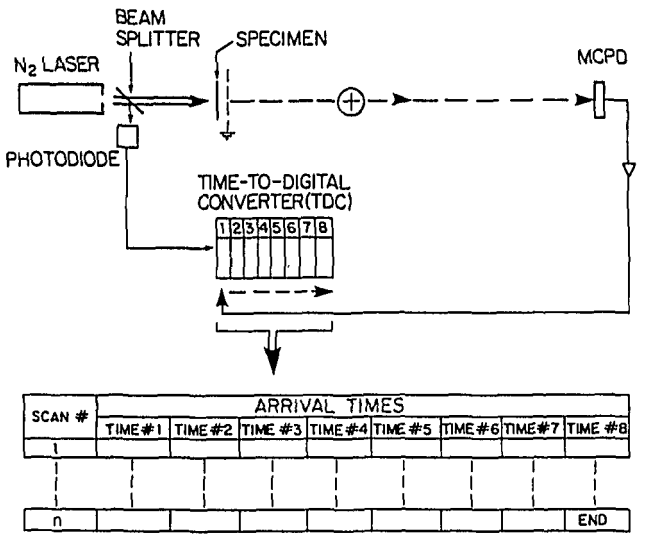

Figure 1. Schematic diagram of experimental data flow where MCPD is the microchannel plate detector.

Presented at the 36th ASMS Conference on Mass Spectrometry and Allied Topics
June 5-10, 1988, San Francisco, CA

SUPERCONDUCTOR ANALYSIS BY GLOW DISCHARGE MASS SPECTROMETRY

J Clark, D J Kirby, N E Sanderson
VG Elemental Ltd, Ion Path, Road Three, Winsford, Cheshire, CW7 3BX, UK

Introduction

High resolution Glow Discharge Mass Spectrometry is routinely used in the analysis of a wide range of bulk solid samples, including metals, semiconductors and insulators. (1)

Recent work on the VG 9000 has demonstrated the extension of this technique to the exciting area of high temperature superconductors. Pin samples of the type $YBa_2Cu_3O_x$ have been analysed whilst maintained at temperatures near liquid nitrogen using standard cell cryo cooling.

The absence of standards for these new materials highlights the importance of the matrix independance of the GDMS technique. Results for the oxygen stoichiometry and impuriy concentration are particularly interesting.

Analytical Protocol

Four different samples of $YBa_2Cu_3O_x$ were analysed on the VG 9000 Glow Discharge Mass Spectrometer. The samples had been processed differently to induce different oxygen contents. Samples A, B and C are from three stages of preparation method 1 and sample D from method 2.

Sample A: An 'as prepared' powder using standard preparation techniques. This sample is superconducting at 90K.
Sample B: Prepared as sample A and subjected to hot pressing - this reduces oxygen content compared to sample A. This sample is not superconducting.
Sample C: A sample of 'B' re-annealed in oxygen - this should increase the oxygen content. This sample is superconducting at 60K.
Sample D: Prepared by a different method to the above samples and expected to be the purest sample. This sample is superconducting at 90K.

Analysis

The samples were received in powder form. They were compressed into pins and immediately loaded into the VG 9000 plasma cell (2), which with the sample is cooled to near liquid nitrogen temperatures. The sample forms the cathode of a DC discharge within the plasma cell. Neutral atoms are sputtered from the sample and subsequently ionized in the plasma. Ions are accelerated through 8KV into a high resolution double focussing mass spectrometer and are collected by a dual Faraday/Daly detector system linear over 11 orders of magnitude. This enables majors (100%-1%), minors (1%-1ppm) and traces (1ppm - 10ppt) to be analysed during one analysis cycle. The majors, (termed matrices) are used as an internal standard against which the minors and traces are ratioed.

Results

Table 1 shows the uncorrected ion beam ratio data for the matrix elements. The internal precision achieved over 5 consecutive analyses is significantly less than 1% of the measured values.

Table 1 - Matrix concentration (wt %)

Element	Sample A	Sample B	Sample C	Sample D
Y	11.74	15.98	11.12	15.22
Ba	56.20	55.57	57.73	53.57
Cu	11.00	9.84	9.94	9.65
O	21.10	18.12	21.20	21.56

Correction factors were derived using the formula $YBa_2Cu_3O_{6.89}$ *to describe* the previously characterised sample D and used to correct the raw data for samples A, B and C. Table 2 shows the corrected results.

Table 2 - Corrected Matrix concentration (wt %)

Element	Sample A	Sample B	Sample C	Sample D
Y	10.1	14.1	9.9	13.38
Ba	42.2	42.6	44.4	41.35
Cu	31.8	29.0	29.4	28.69
O	15.8	13.9	16.3	16.57

Table 3 shows the uncorrected ion beam ratio data for a comprehensive list of impurity elements found in the superconductive ceramics. These values, obtained in one minute/element, reflect sub-ppb limits of detection and are typically within a factor of 3 of the absolute values without standards.

Table 3 - Minor and Trace concentration (ppm wt)

Element	Sample A	Sample B	Sample C	Sample D
F	34	6	12	3
Na	73	85	101	27
Mg	2	5	5	3
Al	878	2083	1780	1526
Si	6	79	48	9
S	19	65	41	13
Cl	905	221	264	78
K	21	2170	1914	20
Ca	57	58	86	86
Sc	0.5	2	0.6	0.8
Cr	6	4	25	5
Fe	12	24	247	8
Mn	1	1	3	1
Co	1	1	2	3
Ni	1	2	3	2
Pb	2	77	3	1
Bi	2	3	3	5
Total Impurities	2020.5	4886	4537.6	1790.8

Discussion

The results clearly demonstrate some important differences between the samples, the most important being the difference in oxygen concentration of the superconductive samples (A, C, D) and the non superconductive sample (B).

From Table 3 is seen that sample D is indeed the purest. Samples A (Tc 90K) and D (Tc 90K) have less than half the total impurities of sample C (Tc 60K) with sample B being of the lowest purity.

The two 90K superconductive samples have significantly lower levels of Si, S and K than the 60K sample, with the non superconductor having the highest levels of these elements. Sample C (Tc 60K) has 247 ppm of iron, approximately 10 times that of the other three samples. Sample B has significanly higher levels of Pb and Al than the other samples.

Conclusion

$YBa_2Cu_3O_x$ samples have been successfully analysed by GDMS. This preliminary data shows differences in oxygen content between superconductive and non superconductive ceramics. Significant levels of impurities have been found in all samples, with the highest temperature superconductors being the samples with the lowest total impurities. Differences in specific element levels between samples have been demonstrated and it may be postulated that these affect the Tc of the ceramic.

References

1) Sanderson N E et al, Mikrochim. Acta (Wien) 1987, I, 275-290
2) Hall D J and Robinson PK, American Laboratory, August 1988

Presented at the 36th ASMS Conference on Mass Spectrometry and Allied Topics
June 5-10, 1988, San Francisco, CA

ENHANCEMENT OF SPARK SOURCE MASS SPECTROGRAPHIC DATA USING STATISTICAL CLUSTER ANALYSIS

Charles R. Wilson, M. Le Roy Jacobs
WAL Inc., 6385 W 52nd Ave., Arvada, CO 80002
and R. M. Hutchinson, Dept. of Geol. Eng.,
Colo. School of Mines, 250 Berthoud Hall,
Golden, CO 80401

Stibnite (antimony sulfide) crystal specimens were analyzed by spark source mass spectrography (SSMS) for trace element content to establish a "trace element fingerprint" for judicative purposes. Removal of many crystal specimens from an antimony mine for surreptitious sale over an extended period of time was suspected. A method was sought for a establishment of the source of certain stibnite crystals and if possible spatial orentiation of crystal specimens in the identified mine.

SSMS was used in this investigation since the technique will give a trace element determination of all elemental constituents from lithium to uranium in as little time as one hour. The SSMS sample preparation involves the grinding of the sample to -200 mesh, mixing with graphite and the addition of an known amount of indium as an internal standard.

It is well known that the absolute concentration of a given trace element can change in similar types of samples matrices on a sample to sample basis. It is also true that elements tend to occur in association with other complimentary elements, i.e., elements which are alike in chemical nature. Even though the absolute concentrations change the inter-element ratios tend to remain constant. Similarities of samples can be established through the use of trace elements, by measuring total concentration of a given trace element in a sample and measuring the same element concentration in a different sample and attempting to correlate the two concentrations. However, if the two absolute concentation levels are different (a frequent occurrence) very little, if any correlation, may be found. Therefore; conversion of absolute element concentrations to inter-element ratios may provide a "finger print" independent of concentration.

Over fifty stibnite crystal samples were examined for trace element ratios or "fingerprints". Direct sample to sample comparison of trace element concentrations was inconclusive. To enhance the similarities and differences between the stibnite specimens, a statistical method was indicated. The determined concentrations of twenty-eight trace elements were converted to inter-element ratios and compared to the same element ratios from reference stibnite samples. The trace elemental ratios derived in this manner gave the sought for unique identifying features, since dependence on absolute trace element concentrations has been mathamatically limited. Further, if one measures many trace element ratios which are characteristic of the sample, a trace element ratio pattern will quickly develop which will be specific to a given sample.

This ratio pattern will uniquely identify a sample much as a fingerprint identifies an individual human. Samples of common origin will have similar trace element ratio patterns. These trace element ratio patterns can then be compared with other ratio patterns to determine any similarities between samples. This process is called clustering and can produce correlation (distance) coefficients which can be used to group samples into similar families.

Graphical representation of this clustering is termed a dendrogram or "tree like" graph. For the stibnite crystals examined, the dendrogram was constructed by grouping together samples that had inter-element ratio similarities. Then by averaging the "distance coefficients" new groupings were constructed until all sample had been grouped into a related branch of the "family tree".

The use of statistical cluster analysis as applied to the elemental ratios of the in-common trace elements of the stibnite crystals allowed the SSMS to differentiate the originating mine from several other known stibnite mines and indeed, to identify the crystal specimens as to specific locations within the mine.

In other words, a very specific "trace element fingerprint" was established for each crystal specimen, which allowed spatial location of individual samples to be correlated with mining production records to establish a probable time-span in which the crystals may have been removed from the mine.

References

(1) Aldenderfer, M. S. and Blashfield, R. K., "Cluster Analysis," Sage Publications, Inc., Beverly Hills, CA, 1984

(2) Davis, John C., Ed., "Cluster and Data Analysis in Geology," J. Wiley & Sons, New York, NY, 1973

The submitted manuscript has been authored by a contractor of the U S Government under contract No W 31-109-ENG-38 Accordingly, the U S Government retains a nonexclusive, royalty free license to publish or reproduce the published form of this contribution, or allow others to do so, for U S Government purposes

Presented at the 36th ASMS Conference on Mass Spectrometry and Allied Topics
June 5-10, 1988, San Francisco, CA

MASS SPECTROMETRIC PROBES OF METAL CLUSTER DISTRIBUTIONS AND METASTABLE ION DECAY*

E. K. Parks, K. Liu, S. K. Cole, and S. J. Riley

Chemistry Division, Argonne National Laboratory, Argonne, IL 60439

The study of metal clusters has provided both an opportunity and a challenge to the application of mass spectrometry. These days the most often-used technique for cluster generation - laser vaporization - leads to extensive distributions of cluster sizes, from one to perhaps thousands of atoms, and most studies reported to date use excimer laser ionization and time-of-flight mass spectrometry for cluster detection. Our apparatus is a simple one-stage TOF design employing Wiley-McLauren spatial focussing and a one-meter drift tube. The double extraction grid (to minimize penetration of the high tube voltage into the extraction region) consists of two 85% transmission molybdenum meshes separated by 0.6 mm. The tube is oriented perpendicularly to the cluster beam, so that deflection plates are needed to direct cluster ions to the detector. Typically, a 20 μsec section of TOF time can be imaged onto the detector for a given set of plate voltages. Our plates are curved to match the round drift tube, and are offset downstream so that larger clusters can be directed to the detector. Even so, for the heaviest masses we see a breakdown of the usual $(\text{mass})^{1/2}$ - time relationship across the 20 μsec window because the ions do not all pass through the center of the plates. The heaviest cluster clearly resolved in this apparatus has been Ni_{366}.

The presence of a nearly continuous distribution of masses has revealed an interesting instrumental effect. The upper panel of Fig. 1 shows a composite (constructed from successive 20 μsec sections) distribution of nickel clusters measured in an earlier version of the apparatus. The undulations in intensity are not a result of the composite construction, but instead are due to interference of some ion trajectories through the double extraction grid (an effect akin to Moiré fringes). The lower panel in Fig. 1 shows a nickel cluster distribution measured in a more recent version of the apparatus (which obviously has higher resolution) in which the double mesh extraction grid is replaced by a double parallel wire grid having the wires parallel to the cluster beam. The interference effects are clearly no longer present.

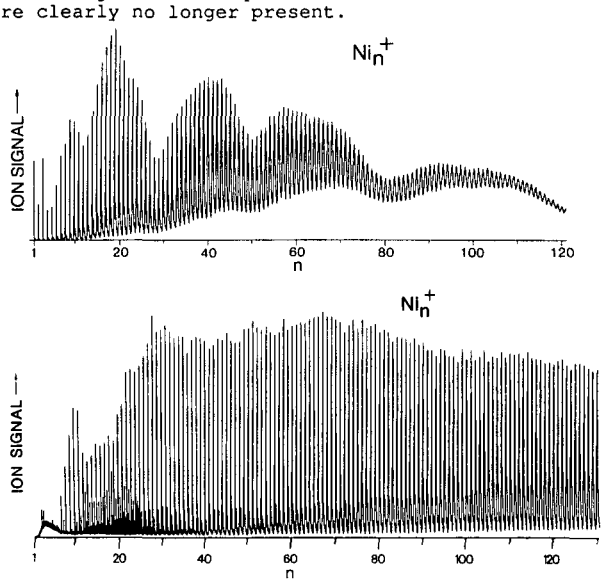

Fig. 1. Upper panel: Spectrum of nickel clusters taken with a double-mesh extraction grid in the TOF mass spectrometer. The small substructure around n = 20 is due to oxide impurities.
Lower panel: Nickel cluster spectrum that is seen when the extraction grid is of parallel-wire type. The mass spectrometer resolution is considerably improved over that in the upper panel. More oxide impurities are evident. Laser ionization conditions were such that only one-photon ionization processes were possible, so the small clusters below n = 7 were not detected.

In a second apparatus employing a pulsed valve in the cluster source, we see asymmetric broadening of niobium cluster mass peaks under multiphoton ionization conditions, indicating metastable decay of parent cluster ions. An example, for Nb_7^+, is shown in the first panel of Fig. 2. Other studies of niobium clusters have shown no such asymmetric peaks. Normally one would fit the peak tail and, using calculated relationships between parent and daughter ion extraction and flight times, determine the decay rates for the parents. In this case, having a continuous distribution of neutral cluster sizes, we do not *a priori* know the parent. Instead, the parent metastable decay can be probed directly by delaying the ion extraction in the TOF spectrometer, allowing the parents to convert to daughters before extraction. The other panels in Fig. 2 show such data. From the disappearance of the tail, the parent decay rate can be determined. Now, from the calculated decay time - TOF relationship, which depends on the parent/daughter mass ratio, the parent mass can be determined.

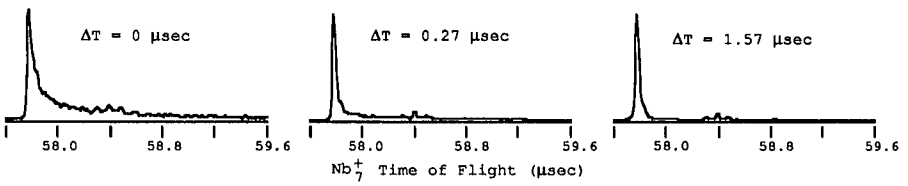

Fig. 2. First panel: The TOF peak for Nb_7^+ with no ion extraction delay. Next two panels: The peaks when extraction is delayed by the times shown.

The results of this procedure are quite surprising. First, fitting the TOF peak tails shows that there are at least two decay pathways. The identification of parents shows that one pathway corresponds to evaporation of one or two atoms, the usual fragmentation process for metal clusters. The other pathway is fission of a larger cluster, a process more characteristic of semiconductor clusters, and suggests there is something unusual indeed about the niobium clusters that are made in this particular cluster source.

Since these are multiphoton ionization/fragmentation processes, there are presumably intermediate neutral electronically excited states involved. We can probe these using a two-color scheme. Following the excimer laser pulse a dye laser at 2 eV photon energy is fired at the clusters. By itself, the dye laser produces no ions, but after the excimer laser pulse it produces a second mass peak arising from excited neutral species. By varying the delay between laser pulses, we find the lifetime of the intermediate neutral is 3.15 μsec, in sharp contrast to the usual picture of transition metal clusters having a "vibronic soup" showing near-instantaneous internal conversion. "Normal" transition metal clusters cannot retain electronic excitation for even picoseconds, yet here are clusters doing so for microseconds.

We believe these unusual clusters result from the pulsed valve used in this source. It opens faster and farther than most, resulting in unusually high carrier gas pressure in the cluster formation area. Under these conditions the metal will be tightly confined, since diffusional loss will be small. The metal is transported out of the growth channel very quickly, so clusters do not grow very large. At the nozzle, we then have a high density of small clusters and a strong expansion because the gas pressure is so high. Thus we have rapid cooling, and many cluster-cluster collisions leading to the formation of unannealed species that might be likened to van der Waals clusters of clusters. Now cluster fission fragmentation can be understood. It represents a decomposition of the "super cluster" into its constituent parts. Also, a mechanism for long-lived storage of electronic excitation is suggested. It could be that the agglomeration leads to isolated electronic bands in a chromophore analogous to typical van der Waals clusters.

*Work supported by the U. S. Department of Energy.

Presented at the 36th ASMS Conference on Mass Spectrometry and Allied Topics
June 5-10, 1988, San Francisco, CA

GUIDED ION BEAM STUDIES OF TRANSITION METAL CLUSTER ION CHEMISTRY:

S. K. Loh, Lian Li, D. A. Hales, and P. B. Armentrout;
Chemistry Department, University of Utah, Salt Lake City, Utah, 84112.

Reactions of size-specific metal cluster ions are examined using guided ion beam tandem mass spectrometry. A continuous beam of cold cluster ions is generated by vaporizing the metal sample with a high repetition rate (6 kHz) Cu vapor laser in a fast flow of helium. Sufficient ions are produced in the laser vaporization step that there is no need for a separate ionization step. Measurement of reaction cross sections and branching ratios characterize the interactions of the clusters with a variety of neutral gases. By examining the variation of these quantities with the kinetic energy of the cluster ions, thermochemical data for both ionic and neutral cluster species can be determined.

In one series of studies, we have examined the collision-induced dissociation (CID) of gas-phase iron cluster ions, Fe_x^+, with Xe. For the dimer ion, the energy dependence of the cross section is consistent with theoretical models and gives $D^o(Fe_2^+) = 2.72 \pm 0.07$ eV,[1] in good agreement with previous studies.[2,3] Combined with the known ionization potentials[4] and electron affinities[5] of Fe and Fe_2, this bond energy also provides $D^o(Fe_2) = 1.15 \pm 0.09$ eV and $D^o(Fe_2^-) = 1.90 \pm 0.09$ eV. For larger cluster ions, up to the decamer, the lowest energy decomposition channel is always loss of an Fe atom. Indeed, our data offers no indication that any molecularly bound neutral products are formed in the dissociation of these cluster ions. Dissociation occurs exclusively by sequential Fe atom loss. This has also been concluded for photodissociation of Fe_x^+ clusters.[3]

This CID behavior contrasts with that of V_x^+ and Nb_x^+. This is most dramatically seen in the CID behavior of the tetramers of these ions.[6] Here, the lowest energy pathway for fragmentation is fission of the molecule into an ionic and neutral dimer. Atom loss does not occur until higher energies, but is the dominant channel at elevated kinetic energies. Thus, the "most probable" process is highly energy dependent, i.e. the relative thermodynamic stability of the dimer and trimer ions is not reflected by the branching ratio at elevated kinetic energies.

These experimental techniques can also be applied to the reactive chemistry of the cluster ions. For example, we have studied the endothermic reactions of D_2 with the monomer, dimer, and trimer ions of iron. The thresholds for production of Fe_x^+-D, the only product observed, differ with cluster size. Analysis of the reaction thresholds lead to bond energies of $D^o(Fe_2^+\text{-D}) = 1.5$ eV and $D^o(Fe_3^+\text{-D}) = 1.8$ eV, which can be compared to $D^o(Fe^+\text{-D}) = 2.2$ eV.[7] These values are very similar to $D^o(Fe_2^+\text{-Fe})$ and $D^o(Fe_3^+\text{-Fe})$, which may imply that the bonding

in Fe^{2+} and Fe^{3+} is largely single σ bonds.

1. Loh, S. K.; Lian, Li; Hales, David A.; Armentrout, P. B. J. Phys. Chem., submitted for publication.
2. Hettich, R. L.; Freiser, B. S. J. Am. Chem. Soc. 1987, 109, 3537.
3. Brucat, P. J.; Zheng, L.-S.; Pettiette, C. L.; Yang, S.; Smalley, R. E. J. Chem. Phys. 1986, 84, 3078.
4. Rohlfing, E. A.; Cox, D. M.; Kaldor, A. J. Chem. Phys. 1981, 81, 3846. Cox, D. M.; Whetten, R. L.; Zakin, M. R.; Trevor, D. J.; Reichmann, K. C.; Kaldor, A. Proc. Int. Laser Sci. Conf. 1986, 527.
5. Leopold, D. G.; Lineberger, W. C. J. Chem. Phys. 1986, 85, 51.
6. Loh, S. K.; Lian, Li; Hales, David A.; Armentrout, P. B. J. Chem. Phys., in press.
7. Elkind, J. L.; Armentrout, P. B. J. Phys. Chem. 1986, 90, 5736-5745.

Presented at the 36th ASMS Conference on Mass Spectrometry and Allied Topics
June 5-10, 1988, San Francisco, CA

STRUCTURE AND REACTIVITY OF CLUSTER IONS

A.P. Baronavski, J.H. Callahan, S.W. McElvany and M.M. Ross
Chemistry Division/Code 6110, Naval Research Laboratory
Washington, D.C. 20375.

Clusters are of great scientific interest because they might bridge the gap between the solid- and gas-phase forms of matter. In order to understand how the transition from atoms to the condensed phase is made, studies have been directed at the determination of the structure and reactivity of clusters as a function of size. The objective of this work is to compare different methods of cluster ion production and to characterize the clusters ions using ion/molecule reactions and collision-induced dissociation (CID).

Cluster ion distributions of bismuth and antimony have been produced by a variety of methods. Direct laser vaporization (DLV) at 532 nm yields distributions which truncate at Sb_5^+ and Bi_5^+. These distributions are strikingly similar to those observed by Duncan [1] using a molecular beam and photoionization of the neutral species. However, Duncan's data for ions from the supersonic expansion extend to Bi_{11}^+. In our work, we have attempted to explain the similarities and differences between (1) Duncan's data and our DLV data, and (2) the distributions of cluster ions of bismuth and antimony produced by particle bombardment (SIMS) and DLV [2], and by condensation from ovens [3].

We have found that the DLV of bismuth depends upon the wavelength of the laser used in vaporization. However, only one additional cluster ion, Bi_7^+, is observed when 1064 nm light is used rather than 532 nm. On the other hand, SIMS produces Bi_x^+ up to x=31. This is dramatically different than the data for DLV or Duncan's data. In Figure 1 we compare the Bi_x^+ distribution observed using SIMS with that observed by Sattler [3] using an oven/ condensation source with electron ionization. The agreement, considering the radically different methods, is remarkable. The enhancements observed for smaller cluster ions (x<=8) can be attributed to dissociations of larger species. This interpretation is borne out by both collision-induced dissociation (CID) experiments in our lab and by photodissociation conducted by Geusic et al. [4] The differences between our DLV data and the SIMS data is believed to be due to dissociations of the larger cluster ions in the plasma produced by the laser.

Similar studies have been carried out for antimony and lead (not Pb) to the conclusion that, unlike larger bismuth cluster ions, the larger antimony cluster ions are produced (using SIMS, DLV, molecular beam) with enough internal energy to unimolecularly dissociate. In high-pressure/SIMS experiments, cluster ions up to Sb_7^+ are collisionally stabilized and observed.

One of the unique aspects of DLV is the ability to induce chemistry in the laser plasma. An example of this is shown in Figure 2 for a sample of tantalum powder in graphite. Cluster ions, $Ta_xC_n^+$ up to x = 18 are observed and for TaC_n^+ with n = 14 have been observed. These types of cluster ions are not produced by SIMS and so are indicative of the extent of chemical reactions in the plasma.

The distribution of cluster ions that can be generated from a solid is dependent upon (1) the production method, due to differences in the magnitude and means of energy deposition, (2) the nature of the sample and the ion source conditions and (3) the time frame in which the cluster ions are formed and detected. Through studies employing several mass spectrometric techniques (FTMS, TOFMS, quadrupole and sector) with laser vaporization and particle bombardment, we have attempted to understand how the experimental conditions affect the size distribution, energies and types of cluster ions observed. Direct laser vaporization of carbon yields abundant and high-mass cluster ions, $[C_n]^+$, in contrast to sputtering, whereas both methods yield similar cluster ion species from some samples such as bismuth and antimony. Similarly, using ion/molecule reactions and MS/MS methods the structures and reactivities of mass-selected cluster ions can be probed. Cluster ions of the forms Bi_x^+, Sb_y^+ and $[Bi_xSb_y]^+$ were studied with low- and high-energy CID, with differences found that are dependent upon instrumental parameters. Our studies have focused on cluster ions of metals, semi-metals and mixed-metal systems.

[1] K. LaiHing, P.Y. Cheng, M.A. Duncan, J. Phys. Chem., 91, 6521 (1987).
[2] M.M. Ross, S.W. McElvany, submitted to J. Chem. Phys.
[3] K. Sattler, J. Muhlbach, E. Recknagel, Phys. Rev. Lett., 45, 821 (1980).
[4] M.E. Geusic, R.R. Freeman, M.A. Duncan, J. Chem. Phys., 88, 163 (1988).

Presented at the 36th ASMS Conference on Mass Spectrometry and Allied Topics
June 5-10, 1988, San Francisco, CA

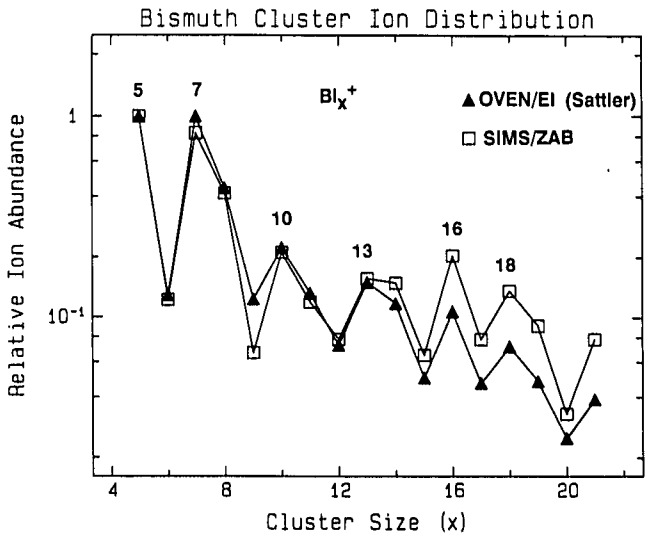

Figure 1.

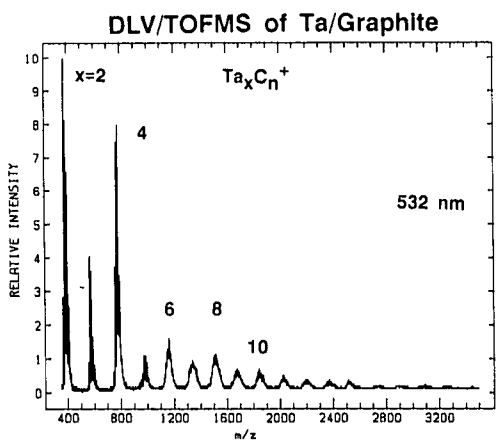

Figure 2.

Presented at the 36th ASMS Conference on Mass Spectrometry and Allied Topics
June 5-10, 1988, San Francisco, CA

HRGC/HRMS ANALYSIS OF BROMINATED/CHLORINATED ANALOGS OF TCDD AND TCDF IN MUNICIPAL INCINERATOR FLY ASH

H.Y. Tong and M.L. Gross, Midwest Center for Mass Spectrometry, Department of Chemistry, University of Nebraska, Lincoln, NE 68588

The fly ash formed during the combustion process in municipal waste incinerators (MWI) is probably the major contributor of polychloro dibenzodioxins and dibenzofurans (PCDD/Fs) to the environment today. However, it is also of interest to analyze other halogenated analogs of PCDD/Fs in fly ash because 1) those planar analogs may have a potential hazardous impact on the environment, and 2) the information on those analogs in fly ash may be helpful for studying the mechanism by which PCDD/Fs are formed. In this presentation, some tetra congeners of brominated PCDD/Fs (BPCDD/Fs) are selected to demonstrate the feasibility and the difficulties in the analysis of fly ash for BPCDD/Fs by using HRGC/HRMS techniques.

The benzene extract of fly ash collected from the bottom of an electrostatic precipitator of a MWI was subjected to two different clean-up methods for comparison. They are the normal phase HPLC fractionation[1] and the multiple open column chromatography[2] which is commonly employed for PCDD/Fs analysis. Consequently, the sample fraction containing PCDD/Fs was analyzed for BPCDD/Fs on a Carlo-Erba GC (30 meter DB-5 column)/Kratos MS-50 MS (70 eV EI, 10,000 resolution). Three characteristic ions were selectively monitored for each BPCDD/Fs analyzed and their mass profiles with 300 ppm span were acquired for qualitative and quantitative analysis.

Our preliminary data from HRGC/HRMS analysis show that BPCDD/Fs elute into the same fraction along with PCDD/Fs in both clean-up procedures used because of the high similarities in structure and polarity between PCDD/Fs and BPCDD/Fs. This observation is consistent with the previous finding of polybromo dibenzodioxins and dibenzofurans present in the PCDD/F fraction obtained in a similar multiple open column chromatographic procedure[3]. Figure 1 shows some mass chromatogram data for several selected PCDD/Fs and BPCDD/Fs found in the extract of fly ash. Notice that 1) $BrCl_3$-DD elutes between TCDD and P_5CDD, and 2) it has the isomer distribution pattern similar to that of TCDD. These observations also apply to other monobromo PCDD/Fs found in the sample, and may provide some interesting information for study of the formation mechanism of PCDD/Fs in incineration process.

One of the primary difficulties in the analysis of trace amount of BPCDD/Fs in fly ash is the interferences caused by PCDD/Fs of high concentration as well as some polyhalogenated aromatic compounds having structures similar to PCDD/Fs. Those interfering compounds are difficult to be separated from BPCDD/Fs by the clean-up methods commonly used and also exhibit GC retention times close to that of BPCDD/Fs. As an example, Table 1 illustrates some potentially interfering compounds in the analysis of fly ash for $BrCl_3$-DF by GC/MS. Based on these MS data, accurate measurements of the masses and particularly, the isotope ratios of molecular ion clusters are essential for identifying BPCDD/Fs in fly ash because the GC retention time data for most of BPCDD/F standard compounds are not available yet. The mass profile data of some selected compounds found in the sample are shown in Figure 2, and indicate that the acquisition of mass profile data is highly recommended in such analyses.

The concentrations of $BrCl_3$-DD and -DF, on the basis of quantitative responses of P_5CDD and P_5CDF standards, were measured to be 18 and 6 ppb respectively, in comparison to 440 ppb of TCDD and 290 ppb of TCDF in the fly ash sample analyzed. Di- and higher bromo PCDD/Fs were not detected at a ppb level in this fly ash sample.

References

1. Tong,H.Y., Shore,D.L., Karasek,F.W., Helland,P., and Jellum,E., J.Chromatogr., 285(1984), 423
2. Weerasinghe,N.C.A., Schecter,A.J., Pan,J.C., Lapp,R.L., Giblin,D.E., Meehan,J.L., Hardell,L., and Gross,M.L., Chemosphere, 15(1986), 1787
3. Donnelley,J.R., Munslow,W.D., Vonnahme,T.L., Nunn,N.J., Hedin,C.M., Sovocool,G.W., and Mitchum,R.K., Biomed. Environ. Mass Spectrom. 14(1987), 465

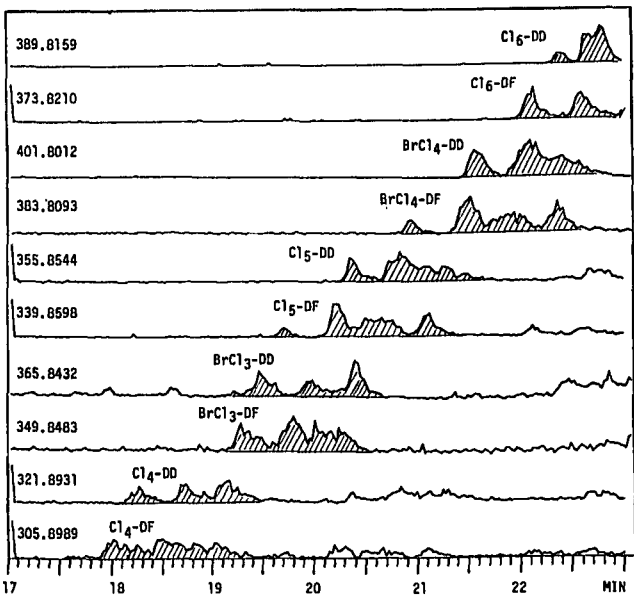

Figure 1: High resolution mass chromatogram data for selected PCDD/Fs and BPCDD/Fs found in the fly ash. DD: dibenzodioxin, and DF: dibenzofuran.

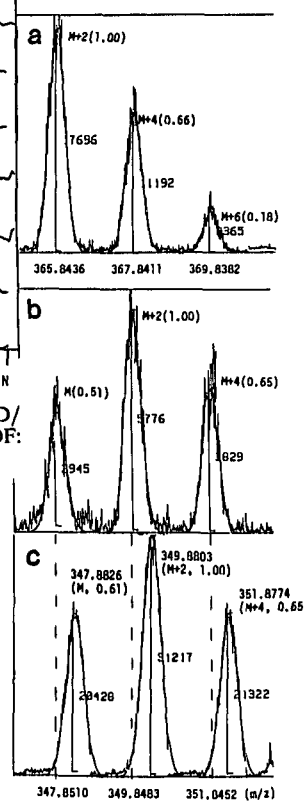

Figure 2: Mass profile data for a) $BrCl_3$-DD, b) $BrCl_3$-DF, and c) interfering compound tentatively identified as Cl_5-anthracene/phenanthrene. The theoretical relative intensities are given in parenthesis.

Table 1. MS DATA FOR $BrCl_3$-DF AND SOME POTENTIAL INTERFERENCES

Compound	*Mass*	*Ion*	*Relative intensity*	*Differentiation[1] by MS*
$BrCl_3$-DF (target analyte)	347.8511	M	0.51	
	349.8487	M+2	1.00	
	351.8459	M+4	0.66	
	353.8440	M+6	0.18	
Cl_5-DF	347.8490	M+10	0.003	IRM HR(170,000)
Cl_5-DD	353.8576	M	0.61	IRM, SDI,
	355.8547	M+2	1.00	HR(26,000)
Cl_5-anthracene/ phenanthrene	347.8834	M	0.61	IRM,
	349.8805	M+2	1.00	HR(10,000)
	351.8777	M+4	0.65	
	353.8750	M+6	0.22	
$BrCl_3$-diphenyl ether	349.8667	M	0.51	IRM,
	351.8643	M+2	1.00	HR(20,000)
	353.8617	M+4	0.66	
$BrCl_3$-fluorene	347.8693	M	1.00	IRM,
	349.8668	M+2	0.65	HR(20,000)
	351.8641	M+4	0.18	
	353.8619	M+8	0.01	
Cl_5-xanthene	351.8783	M	0.61	IRM,
	353.8754	M+2	1.00	HR(10,000)
$BrCl_4$-naphthalene	347.8093	M+6	0.33	IRM,
	349.8065	M+8	0.06	HR(8,000)

1. Differentiation by MS: isotope ratio measurement(ISM), selection of different ions monitored(SDI), and use of high resolution (HR).

Presented at the 36th ASMS Conference on Mass Spectrometry and Allied Topics
June 5-10, 1988, San Francisco, CA

DEVELOPMENT AND APPLICATION OF A THREE-PHASE COUPLED CAPILLARY GC COLUMN FOR GC-MS ISOMER-SPECIFIC DETERMINATION OF BOTH 2,3,7,8-TCDD AND 2,3,7,8-TCDF IN ENVIRONMENTAL SAMPLES

L. A. Harden, T. O. Tiernan, J. H. Garrett, and J. G. Solch
Department of Chemistry and Toxic Contaminant Research Program
Wright State University, Dayton, Ohio 45435

Because of the relative toxicities of 2,3,7,8-tetrachlorodibenzo-p-dioxin (TCDD) and 2,3,7,8-tetrachlorodibenzofuran (TCDF), there is intense interest in measuring these isomers specifically in environmental samples in the presence of other TCDD and TCDF isomers. Our laboratory recently described GC-MS procedures which utilize two separate gas chromatographic columns for this purpose. A DB-5 capillary column is used for detection and quantitation of 2,3,7,8-TCDD uniquely, while 2,3,7,8-TCDF is determined uniquely using a serially-connected DB-225/DB-5 capillary column, which we developed. The objective of the present study was to develop a single GC column which would resolve both 2,3,7,8-TCDD and 2,3,7,8-TCDF from all of their respective congeners, thereby permitting determination of both of these in a single GC-MS analysis.

Initially, the retention times of all 22 TCDD and 38 TCDF isomers on several different capillary GC columns (DB-5, SP-2250, DB-1701, DB-225, SP2401, and DB-WAX) were measured. These data were then used to predict what combinations of columns among those tested (coupled in series) would be effective in completely resolving both 2,3,7,8-TCDD and 2,3,7,8-TCDF. This was achieved by using a computer program, developed in our laboratory, for interpolating retention time data. This program assumes linear flow of each isomer through a given GC column, and the method is similar to that accomplished by graphical "window diagramming" procedures previously described in the literature(1). However, whereas the graphical method is limited to two-dimensional solutions, the computer model can yield multi-dimensional solutions.

The computer model described predicted that there were no possible combinations of pairs of coupled columns among those evaluated here (as listed above) which would uniquely resolve 2,3,7,8-TCDD and 2,3,7,8-TCDF. A three-column combination was therefore sought, and the computer model predicted that a combination DB-225/SP-2250/DB-WAX column would yield the desired resolution. Accordingly, sections of these three columns of appropriate length were coupled in series using butt connectors, and the resultant hybrid column was evaluated for retention or characteristics using all 22 TCDD and all 38 TCDF isomers. The retention data obtained on this initial column was then inserted into the computer program in order to predict optimum combinations of the component coupled column sections. The actual column was then adjusted (fine-tuned) to yield the optimum resolution in a series of successive approximations. This iterative calculation procedure ultimately yielded an experimental approach that compensates for variables in GC parameters, such as the flow gradient through the column.

The resolution of 2,3,7,8-TCDD and 2,3,7,8-TCDF from all of their respective TCDD and TCDF congeners on the finally constructed hybrid three-phase GC column is demonstrated by the mass chromatograms shown in Figures 1 and 2. Clearly, the column developed is quite effective.

Reference:

1. R. J. Lamb and J. H. Purnell, Anal. Chem. 48, 799 (1976).

We acknowledge the contributions of J & W Scientific in support of this work.

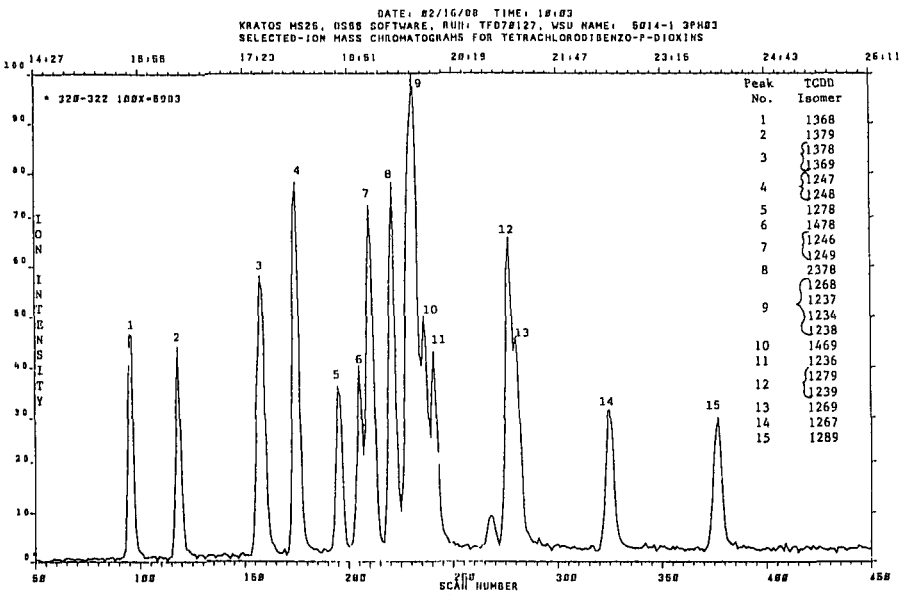

HRGC-LRMS ANALYSIS OBTAINED FOR EPA SAMPLE NO.TCDD PEMIX
FIGURE: 1

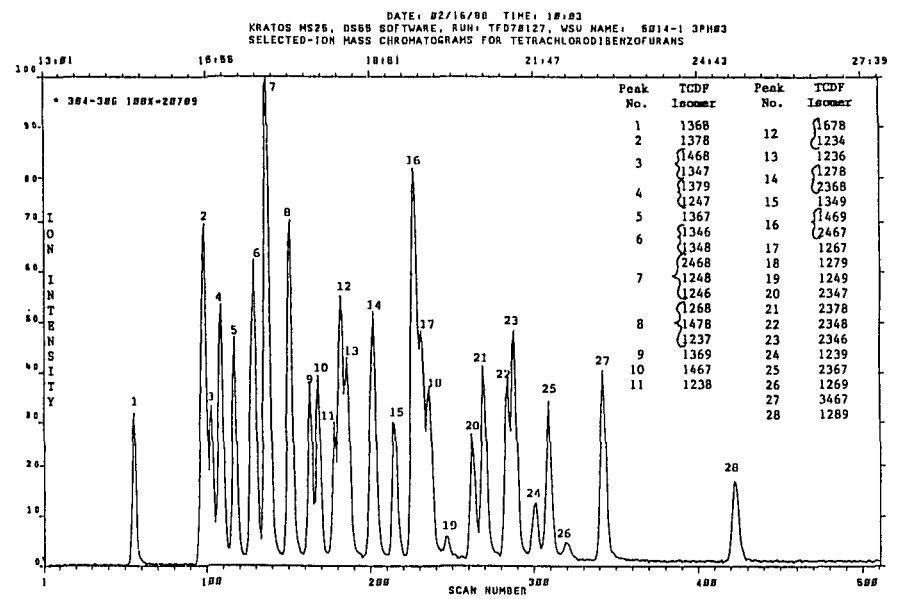

HRGC-LRMS ANALYSIS OBTAINED FOR EPA SAMPLE NO.TCDF PEMIX
FIGURE: 2

Presented at the 36th ASMS Conference on Mass Spectrometry and Allied Topics
June 5-10, 1988, San Francisco, CA

INVESTIGATION OF ANOMALOUS DIOXIN SIGNALS IN DIOXIN ANALYSIS

D.R. Hilker, W.H. Ding, K.M. Aldous, S. Connor, and J. Jurusik
Wadsworth Center for Laboratories and Research
New York State Department of Health,
Albany, NY 12201

Gas Chromatography/mass spectrometry is widely utilized for quantitative analysis of pollutants in environmental samples. The isotopically labelled internal standard method of quantitation has been widely used for quantitation because of its inherent accuracy. This method relies upon a constant relationship between the amount of analyte and the ratio of the instrumental response of the analyte and internal standard. In this presentation we report the observation of the enhancement of the signal due to both 2,3,7,8-TCDD-$^{13}C^{12}$ and native TCDD in the restricted source of a high resolution mass spectrometer when a large amount of native 2,3,7,8-TCDD is present. Our data shows that this particular effect need not threaten the accuracy of quantitation of native TCDD in environmental samples. However, the accuracy of per cent recovery determinations could be significantly impaired as well as the accuracy of quantitation of other isomers. The literature contains references which cite signal enhancement caused by the presence of either known or unknown compounds in the source (1-4). Since this particular type of effect may depend upon source design, its presence or absence must be verified for each instrument. Our investigations to date of the effect and its implications for quantitation on two different mass spectrometers are given.

Five solutions were prepared each containing 1 ppm of 2,3,7,8-tetrachlorodibenzo-p-dioxin-$^{13}C_{12}$ ($^{13}C_{12}$-2,3,7,8-TCDD) and one of the following concentrations of native 2,3,7,8-tetrachlorodibenzo-p-dioxin (2,3,7,8-TCDD): 0.2 ppm (ng/µl), 1.0 ppm, 5.0 ppm, 25.0 ppm, and 45.5 ppm. These compounds had been shown by previous analysis to have a degree of purity commensurate with environmental standards.

Each of these solutions was analyzed with a Kratos MS-50 and a Hewlett-Packard MSD in GC/MS mode with electron impact ionization. The solutions were reanalyzed with the Kratos MS-50 in GC/MS mode with a "restricted" electron impact source. In this source all of the sample entrance ports to the ion chamber are either fitted with a sample introduction device or plugged. Experiments in the GC/MS mode on the MS-50 were done at high resolution (10,000 RP, 10% valley), with a lock mass and monitoring another PFK peak along with the two most intense molecular ions of $^{13}C_{12}$-2378-TCDD and native 2378-TCDD.

The areas of the gas chromatographic peaks in the m/e 334 ion chromatograms ($^{13}C_{12}$-2,3,7,8-TCDD) were obtained. Each of these areas, measured in ADC counts, were divided by the number of nanograms of $^{13}C_{12}$-2,3,7,8-TCDD in the injection to generate a $^{13}C_{12}$-2,3,7,8-TCDD sensitivity.

In another group of experiments a fixed amount of $^{13}C_{12}$-1,2,3,4-TCDD was added to each of the solutions mentioned above. After analysis on the Hewlett-Packard MSD the areas of the $^{13}C_{12}$-2,3,7,8-TCDD were determined and sensitivities were calculated as described above. A response ratio was calculated by dividing the $^{13}C_{12}$-2,3,7,8-TCDD sensitivities by the $^{13}C_{12}$-1,2,3,4-TCDD sensitivities. The response ratios are plotted versus the concentration of native 2,3,7,8-TCDD in the solutions (Figure 1).

Aliquots of the original five solutions were added to glass capillary sample containers. After solvent evaporation these capillaries were introduced into the combined EI/CI source of the MS-50 via the direct insertion probe. The areas of the peaks in the probe elution profiles were obtained and divided by the amount represented by the peaks in the elution profiles($^{13}C_{12}$-sensitivity). The sensitivities for the $^{13}C_{12}$-2,3,7,8-TCDD were divided by the native 2,3,7,8-TCDD to generate a response ratio. The $^{13}C_{12}$ sensitivity data and the response ratios were plotted versus the amount of native 2,3,7,8-TCDD added to the capillaries.

The response ratio data from the MSD versus native 2,3,7,8-TCDD concentration (Figure 1) appears to give a horizontal line despite some scatter. The relative standard deviation of all the response ratios in Figure 1 is less than 13%. The ^{13}C-sensitivity data from the MS-50 fitted with a normal electron impact source plotted versus native 2,3,7,8-TCDD concentration (Figure 2) appears to give a horizontal line despite some scatter. The plot of data taken from the MS-50 fitted with the restricted source does not appear to give a line with a slope of zero. The variance of these two data sets was analyzed using a one way, randomized block design and the hypothesis that the ^{13}C-sensitivity at each concentration is the equal. In the restricted source data set the hypothesis was rejected at the 99% confidence level suggesting that these ^{13}C-sensitivities are varying with native 2,3,7,8-TCDD concentration.

The variation in response ratio on the MSD is small and doesn't necessarily correlate with native 2,3,7,8-TCDD concentration. The coelution of large amounts of native 2,3,7,8-

TCDD into the MSD source has little effect on the response of $^{13}C_{12}$-2,3,7,8-TCDD and little effect on the accuracy of percent recovery calculations and quantitation. The variation in the $^{13}C_{12}$-2,3,7,8-TCDD sensitivity when determined with the MS-50 high resolution mass spectrometer fitted with a normal electron impact source does not appear to vary with native-TCDD concentration. Hence the response factor used in quantitation and percent recovery calculations will not change with the presence of large amounts of native 2,3,7,8-TCDD. Since other factors besides the amount of native 2,3,7,8-TCDD can effect the $^{13}C_{12}$-2,3,7,8-TCDD sensitivity further experiments with both MS-50 EI sources will utilize the $^{13}C_{12}$-1,2,3,4-TCDD containing solutions. The analysis of solutions by direct probe should differentiate "g.c." response enhancement (2) from enhancement effects that occur in the ion source (1). The combined EI/CI source appears to show an increase in response ratio with the amount of native 2,3,7,8-TCDD. The extent of the effect is not as large as reported in reference (1). The decrease in $^{13}C_{12}$-2,3,7,8-TCDD sensitivity with increasing native 2,3,7,8-TCDD may be due to operating without a lock mass at low resolution. In later experiments probe samples which contain $^{13}C_{12}$-2,3,7,8-TCDD and an internal standard will be analyzed at high resolution with a lock mass. A compound such as a higher chlorinated dibenzo-p-dioxin which evaporates from the probe capillary later than 2,3,7,8-TCDD could be used as an internal standard.

FIG.1 NON-CONSTANT RESPONSE EFFECT

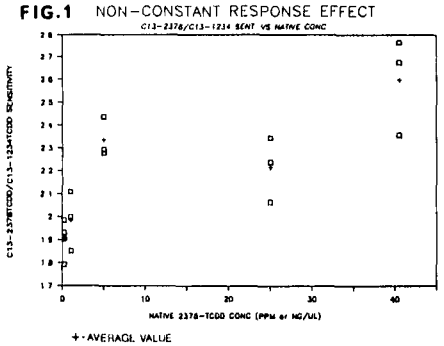

FIG.2 NON-CONSTANT RESPONSE EFFECT

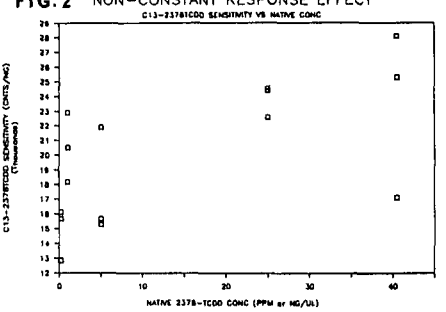

The authors wish to acknowledge the technical assistance of Ernest Mills, Bill Ahearn and Joe Katagiri.

(1) J.R. Tuschall et al, Proceedings of DIOXIN '87, October 4-9, 1987, Las Vegas, NV.
(2) R. D. Voyksner et al, Anal. Chem. 55, 744-749 (1983).
(3) Y. Tondeur et al, Anal. Chem. 56, 1344-1347 (1984).
(4) Y. Tondeur et al, B.E.M.S. 14, 449-456 (1987).

Presented at the 36th ASMS Conference on Mass Spectrometry and Allied Topics
June 5-10, 1988, San Francisco, CA

METABOLISM OF 2,3,7,8-TCDD J.H. McReynolds, J.R. Olson and S. Kumar; Toxicology Research Center, State Univ. of New York at Buffalo and Great Lakes Laboratory, State Univ. College at Buffalo; Buffalo NY 14214

Profound interspecies differences in the toxicity of 2,3,7,8-TCDD may be correlated with the ability of each species to metabolize or excrete the material. Less sensitive species such as the hamster (LD50=5000 ug/kg) show induction of metabolism by TCDD while more sensitive species such as the guinea pig (LD50 = 1ug/kg) lack this ability and rely on direct intestinal elimination for the excretion of TCDD. These differences limit the validity of extrapolations from other species to predict human toxicity of TCDD.

To aid in the identification of metabolites formed from in vivo experiments or from in vitro hepatocyte incubations, we have synthesized as number of potential TCDD metabolites that have been suggested or previously identified.(1,2) TCDD is expected to be metabolized by hydroxylation with and without chlorine elimination and/or migration. Synthetic metabolites were prepared by the condensation of 4,5 dichloro catechol with variously substituted ortho chloro nitro benzenes as reported by others.(3,4) Data are given for the predicted metabolites synthesized to date. Synthetic products were analyzed following diazomethane treatment on a 30m DB-1 column directly coupled to a KRATOS MS80RFA. EI spectra were generally useful for distinguishing the substitution patterns as shown in Fig. 1. Strong M-CH3 ions were produced by 2- or 3- methoxy substitution. Negative ion CI spectra were less useful for distinguishing substitution patterns. The NICI spectrum of metabolite 7 showed a base peak due to M-OCH3 and weak molecular anion in other runs (not shown but similar to that of 2 or 3) indicating that this species is particularly susceptible to oxygen contamination in the system. The dichloro dimethoxy species (10) did not give a useful NICI spectrum and the response of the trichloro mono methoxy product (9) was very weak.

Extracts from feces of rats treated with tritiated TCDD were analyzed by HPLC on a 25cm C-18 column eluted with 90% MeOH, 10% H2O and radioactive metabolite fractions collected and prepared for GC-MS analysis by diazomethane treatment. The fraction eluting at 20 min. corresponds to the HPLC retention time of 2-HO-1,3,7,8 TCDD with this identification confirmed by the GC-MS data shown in Fig. 2. The metabolite fraction collected at 15 min. is more heavily contaminated with endogenous fecal lipids in both the HPLC and GC separations but shows evidence of containing the 2-MeO TrCDD metabolite 9.

The utility of NICI in detecting metabolites of PCDDs is limited by the loss of response that is associated with chlorine loss and methoxy substitution. Identification of other metabolites will require further clean-up of the biological extracts. This effort will be aided by the availability of the synthetic metabolites. Cleaner samples will also alow the use of higer resolution GC conditions. Analysis of urinary extracts and hepatocyte incubations will be the focus of future experiments.

1.Sawahata,T.,Olson J.R. and Neal R.A. Biochem. Biophys. Res. Comm. 105,341,1982.
2.Poiger H. and Buser H.R. Banbury Rept. 18. Biol Mech. of Dioxin Action A. Poland and R.D> Kimbrough ed. Cold SP. Harb. Lab. 39,1984.
3.Poland A.E> and Yang G.C. J. Agric. Food Chem. 20,1093,1972.

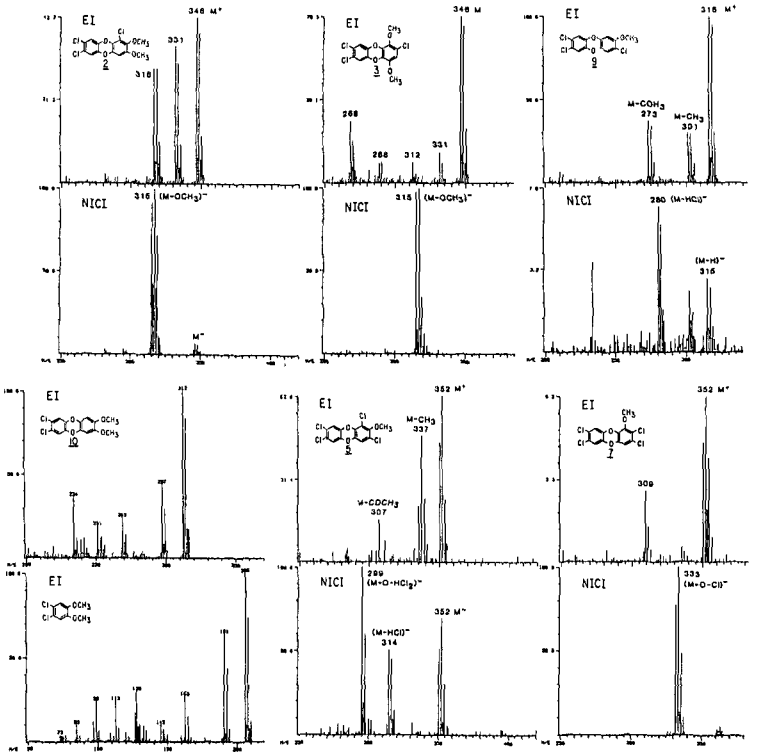

Fig. 1. EI and NICI Spectra of Synthetic Metabolites

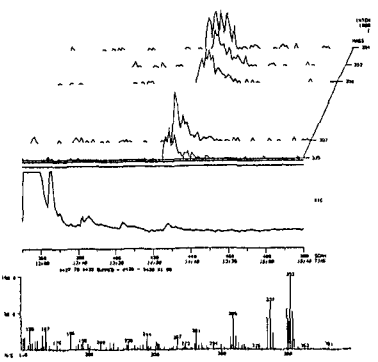

Fig. 2. GC-MS (EI) of 20 min. HPLC Fraction

Presented at the 36th ASMS Conference on Mass Spectrometry and Allied Topics
June 5-10, 1988, San Francisco, CA

OPTIMIZATION OF MS/MS PARAMETERS FOR THE DETERMINATION OF CHLORINATED DIBENZO-p-DIOXINS AND DIBENZOFURANS IN ENVIRONMENTAL SAMPLES

D.H.SCHELLENBERG, B.A. BOBBIE, E.J. REINER AND V.Y.TAGUCHI
Ontario Ministry of the Environment,
Rexdale, Ontario, M9W 5L1, Canada

The determination of chlorinated dibenzo-p-dioxins (CDD) and dibenzofurans (CDF) by tandem mass spectrometry places rigorous demands on the instrumentation because of the sensitivity required to detect ultra-trace quantities and the selectivity needed to eliminate interferences typically encountered in environmental samples. Under these conditions optimization of instrumental parameters is critical.

Optimization of MS/MS instrument parameters is commonly performed using perfluorotributylamine (PFTBA) when analysing for general organic compounds. Unfortunately, the fragmentation of PFTBA under collision induced dissociation (CID) conditions does not parallel the behaviour of all analytes. According to the quasi equilibrium theory [1], the pattern and degree of fragmentation of the parent ion is dependent on its internal energy. Excitation by collision, electron impact, chemical ionization, FAB, etc., forms parent ions with a distribution of internal energies. Kenttamma and Cooks [2] have shown by using breakdown graphs (BG, a plot of the relative ion abundance vs internal energy) that parameters such as collision energy (CE) and collision gas pressure (CGP) have a significant effect on the internal energy of the parent ion and therefore its pattern of dissociation. Catlow et al [3] have shown that the optimum CE and CGP for one reaction will almost certainly not be the same for another reaction of that or any other parent ion. Therefore optimization of a particular fragmentation reaction using the analyte of interest is critical. The optimum values of the above parameters can be determined from the BGs.

Experiments were performed on a Finnigan MAT TSQ-70 triple quadrupole mass spectrometer equipped with a Varian 3400 GC and DEC 11/73 data system. Tuning was performed by introducing 1 ug of the analyte into the ion source using the direct insertion probe. The various tunable instrument parameters were then altered iteratively to maximize response.

BGs were obtained by scanning the instrument in the daughter ion mode and then plotting the % total ion current (%TIC) against CE or CGP. Sample data were collected by monitoring the loss of COCl from the two most abundant parent ions. Each run was split into five groups ranging from Cl_4DD and Cl_4DF in group one to Cl_8DD and Cl_8DF in group five. ^{13}C-CDD internal standards were also monitored.

Figure 1 shows CID-BG of PFTBA and four Cl_4DD isomers. The maximum relative abundance of the m/z 502 to m/z 219 reaction occurs at about 25 eV CE for PFTBA. This value is similar to the 25 eV obtained for 2378-Cl_4DD and values of approximately 21 eV obtained for the other Cl_4DD isomers for the COCl loss reaction. Figure 2 shows the CIDBG for PFTBA, 2378-Cl_4DD and 2378-Cl_4DF plotted vs CGP. The maximum relative (and absolute) abundance for the m/z 502 to m/z 219 reaction occurs at about 0.8mTorr for PFTBA while the maximum relative (and absolute) abundance for the loss of COCl from 2378-Cl_4DD and 2378-Cl_4DF occurs at about 3.3mTorr. A standard CGP setting was difficult to reproduce and a stablization period of a few minutes was required. Although the optimum CE are similar for PFTBA and the Cl_4DD isomers, the considerable difference in the optimum CGP setting and the size of the neutral lost (283 amu for PFTBA and 63 amu for CDD/F) indicates that for optimum instrument performance in multiple reaction monitoring (MRM), tuning on the analyte of interest is required. From the series of Cl_4DD/F to Cl_8DD/F that were determined, the M^+-COCl reaction optimized between 12 and 25 eV for a CGP of 3.3 mTorr. The CE was set for each congener type in each group because it can be set accurately through the keyboard and it does not require a stablization period.

Example 1 shows the mass chromatogram for a mixture of three Cl_4DD isomers (1234, 2378, 1278). Injections (A) and (B) were run at 27.5 eV and 22.5 eV CE respectively. As expected from the BGs, the 2378-Cl_4DD signal strength is enhanced in injection (A) and the 1234-Cl_4DD signal strength is enhanced in injection (B). Example 2 shows a series of Cl_4DD/F to Cl_8DD/F standards injected with a PFTBA tune (top) and a CDD/F tune (bottom). Note

the signal strengths in the CDD/F tune are considerably stronger than in the PFTBA tune. Example 3 shows the tetra region of a 10 g clam sample (top). The largest furan and dioxin peak were determined to be 150 ppt and 60 ppt respectively. The bottom mass chromatogram is of a fish (bass) sample. The largest furan peak is 20 ppt and the dioxin (2378) is 4 ppt. 2/10 ul of the extract were injected with a recovery of 95% for the internal standard giving a limit of detection of 0.2 - 0.5 ppt.

1. H.M. Rosenstock et al, Proc. Natl. Acad. Sci. U.S. 38, 667, (1952).
2. H.I. Kenttamma and R.G. Cooks, Int J Mass Spec Ion Proc, 63, 325, (1985).
3. D.A. Catlow et al, 35th Ann Conf ASMS, Denver, p 1036 (1987).

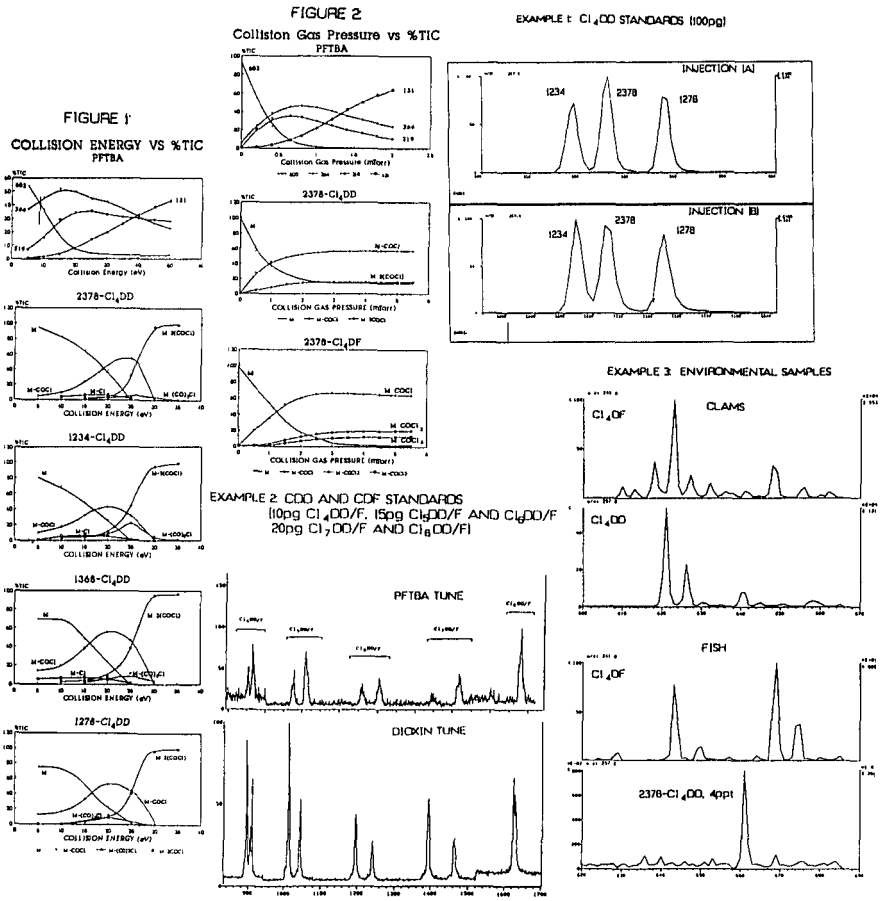

Presented at the 36th ASMS Conference on Mass Spectrometry and Allied Topics
June 5-10, 1988, San Francisco, CA

ACCURATE MASS DETERMINATIONS OF POLYCHLORINATED DIBENZOTHIOPHENES IN SOIL FROM A CAPACITOR PLANT'S INCINERATION SITE

Paul H. Peterman and Jon A. Lebo;
National Fisheries Contaminant Research Center; USDI,
Fish & Wildlife Service, Route 1, Columbia, MO 65201 and
Hilary J. Major
VG Analytical Ltd; Floats Rd; Wythenshawe, Manchester M23 9LE,UK

Chlorinated polycyclic aromatic compounds, e.g. polychlorinated dibenzofurans (PCDFs), dibenzo-p-dioxins (PCDDs) and biphenylenes (PCBPs) have been identified as pyrolysis products from the combustion of PCB-containing capacitors and transformers (1,2). Generally, these compounds are planar and very toxic. The relative compositions of the pyrolysis products vary considerably, depending upon the fire conditions.

From 1946-1964, capacitors containing PCBs, primarily Aroclors 1242 and 1254, were manufactured at a plant located in Crab Orchard National Wildlife Refuge, IL. Waste (defective) capacitors were routinely burned with automobile tires and diesel fuel in open bonfires. As expected, analyses of a soil core sample from the incineration site showed a high concentration of PCBs (3×10^6 ng/g or 0.3%) and lower concentrations of other chlorinated polycyclic aromatic compounds, e.g. PCDFs (570 ng/g), PCDDs (40 ng/g), PCBPs (9 ng/g) and polychlorinated naphthalenes (60 ng/g). Surprisingly, polychlorinated (Cl_2-Cl_7) dibenzothiophenes (PCDTs) and polychlorinated phenanthrene/anthracenes (PCPh/Ans) were both detected at 70 ng/g and were also tentatively identified by quadrupole full-scan GC/MS. Although the PCDTs have the same nominal molecular masses as the PCDDs, they elute 1-4 minutes later from a 30 m DB-5 capillary column. Since the PCDTs have chemical structures very similar to those of highly toxic PCDFs, and likely are also highly toxic and environmentally significant, we felt it necessary to confirm their identity. Unfortunately, no chemical standards of PCDTs exist. The Cl_3-Cl_7-PCDTs do not even have ACS CAS Registry Numbers. Therefore, we chose to obtain accurate mass measurements of the PCDTs.

Air-dried soil was Soxhlet-extracted, first with 60/40 benzene/methanol and then dichloromethane. The extract was processed through an extensive enrichment procedure (3) including a carbon-on-glass fibers separation technique. Initially, both selected ion monitoring and full-scan capillary GC/MS analyses were performed with a Finnigan 4023 GC/MS at 35 eV. Subsequently, capillary GC/high resolution (R.P. 10,000) MS analyses and complementary low resolution (R.P. 1,000) GC/MS analyses were performed with a VG 70-250S GC/MS at 70 eV using the same DB-5 GC column with 0.6 m retention gap. The oven program was 90 °C (1 min)-210 °C @ 15 °C/min, then 210 °C-300 °C @ 4 °C/min. Since the concentrations of PCDT isomers were low (0.05-10 ng/g), 1.3 g equiv. was injected for the high resolution, accurate mass measurements. PFK was constantly bled into the MS to ensure accurate calibration for each scan. To maximize sensitivity and accuracy, the MS was scanned at 360-250 d. @ 5 s/decade, with interscan reset 0.2 s for a total rate of 1 s/scan. The high resolution (R.P. 10,000) was chosen because a minimum of 9,200 would be required to distinguish the $(M+6)^{+\cdot}$ ion (m/z 319.9135) of co-eluting Cl_4-PCPh/Ans from the $M^{+\cdot}$ ion (m/z 319.8788) of Cl_4-PCDTs.

Definitive accurate mass measurements (AMMs) were obtained of those polychlorinated aromatics in the soil extract that exceeded about 1 ng injected. These included 19 peaks resulting from Cl_{2-5} PCDTs, i.e. a majority of the 34 peaks previously detected by quadrupole GC/MS. Several additional PCDT peaks were marginally detected (ion response S:N <4) below the level necessary for definitive AMMs. AMMs were obtained for at least two ions of each PCDT molecular ion cluster to compute its elemental composition. AMMs were typically from one scan, usually at the apex of a GC peak. For a few more highly concentrated PCDT peaks, AMMs were performed on two scans and each AMM was evaluated. All AMMs of PCDT $M^{+\cdot}$ ions and all but one AMM of $(M+2)^{+\cdot}$ ions were within 10 ppm of the exact masses of the PCDTs' elemental compositions. In some cases, the $(M+6)^{+\cdot}$ ion of Cl_4-PCPh/Ans could be detected and accurately distinguished from both the $M^{+\cdot}$ of Cl_4-PCDT and from PFK. Variance ranges are

given in the AMM summary report below:

ACCURATE MASS MEASUREMENTS SUMMARY REPORT

ISOMERS	#	Variance Range (mmu) (Theoretical-Observed) $M^{+\cdot}$	$(M+2)^{+\cdot}$	$(M+4)^{+\cdot}$	Elemental Composition Confirmed
Cl_2-PCDTs	1	-0.3/1.3	-4.0/1.7	ND	$C_{12}H_6Cl_2S$
Cl_3-PCDTs	7	-1.1/1.3	-0.7/0.8	-0.3/1.2 (3)	$C_{12}H_5Cl_3S$
(Interscan Data:		-0.6,0.5	0.8,0.4)	3.5/4.6 (2)	
				ND (2)	
Cl_4-PCDTs	8	-0.7/3.2	-3.0/1.5	0.2/1.9 (2)	$C_{12}H_4Cl_4S$
(Interscan Data:		-0.7,-0.2	1.5,0.1)	ND (6)	
		(-0.7,2.6)			
Cl_5-PCDTs	3	2.0/2.4	-1.7/0.3	2.2 (2)	$C_{12}H_3Cl_5S$
				ND (1)	
Cl_4-PCPh/Ans	6	-0.8/1.3 (5)	-0.4/3.4	-2.0/1.8 (5)	$C_{14}H_6Cl_4$
Cl_4-PCDDs (only 0.7 ng)	1	3.4	9.1	2.4	$C_{12}H_4Cl_4O_2$

Interscan Data denotes AMMs on two scans of an isomeric peak

Thus, the Cl_{2-5} PCDTs as well as some PCPh/Ans are now confidently identified from their elemental compositions. Although PCDT standards are not available, the GC retention times of the identified PCDTs are plausible relative to the retention times of PCDFs, PCDDs and PCPh/Ans.

Full-scan mass spectra of the PCDT and PCPh/Ans from the soil extract show very abundant molecular ion clusters and typical $(M-70)^+$ fragment ions. Quadrupole (at 35 eV) and low resolution magnetic sector (70 eV) mass spectra of peaks from Cl_4-PCDT compared quite closely. The $(M-CSCl)^+$ or $(M-79)^+$ fragment ions of PCDT were < 7% abundant in 35 eV spectra and not discernable in 70 eV spectra. In contrast, the $(M-COCl)^+$ is moderately abundant for both PCDDs and PCDFs. As expected, significant differences between 35 eV and 70 eV PCDT spectra were moderately abundant doubly-charged ions (m/z 160-3; m/z 142.5-144.5; and m/z 125-127) in the 70 eV mass spectra compared with very low abundant doubly-charged ions in the 35 eV mass spectra.

1. Buser, H., Environ. Health Persp. 60:259-268 (1985).
2. Williams, C.H., Jr., C.L. Prescott, and P.B. Stewart in Chlorinated Dioxins and Dibenzofurans in the Total Environment II. L.H. Keith, C. Rappe and G. Choudhary, Ed., pp. 457-468 (1985).
3. Smith, L.M., D.L. Stalling, and J.L. Johnson, Anal Chem 56:1830-1842 (1984).

Presented at the 36th ASMS Conference on Mass Spectrometry and Allied Topics
June 5-10, 1988, San Francisco, CA

A NEGATIVE CHEMICAL IONIZATION GC/MS METHOD FOR THE DETERMINATION OF CHLORINATED PARAFFINS IN ENVIRONMENTAL SAMPLES

David H. Steele, Thomas M. Sack, and Leslie A. Moody
Midwest Research Institute, 425 Volker Blvd, Kansas City MO 64110

Thomas M. Murray Jay A. Glatz, and Joseph J. Breen
U.S. Environmental Protection Agency, Office of Toxic Substances,
401 M. St. S.W., Washington D.C. 20460

Chlorinated paraffins (CPs) are complex mixtures of chlorinated linear alkanes, (typically described by carbon chain length and percent chlorination). Common commercial formulations contain carbon chains in the range of 10 to 30, with percent chlorination ranging from 30 to 70% by weight. The major use for CPs in the United States has been as additives to cutting and machining oils, where they provide a self-sharpening mechanism by forming thin metal chloride films on cutting edges. CPs have been used extensively in Europe as plasticizing additives for polymers and paints, and as flame retardant additives for various materials (1); however, only minor usage for these purposes is noted in the United States.

While toxicological data on CPs is limited, chronic bioassay studies conducted by the National Toxicology Program (NTP) indicated carcinogenic activity for two formulations tested. Other studies have also demonstrated toxicological effects in various species. The available toxicity data and reported widespread aquatic CP contamination in Europe (2) have led to environmental concerns in the United States. Domestic usage patterns indicate that potentially significant CP releases into the aquatic environment will most likely occur from manufacturing operations; however, formulating and end use operations are also of concern.

In the past, such methods as thin-layer chromatography and dechlorohydrogenation followed by gas chromatography have been used for the quantification of CPs (2,3). Although these techniques are reasonably sensitive (ng levels), both suffer from a lack of specificity for the determination of individual CPs. The thin-layer chromatographic procedures use argentation to detect and quantify CPs and are therefore prone to interferences from any chlorinated species present. A lack of resolution between CP formulations has also been noted for the TLC procedure. The dechlorohydrogenation/GC technique quantifies CPs by replacing the chlorine atoms with hydrogen and measuring the alkane levels obtained. All alkanes native to the sample must be completely removed prior to GC analysis to avoid artificially high or false positive results. In addition, information concerning the degree of chlorination of the CP formulation is sacrificed.

Preliminary investigations into the use of negative chemical ionization (NCI) mass spectrometry for the detection of CPs has been performed (4,5). However, optimization of this technique and the demonstration of its effectiveness for use with environmental samples had not been demonstrated. This paper describes the single-laboratory evaluation of an analytical method for the determination of CPs in environmental samples at low to sub part-per-billion levels using GC/NCI-MS.

Based on available toxicity and production data, three CP formulations were chosen for investigation. These were Paroil 1160 (C10-C12, 50-60% Cl), Paroil 152 (C14-C17, 50-60% Cl), and Paroil 142 (C20-C30, 40-50% Cl). Samples of these materials for use as analytical reference standards were generously supplied by the Dover Chemical, Dover, Ohio. Environmental samples for method development and validation were collected from a stream which receives runoff from a CP production facility.

The analytical scheme is shown in Figure 1. Since it was known that CPs adsorb strongly to particulates, suspended solids were filtered from the water samples and analyzed separately. The CPs were removed from the water by liquid/liquid extraction with hexane. Particulate and sediment samples were Soxhlet extracted with hexane to remove the analytes. The extracts were cleaned up on acidic silica gel and activated alumina minicolumns, reduced to dryness and reconstituted in 25 to 50 L of isooctane for analysis. The extracts were chromatographed on a 30-m DB-5 fused silica capillary column, and the CPs were detected using NCI-MS on a Finnigan 4500 GC/MS system operating in a limited mass scan mode. Quantitation ions were chosen from the most abundant ion species for each formulation. Mass chromatograms from the analysis of a standard mixture are shown in Figure 2. Since CPs were determined to decompose in a heated GC inlet, sample extracts were introduced on-column at ambient temperature.

The method validation study was based on quantification results from analysis of a series of environmental samples. The experimental design (6) provided a statistical basis for the estimation of recovery and precision of the method when applied to the matrices. In

general, three replicate analyses at three spiking levels (1, 2.5, and 5 ppb for water; 200, 500, and 1000 ppb for sediments) were performed for each matrix. Four replicate analyses each of the unspiked matrices and the method blanks were also performed. For water, three distilled water spikes (controls) were also analyzed. Since no control sediment was available, four nonmatrix spikes were analyzed as a substitute. A complete discussion of the design, statistical treatment of the data, and the results of the method validation study is contained in the EPA final report (6).

Method recoveries for each CP formulation and matrix are depicted graphically in Figure 3. These recoveries were estimated as the slope (x100) of the calculated regression lines. Ninety-five percent (95%) confidence boundaries were computed based on the standard errors of the slope estimates and the sample sizes. For each matrix, the slope estimates of the three CP formulations were not found to be statistically different at the 95% confidence level; therefore, pooled recoveries were computed. The pooled recovery for water was found to be 106% with lower and upper 95% confidence limits of 92 and 120%, respectively. For sediment, the pooled recovery was 58% with a 95% confidence interval ranging from 52 to 64%. Method precision was estimated for each matrix as the coefficient of variation (100 x standard deviation/mean) of the replicate measured concentrations at each spiking level. Overall, method precision was better for sediments than for water. This is most likely due to the higher spiking levels used for this matrix (20-100 µg for sediments versus 1-5 µg for water). Precision also tended to improve with increasing spiking level. For both water and sediment, none of the background estimates were found to statistically differ from zero at the 95% confidence level.

The analytical method was found to be capable of quantifying CPs in water and sediment at the low to sub part-per-billion levels. While precision was found to be reasonable for this type of analysis, addition of appropriate surrogates and internal standards would be beneficial. This is especially true for the case of internal standards, since instability of the mass spectrometer source was noted throughout these analyses. Acceptable compounds for these purposes could not be identified during this work.

1. Zitco, V. (1980) in the *Handbook of Environmental Chemistry*, O. Hutzinger (Ed.), Vol. 3, Part A, Anthropogenic Compounds, Springer-Verlag, Heidelberg, GFR, pp 149-156.
2. Campbell, I., and McConell, G. (1980) *Environ. Sci. Technol.* 14:10, 1209-1214.
3. Hollies, J.I., Pinington, D.F., Handley, A.J., Baldwin, M.K., and Bennett, D. (1979) *Anal. Chim. Acta* 111, 201-213.
4. Muller, M.D., and Schmid, P.P. (1984) *J. High Resolut. Chromatogr./Chromatogr. Commu.* 7, 33-37.
5. Schmid, P.P., and Muller, M.D. (1985) *J. Assoc. Off. Anal. Chem.* 68:3, 427-430.
6. Murray, T., Frankenberry, M., Steele, D. H., and Heath, R. G. (1987). "Chlorinated Paraffins: A Report on the Findings from Two Field Studies, Sugar Creek, Ohio and Tinkers Creek, Ohio, Volume I - Technical Report," USEPA Publication No. 560/5-87-012.

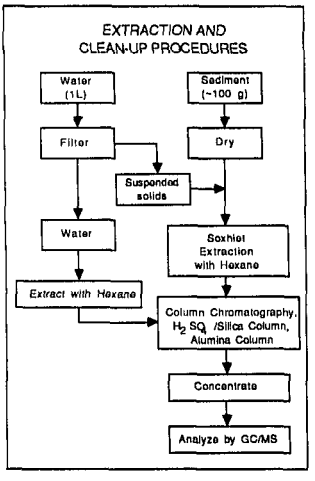

Figure 1

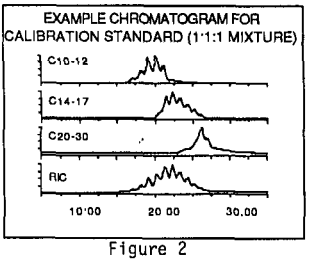

Figure 2

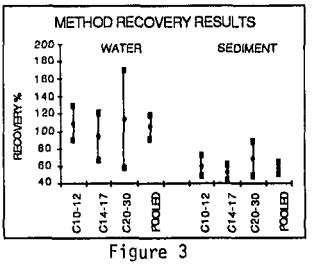

Figure 3

Presented at the 36th ASMS Conference on Mass Spectrometry and Allied Topics
June 5-10, 1988, San Francisco, CA

ANALYSIS OF NITRO-PAH METABOLITES AND THEIR DNA ADDUCTS BY NCI-GC-MS AND FAB-MS WITH B/E LINKED SCANNING

R.S. Annan, J. Bakthavachalam, R. Giese, P. Vouros
Northeastern University, Boston, Ma. 02115

Nitrated polycyclic aromatic hydrocarbons (PAHs) are a common source of environmental pollution. Two of these compounds, NO_2-Fluorene and NO_2-Pyrene account for 40-60% of the mutagenic activity found in automobile diesel exhausts. NO_2-PAHs are heavily metabolized, and a number of these metabolites are known to form covalent adducts with DNA.

An electrophoric derivatization strategy is under development which will allow sensitive detection of the entire metabolic cascade of NO_2-PAHs by NCI-GC-MS. This type of screening is useful as an early warning indicator of exposure. The requirements for the derivatives are that they exhibit good electron capture properties, be formed in high yield and with a high degree of selectivity, form diagnostic ions under NCI conditions and that the EI spectra be structurally informative. Due to the multiplicity of functional groups present in NO_2-PAH metabolism, no simple derivatization reagent was found suitable for all compounds.

Using aminofluorene and aminopyrene as models the reactions of amino PAHs with a variety of elecrophoric reagents were studied. Pentafluorobenzylation (PFB) was found to be unsuitable because of low yields and multiple products. N-acyl derivatives were formed in high yields, but their NCI spectra showed multiple losses of HF, and in some cases high abundance ions resulting from retention of charge on the derivatization tag. Alkylation of the N-acyl compounds with either CH_3I or $F_5C_6CH_2$-Br resulted in simpler NCI in the latter case. There was not, however, a significant improvement in sensitivety under SIM conditions to warrant a two step derivatization.

The formation of a benzylidine derivative using PFB aldehyde occured in near quantitative yield, and resulted in the formation of a molecular anion under NCI. The reaction is specific for primary amines and leaves no reactive sites. The derivative of 2-NH_2-Fluorene is found to be 22 times more sensitive (300 fg S/N = 4) than the corresponding nitro compound.

The reaction of phenols with PFB-Br has been shown (1) to be the method of choice since it occurs in high yield, and results in selective formation of phenoxide ion.

Scheme I shows the strategy for the derivatization of all reported NO_2-PAH metabolites using *p*-aminophenol as a model.

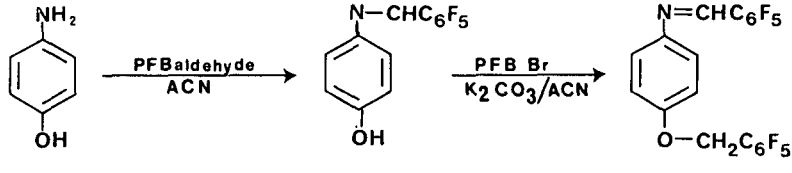

Scheme I

Figure 1 shows an NCI-GC-MS chromatogram of a number of possible me tabolite models including positional isomers. All compounds are easily separated with the exception of *p*-nitrophenol and *o*-N-acetylaminophenol. However, because they have different NCI spectra (m/z 138 and m/z 150 respectively), they can be separated by mass chromatograpy.

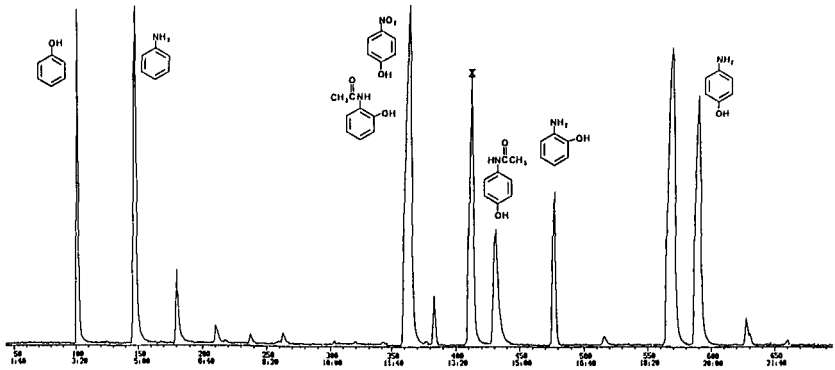

Figure 1. NCI-GC-MS: Separation of NO_2-PAH metabolite models as their electrophoric derivatives.

The analysis of NO_2 and other PAH metabolite-DNA adducts is difficult because of their high polarity, thermal instability, and small sample amounts. The normal FAB analysis of small amounts of these adducts, even after background subtraction, is hampered by the extensive matrix ion in terferences. Generally only M + H and M + alkali ions can be observed. We have found that the use of B/E linked scans for these compounds, even in the 200-500 nanogram range allows elucidation of certain structural features not visible in the normal FAB scan. Figures 2a and 2b show the FAB and B/E FAB scans for the benz(a)pyrene tetrol-deoxyguanine adduct. Ions present in the B/E scan are indicative of the parent (570), the aglycone (453), the PAH (303), and the deoxynucleoside (268). The lack of an M-NH_2 ion shows that the covalent bond is at the exocyclic amine. Figure 2c and 2d show a similar pair of analyses for the N-acetylaminofluorene-deoxyguanine adduct. The B/E scan of the aglycone (373) shows M-NH_2 (357), M-Ac (331), and the deoxynucleoside (267).

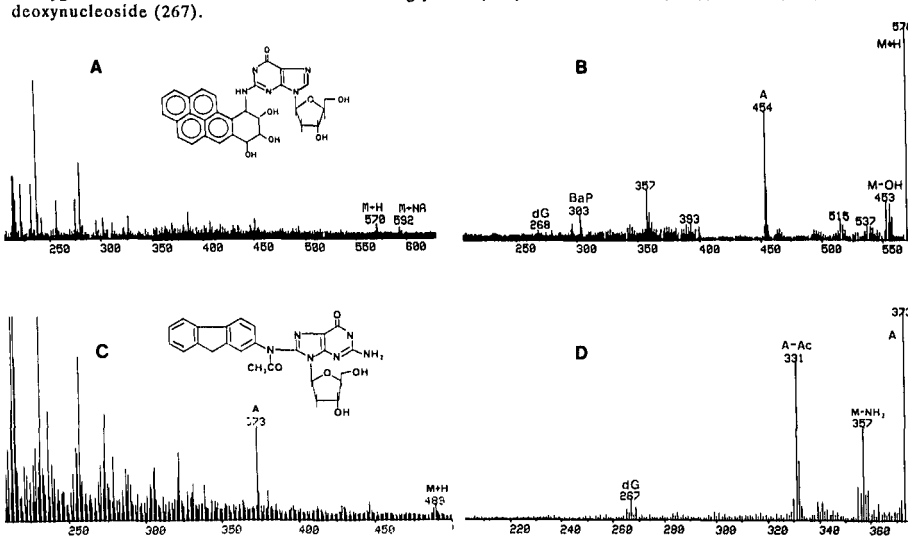

Figure 2. FAB and B/E Linked Scans of PAH-DNA Adducts

1. T. Trainor, P. Vouros, Anal. Chem., **59**, (1987) 601.

Presented at the 36th ASMS Conference on Mass Spectrometry and Allied Topics
June 5-10, 1988, San Francisco, CA

CHARACTERIZATION OF POLYCHLORINATED BIPHENYL PYROLYSIS MIXTURES

C.C. Alley, D.F. Groce, and D.G. Patterson, Jr.; Division of Environmental Health Laboratory Sciences, Center for Environmental Health and Injury Control, Centers for Disease Control, Public Health Service, U.S. Department of Health and Human Services, Atlanta, GA 30333

INTRODUCTION

Elevated polychlorodibenzofuran (PCDF) levels have been found in soot samples that were collected after transformer fires in Canada, the U.S.A., and Sweden (1). Buser and Rappe outlined four reaction routes (Figure 1) by which PCDFs are formed from pyrolysis of individual polychlorinated biphenyls (PCB) isomers (2). Mazer et al. synthesized all 38 tetrachlorodibenzofurans (TCDFs), using these reaction routes to predict which PCB isomer would yield the appropriate TCDFs. We have used these methods and synthesized the 38 TCDFs, the 28 pentachlorodibenzofurans (PnCDFs), and the 16 hexachlorodibenzofurans (HxCDFs).

FIGURE 1

PCB to PCDF Reaction Routes

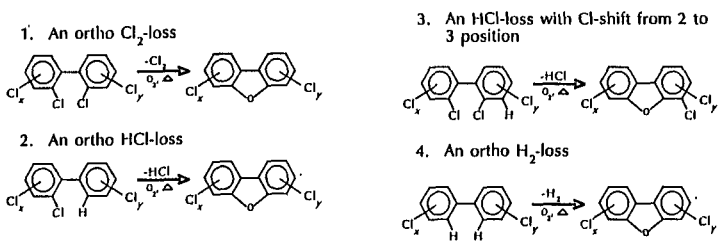

EXPERIMENTAL

Weighed amounts of individual PCBs were pyrolyzed by the method of T. Mazer et al (3). Quantitative aliquots of each pyrolysis mixture were combined with a known amount of $^{13}D_{12}$-2378-TCDF as an internal standard. Each pyrolysis mixture was analyzed using a Finnigan MAT 4500 mass spectrometer operating in full-scan negative chemical ionization mode. The reagent gas was Methane. A 60 m DB-56, 0.25mm, 0.25mm fused silica capillary column was used and temperature programmed as follows: 100 C (2 min) to 260 C at 20 C/min, then to 300 C at 1 C/min and held at 300 C for 5 min. The ionizer temperature was 100 C, the injector temperature was 300 C, the electron energy was 70eV, and the filament was 0.25 mA.

This process allowed each class of congener (e.g., TCDF, PnCDF, HxCDF) to be identified. The principal ion of each individual PCDF was referenced to the m/z 318 ion from the internal standard so that we could quantitatively assess the relative importance of each reaction pathway and calculate the amount of each reaction mixture that should be combined to provide qualitative standards.

Presented at the 36th ASMS Conference on Mass Spectrometry and Allied Topics
June 5-10, 1988, San Francisco, CA

RESULTS

In addition to the four previously determined reaction routes, two more PCB to PCDF routes have been identified: 1) the loss of H_2 with a 2,3-chlorine shift and 2) the loss of H_2 with a double 2,3-chlorine shift (Figure 2). Our method of analysis has allowed a quantitative assessment of the importance of each route for each PCB (Tables 1 and 2). Knowing the importance of each of these routes should allow a more quantitative method of predicting the PCDF levels and fingerprint from transformer accidents.

TABLE 1

PnCDF Isomers Formed by
Pyrolysis of PCB Congeners

PnCDF	RRT	2,3,4,6	2,3,4,5	2,3,5,6	2,3,5,7	2,3,6,7	2,4,5,6	2,3,4,7	2,3,4,5	2,3,4,6	2,3,4,7	2,3,6,7	2,4,5,7	2,3,5,6	2,3,5,7	2,3,4,7	2,3,4,6	2,3,5,6	2,3,5,7	2,3,4,6	2,3,4,5	2,3,4,7	2,3,4,6	2,3,5,7	2,3,4,5	2,3,4,6	2,3,4,5	2,3,4,5	2,3,4,6
		101	131	175	151	135	154	187	100	139	119	104	188	143	141	132	147	103	136	111	129	131	185	126	145	170	87	97	183	181	171	172
13468	1.066	.10	3.90	.01																												
12468	1.068				3.08	1.62																										
23478	1.112						1.84																									
13268	1.117			.28																												
12478	1.119							3.33																								
12467	1.118								.21	.39	4.66																				.14	
13478	1.118						5.88				4																		.16			
12467	1.118															1.19	.72															
13479	1.118						2.49		.11	1.00		.12	4.28																			
23468	1.137	.21												7.33	2.54																	
12479	1.134																3.50															
13469	1.138	.4																.24							.02							
23468	1.140														3.34																	
12469	1.147				1.41	.98													1.89													6.11
13247	1.146									1.34											.92									.38		
13246	1.148																					.60	4.60									
12346	1.187														1.00									6.41								
12378	1.163																												3.72			
13267	1.171									.48														3.82						.34		
23489	1.177																				3.09											
12378	1.179									.78																						
23478	1.205																															
12489	1.211						1.04												3.29													
12389	1.200																					6.08						.68				
12389	1.200															.38	.93								.02		.42					
12467	1.208																									11.38						
13249	1.226													-.15																		
12389	1.239															.36						4.97										

TABLE 2

HxCDF ISOMERS FORMED BY PYROLYSIS
OF PCB CONGENERS

HxCDF	RRT	2,3,4,5,6	2,3,4,5,6	2,3,4,5,6	2,3,4,5,6	2,3,4,5,6	2,3,4,5,6	2,3,4,5,6	2,3,4,5,6	2,3,4,5,6	2,3,4,5,6	2,3,4,5,6	2,3,4,5,6	2,3,4,5,6	2,3,4,5,6
		175	185	141	183	191	187	170	181	171	190	202	145	189	129	205
123468	1.316	.52	3.19	.17												
134678	1.329				.22	12.0										
124678	1.327						.36									
134679	1.341				.08											
124679	1.331	.64					.45									
124689	1.365											45.1				
123467	1.391							4.63	.45	.46	17.7					
123478	1.391				.68											
123678	1.401				.33	13.0		12.6								
123479	1.411								.32							
123469	1.426		2.61	.84												
123679	1.431				.37		.36			.11						
123689	1.443	1.24														
234678	1.446						.45							10.9		
123789	1.518									36		45.1				
123489	1.521														.54	

FIGURE 2

5. A H_2-loss with Cl-shift from 2 to 3 position

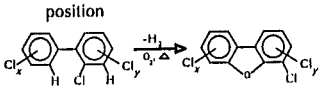

6. A H_2-loss with double Cl-shift from 2 to 3 position

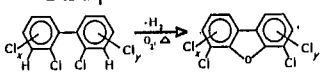

REFERENCES

1. Rappe, C.; Marklund, S.; Bergqvist, P.; Hansson, M. in "Chlorinated Dioxins and Dibenzofurans in the Total Environment," Choudhary, G.; Keith, L.; Rappe, C., Ed.; Butterworth Publishers:Boston, 1983; pp 99-124.

2. Buser, H.R.; Rappe, C. Chemosphere 1979, 3, 157-174.

3. Mazer, T.; Hileman, F.; Noble, R.; Brooks, J. Anal. Chem. 1983, 55, 104-110.

Presented at the 36th ASMS Conference on Mass Spectrometry and Allied Topics
June 5-10, 1988, San Francisco, CA

ANALYSIS OF SELECTED HERBICIDES AND THEIR METABOLITES IN RIVER WATER SAMPLES BY CHEMICAL IONIZATION TANDEM MASS SPECTROMETRY

Colleen E. Rostad, Wilfred E. Pereira, and Thomas J. Leiker
U.S. Geological Survey
P.O. Box 25046, Denver Federal Center
Denver, Colorado 80225

Depth-integrated water samples collected during November and December 1987 from the Mississippi River and its major tributaries were extracted and analyzed initially by gas chomatography/ion trap mass spectrometry. Several commonly used herbicides and their degradation products were identified. In order to detect these compounds in a complex matrix with speed, specificity and sensitivity, a new method for analyzing these compounds was developed utilizing tandem mass spectrometry (MS/MS). The selected compounds included atrazine and its degradation products (deethylatrazine and deisopropylatrazine), simazine, metolachlor, alachlor and its degradation products (2-chloro-2',6'-diethylacetanilide, 2-hydroxy-2',6'-diethylacetanilide and 2,6-diethylaniline) and terbuthylazine (used as the internal standard).

Analytical standards for the selected compounds were analyzed by gas chromatography/positive ion chemical ionization mass spectrometry (GC/+CI/MS). The GC was equipped with a 30 m DB-5 fused silica capillary column. The commonly-used methane reagent gas was replaced with high purity isobutane which increased the ionization efficiency for these compounds 4 to 8 times over that produced by methane. The protonated molecules were then fragmented under collision activated decomposition using a variety of fragmentation conditions of collision energy and collision gas pressure. Argon was used as the collision gas. Collision energy was varied from -15 to -30 V, and collision gas pressure was varied from 1 to 2.5 torr. For each compound, fragmentation conditions were chosen to maximize the generation of one prevalent daughter ion. Because the collision gas pressure was not under data system control, it was set at an optimum value during the entire aquisition. The GC temperature program was set to the maximum rate possible, 20°/min, to minimize sample analysis time.

The scan range used to detect the resulting daughter ions was then limited to just one neutral loss from each protonated molecule. Sensitivity increased significantly. Coeluting or closely eluting compounds were analyzed by splitting the time between each compound. In one area of the chromatogram, four compounds elute very closely. The instrument spent 0.1 sec on the specified neutral loss of each compound sequentially, repeating the sequence throughout the entire elution time window. Sometimes common daughter ions were used simultaneously. It seemed possible that, daughter ions belonging to deisopropylatrazine (at mass 146) would interfere with daughter ions from deethylatrazine (at mass 146). Even at very high concentrations, daughter ion carryover between different compounds with identical daughter ions analyzed simultaneously did not occur.

The neutral loss, from the parent ion to the specified daughter ion, was then used for quantitative analysis. Standard mixtures of the compounds at 20 ng, 2 ng, 200 pg, 20 pg, and 2 pg per microliter were analyzed, with the internal standard, terbuthylazine, at 13 ng/ul. The detection limit (signal to noise, 3 to 1) for deisopropylatrazine and 2-hydroxy-2',6'-diethylacetanilide was 5ng and for diethylaniline and metolachlor it was 50 pg. The detection limit for the remaining compounds was 100 pg. The higher detection limit for deisopropylatrazine and 2-hydroxy-2',6'-diethylacetanilide was due partly to chromatographic and ionization limitations and partly to poor fragmentation in the MS/MS. As a result, sensitivity for these compounds was poor. The rest of the compounds fragmented into one prevalent daughter, which produced excellent sensitivity in the neutral loss mode. Instrument response for most of the compounds was linear over a 200 pg to 20 ng concentration range.

This methodology was then applied to the river water extracts. Reproducibility of the GC/+CI/MS/MS analysis on one of the river water extracts analyzed six times was excellent for some of the compounds. The percent relative standard deviation (%RSD) was less than 10% for diethylaniline, atrazine, and metolachlor. The %RSD was less than 25% for deethylatrazine, simazine, and alachlor, because they were present near detection limit concentrations. The other compounds, deisopropylatrazine, 2-chloro-2',6'-diethylacetanilide, and 2-hydroxy-2',6'-diethylacetanilide, were not found in the river water extract chosen for reproducibility studies.

The entire procedure, including injection, acquisition, and data manipulation, took only 20 min per sample. MS/MS was used to remove interferences, increase sensitivity, and decrease analysis time.

Presented at the 36th ASMS Conference on Mass Spectrometry and Allied Topics
June 5-10, 1988, San Francisco, CA

CONFIRMATION OF FENVALERATE IN ENVIRONMENTAL SAMPLES BY NEGATIVE ION CHEMICAL IONIZATION MS/MS

Charles J. Stafford and Douglas M. Swineford
U.S. Fish & Wildlife Service, Patuxent Wildlife Research Center,
Laurel, Maryland, 20708

A multi-year study was undertaken by the U.S. Fish & Wildlife Service to determine the environmental effects of several agricultural chemicals on the ecology of North Dakota's prairie pothole wetlands. As part of this study the synthetic pyrethroid insecticide fenvalerate was sprayed on agricultural crops adjacent to wetlands and residues of fenvalerate were measured in environmental matrices, including water, sediment, aquatic plants and aquatic invertebrates. Fenvalerate residues were determined in samples by extracting with organic solvents and analyzing the extracts by capillary column gas chromatography (GC) using an electron capture detector (ECD). Further sample cleanup was not necessary due to the separation power of capillary column GC and the specificity of the ECD allowing quantifiable limits on the order of 0.05 ng fenvalerate on column.

Confirmation of fenvalerate residues by electron impact (EI) GC/MS, which we normally employ (1), was difficult however, for two reasons: 1) extensive fragmentation by EI leads to low ion intensities (Fig. 1), and 2) matrix interference from co-extracted materials in environmental samples interferes with the GC/MS analysis. GC/MS analysis of a fenvalerate standard by EI using a Finnigan TSQ-70 required at least 1 ng for acceptable full-scan spectra (70 eV, source temp. 150°C, multiplier 1200 V). Interference from co-extracted materials present in the crude sample extracts made confirmation of fenvalerate at this level difficult. Analysis by methane negative ion chemical ionization (NCI, CH_4 @ 8 torr, 70 eV, source temp. 150°C) however, produced an single intense ion fragment m/z 211 $(C_{11}H_{12}O_2Cl)^-$ (Fig. 2) which allowed confirmation of 10 pg of fenvalerate standard, an approximate 100X increase in sensitivity over EI. Analysis of the same crude sample extracts by NCI produced very little interference.

Collision-induced dissociation of the parent m/z 211 ion by NCI MS/MS (Ar @ 1.4 mtorr, collision offset 4 eV, multiplier 1600 V) produced an intense daughter ion fragment m/z 167 $(m/z\ 211 - CO_2)^-$ (Fig. 3) providing further confirmation of the parent fenvalerate. Residues of fenvalerate in field samples of aquatic plants and snails were able to be confirmed by NCI and NCI MS/MS without cleanup. The selectivity of the negative ion formation processes greatly reduced matrix interference allowing confirmation of residues as low as 0.3 ppm.

Reference:

1. W. L. Reichel, E. J. Kolbe, and C. J. Stafford, JAOAC, 64(5):1196-1200.

Presented at the 36th ASMS Conference on Mass Spectrometry and Allied Topics
June 5-10, 1988, San Francisco, CA

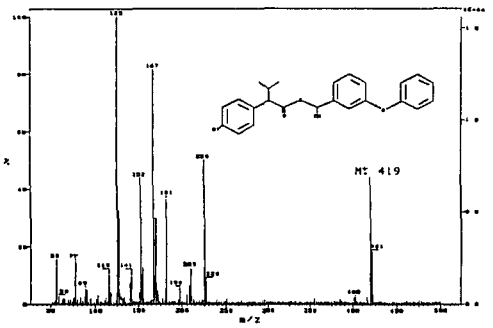

Figure 1. EI spectrum of 10ng fenvalerate standard.

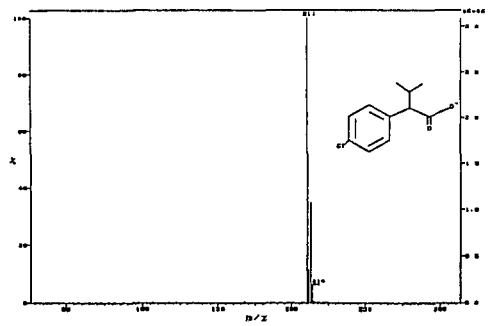

Figure 2. NCI spectrum of 5ng fenvalerate standard.

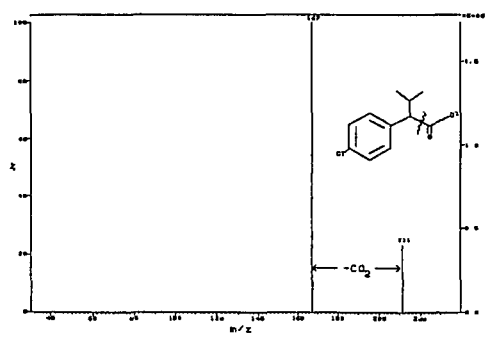

Figure 3. NCI MS/MS spectrum of 5ng fenvalerate standard.

Presented at the 36th ASMS Conference on Mass Spectrometry and Allied Topics
June 5-10, 1988, San Francisco, CA

USE OF MASS SPECTROMETRY IN ENVIRONMENTAL HEALTH EMERGENCIES: LABORATORY INVESTIGATION OF A POISONING EPIDEMIC IN SIERRA LEONE

R.H. Hill, Jr., C.A. Alley, D.L. Ashley, R.E. Cline, S.L. Head, L.L. Needham, and R.A. Etzel
Center for Environmental Health and Injury Control
Centers for Disease Control Public Health Service
U.S. Department of Health and Human Services
Atlanta, Georgia 30333

In June 1986, an epidemic of poisoning occurred in Sierra Leone, West Africa, it involved 49 persons, 14 of whom died (1). These persons had sudden onset of weakness, dizziness, vomiting, and diarrhea that began within half an hour of eating. The most severely affected persons frothed at the mouth, were short of breath, had pulmonary edema, and lost consciousness. The cause of the illnesses was unknown, but it appeared to be a toxicant. We describe our laboratory's part in this investigation.

Experimental - Samples were extracted with ethyl ether. The ether extracts were concentrated and in some cases were subjected to cleanup by using silica gel chromatography. More than 120 samples were received and analyzed. Methane-positive chemical ionization mass spectrometry was performed by using a Finnigan 4500 GC/MS with a direct exposure probe. The mass range was scanned from 50 to 650 amu at 1 sec/scan. Proton nuclear magnetic resonance spectroscopy was carried out by using a Varian XL-300 NMR with a superconducting magnet. Quantitative analyses were performed with a Hewlett-Packard 5880 GC and a Melpar flame photometric detector in the phosphorous mode.

Discussion - Our approach in these types of environmental emergency investigations involves a) examining the available data for clues that suggest particular classes of toxicants; b) preparing samples and testing them for toxicity; and c) after a toxic sample has been identified, using analytical techniques to isolate, identify, and measure the toxicant (2). This poisoning epidemic seemed to be caused by a cholinesterase-inhibiting toxicant. The epidemiologic team showed a striking association with bread consumption 4 hours before the onset of illness (1). A bread sample discarded by villagers was then eaten by some ducks; within minutes these ducks died. Since a toxic sample was identified, we began our laboratory investigation with screening analyses of this sample. When we analyzed an extract of this bread using direct-exposure-probe positive chemical ionization mass spectrometry (see Figure 1.), we found a compound having a pseudo-molecular ion of 292. Among the compounds with molecular weight of 291 was the pesticide parathion (see Figure 2). Parathion is an extremely toxic pesticide with toxic properties that could easily account for the observed epidemic. A simultaneous examination of the bread extract by proton nuclear magnetic resonance confirmed that this pesticide was present. Parathion was also later confirmed by GC/MS. Analysis of various other items by using gas chromatography with flame photometric detection and GC/MS for confirmation supported the epidemiologic team's hypothesis that flour became contaminated during shipment by truck. Subsequent distribution of the contaminated flour to local bakeries in the towns of Kenema and Lalehun led to the sale of bread containing at least 400 ppm of parathion. Modern analytical instrumentation played a major role in this investigation, enabling us to identify an unknown toxicant within hours of receiving the initial bread sample.

References - (1) RA Etzel, DN Forthal, RH Hill Jr, A Demby, Bulletin World Health Organization, 65, 645-49 (1987); (2) RH Hill Jr, LL Needham, JA Liddle, Clinical Toxicology, 24, 363-74 (1986).

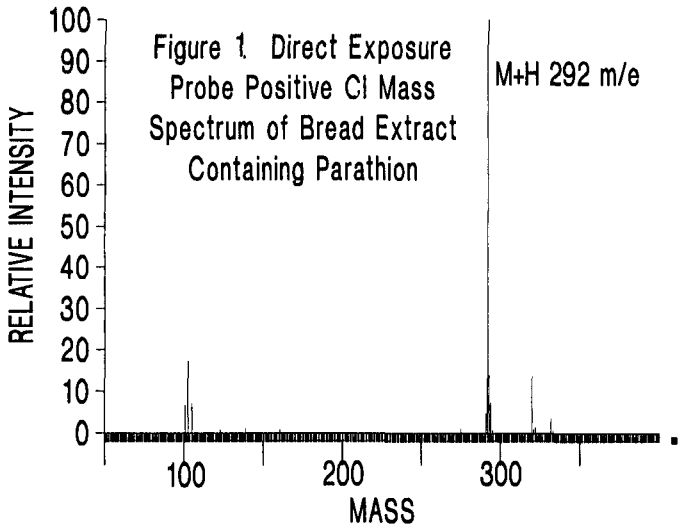

Figure 2. Parathion

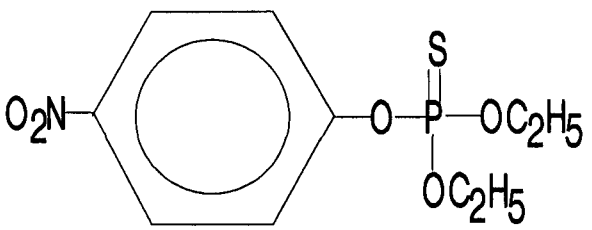

CHOLINESTERASE INHIBITOR MW = 291
EXTREMELY TOXIC
Lethal dose (child) = 0.1 mg/kg

Presented at the 36th ASMS Conference on Mass Spectrometry and Allied Topics
June 5-10, 1988, San Francisco, CA

Application of GC/MS/MS in the Analysis of Nitrosamines in Food and Food Related Products

Dorcas Weber, Nirisinha P.Sen and Benjamin P.-Y.Lau,
Food Research Division, Bureau of Chemical Safety, Food Directorate,
Health and Welfare Canada, Tunney's Pasture, Ottawa,
Ontario, Canada K1A OL2

A VG Analytical model 7070EQ, a hybrid MS/MS system of configuration EBQQ, was used to investigate the analysis of some commonly occuring volatile and non-volatile nitrosamines in food and related products. The instrument's first stage is a conventional EB configuration double focusing sector instrument with an off-axis detector for normal MS operation. For MS/MS operation, the ion beam is directed into a collision cell and another quadrupole mass analyser.

The EI+ spectra of the dialkyl-N-nitrosamines (dimethyl-, diethyl-, dipropyl- and dibutyl-) all show molecular ions with decreasing intensity as the length of the alkyl chain increases. The daughter ion spectra, using Argon as a collision gas, of most dialkyl-N-nitrosamines show a peak corresponding to the loss of 17 (OH) and, in the higher members of the homologous series, a loss of 42 corresponding to the loss of C_3H_6 from the alkyl chain. However, the dimethyl-N-nitrosamine only shows a peak corresponding to the loss of 30 (NO) from the parent molecular ion. The daughter ion spectra of the cyclic nitrosamine (N-nitrosopyrolidine, 1-nitrosopiperidine, and N-nitrosomorpholine) show a loss of 30 (NO) as one of the major ions.

Optimum CID operating conditions were established by two series of experiments. First the collision gas pressure was fixed at 1 x 10^{-6} mbar (total analyser pressure) and the collision energies were varied to obtain the optimum response. Then the collision energy was fixed at the optimum value and the collision gas pressure was varied. An example is shown in Fig. 1

Parent-daughter ion pairs were selected from the daughter ion spectra for multiple reaction monitoring operations (MRM). In most cases, two or more reactions were monitored for each component for confirmation .

Extracts of rubber nipples, rubber netting, smoked meat and apple wax were examined using this method. Typical chromatograms are shown in Fig 2. Most of the traces have little or no interference from different sample matrices indicating the high selectivity of the method. A comparison was also made using low (1K) and medium (5K) resolution for the same sample analysed by both the conventional SIM method and the MS/MS/MRM method. The result is shown in Fig. 3. The MS/MS traces show no interferences in the retention window monitored. As a result, the analysis can be carried out with a shorter GC column and shorter analysis time.

In certain samples, however, some interfering peaks were observed with the front end resolution at 1K. The selectivity can be improved by increasing the front end mass resolution. The result is illustrated in Fig 4 for a rubber nipple extract

In summary, GC/MS/MS has shown to be a sensitive and selective method for trace analyses of nitrosamines. The result is comparable to that obtained by medium (5 - 8 K) resolution using the conventional sector instrument. Selectivity can further be improved by increasing the front end resolution of the instrument.

Presented at the 36th ASMS Conference on Mass Spectrometry and Allied Topics
June 5-10, 1988, San Francisco, CA

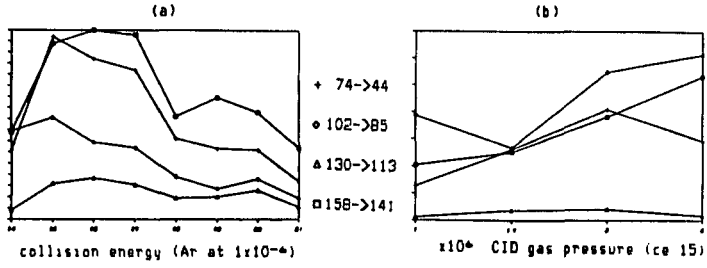

Fig 1 Optimisation of operating parameters (a) collision energy, (b) collision gas pressure

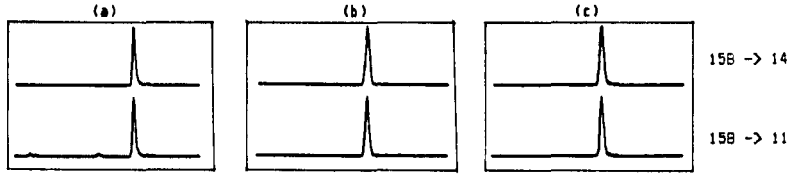

Fig 2 Typical chromatograms obtained from different sample matrices for the analysis of dibutyl-N-nitrosamine using MRM (a) rubber netting, (b) meat(outer), (c) meat(total)

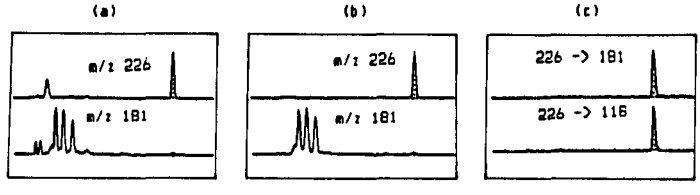

Fig 3 Comparison of low resolution MS, medium resolution MS and MS/MS in the analysis of dibenzylnitrosamine in a rubber netting extract (a) 1K MS, (b) 5K MS, (c) MS/MS

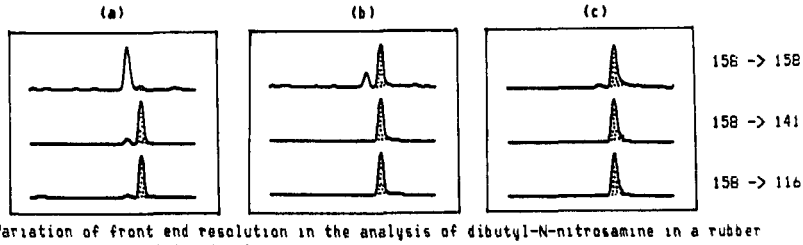

Fig. 4 Variation of front end resolution in the analysis of dibutyl-N-nitrosamine in a rubber nipple extract (a) 1K, (b) 2K, (c) 3.3K

Presented at the 36th ASMS Conference on Mass Spectrometry and Allied Topics
June 5-10, 1988, San Francisco, CA

DEVELOPMENT AND IMPLEMENTATION OF A GC-MS METHOD FOR SIMULTANEOUS DETERMINATION OF THIRTY-EIGHT BIOACCUMULATING COMPOUNDS IN FISH

J. G. Solch, J. H. Garrett, D. J. Wagel, L. A. Harden, M. S. Hanes, G. F. VanNess and T. O. Tiernan, Department of Chemistry and Toxic Contaminant Research Program, Wright State University, Dayton, OH 45435

In collaboration with U.S. EPA, we have recently worked to develop and evaluate a procedure for simultaneous measurement of some 38 organic compounds in fish tissue. This set of target analytes was selected by EPA on the basis of toxicity, bioavailability, metabolism and persistence of these chemicals in fish, as well as the quantities of such chemicals produced annually. The method developed was intended to utilize minimal sample preparation in order to reduce loss of target analytes. The sample extracts were to be amenable to full-scan capillary-column GC-MS analysis, and identification of analytes was to be based on GC retention time, responses at appropriate indicator masses, correct quantitation/confirmation ion intensity ratios, and library matching of mass spectra. The desired GC-MS calibration range was for 1-50 ng/µL of injected analyte.

The sample preparation ultimately developed entailed combining 20 g of ground fish tissue with 80 g of sodium sulfate, adding various surrogate and native standards, and Soxhlet extracting with hexane/methylene chloride. The extract was concentrated to a volume of 2 mL, and was then fractionated on a Biobeads SX-3 GPC column, using cyclopentane/dichloromethane as the mobile phase. The collected effluent fraction was concentrated and the GPC step was repeated. The internal standard was added to the final GPC fraction, after concentration. A set of samples prepared by these procedures for purposes of method validation are described in Table 1.

Initial studies indicated that the GC-MS response factors for the target analytes ranged from 0.011 to 1.200. This range, coupled with the need to analyze 1-50 ng/µL of injected sample, dictated a requirement for a 1:5000 linear instrument response range. To achieve this with the Kratos MS-25 Mass Spectrometer, a 100 volt amplifier was installed in lieu of the standard 10 volt amplifier. This resulted in an eight-fold increase of the usually attainable linear calibration range. A standard EPA software package was to be used for the data acquisition and processing, but this software utilizes a peak detection algorithm which fails when more than one MS peak is present in a given GC retention time window, as was frequently the case here, owing to the large number of compounds and matrix constituents in the fish extracts. This required development of a new algorithm which searches for and identifies the largest quantitation ion in a given window, which also satisfies other peak response and ratio requirements. This new routine correctly identified and measured intensities of analyte indicator ions even in the presence of other interfering peaks. The EPA software quantitation displays were also modified to show the appropriate number of significant figures and to display the measured quantitation/confirmation ion ratios.

Table 2 shows a summary of the data obtained using these methods in a validation study. These results indicate that the procedures described can successfully detect and quantitate 33 of the 38 target analytes in fish, with detection limits of 12.5 ng/g or lower. The calibration range was found to be linear for these analytes from 12.5 to 1250 ng/g. Pentachlorophenol, dicofol, dieldrin, chlorobenzilate and kepone were not reliably detected in fish by these methods.

TABLE 1: METHOD VALIDATION FOR EXTRACTION OF FISH TISSUE FOR 38 ANALYTES

Sample Series	Number Samples	Native Standard Added ng/g	Surrogate Standard Added ng/g	Internal Standard Added ng/g
A	4	12.5	12.5	95.75
B	4	37.5	37.5	93.75
C	4	125.0	125.0	93.75
D	4	1250.0	1250.0	93.75
E	4	0.0	125.0	93.75

Sample size: 20 g; internal standard added prior to analysis

Presented at the 36th ASMS Conference on Mass Spectrometry and Allied Topics
June 5-10, 1988, San Francisco, CA

TABLE 2: SUMMARY OF TARGET ORGANIC ANALYTE DATA OBTAINED FROM FULL-SCAN CAPILLARY GC/MS

R.T.	Analyte Name	Masses	Standard Ave. R.F.	Standard % RSD	Sample Ave. R.F.	% Rec
15:10	1,3,5-Trichlorobenzene	180 182	0.495	3.9	0.419	85
16:30	1,2,4-Trichlorobenzene	180 182	0.500	6.7	0.420	84
17:36	1,2,3-Trichlorobenzene	180 182	0.495	0.9	0.419	85
21:03	1,2,3,5-Tetrachloroben	216 218	1.100	6.0	0.947	86
21:06	1,2,4,5-Tetrachloroben	216 218	1.100	6.0	0.947	86
22:29	Biphenyl	154 152	1.248	10.0	1.120	91
22:31	1,2,3,4-Tetrachloroben	216 218	0.510	7.5	0.432	85
26:34	Pentachlorobenzene	250 252	0.420	4.6	0.334	78
	Internal Standard: D_{10}-Biphenyl					
30:27	Trifluralin	306 264	0.080	30.8	0.079	99
31:12	Alpha-BHC	219 181	0.081	8.7	0.110	134
31:36	Hexachlorobenzene	284 286	0.310	8.5	0.297	96
31:49	Pentachloroanisole	280 265	0.145	7.7	0.128	89
32:42	Pentachlorophenol	266 264	0.017	71.6	0.100	588
32:45	Gamma-BHC	219 181	0.070	11.2	0.088	126
33:01	Pentachloronitrobenzen	295 237	0.029	52.5	0.020	69
34:22	Diphenyl Disulfide	218 109	0.155	4.1	0.244	158
36:06	Heptachlor	272 100	0.037	27.1	0.051	136
37:48	Chloropyrifos	197 314	0.067	15.1	0.100	150
37:55	Dicofol (Kelthane)	250 139	0.015	19.9	0.041	270
38:49	Isopropalin	280 238	0.165	37.8	0.125	61
39:11	Octachlorostyrene	380 382	0.121	8.1	0.086	62
39:22	Heptachlor Epoxide	353 355	0.100	7.5	0.080	80
39:26	Oxychlordane	185 387	0.046	10.9	0.046	99
40:24	Chlordane, trans	373 375	0.143	12.3	0.116	81
40:49	Butachlor	176 161	0.092	15.4	0.053	57
41:02	Chlordane, cis	373 375	0.132	1.5	0.104	79
	Internal Standard: D_{10}-Phenanthrene					
41:15	Nonachlor, trans	409 407	0.179	15.8	0.238	132
41:50	DDE -p-p'	246 318	0.309	14.5	0.428	139
42:02	Dieldrin	79 263	0.042	10.1	0.129	307
42:42	Nitrofen	283 285	0.117	37.1	0.080	68
42:49	Perthane	223 224	0.627	16.3	0.879	140
42:58	Endrin	317 263	0.011	21.0	0.011	96
43:08	Chlorobenzilate	251 139	0.130	15.1	0.335	266
43:52	Nonachlor, cis	409 407	0.173	18.8	0.178	103
44:26	Kepone	272 274	0.018	112.9	0.200	1108
45:50	Triphenyl Phosphate	326 325	0.231	30.7	0.302	131
47:22	Methoxychlor	227 228	0.197	22.6	0.285	144
49:23	Mirex	272 274	0.146	23.9	0.134	92
	Internal Standard: D_{12}-Chrysene					

R.T.	Int/Surr Std Names	Masses	Standard Ave. R.F.	Standard % RSD	Sample Ave. R.F.	% Rec
	Internal Stds:					
22:22	D_{10}-Biphenyl	164 165	--	--	--	--
33:09	D_{10}-Phenanthrene	188 189	--	--	--	--
47:20	D_{12}-Chrysene	240 241	--	--	--	--
	Surrogate Stds:					
21:05	$^{13}C_6$-1,2,4,5-Tetraclb	222 224	0.528	0.0	0.455	86
32:46	$^{13}C_6$-Pentaclphenol	272 270	0.015	56.6	0.075	497
40:38	D_{10}-Pyrene	212 106	0.961	5.1	0.646	67
41:46	D_8-DDE	254 326	0.465	11.7	0.378	82
54:32	D_{12}-Benzo-e-pyrene	264 265	0.942	17.6	0.431	46

We acknowledge the support of this work by the U.S. EPA, under contract No. 68-02-4221, and the cooperation and assistance of EPA/ERL(Duluth), Dr. Douglas Kuehl. We also wish to thank Kratos Analytical for their generous assistance in developing these methods.

Presented at the 36th ASMS Conference on Mass Spectrometry and Allied Topics
June 5-10, 1988, San Francisco, CA

THERMAL DECOMPOSITION OF A SERIES OF 2-CHLOROETHYL ALKYL AND ARYL SULFIDES

Dennis K. Rohrbaugh, Yu-Chu Yang and J. Richard Ward
U.S. Army Chemical RD&E Center, APG, MD 21010-5423

Compounds of the general class $RSCH_2CH_2Cl$ (2-chloroethyl sulfides) are commonly used in the synthesis of radioprotective materials and as simulants for mustard gas (bis[2-chloroethyl]sulfide). Our objective was to define the decomposition pathways of these compounds to determine what hazards are associated with the handling and storage of these compounds. Here we report the application of EI and methane CI GC/MS to characterize the thermal decomposition products of a series of 2-chloroethyl sulfides where R = methyl, ethyl, phenyl and benzyl and present a decomposition mechanism based on the formation of dimeric sulfonium salt intermediates to account for these products.

Samples were analyzed after two years of storage on a Finnigan model 5100 GC/MS using both EI and CI methods. The 15m SE-54 capillary column (split ratio 50:1) was programmed from 60°C to 160°C at 10°C per min. Injector temperature was 200°C and the interface temperature was 230°C. The CI reagent gas was methane (0.6 Torr).

Decomposition products observed are shown in the Table below.

Table. GC/MS Characterization of Aged $RSCH_2CH_2Cl$

Component	Composition, Area %			
	$R=CH_3$ (CEMS)	$R=C_2H_5$ (CEES)	$R=C_6H_5$ (CEPS)	$R=C_6H_5CH_2$ (CEBS)
RCl	0.2	-	0.4	18.2
	-	-	-	trace
	0.4	1.7	-	2.3
$RSCH_2CH_2Cl$	93.0	94.4	95.4	44.8
RSR	-	0.2	0.1	13.5
RSSR	0.6	-	0.6	-
$S[CH_2CH_2Cl]_2$	0.6	0.06	-	5.6
$RSCH_2CH_2SR$	2.6	0.1	1.2	2.8
$RSCH_2CH_2SCH_2CH_2Cl$	1.1	0.1	-	7.9

The samples contained a number of degradation products derived from dimeric sulfonium ions which were absent in the freshly distilled products. These products, common to all four derivatives, can be rationalized by a decomposition mechanism which proceeds through the dimeric sulfonium salt II shown in Equation 1.

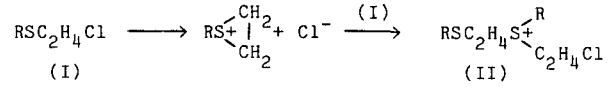

(1)

The products observed can be accounted for in terms of the decomposition of II via nucleophilic substitution. The three carbon atoms alpha to the charged sulfur in II are subject to nucleophilic attack. The two primary nucleophiles present in the neat solution are chloride ion and another molecule of $RSCH_2CH_2Cl$. Attack by chloride results in the three decomposition pathways shown in Equation 2 and attack by $RSCH_2CH_2Cl$ results in the formation of the secondary ions III and IV shown in Eqs. 3 and 4.

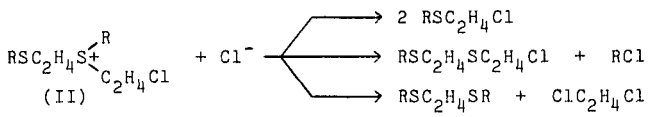

(2)

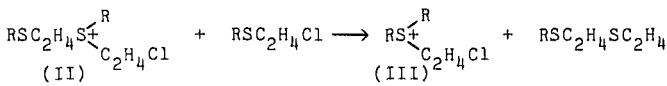

(3)

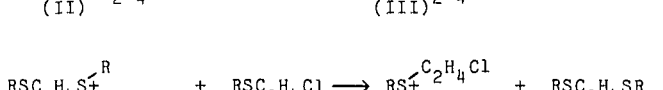

(4)

The sulfonium salt intermediate III can decompose directly to RSR, while IV can decompose directly to mustard and RCl. As shown in the Table, mustard, RSR, RCl and the products in Eqs. 2, 3 and 4 were all observed as products. Dithiane, which can be derived from II, was also detected. Oxidation and hydrolysis products were not observed. Because mustard is produced, safe handling and storage of these compounds is necessary.

The dithioethers produced in these studies are unusual in that more intense molecular ions were observed under EI conditions than under CI conditions. The reason for this is evident in the fragmentation chemistry. During chemical ionization, protonation of the sulfur enhances the leaving group ability and promotes formation of the thermodynamically stable ethylene sulfonium ion as shown below.

$CH_3CH_2SCH_2CH_2SCH_2CH_3$ CI AND EI MASS SPECTRA

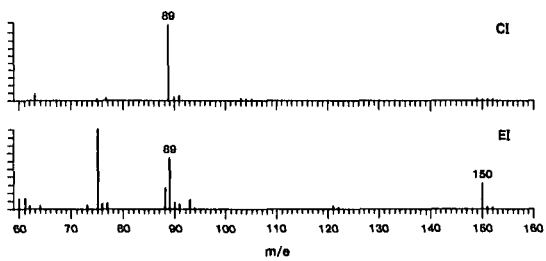

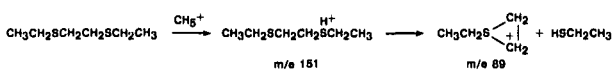

Presented at the 36th ASMS Conference on Mass Spectrometry and Allied Topics
June 5-10, 1988, San Francisco, CA

CHARACTERIZATION OF REACTION PRODUCTS OF CHLORINE DIOXIDE AND FATTY ACIDS OF WHEAT FLOUR USING MASS SPECTROMETRY.

DAVID L. HEIKES, Total Diet Research Center, Food and Drug Administration, Kansas City, MO 64106

The Food and Drug Administration's Total Diet Program surveys table-ready foods for industrial chemicals and pesticides. During examination of several pastry items several unidentified gas chromatographic - microcoulometric and electrolytic conductivity responses were observed. Breads, cakemixes, muffins and soda crackers all contained these compounds at one time or another and at various levels. Since these foods have the common ingredient of flour, a survey of various types of flour was conducted. It was found that only bleached flour contained these unidentified chemicals.

Capillary column GC/MS indicated that these compounds which appeared as single peaks on packed column GC, were in reality comprised of two or more compounds which were nearly coeluting. This phenomenon suggested the presence of structural isomers. Further, most of these compounds showed a common similarity to the unsaturated mass spectral pattern exhibited by linoleic acid (i.e. m/z 41, 55, 67, etc.). Linoleic acid is the predominant fatty acid of wheat. No apparent molecular ions were observed.

Chlorine and chlorine dioxide are used to bleach wheat flour used in pastries and breads. It was therefore suggested, that the compounds observed in the pastries were reaction products of the indigenous linoleic acid and the bleaching agents. Electron impact spectra exhibited no apparent molecular ion and little or no evidence of chlorination (FIGURES 1 and 2). However, each spectra displayed a characteristic ion which could result from the loss of one or more molecules of HCl or cleavage of a former double bond which had received the addition of Cl and OH (1).

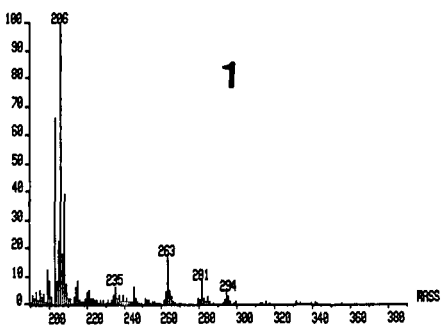

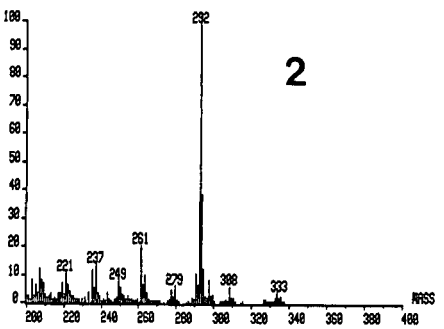

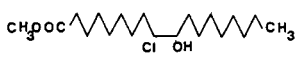

From this information and the proposed reaction products of chlorine and chlorine dioxide with unsaturated acids, a number of feasible compounds (FIGURE 5) were synthesized using classical procedures.

Several reagent gases were employed in the attempt to obtain molecular weight data through chemical ionization techniques. Ethylene oxide (2) proved the most useful (FIGURES 3 and 4).

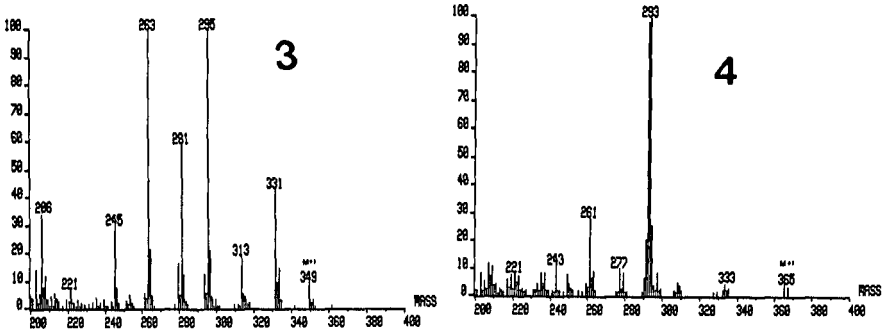

FIGURE 5. SYNTHESIZED PRODUCTS

9,10 - Chlorohydroxyoctadecanoate
9,10 - Chlorohydroxyoctadecenoate
12,13 - Chlorohydroxyoctadecenoate
9,10,12,13 - Trichlorohydroxyoctadecanoate
9,10 - Dichlorooctadecanoate
9,10 - Dichlorooctadecenoate
12,13 - Dichlorooctadecenoate
9,10,12,13 - Tetrachlorooctadecanoate

Two of these compounds have been quantified by gas chromatography with electrolytic conductivity (Hall) detection (FIGURE 6). Confirmation was accomplished using positive ion chemical ionization with ethylene oxide as the reagent gas.

FIGURE 6. TYPICAL FINDINGS

9, 10 - Dichlorooctadecenoic Acid, plus
12, 13 - Dichlorooctadecenoic Acid :
4.2 ppm in White Rolls
48 ppm in Chocolate Cake
49 ppm in Blueberry Muffins
95 ppm in Baking Powder Biscuits

9, 10 - Chlorohydroxyoctadecanoic Acid :
8.1 ppm in Blueberry Muffins
9.6 ppm in Baking Powder Biscuits
5.6 ppm in Chocolate Cake

REFERENCES

(1) Jensen, N.J. and Gross, M.L. "Mass Spectrometry Methods for Structural Determination and Analysis of Fatty Acids", Mass Spectrometry Reviews 1987, 6, 497-536.

(2) Lange, C. "Ethylene Oxide (Oxiran) as a Reagent Gas For Long Chain Compounds and Organic Functional Group Determination by Chemical Ionization Mass Spectrometry", Organic Mass Spectrometry 1986, 21, 524-527.

Presented at the 36th ASMS Conference on Mass Spectrometry and Allied Topics
June 5-10, 1988, San Francisco, CA

ANALYSIS OF AMBIENT AIR SAMPLES UTILIZING AN AIR TOXICS INTERFACE SYSTEM BY MEGABORE CAPILLARY GC/MS/DS

R. L. Porch, J. T. Bursey, D. P. Dayton, R. A. McAllister,
J. Rice, D. E. Wagoner; Radian Corporation,
Research Triangle Park, North Carolina, 27709.

An interface system has been developed for the analysis of ambient air samples collected in 6-liter electropolished stainless steel canisters (see Figure 1). This system delivers a precisely measured volume of ambient air sample to any analytical device. The portable interface is being used with a GC/MS system and a VARIAN™ 3700 gas chromatograph, configured with a PID/FID and an ECD. The interface system can transfer an air sample stored in a canister under pressure, or under vacuum, and preconcentrate the organic content in a cryogenic trap packed with 60/80 mesh glass beads cooled by liquid argon (-189°C). Then the trap is heated to 204°C in 56 seconds and backflushed with helium to sweep the organic compounds directly on-column to a subambient (5°C) DB-624 0.53 mm x 30 m megabore capillary column. The column operates at a flow rate of 15 mL/min with a make-up flow of 15 mL/min into a glass jet separator. The interface system heated transfer line has a standard 2" 26 gauge syringe needle attached which is directed through the GC injection port cap and septum. A heated on-column injector liner allows the needle to fit inside the megabore capillary column.

Calibration canisters containing 90 uL of HPLC water (simulates the 70% humidity at 24°C during the collection of samples) were spiked at various ppbv levels of each target compound and allowed to equilibrate before analysis. The ppbv calibration concentrations vary depending upon whether full scan or MID analysis is required. The approximately 40 target compounds (primarily halocarbons and low boiling aromatic and olefinic compounds) typically have correlation coefficients of >0.99 in the full scan and MID mode. Samples from 34 different sites across the United States have been analyzed on a quadrupole GC/MS/DS and quantitated by linear regression using the Incos data system. GC/MD (multidetector) and GC/MS target compound identification comparisons are summarized in Table 1. Analysis of 15% of the site samples by both the GC/MD system and a GC/MS showed a compound identification confirmation rate of 95.4 percent. Currently the interface system is being modified to allow operation with internal standards.

Presented at the 36th ASMS Conference on Mass Spectrometry and Allied Topics
June 5-10, 1988, San Francisco, CA

TABLE 1. SUMMARY GC/MD AND GC/MS IDENTIFICATION COMPARISONS
UTAP, FOURTH QUARTER 1987

GC/MD vs. GC/MS Comparison	Cases	Percentage
Positive GC/MD - Positive GC/MS	101	8.93
Positive GC/MD - Negative GC/MS	44	3.89
Negative GC/MD - Positive GC/MS	8	0.71
Negative GC/MD - Negative GC/MS	978	86.47
TOTAL	1131	100.00

Correct Identifications, referenced to GC/MS = 95.4%
Incorrect Identifications, referenced to GC/MS = 4.6%

FIGURE 1. SAMPLE INTERFACE SYSTEM

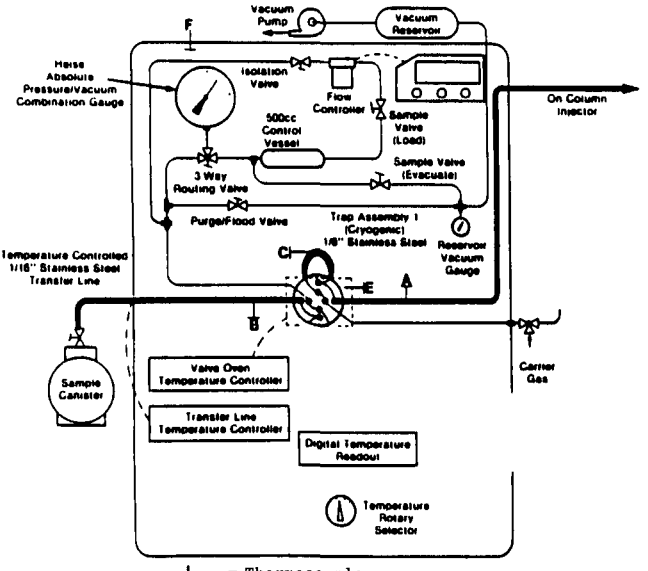

= Thermocouple

Temperatures
- A = Transfer Line to Analytical System
- B = Transfer Line From Sample Canister
- C = Cryogenic Trap
- E = Valve Oven
- F = Room

Presented at the 36th ASMS Conference on Mass Spectrometry and Allied Topics
June 5-10, 1988, San Francisco, CA

MODIFICATION OF A GC/MS SYSTEM TO INCREASE THE LINEARITY OF RESPONSE FOR COMPOUNDS ANALYZED BY EPA METHOD 625

Q. G. Grindstaff, R. E. Slagle, J. C. Vance, and T. N. Ternes

Plant Laboratory
Oak Ridge Y-12 Plant*
Martin Marietta Energy Systems, Inc.
Oak Ridge, Tennessee 37831

ABSTRACT

The compounds analyzed by EPA Method 625 are varied in their chemical and physical properties. These polar and nonpolar compounds range from volatiles to high-boiling compounds; some are thermally labile while others can undergo catalytic decomposition. The problem of nonlinear responses with respect to concentration by these chemical and physical properties is the subject of investigation.

The study was undertaken using a Kratos MS-50 and MS-25E GC/MS/DS system. Two experimental systems have been studied. The first system was composed of a Grob split-splitless injector, SPB-5 column connected to a 1-m deactivated column by a double-ferrule connector, and a stainless steel ionization chamber. The second system was composed of a cooled on-column injector with a 2-m precolumn, an SPB-5 column connected to the precolumn, a 1-m deactivated column by single ferrule connectors, and a gold-plated ionization chamber.

The linearity of the response factors for a range of concentrations for a Grob hot injector versus a cold-on-column injector is shown in Table 1. For the Grob injector (which was heated to 320°C and contained a deactivated glass liner), the difference between the response factor for the 100- and 10-ng/μL concentrations of the listed compounds was approximately two to three times, with no benzidine being detected at 10 ng/μL. However, with the cold-on-column injector with secondary cooling, the response factors showed essentially no change with concentration.

Even after the Grob injector was replaced, the GC peak representing benzidine showed problems with chemical absorption in the GC system. The benzidine peak eluted at 242°C, but still showed a detectable tail at 300°C. The problem was found to be caused by the double-ferrule connector used to connect the column to the precolumn and the interface column. After replacing the double-ferrule connector with a single-ferrule connector, the tailing factor at 25 ng/μL was reduced to 1.5.

The effects on the compounds by the source material were also large. Table 2 shows that in changing from a stainless steel ionization to one plated with gold, the area of the internal standards went up by a factor of 3. The area for phenol increased by a factor of 4, while the area for 4-chloro-3-methylphenol increased by a factor of 6. However, the areas for 2-nitrophenol, 2-methyl-4,6-dinitrophenol, and 2,4-dinitrophenol either stayed the same or dropped. The drop can be correlated with the pKa value. Because of this fact, it was determined that there must be active sites in the gold-plated source. After silylation of the gold source, a marked increase was noted in the areas of the nitro compounds. An overall increase in response factors was indicated by changing from a stainless steel to a gold plated source. This fact coupled with the large increase in absolute areas showed that the gold-silylation source was superior in its ability to produce a lower detection limit and a more linear response over a wider concentration range.

---

*Operated for the U.S. Department of Energy by Martin Marietta Energy Systems, Inc., under contract DE-AC05-84OR21400.

Presented at the 36th ASMS Conference on Mass Spectrometry and Allied Topics
June 5-10, 1988, San Francisco, CA

Table 1. Response factor linearity of Grob injector versus cold-on-column injector

	Response factor			
	Grob		Cold-on-column	
Compound	100 ng/μL	10 ng/μL	100 ng/μL	10 ng/μL
Nitrobenzene	2.814	0.795	0.409	0.337
1,3-Dichlorobenzene	1.527	0.890	0.920	1.016
Benzidine	0.051	0.000	0.388	0.377
3,3-Dichlorobenzidine	0.200	0.099	0.395	0.376

Table 2. Source effects (absolute areas)

	Areas (10 ng/μL)		
Compound	SS	Gold	Gold + Silylation
1,4-Dichlorobenzene-D4	2685085	7945029	8200532
Phenol	2029366	8135956	7943951
2-Chlorophenol	1662789	6769486	6597577
Naphthalene-D8	974067	2858004	3035846
2-Nitrophenol	597395	577546	2328117
2,4-Dimethylphenol	1358350	6311856	5056956
2,4-Dichlorophenol	1130434	6080716	3873915
Acenapthalene-D10	5490952	15099840	15115170
4-Chloro-3-methylphenol	1032001	5898147	3809456
2,4,6-Trichlorophenol	861066	4005762	2693039
4-Nitrophenol	361830	1026351	1099637
2-Methyl-4,6-dinitrophenol	230156	66273	765087
Pentachlorophenol	703438	1326303	1387640
2,4-Dinitrophenol	118889	33071	526266

Presented at the 36th ASMS Conference on Mass Spectrometry and Allied Topics
June 5-10, 1988, San Francisco, CA

DETERMINATION OF ORGANIC COMPOUNDS IN DRINKING WATER USING LIQUID-SOLID EXTRACTION, CAPILLARY COLUMN GAS CHROMATOGRAPHY, AND HIGH SENSITIVITY FULL MASS RANGE MASS SPECTROMETRY

Thomas D. Behymer, James W. Eichelberger, and William L. Budde

U. S. Environmental Protection Agency, Office of Research and Development, 26 W. Martin Luther King Drive, Cincinnati, OH 45268.

A number of pesticides and industrial organic compounds are routinely determined in water using liquid-liquid-extraction, capillary column gas chromatography (GC), and full mass range mass spectrometry (MS). For many monitoring activities including industrial or municipal wastewater, landfill leachate, and groundwater near waste sites, conventional GC/MS methods with quantitation limits of about 10 ug/L (10 parts per billion, ppb) is adequate. But for the determination of organics in drinking water, quantitation limits in the range of 0.1-10 ug/L are needed, and it is highly desirable to retain the full mass range data acquisition of conventional GC/MS to ensure reliable identifications.

The objective of this work was to develop, for drinking water analyses, a general purpose analytical method with the following characteristics: (a) sensitivity for complete electron impact (EI) mass spectra with 0.1 ng injected (corresponding to 0.1 ug/L or 100 parts per trillion after extraction and concentration); (b) applicability to a minimum of 40 organic compounds of concern; (c) isolation of analytes with liquid-solid extraction (LSE) cartridges; (d) minimization of use and worker exposure to solvent (methylene chloride); (e) quantitative accuracy of 70% or better and precision of 30% RSD or better; and (f) strong quality control procedures incorporated into the method.

A group of about 40 compounds (Table 1) which have been found in drinking water supplies, and which are under study for potential adverse health effects, were added to water at 2 ug/L and 0.2 ug/L. These were extracted by passing one liter of water through commercially available LSE cartridges containing 0.9-1.g of reverse phase liquid chromatography packing materials. The compounds were eluted with 10 mL. of methylene chloride, and determined with capillary column high sensitivity full mass range GC/MS. The recoveries of most compounds were greater than 80% with detection limits in the target range. The results from one set of analyses at 2 ug/L (2 ppb) are shown in Table 1.

Table 1. Accuracy and precision data from seven determinations of the method analytes at 2 ug/L with liquid-solid extraction and the ion trap mass spectrometer.

Compound	True conc. (ug/L)	Mean observed conc. (ug/L)	Std. dev. (ug/L)	Rel. std. dev. (%)	Mean method accuracy (% of True conc.)	Method detection limit (MDL) (ug/L)
acenaphthylene	2	1.9	0.2	11.	95	0.6
aldrin	2	1.6	0.2	13.	80	0.6
anthracene	2	1.7	0.1	5.9	85	0.3
atrazine	2	2.2	0.3	14.	110	0.9

Table 1. (continued)

benzo[a]anthracene	2	1.8	0.2	11.	90	0.6
benzo[b]fluoranthene	2	measured with benzo[k]fluoranthene				
benzo[k]fluoranthene	2	4.2	0.3	7.1	105	0.9
benzo[a]pyrene	2	0.8	0.2	25.	40	0.6
benzo[g,h,i]perylene	2	0.7	0.1	14.	35	0.3
butylbenzylphthalate	2	2.0	0.3	15.	100	0.9
chlordane components						
alpha-chlordane	2	2.0	0.2	10.	100	0.6
gamma-chlordane	2	2.2	0.3	14.	110	0.9
trans nonachlor	2	2.7	1.0	37.	135	3.
2-chlorobiphenyl	2	1.9	0.1	5.2	95	0.3
chrysene	2	2.2	0.1	4.5	110	0.3
dibenz[a,h]anthracene	2	0.3	0.3	100.	15	0.9
di-n-butylphthalate	2	2.2	0.3	14.	110	0.9
2,3-dichlorobiphenyl	2	2.3	0.1	4.3	115	0.3
diethylphthalate	2	2.0	0.3	15.	100	0.9
di(2-ethylhexyl) phthalate	2	1.9	0.2	11.	95	0.6
di(2-ethylhexyl)adipate	2	1.6	0.3	19.	80	0.9
dimethylphthalate	2	1.9	0.2	11.	95	0.6
endrin	2	1.8	0.1	5.5	90	0.3
fluorene	2	2.2	0.2	9.1	110	0.6
heptachlor	2	2.2	0.3	14.	110	0.9
heptachlor epoxide	2	2.3	0.2	8.7	115	0.6
2,2',3,3',4,4',6-hepta-chlorobiphenyl	2	1.4	0.2	14.	70	0.6
hexachlorobenzene	2	1.7	0.2	12.	85	0.6
2,2',4,4',5,6'-hexa-chlorobiphenyl	2	1.6	0.4	25.	80	1.
hexachlorocyclo-pentadiene	2	1.1	0.1	9.1	55	0.3
indeno[1,2,3,c,d]pyrene	2	0.4	0.2	50.	20	0.6
lindane	2	2.1	0.2	9.5	105	0.6
methoxychlor	2	1.8	0.2	11.	90	0.6
2,2',3,3',4,5',6,6'-octachlorobiphenyl	2	1.8	0.2	11.	90	0.6
2,2',3',4,6-penta chlorobiphenyl	2	1.9	0.1	5.3	95	0.3
pentachlorophenol	8	8.2	1.2	15.	102	4.
phenanthrene	2	2.4	0.1	4.2	120	0.3
pyrene	2	1.9	0.1	5.3	95	0.3
simazine	2	2.1	0.2	9.5	105	0.6
2,2',4,4'-tetrachloro biphenyl	2	1.5	0.1	6.7	75	0.3
toxaphene	25	28.	4.7	17.	112	15.
2,4,5-trichlorobiphenyl	2	1.7	0.1	5.9	85	0.3
means[1]		1.8	0.2	15.	91	0.6

[1]pentachlorophenol and toxaphene excluded.

Presentod at the 36th ASMS Conference on Mass Spectrometry and Allied Topics
June 5-10, 1988, San Francisco, CA

ANALYSIS OF ORGANIC POLLUTANTS IN AIR AND WATER BY CAPILLARY COLUMN GC/MS

QIAO SHIJUN WU RENMING and GE NINGCHUN
Gansu provincial Institute of Environmental protection.CHINA

Methods for organic volatiles in air and water have been reported(1~5), However faster and simpler methods are needed both sampling and analysis of environmental organic pollutants.

In our experiment,the organic volaties in industrial air are adsorpt on a porous polymer(Tenax GC),the organic volatiles in drinking water are heated and carried out by nitrogen flow,which are adsorpt on Tenax GC.Both pollutants are transferred into a capillary column,and heat desorption onto a GC/MS system.These methods are simple,fast,convenient for analysis of trace organic pollutants in air and water.The methods have beed used for several years.

EXPERIMENTAL

Preparation of Tenax GC Tude.The sampling tude is 20 cm long stainless steel filled with 0.3 g of 60-80 mesh of Tenax GC.Initially,the column is precondtioned at 275°C in a nitroge flow for 24 hours.Befere sampling the tube is heated at 250°C in a flow of pure He for 30 minutes in oeder to eliminate any trace of organic compounds.

Sampling Procedure.For pollutants in industrial air,the Tenax GC tube is connected with a flow-meter and an oilfree air pump.The flow of air is controlled at 0.4 l/min for 30 minutes .The organic volatiles are adsorpt on Tenax GC.This is more simpler.

A schematic diagram of the simpling apparatus is shown in figure 1.The drinking water of 2 l is poured into the class tude,and a constnt temperature water of 50 °C is passed through the inlet of constant temperature water, in the meanwhile,a little flow of nitrogen is introduced into the water sample.Thus the organic volatiles are carried and adsorbed on Tenax GC.

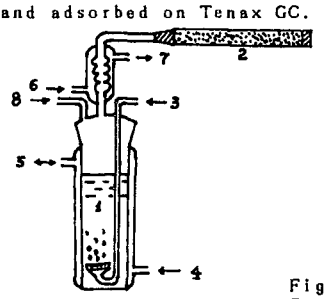

1. water sample
2. Tenax GC tube
3. nitrogen flow inlet
4. 5. inlet.outlet of constant temperature water of 50 °C
6. 7. inlet,outlet of cooled water

Fig.1 Simpling apparatus for water simple

Concentrating and Entering Sample Procedure. The Tenax GC tube is inserted into heat tube,with helium entering from one end for several minutes at a pressure of 0.4 kg/cm². then coil is placed into a lipuid oxygen cup,Tenax GC tube is heated up to 180°C for 15 minutes. So as to

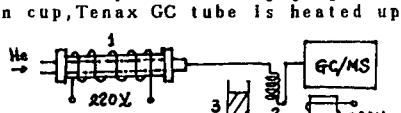

1. heat tube
2. concentration tube
3. liqued oxygen cup
4. heat tube

Fig.2 The arrangement of simple concentration and entering

have the simple inside Tenax GC tube is desorbed and is cooled in the concentration tube.After concentration,the cup is removed and the concentration tube is rapidly inserted into the heat tube, having temperature suddenly rased up to 180 °C, the sample together with helium would enter the GC/MS system.

GC/MS system.The GC/MS system is a JGC-20KEP GC attached with a hydrogen flame detector and a programm temperature device, and a JMS-D100 Mass Sepectrometer with a JMA-0231 DATA processor.The capellary column is squalane column of stainless steel with inner diameter of 0.25 mm and a length of 45 m. An ionic soure of electron impact with ionization voltage of 3000 volts and electron multiplier voltage of 1900 volts is used. The resolution power is 1000.

Blank and Recovery Test. The whole sampling,concentrating and entering for drinking water and air sample are analyzed with blank tests and no foreign matters are found.The recovery test for water is made with chloroform,benzene and n-hepane, the recovery rates reached up to 88%, 91% and100%.While the absorbed method is tested with pentane,benzene,cyclohexane and the recovery rates are 94%,109% and 72%.

RESULT and DISCUSSION

Used these methods,the organic volatiles in Lanzhou drinking water are tested.Fig.3 is the total ionic chromatogram,from which 48 polutants are identified,there are 9 chlorides in drinking water. While 58 pollutants in industrial air are analyzed. These pollutants are ppb level.

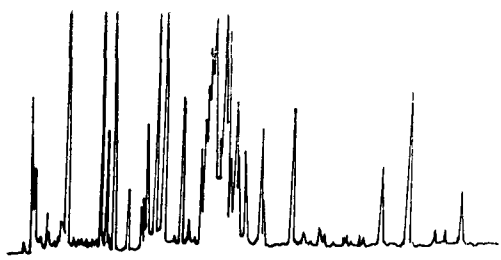

Fig.3 The total ionic chromatogram for drinking water

To analyse organic volatiles in water and air, the Tenax GC has been chose because it is hydrophobic,has a low adsorption strength allowing thermal elution of relatively high boiling compounds at about 250-275 °C,has a good thermal stability and does not react with most of the organic pollutants.

In our experiment,the samples are directly entered into the capillary column withour passing through avapourized chamber, in order to get higher sensidilites(6,7).

The invasion of water vapour or CO_2 in sample would do damage to the mass spectrum, the reason for this,we introduced a few minutes of helium into the Tenax GC tube before heat and concentoation causing the wate rvapour and CO_2 be brought out together helium.

REFERENCES

1. B.Versono et al., J. chromatogr., 122(1986)
2. Liu Aizhu et al., Mass Spectrum,china,7(1),41(1986)
3. B.Versino et al., chromatogr.,7(6),(1984)
4. K.Grob and G.Grob,J.Chromatogr.,90(1974)
5. Yoshio Tsulino,Air pollut., 14(5),1(1979)

Presented at the 36th ASMS Conference on Mass Spectrometry and Allied Topics
June 5-10, 1988, San Francisco, CA

ENVIRONMENTAL CHAMBER/MS TECHNIQUES FOR CONSUMER PRODUCT EMISSIONS

Charlene W. Bayer and Marilyn S. Black
Georgia Tech Research Institute
Atlanta, GA 30332

Volatile organic compounds (VOCs) are one of the major groups of contaminants found in the airborne indoor environment. Total VOC levels of greater than 1.0 mg/m3 indoors indicate inadequate indoor air quality and can result in acute and/or chronic health problems. VOCs are outgassed from a plethora of consumer products such as carpeting, wallpaper, adhesives, paints, fabrics, vinyl flooring, wood products, deodorants, cleaners, etc. (1). Determination of the etiology of VOC emissions is of prime importance for the improvement of indoor air quality.

A wide spectrum of VOCs are generally detected in the indoor environment, and usually the individual VOC detected is in the trace concentration of parts-per-billion volume or less. Often 50 to 100 compounds are observed at individual sampling sites (2). The complexity and trace quantities of the VOCs, as well as the variety of possible sources, creates a difficult sampling, analysis, and source determination problem. The general survey analysis approach can identify many of the airborne VOCs, but provides limited source data. Environmental chamber and mass spectral techniques are essential for the determination of VOC emission sources and for the construction of a data base of consumer product organic emission patterns. The use of an environmental chamber or headspace device eliminates unknown VOC sources, but does not eliminate the basic problems of sampling and analysis.

In this paper, various sampling and analysis techniques for consumer products emissions have been studied and compared. VOC emissions emanating from various consumer products were examined using two different collection techniques: 1) on-line, real-time GC/MS and 2) on-line solid sorbent collection followed by off-line analysis. Two types of direct analyses were investigated. The first consists of direct injection of emissions from a consumer product loaded into an environmental chamber which has been interfaced with a GC equipped with a mass selective detector (MSD) and/or flame ionization detector (FID). The second direct method scrutinized is direct injection of headspace collected emissions into a GC equipped with a MSD. Two types of on-line solid sorbent collection followed by off-line analysis techniques were studied. The first technique consists of loading consumer products into a controlled environmental chamber and collecting consumer product emissions on multi-sorbent tubes which are subsequently analyzed by thermal desorption (TD)/GC/MS. Loading of the consumer product into an ambient headspace chamber followed by collecting the VOC emissions on multi-sorbent tubes with subsequent TD/GC/MS analysis is the second method that was examined. Each of these four techniques were studied and compared to meet the following objectives: 1) optimization of VOCs detection sensitivity; 2) optimization of VOCs collection efficiency; 3) elimination of analyte reaction and decomposition; 4) optimization of individual VOC identification; 5) development of a consumer product emissions data base; 6) determination of VOC emission rates; and 7) correlation between laboratory and field results. Various consumer products emissions were studied to compare the four sampling and analysis techniques. The products studied were drapery material, drapery lining material, carpet, fiberglass insulation coated with a urea-formaldehyde resin, bathroom deodorants, and solid air fresheners.

In general, it was found that environmental chamber/multi-sorbent collection/TD/GC/MS was particularly useful for products outgassing trace

quantities of VOCs in the mid-boiling point range. This method easily detects VOCs in the low ppbv to high pptv range, because of preconcentration of the sample (1 - 25 L are commonly used) on the sorbent tube prior to analysis. The major disadvantages include unknown breakthrough volumes, particularly for the more volatile constituents; irreversible adsorption or inefficient desorption of some analytes; analyte losses and side reactions during sample storage prior to analysis; and thermal decomposition and reactions during desorption. The environmental chamber/GC/MSD is a useful technique for a broad range of analyte structures and volatilities. Lack of sensitivity is the primary disadvantage to this technique. Sample preconcentration is limited to the size of loop compatible with the system (usually 1 to 5 mL). Ambient headspace/multi-sorbent collection/TD/GC/MS is useful for small consumer product samples and for the detection of less volatile VOCs. Heated headspace analyzer/GC/MSD is useful for small consumer product samples and for detection of the less volatile and more reactive VOCs. Headspace techniques cannot be directly correlated to "real-life" conditions. The results are only qualitative. Heated headspace subjects the consumer product to harsher, unnatural conditions resulting in VOC emissions which would not be commonly found in an office or residential setting. The environmental chamber allows the simulation and control of conditions similar to those the sample would experience in actual field use. Tables 1 and 2 illustrate VOC detected in drapery material emission only using the environmental chamber or the ambient headspace. The second major

TABLE 1. Selected VOCs Detected in Drapery Material Emissions Only Detected in Sample Loaded in an Environmental Chamber

Dichlorodifluoromethane
Chloroform
1,2-Dichloroethane
1,4-Dioxane
2-Methylcyclopentanol
Isooctanol
2-Methylcyclohexyl valerate

TABLE 2. Selected VOCs Detected in Drapery Material Emissions Only Detected in Sample Loaded in Ambient Headspace Flask

1-Ethyl-2-methylbenzene
3-Methylfuran
2,5-Dimethylfuran
Thiophene
Dimethyldisulfide

advantage of the environmental chamber over the headspace units is that a larger sample size is analyzed. This allows for realistic results. Consumer products are not homogeneous throughout the entire product. The VOC emissions can vary depending on the portion of the sample that is used for the analysis. The larger the sample size used for the analysis, the more realistic the laboratory emission results will be to the field emission results.

(1) Molhave, L. Indoor air pollution due to organic gases and vapours of solvents in building materials. **Environment International**, 1982, 8 117-127.

(2) Bayer, C.B., and Black, M.S. Indoor air quality evaluations of three office buildings. **ASHRAE Journal**, 1988, in press.

Presented at the 36th ASMS Conference on Mass Spectrometry and Allied Topics
June 5-10, 1988, San Francisco, CA

COMPARATIVE DISTRIBUTION OF HYDROCARBONS IN AIRBORNE PARTICLES COLLECTED BY SIZE FRACTIONATION

***Rafael Infante**, Arnaldo Carrasquillo and Nidia Santiago*
Chemistry Department
Catholic University of Puerto Rico
Ponce, P.R. 00732

The aim of this study is to examine the type and the size distribution of organic compounds present in air particulate matter. Our special concern are the polycyclic aromatic hydrocarbons (PAH's) because of their potential adverse biological effects, including transformation of some of these substances to mutagens and carcinogens by mammalian microsomal enzyme system.

The airborne particulate samples were collected by an Andersen cascade impactor at five sampling sites in Ponce, PR in 1986. The cascade impactor separates particles into five size classifications from < 1.1 to 7.0 um. The cascade impactors were run for 72-hours periods in order to get enough sample for the analysis. A composite sample from four of the five sampling stations was analyzed following the analytical procedure outlined below.

An analytical procedure suitable for the analysis of organic components associated with each of the fraction was developed. It includes ultrasonic extraction with methylene chloride followed by concentration and analysis by high performance gas chromatography/mass spectrometry (HP 5995B GC/MS system). The major peaks in each of the fraction analyzed were identified by comparison of the mass spectra with an online library of over 20,000 spectra and by selective ion monitoring and retention time data. Quantitation was performed by integrating the ion current for the molecular ion for the PAH's and the m/z 85 ion for the normal alkanes. This procedure was tested by extracting a standard mixture of target compounds that included polycyclic aromatic hydrocarbons and normal alkanes and by extracting NBS Standard Reference Material 1649 (Urban Dust Organics). Extraction efficiencies at the 1 ng/ul level were obtained.

The general trends included the observation of low levels of the PAH's in the smallest size particles, < 1.1 uM. They where mostly observed in the west sampling site, which is close to a cement factory that burns coal for their energy demands. PAH's where also observed in the east site, these are probably generated by the agricultural burning activities of this area.

In contrast, aliphatic hydrocarbons both of anthropogenic and natural origin were observed. Their particle size distribution is shown in Figure 1. The distribution remained fairly constant in each of the four sampling stations. The concentration of several higher uneven aliphatic hydrocarbons was found to be higher than that of their even homologues due to contribution from natural sources.

Acknowledgement
Support of this work from MBRS-DRR-NIH Grant No. 0867 and GM-NIH Grant No. 07732 is acknowledge.

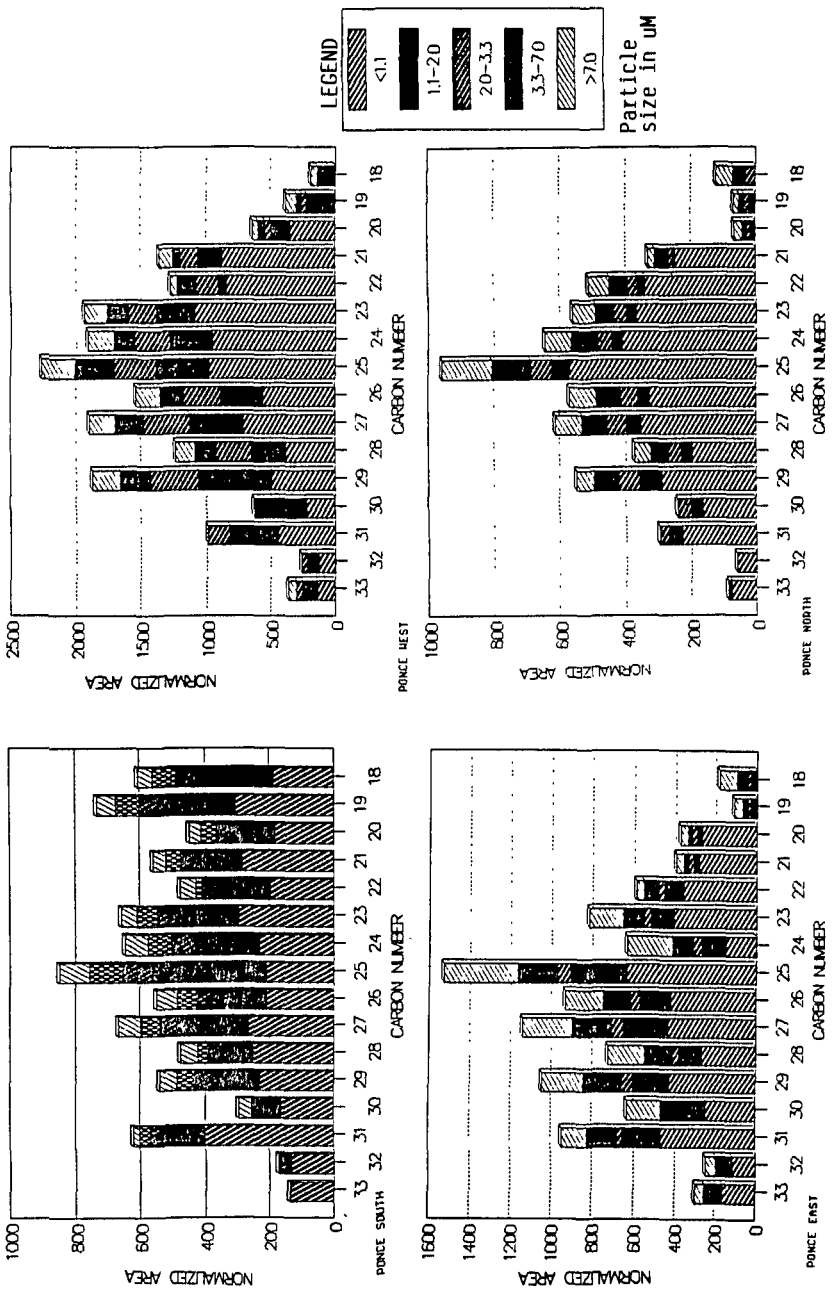

Figure 1. Particle size distribution for n-alkanes in Ponce, PR during 1986

Presented at the 36th ASMS Conference on Mass Spectrometry and Allied Topics
June 5-10, 1988, San Francisco, CA

APPLICATION OF MULTIFUNCTIONAL DERIVATIVE TO THE DETERMINATION OF NITRO-PAH's IN ENVIRONMENTAL SAMPLES BY GAS CHROMATOGRAPHY/MASS SPECTROMETRY

T. A. Dean and C. F. Poole; Wayne State University, Detroit, MI 48202;
J. Auld, The Detroit Edison Company, Engineering Research, Detroit, MI 48210

The N,N-dimethylamino derivative of nitro-PAH's, specifically nitro-pyrenes, provides a powerful analytical tool. Previously the amino derivative has been utilized to enhance the fluorescence of the nitro-PAH under investigation.[1,2] In the case of the amino derivative further sample handling after derivatization is limited by oxygen and light lability. The greater stability of the tertiary N,N-dimethylamine allows a more rigorous sample preparation/clean-up by way of a cartridge type cation exchange(SCX) procedure.[3] It is the SCX procedure that allows greater selectivity and a medium through which the analyte may be concentrated for greater sensitivity.[4]

Experimental

An aliquot of a particulate extract solution is placed in a 5mL vial equipped with a septum cap. If necessary a standard addition is added at this point. Approximately 5mg(½ match head) of Pt/Al_2O_3(5%Pt) catalyst and several drops of 37% formaldehyde solution are added to the reaction vial. After affixing the septum cap the vial is charged with 40psi of hydrogen and placed in a sonicator for 0.5 hour; at which time a fresh charge of catalyst, formaldehyde and hydrogen are added to the reaction vial. The recharge procedure is repeated three times for a total reaction time of 2 hours.

Strong cation exchange cartridges(Supelco SCX) are prepared by first removing the upper frit(it will become plugged by the catalyst fines) and replacing it with a tight plug of glass wool. The SCX surface is activated with 500uL of 0.5M phosphoric acid in 80/20 water/methanol and washed with 50/50 water/methanol. The reaction mixture is passed through the cartridge at a dropwise rate by a low vacuum. The cartridge + mixture is then washed with 500uL of 20/80 water/methanol. The N,N-dimethylamino derivative is eluted from the cartridge with 1.0M ammonia and collected in a 1mL volumetric flask. (See Figure 1)

If no SCX clean-up is to be used, then the derivative must be freed from the surface of the Al_2O_3 catalyst. This is accomplished by the addition of benzene to the reaction mixture, followed by centrifugation. An optimum response, independent of the amount of catalyst was found at a 2 fold dilution(1000uL of benzene added to 500uL of reaction mixture).

Presented at the 36th ASMS Conference on Mass Spectrometry and Allied Topics
June 5-10, 1988, San Francisco, CA

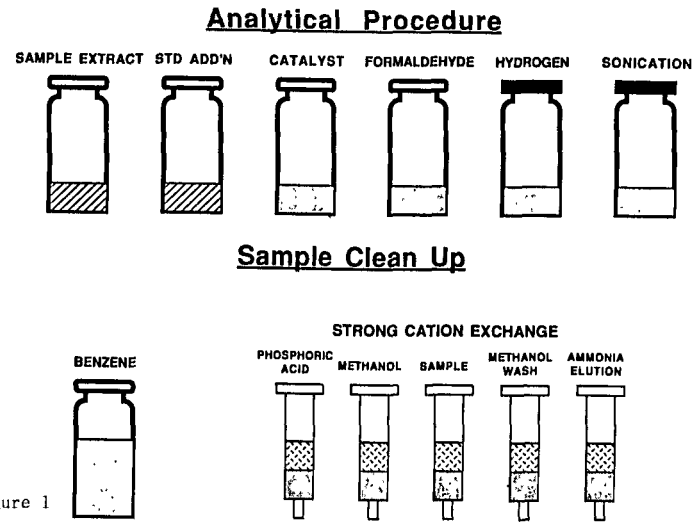

Figure 1

Results

Diesel exhaust, urban air, and coal flyash samples have been successfully analyzed by HPLC/fluorescence. In this particular study analyte concentrations of 50 to 200pg/uL of extract were prepared. Due to the very high fluorescence yield(240ex/370+em) and 10uL injections quantitative HPLC analysis was successful. Unfortunately, due to the limited sample capacity of capillary GC/MS quantitative analysis of these samples was not possible. However, selected ion recording MS analysis did qualitatively indicate the presence of the N,N-dimethylamino derivative at the 50 to 100pg level.

Acknowledgements

D. Schutzle, Ford Motor Company, Dearborn, MI

R. Hood, Central Instrument Facility, Wayne State University, Detroit, MI

References

1. K. K. Brown and C. F. Poole, LC/GC Magzn. 2(1984)526.

2. K. K. Brown and C. F. Poole, HRC&CC 7(1984)520.

3. T. A. Dean and C. F. Poole, JPC-Mod TLC 1(1988)70.

4. T. A. Dean and C. F. Poole, Abstract #585, presented at 14th FACSS Meeting, Detroit, Michigan, 1987.

Presented at the 36th ASMS Conference on Mass Spectrometry and Allied Topics
June 5-10, 1988, San Francisco, CA

A COMPARISON OF GAS, LIQUID AND SUPERCRITICAL FLUID CHROMATOGRAPHIES IN COMBINATION WITH MASS SPECTROMETRY FOR DETERMINATION OF POLYCYCLIC AROMATIC COMPOUNDS IN ENVIRONMENTAL SAMPLES.#

W.D. Jamieson, R.K. Boyd, C.M. Elson*, M.A. Quilliam and P.G. Sim

Marine Analytical Chemistry Standards Program, Atlantic Research Laboratory, National Research Council of Canada, 1411 Oxford Street, Halifax, Nova Scotia, CANADA B3H 3Z1 (* on sabbatical leave from Saint Mary's University, Halifax, Nova Scotia, CANADA B3H 2C3).

Polycyclic aromatic compounds (PACs) are widespread pollutants of well established toxicity. Our interest in analysis for PACs in marine sediments, including development of reference materials, led to a critical evaluation of current protocols for quantitative analyses of 16 polycyclic aromatic hydrocarbons (PAH) designated as priority pollutants by the United States EPA. It was shown (1) that the standard methodology (reversed phase HPLC with single wavelength detection), when applied to real-world complex samples, yields results which combine high precision with high inaccuracy. The latter arises from incomplete chromatographic separations coupled with non-specific detection. We have pursued approaches to this problem which combine different separation selectivities of various chromatographic methods with sensitive and selective detection techniques, of which mass spectrometry (MS) is the most important. As discussed below, some shortcomings of mass spectrometry in this context can be alleviated by simultaneous recording of complete UV spectra using a diode array detector (DAD).

Several chromatographic techniques are available for separations of PACs: **(a)** gas chromatography (GC); **(b)** reversed phase liquid chromatography (RPLC); **(c)** normal phase liquid chromatography (NPLC); **(d)** supercritical fluid chromatography (SFC). Fused silica capillary columns are widely used in GC due to high resolving power and ease of coupling to a wide range of detectors, including MS. LC methods complement very well GC techniques (e.g. LC better for polar PACs, LC vs. GC differences in resolving isomers and interferences in complex mixtures). RPLC and NPLC offer medium resolving power, ability to analyze labile and high molecular weight compounds, excellent quantitative precision, and the possibility of interfacing to selective optical detectors as well as to MS. Though LC techniques are often better at PACs isomer separation than is GC, oxygenated PACs overlap with the PAHs and, given limited resolving power, this can lead to interference problems. Many of the advantages of GC and of LC are combined in SFC, which can be used with either capillary or packed columns (the latter with a wide variety of stationary phases). In our hands the efficiency of SFC is lower than that of the rival methods (almost certainly due to problems of interfacing to detectors); however the polar PACs elute much later than the PAHs, and the resolution within the polar group is also improved. These four separation methods provide complementary separation selectivities for PACs.

Simple ionization detectors, such as the flame ionization detector (FID) in common use with GC, are severely limited (1) in their usefulness in the present context. The photoionization detector (PID) is more selective for PACs; we have shown recently (2) that the PID is also compatible with SFC, and provides excellent sensitivity for PACs, under circumstances (e.g.. high CO_2 flow rates) where FID fails completely. However the PID is also a single parameter detector and is thus of limited

NRCC No. 29012

usefulness in the present context. In the same way, single-parameter detectors based on UV absorption (single wavelength) are reliable only if the chromatographic separation (HPLC or SFC) can guarantee complete separation of all analytes, a practical impossibility (1). Even UV-emission detectors (two parameters) are similarly limited in PACs analysis.

The availability of DADs, permitting complete UV-visible spectra to be acquired across all peaks in a HPLC or (with a high-pressure cell) SFC trace, represents an enormous advance in technology available for trace organic analysis of complex samples. However the information content of a UV-visible absorption spectrum is inherently low, and successful analyses of the present type (1) are not possible using a DAD alone.

The high sensitivity and universal applicability, coupled with high information content (implying high specificity) of MS, makes this technique essential for analyses of complex samples for PACs (1). Interfacing MS to GC and HPLC is now standard methodology; for PACs analyses by HPLC (both normal and reversed phase) we have found the moving belt interface to provide excellent results apart from low transfer efficiencies for the more volatile PACs, e.g. naphthalene (1). Increase in specificity at adequate sensitivity can be achieved by use of medium to high resolving power MS, or in some cases by monitoring the first ^{13}C isotope peak of the doubly-charged molecular ions ("half-massed" MS (3)(4)). The moving belt interface has also proved to be useful for packed column SFC/MS; excellent EI spectra can be thus obtained. Interfacing MS to SFC capillary columns is most easily accomplished by direct insertion of the column to the ion source via a suitable restrictor. We have had good success with this technique by operating the source under CI conditions using the CO_2 mobile phase as reagent gas. In positive ion mode, PACs give essentially only molecular ions with poor ionization efficiencies, presumably via charge exchange. However, in negative ion mode, a rich chemistry is revealed, with evidence for surprisingly effective isomer distinction (5).

Particularly powerful are combinations of several chromatographies plus several detection techniques. For example, a combination of RPLC with DAD plus MS (medium resolving power) in series was shown (6) to be capable of both resolving co-eluting compounds (via the MS reolving power) and also of identifying particular PACs isomers (via the UV spectra). We hope to extend this serial DAD/MS detection strategy to SFC in the near future. Cross-correlation of data from different chromatographies is also a powerful tool in the analysis of complex PACs mixtures (1).

In conclusion, it is emphasised that analysis of real-world samples such as marine sediments for PACs is an exacting task. To obtain reliable data the analyst must call upon all available techniques; simple strategies have been shown (1) to work for only the simplest mixtures.

(1) P.G. Sim et al., Biomed. Env. Mass Spectrom. 14 375 (1987).
(2) P.G. Sim et al., J.Chromatog. (in press).
(3) P.G. Sim et al., Rapid Commun.Mass Spectrom. 1 28 (1987).
(4) P.G. Sim et al., Proc. 11th. Intl. Symp. Polycyclic Aromatic Hydrocarbons, Gaithersburg, MD., (1987), in press.
(5) P.G. Sim and C.M. Elson, Rapid Commun. Mass Spectrom., in press.
(6) M.A. Quilliam and P.G. Sim, J. Chrom. Sci. 26 160 (1988).

Presented at the 36th ASMS Conference on Mass Spectrometry and Allied Topics
June 5-10, 1988, San Francisco, CA

ELECTRON IMPACT MASS SPECTRA OF POLYCYCLIC AROMATIC HYDROCARBONS: A REFERENCE COLLECTION.

Thomas R. Sharp*, Hongmee Lee+, Anna Ferguson#, Kenneth N. Marsh#, Ronald G. Harvey+.

* Center for Chemical Characterization and Analysis, Department of Chemistry, Texas A&M University, College Station, TX 77843.
# Thermodynamics Research Center, Texas Engineering Experiment Station, Texas A&M University, College Station, TX 77843.
+ Ben May Institute, University of Chicago, Chicago, IL 60637.

The polycyclic aromatic hydrocarbons (PAHs) have become an ubiquitous and significant environmental contaminant and, moreover, a major health risk. Although they have been known for many years, and the mass spectra of the basic parent polycyclic systems have been recorded, extensive systematic studies correlating molecular structure with mass spectral details have not been done. Sellier et al. [1] point this out in their recent report on such a study of anthracenes and related compounds.

As a continuation of the Thermodynamics Research Center Spectral Data Program - Mass Spectra (formerly the American Petroleum Institute Research Project 44 - Mass Spectral Data), we report the electron impact mass spectra of a collection of 209 polycyclic aromatic hydrocarbons. Samples which were impure have been purified or otherwise treated in order to include the highest quality data in this collection. The following points have been addressed and summarized as spectra have been collected and examined: the ability to identify compounds by library search procedures; abundance of doubly charged molecular ions; presence of rearrangement reactions; features useful in distinguishing isomeric structures. A significant percentage of these compounds have been found to be carcinogenic in animal tests. The composition of the compound collection is indicated by the class and numbers in Table I. Nomenclature of ring systems is consistent with that of Lee et al. [2].

Table I:

Composition of PAH Collection

# of rings	type	# of compounds
2	naphthalenes	7
2	1,1'-biphenyls	3
2	anthracenes	17
3	phenanthrenes	16
3	fluorenes	6
4	benzanthracenes	77
4	pyrenes	17
4	chrysenes	3
5	benzopyrenes	41
5	cyclopentapyrenes	7
5	dibenzanthracenes	6
	others	9

Our spectra have been searched against the National Bureau of Standards Library on our datasystem (VG 11-250J; 42000 spectra; purity fit search, fit factor 700 or greater). The results are given in Table II. We find that, for the 209 compounds examined, 56% could not be matched to any reference spectrum in the library, and 25% were "erroneously" matched to spectra of other compounds. This "erroneous match" group includes 10% of the compounds which were matched to related isomeric structures, and 15% which were matched to unrelated structures. These results suggest that the PAHs are underrepresented in the NBS library, and that the number of reference spectra in the library needs to be increased.

TABLE II:

NBS Library Search Results

Fits	38	18%
Near fits	21	10%
Wrong fits	32	15%
No fits	117	56%
Total	209	

Observation of doubly charged molecular ions is a nearly universal property in this collection. Jamieson and coworkers [3-5] have recently reported on the analytical utility of these doubly charge ions. 23 compounds exhibit M^{2+} intensities greater than 10% relative abundance. Many of the more highly functionalized compounds produce fragments for which there are observable intensities in the spectrum at 1/2 the mass of the fragment. Although the expectation that the larger PAH systems -- e.g. benzopyrenes -- would exhibit relatively high M^{2+} intensities, the phenanthrenes and fluorenes exhibit high M^{2+} intensities. One third of the phenanthrenes show 10% or higher M^{2+} intensities, and acenaphthylene ($C_{12}H_8$) shows 20% relative abundance of M^{2+}.

Several classes of rearrangements have been observed: neutral loss of CO from carbonyl-containing compounds; loss of H_2 from partially reduced ring systems; loss of HX from certain halogenated compounds: loss of the free acid moiety from esters in which the alcohol

is the PAH. Focusing on the loss of CO, there are 34 compounds in the collection having one or more carbonyl groups. (Esters and free acids are not included in this count.) Over 50% of the aromatic ketones (23 compounds) and aldehydes (7 compounds) exhibited very intense neutral losses of CO from $M^{+\cdot}$, and, for several diones, additional neutral loss of a second CO. Intensities of these $[M-28]^{+\cdot}$ and $[M-28-28]^{+\cdot}$ were typically 50% relative abundance or greater, base peak usually being $M^{+\cdot}$. For three compounds, $[M-28]^{+\cdot}$ is base peak. By contrast, four ketones in which the carbonyl group was located in an aliphatic sidechain exhibited no tendency to fragment by neutral loss of CO.

When possible, series of isomeric compounds have been compared to establish whether the electron impact mass spectrum alone can be used to differentiate between structural isomers or isomer classes. From the large number of benz[a]anthracenes, comparisons have been made of the mass spectra of the mono-, di-, and trimethylbenz[a]anthracenes, which will be described here. Four of the twelve methylbenz[a]anthracenes were recorded here. Eleven of the twelve are represented in the NBS library, and all are selected by library search, with purity fit factors greater than 90%, for each observed spectrum. Only slight differences in the intensities of the two main fragments - $[M-16]^+$, m/z 226 and $[M-27]^+$, m/z 215 - are observed. Differentiation based on mass spectra would not be possible. One would have to rely upon gas chromatography retention times or some other criterion for differentiation.

Spectra for ten of the possible 66 dimethylbenz[a]anthracenes were recorded. Only two isomers are represented in the NBS library - the 1,12- and 7,12- isomers. Ratios of the $[M-15]^+$ (m/z 241) and $[M-17]^+$ (m/z 239) ions change, as well as their relative abundances. Intensities of M^{2+} (m/z 128) and $[M-16]^{2+}$ (m/z 120) also change. Isomers containing a 7-methyl, and especially with a nearby second methyl, produce a large (>25%) $[M-15]^+$, with $[M-15]^+$ also being larger than $[M-17]^+$. These observations suggest that sufficient spectral differences exist to allow identification of these isomers at least into subgroups, if not into individual compounds.

Only eight of the possible 220 trimethylbenz[a]anthracene isomers were examined. Even so, relative abundance changes of $[M-15]^+$ (m/z 255) with respect to $M^{+\cdot}$ (the base peak), and with respect to $[M-31]^+$ (m/z 239) suggest a possible basis for isomer differentiation. The small data set examined, coupled with the fact that the prevalent substitution in the compounds observed is 12- and 7,12-substitution, do not permit our reaching any firm conclusions. However, the striking difference seen is the high $[M-15]^+$ in the one non-12-methylated compound in this data set.

All data were collected on a VG Analytical 70-S mass spectrometer and VG DS 11/250J datasystem. Nearly all of the compounds were crystalline solids, which were introduced into the mass spectrometer on the direct insertion probe. The probe was heated slowly in order to distill the compound being analyzed to evaluate sample purity and to avoid thermal degradation.

Full spectral data of all the compounds in this collection, as well as for a large number of other compounds and compound types, are available from the Thermodynamics Research Center.

Funds from National Science Foundation Grant CHE-8705697 permitted purchase of the mass spectrometer used in this study.

---

1. Sellier, N., Cazaussus, A., Bilger, C., Demerseman, P. (1987). **Org. Mass Spectrom.** 22,719-26.
2. Lee, M.L., Vassilaros, D.L., White, C.M., Novotny, M. (1979). **Anal. Chem.** 51,768-74.
3. Sim, P.G., Jamieson, W.D., Boyd, R.K. (1987). **Rapid Commun. Mass Spectrom.** 1,28-9.
4. Jamieson, W.E., Boyd, R.K., Sim, P.G. (1987). **35th. ASMS Proceedings.** Pp. 123-4.
5. Sim, P.G., Boyd, R.K., Gershey, R.M., Guevremont, R., Jamieson, W.D., Quilliam, M.A., Gergely, R.J. (1987). **Biomed. Environ. Mass Spectrom.** 14,375-81.

Presented at the 36th ASMS Conference on Mass Spectrometry and Allied Topics
June 5-10, 1988, San Francisco, CA

DETERMINATION OF TRANSIENT BIODEGRADATION INTERMEDIATES OF LINEAR ALKYLBENZENESULFONATES (LAS) BY NCI/GC/MS

Michael L. Trehy, William E. Gledhill, Robert G. Orth, Gerry Gasser, Carl B. Roper, B. Mason Hughes, and Victor W. Saeger
Monsanto Company; 800 N. Lindbergh; St. Louis, MO 63167

Hon-Nami and Hanya (1) developed a method to determine alkylbenzenesulfonates by GC/MS after conversion of the sulfonate group to the methyl sulfonate derivative. The derivatization procedure involved treatment with phosphorus pentachloride to form the acid chloride followed by treatment with methanol to convert the acid chloride to the methyl ester. In this paper we describe the advantages of using trifluoroethanol in place of methanol and have extended the derivatization procedure to include both linear alkylbenzenesulfonates (LAS) and the sulfophenylcarboxylates (SPC) which appear as transient intermediates during biodegradation of LAS. The formation and disappearance of the SPC can be followed both in laboratory microcosm experiments and by analysis of wastewater samples. No significant interferences were observed for the GC/MS method which permitted full scan spectra for samples spiked at 0.2 ppm.

The method offers significant improvements in sensitivity and selectivity over methods described in the literature. SPC can be determined by LC with UV detection (2) and by GC/MS after desulfonation (3). However both methods have significant drawbacks. The LC methods lacks sufficient selectivity and the ability to identify the SPC in environmental samples. The desulfonation technique is more complicated and can not differentiate sulfonates other than LAS and their corresponding carboxylic acids from LAS and its corresponding carboxylates. Although derivatization with diazomethane is possible (2) the reaction was difficult to reproduce and is hazardous. The trifluoroethyl ester derivatization procedure is relatively simple and selective for the sulfonates. The presence of the trifluoroethyl group greatly enhances sensitivity for NCI. A full scan mass spectrum is possible for 3 nanograms of sample. The sample derivatization procedure is described below. The derivatives are stable in hexane for at least a month. The method described below has a limit of detection of approximately 0.1 mg/L in full scan mode.

1. Evaporate a 4 ml sample in a Reacti-vial to dryness with a stream of nitrogen.
2. Add approximately 20 mg of phosphorus pentachloride, cap the vial and heat at 110 degrees centigrade for 3 minutes. Allow to cool.
3. Add 1 ml of hexane and extract for 1 minute on a Vortex Genie. Transfer the hexane to another Reacti-vial and evaporate to dryness with a stream of nitrogen.
4. Add approximately 0.3 ml of trifluoroethanol and heat at 70 degrees centigrade for 20 minutes. Allow to cool.
5. Add approximately 1 ml of hexane and 1 ml of deionized water and immediately extract for 1 minute on a Vortex Genie.
6. Transfer the hexane to another vial and concentrate to approximately 0.2 ml with a stream of nitrogen.

The LAS and SPC trifluoroethyl esters all have the m/z ion 163 as a characteristic MS fragment for $SO_3CH_2CF_3$ which can be used to selectively identify the sulfonates in complex environmental matrices. In addition, the mass

spectra for sulfonates also contain the parent ion and a fragment ion corresponding to the loss of trifluoroethanol in the case of SPC while LAS loses m/z 99 corresponding to the loss of the trifluoroethoxy group. In Figure 1 the parent ions corresponding to the SPC are plotted. The presence of the SPC can be detected. When the effluent of more efficient wastewater treatment processes, such as an activated sludge plant were analyzed the SPC were below the limit of detection of the present method. The relative absence of SPC isomers in the activated sludge wastewater treatment plant effluents indicates that all the isomers formed on biodegradation of LAS are further biodegraded. Biodegradation was not hindered by a recalcitrant isomer.

References:

1. H. Hon-Nami and T. Hanya. "Gas-liquid chromatographic-mass spectrometric determination of alkylbenzenesulphonates in river water" J. Chromatography (1978) 161:205-212.
2. Eggert, C.R.; Kaley, R.G.; and Gledhill W.E. Application of a laboratory freshwater lake model in the study of LAS biodegradation. In Proc. of the Workshop: Microbial Degradation of Pollutants in Marine Environments (A.W. Bourquin and P.H. Pritchard, eds.), U.S. EPA Report No.600/9-79-012, 1979, pp. 451-461.
3. Leidner, H.; Gloor, R.; Wuest, D.; and Wuhrmann, K.; "Biodegradation kinetics of LAS" Tenside (1976) 13:122-130.

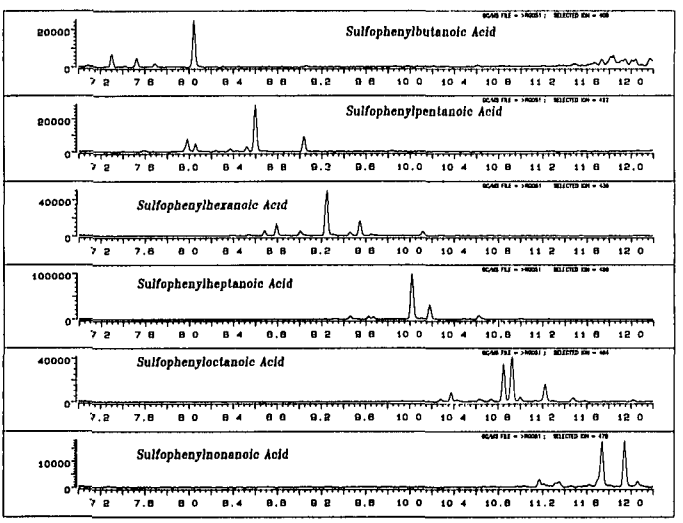

Figure 1. Reconstructed ion chromatogram for the parent ions corresponding to the SPC formed on biodegradation of LAS. The sample is from a trickling filter wastewater treatment plant in Wichita, Kansas.

Presented at the 36th ASMS Conference on Mass Spectrometry and Allied Topics
June 5-10, 1988, San Francisco, CA

THE EFFECT OF SURFACE ACTIVITY ON QUANTITATION OF LINEAR ALKYLBENZENE SULFONATES [LAS] BY FAST ATOM BOMBARDMENT MASS SPECTROMETRY.

J. D. Wernery, D. K. Brain, and D. A. Peake,

The Procter and Gamble Corporation, Cincinnati, OH 45217.

BACKGROUND. Quantitation of sodium linear alkylbenzene sulfonates (LAS) in detergents requires time consuming sample preparation and chromatography steps. Our first attempts to quantitate LAS by FAB MS using a single deuterated C_{12}LAS internal standard (1) resulted in errors of ca. 10-20% for alkyl chainlength distributions, compared to results obtained by desulfonation and GC analysis (DS/GC, 2) of the resulting alkylbenzenes.

Barber and co-workers (3) first recognized the role of surface activity in obtaining FAB mass spectra. Ligon and Dorn (4) used a homologous series of quaternary ammonium salts to demonstrate longer-chain surfactants dominate the glycerol surface, resulting in enhanced sensitivity relative to shorter-chain homologs.

SURFACE ACTIVITY vs CONCENTRATION. Because LAS homologs of different chainlengths have different surface activities and solubilities in the glycerol matrix, the distribution of sputtered LAS anions is skewed relative to the molar ratios of LAS homologs in solution. FAB(-) mass spectra were acquired from 10^{-2} to 10^{-4}M of C_{10}-, C_{12}- and C_{14}LAS in glycerol (Table 1). At lower [LAS], the abundance of C_{14}LAS is enhanced relative to the shorter-chain homologs. As [LAS] increases, the relative abundance of C_{10}LAS increases relative to C_{12}- and C_{14}LAS.

EFFECT OF ACQUISITION TIME. Changes in relative abundances for the equimolar mixture were also observed as a function of scan time. At the beginning of the run, and at lower [LAS], the more surface active species predominate. As the glycerol droplet evaporates, and at higher [LAS], the relative abundance of C_{10}LAS increases. Thus, the relative abundance of LAS homologs is highly dependent on [LAS] and signal averaging time.

QUANTITATION. To compensate for the surface activity differences between the LAS homologs, three deuterated internal standards [d_7-C_{10}, -C_{12}, and -C_{14}LAS] were chosen to bracket the LAS chainlength distribution. Calibration curves were obtained by monitering the d_0/d_7 abundance ratios vs ug LAS standard added. Negative ions monitored were:

C_{10}LAS	(d_0)	m/z 297	(d_7)	m/z 304
C_{11}LAS		m/z 311		
C_{12}LAS		m/z 325		m/z 332
C_{13}LAS		m/z 339		
C_{14}LAS		m/z 353		m/z 360

A series of pure 2-alkylbenzene sulfonate mixtures was analyzed to demonstrate the accuracy of the FAB MS method (Table 2). By using the internal standard approach, the homolog distribution and total amount of LAS determined are typically within ± 5% of the weighed amounts.

A commercial mixture of LAS was analyzed by FAB MS and the results compared with those obtained by DS/GC (Table 3). Without the use of internal standards, the FAB MS data is skewed relative to the DS/GC data. For example, the relative abundance of the C_{10}LAS homolog is 20% higher relative to the GC results. The homolog distribution obtained by FAB MS using the internal standard approach and by the DS/GC method are identical within the experimental error of the two techniques.

CONCLUSION. Bracketing with several isotopically labeled internal standards compensates for differences in surface activity of LAS homologs. FAB MS has major advantages over other methods in specificity, speed of analysis, and eliminates the need for sample cleanup.

Presented at the 36th ASMS Conference on Mass Spectrometry and Allied Topics
June 5-10, 1988, San Francisco, CA

REFERENCES

1. S. R. Ward, J. R. Simms, B. L. Moore, M. M. Bandurraga, T. Keough, Presented at the 35th ASMS Conference, May 24-29, 1987, Denver, CO.
2. Q. W. Osburn, J. Am. Oil Chem. Soc., 1983, 63, 257.
3. M. Barber, R. S. Bardoli, G. J. Elliot, R. D. Sedgewick, and A. N. Tyler, J. Chem. Soc., Faraday Trans. 1, 1983, 79, 1249.
4. W. V. Ligon and S. B. Dorn, Int. J. Mass Spectrom. Ion Processes, 1984, 61, 113.

TABLE 1. RELATIVE ABUNDANCE OF EQUIMOLAR LAS MIXTURE VS. [LAS]

[LAS] M	RELATIVE ABUNDANCE (% ERROR) C10LAS	C12LAS	C14LAS
0.0001	28.2 (-15)	34.6 (+4)	37.2 (+12)
0.0010	29.9 (-10)	35.2 (+6)	34.9 (+5)
0.0100	39.8 (+19)	31.5 (-5)	28.7 (-14)

TABLE 2. ANALYSIS OF MODEL MIXTURES

ug LAS (TOTAL)	WEIGHT % LAS (% ERROR) C10	C12	C14
Added 418	30.6	33.4	36.0
Found 388	29.8	34.2	36.0
% Error = -7	(-3)	(+2)	(0)
Added 151	34.9	33.3	31.8
Found 145	33.1	35.2	31.7
% Error = -4	(-5)	(+6)	(0)
Added 110	20.3	60.2	19.5
Found 113	19.6	60.6	19.8
% Error = +3	(-3)	(+1)	(+1)

TABLE 3. ANALYSIS OF LAS MIXTURE

METHOD	WEIGHT % LAS (% Difference, a) C10	C11	C12	C13	C14
DS/GC	11.2	29.1	32.4	24.9	2.4
FAB MS (Int Stds)	11.6 (+4)	29.7 (+2)	33.0 (+2)	23.5 (-5)	2.2 (-8)
FAB MS (b) (No Std)	13.5 (+20)	31.1 (+7)	31.5 (-3)	22.0 (-12)	2.0 (-17)

(a) Difference between DS/GC and FAB MS Results.
(b) Calculated from Relative Abundance Data.

Presented at the 36th ASMS Conference on Mass Spectrometry and Allied Topics
June 5-10, 1988, San Francisco, CA

ANALYSIS OF SULFONATED AZO DYES USING FAB AND CONTINUOUS FLOW FAB/MS

by

D.L. Miller and L.J. Peterson-Wright

Idaho National Engineering Laboratory, EG&G Idaho, Inc.
P.O. Box 1625, Idaho Falls, ID 83415

Increased interest in the ability to identify and quantitate environmental contaminants not amenable to conventional GC/MS analysis has been displayed by environmental scientists and regulatory agencies. This interest has resulted in the examination of a variety of compound classes not amenable to GC/MS and in the development and application of a variety of new analytical methodologies.

A compound class that has received considerable attention in the literature is that of the sulfonated azo dyes. Even though a great deal of work on azo dyes has been performed additional research is needed due to the large numbers of different dyes and their widely varying properties.

Thirteen sulfonated azo dyes (Aldrich Chemical) containing two, three, or four sodium sulfonate groups were examined as pure compounds and as aqueous solutions. The dyes were used as received from the supplier. All experiments were conducted on a Kratos MS890 equipped with an 8 kV MS50 type FAB source and an Ion Tech 11NF saddle field ion gun. Xenon was used in all experiments for the FAB gas. The thirteen azo dyes examined are given below.

Acid Black 24	Acid Violet 5
Acid Blue 80	Benzopurpurin 4B
Acid Blue 113	Brilliant Yellow
Acid Orange 63	Direct Orange 31
Acid Red 37	Direct Red 81
Acid Red 114	Direct Yellow 50
Acid Red 151	

All of the dyes were examined in both positive and negative ion modes of detection. The various dyes were examined using a variety of FAB matrices which included glycerol, thioglycerol, polyphosphoric acid, 3-nitrobenzyl alcohol, triethanolamine, PEG-600, and tetramethylene sulfone.

Peaks indicative of dyes were observed for nine of the thirteen dyes. For the remaining dyes peaks were observed which did not arise from the matrix but which could not be correlated with the know structure of the various dyes. It is believed that these unknown peaks are from other compounds present in the dye formulations which range from 40 to 100 percent dye. The most successful matrix was found to be thioglycerol which produced spectra for eight of the thirteen dyes, followed by 3-nitrobenzyl alcohol and glycerol which were useful for eight dyes and four dyes respectively. The remainder of the matrices examined were useful for no more than three of the thirteen dyes examined. In general, the best results were obtained using the negative ion detection mode. For the majority of the dyes examined the predominant spectral feature was the loss of a sodium from the intact dye molecule. In the case of the positive ion mode protonated molecular ions were observed as well as other ions indicative of fragmentation of the dyes. In many cases, using both positive and negative ion mode, peaks were observed which were believed to be due to other materials present in the dye formulations, which as was mentioned earlier were as low as forty percent dye. HPLC analysis was performed on a sample of the Acid Blue 80 used in

these experiments to determine the number of components present in the formulation. Acid Blue 80 was chosen due to the fact that this particular dye gave the most intense spectrum in both positive and negative ion mode and worked with five of the six matrices used. The results of the HPLC analysis indicated the presence of at least nine components three of which could be considered major components. Based on these results it was decided to investigate the use of continuous flow FAB/MS for applicability to analysis of azo dyes.

The continuous flow experiments were conducted using a commercially available system obtained from Kratos Analytical. An Isco uLC 500 pump was used to provide flow through the continuous flow probe at rates ranging from one to four microliters per minute. Acid Blue 80 solution (1 microliter) was injected into the flow stream of the probe using the HPLC injection valve supplied with the flow probe system. A variety of solvent systems were investigated but the majority of the work was performed using a 95:5 water/glycerol solution. Good results were obtained using the continuous flow system combined with both positive and negative ion detection modes. Spectra obtained using the flow probe system showed good agreement with those obtained using a conventional FAB probe. Experiments conducted in the positive ion mode were complicated by the fact that sodium dissociated from the dye appears to pass through the flow probe faster that the dye itself, resulting in a high degree of reaction with the glycerol present as the matrix. Repetitive injections of dye build up a large background of sodium/glycerol peaks which require a significant amount of time to purge out of the system (approximately one hour after four one microliter injections of 1 ppm dye solution). This behavior was not observed when negative ion mode was used although the overall sensitivity was lower in the negative ion mode. Based upon these results work is currently underway in which on-line HPLC separation and introduction via the continuous flow FAB system is being investigated. Of particular interest is the question whether dyes that did not yield spectra will do so once they are separated from the remainder of compounds present in the commercially available formulations.

The submitted paper has been authorized by a contractor of the U.S. Government under DOE Contract No. DE-AC07-76ID01570. Accordingly, the U.S. Government retains a nonexclusive, royalty-free license to publish or reproduce the published form of this contribution, or allow others to do so, for U.S. Government purposes.

Presented at the 36th ASMS Conference on Mass Spectrometry and Allied Topics
June 5-10, 1988, San Francisco, CA

Comparison of Dynamic and Equilibrium Head-Space Sampling of EPA Volatile Organic Compounds with Ion Trap Detection

Adam J. Patkin, Perkin-Elmer Corporation Norwalk, CT 06859-0090

The techniques of dynamic, or "purge and trap", and equilibrium head-space with ion trap detection are compared for the analysis of EPA regulated volatiles in water. Dynamic head-space is found to have lower detection limits, while equilibrium head-space is faster, easier, and eliminates carry-over.

INTRODUCTION

The U.S. Environmental Protection Agency (EPA) has promulgated the EPA series 500 and 600 methods for the GC/MS analysis of organic compounds is clean and waste water. Method 624 is for the analysis of waste water and Method 524.2 for clean, or drinking, water. Both methods specify the use of a dynamic head-space, or "purge and trap" sampler.

EXPERIMENTAL - Dynamic Head-space

EPA method 524.2 was used for the experimental conditions. Two modifications were made. First, the LSC-2 trap was desorbed and baked at 225 °C. This was found to improve the chromatographic resolution of early eluting gas peaks be more effective at removing residual water from the trap than the specified 180 °C. Second, the mass range was scanned from 50 to 300 μ instead of the 35 to 300 μ specified in the method. This removed interference caused by the methanol solvent of the standard with the co-eluting bromomethane. The 35 to 300 μ range could be used, but the results would then need to be displayed as a 50 to 300 μ mass chromatogram to show bromomethane at trace levels.

EXPERIMENTAL - Equilibrium Head-space

A 0.32-mm ID column with a 5μm methyl silicone phase was used, in contrast to the 0.53mm ID, 3μm VOCOL phase of Method 524.2. This thick film capillary column was found to give excellent retention of the purgable gases (chloromethane, vinyl chloride, and bromomethane) at 45 °C, eliminating the requirement of sub-ambient cooling found in the EPA 524.2 method. A faster temperature program halved the chromatogram length. The much shorter cycle time of equilibrium head-space makes up to four analyses per minute possible.

DISCUSSION

Table 1 shows the detection limits for dynamic head-space with the Ion Trap Detector, while Table 2 shows the detection limits for equilibrium head-space. Comparing Tables 1 and 2, the dynamic head-space approach is seen to be more sensitive than equilibrium approach. This is for two primary reasons. First, the dynamic method exhaustively purges the water sample, while the equilibrium method only samples a portion of the equilibrated head-space. Second, the dynamic method uses 25 ml of water, and the equilibrium method only 2 ml.

Equilibrium head-space, while not sufficiently sensitive for clean water analysis, has several significant advantages for waste water determinations.

Equilibrium head-space is faster than dynamic. After the sample is thermostatted, the injection cycle takes only 36 seconds. This compares to about one half hour with dynamic head-space. Several samples can be thermostatted at once, and automated analysis of up to 100 samples is possible. The oven cools to 45 °C, rather than 10 °C, eliminating the need for expensive and cumbersome sub-ambient cooling.

Equilibrium head-space is easier than dynamic. Sample preparation consists solely of hermetically sealing the sample in the vial. This can be performed at the analysis site, eliminating possible sample loss during laboratory transfers.

Equilibrium head-space is better suited for dirty or complex samples than dynamic. There are no frits or small diameter openings to become obstructed. Since the sampling vial is disposable, there is no cleaning required. The disposable sample vial eliminates any chance of sample cross-contamination.

CONCLUSIONS

Dynamic head-space with the Ion Trap Detector greatly exceeds the required EPA 524.2 method detection limits.

Equilibrium head-space with the Ion Trap Detector is less sensitive than dynamic, but still exceeds the required waste eater EPA 624 method limits with the Ion Trap Detector. It is also much more suitable than dynamic head-space for the analysis of dirty samples, such as sludges or soils.

Table 1. Dynamic Head – space

Compound Name	Detection Limit	EPA 524.2 MDL
Chloromethane	0 17 ng/L	130 ng/L
Vinyl Chloride	0 63	170
Bromomethane	11.	110
Trichlorofluoromethane	0.79	80
1,1 – Dichloroethene	4.7	120
Methylene chloride	0 073	30
trans – 1,2 – Dichloroethene	2.0	60
1,1 – Dichloroethane	1 6	40
Chloroform	0 25	30
1,1,1 – Trichloroethane	0 22	80
Carbon tetrachloride	2.4	210
Benzene	0 23	40
1,2 – Dichloroethane	0 31	60
Trichloroethene	8 8	190
1,2 – Dichloropropane	5 7	40
Bromodichloromethane	0.94	80
2 – Chloroethyl vinyl ether	0.16	n/a
cis – 1,3 – Dichloropropene	0.52	n/a
Toluene	0 057	110
trans – 1,3 – Dichloropropene	0 56	n/a
1,1,2 – Trichloroethane	0 69	100
Tetrachloroethene	0 54	140
Dibromochloromethane	1 4	50
Chlorobenzene	0 092	40
Ethylbenzene	0.096	60
Bromoform	0 54	120

Table 2. Equilibrium Head – space

Compound Name	Detection Limit	EPA 624 MDL
Chloromethane	0 57 µg/L	nd µg/L
Vinyl Chloride	0.14	nd
Bromomethane	1.5	nd
Trichlorofluoromethane	0 076	nd
1,1 – Dichloroethene	0 56	2.6
Methylene chloride	1 1	2.8
trans – 1,2 – Dichloroethene	1.2	1 6
1,1 – Dichloroethane	0 34	4 7
Chloroform	0 19	1.6
1,1,1 – Trichloroethane	0 13	3 8
Carbon tetrachloride	0 27	2.8
Benzene	0 096	4 4
1,2 – Dichloroethane	0 76	2.6
Trichloroethene	0.52	1 9
1,2 – Dichloropropane	0 57	6.0
Bromodichloromethane	0 25	2.2
2 – Chloroethyl vinyl ether	4.7	nd
cis – 1,3 – Dichloropropene	1 4	5.0
Toluene	0.17	6.0
trans – 1,3 – Dichloropropene	1.4	nd
1,1,2 – Trichloroethane	0 83	5.0
Tetrachloroethene	0 15	4.1
Dibromochloromethane	0 59	3 1
Chlorobenzene	0 14	6.0
Ethylbenzene	0 26	7.2
Bromoform	1.1	4.7

Presented at the 36th ASMS Conference on Mass Spectrometry and Allied Topics
June 5-10, 1988, San Francisco, CA

SUMMARY OF RESULTS FROM THE GC/MS ANALYSIS OF A WASTE BIODEGRADATION STUDY

by
B. Mason Hughes, D. E. McKenzie, M. Bianchini-Akbeg
W. J. Adams, B. J. Simpson, J. M. Lee, and R. A. Kimerle
Environmental Sciences Center
Monsanto Company
St. Louis, Missouri 63167

ABSTRACT

A microbial treatment study was conducted with solid waste from polystyrene manufacturing. Contaminated soil containing polystyrene waste was subjected to microbial degradation using a batch reactor system. The overall experimental design and biological results of this study are not discussed in this summary. This presentation summarizes the capillary GC/MS analysis methods, results of these analyses, and major conclusions which can be drawn from these data. These results indicate that polystyrene wastes can be successfully degraded using this process. Various organic components of the waste were removed with degradation half-lives ranging from 24 to 72 hours.

INTRODUCTION

The primary factor that affects the cost of cleanup of a chemical waste site is the decontamination method used to remove the various contaminants from the site. To date, incineration has been the primary technique for the disposal of organic contaminants. In specific instances where wastes contain almost 100% organic components and have good BTU content, incineration can be both cost effective and environmentally sound. However, when the site consists primarily of soil which contains less than 10% organic components, microbial treatment costs can be lower than incineration costs, since neither incinerator fuel nor large incinerators are required. However, in order to use a potentially less expensive microbial treatment approach, it must be demonstrated that this alternative can actually reduce the amount of organic components below certain acceptable concentrations. The present paper summarizes results from a laboratory scale biological treatment study which was conducted using low-level polystyrene wastes.

SUMMARY

A laboratory batch biodegradation study, using an Aqueous/Soil Biotreatment Approach, was conducted in the spring of 1987. The purpose of this study was to evaluate the biodegradability of polystyrene waste, using indigenous microflora present in the soil. This presentation summarizes the analytical methods used, and important conclusions drawn from this study.

Seven biodegradation reactors (A - G) were analyzed in duplicate over a fourteen-day period. All reactors, except C and G, contained wastes. Reactors A and B were duplicate reactors to which mercuric chloride had been added. (Mercuric chloride was added as a bacteriacide.) Bioreactor D was a closed reactor and contained active microorganisms. Reactors E and F were duplicate reactors and contained active microorganisms. Reactors C and G, extraction glassware, and solvents were used for method blanks in this study. No quality control blanks contained any of the analytes of interest above the instrument level of detection, indicating that no false positives were reported. Anthracene-d_{10} was used as an internal standard and a system performance standard, a standard of crude oil, and a representative styrene waste were analyzed daily. These steps decreased the likelihood that false positives were measured.

Reaction vessels A, B, E, and F were sampled in duplicate on days 0, 1, 2, 3, 4, 5, 6, 7, 10, and 14 of the study. Reaction vessel D was sampled in duplicate on days 0, 7 and 14 Ten-mL sample aliquots were extracted with methylene chloride and the extracts were analyzed for extractable compounds. Instrumental analysis methods were developed so that concentration information for the major extractable chromatographable compounds in the waste could be obtained in each of the extracts. Figure 1 shows that over 95% of chromatographable components of the waste in the key reactors were reduced to non-detectable levels within 120 hours.

EXTRACTABLE ANALYTE IDENTIFICATION

Detailed compound identification can be best accomplished only after all possible isomers of identified compounds are obtained and retention times of authentic standards are compared to the retention times of the components in the waste. However, this detailed identification was not considered critical to the present study since degradation profiles of compounds and relative changes in concentration, were of primary concern. Therefore compounds which were not uniquely identified by standard library search algorithms were identified by molecular formula and/or molecular weight, when possible. No new chromatographable components were detected during the study, indicating that no new chromatographable degradation products were produced during biodegradation. Therefore, from a waste delisting standpoint, no priority pollutants or other chromatographable compounds should be present which could complicate proper disposal of these biodegradation wastes. Four representative degradation profiles are shown in Figure 2.

Figure 1. Total Concentrations of Waste Components in Vessels A, B, D, E, and F

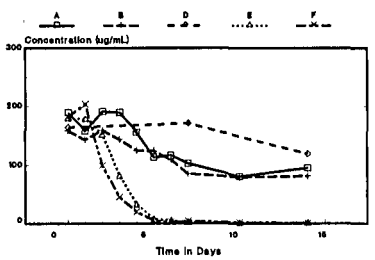

Figure 2. Biodegradation Profiles for Selected Analytes of Vessel E

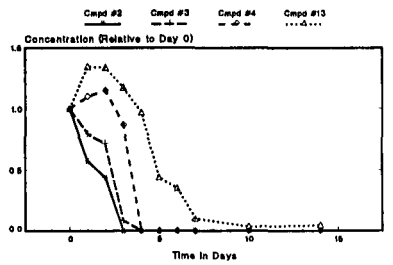

DATA ANALYSIS APPROACH

In order to study the degradation of a large number of compounds in a large number of samples, without sacrificing data quality, the present instrumental analysis approach was devised. Analysis difficulty was increased since many of the organic components were unknown and specific standard reference materials could not easily be obtained within the time constraints of the study. This analysis approach required that sixteen compounds, in seven biodegradation reactors, at ten different days, each be analyzed in duplicate. This resulted in the analysis of sixteen compounds in approximately 100 reactor samples. Approximately two-thirds of these samples contained the sixteen compounds of interest, with the remaining one-third being method blanks, reactor blanks, and QA/QC samples which did not contain the total array of analytes. However, the remaining 100 samples resulted in the generation of 3,200 concentration values and 4,800 additional values which required summing, averaging, and displaying in an efficient manner. Thus the GC/MS study was divided into data acquisition and data analysis phases which were designed to be interrelated and to produce high quality data in a cost effective manner.

Data Acquisition. An internal standard was used to estimate the absolute amounts of each analyte present in each extract. Analyte concentrations were calculated by using the total ion (or selected ion) areas of the analytes, the total ion (or selected ion) area of the internal standard, and the concentration of the internal standard to calculate the "Total Ion Concentrations" or "Selected Ion Concentrations". Figure 3 shows an example of output used to evaluate data quality and Figure 4 shows a portion of the capillary chromatogram and mass spectra of selected waste components.

Data Analysis. Capillary GC/MS analysis of each extract yielded: selected ion areas, total ion areas, retention times, and delta-retention times for all of the analytes in all samples analyzed. Figure 3 gives an example of the graphical data from which this information was obtained. The various digital data was stored in an ASCII file, corrected using EDIT/1000 when errors were observed, transferred to a personal computer, and imported into a LOTUS/1-2-3 template file for further data manipulation and display. Figures 1 and 2 are examples of portions of these reduced data displays. AdvanceLink on the HP-150 and Vectra ES/12 personal computers was used to transfer these ASCII files to the PCs, and 1-2-3 macros were used to assure that these files were placed in specific positions within the template file. Once imported to the template file, a format line was added to define what types of variables were present in the ASCII file and the ASCII data was then parsed into specific 1-2-3 cells. This data analysis approach assured that the primary mass spectrometric data was properly obtained, and that there was a minimum of transcription errors in the data transfer process.

Figure 3. Example of HP-1000 Output Used to Evaluate Data Quality

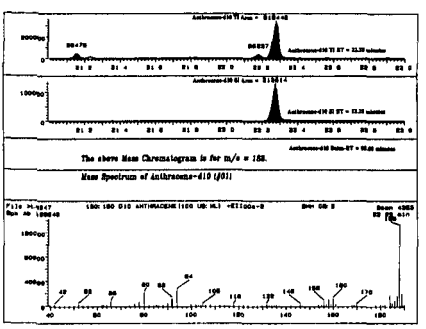

Figure 4. Capillary Chromatogram and Mass Spectra of Selected Components

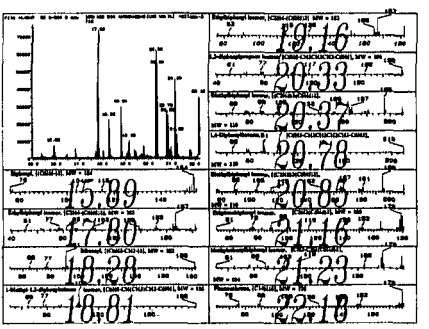

Presented at the 36th ASMS Conference on Mass Spectrometry and Allied Topics
June 5-10, 1988, San Francisco, CA

U.S. EPA NATIONAL DIOXIN STUDY

RESULTS AND CONCLUSIONS FROM PHASE I, INTRODUCTION OF PHASE II

Douglas W. Kuehl, Brian C. Butterworth
U.S. Environmental Protection Agency
Environmental Research Laboratory-Duluth
6201 Congdon Boulevard
Duluth, Minnesota 55804

Donald Bahnick and Ray L. Hanson
CLSES, University of Wisconsin, Superior, WI 54880

In 1981 the Environmental Protection Agency initiated Phase I of the National Dioxin Study (NDS), a survey of sources, fate and distribution of 2,3,7,8-TCDD. The Environmental Research Laboratory at Duluth was responsible for the coordination of samples for Tier 7, an assessment of TCDD background levels, and for the analysis of fish. During the course of this study, we have made several progress reports at this conference[1,2]. that included assessment of QA/QC criteria for both low and high resolution mass spectrometry, and have offered unique ideas for the determination of a minimum level of quantification[3]. A report presenting the results of Phase I has been presented to Congress[4], and Phase II has been initiated. The objective of this presentation is to discuss results and conclusions of Phase I and to introduce Phase II.

Phase I: Samples were collected for analyses in three different categories, statistically selected sites, regionally selected sites, and sites in the Great Lakes. It was found that none of the fish from the statistically selected sites (N=90) were above the action level for human consumption, 25 pg/g, and that no detectable level (1 pg/g) of TCDD was found in 79% of the samples. These results contrast Great Lakes sites where 79% of the samples did contain TCDD (N=29), 8% of which were >25 pg/g. Thirty-one percent (31%) of the regionally selected sites (N=276) were positive with levels ranging to 85 pg/g. It was observed that fish collected near Kraft pulp and paper mills were more frequently positive and contained higher levels of TCDD than those of other watersheds[5].

Phase II: Phase II analytes include all biosignificant PCDDs and PCDFs, mercury, PCBs, and 50 industrial chemicals/pesticides. A primary objective of the PCDD/PCDF analyses is to further investigate the influence of pulp/paper mill discharge upon fish contamination. Over 400 bottom feeding fish are to be analyzed for Phase II. Preliminary results from the analyses of 171 fish showed that 66 samples had a total toxicity equivalent (TEF) value of 2.5 pg/g or greater. Of these samples, 33 of 33 samples collected below pulp and paper mills were positive for 2,3,7,8-TCDD, ranging in concentration from 1-118 pg/g with an average value of 17.4 pg/g. The other 33 positive samples, sites other than pulp/paper discharges, ranged in concentration from 1-34 pg/g, with an average value of 7.2 pg/g.

Analyses of these samples for PCBs and other industrial chemicals indicates that PCBs continue to be a major contaminate in fish. In addition, a mass spectral library of non-target analytes, including both identified and not identified entries, is being compiled. The library includes information on the frequency that a spectrum is observed and information on the types of industrial activities within the sampled watershed. Over 135 entries have been made into this library. An example of an unknown (Figure 1) frequently found in fish from watersheds receiving pulp/paper mill discharge is shown below.

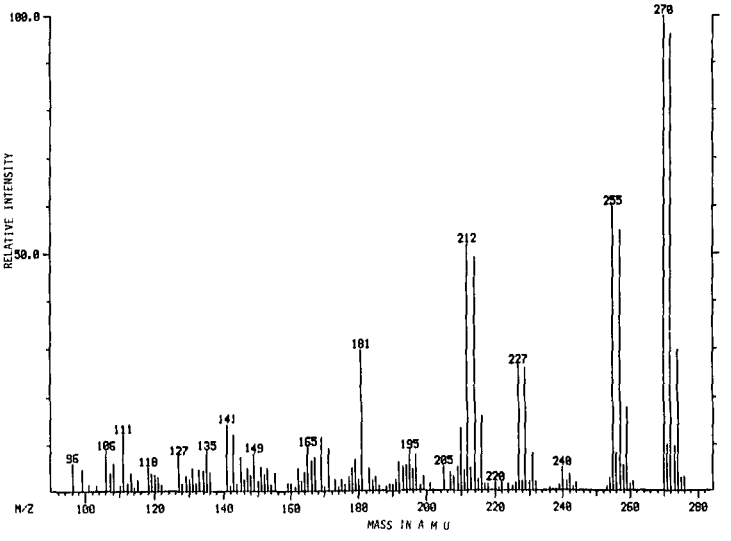

Mass Spectrum of Unknown in Fish
Figure 1

References

1. Kuehl, D.W. et al. 33rd Annual Conf. on MS and Allied Topics, 1985, p 676.
2. Kuehl, D.W. et al. 34th Annual Conf. on MS and Allied Topics, 1986. p. 373.
3. Kuehl, D.W. et al. Analytical Chemistry 58:1598 (1986).
4. U.S. EPA National Dioxin Study: Tiers 3,5,6 and 7. EPA440 14-87-003, February, 1987.
5. Kuehl, D.W. et al. Biomed. and Environ. Mass Spec., 14:493 (1987).

Presented at the 36th ASMS Conference on Mass Spectrometry and Allied Topics
June 5-10, 1988, San Francisco, CA

ISOTOPE DILUTION MASS SPECTROMETRY IN THE ANALYSIS OF ENVIRONMENTAL SAMPLES. A COMPARISON OF EPA METHODS 1624/1625 AND 624/625.

M.C. Shepherd, P.J. Schrynemeeckers, D.A. Hayes, S.K. Mertens, F.L. Shore
Radian Corporation, P.O. Box 201088, Austin, TX 78720-1088

EPA Methods 624 and 625 are the usual required protocols for determining the organic "priority pollutants" in the water and wastewater matrices. Method 624 is the purge-and-trap GC/MS method for volatile organics using internal standard quantitation while Method 625 is the capillary GC/MS method for acid-base/neutral extractable organics. Both of these methods are subject to varying purging/extraction efficiencies of analytes versus internal standards or surrogate compounds from matrix to matrix.

To further improve the performance of GC/MS analyses for priority pollutants, Methods 1624 and 1625 were developed incorporating isotope dilution mass spectrometry for quantitation of target analytes. By spiking the sample with a known amount of a stable isotopically labeled compound for each analyte and quantitating against the labeled compound, the analyses would be automatically corrected for variances in purging or extraction efficiency. The addition of the labeled standards complicates the analysis by doubling the number of quantitation ions to be monitored. The increased number of ions being monitored increases the potential for the analysis to suffer interferences, especially from hydrocarbons. However, the option for internal standard quantitation is always available.

A comparison of the results from the isotope dilution methods versus the internal standard methods was performed for a set of nine wastewater samples. Some of the results of these comparisons are given in Table 1 and 2. Only those compounds that were detected in at least one of the nine samples are reported. The agreement is generally good (within factors of 2). While the target compound quantitation is comparable between the two methods, Methods 1624/1625 also require quantitation of labeled compound recoveries. In several of the samples analyzed in this study the internal standards suffered severe interferences from non-target hydrocarbons, thus making quantitation of labeled compound recoveries difficult if not impossible.

Associated with performing the isotope dilution methods are problems with labeled compound standards. Both expense and stability are critical factors. A complete set of standards which costs in excess of $3000 has a shelf life of approximately 30 days. Also, many of the compounds have limited stability. Acrolein-d_4 decomposes within days, while methyl ethyl ketone-d_3 is present as the d_8-substituted compound. The presence of the d_8-substituted methyl ethyl ketone is perhaps a result of deuterium exchange with the deuterated methanol solvent via tautomeric equilibrium.

A GC/MS/DS capable of automated processing of the data is essential in reducing the large volume of data these analyses produce. The Finnigan-MAT Incos® data system has a program within its AutoQuan® software to perform isotope dilution calculations. The Aquarius® software package used in conjunction with the Hewlett-Packard systems has similar programs. Both software packages were used in our laboratory in this comparison. Calibration curves were established at the beginning of the study and were successfully met over the two month duration of our study.

In conclusion, isotope dilution techniques can provide a more accurate measurement of analyte concentration especially if the analyte experiences losses in the analysis. However, the labeled standards required to perform these analyses are quite expensive and have limited stability. Additionally, the analysis is more susceptible to interferences.

The isotope dilution methods can be applied successfully if set up properly and the problems outlined above are compensated for.

References

1. GRI Report #87/0335, December, 1987.

TABLE 1. COMPARISON OF 1624 VS. 624 (ug/L)

Compound	Sample #1		Sample #9	
	1624	624	1624	624
Acetone	660	270	<3400	<750
Methylethyl ketone	360	110	<3400	<2500
Benzene	<10	<8.8	10,300	8000
Toluene	<10	<12	13,300	18,000
Ethylbenzene	<10	<14	<700	<720

TABLE 2. COMPARISON OF 1625 VS. 625 (ug/L)

Compound	Sample #1		Sample #9	
	1625	625	1625	625
Di-n-butylphthalate	15	5.3	<10	<2.5
Phenanthrene	33	29	<20	<5.4
Acenaphthene	<10	2.3	<10	<1.9
Bis(2-ethylhexyl)phthalate	<10	9.4	<10	6
Phenol	<10	<1.6	442	110
Naphthalene	<10	<1.7	68	87
Pentachlorophenol	<20	<3.8	<20	<3.6
Phenol,2,4-dimethyl	<10	<2.8	305	290
Fluorene	<10	<2.0	<10	<1.9

Presented at the 36th ASMS Conference on Mass Spectrometry and Allied Topics
June 5-10, 1988, San Francisco, CA

GC/MS ANALYSIS OF BSTFA DERIVATIZED POLAR COMPONENTS OF DIESEL PARTICULATE MATTER (NBS SRM - 1650) EXTRACT

Bernd Wenclawiak, University of Toledo, Department of Chemistry, 2801 W. Bancroft St., Toledo, Ohio 43606; Trescott E. Jensen, and Joel F. O. Richert, Ford Motor Company, Analytical Sciences Department, Research Staff, Dearborn, Michigan 48121

Diesel particulate matter contains organic solvent extractable material that is mutagenic in the direct acting Ames assay. A polar HPLC fraction (Fraction 8) of diesel particulate matter (NBS SRM - 1650) dichloromethane extract contains about 11 % of the recovered mutagenicity in the extract (1). Additional separation of Fraction 8 was achieved with acid and base extraction partitioning(2). The GC/MS chromatograms for the polar fraction and the acid, base, and neutral subfractions were not very useful for identification of constituents as shown by the example in Figure 1(a). Benzo(c)cinnoline was the only component easily identified in the underivatized fraction.

N,O-bis(trimethylsilyl)-trifluoroacetamide (BSTFA) derivatization was found to be effective for several aromatic carboxylic acid and hydroxy standards selected as models of compounds expected to be in the polar fraction. The increase in molecular weight of the derivative was offset by the decrease in the polarity of the model compounds resulting in similar chromatographic retention times for the model compounds. Reaction of 10 uL of the BSTFA reagent (Pierce Chemical) with 10 uL each of the four samples at ambient temperature overnight was found to be adequate derivatization for the polar fraction as shown in Figure 1(b). Chromatographic definition of many derivatized components was sufficient for GC and GC/MS (EI and CI) analysis where hydroxy and carboxylic acid functional groups were observed. The components identified in this polar fraction of the extract include p-nitrophenol, benzoic acid, hydroxy benzoic acids, hydroxy benzaldehyde, hydroxyphthalimide, benzene dicarboxylic acids, naphthalene dicarboxylic acids, anthracene/phenanthrene dicarboxylic acids, and for some of these, the C_1 to C_3 alkyl homologs. Also, several methyl esters were observed. These include biphenyl dimethyl ester and benzene trimethyl ester.

Only one, two, and three ring aromatics were observed as trimethylsilane derivatives. The chromatogram in Figure 1(b) shows no peaks in the temperature range of 230 - 300 °C, where larger aromatics would be observed. If aromatics with polar functional groups and four or more rings were present in this polar fraction, they were not observed.

Derivatization of the acid, base, and neutral subfractions was only helpful for identification of components in the acid fraction. No derivatives were present or identifiable in the base or neutral subfraction. Some components observed as derivatives in the original fraction were not found in the acid, base or neutral fractions indicating chemical conversion is taking place during the extraction procedure. Derivatization did not facilitate identification of mutagens in the extract.

1. T. E. Jensen, D. Schuetzle, T. J. Prater, J. C. Ball, and I. Salmeen, "Biological and Chemical Characterization of a Composite Heavy-Duty Diesel Particulate Sample Accumulated Over a Long Period of Time," in "Polynuclear Aromatic Hydrocarbons: Mechanisms, Methods and Metabolism," M. Cooke and A. J. Dennis (Eds.), Battelle Press, Columbus, Ohio (1984), 643-661.

2. D. Schuetzle and J. Lewtas, Anal. Chem. 58 (1986), 1060A.

Presented at the 36th ASMS Conference on Mass Spectrometry and Allied Topics
June 5-10, 1988, San Francisco, CA

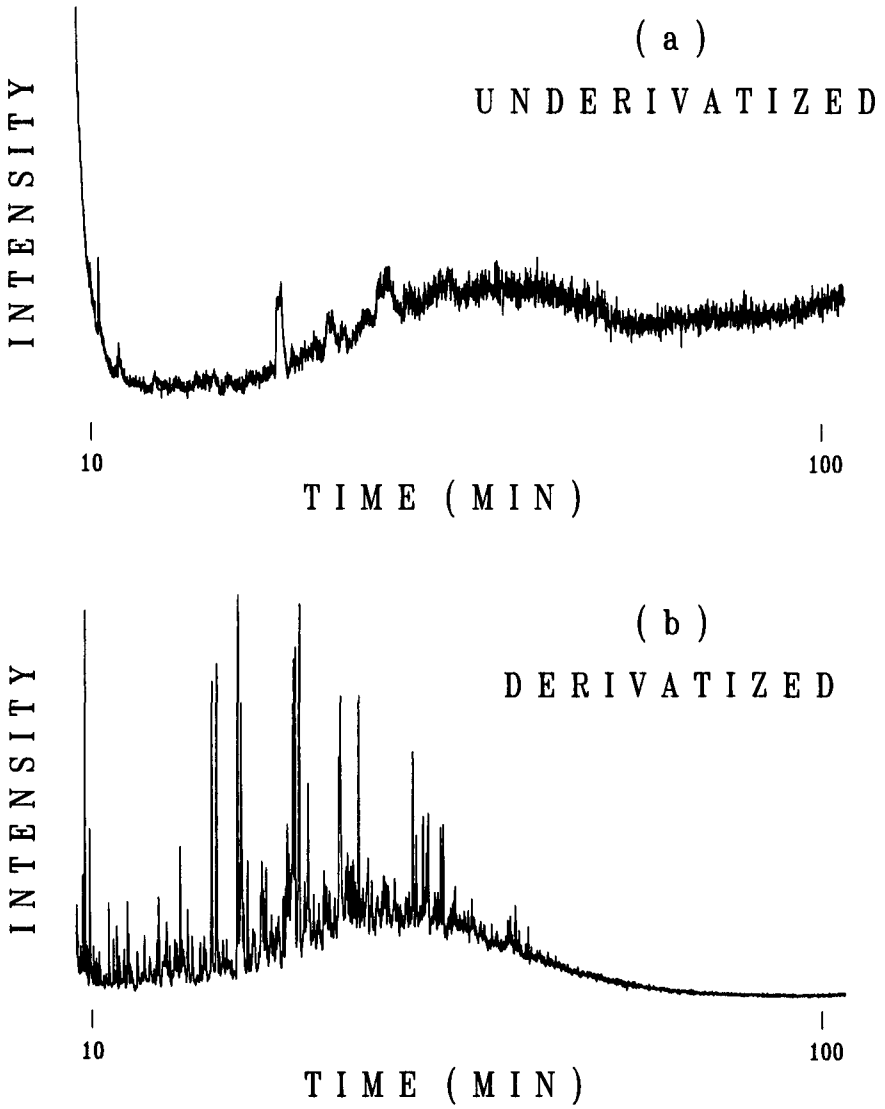

Figure 1. GC/MS total ion chromatograms for the (a) underivatized and (b) BSTFA derivatized HPLC Fraction 8 of a dichloromethane extract of NBS SRM-1650. Chromatography was done with a 30 m X 0.25 mm DB-5 column with on-column injection at 60 °C held for 2 minutes, programmed at 10 °C/min to 100 °C then at 2 °C/min to 300 °C, held for 20 minutes.

Presented at the 36th ASMS Conference on Mass Spectrometry and Allied Topics
June 5-10, 1988, San Francisco, CA

GC/MS ANALYSIS OF HYDROPHOBIC ORGANIC CONTAMINANTS IN CATFISH FROM THE MISSISSIPPI RIVER

Thomas J. Leiker, Wilfred E. Pereira, and Colleen E. Rostad
U.S. Geological Survey, Denver, CO, 80225

INTRODUCTION

The water quality of a given water system is often established by determining the concentrations of the organic contaminants that are contained within the water column. In many instances, this approach produces a false indication of acceptable water quality. Hydrophobic contaminants are often present at concentrations that are often below the detection limits of conventional analytical techniques. These types of compounds usually exhibit high octanol/water partiton coefficients and are selectively partitioned from the water column into the bed sediments and are selectively partitioned into the lipid tissue of stream biota.

The U.S. Geological Survey has been involved in a reconnaissance study to assess contaminant levels in the water column and stream biota from the Mississippi River and its tributaries. This covers a 1200 mile river reach from approximately Naples, Illinois to Belle Chasse, Louisiana. Preliminary data to date indicates that the water column contains relatively low concentrations (ng/L) of hydrophilic organic contaminants while the more hydrophobic contaminants are bioconcentrated in the lipid tissue, specifically catfish, of stream biota and are not detected within the water column.

EXPERIMENTAL

EXTRACTION and CLEANUP: 10 grams of homogenized tissue are mixed with 50 grams of granular anhydrous sodium sulfate, 1 ug D_{10}-Acenaphthene, 1ug Dibromooctafluoro biphenyl and extracted with 100 ml of 20 % (v/v) acetone/hexane using a Sonic Disruptor. After extraction the extract is dried through a column containing 15 grams sodium sulfate and concentrated by K-D. Prior to concentration 25 ml of ethyl acetate is added to the K-D to azetropically remove all hexane from the extract. The lipid material is removed form the extract by passing the extract through a gel permeation column containing 45 grams of Bio-Beads SX-3. The elution solvent is ethyl acetate at a flow-rate of 3.3 ml/min. The extract is further purified by passage through a column containing 20 grams of florisil. The final extract is adjusted to a volume of 10 ml. A 1.0 ml aliquot of the extract is screened by GC/ECD. The remainder of the extract is concentrated to a volume of 100 ul and analyzed by GC/MS.

GC/MS PARAMETERS: GC: HP-5840A, col. 30Mx0.2mm i.d. DB-5, initiial oven temperature; 50°C (hold for 3 min), program rate: 10°C/min., final temperture: 300°C (hold for 10 min.). MS: VG-7035H, resolution: 1000, mass range 150-500, scan-rate: 1 sec/dec, electron-energy: 70eV, emission current: 200 uA, accelerating voltage: 4Kv.

METHOD OF QUANTITATION: Standard Curves. Curves are generated from approximately 5 to 100 ppb using the ratio of diagnostic ions (TABLE I), generated for mass chromatograms, of the compound of interest with the internal standard, D_{10}-acenaphthene.

TABLE I
QUANTITATION ION

COMPOUND	m/z
D_{10}-Acenaphthene	162
Dibromooctafluoro biphenyl	454
Hexachlorobenzene	284
Lindane	217
Aldrin	263
DCPA (Dacthal)	301
tech-Chlordane	373 & 409
DDE	316
Dieldrin	263
Endrin	263
DDD	235
DDT	235
Trichlorobiphenyl	256
Tetrachlorobiphenyl	290
Pentachlorobiphenyl	324
Hexachlorobiphenyl	358
Heptachlorobiphenyl	392
Octachlorobiphenyl	426

Compounds are listed in order of elution from GC.

RESULTS

The Mississippi River and its tributaries exhibit widespread contaminantion with the following compounds: HCB, tech-chlordane, DDE, DDD, DDT, tetra-, penta-, hexa-, hepta-, and octachlorobiphenyl. Other compounds that have been detected include but are not limited too include di-, tri-, tetra-, pentachlorobenzene, pentachloroanisole, hexachorobutadiene, polynuclear aromatics, and chlorinated styrenes. Some areas such as the Missouri River at Hermann, Mo., Mississippi River at Chester,Ill., Helena, Ark., Arkansas City, Ark., and the Mississippi River at the confluence of the White River exhibit eleveted levels of hydrophobic contaminants.

CONCLUSIONS

The hydrophobic contaminants that are present in the water column at concentrations that cannot be detected at conventional detection limits are bioconcentrated to detectable limits within the lipid tissue of stream biota. As a result, stream biota are better indicators of true water quality.

Presented at the 36th ASMS Conference on Mass Spectrometry and Allied Topics
June 5-10, 1988, San Francisco, CA

HYDROCARBONS OF EVOLUTIONARY SIGNIFICANCE IN HOT SPRING MICROBIAL MATS

Jentaie Shiea and David M. Ward
Montana State University, Bozeman, MT, 59717

and Simon Brassell
Stanford University, Stanford, CA, 94305

Ancient microfossils have been interpreted as microorganisms which produced O_2 in photosynthesis (cyanobacteria), and thus might have oxygenated Earth's atmosphere. Alternatively they may have been microorganisms which did not produce O_2 (photosynthetic bacteria). We have studied hot spring microbial mats, built by modern microorganisms of either type, and considered analogs of the ancient communities in which microfossils are often found. By correlating hydrocarbon and microbial distributions in these mats, we hope to interpret whether hydrocarbons found in Precambrian sediments might be used to distinguish between these types of microbes.

METHODS

Cyanobacterial mats were collected from the Orakei Korako thermal area in New Zealand and from "Wiegert's Channel", Lower Geyser Basin, Yellowstone National Park. A mat formed by the green nonsulfur bacterium Chloroflexus sp. was collected from "New Pit" Spring, Mammoth Terraces, Yellowstone National Park. Chloroflexus aurantiacus strain Y400 was provided by Dr. M.T. Madigan (So. Ill. Univ.). Lyophilized samples were extracted with CH_2Cl_2. Hydrocarbons were eluted from alumina with hexane and analyzed by capillary gas chromatography--mass spectrometry (VG MM16 or VG70E-HF).

RESULTS AND DISCUSSION

C_{17} to C_{19} mid-chain branched monomethylalkanes were significant components in both cyanobacterial mats (Figures 1A and 2A). Mass fragmentography of key ions surrounding the site of methylation revealed suites of structural isomers with all possible branching positions (Figure 1B). Most modern cyanobacteria and mats they build contain some mid-chain branched monomethylalkanes (6), but this is the first report of whole suites of these hydrocarbons in cyanobacterial mats. The occurrence of these hydrocarbons as suites in Precambrian sediments and oils (up to 1.7 billion years old, see 3,5) was interpreted as a possible result of diagenetic reactions, but our results suggest that cyanobacteria may have directly contributed these compounds in Precambrian sediments.

Predominant hydrocarbons in the Orakei Korako cyanobacterial mat (Figure 2 A) were tentatively identified as dimethylalkanes. They were more volatile than the corresponding monomethylalkanes and their mass spectra indicated two pairs of fragments presumably generated from bond cleavage at each branch (e.g. m/e 85, 211 and 71, 225 for 4, 13-dimethylheptadecane, Figure 2B). Hydrocarbons tentatively assigned as dimethylalkanes were found in other cyanobacterial mats (4) and in Precambrian oils (3). The similar carbon number range and methylation compared to monomethylalkanes in this sample suggest that cyanobacteria may produce the dimethyalkanes.

The predominant hydrocarbons in Chloroflexus, and the "New Pit" Spring mat built by it, were C_{29} to C_{33} di- and triunsaturated alkenes (Figure 3A). Hydrogenation converted these to the corresponding n-alkanes (Figure 3B) ruling out cyclization. Accurate mass measurement eliminated the possible presence of heteroatoms. The most abundant hydrocarbon, hentriacontatriene ($C_{31:3}$), was also found in the two cyanobacterial mats as well as other hot spring mats containing Chloroflexus (2; unpublished data). Its presence in a lagoonal mat (1) may suggest a low-temperature Chloroflexus strain as an inhabitant. Long-chain alkenes are not known to occur in Precambrian sediments, but if diagenetic products of such distinctive compounds survive, they may be useful "chemical fossils" for the presence of this photosynthetic bacterium.

Presented at the 36th ASMS Conference on Mass Spectrometry and Allied Topics
June 5-10, 1988, San Francisco, CA

REFERENCES

1. Boudou, J.P., Trichet, J., Robinson, N. and Brassell, S.C., Intern. J. Enviro. Anal. Chem. 26:137-155 (1986).
2. Dobson, G., Ward, D.M., Robinson, N. and Eglinton, G., Chem. Geol. 68:155-179 (1988).
3. Klomp, U.C., Org. Geochem. 10:807-814 (1986).
4. deLeeuw, J.W., Sinninghe Damste, J.S., Klok, J., Schenck, P.A., and Boon, J.J., p.350-367 in Hypersaline ecosystems. The Gavish Sabkha (Friedman, G.M.and Krumbein, W.E., eds.), Springer-Verlag, Heidelberg (1985)
5. Summons, R.E., Org. Geochem. 11:281-289 (1987).
6. Ward, D.M., Shiea, J., Zeng, Y.B., Dobson, G., Brassell, S. and Eglinton, G., in Microbial Mats (Cohen, Y. and Rosenberg, E., eds.), Am. Soc. Microbial., Wash. D.C. (in press).

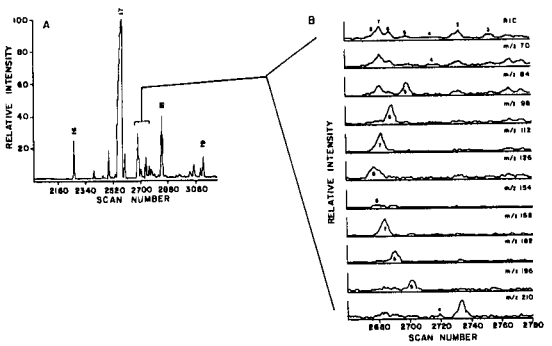

Figure 1. A. Predominant hydrocarbons in the "Wiegert's Channel" cyanobacterial mat. **B.** Mass fragmentography revealing suite of C_{18} mid-chain branched monomethyl-alkanes.

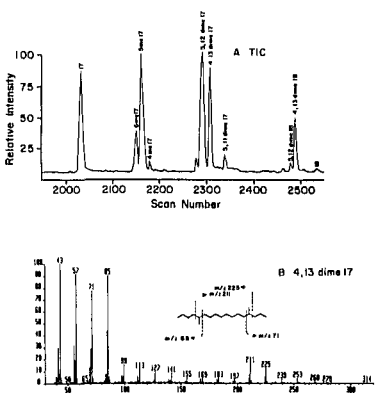

Figure 2. A. Predominant hydrocarbons in the Orakei Korako cyanobacterial mat. **B.** Mass spectrum of 4, 13-dimethylhepta-decane.

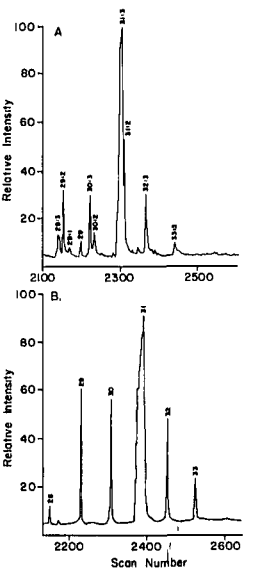

Figure 3. Predominant hydrocarbons in the "New Pit" Spring Chloroflexus mat before (**A**) and after (**B**) hydrogenation.

Presented at the 36th ASMS Conference on Mass Spectrometry and Allied Topics
June 5-10, 1988, San Francisco, CA

STRUCTURAL ANALYSIS OF PORPHYRINS: ANALYSIS OF IN VITRO PREPARED PORPHYRINOGENS USING AN ION TRAP MASS SPECTROMETER

G. J. Van Berkel, G. L. Glish, and S. A., McLuckey
Analytical Chemistry Division, Oak Ridge National Laboratory
Oak Ridge, TN 37831-8121.

Porphyrins are a class of macrocyclic tetrapyrroles important in a number of fields. Detailed structural information on these compounds is often desired, but the structural information available from mass spectrometry is limited by the inability to fragment the extremely stable macrocycle. This problem can be circumvented by converting the porphyrin to the less stable porphyrinogen (hexahydroporphyrin) in vitro (Figure 1) since, using electron ionization (EI), porphyrinogens fragment to yield tri, di-, and monopyrrolic ions from which the pyrrole sequence of the macrocycle can be determined.[1,2] Little information on the structure of the individual pyrrolic units can be determined from these spectra, however, and secondary fragmentation of the substituent groups on the individual pyrrolic units can make spectral interpretation extremely difficult. We have found that analysis of porphyrinogens with the Ion Trap Mass Spectrometer (ITMS), using a variety of ionization techniques and multiple stages of mass analysis (i.e., MS^n, where $n \geq 2$) produces spectra that are less complex and contain more structural information than the EI mass spectra obtained using conventional instruments.

Porphyrinogen mass spectra were simplified through precise control of the ionization process and MS/MS analysis of the protonated porphyrinogen. The mechanism and energetics of the ionization process were controlled using selected reagent ion chemical ionization (SRICI) with both proton transfer reagents (e.g., CH_5^+ from methane) and charge exchange reagents (e.g., $N_2O^{+\cdot}$ from nitrous oxide). The degree of porphyrinogen fragmentation was found to correlate with the exothermicity of the ionization reaction which can be varied via the proton affinity or recombination energy of the selected reagent ion (Figure 2a and b). Using ammonia CI (select NH_4^+) the protonated porphyrinogen was produced without fragmentation. The MS/MS spectra of protonated porphyrinogens were found to contain the same structural information as the EI mass spectra, but in a more interpretable form (Figure 3).

The amount of structural information available from the porphyrinogen mass spectra was increased by using MS/MS and MS/MS/MS (MS^3) analysis. MS/MS analysis of the pyrrolic ions in the EI mass spectra provided information regarding the nature of the substituent groups on these pyrrolic units. The identity of the substituent groups present on the pyrroles can be determined in this manner and such spectra can be used to distinguish between structural isomers of the substituents. MS^3 analysis of the protonated porphyrinogen allows the nature of the individual pyrrolic units making up the tri- and dipyrroles to be determined (Figure 4).

Analysis of in vitro prepared porphyrinogens using the ITMS is a very powerful way to obtain structural information on porphyrins. Compared to conventional EI-MS analyses, analysis of porphyrinogens with the ITMS produces simple and easily interpreted spectra and the amount of structural information obtained is increased because of the ability to perform MS^n analyses.

1. Budzikiewicz, H. and Pesch, R. Org. Mass Spectrom. 11, 821 (1976).
2. Budzikiewicz, H. and Neuenhaus, W. Heterocycles, 7, 251 (1977).

*Research sponsored by the U.S. Department of Energy, Office of Basic Energy Sciences, under contract DE-AC05-84OR21400 with Martin Marietta Energy Systems, Inc.

Figure 1

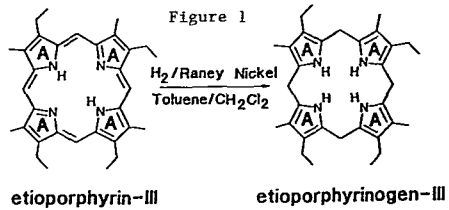

Figure 2

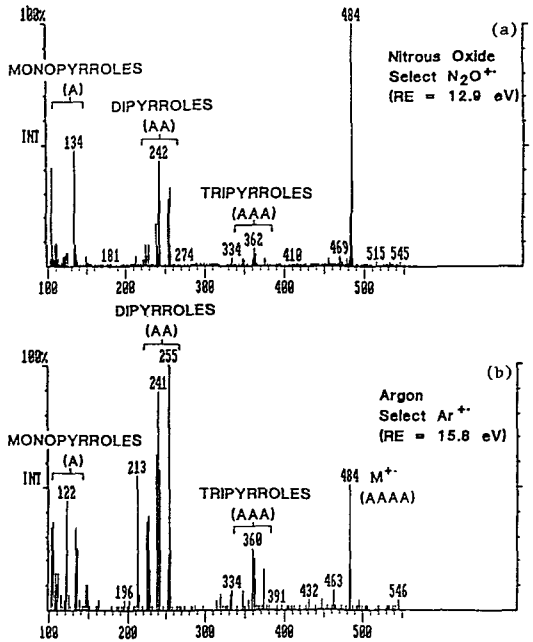

Figure 3. MS/MS Spectrum of MH^+

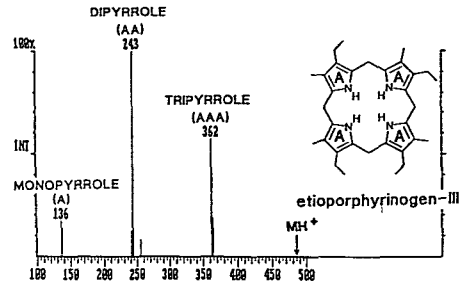

Figure 4. MS/MS/MS Spectrum of MH^+

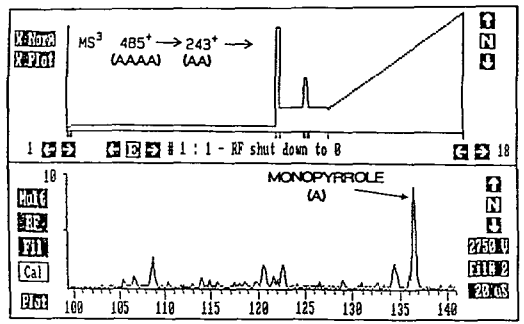

"The submitted manuscript has been authored by a contractor of the U.S. Government under contract No DE-AC05-84OR21400 Accordingly, the U.S Government retains a nonexclusive, royalty-free license to publish or reproduce the published form of this contribution, or allow others to do so, for U.S Government

Presented at the 36th ASMS Conference on Mass Spectrometry and Allied Topics
June 5-10, 1988, San Francisco, CA

Presented at the 36th ASMS Conference on Mass Spectrometry and Allied Topics
June 5-10, 1988, San Francisco, CA

MECHANISM OF PORPHYRIN HYDROGENATION AND DECOMPOSITION IN A CHEMICAL IONIZATION SOURCE

Gary J. Van Berkel, Gary L. Glish, and Scott A. McLuckey
Analytical Chemistry Division
Oak Ridge National Laboratory
Oak Ridge, TN 37831

Several workers have reported evidence for the reduction of porphyrins and extensive fragmentation in the NH_3[1] and H_2[2] chemical ionization (CI) mass spectra, including fragmentation of the macrocycle. This observation is significant in that fragmentation in the electron ionization (EI) mass spectra of porphyrins is typically restricted to the side chains. Fragmentation of the macrocycle permits greater structural characterization of porphyrins via mass spectrometry. We have investigated the CI of selected model porphyrins and porphyrinogens both in a high pressure ion source and in an Ion Trap Mass Spectrometer (ITMS) in conjunction with MS/MS studies of the resulting ions in order to shed further light on the phenomena that underlie the observed reduction/fragmentation.

The MS/MS spectrum of the $(M + 7H)^+$ ion observed in the NH_3 CIMS of the porphyrins that we have investigated match those of the MH^+ ions derived from the corresponding porphyrinogen, the fully reduced form of the porphyrin. This confirms, as expected, that the porphyrin is reduced to the porphyrinogen in the ion source. Several mechanisms for the reduction can be envisioned. We have shown, however, that the reduction does not occur in the ITMS under any conditions normally used for CI. A major difference between CI in a high pressure ion source and the ion trap is the absence of a high concentration of electrons, radicals, and other reactive neutrals in the latter. Furthermore, ion source walls are much more likely to play a role in the chemistry that occurs in the high pressure ion source. We have found that the formation of reduced species in the high pressure source is inversely related to the source temperature (Figure 1). This behavior is consistent the higher volatility of the porphyrinogen relative to the porphyrin. The temperature needed to desorb etioporphyrinogen-III from the solids probe on the ITMS, for example, is 100 K less than that needed to desorb etioporphyrin-III. A plausible mechanism for the reduction of the porphyrin in the CI source is reduction by hydrogen radicals followed by protonation. Reduction of molecules containing the appropriate functional groups by hydrogen radicals under high pressure CI conditions has been shown to occur.[3] The evidence here suggests that the reduction occurs on the walls of the ion source from which the reduced species desorbs and is ionized by proton transfer (in the case of NH_3 CI) or electron transfer (in the case of H_2 CI).

It has been proposed that the fragment ions observed in the CI mass spectrum arise from fragmentation of the ionized porphyrinogen. We have noted, however, that most of the fragment ions observed in the mass spectrum differ by one to several mass units from those observed in the MS/MS spectrum of the $(M + 7H)^+$ ion (Figure 2). This indicates that the majority of the fragment ions in the mass spectrum do not arise from the unimolecular decomposition of the pseudomolecular ions. In light of the proposed mechanism for the reduction reaction, it seems likely that most of the fragment species arise from the thermal decomposition of the porphyrinogen and, to varying degrees, from the lesser reduced species followed by ionization in the CI plasma.

1. B. Tolf, X. Jiang, A. Wegmann-Szente, L.A. Kehres, E. Bunnenberg, and C. Djerassi, J. Am. Chem. Soc., 108, 1363 (1983).
2. G. Shaw, G. Eglington, and J.M.E. Quirke, Anal. Chem., 53, 2014 (1981).
3. C.N. McEwen, Mass Spectrom. Rev., 5, 521 (1986).

This work was supported by the U.S. Department of Energy, Office of Basic Energy Sciences, through Contract DE-AC05-840R21400 with Martin Marietta Energy Systems, Inc.

Figure 2

MS/MS SPECTRUM OF $(M+7H)^+$ FROM ETIOPORPHYRIN-III (5 keV CID)

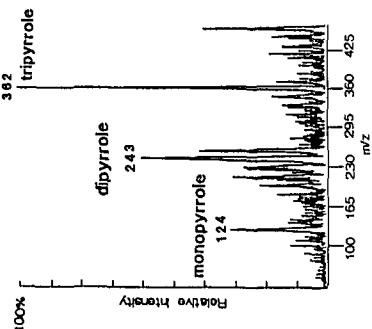

Figure 1

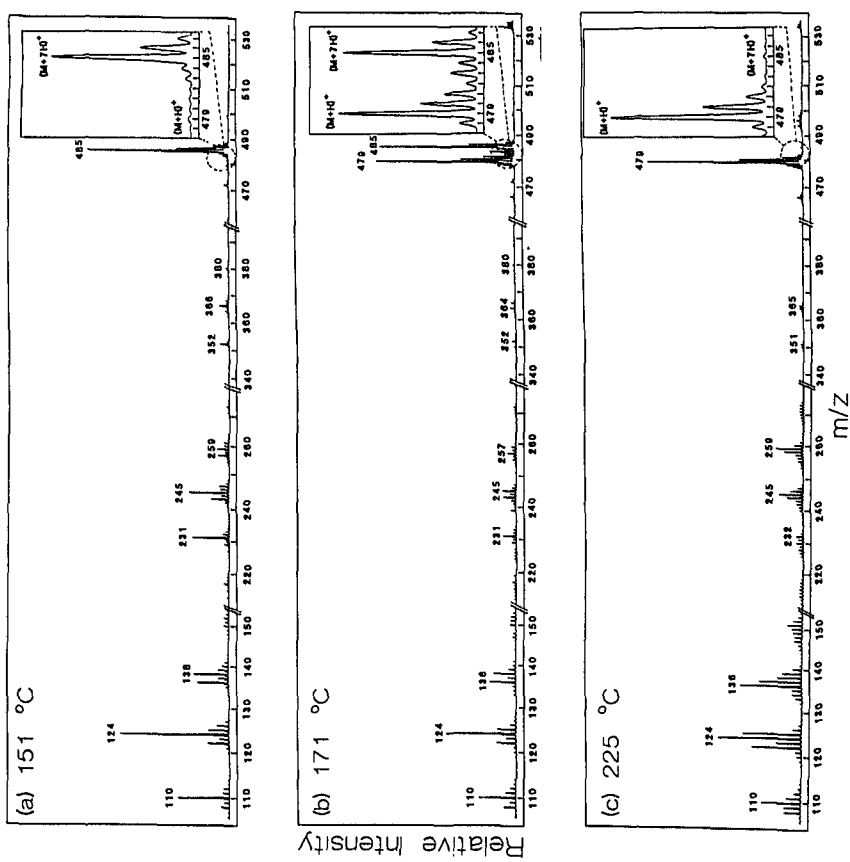

"The submitted manuscript has been authored by a contractor of the U.S. Government under contract No. DE-AC05-84OR21400. Accordingly, the U.S. Government retains a nonexclusive, royalty-free license to publish or reproduce the published form of this contribution, or allow others to do so, for U.S. Government purposes."

Presented at the 36th ASMS Conference on Mass Spectrometry and Allied Topics
June 5-10, 1988, San Francisco, CA

Characterization of Geoporphyrins from New Albany Bitumen and Kerogen by Tandem Mass Spectrometry

B.D. Beato and R.A. Yost, Univ. of Florida, Gainesville, FL 32611
J.M.E. Quirke and M.A. Concha, Florida International Univ., Miami, FL 33199
R.H. Filby and G.E. Mercer, Washington State Univ., Pullman, WA 99164-1300
G.J. Van Berkel, Oak Ridge National Laboratory, Oak Ridge, TN 37831

Geoporphyrins are biological marker compounds which provide information on fossil fuels, such as sample maturation and depositional environment of the sample. Tandem mass spectrometry (MS/MS) has been shown to be a valuable technique in fossil fuel research and exploration by facilitating structural analyses of complex mixtures of geoporphyrins. The Henryville bed of New Albany shale in Clark County, Indiana, is one of the richest sources of both nickel and vanadyl geoporphyrins known, containing about 9000 ppm of each. Shale consists of both bitumen, which is the organically extractable portion, and kerogen, which cannot be extracted with organic solvents by conventional laboratory methods. Very little is known about the composition of kerogen, but porphyrins can be extracted from it via pyrolysis. One primary goal of this research is to compare the porphyrins found in the bitumen with those from the kerogen. This should provide information on how porphyrins are bound to the kerogen matrix. A second goal is to compare nickel porphyrins with vanadyl porphyrins of the same carbon number to determine possible structural differences which are metal-dependant. The last phase of this work involves structure determination of single carbon number fractions of demetalated nickel porphyrins by determining the sequence of pyrroles around the macrocycle. The information obtained from these studies should be useful in oil exploration (porphyrin fingerprinting) and in maturation studies.

All experiments were performed on a Finnigan MAT TSQ45. Samples were introduced via a solids probe (1-2 μg solid sample, 90°C → 400°C @ 120 °C/min) and ionized by either EI (190°C, 70 eV) or hydrogen CI (150 °C, 0.95 torr H_2, 100 eV). Tandem mass spectrometry (MS/MS) was performed with a collision energy of 24 eV and collision gas pressures of 1.8 and 2.9 mTorr nitrogen for the vanadyl and nickel porphyrins, respectively.

Porphyrins from bitumen were separated by thin layer chromatography (TLC) into complex mixtures of nickel porphyrins with a carbon number range of C_{27} to C_{34} and complex mixtures of vanadyl porphyrins with a carbon number range of C_{28} to C_{33}. Similarly, kerogen yielded nickel porphyrins from C_{26} to C_{33} and vanadyl porphyrins from C_{28} to C_{32}. These fractions contained largely the two basic geoporphyrins: etio- and cycloalkano(CAP)-porphyrins. They are differentiated by the CAP porphyrins containing an isocyclic ring.

The EI/MS/MS daughter spectra of the $M^{+\cdot}$ ions of the porphyrins are characterized by β-cleavage of the various alkyl groups from the porphyrin macrocycle (Figure 1). The daughter spectra of the various porphyrins from the bitumen are very similar to those of corresponding porphyrins from the kerogen. This indicates that pyrolysis of the kerogen probably does not result in cleavage of carbon-carbon bonds, which implies that porphyrins are not bound though alkyl linkages to the kerogen.

The daughter spectra of corresponding nickel and vanadyl porphyrins are also very similar (Figure 2). This suggests that both types of metalloporphyrins reflect similar precursors.

Although the EI/MS/MS daughter spectra discussed provide information on the peripheral alkyl substituents on the central porphyrin ring, they do not indicate the relative sequence of the pyrroles in the central ring. Hydrogen CI was found to result in the decomposition of the porphyrins in the ion source to form ions indicative of mono- and dipyrrolic fragments. Single carbon number fractions for six different demetalated nickel porphyrins from both bitumen and kerogen were analyzed by H_2 CI/MS. The pattern of the dipyrrolic fragment ions in the H_2 CI mass spectrum (Figure 3, the labels correspond to the dipyrroles of Figure 4) of one of the fractions resembles that of a well-characterized C_{31} CAP from Serpiano shale (Structure I in Figure 4 from Ref. 1). In earlier H_2 CI/MS studies, dipyrrolic ions were shown to arise out of decomposition pathways which included cleavage of hydrogenated porphyrins. This can lead to a somewhat

complex spectrum further complicated by the fact that each dipyrrolic fragment can contain 0,1, or 2 meso-bridge carbons. The five other demetalated samples analyzed in this way also yielded specific dipyrrolic ion patterns which are useful in structure elucidation and help characterize the New Albany shale more completely.

Although the combination of EI/MS/MS and H_2 CI/MS analyses provides more structural information about geoporphyrins on a micro scale (less than 100 μg) than any other single technique, it does not allow unambigous structure determination except in very limited cases. The next phase of this research will involve the use of ^1H NMR of the demetalated geoporphyrins to further enhance structure elucidation.

REFERENCE 1.
G.A. Wolff, M.I. Chicarelli, G.J. Shaw, R.P. Evershed, J.M.E. Quirke, and J.R. Maxwell (1984) Tetrahedron 40, 3777-3786.

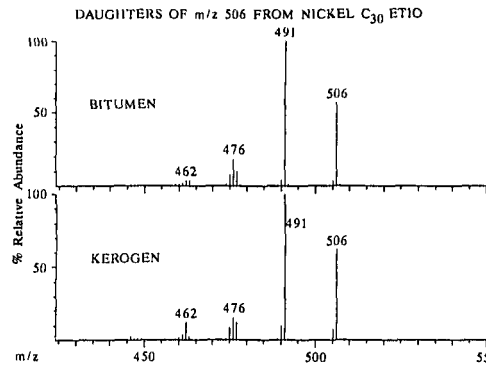

Figure 1.

Figure 2.

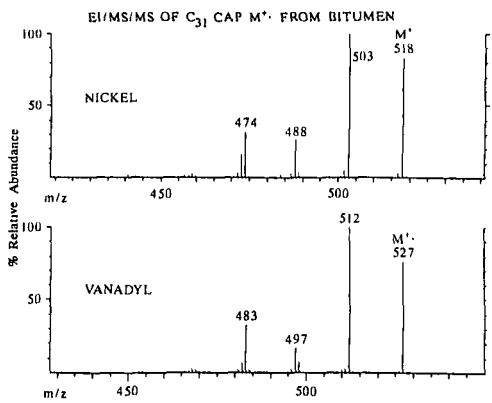

Figure 4.

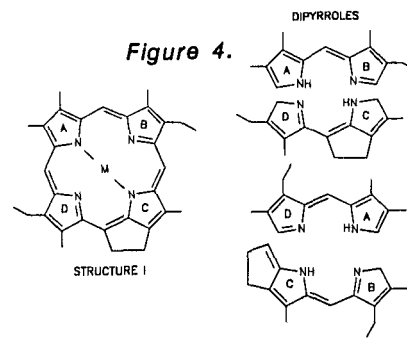

Figure 3.

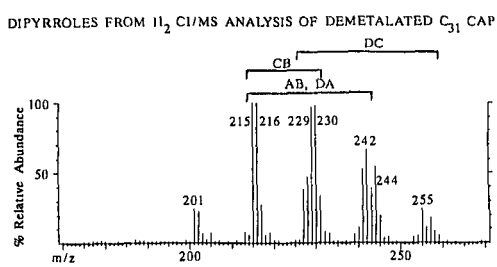

Presented at the 36th ASMS Conference on Mass Spectrometry and Allied Topics
June 5-10, 1988, San Francisco, CA

A CALCULATING METHOD OF PETROPORPHYRIN STURCTURE ISOMERS COMPOSITION BY TANDEN MASS SPECTROMETRY

Xu Lina

Jianghan Petroleum Institute, Hubei, P.R.China

INTRODUCTION

Porphyrins and their congeners constitute near ubiquitious components of life forms at the cellular level and above.Therefore the study of structure of porphyrins has important scientific significance to inquire into the origin of life and petroleum.Petrophyrins is a complex mixture composed of a wide carbon number ranges of several alkyl-porphyrin series. The author analyses the composition of porphyrins in the source rock from Du-65 well of Liaohe Basin in China, for the purpose of clarify application of MS/MS technique in the field of organic geochemistry. Data were obtained on Finnigan MAT triple-stage quadrupole (TSQ-45 Model)GC/MS/MS/DS system.

RESULTS AND DISCUSSION

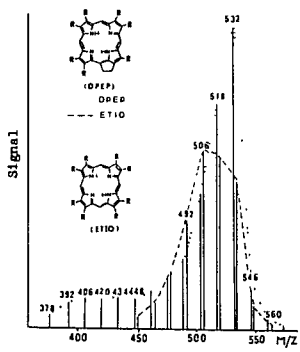

Fig.1 EIMS of the demetallized porphyrins.

EIMS (Fig.1) reveals that the demetallized porphyrins in source rock from Du-65 well include DPEP(58.8%) and ETIO(41.2%).
The EIMS has provided the informations on porphyrin skeletal types present and their canbon number ranges but little data on the structure of the individual components.To correlate the fragment ions with their molecular ions and gain more information about the structure and fragmentation of porphyrin pyrole-alkyl substituents, MS/MS can be employed.
MS/MS of Porphyrin Standards These daughter spectra of standards indicate:1.Porphyrins with extended alkyl substituents(>C_1)will produce MS/MS daughter spectra characterized by the intense daughter ions arising from ß-cleavage of those substituents. 2.Alkyl groups,approching in carbon number,have approximately equal probability of ß-cleaveges. Therefore MS/MS can be used to determine the relative number of n-alkyl substituents,differing in length,present in a compound.
MS/MS of C_{34}-C_{36} DPEP in Source Rock from Du-65 Well The daughter spectra of the C_{34}-C_{36} DPEP reveal the M^+ ions undergoes benzylic cleavage to produce $(M-CH_3)^+$, $(M-2CH_3)^+$ and $(M-CH_3,-C_2H_5)^+$ ions.In addition, C_{35} and C_{36} daughter spectra give $(M-3CH_3)^+$ ion and $(M-2CH_3,-C_2H_5)^+$ ion respectively.Loss of $\geqslant C_3$ groups was not observed.These daughter spectra reveal: 1.The C_{34}-C_{36} DPEP contain ethyl and propyl except for methyl. 2.The ratio of ethyl/propyl can estimate by the intensities of ions in the daughter spectra(see table 1 and Fig.2).
Since the MS/MS analysis of the standards demonstrated exclusive ß-cleavage, it can be assumed that the relative frequency with which a given alkyl group is lost from porphyrins of various carbon numbers does in fact correspond to the relative occurrence of these groups in those porphyrins.(It has one more carbon than the fragment that is lost).Therefore we can calculate the composition of petroporphyrin structure isomers.Calautation includes two steps. First,according to the carbon number of alkyl substituents,the number of substitute pieces and alkyl types, all kind of probable isomers were arranged. Second, the reasonable combination of isomers can be defined by all kinds of probable isomers. For example, out of C_{36} DPEP nucluse has fourteen

Presented at the 36th ASMS Conference on Mass Spectrometry and Allied Topics
June 5-10, 1988, San Francisco, CA

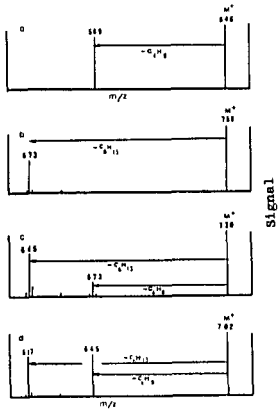

Fig.2 EIMS/MS daughter spectra of molecular ions, M^+, of etiopor phyrin standards: a) tetrame-thyltetrapentylporphyrin; b) tetramethyl tetrahep-tylporphyrin; c) analogous triheptylmonopentylpor-phyrin; d) analogous diheptyldipentylporphyrin.*

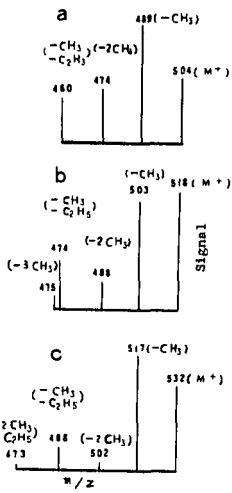

Fig.3 EIMS/MS daughter spectra of the molecular ions, M^+, of the C_{34}-C_{36} DPEP: a) C_{34}; B) C_{35}; c) C_{36}.

Table 1 Estimate of ratios of ethyl/propyl in the C_{34}-C_{36} DPEP

No.	mol. ions	relat. abundance %					Σ-CH_3	Σ-C_2H_5	$\frac{\Sigma-C_1}{\Sigma-C_1}=\frac{C_2}{C_1}$
		$-CH_3$	$-2CH_3$	$-3CH_3$	$-CH_3$ $-C_2H_5$	$-2CH_3$ $-C_2H_5$			
1	m/z 532 C_{36}	100	6	0	24 (12+12)	3 (2+1)	120 (100+6+12+2)	13 (12+1)	120/13 =9.23
2	m/z 518 C_{35}	95	27	13	38 (19+19)	0	154 (95+27+13+19)	19	154/19 =8.11
3	m/z 504 C_{34}	100	45	0	36 (18+18)	0	163 (100+45+18)	18	163/18 =9.05

Table 2 Calculating of isomers composition of C_{34}-C_{36} DPEP

No.	mol. ions	pro-ject	(C_2H_5)	(C_3H_7)	(CH_3)	isomers: mol. ratios	ethyl	prop	C_2/C_3	mol.%
1	M/Z 532 C_{36} n=14	A	7	0	0	6	42	0	48/5 =9.20	75
		B	5	1	1	0	0	0	estimate	0
		C	3	2	2	1	3	2	9.25 error 0.3‰	12.5
		D	1	3	3	1	1	3		12.5
2	M/Z 518 C_{35} n=13	A	6	0	1	14	84	0	106/13 =8.16	63.6
		B	4	1	2	4	16	4	estimate	18.2
		C	2	2	3	3	6	6	8.11 error 0.5‰	13.6
		D	0	3	4	1	0	3		4.6
3	M/Z 504 C_{34} n=12	A	5	0	2	5	25	0	32/4 =8.00	62.5
		B	3	1	3	2	6	2	estimate	25
		C	1	2	4	1	1	2	9.05 error 0.5‰	12.5

carbons (n=36-22=14), seven substitute places and three kinds of alkyl groups (methyl, ethyl and propyl) (cf. Fig.1). It has four kinds of probable isomers (A, B, C, D). When A:B:C:D=6:0:1:1 (molecular rate), the ratio of ethyl/propyl in isomers equal to 9.20 (see table 2). The relative error between this ratio (9.20) and estimating ratio (9.23) is 3‰. The result indicates that C DPEP contains seven ethylporphyrins (75%), triethyldimethyldipro-pylporphyrins (12.5%) and monoethyltrimethyltri-propylporphyrins (12.5%).

CONCLUSION

According to the structural information of por-phyrin pyrole-alkyl substituents provided EIMS/MS daughter spectra, the composition of indivi-dual porphyrin isomers can be calculated.

LITERATURE CITED *

Johnson, J.V.; Britton, E.D.; Yost, R.A.; Quirke, J.M.E; Cuesta, L.L.; Anal.Chem.; 1986, 58, 1325-1329.

Presented at the 36th ASMS Conference on Mass Spectrometry and Allied Topics
June 5-10, 1988, San Francisco, CA

THE DETERMINATION OF FREE ALCOHOLS IN ZINC DIALKYL DITHIOPHOSPHATES BY MASS SPECTROMETRY/MASS SPECTROMETRY

V. P. NERO
Texaco Research Center
Beacon, NY 12508

INTRODUCTION

Zinc dialkyl dithiophosphates, ZDDPs, are used extensively as antiwear agents, corrosion inhibitors, and antioxidants in lubricants. ZDDPs are generally prepared from the reaction of various alcohols with phosphorous pentasulfide, followed by the addition of zinc oxide. The determination of unreacted alcohol in the ZDDP product is important in the optimization of the manufacturing conditions and for developing toxicological information. However, traditional analytical methods either failed to detect alcohols at the low percentage levels normally expected in ZDDPs or cause the product to release alcohols through decomposition.

A mass spectrometry/mass spectrometry method was developed which can detect and quantitate free alcohols in commercial ZDDPs at the subpercent level. The method is based upon a daughter ion analysis which detects possible alcohols along with deuterated surrogate alcohols. This procedure was then applied for the determination of free 2-ethylhexanol in commercial ZDDPs using 2-ethylhexanol (D17, 98%) as a calibration surrogate.

EXPERIMENTAL DEVELOPMENT OF PROCEDURE

The highest observed ion in the total ion mass spectrum for 2-ethylhexanol has a mass of 112.1 representing the loss of water. The highest observed ion for (D17) 2-ethylhexanol has a mass of 128.2 corresponding to the loss of HDO. Both molecules also have identical sensitivities, and corresponding mass spectra, when adjusted for the substitution of deuterium. Considering these findings, a daughter MS/MS method was developed based upon using 112.1 and 128.2 as parent ions. Since the daughter spectra were found to be highly dependent upon collision cell conditions, the collision offset energy in the second quadrupole was optimized to -4 eV and the argon collision gas pressure was optimized to 1.5 torr. These conditions resulted in very reproducible daughter spectra. The summation of fragmentation daughter ions C6H10, C6H11, and C6H12 or C6D10, C6D11, and C6D12 were selected for quantitation purposes. (The quantitation was based on the ratio of the summation of 82.1, 83.1, and 84.1 ion abundances to the summation of 92.2, 94.2 and 96.2 ion abundances.)

EXPERIMENTAL PROCEDURE

A 200 ug ZDDP sample, spiked at the 1.0% level by weight with (D17) ethylhexanol, was maintained at 20C to prevent possible thermal decomposition of the zinc dialkyl dithiophosphate ester at the 250C source temperature. The electron ionization current was maintained at 200 uA with 70 eV. The mass spectrometer, a Finnigan-MAT TSQ70, was operated in a daughter scan mode alternately scanning masses 112.1 and 128.2 as previously described. These alternate scans were reduced to an average scan from which the results were quantitated based upon the summation ratios of the 82 to the 92 series.

RESULTS

ZDDP samples, which were prepared from 2-ethylhexanol, and ZDDP samples, which were not prepared from 2-ethylhexanol, but were spiked with free 2-ethylhexanol at the zero to five percent level, were examined. Figure 1 shows a sample containing no free 2-ethylhexanol. Peaks 82, 83 and 84, representing free 2-ethylhexanol, were not detected. Peaks 92, 94 and 96, representing the deuterated alcohol, are readily observed. Figure 2 shows a sample containing free 2-ethylhexanol. The sample was determined to contain on the average 3.7% of the free alcohol with a 95% confidence interval ranging from 3.4 to 4.0%.

FIGURE 1 A ZDDP CONTAINING NO FREE 2-ETHYLHEXANOL
Ratio (82+83+84)/(92+94+96) = 0.0

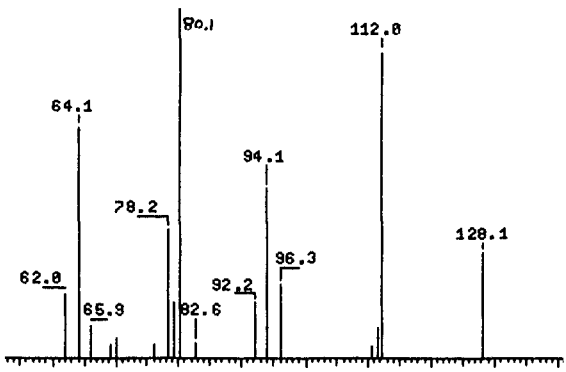

MASS	INTENSITY
46.2	6052
62.0	12506
64.1	45533
65.9	6293
78.2	25107
79.0	10851
80.1	70705
92.2	10676
94.1	33260
96.3	14355
111.5	5866
112.0	60637
128.1	20593

FIGURE 2 A ZDDP CONTAINING FREE 2-ETHYLHEXANOL
Ratio (82+83+84)/(92+94+96) = 3.7

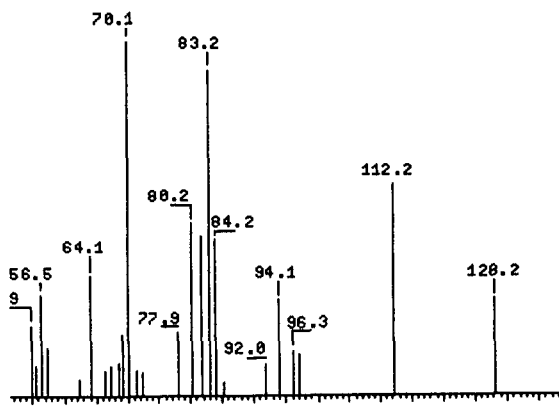

MASS	INTENSITY
54.9	1018
56.5	1470
57.3	699
64.1	1744
68.5	465
69.3	873
70.1	5178
77.9	913
80.2	2418
82.1	2340
83.2	4758
84.2	2275
92.0	458
94.1	1388
96.3	659
97.1	609
112.2	3070
128.2	1391

Presented at the 36th ASMS Conference on Mass Spectrometry and Allied Topics
June 5-10, 1988, San Francisco, CA

MASS SPECTROMETRIC ANALYSIS OF SEDIMENTS FROM AGED JET FUELS

Gene P. Sturm, Jr., Ronald D. Grigsby, John B. Green, and Dennis W. Brinkman

IIT Research Institute, NATIONAL INSTITUTE FOR PETROLEUM & ENERGY RESEARCH
P. O. Box 2128, Bartlesville, OK 74005

INTRODUCTION: The military is experiencing an increasing number of problems with JP-5 fuels provided under current specifications. These problems include formation of solids, increased corrosiveness, development of color, and increased viscosity upon storage of the fuels. With an ultimate objective of an increased understanding of mechanisms or pathways of degradation processes in jet fuels in order to correct those problems, gums and sediments formed during aging of the 350-550° F distillate cuts (JP-5 boiling range) from two West Coast hydrocracker streams were analyzed by GC/MS and low-voltage, high resolution mass spectrometry. For the latter technique, samples were introduced by probe microdistillation (PMD). Stability of hydrocarbon fuels, including aviation fuels, has been a concern for many years and the subject of several reviews[1]. Reactive hydrocarbons and heteroatomic compound types have been implicated in the degradation processes resulting in sediment and gum formation[2-7]. A free radical chain mechanism[8,9], electron transfer mechanism[10,11], condensation of oxidation products, and coupling of substrates by peroxides[6,7], have been proposed as mechanisms.

EXPERIMENTAL: A description of the fuel aging experiments is given in a separate paper[12]. Sediments from fuel A after 19 weeks at 80° C and 44 weeks at 60° C and from fuel B after 8 and 12 weeks at 80° C were analyzed by GC/MS (methylene chloride solution) and PMD/MS. PMD/MS data were acquired with a Kratos MS-50 mass spectrometer at a resolution (static) of 28,000 and an ionizing voltage of 12 eV. The probe temperature was controlled from -80° C to 350° C (sediment 80-95% volatilized). Data were processed by computer programs developed in-house (see paper MPB 50)[13] using a DEC Microvax II computer.

RESULTS/DISCUSSION: The fuel aging experiments at 60° C were characterized by a short induction period, followed by a period of rapid peroxide formation, and finally a period of decreasing peroxide content and increasing sediment formation. GC/MS and PMD/MS composite results for the four sediments are summarized in table 1. The GC/MS peak identifications were made by both retention time and mass spectral matching of authentic samples of the parent and, where available, alkyl-substituted homologs for the compound types shown unless otherwise noted in table 1. The compositions of the four sediment samples were very similar. Prominent compound types observed were alkyl-indenes, -1,2-dihydronaphthalenes, -naphthalenes, -1-tetralones, -indenols, and -1-naphthols. Lesser amounts of indanes, phenols, and indanols were detected. In addition, 2,3-benzofurans and o-phthalic anhydrides were identified by GC/MS. No sulfur or nitrogen compounds were detected in the sediment samples which is consistent with the low elemental S (<7 ppm) and N (<0.3 ppm) content of these fuels. The PMD/MS results indicated broader ranges of compound types and carbon numbers than the GC/MS results. Additional secondary-distributions of hydrocarbons, O-, O_2- and O_3-compounds observed by PMD/MS, were probably dimers of the prominent hydrocarbons and oxygen compounds determined both by GC/MS and PMD/MS. One trend observed was a shift from a prominence of hydrocarbons and O-compound types in the fuel B, 8 week, 80° C sample (consisting primarily of filterable sediment) to a prominence of O- and O_2-compound types in the other sediments (primarily adherent).

CONCLUSIONS: The composition of sediments from two hydrocracked fuels indicates that oxidation of alkyl-indans/tetralins, -indenes/dihydronaphthalenes, -naphthalenes, -benzenes, and their oxidation products results in formation of sediments or gums. The induction period and the inhibiting

effect of antioxidants[12] are consistent with a free radical chain mechanism. The presence of dimers is consistent with the condensation of oxidation products of alkylnaphthalenes and the coupling of substrates by peroxides[6,7].

ACKNOWLEDGMENTS: The authors give thanks to Bob Vrana, Shirley Yu, and Fred Tilley for aid in data acquisition. Financial support for the project provided by the U.S. Navy (Naval Air Propulsion Center) and the U.S. Department of Energy under Cooperative Agreement DE-FC22-83FE-60149 is gratefully acknowledged.

REFERENCES:

1. Goetzinger, J. W.; Thompson, C. J.; Brinkman, D. W. "A Review of Storage Stability Characteristics of Hydrocarbon Fuels 1952-1982."; DOE/BETC/IC-83/3. Available NTIC, U.S. Dept. of Commerce, Springfield, VA 22150.
2. Smith, R. D.; Udseth, H. R.; Hazlett, R. N. Fuel **1985**, 64, 810-815.
3. Pedley, J. F.; Hiley, R. W.; Hancock, R. A. Fuel **1987**, 66, 1646-1651.
4. Bhan, O. K.; Tang, S. Y.; Brinkman, D. W.; Carley, B. Fuel **1988**, 67, 227-237.
5. Bhan, O. K.; Brinkman, D. W.; Green, J. B.; Carley, B. Fuel **1987**, 66, 1200-1214.
6. Mayo, F. R.; Lan, B. Y. Ind. Eng. Chem. Res. **1987**, 26, 215-220.
7. Mayo, F. R.; Lan, B. Y. Ind. Eng. Chem. Prod. Res. Dev. **1986**, 25, 333-338.
8. Mayo, F. R. Acc. Chem. Res. **1968**, 1, 193-201.
9. Ingold, K. U. Chem. Rev. **1961**, 61, 563-589.
10. Beaver, B. D.; Hazlett, R. N.; Cooney, J. V.; Watkins, J. M. Prepr.--Am. Chem. Soc., Div. Fuel Chem. **1987**, 32(1), 538-546.
11. Cooney, J. V.; Hazlett, R. N. Heterocycles **1984**, 22, 1513.
12. Sturm, G. P. Jr. et al. "Sediment Formation in Two Aged Jet Fuels," to be Submitted to Energy and Fuels.
13. Grigsby, R. D. "Processing of High Resolution Mass Spectral Data Recorded from the Probe Microdistillation of Complex Mixtures." Paper MPB 50, 36th ASMS Conference, June 5-10, 1988, San Francisco, CA.

TABLE 1. Compound types identified in sediments

Compound type	Empirical formula	Range of X* GC/MS	Range of X* PMD/MS	Abundance by GC/MS
Indans	C_nH_{2n-8}	0-4	0-5	low
Indenes	C_nH_{2n-10}	0-4	0-6	high
Dihydronaphthalenes	C_nH_{2n-10}	0-2	0-5	high
Naphthalenes	C_nH_{2n-12}	0-4	0-5	medium
Phenols	$C_nH_{2n-6}O$	0-5	1-8	low
Indanols	$C_nH_{2n-8}O$	0-4	0-7	low
Indenols	$C_nH_{2n-10}O$	0-4	0-6	high
Benzofurans	$C_nH_{2n-10}O$	0-4	0-7	low
1-Tetralones	$C_nH_{2n-10}O$	0-2	0-5	high
1-Naphthols	$C_nH_{2n-12}O$	0-4	0-5	high
1-Indenones	$C_nH_{2n-12}O$	?	1-6	‡
1,3-Indandiones	$C_nH_{2n-12}O_2$	?	0-6	‡
o-Phthalic anhydrides	$C_nH_{2n-12}O_3$	0-2	1-7	low

*Range of carbon numbers in alkyl substituents.
‡Presence suspected but unconfirmed.

Presented at the 36th ASMS Conference on Mass Spectrometry and Allied Topics
June 5-10, 1988, San Francisco, CA

THE CHARACTERIZATION OF FUNCTIONAL FLUIDS BY HIGH TEMPERATURE CAPILLARY GAS CHROMATOGRAPHY/MASS SPECTROMETRY

T. H. Wang

Technology Division

Pennzoil Products Company, The Woodlands, TX 77387

A new class of functional fluids, high molecular weight alkylated cyclopentanes were characterized by a novel high temperature capillary gas chromatography/mass spectrometric technique.

A wide-bore fused silica capillary column coated with the polar, thermostable stationary phase PZ-179 (a polyphenylether sulfone) was used for the initial GC separation. Typical programmed runs spanned a temperature range of 150-380°C illustrating the utility of this system in analyzing high boiling functional fluids. The chromatogram of two wax standards on a 60 meter 10% PZ-179 capillary column is shown in Figure 1. The base line was very stable up to C-54. The chromatogram of an alkylated cyclopentane is shown in Figure 2. The isomers of tridecyl-, tetradecyl- and pentadecyl cyclopentane were separated by this PZ-179 fused silica capillary column.

Following GC separation, the structures of alkylated cyclopentane functional fluids were confirmed by electron impact mass spectrometry. However, the parent peaks obtained by electron impact tended to be weak or absent, whereas normal phase liquid chromatography/thermospray mass spectrometry gave an intense $(M-1)^+$ peak and was consequently a better parent ion confirmation than traditional electron impact.

Other high boiling commercial functional fluids containing a large number of isomers were separated on this column and subsequently identified by mass spectrometry. Dibasic acid esters, pentapolyol alkanolates and polyalphaolefins are typical of the types of functional fluids analyzed by this method.

In summation, the combination of mass spectrometry and PZ-179 capillary column chromatography provides a powerful tool for qualitatively and quantitatively analyzing high boiling functional fluids.

Presented at the 36th ASMS Conference on Mass Spectrometry and Allied Topics
June 5-10, 1988, San Francisco, CA

FIGURE 1: CHROMATOGRAM OF TWO WAX STANDARDS ON A 60 METER 10% PZ-179 CAPILLARY COLUMN

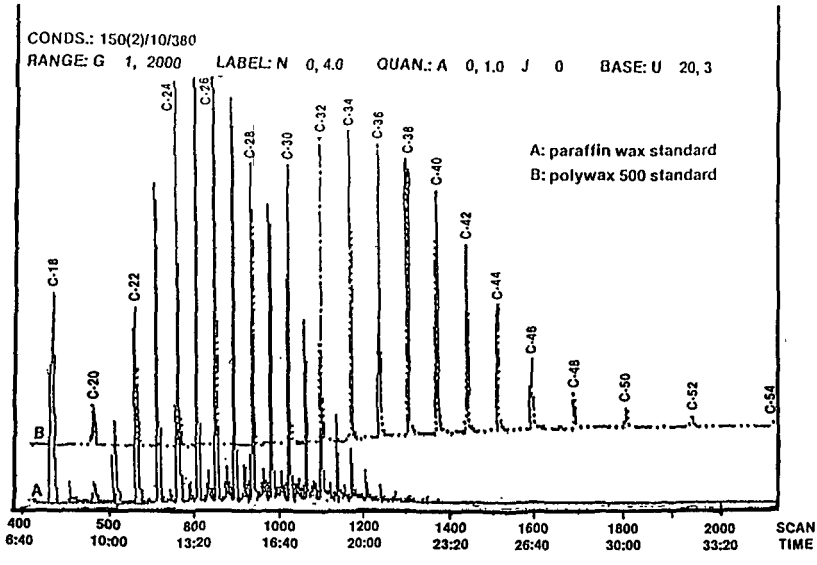

FIGURE 2: CHROMATOGRAM OF ALKYLATED CYCLOPENTANE

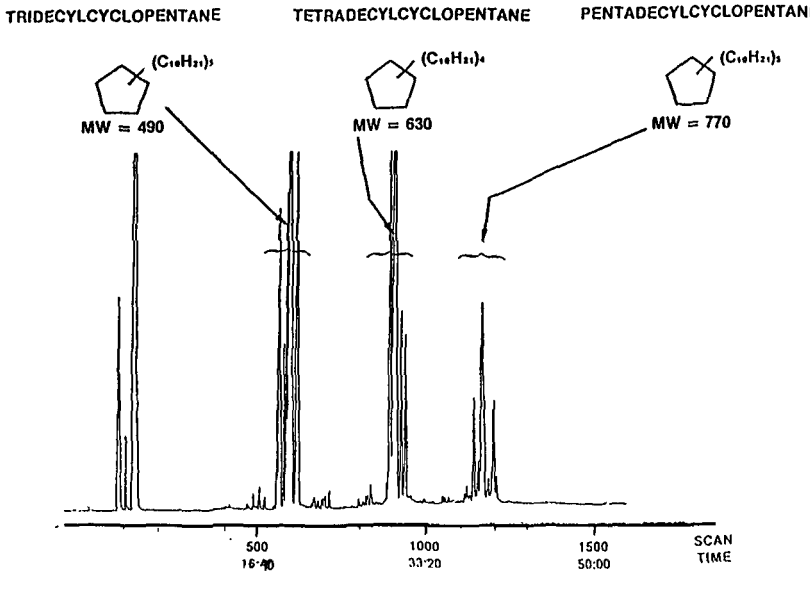

Presented at the 36th ASMS Conference on Mass Spectrometry and Allied Topics
June 5-10, 1988, San Francisco, CA

A MOLECULAR BEAM MASS SPECTROMETRIC INVESTIGATION OF THE COMBUSTION OF SINGLE COAL PARTICLES*

Frank Green, J. Eugene O'Donnell, and David Robaugh

MIDWEST RESEARCH INSTITUTE
Kansas City, MO 64110

Alkali metal species have been identified as principal contributors to the corrosion of heat transfer surfaces and turbines in coal combustion and gasification systems. This corrosion often limits the life and operating temperature of these systems. To date, the information on the behavior of alkali species during coal combustion, particularly at the high pressures typical of pressurized fluidized bed combustors (PFBC) is very limited. This research was therefore undertaken to obtain data on the behavior of alkali species which would be suitable for testing combustion models.

The experimental approach chosen was that of following the reaction of single coal particles with various gas mixtures having temperatures, pressures, and flow rates which simulate PFBC conditions. The species leaving the particle surfaces were measured as a function of time by means of high resolution molecular beam mass spectrometry (MBMS). Particle temperatures were measured by optical pyrometry.

A combustor suitable for the performance of the single particle experiments has been designed and constructed. This combustor has been integrated with an existing MBMS system, which was modified to permit the optical pyrometric measurements and the rapid acquisition of the mass spectrometric data. Measurements have been made using three model coals of three different ranks: Sewickley bituminous coal; Decker subbituminous coal; and Beulah lignite. These measurements were made at temperatures of 1200 to 2000°F, pressures of 1 to 10 atm, and in various gas mixtures at a flow rate of 10 ft/sec. The major alkali species leaving the particle surface were found to be the gaseous metals, with only a small fraction of the total alkali metals present as the hydroxide. The known gaseous sodium oxides were below the limit of detection. Combustion times and combustion products and intermediates were also measured.

---

* This work was supported by the U.S. Department of Energy, Morgantown Energy Technology Center under Contract No. DE-AC-84MC21091.

Experiments were also performed to attempt to determine the behavior of gaseous sodium following its evolution from the coal particles. Measurements were carried out in which the concentration of gaseous Na was measured at different times/distances downstream from arrays containing 19 2-mm Beulah lignite particles. Combustion gases containing 5% and 19% O_2 were used. Although the resulting data showed considerable scatter, which was probably the result of variation in the compositions of the coal particles, good correlations were obtained from the least squares treatment of the data. The "phenomenological" rate law obtained based on these two series of experiments was:

$$-\frac{d\,(Na)}{dt} = 1.06 \times 10^{5}\ (Na)\ (O_2)^{\frac{1}{4}}\ \text{mole cm}^{-3}\ \text{sec}^{-1}$$

Presented at the 36th ASMS Conference on Mass Spectrometry and Allied Topics
June 5-10, 1988, San Francisco, CA

CHARACTERIZATION OF COKE MATERIALS FORMED ON ZEOLITE CATALYSTS: APPLICATIONS OF THERMAL CHROMATOGRAPHY-MASS SPECTROMETRY [1].

Benny R. Richardson, Thomas R. Sharp and James F. Haw
Department of Chemistry, Texas A&M University, College Station, Texas 77843, U.S.A.

Cracking catalysts, such as the Faujasite Y zeolite, are used widely in converting a broad range of various organic feedstocks to branched chain aliphatic and aromatic gasoline-range hydrocarbons. However, a carbonaceous material, called coke, forms in and around the zeolite crystallite, which clogs the passageways through the zeolite and covers its surface, isolating active sites from the hydrocarbon feedstock, and deactivating the catalyst. Application of new "thermal chromatography" [1] techniques to the characterization of these cokes simplifies the analytical task, and promises to provide information leading to a better understanding of the mechanisms involved in coke formation.

The Method: Thermal chromatography [1] is a method for desorbing organic compounds from a solid sample by heat rather than by classical solvent extraction. The technique (Fig 1) consists of placing a solid sample -- e.g., approximately 1 to 5 mg of coked zeolite -- directly into a chamber which is continuously flushed with a flow of helium carrier gas. While flushing is continued, the sample is heated at a predetermined rate from ambient temperature to as high as 600°C. The amount of volatile substances desorbing into the carrier gas is measured by passing it through a flame ionization detector (FID), and correlated with the temperature of the sample at which substances desorb. This experiment is referred to as a Level I thermal analysis, and is used for estimation of total amounts of adsorbed organics.

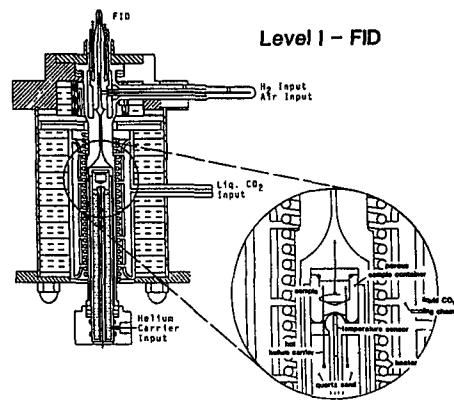

Figure 1: Level I thermal chromatography apparatus. Diagram courtesy of Ruska Laboratories [2].

Identification of specific compounds is achieved using thermal chromatography combined with gas chromatography-mass spectrometry (TC-MS, [1]), known as Level II analysis. A cold trap is placed in the flow path to collect and concentrate thermal fractions desorbing from the sample, e.g. below 200°C. The original solid sample is then cooled to retain any remaining adsorbed materials, while the cold-trapped thermal fraction is introduced onto a gas chromatographic column. Effluent from the column is introduced into an FID detector or, as in Fig 2, a mass spectrometer. After data collection on this first thermal fraction is completed, the original solid sample, having been held in the sample loader, can be reheated, e.g. to 450°C, to collect a second thermal fraction for analysis. This cycle can be repeated to completely characterize the materials adsorbed on the original solid sample.

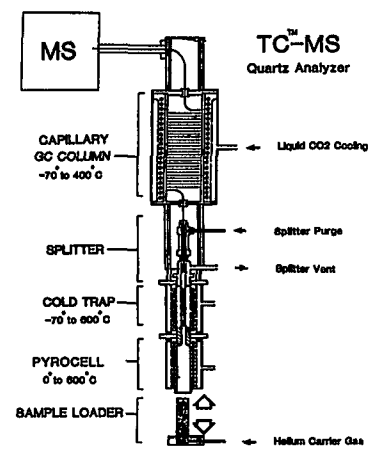

Figure 2: Level II thermal chromatography-mass spectrometry (TC-MS) [1] apparatus. Diagram courtesy of Ruska Laboratories [2].

Level I Characterization of Cokes: Six samples of Faujasite Y zeolite treated with a 1,3-butadiene feedstock were coked at different temperatures -- 150°C, 200°C, 300°C, 400°C, 500°C and 600°C. The results of Level I analyses of adsorbed organic matter on these samples are shown in Fig 3.

They indicate several "thermal classes" of compounds in the cokes, suggested by peaks in the desorption profiles. The amounts of desorbable organics per mg of zeolite are estimated by the areas under the curves, indicating a maximum amount of volatile material on the 200°-coked sample, with less on the samples coked at higher temperatures. These results are in contrast to percentage carbon determinations done on these same samples by an adaptation of standard organic elemental analysis procedures, which indicated a progressive increase in percentage (by weight) of carbon as the coking temperature was increased. The increase in the temperature at which the majority of material is desorbed also suggests that the organics on the samples coked at higher temperature are of progressively larger molecular weight.

Level II Identification of Components: Thermal fractions were collected and subjected to gas chromatography-mass spectrometric analysis. The lower temperature fractions consisted of low molecular weight unsaturated hydrocarbons, identified by mass spectral library matching, which could be logically related to the alkene feedstock used in the coking experiment. The higher temperature fraction contained series of substituted benzenes, naphthalenes, phenanthrenes, and higher polycyclic aromatic compounds, again readily identifiable by chromatographic retention times and mass spectral library matching.

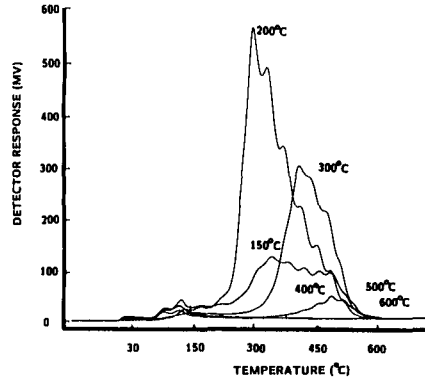

Figure 3: Comparison of amounts of desorbable organic materials on zeolites coked at different temperatures.

Experimental: Faujasite Y zeolite was obtained from Strem Chemical Co., and activated by two overnight exchanges with 1 M aqueous NH_4NO_3, followed by driving the ammonia off by a standard calcination procedure. The 1,3-butadiene feedstock (Matheson Gas Products, 99.0%) was adsorbed to the zeolite by mixing the diene into a stream of dry N_2 flowing over the activated zeolite, while the zeolite was maintained at one of the temperatures indicated above for one hour. Flows of both N_2 and butadiene were each 140 ml/min. The coked zeolite samples were then stored in a sealed inert atmosphere until analyses were performed.

Calibration of the Level I experiments for estimation of total desorbable organics on the zeolites was done using both pure n-C_{30} hydrocarbon and chrysene (Aldrich) as standards. Amounts of the standards were weighed into sample cups, run through Level I desorption, and the area under the FID response curve related to the amount of standard used. Standard curves showed excellent linearity, but different slopes for different standards, as expected.

GC separations of thermal slices during Level II analyses were conducted on non-polar bonded phase fused silica capillary columns (J&W Scientific, DB-1, 15m x 0.32 mm., 0.25 micron film). The mass spectrometer used was a Finnigan/MAT Ion Trap, controlled by an ITDS data system. Full scan spectra were recorded. Identification of components was aided by searching the NBS library version available on that datasystem.

Conclusions: This technique presents an ideal method for characterizing the organic compounds adsorbed on zeolite catalysts, or any solid or semisolid sample which has volatilizable materials adsorbed on its surfaces. It is an alternate, and in certain instances more desirable, technique to solvent extraction procedures in which the ability of the solvent to displace the desired substances from the surface becomes an important additional experimental variable.

Acknowledgement: Funds for this study were provided by National Science Foundation Grant CHE-8700667. We would like to also thank Dr. Chris Sutton, Dr. John Zumberge and Mr. Tim Hartmann of Ruska Laboratories for their continuing support and encouragement.

---

1. Registered trademark or servicemark of Ruska Laboratories [2].
2. Ruska Laboratories, 3601 Dunvale, Houston, TX 77063

Presented at the 36th ASMS Conference on Mass Spectrometry and Allied Topics
June 5-10, 1988, San Francisco, CA

DERIVATIZATION IN COMBINATION WITH LMS AND SIMS FOR ANALYSIS OF OXIDIZED COAL SURFACES.

*Jensen, N.J.; Sharkey, A.G.; Viswanadham, S.K.; Lineman, D.L.; Hercules, D.M. University of Pittsburgh, Pittsburgh, PA 15260

Ambient temperature surface oxidation of coal alters many of its physical and chemical properties important in direct utilization and conversion including heating value, agglomeration, coking quality, liquid yield and beneficiation. Characterization of this oxidation is challenging in that a surface phenomenon is involved. The purpose of this research was to develop methodology for characterization of specific compounds (i.e. functional groups) formed in the oxidation process using in situ derivatization reactions for specific functional groups in combination with the microprobe analytical methods of laser mass spectrometry (LMS) and secondary ion mass spectrometry (SIMS).

A number of potential derivatization reagents were identified for screening. However, to be suitable for coal analysis, these derivatization reactions must be applicable to a wide range of compounds with specific functionality and the reaction must occur at ambient temperature under relatively mild conditions. Mild conditions are essential to minimize extraneous reactions of the coal.

Derivatizations studied included: Girard's reagent, iminium perchlorates, pyridinium salts, -ylium dichloroiodates, bisulfites and 2,4-dinitrophenyl hydrazones for aldehydes and ketones; pentafluorobenzyl esters, carboxyl methylenium chlorides, tetra-ethylammonium salts, and t-butyl dimethylsilyl esters for carboxylic acids; and tri-ethylammonium-1-chloro-2-butene salts (TAB), 2-alkoxy phospholanes, boronates, sulfonate esters and di- and trimethylsilyl derivatives for alcohols and phenols. Many of these derivatives yield salts that are well suited to analysis by LMS and SIMS.

Sets of model compounds were derivatized with the reagents and products were analyzed by LMS and SIMS in both positive and negative ion modes. LMS spectra of the 2,4-dinitrophenylhydrazine derivative of benzaldehyde obtained on a zinc substrait are shown in figure 1. Those derivatives that yielded meaningful spectral data for a range of compounds analyzed on metal foil substraits were then studied on carbonaceous substraits. Both preformed derivatives and model compounds absorbed on charcoal and then derivatized were studied on charcoal to evaluate the effect of a carbon matrix. In general, the carbon matrix is not a problem as derivatization increases the mass of the ions of interest and clearly separates them from the low mass carbon clusters. The negative ion LMS spectrum of benzaldehyde derivatized in situ on charcoal with 2,4-dinitrophenylhydrazine is shown in figure 2.

The specific derivatizations for oxidized coal that were selected on the basis of data obtained for the model compounds included: Reaction with 2,4-dinitrophenylhydrazine followed by negative ion LMS analysis and reaction with Girard's reagent followed by SIMS for analysis of the carbonyl functionality; derivatization at pH > 11 with TAB for characterization of the OH functionality, particularly phenols; and derivatization at pH < 9 with TAB for identification of the acids. Negative ion LMS spectra for (a) nonderivatized, (b) 2,4-dinitrophenylhydrazine treated, and (c) TAB treated oxidized Illinois #6 coal are shown in figure 3.

Considering the list of reagents screened, the number that are applicable to coal analysis is very limited. The ability to form derivatives for a range of compounds under ambient conditions is a demanding requirement. The use of Girard's reagent, 2,4-dinitrophenylhydrazine, and TAB in combination with LMS and SIMS analysis have been shown to be suitable for extraction of specific chemical information from the complex oxidized coal matrix.

Acknowledgement: This work was supported by U.S Department of Energy under Contract No. DE-FG22-86pc90527

Current Address:

*Phillip Morris, USA, Research Center, Richmond, VA 23261

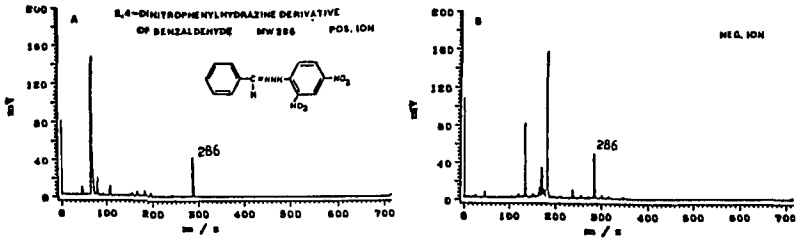

figure 1: LMS Spectra of the 2,4-dinitrophenylhydrazine derivatives of benzaldehyde obtained on a zinc substrate.

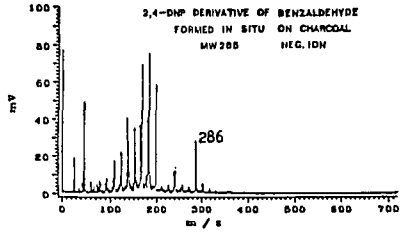

figure 2: Negative ion LMS spectrum of benzaldehyde derivatized in situ on charcoal with 2,4-dinitrophenylhydrazine.

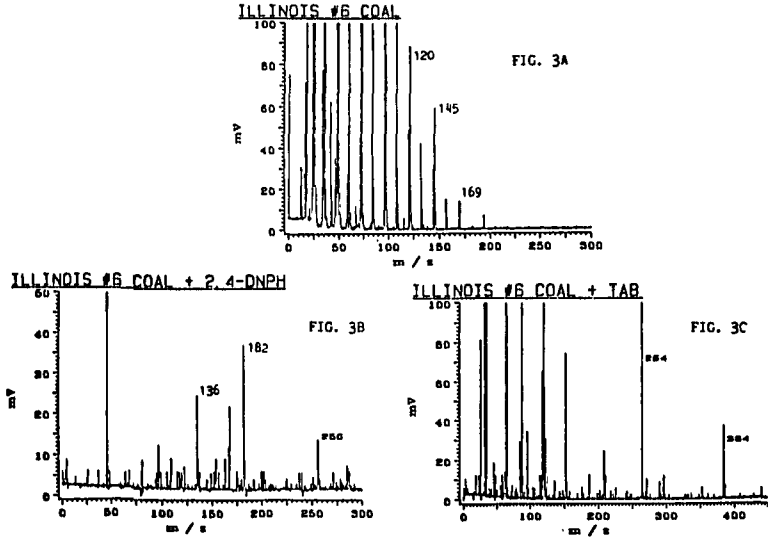

figure 3: Negative ion LMS spectra for (a) nonderivatized, (b) 2,4-dinitrophenylhydrazine treated, and (c) TAB treated oxidized Illinois #6 coal.

Presented at the 36th ASMS Conference on Mass Spectrometry and Allied Topics
June 5-10, 1988, San Francisco, CA

PROCESSING OF HIGH RESOLUTION MASS SPECTRAL DATA RECORDED FROM THE PROBE MICRODISTILLATION OF COMPLEX MIXTURES

by

Ronald D. Grigsby
IIT Research Institute
National Institute for Petroleum and Energy Research
P.O. Box 2128
Bartlesville, OK 74005

Processing and interpretation of the voluminous quantity of high resolution mass spectral data acquired in probe microdistillation experiments (PMD/MS) can be very labor-intensive without the aid of extensive computer software. Recently, modifications to and extensions of programs for processing and interpreting PMD/MS data have been completed. Use of the programs is illustrated with results obtained from the analysis of a jet-fuel sediment.

The sediment, a yellow-colored jelly, was recovered by filtration from a jet fuel aged at 80 deg C for eight weeks. It dissolved readily in carbon tetrachloride. The solution was loaded into a direct-introduction probe, and a stream of nitrogen gas was used to evaporate the solvent at room temperature. The probe and temperature programmer are described in the literature (1).

The sample was distilled into the ion source of a Kratos MS-50 high resolution mass spectrometer over a probe temperature range from -72 to +326 deg C at a programming rate of 10 deg C/min. The ion-source temperature was 250 deg C. Nominal 20eV electron bombardment was used for ionization and and 39 scans of the spectrum were recorded at 100 sec/decade and 25,000 resolving power.

Six FORTRAN programs, run sequentially, allow raw mass/intensity data from as many as 100 scans to be processed into qualitative and quantitative results. These programs are named "SPECTR", "READTAP", "PROB", "CHY", "INTCOR", and "ELMCRV". Another program, "XFER" (Data General software), is required to transfer the data to tape. All programs except "SPECTR" and "XFER" run on a Digital Equipment Corp. MicroVAX-II computer. "SPECTR" and "XFER" execute on a Data General NOVA/4 computer, which is a component part of the Kratos data acquisition system.

Programs "SPECTR" and "XFER" restructure the data into a tape format compatible with the input requirements of the MicroVAX-II. Transfer of data on tape to this computer is handled by program "READTAP". Program "PROB" accepts the data, consisting of 12C masses and intensities in order of decreasing mass, and converts the masses to the Kendrick scale, in which the mass of CH(2) is defined as exactly 14 amu (2). The data are processed to separate the reference peaks (originating from a calibration mixture run simultaneously with the sample) from the sample peaks.

Program "CHY" identifies ions belonging to specified homologous series, e.g., C(n)H(2n+z) or C(n)H(2n+z)O, where z represents the degree of unsaturation. A description of program "CHY" was presented at the 35th ASMS Conference in Denver, last year (3).

Program "INTCOR" uses the intensities of the reference peaks to correct intensities of the sample peaks for variations in ion-source extraction efficiency encountered during a probe microdistillation experiment. The corrections are based on the assumption that the intensities of the reference ions should remain constant during the run. This is an approximation when the reference mixture is introduced through an expansion-volume inlet (the usual procedure).

Program "ELMCRV" calculates elimination curves for the sample ions. By nonlinear regression, the time/intensity (or temperature/intensity) data for each ion are used to evaluate four parameters in a skewed Gaussian equation expressing the intensity of a sample peak as a function of time (or temperature). After they are evaluated, the parameters are used to calculate the maximum intensity of the curve, IMAX, the time (or temperature) at which the maximum occurs, T(IMAX), and the area under the curve, AREA. Ninety percent confidence intervals are included (1). Output from "ELMCRV" consists of line-printer plots of the curves and other results. If the regression analysis is successful, the goodness of fit, values of IMAX, T(IMAX), AREA, and the parameters with ninety percent confidence intervals are included. If a curve cannot be calculated because low intensities cause excessive data scatter, only the points are plotted. In this case, the time (or temperature) centroid and area obtained by adding the areas of trapezoids are calculated and given along with the maximum intensity and corresponding time (or temperature). Program "ELMCRV" also produces a table showing the T(IMAX), IMAX, AREA, and other information for each ion arranged in order of decreasing z number and increasing mass. Ninety percent confidence intervals are included with the statistical output. Table I shows partial results for molecular ions of elemental combination C(n)H(2n-10)O originating from the jet-fuel sediment. Comparison of the areas under the curves provides an estimate of the relative abundances of the components of the given elemental combination. Non-statistical results, i.e., temperature centroids, etc., are printed in a separate table at the end of the output.

Table I. Edited Output from Program "ELMCRV" Showing Statistical and Nonstatistical Results for C(n)H(2n-10)O Assignments in the High-Resolution Mass Spectra of a Jet-Fuel Sediment. Maximum ppm error = 10.

STATISTICAL RESULTS ORDERED BY INCREASING MASS

M/Z	T(IMAX), MIN	IMAX/10000	AREA/10000
118.	36.79 +- 1.69	6.83 +- 0.55	193.46 +- 28.43
132.	33.61 +- 1.15	22.73 +- 10.23	536.84 +- 390.81
146.	36.69 +- 1.38	39.00 +- 3.14	994.44 +- 135.00
160.	39.48 +- 0.92	50.07 +- 2.52	1269.86 +- 100.11
174.	40.20 +- 0.91	43.72 +- 2.24	1072.20 +- 85.42
188.	40.89 +- 1.03	19.51 +- 1.19	471.69 +- 43.34
202.	39.57 +- 1.71	4.82 +- 0.43	127.11 +- 17.80

NON-STATISTICAL RESULTS ORDERED BY INCREASING MASS

M/Z	T(CENTR), MIN	T(IMAX), MIN	IMAX/10000	AREA/10000
104.	41.99	45.15	1.64	24.38
216.	46.28	38.83	1.51	30.80

The sediment from the jet fuel was found to consist predominantly of C(n)H(2n+z) and C(n)H(2n+z)O compound types with values of z ranging from -8 through -12. Other compound types with two and three oxygens were detected. Additional results are presented in paper No. MPB 45 by G. P. Sturm., Jr., R. D. Grigsby, J. B. Green, and D. W. Brinkman.

ACKNOWLEDGMENT

Appreciation is expressed to the Naval Air Propulsion Center, U.S. Navy, and the Pittsburgh Energy Technology Center, U.S. Department of Energy, for support of this work under cooperative agreements DE-FC22-83FE60149 and DE-AC22-86PC90010, respectively.

REFERENCES

1. Schronk, L. R.; Grigsby, R. D.; Scheppele, S. E., Anal. Chem., 1982, 54, 748-755.
2. Kendrick, E. Anal. Chem. 1963, 35, 2146-2154.
3. Grigsby, R. D., presented at the 35th ASMS Conference on Mass Spectrometry and Allied Topics, May 24-29,1987, Denver, CO, paper No. TPA 16.

HYDROCARBON TYPE ANALYSIS BY NITRIC OXIDE CHEMICAL IONIZATION GC/MS

H. A. Petersen, I. Dzidic and H. V. Hart
Shell Development Company, P. O. Box 1380, Houston, Tx 77251

The conventional method of classifying hydrocarbons in mass spectrometry is by the number of hydrogen atoms relative to the number of carbon atoms as expressed by the letter z in the general empirical formula C_nH_{2n+z} (1). All members of a homologous series have the same z number. For paraffins, the most saturated hydrocarbon species, z= +2, for 1-ring naphthenes, z= 0, for 2-ring naphthenes, z= -2, etc.

In our laboratory we have developed a new approach for type analysis based on nitric oxide chemical ionization and GC/MS. The main advantage of this approach is that hydrocarbons of the same nominal molecular weight but different formula can be distinguished by their structurally characteristic ions formed under NO/CI and GC retention times. This method eliminates the need for high resolution mass spectrometry. In addition, hydrocarbons of the same molecular formula, such as acenaphthenes/biphenyls and acenaphthylenes/fluorenes can be distinguished since their GC retention times are different.

The quantification is based on an INCOS procedure which excludes the contribution of alkylbenzothiophenes to alkylbenzenes at z= -6 and the contribution of alkyldibenzothiophenes to alkylnaphthalenes at z= -12. Also z= -18 and z= -20 ion summing ranges are adjusted to include only those species eluting in the specific boiling ranges. The GC/MS is a Finnigan model 4535 equipped with a Townsend discharge mode of ionization. The GC uses a 2mm x 10 ft. glass column packed with 3% OV-101 on 80/100 Supelcoport.

Figure 1 shows that in a catalytically cracked light gas oil (CCLGO) feedstock, within the z= -12 series, the C_4-, C_5-, and C_6-alkylnaphthalenes can be distinguished from the C_0-, C_1-, and C_2-alkyldibenzothiophenes. The same was observed for benzenes and benzothiophenes within the z= -6 series.

Figure 2 shows that different aromatic structures with the same molecular formulas can be chromatographically separated and identified by selective detection of the M+ ions.

The quantitative results of the NO/CI GC/MS method presented by the block diagram are shown in Figure 3. Figure 3 represents the hydrocarbon composition of CCLGO "before" and "after" hydrotreating. Thus, the method reflects the changes in hydrocarbon composition brought about by hydrotreating.

The precision (the percent standard deviation) and the accuracy of the method are about 7-8% relative, for samples boiling in the range 300-900° F. The accuracy was estimated from spiking experiments with pure compounds. Since petroleum samples of accurately known compositions are not available, there is no satisfactory way of determining the accuracy of the method.

For comparison, the total aromatic content by NO/CI GC/MS was found to be higher by an average of 10% relative to the NMR and UV values. From the comparison it was not possible to establish the accuracy limits of the method since there is no satisfactory way of establishing the accuracies of NMR and UV determinations.

1. Richard M. Teeter, "High-Resolution Mass Spectrometry for Type Analysis of Complex Mixtures", Mass Spec. Rev., 1985, 4(1), 123-43.

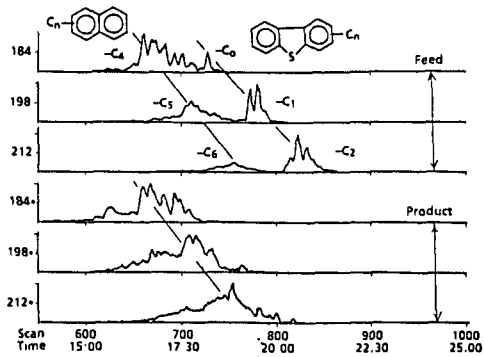

Figure 1. Selective Detection of the M⁺ Ions Shows That C_4^-, C_5^-, C_6^- Naphthalenes Can be Distinguished from Dibenzothiophene and Its C_1^-, C_2^- Homologues in a CCLGO Feed and the Hydrogenated Product Samples
Dibenzothiophenes are not detected in the product sample indicating that the sulfur compounds have been removed by the hydrogenation process.

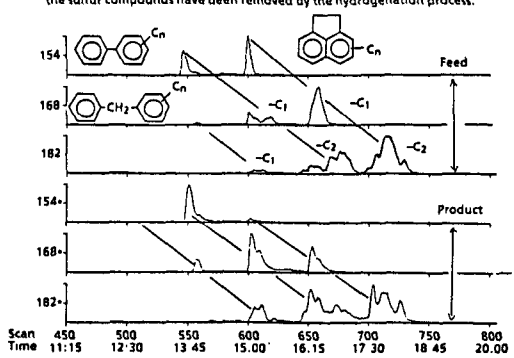

Figure 2. Selective Detection of the M⁺ Ions in a CCLGO Feed and the Hydrogenated Product Shows that Different Structural Homologues of the Same Molecular Weights Can be Chromatographically Separated

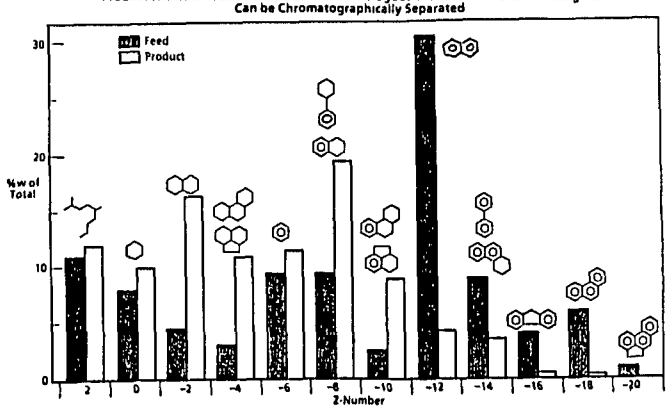

Figure 3. The Percent Total Distribution of Hydrocarbon Types by Z Number in a CCLGO Feed and the Hydrogenated Product Obtained by NO/CI GC/MS

Presented at the 36th ASMS Conference on Mass Spectrometry and Allied Topics
June 5-10, 1988, San Francisco, CA

Solvent Extraction of An Indiana Shale and Characterization of the Oil Extract

K.V. Wood[1], Ramani Narayan[2], K.R. Stringham[1] and Shuyen L. Huang[2]
Campus-Wide Mass Spectrometry Center[1]
Chemistry Building
Laboratory of Renewable Resources Engineering[2]
A.A. Potter Engineering Center

Purdue University
West Lafayette, IN 47907

A novel perchloroethylene solvent extraction scheme has been investigated for obtaining oil from silicate-rich oil shales. While development of oil from oil shale has a lower priority than coal as an energy resource[1], a co-processing scheme using shale oil with coal would make the utilization of oil shale more viable. The proximity of oil shale and coal would enhance the economics of such a process. This combination can be found in both the Illinois and Appalachian basins of the Eastern United States where silicate-rich oil shales immediately overlie commercial coal fields[2]. Surface mining of this coal exposes huge tonnages of oil shale which effects more than 11,000 acres each year in Indiana and Illinois. The purpose of this study is to use mass spectrometry to characterize the specific organic makeup of the oil obtained from a perchloroethylene solvent extraction of a silicate-rich oil shale.

Experimental

The oil shale (Devonian member) was obtained from Daviess County, Indiana (C=5.17%, H=1.07%, N=0.44%). The shale oil was obtained by extraction with perchloroethylene (typically two grams of shale with 25 ml of perchloroethylene at room temperature). The mass spectrometric analyses included: Hydrocarbon type analysis - CEC 103; GC/MS - Finnigan 4000 (DB-1 capillary column); MS/MS - Finnigan TSQ (Collision energy 20 eV; Argon collision gas pressure 1.6 mtorr).

Results and Discussion

The GC/MS analysis shows a number of resolved peaks early in the chromatogram prior to a very intense unresolved envelope at increased column temperatures (Figure 1). The individual resolved peaks were confirmed to be the straight chain alkane series, C_{11} through at least C_{25} at which point the unresolved envelope obscured any remaining straight chain paraffins. The large unresolved envelope was analyzed using a variety of chromatographic conditions but none were found to effect anything resembling a clean separation. The bulk of the ions observed (80%) from an individual mass spectrum obtained from the region of the unresolved envelope, are low mass (i.e., m/z 41, 43, 55, 57) suggesting the presence of a predominance of saturated hydrocarbons. The hopane and sterane biomarkers could be identified on the trailing edge of the unresolved envelope.

Due to the very aliphatic nature of the extracted oil a hydrocarbon type analysis was obtained. The results (Table I) confirm the GC/MS and probe analysis that the predominant chemical constituents in the extracted oil are saturated hydrocarbons (over 40%). As can be seen from Table I the extracted oil also contains a significant amount of olefins/cyclo paraffins. In order to more completely characterize the compounds present in the extracted oil, tandem mass spectrometry was utilized. The parent spectrum of m/z 57 (Figure 2), an intense fragment ion characteristic of alkanes, gives an indication of the paraffin series present in the shale oil extract. Parent spectra of m/z 71 and 85 extend the paraffin carbon number range because the fragment ion used for the parent scan is a correspondingly higher alkyl fragment.

Since both the GC/MS and hydrocarbon-type analysis indicated the abundance of low mass fragmentations, the parent spectra of a number of representative ions (m/z 77, 79, 81, 83, 87, 89, 91) in addition to the previously mentioned paraffin series, were obtained as a preliminary screen in an attempt to determine the organic structure of other components in the unresolved hump. As would be expected from the hydrocarbon-type analysis, the parent spectra of m/z 81, z = -2, dicycloparaffins/cycloolefins, and m/z 83, z = 0, monocycloparaffins/olefins had the most intense series of ions (Figure 3).

The ion at m/z 81 is indicative of having the $C_6H_9^+$ structure. Therefore, the parent spectrum suggests the presence of a compound series having an alkyl chain extending through C_{22} which fragments to m/z 81. There are a number of possible precursor structures which fragment to m/z 81 but daughter spectra suggest a series of long chain alkyl cycloolefins comprise the significant component of the z = -2 series in the extracted oil.

Presented at the 36th ASMS Conference on Mass Spectrometry and Allied Topics
June 5-10, 1988, San Francisco, CA

On the other hand, the ion at m/z 83 is indicative of having the $C_6H_{11}^+$ structure. This parent spectrum suggests the presence of a compound series having an alkyl chain extending through C_{25} which fragments to m/z 83. Daughter spectra suggest that olefins comprise the significant component of the z = 0 series in the extracted oil.

The combination of GC/MS, hydrocarbon-type analysis and MS/MS proved particularly valuable in providing complementary information for characterizing and identifying specific components in a shale oil derived from a perchloroethylene extraction scheme. This degree of characterization is necessary in order to assess the potential of an oil as a co-processing solvent with coal since certain types of hydrocarbons are known to be better proton sources than others.

Acknowledgements

The authors wish to thank Professor R.G. Cooks for access to the Finnigan Triple Stage Quadrupole Mass Spectrometer and D. Charles E. Schmidt of the Pittsburgh Energy Technology Center for performing the hydrocarbon-type analysis.

References

1. Coal and Synfuels Technology, Aug. 18, 1986.
2. Shaffer, N.R., Leininger, R.K., and Ennis, M.V. Shale, Symposium, Nov. 1984, 401.

HYDROCARBON TYPE ANALYSIS

GROUP TYPE (Z NUMBER)	VOLUME %
PARAFFINS (Z=+2)	43.91
OLEFINS/MONOCYCLOPARAFFINS (Z=0)	34.39
CYCLO OLEFINS/DICYCLOPARAFFINS (Z=-2)	8.00
CYCLO DIOLEFINS/TRICYCLOPARAFFINS (Z=-4)	7.18
BENZENES (Z=-6)	3.94
INDANS (Z=-8)	1.21
NAPHTHALENES (Z=-12)	1.36

Table I

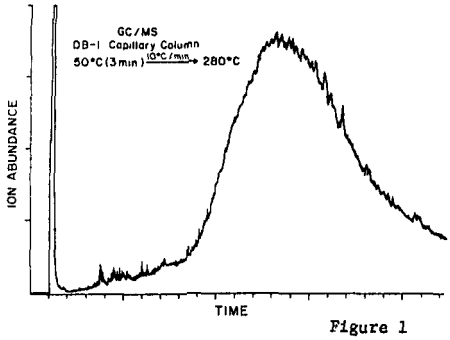

Figure 1

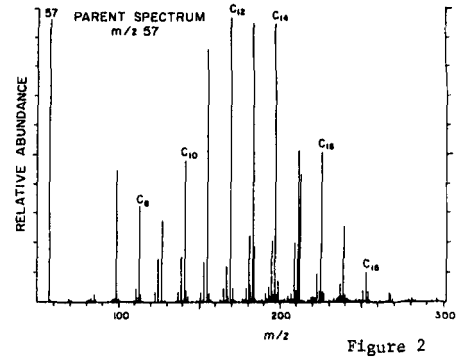

Figure 2

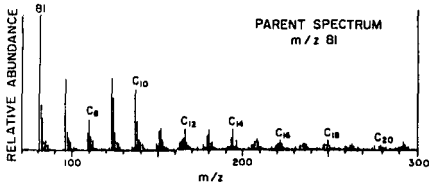

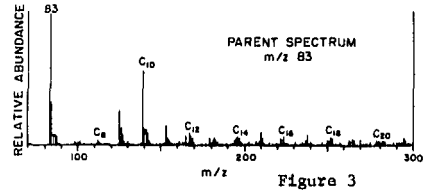

Figure 3

Presented at the 36th ASMS Conference on Mass Spectrometry and Allied Topics
June 5-10, 1988, San Francisco, CA

Hydrocarbon Type Analysis by GC/MS

C. S. Hsu and T. Aczel
Exxon Research and Engineering Company
Route 22 East, Clinton Township
Annandale, New Jersey 08801

T. R. Ashe and J. W. Fedora
Esso Petroleum Canada
Sarnia, Ontario, Canada N7T 7M1

Two recent advances are making GC/MS increasingly valuable for the detailed analysis of complex fossil fuels. Alternate ionization modes allow unequivocal identification of molecular ions; and the demonstrated equivalence of GC/MS data with conventional electron impact spectra, both at high and low voltages, allows accurate and reproducible quantification.

The use of isobutane chemical ionization for isoparaffins and naphthenes, and of low voltage ionization for aromatics and polar aromatics leads to unequivocal identification of molecular ions and improved deconvolution of unresolved GC/MS peaks.

These techniques are equally applicable to the total sample or to individual peaks. In the former case, the methodology allows one to closely relate composition to boiling range, as GC/MS retention times are easily related to boiling points.

Data obtained on various samples and blends also show extremely good agreement between GC/MS and conventional MS analyses using CEC mass spectrometers and ASTM published methods. We have reasons to believe that in fact the GC/MS analyses are slightly more accurate. These findings open a possibility for the of the use of GC/MS for enhanced hydrocarbon type analyses.

The increased scope of GC/MS for the analysis of complex hydrocarbon mixture are illustrated by several examples.

HIGH VOLTAGE EI GC/MS CHROMATOGRAM EXHIBITS OVERALL COMPOUND DISTRIBUTION STRUCTURE OF INDIVIDUAL COMPONENTS IN A COMPLEX MIXTURE CAN BE WELL-DEFINED FROM THEIR FRAGMENTATION PATTERNS.

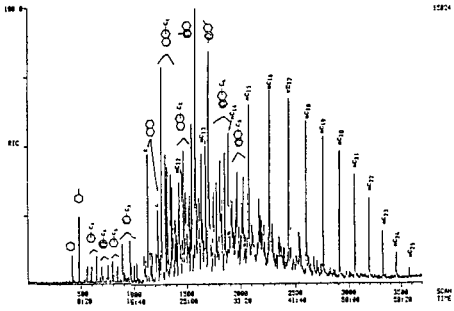

IN LOW VOLTAGE EI, INTERFERING IONS FROM SATURATED COMPONENTS ARE ESSENTIALLY REMOVED AND EACH AROMATIC COMPOUND IS REPRESENTED BY ITS MOLECULAR ION. THESE FACILITATE THE CALCULATION OF AROMATIC COMPOUND DISTRIBUTION.

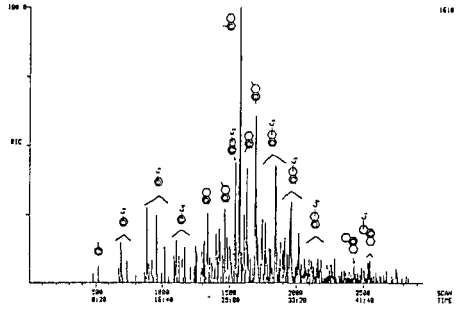

Presented at the 36th ASMS Conference on Mass Spectrometry and Allied Topics
June 5-10, 1988, San Francisco, CA

COMPOUND TYPE AND CARBON NUMBER DISTRIBUTION OF AROMATICS ARE DETERMINED BY MOLECULAR IONS FROM LOW VOLTAGE EI DATA INTEGRATED OVER ENTIRE GC/MS RUN

Series	C_nH_{2n-6}	C_nH_{2n-8}	C_nH_{2n-10}	C_nH_{2n-12}	C_nH_{2n-14}	C_nH_{2n-16}	C_nH_{2n-18}
Typical Molecules	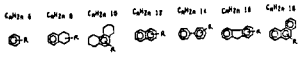						
Carbon No							
C6	0.0						
C7	0.5						
C8	1.3	0.6					
C9	2.9	3.7		0.0			
C10	3.6	22.0		0.0			
C11	3.3	33.8	0.6	1.6	0.0	0.0	
C12	8.6	15.5	4.6	5.5	1.4	2.7	
C13	1.5	4.3	3.9	5.7	3.1	5.1	1.1
C14	0.0	1.4	2.5	3.0	1.6	0.0	3.2
C15	0.3	1.6	1.9	0.0	0.3	0.0	0.3
C16	0.0	0.0	1.1	0.0	0.0	0.0	0.0
C17						1.2	2.7
Totals	16.4	76.6	7.3	4.8	4.2	12.2	16.7
Average CN	10.4	12.0	14.8	12.8	14.1		
Cy/Bic Chain	4.4	2.0	1.8	2.8	2.1		

- MASS SERIES ARE BETTER DEFINED BY GC/MS THAN ASTM TYPE ANALYSIS.

Z = -8 SERIES ARE TETRALINS, NOT INDANS,
-10 SERIES ARE OCTAHYDROPHENANTHRENES, NOT INDENES,
-14 SERIES ARE BIPHENYLS, NOT ACENAPHTHENES,
-16 SERIES ARE FLUORENES, NOT ACENAPHTHALENES

EXCELLENT AGREEMENT IS FOUND BETWEEN GC/MS AND CONVENTIONAL MS IN LOW VOLTAGE OPERATION MODE

A. COMPOUND TYPE DISTRIBUTION

Z NO.	COMPOUND TYPE	WEIGHT PERCENT MS	WEIGHT PERCENT GC/MS
6	BENZENES	17.0	16.8
8	INDANS/TETRALINS	35.8	36.0
10	INDENES/DINAPHTHENOBENZENES	4.3	4.3
12	NAPHTHALENES	38.2	38.0
14	BIPHENYLS/ACENAPHTHENES	4.1	4.1
16	FLUORENES	0.3	0.4
18	PHENANTHRENES	0.3	0.4
		100.0	100.0

LOW VOLTAGE GC/MS ALLOWS US TO DISTINGUISH BETWEEN COMPOUND TYPES WITH THE SAME NOMINAL MASS

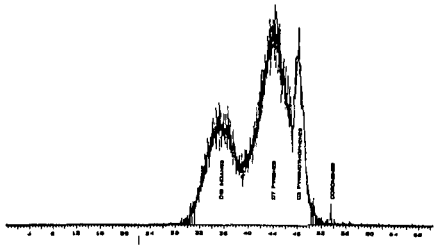

MS AND GC/MS AGREE WITH HPLC ON TOTAL AROMATICS AND AROMATIC RING DISTRIBUTION

COMPOUND TYPE	WEIGHT PERCENT MS	WEIGHT PERCENT GC/MS	WEIGHT PERCENT HPLC
TOTAL AROMATICS	56.7	56.2	55.9
1-RING AROMATICS	32.4	32.1	33.0
2-RING AROMATICS	24.1	23.9	22.5
3-RING AROMATICS	0.2	0.2	0.4

COMBINATION OF LOW VOLTAGE, HIGH VOLTAGE GC/MS ALLOWS DISTINGUISHING BETWEEN ISOMERIC OFFINS AND NAPHTHENES

RATIO OF LOW VOLTAGE MOLECULAR ION INTENSITY TO TOTAL HIGH VOLTAGE IONIZATION IS SENSITIVE TO STRUCTURE.

COMPONENT	RATIO
BENZENE	11.9
TOLUENE	12.1
ETHYL-BENZENE	7.9
O-XYLENE	12.4
ME-PENTENE-2	10.1
3-HEXENE	9.8
ME-PENTADIENE	9.9
3-HEPTENE	8.9
ME-HEXADIENE	8.6
3-ME-PENTANE	0.1
ME-CYCLOPENTANE	1.7
ME-CYCLOHEXANE	0.9
TRIME-CYCLOPENTANE	0.6
DIME-CYCLOPENTANE	1.0

GC/MS DETERMINES EXPERIMENTAL BOILING POINTS FOR ALKYL BENZENES

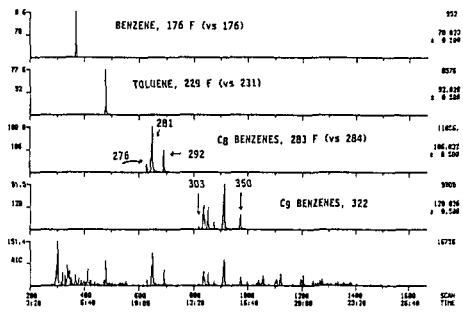

Presented at the 36th ASMS Conference on Mass Spectrometry and Allied Topics
June 5-10, 1988, San Francisco, CA

Petroleum Hydrocarbon Compound Type Analysis By Quadrupole Mass Spectrometer

T.R. Ashe, Imperial Oil Research
Research Division, P.O. Box 3022
Sarnia, Ontario, Canada N7T 7M1

For thirty-five years, quantitative mass spectral hydrocarbon compound type analysis of petrochemical streams has been performed using magentic single-focusing instruments. These instruments were predominantly CEC or DuPont 21-100 series mass spectrometers. In 1976, DuPont ceased manufacturing this type of instrument because of its limited market.

In 1985, EXXON mass spectrometrists formed a committee to identify suitable replacement instruments for both gas and liquids analysis. The major spectrometer vendors were contacted and requested to participate in the evaluation. Five vendors (Extranuclear, Finnigan MAT, Hewlett-Packard, KRATOS, and VG) agreed to analyze the liquid samples. Due to difficulties, only Finnigan MAT, Hewlett-Packard and KRATOS were able to finish the evaluation within the specified time.

Based on the results of the evaluation, a Hewlett-Packard 5970 quadrupole, Mass Selective Detector (MSD), with the large Brunfeldt Inlet system, was chosen to replace the DuPont 21-104 quantitative mass spectrometer at Esso Petroleum Canada, Sarnia, for liquids analysis. This choice also offered the advantage of low voltage ionization for aromatics compositional analysis which could not be performed by the DuPont 21-104.

The MSD has been used to analyze materials with boiling ranges from 50°F to 1050+°F. The first year of operation was spent in developing analysis software and comparisons between the MSD and the DuPont 21-104. The comparisons were excellent for lower boiling materials, naphthas, propylene tetramers and middle distillates. Due to its higher mass range and sensitivity, the replacement system is able to more accurately determine the higher molecular weight materials present in lube aromatic fractions. The aromatics data from the MSD is in excellent agreement with high resolution compound type analyses generated within the EXXON circuit.

Several errors and differences were identified in the saturates analysis software between the DuPont 21-104 and the MSD. Following a comprehensive study, several typographical errors were identified in the ASTM D-2786 published inverses. The method was also extended to higher carbon numbers.

Correlations have been developed between the results from the MSD and the DuPont 21-104 for lube aromatics (ASTM D-3239) and the Robinson Total Oil method.

The instrument has been in daily use with only a minimum of down time associated with mechanical or electrical faults. The long term repeatability of the MSD has surpassed that of the DuPont 21-104.

Presented at the 36th ASMS Conference on Mass Spectrometry and Allied Topics
June 5-10, 1988, San Francisco, CA

DEACTIVATION MONITORING OF CATALYST FROM WILSONVILLE PILOT PLANT BY LOW VOLTAGE PY-MS AND MULTIVARIATE ANALYSIS

Koli Taghizadeh, Rita H. Hardy and Burtron H. Davis
Kentucky Energy Cabinet Laboratory, Lexington, KY 40512

Henk L.C. Meuzelaar
Center for Micro Analysis and Reaction Chemistry, University of Utah
Salt Lake City, UT 84112

The objective of this study is to investigate the deactivation mechanisms of a NiMo catalyst used in the Wilsonville coal liquefaction pilot plant during run 249 (Wyodak coal) while operating in the RITSL (Reconfigured Integrated Two-Stage Liquefaction) mode.

Our approach is to compare and integrate Low Voltage (12 eV) Curie-point pyrolysis/desorption mass spectrometry data with conventional (e.g., elemental analysis and mineral matter) data by means of canonical correlation analysis methods. Both Py-MS and conventional data were obtained on 17 samples collected over a period of 110 days during run 249.

Py-MS conditions were as follows: sample size 100 ug, temperature rise time 5-6 s, equilibrium temperature 610°C, total heating time 10 s, inlet temperature approx. 210°C, electron energy 12 eV, mass range 20-290 amu, scanning rate 1000 amu/s.

In the beginning of the run the organic compounds build up rapidly on the surface of the catalyst. The mass spectrum of sample no. 3 (Figure 1), which was on stream for 12 days, shows the maximum accumulation of organic matter. This organic matter is composed mainly of heteroatomic hydrocarbons (quinolines, phenanthridines, and azapyrenes) which were identified by Py-GC/MS. Subsequently, the concentration of the organics detectable by mass spectrometry decreases gradually. During the later parts of run 249 (88 days and longer) the chemical composition of the remaining organic deposits reveals a shift from heteroatomic hydrocarbons to polynuclear aromatic hydrocarbons.

Canonical correlation analysis of Py-MS and conventional data sets reveals two canonical variates with canonical correlation coefficients of 0.99 and 0.95 respectively. The scores plot of Py-MS and conventional data in the canonical variates I and II subspace is shown in Figure 2 and reveals two trends; (1) a time trend ("catalyst aging") and (2) a nitrogen compound "desorption" trend.

The numerically extracted spectrum along the time axis reveals the accumulation of organic compounds in the early days and the desorption and/or coking of the organic materials in the later days (Figure 3). The spectrum along the nitrogen desorption trend reveals the shift from nitrogen-containing compounds (e.g., quinolines, azapyrenes) to aromatic hydrocarbons (naphthalenes, acenaphthenes and phenanthrenes) in the last few samples (Figure 4).

The loadings of conventional parameters in the canonical variates space (Figure 5) reveal high H, N, and C contents, as well as atomic H/C and N/C ratio's in the early process samples. The later samples, however, show the accumulation of inorganic components such as Na, V, Ni and Ca.

The wellknown rapid deactivation of catalyst during the early stages of the coal liquefaction process appears to be due to adsorption of basic nitrogen compounds on the acid sites of the catalyst. During the later stages of the run these basic nitrogen compounds are gradually replaced by metal cations which increasingly mask the active sites of the catalyst, thereby resulting in slow further deactivation.

The research reported here was supported in part by DOE contract DEFC22-85PC80009 as part of the Consortium for Fossil Fuel Liquefaction Science and by the Commonwealth of Kentucky, Kentucky Energy Cabinet.

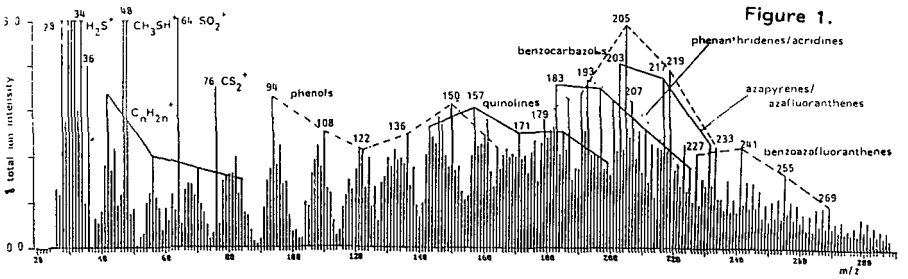

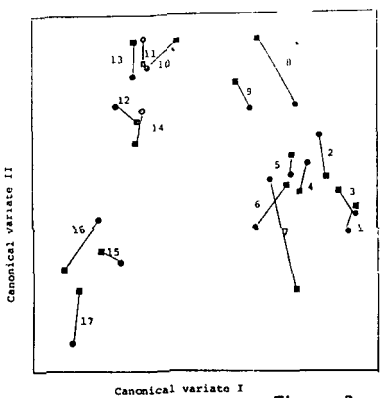

Figure 2.

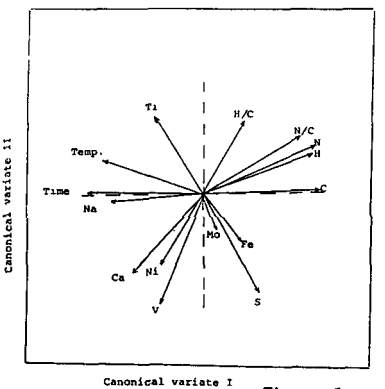

Figure 5.

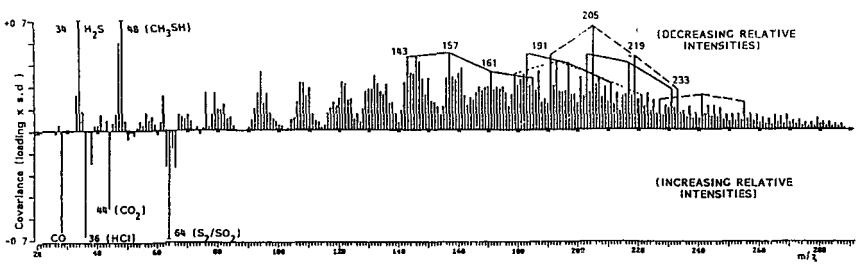

Figure 3.

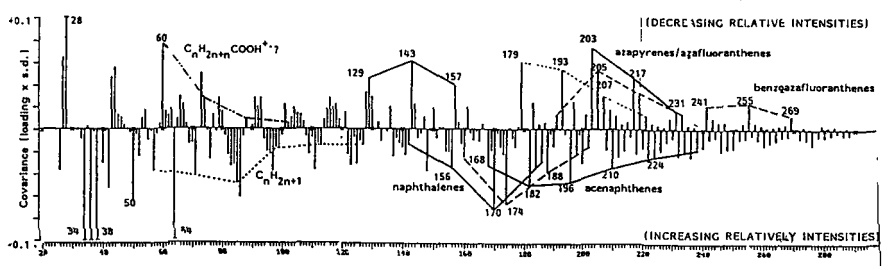

Figure 4.

Presented at the 36th ASMS Conference on Mass Spectrometry and Allied Topics
June 5-10, 1988, San Francisco, CA

STUDY OF NITROGEN CONTAINING COMPOUNDS IN FLUID CATALYTICALLY CRACKED OILS BY NH_3 CHEMICAL IONIZATION GC/MS AND MS/MS TECHNIQUES

D. V. DAVIS, D. B. CARDIN AND J. SCHERZER
Unocal Science and Technology Division, Brea, Ca., 92621

Nitrogen containing compounds play an important role in petroleum refining processes due to their potential as catalyst deactivators and pollutant precursors. In this study we have attempted to characterize the nitrogen containing species in a petroleum fraction (gas oil) both before and after processing thru a pilot plant Fluid Catalytic Cracking (FCC) unit. Preliminary to the study the samples were prepared by first separating both the product and feed into 3 cuts, material boiling below 450 F, material boiling between 450-670 F and material boiling at greater than 670 F. These cuts were further separated by Liquid Chromatography into fractions which were composed of mainly O and N containing species. These LC fractions were then analyzed by a combination of GC/MS and MS/MS techniques using NH_3 chemical ionization.

The Gasoline fraction provided the least amount of information of all fractions studied. The majority of the compounds in the feed were identified by library search as phenols and alkylated phenols. The presence of interfering fragment ions from these phenolic species prevented identification of nitrogen containing compounds in this sample. Many of these interfering ions were not present in the product however and some nitrogen containing compounds could be identified. These were benzamine (aniline) and alkylated benzamines.

The data for the 450-670F fraction and the >670F fraction were not obtained by GC/MS, but rather by MS/MS analysis of different homologous series of ions. The somewhat striking nature of the nitrogen types present before and after FCC processing is apparent in Figures 1A and 1B. These figures are composite NH_3 CI mass spectra of material thermally desorbed from the solid probe after introduction into the ion source. In 1A (feed) series are seen for alkylated indoles (m/z 118+14(n) n=1,2,3...), alkylated quinolines (m/z 130+14(n) n=1,2,3...), and alkylated carbazoles (m/z 168+14(n) n=1,2,3...). As well as an unidentified series (m/z 156+14(n) n=1,2,3...). Close examination of the MS/MS spectra for these series revealed that each single mass consisted of contributions from two isomeric components one of which was amine substituted. In 1B (product) many of the types are no longer present. Only the alkylated carbazoles and indoles are left. MS/MS data on this fraction showed the removal of the amine substituted isomers and that the alkyl substitutents had been altered to much shorter chains predominated by methyl groups.

The data for the >670F fraction is shown in Figures 2A and 2B. These figures are also composite NH_3 CI mass spectra of material thermally desorbed from the solid probe after introduction into the ion source. In 2A (feed) series are seen for alkylated carbazoles (m/z 168+14(n) n=1,2,3...), alkylated benzocarbazoles (m/z 218+14(n) n=1,2,3...), alkylated benzoquinolines (m/z 180+14(n) n=1,2,3...) and alkylated dibenzoquinolines (m/z 230+14(n) n=1,2,3...). Once again MS/MS data revealed the presence of isomeric amine substituted components at these masses. In 2B (product) only two types survive the alkylated carbazoles and benzocarbazoles. Again the alkyl groups are considerably shorter than in the feed usually just methyl groups.

Presented at the 36th ASMS Conference on Mass Spectrometry and Allied Topics
June 5-10, 1988, San Francisco, CA

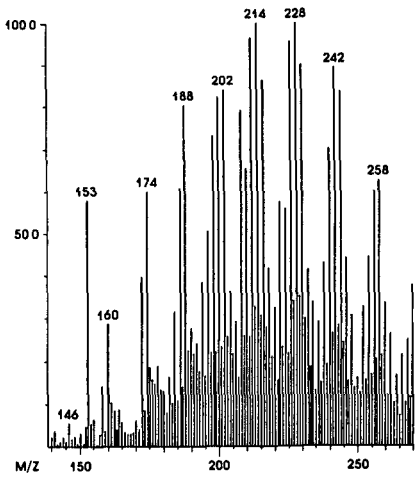

FIGURE 1A

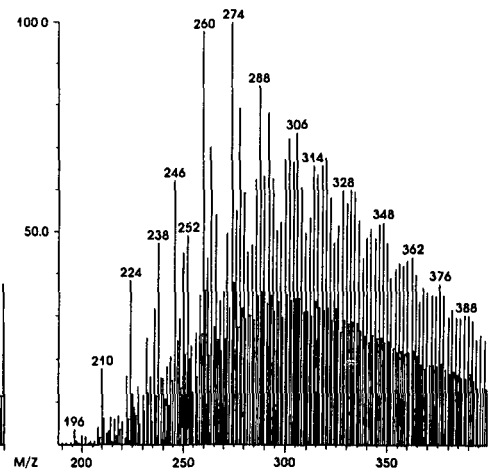

FIGURE 2A

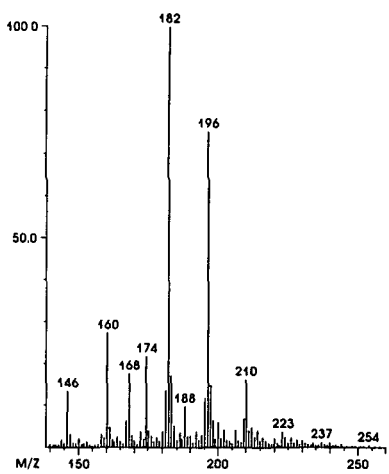

FIGURE 1B

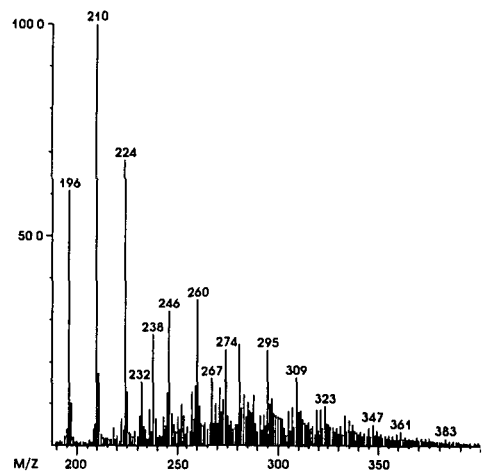

FIGURE 2B

Presented at the 36th ASMS Conference on Mass Spectrometry and Allied Topics
June 5-10, 1988, San Francisco, CA

APPLICATION OF GAS CHROMATOGRAPHY/MASS SPECTROMETRY TO THE STUDY OF BIOSOLUBILIZED COAL

J.A. Campbell, M. McCulloch, R.B. Lucke, R.M. Bean
Battelle, Pacific Northwest Laboratory
Richland, Washington 99352

INTRODUCTION

Biological conversion of low-rank coals by bacteria, fungi, or by enzymes they produce has been receiving considerable attention. These processes occur at ambient temperatures and pressures and may represent a potential cost savings for the processing of certain coals and lignites. In addition, microbial conversion of coal and coal-derived products is potentially an important technology for the production of clean fuels. Current technology for coal conversion requires both high temperatures and pressures which may result in the production of components that are more toxic than the original starting material.

Cohen and Gabriel (1) first reported that fungi could grow directly on, and metabolize leonardite, a naturally oxidized form of lignite coal. Wilson, et al. (2) have shown that the leonardite biodegraded product from C. versicolor was water soluble and contained no detectable polycyclic aromatic hydrocarbons (PAH) having three to six rings. In addition, the bioconverted material was inactive in the microbial histidine reversion assay for mutagenic activity. Campbell, et al., (3) have shown that the average molecular weight of the biodegraded product was 1800 daltons as determined by gel permeation chromatography.

In order to better understand the biosolubilization process, we have oxidized the starting leonardite and the biodegraded product with ruthenium tetroxide and sodium periodate to produce organic fragments that are lower in molecular weight which can then be analyzed. The resulting degradation products were derivatized and analyzed by gas chromatography/mass spectrometry (GC/MS). In addition, we have studied the reactions of model compounds having coal-related functionalities with the total organism, the cell-free filtrate, and the cell-free enzyme of C. versicolor. Many of the degradation products have been identified by GC/MS. Model compounds have the additional advantage of providing a much less complex matrix to examine as compared to the biodegraded product.

EXPERIMENTAL

Oxidation. The method utilized for the oxidation of leonardite coal and its biodegraded product was originally reported by Stock (4). The coal (0.3g) was added to a suspension of sodium periodate (34.2g) and ruthenium chloride trihydrate (30mg) in a mixture of carbon tetrachloride (20 ml), acetonitrile (20 ml), and water (30 ml) and the mixture was stirred vigorously for 12 hours. The aqueous layer was then extracted three times with equal volumes of ether, concentrated, derivatized with diazomethane, and analyzed with a HP 5988A GC/MS.

Model Compounds. The model compounds were prepared by dissolving approximately 10 mg of sample in 10 ml of methanol. Two hundred microliters of sample was added to the total organism, cell-free filtrate, or cell-free enzyme. After a specified incubation period, the solution was extracted with three equal volumes of chloroform, concentrated, and analyzed with a HP 5880 gas chromatograph with a flame ionization detector to determine the amount of degradation and a HP 5988A GC/MS to identify degradation products.

RESULTS AND DISCUSSION

A total ion chromatogram for the oxidized, biodegraded leonardite is shown in Figure 1. The dashed peaks indicate compounds that were tentatively identified. A comparison of the types of carboxylic acids identified for the starting coal and the biodegraded product is shown in Table 1.

No benzenedicarboxylic acids were produced from the oxidation of leonardite, but they were recovered from the biosolubilized product. On the other hand, leonardite produced a higher proportion of tetracarboxylic acids than the biosolubilized product. These results may reflect the action of the fungal enzymes on the leonardite coal to produce the biosolubilized product, or alternatively, the difference may be due to selective oxidation.

We have separated the cell-free filtrate into <10,000 MW and >10,000 MW fractions by ultrafiltration techniques. Gas chromatograms of (a) phenyl benzoate degraded by the <10,000 MW fraction and (b) phenyl benzoate degraded by the >10,000 MW fraction are shown in Figure 2. The peaks labelled (1), (2), and (3) have been identified by GC/MS. The model compound is completely degraded by the >10,000 MW fraction. It should also be noted that most of the coal biosolubilization occurs in the <10,000 MW fraction. These results seem to indicate that at least two mechanisms are responsible for the biosolubilization process, one of which may be hydrolysis.

REFERENCES

1. Cohen, M.S. and Gabriel, P.D., Appl. Environ. Microbiol. 1982, 44, 23-27.
2. Wilson, B.W., Bean, R.M., Franz, J.A., Thomas, B.L., Cohen, M.S., Aronson, H. and Gray, E.T., Jr., Energy and Fuels. 1987, 1, 80-84.
3. Campbell, J.A., Linehan, J.C., Franz, J.A., and Bean, R.M. Submitted to Energy & Fuels.
4. Stock, L.M. and Tse, L. Fuel. 1983, 62, 974-978.

Work supported by the Electric Power Research Institute and the U.S. Department of Energy under contract DE-AC06-76RLO 1830.

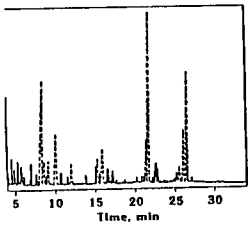

FIGURE 1. TIC of Oxidized Biodegraded Leonardite

TABLE 1

Acids by GC/MS	Percent of Total Leonardite	Percent of Total Product
Succinic	17 04	14.21
Glutaric	4.38	4.01
Methylglutaric	1 19	1.10
Adipic	1 90	1.42
Pimelic	1.42	1.01
Phthalic	2.9	4.1
Benzene dicarboxylic	0.0	3.1
Benzene tricarboxylic	25.8	22 5
Methylbenzene tricarboxylic	1 2	0.61
Benzene tetracarboxylic	19.2	7.2

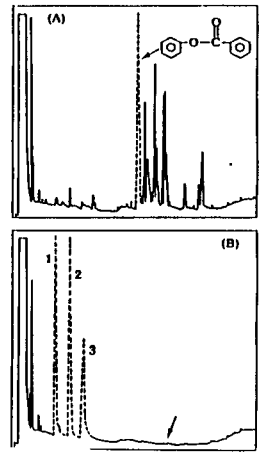

FIGURE 2. Degradation of Phenyl Benzoate by (A) <10,000 MW Fraction and (B) >10,000 MW Fraction

Presented at the 36th ASMS Conference on Mass Spectrometry and Allied Topics
June 5-10, 1988, San Francisco, CA

APPLICATION OF CHROMATOGRAPHY/SECONDARY ION MASS SPECTROMETRY TO FUELS-RELATED MATERIALS: ANALYSIS OF POLYNUCLEAR AROMATIC HYDROCARBONS AND BIOMARKERS

L.K.L. Dean and K.L. Busch; Department of Chemistry, Indiana University, Bloomington, IN 47405 USA
G.J. van Berkel; Analytical Chemistry Division, Oak Ridge National Laboratory, Oak Ridge, TN 37831 USA.

The purification and identification of porphyrins from sediments, bitumens, and crude oils is an integral part in the use of porphyrins as biomarkers. This identification is often accomplished with the use of thin-layer-chromatography (TLC) due to the simplicity, speed, and low cost of this technique. Once these porphyrins are separated, they need to be detected and identified. Some common detection/identification methods include location of the spot under UV light, measurement of the R_f value, detection by fluorescence scanning, and extraction by any of a number of elution techniques. These techniques have the disadvantages that they require the use of standards of known responses, and that the spatial resolution of the separated spots is often compromised. The direct analysis of the chromatograms with a secondary ion mass spectrometer solves these problems.

Chromatography/secondary ion mass spectrometry (SIMS) not only provides identification based on the molecular weight of the sample, but also allows the spatial resolution of the sample to be retained so that selected ion monitoring can be used to obtain an image of the separated spots. In this technique, an extraction matrix is applied to the separated spots on the chromatogram and the chromatogram is introduced into the vacuum chamber. The chromatogram is then bombarded with 5-6 kev Cs^+ ions, and the secondary ions emitted from the intact chromatogram detected. A wide variety of compounds have been analyzed by this technique. The application of this technique to a number of porphyrins and polynuclear aromatic hydrocarbons will be discussed.

A variety of matrices have been used for the FAB analysis of porphyrins including: thioglycerol (1), m-nitrobenzylalcohol (2), and o-nitrophenyloctylether (o-NPOE) (3). Of these three possible matrices, o-NPOE was chosen due to its relatively lower vapor pressure and therefore longer lifetime under low pressure conditions. Free-base octaethylporphine (OEP), free-base deuteroporphyrin IX dimethylester (DME), and a number of metallo-OEP samples were analyzed by SIMS with the use of o-NPOE as the matrix. In each case, an abundant signal was observed for the molecular ion and a small degree of fragmentation was seen (see Figure 1). These results indicate that o-NPOE is a good matrix for the SIMS as well as the FAB analysis of these compounds.

To determine if the o-NPOE matrix was suitable for the extraction of porphyrin samples out of a TLC plate, a 50 µg sample of free-base DME was first spotted onto a silica gel plate and extracted from the face of the plate. The matrix was able to extract the sample; however, there was an apparent increase in background noise and an accompanying decrease in resolution. Samples of the porphyrins listed above were then spotted onto a silica gel TLC plate and developed by conventional methods. The developed spot was then saturated with o-NPOE and analyzed by SIMS. A 50 µg sample of each of the porphyrins produced an $M^{+\cdot}$ ion which could be detected but again there was an increase in background noise and fragmentation (see Figure 2). Even though the fragmentation increases, the molecular ion remains the most abundant peak in this region of the mass spectrum.

In 1984, two different matrices, antimony trichloride (4) and "a high boiling hydrocarbon fraction" (5) were introduced for the FAB analysis of polynuclear aromatic hydrocarbons (PAHs). In the present study of pyrene, benzo(a)pyrene, benzanthracene, coronene and 1,2,3,4-tetraphenylnaphthalene, both antimony trichloride and Santovac 5 (a diffusion pump oil) were tested as possible chromatography/SIMS matrices. The mass spectrum obtained from pyrene out of Santovac 5 contains the molecular ion. However, detection limits were in the high microgram range. The use of antimony trichloride as a matrix also produced abundant $M^{+\cdot}$ ions but the high vapor pressure of

this matrix precluded its extensive use. Due to the success of o-NPOE as a matrix for porphyrins, it was used here for the first time as a matrix for PAHs. A 50 µg sample of pyrene in o-NPOE was analyzed by SIMS and an abundant $M^{+\cdot}$ ion was observed as seen in Figure 3. A 50 µg sample of pyrene was then spotted onto a TLC plate and developed by conventional methods. The sample spot on the developed plate was saturated with o-NPOE and analyzed by chromatography/SIMS. The molecular ion for pyrene was observed with a slight loss in sensitivity (see Figure 4). O-NPOE was then tested as a matrix for the remaining PAHs listed above. All of these PAHs produced $M^{+\cdot}$ ions out of the o-NPOE matrix.

O-NPOE is a suitable matrix for the extraction of porphyrins and polynuclear aromatic hydrocarbons from silica gel TLC plates. Molecular ions ($M^{+\cdot}$) are obtained in each case with a large relative abundance. The adsorbed state of the sample on the TLC plate causes some additional noise and fragmentation in the mass spectra of these compounds; however, the molecular ion is easily distinguishable from the resulting fragments.

1. Kurlansik, L.; Williams, T.J.; Strong, J.M.; Anderson, L.W.; Campana, J.E. Biomedical Mass Spectrometry 1984, 11(9), 475.
2. Barber, M.; Bell, D.; Eckersley, M.; Morris, L.; Tetler, L. Rapid Communications in Mass Spectrometry 1988, 2(1), 18.
3. Meili, J. and Seibl, J. Organic Mass Spectrometry 1984, 19(11), 581.
4. Groenewold, G.S.; Todd, P.J.; Buchannan, M.V. Analytical Chemistry 1984, 56, 2251.
5. Dube, G. Organic Mass Spectrometry 1984, 19(5), 242.

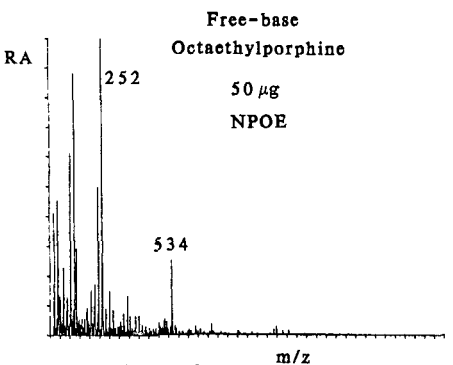

Figure 1

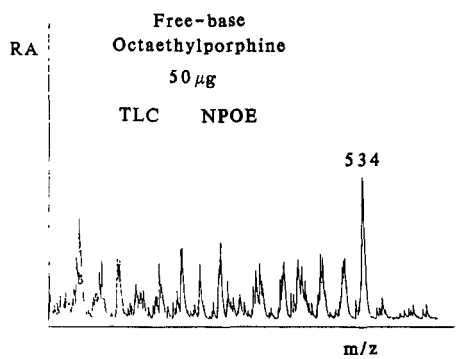

Figure 2

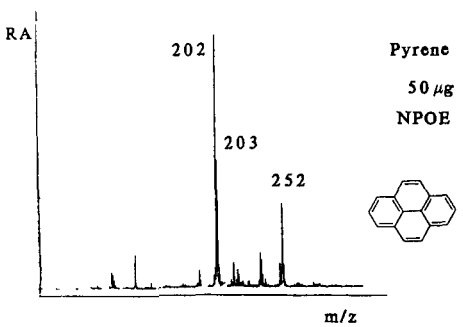

Figure 3

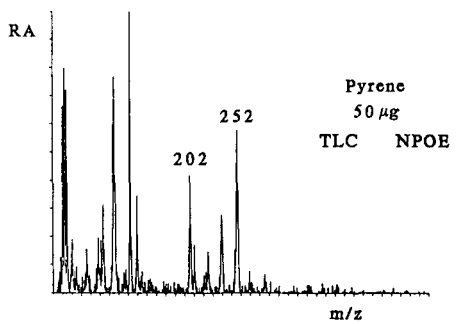

Figure 4

Presented at the 36th ASMS Conference on Mass Spectrometry and Allied Topics
June 5-10, 1988, San Francisco, CA

RADIAL VELOCITY DISTRIBUTIONS OF LARGE SECONDARY MOLECULAR IONS

W. Ens*, B. U. R. Sundqvist, P. Håkansson, A. Hedin and G. Jonsson
Div. of Ion Physics, Dept. of Radiation Sciences, Uppsala University
Box 535, S-751 21 Uppsala, Sweden
**Present address:* Physics Dept., University of Manitoba, Winnipeg, Canada R3T 2N2

For simple linear time-of-flight spectrometers it has usually been assumed that the acceptance of secondary ions desorbed from a solid surface is independent of mass [1]; in the absence of focusing elements, the acceptance is determined by the radial velocity of the secondary ions, the flight path and the size of the detector. In contrast to this picture, we report that the radial velocity distributions for large molecular ions desorbed by high energy (MeV/u) ion bombardment are considerably different from those of light ions and that they are correlated to the incident ion direction. The results have theoretical as well as practical implications.

Radial velocity distributions were measured for secondary ions from valine (117u), LH-RH (1183u), and bovine insulin (5733u). Secondary ions were produced by bombardment with ^{252}Cf fission fragments at normal incidence (on average) from behind the sample foil, with 72 MeV $^{127}I^{18+}$ ions (from the Uppsala EN-tandem accelerator) incident from the front at 45°, and with 18 keV Cs^+ ions incident from the front at 60°. The measurements were made using time-of-flight mass spectrometers equipped with deflection plates in the field-free region after the acceleration stage as illustrated in fig. 1.

Fig. 2 shows the measured intensity of the molecular ion of bovine insulin and a light fragment ion as a function of deflection voltage for fission fragments incident from behind the target foil. The intensity of *low mass* secondary ions shows a single-peaked symmetric distribution around a deflection voltage close to zero. This voltage corresponds

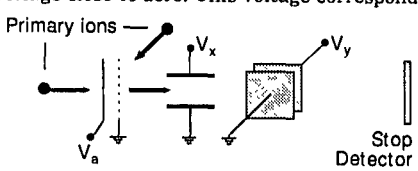

Figure 1 Schematic illustration of the experimental method. In a given experiment, primary ions (see text) were incident from the front *or* from behind.

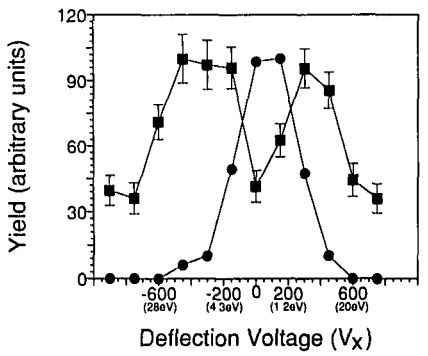

Figure 2 Yield of insulin molecular ions (■) and CH_3^+ ions (●) for fission fragments incident from behind.

to ions that are ejected perpendicular to the target; i.e. with zero radial velocity. However, for molecular ions of insulin, the distribution always shows a local minimum in the perpendicular direction.

Because of the proximity of the ^{252}Cf source to the target, the fission fragments have wide range of incident angles. A much better-defined angle of incidence is obtained from an accelerator beam. For a beam of 72 MeV $^{127}I^{18+}$ ions incident from the front at 45°, the intensity distributions as a function of deflection voltage are single-peaked for both light ions and insulin molecular ions. However, as shown in fig. 3, the distribution for insulin is shifted with respect to that for light ions when the deflection of the secondary ions is in the plane containing the incident beam direction (V_x).

The radial velocities of ions that strike the centre of the detector for the various deflection voltages were calculated assuming that zero radial velocity corresponds to the centroid of the distribution for light ions. The energy corresponding to the radial component of the velocity is indicated in parenthesis in figs. 2 and 3. The ejection angle was deduced from the radial velocity and previously measured axial velocities [2]. The data indicate that the average angle of emission for molecular ions of insulin is considerably

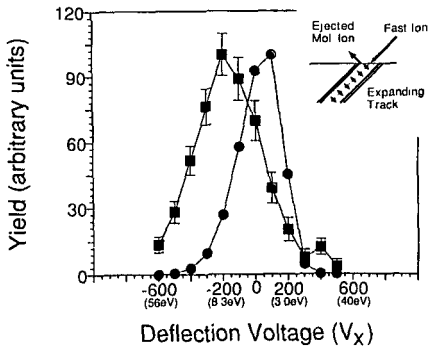

Figure 3 Yield of insulin molecular ions (■) and CH_3^+ ions (●) for $^{127}I^{18+}$ incident from the front at 45° to the normal.

different from that of light ions and that the direction is correlated to the direction of the incident primary ion. In figs. 2 & 3, the maxima of the distributions for insulin correspond to an angle of ejection of approximately 50° to the normal assuming, for the data of fig. 3, that the light ions are ejected perpendicular to the target. (There is some evidence suggesting that the ejection angle of the light ions is also shifted from the perpendicular but in the opposite sense to that of the molecular ions.) In the case of 45° incident ions, the secondary ions are directed away from the incident direction as illustrated in the inset in fig. 3. The same effect was observed to a lesser extent for molecular ions from LH-RH and for cluster ions of valine; the larger the cluster the more pronounced the effect.

It is difficult to reconcile these results with a thermal model of desorption in which the memory of the incident ion direction would be lost. Rather it appears that there is a collective motion of the lattice such as an expansion [3] or a shock wave [4] which transfers momentum outward from the track.

An important consequence of these results is that the required acceptance angle of the detector for large molecular ions desorbed by MeV ion bombardment is much larger than might be expected from measurements with low mass secondary ions. Time-of-flight mass spectra obtained with high energy bombardment have typically used very short flight tubes or an electrostatic particle guide [5] to maximize instrument acceptance. The effect of a simple einzel lens near the target is

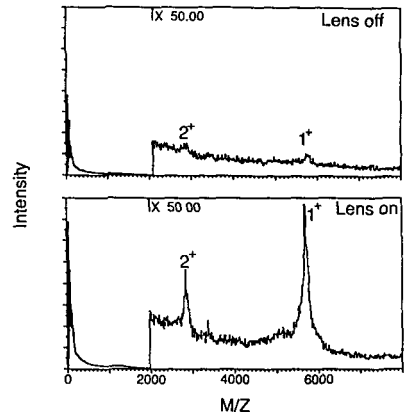

Figure 4 Positive time-of-flight mass spectrum of bovine ionsulin obtained with fission fragments incident from behind without secondary ion focusing (upper) and with focusing. The labels 1^+ and 2^+ correspond to singly and doubly charged molecular ions.

illustrated for a 75 cm flight path, 12 kV acceleration and a 2 cm diameter detector in fig.4. Without the lens, the molecular ions of insulin are barely observable above the background. The lens increases the overall count rate by about 40% but the molecular ion signal is enhanced much more dramatically.

In contrast to the results for MeV ion bombardment the yield of molecular ions of insulin ejected by 18 keV Cs^+ bombardment show the same dependence on deflection voltage as do the light ions. Therefore the effect described above, if present, is much smaller for keV ion bombardment.

References:

1) H. Danigel and R.D. Macfarlane, *Int. J. Mass Spectrom. and Ion Physics* **39** (1981) 157.
2) S. Widdiyasekera, P. Hakansson and B.U.R. Sundqvist, *Nucl. Instrum. Meth.*, in press.
3) P. Williams and B.U.R. Sundqvist, *Phys. Rev. Lett.* **58** (1987) 1031.
4) I.S. Bitenski and E.S. Parilis, *Nucl. Instrum. Meth.* **B21** (1987) 26.
5) R.D. Macfarlane and D.F. Torgerson, *Int J. Mass Spectrom. Ion Phys.* **21** (1976) 81.

Presented at the 36th ASMS Conference on Mass Spectrometry and Allied Topics
June 5-10, 1988, San Francisco, CA

SPUTTERING FROM THE GLASSY STATE AND PRESERVATION OF SPATIAL RESOLUTION IN CHROMATOGRAPHY/SIMS. S.J. Doherty and K.L. Busch; Department of Chemistry, Indiana University, Bloomington, IN 47405

In the direct mass spectrometric analysis of silica gel thin layer chromatography plates, the use of a "phase transition matrix" has been illustrated to increase both the absolute intensity and the duration of analyte signal, as compared to analysis without solvent or with liquid matrices, such as glycerol. These benefits can be obtained without compromising the inherent spatial resolution of the chromatographic separation. Developed TLC plates are overlayered with a low melting point glycerol analog, such as sorbitol (m.p. = 93°C). The TLC plate is heated until the matrix becomes tacky to the touch, and the plate is transferred to an aluminum platform inside the source of the chromatography/SIMS instrument. The temperature of the platform is raised to the appropriate level, using an external temperature controller, and positive or negative ion SIMS spectra can be obtained. Primary ion bombardment can be provided by either a low fluence cesium thermionic emitter, or by a highly focussable gallium liquid metal ion gun. Spatially-resolved extraction images can be generated by moving the xyz manipulator that houses the platform, while simultaneously performing selected ion monitoring experiments.

Figure 1 plots the signal intensity as a function of time for the intact cation of a precharged -onium salt extracted from silica gel TLC. The top plot was obtained using xylitol maintained at its melting point (95°) as the extraction matrix, while the lower plot was obtained with glycerol at room temperature. Xylitol can be seen to provide a much more stable secondary ion flux than glycerol. Though not shown here, the xylitol signal was monitored for over an hour, with no appreciable diminution of signal intensity. The pair of images at the top of Figure 2 illustrate that the phase-transition matrix can extract analyte from the support with limited diffusion in the x and y planes. The image on the left charts the spatial distribution of diphenylmethyl- (left peak) and diphenylethyl- (right peak) sulfonium bromides extracted from TLC with two discrete spots of extraction matrix. The matrix, sorbitol, was maintained just below its melting point. The image on the right was obtained after additional matrix was deposited in the space between spots. The original spatial orientations are maintained, and no analyte is observed to have diffused into the fresh matrix. The lower pair of images in Figure 2 illustrate the importance of rigorous temperature control. The image on the left was obtained from two discrete analyte spots, extracted by a common pool of sorbitol heated to just below its melting point. The analyte peaks are clearly distinguishable. The image on the right was collected from the same TLC plate, heated to just above the matrix melting point. The peaks have obviously diffused through the molten matrix, compromising the inherent spatial resolution of the separation.

The analytical utility of this technique is illustrated in Figure 3. The dipeptide glycylphenylalanine was extracted from a TLC plate with sorbitol maintained just below its melting point. The discrete mass spectrum is seen at the top of the figure. The peak at m/z 223 corresponds to the protonated molecule, while the ions at m/z 166 and 120 arise from the protonated and decarboxylated phenylalanine residue. The spatial distributions of each of these ions are provided below. This illustrates that spatial orientation can serve as an additional dimension of scientific information in the analysis of static forms of chromatography, analogous to the temporal profile typically associated with dynamic chromatographic separations.

The glassy state model is advanced to account for the observed behavior. In this model, thermal energy from the heated platform induces a semi-molten state in the phase-transition matrix. Viscosities, and by extension, diffusion coefficients, are approximately equal to those in the solid. Energy from the impact of energetic primary particles is sufficient to accomplish a localized phase-transition to the liquid state. Diffusional and energy dissipation processes in solution are greater than in the solid, leading to increased signal intensity and duration.

Presented at the 36th ASMS Conference on Mass Spectrometry and Allied Topics
June 5-10, 1988, San Francisco, CA

TLC Extraction images

Signal intensity vs. Time

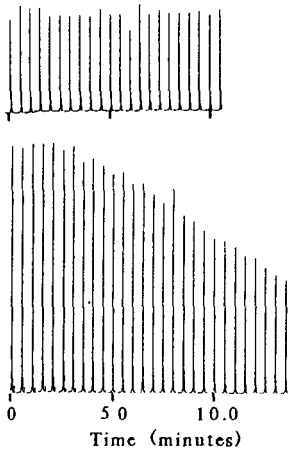

Figure 1

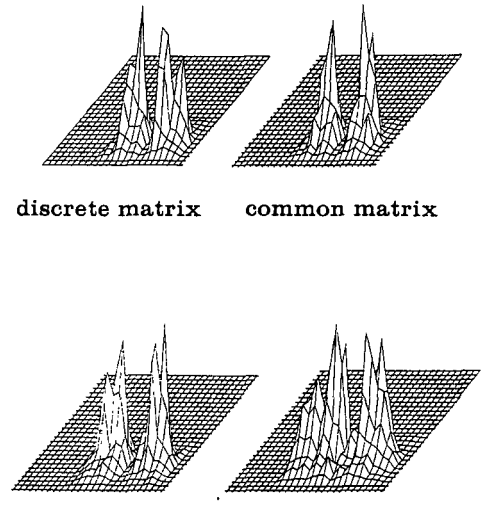

Figure 2

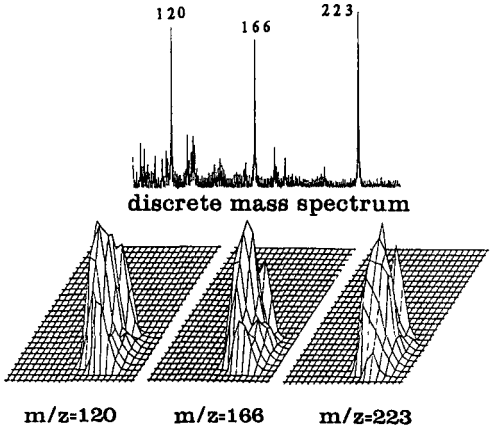

Glycylphenylalanine in sorbitol

Figure 3

Presented at the 36th ASMS Conference on Mass Spectrometry and Allied Topics
June 5-10, 1988, San Francisco, CA

A CCD DETECTION SYSTEM FOR SIMS

Lisa K. Turner, David S. Mantus, Yong-Chien Ling, George H. Morrison;
Baker Laboratory of Chemistry, Cornell University, Ithaca, NY 14853

The ability of SIMS (secondary ion mass spectrometry) to provide images of the elemental composition of sample surfaces makes it a valuable technique for elemental localization in biological, metallurgical, and geological samples. The imaging capability, however, has been greatly underutilized, in part, due to the complexity of extracting quantitative information from an image. While the usual discriminations inherent in the production and transmission of secondary ions are present, imaging SIMS is also plagued by detector or detection system discriminations. The conversion of secondary ion intensities to digitized pixel intensities while retaining absolute geometric and densitometric fidelity is an important step towards achieving quantitative SIMS images.

At present, the CAMECA IMS-3f instrument used in our laboratory has a rather circuitous system of detection and digitization of secondary ion images. The ions strike a microchannel plate (MCP) to produce electrons that are accelerated towards a fluorescent screen (FS). The resulting photon image is recorded on 35-mm film or by video camera and subsequently digitized. This multi-stage approach to acquiring images can introduce non-linearity, degradation of spatial resolution, and signal losses at several points along the path (1). In addition, the responses of the the system's components change over time, and frequent calibration is necessary.

In an attempt to reduce the number of transductions, Odom, et.al.(2), replaced the fluorescent screen and subsequent recording media with a resistive anode encoder (RAE). This provides a more direct means of digitization but it is limited to signals no greater than 10^4 cts/sec.

In our approach, the entire conventional detection system, including the MCP, is replaced by a charge-coupled device (CCD). We use the CCD (Tektronix 512x512, backside-illuminated) to directly detect the ions. Because the CCD is used as an integrating detector, we have built a housing which also incorporates a conventional MCP/FS assembly for tuning and real time imaging (Fig 1). Both detectors are mounted along the same focal plane and can be moved in and out of the path of the beam.

The CCD is an array of MOS-like capacitors. When ions strike the device, electron-hole pairs are generated in the p-type Si, the number of which is proportional to the number of incoming ions. These electrons are swept into potential wells created in the n-type Si buried channel by appropriate voltages placed on the three gates which define each pixel. After the signal is integrated for a specified time, the accumulated charge is read from the chip by the process of charge-coupling.

After draining the signal from the CCD, it is digitized and stored temporarily in an image buffer in the controller unit (Fig. 2) Both the electronics and controller units were purchased (Photometrics, Ltd.) and provide all of the support circuitry for the CCD. These units are interfaced to a PDP 11/34 computer and TRAPIX image processor. The user can display an acquired digitized image within 10 seconds of detecting the ions with the CCD.

In preliminary experiments with this system, we have demonstrated that the CCD is sensitive to keV ions (Fig 3). Past applications of CCDs involved only photons, electrons, and MeV particles. The device has good linearity and very low noise when cooled -- only a few electrons per pixel per second -- and is excellent for long integrations. We are attempting to understand and predict the sensitivity of the CCD. This is dependent upon both the energy loss mechanism of the ions and the efficiency of the device to capture the electrons generated at different depths along the range of the ion. Figure 4 shows the results of calculations performed to model the performance of the CCD and relevant experimental data both as it exists currently (solid curve) and if the collection efficiency of generated electrons were made to be 100% (dotted curve) by a process known as QE-pinning (3).

Although determinative experiments are on-going, we have presented a system which provides spatially quantized secondary ion images directly, quickly, and easily. In addition, we have demonstrated for the first time the sensitivity of CCDs to keV ions.

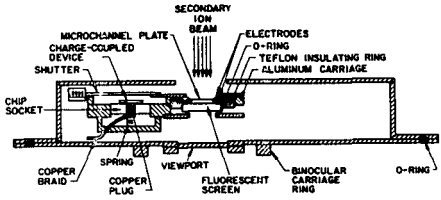

Figure 1 - Schematic of detector housing.

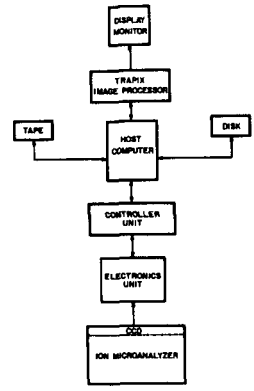

Figure 2 - Block diagram of system.

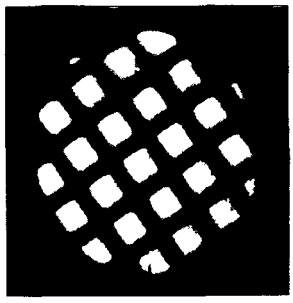

Figure 3 -

$^{27}Al^{+}$ image of Cu grid on Al.

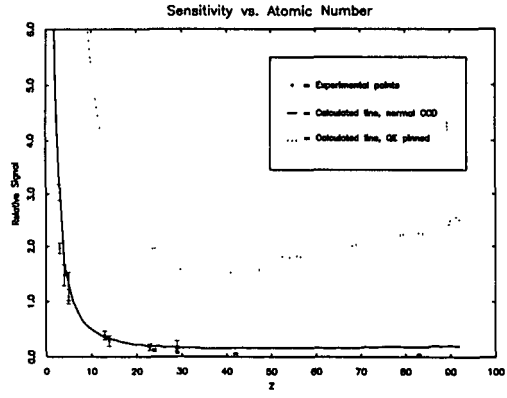

Figure 4 -

Calculated and experimental values for sensitivity.

1. Ling, Y. -C., Bernius, M. T., Turner, L. K., G. H. Morrison, Anal. Chem. (in preparation).
2. Odom, R. W., Furman, B. K., Evans Jr., C. A., Bryson, C. E., Petersen, W. A., Kelly, M. A., Wayne, D. H., Anal. Chem. 55, 574 (1983).
3. Janesick, J. R., Elliot, T., Daud, T., McCarthy, J., Blouke, M., SPIE Vol 570 Solid State Imaging Arrays 1985.

Presented at the 36th ASMS Conference on Mass Spectrometry and Allied Topics
June 5-10, 1988, San Francisco, CA

MOLECULAR COMPOSITIONAL MAPPING BY SECONDARY ION MASS SPECTROMETRY

Greg Gillen and David S. Simons; Center for Analytical Chemistry
National Bureau of Standards, Gaithersburg, MD 20899

INTRODUCTION

A continuing goal of our research is the development of a molecular compositional mapping capability using Secondary Ion Mass Spectrometry. In this study, a Cameca IMS-3F equipped with a resistive anode encoder imaging system was used to acquire high lateral resolution molecular ion images of several organic compounds. Because severe degradation of the analyte molecular structure often occurs during ion bombardment, we have also studied some of the parameters which influence the degradation process.

EXPERIMENTAL

In the IMS-3F an Ar^+ primary ion beam strikes the sample which is maintained at 4.5 kV. The primary ion beam accelerating potential is adjustable, giving an ion impact energy which can be varied from ~2.5-13 keV. For imaging studies an impact energy of 8 keV was used. The beam was focussed to a spot and then rastered over an area of 500x500 µm. Typical current densities were 1-5 $\mu A/cm^2$. Digitized molecular ion images were initially stored on an IBM-AT computer. Subsequently, the image files were transferred to a VAX 11/780 computer for further processing. A DeAnza image processing system was used for display of the images in a thermal scale format.

MOLECULAR SECONDARY ION IMAGING

Molecular secondary ion images were obtained from model systems prepared by evaporating the compound of interest from saturated aqueous or ethanolic solution onto copper TEM grids. In all cases, the images were generated using the secondary ion signal of the intact parent molecular ion. Figure 1 shows a mass spectrum and molecular ion image of acetylcholine chloride generated using the parent molecular cation. Figure 2 shows a mass spectrum and molecular ion image of benzalkonium chloride, also generated using the parent cation. In both images, the spacing between adjacent grid bars is 25 µm. Molecular ion images have also been obtained from a number of other compounds including amino acids.

PRIMARY ION BEAM DAMAGE

The degradation of the parent molecular ion and structurally significant fragment ions can be a major impediment to the acquisition of a molecular ion image. To understand some of the parameters which influence the damage processes in bulk molecular solids, the decay of parent and fragment molecular ion signals were monitored as a function of primary ion dose. A typical decay curve for the parent cation of tetrabutyl ammonium bromide is shown in Figure 3. After an initial rapid decrease in molecular ion signal, the slope of the decay curve flattens (at doses of ~1-4x1014 ions/cm2) and very little decay is subsequently observed as the primary ion dose is increased. Parent molecular ion signals were observed for most compounds at primary doses of >1017 ions/cm^2. Similar behavior has been observed for all compounds studied including amino acids. Detection of significant molecular ion signals, after sputtering several tens of nanometers into the sample, suggests that it may be possible to conduct molecular (imaging) depth profiling experiments. From a practical standpoint, it would be desirable to increase the molecular ion signal in the high dose regime in order to increase the sensitivity of the analysis. One parameter which was found to affect the high dose molecular signal was the primary ion energy. As shown in Figure 4, for the parent molecular ion signal of methylene blue, an increase in the primary ion energy results in a decrease in the molecular ion signal. It might be expected that an increase in primary energy would increase the sputter yield and hence the detected molecular ion signal. By plotting the ratio of fragment ion/parent ion signals as a function of energy, it was found that the ratio increases in proportion to the increase in primary ion energy. Therefore, it appears that the2 decrease in molecular ion signal intensity may result from increased fragmentation of parent molecules by the more energetic primary beam. Studies are now in progress to determine what other parameters may influence the decay process.

Presented at the 36th ASMS Conference on Mass Spectrometry and Allied Topics
June 5-10, 1988, San Francisco, CA

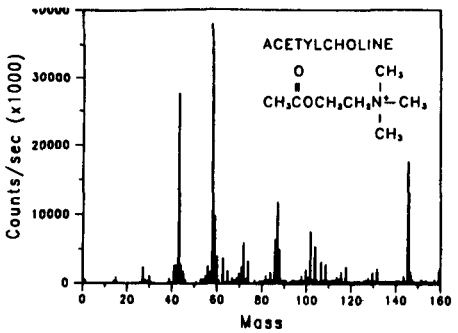

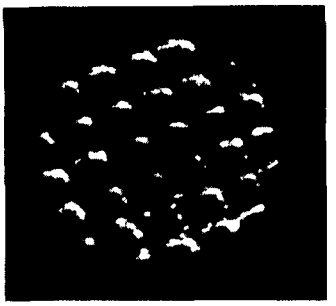

Figure 1. Mass Spectrum and molecular ion image of acetylcholine generated using the parent molecular cation (m/z 146).

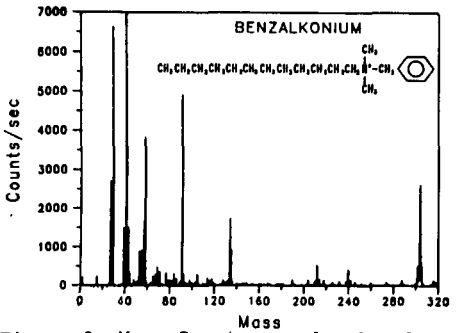

Figure 2. Mass Spectrum and molecular ion image of benzalkonium generated using the parent molecular cation (m/z 304).

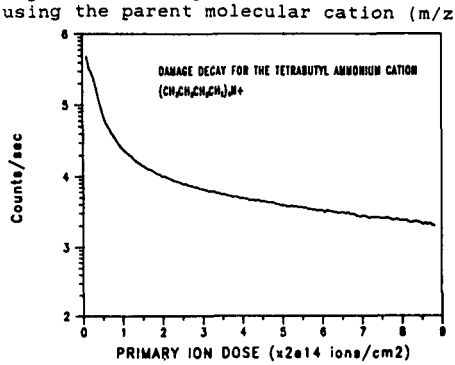

Figure 3. Decay for the tetrabutyl ammonium cation (8 keV, Ar^+).

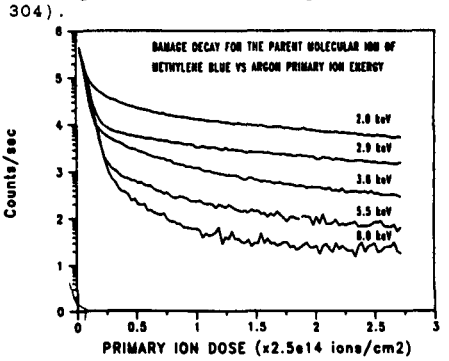

Figure 4. Decay for methylene blue vs Ar^+ primary energy.

CONCLUSION

We have demonstrated that it is possible to generate high lateral resolution molecular ion images from model systems using Secondary Ion Mass Spectrometry. Molecular ion signals were observed at high primary ion doses for all compounds studied. This may allow molecular depth profiling experiments. Studies of the effect of primary ion energy on the decay behavior of organic compounds indicated that a higher primary ion energy decreases the yield of intact molecules. This may result from increased fragmentation of the analyte molecule by the more energetic primary ion beam.

Presented at the 36th ASMS Conference on Mass Spectrometry and Allied Topics
June 5-10, 1988, San Francisco, CA

STATIC SIMS ANALYSIS OF NITROGEN CONTAINING HETEROCYCLIC AROMATIC COMPOUNDS

P.R. Mahaffy, D.N. Harpold and H.B. Niemann

Laboratory for Atmospheres, Goddard Space Flight Center, Greenbelt, Md. 20771

INTRODUCTION: A mass spectrometer is under development at NASA's Goddard Space Flight Center for use in the chemical analysis of the coma of a comet in a future rendezvous mission. In addition to two gas phase ion sources, and a positive and negative ion mode of operation, the instrument includes the capability to generate secondary ions from a cooled collector surface. The SIMS mode of operation is intended to facilitate the search for heavy, non-volatile organic molecules which may be present in the cometary coma. The instrument has been described previously.[1] Static SIMS laboratory studies are presently in progress in order to select optimal collector materials and operating conditions for candidate cometary molecules. The adsorption of three nitrogen containing heterocyclic aromatic compounds on silver and gold surfaces are described.

MASS SPECTROMETRIC ANALYSIS OF COMETARY MATERIAL: A number of missions to comet Halley were carried out in 1986[2]. Although the high flyby velocity of these spacecraft limited the quantitative mass spectrometer measurements to major coma species such as H_2O and CO, there were nevertheless strong indications that cometary organic chemistry is complex. For example, a plasma experiment detected ions of mass greater than 100 amu. The shape of this mass spectra, with peaks separated by alternating 14 and 16 amu has led to the suggestion[3] that polymerized formaldehyde (POM) is a possible cometary constituent. In another experiment[4], time-of-flight mass spectra were obtained of ions produced on dust impact at a surface. These spectra indicate that many cometary dust grains consist of molecules containing only carbon, hydrogen, oxygen, and nitrogen atoms (CHON particles). An extended list has been generated of possible molecules contained in CHON as suggested by the data from the dust impact experiment.[5] Several nitrogen containing heterocyclic aromatic compounds are included on this list.

STATIC SIMS STUDIES: Adsorption of

xanthine = 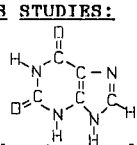 pyridine = 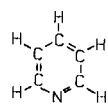 and adenine = 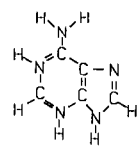

was carried out on polycrystalline gold and silver foil surfaces. Surface cleaning was accomplished by cycles of Ar ion bombardment and 925 K annealing. UHV molecular beams of adenine and xanthine were generated by heating reservoirs of the molecular crystals. Feedback from a small Bayard Alpert gauge near the target and computer control of the reservoir heating power allowed precise dosing levels to be achieved. Pyridine was introduced through a leak valve. The cylindrical mirror energy filter allowed transmission of secondary ions in a band of approximately 16 eV (FWHM).

The xanthine/Au adsorption is characterized in some detail in the following 4 figures. The change with temperature of the parent xanthine peak was obtained with a linear temperature ramp of 0.25 deg/sec.

Presented at the 36th ASMS Conference on Mass Spectrometry and Allied Topics
June 5-10, 1988, San Francisco, CA

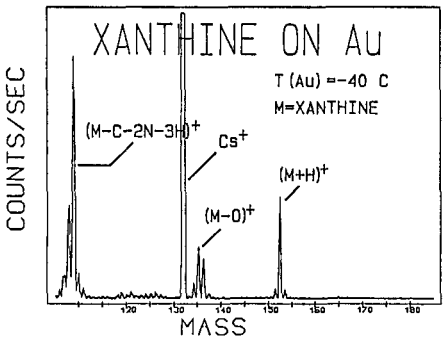

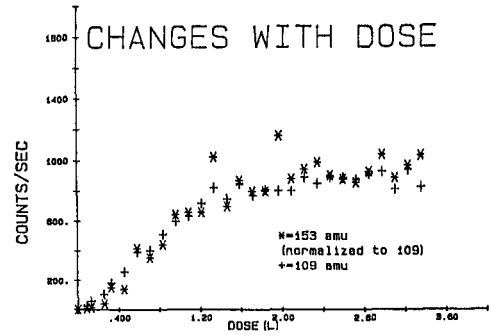

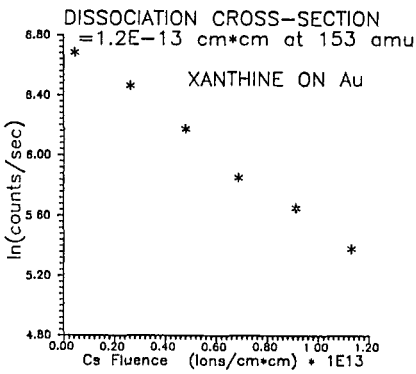

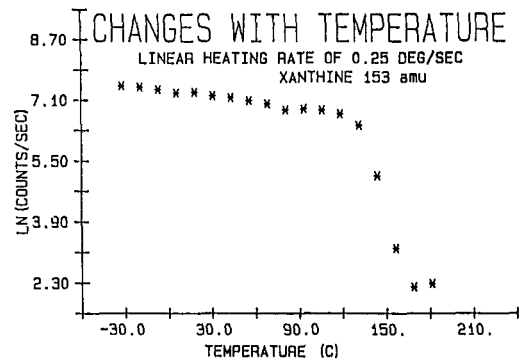

The energy of the cesium excitation ions was approximately 4000 eV in all cases. Adenine adsorbed on gold and pyridine on silver (not shown in the abstract) give strong molecular peaks at $(M+H)^+$ and M^+ respectively for surface temperatures of -40 and -60 C. The fragmentation pattern obtained for xanthine on silver was generally similar to that on gold, with differences in the relative strengths of the major fragment peaks. The strongest negative ion molecular peak for the three species was $(M-H)^-$ for xanthine on gold.

The SIMS mode of operation of the Neutral Gas and Ion Mass Spectrometer on the Comet Rendezvous Mission is expected to provide compositional information which is complementary to that from the gas phase ion sources. The nitrogen containing ring structures studied, to date, can be readily identified using the surface ionization technique. The extent to which detection efficiency is lost in the presence of other strongly adsorbing species needs further investigation.

REFERENCES:

1.) P.R. Mahaffy, D.N. Harpold, and H.B. Niemann, in Secondary Ion Mass Spectrometry, SIMS VI (Springer, in press).
2.) Nature (supplement) 321, 1987.
3.) W.F. Huebner, Science 237, 628 (1987).
4.) J. Kissel and F.R. Krueger, Nature 326, 755 (1987).
5.) J.Kissel and F.R. Krueger, Nature 326, 755 (1987).

Presented at the 36th ASMS Conference on Mass Spectrometry and Allied Topics
June 5-10, 1988, San Francisco, CA

APPLICATION OF A SIMS/TSQ SPECTROMETER FOR ORGANIC SURFACE ANALYSIS IN THE ELECTRONICS INDUSTRY

Bryan L. Bentz and P. Jane Gale

David Sarnoff Research Center
Princeton, New Jersey 08543-5300

A static SIMS instrument based on an extensively modified Finnigan MAT TSQ-15 triple stage quadrupole has been developed at the David Sarnoff Research Center for solid-state organic surface analysis. Surface compositional data for organic solids can be obtained in the positive and negative ion modes. Collisional dissociation of sputtered species is also available. The secondary ion optics for this instrument were designed using the electron optics program ELOP, written in-house. Drawn to scale in Fig. 1 is the geometric configuration of the electrodes. The potentials for the transport and collection of polyatomic ions sputtered from a large surface area by keV primary particles have been calculated. In practice we find that the actual electrode voltages that maximize the transmitted secondary ion signal agree generally to within 3-5% of the voltage values assigned in the computer modelling, except for the deceleration lens following the ESA, where a voltage on the final lens plates of -10V is typically used.

Surface analysis spectra are acquired under low-dose bombardment conditions using a 3 keV xenon neutral beam and an analog electron multiplier as detector. To verify that our many hardware modifications did not reduce the standard mass range of our TSQ instrument (1000 amu), we sputtered a solid CsCl pellet and acquired positive ion spectra of high mass clusters. Fig. 2 shows the mass resolution and peak shapes obtained for the cluster $Cs_5Cl_4^+$ [m/z 805] in the Q3 scan mode. Similarly we could establish that Q1 has the full 1000 amu mass range. Analytical samples are introduced to the homebuilt, 16-port SIMS vacuum chamber via a turbo-pumped load lock which has a base pressure of 2 x 10^{-8} torr.

With this novel SIMS instrumentation we have undertaken surface analytical studies of many insulating and conducting materials of interest in the electronics industry. The surfaces of spin-on glasses, CVD and plasma-deposited thin films, high temperature superconducting materials, conductive thermoplastics, and laminates have been successfully studied for compositional/structural identity or contaminant investigation. To demonstrate the capabilities of our SIMS/TSQ system in organic thin film research, we show in Figs. 3-5 the results of a study of two fluorocarbon-rich surfaces. Fig. 3 presents the positive ion SIMS spectrum of a thin disc of commercial Teflon. The spectrum of a 1000Å film of plasma-polymerized 1,3-perfluorodimethylcyclohexane and N_2 (Fig. 4) contains several peaks in the low mass region of the spectrum identical to those of Fig. 3, with the noted exception of an intense signal at m/z 114. To probe the identity of m/z 114 from this film, a collision-induced dissociation (CID) experiment was undertaken. Interpretation of the daughter ion spectrum of m/z 114 in Fig. 5 suggests that m/z 114 is a nitrogen-containing species and implies that nitrogen was incorporated in the polymer film during its growth in the plasma reactor. In Fig. 6 is shown the SIMS spectrum of the surface of a different type of polymer; poly(ethylene terephthalate) (Mylar). $(M \pm 1)^+$ of the repeating unit are detected in addition to structurally diagnostic fragment ions.

Fig. 1

Computer-Modeled Trajectories of Off-Axis Secondary Ions

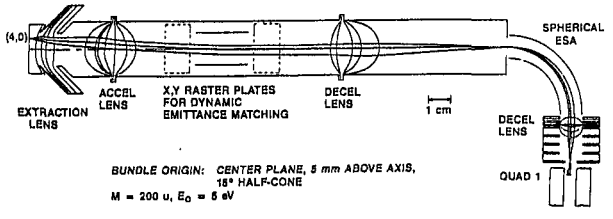

Fig. 2

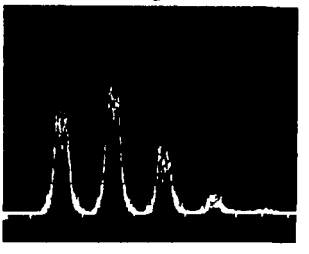

Presented at the 36th ASMS Conference on Mass Spectrometry and Allied Topics
June 5-10, 1988, San Francisco, CA

SIMS SPECTRUM OF TEFLON

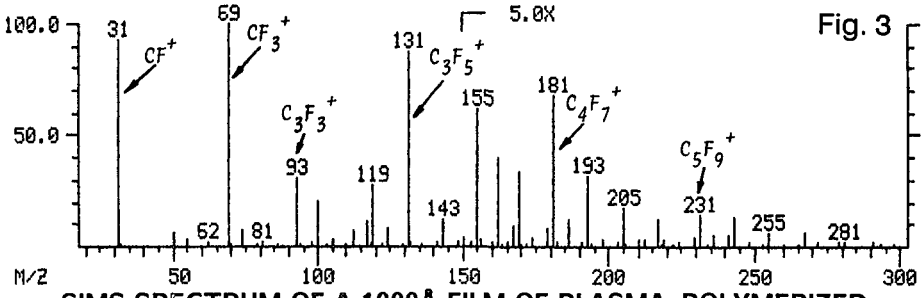

SIMS SPECTRUM OF A 1000Å FILM OF PLASMA-POLYMERIZED 1,3-PERFLUORODIMETHYLCYCLOHEXANE AND N_2

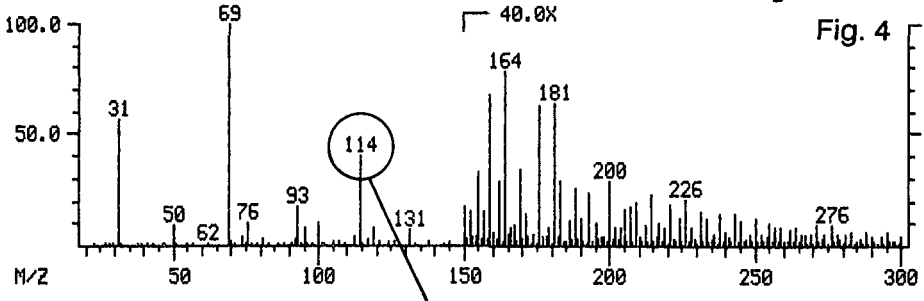

DAUGHTER ION SPECTRUM OF M/Z 114

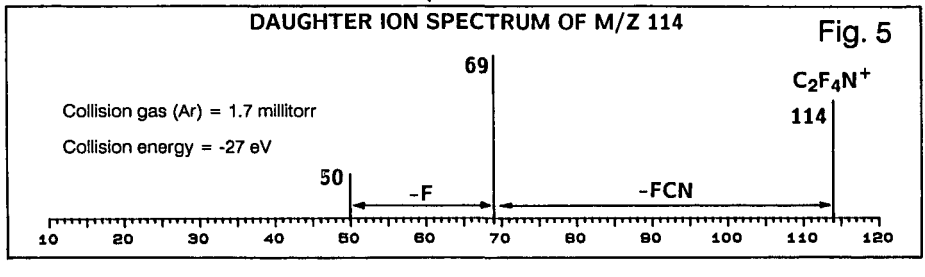

SIMS SPECTRUM OF MYLAR

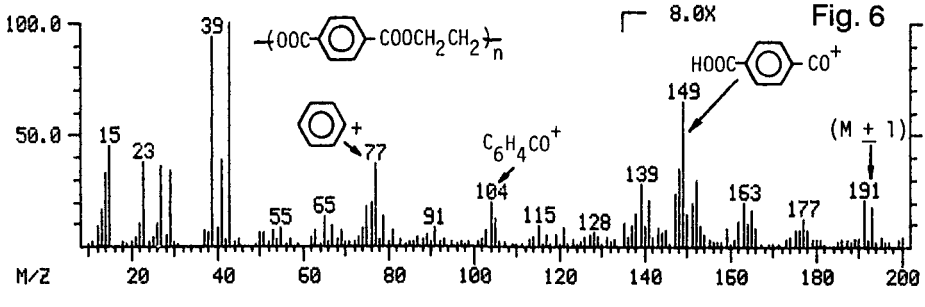

Presented at the 36th ASMS Conference on Mass Spectrometry and Allied Topics
June 5-10, 1988, San Francisco, CA

Characterization of Multilayer Thin Films by Laser-Induced Thermal Desorption Mass Spectrometry

Donald P. Land, Tsong-Lin Tai, John M. Linduist, John C. Hemminger, and Robert T. McIver, Jr. Department of Chemistry and Institute for Surface and Interface Science, University of California, Irvine, California 92717.

We report on the use of laser-induced thermal desorption (LITD) and post-ionization by an electron beam to characterize molecular species absorbed in and on the amorphous carbon layer which covers the surface of a computer magnetic hard disk platter. These hard disks are multilayer structures of which the magnetic layer is a mixed alloy of Co and Cr. A final layer of carbon is sputter deposited on top of the magnetic layer to act as a protective film and lubricant. Adsorption of molecular species in and on this carbon layer has been found to be of great importance to the performance characteristics of the magnetic disk. Identifying these species, however, presents a particularly difficult surface analysis problem since one is interested in detecting small quantities of carbon-containing molecules on an ill-defined carbon surface.

In our experiments, a 1 cm^2 piece of a hard disk is positioned in front of a hole in one of the electrodes of a 6 cm cubic FTMS analyzer cell. A focused laser beam (Lambda Physik model EMG 103 MSC excimer laser, wavelength 248 nm, pulse width 20 ns) enters the cell through a hole opposite the sample and strikes the sample at near normal incidence causing heating of a 0.2 mm^2 area. At low laser power, only neutral species are vaporized from the surface. Some of the neutrals desorbed from the sample pass through a pulsed 10 uA electron beam which traverses the center of the cell. Ions formed in the electron beam are trapped in the cell by the magnetic and electric fields, and are mass analyzed Fourier transform (FT) mass spectrometry.

Previous work in our laboratory has shown that this method can be used to identify a wide variety of organic molecules adsorbed on a single-crystal platinum substrate [1-3]. In most cases, the electron ionization fragmentation patterns were indicative of the original surface adsorbates.

Portions of a computer magnetic hard disk were introduced into a VG ESCALAB MK II for characterization using Auger electron spectroscopy (AES) and X-ray photoelectron spectroscopy (XPS). The data showed the presence of carbon, oxygen, and silicon along with other minor constituents. Also from these data we were able to ascertain that the silicon species was partially oxidized, and that some of the oxygen was similar to that found in graphite exposed to the air [4]. We then placed the samples in our LITD-FT mass spectrometer. Using low laser power densities (<1 MW/cm^2) only CO_2 and water desorb. The CO_2 desorption is consisitent with the XPS data which indicated the presence of oxidized graphite.

At slightly higher incident laser power densities (between 2 and 20 MW/cm^2), laser-induced thermal desorption produces a multitude of peaks up to 341 u, indicating that significantly large species desorb. Figure 1 is a typical mass spectrum that was taken at a power density of about 5 MW/cm^2. Peaks labeled by a star have been identified as poly(dimethylsiloxane) compounds, which are common to many silicon-based oils. At this power level, essentially the same pattern of peaks is observed after as many as 600 laser shots at the same spot on some samples. This indicates that the laser beam is not significantly decomposing these surface species and is not ablating the carbon film. Also, there is evidence that the clusters of peaks between 30 amu and 110 amu are the fragments of an aliphatic alcohol.

Depth profiling using argon ion sputtering with AES detection showed that all the silicon was removed after just one minute of sputtering (about 3 nm of C). The surface nature and amount of sample present indicate that the silicone oil was probably placed on the disk intentionally after manufacturing. Inadvertant contamination of the disk during or after manufacturing is unlikely since most pump oils are phenyl silicon oils which give very different mass spectra in our instrument. Samples of hard disks from different sources showed no evidence of silicon compounds under the same experimental conditions, but some did show evidence of hydrocarbons up to mass 417 u. These spectra obtained from disks manufactured differently show the utility of this technique to monitor

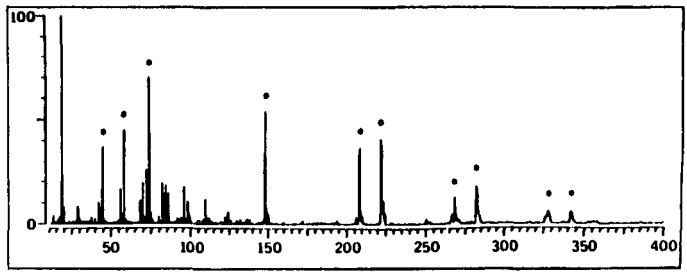

Figure 1: Laser-induced thermal desorption Fourier transform mass spectrum from the sputtered carbon surface of a computer magnetic hard disk.

surface composition on sputtered carbon films.

Since the surface temperature jump is proportional to the incident laser power density, one can use low power densities to desorb only weakly bound species and increase the power density to interrogate increasingly tightly bound compounds. Eventually one reaches power densities (>20 MW/cm^2) which cause ablation of the underlying metal substrates. Under these conditions ions are formed directly by the laser and molecular information about the surface species is lost, but a crude depth profile of the underlying layers can be accomplished. Laser ablation depth profiling is hampered, however, by the widely varying ablation threshholds for the different layers. The ablation threshholds for different materials appear to differ significantly and tend to be very sharp. We are finishing construction on an instrument which would use an ion beam to etch the surface followed by LITD at low power densities to detect the surface species and construct a depth profile.

Both the AES and XPS spectra showed evidence for Si, yet it is clear that the LITD results are far more useful for identifying the nature of the Si species. The ambiguity of vibrational spectroscopies from such surfaces is obvious, and the complications due to species originating from the substrate would hamper interpretation of secondary ion mass spectra or thermal desorp-tion spectra. Laser desorption, however is capable of desorbing large species without ablating the substrate and the FT mass spectrometer allows information to be obtained on a wide mass range for each laser pulse. The combination of these techniques is ideal for the molecular identification of unknown surface species.

ACKNOWLEDGEMENTS

Support for this research was provided by the National Science Foundation under grant CHE8511999 and the Petroleum Research Fund under grant 15664-AC5. J. C. H. would like to acknowledge support from the Alfred P. Sloan Foundation in the form of an Alfred P. Sloan Research Fellowship. D. P. L. and J. M. L. acknowledge support in the form of IBM Graduate Research Fellowships administered by the IBM Almaden Research Center. The authors would like to thank F. J. Feher for helpful discussions of the LITD results.

LITERATURE CITED

(1) Sherman, M. G.; Kingsley, J. R.; Dahlgren, D. A.; Hemminger, J. C.; McIver, Jr., R. T. Surf. Sci. **1985**, 148, L25-L32.
(2) Sherman, M. G.; Kingsley, J. R.; Hemminger, J. C.; McIver, Jr., R. T. Anal. Chim. Acta **1985**, 178, 79-89.
(3) Sherman, M. G.; Land, D. P.; Hemminger, J. C.; McIver, Jr., R. T. Chem. Phys. Lett., **1987**, 137, 298-300.
(4) Barber, M.,; Evans, E. L.; Thomas, J. M. Chem. Phys. Lett. **1973**, 18, 423.

Presented at the 36th ASMS Conference on Mass Spectrometry and Allied Topics
June 5-10, 1988, San Francisco, CA

SIMS MOLECULAR ION IMAGING OF ORGANIC MOLECULES ON SURFACES

Robert W. Odom
CHARLES EVANS & ASSOCIATES
301 Chesapeake Drive Redwood City, CA 94063

Secondary ion mass spectrometry (SIMS) is a sensitive method in the structural analysis of a wide range of organic species. The fast atom bombardment (FAB)[1] and liquid SIMS[2] techniques are often utilized as routine methods in the molecular weight and structural analysis of a number of complex organic and biomolecules dispersed in a glycerol matrix. The static or molecular SIMS technique has demonstrated monolayer detection sensitivities for a number of organic species adsorbed onto a variety of surfaces.[3] Several research groups have begun to employ static SIMS ion imaging techniques for molecular microanalysis.[4] If this SIMS molecular ion imaging technique can be developed to an analytically useful level, it could provide a method for localizing the distribution of molecular species at micrometer (μm) resolutions in such organic solids as polymers and biomaterials. This paper reports the results of SIMS ion imaging of several simple organic compounds dispersed onto Ag substrates. These compounds produce relatively intense, structurally significant secondary ion signals which can be localized at lateral resolutions on the order of a few micrometers.

Spatially dispersed organic layers were produced by an electrospray deposition[5] of dilute methanol/distilled water solutions of the compounds through a TEM finder grid onto the Ag substrate. Approximately 5 μL solutions of the various compounds having concentrations ranging from ~10^{-2} to 10^{-6} M were electrosprayed over a 3mm diameter area. The molecular areal density for the most concentrated solutions was on the order of 3 X 10^{17} molecules/cm^2. The SIMS analyses were performed on CAMECA IMS 3f and 4f instruments. Positive ion SIMS was performed using O_2^+, O^-, and Cs^+ primary ion bombardment and negative ion SIMS employed a Cs^+ primary beam. Secondary ion microscope images were acquired with the resistive anode encoder (RAE) detector which is a two-dimensional pulse counting detector having a spatial resolution on the order of 1 μm.[6] More intense secondary ion signals and better lateral resolutions for the molecular or pseudo-molecular ions were obtained using a microfocused Cs^+ beam on the IMS-4f and positive secondary ion spectroscopy. For these microbeam analyses, a 5 to 20 pA Cs^+ beam was focused to a ~1 μm spot diameter and was rastered over an area 200 μm X 200 μm. The secondary ion signals were detected on the electron multiplier in these analyses. Ion images were acquired using a specially designed primary beam raster circuit along with custom image acquisition hardware and software. The primary ion dose ranged between 8 X 10^{10} and 3 X 10^{11} ions/cm^2 at an impact energy of 5.5 keV.

A number of relatively simple molecules produced structurally significant positive secondary ion signals. These molecules included thymine, γ-aminobutyric acid (GABA), phenylalanine, dopamine hydrochloride, epinephrine, and acetylcholine chloride (ACh^+-Cl^-). Figure 1 illustrates an ion image of the m/z 137 species observed in the analysis of the residue of ~20 picomoles of dopamine HCl. This ion corresponds to the loss of the $NH_3^+ \cdot Cl^-$ from the molecule. This ion signal is not observed in the mass spectrum of a Ag substrate electrosprayed with a methanol/water blank solution. The pattern in this image is the masking produced by the finder grid. The grey scale to the right of the images shows the number of ion counts represented within each grey level. The useful ion yields (number of ions detected/picomoles of molecule deposited) for this ion was determined by performing a "depth profile" analysis of the sample until the signal disappears. The useful ion yield for the 137 ion obtained in this manner was ~1.6 X 10^5 ions/picomole of dopamine.

Figure 2 illustrates the variation in the useful yields for several ions produced from epinephrine as a function of the epinephrine loading on the Ag substrate. The decrease in the useful yield with increased loading suggests that Cs primary ion beam is damaging the sample at these higher loadings. All of these ions produced spatially resolved secondary ion images with lateral resolutions on the order of 2-3 μm.

These results suggest that molecular ions from sub-picomole quantities of these types of compounds can readily be detected in an imaging SIMS analysis. However, these samples are extremely simple compared to the complex chemical compositions of most biological materials. Attempts to

detect structurally significant ion signals of epinephrine, norepinephrine, dopamine and ACh in various regions of ~ 1 μm thick sections of rat brain tissues are underway. These samples are prepared by microtoming cross sections from frozen whole brain tissues and freeze drying these sections on a Si substrate. Sections have been prepared by Ms. Joan Hunter of the Pasarow Analytical Neurochemistry Facility at Stanford University Medical School (Stanford, CA) in collaboration with Dr. Kym F. Faull. Although it is possible to focus the Cs^+ microbeam onto various tissue regions, no structurally significant ions have yet been observed. The samples exhibit varying degrees of sample charging and analysis of these types of tissue sections using an electron flood gun is in progress.

References

1. M. Barber, R.S. Bordoli, R.D. Sedgwick, and A.N. Tyler. J. Chem. Soc. Chem. Commun., 325, 1981.
2. W. Aberth, K.M. Straub and A.L. Burlingame, Anal. Chem. 54:2029, 1982.
3. A. Benninghoven, F.G. Rudenauer, and H.W. Werner, Secondary Ion Mass Spectrometry, New York: John Wiley and Sons, 1987, Chapter 5.
4. R.W. Linton in Secondary Ion Mass Spectrometry, SIMS-V, Eds. A. Benninghoven, R.J. Colton, D.S. Simons, and H.W. Werner, New York: Springer-Verlag, 420, 1985.
5. C.J. McNeal, R.D. Macfarlane and E.L. Thurston, Anal. Chem., 51:2036, 1979.
6. R.W. Odom, B.K. Furman, C.A. Evans, C.E. Bryson, W.A. Petersen, M.A. Kelly, and D.H. Wayne, Anal. Chem., 55:574, 1983.

Acknowledgments: This work was supported by NIH SBIR Grant No. GM39005-01.

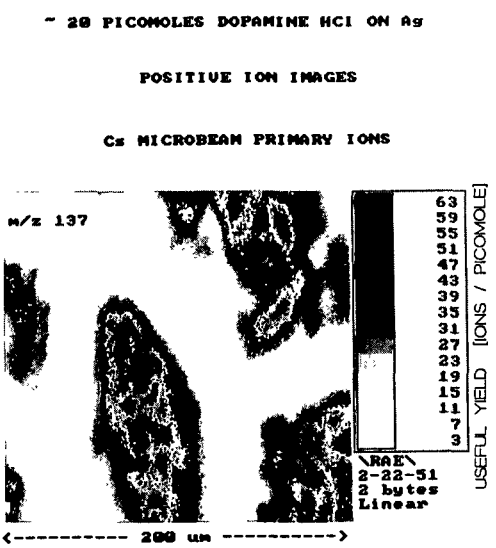

Figure 1

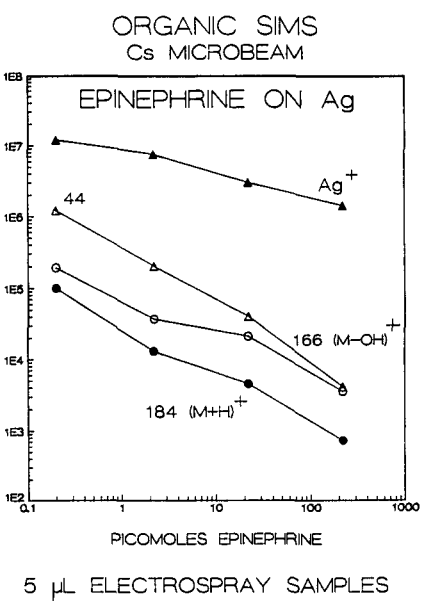

Figure 2

Presented at the 36th ASMS Conference on Mass Spectrometry and Allied Topics
June 5-10, 1988, San Francisco, CA

TIME-OF-FLIGHT MASS SPECTROMETRY: A NEW INSTRUMENT FOR SURFACE CHEMICAL ANALYSIS WITH SUB-MICRON SPATIAL RESOLUTION:

A.R.Waugh, D.R.Kingham, C.H.Richardson and J.Wolstenholme, VG Ionex Ltd., Charles Avenue, Burgess Hill, West Sussex, RH15 9TQ, UK.

INTRODUCTION

When a surface layer is sputtered by a microfocussed ion beam a relatively small number of secondary ions are produced. In order to make the best possible use of the available signal it is necessary to employ a mass spectrometer with parallel detection of all masses, rather than a tuned spectrometer such as a quadrupole or magnetic sector system.

An energy-compensated time-of-flight mass spectrometer is well suited to this purpose. We have combined such a spectrometer with a microfocussed liquid-metal ion source which is able to give a pulsed beam of nanosecond duration. A high stability vacuum chamber and sample manipulator permit a resolution of better than 50nm when the gun is operated in the continuous mode for SEM or total ion imaging. Resolution of the order of 0.25μm can be obtained in mass-selected images in the pulsed mode of operation.

The instrument is also fitted with a Q-switched Nd:YAG laser. An harmonic generator produces second or fourth order radiation (531nm or 266nm) which can be focussed to provide a spot a few microns in diameter at the sample; this provides an alternative means of ionising sample materials.

With the instrument configured in this way the speed of Laser Microprobe analysis is complemented by the precision (extreme surface sensitivity and spacial resolution) of the time-of-flight SIMS (ToFSIMS) technique, so providing an important tool for surface chemical analysis.

PRIMARY SOURCES

The liquid-metal ion gun is currently fitted with a gallium liquid metal ion source operating at up to 30kV. The gun has condenser and focus asymmetric einzel lenses, a Wien mass filter with sufficient resolution to separate $^{69}Ga^+$ from $^{71}Ga^+$, octupole stigmators and scan rods. Auxiliary internal deflector plates can be used to chop the beam (5 to 50ns pulses can be selected by computer control) by scanning it across an aperture. A spatial resolution of <50nm has been achieved using a continuous beam and <0.25μm using a pulsed beam. The ion beam can be pulsed at up to 20kHz, the repetition rate being controlled by the computer.

In the Laser Microprobe mode of operation a "pilot" He:Ne laser is used to select the target area for the Nd:YAG ablating pulse. The laser beams are focussed using a mirror microscope objective which can also be used for viewing the sample via an eyepiece or a TV camera: this is connected to the digital framestore, allowing optical micrographs to be recorded on disk if required.

THE SPECTROMETER

In the time-of-flight mass spectrometer used in this work the secondary ions are accelerated by a high voltage applied between the sample and an extraction electrode. These secondary ions are extracted along the sample surface normal and enter the gridless, toroidal, energy-compensated analyser via a variable iris acceptance aperture. The accelerated ions pass around an energy-compensating electrostatic sector before impinging on a channel-plate detector. This electrostatic sector corrects for the initial kinetic energy spread of the sputtered secondary ions, thereby enabling good mass resolution to be achieved.

The spectrometer has a very high transmission and virtually all the ions leaving the surface may be focussed onto the detector. There is no inherent upper mass limit set by the spectrometer and SIMS spectra may be recorded with good sensitivity up to mass 8,000 and beyond. Post-acceleration may be applied to improve the registration of heavy ions by the channel-plate detector.

Presented at the 36th ASMS Conference on Mass Spectrometry and Allied Topics
June 5-10, 1988, San Francisco, CA

DATA COLLECTION

Time-of-Flight SIMS spectra are collected using a time-to-digital converter with 1ns resolution (LeCroy 4208). Digital delay generators can be used to veto signals from unwanted intense peaks (eg alkali metals) to avoid saturating the acquisition system. A fast CAMAC processor is used to sort the data and transfer it periodically to a PDP 11/73 with a digital frame-store. The datasystem can either acquire mass spectra with acquisition times of typically 10-100 seconds, or can simultaneously acquire both a mass spectrum and multiple mass-resolved secondary ion images of 64^2, 128^2 or 256^2 pixel resolution, with acquisition time typically around 120 seconds. Due to the parallel detection of the time-of-flight spectrometer, images can include ions at different masses (e.g. all the isotopes and all the cluster-ions containing a given element). Laser Microprobe data are generated using a single-shot laser pulse with analogue acquisition using a 200MHz, 8 bit 32,000 channel transient recorder.

INSTRUMENT PERFORMANCE

Examples of the spectral performance of the instrument are presented here:

Fig.1 a) Spectrum from Caesium Iodide demonstrating the mass range of the ToFSIMS showing clusters up to 8000 amu.

Fig.1 b) Spectrum from Silver Bromide showing the isotope distribution of a cluster centred on mass 625. A mass resolution, M/Delta M, of 2500 FWHM at mass 625 has been achieved.

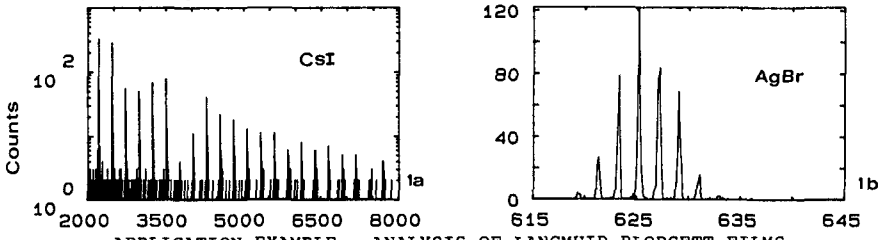

APPLICATION EXAMPLE: ANALYSIS OF LANGMUIR-BLODGETT FILMS

L-B films form as precise, uniform, layers of organic material on the surface of a suitable substrate. Data are presented from films of arachidic acid on silver. Fig.2a shows a positive ToF spectrum from a 3 monolayer film; the cluster ion silver arachidate is clearly seen. Complementary information (Fig.2b) is available from the negative spectrum in which the arachidate ion predominates because of its existing negative charge in the L-B film. (Courtesy of Dr. Joe Gardella, Chemistry Department and Surface Science Center, State University of New York at Buffalo, Buffalo, New York 14214).

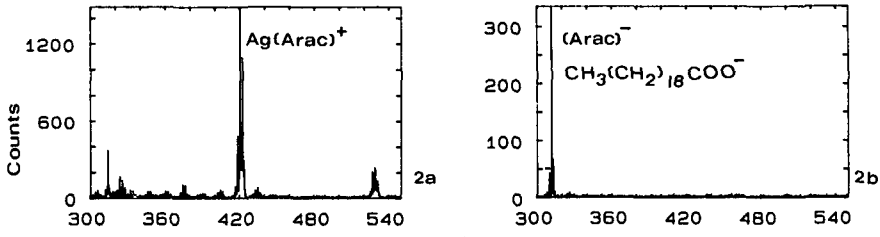

CONCLUSION

A new time-of-flight mass spectrometry instrument has been built which is capable of:

i) surface molecular ion analysis up to at least 8000 mass units;

ii) surface molecular ion imaging with sub-micron spatial resolution under low damage STATIC SIMS conditions.

Presented at the 36th ASMS Conference on Mass Spectrometry and Allied Topics
June 5-10, 1988, San Francisco, CA

THE POSSIBLE RELATION OF STATIC SIMS ION YIELDS FROM Ni_3Mn TO SURFACE ORDERING

K.A. VINEBERG+ and P.H. DAWSON
NATIONAL RESEARCH COUNCIL, OTTAWA, and +McMaster University, Hamilton, Canada

INTRODUCTION

Yields of sputtered ions are known to be sensitive to surface chemistry. The relative yields of different species indirectly reflect the surface composition. Alloys which undergo order-disorder transitions as a function of temperature may provide interesting model systems for study. One limitation is a lack of knowledge of the relationship of the surface behaviour to that in the bulk. However, this in itself is a subject of considerable interest. A number of theoretical studies have been carried out previously (1) and some experimental observations have been made for Cu_3Au using LEED and ion scattering (2). No previous work has been reported on Ni_3Mn surfaces. Using 1 keV argon ion bombardment, "static" secondary ion yields were observed as a function of temperature from clean alloy surfaces. Surface composition and surface cleanliness were monitored using Auger electron spectroscopy. Significant yield decreases were observed above a certain critical temperature. Yields could be restored by annealing at a lower temperature. Different species had different quantitative behaviour. Auxiliary experiments in a sputtered neutral mass spectrometer indicated that the changes were largely in the ionised fraction rather than in the total sputtered yield.

(1) R. Lipowsky, Phys. Rev. Lett. 49, 1575 (1982);
R. Lipowsky and W. Speth, Phys. Rev. B 28, 3983 (1983);
J.L. Moran-Lopez, F. Mejia-Lira and K.H Bennemann, Phys. Rev. B 32, 3534 (1985);
G.H. Vurens, F.C. van Delft and B.E. Nieuwenhuys, Surf. Sci. 192, 438 (1987).
(2) V.S. Sundaram, R.S. Alben and W.D. Robertson, Surf. Sci. 46, 653 (1974);
H.C. Potter and J.M. Blakely, J. Vac. Sci. Technol. 12, 635 (1974);
E.G. McRae and R.A. Malic, Surf. Sci. 148, 551 (1983);
T.N. Buck and G.H. Wheatly, Phys. Rev. Lett. 51, 43 (1983).

BULK PROPERTIES OF Ni_3Mn

For Ni_3Mn, the order/disorder temperature is at 510°C. There is also a magnetic transformation at a lower temperature (~ 465°C). The critical temperatures are highly dependent on the composition, decreasing with nickel enrichment.

EXPERIMENTAL RESULTS

SIMS YIELDS

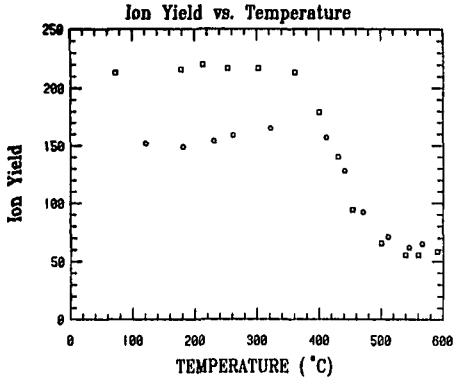

Experiments were carried out on $Ni_3Mn(100)$ surfaces with sufficient time spent at each temperature to ensure thermal equilibration. The figure shows typical yield variations for Mn^+ and Ni^+. There is a significant yield decrease at a temperature near 400°C. The exact temperature was somewhat a function of past history of the surface (say ± 20°C). Similar changes were observed for $Ni_3Mn(111)$, for $Ni_{0.65}Mn_{0.35}$ (Polycrystalline) and for surfaces that had small quantities of the two most common contaminants - S and O. The yield of Mn^{2+} also decreased at the critical temperature but by a much smaller factor than that of Mn^+. Pure Nickel did not show any yield changes in this temperature range.

Similar decreases in yield could be brought about at lower temperatures by excessive ion bombardment.

Yields were restored by extensive annealing at lower temperatures.

Presented at the 36th ASMS Conference on Mass Spectrometry and Allied Topics
June 5-10, 1988, San Francisco, CA

SNMS RESULTS

The yield of Ni atoms remained constant throughout the transition region.

AUGER RESULTS

In the transition region no appearance or disappearance of contaminants at the surface was observed (after the initial cleaning had been carried out). The Auger spectrum indicated no major changes in the Ni/Mn ratio in the surface layers during the transition. Repeated cycling (and the ion bombardment involved in the observations) slowly resulted in a depletion of Mn from the surface.

TEMPORAL BEHAVIOUR

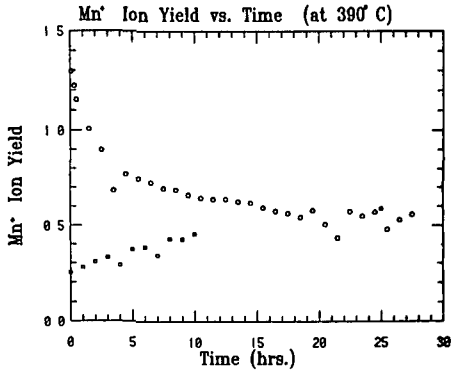

The figure shows the approach to steady state at a temperature in the transition region when the temperature was suddenly increased from 350°C or suddenly decreased from 450°C.

The temporal data can be analysed in an attempt to extract time constants and *activation energies as shown in the two* following figures, one for the heating process and one typical of the cooling process. The data have a large scatter but are consistent with an activation energy of the order of 0.5 eV.

SURFACE PROPERTIES

The simplest situation would arise if the surface were a simple extension of the bulk. e.g. the $Ni_3Mn(100)$ surface would have an outer layer consisting of equal numbers of Ni and Mn atoms and a second layer consisting entirely of Ni atoms in the ordered state. The disordered state would be a completely random arrangement. However, various theoretical treatments suggest that the surface behaviour may differ from that of the bulk (2). For example, the calculations using a lattice gas model in the tetrahedron approximation show that the surface ordering/disordering temperature can differ from the bulk depending on the magnitude of the surface segregation energy to the pairwise interaction energies. Recent Monte Carlo simulations of the outermost eight atomic layers (Vurens et al) show that surfaces can order at very different temperatures from the bulk and that surface enrichment effects must be taken into acount.

DISCUSSION

Large changes in secondary ion yields were observed in a critical temperature range and these do not appear to be related to any changes in composition or impurity segregation that can be observed with the Auger analyser. The changes are predominantly in the yields of ions rather than the total sputtered yield, although the relative yields of different species undergo changes of different magnitudes. The changes have been observed with many different crystals of differing origins. SIMS yields may be sensitive to surface structural changes due to associated changes in electronic structure. Some such electronic changes have been reported in association with order/disorder phenomena (see photoemission results of Jordan and Sohal, J. Phys. C 15, L663 (1982)). The observations reported here occur well below the temperatures expected for the bulk order/disorder transition, but a surface transition is one possible explanation. Clearly a more detailed examination of the Ni_3Mn system would be required in order to demonstrate the validity of this hypothesis.

Presented at the 36th ASMS Conference on Mass Spectrometry and Allied Topics
June 5-10, 1988, San Francisco, CA

INDUSTRIAL APPLICATIONS OF FOURIER TRANSFORM MASS SPECTROMETRY (FTMS)

T G Blease, J H Scrivens, ICI PLC, Wilton Cleveland, UK, TS6 8JE
J J Monaghan, ICI PLC, Runcorn Cheshire, UK, WA7 4QD
D Weil, Nicolet, Madison, WI 5311, USA

The characterisation of polymer formulations which may include increasingly sophisticated additives forms an important part of the work of an industrial laboratory. Modern additives often show substantial increase in molecular weight with decreasing volatility over those used previously. Laser desorption mass spectrometry (LDMS) is a technique that offers considerable promise in the study of these materials.

Fourier transform mass spectrometry (FTMS) is well suited to coupling with pulsed laser desorption and a combination of the two techniques has been used to characterise additives and polymers of industrial interest. Another relevant ionisation technique for these materials is field desorption (FD) and a comparison of these two methods is made.

FTMS spectra were obtained with a Nicolet 2000 FT instrument using a Tachisto 215G pulsed CO_2 laser. FD spectra were obtained on a JEOL HX110 double focussing instrument of forward geometry. LD-FTMS spectra are characterised by abundant cation attachment ions and, to enchance this feature and reduce the ambiguity of the identity of the cation, all samples were doped with KBr.

Fig 1 shows the LD-FTMS spectrum of pentaerythritol tetrabehenate $C(CH_2OCOC_{21}H_{43})_4$ of mol wt 1424. The cation attachment ion at m/z 1464 is clearly seen together with abundant structural information. Demulsifiers are often formed by ethoxylating and/or propoxylating alkyl phenol formaldehyde resins. These materials are difficult to characterise but they do run well by LD-FTMS and an example is shown in Fig 2.

FIG 1

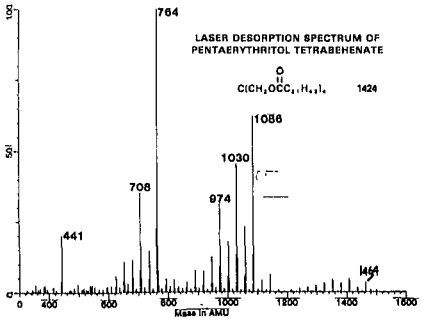

FIG 2

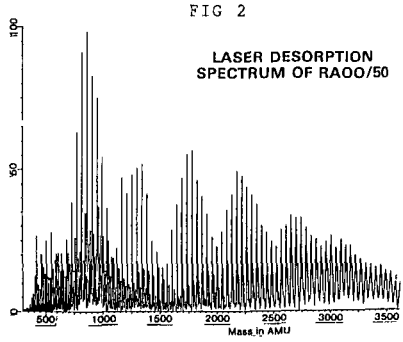

Thus LD-FTMS is a promising technique for the characterisation of polymers and polymer additives. A number of compound classes, of which the foregoing are some examples, have been successfully studied and the future of the approach looks bright.

Presented at the 36th ASMS Conference on Mass Spectrometry and Allied Topics
June 5-10. 1988. San Francisco. CA

Although FTMS has been widely used, published collisionally activated dissociation (CAD) applications are rare. We have compared the results obtainable using a dual cell geometry FTMS instrument together with pulsed valve introduction of collision gas with those obtained previously on a BEQQ hybrid instrument. The problem chosen is the characterisation of the components of an epoxy resin extract. Our original hybrid MS-MS results on this were reported at the Denver ASMS meeting (1).

The collision gas introduction system in the dual cell FTMS instrument leads to the combination of high collision gas pressure with higher resolution conditions (low pressure) for ion detection. This reduces the problem of reaction of daughter ions with neutral molecules.

FIG 3

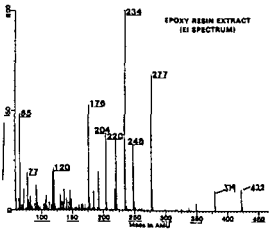

FIG 4

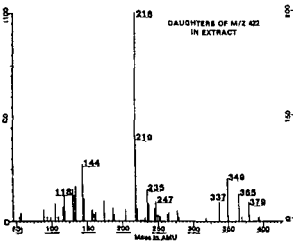

FIG 5

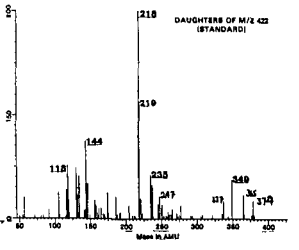

Fig 3 shows the EI spectrum of the extract. Figs 4 and 5 are the CAD daughter ion spectra of m/z 422 from the extract and a standard respectively. Good agreement between the two is obtained. Similar good agreement is found for the daughter ion spectra of m/z 277. For m/z 248, known to be a diaminodiphenylsulphone, the CAD spectra (Figs 6 and 7) confirm the 3,3' isomer to be present in the extract.

FIG 6

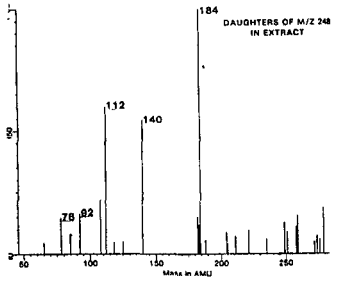

FIG 7

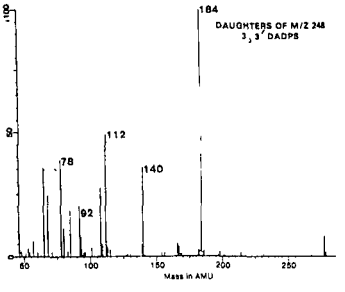

These results can be compared with the daughter ion spectra of m/z 422, 277 and 248 described previously (1) from a VG ZAB HSQ hybrid instrument with ImTorr of argon and 25 eV collison energy.

The CAD FTMS spectra clearly show that analytical problems can be solved by this technique. As currently operated, the energy transfer is greater than that commonly used in hybrid or triple quadrupole experiments. Initial results indicate that higher energy transfers may be possible with CAD FTMS than are possible in hybrid or triple quadrupole collision cells.

1 T G Blease, D A Catlow, E Clayton, J J Monaghan and J H Scrivens, ASMS 1987, Denver, Co.

Presented at the 36th ASMS Conference on Mass Spectrometry and Allied Topics
June 5-10, 1988, San Francisco, CA

METHOD FOR AVOIDING INSTRUMENT RELATED ARTIFACTS IN TRIPLE QUADRUPOLE MASS SPECTRA - A STEP TOWARDS MS/MS CAD DATABASE

S. N. Ketkar and W. L. Fite
Extrel Corporation, Pittsburgh, PA 15238

With the widespread use of triple quadrupole mass spectrometers in analytical applications there is considerable interest in compiling a practical, standardized MS/MS CAD database. One of the key MS/MS parameters that can cause the relative intensities measured in different QQQ instruments for various progeny ions to differ significantly is the Mathieu parameter q_2 (RF voltage on Q2) and restrictive interquadrupole apertures, because of mass dependent focussing effects which determine how effectively parent/daughter ions can be contained within Q2 for emittance (transmission) into Q3.[1]

We report here the use of leaky dielectric endplates in a QQQ instrument as a way of removing the ambiguity associated with the choice of q_2 (RF voltage on Q2). The use of such endplates makes it possible to use all three quadrupoles in a QQQ instrument in a source limited mode.

Figure 1(a) shows the dependence of Q1MS intensity as a function of q_2 for a conventional triple quadrupole mass spectrometer with metallic endplates. Figure 1(b) shows the dependence of Q1MS intensity as a function of q_2 for a conventional triple quadrupole mass spectrometer with leaky dielectric endplates. As can be seen from Figure 1, the Q1MS intensity is independent of the choice of q_2.

We have also measured the cross section for the reaction $N_2^+ + SF_6 \rightarrow SF_5^+ + F + N_2$. Our results are summarized in Table 1. The results agree with the results of Martinez and Ganguli.[2]

Table 1

$$N_2^+ + SF_6 \rightarrow SF_6^{+*} + N_2$$
$$SF_6^{+*} \rightarrow SF_5^+ + F$$
$$E_{cm} = 5.3 \text{ eV}$$

ln Y	P(x10^6 Torr)	σ (Å^2)
0.6	1.17	63.8
0.7	0.88	55
0.8	0.47	62
0.9	0.23	60

[1] Richard I. Martinez and R. Graham Cooks, A Workshop on MS/MS CAD Database: Instrument Design and Operation Apposite to CAD Dynamics. Presented at the 35th ASMS Conference on Mass Spectrometry and Allied Topics, Denver, Colorado, May 24-29, 1987.

[2] R. I. Martinez and B. Ganguli, Rapid Comm. Mass Spectrom., 2, 41 (1988).

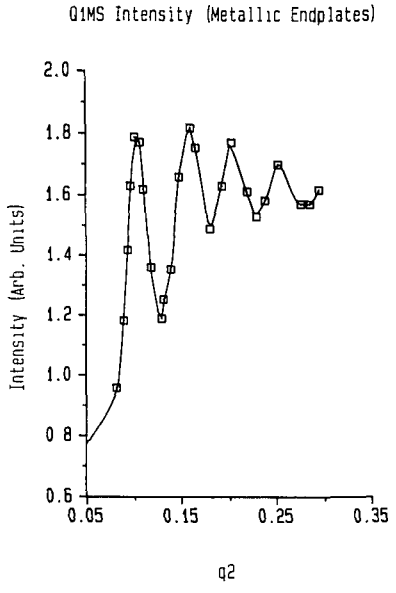

Figure 1(a)

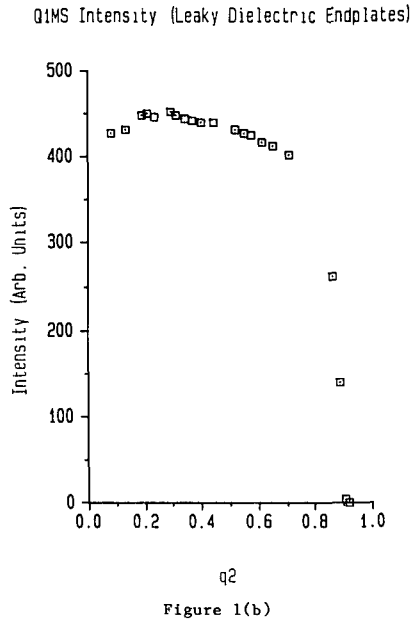

Figure 1(b)

Presented at the 36th ASMS Conference on Mass Spectrometry and Allied Topics
June 5-10, 1988, San Francisco, CA

Pulsed High Pressure Liquid Injection of Small Biologicals Into Time of Flight Mass Spectrometry

David M. Lubman and Ho Ming Pang
Department of Chemistry
University of Michigan
Ann Arbor, MI 48109-1055

The goal of this work is to develop a novel liquid injection method for introducing and ionizing small biological molecules in a time of flight mass spectrometer. This method involves using a high pressure pulsed liquid injection technique followed by resonance enhanced multiphoton ionization (REMPI). A unique feature of this method is that since REMPI depends upon the absorption of a resonant state, one can selectively ionize the analyte based upon the wavelength of the laser source while discriminating against the liquid solvent. Thus, one can achieve a separation of analyte and liquid carrier by the use of laser selectivity without the need for prior physical separation. In addition, REMPI can act as a versatile ionization source which can produce either soft ionization or extensive fragmentation by varying the laser input energy or wavelength. This contrasts to other liquid injection techniques where EI fragmentation methods often cannot be used because of the high pressure which results in the MS. Since the UV photons are transparent to the solvent, extensive fragmentation can be produced for structural studies.

The idea of using a pulsed high pressure liquid injection is particularly well suited for REMPI studies as compared to continuous injection techniques. Since a pulsed laser source is used to produce REMPI, it makes sense to use a pulsed injection source in order to optimize the amount of sample interrogated by the laser pulse and to reduce the duty cycle needed for pumping. Most significantly, though, the degree of solute-solvent cluster formation in this high pressure expansion can be controlled based upon the kinetics of the pulsed jet formation. It has been observed that if the pulsed laser source intersects the liquid jet at the front edge of the molecular beam pulse, then such clustering is minimized. If the delay is adjusted so that the laser probes further into the gas pulse, then extensive clustering is observed. Thus, in these experiments where typically 200 atm of CH_3OH at 70-80°C, or H_2O at 140°C or NH_3 at 130°C serves as the liquid injection carrier for the analyte through a 200 µm orifice into vacuum, there is minimal solute-solvent cluster formation observed. In continuous flow techniques, generally significantly higher temperatures are required in order to prevent clustering.

The experimental apparatus consists of a standard supersonic beam/TOF mass spectrometer device which has been described elsewhere (1). The key to this work is the development of a pulsed injection source for high pressure fluid injection. This valve can operate at up to 200 atm reservoir pressure at 180°C with a pulse width down to 100 µs. The valve is constructed so that it can be used with corrosive, polar fluids such as NH_3. Using this valve and liquid N_2 cryopumping the system can easily pump the injected liquid with an operating pressure of ~ 10^{-5} torr resulting. The laser ionization source is a frequency doubled Nd:YAG pumped dye laser operating at 280 or 320 nm.

In Table I are shown results of using pulsed liquid injection of methanol at 200 atm and 80°C of various catecholamine metabolites. The most salient feature of the tabulated results is that the molecular ion, $M^{+\cdot}$, results in every case at 280 or 320 nm, although often accompanied by several fragments of much lower abundance. There are no solute-solute clusters and minimal solute-solvent cluster ions detected where <2% of the total yield is due to such clusters. Also the mass spectra of Table I shows that at a given laser power the degree of fragmentation generally increases as the photon energy increases. In addition, extensive fragmentation can be induced for structural studies by either increasing the laser frequency or power as shown for tryptamine in figures 2a-c. The detection limit for this method has been

shown to be typically between 10-100 ng for the molecules in Table I and will vary according to the solubility of each compound in the solute and the laser ionization cross section.

(1) C. H. Sin, H. M. Pang, D. M. Lubman and J. Zorn, Anal. Chem. 58, 487 (1986).

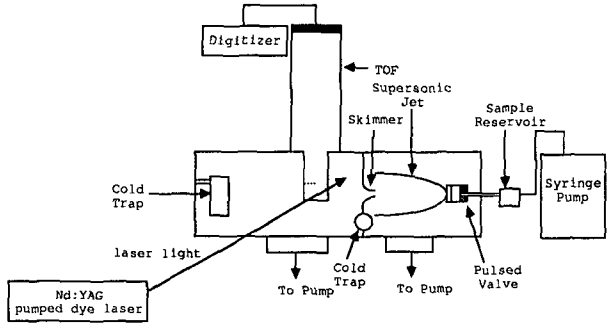

Figure 1: Experimental Setup

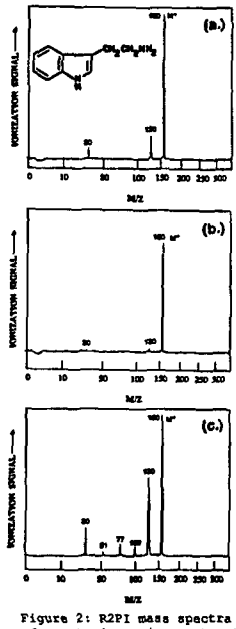

Figure 2: R2PI mass spectra of tryptamine using methanol injection with 200atm backpressure at 80°C using (a) 280nm radiation at $2X10^6 W/cm^2$; (b) 280nm radiation at $8X10^5 W/cm^2$; (c) 266nm radiation at $2X10^6 W/cm^2$.

Table I: R2PI of Catecholamine Metabolites and Related Compounds Injected by Liquid Methanol

Compounds	M.W.	Pressure	Nozzle Temp.	m/z	Relative Intensity* 266nm	280nm
Tyramine	137	200atm	80 °C	137	100	100
				108	26	14
				30	64	30
3-Methoxytyramine	167	200atm	80 °C	167	100	100
				138	22	14
				30	59	31
Octopamine	153	200atm	80 °C	153	75	100
				123	100	38
				30	76	14
Dopamine	153	200atm	120 °C	153	97	100
				123	55	-
				30	100	26
Trans-2-phenylcycle propylamine	133	200atm	80°C	133		
Phenylephrine	167	200atm	80 °C	167	15	78
				123	2	-
				44	100	100
4-Hydroxy-3-methoxy mandelic acid	198	200atm	80 °C	198	100	100
				153	16	16
p-Hydroxy phenyl acetic acid	152	200atm	80°C	152	100	100
				107	38	39
3-(4-Hydroxyphenyl) propionic acid	166	200atm	80 °C	166	100	100
				107	35	26
p-Hydroxy phenyl lactic acid	182	200atm	80 °C	182	100	100
				107	44	44

*laser power 266nm $2x10^6 W/cm^2$ 280nm . $2x10^6 W/cm^2$

Presented at the 36th ASMS Conference on Mass Spectrometry and Allied Topics
June 5-10, 1988, San Francisco, CA

TIME-OF-FLIGHT MASS SPECTROMETRY: MEETING CHROMATOGRAPHY'S CHALLENGE

Christie G. Enke, Department of Chemistry, Michigan State University
East Lansing, MI 48824-1322

As resolution and speed in chromatography have increased, the time available to acquire MS data on each eluting component has decreased. MS scan rates in excess of 10 scans per second are required to produce good peak profiles and non-skewed spectra for one-second wide chromatographic peaks. The technology in sector and quadrupole mass spectrometers are now very near their fundamental limits [1]. For a breakthrough in maximum data rate, non-scanning mass spectrometers such as the linear diode array detector coupled with a magnetic sector MS, fourier transform MS, and time-of-flight MS (TOF-MS) need to be considered. In the NIH/MSU Resource in Mass Spectrometry, we have chosen to explore TOF-MS as a possible answer to chromatography's challenge.*

In TOF-MS, a burst of ions leaving the source simultaneously can produce an ion abundance vs. arrival time (related to mass) signal in about 100 microseconds. Modern high-speed electronic devices, assembled by our group in the form of an integrating transient recorder (ITR), now make possible the digital acquisition of 10,000 TOF spectra per second. This greatly exceeds the data rate requirements of the fastest imaginable chromatography. To reduce storage requirements and improve the signal-to-noise ratio, 500 or more successive TOF transients are summed to provide effective scan rates of up to 20 scans per second [2]. The resulting spectra have no skew since each TOF transient is a true spectrum.

Mass resolution has long been a limiting factor for TOF-MS with gaseous samples. This is due to energy and spatial dispersion of the sample ions in the normal EI source. Current resolution-enhancement techniques are not adequate for chromatography/TOF-MS; time-lag focusing does not work over the entire mass range simultaneously and the reflectron cannot address the energy and spatial dispersion problems simultaneously. The need for an ion source energy and space dispersion compensation method which is mass independent has led us to explore the possibilities of dynamic mid-flight correction techniques. Four properties could be potentially adjusted to achieve simultaneous arrival for isomass ions: flight length, flight time, ion velocity, and ion acceleration These are illustrated in Figure 1. Concentrating on velocity correction first, we have modelled a mid-flight dynamic field system that promises to achieve a mass resolution of 2000 with a 500 K EI source having an ionization depth of 0.2 mm [3]. Our model differs from velocity compaction [4] in that the midpoint correction is designed to produce equal arrival times rather than equal velocities for isomass ions.

Another approach is to combine separate techniques to reduce the effects of energy and spatial dispersion. Pulsing the ion beam after a continuous current ionization source can reduce the spatial dispersion problem (and the reverse energy, or "turn-around" problem). We have used this technique in conjunction with an electric sector energy filter to achieve full range TOF mass spectra with good resolution [5]. A reflectron might have a sensitivity advantage over the electric sector in this application. The signal/noise ratio loss from beam pulsing is equal to the square root of the duty cycle. The number of mass channels simultaneously detected with TOF and ITR more than compensates for the fraction of the ion current not used. Detection limits approaching those of scanning instruments operated under single-ion monitoring mode could potentially be achieved if ions created over a larger fraction of the pulse repetition time could be simultaneously pulsed out of the source.

MS/MS also can benefit from "array-detection" mass spectrometry. The time required to collect the full MS/MS data (daughter spectra of all the parent ion masses) typically requires many minutes with current tandem mass filter instruments. Speeding up the data collection rate and making more efficient use of the sample could extend the benefits of MS/MS to a much broader range of samples. We have combined TOF/ITR with a magnetic sector mass spectrometer in a technique we call time-resolved ion-momentum MS (TRIMS) [6,7]. Each TOF transient provides the velocities of all the ions of a given momentum. Daughter ions have the velocity of their parents, but a lower momentum. Scanning the magnetic field strength once can provide the full set of MS/MS data collection over a one decade mass range in less than 20 seconds. Complete MS/MS data has been

obtained from sample compounds introduced by injection onto a packed column [8]. For still faster data acquisition, TOF could be used for both the selection and analysis stages of MS/MS. The feasibility of adapting a reflectron TOF MS/MS instrument for gaseous samples and high data rates is currently under study.

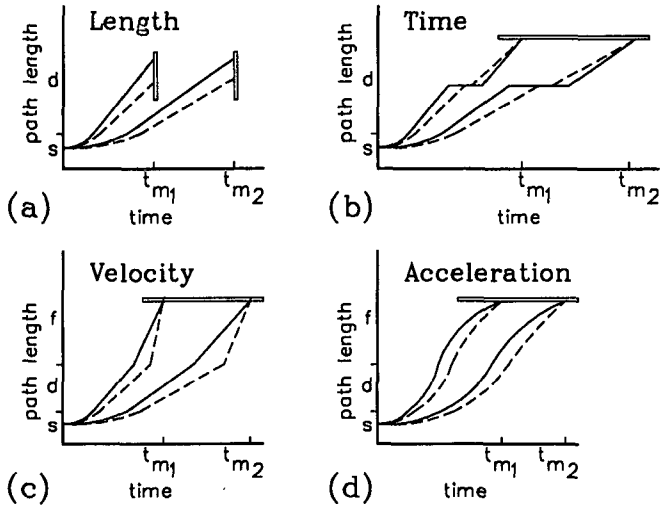

Figure 1. Four possible adjustment techniques to achieve equal arrival times for isomass ions pulsed from a gaseous sample source. The flight path (distance *vs.* time) is shown for ions of two mass values. For each mass, two different ion energies are shown. The source region and two field-free regions are labeled *s*, *d*, and *f*, respectively. In (**a**) the flight length is shorter for ions of lower velocity (some electric sector designs). In (**b**) faster ions are removed from the flight path for a longer time than slower ions (one way of viewing the function of the reflectron). In (**c**) a short dynamically changing acceleration field increases the velocity of slower ions more than that of faster ions. In (**d**) multiple dynamic field gradients adjust ion acceleration for equal arrival times.

*Current investigators involved in this project include John Allison, myself, Jack Holland, Jack Watson, Brian Eckenrode, Eric Erickson, George Yefchak, Ron Lopshire, Mike Davenport, Kevin McNitt, and Gary Schultz.

[1] J. F. Holland, C. G. Enke, J. Allison, J. T. Stults, J. D. Pinkston, B. Newcome, and J. T. Watson, *Anal. Chem.*, 55, (1983) 997A.
[2] J. F. Holland, E. D. Erickson, B. A. Eckenrode, and J. T. Watson, Presented at the 35th ASMS Conference on Mass Spectrometry and Allied Topics, Denver, Colorado, May 24-29, 1987.
[3] G. E. Yefchak, C. G. Enke, and J. F. Holland, *Int. J. Mass Spectrom. Ion Processes*, in press.
[4] M. L. Muga, *Anal. Instrum.*, 16 (1987) 31-50.
[5] J. D. Pinkston, M. Rabb, J. T. Watson, and J. Allison, *Rev. Sci. Instrum.*, 57 (1986) 583-592.
[6] J. T. Stults, C. G. Enke, and J. F. Holland, *Anal. Chem.*, 55 (1983) 1323-1330.
[7] B. A. Eckenrode, J. T. Watson, C. G. Enke, and J. F. Holland, *Int. J. Mass Spectrom. Ion Processes*, 83 (1988) 177-187.
[8] B. A. Eckenrode, J. T. Watson, J. F. Holland, and C. G. Enke, this conference, paper ROC 1000.

Presented at the 36th ASMS Conference on Mass Spectrometry and Allied Topics
June 5-10, 1988, San Francisco, CA

MASS SPECTROMETRIC APPROACHES TO THE ANALYSIS OF BIOPOLYMERS

Charles N. McEwen

Central Research & Development Department
E. I. du Pont de Nemours & Co.
Wilmington, DE 19898

The subject of the 1987 Fall workshop held in Boston was "Mass Spectrometric Approaches to the Analysis of Biopolymers". The speakers for the workshop were John Shively of City of Hope, Klaus Biemann of MIT, Howard Morris of the Imperial College of London, Barbara Larsen of DuPont, Steve Carr of SmithKline & French, Vernon Reinhold of Harvard, and Don Hunt of the University of Virginia. In addition to the speakers, a poster session was held on the evening preceding the main session. The talks covered various aspects of protein and glycoconjugate analysis. Space constraints limit this discussion to methods of protein analysis.

Because proteins are a linear string of amino acids, the most common approach to sequencing is one in which the amino acids are clipped sequentially from the protein and analyzed using liquid chromatography techniques. Methods are available for clipping from either end of the protein, but for practical purposes sequencing is almost always done from the amino-terminus using Edman chemistry. Although the Edman chemistry usually proceeds in high yield, it is less than 100% efficient and some amino acids are not well behaved. As a result, the chemical background builds and after a number of cycles (normally 20 - 40) the results become ambiguous. For this reason, proteins are cleaved into peptide fragments that generally have fewer than 40 amino acid residues. The cleavage is effected by proteases such as trypsin which cleave after lysine and arginine except for lysine-proline combinations and usually arginine-proline combinations. Reverse phase HPLC is used to isolate the peptide fractions. Only about 20 pmole of a pure peptide is needed to sequence 20 - 40 residues. Usually 50 - 100 pmoles of each peptide fraction is submitted for amino acid analysis and 10 - 200 pmoles for molecular weight analysis by mass spectrometry. The sequence analysis, amino acid analysis, and mass spectral results should all agree. The major advantages of Edman gas phase sequencing are the sensitivity (ca. 20 pmoles to sequence 20 - 40 residues), and the reliability (<2% error rate). The Edman method fails if the amino terminus is blocked. Also, posttranslational modifications are frequently difficult to detect and identify using the Edman sequencing method.

Proteins structures can also be determined by sequencing and decoding the gene that codes for the protein of interest. Sequencing DNA is relatively fast and can now be done automatically. Identifying the cDNA that codes for the protein of interest is done by sequencing 5 or 6 amino acid residues from the protein and synthesizing radio labeled oligonucleotide probes that code for the sequence. Because there are 64 distinct codes and only 20 common amino acids, most amino acids have multiple codes. For this reason it is necessary to construct several

oligonucleotide probes, which when placed in the proper medium attach to the single stranded DNA that codes for the protein. Once the cDNA is fished from the matrix it can be sequenced and the code read. Recombinant technology can be used to produce large quantities of protein for further study. The oligonucleotide method is especially useful for large proteins and proteins isolated in small quantities (only about 10 pmoles are necessary to sequence a protein using this method). Drawbacks are occasional problems in obtaining a proper reading frame and frame shift errors. These problems are addressed by using any available mass spectral and sequence data. Posttranslational modifications are not coded for and thus not detected by this method.

Mass spectrometry provides information that is complimentary to the above methods, thus increasing the confidence in the sequencing results and reducing the time of analysis. Mass spectrometry also provides information not readily available from the conventional approaches. For example, identification of blocking groups and posttranslational modifications, sequencing of a blocked peptide, location of sulfur bridges, and sometimes even sequencing of the entire protein is often best accomplished using mass spectrometry. The mass spectrometric method is fast, but requires more material than either of the above methods for sequencing. Another drawback of mass spectrometry is the cost of the instrumentation. The cost is especially high for MS/MS instruments which are used in combination with CID to obtain sequence information.

Fast atom bombardment (FAB) is the ionization method of choice for peptide analysis. Molecular weight information can be obtained at the low picomole level with FAB. The method is fast but does not give sequence information on small amounts of peptide. When working with peptides for FAB analysis, polypropylene should be used for all transfer and storage and if possible the samples should not be allowed to dry or stand around for any substantial period before analysis. Acceptable solvents include acetic acid/water mixtures, methanol/water (0.1% TFA) mixtures, acetonitrile (0.1% TFA), TFA, and propanol. Common FAB matrices include m-nitrobenzyl alcohol (NBA), thioglycerol, thioglycerol/glycerol, magic bullet (dithiothreitol/dithioerythritol), and glycerol. Failures in FAB are often caused by too little sample, the sample sticking to walls, using the wrong matrix, too much salt (remove with SEP PAK), suppression of sample ion current by impurities, too high a mass for the scan range, or too low a mass (ions masked by matrix). The amount of sample needed for FAB analysis depends on the instrumentation available, the peptide, and information desired. Full scan MW information on substance P was obtained by Hunt, et. al. using a tandem QQ/FTMS instrument at the 0.1 pmole level, but some peptides are difficult even at the 100 pmole level. Sequence information requires from <100 pmoles (tandem QQ/FTMS) to several nmoles. Given sufficient sample and the proper conditions, almost all peptides will give MW information by FAB.

Presented at the 36th ASMS Conference on Mass Spectrometry and Allied Topics
June 5-10, 1988, San Francisco, CA

Secondary Mass Spectra from Impacts of Energetic Water Cluster Ions

R. J. Beuhler and L. Friedman
Chemistry Department, Brookhaven National Laboratory, Upton, NY 11973

Impacts of cluster ions containing from 25 to 150 water molecules and accelerated to total energies between 25 and 250 keV provide a means of studying "hot" collision spikes of varying size and depth. These collision zones in the target can be varied by choice of projectile to give spikes that contain thousands of atoms heated to 10's of volts and located close to the surface in dense atomic assemblies. Recently we measured sputtering yields from cluster impacts which were extremely large. Losses from the targets can be on the order of 10^5 to 10^6 atoms per impact which is "visible" by electron micrography (1). Sputtering yields from copper films evaporated on quartz crystal oscillators can be as high as 20,000 Cu atoms/cluster impact (2).

The purpose of the present work is to report preliminary measurements of secondary ions as a function of the size and energy of the impacting cluster. One series of measurements was made with a low resolution, high transmission, time of flight mass spectrometer utilizing the burst of secondary electrons from the projectile impact as the trigger signal. The secondary ions were detected in a modified Daly Detector operating at 20 keV, allowing more efficient detection of higher molecular weight fragments. Our initial results are quite different from other measurements of secondary ions from metallic and frozen gas targets, which usually yield atomic species as the most abundant secondary ions. In the present experiments, from a copper target, yields of copper clusters containing from several to 30 atoms were observed; the mass distribution of the secondary clusters was not sensitive to the projectile cluster size (from 50 to 150 water molecules) or to the cluster energy (from 50 to 250 kilovolts). Cesium Iodide coated carbon surfaces yielded at first a spectrum dominated by the Cs^+ and Cs_2I^+ peaks and including some hydrated species. As the CsI was depleted masses corresponding to carbon clusters containing up to 100 carbon atoms grew in. In general there was a correlation of the maximum cluster size and the heat of vaporization: targets with higher heats of vaporization yielded larger secondary clusters.

Considerations of the fact that an ion lifetime of at least 10^{-6} seconds is required for the detection of cluster ions in these T.O.F. experiments yielded an interesting conclusion on the amount of internal energy that a detectable secondary cluster can hold (2). The classical RRK rate equation can be recast in the form

$$k = \nu\left(1 - \frac{3\varepsilon}{n\rho}\right)^n$$

where ν is a frequency factor taken as approximately 10^{13} s^{-1}, ρ is the energy density in volts/atom, n is the number of internal degrees of freedom in the polyatomic fragment over which the excess energy is distributed, and ε is the threshold energy for decomposition, taken as the heat of vaporization. Rate coefficients on the order of 10^6 s^{-1} or smaller are necessary for the observation of the ion. For energy densities as small as twice threshold energies for decomposition, rate coefficients of 2×10^{12} s^{-1} are calculated for values of n between 12 and 10,000. The excess energy scales with the number of atoms in the polyatomic fragment. For clusters with 20 or more atoms it can be seen that energy densities must be reduced to values less than roughly 20% of threshold energies for decomposition to produce detectable fragments. Initial energy densities resulting from nuclear stopping of water-cluster oxygen atoms in most of the targets are approximately 50 volts/target atom, approximately an order of magnitude above most heats of vaporization. This would indicate that in the earliest stages of the sputtering process, atomic species must be the predominant detectable product.

Preliminary measurements of both the energy and mass of secondary ions are now being made with a quadrupole mass spectrometer. In general, atomic species from the target have higher kinetic energies than polyatomic ions. These observations are now being compared to a model of the hot spike where the atomic species come from the hot central core and the polyatomic species originate from the periphery of the hot spot where the energy density is less because of thermal conductivity away from the central core.

(1) Nucl. Instr. and Methods in Physics Research B14, 448 (1986).

(2) Unpublished results from this laboratory.

*This research was carried out at Brookhaven National Laboratory under contract DE-AC02-76CH00016 with the U.S. Department of Energy and supported by its Division of Chemical Sciences, Office of Basic Energy Sciences.

Presented at the 36th ASMS Conference on Mass Spectrometry and Allied Topics
June 5-10, 1988, San Francisco, CA

Unimolecular Fragmentation of Large Argon Ion Clusters.

P.G.Lethbridge and A.J.Stace, School of Molecular Sciences,
University of Sussex, Falmer, Brioghton BN1 9QJ, U. K.

A high resolution double focusing mass spectrometer in association with a pulsed supersonic nozzle has been used to study the unimolecular fragmentation of Ar_n^+ clusters for n in the range 30 - 200. All cluster ions within this range are observed to undergo the reaction;

$$Ar_n^+ \qquad Ar_{n-1}^+ + Ar$$

Some ions fragment with the loss of up to 4 argon atoms. A systematic study of the above reaction was achieved using both MIKES and linked scanning techniques, this revealed that the relative intensities of the fragment ions fluctuate considerably with n. Many of these fluctuations coincide with depleted or enhanced ion intensities present in the cluster ion normal mass spectrum.

A simple kinetic model based on unimolecular theory (RRKM) has been developed and can reproduce many of the features observed in both the fragmentation spectra and the normal mass spectrum. Of the two main variables involved in the model; reaction symmetry number and dissociation or binding energy, we have been able to show that only the binding energy is important in determining the fragmentation pattern. This was achieved by studying fragmentation patterns of certain mixed isotope cluster ions which have a reaction symmetry number of unity i.e: they have only one way in which they can loss a single argon atom. The range of binding energies used to reproduce the experimental trends indicate that, in large cluster ions, bonding is determined primarily by weak van der waals interactions.

Through the calculations, the experimental data are interpreted in terms of "stable" , "intermediate" and "unstable" cluster ions. Stable cluster ions have enhanced intensities in the normal mass spectrum, whereas unstable ions produce both depletions in the normal mass spectrum, and enhanced fragment ion intensities. The majority of ions can be represented by the intermediate case. The decomposition of these intermediate ions does not produce particularly intense fragment ions, and hence the normal mass spectrum is not significantly enhanced or depleted. The intermediate cluster ions are used as a reference point for the stable and unstable cases.

Presented at the 36th ASMS Conference on Mass Spectrometry and Allied Topics
June 5-10, 1988, San Francisco, CA

it is proposed that unstable cluster ions consist of an atom weakly bound to an underlying stable cluster. A series of hard sphere stuctures are presented to account for some of the observed stable cluster ions. Each of these structures has evolved around a central Ar_2^+ ion, which is in turn contained within a linear trimer or tetramer. This offers the possibility for further charge delocalisation. It is concluded that, since the clusters are forced to accomodate the charge carrying unit, the positive charge appears to have a structural influence which extends well beyond the electrostatic limit. This is reflected in the fact that all of the structures have a waist region connected to two regular polyhedral end caps. These end caps consist of pentagonal and triangular faces which give the structures an overall icosahedral symmetry. An example is shown below.

Ar^+_{126} d_{5h}

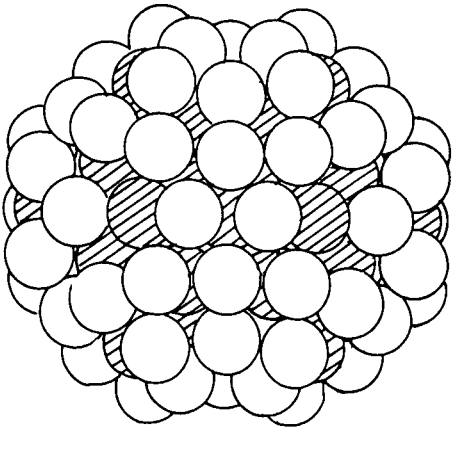

Presented at the 36th ASMS Conference on Mass Spectrometry and Allied Topics
June 5-10, 1988, San Francisco, CA

CROSSED-BEAM STUDY OF THE COLLISION-INDUCED DISSOCIATION OF METHANE ION

S. Howard, K. Qian, J. Biggerstaff, A. Shukla, and J. Futrell
Department of Chemistry, University of Delaware, Newark, DE 19716.

In our continuing efforts to understand the dynamics of ionic dissociation processes activated by collisions with neutrals we have investigated the dissociation of CH_4^+ molecular ions to CH_3^+ and CH_2^+. New results for CH_2^+ obtained at 5.5 eV center-of-mass energy reveal some unique features which are presented here.

The crossed-beam instrument used in this work has been described in detail elsewhere [1] and only a few of its features are mentioned here. The high-pressure ion source customarily used in this apparatus was replaced by a low pressure source operated at 10^{-4}-10^{-3} Torr to generate a propulation of CH_4^+ ions typical of electron impact ion sources utilized in analytical mass spectrometry. The mass-selected ion beam is decelerated to its final collision energy by an apertureless exponential lens and crossed at 90° with a neutral beam of argon seeded with helium and expanded through three differentially-pumped vacuum chambers. Laboratory angular and energy distributions were taken at a series of angles from -3 to 50° for CH_2^+ ions.

Figure 1 shows the scattering contour diagram for the dissociation of CH_4^+ to CH_2^+ at a center-of-mass collision energy of 5.5 eV. There are three distinct maxima in the diagram which can be described as (1) superelastic forward scattering of CH_2^+ along the initial ion velocity vector, (2) strongly inelastic scattering intensity near the center-of-mass, and (3) CH_2^+ ions preferentially scattered at large angles.

Taking into account the sin θ factor by which differential scattering data are multiplied in the integration of Figure 1 to compute the total cross section, the principal mechanism is the feature at 45° (center-of-mass). This feature is predicted by an earlier study [2] of simple hydrocarbon ion dissociation which demonstrated that only a small amount of translational-to-internal energy conversion is required to initiate the lowest energy dissociation process at or near zero angle, but that large angle scattering accompanies the more endothermic CID channels. The linear correlation of energy deposition with scattering angle observed in that study [2] predicts that the highly endothermic (ΔH = 2.8 eV) dissociation process under present investigation would require smaller impact parameter collisions which sample the repulsive core of the potential hypersurface in order to deposit sufficient energy for the reaction to proceed. This results in large angle scattering and we infer the CH_2^+ intensity maximum at 45° results from the dissociation of CH_4^+ ions with modest internal energy proceeding via this impulsive mechanism.

Ions dissociating near zero scattering angle are promoted above the dissociation threshold by a grazing collision (large impact parameter). Such collisions promote a population of highly excited ions that require little or no translational-to-internal energy conversion to stimulate the dissociation process. Since the fragment ions found near the zero scattering angle in the contour diagram are near the circle locating the loci of velocity vectors corresponding to the energy which would be released if electronically excited CH_4^+ ions in the ^2E (D_{2d}) state generated ground state CH_2^+ and H_2, it is speculated that the precursor for these CH_2^+ ions may be CH_4^+ in this state. Since both CH_2^+ and H_2 may be formed with internal excitation, higher excited states could also be involved. The observation of superelastic scattering clearly identifies the precursor ion as from a population of CH_4^+ excited well above the dissociation limit for forming CH_3^+ (+H). These ions, initially formed in the ion source, have survived about 20 microseconds of flight time before

colliding with the neutral beam. Such long lived excited states of CH_4^+ have not previously been reported.

The remaining intensity in Figure 1 near the center-of-mass corresponds to CH_2^+ ions formed with nearly all of the collision energy transferred into internal energy of the fragmenting CH_4^+ ions with little kinetic energy release. This highly inelastic process is distorted by the transformation Jacobian used in constructing the contour diagram. This particular mechanism accounts for only a few percent of total intensity of CH_2^+.

References:

1. C. R. Blakely, P. W. Ryan, M. L. Vestal, and J. H. Futrell, Rev. Sci. Instr. 47 (1976) 15.
2. Z. Herman, J. H. Futrell, and B. Friedrich, Int. J. Mass Spectrom. Ion Proc. 58 (1984) 181.

$$CH_4^+ + Ar \longrightarrow CH_2^+ + Ar + H_2$$

at T = 5.5 eV

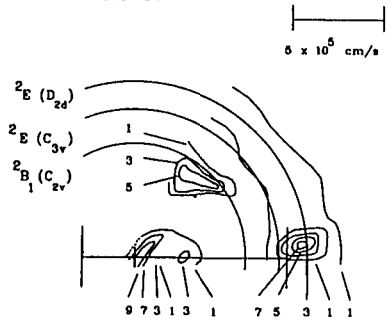

Center-of-mass cartesian velocity, probability contour diagram for the collision-induced-dissociation of CH_4^+ on collision with Ar at 5.5 eV relative energy. Inscribed circles correspond to the velocities of CH_2^+ (and H_2) recoil for the indicated state (and geometry) assuming formation of ground state CH_2^+, H_2 and Ar in the collision process. The vertical bars on the axes correspond to the velocity vectors of the Ar and CH_4^+ reactants and the CM origin of coordinates. Numbers in the diagram label the contours of equal intensity ranging from the highest value (9) to the lowest plotted value (1).

Presented at the 36th ASMS Conference on Mass Spectrometry and Allied Topics
June 5-10, 1988, San Francisco, CA

SEQUENTIAL SOLVATION OF ATOMIC TRANSITION METAL IONS

Peter J. Marinelli and Robert R. Squires
Department of Chemistry, Purdue University, West Lafayette, IN 47907

The structures, properties and reactivity of sequentially solvated transition metal ions have been investigated with use of a flowing - triple quadrupole instrument.[1] Transition metal cations are generated by electron ionization and Penning ionization of volatile metal carbonyl derivatives in the upstream source region of the helium flow reactor (P(He) = 0.3 - 0.5 torr). Solvated metal ions are formed by termolecular association reactions with added H_2O, NH_3 and various other neutral compounds. The following metal ion clusters have been produced:

$M^+(H_2O)_n$	$M^+ = V^+, Cr^+, Mn^+, Fe^+, Co^+, Ni^+$ $n = 1\text{-}3$
$M^+(NH_3)_n$	$M^+ = V^+, Cr^+, Mn^+, Fe^+, Co^+, Ni^+$ $n = 1\text{-}4$
$Cr^+(EtOH)_n$; $Cr^+(NCCH_3)_n$	$n = 1\text{-}6$
$Cr^+(C_2D_4)_n$; $Cr^+(THF)_n$	$n = 1\text{-}3$
	$Mn_2^+(D_2O)_{1,2}$

Unimolecular and bimolecular reactions of mass-selected cluster ions are carried out in the central quadrupole of the triple quadrupole analyzer where both pressure and kinetic energy effects may be characterized.

The thermochemistry for sequential solvation of the metal ions by H_2O and NH_3 has been estimated from the translational energy thresholds for desolvation induced by collision with argon target gas. A remarkable trend is found wherein for most every metal ion the second solvent-binding energy is significantly greater than the first, viz., $D[ML^+\text{-}L] > D[M^+\text{-}L]$ (Fig. 1). This is a striking departure from the normal decrease in successive solvent-binding energies of all other atomic ions for which data are available.[2] This is shown not to be an artifact of our appearance measurements by the reasonable agreement we can achieve in measuring H_2O and NH_3 solvation energies for Na^+, K^+ and other ions by this method.

The origins of the anomalous solvation energy ordering may be in the structures of the clusters and/or special electronic properties of the transition metal ions. We have carried out a variety of isotope labelling experiments aimed at detecting the presence of possible insertion structures. For example, consideration of the known M^+-H and M^+-OH bond energies[3] suggests that both $M^+(H_2O)$ or H-M^+-OH structures are feasible for the monohydrates. Both $M^+(D_2O)$ and $M^+(D_2O)_2$ ($M^+ = V^+, Cr^+, Fe^+, Ni^+$) fail to undergo H/D exchange in the presence of $CH_2{=}CH_2$ and $CH_2{=}CHCH_3$, and both types of ions react with H_2O by thermoneutral ligand exchange <u>without</u> H/D scrambling in the products. Furthermore, the 'mixed-isotope' cluster ions $M^+(H_2O)(D_2O)$ ($M^+ = V^+, Cr^+, Fe^+, Ni^+$) undergo CID by loss of either H_2O or D_2O; essentially no HOD-loss is observed. These experiments (among others) weigh heavily against the presence of structures of the type:

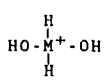

as the static forms for the dihydrates or as intermediates in the (non) exchange reactions. However, they do not rule out the possibility of mobile equilibria among isomeric structures:

Presented at the 36th ASMS Conference on Mass Spectrometry and Allied Topics
June 5-10, 1988, San Francisco, CA

$$M^+\text{-}OH_2 \rightleftharpoons \overset{H}{\overset{|}{M^+}}\text{-}OH; \quad H_2O\text{-}\overset{H}{\overset{|}{M^+}}\text{-}OH \rightleftharpoons H_2O\text{-}M^+\text{-}OH_2 \rightleftharpoons HO\text{-}\overset{H}{\overset{|}{M^+}}\text{-}OH_2$$

A structure for the dihydrate involving one inserted and one non-inserted H_2O ligand could account for the solvation energy orderings since it can be shown that H_2O binds more strongly to metal centers with higher formal oxidation states.

The rich reactivity of atomic metal ions with hydrocarbons and other organic compounds[4] is significantly diminished by partial solvation. Reactions of $M^+(H_2O)_n$ (n = 1-3) ions with various neutral substrates are described including alkanes, alkenes, alcohols and alkyl halides. Simple ligand substitution is evident in most cases, and oxidative insertion reactions by the metal appear to be impeded.

1. Marinelli, P. J., Squires, R. R. manuscript in preparation.

2. Keesee, R. G., Castleman, A. W. J. Phys. Chem. Ref. Data 1986, 15, 1011.

3. a) Elkind, J. L ; Armentrout, P. B. Inorg. Chem. 1986, 25, 1078.
   b) Kang, H.; Beauchamp, J. L. J. Am. Chem. Soc. 1986, 108, 5663.

4. Allison, J. A. Prog. Inorg. Chem. 1986, 627 and references therein.

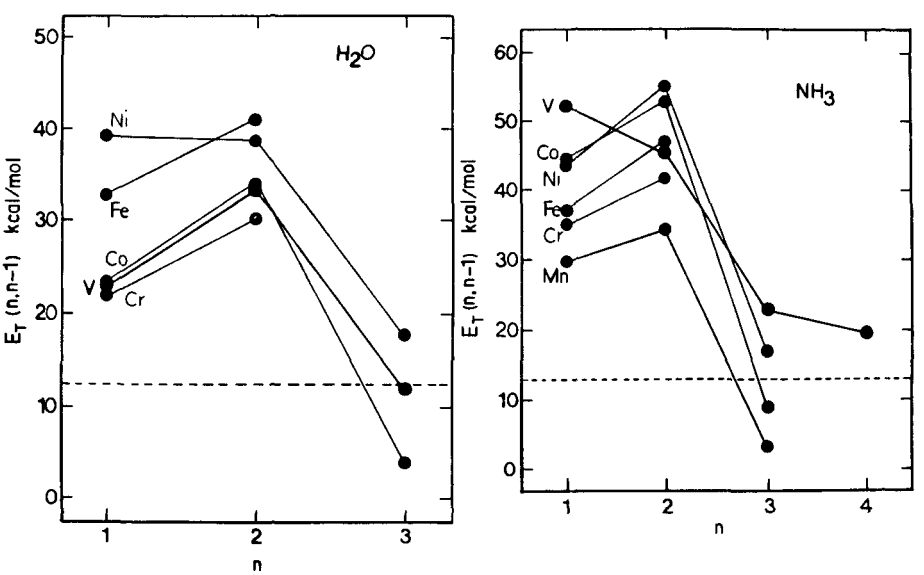

Figure 1. Plot of successive H_2O- and NH_3-binding energies in $M^+(H_2O)_n$ and $M^+(NH_3)_n$ cluster ions.

Presented at the 36th ASMS Conference on Mass Spectrometry and Allied Topics
June 5-10, 1988, San Francisco, CA

ISOMER CHARACTERIZATION VIA NEUTRALIZATION-REIONIZATION MASS SPECTROMETRY (NRMS)

C. Wesdemiotis, R. Feng, M. -Y. Zhang, M. Marchetti, and F. W. McLafferty

Chemistry Department, Cornell University, Ithaca, NY 14853-1301

Collisionally activated dissociation (CAD) has been used successfully in many cases for the characterization of ion structures in the gas phase. However, it may lead to indistinguishable CAD spectra for ionic isomers that can easily interconvert before dissociation because of low isomerization barriers compared to the respective dissociation thresholds. Such behavior is encountered with the 1- and 2-butene molecular cations and the isomeric $C_4H_4^{+\cdot}$ ions. In these cases, the fast equilibration between the ionic isomers, relative to the rate of dissociation, can be slowed down considerably by neutralization. Fragmentation of the neutrals produces structurally diagnostic fragments which can be detected with high sensitivity upon selective reionization to either positive or negative ions with the proper target. Thus, neutralization-reionization (NR) mass spectrometry combined with neutral dissociation provides the structural information that is missing in the CAD spectra.

Spontaneous dissociation of a neutral molecule can be effected upon neutralization with targets of low ionization energy (IE), e.g., Na (IE = 5.1 eV). Na neutralization of 1-butene cations produces 1-butene molecules with an average internal energy equal to the difference of the ionization energies of 1-butene (9.6 eV) and Na. This value lies above the fragmentation threshold of $CH_2{=}CH{-}CH_2{-}CH_3$ to $CH_2{=}CH{-}CH_2\cdot$ + $\cdot CH_3$ (3.2 eV), so that spontaneous dissociation takes place. Na anionization of the allyl radicals formed generates intense structurally characteristic allyl anions whose absolute abundance is 6 times larger than in the similarly obtained spectrum from 2-butene precursor ions.

Alternatively, neutral dissociation can be achieved by CAD of the intact neutral molecules resulting upon neutralization with, e.g., Hg or C_6H_6. Cyclobutadiene, methylenecyclopropene, butatriene, and vinylacetylene $C_4H_4^{+\cdot}$ cations, generated in the gas phase from appropriate precursors, can easily be distinguished on the basis of their neutralization-CAD-reionization spectra. Hg (or C_6H_6) neutralization gives the corresponding neutral molecules that dissociate differently upon CAD; the differences are best made visible by either reionization with He into positive (NR^+ spectra, Figure 1) or with C_6H_6 into negative ions (NR^- spectra, Figure 2). The fragmentation extent in the NR^+ spectra decreases in the order cyclobutadiene > methylenecyclopropene > 1,2,3-butatriene ≈ vinylacetylene, paralleling, thus, the calculated stabilities of these neutral molecules; as expected, cyclobutadiene and vinylacetylene give rise to the most intense $HC{\equiv}CH^{+\cdot}$ (m/z 26) and $H_2C{=}CH^+$ (m/z 27) peaks, respectively. The $C_4H_3\cdot$ radicals formed via $\cdot H$ loss from C_4H_4 are selectively detected upon anionization (Figure 2), and the $C_4H_3^-$ stabilities observed are consistent with the original C_4H_4 neutral structures. The spectra of Figures 1 and 2 are also useful for the characterization of C_4H_4 neutral molecules produced by ionic dissociation.

Additional structural information can be gained by mass-selecting individual ions in a NR spectrum, and subjecting them to CAD. For example, such MS/MS/MS experiments with the $CClH_3^{+\cdot}$ ions in the NR^+ spectra of $CH_3Cl^{+\cdot}$ and $CH_2ClH^{+\cdot}$ clearly show that methylenechloronium ylide, CH_2ClH, can survive intact for 10^{-6} s.

Neutralization of vinylalcohol cations followed by collisional activation of the neutral molecules and reionization to cations leads to recovered $C_2H_4O^{+\cdot}$ ions showing a CAD spectrum which is identical with that of the original vinylalcohol ions. This MS/MS/MS measurement proves that gaseous $CH_2{=}CH{-}OH$ does not tautomerize upon collisional activation to the more stable $CH_3{-}CH{=}O$ in the microsecond time-window.

Presented at the 36th ASMS Conference on Mass Spectrometry and Allied Topics
June 5-10, 1988, San Francisco, CA

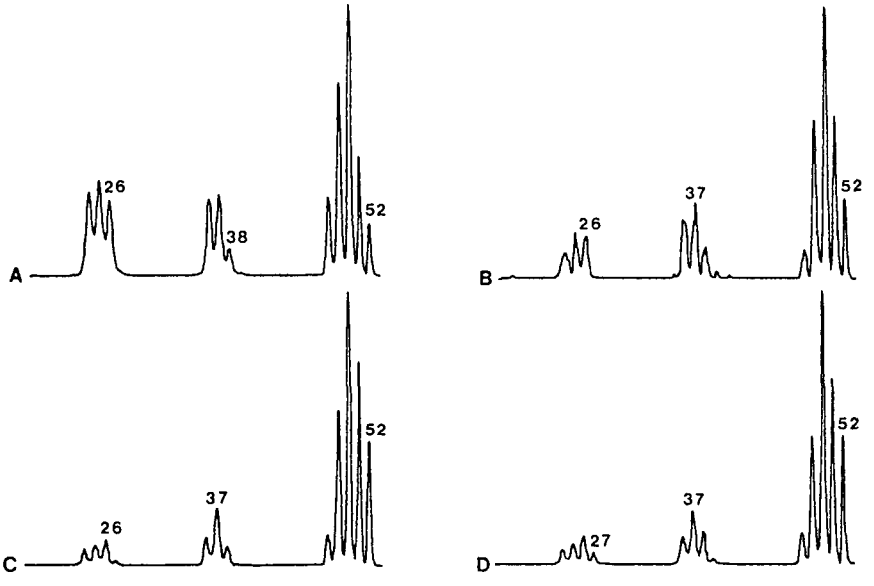

Figure 1. Hg/He NR^+ spectra of (A) cyclobutadiene, (B) methylene-cyclopropene, (C) 1,2,3-butatriene, and (D) vinylacetylene radical cations. The figures on top of the peaks represent m/z values. The transmittances used are 90% for Hg and 30% for He, corresponding to approximately 1 and 2 collisions per affected species, respectively. With He the neutrals can be dissociated in the first collision and the resulting mixture reionized in the second collision.

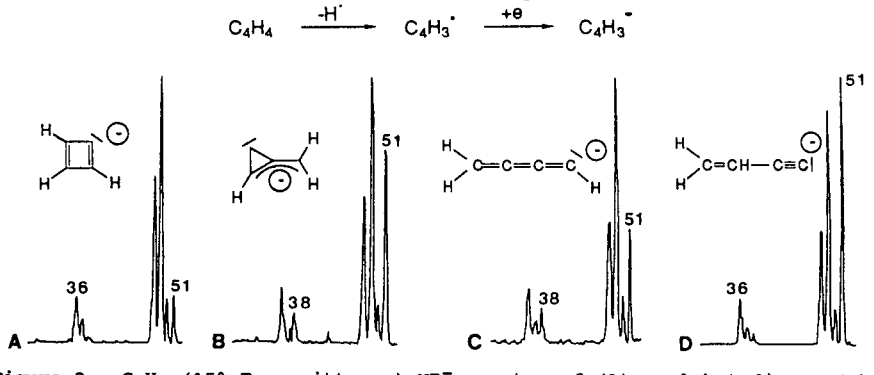

Figure 2. C_6H_6 (15% Transmittance) NR^- spectra of (A) cyclobutadiene, (B) methylenecyclopropene, (C) 1,2,3-butatriene, and (D) vinylacetylene radical cations. The $C_4H_3^-$ structures (m/z 51) are included in the spectra. 15% T corresponds to nearly 3 collisions per affected species, representing the neutralizing, dissociating, and anionizing collisions, respectively. The Hg (90% T)/C_6H_6 (30% T) NR^- spectra are very similar to these spectra.

Presented at the 36th ASMS Conference on Mass Spectrometry and Allied Topics
June 5-10, 1988, San Francisco, CA

ON THE INTERMEDIACY OF ION-MOLECULE COMPLEXES IN UNIMOLECULAR DECOMPOSITIONS OF POSITIVE IONS

Richard W. Kondrat and Thomas Hellman Morton
Department of Chemistry
University of California
Riverside, CA 92521

Over the past decade we have described several ion-molecule complexes that are formed as intermediates in the unimolecular decomposition of alkyl aryl ethers. Two notable examples are [PhO· sec-$C_4H_9^+$] formed from the molecular ion of phenyl n-butyl ether and [PhO· tert-$C_5H_{11}^+$] formed from the molecular ion of phenyl neopentyl ether.[1] In 1987 Sozzi, Audier, Mourgues, and Millet reported MIKES experiments on phenyl sec-butyl ether and phenyl tert-amyl ether that exhibit regioselectivity in their decompositions to phenol molecular ion.[2] They interpret this regioselectivity as being incompatible with the intermediacy of the ion-molecule complexes above. Though it is entirely plausible that ion-molecule complexes may not intervene in these latter decompositions, regioselectivity cannot, by itself, be taken as conclusive evidence against ion-molecule complexes. Suppose that [PhO· tert-$C_5H_{11}^+$] is formed from phenyl tert-amyl ether. Unless it has enough internal energy, it will form only the thermodynamically most favorable products, $PhOH^{\cdot+}$ and $(CH_3)_2C{=}CHCH_3$ regiospecifically. In the case of phenyl neopentyl ether, the intermediate complex has enough energy to form $CH_2{=}C(CH_3)CH_2CH_3$, as well, and the two olefins are produced in the same proportions as in the biomolecular gas phase deprotonation of tert-amyl cation by simple ethers. But there is no necessity that phenyl tert-amyl ether form a complex with so high an energy content, and regioselectivity could be a consequence of the availability of only one thermodynamically accessible reaction channel.

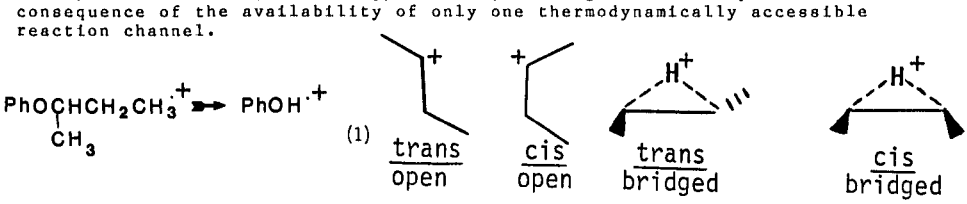

The same argument applies to the decomposition of phenyl sec-butyl ether, reaction 1, with an additional set of complications, for the structure of the sec-butyl cation is by no means certain. Solution phase studies admit of a variety of interpretations,[3] which can be summarized in terms of the four structures above: trans-open, cis-open, trans-bridged, and cis-bridged. The bridged structures might be frozen on the timescale of rigid molecular rotations (which is the lower bound for the lifetime of an ion-molecule complex). If the open structures do not possess enough internal energy to undergo hydride shifts or if the bridged structures should be frozen, then decomposition via [PhO· sec-$C_4H_9^+$] will yield 2-butenes via regioselective proton transfer.

Though the open structures can have chiral equilibrium geometries, it may be assumed that interconversion of enantiomorphic conformations is so rapid as to render them achiral, so that the methylene hydrogens will be enantiotopic. But the methylene hydrogens of sec-butyl ether become chemically nonequivalent (with one of them as the bridging atom) in a frozen, bridged structure. If we deuterate one of the three non-methyl positions in phenyl sec-butyl ether, there are several possible outcomes from an ion-molecule complex:

(i) Hydrogen scrambling that gives the same product distribution from all three d_1 isomers 1-3;

Collisionally Activated Decomposition spectra (8 kV) of molecular ions of racemic isomers of phenyl d_1-sec-butyl ether. Diastereomeric purities were 97% and 89%, respectively, for 1 and 2.

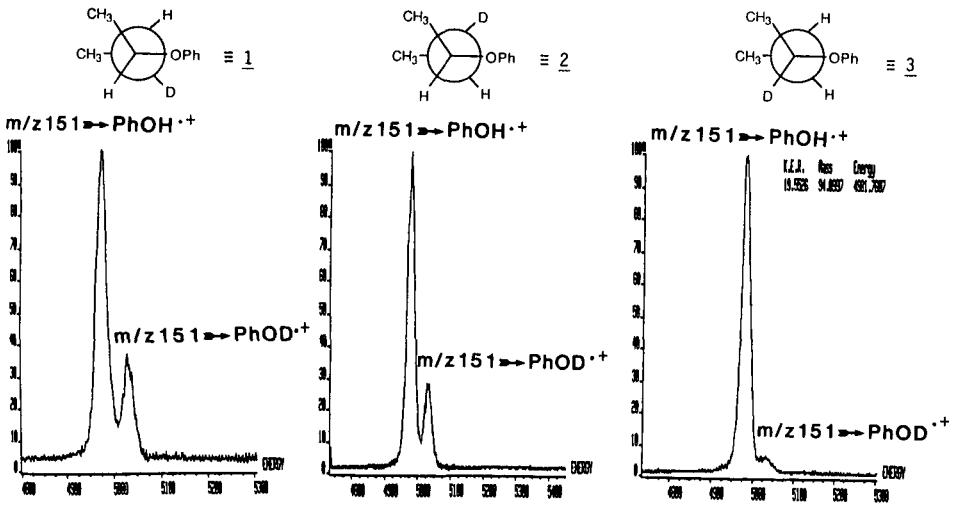

(ii) Open structures that do not scramble, leading to the same product distribution from the two diastereomers of $PhOCH(CH_3)CHDCH_3$, 1 and 2, and a different distribution from $PhOCD(CH_3)CH_2CH_3$, 3;

(iii) Frozen trans-bridged structures producing trans-2-butene as the only expelled neutral, resulting in exclusive D transfer from one $PhOCH(CH_3)CHDCH_3$ diastereomer and exclusive H transfer from the other.

(iv) Interconverting bridged structures, which will give the same outcome as (i).

The 70 eV mass spectra, MIKES, and CAD all give results that are not consistent with any of these outcomes. Each of the three isomers 1-3 gives a mixture of $PhOH^{\cdot+}$ and $PhOD^{\cdot+}$ daughter ions, but a different proportion in each case. The CAD, shown above, gives the result that is closest to ii, with proportions 76.5:23.5 for 1, 79:21 for 2, and 94:6 for 3. This can be interpreted in terms of the following alternatives. Either reaction 1 does not proceed exclusively via ion-molecule complexes, or else there must be a mixture of pathways, iii along with some other option (ii, for example, or frozen cis bridged ions whose proportion varies in response to an isotope effect that favors bridging hydrogen versus bridging deuterium). The first of these alternatives offers the more parsimonious explanation.

References

1. T.H. Morton, J. Am. Chem. Soc. 102, 1596-1602 (1980).
2. G. Sozzi, H.E. Audier, P. Mourgues, and A. Millet, Org. Mass Spectrom. 22, 746-747 (1987).
3. A survey of experimental results is given in J.J. Dannenberg, B.J. Goldberg, J.K. Barton, K. Dill, D.H. Weinwurzel and M.O. Longas, J. Am. Chem. Soc. 103, 7764-7768 (1981).

Presented at the 36th ASMS Conference on Mass Spectrometry and Allied Topics
June 5-10, 1988, San Francisco, CA

LOW-ENERGY DECOMPOSITIONS OF SOME CLOSED-SHELL IONS: NEW INSIGHTS ON CHARGE-REMOTE FRAGMENTATIONS

Jeanette Adams: Department of Chemistry, Emory University, Atlanta, GA 30322.
Michael L. Gross: Midwest Center for Mass Spectrometry, Department of Chemistry, University of Nebraska-Lincoln, Lincoln, NE 68588-0302.

High-energy collisional activation (CA) of closed-shell ions of long-chain fatty alcohols and acids induces decompositions that occur remote from the charge site.[1] One mechanism involves charge-remote 1,4-eliminations of H_2 to give alkenes and terminally unsaturated fatty alcohol and acid ions. The 1,4-eliminations of H_2 do not occur unimolecularly in the fast atom bombardment (FAB) ion source or as decompositions of metastable parent ions. The upper limit for the activation energy for the collision-induced 1,4-eliminations of H_2 was estimated to be 1.3-1.9 eV.[1a]

In contrast, $(M + 2Li - H)^+$, $(M + Li)^+$, and $(M - H)^-$ ions of ricinelaidic and ricinoleic (*trans*- and *cis*-12-hydroxy-9-octadecenoic, respectively) acids, and $(M + Li)^+$ ions of ricinoleyl alcohol and methyl ricinoleate, decompose by charge-remote fragmentations that arise unimolecularly both in the FAB ion source and from metastable ions. The unimolecular decompositions involve loss of H_2O and $C_7H_{14}O$: it is only upon CA that 1,4-eliminations of H_2 occur.

Linked-scanning, MS/CA-MS, and CA-MS/CA-MS, and deuterium labelling provide evidence that the mechanisms for the two unimolecular decompositions are analogous to the mechanisms of thermolytic decompositions of the neutral molecules.[2] The data indicate that the mechanism for the charge-remote loss of $C_7H_{14}O$ is an Ei *O*-hydro-*C*-allyl elimination (eq.1); the mechanism for the charge-remote loss of H_2O is a hydro-hydroxy

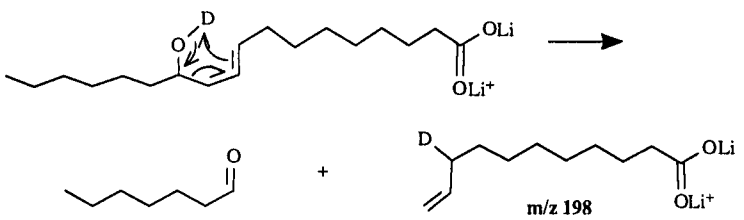

(1)

elimination (eq. 2).

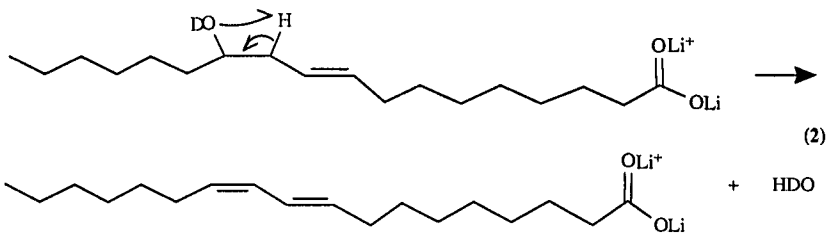

(2)

The energetics of the two reactions can be evaluated from experimental data and from calculated enthalpies. Activation energies for the reverse reactions ($E^o_{rev(cal)}$)can be evaluated from experimentally determined kinetic energy released (KER) in the decompositions,[3] and ΔH_{rxn} can be calculated by using Benson's additivity rules.[4] By adding the $E^o_{rev(cal)}$ and ΔH_{rxn}, approximate activation energies (E^o_{for}) for the two

decompositions can be calculated. These calculated forward activation energies can be compared to experimentally approximated activation energies derived from the competitive loss of alkali cation from the $(M^+ Cat)^+$ ions of ricinoleyl alcohol ($Cat^+ = Li^+, Na^+, K^+, Rb^+$, or Cs^+). These results are shown in Table I.

Table I. Energetics of the unimolecular decompositions.

	$-H_2O$ (eV)	$-C_7H_{14}O$ (eV)
KER ($T_{0.5}$)[a]	0.07	0.06(CID) [e]
$E^o_{rev\ (calc)}$[b]	0 - 0.44	0 - 0.38
$\Delta H_{rxn\ (Benson's\ Rules)}$[d]	0.38	0.55
$E^o_{for} = E^o_{rev\ (calc)} + \Delta H_{rxn}$	0.82	0.93
$E^o_{for\ (Alc + Cat)^+}$[c]	<0.85	<<1.2

[a] KER measurements were made by using the MS-50 Triple Analyzer (Nebraska).
[b] Calculated by assuming either no reverse activation energy and no kinetic shift, or a KER of 0.16 - 1.0 times the reverse activation energy. See ref. 3.
[c] Determined by the competitive loss of alkali cation from $(M + Cat)^+$ ions of ricinoleyl alcohol.
[d] Calculated from tabulation in ref. 4.
[e] Part of the measured peak width is due to a small contribution from CID.

Assuming that the kinetic energy released in the decompositions is only 0.16 of E^o_{rev}, and there is no appreciable excess energy in the transition states, E^o_{for} calculated for the loss of H_2O by using the KER and ΔH_{rxn} (0.82 eV) closely approximates E^o_{for} determined experimentally (<0.85 eV). The calculated value for E^o_{for} for the loss of $C_7H_{14}O$ (0.93 eV) is not in as close an agreement with the experimentally determined E^o_{for} (<<1.2 eV), but there is evidence that this is a result of an experimental over-estimation of the forward activation energy: a competitive shift is probably reducing the detectability of this higher-energy decomposition pathway. The forward activation energy for the loss of $C_7H_{14}O$ is probably less than 1.0 eV.

These results show that charge-remote fragmentations are not limited to high-energy collisional activation because the decompositions can occur by different mechanisms and thus with different energy requirements. The collisionally-induced 1,4-eliminations of H_2 appear to have an activation energy in the range of 1.3-1.9 eV,[1a] whereas the unimolecular losses of H_2O and $C_7H_{14}O$ occur with activation energies less than 1.0 eV. The unimolecular decompositions occur both in the FAB ion source and as metastable ion decompositions. These results show conclusively that the charged site is not involved in the mechanisms of decomposition, and that charge-remote fragmentations are a class of mass spectrometric decompositions that are unequivocally analogous to thermolysis.

References

1.a. Adams, J.; Gross, M.L. *J. Am. Chem. Soc.* **1986**, *108*, 6915. b. Adams, J.; Gross, M.L. *Anal. Chem* **1987**, *59*, 1576.
2.a. Arnold, R.T.; Smolinsky, G. *J. Am. Chem. Soc.* **1959**, *81*, 6443. b. Arnold, R.T.; Smolinsky, G. *Org. Chem.* **1960**, *25*, 129.
3. Holmes, J.L.; Terlouw, J.K. *Org. Mass Spectrom.* **1980**, *15*, 383.
4. Lowry, T.H.; Richardson, K.S. *Mechanism and Theory in Organic Chemistry*; 2nd ed.; Harper & Row: New York; 1981; pp 147-161.

Presented at the 36th ASMS Conference on Mass Spectrometry and Allied Topics
June 5-10, 1988, San Francisco, CA

ENERGETICS OF REMOTE SITE FRAGMENTATION

V.H. Wysocki, M.M. Ross, R.G. Cooks*

Naval Research Laboratory, Washington, DC 20375
* Purdue University, West Lafayette, IN 47907

"Remote site" or "charge-remote" fragmentation is a type of ionic fragmentation for which bond cleavage is thought to be unaffected by the charge site.[1,2] The fragmentation occurs for a wide variety of compound classes and is analytically useful, e.g., for the determination of substituent positions and alkyl chain lengths in functionalized alkanes. Remote site fragmentation is proposed to occur by a 1,4 loss of H_2 and an alkene to produce a terminally unsaturated ion and has been studied extensively by high-energy collision-activated dissociation (CAD).[1] We report here results of our attempts to induce remote site fragmentation by (i) low-energy (0-200 eV) collisional activation with gaseous targets, (ii) surface-induced dissociation, SID (10-90 eV), and (iii) angle-resolved mass spectrometry (3 keV). Several compounds were utilized including $CH_3(CH_2)_{16}CH_2NH_3^+$, $CH_3(CH2)_7CH{=}CH(CH_2)_8NH_3^+$, $[CH_3(CH_2)_{16}CH_2]_2[CH_3]_2N^+$, $CH_3(CH2)_7CH{=}CH(CH_2)_8OHLi^+$, protonated 2- and 4-pentadecylpyridine, $CH_3(CH2)_{11}C_6H_4SO_3^-$, $CH_3(CH2)_{16}CH_2OSO_3^-$, and $CH_3(CH2)_{16}CO_2^-$. The goal of the research is further elucidation of the mechanism and energetics of the reaction. Areas of interest[3] include: (i) the amount of internal energy required to produce detectable remote site fragmentation, e.g. does the reaction have a low activation energy with no significant kinetic shift, a low activation energy and a large kinetic shift, or simply a high activation energy, (ii) the type of excitation required (e.g. electronic vs. vibrational), (iii) the time frame of the fragmentation, (iv) the sequence of bond breaking and bond formation steps which occur, (v) the relationship, if any, between the mechanisms of formation of product ions differing by only one mass unit, and (vi) the role of the charge site of the ion in the fragmentation, including the influence of competitive fragmentation pathways on the extent of remote site fragmentation.

The laboratory collision energy required to produce detectable remote site fragmentation varied from compound to compound in both low-energy CAD and SID experiments. In low energy CAD the fragmentation was observed for selected compounds at energies as low as 50 eV but increased in abundance with increasing collision energy over the laboratory energy range available (maximum 200 eV). In SID experiments, the fragmentation was observed at energies as low as 10 eV and increased or decreased in abundance with increasing laboratory energies depending on the compound. In the low-energy collisional activation experiments, the fragmentation was also found to be quite sensitive to target mass and collision pressure. For example, while abundant remote site fragments are produced upon low-energy collisions of pentadecylpyridine with Ar target, the other positive ions require collisions with the heavier target, Xe, in order to produce abundant remote site fragments (Figures 1 and 2). For all of the positive ions examined by low-energy CAD, single collision conditions appear to be preferable to multiple collision conditions, while for certain anions multiple collision conditions are preferable (competition between electron detachment and fragmentation may be a problem for some of the anions).

The low-energy CAD and SID spectra of lithiated oleyl alcohol were obtained for comparison with the high-energy CAD spectrum since the absence of Li^+ in the high-energy collisional activation spectrum has been interpreted[2] to indicate that the internal energy required to promote remote site fragmentation is lower than that required to form Li^+. The data show that Li^+ is the most abundant ion produced upon activation of lithiated oleyl alcohol at laboratory collision energies as low as 5 eV (CAD) or 10 eV (SID); remote site fragmentation may also be observed at selected collision energies. In contrast to the previously reported high-energy CAD spectrum of lithiated oleyl alcohol, our data (Figure 3) indicate that Li^+ is present following 8 keV collisions with He (it should be noted here that detection of the Li^+ was quite sensitive to the voltage applied to the conversion dynode since the kinetic energy of Li^+ fragment ion [(m/z 7 / m/z 275) x 8 keV] is low.

Angle-resolved mass spectra acquired at 3 keV for three different compounds indicate that the higher mass remote site fragments decrease in abundance as products are collected from progressively higher angles (Figure 4). In ARMS experiments, products detected from higher angles are generally believed to be associated with greater internal energy deposition. As has been observed in certain high-energy CAD experiments,[4] radical ions and even-electron ions are sometimes observed at adjacent masses in both the high- and low energy experiments (e.g. Figures 1 and 4) .

The examples discussed here indicate a complicated dependence of remote site fragmentation on internal energy deposition. Electronic excitation is probably not required since the fragmentation is observed at collision energies (< 100 eV) which correspond mainly to vibrational excitation. They also illustrate the complementary nature of low-energy and high-energy collisional activation data on remote site fragmentation. The results suggest that the energetics, and perhaps the mechanism, of the fragmentation may be more complex than previously suggested based on high-energy data alone. For example, some of the compounds examined might fragment via an ion/molecule complex following activation; this type of fragmentation would be directed by stabilization of the charge site of the molecule and could provide a connection between fragment ions separated by only one mass unit.

Presented at the 36th ASMS Conference on Mass Spectrometry and Allied Topics
June 5-10, 1988, San Francisco, CA

1. N.J. Jensen, K.B. Tomer, M.L. Gross J. Am. Chem. Soc. 1985, 107, 1863.
2. J. Adams, M.L. Gross J. Am. Chem. Soc. 1986, 108, 6915.
3. V.H. Wysocki, M.M. Bier, R.G. Cooks, Org. Mass Spectrom., *in press.*
4. M. Bambagiotti A., S.A. Coran, F.F. Vincieri, T. Petrucciani, P. Traldi Org. Mass Spectrom. 1986, 21, 485.

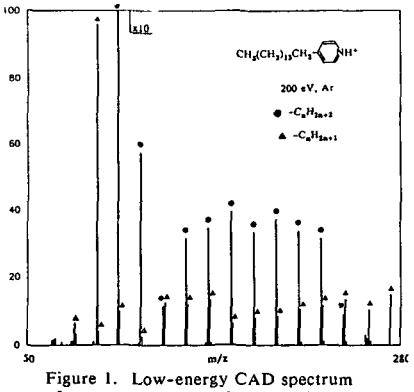

Figure 1. Low-energy CAD spectrum of protonated 4-pentadecylpyridine.

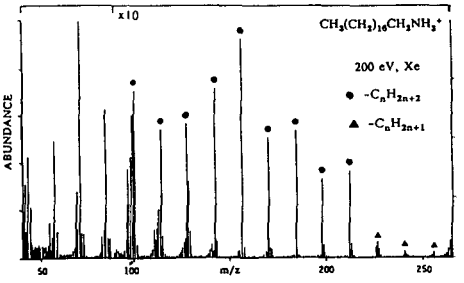

Figure 2. Low-energy CAD spectrum of protonated octadecylamine.

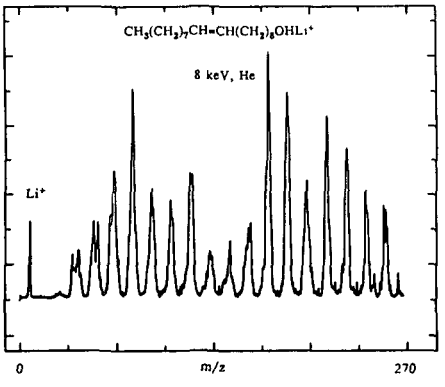

Figure 3. High-energy CAD spectrum of lithiated oleyl alcohol.

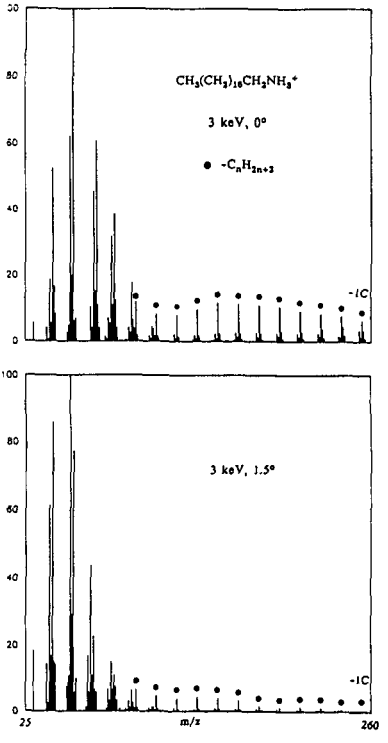

Figure 4. Angle-resolved mass spectra of protonated octadecylamine.

Presented at the 36th ASMS Conference on Mass Spectrometry and Allied Topics
June 5-10, 1988, San Francisco, CA

CHARACTERIZATION OF THE DISSOCIATION OF PROTONATED CYCLIC KETONES USING HIGH AND LOW ENERGY COLLISIONAL ACTIVATION: A PROTOTYPICAL HIGH ENERGY/HIGH ENTROPY DEMANDING REACTION: Jennifer S. Brodbelt-Lustig, R. Graham Cooks, Department of Chemistry, Purdue University, West Lafayette, Indiana 47907

Both enthalpic and entropic barriers are important factors in the dissociation channels of gas phase ions upon collisional activation. The accessible dissociation channels are dependent on the kinetic energy of the selected precursor ion, the nature of the target, the scattering angle through which products are collected, and the number of collisions that the precursor ion undergoes with the neutral target. Differences in product distributions resulting from CAD at keV energies and at eV energies have been accounted for in terms of the energy transfers involved. Larger collision energies promote reactions having higher activation energies since at least some of the precursor ions experience deposition of greater energies. The number of collisions a selected ion undergoes influences the time during which an ion may rearrange and also determines the number of steps of energy input.

A major fragmentation process of protonated 2,2,6-trimethylcyclohexanone after collisional activation under certain reaction conditions results in the protonated acetone ion. This is demonstrated using three methods: 1) deuterium labelling, 2) the sequential scanning capabilities of a hybrid mass spectrometer in which a comparison is made between the consecutive daughter spectrum for protonated 2,2,6-trimethylcyclohexanone and the daughter spectrum of protonated 2,2,6-trimethylcyclohexanone, and 3) by comparison of daughter spectra of m/z 59 ions generated from different precursors in an ion trap mass spectrometer. The reaction in which protonated acetone is formed involves two 1,2-methyl transfers and a ring contraction.

The fragment ion of particular interest in this study, m/z 59, is the most abundant daughter ion present in the daughter spectrum of protonated 2,2,6-trimethylcyclohexanone recorded at low collision energy in a triple quadrupole mass spectrometer, yet it is of low abundance in the high energy MIKES spectrum or in the ion trap spectrum (Figure 1). The striking contrast between the daughter spectra recorded in the different energy regimes can be attributed to the activation conditions used in each instrument. The triple quadrupole employs low energy, multiple collisions, while high energy, single collisions occur in the MIKES and very low energy, multiple collisions occur in the ion trap. When the collision gas pressure in the triple quadrupole instrument is reduced so that single collision conditions are attained, the resulting spectrum resembles the MIKES spectrum. This result implies that the internal energy distributions associated with eV and keV collisions are insufficiently different to cause large differences in product abundances.

It is apparent that the formation of m/z 59 is a high energy process which involves considerable bond reorganization. A process which has stringent enthalpic and entropic demands and involves multiple rearrangements of the cyclic ketone before fragmentation is that proposed by Wolfshutz and co-workers (1). In their report of methane chemical ionization of methylcyclohexanones, the authors proposed that the abundant m/z 59 ion represented a protonated acetone species formed by migration of two methyl groups to the carbonyl position (Figure 2). The decreasing abundance of the m/z 59 ion in the present study as the collision energy or pressure is reduced in the triple quadrupole experiments correlates with the formidable energy and entropic demands of the methyl shifts that occur during the dissociation of the protonated parent ion. In the MIKES instrument, formation of m/z 59 is not as readily accessible to the trimethylcyclohexanone ions because the parent ions experience just one collision before exiting the collision region. Since activation occurs in one step, extensive bond reorganization is not favored, and dehydration by simple cleavage is the preferred process. In the ion trap, the gentle collisions associated with helium as a target gas most likely prevent the parent ions from surmounting the high energy barrier for the dissociation of m/z 141 to m/z 59. In the limit of excitation by stepwise activation, only the <u>lowest</u> energy barrier is traversed as shown by multi-photon (IR) dissociation. Thus, access to m/z 59 requires several relatively energetic collisions to maximize both isomerization and barrier traversal.

Many ions of m/z 59 have been previously characterized and structures have been assigned to various ions formed from different precursors. The CAD behavior of the ion of m/z 59 produced by methane chemical ionization of trimethylcyclohexanone was studied as a function of activation voltage in an ion trap, and the results are compared to the CAD behavior of the m/z 59 ions produced by protonation of acetone, propionaldehyde, and allyl alcohol, and by electron ionization of diethyl ether and 3-methoxy-1-butanol (Figure 3). The plot for dissociation of m/z 59 from protonated trimethylcyclohexanone most closely resembles the plot for protonated acetone. The trends of ions of m/z 31, 41, and 59 follow parallel patterns; none of the plots for the other isomeric ions are remotely similar.

Presented at the 36th ASMS Conference on Mass Spectrometry and Allied Topics
June 5-10, 1988, San Francisco, CA

A study of the complex rearrangement/fragmentation sequence (from which protonated acetone is formed) with respect to the effects of collision energy and number of collisions reveals that it is favored only at high energies and pressures. Large enthalpic and entropic barriers are indicated. High energy (keV) collisions that result in excitation of the parent ion do not favor this rearrangement, while the very low energy multiple collisions occurring in the ion trap are also inadequate for promotion of this dissociation pathway.

Figure 1. Daughter spectra (CAD) of protonated 2,2,6-trimethylcyclohexanone (m/z 141) in (A) a triple quadrupole mass spectrometer, (B) in a MIKES mass spectrometer, and (C) in an ion trap mass spectrometer.

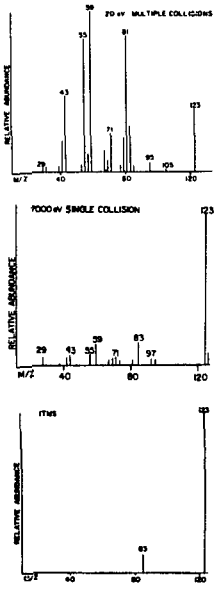

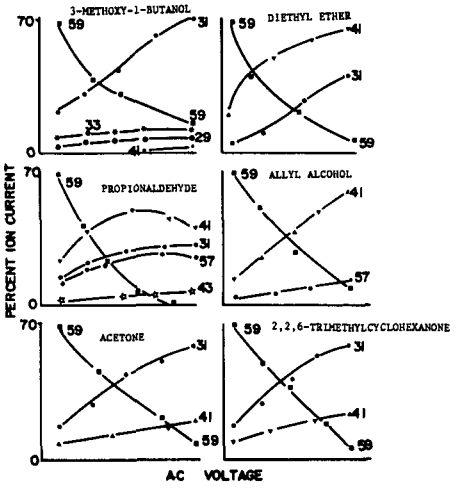

Figure 3. Breakdown curves for m/z 59 ions of isomeric structures as a function of supplementary ac voltage in an ion trap. The range of voltages is 0.5-2.0 V.

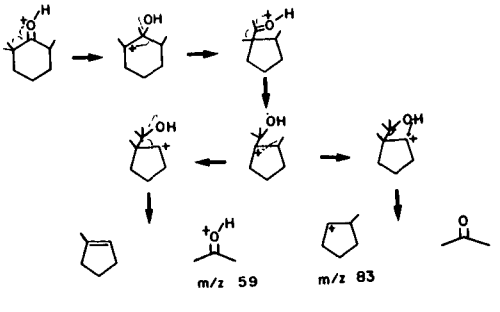

Figure 2. Proposed mechanism for formation of m/z 59 from protonated 2,2,6-trimethylcyclohexanone.

R. Wolfshutz, W. Franke, N. Heinrich, H. Schwarz, W. Blum, W. Richter, Z. Natursforsch, 1982, 37b, 1982.

Presented at the 36th ASMS Conference on Mass Spectrometry and Allied Topics
June 5-10, 1988, San Francisco, CA

ANALYSIS OF CERAMIDE & GLYCOLIPID DERIVATIVES BY HIGH PERFORMANCE TANDEM MASS SPECTROMETRY

C. E. Costello, B. Domon[1] and J. E. Vath
Dept. of Chemistry, Mass. Inst. of Technology, Cambridge, MA
[1]Present address, CIBA-Geigy, Basel, Switzerland.

Ceramides, glycosphingolipids, gangliosides and other glycoconjugates play important roles in biological systems, functioning as components of membranes and cell walls, as intermediaries of cell-cell recognition, as agents in transport and as antigenic determinants, and others too many to enumerate. Delineation of the structural specificities that are required for the various activities is a formidable task. Heterogeneity of the components (N-acyl fatty acids, bases and carbohydrates) is often encountered and results in "average" rather than definitive determinations.

In our initial study (Domon and Costello, *Biochemistry*, 1988) we used high performance tandem mass spectrometry of the native compounds to address this complex problem and have shown that it is possible to assign structural details on the basis of product ions observed in the positive and negative ion FAB CID MS/MS spectra. Now we have extended this investigation to include derivatives, in order to improve sensitivity and to direct fragmentation along pathways that increase the information content of the spectra.

Peracetylated, permethylated (Fig. 1) and reduced derivatives have been prepared and analyzed. Deuterium labeled analogs have been used where necessary to remove ambiguity. Gas phase reagents and a microapparatus (Vath, Zollinger and Biemann, 1988) have been used for most reactions, to minimize sample loss. For ceramides and glycolipids that have only a few sugar residues, reduction alone enhances sensitivity significantly; high quality CID MS/MS spectra are obtained after the reduction of 25 ng (or less) of sample (Fig 2). Concomitant permethylation becomes more appropriate as the number of sugar residues increases, in order to control solubility in the matrix. The fragmentation patterns observed for the reduced and reduced/permethylated samples are consistent with those described for the underivatized samples, with some additions. The major fragments in the reduced compounds are designated U and V (Scheme 1). These occur adjacent to the charge localization site, at the amine. Because the procedure used for the reduction derivatizes olefinic bonds, the method also provides a means for their location. Peracetylated derivatives do not produce informative collision spectra, because ketene and acetic acid losses predominate.

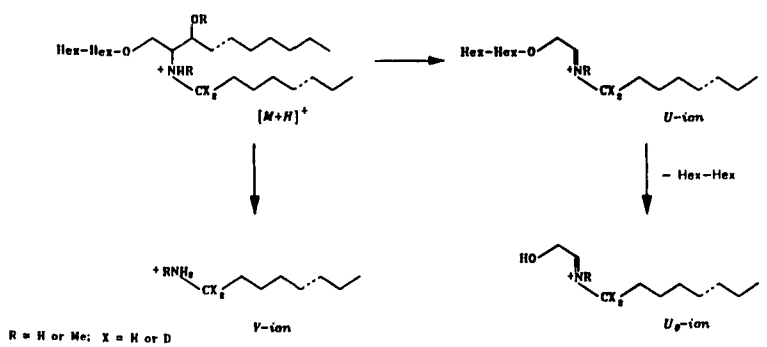

Scheme 1. Fragmentation of reduced glycosphingolipids.

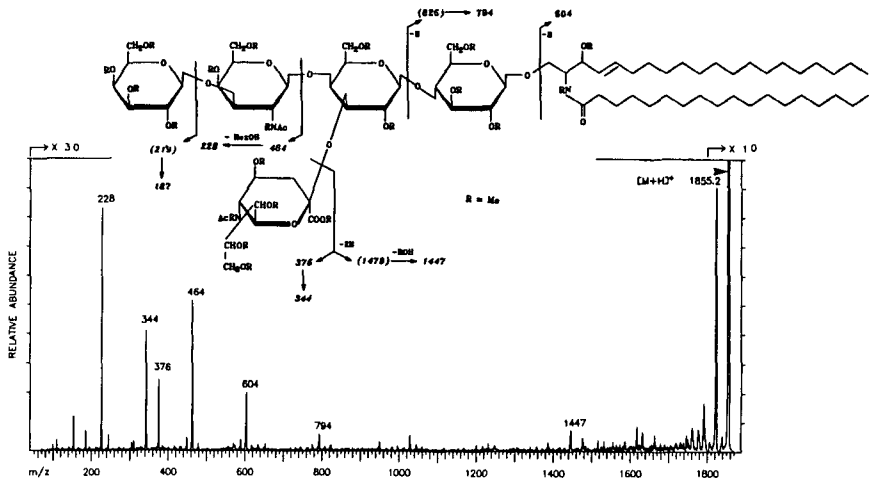

Fig. 1. FAB CID MS/MS spectrum of the $(M+H)^+$ ion, m/z 1855.2 of permethylated GM_1.

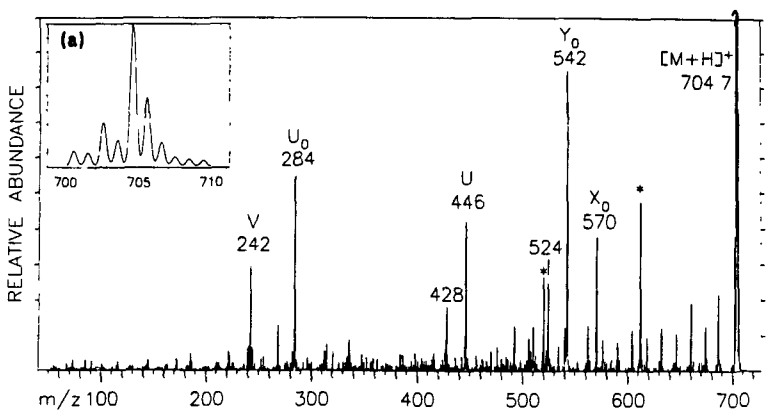

Fig. 2. FAB CID MS/MS spectrum of the $(M+H)^+$ ion obtained after BH_3 reduction of 25 ng N-palmitoyl galactocerebroside. Inset shows the molecular ion region of the 2-sector FAB mass spectrum recorded for the same sample, prior to the 4-sector MS/MS measurement.

Acknowledgement. The MIT Mass Spectrometry Facility is supported by Grant No. RR00317 (to K. Biemann) from the NIH Division of Research Resources. BMD was the recipient of a fellowship from the Swiss Science Foundation.

Presented at the 36th ASMS Conference on Mass Spectrometry and Allied Topics
June 5-10, 1988, San Francisco, CA

Folate and Vitamin B_6 Bioavailability Studies with Human Subjects Using Stable Isotope Labelling and Electron Capture GCMS.

J.P. Toth, P.R. Trumbo and J.F. Gregory, Dept. of Food Science and Human Nutrition, University of Florida, Gainesville, FL.

Folate and Vitamin B_6 are water-soluble B-complex vitamins essential for nucleic acid synthesis, amino acid metabolism and lipid metabolism. The nutritional properties of these vitamins are complicated by the fact that most dietary forms must undergo metabolic conversion to bioactive forms. The proportion of a given dietary form that ultimately undergoes this activation is referred to as its bioavailability. Most of what is understood about this important nutritional parameter is based on animal experiments using radiolabelling. To extend such studies to human subjects we have developed methods based on deuterium labelling and GCMS monitoring of the labelled urinary metabolites.

The analytical procedure we have developed for folate bioavailability studies consists of:

1. Synthesis of d_2- and d_4- labelled folates;
2. Administration of labelled folates to volunteer subjects in amounts corresponding to normal dietary intake;
3. Collection of urine and isolation of folates by affinity chromatography using folate binding protein;
4. Chemical cleavage of all folates to a single analyte, para-aminobenzoyl glutamic acid (pABG), which retains all deuterium labels;
5. Isolation of pABG by reverse-phase HPLC. The isolated pABG is a mixture of labelled and unlabelled (do) forms;
6. Fluorimetric determination of total pABG;
7. Derivatization of pABG by reaction with 2:1 trifluoroacetic anhydride: trifluoroethanol at 90°C for one hour. The major product is a fluorinated lactam of MW 426 whose electron capture negative ion (ECNI) mass spectrum shows the molecular anion with very little fragmentation;
8. Detection of this derivative by ECNI mass spectrometry with selected ion monitoring at m/z 426, 428 and 430;
9. Calculation of the molar ratio of labelled-to-unlabelled derivative from the appropriate mass peak area ratios. For this calculation a calibration curve is prepared from standard mixtures of known isotopic composition. These curves are linear in the range of interest;
10. Calculation of absolute quantities of labelled forms from the results of (6) and (9).

A similar procedure was developed for vitamin B_6: d_2 and/or

d_5 vitamers are administered and urine collected; 4-pyridoxic acid, the major urinary metabolite of all B_6 compounds, is isolated as its lactone, 4-PAL; 4-PAL is acylated by co-injection with trifluoroacetic anhydride into a 250°C GC injection port; ECNI GCMS is performed with selected ion monitoring at m/z 164, 166 and 169, corresponding to $[M-CF_3CO]^-$ for the three isotopic species; isotopic species are quantitated as in the folate procedure.

Experiments thus far have shown that: a) normal dietary doses of labelled vitamers produce detectable and quantifiable signals from labelled urinary metabolites; b) label ratios in administered doses are preserved in urine extracts; c) utilization of pyridoxine-beta-glucoside, a conjugated dietary form of vitamin B_6, by human subjects is different from that observed in rats.

Presented at the 36th ASMS Conference on Mass Spectrometry and Allied Topics
June 5-10, 1988, San Francisco, CA

Negative Ion Fab Analysis of Fatty Acids in Insect Waxes: Cuticular Wax of the Honey Bee

Charles D. Warner, Dept. of Chemistry, Hastings College, Hastings, NE 68901

R. N. Hayes and M. L. Gross, Midwest Center for Mass Spectrometry, Dept. of Chemistry, University of Nebraska-Lincoln, Lincoln, NE 68588

The African honey bee was introduced into the domestic honey bee population of Brazil in 1956. The hybridization of the domestic honey bee with African honey bees is of potential economic impact because the hybridized bees are known to be less prolific producers of honey in comparison to domestic honey bees. Identificaton of subspecies of honey bees has been a difficult taxonomic problem. Traditional morphometric analyses involve time consuming measurement of body parts and statistical analysis. Chemotaxonomic methods are an attractive alternative since cuticular wax contains a variety of substances suitable for chemical analysis. The wax is composed mostly of hydrocarbons and waxes, but also contains fatty acids and more polar materials in lesser amounts[1]. Lavine and Carlson[2] used GC-MS and GC-FID analyses of cuticular hydrocarbons and pattern matching techniques to distinguish between subspecies of honey bees. Smith[3] analysed epoxide derivatives of the alkene fraction of the cuticular wax by GC-MS for this purpose. Chemotaxonomic analysis by mass spectrometry has been reported by Feneslau.[4] Previous work at MCMS[5] has shown the utility of negative ion FAB/MS for mixture analysis and structural identification of fatty acids.

Negative ion FAB analysis of cuticular wax and comb wax was investigated as a potential chemotaxonomic method. It is an attractive one since the analysis of the wax from one insect is very desirable, and the time from extraction of the wax to the analysis is short. Furthermore, the analysis does not require separation of the fatty acids from the wax before analysis. With triethanol amine as the FAB matrix, the fatty acid negative ions are selectively desorbed thus reducing chemical noise from other components of the wax. This is an important consideration, since the 10-25 mg of cuticular wax on each insect contains only about 10% free fatty acids.

The two most abundant fatty acid anions in the samples of cuticular wax analysed were C16:0 and C18:0 carboxylate ions (palmitate and stearate). Spectra reveal the presence of other negative ions at masses corresponding to saturated even numbered fatty acids from m/z 311 to 451 (C20:0 to C30:0). In addition to saturated fatty acids the spectra all show ions corresponding to unsaturated fatty acids. The most prominant ones are those with 16 and 18 carbons. Analysis of comb wax from African honey bees from French Guiana[6] again shows C16:0 and 18:0 fatty acids to be the most abundant fatty acids in the FAB spectrum.

Since the structure of the fatty acids in the wax might be a useful taxonomic marker, MS/MS analysis of some of the ions in the wax was undertaken. In particular, the m/z 367 ion in the cuticular wax of the wild bees was selected in the tandem mass specrometer and collisionally activated. The collisional activation spectrum showed remote-charge site fragmentation characteristic of the saturated fatty acid tetracosanoic acid, C24:0. Likewise, MS/MS analysis of the m/z 281 ion showed fragmentation characteristic of oleic acid. Other ions observed in the FAB spectrum of the wild bees were not subjected to MS/MS analysis because of sensitivity problems.

In all the FAB spectra, considerable background was observed even though the negative carboxylate ions were being desorbed from the triethanol amine matrix in preference to other substances present. As an alternative method for chemotaxonomic analysis the fatty acids in the cuticular wax or comb wax were derivatized as the pentafluorobenzyl (PFB) esters. The PFB esters of fatty acids have been used for analysis of fatty acids by electron capture GC.[7] When

the PFB esters are analysed by negative ion chemical ionization (NICI), loss of the pentafluoro benzyl radical produces fatty acid anions. Although the derivitization increases the analysis time from insect to spectrum, two advantages are obtained.[8] The sensitivity of the method is considerably better than FAB and matrix effects are greatly diminished. The sample of comb wax analysed by FAB which showed m/z 255 and 281 as the predominant anions now shows significantly less noise and the m/z 367 is the most abundant ion. Furthermore, the intensity of other ions at higher masses has dramatically increased. This may be due to surface effects in the FAB matrix. MS/MS analysis of the m/z 281 and 255 ions from this mixture of esters reveals that the acids are oleic and palmitic acids.

FAB, NICI and collisional activation will be useful tools for developing a chemotaxonomic method for fatty acids in insect waxes. FAB will be a fast method for screening wax for particular fatty acids. NICI of the PFB esters of fatty acids improves greatly on the sensitivity and appears to diminish the matrix effect observed with FAB.

---

[1] G. J. Blomquist and L. L. Jackson, *Prog. Lipid Res.*, **17**, 319 (1979).

[2] B. Lavine and D. Carlson, *Anal. Chem.*, **59**, 468A (1987).

[3] R.-K. Smith, private communication.

[4] D. N. Haller, R. J. Cotter, C. Fenselau and O. M. Uy, *Anal. Chem.*, **59**, 2806 (1987).

[5] N. J. Jensen and M. L. Gross, *Lpids*, **21**, 362 (1986); K. B. Tomer, N. J. Jensen and M. L. Gross, *Anal. Chem* , **58**, 2429 (1986).

[6] Samples generously donated by O. R. Taylor, University of Kansas.

[7] J. Adams, M. David, and R. W. Geise, *Anal. Chem.*, **58**, 345-348 (1986).

[8] R. N. Hayes, R. L. Cerny, and M. L. Gross, Paper TOC 1100, 36th ASMS Conference on Mass Spectrometry, San Francisco, Ca, 1988.

Presented at the 36th ASMS Conference on Mass Spectrometry and Allied Topics
June 5-10, 1988, San Francisco, CA

IMAGING ANALYSIS OF BILE ACIDS USING CHROMATOGRAPHY/SIMS

Jocelyn C. Dunphy and Kenneth L. Busch
Department of Chemistry, Indiana University, Bloomington IN, 47405

The analysis of bile acids is often essential for understanding cholesterol metabolism and the role of steroids in biological systems, in addition to being an aid in diagnosing intestinal and liver disorders. Most methods for such analysis involve chromatographic separations followed by mass spectrometric detection. GC/MS following TMS derivatization[1], HPLC/FABMS[2], and radial compression HPLC followed by liquid secondary ion mass spectrometry (SIMS)[3] are a few examples. We have constructed a SIMS instrument for the direct analysis of thin layer chromatograms[4] and demonstrate here the potential of this instrument for direct, spatially resolved SIMS analysis of bile acids separated by silica thin layer chromatography (TLC). Since TLC is often used as a clean-up step prior to GC or LC separation, the direct SIMS analysis of the plate, which can provide qualitative and potentially quantitative information, dispenses with the need for the latter steps.

Positive and negative mass spectra of bile acids contained on thin layer chromatograms were acquired with modified ASYST software, using an average of 50 scans. Glycerol was used as the extraction matrix, and the area of the plate containing the acid of interest was affixed to the probe tip. The 3-dimensional images were obtained by inserting the entire TLC plate into the MS source and rastering the plate via an xy manipulator. A liquid metal gallium gun was used as the source of primary ions, and semi-molten sorbitol was used as the extraction matrix. Data were taken using ASYST software in the single ion monitoring mode, averaging 200 scans per point. Cholic acid, chenodeoxycholic acid and lithocholic acid were purchased from Aldrich Chemicals and used without further purification.

Positive ion spectra of these free bile acids do not show a strong $(M+H)^+$ ion but rather lose two or more molecules of water. Figure 1 shows the positive ion spectrum of cholic acid; m/z 373 is loss of 2 H_2O, and m/z 355 is loss of 3 H_2O. Negative ion SIMS mass spectra, however, give the $(M-H)^-$ ion as the base peak with no fragmentation. Figure 2 is the negative ion spectrum of cholic acid. Because negative ion analysis yields molecular weight information, it is the preferred mode for bile acids and salts. Further work has shown that the glycine and taurine conjugated bile acids give similar results. Figure 3 compares the images of a TLC plate spotted with cholic, chenodeoxycholic and lithocholic acids in the positive and negative ion modes. In the positive ion image, m/z 357 corresponds to loss of 2 H_2O from chenodeoxycholic acid, and m/z 355 comes from cholic acid as discussed above. Lithocholic acid does not show any major ion in the positive ion spectrum, and therefore no signal was obtained for this acid. Lithocholic acid does yield a large $(M-H)^-$ ion and this ion is monitored in the negative ion image. Cholic and chenodeoxycholic acid are imaged using their $(M-H)^-$ ions, 407 and 391, respectively. Comparison of spatial dimensions of the spots is adequate, but can be improved by careful control of the physical state of the sorbitol during analysis. Each spot corresponds to approximately 20 μg of acid; spatial resolution is 0.5 mm. The ability to correlate positive and negative ion analysis enhances selectivity and emphasizes an advantage inherent in TLC/SIMS, that of being able to repeat an analysis at a later time, since separation is accomplished in space rather than in time.

Ongoing work in TLC/SIMS of bile acids includes quantitation of the acids and salts using a deuterated internal standard, analysis of conjugated acids in dog bile, and 2-D HPTLC to resolve structural isomers of the dihydroxy bile acids.

References

(1) Sjovall, J., Eneroth, P., and Ryhage, R. "Mass Spectra of Bile Acids", in The Bile Acids, Vol. 1, Nair, P.O. and Kritchevsky, D., eds. Plenum Press, N.Y., 1971, pp. 209-247.

Presented at the 36th ASMS Conference on Mass Spectrometry and Allied Topics
June 5-10, 1988, San Francisco, CA

(2) Ito, Y., Takeuchi, T., Ishii, D., Goto, M., and Mizuno, T., J. Chromatogr., 358, 201 (1986).
(3) Whitney, J.O., and Burlingame, A.L., Koenshu-Iyu Masu Kenkyukai, (Japan) 7, 3 (1982).
(4). Fiola, J.W., DiDonato, G.C., and Busch, K.L., Rev. Sci. Instrum., 57 (9), 2294 (1986).

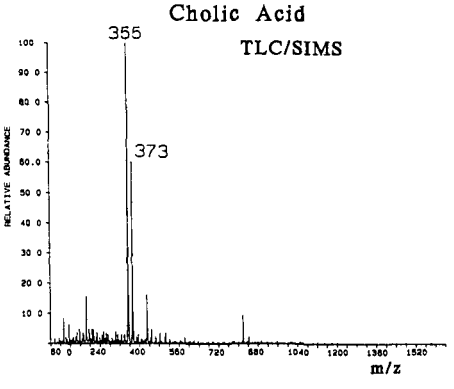

Figure 1

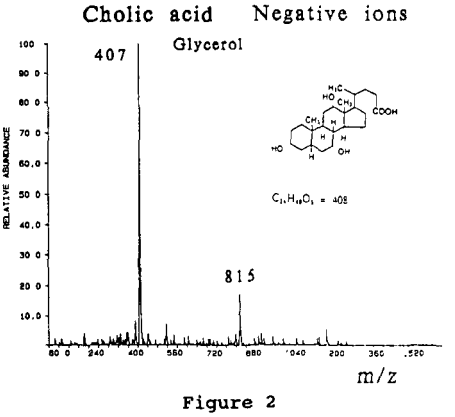

Figure 2

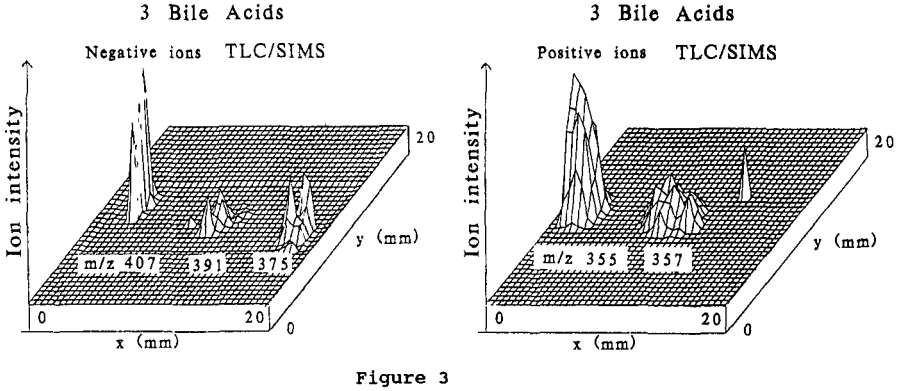

Figure 3

Presented at the 36th ASMS Conference on Mass Spectrometry and Allied Topics
June 5-10, 1988, San Francisco, CA

NEGATIVE ION CHEMICAL IONIZATION-TANDEM MASS SPECTROMETRY OF FATTY ACIDS: IMPROVED SENSITIVITY AND STRUCTURAL INFORMATION

Roger N. Hayes, R.L. Cerny and M.L. Gross, Midwest Center for Mass Spectrometry, Dept. of Chemistry, University of Nebraska, Lincoln, NE, 68588.

The technique of tandem mass spectrometry (MS/MS) has become a widely recognized tool for the rapid screening and analysis of mixtures.[1] Using this technique, a specific ion in a mixture can be mass selected and then collisionally activated (CA) to cause fragmentation of the selected ion. In this manner, the mass spectra of the individual components of a mixture can be determined.

Although FAB is an excellent technique which lends itself to the study of a wide range of compounds, the detection limits for this desorption ionization method are not high (ca. 10 ng for fatty acids). Furthermore, the properties of the matrix with regards to analyte suppression are recognized but not yet fully understood. For example, a 1:1:1 mixture of the fatty acids dodecanoic, 12-hydroxyhexadecanoic and octadecanoic are desorbed from triethanolamine matrix to give very different ion currents for each component of the mixture (Figure 1).

Negative ion chemical ionization (NICI) is known to provide exceptional sensitivity for compounds which contain electron capture groups. In NICI, ionization results from capture of a thermalized electron by an electrophoric analyte in a process known as resonance capture.[2] In this study we examined the utility of the pentafluorobenzyl (PFB) electrophore. PFB-esters of fatty acids were readily synthesized in high yields (> 95%) by using a slight excess of a 1:1 mixture of pentafluorobenzyl bromide and diisopropylamine in acetonitrile solvent. The reaction mixture was heated at 60°C for 1 hour. Excess reagents were evaporated under a stream of nitrogen, and the residue was dissolved in a minimum amount of acetonitrile. No further purification was performed, however, elution of the residue applied to a short silica column with dichloromethane solvent gave a product which was essentially pure as determined by GC/MS.

The PFB-derivatized fatty acids were introduced into the ion source of the mass spectrometer by using a direct insertion probe heated to 100°C. By using toluene as the reagent gas (0.1 Torr) to thermalize electrons, the PFB-ester derivatives yielded abundant $(M - PFB)^-$ anions. Because the energy of the reactive electrons were low, the amount of excess energy available to effect fragmentation was small. Thus, as is often the case for NICI, few structurally informative fragment ions were produced. However, the detection limits for the PFB-esters were very low; typically as little as 100 femtograms was required to observe a carboxylate anion in the mass spectrum.

Presented at the 36th ASMS Conference on Mass Spectrometry and Allied Topics
June 5-10, 1988, San Francisco, CA

Comparison of Fast Atom Bombardment and Negative Ion Chemical Ionization Tandem Mass Spectrometry for the Analysis of Fatty Acids.

Compound	Detection Limit FAB	Detection Limit NICI
Palmitic (C16:0)	25 ng	10 pg
Stearic (C18:0)	30 ng	10 pg
12-Hydroxy Stearic (12-OH C18:0)	45 ng	15 pg
Oleic (C18:1)	30 ng	10 pg

Fatty acid carboxylate anions, desorbed from a triethanolamine matrix by using FAB, decompose upon collisional activation (CA) to yield structurally informative charge-remote fragmentations.[3,4] Various functional groups along the alkyl chain including double bonds, branch points, and hydroxyl groups are readily located. Collisional activation of the fatty acid carboxylate anions produced from the PFB-ester by using NICI gave identical CA mass spectra (Figure 2). The CA mass spectra were, however, obtained with significantly smaller amounts of analyte; typically 10 picograms (Table 1). No suppression of individual analytes from an equimolar mixture was observed. Signal averaging was necessary for quantitative purposes because of slight differences in analyte volatility.

References

1. F.W. McLafferty, Acct. Chem. Res., 13, 33 (1980).

2. H. Budzikiewicz, Angew. Chem. Int. Ed. Engl., 20, 624 (1981).

3. N.J. Jensen and M.L. Gross, Lipids, 21, 362 (1986).

4. K.B. Tomer, N.J. Jensen and M.L. Gross, Anal. Chem., 58, 2429 (1986).

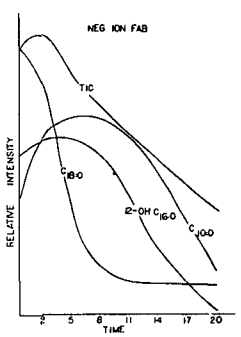

Figure 1

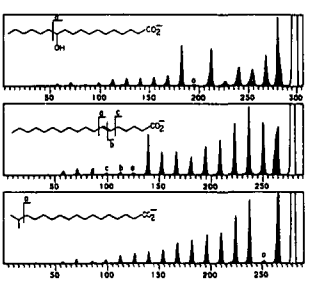

Figure 2

Presented at the 36th ASMS Conference on Mass Spectrometry and Allied Topics
June 5-10, 1988, San Francisco, CA

COMBINED LC-MS ANALYSIS OF NEUTRAL LIPIDS, GLYCOLIPIDS AND PHOSPHOLIPIDS IN TOTAL LIPID EXTRACTS

James E. Evans, Barbara A. Evans and Robert H. McCluer
Eunice Kennedy Shriver Center, Inc., 200 Trapelo Rd., Waltham, MA 02254

Lipids are major components of biological membranes that play important and dynamic roles in mediating the interactions of a cell with its environment. The need for convenient and informative methods for their analysis is apparent. This is a report of our attempts to develop an LC-MS procedure for the combined profiling of all the major components of the neutral lipid and polar lipid classes. This includes analysis of molecular species composition. This work extends the methods we have published (1,2) for LC-MS analysis of phospholipids and for neutral glycosphingolipids with recently developed LC-MS procedures for neutral lipids to provide the complete analysis of the major components of these fractions in a single analysis.

HPLC was performed using a 10cm x 4.6mm Brownlee cartridge column packed with 5um spherical silica. Normal phase chromatography was chosen to provide separation based on lipid polar characteristics rather than heterogeneity of the hydrocarbon chains. If solvents that produced a true solution of the polar sample components were used for injection, broad bands were obtained for the nonpolar components. So sample components were suspended by sonication in n-heptane for injection. Elution was by the gradient illustrated in Fig 1 with a flow rate of 1.0 ml/min. The LC-MS interface used was a Finnigan moving-belt type with an indicated vaporizer temperature of 310°C. Mass spectrometry was performed with a Finnigan 4500 in the positive ion, chemical ionization mode with ammonia as the reagent gas.

The HPLC system established provides separation of about 30 lipids in less than 25 min. The plots in Figs 2, 3 & 4 are plots that identify phospholipids, sphingolipids and neutral lipids present in the TIC shown in Fig 1. This data was obtained by injection of 200 ug of total Folch lower phase lipid (equivalent to 2 mg of fresh tissue) from adult rat brain. The separation of a standard mixture of nonpolar neutral lipids including hydrocarbons, sterol esters and fatty acid esters is shown in Fig 4. Several of these neutral lipids are not resolve well by our HPLC system, but can be analyzed by the use of characteristic ion plots. Molecular species and fatty acid composition data can be obtained for all lipids from their mass spectra.

This work was supported by NIH grant NS16447.

References

1. Jungalwala, Firoze B., Evans, James E., and McCluer, Robert H., J. Lipid Res., 25, 738-749 (1984).

2. Evans, James E. and McCluer, Robert H., Biomed. Environ. Mass Spectrom., 14, 149-153 (1987).

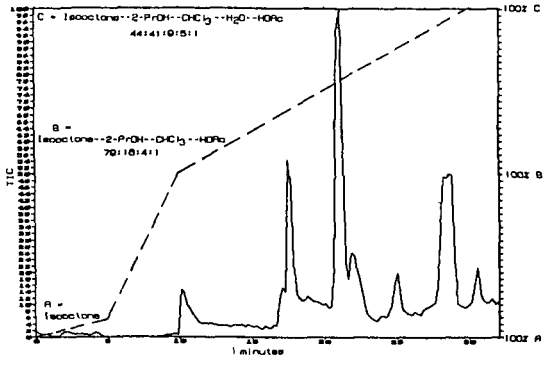

TIC from LC-MS of Cerebellum-Free Rat Brain

Figure 1

Cerebellum-Free Rat Brain Phospholipids

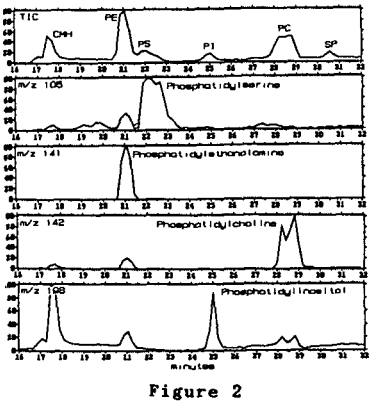

Figure 2

Cerebellum-Free Rat Brain Sphingolipids

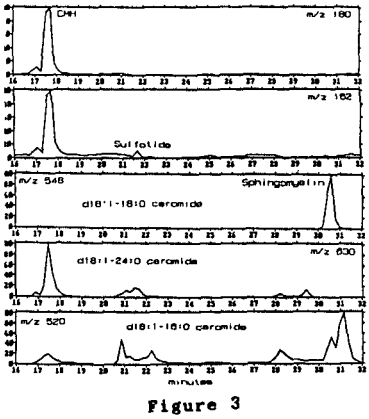

Figure 3

Neutral Lipids from Standard Mixture

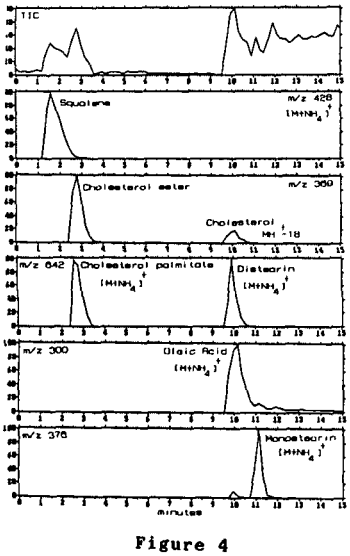

Figure 4

Presented at the 36th ASMS Conference on Mass Spectrometry and Allied Topics
June 5-10, 1988, San Francisco, CA

MASS SPECTROMETRICAL IDENTIFICATION OF TRIMETHYLSILYLATED AND N-METHYLATED STANOZOLOL AND ITS METABOLITES; Schänzer,W.,Opfermann,G. and Donike,M.; Deutsche Sporthochschule Köln, Carl-Diem-Weg 6, D-5000 Köln 41, F.R.G.

Stanozolol (Fig.1,I), an anabolic steroid with a condensed pyrazole ring, was first synthesized by Clinton et al. in 1959 (1). Besides its clinical use it is abused in sports to enhence performance. The use of anabolic steroids is banned by national and international sport federations. Therefore urine samples of athletes are controlled for the presence of stanozolol metabolites. The metabolites of I are isolated from urine (2), trimethylsilylated (TMS) and analyzed after gas-chromatographic separation by mass spectrometry (EI 70 eV). The metabolism of stanozolol was investigated and 10 urinary metabolites were identified. The main metabolites (Fig.1) 3'-hydroxy- (II), 4ß-hydroxy- (III) and 16ß-hydroxy-stanozolol (IV) were synthesized and studied by MS.

Fig.1 Metabolism of stabozolol

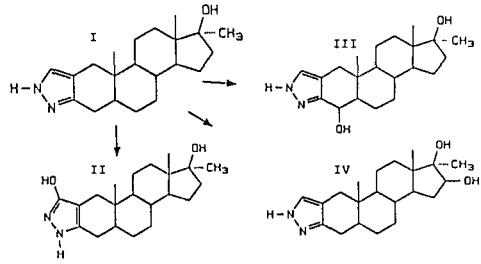

Methylation of I, III and IV with methyliodide in acetone/potassium carbonate (3) yields two N-methyl-isomers each in a ratio of approximately 1:1. The EI-spectrum of 1'-N-methyl-stanozolol is dominated by the ionic fragment m/z 108 which is an A-ring fragment (Fig.2) and can be explained by a retro diels-alder fragmentation. This retro diels-alder fragmentation pattern was reported for stanozolol itself by Budzikiewicz, Djerassi and Williams in 1964 (4). The scission of the A-ring between carbon 1 and 10 and carbon 4 and 5 was proved by deuteration of stanozolol in position 1,4 and 5. The 2'-N-methyl-stanozolol (Fig.3) shows a base peak m/z 110 which was confirmed as an A-ring-fragment with migration of two hydrogen atoms. The origin of this both hydrogen atoms is not quite clear. Deuteration of position 5 and 6 established that approximately 5% of the hydrogen transfer originates from position 5 and 15% from position 6. Deuteration of position 8, 9, 11 and 19 is under study.

Fig.2

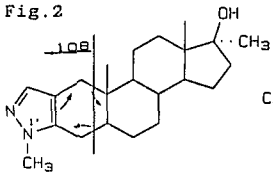

Fig.3

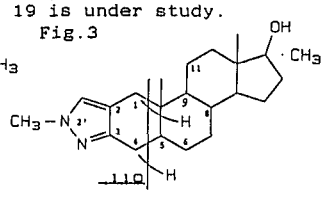

Fig.4

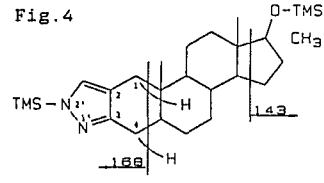

The trimethylsilylation of I, III and IV reacts to only one product each. The EI-spectrum of bis-TMS-stanozolol with a molecular ion m/z 472 shows an abundant D-ring fragment m/z 143 (Fig.4), and an A-ring fragment m/z 168 originating from scissions between carbon 1 and 10 and carbon 4 and 5 with migration of two hydrogen atoms. We assume that the TMS-group is at 2'-N because the location of the double bonds should favour this fragmentation.

Hydroxylation of stanozolol in position 3' yields a pyrazolone derivative which theoretically can exist in eight tautomeric forms, but only three isomers are observed after methylation. The 1',3'-N,O-bis-methyl-derivative (Fig.5) with a molecular ion m/z 372 shows a retro diels-alder fragmentation with an abundant ion m/z 138. The same fragmentation is observed for the 1',2'-N,N-bis-methyl-derivative. The 2',3'-N,O-bis-methyl-derivative shows a different fragmentation (Fig.6). Besides the ion m/z 138 the fragment m/z 140 with approximately the same intensity as m/z 138 is observed. This fragment m/z 140 can be explained with a fragmentation of the A-ring and migration of two hydrogen atoms.

To summarize, the fragmentations of the methyl-isomers of I and II demonstrate that a retro diels-alder fragmentation is preferred when a double bond is located between position 2 and 3 of the A-ring, otherwise an A-ring fragmentation with migration of two hydrogen atoms is apparent.

Fig. 5

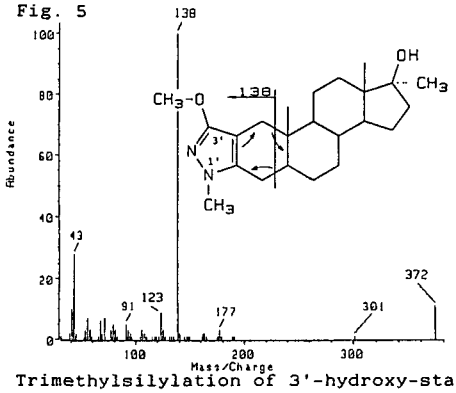

Fig.6

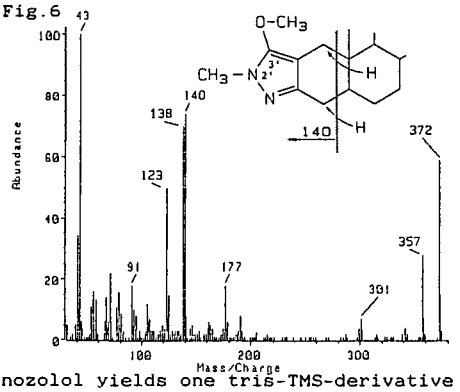

Trimethylsilylation of 3'-hydroxy-stanozolol yields one tris-TMS-derivative with a molecular ion m/z 560, a D-ring-fragment m/z 143 and an intense retro diels-alder fragment m/z 254 (Fig.7) of the A-ring.

Fig. 7

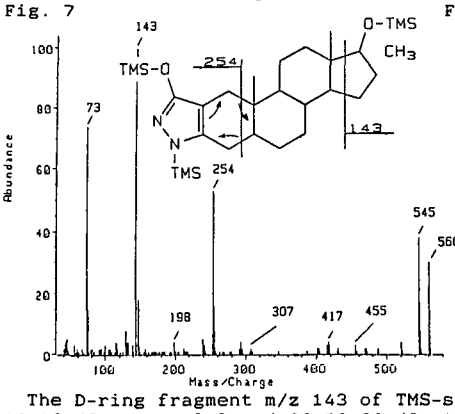

Fig.8

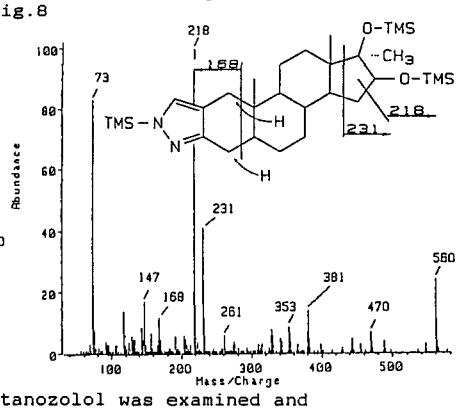

The D-ring fragment m/z 143 of TMS-stanozolol was examined and 16,16-d2-stanozolol and 20,20,20-d3-stanozolol were synthesized. The fragment m/z 143 can be explained with scissions between carbon 13 and 17 and carbon 14 and 15 and an elimination of one hydrogen from carbon 16, the same fragmentation as in tris-TMS-3'-hydroxy-stanozolol (Fig.7). Introduction of a trideuteromethylgroup in position 17 shifts the D-ring ion m/z 143 to m/z 146. Dideuteration in position 16 confirms that carbon 16 is part of the fragment. A base peak m/z 144 elucidates that one deuteium in position 16 is eliminated. But in addition to this ion m/z 144 the fragment m/z 143 is still present, with approximately 30% of the intensity of m/z 144. This ion can be explained by an exchange of the other deuterium atom in position 16 or an other fragmentation not involving carbon 16.

The D-ring fragmentation of 16ß-hydroxy-stanozolol shows the ions m/z 218 and 231 with high abundances (Fig.8). The fragment m/z 231 corresponds to m/z 143 in bis-TMS-stanozolol and originates from a scission between carbon 13 and 17 and between carbon 14 and 15, whereas the ion m/z 218 results from scissions between carbon 13 and 17 and carbon 15 and 16.

References: 1) Clinton et al.,J.Am.Chem.Soc. 81,1513 (1959); 2) Donike et al.,Deutsche Zeitschrift für Sportmedizin 14 (1984); 3) Dunges,W. and Bergheim-Irps,E., Analytical Letters 6, 185 (1973); 4) Budzikiewicz,H., Djerassi,C. and Williams, D.H., Structural Elucidation of Natural Products by Mass Soectrometry , Vol.I, Holden-Day, San Franzisco, London (1964)

Presented at the 36th ASMS Conference on Mass Spectrometry and Allied Topics
June 5-10, 1988, San Francisco, CA

TANDEM MASS SPECTROMETRY, FAB AND EXPERT SYSTEM FOR THE ANALYSIS OF ACYLCARNITINES.

E de Hoffmann*, R. Libert** J. P. Draye** and F. Van Hoof**.

Depts of Chemistry* and Neuropediatry**, University of Louvain, Pl Pasteur 1, 1348 Louvain-la-Neuve, Belgium.

A method has been developed for the analysis of acylcarnitines in urine samples with a Finnigan TSQ70 triple quadrupole instrument. Sample preparation was done by ion exchange chromatography (1). For FAB, the matrix chosen is glycerol acidified with 0.1 M trifluoroacetic acid.

At a Xenon collision gas pressure of 0.08 Pascal and an offset voltage of -2 V, daughter spectra of carnitine conjugates molecular ions are very simple, as illustrated for octanoylcarnitine in Fig. 1. More fragments appear when heteroatoms are present in the conjugated acid chain. The main fragments observed result from neutral losses of either 59 or 161 u or appear at constant masses 85 and 144 u (Schemes 1 and 2). They are all candidates for selective detection of these compounds, but the neutral loss mass of 59 u and the constant ion at 85 u give better sensitivity. Fig. 2 displays the variation of the intensities of these ions with the collision offset voltage. Formation of the 85 u ion shows a broad maximum, and better sensitivity. Further experiments on samples from patients showed that parent scans of 85 u at -10 V collision offset voltage is indeed the best way to selectively detect carnitine conjugates.

An instrument control computer program automatically gets this parents of 85 u spectrum, selects the ten most intense even masses, and then acquires the daughter spectra of these ten ions. Averaging on four scans is performed. The whole acquisition time is about 2.5 minutes.

The left hand spectrum in Fig. 3 is part of the FAB spectrum of the carnitine conjugates extract from a patient with proven 3-hydroxy-3-methylglutaryl-CoA lyase deficiency. Matrix peaks are displayed on a black background. The right hand spectrum is the parent scan of mass 85. From the mass 162 (free carnitine), all the intense ions are carnitine conjugates, as was confirmed by their daughter ions spectra. In this parents scan of mass 85, the most intense peak from the matrix itself above 162 u is at 183 u, almost undetected in this sample. Acetylcarnitine appears at 204 u, and the following homologues at 218, 232 and 246 u. The 260 u peak (hexanoyl) is very weak, but a strong peak appears at 262 u. By comparison of GC/MS analysis of the fatty acids-TMS derivatives before and after hydrolysis of the conjugates, it appears that the only candidate for this mass is 3-OH-isovaleryl-carnitine.

The carnitine conjugates profile (parents of 85 u) from a patient with octanoyl-CoA dehydrogenase deficiency is displayed in Fig. 4. Short-chain fatty acids give only weak peaks. The first two intense ones have masses corresponding to octenoyl- (286 u) and octanoyl-carnitine (288 u). Higher masses can be interpreted either in terms of ω or β-oxydation products. For instance, 304 u can be either ω- or β-hydroxyoctanoylcarnitine, while 302 could correspond to β-ketooctanoyl-carnitine or to ω-hydroxyoctenoylcarnitine. Identification will need reference compounds.

(1): Millington, Bohan, Roe, Yergey and Liberato. Clinica Chimica Acta, 145 (1985), 69-76.

Presented at the 36th ASMS Conference on Mass Spectrometry and Allied Topics
June 5-10, 1988, San Francisco, CA

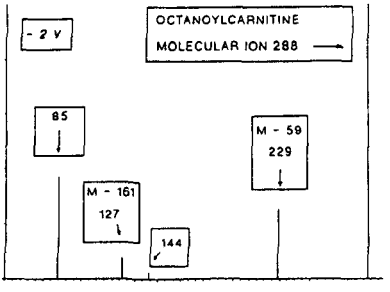

Fig 1

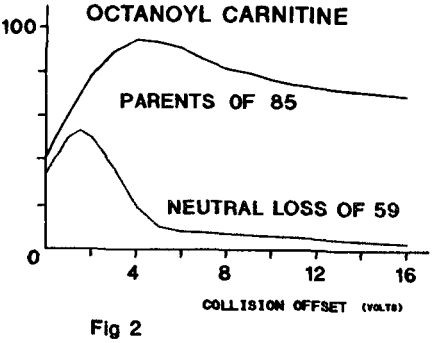

Fig 2

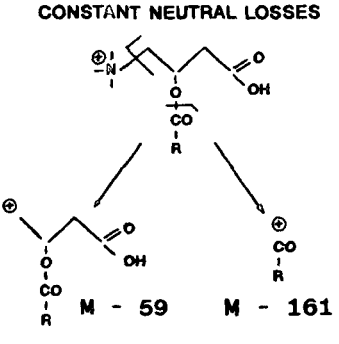

Scheme 1

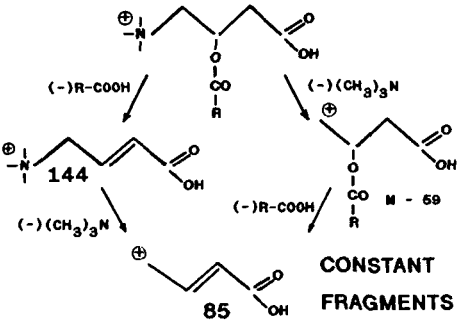

Scheme 2

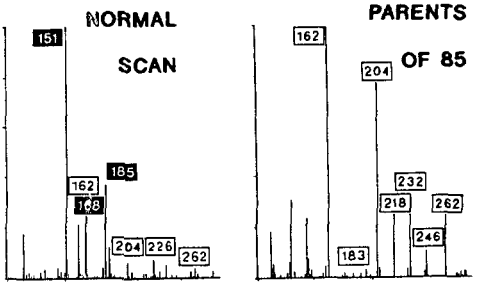

Fig 3

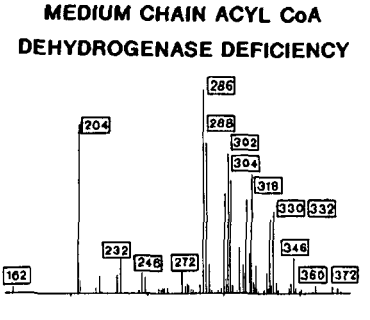

Fig 4

Presented at the 36th ASMS Conference on Mass Spectrometry and Allied Topics
June 5-10, 1988, San Francisco, CA

GENERATION OF FATTY ACID METHYL ESTER PROFILES BY DIRECT CURIE-POINT PYROLYSIS GC/MS OF WHOLE CELL SAMPLES

Jacek Dworzanski* and Henk L.C. Meuzelaar
Center for Micro Analysis and Reaction Chemistry, University of Utah
Salt Lake City, Utah 84112

A novel, on-line pyrolytic derivatization technique has been developed which enables generation of fatty acid methylester (FAME) profiles from microorganisms as well as higher cells by GC/MS without the need for laborious and time-consuming sample preparation. Conventional GC-based methods for obtaining cellular FAME profiles generally require milligram amounts of sample and several hours of successive saponification, methylation and extraction steps [1].

The new pyrolytic technique shown in Figure 1 requires only microgram amounts of sample, thus enabling rapid profiling of a single bacterial colony. Moreover, samples are applied directly to the Curie-point pyrolysis filaments followed by the application of a single drop of derivatizing agent. Using short capillary columns (e.g., 3-5 m) in combination with a Finnigan MAT Ion Trap Detector, complete FAME profiles can be obtained in approximately 6 minutes.

Figure 2 shows a comparison of B. subtilis FAME profiles obtained by means of the conventional saponification, methylation and extraction (SME) method and the new on-line derivatization (OLD) technique, respectively. The two profiles are nearly identical in spite of the major differences in sample treatment. Apparently, under Curie-point pyrolysis conditions the OLD process goes to completion within a fraction of a second. The main origin of the FAME signals in bacterial preparations can be traced back to phospholipid cell wall constituents. As shown in Figure 3, a complex mixture of diglycerides and, to a lesser extent, monoglycerides and free fatty acids is obtained by direct pyrolysis of whole bacterial cells. Addition of the derivatizing agent effectively hydrolizes and methylates these lipid constituents, thereby resulting in the relatively simple FAME pattern.

Further advantages of the pyrolytic approach include high FAME yields from saponification-resistant lipids such as the highly characteristic mycolic acids of Mycobacterium species (see Figure 4). Especially the appearance of the characteristic C32 acid (mycocerosic acid) should be noted in Figure 4. Because mycocerosic acid is found only in mycobacteria a rapid and simple assay would be of great advantage in the diagnosis and treatment of chronic mycobacterial infections such as tuberculosis and lepra [2].

Disadvantages of the new OLD method are degradation of the more labile hydroxy-substituted fatty acids and a higher column background due to pyrolysis products from different cellular components. The latter disadvantage can largely be overcome utilizing the background subtraction capabilities of modern GC/MS software, as shown in Figure 4.

The research reported here was supported in part by DOD subcontract CG1728-88- 001 and by Institutional funds.

REFERENCES:

1. C.W. Moss, J. Chromatography, 203 (1981) 337-347.
2. G. Wieten, J.J. Boon, D.G. Groothuis, F. Portaels, D.E. Minnikin, FEMS Microbiology Letters, 25 (1984) 289-293.

* visiting scientist from Silesian Medical Academy, Sosnowiec, Poland

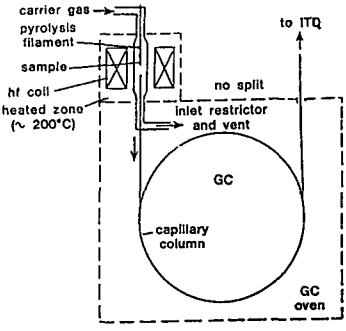

Figure 1. Curie-point pyrolysis GC/MS system.

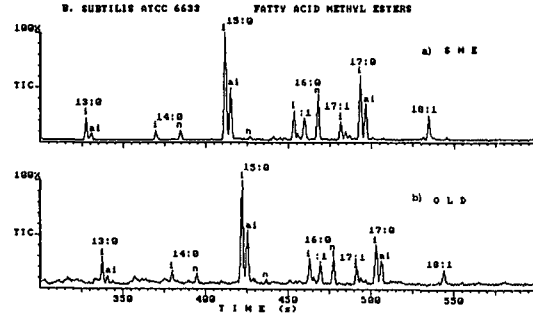

Figure 2. Comparison of FAME profiles from B. subtilis obtained by (a) SME and (b) OLD methods. Note quantitative and qualitative similarity in spite of increased baseline in (b).

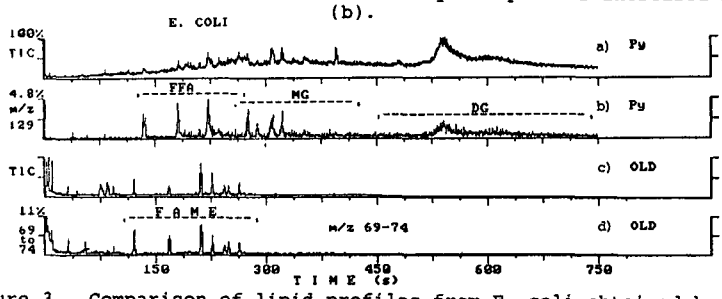

Figure 3. Comparison of lipid profiles from E. coli obtained by direct Curi_ Curie-point pyrolysis (a&b) showing diglycerides (DG) monoglycerides (MG) and free fatty acids (FFA) vs. FAME profiles obtained by OLD method.

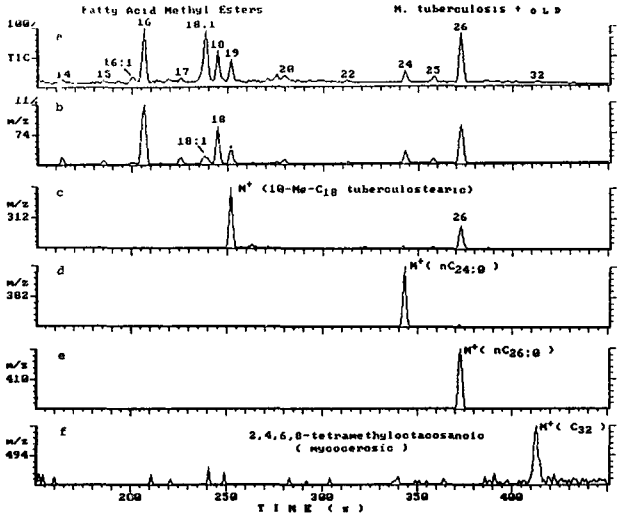

Figure 4. FAME profile of Mycobacterium tuberculosis obtained by OLD method showing baseline removal effect through proper choice of selected ion chromatograms (e.g., m/z 74 in b) as well as the presence of highly characteristic lipid signals at C_{18} (tuberculostearic acid), C_{24}, C_{26} and C_{32} (mycocerosic acid).

Presented at the 36th ASMS Conference on Mass Spectrometry and Allied Topics
June 5-10, 1988, San Francisco, CA

CURIE-POINT DESORPTION, SHORT COLUMN GC/MS OF LARGE POLAR MOLECULES

William H. McClennen, Joseph M. Richards* and Henk L.C. Meuzelaar
Center for Micro Analysis and Reaction Chemistry
University of Utah, Salt Lake City, UT 84112
*Somatogenetics Instruments, Broomfield, CO 80020

The development of a low-dead volume Curie-point pyrolysis GC/MS inlet which maximizes capillary chromatographic resolution by its narrow injection plug has been described [1]. Short column GC/MS has been studied [2,3] as a method which can greatly reduce analysis time while maintaining a useful level of resolution when the column is directly interfaced to the MS vacuum. This work, discusses the utility of this Curie-point pyrolysis inlet as an injection system for relatively large, polar and labile molecules with little or no pyrolysis in flash desorption. The simple injector operation and high linear velocity of a short column with a vacuum outlet permit rapid analyses which rival the ease of direct solids probe techniques with the strong advantage of significant chromatographic resolution. The low dead volume Curie-point pyrolysis inlet (Somatogenetics Instruments) was used with short columns (4m and 5m) directly interfaced to the vacuum of a Finnigan ITD and ITMS. For the analyses on the ITD a 4m x 0.25mm ID CP-Sil5 column (Chrompack) was used which had a linear velocity of 175cm/s and a volumetric flow of 4.0 ml/min (inlet 8 psig, column 60°C, transfer line 250°C). The conditions on the ITMS were a 5m x 0.32mm ID SE-30 column (J&W Scientific) with a linear velocity of 150cm/s and volumetic flow of 7.2ml/min (inlet pressure 3 psig, column 60°C, transfer line 250°C). To accomodate these high flows, the conductances out of the traps were increased by making several additional holes in the teflon spacers of the ITD and by removing the spacers entirely in the ITMS. Flash desorption was performed using 610°C Curie-point filaments with a temperature rise time of ca. 0.2s and 1s total heating time. The remaining analytical conditions (inlet T, GC program, etc) were varied according to sample being analyzed.

The chromatogram from a vulcanized rubber extract representing 5ug of the original solid is shown in Figure 1. Peaks from the antioxidant (di-t-octl-diphenylamine, mw = 339), an antiozonant (N, N-di-s-octyl-phenylene diamine, mw 332), and unreacted sulfur (S_8, mw 256) are indicated. The t-octyldi-phenylamine, which eluted at 4 min. 20s, was most likely an impurity in the antioxidant amounting to less than 2% of the di-octyl material. The molecular ions for these four compounds produced sharp symmetrical peaks with no tailing and clean baselines in their respective single ion chromatograms. The regular series of smaller peaks is due to n-alkanes from a paraffin wax antiozonant.

Figure 2 shows the reconstructed ion chromatogram for a mixture of 5 trichothecene toxins. The numbered peaks are 1:deoxynivalenol, 2:diacetoxy-scirpenol, 3:acetyldiacetoxyscirpenol, 4:J2-tetraol tetraacetate, and 5:T2-toxin. The EI spectra showed no molecular ions with loss of acetic acid to the highest mass ions for compounds 2, 3 and 4. The T-2 toxin lost pentanoic acid to give its highest mass peak at m/z 364 while the deoxynivalenol had a loss of 48 (eg. 18 and 30). H_2O chemical ionization (CI) produced good $(M + H)^+$ ions with extreme fragmentation for compounds 1-3, and isobutane CI still resulted in a loss of water from the T2 toxin with the ITD trap at 200°C.

The analysis of diglycerides is shown in Figure 3. The dipalmitin (mw 568) and distearin (mw 624) eluted while the column was isothermal (300°C). The three n-alkanes, C34, C36, and C44 are included for reference. The EI spectra of the diglycerides gave strong $(M-H_2O)^+$ peaks with abundant fragmentation. Unfortunately, with the traps at such high temperatures (ITMS at 160-180°C and ITD at 225°C), even isobutane CI did not prevent this loss of water in either short column or direct probe analysis. Only when the ion trap was overloaded (self CI occuring) did a small peak appear at m/z 513 for the dimyristin. Thus it remains uncertain whether the dehydration occurs merely in the ion trap or possibly in the inlet. Some pyrolysis of the diglycerides is evidenced by the presence of small free acid and monoglyceride peaks eluting in the first 3.5 min. of Figure 3.

In conclusion, Curie-point flash desorption is an effective injection technique for many moderately large, polar compounds with minimal degra-dation. The use of high linear velocity carrier gas in short capillary

columns with vacuum outlets allows rapid gas chromatography of these types of compounds without derivatization. Finally, the technique is applicable to inexpensive mass spectrometers such as the ITD with minor modification.

The authors acknowledge funding and samples for this work from B.F. Goodrich Company, and the Chemical Research, Development and Engineering Center, U.S. Army.

References

1. H.L.C. Meuzelaar, W.H. McClennen, and Y. Yun, 35th Ann. Conference on MS and Allied Topics, Denver, CO (1987) 1142.
2. C.A. Cramers, G.J. Scherpenzeel, and P.A. Leclerq, J. Chromatogr., 203 (1981) 207.
3. M.L. Trehy, R.A. Yost and J.G. Dorsey, Anal. Chem., 58 (1986) 14.

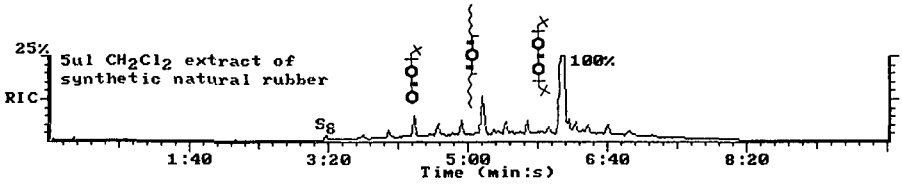

1. Reconstructed ion chromatogram from the analysis of a natural rubber extract. The structures of four major additives are labelled above the series of paraffin wax alkanes and baseline of aromatic and aliphatic processing oil peaks.

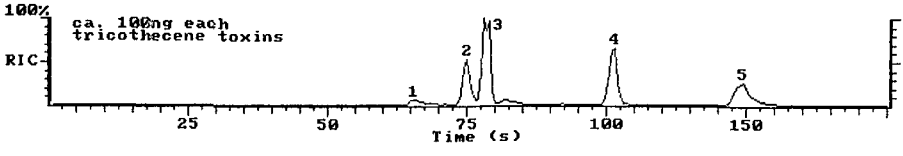

2. Reconstructed ion chromatogram from the analysis of 5 tricothecene toxins. Molecular weight of these underivatized toxins range from 296 for peak 1, deoxynirvalenol, to 466 for peak 5 the T2-toxin and peak 4, the T2-tetraol tetraacetate.

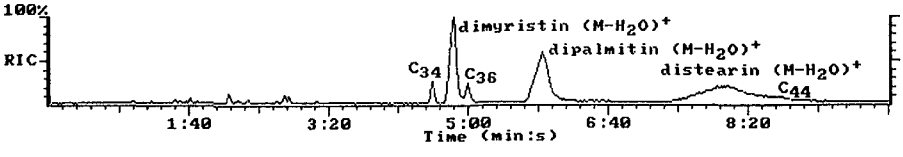

3. Reconstructed ion current from the analysis of 200ng each of three diglycerides and ca. 20ng each of three n-alkanes. The elution of compounds after 5 min. is slowed by the non-standard transfer line which could only be heated to 270°C. Note that the dipalmitin and distearin peaks are relatively symmetrical and free from major tailing.

Presented at the 36th ASMS Conference on Mass Spectrometry and Allied Topics
June 5-10, 1988, San Francisco, CA

Integration of Microsequencing, Mass Spectrometry, and Tandem Mass Spectrometry for Maximum Efficiency in Peptide Sequencing

John T. Stults, William J. Henzel, and John A. Chakel
Genentech,Inc.
460 Point San Bruno Blvd.
South San Francisco, CA 94080

Mass spectrometry has emerged as an essential tool in the protein sequencing laboratory. Mass measurements and sequence determinations by mass spectrometry very often are complementary to conventional amino acid analysis and microsequencing data. As a result, the efficiency and accuracy of microsequencing are improved when the peptide molecular weight is known. Sample amounts required for mass measurement and automated Edman degradation are comparable, on the order of 10-50pmole.

Typically peptides are generated by proteolytic digestion and separated by HPLC. Mass measurement for the collected fractions prior to sequencing identifies the number of peptides present (for coeluting peptides) and provides an estimate of the number of cycles of Edman degradation to program. Following sequencing, knowledge of the molecular weight shows whether the peptide was sequenced to the C-terminus, improves the confidence of residue assignments for low-level signals, and identifies the presence of post-translational modifications when they occur. Sequencing of peptide mixtures is aided when the molecular weight of each component is known; uncertainty of which residue corresponds to which sequence in a particular cycle is greatly reduced.

Confirmation of the sequence of synthetic peptides or peptides produced by recombinant DNA technology can be rapidly performed by mass measurement since the putative sequence is already known. Mass analysis is particularly useful for analyzing recombinant proteins, where the length of the gene product may be uncertain, protease or peptidase processing is likely, or post-translational modifications are possible.

Tandem mass spectrometry is used for sequencing in cases in which Edman degradation fails (e.g., blocked N-terminus) or post-translational modifications are present. Modified residues in synthetic peptides are also readily identified.

Confirmation of microsequencing results is illustrated in Figure 1. Shown are the sequence data and the molecular ion region of the spectrum of a CNBr peptide of bovine brain Protein Carboxyl Methyltransferase (PCMT), Mr~26,500. This enzyme catalyzes L-isoaspartyl/D-aspartyl methylation. The sequence data show diminishing levels near the C-terminus. The measured mass confirms that the sequence is correct and the C-terminus of the peptide was reached. The latter point is important since it shows that the C-terminus of the protein was identified because homoserine would otherwise be expected as the C-terminal residue of a CNBr fragment.

Mass spectrometry is an excellent technique for identifying post-translationally modified amino acids. Conventional microsequencing relies on retention time of the PTH-amino acids for identification, so modified residues are often unidentified or misidentified. Blocking groups at the N-terminus prevent sequencing althogether. Comparison of the peptide mass with the sequencing data usually flags any post-translational modifications. The identity of the modification can then be made by tandem mass spectrometry, amino acid analysis, and or other methods.

Figure 2 shows the sequence data and collision spectrum for a tryptic peptide from the large subunit of muskmelon Ribulose bisphosphate carboxylase/oxygenase (Rubisco), one of the enzymes involved in the dark reaction of photosynthesis. The cDNA sequence codes for ASVGFKAGVK. Initial inspection of the sequence data shows Phe in place of the first Lys. The mass spectrum shows MH^+=1005.7 which is 42u higher than expected from the cDNA sequence. Although acetylation of the Lys immediately comes to mind, thorough examination of the data show the modification to be trimethylation of the Lys. The collision spectrum of 1005.7 shows no significant peaks below m/z 599. The quaternary ammonium group on the Lys fixes the charge and directs the fragmentation as shown. Exact mass measurements as well as subsequent tests with a trimethyllysine standard on both the microsequencer and amino acid analyzer verified the identification.

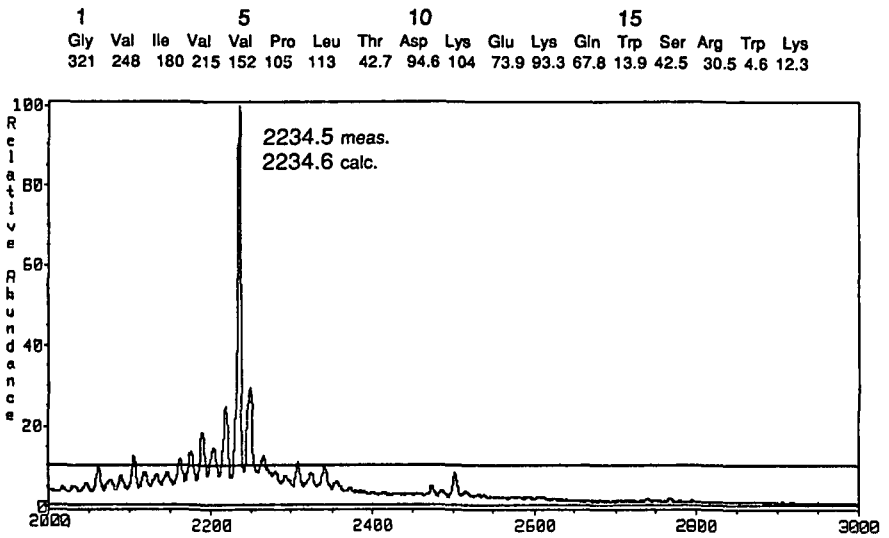

FIGURE 1.

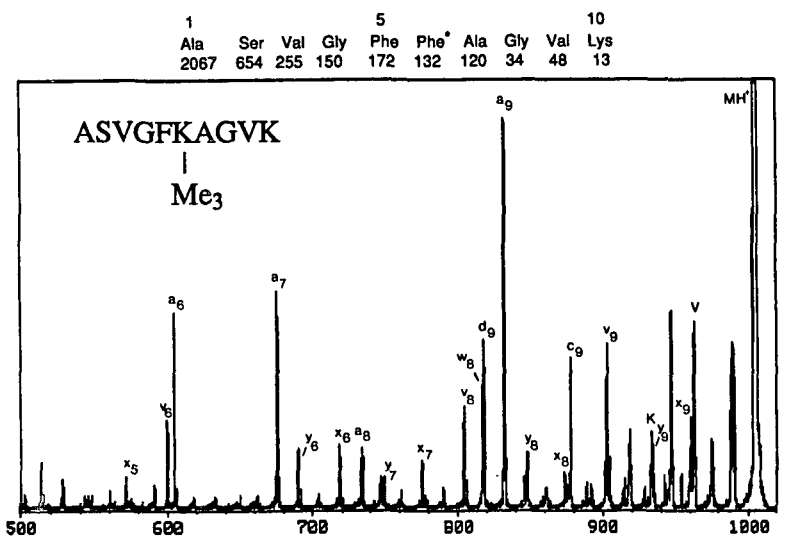

FIGURE 2.

Presented at the 36th ASMS Conference on Mass Spectrometry and Allied Topics
June 5-10, 1988, San Francisco, CA

STYRENE OXIDE ALKYLATION OF HUMAN SERUM ALBUMIN DETERMINED BY FAST ATOM BOMBARDMENT MASS SPECTROMETRY

Richard B. van Breemen and Johnny Creech
Department of Chemistry, North Carolina State University,
Raleigh, North Carolina 27695-8204

Human serum albumin, which weighs 66,439 mass units according to the amino acid sequence determined by Edman degradation (1), is the most abundant protein in the blood plasma and functions as a carrier protein for many drugs, drug metabolites, and endogenous compounds. These properties help make albumin a frequent target molecule for alkylation by activated drug metabolites and other electrophilic compounds. Styrene oxide, an electrophilic epoxide, is the carcinogenic metabolite of styrene, and both are widely used in the manufacturing of plastics and a variety of other compounds (2). Mass spectrometry was used to identify the site(s) of covalent binding of styrene oxide to serum albumin.

[8-^{14}C]Styrene oxide was incubated with human serum albumin (molar ratio = 10:1) for 12 hours at pH 7.4 in 0.1 M phosphate buffer. Because of the high molecular weight of albumin, cleavage by cyanogen bromide followed by tryptic digestion was used to produce peptide fragments weighing less than approximately 5,000 mass units. This procedure enabled the mapping of peptides from albumin by mass spectrometry while preserving as much of the amino acid sequence as possible. This peptide map was compared to one developed for native albumin, which provided a convenient reference for the rapid identification of alkylated peptides. Reversed-phase HPLC was used to purify the seven cyanogen bromide peptide fragments and then the tryptic peptides as previously described (3). Scintillation counting of the HPLC column effluent was used to determine which peptides contained styrene oxide residues.

Positive ion fast atom bombardment (FAB) mass spectra were obtained using a JEOL HX110 double-focussing mass spectrometer equipped with a high field magnet and DA5000 data system. The resolution was 5,000, and the accelerating voltage was 10 KeV. Xenon gas at 3 KV was used for FAB, and the matrix consisted of thioglycerol with 3.5 ug nitrocellulose (4).

Peptide mapping of native human serum albumin by FAB mass spectrometry has confirmed the amino acid sequence of approximately 80% of the albumin molecule, which had been previously determined by Edman degradation. The molecular weights of the three smallest cyanogen bromide peptides (CNBr II, IV, and VII) were determined directly by FAB mass spectrometry and were 4353.50, 3353.65, and 4097.00 mass units compared to the theoretical values of 4352.99, 3353.63, and 4096.89 mass units respectively.

HPLC with scintillation counting indicated that primarily cyanogen bromide peptide IV (CNBr IV) had been alkylated by C14-labelled styrene oxide (Figure 1). CNBr IV of alkylated albumin was purified by HPLC and then analyzed by positive ion FAB mass spectrometry (Figure 2). Because the molecular weight of this peptide increased by 120 mass units compared to native albumin, CNBr IV of albumin had been selectively alkylated by only one styrene oxide molecule. Experiments are in progress to identify the alkylated amino acid(s) in CNBr IV.

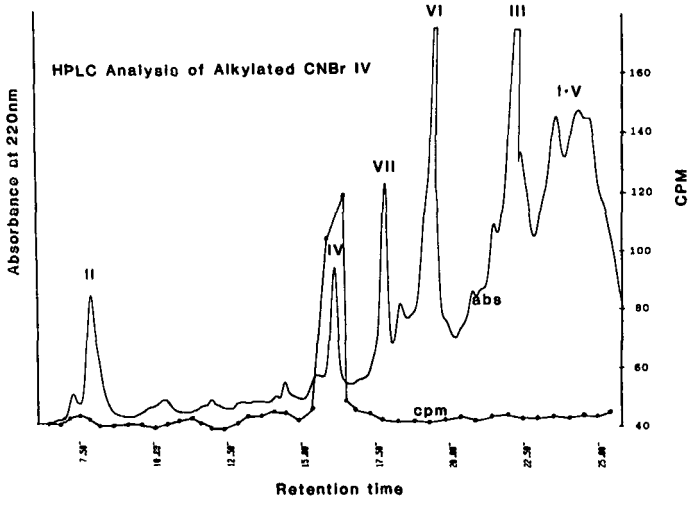

Figure 1. Reversed-phase HPLC purification of the cyanogen bromide peptide fragments of human serum albumin alkylated by [C14]-styrene oxide monitored by UV absorbance and scintillation counting.

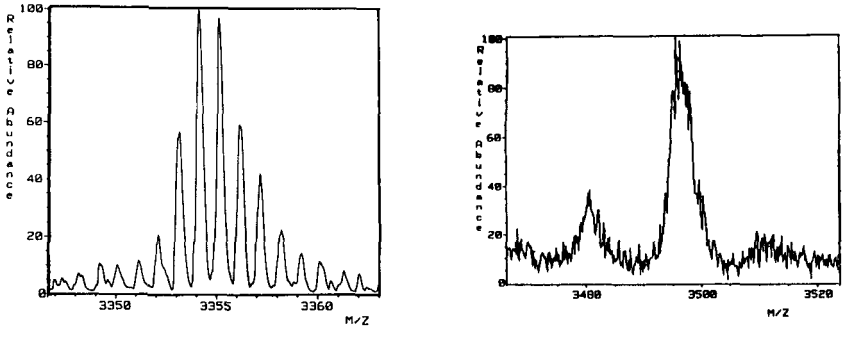

Figure 2. Positive ion FAB mass spectrum of A) native CNBr IV (Resolution = 1,000) and B) styrene oxide-alkylated CNBr IV (Resolution = 5,000) of human serum albumin.

References.

(1) T. Peters, Jr. Adv. Protein Chem., 37, 161 (1985).

(2) "IARC Monographs on the Evaluation of the Carcinogenic Risk of Chemicals to Humans", 19, 275-283 (1979).

(3) P. Iadorola, G. Ferri, M. Galliano, L. Minchiotti, and M. C. Zapponi, J. Chromatogr., 298, 336 (1984).

(4) R. B. van Breemen and J. C. Le, presented at the 36th ASMS Conference on Mass Spectrometry and Allied Topics, San Francisco, CA, June 5-10, 1988.

Presented at the 36th ASMS Conference on Mass Spectrometry and Allied Topics
June 5-10, 1988, San Francisco, CA

FAST ATOM BOMBARDMENT MASS SPECTROMETRY STUDIES OF HUMAN RECOMBINANT GRANULOCYTE-MACROPHAGE COLONY STIMULATING FACTOR

B. N. Pramanik, T. L. Nagabhushan, J. E. Labdon, P. Reichert, Anthony Tsarbopoulos and P. P. Trotta. Schering-Plough Corp. Bloomfield, New Jersey 07003 USA

Human granulocyte-macrophage colony stimulating factor (GMCSF) is one of a family of hematopoietic factors which regulate the differentiation, activation and proliferation of multiple blood-cell types from progenitor stem cells (1). It has been cloned and expressed in various cell lines, including yeast, chinese hamster ovary and E. coli. The E. coli-derived GM-CSF used in this study contains 127 amino acids and has a molecular weight of c. a. 15 kDa.

FABMS mapping of GMCSF involved specific cleavage of GM-CSF with either trypsin or S. aureus V8 protease, followed by mass spectrometric determination of the molecular weights of the resulting mixture of peptides. The experimentally determined molecular weights of the peptide fragments were compared to those predicted from the cDNA-derived amino acid sequence.

The FAB mass spectrum of a tryptic digest of GM-CSF confirmed the presence of all predicted peptides with the exception of those containing cysteine (Table 1). Several incomplete cleavage products were also identified. Most of the predicted peptides from a V8 protease digest of GMCSF were also confirmed (Table 2) with the exception of V9 and V12, which form a high-mass disulfide linked peptide, and V1.

Disulfide bonded peptides were released after the crude tryptic digest was treated with DTT. The free sulfhydryl forms of T4, T10 and T12 were observed at m/z 3202, 2465 and 1950 respectively. This confirmed the presence of 2 disulfide bonds in GMCSF. Enhanced molecular ions were obtained for T4 and T12 after the digest was performed on GM-CSF which was S-alkylated with 4-vinylpyridine (PEC-GM-CSF). In the unreduced V-8 protease digest of GMCSF, an ion at m/z 2273 corresponding to the disulfide-bonded pair V8-S-S-V10 was observed (Table 2). DTT reduction of the digest caused this ion to disappear. These fragments contain half-cystines 54 and 93 respectively. The ion at m/z 3035 (V7-8-SS-V10) resulting from partial cleavage, also disappears after reduction and provides further evidence for this disulfide bond.

CNBr treatment (5 mg/mL in 88% HCOOH for 24 h) of a tryptic digest of PEC-GM-CSF confirmed the presence of two methionine residues in tryptic fragment T4. In a separate experiment, V8 protease peptide V3 was isolated by RP-HPLC and its sequence ions were determined by FABMS.

1. Metcalf, D. (1986) *Blood* **67**, 257-267.

Table 1. FAB/MS Of Tryptic Digest of GMCSF.

Code	Sequence	Expected MW	Ions Observed as $(M+H)^+$ Unreduced	Reduced
T-1	APAR	413.5	+	
T-2	SPSPSTQPWEHVNAIQEAR	2134.4	+	
T-3	(R) LLNLSR	714.9	+[a]	
T-4	DTAAEMNETEVISEMFDLQEPT- -CLQTR	3201.7	-	+
T-5	LELYK	664.8	+	
T-6	QGLR	472.6	+	
T-7	GSLTK	504.6	+	
T-8	LK	259.4	+[b]	
T-9	GPLTMMASHYK	1235.5	+	
T-10	QHCPPTPETSCATQIITFESFK	2465.9	-	+
T-11	ENLK	502.6	+	
T-12	DFLLVIPFDCWEPVQE	1950.3	-	+

[a] also as RLLNLSR m/z
[b] observed as T8-9 m/z 1476.88

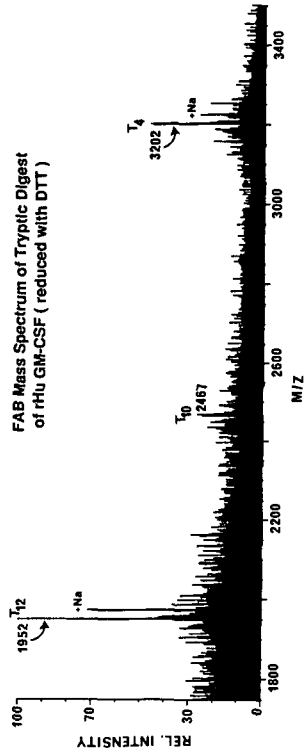

Figure 1.

Table 2. FAB/MS Of V-8 Protease Digest of GMCSF.

Code	Sequence	Expected MW	Ions Observed as $(M+H)^+$
V1	APARSPSPSTQPWE	1510.8	
V2	HVNAIQE	810.0	+
V3	ARRLLNLSRDTAAE	1585.9	+
V4	MNE	392.5	+
V5	TVE	347.4	+
V6	VISE	446.5	+
V7	MFDLQE	782.0	
V8	PTCLQTRLE	1060.4	+
V9	LYKQGLRGSLTKLKGPLT- -MMASHYKQHCPPTPE	3712.9	
V10	TSCATQIITFE	1213.5	+
V11	SFKE	509.6	+
V12	NLKDFLLVIPFDCWE	1852.4	
V13	PVQE	471.6	+
Other Cleavage Products:			
V7-8	MFDLQEPTCLQTRLE	1824.4	+
V12'	NLKD	488.3	+
LQE-V8	LQEPTCLQTRLE	1430.7	+
V7-8-SS-V10		3035.9	+
LQE V8-SS-V10		2642.2	+
V8-SS-V10		2271.9	+
V9'	LYKQGLRGS	1020.6	+

Presented at the 36th ASMS Conference on Mass Spectrometry and Allied Topics
June 5-10, 1988, San Francisco, CA

MAPPING OF COLICIN Ia BY HPLC AND MS/MS

A.M. Falick*, S. F. Mel,** R.M. Stroud,** G. Elliott*** and A.L.Burlingame*

*Mass Spectrometry Facility, Dept. of Pharmaceutical Chemistry, **Department of Biochemistry and Biophysics, University of California, San Francisco, California 94143, and ***Kratos Analytical, Manchester, U.K.

Introduction

Integral membrane proteins are the most common transmitters of information between the extracellular and intracellular environments. Ion channels are found in numerous cell types, playing key roles in nervous system signalling, muscle contraction, and hormone release. Molecular level studies of ion channels have focused on molecules such as the acetylcholine receptor, a large (270kD), multi-subunit transmembrane glycoprotein. Colicin Ia is a smaller (67kD, 626 residues) monomeric bacterial ion channel, which is an excellent model for higher eukaryotic ion channel function.

Colicin Ia is made and released in a water soluble form during the SOS response in the colicin-producing strain of *E. coli*. It then binds to an iron receptor, the *cir* gene product, on the outer membrane of a sensitive (non-colicin-producing) bacterium. The protein subsequently inserts a channel forming region into the inner plasma membrane, thereby killing the cell.

The X-ray structure of the soluble form of colicin Ia is currently being solved in the Stroud laboratory. The structure of the soluble form of colicin Ia will certainly shed light on the membrane conformation of the molecule, but a topographical analysis of the latter form is critical to our understanding of the structure-function of this channel *in vivo*. We have therefore undertaken to map the membrane-bound form of colicin Ia, following which we will identify relevant features of the topography by means of specific labels (Fig. 1).

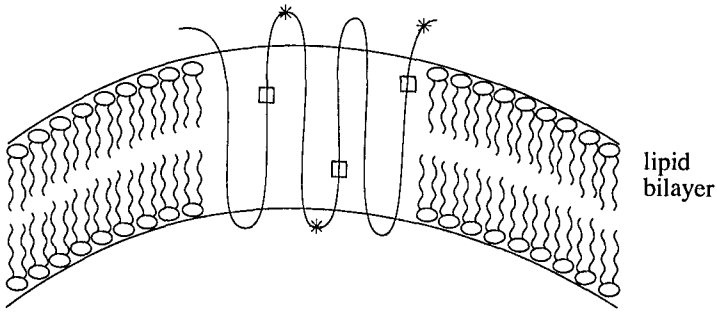

* extramembrane label □ intramembrane label

Fig. 1. Schematic of colicin in transmembrane form.

Experimental

Colicin Ia was purified from *E. coli* strain JK365, according to the method of Konisky, et al. (1970).

Proteolytic digestion was carried out with Endoproteinase Glu-C (*S. aureus* V8 protease) from Boehringer Mannheim. Digestions were done at 37°C for 1 hr in 0.05M phosphate buffer (pH 7.8) and 2.4M urea at an enzyme to substrate ratio of 1:5.

Mass spectrometry was done on a Kratos MS-50S, equipped with a high-field magnet, cesium liquid SIMS source (Falick, et al., 1986a), and cooled probe (Falick, et al., 1986b).

MS/MS experiments were carried out on a Kratos "Concept" 4-sector instrument equipped with a cesium liquid SIMS ion source and an electro-optical array detector (Elliott, et al., 1988).

Results and Conclusion

Proteolytic digestion of a 2 nmol sample of native colicin Ia was carried out with *S. aureus* V8 enzyme to cleave the molecule into a number of peptides. Following separation by HPLC, fractions were analyzed by liquid SIMS. Using this single enzyme, peptides representing 67% of the total 626 amino acid residues in colicin were identified.

Tandem mass spectrometry was carried out on several representative peptides, and the results confirm that the spectra contain sufficient information to allow the sequence of an unknown or modified peptide to be deduced. In addition to sequence information, MS/MS provides a means of distinguishing between different peptides whose masses are very similar or identical. Such pairs occur with moderate frequency in relatively small proteins such as colicin, and with much greater frequency with larger proteins. Some examples from colicin are shown in Table 1.

Sequence	Position	Mass (MH^+)
WITE	551/4	548.2720
IMAVD	24/5	548.2754
KRQKD	188/5	674.3949
KRKQD	440/5	674.3949
SRMLFAD	162/7	839.4085
ALRLHTE	155/7	839.4739
FLKSVSEKYGAKAE	459/14	1556.8324
AGKRLSAAIAAREKD	98/15	1556.8872
RRKGILDTRLSELE	209/14	1685.9662
AGKRLSAAIAAREKDE	98/16	1685.9298

Table 1. Examples of Isobaric Peptides in *S. Aureus* V8 Digest of Colicin Ia

Colicin Ia is an example of a mid-size protein that can be successfully mapped using MS and MS/MS to identify the position of essentially every individual residue. Subsequent modifications for the purposes of determining topography or locating other covalent adducts are precisely locatable, provided that sufficient specificity can be achieved. The mapping and subsequent analysis of the modified form are possible on sub-nanomole quantities of protein, using the high-sensitivity MS techniques employed in this study.

Further work on colicin will first complete the map using other enzymes (endo Lys-C, endo Asp-N), then begin experiments with topographically-selective reagents.

References

Elliott, G., et al. (1988), paper # WPB 38, presented at 36th ASMS Conference on Mass Spectrometry and Allied Topics, June 5-10, 1988, San Francisco, CA.

Falick, A., Wang, G. and Walls, F. (1986a) Anal. Chem. 58, 1308-1311.

Falick, A., Walls, F., and Laine, R. (1986b) Anal. Biochem. 159, 132-137.

Konisky, J. and Richards, F. (1970) J. Biol. Chem. 245, 2972-2978.

Acknowledgements

This work was supported by NIH (Grant RR01614 to ALB and grant GM24485 to RMS) and UCSF (Claypole Fellowship and Graduate Division Mentorship Award to SFM).

Presented at the 36th ASMS Conference on Mass Spectrometry and Allied Topics
June 5-10, 1988, San Francisco, CA

ULTRA-HIGH SENSITIVITY MEASUREMENT OF PEPTIDES AND PROTEINS WITH keV AND MeV ION BOMBARDMENT

Viswanatham Katta, Louis I. Grace, Tanuja Chaudhary and Brian T. Chait
The Rockefeller University, New York, NY-10021.

We have recently made a detailed comparison of the spectra and the relative yields of a series of peptides desorbed from nitrocellulose (NC) surfaces by keV and by Cf-252 fission fragments. We showed that the use of NC significantly reduces the previously reported differences in the relative yield between the two bombardment techniques for electrosprayed samples [1]. In the present investigation we have extended this study to compare the effective sensitivities of the two bombardment techniques for a series of peptides (molecular weight range (1000-6000 u) desorbed from NC. The comparison was made using 30 keV indium ions in a pulsed ion bombardment time-of-flight (TOF) mass spectrometer (PIB-MS) and ca.100 MeV fission fragment TOF mass spectrometer (FF-MS). Both instruments were built at the Rockefeller University [2,3].

The PIB-MS was designed to achieve very high sensitivity by using a tightly focussed (to a diameter of 0.1 mm), high intensity primary ion beam to bombard the sample of interest, which can be concentrated onto a small area (0.3-3.0 mm^2).

The comparisons were made with peptide samples, which include arginine vasopressin (MW = 1083), a 32-residue synthetic peptide analogue of Calcitonin (MW = 3576) and bovine insulin (MW = 5733). The procedure involves deposition of about a micron thick layer of NC on sample insertion probes of PIB-MS (area 3 mm^2) and FF-MS (area 110 mm^2). A microliter of peptide solution (in 0.1% trifluoroacetic acid) was deposited on NC, left for 3 minutes to allow peptide sorption, and then the solvent was removed. Spectra were obtained with both instruments operating under similar conditions (accelerating potential = 2.75 kV and postacceleration potential = 7.5 kV).

As observed earlier [1], both instruments gave very similar spectra. As an example the PIB-MS and FF-MS spectra obtained from 2 picomoles of bovine insulin are compared in Figure 1.

We observed considerably higher effective sensitivity with our PIB-MS compared to our FF-MS. The yields of protonated arginine vasopressin with both instruments are compared in Figure 2 as a function of amount of sample deposited on the probes. It is seen that, of the two instruments the PIB-MS has higher sensitivity (about a factor of 40). This may simply be related to the fact that the same amount of sample is deposited in a 40 times smaller area on PIB-MS probe. Figure 3 shows the spectrum of arginine vasopressin obtained in a 30 minute run from a 20 femtomole sample.

With the PIB-MS, quasimolecular ion yields passed through a maximum when the deposited sample is in the range of 1-10 picomoles. Such a maximum lies in the range of 100-1000 picomoles for FF-MS. This results in considerably shorter run times required with PIB-MS, as is evident from Figure 1.

We observed that with both instruments the relative yield of intact multiply protonated peptide ions increased significantly as the amount of sample deposited decreased. Thus for example, the intensity ratio of $(M+2H)^{2+}$ to $(M+H)^{+}$ observed in the PIB-MS spectrum of bovine insulin increased by an order of magnitude when the deposited sample size decreased from 200 picomoles to 20 picomoles (see Figure 4). We are presently investigating this phenomenon.

REFERENCES: 1. F. LaFortune, R. Beavis, X-Tang, K. G. Standing and B. T. Chait, Rapid commun. mass spectrom., 1987, 1, 114.

2. B. T. Chait and F. H. Field, presented at 32nd ASMS Conf. Mass Spectrom. Allied Topics, May 1984.

3. B. T. Chait, W. C. Agosta and F. H. Field, Int. J. Mass Spectrom. Ion Proc., 1981, 39, 339.

Presented at the 36th ASMS Conference on Mass Spectrometry and Allied Topics
June 5-10, 1988, San Francisco, CA

Bovine insulin
MW = 5733
2 picomoles on PIB probe
Run time = 30 minutes

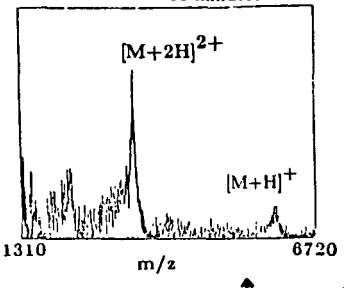

Bovine insulin
MW = 5733
2 picomoles on FF probe
Run time = 660 minutes

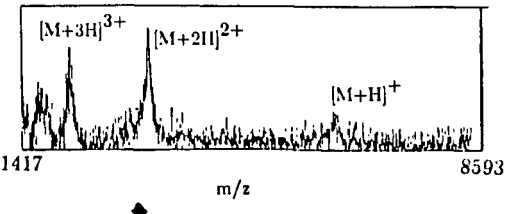

Figure 1

Arginine vasopressin
Quasimolecular ion yield Vs. Amount of sample

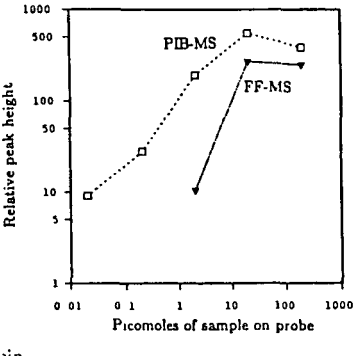

Figure 2

Arginine vasopressin
MW = 1083
20 femtomoles on PIB probe
Run time = 30 minutes

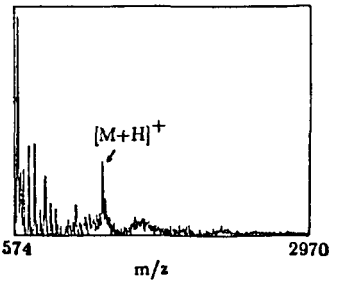

Figure 3

Figure 4

Bovine insulin PIB-MS
Quasimolecular ion yield Vs. Amount of sample

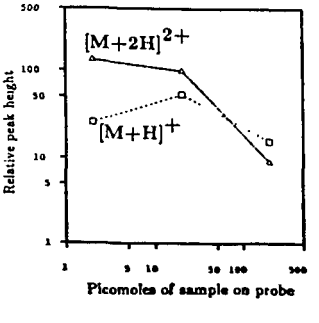

Presented at the 36th ASMS Conference on Mass Spectrometry and Allied Topics
June 5-10, 1988, San Francisco, CA

COVALENT AND NON-COVALENT COMPLEXES ANALYZED BY DESORPTION MASS SPECTROMETRY

L. Chen, C.M. Murphy, R.J. Cotter, Pharmacology, Johns Hopkins University, Baltimore, MD 21205
Y. Osawa and L.R. Pohl, NHLBI, Bethesda, MD 20892

In an effort to elucidate the structures of important biomolecules, we have conducted investigations of covalent bond compounds and extended the study to include non-covalent bond species. Non-covalent linked metal-peptide complexes have been investigated by plasma desorption mass spectrometry while covalent bond heme derivatives have been investigated by FAB.

I. Metal-Linked Dimer of the Cysteine-Rich Region of TAT III Protein from HIV

An 18-amino acid peptide (tat_{21-38}) that contains the cysteine-rich region of the TAT-III protein from HIV has been synthesized [1]. These cysteines serve as metal ligands in the intact protein, causing TAT-III to form metal-linked dimers in vitro. As proposed in Figure 1, four metal ions (M) coordinate in tetrahedral geometries with 14 cysteine thiolate ligands (s) of tat_{21-38} region. This cysteine-rich peptide can also inhibit dimerization of intact Tat-III by forming metal-linked heterodimers. If these heterodimers are unable to transactivate viral transcription, the synthetic peptide could be a lead compound for drugs to treat AIDS.[2]

As shown in Figure 2, plasma desorption spectra permitted direct observation of the metal-linked dimer. The "dimer" peak is less well resolved than the monomer peak but the major species are tat dimers with four bound Cd^{2+} ions adjusted by the addition of Cl^- anions, or subtraction of protons, to achieve a single charge. The "codesorption" of Cl^- is reasonable since $CdCl_2$ was present in these samples. Molecular ions of Zn^{2+}-linked dimer were also observed, however with reduced intensity (not shown). This may indicate a weaker linkage of Zn^{2+}-complexes than Cd^{2+}-complexes.

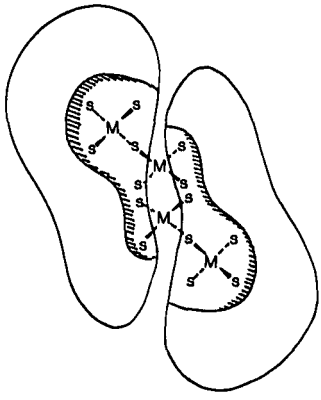

ALA CYS THR ASN CYS TYR CYS LYS LYS-
-CYS CYS PHE HIS CYS GLN VAL CYS PHE

Fig 1. Proposed geometry (top) of a TAT-III metal-linked dimer. The amino acid sequence of the cysteine-rich peptide (tat_{21-38}) is shown at the bottom. [1]

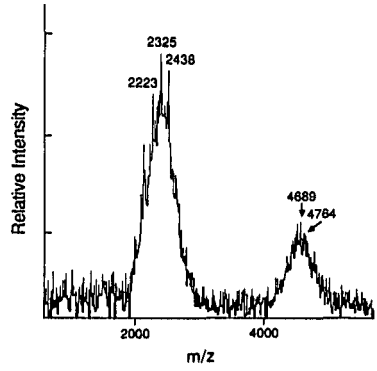

OBS. MASS	ASSIGNMENT	CALCD. MASS
2223	$tat_{21-38}+Cd^{2+}-H^+$	2216.2
2325	$tat_{21-38}+2Cd^{2+}-3H^+$	2326.6
2438	$tat_{21-38}+3Cd^{2+}-5H^+$	2437.0
4689	$2tat_{21-38}+4Cd^{2+}-6H^++Cl^-$	4688.7
4764	$2tat_{21-38}+4Cd^{2+}-4H^++3Cl^-$	4761.7
	$2tat_{21-38}+5Cd^{2+}-9H^+$	4762.7

Fig 2. Plasma desorption mass spectrum (top) and its interpretations (bottom) of the tat_{21-38}-Cd^{2+} complex.

Presented at the 36th ASMS Conference on Mass Spectrometry and Allied Topics
June 5-10, 1988, San Francisco, CA

II. Intermediates Involved in Covalently Bound Heme-Protein Adducts in the Course of Suicide Inactivation of Heme Proteins

During the metabolism of CCl_4 and various other xenobiotics by P-450 cytochromes, these cytochromes become inactivated and produce abnormal hemederived products covalently bound to the protein. Although the molecular mechanism of this process has yet to be elucidated, it appears that in each case a radical intermediate is involved. For example, CCl_4 is reduced by a ferrous P-450 to the trichloromethyl radical. In this study a model system of this reaction, consisting of photoreduced myoglobin and $BrCCl_3$, has been developed to help elucidate the mechanism of the P-450 inactivation.

Myoglobin was reduced under anaerobic conditions by dithionite or by photoreducing system containing EDTA and flavin. The ferrous form was treated with $BrCCl_3$ and a rapid loss of the absorbance due to the ferrous form was observed. The reaction mixture was separated by C_4-reverse phase column into four major soluble components (non-protein associated modified heme) and the protein-heme complexes. The non-protein associated adducts were identified by FAB mass spectrometry (see Fig. 3) as CO_2H, CCl_3OH, and $2(CCL_3)$ adducts of the prosthetic heme (Fig. 4). These products all result from the attack of the trichloromethyl radical on the I-vinyl.

Further study of the protein associated modified heme products will be carried out via PD and FAB mass spectrometry. Information on the covalently bound heme-protein adducts is an important step in understanding the protein inactivation mechanism.

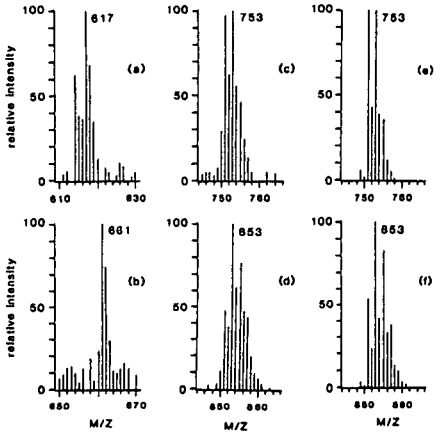

Fig 3. Positive ion FAB mass spectra. Theoretical molecular ion regions are included (e, f) in comparison with the spectra of peaks c and d.

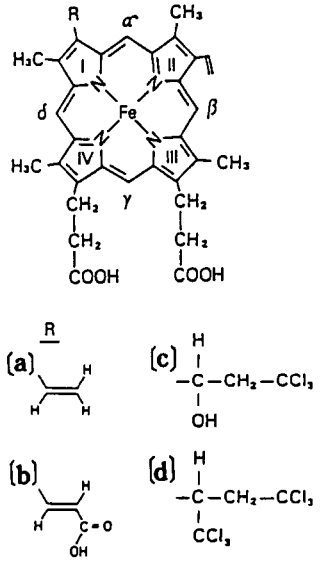

Fig 4. Structures of the heme metabolites. The numbers correspond to those on Figure 3.

REFERENCES

1. A.D. Frankel; D.S. Bredt; C.O. Pabo; Science 240, 70-73 (1988 April)
2. A.D. Frankel; L. Chen; R.J. Cotter; C.O Pabo, submitted to PNAS

Presented at the 36th ASMS Conference on Mass Spectrometry and Allied Topics
June 5-10, 1988, San Francisco, CA

SYNTHESIS OF A DEUTERATED ANALOG OF LEU-ENKEPHALIN FOR FAB QUANTITATIVE ANALYSIS.

Benfenati E., Chen S., Fanelli R., Icardi G. Istituto Mario Negri, 24100 Bergamo and 20157 Milano, Italy.

INTRODUCTION

FAB has become a valuable technique for studying peptides. The FAB mass spectra of many peptides have been interpreted and this technique is useful to elucidate the chemical structure of unknown peptides Only a few quantitative studies have appeared using the FAB technique.
One of the advantages of MS quantitative analysis is that a stable isotope labelled analog of the compound can be used as internal standard. We describe the fast and easy synthesis of a deuterated analog of Leu-enkephalin (LE) by proton exchange of this peptide with CF_3COOD and its use as internal standard.

EXPERIMENTAL

Preparation of internal standard: LE (1 mg) dissolved in CF_3COOD (50 µl) was heated at 70°C for 2 hours, then the acid was evaporated under a stream of nitrogen. This process was repeated four times. The obtained deuterated LE was treated with 25% NH_4OH at room temperature to hydrolize the acetilated peptide formed as contaminant during the reaction.
FAB mass spectrometry: all analysis were done on a VG 70-250 mass spectrometer with standard FAB source and target. Xenon was used as bombarding gas and accelerated at 8 kV. Quantitative measurements were carried out acquiring spectra from m/z 450 to m/z 600, at a scan time of 4 sec/decade
Quantification: a constant amount of internal standard dissolved in H_2O / glycerol (2:1) was added to varying amounts of LE. 2 µl of the solutions, containing 10 ng of internal standard and 10-40 ng of LE, were transferred to the surface of the FAB probe. The water was removed in the vacuum block of mass spectrometer before the introduction of the FAB probe into the ion source. Glycerol remained on the probe as matrix. Scans (15-20) were acquired, and average values of absolute peak intensity were used to make the calibration curve. This procedure was repeated with solutions containing 40 ng/µl of internal standard and 25-250 ng/µl of LE.

RESULTS

The deuterated LE negative FAB spectrum is shown in Fig.1. The main molecular ion contained two deuteria (m/z 556). Is possible to observe the absence of undeuterated specie (m/z 554). We have also treated the deuterated LE with a solution 0.1N HCl because the extractive procedure from biological tissues involve a similar conditions treatment. We didn't observe a proton-deuterium exchange after the acid treatment, therefore the synthetized deuterated LE seems to be an appropriate internal standard for biological samples analysis.
The procedure we described for deuterated LE synthesis introduced a third deuterium, in a rather mobile position, that was eliminated by the treatment with NH_4OH.
We observed two advantages in using negative mode instead of positive mode: the current of LE molecular ion was more stable and the liquid matrix caused a lower noise.

To compare the efficiency as internal standard of deuterated LE with that of a LE analog, we tried to use as internal standard Tyr-DAla-Gly-Phe-DLeu (DADLE). It was no possible to obtain a standard curve due to the different behaviour of the two peptides DADLE is desorbed before LE, and this leads to an unstable ratio of the peak intensity between internal standard and LE.
With the deuterated LE as internal standard this problem doesn't exist. We could obtain two different standard curves. The first one was made using 10 ng/µl of deuterated LE as internal standard and 5-20 ng/µl of LE (Fig 2), the second one with 40 ng/µl internal standard and 25-250 ng/µl LE (Fig 3) In both cases the correlation coefficient is over 0.99.

CONCLUSIONS

In the quantification of LE by FAB, two kinds of internal standard, a chemical analog or a stable isotope labelled LE, may be used. Although the analog is easy to obtain from commercial source, its chemical behaviour, in extraction, purification and instrumental analysis, can be different from the compound of interest.
The use of the stable isotope labelled LE we synthetized as internal standard overcome the problems above. Furthermore, its synthesis is fast, easy and cheap.

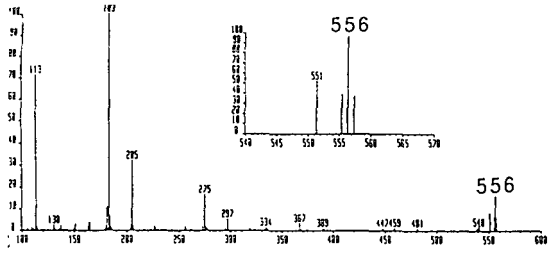

Fig. 1 - SPECTRUM IN FAB NEGATIVE MODE OF 250 ng DEUTERATED LEU-ENKEPHALIN. GLYCEROL WAS USED AS LIQUID MATRIX

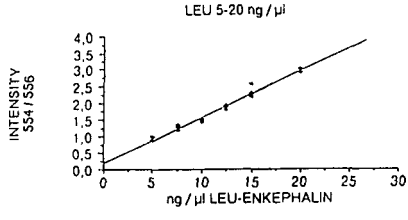

Fig 2 - CALIBRATION CURVE FOR QUANTIFICATION OF LEU-ENKEPHALIN FROM 5 TO 20 ng /µl WITH 5 ng / µl OF DEUTERATED LEU-ENKEPHALIN AS INTERNAL STANDARD

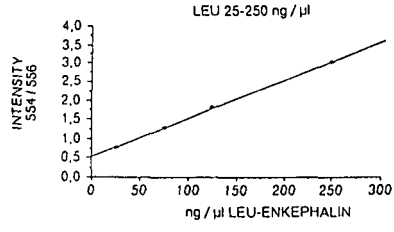

Fig 3 - CALIBRATION CURVE FOR QUANTIFICATION OF LEU-ENKEPHALIN FROM 25 TO 250 ng/µl WITH 40 ng/µl OF DEUTERATED LEU-ENKEPHALIN AS INTERNAL STANDARD

Presented at the 36th ASMS Conference on Mass Spectrometry and Allied Topics
June 5-10, 1988, San Francisco, CA

CHARACTERIZATION OF BIOTECHNOLOGY PRODUCTS AMINO ACID ANALYSIS OF PEPTIDES BY LC/MS

Teng-Man Chen and John Coutant
Merrell Dow Research Institute, Cincinnati,OH 45215

In recent years the use of high performance liquid chromatography (HPLC) for the analysis of derivatized amino acids has become the method of choice over classical techniques, especially in the analysis of protein/peptide hydrolyzates. Several chemistries for derivatization of the amino acids exist but one of the more popular ones has been the use of phenylisothiocyanate (PITC) to form the phenylthiocarbamyl (PTC-) amino acids. The identification of these derivatized amino acids has been based on retention time comparision with standards. This can cause problems for complex mixtures or unique amino acids as the chromophore for UV detection is due to the derivative and differences in UV spectra are minimual. The use of a small dedicated thermospray LC/MS as a routine detector for amino acid analysis can provide qualitative as well as quantitative data.

Acid hydrolysates were derivatized with phenyisothiocyanate (PITC) using the procedures described by Bidlingmeyer et al [1]. The chromatography was performed on a Nova Pak C-18 column using a gradient system of acetonitrile and 0.05 M ammonium acetate. The chromatography was done on a Waters 600-MS system designed for LC/MS and in-line UV detection was acquired with a Waters 490-MS detector. The LC/MS system was a Vestec 101/ Hewlett Packard MSD low cost, dedicated system.

The thermospray (TSP) mass spectra of all the PTC-amino acids are characterized by weak protonated molecular ions, $[M+H]^+$, and intense ions due to the loss of water, $[M+H-H_2O]^+$. A typical mass spectrum is shown in Figure 1A for the PITC derative of isoleucine. It was observed that N-methyl amino acids react to produce the phenylthiohydantion (PTH-) amino acids instead of the PTC-amino acids. The mass spectra of this derivatives are characterized by intense protonated molecular ions as shown in Figure 1B for the PTH-N(methyl)-isoleucine derivative.

The advantages of such a system are in its ability to uniquely identify each amino acid. In cases where peptides contain unique or modified amino acids, the use of LC/MS allows identification of the amino acid or in certain cases, the dipeptide produced by hydrolysates.

[1] B. A. Bidlingmeyer, S. A. Cohen, and T. L. Tarvin, J. Chromatogr., 336 (1984) 93.

Presented at the 36th ASMS Conference on Mass Spectrometry and Allied Topics
June 5-10, 1988, San Francisco, CA

TABLE I

AMINO ACID COMPOSITION OF ANGIOTENSIN I

Amino Acid	Theoretical Value	SIM	UV (247nm)
Arg	1	1.0	0.7
Asp	1	0.8	0.8
His	2	2.3	1.6
Ile	1	0.7	0.9
Leu	1	0.9	1.0
Phe	1	1.0	1.0
Pro	1	0.7	0.8
Tyr	1	0.7	0.7
Val	1	0.9	0.8

Figure I

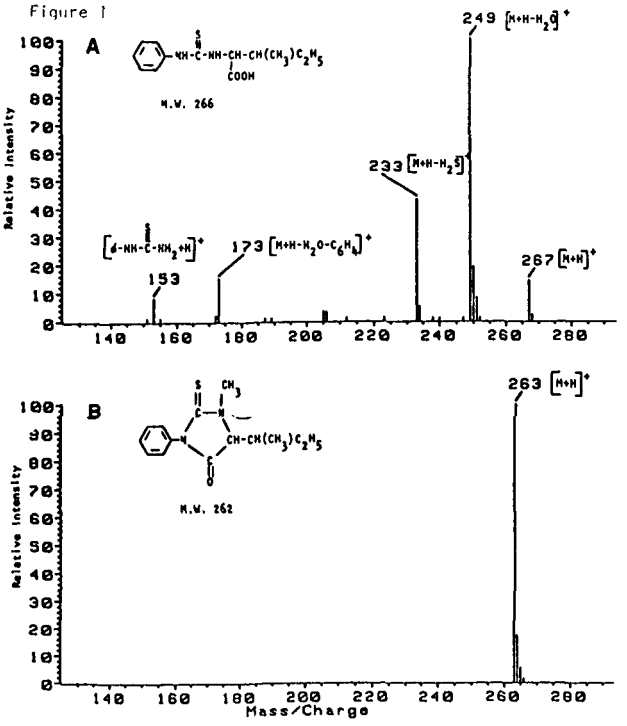

Presented at the 36th ASMS Conference on Mass Spectrometry and Allied Topics
June 5-10, 1988, San Francisco, CA

FAB Mass Spectrometric Investigation of *in vitro* Metabolism Within the Disulfide-Linked Core of Atrial Natriuretic Factor

B.L. Ackermann, T-M Chen, J.E. Coutant, and J.M. Berman
Merrell Dow Research Institute, Cincinnati, OH 45215

Atrial Natriuretic Factor (ANF), a cyclic peptide hormone, is currently under investigation for its potent diuretic and vasorelaxant properties (Fig.1). While several synthetic ANF analogs have shown pharmacological activity, their therapeutic usefulness is limited by rapid metabolism in the kidney (1,2). The current approach to analog design has, therefore, focused on structures less susceptible to protease attack. The results presented here represent an investigation of *in vitro* metabolism within the disulfide-linked core of ANF, with particular attention given to the highly susceptible Cys^7-Phe^8 bond (3,4). For this purpose, two truncated analogs of ANF were digested by the bacterial endopeptidase thermolysin, known to have a specificity similar to the kidney-isolated enzyme EC 3.4.24.11 (5). The resultant degradation products were analyzed using HPLC and FAB-MS.

The structures of the analogs studied are shown in Figure 2 where the arrows indicate the sites of hydrolysis observed under thermolysin digestion. A total of 9 products were identified for $rANF_{5-23}$-NH_2 and 8 for $rANF_{7-23}$-NH_2. However, the difference in stability between the two analogs was rather dramatic as evident from their respective half-lives (Fig.2). This result can be directly related to the relative stability of the Cys^7-Phe^8 bond; this was the site of primary hydrolysis for $rANF_{5-23}$-NH_2 yet remained intact in all products identified for $rANF_{7-23}$-NH_2 (6). These data suggest that the Cys^7-Phe^8 bond may be stabilized towards endopeptidase attack by removing the N-terminal side chain from ANF.

Several methods have been used to identify products from proteolysis of ANF including amino acid analysis (2,3,4), protein sequencing (3,4,7), and RIA (7). FAB-MS offers a convenient alternative to these more time-intensive methods. In the case of ANF, where only a limited number of products are possible, direct identification can be made from the observed MW. An exception occurs, however, for products formed from initial hydrolysis within the disulfide-linked core of ANF as all products have a MW 18u above that for the intact substrate. Fortunately, this problem is easily rectified by reducing the disulfide bond to yield two smaller peptides whose MWs uniquely specify the position of initial hydrolysis. This process is illustrated in Figure 3 for one of three primary hydrolysis products of $rANF_{7-23}$-NH_2. In this case, reduction occured in the thioglycerol matrix during FAB and enabled both the intact substrate (m/z 1724) and the reduced products (m/z 291, 1436) to be observed. The position of hydrolysis specified by the data was Gly^{20}-Leu^{21}.

References

1. J. Tang, R. J. Webber, D. Chang, J. K. Chang, J. Klong and E. T. Wei, Reg. Peptides, 9, 53 (1984).
2. S. L. Stephenson and A. J. Kenny, Biochem, J., 243, 183 (1987).
3. J. A. Koehn, J. A. Normal, B. N. Jones, L. LeSueur, Y. Sakane and R. D. Ghai, J. Biol. Chem., 262, 11623 (1987).
4. G. M. Olins, K. L. Spear, N. R. Siegel and H. A. Zurcher-Neely, Biochem. Biophys, Acta, 901, 97 (1987).
5. M. A. Kerr and A. J. Kenny, Biochem. J., 137, 489 (1974).
6. Manuscript submitted for publication in Biomed. Environ. Mass Spectrom.
7. T. Yandle, I. Crozier, G. Nicholls, E. Espiner, A. Carne and S. Brennan, Biochem. and Biophys. Res. Commun., 146, 832 (1987).

Presented at the 36th ASMS Conference on Mass Spectrometry and Allied Topics
June 5-10, 1988, San Francisco, CA

Figure 1:

Sequence of r-ANF, r = rat; differs from human ANF by the replacement of Ile for Met at position 12.

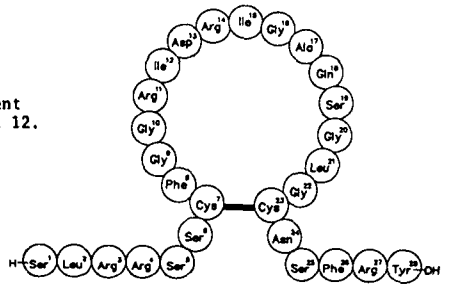

Figure 2:

Truncated rANF analogs; arrows indicate positions of thermolysin-mediated hydrolysis.

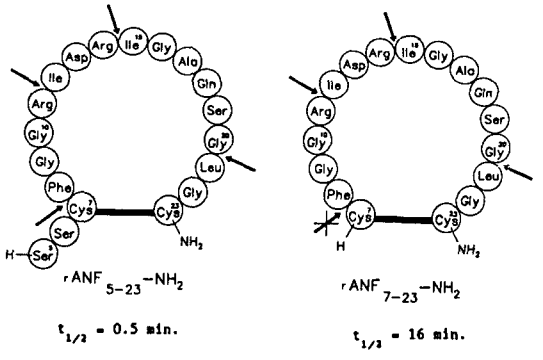

Figure 3:

FAB mass spectrum for primary hydrolysis product 6c from the thermolysin digestion of $rANF_{7-23}$-NH_2.

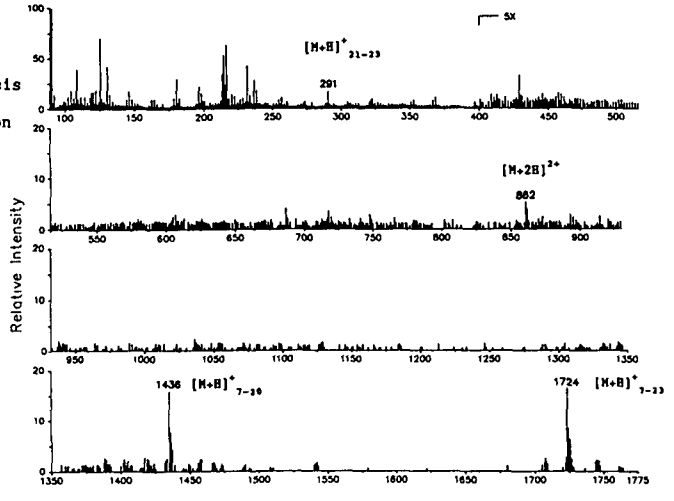

Presented at the 36th ASMS Conference on Mass Spectrometry and Allied Topics
June 5-10, 1988, San Francisco, CA

CHARACTERIZATION OF GUINEA PIG PANCREATIC HORMONES BY MASS SPECTROMETRY

M. Alai and R.J. Cotter, Johns Hopkins University, Baltimore, MD 21205
P C Andrews, Purdue University, Lafayette, IN 47907
D F. Steiner, Howard Hughes Medical Institute, University of Chicago, Chicago, IL 60637

The guinea pig (GP) has several biochemical pecularities in comparison with other mamals. In particular, studies have revealed interesting divergences in the pancreatic hormones of guinea pig; e.g. the sequence of guinea pig insulin has changes in 17 out of 51 residues compared with porcine insulin. Also, guinea pig seems to be the only mamal in which the structure of glucagon is not fully conserved, with 5 of the 9 carboxy terminus amino acids being different. There is also a major difference in the concentrations of pancreatic peptide hormones of GP and other mamals. In addition, guinea pig may exhibit new modes of processing pro-hormones, as in the case of pancreatic polypeptide. The guinea pig pro-pancreatic polypeptide (pro-PP) is predicted to be 126 amino acids (aa), including a 26 residue signal peptide which is followed by the 36 aa PP sequence and a 64 aa C-terminal extension. There is 89% identity between the aa sequence of GP and human PP. In GP pro-PP, however, a Ser for Arg substitution occurs in the processing site at the carboxyl terminal of the PP domain. This substitution converts the dibasic processing site (Lys-Arg) to Lys-Ser. Although, such substitution would seem to inhibit the proteolytic clevage, the amino acid sequence data and radioimmunoassay suggest that efficient proteolytic clevage takes place at the Lys-Ser site and the mature PP is released. Our objective was to verify such abnormal processing by measuring the molecular weight of PP, and also verify the masses of highly substituted peptide hormones of guinea pig pancreas.

By plasma desorption we have verified the molecular weights of GP insulin and glucagon. The measured masses were different by ±1 amu from the expected numbers. We have also isolated and analyzed other GP pancreatic peptides; the assignment of the structures to the ions was made possible by sequencing the amino terminal of unknown fractions, since the full amino acid sequence of many of the peptides analyzed is not known. Guinea pig prosomatostatin (MH^+ 7066) was found to be identical to rat pro-SS in the first 39 amino acids, except for residue 19. The molecular ion of oxyntomodulin suggests presence of an Arg instead of the c-DNA predicted Asn-35. Amino acid sequence analysis also favors presence of an Arg at that site. The amount of oxyntomodulin was found to be higher in guinea pig pancreas than other mamals. The yield of this peptide was approximately equivalent to glucagon.

PDMS analysis of GP-PP confirmed that pro-PP despite a substitution in its processing site, is released as a mature 36 aa peptide. In addition, we have demonstrated that the C-terminal glycine is removed enzymatically to yield a carboxyamidated PP.

REFERENCES:

1) J.M.Conlon, Life Sci., 2: 213 (1984).

2) L.F.Smith, Am. J. Med., 40: 662 (1966).

3) P.C.Andrews and P.Ronner, J. Biol. Chem., 260: 3910 (1985).

4) C.D.Blackstone, S.Seino, T.Takeuchi, T.Yamada and D.F.Steiner, J. Biol. Chem., 263: 2911 (1988).

5) J.Eng, C.-G.Huang, Y.-C.E.Pan, J.D.Hulmes and R.S.Yalow, Peptides, 8: 165 (1987).

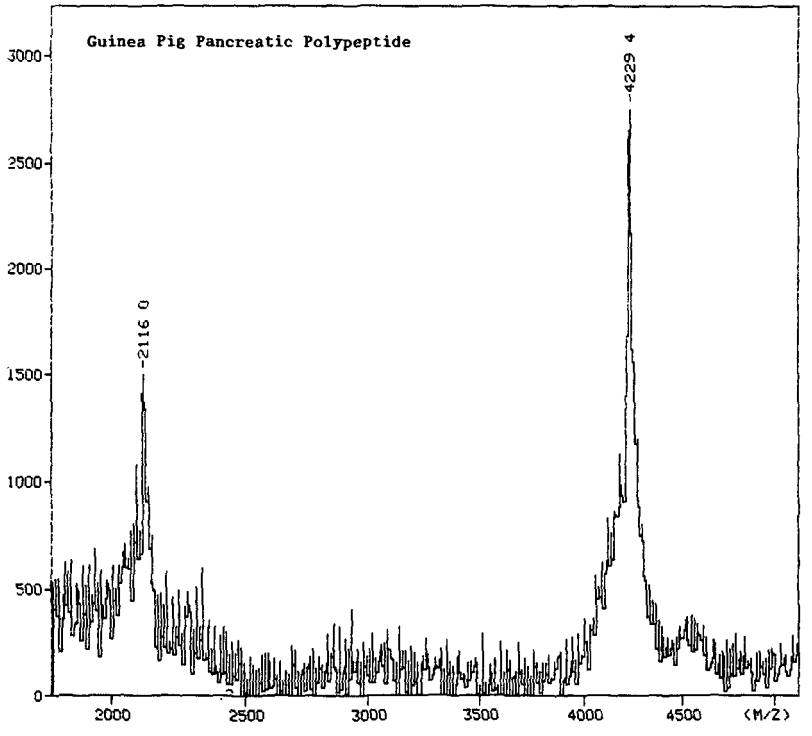

The molecular ion of guinea pig pancreatic polypeptide (PP) indicated that the pro-pancreatic polypeptide despite a substitution in its dibasic processing site, is cleaved to release the mature PP and the C-terminal glycine is removed enzymatically to yield a carboxyamidated peptide. The expected mass of the PP oxidized at the Met residue was calculated to be: 4231.

Presented at the 36th ASMS Conference on Mass Spectrometry and Allied Topics
June 5-10, 1988, San Francisco, CA

STRUCTURAL FINGERPRINTING OF ASN-LINKED CARBOHYDRATES AT SPECIFIC ATTACHMENT SITES IN GLYCOPROTEINS BY MASS SPECTROMETRY, S.A. Carr, G D Roberts, A. Jurewicz, B. Frederick and M. Vettese, Smith Kline and French Laboratories, King of Prussia, PA 19406

Recently we developed a mass spectrometry-based strategy (referred to as carbohydrate mapping) for simultaneously defining the sites of attachment of Asn-linked oligosaccharides in glycoproteins and determining the extent of glycosylation at each site (1). We have now extended this strategy to provide composition (in terms of hexose, deoxyhexose, N-acetylhexosamine and sialic acid) and molecular heterogeneity for oligosaccharide chains from specific attachment sites in glycoproteins (2,3). As in the the carbohydrate mapping strategy, the reduced and alkylated glycoprotein is first cleaved with proteases of known specificity such as trypsin. Approximately 10-20% of this protein digest is then treated with PNGase F to release all Asn-linked oligosaccharides. Potential glycopeptides are identified by comparing the RP-HPLC profiles of the digests obtained prior to and after digestion with the glycosidase. Peaks which disappear or are greatly attenuated in the chromatogram of the sample after digestion with the glycosidase are likely to be glycopeptides with carbohydrate linked to Asn Fractions containing these specific peaks are preparatively isolated from the tryptic digest and analyzed by FABMS to determine the molecular weights of peptides that have been co-purified with the glycopeptides. In favorable cases signals for the glycopeptides may be observed. Subsequently, the fractions are digested with PNGase F and re-analyzed by FABMS to identify the glycosylation-site peptide and its sequence location.

The HPLC-derived fractions consisting of mixtures of peptide and carbohydrate are subsequently peracetylated with acetic anhydride ($^1H_6$ or $^2H_6$) and pyridine, 1:1 (v/v) overnight. Aliquots of the peracetates are examined by FABMS Subsequently, the acetylated extracts are directly permethylated using potassium *tert*-butoxide in dimethyl sulfoxide and analyzed by FABMS. The resulting FAB mass spectra are dominated by $(M+H)^+$ and $(M+H\text{-}MeOH)^+$ peaks for each of the parent oligosaccharides present in the fraction which provide composition in terms of hexose, deoxyhexose, N-acetylhexosamine, and sialic acid. In addition, the relative ratios of these peaks indicate the relative abundances of the various carbohydrate homologs present in the mixture Following analysis by FABMS the permethylated carbohydrate fractions are converted to the partially methylated alditol acetates and analyzed by GC and GCMS for determination of linkage. Carbohydrate structural classes for oligosaccharides at specific attachment sites in the glycoprotein can then be proposed by combining the FABMS and methylation analysis data.

We have applied this strategy in our structural studies of the carbohydrate chains of recombinant tissue plasminogen activator glycoprotein expressed in a variety of mammalian and insect expression systems (3). For example, several potential glycopeptide-containing fractions were obtained from a tryptic digest of ca 10 nanomoles of reduced and carboxymethylated protein (expressed in Chinese hamster ovary cells) by comparative HPLC mapping as described above. Aliquots of each fraction were analyzed by FABMS, but signals readily assignable as glycopeptides were not observed for reasons previously discussed. The remainder of each of these fractions was then digested with PNGase F and analyzed by FABMS For example, Figure 1 compares the FAB mass spectra of fraction 35 from this digest prior to and after digestion with the glycosidase Two new $(M+H)^+_{ave}$ signals were observed in this fraction at m/z 3020 and 2459 that were not present in the FAB mass spectrum of this fraction prior to digestion with glycosidase (Fig. 1, bottom). These masses correspond uniquely to the predicted $(M+H)^+$ for the tryptic peptides Gly_{102}-Arg_{129} and Gly_{102}-Lys_{124} in which Asn_{117} (in the consensus sequence) has been converted to Asp following release of carbohydrate (1-3).

The released carbohydrates in these fractions were detected following peracetylation, extraction and permethylation. The FAB mass spectrum of the derivatized carbohydrate from Asn_{117} (located in HPLC fraction 35, see above) exhibits four clusters of peaks at m/z 1525, 1730, 1934 and 2138 that correspond to $(M+H\text{-}MeOH)^+$ for $(Hex)_n(HexNAc)_2$, where n = 5, 6, 7 and 8, respectively. Methylation analysis of this fraction indicated the presence of 1→2, 1→3, 1→6 and 1→4 linked mannose, but no galactose. These data indicate that the carbohydrate at Asn_{117} in tPA has a high mannose structure The relative ratios of the $(M+H\text{-}MeOH)^+$ peaks in the FABMS data indicate that approximately 45% is Man_5, 40% Man_6, 10% Man_7 and less than 5% Man_8

The carbohydrates attached to Asn_{448} were characterized in a similar manner. FABMS of the peracetylated and permethylated HPLC-fraction shown to contain the glycosylated Asn_{448} site (Fig. 2) yielded five major clusters of peaks at m/z 2584.7, 2947.1, 3396.2, 3757.9 and 4207.5 corresponding to the $(M+H)^+$ for $NANA_m(HexHexNAc)_nHex_3HexNAc_2DeoxyHex$, where m = 1-3, n = 2-4 and NANA represents N-acetylneuraminic acid (Fig. 3). A very weak peak is also observed at m/z 4568.9 which corresponds to m = 4, n=4. The gaps of 449.5 and 361.4 Da between the clusters correspond to the incremental masses for a permethylated lactosamine unit and permethylated N-acetylneuraminic acid, respectively. These data reveal that Asn_{448} has a complex sugar attached that is monofucosylated and has from 1 to 4 NANA units. The relationship of the number of NANA units to HexHexNac units strongly suggests that the carbohydrate attached to Asn_{448} in tPA is is a mixture of bi-, tri- and tetraantennary chains Although the patterns and molecular weights obtained by FAB do not enable one to unambiguously make this distinction, methylation analysis studies of this fraction supports the presence of bi-, tri- and tetraantennary chains, with triantennary dominating

1 S.A. Carr, and G.D. Roberts, Anal. Biochem. **157**: 396-406 (1986).
2 S.A. Carr, M.E. Hemling, and G D Roberts, Macromolecular Sequencing and Synthesis: Selected Methods and Applications, (D.H. Schlessinger, ed.), Alan R. Liss, Inc., New York, pp 83-99. (1988).
3. S.A. Carr, G.D. Roberts, A Jurewicz, and B. Frederick, Biochemie, in press (1988).

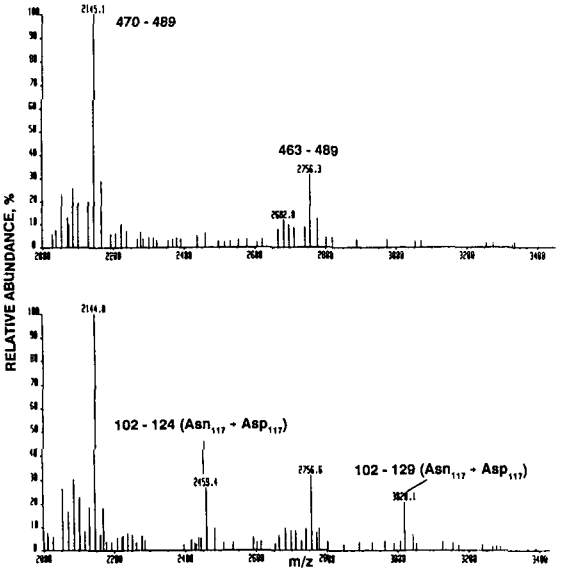

Figure 1. Partial FAB mass spectrum of a glycopeptide HPLC fraction prior to (top) and following (bottom) digestion with PNGase F (see text).

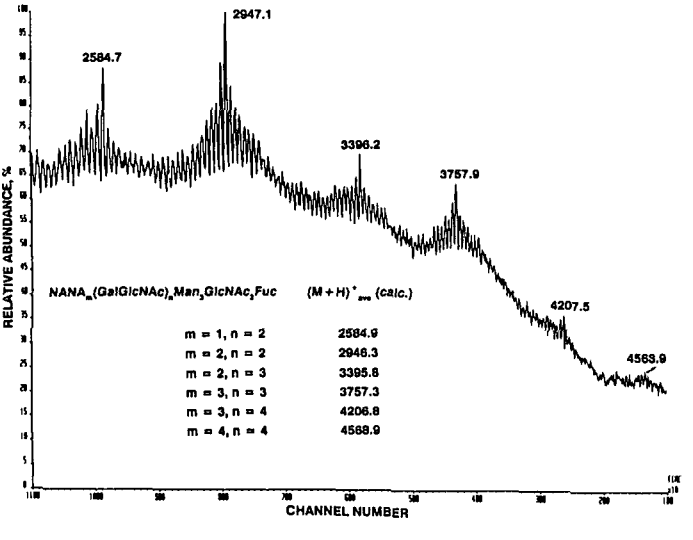

Figure 2. FAB mass spectrum of the peracetylated, extracted and permethylated carbohydrate released from the glycopeptide fraction identified as containing glycosylated Asn_{448} (see text).

Presented at the 36th ASMS Conference on Mass Spectrometry and Allied Topics
June 5-10, 1988, San Francisco, CA

STRUCTURAL ANALYSIS OF INTERLEUKIN-1α AND INTERLEUKIN-1β BY MASS SPECTROMETRY

G. D. Roberts, S. A. Carr, C. A. Meyers, K. O. Johanson, L. M. Miles
Smith Kline and French Laboratories, King of Prussia, PA 19406
and B. N. Green, VG Analytical, Ltd., Manchester, UK

The interleukin-1 (IL-1) family of proteins plays a crucial role in the pathogenesis of many human diseases, functioning as a key mediator in the response of the host to various infectious, inflammatory, and immunologic challenges. This array of activities resides in two distantly related proteins, IL-1β and IL-1α with molecular masses of 17 to 18 kDa. The recent availability of large amounts of recombinant protein will permit extensive structural studies to be undertaken and help to clarify the diverse functions of IL-1 proteins. Fast and reliable analytical procedures are needed to verify structures that have been determined by sequencing of the gene and to identify posttranslational modifications that may be present. FABMS and tandem MS can fill this niche and are especially useful in the structural studies of rationally mutated forms of proteins. We have characterized the primary structures of recombinant IL-1α and IL-1β produced by recombinant methods by direct molecular mass measurements on the intact proteins by FABMS and by FABMS peptide mapping.

Direct mass measurements were performed at VG Analytical, Ltd. using a high voltage (35 kV) CsI FAB gun (B. N. Green, 1987). For IL-1β the mean of five measurements was 17,365.7 +/- 15 Da (expected MH^+_{ave} is 17377.0). The error is -11.3 Da, or 0.06% of expected. For IL-1α the mean of five measurements was 18,026.0 +/- 39.2 Da (expected MH^+_{ave} is 18,048.6). The error is -22.4 Da or about 0.1% of expected. Unfortunately direct MW determination of proteins by MS often lacks sufficient sensitivity and mass measurement accuracy to detect structural variants that may be present at low, but significant levels.

To circumvent these problems limited cleavage strategies employing Asp-N and CNBr were used to obtain large proteolytic fragments (MW ≤ 10,000) that could be detected and mass measured with greater sensitivity and accuracy. Using this approach we obtained 100% sequence coverage of IL-1α with CNBr (Fig.1). Analyses employing CNBr and Asp-N gave less overall coverage of the protein, but provided valuable information on the COOH-terminus and on the site of deamidation (see below). A complementary set of fragments was also obtained by trypsin digestion of CNBr cleaved IL-1α. Complete coverage of the carboxyl-terminus of the protein was not achieved until the protein was reduced and alkylated (see below) The combined FAB mass spectral data from the trypsin and Asp-N digests of carboxamidomethylated and CNBr treated IL-1α cover 97% of the molecule (Fig.1).

The carboxyl-terminal sequence of IL-1α could not be confirmed by conventional approaches because it was completely resistant to digestion with carboxypeptidases. Consequently, digests using other proteolytic enzymes were considered and performed. For example residues 151-159 were shown to be present by the signals at m/z 1077.7 in the FAB mass spectrum of a CNBr/Asp-N digest, while residues 153-159 were confirmed by a strong signal at m/z 815.3 in the FAB mass spectrum of a CNBr/trypsin/chymotrypsin digest. Interestingly, the FAB mass spectra of a CNBr/trypsin digest failed to show the expected tryptic peptide consisting of residues 136-159; similarly, residues 137-150 were not detected in the CNBr/Asp-N digest. However, the expected signals were detected in proteolytic digests of carboxamidomethylated IL-1α (for example, see m/z 2723.5, residues 136-159 in Fig. 1). These observations suggest that the presence of free sulfhydryl groups in a protein that is subjected to CNBr treatment or proteolysis may produce erroneous results and, therefore, when working with cysteine containing compounds, reduction (if necessary) and alkylation is desirable.

An isoform of IL-1α, present at 3% of the level of the expected protein, was isolated by isoelectric focusing and subsequently analyzed by FABMS. The FAB mass spectra of IL-1α and IL-1α isoform were compared. In the spectrum of IL-1α residues 35-53 were indicated by a peak at m/z 2057.7, while this peak in the spectrum of IL-1α isoform was shifted upward one mass unit to m/z 2058.6, suggesting that an amide had been converted to the corresponding acid in this part of the protein. Similarly, the MH^+ peak, m/z 1445.2, for residues 36-48 was found to be shifted upward in mass by one mass unit in the FAB mass spectrum of a CNBr/Asp-N digest of the isoform compared to that of the native material (Fig. 1). Cleavage between residues Ala_{35} and Asn_{36} by the enzyme Asp-N strongly suggests that Asn_{36} has been converted to Asp_{36} in the isoform, which is also consistent with the observed mass shifts To unambiguously establish that Asn_{36} (versus Gln_{38} or Asn_{47}) had deamidated, the peptide of MH^+ 2058.6 from the CNBr/trypsin digest of the isoform was mass selected from the complex mixture (without chromatographic isolation or purification) and analyzed by tandem MS on a VG ZAB SE-4F. A series of amino-terminal B fragments (....NH-CHR_n-CO^+, n = residue number) were obtained that, beginning at the B ion corresponding to cleavage after residue three in this peptide, were shifted upward in mass by one mass unit, establishing that residue 36 is an Asp rather than an Asn, and that residues 38 and 47 have the in-chain masses for Gln and Asn, respectively.

IL-1β was studied less extensively than IL-1α. Signals observed in the FAB mass spectrum of a tryptic digest of reduced and carboxymethylated IL-1β account for 150 of the 153 residues in the protein (98% coverage).

In conclusion, we have shown that FABMS and tandem MS when used together are fast and reliable analytical procedures for verifying the entire amino acid sequences of small proteins and establishing the presence and nature of blocking groups and other posttranslational modifications that may be present.

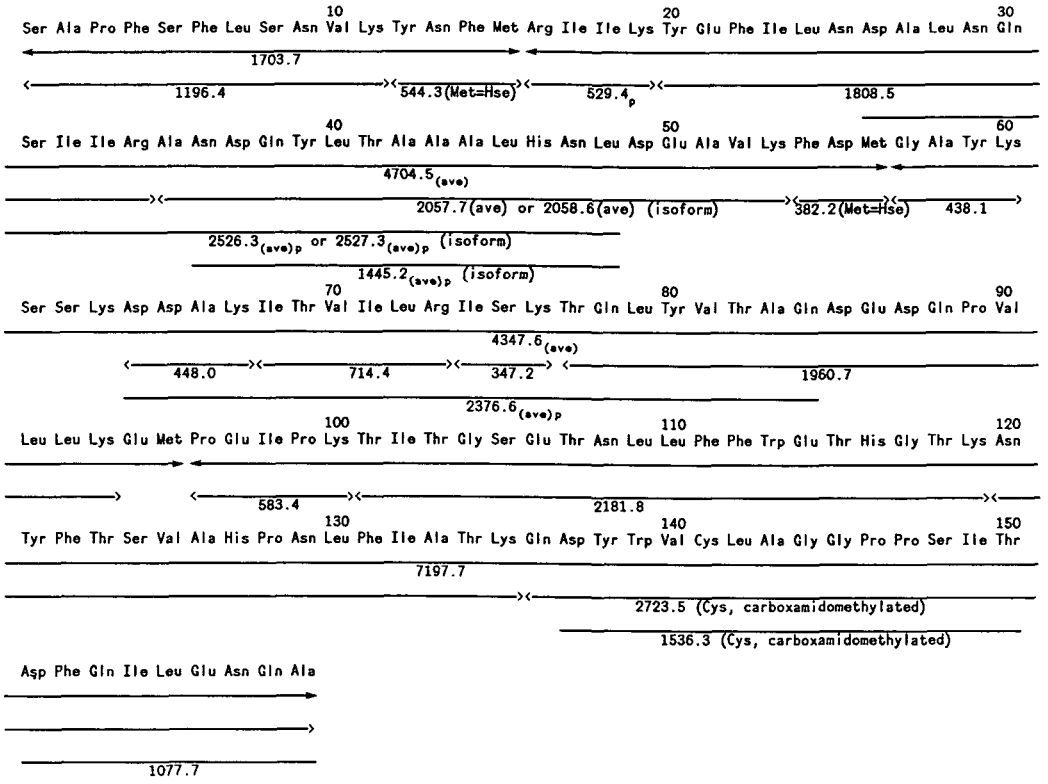

Figure 1. Amino acid sequence of IL-1α and IL-1α isoform indicating the peptides identified by FABMS of a CNBr digest (◄——►), a CNBr/trypsin digest (<——>) and a CNBr/Asp-N digest (——) of the two proteins. Peptides arising by incomplete cleavages are denoted with the subscript p. In cases where overlapping or redundant peptides were observed from the same or from different digests of the proteins, only the largest peptide signals are shown for clarity.

Presented at the 36th ASMS Conference on Mass Spectrometry and Allied Topics
June 5-10, 1988, San Francisco, CA

COMPLEMENTARY APPROACHES TO COMPUTER ASSISTED SEQUENCING OF PEPTIDES FROM FAB MS/MS DATA:

A.J. ALEXANDER, G. ANDERSON, R.K. BOYD,
P. THIBAULT* AND M.J. BERTRAND**

National Research Council, Halifax, Nova Scotia, Canada B3H 3Z1
(*6100 Royalmount Ave. Montreal, Québec, Canada H4P 2R2)
(** Chemistry Dept. University of Montreal, Montreal, Québec
Canada, H3C 3J7)

The elucidation of the primary structure of polypeptides from their FAB mass spectra is a challenging task which would be rather tedious without using computer-assisted strategies. Numerous approaches (1-5) were developed to rationalize the information content of these complex spectra and to reconstruct the peptide molecular structure from it. Unambigious deduction of the amino acid sequence from a FAB spectrum has nonetheless proved to be difficult even for peptides of moderate size (M<2000 Da). Although the information relating to the primary peptide structure can be extracted from the conventional mass spectrum, tandem mass spectrometry (MS/MS) offers considerable advantages when the analyte signal is likely to be suppressed by either matrix ions, salt adducts or impurities. The present work investigates the utility of using MS/MS (Tandem hybrid, BEqQ configuration) in conjunction with two different strategies to characterize the amino acid sequence of small peptides.

The first strategy ("brute force" approach) is an improved version of the program developed by Hamm et al. (2) which generates all possible sequences from a given composition using an efficient recursive procedure. All possible sequences are then compared in turn with the experimentally observed spectrum, using only the number of matches of fragment masses as a selection criteria.

The other strategy ("sequential" approach) generates first the potential peptide composition from the mass measurement, relative isotopic cluster peak intensities and diagnostic ions for the amino acid content (the composition found in this step can be submitted to sequence analysis via the first strategy). From each composition, sequences are generated by subtracting repetitively the masses of five fragments that correspond to 5 fragmentation schemes known for peptides (B,Y",Z",C" A(7)). Whenever a match is found, the intensity of the ion is used as a subscore. During the generation of sequences the averaged intensity for all fragment ions found is calculated, then multiplied by a weighting factor accounting for the number of consecutive sequence ions for a given scheme. Finally sequences with the ten highest scores are retained.

For polypeptides of M<800 Da, the degeneracy of peptidic empirical formulae will be small with respect to the given input provided that some amino acids can be identified to restrict the number of solutions. In fact one can use some approximation on the mass of the compound instead of measuring the exact mass and isotopic abundances in order to generate a list of peptidic empirical formulae. This approximation is possible since any peptide mass will lie between two extremes described by polyleucine and polycysteine, which represent respectively the highest and lowest mass sufficiency for a given nominal mass. Application of this approach for 6 small linear peptides ranging from 555 to 740 Da is shown in Table 1. Only a limited number of peptide empirical formulae and compositions can be generated under these boundaries. However, as the mass of the peptide increases it is crucial to identify as many amino acids as possible since the degeneracy of empirical formulae becomes important. The two most probable peptide

NRCC No. 29080

sequences generated using the two approaches described earlier are reported in Table 2. As can be seen from these results, both approaches were fairly successful in assigning the true sequence. The high number of matches and scores obtained from these potential sequences reflects the validity of the predicted fragmentation schemes and the wealth of information obtainable from the daughter ion spectrum. Similar analyses were conducted on peptides of higher mass. A mass tolerance of 15 p.p.m. from the exact mass was used in the "sequential" approach, whereas the exact amino acid composition was given in the "brute force" approach. The results obtained are presented in Table 3. These results show that for each peptide either the correct or a closely related sequence was generated in both approaches. In this case the number of mismatches is not related to limitations in the computer algorithms but is a direct reflection of the quality of the MS/MS data.

The main limitations are: [1] Degeneracy of sequences containing lysine (K) or glutamine (N), [2] In cases where many compositions are possible matching of only the masses might not provide enough discrimination among possible solutions, [3] The difficulty of experimentally fragmenting higher mass peptides M>800 Da by low collision energy CID processes is reflected by the low number of matches and scores.

(1) Ishikawa K., Niwa Y. Biomed. Mass Spectrom. 13,373 (1986)
(2) Hamm C.W., Wilson W.E., Harvan D.J. Comput. Appl. BioSci. 2,115 (1986)
(3) Siegel M.M., Bauman N. Biomed. Env. Mass Spectrom. 15,333 (1988)
(4) Scoble H.A., Biller J.E., Biemann K. Fres. Z. Anal Chem. 327,239 (1987)
(5) Bertrand M.J., Thibault P., Evans M.J., Zidarov D. Biomed. Env. Mass Spectrom. 13,347 (1986)
(6) Matsuo, T., Matsuda H., Katakuse I. Biomed. Mass Spectrom 8,137 (1981)
(7) Roepstorff P., Fohlman J. Biomed. Mass Spectrom 11,601 (1984)

TABLE 1

LIST OF PEPTIDIC EMPIRICAL FORMULAE AND COMPOSITIONS GENERATED WITH MASS APPROXIMATION AND DIAGNOSTIC IONS

COMPOUNDS		COOH		CONH2	
		EMP FORM	COMP	EMP FORM	COMP
YGGFL-OH	M 555	1	2	1	1
FFGLM-NH2	M 612	0	0	2	2
YGGFLK-OH	M 683	1	2	0	0
KFLGLM-NH2	M 706	1	2	0	0
YGGFLR-OH	M 711	1	2	1	1
MFFGLM-NH2	M 740	10	17	5	14

Underlined elements indicate the amino acids identified from their diagnostic ions (immonium or else) present in the MS/MS spectra

TABLE 2

LIST OF COMPLETE SEQUENCES GENERATED BY TWO DIFFERENT APPROACHES USING THE SELECTED COMPOSITIONS FROM TABLE 1

COMPOUNDS		MASS AND INTENSITIES SELECTION (SCORE)	MASS SELECTION ONLY (# OF HITS)
YGGFL-OH	M 555	YGGFL-OH (5166) YMFL-OH (4794)	YGGFL-OH (10) YDLF-NH2 (8)
FFGLM-NH2	M 612	FFGLM-OH (9265) CFLYM-NH2 (7102)	CYLFM-NH2 (20) CYFLM-NH2 (18)
YGGFLK-OH	M 683	YMFLK-OH (7163) YGGFLK-OH (6753)	YGGFLK-OH (15) YMFLK-OH (12)
KFLGLM-NH2	M 706	KFLGLM-NH2 (1312) KFGLLM-NH2 (1156)	KFLAVM-NH2 (21) KFALVM-NH2 (21)
YGGFLR-OH	M 711	YMFLR-OH (3290) YGGFLR-OH (2982)	YGGFLR-OH (17) YMFLR-OH (14)
MFFGLM-NH2	M 740	MFFGLM-NH2 (8018) KFFGLM-NH2 (6918)	KFFGLM-NH2 (20) GYGFGLM-NH2 (10)

UNDERLINED AMINO ACIDS CORRESPOND TO SEGMENTS OF REEL SEQUENCES

TABLE 3

LIST OF COMPLETE SEQUENCES GENERATED BY TWO DIFFERENT APPROACHES FOR POLYPEPTIDES OF MORE THAN 7 RESIDUES

COMPOUNDS		MASS AND INTENSITIES SELECTION (SCORE)	MASS SELECTION ONLY (# OF HITS)
YGGFLRR-OH	M 867	RLGFGRY-OH (125) RLFGGRY-OH (114)	YGGFLRR-OH (14) GYGFLRR-OH (13)
RPPGFSPL-OH	M: 869	RPPGFSLP-OH (1563) RPPGFSPL-OH (1538)	RPPGFSPL-OH (46) RPPGFSLP-OH (43)
YGGFLRRL-OH	M: 980	YGFGLRLR-OH (1288) YGFGLRRL-OH (1140)	FGLGYRLR-OH (18) FGYGLLRR-OH (18)
YGGFLRRLR-OH	M. 1136	YGFGLRRLR-OH (322) GYFGLRRLR-OH (322)	YGFGLRRLR-OH (24) FGYGLRRLR-OH (23)

Presented at the 36th ASMS Conference on Mass Spectrometry and Allied Topics
June 5-10, 1988, San Francisco, CA

DIGIT PRINTING OF PROTEIN VARIANTS

Hayashi,A.[*1], Wada,Y.[*1], Matsuo,T.[*2], Katakuse,I.[*3], Matsuda,H.[*2]
*1, Osaka Medical Center & Research Institute for Maternal & Child Health
*2, Institute of Physics, College of General Education, Osaka University
*3, Department of Physics, Faculty of Science, Osaka University (JAPAN)

An ultramicro method using secondary ion (SI) mass spectrometry was developed for the structural analysis of protein variants. This method is based on the mass spectrometric detection of the change in molecular weight which is accompanied by amino acid substitution of protein variants, and provides digitalized data on peptide analysis. Since the feature of this method may be comparable with the conventional "Finger Printing", we called it "Digit Printing".

Procedure: Purified and S-aminoethylated proteins were digested with trypsin, directly or after cleavage with cyanogen bromide, and a peptide mixture was examined with mass spectrometer without further purification. In addition to trypsin digestion, lysine endopeptidase, staphylococcal V8 protease, glycinamidation or Edman degradation were used for the modification of proteins. Mass spectra were obtained with a Matsuda-type mass spectrometer with SI mass spectrometric ion source and the data were analized with JMA-2,000 data analysis system on line.

Preliminary Experiment: A study, performed on 4 kinds of normal globin chains (α, β, γ and δ) and several hemoglobin variants whose structural abnormality was already known, proved the accuracy, reliability and reproducibility of this method.

Application to Hemoglobin Variants: As an example, the result on Hb A_2 Honai was shown in this figure. Compared with mass spectra from normal δ(a) and abnormal δ(b), the peak T10 at m/z 1,507 was missing and a new peak at m/z 1,477 appeared in b, showing a shift of 30 mass unit. From this result and the electrophoretic properties of this variant, it was concluded that glycine residue at 69th position was replaced by arginine in the abnormal δ chain of Hb A_2 Honai. The results of structural analyses were summarized in the table.

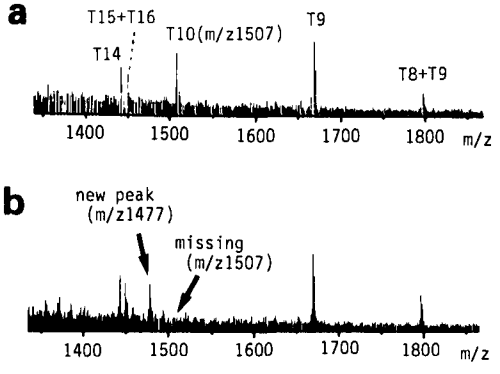

	83	90	95
δT10 (m/z1507)	Gly-Thr- -	- -Ser-Glu-Leu-His-Cys-Asp-Lys	
(m/z1477)	Gly-Thr- -	- -Ser-Val-Leu-His-Cys-Asp-Lys	

Mass Spectra of Hb A_2 Honai: δ 90 Glu → Val

Presented at the 36th ASMS Conference on Mass Spectrometry and Allied Topics
June 5-10, 1988, San Francisco, CA

Structure of Hemoglobin Variants
Determined with Digit Printing

Name of Variant	Structural Abnormality	Cases Examined	New Variant or not
Hb Meilahty	β 36 Pro → Thr	1	new
Hb F Izumi*	$^{A}\gamma$ 6 Glu → Gly	1	new
Hb F Fuchu*	$^{G}\gamma$ 21 Glu → Gln	4	new
Hb F Minoo*	$^{G}\gamma$ 72 Gly → Arg	1	new
Hb A_2 Honai	δ 90 Glu → Val	1	new
Hb Shimonoseki	α 54 Gln → Arg	1	reported
Hb Ube II	α 68 Asn → Asp	2	reported
Hb Hikari	β 61 Lys → Asn	1	reported
Hb Providence	β 82 Lys → Asn,Asp	1	reported
Hb Riadh	β 120 Lys → Asn	1	reported
Hb F Iwata*	$^{A}\gamma$ 72 Gly → Arg	2	reported
Hb F Yamaguchi*	$^{A}\gamma^{T}$ 80 Asp → Asn	40	reported
Hb A_2 Indonesia	δ 69 Gly → Arg	1	reported
Synthetic Variant	α 42 Tyr → Phe	1	
Synthetic Variant	α 42 Tyr → His	1	

* These variants were detected by neonatal mass screening in Osaka Prefecture, Japan.

The structure of 13 natural and 2 synthetic hemoglobin variants were determined or confirmed with this method. Among them, 5 new variants included. All γ chain variants were detected by neonatal mass screening and their structural analysis was performed using dried blood on filter paper.

Application to Other Protein Variants: The method was used for the structural analysis of a prealbumin variant extracted from the plasma of a patient with familial amyloidotic polyneuropathy. The result was identical with the one obtained by the conventional method with valine replaced by methionine residue at 30th position. Further, it was successfully applied to the accurate assignment of amide residues in mammalian calmodulin molecule.

Conclusion

(1) The reliability of Digit Printing was confirmed on various kinds of human hemoglobin variants with known structural abnormality which included electrophoretically and chromatographically silent mutations.

(2) This technique was successfully applied to the structural analysis of human hemoglobin and other protein variants, including several new variants.

(3) In spite of its limit in detecting leucine ≠ isoleucine substitution, this technique showed several advantages over conventional method: very high sensitivity, easy and speedy operation, and accurate detection of abnormal peptide.

Presented at the 36th ASMS Conference on Mass Spectrometry and Allied Topics
June 5-10, 1988, San Francisco, CA

ANALYSIS OF PHENYLALANINE LIBERATED UPON HYDROLYSIS OF THERAPEUTIC PEPTIDES USING CAPILLARY COLUMN GC/NCIMS. D.J. Liberato, E.P. Heimer E.K. Fukuda, M. Ahmad and W.A. Garland, Departments of Drug Metabolism and Peptide Research, Hoffmann-La Roche Inc., Nutley, New Jersey 07110

The requirement for sensitive and selective bioanalytical methods has increased in proportion to the desire for a better understanding of biological processes at the molecular level. In particular, the continued growth in the use of peptides and proteins in biomedical and clinical research has generated an increased need to develop alternative techniques for the quantification of peptides and proteins at low concentrations. Great progress has been made in the sensitive determination of peptides and proteins in biological samples utilizing both immunoassay and bioassay techniques. However, it is recognized that these techniques are not always precise (no reference standard) or specific. The studies detailed here are an exploration of the utility of quantifying Growth Hormone Releasing Factor by GC/NCIMS analysis of phenylalanine (Phe) liberated after hydrolysis of GRF samples that contain stable isotope labelled ($^{13}C_6$-Phe^6)-GRF as the reference.

The most sensitive analytical techniques for the analysis of phenylalanine (Phe) all involve the derivatization of the amine to form an amide, followed by further derivatization of the carboxylic acid to form an electronegative ester. In the studies reported here, the carboxyl group was converted to a pentafluorobenzyl (PFB) derivative and the amine group was acetylated. Table I summarizes results from experiments undertaken to optimize the GC/NCIMS sensitivity of PFB-Phe by comparing the following N-acyl derivatives: acetyl, trifluoroacetyl, pentafluoropropionyl and heptafluorobutyryl (HFB). All derivatives gave spectra characterized by $[M-PFB]^-$ ions. The derivative that gave the greatest ionization efficiency was PFB-HFB-Phe; its NCI mass spectrum is shown in Figure 1.

Figure 2 illustrates using [Ring U-$^{13}C_6$] - Phenylalanine that the GC/NCIMS technique is very sensitive. However, although 1 pg of this stable isotope labelled material injected on column yields a good signal at m/z 366, the data illustrated in Figure 3 demonstrate that there is significant background contamination. The chromatogram in Figure 3 was obtained from an experiment in which 1 ng of $^{13}C_6$-Phe was added per tube prior to derivatization, as the reference standard. In experiments over 4 weeks (N=18 tubes) the mean contamination was found to be 0.8 ng/tube (CV=89%). Experiments to determine if the source of this background contamination was from the solvents or reagents involved separately lyophilizing 10 times the amount used in our procedure into tubes that also contained 1 ng of $^{13}C_6$-Phe as reference. These studies undertaken in duplicate found no increased background.

To determine the feasibility of the quantitative analysis of GRF (1-44)-NH_2, mixtures of GRF and ($^{13}C_6$-Phe^6)-GRF were hydrolyzed, derivatized and subjected to GC/NCIMS. Injections of duplicate samples were made on the GC/MS system and quantitative analysis was carried out by isotope dilution and selected ion monitoring, using the ratio of $[M-PFB]^-$ ions from PFB-HFB-Phe(m/z 360) and PFB-HFB-$^{13}C_6$-Phe(m/z 366). A typical calibration curve for GRF, generated using a stable isotope labelled reference standard, is shown in Figure 4. It is linear over the range 240ng-8µg. Background contamination prevented analysis below approximately 100 ng.

The detection limit for derivatized $^{13}C_6$-Phe was on the order of 100fg-1pg, indicating that the quantification for a peptide of molecular weight 5,000 containing one phenylalanine should be in the range of 10-100pg. However, because of background amino acid contamination of unknown origin, quanatification at these levels is not practical, We are currently attempting to improve the technique for the 1 ng range. In addition, we are also in the process of applying the technique utilizing a peptide that contains a non-naturally occurring amino acid that should not suffer from background interference.

Presented at the 36th ASMS Conference on Mass Spectrometry and Allied Topics
June 5-10, 1988, San Francisco, CA

COMPARISON OF DERIVATIVES

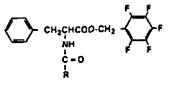

R	RELATIVE INTENSITY $(M-PFB)^-$
CH_3-	0.001
CF_3-	0.001
CF_3-CF_2-	0.16
$CF_3-CF_2-CF_2-$	1.0

TABLE I. COMPARISION OF DERIVATIVES

METHANE NCI MASS SPECTRUM

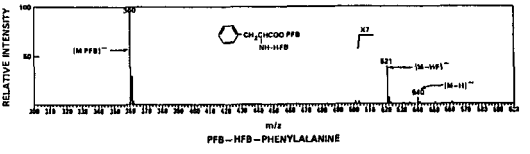

FIGURE 1. NCI MASS SPECTRUM OF PFB-HFB-PHE.

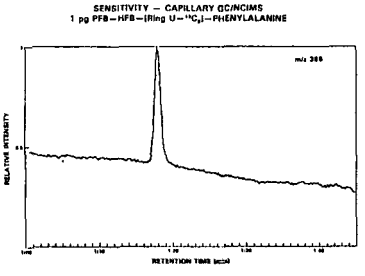

FIGURE 2. SELECTED ION CURRENT PROFILE FROM GC/NCIMS ANALYSIS OF 1 PG $^{13}C_6$-PHE

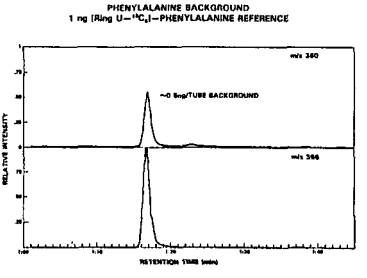

FIGURE 3. SELECTED ION CURRENT PROFILE FROM GC/NCIMS ANALYSIS OF BACKGROUND CONTAMINATION BY PHE USING 1 NG $^{13}C_6$-PHE AS REFERENCE

AMINO ACID SEQUENCE
OF HUMAN PANCREATIC GROWTH
HORMONE-RELEASING FACTOR

Tyr-Ala-Asp-Ala-Ile-Phe-Thr-Asn-Ser-
Tyr-Arg-Lys-Val-Leu-Gly-Gln-Leu-Ser-
Ala-Arg-Lys-Leu-Leu-Gln-Asp-Ile-Met-
Ser-Arg-Gln-Gln-Gly-Glu-Ser-Asn-Gln-
Glu-Arg-Gly-Ala-Arg-Ala-Arg-Leu-NH_2

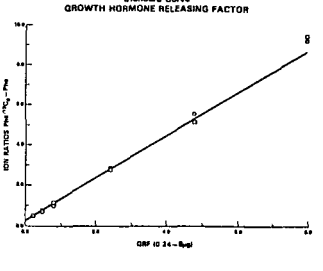

FIGURE 4. CALIBRATION CURVE FOR ISOTOPE DILUTION ASSAY OF GROWTH HORMONE RELEASING FACTOR

Presented at the 36th ASMS Conference on Mass Spectrometry and Allied Topics
June 5-10, 1988, San Francisco, CA

Morphinans in Mammals

K.F.Faull, G.J.Feistner and C.J.Weitz, Departments of Psychiatry and Pharmacology, Stanford University School of Medicine, Stanford, Ca 94305.

The work of Davis and Walsh and others around 1970, which suggested the possibility of morphine biosynthesis in mammals, spawned an investigation for naturally occurring morphine in extracts of mammalian tissues and led to the detection by several groups of substances recognised by antisera raised against morphine. Dr. Avram Goldstein and colleagues at Stanford developed a sequential blank procedure to help in the identification of these compounds in tissue extracts. In the sequential-blank proceedure glassware, reagents and columns were sequestered exclusively for extractions. A tissue-less extraction was always performed with an appropriate volume of extraction solvent. This blank sample was carried through all steps of the purification. Each tissue extraction followed behind its own sequential blank in the same glassware and columns. Using this approach three peaks of immunoreactivity were repeatedly observed when extracts of brain and adrenal were chromatographed on reverse phase HPLC (Figure 1) in the absence of immunoreactivity in the corresponding sequential-blank extracts.

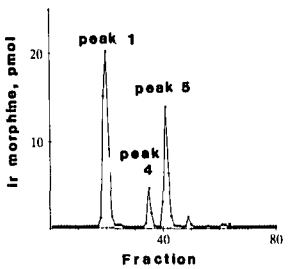

Figure 1. Typical HPLC profile of ir morphinans extracted from Bovine hypothalamus.

Sufficient quantities of these peaks were isolated for unequivocal structural identification by GC/MS. As a further precaution against false positive results, GC/MS experiments were conducted with GC columns naive to the morphinan(s) in question, and retention times and mass spectra of authentic compounds were obtained only after the biological sample had been analysed.

Using this approach two of the immunoreactive peaks in bovine brain were identified as the trifluoroacetyl (TFA) derivatives by GC/MS as morphine (peak 1) and codeine (peak 4) purified from ca. 1200 bovine hypothalami (wet wt. ca 20kg) [Weitz et al., PNAS 83; 9784-9788 (1986), and reported at the 35th ASMS meeting in 1987]. The identity of the third peak of immunoreactivity (peak 5) has recently been established as 6-acetylmorphine by GC/MS and GC/high resolution MS of the TFA derivative from material isolated from ca. 1750 bovine hypothalami (wet wt. ca 28kg) [Weitz et al., PNAS in press]. 6-Acetylmorphine has not been previously described as a natural product in plants or animals. It has long been known as the metabolite in part responsible for the biological properties of heroin (3,6-diacetylmorphine). However, we have excluded slaughterhouse or laboratory contamination by any morphinan as well as derivation from the morphine in tissues during our procedures. 6-Acetylmorphine is more potent than morphine in vivo chiefly by virtue of its greater penetration into the central nervous system, and we conclude that it is a normal constituent of mammalian brain.

In the opium poppy the pathway of morphine biosynthesis (Figure 2) has been elucidated by the incorportion of labelled precursors. Intramolecular coupling of reticuline to form salutaridine is the critical step that generates the morphinan skeleton and defines the stereochemistry of the series. The possibility of morphinan biosynthesis in mammals has been raised by our recent demonstration of the conversion in vivo and in vitro of reticuline to salutaridine by rat liver [Weitz et al., Nature 330:674-677(1987)]. In this work we identified the product synthesised from reticuline by tissues using GC/MS. This necessitated the development of a procedure for the analysis of salutaridine in quantities down to a few picomol.

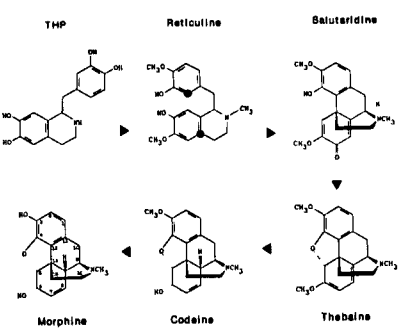

Figure 2. Biosynthetic pathway for morphine in the opium poppy, P. somniferum. THP (tetrahydropapaveroline) is derived from tyrosine and dopamine. The carbons marked by dots in reticuline participate in oxidative coupling to generate salutaridine.

Attempts to chromatograph underivatised salutaridine (free base) were unsuccessful, presumably because it decomposed during passage through the bonded-phase medium-polarity fused-silica capillary column. This result was obtained in spite of the fact that underivatised morphine and codeine (free bases) eluted with reasonable retention times and good peak shapes from the same column. Attempts to derivatise salutaridine on the hydroxyl function by treatment with silylating reagents and perfluoro-acid anhydrides were unsuccessful, presumably because of steric restrictions. However, salutaridine was successfully derivatised by treatment with O-[pentafluorobenzyl]hydroxylamine HCl in pyridine (75°C, 1 hr.). The resulting oxime derivative gave the expected EI mass spectrum, and under electron capture conditions had abundent high mass ions suitable for SIM (Figure 3).

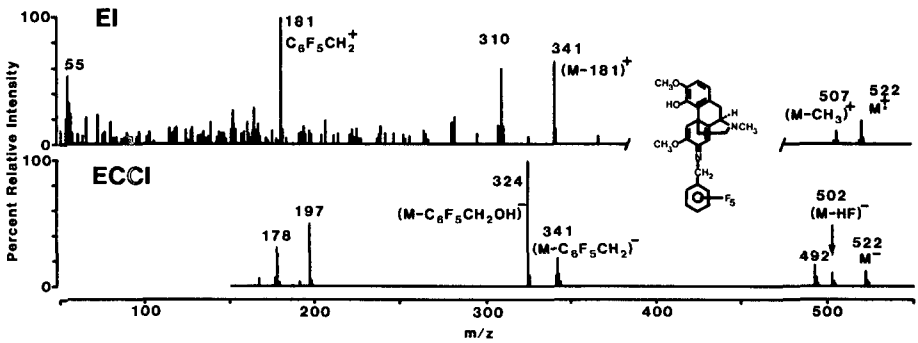

Figure 3. EI and electron capture negative ion mass spectra of the O-[pentafluorobenzyl]-hydroxylamine derivative of salutaridine. Presumed structures of some of the ions are indicated.

The sensitivity obtained for the molecular ion with this derivative under electron capture conditions exceeded that obtained under EI conditions by ca. 200-fold. At the 30 picomol level, under electron capture-SIM conditions, the 4 predominant ions (m/z 522,492,341,324) yielded intense peaks with signal/noise ratios between 23/1 and 33/1.

Analysis of the biosynthetic product obtained from in vitro incubations of reticuline with rat liver homogenate produced the results shown in Figure 4. The biosynthetic product and salutaridine standard produced specific ion currents with retention times and relative peak areas that were identical within experimental error. A pre-boiled control homogenate did not generate selected ion currents with the retention time of interest. The unusual features of the intra-molecular coupling necessary for the conversion of reticuline to salutaridine suggest that it is likely to be catalysed by a specific enzyme.

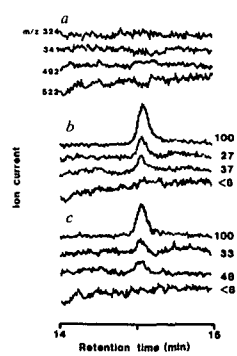

Figure 4. SIM chromatograms obtained under electron capture negative CI conditions for: a)pre-boiled control; b)putative salutaridine biosynthesis product; c)salutaridine standard.

The physiological significance of the naturally occuring morphinans found in mammalian brain is unclear: an essential element necessary for the demonstration of physiological significance would be evidence of control of tissue concentrations or turnover of morphine following experimental manipulation. Furthermore, a complete biosynthetic pathway for morphine in mammals has yet to be demonstrated: essential components of such a demonstration would be: 1)evidence of biosynthesis from putative precursors; 2)evidence for the presence of these biosynthetic precursors as normal constituents of mammalian tissues. Our future work in this area will be directed towards addressing the issue of the natural occurrence in mammals of the morphine biosynthetic precursors.

Presented at the 36th ASMS Conference on Mass Spectrometry and Allied Topics
June 5-10, 1988, San Francisco, CA

CHARACTERIZATION OF SYNTHETIC ADHESIVE DECAPEPTIDES BY FAB-MS AND HPLC-MS;

M.K.Gabriel, D.M.Hindenlang, R.D.Sedgwick, M.D.Swerdloff, and J.I.Williams
Corporate Technology Allied-Signal, Morristown, NJ 07960

Introduction. Natural protein glues are an important aspect of adhesion technology and the proteins responsible for the attachment of marine organisms to surfaces in the presence of water are especially interesting. Recent literature on polyhydroxy and phenolic proteins from intertidal mussels has focused attention of specific repeating decapeptide sequences. In order to further investigate structure activity relationships of these repeat units, a series of related decapeptide glues have been made by soild-phase synthetic techniques. The synthetic decapeptide products have been analyzed by Fast Atom Bombardment-MS and Thermospray HPLC-MS.

Experimental. Protected glue peptides were synthesized on PAM resin using modified Merrifield SPPS chemistries. All terminal amino groups were protected with t-butyloxycarbonyl with side chain amino groups in Lys protected with 2-chlorobenzyloxycarbonyl or triflyoroacetyl. Phenolic groups (Tyr) were protected with 2-bromobenzyloxycarbonyl while aliphatic alcohols in Ser, Thr and Hyp were protected with benzyl groups. The conventional cleavage and deprotectron step was modified to eliminate use of HF. We started with a detailed analysis of the complex reaction products from the modified cleavage/deprotection reactions. This was achieved by combinations of the following techniques. (1) Analytical scale HPLC with diode-array detection (HP 1090) followed by FAB-MS on the crude products using a VG Analytical ZAB-HF mass spectrometer; (2) Preparative scale HPLC (Spectra Physics 8100) followed by HPLC-MS (Varian 5020) using Thermospray ionization on a VG Mass Lab 30-250T Triple Quadrupole mass spectrometer. These techniques were used appropriately in a feedback loop to guide the development of more successful cleavage and deprotection steps.

Modified Cleavage and Deprotection. Initially the method of Yajima et al.* using trifluoromethane sulfonic acid (TFMSA) with trifluoroacetic acid (TFA) was tried. This led to very complex reaction mixtures which HPLC showed to contain as many as 20 components. FAB-MS showed that these components were in fact derivatives of the targeted glue decapeptide sequence. The components were butoxy, benzyloxy, chlorophenoxy and bromophenoxy derivatives of the peptide with combinations of up to any four of these radicals adding to the decapeptide at its phenolic and hydroxlyic amino acids. We conclude that the solid-state synthesis was efficient and that deprotection and cleavage from the resin was complete but that deprotection was followed by complex attack on the peptide by protecting-group radicals to form the observed derivatives. By this procedure we found the underivatized free peptide to be a minor product.

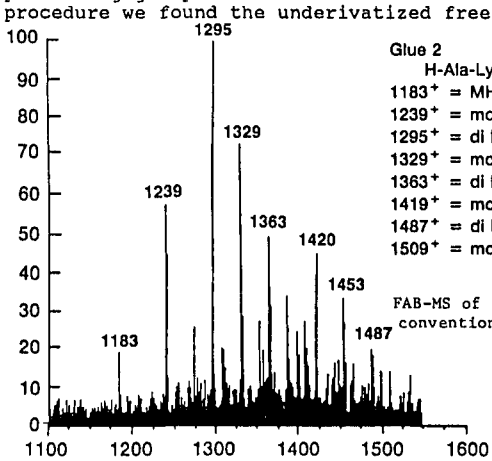

Glue 2
H-Ala-Lys-Pro-Ser-Tyr-Hyp-Hyp-Thr-Tyr-Lys-OH
1183^+ = MH^+
1239^+ = mono butyoxy Glue-2
1295^+ = di butoxy Glue-2
1329^+ = mono butoxy mono benzyloxy Glue-2
1363^+ = di benzyloxy Glue-2
1419^+ = mono butoxy di benzyloxy Glue-2
1487^+ = di benzyloxy mono clorobenzyl oxy Glue-2
1509^+ = mono butoxy tri benzyloxy Glue-2

FAB-MS of complex mixture from conventional synthesis of Glue-2

The one-step TFMSA/TFA cleavage and deprotection was abandoned in favor of a two-step deprotection and cleavage strategy. Both steps were monitored by HPLC and FAB-MS and the following procedures were shown to be effective. (a) Deprotection of the peptide on the PAM resin requires controlled addition of TFMSA to the resin in a m cresol:DMS:TFA mixture at 0°C. (b) Cleavage of the peptide from the resin requires reaction in a thioanisole: 1,2-ethanedithio:TFA mixture with controlled addition of TFA:TFMSA at 0°C. These procedures indicated the complete elumination of all derivatized peptide products. However, cleavage from the resin in acid solution always gave an HPLC trace showing two components. FAB-MS of this mixture showed a single molecular weight at the correct value for the targeted peptide. This was confirmed by on-line HPLC-Thermospray-MS which indicated that the two components were isomers. Preparative HPLC followed by FAB-MS showed the later eluting component to be the true peptide while the earlier eluting isomer was formed by replacement of a backbone peptide linkage by an ester involving the secondary alcohol in threonine. Thus for Glue-12 the true peptide shows an intense 804^+ due to Y_6'' and a weak 815^+ due to C_6''. The isomeric ester also shows 804^+ (Y_6'') but an intense 816^+ in which an amide has been replaced by an ester. Treatment of the isomeric ester with base (NH_4HCO_3) gave a clean sample of the true peptide.

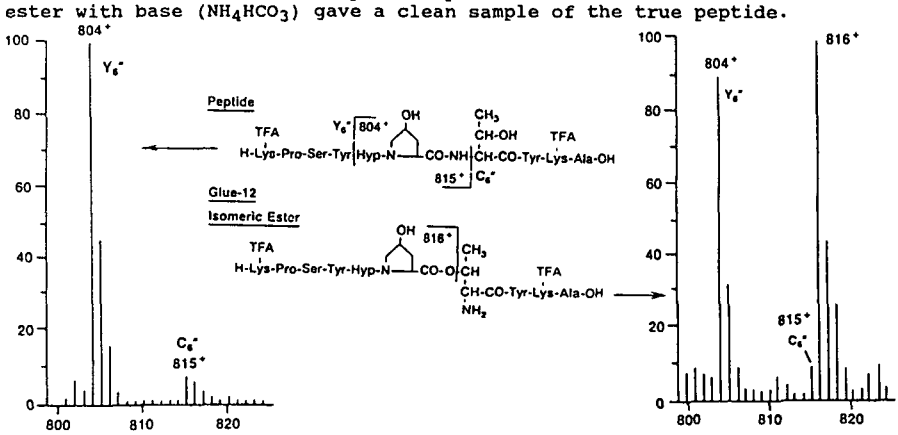

Using these methods we have synthesized a series of decapeptides and some larger analogues and confirmed their sequences by FAB-MS. In general the most intense fragments involve cleavages adjacent to Hyp or Pro giving ions of the type Y_n''. Fragments retaining the N terminus are less intense but frequently gave more complete sequence information. The series A_n was frequently complete for the decapeptides with abundant confirmatory evidence of the sequence coming from partial B_n and C_n'' series.

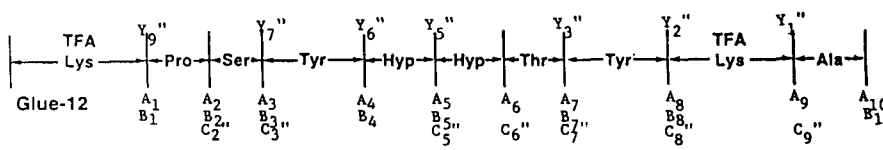

*H. Yajima, S. Funakoshi and K. Akaji, Int. J. Peptide Prot. Res., 26, 336.

Acknowledgement: This work was supported by The Office of Naval Research.

Presented at the 36th ASMS Conference on Mass Spectrometry and Allied Topics
June 5-10, 1988, San Francisco, CA

STRUCTURAL CHARACTERIZATION OF TWO FORMS OF CELLULAR RETINOL BINDING PROTEIN, TYPE II USING A COMBINATION OF FAB AND EI MASS SPECTROMETRY AND EDMAN CHEMISTRY:

W.H. Schaefer*, D.E. Ong, B. Kakkad, and I.A. Blair,
Departments of Biochemistry and Pharmacology, Vanderbilt University, Nashville, TN 37232. and *present address: Department of Drug Metabolism, SmithKline and French Laboratories, King of Prussia, PA 19406.

Vitamin A is essential for the regulation of growth and differentiation of epithelial tissues, as well as for vision . Several forms of vitamin A, including retinol, retinal, retinoic acid, and fatty acid esters of retinol, are involved in its function, transport, and storage. Each of these forms is essentially water-insoluble and the utilization of retinoids appears to require specific carrier or binding-proteins to overcome this hydrophobicity. Cellular retinol-binding protein type II (CRBP II) is the most recently described intracellular retinol-binding protein (Ong, D.E. (1984) J. Biol. Chem. 259, 1476-1582). In adult rats the highest levels of CRBP II are found in the small intestine. It accounts for more than 1% of the soluble protein recovered from the jejunal mucosa, suggesting a role for CRBP II in the absorption of retinol in the small intestine.

CRBP II can be completely resolved into two forms (CRBP IIA and CRBP IIB) that appear to be almost identical. Both forms are present in the same tissues and are present in whole rat pups and rat small intestine in equimolar quantities. CRBP IIA and IIB are very similar in molecular weight and both bind retinal as well as retinol. One observed difference between the two forms was the amount of endogenous retinol recovered bound to the proteins after purification. CRBP IIA was isolated with ten-fold more endogenous retinol bound than CRBP IIB; however, their binding constants and absorption spectra in vitro are indistinguishable.

The gene coding for CRBP II has been isolated from a rat small intestine cDNA library using oligonucleotide probes based on the amino acid sequence of the amino terminus of CRBP IIA (Li, *et al.* (1986) Proc. Natl. Acad. Sci. USA 83, 5770-5783). The nucleotide sequence of the gene was determined and the amino acid sequence deduced for CRBP IIA was identical to the sequence of the amino terminus of the protein established by Edman sequencing. CRBP IIB was found to be resistant to Edman degradation impeding structural characterization. Thus, it was not known whether CRBP IIB was structurally similar, but not identical to CRBP IIA, or whether the two proteins were actually products of the same gene, but had undergone post-translational modification. We have compared the structures of CRBP IIB and CRBP IIA using a combination of techniques including amino acid composition and sequence analyses, and FAB and GC/EI-mass spectrometry to determine the structural features that may be responsible for the differences observed between these two forms of CRBP II. Reduced, carboxymethylated forms of CRBP IIA and CRBP IIB were cleaved with trypsin, and underivatized forms of both proteins were cleaved with cyanogen bromide. . The peptides produced were separated by HPLC prior to structural characterization. Purified tryptic peptides that were too large for FAB mass spectral analyses were digested further with S. aureus V8 protease. Peptides spanning the entire length of both protiens were recovered from the trypsin digests. The sequence of the blocked amino terminal peptide from CRBP IIB was determined by GC/EI-MS following derivatization of the pepitde with BSTFA. Furthermore, these studies provide confirmation for the derived amino acid sequence of CRBP IIA.

Conclusions

1. A combination of methodologies including FAB and GC/EI-mass spectrometry, as well as amino acid composition and sequence analyses was useful for comparing the structures of CRBP IIA and CRBP IIB.
2. GC/EI-mass spectrometry was important for determining the sequence of the blocked amino terminus of CRBP IIB.
3. These structural analyses show that the amino terminus of CRBP IIB is acetylated, but that of CRBP IIA is unmodified. (For example, FAB mass spectra of amino terminal peptides from both proteins are shown in Figure 1.)
4. No differences in the primary structures of the amino terminal regions of either protein were detected that could have directed the acetylation of CRBP IIB, or the deacetylation CRBP IIA. The initiator methionine is absent from both CRBP IIA and CRBP IIB.
5. The amino acid sequences of both proteins are identical and confirm the structure deduced from the sequence of the cDNA for CRBP IIA.

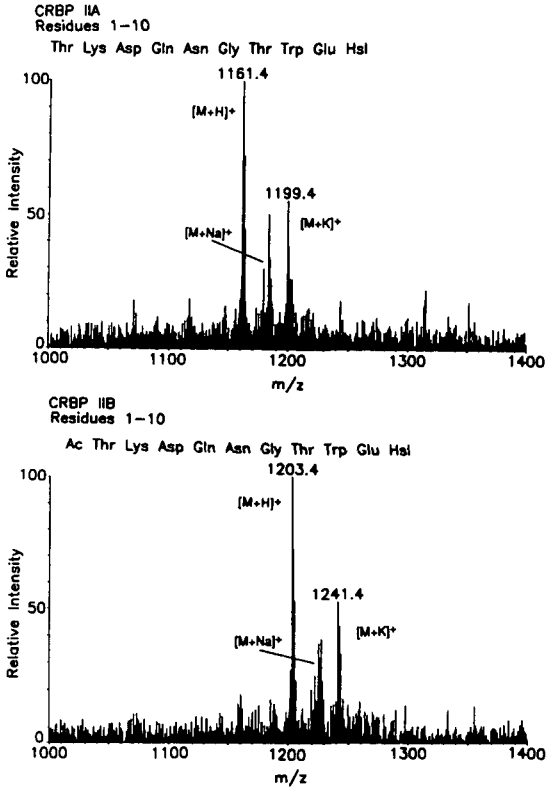

Figure 1. FAB mass spectra of cyanogen bromide peptides spanning residues 1-10 of CRBP IIA (top) and CRBP IIB (bottom). Hsl represents homoserine lactone.

Presented at the 36th ASMS Conference on Mass Spectrometry and Allied Topics
June 5-10, 1988, San Francisco, CA

QUANTITATION OF HIGH MOLECULAR WEIGHT NEUROPEPTIDES BY THERMOSPRAY HPLC/MS.

R. D. Voyksner, T. Pack, and F. Williams, Analytical and Chemical Sciences, Research Triangle Institute, P. O. Box 12194, Research Triangle Park, NC 27709.

Neuropeptides have been found in many regions of the human body. They are in greatest abundance in tissues and fluids of the central nervous system. The fact that these peptides are active in the picomolar range, coupled with the existence of many different individual peptides, places an enormous burden on analytical methodology for their detection.

Thermospray HPLC/MS was successfully applied to a class of neuropeptides called endorphins. The thermospray spectra acquired for α-, β-, and γ-endorphin were simple, showing $[M+H]^+$, $[M+Na]^+$, $[M+2Na-H]^+$ ions and double and triple charged ions ($[M+2H]^{+2}$, $[M+3H]^{+3}$). In negative ion detection $[M-H]^-$, $[M-2H]^{-2}$ and $[M-3H]^{-3}$ were observed. Thermospray spectra exhibited no fragment ions indicative of the amino acid sequence. The presence of multi-charged ions permitted detection of peptides (β-endorphin) which have molecular weights beyond the mass range of the instrument. The thermospray spectra also exhibited a low noise background compared to the FAB/MS spectra for the same compounds.

Thermospray HPLC/MS ion currents for the endorphins were very dependent on the thermospray vaporizor temperature, tip condition, and repeller voltage. For the analysis of the endorphins, the vaporizor was operated at 90-94°C, a 5-10°C lower temperature than conventional thermospray HPLC/MS. The lower temperature results in only 75-85% solvent evaporation. The source temperature was raised to 270°C, about 20-50°C above normal, to provide heat to insure evaporation and prevent freezing from the adiabatic expansion of solvent in the source. The vaporizor tip also plays a critical role in the acquisition of acceptable thermospray spectra. The tip was cut to insure a straight and long stream (10-15 cm) of water at 1 mL/min (at ambient temperature and pressure). These conditions, coupled with the lower vaporizor temperature, appear to enhance the ion evaporation process necessary for the ionization of peptides.

The repeller in the thermospray source plays an important role in the high mass sensitivity and relative intensity of multi-charged ions to single-charged ions in thermospray. Usually a repeller voltage of 100-150V was optimal for the $[M+H]^+$ ion current for α-endorphin (mw 1745). However, these high voltages resulted in reduced ion currents for the double charged ions of β- and γ-endorphin. Ion currents for the multi-charged ions were optimized at lower voltages, usually in the 40-70V range. Due to the variety of peptide molecular weights encountered, the repeller was operated in the 60-80V range to give the best compromise in sensitivities for the single and multi-charged ions.

The development of suitable quantitative methods by thermospray HPLC/MS required the use of internal standards. The internal standards evaluated for the determination of β-endorphin include leu^5-β-endorphin, N-acetyl-β-endorphin, β-endorphin fragment 1-27, β-endorphin (camel), and γ-endorphin. The internal standards α-endorphin, des-try-γ-endorphin and dynorphin-β were evaluated for the quantitation of γ-endorphin. The use of these internal standards improved the injection to injection reproducibility in the HPLC/MS analysis. Usually the relative standard deviation for replicate injections was 5-6%. N-Acetyl-β-endorphin appeared to be the best choice for an internal standard for the determination of β-endorphin. The low relative standard deviation of N-acetyl-β-endorphin (2%) and its co-elution with β-endorphin compensated in part for slight instrumental changes during the analysis. However, most of the test compounds evaluated (except γ-endorphin) were suitable as internal standards for β-endorphin. The three internal standards evaluated for γ-endorphin all proved suitable.

Calibration curve generation and quantitation of plasma extracts and cerebral spinal fluid (CSF) extracts for β- and γ-endorphin was successful by HPLC/MS. Calibrations were generated using multiple ion detection, monitoring the $[M+H]^+$ or $[M+2H]^{+2}$ ions for the internal standard and target endorphin. The calibration for β-endorphin, using N-acetyl-β-endorphin or β-endorphin fragment 1-27 as an internal standard, was linear (correlation coefficient 0.998) over a range of 30 pM to 300 pM. The γ-endorphin calibration, using α-endorphin as an internal standard, was linear from 10 pM to 300 pM (correlation coefficient 0.994). The HPLC/MS chromatogram for the analysis of β-endorphin and γ-endorphin in plasma or CSF exhibited few matrix interferences at the retention time for these endorphins or internal standards. The ratio of the peak areas for the internal standard to the target peptide was used to determine the amount of endorphin from the calibration curve. The measured values (Table I) were usually within 10-20% of the amount spiked.

Presented at the 36th ASMS Conference on Mass Spectrometry and Allied Topics
June 5-10, 1988, San Francisco, CA

The coupling of an immobilized enzyme column (trypsin) after the HPLC improved the specificity and sensitivity for the MS detection of the endorphins. Trypsin hydrolyzes the lysine and arginine amino acid bonds, resulting in several fragment peptides. For example, the hydrolysis of ß-endorphin results in the five tryptic fragment peptides (T_1-T_5) shown below:

YGGFMTSEK	SQTPLVTLFK	NAIIK	NAYK	KGE
T_1	T_2	T_3	T_4	T_5
MW1018	MW1132	MW557	MW493	MW442

The hydrolysis of the peptide has two advantages. First, identification of the peptide such as ß-endorphin does not need to be based on one ion, such as the $[M+2H]^{+2}$, but can be based upon the detection of the tryptic fragments ion. Second, detection of the fragment peptides can result in 10-30 times better sensitivity than the detection of the unhydrolyzed peptide. It appears that the lower molecular weight fragment peptides are more efficiently ionized, transmitted, and detected than the unhydrolyzed peptide.

The HPLC-trypsin hydrolysis-MS methods were used to generate a calibration curve for ß-endorphin. The calibration was based upon tryptic fragment T_1 for ß-endorphin (mw 1018) and fragment T_1 for the internal standard leu^5-ß-endorphin (mw 1000). The calibration was linear (0.97) over the concentrate range of 5-380 pM of ß-endorphin.

Acknowledgements

This research was supported by the National Institute on Drug Abuse, Grant Number 1 RO1 DAC 4202-01.

TABLE I. Quantitative determination of ß- and γ-endorphin in CSF and plasma by thermospray HPLC/MS.

Sample	Amount of Endorphin spiked (pM)	Amounts of each Endorphin Determined by HPLC/MS (pM)	
		ß-Endorphin	γ-Endorphin
Plasma	80	71	65
Plasma	25	27	22
CSF	35	32	29
Average error		9%	16%

(1) Internal standard for ß-endorphin was ß-endorphin fragment 1-27 (60 pM) and the internal standard for γ-endorphin was α-endorphin (30 pM).

Presented at the 36th ASMS Conference on Mass Spectrometry and Allied Topics
June 5-10, 1988, San Francisco, CA

PYROLYTIC AND THERMAL DESORPTION STUDIES OF POLYPROPYLENE.

P J Tayler, D Price, G J Milnes
Department of Chemistry, University of Salford, Salford England M5 4WT
J H Scrivens, T G Blease
ICI PLC Wilton, PO Box 90, Middlesbrough, Cleveland, England TS6 8JE

Formulated polypropylene, like most commercial polymers, is a complex substance. Typically it will contain residual oligomers, various additives and catalyst residues in addition to the polymer itself. Characterisation of commercial polymers can yield useful structural information together with some knowledge regarding the processing history of the polymer. Also, characterisation of the additives present in a compounded polymer can help establish its formulation specification.

Nine polypropylene samples originating from different sources were investigated using two methods; direct pyrolysis-mass spectrometry (Py-MS) and thermal desorption -gas chromatography/mass spectrometry (TD-GC/MS). Computerised pattern recognition methods were used to help interpret the results from both methods. The TD-GC/MS system used consisted of an Envirochem Unacon 810A thermal desorber unit and high temperature furnace interfaced to a VG7070 GC/MS with Finnigan Super Incos data system. The sample loaded into a quartz tube was continuously purged with helium and heated using the programmable furnace (temperature profile RT-150°C @24°C/min, final temperature held for 10 mins). The volatiles released during heating were concentrated by consecutively collecting and desorbing them in two selectively adsorbent trapping devices connected in series before being transferred in the form of a narrow band plug of sample to the capillary column of the GC for analysis. Composite mass spectra were calculated by summing the spectra contained in a chromatogram and correcting for background. This procedure was carried out for each analysis.

The Py-MS system used consisted of a Pye Unicam Curie-point pyrolyser interfaced to a Balzers QMG511 quadrupole mass spectrometer controlled by a Digital PDP 11/23 computer, which was also used for data storage and some pre-processing. Preheating of the pyrolyser (180°C) was required to prevent condensation of the pyrolysis decomposition products, the pyrolysate, consequently the volatiles studied in the thermal desorption experiments were not studied in these analyses. Pyrolysis (770°C for 15s) was carried out under vacuum. 20 scans were performed per analysis and an average mass spectrum was calculated in each case.

Principal component analysis[1] (PCA), a pattern recognition method from the Einsight package (Infometrix Inc.), was used to help interpret and compare the mass spectral results. PCA enables a two-dimensional overview of any relationships that may exist between samples (and/or variables) to be achieved. The principal component plots obtained using the TD-GC/MS mass spectral data, which was normalised with respect to total ion intensity, are presented in figures 1 and 2. Good intra-sample reproducibility is indicated by the clustering of the triplicate analyses for each sample in both plots. In Fig 1. samples B and E are well separated from the others, this was found to be due to an antioxidant, (2,6,di t-butyl 4 methyl phenol), that was only present in these samples. By removing samples B and E and performing a further PCA the relationships between the rest of the samples was explored in more detail, this plot for the reduced set of polypropylene samples is shown in fig 2. The composite mass spectra of several of these samples were indistinguishable to the human eye, but were differentiated with some confidence using PCA. Good inter-sample differentiation is shown for all the samples analysed. PCA carried out using the Py-MS data, however, showed no significant differentiation between the samples.

Conclusions

TD-GC/MS/pattern recognition has been shown to be a successful method for the differentiation of commercial polypropylene samples. These results illustrate the potential of this technique for studying other polymer systems. Direct Py-MS was unable to differentiate these samples due the absence of residual volatiles and the domination of the spectra by relatively uninformative polymer peaks.

Acknowledgement

Financial support from S.E.R.C and I.C.I is gratefully acknowledged.

Reference

1.M.A.Sharaf,D.L.Illman,B.A.Kowalski "Chemometrics" John Wiley and Sons, New York, 1986.

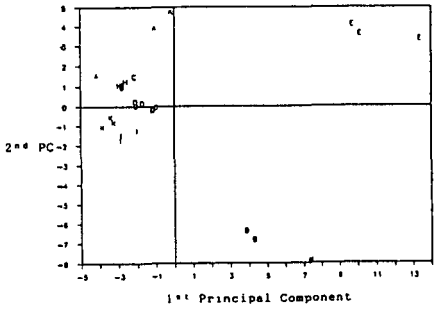

Fig(1) Principal component plot (PC1vPC2) for the 9 polypropylene samples

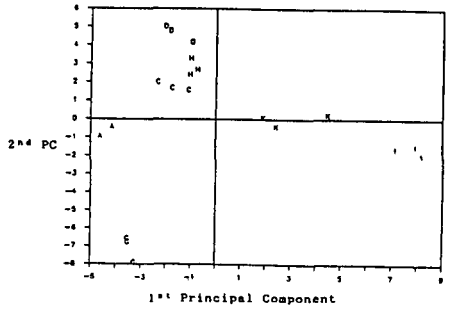

Fig(2)Principal component plot (PC1vPC2) of reduced set of polypropylenes

Presented at the 36th ASMS Conference on Mass Spectrometry and Allied Topics
June 5-10, 1988, San Francisco, CA

PD-MS AND FAB-MS IN THE SEARCH FOR NEUROPEPTIDES

G.J. Feistner[1], P. Roepstorff[2], P. Højrup[2],
K.F. Faull[1], C.J. Evans[1], and D.F. Barofsky[3]
[1]Department of Psychiatry, Stanford Medical Center, Stanford, CA 94305
[2]Department of Molecular Biology, Odense University, DK-5230 Odense M, Denmark
[3]Department of Agricultural Chemistry, Oregon State University, Corvallis, OR 97331

The molecular weights (MWTs) of peptides can conveniently and rapidly be determined by mass spectrometry, even when the sample consists of a mixture of peptides. In the search for novel neuropeptides, MWT information is very powerful in that it allows to quickly identify known peptides and to concentrate efforts on potentially new ones. The benefit obviously will be greatest when the MWTs are known early in the investigation. Fortunately, it appears that only a single reversed-phase HPLC step is needed to obtain the peptides of an acidic tissue extract in a form suitable for either FAB-BE-MS or PD-TOF-MS (Scheme 1, section A). The tissue extract chosen for investigation was bovine posterior/intermediate pituitary. It provided a number of known peptides, which were useful for the evaluation of our methodology, as well as the potential of finding new peptides, especially those which could be predicted to derive from known precursor molecules.

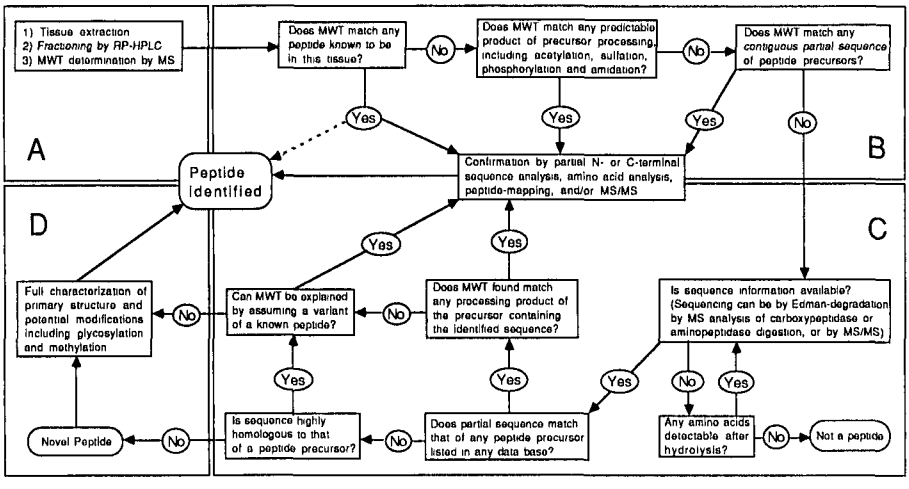

Scheme 1 Algorithm used for the identification of peptides.

The mere knowledge of the MWTs can suggest a known peptide, a peptide arising via a known *processing pattern of a precursor*, or a *peptide arising from a precursor by a yet unidentified* processing pattern (Scheme 1, section B). We screen for the latter possibility by looking for a match of a measured MWT with that of any peptide corresponding to a contigous partial sequence of a precursor peptide using a computer program developed for this purpose. This has, in particular, made the identification of POMC(83-103) (MWT 2081; see Fig. 1) straightforward. Only after all the above options have been exploited without success, do we try to obtain sequence information, screen (if necessary) protein data bases for sequence homology, and try to predict the peptide under consideration from the combined knowledge of partial sequence and MWT (Scheme 1, section C). Always trying to predict a possible candidate helps us to select a suitable confirmative experiment and to

avoid failures such as the attempt to sequence an acetylated peptide. Purification to homology and full characterization of primary structure and possible modifications (Scheme 1, section D) are reserved for those cases where we encounter a novel peptide or modifications such as glycosylation, which prevents prediction of the MWT, or as methylation, where a consensus sequence leading to such a modification is not known.

We found processing products derived from the genes of vasopressin- and oxytocin-neurophysin as well as proopiomelanocortin. In summary, the identified peptides (Fig. 1) account for the entire lengths of the precursor molecules, suggesting that we may indeed detect the majority of the peptides present. Those processing products which, to our knowledge, have been isolated and characterized for the first time from bovine tissue, are highlighted with a dot matrix. It is worthwhile to point out that we could observe peptides regardless of originating precursor and posttranslational modifications. Mass spectrometry therefore provides a unique combination of specificity and broad applicability not offered by any other methodology.

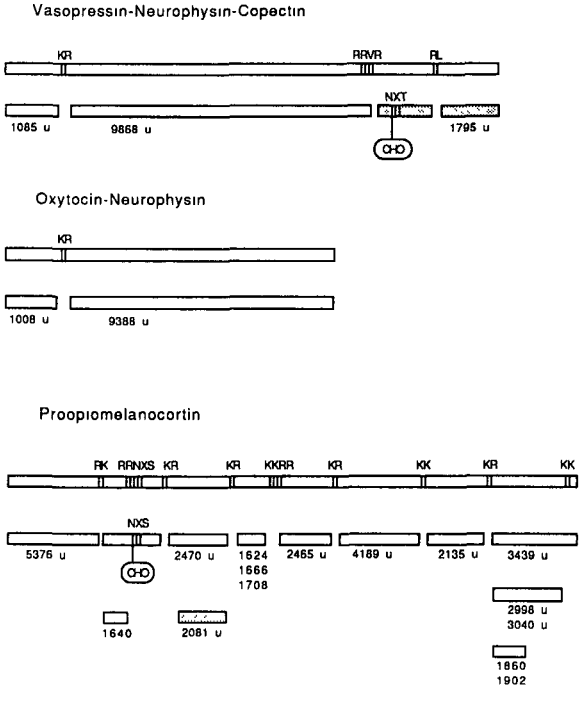

Fig. 1

Processing products from three precursor molecules that were identified following the algorithm outlined in Scheme 1. Multiple mass numbers correspond to acetylated and non-acetylated products.

When comparing PD-TOF-MS versus FAB-BE-MS (R=500) for their usefulness in the routine screening for neuropeptides, using a mass range of 0-22,000 in PD-TOF-MS and of 11,000-1,000 in FAB-BE-MS, we found that due to its integral nature the PD-TOF-MS measurement achieves about an order ofmagnitude greater sensitivity. On the other hand, PD-TOF-MS was somewhat less accurate (± 3 u up to MWT 5,000) than FAB-BE-MS (± 1 u). The accuracy of the measurement for the larger neurophysins (MWT 9,000-10,000) and the N-fragment of POMC (MWT approx. 5400) is not yet known, because they seem to comprise of several closely related compounds, which are still under investigation. An accuracy of ± 3 u is good enough for predicting many peptides, but fails to distinguish between amidated peptides and their corresponding free acids. Also, searching for possible matches of an experimental MWT with a contiguous partial sequence of a precursor will give too many unnecessary suggestions if a window of ± 3 u is allowed. For these types of problems we routinely employ FAB-BE-MS with unit resolution over a mass range of 3,600-600 u, whereupon we achieve an accuracy of better than ± 0.2 u.

Presented at the 36th ASMS Conference on Mass Spectrometry and Allied Topics
June 5-10, 1988, San Francisco, CA

THERMOSPRAY MASS SPECTROMETRY OF METHIONINE ENKEPHALIN

Louis L. Martin and Joseph F. Greer
Drug Discovery Department, Pharmaceuticals Division
CIBA-GEIGY Corporation, 556 Morris Avenue, Summit, New Jersey, 07901

Detection sensitivity limits for the peptide methionine enkephalin (TYR-GLY-GLY-PHE-MET) have been reported to be as low as 250 pg using fast atom bombardment mass spectrometry (Tolun et al., 1987). In this paper, assay conditions and sensitivity levels for the detection of methionine enkephalin by thermospray mass spectrometry are described.

Samples were analyzed on a Finnigan MAT TSQ-70 triple quadrupole mass spectrometer equipped with a Finnigan MAT Thermospray Interface. A Waters model 510 pump was used in combination with a Scientific Systems model LP-21 pulse dampener. Direct liquid injections (10 ul) were made using a Rheodyne model 7125 syringe loading sample injector. A mobile phase consisting of 60% acetonitrile in water was used. Since methionine enkephalin is ionized at neutral pH, it was not necessary to include a buffer in the mobile phase. In fact, sensitivity was lower with a mobile phase consisting of 0.05 M ammonium acetate in 30% methanol. Likewise, the use of either filament or discharge ionization was found to reduce sensitivity.

Maximum sensitivity was obtained in the negative ionization mode under the following conditions: vaporizer temperature, 125°C; repeller, -62.5 V and flow rate, 1.1 ml/min. Manipulation of any one of these parameters dramatically altered sensitivity for methionine enkephalin. On the other hand, varying the aerosol temperature between 170 and 270°C had little effect on sensitivity. Thus, an aerosol temperature of 190°C was selected for routine analyses. Under these conditions, 1.0 ng injections of methionine enkephalin produced peaks which were approximately three times the mean noise level.

Figure 1. Positive thermospray mass spectrum of methionine enkephalin at a vaporizer temperature of 90°C.

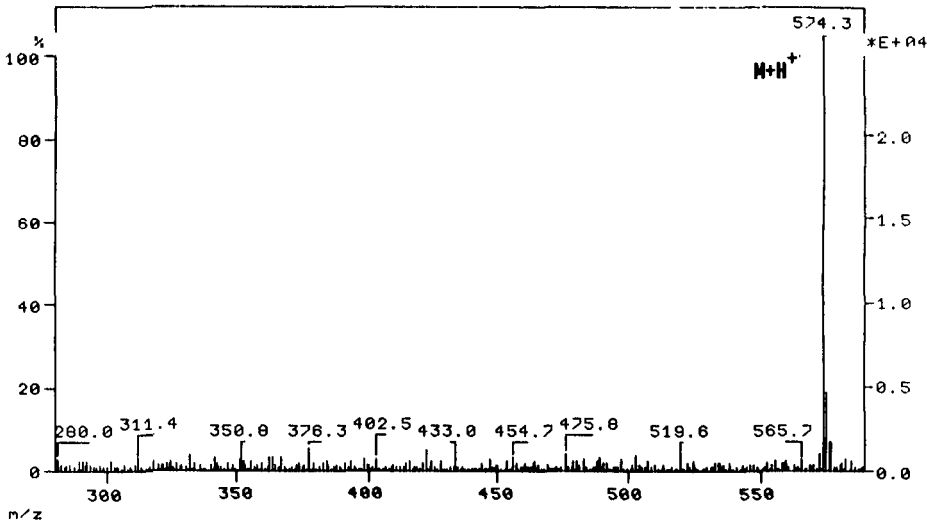

In the positive ion mode, manipulation of the the vaporizer temperature was found to affect not only sensitivity for the molecular ion for methionine enkephalin, but also the degree of fragmentation of the compound. Thus, at a vaporizer temperature of 90°C, only the molecular ion ($M+H^+$) for methionine enkephalin could be seen (Figure 1). On the other hand, at a vaporizer temperature of 120°C, ions corresponding to the peptide fragments, PHE-MET and GLY-PHE-MET, were also prominent in spectra of methionine enkephalin (Figure 2). Varying the vaporizer temperature was found to affect the fragmentation of leucine enkephalin in a similar manner. In the negative ionization mode, the molecular ions $(M-H)^-$ for methionine and leucine enkephalin were found to be much more stable and little or no fragmentation of these compounds was observed even at a vaporizer temperature of 120°C.

These results demonstrate that detection limits for methionine enkephalin by thermospray mass spectrometry are comparable to those obtainable by fast atom bombardment. Sensitivity may be further improved by altering the percentage of acetonitrile in the mobile phase, by the addition of a buffer (other than ammonium acetate), or by substitution of methanol for acetonitrile. Thus, thermospray may prove to be a very useful technique for the analysis of enkephalins and related peptides.

Reference:
Tolun, E., Dass, C. and Desiderio, D.M., Rapid Commun. Mass Spectrom., 1: 77 (1987).

Figure 2. Positive thermospray mass spectrum of methionine enkephalin at a vaporizer temperature of 120°C.

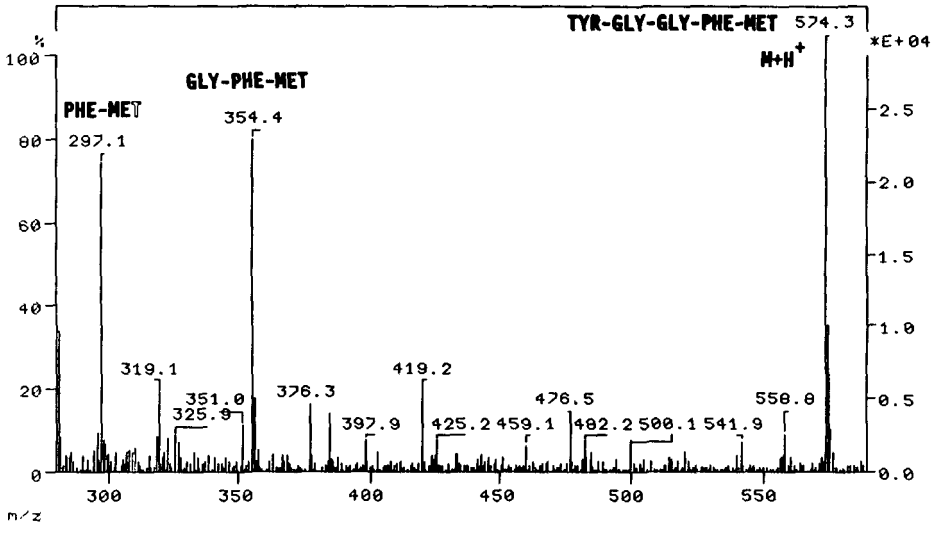

Presented at the 36th ASMS Conference on Mass Spectrometry and Allied Topics
June 5-10, 1988, San Francisco, CA

IMPORTANT FACTORS IN THE FAB/MS ANALYSIS OF LARGER PEPTIDES; G. S. Peterson, J. Elliott, W. J. Roberts, K. Williams, W. J. McMurray; Yale School of Medicine, New Haven, Ct. 06510.

Peptide analysis by mass spectrometry has become a rapidly growing field. Increasing attention has been given to the fast atom bombardment (FAB) technique for this class of biochemicals due to its ease of use and good sensitivity. Despite the facility of this technique, it becomes increasingly important to select the best conditions for the analysis as the molecular weight of the peptide increases and/or sample size decreases.

A large number of peptides with molecular weights above 1800 daltons were analyzed by FAB on a VG ZAB-SE mass spectrometer, and an attempt was made to correlate the following factors with molecular ion abundance: 1) matrix selection, 2) N-terminal acetylation and C-terminal amidation, 3) calculated hydrophobicity index (H.I.)[1], and 4) calculated[2] and measured HPLC retention on a reverse phase C-18 column (RPC).

Matrix selection was found not to be critical, although below 2500 daltons magic bullet (DTT : DTE, 4 : 1) gave better data with hydrophobic peptides. For hydrophilic peptides, and all peptides larger than 2500 daltons, thioglycerol was the matrix of choice. When magic bullet was used with hydrophilic peptides, more intense salt adducts (M+K) were observed. Acetylation and amidation increased the molecular ion abundance in every case, presumably by rendering the peptide less hydrophilic.

The best overall indicator of FAB behavior was the HPLC retention measured by RPC. In general, peptides with longer retention times gave more intense MH+ ions, and in many cases this correlated with a less positive H.I. value for those peptides. Peptides with a large positive H.I. value, in most cases, gave poor FAB sensitivity. Additionally, it was found that a concentration of basic amino acids (LYS, ARG) near the C-terminus enhanced FAB sensitivity compared to the expected values based on HPLC retention, while concentration of the same residues near the N-terminus had the opposite effect. Above 3000 daltons, all indicators failed to predict FAB sensitivity, and it is believed that the ability to desorb the molecule is the overriding concern for these large peptides.[3]

1 H. D. Bull and K. Breese; Arch. Biochem. Biophys.; 166; 655 (1974).
2 D. Guo, C. T. Mant, A. K. Taneja, J. M. R. Parker, R. S. Hodges; J. Chrom.; 359; 499 (1986).
3 B. N. Green and R. S. Bordoli in "Mass Spectrometry in Biomedical Research", (S. Gaskell, ed.); p. 235 (1986).

Applications of Plasma Desorption Mass Spectrometry

M. P. Lacey, T. Keough, D. S. Lucas, R. A. Grant and J. F. Sullivan
The Procter & Gamble Co., Miami Valley Laboratories, P.O. Box 398707
Cincinnati, Ohio 45239-8707

This presentation surveys some of our initial applications of plasma desorption (PD) mass spectrometry. Obviously, the technique is well-suited for determining the molecular weights of biomacromolecules. Molecular weights determined in this fashion can be used to verify and correct DNA sequences (1,2), to confirm reaction products (3), to provide mass balance as a guide during protein modification (4) and to count and locate disulfide bonds in proteins (5). As an example, the PD mass spectrum of a heat-stable serine protease, secreted from Thermomonospora YX, is given in figure 1. We were interested in this material because its reported molecular weight is $\leq$14,500 u (6), determined by HPLC retention behavior and SDS/polyacrylamide-gel electrophoresis, which is much lower than those of other heat-stable proteases ($\geq$20,000 u). PD mass spectrometry established that the correct molecular weight is 19,063 $\pm$ 10 u. Figure 2 contains the PD mass spectrum obtained from 10 nmole of proteinase K, an alkaline protease derived from a fungus, tritirachium album limber. This is the highest molecular weight species that we have successfully analyzed to date. The analysis required ~12 hr integration time and the measured molecular weight was within 1.3% of that calculated based on the known primary structure.

PD mass spectrometry can also be used to complement standard biochemical tools such as amino acid analysis and Edman degradation. Figure 3 contains a PD spectrum of a polypeptide fragment isolated from a proteolytic enzyme of known primary structure. Less than 400 pmoles of the fragment, thought to be an autolysis product, were available for analyses. Ten cycles of automated Edman degradation established the N-terminus of the molecule. PDMS provided the molecular weight. By combining results from both experiments, the identity of the fragment was readily established. Incidentally, this fragment could not have been identified in a single Edman degradation analysis because of it's size (it contains over 100 amino acids).

We have used PD mass spectrometry to verify the structure and assess microhomogeneity of various enzyme inhibitors. These quality control studies were undertaken prior to forming enzyme-inhibitor complexes which often produce single crystals suitable for subsequent x-ray diffraction studies.

We have evaluated the peptide "mapping" capability of PDMS and have compared results with those obtained by static FABMS (7). These experiments are similar to those previously reported by Jardine and coworkers (8). In our studies, several peptide mixtures were prepared by the limited proteolysis of glucagon using the enzymes trypsin, chymotrypsin and pepsin. The mixtures were separated using reverse phase HPLC and each peak was collected, lyophilized and identified using FAB, PD and Edman sequencing (where needed). After the compositions of the mixtures had been established, the unseparated mixtures were analyzed by static-FAB and PDMS. A typical set of results is shown in figure 4. This mixture, produced by the pepsin digestion of glucagon (enzyme/substrate = 3.8×10^{-5} mole/mole, ambient temperature, T=2 hr), contains six major products accounting for more than 80% of the chromatographic area. Of these, only two are hydrophobic (9). Not surprisingly, these are the only two components detected with static-FABMS. Fully two-thirds of the mixture is not detected. The PD mass spectrum, on the other hand, clearly reveals signals for all of the components in the mixture including the intact parent which accounts for less than 1% of the total chromatographic area. A comparison of the peptide "mapping" capabilities of PDMS and continuous-flow FAB (10) is currently in progress in our laboratory.

To date, we've found PDMS to be a very useful complement to static-FABMS. It extends our accessible mass range at least up to 30,000 u. Furthermore, sensitivity is excellent. As little as 1 pmole of material is required in favorable cases. Another major advantage is that the technique does not require the use of a viscous liquid matrix as in static-FAB. Therefore, it is applicable to materials that fail by FAB due to solubility problems.

Furthermore, elimination of the liquid matrix, i.e., requirement of surface activity, minimizes problems associated with the selective detection of components in mixtures. Finally, PDMS is amenable to a high degree of automation and can be efficiently operated unattended.

References

1. K. Biemann, Int. J. Mass Spectrom. Ion Phys. 45, 183 (1982).
2. K. Biemann and S. A. Martin, Mass Spectrom. Rev. 6, 1 (1987).
3. D. V. Myhre, M. S. McCracken, T. Keough, J. C. Hill and R. D. Macfarlane, Biomed. Environ. Mass Spectrom., in press (1988).
4. B. Sundqvist, P. Roepstorff, J. Fohlman, A. Hedin, P. Hakansson, I. Kamensky, M. Lindberg, M. Salephour and G. Sawe, Science 262, 696 (1984).
5. R. Yazdanparast, P. C. Andrews, D. L. Smith and J. E. Dixon, J. Biol. Chem. 262, 2507 (1987).
6. T. W. Gusek and J. E. Kinsella, Biochem. J. 246, 511 (1987).
7. T. Keough, M. P. Lacey, D. S. Lucas, R. A. Grant, L. A. Smith and T. C. Jeffries, "Proceedings of the Fourth Texas Symposium on Mass Spectrometry: Analysis of Peptides and Proteins," John Wiley and Sons, 1988.
8. A. Tsarbopoulos, D. J. Liberato and I. Jardine, Proceedings of the 35th Annual Conference on Mass Spectrometry and Allied Topics, Denver, 1987, p. 80.
9. S. Naylor, A. F. Findeis, B. W. Gibson and D. H. Williams, J. Am. Chem. Soc. 108, 6359 (1986).
10. R. M. Caprioli, W. T. Moore and T. Fan, Rapid Commun. Mass Spectrom. 1, 15 (1987).

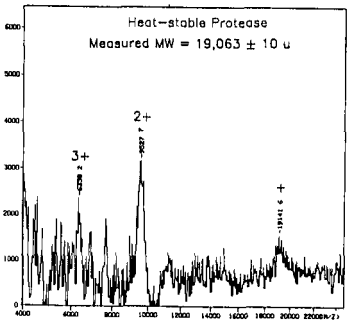

Figure 1

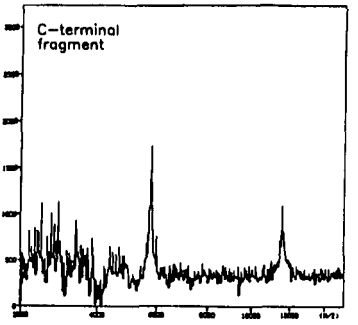

Figure 3

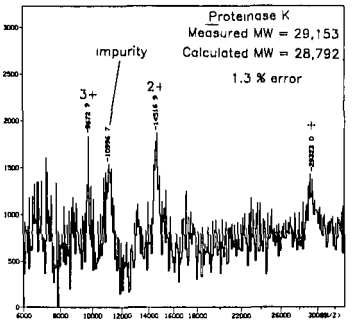

Figure 2

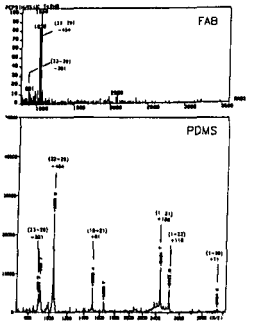

Figure 4

Presented at the 36th ASMS Conference on Mass Spectrometry and Allied Topics
June 5-10, 1988, San Francisco, CA

THE STUDY OF ACETAMINOPHEN CONJUGATE FORMATION BY OXIDATIVE ELECTROCHEMISTRY AND THERMOSPRAY MASS SPECTROMETRY

T.A. Getek and W.A. Korfmacher
National Center for Toxicological Research
Jefferson, AR 72079

ABSTRACT: Since its initial development, thermospray mass spectrometry (TSMS) has proven to be an exceptional interface for liquid chromatography-mass spectrometry (LC-MS) and an unique ionization mode for nonvolatile compounds. Because TSMS utilizes a continuous flow of liquid into the thermospray (TS) source, it may be used as a flow injection analysis (FIA) device for monitoring chemical reactions in solution. In this study, the reaction of acetaminophen (APAP) after electrochemical oxidation with glutathione (GSH) was monitored and evaluated by TSMS at varying pH and mole ratios of GSH:APAP; behavior at varying electrochemical potential was also examined. The mixing of GSH with the electrolyzed APAP, that is, N-acetyl-*p*-benzoquinoneimine (NAPQI), formed on-line the acetaminophen glutathione conjugate (APAP-SG) on the time scale of one second.

EXPERIMENTAL: The configuration of the pumping system is shown in Fig. 1. The syringe pump contained a 3.3 x 10^{-5} M APAP solution in 90/10 H_2O/CH_3OH at 0.1 M ammonium acetate which was pumped through the electrochemical (EC) cell at 0.7 mL/min by the syringe pump. The reciprocal pump carried the same solution but without the APAP at a flow of 0.7 mL/min. GSH was injected and mixed with the APAP after the APAP had been oxidized to NAPQI. The comparison of the expected and observed charge generated by the electrolysis confirmed a two-electron oxidation.

RESULTS AND DISCUSSION: The TS mass spectra of the before and after oxidation of APAP and reaction with GSH are shown in Fig. 2. The peaks at m/z at 457 and 184 (Fig. 2B) are indicative of APAP-SG and APAP-SH, respectively, as reported earlier [1]. The selective ion monitoring (SIM) of the reactants and products is shown in Fig. 3. Note the large dips and valleys in the SIM of m/z 150 and 108 indicating the chemical reaction of NAPQI with GSH. Extensive APAP-SG conjugation began at +0.15V as clearly shown by the appearance of m/z 457 and 184.

Experiments were undertaken to evaluate the effect of varying GSH:APAP mole ratios on the formation of APAP-SG. At mole ratios of 0.2:1 and 1:1 GSH:APAP, m/z 184 is detected but not m/z 457. A minimum of 2:1 mole ratio was necessary to observe $[APAP\text{-}SG+H]^+$ at m/z 457. Observance of m/z 184 prior to detection of m/z 457 suggested that the APAP-SG was formed but due to the lack of intensity of the m/z 457 ion and instability of the APAP-SG conjugate to the TS process, only the fragment for APAP-SH was observed.

Lowering the pH of the ammonium acetate liquid carrier affected the formation of APAP-SG by delaying and inhibiting the reaction. At lower pH, the oxidation of APAP is more difficult, thus a more positive potential for the EC cell is needed before the APAP-SG ion is detected by TSMS.

In summary, the information obtained from this study and similar studies can lead to a better understanding of plausible *in vivo* processes, assist in optimizing the chemical synthesis of conjugates for further experiments, and is a rapid means (ca. 1 sec) to produce on-line thermally labile compounds, such as APAP conjugates, so that thermospray conditions may be adjusted in order to observe maximum intensity for $[M+H]^+$ or a specific fragment. These results are an extension of the utility of solution electrochemistry mass spectrometry (SECYMS) for evaluating redox events by TSMS [2].

REFERENCES:
[1] L.D. Betowski *et al.*, ***Biomed. Environ. Mass Spectrom.***, **14**, 705(1987).
[2] T.A. Getek, presented at ASMS, Denver, CO, 1987, p. 443.

ACKNOWLEDGEMENTS: One of us (TAG) would like to acknowledge the support of the Oak Ridge Associated Universities Postgraduate Research Program. The authors thank Dr. J. Hinson for helpful discussions.

Presented at the 36th ASMS Conference on Mass Spectrometry and Allied Topics
June 5-10, 1988, San Francisco, CA

BLOCK DIAGRAM OF ELECTROCHEMICAL/
THERMOSPRAY FIA SYSTEM

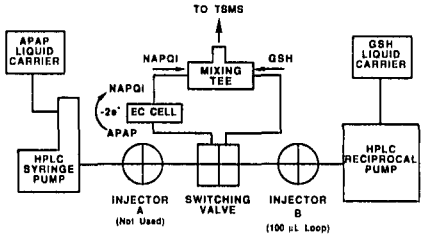

Figure 1

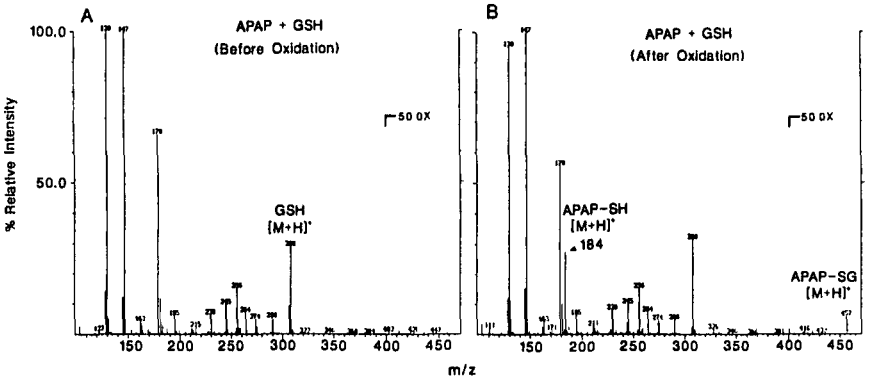

Figure 2

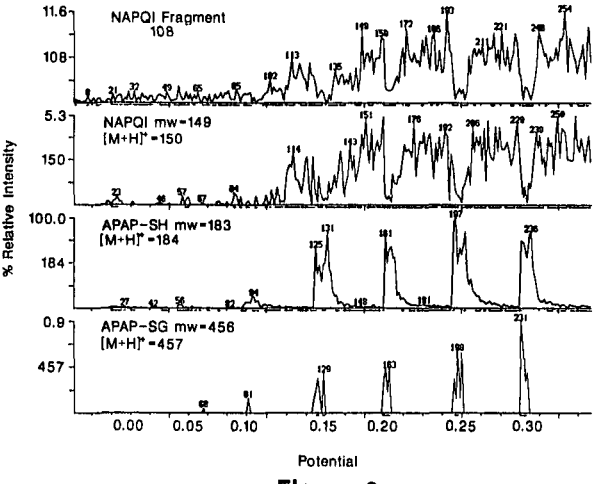

Figure 3

Presented at the 36th ASMS Conference on Mass Spectrometry and Allied Topics
June 5-10, 1988, San Francisco, CA

RECOGNITION AND CHARACTERIZATION OF GLUTATHIONE CONJUGATES USING TRIPLE QUADRUPOLE MASS SPECTROMETRY

V. Gould, M. McDowall, *S. J Gaskell and P. Haroldsen;
VG MassLab Ltd., Tudor Road, Altrincham, WA14 5RZ, UK,
*Baylor College of Medicine, Texas Medical Center,
Houston, TX 77030, USA.

Conjugation with glutathione represents an important route for the detoxification and subsequent excretion of xenobiotics or their metabolites. Structural analysis of these conjugates therefore represents an important approach to the characterization of reactive metabolites and the elucidation of toxic mechanisms of xenobiotics. We have recently described[1] analyses of glutathione conjugates using fast atom bombardment and hybrid tandem mass spectrometry in which characteristically collisionally activated decompositions were observed.

However, the nature of the conjugated moiety has a significant effect on the observed fragmentations, suggesting that recognition of the presence of glutathione conjugates in biological extracts is best achieved by tandem MS using several scan modes. Thus, for example, scanning parents of m/z 130 (derived from the gamma-glutamyl moiety) together with neutral loss (232 u, 129 u) scans indicates the presence of glutathione conjugates of compounds of varying structure.

Here we report the application of triple quadrupole mass spectrometry with mixed mode scanning to the recognition and characterization of glutathione conjugates in biological extracts. The analytical strategy involves: 1) continuous flow FAB/tandem MS analyses with rapid switching between the recording of conventional mass spectra and both parent ion and neutral loss scans characteristic of glutathione conjugates; 2) a second analysis in which daughter ion scans are recorded for relevant parents identified in stage 1.

[1]Haroldsen PE, Reilly M, Hughes H, Gaskell SJ, Porter CJ: Characterization of glutathione conjugates by fast atom bombardment-tandem mass spectrometry: Biomed. Environ. Mass Spectrom. (in press, 1988).

Presented at the 36th ASMS Conference on Mass Spectrometry and Allied Topics
June 5-10, 1988, San Francisco, CA

d0/d3 PHAA-GSH FROM BILE MS MSMS

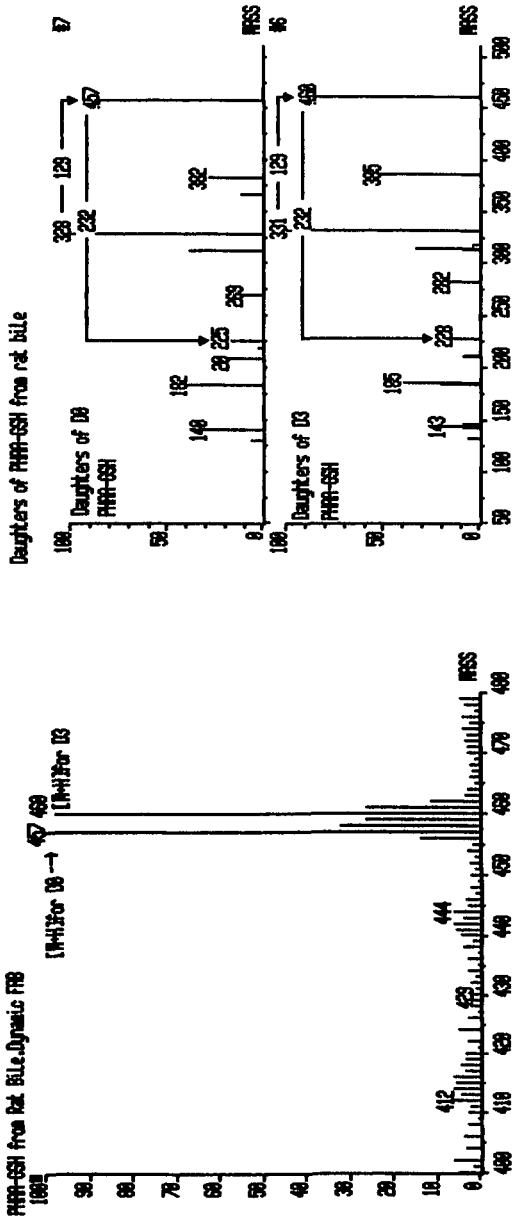

Presented at the 36th ASMS Conference on Mass Spectrometry and Allied Topics
June 5-10, 1988, San Francisco, CA

THERMOSPRAY LC/MS DETECTION OF GLUTATHIONE- AND GLUTATHIONE-DERIVED CONJUGATES IN BILE AND URINE OF MICE TREATED WITH 3-HYDROXYACETANILIDE, A NONHEPATOTOXIC REGIOISOMER OF ACETAMINOPHEN:

Mohamed S. Rashed, Timothy G. Myers, Sidney D. Nelson; Department of Medicinal Chemistry, Univ. of Washington, Seattle, WA 98195.

Introduction

3-Hydroxyacetanilide (AMAP) is a nonhepatotoxic regioisomer of acetaminophen(APAP). Despite lack of toxicity, AMAP produces nearly as much *in vivo* covalent binding to liver proteins as acetaminophen.[1] *In vitro* covalent binding from AMAP occurs four times faster than from APAP.[2] AMAP is metabolized *in vitro* to two diphenolic compounds, 2-acetamidohydroquinone and 3-hydroxyacetaminophen. Further oxidation to quinones was suggested to result in the observed covalent binding. Incubations of AMAP in presence of glutathione (GSH) abolished covalent binding and resulted in the formation of two isomeric *mono*-GSH conjugates of 4-acetamido-*o*-benzoquinone (AOBQ) and 2-acetamido-*p*-benzoquinone (APBQ) and a *bis*-GSH conjugate of the latter. The identity of these conjugates was determined by co-chromatography with synthetic standards.

The objective of the work presented here was to determine if these conjugates or their metabolic breakdown products were biliary or urinary metabolites of AMAP in mice.

Experimental

Synthesis:

N-acetyl-3-methoxy-*p*-benzoquinone imine (MAPQI) was prepared by silver oxide oxidation of 3-methoxyacetaminophen as previously reported for the synthesis of NAPQI.[3]

The synthetic thioether conjugates were prepared by adding the quinone (0.1 mmol) in acetonitrile to the appropiate thiol in phosphate buffer pH 7.4. The mixtures were acidified after 30 min and the conjugates were purified by HPLC. The purified adducts were characterized by 300 MHz ^1H NMR in D_2O. Molecular weight information of some of the conjugates was obtained by LSIMS analysis.

Animal Treatments:

Phenobarbital pretreated male Swiss-Webster mice (16-25g) were fasted for 12 hrs then administered [ring-UL-^{14}C]AMAP (600 mg/kg) ip. The gall bladders were excised 3-4 hrs after injection and the bile collected was acidified to pH 2.0 with formic acid and filtered through a Nylon-66 filter. Urine was collected for 24 hrs in cups containing 15 mg ascorbic acid and immersed in dry ice/acetone. The urine was filtered first through cotton wool then through a Nylon-66 filter.

Analytical:

HPLC was performed with an LKB 2152-2SD dual-pump instrument equipped with an LKB 2152 variable wavelength UV detector set at 254 or 280 nm (LKB, Bromma, Sweden). Analyses and purification were carried out on a 5-u Ultrasphere C_{18} column (10 mm X 25 cm) protected with a 5-u Ultrasphere precolumn. Mobile phase consisted of solvent A: water/acetonitrile/glacial acetic acid (96:2:2 by volume); solvent B: acetonitrile. A linear gradient was employed from 0% B to 20% B in 40 min with a flow rate of 2.0 ml/min.

LC/MS analysis was carried out with an LKB 2150 pump and LKB 2152 controller HPLC sytem interfaced to a Vestec Thermospray LC-MS Model 201 dedicated LC/MS system (Vestec Corp., Houston, TX). The column used was a 5-u Ultrasphere C_{18} (4.6 mm X 15 cm) protected with a 5-u Ultrasphere precolumn. The mobile phase consisted of 90% 0.1 M ammonium acetate and 10% acetonitrile isocratically pumped at a flow rate of 1.0 ml/min. Operating temperatures for the thermospray interface were T_1 (vaporizer) = 140°C; T_2 (tip) = 270°C; source block = 350°C ; jet (vapor) = 320°C. The system was operated in the positive ion mode with the filament off.

Results and Discussion

TSP-LC/MS analysis of the acidified bile samples provided direct evidence for the presence of the GSH conjugates of AOBQ and APBQ. In addition LC/MS provided evidence for the presence of two isomeric GSH conjugates of a novel quinone imine, N-acetyl-3-methoxy-p-benzoquinone imine (MAPQI). The spectra obtained for these compounds showed protonated molecular ions and characteristic fragmentation due to neutral loss of the glutamate moiety. The base peak ions corresponded to cleavage of the thioether bond on the cysteine side of the molecule to yield protonated aryl thiols (fig. 1).

MAPQI was synthesized and found to react with GSH to give one major GSH conjugate which was determined by ^{1}H NMR to be 3-(glutathion-S-yl)-5-methoxy-acetaminophen.

TSP-LC/MS was used for characterisation of products of reactions of the quinones with cysteine or N-acetylcysteine.
The spectra obtained showed protonated molecular ions and other characteristic fragments corresponding to the protonated aryl thiol and the protonated diphenolic moieties (fig. 2).

LC/MS of urine from mice treated with AMAP allowed detection of mercapturates of AOBQ and MAPQI. In addition, glucuronic acid conjugates of the parent compound AMAP and of its diphenolic metabolites were detected in urine by LC/MS.

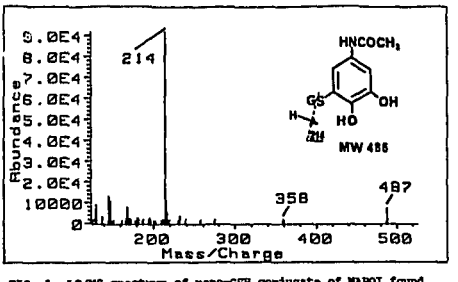

FIG. 1 LC/MS spectrum of mono-GSH conjugate of MAPQI found in bile of mice treated with AMAP.

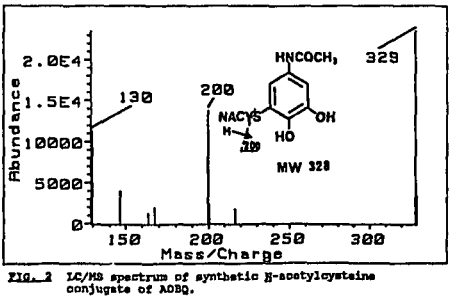

FIG. 2 LC/MS spectrum of synthetic N-acetylcysteine conjugate of AOBQ.

1. Roberts, S.A.; Jollow, D.J. Fed. Proc. 1979, 38, 426.
2. Streeter, A.J.; Bjorje, S.M.; Axworthy, D.B.; Nelson, S.D.; Baillie, T.A. Drug Metab. Dispos. 1984, 12,565.
3. Dahlin, D.C.; Nelson, S.D. J. Med. Chem. 1982, 25, 885.

Presented at the 36th ASMS Conference on Mass Spectrometry and Allied Topics
June 5-10, 1988, San Francisco, CA

APPLICATIONS OF TANDEM MASS SPECTROMETRY TO THE CHARACTERIZATION OF DERIVATIZED GLUTATHIONE CONJUGATES

Paul G. Pearson, William N. Howald, * Michael D. Threadgill and Thomas A. Baillie.

Department of Medicinal Chemistry, School of Pharmacy, University of Washington, Seattle WA 98195, and * Medical Research Council Radiobiology Unit, Didcot, Oxfordshire OX11 ORD, U.K.

Conjugates of the endogenous tripeptide glutathione (γ-glutamyl-cysteinyl-glycine; GSH) represent an important class of metabolite as they may arise from from the interaction of GSH with reactive electrophilic species, which are generated metabolically from drugs or other xenobiotics. Typically these reactive species, which have been implicated in various xenobiotic-induced toxicities, are short-lived and pose complex analytical problems. Consequently, analytical methods to identify GSH conjugates in biological matrices are valuable as the structural information derived provides a unique insight into the chemical nature of the reactive species.

The objectives of the present investigation were two-fold. Firstly, to employ an aqueous phase derivatization procedure to convert glutathione conjugates to either their alkyloxycarbonyl or benzyloxycarbonyl derivatives to permit convenient isolation from a biological matrix. Secondly, to examine the behaviour of the functionalized GSH conjugates by collisionally-activated dissociation (CAD) methods in conjunction with fast atom bombardment (FAB) and tandem mass spectrometry, in order to obtain detailed structural information by examination of their daughter ion spectra. As a model compound for this investigation we chose S-(N-methylcarbamoyl)glutathione (SMG; 1), a metabolite of the anti-neoplastic agent N-methylformamide (NMF ; Threadgill *et al.*, 1987).

Experimental: SMG (1), generated in incubations of rat hepatocytes with either NMF or $^{13}C_2$,^{15}N-NMF (5mM) , was converted to its N-benzyloxycarbonyl dimethylester derivative (3) and purified by HPLC as described previously (Pearson *et al.*, 1988) . Daughter ion spectra of the MH^+ ions from (3), an authentic sample of (1) an N-ethoxycarbonyl dimethylester (2) and a *t* -butyloxycarbonyl dimethylester analog (4), were recorded on a VG 70 SEQ hybrid tandem instrument of EBQQ geometry, equipped with an Ion Tech fast atom gun, and a VG11/250 data system. Samples (5-10μg) were dissolved in methanol (3μl), and added to a glycerol matrix (3μl) containing 0.1N HCl (1μl). Ionization was achieved following bombardment with xenon (6keV) as the primary beam, and conventional FAB spectra were recorded at an accelerating voltage of 8 kV. CAD was performed in the first (rf-only) quadrupole, employing helium as a collision gas (1 x 10^{-6} Torr) with collision energies of 38-40 eV. Daughter ion spectra were recorded, either *via* the data system in the multi-channel-analysis mode and subsequently mass-measured, or by means of an oscillographic recorder.

Results and Discussion: Conventional FAB analysis of(1)-(4) afforded spectra with prominent MH^+ ions. Under CAD conditions structurally-informative fragment ions were observed for (1)-(3), the origins of which are depicted in Figure 1 (adapted from nomenclature proposed by Gaskell. S.J. ; personal communication).(1) underwent loss of the γ-glutamyl moiety (129u) as the major route of fragmentation to yield ion ***e*** ; expulsion of the elements of methylisocyanate (CH_3NCO) from the MH^+ (to yield ion ***i***), or from the ***e*** fragment were also prominent cleavages. Thus, daughter ions indicative of both xenobiotic and tripeptide elements of SMG were clearly observed. Conversion of (1) to (2) or (3) induced a profound change in the relative abundances of ions ***a-k*** , most notably in the intensity of fragment ***a*** (elimination of glycine methyl ester ; see Figure 1), which

dominated the spectrum of (2) and (3; figure1). Ion *e* remained an important mode of fragmentation, as did the expulsion of methylisocyanate (57u) from the respective MH^+ ions. Shifts in m/z values in the spectra of (2) and (3), and isotopic labelling, confirmed these assignments. Therefore, the CAD spectra of (2) and (3), in common with (1), are characterized by ions diagnostic for the drug residue and GSH moiety. In addition, (2) and (3) displayed neutral losses indicative of the functionalized amino and carboxyl groups. In contrast, the CAD spectrum of (4) was dominated by two ions resulting from fragmentation of the *t* -BOC group itself, *viz* m/z 437 $(MH\text{-}C_4H_8)^+$ and m/z 393 $(MH\text{-}CO_2C_4H_8)^+$,and thus conveyed little structural information.

The results of this study demonstrate the value of an aqueous phase derivatization technique. The enhanced HPLC properties, increased lipophilicity, and the introduction of a UV chromophore in (3), served to expediate the isolation and analysis of GSH conjugates. The derivatized GSH conjugates of NMF, when examined under CAD conditions, have mass spectral features similar to underivatized S-aryl and S-alkyl GSH conjugates. One notable exception involved a prominent neutral loss of alkylisocyanate, which appears to be unique to metabolites of the structure "H-Y-CO-SG "(where "Y "is a heteroatom). The prominence of ions *a* and *e* in the CAD spectra of (2) and (3) facilitates neutral loss scans for the elimination of both the derivatized glycine and γ-glutamyl residues, and in principle provides a greater degree of specificity for the detection of GSH conjugates of unknown structure, when compared with a corresponding underivatized conjugate. This approach illustrates the utility of aqueous phase derivatization techniques, accompanied by FAB/MS/MS methodology, in the rapid isolation and characterization of glutathione conjugates from a complex biological matrix.

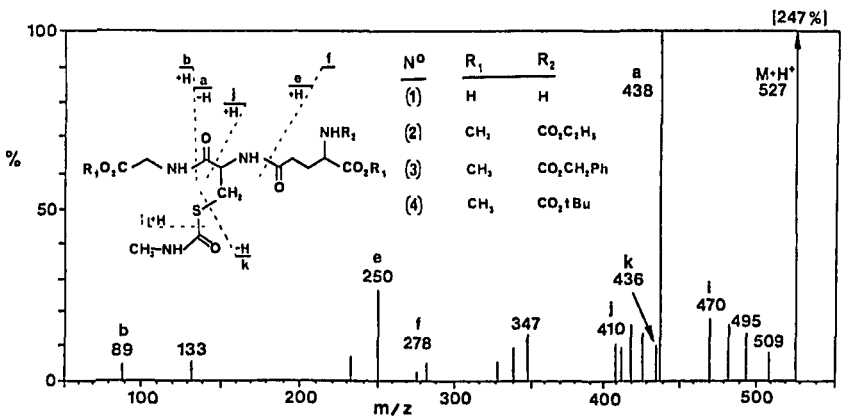

Figure 1. CAD daughter ion spectra of the MH^+ ion of (3); the scheme details the origin of the daughter ions and structures of (1)-(4).

Acknowledgements : This work was supported by grants from NATO and the National Institutes of Health (DK 30699).

Pearson, P.G., Treadgill, M.D., Howald, W.N. and Baillie, T.A., (1988). Biomed. Environ. Mass Spectrom., in press
Threadgill , M.D. , Axworthy, D.B., Baillie, T.A., Farmer, P.B., Farrow, K.C., Gescher, A., Kestell, P., Pearson, P.G., and Shaw, A.J., J. Pharmacol. Exp. Ther., 242, 312 (1987)

Presented at the 36th ASMS Conference on Mass Spectrometry and Allied Topics
June 5-10, 1988, San Francisco, CA

Screening for Mercapturate Conjugates of Xenobiotic Substances in Urine using Negative Ionization and Neutral Loss Scanning

A. Daniel Jones[(1)], Carl K. Winter[(2)], H. J. Segall[(2)], and Michael H. Buonarati[(2)]

(1) Facility for Advanced Instrumentation
(2) Department of Veterinary Pharmacology and Toxicology
University of California, Davis, CA 95616

Mercapturic acids (*N*-acetyl-L-cysteine conjugates) of toxic substances are important end products of detoxification via glutathione conjugation. The appearance of mercapturates of xenobiotic chemicals in urine indicates metabolic conjugation of electrophiles to glutathione *in vivo*. Stereoselectivity in the processes leading to glutathione conjugation can be determined by measuring the amounts of diastereomeric mercapturates excreted in urine[1]. It has also been proposed that the levels of mercapturates in urine can be used as chemical markers of toxic exposure[2].

In the course of an earlier investigation[3], negative FAB ionization was used in conjunction with MIKE spectra for the direct and specific detection of the mercapturic acid conjugate of *trans*-4-hydroxy-2-hexenal (t-4HH) in the urine of rats which had been dosed with t-4HH. The daughter ion spectrum obtained using negative ionization was remarkably simple, characterized by abundant ions which arose from cleavage of the C—S bonds. A significant neutral loss of 129 D appeared to offer the prospect of group-specific detection of mercapturic acids similar to methods developed by Straub and coworkers for other polar conjugates[4].

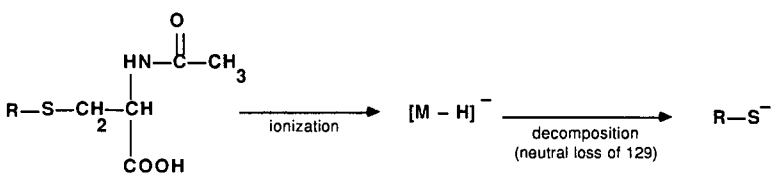

To determine whether this neutral loss scan was applicable to a wide range of mercapturates, full scan and daughter spectra were generated for synthetic mercapturate conjugates of alkyl halides (*cis*-1,3-dichloropropene and benzyl chloride), hydroxyalkenal products of lipid peroxidation (*trans*-4-hydroxy-2-hexenal and *trans*-4-hydroxy-2-nonenal), styrene oxide, and 1,2-naphthalene oxide.

---

1. L.P.C. Delbressine, P. J. Van Bladeren, F. L. M. Smeets, and F. Seutter-Berlage, *Xenobiotica* **1981**, 11, 589.
2. I.G. Sipes and A.J. Gandolfi, in *Casarett and Doull's Toxicology, The Basic Science of Poisons*, Third ed., ed. by C. D. Klaassen, M. O. Amdur, and J. Doull, pp. 64-98, Macmillan, New York, 1986.
3. C. K. Winter, H. J. Segall, and A. D. Jones, *Drug Metab. Dispos.* **1987**, 15, 608.
4. K. M. Straub, P. Rudewicz, and C. Garvie, *Xenobiotica*, **1987**, 17, 413.

Ionization of Mercapturic Acids

Negative ionization methods (FAB, hydroxide CI, and chloride CI) yielded intense $[M-H]^-$ ions for all of the synthetic conjugates. Greater amounts of fragmentation were observed using hydroxide CI relative to the other two ionization methods, and this is attributed to the relatively high proton affinity of OH^-. Small amounts of adduct ions (e.g. $[M+Cl]^-$) were also observed using CI, but alkali metal cation attachment was minimal using FAB even in the presence of 0.1 M NaI in the matrix (dithiothreitol:dithioerythritol). Positive ionization gave intense $[M+H]^+$ except for the hydroxyalkenal and naphthalene oxide conjugates, which gave strong $[M+H-H_2O]^+$ ions. Alkali metal cationization was significant upon addition of NaI to the matrix.

Ion Fragmentation

For all of the mercapturate conjugates studied, decomposition of $[M-H]^-$ resulted in simple daughter spectra characterized by three or fewer principal daughter ions. An abundant daughter corresponding to a neutral loss of 129 D was observed for each mercapturate, and was usually the most abundant daughter ion.

Few generalizations can be drawn regarding decomposition of $[M+H]^+$ ions. Daughter spectra were more complex than observed for negative ionization, and yielded far more structural information. Daughter spectra of $[M+Na]^+$ were even more complex than the daughters of $[M+H]^+$.

Detection of Mercapturates in Urine Extracts

Samples of rat urine were collected and known amounts of authentic mercapturate standards were added. Acidic fractions of ethyl acetate extracts of the urine were analyzed by using chloride desorption chemical ionization, using linked metastable neutral loss scanning (neutral loss of 129) on a VG ZAB-HS-2F mass spectrometer. Sufficient decomposition occurred without addition of collision gas to the first field region to permit detection of all of the added mercapturates at 10 ng/mL levels in the urine.

Current efforts are directed at optimizing sample clean-up procedures and preparing pentafluorobenzyl ester derivatives of the mercapturates, which will be analyzed using electron capture ionization and GC/MS.

Presented at the 36th ASMS Conference on Mass Spectrometry and Allied Topics
June 5-10, 1988, San Francisco, CA

FD and MS/MS studies of high mass polymers,

Moore, C and Barton, E.C
Kratos Analytical, Barton Dock Road, Urmston, Manchester M31 2LD, UK

Fast Atom Bombardment ionization is often used in the analysis of high molecular weight compounds (<1000 mass units). The structure of the pseudo molecular ions generated by this technique may be probed using MS/MS. During the recent analysis of some silicone oils the aforementioned techniques were found to be of little value. However, field desorption ionization and combined with high resolution accurate mass measurements did allow us to partially determine the structure of the oil.

In Figure 1 is a FAB mass spectrum of neat silicone oil of molecular weight 800 mass units. The oil might be expected to have the following general formula;

$$R- \begin{array}{c} CH_3 \\ SiO- \\ CH_3 \end{array}_{n} -R_1$$

As n increases the mass of the ion will increase by 24 mass units e.g. m/z 221, 295, 369 etc. If molecules having different R groups are present then series of ions separated by a common mass difference will be observed eg 207 221, 281 295, 355 369, etc.

In Figure 2 is the field desorption mass spectrum of the same oil sample. Data were obtained by scanning from mass 4000 at 30 sec decade^{-1} at a resolution of 3000. In contrast to the data in Figure 1, no significant ions were observed below mass 739. Once again 2 series of ions differing in mass by 14 mass units were observed and the expanded spectrum in Figure 3 shows that the higher mass series is the most intense above 1700 mass units.

The individual molecular ions do not dissociate unimolecularily or after collisional activation and therefore no MS/MS data have been obtained on them.

By computer assisted peak matching of the m/z 813 ion against a porphyrin reference of mass 770.3526, the accurate mass of this ion was found to be 813.2653 mass units. The most probable elemental composition is therefore,

$(SiOme_2)_9\ C_6H_{13}NO_3$ (m/z = 813.2587)

Other accurate mass measurements confirmed that the nominal mass difference of 74 mass units was due to $(SiOMe_2)$.

Field desorption is obviously a good method for ionizing silicone oils, since very clean spectra are obtained. Data are currently being obtained on higher molecular weight oil samples and these are producing ions around 8000 mass units.

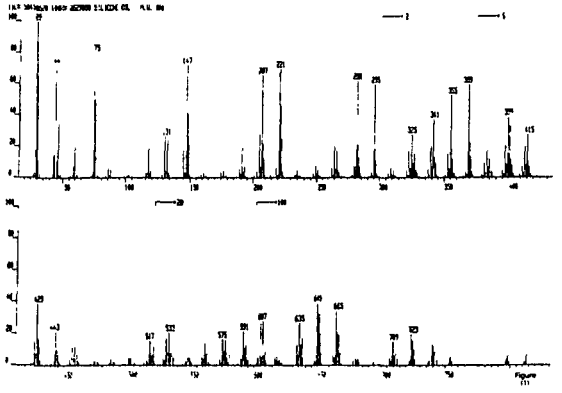

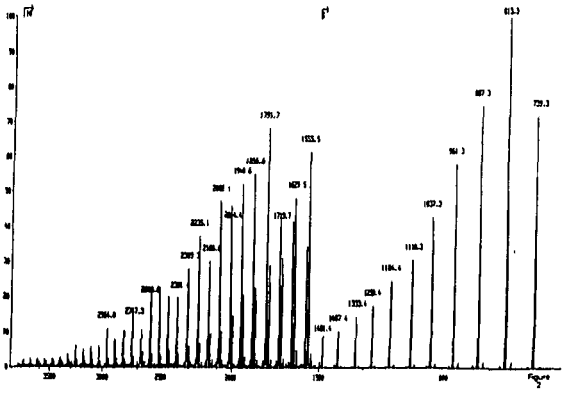

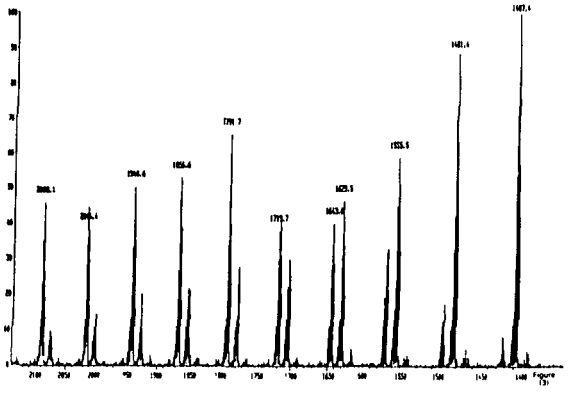

Presented at the 36th ASMS Conference on Mass Spectrometry and Allied Topics
June 5-10, 1988, San Francisco, CA

Electron Impact Ionization Mass Spectra of Polystyrene Oligomers by ThermaBeam LC/MS

G.G. Jones, *R.W. McCoy and R.E. Pauls, Amoco Corporation Naperville, Il 60566; R.C. Willoughby, EXTREL Corporation, Pittsburgh, PA 15238.*

The analysis of polystyrene oligomers by mass spectrometry is made difficult because of their low volatility and ease of thermal degradation. The thermal depolymerization of bulk polystyrene begins at less than 300°C, considerably below the estimated boiling point of MW 2000 polystyrene (1). As a result, the highest reported oligomer detected under electron impact ionization conditions with solids probe introduction is the n = 11 oligomer, mass 1202, in a sample with an oligomer distribution out to at least n = 27 (2). Successful approaches to volatilization-ionization include field desorption, TOF-SIMS, laser microprobe, and chemical ionization. These techniques, applied either directly or with prior LC separation, provide molecular weight information out to beyond 5000 amu, but little or no additional structural information.

Particle beam LC/MS interfaces, in common with moving belt interfaces, remove enough solvent to allow generation of electron impact ionization mass spectra. In the ThermaBeam interface, particles from an aerosol produced by a thermal nebulizer pass through a two-stage jet separator and impact the wall of the ion source, where vaporization occurs. The results of this study, which demonstrate the detection of polystyrene molecular ions out to mass 1930, n = 18, suggest that the vaporization of sub-micron sized particles from a hot source wall is different from and certainly more effective than, bulk vaporization from a heated surface.

Experimental. Polystyrene GPC standard (Mw = 1250), Polymer Laboratories, LTD.) was chromatographed on a 2mm i.d. by 25 cm long Ultrasphere ODS 5 µm column (Beckman Instruments) with the following gradient: 100% methanol to 50%/50% methanol/THF in 40 min.; flow rate 0.4 ml/min. Injection size was typically 50 to 100 µl of a 3.4 mg/ml solution of polystyrene in 80/20 methanol/THF. The LC/MS interface was an EXTREL ThermaBeam (TM) particle beam interface consisting of a thermal nebulizer, expansion region and two-stage jet separator. An EXTREL ELQ-400-2, 2000 amu mass range quadrupole mass spectrometer was used in the EI mode with 70 eV ionization energy. For the maximum molecular weight detection experiment, the mass resolution was adjusted for 2-3 amu wide peaks between 1000 and 2000 amu with a scan range of 80-2000 amu.

Results. Butyl capped polystyrene oligomers were detected out to beyond n = 18, m.w. 1930, by LC/MS with ThermaBeam (TM) particle beam interface and electron impact ionization conditions. As shown in Figure 1, molecular ions were observed up to mass 1930 under very low resolution (2-3 amu wide peaks), high sensitivity conditions. The mass spectrum of the 13-mer, Figure 2, was taken under unit mass resolution conditions. The molecular ion of the 13-mer, mass 1410, is only 0.1% of the mass 91 peak at a source temperature of 250°C.

Source temperature plays an important role in the vaporization of the oligomer particles. At 200°C source wall temperature, only oligomers out to about n = 10 were effectively vaporized, a finding in remarkable agreement with Udseth's determination of 205°C as the evaporization temperature of the decamer from a rapidly heated (1000°C/sec) rhenium filament (2). at a source temperature of 315°C, peaks out to n = 20 were observed in the total ion chromatogram.

References.

1. Ligon, W.V., Jr., Industrial Chemist 8 (No. 10), 4 (October, 1987)
2. Udseth, H.R. and Friedman, L., Anal. Chem 53, 29 (1981)

Presented at the 36th ASMS Conference on Mass Spectrometry and Allied Topics
June 5-10, 1988, San Francisco, CA

Figure 1. Molecular Ion Detection of Polystyrene Oligomers by LC/MS with ThermaBeam Particle Beam Interface.

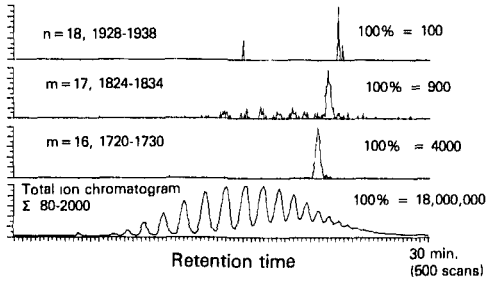

Figure 2. Electron Impact Ionization Mass Spectrum of n = 13 Polystyrene Oligomer.

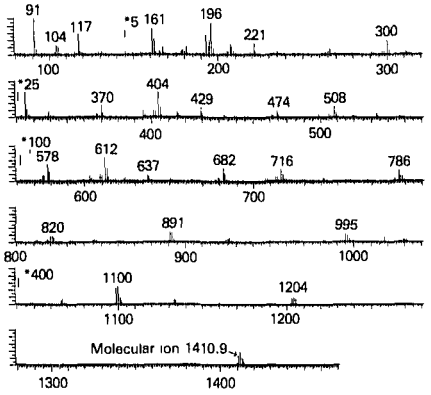

Figure 3. The Effect of Ion Source Temperature on Oligomer Particle Vaporization.

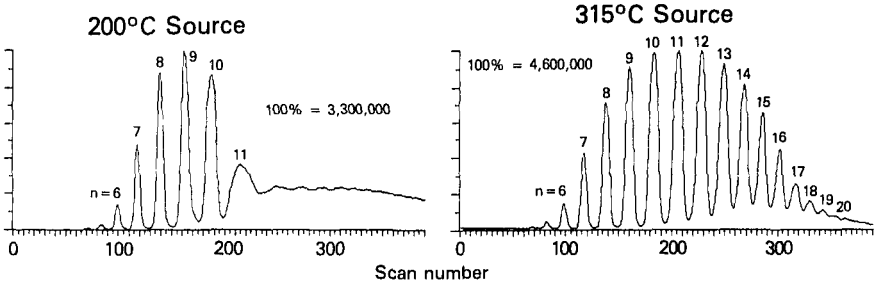

Presented at the 36th ASMS Conference on Mass Spectrometry and Allied Topics
June 5-10, 1988, San Francisco, CA

ASSESSMENT OF RESIDUAL VOLATILES IN PHENOLIC NOZZLE COMPOSITES OF THE SPACE SHUTTLE SOLID ROCKET BOOSTER

J.G. Moncur, P.C. Pinoli, W.P. Holst III, T.L. Ely
Lockheed Missiles and Space Co., Palo Alto, CA 94304

Residual volatiles in ablative tape wrapped carbon and glass phenolic nozzle composites of the Space Shuttle solid rocket booster have been studied. Assessment by helium atmosphere temperature programmed mass spectrometry (Ref. 1) at 25C to 950C, and dynamic headspace gas chromatography mass spectrometry (Ref. 2) at 260C for 15 minutes identified water as the most abundant volatile component present. Carbon dioxide, other entrained atmospheric gases such as nitrogen, and isopropyl alcohol were minor components present.

Quantitative assessment of residual water content and total volatile weight loss were achieved by an automated Karl Fischer proceedure in 260C, two hour inert gas desorptions. Hundreds of test panels, demonstration fired samples, uncured prepreg systems, and witness samples were tested over a one year term. Water was shown to be the major outgassing volatile at 260C, typically 70-90% of the total volatile weight loss. Typical carbon phenolics had moisture contents from 2.5-5.5 wt.%, while glass phenolics had lower moisture and total volatile contents.

The effect of residual water on nozzle components was assessed by thermomechanical analysis. Dynamic crossply expansion curves were shown to clearly exhibit independent response to pore pressure from residual volatiles inititally, and pyrolysis gases secondarily. Pyrolysis gas chromatography mass spectrometry identified phenol, cresols, and dimethyl phenols as the principal pyrolysis gases above 300C. Water induced pore pressure in ablative phenolic composites is beleived to induce "pocket erosion" when ply anlges approach 90° to the gas flow and "ply lift" when the wrap angle approaches the gas flow direction.

References

1. J.G. Moncur, A.B. Campa, P.C. Pinoli, HRC&CC, 5 (1982), 322.
2. J.G. Moncur, T.E. Sharp, E.R. Byrd, HRC&CC, 4 (1981), 603.

Typical Cured Carbon Cloth Phenolic Composite
Temperature Progammed Mass Spectrometry in EI mode

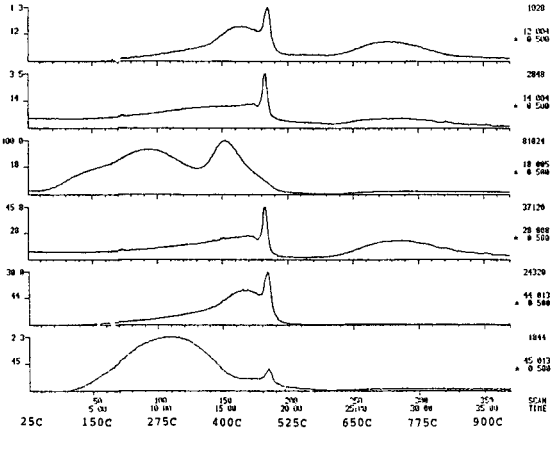

Presented at the 36th ASMS Conference on Mass Spectrometry and Allied Topics
June 5-10, 1988, San Francisco, CA

260C, 15 minute Helium Flow DYNAMIC HEADSPACE/GC/MS
CARBON CLOTH PHENOLIC

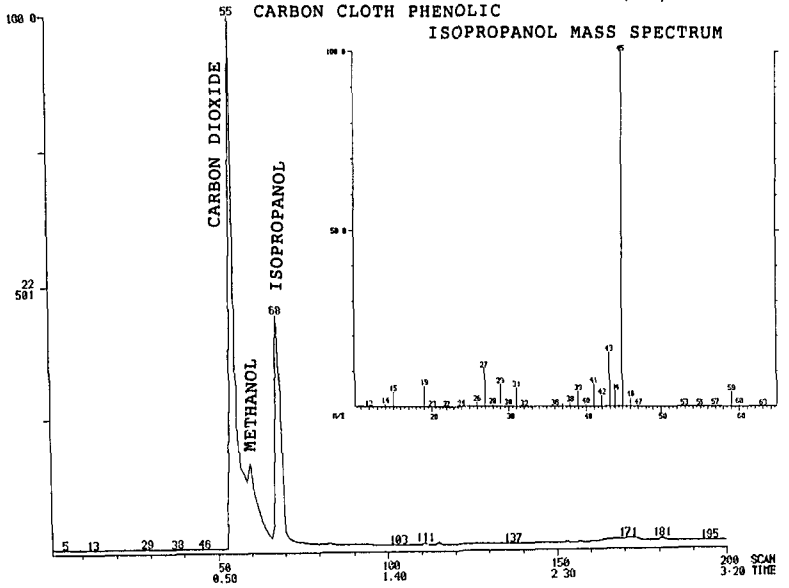

600C, 10 second PYROLYSIS/GC/MS
CARBON CLOTH PHENOLIC

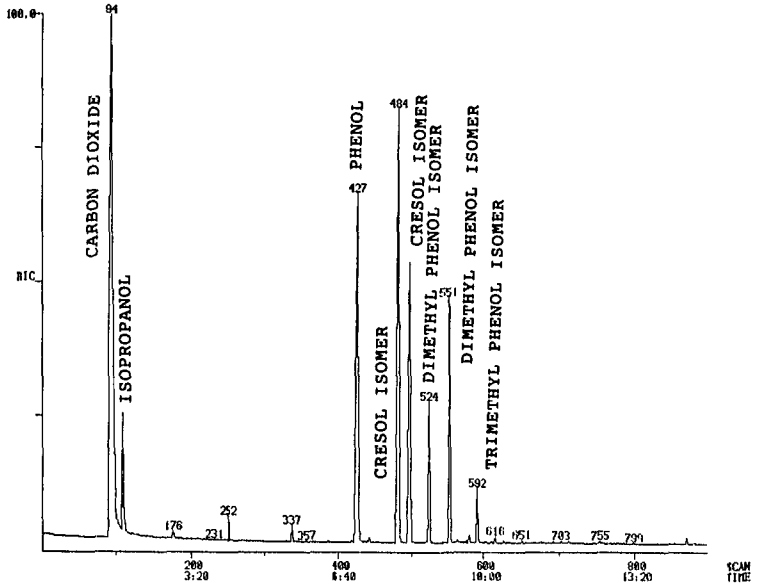

Presented at the 36th ASMS Conference on Mass Spectrometry and Allied Topics
June 5-10, 1988, San Francisco, CA

MONITORING POLYESTER POLYMERIZATIONS BY K^+IDS WITH MASS SPECTROMETRIC DETECTION:

William J. Simonsick, Jr., M. C. Grady
E. I. duPont de Nemours & Co., Ltd.
Philadelphia, PA 19146

Polyesters are the reaction products of polyfunctional acids and alcohols. Many of today's commercial polyester resins are prepared from mixtures of diacids and diols. This mixture of ingredients imparts a desirable balance of physical properties to the finished polyester resin. For example, dipropylene glycol imparts flexibility and toughness to a resin whereas neopentyl glycol provides corrosion resistance. The molecular weights of these starting materials are different. Therefore, a mass spectrometric technique which furnishes molecular weight information would be an excellent tool for sequencing oligomer chains and monitoring the progression of the early stages of a polyester polymerization. Under our operating conditions the recently developed K^+IDS technique affords only molecular weight data of oligomers.

The K^+IDS technique is easy to implement, and requires only a mass spectrometer equipped with a rapid heating probe (>100°C/sec) for sample introduction. Rapid heating makes it possible to desorb intact oligomers. Under our operating conditions, K^+IDS furnishes only molecular weight information in the form of $[M+K]^+$. The simplicity of the spectra, affording only molecular weight information, is sufficient to assign molecular formula to the ions seen in the K^+IDS mass spectra of polyester syntheses. For example, Figure 1 shows a portion of the K^+IDS mass spectrum taken of a polyester synthesis. The hydroxyl terminated trimers with the proposed structures are displayed.

All K^+IDS experiments were performed on a Finnigan 4615B quadrupole GC/MS. The mass spectrometer was tuned using Tris-(perfluoroheptyl)-S-triazine. The mass spectrometer was scanned at 1000 Daltons (Da)/sec. The desorption process of polyesters and the reproducibility of K^+IDS were evaluated using selected ion monitoring.

We used preparative gel permeation chromatography to enrich the high molecular weight fraction of the polyesters followed by K^+IDS analysis. Ions corresponding to eleven units (m/z > 1400 Da) were detected. The raw materials loading was checked using K^+IDS. We monitored the progression of neopentyl glycol, hexanediol, azelaic acid, isophthalic acid polymerization. K^+IDS is well suited for the analysis of low molecular weight polyesters.

Presented at the 36th ASMS Conference on Mass Spectrometry and Allied Topics
June 5-10, 1988, San Francisco, CA

KIDS MS OF TRIMERIC HYDROXYL TERMINATED POLYESTERS

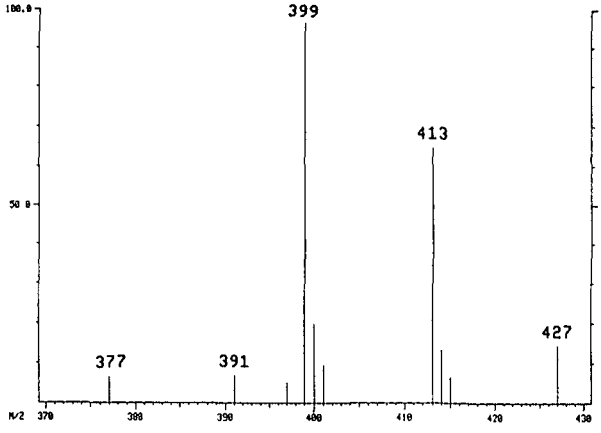

ION (D)	PROPOSED STRUCTURES
377	$HOR_{70}-OCO-R_{76}-OCO-R_{70}OH$
391	$HOR_{84}-OCO-R_{76}-OCO-R_{70}OH$
399	$HOR_{70}-OCO-R_{98}-OCO-R_{70}OH$
413	$HOR_{84}-OCO-R_{98}-OCO-R_{70}OH$
427	$HOR_{84}-OCO-R_{98}-OCO-R_{84}OH$

WHERE: $R_{70} = -CH_2C(CH_3)_2CH_2-$

$R_{98} = -(CH_2)_7-$

$R_{84} = -(CH_2)_6-$

$R_{76} =$ 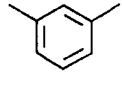

Presented at the 36th ASMS Conference on Mass Spectrometry and Allied Topics
June 5-10, 1988, San Francisco, CA

OLIGOMER ANALYSIS BY POTASSIUM IONIZATION OF DESORBED SPECIES WITH MASS SPECTROMETRIC DETECTION

William J. Simonsick, Jr., Thomas P. Volpe
E. I. duPont de Nemours & Co., Ltd.
Philadelphia, PA 19146

Mass spectrometry has not enjoyed widespread use for polymer analysis. This can be attributed to the low volatility of polymers. There are a variety of methods which have recently become available for the desorption and subsequent ionization of nonvolatile or thermally labile compounds. Unfortunately, many of these techniques are not available with our current mass filtering system, a quadrupole, or they require a substantial capital investment. We modified a direct exposure technique which we have at our disposal to accommodate the analysis of nonvolatile/thermally labile substances. The technique utilizes rapid heating (>100°C/sec) to desorb intact molecules with minimal thermal decomposition.

Once in the gas phase, the analyte must be ionized. Several techniques are available to accomplish this task. Initially we used electron impact MS (EIMS) to study a 90:10 methylmethacrylate (MMA) butylacrylate (BA) low molecular weight macromonomer. The EIMS was rich in fragment ions, however, very little structural information could be gathered because of the extensive fragmentation. Chemical ionization MS using isobutane as the reagent gas imparts less energy to the molecular ion thereby reducing fragmentation. Unfortunately, only monomeric protonated MMA (m/z = 101 Daltons (Da)) and BA (m/z = 129 Da), MMA dimer (m/z = 201 Da), and adduction ions were observed.

To further reduce the observed fragmentation we selected an ionization technique based upon the thermionic emission of potassium from an alumino-silicate matrix. This ionization technique referred to as K^+IDS (K^+ ionization of desorbed species) affords a "pseudomolecular ion" in the form of $[M+K]^+$ hence molecular weight information is easily obtained (1). Little energy is imparted to the molecular ion. Therefore, no significant fragmentation is observed. When directly analyzing oligomeric mixtures, data interpretation is facilitated by a simplified MS. Figure 1 shows the K^+IDS spectrum of the 90:10 MMA/BA macromonomer discussed above. Notice the cationized chains $[M+K]^+$ with no observable fragmentation. Each ion can easily be assigned a molecular composition with a knowledge of the starting monomers. For example, the ion seen at 339 Da corresponds to the potassium cationized MMA trimer terminating in a double bond. Each additional MMA adds 100 Da thereby giving rise to the envelope whose formula can be written 39 + 100n where n is the number of MMA units. If a BA (molecular weight = 128 Da) is substituted for an MMA in the trimer chain a net gain of 28 Da will be observed in the K^+IDS MS (128 Da - 100 Da = 28 Da). Hence, the ion seen at 367 Da corresponds to the potassium cationized chain which contains two MMA units and one BA [(200 Da) + (128 Da)] + K^+ = 367 Da. K^+IDS provides the analyst with an absolute molecular weight distribution, differentiates copolymers from polymer blends, and furnishes data concerning the specific chemical composition and the relative abundance of each oligomeric chain.

Presented at the 36th ASMS Conference on Mass Spectrometry and Allied Topics
June 5-10, 1988, San Francisco, CA

All experiments were performed on Finnigan 4615B quadrupole GC/MS system. An EI source configuration was used in all K^+IDS experiments. The ion source pressure (ion gauge) was $<10^{-6}$ Torr with a source temperature of 200°C. The mass spectrometer was tuned with Tris-(perfluoroheptyl)-S-triazine.

We investigated and optimized the operating parameters involved in the K^+IDS technique and applied the method to the study of oligomeric additives, methylmelamines, low molecular weight epoxy resins, and several synthetic mixtures. Using K^+IDS we have assisted polymer chemists toward the synthesis of targeted materials. The molecular weight snapshot provided by K^+IDS allows one to characterize oligomers by both molecular weight and chemical composition. This is useful data to the polymer chemist and K^+IDS furnishes this information in a five minute experiment.

1. Bombick, D.; Allison, J. Anal. Chem., 1987, 59, 458

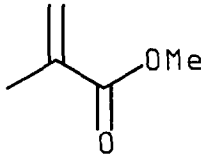

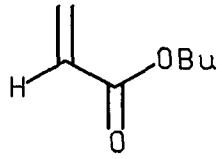

MMA = 100 Da BMA = 128 Da

MMA/BA MACROMONOMER

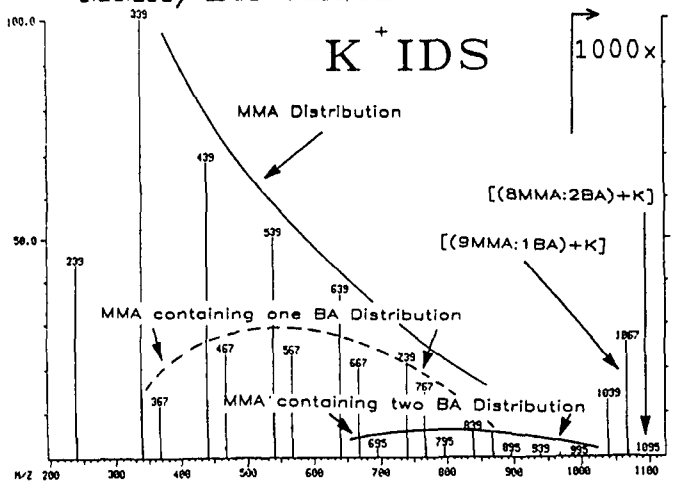

Presented at the 36th ASMS Conference on Mass Spectrometry and Allied Topics
June 5-10, 1988, San Francisco, CA

APPLICATION OF APCI MASS SPECTROMETRIC DETECTION TO PROBLEMS IN MASS TRANSFER

John W. Halliday
U.S. Army Natick R,D&E Center
Natick, Massachusetts 01760

Atmospheric pressure chemical ionization (APCI) mass spectrometry has proven a versatile and valuable detection system in studying the transport of various chemical entities through an assortment of barrier materials. These barriers range from packaging materials designed to protect the soldier's food to materials used in protecting the soldier from the effects of exposure to hazardous chemicals. Packaging barriers such as used in the Meal, Ready to Eat (MRE) are designed to keep food degrading agents (oxygen, moisture, and bacteria, for example) out and quality enhancing factors in. Barriers to permeation or penetration by toxic chemicals are used in the fabrication of garments, shelters, and other structures designed to protect the soldier.

Mechanisms for transport of the undesirable agent through the material encompass both diffusion/permeation and infiltration/penetration. Minute cracks and holes in the barrier material may permit the encroachment of the undesirable agent by physical infiltration, subject to some driving force such as a pressure gradient. In other cases transport is by permeation which, in some cases, approaches ideal Fickian diffusion.

Three areas of application are presented here: detection of packaging defects in MRE pouches, testing of chemical protective fabrics, and development of methodology for evaluating defects in shelter materials. The latter two applications make use of a permeation type experiment. The general features of the apparatus used in such studies is shown below.

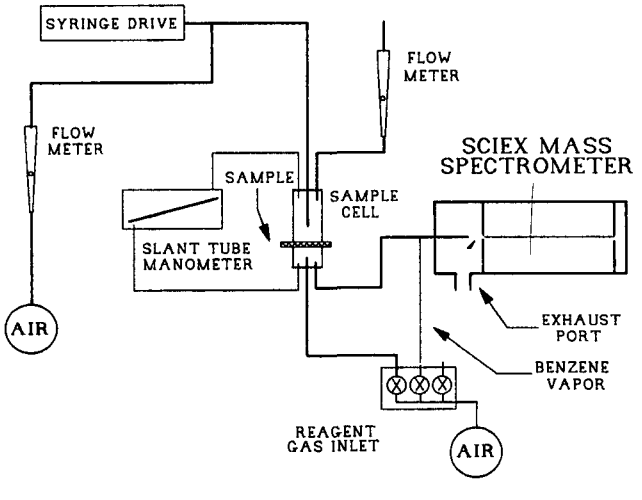

An important feature of the apparatus is the ability to establish a pressure differential across the sample by balancing the exhaust pumping from the Sciex APCI front end with the other gas flows involved. This pressure differential is a driving force for infiltration through discrete fissures and for transport of vapors through air permeable materials containing a sorptive layer.

Transport characteristics for liquid droplet challenge of two materials representing an elastomeric and an air permeable, multilayered fabric are illustrated in the following figure. The permeant used was

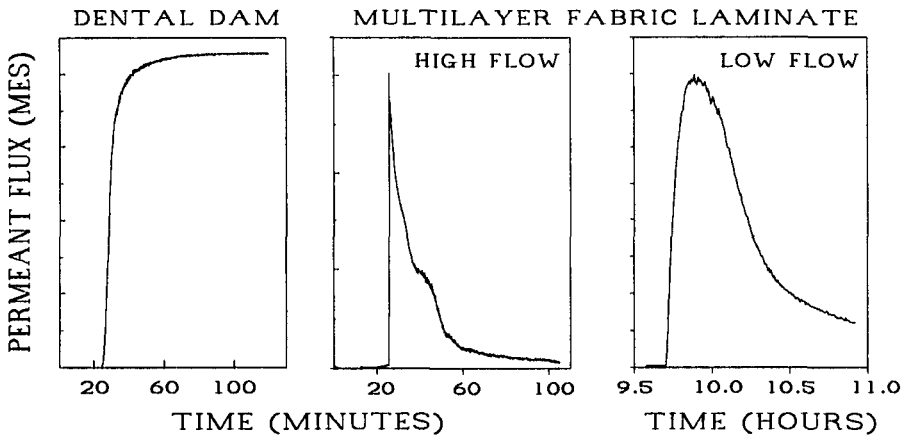

methyl salicylate (MES). Benzene vapor served as the source of $C_6H_6^+$ reagent ions used to form the MES positive ion. Detailed and highly time-resolved transport profiles that are obtained using inocuous, but relevant, compounds supplement the sparser data obtained from testing with the actual toxic compound.

The protective capacity of new, lightweight shelter and tentage materials against these same hazardous compounds would be compromised by the minute defects (cracks, fissures, worn spots) that might be induced by storage, handling, and environmental abuse factors. Using an approach similar to that just described, the pressure dependence of the transport behavior is used to determine components of infiltration and permeation type behavior. This information is used to evaluate impact on the protective capacity.

Incursive defects in packaging materials are evidenced by detection of component(s) of the contained food on the outside of the package. Several sampling approaches were evaluated in a general feasability study. Tomato sauce was used as the food component; the negative ion of acetic acid was monitored. The most effective method involved scanning the pouch surface with a thin "sniffing" tube attached to the Sciex's APCI front end. A small funnel shaped device attached to the probe increased sensitivity significantly. This approach also provides important spatial information.

APCI detection provides, then, the sensitivity, versatility, and time resolution essential to the types of studies outlined here. It can be physically interfaced with a wide variety of apparatuses designed to measure, in real time, the concentration of a host of permeating species of widely differing compositions.

Presented at the 36th ASMS Conference on Mass Spectrometry and Allied Topics
June 5-10, 1988, San Francisco, CA

QUANTITATIVE ANALYSIS OF REACTIVE DECOMPOSITION PRODUCTS USING THERMALLY LABILE SALTS*

John J. Morelli, Michael A. Grayson, Clarence J. Wolf,
McDonnell Douglas Research Laboratories, St. Louis, MO, 63166

Periodic evaluations of raw materials are necessary to detect fluctuations in chemical or physical composition and thus to prevent the manufacturing of substandard goods. Quantitative methods must be developed which address each raw material component. Quantification of reactive decomposition products is often integral to complete understanding of existing interactions among individual components in polymer-based materials. Evolved gas analysis mass spectrometry (EGAMS) can supply qualitative information about polymeric additives and the effects of these additives on thermal decomposition; however, quantitative information is difficult to extract. An EGAMS analysis makes use of a solids probe to heat the sample of interest in the ion source of the mass spectrometer. A linear heating rate is employed. Volatile compounds evolved from the sample during the heating cycle are immediately ionized. The experiments described here covered a temperature range from 40°C to 333°C.

Recently, our attention focused on quantitative analyses of ammonia and hydrogen fluoride (HF) gaseous pyrolysis products from formulated polymer based wire insulations and harness jackets. Ammonia (NH_3) is a pyrolysis product of flame retardants containing ammonium salts and hydrogen fluoride (HF) results from thermal degradation of poly (tetrafluoroethylene ethylene) copolymer-based wire insulations. Both NH_3 and HF are reactive gases with deleterious effects. To quantify these materials, the thermal instability of labile salts was useful. Ammonium bromide (NH_4Br) was used as a reference material for ammonia quantification, whereas, sodium bifluoride ($NaHF_2$) is used to quantify HF evolution. The pertinent thermal degradation reactions are:

1) $NaHF_{2\,(s)} \rightarrow NaF_{(s)} + HF_{(g)}$

2) $NH_4Br_{(s)} \rightarrow NH_{3\,(g)} + HBr_{(g)}$

The reactive nature of NH_3 and HF requires that reference salts and analytes be subjected to nearly identical environments. That is, use of the solids probe is preferred both for the references and samples. A solid diluent must be chosen and a method of homogenizing the analyte within the diluent devised. The diluent material for NH_4Br was 120/140 mesh glass beads and had a thermal window between 150 and 500°C. Alternatively, sodium fluoride (NaF) was chosen as a diluent for $NaHF_2$. TGA analysis indicates NaF is also stable over the temperature range of interest. The diluent is homogenized with the calibrant by gently grinding the mixture with a mortar and pestle.

An important assumption is that variations in ion envelope profiles as a function of temperature will not adversely affect the accuracy of our method. A sample of ammonium sulfamate $NH_4NH_2SO_3$ and NH_4Br were submitted for analysis without the concentrations being communicated to the analyst. The standards used were varying concentrations of homogenized NH_4Br with glass beads.

Figure 1 illustrates that NH_4Br and $NH_3NH_2SO_3$ have very different m/z 17.0265 ion profiles; however, the accuracy of the method is comparable for both the NH_4Br and $NH_4NH_2SO_3$ unknowns.

*This research was conducted under the McDonnell Douglas Independent Research and Development program.

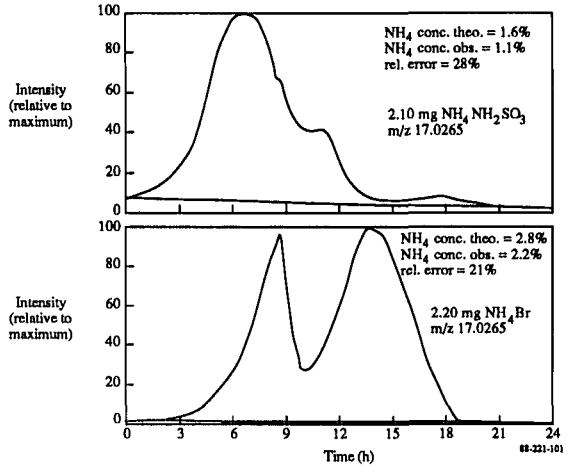

Figure 1.

We have utilized the methodology described to quantify the evolution of HF during thermal degradation of irradiated Tefzel wire insulations manufactured by a variety of suppliers. Of primary concern is the HF evolution between ambient and 200°C, and the variation of this quantity among various suppliers. Wire constructions were obtained from the suppliers of interest in the form intended for use in manufacturing. These constructions were sampled by cutting approximately 2 mm of the wires. The cuttings weighed approximately 1 to 3 mg and had approximately 500 μg of insulation associated with them. Some samples were studied with the conductor absent.

Table I indicates the amount of HF observed among several wire insulations. The yield of HF from the "D" constructions is much lower than that of the other constructions studied. Within the precision of our analysis, we do not see any certain effect on HF evolution by the conductor.

TABLE I

INSULATION	ppm HF evolved to 200°C
A	86
A	226
A NC	309
A outer NC	497
B	306
B	156
B NC	388
C	426
D	44
D NC	48

NC indicates insulations analyzed without conductor.

Presented at the 36th ASMS Conference on Mass Spectrometry and Allied Topics
June 5-10, 1988, San Francisco, CA

LOW-TEMPERATURE THERMAL AGING OF POLY(PHENYLENE SULFIDE) [PPS]*

Michael A. Grayson and Emilie G. Smith
McDonnell Douglas Research Laboratories
St Louis, MO 63166
and
Michael J. Robinson
McDonnell Douglas Astronautics Company
Huntington Beach, CA 92647

Poly(phenylene sulfide) is an important thermoplastic system for the fabrication of parts for many aerospace applications. It has low water uptake and good strength-to-weight ratio characteristics. However, because it is a high-molecular-weight, fully reacted polymer chain, processing temperatures in excess of the melt temperature are used to achieve the low viscosities necessary for void-free composite fabrication. In some cases, the temperature of processing is sufficiently high that thermal decomposition of the resin may occur. This possibility is of greater concern in some processing techniques, such as hot-gas filament winding, than in others, such as compression molding.

In this study, we wished to determine the thermal degradation processes which occur at the lowest temperatures in order to determine the extent of thermal degradation during hot-gas filament winding. Toward this aim, we exposed samples to controlled thermal environments and subsequently performed evolved gas analysis mass spectrometry (EGAMS). The data from these experiments were compared to determine changes in the compounds evolved and selected ions were used to obtain tandem mass spectra for further elucidation of the degradation process.

Samples of Ryton Type 'A' poly(phenylene sulfide) coated on AS4 Carbon fibers were obtained from Phillips Petroleum Co., Chemicals and Catalysts Division, Bartlesville, OK. The PPS/Carbon fiber pre-preg (PPS/C) was dried to constant weight and stored in a dessicating environment until sample treatment or analyses. According to thermogravimetric analysis (TGA) and evolved gas analysis mass spectrometry (EGAMS), approximately 1% of the sample weight was lost by the evolution of trapped indigenous compounds. Consequently, all samples were treated at 387°C for one hour in a dry nitrogen environment to drive off indigenous compounds prior to further studies.

Samples of PPS/C were aged for four hours in dry nitrogen at five different temperatures in the range of 327 to 447°C. Subsequently, EGAMS measurements to 430°C were performed to determine changes in the compounds evolved as a result of the short-term thermal aging. The primary compounds observed from pyrolysis of the as-received sample were hydrogen-deficient oligomers with four to seven repeat units and molecular weights of n*(108). Montaudo et al. (Ref. 1) have observed similar compounds in their studies and determined that the hydrogen deficiency is the result of macrocyclic ring formation. In our experiments with thermally aged PPS/C samples, we observe in addition to the n*(108) series several more series with greater hydrogen deficiency given by the general rules n*(108)-2 and n*(108)-4 (see Figure 1). The abundance of these latter series increases relative to the n*(108) series with increasing thermal aging temperature.

To elucidate the structure, tandem MS experiments were performed on selected ions from the thermal degradation of the aged PPS/C samples. In particular, the MS/MS spectra of the 430 and 432 ions representative of the two series n*(108)-2 and n*(108) for n=4 were studied in detail. Noting the facile loss of a sulfur and the loss of 183, a dibenzothiophene fragment, from the 430 ion, we postulate this compound to have a structure containing two dibenzo-

*This work was performed under the McDonnell Douglas Independent Research and Development program.

thiophene moieties linked by a sulfur atom. Thus, the 430 ion provides evidence for intrachain cyclization in PPS/C samples subjected to thermal aging. When the MS/MS spectrum of the 432 ion is compared with that of the 430, the same losses are observed with nearly the same relative intensities. This result suggests that some portion of the n*(108) series of compounds produced may be due to intrachain cyclization rather than macrocyclic ring formation. Tandem MS spectra of other pairs of products at n=5 (538 and 540 daltons) and n=6 (646 and 648 daltons) have similar fragmentation patterns, suggesting that the formation of the benzothiophene moiety via intrachain cyclization occurs in the higher oligomers as well.

The formation of increasingly hydrogen-deficient oligomeric series as aging temperature is increased clearly indicates the presence of one or more dibenzothiophene moieties in the thermally aged PPS macromolecule. Thus intrachain reactions are important in the low-temperature thermal degradation processes of PPS. Such reactions may actually explain changes in mechanical properties attributed to interchain crosslinking reactions postulated earlier by Brady (Ref. 2).

REFERENCES

1. G. Montaudo, C. Puglisi, E. Scamporrino, D. Vitalini, Macromolecules 19, 2157, 1986.

2. D. G. Brady, J. Appl. Polym. Sci. 20, 2541, 1976.

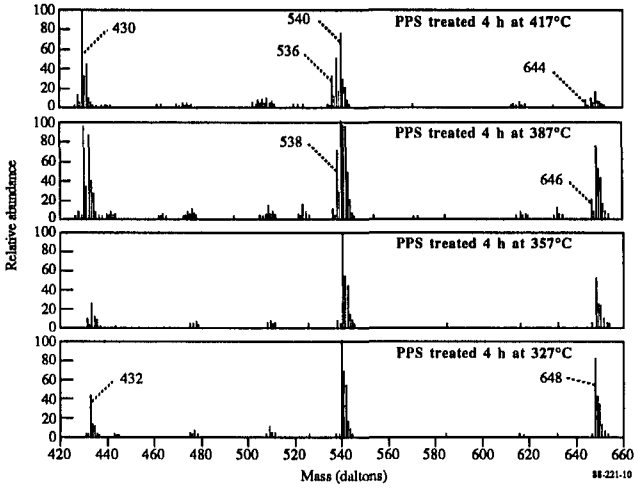

Figure 1. Comparison of composite mass spectra evolved from PPS/C aged at different temperatures for 4 h.

Presented at the 36th ASMS Conference on Mass Spectrometry and Allied Topics
June 5-10, 1988, San Francisco, CA

FRAGMENTATION OF POLYSILOXANES UNDER ELECTRON IMPACT: DIFFERENCES FOR OLIGOMERIC SERIES

P. Jane Gale and Bryan L. Bentz
David Sarnoff Research Center
Princeton, New Jersey 08543-5300

In spite of their broad use--or perhaps because of it--not a great deal of analytical information on polymeric organosilicon materials has been published. In particular, very few mass spectra are included in the commonly available libraries. Since we frequently find ourselves identifying such materials, either because we are interested in them for themselves or because they appear as contaminants in systems we are studying, we have begun to collect the spectra to form our own library. In so doing, we have found evidence for some interesting chemistry in the spectra which we highlight here. The compounds of interest have one of two general structures: linear molecules of the type $R_3SiO[Si(R_2)O]_nSiR_3$ and cyclic species, $[R_2SiO]_n$.

Silicones are easily ionized by electron impact (EI). Fragmentation is often extensive, but it usually follows predictable rules. Thus, the large number of fragment ions actually facilitates identification by aiding in structure elucidation. The compounds are less easily ionized by methane chemical ionization (CI), and, in general, we have not found CI a particularly useful technique for their analysis. Silicones are easily sputtered, however, and secondary ion mass spectrometry (SIMS) has proved an excellent means for determining their presence, either as coatings or as contaminants, on surfaces. The EI spectra presented here were obtained with an HP 5985B GC/MS. The SIMS spectra were obtained with a Finnigan MAT TSQ-15 modified in our laboratory for surface analysis.

On the following page the spectra of four molecules typical of those we encounter are shown. The structures attributed to fragment ions are merely suggested structures. In general, structural assignments for the fragment ions of smaller molecules are fairly certain, since most losses are unique and rearrangements are obvious. Assignment of structures to the fragment ions of larger molecules, particularly those from oligomeric species, is more speculative. In these molecules, several more or less equivalent sites of ionization exist and associated with each of these are a number of fragmentation pathways. In addition, several quite plausible fragment ion structures may have the same nominal mass. In determining empirical formulae for the fragment ions, we are guided by the relative intensities of the silicon isotope peaks. We also check proposed mechanisms for consistency within an oligomeric series. Finally, we compare fragment ion structures for series having different alkyl substitutents, since similar patterns are expected.

Comparison of the spectrum of the ethoxy oligomer with that of the decyl methyl oligomer shows that in general the ethoxy siloxane fragments less under electron impact than does the decyl methyl siloxane. Similar results were found when spectra for each of the n=1,5 oligomers from each series were compared, implying that the ethoxy substitution somehow stabilizes longer Si-O-Si chains. The added stability appears comparable to that imparted by cyclization. We suggest that this increased stability is due to the formation of secondary Si-O-Si bridges within the fragment ion structure when $C_2H_5OC_2H_5$ is split out. Fragmentation to an even number of silicon atoms is favored. This is not surprising, since, with an even number of silicons, each skeletal Si-O-Si triad can be stabilized. All alkoxy siloxanes might be expected to behave in this fashion, since in principle all can eliminate dialkyl ether and form secondary intramolecular oxygen bridges. We did not, however, observe bridged ions in the spectra of methoxy siloxanes; hence, operation of the bridging mechanism in the fragmentation of electron-impact-ionized alkoxy siloxanes must depend in part on the ease with which dialkyl ether can be eliminated. Some measure of the extent to which ether formation is favored can be gained by comparing heats of formation of the potential ethers. For the two ethers discussed here, ΔH_f for $C_2H_5OC_2H_5$ is some 20 kilocalories greater than ΔH_f of CH_3OCH_3.

Presented at the 36th ASMS Conference on Mass Spectrometry and Allied Topics
June 5-10, 1988, San Francisco, CA

EXAMPLES OF FRAGMENTATION PATTERNS FOUND IN POLYSILOXANE MASS SPECTRA

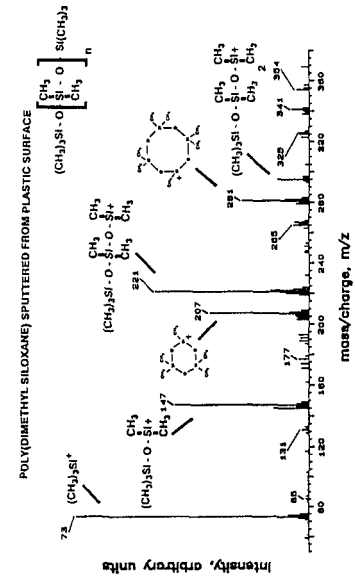

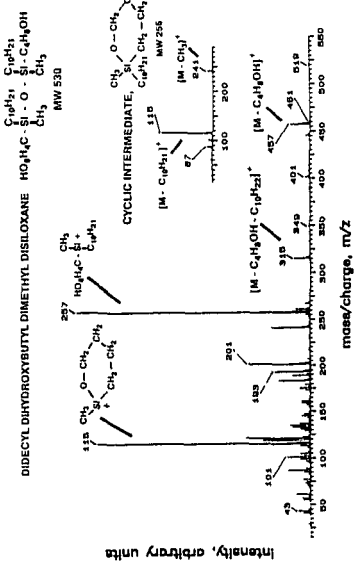

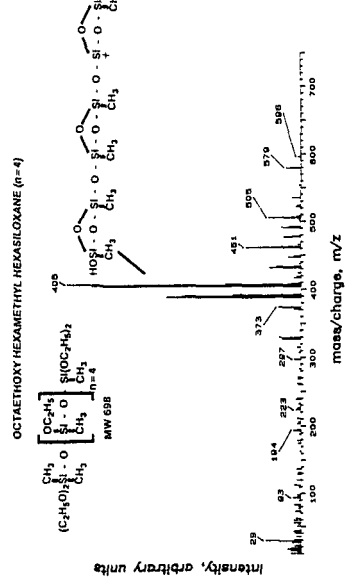

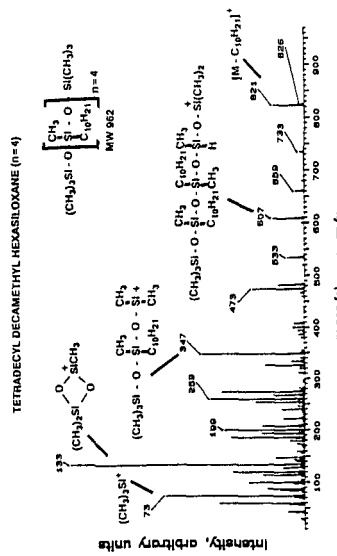

Presented at the 36th ASMS Conference on Mass Spectrometry and Allied Topics
June 5-10, 1988, San Francisco, CA

ORGANIC POLYMER ANALYSIS BY LASER IONIZATION MASS SPECTROMETRY (LIMS)

Filippo RADICATI DI BROZOLO[1], Robert W. ODOM[1],

Peter B. HARRINGTON[2] and Kent J. VOORHEES[2]

[1]Charles Evans & Associates, Redwood City, CA

[2]Departments of Chemistry and Geochemistry, Colorado School of Mines, Golden, CO.

Laser ionization mass spectrometry (LIMS) is a microanalytical materials analysis technique which has been extensively applied to elemental characterization of materials and has more recently found application in the analysis of organic species.[1] Organic characterization of polymeric materials employed in various industrial applications (e.g. semiconductor and optical fiber materials processing and aerospace applications) are particularly interesting since the performance criteria of many devices are ultimately dependant on the materials' micro-composition. We have recently initiated a LIMS characterization of various organic polymers in order to determine the ability of the laser microprobe technique in distinguishing different compositions. This characterization entails acquiring positive and negative ion mass spectra at three different laser irradiances, qualitatively evaluating the spectra for structurally significant or unique peaks and applying principal component analysis (PCA)/discriminant analysis to the data set in order to determine whether the spectra separate into distinctive classes. The laser irradiances employed are designated as low, intermediate, and high corresponding to ion intensities near threshold, ~10X and ~100X above threshold, respectively. These analyses were performed on the model LIMA 2A laser microprobe mass spectrometer manufactured by Cambridge Mass Spectrometry, Ltd (Cambridge, England) which has been described previously.[2] A representative positive ion mass spectrum produced from a thin section (~2 µm thick) of poly(1,4 butylene terephthalate) is illustrated in Figure 1. Two kinds of signals are generally recognized in the mass spectra: C_xH_y cluster ions arising from rearrangement of the molecular structure and structurally significant molecular fragments, such as the aromatic ions C_6H_5, $C_6H_5CH_2$, C_6H_5O, or C_6H_5CO. A weak signal for this latter ion is observed in Fig. 1. Although these molecular fragment ions do provide valuable structural information, the low intensity of these structural ions rarely provide unambiguous identification of the polymer structure.

A principal component analysis (PCA) technique[3] employing canonical variate or discriminant analysis[4] was applied to a limited mass spectral data set produced from seven different polymers in order to determine whether PCA could provide distinctive classification of the spectra. Figure 2 illustrates the canonical variate scores for the first two components produced in a PCA analysis of the high irradiance positive ion data for these polymers. The identification of the various samples in this plot are the following: (1)-Nylon 6, (2)-Nylon 12, (3)-Poly(1,4 Butylene Terephthalate), (4)-Polycarbonate, (5)-Polystyrene, (6)-Spurr's Epoxy Resin, and (7)-Mylar D500 [Poly(Ethylene Terephthalate)]. The data reduced to 12 principal components which described over 80% of the variance while the canonical variate analysis yielded four components which accurately classified over 65% of the spectra. The canonical variate scores for the two components displayed in Fig.2 form distinct clusters which indicates that the canonical variates for the various polymers are reasonably distinct. Each number in the plot represents

the scores for a single mass spectrum in the data file and the spectra from several polymers overlap (i.e. there are less than seven numbers for each polymer type), suggesting that the laser microprobe data are highly reproducible. More accurate classification could result from utilizing a larger data base. A similar analysis of the high irradiance negative ion data yields two canonical variates which accurately classified 55% of the spectra. Thus, the positive ion data seems to provide a more unique pattern of spectral peaks. This type of classification is continuing for other polymer formulations and analysis conditions and ultimately we hope to develop a reference library for laser microprobe polymer analyses.

References

1. L. Van Vlaeck, J. Claereboudt, J. De Waele, E. Esmans and R. Gijbels, Anal. Chem. 1986, 57, 2944.

2. T. Dingle, B.W. Griffiths, J.C. Ruckman and C.A. Evans, Jr., Microbeam Analysis-1982, Ed. K.F. Heinrich, San Francisco Press, Inc. 365

3. Factor Analysis in Chemistry, E. R. Malinowski and D. G. Howery, J. Wiley & Sons, New York, 1980.

4. S.J. DeLucas, K.J. Voorhees, and E.W. Sarver, Anal. Chem. 1986, 58, 2439.

Acknowledgments: This work was supported by a NSF SBIR Grant No. ISI-8760431

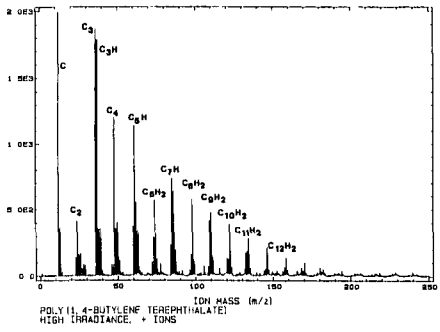

Figure 1

Figure 2

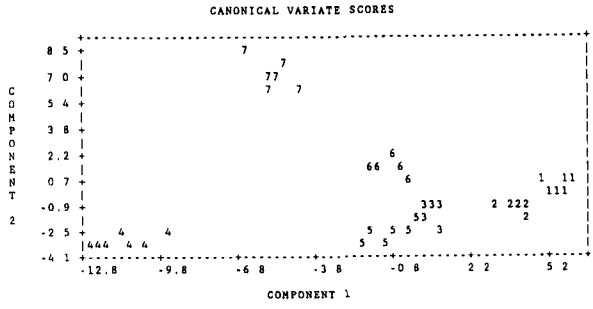

Presented at the 36th ASMS Conference on Mass Spectrometry and Allied Topics
June 5-10, 1988, San Francisco, CA

NEGATIVE ION FAB MASS SPECTROMETRY OF PROCYANIDIN OLIGOMERS

J.J. Karchesy and L.Y. Foo, Department of Forest Products; E. Barofsky
B. Arbogast, and D.F. Barofsky, Department of Agricultural Chemistry
Oregon State University, Corvallis, Oregon 97331

We have previously reported on positive ion FAB mass spectrometry, utilizing linked scanning, of procyanidin oligomers [1]. In the present work we report on a complimentary study of negative ion FAB mass spectrometry of this same group of compounds; as with our positive ion FAB analyses, we have made extensive use of linked scanning to obtain structural information. In recent independent studies, negative ion FAB has been employed to assist in both the structural elucidation and analysis of mixtures of procyanidin oligomers, glucosylated flavanoid oligomers, and derivatives [2-5].

Mass spectra of the dimeric procyanidins B-1, epicatechin(4β→8)catechin (I); B-7, epicatechin(4β→6)catechin (II); epicatechin(4β→2)phloroglucinol (III); A-1, epicatechin(4β→8; 2β→O→7)catechin (IV); and trimeric procyanidins epicatechin(4β→8)epicatechin(4β→8)epicatechin (V); epicatechin(4β→8) catechin(6→4β)epicatechin (VI) were obtained off both a VG 7070E-HF mass spectrometer and a KRATOS MS-50 TC mass spectrometer. Both instruments have standard FAB sources that use Ion Tech saddlefield atom guns. A 5:1 mixture of dithiothreitol and dithioerythritol (commonly referred to as magic bullet) was used as the FAB matrix liquid. Approximately 10 μg of sample compound was dissolved in about 1 μl of magic bullet for analysis; the samples were bombarded with 8 keV xenon atoms. Metastable decomposition pathways were established by B/E linked scanning without collisional activation.

Table 1.

Compound	Ions Observed					
	$(M-H)^-$	RDA	RDA-H_2O	Monomer	Dimer	Other
I.	577(100)	425(25)	407(11)	287(12),289(18)	--	273(-)
II.	577(100)	425(29)	407(8)	287(8),289(24)	--	273(-)
III.	413(100)	261(14)	--	287(7),125(14)	--	--
IV.	575(100)	423(25)	--	285(19),289(10)	--	--
V.	865(100)	713(14) 425(10) 423(7)	695(4) 407(10) 405(4)	287(17),289(20)	575(9),577(10)	--
VI.	865(60)	713(13) 425(29)	695(6) 407(19)	287(20),289(15)	577(100)	--

Retro-Diels Alder (RDA) fission results in characteristic $(M-H-152)^-$ ions for each of the compounds studied (Table 1). In two instances, compounds I and II, a mass peak at m/z 273 (seen only in the B/E spectrum due to a coincident matrix peak) can be rationalized on the basis of a second, consecutive RDA fission from the original RDA fragment ion m/z 425.

A quinone methide (QM) mechanism of interflavanoid bond cleavage is proposed to account for the two different sequence ions that are produced from the $(M-H)^-$ ion of B-1 and B-7 (Scheme 1). The proposed formation of quinone methide from procyanidins under FAB conditions is supported by numerous examples in which gas phase decompositions under mass spectrometric conditions can be accounted for by mechanisms invoked to explain reactions in solution chemistry [6-10]. This mechanism is consistent with the sequence

ions produced by cleavage of B-type interflavanoid linkages in the trimers as well. Most importantly, this mechanism demonstrates that the upper and lower isomeric flavan units can be distinguished after cleavage of the bond between them. This has positive implications for future research on analytical methods that might identify the points of attachment for other groups, such as glycosides, DNA adducts, etc., on a procyanidin oligomer.

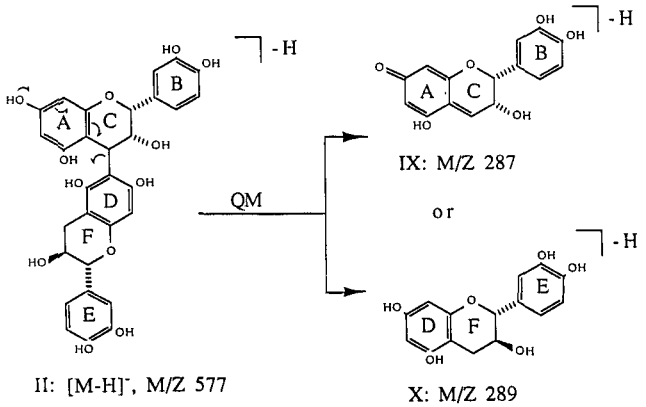

Scheme 1.

Because the QM mechanism results in unsymmetric cleavage about the interflavanoid bond, a linear (V) and a branched trimer (VI) can be distinguished by the dimer ions they produce. With V, cleavage of the upper interflavanoid bond gives a dimer at m/z 577 while cleavage of the lower interflavanoid bond gives a dimer at m/z 575; subsequent RDA fissions of each of these give ions at m/z 425 and m/z 423 respectively. By contrast, VI gives a dimer at m/z 577 (II) upon cleavage of the upper bond and a dimer at m/z 577 (I) on cleavage of the lower bond. Subsequent RDA fissions of I and II give indistinguishable ions at m/z 425.

Acknowledgement. Support for this work was provided by USDA Grant 85-FSTY-0144, by the Forest Research Laboratory, Oregon State University, and by the Chemistry Division, DSIR, New Zealand.

References.

1. J.J. Karchesy, R.W. Hemingway, Y.L. Foo, E. Barofsky, and D.F. Barofsky, Anal. Chem. 58, 2563 (1986).
2. R. Self, J. Eagles, G.C. Galletti, I. Mueller-Harvey, R.D. Hartley, A.G.H. Lea, D. Magnolato, U. Richli, R. Giijer, and E. Haslam, Biomed. Environ. Mass Spectrom. 13, 449 (1986).
3. R. Gujer, D. Magnolato, and R. Self, Phytochemistry 25, 1431 (1986).
4. G. Galletti and R. Self, Annolidichimica 76, 195 (1986).
5. J.J. Karchesy and R.W. Hemingway, J. Agric. Food Chem. 34, 966 (1986).
6. M.R. Attwood, B.R. Brown, S.G. Lisseter, C.L. Torrero, and P.M. Weaver, J. Chem. Soc. Chem. Commun., 177 (1984).
7. L.Y. Foo and H. Wong, Phytochemistry 25, 1961 (1986).
8. P.E. Laks and R.W. Hemingway, J. Chem. Soc. Perkin Trans. I, 465 (1987).
9. R.W. Hemingway and L.Y. Foo, J. Chem. Soc. Chem. Commun., 1035 (1983).
10. L.Y. Foo and R.W. Hemingway, J. Chem. Soc. Chem. Commun., 85 (1984).

Presented at the 36th ASMS Conference on Mass Spectrometry and Allied Topics
June 5-10, 1988, San Francisco, CA

CHARACTERIZATION OF EPOXY DERIVED OLIGOMERS BY FAST ATOM BOMBARDMENT MASS SPECTROMETRY.

James N. Kyranos and Paul Vouros
Barnett Institute Northeastern University,
Boston, Massachusetts 02115

Walter X. Zukas and Gary Hagnauer
Army Material Research Center
Watertown, Massachusetts 02172

The recent general applicability of fast atom bombardment mass spectrometry (FAB/MS) to biopolymer systems has sparked considerable interest in the use of this technique to characterize synthetic polymers. Our laboratory, as well as several others, has begun to examine the fragmentation patterns of oligomers in order to identify and/or confirm the type of structures formed during a particular curing process.

Specifically, we have studied the curing products of methoxyglycidyl ether of Bisphenol A (MGEBA) with 4-aminodiphenyl sulfone (ADS) and 4,4'-diaminodiphenyl sulfone (DDS). The major products of the first reaction mixture (MGEBA/ADS) were first separated by preparative liquid chromatography and enough material collected in order to perform more conventional structural identification techniques (i.e. NMR and IR). Once the structure of each product was established by these techniques, the FAB/MS studies served the dual purpose of confirming the identity of the products and of establishing a data base regarding the relationship between mass spectral patterns and molecular structure. In every case the major fragmentations were directed by the common MGEBA portion(s).

In addition to providing molecular weight information, which confirms the identity of the oligomers, the fragmentation patterns of the mass spectra can also be used to distinguish between different isomeric linkages of the same oligomer. As an example to illustrate this point, the spectra of the two 2:1 (MGEBA:ADS) isomeric products are shown in Figures 1 and 2. Although the molecular weight as well as many of the fragments are common to both isomers, there are two features which distinguishes between the two. The first, and most prominent, is the relative intensity of the peak at m/z 544 compared to the molecular ion. The formation of this ion is favored for the first isomer because the ion is a quaternary amine which is formed by cleavage beta to the nitrogen from either MGEBA moiety and resonance stabilized by the adjacent aromatic electron density. On the other hand, in order for the second isomer to form the ion at m/z 544, cleavage must take place between the methylene and methine carbons adjacent to the ether oxygen resulting with an ion which has a positive charge on the methylene and little adjacent electron density to stablize that charge. The second difference is the peak at m/z 260 for the first isomer (Figure 1) which can only be formed by a tertiary amine and the corresponding ion at m/z 246 for the second isomer (Figure 2) which is indicative of a secondary amine.

By identifying the types of fragmentations which occur in these products, we established a data base which relates fragmentation patterns to molecular structure. We then used this information to characterize the products of the related MGEBA/DDS system using only FAB/MS and the material collected from one HPLC run.

Having the ability to identify reaction products from a chromatographic run, we may envision on-line HPLC-FAB/MS using the moving belt interface in order to identify the minor and trace components of these and other reaction mixtures, as well as the intermediates which are highly reactive or unstable for long periods of time.

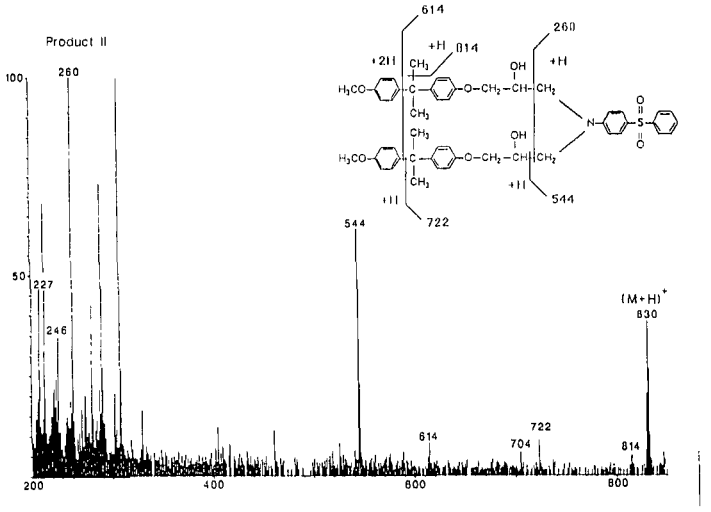

Figure 1. FAB spectrum of 2:1 (MGEBA:ADS) tertiary amine isomer in 3-nitrobenzyl alcohol

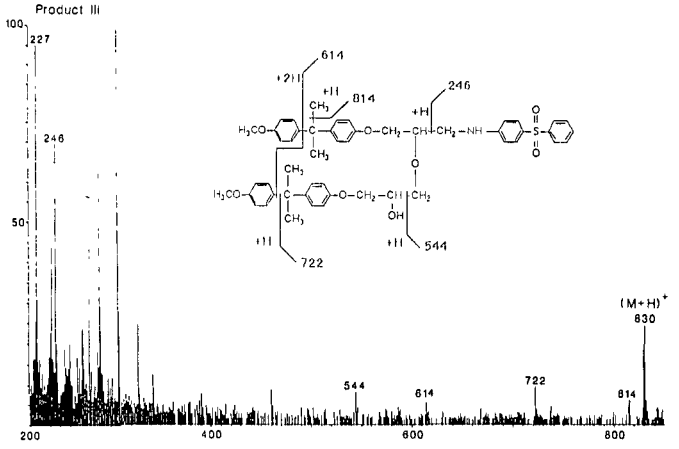

Figure 2. FAB spectrum of 2:1 (MGEBA:ADS) secondary amine isomer in 3-nitrobenzyl alcohol

Presented at the 36th ASMS Conference on Mass Spectrometry and Allied Topics
June 5-10, 1988, San Francisco, CA

Methylation Studies of Protein and Nucleic Acids

W.G. Stillwell, Liang-Shang Gan, John S. Wishnok, Hou-Xiao Xu, and Steven R. Tannenbaum. Department of Applied Biological Sciences, Massachusetts Institute of Technology, Cambridge, MA 02139.

We have begun an investigation of the use of methylated nucleic acids and methylated proteins as indicators of prior exposure to methylating agents in laboratory animals and humans. We chose the carcinogen N-nitrosodimethylamine (NDMA) as the methylating agent for study. NDMA is metabolized in animals to a reactive species capable of methylating nucleic acids and protein. The major DNA adduct formed in vivo and in vitro is 7-methylguanine, however, 3-methyladenine, O^6-methylguanine, as well as methyl phosphotriesters, are found in minor amounts. Methylation is also a naturally occurring process and background levels of methylated nucleic acids and proteins arising from biological sources are observed.

In this work we studied the urinary excretion of 3-methyladenine and 7-methylguanine, as well as methyl esterified amino acids in hemoglobin, as indicators of exposure to methylating agents. The ferret was used in these studies because this species is (1) a better model than the rat for the human stomach and (2) is larger than the rat thus simplifying surgical procedures.

We have also studied the urinary excretion of 3-methyladenine and 7-methylguanine, as well as nitrosoproline and nitrate, in a human population characterized by an increased incidence of gastritis accompanied with elevated levels of urinary nitrate.

METHODS. Male ferrets (600-875 gm) were administered 0.5, 2.0, and 5.0 mg/kg N-nitrosodimethyl-d_6-amine. Urine samples from baseline, 0-24, 24-48 hr post-dosing periods were collected. One ml blood samples were also collected at selected intervals. Isolation and analysis of 3-methyl-d_3-adenine, as well as other purines in urine, were carried out by a modification of a published procedure (1) using 3-ethyladenine as the internal standard. Quantification of 3-methyladenine and 3-methyl-d_3-adenine in extracts of urine was accomplished by GC/MS analysis of the t-butyldimethylsilyl derivatives using selected-ion-monitoring (SIM) at m/z 206 (M-57) for 3-methyladenine, m/z 209 for the d3-analog, and m/z 220 for 3-ethyladenine. Analysis of adducted hemoglobin was conducted after basic hydrolysis of the isolated globin fraction followed by ultrafiltration, extraction, and derivatization of the labeled (d_3) methanol with pentafluorobenzoyl chloride. Negative-ion-chemical-ionization GC/MS was used to quantify the amount of labeled methanol formed from d_6-NDMA.

RESULTS AND DISCUSSION. Analysis of hemoglobin in the ferret showed that methyl ester formation accounted for 25-30% of total hemoglobin modification (approx. 0.6% of the total dose) in the early 24-hr samples. The sensitivity of the GC/MS analysis was such that levels as low as 10 ng of methyl-d_3-ester per gm of hemoglobin could be detected.

Excretion of 3-methyl-d_3-adenine in urine showed a linear dose-response relationship in the range studied and accounted for approx. 0.06% of the total dose administered. Figure 1 shows the SIM traces of the urine extract obtained from the ferret administered 5.0 mg/kg d_6-NDMA; the amount of 3-methyl-d_3-adenine excreted was 1.8 ug. The baseline value of 3-methyladenine excretion was 476 ng/24 hr (the SIM traces for this analysis are shown in figure 1). Ferrets typically excrete 300 to 600 ng of 3-methyladenine per day.

Other purine bases including adenine, guanine, 1-methyladenine, 7-methylguanine, N^2-methylguanine, N^2-dimethylguanine, 8-hydroxyadenine, and 8-hydroxyguanine were also detected in both ferret and rat urine. SIM traces for the analysis of adenine, 7-methylguanine, 8-hydroxyadenine, and N^2-dimethylguanine in control ferret urine are shown in Figure 2.

In the human studies, 3-methyladenine was assayed as described above at m/z 206 and m/z 209 (for the d_3-analog used as internal standard); the corresponding ions at m/z 336 and 339 were used for 7-methylguanine. In a low nitrate group (N=23) a median value of 5.3 ug/24 hr for 3-methyladenine excretion was obtained. In a high nitrate group a wide variation of excretion was noted (range 2.4 to 123.8 ug/24 hr); median values of 8.9 to 9.1 ug/24 hr were observed in this group (N=20). In the highest nitrate

subset, the range of excretion was identical to the range of combined high-nitrate group, but the median value for the excretion of 3-methyladenine was somewhat lower (5.8 ug/24 hr). Excretion of 7-methylguanine for the high nitrate group appeared to be slightly higher than that for the low nitrate group. There was slight correlation between excretion of N-nitrosoproline and 3-methyladenine in these subjects.

1. D.E.G. Shuker, E. Bailey, A. Parry, J. Lamb, and P.B. Farmer. Carcinog. 8, 959 (1987).

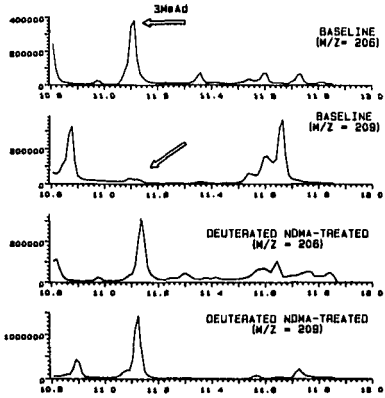

Figure 1

SELECTED-ION-MONITORING TRACES FOR THE ANALYSIS OF 3-METHYLADENINE (m/z = 206) AND 3-METHYL-d3-ADENINE (m/z = 209) ISOLATED FROM FERRET URINE. THE TOP TRACE IS FROM AN UNTREATED (BASELINE) FERRET, THE SECOND SHOWS THE BASELINE VALUE FOR m/z = 209, THE THIRD TRACE SHOWS UNLABELED 3-METHYLADENINE FROM A FERRET TREATED WITH N-NITROSODIMETHYL-d6-AMINE (NDMA) WHILE THE BOTTOM TRACE SHOWS 3-METHYL-d3-ADENINE (m/z=209) FROM THE FERRET TREATED WITH LABELED NDMA (5 mg/kg). 3-ETHYLADENINE WAS USED AS INTERNAL STANDARD IN THESE STUDIES.

Figure 2

SELECTED-ION-MONITORING TRACES OF THE t-BUTYLDIMETHYLSILYL DERIVATIVES OF ADENINE, 7-METHYLGUANINE, 8-HYDROXYADENINE, AND N2-DIMETHYLGUANINE DETECTED IN FERRET BASELINE URINE.

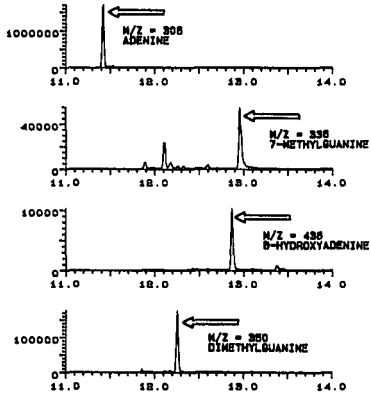

Presented at the 36th ASMS Conference on Mass Spectrometry and Allied Topics
June 5-10, 1988, San Francisco, CA

TIME-OF-FLIGHT SECONDARY ION MASS SPECTROMETRY OF PROTECTED ISOMERIC OLIGONUCLEOTIDES

F.Lafortune[A], W.Ens[C], K.G. Standing[C], J.B. Westmore[B],
M.J. Damha* and K.K. Ogilvie*, Chemistry[B] and Physics Departments[C],
[A]Collège universitaire de Saint-Boniface,
University of Manitoba,Winnipeg, Canada R3T 2N2
and
*Chemistry Department, McGill University, Montreal, Canada H3A 2K6

INTRODUCTION

Particle-assisted desorption ionization techniques have been used sucessfully in mass spectrometry for studies of non-volatile and thermally sensitive biomolecules. In particular, solid SIMS incorporating a time-of-flight (TOF) mass analyzer combines high sensitivity with a very high mass range, and the mass spectra are relatively free from the significant chemical noise that is usually associated with the matrix employed in liquid SIMS, i.e. fast atom bombardment.

We have investigated the use of TOF-SIMS as an analytical tool to characterize and differentiate protected isomeric di and trinucleotides, as shown in Table 1 . These compounds, synthesized at McGill (1), include three pairs of positional isomers of an unusual kind: they contain either 3'-5' or 2'-5' phosphodiester linkages. Also included in these studies is one pair of diastereomeric branching trinucleotides, involved in the maturation process of messenger RNA.

Mass spectrometry was performed on the Manitoba TOF II instrument, which incorporates an ion mirror (2). We will demonstrate how the use of this technique can reveal striking differences between these very closely related biomolecules.

EXPERIMENTAL

1. Sample preparation:

All oligonucleotides were dissolved in methanol at a concentration of ca 1 mg/ml. A few μL of each solution were then deposited on aluminum foil treated to give a boehmite, AlO(OH) , surface (3).

2. Mass spectrometry:

Sample targets were bombarded by a pulsed beam of 23 keV Cs^+ primary ions. The secondary negative ions produced were accelerated to -5 keV, allowed to drift along the field-free region of the flight tube, then detected by microchannel plates. No electric field was applied on the ion mirror in the current study; therefore, only "direct"mass spectra were obtained. An accompanying paper (4) describes how this instrument can also be used as a "tandem-like" mass spectrometer.

RESULTS AND DISCUSSION

Detection of quasimolecular ions and sequence information have been obtained for each oligonucleotide. Contrary to what was observed with unprotected, normal 3'-5' oligonucleotides (5), 5'-phosphate sequence ions (X^- ions(6), see figure 1) are not always more abundant than the corresponding 3'-phosphate sequence ions (Y^- ions). This can be explained in part by the presence of bulky silyl protecting groups in all the compounds studied. On the other hand, indicators of isomeric form have been found in every instance. For example, the ratio of X^- ions/Y^- ions (with or without protecting groups) becomes smaller for positional isomers containing a 2'-5' phosphodiester linkage. In the case of dinucleotides, an increase in the yield of A^{Bz}- is also noted. These observations

may be related, as depicted in scheme 1. In 2'-5' isomers, anchimeric assistance can be provided by neighboring 2'phosphate oxygens, facilitating the loss of the base moiety, therefore competing with X^- ion formation pathways. A similar rationale has been used to explain differences between diastereomeric $A^{U}U$ and arabino-$A^{U}U$, the latter showing both a reduced A^{Bz}- ion yield and an increase in the production of X^- ions (7).

In addition to providing quasimolecular ion detection, base sequence information and protecting group nature and location, many unequivocal indicators of isomeric form were found for each pair of oligonucleotides studied. Time-of-flight SIMS hence constitutes a powerful tool in mass spectrometric investigations of subtly different biomolecules such as these.

REFERENCES

(1) M.J. Damha *et al*, submitted for publication in J.Am.Chem.Soc.
(2) K.G. Standing *et al*, Analytical Instrum. 16(1), (1987) 173;
X. Tang *et al*, Int. J. Mass Spectrom. Ion Processes, in press
(3) R.Beavis *et al*, 35th Annual Conference on Mass Spectrometry and Allied topics, Denver, Col. 1987, p652
(4) F. Mayer *et al*, these proceedings
(5) R. Cerny *et al*, Anal. Biochem. 156, (1986) 424
(6) A. Viari *et al*, Mass Spect. in the Analysis of Large Biomolecules, Ed. C. McNeal, J. Wiley & Sons, (1986) p199
(7) F. Lafortune *et al*, Org. Mass Spectrom. 23, (1988) 228

#	OLIGONUCLEOTIDE	SYMBOL	MOL. WT
1	A^{Bz}3'p5'U	A_pU	1073
2	A^{Bz}2'p5'U	A^pU	1073
3	A^{Bz}3'p5'G^{Bz}	A_pG	1216
4	A^{Bz}3'p5'G^{Bz}	A^pG	1216
5	U3'p5'A^{Bz}3'p5'G^{Bz}	U_pA_pG	1690
6	U3'p5'A^{Bz}2'p5'G^{Bz}	U_pA^pG	1690
7	A^{Bz}(2'p5'U)3'p5'U	A^UU	1469
8	ara-A^{Bz}(2'p5'U)3'p5'U	ara-A^UU	1469

Table 1: List of Oligonucleotides analyzed in the present study

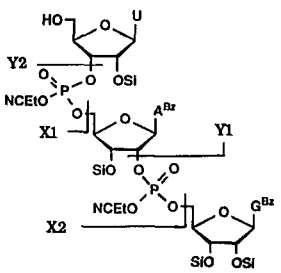

Figure 1: UpAPG

NOTE: Si = t-Bu$(CH_3)_2$Si-
Bz = C_6H_5CO-
NCEt = $NCCH_2CH_2$-
Me = CH_3

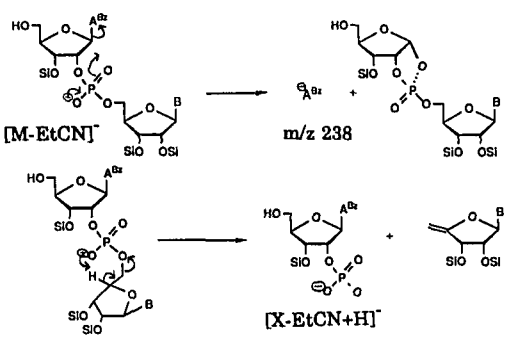

Scheme 1: Anchimeric assistance as a mean to promote formation of A^{Bz}- ions in negative mode mass spectra of 2'-5' dinucleotides.

Presented at the 36th ASMS Conference on Mass Spectrometry and Allied Topics
June 5-10, 1988, San Francisco, CA

MASS SPECTROMETRIC AND CHROMATOGRAPHIC PROPERTIES OF RING-PENTA FLUOROBENZYLATED NUCLEOBASES USED IN THE TRACE DETECTION OF ALKYL DNA ADDUCTS

Gerhard M. Kresbach, R.S. Annan, M.G. Saha, R.W. Giese, and Paul Vouros
Barnett Institute, Dept. of Chemistry, and Dept. of Medicinal Chemistry,
Northeastern University, Boston, Massachusetts 02115

Exposure of humans to chemicals as well as radiation raises the risks of carcinogenesis and mutagenesis due to the formation of adducts in DNA. A specific type of damage is the introduction of small alkyl and hydroxyalkyl groups in nucleobases, e.g. the O^2-methylation of cytosine and the conversion of thymine to 5-hydroxymethyluracil (HMU).

Our laboratory has been interested in the development of chemical derivatization techniques for the trace level detection of modified DNA bases using electrophoric groups and negative chemical ionization mass spectrometry (NCI-MS). The selection of derivatives is based on several requirements, including a) the formation of analyte specific ions under NCI-MS, b) the capability to yield structurally diagnostic ions by EI and/or PCI, c) high yield and adequate chemical stability, and d) good chromatographic performance for GC-MS and LC-MS at trace levels.

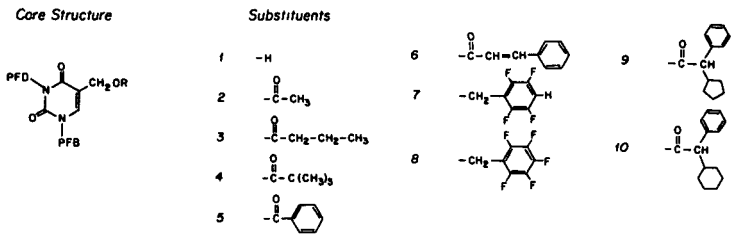

Figure 1: Electrophoric 5-hydroxymethyluracil derivatives

Derivatization with the pentafluorobenzyl (PFB) group as an electrophore was found to comply with most of these demands. N_1,N_3-bis-PFB-HMU with either a free hydroxyl group in position 5 or there further derivatized (Fig. 1) was used as a model compound for hydroxylated nucleobases and demonstrated the impact of PFB in the NCI mode on the main fragmentation pattern and the strong influence of the side chain on the relative ion intensity (Fig. 2). Generally the fragment $[M\text{-}PFB]^-$ was observed as the base peak, serving as diagnostic ion. Fig. 3 shows the separation of 40 fmol each of several of these derivatives by LC-MS using a moving belt interface and selected ion recording of the $[M\text{-}PFB]^-$ -ions. Separation of the same compounds at a 10 fmol level by GC- MS resulted in a comparable signal/noise ratio and demonstrated again the applicability of the transport type interface in trace analysis.

The validity of these results was confirmed in a study of a wide variety of modified bases. $[M\text{-}PFB]^-$ as base peak in NCI is a common feature in all ring-pentafluorobenzylated nucleobases. Well defined protonated molecular ions can be obtained in the PCI mode. Under EI conditions, information about the core struc ture of the base as well as about exocyclic substitution can be obtained, thus facilitating the identification of unknown adducts. Differentiation of positional isomers is possible in some cases.

In summary, pentafluorobenzylation can be used successfully for the detection of alkyl DNA bases at low picogram levels by GC-MS and LC-MS using a moving belt interface.

Presented at the 36th ASMS Conference on Mass Spectrometry and Allied Topics
June 5-10, 1988, San Francisco, CA

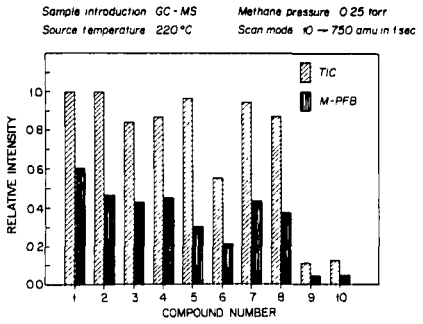

Figure 2:

Relative molar responses of electrophoric HMU derivatives in the NCI mode

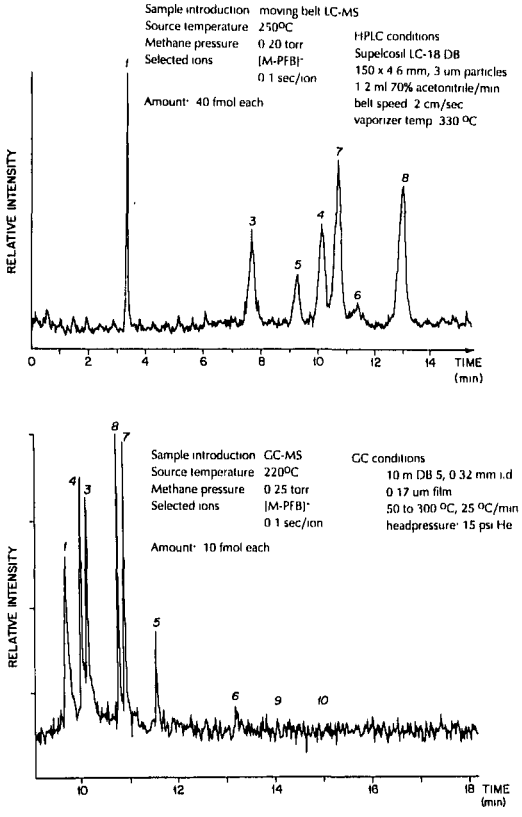

Figure 3:

Comparison of LC-MS (moving belt) and GC-MS near the detection limit

Presented at the 36th ASMS Conference on Mass Spectrometry and Allied Topics
June 5-10, 1988, San Francisco, CA

ISOLATION AND CHARACTERIZATION OF TWO NEW NUCLEOSIDES FROM HUMAN URINE

G.B. Chheda*, H.A. Tworek*, A.K. Bhargava#, J.G. Antkowiak¶, S.P. Dutta* and H.B. Patrzyc*

Departments of Biophysics*, Thoracic Surgery¶, and Laboratory Medicine#
Roswell Park Memorial Institute, Buffalo, New York 14263

In continuation of our studies on urinary nucleosides, we wish to report the isolation and characterization of two new nucleosides, 5-carbamoylmethyluridine I and 5-carbamoylmethyl-2-thiouridine II (Fig. I) from normal human urine. A 24 hour urine (1500 ml) was processed according to the previously described procedure (1). The two unknown nucleosides I and II were purified by HPLC and were obtained in 240 ug and 25 ug respectively. The uv spectra of nucleoside I were similar to those of the 5-substituted uridines [λ_{max} (nm) 266 (pH 1 and 6.0) and 265 (pH 11.0)]. The nmr spectrum in D_2O exhibited resonance at 5.96 ppm for the anomeric proton and at 7.8 ppm for C_6H of uridine. The upfield resonance at 3.35 ppm could be assigned to the methylene protons of the 5-substituent. A trimethylsilyl derivative of I gave a highest mass ion at m/z 646 (Fig. 2) which could be assigned to $M^{+\cdot}-CH_3$ ion of penta TMS derivative (mol. wt. 661) of the nucleoside I. The fragment ion at m/z 546 (M-115) represents the loss of CON-TMS from the side chain while the fragment ion at m/z 386 arises from the silylated base after the cleavage of the glycosidic bond. The ions at m/z 349, 259, 243, 217 and 169 confirm the presence of an unmodified ribose sugar in the molecule. The mass spectra of the penta TMS derivative of authentic I were similar to those of the TMS derivative of unknown urinary nucleoside I, thus supporting 5-carbamoylmethyluridine as the structure of the nucleoside I.

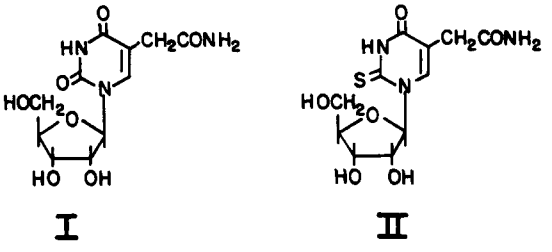

Fig. I

The uv spectra of the nucleoside II exhibited maxima at 275 nm at pH 1 and 7, and at pH 11 maxima shifted to 242 nm with a prominent shoulder at 271 nm. These uv spectra were similar to those of the 5-alkyl-2-thiouridine. A TMS derivative of nucleoside II (Fig. 3) exhibited the highest mass ion at m/z 572. This was assigned to the $M^{+\cdot}-CH_3$ ion of the TMS derivative of dehydration product of II. Authentic 5-carbamoylmethyl-2-thiouridine silylated under identical conditions also exhibited a highest mass ion at m/z 572 assigned to the $M^{+\cdot}-CH_3$ ion of the tetra TMS derivative of the dehydration product. A dehydration product ion ($M-H_2O$) was observed also in the mass spectra of the $(TMS)_5$ derivatives of I. The mass ions m/z 348, 259, 245 and 217 indicate an unmodified ribose sugar. The EI GC/MS spectra for silylated urinary nucleoside II and silylated authentic II are identical, thus supporting the structure II for this urinary nucleoside.

The nucleoside (I) was first isolated from the alkaline hydrolysate of tRNA from Bakers yeast and wheat embryo[2]. More recently, it has been shown to be present in the first position (Wobble) of the anticodons of $tRNA^{Pro}$ and $tRNA^{Val3}$. The isolation of nucleoside II from other biological sources such as tRNA has not been reported. The uridine derivative 5-methoxycarbonylmethyl-2-thiouridine, however, has been isolated from yeast tRNA hydrolysates and has been shown to be present in the Wobble position of the anticodons for $tRNA^{Lys}$ and $tRNA^{Glu}$ from Bakers yeast. Control experiments indicate that the urinary material could originate from

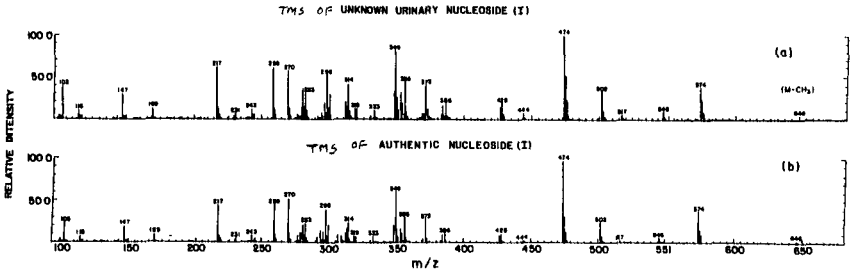

Fig. 2

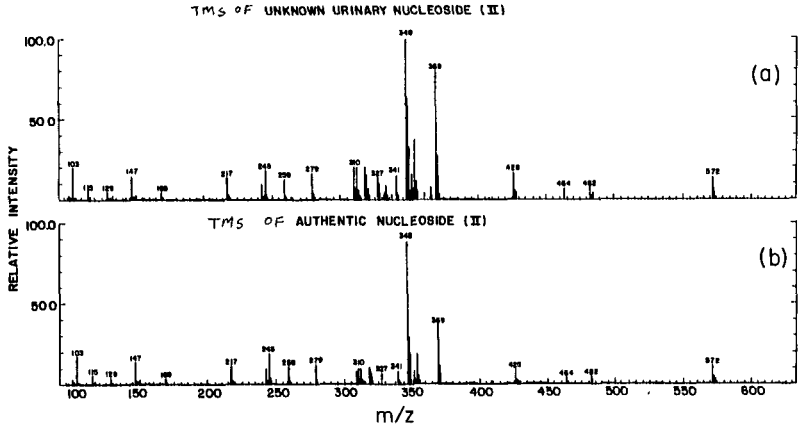

Fig. 3

the 5-methoxycarbonylmethyl-2-thiouridine under the isolation procedure. Nucleoside I, excreted in the urine, is most probably derived from the tRNA turnover. With few exceptions, uridine in the first (Wobble) position of the anticodon in tRNA is replaced by hypermodified uridines or thiouridines substituted at the 5-carbon. It has been demonstrated that some of the hypermodified uridines amplify the Wobble recognition while others such as 2-thio derivatives restrict the recognition. These nucleosides thus, appear to play some role in codon-anticodon interactions. The enzymatic controlled modification mechanism of nucleosides has been shown to be a sensitive indicator for monitoring normal cellular events. Study of the excretion levels of these two modified nucleosides may prove useful in the investigation of the modification phenomena and its role in nucleic acid functions, cell differentiation and turnover rates.

1. G.B. Chheda, H.B. Patrzyc, H.A. Tworek, J.A. McCloskey and S.P. Dutta, in "Chromatographic and Other Analytical Methods in Nucleic Acid Research", Vol. II, C.W. Gherke and K.C. Kuo, eds., Elsevier Science Publishers, Amsterdam, The Netherlands (1988) in preparation.
2. D.B. Dunn, M.D. Trigg, Biochem. Soc. Trans. 3, 656 (1975).
3. N. Yamamoto, A. Mamaizumi, S. Yokoyama, T. Miyazawa, S. Nishimura, J. Biochem. 97, 361 (1985).

Presented at the 36th ASMS Conference on Mass Spectrometry and Allied Topics
June 5-10, 1988, San Francisco, CA

CHARACTERIZATION OF 2'-O-METHYLINOSINE AND OTHER 2'-O-METHYLNUCLEOSIDES IN HUMAN URINE

S.P. Dutta*, H.A. Tworek*, A.K. Bhargava¶, H.B. Patrzyc* and G.B. Chheda*

Depts. of Biophysics* and Laboratory Medicine¶
Roswell Park Memorial Institute, Buffalo, New York 14263

Of more than 65 modified nucleosides known to be present in mammalian tRNA, 21 have, so far, been detected in human urine[1]. Anticodon adjacent modified nucleosides of tRNA, such as N-[(N-9-β-D-ribofuranosyl-purin-6-yl-carbamoyl)-L-threonine (t6A), 1-methylinosine, N2-dimethylguanosine, .. are included in this group. Some of these compounds are known to be present in higher levels in the urines of cancer patients as compared to normal human urine[1]. Ribose modified nucleosides such as the 2'-O-methyl-nucleosides are pesent in mammalian tRNA, mRNA, rRNA and HnRNA. We have been interested in developing suitable clean-up and GC-MS assay procedures for the detection and quantitation of these modified nucleosides in human urine. This report describes a capillary GC-MS procedure for the detection and identification of four 2'-O-methylnucleosides, 2'-O-methyladenosine, 2'-O-methyluridine, 2'-O-methylguanosine and 2'-O-methylinosine in human urine.

A 50 ml sample of urine was fractionated as previously described[2]. The non-cis-diol fraction (0.14 M boric acid eluate) from the DEAE borate column was further fractionated by reverse phase HPLC (ODS C-18 column eluted with 0 → 50% MeOH in water in one hour). An aliquot of each of the collected fraction were lyophilized, dried over P_2O_5 under vacuum at 100° for 2 hours, and then derivatized by heating with 2.5 µl of BSTFA (with 1% TMCS) and 2.5 µl of anhydrous pyridine at 100° for 1.5 hours.

GC-MS analyses were carried out on a Finnigan 4500 GC-MS system using a DB-1 (bonded phase) capillary column (30 M long, film thickness 0.25µ). A splitless injection was made using a Grob injector (temp. 280°) and the column oven was programmed from 80° (2 min hold) to 200° (20°/min) and then to 280° (5°/min; 5 min hold). The mass spectrometer was operated at an ionization voltage of 70 eV and a dynode voltage of -3.0 kV.

Comparison of GC retention times and full mass spectra with those of the authentic standards (Table I) led to the unequivocal identification of the 2'-O-methyladenosine (M^+ m/z 497), 2'-O-methyluridine (M^+ m/z 474), 2'-O-methylguanosine (M^+ m/z 585) and 2'-O-methylinosine (M^+ m/z 498) in one normal human urine and from the urine of a patient with chronic myelogenous leukemia. The identity was further confirmed by spiking the urine samples with appropriate authentic standards.

Table I

GC Retention Times (Minutes) of Silylated 2'-O-Methyladenosine, 2'-O-Methyluridine, 2'-O-Methylguanosine and 2'-O-Methylinosine Isolated from Human Urine and Authentic Standards

	Normal Urine	Leukemic Urine	Normal* Urine	Authentic Standard
1. 2'-O-Methyladenosine $(TMS)_3$	18.02	18.01	18.00	18.07
2. 2'-O-Methyluridine $(TMS)_3$	15.25	15.20	15.28	15.20
3. 2'-O-Methylguanosine $(TMS)_4$	20.35	20.15	20.30	20.20
4. 2'-O-Methylinosine $(TMS)_3$	16.92	16.98	17.05	16.92

*Sample of urine fraction was spiked with approx. 25 ng of appropriate authentic standard before derivatization.

Presented at the 36th ASMS Conference on Mass Spectrometry and Allied Topics
June 5-10, 1988, San Francisco, CA

This paper constitutes the first report on the presence of 2'-O-methylinosine (Fig. 1) in human urine; 2'-O-methyladenosine has earlier been isolated from the urines of immunodeficient children[3] and the presence of 2'-O-methylguanosine (Fig. 2) has been inferred from radioimmunoassay[4].

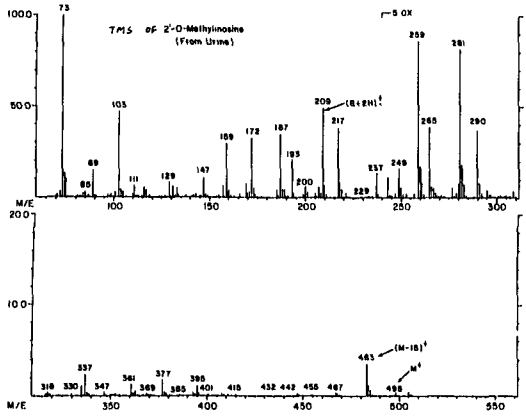

Fig. 1

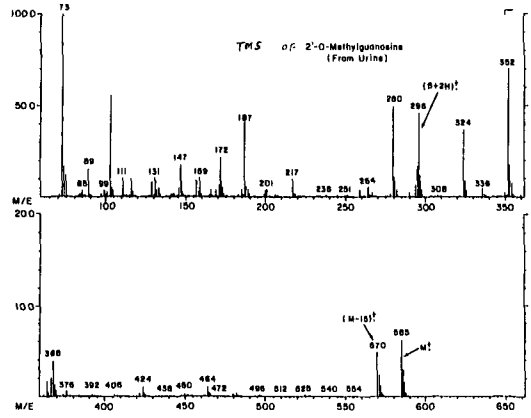

Fig. 2

References

1. G.B. Chheda, H.B. Patrzyc, H.A. Tworek, J.A. McCloskey and S.P. Dutta, in "Chromatographic and Other Analytical Methods in Nucleic Acid Research", Vol. II, C.W. Gehrke and K.C. Kuo, eds., Elsevier Science Publishers, Amsterdam, The Netherlands (1988), in preparation.
2. S.P. Dutta, P.F. Crain, J.A. McCloskey and G.B. Chheda, Life Sciences 24, 1381 (1979).
3. R. Hirschorn, H. Ratech, A. Rubinstein, P. Papageougiou, H. Kesarwala, E. Gelfland and V. Roegner-Mariscalco, Pediat. Res. 16, 362 (1982).
4. B.S. Vold, D.E. Keith and M. Slavik, Cancer Res. 42, 5265 (1982).

Presented at the 36th ASMS Conference on Mass Spectrometry and Allied Topics
June 5-10, 1988, San Francisco, CA

Structural Studies of DNA Covalent Adducts of a Styrene Metabolite by ^{32}P Post-labeling and Liquid Secondary Ion Mass Spectrometry (LSIMS).

S. Kaur, K. Pongracz, W. Bodell and A.L. Burlingame, University of California, San Francisco, CA.

Introduction Epidemiological evidence suggests that many industrial chemicals are carcinogenic. Activation of the parent compound *in vivo* may produce electrophilic intermediates capable of attacking nucleophilic sites in DNA. Structural assignment of covalently modified nucleotides are hence important in elucidating the mechanisms involved in the early stages of chemical carcinogenesis. The presence of DNA-styrene oxide covalent adducts detected by ^{32}P post-labeling[1] has been recently reported in humans occupationally exposed to styrene[2]. This paper reports structural studies of *in vitro* DNA and deoxyguanosine (dGMP) adducts of the metabolite styrene oxide (S.O.) using a combination of ^{32}P post-labeling, chemical synthesis and mass spectrometry.

Results and Discussion DNA (calf thymus, 0.5mg) or 3'-dGMP (0.5mg) in 1ml of 30mM Tris-HCl (pH 7.5) were reacted with 5µl of S.O. (24h, 37°C). Unreacted S.O. was extracted with diethyl ether. The DNA was enzymatically digested using micrococcal nuclease and spleen phosphodiesterase (to yield 3'-dNMPs) and ^{32}P post-labeled (converted to 3'5'-dNDPs at pH 9 by incubation with ^{32}P-ATP, and T_4 kinase, 30 min.; followed by apyrase, 30 min.) The S.O. adducts were separated from the non-modified nucleotides by reversed phase TLC (0.4M ammonium formate, pH 6). After transfer to a PEI cellulose plate, the adducts were resolved by 2-dimensional chromatography (1: 1.8M lithium formate, 4.25M urea, pH 3.5; 2: 0.36M LiCl, 0.22M Tris-HCl, 3.8M urea, pH 8; 3: 1.7M Na_2HPO_4, pH 6; eluting the latter two in the same direction). Autoradiography indicated at least 5 adducts in each case; adducts 1 and 2 accounting for *ca.* 90% of the total radioactivity. Adducts 1 and 2 isolated from the dGMP reaction co-chromatographed with 1 and 2 from the DNA reaction. Reaction products for other mononucleotides were minor and did not elute in this region of the chromatogram.

To identify the major post-labeled adducts 1 and 2 the reaction products from a larger-scale dGMP reaction were fractionated by HPLC and aliquots of each fraction were post-labeled and submitted to LSIMS. Thus, 3'-dGMP (10 mg, 1ml Tris-HCl) was reacted with 100µl S.O. (24h, 37°C). The adducts were isolated by HPLC (10µm, 250x10mm i.d.; solvent A=10 mM NH_4OAc, B=MeOH; t=0 min., A=100, B=0; t=60 min., A=30, B=70; t=70 min. A=0, B=100) and aliquots were ^{32}P post-labeled to locate the fractions containing 1 and 2. 1 (t_R 55-60 min.) and 2 (t_R 50-55 min.) had identical LSIMS mass spectra (mol. ion m/z 586; negative ion mode) indicating structural isomers (Fig.1a). The high resolution spectra showed the elemental compositions $C_{26}H_{30}N_5O_9P$ (∂ 3-5ppm) indicating the presence of 2 S.O. molecules per adduct in each case. Adducts 1 and 2 PEI co-chromatographed with 1 and 2 isolated from the DNA reaction.

One of the minor adducts was identified by PEI co-chromatography with a synthetic standard 6-O-(2-hydroxy-2-phenyl)-2'-deoxyguanosine-3'-monophosphate[3]. The synthetic standard was characterized by high resolution EIMS (as the trimethylsilyl derivative), and UV and ^1H NMR (500 mHz) spectroscopy. One possibility for the major adduct corresponding to alkylation at two sites in the dGMP would be alkylation at the O-6 and N-2 positions. (Alkylation involving the N-7 substituent results in cleavage of the glycosidic bond and the resulting adduct would not be detected by the post-labeling procedure). Thus, in order to obtain an O-6, N-2 diadduct, 6-O-(2-hydroxy-2-phenyl)-2'-deoxyguanosine-3'-monophosphate was reacted with 10 µl S.O. (24h, 37°C). The adducts (t_R 50-55 and 55-60 min.) were isolated by HPLC (as above). ^{32}P post-labeling also showed the same retention behavior as 2 and 1 , respectively, from the DNA and dGMP reactions. The LSIMS spectra (mol. ion m/z 586, negative ion mode) were consistent with the presence of two S.O. moieties (Fig. 1b).

The DNA alkylation reaction was repeated on a larger scale in order to isolate adducts for structural studies. DNA (calf thymus, 100mg; 30mM Tris-HCl, pH 7.5, 100ml) was reacted with 300 µl S.O.(24h, 37°C). In addition, 4x0.5mg (1ml Tris-HCl each) were reacted with ^{14}C-8 S.O.(25 µCi) and 5 µl unlabeled S.O. Unreacted S.O. was extracted with EtOAc and the DNA was further purified by repeated precipitation (5X). After digestion (micrococcal nuclease, spleen phosphodiesterase) the 3'-dNMP adducts were isolated by reversed phase HPLC (as above, Fig. 2). Retention times of the adducts were determined by comparison with those of the labeled ^{14}C adducts. Co-chromatography of 7-(2-hydroxy-2-phenylethyl)guanine identified the major adduct (not detected by post-labeling). ^{32}P post-labeling of aliquots of the HPLC fractions showed 1 and 2 to elute at t_R 50-60 min. 1 and 2 co-chromatographed (PEI) with 1 and 2 isolated from the dGMP reaction (i.e. diadducts, see above). The fractions from the DNA reaction containing 1 and 2 were further purified (reversed phase HPLC, microbore). LSIMS spectra could not be obtained for these fractions, presumably due to the presence of salt impurities still remaining. However, the fact that the major adducts detected by post-labeling from the DNA reaction have identical HPLC retention and PEI co-chromatograph with diadducts 1 and 2 from the dGMP reaction indicates that the structures are similar.

Conclusion (i) *In vitro* DNA-Styrene oxide adducts can be detected by the ^{32}P post-labeling procedure at modification levels of 1 in 10^4 nucleotides (*in vivo* levels of 1 in 10^8 have been reported1), (ii) *In vitro* DNA reactions with styrene oxide result in alkylation mainly at the dG residue, (iii) The major site of alkylation on the dG residue is at the N-7 position. These adducts readily depurinate and are not detected by the ^{32}P post-labeling procedure, (iv) The adducts detected by the ^{32}P post-labeling procedure represent a minor fraction (*ca.* 5%) of the total adducts. Alkylation in the major post-labeled adducts appears to be at both the O-6 and N-2 positions (hydrogen bonding sites in the Watson Crick model) resulting in the formation of diadducts, (v) A minor adduct co-chromatographs with 6-O-(2-hydroxy-2-phenylethyl)-2'-deoxyguanosine-3'-monophosphate[3], (vi) The low level of adduct formation (1 in 10^4 nucleotides) makes it difficult to rationalise the presence of adducts representing alkylation at two sites in a single residue, (vii) While the ^{32}P post-labeling procedure is a highly sensitive method of DNA-adduct detection, no structural information is revealed. The combination of ^{32}P post-labeling and mass spectrometry provides a powerful tool for both the detection and characterization of DNA alkylation products.

Presented at the 36th ASMS Conference on Mass Spectrometry and Allied Topics
June 5-10, 1988, San Francisco, CA

References

1) Randerath K, Haglund K. E., Phillips D. H. and Reddy M. V. (1984). Carcinogenesis, 5, 1613.
2) Lui S. F. and Rappaport S. M. (1987). In, Proceedings of International Conference on ' Detection Methods for DNA-Damaging Agents in Man', Finland, 15.
3) Pongracz K., Kaur S., Burlingame A. L. and Bodell W. (In prep.).

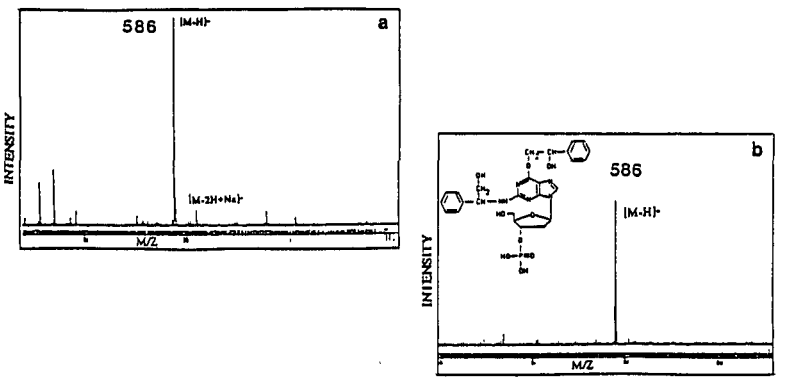

Figure 1. a) LSIMS spectrum (negative ion mode) for compound 1 from the reaction of dGMP with styrene oxide. Identical spectrum obtained for 2. b) LSIMS spectrum (negative ion mode) for compound 1 from the reaction of 6-O-(2-hydroxy-2-phenylethyl)-2'-deoxyguanosine-3'-monophosphate with styrene oxide. Identical spectrum obtained for 2.

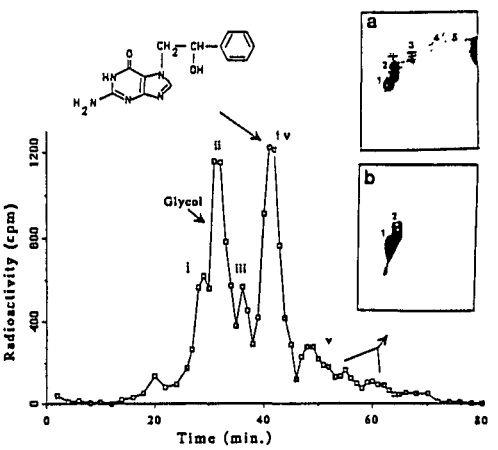

Figure 2. HPLC chromatogram for products from reaction of DNA with ^{14}C-8 styrene oxide. Insets show adducts detected by ^{32}P post-labeling: a) Total mixture. b) Fraction t_R 50-60 min.

Presented at the 36th ASMS Conference on Mass Spectrometry and Allied Topics
June 5-10, 1988, San Francisco, CA

LOW NANOGRAM DETECTION OF NUCLEOTIDES USING FAB-MS

Q.M. Weng, W.M. Hammargren and K.H. Schram, Department of Pharmaceutical Sciences, College of Pharmacy, University of Arizona, Tucson, AZ 85721.
C. Borysko, L. Wotring and L.B. Townsend, College of Pharmacy, University of Michigan Ann Arbor, MI 48109

Despite the success of FAB-MS for analyzing non-volatile compounds, such as nucleotides, lack of sensitivity has been a severe restriction. Reports describing the FAB-MS analysis of nucleotides as the free compounds required sample levels in the ug/ul range[1,2]. The goal of this work was to examine the effect on detection limits in FAB-MS by analysis of the trimethylsilyl derivatives of selected mononucleotides[3].

In order to optimize sensitivity, experimental conditions were determined using adenosine 5'-monophosphate (AMP;**1**) as a model compound. AMP was chosen because it has been studied extensively, both as the free compound and as its TMS derivative. Also, it is amenable to analysis by EI, CI, and FAB-MS[3] and is readily available. After methods were optimized for AMP, reference standards of two clinically important nucleotides were analyzed: tricyclic nucleoside 5'-monophosphate (TCN-MP;**2**)[4], a potential anticancer agent undergoing clinical trials[5] and 5-fluoro-2'-deoxyuridine-5'-monophosphate (FdUMP;**3**), the active metabolite of the widely used anticancer drug, 5-fluorouracil[6].

Table 1 shows the results of the sensitivity studies for the selected mononucleotides analyzed by FAB-MS as both the free compound and TMS derivative. Low detection limits for $AMP(TMS)_3$ (10 ng), $TCNMP(TMS)_3$ (5 ng), and $FdUMP(TMS)_2$ (5 ng) were achieved by FAB-MS. The results were obtained by analysis of the TMS derivatives with m-nitrobenzyl alcohol (NBA) as the matrix and scan averaging in the negative ion detection mode. Figure 1 shows the negative ion FAB-MS spectrum of 5 ng FdUMP as its TMS_2 derivative. Hydrolysis of one or more of the labile TMS groups occurs, with the extent of hydrolysis greatest when glycerol is used as the matrix. Using NBA as the matrix, loss of two TMS groups was observed, while the non-protic tetraglyme matrix usually displayed loss of one TMS group as the most intense peak with the molecular ion of the fully derivatized compound as a minor peak. Complete incorporation of TMS groups for AMP (five), TCNMP (five) and FdUMP (four) was confirmed using EI and CI.

This FAB-MS procedure has been applied to the analysis of TCNMP samples isolated from L1210 cell cultures and purified by HPLC. Samples with quantities (ug levels) of TCNMP estimated at several times the detection limit showed no sample-related peaks, possibly due to the presence of buffers or other artifacts which interfere with derivatization.

Additional sensitivity may possibly be obtained with other derivatizing reagents or by the use of aprotic matrices using a heatable/coolable FAB probe.

This work was supported by NIH grant CA42309.

1. H.R. Schulten and H.M. Schiebel, Fresenius Z. Anal. Chem. **32**, 321 (1985).
2. K.H. Schram, Trends in Anal. Chem. **7**, 28 (1988).
3. K.H. Schram and D.L. Slowikowski, Biomed. Environ. Mass Spectrom. **13**, 263 (1986).
4. K.H. Schram and L.B. Townsend, Tetrahedron Lett. **49**, 4757 (1971).
5. M.J. O'Connell, J. Rubin, R.G. Hahn, L.K. Kvols and C. Moertel, Cancer Treatment Reports **71**, 333 (1987).
6. C. Heidelberger, "Antineoplastic and Immunosuppressive Agents" in Handbook of Experimental Pharmacology, A.C. Sortelli and D.C. Johns, eds. Springer-Verlag, New York, 1974, pp. 193-231.

Presented at the 36th ASMS Conference on Mass Spectrometry and Allied Topics
June 5-10, 1988, San Francisco, CA

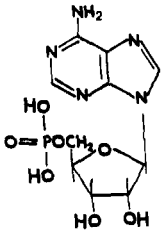

1 AMP

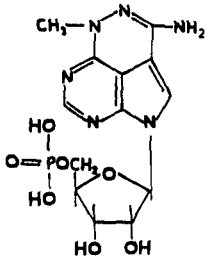

2 TCN-MP

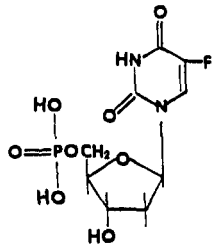

3 FdUMP

TABLE I. SENSITIVITY STUDIES OF NUCLEOTIDES USING FAB-MS

I. FREE

NUCLEOTIDE	MATRIX	DETECTION LIMIT POS	DETECTION LIMIT NEG
AMP	GLYCEROL	250 ng/ul	50 ng/ul
TCNMP	GLY+CR.ETHER	>500 "	500 "
FdUMP	GLYCEROL	500 "	400 "

II. TMS (NBA; using scan averaging over narrow scan range)

NUCLEOTIDE	DETECTION LIMIT POS	DETECTION LIMIT NEG
AMP	5 (TMS4) ng/ul	5 (TMS3) ng/ul
TCNMP	5 (TMS3) "	2.5 (TMS3) "
FdUMP	800 (TMS2) "	2.5 (TMS2) "

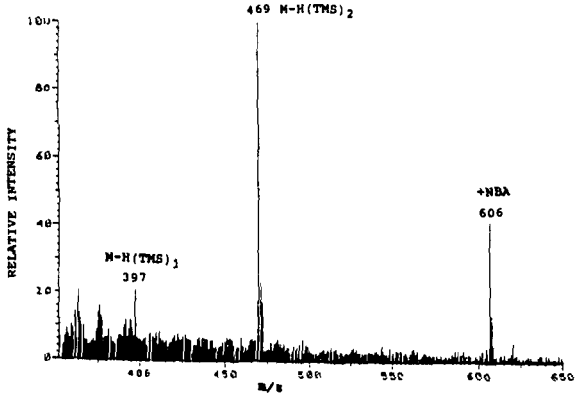

FIGURE 1. NEGATIVE FAB-MS OF 5 ng FdUMP-TMS

Presented at the 36th ASMS Conference on Mass Spectrometry and Allied Topics
June 5-10, 1988, San Francisco, CA

Investigation of the Fragmentation Patterns of the TMS Derivatives of 2', 3' and 5'-Deoxynucleosides

M.L.J. Reimer, T.D. McClure and K.H. Schram
Department of Pharmaceutical Sciences
College of Pharmacy, University of Arizona
Tucson, Arizona 85721

The recent discovery of two novel 5'-deoxynucleosides[1,2] in human urine has generated interest in the mass spectrometry of isomeric deoxynucleosides and their derivatives from the standpoint of both analytical detectability and structural characterization. In an effort to establish the fragmentation pathways of the 5'-deoxynucleosides, a comparative examination of the 2', 3' and 5' isomers of four deoxypurine nucleoside series has been undertaken. The specific compounds under investigation include 2'-, 3'- and 5'-deoxyadenosine (dAdo), deoxyguanosine (dGuo), deoxyxanthosine (dXao) and 2'- and 5'-deoxy-2-fluoroadenosine (d2FAdo), all of which were studied in both free and trimethylsilyl (TMS) derivatized forms. Although the formation and assignment of the ions of TMS derivatized nucleosides has been discussed[3,4], little has been reported concerning the differences in the spectra of the three deoxyisomers, particularly concerning the ions characteristic of each of the compounds. Using the deoxyadenosines as models, low resolution-electron ionization (EI) mass spectra and chemical ionization-collisional activation (CI-CA) daughter ion spectra are reported.

Samples were obtained either commercially (dAdo, 3'-dAdo, 5'-dAdo, dGuo: Sigma Chemical Co.; 3'-dGuo: Yamasa Shoya Co., Tokyo) or synthetically (dXao: deamination of dGuo) or were donated (5'-dGuo, 3'-dXao, 5'-dXao: Dr. K. Nakano, PL Comprehensive Research Institute, Osaka, Japan; d2FAdo, 5'-d2FAdo: Dr. J. A. Secrist, Southern Research Inst., Birmingham, Ala.). TMS derivatives were prepared by standard procedures[3]. All spectra were acquired on a Finnigan MAT 90 mass spectrometer using standard EI (70eV) and CI (NH_3) modes of ionization. Linked scans of daughter ion spectra were obtained using a B^2/E scan law (V constant) with CA (air) in the first FFR of the BE instrument.

Several distinguishing features can be found in comparing the EI mass spectra of the 2', 3', 5' series. The 2'-deoxypurine nucleosides are characterized by a $[M]^{+\cdot}/[M-15]^+$ ratio > 1 (except deoxyguanosines), a base peak at $[B+1]^{+\cdot}$ (except d2FAdo) and an intense peak at m/z 103. The 3'-isomers can be differentiated from the 2'-analogs by a $[B+30]^+$ base peak, a strong $[B+116]^+$ signal and a weakly-abundant ion at m/z 103. The 5'-isomers are easily distinguished from the 2'- by a $[B+30]^+$ base peak (except 5'-dGuo and 5'-d2FAdo) and abundant ions corresponding to $[B+116]^+$, $[S-H]^{+\cdot}$ and $[B+128]^+$. Features of the 5'-spectra that are not present in the 3'-compounds include the ions $[B+128]^+$, $[S-CH_2O]^+$ and $[C_3H_3O_2\ (TMS)_2]^+$.

The CI-CA linked scan spectra of 2', 3' and 5'-dAdo (daughters of $[MH]^+$) also provide a means for differentiating between deoxynucleoside isomers. Intense metastable transitions corresponding to the formation of $[M-90]^{+\cdot}$ and $[C_3H_3O_2(TMS)_2]^+$ distinguishes the 3'-deoxyisomer from its 2'- and 5'-analogs. A unique aspect of the 2'-dAdo spectrum is the absense of $[B+131]^+$ and $[B+116]^+$ daughters, both of which are evident in the spectra of the 3'- and 5'-deoxynucleosides.

In conclusion, significant differences in fragmentation are observed between structural isomers of 2', 3' and 5'-deoxypurine nucleosides. CI linked scanning (with collisional activation) affords complementary structural information when used in conjunction with "normal" EI spectral acquisition.

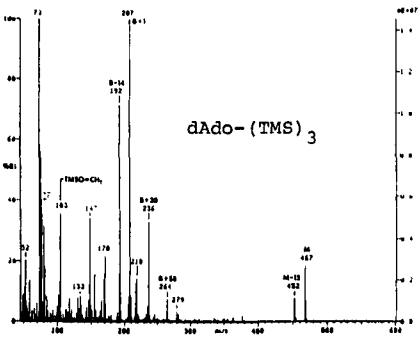

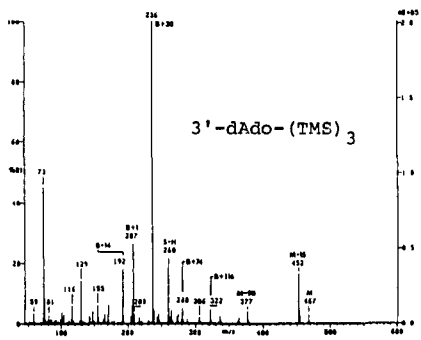

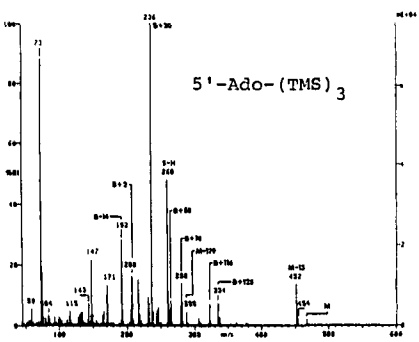

REFERENCES

1. G.B. Chheda, H.B. Patrzyc, A.K. Bhargava, P.F. Crain, S.K. Sethi, J.A. McCloskey and S.P. Dutta, Nucleosides and Nucleotides, 6, 597 (1987).

2. T.D. McClure, K.H. Schram, K. Nakano and T. Yasaka, "Identification of 5'-deoxyxanthosine in Human Urine", Presented at the 36th ASMS Conference on Mass Spectrometry and Allied Topics, San Francisco, CA, June 5-10, 1988.

3. J.A. McCloskey in "Basic Principles in Nucleic Acid Chemistry", Vol. I, P.O.P. Ts'o, Ed., Academic Press, New York, 1974, p. 209-309.

4. H. Pang, K.H. Schram, D.L. Smith, S.P. Gupta, L.B. Townsend and J.A. McCloskey, J. Org. Chem., 47, 3923 (1982).

This work supported by NIH Grant CA43068.

Presented at the 36th ASMS Conference on Mass Spectrometry and Allied Topics
June 5-10, 1988, San Francisco, CA

ANALYSIS OF PRODUCTS FROM THE REACTION OF THE TRIETHYL LEAD KATION WITH A HEXANUCLEOTIDE

E.-M.Rustler and M.Linscheid

Institut für Spektrochemie,
Bunsen-Kirchhoff-Str.11
D-4600 Dortmund 1, POB 101352,
West Germany

INTRODUCTION:

Lead tetraalkylates, used as additives to gasolines and still widespread in the environment, are metabolized in the liver to yield cationic species. The toxic potential of such cations in man has been reported[1].
In addition, it has been shown that mitosis is influenced at lower concentrations, whereas cleavage of chromosomes occurs at higher dose levels of alkylates[2].
For a detailed study of the reaction of lead alkylates on a molecular level, we have synthesized as model target the selfcomplemental hexanucleotide CGATCG in sufficient amounts to allow the necessary biophysical studies.

SYNTHESIS OF THE HEXANUCLEOTIDE:

The systhesis was performed according to a modified phosphotriester method in liquid phase[3] by block condensation (2 + 2) and (4 + 2); purification by RP-HPLC, PRP1-column; the structure confirmation was done by 400 MHz NMR including two dimensional studies, by negative ion FAB mass spectrometry and by UV spectroscopy. The melting point was determined also, to make shure that the reaction at room temperature takes place with the double stranded form rather than the single standed oligonucleotide.

THE REACTION

A twentyfold excess of triethyl lead chloride was allowed to stand with the hexanucleotide for 10 days in a buffer solution at pH 7; a longer reaction time did not change the pattern. The reaction mixture was separated by ion exchange chromatography into fractions, which were directly analyzed by FAB MS; a subsequent separation by HPLC was done only at an analytical scale to correlate the MS results with the chromatography (fig.1). From the fragmentation pattern one can deduce the structures of the smaller oligonucleotides produced in the course of the reaction.

CONCLUSION:

The lead trialkylate cation as the most toxic metabolite of the tetra-alkyl-lead compounds induces cleavage of the DNA stand, apparently predominately between G and A; a sequence priority (GC) may be discussed rather than single strand preference, since in that case the smaller oligonucleotides should occur in larger amounts.. The cleavage of chromosomes by heavy metal species could be caused by the same mechanism.

In general, a well defined model system like the one shown here can serve to study the toxic reactions of xenobiotics as well as the interaction of drugs with DNA (studies are in progress); the results of such reaction models can be used as guides in the course of in vivo studies or in drug design.

Presented at the 36th ASMS Conference on Mass Spectrometry and Allied Topics
June 5-10, 1988, San Francisco, CA

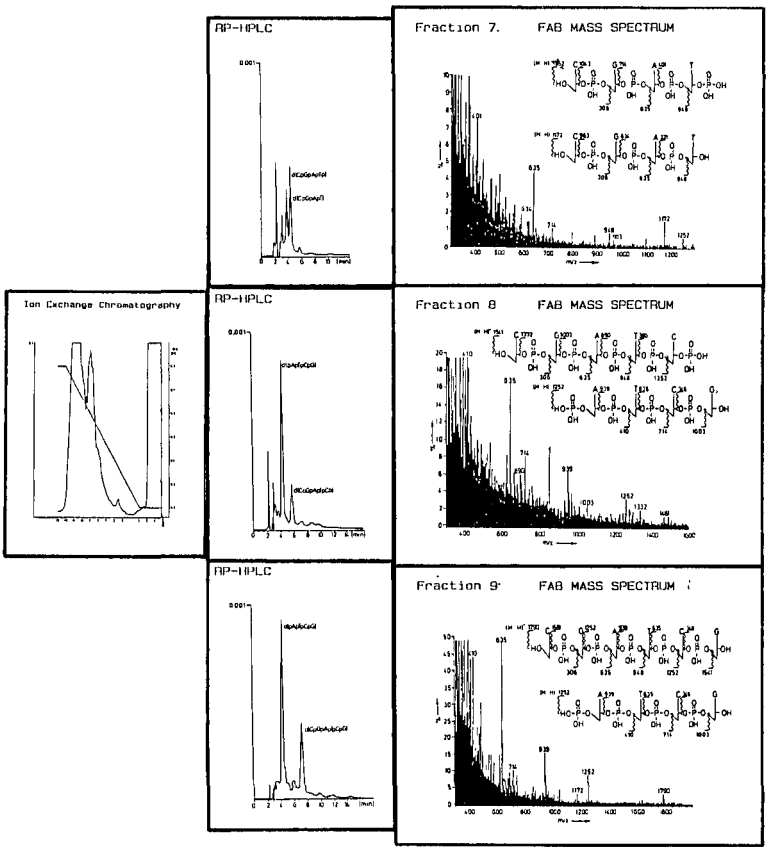

Acknowledgements:
We are indebted to Dr. A.W.H. Jans, MPI fuer Systemphysiologie, Dortmund, for aquisition of the NMR spectra; financial support from the BMFT, Bonn, and the MWF, Duesseldorf, is gratefully acknowledged.

References:

1. Grandjean, P.; Nielsen, T.; Residue Rev. 72, 97 (1979)

2. Ahlberg, J.; Ramel, C.; Wachtmeister, C.A.; Ambio 1, 29, (1972)

3. van Boom, J.H.; van der Marel, G.; van Boeckel, C.A.A.; Wille, G.; Hoyng, C.F.; in: Chemical and Enzymatic Synthesis of Gene Fragments, Eds.: Gassen, H.G.; Lang, A.; VCh Publishers, Weinheim, (1982)

Presented at the 36th ASMS Conference on Mass Spectrometry and Allied Topics
June 5-10, 1988, San Francisco, CA

ANALYSIS OF 5-METHYL-DEOXYCYTIDINE IN DNA BY GCMS

M.Linscheid and C.Randt
Institut für Spektrochemie,
Bunsen-Kirchhoff-Str.11
D-4600 Dortmund 1, POB 101352
West Germany

INTRODUCTION

The methylation of nucleosides in DNA is regarded as an important factor in the regulation of genes in higher organisms[1]. The most frequent modification occurs in adenosine and cytidine (here at the 5-position of the base) and the significance is still subject to investigations. In addition to regulation the activity of endonucleases may be influenced by the degree of methylation. To establish the role of 5-methyl-deoxycytidine (5mdC), sensitive and precise determinations of the base composition of DNA's are necessary and some procedures have been developed, which are usually based on the analysis of the hydrolysis to nucleobases; namely HPLC[2], radioactive labelling, immunoassay, GC-MS[3] and complete sequencing have been used. The problem is that the published procedures are either insensitive, difficult to calibrate or amenable to cross contamination by RNA impurities.
Our method for the quantitative analysis of 5mdC in DNA is based on GC-MS (using electron impact) and multiple / single ion recording. Since we use the trifluoroacetylated derivatives of nucleosides rather than of nucleobases, contamination from RNA-components, which may contain methylated bases, have been excluded. For clean up a sequence of steps for removal of proteins and RNA impurities was developed.
For the MS analysis, a Siemens Sichromat 3 gaschromatograph was directly coupled to a VG 7070E mass spectrometer, run at a resolution of 1000.

THE METHOD

We have chosen the trifluoroacetylation rather than the silylation, since the products were easily purified from excess reagent and stable enough; in addition some intense ions could be used for the single ion recording experiments. As can be seen from the chromatograms, only the pyrimidines are derivatized completely.
In the first step, the chromatographic conditions have been developed using mixtures of deoxynucleosides and were transferred to the separation of hydrolysates (fig.1). Aza-deoxycytidine was chosen as an internal standard, because its chromatographic properties and its mass spectrum are similar enough to 5mdC; to enhance the sensitivity even further, only m/z 152 was detected in single ion mode, which is a minor signal in the mass spectrum of deoxycytidine itself and therfore, it could serve as the final internal standard (fig.2).
We constructed the analysis function (fig.3) using standard addition and the hydrolysate of the DNA from drosophila melanogaster as matrix.
The DNA of the phage ΦX174 was selected[3] to verify the results, because its DNA is fully sequenced and contains 1 5mdC in 5386 nucleotides.

CONCLUSION

We have shown that 5mdC in DNA can be analyzed with very high sensitivity and accuracy.
The full clean up procedure needs c. 5 µg of DNA.
The sensitivity is 13 fmol of the base in a matrix of hydrolyzed DNA.
The accuracy has been established by analysis of the DNA of phage ΦX174.

For drosophila melanogaster the amount is below the detection limit; since the sample is 0.15 µg (=441 pmol), the content is less than 0.3 µmol/mol or less than 1 modified base per 330,000 unmethylated nucleobases. The genom of drosophila contains therefore at maximum 240 5mdC's overall, which renders 5mdC as a factor for the regulation of genes in the DNA of drosophila melanogaster very unlikely.

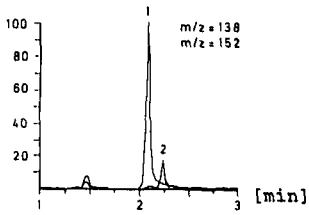

1 = deoxycytidine (m/z 138)
2 = 5mdC (m/z 152)

Fig.1 Pyrimidine - nucleosides from calf thymus DNA ; selected ion recording of m/z 138 and m/z 152 for detection of cytidine and 5mdC

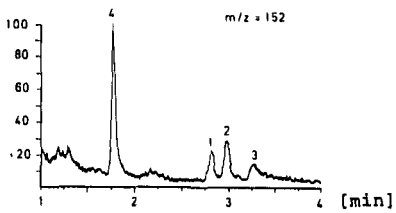

1 = deoxycytidine
2 = 5mdC
3 = Aza deoxycytidine
4 = Thymidine

Fig.2 Nucleosides from the DNA of the phage ΦX174
Using a sample of 200 ng DNA (hydrolysate), we found 105 ± 29 fmol 5mdC. The correct value is 113.8 fmol.

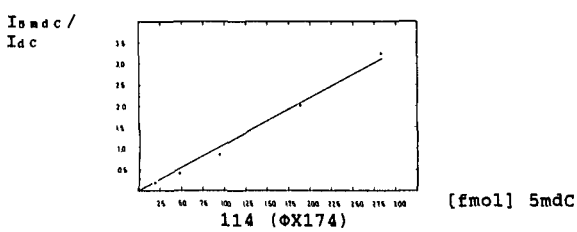

Fig.3 Analysis function for the quantitation of 5mdC in DNA
The detection limit of 13 fmol absolute was calculated using the 3 σ definition by Kaiser[4].

REFERENCES

1. Doerfler, W.; Angew. Chem. 96, 917, (1984)

2. Randt, C.; Linscheid, M.; Fres.Z.Analyt.Chem., (1988), in press

3. Crain, P.F.; McCloskey, J.A.; Anal. Biochem. 132, 124, (1983)

4. Kaiser, H.; Specker, H.; Z. Anal. Chem. 209, 1-18, (1965)

Presented at the 36th ASMS Conference on Mass Spectrometry and Allied Topics
June 5-10, 1988, San Francisco, CA

MAGNESIUM METABOLISM IN HUMANS: QUANTITATION OF STABLE ISOTOPES BY FABMS

Ya-mei Liu[a], David L. Smith[a],
Patricia Neal[b], and James Lemons[b]
Department of Medicinal Chemistry and Pharmacognosy[a]
Purdue University, W. Lafayette, IN 47907
Department of Pediatrics[b]
Indiana University School of Medicine
Indianapolis, IN 46223

Despite the physiological importance of magnesium, the dynamics of magnesium metabolism have not been investigated. This is primarily because the half-life of the longest lived radioisotope of magnesium is only 21.8 hours. Hence, studies extentding over periods of several days, and preferably several months, have not been possible. Although stable isotopes of magnesium are available highly enriched, they have rarely been used as tracers because analytical methods for their quantification in biological materials have not been readily available. We report here on a method for the accurate quantification of stable isotopes of magnesium, which is based on fast atom bombardment mass spectrometry.

These analyses were performed on a Kratos MS-50 high resolution mass spectrometer equipped with a FAB ion source. Magnesium ions are desorbed from the surface of the sample, which is dried on stainless steel probe tips in the prevacuum stage of a standard solids probe introduction inlet. A mass resolution of 3500 was used to prevent the recording of isobaric ions derived from other elements that might be present in the sample. Beams of the isotopes of interest are sequentially focused on the collector by changing the ion accelerating and electric sector voltages. These signals are recorded and manipulated with a data acquisition system, which was developed especially for this purpose.

Urine samples (usually 2 ml) were prepared for isotopic analysis by adding an equal volume of saturated NaOH solution, followed by brief centrifugation 12 hrs later. The $Mg(OH)_2$ precipitate was dissolved in 30 μL of 6 N HCl. Approximately 1 μL of the solution was applied to the probe tip. Plasma samples (600 μL) were freeze-dried, and ashed at 600 ° to remove organic substances. Inorganic residues remaining after ashing were dissolved in 6 N HCl and analyzed as described above.

The precision with which ion abundances can be determined was investigated by measuring the $^{24}Mg/^{25}Mg$ and $^{24}Mg/^{26}Mg$ ratios for a urine sample ten times. The CVs for these replicate measurements were 0.10 % and 0.09%, respectively. The accurate quantification of isotopic tracers of magnesium in urine is demonstrated by results given in Figure 1, which is a plot of the determined enrichment vs the calculated enrichment of ^{25}Mg and ^{26}Mg in four spiked urine samples. The slopes of the lines are 1.01 and 0.99, respectively. The potential applicability of this

method for investigating the dynamics of magnesium metabolism *in vivo* is illustrated in Figure 2, which gives the ^{25}Mg enrichment in the urine of a lactating woman for 125 days after tracer administration.

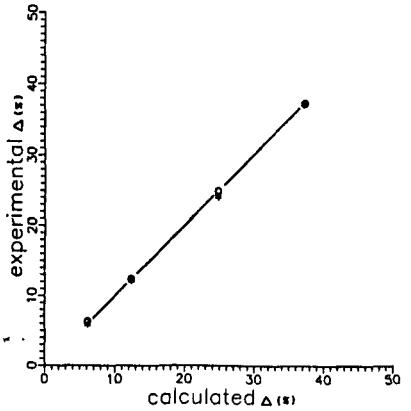

Figure 1 Plot of determined vs calculated enrichments of ^{25}Mg and ^{26}Mg in urine spiked with tracer isotopes.

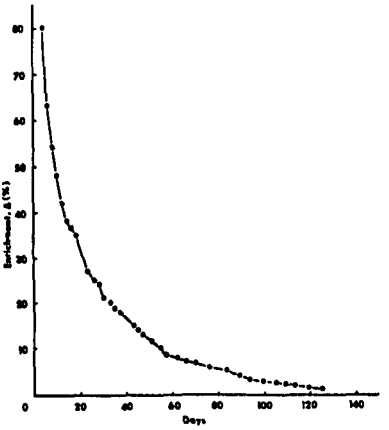

Figure 2 Tracer enrichment in the urine of a lactating woman who received 570 mg of ^{25}Mg intravenously.

Presented at the 36th ASMS Conference on Mass Spectrometry and Allied Topics
June 5-10, 1988, San Francisco, CA

EQUILIBRATION OF CALCIUM ISOTOPIC TRACER IN INFANT FORMULA

Nancy E. Vieira and Alfred L. Yergey
National Institute of Child Health and Human Development, NIH, Bethesda, MD, 20892.

Clinical research using stable isotopic tracers assumes that the tracer is rapidly equilibrated with the naturally occurring material in the system to which the tracer is administered. In our clinical protocols, an oral tracer is administered via food such as milk or infant formula. This tracer is added to the food and allowed to "equilibrate" overnight. While incomplete equilibration in food is not an important issue in studies of children and adults, due to the low stomach pH of 2 (1), it possibly becomes important in studies of premature infants where gastric pH is 3-5. Under such conditions it may be possible that preferential absorption of the tracer could occur due to incomplete equilibration of the tracer and natural calcium. Since the *calculation of fractional absorption assumes all calcium will have the same* bioavailability, preferential absorption of some portion of the calcium in the premature infant's intestine would falsely bias the fractional absorption.

Infant formula, Enfamil with Iron (Meade-Johnson, Evansville, IN.), was used for these experiments. ^{42}Ca (93.77% enriched, Oak Ridge National Resaerch Laboratory, Oak Ridge, TN) was added to 5 ml of formula in amounts expected to a yield standard curve ranging from 0-300Δ% excess based on the total amount of calcium found in the aliquot by standard flame atomic absorption spectrophotometric measurement procedure (Perkin-Elmer Model 5000, Perkin-Elmer Corp., Norwalk, CN)). All ratios were measured relative to ^{48}Ca using a Finnigan MAT THQ thermal ionization quadrupole mass spectrometer (Bremen, FRG). Fractionation correction was made using 43/48 as the normalizing ratio. Precision of the measurements for the 42/48 ratio was 0.8%, and the accuracy of the natural abundance ratio compared to the NBS ratio of 3.519 was -1.5%.

A variety of conditions for equilibration including variation in time, temperature and pH were tested: 1) room temperature at overnight, 1 day, 2 days, and 6 days; 2) refrigerated (4°C) at 1 day, 2 days, and 6 days; 3) pH 3 at room temperature for 1 day; 4) 47°C for 20 minutes

Table I shows the linear regression lines of the various treatment conditions. The expected Δ% excess was calculated based on the total calcium per ml in the formula (Meade-Johnson reported 0.466 mg/ml; our laboratory analysis measured 0.452 mg/ml). The slopes of all the lines suggest either of 2 explanations: a) that the added tracer was preferentially not precipitated, a result opposite to previous observations (2), or b) that the total calcium in the formula was greater than reported and determined.

Following a nitric acid, microwave digestion of the formula using a CEM Microwave Digestion System, Model MDS-81D (CEM Corp.,Indian Trail, N.C.) the total calcium was redetermined by flame atomic absorption spectrophotometry. Duplicate digests yielded total calcium concentrations of 0.566 and 0.554 mg/ml. Recalculation of the expected Δ% excess with the mean of the duplicates (0.560 mg/ml) resulted in the linear regression lines with their respective standard error of the mean ($S_{y.x}$) shown in Table II. As seen, these data suggest that: 1) the added tracer equilibrates with the naturally occurring calcum in the Enfamil, and 2) standard flame atomic absorption spectrophotometry analysis of dilute, undigested formula, directly aspirated into the flame yields a falsely low total calcium concentration.

1. Geigy Scientific Tables Volume 1: Units of Measurement, Body Fluids, Compositon of the Body, Nutrition, (eds.) Lentner, C., Lentner, C., Wink, A., p. 125, 1985.

2. Vieira, N. E., Schmidt, M. P., Yergey, A. L., Proceedings of 33rd Annual Conference on Mass Spectrometry and Allied Topics, p. 615, San Diego, CA., May 26-31, 1985.

Table I: Expected vs Observed Δ% Excess

treatment	linear regression
room temperature	
overnight	y = 0.760x + 0.687
1 day	y = 0.749x + 0.093
2 days	y = 0.713x + 1.759
6 days	y = 0.776x - 1.780
pH 3, 1 day	y = 0.744x + 1.923
refrigerated (4°C)	
1 day	y = 0.751x + 0.601
2 days	y = 0.711x + 0.603
6 days	y = 0.742x - 0.943
heated	
47°C, 20 min.	y = 0.780x + 5.47

Table II: Expected vs Observed Δ% Excess

treatment	linear regression	$S_{y.x}$
room temperature		
overnight	y = 0.942x + 0.689	0.68
1 day	y = 0.928x + 0.095	1.58
2 days	y = 0.884x + 1.760	1.67
6 days	y = 0.962x - 1.779	3.41
pH 3, 1 day	y = 0.922x + 1.924	2.35
refrigerated (4°C)		
1 day	y = 0.931x + 0.602	0.44
2 days	y = 0.881x + 0.604	1.73
6 days	y = 0.919x - 0.942	1.93
heated		
47°C, 20 min.	y = 0.984 + 0.875	2.07

Presented at the 36th ASMS Conference on Mass Spectrometry and Allied Topics
June 5-10, 1988, San Francisco, CA

TRACE-METALS ANALYSIS BY GAS CHROMATOGRAPHY-MASS SPECTROMETRY EMPLOYING VOLATILE CHELATES

S.K.Aggarwal, M.Kinter, M.R.Wills, J.Savory and D.A.Herold
Department of Pathology, University of Virginia Medical Center,
Charlottesville, VA 22908, U.S.A

Introduction

The determination of trace metals in biological specimens is important in view of their clinical, nutritional and toxicological effects. There has been increasing concern in recent years about the accuracy of the published values for the concentrations of trace elements in human body fluids. Since isotope dilution mass spectrometry has the potential of being incorporated into a definitive analytical technique, we have developed a method for measuring the isotope ratios of metals using capillary column gas chromatography - mass spectrometry (GC/MS) employing a general purpose organic mass spectrometer which is more commonly available to various laboratories. Conditions were optimised for the quantitative preparation of metal chelates and for the mass spectrometric analysis by GC/MS. Precision and accuracy was evaluated for isotope ratio measurements of Cr, Ni, Cu and Zn using thermally stable, volatile chelates containing about 10 ng of the metal.

Experimental

Reagents: Chromium acetylacetonate and trifluoroacetylacetone (TFA) were obtained from Alfa Products. Sodium diethyldithiocarbamate (Na(DEDTC)) was obtained from Aldrich Chemical Company. Lithium bis(trifluoroethyl)dithiocarbamate (Li(FDEDTC)) was synthesised using bis(trifluoroethyl)amine, n-butyllithium and carbon disulphide. Aliquots from standard solutions of Cr, Ni, Cu and Zn were diluted with distilled and deionised water (DDW). The solvents n-hexane and methylene chloride were of HPLC grade.

Preparation of metal chelates: A stock solution of $Cr(AA)_3$ in CCl_4 was prepared to give a final concentration of about 10 ng Cr/µL. For the preparation of $Cr(TFA)_3$, Cr(VI) was reduced to Cr(III) using a freshly prepared solution of 0.1 mol/L sodium sulphite. The pH of the solution was maintained at 5.0 using acetic acid - sodium acetate buffer. A 0.1 mol/L solution of TFA in n-hexane was used and the reaction was performed at 60° C for about 2 hours in a water bath. Diethyldithiocarbamates of Cr, Ni, Cu and Zn were prepared by using a 0.1 mol/L solution of Na(DEDTC) in DDW. The reaction conditions consisted of addition of about 1 mL of pH 4 acetate buffer solution to about 100 uL of the metal salt solution (containing about 10 µg of the metal) followed by addition of about 300 µL of 0.1 mol/L solution of Na(DEDTC). The solution was shaken on a vortex shaker for about 2 minutes and the chelate was extracted into methylene chloride. Fluorinated diethyldithiocarbamates were prepared under the conditions similar to those of unfluorinated compounds except for the use of a pH 3.0 acetate buffer solution.

Gas Chromatography/Mass Spectrometry: The mass spectrometer used was a double focusing, reverse geometry instrument (Model 8230, Finnigan MAT) with a SpectroSystem 300 data system. Fragmentation patterns were obtained using exponential scanning mode (1 sec/decade). Data for the isotope ratio measurements were acquired in the selected ion monitoring (SIM) experiment, monitoring m/z corresponding to the various isotopes in the molecular/fragment ion. A resolution of about 1000 was used in either of the two modes. For the SIM experiment, the source and the collector slit widths were optimised to achieve flat peak tops. A DB-1 bonded phase fused silica capillary column was used. One µL of the sample containing about 10 ng of the metal was injected on column at a temperature of 100°C followed by a 25° or 15°C/min ramp to 300°C.

Presented at the 36th ASMS Conference on Mass Spectrometry and Allied Topics
June 5-10, 1988, San Francisco, CA

Results and Discussion

The 70 eV EI mass spectra of various unfluorinated diethyldithiocarbamates and fluorinated diethyldithiocarbamates showed the molecular ions $(M)^{+\bullet}$ for all the chelates studied in this work. The high intensity peaks (molecular ion $M^{+\bullet}$ for Ni, Cu and Zn chelates and fragment ion $(M-L)^{+}$ for Cr chelates) containing the cluster of metal isotopes were used for isotope ratio measurements. For $Cr(DEDTC)_3$ and $Cr(FDEDTC)_3$, measurements were also performed using the molecular ion. The results obtained on isotope ratios measurements are given in the Tables 1 and 2. It can be seen that different isotope ratios can be obtained with a precision of 1-3% (at 95% confidence limits) and there is good agreement between the theoretically expected isotope ratios (calculated using the reported natural abundances of the metals and the contributions of various isotopes of C, N, O and S) and the experimentally measured isotope ratios.

Conclusion

A GC/MS method employing a commonly available organic mass spectrometer and using thermally stable and volatile metal chelates has been developed for the precise and accurate isotope ratios measurements of Cr, Ni, Cu and Zn. The method offers high sensitivity (down to parts-per-billion level) and is promising for the determination of trace metals using isotope dilution technique. The Na(DEDTC) and Li(FDEDTC) chelating agents are attractive compared to the acetylacetonates due to ease of preparation of chelates and the possibilty of multi-element analysis.

TABLE 1

		Chelate used						
	Expected	AA			TFA			
	ratio	Masses	Observed	P	A	Masses	Observed	P	A
	0.0518	248/250	0.0523	1.4	+0.8	356/358	0.0514	1.6	-0.8
Cr	0.2253	251/250	0.2232	0.5	-0.9	359/358	0.2192	0.9	-2.7
	0.0547	252/250	0.0535	0.6	-2.0	360/358	0.0537	1.4	-1.8

TABLE 2

		Chelate used							
		DEDTC				FDEDTC			
	0.0512	494/496	0.0508	1.3	-0.8	818/820	0.0542	2.7	+5.9
Cr	0.3380	497/496	0.3389	1.1	+0.3	821/820	0.3501	1.0	+3.6
	0.3423	498/496	0.3383	1.4	-1.2	822/820	0.3516	1.8	+2.7
	0.0514	346/348	0.0534	2.2	+3.9	562/564	0.0524	3.8	+1.9
Cr	0.2628	349/348	0.3022	0.9	+15.0	565/564	0.2730	2.3	+3.9
	0.2317	350/348	0.2390	1.0	+3.1	566/564	0.2426	3.2	+4.7
	0.5686	356/354	0.5612	1.3	-1.3	572/570	0.5703	0.8	+0.3
Ni	0.0973	357/354	0.0965	0.9	-0.8	573/570	0.0980	0.7	+0.7
	0.1406	358/354	0.1351	1.0	-3.9	574/570	0.1374	1.0	-2.3
	0.0293	360/354	0.0270	1.7	-7.8	576/570	0.0315	2.9	+7.5
Cu	0.6340	361/359	0.6398	1.3	+0.9	577/575	0.6525	0.7	+2.9
	0.7618	362/360	0.7394	0.8	-3.1				
Zn	0.1941	363/360	0.2171	1.5	+11.5				
	0.5213	364/360	0.4909	1.5	-6.0				
	0.0953	366/360	0.0884	1.1	-6.6				

Note: P and A denote precision (%) at 95% confidence limits and accuracy (i.e.% difference between the measured and expected ratios) respectively.

Presented at the 36th ASMS Conference on Mass Spectrometry and Allied Topics
June 5-10, 1988, San Francisco, CA

COPPER ISOTOPE RATIO MEASUREMENT BY LOW TEMPERATURE THERMO-IONIZATION

Y. Fujii, M. Hosoe*, M. Nomura and M. Okamoto
Research Laboratory for Nuclear Reactors
Tokyo Institute of Technology, O'okayama, Meguroku, Tokyo 152 Japan
* The National Defense Academy, Hashirimizu, Yokosuka 239 Japan

There has been a relatively large uncertainty in the value of the atomic weight of copper arising from the difficulty in the measurement of the copper isotope abundance ratio. This tendency appears also in other middle-heavy elements. Usually thermo-ionization is applicable for the precise measurements of isotope ratios, specifically, for metal elements. Thermo-ionization efficiency usually depends on the chemical forms of the samples of the concerned elements. The sample chemical form, therefore, should be closely examined for the thermo-ionization mass spectrometry measurements.

In the previous paper we have found that copper is ionized at low temperatures compared with the ordinary multi filaments method[1]. In the present work more detailed considerations have been directed to the relation between temperature (ionizing filament currents) and the intensity of the created ion beam.

Experimental: Mass spectrometric study on copper isotope analysis was made by using a mass spectrometer Finnigan-MAT 261 equipped with a thermo-ionization ion source incorporated with double filament ionizing units. Copper samples examined were a NBS copper standard sample and a commercially available $Cu(NO_3)_2$ reagent. Three chemically different forms, i.e. electroplated metal, $Cu(NO_3)_2$ and CuI, were examined. The electroplated sample was prepared on an evaporating filament by applying direct current between the filament and an anode inserted in a $Cu(NO_3)_2$ solution. The CuI was prepared also by adding HI to a $Cu(NO_3)_2$ solution on an evaporating filament where Cu(II) was reduced to Cu(I). The amount of each sample

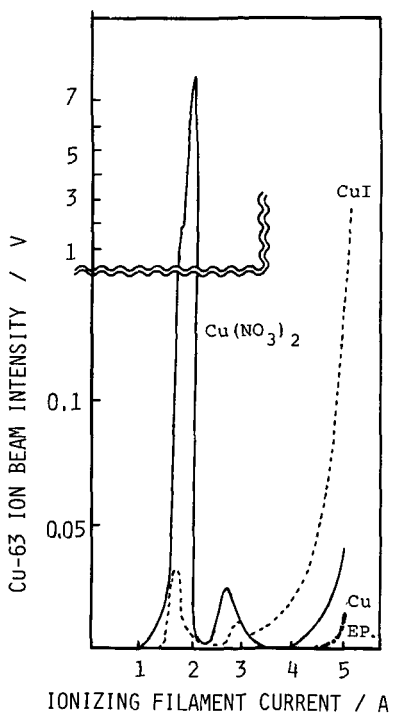

Fig. 1. Cu ion beam vs. filament current (1 V = 10 pA)

was, approximately, in the range of 20 - 100 μg.

Results and Discussion: Fig. 1 shows the relation between the intensities of Cu-63 ion beam and the ionizing filament current. Copper (electroplated) is seen in Fig. 1 to be ionized only at very high temperatures, while CuI is ionized mainly in the high temperature region and produces a week ion beam at around 1.8 A. The ion beam of $Cu(NO_3)_2$ shows a drastic dependency on the temperature of the ionizing filament: the beam intensity significantly increases at the temperature below 1000 °C (ca. 1.5 A). This condition was applied to determine the isotopic abundance ratio of commercially supplied $Cu(NO_3)_2$ reagent(see Fig. 2). The low temperature ionization is not only convenient but also realizes a very small time variation of the measuring data. Thus, the small error range of the copper isotopic ratio is obtained. The determined isotopic ratio ($^{63}Cu/^{65}Cu$) of the commercial reagent is presented in Fig. 2. The directly observed value has shown to well coincide with the value of NBS standard certified as 2.2440 ±0.0021.[2] A detailed isotope measurement study on the NBS standard sample will be given elsewhere[3]. It is another advantage of the present technique that copper nitrate in an aqueous solution can be used as a sample without special pretreatments.

References:
1) Y. Fujii, M. Hosoe and M. Okamoto, Z. Naturforsch. **41a**. 769 (1986).
2) W. R. Shields, T. J. Murphy and E. L. Garner, J. Res. Nat. Bur. Stand., **68a**, 589 (1964).
3) M. Hosoe, Y. Fujii and M. Okamoto, in press.

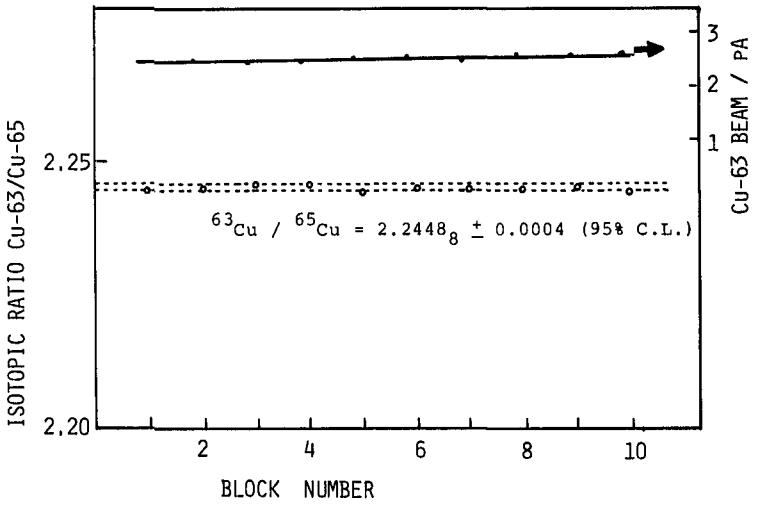

Fig. 2. Copper isotopic ratio of commercial $Cu(NO_3)_2$ reagent measured at the low temperature heating condition.

Presented at the 36th ASMS Conference on Mass Spectrometry and Allied Topics
June 5-10, 1988, San Francisco, CA

MEASUREMENTS OF BORON ISOTOPES BY NEGATIVE ION THERMAL IONISATION MASS SPECTROMETRY

P.J. Turner, J.E. Cantle, P. Barrett, Z. Palacz
VG Isotopes Ltd., Winsford, Cheshire, CW7 3BX, U.K.

The magnetic sector VG 336 has been used to measure the isotopic composition of 1 ug of Boron with a precision of better than 0.1% at the 95% confidence limit, using negative ions. These results are superior to those previously published using a quadrupole analyser and comparable to data obtained on large radius magnetic instruments.

Introduction

The VG 336 can mass analyse both negative and positive ions. The accelerating voltage is easily reversible using the M806 focus unit controlled by the versatile SECTOR software. Boron can be measured either as a positive ion $(Na_2\ BO_2)^+$, $(Cs_2\ BO_2)^+$ or as a negative ion $(BO_2)^-$. The positive ion method can give precise isotope measurements if the mass fractionation can be well constrained. In addition, the positive ion beam is greatly inhibited by the presence of impurities. For example, $Na_2BO_2^+$ is isobaric with ^{88}Sr. Consequently sample processing must produce a highly pure separate - which may not be easy and may introduce blank problems.

With negative ions, there is essentially no interference in the mass range of interest. Several workers have shown that the BO_2 ion beam is greatly improved by 2-3 orders of magnitude by the addition of a weak $Me^2(NO_3)_3$ solution, where Me = Ca,La,Na. Furthermore, the BO_2 signal produced is stable over several hours. Therefore, we have undertaken several experiments to test the effect of various loading procedures on the size of the ion beam and assess the performance of the VG 336 in negative ion mode.

Mass Spectrometry.

The VG 336 thermal ionisation mass spectrometer is equipped with an MS 806 focus control unit, which can reverse the polarity of the 4kV accelerating voltage. The VG 336 has a 36 cm effective radius, and has fixed axial and adjustable off axis Faraday collectors. The collector slit of the axial collector is 0.6mm in width, the off-axis 1mm. (0.6mm is required to obtain resolution of U in positive ion mode). HT reversal does not affect the magnet calibration. Figure 1 shows the excellent peak flat obtained on the off axis collector.

Method & Results

B was run on single Re filaments, with 1 ug B (NBS 951) loaded with lul 100 ng $M(NO_3)_3$ where M = Ca or La. Initial work used La $(NO_3)_3$ as an aid to BO_2 production. However, beam sizes were disappointing. Samples were loaded at filament currents of 0.5A, 0.8A and 1A, and it became noticeable that samples loaded at lowest currents had the highest beam size (8.10^{-13}A). NBS 951 measurements on 6 samples loaded at 0.5A gave a mean of 0.246135, SD 0.22%. The ion beam did not last for very long (20 minutes).

We therefore decided to try Ca $(NO_3)_3$. Samples were loaded at room temperature on outgassed beads. The results were excellent. BO_2 consistently appeared at 1.85-1.9A filament current and a stable beam occured at 2.3A which could last for several hours. A mean of 5 measurements gave 0.24708, SD 0.166%. This was substantially less fractionated than with La, though this may be due to the lack of filament current in the Ca experiment. Furthermore, the ion beam was stable enabling over 100 ratios to be collected. The internal precision over 100 ratios was 0.009% in the best case indicating negligible mass fractionation effects. A subsequent batch of 5 beads using the same loading technique, but using unoutgassed Re gave an external mean of 0.247851, SD 0.28%. The ratio is higher, but within error; however the unoutgassed beads did not give reproducible ionisation characteristics. This may in part be due to the different surface characteristics of an unoutgassed filament relative to an outgassed one. Stable ion beams did not occur until 2.4-2.5A, and some of the runs lasted only 30 ratios. Nevertheless, the internal precision was generally 0.1%, even over 30 ratios.

A further turret of outgassed Re with 1 ul of lug B + 1 ul 100 ng $Ca(NO_3)_2$ loaded at room temperature, gave the following results:- Ion beams were generally 1.10^{-12}A and stable over 1-2 hrs. Mass fractionation was negligible. BO_2 appeared at 1.9A and was stable at = 2.3A. Total warm-up time was 45 mins. The results are presented in Table 1. The mean of 6 beads was 0.24777 with a standard deviation of 0.074%. This is substantially better than previously obtained and indicates that a slow warm-up time and outgassed beads give the best results.

The precision of these data is significantly better than published results taken on a quadrupole analyser, and is comparable with results obtained by positive ion techniques on larger instruments (See references). This method will therefore give excellent results provided filament preparation is well constrained.

Presented at the 36th ASMS Conference on Mass Spectrometry and Allied Topics
June 5-10, 1988, San Francisco, CA

QUANTITATIVE GAS ANALYSIS BY MASS SPECTROMETRY AT THE PART-PER-TRILLION LEVEL: THE HELIUM-3 CONTENT OF ATMOSPHERIC AIR

T. A. Davidson and D. E. Emerson

U.S. Bureau of Mines, Helium Field Operations
Amarillo, Texas 79101

OBJECTIVE

Helium is found in the atmosphere, ground water, ocean water, soil, rock, and natural gas. Because the processes that are known to form the helium isotopes are very different, the relative abundances of helium-3 and helium-4 provide geochemical data that is necessary to the identification of the sources of the helium found in these media.

Quantitative analysis of helium-3 in gases at the part-per-trillion level is required for the determiniation of the helium-3 content of natural gas. Air provides a convenient model system for this analysis. The purpose of this Bureau of Mines study is to establish a direct quantitative determination of helium-3 in near-surface air at the parts-per-trillion level.

EQUIPMENT

Samples were collected in 1-liter stainless steel sample cylinders equipped with stainless steel regulating valves using a portable, non-lubricated air compressor.

Samples were handled with a specially designed stainless steel inlet system with welded connections, metal gasketed fittings, and indium seals. A 180-degree, single focusing mass spectrometer, modified with highly stable electronics and interfaced to a Teknivent 1050 Data System and an IBM XT-286 Personal Computer, was used to analyze the samples.

Presented at the 36th ASMS Conference on Mass Spectrometry and Allied Topics
June 5-10, 1988, San Francisco, CA

METHOD

Aliquots of air were prepared by passing air from the sample container through a drying tube into the inlet system. The dried air was then reduced to 25.00 torr (approximately 4.66 millimoles) with the vacuum pumps to provide the aliquot. The aliquot was then allowed to contact a charcoal trap at -197 °C and then a trap filled with titanium wire at 25 °C. While these traps were removing all gases except helium and neon from the aliquot, the background current readings were made for 3 minutes with the mass spectrometer tuned to the helium-3 peak. After a precise time lapse, the aliquot was admitted to the analyzer. The data collected consisted of two successive 3-minute averages of the electrometer output voltage. The data were corrected for the background and then summed to provide a measure of the helium-3 detected. Each such measurement was compared with identically made measurements using gravimetrically prepared standard mixtures of similar, but precisely known, composition to establish a value for the helium-3 content of the sample.

RESULTS

One hundred measurements were made on seven samples of air collected under various atmospheric conditions at Amarillo, Texas. No variations between samples were detected in helium-3 content. The helium-3 content of atmospheric air is determined to be 7.27 ± 0.20 parts in 10^{12} (parts per trillion).

Presented at the 36th ASMS Conference on Mass Spectrometry and Allied Topics
June 5-10, 1988, San Francisco, CA

CORRECTION OF INTERFERENCES IN THE DETERMINATION OF OXYGEN-18 CONTENT IN ORGANIC MATERIALS

Mourad Aissa, Northrop Services, Inc., Research Triangle Park, NC 27709
and
Gary E. Hatch, US Environmental Protection Agency, Research Triangle Park, NC 27709.

The determination of oxygen-18 content in organic materials requires conversion of the sample oxygen to a suitable compound such as CO_2 for isotope ratio mass spectrometry. Figure 1 shows a schematic diagram of the experimental procedure which is based on the combination of the Unterzaucher method for oxygen determination (1) and isotope ratio mass spectrometry.

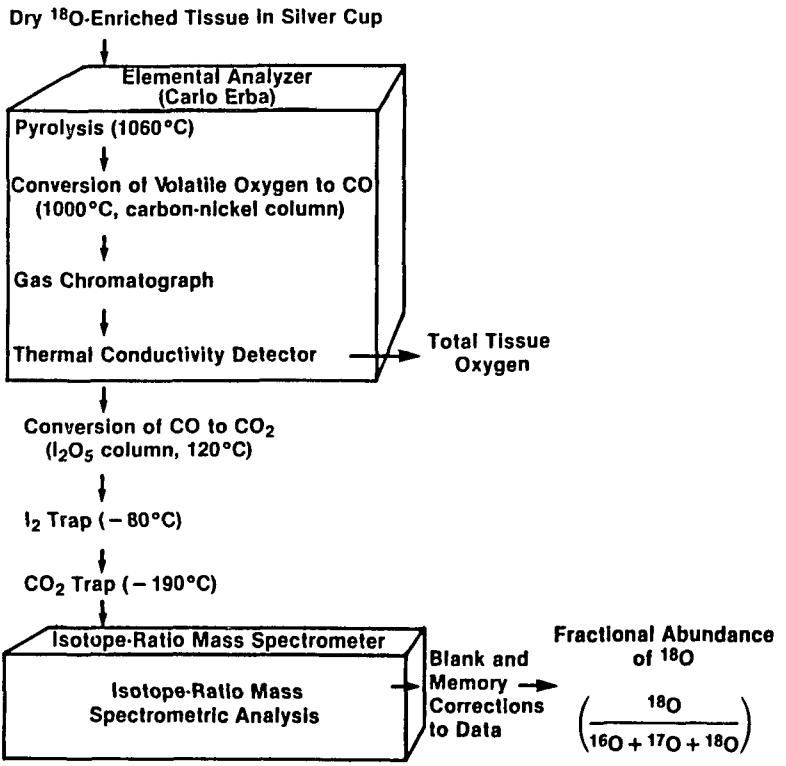

Figure 1. Schematic diagram of the method for determination of oxygen-18 in organic sampler.

Isotopic and mass interferences occur during the CO_2 conversion process where the sample oxygen is first converted to CO by pyrolysis at 1052°C and passage through a specially packed carbon column, and then oxidized to CO_2 in a column of I_2O_5 at 120°C. The main interferences are the blank effects that arise from an oxygen pool unrelated to the sample being analyzed, the CO oxidation, and the memory effect. A published mathematical treatment of this problem that uses mass and isotopic balance equations to derive a model for the correction of the mass spectrometry measurements (2) was modified to include all processes involved. The resulting general model expresses the i-th sample oxygen-18 actual fractional abundance, $F_{s,i}$, as a function of the measured fractional abundance, $F_{c,i}$, and the sample size (in oxygen atoms), $N_{s,i}$:

$$F_{s,i}=\left(2F_{c,i}-F_I\right)+\frac{N_B\left(2F_{c,i}-F_I-F_B\right)+\sum_{j=1}^{i-1}N_{s,i-j}\,ae^{-jb}\left(2F_{c,i}-F_I-F_{s,i-j}\right)}{N_{s,i}\left(1-\sum_{l=1}^{p-i}ae^{-lb}\right)} \qquad i=1,p$$

F_B, F_I are the oxygen-18 fractional abundances of the blank and the I_2O_5 respectively; N_B is the number of oxygen atoms from the blank; a and b are the memory clearance parameters, and p is the number of samples in a batch. Determination of the correction parameters (F_I, F_B, N_B, a and b) is crucial to the accuracy of the method. N_B and F_B are the parameters most likely to fluctuate from batch to batch and most susceptible to vary with such factors as pyrolysis column age and sample composition. For this reason an empty sample container was included in each sample batch and blank related parameters were directly determined. The remaining correction parameters were determined using Santrock's approach (2). Verification of the method was conducted using Benzoic acid isotopic standards which were prepared by exchange with enriched water (3). Results shown in Table 1 indicate close agreement between samples analyzed by pyrolytic decarboxylation and those treated through the analysis system. As expected, the deviation between the two groups increased with sample enrichment. The results confirm the validity of the interference correction procedure, especially for natural abundance samples. Further work is needed to study the effect of impurities and to improve results from highly enriched samples.

Isotopic Standard	n	Pyrolytic Decarboxyl. $^{18}F \times 10^3$	Unterzaucher Procedure $^{18}F \times 10^3$	Δ (percent)
BA-1	10	2.0262 ± 0.0017	2.0227 ± 0.0054	− 0.17
BA-2	10	2.1034 ± 0.0052	2.1114 ± 0.0079	+ 0.37
BA-3	5	2.4716 ± 0.0089	2.5032 ± 0.0188	+ 1.26
BA-4	5	2.9818 ± 0.0121	2.9480 ± 0.0207	− 1.58
BA-5	7	3.9710 ± 0.0071	3.8476 ± 0.1081	− 3.20

n = Number of replicate samples analyzed.

Table 1. Comparison of isotopic analyses of benzoic acid standards using pyrolytic decarboxylaton and the modified Unterzaucher procedure.

References

1. Unterzaucher, J.; Analyst (77) 584-595, 1952
2. Santrock, J. and J. Hayes; Anal Chem (56) 119-127, 1987
3. Roberts, I and H.C Urey; J Am. Chem. Soc. (61) 2580-2584, 1939

(This is an abstract for a proposed presentation and does not represent EPA policy)

Presented at the 36th ASMS Conference on Mass Spectrometry and Allied Topics
June 5-10, 1988, San Francisco, CA

Simultaneous Detection of Multiple Isotopes by Gated Pulse Counting in Resonance Ionization Time-of-Flight Mass Spectrometry

L.W. Green and F.C. Sopchyshyn
Chalk River Nuclear Laboratories, Chalk River, Ont., Canada, K0J 1J0

Resonance ionization mass spectrometry with pulsed tunable dye lasers has attracted much interest from the isotope ratio community in recent years, because of its inherent high selectivity and sensitivity. However, it has a number of features that impede precise quantification of isotope ratios: fluctuating laser beam intensity, isotopic selectivity, duty cycle loss, and fast pulse signal characteristics. In this paper we describe a time-of-flight based mass spectrometry system that overcomes many of these impediments, and isotope ratio results are presented for uranium and barium; the uranium samples were from the NBS uranium isotopic standard series.

The time-of-flight mass spectrometer featured a 1-meter drift tube, a two stage acceleration region with static electrode voltages, and a micro-channel plate detector. A tunable dye laser charged with Rhodamine 590 dye was operated at a repetition rate of 100 Hz and focussed in the source region just above the sample filament. A gated pulse counter was used for signal quantification and it featured 300 MHz bandwidth components for accurate processing of the fast pulse signals. These signals were processed such that each isotope of interest was counted in a separated channel of a counter, and such that all isotopes of interest were processed in each laser pulse. The minimum pulse pair resolution was 4 ns. The detection system did not impose a limit on the pulse repetition rate, and rates as high as 20 kHz could have been used if a copper vapour pump laser had been available.

The resolution and signal-to-noise qualities of the instrument are illustrated by the spectrum of U500 in Figure 1. Background count rates were as low as 0.0001 ions per pulse. Results for replicate measurements of isotopes of approximately equal abundance showed precisions of 0.3% and 0.4% relative standard deviation for Ba and U, respectively. Results for a wide range of uranium ratios are shown in Table 1 and show excellent agreement with certified values in all cases. Precisions for the more extreme ratios were poorer because of the relatively small number of counts obtained for the minor isotope in each case.

For these uranium results the dioxide ion was used as the analyte ion, to avoid large wavelength dependent biases observed for the metal ion. The errors were likely associated with isotope shifts and hyperfine splittings, and are a topic of current study. No such biases were observed for uranium oxides or barium.

Presented at the 36th ASMS Conference on Mass Spectrometry and Allied Topics
June 5-10, 1988, San Francisco, CA

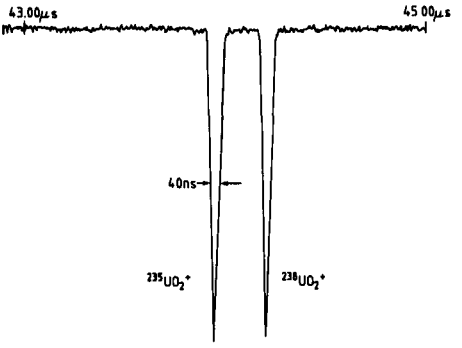

Fig. 1. Time-of-flight mass spectrum of U500. UO_2^+ species; 1400°C. Resolution (FWHM), 496; resolution (5% of max.), 298.

Table 1. Isotope Ratio Results for a Range of Ratios

Sample	Ratio Measured	Observed Ratio ± 1s	Observed/known Ratio ± 1s
Nat. U	235/238	0.00722 ± 0.00015	0.99 ± 0.02
U930	234/235	0.0113 ± 0.0005	0.98 ± 0.04
U500	235/238	1.0005 ± 0.004	1.0008 ± 0.004
U750	235/238	3.164 ± 0.036	0.999 ± 0.01
U930	235/238	17.406 ± 0.19	1.000 ± 0.01

Presented at the 36th ASMS Conference on Mass Spectrometry and Allied Topics
June 5-10, 1988, San Francisco, CA

MODIFICATION OF JMS D-300 TO THE MASS SPECTROMETER FOR PRECISE ISOTOPIC ANALYSIS:

N. Torigoye*, H. Nishimura** and M. Shima***; *Geophys. Inst., Tokyo University, Tokyo 113, **Dept. of Geosci., Naruto University of Education, Tokushima 772, ***National science Museum, Tokyo 110, Japan

The purpose of this work is to analyse precise isotopic ratios by a compact virtual image double focussing mass spectrometer with surface ionization source. New magnetic controll- and data acquisition system was introduced.

Details of the original equipment of JMS D-300 are as follows; 1. It had the virtual image double focussing geometry, which ensured the high mass resolution relative to its small mass analyser, e.g. 15cm radius 60° magnetic field and 120° electrostatic field. 2. For the mass analyser system, the hall probe and the magnetic field stabilizing circuit were contained. 3. The magnetic field scan was available by setting the switches on the front panel, which was made up of one direction and constant speed. It was not suit for precise analyses beacuse a lot of time was spent for background measurement. 4. The ion current is collected by faraday cup or the 16-stage secondary electron multiplier for lower intensity. These currents are converted to voltage by the vibrating reed electrometer, and recorded by the chart recorder.

Modifications in the present work were divided into two parts.

Automatic Magnetic Field Controll: The interface boad with 16 bit-DA converter, shown in Fig.1, was set into 16-bit computer(NEC PC9801). The digital data with 16 bit (0 to 2^{16}) calculated by computer program represented magnetic field intensity. They are sent to DA converter and transfered to voltage which is used as reference value on setting the magnetic field by the stabilizing circuit described above. This new system enabled peak hopping method in which discrete digital data were commanded to the DA converter for changing magnetic field stepwisely.

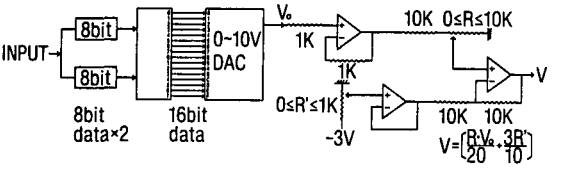

Fig. 1 The magnetic field controll Interface circuit

Data Digitizing: Two separated electrometr, Keithley Model 642 with MOS FET Op-Amp and Takeda Riken TR8401 vibrating reed electrometer, were connected to faraday cup and multiplier respectively, while originally one vibrating reed electrometer controlled both. The out put voltage of these electrometers were measured by digital multimeter with 6 1/2 figuars (Takeda Riken TR6878). The data were collected into computer through GP-IB interface for processing successively. This system excluded any expected error occurred by manual operation.

Presented at the 36th ASMS Conference on Mass Spectrometry and Allied Topics
June 5-10, 1988, San Francisco, CA

Performance of the plan is found to be satisfactory as shown in Table 1., in comparison with the ideal condition for precise isotopic analyses (10^{-4}).

Table 1.
CONDITIONS FOR ANALYSES OF PRECISE ISOTOPIC RATIOS

CONDITIONS	IDEAL	JMS-D300 MODIFIED
High mass resolution	M/ΔM; 400-600	> 350
Width of peak top	$\frac{W(\text{peak top})}{W(1/2\text{hight})} \rightarrow 1$	0.75
Flatness of peak top	< 0.1 %	< 0.5 %
Instant responce of magnetic field	< 1 sec	< 1 sec
Instant responce of detecter	< 1 sec	< 2 sec
Low noise level	$< 10^{-16}$Amp	$< 10^{-15}$Amp
Data processing	digital & analog	digital & analog
scanning of magnet	peak hopping	peak hopping
Stability of magnet	stay on peak top	< 10 % of peak top

Measurement scheme were programmed by computer with following points; 1. The magnetic field scan was made stepwisely for each peak center one after another, which were preset before the each run. 2. To reduce errors of isotopic ratio due to instability of ion current, each peak was measured between reference isotope. 3. In the normal scan, periods of measurement and waiting time of each step were 3 to 5 sec. and 2 to 3 sec., respectively.

To test the performance on precision of analyses, reagents of some elements were measured. As an example, measured data for Sr reagents are shown in Fig. 3. These results shows; 1. The accuracy of analysis was found to be better than 0.01% when the isotope ratio was in the order of unity. 2. For less abundant isotopes, as low as 10^{-4} like ^{40}K, precision and reproducibility of the analyses were within 1%. We conclude that introduction of automatic magnetic controll and on-line data processing system was succesfull in high precise isotopic analyses by the compact virtual image double focussing mass spectrometer.

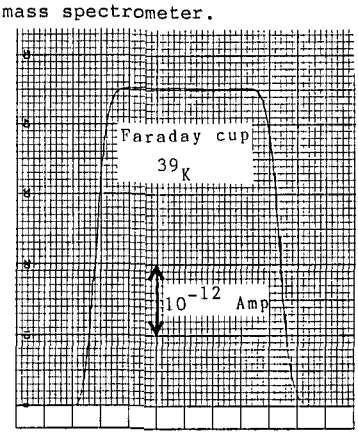

Fig. 2 Peak shape

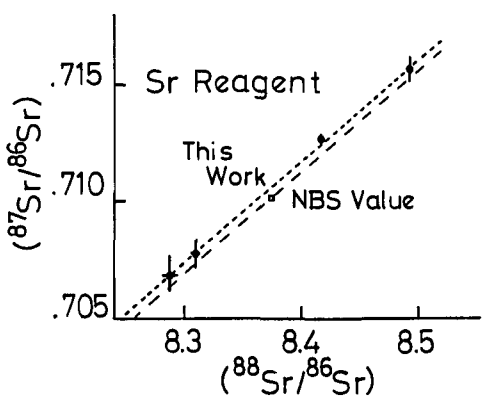

Fig. 3

Presented at the 36th ASMS Conference on Mass Spectrometry and Allied Topics
June 5-10, 1988, San Francisco, CA

SIMULTANEOUS DETERMINATION OF TRACE LEVELS OF GROUP IIIA AND VA HYDRIDES IN SILANE BY SIM GC/MS

Jeffrey M. McGuire
Hercules Incorporated
Research Center
Wilmington, DE 19894

The need for ultrapure raw materials in the semiconductor industry is essential. In particular, high purity silane is critical for silicon device fabrication processes. The purity of this gas must be monitored wherever slight variations in reagent quality can impact process yields dramatically. Group IIIA and VA hydrides, such as diborane, phosphine, and arsine represent particularly undesirable impurities because they can be incorporated as dopants in silicon. This work describes a capillary GC/MS method of analysis for trace levels of diborane, phosphine, and arsine in silane/helium mixtures using the technique of selected ion monitoring (SIM).

An initial literature survey indicated that GC with a photoionization detector (PID) would be highly suitable for detection of phosphine and arsine at ppb levels (1). However, this system would not be applicable to the analysis of diborane or silane, due to the high ionization potential of these inorganic hydrides, and the current limit of UV lamp energies available for the PID. SIM mass spectrometry was chosen as the GC detector, due to the universality of MS and the sensitivity achievable by single ion monitoring.

The analyses were performed on a Hewlett-Packard MSD using a direct interface. Gas samples were introduced using a stainless steel gas sampling valve (2 cc loop at 350 mm Hg) connected in-line with the carrier gas and capillary inlet of the HP Model 5890 GC. Chromatographic separation was accomplished on a fused-silica capillary column (bonded methyl 5% phenyl silicone stationary phase), 50 m long, with an inner diameter of 0.32 mm, and a film thickness of 5.0 µm. A splitless injection mode was used. The column oven was held at -30°C for 5 minutes, and then programmed from -30°C to 100°C at 15°C/min.

For the SIM experiments, the following ions were monitored with a dwell time of 25 milliseconds each: 77.90, 75.80, 34.00, 33.00, 30.90, 29.90, 27.00, and 26.00. These ions were chosen from additional SIM experiments in which areas for a group of five ions at $\pm$ 0.1m/z intervals from the nominal mass were recorded. The m/z value showing the largest background subtracted area was monitored during the SIM quantitation experiment.

Figure 1 shows the combined single ion current chromatograms obtained from the GC/MS analysis of individual standards (~200ppm each in helium) of silane, diborane, phosphine, and arsine.

Calibration curves were constructed from these individual standards and two reference standard mixtures which contained 100ppm (Mole percent) each of silane, phosphine, and arsine in helium and 5ppm each of these hydrides in helium. Due to the reactivity of diborane, this hydride was not included in the reference standard mixtures, and further experiments were suspended. Figure 2 shows the calibration curves for the Group VA hydrides in the presence of silane. As the curves indicate, good linearity was obtained in the 1-200ppm concentration range.

Table I lists the limits of detection, where a concentration was adopted that gave peaks on the SIM trace which exceeded the noise level by a factor of two.

This method has been employed in the analysis of dopants in silane mixtures. Table II shows the results of such an analysis, where a silane mixture containing 5-6ppm of arsine and phosphine dopants was analyzed before and after exposure to a Nanochem^R resin purification system. The Nanochem^R resin consists of reactive organometallic species functionalized on a high surface area support designed to scavenge impurities. As indicated, the analysis clearly demonstrates the ability of this technique to monitor trace levels of the hydride impurities.

A rapid capillary GC/MS method has been developed for the separation of B_2H_6, and quantitation of trace levels of PH_3 and AsH_3 in silane mixtures by the external standard method. SIM mass spectrometry is used for detection. The method shows good linearity and precision between 1ppm and 200ppm, with detection limits of <0.1ppm by volume.

---

1. Driscoll, J.N., Industrial Hygiene News, 3 No. 1 (March 1981)

Figure 1.

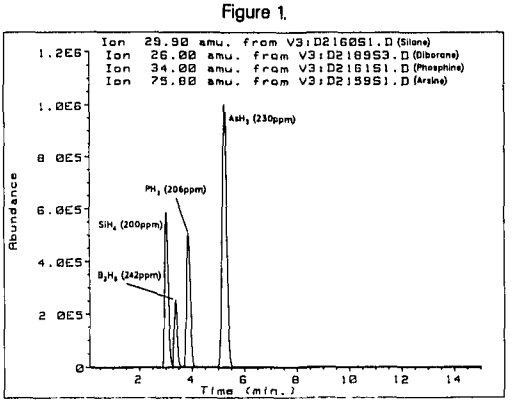

Table I. Detection Limits

	Concentration (ppb)
Silane	60
Phosphine	95
Arsine	65

Figure 2. Calibration curves

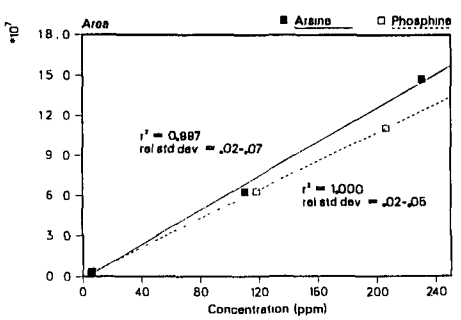

Table II. Analysis of Group VA Hydrides in Silane/Helium Mixtures by SIM GC/MS

	ppm (by volume)	
Component	Feed	Outlet
PH_3	5	<0.3
AsH_3	6	<0.3
SiH_4	150	117
Helium	balance	balance

● Average of four analyses (RSD = 0.11)

Presented at the 36th ASMS Conference on Mass Spectrometry and Allied Topics
June 5-10, 1988, San Francisco, CA

Characterization of nickel complexes by fast atom bombardment mass spectrometry:

Roczko, A.; Viswanadham, S. K.*;, Snarkey, A. G., Hercules, D. M., Department of Chemistry, University of Pittsburgh, Pittsburgh , PA 15260

Mass spectral analysis of metal complexes that are ionic, non-volatile and thermally labile has always been a problem by conventional electron-impact methods. The advent of 'soft ionization ' methods that include secondary ion mass spectrometry, plasma desorption, laser desorption, field desorption and fast atom bombardment (FAB) techniques have allowed a wide range of ionic and non-volatile materials to be analysed by mass spectrometry. The present study is aimed at characterizing nickel complexes of triphenylphosphine (tpp) and related ligands by fast atom bombardment mass spectrometry.

The metal complexes studied are given in table 1 along with their molecular weight. In order to identify a useful matrix for the FAB analysis, FAB spectra of compounds 1,5,6,8 and 10 were investigated using glycerol, thioglycerol, triethanolamine ,tetraglyme and m-nitrobenzylalcohol matrices. Spectra obtained by glycerol and thioglycerol showed peaks due to ligands and adduct ions of the ligands with matrix compounds and matrix generated fragments. Triethanolamine, as a matrix completely suppressed the desorption of the metal complexes. Spectra obtained using tetraglyme and m-nitrobenzyl alcohol as matrix showed ions that are structurally significant and characteristic of the complex compounds. All the spectra reported in this study were obtained using either tetarglyme or m-nitrobenzyl alcohol as a matrix. Fab spectra of compounds 3 and 11 are shown in figs. 1 and 2 respectively as typical examples.

Nickel complexes having NiL_nX_2 type structure (1-9) where L=mono or bidentate .igand and X=Cl,I,Br or CO commonly showed the loss of X when X is chlorine , while loss of HX was observed in the case of compounds having X= I or Br. This $(M-H)^+$ or $(M-HX)^+$ ions subsequently lost another X moiety leading to $(M-2X)^+$ or $(M-HX-X)^+$ ions in their mass spectra. When X=CO , the highest mass peak observed corresponds to $(M-2CO)^+$ ion. Only compounds 8 and 9 showed the formation of ions $(M+H)^+$ and $M^{+\cdot}$ ions respectively. Formation of intact ligand ions is seen in the case of compounds 1 and 3 only.

Fragmentation in these complexes was favored to occur at Ni-ligand bond; ions due to fragmentation within the ligand is not commonly seen. Bis(tpp)nickel dicarbonyl loses a phenyl group from $(M-2CO)^+$ ion leading to an ion at m/z 505. Ion formation due to recombination of some of the structural moieties of the complex were also observed. Bis(tpp)nickel(II) chloride, for example show ions due to $(2tpp-H)^+$ at m/z 523, and $(tpp+Cl)^+$ at m/z 297.

Compounds having a bidentate ligand (5, 6 & 7) showed an interesting ion corresponding to the loss of methylene moieties that are bridging the two phosphorus atoms complexed to the nickel atom, from their $(M-2X)^+$ ion where X=Cl or CO. This ion corresponds to m/z 428 in the case of compound 6. This common fragemnt will aid in gaining insight into the ligand in these complexes.

Complexes having the same four ligands connected to the nickel atom commonly showed ions due to loss of one and two ligands from the molecule. Only tetrakis(triethylphosphite)nickel showed the presence of molecular ion. FAB spectrum of this compound is also an exception in that extensive fragmentation corresponding to the losses of species within the ligand are seen.

FAB spectra of nickel complexes of triphenyl phosphine and related ligands thus show structurally significant and characteristic ions for their characterization. Fragmentation commonly occurs at metal-ligand bond and fragmentation due to bond breakage within the ligands was not common.

Acknowledgement: The authors thank Dr. J. M. Miller and Dr. K.Balasanmugam for providing fab spectra of some of the complexes.

Presented at the 36th ASMS Conference on Mass Spectrometry and Allied Topics
June 5-10, 1988, San Francisco, CA

TABLE 1 · NICKEL COMPLEXES ANALYZED
(M.W. IN PARENTHESES)

1. BIS(TRIPHENYLPHOSPHINE)NICKEL(II) CHLORIDE (652)
2. BIS(TRIPHENYLPHOSPHINE)NICKEL DICARBONYL (638)
3. BIS(TRIPHENYLPHOSPHINE)NICKEL(II) BROMIDE (740)
4. BIS(TRIPHENYLPHOSPHINE)NICKEL(II) IODIDE (838)
5. BIS(1,3-DIPHENYLPHOSPHINO)PROPANE NICKEL(II) CHLORIDE (640)
6. BIS(1,2-DIPHENYLPHOSPHINO)ETHANE NICKEL DICARBONYL (612)
7. BIS(1,2-DIPHENYLPHOSPHINO)ETHANE NICKEL(II) CHLORIDE (528)
8. BIS(TRIPHENYLPHOSPHITE)NICKEL DICARBONYL (734)
9. BIS(TRIETHYLPHOSPHINE)NICKEL(II) CHLORIDE (364)
10. TETRAKIS(DIETHYLPHENYLPHOSPHONITE)NICKEL (660)
11. TETRAKIS(TRIETHYLPHOSPHITE)NICKEL (722)
12. TETRAKIS(METHYLDIPHENYLPHOSPHINE)NICKEL (868)

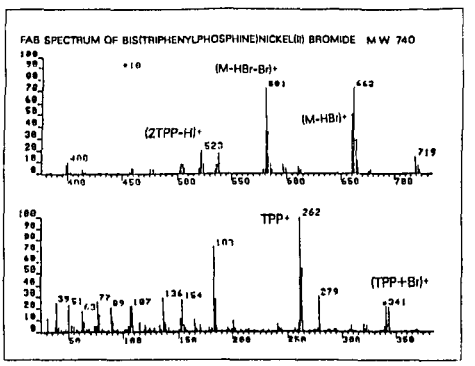

FIG.1 POSITIVE ION FAB SPECTRUM OF BIS(TRIPHENYLPHOSPHINE)NICKEL(II) BROMIDE

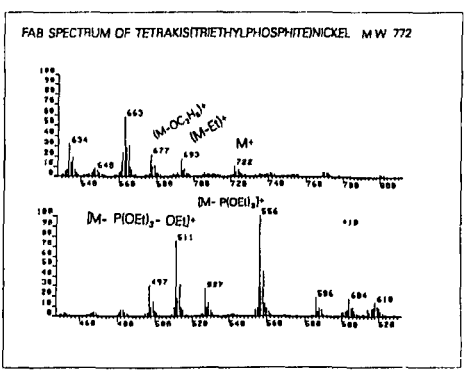

FIG.2 POSITIVE ION FAB SPECTRUM OF TETRAKIS(TRIETHYLPHOSPHITE)NICKEL

Presented at the 36th ASMS Conference on Mass Spectrometry and Allied Topics
June 5-10, 1988, San Francisco, CA

A STUDY OF FABMS OF 2-ETHYLHEXYL PHOSPHONIC ACID MONO-2-ETHYLHEXYL ESTER AND ITS COPPER SALT

M.Yuan, S.Liu*, Y.Zhu and X.Li
(Changchun Institute of Applied Chemistry, Sitalin Str. #109, Changchun, Jilin 130022, China)

Acidic phosphorus compounds are a type of extractants with a good extractability for lanthanide, in which alkyl phosphonic acid monoalkyl esters possess the most excellent separation behaviour. However the application of EIMS to analyze the extractants and extractives has been severely limited. The limitation has arisen due to unsufficient ions in gas phase, thermal decomposition of samples in preference to volatilization. For example, copper salt of 2-ethylhexyl phosphonic acid mono-2-ethylhexyl ester

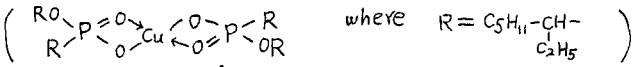

starts to decompose at 190°C under 1 atm. FAB technique is one of the so-called soft ionization methods, which is powerful for the mass spectrometric analysis of low volatility and thermolabile products. However little is known of the FAB ionization mechanism. FAB is an attractive because quasi-molecular ions can be found besides fragment ions.

According to the previously proposed models for FAB ionization,[1] molecules M are ionized by protonation or proton abstraction. This mechanism can be used to explain the formation of $(M+H)^+$ in most FAB cases, but not to the formation of M^+ and $(M+2H)^+$ ions.

All measurements were performed on VG 7070E mass spectrometer. A VG Commercial FAB source was employed. FAB gas was Ar with kinetic energy 8keV. The Ar^+ ion beam current was about 1 m Amp. Glycerol(G), triethanolamine (TEA) and 2-ethylhexyl phosphonic acid mono-2-ethylhexyl ester (HL) were used as matrices. The preparation of CuL_2 was made using the methods described in literature (2).

The positive and negative FABMS of HL (without glycerol) are shown in Figure 1a and 1b respectively. The major ions observed in the spectra are $[(HL)_2+H]^+$ at m/z 613, HLH^+ at m/z 307 and fragment ion $(HLH-C_8H_{16})^+$ at m/z 195 in the positive FABMS of HL as well as $[(HL)_2-H]^-$ at m/z 611, L^- at m/z 305 and fragment ion $(L-C_8H_{16})^-$ at m/z 193.

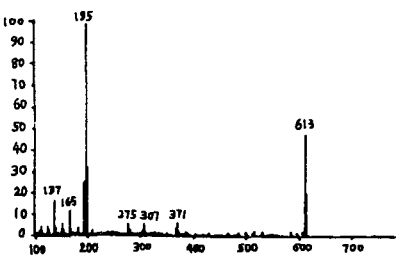

Fig.1a positive FABMS of HL

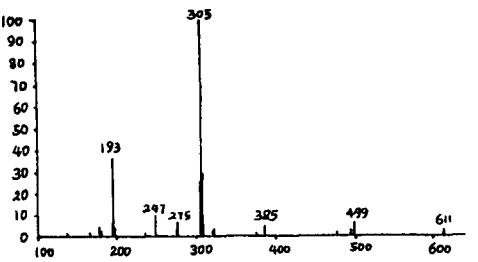

Fig.1b negative FABMS of HL

Presented at the 36th ASMS Conference on Mass Spectrometry and Allied Topics
June 5-10, 1988, San Francisco, CA

The most striking feature of Figure 1a is the intensity of protonated dimer $[(HL)_2+H]^+$ much stronger than HLH^+, which is different from the usual FAB spectra like glycerol. This feature reflects the state of HL in the liquid. Ma and coworkers[2] reported that most of HL molecules in the liquid are dimerized through intermolecular H-bonds i.e.

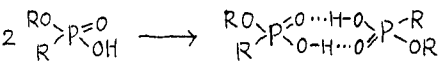

Under fast atom bombardment a proton is captured or abstracted from surrounding molecules to form $[(HL)_2+H]^+$, HL_2^-, HLH^+, L^- ions. The other channel to form HLH^+ is unimolecular decomposition of $[(HL)_2+H]^+$ in gas phase, and HLH^+ further decomposes into $(HLH-C_8H_{16})^+$, which were verified by B/E linked scan technique. In the negative FABMS of HL, intensity of HL_2^- ion are weeker than L^-, which may arise from geometry and H-bond reasons. Therefore FABMS provides the information of liquid phase reactions to a certain extent.

Table I and II list the positive and negative FABMS of CuL_2 respectively. Unusual ion M^+ and $(M+2H)^+$ as well as M^-, $(M-H)^-$ and $(M+H)^-$ were observed. A new FAB ionization mechanism should be proposed, which may contain electron capture, hydrogen radical abstraction and capture processes as follows:

$$CuL_2 \longrightarrow CuL_2^{\ddagger}+e$$
$$CuL_2 \longrightarrow (CuL_2-H)^{\cdot}+H^{\cdot}$$
$$CuL_2+e \longrightarrow (CuL_2)^-$$
$$(CuL_2-H)^{\cdot}+e \longrightarrow (CuL_2-H)^-$$
$$CuL_2^{\ddagger}+2H^{\cdot} \longrightarrow (CuL_2+2H)^+ \quad \text{or} \quad Cu(HL)_2^+$$
$$CuL_2^{\ddagger}+H^{\cdot} \longrightarrow (CuL_2+H)^-$$

From oxidation-reduction point of view, positive FABMS of CuL_2 shows a lack of ions containing Cu(II). The containing copper species observed in the spectra are either Cu(I) or Cu(III), latter is quite rare in solution. Pelzer and coworkers[4] reported that oxidation-reduction processes do occur as a result of the FAB process also.

Table I major ions in positive FABMS of CuL_2

Abundance / m/z / Matrix	$(HO)_2P(=O)OH$ $C_8H_{17}OH$	$[HLH]^+$	$[(HL)_2+H]^+$	$[C_8H_{17}-HL-C_8H_{17}]^+$		$[CuL_2+(n-HL-C_8H_{17})]^+$		$[CuL_2-HL]^+$		$[CuL_2+2H-HL]^+$		$[CuL_2]^+$		$[CuL_2+2H]^+$	
	195	307	613	255	257	257	259	367	369	369	371	673	675	675	677
G	100.0	4.9	4.4	8.0	3.6	9.6	4.3	4.9	2.2	1.9	1.3	2.3	1.0	8.6	4.2
HL	100.0	3.2	7.7	14.1	6.3	24.1	11.0	9.6	4.3	3.1	2.2	25.8	11.6	36.5	17.2
TEA	11.8	0	0	0.7	0.3	2.5	1.0	0.5	0.2	1.2	0.5	0	0	2.6	1.2

Table II *major ions in negative FABMS of CuL_2*

Ions	$(HO)_2P(=O)O^-$ C_8H_{17}	L^-	HL_2^-	$(CuL_2-2H)^-$		$(CuL_2-H)^-$		$(CuL_2)^-$		$(CuL_2+H)^-$	
m/z	193	305	611	671	673	672	674	673	675	674	676
Abundance	14.0	100.0	8.2	11.4	5.1	4.8	2.1	21.1	10.1	9.1	4.9

REFERERENCES

1 M.Barber et al., J.Chem.Soc., Chem.Commun., (1981) 325.
2 E.Ma et al., Scientia Sinica, 24(9) 1237(1981).
3 E.Clayton et al., J.Chem.Soc., Chem.Commun., (1984) 969.
4 G.Pelzer et al., J.Phys.Chem., 88, 5065 (1984).

Presented at the 36th ASMS Conference on Mass Spectrometry and Allied Topics
June 5-10, 1988, San Francisco, CA

MATRIX EFFECTS IN IR-LASER DESORPTION OF NEUTRAL MOLECULES.

R.C. Beavis, J. Lindner, J. Grotemeyer, E.W. Schlag

Institut für Physikalische und Theoretische Chemie, TU München
Lichtenbergstr. 4, D-8046 Garching, Germany.

In the analysis of dipeptides using Infra-Red (IR) laser desorption of neutral molecules followed by resonantly enhanced multiphoton ionization (MUPI), several interesting ionic species were observed:

1) M-18 u : The intensity of this species was dependant on sample preparation, desorption conditions and the peptide sidechains involved.

2) M-16 & M-17 u : These species were only present when the N-terminal residue contained an aromatic group.

The work presented here was an attempt to understand the mechanism of production of these three ion and to see whether the fragmentation of the parent molecule was caused by the desorbing (IR) or the ionizing (UV) laser.

The mass spectrometer used is a BRUKER TOF 1 and has been described elsewhere [1]. For this study, it is important to understand that the desorption and ionization are completely separated in both time and space, with ionization occuring approximately 160 μsec after and 80 mm away from the site of desorption. This separation allows the study of the desorption without intererence from ionization.

A method for affecting the desorption process in a simple way is to change the chemical environment of the sample molecules. In IR desorption of neutral molecules, the threshold for the detectable emmision of molecules is typically 10^4 W/cm^2. Such low photon fluxes do not produce multiphoton effects in a solid and only serve to heat the sample. Therefore, one reaction that may occur is pyrolysis of a peptide at the surface. By changing the chemical enviroment of the molecule during desorption, it should be possible to affect the intensity of species occuring because of a pyrolytic reaction.

The mechanism resulting in $(M-18)^+$ was found to be a pyrolytic dehydration, probably the formation of a C-terminal ketene. Derivatization studies indicated that the C-terminal hydroxyl group participated in the reaction, but the N-terminal amino group did not. Figure 1 demonstrates that the addition of a simple sugar (glucose) can suppress the formation of the $(M-18)^+$ species. The intensity of the $(M-18)^+$ species could not be recovered by changes in the MUPI conditions (i.e. by changes in the UV laser wavelength or power density).

The two additional species, $(M-16)^+$ and $(M-17)^+$, were also studied by this method. Figure 2 shows the effect of adding a sugar to a peptide with an N-terminal aromatic group. The changes in peak intensities can be explained by the suppression of the $(M-18)^+$ species and its C^{13} satellite. The intensities of these species can be altered by changing the ionization condition. Therefore, these two species are true fragment ions, produced by absorption of further UV photons after ionization. The peaks shapes shown in Figure 2 also indicate that the $(M-17)^{+\cdot}$ species has a larger metastable contribution, while the $(M-16)^+$ species has a smaller metastable amount and is relatively stable. A possible reason for this difference is that $(M-16)^+$ was produced by the loss of an $NH_2\cdot$ radical, leaving an even electron ion, while $(M-17)^{+\cdot}$ was formed by the loss of NH_3, leaving a less stable odd electron ion. The necessity of having an N-terminal aromatic species to form these ions also suggests that there may be some resonance stabilization involved in the formation pathway.

These results demonstrate that:

1) Modification of the chemical environment of the sample by the use of a matrix is a useful method of distinguishing between desorption or MUPI induced fragmentations;

2) Sugar matrices eliminate the $(M-18)^+$ species from the mass spectrum by suppression of the formation of an $(M-H_2O)$ neutral species; and

3) The $(M-16)^+$ and $(M-17)^+$ ions are formed from the molecular ion of the peptide after the multiphoton ionization.

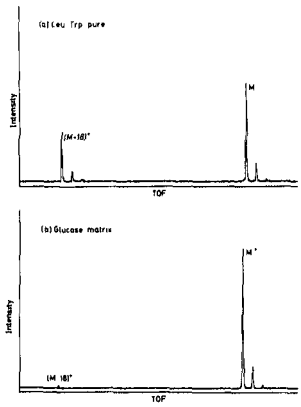

Fig. 1 Partial MUPI-MS of Leu-Trp a) pure; b) glucose added.

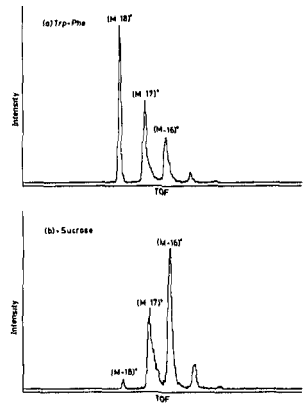

Fig. 2 M-18 region of Trp-Phe a) pure; b) sucrose added.

ACKNOWLEDGEMENTS.

The authors would like to thank dem Bundesministerium für Forschung und Technologie, der Deutschen Forschungsgemeinschaft and Bruker-Franzen Analytik (Bremen) for supporting this work. R.C.B. was supported by a NATO PDF Reseach Grant.

REFERENCES.

[1] U. Boesl, J. Grotemeyer, K. Walter and E. W. Schlag; Anal.Instrum. 16, 151 (1987).

Presented at the 36th ASMS Conference on Mass Spectrometry and Allied Topics
June 5-10, 1988, San Francisco, CA

Uranium Concentration in Fossils

Jun OKANO and Chiaki Uyeda

College of General Education, Osaka Univ., Toyonaka, Osaka, 560 JAPAN

Recently it is known that fossil bones tend to accumulate uranium. The uranium concentrarion, C_u in fossils has been measured so far by γ ray spectroscopy or by fission track method. We applied secondary ion mass spectrometry, SIMS, to detect the uranium in fossil samples. The purpose of this work is firstly to investigate the possibility of semi-quantitative analyses of uranium in fossils, and secondly to study the correlation between C_u and the age of fossil bones. The further purpose of this work is to apply SIMS to measure the distribution of C_u in fossil teeth.

A modified Hitachi IMA 2A ion microprobe was used in this work. The primary ions were 10.5keV $O_2^+(O^+)$ and the probe diameter was 80-300μm. A piece of fossil sample was polished by emery paper to make the analyzing surface flat and the sample was mounted in a stainless steel crucible with pure indium. The sample and the crucible was dried in an oven at 100 °C for 24hrs and then attached to the sample holder of the ion microprobe. Electron spray was applied to compensate the charge on the sample surface induced by the primary ion bombardment.

SIMS mass spectra of uranium in U-glasses and fossil samples have three main peaks of U^+, UO^+ and UO_2^+. Among those, UO^+ is usually most intense although the relative intensities vary to some extent by the change of setting of the energy window. In this work, the energy window was set at the maximum trasmission of UO^+, and the sum of the intensities of U^+, UO^+ and UO_2^+ was taken as the intensity of uranium.

Figure 1 shows the relation between C_u and the SIMS intensity of uranium. The SIMS intensity is normalized to Ca^+ intensity and furthermore corrected for the stoichiometry. G611, G613 and G615 are the standard glasses of National Bureau of Standards. These glasses consist mostly of SiO_2, Na_2O, CaO and Al_2O_3 whose proportions are the same for the three glasses. The C_us are 461.5ppm for 611, 37.38ppm for 613 and 0.823ppm for 615. 120b is the phosphate rock standard of NBS which holds uranium of 128.4ppm. C_us of Dali bone, Arago bone and Barbados coral were determined by γ-ray spectroscopy. It was found that the plots of the standard glasses were well on a straight line as shown in the figure. Althought the plots of the fossil samples and the phosphate rock are scattered to some extent, we adopted the

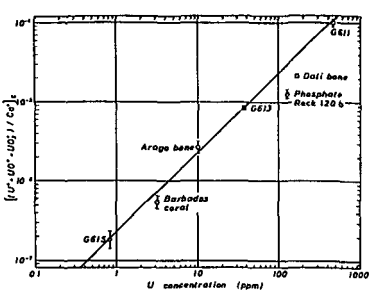

Fig.1 Calibration line for the estimation of C_u

straight line for the glasses as the tentative calibration line to carry out semi-quantitative analyses of uranium in fossil samples. This will be valid with an allowance of a half order of magnitute.

The list of the fossil bone samples and the results are shown in Table I and Fig.2. It is clear that there is a general tendency of increasing C_u with the age of the fossil samples. With a few exception, most data are plotted between the line A, $C_u=1\times10^{-4}t$, and the line B, $C_u=1\times10^{-2}/\sqrt{t}$ as shown in Fig.2.

Figure 3 shows the variation of C_u in the fossil teeth. It has been known that C_u in dentin part of fossil teeth is high and that in enamel part is low. The distribution of C_u from the border of dentine-enamel to the inner part of enamel was measured for three fossil teeth samples. This results seem to show that the diffusion of uranium from dentin to enamel has progressed throuout the fossil age.

References

1) K. Komura and M. Sakanoue, Proc. of the 1st Intern. Symp. on ESR Dating (Ube, Japan 1985) P.9

2) M. Ikeya, ESR Age Determination, p128, IONICS, Tokyo (1987)

Table I

Sample No.	Samples			Age	C_u (ppm)
1	Xenacantus	teeth	(Okulahoma)	Permian	23±5
2	Otodus	dentine	(Morocco)	Eocene	100±18
3	Eohippus	dentine	(Wyoming)	Eocene	1300±260
4	Mericoidodon	jaw bone	(Nebraska)	Oligocene	77±22
5	Leptomeryx	dentine	(Nebraska)	Oligocene	79±9
6	Mesohippus	dentine	(South Dakota)	Oligocene	37±3
7	Hyracodon	dentine	(Nebraska)	Oligocene	570±90
8	Carcharodon	dentine	(South Carolina)	Miocene	750±180
9	Oxyrhina	dentine	(California)	Miocene	43±8
10	Desmostylus	dentine	(California)	Miocene	24±6
11	Horse	dentine	(Chou kou-tien)	$2\sim5.5\times10^4$y	21±3
12	Animal	dentine	(Douara cave)	$6\sim8\times10^4$y	4.5±1.1
13	Animal	bone	(Arago cave)	$2\sim4\times10^4$y	9.8±0.6
14	Animal	bone	(Dali)	$0.5\sim2\times10^4$y	100±10

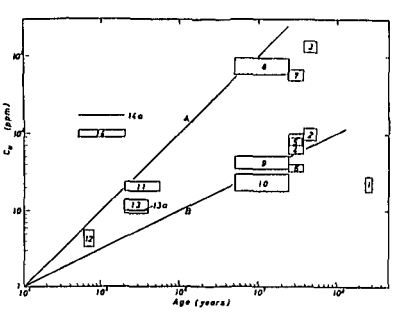

Fig.2 Relation between the age and C_u of the fossil samples

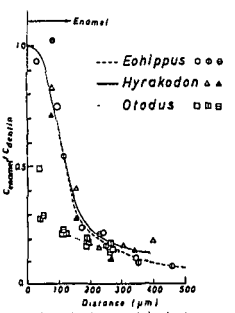

Fig.3 Distribution of C_u in enamel of the fossil teeth

Presented at the 36th ASMS Conference on Mass Spectrometry and Allied Topics
June 5-10, 1988, San Francisco, CA

Evaluation of Fast Atom Bombardment Mass Spectrometry for the Study of Cementitious Stabilized Wastes

J. V. Headley, P. W. Brooks* and P. Hannak

Alberta Environmental Centre, P.O. Bag 4000, Vegreville, Alberta TOB 4LO, Canada
*Geological Survey of Canada, 3303 - 33 St., NW, Calgary, Alberta, Canada

Solidification and stabilization processes(S/S) are of importance for the treatment and disposal of hazardous industrial wastes containing heavy metals, organometallics and polymeric contaminants . Little is known about the mechanism of containment, the nature of contaminant-matrix interactions and the partitioning of the waste in cementitious materials.

Release mechanisms have been investigated using elemental analyses of treated wastes and chemical analyses of leachates. Direct study however, addressing the chemical nature of metal containment in cementitious materials has received little attention.

In this paper, results are reported and evaluated for fast atom bombardment mass spectrometry (FAB/MS) studies of (a) Portland cement standard reference materials and (b) Portland cement standards containing heavy metal contaminated wastes. The wastes contained at least one of four heavy metals (Cd, Cr, Pb, V) covering a range of molar concentrations (0.01 M - 0.4 M), with known moisture content (27-32%). Binder systems studies included normal Portland cement type II and cement kiln dust with sodium silicate additives. The latter were selected to promote heavy metal-silicate interactions.

The studies were conducted on a hybrid VG 70S mass spectrometer with EBQQ geometry, using methanolic suspensions of the cementitious materials deposited on the FAB target. Negative ions and positive ions were collected using continuous mode detection.

The major components of the Portland cement standards yielded abundant positive ions; the corresponding negative ions were poorly observed. For example, standard reference material containing CaO, (64.5% by weight), yielded abundant ions for the series Ca^+, CaO^+, $CaCaOCaO^+$. Likewise for cementitious material containing lead contaminated waste, Pb^+, $PbOH^+$, $PbCaO^+$, $PbSiO^+$, $PbOHCaO^+$, and $PbOSiO^+$ are the major ions observed. Similar species were observed for waste containing Cd, Cr, and V.

Conditions were attained in which matrix species are tagged by ion-molecule reactions occurring in the FAB ion source. The reproducibility of the FAB mass spectral data (Table 1) is thus dependent on (a) the homogeneity of the subsamples and (b) the stability and duration of the ion beam. As shown in Table 1, the reproducibility of the technique is satisfactory.

The results indicate that FAB/MS is a viable technique for the study of cementitious stabilized wastes. For example the FAB mass spectra contained a preponderance of metal ions associated with SiO groups, for binders with sodium silicate additives. Likewise the abundance of the metal hydroxide ions were observed to be dependent on the S/S process. Future work is warranted to correlate the abundance and distribution of the metal-ligand species with containment mechanisms for S/S processes.

Table 1 Reproducibility data for FAB/MS of cementitious stabilized waste contaminated with lead

Ion	Relative Abundance	%RSD	Range	No. of Determinations
Pb^+	100			8
$PbOH^+$	18.6	10	16.3- 21.4	8
$PbCaO^+$	4.1	8.6	3.8 - 4.7	8
$PbSiO^+$	0.6	17	0.5 - 0.8	8
$PbOHCaO^+$	2.4	6.3	2.2 - 2.6	8
$PbOSiO^+$	1.0	11	0.8 - 1.2	8
Ca^+/Si^+	1.12	2.17	1.10- 1.16	8
*Ca/Si	1.16	-	-	12

*Neuwirth et al. (1986) STEM, EDAX experiments

Acknowledgements:

This research is part of a program on "Research into immobilization of hazardous heavy metal waste with chemically bonded ceramics (cements)". Participants include:
Alberta Environmental Centre, University of Alberta, Energy, Mines and Resources Canada, and Alberta Research Council. Dr. R. D. Smillie and Dr. J. G. Hardy are thanked for their support.

Reference:

M. Neuwirth, R. Mikula and P. Hannak, 4th Int. Hazardous Waste Symposium on Environ. Aspects of S/S of Hazardous and Radioactive Wastes (1986).

Presented at the 36th ASMS Conference on Mass Spectrometry and Allied Topics
June 5-10, 1988, San Francisco, CA

ANALYSIS OF AIR AND MOISTURE SENSITIVE ORGANOMETALLIC COMPOUNDS USING AN ARGON STREAMING INTRODUCTION SYSTEM

L. M. Mallis

High Resolution Mass Spectrometry Facility
The University of Iowa
Iowa City, Iowa 52242

C. Ting, M. S. Hammer and L. Messerle

Department of Chemistry
The University of Iowa
Iowa City, Iowa 52242

The reaction chemistry of a new class of metal-metal doubly-bonded species $(Cp^*MX_2)_2$ [M = Ta; X = Cl, Br, BH_3; Cp^* = η-$C_5(CH_3)_5$] has been under development. These species, which are prepared by reductive dimerization of high-valent mononuclear precursors, are highly air and moisture sensitive. The emphasis on reactivity studies with small molecules (e.g., H_2, C_2H_4) have resulted in a need for routine mass spectrometry of these highly sensitive, high mass organodimetallics The principal impediment to these studies is routine sample introduction under conditions which preserve the integrity of the sample.

The development of dinuclear early transition metal organometallic chemistry, particularly of species with metal-metal bonds, has been slowed by a reliance on relatively slow X-ray diffraction methods in characterization of the dinuclear unit. In addition, the use of X-ray diffraction also suffers from potentially severe sampling errors. Mass spectrometric methods would be of tremendous value in determining the nominal mass, nuclearity of reaction products (through isotope patterns) and fragmentation patterns of organodimetallics. The extreme air and moisture sensitivity of early transition metal organodimetallics has limited the routine application of mass spectrometric methods in compound characterization.

In this paper, a technique for introduction of such air and moisture sensitive compounds is presented. This technique uses argon to purge the sample introduction environment. In general, the compounds mentioned above show a significant increase in molecular ion formation when this argon streaming sample introduction technique is used. In addition, for some of the dimetallic compounds sample introduction with argon provides the opportunity to observe the intact molecular ion. In all cases, the spectra were obtained using a VG ZAB-HF mass spectrometer in the electron-impact ionization mode.

Three different organo-dimetallic species were analyzed. In general, the structure of these compounds is thought to contain a metal-metal double bond The X-ray structure of $(Cp^*TaBr_2)_2$ is shown in Figure 1. A 4.05 fold increase in sensitivity is observed for the selected molecular ion (m/z 952) of this compound (see Table 1). For the BH_3 adduct of this compound, a 3.27 fold increase in sensitivity was observed (m/z 688, see Table 2). The Cl adduct of this series produced a 15.3 fold increase in sensitivity for the selected molecular ion (m/z 774; see Table 3).

The technique of argon streaming increases the chance of observing the molecular ion cluster for such compounds. Further modifications on the method of sample preparation and introduction are currently underway. In addition, a method for sample introduction during a fast atom bombardment experiment is currently under development.

FIGURE 1 This is an X-ray crystallographic representation for the structure of $Ta_2Br_4Cp^*_2$ (m/z 952).

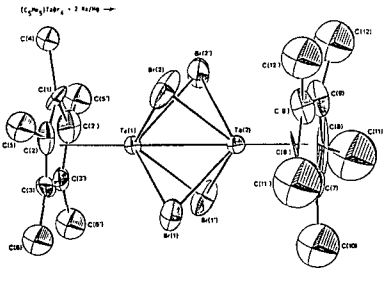

TABLE 1.

$Ta_2Br_4Cp^*_2$ Experiment Without Argon (m/z 952 isotope of Molecular Ion Cluster; Area Counts-arbitrary units, see Figures 4 and 5, Spectrum 1)

5,566,061 (± 1.8 %)
4,092,251 (± 1.9 %)
Ave: 4,829,156 (± 18.0 %)

$Ta_2Br_4Cp^*_2$ Experiment With Argon Protection

20,884,105 (± .72 %)
16,998,869 (± .94 %)
22,281,467 (± .86 %)
17,977,260 (± 1.7 %)
Ave: 19,535,425 (± 10.5 %)

Increase in Sensitivity Towards Molecular Ion Observation

$$\frac{19,535,425}{4,829,156} = 4.05 = 405\ \%\ \text{Increase}$$

TABLE 2.

$Ta_2B_4H_{12}Cp^*_2$ Experiment Without Argon (m/z 686 isotope of Molecular Ion Cluster; Area Counts-arbitrary units, see Spectrum 2)

30,684,682 (± 5.5 %)
33,305,533 (± 1.1 %)
Ave: 31,995,108 (± 8.2 %)

$Ta_2B_4H_{12}Cp^*_2$ Experiment With Argon Protection

122,195,861 (± 1.5 %)
106,593,450 (± 1.2 %)
84,893,368 (± 1.9 %)
Ave: 104,560,890 (± 12.5 %)

Increase in Sensitivity Towards Molecular Ion Observation

$$\frac{104,560,890}{31,995,108} = 3.27 = 327\ \%\ \text{Increase}$$

TABLE 3.

$Ta_2Cl_4Cp^*_2$ Experiment Without Argon (m/z 774 isotope of Molecular Ion Cluster; Area Counts-arbitrary units, see Spectrum 3)

4,743,267 (± .90 %)
4,841,000 (± 1.1 %)
Ave: 4,792,134 (± 1.1 %)

$Ta_2Cl_4Cp^*_2$ Experiment With Argon Protection

71,154,397 (± 1.3 %)
78,178,408 (± .44 %)
69,858,708 (± 2.7 %)
Ave: 73,063,838 (± 4.7 %)

Increase in Sensitivity Towards Molecular Ion Observation

$$\frac{73,063,838}{4,792,134} = 15.3 = 1530\ \%\ \text{Increase}$$

Presented at the 36th ASMS Conference on Mass Spectrometry and Allied Topics
June 5-10, 1988, San Francisco, CA

CHARACTERIZATION OF AIR-SENSITIVE METALLOPORPHYRINS BY FABMS

Emirgul Tolun and Julie A.Leary

Chemistry Dept. University of California, Berkeley, CA 94720

There is significant interest in metalloporphyrins for both biological and industrial reasons.The difficulty in obtaining large X-ray quality single crystals of these compounds, particularly the metal-metal multiply bonded metalloporphyrin dimers have necessitated the use of mass spectrometry to establish their dinuclearity. The octaethyl porphyrin (OEP) and meso-tetratolyl porphyrin (TTP) dianionic complexes containing tungsten and rhenium are extremely oxygen sensitive and begin to decompose in the presence of small levels of oxygen in solution.

In this presentation we report the development of specific handling procedures for FABMS of oxygen and water sensitive organometallic compounds and its application to the analysis of tungsten and rhenium porphyrins.

All samples run on a Kratos MS-50 double focussing mass spectrometer equipped with a DS-55 data system. Vacuum distilled tetramethylene sulfone (sulfolane) was used as a matrix.Sample preparation and loading were done under nitrogen or argon in a Vacuum Atmospheres HE 43-2 dry-box.

Table 1 is a summary of the results obtained for the positive ion FABMS of W and Re metalloporphyrins. In general, molecular ion was present in each spectrum.

All spectra also exhibited some oxygenated form of the metalloporphyrin. At this point it has not yet been determined whether the oxygenated products were produced in the mass spectrometer, during sample preparation and mounting or whether these by-products were already present in the original samples.

The major ions observed for the dinuclear complexes $[Re(OEP)]_2$ and $[W(OEP)]_2$ include the molecular ion, the Metal(OEP) ion and the ions corresponding to M+14, M-14 and M-28 (Figure 1).M-14 and M-28 type ions probably arise from the loss of CH_3 and C_2H_5 respectively, with the transfer of hydrogens to the macrocycle. Ions corresponding 14 mass unit additions either to the molecular ion or fragment ions, may be metal carbenes forming as a result of methyl losses from one molecule and attachment of the metal of another molecule in the gas phase.

Computer simulated isotope patterns were in excellent agreement with molecular, oxygenated and fragment ions.

Presented at the 36th ASMS Conference on Mass Spectrometry and Allied Topics
June 5-10, 1988, San Francisco, CA

FIGURE 1

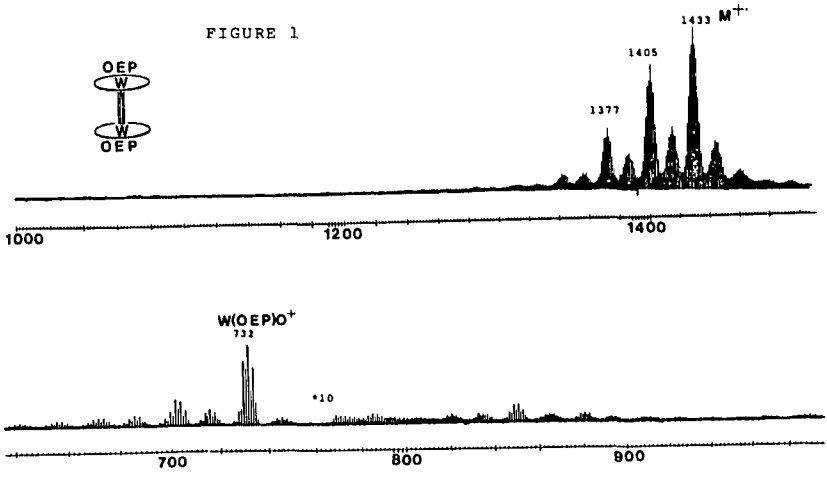

TABLE 1

Complexes	[M]+	Predominant fragment ions	Oxygenated by-products
$W(TTP)(F_5C_6C{=}CC_6F_5)$	1210	1192 $(M-F+H)^+$, 852 $W(TTP)^+$	868 $[W(TTP)O]^+$
$W(OEP)(F_5C_6C{=}CC_6F_5)$	1074	1056 $(M-F+H)^+$, 1046 $(M-C_2H_4)^+$ 716 $W(OEP)^+$, 702 $[W(OEP)-CH_3+H]^+$	732 $[W(OEP)O]^+$
$W(OEP)Cl_2$	-	751 $[M-Cl]^+$, 716 $[W(OEP)-CH_3+H]^+$ 702 $[W(OEP)-CH_3+H]^+$	766 $[M-Cl+O]^+$ 748 $[W(OEP)O_2]^+$, 732 $[W(OEP)O]^+$
$W(TTP)Cl_2$	-	887 $[M-Cl]^+$, 852 $[W(TTP)]^+$	939 $[M+O]^+$, 903 $[M-Cl+O]^+$ 884 $[W(TTP)O_2]^+$, 868 $[W(TTP)O]^+$
$Re(OEP)Cl_2$	-	754 $[M-Cl]^+$, 719 $[Re(OEP)]^+$	735 $[Re(OEP)O]^+$
$[W(OEP)]_2$	1433	1419 $[M-CH_3+H]^+$, 716 $[W(OEP)]^+$ 1405 $[M-C_2H_4]^+$, 1377 $[M-(C_2H_4)_2]^+$	737 $[W(OEP)O]^+$
$[Re(OEP)]_2$	1437	1409 $[M-C_2H_4]^+$, 719 $[Re(OEP)]^+$	1453 $[M+O]^+$
$[Re(TTP)]_2$	1710	855 $[Re(TTP)]^+$	887 $[Re(TTP)O_2]^+$, 871 $[Re(TTP)O]^+$
$Re(OEP)(PEt_3)_2$	955	837 $[M-PEt_3]^+$, 719 $[Re(OEP)]^+$	-
$Re(TTP)(PEt_3)_2$	1091	973 $[M-PEt_3]^+$, 855 $[Re(TTP)]^+$	1107 $[M+O]^+$, 989 $[M-PEt_3+O]^+$

Presented at the 36th ASMS Conference on Mass Spectrometry and Allied Topics
June 5-10, 1988, San Francisco, CA

DESIGN AND CHARACTERIZATION OF A RADIO FREQUENCY (RF) POWERED GLOW DISCHARGE SOURCE FOR SOLIDS MASS SPECTROMETRY

R. Kenneth Marcus, D. Duckworth, and W. Kolar
Department of Chemistry, Clemson University
Clemson, SC 29634

Glow discharge mass spectrometry has evolved into one of the most powerful of methods for performing direct solids elemental analysis. While the technique is applicable to a wide range of alloy and semiconductor systems, one limiting factor is the inability to analyze insulating (non-conducting) materials without some form of matrix modification. The approach typically taken for such analyses, is to mix the sample specimen (in powder form) with a metal powder such as Cu, Ta, or graphite. In doing so, the sample becomes diluted and the ability to obtain depth-resolved analyses is lost.

In this laboratory we have designed and constructed a radio frequency powered glow discharge source to perform direct solids elemental analysis of metals and insulators. By applying a radio frequency (13.56 MHz in this case) potential to an insulating surface, the rate of the capacitor-like decay response to a voltage pulse is overcome, resulting in a psuedo-continuous plasma. By choosing the appropriate electrode geometry, a d.c. bias potential develops on the cathode (sample) resulting in its bombardment by positively charged argon discharge gas ions. In addition to the advantage of being able to sputter insulating materials directly, it is expected that the lower operating pressures of the rf glow discharge (mtorr vs. torr for the d.c. case) will provide enhanced depth profiling capabilities.

EXPERIMENTAL

Figure 1 is a diagrammatic representation of the instrumentation employed in the rf glow discharge system. The rf glow discharge is powered by a 1 kW generator (Model RF-10, RF Plasma Products) which is coupled via an automatic LC matching network (Model AM-10) for efficient power transfer. The operating power of the plasma is continuously variable over the 5-50 watt operating range employed here. Analytical samples are in the form of 0.5" diameter, 0.4" thick, disks which are mounted on a water cooled stainless steel holder. The holder is encapsulated in a Macor sleeve with a steel shutter employed to restrict the sputtering to the sample surface. The sample holder is flange mounted to a stainless steel six-way cross which forms the source region.

A quadrupole-based glow discharge mass spectrometer system designed and assembled in this laboratory is employed to sample the rf plasma ions. The system consists of Extrel C-50/400 components housed in a vacuum chamber which is differentially pumped by a pair of Leybold Hereaus RPK series cryopumps. Ions exiting the source region pass through the first pumping stage into the analyzer region where they are focussed by a two-element lens into a Bessel Box energy analyzer. The Bessel Box is employed both as a means of normalizing ion energies and of determining relative kinetic energies of the various plasma species. Ions are detected by a conversion dynode-channeltron pair in both analog and ion counting modes. Output from the electrometer is fed to an X-Y plotter to record spectral scans. Relative ion intensity measurements are performed through a Hewlett Packard 9835A computer with Extrel peak-hopping measurement routines.

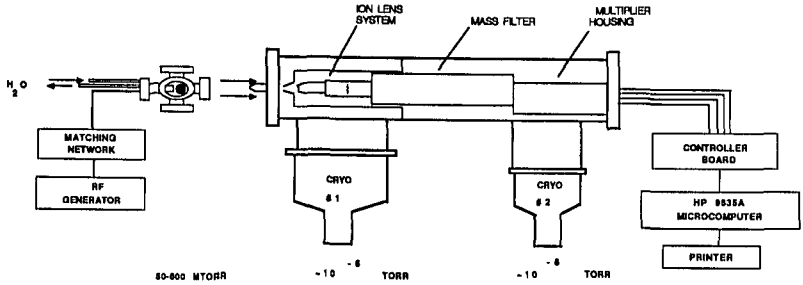

Figure 1. RF powered glow discharge mass spectrometer system.

RESULTS AND DISCUSSION

Figure 2 is an rf glow discharge mass spectrum of NBS C1122 copper-beryllium alloy. The mass spectra produced by the rf glow discharge source are quite similar to those of the d.c. glow discharges with ion currents on the same order of magnitude (3X10-11 amps for $^{63}Cu^{+}$ here). Certified minor components of this alloy are shown in expansions of the spectrum with their respective elemental concentrations. The plasma source operates stably with a variation of the ^{54}Fe ion signal of ~3% over a 40-minute time period. Detection limits are difficult to assign, at this point, due to non-ideal rf grounding (noise) and an inability to optimize the sample-to-skimmer cone distance.

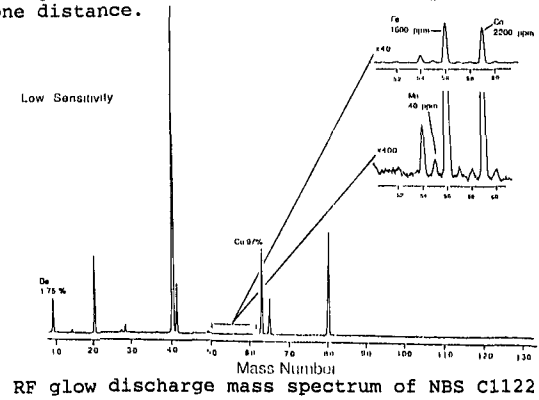

Figure 2. RF glow discharge mass spectrum of NBS C1122.

As was expected, the operating regime of the rf glow discharge ion source is much different from its d.c. counter part. Also different from the normal d.c. source is the relatively limited range of operating parameters (0.1-0.4 torr, 5-50 watts) over which high ion populations are extracted. It should be noted that the plasma operates stably at higher powers at each pressure and in fact the conditions of higher pressure and powers would seem to be those employed for atomic emission spectroscopy. We believe that these pressure-power relationships indicate a shift in the optimal sampling position in the plasma negative glow.

Future studies of the rf glow discharge source will focus on its application to the analysis of insulating materials and in reducing electronic noise pick-up from the plasma generator. Given the magnitude of the matrix ion current and the source stability (after only weeks of investigation), it is believed that the rf glow discharge operating as an atomization/ionization source may be a viable method for direct solids elemental analysis of both conducting and insulating sample matrices.

Presented at the 36th ASMS Conference on Mass Spectrometry and Allied Topics
June 5-10, 1988, San Francisco, CA

ATMOSPHERIC PRESSURE PLASMA MASS SPECTROMETRY - CONSIDER THE SOURCE

R.D. Satzger

U.S. Food and Drug Administration
Cincinnati, Ohio 45202

Atmospheric pressure plasma mass spectrometry is a multi-element technique with excellent detection limits and the capability to provide isotope ratio information enabling isotope dilution. The commercially availabe Ar ICP ion source principally generates singly charged monatomic species. Its high gas temperatures facilitate liquid sample introduction with few ionization suppression problems which cannot be handled through dilution due to the excellent sensitivity of the technique.

However, argon containing molecular background ions can interfere in the determination of the principle isotopes of K, Ca, V, Cr, Mn, Fe, Ni, Co, Ge, As and Se. Also, the Ar plasma does not generate substantial quantities of Br^+, Cl^+, and F^+ which are only partially ionized. Therefore, in an attempt to reduce the argon containing molecular background and provide the capability to determine the halogens as positive ions, the He microwave induced plasma (MIP) source is being investigated in this laboratory using a laboratory built atmospheric pressure plasma sampling mass spectrometer.

In this work an electrothermal vaporizer (ETV) is investigated as a means of sample introduction to the He-MIP. Use of ETV in conjunction with a He plasma provide several advantages. Background peaks in the mass spectrum due to the presence of water when using aqueous solution nebulization as a means of sample introduction are reduced. Major background ions present in a 350W He-MIP are dependent on sampling position. $^4He_2^+$ is the principal ion in the backgound spectrum when sampling the plasma on center at a distance of a few millimeters. A second advantage of the ETV/He-MIP is the ability to reduce the matrix effects observed during solution nebulization into the He plasma, through selective volatilzation of interferents. In many cases the volatility of major matrix species differs from that of the analyte enabling a separation before introduction to the plasma source. A third advantage is the ability to analyze samples which present great difficulties to solution nebulization techniques. Volume limited samples, viscous samples and solid samples may be introduced to the plasma using electrothermal vaporization.

The electrothermal vaporizer assembly is a modified HGS-500 graphite furnace which was formerly used for atomic absorption analyses. The distance between the center of the graphite tube vaporizer and the plasma is approximately 13 cm. The MIP torch assembly requires two He gas flow. A tangential He flow rate of 8.5 L min^{-1} sustains a 350W plasma during all phases of sample introduction (sample loading, drying, ashing, vaporization). The sample aerosol carrier gas flow rate is 1.5 L min. The plasma is sustained in a 1 cm deep TM^{010} resonant cavity at a frequency of 2455 MHZ. All data acquisition was in the analog mode. Optimum sampling position, gas flows, ion lens potentials and mass filter tuning were accomplished during continuous introduction of methyl chloride, methyl bromide, methyl iodide or Hg vapor, depending on the mass of interest.

Initial experiments have demonstrated that the optimum sampling position at 350W is approximately 2 mm above the center of the plasma with a microwave cavity/sampler separation of 4 mm. At this position, NO^+ and O^+ are the principal ions in the mass spectrum. An estimated detection limit for all elements investigated (Se, Cd, Sn, Au, Pb) based on the response for a 5 ng injection is below 50 pg. Relative standard deviation of successive manual injections of Pb was 14%. Peak widths for Pb and Au were approximately 8 sec when using a 5 second ramp to 2000°c. Separation of matrix interferences and isoboric overlaps using the ETV will be discussed.

Presented at the 36th ASMS Conference on Mass Spectrometry and Allied Topics
June 5-10, 1988, San Francisco, CA

76 Carbon And Oxygen Stable Isotope Geochemistry Of Ammonia Beccaril In China Seas And Its Geological Implicatons. He Zhe, Wang Xung And Kau Ya Ping, P. O. Box 18, Qingdao, China.

Ammonia Beccaril Samples from the China Seas and Huanghe River Delta have been determined in carbon and oxygen stable isotopes. Results are so obvious to indicate that the carbon and oxygen stable isotopes are implication of sedimentary environments, so that they are useful tools for facies analysis of carbonate deposits.

The oxygen stable isotopic of foraminifera is related to temperature and salinity of sea water. Foraminifera will deplete oxygen-18 with increasing temperature and decreasing salinity. Therefore, the foraminifera in transitional environments will show lighter values both in carbon and oxygen stable isotopic composition. For example, the oxygen-18 of Ammonia is the lightest in Ginyin Island to the south China Sea, and at the mouth of Changjian River, $\delta^{13}C$ and $\delta^{18}O$ are lightened owing to the flux of fresh water. Samples from Gingdao No.1 Bathing Beach and Leichou Bay show values at level in $\delta^{13}C$ and $\delta^{18}O$ indicating same boundary conditions occurred in the two bays. Results reconfirm the conclusion that the carbon-13 values are closely related to photosynthesis.

The results from the Huanghe River Delta demonstrate that the ammonia beccaril lived in a transitional environment, very typical isotopic values were observed. In a plot of carbon-13 vs. oxygen-18, it was noted that all of the results were concentrated in small area. This is typical for foraminifera from transitional enviroments. Samples plotting far from this area may result from diagnesis of fresh water.

76

Table 1 $\delta^{13}C$ And $\delta^{18}O$ Of Ammonia Beccaril In China Seas

Sample No.	Environment	$\delta^{13}C$ ‰	$\delta^{18}O$ ‰
H016 Jinyin Island	Reef Flat	-1.466	-4.185
H004 Yongxiong Island	"	-0.865	-4.096
H042 Yalong Peninsula	Intertidal Zone	-0.906	-3.674
Zhejiang Mount Of Putuo	"	-0.855	-1.885
8431-3 South Yellow Sea	31.7m In Water Depth	-1.001	-1.333
8102 Mouth Of Changjiang	27m In Water Depth	-1.245	-3.033
Qingdao No.1 Bathing Beach	3m In Water Depth	-2.192	-1.972
M008 Jiaozhou Bay	Intertidal Zone	-1.543	-0.847
M016 Jiaozhou Bay	"	-0.837	-0.568
007 Laizhou Bay	2.55 Below Sea Level	-2.430	-2.333

Table 2 $\delta^{13}C$ and $\delta^{18}O$ of Ammonia Beccaril From Drill Hole ZK228 Of Huanghe River Delta

Sample No.	Depth	$\delta^{13}C$ ‰	$\delta^{18}O$ ‰	Environment Inferred From Forams and Ostracods
F4	7-7.08	-3.647	-4.365	River Mouth
F6	10.98-11.05	-4.111	-4.642	"
F9	16.29-16.33	-3.873	-4.216	Intertidal Zone
F9-1	17.28-17.34	-5.710	-8.040	"
F9-2	18.22-18.27	-3.504	-4.423	"
F11	21.46-21.53	-6.447	-10.027	Suhtidal Zone
F21	38.85-39.92	-3.295	-3.401	"
F22	42-42.10	-3.502	-2.314	"
F22-1	42.14-42.59	-3.817	-2.434	"
F24	45.03-45.06	-4.216	-3.102	"
F25	45.25-45.32	-3.689	-3.623	"
F27	49.92-49.44	-4.207	-4.470	Intertidal Zone
F28	49.53-49.65	-4.376	-5.205	"

Presented at the 36th ASMS Conference on Mass Spectrometry and Allied Topics
June 5-10, 1988, San Francisco, CA

MASS SPECTROMETRIC STUDIES OF AIR/MOISTURE SENSITIVE COMPOUNDS BY CF-FAB

M.Barber, D.J.Bell, M.Morris, L.W.Toller, M.Woods, G.A.Gott, P.P.MacRory, C.A.McAuliffe, UMIST, Sackville St., Manchester, UK.

INTRODUCTION

In standard probe FAB analysis, a liquid matrix is used to dissolve the sample under investigation. This has given rise to problems in some cases where interaction between sample and matrix occurs [1]. Sample introduction via a continuous flow FAB is an alternative approach where the amount of matrix present may be reduced or eliminated [2,3].

The study of manganese/phosphine compounds is of particular interest because of their ability to bind small molecules, e.g. they reversibly bind dioxygen in a manner that closely resembles the properties of both haemoglobin and myoglobin. Gas separations are also possible using these complexes [4]. Previous attempts at FAB mass spectrometric analysis of analogous phosphine oxide complexes proved unsuccessful, with suspected sample disproportionation in the matrix.

EXPERIMENTAL

A commercially available (Kratos Analytical) continuous flow FAB probe [5] was used in conjunction with a Kratos MS50RF-TC. The spectrometer was operated at 6kV, and scanned at 3 $s.dec^{-1}$ under data system (DS90) control. The instrument was equipped with an Ion Tech FAB gun operated at 8kV with Xenon gas.

Samples were introduced to the probe tip by passing the capillary through a septum into the sample system under investigation. The pressure was stabilised by heating the source block accordingly, thus preventing sample freezing and capillary choking. Between sample introductions, the capillary was flushed with dry toluene for five minutes, so eliminating any memory effects.

The normal FAB sample preparations were carried out in a fume cupboard by syringing sample from the sealed system and applying to the probe tip. The introduction and acquisition was done as quickly as possible to reduce the air exposure time. The source heating was turned off.

RESULTS AND DISCUSSION

a) Tertiary Phosphines

The mass spectra of two tertiary phosphines (Fig. 1), both air sensitive, show intense ions relating to the $M^{\cdot +}$ entity, with little or no oxidation evident when using continuous flow FAB. Structural confirmation of the phosphines may be derived from the fragmentation patterns, and no clusters or adducts of the phosphines are manifest.
In contrast, on normal FAB analysis with limited exposure to air, the ion pertaining to the protonated phosphine oxide species predominates.

b) Manganese Halide / Phosphine Complexes

The mass spectra of the manganese halide/phosphine mixtures (Fig. 2) show ions suggesting that the phosphine(L) contains a minute

amount of phosphine oxide(OL). Copper (from the probe tip) is found to complex as Cu(I) with L, and the Mn(II) reacts with OL in preference to L. Both $Mn(OL)X_2$ and $Mn(OL)_2X_2$ have been isolated. The unexpected result is the appearance of an ion sixteen daltons higher than the $(Mn(OL)_2X)_+$ entity that suggests the presence of either $Mn(OL)(L)(O_2)X_2$, or the less likely $Mn(OL)_2X_2O$.

CONCLUSION

Continuous flow FAB mass spectra of a number of air/moisture sensitive compounds were attained with relative ease. This method permitted facile analysis of some sensitive and extremely odorous compounds with contamination of neither the sample nor the laboratory. A species was observed that suggested the possible binding of molecular oxygen to a manganese phosphine/phosphine oxide complex.

REFERENCES

1 M.Barber et al., submitted for publication.
2. Y.Ito et al., J.Chromatogr., 346 (1985) 161.
3. R.M.Caprioli et al., Anal.Chem., 58 (1986) 2949.
4. C.A.McAuliffe, J.Mol.Cat., 44 (1988) 35.
5. M.Barber et al., Org.Mass Spectrom., 22 (1987) 647.

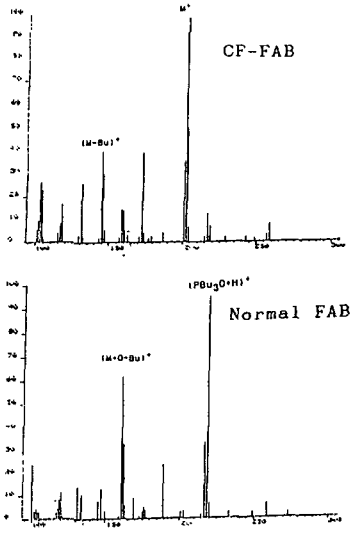

Figure 1.

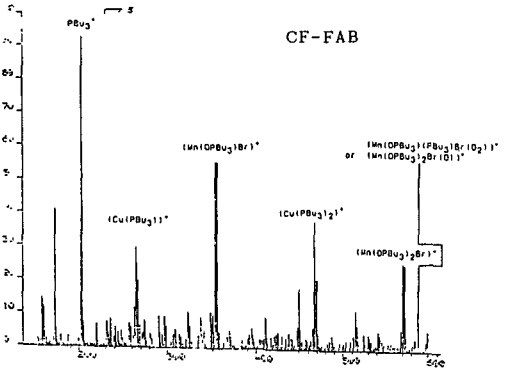

Figure 2.

Presented at the 36th ASMS Conference on Mass Spectrometry and Allied Topics
June 5-10, 1988, San Francisco, CA

ANALYSIS OF SYNTHETIC AND NATURAL POLYMERS USING PYROLYSIS SHORT COLUMN GC/MS

J.M. Richards, Somatogenetics Instruments Inc., Broomfield, CO 80020; W.H. McClennen, J.A. Bunger, and H.L.C. Meuzelaar, Center for Micro-Analysis and Reaction Chemistry, University of Utah, S.L.C. UT 84112.

Pyrolysis-gas chromatography-mass spectrometry (Py-GC-MS) has long been used in the analysis of synthetic and natural polymers for quality control, material characterization and in the study of degradation and biomass conversion. However; Py-GC-MS has the disadvantage of often very long analysis times (>100min), and the loss of highly polar and high MW pyrolysis products on the column. Decreasing the analysis time, and increasing the throughput of polar and high MW compounds would greatly enhance this technique for the analysis of polymers and biopolymers.

Short column-gas chromatography mass spectrometry (SC/GC-MS) has been studied and demonstrated [1,2] as a method which can greatly reduce the time required for analysis while maintaining a useful level of resolution. Further increases in analysis speed can be achieved by interfacing the column directly with the vacuum of a mass spectrometer since the optimum carrier gas velocity for a column with a vacuum outlet is higher than for a column with an atmospheric outlet (ca. 2 times higher for 2.5m x 0.25mmID column [2]). Thus, a short column which is interfaced directly with the vacuum of the mass spectrometer allows increased analysis speed by virtue of the reduced column length and the increased carrier gas velocity. A short column GC-MS system with a vacuum column outlet and a pyrolysis inlet should be capable of rapid analyses of polymers and biopolymers.

A low dead volume Curie-point pyrolysis inlet (Somatogenetics Instruments) was used with short columns (4m and 5m) directly interfaced to the vacuum of a Finnigan ITD and ITMS. For the analyses on the ITD a 4m x 0.25mm ID CP-Sil5 column (Chrompack) was used which had a linear velocity of 175cm/s and a volumetric flow of 4.0ml/min (inlet 8psig, column 60°C, transfer line 250°C). The conditions on the ITMS were a 5m x 0.32mmID SE-30 column (J&W Scientific) with a linear velocity of 150cm/s and volumetric flow of 7.2ml/min (inlet pressure 3psig, column 60°C, transfer line 250°C). Pyrolysis was performed using 610°C Curie-point filaments with a temperature rise time of ca. 0.2s, and 1s total heating time. The remaining analytical conditions (inlet T, GC program, etc) were varied according to sample being analyzed.

Analysis of synthetic polymers shows the ability to rapidly characterize these samples and detect relatively high MW compounds without derivatization. The analysis of Biomer rapidly identified the diisocyanate, polyol and chain extender components used in the synthesis of Biomer (4,4'-methylene-bis-(phenyl isocyanate), poly(tetramethylene oxide) and ethylene diamine respectively). Also a hindered amine light stabilizer, an antioxidant (poly(2,2'-diisopropylamino ethylmethacrylate) and 4,4'-butylidene-bis-(6-*t*-butyl-*m*-cresol) respectively) and phthalate additives or contaminants were detected in under 10 minutes. Large polyol oligomers up to n=7 (MW=522) are detected in this analysis.

The analysis of Silastic yields a series of polymer fragments which includes high MW fragments (figure 1). This series of fragments begins with the tetramer fragment which elutes in ca. 20s and concludes with the dodecamer (n=20) at 7min 40s. This dodecamer fragment (MW~1480) is one of the highest molecular weight compounds which has been detected by gas chromatography methods without derivatization.

The speed with which underivatized polar compounds can be analyzed is demonstrated by the analysis of cellulose (figure 2). Both the polar monomer (levoglucosan m/z163) and isomers of the dehydrated monomer (levoglucosenone, m/z145) are detected in under one minute. The separation of isomers of levoglucosenone and the small amount of tailing of the levoglucosan peak show that resolution and chromatographic quality are not sacrificed for the sake of rapid analyses.

Diketopiperazines characteristic of amino acid pairs are detected in the analysis of oligopeptides. Diketopiperazines characteristic of Gly-Pro, Phe-Pro, and Tyr-Pro are detected in the analysis of β-Casomorphin acetate. In principle these compounds can be used in the sequencing of proteins.

The analysis of Walnut wood produced a complex chromatogram which contains peaks characteristic of the saccharide (xylose, hexose and cellulose) and lignin portions of the wood. Compounds characteristic of the syringol and guaiacol units are the dominant lignin fragments. Also, a naphthol wood preservative is detected (figure 3).

The analysis of a dichloromethane extract from a styrene/butadiene rubber compound shows the ability to rapidly detect additives present in the rubber compound. Relatively polar and high MW compounds, such as antioxidants (di-*t*-octyldiphenylamine mw=332 and poly(2,2,4-trimethyl-1,2-dihydroquinoline) dimer detected

at mw=376), antiozonant (N-(1,3-dimethylbutyl)-N'-phenyl-*p*-phenylenediamine mw=268), sulfur (S_8 mw=256) and fatty acids (myristic acid mw=228, palmitic acid mw=256, and stearic acid mw=284), are eluted in under 10 minutes.

The results of this study show the capability of Py-SC/GC-MS to rapidly analyze complex polymeric materials. The combination of pyrolysis and SC/GC-MS (with a vacuum GC outlet) enables rapid detection of relatively high MW and polar compounds which are difficult or impossible to detect using longer columns with an atmospheric pressure outlet. There is relatively little loss of resolution due to the shorter column, while ample information can be collected for the characterization of complex materials.

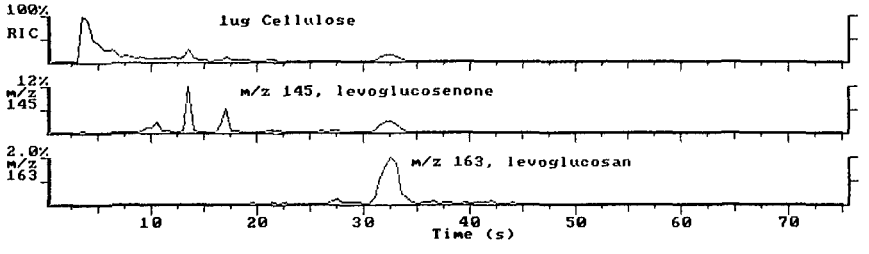

Figure 1. Reconstructed ion current and selected ion chromatograms from the analysis of cellulose. The polar monomer compound, Levoglucosan (*m/z* 163) and the dehydration product of the monomer, levoglucosenone (*m/z* 145), are detected in under 1 minute. Note that isomers of levoglucosenone are resolved. Isobutane chemical ionization.

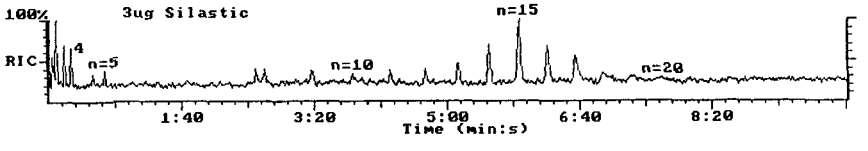

Figure 2. Reconstructed ion current from the Py-SC/GC-MS analysis of Silastic. Fragments of the polymer up to 20 repeat units in length are detected. The n=20 fragment (MW~1480) is one of the highest MW compounds detected via GC *without* derivatization.

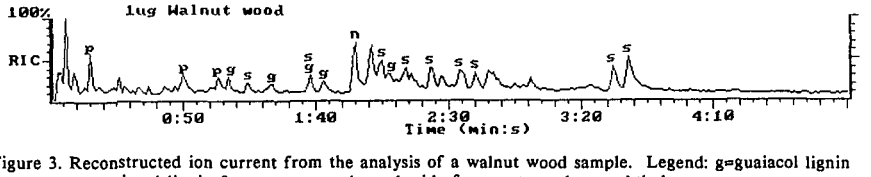

Figure 3. Reconstructed ion current from the analysis of a walnut wood sample. Legend: g=guaiacol lignin fragments, s=syringol lignin fragments, p=polysaccharide fragments, and n=naphthol.

1. C.A. Cramers, G.J. Scherpenzeel, and P.A. Leclercq, *J. Chromatogr.*, 203 (1981) 207.
2. M.L. Trehy, R.A. Yost, and J.G. Dorsey, *Anal. Chem.*, 58 (1986) 14.

Presented at the 36th ASMS Conference on Mass Spectrometry and Allied Topics
June 5-10, 1988, San Francisco, CA

PEPTIDE ANALYSES USING CONTINUOUS-FLOW FABMS

Richard M. Caprioli
The University of Texas Medical School
Houston, TX 77030

Continuous flow (CF) FABMS (1) has been used for the analysis of peptide mixtures which were obtained from enzymic digests of proteins as well as those that have been synthetically prepared. Typically, CF-FAB will involve injection of aqueous samples into a carrier-flow solution containing 95% water, 5% glycerol, and 0.1% TFA. In comparison, standard FAB involves dissolving a small amount of aqueous or solid sample in 80-90% glycerol containing TFA or oxalic acid. The CF-FAB technique has several advantages over the standard FAB technique for peptide analyses. These include higher sensitivity and lower limit of detection because of reduced background chemical noise, reduced ion suppression effects, compatibility with aqueous samples, and capability as an on-line interface for gradient microbore LC/MS applications. The major disadvantages are the initial time required to set up the pump and flow solvent and stabilization of the probe in the source, typically about 15 min. Also, because microcapillary methods are being used, solutions should be filtered to remove solid particles and microbore capillary plumbing carefully done to avoid connections with large dead-volumes.

Depending on the nature of the information sought, the analyses of peptide mixtures using the CF-FAB technique can be accomplished in a number of different modes of operation. In the case where there are a great number of samples to be analyzed, direct injection via a microinjection valve provides a fast and facile method for the introduction of a sample every 2-3 min without cross-contamination. Individual samples may also be analyzed in this way to take advantage of the higher sensitivity of the technique. Reaction mixtures such as those produced from proteolytic digests can be analyzed by direct injection, a one-step elution from a C-8 column or other support medium to which it has been absorbed, or by gradient elution HPLC methods. Again, each method has particular advantages and drawbacks relative to the others. Briefly, direct injection is simple and fast, and since it does not require binding to any media, has the least potential for loss of samples through irreversible adsorption. However, ion suppression effects are maximized since all the peptides are present at the same time and peptides having the same mass cannot be distinguished. Single-step elution of a peptide sample previously adsorbed to a solid phase with a high percentage of organic solvent allows pre-purification and concentration of the sample. One obtains a gross fractionation of the sample so that all the peptides are not present at the same time, although it may still be difficult to distinguish peptides of the same nominal mass. Microbore gradient LC/MS techniques provides better separation of individual components of a mixture over time, minimizing ion suppression effects and providing maximum resolution of individual peptides. However, such an analysis is more time-consuming, ranging from 20-40 min or more for a typical gradient separation.

These points are illustrated for the analysis of the tryptic digest of human apolipoprotein A-I (apo A-I). In a 20 min LC/MS analysis, 25 tryptic fragments were identified in the mass range m/z 2000 - 400. The overall response and sensitivity for this mass range was determined by analyzing the digest at different dilutions, allowing 240, 24 and 2.4 pmol to flow into the MS source. Most of the peptides were readily identified at good signal-to-noise levels even at the lower concentration. Figure 1 shows the CF-FAB mass spectrum of one of these tryptic fragments.

Minimization of ion suppression effects using CF-FAB is illustrated for the analysis of a mixture of seven heptapeptides that have been synthetically prepared. The sequences are similar; the N-termini are Ala-Phe-, the C-termini are -Asn-Gly, and the middle three residues varied from hydrophobic to hydrophilic residues. Figure 2 shows the CF-FAB and standard FAB analyses of this mixture. It is seen that major ion

suppression effects are operating in the case of standard FAB for peptides I, III, and V. This is greatly reduced in the analyses utilizing CF-FAB. The results are also interesting because the peptides suppressed the greatest are the more hydrophobic of the group, although all the peptides have hydrophilic indices. This suggests that for these types of peptides, other factors such as peptide-peptide interactions and secondary structure may also play a major role in the production of ions from the liquid sample. This is discussed in more detail elsewhere (2).

We have shown that CF-FAB can be used effectively for the analysis of mixtures of peptides and has several advantages over standard FAB techniques. When used as an LC/MS interface, complex mixtures can be analyzed at the 1-5 pmol level using wide mass range scans. We believe that this technique provides a most effective means for analyzing protease digests and other peptide mixtures.

ACKNOWLEDGEMENTS:

The author acknowledges the expert assistance of Beverly DaGue, Millie Martin and William T. Moore in obtaining the data presented in this paper.

REFERENCES:

1. R. M. Caprioli, T. Fan and J. S. Cottrell, Anal. Chem. 58, 2949 (1986).
2. R. M. Caprioli, W. T. Moore, G. Petrie and K. Wilson, Int. J. Mass Spectrom. & Ion Phys.(1988) in press.

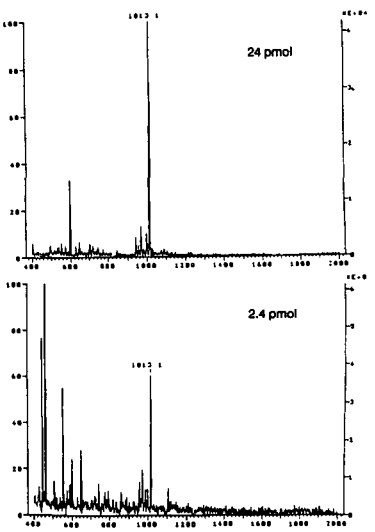

Figure 1

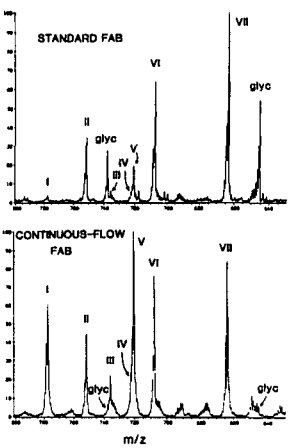

Figure 2

Presented at the 36th ASMS Conference on Mass Spectrometry and Allied Topics
June 5-10, 1988, San Francisco, CA

OPIOID PEPTIDE MEASUREMENTS WITH FAB-MS

Dominic M. Desiderio
Departments of Neurology and Biochemistry,
University of Tennessee, Memphis,
800 Madison Avenue, Memphis, Tennessee 38163

State-of-the-art mass spectrometric (MS) methods are used effectively to identify and to quantify neuropeptides in biological CSF, plasma, and tissue extracts with excellent sensitivity and specificity. RP-HPLC gradient elution (1-3) is performed on a Sep-Pak treated peptide-rich fraction from a biologic extract, and the eluent is monitored by a variety of post-HPLC detectors to maximize amino acid sequence information: UV (200 nm) provides the analog absorption trace; receptorassay analysis (RRA) of 90 one-minute fractions provides the metabolic profile of opioid receptoractive peptides (4); radioimmunoassay (RIA) of selected fractions provides immunoreactivity information; and two modes of fast atom bombardment mass spectrometry (FAB-MS) provide additional structure information: corroboration of the (M+H)+ of the expected peptide (5), or MS/MS in the selected ion monitoring (SIM) mode to monitor an amino acid sequence-determining fragment ion unique to that peptide, for quantification with maximum specificity. FAB-MS-MS-SIM of solutions of synthetic leucine enkephalin is sensitive to the 70 femtomole (6) and attomole level (7).

The objective of this research program is to identify and measure endogenous opioid peptides that are extracted from biologic tissues and fluids at the maximum level of molecular specificity and detection sensitivity. At present, the greatest need in neurochemistry is not necessarily detection sensitivity but rather the more crucial parameter, molecular specificity, which is an experimental parameter that can be provided only by amino acid sequence information derived from gas-phase, wet-chemical, or MS/MS sequencing methods. It is our opinion that MS methods maximize molecular specificity and attain a detection sensitivity that rivals that of immunoassay (6,7).

METHODS

Tissue preparation. After acquisition, post-mortem human pituitaries, pituitary tumors, placental tissues, and human teeth are frozen rapidly in liquid nitrogen, and stored at -70° C. Tissue is homogenized in acetic acid. Acidified acetone further precipitates proteins. The peptide-rich fraction is eluted from a Sep-Pak with 50% acetonitrile in TFA, and lyophilized.

Radioreceptor assay (RRA). A radioreceptor assay is used to measure opioid receptoractivity, which is contained in the HPLC fractions (4), to obtain a metabolic profile. Tritiated etorphine is a broad-based ligand that competes with a wide range of opioid peptides for binding to opioid receptors in a canine limbic system P2 preparation.

Radioimmunoassay (RIA). Commercial RIA kits are used to measure immunoreactivity (ir-) eluting from the gradient HPLC.

Mass spectrometry. FAB-MS produces a (M+H)+ ion of peptides in those HPLC fractions demonstrating immuno- and receptoractivity. VG 7070E-H and Finnigan MAT 731 instruments are used.

Mass spectrometry/mass spectrometry (MS/MS). MS/MS selects a unique amino acid sequence-determining fragment ion arising from a peptide, defines more accurately the amino acid sequence of the peptide to be measured in the biological extract, and extends the information beyond only the nominal mass of the peptide (2). In principle, a first MS produces the (M+H)+ ion, and a second MS produces the mass spectrum of that selected ion. In a two-sector MS instrument, equivalent data are obtained with a B/E linked-field scan, which collects product ions

arising from a precursor ion. A known amount of stable isotope -incorporated peptide internal standard, which posses identical HPLC and MS properties with the endogenous peptides, is added to quantify the endogenous peptide.

RESULTS AND DISCUSSION

Opioid receptoractivity in a human chromophobe adenoma obtained from pituitary neurosurgery was profiled (1). All HPLC fractions were also assayed for ir-ME content using a commerical RIA kit. The fractions near the HPLC retention time of synthetic ME showed immuno- and opioid receptoractivities. An additional unidentified ME-like immunoreactive peak, which also demonstrates receptoractivity, was found in a more hydrophobic (later-eluting) area of the gradient elution. Those data demonstrate the limited structure information and molecular specificity that can be provided by RIA (2). Furthermore, the two HPLC areas are still not proven to contain only one compound.

In other studies, FAB-MS/MS confirmed the presence of ME in the appropriate fractions from an HPLC-gradient from the calcified portion of human teeth (3), and demonstrated that ten times more ME-receptoractivity occurs in the calcified portion versus the soft pulp tissue of human teeth. FAB-MS demonstrated an (M+H)+ corresponding to dynorphin 1-8 extracted from human placenta (5).

HPLC, RIA, RRA, and the MS-determined molecular weight of a peptide - when those analytical methods are used either individually or in combination - provide insufficient information concerning the structure of a peptide; only amino acid sequence-determining information provides structure certainty. MS/MS provides the highest level of molecular specificity to ensure identification of peptides in biological tissues (2,3), and recent FAB-MS/MS results indicate femtomole (5) to attomole sensitivity (6). We are extending these studies to the analysis of beta-endorphin by the use of a trypsin-generated peptide fragment NAIIK (7), peptides in cornea tissue (8), and tuftsin in human plasma (9).

References

1. G. Fridland and D.M. Desiderio. J. Chromatogr. 379, 251-268 (1986).
2. D.M. Desiderio, Analysis of Neuropeptides by Liquid Chromatography and Mass Spectrometry, Elsevier, Amsterdam, 1984.
3. F.S. Tanzer, E. Tolun, G. Fridland, C. Dass, J. Killmar, P. Tinsley, and D.M. Desiderio. Methionine-enkephalin Peptides in Human Teeth. Int. J. Pept. Prot. Res., in press.
4. H. Takeshita, D.M. Desiderio and G. Fridland Biomed. Chromatog. 1126-139 (1986).
5. M.S. Ahmed, L.W. Randall, B. Sibai, C. Dass, G. Fridland, D.M. Desiderio and E. Tolun. Life Sci., 40, 2067 (1987).
6. D.M. Desiderio and C. Dass. Analyt. Lett. 19, 1963- 1971 (1986).
7. E. Tolun, C. Dass, and D.M. Desidero. Rapid Commun. Mass Spectrom. (1987).
8. C. Dass, G.H. Fridland, P.W. Tinsley, J.T. Killmar and D.M. Desiderio, Structural Characterization and Quantitation of b-Endorphin in Human Pituitary by Fast Atom Bombardment Mass Spectrometry of Trypsin-Generated Fragments. Analyt. Biochem., submitted.
9. P. Tinsley, C. Dass, J. Trimble, and D.M. Desiderio. Identification of methionine enkephalin in the bovine cornea by fast atom bombardment-mass spectrometry. Biochem. Biophys. Res. Commun., submitted.
10. J. Naim, R. Hinshaw, J. Trimble, and D.M. Desiderio. Analyt. Biochem. 164, 221 (1987).

Presented at the 36th ASMS Conference on Mass Spectrometry and Allied Topics
June 5-10, 1988, San Francisco, CA

OLIGOPEPTIDE ANALYSIS BY FT-MS

Jeffrey Shabanowitz, Patrick R. Griffin, Nian Zhou Zhu,
John R Yates, III, and Donald F. Hunt
Department of Chemistry, University of Virginia,
Charlottesville, Virginia 22901

Molecular weight analysis of oligopeptides and small proteins in the mass range, 1-13 kDa, by liquid secondary ion mass spectrometry on a tandem quadrupole Fourier transform mass spectrometer (QFTMS) has been described in an earlier publication from this laboratory (1). Use of laser photodissociation on the above instrument to obtain the complete sequence of amino acids in small oligopeptides of unknown structure has also been reported (2,3). To obtain data of this type, peptide (10-50 pmol) in 0.5 ul of 5% acetic acid and 0.5 ul of 3:1 thioglycerol/glycerol is bombarded with 10 keV Cs^+ for 2-4 msec resulting in the peptide being sputtered into the gas phase as $(M+H)^+$ ions. These ions are then transferred through the fringing fields of a 7-T superconducting magnet via rf-only quadrupole rods, trapped in an elongated ion cyclotron resonance cell, and photodissociated with a 10 nsec pulse from an ArF excimer laser. The resulting trapped ions are excited by a rf pulse containing a range of frequencies that causes the ions to move coherently in orbits at cyclotron frequencies characteristic of their individual masses. Image currents produced by this motion are amplified, digitized, and Fourier transformed to generate a mass spectrum. Data from 50-200 such experiments on the same 10-50 pmol sample are acquired and summed in seconds to produce the desired mass spectrum. The total experiment time to produce the required data is seconds, and the total sample consumption time is less than a second. Examples of the kind of sensitivity and sequencing information obtainable by this technique are described below.

Molecular weight determination requires only 2-10 pmol of peptide for routine analysis up to 6000 amu as illustrated by the low resolution mass spectrum from 10 pmol of porcine insulin in Fig. 1. A detection limit of high femtomoles (loaded on the probe) is possible for most peptides below 2000 molecular weight as shown by the mass spectrum obtained on 100 fmol of substance P in Fig. 2.

Although use of laser photodissociation with the quadrupole Fourier transform mass spectrometer to obtain oligopeptide sequence information is successful, only 30% of the peptides give complete sequence analysis. However, some sequence information is always discernable and only 10-50 pmol of peptide is necessary. As illustrated in Fig. 3 and Fig. 4 the majority of the sequence can be read directly from the spectrum, which only takes seconds to acquire. The oligopeptide shown in Fig 3. resulted from an acid hydrolysis reaction on a larger fragment generated by an endopeptidase Glu-C digest of the major isoform of a small calcium binding protein. The majority of Y-type ions can be read directly from the spectrum obtained on 50 pmol of sample derived from a 200 pmol endopeptidase Asp-N digest of rabbit sex steroid binding protein that is being sequenced in our laboratory.

The final example, shown in Fig. 5, is the nearly complete sequence obtained from the methyl ester of 10 pmol of a tryptic fragment derived from a total of just 40 pmol of apolipoprotein A-1. The protein was isolated using 2D-gel electrophoresis from cerebral spinal fluid, which contains thousands of proteins at the 0.02-10 pmol level. After separation the apolipoprotein A-1 spot from several gels were electroblotted onto nitrocellulose, eluted, digested with trypsin, HPLC'd, and screened using the QFTMS. The sequence of apolipoprotein A-1 is already known but was chosen to check feasibility of the methodolgy. An aliquot of the digest was used to screen for molecular weight of the predicted tryptic fragments. 12 out of 37 residues were readily identifiable, accounting for over 50% of the molecular weight of the protein. The sequence derived from the oligopeptide fragment shown in Fig. 5 yielded a series of amino acids which would be excellent candidates for manufacturing a probe for DNA cloning experiments.

Even though the complete unambiguous sequence is not always attainable, a wealth of sequence information is always obtained using the QFTMS.

(1) D. F. Hunt, et.al, Proc. Natl. Acad. Sci., USA (1987) 84, 620-623.
(2) D. F. Hunt, et.al, J. Chem. Soc., Chem. Comm. (1987) 548-550.
(3) D. F. Hunt, et.al, J. Biol. Chem. (1988) 263, 1123-1130.

Presented at the 36th ASMS Conference on Mass Spectrometry and Allied Topics
June 5-10, 1988, San Francisco, CA

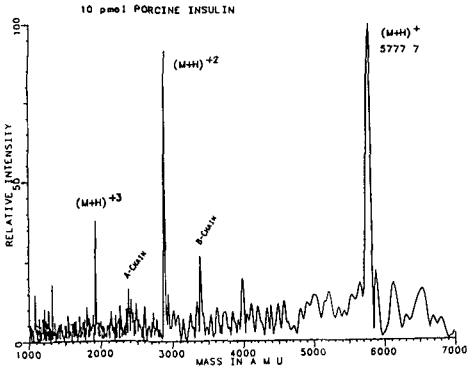

Fig. 1

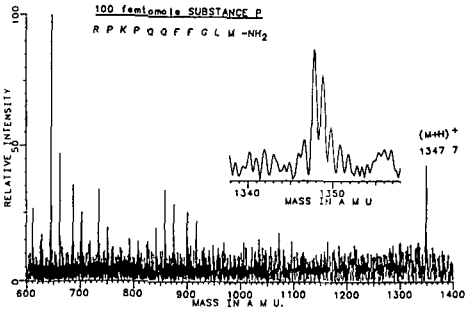

Fig. 2

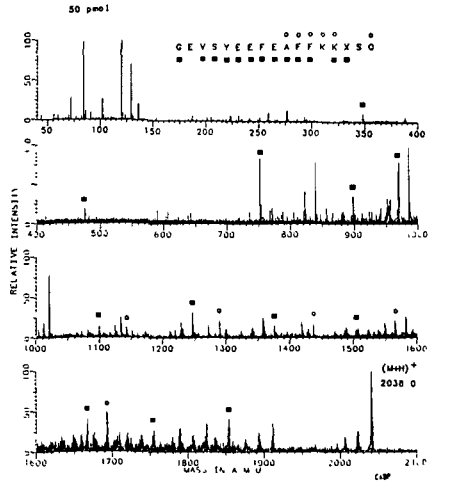

Fig. 3

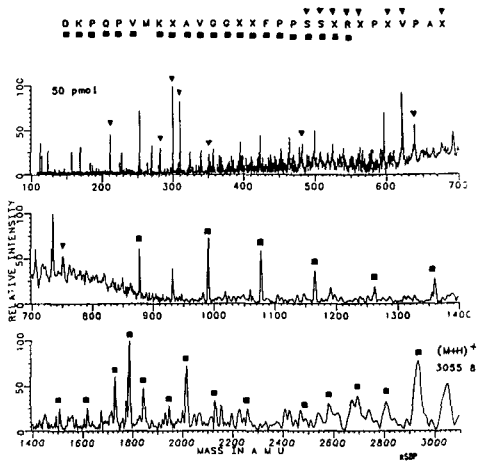

Fig. 4

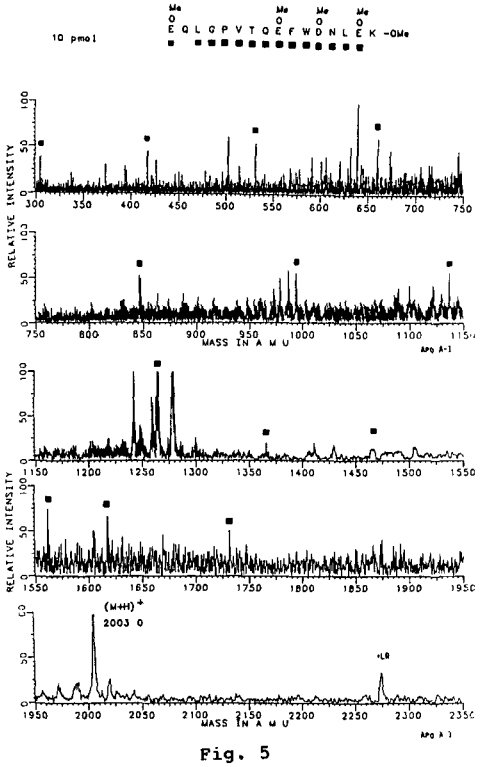

Fig. 5

Presented at the 36th ASMS Conference on Mass Spectrometry and Allied Topics
June 5-10, 1988, San Francisco, CA

Progress in the Mass Spectrometric Analysis of Peptides and Proteins at the Picomole Level

Bradford W. Gibson, Zhonghua Yu, A.L. Burlingame and William Aberth

Department of Pharmaceutical Chemistry, University of California, San Francisco, CA., 94143

The analysis of peptides and proteins by mass spectrometry has undergone major improvements since the introduction of liquid secondary ion mass spectrometry (LSIMS). The application of LSIMS (or FABMS) to the structure determination of proteins has been used to sequence proteins directly and to verify the correctness of DNA-deduced protein sequences [1]. The success of these efforts were largely dependent on the ability to determine the molecular weights of peptides in complex mixtures; a procedure often referred to as 'peptide-mapping'. Recently, we have attempted to improve upon the sensitivity of mass spectrometric 'peptide-mapping' for the analysis of proteins and bio-active peptides. Several areas in the current protocols for peptide analysis has been investigated with emphasis on improving sample preparation, ionization efficiency and ion detection systems. In these studies, considerable use has been made of a prototype Wien mass spectrometer with a channel electron multiplier array (CEMA) [2].

One of the major advantages of the Wien instrument is its ability to expand (zoom-out) and contract (zoom-in) the observed mass range. The mass range that is focused on the detector is dependent on the E and B fields. At maximum B, the E field determines the masses that will pass through and strike the detector, giving the smallest mass range at the highest resolution possible. In this mode, several high mass peptides and small proteins were analyzed at the sub-nanomole level, including EGF [3], tryptic peptides isolated from FABP [4] and a rat trypsinogen mutant [5]. However, by lowering the magnetic field, a larger mass range can be simultaneously focused on the detector. This allows one to first zoom-out for simultaneous detection over a very large mass range (e.g. m/z 500-3,000) and then zoom-in on a smaller mass range of particular interest

In order to apply the 'zoom-in/zoom-out' approach, we digested 100 pmoles of rat heart FABP with trypsin and isolated 16 fractions by microbore HPLC. Under these conditions, each peptide fraction had a elution volume of approx. 50 µL. In the first experiment, a 2 pmole equivalent (1µL) was directly analyzed over a mass range of m/z 650-1,700 (Fig. 1). For these experiments, the primary Cs^+ current was reduced 100 fold (10^{-9}A) such that the CEMA detector would not be overloaded by a excessive count rate. However, even with this small Cs^+ flux, a spectrum was obtained which contained a significant ion cluster centered at m/z ≈1030. Now, by adjusting B to its maximum and selecting a value for E to pass this ion cluster through, a zoom-in scan can now be obtained showing a resolved, more abundant molecular ion (Fig. 2). Thus, in screening a series of peptides of unknown mass, a 'zoom-out/zoom-in' strategy is an extremely effective approach. As previously stated, the zoom-out scans often required that the Cs^+ beam be operated at a very small flux. While this had the effect of reducing the overall sensitivity, it had the advantage of conserving sample since little sample is consumed under these conditions. Thus, by using an initial large mass range accumulation to detect the presence of peptide ions with a weak Cs^+ beam, the remaining sample still on the probe tip can be used more efficiently in the zoom-in scan.

The sensitivity of combined microbore-HPLC and Wien MS 'zoom-in' analysis was evaluated by analyzing a several 100 pmole peptide fractions. Small aliquots (10%, 1% and 0.1%) were directly analyzed on the Wien MS and MH^+ ions were clearly defined at the 1 and 10 pmole levels, but were generally weak in the 0.1 pmole spectra. A comparison was also made between directly applying a 1 pmole aliquot to the probe and loading a 1 pmole aliquot of a peptide sample tube that was first dried and then re-dissolved. This drying procedure reduced the MH^+ abundances between 3-10 fold for most peptides. Clearly, it is essential that the smallest possible volume be obtained in the last chromatographic step so drying and concentrating steps can be avoided.

Recently, a 1 inch diode array detector with superior resolution and counting efficiency to the CEMA has been constructed and equipped on a double focusing Kratos MS 50 RF mass spectrometer. In this configuration, it has been shown to increase ion detection efficiency by at least a factor 50 or more [6]. Our own experience using this instrument has allowed us to successfully analyze a series of high mass protein fragments from cytochrome b_5 (m/z 10,000) using 100-300 pmoles of sample. To fully take advantage of this ion detection system, a tandem four sector mass spectrometer has been constructed which has this diode array detection system for MS-II. In order to accumulate an entire daughter ion scan, the mass range is covered in sequential steps of 4% of the mass range under computer control. In this configuration, we have obtained mass spectra of peptides in the 10-100 pmole range with excellent signal to noise characteristics.

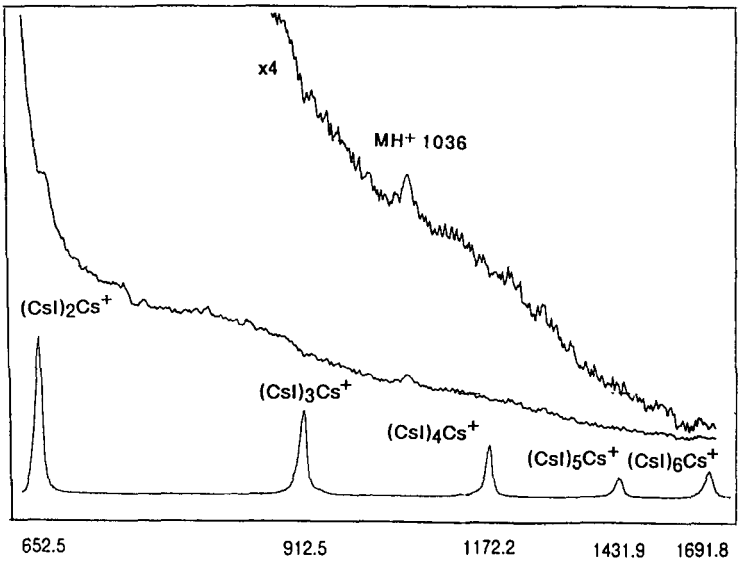

Figure 1. Wien 'zoom-out' spectrum of 1 picomole of peptide fraction 15 from FABP tryptic digest.

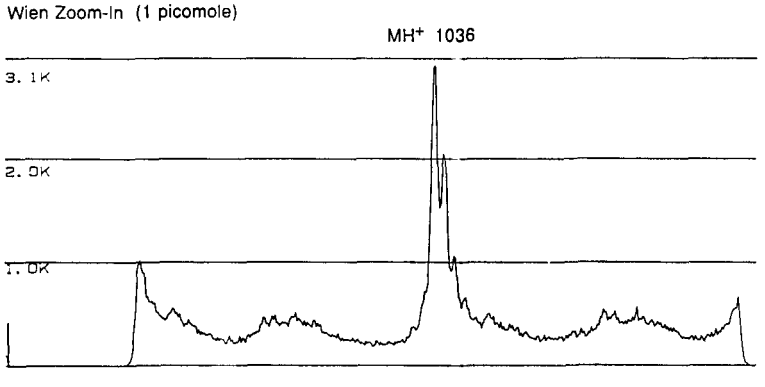

Figure 2. Wien 'zoom-in' spectrum of molecular ion region for same sample (1 pmole).

1. K. Biemann and S.A. Martin (1987) *Mass Spectrom. Revs.*, 6, 1-76
2. W. Aberth (1981) *Int. J. Mass Spectrom. Ion Phys.* 37, 379-382
3. B.W. Gibson *et al.* (1988) *J. Biol. Sci.*, 263, 4182-4185
4. R. DiAugustine *et al.* (1987) *Anal. Biochem.*, 165, 420-429
5. J. Higaki *et al.* (1988) In: Evolution of Catalytic Function, p. 615-621
6. J. Cottrell and S. Evans (1987) *Anal. Chem.*, 59, 1990-1995

This work was supported by grants from the University of California, Academic Senate (B. Gibson) and the NIH (RR 01614, A.L. Burlingame).

Presented at the 36th ASMS Conference on Mass Spectrometry and Allied Topics
June 5-10, 1988, San Francisco, CA

THE McLAFFERTY REARRANGEMENT IN THE UNIMOLECULAR DISSOCIATION OF FORMATE ESTERS

Qingmei Zha, R. N. Hayes, M. L. Gross and G. G. Meisels
Department of Chemistry University of Nebraska-Lincoln Lincoln NE 68588
T. Nishimura
Control Spectroscopy Development The Upjohn Co. Kalamazoo MI 49001

The unimolecular dissociation of propyl formate ion was studied using both photoelectron photoion coincidence (TPEPICO) and tandem (MS/MS) mass spectrometry. The major fragment ions observed in the breakdown graph (Fig. 1) are $C_3H_7OH^+$ (m/z 60), $HC(OH)_2^+$ (m/z 47), $C_3H_6^{+\cdot}$ (m/z 42), $C_3H_5^+$ (m/z 41) and CH_2OH^+ (m/z 31). The main feature of the dissociation of propyl formate that differs from the dissociation of methyl formate[1] and ethyl formate[2] is that the appearance potentials of the three fragment ions of m/z 60, m/z 47 and m/z 42 are identical to the ionization energy of the propyl formate molecule. This means that the dissociation of the propyl formate ion occurs nearly simultaneously with ionization, and that the molecular ion dissociates without the need to acquire significant internal energy.

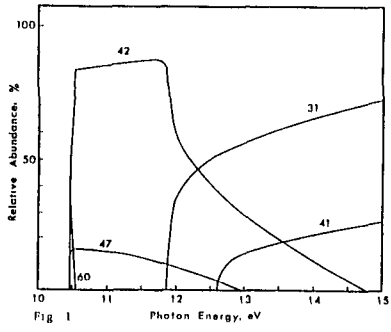

Fig 1

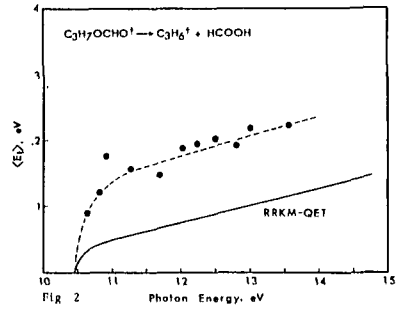

Fig 2

The average kinetic energy release (KER) for the formation of $C_3H_6^{+\cdot}$ derived from the TPEPICO experiment is compared with the calculated value based on statistical theory (Fig. 2). RRKM-QET predicts that about 4 % of the available excess internal energy should be converted to translational energy. The experimental data indicate a conversion that is approximately 0.1 eV higher than that predicted by the RRKM-QET calculation, in reasonable agreement with statistical theory.

$C_3H_6^{+\cdot}$ (m/z 42) has the highest relative abundance in the breakdown graph. A plausible mechanism for the formation of $C_3H_6^{+\cdot}$ is the McLafferty rearrangement.

Presented at the 36th ASMS Conference on Mass Spectrometry and Allied Topics
June 5-10, 1988, San Francisco, CA

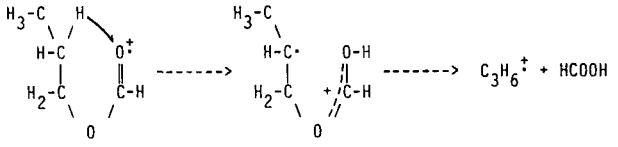

The observed kinetic energy release for the formation of $C_3H_6^{+\cdot}$ suggests a reverse activation energy of about 0.1 eV. The concurrent formations of parent ion and $C_3H_6^{+\cdot}$ at threshold suggest that the molecular ion rearranges to an intermediate isomeric structure prior to decomposition. Moreover, this would allow for the existence of a potential energy barrier between the molecular ion and fragment ion. The formation of this intermediate isomer, the distonic radical cation formed by a gamma-hydrogen transfer, is the first step of the stepwise McLafferty rearrangement.

This reaction mechanism is also observed for the formation of $C_2H_4^{+\cdot}$ (m/z 28) from ethyl formate ion[2]. The only fragment ion observed in the MIKE spectrum of butyl formate (Fig. 3) is $C_4H_8^{+\cdot}$ (m/z 56). These fragment ions correspond to $[R-H]^{+\cdot}$ (for HCOOR, where R is alkyl).

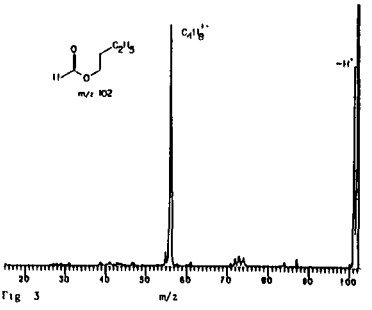

Fig 3

This dissociation behavior, which appears to be the predominant mode of formate ester decomposition at low internal energies differs from a model proposed previously[3]. The first band in the He I photoelectron spectra of formate esters corresponds to the excitation of the nonbonding electron from carbonyl oxygen, which favors the gamma-hydrogen transfer to carbonyl oxygen required by the McLafferty rearrangement. The $[R-H]^{+\cdot}$ ion is thus readily formed at low internal energies.

REFERENCES

1. Nishimura, T.; Zha, Q. and Meisels, G. G. J. Chem. Phys. **87(8)**, 4589 (1987).
2. Zha, Q.; NIshimura, T. and Meisels, G. G. to be published.
3. King, A. B. and Long, F. A. J. Chem. Phys. **29**, 374 (1958).

Presented at the 36th ASMS Conference on Mass Spectrometry and Allied Topics
June 5-10, 1988, San Francisco, CA

THE INVOLVEMENT OF RING HYDROGENS IN THE REACTION $C_6H_5NH_2^{+\cdot} \longrightarrow C_6H_5^{+\cdot} + HNC$

Jeffrey A. Zimmerman and Rebecca M. O'Malley
University of South Florida, Tampa, Florida 33620.

The metastable decomposition reaction of the aniline radical cation $C_6H_5NH_2^{+\cdot} \longrightarrow C_6H_5^{+\cdot} + HNC$ has been well studied by single and multiphoton ionization (MPI) and also by electron impact. Burgers et al. have confimed experimentally that the identity of the neutral produced in the reaction is HNC and not HCN (1). More recently the cyclopentadienyl structure of the ionic product has also been confirmed (2). In this paper we present electron impact and 266 nm MPI data obtained using an aniline/aniline 2,3,4,5,6-d_6 mixture which indicate clearly that the reaction has two components. The major component involves the loss of a hydrogen atom originally attached to the nitrogen atom in the aniline molecule, whereas the minor component involves the loss of a hydrogen atom originally attached to the ring.

The data shown here were obtained using a laser/time-of-flight mass spectrometer. Ion acceleration is achieved with a system of three grids. The first of these, the ion draw-out grid, initiates ion acceleration and is pulsed to a voltage of -200 V at a known and variable time after the laser light crosses the source. This delay time (time-lag) can be set at 0.1 μs intervals in the range 0-5.0 μs and can be varied in order to vary the allowed reaction time. All data shown were obtained using an approximately 1:1 aniline/aniline 2,3,4,5,6-d_6 mixture.

Electron Impact 70 eV and 20 eV electron impact spectra are shown for comparison purposes. The 20 eV spectrum shows clearly that in the aniline-d_5 system two reactions are occurring

$$C_6D_5NH_2^{+\cdot}\ (m/z = 98) \longrightarrow C_5D_5H^{+\cdot}\ (m/z = 71) + HNC$$

$$C_6D_5NH_2^{+\cdot}\ (m/z = 98) \longrightarrow C_5D_4H_2^{+\cdot}\ (m/z = 70) + DNC$$

Metastable $C_5(H,D)_6^{+\cdot}$ Formation: MPI at 266 nm. It is known from our previous studies that using a low intensity 266 nm laser beam it is possible to excite a large fraction of the neutral molecules with three photons such that the molecular ion is in the energy range for metastable decomposition to occur. The 266 nm unfocussed spectrum shown indicates that the two reactions identified under electron impact were again observed.

Measurement of Relative Rate Constants for the Two Aniline-d_5 Reactions. MPI spectra of the same aniline/aniline-d_5 mixture were recorded as a function of reaction time using an unfocussed, low intensity (0.25 mJ) 266 nm laser beam. Peak heights for m/z = 66 from aniline and m/z = 70 and 71 are plotted versus time-lag. Assuming that ion loss effects are negligible and that ion focussing effects are similar for these similar mass ions relative rate constants for the reactions were obtained from a first order plot of $-\ln(1-B/B_\infty)$ versus time. (B is the product ion intensity). The rate constant for the production of $C_5H_6^{+\cdot}$ (from $C_6H_5NH_2^{+\cdot}$) is approximately equal to that for the production of $C_5D_5H^{+\cdot}$ (from $C_6D_5NH_2^{+\cdot}$). However the rate constant for the production of $C_5D_4H_2^{+\cdot}$ (from $C_6D_5NH_2^{+\cdot}$) is approximately 0.75 times that for the production of $C_6D_5H^{+\cdot}$ (from $C_6D_5NH_2^{+\cdot}$). It appears that in the deuterated aniline two different reactions are occurring, one of which involves the breaking of a carbon-deuterium bond.

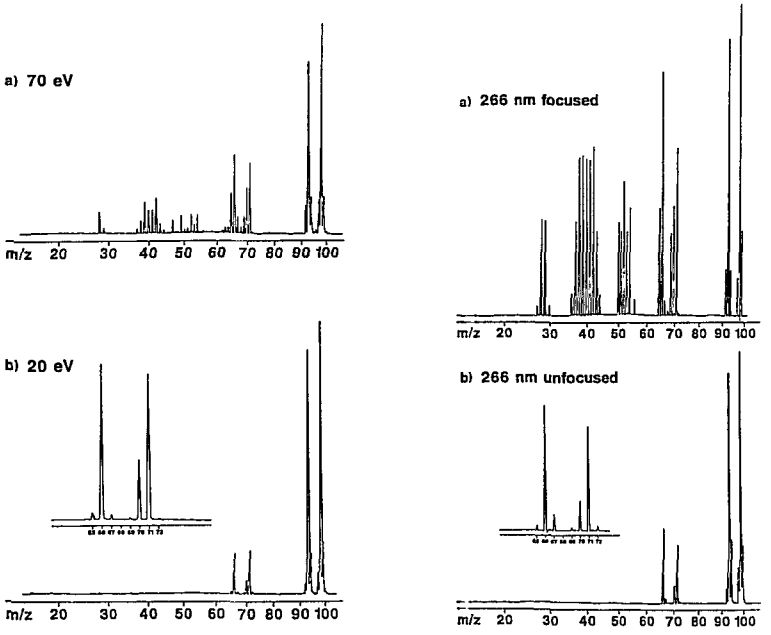

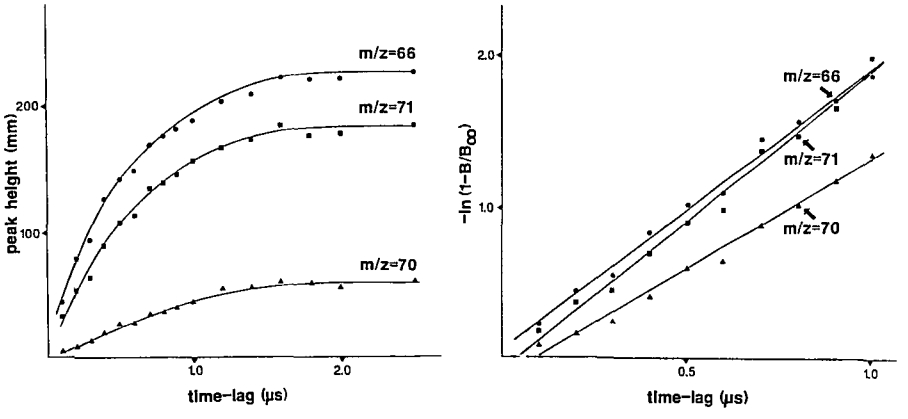

References:

1. P.C. Burgers, J.L. Homes, A.A. Mommer and J.K. Terlow, Chem. Phys. Lett., 102 (1983) 1.

2. R. Flammang, P. Meyrant, A. Maquestiau, E. Kingston and J.H. Beynon, Org. Mass. Spectrom. 20 (1985) 253.

Presented at the 36th ASMS Conference on Mass Spectrometry and Allied Topics
June 5-10, 1988, San Francisco, CA

The application of butyl nitrite CI and linked scans to study the deprotonation of alcohols.

Ibrahim, S, Wilson, J.M. and Moore, C.
Kratos Analytical, Barton Dock Road, Urmston, Manchester M31 2LD, UK.

This study looked at the fragmentation of alkoxide anions eg

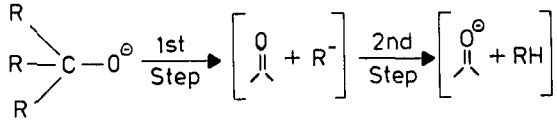

In particular, at the relative energetics of the two steps of the process. Data are available in the literature for the tert-Butoxide Anion[1].

The alkoxide anion was prepared by hydrogen abstraction from tertiary alcohols using butyl nitrite as the reagent gas in the chemical ionization source of a mass spectrometer.

i.e.

$$BuONO + e^- \quad BuO^- + NO \qquad (1)$$

$$BuO \quad + R_3COH \quad R_3CO \quad + BuOH \qquad (2)$$

The butyl nitrite was introduced into the CONCEPT IS mass spectrometer via a length of silica tubing which sampled the vapour in a vial half filled with liquid butyl nitrite[2]

First consider fragmentation of 1,3 dideuteroalkoxide (Scheme 1), assuming that the first step is reversible, cleavage of the bonds α to the oxygen gives 2 identical products. These two ion-dipole complexes lead to one of two products. The ratio of the two product ion abundances are a direct measure of the primary kinetic isotope effect.

i.e.
$$\frac{I_{196}}{I_{195}} = \frac{k_H}{k_D} = \underline{2{\cdot}4}$$

The ratio was obtained by a B/E linked scan from the $(M-1)^-$ ion (Figure 1). Looking now at the 1,1 dideuteroalkoxide (Scheme 2), α-cleavage gives two different ion-dipole complexes. The relative rates of decomposition of these two complexes is / which was determined in the previous experiment.

For the 1,1 dideuteroalkoxide therefore,

$$\frac{I_{196}}{I_{195}} = \frac{k_H}{k_D} \cdot \frac{K_{\alpha D_2}}{K_{\alpha H_2}} = 0{\cdot}7$$

From which the magnitude of the secondary isotope effect is,

$$\frac{K_{\alpha H_2}}{K_{\alpha D_2}} = \underline{1{\cdot}7}$$

These data show that,

(1) Butyl nitrite CI is a good method for obtaining alkoxide ions in good yield.

(2) Using linked scans ion labelled materials to selectively follow the decomposition of the alkoxide ions we have obtained,

(a) A direct measurement of a primary kinetic isotope effect of 2.4.

(b) An indirect measurement of a secondary isotope effect of 1.7.

(3) It follows from (a) and (b) that our assumption of reversibility in the 1st step is valid and that the 2nd step is rate determining.

References

(1) W. Tumas, R.F. Foster, M.J. Pellerite, J.I. Brauman, J. Am. Chem. Soc., 109, 961 (1987)

(2) J.H. Moncur, R.S. Brown, S. Ibrahim, J.M. Wilson, Rapid Comm. Mass Spectrom., 2, 77 (1988)

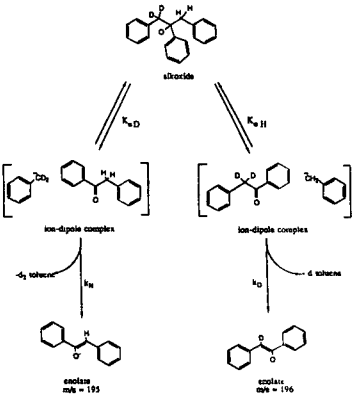

Enolates from 1,1-dideuteriodiphenylmethanolate

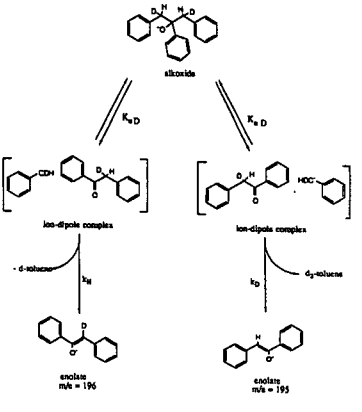

Enolates from 1,3-dideuteriodiphenylmethanolate

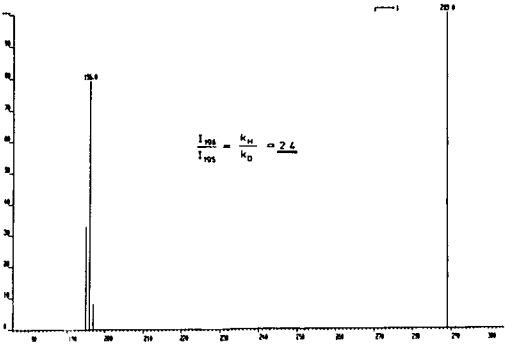

Presented at the 36th ASMS Conference on Mass Spectrometry and Allied Topics
June 5-10, 1988, San Francisco, CA

The effect of strong anharmonic potential on unimolecular dissociation dynamics: The energy selected n-butanol and i-butanol ions

Jian-dong Shao, Tomas Baer, and David K. Lewis
Chemistry Department, University of North Carolina, Chapel Hill, NC 27514

Photoionization and threshold photoelectron photoion coincidence (TPEPICO) methods[1] were used in this study.

The PIE spectra show that the only dissociation channel of the n-butanol ion below 11.2 eV is the loss of H_2O. The activation energy for the H_2O loss channel is 0.19 eV. According to statistical theory fast dissociation rates would be expected. However, in Fig.1 a number of fragment ion time of flight (TOF) distributions near the dissociation limit show slow dissociation feature. Furthermore, the asymmetric TOF distributions cannot be fitted with a single exponential decay. A two component decay, $P(t) = \exp(-k_+t) + \exp(-k_-t)$ (1), was used in the data analysis and results are listed in Table I.

Four major fragmentation paths can be seen from the PIE spectra of i-butanol. The corresponding reactions are, in order of increasing threshold energy:

$$(CH_3)_2CHCH_2OH^+ \rightarrow \begin{cases} C_4H_8^+ + H_2O \\ CH_3OH_2^+ + C_3H_5 \\ C_3H_6^+ + H_3COH \\ C_3H_7^+ + H_2COH \end{cases}$$

The first two reaction channels involve slow dissociations even though the activation energies are only 0.31 and 0.41 eV respectively. Several of their TOF distributions are shown in Fig.2. The H_2O loss channel can be well represented by a single exponential decay. On the other hand, the loss of C_3H_5 proceeds via a non-exponential decay. Also, the data were fitted with Eq.(1). The results are listed in Table II.

The loss of H_2O in both n-butanol and i-butanol ions suggests the formation of $C_4H_8^+\cdots OH_2$ complex before the dissociation. According to the thermochemical data and the observation of slow dissociation rates, the product ion most likely has the structure of methylcyclopropane. The ground state of a similar ion-dipole complex, $c\text{-}C_3H_6^+\cdots OH_2$, was found[2] to be between 0.4 and 0.6 eV more stable than the dissociation products. With these assumptions, the potential energy surfaces can be constructed as shown in Fig.3 and 4. The dissociation limit 2-butene ion-water complex is much lower than the activation energy barrier of n-butanol ion. Therefore, statistically, the k_4 is fast and shown as the fast component in the TOF spectra. The both ions dissociate through the methylcyclopropane ion-water complex on much like potential energy surfaces. According to the TOF spectra of i-butanol ion, the methylcyclopropane ion-water complex can be counted for the slow component shown as the peak tails. The slow component for the C_3H_5 loss in the i-butanol ion dissociation can be understood with the double well model[3].

Nevertheless, the conventional RRKM calculation predicts much faster dissociation rates for the methylcyclopropane ion-water complex. The minimum calculated rate is 10^8 sec^{-1} for a very tight activated complex and 10^9 sec^{-1} for a more reasonably loose complex. These rates are two to three orders of magnitude greater than is experimentally observed. The discrepancy may be caused by the assumption of harmonic oscillators in calculating densities of states. However, simple first order corrections to the harmonic potential, such as the van der Waals potential, are not sufficient to resolve this problem because the ion-dipole potential is far more anharmonic than a van der Waals potential. Further theoretical work is required to understand this problem more completely.

References

1. J.J. Butler and T. Baer, J. Am. Chem. Soc. 102, 6764(1980).
2. J.D. Shao, T. Baer, J.C. Morrow and M.L. Fraser-Monteiro, J. Chem. Phys. 87, 5242(1987).
3. T. Baer, W.A. Brand, T.L. Bunn, and J.J. Butler, Faraday Discuss. Chem. Soc., 75, 45(1983).

Presented at the 36th ASMS Conference on Mass Spectrometry and Allied Topics
June 5-10, 1988, San Francisco, CA

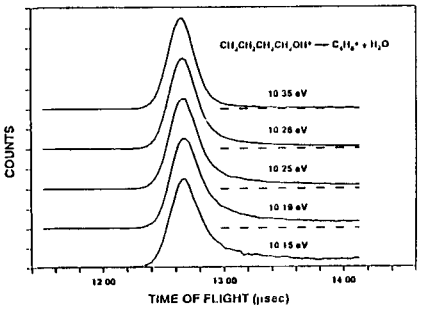

Figure 1

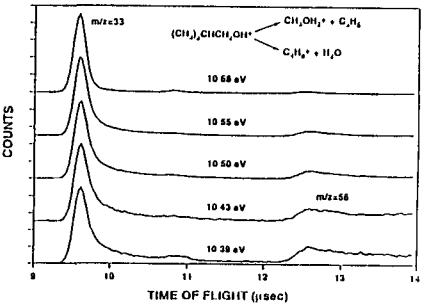

Figure 2

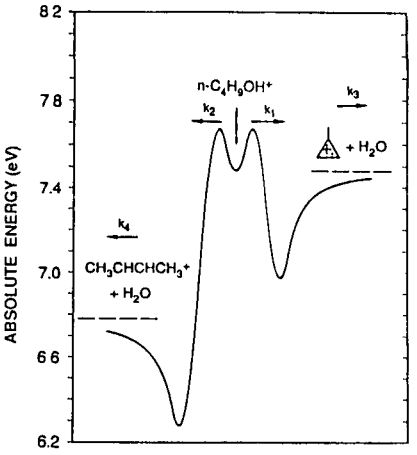

REACTION COORDINATE

Figure 3

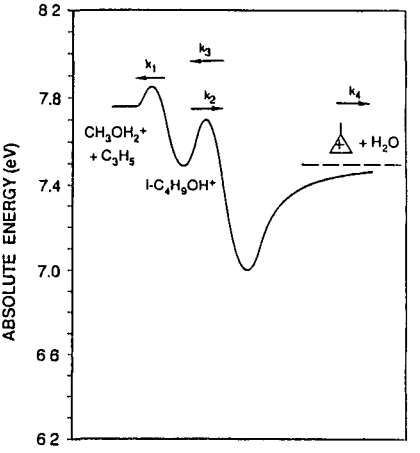

REACTION COORDINATE

Figure 4

TABLE I. Dissociation rates (μs^{-1}) of n-butanol ions.

Ion energy (eV)	H_2O loss k_+	B	k_-
10.15	>5	.085	.33
10.19	>5	.085	.38
10.25	>5	.058	.45
10.28	>5	.053	.55
10.35	>5	.018	.70

TABLE II. Dissociation rates (μs^{-1}) of isobutyl alcohol ions

Ion energy (eV)	H_2O loss k	C_3H_5 loss k_+	B	k_-
10.39	0.12	>5	0.09	0.6
10.43	0.20	>5	0.06	0.5
10.50	0.33	>5	0.05	0.6
10.55	0.48	>5	0.04	0.6
10.68	1.10	>5		

Presented at the 36th ASMS Conference on Mass Spectrometry and Allied Topics
June 5-10, 1988, San Francisco, CA

Stereochemical Control of CID Reactions of Peracetylated Hexoses and Amino-Hexoses.

J.L.C.Wright and R.Guevremont,
National Research Council of Canada, 1411 Oxford St., Halifax,
Nova Scotia, Canada B3H 3Z1.

Sequential mass spectrometry (MS/MS and MS/MS/MS) has been shown to be useful for the identification of hexose and amino-hexose stereoisomers (1,2) in glycoconjugates. The fast atom bombardment (FAB) spectrum of a simple conjugate includes an abundant, even-electron ion (m/z 331 for hexoses and 330 for amino-hexoses) formed by the loss of the aglycone from the anomeric position (C-1) of the terminal sugar group. The relative abundances of fragment ions formed in collision induced dissociation (CID) reactions of these ions appears to be a function of the stereochemistry of the ion. The mechanism of the CID reaction and the reason for this stereochemical specificity have been studied using sequential mass spectrometry and isotope labelling experiments on a hybrid mass spectrometer (VG Analytical ZAB-EQ, BEqQ geometry). Modifications of this system to permit unlinked E-Q scans have been described (3).

The daughter spectra of m/z 331 of the hexoses are deceptively simple. This spectrum contains abundant fragments at m/z 271, 211, 169 and 109, which would suggest a mechanism of sequential losses of two acetic acid molecules, a ketene (CH_2CO), and a final acetic acid moiety. Anomalies in this pattern have been noted (4,5) and mechanisms proposed to account for a single, concerted loss of acetic acid and ketene (without a long-lived intermediate ion).

MS/MS/MS experiments have shown that the CID reaction of acetylated hexoses is characterized by two major competing parallel pathways. The grand-daughters of m/z 271 (m/z 331 to m/z 271 to grand-daughters) include ions with m/z 211, 169, and 109, whereas the grand-daughters of m/z 211 include m/z 169 and 127 but with low abundance of m/z 109. This indicates that separate pathways lead from the parent m/z 331 to each of m/z 271 and m/z 211. If these ions were part of a single, common sequential mechanism, the grand-daughters of m/z 211 would necessarily include all those of m/z 271, including abundant m/z 109.

MS/MS and MS/MS/MS experiments with per($^2H_3$)acetylated hexoses further supported the observation of two parallel CID reaction pathways. The CID daughter ion spectrum of these compounds included a pair of ions at m/z 172 and m/z 173, shown in Fig.1. The grand-daughter spectrum of m/z 280 (d_9 of m/z 271) yielded only the fragment of m/z 172 and the grand-daughter spectrum of m/z 217 (d_6 of m/z 211) yielded only m/z 173. Possible reactions(4,5) are shown in Fig.2. Since the grand-daughters of m/z 280 (d_9) included low abundance of m/z 173, the ion m/z 280 (d_9) cannot be a precursor of m/z 217 (d_6). The fragments m/z 280 (d_9) and 217 (d_6) are therefore formed independently from the parent ion. This pathway is illustrated in Fig.3.

Isotope label experiments with ($^2H_3$)acetates at C-4, at C-6, and at both C-4 and C-6 simultaneously have suggested further complexity of the CID reaction process. Fig.4 illustrates unimolecular decomposition of m/z 337 (d_6) in the 2nd field free region of a BEqQ geometry instrument, and the quadrupole resolved version of the same spectrum near m/z 169. The low-energy quadrupole spectrum (below 10eV collision energy) is the same as shown in Fig.4. There are no less than 4 different species which would have a m/z ratio of 169 (without deuterium labels). Similarly (not shown) m/z 211 appears as 3 distinct species.

The abundances of ions in the daughter spectra of m/z 331 of the hexoses will be a combined result of the relative importance of the two CID reaction pathways, and the stability and lifetimes of the various ions in each pathway. These parameters appear to vary for each stereoisomer, and are possibly controlled by the tertiary structures of the ions. For example, the single-step concerted reaction leading from m/z 271 to 169 (Fig.2,3) involves interaction between acetates at C-2 and C-4 of the hexoses. Molecular models show that, for the most favourable conformation

NRCC No 29011

of the hexose ring, these acetates are considerably closer together in galactose than glucose. The proximity of these acetates may facilitate the decomposition reaction, and explain the low yield of m/z 271 from galactose.

The above explanation fails for allose (which differs from glucose only at C-3). The lower abundance of m/z 172 shown in Fig.2 suggests decreased importance of the 331 to 271 to 169 to 109 pathway in the case of allose. The elimination of acetic acid from the allose C-3 position (m/z 331) may be restricted because the hydrogens at C-2 and C-4 are both trans relative to the acetate at C-3.

(1) D.R.Mueller, B.M.Domon, W.Blum, R.Raschdorf, W.J.Richter, Biomed. Environ. Mass Spectrom., 15, 441 (1988)
(2) R.Guevremont, J.L.C.Wright, Rapid Comm. Mass Spectrom., 2,50 (1988).
(3) R.Guevremont, Rapid Comm. Mass Spectrom., 1, 19 (1987).
(4) T.C.Smale, E.S.Waight, Chem. Comm., 680 (1966).
(5) K.Heyns and D.Muller, Tetrahedron Letters, 6061 (1966).

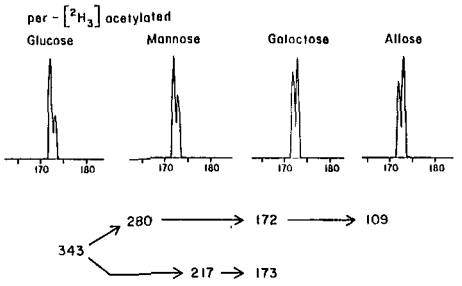

Fig.1. Part of the CID spectrum of m/z 343 of per($^2H_3$)acetylated hexoses. Reactions which lead to m/z 172 and 173 are indicated.

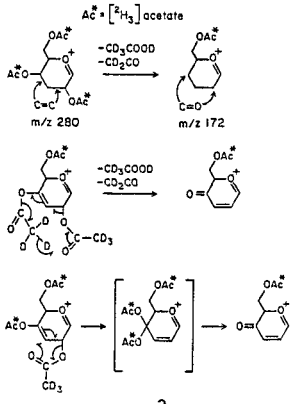

Fig.2. Reactions (4,5) of m/z 280 (d_9) from per($^2H_3$)acetylated hexoses leading to m/z 172 (d_3).

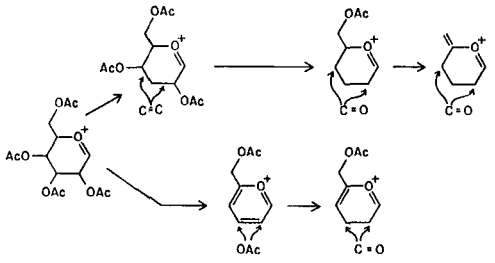

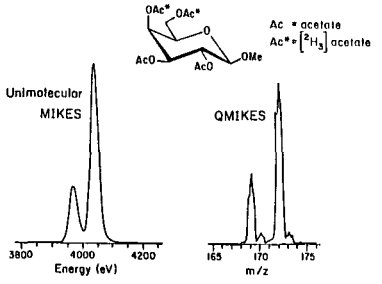

Fig.3. CID reaction pathways of m/z 331 of the hexoses.

Fig.4. (a) Part of a unimolecular MIKE spectrum of m/z 337 (d_6) of glucose labelled at C-4 and C-6 with ($^2H_3$)acetate. (b) quadrupole resolved (QMIKES) version of the MIKE spectrum.

Presented at the 36th ASMS Conference on Mass Spectrometry and Allied Topics
June 5-10, 1988, San Francisco, CA

GC/MS Identification of Macrocycles;

George R. Dubay, Vincent Chang, Ned A. Porter; Dept. of Chemistry, Duke University, Durham, NC 27706; 919-684-3549

INTRODUCTION:

Macrocyclic rings are found in many natural products including muscone. A general synthetic approach was developed by Porter and co-workers using an intramolecular radical cyclization to form the macrocyclic ring (Figure 1). This scheme affords efficient preparation of the desired products. The reaction does give a mixture containing several cyclic and acyclic products. Characterization of this mixture frequently required HPLC separation followed by NMR analysis. In general, this is slow and time consuming. NMR analysis is complex for muscone and analogous macrocycles because they are such simple compounds. At times the methylene portion of the NMR at high resolution is quite complicated and unambiguous structure assignment is not possible.

Figure 1. Formation of Macrocyclic Rings

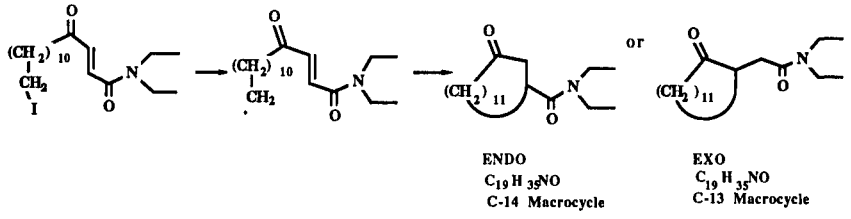

In these radical cyclizations macrocycles of two different sizes are formed (Figure 1). They are referred to as endo, all methylenes inside the macrocycle, and exo, one methylene between the ring and the amide carbonyl. In both cases, a methylene is adjacent to a carbonyl and the carbon bearing the amide side chain. Thus, the methylenes are observed at similar positions in the NMR. Indeed, for some products NMR is not able to be used for an unambiguous structure assignment. As a result, some other technique was required for structure assignment.

In this paper we report that capillary GC/MS using EI and PCI is capable of distinguishing the products formed during reaction. Separation and quantitation of the major products was achieved using the capillary GC. Mass spectrometry was then used to identify the macrocyclic and acyclic compounds formed. This provided a very rapid and specific method of analysis to test the efficiency of the cyclization reaction.

EXPERIMENTAL:

Instrumentation:	Hewlett Packard 5988A GC/MS/DS	
GC:	Samples from reaction were diluted with ethyl acetate for injection upon the GC after radical initiators were removed. HP-5890 with a split/splitless injector	
Column:	15 m by .25 mm i.d. SPB-1 (Supelco, Inc.) or 12 m by .20 mm i.d. HP-1 (Hewlett Packard)	
Pressure:	10 psi	split ratio: 10:1
Temps:	Inj. Port	250°C
Oven:	Initial Temp	70°C pgm 210° at 25°/min pgm 280° at 5°/min
MS: Temps:		
Interface:	275°	
Ion source:	200°	
Ionization:	EI at 70eV or PCI Methane(g) at 1 torr	

Presented at the 36th ASMS Conference on Mass Spectrometry and Allied Topics
June 5-10, 1988, San Francisco, CA

RESULTS AND DISCUSSION:

The mass spectra of the endo and exo cyclization products showed characteristic fragment ions in the EI which allow us to differentiate between the two ring sizes formed. In Figure 1 it can be seen that the endo product has no methylene adjacent to the ring on the amide side chain. The exo product has a methylene between the amide and the macrocyclic ketone. Most of the spectra for these two compounds are very similar as expected. Yet, a distinctive difference is found in the relative abundance of two ions. The exo compound fragments with a McLafferty type rearrangement giving an abundant ion at m/z = 115. An ion was present in the spectra of the endo product at m/z = 115, but the abundance of this ion was 8 times smaller. By contrast, the endo product has its base peak at m/z = 128; this ion is explained by a similar McLafferty type rearrangement and cleavage of two C-C bonds to give an even electron ion as shown (Figure 2). This reaction is relatively rapid due to the stability of the products formed. In contrast, the fragment ion at m/z = 128 for the exo product is 5 times less abundant. This is consistent with the fact that formation of this ion requires more complex fragmentation chemistry for the exo structure.

The PCI-MS spectra confirm these observations. Protonation of the amide to give the MH^+ ion is the dominate reaction for both in PCI and few fragment ions are present. In the spectra of the exo product an ion is observed at m/z = 116. This is a simple cleavage which follows the same hydrogen migration pathway observed in the EI-MS. In the PCI-MS spectra of the endo compound this ion is not observed. There is not enough energy available to produce the complex fragmentation required to form this ion in the latter case. This strongly supports the assignment made from the EI spectra. Thus, the use of routine EI- and PCI-MS spectra allows identification of the products of reaction.

Capillary GC was shown to provide separation and quantitation of the reaction mixture. This is extremely useful because it eliminated the time consuming use of HPLC and NMR. In addition, NMR failed to characterize the amides studied here. So, GC/MS analysis is the method of choice.

This work was extended to another case in which a chiral amide was used to control the stereochemistry of the products. Two chiral centers were present near the reactive site. The endo and exo products in this case are mixtures of diastereomers. Capillary GC was able to separate the four diasteromers with baseline separation. The EI-MS spectra were able to distinguish the endo and exo conformers formed and show that a cyclization was stereoselective for the endo products. Here too, NMR was unable to differentiate the products and mass spectrometry was the method of choice.

In conclusion, we have shown the power of capillary GC/MS to solve problems that were not solved by NMR and HPLC. It is our goal to understand the fragmentation of synthetic products to determine where mass spectrometry can be employed to aid in the solution of structural problems.

Figure 2. Fragmentations Characteristic of Endo & Exo Products

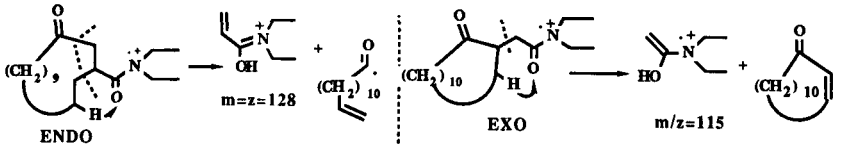

Presented at the 36th ASMS Conference on Mass Spectrometry and Allied Topics
June 5-10, 1988, San Francisco, CA

ELECTRON IONIZATION-INDUCED FRAGMENTATION OF α,β-UNSATURATED ESTERS: A STUDY ON THE *META* AND *PARA* DERIVATIVES OF ETHYL α-FLUOROCINNAMATE*

C. Dass[1], C. N. Robinson[2], J. L. Pflug[3], and D. M. Desiderio[1,4]

Departments of Neurology[1] and Biochemistry[4], University of Tennessee, Memphis, TN 38163; Department of Chemistry[2], Memphis State University, Memphis, TN 38152; Frank J. Seiler Research Laboratory[3], United States Air Force Academy, Colorado Springs, CO 80840.

The present study was undertaken to understand mass spectral fragmentation pathways of the gas-phase ions generated by electron ionization (EI) of 21 *meta* and *para* benzene ring substituted ethyl α-fluorocinnamates of the general formula RC_6H_4-CH=CF-$COOC_2H_5$, where R=H, m- and p-CH_3, p-NMe_2, m- and p-OCH_3, p-C_6H_5, m- and p-OC_6H_5, m- and p-CN, m- and p-NO_2, m- and p-CF_3, m- and p-F, m- and p-Cl, and m- and p-Br. The specific goal was to understand the influence on fragmentation of the fluorine atom attached to the α-carbon atom and of the various aromatic ring substituents.

The research was accomplished by acquiring 70 eV low-resolution EI mass spectra (on HP 5985 GC/MS). The elemental compositions of the fragment ions were confirmed by the accurate mass data. The B/E linked-field scan coupled with CAD was used to corroborate the assigned fragmentation pathways. The genesis of the fragment ions was also confirmed by acquiring the B/E and B^2/E linked-field scans (Table 1) of a few selected fragment ions formed from p-methyl derivative. The accurate mass and linked-field scans data were obtained on VG 70E-HF.

All the compounds yielded $M^{+\cdot}$ as the base peak except the p-NMe_2 and m-CF_3 derivatives and followed a common fragmentation pattern. Direct cleavage of the bonds *a*, *b*, and *c* resulted in the elimination of $\cdot OC_2H_5$, $\cdot COOC_2H_5$, and $\cdot C_2H_5$ radicals, respectively (Scheme 1) to yield ions **a**, **b** and **c**. The cleavage of bonds *a* and *c* also generated ions of m/z 45 and 29, respectively. Alternative routes leading to ion **b** were the losses of CO and COOH from ions **a** (Scheme 1) and **d** (Scheme 2), respectively. Ion **a** also fragmented to **a'** by HF loss. Direct expulsion of HF from the $M^{+\cdot}$ of these esters was energetically unfavorable, but occurred frequently from the product ions that were formed in the primary fragmentation steps of the $M^{+\cdot}$. For example, ion **b'** was formed from the styryl ion (**b**) by the loss of a molecule of HF.

These compounds also participated in a variety of structural rearrangements. For example, the McLafferty rearrangement (Scheme 2) yielded ion **d**, which decomposed further to structure **d'** by expulsion of HF. Another interesting H rearrangement involved the ethyl group and the C=C of the fluoroacrylate side chain. A concomitant loss of the $COOCH_2CH_2$ moiety, or equivalently the simultaneous expulsion of CO_2 and ethylene from the resulting intermediate structure **e** yielded ion **e'**. The driving force for this reaction was the resulting stable styrene ion (**e'**). Subsequent elimination of H_2 or HF from **e'** resulted in the generation of phenylacetylene ions $\mathbf{e'_1}$ or $\mathbf{e'_2}$, respectively. Intramolecular acylation of the aromatic ring (Scheme 3) in the acylium ion **a** and concomitant loss of the *ortho* ·H radical was also observed to yield an ion **f**. Alternatively, a similar cyclization may also occur in **d** with the concomitant loss of H_2O.

The rearrangement involving bond formation between the fluoroacrylate side chain and the R group with subsequent elimination of benzyne yielded ion **g** of general formula R-CH=CF-$CO_2C_2H_5$. Migration of F atom was also observed in the $M^{+\cdot}$ (1,2-F shift with the subsequent loss of $C_4H_5O_2$ moiety) and in **b**, although these reactions were not very prominent.

In conclusion, (a) EI of the α-fluoro cinnamates leads to extensive fragmentation, (b) the substtution of α-fluorine atom stabilizes the cinnamates (c) an electron-donating group stabilizes the $M^{+\cdot}$ of the fluoroesters compared to the electron-withdrawing groups; the effect was more pronounced in the *meta* isomers.

* The research will appear in *Org. Mass Spectrom.* **23**, (1988)- in press.

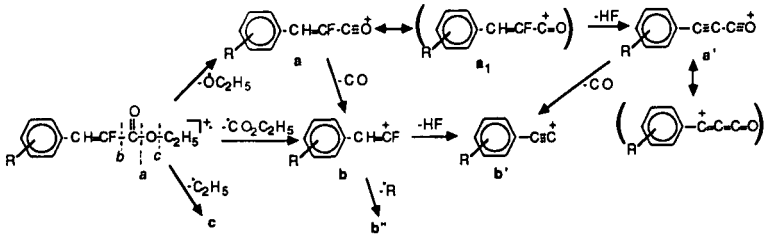

SCHEME 1

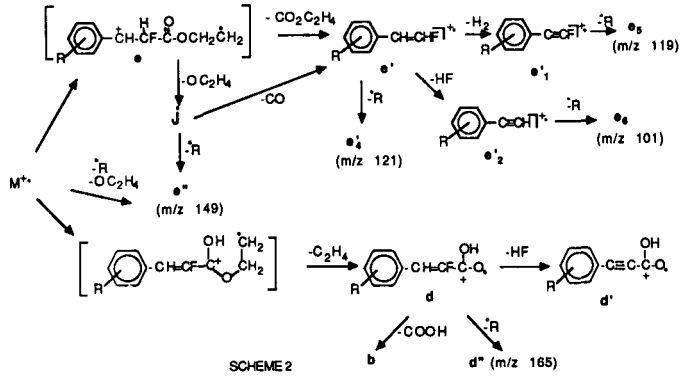

SCHEME 2

Table 1-Linked Scans of Selected Fragments from p-CH_3 derivative

(a) B/E - CAD Precursor	Corresponding Product Ions					
180 (d)	165 (d")	162 (f)	160 (d')	135 (b)	116 (e'2)	115 (b')
163 (a)	143 (a')	135 (b)	120 (b")	115 (b')		
135 (b)	115 (b')	109 (l)				

(b) B^2/E Fragment	Corresponding Precursor Ions				
165 (d")	180 (d)				
160 (d')	180 (d)				
149 (e")	208 ($M^{+\cdot}$)		164 (j)		
136 (e')	208 (e)	164 (j)			
135 (b)	208 ($M^{+\cdot}$)		180 (d)	163 (a)	
116 (e'2)	188	180 (d)	160 (d')	144	136 (e')
109 (l)	135 (b)				

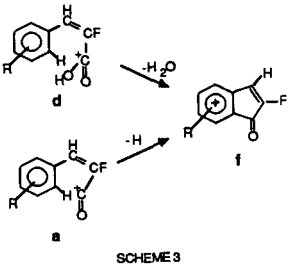

SCHEME 3

Presented at the 36th ASMS Conference on Mass Spectrometry and Allied Topics
June 5-10, 1988, San Francisco, CA

MECHANISM OF FRAGMENTATION OF DIQUATERNARY AMMONIUM SALTS BY FAST ATOM BOMBARDMENT;

M. T. Cheng; ICI Americas Inc., Richmond, CA

Multiple charged ions are often observed in mass spectra obtained with desorption ionization methods. By observing doubly charged ions one essentially doubles the mass range of a sector type mass spectrometer. Cooks in 1980 (1) reported the study of diquaternary ammonium salts by secondary ion mass spectrometry, and reported three major processes: dication emission, electron capture, and charge separation. This report investigates the requirements for dication emission, and the mechanism of charge separation in saturated systems by FAB mass spectrometry.

Experimental:

All compounds were synthesized by alkyliodide alkylation in acetonitrile; the structures were confirmed by NMR and mass spectrometry. FAB mass spectra were obtained on a VG7070E-HF mass spectrometer with an Ion Tech gun, and the samples were dissolved in glycerol.

Results and Discussion:

The FAB mass spectra of compounds I, II, and III show the expected loss of methyl as the highest mass peak due to charge

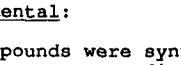

$Me_3\overset{+}{N}(CH_2)_n\overset{+}{N}Me_3$

I n = 2

II n = 6

III n = 12

separation mechanism. No singly charged molecular cation is observed because electron capture cross section is virtually zero for these saturated compounds. For compound III where the charge sites are separated by 15.9A a doubly charged molecular ion is observed. This is confirmed by the observation of the ^{13}C isotope peak one-half mass unit above the dication peak at m/z 143.5. In order to observe dication emission, the two cationic sites must Be separated by at least 9.5A, therefore for compound II where the charge sites are separated by 8.7A, no dication is observed. Unfortunately I presently do not have data for compounds where n = 7, 8, 9, 10, or 11 to confirm the 9.5A separation requirement. Nevertheless, one should begin to observe doubly charged ions at n = 8, where the charge separation is approximately 10A.

To investigate the charge separation mechanism, compounds IV, V, VI were synthesized.

$Me_2\overset{+}{R}N(CH_2)_6\overset{+}{N}RMe_2$

IV R = ethyl

V R = *n*-propyl

VI R = *i*-propyl

The FAB mass spectra for these compounds show the loss of methyl cation due to charge separation as the highest mass peak. For Compound IV, the peak at m/z 215 is due to the loss of methyl cation, and the m/z 201 peak is due to the loss of ethyl cation (Figure 1). The ratio of the loss of ethyl to the loss of methyl is approximately 0.8, if the processes are completely random, the ratio is 0.5, therefore, there is a definite preference towards the loss of ethyl cation. For compound V, the ratio of the loss of *n*-propyl to the loss of methyl is approximately 0.8 (Figure 2), similar to compound IV, and for statistical losses, the ratio is 0.5. These results are not unexpected, both ethyl and *n*-propyl cations are primary cations with approximately the same stability (2) and are more stable than methyl cation. Therefore, the loss of ethyl and *n*-propyl are favored over the loss of methyl cation. This result is

confirmed by the mass spectrum of compound VI (Figure 3), where a secondary alkyl (*i*-propyl) replaces the primary alkyl group. The ratio of the loss of *i*-propyl cation to the loss of methyl cation is approximately 1.2, where as for a random process the ratio is 0.5. This is so because the secondary *i*-propyl cation is much more stable then the primary *n*-propyl cation (Table 1).

(1) Ryan, T. M.; Day, R. J.; Cooks, R. G., Anal. Chem. 1980, 52, 2054.

(2) Franklin, J. L. Carbonium Ions; Olah, G. A.; Schleyer, P. von R., Ed., Wiley: New York, 1968.

Table 1. Ratio of Losses and Stabilities of Gaseous Alkyl Cations

Compound	M-Alkyl/M-Ethyl	Heats of Formation of Alkyl (KCAL/MOLE)
IV	1.33	225
V	1.32	218
VI	2.41	194

Figure 1. FAB Mass Spectrum of Compound IV

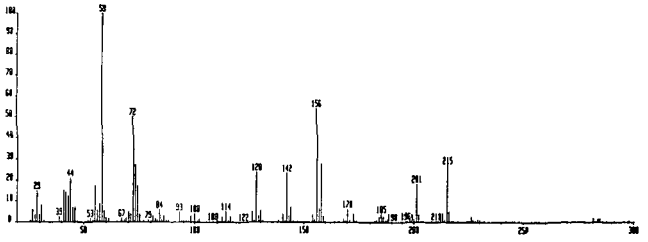

Figure 2. FAB Mass Spectrum of Compound V

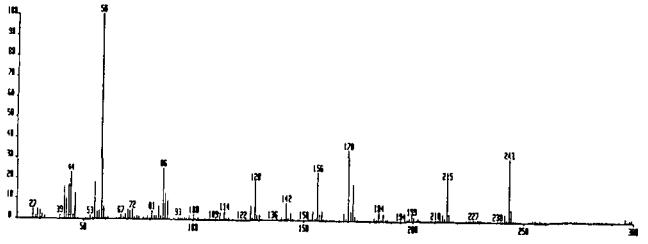

Figure 3. FAB Mass Spectrum of Compound VI

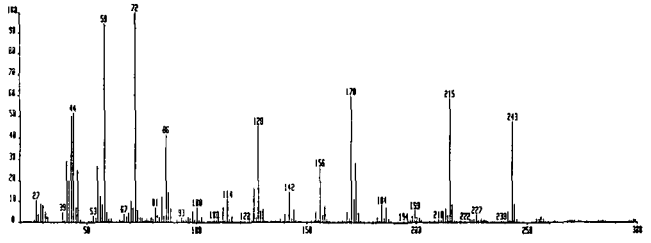

Presented at the 36th ASMS Conference on Mass Spectrometry and Allied Topics
June 5-10, 1988, San Francisco, CA

BORATE IONS IN THE GAS PHASE. FAST-ATOM BOMBARDMENT OF CONDENSED-PHASE BORATES

Robert J. Doyle, Jr.
Chemistry Division
Naval Research Laboratory
Washington, DC 20375-5000

The intractable properties of crystalline and vitreous, condensed-phase, boron-oxygen compounds have always hindered the generation and analysis of gas-phase, boron-oxygen species. Recently, structures of gas-phase boron oxide cations, generated by fast-atom bombardment (FAB) of boron trioxide (B_2O_3), were proposed on the basis of collision-induced dissociation (CID).[1] The experiments employed a high-temperature FAB sample holder which eliminated problems with hygroscopicity and provided a molten sample for fast-atom bombardment by xenon atoms.[2] It was concluded that boron oxide cations typically contain integral BO_3 triangles and terminal -B=O units, in which case boron is exclusively 3- or 2- coordinated with oxygen.

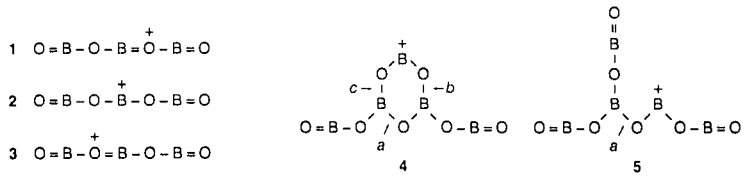

Figure 1. Proposed structures for $B_3O_4^+$ and $B_5O_7^+$.

Figure 1 shows proposed structures for $B_3O_4^+$ and $B_5O_7^+$. Structures 1-3 represent the three equivalent forms of $B_3O_4^+$ in which electron sharing and resonance serve to enhance the stability of this species. Structures 4 and 5 show the possible cyclic and acyclic isomeric forms of $B_5O_7^+$. Both proposed structures are reasonable in light of the collisional-activation spectrum of $B_5O_7^+$. Structures 4 and 5 illustrate a significant problem with the CID of boron oxides; it cannot be determined by CID techniques whether or not the boron oxide ions generated by FAB of B_2O_3 contain the partially aromatic boroxol ring that is found in condensed-phase B_2O_3.

The present study involves the determination of the structures of boron-oxygen anions (borates). Borates generated by the fast-atom bombardment of vitreous boron trioxide are found to contain integral BO_3 triangles and terminal -B=O units, in common with boron oxide ions. The most abundant species observed were BO^-, BO_2^-, $B_2O_4^{-\cdot}$, $B_3O_5^-$, and $B_5O_8^-$. The fast-atom bombardment of crystalline samples of $Li_2B_4O_7$,

Presented at the 36th ASMS Conference on Mass Spectrometry and Allied Topics
June 5-10, 1988, San Francisco, CA

$Na_2B_4O_7$, $Zn_3B_4O_9$, $Zn_2B_6O_{11}$, and $K_2B_{10}O_{16}$ also yielded BO^-, BO_2^-, and $B_3O_5^-$. Collision-induced dissociation and collision-induced charge inversion were used to examine $B_3O_5^-$ and $B_5O_8^-$ generated from all of the above mentioned samples. Two diagnostic charge-inversion reactions are:

$$(1)\quad B_3O_5^- \text{ ----> } B_2O_2^{+\cdot} + {}^{\cdot}BO_3 + 2e^-$$
$$(2)\quad B_5O_8^- \text{ ----> } B_3O_4^+ + B_2O_4 + 2e^-.$$

The significance of these reactions lies in the structures of the neutral products. The proposed structures of the ${}^{\cdot}BO_3$ molecule (stabilized by six equivalent forms) and the B_2O_4 molecule (stabilized by two equivalent forms) are shown in Figure 2. The direct loss of ${}^{\cdot}BO_3$ must occur from an acyclic parent anion containing a terminal BO_3 unit or a cyclic parent anion (Figure 2).

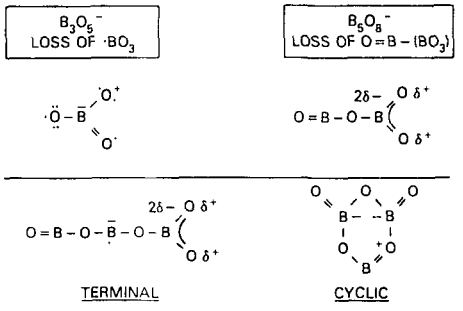

Figure 2. Proposed structures of ${}^{\cdot}BO_3$, B_2O_4 and $B_3O_5^-$.

The acyclic $B_3O_5^-$ anion, with a terminal BO_3 unit, does not exhibit canonical structures that allow for delocalization (and hence stabilization) of the negative charge. The cyclic $B_3O_5^-$ anion, however, exhibits several resonance forms that would provide delocalization (similar to that found in boroxol rings) and it is therefore suggested that the parent anion is cyclic. Similar arguments may be made for the $B_5O_8^-$ ion based upon the neutral loss of B_2O_4.

(1) Doyle, R.J., Jr. J. Am. Chem. Soc., In Press, June 1988 Publication.
(2) Doyle, R.J., Jr. Anal. Chem. 1987, 59, 537-539.

Presented at the 36th ASMS Conference on Mass Spectrometry and Allied Topics
June 5-10, 1988, San Francisco, CA

CHLOROFLUOROCARBONS IN THE ENVIRONMENT:

A REVIEW

Mario J. Molina
Jet Propulsion Laboratory
Pasadena, California 91109

It has been 14 years since the publication of the first paper on depletion of stratospheric ozone due to the release of chlorofluorocarbons (CFC's) to the atmosphere (1). Because of their unusual stability and low toxicity, CFC's were regarded as ideal industrial chemicals and are widely used in refrigeration, as solvents for cleaning electronic boards, for foam insulation, etc. Ironically, it is this chemical inertness that allow the CFC's to survive for long periods of time in the environment and to eventually diffuse above the ozone layer where they are broken apart by solar UV radiation. The decomposition products include chlorine atoms, which speed up the destruction of ozone through a catalytic cycle: each chlorine atom may destroy tens of thousands of ozone molecules before leaving the stratosphere, mostly in the form of hydrogen chloride, which is efficiently scavenged by rain.

Numerous laboratory studies, field measurements and computer modeling calculations have essentially confirmed the validity of the CFC's - ozone depletion theory. Both atomic chlorine and chlorine monoxide have been detected in the stratophere, demonstrating that the postulated catalytic chain reactions are actually occurring. Many other species have also been measured, e.g., hydrogen chloride (HCl), chlorine nitrate ($ClONO_2$), hydrogen fluoride (HF), hydroxyl radicals (OH), etc. Stratospheric ozone levels are predicted to decrease by several percent towards the end of the century, assuming that the emission of CFC's continues at current rates. This depletion is predicted to occur mostly in the upper stratosphere, where ozone is being produced in largest quantities. In the lower stratosphere, ozone in predicted to increase somewhat, partially compensating the losses higher up. Even if the total amount of ozone were to remain the same, a substantial redistribution could have a serious impact on the climate by changing the temperature profile of the atmosphere. One of the worrisome aspects of this CFC theory is the long time scale involved: the effect of a release of CFC's at any given time is only felt about a decade later, and it persists for a period of over a century. Levels of chlorine in the stratosphere are expected to continue increasing for many decades even if production and release of CFC's were to level off.

In response to public concern over the effects of CFC's on stratospheric ozone, the United States banned the use of CFC's as propellants in aerosol sprays in 1978; Canada, Sweden, Denmark and Norway subsequently imposed similar regulations. In September 1987, 24 nations - including the United States and nearly all the major industrial countries - signed an agreement to freeze the consumption of CFC's at 1986 levels and to halve the usage by 1999. This historic agreement, known as the "Montreal Protocol", must be ratified

by at least eleven countries before it becomes official in 1989.

It has been established that a statistically significant drop in ozone levels has already occurred, particularly in the winter months at high latitudes. Also, ozone depletion has already been detected in the upper stratosphere. Furthermore, the ozone levels over Antaractica dropped last October to the lowest ever observed anywhere in the atmosphere -- more than 50% total column ozone depletion, with more than 95% disappearing around 18 km altitude. The discovery of this mysterious "hole" was unexpected. A change in ozone concentration of this magnitude was not anticipated by atmospheric scientists, suggesting that the ozone layer is influenced by processes not previously recognized. Two sets of theories were competing to explain this phenomenon. The dynamical or meteorological theories consider the hole to be the result of ozone redistribution in the atmosphere. In contrast, proponents of a chemical origin assume man-made pollutants as the cause and they believe that ozone is actually being destroyed through some unusual chemical processes. Recent findings have shown conclusively that this "ozone hole" is due to the release of man-made CFC's. Laboratory measurements demonstrated how catalytically active chlorine can be released in the presence of ice particles, which exist over Antarctica as "polar stratospheric clouds". Ground-based and aircraft measurements have yielded large amounts of information supporting the chlorine-ozone destruction mechanism.

---

(1) M. J. Molina and F. S. Rowland, Nature, 249, 810, 1974.

Presented at the 36th ASMS Conference on Mass Spectrometry and Allied Topics
June 5-10, 1988, San Francisco, CA

ATMOSPHERIC TRANSPORT OF PESTICIDES BY FOG

Majewski, M.S.[1], Glotfelty, D.W.[2] and Seiber, J.N.[1]

[1]Department of Environmental Toxicology, University of California, Davis, CA 95616

[2]Soil Nitrogen and Environmental Chemistry Laboratory, Agricultural Environmental Quality Institute, U.S. Department of Agriculture, Beltsville, MD 20705

We are examining the vapor-moisture-particulate distribution of atmospheric organic compounds in fog in several rural locations in California, and in residential districts in Maryland. Fog water was collected using a rotating screen type sampler, while the interstitial gases, aerosols and particulates were collected using a dichotomous impactor. Each fog water sample was filtered through a glass fiber (GF) filter before being extracted using a multi-residue extraction procedure. The extracts were fractionated into chemical classes of increasing polarity using HPLC techniques. Each sample was analyzed by GC using various element selective detectors.

The MD fogs had a greater particulate load than did the CA fogs which is most likely due to the manner in which the homes are heated (oil, coal and wood). All of the fog samples foamed when shook indicating the presence of surface-active materials contained in the fog droplets. The filtered samples were also pale yellow in color with a major portion of this color being removed in the dichloromethane extraction.

The pH of the MD fog ranged from 2.5 - 4.5 with the major ionic species being SO_4^{2-}. The pH of the CA fog ranged from 5-7 with the acidity being reported to be controlled by a balance between sources of SO_4^{2-} and NO_3^-, and agricultural sources of NH_3.

Various types of organic compounds were found including plasticizers, flame retardants, PAH's, and pesticides. The CA fog yielded a greater variety and higher concentrations of pesticides than did the MD fog. The organophosphorus (OP) pesticides including parathion, diazinon, chlorpyrifos, and methidathion, were found in the greatest abundance in CA which may be attributed to their use as dormant sprays during the winter months. The OP pesticide concentrations frequently exceeded 10 ppb in the fog which is 2-3 orders of magnitude greater than commonly reported for pesticides and other neutral organics in rain from other locations.

The measured pesticide distribution between fog water and the interstitial air strongly favored the water phase resulting in large aqueous phase enrichments (EF) (Table 1). Table 1 represents averaged values of samples taken at three CA locations. EF is defined as the ratio of the pesticide concentration in fog water to that in air, divided by the Henry's law coefficient (H) of the pure compound. The enrichment in the fog droplets for those pesticides that are more volatile and/or less water soluble (DEF and pendimethalin) seem to be more pronounced.

The reason for this enrichment is unknown at this time. Temperature effects and sampling artifacts have been ruled out because of the similar EF values for each pesticide at the various CA sampling locations. One explanation may be the presence of surface active materials which would enhance the uptake of the pesticides into the droplets. The

acidity of the fog may also enhance the uptake of certain N-containing and even neutral compounds by altering the character of the surface active materials. These enrichment factor results imply that H is not a good quantitative estimate of the distribution of pesticides between fog droplets and the interstitial air.

The toxic oxygen analogs (OA) of a number of the OP's were also found in the fog water. Their source is uncertain. It is known that these OAs form in gas phase reactions between the parent compound and ozone. The OA's also occur in high concentrations in dry surface dust which, subsequently, may act as condensation nuclei for the fog droplets. Also, high oxidant levels are possible within the fog droplets, indicating that *in situ* conversion of the parent compound may occur. We found that high OA levels occur during clear, sunny days with lower levels during the following night time fog. These data suggest that the oxons are formed primarily during the day and are taken up into the fog after it forms. The lower OA concentrations under foggy conditions may result from slower formation at night, or from preferential scavenging of the oxons by fog and transport to the surface early during the fog event.

The dichotomous sampler filtered the interstitial fog air and trapped the suspended particulate matter. These particulates were also analyzed for their pesticide concentration, however, it is not clear whether these results accurately reflect the fraction of pesticide present on the dry, unactivated aerosol particles in the foggy air. It is possible that some adsorption from the vapor onto the trapped particulates, or conversely, desorption from the trapped particulates to the vapor may have occurred.

The concentration on the particulates ranged from 4-40% of the total pesticide distribution between the fog water, vapor, and particulates, depending on the compound and fog event. Conversely, only traces of pesticides were found on the particulates filtered out of the collected fog water. This implies that if the pesticides were originally present on the particulates, then almost complete desorption to the solution occurred by the time the samples were extracted. The extractions were done usually within 2-3 hours from the time of collection.

TABLE 1. Distribution and EF for selected pesticides in CA fog.

Pesticide	Concentration Fog water ($\mu g\ L^{-1}$)	Concentration Air ($\mu g\ L^{-1}$)	Air-to-Water Distribution ($ng\ m^{-3}$)	Enrichment Factor (EF) ($x10^{-6}$)
Parathion	23.2	4.0	0.24	310
Chlorpyrifos	2.6	6.2	2.5	190
Diazinon	16.8	3.9	0.24	310
DEF	0.52	0.08	0.15	2200
Pendimethalin	2.5	2.1	0.74	2400

Presented at the 36th ASMS Conference on Mass Spectrometry and Allied Topics
June 5-10, 1988, San Francisco, CA

BACKGROUND ENVIRONMENTAL CONCENTRATIONS OF DIOXINS AND FURANS

Brian Eitzer and Ronald A. Hites, School of Public and Environmental Affairs and Department of Chemistry, Indiana University, Bloomington, Indiana 47405

Abstract. A method of analyzing ambient air for dioxins and furans in the femtogram per cubic meter range has been developed. The method is used to compare dioxin and furan concentrations in air collected at three locations with the concentrations found in rain and sediment. These comparisons suggest that atmospheric transport followed by particle deposition is a primary method of dispersing these compounds throughout the environment.

Introduction. The incineration of municipal waste leads to the production and emission to the atmosphere of polychlorinated dibenzo-p-dioxins (PCDD) and dibenzofurans (PCDF) (*1-10*). Once in the atmosphere, these compounds can travel long distances before being deposited into the environment; this is demonstrated by their presence in the sediment of a remote lake whose only input of these compounds could be from atmospheric sources (*11*). To understand these transport and depositional processes, it is necessary to examine these compounds in each of the various compartments so transformations which occur between the sources and sinks can be studied. Previous work has focused on either combustion sources (*1-10*) or sinks such as sediment (*11-13*), leaving the transport medium, the atmosphere, to be studied.

We have undertaken a study aimed at determining the concentration of these compounds in the ambient air of Bloomington, Indiana. Bloomington was chosen because it is the proposed location for an incinerator designed to burn a mixture of municipal waste and polychlorinated biphenyl (PCB) contaminated materials. Thus, this study will provide baseline atmospheric concentrations of these compounds which can be used later to evaluate the performance of the incinerator. In addition, we will be able to improve our understanding of the atmospheric transport and depositional processes.

Experimental. Air has been sampled at three sites in Bloomington. These sites include two sites which had the highest predicted particulate concentrations from the incinerator proposer's computer model and one site in the downtown area about which the local population is centered. All sampling sites are located on roofs of buildings which are 2-4 stories tall. Sets of samples have also been taken at two comparison locations. These are a much more rural site, Trout Lake, WI, and a more urban site, indianapolis, IN.

Air has been sample with a modified high-volume air sampler. Air is drawn through a glass fiber filter and then a polyurethane foam (PUF) plug. These materials are analyzed separately giving a determination of particulate bound (on the filter) and vapor phase (in the PUF plug) compounds. It is important to note that vapor phase compounds could absorb to the filter or particulate bound compounds can be "blown-off" the particulate matter or pass through on very small particles; thus, the two phases are operationally defined.

Rain is sampled with a one square meter wet only collector. The sampler is designed so that as rainwater is collected it is pumped through a glass fiber filter to create operationally defined particulate bound and dissolved phases.

The sample clean-up procedure is described more completely elsewhere (*14*) and consists of Soxhlet extraction followed by column chromatography. Prior to extraction, samples are spiked with two carbon-13 labeled isotopic compounds (OCDD and 1,2,3,7,8 PCDF) which are used as internal standards. A series of external standards are used to measure response factors for each level of chlorination as compared to the internal standard. These external standards are also used in conjunction with published retention indices for PCDD (*15*) and PCDF (*16*) to get isomer specific information for some of the congeners. Only congeners containing four or more chlorines are examined. After clean-up, the samples are analyzed by high resolution gas chromatographic low resolution mass spectrometry; the mass spectrometer is operated in the electron capture, negative ion mode with selective ion monitoring (SIM). It is important to note that this ionization mode gives a poor response for 2,3,7,8-TCDD.

Results. Previous work has shown that the chloro-homologue profile of dioxins and furans changes as one progresses from source to sink (*12-13*). The profile changes from one in which no chloro-homologue dominates to one in which OCDD is predominate. if it is assumed that the quantity of combustion sources at a close proximity are greatest for a large city (Indianapolis), second for a smaller city (Bloomington), and smallest for a rural community (Trout Lake), then a hypothetical transect of chloro-homologue profiles with distance from source can be created by examining the chloro-

significant portion of the atmospheric burden. Third, as the air is "transported" from the "source" region, it undergoes a transformation to a profile dominated by the OCDD. Fourth, as the air is "transported," the concentrations decrease by either degradational or dilution processes. It should be noted that the Indianapolis and Trout Lake concentrations are sets of samples taken over a two week average vs. the long term average for Bloomington.

Figure 2 compares the chloro-homologue profile in the Bloomington average air with Bloomington rain and average Great Lakes sediment. The fact that the chloro-homologue profile in the sediment closely resembles that for the particular bound material suggests that particle deposition (wet or dry) is the primary depositional mode of these compounds from the atmosphere.

To further examine depositional processes the flux to the sediment measured previously (*12*) is compared to the flux implied by the measured air concentrations. The implied flux is determined by multiplying the air concentration by the depositional velocity and proper conversion factors. Other work has given an estimated depositional velocity of 1 cm/sec for organic compounds (*17*). This data comparison is given in Table I for fluxes implied by either the total or particulate bound only concentration. If the two rural sites are compared, it is seen that the Trout Lake flux is less than Siskiwit Lake but it should be noted that Thunder Bay, Ontario (a city of 100,000) is approximately 40 miles Northwest of Siskiwit Lake. The average Great Lakes flux lies somewhere between Indianapolis and Bloomington which seems correct as there are both urban and rural areas in the Great lakes area.

Table I. Comparison of measured and implied fluxes.

	PCDD & PCDF CONCENTRATION		IMPLIED FLUX	
	TOTAL	PART. ONLY	TOTAL	PART. ONLY
	pg/m^3	pg/m^3	pg/cm^2yr	pg/cm^2yr
TROUT LAKE	0.53	0.28	17	9.0
BLOOMINGTON	2.2	1.6	70	51
INDIANAPOLIS	5.2	4.1	165	130

MEASURED AVERAGE GREAT LAKES SEDIMENT FLUX = 120 pg/cm^2yr

MEASURED SISKIWIT LAKE FLUX = 20 pg/cm^2yr

The data shown suggest the following scenario. Combustion produces a large variety of chloro-homologues. As these compounds are transported through the atmosphere, a degradation process occurs on the vapor phase. This process reduces the total air concentration, but significant amounts remain in the vapor phase due to equilibrium with particulate bound material. This equilibrium favors the particulate bound material for the higher chlorinated homologues, and thus they undergo less degradation. Eventually. the particulate matter deposits from the atmosphere and enters the biosphere where it can be deposited in sediment or on plant matter which can be taken up through the food chain.

Acknowledgments. We thank the Westinghouse Electric Corporation and the U.S. Environmental Protection Agency for support.

REFERENCES

1. R. R. Bumb, W. B. Crumett, S. S. Cutie, J. R. Gledhill, R. H. Hummel, R. P. Kagel, L. L. Lamparski, E. V. Luoma, D. L. Miller, J. J. Nestrick, L. A. Shadoff, R. H. Stehl, and J. S. Woods, Science 210, 385-390 (1980).

2. H. R. Buser and H. P. Bosshardt, Mitt. Gibiete Lebensm. Hyg. 69, 191-199 (1978).

3. A. Cavallaro, L. Luciani, G. Ceruni, I. Rucchi, G. Ivernizzi, and A. Garin, Chemosphere 11, 859-868 (1982).

Presented at the 36th ASMS Conference on Mass Spectrometry and Allied Topics
June 5-10, 1988, San Francisco, CA

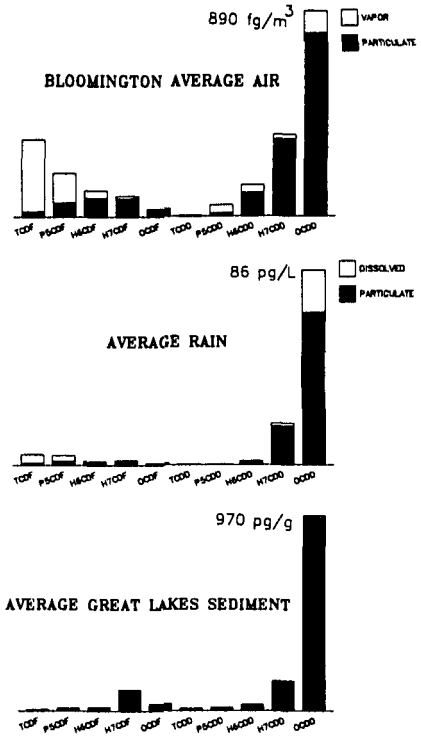

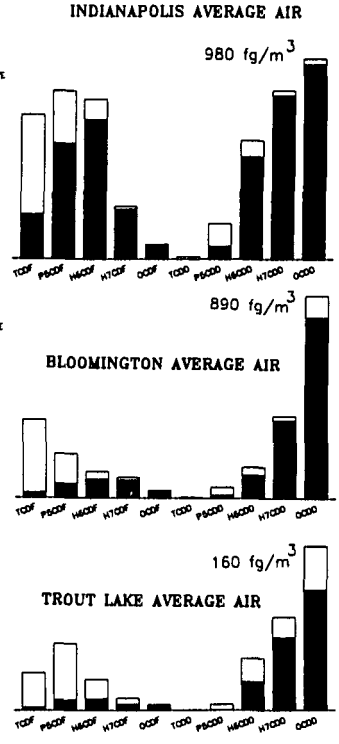

Figure 1. (left) Chloro-homolog profiles for average air from Indianapolis, IN; Bloomington, IN; and Trout Lake, WI. The total OCDD concentration is given as a scaling factor.

Figure 2. (right) Chloro-homolog profiles for average Bloomington air; Bloomington rain; and Great Lakes Sediment. The total OCDD concentration is given as a scaling factor.

Presented at the 36th ASMS Conference on Mass Spectrometry and Allied Topics
June 5-10, 1988, San Francisco, CA

Determination of the Photoinduced Loss Rate of Low Vapor Pressure Molecules by Mass Spectrometry.

Robert Orth

Environmental Sciences Center, Monsanto Company, 800 N. Lindbergh Blvd., St. Louis, Missouri 63167.

The fate of compounds such as chlorinated organic compounds in the environment depend on their rates of biodegradation and chemical degradation. This paper discusses the photodegradation of polychlorinated dibenzo-p-dioxin(PCDDs) and dibenzofurans (PCDFs). The PCDDs and PCDFs have vapor pressures which are lower than 10^{-4} torr which limits the experimental method for determining the photoloss in the vapor phase. An apparatus which minimizes the problems associated with studying low vapor pressure photoinduced loss was constructed. The apparatus and the associated dynamics has been described previously(1,2) in which a mass spectrometer is directly coupled to a quartz gas cell. PCDDs and PCDFs are passed through the cell which may or may not be irradiated with various wavelengths of light The mass spectrometer monitors the gas phase concentration of the analytes allowing the kinetic studies to be conducted.

The objectives of the study are; to determine the photoinduced quantum yield for 2,3,7,8 tetrachlorodibenzo-p-dioxin, 2,3,7,8-TCDD, over the region of the light spectrum from 200 nm to 300 nm; to examine the variation between various PCDDS isomers with respect to 2,3,7,8-TCDD; and to finally determine the relative rate difference between tetrachlorodibenzofuran, TCDF, and 2,3,7,8-TCDD. The variability among TCDD isomers was examined by varying the number of Cl on each benzene ring i.e. all the chlorines on the first ring (1,2,3,4-TCDD), 3 on first ring and 1 on the second ring (2,3,4,8-TCDD), and the symmetric 2 by 2 (2,3,7,8-TCDD). The variation between congeners involve the determination of the photoinduced loss rate 1,2,3,4,7 pentachlorodibenzo-p-dioxin with the TCDDs. The relative rate between TCDF and TCDD was examined using 2,3,6,8-TCDF vs 2,3,7,8-TCDD.

As can be seen in Figure 1 the light on curve using the 325 broad band filter does induce a loss for TCDD as compared to the no light loss curve. The two loss curves are for 2,3,7,8 and 2,3,4,8-TCDD. The 2,3,7,8-TCDD is lost at a faster rate than the 2,3,4,8-TCDD The photon flux was measured using acetone as a reference. Therefore the quantum yield for 2,3,7,8-TCDD was calculated to be 0.03 ±70%. The major uncertainty in the quantum yield arises from difficulty in measuring the photon flux. The relative rate constants have a better precision of ±15%.

Figure 2 shows the relative half life obtained from the rate constants for loss with respect to 2,3,7,8-TCDD for each of the PCDDs and PCDFs examined. The results shows that for this group the 2,3,7,8-TCDD has the shortest half life of the group while the pentaCDD is 2.3 times longer then the 2,3,7,8-TCDD. Thus as the chlorination increases the half life increases. The other isomers have a longer half life than 2,3,7,8-TCDD but are comparable between themselves.

Figure 3 shows the results obtained for the photoloss of 2,3,7,8-TCDD and 2,3,6,8-TCDF as a function of wavelength. 2,3,6,8-TCDF has two apparent maxima at 300 nm and 260nm. The 2,3,7,8-TCDD shows a maximum photoloss at 300nm. The maximum for 2,3,7,8-TCDD corresponds with the maximum observed for the absorption of light in a hexane solution. Considering the observed wavelength dependence for photoinduced loss for TCDF and TCDD and the sunlight flux in this region of the light spectrum, the life time of these molecules in the vapor phase with sunlight present is going to be finite.

With the low vapor pressures experienced with these compounds the amount of sample on the surface of the photolysis cell can be larger than that in the gas phase. The loss due to light could therefore be arising from the molecules on the surface photodegrading, not the vapor phase molecules. A second surface photodegradation could also arise from a molecule which is photo-excited in the gas phase but requiring a surface interaction for degradation to occur. To determine if the surface is a major contributor to the above photoloss determinations the surface area of the photocell was decreased by a factor of two. By keeping the photon flux the same as in the larger cell an observed change in the rate constant of 0.5 times should be observed if the above mechanisms are the major contributor The rate constant did not change within experimental error. Thus this surface process is not a major contributor to the observed loss.

In conclusion the TCDD and pentaCDDs were found to photodegrade in the UV region with a maximum for photoloss occurring at 300nm for the TCDDS and TCDFs. The quantum yield for 2,3,7,8-TCDD was 0.03±0.02. 2,3,7,8-TCDD was found to have the shortest relative life time compared to the other PCDDs. Also as the number of chlorines increase from 4 to 5 the relative half life compared to 2,3,7,8-TCDD increases by a factor of 2.3.

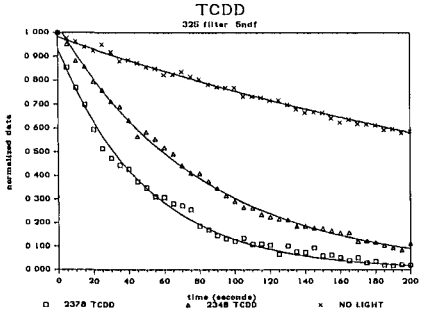

Figure 1. Light off and on loss curves from photocell for 2,3,7,8 and 2,3,4,8-TCDD.

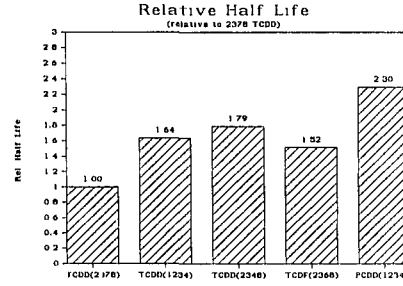

Figure 2. Relative half life for each PCDD and PCDF.

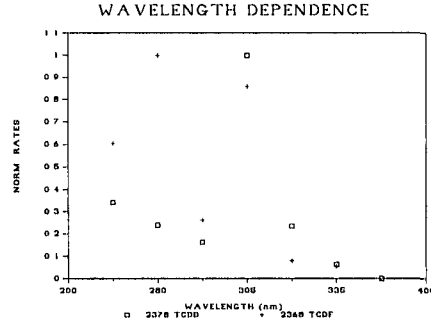

Figur 3. Wavelength dependence for TCDD and TCDF.

References

1. Orth, R.G.; Ritchie, C.; Hileman F.; Measurement Of Photoinduced Loss of Low Vapor Pressure Molecules by Mass Spectrometry, Presented at the 35th Conf. on Mass Spectrometry and Allied Topics May 24-29, 1987, Denver Co.

2. Orth, R.G.; Ritchie, C.; Hileman F. Chemosphere in press.

Acknowledgments: The author would like to acknowledge the helpful discussions of Fred Hileman. Also the technical assistance of Cheryl Ritchie.

Presented at the 36th ASMS Conference on Mass Spectrometry and Allied Topics
June 5-10, 1988, San Francisco, CA

PEAK EXPOSURE AND DISSIPATION RATE MEASUREMENTS OF HALOGENATED VOLATILE ORGANIC COMPOUNDS IN INDOOR AIR

Joachim D. Pleil,* William A. McClenny
Environmental Monitoring Systems Laboratory
U S. Environmental Protection Agency
Research Triangle Park, NC 27711

Karen D. Oliver
Northrop Services, Inc. – Environmental Sciences
Research Triangle Park, NC 27709

The indoor breathing space is often subjected to various volatile organic compounds (VOCs) from human activity, which can greatly impact the quality of the air. Because the indoor environment is restricted in volume and the exchange rate between indoor air and outdoor air is generally low, even seemingly small emissions (high-level and short-term or low-level and long-term) can cause human exposures of concern. The ambient (outdoor) air can also be similarly affected when local point sources emit large volumes of VOCs into the considerably larger local air volume.

Measurement of VOCs is generally performed with time-integrated sampling and subsequent detailed analysis. The two predominant sampling methods are solid absorbent sampling with Tenax-gas chromatography (GC) and whole-air sampling with SUMMA® polished canisters or Tedlar® bags. Typical sampling periods are 12 and 24 h.

The currently used methodology for VOC determination does not address the time-dependent nature of such emissions, with the exception of screening devices such as real-time systems that include photoionization detectors (PIDs) or portable GCs. Though such instruments can yield some time-resolved data, the "total response" nature of the former and the low-quality resolution of the latter method tend to result in ambiguous VOC data.

Our laboratory has developed three related high-resolution GC methods to address the need for time-resolved measurement of VOCs. These are

1. automated, repetitive sampling and analysis performed on-site;
2. multiple, sequential grab sampling with subsequent laboratory analysis; and
3. automated sequential syringe sampling (SSS) with subsequent automated multiple analyses in the laboratory

These methods have been used in a variety of situations to demonstrate their utility and to document the variations in concentration of halogenated VOCs.

For the first method, the analytical instrumentation must be in place at the sampling site and is thus of limited utility for other than developmental work. An automated repetitive analytical cycle was used to measure hourly concentrations of VOCs in our laboratory building; some representative data for tetrachloroethene are given in Figure 1. This system, employing high-resolution GC with parallel flame ionization and electron capture detectors, was then installed in a mobile laboratory for use in ambient (outdoor) sampling. Also, the mobile laboratory can be parked next to a building and with appropriate sample delivery can be used for indoor air VOC determination.

The second method, sequential canister sampling and analysis, removes the necessity for on-site analytical equipment; however, the method requires a great deal of operator intervention. Here, a number of evacuated SUMMA® polished sampling containers are manually opened at certain intervals to collect whole-air grab samples for subsequent detailed GC/MS laboratory analysis. This method was applied to an indoor situation involving the use of a "hot tub" spa wherein bromine pool chemicals are used as an algicide. Representative data are presented in Figure 2.

Finally, the third method was developed to streamline and fully automate both the sampling and analytical phases of time dependent VOC determination. By using a modified, commercially available SSS system, 12 consecutive 150-cm^3 whole-air samples could be collected and then transported to the laboratory for fully automated GC/MS analysis. The SSS system is pre-programmable in the laboratory to collect samples on a variety of time scales ranging from 2 to 90 min/sample The only work required from the field operator is sampler transportation and placement at the site of interest Upon return to the laboratory, the SSS is connected to a manifold, and the analytical system automatically performs analyses of all 12 collected samples and prints

calibrated reports for 40 compounds of interest. Because the analytical phase requires no ongoing operator intervention, it is generally performed overnight to free the instrumentation for other workday analyses. Representative data from two tests, bathroom air during shower activity and residential air during use of household spray products, are given in Figures 3 and 4. Figure 3 shows the temporal variability of chloroform correlated to water use and shows para-dichlorobenzene (presumably from an air freshener) as unaffected. The household product test showed many use-correlated variations; dichloromethane and methyl chloroform had maximum levels exceeding 300 ppbv and 200 ppbv, respectively. Other correlated variations for carbon tetrachloride, methyl chloride, and trichloroethylene are presented in Figure 4.

The results from this variety of experiments demonstrated that (1) halogenated VOCs often exhibit order of magnitude changes in concentration, (2) time scales of changes vary and depend upon the compound, (3) absolute magnitudes of concentrations and dissipation rates can vary widely for different compounds in the same test, and (4) unexpected compounds (such as carbon tetrachloride) can occur. All three methods described here were capable of producing high-quality peak exposure and dissipation rate measurements for halogenated VOCs despite the variabilities inherent in indoor air situations.

(This is an abstract of a presentation and does not necessarily reflect EPA policy.)

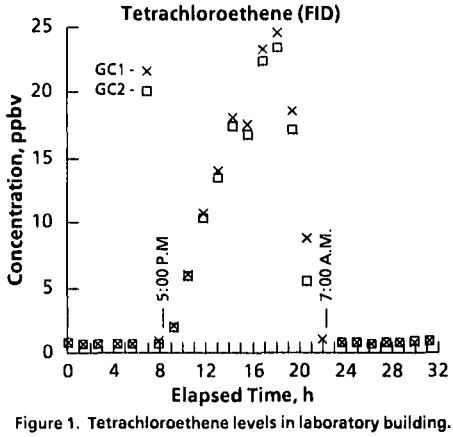

Figure 1. Tetrachloroethene levels in laboratory building.

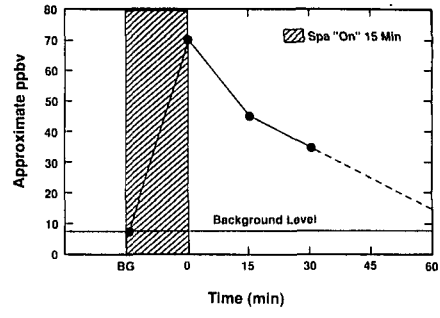

Figure 2. Bromoform – indoor spa, individual canisters.

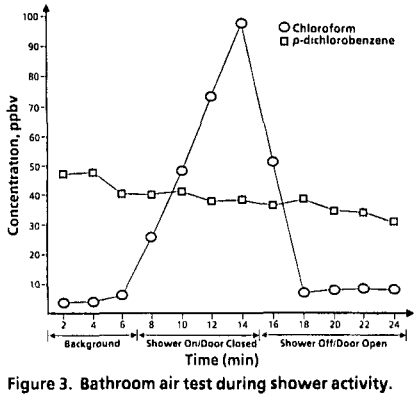

Figure 3. Bathroom air test during shower activity.

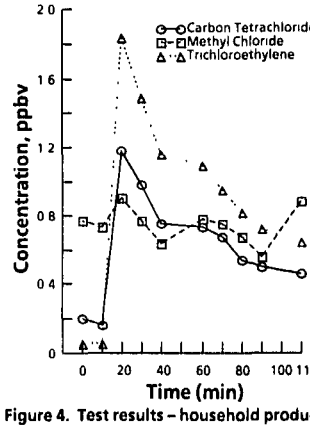

Figure 4. Test results – household products.

Presented at the 36th ASMS Conference on Mass Spectrometry and Allied Topics
June 5-10, 1988, San Francisco, CA

EXACT MASS ERRORS IN FOURIER TRANSFORM MASS SPECTROMETRY: EXPERIMENTAL EVIDENCE FOR INDIRECT COULOMBIC MECHANISMS

S. S. Yang, D. L. Rempel and M. L. Gross
Midwest Center for Mass Spectrometry,
Department of Chemistry, University of Nebraska, Lincoln, NE 68588-0304

New calibration procedures based on accurate ion dynamic models are a means to reduce systematic mass measurement errors in Fourier transform mass spectrometry. Systematic errors have been shown to increase with ion number.[1,2]

The fact that errors increase with ion number might be attributable to coulombic interaction amongst the ions. There are two developments upon which models of coulombic interaction might be based: one makes use of uniform ellipsoidal ion clouds[3] and the other exploits averaging[4].

To the extent that the errors can be explained or removed by applying these developments to the ion motion during the detection time, the errors will be said to be due to "direct" mechanisms. Otherwise, the errors will be said to be due to "indirect" mechanisms.

Experimental evidence is given for two mechanisms which are thought to be indirect. The first appears as a correlation between ionization period processes and changes in the dependence of error on ion number. The second appears as a correlation between trap field shape and dependence of error on ion number. The experimental evidence of these mechanisms is most visible in experiments designed to test the veracity of models based on the developments.

General parameters were: magnetic field = 1.2 T; trap disk = 1.007 V, outer segment = 1.705 V; filament bias = -70 V. Trap was a .0254 m cubic trap which was compensated by segmenting the trap plates into two parts.[7] The material was 304SS. Excitation was three sequential rf bursts, .345 V b-p for 700 us applied at the calibrant ion frequencies corresponding to m/z = 77 and m/z = 120 of acetophenone and at the test ion frequency corresponding to m/z = 105, except the test ion was excited for 650, 700, or 750 us.

Exact mass measurement errors were obtained by first fitting the equation $m = (a/f) + (b/f^2)$ to the known masses and measured frequencies of the two calibrant ions. Then the measured frequency of the test ion was used in the fitted equation to calculate the calibrated mass. The difference between the calibrated mass and the true mass is the mass measurement error.

In fig. 1, the error as a function of the electron beam time-current product varied with changes in beam time when the test and calibrant ion orbit sizes were different. This observation would suggest that a factor other than ion number was also influencing the errors as the ion number is varied. This effect confounds efforts to test ion-ion coupling models in circumstances involving different orbits.

As a parameter in this factor, time does not play a significant role. Extending the beam time from 3 ms to 18 ms had little effect. This would suggest that electron-ion collisions or ion-ion collisions during the ionization period were not responsible for the effect. Time delay between the ionization and excitation periods produced only small changes in the high orbit error behavior. This would suggest that evolutionary processes after the ionization period were not responsible as well. One possible mechanism is the modification of the ion cloud state by the electric field of an electron beam that is not perfectly coaxial with the trap electric field center. Magnetron motion did affect the error dependence in the case where the trap electric field center was shifted by using bias on the transmitter plates, and in the case where overt magnetron excitation was applied. Electron beam trapping of ions[6] at 500 nA is suggested appearance of asymmetry with respect to magnetron excitation. As a check, asymmetry was observed when the trap field center was moved by using transmitter plate bias.

The shape of the trap electric field affects the dependence of error on ion number. The error dependence for the compensated trap conforms more closely to an affine function. This observation supports the notion that the errors recorded here are electric in origin.

A tentative explanation for the difference between compensated and uncompensated trap performance can be found in the notion that only a fraction of the ion population is detected. The detected fraction is determined by the shape of the electric fields.[7] As the electric fields are modified by increasing ion number, the detected portion of the ion population can change. As the relationship of the detected portion to the whole cloud changes, the effect of ion-ion coupling changes, and a different frequency shift per ion number is produced.

For the uncompensated trap, it is known that the detected fraction for low ion number is a subpopulation with moderately high z-mode amplitudes. For high ion number, the uncompensated trap behaves like a compensated trap, in which the detected ion fraction is a subpopulation with moderately low z-mode amplitudes for all ion number.[7] In fig. 2, the frequency slope changes only for the uncompensated trap as expected.

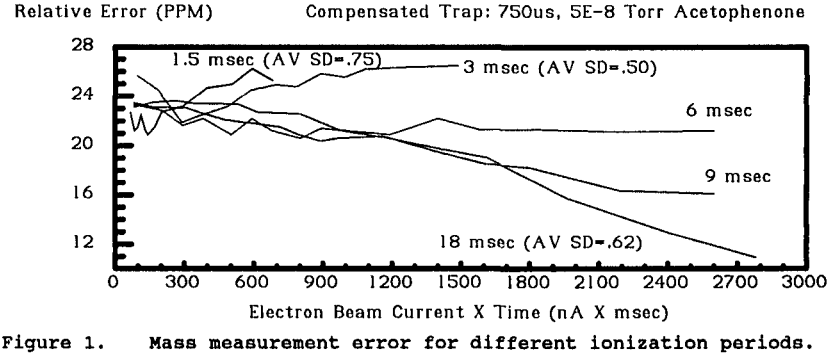

Figure 1. Mass measurement error for different ionization periods.

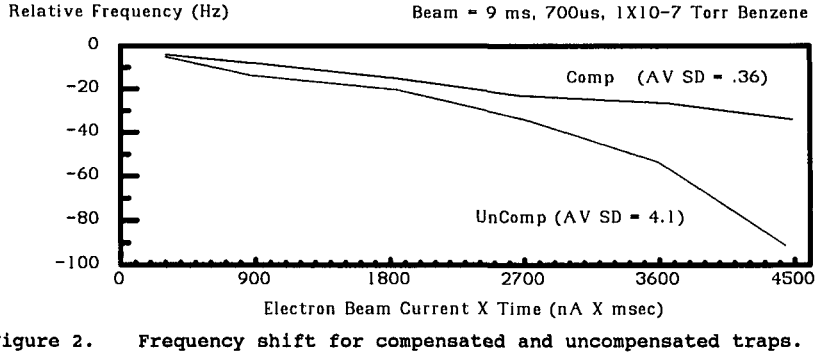

Figure 2. Frequency shift for compensated and uncompensated traps.

References

1. E. B. Ledford, D. L. Rempel and M. L. Gross, Anal. Chem., **56** (1984) 2744.
2. T. M. Sack and D. L. Rempel in Proceedings of the 33rd Annual Conference on Mass Spectrometry and Allied Topics, 1985, pp. 715-716.
3. J. B. Jeffries, S. E. Barlow and G. H. Dunn, Int. J. Mass Spectrom. Ion Phys., **54** (1983) 169.
4. V. L. Talrose and E. N. Nikolaev, Adv. Mass Spectrom., **10A** (1985) 343.
5. D. Wineland and H. Dehmelt, Int. J. Mass Spectrom. Ion Phys., **16** (1975) 338.
6. B. S. Freiser, Int. J. Mass Spectrom. Ion Phys., **26** (1978) 39.
7. D. L. Rempel in Proceedings of the 35th Annual Conference on Mass Spectrometry and Allied Topics, 1987, pp. 1124-1125.

Presented at the 36th ASMS Conference on Mass Spectrometry and Allied Topics
June 5-10, 1988, San Francisco, CA

NEW AND IMPROVED MASS CALIBRATION LAW FOR FT/ICR MASS SPECTROMETRY

Mingda Wang and Alan G. Marshall

Deartment of Chemistry (and Dept. of Biochemistry)
The Ohio State University
120 W. 18th Avenue
Columbus, OH 43210

For a trapped-ion cell with quadrupolar potentials, Ledford et al. were able to relate ICR frequency (ν) to ionic mass (m) in the absence of ion-molecule collisions according to:[1]

$$m = A/\nu + B/\nu^2 \qquad [1]$$

It has proved remarkably successful for wide-range mass calibration, presumably because: (a) most FT/ICR ion traps closely approximate the quadrupolar potential, and (b) the additional ion-ion Coulomb "space-charge" potential in actual experiments is evidently approximately quadrupolar.[2]

Nevertheless, collisions can shift an FT/ICR spectral peak, as shown in Figure 1. The Fourier transform of a causal, linearly-polarized (i.e., mathematically real) exponentially-damped sinusoidal signal yields the usual spectral peak at positive frequency, but also a mirror-image peak at negative frequency. Ordinarily, we ignore the negative-frequency peak, because it has no direct physical significance. However, as the collision rate increases (so that the frequency-domain peak(s) broaden), the "tail" of the negative-frequency peak shifts the positive-frequency spectral peak maximum slightly to lower frequency.

For a magnitude-mode Lorentzian spectral peak, the frequency shift, $\Delta\omega = 2\pi\Delta\nu$, resulting from ion-molecule collisions can be shown to be

$$\Delta\omega \approx -1/(2\omega_0\tau^2) \approx -\xi^2/(2\omega_0) \qquad [2]$$

in which $\tau = 1/\xi$ is the time-domain exponential damping constant, and ν_0 is the observed ICR frequency in the absence of ion-molecule collisions.

The remarkable result of this treatment is that the usual approximations lead to a four-term mass calibration (Eq. 3).

$$m = A/\nu + B/\nu^2 + C/\nu^3 + (BC)/(A\nu^4) \qquad [3]$$

Although there are two new terms, there is only one new parameter, C, which can be obtained from the FT/ICR magnitude-mode peak width in the high-pressure limit.[3] Several interesting conclusions follow from Figure 1. First, most of the frequency shift arises from overlap of the dispersion components of the magnitude-mode spectrum. Thus, phasing of the spectrum to give absorption-mode display reduces collision-induced frequency shifts to a negligible level. Second, the negative-frequency peak is a direct consequence of linearly-polarized detection. Thus, quadrature detection also eliminates collision-induced shifts, by detecting a circularly-polarized signal with no negative-frequency component.

We have compared iterative best-fits (with various weight factors) of actual ICR mass/frequency data to Eqs. 1 and 3. The new 4-term mass calibration law typically improves mass calibration accuracy by a factor of ~2 over the 2-term law. Moreover, the 4-term fit gives random errors throughout the mass range, whereas the 2-term equation typically gives systematic mass errors (e.g., positive at the high end of the calibrated mass range).

The authors thank W. J. van der Hart for helpful discussions. [This work was supported by grants (to A.G.M.) from N.S.F. CHE-8721498 and The Ohio State University.]

1. Ledford, E. B., Jr.; Rempel, D. L.; Gross, M. L. *Anal. Chem.* **1984**, *56*, 2744-2748.
2. Jeffries, J. B.; Barlow, S. G.; Dunn. G. H. *Int. J. Mass Spectrom. Ion Proc.* **1983**, *54*, 169-187.
3. Marshall, A. G.; Comisarow, M. B.; Parisod, G.; *J. Chem. Phys.* **1979**, *71*, 4434-4444.

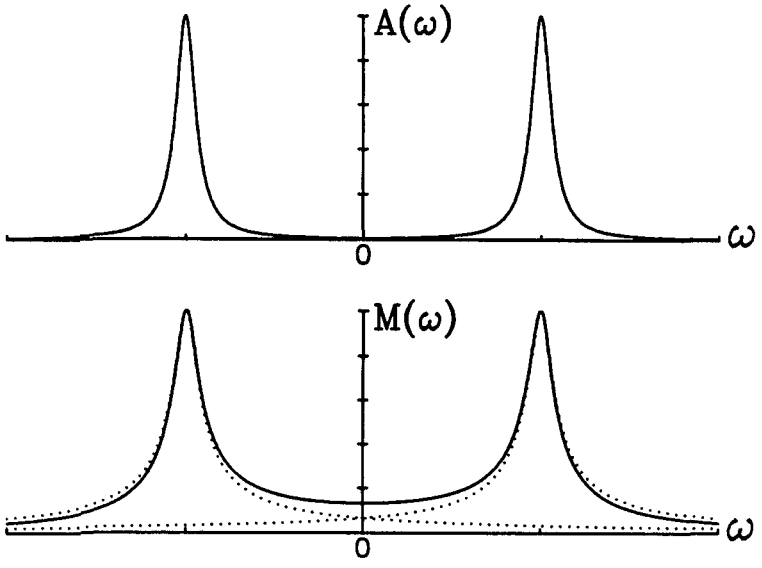

Figure 1. Absorption-mode (top) and magnitude-mode (bottom) spectra obtained by Fourier transformation of a linearly-polarized exponentially damped sinusoidal time-domain signal. Although the negative-frequency peak has no direct significance, its spillover into the positive-frequency spectrum can shift (to lower frequency) the maximum of the positive-frequency peak. In each spectrum the dotted curves represent the right- and left-circularly polarized components, and the solid curves represent the linearly polarized spectrum. Practically speaking, the shift is negligible in absorption-mode, but can reach several ppm in magnitude-mode.

Presented at the 36th ASMS Conference on Mass Spectrometry and Allied Topics
June 5-10, 1988, San Francisco, CA

EXTENSION OF LOWER MASS LIMIT IN DIRECT-MODE FT/ICR MASS SPECTROMETRY BY MEANS OF ALTERNATE DELAY SAMPLING

Francis R. Verdun, Tom L. Ricca, and Alan G. Marshall

Department of Chemistry (and Dept. of Biochemistry)
The Ohio State University
120 W. 18th Avenue
Columbus, OH 43210

According to the Nyquist theorem, the highest signal frequency which can be represented without foldover (aliasing), in a Fourier transform frequency-domain discrete spectrum is one half of the time-domain sampling frequency. For example, since ion cyclotron resonance (ICR) frequency is inversely related to ionic mass-to-charge ratio m/z, the highest ICR frequency (corresponding to the lowest correctly represented m/z) in direct-mode FT/ICR mass spectrometry is restricted to one-half of the maximum sampling frequency, or m/z ~18 at ~3.058 T, for a maximum sampling frequency of about 5.2 MHz. We now show that interleaved addition of two digitized time-domain transient signals, one of which is delayed by one-half of one sampling period with respect to the other, generates a time-domain discrete waveform which is indistinguishable from a single waveform produced by sampling at twice the original sampling rate. Thus, provided that the two time-domain transients have (or have been normalized to) the same magnitude, one can double the Nyquist-limited frequency range by means of interleaved sampling.. If the sampling period is divided into three or more equal parts, with interleaved addition of three or more correspondingly delayed transients, the same method can further increase the upper frequency limit. With respect to signal-to-noise ratio, the interleaving method is equivalent to two-fold oversampling of the time-domain signal.

Experimental

FT/ICR spectra were acquired with a Nicolet FTMS-1000, operating at 3.058T [1]. Ions were produced by electron impact in a standard FT/ICR event sequence. Methane and perfluoro-tri-n-butylamine were introduced at partial pressures of 10^{-9} torr.[2] Software-programmed delays proved suitable for testing the method at relatively low sampling rates (<500 kHz), but were not applicable at high sampling rate. The maximum speed of our Nicolet analog-to-digital converter (ADC) is 1/3 of 16 MHz, or 5.33×10^6 samples per second. Thus, extension of the Nyquist limit by means of interleaved sampling requires a delay increment of ~100ns. Unfortunately, the smallest programmable delay increment for the Nicolet 1280 hardware is 8 cycles of an 8 MHz clock, or 1 ms. Therefore, the receiver amplifier output was routed to an external module, through which the signal was either passed without further delay, or manually switched through a series of linked gates of appropriate duration. The different time-domain digitized transients were stored in memory and interleaved afterwards by a simple Fortran routine. No noticeable artifacts were detected during our experiments. Simulations showed that differences of less than 5% (in delay time or magnitude) between the two time-domain data sets are not critical.[2]

Results

In FT/ICR spectrum A, singly-charged ions from 11.73 to 3000 μ were coherently excited and their composite time-domain signal was sampled directly at 4 MHz (to give a Nyquist low-mass limit of 23.47 μ). The ICR signals arising from ions with m/z values below that limit appear folded-over into the displayed mass range.

Spectrum B was produced by FFT of a data set formed by interleaving the time-domain data of the previous Figure with a second time-domain data set acquired with an additional delay of 125 ns between the excitation and reception events. ICR spectral peaks which were folded-over in spectrum A are now displayed at their correct frequencies (and m/z-values). The expanded scale inset reveals the expected CH_2^+ at m/z = 14.015 μ and a small artifact peak due to imaging of CF_3^+ at an apparent m/z = 14.145.

Conclusion

For a given maximum ADC rate, the FT/ICR lower mass limit varies directly with magnetic field strength. For example, at 7.0 T, our maximum ADC rate of 5.33 MHz would limit the lowest observable (without foldover) m/z to ~43 μ. For that same ADC maximum rate, interleaved acquisition can reduce the lower mass limit by a factor of 2 (or 4 or more). Thus, the present method offers a useful alternative to quadrature detection (see paper # ROC 1115).

This work was supported by grants (to A.G.M.) from the U.S. Public Health Service (N.I.H. GM-31683), the National Science Foundation (8721498), and The Ohio State University. F.R.V. is supported by an Ohio State University Postdoctoral Fellowship.

1. Nicolet Instrument Co., P.O. Box 4508, Madison, WI 53711-0508.
2. Verdun, F. R.; Ricca, T. L.; Marshall, A. G. *Appl. Spectrosc.* **1988**, 42, 199-203.

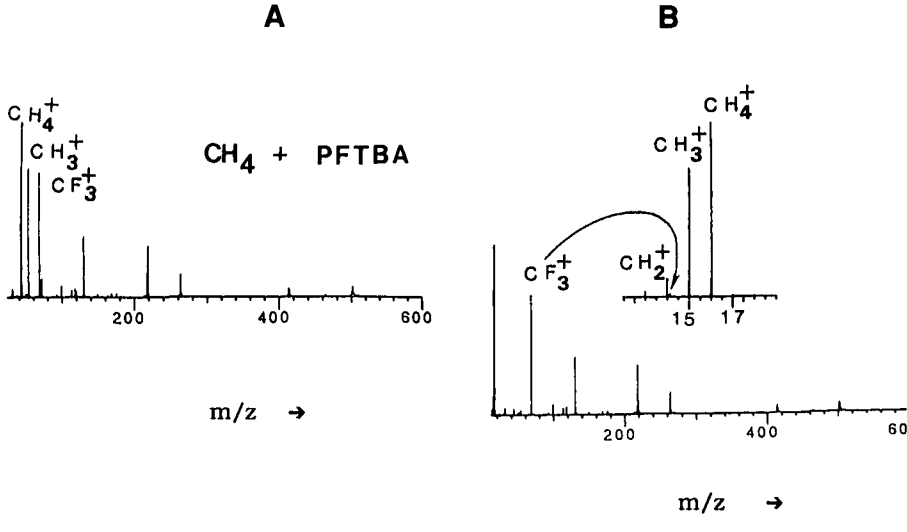

Presented at the 36th ASMS Conference on Mass Spectrometry and Allied Topics
June 5-10, 1988, San Francisco, CA

UPPER MASS AND ENERGY LIMITS IN FT/ICR MASS SPECTROMETRY: DESIGN AND TESTING OF NEW ION TRAPS

Peter B. Grosshans#, Mingda Wang#, Tom L. Ricca#,
Edward B. Ledford, Jr.@, and Alan G. Marshall#

#Dept. of Chemistry (and Dept of Biochemistry)
The Ohio State University
120 W. 18th Avenue
Columbus, OH 43210

@ICR Research Associates, Inc.
201 N. 8th Street, Suite 201
Lincoln, Nebraska 68508

In Fourier transform ion cyclotron resonance (FT/ICR) mass spectrometry, ions are conventionally detected in a single-section ion trap typically consisting of two end cap electrodes and four side plate electrodes. Up to now, it has generally been assumed that the optimal electric field profile in an FT/ICR ion trap is the quadrupolar potential provided by hyperbolically curved side and end plates.[1] We have shown that such a design does in fact reduce the variation of ICR frequency with ion cyclotron orbital radius.

However, the same end-cap d.c. voltage that traps the ions from escaping along the magnetic field direction also forces ions radially outward, thereby setting an absolute limit to the highest m/z value observable by FT/ICR. The ultimate upper mass limit is the m/z value at which a stable orbit no longer exists (i.e., the quadrupolar electric outward radial force is larger than the Lorentz inward radial force, independent of initial ion velocity).[1] That upper mass limit is shown as the 100%-ejection curves in Figure 1, for three representative magnetic field strengths. However, in this work, we note that a more severe constraint is that the ICR orbital radius of a thermal ion of sufficiently high mass may exceed the transverse radius of the ion trap (~2-5 cm). Since thermal ions have a Boltzmann distribution in speeds, a calculable fraction of ions of a given m/z will be ejected at any given trapping potential and magnetic field strength. As a practical guide, Figure 1 also shows the effective upper mass limit for which 99% of the (room temperature) thermal ions of that m/z will have ICR orbital radii less than the transverse dimension of the trap. The new upper mass limit should be a better practical estimate, since a trapped ion must be further excited by ~1 cm in radius in order to be detected. The present results go far toward explaining why FT/ICR sensitivity and mass resolution for ions of high m/z fall well below the values extrapolated from those observed for ions of low m/z.

We are therefore led to consider non-quadrupolar electric potentials for FT/ICR ion traps. Figure 2 shows one of our recent designs, consisting of an elongated (6:1 aspect ratio) three-section cell, compared to a more conventional cubic cell. A plot of electric potential along the z-axis shows that the electric potential drops to less than 10 μV in the center of such a cell, when 1 V is applied to the two end plate electrodes! We have experimentally confirmed that electric field-induced ICR frequency shifts are significantly reduced when ICR detection is limited to the central field-free region of the three-section cell. These and other new ion trap designs will be discussed in an upcoming publication.

This work was supported by grants (to A.G.M.) from N.S.F. CHE-8721498 and The Ohio State University.

1. Jeffries, J. B.; Barlow, S. G.; Dunn. G. H. *Int. J. Mass Spectrom. Ion Proc.* **1983**, *54*, 169-187.
2. Ledford, E. B., Jr.; Rempel, D. L.; Gross, M. L. *Anal. Chem.* **1984**, *56*, 2744-2748.

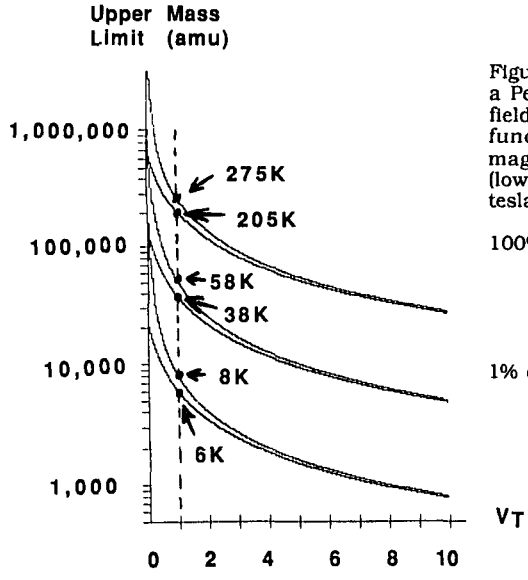

Figure 1. Upper mass limit for an ion in a Penning trap (i.e., quadrupolar electric field and constant magnetic field), as a function of trapping voltage, V_T, for magnetic field strengths of 1.2 tesla (lowermost pair of curves) 3.0, and 7.0 tesla (uppermost pair of curves)

100% ejection: highest m/z for which an ion has a stable cyclotron orbit. The upper value for each pair of curves is the upper mass limit for V_T = 1 V.

1% ejection: highest m/z for which the ICR orbit does not intersect the cell detector plates, for 99% of thermal room-temperature (25 °C) ions.

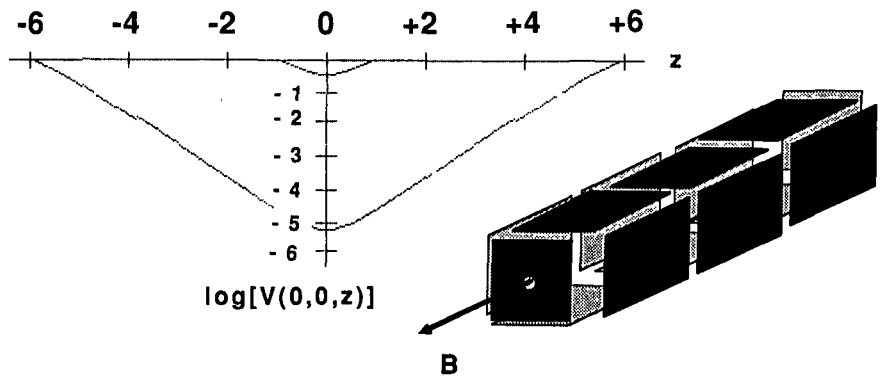

Figure 2. Cubic and elongated (6:1 aspect ratio) ICR ion traps of 1" square cross-section (right) and a semi-log plots (left) of z-axis electric potential, V(0,0,z) in V, versus axial distance, z, measured from the center of the cell. Note the 10^5-fold reduction in electrostatic potential (and thus substantially reduced "trapping" shift in ICR frequency) at the center section of the three-section cell compared to the center of the cubic cell.

Presented at the 36th ASMS Conference on Mass Spectrometry and Allied Topics
June 5-10, 1988, San Francisco, CA

HARTLEY TRANSFORM ION CYCLOTRON RESONANCE MASS SPECTROMETRY

Christopher P. Williams and Alan G. Marshall

Dept. of Biochemistry (and Dept. of Chemistry)
The Ohio State University
120 W. 18th Avenue
Columbus, OH 43210

In FT/ICR mass spectrometry, a linearly-polarized (i.e., mathematically "real") time-domain signal, f(t), is converted to its corresponding frequency-domain spectrum, F(v) (which is re-scaled to give a mass spectrum), by use of a complex Fourier transform.[1] The complex FT and its inverse differ by a sign in the exponent:

$$F(v) = \int_{-\infty}^{+\infty} f(t)\, e^{-2\pi i v t}\, dt = \int_{-\infty}^{+\infty} f(t)\, [\cos(2\pi v t) - i \sin(2\pi v t)]\, dt$$

$$f(t) = \int_{-\infty}^{+\infty} F(v)\, e^{2\pi i v t}\, dv = \int_{-\infty}^{+\infty} F(v)\, [\cos(2\pi v t) + i \sin(2\pi v t)]\, dv$$

The same spectrum can be obtained without resorting to mathematically complex notation, by use of the "Hartley" transform, to give the Hartley spectrum, H(v):

$$H(v) = \int_{-\infty}^{+\infty} f(t)\, [\cos(2\pi v t) + \sin(2\pi v t)]\, dt = \int_{-\infty}^{+\infty} f(t)\, \mathrm{cas}(2\pi v t)\, dt$$

The Hartley spectrum (see Figure) can thus be thought of as the sum of the usual absorption and dispersion spectra, and contains the same information as the conventional complex FT spectrum. For example, the real and (negative of the) imaginary components of the FT spectrum may readily be recovered from the even and odd components, E(v) and O(v), of the Hartley spectrum:

$$E(v) = \frac{H(v) + H(-v)}{2} = \int_{-\infty}^{+\infty} f(t) \cos(2\pi v t)\, dt$$

$$O(v) = \frac{H(v) - H(-v)}{2} = \int_{-\infty}^{+\infty} f(t) \sin(2\pi v t)\, dt$$

Similarly, the magnitude and phase spectra, M(v) and $\phi(v)$, may be computed as easily from the HT spectrum as from the FT spectrum:

$$M(v) = \sqrt{\frac{H(v)^2 + H(-v)^2}{2}} \quad ; \quad \phi(v) = \arctan\left[\frac{-O(v)}{E(v)}\right] = \arctan\left[\frac{H(-v) - H(v)}{H(v) + H(-v)}\right]$$

The Hartley transform is interesting for both conceptual and computational reasons. The fundamental principle is that cosine and sine are already orthogonal functions; therefore, there is no need to separate them as the real and imaginary parts of a complex number. Stated another way, if the Fourier transform gives the projection of a frequency-domain vector (length = magnitude and angle = phase) onto two orthogonal (cosine and sine) axes, then the Hartley transform is the projection of that same vector onto a single axis bisecting the sine and cosine axes:

$$\mathrm{cas}(\theta) = \cos(\theta) + \sin(\theta) = \sqrt{2} \cos[\theta - (\pi/4)] = \sqrt{2} \sin[\theta + (\theta/4)]$$

It is also interesting to note that, unlike the Fourier transform, the Hartley transform and its inverse are identical in form:

$$f(t) = \int_{-\infty}^{+\infty} H(\nu)\, \mathrm{cas}(2\pi\nu t)\, d\nu$$

For real data, a complex FFT takes twice as long as a (real) FHT, when both are similarly optimized (e.g., precalculation of trigonometric identities). However, one should be aware that it is possible to construct an FFT algorithm for real data, in which the original N time-domain (real) data points are first separated ("shuffled") into two halves consisting of the odd-numbered and even-numbered data points. The two time-domain data halves are then treated as real and imaginary parts of a complex data set, transformed by the conventional complex FFT, and the final frequency-domain spectrum recovered from the result. For a real data set, such a "real FFT" algorithm also runs twice as fast as a complex FFT. We have confirmed (on an Atari 1040 ST computer, 8 MHz, 1 megabyte RAM, 68000 processor) that the Bracewell radix-2 FHT[2] is essentially the same in computational speed to a similarly optimized radix-2 FFT, for real data sets from 1K to 8K in size. We have also implemented the FHT on our Nicolet 1280 computer and applied it to experimental time-domain ICR transients to obtain *magnitude-mode spectra identical to those obtained by FFT.*

[This work was supported by grants (to A.G.M.) from N.I.H. GM-31683 and The Ohio State University.]

1. Marshall, A. G.; Acc. Chem. Res. **1985**, 18, 316-322.
2. Bracewell, R. N.; "The Hartley Transform" (Oxford Univ. Press, NY, 1986).

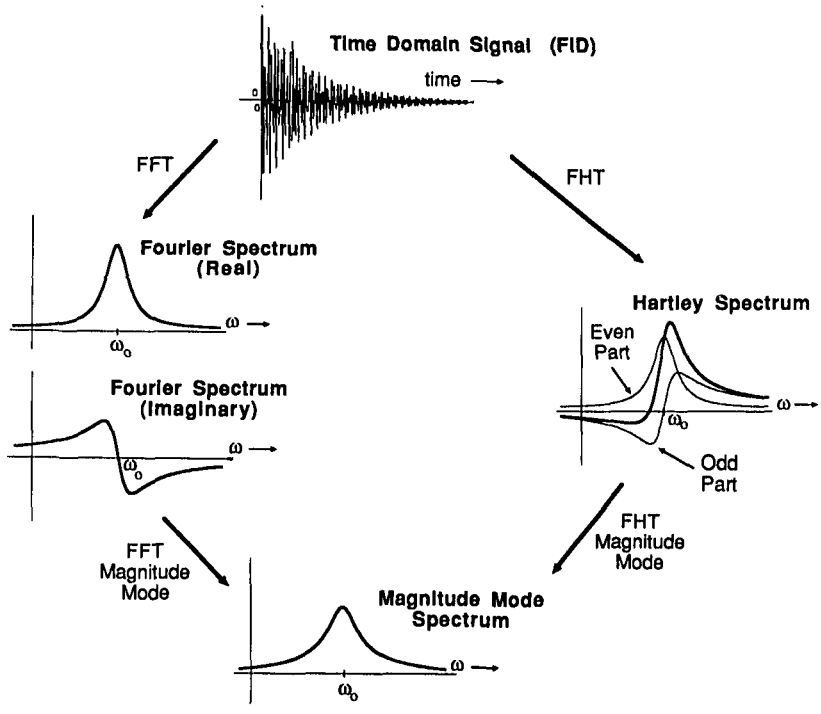

Presented at the 36th ASMS Conference on Mass Spectrometry and Allied Topics
June 5-10, 1988, San Francisco, CA

HIGH-RESOLUTION MULTIPLE ION SIMULTANEOUS MONITORING BY MEANS OF MULTIPLE FOLDOVER FT/ICR MASS SPECTROMETRY

Mingda Wang and Alan G. Marshall

Dept. of Chemistry (and Dept. of Biochemistry)
The Ohio State University
120 W. 18th Avenue
Columbus, OH 43210

In any form of Fourier transform spectrometry, the Nyquist criterion requires that a sinusoidal signal be sampled at least twice per cycle in order that its apparent frequency (after discrete FT) represent its true frequency. If the sampling frequency, $\nu_{sampling}$, is less than the true signal frequency, then the apparent peak frequency in the FT spectrum will be "folded over" into the displayed frequency range from $\nu = 0$ to $\nu_{sampling}$

In particular, for FT/ICR mass spectrometry[1], ultrahigh mass resolution requires a long time-domain data acquisition period, whereas coverage of a wide mass range requires a rapid time-domain sampling rate, if foldover is to be avoided. For typical FT/ICR data sets (e.g., 16K-256K time-domain data points), one is usually forced to choose between wide mass range (at relatively low resolution because of the limited number of data points per peak) and high mass resolution (over relatively narrow mass range, in order to define each peak position more precisely).

In general, high-resolution FT/ICR mass spectra are acquired in heterodyne mode over a narrow mass range, as shown in Figure 1 (middle). However, when the true ionic **mass-to-charge (m/z) values** (and thus the ICR frequencies) are known but the relative **abundances** of ions of different m/z are not (as in multiple-ion monitoring), then time-domain sampling at a frequency well below the Nyquist limit can "fold over" the ICR signals from ions of widely separated m/z-values into a single narrow band (and thus high-resolution) spectrum. Applications for intentional undersampling to induce foldover include:

(a) **Increased mass calibration precision**, by folding over low-mass calibrant peaks into a narrower mass range (with higher digital resolution).[2]

(b) **Extension of FT/ICR low-mass limit**. For example, Cody et al.[3] employed a single foldover to detect and identify ions whose m/z-values were too low (and whose ICR frequencies are therefore too high) to satisfy the Nyquist limit. Such procedures should be especially useful at higher magnetic field strength (e.g., 7 tesla).

(c) **High-resolution multiple-ion monitoring of ions of widely different m/z.**[4] For example (see Figure 2), we have produced a single direct-mode (i.e., no heterodyning) mass spectrum of an electron-ionized mixture of respiratory gases (H_2O, N_2, O_2, CO_2, N_2O) at a resolution sufficient to resolve CO from N_2 and CO_2 from N_2O. The number of foldovers (up to >1000) differs for different ions.

(d) **Isotopic resolution for ions of widely different m/z.** In gas-phase ion-molecule reaction kinetics and equilibria measurements, it is desirable to be able to resolve $(M+H)^+$ from the M^+ ions which contain one carbon-13, particularly when (as for unknown and reference bases of widely different basicity) the two ions are of comparable abundance.

Presented at the 36th ASMS Conference on Mass Spectrometry and Allied Topics
June 5-10, 1988, San Francisco, CA

This work was supported by grants (to A.G.M.) from the U.S. Public Health Service (N.I.H. GM-31683), the National Science Foundation (8721498), and The Ohio State University.

1. Marshall, A. G., *Acc. Chem. Res.* **1985**, *18*, 316-322.
2. Cody, R. B.; Kinsinger, J. A. *Anal. Chem.* **1986**, **58**, 670-671.
3. Cody, R. B.; Kinsinger, J. A.; Goodman, S. D. *Anal. Chem.* **1987**, *59*, 2567-2569.
4. Wang, M.; Marshall, A. G. *Anal. Chem.* **1988**, *60*, 341-344.

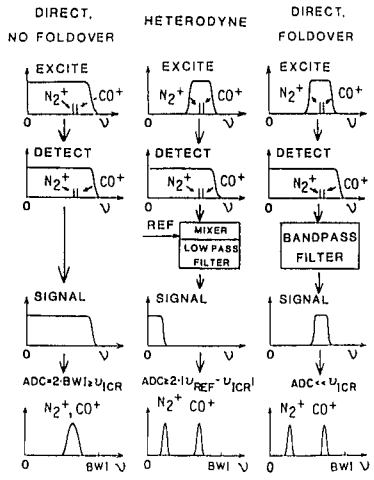

Figure 1. Three FT/ICR detection modes. In each case, the time-domain signal is sampled at a frequency of 2.BWI.

Left: Direct mode without foldover.

Middle: Heterodyne mode. The amplified ICR signal is mixed (i.e., effectively multiplied by) a reference sinusoid of nearly the same frequency. The mixer output, consisting of signals at the sum and difference of the ICR and reference frequencies sum and difference frequencies of the ICR and reference signals, is then passed through a low-pass filter to eliminate the higher (summed) frequency component. The desired (initially high-frequency) ICR signal is thereby converted to a relatively low frequency signal which can thus be sampled a low digitizing rate for a long time, to produce a narrow-range mass spectrum with high analog and digital resolution.

Right: Direct mode with foldover.

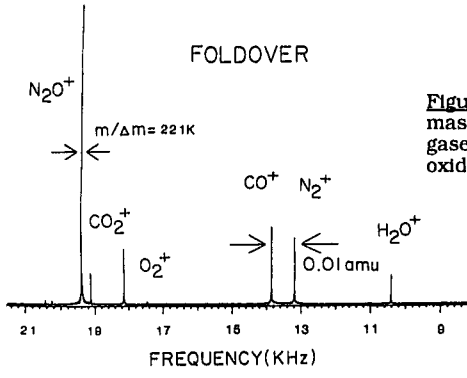

Figure 2. High-resolution foldover FT/ICR mass spectrum of a mixture of respiratory gases with carbon monoxide and nitrous oxide general anesthetic.

Presented at the 36th ASMS Conference on Mass Spectrometry and Allied Topics
June 5-10, 1988, San Francisco, CA

RESOLUTION IMPROVEMENT IN FTMS BY HARMONIC DETECTION

Y. Pan, D.P. Ridge, Alan L. Rockwood

Department of Chemistry, Univ. of Delaware, Newark, DE 19716

Recently we have developed a technique for obtaining higher resolution in an ion cyclotron resonance (ICR) mass spectrometry by observing harmonic signals. The experiment has been done both in the continuous wave (CW) mass spectrometer and Fourier Transform mass spectrometer. In the CW experiment the second harmonic signal was detected and the resolution was shown to be two times better than the fundamental one[1]. On a Nicolet FTMS-2000 spectrometer the third harmonic signal was clearly observed and the resolution was three times better than the fundamental one. The harmonic signal is especially useful in resolving high mass peaks because it does not require increasing the magnetic field or acquisition time.

Harmonics originate in the fact that the field of the orbiting ions sensed by a finite electrode varies nonlinearly with distance. The signal detected is therefore not a pure sinusoidal wave and contains higher harmonics.

Figure 1 shows the fundamental, the third harmonic, the fifth harmonic and the seventh harmonic of the m/z 128 signal in naphthalene. In these spectra the linewidth is determined by the observation time. For each harmonic the width of the x axis is one amu. The improvement in resolution with harmonic order is evident. The enhanced resolution also comes at the cost of signal to noise ratio.

If the linewidth is determined by observation time or by collision frequency or other homogeneous mechanism, then the widths (δf) of all the harmonics are the same as that of the fundamental. Since the frequency (nf) of the nth harmonic is higher than that of the fundamental (f), the resolution will be correspondingly higher ($nf/\delta f$). The resolution increases in proportion with harmonic order. This is evident in Fig. 1.

A cell may be designed to optimize a particular harmonic[2]. An array of M receiving electrodes arranged to have D_{mh} symmetry can be used to detect certain harmonics selectively. The sum of the signals from all the electrodes will contain harmonics of order M, 2M, 3M, etc. If the sum of signals from alternating pairs of electrodes are subtracted from the sum of signals from the remaining electrodes, harmonics of order M/2, 3M/2, 5M/2, etc.(M must be even in this case). The two arrangements are indicated schematically in Fig 2.

1. Y. Pan, D. P. Ridge, J. Wronka and A. L. Rockwood, Rapid Commun. Mass Spectrom., 1987, 1, 120.

2. Y. Pan, D. P. Ridge and A. L. Rockwood, Int. J. Mass Spectrom. and Ion Proc., 1988, in press.

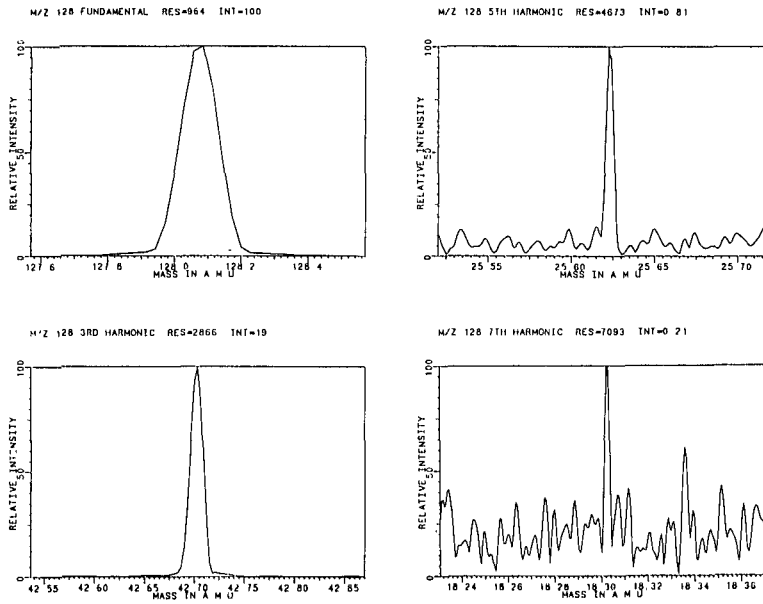

Figure 1

M = Number of Electrodes

M = 8

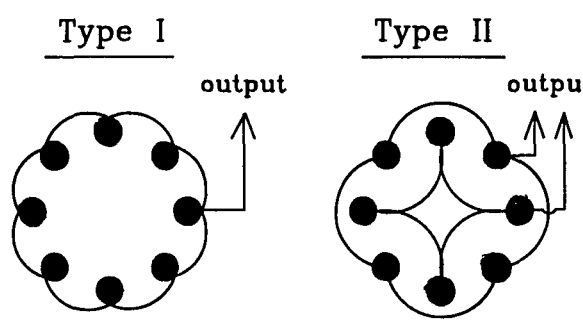

Figure 2

Presented at the 36th ASMS Conference on Mass Spectrometry and Allied Topics
June 5-10, 1988, San Francisco, CA

IMPROVED MASS RESOLUTION IN FOURIER TRANSFORM ION CYCLOTRON RESONANCE MASS SPECTROMETRY BY DATA FILLING

C.H. Watson and J.R. Eyler, Department of Chemistry,
University of Florida, Gainesville, Florida 32611

This work presents a new method of data processing for Fourier transform ion cyclotron resonance (FTICR) mass spectrometry that results in improved mass resolution for a time-domain data set of given size. The time-domain signal x(t) arises from the superposition of n periodic signals, one for each ionic species present, all having a characteristic period (frequency). A single period of the resulting time-domain waveform x(t) of length (t_2 - t_1) not only represents the signal over the interval t_1 to t_2, but it also represents x(t) for all values of t. One such period contains all the information necessary to obtain the desired frequency-domain spectrum. In order to obtain improved resolution, a single period can be used as a basis to reconstruct or extend the time-domain signal x(t) to any desired length yielding much improved frequency resolution. This technique of signal extension will be referred to as data-filling.

The main benefit of the technique is to extend the length of transient signals that otherwise would decay rapidly with time or in cases where the total acquisition time is limited. High resolution is normally obtained by operating the FTICR mass spectrometer in the heterodyne mode, allowing transient image current signals to be digitized for extended lengths of time. Unfortunately, during long acquisition times ion/neutral collisions dephase the ion's motion resulting in a loss of signal and ultimately limiting the resolution. In some cases the signal decay is not significant over the acquisition time, but the resolution is limited by the finite amount of fast digitizer memory available. Especially when working at lower magnetic fields much longer data acquisition times are desired to compensate for the lower magnetic field values.

Once the time-domain spectrum has been recorded the length of one period must be determined. Initial results were obtained by manual inspection of the time domain spectrum. This approach is not practical for rapid analysis or for when the signal decays rapidly and exhibits a generally noisy appearance. If the periods of the individual signals are known in advance, then the period of the resulting waveform is given by the lowest common multiple of periods. However, when a number of components comprise the time domain waveform calculation of the lowest common multiple for the n periods can be time-consuming. Pattern recognition techniques are currently used to determine the overall periodicity.

The periodicity is determined by the computer using a simple search routine. A pattern vector is obtained by assigning each time domain point a value of one or zero depending on the sign of each point. This reduces the problems associated with slowly decaying transient signals. Feature extraction is accomplished by assigning a portion of the pattern vector as a search interval and searching the rest of the pattern vector for repeating units. Care must be taken when selecting the search interval in order to avoid aliasing. The search interval is typically chosen as a fraction (1/10 to 1/20) of the total number of points.

After the period has been determined a reconstruction of the time domain waveform x(t) is possible. The heterodyne time-domain spectrum of CO and N_2 is shown in Figure 1. A portion of the original data one period in length is extracted as shown in Figure 1C. These data are duplicated and added together (see figures 1D and 1E) phase consistently. This process is repeated and the reconstructed data set doubles in size with each step. The size of the reconstructed data set is limited only by the amount of computer memory available. The FWHM resolution for CO has been increased from 78000 for the original data to 8,200,000 for the data-filled spectrum.

Problems arise when the period does not fall on a integer multiple of the digitizer time step. This can cause a phase discontinuity resulting in distorted peak shapes after Fourier transformation or in "ringing", the presence of additional low amplitude frequency components through the frequency spectrum. The effects of such a discontinuity can be lessened by digitizing at a higher rate. Figure 2 shows a data-filled mass spectrum for carbon monoxide and nitrogen identical to that shown in Figure 1 except that the transient signal was sampled at twice the digitization rate. Note in Figure 2 the "ringing" observed in Figure 1 is absent. Further increases in resolution are possible by further data-filling to larger-sized data sets.

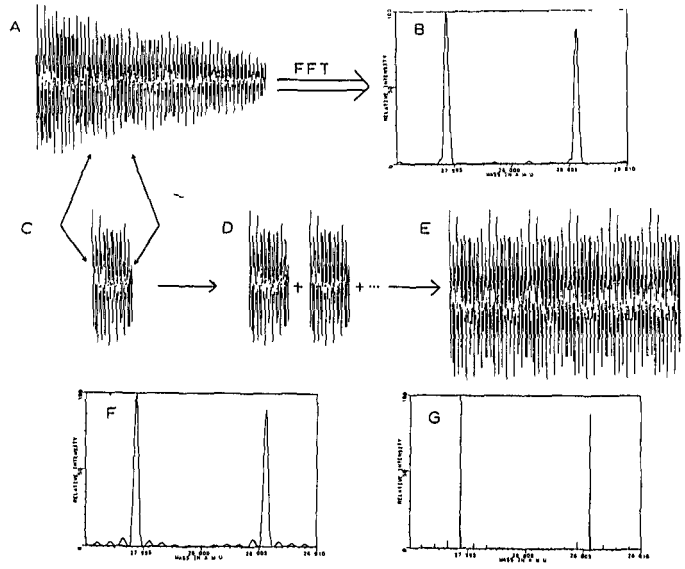

Figure 1.
A) A 512 point heterodyne time-domain spectrum of CO and N_2.
B) Mass spectrum of CO and N_2 obtained by Fourier transformation.
C) A representative portion of the data is extracted to serve as a basis for data-filling.
D) Data-filling of the time-domain waveform is accomplished by duplicating the basis with phase continuous addition of the data.
E) A 512 point time-domain waveform obtained by data-filling.
F) Mass spectrum of CO and N_2 obtained from a 512 point data-filled time-domain spectrum.
G) Mass spectrum of CO and N_2 obtained from a 65536 point data-filled time-domain waveform.

Figure 2.
Mass spectrum of CO and N_2 obtained by data-filling the time-domain spectrum to 65536 points prior to Fourier transformation. The FWHM resolution for the Co and N2 peaks is 8 X 10^6.

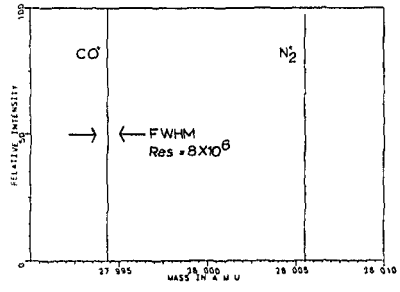

Presented at the 36th ASMS Conference on Mass Spectrometry and Allied Topics
June 5-10, 1988, San Francisco, CA

TWO DIMENSIONAL FTMS

M. Bensimon, T. Gäumann, J. Rapin and G. Zhao
Department of physical chemistry
Federal School of Technology
CH-1015 Lausanne, Switzerland

In Fourier Transform Mass Spectrometry (FTMS), the movement of the ions can be treated in an analogous manner to the spin precession in the "NOESY" 2D-NMR technique. The possibility of easily changing the pulse sequence on a standard instrument with software modifications only, allows the established NMR techniques to be carried over to the field of mass spectrometry. The two dimensional Fourier transform mass spectrometer [2D-FTMS] permits one to measure in one experiment all the ion-molecule reactions and fragmentations that take place in a mass spectrometer cell during a reaction period varying between one ms and several seconds. The ion movement is shown in Fig. 1 where a and c are the two exciting pulses, separated by the variable time t_1, (b). d corresponds to the resulting ion amplitude. During this time the ions may react, photofragment, etc. The modulation of the ion amplitude is shown in Fig. 2 for the reaction of CH_4^+ with CH_4 : the resulting CH_5^+ carries the same modulation frequency as CH_4^+, contrary to CH_3^+. Heterodyne (high resolution) [1] and broadband [2] mode are possible in both dimensions as far as the capacity of the memory will allow. Ion-molecule reactions in mixtures of differently labelled toluenes show one application of the method. In a relatively short time a good overview of the different type of reactions can be obtained. Irradiation with a CO_2-laser (10 μm) allows to simulate metastatable decays in an ICR spectrometer. For the moment, the main difficulties are the incompatibility of the MS-software with 2D, the conditions for an optimum signal-to-noise ratio without excessive harmonics and the choice ot the most useful presentation of the results.

References

[1] P. Pfändler, G. Bodenhausen, J. Rapin, R. Houriet and T. Gäumann : "Two-dimensional Fourier Transform Ion Cyclotron Resonance Mass Spectrometry", Chem. Phys. Letters 138, 195-200 (1987)

[2] P. Pfändler, G. Bodenhausen, J. Rapin, M.-E. Walser and T. Gäumann, "Broadband Two-Dimensional FT Ion Cyclotron Resonance", J. Am. Chem. Soc. 110 (Sept. 15, 1988)

Presented at the 36th ASMS Conference on Mass Spectrometry and Allied Topics
June 5-10, 1988, San Francisco, CA

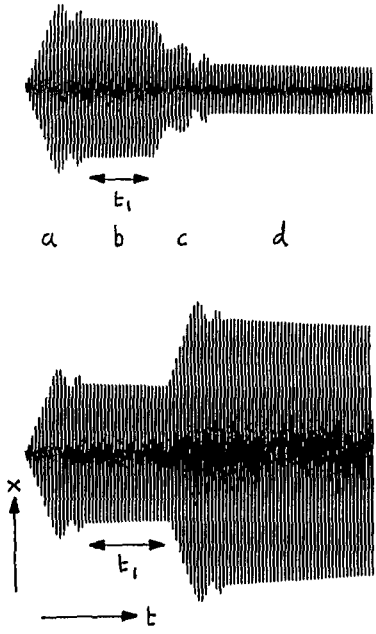

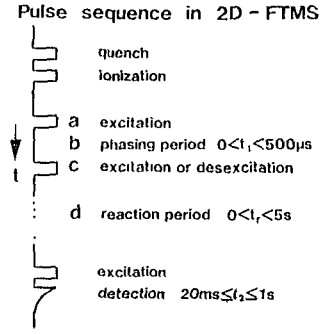

Figure 1

$$CH_4 + e^- \rightarrow CH_4^{+\cdot}, CH_3^+$$

$$CH_4^{+\cdot} + CH_4 \rightarrow CH_5^+ + CH_3^{\cdot}$$

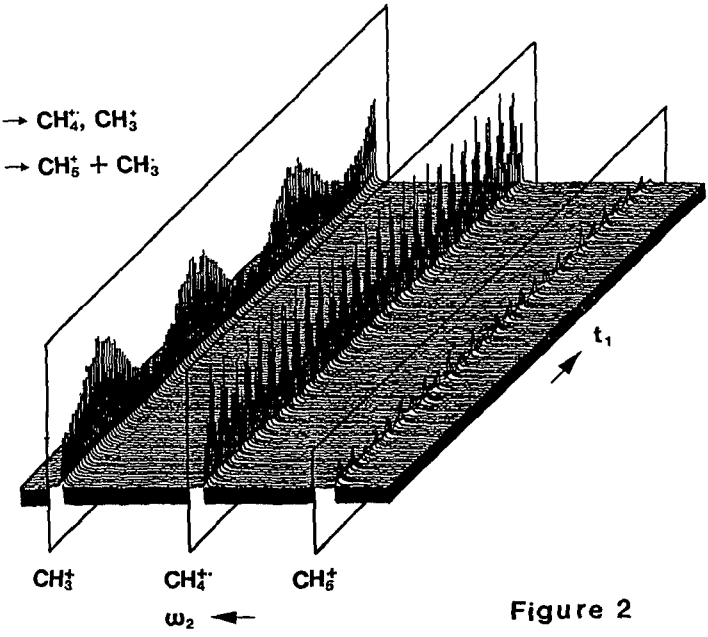

Figure 2

Presented at the 36th ASMS Conference on Mass Spectrometry and Allied Topics
June 5-10, 1988, San Francisco, CA

AN ION TRAJECTORY MODEL FOR FOURIER TRANSFORM ION CYCLOTRON RESONANCE MASS SPECTROMETRY.

B.A. Hearn, C.H. Watson, G. Baykut, and J.R. Eyler
Department of Chemistry, University of Florida
Gainesville, Florida 32611.

An ion trajectory model was developed from an analytical solution of the equations of motion for Fourier transform ion cyclotron resonance mass spectrometry in two dimensions for an ion subjected to a swept-frequency excitation. The motion of ions as a function of time was calculated using various excitation waveforms, which provided the final coherent radius of an ensemble of ions, the center of motion of the ensemble of ions, and the number of ions that exceeded the cell boundaries. The model allowed the randomization of the phase of the initial thermal velocity of each ion with respect to the excitation waveform. The magnetic field, the number of ions for each ensemble, the mass of the ions, and various ion excitation parameters could be varied.

As an example of the utility of the model, the x-y motion for m/z 100 using a chirp of 12.5 volts from 0 to 944128 Hz consisting of 4096 steps over a time period of 0.5 ms is shown in figure 1. Initially, the ion has a small radius from its thermal velocity. Due to the changing frequency, each step is not broadcast for an entire period. Early in the chirp excitation, as the low frequency voltages are output, the average potential the ion experiences is not zero, so the ion drifts in the y direction due to the forces from crossed electric and magnetic fields. This drift is not desirable because it limits the maximum radius that the ion can be excited to without being ejected. The radius should be as large as possible because in FT ICR mass spectrometry, the signal is proportional to the radius of the ion[1]

$$v = kNq^2rB / m$$

where v is the instantaneous ICR voltage signal, k is a constant, N is the number of excited ions, q is the charge of the ion, r is the radius of the ensemble of ions, B is the magnetic field, and m is the ion's mass. Changing the chirp's lowest frequency to 47972 Hz enabled an 18 volt excitation waveform to be broadcast without ejecting the ions. The result was a larger radius, thus a larger signal.

A comparison of chirp excitation with SWIFT[2] excitation was performed, with an excitation window chosen for a range of m/z 100 to 500 for the two techniques. The mass cutoff for the two techniques, shown in figure 2, indicates that SWIFT gives much more selective excitation. The model was also used to give an upper limit for the excitation voltage for a pulsed excitation, which was approximately 20% higher than that determined experimentally.

[1]Comisarow, M.B., J. Chem. Phys 69(9), 1978, 4097.
[2]Marshall, A.G., Wang, T.-C.L., Ricca, T.L. J Amer Chem Soc 1985 107 7893.

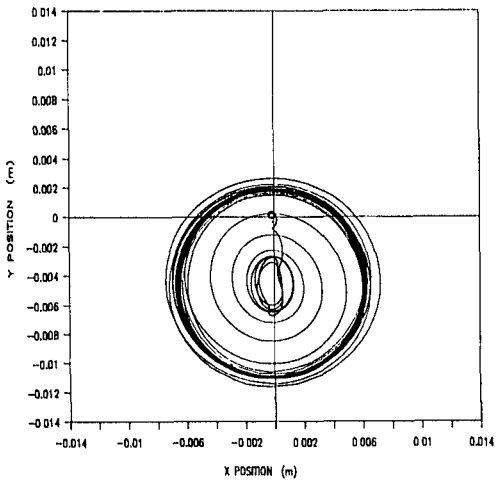

Figure 1. The x-y motion for an ion of m/z 100 at 1 T excited with a chirp waveform from 0 to 944128 Hz consisting of 4096 steps over 0.5 ms at 12.5 volts. Note the large drift of the center of motion of the ion.

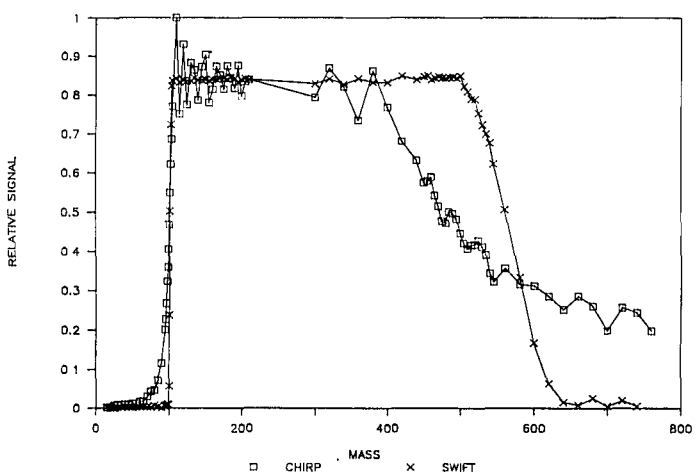

Figure 2. The cutoff for SWIFT and chirp waveforms over a range of m/z 100 to 500. The SWIFT excitation allows a much more selective excitation over the desired range of masses.

Acknowledgements:
This material is based upon work supported under a National Science Foundation Graduate Fellowship and by a grant from the Department of the Navy.

Presented at the 36th ASMS Conference on Mass Spectrometry and Allied Topics
June 5-10, 1988, San Francisco, CA

STUDIES OF ION MOTION IN AN ICR CELL BY DUAL CELL FTMS

J.P. Honovich and S.P. Markey
National Institute of Mental Health, Bethesda, Maryland 20892

The Nicolet FTMS-2000 contains two nearly identical cubic (1 7/8") ICR cells separated by a common trap plate (conductance limit). A 2 mm hole allows ion transfer between the differentially pumped cells. The trapping oscillation (Z axis motion) is studied by creating ions by electron impact ionization in the high pressure source cell followed by pulsing the common trap plate to ground potential. Ions are then free to move on a new potential surface over both cells. After the variable transfer period the ion population in either the source or analyzer cell is sampled.

Figure 1 shows the experimental results for the detection of m/z 128 (naphthalene) in the analyzer cell as a function of grounding time on the conductance limit. We have worked on modeling three features of these curves: 1) peak locations (transfer time), 2) shape of peaks, and 3) approach to a 50% randomization.

A numerical integration model (4th order Runge-Kutta) allows ions to be formed in a quadrupolar source cell followed by a transfer period where ions are allowed to oscillate on a specified potential surface over both cells. The potential V(z) is represented by the form $V = K_1Z^2 + K_2Z^4$ where the higher order term is required due to the nonharmonic nature of the dual cell when the conductance limit is grounded. Ions are created in the source cell with a position and velocity distribution using the aid of random number generator. Theoretical transfer curves use up to 800 initial ions and their z axis position is calculated as a function of transfer time.

The potential along the centerline z axis in a cubic six-sided box with one non-zero face voltage (V_t) can be calculated as below.

$$V(z) = \sum_{n=1,3,\ldots}^{\infty} \sum_{m=1,3,\ldots}^{\infty} \frac{16V_t \operatorname{Sinh}(\gamma z)}{mn \operatorname{Sinh}(\gamma c)} \operatorname{Sin}(n\pi/2) \operatorname{Sin}(m\pi/2)$$

$$\text{where} \quad \gamma = \sqrt{n^2 + m^2}$$

The cell potential was calculated at 5% intervals along the cell axis and a simplex curve fitting routine gave the following best fit (K_1 = .55, K_2 = .45). Using this potential in the numerical model yielded the transfer curve shown in Figure 2. This model gives good results for the transfer time but is apparently "too anharmonic" by comparison with the experimental results shown in Figure 1, in terms of early randomization between cells.

Figure 3 shows the calculated effect of increasing the anharmonic z^4 term. By inspection, the experimental results shown in Figure 4 for m/z 78 from benzene are most consistent with calculated results using K_1 = .75, K_2 = .25 as in Figure 5. This agreement between the calculated and observed results allows the use of K_1 = .75, K_2 = .25 to define the effective cell potential experienced by the ions.

CONCLUSIONS OF MODEL

1) The ability to randomize ions made in the source cell is highly dependent on the anharmonicity, and hence, on the geometric dimensions of the ICR cell. 2) If rapid randomization is desired, as in the case of high losses through the conductance limit, one should lengthen (or narrow) the ICR cell. 3) If it is desired to keep the ion packet together the cell should be slightly shortened (or broadened). 4) This model gives a sensitive measure of the "effective" cell potential within the dual cell ICR.

Presented at the 36th ASMS Conference on Mass Spectrometry and Allied Topics
June 5-10, 1988, San Francisco, CA

Fig. 1

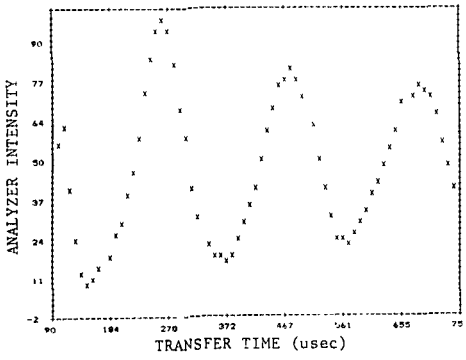

Fig. 2

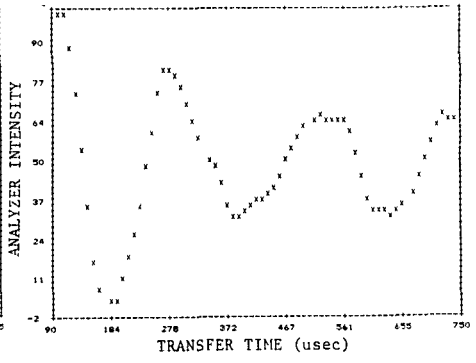

EFFECT OF Z^4 TERM

Fig. 3

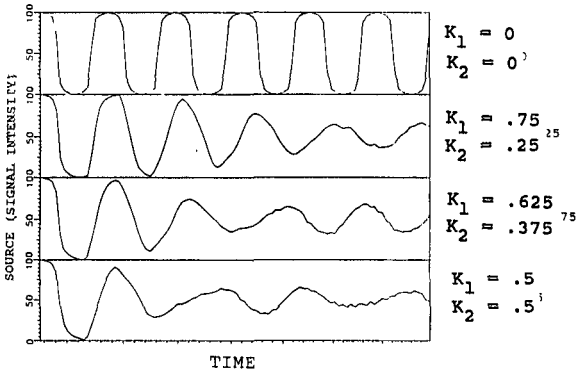

Fig. 4

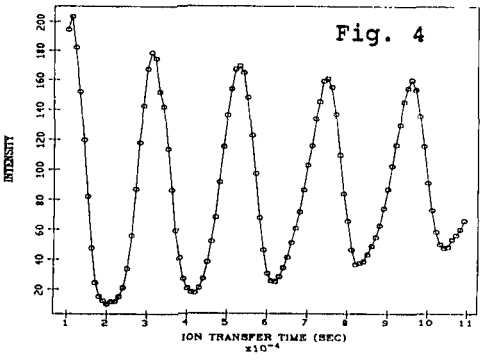

Fig. 5

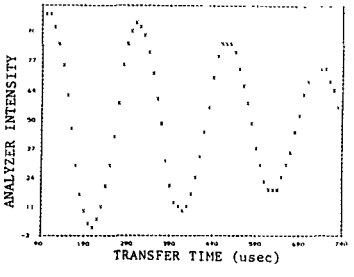

Presented at the 36th ASMS Conference on Mass Spectrometry and Allied Topics
June 5-10, 1988, San Francisco, CA

IMPROVEMENT OF THE ELECTRIC FIELD IN FT-ICR TRAPPED ION CELL.

Y. Naito and M. Inoue,
Department of Applied Physics and Chemistry, The University of Electro-Communications, Chofu-shi, Tokyo, 182 Japan.

In FT-ICR trapped ion cell ions are confined by a magnetic field and an electrostatic field. The conventional FT-ICR cell has a cubic or a cylindrical geometry and consists of six electrodes. The pattern of the electrostatic potential surfaces formed in the cell is quite complex and results in a complicated motion of ions. It is characterized by three periodic motions; cyclotron, magnetron and oscillation in the direction parallel to the magnetic field. The magnetron motion is the precession of the center of the cyclotron trajectories about the cell axis and produces undesirable effects such as shift in the cyclotron resonance frequency and appearence of sidebands in the frequency domain spectrum. The motion results from the forces exerted on ions by the magnetic field and electric field component perpendicular to the magnetic field.

We have found that the electric field in the cylindrical cell can be improved by dividing the conventional trapping electrodes in a concentric manner and by applying appropriate potentials to the divided electrodes. Using the cylindrical coordinates the radial (Er) and the axial electric field component (Ez) are given by

$$E_r = \sum_{\ell=1}^{\infty} \frac{2V_t J_1(k_\ell r)\cosh(k_\ell z)}{A J_1(k_\ell A)\cosh\{k_\ell (L/2)\}}, \quad E_z = -\sum_{\ell=1}^{\infty} \frac{2V_t J_0(k_\ell r)\sinh(k_\ell z)}{A J_1(k_\ell A)\cosh\{k_\ell (L/2)\}}$$

where A is the inner radius of the cell, Vt is the trapping potential, J_0 and J_1 are Bessel functions and $J_0(k_\ell A)=0$

Note that Er/Ez ratio deponds on r and z, but is independent of Vt. In case of the improved cell, Er and Ez are given by

$$E_z = -\sum_{\ell=1}^{\infty} \frac{2k_\ell J_0(k_\ell r)\sinh(k_\ell z)}{A^2\{J_1(k_\ell A)\}^2\cosh\{k_\ell (L/2)\}} (C_{1\ell} V_{t1} + C_{2\ell} V_{t2} + \cdots)$$

$$E_r = \sum_{\ell=1}^{\infty} \frac{2k_\ell J_1(k_\ell r)\cosh(k_\ell z)}{A^2\{J_1(k_\ell A)\}^2\cosh\{k_\ell (L/2)\}} (C_{1\ell} V_{t1} + C_{2\ell} V_{t2} + \cdots)$$

where Vt1, Vt2, ... are trapping potentials applied to each divided trapping electrodes. It has shown that the electric field in the improved cell is expressed by a linear combination of the applied potentials and Er/Ez ratio is variable. Therefore the radial electric field component Er can be reduced without decreasing the trapping efficiency.

We have constructed a cylindrical cell which has three pairs of trapping electrodes with different apertures arranged on both sides of the cell.[1] Measurements of magnetron frequencies were made with various combinations of the trapping potentials using an FT-ICR spectrometer built in this laboratory.[2]

We have confirmed that the magnetron frequency is greatly decreased and can be controlled by a linear combination of the trapping potentials. The

results suggests that homogeneity of the electric field is significantly improved.

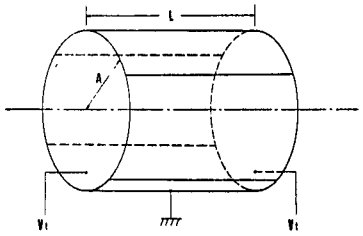

Fig.A. Configuration of electrodes of the conventional cylindrical cell

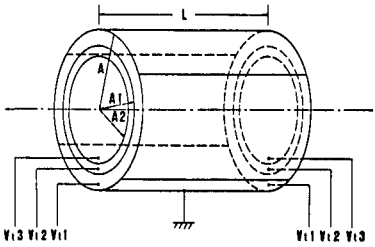

Fig.C. Configuration of electrodes of the improved cylindrical cell

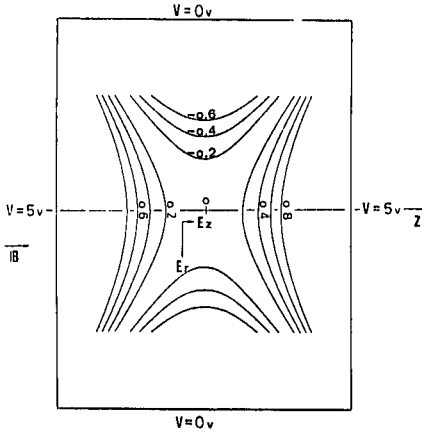

Fig.B. Example of equipotential lines in the cross section containing the axis of the conventional cylindrical cell

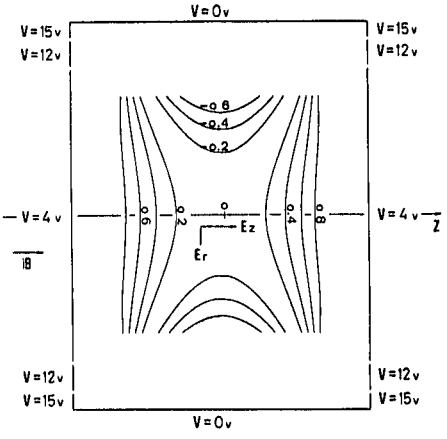

Fig.D. Example of equipotential lines in the cross section of the improved cylindrical cell

References

1) Y. Naito and M. Inoue, Proc. Asian Chem. Congress '87 Seoul (ASCHEM SEOUL), PP.506-507 (1987)
2) M. Inoue, M. Fujiwara, M. Onoyama, Y. Goto, Shitsuryo Bunseki, 35, 42 (1987)

Presented at the 36th ASMS Conference on Mass Spectrometry and Allied Topics
June 5-10, 1988, San Francisco, CA

HIGH PRESSURE ION SOURCE FOURIER TRANSFORM ION CYCLOTRON RESONANCE SPECTROMETRY

P. Kofel and T.B. McMahon
Department of Chemistry, University of Waterloo, Waterloo, Ont., Canada, N2L 3G1.

The technique of high pressure ionization combined with a magnetic sector mass analyzer has provided an abundance of thermochemical data on gaseous ions and molecules during the past two decades [1,2]. However, the analysis of the ions leaving the high pressure sources was limited to nominal mass analysis and relatively low masses.

High mass capability, high mass resolution, the possibility of structural characterization by dissociation experiments and of extended ion molecule reactions makes the FT-ICR technique [3] a superior tool to study ions. But only with the development of the external ion source [4,5] the FT-ICR instruments became attractive for ionization techniques with high gas loads, such as high pressure ionization

A high pressure ion source and ion transfer system was built and coupled (Fig 1) to a CMS 47 FT-ICR spectrometer equipped with a 4.7 T superconducting magnet [6]. The pressure differential between the ion source at 5 mbar and the ICR cell at $5x10^{-9}$ mbar is achieved by four pumping stages, including three turbomolecular pumps

The design of the high pressure ion source is similar to those described in the literature [1] Ions are produced by impact with electrons from a magnetically shielded, pulsed 2 keV electron gun The primary ions diffuse through the field free ionization chamber, thereby undergoing subsequent reactions in hundreds of ion molecule collisions. Thermal equilibrium conditions for these ion molecule reactions can be established between room temperature and 300° C . Ions reaching the exit aperture of the source are accelerated and transferred through gas flow restrictions and the fringing fields of the magnet to the ICR cell and trapped therein. Once trapped in the ICR cell, the ions can either be observed directly with high resolution, be structurally characterized by collision induced dissociation or react with species introduced only into the ICR cell region.

A novel injection lens / decelerator assembly was designed. It consists of an einzel lens followed by a cylindrical decelerator with 20 mm radius and 100 mm long, 0.55 m from the ICR cell at a field strength of 0.10 T . In our ion optics calculations this combination showed excellent qualities in decelerating and injecting the ions through the fringing fields of the superconducting magnet. The amount of energy, which is transferred from the axial to the radial velocity components of the ions by the magnetic mirror effect, can be kept below 1 eV with such a combination, increasing the number of ions that are trapped in the ICR cell [7].

An overview spectrum of air with traces of water is displayed in Fig 2. Due to the high pressure and long residence time in the ion source, most of the O_2^+ typically present in CI spectra has reacted with the water trace molecules and formed water cluster ions $H_3O^+(H_2O)_n$ at m/z=37, 55, 73, 91 and 109, corresponding to n=1,2,3,4 and 5, resp.

Reaction of the water cluster ions of air (Fig. 2) with acetone molecules at $2x10^{-7}$ mbar for 0 25 s in the ICR cell resulted in the spectrum of Fig 3. The complex reaction sequences involved are subject of our continuing experiments.

A negative ion high resolution spectrum of m/z=71 from traces of carbon tetrachloride and water in air (Fig 4) resolved the two peaks $ClHCl^-$ and $Cl^-(H_2O)_2$, as was confirmed by both accurate mass measurements and high resolution isotope peak analysis.

These preliminary experiments show the wide range of applications of the instrument to exact mass measurements, structural characterization and reaction mechanisms of ions from a high pressure ion source

REFERENCES

[1] M. Arshadi, R. Yamdagni and P. Kebarle, J. Phys. Chem. 74 (1970) 1475.
[2] J.E. Szulejko, J.J Fisher, T B. McMahon and J. Wronka, Int. J. Mass Spectrom Ion Processes, 83 (1988) 147
[3] K -P. Wanczek, Int. J. Mass Spectrom. Ion Processes, 60 (1984) 11.
[4] R T McIver, R.L. Hunter and W.D. Bowers, Int. J. Mass Spectrom. Ion Processes, 64 (1985) 67.
[5] P Kofel, M. Allemann, Hp Kellerhals and K -P. Wanczek, Int. J. Mass Spectrom. Ion Processes, 65 (1985) 97
[6] Spectrospin AG, Faellanden, Switzerland
[7] P. Kofel, M. Allemann, Hp. Kellerhals and K.-P. Wanczek, Int. J. Mass Spectrom. Ion Processes, 72 (1986) 53.

Presented at the 36th ASMS Conference on Mass Spectrometry and Allied Topics
June 5-10, 1988, San Francisco, CA

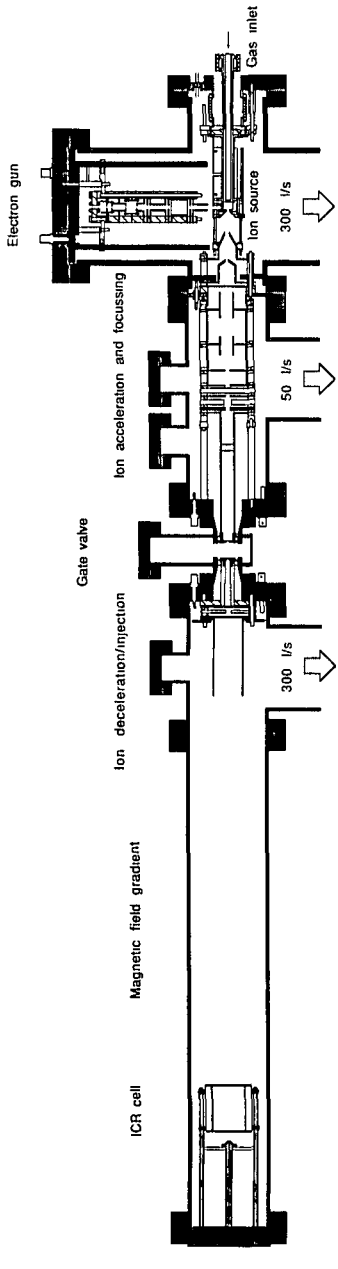

Fig. 1 Cross section of the instrument.

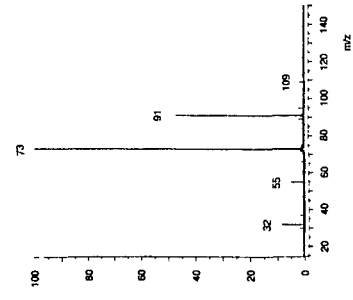

Fig. 2 Water cluster ions $H_3O^+(H_2O)_n$.

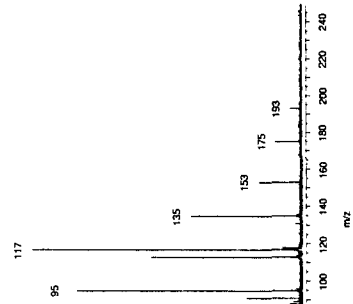

Fig. 3 Reactions of water cluster ions with $2x10^{-7}$ mbar acetone for 0.25 sec.

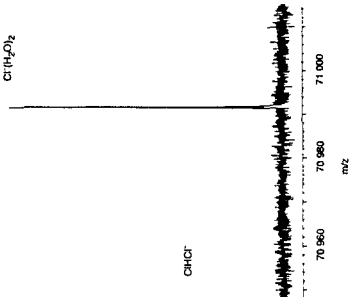

Fig. 4 High resolution spectrum of m/z=71 from carbon tetrachloride, negative ions.

Presented at the 36th ASMS Conference on Mass Spectrometry and Allied Topics
June 5-10, 1988, San Francisco, CA

THE IMPLICATIONS OF ION INJECTION FROM AN EXTERNAL ION SOURCE ON THE DYNAMICS OF TRAPPING AND DETECTION IN FT-ICR

C.D. Hanson, E.L. Kerley, M.E. Castro, and D.H. Russell
Department of Chemistry, Texas A & M University
College Station, Texas 77843.

Although the high resolution and high sensitivity of FT-ICR for the analysis of biomolecules was recognised early, the theoretical potential of the technique has not yet been realized. Ionization methods incompatible with the high vacuum requirements for detection by FT-ICR methods, have led to the development of differentially pumped external ion sources. Ions produced in an external source must be injected into the ICR cell by electrostatic methods. To accomplish injection, the ions are given appreciable translational energies. The effect of the kinetic energy on ion trapping and detection is difficult to study in simple cubic ICR cells. The complicated issue of ion motion and ion kinetic energy can be modeled in a two-section cell. By giving ions translational energy prior to the partitioning event, the effect of moving ions from an external source to ICR cell can be systematically studied. The impact of kinetic energy on partitioning efficiency and ion detection can be related to ion transfer from an external source.

The effect of radial translational energy imparted to the ions during the injection from an external ion source can be modeled in a two-section cell. By utilizing the conductance limit orifice as an ion skimmer, it is possible to differentiate between ions of different radii upon partitioning[1]. During the partitioning event, ions having cyclotron radii smaller than the orifice of the conductance limit will be transferred efficiently from the source to analyzer region. If an ion is accelerated into a larger cyclotron radius prior to partitioning, when the ensemble of ions are partitioned through the orifice, the ion of larger radius will be selectively discriminated against. The use of this selective ion partitioning has been studied both theoretically and experimentally. By using this technique, it is possible to profile an ions radius (i.e., translational energy) by monitoring its partitioning efficiency.

It has been demonstrated that an ion which is translationally excited to a larger cyclotron radius by a resonant oscillating electric field can be de-excited (*i.e.*, lose translational energy in the X-Y plane) by inverting the phase of the applied rf field with respect to the phase of the cyclotron orbit.[2,3] In this manner the translational energy of selected ions can be systematically regulated by an excitation/de-excitation technique.[4] Ions which are originally excited to radii which exceed the dimensions of the conductance limit orifice can be de-excited to radii acceptable for partitioning. Contained in figure 1 is a schematic of the procedure for investigating the effect of translational energy and relative phase angle in a two-section cell. Following ion production in the source region (A), all ions are excited to larger cyclotron radii by an rf excitation sweep (B) Selected ions are de-excited to the original radii by applying a second rf sweep which is 180° out of phase with respect to the cyclotron motion of the selected ions (C). The phase of the second pulse is selected by a variable delay between the first and second excite pulses. If the delay between the pulses corresponds to an odd integral of $n\tau/2$ (where τ is the period of the cyclotron orbit) the second excite pulse will be phase inverted. The radius of the de-excited ion can be analyzed by utilizing the orifice of the conductance limit. Only ions de-excited to energies corresponding to the dimensions of the orifice of the conductance limit will be partitioned into the analyzer region of the two-section cell (D).

The effects of excess translational energy have also been modeled theoretically. Contained in figure 2 is a computer simulation of a ensemble of ions of a specific m/z being excited by resonant excitation in a 3 T magnetic field. The ions were given thermal energies (*i.e.*, translational energy corresponding to electron impact ionization) and random phases with respect to the phase of the rf excitation. The resulting packet of ions (A) have a small radial and phase distribution cycloiding about a well defined center of rotation (B). Ions which are initially given

significant translational energies *prior to excitation* (*i.e., energies* corresponding to injected ions of *ca.* 3 eV) produce a poorly defined ion packet (figure 3). Owing to the extreme significance of the definition of the ion packet on ion detection, initial translational energy of ions trapped in an ICR cell is of profound importance.

Before FT-ICR analysis of high mass biomolecules can be considered as routine, *information as to the nature of trapping*, detection, and quantification of the technique must be understood. Preliminary *results from studies* performed on a system equipped with a two-section cell indicates that quenching of excess kinetic energy is important before a stable detection orbit can be achieved.

References Cited:

1. Kerley,E.L. and Russell,D.H. *Submited for* publication to *Anal. Chem*

2. Marshall, A.G.; Wang,T.L.; and Ricca, T.L Chem. Phys. Lett. 1984,105,233

3. Pfandler, P.; Bodenhausen, G.; Rapin, J.; Houriet, R.; and Gaumann, T. Chem. Phys. Lett., 1987,138,195

4. Hanson,C.D.; Kerley,E.L.; and Russell,D.H. submitted for publication to *Anal. Chem.*

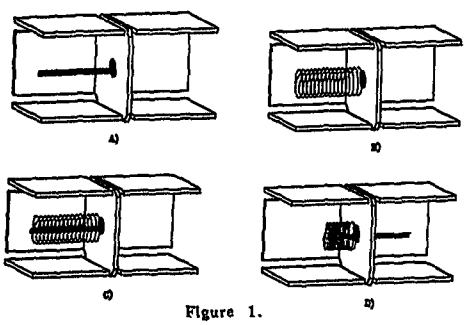

Figure 1.

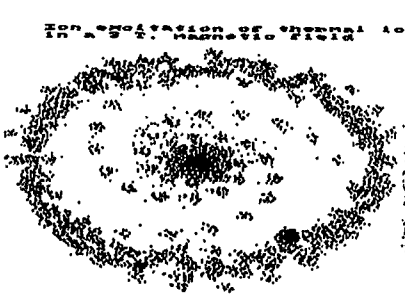

Figure 2.

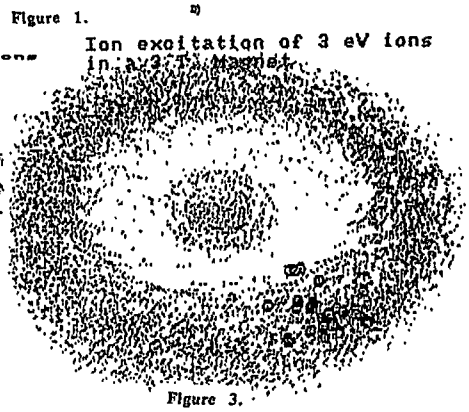

Figure 3.

Presented at the 36th ASMS Conference on Mass Spectrometry and Allied Topics
June 5-10, 1988, San Francisco, CA

FOURIER TRANSFORM ION CYCLOTRON RESONANCE MASS SPECTROMETRY OF METAL IONS GENERATED BY LASER DESORPTION IN AN EXTERNAL SOURCE

Robert R. Weller[a], Sahba Ghaderi[b], Othmar Vorburger[c] and Ben S. Freiser[a]

[a]Department of Chemistry, Purdue University, West Lafayette, IN 47907
[b]IBM General Products Division, San Jose, CA 95193
[c]Nicolet Instrument Corp., P.O. Box 4508, Madison, WI 53711

Fourier transform ion cyclotron resonance mass spectra have been obtained for metal ions generated by laser desorption in a source external to the ICR analyzer cell and high magnetic field. Prior work (1-4) has demonstrated the potential advantages of external ion generation and has thus far utilized SIMS, FAB, EI, and MPI sources. In contrast to these methods, LD generated ions required no acceleration or special ion optics to produce an ion signal comparable to that obtained using the conventional configuration where the ions are desorbed from a target inside or immediately adjacent to the analyzer cell. Metals that have been generated in the external source include Fe, Cr, Co, Cu, Pd, Rh, Pt, Au, La, and Al.

The experimental arrangement consists of an extension to the analyzer flange of a Nicolet FTMS-2000 dual cell FT-ICR to which a four way cross was connected. Metal samples were either mounted permanently on a screen in the external source or were mounted on the 45° beveled end of a solids probe (Figure 1). LD was accomplished using the focussed fundamental beam from a Nd:YAG laser.

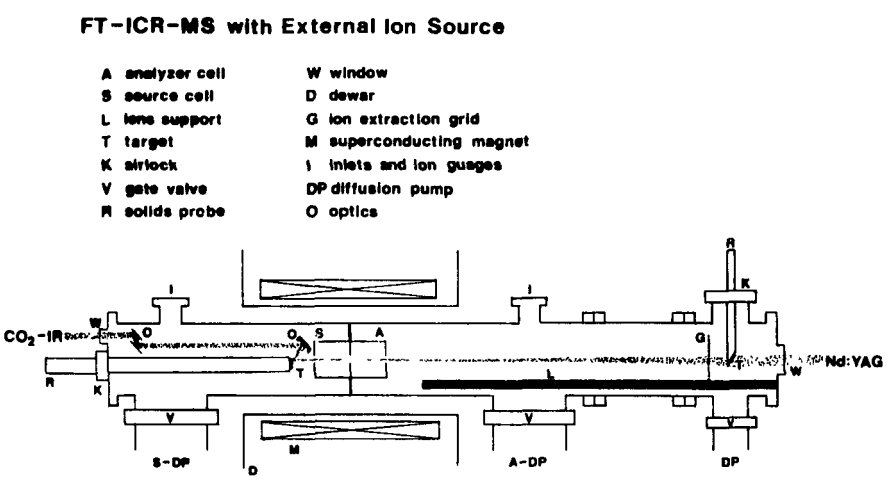

Figure 1.

The positive ions produced could be blocked from entering the analyzer cell with the application of a +35 V potential on a grid located just inward of the target. No signal was observed at the cell unless at least a 2.5 to 3 ms delay was placed between the laser pulse and the detect sequence, suggesting that the ions which have the proper energy spread to be trapped in the ICR cell are travelling a long (spiral?) slow path. Studies with a movable aperture show that the ions are focussed as expected by the magnetic field, but come from a broad source. For example, in contrast to the unrestricted 10 cm bore of the vacuum system, only 75% of the ions pass through a 5 cm diameter aperture located 10 cm from the target.

There are several advantages with being able to produce LD ions in an external source. First, the optics are very simple due to the short beam path once inside the vacuum chamber. Second, many studies of metal ion chemistry have had interferences due to background oxygen. Permanently mounted samples in the external source allow the system to be operated at base pressures (10^{-9}torr) since a solids probe does not have to be used. Third, the presence of two low pressure analyzer cells allows for more complex reaction schemes to be studied, e.g. LD metal ions are trapped and reacted in the source cell, product isolated and transferred back to the analyzer cell where further reactivity or photochemical studies can be undertaken.

Future work involves modifying the experimental arrangement so the laser plume is towards the analyzer cell. Also being developed is a Cs^+ source for SIMS studies. Further down the line the system will be greatly expanded with a cluster source patterned after that in ref. 3. All of these techniques combined with the advantages of FT-ICR-MS will greatly enhance the studies of the chemistry of metal ions.

1) R.T. McIver, Jr. and R.L. Hunter; presented at 31st ASMS Conference on Mass Spectrometry and Allied Topics; Boston, MA; May 8-13, 1983.

2) D.F. Hunt and J. Shabanowitz; presented at 35th ASMS Conference on Mass Spectrometry and Allied Topics; Denver, CO; May 24-29, 1987.

3) J.M. Alford, P.E. Williams, D.J. Trevor, and R.E. Smalley; Int'l. J. of Mass Spectr. and Ion Proces. 72 33-51 (1986).

4) P. Kofel, M. Allemann, Hp. Kellerhals, and K.-P. Wanczek; Int'l. J. of Mass Spectr. and Ion Proces. 72 53-61 (1986).

Presented at the 36th ASMS Conference on Mass Spectrometry and Allied Topics
June 5-10, 1988, San Francisco, CA

FAST ATOM BOMBARDMENT COMBINED WITH FOURIER TRANSFORM MASS SPECTROMETRY

P. Grossmann, P. Caravatti, M. Allemann, H.P. Kellerhals
Spectrospin AG, Industriestrasse 26, 8117 Fällanden, Switzerland

Fast atom bomardment (FAB) uses a beam of high energy atoms (kilovolts energy), to desorb the sample from a liquid matrix. Typically glycerol or some other suitable liquid is used as a matrix, argon or xenon is used as fast atoms. FAB turned out to be very successful for many compounds which are intractable by the commonly used ionization modes electron impact (EI) and chemical ionization (CI). FAB produces quasi-molecular ions and significant fragment ions of many thermally labile and/or polar compounds. FAB-MS was therefore readily accepted and is nowadays routinely used in analytical mass spectrometry.

Fourier transform mass spectrometry (FTMS) has seen rapid developments during the last five years (1-3). Traditionally used and appreciated as one of the best methods for studying ion-molecule reactions, FTMS is nowadays more and more used as a reliable analytical method for structural elucidations. This is due to the well proven capability of FTMS for high resolution, exact mass determination and MS/MS-experiments.

The combination of FAB with FTMS provides therefore some attractive features for structural analysis. However, FTMS requires ultra high vacuum for high resolution (better than 10^{-8} mbar) and FAB is dependant on a large concentration of glycerol or a similar liquid resulting in a vapor pressure higher than 10^{-5} mbar. A direct coupling of FAB with FTMS is therefore not feasible.

One possibility of solving this pressure associated problem is to separate the ion generation and ion detection in space. We developed a differentially pumped, external ion source used for GC-FTMS (3) and presented in Figure 1. Ions are extracted from the ion source and transferred into the ICR-cell with 3 keV. The ions are decelerated shortly before entering the detection cell, are trapped within the cell and subsequently measured. In this work we removed the GC and mounted the FAB gun on the ion source. 7 keV argon atoms were used to produce the FAB-FTMS spectra. The pressure in the ion source was typically $2 \cdot 10^{-4}$ mbar, in the ICR cell about $5 \cdot 10^{-9}$ mbar. High resolution spectra of glycerol will be presented to demonstrate the resolving power of this FAB-FTMS-configuration. Resolutions of over 400'000 (for m/z 93) and 100'000 (for m/z 277) could be achieved. The FAB-FTMS spectrum of Leu-enkephalin is shown in Fig. 2. The protonated molecular ion (m/z 556) and sequence fragments like in classical FAB-MS are observed. Broad band and high resolution FAB-FTMS spectra of Tetra-Alanine will be presented to show the advantage of high resolution and the similarities with the classical FAB-mass spectrum.

1) N.M.M Nibbering, Advances in Mass Spectrom., 1985 p. 417-435

2) D.H. Russel, Mass Spectrom. Rev. 1986, 5, p. 167-189

3) D.A. Laude, C.L. Johlman, R.S. Brown, D.A. Weil, Ch. L. Wilkins, Mass Spectrom. Rev. 1986, 5, p. 107-166

4. P. Grossmann, P. Caravatti, St. Dütsch, M. Allemann, H.P. Kellerhals, Lab. Pract. V.36 N.11, 1987, p. 63-65

Presented at the 36th ASMS Conference on Mass Spectrometry and Allied Topics
June 5-10, 1988, San Francisco, CA

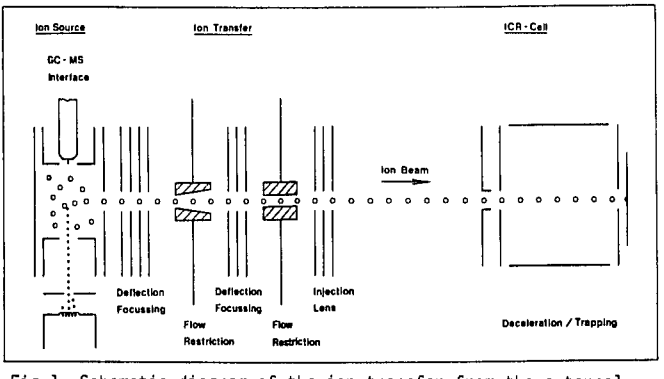

Fig.1: Schematic diagram of the ion transfer from the external ion source into the ICR cell

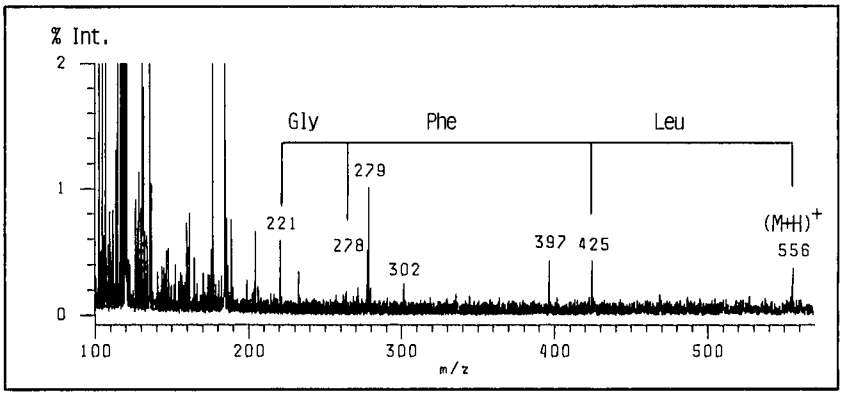

Fig.2: FAB - FTMS of Leu-enkephalin (MW 555; Tyr-Gly-Gly-Phe-Leu)

Presented at the 36th ASMS Conference on Mass Spectrometry and Allied Topics
June 5-10, 1988, San Francisco, CA

High Precision Multipurpose Solid Sample Probe for Field Desorption Ion Cyclotron Resoonance Spectrometry

I. Pezsa, H. Knoll and K. P. Wanczek,
Inorganic Chemistry, NW 2, University of Bremen, D-28 Bremen 33,
and H. B. Linden,
Linden-ChroMasSpec, D-28 Bremen 61, West Germany

For the use with ultra high vacuum ion cyclotron resonance spectrometry a high precision multipurpose solid sample probe has been developed. The probe is suited for the use with high magnetic field ICR. The probe is introduced in the ultra high vacuum system with the aid of a differentially pumped vacuum lock, such that the probe tip is located directly in front of the ICR cell in the region of highest magnetic field. The probe has an exchangeable tip, where different kinds of targets, a sample evaporator, or a field desorption emitter can be fixed.

The Fourier transform ICR spectrometer utilized in the study is based on the Spectrospin CMS 47. It is equipped with a 7 Tesla magnet with 89 mm room temperature bore and a cylindrical ICR cell. The instrument is controlled by an Aspect 3 000 minicomputer. The ICR ultra high vacuum system is pumped by a 600 l/s diffusion pump, equipped with a liquid nitrogen baffle. The base pressure is below 10^{-9} mbar.

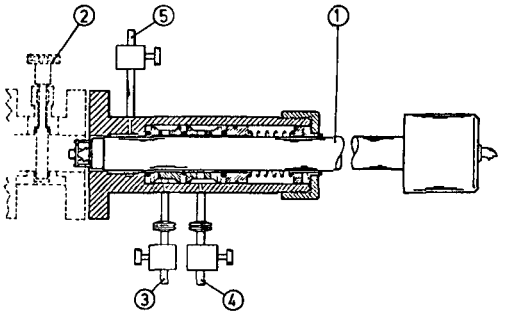

Fig. 1. Vacuum and pushrod arrangement.

In Fig.1 the vacuum and pushrod arrangement are shown. The pushrod (1) is prepared for the FD operational mode and shown in the withdrawn position with the gate valve (2) closed. The length of the pushrod is 1,000 mm, its diameter is 20 mm. It is manufactured from nonmagnetic stainless steel tube. The vacuum lock is differentially pumped. Vacuum lines (3) and (4) are connected with one two stage rotary pump, vacuum

line (5) with another. The down pumping time after introducing the pushrod in the vacuum lock is only a few seconds. Similarily, after opening the gate valve (2), a base pressure below 10^{-9} mbar necessary for ultra high resolution is reached in a few seconds. This is, in addition to the high pumping speed, mainly due to the elaborate arrangement of the sealing elements and the differential pumping system, and to the ultrahigh precision manufacturing of the pushrod surface. The dead volume of the vacum lock is very small. Surface roundness and unevenness are much better than 1 µm.
Vacuum lock and pushrod are developed in cooperation with and manufactured by Hanseatische Präzisions- und Orbit-Technik, Bremen, West Germany.
The probe has a relatively large diameter. This is of great advantage and does not cause any problem if utilized with an ICR spectrometer. The mechanical stability is great. The probe can be located reproducibly in front of the ICR cell with a deviation of less than 0.5 mm, only guided by the vacuum lock. The diameter of the tip is also larger than usual. Therefore four standard high voltage vacuum feedthroughs can be used. Potential differences of more than 12 kV can be generated between the feedthroughs and to ground. The probe tip is designed to fit various types of sample carriers, probe targets, and ionization systems. In the Fig. 2 the setup for field desorption is shown. The emitter (1) is held by two demountable supporting rods (2); (3) is the counter electrode, (4) is a shielding electrode.
Emitter and FD electronics are manufactured by Linden-ChroMasSpec, Bremen, West Germany.

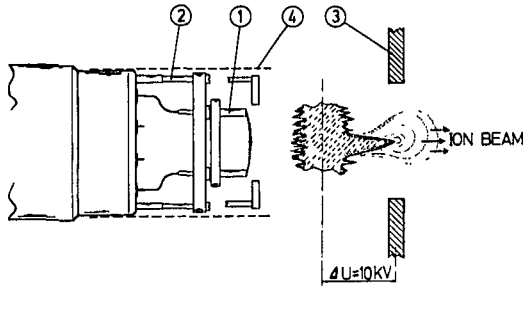

Fig. 2. Interchangeable probe tip with FD emitter.

The FD mode of operation is tested with several organic compounds and with cesium iodide.

Presented at the 36th ASMS Conference on Mass Spectrometry and Allied Topics
June 5-10, 1988, San Francisco, CA

DIRECT DETERMINATION OF SURFACTANTS ON TEXTILES BY LASER DESORPTION FOURIER TRANSFORM MASS SPECTROMETRY. M.P. Chiarelli[1], D.A. Peake[2], and M.L. Gross[1] [1]. Department of Chemistry, University of Nebraska-Lincoln, Lincoln, NE 68588. [2]. Procter and Gamble Corporation, Cincinnati, Ohio 45217.

The purpose of these investigations is to determine if laser desorption can be applied to the analysis of surfactants on textiles. Laser desorption of mono- and dipeptides was shown to proceed independently of the sample support at sufficiently high laser power densities (1). Thus LD/FTMS should be well-suited for the direct analysis of surfactants on textiles.

All experiments were executed on a home-built FTMS interfaced to a Nicolet 1000 data system (2). The cloth to be analyzed was about 0.5 cm square and was stretched over a copper support with a teflon sleeve. Solutions were allowed to saturate the cotton cloth before analysis. The laser power densities employed throughout this study were in the range of 3-6 x 10^8 W/cm^2 at a wavelength of 266 nm, 1-3 x 10^9 W/cm^2 at 532 nm, and 5-10 x 10^9 W/cm^2 at 1064 nm.

Dimethyl-distearyl ammonium chloride was chosen for an initial demonstration because it is a surfactant normally found in detergents. Desorption was executed from a copper substrate and cloth to compare the working power density ranges over which spectra could be acquired for the two supports. The working range of the copper was larger than that of the cloth due to a larger sample thickness on the copper resulting from a smaller surface area. Spectra obtained from both supports were the same, showing ions resulting from methyl and stearyl losses in addition to a molecular ion. Detection limits were ca. 125 μg/gram cloth.

Homolog Mixture Determination: Next we wanted to determine if relative quantities of surfactants could be analyzed by LD/FTMS. A five component mixture of C_{10}-C_{14} sodium alkyl benzene sulfonates was utilized. The percent relative abundances of the $(M - Na)^-$ ions were assessed at 3 different wavelengths and energies from both cloth (Table I) and copper (Table II) supports. The LD ion distributions are compared to homolog distributions determined by GC/FID to judge accuracy. Laser desorption from the copper showed better sensitivity than LD from the cloth where no C_{14} homolog was observed in most determination. This is due to the difference in surface areas between the two supports as discussed above. Ion distributions from the cloth are more accurate than those obtained from the copper at 1064 nm. Sample depositions on the cloth is not preceeded by solvent evaporation as is the case for copper, where slight differences in solubility may cause discrimination in sample precipitation. Resonant desorption compared to LD at 1064 nm. This may be caused by slight differences in the homologs absorbtivities or the relative energies of the homologs' S_1 states.

Quantification Range Determination: Next we wanted to ascertain the range over which an analyte may be quanitated. Solutions of $C_{12}H_{25}SO_4Na$ and $C_{12}D_{25}SO_4Na$ were deposited on the cloth in different ratios and laser desorbed at a wavelength of 1064 nm. The ions observed were of the $(M - Na)^-$ and $(2M - Na)^-$ type, one of the latter being a mixed dimer. The theoretical, monomer, and total ion abundance ratios from LD are plotted against the ratio of the compounds on the cloth. The monomer ratio (m/z 290 and m/z 265) best approximates the theoretical one. The data indicates that the analyte may be detected in the mixed dimer, m/z 578, when present as low as 1:40 to the deuterated standard.

1. F. Hillenkamp, M. Karas, D. Holtkamp, and P. Klusner, Int. J. Mass Spectrom. Ion Proc., **69**, 265 (1986).

2. D. A. McCrery, E.B. Ledford, Jr., and M.L. Gross, Anal. Chem., **54**, 1437 (1982).

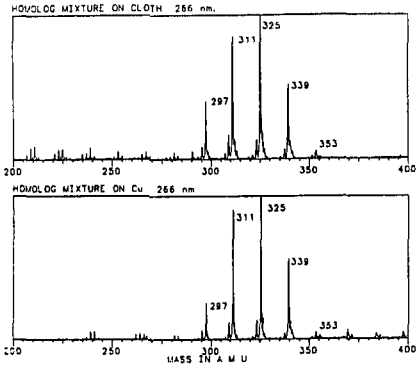

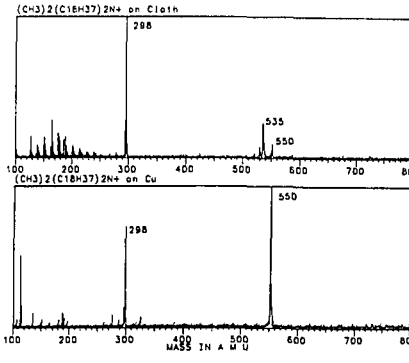

Table I: Relative abundances of ions laser desorbed from a sodium linear alkyl benzene sulfonate mixture on a cotton cloth.

C NO.	GC/FID[2]	WAVELENGTH[1] 1064nm. 125mJ.	532nm. 17mJ	532nm. 42mJ.	266nm. 5mJ.	266nm. 9mJ.
10	11.2[11.5]	13.4(0.5)	11.3(0.3)	15.2(0.5)	11.5(0.3)	15.0(0.8)
11	29.1[29.8]	29.5(0.7)	29.7(0.5)	30.7(1.4)	25.3(0.8)	33.6(0.9)
12	32.4[33.2]	33.3(1.1)	35.8(0.7)	30.6(1.4)	36.4(0.7)	31.3(0.6)
13	24.9[25.5]	22.4(0.8)	23.2(0.7)	23.5(2.3)	24.8(0.7)	19.7(0.6)
14	2.4[--]	------	------	------	2.5(0.5)	------

[1]Values in parentheses are the relative standard deviations associated with the relative abundances given. N=8 determinations.

[2]Relative abundance values in brackets are renormalized to account for the absence of the C_{14} homolog in the laser desorption spectra.

Table II: Relative abundances of ions laser desorbed from a sodium linear alkyl benzene sulfonate mixture on a copper surface.

C NO.	GC/FID[2]	WAVELENGTH[1] 1064nm. 125mJ.	532nm. 17mJ	532nm. 42mJ.	266nm. 5mJ.	266nm. 9mJ.
10	11.2[11.5]	9.4(.04)	8.6(0.4)	9.2(0.4)	10.9(0.4)	9.5(0.6)
11	29.1[29.8]	23.6(0.6)	24.9(0.8)	25.6(0.9)	27.2(1.1)	27.2(0.5)
12	32.4[33.2]	43.6(1.5)	43.4(0.7)	39.1(1.6)	37.9(1.6)	40.0(1.2)
13	24.9[25.5]	23.1(0.6)	20.3(0.7)	23.1(1.3)	20.9(1.3)	20.6(0.7)
14	2.4[--]	------	2.8(0.2)	3.3(0.4)	3.2(0.4)	2.8(0.2)

[1]Values in parentheses are the relative standard deviations associated with the relative abundances given. N=8 determinations.

[2]Relative abundance values in brackets are renormalized to account for the absence of the C_{14} homolog in the laser desorption spectra.

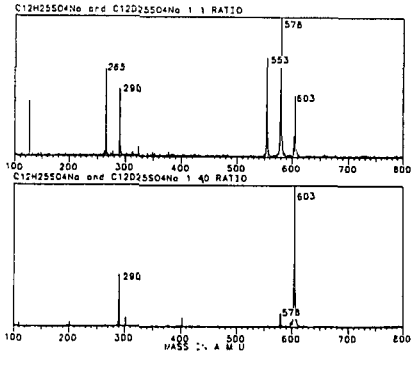

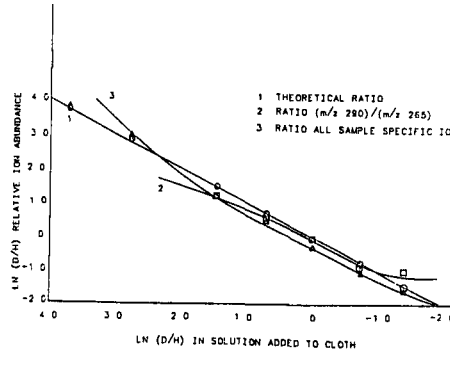

Presented at the 36th ASMS Conference on Mass Spectrometry and Allied Topics
June 5-10, 1988, San Francisco, CA

Strategy for Sequencing Oligopeptides Using Laser Desorption Fourier Transform Mass Spectrometry

Liub-Chii Yang and Charles L. Wilkins*
Department of Chemistry, University of California, Riverside, CA 92521

Introduction

Gramicidin D has been studied by Cody[1] and coworkers as well as Drochon[2]. Cody and coworkers[1] identified 12 of the 15 amino acids in Gramicidin D using laser desorption Fourier transform mass spectrometry (LD/FTMS) with Collision-Activated Dissociation (CAD). Drochon[2] identified all of the 15 amino acid residues in gramicidin D by using direct chemical ionization triple quadrupole mass spectrometry with CAD. Although Cody used only positive ion LD/FT mass spectra, several papers[4-7] suggest that complementary information can be obtained by concurrent consideration of negative ion spectra. That premise is explored in the research reported here, which investigates use of the complementary information derived from positive and negative ion LD/FT mass spectra and CAD as an oligopeptide sequence tool.

Results and Discussion

Strategy for Sequencing Linear Oligopeptides. Nomenclature used here is that proposed by Roepstorff[8]. Detailed procedures for sequencing oligopeptides by using both positive and negative ion LD/FT mass spectra obtained with CAD are as follows:

1. the molecular mass is determined by locating $[M+H]^+$, $[M-H]^-$, $[M+K]^+$, and $[M+Na]^+$ ions.
2. characteristic fragmentation patterns are used to identify particular amino acid residues. For example, if ions $[M+H-17]^+$, $[M+H-42]^+$, and $[M+H-60]^+$ are present, then the oligopeptide contains at least one arginine at the carboxylic acid terminus.
3. sequencing is begun by identifying corresponding series of ions in the positive and negative ion spectra. One series, $[Y_n+2H]^+$ and $[Y_n]^-$ ions, can be distinguished because the positive ions are 2 dalton higher than the corresponding negative ions.
4. the $[B_n]^+$ and $[B_n]^-$ series of ions are assigned. These ions have the same masses in both positive and negative ion spectra.

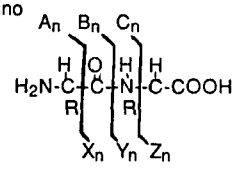

Because Y series ions indicate the oligopeptide sequence starting from the carboxyl terminus and the B series the sequence beginning with the N-terminus, the two will overlap. Thus, in most cases a complete sequence can be derived, even though neither series is necessarily complete.

Examples. Figures 1 (a) and (b) show the molecular mass region of the LD/FT mass spectra for gramicidin D. From the Y series of ions in the negative and positive ion spectra, the sequence can be read as 29-Val-Gly-Ala-Leu-Ala-Val-Val-Val-Trp-Leu-Trp----. The mass difference between the B_{max} ion and the molecular ion is 60 daltons. From the B series, the sequence can be read as 60-Trp-Leu-Trp-Leu-Trp-leu-Trp-Val-Val-Val-Ala-Leu----. Because a portion of the sequence in the Y series overlaps a portion of the B series sequence, the complete sequence can be read as 29-Val-Gly-Ala-Leu-Ala-Val-Val-Val-Trp-Leu-Trp-Leu-Trp-Leu-Trp-60. Mass spectra of cyclic oligopeptides do not display the same relationship between positive and negative ion spectra as linear oligopeptides. For example, the negative ion spectrum of gramicidin S reveals one partial sequence, 130-Leu-Orn-Val-Pro-Phe-Leu----. The positive ion spectrum displays another partial sequence Leu-Phe-Pro-Val-Orn-Leu-Phe----. Based upon the two sequences derived from the positive and negative ion spectra, a complete sequence, cyclo(Leu-Orn-Val-Pro-Phe-Leu-Orn-Val-Pro-Phe) can be proposed.

"Unknown"s. 18 "unknown" oligopeptides, selected and purchased by a third party and supplied to us as "blind" samples were examined to test the method. Correct structures were deduced for 14 of these. Using "unknown" A as an example, it is possible to distinguish lysine from glutamine by analyzing the negative ion spectrum. Glutamine loses 18 and 74 dalton fragments from

the deprotonated molecular ion, whereas lysine does not show such a fragmentation pattern. The triplet fragmentation pattern consisting of consecutive loss of two 18 dalton fragments from the Y series of ions is observed throughout the negative ion spectrum. After the loss of the first glutamine, only one peak corresponding to the loss of 18 daltons from the Y series of ions is observed. After the loss of the second glutamine, no peak corresponding to the loss of an 18 dalton fragment appears.

Conclusion

Use of both positive and negative ion laser desorption Fourier transform mass spectra for the analysis of oligopeptides has been demonstrated. For gramicidin D, all 15 amino acid residues were identified and the correct sequence deduced. By examining the relationships between the positive and negative ion spectra, it is possible to distinguish linear oligoeptides from cyclic oligoepeptides. Finally, complete structures of 14 of the 18 "unknown" oligopeptides were sucessfully determined using this method.

Acknowledgement

We gratefully acknowledge the support of a grant GM-30604 from National Institutes of Health.

References

1. Cody, R.B., Amster, I.J., McLafferty, F.W., Proc. Natl. Acad. Sci., 1985, 82, 6367-6370.
2. Drochon, B., Spectra, a Finnigan MAT publication, 1987, 11(1), 31-37.
3. Seki, S., Kambara, H., Org. Mass Spectrom., 1985, 20, 18-24.
4. Williams, D.H., Santikarn, S., DeAngelis, F., Smith, R.J., Reid, D.G., Oelrichs, P.B., Macleod, J.K., J. Chem. Soc. Perkin Trans., 1983, 1, 105-117.
5. Dass, C., Desiderio, D.M., Anal. Biochem., 1987, 163, 52-66.
6. Konig, W.A., Aydın, M., Schulze, U., Rapp, U., Hohn, M., Pesch, R., Kalikhevitch, V.N., Int. J. Mass Spectrom. Ion Phys., 1983, 46, 403-406.
7. Yang, C.L.C., "Laser desorption Fourier transform mass spectrometric study of oligopeptides in the presence and absence of collision-activated dissociation", 35th ASMS Conference on Mass Spectrometric and Allied Topics, May 24-29, 1987, Denver, CO., page 1118-1119.
8. Roepstorff, P., Fohlman, J., Biomed. Mass Spectrom., 1984, 11, 601.

Figure 1. LD/FT mass spectra of Gramicidin D. (a) negative ion and (b) positive ion spectra obtained with CAD for the mass range from 1600 to 1950 daltons.

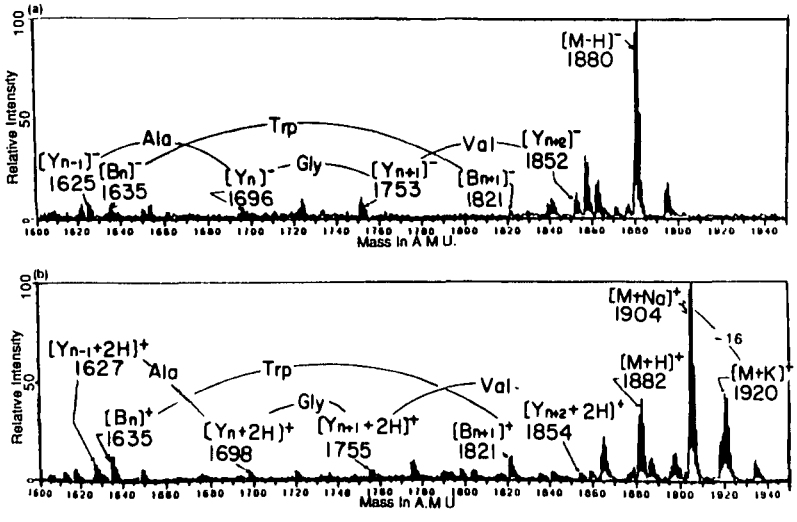

Presented at the 36th ASMS Conference on Mass Spectrometry and Allied Topics
June 5-10, 1988, San Francisco, CA

STORED WAVEFORM INVERSE FOURIER TRANSFORM EXCITATION: ANALYTICAL APPLICATIONS FOR FOURIER TRANSFORM MASS SPECTROMETRY

R. B. Cody*, S. D. Goodman, R. E. Hein, D. A. Weil
Nicolet Analytical Instruments
5225 Verona Rd., Madison, WI 53711

Stored waveform inverse Fourier transform (SWIFT) excitation [1-4] is a powerful method for controlling excitation, acceleration, and excitation of ions infrequency-based mass spectrometric techniques such as Fourier transform mass spectrometry (FTMS). In the SWIFT method, the operator defines the requested excitation spectrum in terms of desired resolutions, masses, and energies. Inverse Fourier transform methods are used to automatically design the time domain excitation waveform which will produce the desired effect.

SWIFT provides a number of benefits including simplified operation and increased control for all FTMS experiments, increased selectivity for excitation, improved selectivity for single- or multiple-ion-monitoring, and capabilities for performing very complex experiments such as Hadamard transform MS/MS [8].

One application of SWIFT involves increased parent ion selectivity in MS-MS experiments [4]. The resolution for excitation depends on the same factors as resolution for detection: increasing the excitation time increases the selectivity of ion excitation in the same way that increasing the observation time increases the resolution for ion detection. We have used a prototype SWIFT apparatus to separate the carbon 13 isotope from acridine from the molecular ion of 9-methylfluorene in an MS/MS experiment. For this example, a resolution of 10,000 is required to separate the parent ions. Much higher resolution is expected once heterodyne capabilities are implemented.

Isolation of trace components in complex mixtures is possible by using SWIFT even in the presence of interferences at the same nominal mass. A an example, we have isolated benzothiophene from butylbenzene in a petroleum fraction with added perfluorotributylamine (internal calibrant). Prior to ejection, the abundance of benzothiophene was only 0.2% (relative to the base peak at 69 u). SWIFT has also been used to obtain MS/MS and MS/MS/MS spectra for several major and minor components in an asphaltene sample.

By removing many of the variables associated with swept frequency excitation, ultrahigh resolution measurements over a narrow mass range are facilitated by using SWIFT. As an example, we collected ultrahigh resolution spectra for a complex petroleum distillate. Spectra were obtained at >100,000 resolution over a 3 u mass range about m/z 190 and a 10 u mass range about m/z 300 in the mixture.

Multiple ion monitoring provides increased selectivity by only exciting ions of interest. In addition, increased sensitivity is possible because ions can be excited to a higher orbit by using SWIFT than by using broadband chirp excitation [7]. As an example, high resolution multiple ion monitoring was used to detect characteristic ions from methyl stearate in the presence of background interferences.

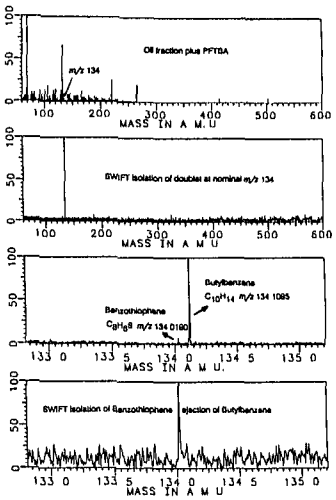

Selective excitation and high resolution mass measurements

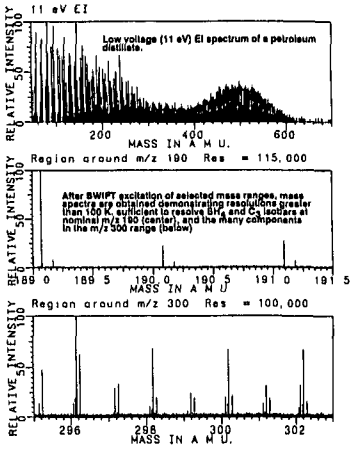

SWIFT GC/MS SELECTED ION MONITORING

Screening for 2, 3, 7, 8 - tetrachlorodibenzo-p-dioxin (TCDD) in the presence of Arochlors

Monitor. 2, 3, 7, 8 - TCDD Molecular Ions 320 and 322 (319 9865 and 321 9836)

2, 3, 7, 8 - TCDD Confirmation ions $(M - COCL)^+$ at 257 and 259 (256 9328 and 258 9298)

$^{13}C_{12}$ - 2, 3, 7, 8 - TCDD Internal Standard Molecular Ions at 332 and 334 (331 9868 and 333 9839)

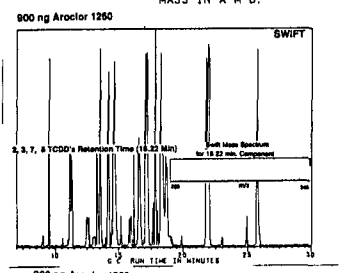

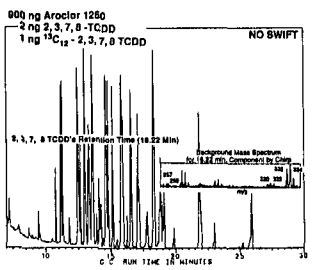

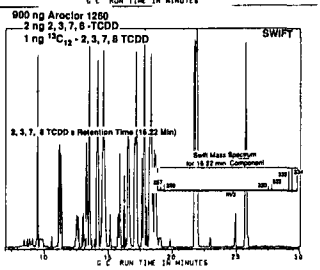

REFERENCES

1. Chen, L. and A. G. Marshall, Rapid Comm. Mass Spectrom., vol. 1, no. 3, pp. 39-42, 1987.
2. Chen, L. and A. G. Marshall, Int. J. Mass Spec. Ion Proc., vol. 79, pp. 115-125, 1987.
3. Chen, L., T.-C. L. Wang, T. L. Ricca, and A. G. Marshall, Anal. Chem., vol. 59, pp. 449-454, 1987.
4. Cody, R. B., R. E. Hein, and S. D. Goodman, Rapid Comm. Mass Spectrom., vol. 1, pp. 99- 102, 1987.
5. Marshall, A. G., T. -C. L. Wang, and T. L. Ricca, J. Am. Chem. Soc., vol. 107, pp. 7893-7897, 1985.
6. Wang, T.-C. L., T. L. Ricca, and A. G. Marshall, Anal. Chem., vol. 58, pp. 2935-2938, 1986.
7. Cody, R. B., R. E. Hein and D. A. Hanna, presented at the 35th ASMS Conference , May 24-29, 1987, Denver, CO. (collected abstracts p. 259)
8. Loh, S. Y., E. R. Williams, F. W. McLafferty and R. B. Cody, presented at the 36th ASMS Conference, May6-10, San Francisco, CA. (Paper ROD 400)

Presented at the 36th ASMS Conference on Mass Spectrometry and Allied Topics
June 5-10, 1988, San Francisco, CA

LASER MICOPROBE FOURIER TRANSFORM MASS SPECTROMETRY: INSTRUMENTATION AND APPLICATIONS:

M. Pelletier, G. Krier, F. Tollitte, J. F. Muller; Laboratoire de Spectrometrie de Masse de Chimie Laser, Universite de Metz, Metz, Cedex, 01 France
D. Weil and M. Johnston, Nicolet Instrument Corporation, Madison, WI 53711 U. S. A.

Laser desorption/ionization was the first soft ionization method coupled to a Fourier transform mass spectrometer for the introduction of nonvolatile thermally labile compounds. Laser desorption/FTMS (LD/FTMS) was initially used to generate metal ions for metal ion chemistry studies, later as an alternative to FAB, and recently for surface analysis. Herein, we report preliminary data obtained on a modified Nicolet FTMS-2000. Three-dimensional sample manipulation, small laser spot size and viewing optics (Figure 1) have been added to the instrument.[1]

To reproducibly and precisely position a sample, an x, y, z sample-stage manipulator was constructed, using bimetallic materials which are unaffected by strong magnetic fields of 3.0 Tesla. The prototype manipulator has a maximum translational displacement of 5 mm and minimum x, y translational displacement of 6 microns. Z-axis manipulation allows maintenance of laser focus with variations in surface topography.

Laser desorption/ionization is performed using an excimer laser charged with KrF, (λ = 249 nm) with a pulse energy of 3.5 mJ delivered in 20 ns. The laser energy is controlled by an iris attenuator and measured with a photoelectric detector (Joulemeter) positioned after the iris. Energy at the sample surface is approximately 70 mJ with a power density of 2×10^9 W/cm^2. A 10.6 cm focal length quartz lens focuses the laser beam through the conductance limit, to a minimum 6 micron spot size diameter. The sample stage is illuminated by light transmitted by using a flexible polymer lightpipe. A magnified (20X) image of the sample stage is viewable through an endoscope.

The performance of the laser microprobe/FTMS was compared with results obtained using a laser microprobe Time-Of-Flight mass spectrometer.

A glass sample was analyzed in order to separate metal (rare earth) ions from metal oxide ions. The glass sample was prepared from mainly SiO_2 and PbO with 10% impurities: 2% chromium, 2% cobalt, 2% tin, 1% neodymium, 1% samarium, 1% europium and 1% gadolinium. To separate $^{142}NdO^+$ ions from $^{158}Gd^+$ ions, a resolution of 7,250 is required. Figure 2a shows the positive ion mass spectrum of the glass sample obtained by the TOF instrument. All of the rare earth impurities metal ions were observed, but poor mass resolution makes the separation of metal oxide ions from metal ions difficult. For comparison, Figure 2b was obtained with the FTMS at medium resolution. Partial ejection of Pb^+ enhances the detection of the rare earth ions. Figure 2c was obtained at high resolution >26,000 (FWHH) over a 35 Daltons mass range and the doublets at mass 158 and 160 can be identified as NdO^+ and Gd^+ (Figure 2d). Accurate mass measurements and an elemental composition program permitted the assignment of most peaks in the 142 - 176 Dalton mass range to a unique molecular species. For the remaining peaks, theoretical isotope abundances were used to eliminate one of the peaks. For example, at nominal mass 144: $^{144}Sm^+$ and $^{144}Nd^+$ are possible. From the theoretical isotope abundaces (11% and 88%), one can eliminate the $^{144}Sm^+$ ion.

As an additional test of the mass resolution for the microprobe FTMS, a nickel-chromium alloy with 2% of titanium was examined. With chromium and titanium in the same sample, a doublet consisting of $^{50}Cr^+$ and $^{50}Ti^+$ is present, requiring ~40,000 resolution for separation. This doublet was separated by the high resolving power of the FTMS instrument (Figure 3) with a measured resolution (FWHH) of > 100,000.

Surface profile analysis of integrated circuit chips requires high spatial resolution, small laser spot diameters and accurate sample positioning. To demonstrate the usefulness of the laser microprobe FTMS for such applications, positive and negative ion mass spectra were obtained from four separate components of a circuit chip. On the metallic part, doubly-charged tin was separable from singly-charged cobalt and nickel metal ions.

Conclusion:

The high mass resolution and mass accuracy of FTMS coupled with a prototype laser microprobe interface and sample introduction method demonstrate the usefulness of FTMS for surface characterization and the ability to eliminate mass spectral interferences.

1. M. Pelletier, G. Krier, J. F. Muller, M. Johnston, and D. Weil; *Rapid Comm. Mass Spectrom.*, 1988 (in press)

Presented at the 36th ASMS Conference on Mass Spectrometry and Allied Topics
June 5-10, 1988, San Francisco, CA

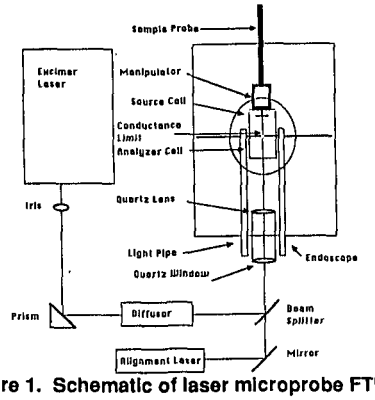

Figure 1. Schematic of laser microprobe FTMS

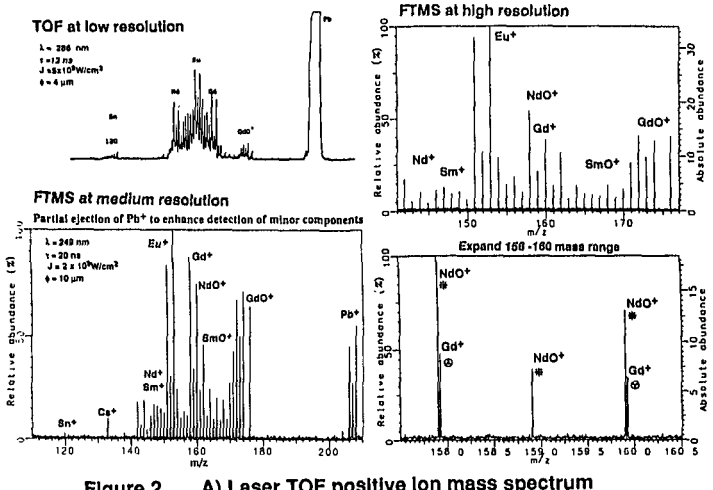

Figure 2. A) Laser TOF positive ion mass spectrum
B) FTMS partial ejection of Pb^+
C) High resolution positive ion mass spectrum
D) Expansion of 158-160 u region

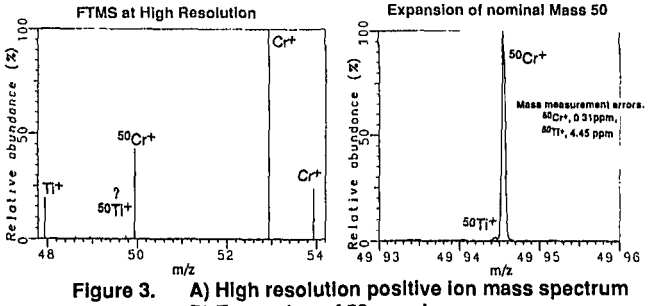

Figure 3. A) High resolution positive ion mass spectrum
B) Expansion of 50 u region

Presented at the 36th ASMS Conference on Mass Spectrometry and Allied Topics
June 5-10, 1988, San Francisco, CA

THE APPLICATION OF NOVEL ION TRAP SCAN MODES FOR HIGH SENSITIVITY GC/MS

D.B. Tucker, C.H. Hameister, S.C. Bradshaw, D.J. Hoekman, and M. Weber-Grabau
Finnigan MAT, San Jose, California 95134

The quadrupole ion trap mass spectrometer has the capability to simultaneously store ions over a wide range of m/z values prior to analysis. A practical limitation exists, however, in the number of ions that can be mass analyzed with unit resolution. Excess ions create space charging within the trap volume, shielding some ions from the RF level that would normally expel them and thus degrading resolution (Figs. 1a-b). The application of two different scan modes, axial modulation and Selective Mass Storage, overcome this limitation.

The physical description and explanation of axial modulation is described elsewhere (1). Briefly, the technique involves the application of an AC voltage signal to the endcap electrodes of the ion trap analyzer assembly during the data acquisition phase of the scan function. Resolution is improved dramatically, allowing the use of much longer ionization times to improve sensitivity (Fig. 1c). A series of analyses of Peregrine falcon egg extract demonstrates the detection of pesticides and polychlorinated biphenyls (Figs. 2a-b). The amounts injected were quantitated with external standards to be 8.5 ng p,p'-DDE (43 ppm/dry sample), 35 pg trans-nonachlor (175 ppb), and 29 pg nonachlorobiphenyl (145 ppb). Background substracted spectra of these compounds are correctly identified in a search of the NBS library (Figs. 3a-b).

There are several significant advantages of axial modulation as applied to ion trap mass spectrometry. The most important, of course, is the order of magnitude improvement in sensitivity achieved while maintaining unit mass resolution. But further, as a result of improved ion statistics, quantitation at low levels is more accurate. Linear quantitation curves can be obtained down to the picogram level (Fig. 4a-b). Isotope ratio patterns are readily discernible against background noise, improving the comparison with the NBS library.

Normal full scan function of the ion trap utilizes only RF voltages to isolate and analyze ions. Selective Mass Storage involves the application of a DC pulse, momentarily operating the trap near the apex of the stability diagram (q=0.78 and a=0.15). As a result, only ions of a single m/z value remain stored in the trap to be mass analyzed in RF-only mode. The expulsion of the majority of ions prior to mass analysis greatly reduces space charging effects. In selective ion monitoring mode, this reduction allows the use of very long ionization times to accumulate ions of the desired mass to charge ratio. An example of this effect is seen in the chromatogram of 1 pg of hexachlorobenzene (Fig. 5). With SMS of the molecular ion (m/z=284), a signal-to-noise ratio of 50:1 is achieved.

Selective Mass Storage can also be used in chemical ionization experiments to isolate a particular reagent ion and expel any EI fragments prior to mass analysis. In this case, the DC pulse is applied after the ionization pulse but prior to the reaction period. The ions that are then mass analyzed are generated solely by reagent ion/analyte reactions.

Acknowledgements:

We would like to thank Brock DeLappe and Walter Jarman of the Joseph M. Long Marine Laboratory at U.C. Santa Cruz for the standards and samples used in the axial modulation experiments.

References:

(1) Advances in MS/MS Analysis with the Ion Trap Mass Spectrometer, M. Weber-Grabau, P.E. Kelley, S.C. Bradshaw, D.J. Hoekman, presented at the 36th ASMS, San Francisco, California, 1988.

Presented at the 36th ASMS Conference on Mass Spectrometry and Allied Topics
June 5-10, 1988, San Francisco, CA

Figure 1

Axial Modulation

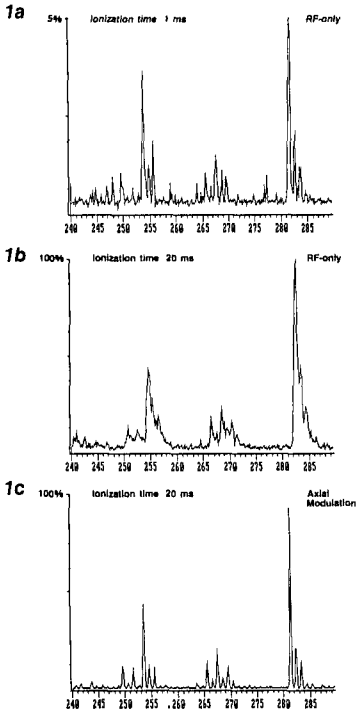

Figure 2

Reconstructed Ion Current Chromatogram

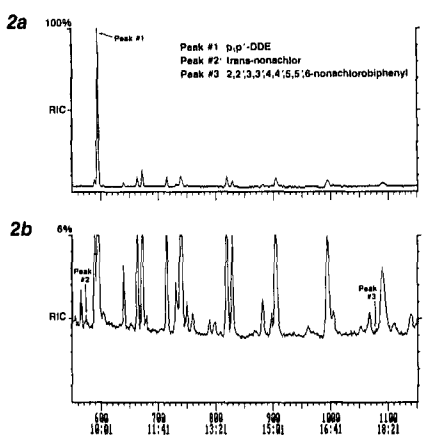

Figure 3

Identification and Quantitation of a Nonachlorobiphenyl at the ppb Level

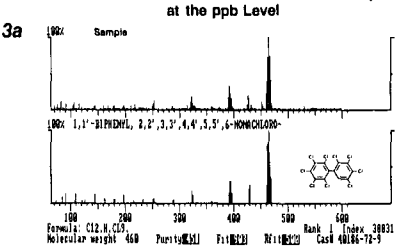

Identification and Quantitation of *trans*-nonachloro at the ppb Level

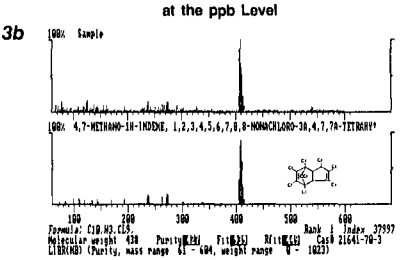

Figure 4

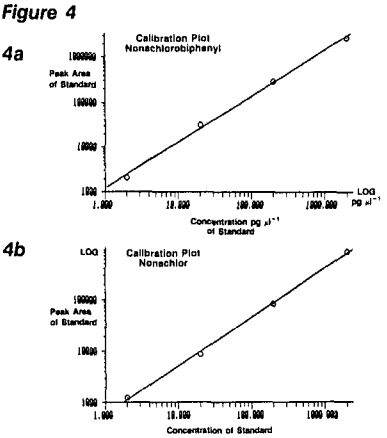

Figure 5

Detection of 1 pg of Hexachlorobenzene

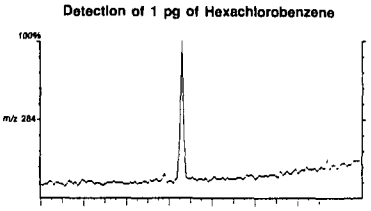

Presented at the 36th ASMS Conference on Mass Spectrometry and Allied Topics
June 5-10, 1988, San Francisco, CA

Characterization of Tandem Mass Spectrometry in the Quadrupole Ion Trap

Jodie V. Johnson and Richard A. Yost
Chemistry Department, University of Florida
Gainesville, FL 32611

Tandem Mass Spectrometry (MS/MS) consists of five processes: (1) ionization of the sample, (2) mass selection of an ion characteristic of the analyte, (3) collisional activated dissociation (CAD) of this parent ion with neutral gas molecules or surfaces to produce daughter ions followed by (4) mass analysis and (5) detection of these daughter ions. Most of the applications of MS/MS to the determination of trace analytes have been performed with Tandem-in-Space instruments (e.g. triple quadrupoles) where the MS/MS processes occur in separate, distinct regions of the instrument. The ion trap mass spectrometer (ITMS) represents a new approach to instrumentation for MS/MS. With the ITMS, the MS/MS processes all occur sequentially in the same physical space, and thus, MS/MS is Tandem-in-Time. Here we report the results of the characterization of the different ITMS parameters which affect MS/MS, as well as evaluations of the MS/MS efficiencies and sensitivity.

Operation of the ITMS. The Finnigan MAT Ion Trap Mass Spectrometer is a quadrupole ion trap consisting of a ring electrode and two electrically connected end-cap electrodes. Application of a radio frequency (RF) voltage to the ring electrode of the quadrupole ion trap relative to the end caps creates a symmetrical three-dimensional quadrupole electric field within the electrode surfaces. When ions are created within this quadrupole field, they are either trapped or ejected depending upon the specific mass-to-charge ratio (m/z) of the ion and the applied field parameters (the magnitude and frequency of the RF voltage). Those ions which are trapped will obtain an oscillatory motion with a unique secular frequency which is again dependent upon an ion'z m/z and the applied field parameters. In order to perform MS/MS of a particular ion, all ions below the parent ion of interest are ejected from the ion trap. This parent ion is "tickled" by applying an auxillary AC (tickle) voltage to the end caps. When the frequency of the tickle voltage has the same frequency as the secular frequency of the parent ion of interest, that ion begins to resonate, increasing its kinetic energy and orbit and undergoing collision with the helium buffer gas present in the ion trap. Provided the magnitude of the tickle voltage is sufficient, the ion will undergo CAD to produce daughter ions.

Experimental. All experiments were performed on a Finnigan MAT Ion Trap Mass Spectrometer (ITMS) operated at 100 °C with approximately 1 mtorr helium buffer gas under methane positive chemical ionization (PCI) conditions with approximately 2-3 X 10^{-5} torr methane. For studies on the effect of CAD parameters, diethylethylphosphonate (DEEP) was introduced via a Granville-Phillips fine metering valve to give a constant indicated pressure of approximately 0.1 X 10^{-5} torr. For the evaluation of MS/MS sensitivity, GC/methane PCI-MS/MS analyses were performed on a series of diisopropylmethylphosphonate (DIMP) in methanol standards of varying concentrations.

Results and Discussions. The methane PCI-CAD daughter spectrum of the $(M+H)^+$ ion of DEEP is characterized by daughter ions at m/z 65, 93, 111, and 139 (Figure 1). It was found that the efficiency of CAD is very dependent upon the frequency and magnitude of the tickle voltage and the time (CAD reaction time) for which it is applied. Variation of the tickle frequency demonstrated that the efficiency of CAD varied rapidly over a narrow range of frequencies with the maximum CAD occurring at the secular

frequency of the parent ion (Figure 2). Although the width of the tickle frequency band increased with increasing tickle voltage, it was possible to "tickle" the parent ion with unit mass resolution. It was also found that the length of the CAD reaction time and the magnitude of the tickle voltage required for the onset of CAD are inversely related. Following the onset of CAD, the amount of CAD increased with increasing tickle voltage and CAD reaction time (Figures 3 and 4). However, a maximum level of CAD was reached which was dependent upon the applied CAD parameters. With optimized CAD parameters, greater than 80% overall CAD efficiency could be obtained. The sensitivity of the ITMS was evaluated by the GC/PCI-MS/MS analyses of standard solutions of diisopropylmethylphosphonate (DIMP). A limit of detection of approximately 7 pg injected was obtained with a linear dynamic range of 3 orders of magnitude. It was possible to obtain full mass range daughter mass spectra of the $(M+H)^+$ ion on only 15 pg injected (Figure 5). The linear dynamic range was limited in the upper range by space charging. Space charging resulted in broadening of the ion profile and reduced CAD efficiencies due to a shift in the secular frequency of the parent ion to lower frequencies; thus, effectively reducing the coupling of the tickle voltage into resonating the parent ion.

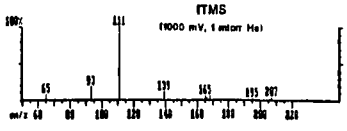

Figure 1

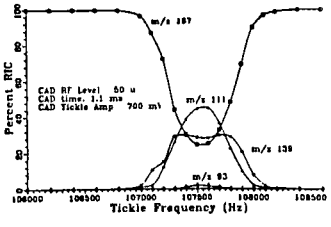

Figure 2

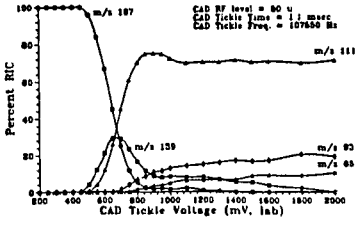

Figure 3

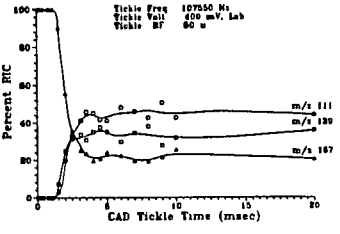

Figure 4

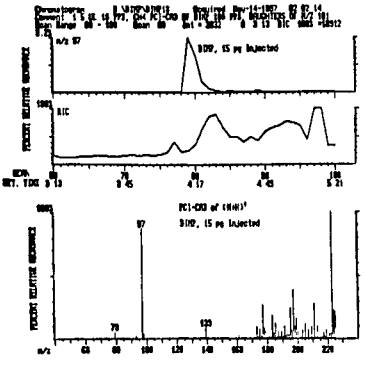

Figure 5

Presented at the 36th ASMS Conference on Mass Spectrometry and Allied Topics
June 5-10, 1988, San Francisco, CA

COMPUTER SIMULATION OF ION TRAJECTORIES IN A QUADRUPOLE ION TRAP MASS SPECTROMETER

Randall E. Pedder and Richard A. Yost
Department of Chemistry, University of Florida
Gainesville, Florida 32611

Introduction. Ion motion in a quadrupole ion trap mass spectrometer (ITMS) is described by the Mathieu equation. BASIC computer programs were created which calculate the trajectory of an ion in an ion trap by solving a modified form of this equation using a Fourth order Runge-Kutta algorithm. These programs were compiled using Borland's Turbo BASIC on an IBM PC compatible

Theory. A modified form of the Mathieu equation is used to calculate the motion of an ion in the 'z' direction of an ITMS:

$$\frac{d^2z}{d\xi^2} + (a_z - 2\, q_z \cos 2\xi)z = (\, b_z \cos \alpha\, \xi\,)z$$

with 'a', 'q', 'b', and 'α' defined as follows:

$$a_z = \frac{-\,4eU}{mz_0^2\omega^2} \qquad q_z = \frac{-\,2eV}{mz_0^2\omega^2}$$

$$b_z = \frac{-\,4eV_t}{mz_0^2\omega^2} \qquad \alpha = 2\,\omega_t/\omega$$

where ξ is the phase of RF voltage, e is the charge on an electron, U is the applied DC voltage, V is the zero to peak RF voltage, m is the mass-to-charge-ratio of a given ion, ω is the angular frequency of the field applied to the ring electrode, z_0 is the trap radius in the z direction, V_t is the zero to peak tickle voltage, and ω_t is the tickle frequency.

This equation assumes the superposition of two hyperbolic fields: the field caused by the RF voltage applied to the ring electrode, and the field caused by the application of a tickle voltage to the endcap electrode. The right hand side of this perturbed Mathieu equation contains the term for tickle voltage; if no tickle voltage is applied, this equation reduces to the more traditional unperturbed Mathieu equation. The computer programs which use this equation assume that the tickle voltages applied to the two endcap electrodes are 180° out of phase.

Motion in the 'x' and 'y' directions are described by the traditional unperturbed Mathieu equation.

Resonant Excitation. When a tickle voltage is applied across the endcaps of an ITMS any ions whose secular frequency corresponds with the tickle frequency will resonate, increasing the magnitude of their excursions in the 'z' direction with a corresponding increase in acceleration and kinetic energy. Collisions of these energized ions result in Collisionally Activated Dissociation (CAD). The application of a tickle voltage is modeled by solving the perturbed Mathieu equation. While maximum kinetic energy (most energetic daughter spectra) is obtained while exciting an ion at its secular frequency, excitation at frequencies near this secular frequency also result in excitation. Figure 1 shows the resolution of resonant excitation from a daughter experiment performed on the molecular ion of n-butylbenzene (m/z 134) in a Finnigan MAT ITMS. Figure 2 shows the simulated final kinetic energy of an ion based on the same experimental conditions, resulting in similar peak shape and bandwidth when compared with the experimental data. Note that typical ITMS MS/MS experiments employ much lower voltages and longer tickle times, resulting in narrower bandwidths (higher resolution) than shown in this example.

Electron Energy. The trajectory of a 12.5 eV electron injected through an endcap into an ion trap mass spectrometer was modeled by solving the Mathieu equation of motion for this very light "ion". The electron trajectory is unstable (electrons are too light to be stored in an ITMS) but the electron has a brief but finite residence time in the ion trap (low nanosecond range). Only electrons injected when the ring RF voltage is positive

result in ionization (see Figure 3); during negative RF phases, the electron is repelled back toward the endcap electrode resulting in a very short residence time and low electron energy (less than 6eV). In Figure 4 it can be seen that electron energy in an ITMS is dependent upon the ionization RF voltage. When the Automatic Gain Control (AGC) software of the Finnigan MAT Ion Trap Data System is used, the average electron energy is about 54 eV. EI mass spectra obtained with this electron energy should be extremely similar to standard 70 eV EI mass spectra.

Acknowledgement. We wish to thank Professor John Eyler of the University of Florida, and William Fies Jr. and Michael Weber-Grabau of Finnigan MAT Corp. for their contributions to this work.

Reference.

(1) P.E. Kelley, G.C. Stafford, Jr., W.J. Fies, Jr., J.E.P. Syka, R.T. McIver, Jr., R.L. Hunter, J.F.J. Todd, J.J. Bexon; Presented at the 32nd Annual Conference on Mass Spectrometry and Allied Topics, San Antonio, TX, May 27 - June 1, 1984. p. 505

This work was sponsored in part by a grant form the U.S. Army Chemical Research Development and Engineering Center.

Figure 1.

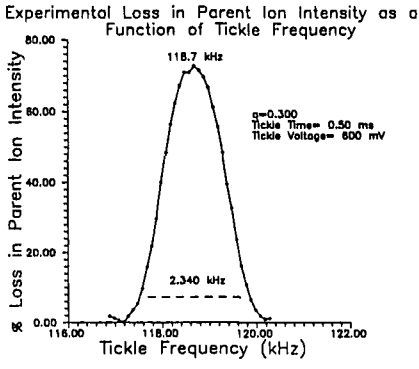

Figure 2.

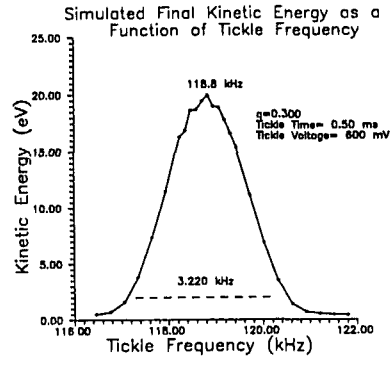

Figure 3.

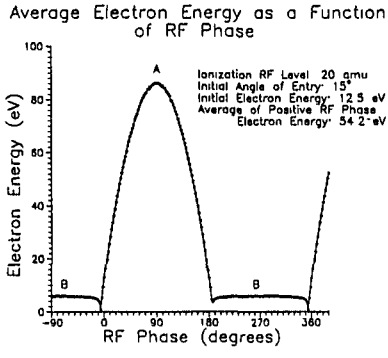

Figure 4.

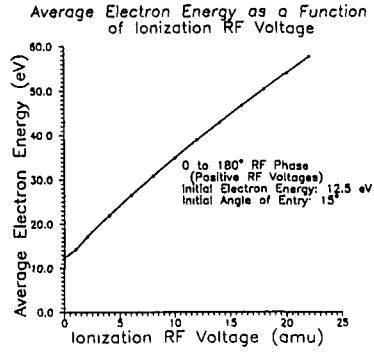

Presented at the 36th ASMS Conference on Mass Spectrometry and Allied Topics
June 5-10, 1988, San Francisco, CA

QUANTITATIVE EVALUATION OF ION INJECTION INTO A QUADRUPOLE ION TRAP

J.C. Schwartz and R.G. Cooks
Chemistry Department, Purdue University, W. Lafayette, IN 47907

M. Weber-Grabau and P.E. Kelley
Finnigan MAT, 355 River Oaks Parkway, San Jose, CA 95134

The ion trap operated in the mass selective instability mode has proved to be a relatively simple, yet versatile instrument for mass spectrometric studies. Ionization traditionally takes place inside the trap by injecting ionizing electrons, and thus excludes the use of methods not compatible with internal ionization such as FAB, glow discharge, etc. Successful trapping of externally generated ions which are then injected into the ion trap allows many different ionization methods to be coupled with the quadrupole ion trap.

To study in detail the operating parameters and characteristics of the process of ion injection into an ion trap, a simple apparatus consisting of an external EI source, ion injection lens assembly, and a quadrupole ion trap was constructed (Figure 1)[1].

The SIMION program was used to investigate the ion optics of the entire system including the source, injection lens system, and trap end-cap electrode. The results confirmed that the injection lenses can indeed focus the ion beam into the trap as designed and that the middle injection lens can be used to gate the ions into the trap at the appropriate time (Figure 2). Ion currents were measured at various points in the system in order to determine transmission and trapping efficiencies. The transmission of the injection lens system was 9%. Overall intensity of spectra obtained by injection vs. ionization <u>in situ</u> was 4 %. Therefore an efficiency of trapping injected vs. internally formed ions of 44% is implied, with the transmission characteristics of the injection system limiting the sensitivity.

Mass spectra for both positive and negative ions after injection were recorded over a range of ion energies from 10 to 60 eV. Spectra for FC-43 and 1,1,2,-trichloroethane are shown in Figure 3. Background ion intensity observed in earlier experiments was eliminated and ion intensity improved by including a source magnet. Due to the high ion energies and high pressures, CID accompanies ion injection as evidenced by the low abundance of the m/z 219 fragment and the large m/z 131 ion abundance in the positive FC-43 spectra, and the large m/z 169 ion abundance in the negative ion spectrum of FC-43, determined to be a daughter of m/z 452 ion.

Several parameters were found to have dramatic effects on the trapping of injected ions. Argon ions were used to investigate these parameters. The gate lens potential behaves as the ion optics predicts for focussing different energy ions into the trap (Figure 4.). A damping gas (He) is <u>essential</u> for successful trapping of injected ions, while it only <u>improves</u> performance of the trap for ions formed within it (Figure 5).

The Rf level during injection is a very important parameter. If an ion oscillates at a subharmonic of the Rf frequency, it can gain energy from the Rf and be ejected from the trap causing a local minimum in the intensity vs. q curve. For example at a **q** of .635, the ion oscillates at exactly 1/4 the Rf frequency and therefore a drop in intensity is observed (Figure 6). In comparing these curves for different ion energies, one notices that the onset of successful trapping occurs at higher Rf values for higher ion energies (Figure 7). This is to be expected as the Rf amplitude determines the depth of the potential well formed inside the trap.

Preliminary computer modelling studies show successful trapping occurs only during a narrow range of phases of the Rf around the downward zero crossing of the Rf amplitude and that approximately 5 or more stabilizing collisions are required.

This work demonstrates that ion injection is a viable method of coupling an external ion source with the ion trap. It should be possible to use any type of ion source. Ample sensitivity is observed in ion injection spectra and the data is of comparable quality to normal ion trap spectra. Under the conditions used, CID occurs as a result of the injection process. Several parameters have profound effects on the injection spectra and must be optimized when performing ion injection.

---

1 J.N. Louris, J.W. Amy, T.Y. Ridley, R.G. Cooks, Int. J. of Mass Spec. Ion Proc., in press.

Presented at the 36th ASMS Conference on Mass Spectrometry and Allied Topics
June 5-10, 1988, San Francisco, CA

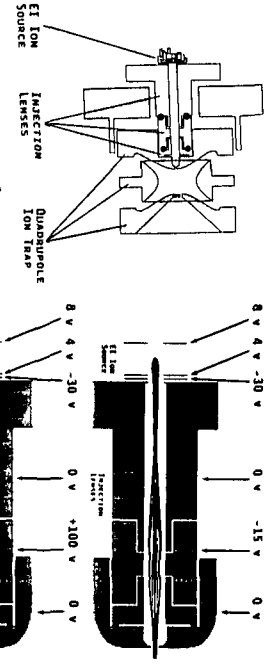

Figure 1

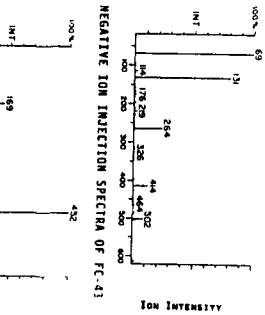

Figure 2

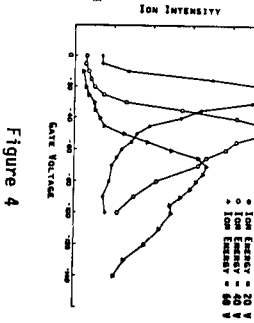

Figure 3

Figure 4

Figure 5

Figure 6

Figure 7

Presented at the 36th ASMS Conference on Mass Spectrometry and Allied Topics
June 5-10, 1988, San Francisco, CA

COUPLING OF AN ATMOSPHERIC SAMPLING ION SOURCE WITH AN ION TRAP MASS SPECTROMETER

Keiji G. Asano, Gary L. Glish, and Scott A. McLuckey
Analytical Chemistry Division
Oak Ridge National Laboratory
Oak Ridge, TN

The Ion Trap Mass Spectrometer (ITMS) is characterized by a number of features that make it potentially useful as the MS/MS instrument in a device that analyzes for trace organics in air. Among these features are its high MS/MS efficiencies, relatively small size, ruggedness, capability for mass-selective storage, and flexibility in scan modes. The present approach to ionization in the ITMS, viz. formation of ions within the ion trap, is not, however, optimal for the direct sampling of ambient air. We have developed an atmospheric sampling glow discharge ionization (ASGDI) source that has proved to be very useful for real-time trace analysis of organics in air when coupled with a beam-type MS/MS instrument. We have therefore interfaced this ASGDI source with an ITMS. The success of this combination hinges on how well ions that issue from the ion source can be injected and trapped in the ITMS.

Figure 1 shows a schematic of the ASGDI source/ITMS combination. A three elememt lens situated between the ion source and the ion entrance end cap of the ITMS serves the dual role of facilitating the transport of ions to the ion trap and pulsing the ion beam. Two half-plates constitute the center element of the lens. When both half-plates are held at the same potential either positive or negative particles are injected into the ion trap. Charged particles are deflected from entering the ion trap by changing the voltage of one of the half-plates. An off-axis conversion dynode electron multiplier is used to detect the ions and to avoid background noise arising from photons that issue from the glow discharge.

Both positive and negative ions have been successfully injected from the ASGDI source and trapped in the ITMS. We have found that the efficiency with which positive ions are trapped increases rapidly with He background pressure as indicated in Figure 2. Total positive ion signal increases by a factor of 40 over the pressure range indicated. We have noted several ways in which positive ions can be observed in these studies. These include: electron ionization in the trap, positive ion injection, and charge transfer within the ion trap from injected ions to ambient neutrals. Products from electron ionization are observed at low background pressures where injected ions are not efficiently trapped. At higher pressures, the mass spectrum is dominated by injected ions. Charge transfer to organic neutrals in the ion trap is observed when large concentrations of reagent ions formed in the ion source are allowed to accumulate. Organic ions formed in the ion source unaugmented by ions from charge transfer in the ion trap can be observed by operating the ion trap so that reagent ions are not trapped.

Electrons are injected under the same conditions for negative ion injection resulting in electron ionization within the trap. The positive ions formed in the trap can rapidly neutralize injected anions if they are allowed to accumulate. This situation can be avoided either by operating

the trap so that ions of m/z<34 are not stored or by applying a DC voltage to the ring to reject positive ions. The total negative ion signal observed, like the positive ion signal, also increases with He background pressure but tends to level off at about 10 mtorr. In these preliminary studies we have been able to obtain mass spectra and MS/MS spectra from anions formed from low levels (ppb and less) of nitro compounds in periods of 1 s and less.

These studies indicate that positive and negative ions can be injected from a high pressure ion source and trapped in the ITMS with sufficient efficiency to be analytically useful. These preliminary results indicate that the ASGDI source/ITMS will be a powerful combination for determination of trace organics in air. It seems likely that optimization of the injection experiment and measures to better accommodate the high background pressures required for trapping will improve the performance of this combination.

Research sponsored by the U.S. Department of Energy, Office of Basic Energy Sciences, under Contract DE-AC05-840R21400 with Martin Marietta Energy Systems, Inc.

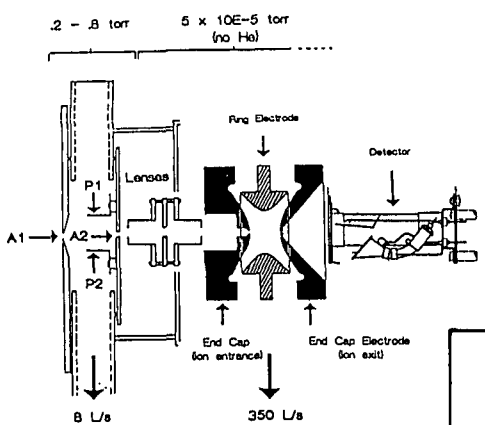

Fig. 1 Schematic diagram of the ASGDI source/ITMS

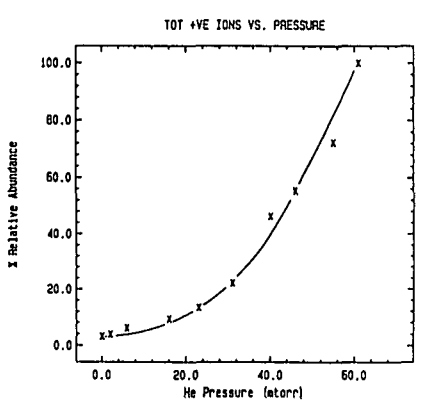

Fig. 2 He pressure effect on trapping efficiency

"The submitted manuscript has been authored by a contractor of the U.S. Government under contract No. DE-AC05-84OR21400. Accordingly, the U.S. Government retains a nonexclusive, royalty-free license to publish or reproduce the published form of this contribution, or allow others to do so, for U.S. Government purposes."

Presented at the 36th ASMS Conference on Mass Spectrometry and Allied Topics
June 5-10, 1988, San Francisco, CA

NON-CHROMATOGRAPHIC APPLICATIONS OF ION TRAP MASS SPECTROMETRY

P. H. Hemberger, W. D. Spall, C. P. Leibman, and T. M. Cannon
Los Alamos National Laboratory
Los Alamos, NM 87545

Instrumentation based on the Finnigan Ion Trap Detector is being developed at Los Alamos National Laboratory for real-time, in situ point monitoring of (1) combustion products and (2) vapor phase sub-surface transport of volatile organics at chemical waste areas. The sensitivity of the ion trap detector was determined for a variety of compounds to assess its suitability for these applications. An exponential dilution method was used to determine the detection limits for trace organic vapors in air. This is a dynamic calibration where a known concentration of organic vapor in a calibrated volume is continuously diluted by a constant flow of air to the vessel. The concentration of organic vapor (C) at any time is $C=C_0 \exp[-(Ft/V)]$, where C_0 is the initial concentration, F is the flow rate of the diluent gas, t is the elapsed time of dilution, and V is the flask volume.

Two gas-sampling systems for the ion trap detector have been evaluated. The first is the direct sampling of gases at atmospheric pressure through a leak valve. The limits of detection for organic compounds using this method approach 1 part per million. For environmental monitoring, lower detection limits can be achieved by replacing the leak valve with a silicon membrane. This provides an enrichment of the organic vapors over permanent atmospheric gases with a concomitant lowering in detection limits. Detection limits with membrane sampling were typically in the low part-per-billion range. Operation of the membrane at elevated temperatures did not improve the overall sensitivity because the diffusion of permanent gases through the membrane was enhanced as the temperature was increased.

SIGNAL INTENSITY VERSUS TIME AND CONCENTRATION FOR THE EXPONENTIAL DILUTION OF 500 ppm ORGANIC IN AIR. SAMPLING THROUGH A SILICON MEMBRANE AT 30 °C.

p (SAMPLE) = 2 x 10^{-6} Torr p (HELIUM) = 1 x 10^{-4} Torr

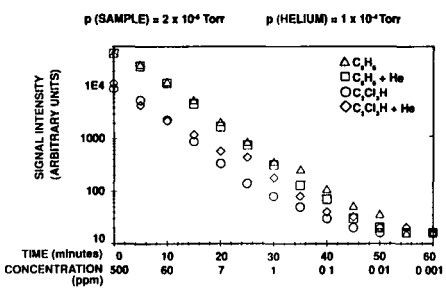

DETECTION LIMITS IN PARTS PER MILLION FOR ORGANICS IN AIR AT THE 3/1 (S+N) /N LEVEL.

	SAMPLING	
	DIRECT (LEAK VALVE)	MEMBRANE (30 °C)
C_2H_6	4	0.3
C_2H_6 + He	3	0.09
C_2Cl_3H	3	0.04
C_2Cl_3H + He	4	0.04
n - C_6H_{14}	40	
n - C_6H_{14} + He	30	
$(CH_3)_2CO$	40	
$(CH_3)_2CO$ + He	20	

Presented at the 36th ASMS Conference on Mass Spectrometry and Allied Topics
June 5-10, 1988, San Francisco, CA

ANALYSIS OF PORPHYRINS USING AN ION TRAP MASS SPECTROMETER

Gary J. Van Berkel, Gary L. Glish, and Scott A. McLuckey
Analytical Chemistry Division, Oak Ridge National Laboratory
Oak Ridge, TN 37831-8121

A major focus of our work with porphyrins is development of mass spectrometric analysis methods that provide more detailed structural information, and greater sensitivity and selectivity than obtainable from current mass spectrometric methods. We have found the ion trap mass spectrometer (ITMS) to be a promising tool in this effort due to its high sensitivity, multiple ionization modes, and MS^n capability. Using the ITMS, we have achieved a better understanding of the mass spectrometric behavior of porphyrins, thereby increasing the analytical utility of mass spectrometry for porphyrin analysis.

Electron ionization (EI) and chemical ionization (CI) in conjunction with multiple stages of mass analysis (i.e., MS^n, where $n \geq 2$) were investigated. The EI mass spectra obtained were very similar to those obtained on conventional instruments. For CI, common proton transfer reagent gases (CH_4, i-C_4H_{10}, and NH_3) and charge exchange reagent gases (N_2O and Ar) were used. In conventional CI, the mechanism of ionization and the extent of fragmentation can only be crudely controlled since several ions are often present to affect the mass spectrum. A particular reagent ion can be selected with the ITMS, however, allowing the mechanism and energetics of the ionization process to be more precisely controlled (Table 1). In conventional methane CI the major reagent ions present (CH_5^+ and $C_2H_5^+$) ionize the porphyrins <u>via</u> proton transfer and electron transfer respectively, complicating the molecular ion region of the spectrum. When CH_5^+ or $C_2H_5^+$ were selected to perform the ionization, the spectra were simplified producing only MH^+ or $M^{+\cdot}$, respectively. The degree of porphyrin fragmentation could be controlled by using charge exchange ionization via the recombination energy of the selected reagent ion. The ionization exothermicity was found to correlate with the degree of fragmentation.

MS/MS of porphyrin molecular ions and protonated molecules was used to determine the fragmentation pathways of alkylporphyrins (Figure 1). The MS/MS spectra contain a daughter ion characteristic of each substituent group of different mass on the macrocycle. The fragment characteristic of a particular substituent depends on the metallation state of the porphyrin and whether $M^{+\cdot}$ or MH^+ is analyzed. MS^n analysis was also used to investigate the nature of the substituent groups on the porphyrin macrocycle and the substituent group fragmentation pathways. MS^7 and MS^8 spectra were obtained.

The analytical utility of these ITMS techniques was demonstrated by the analysis of a complex vanadyl geoporphyrin mixture isolated from the New Albany Oil Shale Bitumen (Clark Co., IN). Using nitrous oxide (select $N_2O^{+\cdot}$) and ammonia (select NH_4^+) CI, the molecular ions and protonated molecules were produced, respectively, with no fragmentation (Figure 2a). The MS/MS spectra of each parent ion reveals the nature of the substituent groups on the porphyrins present at that mass (Figure 2b).

Selected reagent ion chemical ionization combined with multiple stages of mass analysis make the ITMS extremely useful for porphyrin identification, quantification, and structure determination. For example, "soft" ionization in combination with MS/MS could be of great utility in geoporphyrin mixture analysis. MS/MS spectra of all the porphyrins present in a mixture can provide a detailed substituent group "fingerprint" that might aid the use of porphyrins as biomarkers.

*Research sponsored by the U.S. Department of Energy, Office of Basic Energy Sciences, under contract DE-AC05-84OR21400 with Martin Marietta Energy Systems, Inc.

Table 1

Reagent Gas	Reagent Ion	Proton Transfer	Electron Transfer	PA (kcal/mol)	RE (eV)	Base Peak	Fragments
methane							
	CH_5^+	+	–	130.5		MH^+	–
	$C_2H_5^+$	–	+	163.5	8.13	$M^{+\cdot}$	–
isobutane							
	$C_3H_7^+$	+	–	184.9		MH^+	–
	$C_4H_9^+$	+	–	196.9		MH^+	–
water							
	H_3O^+	+	–	173		MH^+	–
ammonia							
	NH_4^+	+	–	205		MH^+	–
nitrous oxide							
	$NO^{+\cdot}$	–	+		9.25	$M^{+\cdot}$	–
	$N_2O^{+\cdot}$	–	+		12.9	$M^{+\cdot}$	$(M-15)^+$
argon							
	$Ar^{+\cdot}$	–	+		15.8	$(M-15)^+$	$(M-15)^+$

Figure 1

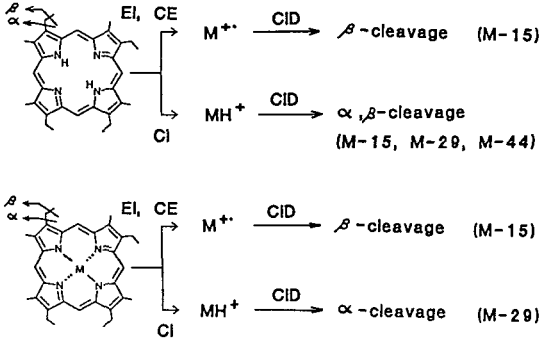

Figure 2. New Albany Geoporphyrins

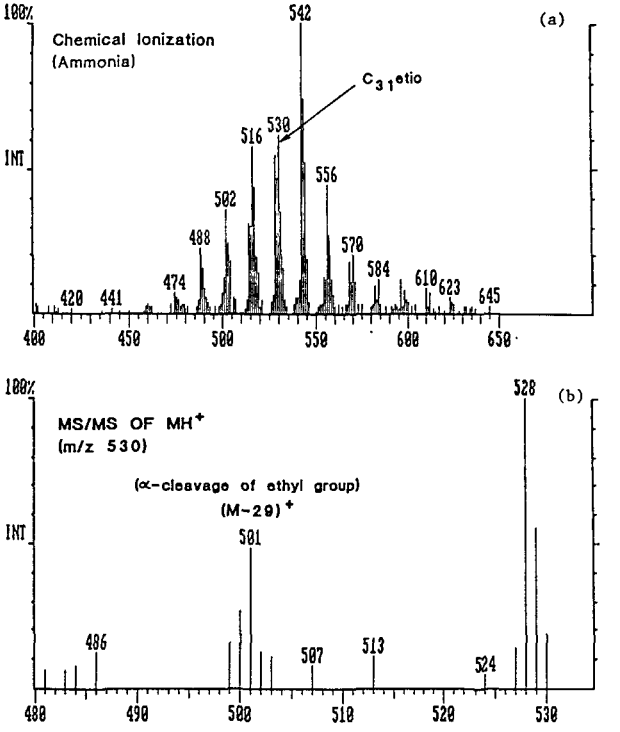

Presented at the 36th ASMS Conference on Mass Spectrometry and Allied Topics
June 5-10, 1988, San Francisco, CA

Presented at the 36th ASMS Conference on Mass Spectrometry and Allied Topics
June 5-10, 1988, San Francisco, CA

RAPID MICROORGANISM CHARACTERIZATION WITH PYROLYSIS, SHORT-COLUMN GC-ION TRAP MASS SPECTROMETRY

A. Peter Snyder
U.S. Army Chemical Research, Development and Engineering Center,
Aberdeen Proving Ground, Maryland 21010-5423

William H. McClennen and Henk L.C. Meuzelaar
Biomaterials Profiling Center, University of Utah,
Salt Lake City, Utah 84108

The analysis of complex compounds such as microorganisms is a formidable challenge, especially for the field of mass spectrometry (MS). The microbiological, medical and biotechnological communities have taken highly complex living systems and tailored the in-vivo/in situ experimental conditions to yield precise, yet trivial response characteristics, i.e., a go/no-go, present/absent or positive/negative analysis, expressed as a color (spectral) change as indicators of viability, process robustness and identification. Mass spectrometry, on the other hand, essentially uses abiological techniques in sample interrogation and must necessarily contend with analyzing parts and pieces of these large molecular weight entities. Lengthy extraction and derivatization of lipids from organisms with subsequent GC or GC/MS have provided an extensive database that accurately portrays their differentiation. Pyrolysis-short column GC-EI-ITMS is explored as a rapid (<6 min) and convenient means of producing information for generic and specific discrimination of microbes.

Microgram amounts of virulent (V) and low virulence (LV) B. anthracis (BA), B. licheniformis (BL) and F. tularensis (FT) were tested for strain response. The three species can be distinguished by a visual inspection of the TICs (Figure 1) and the latter part of each chromatogram was identified as the lipid TIC region. The microbiological literature attests to the diversity of lipid material in organisms, and extracted ion mass spectra were obtained (Figure 2) for a number of organisms including B. cereus (BC), B. thuringiensis (BT), B. subtilis (BS), L. pneumophila (LP), E. coli (EC) and S. aureus (SA). The mass spectral patterns are thought to represent the dehydrated diglyceride lipids. The possibility of discriminatory evidence between the virulent and low virulence strains of B. anthracis is noted in the reproducible differences associated with the extracted m/z 508, 522 and 536 mass spectra. This concept is of particular importance, and is a non-trivial exercise which requires a battery of plate growth and biochemical reaction tests for an accurate discrimination for virulence.

Figure 2 also shows distinct mass spectral differences as well as similarities within the Bacillus group, SA and Gram (-) organisms. Figure 3 presents a positive identification of the DNA/RNA nucleic acid and ATP adenine moiety, which is found in virtually all living systems, and is representative of all bacteria examined.

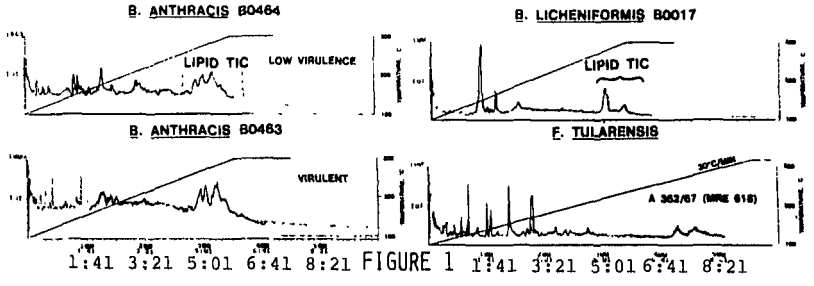

FIGURE 1

EXTRACTED MASS SPECTRA
FROM THE m/z 494 RIC

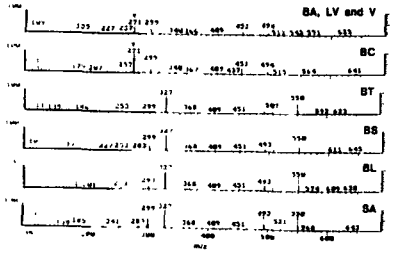

NOTE RIC NOT PRESENT FOR LP, EC AND FT

EXTRACTED MASS SPECTRA
FROM THE m/z 508 RIC

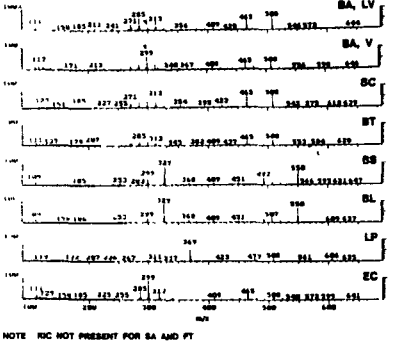

NOTE RIC NOT PRESENT FOR SA AND FT

EXTRACTED MASS SPECTRA
FROM THE m/z 522 RIC

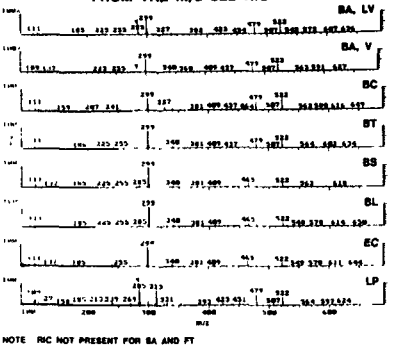

NOTE RIC NOT PRESENT FOR SA AND FT

FIGURE 2

EXTRACTED MASS SPECTRA
FROM THE m/z 536 RIC

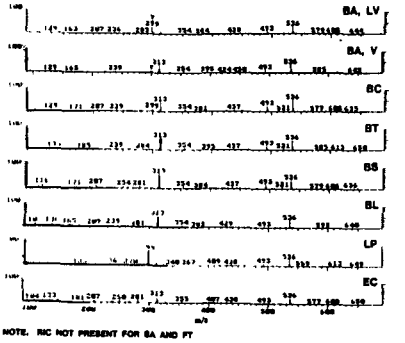

NOTE. RIC NOT PRESENT FOR SA AND FT

EXTRACTED MASS SPECTRA
FROM THE m/z 550 RIC

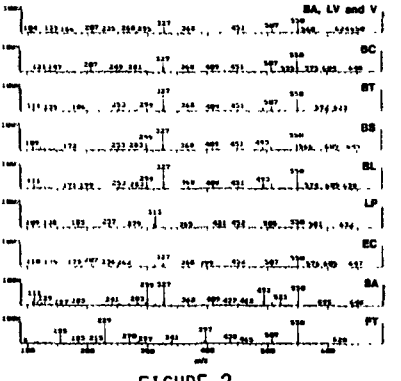

FIGURE 2

m/z 135 IDENTIFICATION

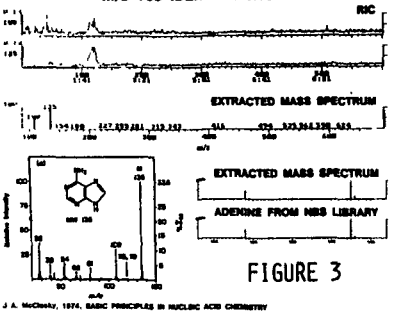

FIGURE 3

J. A. McCloskey, 1974, BASIC PRINCIPLES IN NUCLEIC ACID CHEMISTRY

Presented at the 36th ASMS Conference on Mass Spectrometry and Allied Topics
June 5-10, 1988, San Francisco, CA

ANALYSIS OF FRAGRANCE MATERIALS USING AUTOMATIC REACTION CONTROL™ CHEMICAL IONIZATION ON THE ION TRAP DETECTOR™

P. R. Keller, G. J. Harvey and D. J. Foltz
The Procter and Gamble Company, Cincinnati, OH, 45241

Fragrances play an important role in the acceptance of many consumer products and thus, analytical characterization and quantitation of fragrance materials have become extremely important. Analytically, fragrances are challenging due to their complexity and the presence of numerous trace components. Chemical ionization has long been recognized as a useful tool for obtaining molecular weight information and selective/sensitive quantitation. For this application, the CI instrument should be capable of providing molecular weight information on trace components and quantitation of many components in a single GC run (i.e., good full scan sensitivity and dynamic range). With these considerations in mind, the chemical ionization capabilities (Automatic Reaction Control mode) of the Finnigan Ion Trap Detector (ITD) have been investigated for a number of common fragrance components.

Experimental

A 25 component perfume mixture was used to evaluate the CI capabilities of the ITD. The chromatographic separation was accomplished through the use of a 30 m DB–5 capillary column. The standard ITD open split interface was used throughout this work. Full scan data (100–300 Daltons) using the ARC CI scan function[1] was obtained for both qualitative (molecular weight determinations) and quantitative evaluations. Ammonia, isobutane and methane were all investigated as reagent gases. This perfume mixture was also analyzed on our Finnigan 4500 quadrupole mass spectrometer in order to obtain data for a direct comparison.

Molecular Weight Information

With the exception of one component, linalool, molecular weight information was obtained for each of the perfume components in the mixture with at least one of the reagent gases. High quality spectra were obtained in the low picogram range for most components. Linalool, a tertiary alcohol of molecular weight 154 Daltons, exhibited a major ion at m/z 137. This loss of water was also evident in the quadrupole CI spectra. Only ammonia CI on the quadrupole produced any ions with mass higher than the molecular weight (M+H, M+18, and M+35). In general, the CI spectra obtained on the ITD were similar to those obtained on our quadrupole MS (see Figure 1). The differences that were observed were in the areas of fragmentation and adduct ion formation. The ITD CI spectra exhibited somewhat more fragmentation than those obtained on our quadrupole. This increased fragmentation is likely due to the longer residence time (milliseconds vs. microseconds) for ions in the ITD vs. a beam instrument. With respect to adduct ions, the ITD spectra exhibited less adduct ion formation than our quadrupole. No methane adduct ions (M+29, M+41) were observed in any of the ITD spectra. However, ammonia CI did yield some adduct ion formation (M+18), although no higher adducts (M+35) were observed. It was generally observed that ammonia adducts were produced with molecules that were not stable to protonation.

Quantitation

The quantitative capabilities of ARC CI were evaluated by obtaining full scan data as above, followed by selected ion quantitation. Typically, the protonated molecular ion, an adduct ion, or the largest fragment ion was used for the quantitation. Isobutane was found to provide the best detection limits. This superiority is likely due to the minimal fragmentation induced by this reagent gas and the higher RF levels (i.e., higher trapping efficiencies) that are used with isobutane. Detection limits, using isobutane were in the 5 to 50 picogram range (injected). The linear dynamic range extends from the detection limits up to at least 100 nanograms, the highest level employed in

the experiment. This full scan sensitivity makes it possible to quantitate, at picogram levels, a large number of perfume components (20–60) in a single GC run.

References:
1. M. Weber, P. E. Kelley, J. E. P. Syka, S. C. Bradshaw, J. S. Brodbelt, 35th ASMS Conference on Mass Spectrometry, 1987, 1114.

FIGURE 1: COMPARISON OF QUADRUPOLE AND ITD CI SPECTRA

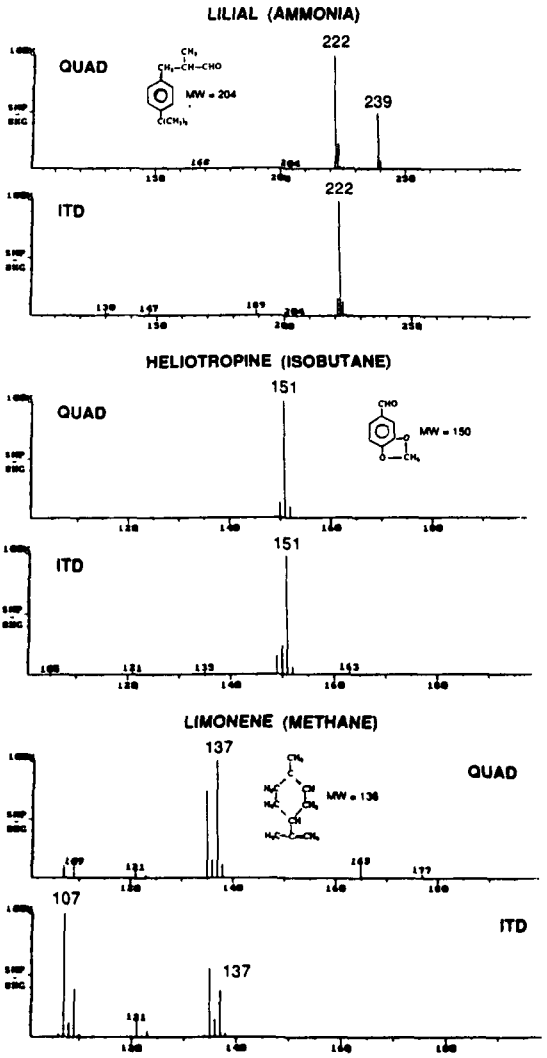

Presented at the 36th ASMS Conference on Mass Spectrometry and Allied Topics
June 5-10, 1988, San Francisco, CA

TRACE ANALYSIS OF ORGANIC COMPOUNDS IN AQUEOUS SOLUTIONS USING A MEMBRANE PROBE AND A QUADRUPOLE ION TRAP

Anita K. Lister, R. Graham Cooks,
Purdue University
West Lafayette, IN 47907

Trace analysis of organic molecules directly from water poses many problems. Liquid chromatography/mass spectrometry and semipermeable membranes have been developed to allow fluid samples to be introduced into a mass spectrometer. Membrane probes have been interfaced to a triple quadrupole mass spectrometer for the analysis of organics in blood (1), for reaction monitoring and environmental analysis (2), and for off-line analysis of fermentation broths. Here, a membrane probe is interfaced to an Ion Trap Detector for the qualitative and quantitative analysis of organics directly from water.

Experimental:

A modified Finnigan 700 Ion Trap Detector (ITD) is used in this experiment (Figure 1). The software used is a special version of the standard ITD software supplied by the manufacturer.

Aqueous samples are introduced into the ITD through a simple membrane probe via the Granville-Phillips valve. The small amount of water which permeates the membrane is used as the chemical ionization reagent gas.

The membrane probe is constructed from Dow Corning silicon capillary tubing which is fashioned in a loop and sealed to a metal tube with vacuum epoxy (Figure 2). The probe is coupled to the ITD via a Granville-Phillips valve.

Results:

Ten organic compounds in the ppb to low ppm concentration range are analyzed directly from water. All solutions are analyzed with no sample preconcentration, and the most abundant ion in the $CI(H_2O)$ mass spectrum, typically $(M+H)^+$, is used for quantitation.

The detection limit for these compounds is established when the signal-to-noise ratio for the monitored ion is 2. Table 1 summarizes the monitored ion and the detection limit for each compound. Note that N,N-dimethylformamide is the only compound not detected in the concentration range of interest.

The linearity of the ion intensity over this concentration range is illustrated by the response curve of toluene (Figure 3). The rise time of most of the compounds is less than 60 seconds, and the fall times are generally less than 120 seconds (Table 2). Thus, analysis of a sample is complete within minutes.

Aqueous solutions of these compounds have also been analyzed using a triple quadrupole mass spectrometer. The chemical ionization mass spectra obtained on both instruments are similar.

One application of this technique is the analysis of mixtures. In two test mixtures containing three components, the response of each compound in the mixture appears to be unaffected by the presence of the other components. Table 3 summarizes the results of one of the mixtures.

Conclusion:

A membrane probe has been successfully interfaced to an ITD. The membrane/ITD combination is capable of rapidly detecting ppb levels of organics directly from water with no sample preconcentration.

Literature Cited:

(1) Tou, J. C.; Kallos, G. J.; Dryzga, M. D.; Brodbelt, J. S.; Cooks, R. G. Anal. Chem., 1987, 59, 454-458.

(2) Brodbelt, J. S.; Cooks, R. G. Anal. Chem., 1985, 57, 1153-1155.

(3) Bier, M. E.; Cooks, R. G. Anal. Chem., 1987, 59, 597-601.

Presented at the 36th ASMS Conference on Mass Spectrometry and Allied Topics
June 5-10, 1988, San Francisco, CA

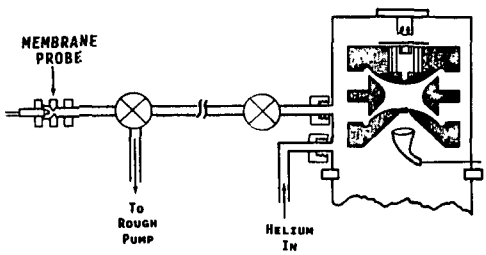

Figure 1 Ion Trap Detector with a Membrane Probe

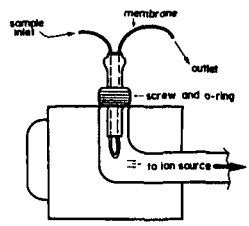

Figure 2 Simple Membrane Probe

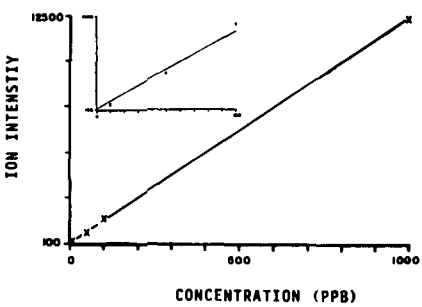

Figure 3 Response Curve of Toluene

COMPOUND	CONC(PPB)	ION MONITORED
ACETONE	100	59
AMYL ACETATE	10	61
BENZENE	1	79
CHLOROBENZENE	100	113
DIETHYL ETHER	10	75
ISOBUTYL CHLORIDE	10	57
METHYLENE CHLORIDE	50	49
N,N-DIMETHYLFORMAMIDE	>10000	74
TETRAHYDROFURAN	100	73
TOLUENE	10	93

Table 1 Detection Limits of 10 Organic Compounds using CI(H_2O) in an ITD interfaced with a membrane probe

COMPOUND	ARISE TIME (SEC)	BFALL TIME (SEC)
ACETONE	112	>300
AMYL ACETATE	24	208
BENZENE	26	61
CHLOROBENZENE	43	80
DIETHYL ETHER	87	118
ISOBUTYL CHLORIDE	91	153
METHYLENE CHLORIDE	8	75
TETRAHYDROFURAN	43	80
TOLUENE	24	113

ARISE TIME IS THE TIME IT TAKES FOR THE SIGNAL TO GO FROM 10% TO 90% OF THE MAXIMUM NORMALIZED SIGNAL.

BFALL TIME IS THE TIME IT TAKES FOR THE SIGNAL TO GO FROM 90% TO 10% OF THE MAXIMUM NORMALIZED SIGNAL.

Table 2 Typical Rise and Fall Times

Individual 100 ppb Solutions

COMPOUND	m/z	INTENSITY
DIETHYL ETHER	75	94 COUNTS
METHYLENE CHLORIDE	49	6 COUNTS
TETRAHYDROFURAN	73	16 COUNTS

Mixture of 100 ppb of each compound

COMPOUND	m/z	INTENSITY
DIETHYL ETHER	75	95 COUNTS
METHYLENE CHLORIDE	49	6 COUNTS
TETRAHYDROFURAN	73	15 COUNTS

Mixture of 50 ppb diethyl ether, 100 ppb methylene chloride and 100 ppb tetrahydrofuran

COMPOUND	m/z	INTENSITY
DIETHYL ETHER	75	48 COUNTS
METHYLENE CHLORIDE	49	6 COUNTS
TETRAHYDROFURAN	73	16 COUNTS

Table 4 Mixture Analysis

Presented at the 36th ASMS Conference on Mass Spectrometry and Allied Topics
June 5-10, 1988, San Francisco, CA

REMEASUREMENT AND DETECTION OF HIGH MASS IONS IN FOURIER TRANSFORM MASS SPECTROMETRY

E. R. Williams, B. H. Wang, J. A. Loo, K. D. Henry,
and F. W. McLafferty
Chemistry Department, Cornell University, Ithaca, NY 14853-1301

Fourier transform mass spectrometry (FTMS) has numerous advantages in the analysis of larger molecules, including multichannel detection, high resolution, and extensive MS/MS capabilities. However, FTMS requires a minimum of about 10 ions to produce a detectable signal with a single measurement [1], a severe disadvantage over other detection methods, i.e., electron multipliers, capable of single ion detection. We now offer evidence for repeated FTMS measurements of the same ions resulting in substantial gains in sensitivity.

A 50 μCi ^{252}Cf source and a 60+ keV μMEVVA (MEtal-Vapor Vacuum Arc) SIMS gun in conjunction with a prototype FTMS-2000 provide continuous [2,3] and pulsed ion sources respectively [4]. Removal of the conductance limit and doubling the length of the cell improves the pumping capability but has negligible effect on sensitivity and resolution. However, elimination of the quench pulse can result in greater than 35 times increased signal for high mass ions measured with 40 scans (figure 1) and over 100 times with 800 scans. Collisional relaxation of large ions back to the center of their orbits makes these ions available for subsequent redetection. For gramicidin S (MW 1140.7) molecular ion species at 2 x 10^{-9} torr, the efficiency of relaxation is nearly 100% after approximately 180 sec. Higher pressures decrease the time necessary for relaxation; lower mass ions increase the relaxation time, consistent with the corresponding decreased collisional cross section. In addition, increasing the excitation power thereby increasing the ion orbit results in longer relaxation times. The high efficiency for ion relaxation is confirmed using a pulsed SIMS gun. Excitation of ions 2 times before the excite/detect sequence results in little loss of ion signal provided an adequate delay is allowed after both excite events to allow the ions to relax down to the center of their orbits.

Decreasing the system pressure through the use of an ion pump results in longer relaxation times and also longer RF transient lengths making possible high resolution measurements with plasma desorption (PD) (figure 2). The much shorter transients of large organic ions can provide useful mass spectral data by using special methods. In this regard the Hankel matrix singular value decomposition of Barkhuijsen and de Beer appears particularly promising.

[1] Comisarow, M. B. Anal. Chim. Acta 1985, 178, 1-15.
[2] Loo, J. A.; Williams, E. R.; Amster, I. J.; Furlong, J. J.; Wang, B. H.; McLafferty, F. W.; Chait, B. T.; Field, F. H.; Anal. Chem. 1987, 59, 1880-1882.
[3] Loo, J. A.; Williams, E. R.; Furlong, J. J. P.; Wang, B. H.; McLafferty, F. W.; Chait, B. T.; Field, F. H. Int. J. Mass Spectrom. Ion Proc. 1987, 78, 305-313.
[4] Brown, I. G.; Galvin, J. E.; MacGill, R. A.; Wright, R. T. Appl. Phys. Lett. 1986, 49, 1019-1021.

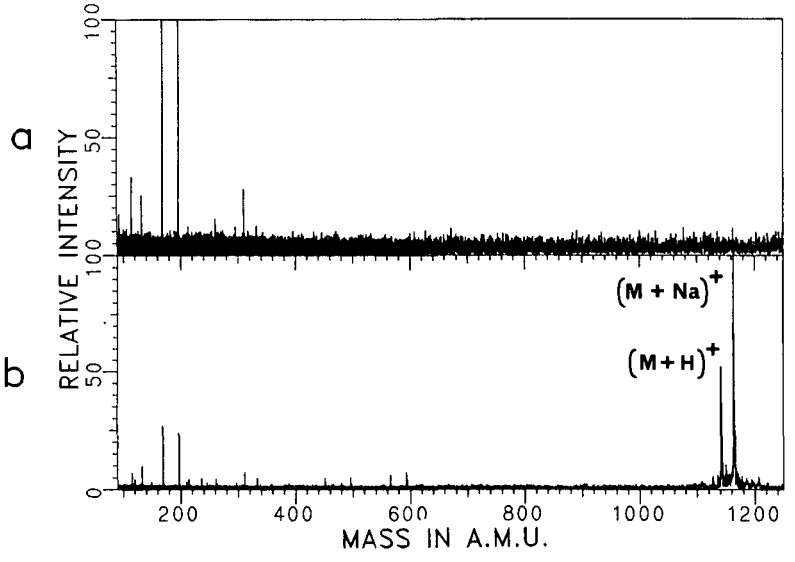

Figure 1: ^{252}Cf-PD spectrum of Gramicidin S using 45 s ion collection time and 40 scans (30 min. total) with a) quench on, b) quench off.

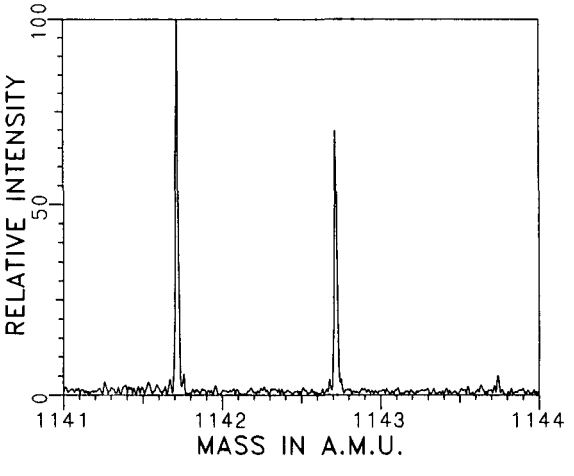

Figure 2: ^{252}Cf-PD high resolution spectrum of gramicidin S $(M + H)^+$ showing 65,000 resolution (FWHH). Spectrum collected using 500 s ion collection time and 1 scan.

Presented at the 36th ASMS Conference on Mass Spectrometry and Allied Topics
June 5-10, 1988, San Francisco, CA

CROSSED-BEAM STUDIES OF ENERGY TRANSFER IN LOW ENERGY ION-MOLECULE COLLISIONS

S. Howard, A. Shukla, K. Birkinshaw, J. Wang, and J. Futrell
Department of Chemistry, University of Delaware, Newark, DE 19716

The crossed molecular beam method was used to investigate energy transfer in ion molecule collisions. The measurement of angular scattering along with translational energy exchange in these systems provide detailed information on energy transfer during the collision. The basic mechanisms for energy transfer in low energy collisions have been a subject of debate for several years. The role of short-range repulsive interactions, transient complexes,[1] or the effects of a forced harmonic oscillator[2] are some of the possibilities for discussion. The reaction of oxygen ions with methane has received much study[1,3] as has the reaction of argon ions with nitrogen.[4]

Ion molecule reaction studies using well-defined beams are favorable for reaction dynamics investigations since they provide the possibility to examine the transfer of translational and internal energies in an elementary process. The basis for analyzing the dynamics of these studies lies in the expressions connected with conservation of energy, as discussed in more detail elsewhere.[5]

The crossed beam apparatus used in this study has been described in detail elsewhere.[6] Key features for present investigation include: a mass-selected ion beam decelerated to the chosen collision energy, a neutral beam generated by a supersonic expansion, and a detector capable of mass, energy and angular analysis.

Laboratory angular and energy distributions were taken at a series of angles from 0° to 90° for the product ion. These data were graphically transformed into Cartesian probability densities, $P_c(u_1,u_2,u_3)$, required to construct scattering diagrams.[7]

At energies near 1 eV, the scattering diagram for oxygen ions scattering from methane (Figure 1) shows that scattering is approaching the isotropic distribution predicted by the transient complex model by Ferguson et al.[1] This diagram is the first to our knowledge which has a neutral velocity greater than the ion velocity. The diagram suggests that the excited a $^4\Pi_u$ state contributes to the overall scattering in addition to the vibrationally excited (v = 2) ground state. Ground-state oxygen quite effectively transferred between 0.2 and 0.9 eV translational energy to methane.

The absence of signal at the location where product would be found from initially $O_2^+(X^2\Pi_g)$ could be interpreted as reaction competing effectively with energy transfer. If this reaction occurs, product ions of different mass would be formed (the second mass analyzer was set to transmit only m/e = 32 ions). Tanaka et al.[3] have shown that reactive channels can be vibrationally enhanced for this system.

The reaction of $Ar^+(^2P_{3/2})$ with oxygen at 2.2 eV CM as shown in Figure 2 shows that charge transfer can also transfer both electronic and vibrational energy. Product oxygen ions are formed both in highly vibrationally excited ground states and in electronically excited states. Charge transfer can, therefore, be very effective in transferring energy during ion molecule collisions.

Presented at the 36th ASMS Conference on Mass Spectrometry and Allied Topics
June 5-10, 1988, San Francisco, CA

References:

1. E. Ferguson, J. Phys. Chem., 90, 731 (1985).
2. P. Cosby and T. Moran, J. Chem. Phys., 52, 6157 (1970).
3. K. Tanaka, T. Kato, and I. Koyano, J. Chem. Phys., 84, 750 (1986).
4. K. Birkinshaw, A. Shukla, S. Howard, and J. Futrell, Chem. Phys., 113, 149 (1987).
5. D.-W. Hu, B. Friedrich, A. Rockwood, S. Howard, W. Lindinger, and J. Futrell, Proc. Sympos. on Atomic & Surf. Phys., 106 (1984).
6. M. Vestal, C. Blakeley, and J. Futrell, Phys. Rev. A, 17, 1321 (1978).
7. B. Friedrich and Z. Herman, Coll. Czech. Chem. Commun., 49, 570 (1984).

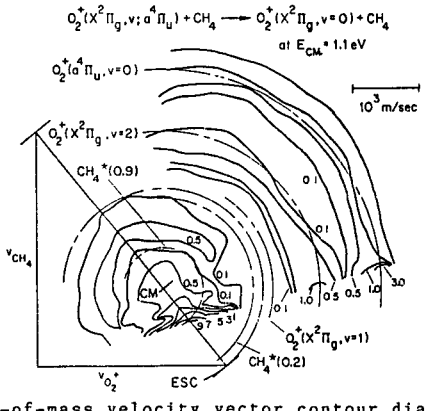

Fig. 1 Center-of-mass velocity vector contour diagram for the reaction $O_2^+(X^2\Pi_g, v;\ a\ ^4\Pi_u) + CH_4 \rightarrow O_2^+(X^2\Pi_g, v=0) + CH_4$ at 1.1 eV collision energy. The circles outside the elastic scattering circle (ESC) indicate the location of velocity vectors for O_2^+ products with conversion of electronic or vibrational energy into translational energy and no energy deposited in rotation.

$$Ar^+(^2P_{3/2}) + O_2 \longrightarrow Ar(^1S_0) + O_2^+$$

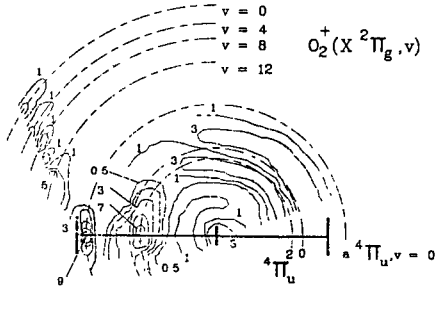

Fig. 2 Center-of-mass velocity vector contour diagram for the reaction $Ar^+(^2P_{3/2}) + O_2 \rightarrow O_2^+ + Ar(^1S_0)$ at 2.2 eV collision energy. The circles indicate the location of velocity vectors for O_2^+ products with translational to internal energy conversion.

Presented at the 36th ASMS Conference on Mass Spectrometry and Allied Topics
June 5-10, 1988, San Francisco, CA

The Kinetic Energy Dependences of the Rate Constants for the Reactions of O^- with CH_4, N_2O, and SO_2 at Several Temperatures: Deriving Rotational Energy Dependences

A.A. Viggiano, Robert A. Morris, John F. Paulson, and F. Dale
Air Force Geophysics Laboratory, Ionospheric Interactions Branch
Hanscom AFB MA 01731-5000

The kinetic energy dependences of the rate constants for the reactions of O^- with CH_4, N_2O, and SO_2 have been measured at several temperatures over the range 85-500 K. The main ionic products are OH^-, NO^-, and e^-, respectively. The rate constants were measured in a selected ion flow drift tube. A similar apparatus has been described in detail[1] and will not be discussed here.

Figures 1-3 show the kinetic energy dependences of the rate constants for the reactions of O^- with CH_4, N_2O, and SO_2, respectively. The reactions of O^- with N_2O and SO_2 show little dependence of the rate constant on temperature, although there are appreciable kinetic energy dependences. The reaction of O^- with CH_4 is in contrast to this behavior, and the rate constants show substantially different kinetic energy dependences at various temperatures.

The data can be used to derive rotational temperature dependences of the rate constants for the reactions. When a reaction involving a monatomic ion is studied in the drift tube, varying the electric field results only in changing the ion translational energy and therefore the center of mass kinetic energy (which depends both on the electric field and temperature). Thus, the translational energy dependence of the rate constant at a particular temperature of the reactant neutral is obtained. The temperature of the reactant neutral is equal to the bath gas temperature, defining the internal temperature of the neutral. For neutral species with vibrational modes not appreciably excited at the temperatures used in the experiment, the only significant internal energy is that of rotation. By comparing rate constants measured at a particular kinetic energy at several temperatures, we obtain the dependence of the rate constant on the rotational (or internal) temperature of the neutral.

The data in Fig. 1-3 indicate that, for the three reactions in this study, only for the reaction of O^- plus CH_4 does the rate constant have a substantial dependence on internal temperature of the reactant neutral . The other two reactions have rate constants that depend only slightly on the internal temperature of the reactant. The vibrational frequencies of CH_4 are sufficiently high that the CH_4 in our experiments is mainly in the ground vibrational state, and the internal energy dependence therefore corresponds to a purely rotational effect. The rotational temperature dependence of this reaction is shown in Fig. 4 at 0.06 and 0.25 eV center of mass kinetic energy. The temperature dependence of the rate constant for this reaction was found to be $T^{-0.56}$ at 0.06 eV and $T^{-0.40}$ at 0.25 eV. The rate constants vary by a factor of 2.7 and 2.0 over the temperature range 85 to 500 K at 0.06 and 0.25 eV, respectively. To the best of our knowledge these represent the first measurements of the dependence of an ion-molecule rate constant on the rotational temperature of the neutral.

1. D. Smith and N.G. Adams, *Adv. At. Mol. Phys.*, 23 (1988).

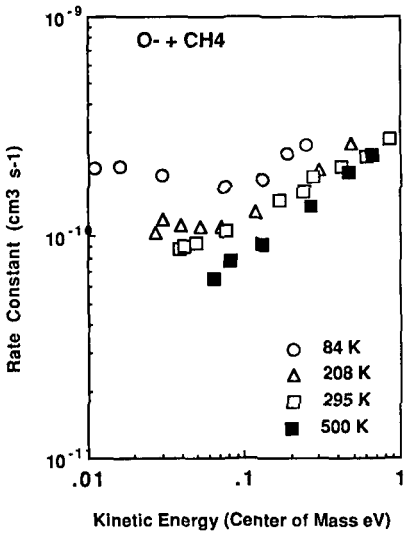

Fig. 1 Rate constants for the reaction of O^- with CH_4 vs. energy at various temperatures.

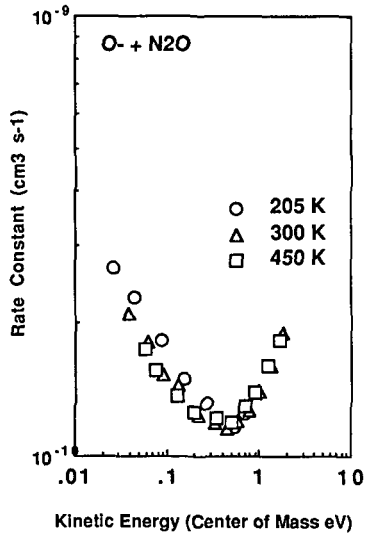

Fig. 2 Rate constants for the reaction of O^- with N_2O vs. energy at various temperatures.

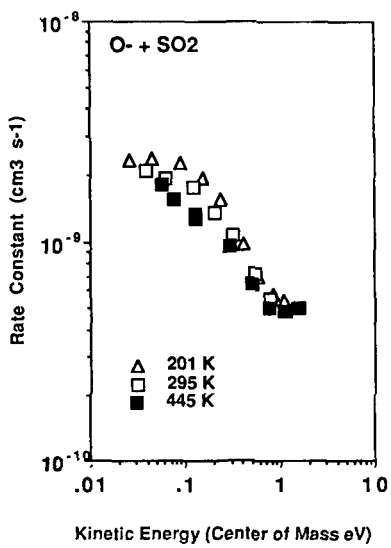

Fig. 3 Rate constants for the reaction of O^- with SO_2 vs. energy at various temperatures.

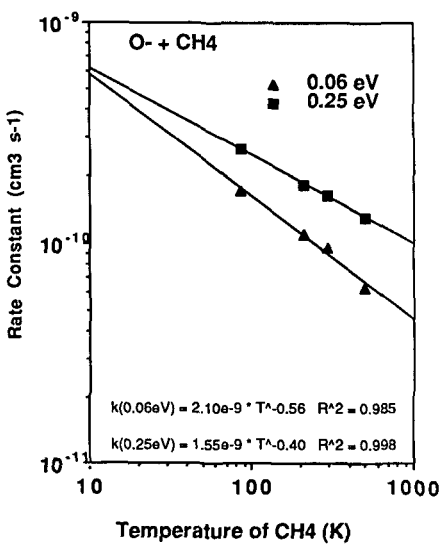

Fig. 4 Rate constants for the reaction of O^- with CH_4 *vs. rotational temperature at 0.06 and 0.25* eV.

Presented at the 36th ASMS Conference on Mass Spectrometry and Allied Topics
June 5-10, 1988, San Francisco, CA

RATE CONSTANTS FOR ION-MOLECULE REACTIONS OF ATMOSPERIC SULFUR COMPOUNDS

T.F. Thomas, Dept. of Chemistry, University of Missouri-Kansas City, Kansas City, MO 64110; A.A. Viggiano, F. Dale, J.F. Paulson, Air Force Geophysics Laboratory, Hanscom AFB, MA 01731

In an effort to better understand the role of sulfur-compounds in the ion chemistry of the stratosphere rate constants for 24 reactions have been measured on the Selected Ion Flow Tube at AFGL. Figure 1 shows typical-looking data in the atypical case of an endothermic reaction (presumably due to many SO_2^+ ions retaining their vibrational excitation during their passage down the SIFT). Table I shows the rate constants obtained at 298°K for some of charge transfer reactions studied (only the major product formed is shown).

Table I. Rate Constants for Charge Transfer.

Reaction	$10^{10} \times k_{exp}$ ($cm^3 \cdot s^{-1}$)	$10^{10} \times k_{lit}$ ($cm^3 \cdot s^{-1}$)	ΔH (ev)
$SO_2^+ + NO \rightarrow NO^+ + SO_2$	1.0	0.7[1]	-3.0
$SO_2^+ + NO_2 \rightarrow NO_2^+ + SO_2$	3.6	-----	-2.7
$OCS^+ + NO \rightarrow NO^+ + OCS$	1.0	0.7[2]	-1.9
$OCS^+ + NO_2 \rightarrow NO_2^+ + OCS$	1.6	-----	-1.6
$O_2^+ + OCS \rightarrow OCS^+ + O_2$	11.0	10.[3]	-0.9
$H_2O^+ + SO_2 \rightarrow SO_2^+ + H_2O$	28.	-----	-0.3
$SO_2 + H_2O \rightarrow H_2O^+ + SO_2$	12.	-----	+0.3

Figure 2 displays the dependence of our measured rate constants for charge transfer, relative to theoretical values calculated by the method of Su and Chesnavich,[4] upon the enthalpy of reaction (ΔH). The data suggest a near-resonance condition $0 \leq -\Delta H \leq 1$ev for efficient charge transfer, which is a special case of energy transfer from an electronically excited molecule.

Some of the results obtained for clustering reactions at 298°K are shown in Table II.

Table II. Rate Constants for Clustering Reactions.

Reaction	$10^{-16} \times N_{He}$ (cm^{-3})	$10^{27} \times k_{ter}$ ($cm^6 \cdot s^{-1}$)	$10^{10} \times \tau$ (s)
$SO_3^+ + H_2O \rightarrow H_2SO_4^+$	1.14-1.70	4.5	36
$SO_2^+ + SO_2 \rightarrow S_2O_4^+$	1.30	2.1	24
$SO^+ + SO_2 \rightarrow S_2O_3^+$	1.30	1.0	10.5
$OCS^+ + H_2O \rightarrow H_2CO_2S^+$	1.29-1.85	1.2	9.0

In Table II $k_{ter} = k_{exp}/N_{he}$ and τ is the calculated lifetime of the ion-neutral collision complex in the usual mechanism for a termolecular reaction.

Acknowledgement: T.F. Thomas was supported by Air Force Systems Command Contract No. F19628-84-K-0038 while making these measurements.

Presented at the 36th ASMS Conference on Mass Spectrometry and Allied Topics
June 5-10, 1988, San Francisco, CA

1) M. Durup-Ferguson, et al., J. Chem. Phys. 79, 265 (1983).
2) D. Smith, N.G. Adams, and W. Lindinger, J. Chem. Phys. 75, 3365 (1981).
3) D. Smith, N.G. Adams, and T.M. Miller, J. Chem. Phys. 69, 308 (1978).
4) T. Su and W.J. Chesnavich, J. Chem. Phys. 76, 5183 (1982).

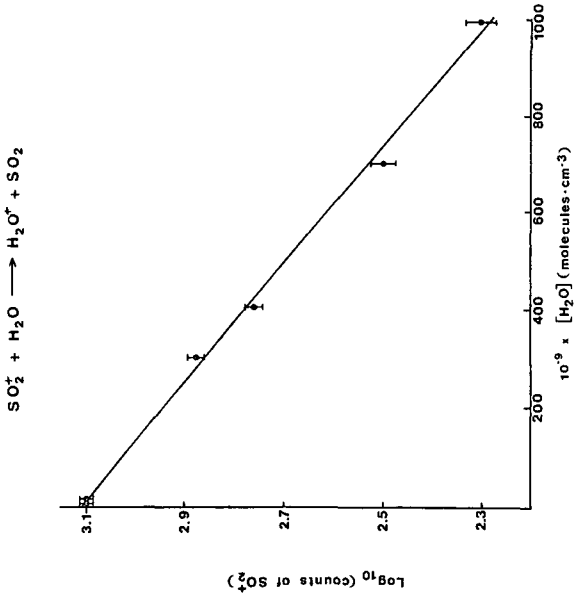

Fig. 1. Pseudo 1st order plot of data for $SO_2^+ + H_2O \rightarrow H_2O^+ + SO_2$

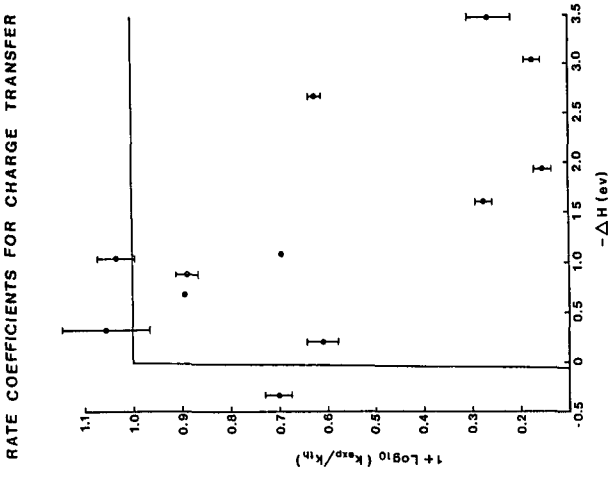

Fig. 2. Rate constants for charge transfer plotted versus reaction enthalpy (ΔH).

Presented at the 36th ASMS Conference on Mass Spectrometry and Allied Topics
June 5-10, 1988, San Francisco, CA

EMPIRICAL AND *AB INITIO* ESTIMATES OF THE STABILITIES OF FLUORINE-CONTAINING CATIONS

Dion A. Stams,[a] T. Darrah Thomas,[b] Duncan C. MacLaren,[b] De Ji[b] and Thomas Hellman Morton[a]

[a]Department of Chemistry, University of California, Riverside, CA 92521
[b]Department of Chemistry, Oregon State University, Corvallis, OR 97331

Since its introduction in 1970,[1] the concept of the isodesmic process has been proved as a useful way to analyze *ab initio* calculations and to compare them with experiment. In 1977 Jolly and Gin introduced the method of equivalent cores, which is a fully empirical approach for extracting thermochemical information from isodesmic processes involving positive ions.[2] The metathesis shown in equation 1 represents a hypothetical reaction that corresponds to an isodesmic process. The experimental value for ΔH, based on the gas phase heats of formation of the reactants and products, is 68 kJ/mol, with an experimental uncertainty on the order of ±8 kJ/mol.

$$(CH_3)_2C{=}O \quad + \quad CH_3CHO \quad \rightarrow \quad (CH_3)_2C{=}O \quad + \quad CH_3CHF^+ \qquad (1)$$

The method of equivalent cores equates ΔH of equation 1 to that of equation 2 estimated from ESCA core ionization energies. Since the O_{1s} core ionization energy of acetone is reported to be 0.66 eV lower than that of acetaldehyde, the value of ΔE_{ESCA} for equation 2 is 64 kJ/mol.

$$(CH_3)_2CO^{\cdot+}(1s) + CH_3CHO \rightarrow (CH_3)_2CO + CH_3CHO^{\cdot+}(1s) \qquad (2)$$

The implicit assumptions of the method of equivalent cores include the following shortcoming, which should be viewed as a caveat to its application:

(i) The ion may have bond lengths and bond angles different from its isoelectronic, electrically uncharged analogue. For example, constraining the ions in equation 1 to the geometries of the corresponding carbonyl compounds may involve different energetic costs on the two sides of the equation.

Additional caveats that apply to the method of equivalent cores are not implicit in its underlying assumptions:

(ii) The ion may have a different conformational minimum than does its isoelectronic, electrically uncharged analogue;

(iii) Covalent or hydrogen bonds in the isoelectronic, electrically uncharged analogue may be absent in the ion (or vice-versa).

To examine these effects more deeply we have combined empirical and *ab initio* approaches for α-fluoro carbocations (equation 3) and fluoronium ions (equation 4).

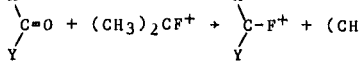

$$\text{X,Y}{=}C{=}O + (CH_3)_2CF^+ \rightarrow \text{X,Y}{-}C{-}F^+ + (CH_3)_2C{=}O \qquad (3)$$

Equation 3 is a generalized example of equation 1 (the *ab initio* value for whose ΔH is 67 kJ/mol). Additional equivalent cores estimates for different choices of X and Y are given in the table. The *ab initio* changes in electronic energy are in good agreement with the empirical estimates, ΔE_{ESCA}.

$$R_1OR_2 + (CH_3)_2F^+ \rightarrow R_1F^+R_2 + (CH_3)_2O \qquad (4)$$

Presented at the 36th ASMS Conference on Mass Spectrometry and Allied Topics
June 5-10, 1988, San Francisco, CA

Empirical (method of equivalent cores) and *ab initio* (6-31G**//6-31G**) estimates of energy changes (in kJ/mol) for equations 3 and 4.

Equation 3			*ab initio*	Equation 4			*ab initio*
X	Y	ΔE_{ESCA}	ΔE	R_1	R_2	ΔE_{ESCA}	ΔE
CH_3	H	+64	+67		$-CH_2CH_2-$	+24	+17
					$-CH_2CH_2CH_2-$	-53	-56
$-CH_2-$		+218	+238	CH_3	$CH_2=CH$	+38	+38
H_2N	H	-23	-39	CH_3	$CH_2=CCH_3$	+22	+7
					$-CH(CH_3)CH_2^-$	-16	-91
CH_3	Cl	+107	+101	$CH_2=CHCH_2$	H	+16	-86

Dialkyl fluoronium ions, $F_1FR_2^+$, can be expected to manifest substantial distortions relative to their isoelectric oxygen analogues. As we have previously discussed,[3] the two bonds to fluorine often have widely different heterolytic dissociation energies when $R_1 \neq R_2$. Only when $R_1 = R_2$ or when the two C-F bond strengths happen to be nearly the same should agreement between equivalent cores and *ab initio* estimates be anticipated.

For equation 4 the *ab initio* ΔE is within experimental uncertainty of ΔE_{ESCA} for oxirane and oxetane and their isoelectronic fluoronium ions, fluoriranium and fluoretanium. All are calculated to have symmetrical, planar geometries (even though no such constraints were imposed upon the geometry optimization). For methyl vinylfluoronium ions the heterolytic C-F bond dissociation energies are close to one another. Equivalent cores and *ab initio* estimates are in good agreement here, as well. The conformational minima for the methyl vinyl ethers (planar *s*-cis geometry) correspond to local maxima for the isoelectronic dialkyl fluoronium ions. The conformational energy barriers are not large, however, and it is not surprising that caveat ii does not lead to a large discrepancy in these instances.

In the last two cases summarized in the table, bond distortions are severe enough to correspond to caveat iii. The fluoronium ion that is isoelectronic to propylene oxide (which was calculated to possess a stable bridged geometry at 3-21G[3]) adopts a planar, acyclic *s*-cis conformation when the geometry is optimized using Hartree-Fock calculations with the 6-31G** basis set. Therefore ΔE_{ESCA} underestimates the stability of $CH_3CH^+CH_2F$ by 75 kJ/mol relative to the *ab initio* computation. A similar distortion is seen in the fluoronium ion that is isoelectronic with allyl alcohol. Here the fluoronium ion becomes an ion-molecule complex of allyl cation plus hydrogen fluoride, which is calculated to be >100 kJ/mol more stable than estimated by ΔE_{ESCA}. The discrepancies between empirical and *ab initio* estimates due to caveat iii can therefore be quite large.

References

1. W. J. Hehre, R. Ditchfield, L. Radom, and J. A. Pople, *J. Am. Chem. Soc.*, *92*, 4796-4801 (1970); W. J. Hehre, L. Radom, P. v. R. Schleyer, and J.A. Pople, "Ab Initio Molecular Orbital Theory," John Wiley, New York, 1986.
2. W. L. Jolly and C. Gin, *Int. J. Mass Spectrom. Ion Phys.*, *25*, 27-37 (1977).
3. D. A. Stams, K. K. Johri and T. H. Morton, *J. Am. Chem. Soc.*, *110*, 699-706 (1988).

Presented at the 36th ASMS Conference on Mass Spectrometry and Allied Topics
June 5-10, 1988, San Francisco, CA

THERMOCHEMISTRY AND GAS-PHASE ION/MOLECULE REACTIONS OF BOROHYDRIDE IONS

Derek B. Workman and Robert R. Squires
Department of Chemistry, Purdue University, West Lafayette, IN 47907

The properties and reactivity of borohydride negative ions have been investigated with a flowing afterglow - triple quadrupole apparatus.[1] Borohydride ion (BH_4^-), substituted borohydride ions (XBH_3^- and HBR_3^-), and polyborohydride cluster ions (ie., $B_2H_7^-$, $B_3H_8^-$, etc.) are generated in a helium flow reactor at 298K, 0.4 torr by ion/molecule reactions with the volatile borane complex Me_2S^+-BH_3^- ("BMS") (eq 1), or by hydride transfer to neutral boranes (eq 2). Trimethoxyborohydride ($HB(OMe)_3^-$) can be

$$(1) \qquad X^- \xrightarrow{BMS} XBH_3^- \xrightarrow{BMS} BH_4^- \xrightarrow{BMS} B_2H_7^-,\ B_3H_8^- \ldots$$

$$(2) \qquad H^- \xrightarrow{BuSiH_3} BuSiH_4^- \xrightarrow{BEt_3} HBEt_3^-$$

produced from the sequence of ion/molecule reactions accompanying direct electron ionization of $B(OMe)_3$ (eq 3).

$$(3) \qquad B(OMe)_3 \xrightarrow{e^-} (CH_3O^-)^* \xrightarrow{B(OMe)_3} HB(OMe)_3^- + CH_2O$$

The BH_4^- and $B_2H_7^-$ ions, and most all of the substituted borohydride ions are completely unreactive in the presence of simple aliphatic carbonyl compounds[2], substituted olefins, CO_2 and other potential H^- acceptor reagents. Neither H^- transfer nor adduct formation can be observed. Furthermore, reactions between neutral, monomeric boranes such as BEt_3 or $B(OMe)_3$ and potential hydride donor anions such as CH_3O^-[3] and c-$C_6H_7^-$[4] produce mainly or exclusively the corresponding adduct ions by efficient termolecular association. This behavior precludes the use of conventional ion/molecule equilibrium and bracketing experiments for determining the relative hydride affinities (HA) of neutral boranes under flowing afterglow conditions. However, we have found that endothermic hydride transfer reactions between mass-selected, translationally-excited borohydride ions and CO_2 (HA = 51.6 ± 2.5 kcal/mol)[5] can be observed in the triple quadrupole collision cell. From careful analysis of the energy thresholds for appearance of HCO_2^-, estimates of hydride binding energies of the borohydride reactant ions can be obtained.

Table 1 presents a summary of the resulting thermochemical data for five borohydride ions. The apparent differences are consistent with expected substituent effects,[6] high-level ab initio calculations,[7] and the known reducing activities of these species in solution.[8]

The hydride affinities of simple aliphatic ketones and aldehydes are ca 30-40 kcal/mol less than HA(BH_3) = 74.2 kcal/mol.[5] Thus, H^- transfer from BH_4^- to these compounds is strongly endothermic. The well-known facility with which borohydride reagents reduce ketones in alcohol solution suggests a pivotal role of the solvent and (alkali metal) counter-ion in the reduction mechanism. We have examined the effects of partial solvation of BH_4^- on its reactions with simple ketones in the gas phase. Solvated borohydride ions can be formed in the flow reactor by termolecular association of BH_4^- with H_2O, alcohols, and carboxylic acids (eq 4). The

$$(4) \qquad BH_4^- + HX \xrightarrow[\text{[He]}]{} BH_4^-(HX)$$

$$HX = H_2O,\ MeOH,\ CH_3CO_2H \quad \text{etc.}$$

$BH_4^-(MeOH)$ cluster ion reacts with acetone to yield an apparent switching product (eq 5) The observed reactivity of this product ion clearly shows

$$(5) \qquad BH_4^-(MeOH) + (CH_3)_2CO \longrightarrow BH_4^-((CH_3)_2CO) + MeOH$$

it to be a simple electrostatically-bonded cluster ion, rather than the lower energy $^iPrOBH_3^-$ form in which reduction of the ketone has occurred. We therefore conclude that one alcohol solvent molecule is insufficient to catalyze the strongly exothermic addition of the borohydride ion to the carbonyl group.

References

1. Workman, D. B., Squires, R. R. Inorg. Chem. 1988.

2. Kayser, M. M.; McMahon, T. B. Tet. Lett. 1984, 25, 3379.

3. Ingemann, S.; Kleingeld, J. C.; Nibbering, N.M.M. J. Chem. Soc. Chem. Commun. 1982, 1009.

4. DePuy, C. H.; Bierbaum, V. M.; Schmitt, R. J.; Shapiro, R. H. J. Am. Chem. Soc. 1978, 100, 2920.

5. Squires, R. R. in "Structure/Reactivity and Thermochemistry of Ions", Ausloos, P.; Lias, S. G. Eds. Dordrecht, 1987, pg 373.

6 Larson, J. W.; McMahon, T. B. J. Am. Chem. Soc. 1985, 107, 766.

7. Eisenstein, O.; Kayser, M.; Roy, M.; McMahon, T. B. Can. J. Chem. 1985, 63, 281.

8. Lane, C F. Synthesis, 1975, 135.

Table 1

Thermochemical Data for Gas-Phase Borohydride Ions

borohydride ion	borane	HA(kcal/mol)	$\Delta H_f[BHR_3^-,g]$(kcal/mol)
BH_4^-	BH_3	74.2	-14.8
$HBEt_3^-$	BEt_3	69.4	-71.2
$B_2H_7^-$	B_2H_6	74.0	-28.5
BH_3CN^-	BH_2CN	96.3	-18.6
$HB(OMe)_3^-$	$B(OMe_3)$	~60	-240

Presented at the 36th ASMS Conference on Mass Spectrometry and Allied Topics
June 5-10, 1988, San Francisco, CA

TEMPERATURE AND METHYL H3/D3 ISOTOPE EFFECTS ON THE ENTHALPY AND ENTROPY CHANGES OF METHYLATED ACETONE ONTO ACETONE AND DIMETHYL ETHER.

J.E. SZULEJKO AND T.B. McMAHON
DEPARTMENT OF CHEMISTRY, UNIVERSITY OF WATERLOO, WATERLOO, ONTARIO, CANADA. N2L 3G1

EQUILIBRIUM ISOTOPE EFFECTS [EIE] HAVE BEEN OBSERVED FOR IONS IN SOLUTION [1] AND IN THE GAS PHASE [2-4.] MOST OF THE PREVIOUSLY REPORTED WORK WAS OBTAINED BY ICR MS [2,3]. SOME EIE HAS BEEN OBTAINED BY PULSED ELECTRON BEAM HIGH PRESSURE MASS SPECTROMETRY [HPMS] [4.] LITTLE OR NO TERMOLECULAR ION CLUSTERING EIE HAS BEEN REPORTED BY HPMS.

THE EXPERIMENTS WERE CONDUCTED ON A HPMS [5]. TYPICAL SAMPLE COMPOSITIONS USED WERE; (A) CH4 (OR N2) 700 τ, CH3Cl (OR CH3F) 5-15 τ, ACETONE 0.5-10 τ AND DIMETHYL ETHER 5-200 τ; OR (B) CH4 700τ, ACETONE 1-50 τ AND 2,2 DIMETHOXYPROPANE 2-5 τ.

THE FOLLOWING CLUSTERING REACTIONS WERE STUDIED AND THE DATA SUMMARIZED IN TABLE 1. Van't HOFF PLOTS ARE SHOWN IN FIGS 1 AND 2 FOR REACTIONS (1) IN FIG1; AND (5), (6), (7) IN FIG.2.

(CH3)2COCH3+ + (CH3)2CO		(1)
(CH3)2COCH3+ + (CH3)2CO		(2)
(CD3)2COCH3+ + (CD3)2CO		(3)
(CH3)2COCD3+ + (CH3)2CO		(4)
(CH3)2COCH3+ + (CH3)2O		(5)
(CD3)2COCH3+ + (CH3)2O		(6)
(CH3)2COCH3+ + (CD3)2O		(7)
(CH3)2COCH3+ + CH3OCD3		(8)

TWO SALIENT FEATURES ARE READILY OBSERVED FROM THE van't HOFF PLOTS; (1) SIGNIFICANT EIE AT LOW TEMPERATURES WITH LARGE ΔH AND ΔS AND AT HIGHER TEMPERATURES SMALLER ΔH AND ΔS VALUES. THE TWO LINES CROSSED AT Tc WHICH IS DETERMINED WHEN ΔG FOR THE TWO ISOMERIC CLUSTER IONS BECOME EQUAL. THE HIGH TEMPERATURE REGION HAS LITTLE EIE EXCEPT FOR (7). THE 2 ISOMERIC FORMS ARE PROPOSED TO HAVE (1) A COVALENTLY BONDED CLOSELY PACKED CONGESTED STRUCTURE AS REVEALED BY SPACE FILLING MODELS WITH MOST OF THE INTERNAL ROTORS SEVERELY RESTRICTED [6] AND THE OTHER (2) IS A LOOSELY BOUND CH3+ BRIDGED STRUCTURE [7]. THE EIE CAN BE RATIONALIZED IN TERMS OF THE GREATER ROTATIONAL ENTROPY OF A -CD3 OVER A -CH3 ROTORS (CIRCA 0.8 EU). THE ΔS OBSERVED WITH ACETONE AS THE NEUTRAL IS MUCH LESS THAN FOR DIMETHYL ETHER DUE TO A LESS CONGESTED FORM.

IN CONCLUSION, IT HAS BEEN DEMONSTRATED BY HPMS, TERMOLECULAR CLUSTERING EIE AND ISOMER DIFFERENTIATION. THE C2H5+ + H2 CLUSTERING (BY HPMS) HAS 2 ISOMERS [8].

Presented at the 36th ASMS Conference on Mass Spectrometry and Allied Topics
June 5-10, 1988, San Francisco, CA

REFERENCES

1 V. GOLD AND S. GRIST J.CHEM.SOC (1971) *13* 1665
2 J.W. LARSON AND T.B. McMAHON J.PHYS.CHEM. (1988 *91* 554
3 J.W. LARSON AND T.B. McMAHON J.AMER.CHEM.SOC (1988) *110* 1087
4 M. MEOT-NER J.AMER.CHEM.SOC. (1987) *109* 7947
5 J.E. SZULEJKO, J.J. FISHER, T.B. Mc.MAHON AND J. WRONKA
INT.J.MASS SPECTROM ION PROC. (1988) *83* 147
6 K. HIRAOKA AND P. KEBARLE J.AMER.CHEM.SOC. (1976) *98* 6119
7 M. MEOT-NER AND C.A. DEAKYNE J.AMER.CHEM.SOC. (1985) *107* 469
8 D.K. SEN SHARMA, S. IKUTA AND P. KEBARLE
CAN.J.CHEM. (1982) *60* 2956

TABLE I

REACTION	ΔH_1	ΔS_1	ΔH_2	ΔS_2	No
$(CH_3)_2COCH_3^+ + (CH_3)_2CO$	-22.2	-42.0	-14.8	- 23.0	1
$(CH_3)_2COCH_3^+ + (CD_3)_2CO$	-22.2	-42.8	-14.8	-22.8	2
$(CH_3)_2COCD_3^+ + (CH_3)_2CO$	-22.2	-42.2	NOT MEASURED		3
$(CD_3)_2COCH_3^+ + (CD_3)_2CO$	-22.2	-44.0	-14.8	-22.6	4
$(CH_3)_2COCH_3^+ + (CH_3)_2O$	-26.4	-58.0	-14.0	-24.5	5
$(CH_3)_2COCH_3^+ + CH_3OCD_3$	-26.4	-60.5	-14.0	-24.0	6
$(CH_3)_2COCH_3^+ + (CD_3)_2O$	NOT SEEN		-14.0	-22.5	7
$(CD_3)_2COCH_3^+ + (CH_3)_2O$	-26.4	-60.8	-14.0	-24.5	8

UNITS: ΔH kcal mol $^{-1}$ ΔS cal mol K^{-1}

FIGURE 1

VAN'T HOFF PLOT
$(CD_3)_2C^+OCH_3 + (CH_3)_2O$ CLUSTERING

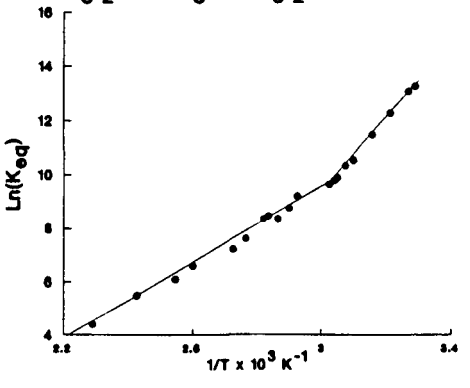

● $(CH_3)_2COCH_3^+ + (CH_3)_2CO$ CLUSTERING

■ $(CD_3)_2COCH_3^+ + (CH_3)_2O$ CLUSTERING

◊ $(CH_3)_2COCH_3^+ + (CD_3)_2O$ CLUSTERING

FIGURE 2

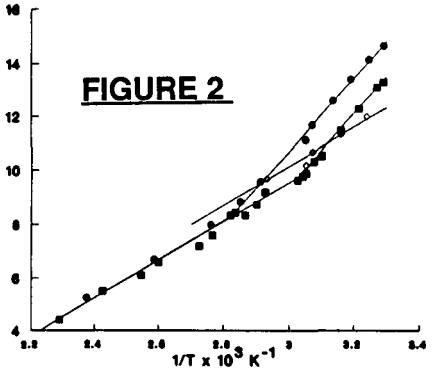

Presented at the 36th ASMS Conference on Mass Spectrometry and Allied Topics
June 5-10, 1988, San Francisco, CA

GAS-PHASE ACIDITIES FROM ENDOTHERMIC REACTIONS

Susan T. Graul and Robert R. Squires
Department of Chemistry, Purdue University
West Lafayette, IN

The gas-phase acidity of a compound is defined as the heat of reaction H (or free energy G) for deprotonation (eq.1). This fundamental property is

$$RH \quad R^- + H^+ \quad H_{acid}(RH) \tag{1}$$

useful index of reactivity and has been measured for a variety of species. Well-established experimental techniques for determining acidities include bimolecular ion/molecule proton transfer equilibrium measurements or acidity bracketing and collision-induced dissociation (CID) of cluster ions, as well as electron affinity measurements (corresponding to R^-). Although these methods are widely applicable, there are certain limitations that restrict their usage. For example, proton transfer reactions are selective for the most acidic proton in the substrate. Moreover, the most basic of the readily available reagent anions is H_2N^- ($H_{acid}(NH_3)$ = 403.6 kcal/mol), but even this anion fails at thermal energy to deprotonate weak acids such as ethylene and cyclopropane. Thus, it is a worthwhile endeavor to develop experimental techniques that provide data for a specific proton in a given substrate, and that can be applied to even the weakest acids.

We recently introduced a method that allowed us to estimate gas-phase acidities for specific protons in a substrate(1). The acidity is derived by way of a simple thermochemical cycle from an experimental threshold energy for a decarboxylation reaction leading to the anion of interest (eq. 2).

$$RCO_2^- \quad R^- + CO_2 \tag{2}$$

$$H_{acid}(RH) = E_T + H_f(RCO_2H) - H_f(RH) - H_f(CO_2) + H_{acid}(RCO_2H) \tag{3}$$

We have applied this method to a number of anions with known proton affinities (note $PA(R^-) = H_{acid}(RH)$), and found in most cases very good agreement with accepted literature values(1). In the course of these studies, we had occasion to observe that the anions formed by decarboxylation of RCO_2^- could also be generated by CID of the appropriate alkoxide anion, e.g., RCH_2O^- (eq. 4).

$$RCH_2O^- \quad CID \quad R^- + CH_2O \tag{4}$$

Therefore, we undertook to extend the methods to estimate proton affinities for several previously unknown anions.

Our experiments are carried out in a flowing afterglow-triple quadrupole instrument. The precursor anion is generated by ion/molecule reactions in the flow tube and mass-selected at the first quadrupole (Q1). CID is effected in the second quadrupole (Q2) at single-collision conditions. By monitoring the intensity of a given fragment ion as a function of collision energy, we obtain a first-order estimate for the appearance energy of that fragment. This value is corrected for Doppler broadening due to thermal motion of the target gas to give our final CID threshold energy.

As an example of these techniques, we have observed the methyl anion CH_3^- resulting from CID of $CH_3CO_2^-$, $CH_3CH_2O^-$, $(CH_3)_2CHO^-$, and $(CH_3)_3CO^-$. Table I lists the observed threshold energies for these species and the resulting acidity for methane. The average value (417 kcal/mol) is in excellent agreement with the established literature value of 416.6 kcal/mol (2). We have estimated acidities for several other species; these results are shown in Table II.

We have augmented these activated unimolecular reactions with bimolecular reactions. One of these methods is a proton transfer reaction,

and like the thermal energy proton transfers, this method is selective for the most acidic proton. However, unlike the thermal energy counterparts, the technique is not limited to species that are more acidic than NH_3. This limitation is removed by balancing the energy deficit with kinetic energy. The reference base B^- is generated in the flow tube and accelerated into Q2 where it collides with and can deprotonate the reactive collision gas AH. By monitoring the intensity of A^- as a function of the collision energy, an appearance energy is obtained that can be related to the acidity of AH:

$$H_{acid}(AH) = H_{acid}(BH) + E_T \quad (5)$$

This method was applied to measuring the acidity of ethylene and methyl fluoride and yielded values of $H_{acid}(C_2H_4) = 406 \pm 2$ kcal/mol and $H_{acid}(CH_3F) = 407 \pm 3$ kcal/mol, in good agreement with values derived from decarboxylation thresholds and from CID of alkoxides.

The second bimolecular reaction is related to a method developed by DePuy, Bierbaum, and Damrauer (3) for estimating gas-phase acidities, in which the branching ratio for loss of CH_4 and RH from the addition/elimination reaction of OH^- with $RSiMe_3$ was correlated to the relative acidities. We used vinyltrimethylsilane as the collision gas, and Cl^- generated in the flow tube was accelerated into the collision chamber. Both CH_3^- and $C_2H_3^-$ can be detected, but their appearance energies are significantly higher (by 0.5 to 1.5 eV) than would be expected on the basis of simple thermochemistry. Moreover, the yield is low and the ion signals are weak, making accurate measurements difficult. Analogous reactions with other nucleophiles and silanes (e.g., CH_3O^- with Me_3SiPh) were attempted, but the energetics of displacement did not reflect thermochemistry. When the adduct of F^- with vinyltrimethylsilane is formed in the flow tube and subjected to CID, fragmentation results in loss of CH_4 and C_2H_4 and formation of $C_2H_3^-$. The $H_{acid}(C_2H_4)$ derived from the threshold energy for $C_2H_3^-$ is in fair agreement with our other measurements, although it is lower than expected. These silane-based methods proved more difficult to implement than the others discussed here due to low signal intensities.

Table I.

precursor ion	E_T, eV[a]	$\Delta H_{acid}(CH_4)$[b], kcal/mol
$CH_3CO_2^-$	2.74	420
$CH_3CH_2O^-$	2.27	416
$(CH_3)_2CHO^-$	2 10	416
$(CH_3)_3CO^-$	1.93	414
	average	417

Table II. Acidity Scale

Anion (R^-)	Neutral (RH)	$\Delta H^\circ_{acid}(RH)$, kcal/mol
$(CH_3)_3CCH_2^-$	$C(CH_3)_4$	423 ± 7
CH_3	CH_3	418 ± 3.5
CH_3^-	CH_4	417 ± 3
H	H	413 ± 3.5
FCH_2^-	FCH_3	411 ± 3.5
$CF_3CH(CH_3)CH_2^-$	$CF_3CH(C\underline{H}_3)C\underline{H}_3$	410 ± 4.5
$C_6H_5CH_2CH_2^-$	$C_6H_5CH_2C\underline{H}_3$	408 ± 6
$CH_2=CH^-$	$CH_2=CH_2$	406 ± 3
$CH_3CH=CH^-$	$CH_3CH=C\underline{H}_2$	405 ± 3.5
$CF_3CH_2CH_2^-$	$CF_3CH_2C\underline{H}_3$	402 ± 3.5
$C_6H_5^-$	C_6H_6	400 ± 6

1. Graul, S. T.; Squires, R. R. J. Am. Chem. Soc. 1988, 110, 607.
2. Ellison, G. B.; Engelking, P. C.; Lineberger, W. C. J. Am. Chem. Soc. 1978, 100, 2556.
3. DePuy, C. H.; Bierbaum, V. M.; Damrauer, R. J. Am. Chem. Soc. 1984, 106, 4051.

Presented at the 36th ASMS Conference on Mass Spectrometry and Allied Topics
June 5-10, 1988, San Francisco, CA

Π-BOND STRENGTHS IN FLUORO, METHYL SILAETHYLENES

C.E. Allison and T.B. McMahon.
Department of Chemistry, University of Waterloo.
Waterloo, Ontario, CANADA N2L 3G1.

The strength of the Si=C double bond (E(Π)) in substituted silaethylenes has been investigated using Fourier transform ion cyclotron resonance (Spectrospin CMS-47). Proton transfer and fluoride transfer reactions from appropriately substituted silane precursors yielded proton affinities, fluoride affinities and the Π-bond strengths for the silaethylenes I, II and III.

Previous estimates of E(Π) in I have ranged from 38 kcal mol^{-1} (ICR bracketing) **[1]** to 47 kcal mol^{-1} (*ab-initio* calculation) **[2]**. Using the proton affinities measured in this work for I, II and III (Table) and other thermochemical quantities, E(Π) for I, II and III were calculated to be 43, 68 and 54 kcal mol^{-1} respectively (see Schemes). Using the fluoride affinities (Table), values of 51, 57 and 63 kcal mol^{-1} were obtained for E(Π). The disagreement between E(Π) obtained using the two approaches can be rationalized using a new value for the Si-F bond strength (134 kcal mol^{-1} - required in the calculation of E(Π) using the measured fluoride affinities - literature : 142 kcal mol^{-1} **[3]**) to give 43, 49 and 55 kcal mol^{-1} for I, II and III respectively. The two approaches then agree for I and III but provide vastly different estimates for the value of E(Π) in II.

Ab-initio calculations **[4]** indicate I and III are more stable than the isomeric silylene structures (Ia and IIIa) by 12 kcal mol^{-1} and by 37 kcal mol^{-1}, whereas II is 55 kcal mol-1 more stable then the methyl, fluoromethyl silylene (IIa), but 5 kcal mol^{-1} <u>less</u> stable than the fluoro, ethyl silylene (IIb). This arises from the stabilizing effects of both methyl and fluoro at the silicon and carbon centres **[5]**. Both groups have stabilizing effects, but the effects due to having fluorine on silicon and methyl at the carbon stabilizes the fluoro, ethyl silylene to a greater extent. (Methyl on silicon and fluorine on carbon destabilizes the silylene.) Where the substitution is for the same species (I and III) the stabilization is greatest for the silaethylene isomer. This indicates that the disagreement between the two approaches to E(Π) for II arises from the stability of the silylene isomer IIb. The proton affinity measured for II is thus that of the more stable species - the silylene. Using this information it is possible to estimate the proton affinity for II by using the value of E(Π) calculated from the fluoride affinity measurements. This gives a revised value of **206** kcal mol^{-1} for the proton affinity of II.

Presented at the 36th ASMS Conference on Mass Spectrometry and Allied Topics
June 5-10, 1988, San Francisco, CA

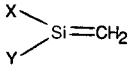

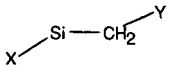

X = Y = CH_3	(I)	X = Y = CH_3	(Ia)
X = F ; Y = CH_3	(II)	X = CH_3 ; Y = F	(IIa)
X = Y = F	(III)	X = F ; Y = CH_3	(IIb)
		X = Y = F	(IIIa)

Table : Proton affinities and fluoride affinities for the silaethylenes.
(All in kcal mol^{-1})

SILAETHYLENE	PROTON AFFINITY	E(Π)	FLUORIDE AFFINITY	E(Π)	(revised)
I	228	43	37	51	(43)
II	187	68	40	57	(49)
III	178	54	46	63	(55)

Schemes : Thermochemical cycles for the estimation of E(Π).
(a) From proton affinity measurements.

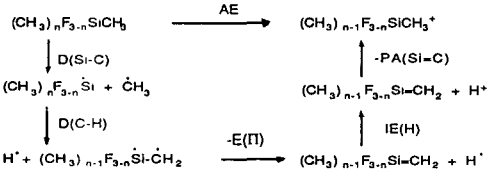

$$E(\Pi) = D(Si\text{-}C) + D(C\text{-}H) + IE(H) - AE((CH_3)_{n-1}F_{3-n}SiCH_3^+) - PA(Si{=}C)$$

(b) From fluoride affinity measurements.

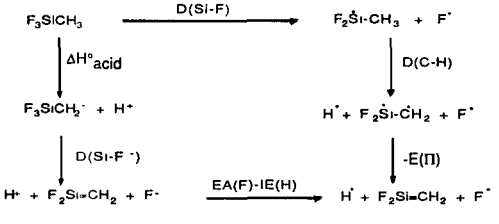

$$E(\Pi) = D(Si\text{-}F) + D(C\text{-}H) + IE(H) - \Delta H^\circ_{acid} - D(Si\text{-}F) - EA(F)$$

REFERENCES

1. W.J. Pietro, S.K. Pollack and W.J. Hehre, *J. Am. Chem. Soc.*, **105**, 16 (1983).
2. M. Hanamura, S. Nagase and K. Morokuma, Tetrahedron Lett. **22**, 1813 (1981).
3. A. Campanaro, C.H Marvin, S.P. Morehouse and T.B. McMahon, *Org. Mass Spectrom.*, in press
4. GUASSIAN 82, J.S Binkley, M.J. Frisch, D.J. DeFrees, K. Rahgavachari, R.A. Whiteside, H.B. Schlegel, E.M. Fluder and J.A. Pople, Department of Chemistry, Carnegie-Mellon University, Pittsburgh, PA.
5. M.S. Gordon, *J. Am Chem. Soc.*, **104**, 4352 (1982).

Presented at the 36th ASMS Conference on Mass Spectrometry and Allied Topics
June 5-10, 1988, San Francisco, CA

Structural Factors That Effect The Extent Of Deuterium Exchange When Using ND_3 As A CI Reagent Gas:

Killmer,L. SK&F R&D Laboratories, King of Prussia, PA 19406-0939

Introduction:

For most organic compounds, ND_3/CI/MS is an easy and unambiguous technique for determining the number of exchangeable (active) hydrogens. ND_3/CI/MS can also be used to support the proposed structures of unknowns and fragment ion assignments.

Theory:

H/D exchanges results from the collisions of the sample ions with the ND_3 reagent gas neutrals in the CI ion source. At typical ND_3/CI source pressures, each sample ion undergoes several hundred collisions before exiting the ion source. Multiple collisions between sample molecules and ND_3 reagent gas ions are highly unlikely due to their relatively low concentration in the ion source. $[M+D]^+$ and $[M+ND4]^+$ are the typical molecular ion species observed when using ND_3 as the CI reagent gas.

Experimental Conditions:

All of the mass spectra were obtained using either a Finnigan/MAT model 3625 or 4610 quadrupole mass spectrometer. The ND_3 (99.5%) was purchased from Cambridge Isotope Laboratories (CIL) Woburn,MA 01801. The source pressure was 450-475 microns and was measured using a Datameterics Model 1400 Barocel manometer. The source temperature was 150-175° C. All of the mass spectra were generated using a DCI or direct probe. When determining the number of active hydrogens in organic compounds it is critical to evaluate the compound first using NH_3 , then using ND_3. This technique makes determining the number of exchangeable hydrogens and fragment ion structure assignments an easier task.

Results:

1. Polyhydric Aromatic Compounds:

Hydroxyl groups are strongly activating ortho para directors. Aromatic ring hydrogens can be exchanged if they are activated by more then one OH group. Table #1 lists the number of exchangeable hydrogens for a series of aromatic diols and triols.

TABLE #1

COMPOUND	ACTIVE HYDROGENS	DEUTERIUM EXCHANGES
Catechol(1,2)	2-OH	2D (100.0%)
Resorcinol(1,3)	2-OH	2D (100.0%)
Hydroquinone(1,4)	2-OH	2D (100.0%)
Pyrogallol(1,2,3)	3-OH	3D (100.0%)
Hydroxyhydroquinone	3-OH	3D (77.6%)
(1,2,5)	1-H	4D (22.4%)
Phloroglucinol(1,3,5)	3-OH	3D (11.6%)
	3-H	4D (19.0%)
		5D (28.4%)
		6D (52.6%)

Note: In the case of phloroglucinol, each of the ring hydrogens are activated by all three OH groups.

Polyhydric aromatic compounds are the most difficult class of compounds to determine the number of exchangeable hydrogens when using ND_3. Catechin provides an example of the problems that one can encounter with polyhydric aromatic compounds. Catechin has 5 OH groups but exchanged 7 rather then 5 deuteriums since two of the aromatic ring hydrogens were also exchanged.

2. Polyamino Aromatic Compounds:

   Like OH groups, NH_2 groups are strongly activating ortho para directors. If an aromatic ring hydrogen is activated by more then one NH_2 group it can be exchanged. Table #2 details the extent of deuterium exchange for a group of di and triamino benzenes and aminophenols.

TABLE #2

COMPOUND	ACTIVE HYDROGENS	DEUTERIUM EXCHANGES
1,2 Benzenediamine	2-NH2	4D 100.0%
1,3 Benzenediamine	2-NH2	4D 52.0%
	2-H	5D 26.4%
		6D 21.6%
1,4 Benzenediamine	2-NH2	4D 100.0%
1,2,4 Benzenetriamine	3-NH2	6D 75.0%
	1-H	7D 25.0%
2-aminophenol	1-OH	3D 100.0%
	1-NH2	
3-aminophenol	1-OH	3D 52.7%
	1-NH2	4D 35.7%
	2-H	5D 11.6%
4-aminophenol	1-OH	3D 100.0%
	1-NH2	

3. Alkynes:

   Alkynes with the triple bond at the end of a chain are very weak acids. In the presence of ND_3 many terminal alkynes will undergo H/D exchange.

4. Keto-Enol Tautomers:

   Since the two forms of these tautomers differ by one exchangeable hydrogen, each form of the keto-enol equilibrium can be observed via ND_3/CI/MS.

5. ß-Diketones:

   The methylene hydrogens in ß-diketones are acidic and therefore exchangeable. The H/D exchange for ß-diketones is a two step process.. The addition of the second deuterium is a function of probe temperature and reaction time within the ion source.

6. Negative Ion Deuterium Exchange:

   ND_3 can be used to determine the number of active hydrogens in the negative in the negative ion mode. The main advantage of ND_3 in the negative ion mode is that the deuterium exchange tends not to involve aromatic ring hydrogens. This in turn generates simpler spectra that can be easily interpreted.

Presented at the 36th ASMS Conference on Mass Spectrometry and Allied Topics
June 5-10, 1988, San Francisco, CA

THE BICYCLOBUTYL ANION: AN ALKYL CARBANION

Phillip Chou and Steven Kass
Department of Chemistry
University of Minnesota, Minneapolis, MN 55455

Alkyl anions are extremely rare in the gas phase. They are extremely basic and many are thought to have negative electron affinities.[1] It therefore is not surprising that only a few alkyl anions, methyl, cyclopropyl, methylcyclopropyl and neopentyl have been reported to date.[2] None of them have been produced by proton abstraction from the parent alkane. In fact, methyl anion has the largest known proton affinity, 416.6 ± 0.9 kcal/mole.[3]

We have recently generated a new alkyl anion derived from bicyclobutane. This hydrocarbon is highly strained but thermally quite stable. The rigid ring system results in the bridgehead carbon-hydrogen bonds having a high degree of s-character (~$sp^{1.5}$) thereby enhancing their acidity. As a result, we have been able to deprotonate an alkane for the first time.

Proton abstraction from bicyclobutane affords the 1-bicyclobutyl anion and does not lead to any ring opening (eqn. 1). The proton affinity (397 ± 4 kcal/mole) and electron affinity (0.77 ± .34 eV) were measured and the reactivity of this novel ion with reagents such as O_2, CS_2 and N_2O was explored.

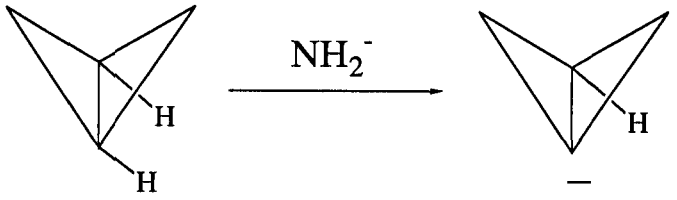

1)

In the process of carrying out this work it was noted that there is a correlation between gas phase acidity and ^{13}C-^{1}H NMR coupling constants (figure 1). This observation leads to the prediction that other strained hydrocarbons, such as bicyclo(2.1.0)pentane, should be suitable precursors for the generation of alkyl anions. Further investigations are in progress

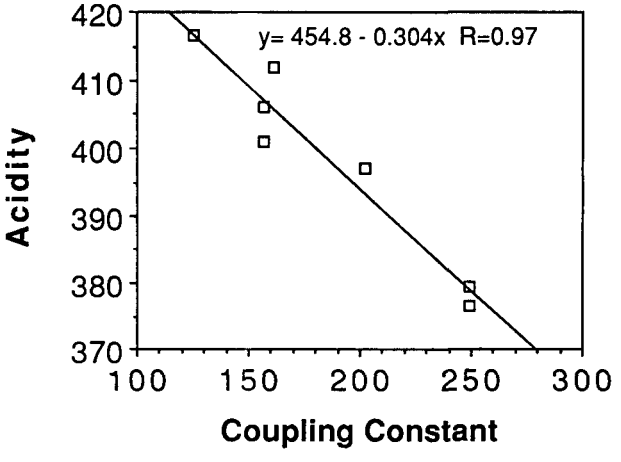

Compounds	ΔHAcid (kcal/mole)	J (Hz)
Methane	416.6	125
Ethylene	406	157
Benzene	401	157
Cyclopropane	412	161
Acetylene	379.6	249
Methylacetylene	376.7	249
Bicyclobutane	397	202

Figure 1. Gas Phase Acidities versus ^{13}C-H NMR coupling constants.

1. Charles H. Depuy, Veronica M. Bierbaum, and Robert Damrauer, J. Am. Chem. Soc., 106, 4051(1984).
2. Susan T. Graul and Robert R. Squires, J. Am. Chem. Soc., 110, 607(1988).
3. J.E. Bartmess and R.T. McIver Jr., "Gas Phase Ion Chemistry", M.T. Bowers, Ed., Academic Press: New York, 1979; Vol.2, Chapter 11.

Presented at the 36th ASMS Conference on Mass Spectrometry and Allied Topics
June 5-10, 1988, San Francisco, CA

The Detection of Neutral Products of Chemical Ionization Reactions

Charles Allgood and Burnaby Munson
Department of Chemistry and Biochemistry
University of Delaware
Newark Delaware 19716

The neutral products formed in chemical ionization reactions can be detected and provide additional information to that obtained in a conventional CI mass spectrometry experiment.

Initial experiments were carried out with bibenzyl, $C_6H_5CH_2CH_2C_6H_5$ which has a simple CH_4 CI mass spectrum: the base peak at m/z 105 and an abundant MH^+ at m/z 183. In agreement with previous experiments[1] the neutral product of benzene could be detected by the increase with increasing electron current of the ratio of ion currents, $C_6H_7^+/C_8H_9^+$, according to the following reactions:

$$CH_5^+ + C_6H_5CH_2CH_2C_6H_5 \longrightarrow C_8H_9^+ + C_6H_6 + CH_4$$

$$CH_5^+ + C_6H_6 \longrightarrow C_6H_7^+ + CH_4$$

The ratio of ion currents I(183)/I(105), or $[MH^+]/[C_8H_9^+]$, was independent of variations in electron current, as one would expect for two ions which were formed by competing bimolecular reactions of CH_5^+ and $C_2H_5^+$ ions with the sample.

The ratio of I(79)/I(105) was observed to increase as expected while the ratio I(183)/I(105) remained essentially constant as the reaction time increased with increasing source pressure.

The CH_4 CI mass spectrum of p,p'-DDT contains fragment ions corresponding to the loss of C_6H_5Cl, HCl, and $CHCl_3$ molecules from the protonated molecule.[2] The neutral product of chlorobenzene is easily detected as the MH^+ ion at m/z 113 and the $(M+C_2H_5^+)$ ion at m/z 141. The relative intensities show the characteristic dependence on electron current.

Small amounts of CCl_3^+, the dominant ion in the CH_4 CI spectrum of chloroform, were also detected in the spectra of DDT but only at the highest electron currents used in these experiments.

The neutral product from the other major fragmentation reaction of DDT is HCl; however, no significant amounts of H_2Cl^+ are observed under any conditions. We presume that the HCl reacts rapidly with the walls of the source of the mass spectrometer. The dominant ionic products in the CH_4 CI mass spectra of aliphatic chlorides are $(M+H-HCl)^+$ ions; however, no significant amounts of H_2Cl^+ were detected with these compounds either.

Ratios of other primary fragment ions in p,p'-DDT as well as chlorine isotopic peaks are independent of electron current consistent with the proposed mechanism of formation.

For benzil, $C_6H_5COCOC_6H_5$, the CH_4 CI mass spectrum contains predominantly $C_6H_5CO^+$ at m/z 105 which can be formed by two equally reasonable mechanisms that cannot be differentiated from the ionic species formed:

$$\text{---> } C_6H_5CO^+ + C_6H_5CHO$$

$$C_6H_5COCOC_6H_5 + CH_5^+ \text{ --}$$

$$\text{---> } C_6H_5CO^+ + C_6H_6 + CO$$

The correct mechanism can be determined by detecting the neutral products by subsequent reaction with methane reagent ions, either benzaldehyde or benzene and carbon monoxide.

The experimental results clearly show that formation of benzaldehyde is the correct pathway as the ionic ratio $C_6H_5CHOH^+/C_6H_5CO^+$ or I(107)/I(105) increases with increasing electron current while only very small amounts of protonated benzene are detected at m/z 79 and the ratio I(79)/I(105) is independent of electron current. Protonated carbon monoxide, HCO^+ cannot be detected at m/z 29 due to interference from a methane reagent ion, $C_2H_5^+$.

In conclusion it appears that this two step mechanism is occuring to some extent in forming ions for these samples under chemical ionization conditions. The detection of these neutral products may be useful in structure confirmation as well as in studies of the mechanisms of chemical ionization reactions.

References

1. Blom. K.; McGuire, J.M.; Hauer, C.R.; Munson, B. Org. Mass Spectrom., 1982, 17, 345.

2. Safe and Huntzinger Mass Spectrometry of Pesticides and Pollutants, CRC Press, 1973, p. 24.

To be published in Analytical Chemistry, 1988.

Presented at the 36th ASMS Conference on Mass Spectrometry and Allied Topics
June 5-10, 1988, San Francisco, CA

THE REACTION OF THE BUTADIENE RADICAL CATION AND METHYL VINYL KETONE: a GAS PHASE ANALOGOUE OF A [4 + 2] CYCLOADDITION

L.W. Castle, and M.L. Gross, Midewest Center for Mass Spectrometry, Dept. of Chemistry, University of Nebraska, Lincoln, NE 68588

The ability of tandem mass spectrometry to moniter a single ion for collisional activation (CAD) makes it an effective tool for studying bimolecular gas-phase reactions. Using a chemical ionization (CI) source as a reaction vessel. An adduct can be generated and then its structure determined by measuring its CAD mass spectrum. In order to determine possible changes in an adduct structure over time, we can conduct the reaction in an FTMS. With these two complimentary tools we are able to obtain structural and kinetic information concerning the reaction products and intermediates.[1,2]

We have used this strategy to study the reaction between the butadiene radical cation and methyl vinyl ketone. Assignment of adduct structures were based on the comparison of adduct CAD spectra with those of appropriate model compounds. Due to interference at the exact mass from a competing adduct we have generated specifically labeled adducts at masses free from interference by other ions.

The reaction of D_6-butadien radical cation plus methyl vinyl ketone gives an adduct at m/z 130 which fragments to generate ions of m/z 43, m/z 60, m/z 87, m/z 113 and 115. The ion of m/z 43 corresponds to $[CH_3 - C = O]^+$ which is a loss of $[C_6H_3D_6\cdot]$. The peak at m/z 60 corresponds to $C_4D_6^{+\cdot}$ which is D_6-butadiene; or reversion to starting material. The ion of m/z 87 corresponds to $[C_6D_6H_3]^+$. The peaks at m/z 115, and 113 correspond to losses of methyl; m/z 115 is loss of CH_3; and m/z 113 is loss of $CD_2H\cdot$, respectively. The fragments m/z 113 and 115 occur in almost identical proportion. These fragments can be explained when the (CAD) spectra of certain model compounds CAD spectra are used for comparison. The model of 1(3-cyclohexenyl)-ethanone fragment. to give m/z 43, m/z 81, and m/z 109 as its major fragments. The model compounds of 1-(3-cyclohexenyl) ethanone fragments to form m/z 43, m/z 81, and m/z 109 as its major fragments. The ion of m/z 43 corresponds to $[CH_3CO]^+$ in both the adduct and the model compound; the ion of m/z 81 is $[C_6H_9]^+$ whereas the adduct gives m/z 87 which is $[C_6D_6H_3]^+$; the ion of m/z 109 corresponds to loss of methyl, the adduct forms m/z 115 and 113 which is the loss of $CH_3\cdot$ and $CD_2H\cdot$, respectively. The ratio of these fragments to each other in the model compound, and in the adduct, are very close suggesting thay they are generated from the same structure.

However, there is one fragment peak unaccounted for by this model compound; i.e., m/z 60, which corresponds to $[C_4D_6]^{+\cdot}$ and is a reversion to starting materal. The only model compound which we found to give rise to m/z 54 $[C_6H_6]^{+\cdot}$ was 2 ethenyl 3,4-dihydro pyran via the retro Diels Alder (RDA) reaction. It is known that ethenyl 3,4 dihydro pyran systems can isomerize to form 4-cyclohexen substitude aldehydes or ketones dependant on the substitution at the six position.[3,4]

From this information we propose that D-6-Butadiene radical cation reacts with methyl vinyl ketone to form 2 ethenyl 3,4-dihydro 6-methyl pyran radical cation this then can decompose by two paths; either the (RDA) to generate m/z 60 or the Claisen rearrangement to form 1-(3-cyclohexene) ethanone which can then fragment to form ions of m/z 43, m/z 87, m/z 115 and 113.

We were able to establish by appropriate double resonance experiments in FTMS that the reactant species is the butadiene radical cation in the butadiene/methyl vinyl ketone system. In the FTMS we were able to adjust reation conditions (i.e., ionization voltage, and partial pressures of reactants) in such a way as to favor the butadiene/methyl vinyl keton reactions over methyl vinyl keton/methyl vinyl ketone reaction. With this obstacle overcome we were able to use unlabeled butadiene plus methyl vinyl ketone. We then did the reaction as a function of delay time between

ionization and detection, starting at 50 mS and ending at 600 mS. We monitered the ion of m/z 54 (butadiene radical cation) and the ions of m/z 43, m/z 81, and m/z 109 which correspond to fragments of 1-(3-cyclohexenyl) ethanone. We also mointored the methyl vinyl ketone radical cation (m/z 70).

When the data is plotted with time in mS versus relative abundance we find that the ion of m/z 54 declines linearly while m/z 43, 81, and 109 all increase steadily from 50 mS to 600 mS. It was noted that the ion of m/z 70 is only present in low abundance during the first two data points (i.e., 50 and 100 mS).

The conclusion then is that a [3 + 2] cycloaddition is occuring; furthermore, the reaction has first order rate kinetic with respect to the butadiene radical cation.

1 Groenewold, G.S.; Gross, M.L., J. Am. Chem. Soc. 1984, 106, 6575.

2 Groenewold, G.S.; Gross, M.L., J. Am. Chem. Soc. 1984, 106, 6569.

3 Buchi, G. and Powell J. E., Jr., J. Am. Chem. Soc. 1970, 92, 3126.

4. Sarraf, M.; Andier, H. and Morizer, J. P., Bull. Soc. Chim. Fr. 1983, 78-82.

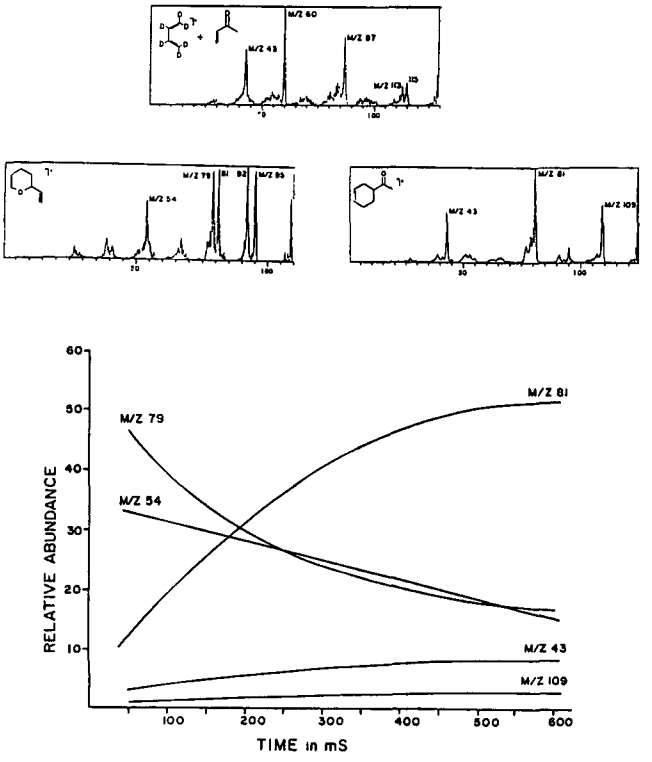

Presented at the 36th ASMS Conference on Mass Spectrometry and Allied Topics
June 5-10, 1988, San Francisco, CA

Gas-Phase Ion Chemistry of Benzene Radical Cation and Cyclic Ethers

Charles D. Warner, Dept. of Chemistry, Hastings College, Hastings, NE 68901;
R. W. Holman and M. L. Gross, Midwest Center for Mass Spectrometry, Univ. of Nebraska-Lincoln, Lincoln, NE 68588

The principle aim of this study is to investigate whether gas-phase ion molecule reactions take place between benzene radical cation and cyclic ethers, and if so characterize the adducts. These reactions are of interest because the adduct formed may initially exist as a distonic radical cation (charge-radical site separate radical cations). Previous work showed that benzene radical cation formed distonic ions when reacted with dienes[1], alkenes[2], and cyclic alkanes[3]. In addition, these reactions may serve to further the understanding of the nature of radical cation adducts, and add to the growing body of bimolecular radical cation reactions.

When the reaction of an unionized mixture of benzene and either ethylene oxide, oxetane, or tetrahydrofuran (THF) is conducted in the high pressure source of a tandem mass spectrometer (Kratos MS-50 TA), adduct ions are formed. In these reactions it is benzene that reacts as the radical cation (proven by FTMS pulsed valve experiments).

The efficiency of adduct formation for the reaction of benzene radical cation with each of the neutral cyclic ethers was determined semiquantitatively so that relative reaction efficiency could be assigned. The following reaction efficiency order is obtained:

Table 1

	Ethylene oxide		Oxetane		THF
$(Adduct^{+\cdot}/C_6H_6^{+\cdot})$	6	:	1	:	~ 0

This relatively small differential in relative reactivity between ethylene oxide and oxetane contrasts sharply with the 100:1 differential in reactivity observed when comparing the reaction of the benzene radical cation with cyclopropane versus that with cyclobutane. The relatively small differential in reactivity for the cyclic alkanes must mean that oxygen coordination must take place (at least in part) in the formation of adduct ions.

To test further the nature of the bonding in these adduct ions the CAD spectra of the various benzene radical cation/cyclic ether adducts were obtained as a function of internal energy. The methodology employed to study bimolecular reactions as a function of internal energy involves conducting the reaction in the high pressure source with variable partial pressure of a third body collision gas, in this case, CS_2. By incrementing the partial pressure of the third body the degree of collisional stabilization of the adduct becomes greater, and hence average internal energy lower.

The benzene/ethylene oxide CAD spectra change dramatically with internal energy.

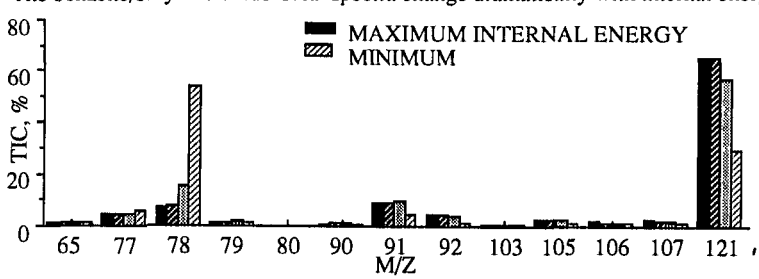

For low internal energy adducts the predominant process is either return to starting material or charge exchange.

Table 2:

$$\text{Benzene}^{+\cdot} + C_nH_{2n}O \longrightarrow C_nH_{2n}O\text{-}C_6H_6^{+\cdot}$$

$C_nH_{2n}O$	$C_nH_{2n}O^+/C_6H_6^{+\cdot}$	Ionization Potential
ethylene oxide	0.011	10.57
oxetane	0.1	10.26
THF	2.1	9.63

The extent of charge exchange parallels the ionization potential of the various cyclic ethers. It is concluded that the low energy benzene radical cation/cyclic ether adduct ions are predominantly ion-dipole complexes (possibly involving oxygen coordination). For high internal energy adducts the contribution from ion-dipole complexes is greatly reduced as evidenced by only minor $C_6H_6^{+\cdot}$ or $C_2H_2O^{+\cdot}$ formation. The predominant dissociation pathways for the high energy adduct is to form $C_7H_7^{+\cdot}$, $C_7H_8^{+\cdot}$, and $C_6H_5C_2H_2O^{+\cdot}$ at m/z 91, 92, and 121, respectively. Hence, the high internal energy adducts are predominantly covalent species.

The structure of the initial covalent benzene radical cation/ethylene oxide adduct may be either structure 1, 2, or 3 (see figure 2). A comparison of the initial CAD mass spectra of appropriate model compounds with that of the adduct can be

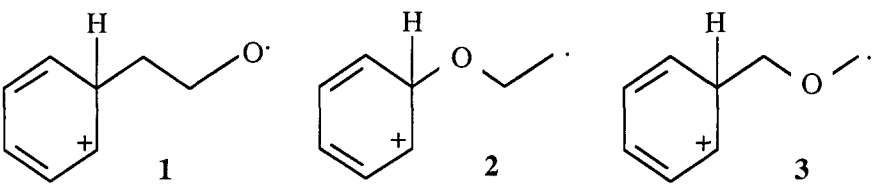

used to elucidate the structure. The model compounds studied include the phenyl ethyl ether radical cation and phenylethanol radical cation. The CAD spectra of the model compounds do not match well with the spectrum of the adduct, and hence it is unlikely that the adduct that is collisionally activated is linear. This is not surprising since rearrangements such as from 1, 2, and 3 are quite fast.

Two processes account for the spectra obtained from the reaction of benzene radical cation and cyclic ethers. At low internal energy, the initially formed ion-dipole complex is the dominant process. This complex either dissociates to benzene radical cation or, if the IP of the ether is low, charge exchange occurs and the radical cation of the ether dissociates from the complex. At higher internal energy and to a certain extent at lower energy, a covalent adduct is formed. This adduct rearranges to a structure for which the dominant process is loss of H. The structure which reaches the collision cell does not appear to be a linear structure such as 1, 2, or 3.

---

[1] R. W. Holman, M. D. Rozeboom, M. L Gross, and C. D Warner, Tetrahedron, 42, (22), 6235-6244, (1986).

[2] R. W. Holman, M. L. Gross, and C. D Warner, 34th Annual Conference, American Society for Mass Spectrometry, Cincinnati, Ohio, June 1986.

[3] C D. Warner, R W. Holman, and M L Gross, 35th Annual Conference, American Society for Mass Spectrometry, Denver, Colorado, May 1987.

Presented at the 36th ASMS Conference on Mass Spectrometry and Allied Topics
June 5-10, 1988, San Francisco, CA

GAS PHASE SYNTHESIS OF DODECAHEDRENE AND DETERMINATION OF ITS DOUBLE BOND ENERGY

Jeffrey P. Kiplinger, Alan G. Marshall, Tomoshige Kobayashi, and Leo A. Paquette

Departments of Chemistry and Biochemistry
The Ohio State University
120 W. 18th Avenue
Columbus, OH 43210

The synthesis of dodecahedrane (**1**, $C_{20}H_{20}$) in 1982[1] generated a great deal of interest in highly symmetric and strained hydrocarbons. We have recently synthesized dodecahedrene (**2**, $C_{20}H_{18}$) in the gas phase. This molecule is the neutral product of an ion-molecule reaction carried out in a Nicolet FTMS-2000 FT-ICR spectrometer, and our evidence for its formation is thus indirect.

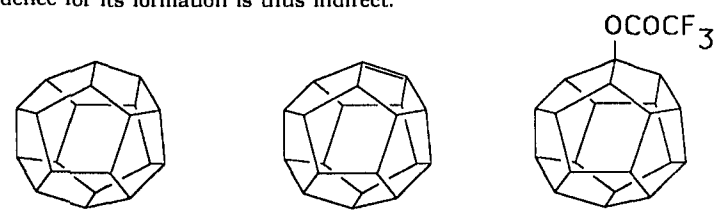

1 **2** **3**

Dodecahedrene is produced as the product of a gas-phase β-elimination reaction when trifluoroacetoxydodecahedrane (**3**) reacts with strong bases (e.g., hydroxide ion). The observed ionic product of this reaction is trifluoroacetate ion, m/e 113^-. Trifluoroacetate is also produced in small quantities on impact of near-thermal electrons, but not on impact of the 5.3 eV electrons used to produce hydroxide from water. In addition, prior ejection of the anionic base produces a >90% reduction in the abundance of m/e 113^- ions.

Reaction of hydroxide ion with **3** to produce trifluoroacetate may take place via a different mechanism, however. Bimolecular substitution is indistinguishable from elimination in the FT-ICR spectrometer since both produce the same ionic product, but in the case of the dodecahedrane system this reaction is sterically unreasonable due to the impossibility of backside attack by the base. Trifluoroacetate may also be produced via a $B_{AC}2$ mechanism, as illustrated in Equation 1. The activated tetrahedral intermediate formed would decompose preferentially to yield trifluoroacetate rather than the dodecahedrane alkoxide due to the greater acidity of trifluoroacetic acid. Reaction of **3** with $^{18}OH^-$ produced from labeled water allows us to differentiate between this mechanism and β-elimination, since the former incorporates the oxygen label into the product ion while the latter does not. The ratio of 113^- to 115^- produced in this experiment is approximately 2.5:1, and this ratio is a direct measurement of the branching ratio for elimination vs. $B_{AC}2$ pathways. Elimination is therefore the preferred pathway, and dodecahedrene is the reasonable neutral product.

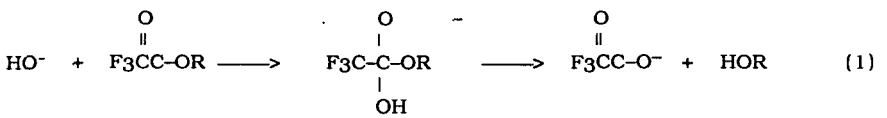

(1)

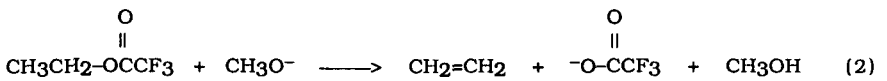

(2)

Examination of the thermochemistry involved in this reaction yields a measurement of the amount of energy necessary to incorporate the strained double bond into this molecule. The elimination reaction takes place easily and with comparable rate constants with the bases hydroxide and methoxide, but does not take place even at very long ion trapping times with ethoxide, which is 13 kJ/mol less basic in the gas phase than methoxide. Such a dramatic change in kinetics with a relatively small change in thermochemistry suggests a kinetically facile mechanism with a small barrier, and allows us to assign a thermochemical threshold for the reaction with confidence. The 1,2 elimination of trifluoroacetate from its ethyl ester (Eq. 2) is calculated[2] to be 174 kJ/mol exothermic with methoxide and 161 kJ/mol exothermic with ethoxide as base. The increased endothermicity involved in the dodecahedrane system represents the extra energy (relative to ethene) necessary to form the strained olefin; our measurement allows a bracketing of this "strain energy" at 168 +/- 12 kJ/mol. This is the additional energy cost of the pyramidalized π-system, and is similar to the energy associated with other strained π bonds.[3]

References

1. (a) Ternansky, R. J.; Balogh, D. W.; Paquette, L. A. J. Amer. Chem. Soc. **1982**, 104, 4503. (b) Paquette, L. A.; Ternansky, R. J.; Balogh, D. W.; Kentgen, G. ibid. **1983**, 105, 5446.

2. Neutral molecule gas phase heats of formation are available from standard references or may be calculated from group additivity rules. See Benson, S. W. *Thermochemical Kinetics*, 2nd Ed., Wiley: New York 1976. Anion gas phase heats of formation are available in J. Phys. Chem. Ref. Data Supp. 1, **1988**, in press.

3. Radzizewski, J. G.; Yin, T.-K.; Mayike, F., Renzoni, G. E.; Borden, W. T.; Michl, J. J. Amer. Chem. Soc. **1986**, 108, 3544.

Acknowledgments

Work supported by National Science Foundation grant CHE-8721498 (AGM) and by National Institutes of Health grant AI-11490 (LAP), and the Ohio State University.

Presented at the 36th ASMS Conference on Mass Spectrometry and Allied Topics
June 5-10, 1988, San Francisco, CA

ACIDIFICATION-NEUTRALIZATION OF CARBONYL COMPOUNDS IN THE GAS PHASE

Thomas A. Shaler and Thomas Hellman Morton
Department of Chemistry
University of California
Riverside, CA 92521

The Brønsted basicity of carbonyl compounds strongly influences their reactivity in a wide range of organic reactions. In many cases protonation on oxygen predominates over protonation at other basic sites. We have investigated this using acidification-neutralization in the FTMS. A neutral molecule, M, is deuterated with a D^+ donor to prepare the [M+2] conjugate acid. Hydron is subsequently removed by reaction with a Brønsted base, B, and the BH^+/BD^+ intensity ratio is measured to assess the degree of isotopic scrambling that must have taken place within the [M+2] conjugate acid. In favorable instances we can detect isomeric conjugate acids and assess which is thermodynamically favored.

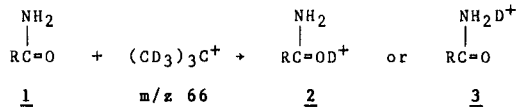

(1)

If the nitrogen of simple amides were deuteronated, 1 → 3 in reaction 1, then one deuterium would become equivalent with two hydrogens. Subsequent removal of hydron from the [M+2] conjugate acid with a Brønsted base (B:) would yield approximately twice as much proton transfer as deuteron transfer. Under typical experimental conditions, the d_9-t-butyl cation (m/z 66, prepared by electron impact on d_{12}-neopentane) reacts with acetamide (1, R=CH_3) to form [M+2] conjugate acid, which yields predominantly BD^+ when a pulse of base is added after trapping. This implies that the [M+2] conjugate acid is O-protonated (structure 2), in accord with what is known for amides in solution. When a mixture of pyridine is used to dehydronate a 4.0:1 mixture of [M+2]:[M+1] from acetamide, the BD^+:BH^+ ratio is 2.8:1 for B = pyridine and 3.6:1 for B = N,N-dimethylacetamide. After correction for the presence of [M+1], this means the 92% of the product of reaction 2 is BD^+ for the former base and 98% is BD^+ for the latter.

Vinylogous carbamate 4 has a basic carbon atom as well as basic heteroatoms. From gas phase equilibrium measurements we find that 4 is more basic than pyridine and less basic than 2-methoxypyridine. Tautomeric [M+2] conjugate acids are shown in reaction 3. Deuteronation on carbon yields 5, in which it scrambles with one hydrogen. Deposition on oxygen yields 6, which, if equilibration proceeds among internally hydrogen-bound species, scrambles one deuterium with two hydrogens via 7 and 8.

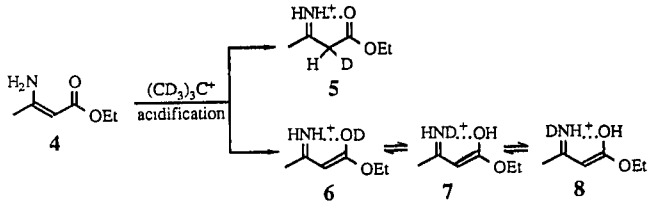

(3)

Presented at the 36th ASMS Conference on Mass Spectrometry and Allied Topics
June 5-10, 1988, San Francisco, CA

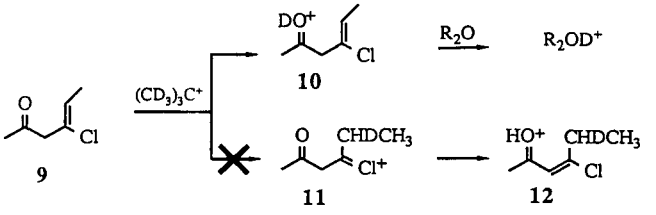

(4)

The results for a 4.9:1 mixture of [M+2]:[M+1] from 4 (vapor from the crystalline Z-isomer) yield more BH^+ than BD^+. The [M+1] conjugate acid from the bimolecular reaction between $M^{+\cdot}$ and M does not react with N,N-dimethylacetamide, while both [M+1] and [M+2] react with 2-methoxypyridine. If the conjugate acids are dehydronated by a 50:1 N,N-dimethylacetamide:pyridine, mixture the BD^+:BH^+ ratio from 2-methoxypyridine is 0.39:1, while the ratio from N,N-dimethylacetamide is 0.93:1. Since neither base is much stronger than 4, reaction of any of the ions in reaction 3 must return it to 4. The most parsimonious explanation of our result is that the [M+2] conjugate acid of 4 consists of a mixture of tautomers 5-8, with 5 less than the others. 2-Methoxypyridine is a strong enough base to dehydronate all of the tautomers, while N,N-dimethylacetamide (which is 4 kcal/mol weaker) only reacts with the high energy tautomer. Since the BD^+:BH^+ ratio is close to unity for the less stable [M+2] conjugate base, we conclude that this must be 5. Therefore deuteronation on carbon occurs, but it is neither kinetically nor thermodynamically favored. This contrasts to the solution phase result, in which we confirm the previously reported observation by Witkop that 4 protonates solely on carbon in $CDCl_3$.

In CD_3OH/HCl solution the ^1H NMR spectrum is much more complex, as a number of species appear to be present. These could be due to the presence of heteroatom-protonated forms, although no assignments are yet conclusive.

Finally we turn to the β,γ-unsaturated chlorohexenone 9. We prepare this with high regio- and stereoselectivity by an "ene" reaction of acetyl chloride/$AlCl_3$ with 2-chloro-1-butene. Three tautomers of the [M+2] conjugate acid are shown in reaction 7. If internal proton transfer were facile, interconversion of 10 with 11 would scramble the deuterium with a hydrogen. Further internal transfer could convert 11 to 12, which might transfer only protons to base. Experimentally, however, we find that the [M+2] conjugate acid of 9 gives ≥95% BD^+ when B = diethyl ether. Therefore 10 is formed and does not interconvert with 11. The sort of transfer that occurs rapidly between oxygen and nitrogen (e.g. 6 ⇄ 7 ⇄ 8) does not readily take place between oxygen and carbon. Reaction of 9 with D_3O^+ in solution leads eventually to exchange of the α-hydrogens for deuterium with no detectable isomerization.

Acknowledgment. We are grateful to Dr. Robert Brown and Ms. Lydia M. Nuwaysir for assistance in writing the FTMS pulse sequence. This work was supported by NSF Grant CHE85-09557.

Presented at the 36th ASMS Conference on Mass Spectrometry and Allied Topics
June 5-10, 1988, San Francisco, CA

FOURIER TRANSFORM MASS SPECTROMETRIC GENERATION AND STUDIES OF CARBOETOXY RADICAL ANION, EtOCOCH·⁻

A. Kasem Chowdhury and Charles Wilkins
Department of Chemistry
University of California, Riverside
Riverside, CA 92521

Introduction:

In contrast to results from Flowing afterglow studies[1], we report here that ethyl- diazo acetate undergoes dissociative electron attatchment under low pressure FTMS conditions, yielding abundant carboethoxy radical ion, EtOCOCH·⁻ (1). In addition to qualitative characterization of its reactions, proton affinity (PA), H atom affinity, and heats of formation of (1) are reported.

Experimental:

All experiments were performed on a Nicolet FTMS-1000 Fourier transform mass spectrometer equipped with a 4.76 cm^3 cell and 3.0 tesla superconducting magnet. A potential of -0.7V was applied to the trap plates to retain negative ions in the cell. Carboethoxy radical anion was generated by a 200 ms beam of 0.199 eV electrons with a filament emission current of approximately 1-2 uA. The anions were trapped in the cell for variable times (from a few millisecond to 1 second) to allow ion-molecule reactions with selected neutral reagent gas.

Results and Discussion:

Dissociative electron attatchment with EtOCOCHN2 in the FTMS yields abundant carboethoxy radical anion (reaction 1). This is in contrast to high pressure FA results where formation of molecular diazo anion was observed[1]. Flowing afterglow systems operate at relatively high pressure (0.3 - 1.0 torr), the electron energy distribution is significantly broader, and fragmentation of molecular ion is less evident. Furthermore, multiple collisions with He buffer gas also contribute to collisionally stabilize vibrationally excited molecular ions. Such collisional stabilization, however, is inefficient in the low pressure FTMS system and the fragmentation of molecular ion is more likely.

$$\text{EtOCOCHN2} \xrightarrow{e^-} [\text{EtOCOCHN}_2^-] \longrightarrow \text{EtOCOCH}^{\cdot -} + N_2 \qquad (1)$$

Upon collision induced dissociation, EtOCOCH·⁻ appears to eliminate C_2H_4 via a six membered transition state, yielding m/z 58. The reaction of EtOCOCH·⁻ with the neutral diazoester produces EtOCOCHCHCO2Et⁻ anion (m/z 172) by attacking at C1, with subsequent loss of N_2 (reaction 2).

$$EtOCOCH^{\cdot -} + EtOCOCHN_2 \rightarrow \begin{cases} EtOCOCHCHCO_2Et^- + N_2 \\ m/z\ 172 \\ EtOCOCN_2^- + EtOCOCH_2^{\cdot} \\ m/z\ 113 \end{cases} \quad (2)$$

The product with m/z 113 is the result of proton abstraction from the diazo ester.

To determine the PA of (1), the reactions of $EtOCOCH^{\cdot -}$ with a series of potential proton donors of known gas phase acidity were investigated. Thus, the PA of $EtOCOCH^{\cdot -}$ was bracketed between the ΔH_{acid}'s of C_2H_5OH and CH_3OH giving PA ($EtOCOCH^{\cdot -}$) = 377.7 ± 2 kcal/mol. By relating the PA with other thermochemical data, ΔH_f ($EtOCOCH^{\cdot -}$) = 48.5 ± 3 kcal/mol was calculated[2]. As a free radical $EtOCOCH^{\cdot -}$ abstracts H· atom from potential H· atom donors. Bracketing such reactions yielded D(EtOCOC-H $^-$) = 104 ± 4 kcal/mol.

Both $CF_3CO_2CH_3$ and $CF_3CO_2C_2H_5$ react rapidly with $EtOCOCH^{\cdot -}$, yielding two products (reaction 3).

$$EtOCOCH^{\cdot -} + CF_3CO_2R \rightarrow \begin{cases} 0.99 & EtOCOCHCOCF_3^- + \cdot OR \\ 0.01 & EtOCOCHCO_2R^- + \cdot CF_3 \end{cases} \quad (3)$$

The major reaction channel is considered to be the product of carbonyl addition followed by radical β-fragmentation of the alkoxy radical. The minor product appears to be formed via loss of $\cdot CF_3$ radical from the tetrahedral intermediate produced by carbonyl attack. Although no reaction was observed with O_2 and N_2O, $EtOCOCH^{\cdot -}$ reacted rapidly with CS_2 via S atom abstraction to yield $EtOCOCHS^-$.

References:

1. McDonald, R.N.; Chowdhury, A.K. ,Tetrahedron, 42, 6253, 1986.
2. Bartmess, J.E.; McIver,Jr., in M.T. Bowers (Ed.), Gas Phase Ion Chemistry, Vol.2, Academic Press, New York, 1979, pp. 87-121.

Presented at the 36th ASMS Conference on Mass Spectrometry and Allied Topics
June 5-10, 1988, San Francisco, CA

ION/MOLECULE REACTIONS OF $C_5H_3^+$ AND $C_7H_7^+$ IN THE GAS PHASE

F. Ozturk and J. R. Eyler
Department of Chemistry
University of Florida
Gainesville, Florida 32611

Introduction:

The $C_5H_3^+$ and $C_7H_7^+$ ions have been proposed as two species involved in an ion/molecule mechanism of soot formation.[1,2] Results of previous experimental work suggested[3] two different linear structures for the $C_5H_3^+$ ion, each produced from a different precursor. Previous experimental studies[4] on structural characterization of $C_7H_7^+$ ions indicated that these ions exist in the gas phase with at least two structures; tropylium, and benzyl, which were also identified as the two most stable structures by theoretical studies.[5] Unreactive and reactive $C_7H_7^+$ observed in ion/molecule reactions have been attributed[6] to tropylium and benzyl structures respectively.

Experimental:

A Nicolet FTMS-1000 Fourier transform ion cyclotron resonance (FTICR) mass spectrometer was used. Reaction pathways were delineated using the ejection capabilities of FTICR which make it possible to eject one ion from a complicated reaction mixture to determine its contribution to the mass spectrum of all the other ions. Reaction rate coefficients were determined by monitoring the intensity of the $C_5H_3^+$ and $C_7H_7^+$ ions as a function of time after ejection of all other ions from the analyzer cell. $C_5H_3^+$ ions were produced by 50 eV electron ionization of 2,4-hexadiyne and by the reaction of $C_3H_3^+$ with diacetylene. $C_7H_7^+$ ions were produced from toluene, cycloheptatriene and norbornadiene by dissociative chemical ionization using different charge transfer agents ($C_4H_2^+$, Xe^+, Kr^+, and Ar^+).

Results:

$C_5H_3^+$ Reactions with Acetylene and Diacetylene: Although almost all of the $C_5H_3^+$ ions produced from 2,4-hexadiyne reacted with the neutral precursor, no reaction of these ions was observed with either C_2H_2 or C_4H_2. $C_5H_3^+$ ions produced as products of the reaction of $C_3H_3^+ + C_4H_2$ were 100% reactive with both propargyl iodide and diacetylene (the neutrals present in the reaction medium). The rate coefficient for the reaction of $C_5H_3^+$ with diacetylene was found to be $(5.6 \pm 1.7) \times 10^{-10}$ cm^3/s.

$C_7H_7^+$ Reactions with Acetylene and Diacetylene: $C_7H_7^+$ ions produced from different precursors had both reactive and unreactive populations. While $C_7H_7^+$ produced from cycloheptatriene and norbornadiene reacted with acetylene with rate constants in the range of $(1\text{-}4) \times 10^{-11}$ cm^3/s to form $C_9H_9^+$, no reaction was observed with $C_7H_7^+$ ions produced from toluene. $C_7H_7^+$ ions produced from different precursors reacted with diacetylene with different rate coefficients.

Discussion:

$C_5H_3^+$: Higher reactivity of $C_5H_3^+$ ions produced by the $C_3H_3^+ + C_4H_2$ reaction compared to those produced by electron ionization of 2,4-hexadiyne suggests that the former has a higher heat of formation with a stable structure <u>different</u> from those reported earlier for $C_5H_3^+$ ions from both 2,4-hexadiyne <u>and 1,3-pentadiyne</u>. Although no structural assignment can be made for the $C_5H_3^+$ ion produced by reacting $\ell\text{-}C_3H_3^+$ with diacetylene based on the results of this study, several structures can be considered possible on the basis of initial charge distribution on $\ell\text{-}C_3H_3^+$. Thus, reaction of the propargylium cation with diacetylene with resultant loss of acetylene, might proceed according to either Scheme I or Scheme II leading to the formation of three different $C_5H_3^+$ ion structures.

Presented at the 36th ASMS Conference on Mass Spectrometry and Allied Topics
June 5-10, 1988, San Francisco, CA

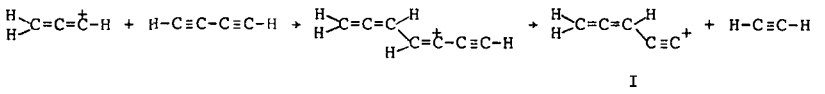

I

Scheme I

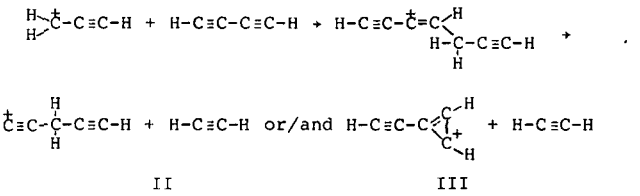

II III

Scheme II

$C_7H_7^+$: Based on the differences in behavior observed in this study of $C_7H_7^+$ ions produced from three precursors, the possibility of stable structure(s) other than benzyl and tropylium must be considered. As suggested by AM1 calculations for the $C_7H_7^+/C_7H_8^+$ surface,[7] the ion produced by hydrogen loss from the bicyclo [3.2.0] heptadiene radical cation is a stable $C_7H_7^+$ isomer accessible at about 2.8 eV above the appearance potential of tropylium from cycloheptatriene. Table I summarizes the proposed $C_7H_7^+$ structures for different precursors on the basis of previous and present studies.

Table I.

Precursor of $C_7H_7^+$	Unreactive Structure (ΔH_f = 207 kcal/mole)	Reactive Structure	ΔH_f (kcal/mole)
Toluene	Tropylium$^+$	Benzyl$^+$	211 (Ref. 8)
Cyclohpetatriene	Tropylium$^+$	(BCH-H)$^{+a}$	271 (Ref. 7)
Norbornadiene	Tropylium$^+$	(MCH-H)$^{+b}$	?(236) (Ref. 5)

[a] Structure produced by hydrogen loss from bicyclo[3.2.0]heptadiene radical cation.
[b] Structure produced by hydrogen loss from 5-methylene-1,3-cyclo hexadiene ion.

References:

1. Olson, D. B.; Calcote, H. F. in "Particulate Carbon Formation during Combustion" Siegla, D. C.; Smith, G. W., Eds.; Plenum: New York, 1981, 177-205.
2. Calcote, H. F. Combust. Flame 1981, 42, 215.
3. Dannacher, J.; Heilbronner, E.; Stadelmann, J.-D.; Vogt, J. Helvetica Chimica Acta 1979, 62, 2186.
4. Bombach, R.; Dannacher, J.; Stadelmann, J.-P. J. Am. Chem. Soc. 1983, 105, 4305, and the references therein.
5. a. Cone, C.; Dewar, M. J. S.; Landman, D. J. Am. Chem. Soc. 1977, 99, 372. b. Dewar, M. J. S.; Landman, D. Ibid, 1977, 99, 2446.
6. Ausloos, P. J. Am. Chem. Soc. 1982, 104, 5259 and the references therein.
7. Bartmess, J. E. private communication.
8. Lossing, F. P., Can. J. Chem. 1971, 49, 357.

Presented at the 36th ASMS Conference on Mass Spectrometry and Allied Topics
June 5-10, 1988, San Francisco, CA

ION-MOLECULE REACTIONS OF ISOMERIC TERPENE DERIVATIVES UNDER POSITIVE AMMONIA CI: STUDY OF STEREOCHEMICAL EFFECTS

Richard B. Cole, Chantal Prevost and Jean-Claude Tabet*

Laboratoire de Chimie Organique Structurale, U.A. 455, Université Pierre et Marie Curie, 75230 Paris Cedex 05 and Laboratoire de Synthèse Organique, Ecole Polytechnique, 91128 Palaiseau, FRANCE

The following epimeric 16-hydroxy-13-ketal modified tetracyclic terpene derivatives (exo 1a and endo 1b) undergo competitive ion-molecule reactions in a high pressure chemical ionization (> 10^{-1} torr ammonia) source of a Triple Quadrupole (Nermag R30-10). Among the predominating processes (Fig. 1) are protonation and aminolysis of the ketal group to form MH^+ (m/z 335), as the proton affinity of the ketal group is superior to that of ammonia, and $(M+NH_4-C_2H_4O)^+$ (m/z 308, denoted MaH^+), respectively.

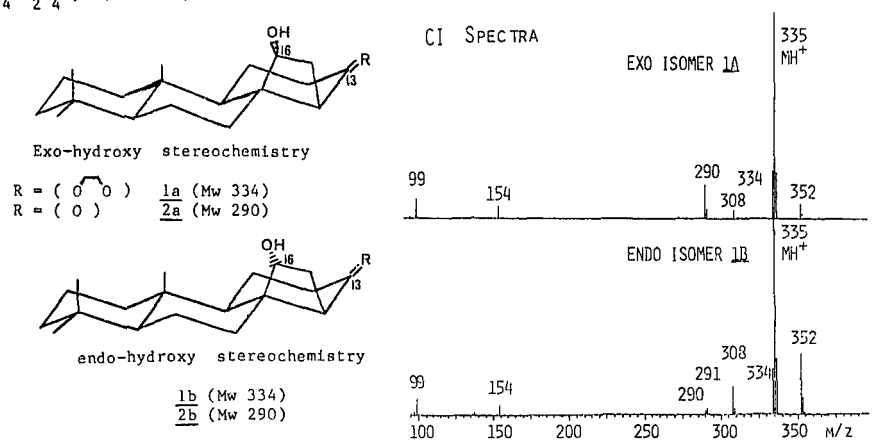

Figure 1

Comparison of low-energy (10 eV lab.) CAD spectra of MaH^+ ions with those of ammonia adducts of the corresponding hydroxy-ketone isomeric forms (i.e., a carbonyl group at C_{13} in place of the ketal group) reveals identical structures for each pair of ions with the same hydroxyl spatial orientation. This confirms that the stereochemistry of the hydroxyl group is not affected by the aminolysis reaction. A solvated adduct structure appears to be involved in preference to geminal hydroxyl and ammonium groups at C_{13}. Under higher collision energy (60 eV lab.), the CAD spectra are superimposable at low m/z values indicating that the polycyclic skeleton is preserved intact in all cases. The MaH^+ ion is most likely produced by ammonia solvation of the protonated ketone fragment ion in the ion source and not by direct ammonia attack upon the m/z 352 adduct ion.

In comparing the fragment ions at m/z 290, produced from hydroxy-ketal $(M+NH_4-C_2H_6O_2)^+$ and hydroxy-ketone (mol. wt. 290) stereoisomers, structural differences involve more than just hydroxyl stereochemistry. From ketal isomers, m/z 290 is characterized by immonium (as

opposed to ammonium) ion structures. The immonium ion could be produced from an opened-ring form of the ketal adduct ion which reacts with NH_3 leading to aminolysis. In contrast, for the hydroxy-ketone, a direct nucleophilic substitution occurs at the hydroxylic site to form m/z 290. This reaction is favored because the proton affinity of the hydroxyl group is lower than that of ammonia. Consequently, formation of MH^+ from an adduct form where the hydroxyl group solvates NH_4^+, is endothermic. Exothermic nucleophilic substitution thus occurs preferentially. Similarly, nucleophilic substitution also occurs to a minor extent at the C_{16} hydroxyl group of hydroxy-ketal derivatives to form $(M+NH_4-H_2O)^+$, m/z 334 denoted MsH^+. Low-energy (30 eV lab.) CAD spectra (below) reveal that the structure of this substituted MsH^+ ion is the same for both reactant stereoisomers and corresponds to an exo ammonium form.

Figure 2.

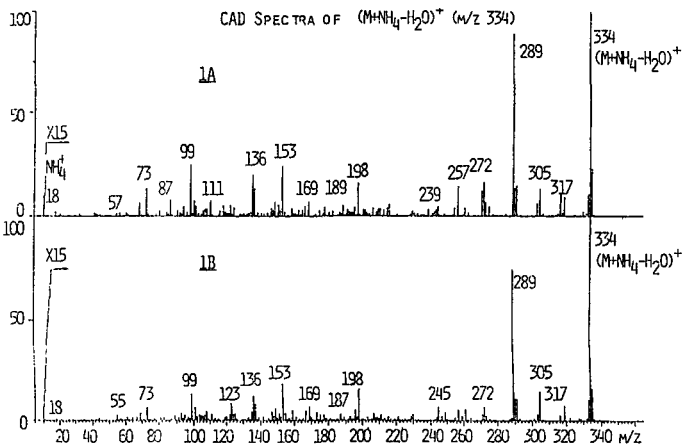

This indicates that the substitution reaction is bimolecular (S_N2) with inversion of configuration for the endo isomer (1b+NH_4)$^+$; for the exo isomer (1a+NH_4)$^+$, steric constraints on the NH_3 approach (endo side) permit only intramolecular (S_Ni) reaction with retention of configuration.

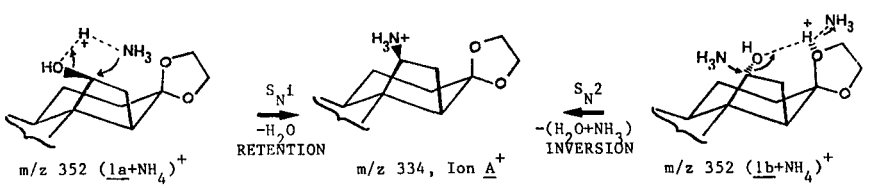

Presented at the 36th ASMS Conference on Mass Spectrometry and Allied Topics
June 5-10, 1988, San Francisco, CA

ENERGY DEPOSITION VIA COLLISIONALLY INDUCED DISSOCIATION IN A HYBRID MASS SPECTROMETER

T G Blease, J H Scrivens, ICI PLC, Wilton, Cleveland, UK, TS6 8JE
J J Monaghan, ICI PLC, Runcorn, Cheshire, UK, WA7 4QD
E Schöder, Finnigan MAT, 2800 Bremen, FRG

In MS-MS various methods of inducing a selected ion to fragment have been proposed. These include collision induced dissociation (CID), photodissociation, surface induced dissociation (SID) and electron induced dissociation. Of these, CID has proven of widest utility due to the relatively large cross-sections for excitation and subsequent dissociation and the ability to vary the density of the target gas readily.

The fragmentation induced by CID in a low energy MS-MS experiment has been found to depend on the number of collisions in the collision region (gas pressure), the collision energy of the parent ion, the energy level of the collision quadrupole with respect to the analysing quadrupole, the nature of the target gas, the design parameters of the collision quadrupole (including interquadrupole apertures and rf level) and the type of detector used.

In addition to fragmentation efficiency and CID efficiency, recent literature discussions have highlighted another important parameter affecting CID performance, namely the internal energy deposition of the selected ion after activation. Cooks and co-workers have outlined an objective approach to the measurement of this parameter. This involves the study of compounds that undergo consecutive fragmentations of known activation energies.

We have used this approach with tetraethylsilane to characterise energy deposition in a Finnigan HSQ30 hybrid mass spectrometer of geometry BEQQ. We have found that the Finnigan instrument allows access to significantly higher energy transfer conditions than other hybrids. Since these conditions are only analytical useful if adequate sensitivity is available, we have compared results obtained previously on a VG ZAB HSQ instrument for the detection of alkyl sultones in detergent formulations (1) with those obtained on the Finnigan instrument under these high energy transfer conditions.

The decomposition/appearance potentials for tetraethylsilane are well established: $SiEt_4^+$ (m/z 144, 10.5eV), $SiEt_3^+$ (m/z 115, 11.0eV), $HSiEt_2^+$ (m/z 87, 12.5 eV), H_2SiEt^+ (m/z 59, 14.0 eV), SiH_3^+ (m/z 31, 20.6 eV), $SiEt^+$ (m/z 57, 19.4 eV), SiH^+ (m/z 29, 26.8 eV), and serve as a useful indicator of the energy transfer possible in any instrument.

Fig 1 shows the daughter ion spectrum of m/z 144 obtained using the Finnigan HSQ30 with 3mTorr of argon and 30 eV collision energy. This corresponds to multiple collision conditions and, by increasing the target gas pressure and thus the average number of collisions experienced, more energy may be transferred. Fig 2 shows the spectrum obtained at 30mTorr of argon and 30 eV. As can be seen, very significantly more energy is transferred. Fig 3 shows the effect of increasing the collision energy to 100 eV when extensive fragmentation is observed.

Fig 4 gives the variation of fragment ion intensities obtained from 0-100 eV collision energy at an argon gas pressure of 30mTorr. These may be compared with Cooks' results (Fig 5) obtained from the same molecule using SID. Very similar results are obtained although the absence of m/z 57 from our CID results is interesting.

FIG 1

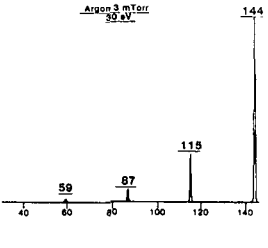

FIG 2

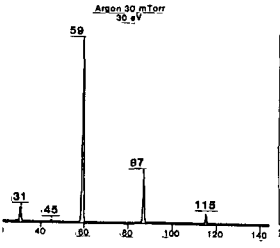

FIG 3

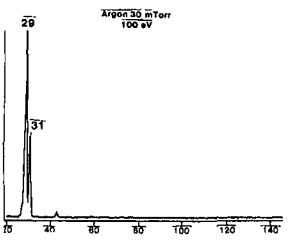

FIG 4

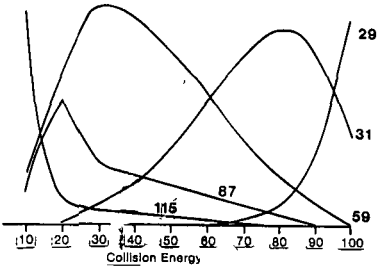

FIG 5

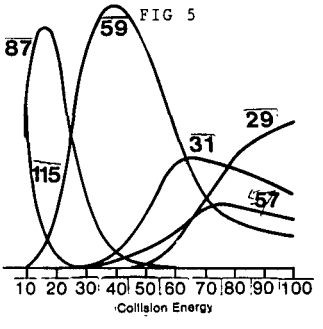

Although these results indicate that, under experimentally extreme collision conditions, energy transfer may be induced beyond that normally obtained with low energy CID, it is important to achieve adequate sensitivity using a well characterised sample.

The analysis of 1,3 and 1,4 alkyl sultones in an anionic surfactant matrix, $RO(CH_2CH_2O)_n\ SO_3^-Na^+$ where n = average of 3, using hybrid MS has been described earlier (1). Negative CI using ammonia is used to discriminate in favour of the uncharged sultone species which give $(M-H)^-$ ions for the 1,3 species and M^- ions for the 1,4 sultones.

Using a VG ZAB HSQ hybrid mass spectrometer, a daughter ion spectrum of $(M-H)^-$ from hexadecane 1,4 sultone (m/z 303) gave a detection limit of <1 ppm for the sultone in the surfactant matrix.

Using the HSQ30 under these high energy transfer conditions, at least equivalent sensitivity to the lower pressure data is obtained for the detection of the sultone in the matrix. Subsequent work using the parents of m/z 80 (SO_3^-) as a general analysis for both 1,3 and 1,4 sultones yielded the required sensitivity.

The use of collision cell pressures of 30mTorr of argon and collision energies of 100 eV can, with suitable instrumentation, result in a combination of high energy transfer via multiple collisions and adequate analytical sensitivity. This increased range of energy transfer will improve the applicability of MS-MS approaches in areas where stable ions are involved or where greater flexibility in directed fragmentation is required.

1 T G Blease, D A Catlow, E Clayton, J J Monaghan and J H Scrivens, ASMS 1987, Denver, Co

Presented at the 36th ASMS Conference on Mass Spectrometry and Allied Topics
June 5-10, 1988, San Francisco, CA

A COMPARISON OF THEORETICAL AND EXPERIMENTAL RELATIVE SENSITIVITIES IN GAS CHROMATOGRAPHY/CHEMICAL IONIZATION MASS SPECTROMETRY

Ron Orlando and Burnaby Munson
Department of Chemistry and Biochemistry
University of Delaware
Newark, Delaware 19716

One problem in the quantitation of complex mixtures by any technique is the availability of the standards which are needed to establish either the sensitivities or the relative sensitivities of the compounds in the mixtures. The more complex the mixture, the more difficult it becomes to obtain all of the compounds. Therefore, methods of predicting relative sensitivities of compounds or correlating sensitivities with molecular structures are of great importance in reducing the necessary number of standardization experiments.

In chemical ionization mass spectrometry, the sample ions are produced by ion/molecule reactions of the reagent ions with the sample molecules; consequently, the sensitivities (or calibration factors) are proportional to the rate constants for these ion/molecule reactions.[1] The rate constants (or collision frequencies) for these reactions can be calculated either from the Langevin theory which uses only the molecular polarizabilities[2], or from another theoretical model which includes both the molecular polarizabilities and dipole moments.[3] The relative sensitivities, based on total sample ionization, can then be calculated for all compounds from the ratios of these rate constants.

The relative sensitivities for a number of compounds in chemical ionization mass spectrometry with tetramethylsilane (TMS) as the reagent gas have been accurately represented by the ratios of calculated rate constants. The agreement between the calculated and experimental relative sensitivities is good for both theoretical models for a diverse set of compounds (ketones, phenols, aliphatic alcohols, di-alkyl ethers, cyclic ethers, sulfides, and thiols). The average difference between the calculated and experimental relative sensitivities is 9.2% for the Langevin model and 5.8% for the Su and Chesnavich model. These errors are slightly smaller than the sum of the errors in the experiments, and the calculated values usually lie within one standard deviation of the experimental value. However, it is apparent that the relative sensitivities calculated from the Su and Chesnavich model (which includes a contribution from the dipole moment) are in much better agreement with the experimental data for the ketones than the relative sensitivities calculated on the basis of the Langevin theory (polarizabilities only).

The deviation between the two models decreases with decreasing dipole moment and with increasing polarizability (molecular weight) of the sample molecules. Plots of the relative deviation, [k(exp) - k(L)]/k(L), as functions of molecular weight for different compounds with various values of dipole moments are in excellent agreement with the theoretical curves for the calculated relative deviations, [k(SC) - k(L)]/k(L), using the appropriate dipole moment[4] for each individual compound. k(SC) refers to the rate constant calculated from the Su and Chesnavich model[3] and k(L), from the Langevin model,[2] both relative to 1-hexanol. Even for very polar species, the relative sensitivities calculated with the two models differ by no more than 10% for compounds with molecular weights greater than 200. In addition, for compounds of the same type, the deviations between these two models change very slowly with increasing molecular weight above 200;

consequently, the ratio of rate constants or the relative sensitivity for two compounds, k_2/k_1, will be approximately the same when calculated using the Su and Chesnavich or the Langevin model.

The TMS CI spectra of the primary, secondary, and tertiary alcohols are very different and show strikingly different variations with sample size because of different sample ion/sample molecule reactions.[5] However, the sensitivities, which are determined by the reactions of $(CH_3)_3Si^+$ with compounds of the same polarizabilities and nearly identical dipole moments, are essentially identical.

One possible problem with this procedure for calculating relative sensitivities results from different mechanisms for the formation of sample ions for different compounds. These different mechanisms lead to different temperature dependences of the relative sensitivities. It was shown earlier that the relative sensitivities of aliphatic alcohols and ethers which undergo dissociative addition reactions with $(CH_3)_3Si^+$, are independent of temperature.[5,6] The Si-containing ions, produced in the primary reactions, have been shown to react by trimethylsilyl ion transfer with a second sample molecule to form the adduct ion, $(M+73)^+$. However, the relative sensitivities for those compounds which form adduct ions by collisionally stabilized addition, have strong negative temperature coefficients, in agreement with earlier work on association reactions on simple system[7]. Consequently, the calculated relative sensitivities for these compounds will be reliable only at relatively low temperatures when the rate of sample ion formation is determined by the rate of collisions of the trimethylsilyl ion with the samples.

Additional problems may be encountered because the relative sensitivities may not be independent of the source configuration, although this would not effect the rate constants. More experimentation with different instruments is needed to test this possible source of error.

Because the relative rate constants can be calculated for the reactant ions from any CI reagent gas, we would like to suggest the use of this method for other systems.

To be published in Analytical Chemistry, 1988.

LITERATURE CITED

1. Munson, B. Interactions Between Ions and Molecules ed. by P. Ausloos, Plenum Press, New York, 1975, 505.

2. Harrison, A. Chemical Ionization Mass Spectrometry CRC Press, Boca Raton, FL 1983.

3. Su, T.; Chesnavich, W. J. Chem. Phys. 1982, 76, 5183.

4. McClellan, A. Tables of Experimental Dipole Moments, W. H. Freeman and Company, San Francisco, 1963.

5. Orlando, R.; Strobel, F.; Ridge, D.P; Munson, B. Org. Mass Spectrom. 1987, 22, 597.

6. Orlando, R.; Ridge, D.; Munson, B. Org. Mass Spectrom. in press.

7. Meot-ner (Mautner), M. Gas Phase Ion Chemistry Vol. 1 ed. by M.T. Bowers, Academic Press, New York, 1979, 198.

Presented at the 36th ASMS Conference on Mass Spectrometry and Allied Topics
June 5-10, 1988, San Francisco, CA

ION MOLECULE REACTIONS OBSERVED FOR NITRO AROMATIC COMPOUNDS IN NEGATIVE ION FAST ATOM BOMBARDMENT MASS SPECTROMETRY

K. Balasanmugam[1], J. M. Miller[1], and R. W. Smith[2]

[1] Dept. of Chemistry, Brock University, St. Catherines, Ont., L2S 3A1, Canada

[2] McMaster Regional Centre for Mass Spectrometry, Dept. of Chemistry, McMaster University, 1280 Main St. W., Hamilton, Ont., L8S 4M1, Canada.

Nitro aromatic compounds (NACs) have been identified in various environmental samples such as air particulates, diesel exhaust paricles and carbon black. Since NACs have been characterized as direct mutagens there is considerable interest in their identification. Consequently, NACs have been extensively investigated using mass spectrometric techniques such as electron impact, electron capture negative ion chemical ionization, high pressure mass spectrometry, and atmospheric pressure ionization mass spectrometry. More recently, laser mass spectrometry (LMS) has been employed to characerize NACs[1]. In this study[1] an interesting ion-molecule reaction was observed (a).

$$NAC + NO_2^- \longrightarrow (NAC + O\text{-}H)^- + HNO \quad (a)$$

In this paper we have studied a series of twenty NACs by positive and negative ion fast atom bombardment mass spectrometry (FAB) in an attempt to assess the potential of the technique both as a means to characterize NACs and to detect any ion-molecule reactions that may be occurring during the FAB ionization process. All experiments were performed on a VG ZAB-E mass spectrometer. Xenon was used as the primary atom beam and the FAB gun was operated at 8keV/mA. Depending on the solubility of the samples, either 3-nitrobenzyl alcohol (NBA) or 2-nitrophenyl octyl ether (NPOE) were used as the matrices. Samples were dissolved in the matrix (10-15 mg/ml) and, in some cases, a small amount of dimethyl sulphoxide was used to enhance solubility. All spectra presented are the average of at least 10 scans. The variation in peak intensities from scan to scan is on the order of 6-10%.

In general, the negative ion FAB spectra of the NACs studied are more useful than the positive ion spectra for compound characterization. The negative ion spectra (Table 1) all exhibit ions corresponding to $M^{-\cdot}$ and/or $(M\text{-}H)^-$ except for compounds 8 and 13. Compounds 7, 16, and 17 undergo hydrolysis in these experiments, for example, 4-nitrobenzyl bromide yields a very weak molecular anion in NBA matrix. The spectrum is dominated by ions characterized as Br^-, $(NBA+Br)^-$, and $(2NBA+Br)^-$. Interestingly, an ion-molecule reaction seems to be occurring between the Br^- ion and the matrix. Some of the NACs studied yield ions corresponding to $(M+NO_2)^-$ and/or $(M+O\text{-}H)^-$ (Table 1). Formation of the molecular anion, $M^{-\cdot}$, is presumeably by electron exchange with the NO_2^- ion whilst the $(M\text{-}H)^-$ ion is formed by proton abstraction by the NO_2^- ionic species. In positive ion FAB, only compounds 1-6, 8, 14, and 15 yielded ions indicative of structure. In these cases, $(M+H)^+$ ions dominate although $M^{+\cdot}$ ions are also observed. Formation of the $M^{+\cdot}$ ions, again by electron exchange, only occurs for those samples with ionization potentials less than 9eV.

The linked scan and CID spectra of the ion at m/z 199 $(M+NO_2)^-$ in the spectrum of NBA shows that the ions characterized as $(M+O\text{-}H)^-$ m/z 168, $M^{-\cdot}$ m/z 153, $(M\text{-}H)^-$ m/z 152, $(M\text{-}2H)^{-\cdot}$ m/z 151, and $(C_6H_4NO_2)^-$ m/z 122 are formed in part from the ion-molecule adduct (Figure 1). Addition of an NO_2^- source to the matrix (eg. 1,3,5-trinitrobenzene) increases the intensity of all ions associated with NO_2^- formation. This observation further supports the contention that the $(M+NO_2)^-$ ion is formed through an ion-molecule reaction.

Presented at the 36th ASMS Conference on Mass Spectrometry and Allied Topics
June 5-10, 1988, San Francisco, CA

Table 1 Negative ion FAB mass spectra of compounds studied

	COMPOUND (MW)	M /(M H)	(M+NO_2) / (M+O-H)	NO_2	OTHER IMPORTANT IONS (M/Z, RELATIVE INTENSITIES)[b]
1	2-(4-nitrobenzyl) pyridine[a] (214)	33.5/27.9	0/3.4	82.1	
2	4-nitrobenzamide (166)	100/69	21.4/7.1	70.0	(M - $CONH_2$) (122, 11.9), (M+NO_2) (212, 2.4)
3	2,4-dinitrodiphenylamine (259)	79.1/60.9	35.6/2.7	81.4	$NO_2C_6H_3NH^-$ (136, 8.5), $(NO_2)_2C_6H_4^-$ (168, 11.9) $(NO_2)_2C_6H_4$- NH (182, 3.3)
4	2,4-dinitrophenylhydrazine (198)	41.6/95.7	4.4/1.3	99.5	$(NO_2)_2C_6H_4NH^-$ (182, 11.5) $NO_2C_6H_3NH^-$ (136, 11.5) $C_6H_5NH^-$ (92, 5.3)
5	3-methyl 2-nitrobenzoic acid (181)	37.6/100	0/2.1	20.2	(M - NO_2) (135, 3.4) (M - H - CO_2) (136, 24.0)
6	3-nitrophthalic acid (211)	33.7/100	0/0	17.2	(M - H - $2CO_2$) [c] (122, 35.5), (M - H - CO_2) (166, 58.6)
7	3-nitrophthalic anhydride[d] (193)	34/100	0/0	10.0	(M - H - $2CO_2$) [c] (122, 34), (M - H - CO_2) (166, 39.1)
8	4-nitrophenylphosphate (227)	100/0	0/12.0	56.8	
9	1,3-dinitrobenzene (168)	100/6.9	0/6.6	38.5	
10	1,3-dinitrobenzoylchloride[a] (151)	56.6/4.7	0/3.2	76.8	
11	4-nitrophenylacetonitrile (162)	35.7/100	1.2/4.8	70.0	
12	4-nitrobenzonitrile[a] (148)	85.5/6.9	0/6.6	79.1	
13	4-chloronitrobenzene[a] (157)	39.1/0	0/0	70.7	
14	2-nitrophenyl octyl ether (251)	81.7/20.1	5.7/16.7	73.1	$NO_2C_6H_4O^-$ (138, 100)
15	3-nitrobenzyl alcohol (153)	100/55	31.2/23.5	50.4	(2M + NO_2) (152, 3.7) 4M (612, 1.2) 3M (459, 7.5) (M - H_2) (151, 50.7)
16	4-nitrobenzyl chloride[a] (171)	51.0/12.8	0/0	78.6	$O_2NC_6H_4CH_2OH^-$ (153, 7.4) Cl (35, 80.6)
17	4-nitrobenzyl bromide[a] (215)	4.8/4.5	0/0	45.8	$NO_2C_6H_4CH_2OH^-$ (153, 16.8), $(O_2NC_6H_4CH_2OH + NO_2^-)$ (199, 4.2) $(O_2NC_6H_4CH_2OH + Br)$ (232, 20.6) Br (79, 100)
18	2-nitrobenzoic acid[b] (167)	60.0/94.9	5.0/1.8	58.2	(M - H - CO_2) (122, 48.1) (M - CO_2) (123, 8.9)
19	3-nitrobenzoic acid (167)	20.2/100	3.8/6.3	24.0	(M - H - CO_2) (122, 22.8) (M - CO_2) (123, 3.8)
20	4-nitrobenzoic acid[b] (167)	24.0/62.0	2.5/2.5	40.5	(M - H - CO_2) (122, 37.9) (M - CO_2)$^-$ (123, 8.7)

a. matrix used in these cases is NPOE where ions corresponding to $NO_2C_6H_4O^-$ (m/z = 138, 100%) from the matrix dominate the spectra. NBA is used for all other cases with the NBA (m/z = 153) ion dominating the spectra of 3 and 4

b. ions corresponding 2M - (2M - H) (M + NBA) (M + NBA - H) (M - O) and $O_2NC_6H_4^-$ are generally observed in majority (molecular cluster ions are absent for 10, 12, 13, 16 and 17) of the examples studied

c. includes a small contribution from the matrix peaks.

d. spectrum is identical to that of 3-nitrophthalic acid with respect to ion masses (m/z), where M refers to m/z = 211 rather than 193 (see text)

LINKED SCAN (B/E, CID) M/Z 199 NBA -FAB

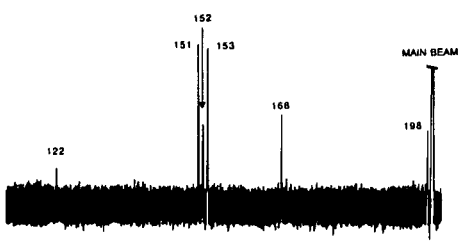

Figure1

[1] K. Balasanmugam, S.K. Viswanadham, and D.M. Hercules; Anal. Chem., **55**, 2424, (1983).

Presented at the 36th ASMS Conference on Mass Spectrometry and Allied Topics
June 5-10, 1988, San Francisco, CA

EFFECT OF COLLISION GAS PRESSURE AND ENERGY ON THE MASS SPECTRA OF SOME TRICHOTHECENES OBTAINED BY REACTIVE COLLISIONS WITH AMMONIA

R. Kostiainen

Finnish Research Project on Verification of Chemical Disarmament, Department of Chemistry, University of Helsinki, Vuorikatu 20, Helsinki 10, Finland

The use of reactive collisions with ammonia provides a highly specific method for the characterization of trichothecenes. In this method the trichothecenes are introduced to the ion source by direct exposure probe and ionized by isobutane CI. The protonated molecule is mass-selected by the first quadrupole and enters the collision chamber (quadrupole 2, Q2), where ammonia is used as neutral reagent instead of inert collision gas. Interaction of the protonated molecule with ammonia in Q2 produces not only ions formed by the collisionally activated dissociation (CAD) $[M+H-HX]^+$, but also ions formed by collisionally activated reactions (CAR): the adduct ion $[M+H+NH_3]^+$, ions formed by substitution reactions $[M+H+NH_3-HX]^+$, solvated ions $[M+H+(NH_3)_2]^+$ and $[M+H+(NH_3)_2-HX]^+$ (1). The ions formed by the collisionally activated reaction (CAR) process provide additional information for structural characterization and can also be used for monitoring (2). Figure 1. shows, as an example, collisionally activated reaction spectra of diacetoxyscirpenol (DAS) and deoxynivalenol (DON) using ammonia as a collision gas.

The collision pressure and energy have a great effect on the formation of ions in the reactive collisions. On the basis of the energy and pressure resolved curves, suitable collision conditions can be chosen for analytical purposes. The formations of adduct, substitution and solvated ions are favoured by high collision pressures and low collision energies, whereas the formation of CAD ions is favoured by high collision energy and pressure (Fig. 2). By choosing a relatively low collision energy and high collision pressure, the ions formed in the reactions between ammonia and protonated molecule and the ions formed by collisionally activated dissociation can be clearly detected.

<u>references</u>

(1) R. Kostiainen, Biomed. & Environ. Mass Spectrom., International Symposium on Applied Mass Spectrometry in the Health Sciences, Barcelona, September 28-30, in press.

(2) R. Kostiainen, A. Rizzo, and A. Hesso, Arch. Environ. Contam. Toxicol, in press.

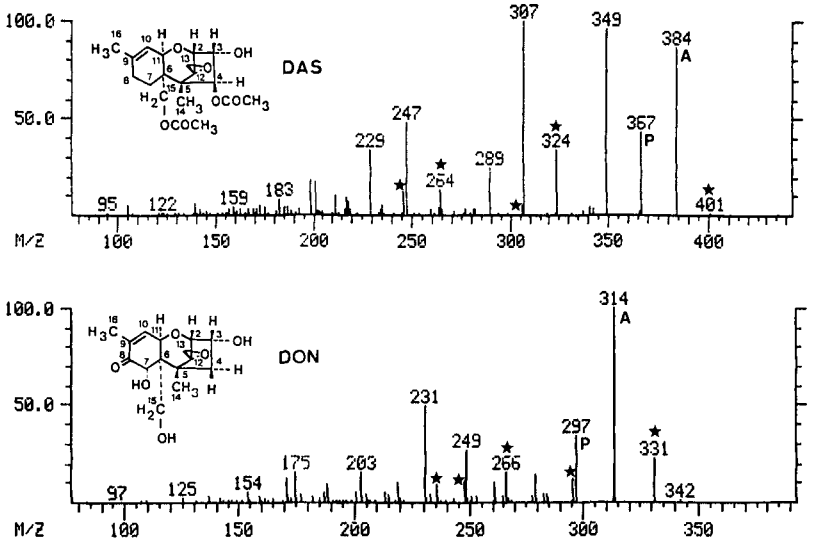

Fig. 1. Low energy (7 eV) collisionally activated reaction spectra of protonated (isobutane CI) trichothecenes DAS and DON using ammonia (8 mTorr) as a collision gas. P=parent ion, A=adduct ion, *=substitution ion and solvated ion. The other ions are formed by CAD process.

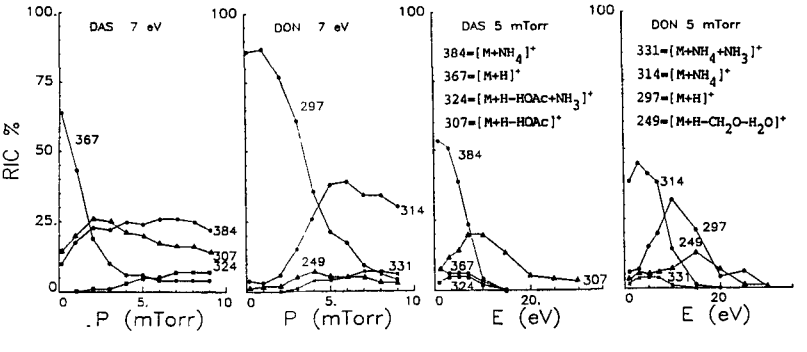

Fig.2. Pressure (Figs. a and b) and energy resolved curves (Figs. c and d) of the protonated molecule of DAS and DON. Collision gas (ammonia) pressure was 5 mTorr in the energy resolved experiments and collision energy was 7 eV in pressure resolved curves.

Presented at the 36th ASMS Conference on Mass Spectrometry and Allied Topics
June 5-10, 1988, San Francisco, CA

GOLD CHEMICAL IONIZATION MASS SPECTRA OF ALKANES AND ALKENES USING FOURIER TRANSFORM MASS SPECTROMETRY

A. Kasem Chowdhury and Charles L. Wilkins
Department of Chemistry
University of California, Riverside
Riverside, CA 92521

Introduction:

Use of metals or metal complex ions as CI reagents is emerging as an area of active current research interest. In this report, we describe the results of our investigation on the utility of Au as reagents for obtaining chemical ionization mass spectra of alkanes and alkenes.

Experimental:

Experiments were carried out using a Nicolet FTMS-2000 Fourier transform mass spectrometer equipped with a dual 4.78 cm^3 cell and a 7 tesla superconducting solenoid magnet. Gold ions were generated by focussing the beam of a Tachisto 215G pulsed TEA CO_2 laser onto a gold foil. Following the ion formation laser pulse, gold ions were trapped in the cell for variable times to allow chemical ionization reactions with the selected neutral gases.

Results and Discussion:

Two fundamental processes, hydride abstraction and dehydrogenation, are involved in the reaction of gold ions with alkanes and alkenes. The processes are summarized in reactions 1-3.

$$Au^+ + \text{Alkane} \begin{cases} \text{Hydride abstraction} \longrightarrow [\text{Alkyl cation}] \longrightarrow (C_nH_{2n+1})^+ \\ \text{Dehydrogenation} \longrightarrow [Au + \text{Alkane} - nH_2]^+,\ n = 0\text{-}1 \end{cases} \quad (1)$$

$$Au^+ + \text{Alkene} \begin{cases} \text{Hydride abstraction} \longrightarrow [\text{Alkenyl cation}] \longrightarrow (C_nH_{2n-1})^+ \\ \text{Dehydrogenation} \longrightarrow [Au + \text{Alkene} - nH_2]^+,\ n = 0\text{-}1 \end{cases} \quad (2)$$

$$Au^+ + \text{Cycloalkane} \begin{cases} \text{Hydride abstraction} \longrightarrow [\text{Cycloalkyl cation}] \longrightarrow \text{no fragmentation} \\ \text{Dehydrogenation} \longrightarrow [Au + \text{cycloalkane} - nH_2]^+,\ n = 0\text{-}1 \end{cases} \quad (3)$$

Hydride abstraction by Au^+ produces excited alkyl cation which fragments to yield a series of ions (C_nH_{2n+1}) characteristic of alkanes. Figure 1 shows mass spectra of 2,2-dimethyl hexane and 2,5-dimethyl hexane which demonstrate the utility of Au^+ as a CI reagent to characterize branched isomers. In the presence of C_6F_6 (1×10^{-6} torr) in the FTMS system, all alkanes produce abundant (Au + alkane) ions to give molecular weight information. Figure 2 shows mass spectra of 1- and 3-heptene. In addition to characteristic alkene series, (CnH2n-1) ions and (Au + Alkene) ions the relative abundances of m/z 98, m/z 225, and m/z 253 clearly distiguish each isomer.

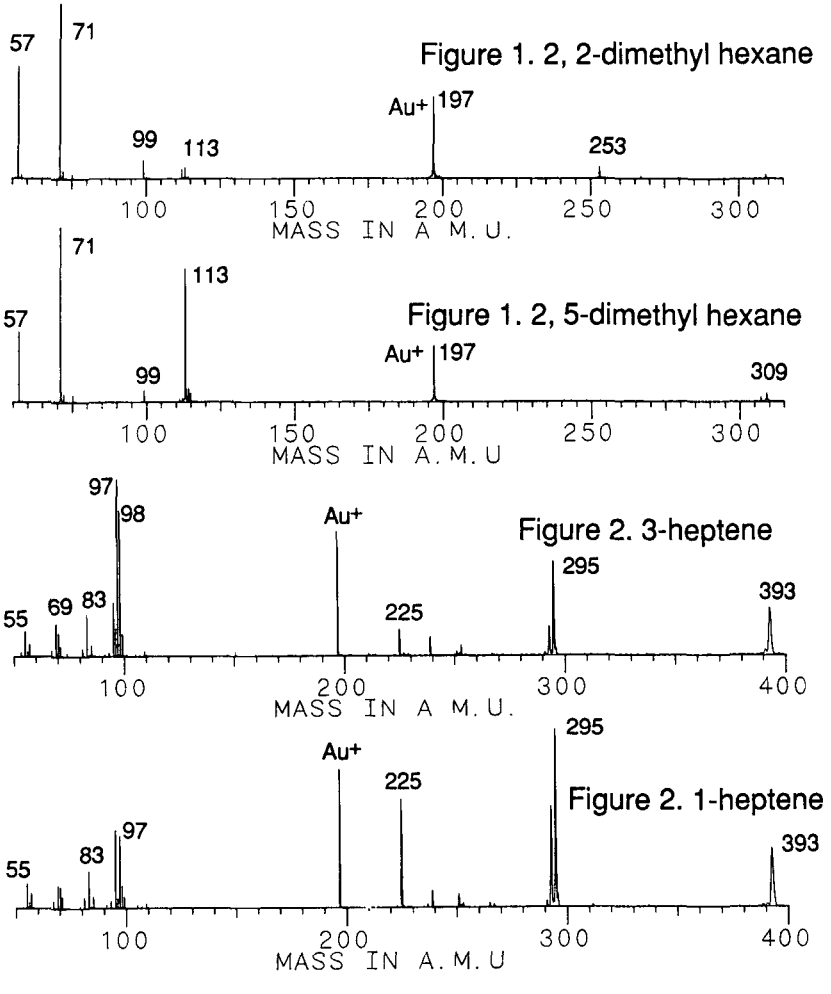

Figure 1. 2, 2-dimethyl hexane

Figure 1. 2, 5-dimethyl hexane

Figure 2. 3-heptene

Figure 2. 1-heptene

Presented at the 36th ASMS Conference on Mass Spectrometry and Allied Topics
June 5-10, 1988, San Francisco, CA

METHYLENE CHLORIDE - A USEFUL REAGENT FOR POSITIVE ION CI/MS OF ALCOHOLS, ALDEHYDES AND KETONES:

Harri G. Ramjit and Roger E. Powers;
Merck Sharp & Dohme Research Laboratories, West Point, Pennsylvania 19486

The potentials of negative ion CI/MS have been investigated using methylene chloride as the CI reagent; carboxylic acids, amino acids, amines, phenols and amides gave the $[M+Cl]^-$ ion as the base peak in most cases.(1) Yields of chlorine attachment have been explored as probes in HPLC/CI/MS, where methylene chloride has been added as mobile phase modifiers.(2) The effectiveness of chlorine attachment in the production of $[M+Cl]^-$ has been studied using mixed reagents such as methylene chloride/chloroform, carbon tetrachloride/methane.(3,4) However, Positive Ion Chemical Ionization using halogenated solvents has not been investigated. Accordingly, the object of this study was to assess the influence of methylene chloride as a CI reagent with primary, secondary and tertiary alcohols, aldehydes and ketones, employing the VG MM7035 mass spectrometer.

Methylene chloride CI mass spectra of the primary alcohols C_6-C_{12} show that protonation $(M+H)^+$ is a relatively insignificant reaction pathway, while deprotonation $(M-H)^+$ exhibits a well defined trend with increasing carbon number (Fig. 1). The intensities of $[M+H-H_2O]^+$ and $[M-H-H_2O]^+$ suggest that the $[M+H]^+$ and $[M-H]^+$ species are relatively unstable and readily dehydrate to give the carbonium ion R^+, and the alkenyl ion $[R'-CH=CH_2]^+$.

Secondary Alcohols: Alcohols such as 2-octanol and 4-heptanol exhibited $[M+H]^+$ ion intensities of less than 0.5% with $[M+H-H_2O]^+$ as the base peak; $[M-H]^+$ intensities were about 12% and $[M-H-H_2O]$ between 12 and 30%.

Tertiary Alcohols such as 3-ethyl-3-pentanol and t-butanol exhibited $[M+H]^+$ intensities at 0.1 and 0.7%, with $[M+H-H_2O]^+$ as the base peak. The $[M-H]^+$ was found to be between 4 and 9% with $[M-H-H_2O]^+$ at about 2 and 4% relative intensity.

Ketones: For the 2-ketones (C_6-C_{12}), $[M+H]^+$ increased in intensity between C_8 and C_{10}, then dropped off to about 42% at C_{12}, while the $[M-H]^+$ intensity increased somewhat linearly up to C_{10}, then formed the base peak at C_{11} and C_{12}. $[M+H-H_2O]$, on the other hand, formed the base peak up to C_9, then decreased linearly to 31% at C_{12}, while $[M-H-H_2O]^+$ plateaued between C_9 and C_{11} and decreased at C_{12} to 32% (Fig. 2). The ratio of $[M-H]^+/[M+H]^+$ (Fig. 3) shows a definite trend with increasing carbon number. This could be a reflection of keto-enol tautomerism prevalent in these compounds. The most interesting feature is the attachment of $[CHCl_2]^+$ to these ketones; the effectiveness of attachment increases from C_6 to C_{12} linearly (Fig. 2). This attachment process does not occur with the alcohols as illustrated in Fig. 4.

Aldehydes: The C_8, C_{10} and C_{12} aldehydes show $[M+H]^+$ with increasing intensity from 9% to 34%, while $[M-H]^+$ formed the base peak. Although chlorine-containing radicals yielded attachment products at intensities less than 5%, the most significant observation is the formation of the $[M-3H]^+$ species with intensities from 46 to 35%.

The reaction of methylene chloride under CI conditions with substrates such as alcohols, aldehydes and ketones where protonation, deprotonation and radical attachments are favored could be exemplified by the proposed mechanism Scheme 1.

We are currently evaluating other halogenated solvents such as chloroform and tetrachloroethylene on various classes of compounds. Our objectives accommodate such approaches as GC/MS/CI, HPLC/MS/CI and DCI. It is anticipated that qualitative and indeed quantitative procedures would be enhanced. These approaches are seen as complementary to negative ion CI studies using halogenated solvents.

References:

1. Harvey P. Tannenbaum, J. David Roberts and Ralph C. Dougherty. Anal. Chem., 47 (1), 49-54 (1975).
2. C. E. Parker, K. Yamaguchi, D. J. Harvan, R. W. Smith and J. R. Hass, J. Chromatography, 319 (3), 273-283 (1985).
3. Deng Yan and Peng Rongkun. Youji Huaxue (3), 254-260 (1985), Chinese.
4. Daishima Shigoki, Ioda Yoshio and Ishimori Toshihiro. Shitsuryo Bunseki, 33 (6), 343-350 (1985), Japanese.

Presented at the 36th ASMS Conference on Mass Spectrometry and Allied Topics
June 5-10, 1988, San Francisco, CA

FIGURE 1
POSITIVE ION CI - METHYLENE CHLORIDE REAGENT
PRIMARY ALCOHOLS C6 - C12

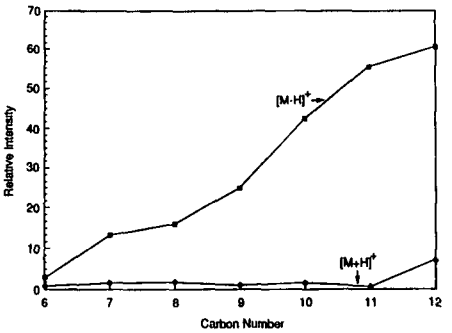

FIGURE 2
POSITIVE ION CI - METHYLENE CHLORIDE REAGENT
2 - KETONES C6 - C12

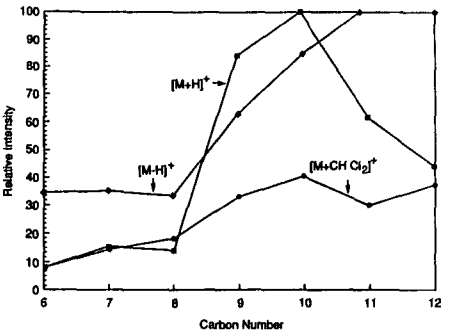

FIGURE 3
POSITIVE ION CI - METHYLENE CHLORIDE REAGENT
2 - KETONES C6 - C12

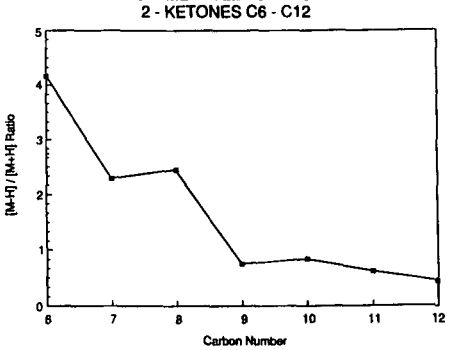

FIGURE 4
METHYLENE CHLORIDE CI MASS SPECTRA

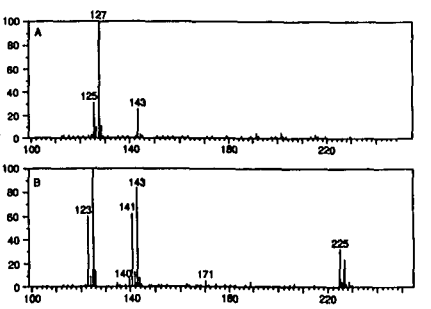

A) 1- Nonanol (mw = 144) 70ev, 1x10^{-4}Torr
B) 2- Nonanone (mw = 142) 70ev, 1x10^{-4}Torr

PROPOSED MECHANISM FOR POSITIVE ION METHYLENE CHLORIDE CHEMICAL IONIZATION

Initiation Reaction

$CH_2Cl_2 + [CH_2Cl_2]^{\dagger} \rightarrow [CH_2Cl_3^{\bullet}]^+ + [CH_2Cl]^{\bullet}$ complex

$\rightarrow [CH_3Cl_2^{\bullet}]^+ + [CHCl_2]^{\bullet}$ complex

Product Formation

a. Attachments and Protonation

1. $M + [CH_2Cl_3^{\bullet}]^+ \rightarrow [M+CH_2Cl]^+ + Cl_2$
   $\rightarrow [M+CHCl_2]^+ + HCl$
   $\rightarrow [M+Cl]^+ + CH_2Cl_2$

2. $M + [CH_3Cl_2^{\bullet}]^+ \rightarrow [M + CHCl_2]^+ + H_2$
   $\rightarrow [M + CH_2Cl]^+ + HCl$
   $\rightarrow [M+H] + CH_2Cl_2$

b. Hyrdride Abstraction

1. $M + [CH_2Cl_3]^+ \rightarrow [M - CHCl_2^{\bullet}]^+ + HCl$
   $\downarrow$
   $[M-H]^+ + CH_2Cl_2$

2. $M + [CH_3Cl_2^{\bullet}]^+ \rightarrow [M - CH_2Cl]^+ + HCl$
   $[M-H]^+ + CH_3Cl$

Presented at the 36th ASMS Conference on Mass Spectrometry and Allied Topics
June 5-10, 1988, San Francisco, CA

REACTIVITY AND COLLISIONAL DE-EXCITATION OF ELECTRONICALLY EXCITED METAL IONS

Fred Strobel and D. P. Ridge
Department of Chemistry and Center for Catalytic Science and Technology
University of Delaware, Newark, DE 19716

Electron impact on $Mn_2(CO)_{10}$ produces electronically excited Mn^+. This electronically excited Mn^+ has a lifetime long enough to be studied under ICR conditions. The evidence for the electronically excited Mn^+ is the ratio of MnI^+ to $MnCl^+$ produced when Mn^+ reacts with ICl. Mn^+ produced by electron impact on $Mn_2(CO)_{10}$ gives 37±2% MnI^+. Mn^+ formed by surface ionization gives 19±3% MnI^+. Surface ionization presumably forms only ground state ions so the difference can be attributed to excited state ions produced by electron impact.

A measurement of the lifetime of the excited state was done on a Nicolet FTMS-2000. Mn^+ is formed in the source side by electron impact on $Mn_2(CO)_{10}$ and then is transferred to the analyzer side and isolated by ion ejections. The pressure in the analyzer side, $3X10^{-9}$Torr, assures a long mean free time between collisions. The Mn^+ was allowed to remain in this region for a variable length of time, T_d, before $Cr(CO)_6$ is pulsed into the analyzer side. The Mn^+ is allowed to react with the $Cr(CO)_6$ for 1 second before a spectrum is taken. One of the products observed is $Cr(CO)_6^+$, the result of charge transfer which is endotermic for the ground state species by .707eV. The intensity of the $Cr(CO)_6^+$ thus indicates the amount of electronically excited Mn^+ present after the variable delay T_d. A plot of ($Cr(CO)_6^+$/Total ion current) vs T_d. gives a exponential decay with a first order rate of $.17\pm.02s^{-1}$ which corresponds to a lifetime of 5.8±.7 seconds.

The lifetime that was measured may be a lower limit on the actual radiative lifetime since it is comparable to the time between collisions for Mn^+ and the background gas at $3X10^{-9}$ Torr. Dividing the unimolecular rate ($.17\ s^{-1}$) by the neutral number density gives a second order rate constant of $1.7X10^{-9}$molecules^{-1}cm^{3}s^{-1}. The background is hydrocarbons and as discussed below it is not unreasonable that the excited Mn^+ could be collisionaly relaxed by hydrocarbons at this rate constant.

The possibility that quenching of the electronically excited Mn^+ occurs was investigated by monitering the MnI^+ to $MnCl^+$ ratio for the reaction of Mn^+ produced by electron impact with ICl as N_2 and CH_4 are added to a drift cell ICR. The result indicates that N_2 is an inefficient quenching gas but CH_4 is very efficient(k_Q= $1.88\pm.35X10^{-9}$ molecules^{-1}cm^{3}s^{-1}).

A qualitative potential surface is shown in fig. 1 for the low lying states of Mn^+ reacting with CH_4. As indicated in the figure surface crossings will result if the ^5D surface is attractive. This provides the means for crossing to the repulsive ground state surface. Since the excited states are quintets and the ground state is a septet the quenching process implies that spin is not a good quantum number. The quenching process also substantiates that one of the excited states is attractive.

These results can explain why the Mn^+ produced by electron impact on $Mn_2(CO)_{10}$ did not react with alkanes even though there is evidence for the presence of excited states which are expected to react with the alkanes efficiently. Evidently reaction cannot compete with the de-excitation process.

Presented at the 36th ASMS Conference on Mass Spectrometry and Allied Topics
June 5-10, 1988, San Francisco, CA

Potential Surfaces

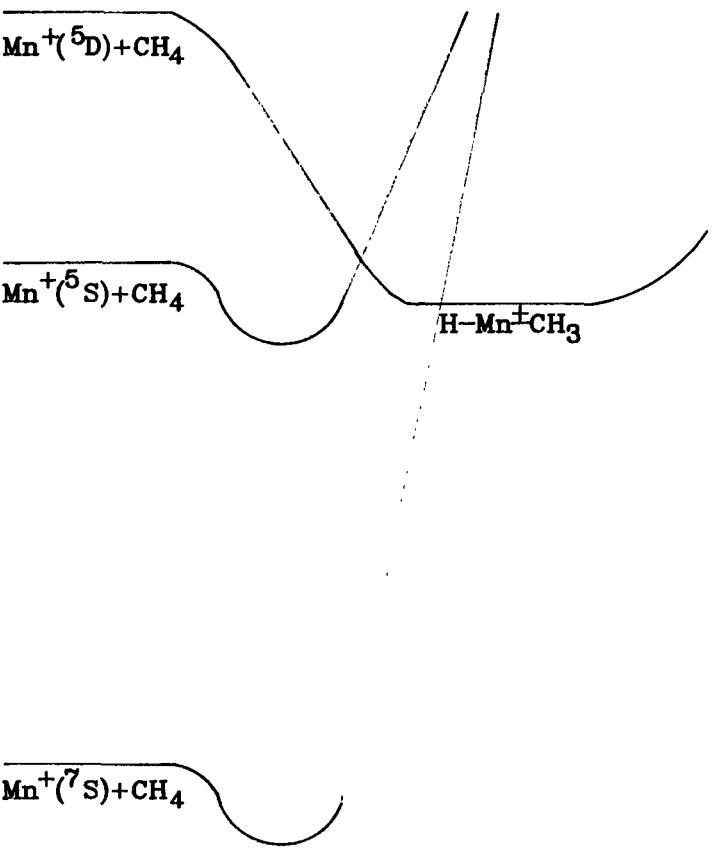

figure 1

Presented at the 36th ASMS Conference on Mass Spectrometry and Allied Topics
June 5-10, 1988, San Francisco, CA

GAS-PHASE REACTIONS OF BIS(CYCLOPENTADIENYL)METHYL-ZIRCONIUM(1+) WITH UNSATURATED HYDROCARBONS

Christ, Jr. C.S.;Eyler, J.R.;Richardson, D.E.
University of Florida, Gainesville, FL

Recently the solution phase investigation of electron deficient transition metal complexes such as $Cp_2ZrCH_3(L)_n^+$ (n=1,2)[1,2] and $Cp^*_2ScCH_3$[3,4] has revealed a high reactivity toward hydrocarbon and nitrogen containing hydrocarbon substrates. A similar reactivity can be observed in the gas-phase for the d^0 complex $Cp_2ZrCH_3^+$ (1), allowing a direct comparison. Our work with alkenes and nitriles shows products observed in solution reactions are in many cases intermediates in gas phase reactions whereas products of the analogous gas phase reactions may provide insight into thermally accessible higher energy products or intermediates in solution.

We applied Fourier Transform Ion Cyclotron Resonance Mass Spectrometry to study the gas-phase reactions of $[Cp_2ZrCH_3]^+$ (1, Cp=cyclopentadienyl). Collision induced dissociation (CID) experiments on 1 show the loss of CH_3, strongly implying a metal-methyl structure. No evidence was found for the involvement of the Cp rings in the reactions examined, therefore the transformations below are assumed to retain the Cp_2Zr unit.

Jordan, et al.,[1] have observed ethylene polymerization by $[Cp_2ZrCH_3(THF)]^+$ in CH_2Cl_2 solution, but polymerization of ethylene by the solvent-free ion 1 is not observed in the gas phase. Instead, the energy released upon formation of $[Cp_2Zr(n\text{-}C_3H_7)]^+$ causes an intramolecular decomposition of the insertion product and produces a metal-allyl complex, $[Cp_2ZrC_3H_5]^+$(2), and H_2 (eq 1). CID experiments performed on 2 are consistent with allyl formation,as fragments corresponding only to the loss of one and two molecules of H_2 as well as C_3H_5 are produced. Reaction of 1 with ethylene

$$Cp_2ZrCH_3^+ + C_2H_4 \longrightarrow Cp_2ZrC_3H_5^+ + H_2 \qquad (1)$$

does not produce $[Cp_2ZrH]^+$, thus B-hydride abstraction followed by alkene elimination[5] is not observed in the gas-phase.

An investigation of mechanistic aspects of the ethylene reaction by using C_2D_4 shows a significant amount of hydrogen-deuterium scrambling, eliminating 11% D_2, 74% HD, and 15% H_2, which is somewhat different from the statistical distribution of 28.6% D_2, 57.1% HD, 14.3% H_2. A possible mechanism for the reaction of 1 with ethylene to produce 2 is given in Scheme I. Scrambling probably occurs during interconversion of the insertion product (3) and hydride intermediate (4) via successive hydride shifts along the three carbon framework of intermediate (5).

Scheme I

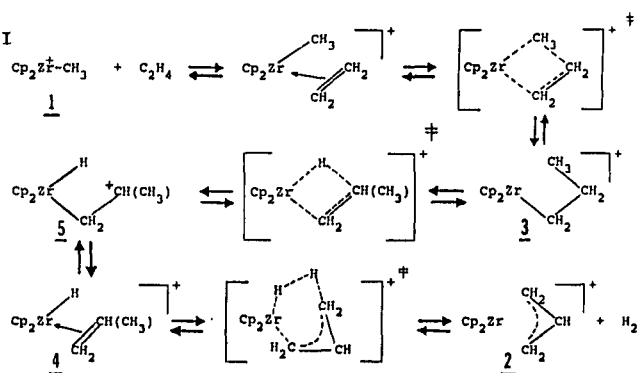

In the gas-phase rapid insertion of CD_3CN and elimination of CH_3CN occurs before the mono-adduct $Cp_2Zr(CH_3)(CD_3CN)^+$ is observed (eq 2).

$$Cp_2ZrCH_3^+ \ (1) \ + \ CD_3CN \longrightarrow Cp_2ZrCD_3^+ \ + \ CH_3CN \quad (2)$$

The insertion/elimination process yields products with no H-D scrambling observed implying an intact transfer of CD_3.

$Cp_2ZrCH_3^+$ (1) adds one molecule of acetonitrile yielding two isomers (m/z 276), $Cp_2ZrCH_3(NCCH_3)^+$ (6) and $Cp_2Zr(NC(CH_3)_2)^+$ (7) (eq. 3,4). Only (7) is reactive to coordination of a second acetonitrile molecule (eq 5).

$$Cp_2ZrCH_3^+ \ (1) + CH_3CN \longrightarrow Cp_2ZrCH_3(CH_3CN)^+ \ (6) \quad (3)$$

$$Cp_2ZrCH_3^+ \ (1) + CH_3CN \longrightarrow Cp_2Zr(NC(CH_3)_2)^+ \ (7) \quad (4)$$

$$Cp_2Zr(NC(CH_3)_2)^+ \ (7) + CH_3CN \longrightarrow Cp_2Zr(NC(CH_3)_2)(CH_3CN)^+ \ (8) \quad (5)$$

Structures were assigned to the isomers, (6) and (7), based on known solution structures and our gas-phase experimental results. Jordan et al. have reported similar product formation, i.e. the isolation of $Cp_2ZrCH_3(CH_3CN)^+$ as a salt of BPh_4^- and the observation of $Cp_2Zr(NC(CH_3)_2)(CH_3CN)^+$ detected by nmr after irreversible acetonitrile insertion.[2] Several experimental facts support the assignment of structurally isomeric products (6) and (7). Coordination of a second acetonitrile molecule to (m/z 276) occurs initially producing (m/z 317), however the addition stops leaving only the inert isomer (6) (m/z 276). The inert isomer (6) may be isolated and translationally excited; upon collision a rearrangement occurs forming the reactive isomer (7) and after an appropriate reaction time coordination of acetonitrile takes place producing $Cp_2Zr(NC(CH_3)_2)(NCCH_3)^+$, (8). Experiments to determine the effect of acetonitrile pressure have also been performed and indicate that an approach to equilibrium is not a reasonable explaination for the decrease in the rate of conversion of the (m/z 276) to (m/z 317).

Our observations suggest that intermediates of polymerization and metathesis reactions also occur in the solvent-free reactions of electron deficient d^0 transition-metal complex ions. Complexes formed following elimination of H_2 from these chemically activated gas-phase intermediates are possible products of chain termination in the polymerization of alkenes by solvated d^0f^n transition-metal catalysts. In addition, the formation of allyl species in solution and the possible role of this process in introducing unsaturation into polymers warrants further investigation. Reactions of acetonitrile are consistent with mechanisms proposed for analogous reactions in solution. This implies similar mechanisms may be used to understand these and related reactions in the gas-phase.

1. Jordan, R.F.;Chandrasekhar, S.B.;Willet, R.;Scott, B. J. Am. Chem. Soc. 1986, 108, 7410.
2. Jordan, R.F.;Chandrasekhar, S.B.;Dasher, W.B.;Rheingold, A.L. Organometallics 1987, 6, 1041.
3. Thompson, M.E.;Bercaw, J.E. Pure Appl. Chem. 1984, 56, 1.
4. Bercaw, J.E.;Davies, D.L.;Wolczanski, P.T. Organometallics 1986, 5, 443.
5. Boor, J. Ziegler-Natta Catalysts and Polymerizations; Academic: New York, 1979.

Presented at the 36th ASMS Conference on Mass Spectrometry and Allied Topics
June 5-10, 1988, San Francisco, CA

AN FTMS STUDY OF THE GAS-PHASE CHEMISTRY OF THE METAL DIMER $ScFe^+$

Leo M. Lech and Ben S. Freiser
Department of Chemistry
Purdue University
West Lafayette, IN 47907

The interest in both ionic and neutral metal clusters has increased tremendously in the past decade. Our laboratory has been actively studying the chemistry of various metal dimers. In one of these studies it was determined that the Sc^+-Fe bond strength was the lowest of a series of MFe^+ bond strengths (M = Ti, V, Cr, Fe, Co, Ni, Cu, Nb, Ta). The focus of this work was to determine if this weak dimer bond strength resulted in any unique chemistry between the dimer and various small organics. Reactions of $ScFe^+$ with both the linear butenes and isobutene reflect the weak cluster bond strength as do virtually all of the collision-induced dissociation (CID) spectra of various $ScFe^+$-ligand species.

The $ScFe^+$ dimer was generated and isolated in the gas-phase using Fourier transform mass spectrometry (FTMS), equation 1.

$$Sc^+ + Fe(CO)_5 \longrightarrow ScFe(CO)_3^+ \xrightarrow{CID} ScFe^+ \qquad (1)$$

By trapping the dimer in the presence of an organic, we can study the chemistry of $ScFe^+$. As expected, the observed chemistry of $ScFe^+$ is significantly different from the chemistry of the bare metal ions Sc^+ and Fe^+. There are much fewer reactive processes seen for the dimer and, when these reactive processes are observed, they involve predominantly, activation of C-H bonds. The single metal ions on the other hand are more reactive and have a higher affinity for C-C bond activation, especially in the case of Fe^+. One of the most interesting reactions observed for $ScFe^+$ is with the butenes. For example, in the reactions with 1-butene, Fe is displaced from the cluster generating the stable Sc^+-butadiene, equation 2. The Sc^+-butadiene can react with a second butene generating $Sc(C_4H_6)_2^+$ which is

$$ScFe^+ + C_4H_8 \longrightarrow ScC_4H_6^+ + FeH_2 \qquad (2)$$

isobaric with $ScFe(C_4H_4)^+$, a possible double dehydrogenation product of butene by $ScFe^+$, equation (3). The positive identification of this ion was obtained by implementing two different experiments. First, double resonance

$$ScFe^+ + C_4H_8 \longrightarrow ScFe(C_4H_4)^+ + 2H_2 \qquad (3)$$

ejection was used, Figure 1. When $Sc(C_4H_6)^+$ was continuously ejected during the reaction period, the product ion was not formed thus indicating that it arises directly from $Sc(C_4H_6)^+$. Also, when the product ion was collisionally activated, it lost a fragment corresponding to 54 a.m.u. which would not be possible if the ion was $ScFe(C_4H_4)^+$, equation 4.

$$Sc(C_4H_6)_2^+ \xrightarrow{CID} Sc(C_4H_6)^+ + C_4H_6 \quad (4)$$

$$ScFe(C_4H_4)^+ \xrightarrow{CID} \text{can not lose 54 a.m.u.}$$

The other reactions of $ScFe^+$ with alkenes show almost exclusive dehydrogenations. The weak nature of the cluster bond is again observed when the $ScFe^+$-ligand product ions from these reactions are collisionally activated. In virtually all of the CID processes observed, the cluster is broken apart resulting in a neutral loss of Fe,FeH, or FeH_2 implying in general that $D^\circ(Sc^+\text{-ligand}) > D^\circ(Sc^+\text{-Fe})$.

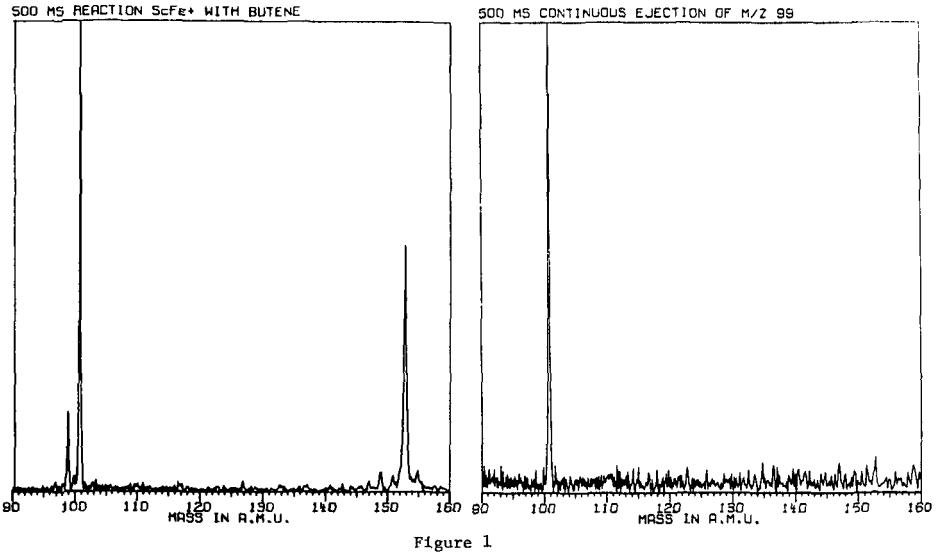

Figure 1

Presented at the 36th ASMS Conference on Mass Spectrometry and Allied Topics
June 5-10, 1988, San Francisco, CA

BIMOLECULAR REACTIONS OF DOUBLY CHARGED METAL IONS IN THE GAS PHASE

S.W. Buckner, T.J. MacMahon, Y. Huang, J.R. Gord, and B.S. Freiser
Department of Chemistry
Purdue University
West Lafayette, IN 47907

There has been much interest in the reactivity of gas-phase metal ions with small organic molecules as seen in the extensive literature relating to this topic. Multiply charged metal ions have not received much attention, however, due in part to the belief that rapid charge exchange would occur exclusively. In a very interesting recent paper, Tonkyn and Weisshaar [1] have observed clustering reactions of Ti^{2+} with methane and hydride abstraction from ethane in a flowing afterglow. This has prompted us to look at some bimolecular reactions of doubly charged early transition metals with various organic molecules under low pressure conditions in a Fourier transform mass spectrometer (FTMS). In this paper we present a "progress report" on our efforts in this area, including some recent results on (i) the reactions of M^{2+} (M = Nb, La, Zr, Ta) with methane, ethane and propane; (ii) the formation and reactions of the first doubly charged heteronuclear dimer species $LaFe^{2+}$; and (iii) the determination of kinetic energy release in the charge transfer reaction $M^{2+} + A \rightarrow M^{+} + A^{+}$ using FTMS methods.

Nb^{2+}, Zr^{2+} and Ta^{2+} are observed to react via other routes besides charge exchange, as in reactions 1 and 2 with methane. La^{2+}, however, is

$$M^{2+} + CH_4 \rightarrow \begin{cases} MCH_2^{2+} + H_2 & (1) \\ MH^{+} + CH_3^{+} & (2) \\ M^{+} + CH_4^{+} & (3) \end{cases}$$

unreactive with methane. Observation of MCH_2^{2+} from methane implies $D(M^{2+}-CH_2) > 112$ kcal/mol. In fact, we have assigned $D(Nb^{2+}-CH_2) = 197 \pm 10$ kcal/mol which can be compared to $D(Nb^{+}-CH_2) = 109 \pm 7$ kcal/mol [2].

$NbCH_2^{2+}$, $ZrCH_2^{2+}$ and $TaCH_2^{2+}$ all react further with CH_4. For example, $NbCH_2^{2+}$ reacts sequentially with CH_4, reaction 4, generating a variety of products. It is interesting to note that products further along in the reaction sequence undergo more extensive dehydrogenation. This may be

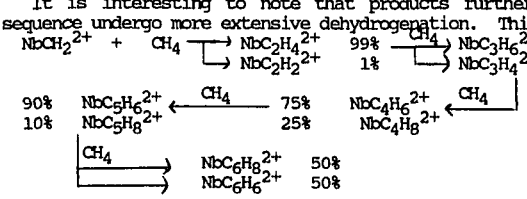

(4)

indicative of ligand coupling, as would be expected in a reaction which incorporates six separate C_1 units. Nb^{2+} reacts with C_2H_6 at least three times, reactions 5-11.

Presented at the 36th ASMS Conference on Mass Spectrometry and Allied Topics
June 5-10, 1988, San Francisco, CA

$$Nb^{2+} + C_2H_6 \rightarrow NbCH_2^{2+} + CH_4 \quad (5)$$
$$\rightarrow NbC_2H_2^{2+} + 2H_2 \quad (6)$$
$$\rightarrow NbC_2H_4^{2+} + H_2 \quad (7)$$
$$\rightarrow Nb^{+} + C_2H_6^{+} \quad (8)$$
$$\rightarrow NbH^{+} + C_2H_5^{+} \quad (9)$$

$$NbCH_2^{2+} + C_2H_6 \rightarrow NbC_3H_4^{2+} \xrightarrow{C_2H_6} NbC_5H_6^{+} \quad (10)$$

$$NbC_2H_2^{2+} + C_2H_6 \rightarrow NbC_4H_4^{2+} \; 75\% \xrightarrow{C_2H_6} NbC_6H_6^{2+} \quad (11)$$
$$\rightarrow NbC_4H_6^{2+} \; 25\%$$

A natural extension of this work is the study of doubly charged cluster ions. Recently, Tsong and coworkers [3] provided evidence for the first reported doubly charged metal dimer species, Mo_2^{2+}. The lifetime of this species was given a lower limit of several tens of nanoseconds, and it was not clear whether or not the species was metastable. We have successfully generated $LaFe^{2+}$ and shown it to be stable for at least on the order of seconds. The $LaFe^{2+}$ was generated <u>in situ</u> by collision-induced dissociation on $LaFe(CO)_2^{2+}$, which was formed from the reaction of La^{2+} with $Fe(CO)_5$. This method may be generalized to other systems, and, for example, we have generated YFe^{2+} in a similar manner. Nb^{2+} and Ta^{2+} react with $Fe(CO)_5$ only by charge transfer, and, thus, the corresponding dimers could not be synthesized. The nature of the bonding in $LaFe^{2+}$ is of real interest and calculations are underway in collaboration with Dr. Bauschlicher at NASA-Ames. Preliminary results indicate that the bonding is somewhere between the two possibilities La^{2+}-Fe and La^{+}-Fe^{+}, i.e. with La having most but not all of the charge.

Finally, in order to obtain additional information on the thermochemistry and reaction dynamics of these species, we have successfully transferred the methodology of Marx [4] and Bowers [5] to our FTMS to determine the kinetic energy released when a doubly charged ion undergoes charge exchange (or abstracts a negatively charged fragment) with a neutral to form two singly charged ions, which subsequently repel each other. As a model system, the reaction of Nb^{2+} with benzene to form Nb^{+} and $C_6H_6^{+}$ has been studied. Not surprisingly, a range of kinetic energies is observed indicating that the products are generated with a variety of internal energies.

[1] Tonkyn, R.; Weisshaar, J.C. <u>J. Am. Chem. Soc.</u> **1986**, <u>108</u>, 7128.
[2] Buckner, S.W.; Freiser, B.S. <u>J. Am. Chem. Soc.</u> **1987**, <u>109</u> 1247.
[3] Tsong, T.T. <u>J. Chem. Phys.</u> **1986**, <u>85</u>, 639.
[4] a) Mauclaire, G.; Derai, R.; Fenistein, S.; Marx, R. <u>J. Chem. Phys.</u> **1979**, <u>70</u>, 4017.
b) Mauclaire, G.; Derai, R.; Fenistein, S.; Johnsen, R.; Marx, R. <u>J. Chem. Phys.</u> **1979**, <u>70</u>, 4023.
[5] a) O'Keefe, A.; Parent, D.; Mauclaire, G.; Bowers, M.T. <u>J. Chem. Phys.</u> **1984**, <u>80</u>, 4901.
b) O'Keefe, A.; Mauclaire, G.; Parent, D.; Bowers, M.T. <u>J. Chem. Phys.</u> **1986**, <u>84</u>, 215.

Presented at the 36th ASMS Conference on Mass Spectrometry and Allied Topics
June 5-10, 1988, San Francisco, CA

CLUSTERING REACTIONS AND THERMOCHEMISTRY OF LASER ABLATED METAL IONS

F. Bouchard, J.W. Hepburn and T.B. McMahon,
Department of Chemistry, University of Waterloo, Waterloo, Ont.,Canada, N2L 3G1

In this experiment, we are using a conventionnal High Pressure Mass Spectrometer(1) suitably modified to allow a laser beam to penetrate the high pressure region(Fig. 1). A metal target located inside is the source for laser generated metal ions. Those ions diffuse randomly, undergoing thousands of collisions which efficiently cool them to the temperature of the gas. Furthermore, they can react in the bath with ligands of interest, cluster and equilibriate. The ions can diffuse freely through a small aperture of about 100 μm into a low vacuum region. They are then extracted, separated with a magnetic sector mass spectrometer and detected using a multichannel technique which provides a time profile of each ion. The entire experiment is pulsed.

The scope of our experiment is to generate metal ions in the HPMS using an excimer laser(308 nm) and to look at clustering equilibria between the metal ions and the ligand of interest. Up to now, $[Cu(X)_n]^+$ was observed for n=1 to 2 for X = Ar and Ne, n=1 to 3 for Xe and Kr and n = 1 to 4 for H_2O, N_2, CH_3OCH_3 , CO, CO_2, N_2O, CS_2 and CH_3OH. We have also observed various clusters containing aluminum, platinum or iron as the metal ion.

Under conditions of a mild supersonic expansion which is achieved by using 1 mm apertures, equilibrium time profiles were obtained when a xenon bath (5 torr) was allowed to react with copper ions (Fig. 2).

Using a gas tight source (100 μm apertures), water-copper ion equilibria have been observed and studied. Laser generated ions were allowed to react with 0,06 torr of H_2O in ≈ 4 torr of N_2. The ion time profiles are shown on Figure 3. For the first equilibrium: $Cu^+ + H_2O \leftrightarrow [Cu(H_2O)]^+$, the equilibrium constant is 1900 at 300K. This yields a ΔG value of 4,5 kcal/mol. Estimating ΔS to be about 20 cal/molK, we find ΔH to be 10.5 kcal/mol. In the case of the second equilibrium, $[Cu(H_2O)]^+ + H_2O \leftrightarrow [Cu(H_2O)_2]^+$, K is $1x10^6$, ΔG is 8,2 kcal/mol. Taking ΔS to be 25 cal/molK, ΔH is thus 15.7 kcal/mol for the second water-copper bond.

In the near future, temperature dependent studies will be conducted to definitely assess the bond energies and entropy changes involved in the clustering of water onto copper. Furthermore, other metals and others ligands will be studied. A cooled source is also being constructed. This source will allow the determination of the energetics of rare gases attachement onto metal ions.

1- J. E. Szulejko, J. J. Fisher, T. B. McMahon and J. Wronka, **Int. J. Mass Spectrom. Ion Processes**, 83 (1988) 147

Presented at the 36th ASMS Conference on Mass Spectrometry and Allied Topics
June 5-10, 1988, San Francisco, CA

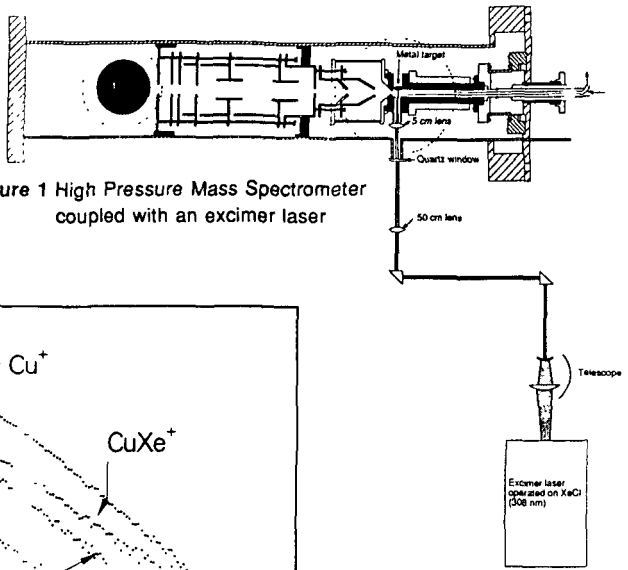

Figure 1 High Pressure Mass Spectrometer coupled with an excimer laser

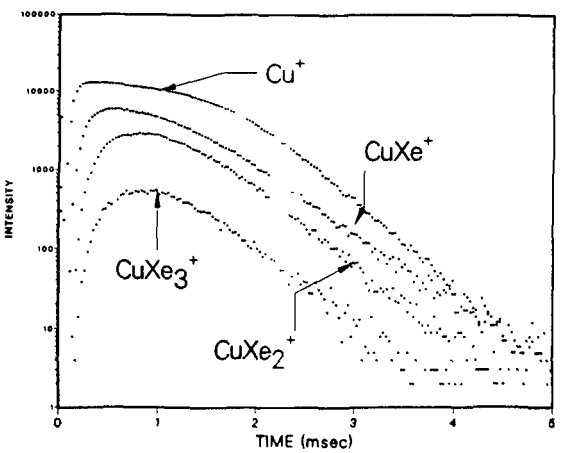

Figure 2 Ion time profiles for the reaction of 5 torr of xenon with copper ions

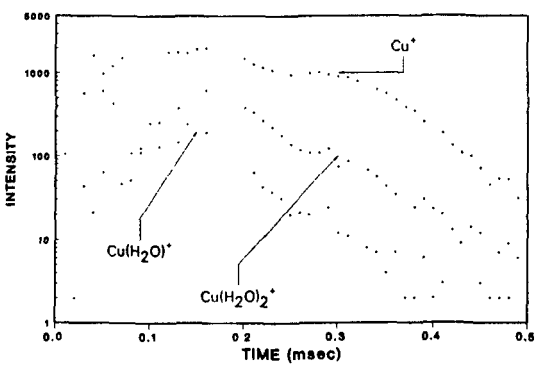

Figure 3 Ion time profiles for the reaction of 0,06 torr of water with copper ions at 300K

Presented at the 36th ASMS Conference on Mass Spectrometry and Allied Topics
June 5-10, 1988, San Francisco, CA

TRANSITION METAL CATION MEDIATED CARBON-CARBON BOND FORMATION IN A MULTIQUADRUPOLE MS/MS/MS INSTRUMENT

Claude Beaugrand,
Nermag, 49 quai du Halage, 92500 Rueil-Malmaison, France
Hélène Mestdagh, Nicole Morin and Christian Rolando,
Ecole Normale Supérieure, 24 rue Lhomond, 75005 Paris, France

Most of the known reactions of transition metal cations with organic molecules involve chemical bond cleavage. For instance 2-methylpropane reacts with Fe^+ or Ni^+ by dehydrogenation or methane loss. For an organic chemist carbon-carbon bond formation looks more exciting ! We report here that reactive alkyl halides can be coupled by iron carbonyl cations ; typically allyl chloride leads to the formation of hexadiene radical cation :

$$Fe(CO)_n^+ + C_3H_5Cl \longrightarrow C_6H_{10}^{+\cdot} + n\ CO + FeCl_2$$

$Fe(CO)_n^+$ ions were generated in source by electron impact on $Fe(CO)_5$, mass selected using the first quadrupolar analyzer, and reacted with allyl chloride (1 mtorr) in the first RF-only collision cell. After mass selection by the second analyzer, the reaction products could be submitted to CAD (or to new reaction) in the second RF-only collision cell. The resulting fragments were finally scanned in the third analyzer.

Whereas bare Fe^+ leads mainly to $C_3H_5^+$ ion, which reacts further with allyl chloride, the presence of CO ligands allows fixation of the elements of allyl chloride on the transition metal ion, as indicated by the following major reaction pathways :

$$Fe^+ + C_3H_5Cl \longrightarrow C_3H_5^+ + FeCl \xrightarrow{C_3H_5Cl} C_6H_9^+,\ C_6H_7^+$$

$$Fe(CO)_2^+ + C_3H_5Cl \longrightarrow FeC_3H_5Cl^+ + 2CO$$

$$Fe(CO)_4^+ + 2C_3H_5Cl \longrightarrow FeC_6H_{10}Cl_2^+ + 4CO$$

$Fe(CO)^+$ and $Fe(CO)_3^+$ give intermediate results. $Fe(CO)_5^+$ is less reactive and undergoes mainly CO loss.

Ion $C_6H_{10}^{+\cdot}$, corresponding to the coupling of two allyl units, was found among the reaction products for n>2. Its CAD spectrum was very similar to the fragmentation pattern of hexadiene radical ions. CAD of $FeC_3H_5Cl^+$ ion gives mainly the following products, suggesting structure 1 :

$$FeC_3H_5Cl^+ \longrightarrow FeCl^+ + C_3H_5 \text{ (favored by high collision energy)}$$
$$\searrow FeC_3H_4^+ + HCl \text{ (favored by low collision energy)}$$

CAD of $FeC_6H_{10}Cl_2^+$ ion shows that it is the actual precursor of $C_6H_{10}^{+\cdot}$ ion :

$$FeC_6H_{10}Cl_2^+ \longrightarrow C_6H_{10}^{+\cdot} + FeCl_2$$
$$\searrow FeC_3H_5Cl^+ + C_3H_5Cl$$

A mixture of structures 2 and 3 would account for both fragmentation pathways of $FeC_6H_{10}Cl_2^+$ ion. Ligand exchange experiments confirmed this hypothesis : when $FeC_6H_{10}Cl_2$ was submitted to reaction with methallyl chloride C_4H_7Cl in the second collision cell (a variable reaction time was allowed, using ion confinement technique), replacement of one C_3H_5Cl ligand by one C_4H_7Cl ligand, expected to take place on structure 3, occurred at first very rapidly, but remained incomplete.

The coupling reaction occurring within the $FeC_6H_{10}Cl_2^+$ complex and leading to $C_6H_{10}^{+\cdot}$ ion is analogous to the transition metal promoted coupling of allylic halides in solution (Corey reaction). As in solution it does not occur on saturated alkyl halides. These results also show the key role of the CO ligands for the formation of the intermediate iron complex in the coupling reaction.

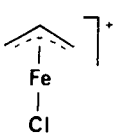

1

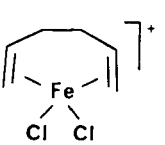

2

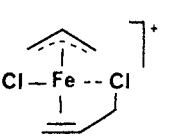

3

Presented at the 36th ASMS Conference on Mass Spectrometry and Allied Topics
June 5-10, 1988, San Francisco, CA

EXPERIMENTAL AND THEORETICAL INVESTIGATIONS INTO CHAINLENGTH EFFECTS IN THE CHEMISTRY OF TRANSITION METAL IONS WITH ORGANIC MOLECULES; John Allison, Deborah J. Hankinson, Cliff B. Miller, Eric J. Hooper, Anthony Tsarbopoulos, Tammy L. Wyatt, Department of Chemistry, Michigan State University, East Lansing, MI 48824

We have been using a simple electrostatic calculation to model possible interactions that occur between a metal ion and an organic molecule "before the chemistry starts". These interactions are being investigated to determine whether early events can be correlated to final product distributions. We have proposed the following: Initial ion/molecule interactions are largely electrostatic in nature. Such interactions will create "hot spots" - sites within the molecule that are highly attractive to a transition metal ion. The hot spots that correspond to the deepest potential wells represent those parts of the molecule about which the ion may reside, and hence positions from which chemistry (i.e., M^+ insertion into a bond) may occur. In the model used here, we consider interactions of the ion with each bond (using a bond-polarizability model), and with each atom (considering both partial charges on the atoms, and repulsive interactions).

In previous ASMS meetings[1], we have discussed these calculations for Cr^+ interacting with butane and butyl chloride. In the case of butane, it was found that positions about the interior C-C bond were more attractive than those in close proximity to the terminal C-C bond. This correlates with the observation that first row transition metal ions (M^+) form the product $MC_2H_4^+$ to a greater extent than the product $MC_3H_6^+$. In the case of butyl chloride, the most attractive molecular environment was atop the C-Cl bond, which again correlates with the observed chemistry, which is dominated by attack of that bond.

Here we report preliminary results for chlorohexane. The interaction of Cr^+ with a number of configurations of chlorohexane have been studied. The molecule is sufficiently large that hot spots analogous to those found in both butane and butyl chloride are present. The unique feature of these larger molecules is their ability to participate in multiple interactions with the metal ion. We had previously proposed[2] that when M^+ reacts with a molecule such as chlorohexane, the first interaction is with the electronegative Cl- end. Then, if the complex is sufficiently long-lived, parts of the alkyl chain can be accessed by M^+ via 5- and 6-membered rings. Through such multiple interactions, parts of the alkyl chain far from the functional group can be brought close to the metal ion, and thus become candidates for insertion to occur. In the electrostatic model presented here, the potential energies associated with such 5- and 6-membered ring intermediates are larger than those for simpler interactions.

If one considers attractive potentials close to the molecule, it appears that M^+ could access every bond, although this is not observed experimentally. However we find that, for molecules possessing permanent dipole moments, regions of positive potential exist at longer range about some parts of the alkyl group (e.g., close to the methylene unit adjacent to the Cl-, since this carries a substantial positive charge). These repulsive regions may prevent access of the attractive regions that lie closer to the atoms in the molecule.

The figure shows a family of potential curves for the Cr^+/chlorohexane system, for one of the configurations that we have studied. The points on the curve marked -10 kcal/mol indicate those positions where Cr^+ could be placed to yield this interaction energy. While the actual energies determined by this simple model appear to be higher than those determined experimentally, we have found the relative values to be extremely useful in suggesting the relative importance of the various molecular environments that the molecule presents to an incoming metal ion.

---

1. D.J. Hankinson, E.J. Hooper, J. Allison, Presented at the 35th ASMS Conference on Mass Spectrometry and Allied Topics, Denver, CO, May 24-29, 1987.

2. A. Tsarbopoulos, J. Allison, J. Amer. Chem. Soc., 107, 5085 (1985).

Presented at the 36th ASMS Conference on Mass Spectrometry and Allied Topics
June 5-10, 1988, San Francisco, CA

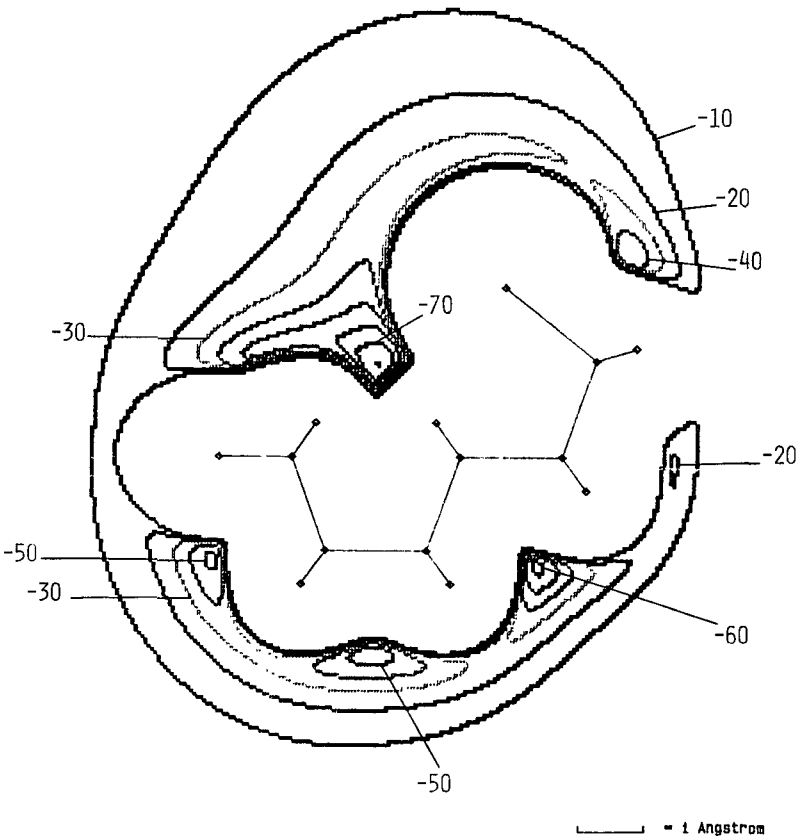

Shown above is a family of potential curves about a configuration of chlorohexane, as it interacts with Cr^+. This configuration was selected to investigate the relative stability of a 5-membered ring type of intermediate, in which the Cr^+ interacts with both the chlorine and a methylene unit in the hexyl group. This creates a region in space that is more attractive than any other "hot spot" about the molecular framework.

Presented at the 36th ASMS Conference on Mass Spectrometry and Allied Topics
June 5-10, 1988, San Francisco, CA

THE GAS PHASE CHEMISTRY OF NICKEL AND NICKEL-CONTAINING IONS WITH AROMATIC COMPOUNDS; Richard M. Stepnowski, John Allison, Department of chemistry, Michigan State University, East Lansing, MI 48824

The gas phase chemistry of transition metal ions with organic molecules has been extensively studied in recent years, using ion cyclotron resonance (ICR) and ion beam techniques. The organic molecules that have been studied include alkanes, as well as molecules that contain the basic alkyl structural features (straight chain, cyclic, branched) and functional groups of organic chemistry (halogens, alcohols, acids, esters, ketones, ethers, amines, nitro-compounds and nitriles)[1]. Some multifunctional compounds have also been studied.[2,3] The major reaction mechanisms have been discussed and reviewed.[1]

For small compounds such as alkyl halides (RX)[4], reaction products appear to be formed via a series of elementary steps. First, a transition metal ion such as Fe^+ inserts into the C-X bond to yield the intermediate $R\text{-}Fe^+\text{-}X$. If the R- group is an ethyl group or larger, a β-H shifts to yield a complex of the form $(C_nH_{2n})Fe^+(HX)$. The complex dissociates in a competitive ligand loss step.[3] For more complex functional groups (e.g., carboxylic acids), insertion into bonds within the functional group can also be important.[5,6]

This study involves the reactions of Ni^+, $NiCO^+$, $NiPF_3$, and $NiCp^+$ with a variety of aromatic compounds, including phenyl, benzyl, and aromatic carbonyl compounds. Reaction products and pathways were determined by Ion Cyclotron Resonance (ICR) Mass Spectrometry.

The phenyl group in some aspects behaves chemically intermediate to the methyl and ethyl groups. H transfer from the phenyl group is a high energy process, closer to the energy required for H transfer from a methyl group than an ethyl group. Nonetheless, reactions such as:

$$Ni^+ + C_6H_5X \rightarrow NiC_6H_4^+ + HX$$

are observed. The formation of a strong benzyne-Ni^+ bond makes this reaction possible in a few cases. When other pathways are open, such as the elimination of a small neutral molecule from the functional group, this pathway is preferred. For example, nitrobenzene reacts with Ni^+ via a nitro to nitrile isomerization[6] to first lose NO, then CO, leaving C_5H_5 retained by the metal ion:

$$Ni^+ + C_6H_5NO_2 \rightarrow NiC_5H_5^+ + NO + CO$$

A major effect of the phenyl group is its inductive effect. This can be seen in reactions of substituted benzyl compounds. The weak $C_6H_5CH_2\text{-}X$ bond plays an important role in these reactions. This bond is the only bond attacked for most of the benzyl compounds studied. Charge transfer to the $C_6H_5CH_2$ moiety following insertion into this bond occurs for benzyl chloride, benzyl bromide, and benzyl alcohol, due to the low ionization potential of the benzyl radical.

Most of the trends in reactivity can be explained by the steric effects of the ligand. By size, Cp > PF_3 > CO. This is also the same order as for the metal-ligand bond energies. The reactivity of the ligated metal ions $NiCO^+$, $NiPF_3^+$, and $NiCp^+$ may be related to both these factors. The NiL^+ ions often insert into bonds where steric interactions will be minimized in the insertion imtermediate.

The reactions of $NiPF_3^+$ follow closely the reactions of $NiCO^+$, with slightly less reactivity observed for the $NiPF_3^+$ ion. The bonding of the ligand in $NiCO^+$ and $NiPF_3^+$ is similar (primarily electrostatic, according to recent theoretical studies[7]) so this is not surprising. The slightly less reactivity of $NiPF_3^+$ reflects the steric crowding involved for insertion produced by this larger ligand. Much of the chemistry of the NiL^+ ions can be explained by the formation of intermediates with low steric interactions. The reactivity of $NiCp^+$ with the halobenzenes indicate that the Cp ligand affects the metal ion much differently than either CO or PF_3. Charge transfer to the cyclopentadienyl group may occur, to increase its aromatic character (giving it 6 π electrons) explaining why this ion is more reactive than the other NiL^+ species in some cases. In other cases, such as the aromatic carbonyls the steric hindrance of the bulky Cp group appears to prohibit reactions from occuring.

We also observed that Ni^+, produced by 70 eV electron ionization on the organometallic compounds $Ni(CO)_4$, $Ni(PF_3)_4$, and NiCpNO, have somewhat different reactivity. For example, Ni^+ produced from NiCpNO reacts with iodobenzene to form only the adduct $NiC_6H_5I^+$, while Ni^+ produced from $Ni(CO)_4$ and $Ni(PF_3)_4$ reacts according to:

$$Ni^+ + C_6H_5I \rightarrow NiC_6H_4^+ + HI \quad (1)$$

$$Ni^+ + C_6H_5I \rightarrow NiC_6H_5^+ + I \quad (2)$$

The ratio of products 1 and 2 is 1:1 for Ni^+ produced from $Ni(CO)_4$ and 1:2 for Ni^+ produced from $Ni(PF_3)_4$. Future work in our lab will determine if the Ni^+ ions, produced from different precursor molecules, are formed in excited states and what the relative population of those states are.

1. Allison, J. Prog. Inorg. Chem., **1986**, 34, 627.

2. Lombarski, M.; Allison, J. Int. J. Mass Spec. Ion Phys., **1983**, 49, 281.

3. Tsarbopoulos, A.; Allison, J. Organometallics, **1984**, 3, 86.

4. Allison, J.; Ridge, D.P. J. Am. Chem. Soc., **1979**, 101, 4998.

5. Lombarski, M.; Allison, J. Int. J. Mass Spec. Ion Proc., **1985**, 65, 31.

6. Cassidy, C.J.; Freiser, B.S.; McElvany, S.W.; Allison, J. J. Am. Chem. Soc., **1984**, 106, 6125.

7. Alvarado-Swaisgood, A.E.; Harrison, J.F. J. Phys. Chem., in press.

Presented at the 36th ASMS Conference on Mass Spectrometry and Allied Topics
June 5-10, 1988, San Francisco, CA

TIME-RESOLVED METASTABLE FRAGMENTATIONS OF METHYL ACETATE IONS

R. Arakawa
Institute of Chemistry, College of General Education,
Osaka University, Toyonaka 560, Japan

The unimolecular gas-phase chemistry of ionized methyl acetate has been the subject of a number of studies.[1-5]

$$CH_3COOCH_3^{+\cdot} \longrightarrow CH_3CO^+ + COH_3^{\cdot} \qquad (1)$$

The main interest consists in what configuration is a reacting precursor in complexity of isomerization/dissociation paths. Extensive labeling experiments[2,4] on methyl acetate and its enol isomer have proposed that the distonic ion, $CH_3\overset{+}{C}(OH)O\dot{C}H_2$, in which the charge and radical site are separated by more than one atom, is a key intermediate. This intermediate accounts for the considerable loss of positional identity of H and D atoms in the labeled isomers. However, the time-resolved mass spectra of ionized methyl acetate[4] indicated that the isomerization of methyl acetate ion is a rate-determining step in a μsec time-frame. On the other hand, ab initio calculations showed that the hydrogen-bridged ion/dipole complex, $CH_3CO\text{-}H\text{-}OCH_2^{+\cdot}$ is probably a precursor ion decomposing to CH_3CO^+ and $\dot{C}H_2OH$.[5] In this way, the reaction path of ionized methyl acetate is still an unsettled problem.

The reaction (1) has a strong metastable peak in a μsec time-frame. The apparent appearance energy is only 0.7 eV higher than ionization energy, and thus RRKM theory predicts no metastably slow rate. One way of accounting for such unusual characteristics is to assume a mechanism that the reaction path involves isomerization to a more stable structure prior to the dissociation.[6] We have investigated which isomer serves as the intermediate precursor, when assuming the prior isomerization mechanism, so as to explain the experimental time-resolved metastable fragmentation. The metastable ion intensities were measured as a function of ion-source-residence time by trapped ion mass spectrometry[7].

Figure 1 shows the metastable-to-main beam intensity ratio against the ion-residence time at electron impact energy of 40eV. The decay of metastable ion is principally dependent on rate vs. energy. Along a potential energy profile (Fig. 2) obtained by Heinrich et el.[5] using a high level of ab initio calculations, we suppose two prior isomerization models accounting for the unimolecular dissociation rate; the distonic ion and the hydrogen-bridged complex serve as a precursor ion. The vibrational frequencies for RRKM calculations are obtained from a

vibrational analysis for the assumed geometries and approximate simple valence fields. The experimental results are well reproduced by the distonic ion model(———) compared with the hydrogen-bridged complex model(----). The prior isomerization can yield slow dissociation rates($\lesssim 10^5$ s^{-1}). This is because the distonic ion model exhibits the high activation energy, and the hydrogen-bridged complex model has a loose structure in spite of low activation energy. Both models provide the higher state-density of the reactant at threshold energy. Finally, it is suggested from the present results of time-resolved metastable fragmentations that the distonic structure among the several isomers is the plausible precursor decomposing metastably to CH_3CO^+ and $\dot{C}H_2OH$.

References

1) J. K. Terlouw, J. L. Holmes, and P. C. Burgers, Int. J. Mass Spectrom. Ion Processes, 66, 239 (1985).
2) C. Wesdemiotis, R. Csenscits, and F. W. McLafferty, Org. Mass Spectrom., 20, 98 (1985).
3) J. L. Holmes, C. E. C. A. Hop, and J. K. Terlouw, Org. Mass Spectrom., 21, 776 (1986).
4) P. C. Burgers, J. L. Holmes, C. E. C. A. Hop, and J. K. Terlouw, Org. Mass Spectrom., 21, 549 (1986).
5) N. Heinrich, J. Schmidt, H. Schwarz, and Y. Apeloig, J. Am. Chem. Soc., 109, 1317 (1987).
6) L. F. Monterio, M. L. F. Monterio, J. J. Butler, and t. Baer, J. Phys. Chem., 86, 752 (1982).
7) C. Lifshitz, Mass Spectrom. Rev., 1, 309 (1982).

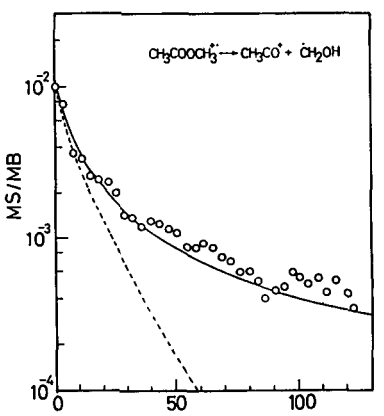

Fig.1

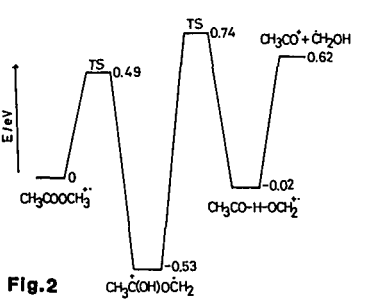

Fig.2

Presented at the 36th ASMS Conference on Mass Spectrometry and Allied Topics
June 5-10, 1988, San Francisco, CA

USE OF A VG 70-4SE TANDEM FOUR-SECTOR MASS SPECTROMETER IN STRUCTURAL STUDIES

R.M. Milberg*, J.M. Curtis, L.S. Rong, and K.L. Rinehart, School of Chemical Sciences, University of Illinois, Urbana,IL 61801; R.H. Bateman, B.N. Green, and G.W.T. Lee, VG Analytical Ltd., Floats Road, Wythenshawe, Manchester, M23 9LE, United Kingdom.

Introduction

The VG Instruments 70-4SE, a new double focusing, four-sector tandem mass spectrometer of E-B-E-B geometry (mass range to 3000 amu at 8-kV accelerating potential), has been in use since November 1987 at the University of Illinois. The MS1 section of the instrument is a standard VG 70-SE and meets all of the 70-SE performance specifications. The MS2 section is a modified 70-SE. The 70-4SE has a calibration-only FAB ion source and a high efficiency gas collision cell between MS1 and MS2. MS1 is used for EI and CI GC-MS and probe sample service work in our laboratory. The 70-4SE is interfaced to a VG 11-250J data system which provides control for MS/MS measurements. The four-sector tandem FAB sensitivity is greater than 6 x 10^{-9} amp for the m/z 133 ion of CsI at the MS2 detector for ions from MS1 and the CID collection efficiency is greater than 10% for the daughter ions of the m/z 142 precursor ion of n-decane from MS1 in the EI mode with the gas cell grounded.

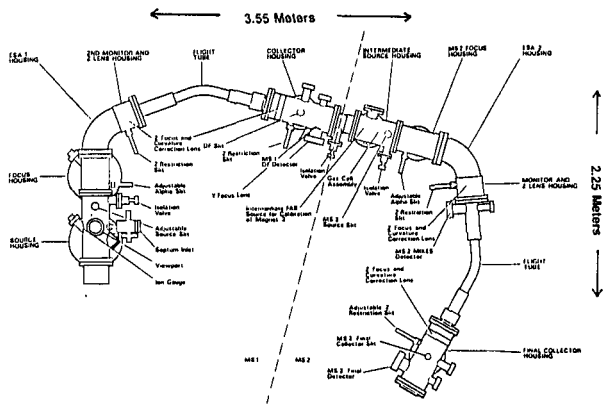

VG 70-4SE

Results

We have employed the 70-4SE for the study of the fragmentation of a number of peptides, marine natural products, and antibiotics, employing samples as small as 300 ng.

A neuroactive decapeptide, HTF-II, was isolated from Carausius morosus, an Indian stick insect. From FABMS, FAB-MS/MS, and amino acid analysis the sequence below was determined:

pGlu-Leu-Thr-Phe-Thr-Pro-Asn-Trp-Gly-Thr-NH_2

The analog HFT10 (with a hydroxyl C-terminus) was then generated on a peptide synthesizer in a structure-activity realationship study. The FABMS spectrum of HFT10 has a (M+H) peak at m/z 1147.5 and a large fragment at m/z 574.2. The MS/MS spectra of m/z 1147.5, shown below, has a large daughter ion at m/z 574. High resolution FABMS measurements found that the m/z 574 peak was a doublet at 574.2877 and 574.2625. The MS1 section was tuned to 15,000 resolution (10% valley) and MS/MS spectra,

shown below, were obtained of the two isobaric peaks. The data indicate that the daughters of m/z 574.2877 are derived from the C-terminal pentapeptide sequence and the daughters of m/z 574.2625 are derived from the N-terminal pentapeptide sequence.

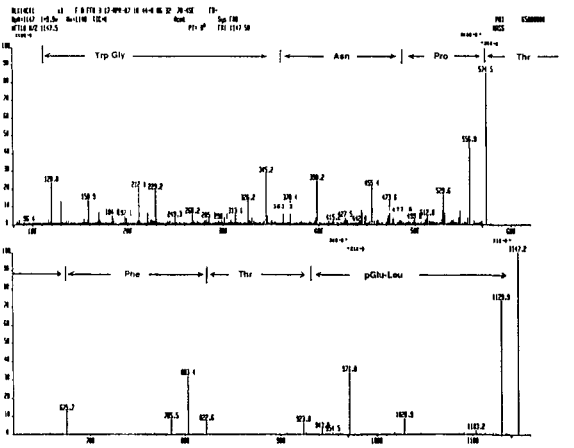

MS/MS of HFT10

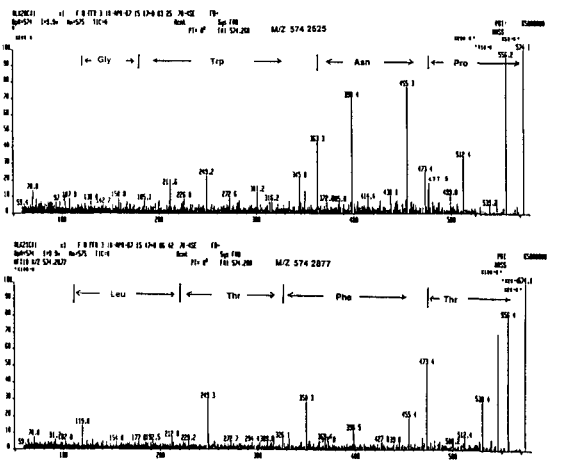

MS/MS of Peaks at m/z 574

Conclusions

The VG 70-4SE is a versatile tandem mass spectrometer which occupies the same floor space as a VG ZAB-SE instrument. The 70-4SE is used for routine probe and GC/MS service work employing EI and CI as well as performing MS/MS studies using FAB and EI.

This work supported by NIH grant GM27029.
*Author to whom correspondence should be directed.

Presented at the 36th ASMS Conference on Mass Spectrometry and Allied Topics
June 5-10, 1988, San Francisco, CA

AN EXPERIMENTAL INVESTIGATION OF FACTORS AFFECTING THE EFFICIENCY OF COLLISION-INDUCED DISSOCIATION OF PROTONATED PEPTIDE IONS.*

A.J.Alexander and P.Thibault**
National Research Council of Canada, 1411 Oxford St., Halifax, Nova Scotia, Canada B3H 3Z1; ** 6100 Royalmount Avenue, Montreal, Quebec, Canada H4P 2R2.

Tandem mass spectrometry under high (1) and low (2) collision energy regimes is a powerful tool in the characterization of peptides. Tandem sector instruments have proved more successful at generating diagnostically useful fragments from higher mass precursor ions (>1000 Da), and such MS/MS spectra are less dependent on instrumental parameters than those generated using XqQ instruments. In the latter the collision energy E(Lab), the amplitude of the RF power in q, the type of target gas (Tg) and its thickness P(Tg) are some of the parameters influencing the quality of the spectra (3).

Results from a study of Leu-Enkephalin (Tyr-Gly-Gly-Phe-Leu, MH+ 556), using an instrument of BEqQ geometry, show that different combinations of E(Lab) and P(Tg) with either argon or xenon target gas can be used to generate comparable daughter ion spectra (4), e.g. very similar MS/MS spectra were obtained with argon or xenon using E(Lab) values of 40 or 20 eV respectively, and 20% attenuation of the precursor ion. The degree of collisional activation in q could be easily controlled via changes in either E(Lab), P(Tg) or Tg. Xenon was more efficient than argon for generation of fragment ions at a given value of E(Lab), under both single and multiple collision conditions.

The combined influence of the RF amplitude and E(Lab) on the transmission of both precursor and fragment ions through q were in accord with established principles, given the significantly higher mass of the precursor ion studied here than in previous evaluations of the performance of XqQ tandem instruments.

However, studies on a series of Dynorphin peptide fragments (Leu-Enkephalin plus n residues, where n = 1,2 and 3) showed that with increasing precursor ion mass it becomes more difficult to obtain useful spectra for CID reactions conducted at low values of E(Lab) in q (Figure 1). This is only in part due to the fall-off in transmission of the deceleration lens/qQ assembly. The change in amino acid content also contributes to the observed change in fragmentation behaviour. For example Leu-Enkephalin-Arg and Leu-Enkephalin-Lys were found to exhibit quite different unimolecular and CID fragment ion spectra.

The exceptions observed thus far to this trend of lower efficiency CID with increasing mass (e.g protonated Gramacidin S, m/z MH+ 1141) have in common one significant feature, viz. an intense spectrum under unimolecular conditions (Figure 2). This suggests that collisional activation of large ions (MH+ approximately 800 Da or higher) at E(Lab) values less than 120 eV or so results in only a small <u>fractional</u> increase in the internal energy of the precursor. Under such conditions the pre-collision internal energy, assessed by the extent of unimolecular dissociation, largely determines the quality of the fragment ion spectrum generated by CID. This disparity between pre-collision internal energy and additional energy gained from the collision will increase as the mass (and thus number of vibrational modes) of the precursor ion increases.

(1) Martin et al., Int. J. Mass Spectrom. Ion Proc.<u>78</u> (1987) 213; Sato et al., Anal Chem.<u>59</u> (1987) 1652.
(2) Hunt et al., Proc. Natl. Acad. Sci. USA <u>83</u> (1986) 6233
(3) Martinez R.I., Rapid Comm. Mass Spectrom. <u>2</u> (1988) 8.
(4) Alexander A.J. and Boyd R.K., Int. J. Mass Spectrom. Ion Proc. (submitted)

* NRCC# 29079

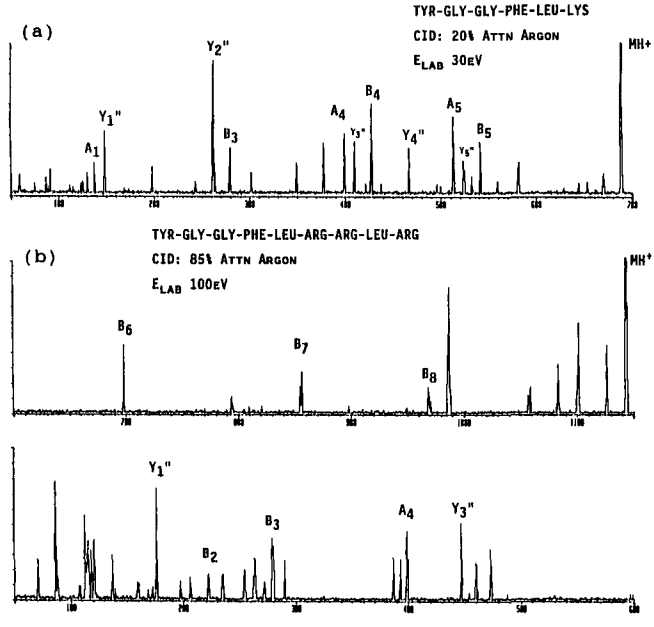

Figure 1: Fragment ion spectra of precursor ions MH+ obtained by CID in RF-only quadrupole collision cell. (a) Leu-Enkephalin-Lys [MH+ m/z 684.4], (b) Dynorphin A: Frag. 1-9 [MH+ m/z 1137.7].

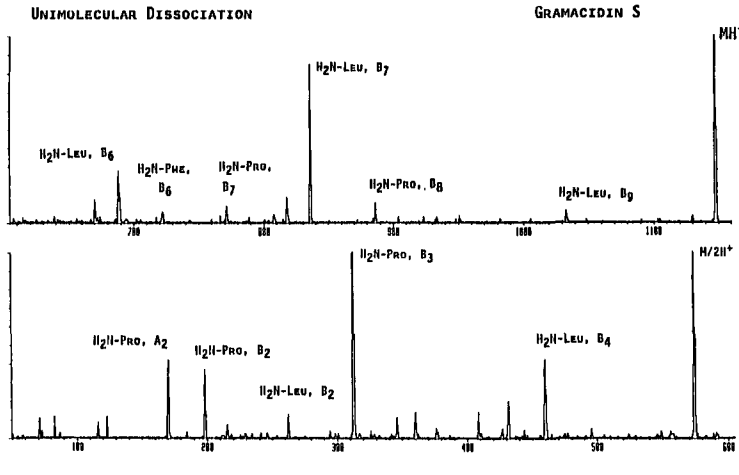

Figure 2: Fragment ion spectrum of MH+ from Granacidin S. Quadrupole mass-filter scan, no gas in rf-only collision cell.

Presented at the 36th ASMS Conference on Mass Spectrometry and Allied Topics
June 5-10, 1988, San Francisco, CA

A New Totally Automated Hybrid MS/MS System

M.R. Clench, R.Owen, V.C. Parr and D. Wood
VG Tritech Ltd., Crewe Rd., Wythenshawe, Manchester, England

Objective

To design a hybrid MS/MS system which offers a comprehensive set of MS/MS experiments at both high and low collision energies. Parent ion resolutions of up to 7500 should be achieved.

In addition the instrument control system should offer total flexibilty in choice of conditions without being overly complicated.

Introduction

The TS-250, with its air cored magnet [1] has become accepted as a flexible and easy to use general purpose GC/LC-MS instrument. Only in the field of MS/MS are there limitations in the available performance. This area has been addressed by TRIBRID, a unique MS/MS workstation based upon the successful TS-250 design. It has three collision cells and three analysers to allow complete freedom of choice of collision energies and modes of analysis.

This paper illustrates the implementation of this concept into an integrated system design.

Background

The TS-250 double focussing mass spectrometer uses a unique air cored electromagnet capable of rapid scanning (< 7 ms/decade ultimate) and switching. Also, by virtue of its air core, it does not suffer from magnetic hysteresis. This allows masses to be predicted and set by reference to the equation below.

$$m = k (I - dI)^2$$

where:

k is a constant of proportionality, I is the coil current, dI is an offset.

The basic performance of the electromagnet system is illustrated by the figures below. The ultimate scan speed of less than 7 ms/decade is some ten times faster than for any other commercially available sector mass spectrometer. The switching example illustrates the absence of hysteresis in the system. These two features will allow fast and predictable parent ion selection, even at elevated resolving powers.

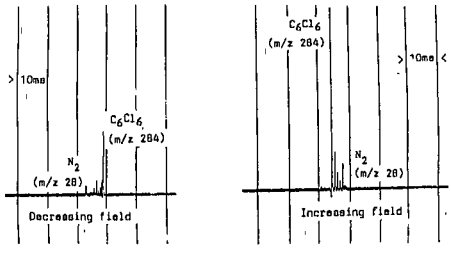

Maximum magnetic field rise and decay rates

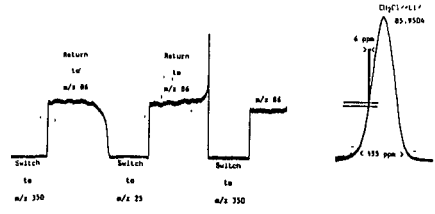

Magnet hysteresis at mass 86

The TRIBRID comprises a standard TS-250 analyser system (MS1) followed by a high energy collision cell and ESA for MIKES analysis. This is followed by retardation and beam shaping lenses which introduce the ions into an RF only collision quadrupole with energies selectable from 0 to 250 electron volts. A high performance quadrupole with 2-2000 dalton mass range and better than unit mass resolution characteristics analyses the daughter ions produced.

Because of the predictability of the analysers the scan functions for daughter, parent, mass loss and reaction monitoring can simply be programmed from a microprocessor control system in accordance with theory.

The analyser configuration is illustrated in the next figure.

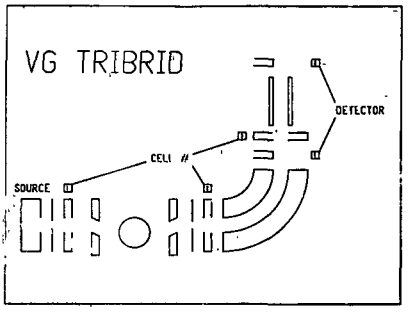

The performance in each of the three cells is summarised below

	Cell 1	Cell 2	Cell 3
Parent R.P.	- 100	up to 7500	up to 7500
Daughter R.P.	2-500	- 50	unit mass
collision energy	high	high	0 to 250 eV

The control system adopted for the system is based upon a VME bus supporting three 68000 series micro's. Communication to a Vaxstation™ 2000 host is via a thinwire ethernet. Peak display for tuning is generated in a "scope" window on the VS2000 screen. The particular cell used and the collision conditions are illustrated in the "system visual". This is an interactive display which not only informs the operator of the current experiment, but also allows him to change the method by simply using the mouse to "click" on the appropriate cell or detector. Any sequence of experiments can be pre-programmed, although manual intervention can take place at any time.

Conclusion

A system has been developed which allows selection of any one of a wide menu of MS/MS experiments via interactive control from a Vaxstation 2000 workstation. Software aides such as the SMILES graphical structure system allow the MS/MS data generated to be interpreted more easilly. The use of both high and low collision energies offers structural information and selectivity for a wide range of applications.

Presented at the 36th ASMS Conference on Mass Spectrometry and Allied Topics
June 5-10, 1988, San Francisco, CA

STRUCTURAL STUDIES OF OLIGOMERIC AND POLYMERIC AROMATIC SYSTEMS BY TANDEM MASS SPECTROMETRY

T G Blease, J H Scrivens, ICI PLC, Wilton, Cleveland, UK, TS68JE
J J Monaghan, W E Morden, ICI PLC, Runcorn, Cheshire, UK, WA7 4QD

The use of MS in the characterisation of synthetic oligomeric and polymeric systems has, until recently, been limited to monomer purity studies and pyrolysis (either direct py-MS or py-GC-MS). These areas have given important results but their applicability is limited.

The advent of new types of high performance materials utilising poly aryl ethers, ketones, sulphones and sulphides has highlighted the need for MS methods capable of fully characterising these polymeric species. Specifically these methods should enable us to

1 obtain an accurate mol wt distribution of any synthetic polymer species, and
2 carry out detailed sequencing of the individual monomers which make up such a polymer.

Characterisation of these non-polar, highly involatile, relatively intractable materials is difficult using conventional methods. However, high temperature (>600°C) direct probe EI MS has enabled us to obtain spectra of oligomers of these materials up to >1200 Daltons in mass.

MS-MS daughter ion spectra have been obtained, using a VG ZAB-HSQ hybrid mass spectrometer, from molecular ions of these oligomers and detailed sequencing information has been derived from these spectra.

Compounds of general structure 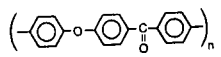 have been studied in detail and the effects of variation of the end group (phenyl, F, Cl) on the direction and ease of the fragmentation noted.

Fig 1 shows the sequence information available from the daughter ion spectrum of an oligomer of mol wt 1006 containing ether, ketone and sulphone linkages. As can be seen from the spectrum, complete sequencing is relatively straightforward with cleavages occurring preferentially at the carbonyl groups followed by the ether and sulphone linkages.

FIG 1

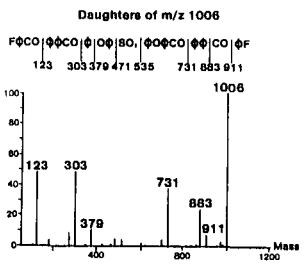

The sequencing rules derived from the study of such model compounds have enabled us to obtain structural information from the components of oligomeric synthetic reactions. From the reaction shown in Fig 2, two major products were obtained of mol wt 926 and 730 respectively. Application of the sequencing rules to the daughter ion spectra of m/z 926 (Fig 3) and m/z 730 (Fig 4) enabled us to determine the structures of both products unequivocally.

FIG 2

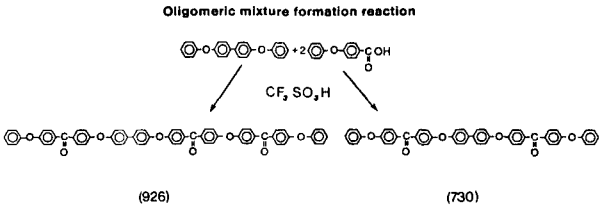

FIG 3

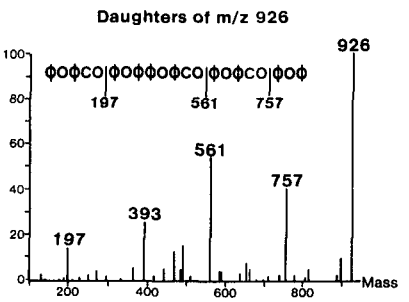

FIG 4

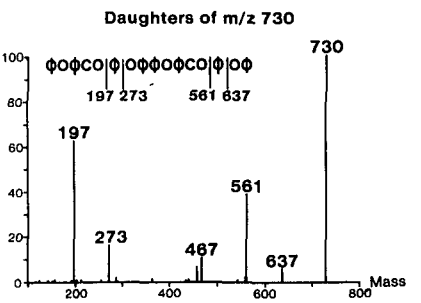

Thus high temperature direct probe EI-MS-MS has been shown to provide useful structural information on the components of synthetic oligomeric reaction mixtures.

It becomes increasingly difficult, however, at higher mol wts to obtain EI spectra of these aromatic materials and alternative ionisation techniques are needed to permit the study of such species. As part of our MS study of these materials we have used Field Desorption (FD) to study several typical aryl polymers. These FD spectra have enabled us to study related oligomeric species of the type $ClØSO_2(ØSØSO_2)_nØCl$. As well as clearly indicating the monomer spacing and differences in mol wt distribution between the samples, the spectra also show the presence in one of the samples of additional end groups, shown by satellite peaks corresponding to the replacement of Cl by F and OH.

Daughter ion spectra of these ions could easily be obtained so confirming these theories and giving detailed structural information.

We have also obtained FD spectra of similar aryl polymers showing a mol wt distribution up to 9000 Daltons.

Thus these non-polar, highly involatile, novel high performance species can be characterised by FD. Use of a high mass range FD MS-MS instrument should enable good sequence information to be obtained from such materials.

Presented at the 36th ASMS Conference on Mass Spectrometry and Allied Topics
June 5-10, 1988, San Francisco, CA

Molecular Orbital Study of Remote Charge Site Decompositions in the Collision Induced Decomposition Mass Spectra of Fatty Acid Carboxylate Anions

Marshall M Siegel* and Norman B. Colthup

American Cyanamid Company, Medical Research Division,
Lederle Laboratories, Pearl River, NY 10965

INTRODUCTION

In a series of papers, Gross, Tomer, Jenson and co-workers [1] demonstrated that a new class of decomposition ions is produced when closed shell positive and negative ions undergo collision induced decomposition (CID). The decomposition ions are formed remote from the charge site and are related to ions produced by thermal decomposition processes

The earliest observations of remote charge site decompositions were in FAB CID mass spectra of saturated and unsaturated fatty acid carboxylate anions [2] Similiar observations were made by Bambagiotti and co-workers [3] in CI CID mass spectra of saturated and mono-unsaturated fatty acid anions. Four major observations in the FAB and CI CID mass spectra of saturated fatty acid carboxylate anions were: (1) a characteristic homologous series of olefin carboxylate anions of moderate abundance, (2) an homologous series of radical anions of lower abundance, (3) losses of methane and (4) water from the fatty acid carboxylate anion. Semi-empirical molecular orbital (MO) calculations were performed in order to obtain a greater in depth understanding of the energetics involved in the four types of decomposition reactions thought to be involved in the production of these CID mass spectra.

RESULTS AND DISCUSSION

A) Formation of Terminally Unsaturated Fatty Acid Carboxylate Anions. Main Anion Decomposition Series

Reaction mechanism 1 was modeled using MO calculations with lauric acid carboxylate anion, $CH_3(CH_2)_{10}CO_2^-$. In order for reaction mechanism 1 to proceed, a CCCC segment of the molecule must be in the *gauche* configuration and distorted, as illustrated in Figure 1, where the central C-C bond length is stretched and the two C-H bond lengths are equally stretched. MO calculations were performed for a series of C_5-C_6 , C_4-H and C_7-H bond lengths, where the two C-H bond lengths were kept equal. The rest of the molecule was optimized for minimum MO energy The potential energy surface exhibited a saddle point 92 4 kcal/mol above the minimum energy *gauche* structure for lauric acid carboxylate anion. This energy corresponds to the calculated activation energy for reaction mechanism 1. The structure at the saddle point for the reactive segment of the hydrocarbon backbone is illustrated in Figure 1

B) Formation of Radical Anions by Cleavage of C-C Bonds of Fatty Acid Carboxylate Anions

Unlike the *gauche* case, the *anti* configuration for the hydrocarbon backbone of the lauric acid anion cannot lose a hydrogen molecule. If given sufficient energy, the C-C bonds will cleave to give two radical fragments. However, the high energy required for cleavage by this mechanism, calculated to be ~140 kcal/mol, compared to 92.4 kcal/mol for reaction mechanism 1, suggests that it should generate FAB CID ions of lower abundance FAB CID anions at m/z 58, 86 and 100 are of low abundance and are only seen because the main decomposition ion series becomes weak in this region It is suggested that all the CCCC *anti* segments can undergo homolytic cleavage, but that most of the peaks are too weak to be seen. These types of ions are observed at higher mass in the CI CID spectra of carboxylate anions [3], generated under higher resolution than the FAB CID experiments.

C) Methane Loss from Fatty Acid Carboxylate Anions

Figure 2A shows the optimized structure for the high energy intermediate for the terminal hydrocarbon segment of lauric acid carboxylate anion undergoing methane loss via mechanism 2. Figure 2B shows what happens when this $C_{1'}$-H distance is reduced to 1.45 Å, which is just past the high energy intermediate point. The methyl group rotates sharply, breaking the $C_{1'}$-$C_{2'}$ and the $C_{3'}$-H bonds, forming the $C_{1'}$-H bond to produce methane. These results show that reaction mechanism 2 is a plausable explanation for the $C_{1'}$-$C_{2'}$ bond cleavage. The calculated activation energy for this reaction is 119.0 kcal/mol indicating that this reaction is not forbidden. Figure 2 suggests why mechanism 2 is not a suitable mechanism for non-terminal C-C bond cleavages. In

order to form methane by mechanism 2, the methyl group must rotate sharply. The methyl group has a low moment of inertia and can rotate easily However, if a methyl hydrogen atom is replaced by a carbon chain, the molecule has a considerably lower probability for achieving the proper geometric configurations required for cleaving non-terminal C-C bonds, thereby, effectively preventing reactions by mechanism 2

D) Water Loss from Fatty Acid Carboxylate Anions

The m/z 237 anion in the FAB CID mass spectrum of palmitic acid is assigned to be the dehydration product of the parent carboxylate anion [2]. Jenson, *et al* [2] determined by deuterium substitution studies that both hydrogen atoms which form H_2O come from a single CH_2 group which is either α or β from the carboxylate carbon. MO calculations show that the two hydrogens are most likely removed from the α carbon.

1. H. J. Jenson, M. L. Gross Mass Spectrom. Rev. 6, 497 (1987).
2. H. J. Jenson, K. B. Tomer, M. L. Gross J. Am. Chem. Soc. 107, 1863 (1985).
3. M. Bambagiotti A., S. A. Coran, F. F. Vincieri, T. Petrucciani, P. Traldi Org. Mass Spectrom. 21, 485 (1986).

SIX ELECTRON REACTION MECHANISM

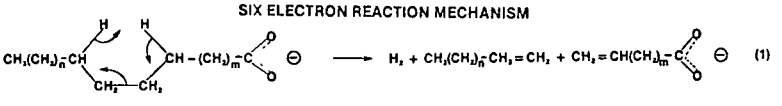

FOUR ELECTRON REACTION MECHANISM

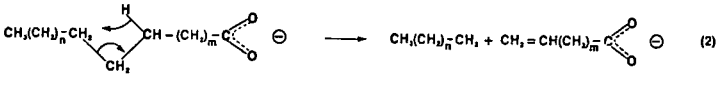

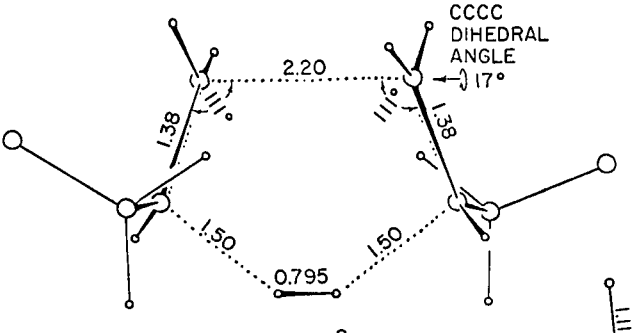

Figure 1. Small and large circles are hydrogen and carbon atoms respectively. Partial bonds are shown as dotted lines. The high energy intermediate structure for a formerly *gauche* hydrocarbon segment of a lauric acid carboxylate anion. The central C-C bond and the two C-H bonds are in the process of breaking to form two vinyl bonds and a hydrogen molecule.

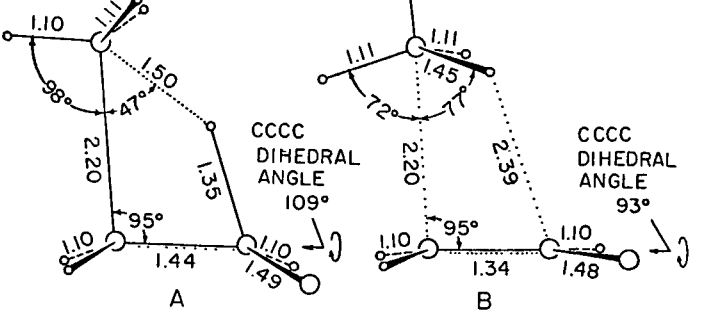

Figure 2. A) The high energy intermediate at the saddle point for methane loss from the hydrocarbon end of a lauric acid carboxylate anion. The terminal carbon C_1, is shown in the upper left. B) The structure just after the high energy intermediate stage. Note the rotation of the terminal methyl group, the lengthening of the $C_{3'}$-H bond, and the shortening of the $C_{2'}$-$C_{3'}$ bond.

Presented at the 36th ASMS Conference on Mass Spectrometry and Allied Topics
June 5-10, 1988, San Francisco, CA

"SELF-CI" IN THE ION TRAP DETECTOR.

L. K. Pannell, Q-L. Pu, Lab. of Bioorganic Chemistry, NIDDK, NIH, Bethesda, MD 20892; H.M. Fales, R.T. Mason, Lab. of Chemistry, NHLBI, NIH, Bethesda, MD 20892; and J.L. Stephenson, Finnigan MAT, Frederick, MD 21701.

AIM: To Investigate the Formation of Chemical Ionization Peaks in a Finnigan Ion Trap Detector and to Determine Inhibition of the McLafferty Rearrangement During Collisional Activation.

HISTORY: Those familiar with the Ion Trap detector will be aware of the existence in routine EI spectra of M+1 ions in the parent ion region. A recent communication (Eichelberger, Budde and Slivon, Anal. Chem 1987, 59, 2732-2734) examined this problem using anthracene. By observing real time ion profiles of the eluting peaks, they concluded that this phenomenon resulted from ion-ion repulsions in an overloaded orbit within the trap. However this explanation did not adequately account for our observations of M/M+1 ratios in relatively small peaks on a typical chromatogram using the AGC programs. Furthermore, it appeared that only the parent ion showed this effect, and fragment ions which were considerable more intense, did not show any abnormal carbon-13 isotope peaks. We decided to investigate this phenomenon further after repeating their experiment on a related compound.

EXPERIMENTAL: Normal mass spectra were acquired on both a Finnigan Ion Trap Detector (ITD) and on a Finnigan Ion Trap Mass Spectrometer (ITMS). Results were the same on both instruments. The ion trapping experiments were performed only on the ITMS. Except where otherwise noted, the samples were run in "AGC OFF" mode. Quantities noted on plots were actual amounts reaching the Trap. Deuterated compounds were obtained from Cambridge Isotope Laboratories in Woburn, Massachusetts. The methyl palmitate originated from Chem Service, West Chester, Pennsylvania.

OBSERVATIONS: Perdeuterio-naphthalene: This compound was chosen to relate closely to the experiments of Eichelberger, et al. When 77ng was injected onto the column with a filament "on" time of 1 microsecond, the parent ion at m/z 136 exhibited only a normal M+1 ratio. Even with ten times the ionization time, there was little if any change observed. However, with a B time of 25000, the M+1 ion dominated the spectrum. The prediction that this is "self-CI" was ruled out by Eichelberger, et al. on two accounts: first one would expect that the ion formed by "self-CI" would be an M+2 as the only source of protons must be the compound itself and the perdeuterio-naphthalene was nearly completely deuterated; second, an examination of the ion profiles showed that the M+1 resulted from poorly shaped ion peaks. We observed a similar result in that 77ng of perdeuterio-naphthalene with a filament time of 25 microseconds gave a good ion profile at the start of the peak but showed no integer resolution at the chromatographic peak apex. Therefore for these observations it seems easy to interpret the results in terms of overloaded ion orbits in the Ion Trap and certainly this is also true in our experiments run at very high sample ionization levels.

Contrary to this, however, we have observed that compounds which show considerable fragmentation in the EI spectra (in contrast to those used by Eichelberger et al.) tended to be the best candidates for M+1 formation. Following this idea we decided to investigate the spectra of fatty acid methyl esters and chose methyl palmitate (molecular weight 270) for this study. In a typical spectrum of methyl palmitate with increased parent ion + 1, the M+1 ratio of the fragment ions is not changed so the M+1 peak of the parent ion does not result from peak assymetry due to overloaded ion orbits. Furthermore, as the Ion Trap scans masses out of the trap from low mass to high mass, those ions most likely to be effected by space-charge saturation are indeed the lower masses. If the source of the M+1 is an ion-molecule reaction then we would expect perdeuterio-methyl palmitate to show M+2 instead of M+1. With 6ng of d34-methyl palmitate (m/z 304) only

an ion at 304 is present accompanied by fragment ions. However at 12ng, the ion at m/z 306 is as high as the parent ion and at 24ng, the M+2 dominates. As there is no large change to the M+1 and M+3 ratios, the explanation must be that the effect results from "self-CI", ie. an ion-molecule reaction. With an injection of 48ng of d34-palmitic acid, the ion profile was observed and it clearly showed resolved peaks and not a broadened hump as was observed in the overloaded case with naphthalene.

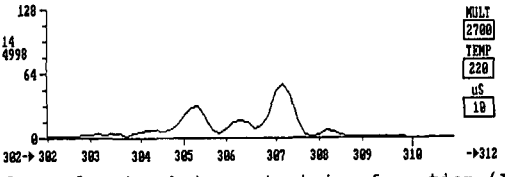

With increased sample size but constant ion formation (AGC ON), we found that the amount of M+2 increased and this led to the hypothesis that this was a reaction between ions in the trap and the neutral compound which is continually eluting into the trap during the analysis section of the trap cycle.

Some aditional experiments were run on the ITMS which involved the "trapping" of individual ions in the mass spectrum of methyl palmitate. The ions chosen were the parent ion at 270 and fragment ions at 143, 87 and 74. In separate experiments, all ions other than the ion of interest were ejected from the trap with a combination of RF and DC fields. The selected ion was then held in the trap for a period of 20 milliseconds before being scanned out. All fragment ions did show protonated molecular ion formation with m/z 74 being the best. Therefore, the fragment ions DO react with the neutral molecule to give M+H as an ion-molecule reaction product. However no such product was observed from the storage of the parent ion itself at m/z 270; instead a protonated dimer ion was observed at m/z 541.

MC LAFFERTY REARRANGEMENT WITH ION TRAP MS/MS: During these experiments, we also examined the ms/ms of the parent ion (m/z 270). After sweeping out all other ions, the collisionally activated ion produced the fragments shown below. We were suprised to note that the McLafferty rearrangement ion at m/z 74 was completely absent. Presumably this ion results from a more short-lived species formed during ordinary electron impact mass spectrometric conditions. This phenomenon is currently being investigated with other species such as ketones.

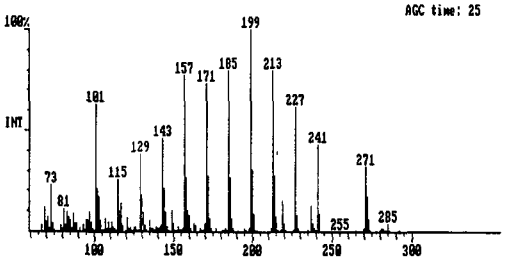

SUMMARY: "Self-CI" does occur in the Ion Trap mass spectrometer as a result of fragment ions reacting with the neutral molecule entering the trap during the storage and analysis phase. It appears that this only occurs with fragment ions and not with the parent ion. Hence in the previously reported results of Eichelberger, Budde and Slivon, no "self-CI" was observed because the compound gave few fragment ions. With such compounds, ion saturation occurs and causes broadened peaks which are interpreted by the software as higher mass ions. In our hands, we have only observed a changed C-13 isotope ratio for a non parent ion in a compound where facile loss of water occurred. Here the M-water ion also showed an increased isotope ratio.

Presented at the 36th ASMS Conference on Mass Spectrometry and Allied Topics
June 5-10, 1988, San Francisco, CA

Mass Spectrometry and Structural Biology - An Exciting Symbiosis

A.L. Burlingame
Department of Pharmaceutical Chemistry and the Liver Center, University of California, San Francisco, CA 94143-0446

Present challenges in protein biochemistry, rational drug design and biotechnology involve the need for determination of structurally precise structure-function relationships at the picomole sample level. Often the unavailability of sufficient quantities of protein or protein crystals precludes use of 2-d NMR and X-ray crystallographic methods. Immunochemical methods are sufficiently sensitive, but structurally imprecise.

Many of these problems in structural biology may be solved by concerted use of a variety of new mass spectrometric-based technologies in conjunction with micro methods of protein sample handling, viz. the isolation, e.g. 2-d gel electrophoresis, enzymic digestion and microbore HPLC. Success in integrating these methods requires picomole sensitivities for all of the steps in the overall structural characterization and sequencing strategy.

In this laboratory we have invested considerable effort in development of both sample handling and mass spectrometric technologies to meet these goals. We have now achieved an operational ability to solve sequencing, structural and topographic issues in protein and glycoprotein problems at the subnanomole to picomole level.

We are studying three classes of proteins which represent the types of structural and topographic issues which must be tackled: 1) cytosolically soluble, 2) amphipathic, and 3) integral membrane proteins. We have illustrated our strategy on sequence revision studies of rat heart fatty acid binding protein [1] using 100-500 pmol total sample. Mapping molecular weights of proteolytic digest HPLC fractions was carried out using the wide mass range zoom capabilities and subpicomole sensitivity of the Wien mass spectrometer [2]. Peptide sequencing was carried out by ultra-high sensitivity 4-sector MS-MS using the Kratos Concept with 35 Kev cesium liquid sputtering ion source and computer-controlled electro-optical multi-channel array detection system [3]. For example, correction of the published sequence of peptide 45-52 [4] was verified using a high energy CID spectrum of MH^+ 861, which coeluted with another peptide of MH^+ 875.

Figure 1a illustrates the quality of high energy CID-array spectra yielding full sequence information obtained on one compound of this mixture using only 10 pmol of sample. Previous 4-sector results without cesium source and array detection required 700 pmol in the case of the N-terminally blocked peptide MH^+ 1036 [1]. Figure 1b illustrates the sensitivity of the Kratos 4-sector array detection instrumentation using 10 pmol of substance P to obtain a high energy CID spectrum and full sequence. Previous results using a Jeol 4-sector instrument without array detection required 1-2 nmol of substance P [5], while recent results on the same instrument with array detection required 0.2 nmol of substance P [6] to obtain the entire CID spectrum.

Studies are in progress on the mapping of colicin 1a, a model amphipathic protein [7]. We will use 4-sector CID spectra to study photoaffinity binding to the integral membrane form of this protein to ascertain topographic information with respect to the membrane.

Studies of the nicotinic acetylcholine receptor have been carried out to delineate post-translational modifications, i.e. glycosylation and phosphorylation, and obtain topographic information [8]. Results on photoaffinity labelling of colicin 1a will be used to guide analogous studies of the acetylcholine receptor.

This research was supported by NIH DRR Grant RR01614, GM 32315 (to W. Aberth), AM 24643 and The Biological Instrumentation Program, NSF.

1. B.W. Gibson, Z. Yu, W. Aberth, A.L. Burlingame and N. Bass, J. Biol. Chem., 263, 4182-4185 (1988).

Figure 1

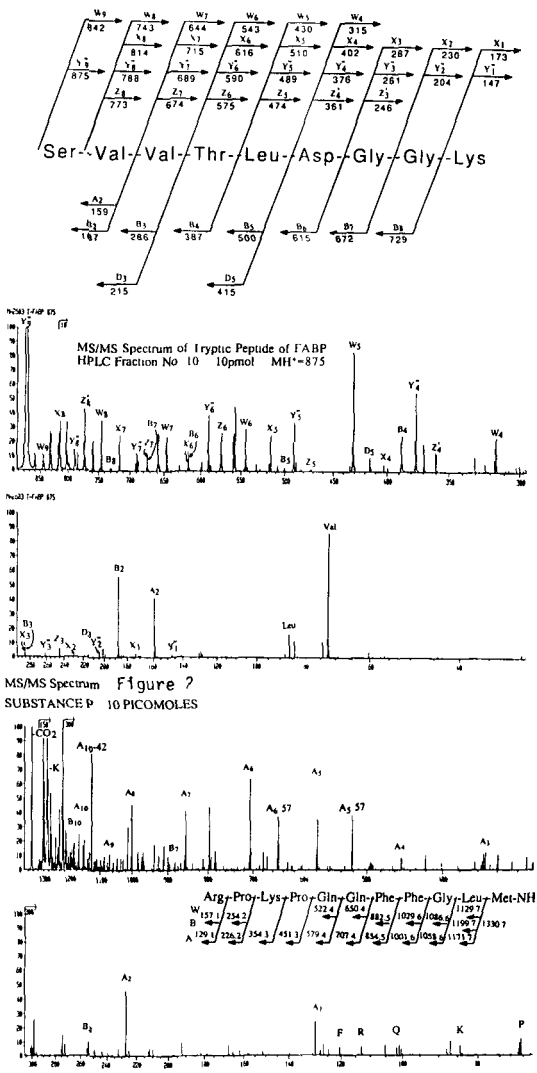

2. B.W. Gibson, Z. Yu, A.L. Burlingame, and W. Aberth in Texas Symposium on Mass Spectrometric Analysis of Peptides and Proteins, C. McNeal and R. MacFarlane, Eds., Elsevier, in press; ibid., this conference, paper TOD445.

3. G. Elliott, R. Gallagher, S. Evans, A. Ashcroft, G. Gooch, A.O. Wright, presented at the 36th Annual Conf. on Mass Spectrometry and Allied Topics, San Francisco, CA, June 5-10, 1988, poster WPB38.

4. Sacchettini et al., J. Biol. Chem., 262, 5428-5430 (1987).

5. S.A. Martin and K. Biemann, Int. J. Mass Spectrom. Ion Proc., 78, 213-228 (1987).

6. J.A. Hill, S.A. Martin and K. Biemann, presented at this conference, poster WPB39.

7. A.M. Falick, S. Mel, R.M. Stroud and A.L. Burlingame, presented at this conference, poster TPA4.

8. L. Poulter, J. Earnest, R.M. Stroud and A.L. Burlingame, Biomed. Environ. Mass Spectrom., in press.

Presented at the 36th ASMS Conference on Mass Spectrometry and Allied Topics
June 5-10, 1988, San Francisco, CA

CONTINUOUS-FLOW FABMS - AN OVERVIEW

Richard M. Caprioli
The University of Texas Medical School
Houston, TX 77030

Continuous-flow (CF) FAB provides a means for the analysis of polar compounds in aqueous solution without the need for glycerol in the sample (1). Low concentrations (about 5%) of glycerol or other viscous liquid present in the carrier solution are adequate to provide a fluid stage for the bombardment process. The ability to continuously feed samples and solutions into the ion source of a mass spectrometer opens up many areas for the mass specific analysis of compounds. The use of CF-FAB provides some significant advantages over standard FAB techniques, including higher sensitivity and lower limit of detection due to the decreased background chemical noise and decreased ion suppression effects. In addition, it provides a means for the rapid analysis of large numbers of samples present in aqueous solutions as well as those dissolved in volatile organic solvents such as acetonitrile or methanol.

The CF-FAB probe has been used in this laboratory on three different instruments; a Finnigan MAT 90 high field magnetic instrument, a Finnigan MAT TSQ 70 MS/MS instrument, and a Kratos MS50RF high field instrument. The technique was found to perform essentially the same on these instruments although each device is somewhat different and has minor advantages. However, a significant advantage of the probe for the MAT 90 is the incorporation of a mechanism to allow the capillary to be moved while in the ion source and also the placement of a small filter pad below the probe tip which acts as a wick to remove solution from the tip and provide a thin surface and smooth flow. The filter pad has the additional advantage of allowing the recovery of a sample if necessary through removal and extraction of the pad.

We have used CF-FAB for the analysis of compounds from a wide array of applications in the field of biological chemistry. These include on-line monitoring techniques for the analysis of drugs directly in the bloodstream of live animals using microdialysis methods, direct injection of aqueous samples and urine using MS/MS methods for drug analyses, enzymic reaction analysis to determine kinetic parameters, and LC/MS applications.

The on-line reaction monitoring application is illustrated for the tryptic digest of a solution containing 11 different peptides in a study aimed at the investigation of the catalytic properties of trypsin. The relative rates of cleavage of the peptides were of interest as the specific reaction conditions were altered. The CF-FAB system was operated in the flow-injection mode whereby a micro-autoinjection valve was used to constantly inject sub-microliter samples of the aqueous enzymic reaction into a carrier flow solvent. This solvent is typically composed of 95% water, 5% glycerol, and 0.1% TFA. The reaction solution contained 100 pmol of each of eleven peptides, 50 mM Tris (pH 8.4), and trypsin in a substrate: trypsin ratio of 200 : 1 (w/w). As the reaction proceeded, individual molecular species were monitored, i. e., the decrease in the $(M+H)^+$ of the reactants and increase in that of the products was followed over a period of about 50 min. Figure 1 shows the selected ion chromatograms for the molecular species of physaleamin at m/z 1265 and its tryptic fragment at m/z 629. The relative rate curves for the hydrolysis of this peptide as well as several others are shown in Figure 2.

We have used CF-FAB for the microbore LC/MS analysis of peptide mixtures. This is illustrated for the analysis of the tryptic digest of β-lactoglobulin A. An Applied Biosystems model 130A microbore LC system was linked to a Finnigan MAT 90 mass spectrometer through the CF-FAB probe as an interface. The LC was fitted with a Brownlee RP-300 1x50 mm column which was eluted at a rate of 25 μL/min with 0-60% acetonitrile gradient. The eluate was split 4:1 to the UV and MS detectors, respectively. The MS was continuously scanned from m/z 600-2900 at 10 sec/scan in the analysis

of 40 pmol of the digested protein. Individual ion searches were used to locate peptides in the total ion chromatogram. In all, fifteen peptides were identified in this single analysis. Simultaneous UV detection and sample collection of the effluent permits additional sample work-up on the mass identified peak fractions. Other aspects of the use of CF-FAB as an LC/MS interface are described in the paper by W. T. Moore et al. in this volume.

The direct sampling of blood in a live rat using a microo[illegible] probe implanted in the jugular vein and connected to the CF-FAB probe in a TSQ 70 MS/MS instrument permitted pharmacokinetic measurements to be obtained directly and on-line. Negative ion MS/MS techniques together with on-line sample enrichment methods provided the required sensitivity and selectivity to perform the analysis in the perfusate without the need for extraction and derivatization steps or other sample handling. Additional details of this application are found in the paper by S. Lin and R. M. Caprioli in this volume.

Direct analysis of drugs and drug metabolites in aqueous solution including urine have been demonstrated using CF-FAB and MS/MS techniques. The compounds analyzed include cocaine, benzoylecognine, phentolamine, penicillin G, THC, morphine and phenobarbital. The high sensitivity of the procedure was demonstrated, for example, with the analysis of phentolamine at 50 pg injected into the spectrometer. Additional details of this work can be found in the paper by W. E. Seifert et al. in this volume.

CF-FAB has been shown to be an effective means to introduce samples in volatile liquids into a FAB mass spectrometer. It is amenable to on-line operation for the analysis of batch reactions and also for a wide variety of applications where a continuous analysis is required. In this regard, it serves as an efficient and effective interface for microbore LC/MS applications.

ACKNOWLEDGEMENTS

The author recognizes the expert assistance of S. Lin, W. T. Moore, W. E. Seifert, A. Ballatore, B. DaGue, and M. Martin for obtaining the data presented in the paper.

REFERENCES

1. R. M. Caprioli, T. Fan and J. S. Cottrell, Anal. Chem. 58, 2949 (1986).

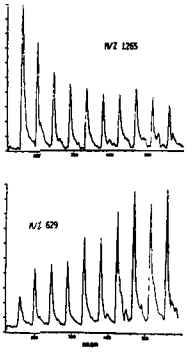

Figure 1

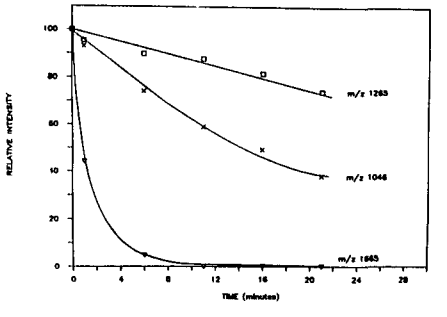

Figure 2

Presented at the 36th ASMS Conference on Mass Spectrometry and Allied Topics
June 5-10, 1988, San Francisco, CA

QUANTITATION BY LC/MS OF ENDOGENOUS NEUROPEPTIDES ISOLATED BY IMMUNOAFFINITY CHROMATOGRAPHY

C.A. Lisek, T.L. Yaksh and I. Jardine

Depts. of Pharmacology and Neurologic Surgery
Mayo Clinic, Rochester, MN 55905

Neuropeptides are important biologically active molecules which function as intracellular messengers, i.e. neurotransmitters, in the nervous system. Neurotransmitters are usually quantitated by radioimmunoassay (RIA), an immunological method which affords high sensitivity (fmol range) of analysis but lacks complete specificity. We have developed a strategy (Figure 1) for the quantitative analysis of neuropeptides which combines immunological methods with the sensitivity and specificity of LC/selected ion monitoring (SIM) mass spectrometry. This strategy is detailed below.

Cat spinal cords were boiled in 0.1 N HCl, homogenized, concentrated in vacuo, then dissolved in phosphate-buffered saline (PBS) solution (0.5 M KH_2PO_4, 0.9% NaCl, pH 6.5). An aliquot of the PBS solution of the extract was assayed for neuropeptide activity by RIA using the I^{125}-analog of the neuropeptide (recoveries: 85-91% for authentic methionine enkephalin, substance P, and VIP). For substance P, the rest of the extract was then applied to an immunoaffinity column containing rabbit polyclonal antibodies (IgG fraction) immobilized on cyanogen bromide-activated Sepharose 4B. Substance P was eluted with 20% aqueous formic acid. The formic acid fractions from several runs were pooled and lyophilized, and a small aliquot was assayed by RIA for SP activity (yield: 100 pmol). A second SP extract (126 pmol) was subjected to the above immunoaffinity purification in the presence of a 10-fold molar excess (1260 pmol) of deuterated (d_8-Phe^8) substance P as internal standard (yield: 40.7 pmol d_0-SP).

Standard solutions of d_0- and (d_0 + d_8)- methionine enkephalin (MW 573.7) and substance P (MW 1347.6) were analyzed by combined HPLC/thermospray mass spectrometry. The MH^+ and MNa^+ ions were selectively monitored. The limit of detection was 100 pmol. In contrast, analysis of standard solutions of d_0-SP by dynamic FAB SIM MS (Figure 2) resulted in a limit of detection of 0.1 pmol.

The immunoaffinity purified endogenous substance P samples were desalted on a C4 wide pore (40 μm) disposable filtration column, then quantitated by microcolumn LC/dynamic FAB SIM MS. An aliquot (0.1 or 0.5 μL) of sample was injected onto a C18 packed fused silica microcolumn (0.32 mm ID) fitted to a VG 30-253 quadrupole mass spectrometer dynamic FAB-MS inlet. The mobile phase was 0.1% TFA and 5% glycerol in 75:25 MeOH:H_2O and the flow rate was 5 μL/min. The protonated molecular ions of d_0- and d_8-SP were selectively monitored.

A comparison of the results from the analysis of one immunoaffinity purified endogenous sample (40.7 pmol by RIA) with those results from standard solutions of (d_0 + d_8)-SP is depicted in Figure 3. From the d_0/d_8 ratios obtained from the standard solutions, a response curve (Figure 4) was generated. The d_0/d_8 ratio for the endogenous sample corresponds to 39.0 pmol of d_0-substance P, which is in agreement with that value (40.7 pmol) determined by RIA. Quantitation of the second immunoaffinity purified endogenous SP sample (100 pmol) also gave results complementary to the RIA results.

In conclusion, (1) endogenous substance P was quantitated by combined microcolumn LC/dynamic FAB SIM MS; (2) the dynamic FAB SIM MS results for substance P were in agreement with those determined by RIA; (3) the limit of detection of substance P by dynamic FAB SIM MS was three orders of magnitude lower than that obtained by thermospray SIM MS and (4) the combination of immunoaffinity chromatography with both RIA and microcolumn LC/dynamic FAB SIM MS detection provides an optimal analytical methodology for endogenous neuropeptides.

Presented at the 36th ASMS Conference on Mass Spectrometry and Allied Topics
June 5-10, 1988, San Francisco, CA

FIG. 1 STRATEGY FOR ANALYSIS OF ENDOGENOUS NEUROPEPTIDES

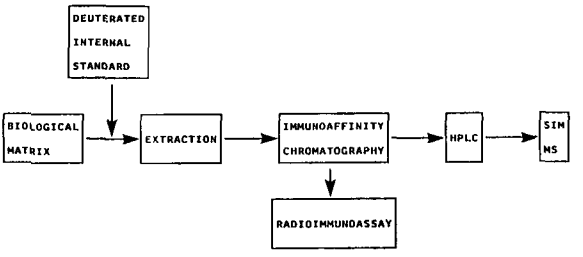

FIG. 2 DYNAMIC FAB SIM MS ANALYSIS OF d_0-SUBSTANCE P (MH^+: 1348.7)

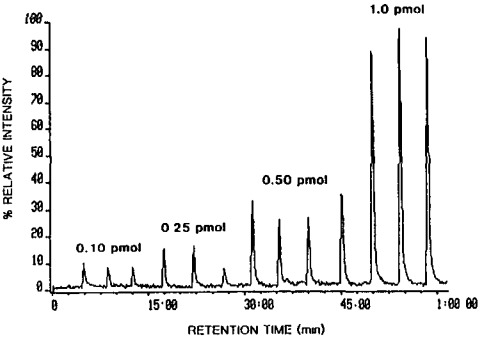

FIG. 3

MICROCOLUMN LC/DYNAMIC FAB SIM MS ANALYSIS OF ENDOGENOUS SUBSTANCE P

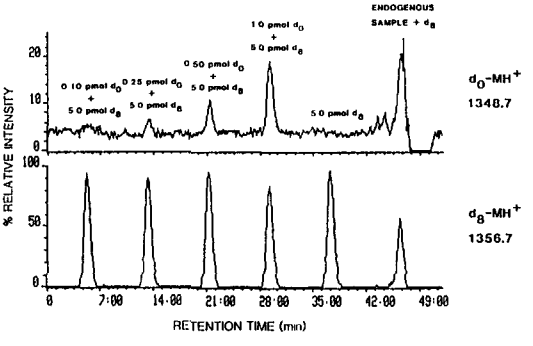

FIG. 4

QUANTITATION OF ENDOGENOUS SUBSTANCE P - RESPONSE CURVE

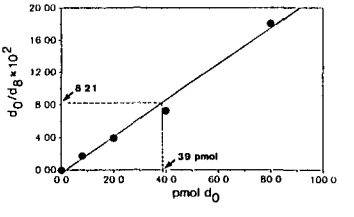

Presented at the 36th ASMS Conference on Mass Spectrometry and Allied Topics
June 5-10, 1988, San Francisco, CA

CONTINUOUS FLOW FAST ATOM BOMBARDMENT MASS SPECTROMETRY OF PEPTIDES AND PEPTIDE DIGESTS

Keith R Jennings, David W Hutchinson and Adrian R Woolfitt
University of Warwick, Coventry, England.

The analysis of peptides and peptide digests by continuous flow fast atom bombardment (CF-FAB) ionisation offers a number of advantages over static FAB. Following preliminary work at Kratos [1] using Dipeptidyl Peptidase (DPP) I and IV for cleaving dipeptides from the N-terminus end of peptides, CF-FAB has been implemented on the MS50 instrument at Warwick during the past year. Investigations have been concentrated on the widely dispersed peptide ubiquitin which is unusual in that all ubiquitin extracted from animal sources has an identical sequence whereas that derived from plant sources shows very slight changes in the residues present. Ubiquitin has a RMM of 8560.6 and comprises 76 amino-acid residues (Fig.1). It has recently been shown [2] that it may be denatured in 6M urea and that under these conditions, a tryptic digest will yield approximately 12 smaller peptides ranging in mass from m/z 133 to m/z 1788 which can be separated off-line by means of reverse-phase HPLC.

To date, 9 of the expected 12 peptides have been recognised using CF-FAB. Those of m/z 133 and m/z 1788 were outside the calibrated mass range and the fragment ALA-LYS with a Bull and Breeze index of 535 would be difficult to detect. In a number of cases, it was noticed that after several runs in which the MH^+ ions of a peptide dominated the spectrum, the peak was replaced by one which was 62 amu higher in mass. This was attributed to the replacement of H by Cu which would occur only after the peptide had flowed beyond the stainless steel central section of the probe tip to the copper surrounding this section. Further confirmation of the identity of peaks ascribed to peptide ions was obtained by treating the fraction of the digest with acetic anhydride which adds 42 amu to the mass of the MH^+ ion, readily distinguishing between peaks arising from peptides and those due to the background (Fig. 2). Two unexpected peptides were observed but could be interpreted as being due to tryptic peptides 11+12 and 5+6, the bonds between these pairs being somewhat resistant to tryptic cleavage.

It is important positively to identify each tryptic peptide appearing in the mass spectra of the HPLC fractions. The products of collision-induced decomposition of each of the peptides will be investigated using tandem mass spectrometry in the near future but valuable information may be gained by investigating the products of various secondary enzyme digests. Chymotryptic digests of 3 HPLC fractions have been carried so far and additional information on the sequence of amino-acid residues has been obtained (Fig. 3); DPPI has also been used to obtain information on the peptide believed to be due to tryptic digests 5+6.

In summary, considerable progress has been made using CF-FAB in obtaining sequence information for the peptide ubiquitin. The sensitivity of the technique has not yet been established for these peptides but in the case of bradykinin, it is in the picomole range. Further work on enzyme digests is in progress and it is planned to investigate ubiquitin isolated from plant sources with a view to searching for the slight variations in amino-acid sequences which have been reported.

1. D W Hutchinson, A R Woolfitt, K R Jennings and A E Ashcroft, 35th ASMS Conference, Denver, 1987.

2. M J Cox, R Schapira and K D Wilkinson, Analyt. Biochem. 1986, 154, 345.

Presented at the 36th ASMS Conference on Mass Spectrometry and Allied Topics
June 5-10, 1988, San Francisco, CA

UBIQUITIN

76 residues C378 H630 O118 N105 S m/z = 8560.6

100[(M+1)]/(M) = 476.3 B and B Index = -51

MET - GLN - ILE - PHE - VAL - LYS -*
THR - LEU - THR - GLY - LYS -*
THR - ILE - THR - LEU - GLU - VAL - GLU -(PRO)- SER - ASP -
THR - ILE -(GLU)- ASN - VAL -(LYS)-*
ALA - LYS -*
ILE - GLN - ASP - LYS -*
GLU - GLY - ILE - PRO - PRO - ASP - GLN - GLN - ARG -*
LEU - ILE - PHE - ALA - GLY - LYS -*
GLN - LEU - GLU - ASP - GLY - ARG -*
THR - LEU -(SER)- ASP - TYR - ASN - ILE - GLN - LYS -*
GLU - SER - THR - LEU - HIS - LEU - VAL - LEU - ARG -*
LEU - ARG -*
GLY - GLY

Expected points of cleavage by trypsin indicated by *

Residues for which variants have been reported are indicated as follows -(PRO)-

Fig. 1. Sequence of Amino-acid Residues in Ubiquitin with expected points of cleavage by trypsin indicated.

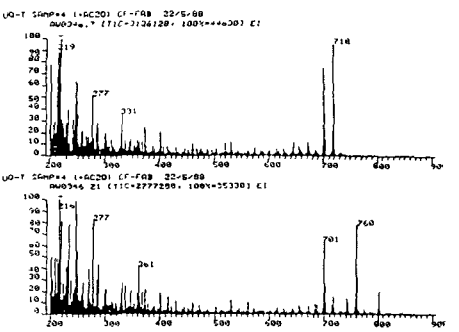

Fig. 2. CF-FAB spectra of Fragment 7 of tryptic digest of Ubiquitin without (upper) and with (lower) addition of acetic anhydride.

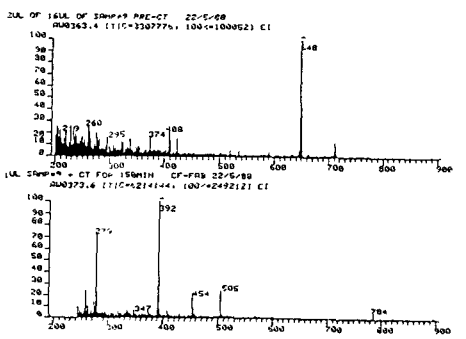

Fig. 3. CF-FAB spectra of Fragment 6 of tryptic digest of Ubiquitin before (upper) and after (lower) further digestion by chymotrypsin.

Presented at the 36th ASMS Conference on Mass Spectrometry and Allied Topics
June 5-10, 1988, San Francisco, CA

ANALYSIS OF PERMETHYL-OLIGOSACCHARIDES BY CONTINUOUS-FLOW FAB-MS AND BY COUPLING LC-MS WITH CONTINUOUS-FLOW FAB AS INTERFACE

Bernard FOURNET,* Yves LEROY,* Guy RICART,§ and Jean MONTREUIL*
*Laboratoire de Chimie Biologique de l'Université des Sciences et Techniques de Lille Flandres-Artois (UA du CNRS No 217), 59655 Villeneuve d'Ascq Cedex, France; §Laboratoire de Spectrométrie de Masse de l'Université des Sciences et Techniques de Lille Flandres-Artois, 59655 Villeneuve d'Ascq Cedex, France

Conventional positive fast atom bombardment (FAB) and continuous-flow FAB analysis were carried out with permethylated lacto-N-tetraose. This latter method, a new approach, has been used to analyse a mixture of permethylated oligosaccharides by liquid chromatography-mass spectrometry (LC-MS) with a packed capillary fused-silica column and the continuous-flow probe as interface. Under these conditions, we found the continuous-flow probe to be superior to the conventional probe because its low matrix level increased the signal-to-noise ratio. The analysis of the mixture of permethylated oligosaccharide alditols obtained from hen ovomucoid by LC-MS using the continuous-flow probe as interface is described.

EXPERIMENTAL

Mass spectrometer. A Kratos MS 50 RF equipped with a DS 90 data system was used in these studies. The mass spectrometer was operated at a 8 keV accelerating potential. An Ion Tech fast atom source was used with xenon (7.3 kV, 1.2 mA). For classical FAB analysis, permethylated lacto-N-tetraose dissolved in methanol was introduced with a Rheodyne Model 7520 injection valve. The solvent, methanol:thioglycerol:water, (90:10:5, v/v/v) was delivered by a Brownlee syringe pump operated at 5 µl/min. The continuous-flow probe is described in Ref.(1). For the analysis of the permethylated lacto-N-tetraose, the mass range 1000 to 200 was scanned at 10 s/decade with a mass resolution of 3000. For the LC-MS analysis of the permethylated oligosaccharide alditols from ovomucoid, the mass range 3200 to 900 was scanned at 10 s/decade with a mass resolution of 3000.

Micro-LC with a packed fused-silica column. The microdelivery system consists of a Brownlee syringe pump equipped with a 60-nl Valco injection valve. The analysis of permethylated oligosaccharides from hen ovomucoid (4.5 µg) was performed on a fused-silica micro-LC column (250 X 0.32 mm) packed with 5 µm RoSil C 18D (RSL/Alltech). the flow rate was 5 µl/min. The column was connected directly to the capillary of the continuous-flow probe. The elution was carried out with the following gradient: 80% of solvent A (methanol:thioglycerol:water, 90:10:5, v/v/v) and 20% of solvent B (thioglycerol:water, 10:90, v/v) to 100% of solvent A in 20 min followed by isocratic conditions for 1 h.

RESULTS AND DISCUSSION

Positive FAB analysis of permethylated lacto-N-tetraose clearly shows that for detection of $(MH)^+$ in permethylated LNT, continuous-flow FAB is 1.5 times more sensitive with 0.1 µg and 3.4 times more sensitive with 1µg than conventional FAB. The quality of the separation by micro-LC coupled to FAB-MS (Fig.1) is illustrated by the very slight deformation of peaks due to the suitability of the probe and the good separation of a mixture of permethylated oligosaccharide alditols from hen ovomucoid and characterizes oligosaccharides 1, 7, 11, and 14 (2). In Fig. 2, we give the LC-MS continuous-flow FAB mass spectra of oligosaccharides 7 and 14.
These first results obtained by using the packed capillary LC-FAB-MS with continuous-flow probe as interface are very promissing. indeed, the good resolution of a packed capillary column allows the analysis of microquantities of very complex mixtures of oligosaccharides (less than 200 ng per peak) with a suitable intensity of molecular ion.

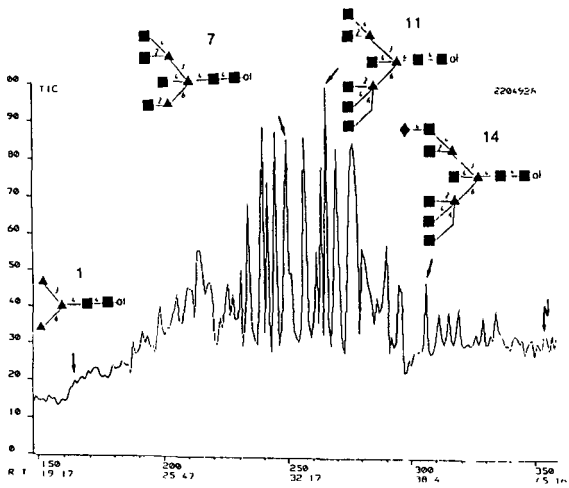

Fig. 1. Total ionic current of the permethylated oligosaccharides from hen ovomucoid on a packed fused-silica capillary column. Oligosaccharides 1, 7, 11, and 14 are localized and their structures are shown. (■) GlcNAc, (▲) Man, (♦) Gal.

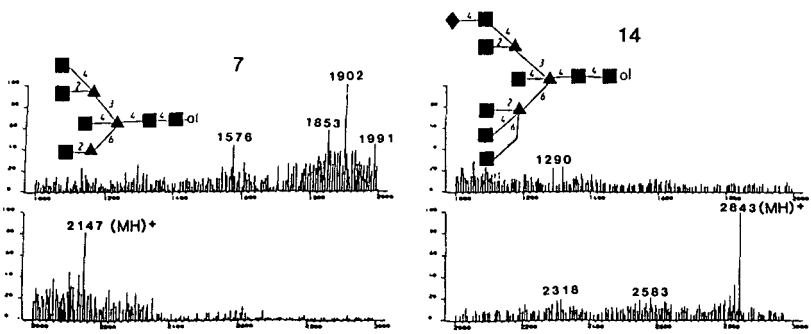

Fig. 2. Positive FAB mass spectra of oligosaccharides 7 $(MH)^+$ m/z 2147 and 14 $(MH)^+$ m/z 2843.

REFERENCES

1. Caprioli, R.M., Fan, T., and Cottrell, J.S. (1986) Anal. Chem. **58**, 2949-2954.

2. Paz-Parente, J., Strecker, G., Leroy, Y., Montreuil, J., Fournet, B., van Halbeek, H., Dorland, L., and Vliegenthart, J.F.G. (1983) FEBS Lett. **152**, 145-152.

Presented at the 36th ASMS Conference on Mass Spectrometry and Allied Topics
June 5-10, 1988, San Francisco, CA

TANDEM MASS SPECTROMETRY OF BIOMOLECULES BY USING CONTINUOUS FLOW FAB.

R.L. Cerny, R.N. Hayes and M.L. Gross, Midwest Center for Mass Spectrometry Dept. of Chemistry, University of Nebraska, Lincon, NE 68588

One problem encountered in using FAB has been the generally poor sensitivities obtainable as compared to those achieved for samples amenable to EI. A major contribution to this problem has been the level of chemical noise due to the matrix background. Another characteristic of FAB is the short-lived ion currents obtained when small amounts of sample are used. This can be problematic when FAB is used in conjunction with tandem mass spectrometry (MS/MS).

Continuous flow FAB[1] reduces the amount of background chemical noise present and thus leads to increased sensitivity for the molecular species. In addition, continuous introduction of the analyte leads to steady production of these ions for long periods of time. As in conventional FAB, however, few structurally informative fragments are produced. FAB combined with tandem mass spectrometry has been shown to be a powerful tool in the structure elucidation of biomolecules such as peptides and oligonucleotides. CF FAB and MS/MS are now combined to exploit the advantages of the individual methods. Of major interest are the importance of factors such as reduced chemical background and the continuous sample introduction to success of the MS/MS experiment.

For MS/MS studies, it is desirable to produce stable ion current for long periods of time for the species of interest. This allows improved S/N through either signal averaging or long scan times with high filtering. In these experiments the mass is known; the most important aspect is the ion yield for a given amount of material. A comparison of the ion currents for the $(M + H)^+$ species produced from 10 ng of Leu-Enkephalin by the direct probe method and by CF FAB is shown in Fig. 1.

For the direct probe experiments, 1 µl of a 10 ng/µl solution of the peptide in methanol was placed on the probe with 1 ul of DTE/DTT matrix. The CF-FAB experiments used a solution of 5% DTE/DTT in water with .1% TFA added. The analyte was present at a level where 10 ng would be delivered to the probe over 6 min at a flow rate of 3 µl/min.

As expected, the initial ion production in the probe experiment is higher. This tails off as the sample is depleted. In the CF FAB experiments a lower but more stable ion production is observed. The integrated ion current is greater for the probe experiment than for CF FAB; it is likely that conditions are not yet optimized for the CF FAB experiments. These preliminary results, however, hold promise for increased ion production by using CF-FAB.

For higher mw peptides we have observed > an order of magnitude increase in sensitivity in MS/MS experiments incorporating CF FAB (see Fig. 2). As shown in this example, a characteristic spectrum of Gramicidin S can be obtained for as little as 200 p mole of the peptide with CF FAB.

The reduction of chemical interferences is most important when studying a low abundance species in the presence of others with much greater abundance. Such a situation arises when using naturally occuring isotopic abundances as sources of "labeling experiments" in mechanistic studies. This practice is common with EI and CI ionization but not with FAB.

In the MS/MS spectra of cationized peptides, the most abundant fragment involves the C-terminus amino acid. Two different mechanisms can be postulated which include the loss of either O and NH_2 or 2 O. This could be resolved by MS/MS of the ^{18}O containing species. Background interferences preclude this experiment using conventional FAB (see Fig. 3). CF FAB produces much less interference.

Presented at the 36th ASMS Conference on Mass Spectrometry and Allied Topics
June 5-10, 1988, San Francisco, CA

Shown in Fig. 4 is the MS/MS spectrum in the mass range of the fragmentation under study. For the monoisotopic species (^{16}O containing) a singlet is observed of m/z 82. The MS/MS spectrum of the ^{18}O-containing isotope consists of a doublet of m/z 82 and 84. The peptide studied contains three oxygens; if the mechanism involves loss of 2 oxygens the ratio of 82:84 should be 2:1 - if only 1 oxygen is lost the ratio should be 1:2.

Although the S/N is low; it is evident that the observed ratio favors the mechanism which involves elimination of only one oxygen.

1 R.M. Caprioli, T. Fan, J.S. Cottrell Anal. Chem., **58**, 2949 (1986).

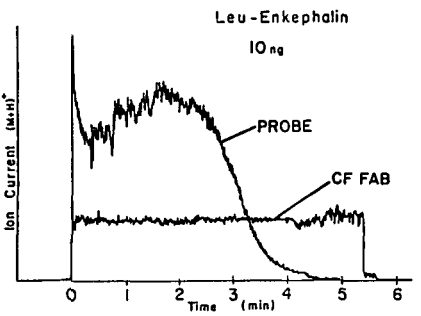

FIGURE 1

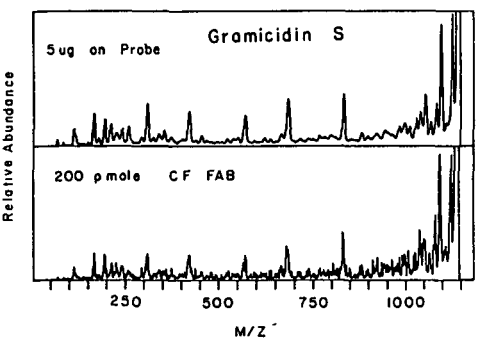

FIGURE 2

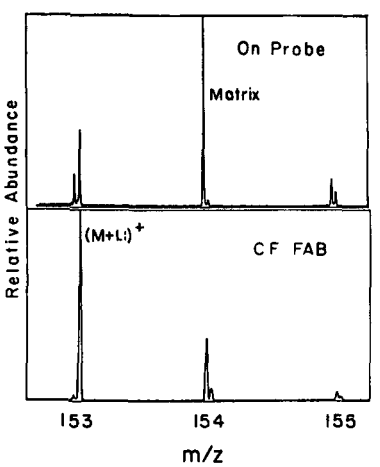

FIGURE 3

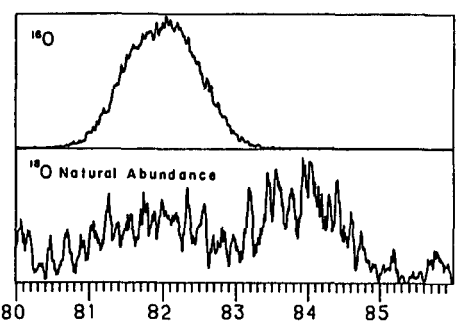

FIGURE 4

Presented at the 36th ASMS Conference on Mass Spectrometry and Allied Topics
June 5-10, 1988, San Francisco, CA

QUANTITATIVE ANALYSIS OF POLAR COMPOUNDS BY CONTINUOUS FLOW FAB

S.P. Markey, T.-C.L. Wang, M. Shih, R. Boni, M. Duncan, S.-C. Yang
Laboratory of Clinical Science, NIMH, Bethesda, MD 20892 and
D.C. Bradford, Finnigan MAT, San Jose, CA 95134

Ease of analysis and achievement of accuracy in the quantification of polar biologicals can be realized best without chemical transformation. For example, the norepinephrine metabolite MHPG (3-methoxy-4-hydroxyphenylethylene glycol) is found as a sulfate ester, a glucuronide, or as the free compound in biological fluids. The high precision attainable within a laboratory using GC/MS to quantify MHPG after hydrolysis of the conjugates highlights the systematic discrepencies in the literature regarding interlaboratory differences for normal versus clinically different diagnostic groups. One means of addressing the accuracy issue is direct analysis of each conjugate by continuous flow-FAB (CF-FAB). In the process of testing a prototype Finnigan Bioprobe system on a triple quadrupole mass spectrometer, we have determined this system's general applicability to a variety of analytical problems.

Our system uses a pulse-dampened HPLC pump to deliver a 20% glycerol/-water solution to a 0.5 µL loop injector and then through 75 micron i.d. fused silica tubing into the ion source region through a flange on the side of the vacuum manifold. The fused silica tubing is guided through a temperature controlled aluminum cylinder in the ion source, from which a 3-6 mm portion protrudes to make contact with a standard static FAB probe tip. The liquid emerging from the fused silica wets the congruent surface of the copper FAB tip, and mechanical adjustment is monitored optically in order to maintain a stable film. Typically, with the chamber and source block at ambient temperature, a stable film is obtained at 5.5-6.5 µL/min. Important factors effecting stability and sensitivity include maintaining thermal contact to the fused silica near to the region of evaporative cooling; orientation of the probe tip relative to the capillary (Fig. 1); composition of the sample with regard to surface tension; and film thickness or flow rate (Fig. 2).

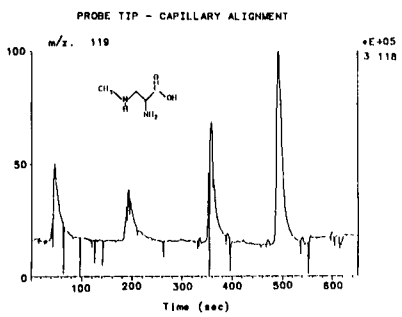

Fig. 1. Small rotational changes of the probe tip influence the flow of sample and the secondary ions, altering both peak shape and sensitivity as indicated by repetitive injections of BMAA.

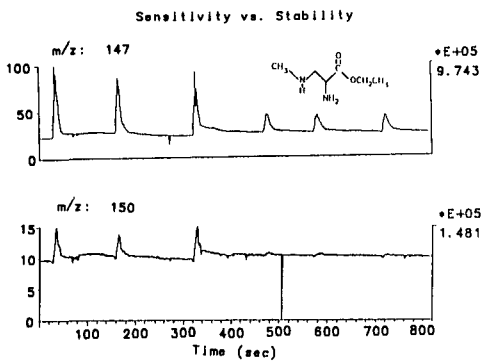

Fig. 2. Repetitive injections of BMAA-Et made while increasing glycerol-water flow rate from 6 to 6.5 µL/min show that higher sensitivity as indicated for m/z 147 (MH^+) is due to film instability evidenced by spurious baseline rise detected at m/z 150. At higher flow, signal at m/z 147 is less intense, but baseline at m/z 150 is stable.

Repeated injections (n = 10) of standards of 1-methyl-4-phenylpyridine (mw 170) and its $^2H_3$-isotopomer (mw 173) demonstrate the consistent reproducibility of the system (Fig. 3). The sample peaks were 50 sec wide at baseline, 15 sec wide at half-height, allowing sample introduction every 2 min. Routine chromatographic data processing was applied, including background subtraction and peak ratio analyses so that CF-FAB combines the benefits of liquid chromatography with the power of fast atom bombardment ionization even at low m/z. The mean ratio of m/z 170/173 integrated ion current peak areas was 0.3983 ± 0.002 S.D. with a range of 0.3955-0.4011.

Other examples to which we have applied CF-FAB include: quantitative tryptophan analysis from 5-500 ng; sensitive MHPG-sulfate detection in negative ion mode, (5 ng/sample); and the quantification of β-N-methylamino-alanine (BMAA) in plant extracts by CF-FAB MS/MS. For the latter problem, we compared the results of a capillary GC-selected ion assay of derivatized BMAA with a direct CF-FAB analysis of crude plant extracts. As expected, the CF-FAB-MS did not exhibit sufficient selectivity when ions at m/z 119 were monitored with respect to the $^2H_3$ isotopomer at m/z 122. Two steps were added to provide the requisite selectivity and sample concentration prior to CF-FAB MS/MS. Formation of BMAA-ethylester (mw 147) permitted acid-base extraction as well as concentration in chloroform prior to drying and dissolution in glycerol-water. Subsequently, excellent selective and quantitative results (Fig. 4) were obtained from plant extracts which contain BMAA (Cycas spp.) in contrast to those which do not (Macrozamia spp.) by monitoring alternately m/z 147 fragmenting to 44 and the $^2H_3$ isotopomer m/z 150 to 47.

Areas of active research in CF-FAB include focussing a cesium ion beam to maximize liquid-SIMS performance; improvement of liquid film stability by providing a better wetting mechanism; and design of an alternative and rugged probe assembly.

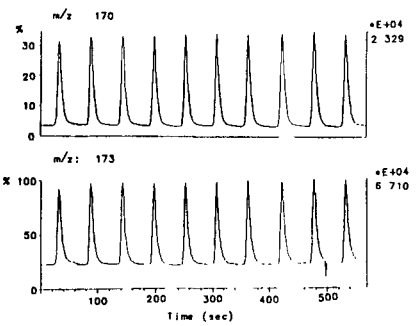

Fig. 3. Repetitive injections of MPP^+ and $^2H_3$-MPP mixtures indicate system stability for repeated measures.

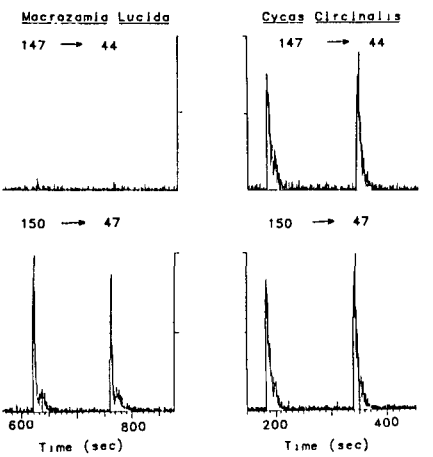

Fig. 4. CF-FAB MS/MS of plant extracts indicate the absence of BMAA-Et in Macrozamia relative to the amount detected in Cycas, both having been spiked with identical amounts of $^2H_3$-BMAA.

Presented at the 36th ASMS Conference on Mass Spectrometry and Allied Topics
June 5-10, 1988, San Francisco, CA

AN RRKM EXPLORATION OF WHETHER THE MCLAFFERTY REARRANGEMENT OF IONIZED N-BUTANAL IS STEPWISE OR CONCERTED: Lawrence L. Griffin,[a] David J. McAdoo[b] and Charles E. Hudson[b]
[a]Department of Marine Sciences, Texas A&M University at Galveston, Galveston, Texas 77553,
[b]Marine Biomedical Institute, University of Texas Medical Branch, Galveston, Texas 77550.

A long-standing issue in gas phase ion chemistry is whether the McLafferty rearrangement is stepwise or concerted [1]. Hydrogen/deuterium exchange accompanying this reaction at low energies has been taken to prove a stepwise mechanism [1,2]. A belief has since developed that reactions of ions in the gas phase are in general stepwise [3]. However, recent ab initio calculations by Ha and coworkers [3] gave a critical energy for concerted loss of ethene from ionized n-butanal (1) lower than that for loss of ethene from $^{\cdot}CH_2CH_2CH_2CH{=}OH^+$ (2), the intermediate in the stepwise process. They concluded that the reaction is concerted. Also, the critical energy calculated by Ha et al [4] for hydrogen exchange by $1 \rightleftharpoons 2$ is considerably lower than the barrier to decomposition by either concerted or stepwise processes. Therefore this hydrogen exchange might precede either stepwise or concerted decomposition. This reopens the issue of whether the McLafferty Rearrangement is stepwise or concerted. To further explore this, we carried out RRKM calculations (program of Bunker and Hass [5]) utilizing the potential surface of Ha et al. [4], and one modified based on our own ab initio calculations [6].

Our calculations indicated no reverse activation energy for $2 \rightarrow 3$, in contrast to those of Ha et al [4]. Their transition state was constrained to have a plane of symmetry; ours was not.

SPECIES	RATE CONSTANTS	RELATIVE ENERGIES (KCAL/MOL^{-1})	
		Ha et al. [4]	This work
$CH_2CH_2CH_2CHO^{+\cdot}$ (1)		0.0	0.0
$^{\cdot}CH_2CH_2CH_2CH{=}OH^+$ (2)		-3.6	-3.6
$CH_2{=}CH_2 + CH_2{=}CHOH^{+\cdot}$ (3)		16.9	16.9
TS($1 \rightarrow 2$) (B)	k_1, k_2	8.5	8.5
TS($2 \rightarrow 3$) (F)	k_3	37.6	16.9
TS($1 \rightarrow 3$) (H)	k_4	31.5	31.5
TS($2 \rightarrow 3$) (B,H)	k_5	37.6	

In most calculations vibrational frequencies were taken to be similar to those of the corresponding groups in other molecules. RRKM calculations utilizing harmonic frequencies for 1 obtained with Gaussian 86 [6] at the 3-21 level gave results only slightly different from ones obtained using estimated frequencies. The following table gives RRKM-calculated rate constants as a function of energy in the ion.

ENERGY	LOG(K1)	LOG(K2)	LOG(K3)		LOG(K4)	LOG(K5)
			Ha et al	This work		
8.6	7.37	5.55				
9.1	7.63	5.99				
16.6	9.18	7.91				
17.1	9.23	7.97		4.97		
17.6	9.29	8.04		5.39		
19.10	9.44	8.22		6.13		
31.1	10.25	9.18		8.44		
31.6	10.28	9.21		8.49	3.72	2.59
32.1	10.30	9.23		8.55	4.05	3.10
37.1	10.52	9.48		9.00	5.99	5.33
37.6	10.54	9.51		9.04	6.12	5.45
38.1	10.55	9.53	1.55	9.08	6.25	5.59
38.6	10.57	9.55	1.90	9.12	6.38	5.72
48.1	10.88	9.91	4.81	9.71	8.08	7.48
58.1	11.13	10.19	6.25	10.15	9.18	8.60

On the surface of Ha and coworkers [5], the calculated rates predict concerted decomposition (1 → H → 3 and 2 → B,H → 3) to be much faster than stepwise decomposition, and gamma hydrogen exchange to be much faster than either. Thus hydrogen exchange is not necessarily proof of a stepwise process. Assuming that 1 and 2 reach a steady state (a plausible assumption at long times) yields a relative concentration of 2 an order of magnitude greater than that of 1. Concerted 1 → 3 and 2 → 3 would be the dominant decompositions of Ha's surface. However, in our model 2 → 3 becomes orders of magnitude more frequent than concerted 1 → 3 and 2 → 3. We believe our model to be closer to reality, and hence conclude that the decomposition of 1 via the McLafferty rearrangement is stepwise.

1. J.S. Smith and F.W. McLafferty, Org. Mass Spectrom., 5 (1971) 483.
2. For references, see D.J. McAdoo, Org. Mass Spectrom. 23 (1988) 350.
3. D.J. McAdoo and C.E. Hudson, Int. J. Mass Spectrom. Ion Processes, 62 (1984) 269.
4. T.-K. Ha, C. Radloff and M.T. Nguyen, J. Phys. Chem. 90 (1986) 2991.
5. W.K. Hase and D.L. Bunker, Quantum Chemistry Program Exchange, No. 234, Chemistry Department, Bloomington, IN.
6. H. Frisch, J.S. Binkley, H.B. Schlegal, K. Raghavachari, R. Martin, J.P. Stewart, F. Bobrowiscz, D. Defrees, R. Seeger, R. Whiteside, D. Fox, E. Fluder and J.A. Pople, Gaussian 86, Release C, Carnegie Mellon University.

Presented at the 36th ASMS Conference on Mass Spectrometry and Allied Topics
June 5-10, 1988, San Francisco, CA

COMPETING REACTIONS OF THE ACETONE CATION-RADICAL, RRKM-QET CALCULATIONS ON AN *AB INITIO* POTENTIAL ENERGY SURFACE

Chava Lifshitz and Frank Louage
Department of Physical Chemistry and
The Fritz Haber Center for Molecular Dynamics
The Hebrew University of Jerusalem, Jerusalem 91904, Israel

and

Nikolaus Heinrich and Helmut Schwarz
Department of Chemistry
Technical University, D-1000 Berlin 12, W. Germany

We have employed, for the first time in RRKM-QET calculations, sets of reactant and transition state frequencies as well as energetics based on *ab initio* calculations of a reaction potential energy profile The reaction system involves two parallel dissociations of the acetone cation radical

$$CH_3COCH_3^{+\cdot} \xrightarrow{(1)} CH_2CO^{+\cdot} + CH_4$$
$$CH_3COCH_3^{+\cdot} \xrightarrow{(2)} CH_3CO^{+} + CH_3$$

Ab initio calculations demonstrate the intermediate existence of a hydrogen-bridged $[CH_3CO^+/CH_3]$ complex for both reactions Assumptions made and data used in the RRKM calculations are as follows: 1) Dissociation takes place from the acetone cation radical potential well, i.e., the reactant, even if going through the H-bridged complex, has available to it the high density of states of the acetone well. 2) The energetics of the dissociations conform to those of the highest level *ab initio* calculations, MP3/6-31G(d,p)//6-31G(d) + ZPVE. 3) Reaction (1) can take place at its endothermic threshold by quantum-mechanical tunneling through the barrier. An unsymmetrical Eckart barrier has been assumed with tunneling taking place between the H-bridged complex and a ketene ion/methane complex. By invoking tunneling in the first unimolecular reaction channel (CH_4 elimination) we were able to reproduce several experimental observations: (a) Reaction channel (1) is the major channel for so-called "metastable ion" fragmentations in the microsecond lifetime range; (b) Channel (2) becomes the major reaction channel at high internal energies of the reactant ion. Photoionization efficiency (PIE) curves for the two competing channels calculated on the basis of RRKM-QET microcanonical rate coefficients k(E) reproduce experimental results[1] rather well (see Figure 1).

The reaction system is a quite general example in mass spectrometry for two parallel reaction paths with slightly different critical energies and different activation entropies. The special interest in this system is two-fold: The formation of a single intermediate through which both reaction paths proceed, and the possibility of tunneling through a barrier other than a centrifugal one.

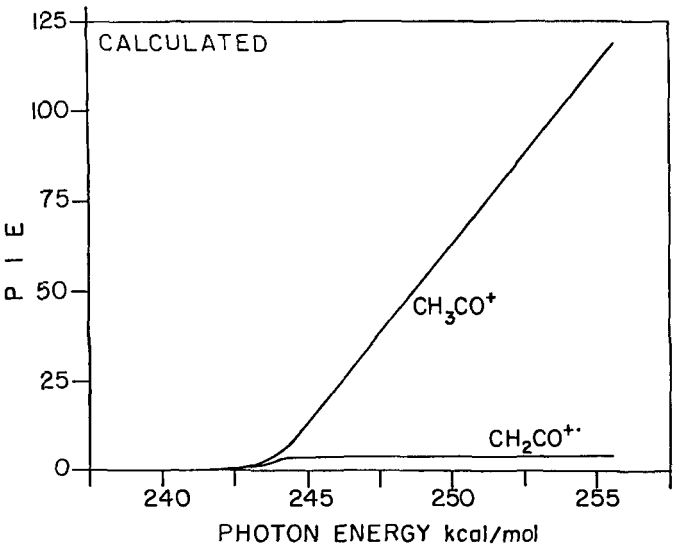

Figure 1

[1] J C Traeger, C.E. Hudson and D.J. McAdoo, J. Phys. Chem. 92 1519 (1988)

Presented at the 36th ASMS Conference on Mass Spectrometry and Allied Topics
June 5-10, 1988, San Francisco, CA

THE UNIMOLECULAR DISSOCIATION MECHANISM OF METHYLNITRITE

Qingmei Zha, R. N. Hayes, M. L. Gross and G. G. Meisels
Department of Chemistry, University of Nebraska-Lincoln
Lincoln NE 68588-0312

The fragmentation mechanism of methylnitrite ion has been the subject of considerable interest, especially with regard to the formation of the ion at 31 daltons. Gilman et al[1] investigated this process by TPEPICO and reported that the fragmentation of the parent ion at a constant internal energy produced ions at 30 and 31 daltons at greatly different rates, with that for the production of the latter ion much too slow to be accounted for by single-state statistical theories (RRKM/QET). They suggested therefore that this ion was formed by a state-specific channel. They also suggested that the ion at 31 daltons might be CH_3O^+. Burgers and Holmes[2] measured kinetic energy release accompanying metastable ion formation in methylnitrite, and concluded that the ion at 31 daltons is CH_2OH^+ and is formed by a hidden hydrogen migration. Baer and Hass[3] attempted to account for the difference in rate constants of the formation of ions at 30 and 31 daltons by proposing that a stable isomeric structure $HNC(OH)_2^+$ is formed prior to dissociation of the molecular ion at low internal energies. The product ion would also have the structure CH_2OH^+. The assumption of the intermediate, stable isomeric ion allowed statistical calculations to be brought into agreement with observations. However, Ferguson[4] noted that the formation of the proposed intermediate required the simultaneous breaking and re-making of five bonds and was therefore probably energetically not feasible.

We have reexamined the mechanism of methylnitrite dissociation using a triple-sector Kratos MS50TA tandem mass spectrometer by analyzing the isotopic composition of reaction products resulting from the metastable dissociation of CH_3ONO^+ and specifically labeled $CH_3{}^{18}ONO^+$. The latter was prepared from $CH_3{}^{18}OH$ and $NaNO_2{}^1$.

The major peaks in the metastable mass spectrum of CH_3ONO (Figure 1) are at 60 (CH_2ONO^+), 31 (CH_3O^+ or CH_2OH^+), 30 (NO^+) and 29 (HCO^+) daltons. A precursor ion spectrum of HCO^+ indicates that its predominant precursor is the ion at 31 daltons. The ratio of the peaks at 31 and 29 daltons, respectively, is about 14:1.

If a long lived intermediate of structure $HNC(OH)_2^+$ were the only precursor of the ion at 31 daltons, one would expect that the two oxygen atoms would be equivalent and that either the labeled or unlabeled oxygen would be lost with equal probability, and the peak at 31 daltons in the unlabeled methylnitrite should split into ions at 31

Presented at the 36th ASMS Conference on Mass Spectrometry and Allied Topics
June 5-10, 1988, San Francisco, CA

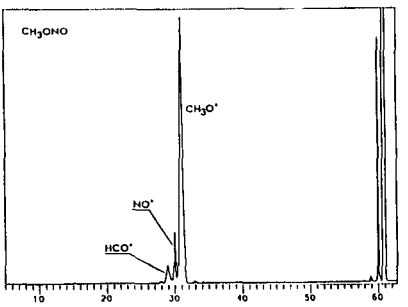

Figure 1.

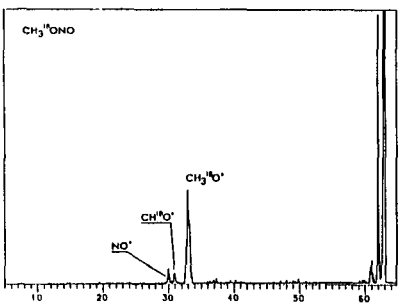

Figure 2.

and 33 daltons with approximately equal intensities. Similarly, the peak at 29 daltons in the unlabeled compound should lead to ions at 29 and 31 daltons in approximately equal intensities.

The metastable mass spectrum of $CH_3{}^{18}ONO$ (Figure 2) does not show such behavior. The peak at 29 daltons in CH_3ONO essentially disappears and is presumably shifted to 31 daltons. The new peak at 33 daltons becomes the major peak (other than for unchanged NO^+); the ratio of the peaks at 33 and 31 daltons is about 10:1. After correction for the contribution of $CH_3{}^{18}O^+$ to the peak at 31 daltons, not more than 6 % of the CH_3O^+ peak could have been formed via an intermediate structure in which the two oxygen atoms are equivalent. This suggests strongly that there is very little if any scrambling and certainly that in the dominant dissociation process the two oxygen atoms have not become equivalent.

We note here also that the formation of 31 daltons occurs only over a very narrow range of about 0.5 eV[1]. Hence, the ion is not formed with more than 0.5 eV excess internal energy above ionization threshold. Since a MIKE investigation has reported the kinetic energy release to be measured to be 0.3 eV[2], kinetic energy release would be about 60 % if the nascent fragment ion had the CH_3O^+ structure. Direct dissociation without participation of internal modes would predict a kinetic energy release of 68 %. This would be consistent with a similarly high proportion of excess energy appearing as kinetic energy reported in the dissociation of dimethyl ether[5].

REFERENCES

1. Gilman, J. P.; Hsien, T. and Meisels, G. G. J. Chem. Phys. **78**, 3767 (1983).
2. Burgers, P. C. and Holmes, J. L. Org. Mass Spectrom. **19**, 452 (1984).
3. Baer, T. and Hass. J. R. J. Phys. Chem. **90**, 451 (1986).
4. Ferguson, E. E. Chem. Phys. Let. **138**, 450 (1987).
5. Nishimura, T.; Das, P. R.; Zha, Q. and Meisels, G. G. to be published.

Presented at the 36th ASMS Conference on Mass Spectrometry and Allied Topics
June 5-10, 1988, San Francisco, CA

SELECTIVITY IN THE REACTIONS OF ANIONS WITH DIMETHYLDISULFIDE

Joseph J. Grabowski and Lijian Zhang
Department of Chemistry, Harvard University
Cambridge, MA 02138

The importance of sulfur, demonstrated by the existence of a vast literature, is due to the variety of valence states for sulfur and sulfur's widespread occurrence in chemistry, in biology, in industry, in agriculture and in air pollution among others. It appeared to us that a gas phase ion-molecule investigation into the intrinsic chemistry displayed by unsolvated, uncomplexed anions reacting with unsolvated, unaggregated reduced sulfur systems would make an important contribution to efforts to thoroughly understand the chemistry of sulfur in all its applications. In the study reported here, we have allowed a series of anions to react with dimethyldisulfide in the gas phase, under thermally-equilibrated (300K) reaction conditions. The results presented below were obtained utilizing the flowing afterglow technique, in 0.3 Torr of helium buffer gas.

A sample branching ratio plot for the reaction of H_2N^- with CH_3SSCH_3 is shown in the first figure below, while the data from repeated measurements is summarized in eq 1.

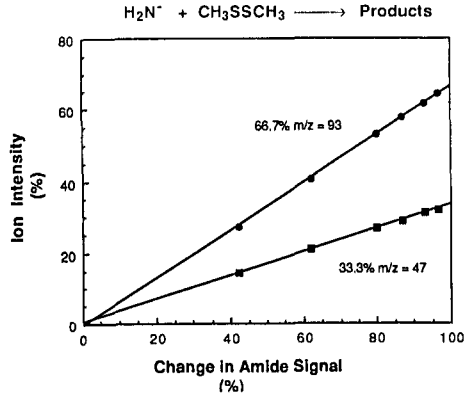

$$H_2N^- + CH_3SSCH_3 \longrightarrow 34\%\ CH_3S^- + [CH_5NS] \quad (1a)$$
m/z = 16 m/z = 47

$$H_2N^- + CH_3SSCH_3 \longrightarrow 66\%\ (C_2H_5S_2)^- + NH_3 \quad (1b)$$
m/z = 16 m/z = 93

While there can be no doubt as to the structure of the ion at m/z = 47 or the chemical composition of the ion at m/z = 93, the structure of the latter ion is not obvious from this one experiment. Based on an extensive series of experiments that examined the chemical reactivity of the m/z = 93 ion synthesized by amide (and by other reagent ions with dimethyldisulfide) and compared to the reactivity of model anions of known chemical structure, we were able to show that the m/z = 93 ion has the thiolate ion structure, $CH_3SCH_2S^-$. The data from a number of analogous reactions are summarized in the Table.

Presented at the 36th ASMS Conference on Mass Spectrometry and Allied Topics
June 5-10, 1988, San Francisco, CA

$HA^- + CH_3SSCH_3 \longrightarrow$

PA (kcal/mole)	HA^-	CH_3SA^-	CH_3S^-	$CH_3SCH_2S^-$
356 4	$CH_2NO_2^-$	100%	0%	0%
369 1	$H_3C\text{-}\overset{O^-}{\overset{\vert}{C}}{=}CH_2$	82%	18%	0%
373 9	CH_2CN^-	75%	25%	0%
379 8		0%	99%	1%
390 7	$H_2C{=}CH\text{-}CH_2^-$	0%	94%	6%
403 6	H_2N^-	34%	0%	66%
390 7	HO^-	36%	7%	57%
380 6	CH_3O^-	13%	11%	76%

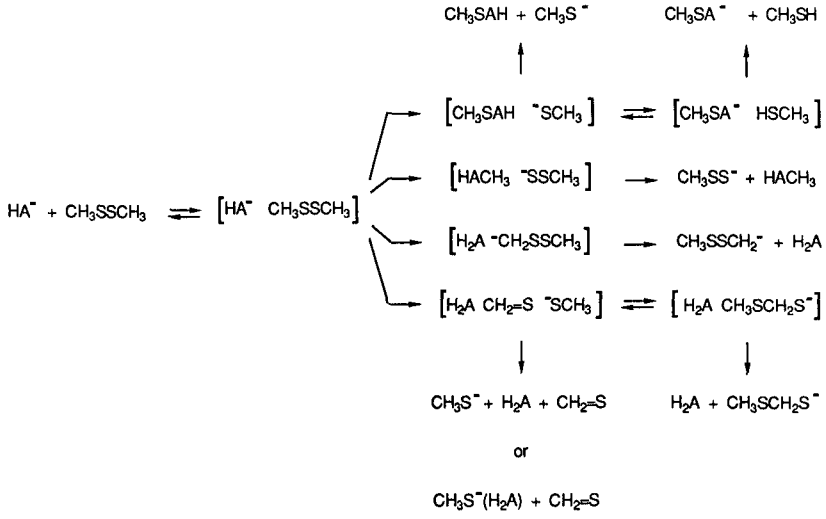

In general, we find that anions react with dimethyldisulfide either by displacement at sulfur or by elimination across a carbon sulfur bond. Anions which can be described as being localized in nature appear to react principally (if not exclusive) by elimination (bottom pathway of general scheme) while anions that are best described as being delocalized react almost entirely by displacement at sulfur (top pathway of general scheme). The reaction pathway selected for any particular ion appears to depend solely on the structure of the ion and not the energetics (e.g., compare reactivity of hydroxide and allyl anions; both reactions proceed at near the collision efficiency). Displacement at carbon to yield the disulfide anion and proton abstraction to yield the stable conjugate base of dimethyldisulfide was not observed for any anion examined.

Presented at the 36th ASMS Conference on Mass Spectrometry and Allied Topics
June 5-10, 1988, San Francisco, CA

Ion-Molecule Reactions of Ethyl Vinyl Ether With Various Oxygen-Containing Cations in a Triple Quadrupole Mass Spectrometer and a Quadrupole Ion Trap

H.I. Kenttämaa and R.G. Cooks
Purdue University
West Lafayette, IN 47907

Gas-phase reactions of ethyl and methyl vinyl ether with different oxygen containing cations were examined by employing a triple quadrupole tandem mass spectrometer, and a quadrupole ion trap capable of tandem experiments. A product ion which formally corresponds to exchange of a proton of the reactant ion to a vinyl group (loss of ethanol/methanol from the ion-molecule complex with ethyl vinyl ether/methyl vinyl ether) is of special interest. An abundant vinylation product was obtained in both instruments for ions which contain a protonated carbonyl group and a hydroxy group in close proximity (e.g., 1 and 2; 3 to a minor extent). The reaction seems to be specific to this combination of oxygen-containing functional groups; no vinylation product was observed for various protonated ethers, epoxides, aldehydes, ketones, esters and lactones studied.

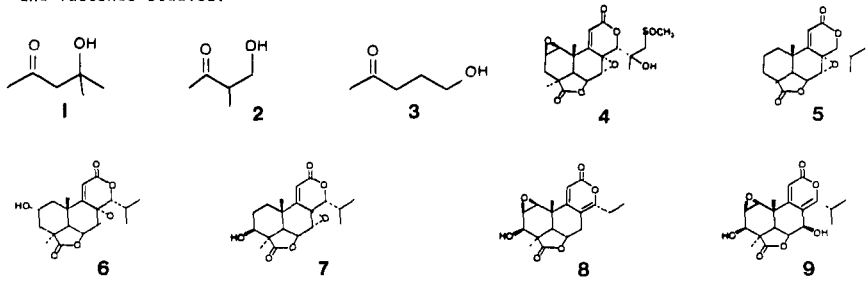

The general behavior described above applies to complex polyfunctional molecules, as well. After protonation, the molecules 4-9 were allowed to collide with ethyl vinyl ether in the center quadrupole of the triple quadrupole mass spectrometer. While an abundant vinylated molecule was observed for 7-8 which have a hydroxy group close to the lactone ring, protonated 4-6 do not give the corresponding product ion (Figure 1).

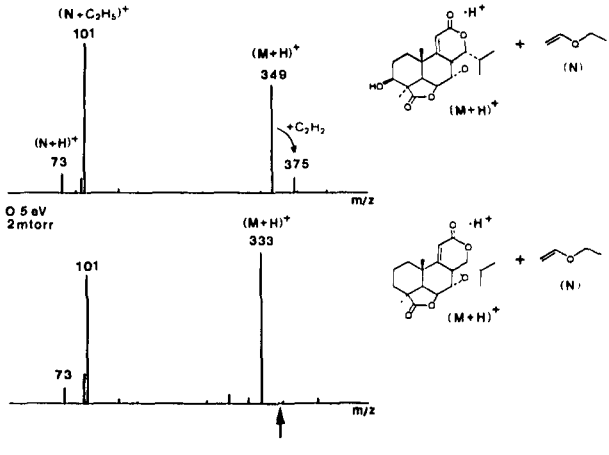

Figure 1

Studies employing various ionic reagents indicate that the reactant ion is the protonated carbonyl compound and not the protonated ether. The yield of the reaction (Figure 2) appears to be first order with respect to ethyl vinyl ether at pressures below 2 mtorr in the triple quadrupole mass spectrometer. The reactions of simple ions as well as complex polyfunctional ions show a negative kinetic energy dependence which indicates that the reaction is exothermic, and that it has no significant energy barriers in the cases studied.

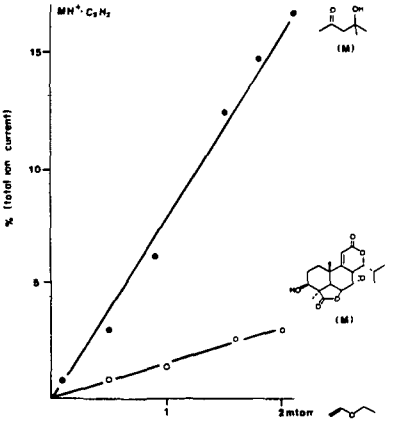

Figure 2

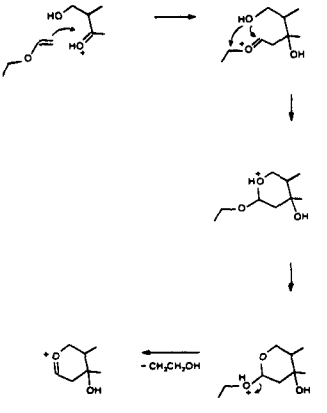

Figure 3

A mechanism unified with the experimental results is presented in Figure 3. Results obtained by deuterium labelling experiments, and MS/MS/MS employing collision-activated dissociation of the product ion (major loss of acetaldehyde) in the ion trap provide support for the proposed product ion structure.

Presented at the 36th ASMS Conference on Mass Spectrometry and Allied Topics
June 5-10, 1988, San Francisco, CA

THE STRUCTURE OF IONIZED n-PROPANOL PRECEDING THE LOSS OF WATER

Qingmei Zha and G. G. Meisels
Department of Chemistry University of Nebraska-Lincoln Lincoln NE 68588
T. Nishimura
Control Spectroscopy Development The Upjohn Co. Kalamazoo MI 49001

The unimolecular dissociation of energy-selected normal propanol ion was investigated by photoelectron photoion coincidence (TPEPICO) mass spectrometry. Asymmetric time-of-flight (TOF) distributions were observed for the formation of cyclopropane ion resulting from the loss of H_2O. The observed rate constants were about 10^6 s^{-1} at threshold.

There are two possible isomeric structures of ionized n-propanol. Holmes et al[1] concluded that the distonic radical cation ($\cdot CH_2CH_2CH_2OH_2^+$) is the proper reacting configuration for dissociation leading to the loss of H_2O at low internal energies. The heat of formation for this structure was determined to be 714 ± 5 kJ mol^{-1}, 17 kJ mol^{-1} lower than that of the molecular ion. Shao, Baer et al[2] suggested that the stable isomeric structure is the ion-dipole complex ($c\text{-}C_3H_6^{+\cdot}\text{---}OH_2$), and that the heat of formation of this complex can be taken to be the same as that of the distonic radical.

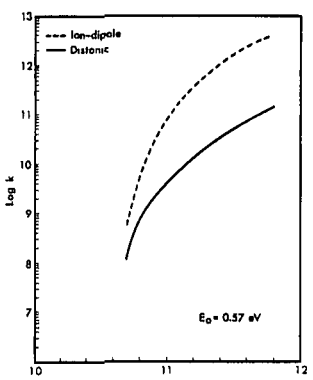

Fig. 1.

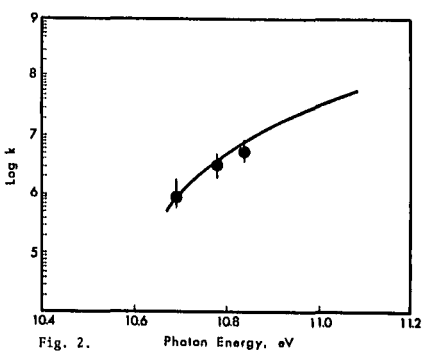

Fig. 2.

The results of RRKM/QET rate calculations are shown in Fig. 1. The calculated rate constants for ion-dipole assumption are of the magnitude of 10^9 s^{-1}, much higher than observed experimentally. This is also higher than the calculated rate constants of an order based on the distonic radical as the assumed intermediate.

However, the latter calculation still leads to calculated rates higher than those

observed. A modification of the calculation was attempted by multiplying the vibrational frequencies of the reactant by a reactant frequency factor R ($R < 1$). The result is shown in Fig. 2, where factor R was taken as 0.7 at the same activation energy of 0.57 eV.

The relationship between R and the minimum rate constant k_{min} at threshold can be derived from the rate expression:

$$\frac{[k_{min}]_o}{[k_{min}]_r} = \frac{[N(E_o)]_r}{[N(E_o)]_o} \approx \frac{1}{R^v}$$

where subscripts o and r represent the situations without and with adopting R factor, $N(E_o)$ is the density of states of reactant with energy between critical energy E_o and E_o+dE, and v is the number of independent oscillators for a given reactant.

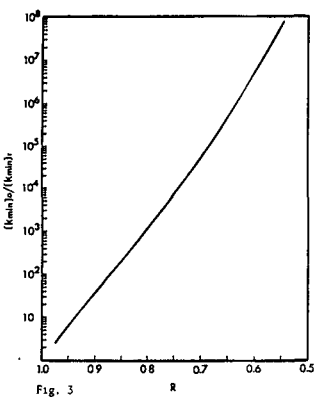

Fig. 3

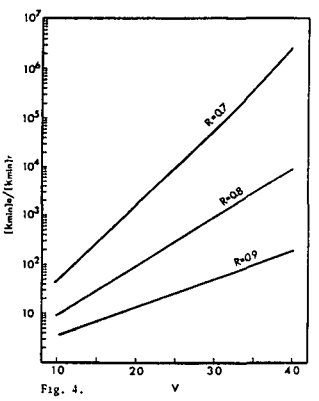

Fig. 4.

Fig. 3 shows the ratio of $[k_{min}]_o$ / $[k_{min}]_r$ vs. R for n-propanol ion in which v is 30. When R is taken as 0.7, k_{min} is reduced by about 10^4. This corresponds to an increase in the state density of the reacting ion as shown in the above equation. The relationship between the ratio of $[k_{min}]_o$ / $[k_{min}]_r$ and molecular complexity is shown in Fig. 4 where R is fixed while the variable is the number of independent oscillators v. The ratio of $[k_{min}]_o$ / $[k_{min}]_r$ increases greatly for large number of v, i.e. big molecules. The need for the reduction of vibrational frequencies may reflect the involvement of an isomerization process in the unimolecular dissociation.

REFERENCES

1. Holmes, J. L.; Mommers, A. A.; Szulejko, J. E. and Terlouw, J. K. J. Chem. Phys. Soc. Chem. Commum. 165 (1984).
2. Shao, J.-D.; Baer, T.; Morrow, J. C. and Fraser-Monteir, M. L. J. Chem. Phys. **87**, 5242 (1987).

Presented at the 36th ASMS Conference on Mass Spectrometry and Allied Topics
June 5-10, 1988, San Francisco, CA

SEPARATION OF PHOTOOXIDATION PRODUCTS OF TOLUENE BY MEDIUM RESOLUTION ATMOSPHERIC PRESSURE IONIZATION MASS SPECTROMETRY

Andrew H. Grange, Oregon Graduate Center, Beaverton, OR 97006
Robert J. O'Brien, Portland State University, Portland, OR 97207
Douglas F. Barofsky, Oregon State University, Corvallis, OR 97331

Atmospheric photooxidation of toluene, an important industrial solvent and a major component of gasoline, contributes to the severity of smog episodes. Recent studies have utilized GC/MS, CI tandem MS, or atmospheric pressure ionization (API) MS to identify photooxidation products of toluene generated in simulated atmospheres. The resolution provided by the quadrupole mass filters used was insufficient to distinguish between ring fragmentation products differing in composition by a -C=O vs a -CH2CH2- group. Identities of several products remain uncertain.

Of the aforementioned mass spectrometric techniques, only APIMS has sufficient sensitivity to detect photooxidation products generated in simulated atmospheres without prior separation or concentration steps, which have altered products in past studies. To analyze these products directly and to enhance resolution we built a corona discharge, API source for a VG 7070E-HF double focusing mass spectrometer.[1,2] Operating with a resolution of 2,800 (m/z 101, <1% valley, 1/6 maximum transmission) multiple peaks were resolved at numerous nominal masses. Three species were resolved at both m/z 97 and m/z 99 (Figure 1). The different kinetic behavior of each peak allows them to be distinguished as photoproducts and two types of background components.

Table 1 lists experimentally determined masses for these peaks and the computed masses for molecular formulae containing C, H, O, or N that are chemically reasonable and whose exact masses agree to within two standard deviations (peak a3 is the lone exception to the latter criterion). The errors associated with experimental masses of peaks a1, b1, and b3 are nearly small enough to establish the elemental compositions of the corresponding ions without invoking supplementary information. For peaks a2 and b2 the first molecular formulae listed are most likely since compounds containing N are inconsistent with the known photochemistry of toluene. The products identified in other studies listed in the right column have the molecular formulae determined in our study.

In normal operation, a small potential is applied across the differentially pumped region in the API source to maximize the signal from molecular ions by dehydrating molecular ions associated with water molecules. Figure 2 illustrates an additional use of the CID potential to clarify the structure of the compound producing the principal peak at m/z 103. Both 1,4-butenedial and hydroxy-3-oxobutanal have been identified as toluene photooxidation products in past studies. This peak could arise from protonated hydroxy-3-oxobutanal or from protonated, monohydrated 1,4-butenedial. A modest increase in the CID potential, insufficient to induce significant fragmentation of molecular ions, (row three) substantially diminished the principal peak at m/z 103, while the peaks due to non-hydrated ions at m/z 99 showed little change. Hence, the majority of this peak's ion abundance is due to the hydrated ion.

[1] Grange, A.H.; O'Brien, R.J.; Barofsky, D.F. Rev. of Sci. Instrum. 1988, 59, 573-579.
[2] Grange, A.H.; O'Brien, R.J.; Barofsky, D.F. Rev. of Sci. Instrum. 1988, 59, 656-658.

Presented at the 36th ASMS Conference on Mass Spectrometry and Allied Topics
June 5-10, 1988, San Francisco, CA

MASS SPECTRAL DATA FOR SPECIES OBSERVED AT m/z 97 AND m/z 99

TABLE 1.

Peak	Experimental Mass, mu ± mu/ppm	Possible Composition (exact mass)		Deviation, mu/ppm	Possible Structure of Analyte (formula)
a1	97.0290 ± 0.0020/20.6	$C_5H_5O_2^+$	(97.0290)	-0.00005/0.5	furfural ($C_5H_4O_2$)
a2	97.0564 ± 0.0113/116 4	$C_6H_9O^+$	(97.0653)	+0.0089/92.1	5-oxo-1,3-hexadiene (C_6H_8O)
		$C_5H_7NO^+$	(97.0528)	-0.0036/37.4	
a3	97.0968 ± 0.0024/24.7	$C_7H_{13}^+$	(97.1017)	+0.0049/50.7	
		$C_6H_{11}N^+$	(97.0892)	-0.0077/78.8	
b1	99.0079 ± 0.0020/20 2	$C_4H_3O_3^+$	(99.0082)	+0.00032/3.2	maleic anhydride ($C_4H_2O_3$)
b2	99.0447 ± 0.0014/14.1	$C_5H_7O_2^+$	(99.0446)	-0.00010/1.0	4-oxo-2-pentenal ($C_5H_6O_2$)
		$C_3H_5N_3O^+$	(99.0433)	-0.0014/14.6	3,4-dioxo-1-pentene ($C_5H_6O_2$)
b3	99.0797 ± 0.0042/42 4	$C_6H_{11}O^+$	(99.0810)	+0.0013/13.1	

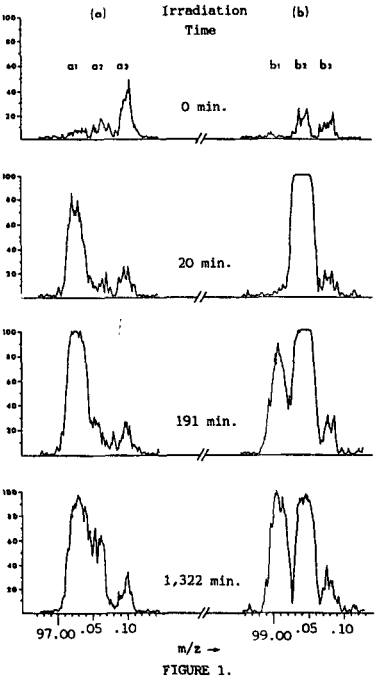

FIGURE 1.

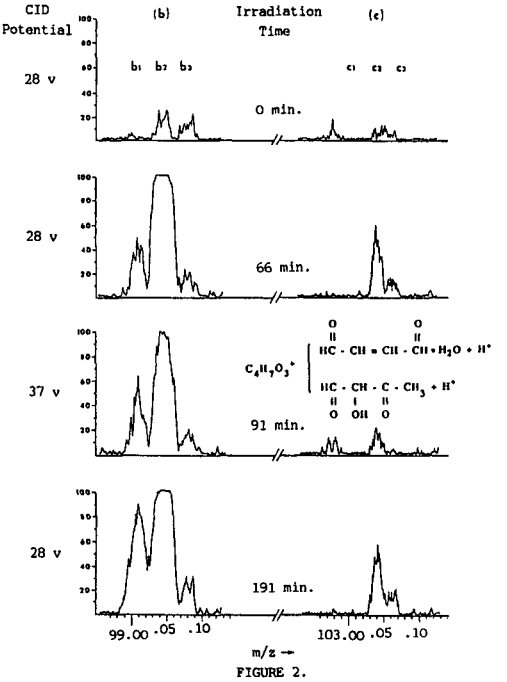

FIGURE 2.

Presented at the 36th ASMS Conference on Mass Spectrometry and Allied Topics
June 5-10, 1988, San Francisco, CA

FAST ATOM BOMBARDMENT MASS SPECTROMETRY AS A PROBE FOR THE ANALYSIS OF SHORT LIVED REACTION INTERMEDIATES

Larry M. Mallis[1] and William J. Scott

[1]High Resolution Mass Spectrometry Facility
and Department of Chemistry
The University of Iowa
Iowa City, Iowa 52242

A growing body of synthetic methodology has been developed in the last two to three decades which involves the use of stoichiometric or catalytic amounts of transition metals to mediate carbon-carbon bond forming reactions. In this paper, we report on a palladium catalyzed coupling reaction of 4-*tert*-butyl-cyclohexenyl triflate with vinyltributylstannane in the presence of tetrakis(triphenylphosphine)palladium(0) [$Pd(PPh_3)_4$] and lithium chloride to give 1-vinyl-4-*tert*-butylcyclohexene. While there is precedent in the literature for each step of the mechanism for this reaction there remains no direct evidence for the formation of many of the postulated palladium(II) intermediates.[2]

Recently, Daves and co-workers showed that fast atom bombardment mass spectrometry (FAB-MS) could be used to probe the short lived intermediates involved in the Pd(II) catalyzed olefination of organomercury compounds.[3] Thus, to better understand the mechanism of the Pd(0) catalyzed coupling reactions with electrophiles the reaction was performed on a standard FAB probe tip.

A suitable FAB matrix for this reaction had to be inert with respect to the components of the reaction mixture yet be able to aid in ionization of the reaction intermediates being studied. Triethanolamine was the only matrix compound tried that produced PdL_n^+ ions while inhibiting the decomposition product ions $Pd_nL_n^+$ observed for all other matrix compounds.

The first step of the catalytic reaction is an oxidative addition of tert-butylcyclohexene to $Pd(0)L_n$ in the presence of LiCl to form an organoPd(II) chloride species (Figure 1). An ion at m/z 958 is observed in the catalytic reaction and assigned as organoPdL_2Cl·LiOTf, an intermediate in the oxidative addition process (see Figure 3). In addition, an ion at m/z 767, shown under stoichiometric conditions to be organoPdL_2, was observed in the catalytic process. It is interesting to note that an ion at m/z 399 corresponding to $RPPh_3$ was observed only in the presence of palladium. Further studies to elucidate the mechanism of the transmetallation step are currently under way.

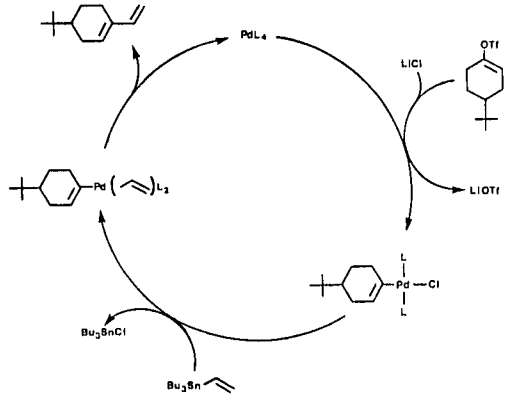

Figure 1. Schematic representation of the palladium catalyzed reaction pathway. Although the mechanism is generally accepted, reaction intermediates have not been fully elucidated.

[2]Scott, W. J.; Stille, J. K. *J. Am. Chem. Soc.* **1986**, *108*, 3033.
[3]Kalinoski, H. T.; Hacksell, U.; Barofsky, D. F.; Barofsky, E.; Daves, G. D., Jr. *J. Am. Chem. Soc.* **1985**, *107*, 6476.

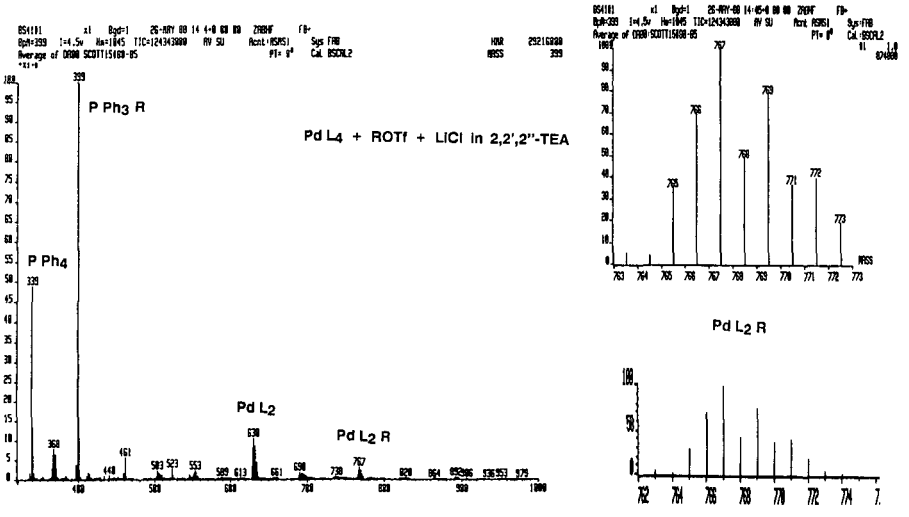

Figure 2. (A) FAB spectrum resulting from the mixture of PdL_4, ROTf and LiCl in a THF/TEA solution. The ion at m/z 767 is assigned as the product of oxidative addition to form an organoPdL_2 species. This is the first major intermediate formed in the catalytic process.
(B) Observed (top) and calculated isotopic distribution for ion cluster at m/z 767.

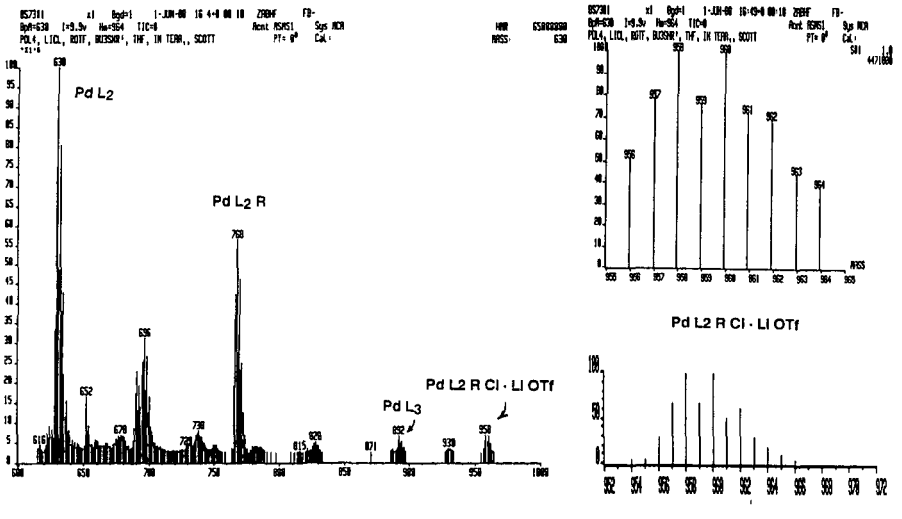

Figure 3. (A) FAB spectrum resulting from the mixture of PdL_4, ROTf, LiCl and Bu_3SnR'in a THF/TEA solution. The ion at m/z 958 is assigned as the primary intermediate of the oxidative addition to form the organoPdL_2 species (m/z 767). (B) Observed (top) and calculated isotopic distribution for ion cluster at m/z 958.

Presented at the 36th ASMS Conference on Mass Spectrometry and Allied Topics
June 5-10, 1988, San Francisco, CA

CLUSTER IONS AS A PROBE FOR BIMOLECULAR SUBSTITUTION REACTIONS UNDER SIMS CONDITIONS--CHOLINES--

Mamoru Ohashi, Takashi Iino, and Takeshi Tani
Department of Applied Physics and Chemistry, The University of Electro-Communications, Chofu, Tokyo 182 Japan

Recently particle bombardment-induced reactions in a matrix under SIMS conditions attract considerable attention. Because of the widespread use of desorption ionization methods, it must be essential to clarify the scope and limitation of those reactions. This paper deals with the particle bombardment-induced intermolecular reactions of choline and acetylcholine halides under SIMS conditions. Structures of the reaction products contained in cluster ions were characterized by means of linked scannings at constant B/E and B^2/E.

As an example, dry SIMS and liquid SIMS(glycerol matrix) spectra of choline bromide(C^+(a) Br^-) are shown in Fig. 1A and 1B, respectively. In Fig. 1A the peak corresponding to transmethylation product at m/z 118 is prominent and the linked scanning at B/E constant showed its daughter ions at m/z 90, 74, 60, 59, 58, and 42, which clearly indicated its structure as the transmethylation product $MeOCH_2CH_2\overset{+}{N}Me_3$(b). On the other hand, Fig. 1B exhibits many cluster ions whose structures were characterized as (C^++nM, where M=C^+X^-); m/z 104, (287 and 289), (470, 472 and 474), (653, 655, 657 and 659): (b)+nM; m/z 118, (301 and 303): $Me_3\overset{+}{N}CH_2CH_2O^-$ (c) $Me_3\overset{+}{N}CH_2CH_2OH$ +nM; m/z 207, (390 and 392), (573, 575 and 577): $^-BrCH_2CH_2\overset{+}{N}Me_3$(d)+nM; m/z(166 and 168), (349, 351 and 353), (532, 534, 536 and 538), (715, etc.). Comparison of these two spectra lead us to conclude that transmethylation is more favorable under dry conditions than in glycerol, and that the brominated compound was detected only in glycerol. In the cases of choline chloride, transmethylation occurs in a similar tendency, but the chlorinated cation corresponding to (d) was not detected even in glycerol. Cluster ions of (a),(b) and (c) were also observed on liquid SIMS of choline chloride but not on dry SIMS.

On the liquid SIMS spectra of acetylcholine halides(C^+X^- X=Cl, Br, I) the following cluster ions were characterized in commom with the use of linked scannings; in the case of chloride: C^+(e)+nM; m/z 146, 327, 508, 689 and 872: $HOCH_2CH_2\overset{+}{N}Me_3$(a)+nM; m/z 104, 285, 446, 647 and 830: $CH_2{=}CH\overset{+}{N}Me_3$(f)+nM; m/z 267, 448, 629 and 813. While on the dry SIMS spectra of acetylcholine chloride, a transmethylation product(g, m/z 160) but not (f) was observed. In the case of benzoylcholine iodide, a series of peaks due to C^+ +nG(G; glycerol molecule, MW 92), m/z 208, 300, 392, 484, 576, 668, 760, 852 and 944, have been observed besides the C^++nM(m/z 208, 543, 878).

In summary, ions indicating the following reaction products of choline and acetylcholine halides have been recognized under liquid SIMS conditions;

1) $2HOCH_2CH_2N^+Me_3$(a) ⟶ $MeOCH_2CH_2N^+Me_3$(b) + $HOCH_2CH_2NMe_2$

2) $HOCH_2CH_2N^+Me_3\ X^-$ ⟶ $^-OCH_2CH_2N^+Me_3$(c) + HX

3) $HOCH_2CH_2N^+Me_3\ Br^-$ ⟶ $BrCH_2CH_2N^+Me_3$(d)

4) $AcOCH_2CH_2N^+Me_3$(e) ⟶ $CH_2{=}CHN^+Me_3$(f) + AcOH

5) $2AcOCH_2CH_2N^+Me_3\ X^-$ ⟶ ($CH_2{=}C(OMe)OCH_2CH_2N^+Me_3$(g)) + $AcOCH_2CH_2NMe_2$

6) $AcOCH_2CH_2N^+Me_3$ ⟶ $HOCH_2CH_2N^+Me_3$

Presented at the 36th ASMS Conference on Mass Spectrometry and Allied Topics
June 5-10, 1988, San Francisco, CA

Although all processes from the molecular cations(C^+) to fragment ions(F^+) were confirmed by linked scan techniques, no metastable transitions from (C^++nM) to (F^++nM) in the first field free region have been observed except for reaction 2. This means that transmethylation occurs mainly in the liquid phase but scarcely in the cluster ion forms in the vapor phase. Commercial samples of choline halides we used turned out to contain a small amount of $HOCH_2CH_2OCH_2CH_2\overset{+}{N}Me_3$ cation whose structure has been confirmed by liquid SIMS linked scannings.

Figure 1. SIMS spectra of choline bromide, 1A; dry SIMS, 1B; liquid SIMS(glycerol).

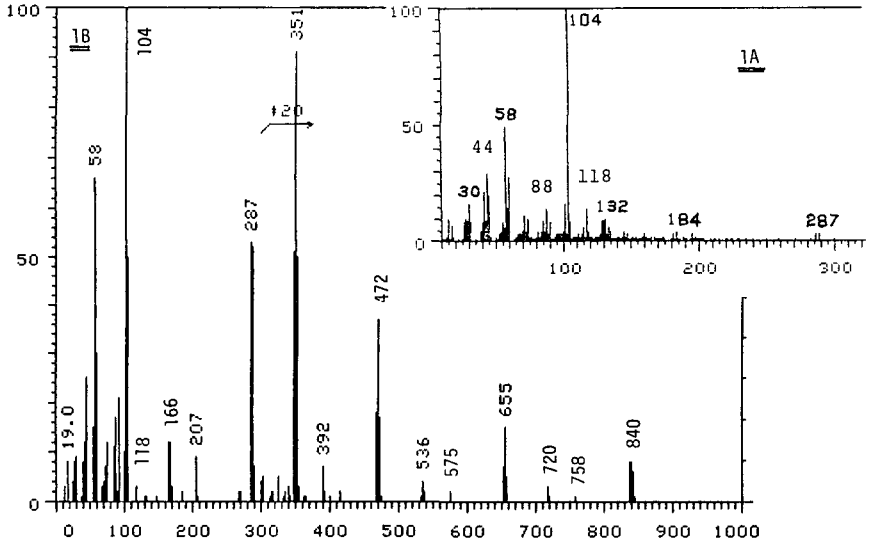

Figure 2. SIMS spectra of choline chloride, 2A; dry SIMS, 2B: liquid SIMS(glycerol).

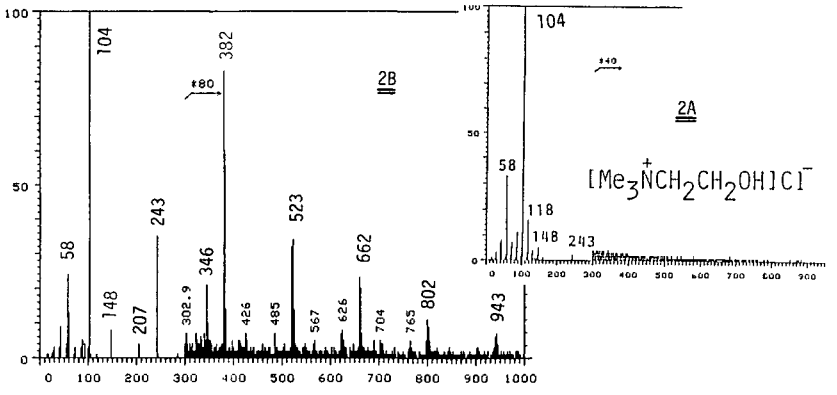

Presented at the 36th ASMS Conference on Mass Spectrometry and Allied Topics
June 5-10, 1988, San Francisco, CA

Mass Spectrometric Measurement of Isotopic Oxygen Abundances Occurring within Transient Products Generated from Hot $^{18}O(^3P)$ Atom Reactions with Formaldehyde

Richard A. Ferrieri and Alfred P. Wolf

Brookhaven National Laboratory, Department of Chemistry,
Upton, New York 11973.

Our recent interest in the reactions of translationally hot ground-state (^3P) oxygen atoms with aldehydes, and other related compounds, stems from the realization that high temperature OH radical formation from such systems remains as one of the fundamental aspects of oxygen atom chemistry not clearly understood.(1) However, the major role these processes play in the many facets of today's growing technology, such as in combustion, laser chemistry, rocket propulsion, atmospheric chemistry and in space materials research, creates practical problems that require solutions as well.

Within the last two years, we have developed a novel oxygen atom source that is well-suited for conducting high energy chemical studies of this nature.(2) This source relies on kilovolt atomic ion sputtering for the generation of macroscopic concentrations of oxygen atoms sputtered from appropriate metal oxide targets through one or more mechanisms.(3) By virtue of the nature of this sputtering mechanism, some degree of control can be affected over the state and energy of the sputtered atom. For example, low mass-medium energy (<100 KeV) atomic ion sputtering of a Ta_2O_5 target yields a clean source of neutral ground-state oxygen atoms that possess a distribution of translational energies centered about 6 eV. This behavior was shown to be characteristic of a sputtering mechanism dominated by linear collision cascades where nuclear stopping of the impinging ion beam was important. However, these characteristics could have been altered by promoting a different mechanism through retuning the impinging ion beam to a different mass and energy, or by selecting a different target material that exhibited different surface binding properties.

Surrounding the above source was a high vacuum chamber that permitted the controlled introduction of substrate gases over a broad range of pressures. Also attached to this chamber in an orientation 90° to the axis of the impinging ion beam was a differentially pumped quadrupole mass spectrometer equipped with an electron impact ionizer and electron multiplier detector. This system enabled the measurement of both transient and stable products that could be related to primary reactions involving the hot atom and the substrate molecule. In operating this detector, background signals from the substrate gas were minimized by modulating the oxygen atom source through chopping the incident ion beam. A difference in the product ion signal was then measured from this modulation sequence and was equated to reactive channel contributions and background beam scatter contributions within the chamber. The latter was removed through separate background calibrations.

Most recently, we investigated the reactions of hot $^{18}O(^3P)$ atoms with formaldehyde containing oxygen-16. Formaldehyde represents the smallest homolog of the aldehyde class. The isotopically enriched atomic source, generated by sputtering oxygen-18 from $Ta_2{}^{18}O_5$, enabled us to probe the mechanisms for OH radical formation through mass spectrometric measurement of the isotopic oxygen abundances in transient and stable products. Near-single collision conditions were achieved, in part by conducting the studies at 1×10^{-5} Torr, and in part by acquiring reactive ion signals on a 4 msec time basis.

It is generally accepted that abstraction of the weak aldehydic hydrogen atom of formaldehyde is the only important reaction at thermal energy.(4) Under these circumstances, we would expect no isotopic mixing to occur in the OH and HCO radical products.

Presented at the 36th ASMS Conference on Mass Spectrometry and Allied Topics
June 5-10, 1988, San Francisco, CA

$$^{18}O(^3P) + H_2C^{16}O \longrightarrow {}^{18}OH + HC^{16}O$$

However, atom attachment to the carbonyl double bond may be of sufficient importance to be seen as a reaction channel (5), if sufficient energy could be deposited within the newly formed triplet dioxymethylene intermediate to promote migration of a hydrogen atom across one of the two C-O bonds and yield triplet formic acid.

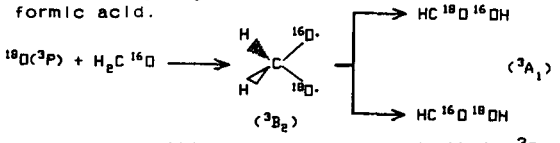

Although a recent ab initio study suggested that $^3B_2$ dioxymethylene isomerization to $^3A_1$ formic acid would require at least 30 kcal/mol (6), this energy restriction may not apply here.

Once formed, the excited acid will unimolecularly dissociate by one of several pathways--one in particular yielding HCO and OH radicals.(7)

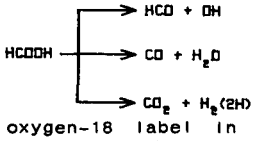

The distribution of the oxygen-18 label in these products would then reflect its' position in the excited acid.

Results from our mass spectrometric measurements showed that the intermediate migration pathway to OH formation was not only operative at these high kinetic energies, but also accounted for a major portion of those radicals detected. Similiar pathways have been proposed by us for this species formation when hot $O(^3P)$ atoms react with alkenes.(2b,8)

Research carried out at Brookhaven National Laboratory under contract with the U.S. Department of Energy and supported by its Office of Basic Energy Sciences.

References

1. (a) R.J. Cvetanovic and D.L. Singleton, "Reviews of Chemical Intermediates", 1984, 5, 183.
(b) R.J. Cvetanovic, "Adv. in Photochemistry", Interscience Publishers, John Wiley and Sons, New York, 1963, pp 117-149.

2. (a) R.A. Ferrieri, Y.Y. Chu and A.P. Wolf, NASA Workshop on Atomic Oxygen Effects [Proc.] Nov 10, 1986, 119, JPL Pub. 87-4.
(b) R.A. Ferrieri, Y.Y. Chu and A.P. Wolf, 13th Intern. Hot Atom Symp. [Proc.], Radio Chim. Acta. (in press).
(c) R.A. Ferrieri and Y.Y. Chu, "Ion Sputtering on Metal Oxides:A Source of Translationally Hot $O(^3P)$ Atoms for Chemical Studies Above 1 eV," Rev. Sci. Instru. (submitted).

3. R. Kelly and N.Q. Lam, Rad. Effects, 1973, 19, 39.

4. R.J. Cvetanovic, Can. J. Chem. 1956, 34, 775.

5. J.S. Chang and J.R. Barker, J. Phys. Chem., 1979, 83, 3059.

6. M. Dupuis and W.A. Lester, J. Chem. Phys. 1984, 80(9), 4193.

7. J.T. Herron and R.E. Huie, Int. J. Chem. Kinet., 1978, 10, 1019.

8. (a) R.A. Ferrieri, Y.Y. Chu and A.P. Wolf, "Hot $O(^3P)$ Atom Reactions with Trans and Cis Butenes," J. Phys. Chem. (submitted).
(b) R.A. Ferrieri, Y.Y. Chu and A.P. Wolf, "Regiospecific Addition of Hot $O(^3P)$ Atoms to Trans and Cis Butenes," J. PHys. Chem. (submitted).

Presented at the 36th ASMS Conference on Mass Spectrometry and Allied Topics
June 5-10, 1988, San Francisco, CA

CALCULATED ION STRUCTURES FOR SMALL COPPER- AND SILVER-CONTAINING IONS: COMPARISON WITH RESULTS FROM MS/MS EXPERIMENTS. R. A. Flurer and K. L. Busch; Department of Chemistry, Indiana University, Bloomington, Indiana 47405

Busch et al. [1] have recorded the daughter and parent ion MS/MS spectra of several small silver-containing ions formed from silver carboxylates. On the basis of the observed fragmentation pathways, it was concluded that certain of the fragment ions contained metal-metal bonds and others did not, based on the distribution of parent ions of the Ag_2^+ dimer ion. Specifically, it was concluded that $Ag_2CH_3^+$, Ag_2O^+, and Ag_2CO^+ probably contain metal-metal bonds to some degree, and that Ag_2H^+ does not.

DeKock et al. [2] have recently calculated the equilibrium geometries and fragmentation energies of the Ag_2H^+ and $Ag_2CH_3^+$ species using the Hartree-Fock-Slater method. They concluded that both of these species should have a bent geometry and contain metal-metal bonds. Gaspar and Tamassy-Lentei [3] have also investigated the Ag_2H^+ species using a simple pseudopotential method and have also predicted that this species should have a bent equilibrium geometry, but do not speculate on the presence or absence of a metal-metal bond. The present work applies the Hartree-Fock SCF method with effective core potentials to the calculation of the equilibrium geometries and dissociation energies of several copper- and silver-containing species observed in the electron ionization mass spectra of copper(II) propionate and silver propionate.

Calculations have been carried out for the following copper- and silver-containing species: Ag_2, AgH, Ag_2H^+, Ag_2O^+, AgO, $Ag_2CH_3^+$, Cu_2, CuH, and Cu_2H^+. Full geometry optimizations were carried out for all species at the Hartree-Fock SCF level of theory using relativistic effective core potentials for the silver-containing species and non-relativistic effective core potentials for the copper-containing species. For all species, the outer core orbitals on silver (4s and 4p) and copper (3s and 3p) were not included in the effective core potential, but were treated explicitly in the HF SCF calculations. The basis set used on copper consisted of a (5s5p/5s3p5d) basis contracted to [1s1p/3s2p3d], and for silver a (5s5p/5s3p4d) basis contracted to [1s1p/3s3p3d] was used. The basis sets for carbon and oxygen were STO4-31G*, and the basis set used for hydrogen was STO6-31G**. The calculated equilibrium geometries for all species studied are shown in Figure 1. The experimental geometries for the diatomic species are listed in parentheses for comparison.

The Ag_2H^+ and Cu_2H^+ species are predicted to be linear, and therefore not to contain metal-metal bonds, by calculation, which is consistent with the absence of these two species in the corresponding parent ion spectra of the metal dimer ion. In contrast, DeKock et al. predict the Ag_2H^+ species to have a bent geometry, and thus the possible presence of a metal-metal bond, which is not consistent with the fact that this species does not appear in the parent ion spectrum of the silver dimer ion. The authors cite several possible reasons for this discrepancy in their conclusions; however, none of them is really satisfying. The Ag_2O^+ species is also predicted to have a linear geometry, and therefore not to contain a metal-metal bond; however, this is not consistent with the presence of this ion in the parent ion spectrum of the silver dimer ion, which suggests that either this species has a much lower barrier for fragmentation to the dimer ion than do the Ag_2H^+ and Cu_2H^+ species or that the calculated results are not trustworthy for this particular species. However, the calculations do predict a significantly lower dissociation energy for the Ag_2O^+ species (28 kcal/mole) relative to the Ag_2H^+ (44 kcal/mole) and Cu_2H^+ (54 kcal/mole)species, a trend that is at least in agreement with the MS/MS results. These dissociation energies should not, however, be taken as quantitative due to the fact that electron correlation has not been included in the computations. The calculated geometries for the diatomic species AgO and CuH suggest that this computational method generally predicts bond lengths to be somewhat too long; this could probably be corrected to a large extent by including the effects of electron correlation in the computations by perturbation theory [4].

As shown in Figure 1, the $Ag_2CH_3^+$ species is predicted to have a bent Ag-C-Ag framework and thus a metal-metal bond to some degree, which is consistent with the presence of this species in the parent ion spectrum of the Ag_2^+ dimer ion. This is also consistent with the results of DeKock et al., which also predict a bent Ag-C-Ag framework with a Ag-C-Ag bond angle of 77 degrees. However, the present calculations predict a Ag-Ag distance that is 0.22 angstroms longer than that calculated by DeKock et al. This notwithstanding, it still seems possible that a metal-metal bond could be present in this species.

In summary, it can be stated that in general the Hartree-Fock method using effective core potentials provides geometric predictions for ionic species, which contain transition metal atoms, that are consistent with the results of MS/MS experiments. However, it appears that in some cases (the Ag_2O^+ species), transition state calculations that yield barrier heights for chemical processes, are necessary to obtain a full understanding of the gas-phase ion chemistry of transition metal containing species.

References

1. K.L. Busch, R.G. Cooks, R.A. Walton, and K.V. Wood, Inorg. Chem. 23, 4093, (1984).
2. R.L. DeKock, R.D. van Zee, and T. Ziegler, Inorg. Chem. 26, 563 (1987).
3. R. Gaspar and I. Tamassy-Lentei, Acta Phys. Acad. Sci. Hung. 50, 343 (1981).
4. R.L. Martin, J. Chem. Phys. 86, 5027 (1987).

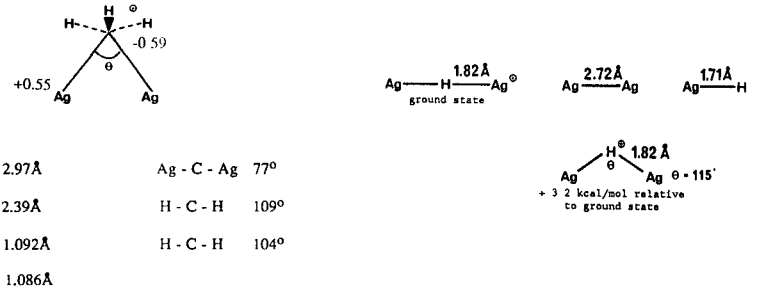

Figure 1

Presented at the 36th ASMS Conference on Mass Spectrometry and Allied Topics
June 5-10, 1988, San Francisco, CA

PLASMA DESORPTION MASS SPECTROMETRY OF SUCROSE POLYESTERS, T. Keough, M. Lacey, R. A. Sanders and D. R. Gardner, Winton Hill Technical Center, 6071 Center Hill Road, Cincinnati, OH 45224

Introduction: Molecular weight determination of large non-polar molecules is a continuing challenge of interest to lipid chemists. Techniques such as fast atom bombardment (FAB) and field desorption (FD) are most applicable to polar or ionic species. Non-polar lipids are ionized with low efficiency or not at all so that very little molecular weight information is obtained. The goal of this work was to investigate the applicability of plasma desorption mass spectrometry to molecular weight determination of non-polar lipids, especially sucrose polyesters.

A sucrose polyester structure is shown in Figure 1. When the C-C double bond is cis 9, this is sucrose octaoleate. Such sucrose polyesters have properties similar to triglycerides in food products. Mass spectral applications to sucrose polyesters include verification of identity and characterization of lower esters, such as hepta or hexaesters.

FAB and FD have been applied to sucrose polyesters with substantial success(1,2). FD of sucrose octaoleate produces a protonated molecule containing one C-13 as the most abundant ion in the molecular weight region. Though this was a significant breakthrough that allowed acquisition of mass spectra from sucrose polyesters for the first time, the approach was only applicable, for sensitivity reasons, to relatively simple, one or two component systems. And, the transient nature of the signal precluded observation over the wide mass range necessary for determining ester distributions. This latter problem was largely solved by using fast atom bombardment. In a DTT/DTE matrix, with approximately 1 ppm NaI, sucrose polyesters give interpretable FAB spectra in which Na adduct ions provide the required molecular weight information. Though S/N is no better, the persistent signal allows semi-quantitative ester distribution measurement and the use of MS/MS techniques. However, the sensitivity is such that large amounts of pure samples are required -- making it difficult to characterize isolates from HPLC. In particular, we were unable to obtain molecular weight information on minor components (suspected to be sucrose polyester dimers formed in heated samples) in the 4000-5000 molecular weight range as estimated from size-exclusion chromatography retention data.

Experimental: The plasma desorption (PD) data reported were obtained through the use of a Bio Ion 20 PD mass spectrometer. The nitrocellulose substrate was treated with NaI by evaporation from aqueous solution (10 uL of a 75 ug/mL solution). The 1-10 nmoles of sucrose polyester were deposited on the foil from solution in a 70/30 hexane/benzene mixture.

Results and Discussion: Figure 2 displays a PD spectrum of sucrose octalaurate (C12 fatty acid with no C-C double bonds). The parent + 23 peak at 1824 defines the molecular weight (nominal mass 1798 + 23 + 2 for H mass defect + 1 for C13) and the fragment at 893 corresponds to cleavage at the oxygen between the glucose and fructose rings. When a mixture of fatty acids is used and when hepta and hexaesters exist, a spectrum like the one shown in Figure 3 is obtained. The fatty acids are C16 and C18 with 0, 1 or 2 C-C double bonds. The peaks at approximately 2466, 2203 and 1940 daltons are parent + 23 for octa, hepta and hexaesters, respectively. Cleavage between the sucrose rings is observed as before -- peaks at approximately 1200 and 900 daltons corresponding to tetraester and triester, respectively. An expanded view of the molecular ion region of a similar mixture is shown in Figure 4. It is clear that the hexa, hepta and octaester peaks are split into components that differ in molecular weight due to the different numbers of carbons in the fatty acids. The highest mass octa component corresponds to eight C18 fatty acids; the next highest contains one C16 fatty acid, etc. Compared to FAB data on similar samples, PD suffers in terms of mass resolution. It is not possible to distinguish species which differ only in degree of unsaturation by PD. However, better S/N is achievable on lower levels (10 nmoles were required for this analysis) making it more applicable to HPLC and TLC isolates. Figure 5 shows the PD spectrum of a heptaester LC fraction from a sucrose polyester mixture very similar to the one analyzed above. The S/N is substantially better than that achievable by FAB and the sample preparation is more straightforward. The requirement of sample solubility in the FAB matrix was quite restrictive in the FAB approach; the PD approach only requires solubility in a non-chlorinated solvent (we found that chlorinated solvents disrupted the nitrocellulose surface).

Another advantage of the PD approach to sucrose polyester analysis parallels its advantage over FAB for high-mass, polar compounds. We have been able to obtain molecular weight information, for the first time, on dimeric sucrose polyester species isolated from heated samples by size-exclusion chromatography. Figure 6 shows the PD spectrum of this dimer. Peaks in the 2400 region are due to the monomer, which is not completely resolved by the chromatography. Components in the 4800 region are parent + 23 peaks for dimers. The peaks in the 3600 region are dimer fragments at the ring-joining oxygen, analogous to those fragments observed in the 1200 dalton region of the monomer.

Conclusion: Plasma desorption mass spectrometry offers the advantages of better high mass sensitivity as well as simpler and more universal sample preparation when compared to fast atom bombardment of sucrose polyesters. These come at the expense of mass resolution and accuracy. A combination of both techniques, applied in the appropriate circumstances, is recommended.

1) "Field Ionization/Desportion Mass Spectra of Sucrose Polyesters", R. A. Sanders, A. J. DeStefano, R. S. Ampulski and K. R. Compson, Presentation at 25th Annual Conference on Mass Spectrometry and Allied Topics, 1977, p. 57.

2) "Analysis of Food Lipids by Fast Atom Bombardment", T. Keough and R. A. Sanders, Presentation at 33rd Annual Conference on Mass Spectrometry and Allied Topics, 1985, p. 688.

Figure 1

Sucrose Octaoleate

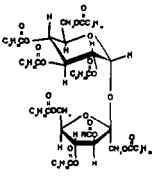

Figure 2

Plasma Desorption Mass Spectrum Of Sucrose Octalaurate

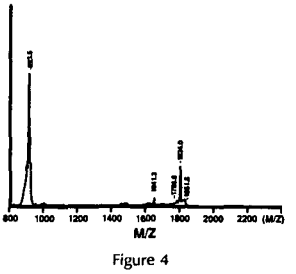

Figure 3

PDMS Of Sucrose Polyester Mixture

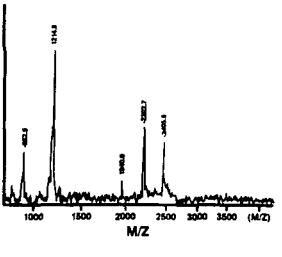

Figure 4

Molecular Ion Region Of Sucrose Polyester Mixture

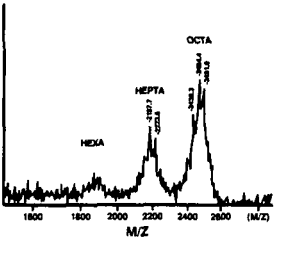

Figure 5

PDMS Of Heptaester Fraction

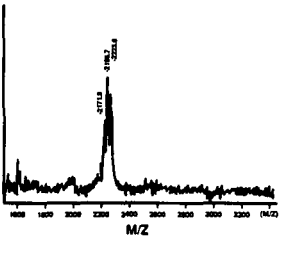

Figure 6

PDMS Of Sucrose Polyester Dimer

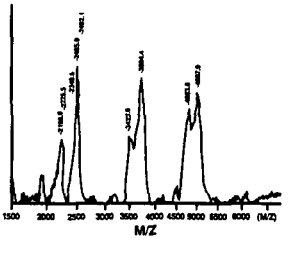

Presented at the 36th ASMS Conference on Mass Spectrometry and Allied Topics
June 5-10, 1988, San Francisco, CA

COMPARISON OF FAB WITH CI USING GLYCEROL AS A REAGENT GAS: K.L. Duffin and K.L. Busch; Department of Chemistry, Indiana University, Bloomington, IN, 47405.

Positive ion mass spectra generated by fast atom bombardment mass spectrometry using glycerol as a liquid matrix are compared to mass spectra recorded with chemical ionization using glycerol as a reagent gas. Comparison of mass spectra and daughter ion MS/MS spectra of protonated molecules suggest both similarities and differences in the mechanisms underlying these two ionization methods. In the first part of this study, FAB and CI mass spectra of leucine and glutamine are compared. When the glycerol vapor pressure is sufficiently high, CI mass spectra of these two compounds are very similar to the corresponding FAB mass spectra [Figure 1]. At these pressures, glycerol dimer ions are also present in the mass spectra. Adjustment of the reagent gas pressure to yield fragment and dimer ion abundances similar to those observed in FAB mass spectra provides a pressure reading of 2-5 Torr. However, even at these high CI gas pressures, glycerol cluster ions greater than n=2 are not observed. As expected, CI spectra also do not contain the chemical noise at every mass unit that is common in FAB mass spectra and has been attributed to radiation chemistry resulting from bombardment by the primary fast atom beam [1].

Energy-resolved daughter ion MS/MS spectra of the $(M+H)^+$ ethopropazine obtained at different CI gas pressures indicate that the relative abundances of the respective daughter ions depends dramatically on the source pressure at which the protonated molecule is initially formed and, to a much lesser extent, on the parent ion collision energy. At low CI reagent gas pressures (<0.5 Torr), daughter ions of protonated ethopropazine are produced in high abundance at m/z 100 and 214, corresponding to cleavage of a carbon-carbon bond [Figures 2 and 3]. However, at high CI reagent gas pressures (>2 Torr), daughter ion MS/MS spectra obtained at the same collision energy contain ions at m/z 114, 198, and 240, corresponding to cleavage of carbon-nitrogen bonds. Collisional stabilization at higher source pressures appears to make cleavage of a carbon-carbon bond inaccessible, whereas large internal energy deposition at low source pressures favors cleavage of the carbon-carbon bond to yield different daughter ions. Correlation of the daughter ion MS/MS spectra obtained by fast atom bombardment ionization from a glycerol matrix and by chemical ionization using glycerol reagent gas [Figure 3] independently confirms that fast atom bombardment ionization simulates high pressure chemical ionization. Daughter ion MS/MS spectra of protonated ethopropazine are also obtained using methane, ammonia, water, and triethanolamine as CI reagent gases, and thioglycerol and triethanolamine as FAB matrices. In general, small differences in the daughter ion MS/MS spectra can be correlated to differences in exothermicities of protonation of the various reagent and matrix compounds [2]. However, this effect is far outweighed by changes in source pressure. Deuterated ethopropazine obtained by using deuterated glycerol as a FAB matrix helped confirm daughter ion assignments. In conclusion, the occurrence of high pressure gas phase protonation reactions in FAB is confirmed, and further, it is shown that source conditions can have a dramatic effect on daughter ion MS/MS spectra.

1. F.H. Field, J. Phys. Chem., 86, 5115 (1982).
2. C.W. Tsang and A.G. Harrison, J. Amer. Chem. Soc., 98, 1301 (1976).

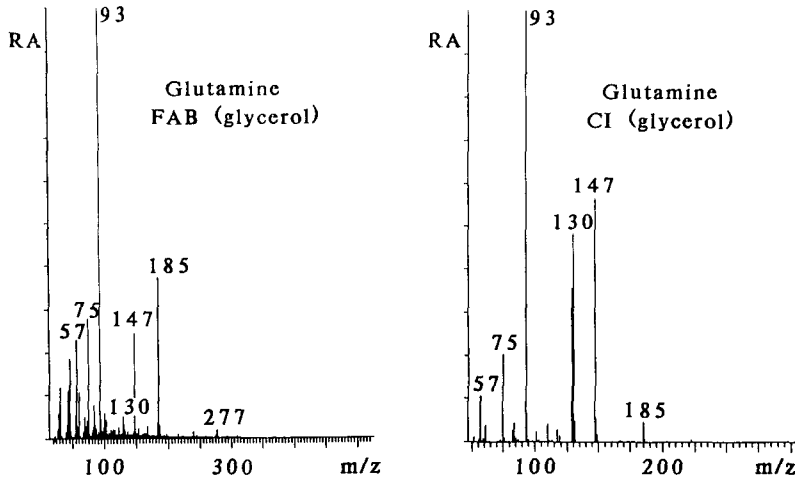

Figure 1

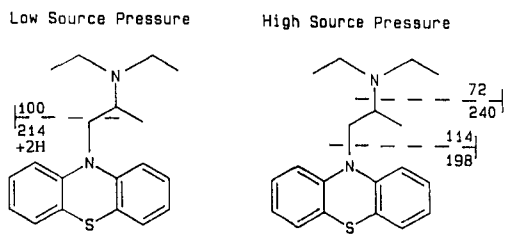

Figure 2

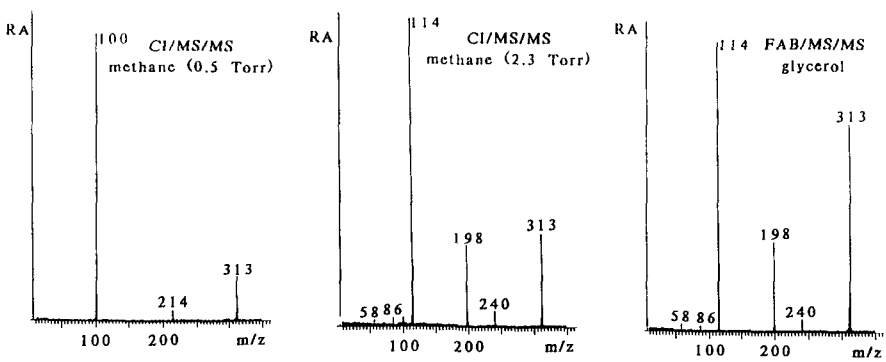

Figure 3

Presented at the 36th ASMS Conference on Mass Spectrometry and Allied Topics
June 5-10, 1988, San Francisco, CA

GAS-PHASE ION-MOLECULE AND SURFACE-CATALYZED OXIDATION REACTIONS OF PAH UNDER NEGATIVE ION CHEMICAL IONIZATION CONDITIONS*

M.V. Buchanan and E.A. Stemmler
Oak Ridge National Laboratory, Oak Ridge, TN 37831-6120

The negative ion chemical ionization (NICI) mass spectra of polycyclic aromatic hydrocarbons (PAH) often show unusual ions that can be used for isomeric differentiation. One such ion appears at $[M+14]^-$ in the spectra of PAH with an exposed methylene group, such as fluorene (1). Previous studies in this laboratory using deuterium labelled analogues, isotopically labelled buffer gases, Fourier transform mass spectrometry (FTMS), and MS/MS showed that the $[M+14]^-$ ion corresponds to $[M+O-2H]^-$, where oxygen substitution occurs at the 9-carbon and the anion structure resembles the molecular anion of 9-fluorenone (1).

One question regarding formation of the $[M+O-2H]^-$ ion that remained unanswered resulted from the inability to identify ionic precursors to this ion using swept double resonance (SDR) experiments on the FTMS. Additional experiments were conducted on a quadrupole instrument to determine the source of oxygen in the $[M+O-2H]^-$ ion. Fluorene was introduced through a gas chromatograph and oxygen containing reagents, including H_2O and O_2, were doped into the N_2 buffer gas. The addition of H_2O enhanced the $[M-H]^-$ ion from fluorene; however, $[M+O-2H]^-$ was enhanced by the addition of O_2. Experiments with ^{18}O-labelled O_2 verified that oxygen was being incorporated in the $[M+O-2H]^-$ ion; however, the degree of incorporation was lower than expected from the ^{18}O enrichment.

During the course of these studies, it was found that ion chromatograms corresponding to the $[M+O-2H]^-$ ion tailed relative to those observed for the $[M-H]^-$ ion (see Figure 1). It was also found that elevation of the ion source temperature increased the abundance of the $[M+O-2H]^-$ ion, and reduced the degree of chromatographic peak tailing exhibited by this ion (see Figure 2). In contrast, the peak shape for the $[M-H]^-$ ion showed no variation as a function of ion source temperature. Recent reports (2) have indicated that tailing ion chromatograms in NICI mass spectra are associated with solute-surface interactions in the ion source region that are followed by electron capture ionization. Our experiments indicate that the formation of 9-fluorenone from fluorene proceeds by a surface-catalyzed reaction with oxygen that occurs after fluorene elutes from the chromatographic column (see Scheme 1). Further results that support this conclusion come from experiments made under positive chemical ionization (PCI) conditions. The O_2/N_2 PCI mass spectrum of fluorene shows the expected ions at M^+ and $[M+H]^+$, which exhibit normal chromatographic peak shapes. Ions at $[M+14]^+$ and $[M-14]^+$ are also observed, and correspond to the M^+ and $[M-CO]^+$ from 9-fluorenone. Both of these ions exhibit tailing chromatographic peaks.

Additional studies were conducted to determine if similar reactions occur for other PAH, such as anthracene. In addition to the formation of M^-, anthracene was found to undergo various ion-molecule reactions in the presence of oxygenated compounds such as H_2O, N_2O and O_2. For example, $[M-2H]^-$ and $[M+O-H]^-$ were observed in the FTMS spectra of anthracene using N_2O, and were found to be linked to O^- by SDR experiments. In addition, SDR experiments indicated that ions corresponding to $[M-H]^-$ resulted from reactions with OH^-.

Using the quadrupole system, the $[M-H]^-$ from anthracene was enhanced by the addition of water to generate OH^-, and an ion at $[M+OH]^-$ was also

The submitted manuscript has been authored by a contractor of the U.S. Government under contract No. DE-AC05-84OR21400. Accordingly, the U.S. Government retains a nonexclusive, royalty-free license to publish or reproduce the published form of this contribution, or allow others to do so, for U.S. Government purposes.

observed. Upon addition of N_2O, the ion at $[M+O-H]^-$ was enhanced. When oxygen was added to the reagent gas at low ion source temperatures, an ion at $[M+O_2]^-$ was formed. All four of these ions gave normal chromatographic peak shapes and ion formation was attributed to gas-phase ion-molecule reactions. In contrast, the O_2/N_2 NICI mass spectrum of anthracene, measured with the ion source temperature at 300° C, showed an ion at $[M+30]^-$ that exhibited a tailing chromatographic profile. Upon addition of $^{18}O_2$, incorporation of two oxygen atoms was indicated. These results, in conjunction with experiments using fully deuterated anthracene, showed that the $[M+30]^-$ ion resulted from $[M+2O-2H]^-$. This ion corresponds to the M^- ion of anthraquinone, where anthraquinone is formed by a surface-catalyzed oxidation reaction. This assignment is supported by measurements made in the PCI mode, where ions corresponding to the M^+, $[M-CO]^+$, and $[M-2CO]^+$ ions from anthraquinone appeared in the spectrum of anthracene.

These studies have shown that PAH undergo gas-phase electron-capture and ion-molecule reactions, in addition to surface-catalyzed oxidation reactions. These latter reactions are enhanced by addition of O_2 and elevation of the ion source temperature. The oxidized products, such as ketones and quinones, appear in the NICI mass spectra when they are ionized by electron-capture reactions.

(1) M. V. Buchanan, I. B. Rubin, M. B. Wise, and G. L. Glish, Biomed. Environ. Mass Spectrom. 14, 395 (1987).
(2) L. J. Sears, J. A. Campbell, and E. P. Grimsrud, Biomed. Environ. Mass Spectrom. 14, 401 (1987).

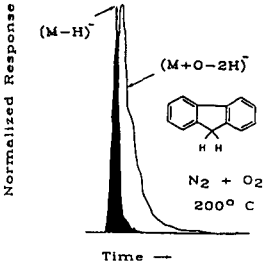

Figure 1.

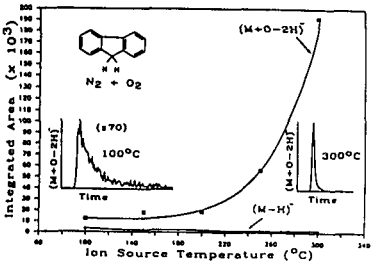

Figure 2.

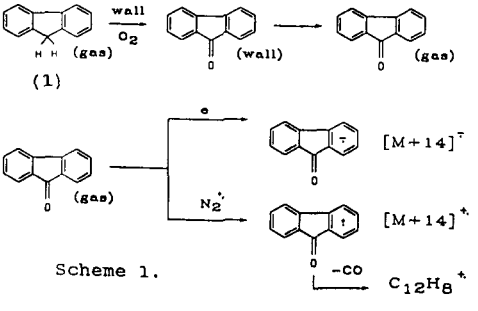

Scheme 1.

*Research sponsored by the Office of Health and Environmental Research, U.S. DOE under contract DE-AC05-84OR21400 with Martin Marietta Energy Systems, Inc and the Postgraduate Research Training program under contract DE-AC05-76OR00033 between the U.S DOE and Oak Ridge Associated Universities.

Presented at the 36th ASMS Conference on Mass Spectrometry and Allied Topics
June 5-10, 1988, San Francisco, CA

ISOMERIC DIFFERENTIATION OF PAH AND METHYL-PAH USING SURFACE-CATALYZED OXIDATION REACTIONS*

E.A. Stemmler and M.V. Buchanan
Oak Ridge National Laboratory, Oak Ridge, TN 37831-6120

Recent studies have shown that surface-catalyzed oxidation reactions followed by electron-capture ionization produce unusual ions that dominate the O_2/N_2 negative ion chemical ionization (NICI) mass spectra of polycyclic aromatic hydrocarbons (PAH) at an ion source temperature of 300° C. These oxidation reactions yield products that can be used to differentiate isomeric PAH.

The spectra of unsubstituted PAH show three types of oxidized products. Compounds with methylene groups, like fluorene, undergo $-CH_2-$ to $-CO-$ conversion giving an $[M+O-2H]^-$ ion that appears at $[M+14]^-$. Ring oxidation reactions produce quinones and anhydrides. Most PAH undergo ring oxidation to give an $[M+2O-2H]^-$ ion that appears at $[M+30]^-$ (see Scheme 1A). PAH with an exposed ethene group undergo a unique oxidation reaction to give an $[M+3O-2H]^-$ ion that appears at $[M+46]^-$ (see Scheme 1B). These ring oxidation reactions permit differentiation of isomeric PAH such as benzo[ghi]fluoranthene, which gives an $[M+30]^-$ ion, from cyclopenta[cd]pyrene, which has an exposed ethene bridge and gives an $[M+46]^-$ ion. PAH also undergo oxidative ring cleavage reactions that produce anhydrides and ketones. Anhydride formation is observed when oxidation occurs in conjunction with loss of part of the aromatic ring. For example, naphthalene oxidizes to give an ion at m/z 148 that corresponds to phthalic anhydride. This reaction can be used to determine the number of methyl substituents on each aromatic ring of dimethylnaphthalenes because the isomers with methyl groups substituted on both aromatic rings give a single ion at m/z 162 (corresponding to methyl-substituted phthalic anhydride), while the isomers with both methyl groups substituted on the same ring give two ions at m/z 148 and 176 (corresponding to phthalic and dimethylphthalic anhydride, respectively). Ketone formation occurs in conjunction with loss of CH_2 to give an ion at $[M+2]^-$. The fact that these reactions occur to different a different extent for isomeric PAH with different structures permits differentiation of isomers, such as benz[a]anthracene, chrysene, and triphenylene (see Figure 1).

Methyl-substituted PAH undergo a variety of oxidation reactions involving oxidation of the methyl group, displacement of the methyl group during ring oxidation, and proximity reactions that take place between the methyl group and the aromatic ring or another methyl group. Methyl group oxidation involves conversion of the methyl group to an aldehyde to give an $[M+O-2H]^-$ ion that appears at $[M+14]^-$. Ring oxidation gives an ion at $[M+30]^-$ if the methyl group is not substituted at the site of oxidation. When methyl group and ring oxidation both occur, an ion at $[M+3O-4H]^-$ appears at $[M+44]^-$. These ions are all observed in the spectrum of 2-methylanthracene (see Scheme 2). If a methyl group is substituted at the site of ring oxidation, methyl group displacement occurs. For example, the spectrum of 9-methylanthracene is dominated by an ion at $[M+16]^-$, which corresponds to $[M+2O-CH_3-H]^-$ (see Scheme 3). In the case of 9,10-dimethylanthracene, the spectrum is dominated by an ion at $[M+2]^-$, which corresponds to $[M+2O-2CH_3]^-$. These reactions can be used to differentiate positional isomers of methyl-PAH. For example, 3,9-dimethylbenz[a]anthracene can be differentiated from the 7,12-isomer because of the $[M+2]^-$ ion that appears in the spectrum of the latter compound (see Figure 2). Ions are also observed that result from interactions of between the methyl group and the aromatic ring. For example, the spectrum of 4-methylchrysene is dominated by an ion at $[M+12]^-$, which is not observed in the spectra of the 1-, 2-, 3-, or 6-methyl isomers. This ion corresponds to $[M+O-4H]^-$ and would result from an oxidative ring closure to produce a cyclopentenone ring. This reaction, in conjunction with methyl group oxidation, accounts for the $[M+26]^-$ ion observed in the spectrum of 7,12-dimethylbenz[a]anthracene.

Presented at the 36th ASMS Conference on Mass Spectrometry and Allied Topics
June 5-10, 1988, San Francisco, CA

In summary, the O_2/N_2 NICI mass spectra of PAH and methyl-substituted PAH, measured with an ion source temperature of 300° C, are dominated by unusual ions that result from surface-catalyzed oxidation reactions, followed by electron-capture ionization. These reactions yield products that can be used to distinguish isomeric PAH and help determine the position of substitution for methyl-PAH.

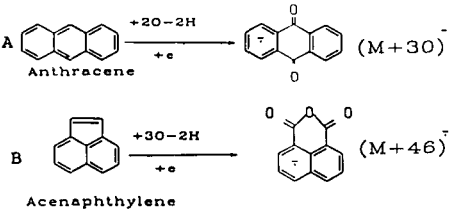

Scheme 1

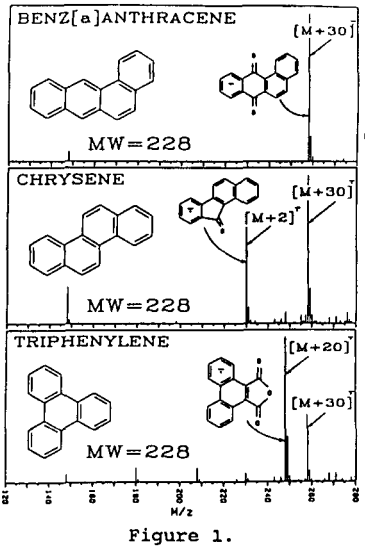

Figure 1.

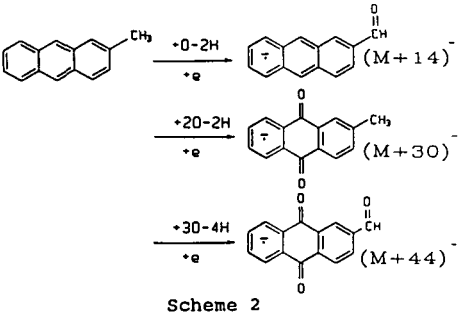

Scheme 2

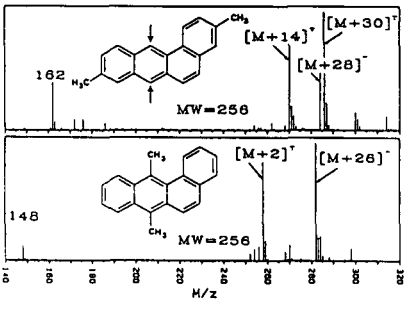

Figure 2.

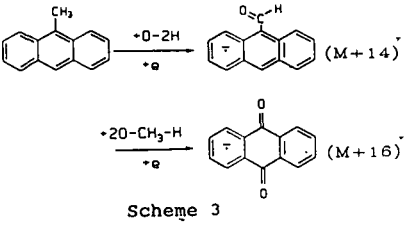

Scheme 3

"The submitted manuscript has been authored by a contractor of the U S Government under contract No DE-AC05-84OR21400 Accordingly, the U S Government retains a nonexclusive royalty-free license to publish or reproduce the published form of this contribution, or allow others to do so, for U S Government purposes."

*Research sponsored by the Office of Health and Environmental Research, U.S. DOE under contract DE-AC05-84OR21400 with Martin Marietta Energy Systems, Inc and the Postgraduate Research Training program under contract DE-AC05-76OR00033 between the U.S DOE and Oak Ridge Associated Universities.

Presented at the 36th ASMS Conference on Mass Spectrometry and Allied Topics
June 5-10, 1988, San Francisco, CA

ELECTROSPRAY IONIZATION OF SOME POLYPEPTIDES AND SMALL PROTEINS

Chin Kai Meng, Matthias Mann and John B. Fenn
Department of Chemical Engineering
Yale University, New Haven, CT 06520-2159

Previously we have reported results obtained with Electrospray (ES) mass spectrometry of poly ethylene glycols (PEG) having nominal values of Molecular Weight (M) from 400 to 17,500. At M greater than about 4000 there were so many combinations of m and z within a small interval of m/z that our analyzer was unable to resolve the individual peaks because the spectra were so congested. Even so, the results indicated that the largest of the oligomers (M = 20,000) could accommodate as many as 23 charges (Na^+). (1) Such multiple charging is most attractive because it can substantially extend the effective mass range of any analyzer. Consequently, we have extended our studies and report here some of the results obtained by ES ionization of polypeptides and small proteins with M up to about 40,000.

The ES mass spectrometer was the same one used in the PEG studies and has been previously described (1,2). Samples of varying purity were obtained from various sources. Solvents usually comprised a mixture of methanol, acetonitrile and water but sometimes a propanol water mixture was used. Acidification with small quantities of acetic acid (HAc) or trifluoro acetic (TFA) acid was most helpful. Solutions at sample concentrations ranging from 0.05 to 2.0 mg/ml were introduced at a uniform flow rate of 8 ul/min.

The results are conveniently summarized in the accompanying figures showing illustrative examples of the spectra that were obtained. Each spectrum is the result of a single 30 second scan over the indicated range of m/z values and comprised a family of peaks in which adjacent members differ by one in the number of charges, each of which is an H^+ in these experiments. This number of charges per ion, shown for two peaks in each spectrum, reaches a value of at least 46 in the case of alcohol dehydrogenase from equine liver which has an M of about 40,000 and is the largest species we have yet run successfully. In this case, as for some other large species, the individual peaks seem to be too broad to be completely resolved. We do not yet fully understand why this broadening occurs in but we are fairly certain that it is not due to internal excitation as has been found to be the case when similar species have been ionized by bombardment with 35 kV cesium ions. (3)

References

1. S. F. Wong, C. K. Meng, and J. B. Fenn, J. Phys. Chem. 1988, 92, 546.

2. C. M. Whitehouse, R. N. Dreyer, M. Yamashita and J. B. Fenn, Anal. Chem. 1985, 57, 675.

3. M. Barber and B. N. Green, Rapid. Commun. in Mass Spectrom. 1987,1,80.

We acknowledge the support from NIH.

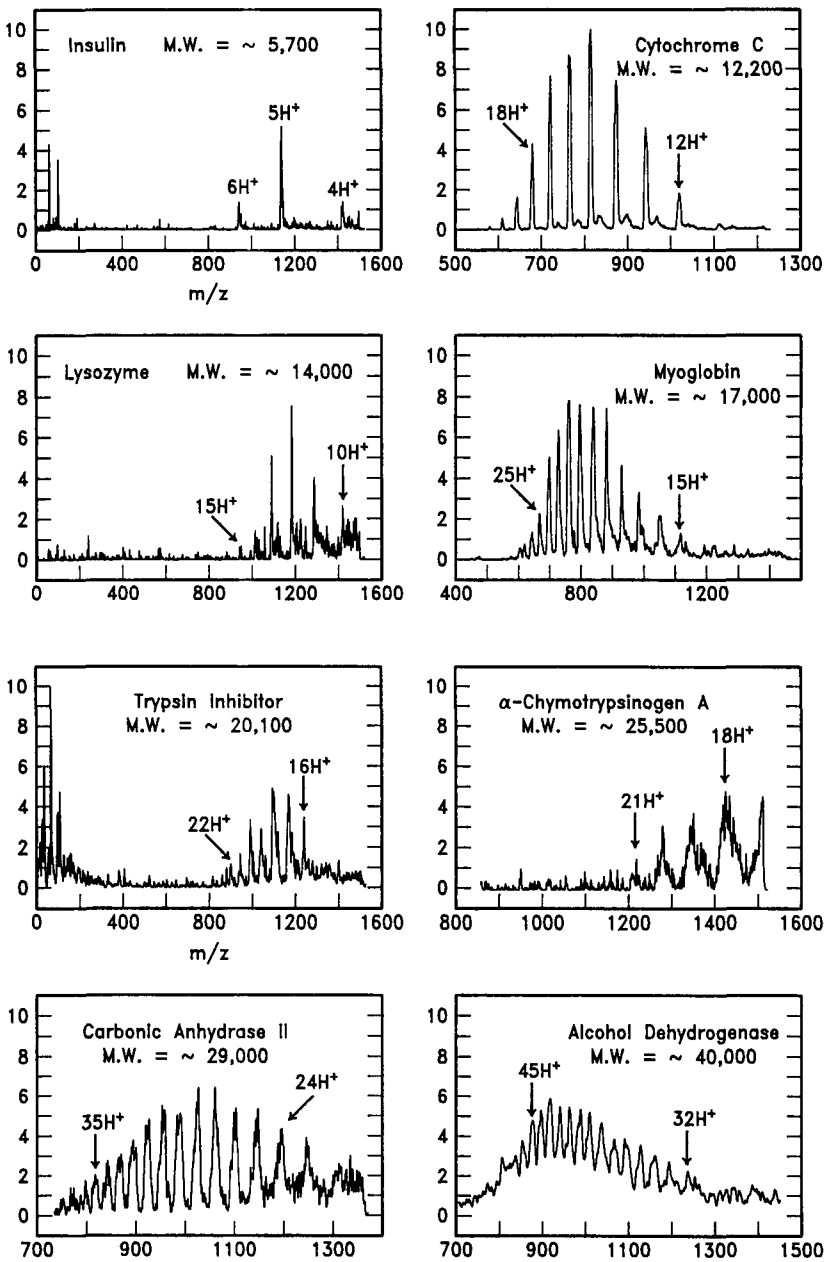
Insulin M.W. = ~ 5,700
5H+
6H+
4H+
m/z
Cytochrome C
M.W. = ~ 12,200
18H+
12H+
Lysozyme M.W. = ~ 14,000
10H+
15H+
Myoglobin
M.W. = ~ 17,000
25H+
15H+
Trypsin Inhibitor
M.W. = ~ 20,100
16H+
22H+
m/z
α-Chymotrypsinogen A
M.W. = ~ 25,500
18H+
21H+
Carbonic Anhydrase II
M.W. = ~ 29,000
24H+
35H+
Alcohol Dehydrogenase
M.W. = ~ 40,000
45H+
32H+

Presented at the 36th ASMS Conference on Mass Spectrometry and Allied Topics
June 5-10, 1988, San Francisco, CA

Photo-Assisted Fragmentation Spectroscopy by Neutralization-Reionization Mass Specroscopy

Susan F. Selgren and Gregory I. Gellene
Department of Chemistry
University of Notre Dame
Notre Dame, IN 46556

A new technique where by the high resolution absorption spectrum of unusual metastable radicals in a high velocity beam can be obtained by monitoring photoinduced changes in their neutralization-reionization mass spectra has been developed. H_3^* radicals can be produced in an unusual metastable ($2p^2A''_2$, N=K=0, where N and K are the rotational quantum numbers of a symmetric top molecule) by an H_3^+/K electron transfer reaction. These radicals have lifetimes in excess of 10μs and can be collisionally reionized to give rise to the neutralization-reionization mass spectra in Fig. 1.

The integrated intensity of the parent ion signal in the secondary mass spectrum is a direct indication of the extent to which the neutral H_3^* molecules survived the transit time from the neutalization to the reionization chamber. In the present experiment, the stability of H_3^* in this region is affected by photo-assisted fragmentation (PAF) induced by the resonant absortion of a photon provided by tunable dye laser system using a modified version of the apparatus as shown in Fig. 2. The laser is chopped at a frequency of about 100Hz, allowing secondary ions to be counted alternately with the laser on (N_{on}) and (N_{off}). The ion counting data is used in the relationship: $A=1-N_{on}/N_{off}$ to provide a normalized measure of the effect of laser radiation on the mass resolved secondary ion signal.

Figure 3 shows a plot of A vs. photon energy for secondary H_3^+ ions. The peak at 16694.96 cm^{-1} is the previously known $R_0(0)$ transition of the $3s^2A'_1 \leftarrow 2p^2A''_2$ band. The result is readily understood in terms of a metastable H_3^* radical absorbing a photon, making a transition to the $3s^2A'_1$, N'=1, K'=0 state which then fluoresces back to the $2p^2A''_2$ electronic state branching between the (N",K")=(0,0) and (2,0) rotational levels in a 1:2 ratio. Although those molecules returning to the N"=K"=0 level are again metastable, those in the N"=2,K"=0 level predissociate with a lifetime of about $2x10^{-11}$s. Thus at least two thirds of the H_3^* radicals which undergo the optical absorption dissociate following fluorescence, but because the upper state is spectroscopically long-lived, the lifetime broadening of the transition, determined by the molecular transit time through the radiation field, is less than $2x10^{-4}$ cm^{-1}.

Although application of this technique would appear to be limited, all that is actually required is a lower state having a greatly decreased lifetime with increased internal energy and an upper state which is radiatively stable. These stability characteristics have been identified theoretically and experimentally for the second row hypervalent hydrides, NH_4, H_3O, H_2F, NeH, which will be the focus of future PAF spectroscopic investigations in this laboratory

This work was funded by Finnegan MAT through the ASMS reearch awards program.

Presented at the 36th ASMS Conference on Mass Spectrometry and Allied Topics
June 5-10, 1988, San Francisco, CA

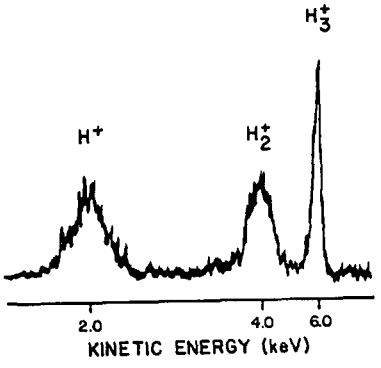

Fig. 1) Neutralization-reionization mass spectra of H_3^+ obtained using K as the neutralization target and N_2 as the reionization target.

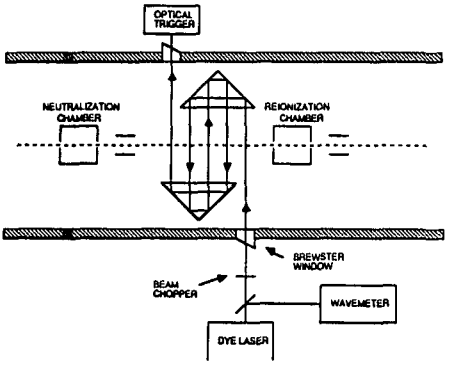

Fig. 2) Partial schematic of the apparatus depicting modifications for obtaining photo-assisted fragmentation (PAF) spectra.

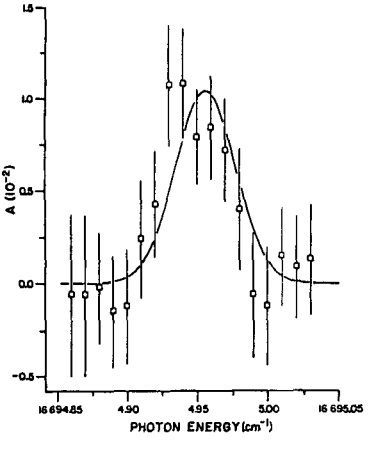

Fig. 3) Photo-assisted fragmentation spectrum of the H_3 radical. Vertical lines represent one standard deviation error bars. The smooth curve represents a least squares fit of the data to a gaussian function with a 0.05 cm^{-1} full width at half maximum.

Presented at the 36th ASMS Conference on Mass Spectrometry and Allied Topics
June 5-10, 1988, San Francisco, CA

Laser Ionization Spectroscopy of Amino Acids and Peptides Using Supersonic Jet Injection Into a Time-of-Flight Mass Spectrometer

David M. Lubman and Liang Li
Department of Chemistry
University of Michigan
Ann Arbor, MI 48109-1055

Resonant two-photon ionization (R2PI) spectroscopy has been shown to be a means of preselecting ions for mass spectrometry. Although ions are produced as the final product of R2PI, the ionization cross-section as a function of wavelength reflects the absorption-excitation spectrum of the $S_0 \rightarrow S_1$ transition of a molecule. Thus by tuning the laser frequency to a given rovibronic transition, one can in principle selectively excite a target molecule in a complicated mixture. The problem here is that the UV-VIS spectra of most large polyatomics consists of an unresolvable contour due to a broad thermal congestion of unresolvable rotational lines in the electronic transition. We therefore use the supersonic jet technique to provide ultracold molecules with sharp spectral features for selective chemical analysis.

The above combination of techniques has generally been limited to reasonably volatile molecules. In this work we use pulsed laser desorption as a means of volatilizing nonvolatile and thermally labile molecules for entrainment into a supersonic jet expansion. A relatively low-powered CO_2 laser (~ 10^6 W/cm^2) is used to desorb neutral molecules without decomposition. The resulting plume is synchronized with a pulsed supersonic flow of Ar or CO_2 and carried into a time-of-flight device where the molecules are detected using R2PI spectroscopy. This desorption technique provides a simple repetitive method for obtaining cold biological molecules in a supersonic jet for spectroscopic scanning purposes. Using this method we demonstrate the ability to obtain cold, sharp spectral features using R2PI spectroscopy in a TOFMS for tyrosine, tryptophan, catecholamines and their related analogs as well as several dipeptides as shown in Figure 1.

The key to this method is that R2PI spectroscopy serves as a sensitive probe, revealing small differences in molecular structure (Figure 2). This figure shows R2PI spectra of octopamine and synephrine obtained by monitoring only the molecular ion as a function of wavelength. These two compounds are very similar in structure, the difference being an extra $-CH_3$ group attached to the linear substituent chain. Nevertheless, each spectrum has distinctive sharp spectral features which are shifted by several tenths of a nm relative to one another, but which can clearly be resolved by the laser. In combination with the mass spectrometer, this technique provides a powerful tandem method of discriminating molecules. This capability is demonstrated in Figure 3 which illustrates the mass spectrum of a 1:1 mixture of tryptophol:tryptamine dissolved in a glycerol matrix and desorbed from the probe using pulsed laser desorption. The relative abundance of the mass peaks corresponding to the compounds are monitored as a function of wavelength at (Figure 3): (a) 286.30 nm, (b) 285.27 nm, and (c) 285.59 nm. Using this method, an optical discrimination of 1:100 of tryptamine in tryptophol has been demonstrated. A series of mixtures of tryptamine in tyramine were also examined at 286.30 nm and an optical discrimination of $1:10^5$ was achieved since cold tyramine does not absorb radiation at this wavelength.

Presented at the 36th ASMS Conference on Mass Spectrometry and Allied Topics
June 5-10, 1988, San Francisco, CA

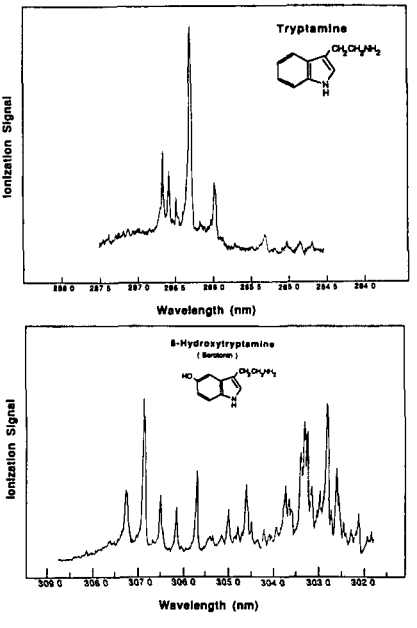

Figure 1. Resonant two-photon ionization (R2PI) spectra of tryptamine and 5-Hydroxy-tryptamine.

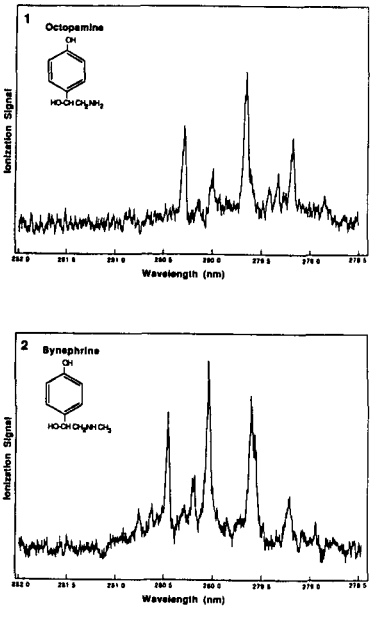

Figure 2. Resonant two-photon ionization (R2PI) spectra of (1) octopamine and (2) synephrine.

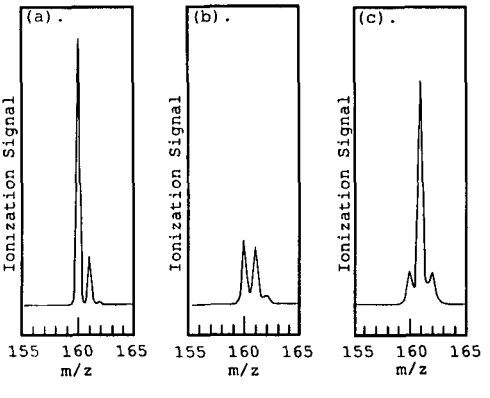

Figure 3. R2PI mass spectra of a 1:1 mixture of tryptophol (m/z 161):tryptamine (m/z 160) obtained as a function of wavelength:
(a) 286.30 nm, (b) 285.27 nm, and (c) 285.59 nm.

Presented at the 36th ASMS Conference on Mass Spectrometry and Allied Topics
June 5-10, 1988, San Francisco, CA

Sequence Specific Fragmentation of Derivitized Dipeptides Using Resonance Enhanced Multiphoton Ionization

Kimberly R. Segar and Murray V. Johnston; C.I.R.E.S. and Department of Chemistry and Biochemistry
University of Colorado, Boulder, Colorado, 80309-0215

We have studied the REMPI fragmentation at 266 nm of benzyloxycarbonyl (CBZ) derivatized dipeptide methyl esters of nonaromatic amino acids:

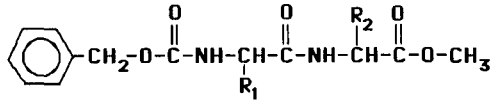

These compounds represent simple examples of chromophore derivatives of nonabsorbing compounds that permit detection by REMPI. If chromophore derivatization is to be of use in REMPI, it will be important to understand how the chromophore perturbs the fragmentation processes of the underivatized compound and whether or not the information content of the mass spectrum is enhanced or diminished.

<u>Types of Fragment Ions Observed in REMPI</u> Prominent ions in the REMPI mass spectra of all of the CBZ dipeptides are given in Table 1. Ions present at low laser intensities are the parent ion ($M^{+\cdot}$), ions corresponding to the loss of the amino acid side chains ($M-R_i^{+\cdot}$), ions corresponding to the N-terminal type A and A+H sequence ions, and $C_7H_7^+$ (m/z 91) corresponding to fragmentation of the CBZ moiety. The mass spectra taken with higher laser pulse energies exhibit increased abundance of m/z 91 and additional fragment ions identified as $A-C_7H_6^+$, $A-CO_2^+$ and $A-C_7H_6-CO_2^+$. Many of the dipeptides also give a weak Y sequence ions as well.

<u>REMPI Fragmentation Mechanisms</u> To understand the mechanism of ion formation in REMPI, one would like to determine the number of photons required to produce a given ion and whether or not all ions arise from ionization/dissociation of the same neutral precurser. An indication of the number of photons required to produce a given ion can be obtained from the dependence of the ion current on laser pulse energy. The number of photons involved in fragment ion formation can be obtained by plotting the ratio of the fragment ion to parent ion current vs. laser pulse energy. From such power dependent studies we have found that the parent ion is created by resonant two photon ionization (R2PI). Power dependent studies have also allowed us to classify the fragment ions observed as being produced by either a 2+0 or 2+1 photon process. A 2+0 fragmentation mechanism is defined as R2PI of the neutral molecule to form the parent ion with sufficient internal energy to cause spontaneous decomposition to the 2+0, low appearance energy , fragments ions. $A^+/A+H^+$ and $M-R_i^{+\cdot}$ are examples of 2+0 fragments. High energy fragments such as m/z 91, $A-CO_2^+$, $A-C_7H_6^+$ and $A-C_7H_6-CO_2^+$, were found to be formed by a 2+1 photon mechanism, one photon dissociation of the parent ion which was previously created by resonant two photon ionization. A summary of the mechanisms of ion formation for all compounds studied is given in Table 1. Relative abundancies of the ions are also given in Table 1. At low laser intensities both the molecular ion and the A type sequence ion are produced in large amounts. The molecular ion is usually the base peak (never lower than 20 % relative abundance) while the intensity of the sequence ion ranges from 8% to 86% of the base peak (usually averaging <50% relative abundance). This contrasts with 70 eV electron impact (EI) data of these compounds. Although the same types of fragment ions are observed in both the REMPI and EI mass spectra the relative intensities vary greatly. For 70 eV EI the parent and the sequence ions are

seldom greater than 3% and 20% respectively of the base peak. The base peak in the EI mass spectra for all the CBZ dipeptides is m/z 91which is due to fragmentation of the chromophore and provides no sequence information.

Isomer Differentiation From our work we have determined that the isomers CBZ-ile-ala-OCH_3 and CBZ-leu-ala-OCH_3 can be distinguished by their REMPI mass spectra shown in Figure 1. It is evident from the REMPI mass spectra that the peak ratios for m/z 220 to 294 ($A^+/M\text{-}R_1^{+\cdot}$) are different and could be used to differentiate between the two isomers. The 70 eV EI spectra for these isomers are identical.

Table 1

Assignment	Ala-Gly	Ala-Val	Val-Gly	Val-Ala	Val-Leu	Ile-Ala	Leu-Ala	Leu-Leu
			(2 + 0) FRAGMENTATION MECHANISM					
$M^{+\cdot}$	100(294)	100(336)	100(322)	100(336)	69(378)	25(350)	20(350)	25(392)
$M\text{-}R_1^+$	------	------	2.5(281)[b]	9(294)[b]	16(336)[b]	100(294)[b]	100(294)[b]	100(336)[b]
$M\text{-}R_2^+$	------	------	------	------	100(322)[b]	------	------	
$A^+/A+H^{+\cdot}$[c]	8(178)	20(179)[b]	65(206)[b]	86(206)[b]	52(206)[b]	72(220)[b]	62(220)[b]	28(220)[b]
			(2 + 1) FRAGMENTATION MECHANISM					
$A\text{-}CO_2^+$	------	7(134)	35(162)	7(162)	47(162)	23(176)	17(176)	16(176)
$A\text{-}C_7H_6^+$	17(88)[d]	17(88)	13(116)	20(116)[b]	72(116)[b]	53(130)[b]	52(130)[b]	100(130)[b]
$A\text{-}C_7H_6\text{-}CO_2^+$	27(44)	100(44)[b]	13(72)	8 4(72)	26(72)	19(86)	11(86)	51(86)[b]
$C_7H_7^+$(91)	100	46	100	100	100	100	100	48
Y^+	17(88)[d]	10(130)	4(88)	4(102)	14(144)	12(102)	-----	-----

[a]Peak areas are calculated relative to the most abundant ion produced by each mechanism. Mass-to-charge ratios are shown in parentheses.
[b]Metastably broadened ions.
[c]Total peak area for both A+ and A + $H^{+\cdot}$.
[d]Unambiguous assignment cannot be made.

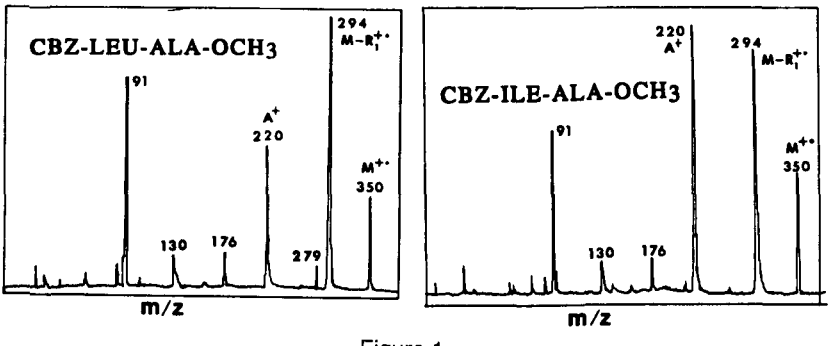

Figure 1

Presented at the 36th ASMS Conference on Mass Spectrometry and Allied Topics
June 5-10, 1988, San Francisco, CA

LITHIUM METAL PROBE TIP: PRODUCTION OF LITHIUM CATIONS AND LITHIATION OF NEUTRAL MOLECULES DURING FABMS

Julie A. Leary and Emirgul Tolun

Chemistry Dept., University of California, Berkeley

We have developed a lithium probe tip from which a continuous lithium bean can be generated by bombarding the metal surface with 8 keV Xenon atoms. This beam provides a mechanism whereby lithium can efficiently cationize neutral organic molecules thereby generating positively charged ions. Our results with a series of symmetrical and unsymmetrical vicinal diols (Table 1) show that lithiated molecular ions (MLi+) are obtained when crystals of the sample are impregnated into the lithium metal tip. The spectra are then recorded without the use of a liquid matrix. These vicinal diols do not give molecular ions using conventional EI or FAB techniques but instead the molecular ion minus water is seen.

Construction of the lithium tip and all sample preparation and deposition onto the tip was done under inert atmosphere in a dry box using argon. A uniform layer of lithium metal shavings are deposited onto the stainless steel tip in much the same way as putty is applied to surfaces. A few crystals of the sample are then placed into indentations made in the lithium metal. Although spectra generated from the litium tip have a tendency to show only MLi+ and no fragment information (Fig. 1), we have been able to show that subsequent BEQQ scans provide structural detail (Fig.2). These data clearly show that a matrix is not required when desorption and ionization take place from a lithium surface, and may be beneficial in cases where samples either react with or do not dissolve in the available solvents used as FAB matrices.

FIGURE 1.

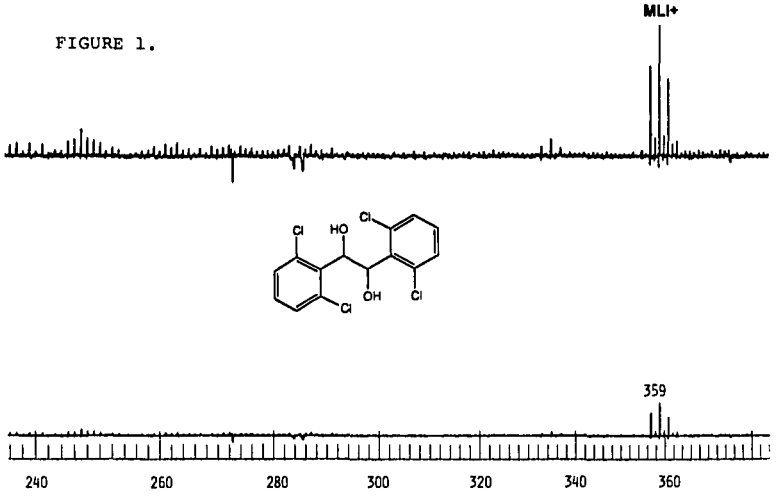

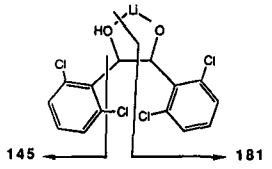

FIGURE 2.

MS/MS, P = 359, BEQQ with Argon,

TABLE 1.

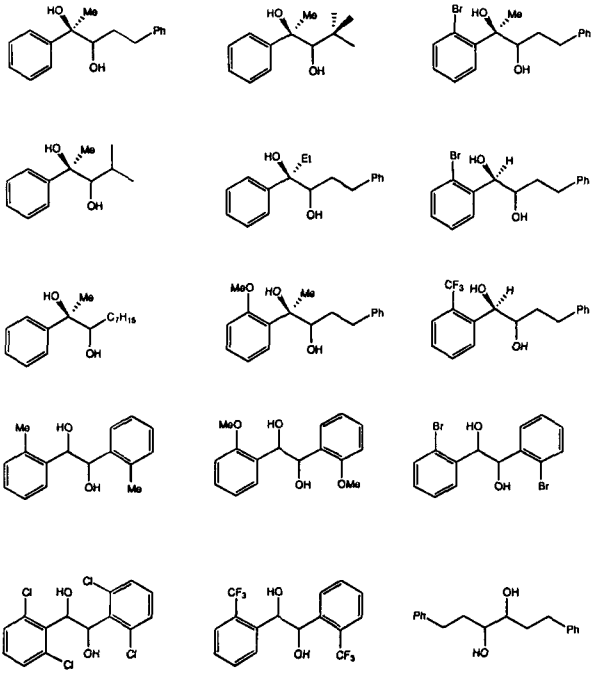

Presented at the 36th ASMS Conference on Mass Spectrometry and Allied Topics
June 5-10, 1988, San Francisco, CA

NONLINEAR SECONDARY ION YIELD ENHANCEMENT WITH FAST INCIDENT MOLECULAR IONS*:

Mehran Salehpour, Derry Fishel and Jerry Hunt, Chemistry Division, Argonne National Laboratory, 9700 South Cass Avenue, Argonne, Illinois 60439, U. S. A.

Incident ions with velocities greater than the Bohr velocity ($v_o \approx 0.2$cm/ns), referred to here as fast ions, interact mainly with the electrons of the medium in which they are traversing. This distinguishes the mechanism from the low energy processes such as those observed in conventional SIMS (Secondary Ion Mass Spectrometry) and FAB (Fast Atom Bombardment). From an application point-of-view, the use of fast ions has been very successful in the high molecular weight mass spectrometry. Plasma Desorption Mass Spectrometry has been responsible for detection of intact protein molecular ions such as pepsin (MW≈34000) [1]. The use of high energy accelerators (≈ 1MeV/nucleon) has facilitated more insight into the physics of the desorption process. All experiments, until recently, had concerned incident atomic ions. Thomas et al. has reported measurements with H_n^+ clusters in a velocity region around v_o [2].

The yield is defined as the number of detected secondary ions per incident ion. The experimental details are explained elsewhere [3]. A 4.5 MV dynamitron accelerator at the physics division, Argonne National Laboratory has been used to accelerate the incident ions. Measurements on the secondary ions are performed using a time-of-flight technique. The yield of valine molecular ions, $(M-H)^-$, has been measured as a function of the velocity of a number of different incident atomic and molecular ions.

Figure 1 shows the yield of valine molecular ions as a function of the velocity of C^+, O^+, CO^+, O_2^+ and CO_2^+ incident ions. Let Y(X) be the yield of the valine secondary molecular ions for an incident ion X. The inherent nonlinearity of the desorption process can be seen in comparing $Y(C^+)$ and $Y(O^+)$ to the molecular ions, $Y(CO^+)$ and $Y(O_2^+)$, i.e., $Y(O_2^+) >> 2 \cdot Y(O^+)$ and $Y(CO^+) >> Y(C^+) + Y(O^+)$. Desorption by atomic ions in this velocity region varies with the square of the electronic stopping power [3]. However, the yield enhancements with incident molecular ions can not be solely explained on the basis of a quadratic dependence of the yield on the electronic stopping power. Thus, collective effects exist for incident molecular ions which are due to the vicinage of the moving charges in the medium. Spatially and temporally correlated fast moving charges in solids have been experimentally shown to display collective effects in the form of enhancement in the electronic stopping power per atom [4]. Another interesting feature is the high yield due to incident CO_2^+ ions.

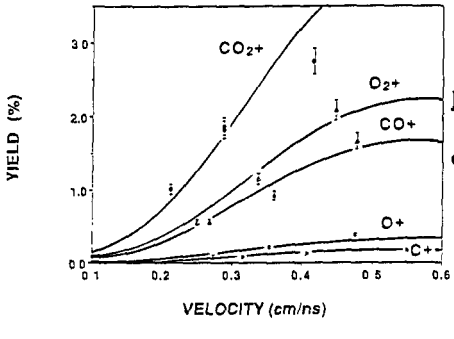

Figure 1. The yield of valine molecular ions, $(M-H)^-$, as a function of the velocity of C^+, O^+, CO^+, O_2^+ and CO_2^+ incident ions.

Figure 2 shows the yield of valine (amino acid, MW=117) molecular ions as a function of the velocity of incident C^+, CF^+, CF_3^+, $C_3F_5^+$ and $C_4F_7^+$ ions. As with the ions discussed above, collective molecular effects exist for all the incident ions. From an applied point-of-view, it is interesting to note that strong yield enhancements are measured with the heavy incident molecular ions such as $C_3F_5^+$ and $C_4F_7^+$. The absolute value of $Y(C_4F_7^+)$ is about 5% which is comparable to yield obtained with fission fragments from a ^{252}Cf. In fact this particular sample was removed from vacuum repeatedly due to unavoidable experimental problems prior to the start of the measurements. Thus, the yield from a fresh sample could be an order of magnitude higher.

For heavy molecular ions such as $C_3F_5^+$ and $C_4F_7^+$, comparison to incident C^+ at the same velocity is not possible, however, we can compare to the C^+ data point at the lowest velocity. Results shows that $Y(C_4F_7^+) > 60 \cdot Y(C^+)$. Such dramatic enhancements in the secondary ion yield are very important for mass spectrometry of large organic molecules. Håkansson et al. [5] have shown that the inherent nonlinearity in desorption with atomic ions, becomes more pronounced for larger secondary ions. This makes it very important to utilize projectiles with high electronic stopping powers. The use of incident molecular ions, as shown here, could prove to be very important in mass spectrometry.

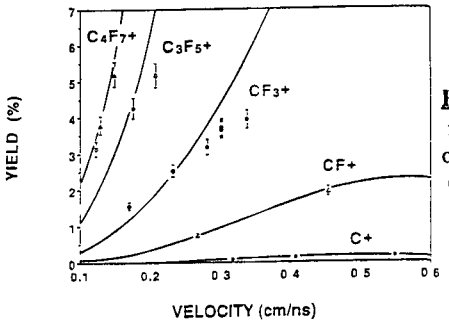

Figure 2. The yield of valine molecular ions, $(M-H)^-$, as a function of the velocity of incident C^+, CF^+, CF_3^+, $C_3F_5^+$ and $C_4F_7^+$ ions.

1- Ivan Kamensky, Bio-Ion Nordic AB, Box 15045, S-750 15 Uppsala, Sweden.
2- J. P. Thomas,et al., Phys. Rev. Lett. **55**, 103 (1985).
3- M. Salehpour, D. L. Fishel and J. E. Hunt, to appear in J. Appl. Phys.
4- W. Brandt, A. Ratkowski and R. H. Ritchie, Phys. Rev. Lett. **33**, 1325 (1974).
5- P. Håkansson et al., Rad. Eff. **80**, 141 (1984).

*Work performed under the auspices of the Office of Basic Energy Sciences, U.S. Dept. of Energy under contract number W-31-109-ENG-38.

Presented at the 36th ASMS Conference on Mass Spectrometry and Allied Topics
June 5-10, 1988, San Francisco, CA

A ROBOTIC BASED SAMPLE PREPARATION AND INTRODUCTION SYSTEM FOR AUTOMATED EI AND CI PROBE ANALYSIS

D.C. Smith, V. Gould, M.J. Hammond and D.E. Todd*.

VG MassLab Ltd., Tudor Road, Altrincham, WA14 5RZ, UK. Phone 061 941 3552. Tlx 669964. *Zymark Ltd., The Genesis Centre, Science Park South, Birchwood, Warrington, WA3 78H. Phone 0925 826600. Tlx 629343.

A high throughput of routine samples is a common feature of many laboratories such as those in the pharmaceutical industry. Sample preparation and injection onto a probe and introduction of the probe into a mass spectrometer is generally a repetitive process involving very little operator skill. As such the process is ideally suited to some form of automation.

We have developed an integrated robot-MS-DS instrument capable of performing complete analyses on a series of such samples.

A laboratory robot is used to prepare the sample prior to injection. The robot is fed with screw topped sample bottles placed in a rack. Samples may be dry or already in solution. The robot will automatically perform a number of functions such as screw cap removal, addition of solvent, ultrasonic agitation and injection. Sample workup can easily be extended to include extraction, purification and derivatisation steps. Internal standards may also be added. Programming of the robot is through a high level language so the operator can readily change the preparation stages.

If sample workup is not required, the laboratory robot can be replaced by a conventional GC autosampler. Each sample bottle in turn is transferred to the injection station from the 100 position rack. After injection normal syringe washing routines are performed and the sample bottle is returned to the rack.

The sample insertion probe is automatically admitted to and withdrawn from the ion source using a pneumatically driven multi-position linear actuator. Sample is injected onto a coil of platinum wire mounted at the tip of the probe. The coil can be heated to aid sample desorption and, after completion of the analysis, to eliminate memory effects.

The introduction lock is of conventional design. The ball valve is pneumatically operated and the rough pumping is controlled by a solenoid valve. The complete system has been designed to be fitted permanently to the mass spectrometer without interfering with other inlets.

All operations are controlled automatically by the mass spectrometer datasystem, although an override facility has been incorporated for manual control. Valve and probe operations are governed by the vacuum system interlock.

If desired, sample heating may be regulated by feedback of the total ion current signal to give a controlled evaporation profile.

Operation is fully compatible with normal datasystem functions such as spectral acquisition, library searching and output.

Spectra may be acquired in either the EI or CI mode. When fitted to an instrument equipped with the ACE facility, alternate EI and CI spectra may be acquired.

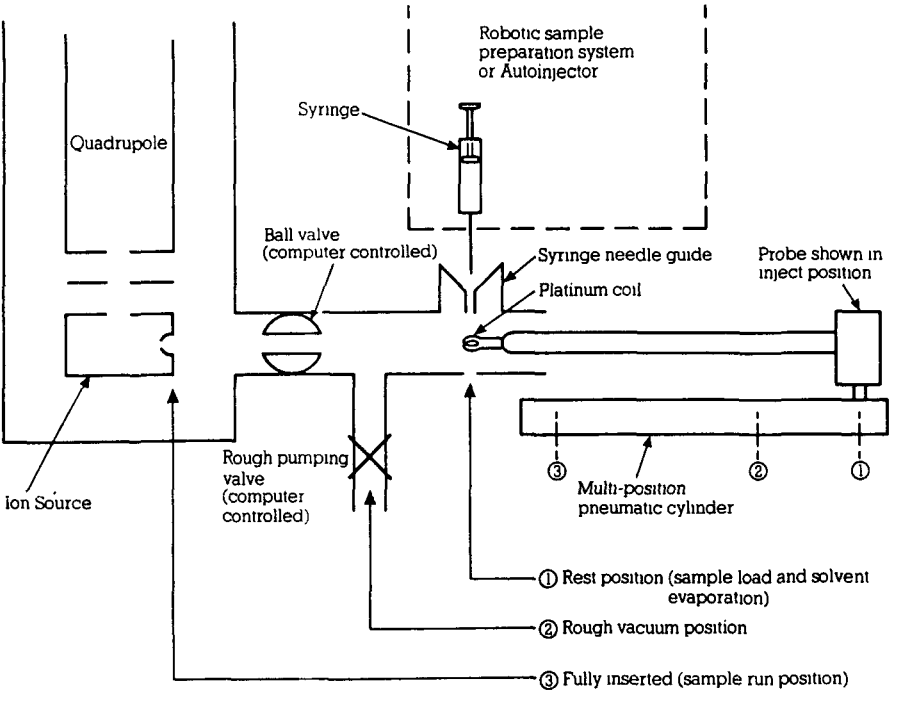

The sequence of operation following syringe loading is as follows:

1. 1 microlitre of dissolved sample is injected onto the probe tip. Sufficient time is allowed for solvent evaporation.
2. The probe moves to the first stage of the vacuum lock and the roughing valve opens.
3. When the roughing pressure is sufficiently low the ball valve opens. The probe moves into the ion source.
4. The sample is desorbed, and data is acquired in the normal manner.
5. The heating current is increased to 1.5 Amps to clean the coil.
6. The probe is withdrawn to the intermediate position and then, after the valves have closed, to the inject position ready for the next sample.

The cycle time for the above sequence is typically three minutes.

The robot MS-DS system described above allows repetitive, routine sampling to be carried out automatically, leaving the operator free to concentrate upon evaluating the results. In addition to relieving the tedium of manual probe operation, laboratory productivity can be significantly improved.

Presented at the 36th ASMS Conference on Mass Spectrometry and Allied Topics
June 5-10, 1988, San Francisco, CA

A NEW DEVICE FOR PYROLYSIS MASS SPECTROMETRY OF BIOLOGICAL MATERIALS

William M. Lagna
U.S. Army Chemical Research, Development and Engineering Center (SMCCR-DDT)
Aberdeen Proving Ground, Maryland 21010-5423.

Pyrolysis mass spectrometry has been utilized as an analytical technique for the profiling of biological materials which are well beyond the mass range associated with traditional mass spectrometry. The biomaterials, which include fungus, pollen, bacteria and viruses, are pyrolyzed for the release of characteristic compounds or groups of compounds. These chemical signatures can be used as the basis for identification of the compounds.

Recently, a pyrolysis device based on infrared heating has been integrated with a mass spectrometer and successfully implemented as an experimental biological sample processing system. As an extension of this technology, a low cost version of this pyrolyser was constructed using commercially available components (Figure 1). The new device was designed with provisions for batch sample introduction, interface to an aerosol sampling device or for direct sampling of airborne biomaterials within the pyrolyser volume. A programmable temperature controller is used for either isothermal or temperature-ramped heating and is programmed through the serial communications adapter of the data system of the mass analyzer. A section of quartz tubing is used for the construction of the pyrolysis cell. Quartz wool is placed within the cell and acts as the pyrolysis surface for batch samples, or as a filter when the device is interfaced with an aerosol sampler. The cell is wound with either platinum or nichrome wire and mounted within a larger quartz tube. A four-way tee is used to connect the unit to the capillary inlet of the gas chromatograph or mass spectrometer. The heater and thermocouple leads are passed through the connector with a feedthrough designed for such purposes, and a small vacuum pump is connected to the tee. The unit can be placed within the oven of a gas chromatograph, or insulated for stand-alone applications. A three way-tee on the opposite end can be used as an inlet for helium, as an interface to the capillary output line of an aerosol sampler or deleted for oxidative pyrolysis.

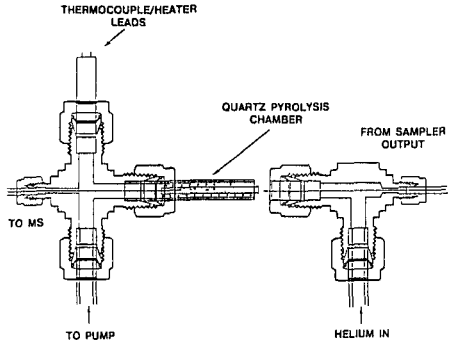

FIGURE 1
CUTAWAY VIEW OF THE NEW PYROLYSIS DEVICE

Initial runs were performed on batch introduced samples in a temperature programmed pyrolysis mode. The output was initially profiled on a flame ionization detector. Full gas chromatographed mass

spectrometry (GC/MS) was performed to determine if the nature of the pyrolysates were unique to each group. Mass spectra were acquired on a Finnegan Ion Trap detector using electron impact ionization.

Results in the batch introduction mode from samples of bee pollen, brewer's yeast, Acidophilus milk culture bacteria and urban particulate dust indicate that the temperature programmed pyrolytic signatures are reproducible and visually differentiable (Figure 2). Examination of the GC/MS data revealed that the pyrolytic components correlate well with the published data obtained using other pyrolytic methods on related materials (Figure 3). In addition, the lower temperature (up to 240 ^{o}C) pyrolysis data included a large number of higher molecular weight compounds.

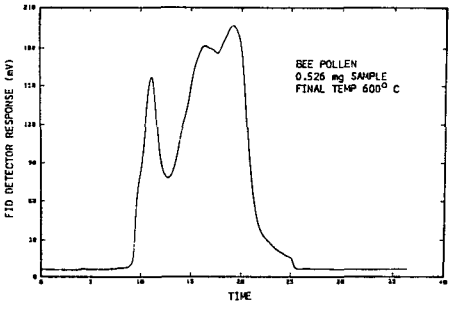

FIGURE 2
PYROGRAM OF BEE POLLEN

When interfaced with a virtual impaction aerosol sampler, isothermal operation of the pyrolyser resulted in signatures which appeared to vary with ambient conditions. The complex data sets require statistical analysis for interpretation. With the device connected to a small vacuum pump, very slow sample acquisition precludes simultaneous isothermal operation of the pyrolyser. In this mode, sample is collected for an extended period into the pyrolyser cell which is then heated in a temperature programmed mode. The resulting spectra are similar to those observed using the batch introduction method. However, substantial interferences from larger background particulates are observed and tend to mask the presence of the lower level biological materials. A coarse prefilter appears necessary to establish an upper-limit size cutoff and MS/MS could be utilized to increase the specificity of the method.

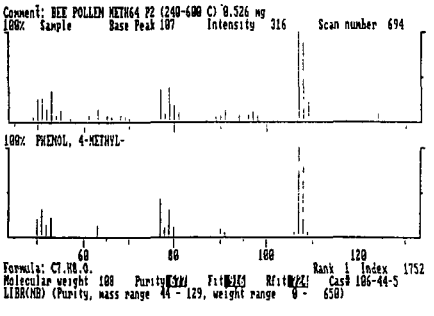

FIGURE 3
UPPER FIGURE IS A SAMPLE SPECTRA OF ONE OF THE PRINCIPAL PYROLYTIC COMPONENTS OF BEE POLLEN. LOWER FIGURE IS COMPUTER SEARCH LIBRARY MATCHED SPECTRA.

In conclusion, this device appears useful for general pyrolysis mass spectrometry applications on biological materials. The direct aerosol sampling method, although non-specific in nature, requires a minimal amount of sample preparation and could be used as a fast method of classifying airborne biological materials.

Presented at the 36th ASMS Conference on Mass Spectrometry and Allied Topics
June 5-10, 1988, San Francisco, CA

DEVELOPMENT OF A SELECTIVE SECONDARY ION ENHANCER FOR SIMS

M. Inoue, Y. Sugiyama, S. Nishigaki and T. Noda

Toyohashi University of Technology, Toyohashi 440, JAPAN

In SIMS (Secondary Ion Mass Spectrometry) measurements, it is well known that the detection sensitivity for positive or negative element is enhanced by flooding oxygen or cesium on the specimen surface. Therefore, oxygen or cesium ions have often been used as the primary ion. This method has a merit that the surface concentration of dosed elements is dependent only on the sputtering yield and not affected by the fluctuation of the beam current density. Contrary speaking, however, this method has a demerit that the concentration of dosed elements is hardly variable and the optimum condition is not usually established. Furthermore, in-situ detection of positive and negative elements is difficult because different ion guns are required. In the present study, we developed a compact secondary ion enhancement hardware that allows us to conveniently dose proper amount of oxygen gas and/or cesium vapor selectively onto the specimen surface, while retaining the same ion gun in operation. In this method, the surface concentration of dosed elements is easily controlled by varying the dose rate.

Since the secondary ion yield is very sensitive to the amount of dosed elements on the surface, it is important to monitor the elemental composition at the sputtering front under the ion bombardment for the reproducible SIMS measurement. ISS (Ion Scattering Spectroscopy) is, as well known as a very sensitive technique for outermost atomic layers, particularly adequate for this purpose. We recently developed a new technique for the sequential SIMS-ISS measurement[1)] by means of a double focusing mass analyzer of a commercial SIMS instrument operated with B^2/E linked scan method and AC modulation for the magnetic field B.

Figure 1 shows the construction of the newly developed O_2/Cs flooder. Oxygen gas is introduced into an experimental chamber through a variable leak valve and a stop valve, and then flooded onto the specimen surface through a capillary. The dose rate of oxygen was controlled with valve manipulation so

as to maintain the oxygen pressure unchanged. Actual oxygen pressure at the specimen surface was nearly three times of that indicated on a pressure gauge for the experimental chamber.

Cesium vapor is obtained by heating a powder mixture of Cs_2CrO_4 and Si in a crucible made of boron nitride. The dose rate of cesium was stabilized by feedback control of the crucible temperature. Figure 2 shows variations of the temperature and the ISS signal intensity from cesium on the specimen surface with time. It is obvious that the preset temperature is attainable within 20 seconds, and that the cesium concentration at the surface reaches stationary within a minute. It is thus concluded that enhanced measurement in SIMS can reproducibly be established by means of this O_2/Cs flooder unit in combination with the ISS technique.

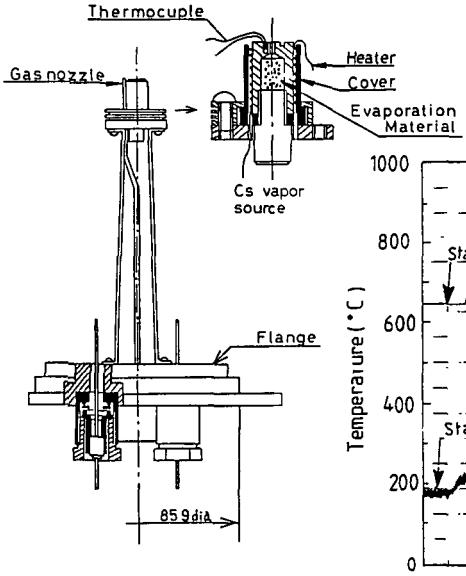

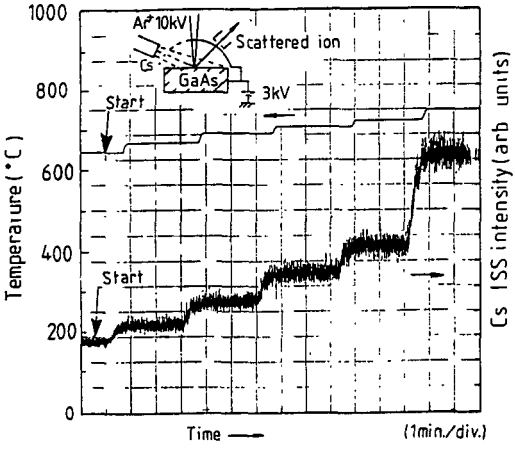

Fig.1. Construction of O_2/Cs flooder. Fig.2. Characteristics in Cs dose.

Reference

1) M.Inoue, Y.Sugiyama, S.Nishigaki and T.Noda:
To be published in Appl. Surf. Sci. (1988)

Presented at the 36th ASMS Conference on Mass Spectrometry and Allied Topics
June 5-10, 1988, San Francisco, CA

AN AUTOMATED REDUCED-PRESSURE INTERFACE DEVICE FOR THE HEWLETT-PACKARD MASS SELECTIVE DETECTOR. Patrick W. Langvardt, Michael J. Bartels, The Dow Chemical Company, Midland, Michigan, 48674.

An automated reduced-pressure interface device (RPID) has been developed for the Hewlett-Packard 5970 Mass Selective Detector (MSD). Because the MSD has no interface oven, considerable modifications of the original RPID design(1) were necessary. The result was a device that has all of the characteristics of the original RPID: chromatographically efficient, inert, complete analyte transfer, suppression of unwanted sample components, rapid column changing, pressure control at end of analytical column, low maintenance, and inexpensive.

The MSD design required that the interface be positioned in the oven of the gas chromatograph (see diagram). A custom-built (Scientific Glass Engineering, Austin, TX) glass-lined tee connects directly to the transfer line of the MSD. The MS restrictor tube (150 μ x 35 cm) determines the ratio of column effluent that can be diverted. The GC restrictor (120 μ x 40 cm) provides a 15 psi pressure drop such that the end of the analytical column is near atmospheric while the tee operates at reduced pressure at all times. It is important that the 1/16 inch tubing leading from the tee to the divert valve is coiled to provide a tightening of the seal to the MSD.

In operation, analytical columns can be changed in minutes by diverting gases away from the ion source. Ion gauge pressures of 10^{-6} torr are typical during that procedure. Analytical columns (0.18 to 0.53 mm id) are threaded over the protruding GC restrictor and butted inside the column connector.

The divert solenoid valve is powered by the GC injector A purge control circuitry and can be controlled manually from the GC front panel or by entries in the MSD computer Run Table via an optional A111 control board. Thus, the ion source is protected from unwanted sample components and column bleed, considerably reducing source maintenance.

The described MSD RPID has been installed on four instruments in our organization for several months. The devices have been applied primarily to automated trace analyses of complex matrices and have operated with little maintenance efforts. The RPID is a universal device for coupling capillary gas chromatography with mass spectrometry.

(1) Langvardt, P. W., Shadoff, L. A., Kastl, P.E., "Design and Applications of a Reduced-Pressure Interface Device for Capillary Gas Chromotography-Mass Spectrometry," ASMS, San Diego, CA, pp 837-38 (1985)

Presented at the 36th ASMS Conference on Mass Spectrometry and Allied Topics
June 5-10, 1988, San Francisco, CA

SCHEMATIC DIAGRAM OF THE MSD REDUCED-PRESSURE INTERFACE SYSTEM

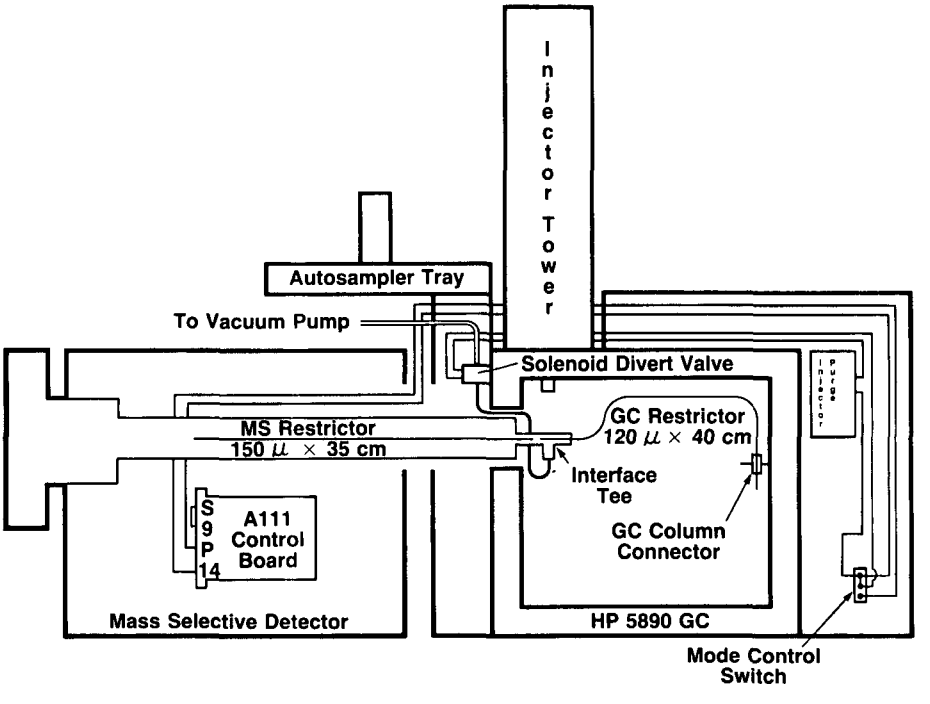

Presented at the 36th ASMS Conference on Mass Spectrometry and Allied Topics
June 5-10, 1988, San Francisco, CA

DYNAMIC FAB WITH A DIP GUN

Julius Perel and John F. Mahoney
Phrasor Scientific, Inc.
Duarte, CA 91010

INTRODUCTION

Continuous flow systems allow for the delivery of aqueous solutions with buffers and samples to a FAB sample target in a mass spectrometer at controlled rates [1]. To retain a thin liquid coating, flow and evaporation balance are achieved by control of the flow rate and the target temperature. The continuous flow system may be used as an LC interface or a batch load inlet for separate samples. It can also be used to monitor selected ions reflecting the progress of a biochemical reaction, and has been shown to greatly reduce chemical noise often observed with regular FAB.

A new device combining these advantages with those of a DIP Gun [2] used for FAB has been developed. The DIP Gun, which combines the ion gun and the sample target onto a single probe, offers several advantages over other designs. It requires only a single vacuum inlet part, rather than two. The gun-to-target distance is small (increasing flux), and alignment is fixed (facilitating alignment). The probe can be used with an EI source, allowing instantaneous calibration and molecular ion fragmentation. Furthermore, enhanced signal-to-noise has been found with the DIP Gun used on quadrupoles, evidently due to a reduction in fast particle scatter noise [3].

The DynaFAB Probe, a DIP Gun modified to accommodate continuous flow FAB, has all of the above advantages and is also capable of performing both dynamic and static FAB. A single probe replaces the FAB gun, the dynamic probe and the static FAB probe.

DynaFAB CONFIGURATION

A DIP Gun was modified to include a fused silica capillary (0.075 mm I.D. x 700 mm long) to deliver solution to the target. The capillary is brought into the probe shaft through an LC fitting using a special adapter, which is the major modification of a regular DIP Gun (see Fig. 1). The capillary traverses the shaft between the Teflon insulation and the inside of the shaft wall and passes through the extractor button about 3 mm from the Capillaritron nozzle. It threads through the inside of the sample tip and terminates at the target.

TEST RESULTS

The prototype DynaFAB Probe described above was tested on an HP5982 mass spectrometer using a solution containing 80% H_2O, 20% glycerol and 0.1 M ammonium acetate. A flow rate of 4.7 μℓ/min. was attained using atmospheric pressure to feed the solution in reasonable agreement with calculation for Pousille flow.

When the target was rotated to face 90° or 180° from the analyzer axis, fewer fast beam particles were scattered toward the detector, but the slow desorbed sample ions were still effectively collected for analysis by means of repeller and draw out fields in the source. While the sample signal was attenuated slightly, the scatter noise was greatly reduced by this rotation and the signal-to-noise ratio was greatly enhanced consistant with results for the unmodified DIP Gun [3].

Spectra were measured to demonstrate use of the probe in the various FAB modes. In the static mode the results showed no discernable difference from those obtained using a regular DIP Gun. A dynamic FAB spectrum of Stateze, a surfactant with a molecular weight of 256 amu, is shown in Fig. 2. The ionization source was maintained at 80°C and only minimal effort was made to optimize the temperature/flow relationship. Fig. 3 shows the spectrum of the same sample in the filament on (EI mode), thus showing glycerol peaks which could be useful for calibration.

Future tests are planned to optimize the operating variables and to allow for the direct and simple threading of the capillary tubing into the DynaFAB Probe.

REFERENCES

1. R.M. Caprioli, T. Fan and J. Cottrell, 34th Annual Conf. on Mass Spec. & Allied Topics, p. 213, Cincinnati, Ohio (June 1986).
2. J. Perel, K.F. Faull, J.F. Mahoney, A.N. Tyler and J.D. Barchas, American Lab, p. 94 (Nov. 1984).
3. J. Perel and J.F. Mahoney, 33rd Annual Conf. on Mass Spec. & Allied Topics, p. 853, San Diego, CA (May 1985).

Presented at the 36th ASMS Conference on Mass Spectrometry and Allied Topics
June 5-10, 1988, San Francisco, CA

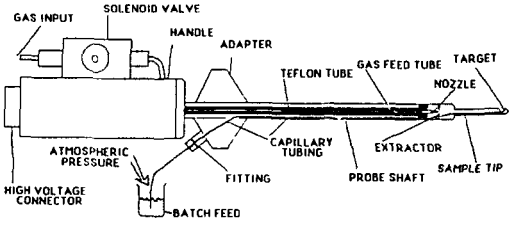

Fig. 1. Schematic of DynaFAB Probe

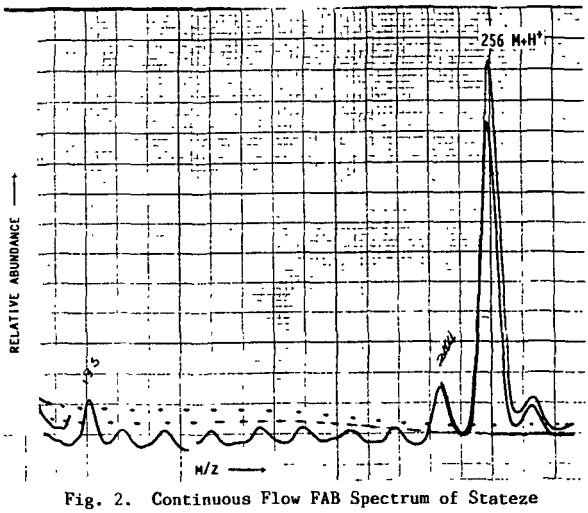

Fig. 2. Continuous Flow FAB Spectrum of Stateze

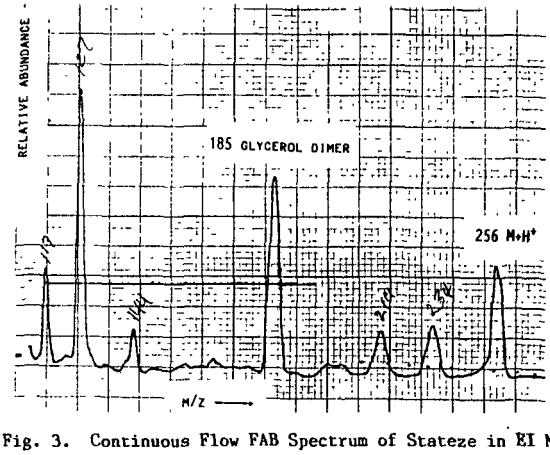

Fig. 3. Continuous Flow FAB Spectrum of Stateze in EI Mode

Presented at the 36th ASMS Conference on Mass Spectrometry and Allied Topics
June 5-10, 1988, San Francisco, CA

Design and Characterization of a Continuous Flow FAB Probe and an Ion Source Modified for Dynamic Sample Introduction

Mark R. Bauer and Mark F. Yancey

Battelle Columbus Division, Columbus, Ohio 43201

A simple, inexpensive continuous flow FAB probe was designed and tested which obviates several of the physical short comings of standard probe techniques. The new probe, which fits into a conventional VG FAB source, uses a 50 μm i.d. fused silica capillary column to deliver a constant flow of analyte and matrix to the probe tip for continuous analysis.

The probe, shown in Figure 1, is constructed from a 22 inch length of 1/2 inch stainless steel tubing. One end is threaded to accept a bullet-shaped polished copper tip, separated from the probe body with a hollow teflon insulator. A piece of 50 μm i.d. fused silica tubing runs inside the probe and extends about 0.1 mm through a 0.060 inch hole in the copper tip. The capillary is held in place by a septum sandwiched between the insulator and the inside of the copper tip. A 1/16 inch swagelock fitting is soldered to the other end of the probe to provide the vacuum seal.

The probe design mandated several modifications to the existing FAB source block so heat could be applied to the probe. These modifications are shown in Figure 2. Two holes were drilled through the block to accommodate EI-style cartridge heaters. To prevent the heater connections from protruding into other interfaces present in the source chamber, two 5x7 mm slots were milled into the bottom of the source block, thus allowing the heater connections to be made underneath the block.

There are no provisions in the conventional FAB source for heater or thermocouple connections. These connections, which are available for the EI source, were added by installing the appropriate leads to the FAB mounting plate and utilizing the EI control electronics. Figure 3 shows the positions of the connections added to the mounting plate. Because the FAB source block is held at the repeller potential, the thermocouple must be isolated from the block with ceramic insulators. The thermocouple is floated at the accelerating voltage by adding a short to the source potential feedthrough. These modifications to the source do not interfere with using the source in the conventional manner.

A variety of FAB applications may be accomplished with this new probe. The capillary which carries analyte to the probe tip can simply be dipped into the sample. Analyte can be continually introduced into the source using this "dip-and-suck" method. Dip-and-suck is typically accomplished by dissolving the analyte in a 5% glycerol in water solution, dipping the capillary into the sample and allowing the vacuum to aspirate the sample into the source. The flow rate is controlled by adjusting the length or diameter of capillary tubing used. A flow rate of 1 μL/min is typically achieved with a 1 meter, 50 μm i.d. capillary.

This mode of operation is especially useful for long experiments and MS/MS work which require the analyte signal to be present for extended periods. Dip-and-suck is also useful when analyzing many consecutive samples; it eliminates the constant insertion and removal of the probe. Kinetic and other dynamic experiments can easily be monitored, as there is always a fresh supply of the reaction mixture to the ionization surface. An HPLC loop injector can also be added to improve the reproducibility of small volume injections.

Chromatographic separations can be accomplished inside the probe by replacing the 50 μm tubing with a 250 μm i.d. packed capillary column filled with 3-5 μm packing material. By placing the column inside the probe, only a 2 cm length of 50 μm tubing is needed as an interface to the probe tip.

The short interface results in a minimum amount of peak broadening. Due to backpressure of the column, a pump is required to deliver a flow of about 1 μL/min. Figure 4 shows a selected ion chromatogram of the protonated molecular ion from pyridostigmine generated using the packed capillary interface. The mobile phase used was 100% acetonitrile; no glycerol was added.

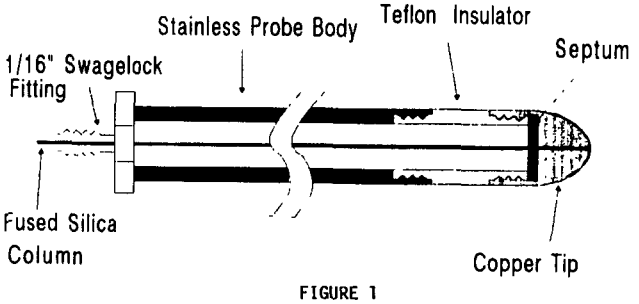

FIGURE 1

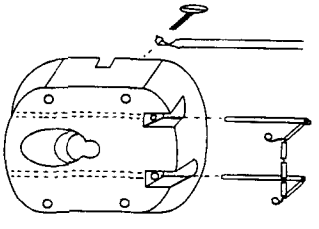

FIGURE 2

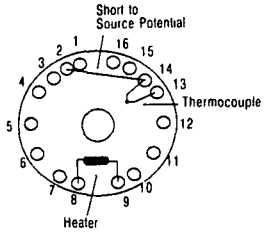

FIGURE 3

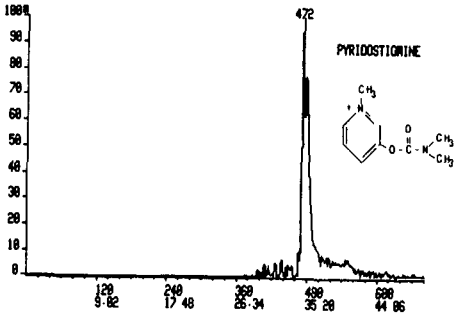

FIGURE 4

Presented at the 36th ASMS Conference on Mass Spectrometry and Allied Topics
June 5-10, 1988, San Francisco, CA

THERMOELECTRICALLY COOLED SAMPLE PROBE FOR FABMS (LSIMS)

S.A. Martin*, J.A. Hill, K. Biemann
Dept. of Chemistry, Massachusetts Institute of Technology, Cambridge,MA 02139
*on leave of absence Dept. Pharmacology, Med. Univ. of South Carolina

Since the introduction of FAB the effect of temperature on the secondary ion yield of samples has been noted (1) and recently the design and construction of a chilled probe employing freon was described (2). We report here the design, construction and operation of a thermoelectric (Peltier) cooler in which surface temperature, above or below ambient, is precisely regulated by applied current.

In a thermoelectric (Peltier) cooler, current is applied to semiconductor junctions between two layers of beryllium oxide which results in the cooling of one surface and the heating of the other. These devices are commercially available and can be obtained in sizes small enough to be incorporated in the tip of a sample probe that fits through the normal vacuum lock of a FAB probe.

The ability to cool the matrix has several advantages. First, it allows the use of a wider variety of matrices because their vapor pressure can be reduced to the point that the evaporation rate is sufficiently slow to obtain a long lasting secondary ion current. Second, the Peltier cooler has a reproducible current *vs.* temperature curve which allows reproducible fast attainment of surface temperatures. Third, by reversing the potential, the probe tip can be heated and thus permits the use of low melting matrices. Such a system is more convenient to use and more reliable than chilled probes operating with cold gases or low boiling liquids (Freon).

We have built and tested such a thermoelectrically cooled sample probe (Fig. 1) and use it routinely on our JEOL HX110/HX110 tandem mass spectrometer (EBEB). The thermoelectric heat pump modules are purchased from MELCOR Corp, Trenton, NJ 08648, part no. FC0.45-4-05L. The thermoelectric sample probe is calibrated for cooling (Fig. 2) and heating (Fig. 3) by recording the sample surface temperature under vacuum as a function of applied current. As a test case, the ion current of of the $(M+H)^+$ isotope cluster of aprotinin (MW 6507.0) in thioglycerol kept at -4 °C showed a twentyfold increase in ion current as compared to operation at ambient temperature. It also lasted for more than 6 min as compared to less than 2 min. The S/N of the data is also improved by the lower temperature. Measurements have also been made of the secondary ion yield of various matrices at various temperatures. A comparative study of the relationship of the secondary ion yield of various peptides and small proteins *vs.* probe tip temperature has been carried out.

The thermoelectric temperature regulated sample probe was inexpensive to build and has been in routine use in our laboratory for more than 8 months with only a single structural failure. During this period its applications have ranged from two sector high mass to negative ion MS/MS studies providing longer lasting secondary ion signals and a wider range of matrix options.

Acknowledgement. This work was supported by a grant from NIH (RR00317). The authors would like to thank Dr(s). I.A. Papayannopoulos and C.E. Costello for data used in this study.

(1) D. F. Hunt, W. M. Bone 29th ASMS, 357-358 (1981).
(2) A.M. Falick, F.C. Walls, R.A. Laine Anal. Biochem. 159(1), 132-137 (1986).

Presented at the 36th ASMS Conference on Mass Spectrometry and Allied Topics
June 5-10, 1988, San Francisco, CA

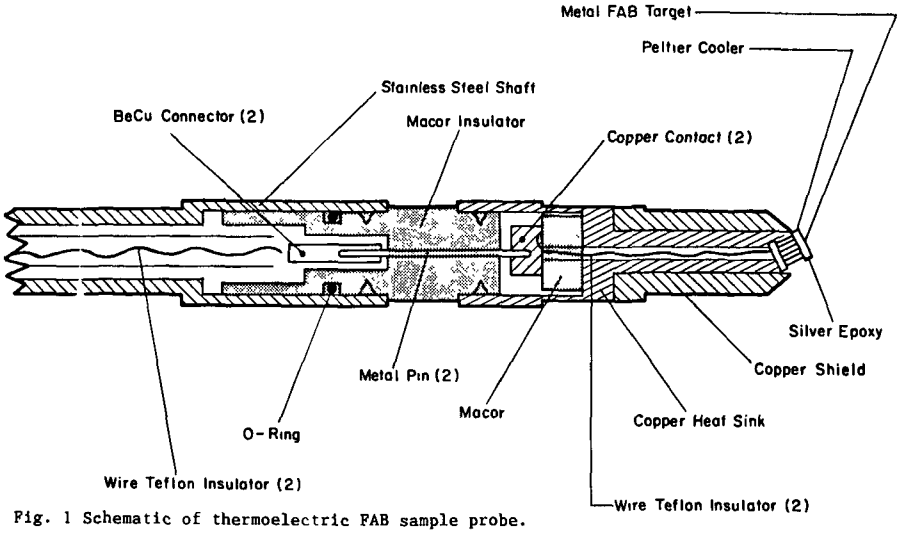

Fig. 1 Schematic of thermoelectric FAB sample probe.

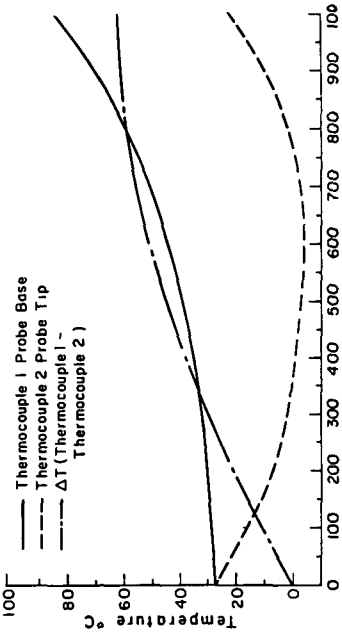

Fig. 2 Plot of the effect of varying the applied current to the thermoelectric module on the sample surface temperature in the cooling mode. These measurements were done in vacuum in which thermocouple 1 is attached to the probe base and thermocouple 2 is attached to the sample surface.

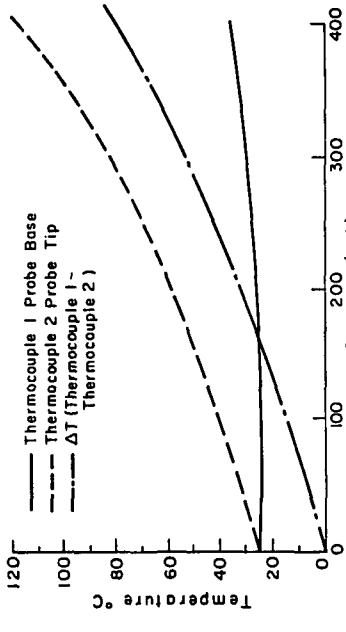

Fig. 3 Plot of the effect of varying the applied current to the thermoelectric module on the sample surface temperature in the heating mode.

Presented at the 36th ASMS Conference on Mass Spectrometry and Allied Topics
June 5-10, 1988, San Francisco, CA

STUDIES WITH FAST ATOM BOMBARDMENT PROBE TARGETS

Marshall M. Siegel*, Rushung Tsao, William Boulay

American Cyanamid Company, Medical Research Division,
Lederle Laboratories, Pearl River, NY 10965

1) ENCLOSURES FOR PLANAR AND ARTICULATED FAB PROBE TARGETS

Sputtering and splattering of both the FAB matrix and sample from a planar FAB probe target often occurs at an excessive rate resulting in short sample lifetime, source contamination and losses in sensitivity and resolution. When using an articulated FAB probe target for exact mass measurements, the uncontrolled sputtering and splattering occasionally quench the signal of the unknown or reference compound.

To alleviate the above problems, a variety of enclosures were designed for the planar and articulated FAB probe targets. FAB target styles I and II were found to enhance sample lifetime and reduce source contamination. Style I is effectively a three walled enclosure about the planar FAB target where the top is opened and the fourth side is absent enabling the fast atom beam to strike the sample. Style II is similar to style I except that the top is covered and a slit is provided for the exit of the ion beam. Dimensions for these probe targets when used on a VG ZAB-SE FAB source are: length - 0.25", width - 0.08" (0.18"), height - 0.13" (0.25") and slit width - 0.015".

The effect of sample lifetime was studied for a variety of FAB targets of similar dimensions on which was applied 5.0 ul of sulfolane, a more volatile FAB matrix. The sample lifetime was about two times longer with target style IA vs. the planar target. The sample lifetime was about four times longer for target style IIA vs. the planar target, the initial total ion current was reduced by a factor of about four times and the net resolution increased from 1000 to 1500. (The beam from the FAB gun must be alligned with the opening on the side of the style II target for optimum ionization of the sample. The ions can then exit through the slit on the cover of the FAB target.)

The use of especially style IA FAB target in our laboratory has enabled us to use volatile matrices, run large numbers of routine samples with reduced source contamination and arcing, and enhance the lifetime of samples for nominal and exact mass measurements. With the targets, polyethylene glycols and their derivatives (neutral surfactants adulterated with potassium ions) which seriously contaminate the FAB source, can be used with minimal source contamination as internal standards for exact mass measurements. The behaviour of the FAB target enclosure mimics some of the characteristics of commercially available exchangeable ion volumes for FAB sources.

2) PROBE TARGET DESIGNED FOR DYNAMIC FAB

Target style III was designed for dynamic FAB based upon the three sided enclosure of the style I target. The sample is confined to flow in a recessed narrow region of the target (depth - 0.05", length - 0.10", width - 0.05") in order to achieve optimum sensitivity and minimization of sputtering and splattering of the liquid sample so as to control the sample lifetime. The collar around the target serves to shield the bottom surface of the inner dynamic FAB target from the fast atom beam, thereby, minimizing memory effects. It also serves to trap any liquid which may acculmulate, after flowing over the dynamic FAB target, and to channel it away from the fast atom beam to the drain hole.

3) HEATED FAB PROBE TARGETS

Heated FAB targets were fabricated utilizing nichrome wire (0.010" and 0.004" diameter) as the heating element. The VG DCI power supply was used to generate the heating current. Style IV heated FAB target consists of a heater coil which coaxially surrounded the planar FAB target upon which the sample is placed. Style V heated FAB target consists of nichrome wire folded to form a plane upon which the sample resided so as to be heated directly by the nichrome wire. Style VI heated FAB target is a nichrome coil mounted inside a FAB target enclosure. The matrices evaluated were mannose, polyphenyl ether and fomblin oil. The properties of the latter two materials, viz., high

boiling points, very low vapor pressures and high thermal stabilities, enable samples to be analyzed in these liquids at relatively high temperatures.

Figure 1A illustrates the FAB mass spectrum of tri-tyrosine methyl ester acquired at room temperature with "magic bullet" matrix and Figure 1B illustrates the spectrum at elevated temperature with style IV target and mannose as the matrix. In the high temperature spectrum, note the absence of matrix ions and the additional fragmentation relative to the room temperature spectrum. For the model compounds studied to date, no significant spectral differences were observed at elevated temperatures as a function of tip style or high temperature FAB matrix. These observations are similar to those reported by Ackermann et al [1,2]

[4] INSERT FOR THE VG EI/CI DIRECT PROBE

A stainless steel insert was fabricated and placed within the boron nitride sample holder assembly of the VG EI/CI direct probe. This insert provides for rapid heat transfer to the sample cup from the heatable/water cooled end of the direct probe.]

1. B. L. Ackermann, J. F. Holland, J. J. Watson Anal. Chem. 57, 2656 (1985).
2. B. L. Ackermann, J. F. Holland, J. J. Watson Biomed. Envir. Mass Spectrom. 14, 501 (1987).

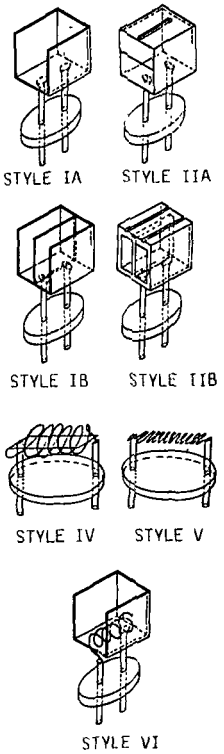

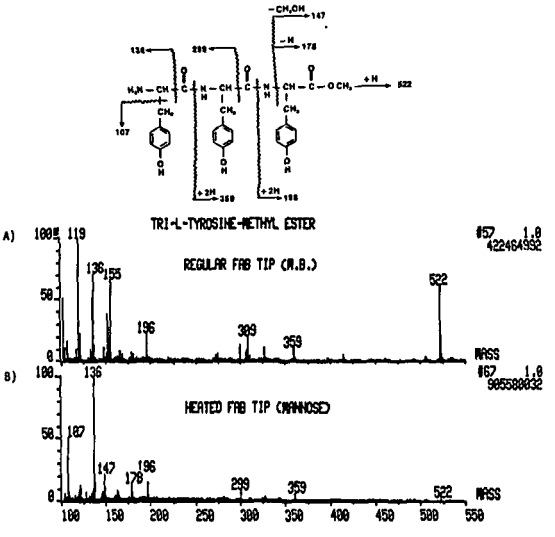

Figure 1. A) "Magic Bullet" background peaks: 103, 119, 135, 155 and 309.
B) Mannose background peaks: 127, 145 and 163.

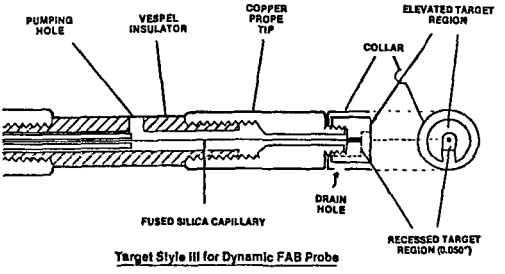

Target Style III for Dynamic FAB Probe

Presented at the 36th ASMS Conference on Mass Spectrometry and Allied Topics
June 5-10, 1988, San Francisco, CA

MINIATURIZED SOLID-STATE EI/FI ION SOURCE

Steve Young and Michael J. Coggiola
SRI International, Menlo Park CA, 94025

A miniaturized ion source has been developed and tested that is capable of performing either electron impact or field ionization depending on the polarity of the voltage applied across the device. The basis for this source is a solid-state, micromachined structure that is fabricated using techniques similar to those employed for integrated circuit fabrication. The device consists of an array of 10,000 2 μm diameter wells etched in silicon dioxide on a silicon substrate. Each well contains a molybdenum cone whose tip is coplanar with a molybdenum gate film deposited on the top of the silicon dioxide. Th application of a modest voltage (50-150 volts) between the tips and the gate film produces very high (10^8 v/cm) local electric fields. As originally developed, these devices were designed as cold electron sources producing electrons via field emission. However, by reversing the polarity of this voltage, the high field can also produce positive ions via field ionization.

A compact ion source was designed and built by placing the 1x1 mm emitter array in an enclosed volume of 1 cc, opposite to an ion extraction aperture. Sample gas was admitted directly into the source volume. A number of source designs were investigated using ion trajectory simulations (SIMION) and the optimum configuration was selected for fabrication. For test purposes, the source was mounted on an Extrel quadrupole, and electrically floated so that the ion energy could be established between 10 and 100 volts. The emitter tips were driven in a pulsed mode with 60 Hz half wave rectified ac of variable amplitude.

When operated in the EI mode, typical electron currents were 10-20 μA. Organic vapor samples exhibited mass spectra very similar to standard electron impact spectra. Some small differences were noted, however, these are likely due to differences in the electron energy and the source temperature. With the polarity across the emitter array reversed, characteristic positive FI mass spectra were observed consisting primarily of organic sample parent ions. Because of the very small dimensions of the active field emission sites, the voltages required to produce field ionization are very low. A typical plot of ion current as a function of the applied voltage is shown in Figure 1. It is noteworthy that a potential as low as 70 volts was able to generate an electric field strength sufficient to produce field ionization.

Sensitivity for this source was higher in the EI mode than the FI mode. Typical total ion signal levels for a 1 x 10^{-6} Torr sample pressure of n- propyl benzene were 400 kHz in the EI mode and 10 kHz in the FI mode. As a result of prolonged operation in the FI mode, it was observed that higher voltages were required to obtain the same ion currents. This behavior is most probably associated with the deposition of conductive organic polymers on the device. These materials lead to a leakage path between the emitter tips and the gate film, thus requiring higher potentials to establish the same local electric field strength. Even if a leakage path is localized to a few emitter cones, it will affect the entire array since all tips are electrically connected in parallel.

These preliminary studies have shown that a miniaturized EI/FI source can be based upon a microfacbricated, solid-state device. Such a source could potentially be made much smaller than the version described here since the active area of the array is only 1x1 mm. In addition, the low sensitivity of this source in the FI mode could be enhanced by improving the sample introduction method. At present, FI depends on the diffusion of sample vapors into the regions of high field strength near the emitter tips. A more efficient mechanism of sample delivery would thus improve the FI sensitivity.

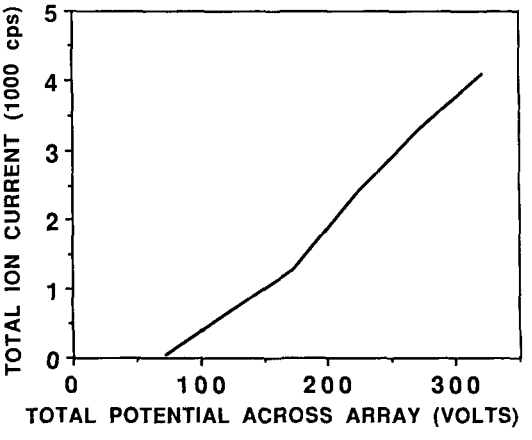

Figure 1. Total ion current for *n*-propyl benzene in the FI mode as a function of the potential across the source.

Presented at the 36th ASMS Conference on Mass Spectrometry and Allied Topics
June 5-10, 1988, San Francisco, CA

A GAS TRAP FOR HEADSPACE GC/MS ANALYSIS.

Jia-shen Wang*, Avelina Qua, and Ira E. Rosenberg
Clairol Inc., Stamford, CT 06922

Headspace/gas chromatography (HS/GC) or headspace/gas chromatography/ mass spectrometry (HS/GC/MS) have been widely applied for the analysis of volatile compounds in the presence of non-volatile matrices. At Clairol we have constructed a gas trap which can be directly coupled with a Finnigan GC/MS system for headspace analysis. The advantages of this set-up are: the device is very easy to install and remove from the GC/MS system, will not effect the performance of the system, no modification of the GC inlet system is necessary, and the whole unit is very compact, inexpensive and easy to fabricate. The set-up is shown in Figure 1. The device can be divided into three portions: the desorber, the power and temperature control unit (P/T unit), and the

Figure 1. Gas Trap & GC Configuration

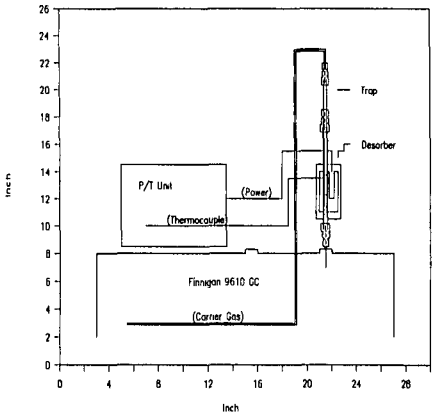

Figure 2. Desorber & Trap

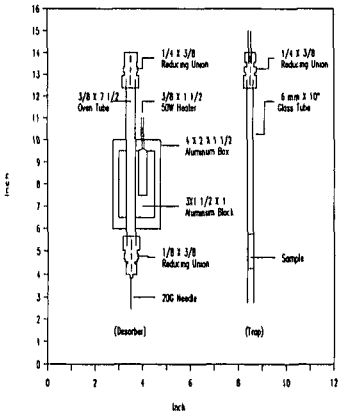

trap. The dimensions of the desorber are similar to that of Priestley's design[1]. Modifications, however, have been made to simplify construction and operation. The desorber and the trap are shown in Figure 2.

The desorber is made with a piece of 1"X1.5"X3" aluminum block and was enclosed with a 1.5"X2"X4" aluminum box. Glass wool was packed between the box and the block for insulation. A 3/8" i.d. hole was drilled through the block and the box for an oven tube. A 3/8" i.d. blind hole was drilled for a cartridge heater. The heater is a 3/8"X1.5" 50 watt cartridge heater. The oven is a 3/8" o.d. and 7.5" long stainless

steel tube. Two Swagelok reducing unions were attached at the ends of the tube. The center of the top union was enlarged to 1/4" in order for a trap to pass through. A 20 gauge needle surrounded with a piece of 1/8" o.d and 1/2" long copper tube was inserted into the 1/8" end of the lower union.

The trap was made of a 10" long 6 mm glass tube with one end attached to the 1/4" side of a 1/4 X 1/8 Swagelok reducing union. The 1/8" side of the union was connected with a piece of 1/8" o.d and 3" long copper tube which was then connected with a Tygon tube for carrier gas. Either the adsorbent or a sample should be packed near the end of the tube which would sit in the heating zone when a trap was fully inserted in the heating block.

The temperature of the heating block was controlled by the P/T unit. The J-type thermocouple was used for temperature mesurement. The P/T unit is a 10 ampere analog temperature controller (Thermon Manufacture Company) enclosed with a 6" X 8.5" X 9" metal box. A jack for the J-type thermocouple was mounted on the front of the box. A jack for the 120 v. power line was mounted on the side of the box.

The trap was operated in two modes: trapping and desorption. In the trapping mode, the glass column was packed with an adsorbent. In the other mode the column will be packed with sample only. In either case, once a tube was loaded, the subsequent procedure is the same. The sample end of the tube was inserted into the oven about 1". The other end was connected to a gas outlet of the GC which was used for measuring the carrier gas flow rate of the packed GC. The heating block was then connected to the GC by punching the needle into the injection port of the Packed GC. The next step is to set the GC in the carrier gas measuring mode. The carrier gas will enter into the trap and then into the GC. After 30 seconds (to remove the air in the trap), the trap was inserted into the oven tube totally and the GC/MS set to run. The volatiles were desorbed by heat. The carrier gas carried the volatiles into the GC for a GC/MS analysis.

This device in conjunction with the GC/MS system had been used to perform headspace analysis for malodorous samples (e.g. to detect the hardener in the plastic used to manufacture rollers). The device has also been used to analyze directly samples (0.2 gram of non-volatile) where the contaminats (volatiles) were in the range of fractions of ppm. Most important, however, is that the device enables us to analyze samples which are chemically unchanged prior to the MS analysis. Therefore, contamination due to sample preparation is minimal.

1. L. J. Priestley, Jr. and B. E. Wilkes, Microchemical J., 24, 88 (1979).

Presented at the 36th ASMS Conference on Mass Spectrometry and Allied Topics
June 5-10, 1988, San Francisco, CA

CONCEPTS AND APPLICATIONS OF SHORT OPEN TUBULAR COLUMNS IN GAS CHROMATOGRAPHY/MASS SPECTROMETRY

Mark E. Hail, and Richard A. Yost, University of Florida,
Department of Chemistry, Gainesville, FL 32611.

The multidimensional information provided by mass spectrometry and tandem mass spectrometry reduces the necessity of chromatographic resolution for mixture analysis. The use of short (e.g. 3 meter) open tubular columns in GC/MS provides several notable advantages (1). Chromatographic theory predicts that optimum carrier gas velocities are higher when the column outlet is at vacuum, and with short open tubular columns higher flow velocities can be used without much loss of chromatographic efficiency. Analysis times are reduced by a factor of 30, if a 3 m column is used instead of a 30 m column, and both are operated at their optimum gas velocities. The reduced analysis times are due to the reduction of the column length by a factor of 10, as well as the increase in the optimum gas velocity by a factor of 3 for the shorter column. In addition, the resolution lost by a using a column that is 10 times shorter is only a factor of the square root of 10.

The increased optimum carrier gas velocities obtained with short columns with vacuum outlet is due to the reduction of the average column pressure. A better understanding of this phenomenon can be obtained by observing the effects of the outlet pressure on the calculated pressures at each point along a 3 m column, as shown in Figure 1. Figure 2 shows the theoretical dependence of the plate height on the average gas velocity for the same outlet pressures used in Figure 1. Note that the behavior is essentially the same for 100 Torr and 1 Torr outlet pressures. Thus, any GC detector which could be operated at the reduced outlet pressures would offer significant advantages in terms of speed of analysis.

The limitation is that short columns with vacuum outlet require sub-atmospheric inlet pressures, if optimum gas velocities are to be obtained. This is demonstrated in Figure 3 for both He and H_2 carrier gases. Most capillary GCs use pressure regulators, thus optimum velocities can not be obtained with short columns operated with reduced outlet pressures. Alternatively, a flow-controlled system can be used, as shown in Figure 4. This system allows the injection port to be operated at reduced pressures in the split or splitless mode. In particular, during splitless operation, the sample is injected at pressures slightly above atmospheric, and then the pressure is sharply reduced after a few seconds (i.e. after allowing all of the sample to be loaded onto the column).

Flow programming of the carrier gas has been evaluated as an alternative to temperature programming for use with chemical ionization (CI). In fact, exponential flow programming of the carrier gas results in peak distributions similar to those obtained with linear temperature programming (2). This is demonstrated in Figure 5, which shows a comparison of temperature and flow programmed runs. The sensitivity under electron ionization (EI) conditions decreases dramatically with increasing flow rates of carrier gas into the ion source. Thus, vacuum inlet pressures (and thus lower flow velocities) are preferred for the use of EI and short columns. However, studies have shown that carrier gas flow rates as high as 30 mL/min can be used without degrading CI mass spectra. Even when H_2 is used as a carrier gas and is present in the source at pressures of 0.5 Torr, methane CI spectra are unaffected. This is apparently due to the fact that the hydrogen reagent ions (H_3^+) are used in the protonation of methane gas, since methane has a higher proton affinity than hydrogen.

One advantage of flow rate programming is that lower temperatures can be used to separate thermally labile components. Another advantage is that a high sample throughput can be obtained, since column equilibration is accomplished by an essentially instaneous resetting of the column flow rate. These concepts are being applied toward the development of a compact GC, which utilizes short open tubular columns and is approximately the same size as a conventional direct insertion probe. Flow programming would be particularly attractive for isothermal operation of the probe-type GC, since it would not be necessary to cool the probe between injections.

Presented at the 36th ASMS Conference on Mass Spectrometry and Allied Topics
June 5-10, 1988, San Francisco, CA

References:
(1) Trehy, M. L.; Yost, R. A.; Dorsey, J. G. Anal. Chem. 1986, 58, 14.
(2) Nygren, S.; Anderson, S. Anal. Chem. 1985, 57, 2748.

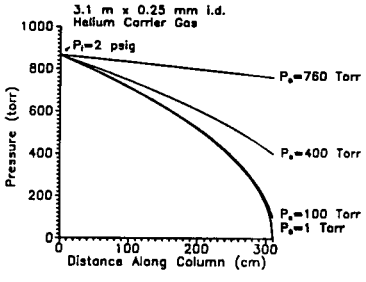

Figure 1. Effect of the outlet pressure on the pressure calculated at each point along a 3.1 m open tubular column.

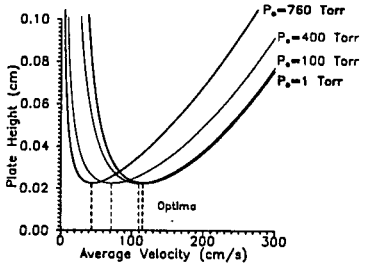

Figure 2. Plots of plate height vs. average velocity illustrating increase in optimum gas velocity associated with decreased outlet pressures.

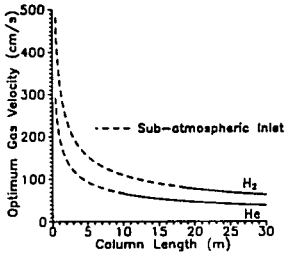

Figure 3. Plot of optimum gas velocity vs. column length illustrating need for reduced inlet pressures with short columns.

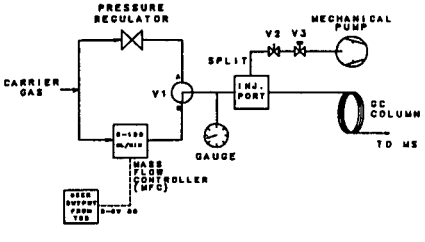

Figure 4. Schematic of flow control system designed for operation of the injection port at reduced pressures and for flow rate programming.

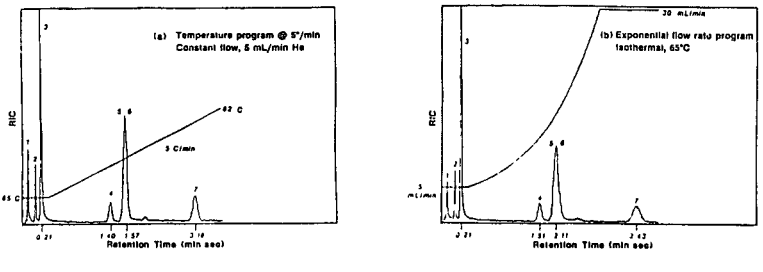

Figure 5. Comparison of (a) temperature programming and (b) flow rate programming on a 3 m column.

Presented at the 36th ASMS Conference on Mass Spectrometry and Allied Topics
June 5-10, 1988, San Francisco, CA

CAPILLARY GC/MS FOR THE DETECTION OF ORGANIC FIREARMS DISCHARGE RESIDUE

Dean D. Fetterolf and Robert D. Koons
FBI Laboratory, Forensic Science Research Unit
FBI Academy, Quantico, Virginia 22135

The most common method to indicate the handling or discharging of a firearm involves the analysis of hand swabs for antimony, barium and/or lead, components of the primer mixture. Another popular method involves particle analysis of primer residue by scanning electron microscopy. Interpretation of the forensic significance of the elemental concentrations is compounded by their ubiquitous environmental presence. Particle analysis methods are time consuming.

The majority of firearms propellants are double-based composition; containing nitroglycerine (NG), nitrocellulose and stabilizers such as ethylcentralite or diphenylamine. Typical ammunition ranges from 10% to 40% by weight NG. Due to its limited usage, NG is not a common environmental contaminant. Attempts at determining the organic residue on hands has met with limited success and application. Most procedures involve the use of HPLC with reductive electrochemical detection.

Using solid phase extraction and GC/MS we have developed a rapid and simple procedure for the detection of NG on hand swabs. Cotton swabs moistened with methyl tertiary butyl ether (MTBE) are rubbed across the back of the hands of suspected shooters. NG is extracted from the swabs with 2 x 1 mL pentane washes. Sample clean-up is carried out using a preconditioned (pentane/ethyl acetate) disposable diol (Supelclean, LC-Diol) extraction column. Following a 1 ml pentane wash, the NG is eluted with 1 mL ethyl acetate into a silanized screw cap vial.

Results of recovery studies from various packing materials indicated that the diol or CN packing provided complete recovery from the column (100% and 98% respectively). Micropacked XAD-7 columns showed 62% recovery while SAX columns only 14%. Recovery of 92 ng NG from spiked swabs ranged from 80% to 90%. The effect of contamination on recovery was studied by spiking swabs with 92 ng NG along with 100 μL of contaminant. Recoveries from swabs contaminated with gasoline, hand lotion and floor sweepings were 80%, 85%, and 87% respectively.

Using cold on-column injection 1 μL of the eluant is chromatographed on a 0.1 micron film, 15M DB-5 x 0.25 mm ID capillary column temperature programmed from 100 C to 250 C. Using electron capture negative chemical ionization, the NG is detected by multiple ion detection at m/z 46 $(NO_2)^-$ and 62 $(NO_3)^-$ on a Finnigan-MAT TSQ-45 operated in the Q3 MS mode. Relative sensitivities observed for EI (m/z 46,76), PCI (m/z 46,76), and NCI (m/z 46,62) were 1.0, 1.6 and 352 respectively. A limit of detection of 0.3 pg NG has been obtained. This corresponds to 0.3 ng NG on the hand. Hand blanks from non-shooters showed no interference with the NG peak using the above procedure. Figure 1 shows the chromatographic results of the injection of a hand blank, swab extracts from a shooter after firing three shots with a Smith and Wesson (S&W) 38 Special and a 92 pg NG standard.

A number of studies relevant to the forensic utility and interpretation of the data are underway. Where is NG deposited on the hand? What are the effects of weapon choice and firing method? What effect does activity have on the recovery of NG from the shooter's hand?

The highest amounts of NG are typically recovered from the thumb-web-forefinger area of the shooting hand. Test firing a variety of weapons has shown NG deposition ranging from 1.2 ng to 1,600 ng. Some typical results from swabing the left and right backs of shooter's hands are shown in Figure 2. As expected, the choice of weapon (38 caliber Smith and Wesson vs. 22 caliber RG) and the firing method (right handed vs. 2 handed) effect NG deposition. In addition, no NG was recovered from the hand of a non-shooter moving throughout the firing range or from the hands of a person having fired 6 shots the previous day.

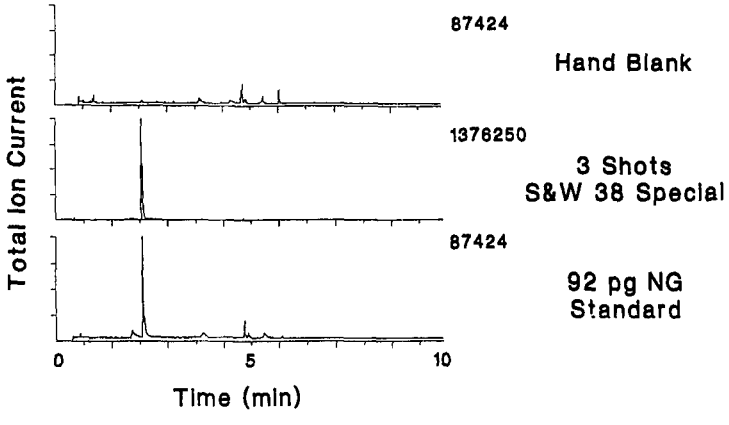

Figure 1. Chromatographic results for hand blank, 3 shots - Smith and Wesson 38 Special and 92 pg NG standard.

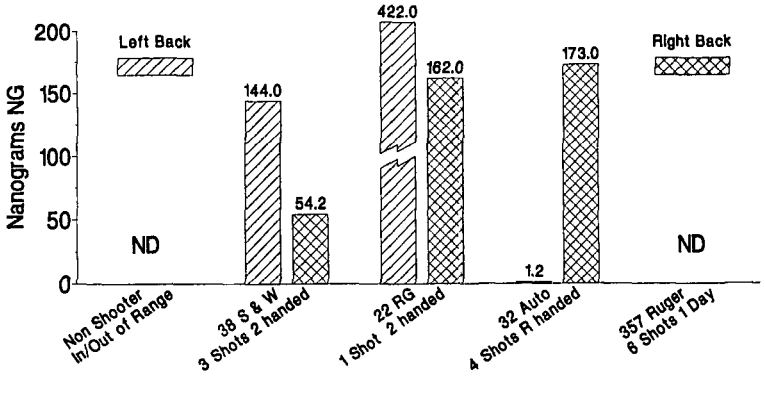

Figure 2. Typical results demonstrating effect of weapon, firing method and activity on NG deposition.

Presented at the 36th ASMS Conference on Mass Spectrometry and Allied Topics
June 5-10, 1988, San Francisco, CA

CAPILLARY SUPERCRITICAL FLUID CHROMATOGRAPHY NEGATIVE ION CI MASS SPECTROMETRY OF TRICHOTHECENE MYCOTOXINS

John A. G. Roach, Denis Andrzejewski and James A. Sphon, Damico MS Lab,
Division of Contaminants Chemistry, Food and Drug Administration,
Washington, DC 20204

Purpose

Trichothecene mycotoxins are produced by various fungi which attack agricultural products. These compounds can be detected in food extracts by mass spectrometry (MS) but they are difficult to gas chromatograph. Extensive sample preparation is usually required for combined gas chromatography/MS. Supercritical fluid chromatography (SFC) is an alternative to gas chromatography (GC). Thus, there are three purposes for this work:

(A) To determine if it is advantageous to use SFC rather than GC for trichothecene analyses.
(B) To design an SFC/MS interface and define parameters suitable for trichothecene analyses.
(C) To determine if SFC is compatible with negative ion MS of trichothecenes.

SFC/MS Interface Design Criteria

(A) SFC/MS interface would not impede GC/MS or probe analyses.
(B) Fabrication used existing equipment and available materials.
(C) Adequate control of interface and restrictor temperatures.

Need for SFC Restrictor Temperature Control

A restrictor is required at the end of the capillary column to maintain SFC conditions throughout the column. In an SFC/MS interface, the restrictor must separate the high vacuum of the MS from the high pressure of the SFC column and still permit the transmission of sample into the MS. The expansion of mobile phase at the exit of the column cools the tip. Therefore, heat must be added to the restrictor to assist in vaporization of the effluent.

Our interest in thermally labile samples caused us to use two heated zones in the SFC/MS interface. The tip of the restrictor is heated independently of the rest of the interface. The two zones permit the selection of interface temperatures which minimally heat the SFC effluent.

Component Parts of SFC/MS Interface

The fabricated parts of the interface are a block heater on the ion source, a hollow direct inlet probe and a flexible coupling between the probe and the SFC oven.

A standard porous frit supplied by the SFC manufacturer acts as the restrictor. The restrictor is coupled to the column with a zero dead volume butt connection and threaded through the interface until the frit is at the tip of the direct inlet probe. A swagelock tee in the handle of the probe supplies CI reagent gas coaxially to the source through the probe.

The major portion of the SFC/MS interface is maintained at or near the SFC oven temperature. The frit in the tip of the restrictor is independently heated by a block heater that replaces the standard ion source inlet adapter on the ion source.

Experimental

The trichothecene mycotoxins T-2 toxin, deoxynivalenol and roridin A were used to evaluate the effect of restrictor temperature and carbon dioxide mobile phase on the negative ion CI spectra of these compounds under electron capture, proton abstraction and chloride attachment conditions. The reagent gases employed were:

(A) methane - resonance electron capture CI
(B) methane/nitrous oxide - hydroxide ion CI
(C) methane/difluorodichloromethane - chloride CI

Split and splitless 0.2 ul injections were made. A 10:1 splitter was used for the split injections. An uncoated 40 cm length of 0.075 mm i.d. fused silica tubing was used to couple the injector valve to the 10 m x 0.050 mm i.d. fused silica methyl silicone capillary column for splitless injections.

Column temperature was maintained at 100 C. The width of each mycotoxin response narrowed as the temperature of the frit was raised to approximately 100 C above the published melting point of each mycotoxin. As examples: the width of a T-2 response was 50 sec at 225 C and 10 sec at 245 C; a roridin A response continued for 9 minutes at 245 C, but an equal amount of roridin A eluted in 20 sec at 295 C.

The negative ion mass spectra of the trichothecenes obtained by SFC/MS were comparable to those obtained by direct probe. No significant interferences were observed to arise from the carbon dioxide mobile phase. Repetitive scans of a 500 dalton window readily detected 40 ng of the trichothecenes using the 3 negative ion CI reagent species chosen for this study.

Conclusions

Combined SFC/MS can be used for the confirmation of trichothecene mycotoxins in the negative ion mode. Restrictor temperatures less than 100C above the melting point of the samples retard sample transfer into the MS, but neither restrictor temperature nor carbon dioxide mobile phase significantly affect negative ion CI conditions.

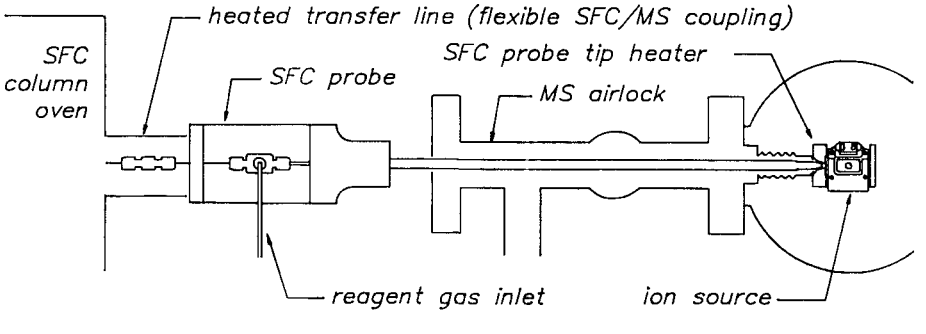

Presented at the 36th ASMS Conference on Mass Spectrometry and Allied Topics
June 5-10, 1988, San Francisco, CA

DESIGN AND PERFORMANCE OF A CONTINUOUS FLOW PROBE HPLC INTERFACE FOR A LIQUID SIMS TIME OF FLIGHT MASS SPECTROMETER

Kai-Hsien Chen, Peter Marcus, and Robert J Cotter
Department of Pharmacology, Johns Hopkins University, Baltimore, MD 21205

OBJECTIVES

We recently reported the design of a liquid SIMS time of flight mass spectrometer (1,2) which enables the use of liquid matrix with a high flux primary ion beam. With a grounded source and relatively low voltage extraction pulses, it was possible to incorporate with a TOF a continuous flow probe with a rather simple design. The objectives of this report are to describe the design of such a probe for the future development of LC-TOF and to detail our studies of the dynamic processes of LSIMS desorption with regard to ion yield, mass spectra and chromatogram performance.

EXPERIMENTS

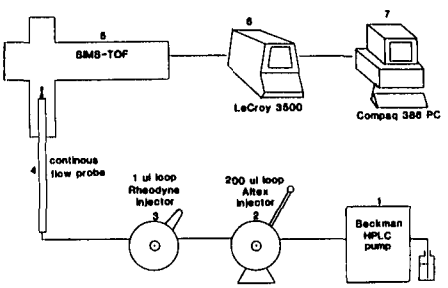

Figure 1 System setup

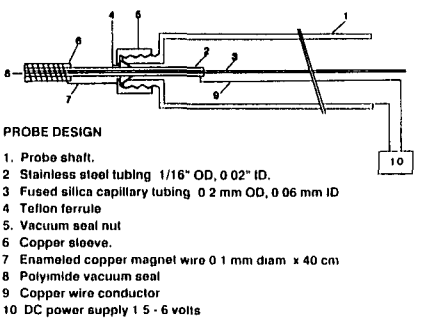

Figure 2 Probe design

The HPLC pump was operated at 1 - 3 ul/min, different solvents were injected into the 200 ul solvent loop, and the temperature of the probe was maintained at 30 - 40 C. After the pressure was stabilized in LSIMS-TOF, 1 ul of sample was injected into the system through the Rheodyne 7520 injector. The transient signals from the LSIMS were analyzed by a LeCroy 3500 wave form analyzer then transferred to a Compaq 386 PC for later processing.

RESULTS AND DISCUSSIONS

1. Low molecular weight ions were greatly suppressed by a longer primary ion pulse, while higher molecular weight ions were less affected (Table 1). This may indicate that, with the continuous flow probe, lower molecular weight species like the solvent and matrix leave the source faster under higher flux conditions prior to ion extraction. A longer primary ion pulse also resulted in less background and less memory effects in the selected ion chromatogram than when a shorter ion pulse was used (Fig. 4a, 4d). This may indicate that with a shorter ion pulse the sample on the probe surface was not completely removed by bombardment, thus a small amount of sample was deposited at the probe tip and resulted in the tailing seen on the chromatogram (fig. 4b, 4e).
2. Reducing the duty cycle of both the ion pulse and extraction pulse from 800 Hz to 400 Hz resulted in a small increase in the ion yield but greatly increased the tailing of the the selected ion chromatogram especially when shorter ion pulse was applied (Fig. 4b, 4e). Maintaining the extraction pulse at 400 Hz but increasing by ten times the frequency of the ion pulse greatly improved the chromatogram without losing the ion yield (Fig. 4e, 4f), while double the extraction duty to 800 and ion duty cycle to 8000 resulted in a good chromatogram but very low ion yield (Fig. 4b, 4c). These

results indicate that a proper balance between the duty cycle of the extraction and primary ion pulse and the width of the ion pulse is required for both good chromatogram and ion yield

CONCLUSION

The performance of continuous flow probe for LSIMS-TOF depends on a proper probe design and a combination of various proper controls such as probe temperature, flow rate, solvent compositions, extraction pulse duty cycles, ion pulse width, ion pulse duty cycle and vacuum pump evacuation rate. The selected ion chromatogram are highly reproducible as shown by multiple injection Thus, the design of this continuous flow probe is well adapted to our LSIMS-TOF and is a promising LC interface for high mass molecules analysis.

Table 1. Ion yields at two primary ion pulse width

m/z	ion yields (counts)	
	5 us[1]	13 us[2]
18.0	19,455	1,401
31.0	67,635	6,004
93.0	5,360	1,003
195.0	1,564	777
1142.3	877	1,067

1. 4000 scans collected
2. 8000 scans collected

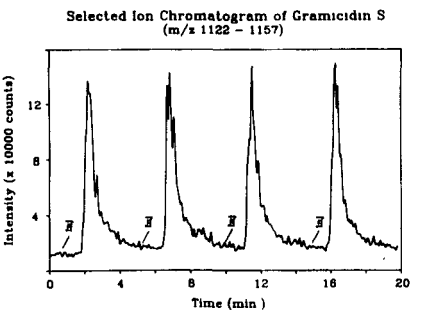

Figure 3 Selected ion chromatogram for multiple injections of gramicidin S

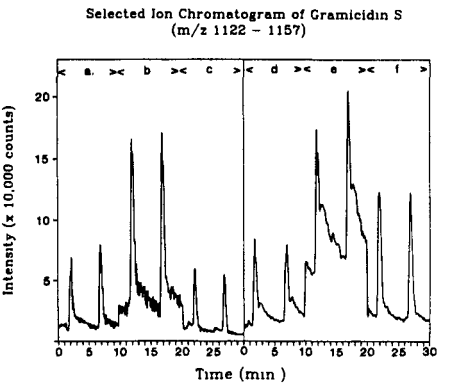

Figure 4 Selected ion chromatogram of gramicidin S with different duty cycles and primary ion pulse widths

a Extraction pulses rate 800 Hz
Ion gun pulse rate 800 Hz
Ion gun pulse width 12 us

b. Extraction pulses rate. 800 Hz
Ion gun pulse rate: 800 Hz
Ion gun pulse width: 5 us

c Extraction pulses rate 800 Hz
Ion gun pulse rate 8000 Hz
Ion gun pulse width 5 us

d. Extraction pulses rate: 400 Hz
Ion gun pulse rate 400 Hz
Ion gun pulse width 12 us

e Extraction pulses rate 400 Hz
Ion gun pulse rate 400 Hz
Ion gun pulse width 5 us

f Extraction pulses rate 400 Hz
Ion gun pulse rate 4000 Hz
Ion gun pulse width 5 us

REFERENCE

1. J. K. Olthoff, I. Lys, and R. J. Cotter, 35th ASMS conference proceedings, Denver 1987, pp. 735-6.
2. J. K. Olthoff, J. P Honovich, and R. J. Cotter, Anal. Chem. 1987 (59) 999.
3. R. M. Caprioli, T. Fan, and J. S. Cottrel, Anal. Chem. 1986 (58) 2949-2954.
4 R. M. Caprioli, and T. Fan, Biochem. Biophy. Res. Comm 1986 (141) 1058-1065.

Presented at the 36th ASMS Conference on Mass Spectrometry and Allied Topics
June 5-10, 1988, San Francisco, CA

ION CONFINEMENT IN THE RF-ONLY QUADRUPOLE COLLISION CELL OF TANDEM QUADRUPOLE MASS SPECTROMETERS : ACCESS TO THERMODYNAMIC EQUILIBRIUM AND ION REJECTION

Claude Beaugrand and Gérard Devant,
Nermag, 49 quai du Halage, 92500 Rueil-Malmaison, France
Daniel Jaouen, Hélène Mestdagh and Christian Rolando,
Ecole Normale Supérieure, 24 rue Lhomond, 75231 Paris Cedex 05, France

We have shown last year that ion confinement in the RF-only collision cell of a tandem quadrupole instrument, using the entrance and exit lenses as electrostatic mirrors (Figure 1), is very efficient. The CAD efficiency under monocollision conditions was checked to depend only on the number of collisions, i.e. the product of confinement time and pressure, in a wide range of each parameter. We present here an important application of this device : access to thermodynamic equilibrium, and a new possibility : selective ion ejection.

Applied to ion-molecule reactions, the ion confinement technique allows for a variable interaction time, therefore for the measurement of kinetic and in some cases thermodynamic parameters of the reactions. The chemical system chosen for testing this method was the interaction of ammonium ion with a mixture of piperidine (Pi) and pyrrolidine (Py), involving the following successive steps :

- Kinetic protonation of the amines by NH_4^+ ion :

(k_1) $NH_4^+ + Py \longrightarrow PyH^+ + NH_3$; (k_2) $NH_4^+ + Pi \longrightarrow PiH^+ + NH_3$

- Proton exchange leading to acid-base equilibrium :

(k_3) $PyH^+ + Pi \rightleftharpoons PiH^+ + Py$ (k_{-3}) $K_3 = k_3/k_{-3}$

- Formation of proton-bound dimers :

$$PyH^+ + Py \longrightarrow PyHPy^+$$

$$PyH^+ + Pi \text{ or } PiH^+ + Py \longrightarrow PyHPi^+$$

$$PiH^+ + Pi \longrightarrow PiHPi^+$$

$$\begin{array}{ccc} Py & \rightleftarrows & Pi \end{array} \quad \text{fast equilibrium } (K_4)$$

$$\begin{array}{ccc} Py & \rightleftarrows & Pi \end{array} \quad \text{fast equilibrium } (K_5)$$

The variation of relative abundance of parent and fragment ions with confinement time was recorded for several reactant gas pressures (10^{-5} to 2.7 x 10^{-4} torr) in a wide time range (0.035 to 10 ms, up to 220 ms for one pressure). Figure 2 displays an example of these abundance curves. As shown in Figure 3, the PiH^+/PyH^+ ratio becomes constant for large enough reaction time and/or pressure, indicating that chemical equilibrium is actually reached for reaction [3]. This ratio corresponds to the equilibrium constant $K_3 = 3.5 \pm 0.5$, in agreement with literature values. Base-exchange equilibrium is rapidly achieved among the dimers (equilibrium constants K_4 = 2.3, K_5 = 0.38). Several rate constants were also measured. Figure 4 displays the linear variation of $\ln(NH_4^+)$ with confinement time for the different pressures used. As expected the slope of these curves is proportional to pressure, allowing to derive the rate constants k_1 and k_2 (2.3 x 10^{-9} and 2.1 x 10^{-9} s^{-1} molec.$^{-1}$ cm^3).Rate constants of other reactions involved were determined in a similar way : k^3 and k^{-3} = 2.8 x 10^{-10} and 8.1 x 10^{-11} s^{-1} molec.$^{-1}$ cm^3, k_d (total dimerization third-order rate constant) = 3.0 x 10^{-24} s^{-1} molec.$^{-2}$ cm^6.

Selective ion rejection from the collision cell can be effected using an auxiliary radiofrequency field applied on the RF-only quadrupole and tuned on the transverse frequency characteristic of the considered ion. The efficiency of this method was studied on a mixture of $Fe(CO)_n^+$ (n=0 to 5, m/z 54 to 196) ions confined (0.5 ms) in the collision cell. For instance, optimization of radiofrequency power allows nearly complete rejection of $^{56}Fe^+$ ion (intensity reduced to 2.5% of its initial value) with no distortion on other $Fe(CO)_n^+$ ions. The slight intensity decrease of the minor isotope $^{54}Fe^+$ ion (intensity reduced to 75% of its initial value) shows that the band width of ion ejection is in fact less than two mass units.

Figure 5 demonstrates the application of ion rejection to elucidation of reaction mechanisms in the case of Fe^+ ion-allyl chloride reaction. Excitation of ion $C_3H_5^+$ (m/z 41) leads to a large decrease not only of this ion, but also of m/z 55, 75, 79, 81, 89 ions,indicating that these ions are subsequent reaction products of $C_3H_5^+$ with allyl chloride. Ions which remain

unaffected (m/z 67, 76, 78, 82, 91, 93, 96, 132, 134) must be formed in another way.

In conclusion, use of variable confinement time, and its association with selective ion rejection, appear as powerful tools for studying complex ion-molecule processes.

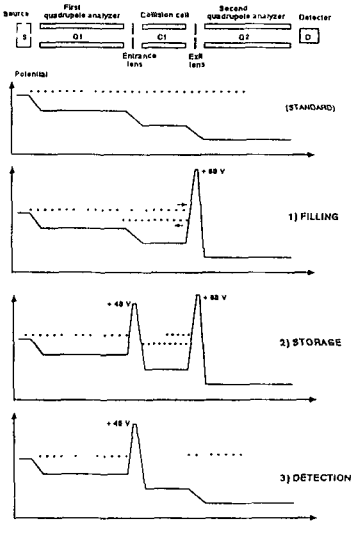

Figure 1 : Successive stages of a confinement cycle.

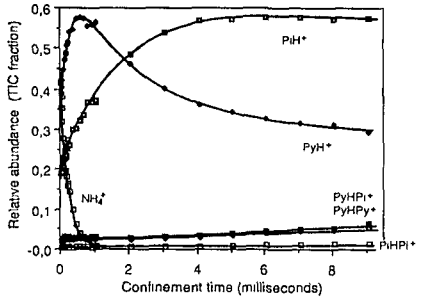

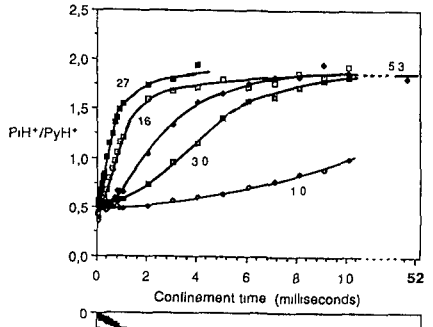

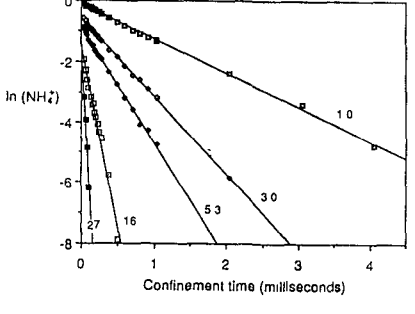

Figure 2 (up): Variation of relative abundance of reactant and product ions with confinement time at a 0.053 mtorr pressure, for medium confinement times.

Figure 3 (middle): Variation of the PiH^+/PyH^+ ratio with confinement time for the different pressures used (pressures indicated in 10^{-5} torr units).

Figure 4 (down): Variation of $\ln(NH_4^+)$ with confinement time for the different pressures used (pressures indicated in 10^{-5} torr units).

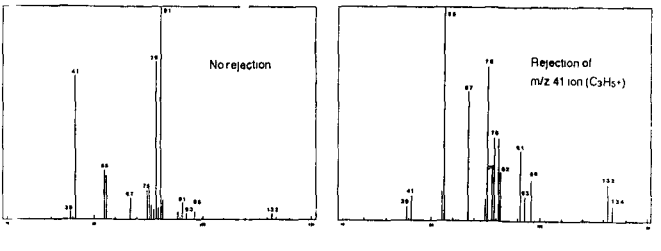

Figure 5 : Reaction spectrum of Fe^+ with allyl chloride (approximate pressure 1 mtorr, confinement time 0.5 ms) without and with rejection of m/z 41 ion.

Presented at the 36th ASMS Conference on Mass Spectrometry and Allied Topics
June 5-10, 1988, San Francisco, CA

CHARACTERIZATION OF MULTIPOLE FRAGMENTATION CHAMBERS USING COMPUTER SIMULATIONS OF ION TRAJECTORIES: Sherri-Sue Delbert and Chris G. Enke; Michigan State University, Department of Chemistry, East Lansing, MI 48824

Optimal characteristics for a reaction/fragmentation chamber include minimal gain of radial energy, efficient ion trapping and wide mass range. We have modified a lens analysis and design program called SIMION[1] to characterize a hexadecapole chamber. Program modifications include the application of a cosine function to the potential gradient, insertion of a frequency dependent, time-step size limit, insertion of a maximum integration time and implementation of a batch run capability.

Although analytical solutions are possible for the Mathieu equations representing the quadrupole system, they are not available for multipole systems[2,3] due to the coupling of the ion motion. Computer simulation is used to characterize "non-standard" multipole systems because it can represent the "real" features of the chamber; the rods can be any shape or size placed in any geometrical position.

Computer simulations of ion trajectories in rf-only quadrupole chambers have shown that ions can gain five to ten volts of radial energy due to the electric field potentials extending into the central region. Our simulations for the hexadecapole chamber indicate that, as the number of poles increases, the field potential becomes increasingly flat in the center. In addition we show that better ion containment can be achieved by increasing the applied voltage or decreasing the voltage rf. Thus, for tandem mass spectrometry applications, a multipole reaction chamber is expected to be superior to the now-standard quadrupole system.

According to the theory of quadrupoles, a stable ion trajectory occurs when the radial position remains finite as time approaches infinity. Thus, we have defined a stable trajectory as one in which the change in radial position over time remains constant or decreases. On the other hand, a transmitted ion is one which did not hit an electrode or escape from the chamber during the time it requires to travel the chamber length. As a result, there are four possible types of ion trajectories: transmitted/stable, transmitted/unstable, nontransmitted/stable and nontransmitted/unstable.

We have investigated the ion transmission/stability characteristics of a quadrupole and a hexadecapole system as a function of the ion's initial off-axis energy (Figs. 1 & 2). The boundaries between transmission and nontransmission for the quadrupole system are well defined as expected from the a,q diagram. However, the hexadecapole system does not exhibit clear boundaries for transmission or stability. This result is also expected considering the diffuseness of the a,q diagrams generated by Szabo[3] for various multipole systems.

SIMION has proved invaluable in the characterization of "non-standard" multipole chambers. We have also shown that quadrupole systems exhibit predictable transmission/stability characteristics while hexadecapole systems exhibit chaotic behavior. As a result of the chaotic behavior of hexadecapole systems at the transmission boundary, attempting to define the relationship between various instrumental/ ion parameters which will produce the best ion transmission in multipole chambers may be more complex than previously thought. However, because of the improvement in ion containment and the reduction of radial energy gain relative to the quadrupole system, multipole chambers are useful as ion/molecule or ion/photon reaction chambers.

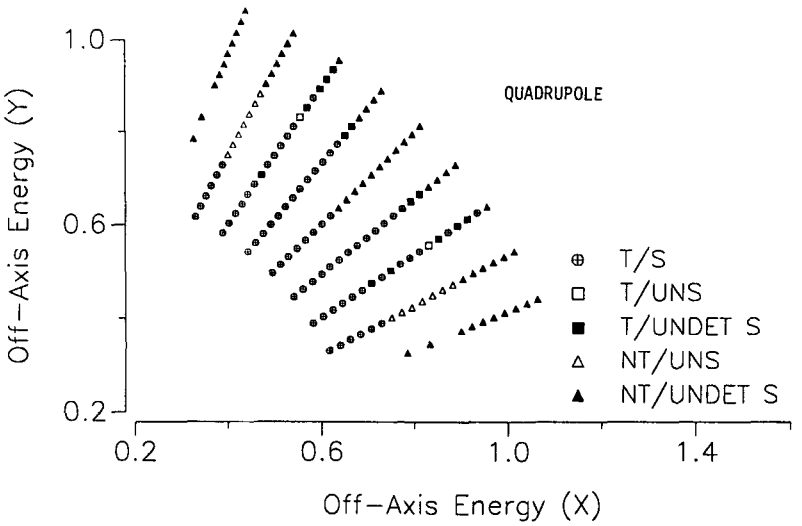

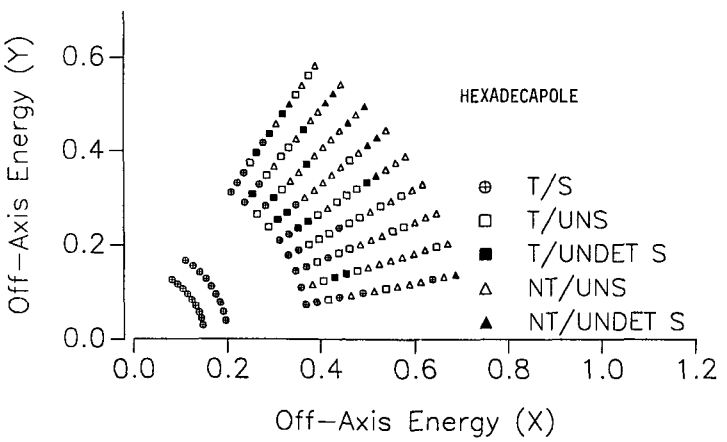

[1] Developed by D.A. Dahl and J.E. Delmore at Idaho National Engineering Laboratories.
[2] P.H. Dawson, Quadrupole Mass Spectrometry and Its Applications, Elsevier Scientific Publishing Company, New York, 1976.
[3] C. Hägg and I. Szabo, Int. J. Mass Spectrom. Ion Phys., 73 (1986) 197.

Presented at the 36th ASMS Conference on Mass Spectrometry and Allied Topics
June 5-10, 1988, San Francisco, CA

LONGITUDINAL FIELD FAULTS IN QUADRUPOLE MASS FILTERS

P.H. DAWSON
NATIONAL RESEARCH COUNCIL, OTTAWA, CANADA

INTRODUCTION

Quadrupole mass filters may have longitudinal field faults (i.e. along the length) due to converging or diverging rod sets. A similar effect could be produced by very rapid scanning giving a varying q as the ions pass through the filter. A more complex longitudinal field fault is produced by rod sets that are bowed out or bent in at the centre. Using phase space techniques, it is shown how these faults can influence performance and produce non-ideal peak shapes. Even very small geometric deviations can have significant effects for slow ions under high resolution conditions.

METHOD OF CALCULATION

The $+r_0$ and $-r_0$ limits to oscillation at each zero phase of the rf field were transformed back to the quadrupole entrance in order to find the restrictions placed on ion entry conditions. The results are shown as superimposed plots on phase plane diagrams (transverse velocity versus transverse position).

The longitudinal field faults were included by inserting different a and q values along the length of the quadrupole. Where a,q values are quoted they refer to those at the entrance of the quadrupole.

For quadrupoles operating under analyser limited conditions peak shapes can be examined by multiplying together x and y acceptance areas and examining them as a function of q.

NOMENCLATURE

a and q are the Mathieu parameters.

n_0 is the number of rf cycles that the ions spend in the field.

δq is the change in q <u>per rf cycle</u> due to the field fault, e.g. for diverging or converging rods the total change in q will be $n_0\delta q$.

Note that $\delta q/q = -2\delta r_0/r_0$ where r_0 is the radius of the field.

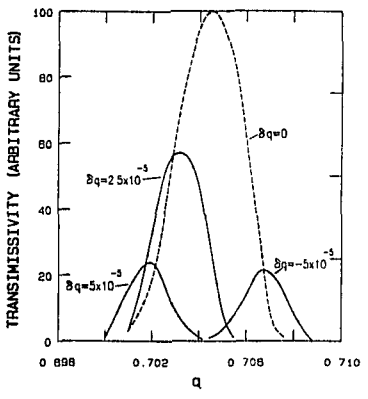

Converging rod sets give an increase in a and q as the ions pass through. A similar effect could be caused by very fast mass scanning.

For analyser limited transmission, peak shapes can be calculated. Examples are shown in the figure for δq positive. Note the tendency to produce a tail on the high mass side as the magnitude of the field fault increases.

Diverging rod sets give decreases in a and q as the ions pass through.

For analyser limited operational conditions, the resulting peak shape for 100 cycles in the field and $\delta q = 5\times10^{-5}$ is shown. This corresponds to a total fractional change in q (from entrance to exit) of 0.7% (or a fractional change in rod separation of 0.35%.
Note the asymmetry of the peak.

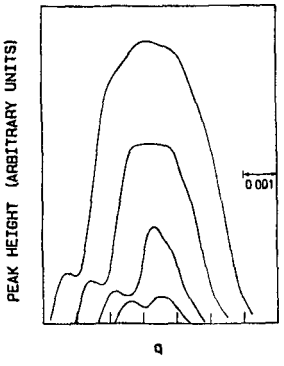

Peaks with differing resolution

For rod sets bent in at the centre

For a given field fault and 100 cycles in the field, the peak shapes vary with the resolution. At high resolutions the shoulder becomes dominant. With very large field faults, multiple structure can appear. $\delta q = 5\times10^{-5}$

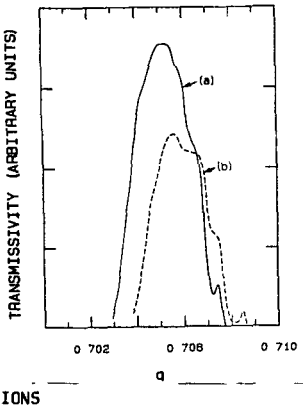

For rod sets bowed out at the centre

Under analyser limited transmission conditions peak shapes can be calculated. Bowed rod sets lead to satellite structures on the high mass side. Even satellite peaks may be observed.
(a) $n = 100$ $\delta q = 2.5\times10^{-5}$
(b) $n = 100$ $\delta q = 5\times10^{-5}$

CONCLUSIONS

As quadrupole mass filter performance is pushed to high levels, peak shape problems due to non-parallel rod sets are likely to be observed.

The characteristics predicted for bent and bowed rod sets are very similar to certain features observed experimentally. i.e. shoulders or even satellite peaks that become more and more dominant as the resolution is increased and the main peak decreases in magnitude.

Presented at the 36th ASMS Conference on Mass Spectrometry and Allied Topics
June 5-10, 1988, San Francisco, CA

ISOBARIC DOUBLET ION SEPARATION ON QUADRUPOLAR SINGLE AND TANDEM MASS SPECTROMETERS

Frederic de Maack, Gérard Devant, Gérard Lepetit,
Nermag, 49 quai du Halage, 92500 Rueil-Malmaison, France
Christian Rolando,
Ecole Normale Supérieure, 24 rue Lhomond, 75231 Paris Cedex 05, France

Analytical experiments using a quadrupolar mass spectrometer are normally recorded with a constant peak width, typically 0.5 u at half height all over the mass range. This operating mode leads to a variable resolution R (R=M/ M) equal to 2M at mass M. A new method has been developed in order to improve the resolution of quadrupole analyzers. An electronic device called "Resolver™" has been developed to implement this new technique in analytical mass spectrometers. Using this method a peak width of 0.15 u at half height is obtained over the mass range of 10 to 1500 mass units;thus the higher achievable resolution is ten thousand. This improvement was obtained by association of the classical AC-DC resolving mode of the quadrupolar analyzer and a periodically over-resolving modulation.

Figure 1 shows the results obtained on the $[M - 19]^+$ isotopic ions of 2,4,6-tris(perfluorononyl)-1,3,5-triazine at m/z 1466. This resolution better than ten thousand at 50% valley, was obtained with a decrease in signal intensity less than a factor of ten from the normal operating conditions. Furthermore the isotopic ratio M + 1 to M that could be measured from this figure fits the theoretical value with a precision better than 1%.

Figure 2 shows the reconstructed ionic currents at m/z 253.19 and 253.29 obtained during the capillary GC/MS separation of a crude oil from Hungary. These data were obtained in multiple ion monitoring mode with a scanning rate of 200 ms per ion. Using the "Resolver™", isobaric doublet of aromatic (253.19) and aliphatic (253.29) hydrocarbons base peaks are cleanly separated; this increases the analysis specificity whithout any limitation of the fast scanning rate of quadrupole instruments.

Obviously this technique can be easily implemented on the first analyzer of a tandem quadrupole MS/MS instrument. The second analyzer works under more harder conditions due to kinetic energy spread after collision. In spite of these difficulties we demonstrate here that a medium resolution can also be obtained from CAD fragment ions. Figure 3 displays a part of the daughter spectrum of two isobaric parent ions from a mixture of diazepam (m/z 284.07) and hexachlorobenzene (m/z 283.87) introduced by the direct inlet probe. We used a "classical" resolution (c.a 500) on the first analyzer and a medium resolution (c.a 3000) on the second analyzer. The resolution of the second analyzer is such that even after collision with neutrals the common isobaric daughter doublet resulting from the loss of chlorine is cleanly separated.

These experimental results demonstrate that a medium resolution (c. a. peak width 0.15 u) on the entire mass range can be obtained on quadrupole analysers either in GC-MS or in tandem MS/MS instruments using the "Resolver™".

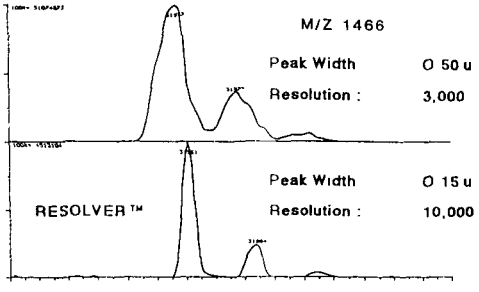

Figure 1 : $[M - 19]^+$ isotopic ions of 2,4,6-tris(perfluorononyl)-1,3,5-triazine (m/z 1466); (up) Resolver™ off, (down) Resolver™ on.

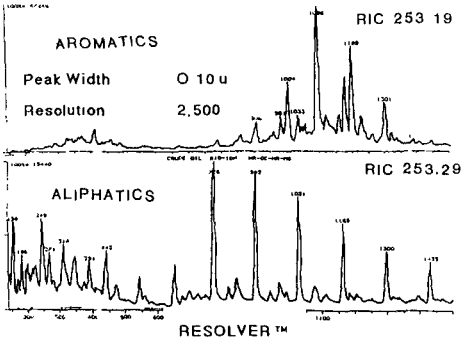

Figure 2 : reconstructed ionic currents at m/z 253.19 (aromatic compounds) and 253.29 (aliphatic compounds) obtained during the capillary GC/MS separation of a crude oil from Hungary.

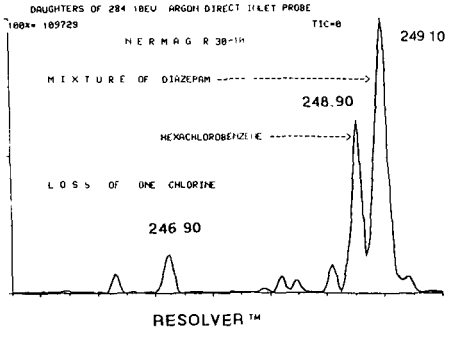

Figure 3:common isobaric daughter doublet in the daughter spectrum of two isobaric parent ions from a mixture of diazepam (m/z 284.07) and hexachlorobenzene (m/z 283.87).

Presented at the 36th ASMS Conference on Mass Spectrometry and Allied Topics
June 5-10, 1988, San Francisco, CA

Improved Performance from a Hybrid Mass Spectrometer

J.J. Monaghan, I.C.I
B. Wright, Kratos Analytical

Introduction

RF-only quadrupoles have widespread applications including MS/MS (Triple Quadrupole[1] and Hybrid Mass Spectrometers), focusing elements for ICP/MS instruments and some quadrupole based GC/MS system[2]. The principal use of the RF-only quadrupole is in ion containment and focusing devices for obtaining collisionally induced dissociation spectra for MS/MS. They are still widely regarded as total ion transmission devices despite the lack of experimental data regarding the extent of mass discrimination. Miller and Bonner Denton[3] have recently pointed-out some of the problems associated with ion transmission through RF-only quadrupoles and our experimental work broadly agrees with their theoretical and experimental data.

We have constructed a new type of collision cell, utilising the strong focusing action of RF fields, which is capable of replacing the conventional quadrupole collision cell and which shows significant improvements in ion transmission properties.

Ion Transmission Efficiency

Ion transfer efficiencies in RFonly quadrupoles (after RF optimisation) can be made quite large (typically 50-90%) over a wide mass range. However, Miller and Bonner Denton[3] have shown that spatial focusing effects cause RF-only quadrupoles to exhibit mass discrimination effects of an oscillatory nature that are of importance even over a narrow mass range.

Ion intensity comparisons are frequently made by users of MS/MS instruments and, in such cases, the RF-only quadrupole should be operated under conditions such that both the flight time and the operating point of all ions in a,q space are the same. These restrictions impose difficult practical limitations on the users of such instruments. A more productive approach is to make an improved collision cell which is not subject to these restrictions.

New Collision Cell

Data for CsI was obtained using a FAB ion source. A parent ion of m/z 912 and a daughter ion of m/z 393 were chosen as representative examples. The mass spectrometer was a CONCEPT ISQ hybrid, produced by KRATOS ANALYTICAL, with an EBQQ configuration.

Figure 1 shows the effect of varying the applied RF voltage on the parent ion transmission in both the traditional quadrupole and the new collision cell. The overall shape[4] [5] and fine structure of the curve in the case of the collision quadrupole agrees with Miller and Bonner Denton[3]. Note the curve for the new collision cell is linear and the cell is capable of operating over a larger RF voltage range.

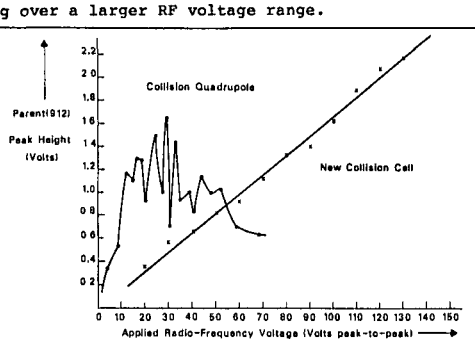

Fig. 1 Effect of RF Voltage on Parent Peak Height

Presented at the 36th ASMS Conference on Mass Spectrometry and Allied Topics
June 5-10, 1988, San Francisco, CA

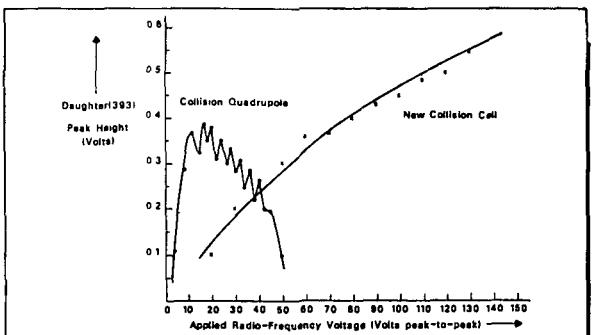

Fig.2 Effect of RF Voltage on Daughter Peak Height

Figure 2 shows the effect of varying the applied RF voltage on the daughter ion transmission. Note, in the collision quadrupole case, that the fine structure in the curve persists, but is reduced in amplitude. Again, the curve for the new collision cell is more linear over a wider voltage range.

Figure 3 shows the combined effects of Figures 1 and 2 by plotting the daughter/parent ion current ratio as a function of applied RF voltage.

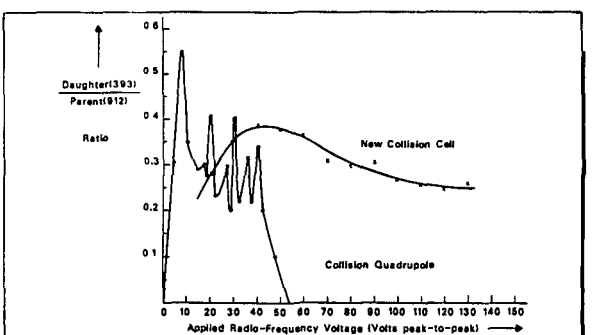

Fig.3 Effect of RF Voltage on Daughter/Parent Ratio

Conclusions

The new collision cell shows a far more stable daughter/parent relationship as the RF voltage is changed and indeed our best results have shown about a 10% relative change in ratio over the useful RF voltage range. In the future, it is hoped that the new collision cell will help in producing more precise daughter/daughter and daughter/parent ratios, so that such data may be conveniently used for instrument comparisons and quantitative applications.

References

1. R.A. Yoat and C.G. Enke, J. Am. Chem Soc. 100, 2274 (1978)

2. W.H. McFadden, Techniques of Combined Gas ChromatographyMass Spectrometry, Wiley-Interscience, New York, 1973

3. P.E. Miller and M. Bonner Denton, Int. J. Mass Spectrom. Ion Pro., 72, 223-238 (1986)

4. P.H. Dawson and J.E. Pulford, Int. J. Mass Spectrom. Ion Phys., 42, 195 (1982)

5. A.G. Harrison, R.S. Mercer, E.J. Reiner, A.B. Young, R.K. Boyd, R.E. March, C.J. Porter, Int. J. Mass Spectrom. Ion Pro., 74, 13-31 (1986)

Presented at the 36th ASMS Conference on Mass Spectrometry and Allied Topics
June 5-10, 1988, San Francisco, CA

A Comparison of the Use of Low and High Energy Collisions for the Analysis of Oligopeptides by Tandem Mass Spectrometry

M. Barber, D. Bell, M. Morris, and L. Tetler
M. Clench, R. Owen, V. Parr, O. Weir, and D. Wood
Dept. of Chemistry, University of Manchester
Institute of Science and Technology, UK
VG Tritech, Cewe Road, Wythershawe, Manchester, UK

Introduction

Normal FAB mass spectra of small peptides often do not contain sufficient sequence information to allow complete structural elucidation (1). Collisionally Induced Dissociation (CID) of the (M + H) species has been suggested as a *means to overcome this problem. Two collision regimes are available ie high* (kev) and low (ev) collision energies. In order to asses the usefullness of the technique we have chosen to investigate the daughter ion spectra generated from small peptides. For high energy collisions First Field Free Region collisions and Linked B/E scans were employed. Low energy collisions were generated by the use of a RF only quadrupole collision cell and mass analysed with a quadrupole mass filter.

Experimental

Spectra were obtained on a VG Tribrid mass spectrometer. Samples presented in a matrix of 2:1 thioglycerol/glycerol were ionised by Fast Ion Bombardment with an 11 kev Csi primary ion beam.

Result and Discussion

The data from high energy collisions along with a normal mass spectrum for Beta Casomorphin (YPFPGPI RMM 789) are shown in Figs (1-3). Data from a range of collision gas pressures was recorded, all data being obtained at 4kev collision energy. As can be seen the B/E scan combined with high energy CID generates good quality data containing a great deal of structual information. The relative instensity of specific ions in the spectrum as a function of collision gas pressure Fig. 6 shows the expected trends. The only effect of increasing collision gas pressure is to decrease the intensity of the higher mass ions relative to those at lower mass. At the high gas pressures beam scatter reduces all signal intensity. The low energy CID spectra Figs. 4 and 5 also show intense sequence ions at high mass however in this case it proved difficult to obtain good quality data containing both intense sequence and diagnostic immonium ions in one spectrum. For smaller peptides it was possible to produce a low energy collision regime that gave as much structural information as the high energy work. This work will be extended for peptides in the 1000 - 2000 moleular weight range.

Conclusion

The method of B/E linked scanning in conjunction with high energy CID offers an excellent method for structural analysis of small peptides.

1) Roepstorff P., Hojrup P. and Moller J. Biomed Mass Spectrum 12 (1985) 181

Presented at the 36th ASMS Conference on Mass Spectrometry and Allied Topics
June 5-10, 1988, San Francisco, CA

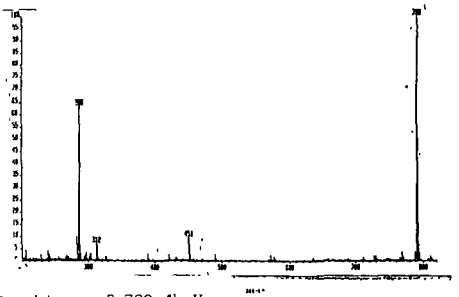

Figure 1.
Beta Casomorphin
Normal Scan

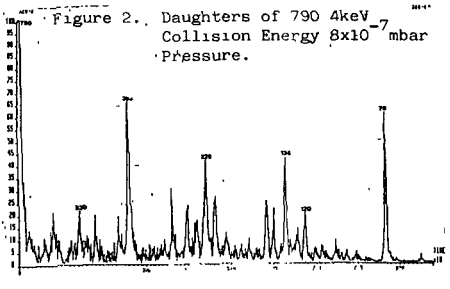

Figure 2. Daughters of 790 4keV Collision Energy $8x10^{-7}$ mbar Pressure.

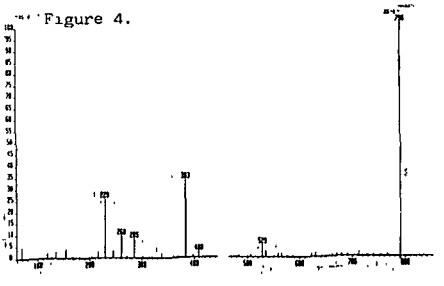

Figure 4.

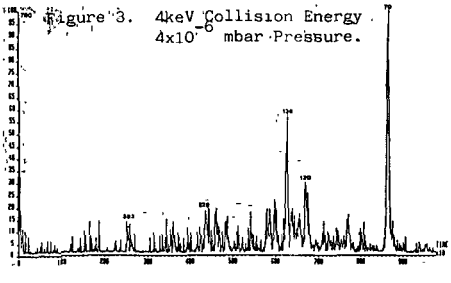

Figure 3. 4keV Collision Energy $4x10^{-6}$ mbar Pressure.

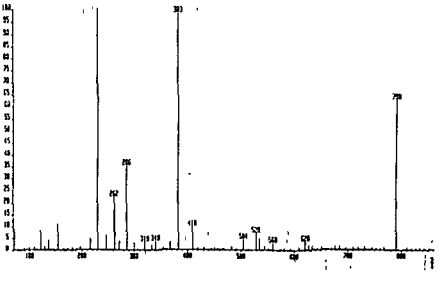

Figure 5.

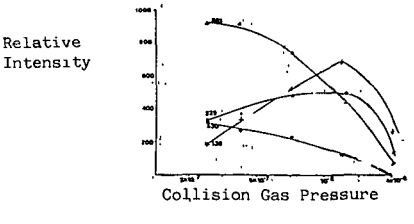

Figure 6. Effect of Collision Gas Pressure on Intensity of Daughter Ions in High Energy CID Daughter Ion spectra.

Presented at the 36th ASMS Conference on Mass Spectrometry and Allied Topics
June 5-10, 1988, San Francisco, CA

SCAN MODES FOR HYBRID MASS SPECTROMETERS

Gary L. Glish and Scott A. McLuckey
Analytical Chemistry Division, Oak Ridge National Laboratory
Oak Ridge, TN 37831

Hybrid mass spectrometers consisting of a quadrupole combined with a magnetic and/or electric sector are becoming increasingly popular. One of the advantages of such instruments is that they have reaction regions in which high kinetic energy (3-10 keV) collision-induced dissociations (CID) can be performed and reaction regions in which low kinetic energy (5-500 eV) CID can be performed. However, to date, almost all the reported data has used the low collision energy reaction region. This is due in part to the fact that the scanning modes necessary to acquire such data are simple.

This paper describes the scanning modes necessary to acquire daughter ion, parent ion and neutral loss spectra from any reaction region in eight different hybrid mass spectrometers composed of a magnetic and/or electric sector followed by a quadrupole and vice versa. Several of these scans require scanning all three analyzers simultaneously and, in geometries in which the sector(s) precede the quadrupole, often also the decelerating voltage . The scan equations are listed in the tables below.

Table I. Scan equations for the EQ geometry.[a]

Reaction region	1 (E)	(decel) (Q)
Ion kinetic energy	keV	
Daughter ion scan	Q/E=C	
Parent ion scan	SCAN E	
Neutral loss scan	(Q/E)-Q=C	

[a] The reaction regions are numbered consecutively from the source to detector. B,E and Q are proportional to the field of the appropriate analyzer.

Table II. Scan equations for the BQ geometry.

Reaction region	1 (B)	2 (decel)	3 (Q)
Ion kinetic energy	keV	keV	eV
Daughter ion scan	$Q^2/B^2=C$	SCAN Q	SCAN Q
Parent ion scan	SCAN B	SCAN B	SCAN B
Neutral loss scan	$(Q^2/B^2)-Q=C$	$B^2-Q=C$	$B^2-Q=C$

Table III. Scan equations for the EBQ geometry

Reaction region	1 (E)	2 (B)	3 (decel)	4 (Q)
Ion kinetic energy	keV	keV	keV	eV
Daughter ion scan	$B/E=C_1$ $Q/E=C_2$	$Q^2/B^2=C$	SCAN Q	SCAN Q
Parent ion scan	$B^2/E=C$	SCAN B	SCAN B	SCAN B
Neutral loss scan	$B^2(1-E)/E^2=C_1$ $(Q/E)-Q=C_2$	$(Q^2/B^2)-Q=C$	$B^2-Q=C$	$B^2-Q=C$

Table IV. Scan equations for the BEQ geometry.

Reaction region	1 (B)	2 (E)	3 (decel)	4 (Q)
Ion kinetic energy	keV	keV	keV	eV
Daughter ion scan	$B/E=C_1$ $Q/E=C_2$	$Q/E=C$	SCAN Q	SCAN Q
Parent ion scan	$B^2/E=C$	$B^2E=C$	SCAN B	SCAN B
Neutral loss scan	$B^2(1-E)/E^2=C_1$	$B^2-EB^2=C_1$	$B^2-Q=C$	$B^2-Q=C$

Table V. Scan equations for the QE geometry.
Reaction region(Q)(accel) 1 (E)

Ion kinetic energy	keV
Daughter ion scan	SCAN E
Parent ion scan	QE=C
Neutral loss scan	Q-QE=C

Table VI. Scan equations for the QB geometry.
Reaction region (Q) 1 (accel) 2 (B)

Ion kinetic energy	eV	keV
Daughter ion scan	SCAN B	SCAN B
Parent ion scan	SCAN Q	$QB^2=C$
Neutral loss scan	$Q-B^2=C$	$Q-QB^2=C$

Table VII. Scan equations for the QEB geometry.
Reaction region (Q) 1 (accel) 2 (E) 3 (B)

Ion kinetic energy	eV	keV	keV
Daughter ion scan	SCAN B	B/E=C	SCAN B
Parent ion scan	SCAN Q	$QE=C_1$ $B^2/E=C_2$	$QB^2=C$
Neutral loss scan	$Q-B^2=C$	$Q-QE=C_1$ $B^2(1-E)/E^2=C_1$	$Q-QB^2=C$

Table VIII. Scan equations for the QBE geometry.
Reaction region (Q) 1 (accel) 2 (B) 3 (E)

Ion kinetic energy	eV	keV	keV
Daughter ion scan	SCAN B	B/E=C	SCAN E
Parent ion scan	SCAN Q	$QE=C_1$ $B^2/E=C_2$	$QE=C_1$ $B^2E=C_2$
Neutral loss scan	$Q-B^2=C$	$Q-QE=C_1$ $B^2(1-E)/E^2=C_1$	$Q-QE=C_1$ $B^2-EB^2=C2$

To use the keV reaction regions in the sector/quadrupole geometry instruments, the deceleration voltage must also be scanned with the sectors. Also, with these instruments, some type of crude energy filter has to be present to allow the reaction region between the last sector and the deceleration lens to be used. Otherwise, severe background and artifact peak problems will make these reaction regions useless. RR1 in the EBQ and BEQ provides no improvement to the as compared to using just the sectors and detecting prior to the deceleration. In fact, using the quadrupole is detrimental due to the reduced sensitivity from transmission losses.

In summary, no single instrument or geometry will be best for all applications. The sector/quadrupole instruments will have better parent ion resolution for reactions occurring at eV energies. This is the main advantage these instruments have over quadrupole/sector instruments for the basic MS/MS experiments. The latter will be less prone to artifact peaks, have higher daughter ion resolution for eV reactions and some keV reactions, and will not have to scan any lens voltages such as the deceleration voltage in the sector/quadrupole geometry instruments.

*Research sponsored by the U. S. Department of Energy, Office of Basic Energy Sciences, under contract DE-AC05-84OR21400 with Martin Marietta Energy Systems, Inc.

Presented at the 36th ASMS Conference on Mass Spectrometry and Allied Topics
June 5-10, 1988, San Francisco, CA

KINETIC ENERGY RELEASE EFFECTS ON RESOLUTION IN MS/MS

Gary L. Glish and Scott A. McLuckey
Analytical Chemistry Division, Oak Ridge National Laboratory
Oak Ridge, TN 37831

Artifact peaks occur in many types of MS/MS scans due to the fact that when an ion dissociates part of its internal energy is partitioned into energy of separation, the so-called kinetic energy release, which manifests itself as a change in ion velocity. Since sectors analyze properties which are a function of velocity (momentum or kinetic energy), scans which have velocity as a parameter are subject to artifact peaks and/or have decreased resolution. Such scans are performed with sector instruments and hybrid instruments (instruments with sector(s) and quadrupole(s)).

The effects of kinetic energy release can be grouped into two categories which cover all scans on sector and hybrid instruments. The first category is that in which the dissociation occurs prior to the last sector, which is also the last analyzer (i.e. quadrupole/sector geometry hybrid instruments). In this case, the kinetic energy release affects the daughter ion resolution. The second category is that in which the dissociating ion must pass through two or more analyzers before arriving at the detector. In such cases, the kinetic energy release leads to artifact peaks, which can be thought of as being due to a decrease in parent ion resolution.

For the daughter ion resolution case, the kinetic energy release (T), measured at some defined percentage of the peak maximum, necessary to cause a signal to be obtained at the centroid of the next mass can be calculated, to a close approximation, from the following equations for an electric sector and magnetic sector, respectively

$$T=V/4m_d m_n \qquad T=V/m_d m_n$$

where V is the accelerating voltage, m_d is the daughter ion mass and m_n is the neutral fragment mass. It can be seen from these equations that when kinetic energy release is the daughter ion resolution limiting factor that a magnetic sector will have four times the resolution of an electric sector.

For parent ion resolution, the same equation applies for both types of sectors. It is

$$T=m_d V/4m_p{}^2 m_n$$

From these equations, one can get the relationships between the various parameters and kinetic energy release. Six plots are shown on the next page.

*Research sponsored by the U.S. Department of Energy, Office of Basic Energy Sciences, under contract DE-AC05-84OR21400 with Martin Marietta Energy Systems, Inc.

Presented at the 36th ASMS Conference on Mass Spectrometry and Allied Topics
June 5-10, 1988, San Francisco, CA

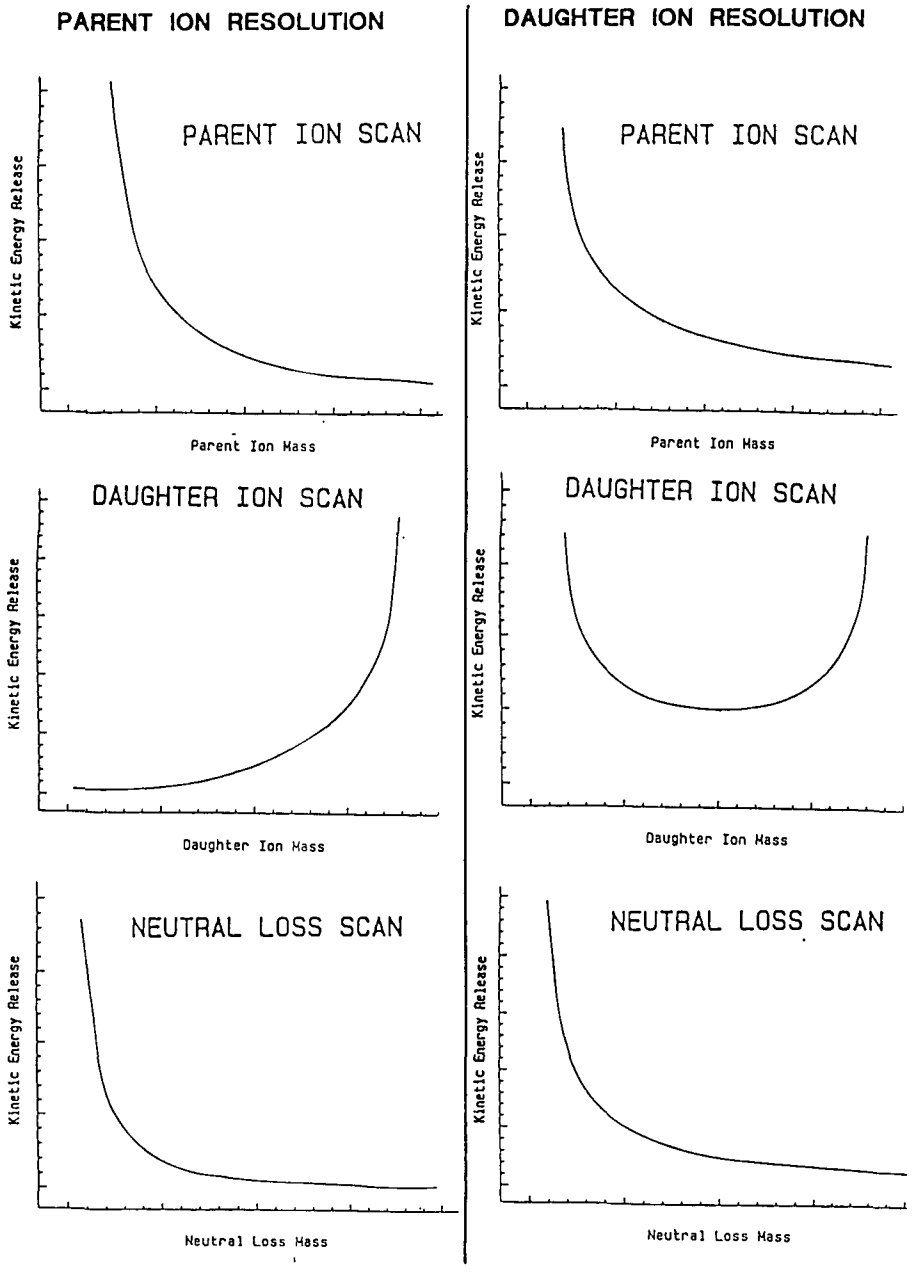

Presented at the 36th ASMS Conference on Mass Spectrometry and Allied Topics
June 5-10, 1988, San Francisco, CA

A GRAND SCALE MASS SPECTROMETER "GEMMY" AT OSAKA UNIVERSITY

T. Matsuo, T. Sakurai, M. Morris, I. Katakuse, H. Matsuda.
Institute of Physics, College of General Education, Osaka University, Toyonaka 560, Japan.
M. Azuma, Y. Kammei, E. Kubota, Analytical Instrument Technical and Engineering Devision, JEOL, Tokyo, Japan.

INTRODUCTION

The advent of the soft ionisation techniques (FD, FAB, LSIMS, PD, LD) has opened the pathways for the mass spectrometric studies of high molecular weight compounds, such that the demand for accurate mass measurement of such heavy species has also increased. For such analysis, an instrument that satisfies the criteria for high mass range, high mass resolution and high sensitivity simultaneously is required. We know the four equations that determine the ion optical characteristics of a mass spectrometer: 1) Mass spectrometry equation, 2) Abbe's sine law. 3) Q-value concept, and 4) Theoretical mass resolution as expressed by the transfer matrix elements. A grand scale instrument is one of the solutions that satisfied the above requirements, a geometrically large size being essential. We have designed and constructed such a machine of QQBQE [1] arrangement GEMMY at Osaka University. The ion optical block diagram of GEMMY is shown in Fig. 1.

RESULTS AND DISCUSSION

First, a comparison of the theoretical and experimental mass resolutions was made using an EI source, and found to be 24,300 by experiment and 28,000 by theoretical calculation, both with a 100μm source slit width. This agreement is satisfactory. Second, the detectable mass range was examined using CsI and Ag clusters, and was found to be 50,000 daltons at 5kV. Third, the mass determination was assessed for each isotopically separated peak of an organic compound, and was found to be better than 0.2 mass units in routine measurement mode. We are concerned with the analysis of peptide mixtures, including mutants, which are obtained from enzymatic digestion of proteins. The molecular weights of the components of such a mixture are usually less than 5,000 daltons, and the present accuracy of GEMMY is adequate for this type of analysis. The mass spectrum of bovine insulin is shown in Fig. 2.
Our current project is concerned with the detection of heavy biomolecules (great than 10,000 daltons) in low resolution mode.

REFERENCE

[1] H. Matsuda, Int. J. Mass Spectrom. Ion Proc. 66 (1985) 209.

Presented at the 36th ASMS Conference on Mass Spectrometry and Allied Topics
June 5-10, 1988, San Francisco, CA

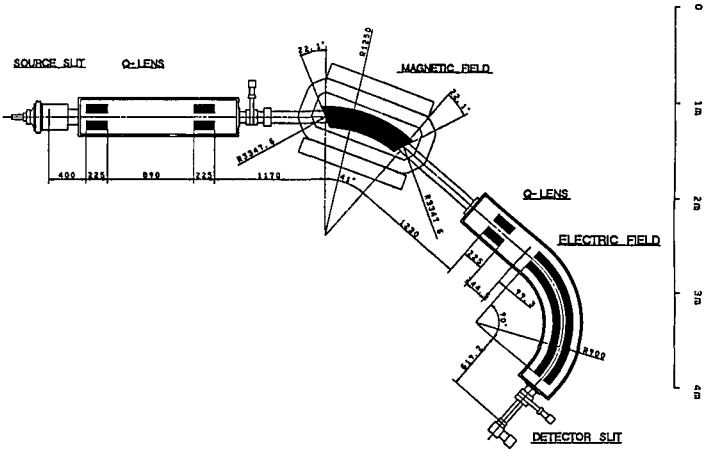

Fig. 1 Ion optical block diagram of GEMMY.

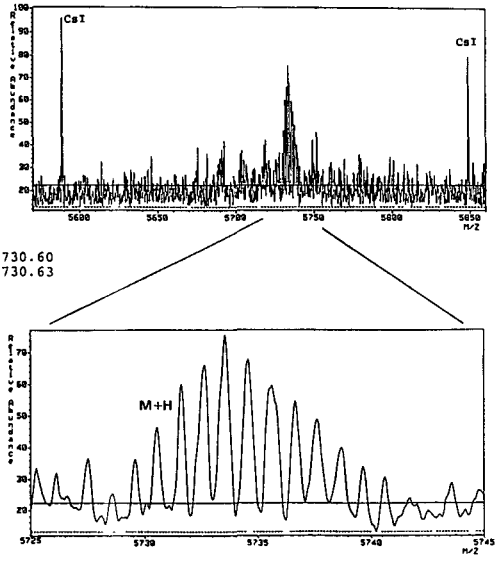

Theoretical 5730.60
Experimental 5730.63

Fig. 2 Mass spectrum of bovine insulin in routine measurement mode.

Presented at the 36th ASMS Conference on Mass Spectrometry and Allied Topics
June 5-10, 1988, San Francisco, CA

CALIBRATION AND OPTIMIZATION OF AN EBQQ SYSTEM FOR QUANTITATIVE ANALYSIS - A NOVEL APPROACH

Paul E. Farrow and Lauren M. Yelle, Arthur D. Little, Inc., Cambridge, MA 02140 and Gerald Dudek, Brandeis University, Waltham, MA.

OBJECTIVE

A large amount of our work involves trace analysis of specific analytes in complex matrices. The matrix may be a polymer, food, soil, sludge or slurry extract. MS/MS has proved very successful in our laboratories and others for this type of analysis (1,2,3). However, we, and others, have found that several key MS/MS parameters can cause significant changes in relative intensities of daughter ions obtained from XQQ systems (QQQ, BEQQ, EBQQ, etc.). The increasing need to carry out qualitative and quantitative experiments by GC/MS/MS and LC/MS/MS means that standardizing instrument set-up is critical for obtaining reproducible results. Our objective was to find a compound, or compounds, suitable for the standardization and fine tuning necessary to achieve such results.

INSTRUMENTATION

All experiments were carried out on a VG 70SEQ hybrid (EBQQ) mass spectrometer (VG Instruments, Inc., Danvers, MA). Typical operating conditions were:

Accelerating Voltage: 8kV
Source Temperature: 200° C
Emission Current: 200 A
Electron Energy: 70 eV
Solid Probe Temperature: 45°C

SUMMARY

The Electron Impact (EI) ionization of sulfur, S_8, gives an interesting spectrum. The successive losses of 32 amu (S^+) gives a repetitive fragmentation pattern ideal for linear calibration of a quadrupole system. In addition, the daughter ion spectrum is responsive to changes in the quadrupole system (e.g., gas type, pressure and collision energy). Sulfur is readily available, inexpensive and easy to handle (a solid). By controlling the solid probe temperature, a steady bleed of sulfur vapor is introduced into the ionization chamber.

The following figure demonstrates the relationship between gas pressure and relative response of two daughter ions in the sulfur spectra. We have arbitrarily chosen the relative response of m/z 160 to m/z 192 for these illustrations. Each plot shows the response for a given gas at varying pressure (log torr) with collision energy kept constant.

METHOD

Initially we obtain a standard daughter ion spectrum of the analyte(s) of interest. Parameters such as collision energy, collision gas type and gas pressure are optimized for the analyte. We then introduce sulfur into the system and record its daughter ion spectrum under these conditions. When the analysis is to be repeated, the conditions are optimized for the sulfur spectrum previously stored.

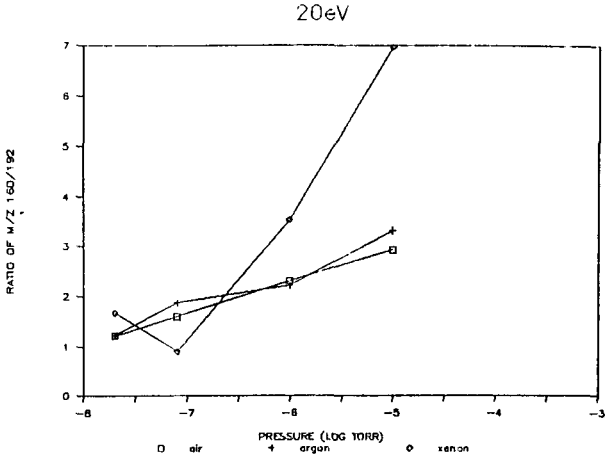

EXAMPLE

An example of data obtained by using this approach is the detection of a chlorophenol in a food extract. Interference rules out the identification and the desired quantification of this analyte.

The daughter ion spectrum of the chlorophenol was optimized and recorded along with the standard sulfur spectrum.

By selecting suitable daughter ion transitions, a MRM (multiple reaction monitoring) experiment was set up for this analysis. A positive identification was made and quantification in the ppb range was possible.

CONCLUSION

Whenever a compound is analyzed by MS/MS, we record a standard sulfur daughter ion spectrum along with the data and operating conditions. When the analysis is to be repeated, possibly months later, sulfur is used to fine tune the operating parameters (energy, gas, pressure) to give the same daughter ion spectrum as before. The system is then ready for the analysis without having to introduce a standard of the analyte again.

As a result of this work, we are able to obtain reproducible daughter ion spectra from one experiment to another. This has led to consistent detection limits and the ability to obtain quantitative data at the ppb level from MS/MS experiments.

REFERENCES

1. Busch, K., Kroha, K., "Characterization and Measurement of Flavor Compounds,'" ed. Bills, D., Mussinan, C., ACS Symposium Series 289, pp. 121-137.

2. Yelle, L., Farrow, P., Taylor, R., "Characterization of Carotenoids and Retinoids by HPLC-MS-MS," ASMS, Denver, CO, 1987.

3. Hunt, D., Shabanowitz, J. and Giordani, A.B., Anal. Chem., 1980, 52, 386.

Presented at the 36th ASMS Conference on Mass Spectrometry and Allied Topics
June 5-10, 1988, San Francisco, CA

Operation of a Hybrid Tandem Mass Spectrometer of BEqQ Configuration in Unlinked Scan Modes: Theory and Applications.

A.J.Alexander, R.K.Boyd, R.Guevremont, P.Thibault,
National Research Council of Canada, 1411 Oxford St., Halifax,
Nova Scotia, Canada B3H 3Z1.

Mass analyzed ion kinetic energy spectroscopy (MIKES) (1) is widely used for the study of collision induced dissociation (CID) at keV energy. Limitations of MIKES include (i) lack of mass resolution in the fragment ion spectrum, (ii) uncertainty in mass due to appreciable energy losses during collisional activation, and (iii) occurrence of artifact peaks. A hybrid tandem instrument of BEqQ configuration can provide unit-mass (Q-defined) fragment spectra for keV collisions, essentially artifact-free, via a linked-scan at constant E/Q. Problems (i) and (iii) are thus avoided. Unfortunately the linked E-Q scan does not solve problem (ii), and may introduce new problems such as drift (electronic) in the E/Q ratio with time, and inaccuracy in the q deceleration lens and the qQ float voltages.

The experiments reported here were conducted using a VG Analytical ZAB-EQ hybrid instrument. Changes to the instrumentation were made to permit selection of a series of operating states wherein the computer and the console could simultaneously retain control of different parts of the instrument; eg. the electric sector could remain under console control while the computer controlled the functions necessary for the acquisition of data using a normal Q scan (eg. MS/MS/MS,(2)).

All benefits of the linked E-Q scan may be retained, with minimization of electronic problems, if the scans of E and Q are uncoupled. In this mode E and Q are both scanned during acquisition, but the scan functions are unrelated. The quadrupole analyzer is scanned under computer control, to utilize existing capability of the system to collect data into a multichannel analyzer (MCA) file. The electric sector is scanned under console control. Although the E scan is completely uncoupled from the computer controlled quadrupole scan, a Quadrupole-resolved MIKES (QMIKES) spectrum is acquired. QMIKES is best described as mapping of the 2-dimensional E-Q space onto the Q axis. The areas of simultaneous transmission through E and Q fall on a line through E-Q space; the peaks are broad if viewed from the E axis, and narrow when viewed from the Q axis. Unlinked, random, scans of E and Q will eventually pass over every area of E-Q space. If all the quadrupole scan data is acquired into a MCA data file, this file will be a record of all occurrences of simultaneous transmission of ions through E and Q, and more important, the MCA data will be accurately mass analysed, with unit resolution. Fig.1 illustrates a comparison of MIKES and QMIKES spectra of the same group of fragment ions.

The unlinked E-Q scan is simple to implement, but inappropriate for scans over a wide mass range. A version of 'partially linked E-Q scans' has been designed to improve the efficiency of scans over a wider mass range, and to avoid the limitations of completely linked scans. This approach uses a small (50V) low frequency (100Hz) modulation of the electric sector added to a constant E/Q scan. Electronic deviations from the ideal E-Q link, and shifts of the MIKES peaks caused by kinetic energy (Derrick) effects, can be accommodated without loss in ion intensity. The electric sector will pass through the optimum energy of transmission of fragments during the course of the E modulation, even though the calculated E-Q link is slightly in error.

Fig.2 is a schematic representation of the modifications to the VG Analytical ZAB-EQ which enable operation in the 'partially linked E/Q' mode. The electric sector voltage is 'slaved' to the quadrupole analyzer scan so as to maintain constant E/Q ratio, and a modulation is added to the E voltage. The modulation is not coupled to the E-Q scan function. (The quadrupole float voltages remain 'slaved' to E.) In addition, these circuits drive the mass display unit and provide appropriate values to the quadrupole energy partition circuitry. During the operation of the

NRCC No . 9010

partially linked E/Q scans, the computer is allowed to control only the quadrupole scan; all other control remains with the console units and the circuits in Fig.2.

QMIKES and the partially linked E-Q scans have been used to identify artifact ions in MIKES spectra (Fig.3), obtain unit mass resolved MIKES spectra of isotope labelled compounds, and to assess the CID reactions of larger molecules(3) where a so-called Derrick shift (kinetic energy loss) can lead to uncertainty in the assigned masses of fragment ions (Fig.4).

(1) R.G.Cooks, J.H.Beynon, R.M.Caprioli, G.R.Lester, "Metastable Ions", Elsevier (1973).
(2) R.Guevremont, Rapid Commun. Mass Spectrom., 1 19 (1987).
(3) R.Guevremont, J.L.C.Wright, Rapid Commun. Mass Spectrom., 2 50 (1988).
(4) R.Guevremont, R.K.Boyd, Rapid Commun. Mass Spectrom., 2 1 (1988).

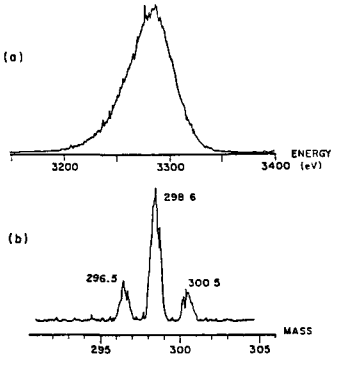

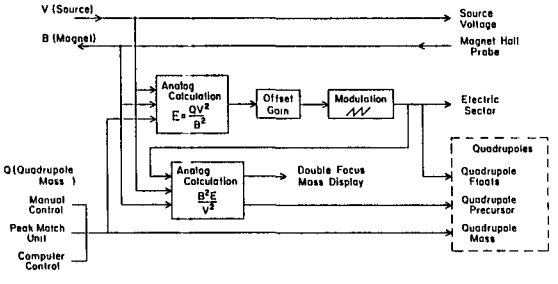

Fig.2. Schematic of control circuitry developed to permit accurate linking for E-Q scans with the option of modulation of the electric sector field E.

Fig.1. Spectra obtained for $^{85}Rb_2{}^{87}Rb_2I_3{}^+$ precursor ions forming Rb_2I^+ fragments (8keV, He) (a) MIKE spectrum, (b) QMIKE spectrum.

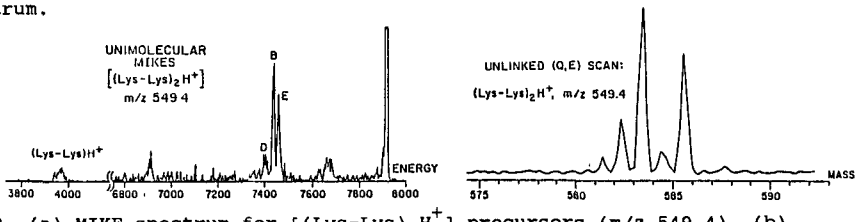

Fig.3. (a) MIKE spectrum for [(Lys-Lys)$_2$H$^+$] precursors (m/z 549.4), (b) quadrupole-resolved spectrum of the region corresponding to peaks B, D, and E in (a) obtained using the unlinked scan technique. Note m/z higher than the MIKES precursor!

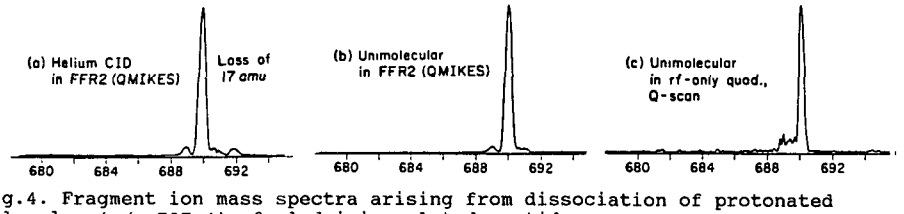

Fig.4. Fragment ion mass spectra arising from dissociation of protonated molecules (m/z 707.4) of eledoisin-related peptide: Lys-Phe-Ile-Gly-Leu-Met-NH_2 (a) unlinked scans (QMIKES), He collision gas, (b) same as (a) but no He, (c) low energy collision of the same parent, rf-only quadrupole and quadrupole mass filter.

Presented at the 36th ASMS Conference on Mass Spectrometry and Allied Topics
June 5-10, 1988, San Francisco, CA

A MODEL FOR MASS-INDEPENDENT SPACE AND ENERGY FOCUSING IN TIME-OF-FLIGHT MASS SPECTROMETRY USING DYNAMIC POST-SOURCE ACCELERATION

GEORGE E. YEFCHAK AND CHRISTIE G. ENKE
Department of Chemistry, Michigan State University, East Lansing, MI 48824

JOHN F. HOLLAND
Department of Biochemistry, Michigan State University, East Lansing, MI 48824

Conventional time-of-flight mass spectrometers suffer from poor resolving power with gaseous samples due to the initial spatial and kinetic energy distributions of ions at the time of their formation. It has been shown that mass-independent compensation for both the spatial and energy effects cannot be achieved concurrently using static acceleration fields [1]. Mass independent space and energy focusing is needed, however, to gain the advantage of monitoring the full spectrum of arrival times for each pulse of ions from the source.

Exploration into the use of non-static fields has resulted in techniques which incorporate dynamic acceleration either in the source [2] or in a region past the source [3]. To further develop dynamic post-source acceleration, a computer model has now been developed which incorporates all pertinent parameters including the extraction voltage, the accelerating and field-free region lengths, and the dynamic acceleration function. Analytical equations and ion flight-time simulations using this model have led to the development of a new post-source acceleration technique, *dynamic-field focusing* (DFF), which provides mass-independent space and energy focusing [4].

The DFF focusing principle is illustrated in Fig. 1. Ions are extracted from a single-field source and enter the first of two field-free regions (FF1). As the ions approach the space-focus plane, there is no simple relationship between their positions and velocities. Farther along the flight path, however, velocity becomes related to position in such a way that the velocity adjustment necessary to achieve simultaneous arrival at the detector (within the isomass packet) is a monotonic function of arrival time at the DFF region. Ions are accelerated as they pass through the DFF region and enter the second field-free region (FF2). The magnitude of this acceleration is a function of the ion's arrival time at the end of FF1; ions arriving later receive more energy than leading ions. Thus in FF2, the relationship between position and velocity is inverted (*i.e.*, within any isomass group, the leading ions are the *slowest*). The applied acceleration is tailored at each instant to make the trailing ions just catch up to the leading ones at the detector.

To obtain the functional form of the required dynamic acceleration, equations were derived which yield the voltage rise, dV/dt, needed to focus isomass ions. A separate equation was derived for each of three cases: Case **S** results from ions initially located away from the center of ionization; cases **E+** and **E-** result from ions having initial thermal motion directed toward or away from the detector, respectively. These three equations were reconciled by inspection, combined with simplex optimization of an "overall resolving power" response function, to yield instrument parameters which make dV/dt similar for the three cases. The resulting average dV/dt

function was then numerically integrated to yield the DFF voltage function. A Monte-Carlo simulation of DFF-TOFMS peak shapes for 1000 and 1001 u ions is shown in Fig. 2. Predicted resolving power as a function of mass for DFF-TOFMS is shown in Fig. 3. Unit resolving power is achieved for ions up to 2000 u.

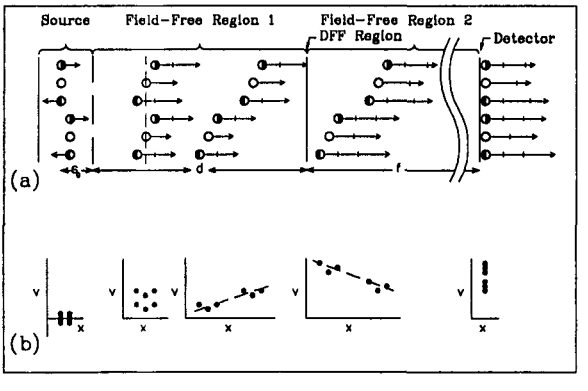

Fig. 1

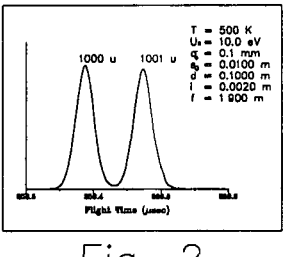

Fig. 2

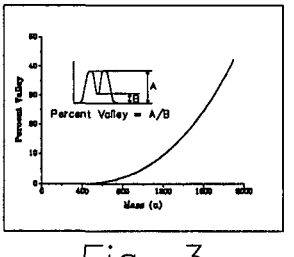

Fig. 3

1 R. Stein, *Int. J. Mass Spectrom. Ion Phys.*, 14 (1974) 204-218.
2 J. A. Browder, R. L. Miller, W. A. Thomas, and G. Sanzone, *Int. J. Mass Spectrom. Ion Phys.*, 37 (1981) 99-108.
3 M. L. Muga, *Anal. Instrum.*, 16 (1987) 31-50.
4 G. E. Yefchak, C. G. Enke, and J. F. Holland, submitted for publication in *Int. J. Mass Spectrom. Ion Processes.*

Presented at the 36th ASMS Conference on Mass Spectrometry and Allied Topics
June 5-10, 1988, San Francisco, CA

INSTRUMENTATION FOR MASS SPECTROMETRY/COINCIDENT FRAGMENT DETECTION

D.E. Goeringer, S.A. McLuckey, and L.K. Bertram
Analytical Chemistry Division
Oak Ridge National Laboratory
P.O. Box 2009, Oak Ridge, TN 37831-8121

Mass spectrometers of various geometries are used to study the collision-induced dissociation (CID) of mass-selected molecular ions (M^+) into fragments (m_1^+, m_2), with the charged fragment subsequently mass/energy analyzed. However, much of the M^+ beam current in MS/MS instruments is lost via neutralization

$$M^+ + N \text{ ---> } M + N^+$$

or dissociative charge exchange (DCE)

$$M^+ + N \text{ ---> } M^* + N^+$$
$$\quad\quad\quad\quad\quad\quad\quad\quad \text{---> } m_1 + m_2$$

It seems likely that we can improve the detection of fragments in MS/MS by optimizing DCE and detecting the neutral fragments. Therefore, we propose to develop a new type of instrument for mass and energy analysis of neutral fragments.

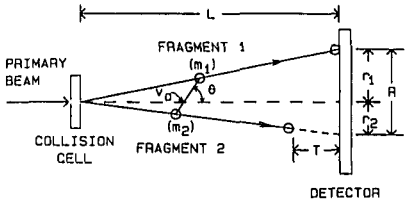

The general experiment depicted above involves the measurement of time delay (T) and spatial separation (R) for the (nearly) coincident detector impacts of two neutral fragments resulting from the dissociation of a mass-selected molecule having center-of-mass velocity, v_0, and initial energy, E_0. For our instrument design, delay and position measurements must be made with a resolution of ~1 ns and ~200 μm, respectively. The experimentally determined time delay and spatial separation for the detector impacts can be used to calculate the kinetic energy release (ϵ) and recoil angle (θ) for the dissociation; because the precursor mass (M) is known, the masses of the fragments (m_1, m_2) can also be determined using the corresponding distances (r_1, r_2) from the center of the detector.

The proposed instrument consists of a first stage mass spectrometer (single magnetic sector) for mass selection of the parent molecular ion, a collision cell for DCE, deflection plates for removal of charged species, a flight tube (straight) for separation of the neutral fragments, and a two-dimensional detector for time and position measurements. The detector for the instrument is a dual microchannel plate (75 mm dia.) located in front of a specially designed anode consisting of two semicircular sections of concentric rings. The fragment impact positions are determined by charge division and the time delay by direct time measurement. The schematic diagram for the detector and the anode design is shown below.

Presented at the 36th ASMS Conference on Mass Spectrometry and Allied Topics
June 5-10, 1988, San Francisco, CA

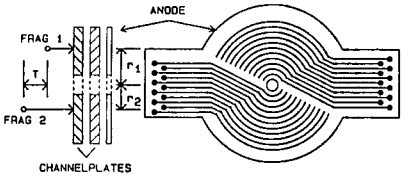

The data acquisition system is based on the computer automated measurement and control (CAMAC) concept; a DEC LSI-11/73 microcomputer system is used to control four analog-to-digital converters (ADCs), a time-to-digital converter (TDC), and associated memory modules housed in a CAMAC crate. A schematic diagram for the data system is shown below.

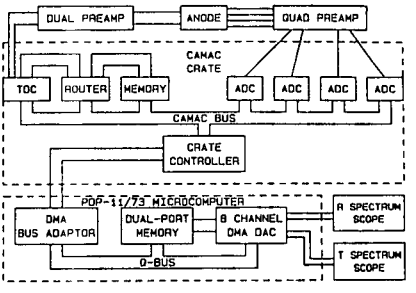

Data acquisition for each dissociation event involves the coordination of four ADC conversions and one TDC conversion. It is possible for the CAMAC system to autonomously acquire such data in blocks of 5 x 1024 points (fragmentation events) at burst rates of 150 kHz. The data block is then transferred via direct memory access (DMA) to the microcomputer where it is histogrammed and displayed in near real-time while another block of data is being acquired via the CAMAC system. Special memory and digital-to-analog converter (DAC) boards, with private DMA interconnection, enable the data to be displayed without using microcomputer DMA cycles. Therefore, the DMA capability for the microcomputer is totally available for data transfer from the CAMAC system.

Because this technique can detect charged fragments from CID as well as neutral fragments from DCE, we will study CID of well-characterized molecular ions such as ionized acetone for proof-of-principle demonstrations. Following this, we will repeat experiments performed on a similar instrument by de Bruijn and Los (1) involving the DCE of H_2^+. We will then proceed to investigate the unimolecular chemistry of neutralized beams of larger polyatomics. The systems created via ion formation/neutralization could be very interesting and unusual, e.g. $MH^{\cdot}$ from MH^+ or other ions for which no stable neutral counterpart is known to exist. The instrument could also be very useful for fundamental studies of neutralization-reionization mass spectrometry (NRMS) since the charge exchange reaction is the first step in that process.

(1) D.P. de Bruijn and J. Los, **Rev. Sci. Instrum.** 53, 1020 (1982).

Research sponsored by the U. S. Department of Energy, Office of Basic Energy Sciences, under Contract DE-AC05-84OR21400 with Martin Marietta Energy Systems, Inc.

"The submitted manuscript has been authored by a contractor of the U.S. Government under contract No DE-AC05-84OR21400 Accordingly the U S Government retains a nonexclusive royalty-free license to publish or reproduce the published form of this contribution, or allow others to do so, for U S Government purposes."

Presented at the 36th ASMS Conference on Mass Spectrometry and Allied Topics
June 5-10, 1988, San Francisco, CA

A Direct Comparison of Two-, Three-, and Four-Sector Mass Spectrometers for Measuring CID Spectra of Peptides

John T. Stults and John A. Chakel
Genentech, Inc.
460 Point San Bruno Blvd.
South San Francisco, CA 94080

Tandem mass spectrometry utilizing four-sector instruments represents one of the best means of obtaining sequence data for peptides by mass spectrometry. The mass range and resolving power permit reliable data to be obtained for a variety of peptides of up to about 25 residues in length. Newer techniques are pushing the mass range upward and reducing the amount of sample required. Typically 0.5-1.0 nmole of peptide is necessary for obtaining collision spectra with reasonable ion signal levels.

A successful MS/MS experiment is most dependent on the precursor ion intensity, so sample quantity, precursor mass, and instrument resolving power all play a role. When adequate precursor intensity is available, the EB-EB CID spectrum with unit resolution of both precursor and daughter ions is most desirable. Quite often, the desired quantity of sample is not available, particularly when the peptides are isolated from natural sources. With our present instrumentation, this necessitates reduction in resolving power to increase the signal. When the precursor ion intensity is less than desired, compromises in resolution need to be made.

Generally the resolution of MS1 is set to transmit only the ^{12}C isotope of the precursor. This value separates the peptide of interest from other peptides and matrix ions, and provides monoisotopic peaks in the daughter spectrum. Resolution in MS2 is normally set to resolve all daughter ion peaks. For compounds with mass <2000Da, available in >0.5nmole amounts, these conditions usually provide sequence-rich spectra. The resolution requirements are low and the ^{12}C isotope is the largest peak in the precursor ion cluster. Larger peptides typically fragment less efficiently, require greater resolving power, and display less intense ^{12}C isotope peaks. In these cases, and for smaller peptides which are available in low quantity, compromises in resolution may be necessary. However, the integrity of the sequence information must be preserved.

Several peptides of different masses have been examined to determine what operating conditions (including 2- and 3-sector operation) provide the best signal levels without sacrificing the sequence information content of the spectra. These peptides were:

FPTIPLSR, MH^+=979.5, 30pmole

DLEEGIQTLMGR, MH^+=1361.7, 30pmole

LHQLAFDTYQEFEEAYIPK, MH^+=2342.1, 1.2 nmole

<ELYSALANKCCHVGCTKRSLARFC, MH^+=2657.3, 1.3 nmole

The first three peptides were isolated from a tryptic digest of recombinant human Growth Hormone. The fourth peptide is the A-Chain of synthetic human Relaxin. Spectra were obtained with a JEOL JMS-HX110HF/HX110HF Tandem Double-Focusing Mass Spectrometer (E_1B_1-E_2B_2 configuration), equipped with a JEOL DA-5000 data system. Samples were dissolved in 0.1%TFA and 0.5ul of each mixed 1:1 on the probe tip with 0.5ul glycerol:DTT:DTE (6:5:1). Ionization was by fast atom bombardment using a JEOL FAB gun, 6keV Xe atoms, 10mA emission current. For EB-EB and EB-E experiments, precursor ions were selected with MS1 and fragmented by CID in the grounded collision cell-2 (10keV energy, 75% attenuation of the precursor beam with helium). For EB (constant B/E linked scan) measurements, ions were formed in the MS2 ion source; fragmentation by CID or metastable decomposition took place in collision cell-2.

Based on examination of the measured spectra, several conclusions can be drawn about the different modes of operation:

For precursor mass <~2000u:

EB-EB

Unit resolution of the precursor ^{12}C peak should be maintained. This yields monoisotopic daughter ion peaks and it is easy to achieve because MS1 resolution <1000 is required [S.A.Martin et al, 1987 ASMS, Denver, bound volume pp.78-79]. Reduction of MS2 resolution will give unresolved peaks only at the high mass end of the spectrum, but this is generally not a problem (except for z,z+1; a,a+1; etc.).

EB-E

Signal intensities for the three- and four-sector experiments are similar. The much poorer daughter ion resolution, and the observed translational energy release and translational energy loss make this mode of operation of little utility. A non-uniform baseline makes mass assignment by the data system difficult.

EB (B/E linked scan)

Signal intensities are 10-20 times larger than those observed in the four-sector experiments, and for precursor mass <1000, where the ^{13}C peaks are minimal, the spectra are readily interpretable. However, for low sample quantity, matrix ion interferences often mask the peptide daughter ions. Much of the matrix interference is due to metastable decompositions.

For precursor mass >~2000u:

EB-EB

When possible, maintain unit resolution in MS1. As the mass increases, however, unit resolution of the precursor becomes harder to achieve while yielding good daughter ion spectra. The precursor abundances are less, the ^{12}C isotope peak becomes increasingly smaller, the collision efficiency decreases, the total daughter ion intensity is spread over a larger number of ions, and the resolution required increases. Selection of the ^{13}C precursor peak or the isotope envelope produces daughter ion peaks that are weighted averages of the precursor isotopic components and require mass correction before interpretation. However, if the mass differences between peaks are used for interpretation [Scoble, Biller, and Biemann, Fresenius Z. Anal. Chem. **1987**, 327, 239-245], the mass shifts are not a problem. Reduction of MS2 resolution is acceptable if the ^{12}C precursor peak is selected. Low resolution in both MS1 and MS2 can be used for those sample where intensity is at a premium.

EB-E

The increased complexity of the spectra in addition to the reasons mentioned above make the three-sector mode of operation of limited value for peptides of this size.

EB (B/E linked scan)

The poor parent resolution inherent to two-sector B/E scans results in daughter ion masses that are weighted functions of the precursor isotopic envelope. However, the increase in signal is substantial and matrix contributions in this mass range are minimal. The metastable spectrum is strong and is simpler than the CID spectrum (no w ions), making it potentially useful for higher mass precursor ions.

Although two-sector B/E spectra provide useful data for low mass peptides (<1000Da) and higher mass peptides (>2000), data from the four-sector mode of operation give superior results in most cases, providing maximum sequence information with the best resolution. The ability of the four-sector mode of operation to eliminate artifact peaks and to utilize a floating collision cell also weigh in the comparison.

Presented at the 36th ASMS Conference on Mass Spectrometry and Allied Topics
June 5-10, 1988, San Francisco, CA

A FOUR SECTOR MASS SPECTROMETER FOR NEUTRALIZATION-REIONIZATION (NR) STUDIES

R. Feng, M. -Y. Zhang, C. Wesdemiotis, M. A. Baldwin, D. E. Drinkwater, B. Leyh, M. Marchetti, and F. W. McLafferty

Chemistry Department, Cornell University, Ithaca, NY 14853-1301

The prototype Cornell EBEB mass spectrometer has been modified to permit high performance neutralization-reionization (NR) experiments. Precursor ions, mass-selected by MS-I (EB), enter the interface region between MS-I and MS-II and undergo neutralizing collisions at collision cell I (Cls-I). A deflector electrode (Dfl-I) is situated immediately after Cls-I to remove unneutralized ions. Cls-II follows, and is used for reionization, or neutral dissociation. In the latter case, newly formed ions are removed by Dfl-II, and the neutral beam is reionized in Cls-III. Cls-I and Cls-II have differential pumping systems, with a 10" diffusion pump on the entire interface region. Cls-III can be replaced by a field ionization chamber for the selective reionization of neutrals in Rydberg states. NR spectra are detected after mass-analysis through ESA-II; alternatively, ESA-II can be used to mass-separate individual ions from the NR spectra for collisionally activated dissociation (CAD) at Cls-IV in the field-free region between ESA-II and Magnet-II. Fragment ions from such MS/MS/MS experiments are recorded after mass-analysis in the final magnet.

A new data system based on an IBM personal computer (PC/AT) is interfaced to the instrument. It enables accurate determination of absolute abundances for neutralization and reionization cross-section measurements.

He is the best target for CAD of neutral species. Spontaneous and extensive fragmentation of the neutrals produced can also be achieved by neutralization with targets of low ionization energy, such as Na or Cs. Individual neutral components in neutral mixtures can be detected selectively via reionization and CAD in Cls-IV. Closed-shell molecules are best made visible by cationization (NR^+) with O_2 or He, while for many radicals anionization (NR^-) with C_6H_6, Hg, or Na exhibits high relative efficiency. For example, extensive dissociation of 1- and 2-butene molecules is effected upon Na neutralization of their molecular cations; the resulting allylic radicals are selectively anionized with Na (Figure 1). As expected, 1-butene yields more abundant allyl anions (m/z 41) than 2-butene.

Field ionization conditions that produce $Ar^{+\cdot}$ ions from Rydberg Ar atoms fail to reionize $H_2Cl\cdot$, obtained via H_2Cl^+ neutralizaion with Hg, indicating that this hypervalent radical is not generated in a Rydberg state. Semiempirical calculations suggest that this radical has the structure H-H-Cl, formed in its ground state via vertical neutralization from the first triplet state of H_2Cl^+, for which the $H\text{-}H\text{-}Cl^+$ is more stable than the $H\text{-}Cl\text{-}H^+$ conformation.

Often, the structural identity of a molecular ion is hidden in the neutral CAD fragments. The He CAD spectra of the protonated molecules of N,N-dimethyl- and N-ethyl-β-phenylethylamine are identical within experimental error, showing intense $C_8H_9^+$ fragments (loss of C_2H_7N). However, the O_2 reionization spectra of their neutral dissociation products display structurally diagnostic differences (Figure 2): the appearance of intense ions at m/z 44 in the upper, and at m/z 30 in the lower spectrum are consistent with the presence of $(CH_3)_2NH$ and $CH_3CH_2NH_2$ in the corresponding neutral CAD beams.

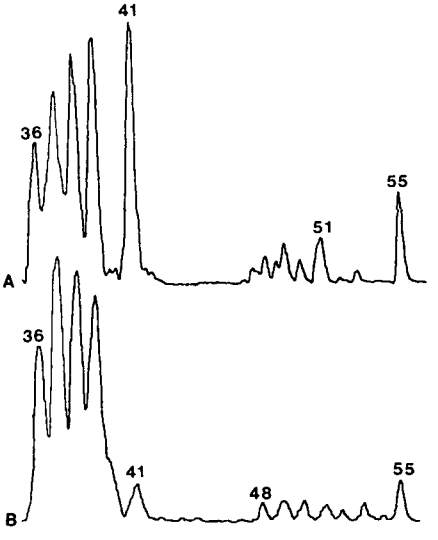

Figure 1. Na (30% Transmittance) NR^- spectra of the molecular cations of (A) 1-butene and (B) 2-butene.

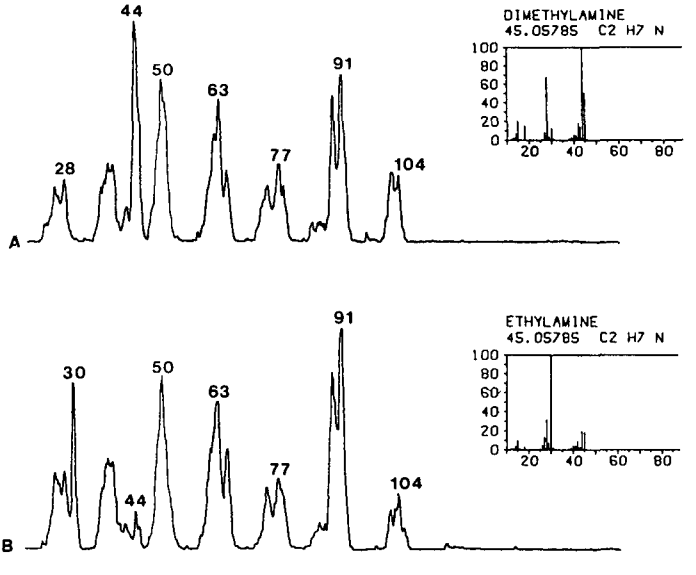

Figure 2. He (30% T)/O_2 (30% T) NR^+ spectra from the protonated molecular cations (methane chemical ionization) of (A) $C_6H_5CH_2CH_2N(CH_3)_2$ and (B) $C_6H_5CH_2CH_2NHCH_2CH_3$. Insets are the EI spectra of dimethylamine and ethylamine.

Presented at the 36th ASMS Conference on Mass Spectrometry and Allied Topics
June 5-10, 1988, San Francisco, CA

DESIGN AND PERFORMANCE OF A NEW REVERSE GEOMETRY MASS SPECTROMETER WITH HIGH SENSITIVITY AND HIGH ION TRANSMISSION

F.KUNIHIRO, M.ISHIHARA, Y.KAMMEI, E.KUBOTA, Y.ITAGAKI
AID, JEOL LTD. 3-1-2 Musashino Akishima, Tokyo 196 JAPAN
B.D.MUSSELMAN, T.HIGUCHI,
JEOL USA INC. 11 Dearborn Road, Peabody,MA 01960 USA

High resolution selected ion monitoring (HR/SIM) in GC/MS becomes regularly used[1] to advance detection limits in trace analysis. Furthermore, FAB/MS has been routinely used for the analysis of high molecular weight compounds. In both, a magnetic sector mass spectrometer is commonly utilized, and that under higher mass resolutions. However, a magnetic mass spectrometer has an inherent problem that sensitivity decreases proportionally when the main slit width is decreased for the purpose of increasing resolution.

We have designed and constructed a highly sensitive, medium sized double focusing mass spectrometer, the JMS-SX102, which allows for a wider main slit width than that on conventional instruments.

The ion optics of the JMS-SX102[2] is shown in Fig.1 and the major ion optical parameters are shown in Table 1. The $A\gamma/Ax$ ratio ($A\gamma$:mass dispersion, Ax:image magnification) is 5 times as large as that of ordinary optics($A\gamma/Ax$=1.0). This means that a wider main slit can be used not only under low resolution conditions but also under high resolution conditions. Fig.2 shows horizontal(X) and vertical(Y) ion trajectories. The pair of electrostatic quadrupole lenses(Q_1,Q_2) vertically focuses the ion beam so that it can be transmitted through the narrow magnet gap, and the third quadrupole lens(Q_3) refocuses the beam stigmatically at the collector slit. Consequently, high ion transmission is obtained.

Table 1 Ion Optical Parameters

deflection angle of magnetic field	40°
deflection angle of electric field	85°
image magnification(Ax)	0.20
mass dispersion($A\gamma$)	0.98
$A\gamma/Ax$	4.9

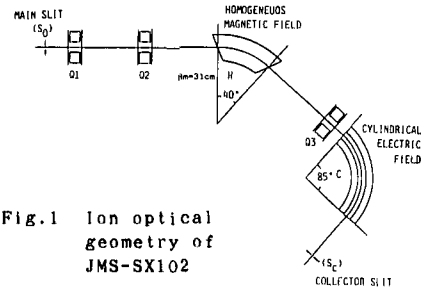

Fig.1 Ion optical geometry of JMS-SX102

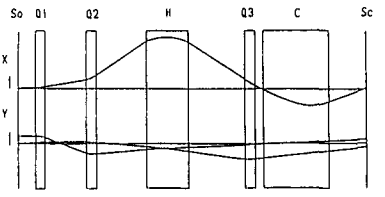

Fig.2 Horizontal(X) and vertical(Y) ion trajectories

Second- and third-order optical aberrations are minimized[2] using the computer code "TRIO"[3].
Fig.3 shows a high resolution spectrum of CH_2Cl_2 and $CDCl_2$ over 60,000 (The resolution required to separate the two peaks is R=54,260).
The main slit was set at 11μm which closely coincides with the calculated value of 13μm.

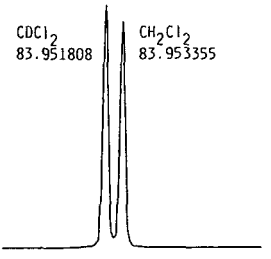

Fig.3 High resolution spectrum over 60,000

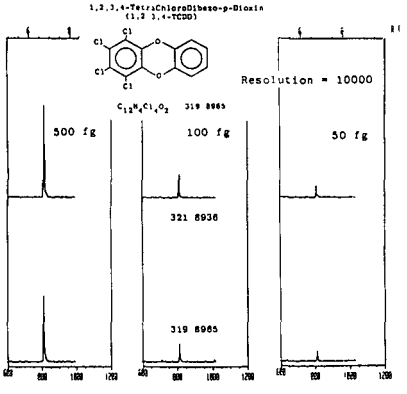

Fig.4 HR/SIM profile of 1,2,3,4-TCDD(m/z319.8965, 321.8936)

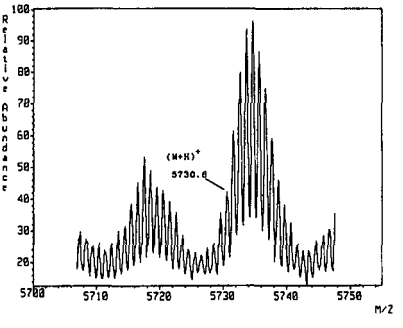

Fig.5 FAB spectrum of bovine insulin (moleculer ion region)

Fig.4 shows HR/SIM chromatograms of fentogram range TCDD. The resolution was set at R=10,000 which is enough to eliminate interferences from adjacent mass peaks.
Fig.5 shows the molecular region FAB spectrum of bovine insulin. The spectrum was obtained at 4KV accelerating voltage and with R=6,000.

These results show that the JMS-SX102 is extremely sensitive under even high resolution conditions and in any mass regions, compared to conventional instruments.

1) D.G.Patterson, Jr., L.Hampton, C.R.Lapeza, Jr., W.T.Belser, V.Green, L.Alexander, and L.L.Needham, Anal. Chem. 59 2000 (1987)
2) H.Matuda, Int.J.Mass Spectrom. Ion Processes 66 209 (1985)
3) T.Matsuo, H.Matuda, Y.Fujita and H.Wollnik, Mass Spectroscopy (Jap.) 24 19 (1976)

Presented at the 36th ASMS Conference on Mass Spectrometry and Allied Topics
June 5-10, 1988, San Francisco, CA

IMPROVEMENT IN HIGH MASS ION DETECTION OF A TANDEM QUADRUPOLE MASS SPECTROMETER USING A HIGH VOLTAGE POST-ACCELERATION DETECTOR

A.E. Schoen and John E.P. Syka, Finnigan MAT
355 River Oaks Parkway, San Jose, California 95134

Recent advances in quadrupole technology have enabled the use of soft ionization techniques such as liquid SIMS and thermospray to be utilized effectively on triple quadrupole instruments for the analysis of molecules larger than 2000u. However, these instruments suffer due to mass dependent detection efficiencies far less than unity. A new detector employing post analysis acceleration to 20 kilovolts of ion energy increases the detected analog signal at mass 4030 by more than a factor of twenty.

Detectors employing post analysis acceleration have been used in many mass spectrometers. Our goal was to design an implementation for a triple quadrupole system which allows investigation of higher conversion energies while reducing noise from field emission. The system uses a single, large, concave dynode mounted 90 degrees off axis from the beam exiting the final quadrupole. The entrance to the electron multiplier is directly opposite the dynode such that fast neutrals and photons may pass between the dynode and the multiplier without striking any surfaces.

The detector is similar to the one found on a sector field instrument. The difference is the nature of the ion beam. In sector instruments, the ion beam has a high kinetic energy at ground potential. Sector instruments without post acceleration detectors have a conversion energy equal to the difference between the ion source potential and the electron multiplier bias which has historically contributed to the observation of larger high mass peaks compared to peaks on quadrupole systems. The post acceleration detector eliminates this distinction between sector field and quadrupole mass spectrometers. In addition, this detector has essentially no dark current for dynode voltages up to 15 kilovolts and less than 20 ion counts per second at 20 kilovolts.

Figure 1 shows the gain in peak intensity as a function of mass for 10, 15, and 20 kilovolts relative to 5 kilovolts. The data is for cesium iodide and glucagon, however, other data for florinated reference compounds show indentical results. Not shown are results for a negative ion at mass 452 which exhibit a ninefold improvement when the dynode voltage is increased form 5kV to 20kV. SIMION was used to model the ion trajectories to the dynode and the collection of secondaries from the dynode. It was found that the high dynode voltage dominates the ion motion. Quadrupole exit conditions and lens settings have little effect.

Inspection of profile data acquired for daughters of substance P and the molecular cluster region of glucagon reveals an improvement in the subjective quality of data obtained while data taken at low mass shows no noticable change. Conversion efficiency alone cannot account for the improvement and overall detector gain should only affect peak height ratios. Indications that conversion efficiency does not increase as much as gain is contradicted by the obvious decrease in jitter on the peaks.

Since 20kV is insufficient to reach the threshold velocity for conversion efficiency to be greater than unity at mass 2000 (1), a statistical evaluation of the improvement was attempted. Measurements to compare the relative standard deviation of a measured ion signal at mass 502 as a function of dynode voltage revealed only a modest improvement in ion statistics. To determine whether the improved high mass detection is due to improved conversion efficiency or mass dependent gain, low ion flux was observed with a bandwidth of 23000Hz. At mass 1951, 32 ions are seen in 0.5 seconds at 5kV and 43 are seen at 20 kV. The conversion efficiency improves by a ratio of 1.34. The maximum pulse height increases by a factor of 6.33 to give a total gain of 1.34 x 6.33 = 8.48 which compares low to 11.1 as measured by conversion efficiency increase. Pulse pile up probably obscures some conversion efficiency increase and the relative pulse height distribution is slightly narrower at high voltage giving more gain compared to the ratio of maximum pulse heights.

The crude pulse height test confirms that most signal increase is due to mass dependent gain accompanied by a small improvement in the relative pulse height distribution and conversion efficiency. It should also be noted that for masses below 2000u, which can reach the threshold velocity, there are no breaks in the curves for the effect of dynode voltage on peak height.

The following conclusions may be drawn from these observations. Consistent with work by many others, higher conversion dynode voltage increases the detection of high mass ions relative to low mass ions. The improved high mass detection allows quadruople or other low energy instruments to yield spectra more similar to magnetic sector systems. The increase is due to a combination of increased conversion efficiency and mass dependent gain. An improvement in pulse height distribution may also contribute to better signal quality. Where detected noise is due to residual low mass ions or neutrals, the mass dependent gain will directly improve the signal to noise ratio. And finally, the simple dynode design eliminates most of the dynode noise from field emission expected with high voltage systems.

(1) J. Beuhler and L. Friedman, Int. J. Mass Spectrom. Ion Phys., 23 (1977) 81-97.

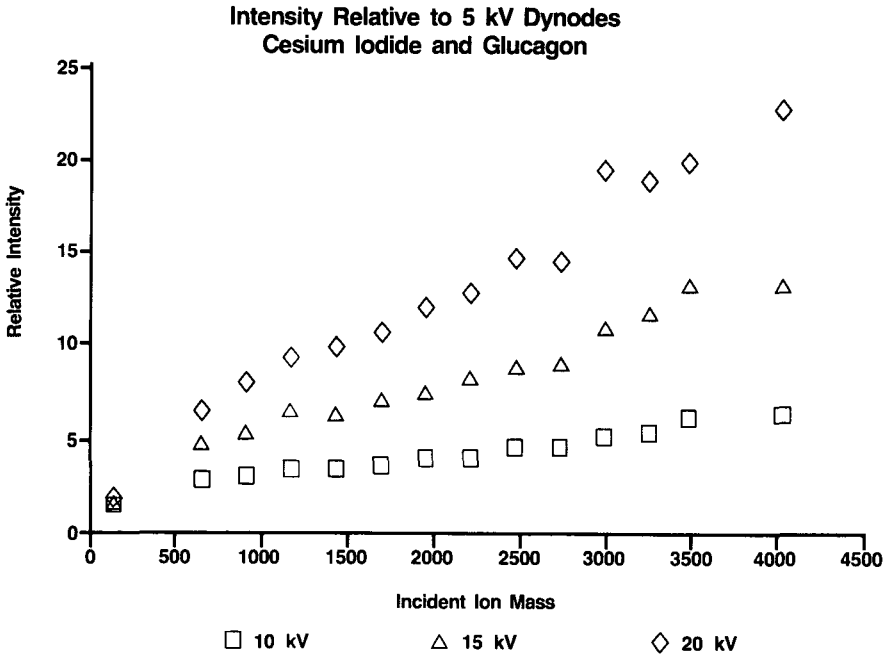

Presented at the 36th ASMS Conference on Mass Spectrometry and Allied Topics
June 5-10, 1988, San Francisco, CA

IMPROVING THE DETECTION SENSITIVITY FOR HIGH MASS IONS

J.F. Mahoney[1]*, J. Perel[1], T.D. Lee[2] and K. Legesse[2]

[1]Phrasor Scientific, Inc., 1536 Highland Ave., Duarte CA 91010
[2]Div. of Immunology, City of Hope, Duarte CA 91010

A needexists in mass spectrometry for a more sensitive method of detecting high mass ions of biologically important compounds. Conventional means for the detection of ions have relied on the production of secondary electrons released when incident ions impact an electron multiplier or post-acceleration dynode. Both methods are limited by an incident ion threshold velocity below which efficient ejection of secondaries is poor (1). In general, ion detection based on the kinetic ejection of secondary electrons becomes progressively more difficult to achieve with increasing ion mass. Recent approaches for improving detection sensitivity depend on post-dynode elements to achieve current amplification. This present study reports on the feasibility of improving the yield of secondary negative particles at the ion impacted dynode by forming a low work function overlayer on the dynode surface. Typically, low work function dynode surfaces are prepared by alternate or co-deposition of cesium and oxygen (2).

By forming a low work function, semiconducting photoemissive surface, the yields of secondary negative particles induced by impact of high molecular weight ions can be increased by several mechanisms. Sinceorganic ions undergo fragmentation after colliding with solid targets (3), enhanced yields of desorbed negative fragment ions can be achieved by establishing conditions at the dynode surface favorable for electron capture by the low mass, molecular fragments. These conditions are met by providing a low work function surface and molecular fragments having high electron affinities. Additionally, low energy ion-surface collisions can induce optical radiation (4). By irradiation of a thick cesium-oxide film with photons formed in the collisional interaction between incident biomolecular ions and a dynode surface, photoemissive electrons can be ejected. Photon emission can occur by excitation of backscattered ions, by excitation of adsorbed surface molecules and by excitation of fragmentation products. Thermionic emission arising from localized thermal spikes in low work function regions may also contribute to signal enhancement.

To examine the effects on increased ion detection sensitivity arising from the mechanisms described above, the apparatus shown in Fig.1 was constructed. A highly polished nickel dynode was machined to duplicate the dynode configuration supplied with a JEOL HX100 HF double focusing MS and mounted on a movable shaft. Retracted to the deposition position, the dynode was exposed to alternate doses of cesium supplied by a heated dispenser and oxygen was introduced through a leak valve. After each dosage, the activated dynode was re-positioned and FAB spectra acquired for melittin (MW=2846). The increase in sample ion intensity for the treated dynode over the bare nickel dynode is expressed as a ratio in Table I. For the last deposition condition (Cs+O+Cs+O+Cs), the sample ion intensity reached a value over 30 times that measured for the untreated dynode. Fig.2 illustrates the melittin spectra for the bare nickel singly, doubly and triply dosed dynode. Low mass, matrix ions show similar increases. In these studies the chemical background was proportionally amplified with the overall signal-to-noise remaining nearly constant. The Cs-O activated dynode exhibits higher cold emission or thermionic noise under applied voltage but remained below the chemical background. Quantification and discrimination involving the mechanisms postulated for the increases observed in signal enhancement are under investigation.

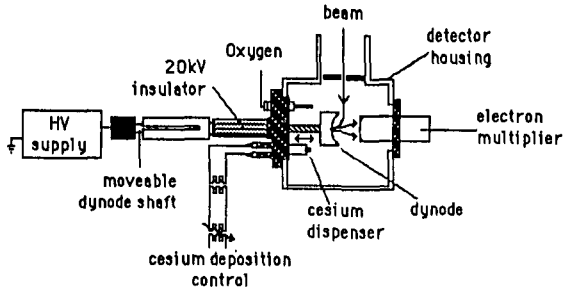

Fig. 1. Detector Test Configuration

Table 1. Sample Ion Intensity Ratio I/I_0 For Treated (I) vs. Standard Dynode (I_0).

Dynode Voltage			Deposition Condition
-10 kV	-15 kV	-19 kV	
1	1	1	Bare Nickel
12.3	13.3	12.8	Cs
32.3	21.5	21.9	Cs - O - Cs
37.4	34.4	---	Cs - O - Cs - O - Cs

Sample Ion (melittin, m/z 2846) intensities are the average of 10 scans. Standard Dynode = Bare Nickel

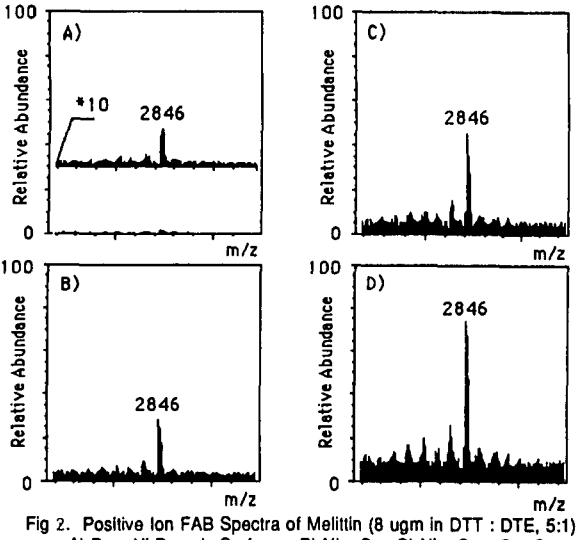

Fig 2. Positive Ion FAB Spectra of Melittin (8 ugm in DTT : DTE, 5:1)
A) Bare Ni Dynode Surface. B) Ni + Cs. C) Ni + Cs + O + Cs
C) Ni + Cs + O + Cs + O + Cs.

References

1. R.J. Beuhler and L. Friedman, Nucl. Instrum. Meth., 170, 309 (1980).

2. F.N. Huffman and P.E. Oettinger, Proc. 2nd Symp. On The Production and Neutralization Of Negative Hydrogen Ions And Beams, BNL 51304 (Brookhaven National Laboratory, Oct. 1980) p.119.

3. Md.A. Mabud, M.J. DeKrey and R.G. Cooks, Int. J. Mass Spectrom. Ion Processes, 67, 285 (1985).

4. C.W. White, E.W. Thomas, W.F. Van der Weg and N.H. Tolk in Inelastic Ion-Surface Collisons, Academic Press, New York (1977) p.201.

Presented at the 36th ASMS Conference on Mass Spectrometry and Allied Topics
June 5-10, 1988, San Francisco, CA

AN IMPROVED ^{252}Cf PLASMA DESORPTION MASS SPECTROMETER FOR LARGE BIOMOLECULES

P.D. Mudgett, J.C. Hill, and R.D. Macfarlane
Texas A&M University, College Station, TX 77843

^{252}Cf Plasma Desorption Mass Spectrometry (PDMS) has developed into a highly useful technique for the mass analysis of involatile biomolecules. It is, however, desirable to extend the sensitivity of the technique into the picomole to femtomole range [1]. There are many factors which determine the sensitivity of PDMS for large molecules, and the research in this area of PDMS involves determining the necessary conditions for detecting massive ions, as well as the sources of the large background associated with the PD mass spectra. A more complete understanding is necessary in the design of the instrumentation required for optimal sensitivity and mass accuracy for PDMS of high mass molecules. In this report, several sensitivity considerations will be discussed, and improvements to PDMS time-of-flight instrumentation presented along with spectrometric results using bovine insulin (m/z 5735) as a test molecule.

The analyte peaks of interest in a PDMS spectrum appear superimposed on the background continuum which affects the mass assignment. It is thus desirable to "decouple" in real time the peak from the background via the hardware. The background continuum generally increases in relative intensity with mass and is a composite of energetic neutrals, metastable ions, uncorrelated or mixed events, and electronic noise (generally minimal). Retarding fields [2] have been used to partially resolve a given peak into its molecular ion, metastable and neutral components. Parallel electrostatic deflector plates can also be used to separate the ions and neutrals into two "beams" which can be monitored individually. The mixed event problem has been investigated and may contribute up to 50% to the background [3].

In an effort to decrease the significant component of the background due to neutrals, the ion flight length was doubled to reduce the acceptance angle of the detector for the divergent neutrals beam. The fraction of the total ion counts per unit time due to neutrals from a bovine insulin on nitrocellose were recorded vs. the diameter of a collimating iris with +3kV across the deflector plates. The results are shown in Fig 1. The fraction due to neutrals is indeed decreased with length; however, there is a ten-fold decrease in the intensity of the $(M + H)^+$ ion. Apparently, the insulin ion has a lifetime limitation and/or the ion beam diameter was larger than the detector active diameter. (A einzel focusing lens was employed to control the ion beam diameter but its effect on the very divergent beam off nitrocellulose was marginal at best).

In PDMS the analyte molecule is detected if the corresponding ions obtain sufficient velocity for detection and assume trajectories which intersect the active area of the detector. Thus, the threshold velocity and detection efficiency [4], the characteristic beam diameter [5], and the detector active area are important parameters in the design of a PDMS system for large molecules. Recent work by Geno and Macfarlane [1,4] has yielded a practical model for predicting the detection probability of a given biomolecular ion based on its mass and velocity. Fig 2 illustrates the effect of velocity on detection efficiency. The velocity that an ion attains is a function of its m/z and the total acceleration potential, which is the sum of the primary acceleration and post-acceleration potentials.

For this system, a detector with large active diameter and high of post-acceleration capability is desirable. Because of the relatively divergent ion beam characteristic of the PDMS system, the active diameter of the ion detector must accomodate the beam for optimal sensitivity. The actual diameter of the anode in a commercially-available dual 40mm microchannel detector with a 50 ohm anode is 20mm. (The advantage of the impedance-matched anode over the flat collector with RC "pickoff" circuit is well-known [6].) To aid in the design of such a detector, the ion optics simulation program "SIMION" [7] was employed to optimize the authors' ideas. Two such "SIMION" designs as well as the conventional detector, in which about half of the secondary electrons strike the anode, are included for comparison. Using three microchannel plates (MCP), a detector capable of-10kV post-acceleration voltage was designed (Fig 4), implemented, and tested. (Note that the electrons emitted from the front MCP are focused onto the

center portion of the chevron, thus providing a full 40mm active diameter.) The data set given previously in Fig 2 was acquired using this detector configuration in which the post-acceleration voltage could be varied while maintaining a constant voltage across the front MCP. In spite of the positive results for this novel detector, there are problems with noise and saturation of the chevron which limit its practicality for routine use.

Fig 5 shows a more practical detector with a full 40mm active diameter and a wide range of possible post-acceleration potentials in either polarity. Here, focusing occurs behind the chevron rather than in front as before. This electron focusing chevron detector (EFCD) configuration is similiar to that of Olthoff and Cotter [9] in that it utilizes a ring to focus the electrons onto the conical anode. The present configuration rather unconventionally uses a voltage on the anode in addition to that on the focusing ring. The signal is "picked off" via an R-C circuit(in vacuum and in close proximity to the anode). With the use of 50 ohm coaxial cable and a BNC-to-BNC vacuum signal feedthrough, the signal shape is preserved. The spectra for insulin using the EFCD at two anode voltages (Fig 6) serve demonstrate the focusing action. These results are preliminary - the details and further test results are forthcoming [10].

In summary, this report has reviewed the problem of background in PDMS and the relatively poor detection efficiency of high mass molecules. With these restrictions in mind, various detector configurations, and other hardware features to enhance the sensitivity of ^{252}Cf-PDMS were presented.

Acknowledgements: The authors are grateful to Dennis Shelton for assisting with the electronics, to Mark Miller for maintaining the computer, and to the National Institutes of Health (GM-26096) and the Robert A. Welch Foundation (Grant A-258), for supporting this work.

Fig 1 Profile of the beam of undeflected species for the 0.5m (a) and the 1.1m (b) flight lengths

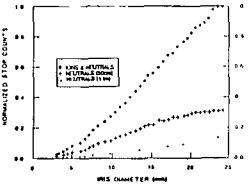

Fig 2 Effect of the total acceleration potential (or ion velocity) on insulin (M+H) yield

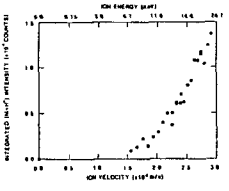

Fig 3 Simulation of a conventional chevron detector configuration using a 50 ohm conical anode

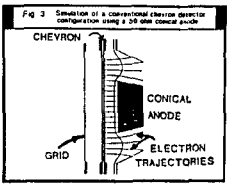

Fig 4 A high post-accelerator detector with electron focusing between the front MCP and the chevron

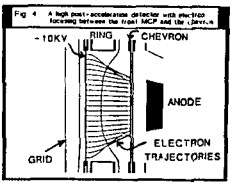

Fig 5 A model of the electron focusing stop detector configuration with -2.2 kV post-accelerator

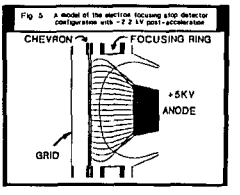

Fig 6 Spectra of bovine insulin on nitrocellulose acquired for 30 min using the focusing detector of Fig 8 with 0 V (a) and +5000 V (b) on the conical anode

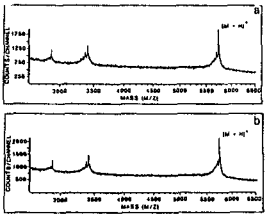

1. R.D.Macfarlane, J.C. Hill, P.W. Geno, and P.D. Mudgett, in Proc. 4th Texas Symposium Conference, C.J McNeal, ed., Wiley, 1988 (in press).
2. B.T. Chait, Int. J. Mass Spectrom. Ion Physics, 53 (1983) 227.
3. A. Hedin, P. Hakansson and B.U.R. Sundqvist, Int. J. Mass Spectrom Ion Processes, 70 (1986) 203.
4. P.W. Geno "^{252}Cf Plasma Desorption Mass Spectrometry in a Low-voltage Regime" (Ph.D. Dissertion, Texas A&M University, 1988).
5. H. Danigel and R.D. Macfarlane, Int. J. Mass Spectrom. Ion Physics, 39 (1981) 157.
6. J.L. Wiza, Nucl. Inst. and Meth., 162 (1979) 587.
7. An electrostatic lens design program by D.A. Dahl and J.E. Delmore, Idaho National Engineering Laboratory, Idaho Falls, ID.
8. E.C. Pollaco, J.C. Jacmart, Y. Blumenfeld, P. Chomaz, N. Frascaria, J.P. Garron, J.C. Roynette, Nucl. Instr. and Meth. in Physics Res. 225 (1984) 51.
9. J.K. Olthoff and R.J. Cotter, Proc. 35th Annu. Conf. on Mass Spectrometry and Allied Topics, ASMS, 1987, p.735.
10. to be submitted to Int. J. Mass Spectrom Ion Processes.

Presented at the 36th ASMS Conference on Mass Spectrometry and Allied Topics
June 5-10, 1988, San Francisco, CA

USE OF A MICROCHANNEL ARRAY DETECTOR IN A FOUR-SECTOR TANDEM MASS SPECTROMETER

J. A. Hill, S. A. Martin and K. Biemann
Dept. of Chemistry, Mass. Institute of Technology, Cambridge, MA 02139

Mass spectra generated by collision induced dissociation (CID) of a selected precursor ion are characterized by a relatively low ion current but the "chemical noise" observed in normal FAB spectra is absent. Integration of the signal is the best way to increase the sensitivity and to average out the electronic and ion noise. This is best achieved by placing an array detector in the limited focal plane of the spectrometer and recording the spectrum by integrating the ion current of consecutive segments for the proper length of time repeatedly. The data are then assembled to the full spectrum. The array detector can also be used to record a normal FAB spectrum[1] in a similar manner or in the "enhanced resolution mode"[2].

We have constructed an array detector consisting of a 2" microchannel plate and a 2" Reticon photodiode array consisting of 2048 diodes (Fig. 1). It is placed in the focal region of the JEOL HX110/HX110 tandem mass spectrometer, which has a 3" focal plane at an angle of approximately 20° to the incident ion beam[3]. The 2" array covers 6.6% of any given mass range.

The detector can record signals generated in any of three modes: 1) MS/MS (sample in ion source of MS-1), 2) Molecular ion region at "enhanced resolution" (sample in the ion source of MS-1), and 3) Normal FAB or EI spectra (sample in the ion source of MS-2). Because of the high increase of sensitivity, the array detector is particularly useful in the MS/MS mode. Fig. 2 shows the CID spectrum of the $(M+H)^+$ ion of a peptide, Substance P (M_r = 1346.7), 0.2 nmol in glycerol, at an accelerating voltage of 10 kV, the collision cell at 5 kV and recorded with the array detector.

The potential applied to E_2 and the magnetic field B_2 were stepped (by the JEOL DA5000 data system) in such a way that an imaginary ion beam ("center mass") is consecutively focused at the center of the MCP in increments of 6% of mass, to provide some overlap of the consecutive segments. To assure efficient transmission through E_2 of product ions differing in kinetic energy by 6%, the collision has to be carried out after significant deceleration and before reacceleration. For this reason, the collision cell is floated at 5 kV. The spectrum shown in Fig. 2 was recorded in 48 steps to cover the mass range from m/z 68 - 1326. For each step the ion current was integrated for 200 msec repetitively. The photodiode readout (ten 0.2 sec integrations per step) was acquired by a dedicated data system before transfer to a VAX 750 for processing. The center mass and the dispersion of the spectrometer permits conversion to mass and alignment of the consecutive segments to the complete mass spectrum. Figure 3 shows the good signal-to-noise ratio at sample concentrations down to 500 fmol (Fig. 3C).

Resolution of a normal spectrum is considerably increased when using all 4 sectors in the "enhanced resolution" mode[2]. In this mode the focal plane is even further inclined, at an angle of approximately 14° to the incident ion beam[3]. This is one of the reasons why the array detector is designed for changing position and angle without breaking the vacuum. The achieved resolution is evident in Fig. 4, the molecular ion region of glucagon.

This work was supported by a grant from the National Institutes of Health (RR00317).

1. J.S. Cottrell and S. Evans, Anal. Chem., 59, 1990 (1987).
2. T. Matsuo, M. Ishihara, S.A. Martin, K. Biemann, Int. J. Mass Spectrom. Ion Processes, in press.
3. E. Kubota, Y. Kammei, M. Ishihara, JEOL LTD., Tokyo, Japan, private communication.

Presented at the 36th ASMS Conference on Mass Spectrometry and Allied Topics
June 5-10, 1988, San Francisco, CA

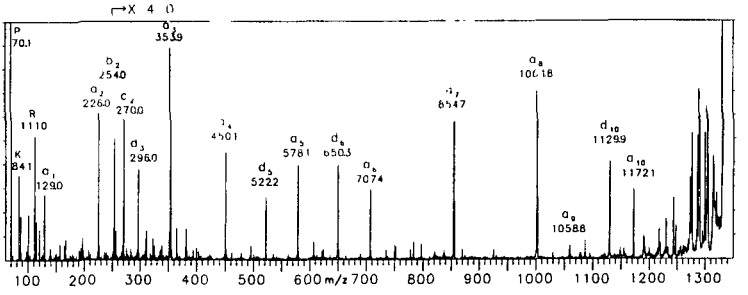

Fig. 2 Tandem mass spectrum of 0.2 nmol Substance P (Arg-Pro-Lys-Pro-Gln-Gln-Phe-Phe-Gly-Leu-Met-NH_2, M_r 1346.7) recorded with an array detector.

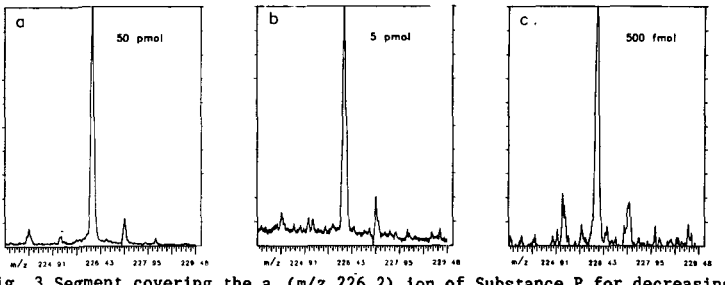

Fig. 3 Segment covering the a_1 (m/z 226.2) ion of Substance P for decreasing amounts of sample: (a) 50 pmol (10 integrations of 0.5 sec duration): (b) 5 pmol (5 x 1.0 sec); and (c) 0.5 pmol (5 x 2.0 sec). The x-axis is diode numbers converted to m/z values.

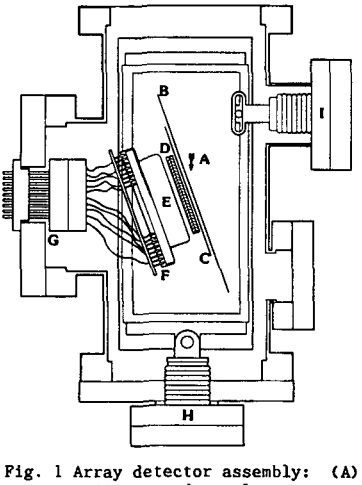

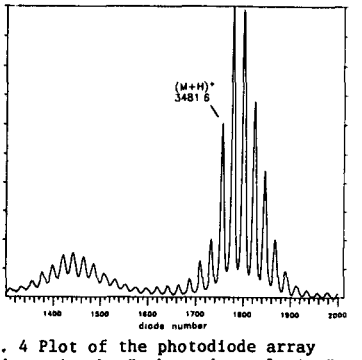

Fig. 4 Plot of the photodiode array read-out in the "enhanced resolution" mode of the region of m/z 3461-3493 of the FAB spectrum of glucagon. The calculated resolution (extrapolated from FWHH to 10% valley to eliminate flare) is 1:5500.

Fig. 1 Array detector assembly: (A) incident central ion beam; (B) grounded screen; (C) secondary electron suppressor screen; (D) two 2" micro channel plates (MCP) in "chevron" arrangement; (E) fiberoptics coated with phosphor in front; (F) 2" reticon array of 2048 photodiodes; (G) connector to feedthrough of vacuum envelope; (H) position adjustment; (I) angle adjustment.

Presented at the 36th ASMS Conference on Mass Spectrometry and Allied Topics
June 5-10, 1988, San Francisco, CA

TIME RESOLUTION AND MS/MS ANALYSES OF GROUP A STREPTOCOCCUS PYROLYSIS MASS SPECTRA UNDER ATMOSPHERIC PRESSURE IONIZATION

A. Peter Snyder, U.S. Army Chemical Research, Development and Engineering Center, Aberdeen Proving Ground, MD 21010-5423

Willem Windig, GEO-CENTERS, INC., 10903 Indian Head Highway, Ft. Washington, MD 20744

Analysis of macromolecular biological compounds in solid and solution/liquid suspension is of concern to a number of scientific disciplines. Because of their high molecular weight these substances (biopolymers and microorganisms) must be reduced in size so as to form low yet informative molecular weight products for effective mass spectral analysis. Other objectives desired from the sample preparation, processing and data analysis methods are that they are simple, rapid, convenient and produce information that is characteristic to the biological substance whether it be generic or specific in nature. Ribbon oxidative pyrolysis was the method of choice for sample introduction (1) while the Atmospheric Pressure Chemical Ionization (APCI) conditions in the ion source provided attractive benefits to the process. Ramped heating conditions prevailed at 300 °C/min to a final set temperature of 600°, and an air flow of 150 ml/min was directed over the heating zone.

In the interest of rapid data analysis, a univariate method for component deconvolution was developed, called the Scaled-Power-Total Ion Current (SP-TIC). It is approximately 20-100 times faster than multivariate analysis techniques (2) and is highlighted by a minimum of operator interaction. The theory is pictorially represented in Figure 1, and practical application is then applied to a pyrolysis (Py)-APCI-time resolved, mass spectrum (Figure 2) of a Group A Streptococcus strain. Three main components (Figure 3) were isolated with the SP-TIC technique and each main component was observed to consist of a number of individual components.

This distillation of the mass spectral data provided a clearer visual analysis for component identification. Muramic acid is found only in the cell walls of bacteria and its Py-APCI-mass spectrum is shown in Figure 3. The late eluting component C (Figure 4) consisted of a pattern highly similar in m/z and intensity distribution to that of proteinaceous substances. The first component consisted of, among other features, m/z 90 and 108. Daughter ion analysis (Figure 5) confirmed their identities as arising from muramic acid. A similar analysis of m/z 127 (Figure 6) shows that it arises from the thymine (MH^+) base from deoxyribonucleic acid along with a contribution from the hexose sugar components.

1. Liebman, S.A.; Snyder, A.P.; Kremer, J.H.; Reutter, D.J.; Schroeder, M.A.; Fifer, R.A. J. Anal. Appl. Pyrolysis 1987, 12, 83.

2. Windig, W.; Liebman, S.A.; Wasserman, M.B.; Snyder, A.P. Anal. Chem. 1988.

Presented at the 36th ASMS Conference on Mass Spectrometry and Allied Topics
June 5-10, 1988, San Francisco, CA

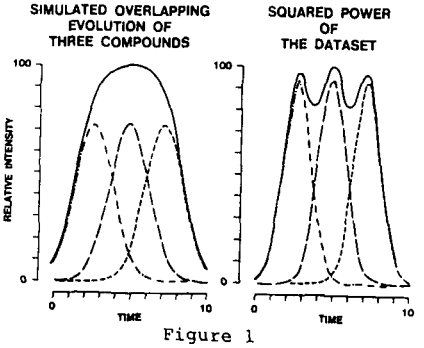

Figure 1

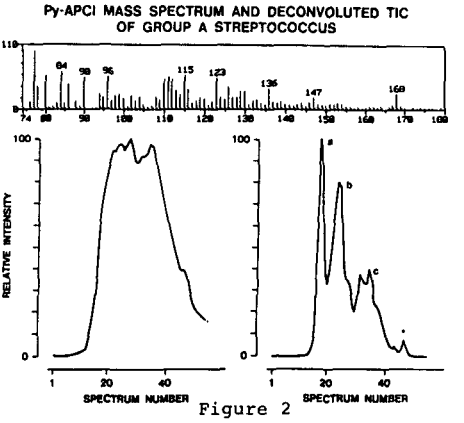

Figure 2

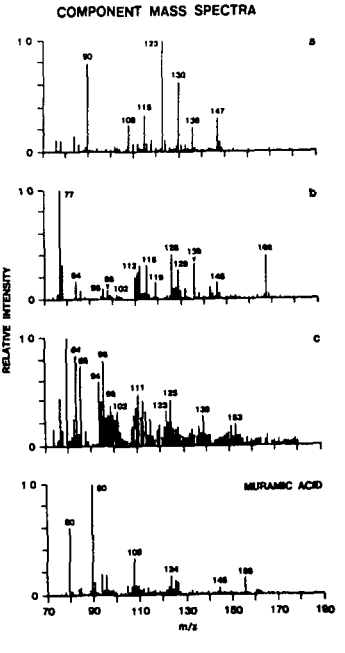

Figure 3

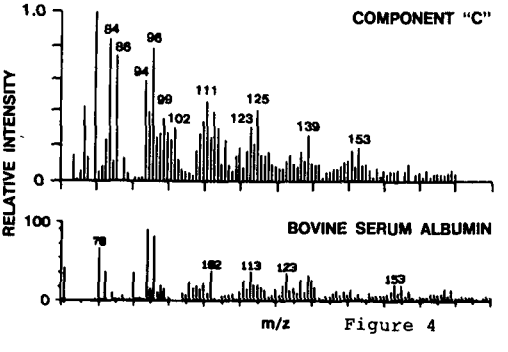

Figure 4

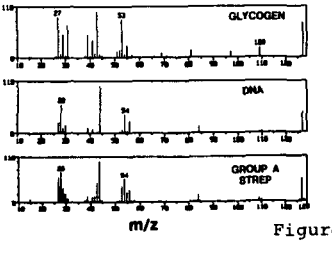

Figure 6

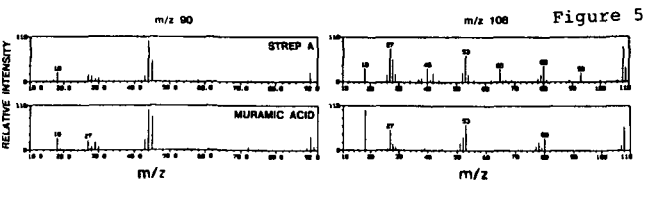

Figure 5

Presented at the 36th ASMS Conference on Mass Spectrometry and Allied Topics
June 5-10, 1988, San Francisco, CA

AN ION-OPTICAL BENCH FOR TESTING ION SOURCE LENSES

J. J. Stoffel(s) and D. R. Ells
Pacific Northwest Laboratory
Richland, WA 99352

An ion-optical bench (see figure below) has been designed and constructed to obtain experimental data on the focusing properties of ion lenses in three dimensions. The heart of the apparatus is a position-sensitive detector (PSD) that gives output signals proportional to the x and y positions of each ion impact. The position signals can be displayed on an oscilloscope screen to give a visual picture of the ion beam cross section. The effect of tuning the voltages on the lens plates can be viewed in real time. The position signals can also be analyzed by a two-parameter pulse-height analyzer to give a three-dimensional picture of the ion intensity distribution.

The PSD itself is mounted on a track and is movable during operation from a position following the ion lens to 30 cm away. This enables the rapid collection of accurate data on the intensity distribution and divergence angles of ions leaving the source lens. A movable Faraday cup can be inserted into the beam to measure ion transmission efficiency of the lens.

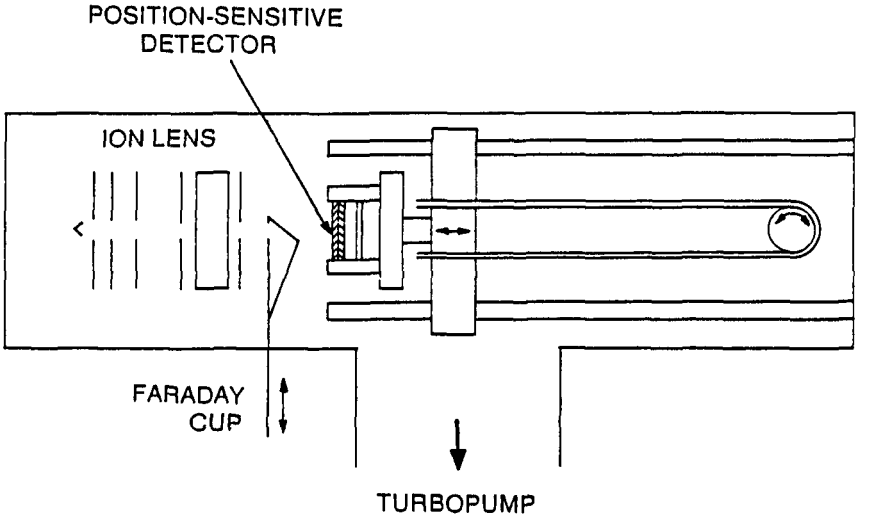

An example of the measurements that can be made with the ion-optical test bench is given below. The ion lens used is one designed at the National Bureau of Standards [1]. The lens was equipped with a single V-filament surface ionization source loaded with cesium. Ion beam cross sections are shown as they appeared on the oscilloscope screen at different distances from the exit of the lens. From the 'scope photos, we can determine that the beam was diverging in the horizontal plane at an angle of 1.0 degree about the axis. The beam was also brought to a focus in the vertical plane by adjustment of the voltage on vertical focus plates.

This example demonstrates the ease, rapidity and accuracy with which ion beam parameters can be measured. With the ability to show instantaneously the effect of tuning the lens voltages, the ion-optical bench is a powerful tool for electrostatic lens evaluation.

We thank J. D. Fassett for use of the NBS ion lens and voltage divider.

REFERENCE

1. W. R. Shields, editor, NBS Technical Note 426, 1967, pp. 7-9.

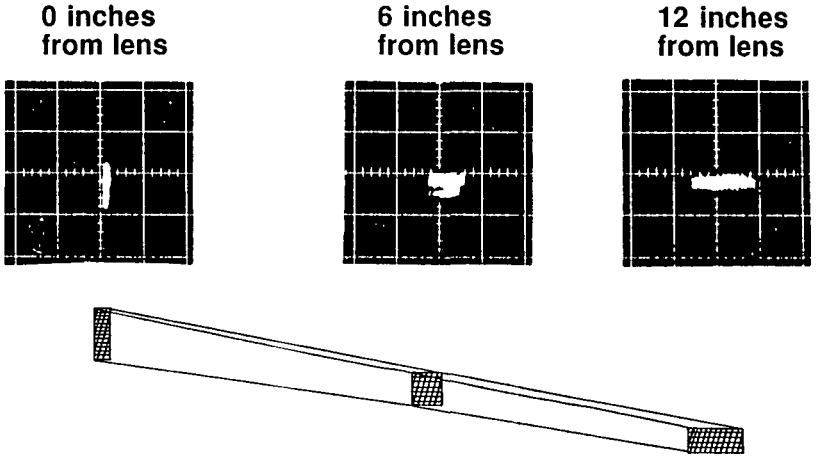

Ion beam cross sections from the NBS lens with a single V-filament. The vertical focus control was adjusted to give a crossover 12 inches from the lens.

Presented at the 36th ASMS Conference on Mass Spectrometry and Allied Topics
June 5-10, 1988, San Francisco, CA

GAS ANALYSIS OF LOW-PRESSURE MERCURY-ARGON DISCHARGE

EDWARD PANG GTE ELECTRICAL PRODUCTS, DANVERS, MA 01923
ARMIN EICH GTE ELECTRICAL PRODUCTS, ERLANGEN, WEST GERMANY

An electric discharge between two electrodes within a glass tube filled with argon (2 ~ 3 torrs) and mercury (3 ~ 5 x 10^{-3} torr) produces UV radiation. It is emitted by excited mercury atoms returning to their ground state. The surplus energy (excited state --> ground state) is released by the atom as UV at 253.7 nm. This radiation strikes special phosphors producing visible radiation. Gaseous impurities can affect the discharge. For example, molecular hydrogen interacts with some meta-stable argon atoms transferring off the excitation energy and then dissociates. Electrons that strike hydrogen molecules lose part of their kinetic energy and are slowed down. As a result, the number and the kinetic energy of the electrons have to be increased to compensate for the loss. Discharges with high and normal operation voltages were monitored using mass spectrometry.

EXPERIMENTAL

The experimental system and the circuit for discharge operation are shown schematically in Figures 1 and 2, respectively. A well-degassed heated stainless steel inlet system was connected to a VG MM14-80 magnetic sector mass spectrometer for analysis. Typical background pressure in the source was about 6 x 10^{-9} torr. The inlet manifold was evacuated to 8 x 10^{-8} torr. Each discharge tube was operated for at least two hours before analysis. High purity argon was used as carrier gas for impurities evolved during operation. m/e = 2, 12, 14, 18, 28, 32, 43, 44 peaks were monitored.

RESULTS

1. Normal discharge tubes showed an operating voltage of 25.0 volts. Discharge tubes with high voltages were operated at 28.0 volts.
2. Mass/Charge = 2, 18, 32, 43, 44 peaks did not change significantly.
3. Typical CO concentration-time profiles are shown in Figure 3.
4. In discharge tubes with normal operating voltage, the average rate of CO evolution was 2.7 x 10^{-9} torr·liter·second^{-1}.
5. In discharge tubes with high operating voltage, the average rate of CO evolution was 67.0 x 10^{-9} torr·liter·second^{-1}.

DISCUSSION

1. This invsetigation strongly suggests that CO evolution is related to increasing operating voltage in low pressure mercury-argon discharge.
2. Excitation of CO molecules to higher vibrational states may low the energy of accelerated electrons in the discharge.
3. The presence of CO may lead to Mercury oxide formation.
4. Possible poisoning of electrodes by CO increases the work function of electron emission.

REFERENCES

1. E.K. Pang, P.L.Fortucci, and V.D. Meyer, *Anal. Chem.*, 57, 2995(1985).
2. E.K. Pang , *Proceedings of the 34th Annual Conference on Mass Spectrometry and Allied Topics*, pp.833-834(1986).
3. J. Waymouth, *Electric Discharge Lamps*, Cambridge, Mass., M.I.T. Press, 1971.

Presented at the 36th ASMS Conference on Mass Spectrometry and Allied Topics
June 5-10, 1988, San Francisco, CA

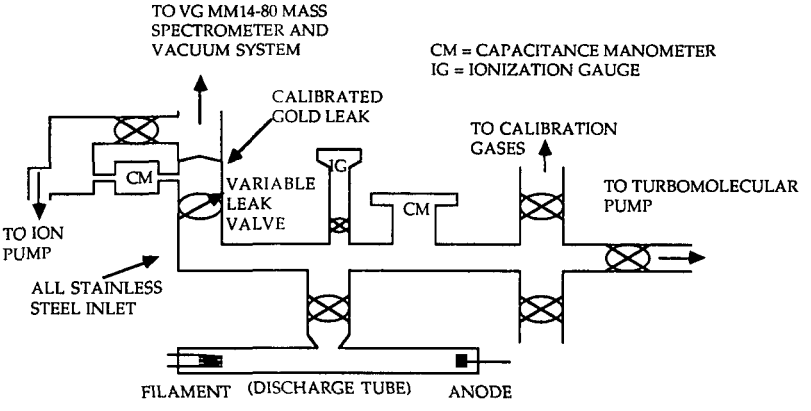

FIGURE 1. EXPERIMENTAL SYSTEM

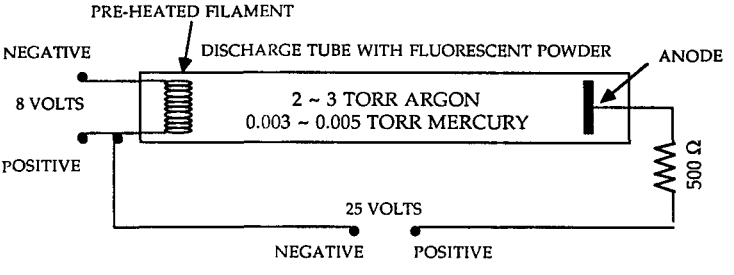

FIGURE 2. OPERATION OF DISCHARGE TUBE

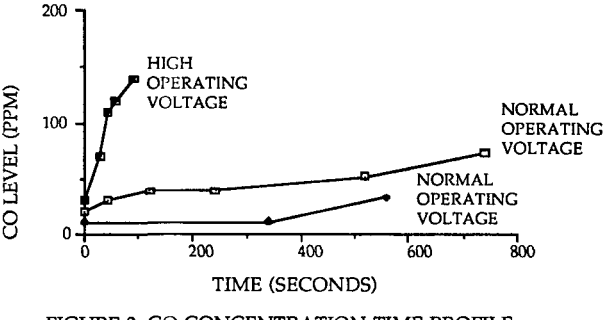

FIGURE 3. CO CONCENTRATION-TIME PROFILE

Presented at the 36th ASMS Conference on Mass Spectrometry and Allied Topics
June 5-10, 1988, San Francisco, CA

A SINGLE COLLECTOR MAGNETIC MASS SPECTROMETER FOR RESPIRATORY APPLICATIONS

Rosemarie A. Ungarelli, John L. Lehr, Donald J. Marshall

Boston University, Boston, MA 02215; Brigham and Women's Hospital, Boston, MA 02115; Measurement and Analysis Systems, Inc., Acton, MA 01720

The objective of this project is to adapt a single collector magnetic sector mass spectrometer for respiratory studies. The desired performance characteristics include a time response of less than 100 ms, minimal calibration, a mass range including all normal respiratory gases as well as tracer gases, and a dynamic partial pressure range of 10^5 or greater. Existing respiratory machines include multiple detector magnetic and quadrapole instruments. The single collector magnetic instrument offers advantages of good long term stability, wide dynamic range, continuously selectable mass range, and adjustable resolving power. An interface has been designed to operate a 3 inch, 60 degree Nuclide magnetic instrument with multiple peak stepping among up to five gases (He, N_2, O_2, CO_2, SF_6) by a DEC PDP-11 computer. The system can control the electric and magnetic fields, and can vary electrometer gain in log steps over a range of 10^6. The output of the mass spectrometer is digitized and results are processed on line in real time. The entire operation is well-prompted: the user initiates operation by specifying gases and introducing an appropriate standard mixture containing each of the gases to be analyzed. Thereafter, the instrument selects all parameters, locates the peaks, and determines the required electrometer gains. The system then goes into the automatic analysis mode and cyclically steps through each component of the mixture in 10 ms per gas -- compensating for the response time of the instrument in each gas -- while solving the mixture analysis matrix. For example, the instrument corrects for the contribution of SF_6 to the O_2 peak, as well as for the CO_2 produced by the filament in the presence of O_2 in the analyzer. The automatic gain correction for instrument sensitivity variation is made every cycle, as well. Since the stepping among gases must be as rapid as possible (10 ms), the electric field, rather than the magnetic field, is varied; however, this limits the mass range of the instrument. Hence, in order to read both He and SF_6, SF_6 must be examined as mass 54, the fragment SF_4^{++}, which greatly reduces the sensitivity of the analyzer. Although its output is limited under these conditions, the instrument is still capable of detecting concentrations as low as 0.2% SF_6 with a signal-to-noise ratio of one.

The automatic gain correction adjusts for variations in instrument sensitivity by multiplying the partial pressure of each of the gases by its sensitivity constant, and subtracting the crosstalk effects of the remaining gases in the mixture. The sensitivity constants are derived by summing the partial pressures of the gases and comparing the result to atmospheric pressure. The deviation of the calculated sum from the theoretical sum is denoted by ERROR. A new sensitivity constant is then derived for each gas as:

$$\text{NEW K} = \text{OLD K/ERROR}$$

where OLD K is a pre-determined, measured constant. The automatic gain

correction then adjusts each component of the gas mixture by solving the equation:

$$\text{NEW P} = \text{NEW K}(\text{OLD P} - \text{CROSSTALK})$$

where OLD P represents the partial pressure of the gas prior to the gain correction. The sensitivity constants (NEW K) are updated each complete peak stepping cycle.

The time response of any type of mass spectrometer is a complex function of inlet response, and source, analyzer, and detector response; it is different for every gas. The observed time response of the instrument for each gas is corrected in the time domain using the measured step response of the instrument and classical inverse filtering techniques.* The output data string is derived from the instrument's output using the deconvolution formula:

$$Y(I) = \sum_{j=-m/2}^{m/2} (H(J) \cdot X(I - J))$$

where X(I - J) denotes the mass spectrometer output after correction for the delay, H(J) is the impulse response of the inverse filter of length m, and Y(I) represents the desired deconvolved signal.

The impulse response of the inverse filter is determined by measuring the step response of the instrument and solving the system of equations:

$$Y^T \cdot X = Y^T \cdot Y \cdot H$$

where H is a vector of length m representing the impulse response of the inverse filter, X is a vector of length n representing the step input, and Y is a matrix of dimensions m by n, representing the mass spectrometer step response.

The final data for each of the gases, corrected for response time and instrument sensitivity variations, can be displayed, stored, or output as analog signals.

* Ref: Shykoff, B.E.,and H.T. Swanson. A model-free method for mass spectrometer response correction. J. Appl. Physiol. 63(5):2148-2153, 1987.

Presented at the 36th ASMS Conference on Mass Spectrometry and Allied Topics
June 5-10, 1988, San Francisco, CA

A Magnetic Field Selector (MFS) for a VG 7070F Double Focussing Mass Spectrometer to enable Multiple Program High Resolution Selected Ion Monitoring (HRSIM).

D. A. Durden
Neuropsychiatric Research Unit, University of Saskatchewan, Saskatoon, Saskatchewan, Canada S7N 0W0

Introduction

The VG 7070F Mass Spectrometer was designed to be able to perform a wide variety of analyses under both low and high resolution conditions. As with most older double focussing mass spectrometers High Resolution Selected Ion Monitoring (HRSIM) is achieved by changing the Accelerating (V) and Electric Sector field (E) at constant Magnetic Field (B). If a range of ion masses is selected so that a series of compounds can be detected during a GC-MS analysis, the sensitivity of the instrument towards the high masses is reduced drastically due to the reduction of V. If, however, B is changed periodically during the GC run so that the high mass ions are detected at close to the maximum acceleration potential the sensitivity is increased for these ions.

A Magnetic Field Selector unit has been constructed to operate in conjunction with the VG digital multiple ion detector (DIGMID which controls V and E) and the Hall effect field control unit to select up to 8 magnetic fields (B) during the analysis time and enable up to 64 ions to be detected at maximum sensitivity. The operation is similar to a recently reported computer controlled system (1) but is much simpler to construct and allows independent monitoring of the ion masses being detected which can be verified by peak matching.

The system can also be used for Seleced Metastable Peak Monitoring (SMPM) of up to 8 transitions.by controlling B while the DIGMID controls E at constant V.

Instrumentation

The schematic diagram of the MFS is shown in fig 1.The output of a ±10.000V precision voltage source is fed into eight digital pots each of which is in series with an analog ten turn pot. These latter pots permit fine tuning of the mass position during the GC run. The outputs of the digital pots are sampled by an analog multiplexer followed by a low noise amplifier to removes the effect of the "on" resistance of the multiplex gates. The channel voltage is then buffered by a second amplifier which allows a span signal from the DIGMID to be added so that the ion peak can be scanned by B or by E and V. This output is connected to the Mode Selector of the 7070F so that the MFS will control the magnetic field when the settings are LRMID and KV/ESA and the magnet is under Scan control.

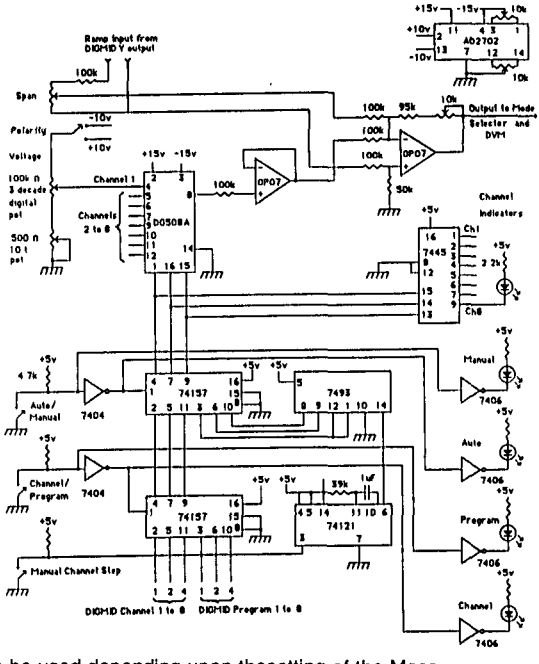

Either current or field control can be used depending upon thesetting of the Mass Indicator Mode switch. The channel of the MFS is controlled by either the Program or Channel number of the DIGMID unit or can be selected manually from the MFS itself.

Program control is used for the HRSIM analyses for which the MFS controls the magnet and the DIGMID controls E and V (at constant E/V ratio).

Channel control is used for (SMPM) for which V is kept constant and the DIGMID controls E alone. The ratio B/E is kept constant by the respective settings of the MFS and DIGMID values. The Mode is set to LRMID and ESA with the magnet under Field control.

Results

The output is very stable and enables operation of the mass spectrometer at resolutions in excess of 10,000. Fig 2 shows the analysis by HRSIM at 5000 resolution of a biological sample, in this case human plasma, for putative neurotransmitter metabolites phenylacetic acid (PAA), mandelic acid (MA), meta and para hydroxyphenylacetic acids (mHPAA and pHPAA), para-hydroxymandelic acid (pHMA), homovanillic acid (HVA), vanilmandelic acid (VMA), indoleacetic acid (IAA) and 5-hydroxyindoleacetic acid (5-HIAA) as either trifluoroethylesters or methyl esters of the acidgroups and pentafluoropropionyl esters of the phenolic and alcoholic groups using deuterated internal standards (3). The ions selected range in mass from 218.0555 to 547.0394 and by grouping them into eight programs with eight reference ions ranging in mass from 213 9903 to 463.9743 (from perfluoro-tri-n-butylamine) it has been possible to keep the mass ratios within 20% of unity.

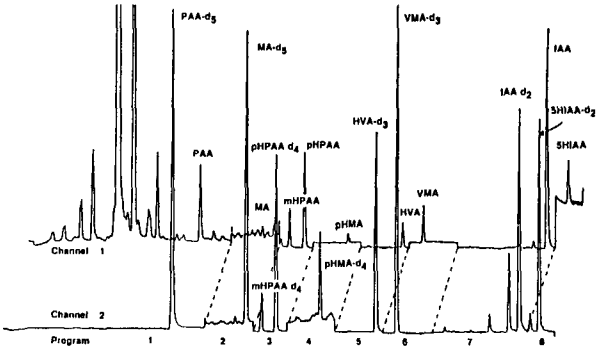

If the instrument is operated in the original mode using a single mass reference ion a high mass ion such as that of pHMA (m/z 474) looses sensitivity by a factor of about 3 when it is run against a low mass reference ion m/z 214 at an accelerating voltage ratio of 0.45144 (1.81 KV) instead of against a higher mass reference ion such as m/z 464 at a ratio of 0.97881 (3.91 KV). The other limitation of the single reference mass system is the loss of mass spectrometer resolution as the accelerating potential is reduced and the ion beam becomes less precisely focussed.

For SMPM (at constant V) the values of E and B for 6 metastables selected for the compounds mHPAA, pHPAA (same ions), HVA and IAA and for their deuterated isotopomers.may be loaded onto the same DIGMID program. The cycle time of 1 18 sec was considerable greater than the aggregate of the dwell times 0.72 sec due to the magnet settling time and the chromatographic peaks of the eluting compounds were sampled unsatisfactorily If, however, the 8 metastable transitions in pairs (protio and deutero) are put into four programs that change during the GC run, the cycle time is shortened to 0.36 sec for three channels (including a reference mass) and the GC peaks are sampled optimally

References

1. J.C. Bill, B.W. Gray, B.N. Green, J.A. Yoffe; 35th A.S.M.S Conference, Denver, 1987. p 142.
2. R.K. Boyd, J.H. Beynon; Org. Mass Spectrom. 1977. 12, 163-165
3. B.A. Davis, D.A. Durden, A.A. Boulton; J. Chromatogr.: Biomed Appl., 1986.374, 227-238.

Presented at the 36th ASMS Conference on Mass Spectrometry and Allied Topics
June 5-10, 1988, San Francisco, CA

THE USE OF CYCLIC NITROBENZAL ACETAL DERIVATIVES IN NEGATIVE ION MASS SPECTROMETRY OF LONG CHAIN 1,2 AND 1,3 DIOLS.

Mallet A.I., Rendell N.B. and Minnikin D.E.*
St Thomas' Hospital, London and
*University of Newcastle on Tyne**, UK.

Sensitive methods for the characterisation and quantitation of diols have been required in our laboratories for two classes of naturally occurring diols. One consists of the family of 1-O-alkyl glycerols produced by degradation of *lyso*-platelet activating factor and the other are the 1,3 diols, phthiocerols, which result when the high molecular weight lipid which is characteristic of the organism *Mycobacterium leprae*, the causative agent of leprosy, is reductively hydrolysed.

This presentation describes preliminary approaches to the production of volatile, stable derivatives which on NICI-MS produce molecular weight information. While a number of methods are available for the derivatisation of each hydroxyl group separately, those giving good NICI signals in the molecular ion region gave molecules with excessively high molecular weights, especially in the case of the phthiocerols. We have examined the production of cyclic benzylidene acetals from these diols and have found these derivatives to be prepared easily and in high yield by the action of a solution of the appropriate aldehyde in toluene together with a trace of p-toluenesulphonic acid as a catalyst. The aldehydes chosen included o-, m- and p-nitrobenzaldehydes and *bis*-trifluoromethylbenzaldehyde. Analyses were carried out on non-polar capillary gc columns interfaced directly to a VG Masslab Ltd Trio-2 quadrupole mass spectrometer operating in NICI mode with methane as the moderating gas.

The meta-nitro derivatives performed consistently worse, in terms of chromatography and mass spectrometric signal, than the ortho- and para-nitro derivatives, but all three gave base peaks of the molecular anion with both families of diols. The bis-trifluoromethyl derivative gave a base peak at m/z 242 ($C_9F_6H_4O$) and a small molecular ion when formed from the alkyl-glycerol. The sensitivities for detection of the derivatives was not better than in the 100 pg range (Figure 1) and this lack of signal would appear to be a result of poor chromatographic performance especially during the 'splitless' mode injection, during which decomposition appears to occur. Figure 2 shows the result of an analysis of the extracted and derivatised products from a sputum sample from a tuberculosis patient. In this disease mycobacteria are also found and these too have phthiocerol containing lipids in their cell envelopes. The trace of the expanded region shows the presence of a n=22 phthiocerol A component (m/z 687).

These derivatives show excellent molecular weight information for the diols examined here and were simple to prepare in good yields. The chromatographic performance was poor and further experimentation is required to optimise this aspect of the method with attention being given to alternative methods of sample injection such as cool, on-column techniques.

Figure 1

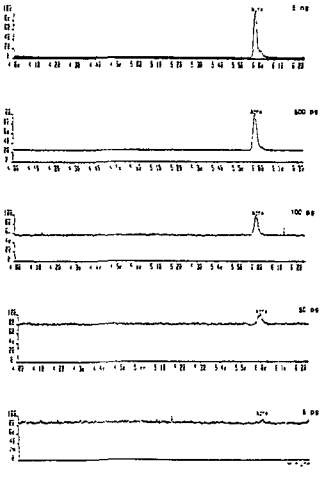

Figure 2

(A) 25 minute scan data TIC profile.

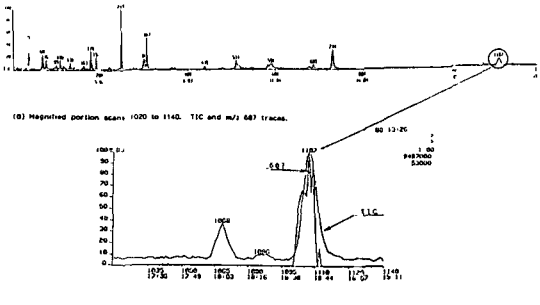

(B) Magnified portion scans 1020 to 1140. TIC and m/z 687 traces.

Presented at the 36th ASMS Conference on Mass Spectrometry and Allied Topics
June 5-10, 1988, San Francisco, CA

QUANTITATIVE DETERMINATION OF FUNGAL STEROLS BY GC-MS-SIM AND ITS APPLICATION TO THE CHEMOTAXONOMY OF DERMATOPHYTES.

A.I. Mallet and S.A. Howell.
St Thomas' Hospital, London U.K.

The dermatophytes are a closely related group of fungi which are responsible for skin and nail infections, including ringworm and athletes' foot. This group consists of three genera, *Trichophyton, Microsporum* and *Epidermophyton* which are currently identified on the basis of morphological criteria. Two other species of fungi which cause infections similar to those produced by dermatophytes, are members of a different taxonomic class and are *Hendersonula toruloidea* and *Scytalidium hyalinum*. Three colonial variants have been described for *H. toruloidea*, on the basis of growth rate and morphological characteristics. We present a study of the sterol composition of these fungi and describe the application of these analyses as a taxonomic tool.

All the fungal cultures were from clinical isolates obtained from within the Institute of Dermatology. Fungi were grown for ten days at 30°C on Sabouraud's dextrose broth. The mycelia were collected and freeze-dried and the sterols were extracted by an alkaline saponification for 2 hours at 60°C. The sterols were derivatised with MTBSTFA in acetonitrile, to produce the tBDMS ethers. Analysis was carried out by SIM of the m/z values expected for the $[M-57]^+$ ions using on-column injection onto capillary columns coupled to the source of a VG Analytical Ltd 305 mass spectrometer. SE-30 stationary phases were employed with temperature gradients, starting at 175° for 2 mins and increasing to 245° at 30°/min and then to 300° at 7°/min. The sterols eluted between 10 and 18 mins. All data was collected by and presented on, a Technivent Data system. Principal component analyses were performed using the SIMCA package (Sepanova AB, Sweden).

It was possible to identify eight sterols on the basis of their mass spectra and by comparison with the GC-MS behaviour of standard sterols. Several other sterol-like substances were observed in the extracts and for the ten ions monitored a total of 80 distinct peaks were observed. While it was possible to identify qualitative differences in the ion chromatograms, for all ten ions and all the genera and species analysed, visual observation was too inexact and a more objective method was sought. This was provided by the use of the SIMCA package, with which principal component analysis and class modelling could be achieved. The height of each peak in the ion chromatograms was corrected for isotopic cross contribution and expressed as a percentage of the total peak heights for each strain. In principal component analysis each measured variable (time resolved, m/z peak height) provides a dimension of comparison with other objects, (in our case fungal strains) and the principal component plot displays two dimensions at a time.

Figure 1 illustrates the ability to distinguish between the three colonial forms of *H. toruloidea* and the *S. hyalinum* isolates. Form 3 strains are clearly separable from the other morphological variants. While two of the *S. hyalinum* isolates appear mixed in panel (i) they can be clearly distinguished on a different plane, panel (ii).

Further analysis was carried out using the class modelling feature of SIMCA. This procedure is illustrated in Figure 2. *H. toruloidea* form 1 is chosen as one class (x-axis) and this is tested for similarity against a second chosen class, in this case *S. hyalinum* expressed as distance between the classes. The diagram records four regions, A contains strains with sterol patterns similar to form 1 isolates and B those similar to *S hyalinum*. Region C would contain strains not identifiable as either and D, those outside the confidence limits. The lines represent 95% confidence limits.

The procedure has proven an effective one for distinguishing fungal strains on the basis of their sterol patterns and is now being applied to studies of the development of resistance to imidazole drugs which are thought to act on sterol synthesis pathways.

Figure 1. Principal component analysis of *H. toruloidea* forms 1(1), 2(2), 4(3) and *S. hyalinum* (4).

Figure 5(a). Plot of the first and second principal components.

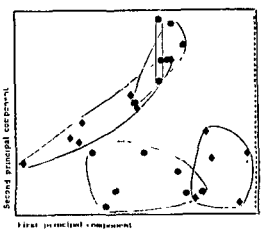

Figure 5(b). Plot of the second and fourth principal components.

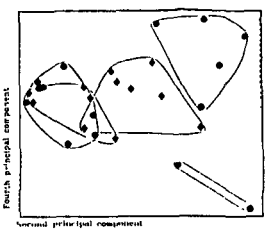

Figure 2. Class distance plots from *H. toruloidea* and *S. hyalinum*

Figure 6(a). *H. toruloidea* form 1 (class 1) and *S. hyalinum* (class 2)

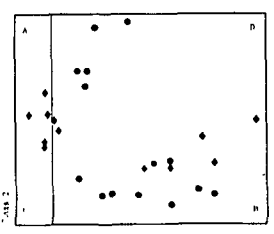

Figure 6(b). *H. toruloidea* form 1 (class 1) and *S. hyalinum* (class 2)

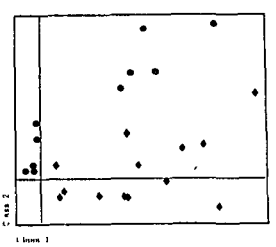

Presented at the 36th ASMS Conference on Mass Spectrometry and Allied Topics
June 5-10, 1988, San Francisco, CA

HOW PURE IS PURE? THE CERTIFICATION OF SRM 911b CHOLESTEROL

Michael J. Welch, Alex Cohen, and Edward White V
Center for Analytical Chemistry, National Bureau of Standards
Gaithersburg, Maryland 20899

Determination of the purity of an organic compound is frequently not straightforward. The process may involve a variety of analytical techniques, each of which is used to detect and/or quantify impurities in the material. In that sense, it becomes a problem of trace analysis. This paper describes the process involved in certifying the purity of a new batch of cholesterol to be issued as Standard Reference Material (SRM) 911b.

Initial Screening Suppliers of chemicals were contacted to determine if they had high purity cholesterol from a single lot that might be suitable as an SRM. Samples of three candidate materials were obtained and subjected to chemical analysis to identify the purest material.

The materials (X, Y, and Z) were examined by GC, GC/MS, Direct Probe MS, TLC, and UV. When compared to the existing SRM (911a), material Z was clearly inferior; the other two were comparable. Material X appeared to be slightly better and it was examined further. However, when this material was subjected to NMR analysis it was found to contain a significant silicone impurity (probably silicone grease). Thus material X was rejected.

Material Y was then examined further. NMR analysis did not find any silicones. Impurities found by GC/MS appeared to be present at marginally higher levels than in SRM 911a, but the material was judged to be sufficiently pure for the lot to be conditionally accepted as the candidate material. The lot was then vialed (5 grams/bottle) and the vials subjected to further testing.

Testing of the Candidate Material

Direct Probe MS The material was examined by direct probe mass spectrometry as a test for solvents and other volatile impurities. No solvents were detected but evidence was found for the presence of some other steroids in the material.

GC/MS Samples, treated with N,O-bis-trimethylsilylacetamide to convert cholesterol and other steroids to their TMS derivatives, were examined by GC/MS. Low levels of three other steroids were found in the material. The retention times and molecular weights of these impurities were consistent with campesterol (mw 400), sitosterol (mw 414), and 7-dehydrocholesterol (mw 384). Two suspected impurities in cholesterol, cholestanol and lathosterol, were tested for, but were not found. A standard additions experiment using campesterol was performed to estimate the concentration of the impurities that were found. The levels for campesterol, sitosterol, and 7-dehydrocholesterol were estimated to be 0.05%, 0.05%, and 0.03%, respectively.

GC/MS was also used to investigate the vial-vial homogeneity of the candidate material. Samples from seven vials were derivatized and analyzed. The sizes and number of impurity peaks were compared. No significant differences were found. Thus, the material is homogeneous at least with respect to the impurities detected by GC/MS.

ID/MS Samples of the candidate material and SRM 911a were spiked with a solution of cholesterol-$^{13}C_3$ and their isotopic ratios carefully measured by our ID/MS definitive method for cholesterol. No significant differences were found, but differences of <0.1% probably would not be detected by this technique.

Infrared Spectra IR spectrum of the candidate material in Nujol was not significantly different from that of SRM 911a.

Thin-layer Chromatography TLC of both the candidate material and SRM 911a found traces of three impurities and these had the same rf values for both materials.

Differential Scanning Calorimetry DSC analysis of the candidate material found a total impurity of 0.095 ± 0.039 mole % compared with 0.150 ± 0.035 mole % for SRM 911a. This technique measures impurities which are soluble in the melt but insoluble in the crystalline material. This was the only case where the candidate material was found to be purer than SRM 911a.

Melting Point Candidate material melted at 149.0-149.2 °C. compared with SRM 911a which melted at 149.0-149.1 °C.

Insoluble Matter Chloroform solutions of the candidate material were filtered through a preweighed teflon membrane (0.5 um porosity), yielding an average increase in weight of the membrane corresponding to 0.036% of the weight of cholesterol. Filtering solutions through porcelain crucibles (1.5 um porosity) yielded an average of 0.017%. The former is probably high because cholesterol was detected on the membrane after filtering; the latter is probably low because of the large pore size.

Volatiles Weight loss for samples of the candidate material heated at 60° in vacuum were 0.020%, identical to the losses measured for SRM 911a.

Total Ash Content Two 3 gram samples of the candidate material were heated in a muffle furnace, yielding ash weights of 0.0048 and 0.0061%.

Halogens Neutron activation analysis was used to determine the chlorine, bromine, and iodine in the candidate material. The average results for two samples were: 6 ppm, 38 ppm, and <0.1 ppm for chlorine, bromine, and iodine, respectively. For SRM 911a the results were 7 ppm, 12 ppm, and <0.1 ppm. Traces of sodium and manganese were also observed, but zinc, which is used in the purification of cholesterol, was not found.

The form of the halogens affects their contribution to the weight of impurities. If they are predominantly in the form of sodium halides, the total impurity (NaCl + NaBr) would be 59 ppm or 0.006%. In contrast if the form is cholesteryl halides the total would be 280 ppm or 0.028%. These two cases represent the extremes among the reasonable possibilities for the halide forms.

Ultraviolet Spectra Four maxima from 296-350 nm were found in the UV spectrum of a 4% solution of the candidate material in CH_2Cl_2. The peak at 296 nm is probably from the 7-dehydrocholesterol believed to be present at about 0.03%. The other peaks are probably from some impurities with longer conjugated pi systems, possibly including a triene.

Conclusion We evaluated the data to determine reasonable upper and lower limits for the total impurity The lower limit is set by the DSC data and is 0.1%. The upper limit is from the sum of the GC/MS, halide, volatiles, ash, and insolubles data and is 0.3%. The DSC data is probably low because certain types of impurities will not be detected. The upper limit is probably high because some of the impurities probably contribute to more than one analysis. We therefore believe the best estimate of the total impurity is 0.2 ± 0.1 %, identical to the certified level of impurity for SRM 911a.

Acknowledgements Some of the analyses above were performed by other members of the Center for Analytical Chemistry, NBS as follows: NMR, Bruce Coxon; DSC, Richard Christensen, Total Ash, George Marinenko; and Halogens, Donald Becker.

Presented at the 36th ASMS Conference on Mass Spectrometry and Allied Topics
June 5-10, 1988, San Francisco, CA

QUANTITATION OF PLATELET ACTIVATING FACTOR BY FAB/MS/MS

E. D. Bush, D. L. Stevens and D. L. Miller

Clin. Pharmacol. and Gerontol. Res. Unit, VA Medical Center, Boise, ID;
Coll. of Pharm., ISU, Pocatello, ID;
Sch. of Med., Univ. of Wash., Seattle, WA;
Chemical Sciences Group, INEL, Idaho Falls, ID;

INTRODUCTION

Platelet Activating Factor (PAF) is a potent mediator of biological activity. PAF has been implicated in the onset of several physiological disorders including inflammation, asthma and shock. Work in our laboratory on the mechanism and treatment of septic shock led to the belief that PAF could play a major role in its development. In order to test this hypothesis an accurate, sensitive and reproducible method was needed to quantitate PAF. Recently several analytical methods have been reported with the apparent sensitivity needed for such a potent compound. However, these methods include the degradation of the parent compound to a molecule that is amenable for derivatization and GC/MS analysis. This process requires that the sample be highly purified in order to obtain artifact free results. Thus the multiple purification, degradation and derivatization steps required for the existing methods make them cumbersome for large scale animal or clinical studies.

OBJECTIVES

Develop a simple, fast and reliable method to quantitate PAF and eventually lyso-PAF from biological matrixes. Develop a method which does not require that the parent compound be purified, degraded and derivatized before analysis. Develop a method with a limit of detection (LOD) of approximately 10 femtomoles per sample.

MATERIALS AND METHODS

PAF was purchased from Sigma Chemical Company as the product isolated from natural sources. Deuterated PAF was synthesized by the reaction of lyso-PAF (Sigma) and d6-acetic anhydride (MSD Isotopes). Although several FAB matrixes were utilized the optimum results were obtained with a 1:1:1 mixture of methanol:glycerol:thioglycerol. Standard curves were prepared by adding a fixed volume of d3-PAF in the matrix to varying concentrations of d0-PAF in the matrix. Final concentrations were 50pg/µl d3-PAF and 5,10,50,100,500 pg/µl of d0-PAF. Clinical samples of puss fluid were extracted utilizing Bley and Drier conditions, chromatographed on TLC plates and the PAF band extracted with a 1:1 mixture of methanol:chloroform. These samples were dried under a stream of nitrogen and resuspended in a minimum volume of the matrix just before the analysis.

INSTRUMENTATION

Experiments were conducted on three different instruments: 1) The Kratos MS-890 was located at the Idaho Nuclear Engineering Laboratory in Idaho Falls, ID. The instrument's accelerating potential was set at 6 keV and Xenon was used as the FAB gas. Data was collected and analyzed utilizing the DS-90 data system. 2) The VG-70SQ was located at the Burroughs Wellcome Research Laboratories in Research Triangle Park, NC. This instrument's accelerating potential was set at 8 keV and Xenon was used as the FAB gas. During the MS/MS experiments the collision energy was set at approximately 25 volts and the collision gas was Argon (when used). Data was collected and analyzed utilizing the VG-250 data system. 3) The VG-70SEQ was located in the Dept. of Med. Chem., Univ. of Wash., Seattle, WA. Operating parameters were the same as those given for the VG-70SQ above.

All the instruments were calibrated using CeI clusters in positive ion FAB mode with the resolution nominally set at 1000. The MS/MS experiments were conducted with and without collision gases (collision induced decompositions, CID and unimolecular decompositions).

Results

Initial attempts to quantitate PAF by FAB/MS utilizing either selected ion monitoring or narrow scan mode found limits of detection in the range of 1-10ng applied to the probe. These limits were only marginally affected by the type of FAB matrix employed. A variety of matrixes were utilized including triethanolamine, glycerol, 'magic bullet', glycerol:thioglycerol and phosphoric acid. A 1:1:1 mixture of methanol:glycerol:thioglycerol was judged superior based on its apparent increased ability to solvate PAF. However, analysis of the full scan FAB spectra of PAF revealed that two ions were predominate in all matrixes. These were the M+H of the parent compound and a 184 fragment ion which was the base peak. The structure of the 184 fragment ion has been assigned as the protonated phosphocholine head group. In addition these full scan FAB spectra demonstrated a great deal of the usual back-ground or 'grass' noise. Thus, to take advantage of this facile fragmentation pathway and to increase the methods sensitivity by eliminating the FAB background, FAB/MS/MS was attempted. Initially, we choose to look at the full scan daughter ions of the M+H parent ion. These experiments indicated that a recognizable spectra could be achieved with as little as 2 pg of PAF loaded onto the FAB probe. Although results could be obtained in MS/MS mode under unimolecular decomposition conditions, the quantity of the 184 ion increased by more than an order of magnitude when a collision gas was introduced into the RF only quadrupole region. Therefore the CID conditions were chosen for most of the succeeding studies.

A deuterated internal standard was synthesized from lyso-PAF and d_6 acetic anhydride. The full scan FAB spectra of this compound displayed the expected plus three M+H ion, but the daughter ion was 185, indicating a shift of a deuterium from the acetate to the phosphocholine group during fragmentation. Therefore by alternately monitoring the 524->184 and the 527->185 decompositions in Multiple Reaction Monitoring (MRM) mode we are able to quantitate PAF at the 5 pg level. The standard curves were linear as long as the concentration of the internal standard did not exceed 10 times that of the unlabeled compound.

Preliminary, analysis of puss fluid extracts from patients with active bacterial infections exhibited levels of 0-5pg/100ul of PAF. With future studies we hope to better characterize and validate the method as well as add lyso-PAF to the list of compounds quantitated.

Conclusions

Based on these results, we can make the following preliminary conclusions: 1) that PAF can be quantitated to the low pg level without extensive purification and degradation; 2) that FAB can be a sensitive analytical technique if the background can be eliminated; and, that the fragmentation of PAF to the 184 daughter ion involves the transfer of a proton from the acetate group.

The authors would like to acknowledge the generous assistance of William Trager and William Howard at the University of Washington, and David Brent, Lester Taylor and Robert Johnson at the Burroughs Wellcome research laboratories.

Presented at the 36th ASMS Conference on Mass Spectrometry and Allied Topics
June 5-10, 1988, San Francisco, CA

MASS SPECTROMETRIC DETERMINATION OF PLATELET-ACTIVATING FACTOR FROM HUMAN SUBJECTS

Kiyoshi SATOUCHI, Makoto ODA* and Kunihiko SAITO

Department of Medical Chemistry
Kansai Medical School, Moriguchi, Osaka 570, JAPAN

Platelet-activating factor (PAF) is now recognized as one of the most potent chemical mediators of allergy and inflammation (Fig. 1). In fact, evidences are now accumulating that drugs affecting the PAF action have a potential as a therapeutic agent in the fields of anaphylatic and endotoxin shocks (1).

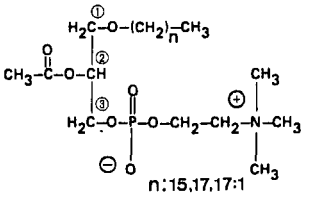

Fig. 1 The chemical structure of PAF

For evaluating PAF role in the disease process, it is essential to detect and quantitate PAF exactly. However, the concentration of PAF in the body is extremely low, and the available volume of blood or body fluid from patient is limited. Furthermore, there is a system in our body to quickly metabolize newly-synthesized PAF into an inactive form (2). For above reason, PAF detection from patients has been hampered.

We have applied a gas chromatography/electron impact selected ion monitoring (GC/EISIM) technique to PAF determination using a stable isotope labelled internal standard and tert-butyldimethylsilyl derivative. Recently, Ramesha and Pickett have also developed a gas chromatography/negative ion chemical ionization selected ion monitoring (GC/NICISIM) technique using pentafluorobenzoyl derivative. These mass spectrometric methods are now useful as a strategy of PAF determination because of their high specificity and sensitivity (3).

We have examined PAF activity of various body fluids, such as pleural effusions, bronchoalveolar lavage fluid, middle ear effusion and so on. However, as stressed above, the volumes of these fluids from patients were limited. Accordingly, PAF was detected on the basis of its ability to cause the immediate aggregation of washed rabbit platelets, and identified on the bases of its behaviors on thin-layer chromatography and against the pretreatment of platelets with the specific PAF antagonists, CV-3988 and L-652, 731 (4). Detection and identification of PAF in brochoalveolar lavage fluid from asthmatic patient is shown (Fig. 2)

Among the body fluids, pyothorax, an infectious lung disease with abscess, was further subjected to PAF assay by GC/EISIM technique

By the monitoring at m/z 117, the ion due to acetic acid, and the comparison of retention times on GC with standards, PAF and acyl-form PAF were detected. By the calculation using internal standards, major species were 16:0 in chain length in both PAF and acyl-form PAF, and the content of 1-hexadecyl-2-acetyl-sn-glycero-3-phosphocholine was 10 times more abundant than that of 1-palmitoyl-2-acetyl-sn-glycero-3-phosphocholine.

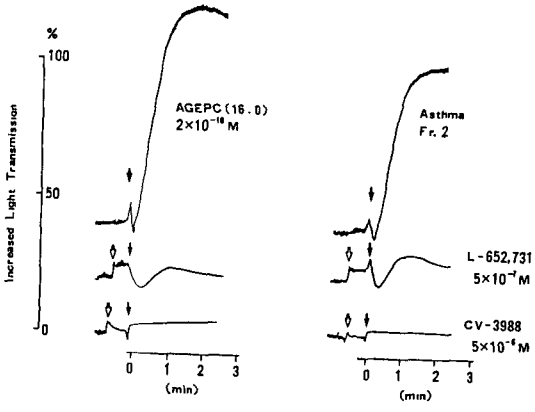

Fig. 2 The identification of PAF in BALF from asthmatic patient

By bioassay, PAF can be detected as little as picogram quantity. Furthermore, specific receptor antagonist to PAF molecule is now available. Accordingly, identification and determination of PAF are easily attainable. However, it is recently known that substantial amount of acyl-form PAF produced concomitantly with PAF. Unfortunately, acyl-form PAF has nearly negligible activity of platelet activation compared with that of PAF. This indicate the limitation of bioassay.

In contrast, SIM technique can achieve the separate quantitation of PAF and acyl-form PAF. In the present experiment of pyothorax, PAF and one-tenth amount of acyl-form PAF were detected. Human neutrophil produce PAF and one-fifth amount of acyl-form PAF when stimulated with calcium ionophore A23187 (5). Pyothorax is an infectious disease, characterized by the infiltration of neutrophils. Taken together, it is suggested that neutrophil is the origin of PAF detected.

Only SIM technique, information above can be gained. GC/SIM coupled with capillary GC will prove to improve the sensitivity. Another approach to improve the sensitivity in the mass region is to apply high resolution MS or tandem MS.

In any event, PAF detected by bioassay shoud be subjected to SIM assay. If not, we can not have any information other than that PAF is there.

REFERENCES

(1) Braquet, P., Touqui, L., Shen, T.Y., & Vargaftig, B.B. Pharmacol. Rev., 39, 97-145 (1987)
(2) Farr, R.S., Wardlow, M.L., Cox, C.P., Meng, K.E., & Greene, D.E. Fed. Proc., 42, 3120-3122 (1983)
(3) Satouchi, K., & Saito, K. JEOL NEWS, 23A, 17-20 (1987)
(4) Doebber, T.W., Wu, M.S., & Biftu, T. J. Immunol., 136, 4659-4668 (1986)
(5) Satouchi, K., Oda, M., & Saito, K. Lipids, 22, 285-287 (1987)

* Current address: Department of Internal Medicine, Saisekai Izuo Hospital, Osaka 551 JAPAN

ACKNOWLEGEMENT: This work was supported in part by a Grant-in-Aid for Special Project Research from the Ministry of Education, Science and Culture of Japan. The expense to attend the meeting was sponsored by Fugaku Foundation.

Presented at the 36th ASMS Conference on Mass Spectrometry and Allied Topics
June 5-10, 1988, San Francisco, CA

MASS SPECTROMETRIC ANALYSIS OF PLATELET ACTIVATING FACTOR (PAF) IN MOUSE URINE.

Benfenati E., Bettazzoli L., Davoli E., Gavinelli M., Macconi D., Noris M.
Istituto Mario Negri,24100 Bergamo and 20157 Milano Italy

INTRODUCTION

PAF is a phospholipid mediator of inflammatory reactions which has been recently suggested to play a role in immune glomerulonephritis. Given its short plasma half-life, PAF measurement in the urine is likely to reflect events taking place in the kidney. Thus, we have developed a GC-MS quantitative method for PAF analysis in mouse urine which will allow to evaluate the role of this autacoid in immune injury.

EXPERIMENTAL

Chemicals

- PAF C 16 : 0	1-O-hexadecyl-2-O-acetyl-sn-glycero–3-phosphocholine
- PAF d_3	1-O-hexadecyl-2-O-acetyl-d_3-sn-glycero-3-phosphocholine
- ALP	1-O-octadecyl-2-O-methyl-glycero-3-phosphocholine

Preparation of deuterated PAF
1.5 mg of lyso-PAF was added with 200 µl of acetic anhydride-d_6 and heated at 80° C for 3 h. The purity of PAF d_3 was checked with TLC, GC-MS and FAB-MS.

Animals
Female Crl:CD-1 (ICR) BR mice had free access to standard diet and water. The animals were housed in metabolic cages that allowed collection of the 24 h urine sample.

Extraction of urine
24 h urine samples were added with internal standard (20 ng of PAF d_3 or 5 ng of ALP) and methanol to a final rate of 3:2 CH_3OH/urine. After gentle mixing for 30', the samples were centrifuged. Chloroform and water were added to the supernatant to obtain a solvent mixture containing chloroform, methanol and water (1:1:0.9 vol/vol). The chloroform layer was removed and evaporated under N_2.

Silicic acid column
The extract was applied to a silicic acid column (0.5 g) and eluted using a sequential solvent system of chloroform, acetone, acetone/methanol (1:1), chloroform/methanol (1:4). The fourth fraction containing PAF was evaporated under nitrogen.

Hydrolysis and derivatization
Purified samples were treated with 0.2 ml of 50% HF at room temperature for 4 h. Hydrolized PAF was extracted twice with 0.5 ml of hexane. After removing the solvent under N2 , 50 µl of PFBCl were added to each sample. The system

was heated at 100° C for 40'. The exceeding reagent was removed and the residue was dissolved in iso-octane for GC-MS analysis.

Mass spectrometry

GC-MS analyses were carried out on a VG 70-250 mass spectrometer coupled to a DANI 6500 gas chromatography . A silica capillary column CPSil 25 m 0.32 mm I.D. was used . Oven temperature was: 140° C isothermal for 1.3 min; then programmed from 140° to 280° C , 18°C min. For chemical ionization ammonia was used as reagent gas. SIR analyses were done on derivatized samples , monitoring the ions at m/z 552 for PAF and ALP, and 555 for PAF-d_3.

RESULTS AND CONCLUSION

SIR traces of PAF in mouse urines are shown in figures 1-2. In both cases PAF produced two separated peaks with a characteristic shape and relative intensity ; this contributed, with masses and retention time, to the identification of the compound .

The same chromatographic pattern appeared for the PAF-d_3 too. Calibration curves using PAF-d_3 (400 pg) was linear from 2 to 800 pg (fig. 3). A similar linearity was found for the curve built with ALP (data not shown) .

PAF excretion in 24 h fresh urine samples, measured by GC-MS using two different internal standards, PAF-d_3 and ALP, was comparable (2.81 ± 1.25 ng and 3.60 ± 0.84 ng respectively) . Similarly no significant difference was found in frozen samples (3.69 ± 2.15 ng).

In conclusion we developed an analytical method useful for quantitation of PAF in urines that represents the first quantification of PAF in urine using GC-MS.. The method appears selective and sensitive, able to quantify very low amounts of PAF. This technique will be used to investigate the biological origin of PAF in urine and its significance in different models of disease.

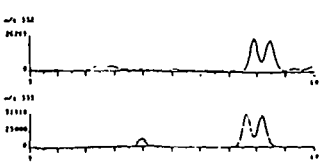

fig 1 - Selected ion recording at m/z 552 of the M^- ion of the penthafluoride benzoyl derivatives of PAF, excreted in a 24 h urine sample and at 555 for PAF-d3 internal standard

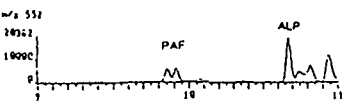

fig 2 - Selected ion recording at m/z 552 of the M^- ion of the penthafluoride benzoyl derivatives of PAF, excreted in a 24 h urine sample and of ALP , added to the urine samples as internal standard

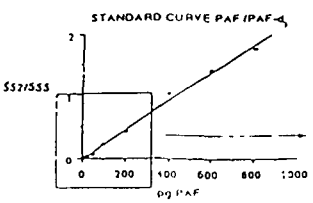

Fig 3 - The calibration curve for quantification of PAF by GC-MS using 400 pg of PAF-d_3 as internal standard and different amounts (2-800 pg) of PAF

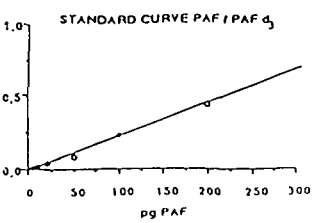

- Particular of the calibration curve shown in Fig 3

Presented at the 36th ASMS Conference on Mass Spectrometry and Allied Topics
June 5-10, 1988, San Francisco, CA

Quantitative analysis of Lysophosphatidylserine (LPS) by FAB-MS

Benfenati E., Bettazzoli L., Chen S., De Bellis G., Fanelli R. and Pege G.°

Istituto Mario Negri, 24100 Bergamo and 20157 Milano, Italy
°Fidia Research Laboratories, 35051 Abano Terme, Padova, Italy

Since it first appeared, FAB has been used to study phospholipids (PL), a class of biomolecules of fundamental importance. A review on PL analysis with FAB and other ionization techniques recently appeared (1). However quantitative studies of these substances by FAB are scant; other methods routinely used to quantify PL are old and require many steps.
LPS is difficult to be analyzed using usual methods; nevertheless it could be of particular biological importance. Extending our work on PL analysis by FAB (2-4) we present here a method for quantifying LPS by negative FAB in biological samples (rat brain).
We used a VG 70-250 mass spectrometer with its standard FAB source and target, and Xenon accelerated at 8kV as bombarding gas. Quantitative measurements were done scanning from m/z 450 to m/z 600 at scan speed of 4 sec/decade. The samples were dissolved in $CHCl_3$ / MeOH / H_2O (10:1:0.1) and deposited on a surface of diethanolamine (DEA), used as liquid matrix. This solvent/matrix pair gave good sensitivity. It is important not to mix the sample with the matrix. This technique is similar to the "surface precipitation" technique and has provided good results for other PL (4).
Since in FAB spectra of rat brain, the biological material of our interest, we didn't detect ions corresponding to LPS 16:0, we used this as internal standard. The standard LPS was obtained from PS (bovine brain) treated with phospholipase A_2. This class is mainly LPS 18:0, no significant peak corresponding to LPS 16:0 appeared. The standard curve was prepared adding a constant amount of LPS 16:0 (250 ng) to varying amount of LPS standard (10,20,50,100,250,500,1000 ng). Scans (at least 40) were acquired and peak intensity of $(M-H)^-$ ions, m/z 524 (18:0) and 496 (16:0), were recorded by usual scan mode. The average value over 25 scans (from scan 5 to 30) of absolute peaks height were used to design the curve. We obtained stable ion current and constant intensity ratio. The standard curve was linear with a correlation coefficient (squared) of 0.999 from 10 to 1000 ng. This curve was used for the quantification of LPS in rat brain; in particular we extracted cortex (40 mg) according to Bligh and Dyer (5) after addition of 25 µg of LPS 16:0. After purification on TLC analysis has been performed as above described. The quantity of LPS 18:0 in cortex of rat brain is 475 (+/-40) ng / mg of cortex. This value is very close to that obtained using phosphorus assay (597 (+/-79) ng / mg of cortex).
A major difference between the two methods is that in our experience N-FAB MS analysis is at least 50 times more sensitive than phosphorus assay.
In conclusion we provided an effective analytical method for LPS quantification by N-FAB MS. This method appears to be more sensitive than the ones currently available and provide also informations on the fatty acid chains present in the molecule.

Acknowledgements:
We thank Dr Tacconi who kindly performed biological samples preparation and FIDIA Research Laboratories, Italy for LPS 16:0 gift.

REFERENCES

1) N. J. Jensen, M. L. Gross, *Mass Spectrom. Rev.*, 1988, Vol. 7, 1, 41
2) E. Benfenati, R. Reginato, Mass spectrometry in the health and life sciences, Int. Symp., San Francisco, USA, 1984
3) E. Benfenati, R. Reginato, *Biomed. Mass Spectrom.*, 1985, 12, 643
4) S. Chen, E. Benfenati, R. Fanelli, G. Kirschner, F. Pregnolato, *Biomed. Environ. Mass Spectrom.*, 1988 (in press)
5) E. G. Bligh, W. J. Dyer, *Can. J. Biochem. Physiol.*, 1959, 37, 911

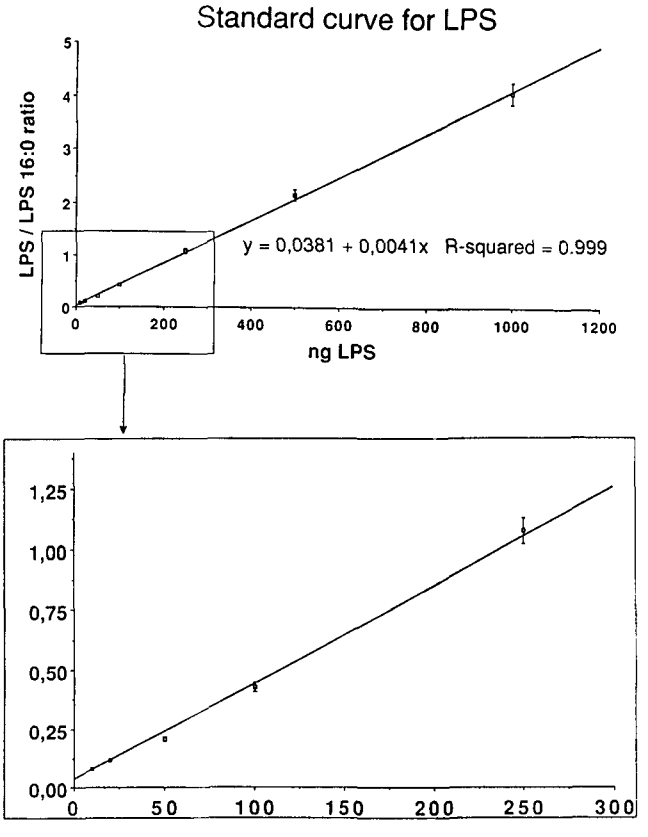

Fig 1 Standard curve for LPS from 10 to 1000 ng
250 ng of LPS 16:0 as I.S.

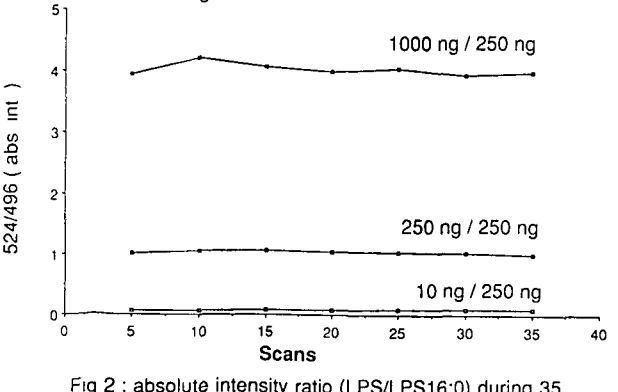

Fig 2 : absolute intensity ratio (LPS/LPS16:0) during 35 scans at different concentration

Presented at the 36th ASMS Conference on Mass Spectrometry and Allied Topics
June 5-10, 1988, San Francisco, CA

CHARACTERIZATION OF EPOXIDES OF UNSATUTRATED FATTY ACIDS BY MASS SPECTROMETRY VIA PICOLINYL ESTERS

M. BALAZY AND A.S. NIES
Division of Clinical Pharmacology, University of Colorado, HSC
Denver, CO 80262

INTRODUCTION

The goal of this poster is to describe a convenient gas chromatographic-mass spectrometric method for qualitative analysis of regioisomeric epoxides of unsaturated fatty acids. These epoxides are products of cytochrome P-450 monooxygenase mediated metabolism and are found in incubates from hepatic or renal microsomal preparations stimulated with NADPH. Linoleate epoxides are found in leukocytes from hyperoxic lung. Epoxyeicosatrienoic acids (EET) also occur in human urine and in phospholipids of rat liver and rabbit kidney. Human platelets convert arachidonoylphosphatidylinositol into 14,15-EET.

Epoxyeicosatrienoic acids are potent mediators of diverse biological activities including for example inhibition of platelet aggregation and cyclooxygenase activity, and inhibition of vasopressin stimulated osmotic water flow. EETs are also involved in the release of somatostatin, leutinizing hormone, insulin and glucagon. Microsomal calcium mobilization as well as ion transport in the rabbit cortical collecting tubule are also believed to be altered by arachidonic acid epoxides. These epoxy acids can be succesfully analysed by GC/MS as methyl or pentafluorobenzyl esters but these derivatives do not easily distinguish between regioisomers.

We report here a rapid and mild procedure for the synthesis of picolinyl (with 3-pyridylcarbinol) esters of fatty acid epoxides. These esters had characteristic mass spectra and allowed differentiation between isomeric epoxides at the nanogram level. The picolinyl esters were previously applied to GC/MS analysis of fatty acids (D.J. Harvey, Biomed. Mass Spectrom. 9, 33, 1984) and presented here method extends the application of this unique derivative in GC/MS to another group of compounds, e.g. epoxides of unsaturated fatty acids.

METHODS

Epoxides were prepared by the reaction of metachloroperbenzoic acid (MCPBA) with linoleic, arachidonic and docosahexaenoic acids as described (Chung and Scott: Tetrahedron Lett. 35, 3023, 1974).

SP-HPLC: column: Altex Ultrasphere Si 250*4.6 mm, 5um; solvent: hexane/isopropanol/acetic acid (500:0.5:0.25) isocratic 15 min then isopropanol increased to 50% in 15 min; flow: 1 mL/min; detection: UV at 200 nm with Waters HPLC system.

Derivatization: To 0.15-1.5 nmol (50-500 ng) of epoxide dissolved in 100 uL of methylene chloride 10 uL of 1,1'-carbonyldiimidazole solution (50 ug/mL) was added and after 1 min 10 uL of 1% 3-pyridylcarbinol (Aldrich) solution was added along with 10 uL of triethylamine. After 10 min at room temperature the solvents were evaporated and the residue dissolved in hexane/ethyl acetate (3:1) and chromatographed on silica. The yield was quantitative based on the recovery of radioactive arachidonate epoxides.

Rat liver microsomes isolation and incubations were performed as described (Oliw, Guengerich, and Oates, J. Biol. Chem. 257, 3771, 1984). The incubate was subjected to TLC and SP-HPLC, and fractions containing epoxides (E1 to E4) were derivatized as described above.

Presented at the 36th ASMS Conference on Mass Spectrometry and Allied Topics
June 5-10, 1988, San Francisco, CA

Gas chromatography-mass spectrometry: 15 m DB-1+ column was temperature programmed from 200 deg C at 15 deg min-1. Injections were made with solvent-less injector. Mass spectra were recorded with VG 7070H spectrometer interfaced to a Teknivent data system. Operating conditions were: electron energy, 70 eV; trap current, 200 uA; accelerating voltage 4 kV, scan 2s per decade-1, exponential.

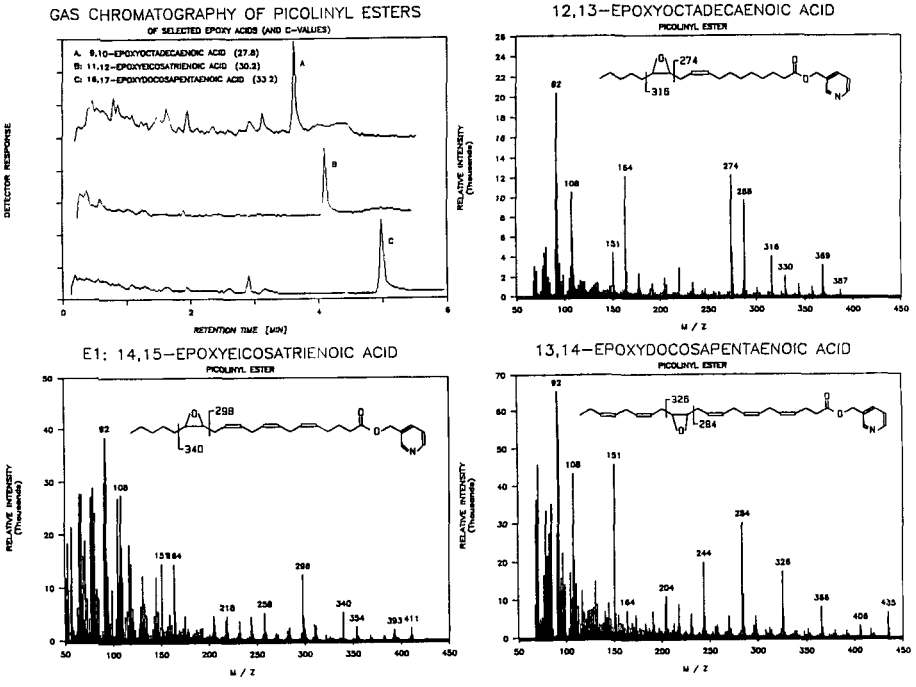

CONCLUSIONS

1. Mass spectra of picolinyl derivatives of epoxides of linoleic, arachidonic and docosahexaenoic acids showed two characteristic abundant ions produced by formal cleavage of alfa carbon bonds at oxirane ring and were therefore characteristic for each regioisomer studied providing easy and sensitive way of differentiating between them.

2. The spectra not only provided the information about the position of the epoxy group, but also the position of double bonds in the unsaturated chain can be concluded.

3. Other nitrogen containing esters, e.g. N,N-dimethylaminoethyl 3-pyridyl were studied but their spectra were not as characteristic as picolinyl derivatives.

4. Described here method can be appplied to the analysis of epoxides extracted from biological fluids.

Presented at the 36th ASMS Conference on Mass Spectrometry and Allied Topics
June 5-10, 1988, San Francisco, CA

STRUCTURAL ELUCIDATION OF CAROTENOID PIGMENTS BY FAB-CAD-MS/MS

Douglas A. Gage, Chris Rock, Jan A D. Zeevaart and J.T. Watson
Michigan State University, East Lansing, Michigan 48824

INTRODUCTION

EIMS has played an important role in the structural elucidation of carotenoid pigments (1, 2, 4, 5). Fragmentation pathways have been determined which provide information on substitution pattern in both the end groups and polyene chain (1, 2, 4, 5). However, because carotenoids are thermally unstable, reproducible EI spectra are difficult to obtain. Factors such as probe temperature, heating rate and position, as well as source temperature and pressure can dramatically affect the spectra obtained (5). Furthermore, EI spectra of carotenoids are often contaminated with ions from pyrolysis products produced during sample volatilization. Metastable analysis techniques (linked scans at constant B/E) have been applied to eliminate some of these problems (3, 4). Structurally significant ions have been observed in the daughter ion spectra of the $M^{+\bullet}$ decomposition, but these ions are rarely seen more than about 230 mass units below the $M^{+\bullet}$ ion. Other diagnostic ions found at lower m/z values are not observed.

Recently, the positive FAB mass spectrum of ß-carotene in 3-nitrobenzyl alcohol (with trichlorobenzene as a cosolvent) was reported (6). A strong $M^{+\bullet}$ ion was observed, instead of an $[M+H]^+$ ion Few fragment ions were present in the spectrum.

We have examined a series of oxygenated carotenoid pigments by positive FAB CAD MS/MS of the $M^{+\bullet}$ ion using linked scans at constant B/E to increase the amount of fragmentation in the spectrum

RESULTS AND DISCUSSION

All carotenoid compounds examined to date produce a dominant $M^{+\bullet}$ ion, rather than $[M+H]^+$, in FABMS when using 3-nitrobenzyl alcohol as the matrix. In glycerol, however, the more typical $[M+H]^+$ ion is dominant. Using the strong $M^{+\bullet}$ ion as the parent ion, the CAD MS/MS spectra of violaxanthin, lutein and neoxanthin contain fragments which are structurally diagnostic. Most of the fragment ions observed in these spectra are also found in the EI spectra of these compounds (1) It is possible to distinguish the two isomeric compounds violaxanthin and neoxanthin by their FAB CAD MS/MS spectra.

The CAD MS/MS technique was also useful in determining the structure of an unusual violaxanthin ester. The shift of several key end group containing fragments in the CAD MS/MS spectrum clearly showed that the new compound is a C_{14} fatty acid ester of violaxanthin (violaxanthin myristate). This was confirmed by hydrolysis and CAD MS/MS and VIS spectroscopy of the carotenoid product.

Several fragment ions are observed in the FAB CAD MS/MS spectra of these compounds which are not present in their EI spectra. For example, in the spectrum of violaxanthin one such prominent ion is seen at m/z 446. This ion shifts to m/z 488 in the spectrum of the monoacetate of violaxanthin, and to m/z 530 in the spectrum of its diacetate. These results suggest the unknown fragment contains both end groups of the molecule. An unknown ion at m/z 526 in the spectrum of violaxanthin myristate cannot be easily related to the ion at m/z 446 in the CAD MS/MS spectrum of violaxanthin At present, the structures of these ions remain unclear.

CONCLUSIONS

Positive FAB CAD MS/MS of the molecular ion of carotenoids is a convenient method to obtain structurally significant fragment ions. The spectra are easy to acquire and are reproducible. This is an important advantage over EIMS All of the diagnostic fragment ions found in the EI spectra of these compounds are also observed inthe FAB CAD MS/MS spectra. However, a few prominent, as yet unidentified, fragment ions are seen in the CAD MS/MS spectra that are not found in the EI spectra of these compounds. Some preliminary evidence suggests that at least one of these fragments contains both end groups of the compound. Additional studies with isotope labelled carotenoids will be required to determine the structure of these unknown ions

EXPERIMENTAL

Carotenoids: Compounds were isolated from fresh roots of *Xanthium strumarium* by extraction with methanol Extracts were partitioned into diethyl ether after dilution with aq 10% NaCl. Carotenoids were purified from the root extracts by semiprep normal phase HPLC using a hexane-ethyl acetate gradient. FAB CAD MS/MS: Carotenoid solution in methanol (1-10 nmol/µl) was mixed with 2 µl of matrix (3-nitrobenzyl alcohol) on the FAB probe tip. The precursor ions ($M^{+\bullet}$) were formed by fast atom bombardment using 6 keV Xe atoms in a JEOL HX 110 double focussing mass spectrometer. The accelerating voltage was 10 kV and the resolving power was 1000. Helium was used as the collision gas in a cell located in the first field free region. The helium pressure was adjusted to reduce the abundance of the precursor ion ($[M]^{+\bullet}$) by 50% A JEOL DA-5000 data system generated a linked scan at constant B/E. The data profiles were acquired at 30 sec/decade. The spectra shown were produced from a single scan.

REFERENCES

1. Budziklewicz, H., Brzezinka, H and Johannes, B. (1970) Monatsh. Chem 101, 579.
2. Enzell, C.R. and Wahlberg, I. (1980) in Biochemical Applications of Mass Spectrometry (Waller, G.R. and Demmer, O.C., Eds.) p. 407. Wiley, N.Y.
3. Rose, M.E. (1982) in Carotenoid Chemistry and Biochemistry (Britton, G. and Goodwin, T.W., Eds.) p 167. Pergamon, London.
4. Schweiter, U., Englert, G., Rigassi, N. and Vetter, W (1970) Pure Appl. Chem. 20, 365.
5. Vetter, W., Englert, G , Rigassi, N. and Schweiter, U. (1970) in Carotenoids (Isler, O., Ed.) p. 189. Berkhauser Verlag, Basel.
6. Vetter, W and Meister, W. (1985) Org. Mass Spec. 20, 266.

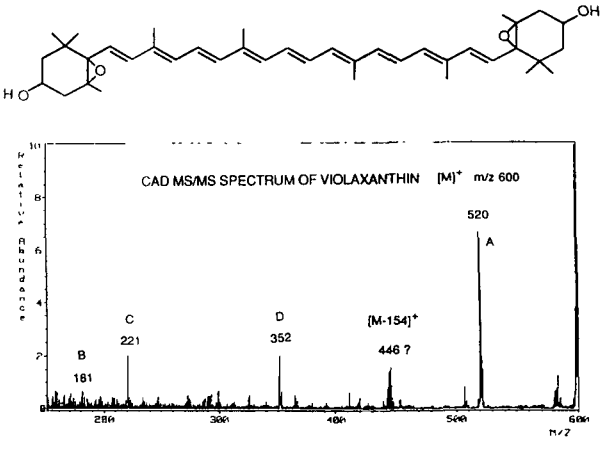

Figure 1. FAB CAD MS/MS spectrum of the $M^{+\bullet}$ ion of violaxanthin at m/z 600. Ion A $[M-80]^+$ is characteristic of carotenoid epoxides, while the ions labelled B, C and D are end group containing fragments (1, 2, 5). The later three ions displayed diagnostic shifts in the monomyristate, monoacetatae and diacetate esters of violaxanthin In the monoacetates the unshifted fragments (from the unesterified end group of the molecule) were also present in the spectrum

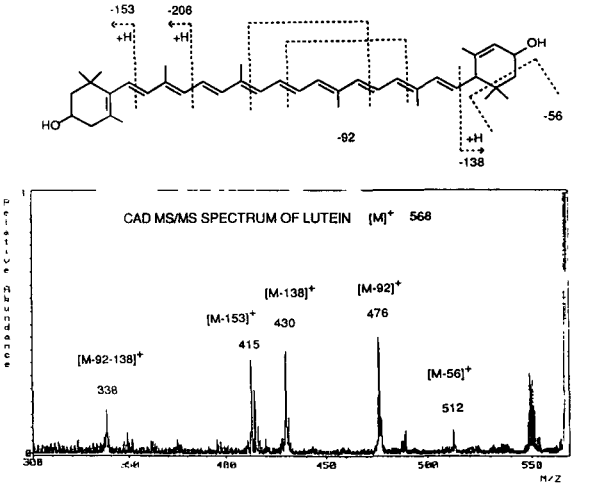

Figure 2. FAB CAD MS/MS spectrum of the $M^{+\bullet}$ ion at m/z 568 of lutein. The labelled ions are characteristic of the fragmentation of this compound

Presented at the 36th ASMS Conference on Mass Spectrometry and Allied Topics
June 5-10, 1988, San Francisco, CA

QUANTITATIVE ANALYSIS OF PLATELET ACTIVATING FACTOR BY TANDEM MASS SPECTROMETRY. Peter E.Haroldsen and Simon J. Gaskell, Center for Experimental Therapeutics, Baylor College of Medicine, Houston, Texas 77030

Platelet activating factor (PAF) is a unique biologically active phospholipid (1-0-alkyl-2-acetyl-sn-3-glycerophosphocholine) synthesized from cellular lipid stores and implicated as an important mediator of inflammatory reactions. The detection and quantitation of PAF is of great importance to gain a better understanding of inflammatory events and for potential pharmacologic intervention. Various physiochemical techniques have been used to analyze PAF (1) and have relied upon scrupulous purification procedures as well as molecular alteration and derivatization. Tandem MS analysis of individual components in complex mixtures can be achieved with retention of a high degree of selectivity and specificity often obviating the need for extensive purification. Here we report the use of a hybrid instrument of BEqQ design (VG-ZAB-SEQ)to detect and quantitate biologically derived PAF by parent ion scanning.

In common with other phosphatidylcholine molecular species, PAF fragments to produce a protonated choline phosphoester (m/z=184) in the source, as a metastable transition or under CAD conditions with FAB ionization. CAD analyses were performed on MH^+ ions using argon as collision gas in the first quadrupole (q, rf only) employing the second quadrupole filter (Q) for daughter ion separation. Daughter ion spectra of authentic standards of hexadecyl (C16:0) PAF and its trideutero analog ($^2H_3$-acetyl) contained one major ion at m/z=184 and 185, respectively. The 1 amu shift observed for $^2H_3$-PAF indicates a rearrangement process involving one of the acetate methyl hydrogens upon formation of the phosphocholine fragment. A high conversion of PAF parent ions to a single daughter ion in q (representing up to 16% of the ion intensity at BE) is observed suggesting that PAF can be detected and quantitated based on selected reaction monitoring of parent ions → daughter ion (parent ion scanning). For quantitation, dual reaction monitoring was performed to detect both PAF and $^2H_3$-PAF internal standard (IS) by alternate switching of the Q mass filter to transmit m/z=184 or 185 during repetitive magnet scans. This technique is sufficiently sensitive to allow detection of <100pg of a C16:0 PAF standard on probe (S/N=10/1).

The application of this methodology to the analysis of biologic samples has been made using Ficoll-HyPaque purified human neutrophils. Cells were incubated with (stimulated) or without (control) 10μm calcium ionophore (37°, 20 min) and lipids extracted (chloroform/methanol/water). Lipid classes were initially separated by open column chromatography (aminopropyl Bond Elut). PAF was purified from other phospholipids by TLC (2). Analysis of a biological sample derived from stimulated neutrophils by parent ion scanning indicates the presence of both C16:0 PAF and IS (Fig. 1). Measurement of ion ratios in conjunction with a standard curve indicated the levels of PAF in stimulated cells to be 75-169 ng per 10^7 cells and nondetectable in controls. Other PAF species, (C18:0, C18:1) were detected representing < 5% of the major C16:0 PAF species. Comparison of the parent ion scan of biologically derived PAF (Fig. 1) with that of the same sample analyzed by a conventional mass scan (Fig. 2) can be made. A significantly increased signal to noise ratio is observed with parent ion scanning. A lack of matrix ions results in a 20 fold increased signal to noise response and greatly improved sensitivity. The results of this study demonstrate tandem mass spectrometry to be well suited to the detection and quantitation of the inflammatory lipid mediator PAF.

[1]Murphy, RC and Clay, KL. Am.Rev.Respir.Dis. 136:p.207, 1987.
[2]Haroldsen, PE, Voelkel, NF, Henson, JE, Henson, PE and Murphy, RC. J.Clin.Invest. 79:p.1860, 1987.

Presented at the 36th ASMS Conference on Mass Spectrometry and Allied Topics
June 5-10, 1988, San Francisco, CA

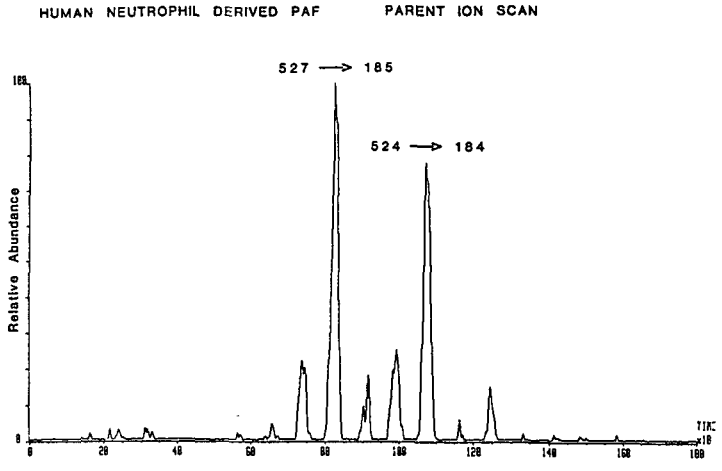

Figure 1

Figure 1. FAB parent ion scan of C16:0 PAF and $^{2}H_{3}$-PAF internal standard derived from stimulated human neutrophils. Triethanolamine FAB matrix, 30eV collision energy and $4x10^{-6}$ torr argon in q collision cell.

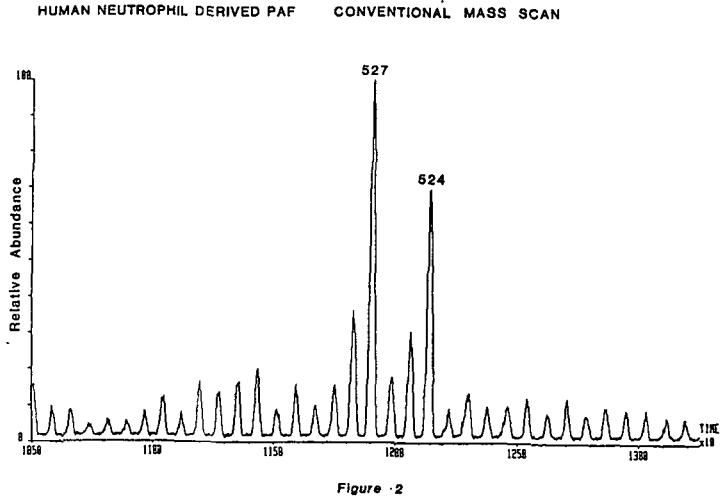

Figure 2

Figure 2. Conventional FAB mass scan of C16:0 PAF and $^{2}H_{3}$-PAF from the same sample as in Figure 1.

Presented at the 36th ASMS Conference on Mass Spectrometry and Allied Topics
June 5-10, 1988, San Francisco, CA

A COMPARISON OF PROSTAGLANDIN LEVELS IN HUMAN AND RHESUS MONKEY CEREBROSPINAL FLUID:

James A. Yergey, Norman Salem, Jr., John W. Karanian, Markku Linnoila, Laboratory of Clinical Studies, DICBR, NIAAA, Bethesda, MD 20892, and Melvyn P. Heyes, Laboratory of Neurophysiology, NIMH, Bethesda, MD 20892.

INTRODUCTION:

The ability of central nervous system tissue to produce prostaglandins (PG) *in-vitro* has been known for quite some time, and they appear to be involved in many brain functions. It has been assumed that measurement of PG in cerebrospinal fluid (CSF) are indicative of their brain production, although there have been disparate results for PG concentrations in the CSF of healthy human volunteers. Literature values range from undetectable (e.g. < 10 pg/mL CSF) to as much as 1 ng/mL CSF. We have developed an assay based on the selected-ion-monitoring, negative chemical ionization GC/MS detection of the MO-PFB-TMS derivative of prostaglandins E_2, E_1, $F_{2\alpha}$, $F_{1\alpha}$, and 6-keto-$F_{1\alpha}$. This assay has been used to measure PG concentrations in lumbar CSF of healthy human volunteers and abstinent alcoholic patients, cisternal CSF of Rhesus monkeys, and in continuously sampled lumbar CSF of awake Rhesus monkeys.

METHODS:

Sampling: Human lumbar CSF samples were drawn on ice and the 22-23 mL of a 30 mL tap was transferred to a tube containing tetradeuterated internal standards ($^2H_4$-PGE_2, $^2H_4$-$PGF_{2\alpha}$, and $^2H_4$-6-keto-$PGF_{1\alpha}$). Initially, sampling tubes contained indomethacin to inhibit PG formation, however, this was found to be unnecessary. Rhesus monkey CSF samples were acquired in order to investigate another closely related source of CSF, which had the possibility for larger sample sizes and timed profiles . Rhesus monkey lumbar CSF samples were drawn from an indwelling lumbar catheter. Sampling began after ketamine anesthesia wore off and continued for 3-4 days. Rhesus monkey cisternal CSF was drawn following administration of ketamine. Samples were frozen at -70°C and deuterated internal standards added to weighed samples just prior to extraction

Derivatization and Extraction: Thawed samples were methoximated at room temperature overnight (1% MOX-HCl in KH_2PO_4). Solid phase extraction, using 1 mL Bond-Elut C_{18} cartridges, proceeded as follows: condition with 2 mL of CH_2OH and 2 mL of H_2O, apply sample, rinse with 2 mL of 80:20 H_2O:CH_2OH, dry with vacuum for 10 min, rinse with 2 mL of CH_2Cl_2, elute PG with 1 mL of CH_2OH into silanized glass vials. Samples were further derivatized to the pentafluorobenzyl ester (0.1% PFBB, 10% DIEA in CH_3CN, 60°C for 15 min), trimethylsilyl ether (BSTFA in CH_3CN, 60°C for 15 min) and dried samples dissolved in 10 µL of dodecane.

GC/MS Determination: Separations were performed on a 15 m, 0.25 mm i.d., 0.25 µm film thickness DB-5 column. Samples (2 µL of 10 µL) were injected into the Carlo-Erba 4160 gas chromatograph using the cooled on-column injector, with the column oven at 215°C. The column was immediately heated to 315°C at 50°C/min, and the PG eluted between 3 and 4 min. The column was fed directly into the ion source of a Kratos MS-80 mass spectrometer which was kept at 250°C. The mass spectrometer was operated in selected-ion-monitoring, electron-capture negative ionization mode using CH_4 reagent gas and the $[M\text{-}PFB]^-$ ions of the PG and internal standards were monitored.

Assay Improvements: Indomethacin was found to be unnecessary during sampling, thereby eliminating its interference with the GC/MS determinations. Aqueous oximation avoids the use of pyridine, and allows methoximation by-products to be separated from PG during extraction. Using 100-fold less pentafluorobenzyl bromide during esterification greatly reduces electron capturing contaminants. Dodecane was used as the final solvent, allowing reduction of the GC/MS cycle time to less than 7 min/sample (RT 3-4 min).

RESULTS AND DISCUSSION:

The concentrations of PGE_2, PGE_1, $PGF_{2\alpha}$, $PGF_{1\alpha}$ and 6-keto-$PGF_{1\alpha}$ are below the assay detection limit of 5-pg/mL CSF in cerebrospinal fluid of healthy human volunteers and Rhesus monkeys (Figure 1 and 2, Table 1). Alcoholics sampled following a three week period of abstention also had prostaglandin levels below 5 pg/mL CSF. Literature reports of much higher levels in healthy humans are in error, most likely due to methodological problems. Future studies of prostaglandins in the human central nervous system should include samples from healthy volunteers in order to demonstrate similarly low levels for these PG. The low levels observed are most likely due either to very low production rates in the healthy brain and/or transport phenomena which limit their bulk CSF concentrations.

TABLE 1: Prostaglandin Concentrations in CSF of Humans and Rhesus Monkeys (pg/mL)

Sample	n	PGE_2	PGE_1	$PGF_{2\alpha}$	$PGF_{1\alpha}$	6-keto-$PGF_{1\alpha}$
Human[1]	37	nd	nd	?	nd	nd
Monkey[2]	6	nd	nd	?	nd	nd
Monkey[3]	9	400±109	nd	>200	nd	200±87

[1]Healthy volunteers and abstinent alcoholics; lumbar samples
[2]Acute cisternal sample
[3]Continuous (3-4 day) lumbar samples from a single animal

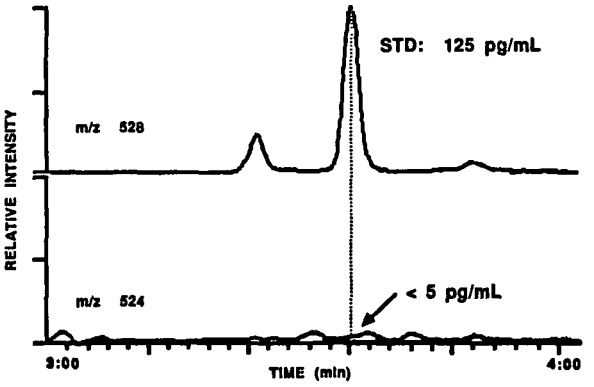

FIGURE 1: Prostaglandin E_2 in Healthy Human CSF.

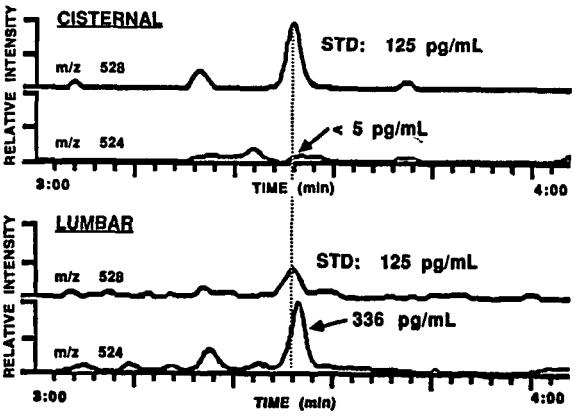

FIGURE 2: Prostaglandin E_2 in Rhesus monkey CSF.

Presented at the 36th ASMS Conference on Mass Spectrometry and Allied Topics
June 5-10, 1988, San Francisco, CA

QUANTIFICATION OF 12S-HYDROXYEICOSATETRAENOIC ACID RELEASE FROM HUMAN PLATELETS BY NEGATIVE ION MASS SPECTROMETRY

K. Yamashita, J. Capdevila and I. A. Blair
Departments of Pharmacology and Medicine, Vanderbilt University
Nashville, TN 37232

It is well known that the major product of arachidonic acid derived from platelet lipoxygenase is 12S-hydroxyeicosatetraenoic acid (12S-HETE).[1] Stimulation of human platelets with a number of pro-aggregatory stimuli results in release of arachidonic acid and synthesis of 12S-HETE together with products of the cyclooxygenase pathway of metabolism. Published data reporting the quantification of 12S-HETE during platelet aggregation are confusing and contradictory.[2-4] To clarify the consequences of lipoxygenase activation during platelets aggregation, it was considered essential to develop a precise and sensitive method for quantification of 12S-HETE. We have developed a stable isotope dilution assay based on the use of negative ion chemical ionization mass spectrometry (NICIMS) for 12S-HETE. The method has been applied to the analysis of 12S-HETE released during platelet aggregation stimulated by thrombin and collagen in the presence and absence of a cyclooxygenase inhibitor.

Oxygen-18 labelled 12-HETE for use as an internal standard was prepared by the method of Murphy et al.[5] The methyl ester of 12-HETE was saponified with 0.2 N $Li^{18}OH$ in 50 μL tetrahydrofuran/water (1:1). Successive exchange of oxygen-16 in the carboxyl moiety to the corresponding oxygen-18 was performed by repeating the procedure of methylation and subsequent saponification. Carrying out the exchange reaction for six cycles resulted in the formation of ^{18}O labelled 12-HETE with overall yield of 40% ($^{18}O_2$, 88.3%; $^{18}O^{16}O$, 11.4%; $^{16}O_2$, < 0.3%).

Washed human platelets (10^8/mL) were stimulated with thrombin (1 unit/mL) or collagen (0.5 mg/mL) in a Payton aggregometer and aggregation allowed to proceed for 10 min. The platelet suspension was added to ethyl acetate (1 mL) containing the internal standard (10 ng in 50 μL of ethanol). The ethyl acetate layer was separated and the aqueous layer was extracted with a further 1 mL of ethyl acetate. The combined organic extracts were evaporated under nitrogen. The residue was dissolved in methanol (0.5 mL) and then hydrogenated at room temperature for 5 min using PtO_2 (1 mg/mL) or Rh/Al_2O_3 (1 mg/mL) as catalyst. The catalyst was removed by filtration through a small column containing glass wool and the hydrogenated product was esterified with 5% pentafluorobenzyl (PFB)-bromide in acetonitrile (40 μL) containing diisopropylethylamine (10 μL). After evaporation of excess reagent, the PFB ester was extracted with n-hexane (1 mL) and H_2O (1 mL). The aqueous layer was extracted with a further 1 mL of n-hexane. The combined organic layer was evaporated under nitrogen. The product was purified by silica gel TLC (Whatman LK6DK) using n-hexane/ethyl acetate (90:10) as a developing solvent. The purified PFB ester of 12S-HETE was silylated with BSTFA at 60 °C for 30 min. Samples were analyzed on an SPB-5 fused silica capillary (30 m) in the NICI mode using methane as reagent gas.

The PFB ester-trimethylsilyl (TMS) ether derivative of hydrogenated 12S-HETE had excellent gas chromatographic properties, particularly when compared with the non-hydrogenated derivative. The amount of catalyst used in the hydrogenation was critical. Optimal yields were obtained with 1 mg/mL of catalyst (PtO_2 or Rh/Al_2O_3). A fully saturated C-20 acid was always formed as a by-product during hydrogenation with PtO_2, however, the formation of this compound was minimized by the use of Rh/Al_2O_3 as catalyst. Figure 1 shows the NICI mass spectrum of the PFB-TMS ether derivative of hydrogenated 12S-HETE. The mass spectrum was characterized by the ions at m/z 399 and 309, which were formed by the loss of PFB moiety and subsequent elimination of TMSOH from the molecular ion, respectively. The structure of the fragment ion at m/z 178 was thought to be $[C_6F_4CH_2O]^-$. A good linearity was observed between the peak area ratio of m/z 399 (M-PFB of hydrogenated 12S-HETE-PFB ester) to m/z 403 (M-PFB of hydrogenated $^{18}O_2$-12S-HETE-PFB ester) and weight ratio of 12S-HETE to $^{18}O_2$-12-HETE in the range of 0.5 ng to 10 ng/mL. This confirmed that no significant back exchange of labelled ^{18}O took place during the extraction and derivatization processes described above.

The method was applied to the analysis of 12S-HETE released from human platelets in response to thrombin and collagen stimulation. The amounts of 12S-HETE released from platelets increased after stimulation in a time-dependent manner. Concentrations of 12S-HETE in human platelets suspension at 10 min after and thrombin and collagen stimulation were 80.0 ng/10^8 platelets and 29.6 ng/10^8 platelets respectively. In the presence of aspirin these concentrations increased to 131.5 ng/10^8 platelets and 100.9 ng/10^8 platelets respectively. Thus, pre-treatment of platelets with aspirin resulted in remarkable enhancement of 12S-HETE production. This was attributed to the specific blockade of the platelet cyclooxygenase with aspirin and a consequent increase in the amount of substrate available for the lipoxygenase.[6] There was no significant effect on 12S-HETE production by labelling with ^{14}C-arachidonic acid prior to stimulation.

In conclusion, the development of a precise and sensitive analytical method based on the use of ^{18}O-labelled internal standard and NICI mass spectrometry enabled us to determine low concentration of 12S-HETE in human platelet suspension. The present methodology for 12S-HETE promises to provide a wealth of information on the role and function of the platelet lipoxygenase products during platelet activation.

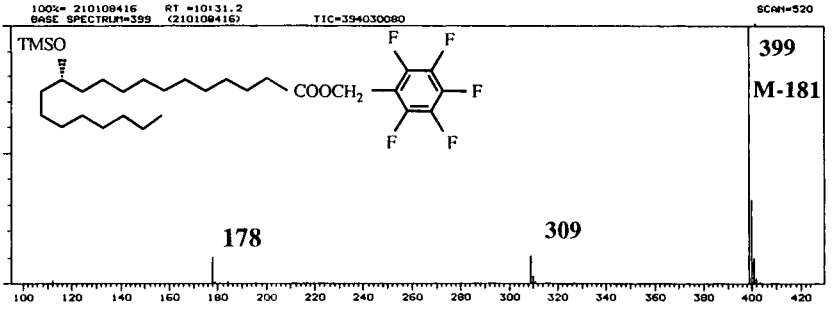

Figure 1: Mass spectrum of the PFB-TMS ether derivative of hydrogenated 12S-HETE released from human platelets in response to thrombin stimulation.

ACKNOWLEDGEMENT

This work was supported by NIH grant DK-39261.

REFERENCES

1. M. Hamberg and B. Samuelsson, Proc. Natl. Acad. Sci., 71, 3400 (1974).
2. M. Hamberg, J. Svensson and B. Samuelsson, Proc. Natl. Acad. Sci., 71, 3824 (1974).
3. E. Malle, J. Nimpt, H. J. Leis, H. Wurm, H. Gleispach and G. M. Kostner, Prostaglandins Leukotrienes and Medicine, 27, 53 (1987).
4. M. R. Buchanan, R. W. Butt, J. Hirsh, B. A. Markham and D. J. Najir, Prostaglandins Leukotrienes and Medicine, 21, 157 (1986).
5. J.Y. Westcott, K.L. Clay and R.C. Murphy, Biomed. Mass Spectrom., 12, 714 (1985).
6. M. Hamberg and G. Hamberg, Biochem. Biophys. Res. Commun., 95, 1090 (1980).

Presented at the 36th ASMS Conference on Mass Spectrometry and Allied Topics
June 5-10, 1988, San Francisco, CA

STRUCTURAL CHARACTERIZATION OF THREE ENDOTOXINS FROM *Salmonella minnesota* RESPONSIBLE FOR HUMAN PLATELET ACTIVATION:

V.N. Reinhold, G.R. Her, R.S. Johnson, J. Grabarek, J. Hawiger,
Harvard Schools of Public Health and Medicine, Boston, MA

Introduction

Gram-negative bacteria have many cellular targets, including blood platelets, granulocytes, monocytes, lymphocytes, erythrocytes, and endothelial cells. Some of these effects contribute to the development of intravascular coagulation and septic shock, and it is estimated that approximately 71,000 patients per year in the United States develop gram-negative bacteremia, resulting in 18,000 deaths. The most frequent cause of death is disseminated intravascular coagulation and shock. Therefore, efforts have been focused on *in vitro* evidence of human platelets interact with the endotoxic principle, Lipid-A. Lipid-A is the name given to a chloroform-methanol extract of partially hydrolyzed lipopolysaccharides. The extract is complex and the major components are a series of multiply acylated 2-amino-2-deoxy diglucose homologs which once constituted the membrane anchor for the outer cell wall polysaccharides of gram-negative bacteria. Under conditions of isolation, this fraction occurs as a complex mixture with varying degrees of O-deacyltion and aminoethylation.

Results & Discussion

Using a combination of TLC and FAB-MS, eight individual components have been detected in the Lipid-A fraction obtained from *Salmonella minnesota*. Three of the fractions have been shown to activate human platelets. This activity is manifested by platelet secretion of serotonin and subsequent aggregation: a process which may be analogous to human intravascular coagulation and septic shock upon gram-negative bacteremia. The extracts were analyzed directly by FAB-MS as the monophosphoryl analogs from the complex extract by FAB-MS The most active component (I) provided the mass spectrum shown in Figure 1, suggesting it to be the heptaacyl monophosphoryl Lipid-A (1). FAB-MS of the other two fractions (II, III) proved to be somewhat less active and their structures are presented below. Most interestingly, compound I was not detected in the original extracts when analyzed by FAB, but it was easily detected by FAB-MS following TLC purification. Moreover, addition of small amounts of the original extract completely suppressed desorption of this biologically active component. FAB spectra from complex matricies are frequently biased by the components exhibiting enhanced surface activity and this continues to be a matter of great concern with impure biological isolates. To approach this problem we are currently applying SFC and SFC-MS. Preliminary data indicates that quantification of these materials by an SFC using an FID detector is comparable to independent tests for phosphate. To position points of acylation (2,3) we have combined a series of O-deacylation steps with positive FAB-MS to position each residue. Under positive FAB-MS a glycosidic cleavage fragment provides molecular weight information for each monosaccharide residue and this in combination with C-3 and C-3' de-O-acylation differentiates the varying possibilities of N- and O-acyl groups.

References

1.) N. Qureshi, P. Mascagni, E. Ribi, K. Takayama. J. Biol. Chem., 260:5271-5278(1985).
2.) N. Qureshi, K. Takayama, D. Heller, & C. Fenselau. J. Biol. Chem., 258:12947-12951(1983).
3.) K. Takayama, N Qureshi, K. Hyver, J. Honovich, R.J. Cotter, P. Mascagni, H. Schneider. J. Biol. Chem., 261:10624-10631(1986).

Presented at the 36th ASMS Conference on Mass Spectrometry and Allied Topics
June 5-10, 1988, San Francisco, CA

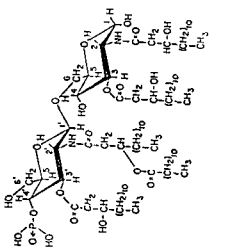

STRUCTURE OF III

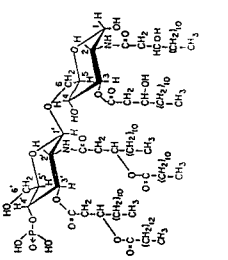

STRUCTURE OF II

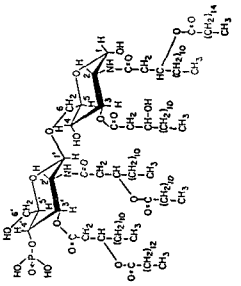

STRUCTURE OF I

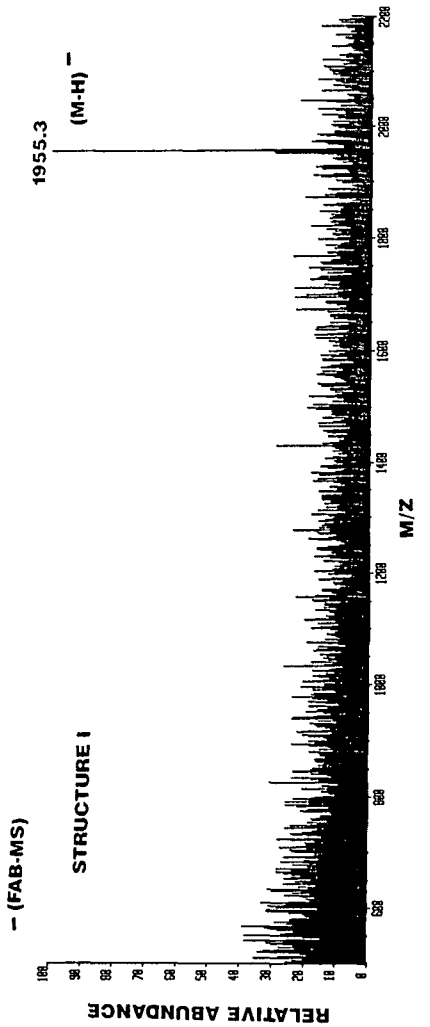

Presented at the 36th ASMS Conference on Mass Spectrometry and Allied Topics
June 5-10, 1988, San Francisco, CA

IMPROVEMENTS IN STRUCTURAL DETAIL FOR GLYCOSPHINGOLIPID SAMPLES USING CO_2 & CO_2/CH_3OH MIXTURES AS A DCI REAGENT GAS:

G.R. Her, D.M. Sheeley, V.N. Reinhold.
Harvard School of Public Health, Boston, MA 02115.

Introduction

Glycosphingolipids (GSLs) are amphoteric conjugates of a long chain base, a simple fatty acid, and one or more carbohydrate residues. The base and its fatty acid conjugate frequently impart heterogeneity to the molecular ion region as a consequence of alkane chain modifications in one or both of these residues. The molecular ion distribution can most frequently be related to variations in chain length, unsaturation, hydroxylation or their combinations in either the long chain base or the fatty acid. Negative FAB-MS has been successfully applied to underivatized GSLs, often producing many sequence related fragment ions. However, no fragment ions that can be used to determine the ceramide composition. Although positive FAB has shown little value in the analysis of underivatized GSLs, it has proven very useful for permethylated samples. Despite some reports in the literature (1), positive FAB-MS of permethylated GSLs rarely show intense fragment ions which can be used to determine the ceramide composition (2). Recently, MS/MS has shown that it could be used to determine ceramide composition (3).

As a consequence of independent SFC-MS studies, using CO_2 or CO_2/CH_3OH as mobile phases, we have looked closely at using these gases for DCI analysis of GSLs. When evaluated with these samples, these gases show one major advantage over the commonly used ammonia reagent gas, a unique α-cleavage fragment of the long chain base allows the assignment of contributing molecular heterogeneity. In addition, the ions defining the carbohydrate sequence are often clearer and more abundant.

Figure 1 shows the CO_2/CH_3OH (4:1) DCI mass spectrum of permethylated GM1. The pair of protonated molecular ions (m/z 1854 and 1826), with a 28 dalton interval, indicates that this fraction occurs with approximately half the sample containing an alkane side chain shortened by two methylene units. The ions at m/z 1479 and 1451 can be ascribed to loss of a neuraminyl residue from the molecular ion $(MH-375)^+$. Since this loss does not alter the ceramide moiety, the alkane heterogeneity is still observed. The ion at m/z 1573 does not show the alkane heterogeneity and can be accounted for by considering cleavage α to the nitrogen with elimination of the aliphatic sphingoid residue. The corresponding events, loss of heterogeneity and sphingoid residue elimination, indicate that the alkane chain variation resides with this residue. This fragment also shows the facile loss of a neuraminyl group, at m/z 1198. In the absence of methanol (100% CO_2), these two fragments (m/z 1573 and 1198) are the most abundant ions (Fig. 2).

This technique has been tested on other GSLs such as GD1a, GD1b, ceramide trihexoide, globoside(GL4) and lignoceroyldihydrolactocerebroside, α cleavage fragments were observed for every sample tested. Based on these fragments, fatty acid composition of each compound can be assigned.

References

1. Fukuda, M. N.; Dell, A.; Oates, J. E.; Wu, P.; Klock, J. C.; Fukuda, M. J. Biol. Chem. 1985, 260, 1067
2. Egge, H., Peter-Katalinic, J. Mass Spectrom. Rev., 1987, 6, 331
3. Costello, C. E.; Domon, B. Biochemistry 1988, 27, 1543

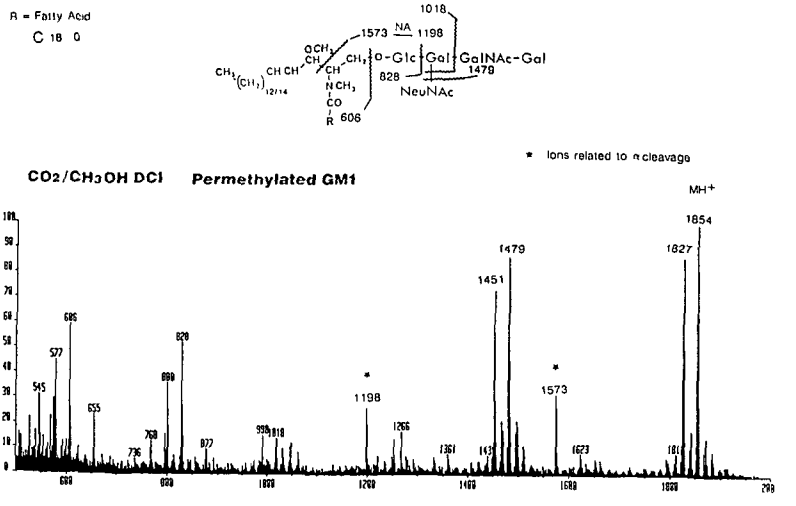

Figure 1. CO_2/CH_3OH DCI mass spectrum of permethylated GM1

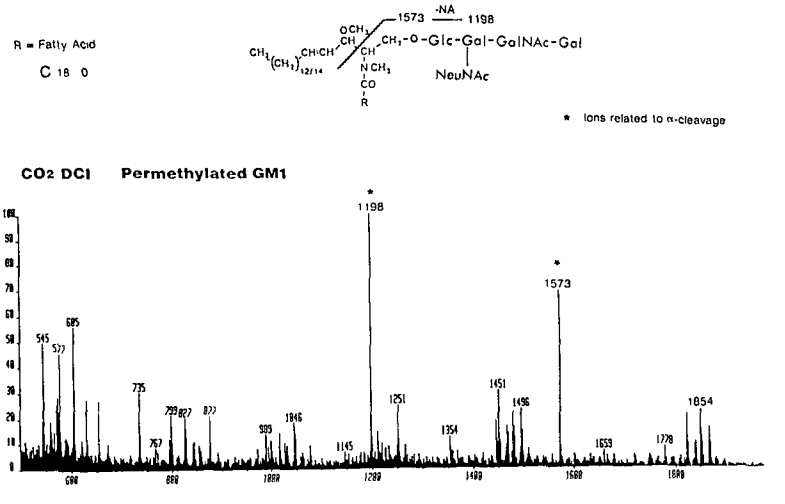

Figure 2. CO_2 DCI mass spectrum of permethylated GM1

Presented at the 36th ASMS Conference on Mass Spectrometry and Allied Topics
June 5-10, 1988, San Francisco, CA

MEASUREMENT OF PROSTAGLANDIN E_2 (PGE_2): IMMUNOAFFINITY PURIFICATION WITH GC/MS, GC/MS/MS AND DCI/MS/MS

T. A. Gillespie, M. E. Hail and R. A. Yost
Department of Chemistry, University of Florida, Gainesville, FL 32611

J. J. Vrbanac and D. R. Knapp
Department of Pharmacology, Medical University of South Carolina, Charleston, SC 29425

Detection of urinary arachidonic acid metabolites (AAMs) by capillary GC/MS involves extensive sample preparation. The methoxime-pentafluorobenzyl ester-trimethyl silyl (MO-PFB-TMS) derivative used with electron-capture negative chemical ionization (EC-NCI) is the most sensitive and specific technique for the trace determination of prostaglandins (PGs). Immunoaffinity (IA) purification using polyclonal antibodies has been shown to provide sufficient sample purification prior to analysis of urinary PGs by electron ionization (EI) GC/MS/MS (1). This method of analysis reduces the need for extensive sample clean-up and utilizes the increased selectivity and reduced chemical noise inherent with MS/MS. However, the time required for derivatization and GC dominates the overall analysis time.

Evaluation of the relative trade-offs between analysis time and selectivity with respect to sample preparation, sample introduction and mass spectrometry in the determination of urinary PGs was accomplished. All GC/MS and GC/MS/MS experiments were performed using a Finnigan MAT TSQ 45, while the direct chemical ionization (DCI) experiments were performed on a Finnigan MAT TSQ 70. Methane EC-NCI of the MO-PFB-TMS derivative of PGE_2 and $^2H_4$-PGE_2 in urine was examined.

In the GC/MS (SIM) studies performed on a 10 m capillary column, the $(M\text{-}PFB)^-$ ion of both PGE_2 (524^-) and $^2H_4$-PGE_2 (528^-) were monitored. The comparison between the single-ion monitoring (SIM) profiles demonstrates that increased selectivity is required in the sample preparation for the GC/SIM determination of PGE_2. The increased selectivity obtained with IA solid phase extraction (Figure 1) is obtained at the expense of increased sample preparation time. Nevertheless, it appears that IA in combination with high resolution GC/MS (e.g. use of a 30 m column) would work quite adequately.

The GC/MS/MS selected-reaction monitoring (SRM) profiles were obtained by monitoring the selected reactions of $524^- \rightarrow 268^-$ for PGE_2 and $528^- \rightarrow 348^-$ for $^2H_4$-PGE_2. Figure 2 illustrates the advantages of using SRM for the determination of PGE_2. The increased selectivity of SRM results in a reduction of the chemical noise. The 845 pg of $^2H_4$-PGE_2 injected on the column is slightly above the detection limit, while PGE_2 is below the limit of detection. A possible explanation for the poor sensitivity of PGE_2 is that other components in the sample, eluting from the column at the same time, may quench the formation of the parent ion. However, despite the increased selectivity of SRM, better chromatographic separation is required to avoid the quenching problem. Figure 3 illustrates the ultimate trade-offs between selectivity, the time spent for sample preparation, sample introduction (GC) and MS/MS. Some of the additional time spent on sample preparation (IA) is recovered by using a short capillary column (e.g. 3 m instead of 10 m).

Analysis times can be further reduced by coupling IA with direct chemical ionization (DCI)/MS/MS. In this method, an abbreviated derivatization step using only the PFB derivative of PGE_2 is employed. If proceeded by IA, it appears that DCI with SRM would be the ultimate method in terms of speed of analysis. The SRM profile for $^2H_4$-PGE_2 ($355^- \rightarrow 335^-$) demonstrates that it may be possible to detect PGs in the low nanogram levels (4 ng on the probe) in urine with DCI/MS/MS (Figure 4). Levels lower than the nanogram range may be extremely difficult to detect as observed

when monitoring the $(M-PFB)^-$ ion $351^- \rightarrow 315^-$ for PGE_2. Monitoring other characteristic reactions for SRM did not seem to solve the problem. Although DCI allows for rapid analysis times, it is possible, with rapid heating of the probe, to vaporize undesirable components of the urine, which can interfere with the analysis. This creates problems with contamination of the ion volume and the source region, and leads to a drastic reduction in sensitivity. Another reason for the poor sensitivity is the possibility of quenching effects, which may occur when many components are vaporized at the same time.

In summary, GC/SIM determination of PGE_2 can be successfully performed when using both SEP-PAK and IA solid phase extractions with a sufficient length of capillary GC column to yield adequate separation. Reduced sample preparation (SEP-PAK only) should be possible, if conventional lengths of capillary GC columns (20-30 m) are used with MS/MS (SRM). A useful trade-off between selectivity and analysis time can be achieved with IA and short capillary GC columns coupled with MS/MS (SRM). DCI/MS/MS is a rapid analysis technique which may reduce lengthy derivatization procedures, but requires further investigation if it is to become a viable technique for the determination of urinary PGs.

Reference

1. Vrbanac, J. J. and Knapp, D. R., 35th ASMS Conference on Mass Spectrometry and Allied Topics, p. 7-8, 1987.

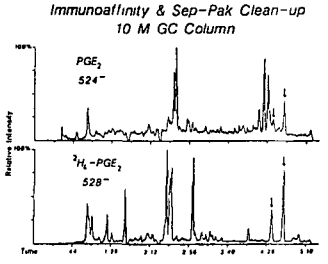

Figure 1: GC/SIM with 10 m GC column:IA & SEP-PAK

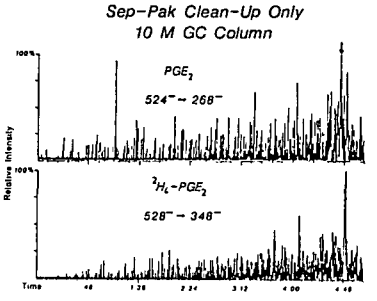

Figure 2: SRM with 10 m GC column SEP-PAK Only

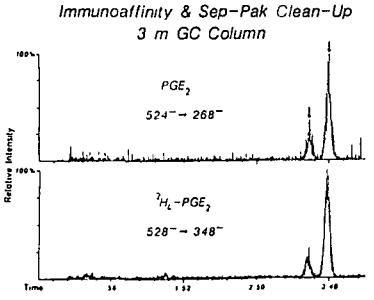

Figure 3: SRM with 10 m GC column IA & SEP-PAK

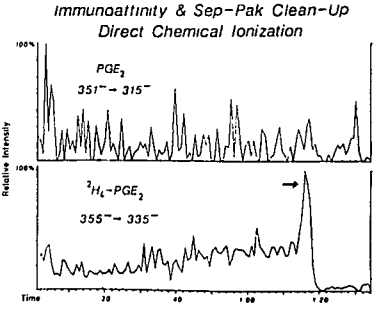

Figure 4: DCI/SRM - IA & SEP-PAK

Presented at the 36th ASMS Conference on Mass Spectrometry and Allied Topics
June 5-10, 1988, San Francisco, CA

COMPARATIVE GC/MS TECHNIQUES FOR THE IDENTIFICATION OF FATTY ACIDS AND ALCOHOLS FROM HUMAN CERUMEN.

D.J. Harvey,

University Department of Pharmacology, South Parks Road, Oxford, OX1 3QT, UK.

Cerumen, or ear wax, consists of wax esters and cholesterol esters which, on hydrolysis yield complex mixtures of fatty acids, alcohols and cholesterol. The structures of the constituent acids and alcohols have not been well studied although it is known that they resemble those in sebum, the main constituent of skin-surface lipids. This paper compares various GC/MS techniques for structural identification of these compounds and an examination of constituents in a typical cerumen sample.

Lipids were extracted from the cerumen with ethyl acetate and hydrolyzed with ethanolic potassium hydroxide. Direct derivatization for GLC and GC/MS involved preparation of TMS, [$^2H_9$]TMS, methyl ester/TMS, picolinyl/TMS (1,2), nicotinate/TMS (3), picolinyldimethylsilyl/TMS (4) and pyrrolidide (directly from the cerumen extract) derivatives. The unsaturated compounds were also converted into cis-diols with osmium tetroxide and acids were reduced to alcohols with lithium aluminium deuteride. These derivatized compounds were examined by GLC using a 50 m x 0.3 mm OV-1 fused silica capillary column and by GC/MS using a VG 70/70F mass spectrometer (70 eV) fitted with a 25 m x 0.2 mm OV-1 fused silica capillary column terminating inside the ion source.

Fig. 1 shows a chromatogram of the TMS derivatives of the constituent lipids from the hydrolyzed cerumen. Nearly 100 compounds were identified; these consisted of straight-chain, branched-chain, saturated and unsaturated acids and alcohols. Although the TMS and Me/TMS derivatives were the best for gas chromatography, they gave little structural information on the aliphatic chains of the acids and alcohols. This information was best obtained by preparation of other derivatives. Hydroxylation of the double bonds with osmium tetroxide and conversion of the resultant glycols into TMS derivatives was the most satisfactory method for double bond location in the mono-unsaturated acids and alcohols but was very much less satisfactory as the number of double bonds increased. This was mainly the result of the great mass increment of the TMS group giving, after hydroxylation and TMS ether formation, an increase of 178 mass units for each double bond. The main advantage of these derivatives for mixture analysis was that differences in double bond position were indicated by only two very abundant ions at distinctly different masses in the mass spectra of isomeric compounds. This method did not, however give structural information on methyl branch points.

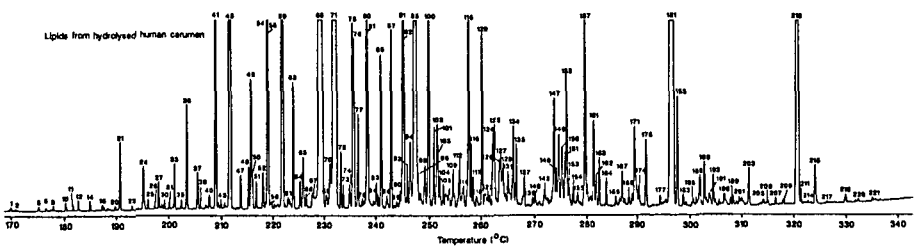

Fig. 1. Gas chromatogram (50 m fused silica capillary column) of the fatty acids and alcohols from human cerumen separated as TMS derivatives.

Both pyrrolidide and picolinyl (Fig. 2) derivatives gave structural information on the full range of acids present. These derivatives initiate a radical-site fragmentation following hydrogen abstraction from any position of the chain resulting in a series of ions spaced by 14 mass units from saturated compounds. Positions of methyl branch-points are indicated by the absence of a peak and unsaturation can be determined both by the mass numbers and by the presence of two ions of higher abundance produced by abstraction of either of the two allylic hydrogen atoms. Of the two derivatives of this type, the picolinyl esters gave spectra with much more abundant ions than the pyrrolidides. However for structural determination of isomers that were not separated by GLC, these derivatives were not as satisfactory for double bond location as the isomers produced ions at common masses and the largest differences in the spectra were those of ion abundance rather than mass.

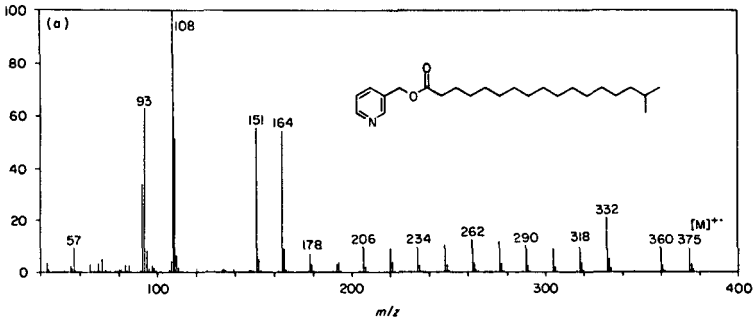

Fig. 2. 25 eV Mass spectra of the picolinyl derivatives of iso-octadecanoic acid.

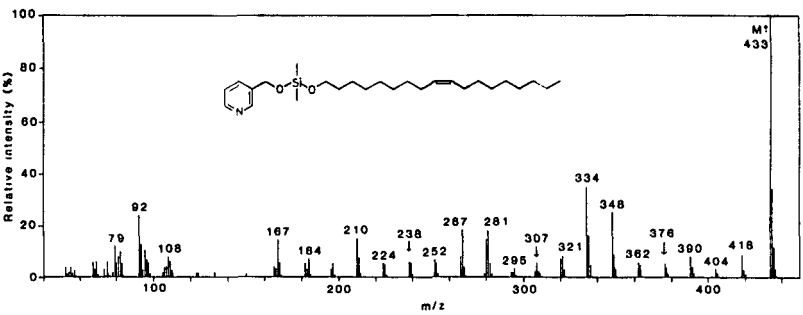

Fig. 3. 25 eV mass spectrum of the PICSI derivative of n-octadecanol.

Nicotinate derivatives were among the most satisfactory for identification of alcohols. These fragmented in the same way as the picolinyl esters and could, thus, be used for both unsaturated and branched-chain compounds. PICSI Derivatives fragmented in a similar way and had the additional advantage of producing abundant molecular ions.

The major carboxylic acids in the cerumen sample were n-16:1,delta-6 (peak 68, Fig. 1), n-16:0 (peak 71), n-18:1,delta-9 (peak 95), n-14:0 (peak 45). n-15:0 (peak 59), ai-15:0 (peak 54), n-14:1,delta-6 (peak 41), 17:1, delta-6 (peak 76), n-17:1,delta-6 (peak 80) and n-18:2,delta-9,12 (peak 90). The major alcohols were n-20:0,delta-10 (peak 115), n-18:0 (peak 87), n-19:0 (peak 103), n-20:0 (peak 120), n-22:1,delta-12 (peak 147), n-24:1,delta-14 (peak 171) and 16:0 (peak 63). Peak 181 was squalene and peak 210 was cholesterol.

This work was supported by the Wellcome Trust.

1) D.J. Harvey, Biomed. Mass Spectrom., 1982, 9, 33.
2) D.J. Harvey, Biomed. Mass Spectrom., 1984, 11, 340.
3) D.J. Harvey and J.M. Tiffany, Biomed. Mass Spectrom., 1984, 11, 353.
4) D.J. Harvey, Biomed. Mass Spectrom., 1987, 14, 103.

Presented at the 36th ASMS Conference on Mass Spectrometry and Allied Topics
June 5-10, 1988, San Francisco, CA

Determination of the Phosphocholine Molecular Species Which are Direct Precursors of Platelet Activating Factor

Keith L. Clay and C. A. Johnson

University of Colorado Health Sciences Center
Department of Pharmacology
4200 E. 9th Avenue
Denver, CO 80262

In response to appropriate stimulation, human and animal neutrophils synthesize platelet activating factor (PAF, 1-O-alkyl-2-O-acetyl-glycero-3-phosphocholine) which is predominantly hexadecyl in the sn-1 alkyl chain (1,2). By contrast, the putative precursor pool of ether-linked phosphocholine in human neutrophils is almost an equal mix of alkyl chains which contain 16 carbon atoms and alkyl chains with 18 carbons atoms (3). This fact implies that there is significant selection in the acetylation of lyso-PAF species to give PAF. The basis for that selectivity was the subject of this investigation.

Specificity in the synthesis of a unique molecular species of PAF in the presence of a rather heterogeneous precursor pool could arise at any point in the synthetic or degradative pathways. The major pathways for the synthesis of PAF and its subsequent catabolism are diagrammed in Fig. 1.

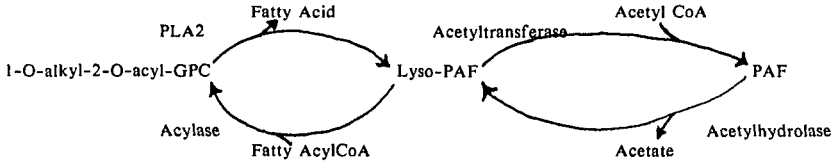

None of the enzymes shown to be involved in this cyclic process have shown specificity based on the alkyl chain length, but there is at least one report that the initial hydrolysis mediated by Phospholipase A2 may have some specificity for a specific acid, arachidonic acid, in the sn-2 position, (4). The possibility, therefore, exists that the basis for specificity in the synthesis of PAF is in the specific molecular species of phosphocholine which serves as substrate for PAF biosynthesis.

To define the presursor alkyl-linked GPC which serves as proximate substrate for PAF biosynthesis, we labelled those ether phospholipids with deuterium by incubation with stable isotopically labelled variants of normal phospholipid precursors. PAF synthesis was then initiated with appropriate stimulus, the PAF and phosphocholine pools were then isolated, the PC was further fractionated by HPLC into its constituent molecular species and the isotopic composition of the alkyl ether chains in PAF and each of the molecular species was determined. Comparison of isotopic composition of the PAF with a putative precursor pool then allowed some estimation of the contribution of that molecular species to the synthesis of PAF.

Deuterated lyso-PAF was synthesized from beef heart phosphochoine by reduction with deuterium gas in the presence of platinum on carbon. Deuterated alkylgycerol was then derived from this lyso-PAF by hydrolysis with concentrated hydrofluoric acid. Tritiated lyso-PAF was added to the deuterated lyso-PAF prior to incubation with the cells to allow easy visualization of the areas of incorporation of label (both deuterium and tritium) into the cellular phospholipids.

Human neutrophils were isolated from blood of healthy volunteers and then re-suspended in Hank's balanced salt solution to which the labelled precursors had been added. The incubation was carried out for various lengths of time and then terminated by the addition of methanol. Cellular lipids were extracted and a PAF and PC fraction were obtained by TLC. The PAF fraction was then derivatized with pentafluorobenzoyl chloride for negative ion chemical ionization GC/MS. The PC fraction was further fractionated by reverse phase HPLC into its constituent molecular species. The identity of each of the fractions was determined by fast atom bombardment mass spectrometry.

These separated fractions were then degraded to alkylglycerols and derivatized with acetone to the *corresponding isopropylidene derivatives. The isotopic composition of the alkyl ether chains in* these molecular species was then determined by positive ion GC/MS.

As illustrated by the data in tables 1 and 2, the basic conclusion which can be derived from this study is that PAF is synthesized from a pool of phosphocholine which is much more highly enriched than any of the identified pools of PC molecular species. The most highly enriched pool of alkyl-acyl-PC is that containing arachidonic acid in the sn-2 position, and this data therefore supports the hypothesis that alkyl-arachidonyl-GPC is the primary pool used as precursor for the synthesis of PAF in the human neutrophil, and probably in other cells.

Table 1. Isotopic Composition of PAF and PC
Molecular Species after Incubation with Deuterated lyso-PAF

Sample	Ratio, D_2/D_0 Hexadecyl	Ratio, D_2/D_0 Octadecyl	Mol. Species**
D_2-Lyso-PAF	2.54(80%)	1.61(20%)	
PC, from TLC	0.06	0.06	
HPLC Fractions*			
46,47	0.17		16/20:4
48,49	0.06		16/18:2
57,58	0.15	0.15	16/20:3 + 18/18:3
64,66	0.04	0.11	16/16:0 + 18/?
78,79		0.14	18/20:4
83,84		0.07	? (18/18:2?)
PAF	0.47	0.09	

Table 2. Isotopic Composition of PAF and PC
Molecular Species after Incubation with Deuterated Alkylglycerol

Sample	Ratio, D_2/D_0 Hexadecyl	Ratio, D_2/D_0 Octadecyl	Mol. Species**
PC, from TLC'	0.07	Not measurable	
HPLC Fractions*			
35,36	0.05		16/20:4
48	0.04		16/16:0
49,50	0.03		16/16:0 + 16/16:1
55,56	0.03	0.5	16/20:2 + 18/20:4
PAF	0.09	Not measurable	

* Slightly different mobile phase conditions were used for these sets of HPLC separations
** Data are shown as alkyl ether chain length/acyl species. i.e. 16/20:4 = hexadecyl-arachidonyl-PC

In the study with lyso-PAF incubation, most of the precursor was acylated with arachidonic acid in the sn-2 position, and the PAF synthesized came from that pool. In the incubations with alkylglycerol, most of the precursor was synthesized to a hexadecyl-palmitoyl-GPC species, and the PAF synthesis was not from that pool. These data are most consistent with the synthesis of PAF being from a sub-pool of hexadecyl-arachidonyl-GPC.

This work was supported in part by a grant from the National Institues of Health (HL 34303)

1. Clay, K.L., Murphy, R C., Anders, J.L., Lynch, J.L. and Henson, P.M. Biochem. Biophys. Res. Commun. 121:815 (1984).
2. Ramesha, C.S. and Pickett, W.C. J. Immunol. 138:1559 (1987).
3. Muller, H.W., O'Flaherty, J T. and Wykle, R.L. J. Biol. Chem. 259:14554 (1984).
4. Leslie, C.C., Channon, J.Y , Wall, M.M. and Zelarney, P.T. J. Cell. Biochem. S-12E:S121, (1988).

Presented at the 36th ASMS Conference on Mass Spectrometry and Allied Topics
June 5-10, 1988, San Francisco, CA

ANALYSIS FOR LEUKOTRIENE B_4 IN HUMAN SERUM BY GC-MS

Helen Hughes, Jerry R. Mitchell and Simon J. Gaskell
Center for Experimental Therapeutics
Baylor College of Medicine
Houston, Texas

Leukotriene B_4 (LTB_4, (5S, 12R)-5,12-dihydroxy-(ZEEZ)-6,8,10,14-eicosatetraenoic acid) is formed from arachidonic acid via the 5-lipoxygenase pathway. It is a potent chemotactic agent for polymorphonuclear leukocytes and is thought to be an important mediator in several pathological processes involving inflammatory and allergic responses. The analysis of LTB_4 in vivo poses significant problems. First the role of ex vivo formation during blood sampling and serum preparation must be assessed before the circulating concentration can be determined. The method must have both high sensitivity and the specificity to distinguish between LTB_4 and several isomeric dihydroxyeicosatetraenoates which have been identified in different cell incubation systems. We have developed a method based on electron capture negative ion mass spectrometry for the analysis of LTB_4 in serum at low pg/ml concentrations.

Blood is collected into the 5-lipoxygenase inhibitor nordihydroguaiaretic acid (NDGA) to suppress ex vivo formation. Serum is isolated, equilibrated with the internal standard [$^2H_4$] LTB_4, and extracted using C-18 cartridges. Following derivatization to the pentafluorobenzyl esters, the extracts are purified by straight-phase HPLC (Figure 1). Gas chromatographic-mass spectrometric analysis was accomplished on the tert-butyldimethylsilyl ether derivatives. A DB-1 capillary column (30 m x 0.32 mm) was used for the analyses and was programmed from 210° to 310° at 5°/min. Ions were monitored at m/z 431 and 435, which correspond to loss of tert-butyldimethylsilanol from the M-PFB anions of endogenous and [$^2H_4$] LTB_4 respectively.

This method takes advantage of the high sensitivity under electron capture negative ion MS conditions rendered on the eicosanoids by virtue of the PFB ester moiety. The limit of detection for LTB_4 standards was well below 5 pg, injected on column. The concentration of LTB_4 in human serum, collected with NDGA, was 11.0 pg/ml (Figure 2). At this concentration the interassay coefficient of variation was 16.7%. The method showed a high degree of accuracy as determined by the analysis of five 25 ml serum samples spikes at concentrations of 5, 10, 25, 50, and 100 pg/ml with unlabeled LTB_4 and carried through the analysis (Figure 3). The serum concentration of LTB_4 measured in this study is less than 10% of that previously reported by Blair and colleagues (1985) where no lipoxygenase inhibitor was used. Ex vivo formation of LTB_4 can therefore be a major obstacle when assessing the circulating concentration.

Blair, I.A., Brash, A.R., Daugherty, J., Fitzgerald, G.A. (1985) in Advances in Prostaglandin, Thromboxane and Leukotriene Research (Hayaishi, O., Yasmamoto, S., eds.), Vol. 15, pp. 61-65, Raven Press, New York.

Presented at the 36th ASMS Conference on Mass Spectrometry and Allied Topics
June 5-10, 1988, San Francisco, CA

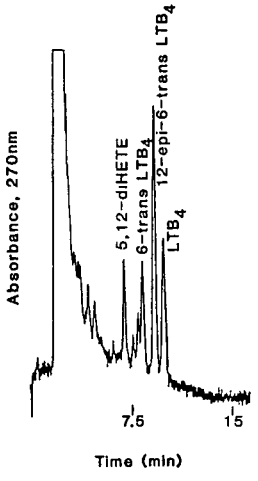

Figure 1. Straight-phase HPLC separation of LTB_4 and isomeric 5,12-diHETEs as their PFB esters.

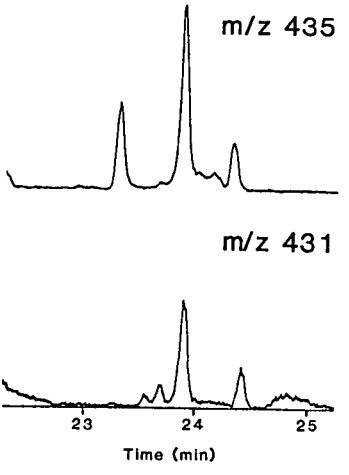

Figure 2. Selected ion chromatograph of a 25 ml serum extract. Ions at m/z 431 and 435 correspond to endogenous and deuterated LTB_4 respectively. The concentration of LTB_4 in this sample was 11.0 pg/ml.

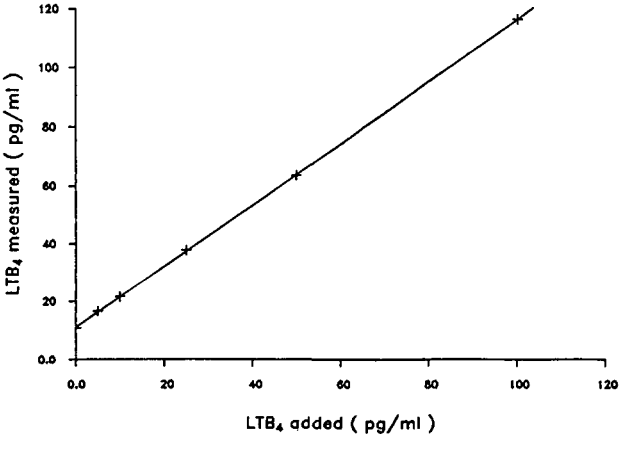

Figure 3. Aliquots of pooled serum were spiked with differing concentrations of LTB_4. The linear regression analysis, shown here, for LTB_4 measured versus LTB_4 added gave a correlation coefficient of 1.000, slope 1.050 and Y intercept 11.26.

Presented at the 36th ASMS Conference on Mass Spectrometry and Allied Topics
June 5-10, 1988, San Francisco, CA

ANALYSIS OF LTB_4 AND 20-HYDROXY-LTB_4 IN WHOLE BLOOD CHALLENGED WITH ZYMOSAN

J.A. Zirrolli, A. Fradin, J. Maclouf, and R.C. Murphy

University of Colorado Health Sciences Center
Department of Pharmacology
4200 E. 9th Avenue
Denver, CO 80220

Various oxygenated metabolites of arachidonic acid are known to be generated by cells following stimulation *in vivo* (1). For example, leukotriene B_4, an important 5-lipoxygenase metabolite of arachidonic acid is known to be synthesized by the human polymorphonuclear leukocyte which is undergoing phagocytosis (2). While there is a great deal of interest concerning the generation of such lipid mediators derived from arachidonic acid, it has been a challenging analytical problem to develop means by which one can accurately and specifically measure these molecules produced in picomolar amounts. We have been interested in the potential for generation of leukotrienes by a transcellular metabolic process which would involve the synthesis of one intermediate, for example leukotriene A_4, within one cell which is then transferred to another cell for subsequent processing into leukotriene B_4 or leukotriene C_4 (3). Some evidence has been obtained to suggest that such a complex route of synthesis for leukotrienes may take place in tissues including whole blood (4). A major objective of the work presented here was to develop means by which one could accurately measure LTB_4 and 20-hydroxy-LTB_4, a subsequent metabolite of LTB_4, using stable isotope dilution and mass spectrometry. An extraction based method has been developed which results in substantial purification by taking advantage of the unique chemistry inherent in the 5-lipoxygenase products and facile formation of neutral δ-lactones.

Human blood was collected from healthy volunteers who had not previously taken nonsteroidal antiinflammatory agents for at least one week prior to donation. It was immediately anticoagulated with 3.8% sodium citrate in polypropylene tubes. Differential cell counts of neutrophils, platelets, monocytes, and red blood cells were carried out for each blood sample taken for study. Incubations were performed at 37°C in 15 ml sterile polypropylene tubes, placed in a shaking bath after a 5 min equilibration period. Zymosan was boiled in saline for 2 hrs, washed, and sonicated twice before being suspended in HBSS at 50 mg/ml. Zymosan was added to whole blood at a final concentration of 2 x 10^3 particles per neutrophil. Incubations were carried out for 30 min. Following the incubation period, stable isotope labeled LTB_4 and 20-OH-LTB_4 were added and cell suspensions were centrifuged. The supernatants were treated with 4 volumes of ethanol to precipitate proteins followed by centrifugation. Supernatant was acidified to pH 3 with formic acid and diluted with 4 volumes of water. The leukotrienes were partially purified by solid phase extraction (5).

Formation of the LTB_4 lactone was carried out by treating the residue with 100 μl of 1% isobutyl chloroformate and 10% diisopropylethylamine in acetonitrile at room temperature for 30 min (Figure 1, Step A). After evaporation to dryness, the sample was suspended in .1 M phosphate buffer (pH 7.5) and extracted with methylene chloride. The organic layer was separated, taken to dryness, then treated with a solution of 50 μl pyridine, 20 μl 1.0 normal LiOH and 200 μl 0.1 M phosphate buffer (Figure 1, Step B). Lactone hydrolysis was carried out for 15 min at room temperature followed by the addition of 1.8 mls of water. This alkaline solution was extracted with methylene chloride to remove neutrals and the aqueous layer acidified with 20 μl of 10 N HCl. After extraction with 2 mls of methylene chloride, the organic layer was removed and taken to dryness (Figure 1, Step C). This residue was then derivatized to the pentafluorobenzyl ester, trimethylsilyl ether derivatives (Figure 1, Step D as previously described) (5).

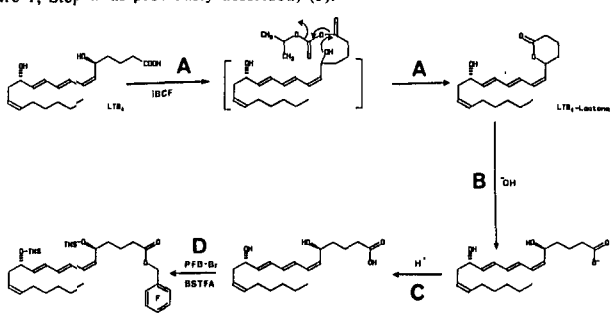

Figure 1. Transformations of LTB_4 during the extractive isolation procedure for LTB_4 and 20-OH-LTB_4.

The leukotrienes in this sample were quantitated by selected ion monitoring, capillary gas chromatography/mass spectrometry as previously described (5). Table 1 shows the recovery of LTB_4 as assessed by radiolabeled LTB_4 added to the biological matrix prior to the various organic extractions steps and formation of the lactone. Overall, the yield was 65% starting from the biological mixture as compared to a typical yield following an HPLC purification protocol which yielded only 30% of the starting LTB_4 (Table 1). Figure 2 shows the selected ion monitoring trace of LTB_4 and deuterium labeled LTB_4 obtained by the extractive technique monitoring ions at m/z 479 and 483. This LTB_4 was generated by zymosan phagocytosis in whole blood.

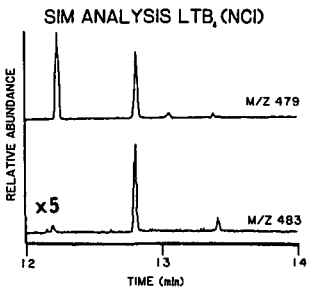

Figure 2. Selected ion monitor recordings for m/z 479 (LTB_4) and m/z 483 (D_4-LTB_4) by negative ion electron capture mass spectrometry. LTB_4 was produced by zymosan challenged whole blood and isolated by the extractive techniques.

Table 1

Recoveries (LTB_4)

Step	HPLC Method		Step	Extractive Method	
1	Sep Pak	80%	A	Sep Pak	80%
2	HPLC	30%	B	Alkaline Wash	75%
			C	Acidic Wash	65%

The facile formation of δ-lactones of LTB_4 and 20-hydroxy-LTB_4 can be used in an extractive technique for the isolation of these molecules. Very high yields can be achieved and substantial purification is realized.

ACKNOWLEDGEMENT

This work was supported in part by a grant from the National Institutes of Health (HL25785).

REFERENCES

1. Lewis, R.A., and Austen, K.F. (1981) *Nature* 293, 103-108.
2. Borgeat, P., and Samuelsson, B. (1979) *Proc. Natl. Acad. Sci. USA* 76, 3213-3217.
3. Maclouf, J.A., and Murphy, R.C. (1988) *J. Biol. Chem.* 263, 174-181.
4. Gresele, P., Arnout, J., Coene, M.C., Deckmyn. H., and Vermylen, J. (1986) *Biochem. Biophys. Res. Commun.* 137, 334.
5. Westcott, J., Chang., S., Balazy, M., Stene, D.O., Pradelles, P., Maclouf, J., Voelkel, N.F., and Murphy, R.C. (1986) *Prostaglandins* 32, 857-873.

Presented at the 36th ASMS Conference on Mass Spectrometry and Allied Topics
June 5-10, 1988, San Francisco, CA

EI,CI LC/MS THROUGH FRIT VAPORIZATION SYSTEM

K.Matsuura, K.Otsuka, T.Kobayashi, E.Kubota, Y.Itagaki,
B.D.Musselman and T.Higuchi
MSG JEOL, 3-2-1 Musashino Akishima Tokyo 196 Japan

Introduction

Development of a multipurpose LC/MS interface which enables ionization of various types of compounds has been expected. The authors reported the FRIT-FAB LC/MS interface as a new LC/MS technique (1). And now, a LC/MS interface with a frit which enables EL and CI has been developed. Using this interface, LC/MS analysis of glycerides and polyaromatic hydrocarbons were performed.

Experimental

This interface has improved the FRIT-FAB LC/MS interface ionization chamber heating to a high temperature of over 400℃. A frit was installed at the ionization chamber of the EI/CI/FAB combination ion source. The effluent from the HPLC column is vaporized on the heated frit and ionized by EI and CI. The mobile phase solvent is used as a reagent gas for CI, and also it is possible to add a reagent gas like ammonia. The equipment used was the JMS-DX303 mass spectrometer with a DA5000 data processing system(JEOL). The effluent from the column was precisely split and introduced at 5μl/min to the frit. The column outlet and ion source were connected by a 60μm I.D x 1m fused silica capillary tube. Ionization current was 300μA. The column was a SFPAK ODS-5S25 1.7mm I.D. x 25cm(JEOL) and the flow rate was 150μl/min.

Results and Discussion

1. Polyaromatic hydrocarbons(PAHs)

LC/MS analysis of PAHs is difficult by LC/MS based on CI because of the property of their lower proton affinity. PAHs are easily ionized by EI. Using EI LC/MS with a frit PAHs containing naphthalene, anthracene, pyrene, chrysene, 3,4-benzopyrene, dibenzoanthracene and coronene were analysed. Separation of these compounds was carried out by a ODS column under a gradient elution from 70% acetonitrile in water solution to 100% acetonitrile. Ionization chamber temperature was kept at 350℃. Fig.1 shows a mass chromatogram of M^+ for each compound. Their compounds were separated and detected at the same sensitivity. The chromatogram showed a stable and symmetrical peak shape and it means that the sample is smoothly vaporized and ionized on the frit. Fig.2 shows the EI mass spectra of 3,4-benzopyrene, dibenzoanthracene and coronene giving an intense molecular peak and a doubly charged peak.

2. Trilaurin

The mobile phase used was acetone. In order to enhance soft ionization of the sample, ammonia gas was added to the ionization chamber. The ionization chamber temperature was kept to 320℃. Figure 3 shows a mass chromatogram of $M+NH_4$ for trilaurin and the impurities. Figure 4 shows the mass spectrum of trilaurin. A m/z 656($M+NH_4$) is the base peak and m/z 439 ($M-C_{11}H_{23}CO_2$) shows the existence of fatty acid moieties.
Since minor components showed a similar mass spectral pattern, the constitutive fatty acids were easily identified. Peak 1 was dilaurin, peak 2 decanoyl didodecanoin, and peak 4 was tetradecanoyl didodecanoin.

A non-aqueous mobile phase such as tetrahydrofuran or acetonitrile is used generally in the case of LC runs of fat oil containing triglycerides. The FRIT-CI LC/MS technique is suitable for such analysis.

Conclusions

Using the frit,a LC/MS interface which enables EI and CI has been developed. The interface has a simple structure and gives stable chromatograms, thus allowing molecular weight determination and structural analysis of volatile compounds.

Reference

(1) Y.Ito, T.Takeuchi, D.Ishii, M.Goto and T.Mizuno, J.Chromatogr., 358, 201 (1986)

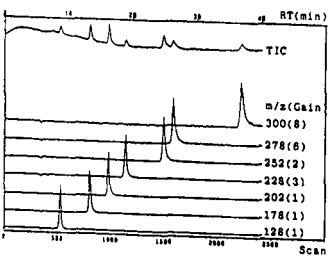

Fig.1 Mass chromatogram of M for PAHs.

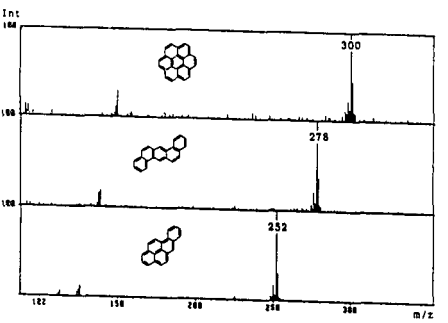

Fig.2 EI mass spectra of 3,4-benzopyrene, dibenzoanthracene and coronene

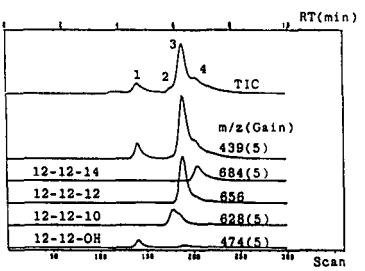

Fig.3 Mass chromatogram of M+NH4 peak for trilaurin and the impurities

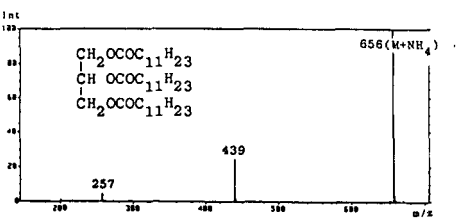

Fig.4 Mass spectrum of trilaurin

Presented at the 36th ASMS Conference on Mass Spectrometry and Allied Topics
June 5-10, 1988, San Francisco, CA

CAPILLARY ZONE ELECTROPHORESIS/MASS SPECTROMETRY OF SULFONATED AZO DYES

Thomas Covey, Sciex Inc., 55 Glencameron Road, Thornhill, Ontario, Canada, L3T 1P2

Edgar Lee and Jack Henion, Equine Drug Testing and Toxicology, Cornell University, 925 Warren Drive, Ithaca, NY 14850

Zone electrophoresis in open tubular capillaries (capillary zone electrophoresis, CZE) has been shown to be a promising technique for the high resolution separation of charged substances in solution (1). A high voltage (10-50 kv) is applied across a length of open tubular capillary (30 cm) and positively charged ions, neutral molecules, and negatively charged species migrate toward the cathode through the combined effects of electromigration, and electrosmotic flow. Typically, both the anode and cathode are immersed in buffer resevoirs with UV or fluorescence detectors constructed around short lengths of the separation capillary. Smith and co-workers (2) demonstrated that the cathode need not be in a buffer but only at a negative potential relative to the anode.

The ion spray interface for liquid chromatography-mass spectrometry (3) is a device which produces gas-phase ions from charged species in solution by the ion evaporation mechanism (4). This combination is ideally suited for the detection of ionic compounds separated in capillary zone electrophoresis (5). It consists of a modified electrospray interface enhanced with pneumatic nebulization for the production of ions at atmospheric pressure. Ion evaporation is an extremely mild form of ionization producing predominately pseudo-molecular ions and multiply charged species in accordance with the number of charged functional groups on the molecule. Because this system operates at atmospheric pressure, the interfaceing is relatively simple to construct and operate with no accommodations required to counteract a vacuum system pulling on the CZE separation capillary. Smith (2) has previously demonstrated CZE/MS with an electrospray interface on an API source.

A Sciex TAGA 6000E MS/MS equipped with an API source was used to sample ions generated from the API interface. The electrophoresis system consisted of a Spellman 0-60 kv power supply and a 100 um i.d. x 100 cm fused-silica capillary. High voltage was applied to the anode through a graphite vessel containing 60/40 methanol/20 millimolar NH_4OAc. Five to ten second hydrodynamic injections were made (5 cm elevation) resulting in injection volumes of 10-20 nanoliters (2.1 nanoliters/second). Figure 1 shows triplicate 10 second hydrodynamic injection at 4 levels. CZE voltages of 15-40 kv with operating currents of 10-50 micro amps were maintained.

The above-described instrumentation was tested for its capability to separate standard sulfonated azo dyes and a solid-liquid extract of the raw sewage influent to the greater Cincinnati sewage treatment plant. Standard dye mixtures demonstrated resolution capability of 100,000 theoretical plates with SIM detection limits in the high femptomole range of material injected on-column. Figure 2 is a selected ion monitoring electropherogram of a mixture of 6 standard azo dyes at 3 picomoles/component. Figure 3 is the full-scan spectrum (30 picomoles) of acid orange 7 (peak 3). Using parent ion screening techniques and monitoring the daughter ion common to sulfonated aromatic rings (m/z 80, SO_3^-), three dyes were observed in the waste water. Full-scan daughter ion spectra were used for confirmation.

References

1. Jorgenson, J.W.; Lukas, K.D., Anal. Chem., 1981, 53, 1298-1302.
2. Olivares, J.A.; Nguyen, N.T.; Yonker, C.R.; Smith, R.D., Anal. Chem., 1987, 59, 1232-1236.
3. Bruins, A.P.; Covey, T.R.; Henion, J.D., Anal. Chem., 1987, 59, 2642-2546.
4. Thomson, B.A.; Iribarne, J.V., J. Chem. Phys., 1979, 71, 4451-4463.
5. Lee, E.D.; Edlund, P.O.; Henion, J.D., Pitts. Conf. and Exp., 1988, 907.
6. Edlund, P.O.; Lee, E.D.; Henion, J.D.; Budde, W.L., Biomed. and Environ. Mass Spectrom., submitted.

Presented at the 36th ASMS Conference on Mass Spectrometry and Allied Topics
June 5-10, 1988, San Francisco, CA

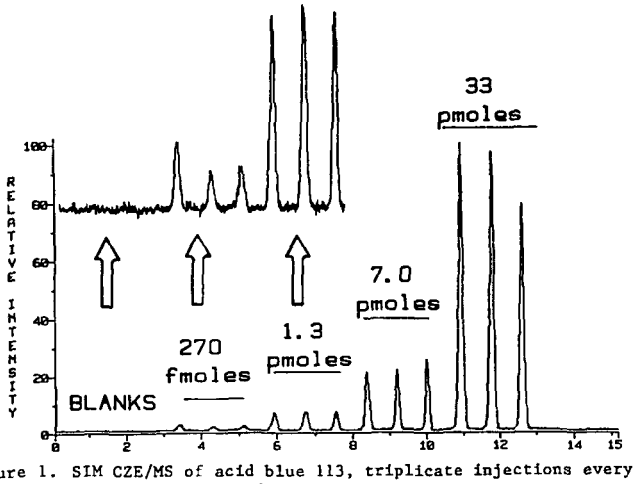

Figure 1. SIM CZE/MS of acid blue 113, triplicate injections every minute. Twenty nanoliters injected

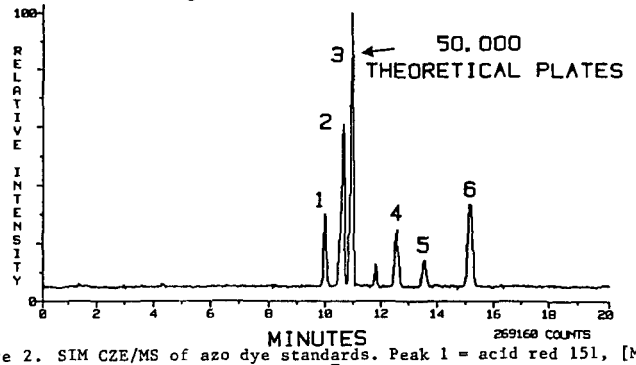

Figure 2. SIM CZE/MS of azo dye standards. Peak 1 = acid red 151, $[M-H]^-$ = 431; peak 2 = acid red 88, $[M-H]^-$ = 377; peak 3 = acid orange 7, $[M-H]^-$ = 327; peak 4 = acid blue 113, $[M-2H]^{2-}$ = 317; peak 5 = acid black 1, $[M-2H]^{2-}$ = 285; peak 6 = acid red 14, $[M-2H]^{2-}$ = 228.

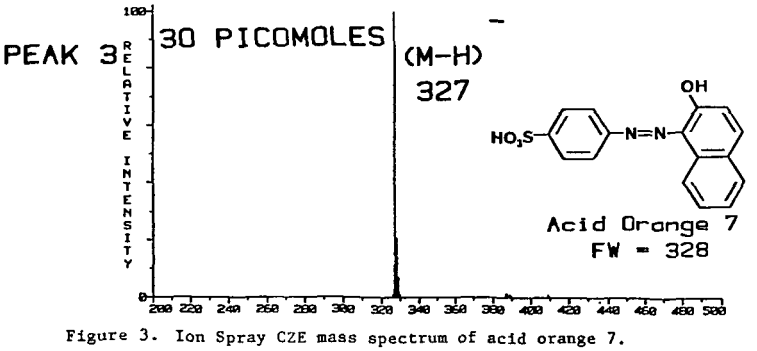

Figure 3. Ion Spray CZE mass spectrum of acid orange 7.

Presented at the 36th ASMS Conference on Mass Spectrometry and Allied Topics
June 5-10, 1988, San Francisco, CA

ANALYSIS OF SULFONATED AZO DYES USING SELECTED ION MONITORING AND LIQUID CHROMATOGRAPHY/THERMOSPRAY IONIZATION MASS SPECTROMETRY

MATTHEW A. MCLEAN[a], DONALD A. FLORY[a], MARVIN L. VESTAL[b], ROYAL B. FREAS[a]
[a] DEPARTMENT OF CHEMISTRY, UNIVERSITY OF HOUSTON, TX 77204-5641
[b] VESTEC CORPORATION, 9299 KIRBY DR., HOUSTON, TX 77054

INTRODUCTION: There has been increased concern in recent years over the release of azo dyes and aromatic amines into the environment. This concern arises from the toxic nature of these compounds and their ability to travel large distances in ground and surface water without being degraded. The Environmental Protection Agency has listed a number of azo dyes, particularly sulfonated azo dyes, on the Appendix VIII Hazardous Constituent List. A method to identify and measure these compounds has not yet been developed. Methods involving chromatographic separations and mass spectrometric detection are attractive because species can be tentatively identified by chromatographic retention time and in many cases confirmed using mass spectral data. Several mass spectrometric techniques including FAB, electrospray/API and thermospray are compatible with on-line liquid chromatography/mass spectrometry and have shown promise in analyzing polysulfonated azo dyes.[1-3]

Thermospray has proven useful in analyzing nonsulfonated dyes using tandem mass spectrometry for detection and confirmation.[4] However, sulfonated azo dyes have been more difficult to analyze using this technique, presumably due to their lack of volatility. Some instrumental parameters have been changed to increase the sensitivity of thermospray with regard to sulfonated azo dye analysis. These instrumental changes include: (a) restriction of the thermospray vaporizer exit orifice which is done to increase the initial charge per unit area on the thermospray droplet and (b) addition of a needle-tip repeller to a conventional thermospray ion source to increase ion extraction efficiency. In addition to these modifications, a liquid chromatographic procedure was developed that is highly efficient in separating the sulfonated dyes and is compatible with thermospray mass spectral detection.

EXPERIMENTAL: A Hewlett-Packard Model 5988A mass spectrometer was used and operated in the negative-ion mode. The mass spectrometer was coupled to a Scientific Services Inc. high-performance liquid chromatography (HPLC) gradient system via a Vestec Thermospray™ liquid chromatography/-mass spectrometry (LC/MS) interface. The Vestec ion source was modified by machining away the step restriction in the ion volume thus making a more open region around the sampling cone. A needle-tip repeller was added opposite the sampling cone to enhance ion extraction efficiency from the ion source. The thermospray vaporizer was modified so that the orifice size could be varied using different sizes of fused silica tubing held in place by a graphite/vespel ferrule and a screw-on cap. All chromatograms were obtained using selected ion monitoring (SIM) at a flow rate of 1.2 mL/min with a exit orifice of 100 microns. The HPLC procedure consisted of the following linear gradient elution:

TIME(min)	%A (0.01M NH_4OAc)	%B (35/65 ACN/H_2O)
0	100	0
1	100	0
4	0	100

RESULTS: An LC/MS procedure was developed to separate and detect sulfonated azo dyes after instrumental parameters were optimized for sulfonated azo dye detection. Restriction of the thermospray vaporizer and addition of a repeller in the ion source are necessary to obtain mass spectra of disulfonated azo dyes. A number of important problems were encountered in developing a suitable LC/MS procedure for sulfonated azo dyes. Foremost was developing an LC procedure that would separate sulfonated azo dyes while still being compatible with thermospray detection. Previous results indicated that ammonium acetate concentrations higher than 0.01M were detrimental to sulfonated azo dye detection due to neutralization reactions occurring in the ion source.[3] As a result, a reverse-phase LC procedure was developed using a low concentration of ammonium acetate as an ion-pairing agent.

Full-scan mass spectra of selected disulfonated azo dyes in a mobile phase of 30:28:42 0.01M $NH_4OAc_{(aq)}$/acetonitrile/water are shown in Figs. 1 to 3. Characteristic ions were obtained in all spectra. These diagnostic ions include $[M-2Na]^{2-}$, $[M-2Na+H]^-$, and $[M-Na]^-$ ions. In some mass spectra, other diagnostic ions such as $[2M-3Na]^{3-}$ and $[2M-3Na+H]^{2-}$ were observed.

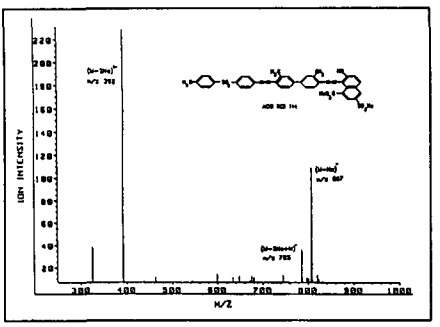

Figure 1. Full scan thermospray mass spectrum of Acid Red 114.

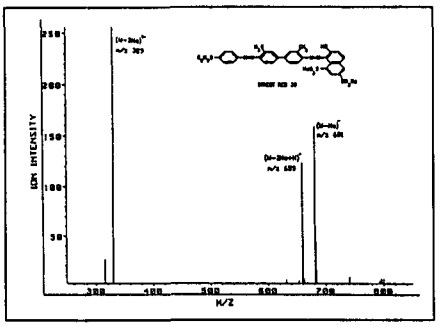

Figure 2. Full scan thermospray mass spectrum of Direct Red 39.

Molecular weight information is therefore available and in many cases can be used to identify a dye or to narrow down the possibilities for an unknown. Further mass spectral fragmentation and matching the retention time of a standard are needed for confirmation. An SIM trace of five dyes is shown in Fig. 4. All dyes were present in concentrations of about 500 ng assuming 50% purity. Only the $[M-2Na+H]^-$ ion was monitored for each dye. Selected ion chromatograms show that other characteristic ions such as $[M-2Na]^{2-}$ and $[M-Na]^-$ ions can also be used to confirm the presence of a dye in a particular sample even though their abundance is generally less than that of the $[M-2Na+H]^-$ ion.

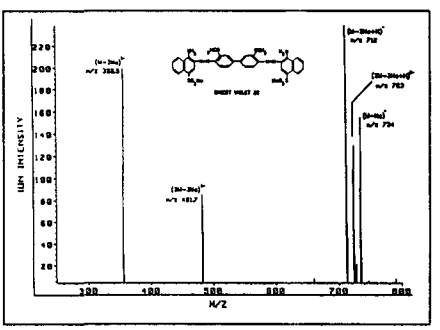

Figure 3. Full scan thermospray mass spectrum of Direct Violet 32.

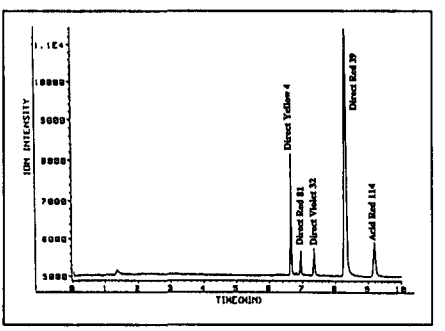

Figure 4. Selected ion chromatogram for a mixture of five disulfonated azo dyes monitoring the $[M-2Na+H]^-$ ion for each dye.

CONCLUSIONS: Modifications to a thermospray ion source and vaporizer are needed to obtain mass spectra for sulfonated azo dyes. These modifications include restricting the exit orifice of the thermospray vaporizer and the addition of a needle repeller in the thermospray ion source. A linear HPLC gradient of 100% 0.01M aqueous ammonium acetate to 100% 35:65 mixture of acetonitrile/water can be used to efficiently separate a mixture of disulfonated azo dyes using SIM detection. Mass spectra obtained under these conditions give pseudomolecular ions which can be used to determine the molecular weight of an unknown dye species.

REFERENCES

1. Monaghan, J.J.; Barber, M.; Bordoli, R.S.; Sedgwick, R.D.; Tyler, A.N. *Org. Mass Spectrom.* **1983**, *18*, 75.
2. Henion, J.; Bruins, A. presented at the 34th Annual Conference on Mass Spectrometry and Allied Topics, Cinncinati, OH, 1986.
3. Flory, D.A.; McLean, M.A.; Vestal, M.L.; Betowski, L.D. *Rapid Comm. Mass Spectrom.* **1987**, *1*, 59.
4. Ballard, J.M.; Betowski, L.D. *Org. Mass Spectrom.* **1986**, *21*, 575.

Presented at the 36th ASMS Conference on Mass Spectrometry and Allied Topics
June 5-10, 1988, San Francisco. CA

IDENTIFICATION OF CARBONYL COMPOUNDS IN TOBACCO SMOKE BY LIQUID CHROMATOGRAPHY/MASS SPECTROMETRY

Henry L. Chung, Michael F. Borgerding, and Rebakah S. Dunn

R. J. Reynolds Tobacco Company, Bowman Gray Technical Center
Winston-Salem, NC 27102

An improved LC method for the determination of low molecular weight carbonyl compounds in tobacco smoke has been developed. A variety of reagents have been used to derivatize carbonyl compounds for subsequent chromatographic analyses. The reagent chosen for this work was 2-diphenylacetyl-1,3-indandione-1-hydrazone which reacts with carbonyl compounds to form an azine derivative and water. This method was based on work reported by Swarin and Lipari (1) which indicated the following advantages when using the hydrazone reagent: (a) The reagent is carbonyl specific; (b) Derivatives are formed rapidly and quantitatively with a minimum of sample preparation; (c) The derivatives fluoresce enabling detection at ppb levels; and (d) Accurate and precise quantitation is possible with liquid chromatography.

Although the hydrazone reagent appears ideal based on literature reports, additional chracterization was necessary before a useful, valid method could be developed. An on-line liquid chromatographic/mass spectrometric (LC/MS) system with a direct liquid introduction (DLI) LC/MS interface was used to identify the derivatized carbonyl compounds.

Carbonyl compounds in the smoke samples were collected and reacted with the derivatizing reagent under catalytic condition. A reversed-phasé C-18 column with an acetonitrile/water gradient as mobile phase at 1.2 ml/min was used for separation. All compounds of interest were sufficiently resolved. Positive chemical ionization mass spectra were obtained with protonated molecular ions for all the carbonyl-azine derivatives.

Fifteen carbonyl compounds were identified in mainstream tobacco smoke. Of interest is the identification of the existence of two isomers of acrolein-azines which have not been reported in the literature. These two isomers of acrolein-azine in the standard and the tobacco smoke were observed at m/z 393 by using the selected ion monitoring.

Reference

1. F. Lipari, and S. J. Swarin, J. Liq. Chrom., 6, 425-444, 1983.

Presented at the 36th ASMS Conference on Mass Spectrometry and Allied Topics
June 5-10, 1988, San Francisco, CA

DLI- AND OTLC-MS ANALYSIS OF METRIBUZIN AND ITS METABOLITES

B.H. Escoffier, C.E. Parker, J.S.M. deWit, T.C. Mester, and K.B. Tomer

Laboratory of Molecular Biophysics, National Institute of Environmental Health Sciences, Research Triangle Park, NC 27709

Metribuzin (MZN) is a 1,2,4-triazine herbicide which has been widely used on foodcrops, including soybeans, tomatoes, and sugarcane. Differences in crop tolerance to this herbicide has led to studies of its metabolism. Three metabolites are presently known: DA, deaminated metribuzin; DK, diketo metribuzin and DADK, deaminated diketo metribuzin.

The objective of this study was to compare Open Tubular Liquid Chromatography (OTLC) and Direct Liquid Introduction (DLI) LC/MS for the analysis of metribuzin and its metabolites in soybean plant extracts, and to evaluate LC/MS as a confirmatory technique when the presence of these metabolites is indicated by other less-selective detectors.

All four of the metabolites could be separated by DLI; three could be separated by OTLC on the available column. The fourth compound was of very low sensitivity, however, which would limit its detectability in either LC/MS mode. On column detection limits in the negative ion mode for MZN, DA, and DK were 10-30 pg in OTLC and 2-5 ng by DLI.

The positive and negative ion spectra obtained by OTLC/MS, which uses a heated interface were essentially identical to those obtained by DLI, where the interface is cooled. Since no additional fragmentation was observed in OTLC/MS, there is no evidence of thermal degradation of these compounds. For on-line injection of standards, OTLC had a sensitivity advantage of ~200. This can be partly explained by the absence of a solvent stream split in OTLC (<20% of the injected sample enters the source in DLI), and partly by the greatly reduced peak width in OTLC, leading to a higher mass flow per scan. Also, in DLI some of the sample may be lost with the solvent as the source pressure is adjusted by moving the probe inside the desolvation chamber.

The original OTLC injection system wasted too much sample (~200 ul was needed in order to inject 1 nl). A "dip" technique, analagous to on-column injection in capillary GC/MS, was developed in which the vacuum in the mass spectrometer is used to suck a known small volume (~1 nl) into the OTLC column. This low injection volume of OTLC (~1 nl) means that LC/MS analysis can be performed on very small sample volumes. This small injection volume, however, severely limits the amount of analyte that can be delivered to the source. Concentrating the sample prior to injection helps somewhat, but may lead to analyte solubility problems, and, since the matrix components are concentrated as well, may lead to plugging of the capillary column. A better LC/MS system may involve the use of packed capillary LC columns, which are presently under development.

Sensitivities of both OTLC and DLI LC/MS were sufficient to allow detection in extracts of soybean plants treated with 0.04 ppm metribuzin in the culture medium. Due to the limited injection volume of OTLC, however, the plant extract had to be concentrated by a factor of almost 100 compared to DLI before the metabolites could be detected. One would expect that the sample preconcentration and the relative sensitivity advantage of OTLC over DLI would compensate for the small injection volume of OTLC and result in similar responses between the two techniques for the plant extract analyses. DLI, however, gave a much better response than did OTLC. The plant matrix apparently has an extremely deleterious effect on the performance of the OTLC/MS system, and some of the analyte may have been lost during the extensive sample concentration process. Matrix effects in conventional HPLC have been observed in previous studies on these metabolites (1,2). Matrix effects are reduced in DLI LC/MS both by the inherent sample loading

characteristics of the larger column and by the injection system developed for on-line sample concentration and cleanup. This injection system combines the principles of "back cutting" (3) with column switching (3,4). An extra LC pump is used so that flow is not interrupted to the DLI probe during sample concentration and cleanup.

The major metabolite detected in both diploid (MZN-sensitive) and tetraploid (MZN-tolerant) soybean shoots was DA. A trace of DK was also detected. This pattern of metabolites was confirmed by radiochemical detection, which also indicated the presence of additional later-eluting metabolites. No consistent differences in the ratio of DA and MZN between the diploid and tetraploid soybeans could be detected by DLI, mainly due to the lack of suitable internal standards for quantitation. The major differences appeared to be in the late-eluting metabolites, detected by radiochemical detection. These metabolites did not show masses characteristic of the previously-identified metabolites. The structure of these metabolites have not been determined and are the subject of continuing investigation.

1. C.E. Parker, G. Degen, E.O. Abusteit, and F.T. Corbin, J. Liquid Chromatog., 6(4), 725(1983).
2. C.E. Parker, A.V. Geeson, D.E. Games, E.D. Ramsey, E.O. Abusteit, F.T. Corbin, and K.B. Tomer, J. Chromatog., 438, 359(1988).
3. R.C. Ludwig and R. Eksteen, LC-GC, 6(3) 250(1988).
4. S.R. Bakalyar and B. Spruce, Rheodyne Technical Note 8, Feb. 1987.

SEPARATION OF STANDARD MIXTURE
DLI, MID-NCI

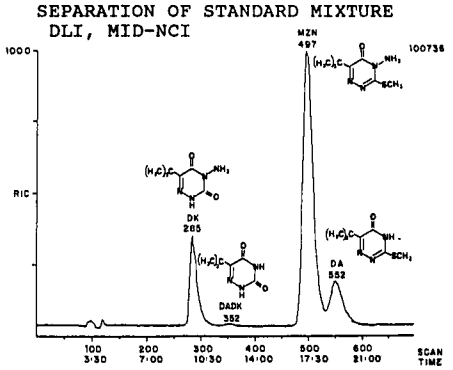

SEPARATION OF STANDARD MIXTURE
OTLC, MID-NCI

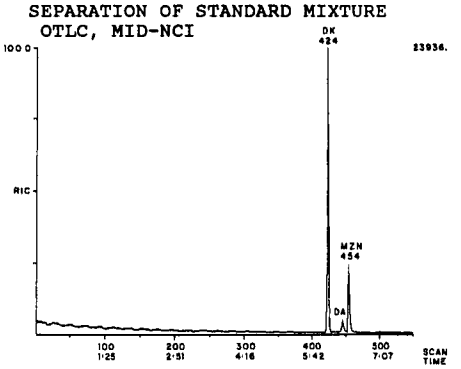

SOYBEAN SHOOT EXTRACT
DLI, MID-NCI

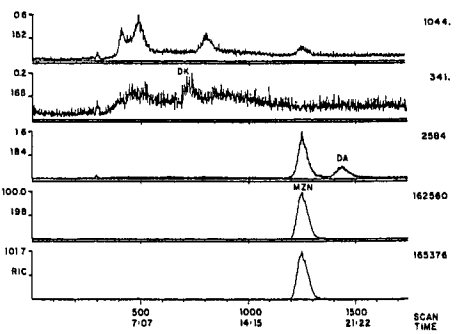

SOYBEAN SHOOT EXTRACT
OTLC, MID-NCI

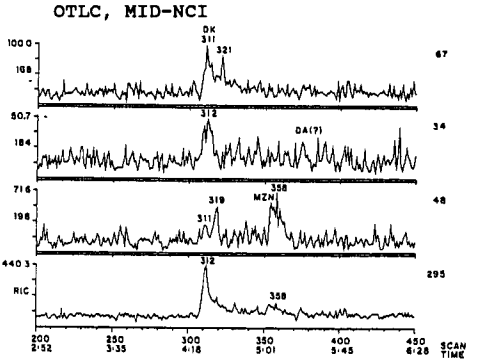

Presented at the 36th ASMS Conference on Mass Spectrometry and Allied Topics
June 5-10, 1988, San Francisco, CA

POSITIVE- AND NEGATIVE- ION CHEMICAL IONIZATION MASS SPECTROMETRY OF ALDICARB AND ITS DERIVATIVES BY PARTICLE BEAM HPLC/MS

Bert C. Lynn, Jr., G.D. Marbury, J.R. Tuschall, Jr., Northrop Services, Inc., Research Triangle Park, NC 27709
R.C. Willoughby, Extrel Corporation, Pittsburgh, PA 15238
E.J. Kantor, U.S. Environmental Protection Agency, EMSL/QAMDD, Las Vegas, NV 89193

The oxime carbamate pesticide, aldicarb and its oxygenated derivatives, aldicarb sulfoxide and aldicarb sulfone present a diffcult problem for the analytical chemist due to their relative instability of these compounds. To overcome these analytical problems, an HPLC/MS method was evaluated using the Thermabeam^R interface. Using flow injections, these aldicarb compounds were found to exhibit classic EI spectra, free from solvent interferences. However, the EI spectra, as with other sample introduction means, were highly fragmented, and there was very little structural information obtained for the three compounds. Therefore, chemical ionization (CI) was explored using a variety of reagent gases. With methane as a reagent gas in positive CI (PCI), the aldicarb compounds produced protonated molecular ions and ions resulting from the loss of the N-methylcarbamic acid group. For example, aldicarb showed $[M+H]^+$ (m/z 191), $C_5H_{10}SN^+$ (m/z 116), and $C_4H_7NO^+$ (m/z 85). Under negative CI (NCI), these compounds were found to produce unusual adduct ions. For example, aldicarb produced an anion at m/z 74 in the form of an N-methylcarbamic acid anion and an ion at m/z 264 (Figure 1) The anion at m/z 264 appears to arise from a "self CI" process in which a N-methylcarbamic acid anion reacts with an aldicarb molecule to form this adduct ion. To confirm that this process was not an artifact of the particle beam HPLC/MS interface and establish the parameters involved in this process, the NCI of aldicarb was investigated using solid probe and desorption CI (DCI) sample introduction.

The adduct formation was found to be concentration dependent appearing at levels greater than 0.1 ug and increasing through 20 ug. The formation of adduct ions was also dependent on the source pressure and type of reagent gas. Isobutane was found to produce the highest relative percentage of adduct to N-methylcarbamic acid anions between 0.25 and 0.50 torr, indicated source pressure. Electron energy had little or no effect on the ratio of m/z 264 to m/z 74, discounting classic CI processes. Based on these data, we hypothesize that the mechanism of this reaction involves aldicarb's ability to produce a flux of reactive n-methylcarbamic acid anions; these reactive anions interact with aldicarb molecules and are stabilized by energy transfer to reagent gas molecules resulting in the formation of the m/z 264 ion observed under NCI conditions.

To develop a selective reagent anion for aldicarb and its derivatives, experiments were conducted to exploit the process of adduct formation. Because the formation of N-methylcarbamic acid anions were observed from oxime carbamates, we investigated compounds that would , upon ionization, produce stable cationic leaving groups and carbamic acid anions. Benzyl carbamate formed a tropylium cation and a carbamic acid anion under CI conditions using methane as a reagent gas. Co-ionization of aldicarb and benzyl carbamate produced ions which could only arise from "cross CI" reactions (Figure 2). The ion at m/z 250 resulted from combination of a carbamic acid anion and an aldicarb molecule.

We are continuing experiments in the area of post column introduction of benzyl carbamate into the HPLC mobile phase to produce a steady state flux of carbamic acid anions for selective reaction with aldicarb and its derivatives.

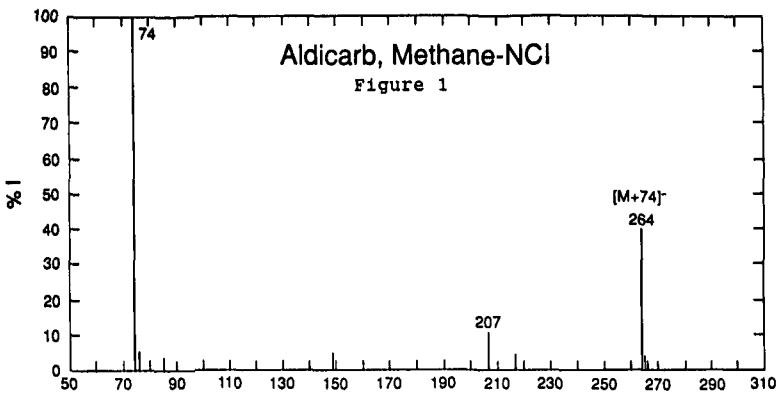

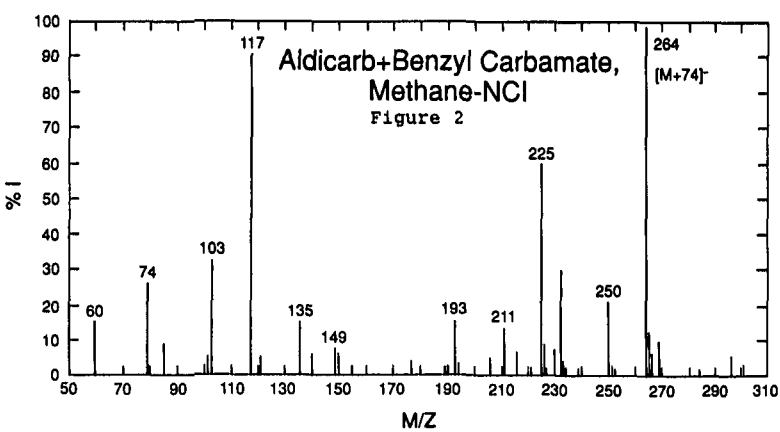

Presented at the 36th ASMS Conference on Mass Spectrometry and Allied Topics
June 5-10, 1988, San Francisco, CA

A COMPARISON BETWEEN POSITIVE AND NEGATIVE ION MODES IN THERMOSPRAY LIQUID CHROMATOGRAPHY-MASS SPECTROMETRY FOR THE DETERMINATION OF CHLOROPHENOLS AND HERBICIDES.

D. Barceló
Environmental Chemistry Dept. CID-CSIC
c/ Jorge Girona Salgado, 18-26. 08034 Barcelona (Spain)

INTRODUCTION

The thermospray (TSP) technique is becoming the most popular method for interfacing a liquid chromatography (LC) column with a mass spectrometer (MS) and typically involves the use of reversed-phase columns and volatile buffers such as ammonium acetate. TSP LC-MS has been employed for analyzing a large variety of pesticides and herbicides such as organophosphorus and pyrethroid insecticides and urea, triazine and chlorinated phenoxy acid herbicides (1-4). As the PI mode is the most popular way of operating TSP LC-MS, it is of interest to devote more attention to NI formation, specially for compounds of stronger acidity than acetic acid in the gas phase (1458 $KJ.mol^{-1}$). The ion-forming reactions observed in NI, TSP LC-MS are of a similar type to those in NICI-MS, with mechanims of proton abstraction $[M-H]^-$, resonance capture, dissociative capture and ion-molecule reactions (2,3).
In order to demonstrate the utility of NI, TSP LC-MS and examine the formation of adducts, 2,4-dichlorophenol, 2,4,5-trichlorophenol, pentachlorophenol, Linuron and Cyanazine were chosen as model compounds. The results are compared with those obtained using PI. Attention will be paid to the use of ammonium formate as ionizing additive in thermospray operation for characterizing the triazine herbicides Simazine, Atrazine and Propazine.

RESULTS AND DISCUSSION

For the first time, the NI, TSP-MS spectra of 2,4-dichlorophenol, 2,4,5-trichlorophenol, pentachlorophenol, Linuron and Cyanazine are reported. The effectiveness of NI versus PI in TSP LC-MS is demonstrated for compounds which are gaseous acids stronger than acetic acid, such as the chlorophenols, which are not even detected in the PI mode. For compounds which give higher signals in the PI mode than in NI mode (about 1 order of magnitude) such as Linuron and Cyanazine, the use of the NI mode offers valuable complementary information for the MS identification of these analytes Concerning the use of ammonium formate in the LC eluent it has been proved that this was an adequate buffer choice for analyzing triazine herbicides with slightly better sensitivities than when ammonium acetate was employed The generation of ammonium and formate or acetate ions as reactant ions for a gas-phase chemical process should be considered with different adduct ions formation in each case.

ACKNOWLEDGEMENTS

The author is grateful to the Consejo Superior de Investigaciones Científicas (C.S.I.C.) and to the Association Gaspar de Portolá for financial support of this project.

REFERENCES

1. K Levsen, Org Mass Spectrom , 23 (1988) 406
2. R. D. Voyksner in Applications of New Mass Spectrometry Techniques in Pesticide Chemistry, J D. Rosen, ed; John Wiley, New York, Chap.11 (1987).
3. D Barceló, LC-GC, 6 (1988) 324.
4. D. Barceló, Chromatographia, 25 (1988) 295.

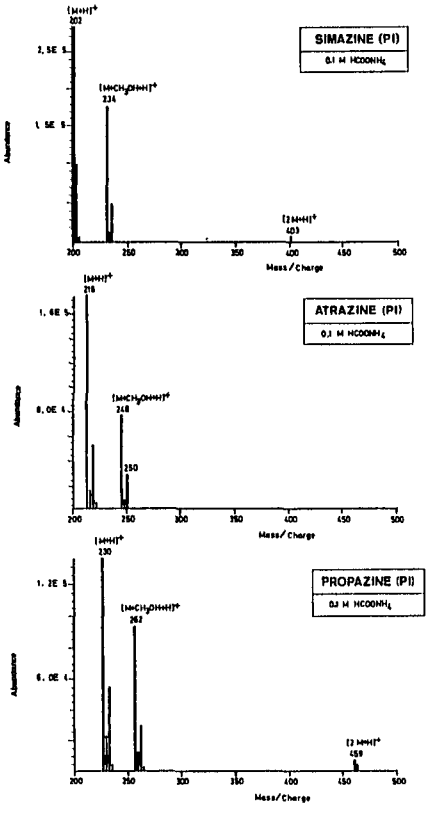

Figure 1. Direct flow injection TSP PI MS spectra of Simazine, Atrazine and Propazine Carrier stream methanol water (50 50) + 0 1M ammonium formate Flow rate 1 2 ml/min Injection 300 ng

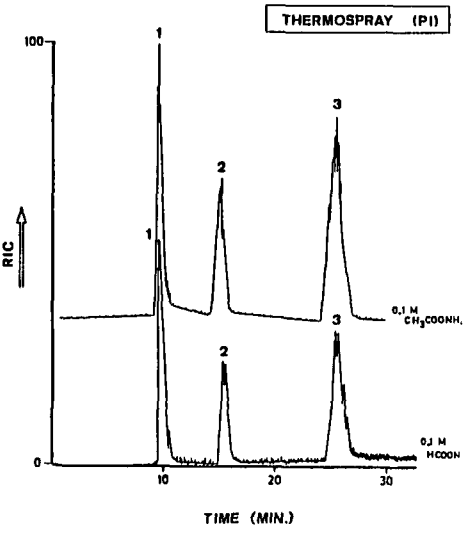

Figure 2. TSP PI LC-MS using SIM of a sediment sample spiked with 5 ppm of (1) Simazine, (2) Atrazine and (3) Propazine using an LC eluent of methanol water (50 50) + 0 1M ammonium formate or 0 1M ammonium acetate Flow rate 1 2 ml/min Injection 100 ng each compound

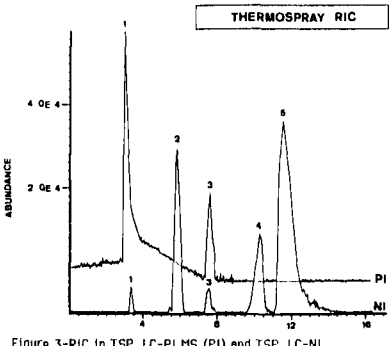

Figure 3-RIC in TSP, LC-PI MS (PI) and TSP, LC-NI MS (NI) for mixture (1) Cyanazine, (2) *2,4-dichlorophenol*, (3) *Linuron*, (4) 2,4,5-trichlorophenol and (5) pentachlorophenol

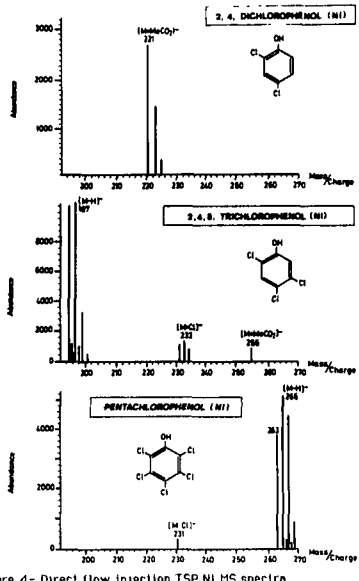

Figure 4- Direct flow injection TSP NI MS spectra of 2,4-dichlorophenol, 2,4,5-trichlorophenol and *pentachlorophenol Carrier stream methanol water* (70 30) + 0 1M ammonium acetate + 0 2% acetic acid Flow rate 1 2 mL min^{-1} Injection 200 ng

Presented at the 36th ASMS Conference on Mass Spectrometry and Allied Topics
June 5-10, 1988, San Francisco, CA

THE ROLE OF MASS SPECTROMETRY COMBINED WITH REVERSED PHASE HPLC IN THE IDENTIFICATION OF AN UNUSUAL SHELLFISH TOXIN#

R.K. Boyd, L.R. Hogge*, W.D. Jamieson, J.W. McLaren**, M.A. Quilliam, P.G. Sim, P. Thibault*** and J.L.C. Wright

National Research Council of Canada, 1411 Oxford Street, Halifax, Nova Scotia, B3H 3Z1 (* 110 Gymnasium Road, Saskatoon, Saskatchewan, S7N 0W9; ** Montreal Road, Ottawa, Ontario, K1A 0R6; *** 6100 Royalmount Ave., Montreal, Quebec, H4P 2R2), CANADA.

In November, 1987, an outbreak of shellfish poisoning occurred which was traced to cultured blue mussels (Mytilus edulis) from a very localized area of eastern Prince Edward Island. Symptoms induced in affected humans and in test mice used in the AOAC standard bioassay for paralytic shellfish toxins (1) indicated an excitatory neurotoxin but were unlike those induced by known toxins. Initially, several laboratories participated in screening contaminated and control mussels for known anthropogenic xenobiotics (methods such as ICP/MS for metals, GC/MS for organics) without success. By December 13, bioassays showed the toxin(s) not to have been lipophilic and our approach changed to concerted and parallel extraction, fractionation and characterization of contaminated and control mussels by quantitatively comparable bioassays, and by chemical assays. A team of more than 40, chemists as well as biologists and experts from Fisheries and Oceans Canada, cooperated in this work based at our Atlantic Research Laboratory in Halifax. The main chemical methods used were reversed-phase HPLC with UV diode-array detection (DAD), high voltage paper electrophoresis, micro-FTIR spectroscopy of thin dried films, and FAB-MS (VG Analytical ZAB-EQ) using a glycerol/water/HCl matrix.

As the toxicity was progressively concentrated, toxic extracts were marked by a peak in the HPLC/DAD chromatogram which gave a UV spectrum with a 242 nm maximum, while FAB positive mass spectra showed an increasingly characteristic ion at m/z 312 (m/z 310 in negative mode) suggesting a molecular mass of 311. The mass of the m/z 312 species was measured to be within 5 ppm of 312.146. Tandem mass spectrometry on ions of m/z 312 showed two and possibly three successive losses of 46 Da, attributable to HCO_2H, a characteristic (2,3) of protonated amino acids. Tentative identification of the toxin as an amino acid was supported by an intense fragment (CID spectrum) of m/z 312 at m/z 74, probably (2,3) due to $HCO_2CH{:}NH_2^+$. From the accurate mass and the evidence of at least four oxygen atoms, the molecular formula was taken to be $C_{15}H_{21}NO_6$.

Linked searches of chemical and toxicological databases suggested the unknown toxin was probably domoic acid 1, previously described (4,5) as occurring in Chondria armata, a marine alga native to Japan. Though mass spectra of domoic acid had not been reported, the data we had recorded were consistent with its structure, and the formula agreed as did other chemical characteristics such as the UV spectrum (4,5) shown in Fig. 1 (peak E). Later preparative HPLC isolated enough adequately pure toxin for NMR (proton, carbon-13) and FTIR spectra to confirm the toxin structure as 1. That these confirmatory results were obtained on December 16, and confirmed independently by Health and Welfare Canada the following day, shows the dedication, skill and stamina of the many who were involved. This work will be described fully elsewhere (6). Though the aquaculture industry must be interested in this new toxin, it will also be important in neurobiological research as it is the most potent known substrate for the kainate receptors of the central nervous system (7).

Further work on the mass spectrometry of 1 has shown: a positive FAB-MS ion at m/z 314 is due to beam-induced transformation of 1; tandem

NRCC No. 29014

mass spectrometry (Fig. 2) will be useful in discriminating between several of the isomers of 1 found at low levels in extracts of mussel tissue; thermospray-MS (Finnigan/Vestec) or plasmaspray-MS (VG ZAB-HF) of 1 yield few ions; continuous-flow HPLC-FAB-MS determinations of 1 should have a detection limit of 30 ng (full scan, lower in selected-ion mode; compare with 3 ng with full UV spectrum by HPLC-DAD, 0.3 ng for detection at 242 nm); GC/MS determinations should be feasible following conversion of 1 to the tert-butyldimethylsilyl (8) derivative. Relevant analytical procedures have been communicated to several laboratories in Canada, the U.S.A. and Europe who have been provided with an interim instrument calibration solution and reference samples, pending availability of certified reference materials.

(1) "Official Methods of Analysis", Association of Official Analytical Chemists, Arlington, VA, 18.086-18.092 (1984); W.N. Adams and J.J. Miescier, J. Assoc. Off. Anal. Chem. 63 1336 (1980).
(2) G.W.A. Milne et al., J. Am. Chem. Soc. 92 5170 (1970).
(3) C.W. Tsang and A.G. Harrison, J. Am. Chem. Soc. 98 1301 (1976).
(4) T. Takemoto and K. Daigo, Chem. Pharm. Bull. 6 578 (1958).
(5) Y. Ohfune and M. Tomita, J. Am. Chem. Soc. 104 3511 (1982).
(6) J.L.C. Wright et al., in preparation.
(7) J.T. Slevin et al., Brain Research 265 169 (1983).
(8) M.A. Quilliam and J.B. Westmore, Anal. Chem. 50 59 (1978).

FIGURE 1 RPLC/DAD OF TOXIC MUSSEL EXTRACT.

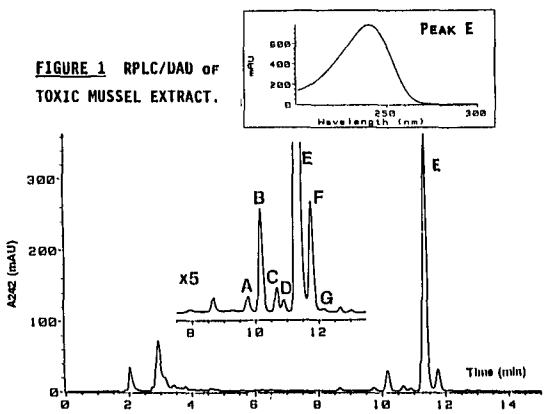

FIGURE 2

FRAGMENT ION SPECTRUM OF MH^+, DOMOIC ACID

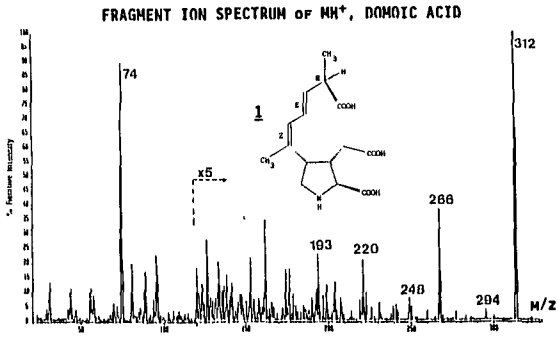

Presented at the 36th ASMS Conference on Mass Spectrometry and Allied Topics
June 5-10, 1988, San Francisco, CA

RESIDUE ANALYSIS OF FOSAMINE AMMONIUM IN SOIL BY LIQUID CHROMATOGRAPHY/MASS SPECTROMETRY

L. M. Shalaby and J. E. Eble
E. I. du Pont de Nemours and Company, Inc.
Wilmington, DE

INTRODUCTION

In the area of agricultural products, crops and soils are analyzed for parent and metabolites. These analyses are necessary to understand the manner in which the compound behaves in the environment. These levels are normally low. The highest acceptable limit of quantitation is generally 0.05 parts per million (ppm). Due to the low levels in difficult matrices, we look for high selectivity and high sensitivity in an analytical technique. We found the thermospray LC/MS to offer both.

Krenite® Brush Control Agent is a product which is applied as a foliar spray for control and/or growth suppression of many woody species. A field dissipation study is one of the studies run to monitor the behavior of the compound in soil. In this study, the dissipation of the active ingredient, fosamine ammonium, and the formation and dissipation of the major degradation product must be monitored under actual field conditions down to the 0.05 ppm level.

Both of these compounds are difficult to analyze in a soil matrix. The molecules are highly ionic and are not extracted into non-aqueous media. Also, due to their ionic nature, gas chromatography cannot be used. Numerous attempts at derivitization of fosamine ammonium to improve detection or allow the use of gas chromatography have led to more than one product and/or irreproducible results.

The compounds can be quantified with an ion exchange chromatography method. However, since the molecules have relatively low absorptivity, the compounds cannot be quantified down to the necessary 0.05 ppm limit in soil. We are able to quantify fosamine ammonium using an ion exchange liquid chromatographic method in tandem with thermospray mass spectroscopy.

STRUCTURE

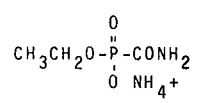

Fosamine Ammonium
(mol. wt. = 170.1)

METHODOLOGY

The samples are received frozen and are maintained frozen unless being prepared or analyzed. The preprocessing is done as quickly as possible to minimize degradation of fosamine ammonium. The samples are prepared by placing the entire contents of a sample into a bag which is pounded with a wooden mallet until the contents are broken into small pieces. The bag is shaken and the entire sample, except for stones and plant matter, is passed through a mesh sieve by rubbing the thawing soil against the mesh.

A representative amount of the wet sample is immediately weighed into a large centrifuge tube. The first portion of extracting solvent is added as described below. At the same time moisture content of the soil is determined so that calculations made be done on a dry-weight basis.

The sample is extracted on a wrist action shaker with a mixture of ammonium carbonate and methanol. After centrifugation, the supernatant is passed through a C18 solid phase extraction (SPE) cartridge into a round-bottom flask. The combined extracts are concentrated on a rotovap and passed through a C18 SPE cartridge connected to a SAX SPE cartridge. Any residual fosamine ammonium remaining on the SAX cartridge is eluted by rinsing the cartridge with 0.2 M ammonium acetate. The combined rinses are evaporated to dryness. The dry tubes have been held in the refrigerator for three weeks with no sign of degradation.

The chromatographic system is an anion exchange system using a 25-cm Zorbax® SAX analytical column with a mobile phase of 0.05 M ammonium acetate plus glacial acetic acid to a pH of about 6.5. The HPLC pumps used were Spectroflow 400 models from ABI Analytical, Kratos Division. The thermospray LC/MS unit is the Vestec 201 form Vestec Corporation.

After the system is equilibrated an injection is made with the effluent from the column being directed to waste. The effluent remains directed to waste until 1 to 2 minutes before the elution of fosamine ammonium. The retention time of fosamine ammonium is about 13 to 15 minutes. When the elapsed time is within about two minutes of the elution of fosamine ammonium, the eluent is directed into the thermospray interface and the tip temperature brought to the predetermined optimal value. The timing is kept as consistent as possible from injection to injection. This procedure minimizes source contamination and eliminates matrix effects. Data is acquired by SIM at m/e of 171.

RESULTS

Investigations on the optimum stem temperature indicate a plateau of less than 7°C before reaching the take-off temperature. Recoveries were run on spiked control soil from two separate sites over a range of 0.05 ppm to 1.0 ppm. The average recovery was 84% +/- 19% with a limit of quantitation of 0.05 ppm. The use of SIM allowed us to obtain selectivity and sensitivity that we were unable to accomplish with any other technique.

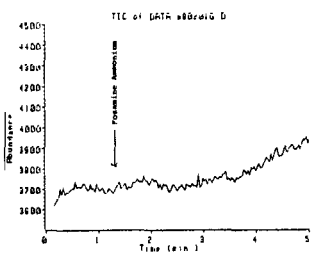

Chromatogram of a Soil Control Sample

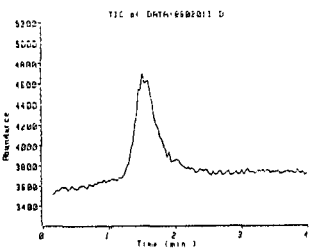

Chromatogram of a Recovery of Fosamine Ammonium at 0.050 ppm to Soil

Presented at the 36th ASMS Conference on Mass Spectrometry and Allied Topics
June 5-10, 1988, San Francisco, CA

A Comparative Evaluation of Liquid Chromatography/Thermospray Mass Spectrometry and Immunochemical Assay for Paraquat and Monoquat

T. L. Jones, L. D. Betowski, and J. M. Van Emon, U.S. Environmental Protection Agency, Las Vegas, NV 89114.

INTRODUCTION

Paraquat is an extensively used bipyridinium herbicide that is water soluble and has a low vapor pressure. Evidence of paraquat's acute oral toxicity to humans has been reported[1]. It has also been recently suggested that Parkinson-type disorders may be linked to paraquat exposure[2].

An enzyme-linked immunosorbent assay (ELISA) was developed for the determination of paraquat in various matrices[3,4]. A study was undertaken to use liquid chromatograph/mass spectrometric (LC/MS) and LC/MS/MS methods to monitor the purity of the compounds, the synthesis of the haptens, and the results from ELISA with another analytical technique. Other compounds that can cross-react within the immunochemical assay were also targeted for LC/MS monitoring.

EXPERIMENTAL

The paraquat dichloride standard was obtained from Sigma Chemical Co. (St. Louis, MO). Monoquat and paraquat hapten were synthesized by Dr. Van Emon[3]. The diquat dibromide was obtained from the U.S. EPA Repository (RTP, NC).

Thermospray LC/MS was performed with a Finnigan MAT 4500 Triple Stage Quadrupole (TSQ) interfaced with a Vestec Corp. thermospray system and a Spectra Physics SP8700-XR solvent delivery system. The HPLC flow rate was set to 0.4 mL/min with the following gradient elution conditions: 0 minutes, 50% methanol, 50% water; 5 minutes, 20% methanol, 40% water, and 40% ammonium acetate; 5 min hold time. A post-column addition of water was used to make up a total flow rate of 1.3 mL/min.

FAB mass spectra was obtained with a VG model ZAB-3F(8kV, Xe FAB reagent gas, He CAD reagent gas).

RESULTS AND DISCUSSION

The solvent environment played an important role in the final analysis of the paraquat structure as determined by LC/MS and LC/MS/MS. The predominant ion was m/z 186 when water was used as the post-column solvent. However, the use of ammonium acetate as a post-column solvent resulted in the disappearance of m/z 186 ion and the emergence of m/z 187 ion. It was proposed that the attachment of a hydride ion forms the m/z 187 ion[5]. The lack of evidence for the m/z 93 dication and the appearance of the m/z 186 ion, in an aqueous environment, would suggest a one-electron reduction of the dication.

It is interesting to note the difference in their CAD spectra between the m/z 186 ion and the m/z 187 ion. Initially the m/z 186 ion and the m/z 187 ion both lose 15 amu to give m/z 171 and m/z 172 respectively. Further CAD experiments on these ions are instructive in the fact that the m/z 171, an even-electron ion, loses methane(CH_4) and the m/z 172, an oddelectron ion, does not show this behavior as the major channel is loss of a methyl radical ($CH_3^{\cdot}$).

CONCLUSIONS

The results demonstrate that the use of water as a post-column solvent enhances the paraquat m/z 186 ion detection. LC/TSP/MS, though not as sensitive as ELISA, provides a selective detection method for cross-validating immunochemical assays, while the specificity of MS/MS provides for greater compound identification.

Future experiments will include analysis of various matrix extracts for immunochemical assay comparisons.

Presented at the 36th ASMS Conference on Mass Spectrometry and Allied Topics
June 5-10, 1988, San Francisco, CA

NOTICE: Although the research described in this article has been supported by the United States Environmental Protection Agency, it has not been subjected to Agency review and therefore does not necessarily reflect the views of the Agency and no official endorsement should be inferred. Mention of trade names or commercial products does not constitute endorsement or recommendation for use.

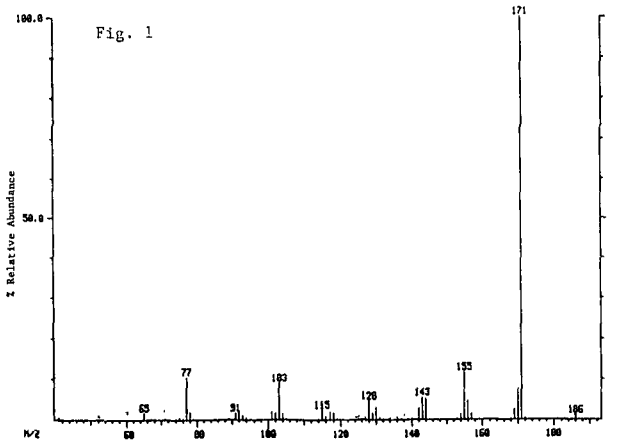

Fig. 1
Thermospray MS/MS (CAD) of m/z 186 of Paraquat

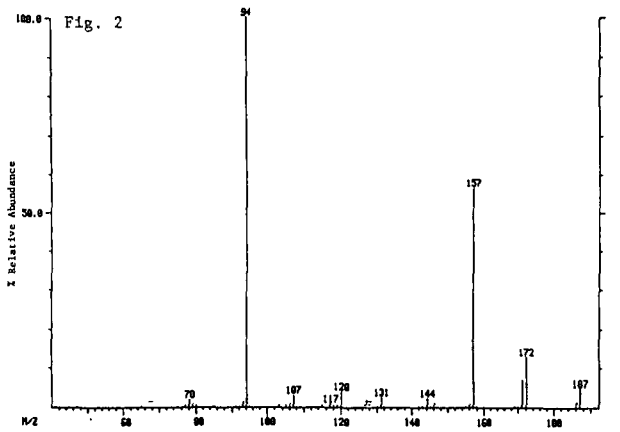

Fig. 2
Thermospray MS/MS (CAD) of m/z 187 of Paraquat

REFERENCES

1. Bullivant, C.M. Br. Med. J. 1966, 1, 1272-1273

2. Lewin, R. Science 1985, 229, 257-258

3. Van Emon, J., B. Hammock and J. Seiber, Anal. Chem. 1985, 58, 1866-1873.

4. Van Emon, J., J. Seiber and B.Hammock, Bull. Environ. Contam. Toxicol.

5. Vestal, C., Vestec Thermospray Newsletter, Feb. 1987.

Presented at the 36th ASMS Conference on Mass Spectrometry and Allied Topics
June 5-10, 1988, San Francisco, CA

SURFACE ANALYSIS WITH A TIME-OF-FLIGHT MASS SPECTROMETER WITH CHARGE COMPENSATION FOR SECONDARY IONS AND POSTIONIZATION OF NEUTRALS

E.Niehuis, B.Hagenhoff, T.Heller, G.Kampwerth,
D.van Leyen and A.Benninghoven

Physikalisches Institut, Universität Münster
4400 Münster, FRG

Secondary ion mass spectrometry (SIMS) has become a well established surface analytical technique. A variety of e/m-analyzers are applied for mass analysis of the generated secondary ions: magnetic sector fields, quadrupols, and, more recently, ion cyclotron resonance (ICR) and time-of-flight (TOF) instruments.

Time-of-flight features some important properties, which make this technique most attractive for secondary ion mass spectrometry: high transmission, unlimited mass range, and quasisimultaneous detection of all masses.

We built a number of TOF-SIMS instruments which we apply successfully to a wide variety of analytical problems. Main fields are:

- detection, identification and structural analysis of biomolecules
- characterization and surface analysis of polymers
- characterization and surface analysis of electronic materials
- detection of organic as well as inorganic traces

The successful application of TOF-SIMS in these different fields is based on instrumental developments in the following directions:

- high mass resolution,
- charge compensation for insulating materials, and
- postionization of sputtered neutrals for quantitative element analysis

1. High mass resolution

The mass resolution of a time-of-flight instrument is determined by the quality of the primary ion pulse, the energy focusing properties of the drift path, and the time resolution of the detection and registration unit.

In our TOF-SIMS instruments the primary ion pulse is generated by an EI gas ion source combined with a pulsed 90°-deflector, a bunching system and a lense. For 10 keV Ar^+-primary ions we obtain mass separated ($m/\Delta m = 350$) ion pulses below 1 ns with a repetition rate between 5 and 10 kHz. Each pulse contains up to 10.000 ions. The beam diameter on the target surface is typically 100 µm.

Secondary ions are accelerated by a 3 kV extraction voltage and separated in a single stage reflectron with first order energy focusing properties.

Figs 1 and 2 present sections of the positive secondary ion spectrum in the low mass range for a contaminated GaAs surface (Fig. 1) and a polymer surface (Fig. 2). The high mass resolution allows the separation of Fe^+ and CaO^+ as well as the separation of metal ions from the corresponding hydrocarbon ions emitted from the GaAs surface. In the PMMA-spectrum pure hydrocarbon ions are separated from those containing oxygen.

2. Charge compensation

During ion bombardment of insulating materials charging of the bombarded surface occurs. This results in a loss of resolution and transmission. We have developed a pulsed charge compensation device which avoids completely these effects /1/. Charge compensation is realized by low energy (5 eV) electron injection into the target region during the time between two ion pulses. By an appropriate pulsed field modification in the target region all disturbing effects of postaccelerated electrons, as EI of particles in the gas phase, electron bombardment induced ion emission, etc. can be avoided. We have

applied this charge compensation device successfully to many insulating samples as glasses, polymers, oxides, etc.

3. Postionization of sputtered material

The majority of sputtered particles emitted from a solid surface during ion bombardment are neutral. Their postionization can be realized most efficiently by EI or by laser irradiation. We have applied the technique of UV-multiphoton postionization described by Becker and Gillen /2/ by attaching an Excimer laser to our TOF-SIMS. We obtained useful yields for atomic particles in the 10^{-3} range for metals and semiconductors /3/.

/1/ B.Hagenhoff, D.van Leyen, E.Niehuis and A.Benninghoven, in SIMS VI, John Wiley & Sons, Chichester 1988, p. 235
/2/ C.H.Becker and K.Gillen, Anal.Chem. 56, 1671 (1984)
/3/ E.Niehuis, T.Heller, G.Kampwerth and A.Benninghoven, in SIMS VI, p. 255

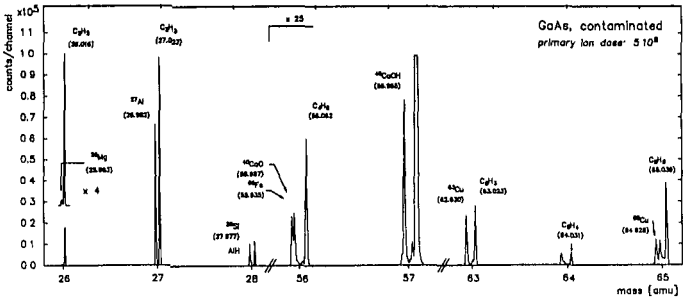

Fig. 1
High resolution TOF-SIMS spectrum of a contaminated GaAs wafer

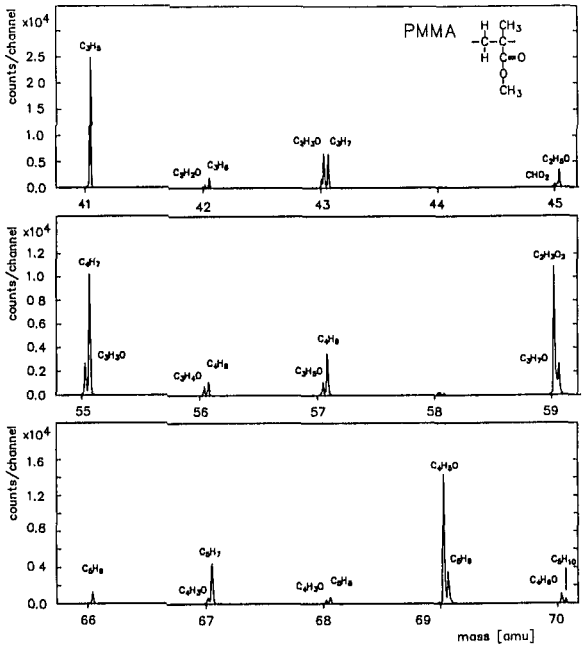

Fig. 2
High resolution TOF-SIMS spectrum of a polymethylacrylate (PMMA) surface

Presented at the 36th ASMS Conference on Mass Spectrometry and Allied Topics
June 5-10, 1988, San Francisco, CA

ANALYSIS OF DRUGS OF ABUSE BY PARTICLE BEAM LC/MS

A. Apffel; Hewlett-Packard Company, Palo Alto, California 94304

The introduction of Particle-Beam based LC/MS (PB LC/MS) interfacing techniques opens the opportunity of utilizing high performance liquid chromatography on a wide range of applications in which GC/MS is not applicable, while retaining high information content EI spectra at low detection limits (mid-pg).

The analysis of drugs of abuse (e.g. LSD, Amphetamines, and Fentanyl) by GC/MS requires extensive pre-treatment involving extraction, preconcentration and derivatization. The use of precolumn technology in HPLC automates cleanup procedures of large volumes of physiological fluids, negating the need for labor intensive sample work-up. Furthermore, PB LC/MS generates EI or CI spectra for thermally labile or low volatility compounds, negating the need for derivatization

The following three applications demonstrate these advantages.

1. LSD has been analyzed with derivatization, generating library searchable EI spectra below 10ng Automated preconcentration procedures allow SIM detection below 1 ppb.

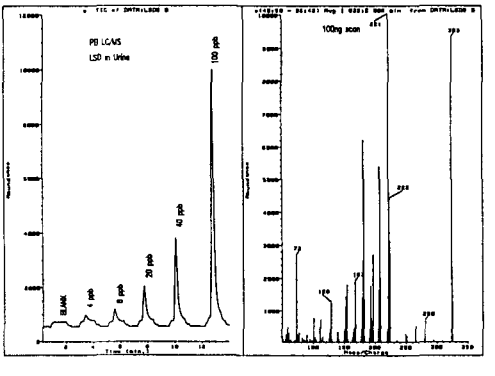

2. A mixture of amphetamines has been analyzed in biological fluids generating EI spectra below 100ng. The use of automated on-line precolumn concentration allows large volumes of physiological fluids to be analyzed for these drugs at low levels with positive confirmation.

3. Fentanyl and Sufentanyl have been rapidly cleaned up from plasma samples with off-line solid phase extraction procedures. Analysis of the extracted fraction yields rapid identification of the components in this complex matrix.

Presented at the 36th ASMS Conference on Mass Spectrometry and Allied Topics
June 5-10, 1988, San Francisco, CA

LSIMS of Intact Oligosaccharides: Comparison of Sensitivity and Spectral Quality Among Selected Derivatives

L. Poulter, R. Karrer, K. Jiang, B.L. Gillece-Castro and A.L. Burlingame
Department of Pharmaceutical Chemistry, University of California, San Francisco, CA 94143-0446

In this laboratory we are pursuing a comprehensive strategy to separate and characterize oligosaccharides isolated from low levels of glycoproteins. To increase sensitivity in the LSIMS analysis it is necessary to derivatize oligosaccharides, thereby increasing their surface activity within the liquid matrix. However, before mass spectrometry can be applied, the oligosaccharides need to be purified. An ideal derivative would therefore incorporate a radiolabel or a chromophore to aid detection during chromatography, as well as a hydrophobic group to increase surface activity. To address this issue we have extended our work[1] and that of others[2], by using a series of alkyl esters of p-aminobenzoic acid to derivatize the reducing termini of oligosaccharides.

All esters that were not commercially available were synthesized from p-aminobenzoic acid and the corresponding alcohol[3] and reductively coupled to the reducing termini of oligosaccharides as shown in Figure (1). Reverse phase HPLC (Vydac, C4 or C18) using water and acetonitrile was effective in desalting samples prior to mass spectrometry with monitoring at λ = 304 nm to detect the derivatized oligosaccharides.

Maltoheptaose (M7) was derivatized with all esters from methyl to tetra-decyl and the relative sensitivities of these derivatives were compared. Figure (2) shows the time courses obtained for protonated molecular ions using 0.1 µg of M7-ABXE in 1 µl of glycerol:thioglycerol (1:1). From the graph it is clear that increasing alkyl chain length does have a profound effect on sensitivity in LSIMS. Esters higher than octyl did have greater absolute sensitivity, however the yields obtained in the derivatization were considerably reduced, largely due to problems of solvent incompatibility.

Figure (3) shows the negative-ion spectrum obtained on 0.2 µg of a hexasaccharide derivatized with the octyl ester. Glycosidic bond cleavages are observed with charge retention at the derivatized reducing terminus providing the structural information shown. The chemical noise arising from the matrix was eliminated by resorting to positive-ion MS/MS (carried out on a four sector Kratos Concept with array detection) which provided clear glycosidic bond cleavages with charge retention on both reducing and non-reducing termini[3].

Studies carried out within our group have shown that derivatization with the ethyl ester of p-aminobenzoic acid provides a sensitivity in LSIMS comparable to that achieved by permethylation or peracetylation. While one might not expect this ester derivative to be as surface active as a permethylated or peracetylated sample, the reverse-phase HPLC step used after derivatization provides an extremely clean sample for MS analysis. By using the octyl ester, the amount of sample needed is decreased by approximately a factor of ten. The small increase in mass obtained upon derivatization is an important factor when larger oligosaccharides are of interest, while the lack of under- or over-derivatized products and salt adducts makes mass spectral interpretation much easier, particularly in the case of oligosaccharide mixtures. Reducing terminal fragments predominate in the negative-ion mass spectra of the ester derivatives, as opposed to non-reducing terminal fragments in the case of permethylated or peracetylated samples; however by using MS/MS methods on the ester derivatives both reducing and non-reducing terminal fragments can be obtained.

Presented at the 36th ASMS Conference on Mass Spectrometry and Allied Topics
June 5-10, 1988, San Francisco, CA

Figure (1)

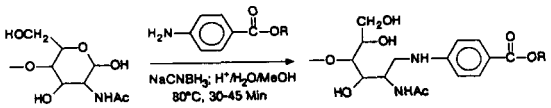

R = Me, Et, Bu, Hex, Oct, Dec, Tetradec.

Figure (2)

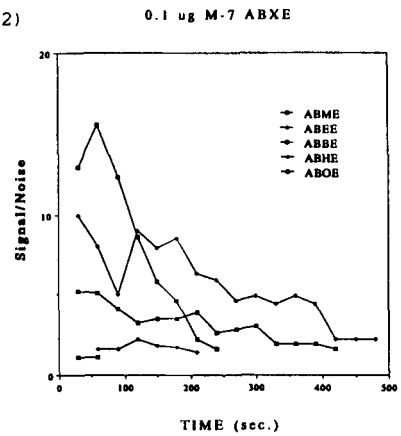

1. J.W. Webb et al., Anal. Biochem., 169, 337-349 (1988).
2. W.T. Wang et al., Anal. Biochem., 141, 366-381 (1984).
3. R. Karrer, L. Poulter and A.L. Burlingame, in preparation.

Research supported by NIH DRR Grant RR01614. LP is the recipient of a NATO Postdoctoral Fellowship.

Figure (3)

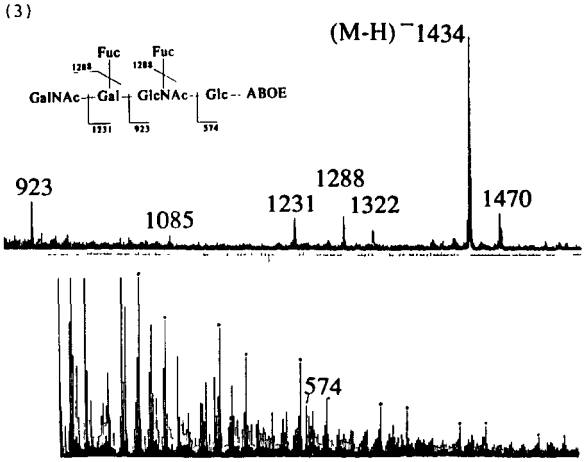

Presented at the 36th ASMS Conference on Mass Spectrometry and Allied Topics
June 5-10, 1988, San Francisco, CA

CHARACTERIZATION OF A PRE-S2 GLYCOPEPTIDE FROM HEPATITIS B SURFACE ANTIGEN BY LIQUID SECONDARY ION MASS SPECTROMETRY

B. L. Gillece-Castro and A. L. Burlingame, Dept. of Pharmaceutical Chemistry and the Liver Center, University of California, San Francisco, CA 94143-0446 and D.L. Peterson, Dept. of Biochemistry, Medical College of Virginia, Richmond, VA 23298

The comparison of protein and carbohydrate structures of vaccines for Hepatitis B is the goal of this work. Hepatitis B surface antigen (HBsAg) used in vaccination is a complex macromolecular structure containing glycoproteins embedded in a lipid bilayer. The protein components are all derived from a single open reading frame in the viral genome, referred to as the S+Pre-S2+Pre-S1 gene. The majority of the proteins contain only S sequences however 10% or less contain both Pre-S2 and S sequences. HBsAg from human plasma and that expressed in Chinese Hamster Ovary (CHO) cells were analyzed to confirm the amino terminal sequence, determine the amino terminal blocking groups, and determine the structures of the asparagine linked oligosaccharides of the Pre-S2 region.

The amino terminal Pre-S2 glycopeptide was isolated from the antigen by tryptic digestion of the intact antigen and HPLC isolation of peptides. The 16 amino acid amino terminal peptide could not be sequenced by Edman chemistry without the removal of the N-terminal Met which was blocked. A strategy of enzymic (PNGase F) deglycosylation of glycopeptides followed by separation of the peptide and oligosaccharide portions by reverse phase HPLC and LSIMS analysis of the products was followed. MH^+ ions for cloned and human peptides were found at *m/z* 2033 or 43 Da greater than predicted. In this manner it was determined that both plasma and CHO derived peptides were acetylated on their amino termini and the glycosylated Asn was converted to Asp.

The oligosaccharides which eluted in the void volume of the previous HPLC were derivatized at their reducing termini with p-amino benzoic acid esters ABEE or ABOE (1,2,3) to introduce a hydrophobic chromophore and site of charge localization. Acidic and neutral fractions of the derivatized oligosaccharides were separable by reverse phase HPLC (Figure 1) and LSIMS data is shown for the neutral fraction of the cloned antigen oligosaccharides. Molecular anions (not shown) at *m/z* 2226 and 2064 were observed from the acidic fraction of the cloned HBsAg as the ethyl ester (ABEE) derivative. These correspond to biantennary complex oligosaccharides with one fucose and one N-acetyl neuraminic acid (sialic acid). The larger oligosaccharide is shown while the other is truncated by the loss of one hexose. The neutral oligosaccharides are shown (Fig 2) as the octyl ester derivatives (ABOE) which gives an improved signal to noise. The major component is the fucosylated biantennary structure (*m/z* 2019) shown. However a higher molecular weight triantennary structure is also present (*m/z* 2384) as is a bifucosylated biantennary oligosaccharide (*m/z* 2165). Evidence for truncated structures is subtle in this spectrum and is represented by the abundance of the ions at m/z 1857, 1653 and 1492. The oligosaccharides from plasma derived HBsAg were similarly treated and the LSIMS data included the molecular anion is m/z 1873 and fragments of this biantennary oligosaccharide are noted. It is significant to note that no fucosylated or triantennary structures are presented by the human antigen, but are present on the CHO cell antigen. The strategy of enzymatic deglycosylation followed by HPLC isolation of peptide and oligosaccharide portions and subsequent LSIMS analysis of peptides and reducing terminal derivatives of oligosaccharides was successful in identifying peptide modifications as well as characterizing the oligosaccharides attached at a paricular site.

1) Wang, W.T., LeDonne, N.C., Ackerman, B. Jr., and Sweeley, C.C. (1984) *Anal. Biochem.* 141, 366-381.

2) Webb, J.W., Jiang, K., Gillece-Castro, B.L., Tarentino, A.L., Plummer, T.H., Byrd, J.C., Fisher, S.J. and Burlingame, A.L. (1988) *Anal. Biochem.* 169, 337-349.

3) Poulter, L., Karrer, R. Jiang, K., Gillece-Castro, B.L. and Burlingame, A.L., Presented at the 36th Annual Conf. on Mass Spectrometry and Allied Topics, San Francisco, CA, June 5-10, 1988.

Research supported by NIH DRR Grant RR01614, and NIH Grant AM 27643. B. Gillece-Castro is supported by NIH Training Grant GM 07175.

Figure 1

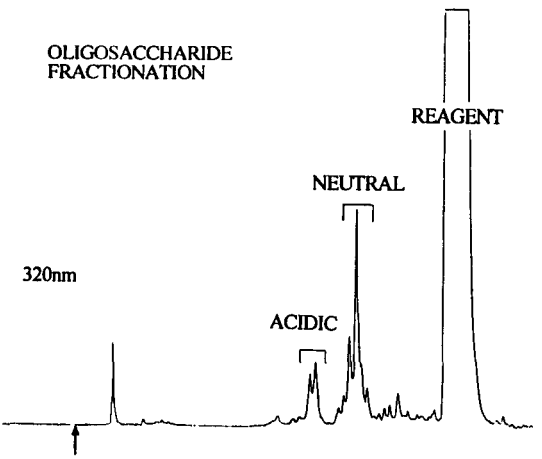

Figure 2

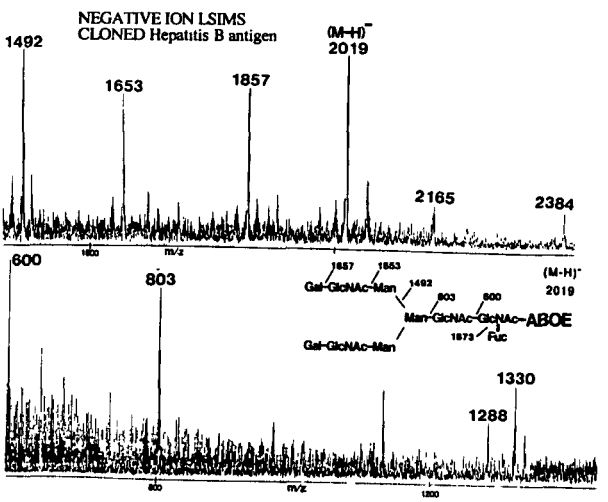

Presented at the 36th ASMS Conference on Mass Spectrometry and Allied Topics
June 5-10, 1988, San Francisco, CA

LSIMS Analysis of High Mannose and Complex Sialylated Oligosaccharides Isolated from Low Levels of Glycoprotein: Application to α_1 Acid Glycoprotein and the Nicotinic Acetylcholine Receptor

Linda Poulter and A.L. Burlingame
Department of Pharmaceutical Chemistry, University of California, San Francisco, CA 94143-0446

The full characterization of N-linked oligosaccharides from membrane-bound glycoproteins, such as insulin receptor and epidermal growth factor receptor, is a goal of our research group. Since typically only picomole to nanomole quantities of these proteins are available from most sources, a successful approach requires high recovery in the isolation and purification of oligosaccharides as well as excellent sensitivity in the subsequent mass spectral analyses.

We first developed a protocol using 2 nanomoles of α_1-acid glycoprotein from human plasma which, although not an integral membrane protein, possesses large and highly sialylated oligosaccharides. Having established the appropriate methods, we then turned to the more challenging analysis of 2 nanomoles (500 µg) of the nicotinic acetylcholine receptor (nAChR) from Torpedo californica[1]

In the generalized procedure, glycoproteins were deglycosylated using peptide-N-glycosidase F (PNGase F) in ammonium bicarbonate buffer (100 mM, pH 8.6) in the presence of 0.1% sodium dodecyl sulphate (SDS) and 0.6% Nonidet P-40 (NP-40). Analytical SDS-polyacrilamide gel electrophoresis was used to test for complete deglycosylation. SDS was precipitated by adding guanidine hydrochloride (1.0 M) dropwise, and after cooling and centrifugation, the supernatant was applied to a C-18 Sep pak cartridge. Oligosaccharides were eluted with water, and the protein was removed subsequently with 80% acetonitrile/0.1% TFA. The aqueous phase was lyophilized and the reducing termini of all oligosaccharides were derivatized with p-aminobenzoic acid hexyl ester in the presence of sodium cyanoborohydride, and then chromatographed by reverse phase HPLC. Derivatization introduces a chromophore (λ_{max} = 304 nm) and also a hydrophobic tail to aid sensitivity in the LSIMS analysis[2,3], while RP-HPLC desalts the samples effectively and separates the oligosaccharides largely on the basis of net charge.

Positive-ion LSIMS, using 200 pmol - 500 pmol of oligosaccharide, gave molecular weight information only, while negative ion spectra provided extensive fragmentation with cleavage of glycosidic bonds and charge retention at the derivatized reducing termini of all oligosaccharides. Figure (1a) shows the negative-ion spectrum of the monosialylated fraction from nAChR revealing no less than eight molecular ions [$(M-H)^-$ = 1932, 2094, 2135, 2176, 2338, 2379, 2500 and 2541, nominal masses]. The molecular weights provide monosaccharide compositions (on the basis of deoxyhexose : hexose : hexosamine : sialic acid), while fragment ions confirm proposed structures [e.g. see $(M-H)^-$ = 1932 and 2094 in Figure (1b)]. Table (1) lists data on all of the oligosaccharides found in this analysis. Negative-ion spectra on oligosaccharide mixtures or on further purified components provided branching information.

The lack of mass spectral complexity, such as that brought about by under- or overderivatized oligosaccharides or the presence of salt adducts, is notably absent using our procedure. The application of this method when dealing with heterogenous mixtures of oligosaccharides is therefore particularly useful. The small increase in mass of oligosaccharides upon derivatization is also an important factor when larger structures are to be analyzed.

Presented at the 36th ASMS Conference on Mass Spectrometry and Allied Topics
June 5-10, 1988, San Francisco, CA

Figure 1: a) Negative-ion mass spectrum of monosialylated oligosaccharides from nAChR; b) Proposed (hybrid) structures for oligosaccharides M_r = 1933 and 2095 detailing fragmentation observed.

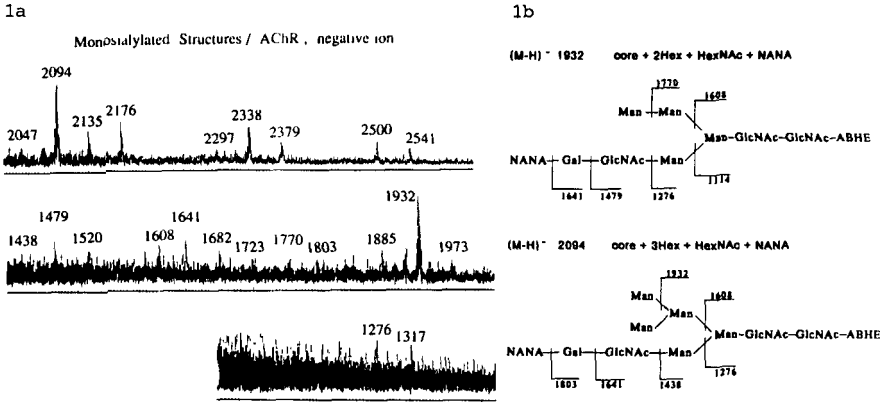

Table 1: Oligosaccharides isolated from 500 µg (2 nmoles) of nAChR

Fraction	Mr (as ABHE)	Composition	Approx. Molar %
Neutral	1925	8Man+2GlcNAc	40
	2087	9Man+2GlcNAc	28
Monosialylated	1933	Core+2Hex+ HexNAc+ NANA	<1
	2095	Core+3Hex+ HexNAc+ NANA	<1
	2135	Core+2Hex+2HexNAc+ NANA	<1
	2177	Core+ Hex+3HexNAc+ NANA	<1
	2339	Core+2Hex+3HexNAc+ NANA	<1
	2380	Core+ Hex+4HexNAc+ NANA	<1
	2501	Core+3Hex+3HexNAc+ NANA	<1
	2542	Core+2Hex+4HexNAc+ NANA	<1
Bisialylated	2427	Core+2Hex+2HexNAc+2NANA	<1
	2630	Core+2Hex+3HexNAc+2NANA	<1
	2792	Core+3Hex+3HexNAc+2NANA	<1
Trisialylated	2920	Core+2Hex+3HexNAc+3NANA	3
	3082	Core+3Hex+3HexNAc+3NANA	10
	3123	Core+2Hex+4HexNAc+3NANA	<1
	3285	Core+3Hex+4HexNAc+3NANA	5
Tetrasialylated	3738	Core+4Hex+4HexNAc+4NANA	2

*Core = 2GlcNAc+3Man

1. L. Poulter and A.L. Burlingame, in preparation.
2. R. Karrer, L. Poulter and A.L. Burlingame, in preparation.
3. L. Poulter, R. Karrer, K. Jiang, B.L. Gillece-Castro and A.L. Burlingame, presented at the 36th Annual Conf. on Mass Spectrometry and Allied Topics, San Francisco, CA, June 5-10, 1988.

Research supported by NIH DRR Grant RR01614. LP is the recipient of a NATO Postdoctoral Fellowship.

Presented at the 36th ASMS Conference on Mass Spectrometry and Allied Topics
June 5-10, 1988, San Francisco, CA

IDENTIFICATION OF 5'-DEOXYXANTHOSINE IN HUMAN URINE:

Thomas D. McClure and Karl H. Schram, Department of Pharmaceutical Sciences, College of Pharmacy, University of Arizona, Tucson, Arizona, 85721 and K. Nakano and T. Yasaka, PL Comprehensive Institute, 1 Kamiyamacho, Tondabayashi, Osaka 584, Japan.

Introduction

The occurrence of 5'-deoxynucleosides or nucleotides as natural components of biological systems is rare. Until recently, the only known member of this class was 5'-deoxyadenosine (5'-dA), which occurs as a result of the metabolism of nicotine adenine dinucleotide. Chheda, et. al. have isolated the second such compound, 5'-deoxyinosine(5'-dI)[1], from the urine of chronic myelogenous leukemia patients. This report describes the isolation and identification of 5'-deoxyxanthosine(5'-dX) the third compound of this class, from human urine.

Isolation and Preparation

5'-dX was isolated and identified from normal human urine by the following methods. The urinary nucleosides were separated from other urinary components using the boronate-gel method of Gehrke, et. al.[2]. A preliminary separation of the nucleoside mixture was then accomplished using HPLC[3]. The HPLC fractions were converted to their trimethylsilyl(TMS) derivatives[4] for GC/MS analysis.

GC conditions include: linear temperature programing from 150 to 300 deg. at 6 deg. per minute using a bonded phase 30m capillary column; splitless injection; and direct inlet into the ion source of the mass spectrometer. Mass spectrometer conditions include: low resolution (R=1000); GC/MS scanning a range of m/z 70 to 1000 at 2 scans per second; high resolution studies (R=7200) on the reference compound were acquired by peak matching from the direct inlet probe. The instrument used was a Finnigan MAT90 with a Varian 3400 GC.

Reference Compound Synthesis

A reference compound of 5'-dX was prepared using a combination of biochemical and chemical methods. Initially it was believed that 5'-dX might be the product of purine metabolism involving first the adenosine deaminase (ADA) conversion of 5'-dA to 5'-dI. 5'-dI is then oxidized by xanthine oxidase (XO) to 5'-dX. Under these experimental conditions, 5'-dI was not converted to 5'-dX, leading to the conclusion that 5'-dI is not a substrate for XO. The next attempt to produce 5'-dX involved the use of purine nucleoside phosphorylase (PNP) to couple xanthine to 5'-deoxyribose-1-phosphate (5'-dR-1-P)[5]. No reaction occurred. PNP did couple guanine to 5'-dR-1-P to form 5'-dG, which was then deaminated chemically to 5'-dX.

Discussion

Major points of interest[6] in the low resolution mass spectra of the TMS derivative of 5'-dX include a) m/z 556 which is a very weak ion, and m/z 541 assigned as the $M^{+\cdot}$ and M-15 ions for 5'-dX; b) m/z 260 (S-H), m/z 217 ($C_3H_3O_2TMS_2$), and m/z 171 (S-90) which indicate the presence of a deoxypentofuranose. The very low intensity of m/z 103 (CH_2OTMS) suggests the 5' position is lacking a hydroxyl group; c) m/z 423(B+128), m/z 369(B+74), m/z353(B+58), m/z 325(B+30), m/z 297(B+2H) and m/z 281(B-14) assigned as containing the base plus portions of the sugar. A comparison of the spectra of the reference and urinary compounds is found in fig.1. Structures of the above ions were further substantiated by preparation of the TMS-$^2H_9$ analog and analysis of the resulting spectrum.

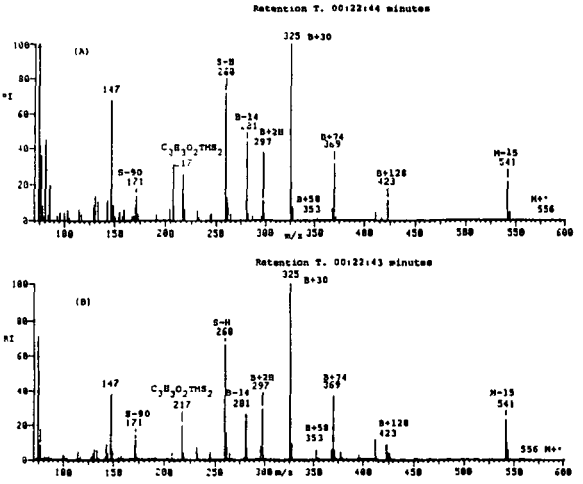

Fig. 1 Low resolution mass spectrum of (a) urinary 5′-dX and (b) biochemically synthesized 5′-dX.

In order to eliminate 2′- and 3′- dX from consideration, the low resolution spectra of these compounds were compared to that of 5′-dX. Important differences in the mass spectra of 2′,3′ and 5′-deoxynucleosides have been noted[7], and this comparison establishes the 5′ position as the site of deoxygenation.

High resolution MS was performed on the reference compound for the ions listed above. Elemental composition for these ions is established and is consistent with the assigned structures.

The LC and GC retention times for the reference compound and the urinary component were in agreement within experimental error, further verifying the identity of the urinary component as 5′-deoxyxanthosine.

Acknowledgment

This work supported by NIH grant CA43068, a grant from Patriarch Takahito Miki, and a grant from the 'Perfect Liberty' organization.

References

1. G.B.Chheda, H.B.Patrzyc, A.K.Bhargava, P.F.Crain, S.K.Sethi, J.A.McCloskey and S.P.Dutta, Nucleosides and Nucleotides, **6**, 597 (1987).
2. C.W.Gehrke, K.C.Kuo, G.E.Davis, R.D.Suits, T.P.Waalkes and E.Borek, J. Chromatogr., **150**, 455 (1978).
3. K.Nakano in J.C.Giddings (Ed.), 1986, Advances in Chromatography, Vol. 25, Marcel Dekker, New York, pp. 245.
4. J.A.McCloskey, R.N.Stillwell and R.M.Lawson, Anal.Chem., **48**, 233 (1968).
5. J.D.Stoeckler, C.Cambor and R.E.Parks Jr., Biochemistry, **19**, 102 (1980).
6. H.Pang, K.H.Schram, D.L.Smith, S.P.Gupta, L.B.Townsend and J.A. McCloskey, J. Org. Chem., **47**, 3923 (1982).
7. M.Reimer, T.D.McClure and K.H.Schram, "Investigation of the Fragmentation of the TMS Derivatives of 2′,3′ and 5′ Deoxynucleosides", Presented at the 36th ASMS Conference in San Francisco, 1988.

Presented at the 36th ASMS Conference on Mass Spectrometry and Allied Topics
June 5-10, 1988, San Francisco, CA

MASS SPECTRAL CHARACTERIZATION OF ACRYLONITRILE OXIDE DNA ADDUCTS. ALKYLATION AT N-3 OF CYTOSINE RESULTS IN HYDROLYTIC DEAMINATION TO A URACIL ADDUCT.

Jerome J. Solomon, K. Decker, F. Mukai and A. Segal

Institute of Environmental Medicine, New York University Medical Center, New York, NY 10016

Acrylonitrile epoxide (2-cyanoethylene oxide, ANO) is a mutagenic 3-carbon epoxide. ANO has been suggested to be the ultimate carcinogenic metabolite of the rodent carcinogen acrylonitrile (AN, CH_2=CH-C≡N) in part due to its structural similarity to vinyl chloride. AN is extensively used in industrial applications with a production in 1986 of 2.3 X 10^9 lbs. OSHA has estimated that 278,000 workers are potentially exposed to AN. AN requires metabolic activation to cause mutations with S. typhimurium but has also been found to be a weak direct-acting mutagen in E. coli WP2. We previously examined the ability of AN to form adducts with calf thymus DNA without metabolic activation. Alkylation via Michael addition was very slow at physiological pH and temperature and adducts were reported after a 40 day reaction. Cyanoethyl (CNE, -CH_2CH_2CN) adducts were detected at N-7 guanine and N-3 thymine but carboxyethyl (CE, -CH_2CH_2COOH) adducts were produced at sites adjacent to an exocyclic nitrogen (N-1 adenine and N-3 cytosine). We proposed a mechanism for the rapid hydrolysis of CNE adducts to CE adducts. The CE adducts that result at N-1 of A and N-3 of C are common lesions that we have shown to be produced by several rodent carcinogens including β-propiolactone, AN, acrylamide and acrylic acid.

The purpose of this study was to characterize how ANO modifies DNA. ANO was reacted at pH 7.0-7.5 and 37°C for 3 h with 2'-deoxynucleosides and formed a variety of adducts. Figure 1 gives the structure of the adducts detected and includes the yields determined after 3 h reaction. Attempts to obtain EI and CI spectra for several of these adducts were unsuccessful due to the polarity of the adducts. Derivatization resulted in volatile products whose EI mass spectra are shown in Figure 2. Table I lists the results of accurate mass measurement studies on M and M-CH_3 ions for the trimethylsilyl (TMS) derivatives of ANO-DNA adducts. A proposed pathway for the formation of 1,N^6-etheno-dAdo (ε-dAdo) and N^6-(2-hydroxy-2-carboxyethyl)-dAdo (N^6-HOCE-dAdo) is given in Figure 3. Conversion of 1-(2-hydroxy-2-cyanoethyl)-dAdo (1-HOCNE-dAdo) to 1-HOCE-dAdo occurs as with AN at N-1 of A where the nitrile group was hydrolyzed to a carboxylic acid. The formation of ε-dAdo from ANO and dAdo is similar to the formation of ε-dAdo from the reaction of the structurally related epoxide of vinyl chloride with dAdo. A scheme for the alkylation at N-3 of dCyd which results in a dUrd adduct, 3-HOCE-dUrd, is shown in Figure 4. The initial ANO adduct contains a OH group in the 3-carbon side chain which catalyzes the hydrolytic deamination of 3-HOCE-dCyd to 3-HOCE-dUrd.

ANO was reacted with calf thymus DNA (pH 7.0-7.5, 37°C, 3 h) and yielded N^6-HOCE-dAdo (2 nmol/mg DNA), ε-dAdo (11 nmol/mg DNA), 3-HOCE-dUrd (80 nmol/mg DNA), 7-(2-oxoethyl)-Gua (7-OXE-Gua, 110 nmol/mg DNA) and 3-OXE-dThd (1 nmol/mg DNA). The ANO adduct which results from hydrolytic deamination of an initially formed adduct at N-3 of dCyd is a major lesion in DNA. Experiments with other 3-carbon epoxides including propylene oxide, epichlorohydrin and glycidol indicate that this C to U conversion may be a common phenomenon with aliphatic epoxides containing a primary carbon in the oxirane ring and may play an important role in the biological activity of this class of compounds.

Supported by NCI Grant CA 13343 and NIEHS Grants ES 00260 and ES 03563.

Presented at the 36th ASMS Conference on Mass Spectrometry and Allied Topics
June 5-10, 1988, San Francisco, CA

FIGURE 1
STRUCTURE OF ACRYLONITRILE EPOXIDE (ANO) ADDUCTS WITH 2'-DEOXYNUCLEOSIDES

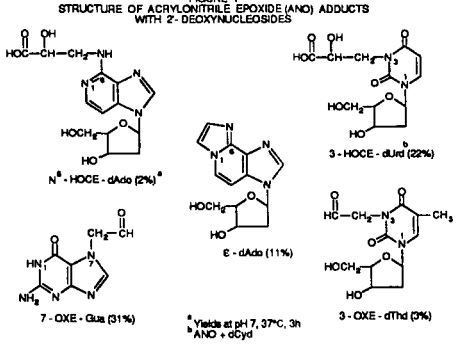

FIGURE 2
EI MASS SPECTRA OF TRIMETHYLSILYL (TMS) DERIVATIVES OF ANO - DNA ADDUCTS

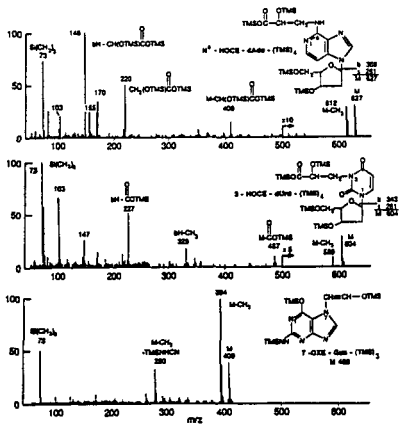

FIGURE 3
PROPOSED PATHWAY FOR FORMATION OF ACRYLONITRILE EPOXIDE (ANO) - ADDUCTS WITH 2'-DEOXYADENOSINE (dAdo)

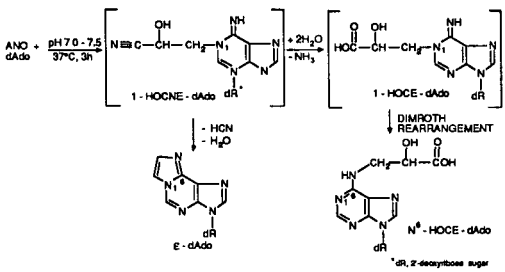

FIGURE 4
PROPOSED SCHEME FOR FORMATION OF 3 HOCE-dUrd FROM ACRYLONITRILE EPOXIDE (ANO) AND 2'-DEOXYCYTIDINE (dCyd)

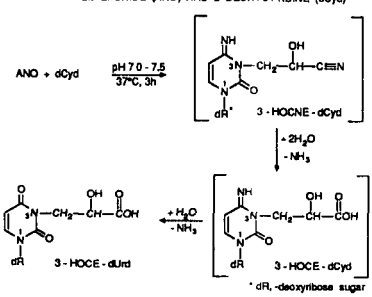

TABLE I
ACCURATE MASS MEASUREMENT

TRIMETHYLSILYL (TMS) DERIVATIVES OF ANO-DNA ADDUCTS

COMPOUND	ELEMENTAL COMPOSITION	IONIC SPECIES	CALCULATED MASS	MEASURED MASS
N^6 - HOCE - dAdo - $(TMS)_4$	$C_{25}H_{48}N_5O_6Si_4$	M	627.2760	627.2764
		M - CH_3	612.2525	612.2528
ε - dAdo - $(TMS)_2$	$C_{16}H_{29}N_5O_3Si_2$	M	419.1809	419.1814
		M - CH_3	404.1574	404.1574
3 - HOCE - dUrd - $(TMS)_4$	$C_{26}H_{48}N_2O_8Si_4$	M	604.2488	604.2490
		M - CH_3	589.2253	589.2251
7 - OXE - Gua - $(TMS)_3$	$C_{16}H_{31}N_5O_3Si_3$	M	409.1786	409.1779
		M - CH_3	394.1551	394.1552

Presented at the 36th ASMS Conference on Mass Spectrometry and Allied Topics
June 5-10, 1988, San Francisco, CA

FAB-MS/MS AS A SCREENING METHOD FOR DETECTING TRACE AMOUNTS OF BIOMOLECULES IN HPLC FRACTIONS

Andrea M. Dietrich[1], Christian R. Guenat[2], Kenneth B. Tomer[3], Louise M. Ball[4]
[1] Div. of Envir. Engr. and Envir. Sci., Virginia Polytechnic Institute, Blacksburg, VA 24061-0246; [2] CIBA-GEIGY AG, Basel, Switzerland; 3 Laboratory of Molecular Biophysics, NIEHS, Research Triangle Park, NC 27709; [4] Dept. Environmental Sciences and Engineering, University of North Carolina, Chapel Hill, NC 27599-7400

FAB-MS/MS is a useful technique to generate characteristic fragmentation data from specific molecules in complex mixtures/matrices. In this research FAB-MS/MS was applied to successfully detect and identify the DNA nucleoside adduct **N-(deoxyguanosin-8-yl)-3-aminofluoranthene (MW 482)**. This biomolecule was produced from reacting calf thymus DNA with reduced 3-nitrofluoranthene under acidic conditions, followed by aqueous enzymatic hydrolysis of the DNA to 2'-deoxynucleosides. The digested DNA, which contained both modified and normal nucleosides, was extracted with n-butanol which preferentially concentrates the nucleosides containing the non-polar fluoranthene moiety.

The n-butanol extract, which was taken to dryness and redissolved in methanol, was subjected to +FAB-MS and +FAB-MS/MS. Mass spectrometric experiments were performed on a VG ZAB-4F (BEEB configuration) with an 11-250 datasystem. The xenon FAB gun was operated at 8 kV and 1 mA current with a matrix of dithiothreitol/dithioerythritol (DTs). Full scan mass spectrometric data, acquired at a scan rate of 10 sec/decade, 8000 kV accelerating voltage, and 1000 resolution, indicated the presence of the protonated molecular ion at m/z 483, and a major fragment ion at m/z 367 due to loss of the deoxyribose moiety and migration of a deoxyribose proton to the modified guanine base (see structure in Figure 2). Collisionally activated decomposition (CAD) spectra were obtained by collision of m/z 483 and m/z 367 with helium in the grounded collision cell of the third field free region. Mass analysis of the daughter ions was achieved by a B_2/E_2 linked scan of MS_2. The scan rate was 30 sec/decade. The MS/MS spectrum of m/z 483 lead to a single daughter ion at m/z 367. The MS/MS spectrum of m/z 367 yielded numerous characteristic daughter ions, including ions related to cleavage of the C-N bonds of guanine-aminofluoranthene, and a series of ions due to loss of fragments from the purine ring.

Initial chromatographic separation of the n-butanol extract demonstrated a complex, poorly resolved UV/VIS HPLC chromatogram containing approximately 30 components (Figure 1). Only one of these components was the desired adduct, and only about 100 ug were present. In order to isolate the adduct and recover as much N-(deoxyguanosin-8-yl)-3-aminofluoranthene as possible, HPLC fractions were collected and then screened for the presence of this adduct using FAB-MS/MS analysis of m/z 483 and m/z 367. Initially four HPLC fractions (7-14 minutes each) were collected during a 40 minute HPLC separation program, and the adduct was identified in Fraction 3 (Figures 1 and 2). The impurity at m/z 329 in Figure 2 was not present in the unfractionated sample, and was shown to be both an artifact primarily due to a DTs adduct of dimethyloctadecylsilanol from the C_{18} column (328 + 154 + 1).

Fraction 3 was still a complex sample, so it was further chromatographed from 70% methanol/30% water to 83% methanol/17% water in 20 minutes, and six HPLC fractions were collected. These fractions were again screened by MS/MS for the presence of m/z 483 fragmenting to m/z 367. If m/z 367 was present, then the daughter ion spectrum was obtained to confirm the presence of N-(deoxyguanosin-8-yl)-3-aminofluoranthene in the fraction. A third level of chromatographic separation using a methanol/water gradient from 60% methanol to 75% methanol in 30 minutes was necessary to resolve and isolate purified N-(deoxyguanosin-8-yl)-3-aminofluoranthene. The final purified adduct yielded spectra similar to those obtained for the unpurified adduct in the initial n-butanol extract. The major differences were due to the presence on impurities such as the DTs/dimethyloctadecylsilanol adduct cited above. Although several iterations of HPLC separation, fraction collection, and FAB-MS/MS screening were necessary, the chromatographic peak containing the adduct was identified, and N-(deoxyguanosin-8-yl)-3-aminofluoranthene was successfully isolated and purified.

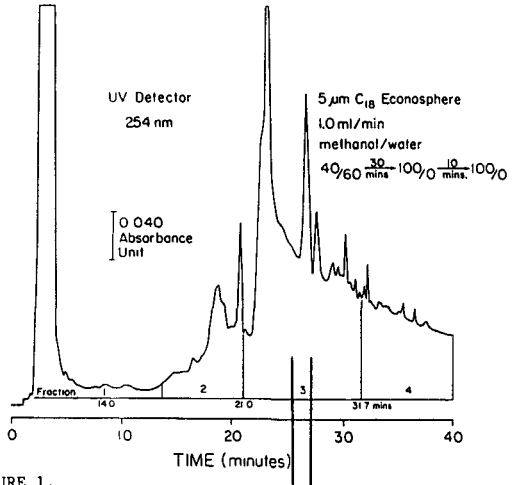

FIGURE 1.

Fraction 3, Level I Chromatography, Impure dG:C8-3-AF

(from Chemically Mediated Formation)

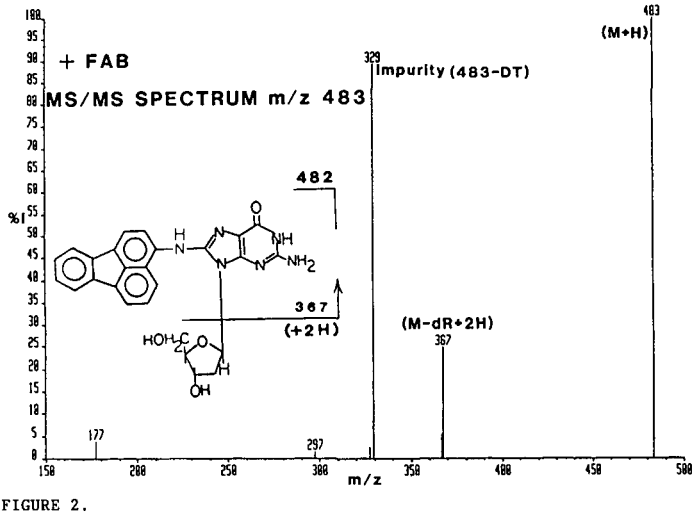

FIGURE 2.

Presented at the 36th ASMS Conference on Mass Spectrometry and Allied Topics
June 5-10, 1988, San Francisco, CA

FRAGMENTATION OF OLIGODEOXYNUCLEOTIDES

J.A. Laramée[1], B. Arbogast[1], G. Stirchak[3], D. Weller[2], and M.L. Deinzer[1]
Departments of Agricultural Chemistry[1] and Chemistry[2]
Oregon State University, Corvallis, Oregon 97331 and
Antivirals, Inc.[3], Corvallis, Oregon 97333

Predictable fragment ions from oligonucleotide carbamate analogs (A) can be used to confirm their base sequence (Griffin et al., 1988). Primary cleavage occurs at the carbamate linkage between the carbonyl carbon and ether oxygen at the 3'-ribose position (cleavage A). Fragmentation results in a regular anion series with the negative charge borne by the 3'-oxygen and formation of an isocyanate moiety at 5'-carbon on the next base unit. This mechanism should proceed if ionization occurs from the amide nitrogen to yield $(M-H)^-$ anions (Eq. 1). The presence of a methyl carbamate unit in the backbone of the oligonucleotide carbamate analog (B) yields the same ion series despite the absence of weakly ionizable amide protons. Capture of thermal electrons generated in the matrix (Williams et al., 1987) to generate the radical anion and subsequent dissociation to form the alkoxide ion is proposed (Eq. 2). Calculation of $(M-H)^-$ isotope distribution shows poor fit with experimental measurements, but inclusion of calculated isotopic abundance for $M^{+\cdot}$ in the molecular ion composition, shows much better agreement with experimental isotopic patterns.

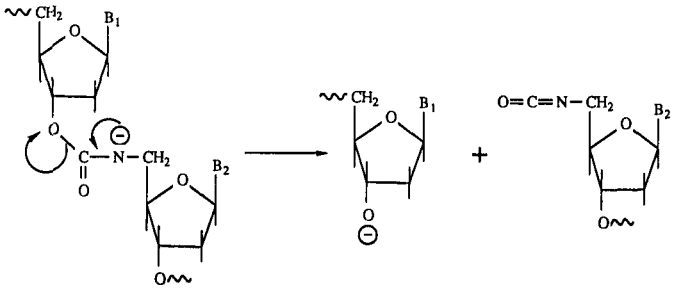

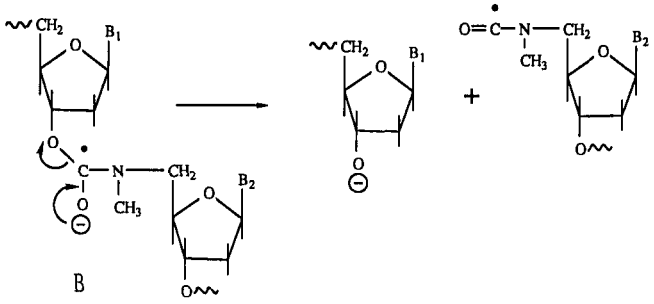

The presence of low-lying molecular orbitals seems to enhance formation of $M^{\pm}$ relative to $(M-H)^-$ ion. The experimental results for p-nitrophenyl ester of a morpholino nucleic acid (C) molecular ion cluster, for example, suggests considerable contribution of $M^{\pm}$ ion. The fragment ion with m/z 571.2, on the other hand, shows good agreement between calculated and experimental isotope cluster patterns.

Electron capture in negative ion FABMS or LSIMS may be more general than previously realized. For example, molecular ion centroid clusters are shifted to higher mass for oligodeoxynucleotides and this shift seems mass dependent (Fig. 1). Oligodeoxynucleotides, therefore, may fragment from the $M^{\pm}$ ion yielding the expected 3' and 5' ion series (Grotjahn et al., 1982) (Eq. 3).

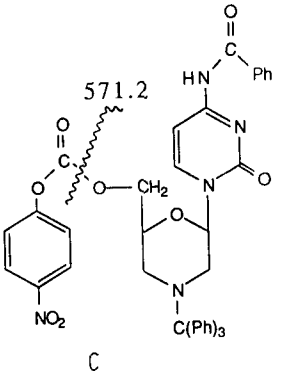

Figure 1. Molecular Ion Cluster Centroids

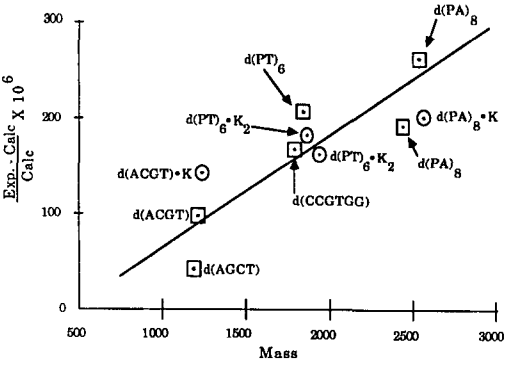

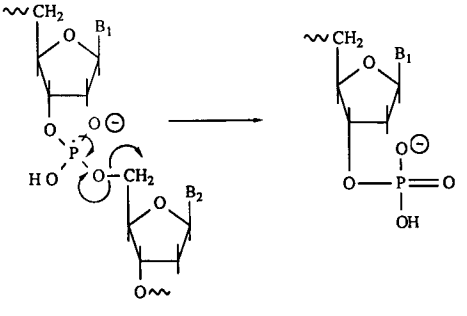

(3)

References

1. Griffin, D.; Laramée, J.; Stirchak, E.; Weller, D.; Deinzer, M. Biomed. Environ. Mass Spectrom. in press.

2. Williams, D.H.; Findeis, A.F.; Naylor, S.; Gibson, B.W. J. Am. Chem. Soc. 109, 1980 (1987).

3. Grotjahn, L.; Frank, R.; Blöcker, H. Nucleic Acids Res. 10, 4671 (1982).

Presented at the 36th ASMS Conference on Mass Spectrometry and Allied Topics
June 5-10, 1988, San Francisco, CA

MASS SPECTROMETRIC APPROACHES TO THE CONFIRMATION OF MADURAMICIN α IN CHICKEN FAT

S. J. Stout, L. A. Wilson, A. I. Kleiner, A. R. daCunha, and T. J. Francl

American Cyanamid Company, Agricultural Research Division, Princeton, New Jersey 08540

Introduction

Maduramicin, a polyether ionophore antibiotic, is a potent coccidiostat effective at a level as low as 5 ppm. Regulatory agency requirements state a confirmatory assay should yield high chemical specificity concomitant with providing structural information for unambiguous drug residue identification. Because mass spectrometry meets these criteria, it has gained widespread acceptance as the preferred analytical technique for confirmatory methods of analysis. For a confirmatory assay, coupling the thermal instability and low volatility of the ionophores with matrix coextractives essentially precludes the more routine mass spectrometric confirmatory approaches of GC/MS and solid probe/MS. Fast atom bombardment (FAB) was recently used for the quantitation of the polyether ionophore, monensin, in chicken fat, but did not provide sufficient fragmentation data for a confirmatory analysis(1). Additionally, FAB contributes further matrix to that already present from the tissue coextractives. Desorption chemical ionization (DCI) in conjunction with tandem mass spectrometry (MS/MS) has been reported for the confirmation of ivermectin, an antiparasitic compound, in cattle tissue. However, extensive sample cleanup was required prior to mass spectrometric analysis(2).

Objective

To develop a mass spectrometric confirmatory method for maduramicin α in chicken fat at the 0.5 ppm level.

Sample Preparation

The analyte is extracted from chicken fat using CH_3CN. After filtration, the CH_3CN extract is partitioned with hexane and then deposited on an acid alumina column for final cleanup. The analyte is eluted from the alumina with 10% H_2O in CH_3CN, the solvent is evaporated, and the residue redissolved in an aliquot of CH_3OH for analysis.

Results and Discussion

With the success in using DCI in conjunction with MS/MS for the confirmatory analysis of ivermectin(2), DCI appeared to offer a simple and straightforward approach to a confirmatory method for maduramicin α in chicken fat. While standards gave excellent DCI (NH_3) mass spectra, extracts prepared by the cleanup procedure left visible residues filling the loop of the emitter wire and generated ions at every mass during analyte vaporization. Coupling the matrix interferences with a low analyte recovery (only 6%) would probably doom efforts at MS/MS without an exhaustive cleanup. However, developing a prep-LC cleanup prior to DCI would prove difficult owing to the lack of a decent UV chromophore on the analyte.

While DCI did not succeed because of matrix coextractives, the favorable CI(NH_3) mass spectrometric data did suggest thermospray (TSP) LC/MS as a potential approach. Not only could TSP LC/MS serve as an ionization technique similar to CI(NH_3)(3), but it could also provide a much needed chromatographic cleanup prior to mass spectrometric analysis(4). Establishing acceptable thermospray conditions for the analyte was the most demanding challenge. A 10°C change in the vaporizer temperature was the difference between obtaining molecular species and thermally degrading the analyte in an irreproducible fashion. After establishing acceptable thermospray conditions, preliminary TSP LC/MS experiments on control and fortified chicken fat tissues were very encouraging. Ions at nominal masses of m/z 939, 934, 895, 890, and 805 were monitored to ensure compliance with confirmatory criteria(5). The response at m/z 939, used for quantitation and recovery calculations, was linear from 50 to 500 ng injected on-

column (corresponding to 0.25 to 2.5 ppm of analyte in tissue) and all confirmatory ions were present. The molecular species could be readily detected down to 10 ng on-column (0.05 ppm in fat) but the confirmatory ions were no longer present.

After seemingly having a successful route to a confirmatory method, the tip of the thermospray vaporizer had to be cut after plugging, a normal maintenance procedure. Upon restoring thermospray conditions, the fragment ions previously monitored could not be generated. Either only molecular species were generated, or the analyte was thermalized into irreproducible fragment ions. Apparently the fragment ions previously monitored had at least some origins in thermal and/or catalytic processes dependent upon the exact nature of the cut vaporizer tip. Approaches considered for inducing reproducible fragmentation included use of the filament, which did nothing, and use of repeller-induced CAD using a discharge electrode(6,7), which was not available at the time. Further analyses of the fat extracts in the full scan mode indicated that lower mass fragment ions generated for single stage MS analysis would not work owing to intense chromatographic peaks containing lower mass ions and a continuous background of ions below m/z 800 after several extract injections.

Consequently, coupling TSP LC/MS with MS/MS was considered in order to generate reproducible fragment ions from the molecular species obtained from thermospray. By using the program RF mode to pass all ions above m/z 900, implementation of MS/MS was far easier than getting TSP LC/MS to work. Because of the high molecular weight of the analyte and the absence of interferences in that mass region, using program RF circumvented the need to detune the Q_1 resolution to provide adequate response for MS/MS(8). Compared to TSP LC/MS of the analyte, the program RF mode without collision gas in Q_2 attenuated the parent ion responses about 50%. The conditions chosen for the CAD experiment in Q_2 (Ar @ 1 mT; collision energy, -15 V) provided an acceptable compromise between retention of the molecular species, sufficient fragmentation, and overall response.

CAD fragment ions at m/z 895 and 877 from the protonated sodium salt (m/z 939) in addition to CAD fragment ions at m/z 647 and 629 from the protonated ammonium salt (m/z 934) were monitored along with the molecular species. Control extracts were clean at all monitored ions. Analyses of five fortified tissues gave an average recovery of 68.9% (range 61.3 to 79.6%). While recoveries are not as important to a confirmatory method as the structural information provided, these values are within guidelines for regulatory methods(5). Analyses of five biologically incurred tissues confirmed the presence of the analyte in each case and gave an average residue level of 0.33 ppm (std dev = 0.041 ppm) in excellent agreement with a value of 0.40 $\pm$ 0.028 ppm from the LC/fluorescence determinative method.

References

(1) Blomkvist, G.B.; Jansson, K.M.; Ryhage, E.R.; Osterdahl, B.-G. J. Agric. Food Chem. 1986, 34, 274-276.

(2) Tway, P.C.; Downing, G.V.; Slayback, J.R.B.; Rahn, G.S.; Isensee, R.K. Biomed. Mass Spectrom. 1984, 11, 172-176.

(3) Voyksner, R.D.; Haney, C.A. Anal. Chem. 1985, 57, 991-996.

(4) Covey, T.R.; Lee, E.D.; Bruins, A.P.; Henion, J.D. Anal. Chem. 1986, 58, 1451A-1461A.

(5) Sphon, J.A. J. Assoc. Off. Anal. Chem. 1978, 61, 1247-1252.

(6) McFadden, W.H.; Lammert, S.A.; J. Chromatogr. 1987, 385, 201-211.

(7) McFadden, W.H.; Garteiz, D.A.; Siegmund, E.G. J. Chromatogr. 1987, 394, 101-108.

(8) Hunt, D.F.; Buko, A.M.; Ballard, J.M.; Shabanowitz, J.; Giordani, A.B. Biomed. Mass Spectrom. 1981, 8, 397-408.

Presented at the 36th ASMS Conference on Mass Spectrometry and Allied Topics
June 5-10, 1988, San Francisco, CA

INFLUENCE OF DIET ON THE OXIDATION OF FATTY ACIDS IN HUMANS USING ISOTOPE RATIO MASS SPECTROMETRY

M.A. French, E. Kielo, S. Pharazyn, A.B.R. Thomson, L. Wang, R. Rajotte and M.T. Clandinin
Nutrition and Metabolism Research Group, 533 Newton Research Building
University of Alberta
Edmonton, Alberta, CANADA T6G 2C2

Animal studies have shown that diets high in polyunsaturated fats increase absorption of medium and long chain fatty acids (1,2). The present study was undertaken to determine the effects of the quantity of fat and degree of polyunsaturation on absorption and whole body oxidation of fatty acids in humans.

Six healthy adult males were placed on a diet to meet maintenance energy requirements for 15 days in four test periods. During each test period, the subjects were provided with a different diet treatment. The diet was formulated (3) to contain 40% fat by energy in the high fat diets and 30% fat in the low fat diets. The polyunsaturated to saturated fat (P/S) ratio fed was either 0.2 or 1.0 at both levels of fat intake. The ratio of 10:0/16:0 was kept constant at 0.14 for all the diets and this was achieved by adding MCT oil to the diets.

Within each diet treatment, three menus were used. The same menu was always consumed one day prior to and on all test days. Meals were prepared in a metabolic kitchen and consumed at fixed times. On the test days duplicates of each subject's meals were prepared, homogenized and freeze-dried. Subsequently total fat and fatty acid content were analyzed by GLC of the fatty acid methyl esters (4,5).

The first 9 days of each test period served as a stabilization period. During days 9, 10 and 13 of each test period, the subjects were confined to the metabolic laboratory and provided hourly breath samples from 0730 to 1630 h for 6 minutes. On day 9 analysis of the $^{13}CO_2$ background enrichment enabled measurement of ^{13}C abundance due to the diet alone. On days 10 and 13 of each test period either [1-^{13}C] palmitic acid or [1-^{13}C] decanoic acid was ingested in capsule form by the subjects with the breakfast meal. The labeled fatty acids were administered at a dose of 15 mg of 99% [1-^{13}C]16:0 per kg of body weight and 3 mg of 99% [1-^{13}C]10:0 per kg of body weight, respectively.

The CO_2 in the expired breath was trapped in 1N NaOH. The CO_2 was regenerated under vacuum with phosphoric acid and the ^{13}C enrichment was measured by a Finnigan MAT 251 Isotope Ratio Mass Spectrometer against a laboratory CO_2 standard.

The average response to [1-^{13}C]10:0 was approximately ten times that of [1-^{13}C]16:0. Figure 1 shows that increasing the P/S ratio from 0.2 to 1 increased the Atom Percent Excess (APE) of ^{13}C in breath CO_2 by an average of 12%, and on the low fat diet increasing the P/S ratio increased the APE by 18% when the substrate fed was C10:0. When [1-^{13}C]16:0 was fed the APE increased by 25% on the low fat diet when the P/S ratio was increased.

The rate constants for the disappearance of ^{13}C from the breath were calculated when the substrate was C10:0. Figure 2 show the ratio of the rate constants for the low P/S diet compared to the high P/S diet at the two fat levels. The rate of disappearance of ^{13}C from the breath is consistently higher on a low P/S high fat diet for all subjects.

The results of this study suggest that the type and amount of fat in the diet affect the absorption and oxidation of fatty acids in normal subjects. This may have implications for nutritional therapy of individuals with chronic malabsorption diseases.

References

1. Thomson ABR, Keelan M, Clandinin MT. Onset and persistence of changes in intestinal transport following dietary manipulation. Lipids 1987;22:22-7.
2. Thomson ABR, Keelan M, Clandinin MT, Walker K. A high linoleic acid diet diminishes enhanced intestinal uptake of sugars in diabetic rats. Amer. J. Physiol. 1987;252:G262-71.
3. Agriculture handbook No. 8-1 to 7, Agricultural Research Service, U.S. Department of Agriculture, Washington, D.C. 1963-80.
4. Folch J, Lees M, Sloane SGH. A simple method for the isolation and purification of total lipids from animal tissues. J. Biol. Chem. 1957;226:497-509.
5. Bannon DC, Craske JH, Man NT, Harper NL, O'Rourke KL. Analysis of fatty acid methyl esters with high accuracy and reliability. II. Methylation of fats and oils with boron trifluoride-methanol. Chrom 1982;15:63-9.

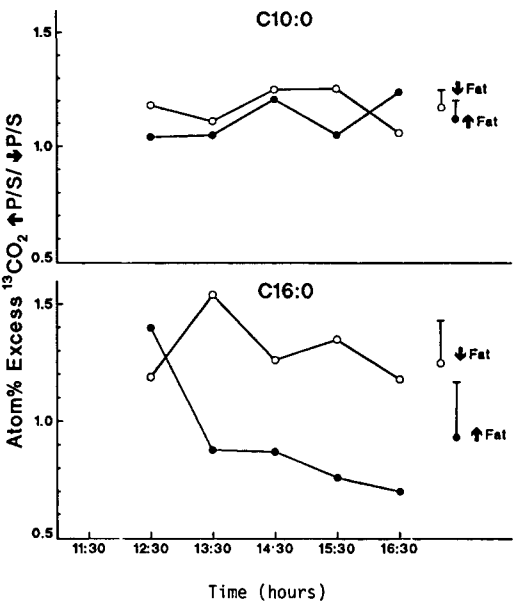

Figure 1. Ratio of response on high P/S diet to low P/S diet.

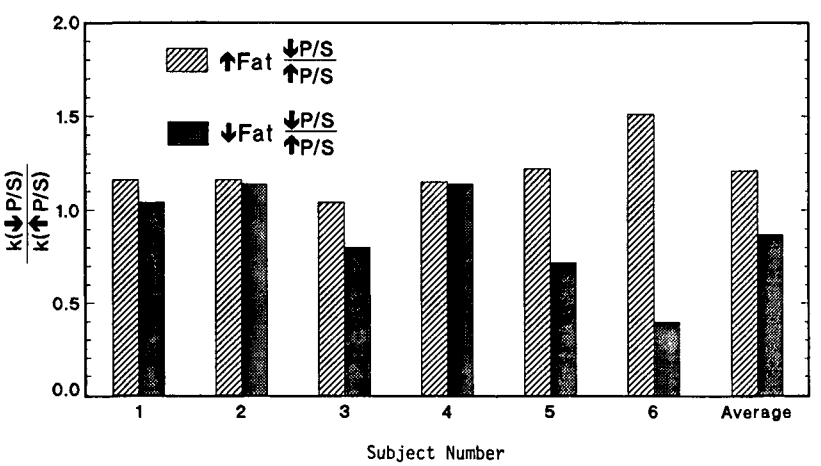

Figure 2. Ratio of rate constants for decay of $^{13}CO_2$ on C10:0 test day.

Presented at the 36th ASMS Conference on Mass Spectrometry and Allied Topics
June 5-10, 1988, San Francisco, CA

THE ROLE OF SOLVENT CHEMISTRY IN DESORPTION IONIZATION MASS SPECTROMETRY

Kelsey D. Cook
Department of Chemistry, University of Tennessee, Knoxville, TN 37996-1600

Developments in matrix-assisted desorption ionization (DI) have extended not only the range of chemicals to which mass spectrometry can be applied, but also the range of chemistry subject to characterization. The detailed speciation of solution components made possible through DI is often unrivaled by other analytical techniques, providing great potential for both qualitative and even quantitative investigations of reacting and equilibrated systems. However, care must be taken to account for variations in sensitivity and for the invasiveness of the probe in such spectral interpretations. In particular, careful studies by several workers have demonstrated that a bombarding particle beam can induce chemical changes (e.g., reductions and rearrangements) that could be severely misleading in the interpretation of a spectrum of an unknown. Even in the absence of a probe beam (as in the case of electrohydrodynamic (EH) MS), important "matrix effects" can complicate spectral interpretation. Work in our laboratory has sought to assess the impact of these effects in EH MS, for subsequent comparison with corresponding FAB data. This should ultimately allow resolution of bombardment artifacts.

To investigate the role of sample redox chemistry, EH spectra of a series of transition metals and their complexes were compared with corresponding published FAB data (Tables 1-2). Evidence of reduction was generally less extensive in EH than in FAB, confirming the role of bombardment-induced radicals invoked elsewhere to explain aspects of FAB spectra. A key example is Cu^{2+}, whose reduction by glycerol is known to be prevented by Cl^-. While reduction products are nevertheless evident in FAB spectra of $CuCl_2$, they are absent in corresponding EH spectra (Table 1). Reduction products were strongly evident in EH mass spectra only of those transition metals and complexes with $E^o > 0.1$ V, indicating that the EH spectra may accurately reflect the unperturbed redox chemistry of glycerol.

A conclusion that solution chemistry is not substantially perturbed by EH sampling does not constitute a "declaration of independence" from the effects of variations in sampling efficiencies. Two examples of chemical effects on sampling efficiencies were illustrated in a study of a series of quaternary ammonium salts described elsewhere in this Volume. In that study, ion pairing was noted to depend predictably on counterion identity. While extensive pairing reduced sensitivities by neutralizing singly charged ions, it actually enhanced sensitivity by reducing solvation of (otherwise) multiply charged ions. The implication that solvent dielectric constant and electrolyte selection are important parameters of matrix design may also pertain to other DI experiments (an hypothesis still largely untested).

A second chemical implication of matrix selection evident in the study of quaternary ammonium salts arises from the role of mass transport in affecting sampling efficiencies. In order to "cross the solution-vacuum barrier," an analyte ion or molecule must reach the interface. In EH MS, this occurs largely through convection and diffusion, both of which depend on matrix viscosity. While convection should supply all analytes at an equal rate, diffusion coefficients of components of a mixture may differ, introducing sampling bias against those components which diffuse more slowly. This rationale was invoked to account for the persistence of sampling bias against heavier members of the homologous series of quaternary ammonium salts, even in solutions where ion pairing was expected to be negligible. The bias was found to be amplified by the introduction of electrolytes which increased solvent structure (and therefore viscosity). For a given viscosity, the bias (a difference in relative sensitivities) was unaffected by a change to a counterion expected to pair less extensively; the members of the series were evidently all affected by ion pairing to the same extent.

Presented at the 36th ASMS Conference on Mass Spectrometry and Allied Topics
June 5-10, 1988, San Francisco, CA

TABLE 1: Reduction of Transition Metals and Complexes Evident in in EH Mass Spectra

Analyte	% Reduction	Reduction Product	E°	Comment
$Ru(bpy)_3^{3+}$	100%	Ru(II)	1.30 V	
$Cu(NO_3)_2$	(a)	Cu^o	0.34 V	$Cu^{2+/o}$
	15%	Cu(I)	0.16 V	$Cu^{2+/1+}$
$Cu(bpy)_2^{2+}$	43%	Cu(I)	0.12 V	NO_3^- counterion
	10%	Cu(I)		Cl^- counterion

Not Reduced: $CuCl_2$ (<0.16 V); $Ni(NO_3)_2$) (-0.23 V);
$Cr(bpy)_3^{2+}$ (-0.52 V^b); $Co(bpy)_3^{2+}$ (-0.73 V^b);
$Ru(bpy)_3^{2+}$ (-1.28 V^b).

a: Cu^o observed as precipitate; not evident in spectrum.
b: Measured in acetonitrile.

TABLE 2: Reduction of Transition Metals and Complexes Evident in in FAB Mass Spectra

Analyte	% Reduction	Reduction Product	E°	Comment
$Fe_2(SO_4)_3$	80%	Fe(II)	0.77 V	Also $FeCl_3$ (a,b)
$CuCl_2$	82%	Cu(I)	<0.16 V	(b)
$Cr(NO_3)_3$	46%	Cr(II)	-0.41 V^c	(b)
$Ru(bpy)_3^{2+}$	51%	Ru(I)	-1.28 V^c	(d)
	56%	Ru(I)	-1.28 V^c	(e)

a: Williams, Findeis, Naylor, and Gibson, JACS 109, 1980 (1987).
b: Pelzer, De Pauw, Dung, and Marien, J. Phys. Chem. 88, 5065 (1984).
c: Measured in acetonitrile.
d: Bojessen, Org. Mass Spec. 20, 413 (1985).
e: Miller, Balasanmugam, Nye, Deacon, and Thomas, Inorg. Chem. 26, 560 (1987); measurements made in m-nitrobenzylalcohol.

Presented at the 36th ASMS Conference on Mass Spectrometry and Allied Topics
June 5-10, 1988, San Francisco, CA

ELECTROSPRAY IONIZATION PHENOMENA AND THE INTERFACE OF CAPILLARY ELECTROPHORESIS AND MASS SPECTROMETRY

Richard D. Smith, Charles J. Barinaga, and Harold R. Udseth
Chemical Methods and Separations Group
Chemical Sciences Department
Pacific Northwest Laboratory (operated by Battelle Memorial Institute)
Richland, WA 99352

The electrospray ionization (ESI) for mass spectrometry was first explored by Dole and coworkers. Recently, Fenn and coworkers have contributed extensively to the understanding of ESI and its potential applications for LC-MS interfacing. The interest in our laboratory has been to use ESI as an interface between capillary electrophoresis and mass spectrometry. The success of this application depends strongly upon our ability to manipulate and exploit the ESI process.

Capillary electrophoresis refers to a set of micro-scale analytical and preparative separations methods which include capillary zone electrophoresis (CZE), gel electrophoresis, isotachophoresis, isoelectric focusing and electrokinetic chromatography (although the latter is more strictly considered a chromatographic method, since it involves analyte partitioning with an electrophoretically migrating micellar phase). Capillary zone electrophoresis is a form of free zone electrophoresis conducted in small diameter capillaries and capable of ultra-high resolution separations. Separations are based on differences in the electrophoretic mobilities of analytes and more than 10^6 theoretical plates can be obtained in less than twenty minutes. Electroosmotic flow of the buffer mediums makes it an elution technique which resembles chromatography, although the use of capillaries filled with gels is also feasible. Thus, CZE provides high-resolution separations and selectivities which can be manipulated by changing the electrophoretic medium (i.e., typically pH and buffer composition, as well as equilibria with electrophoretically migrating micellar phases).

Recently a new electrospray ionization interface for capillary electrophoresis-mass spectrometry (CE-MS) has been developed. The interface uses a sheath flow of liquid to make the electrical contact at the CZE terminus, thus defining both the CZE and electrospray field gradients. This allows the composition of the electrosprayed liquid to be controlled independent of the CZE buffer, providing operation with buffers which could not be used previously (e.g., aqueous and high ionic strength buffers). The interface operation is substantially independent of CZE flow rate, CZE capillaries are easily replaced, and require no additional preparation. Since the electrospray occurs directly from the CZE capillary terminus, additional mixing volumes and metal surfaces are avoided and electrophoretic separation efficiency appears unperturbed. The dead volume associated with the electrospray interface is < 10 nL, corresponding to < 0.1 s for typical flow rates of the sheath electrode liquid.

Ions created by the ESI process are sampled through a 1 mm orifice (nozzle) into a region mechanically pumped at 50 L/s using a single-stage roots blower. The ions entering this region are sampled through a 2 mm diameter skimmer orifice located 0.5 cm behind the nozzle orifice. Ions passing through the skimmer enter a radio frequency focusing quadrupole. This region is pumped by a cryopump, consisting of a standard compressor and cold head with a custom cylindrical second stage baffle (cooled to ~14 K) which encloses the quadrupole and provides an effective pumping speed of >30,000 L/s for N_2. The analyzer quadrupole chamber was pumped at 500 L/s with a turbomolecular pump. A single ion lens with an 0.64-cm aperture separated the ion focusing and analysis quadrupole chambers. The pressures in the focusing and analysis chambers were ~1 x 10^{-6} and 2 x 10^{-7} Torr, respectively. The countercurrent flow of N_2 (at ~70 °C) for desolvation of the electrospray was in the range of 3 to 6 L/min.

In the following we use a simple mixture of four quaternary phosphonium salts to illustrate the characteristics of capillary electrophoresis separations with mass spectrometry and to illustrate the potential analytical value of these new methods. The CZE-MS total and single ion electropherograms for the quaternary phosphonium salts are shown in Figure 1. The separation was conducted in a relatively short 60 cm capillary, using an 11 kV CZE voltage drop. Buffer conductivities were generally chosen to be on the order of 10^3 µmho/cm. The separation in Figure 1 was obtained using a 0.05 M potassium hydrogen phthalate aqueous buffer with 10^{-4} M KCl adjusted to pH 4.8 by titration with NaOH. The sheath electrode liquid was 8.7% water in isopropanol containing 0.1 M ammonium acetate and 2 x 10^{-5} HCl at a pH of 8.9. Although 40,000 to 80,000 theoretical plates are obtained in the separation of the individual components, as shown for the single ion electropherograms, the four component mixture is resolved into only two peaks. It is not surprising that the vinyltriphenyl and ethyltriphenyl phosphonium ions elute simultaneously due to the expected similarities in their electrophoretic mobilities; it was somewhat less expected that the tetrabutyl and tetraphenyl phosphonium ions coelute.

Isotachophoresis in a capillary format is an alternative electrophoretic method which provides an attractive complement to CZE. The instrumentation used for capillary isotachophoresis (CITP) can be nearly identical to that of CZE. In CZE analyte bands separate on the basis of differences in electrophoretic mobilities in an electric field gradient, which is ideally unperturbed by their presence (due to the much lower effective concentrations). In contrast, for isotachophoresis the analyte mobilities define the electric field strength.

Two different electrolyte solutions are chosen as the leading and terminating electrolyte solutions which have sufficiently high and low electrophoretic mobilities, respectively, to bracket the electrophoretic mobilities of the sample components of interest.

A direct CITP-MS combination is an attractive complement to CZE for a number of reasons. First, the sample size which can be introduced is greater by several orders of magnitude than can be tolerated in CZE and is limited primarily by the volume of the capillary and the time allowed to obtain a separation (which is inversely related to voltage). Second, CITP generally results in concentration of analyte bands (depending upon concentration relative to the leading electrolyte), which is in contrast to the inherent dilution obtained with CZE. These two features can provide a substantial improvement in detection limits compared to CZE. A third benefit of CITP is derived from the nature of separations compared to CZE or chromatographic methods. The chromatographic peak capacity needed to separate all the components of a sample greatly exceeds the number of sample components. In other words, to obtain conditions such that no two components coelute most of the detector observation time during a separation is wasted. In contrast, for isotachophoresis one sample band immediately follows another (once a separation is obtained).

The application of CITP-MS to the same phosphonium salt mixture used for the CZE-MS experiments is shown in Figure 2. The separation was conducted using a 2 m x 100 μm i.d. untreated fused silica capillary and the separation conducted at 35 kV. The leading electrolyte was 10^{-3} M ammonium acetate and the trailing electrolyte was 10^{-3} M tetraoctyl ammonium bromide in a 1:1 water-methanol solvent mixture. The separation is well developed with minimum band overlap and sharp edges. The widths of the four bands are nearly equivalent, consistent with the similar sample concentrations and the minor discrimination expected using electromigration for introduction of this mixture.

The most striking feature of the separation shown in Figure 2 is the excellent resolution of the four phosphonium salts, which were not resolved in the short CZE separations, and even in longer separations on a 2 m capillary. The fact that the vinyltriphenyl and ethyltriphenyl phosphonium ions are clearly resolved illustrates the potential of CITP-MS to generate high resolution separations. Another advantage is the greater signal-to-noise ratios. The development of capillary isotachophoresis-MS promises to provide a powerful complement to CZE-MS. Other variations of capillary electrophoresis, including isoelectric focusing, gel electrophoresis and capillary electrokinetic chromatography also appear amenable to mass spectrometric detection using the new interface methods. The rapid developments in injection techniques and the use of buffer media providing enhanced selectivities promise increasing interest in these attractive instrumental methods.

We thank the U.S. Department of Energy, Office of Health and Environmental Research, for support of this research under Contract DE-AC06-76RLO 1830.

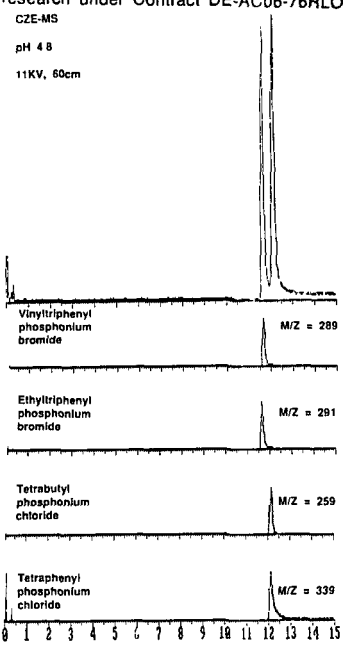

Fig. 1

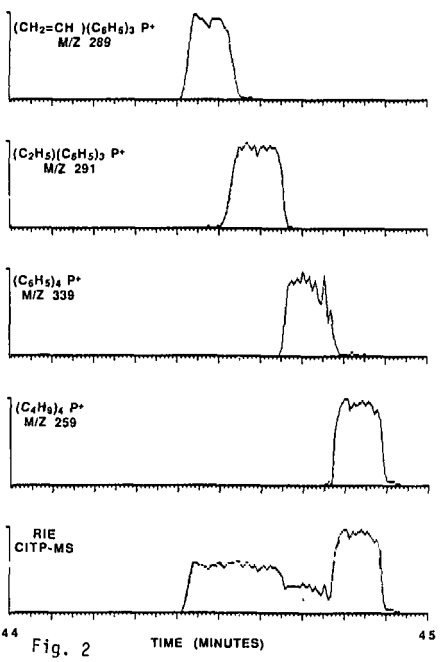

Fig. 2

Presented at the 36th ASMS Conference on Mass Spectrometry and Allied Topics
June 5-10, 1988, San Francisco, CA

MAGIC-LC/MS: A VERSATILE SAMPLE INTRODUCTION PATH FOR MASS SPECTROMETRY

Richard F. Browner, J. Daniel Kirk, W. Eric Harris and Deborah D. Perkins
School of Chemistry, Georgia Institute of Technology, Atlanta, Georgia 30332-0400

MAGIC-LC/MS provides a simple, mechanical means of interfacing LC effluents of virtually any composition with a mass spectrometer. Controlled drop size aerosol is formed from the LC effluent, and after dispersion with helium, the solvent evaporates under kinetic conditions controlled by thermal transport to the evaporating aerosol drops. The resulting mixture of essentially solvent-free analyte particles, solvent vapor and helium then passes to a momentum separator, where after supersonic nozzle expansion, the analyte particle beam is preferentially skimmed from the jet in a two-stage process. The highly enriched, largely solvent free analyte particle beam then passes to the mass spectrometer ion source area, where various ionization techniques may lead to the generation of mass spectra.

The process of aerosol generation is not yet totally characterized, but is believed to involve a two-step process, whereby a stream of drops initially approximately twice the diameter of the liquid injection capillary is further shattered by a stream of He to produce a laminar flow stream of drops with diameters roughly the same as the diameter of the liquid capillary. The drop size distribution of this drops stream is still quite narrow, although under certain conditions some multimodality may be introduced. Collection of the desolvated particles, and size measurement using electron microscopy, shows that the diameters of the dry particles entering the mass spectrometer ion source region are precisely as predicted from calculations based simple solvent evaporation theory. Consequently, there appears to be very little agglomeration or other process taking place to increase particle size after initial aerosol formation takes place. The manner in which particle vaporization in the ion source is able to give rise to classical EI and CI spectra is a direct consequence of the rapid vaporization step which occurs when the small particles flash vaporize in the ion heated source.

Presented at the 36th ASMS Conference on Mass Spectrometry and Allied Topics
June 5-10, 1988, San Francisco, CA

MECHANISM OF FAB SPECTRA FORMATION TEMPERATURE DEPENDENCE

J. Sunner, Department of Chemistry,
Montana State University, Bozeman, MT 59717.
A. Morales and P. Kebarle, Department of Chemistry,
University of Alberta, Edmonton, Alberta, Canada T6G 2G2

Fast Atom Bombardment (FAB) spectra frequently reveal strong matrix effects. For example, an analyte with a low concentration in the near-surface region of the liquid matrix may dominate the FAB spectrum. A kinetic scheme, based on ion/molecule reactions occurring in high-pressure mass spectrometry, was previously shown to be able to reproduce FAB spectra of varying concentration diethanol-amine (DEA) in glycerol (1). The presence of an intermediate gas-like state is supported by the observation that the protonation of the analyte is determined by gas-phase energetics and by the indications that extensive +/-ion recombination occurs during the desorption event. We have explained the formation of the gas-like state in desorption ionization in terms of fundamental thermodynamic properties of liquids in the Phase Explosion model (2). However, in its first version this model could not explain the very strong dependence of FAB spectra on the temperature of the bulk matrix, T_b, observed by Field et al. (3). We here report investigations into the temperature dependence of FAB spectra of some simple systems. The spectra of glycerol and of DEA in glycerol were successfully modelled by the same kinetic scheme that was previously used (1). In a refined Phase Explosion model, interactions of the gas-like state with the surrounding liquid is considered.

Fast Atom Bombardment (FAB) spectra of glycerol and of solutions of analytes in glycerol were studied as a function of the temperature of the FAB matrix, from -30°C to +40°C. In agreement with Field et al. (3) it was found that the spectra deteriorated towards a series of nondescript peaks as the matrix temperature (T_b) decreased. It was also found that the intensities of analyte ions decreased more rapidly with decreasing T_b than even the glycerol cluster ions.

Figure 1 shows the temperature dependence for major ions in FAB spectra of neat glycerol. It is seen that the dependence on T_b is quite regular. Noteworthy is the very strong decrease for the "noise-ions" (which includes all background peaks) with increasing T_b and the corresponding increase for the molecular ion. With regard to their temperature dependence, the ions on the glycerol spectrum follow the order:

$$\text{"noise-ions"} < F_G^+ < GlH^+ < (Gl)_2H^+ < (Gl)_nH^+;\ n \geq 3 \qquad (1)$$

This is the same order that was previously observed (1) for the attenuation of the different ions as DEA was gradually added to the glycerol matrix. Figure 2 shows the temperature dependence of ions for a 10 mol% solution of DEA in glycerol. The DEA ions are seen to have a very strong temperature dependence.

Results like those shown in Figures 1 and 2 were reproduced by the kinetic model. The modelling required the assumption that t_{max} increased with T_b, where t_{max} is the time after the atom impact when ions emission ceases, Figure 3. The results of the kinetic modelling are shown by the dotted lines in Figures 1-2.

The strong dependence on t_{max} on T_b can be understood qualitatively as a consequence of the radial expansion of the gaseous cavity formed by the fast atom. At low temperature, when the glycerol viscosity is high, a high temperature, high pressure gas that has considerable radiation damage is very rapidly expelled from the cavity. At higher matrix temperature, the lower viscosity allows for an initial radial expansion of the cavity gas. As a result this gas cools very considerably and the pressure decreases. The rate of expulsion decreases and the rate of heat transport to the surrounding liquid becomes competitive. The conditions described by the initial phase explosion model are asymptotically reached.

Presented at the 36th ASMS Conference on Mass Spectrometry and Allied Topics
June 5-10, 1988, San Francisco, CA

1. Sunner, J.; Morales, A.; Kebarle, P. Anal. Chem., **1988**, 60, 98.
2. Sunner, J.; Ikonomou, M.; Kebarle, P. Int. J. Mass Spectrom. Ion Proc., **1988**, 82, 221.
3. Katz, R.N.; Chaudhary, T.; Field, F.H. Int. J. Mass Spectrom. Ion Proc., **1987**, 78, 85.

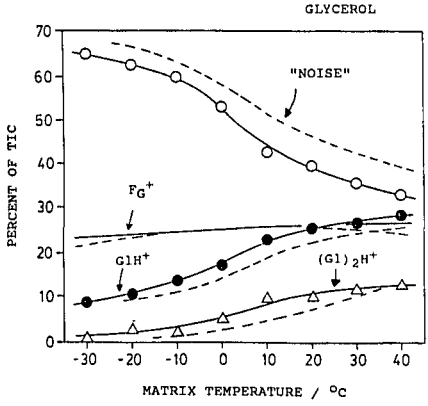

Figure 1. Temperature dependence of intensities of ions in FAB spectra of glycerol; Gl=glycerol; F_G^+=major fragment ions; "noise" includes all background ion peaks. Dashed lines show calculated results.

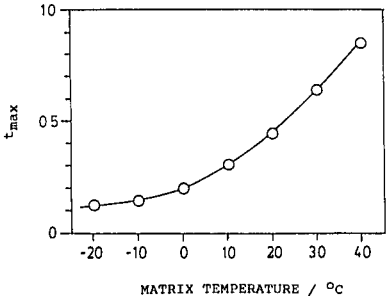

Figure 3. Dependence of t_{max} on bulk matrix temperature. Timescale in ns if it is assumed that the protonation reaction leading to $DEAH^+$ occurs with a diffusion limited rate constant.

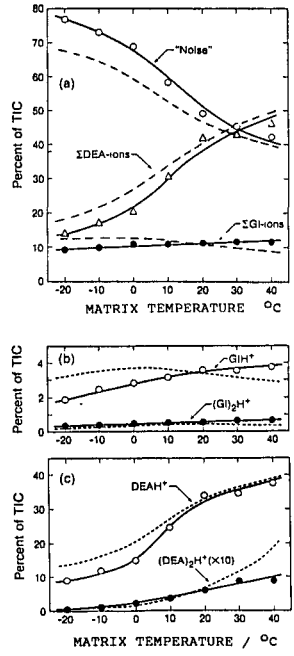

Figure 2. Temperature dependence of major ions in FAB spectra of 10 mol% DEA in glycerol; ΣDEA and ΣGl refer to the sum intensity of major fragments, pseudo-molecular and cluster ions; F_D^+ = major DEA fragments; Dashed lines show calculated results.

Presented at the 36th ASMS Conference on Mass Spectrometry and Allied Topics
June 5-10, 1988, San Francisco, CA

MASS TRANSPORT IN LIQUID SIMS

Peter J. Todd
Analytical Chemistry Division
Oak Ridge National Laboratory
Oak Ridge, Tennessee 37831-8121

Secondary ion emission occurs only from the sample surface. From glycerol solutions containing involatile solutes, enhanced emission of solute-characteristic ions occurs because the solutes become adsorbed to the surface from the bulk solution. The flow of solutes to the surface is controlled by diffusion. This mechanism of mass transport was investigated by using the method of finite differences[1] to evaluate Fick's equations and comparing the results to SIMS spectra. The results show that flow of solute to the surface is influenced by a number of factors which can neither be controlled nor evaluated with any confidence. Volatile solutes, such as amines can be adsorbed to a glycerol surface from the gas phase at a rate independent of diffusion. SIMS spectra of such surfaces appear much like Langmuir isotherms, and are highly reproducible. Furthermore, from a knowledge of the amine surface activity and Henry's Law constant, the actual surface concentration can be determined. This feature permits an explicit comparison between SIMS spectra and surface activity.

For diffusion, calculations were made by assuming the sample to consist of two phases. In the bulk phase, diffusion coefficients, D were assumed to be between 10^{-11} and 10^{-9} cm^2/s. A surface phase was assumed to have no thickness and infinite diffusion. That is, the surface phase was assumed to behave as a two dimensional gas. Mass transport between the surface phase and the bulk was determined by assuming the surface phase to have an effective concentration, C_s, related to the actual surface concentration, Γ(moles/cm^2), by the Gibbs Equation, (1)

$$\Gamma = -(C_s/RT)(d\gamma/dC) \quad (1)$$

where R= Gas constant
T = Temperature
$(d\gamma/dC)$ = variation of surface tension with analyte concentration.

The surface concentration can be mathematically generated by diffusion and depleted at different rates as a fraction of surface coverage to mimic sputtering by different primary ion currents. The surface concentration does not reflect the bulk concentration, as might be expected from the Gibbs equation, but rather to a fraction, between 1 and 10% of the bulk concentration. Figure 1 shows plots of concentration vs depth for a sample under 1 $\mu A/cm^2$ primary ion bombardment, where it can be seen that the origin of this effect is the depleted region of the bulk solution near the surface. Furthermore, as the surface is depleted by the primary ion beam, surface concentration is determined by the flux of solute to the surface, a function of dC/dx, which is itself time-dependent.

To ensure that the flow of surfactant was not a function of time, amines were introduced as vapors onto the surface of glycerol under bombardment. Figure 2 shows plots of protonated octylamine ion intensity vs. amine pressure. The shape of this curve is that of a Langmuir isotherm. Such behavior is described by equation (2)

$$P/I = P/I_{max} + 1/(bI_{max}) \quad (2)$$

where P = amine pressure
I = fractional secondary ion current carried by protonated amine
b = ratio of adsorption/desorption rate constants

Presented at the 36th ASMS Conference on Mass Spectrometry and Allied Topics
June 5-10, 1988, San Francisco, CA

When data such as that plotted in Figure 2 are plotted in the terms of equation (2), straight lines are obtained for each plot. For a series of data taken under different primary ion current density, lines are parallel, with intercepts that differ by a constant proportional to primary ion current density. From the intercept data, erosion of the surface monolayer occurs at a rate of 1 monolayer/7s. for a primary ion current density of 1 $\mu A/cm^2$. Furthermore, the data indicate that if there is an amine molecule within a radius of approximately 250 Angstroms from a primary ion impact point, that amine will be ejected as a protonated secondary amine ion.

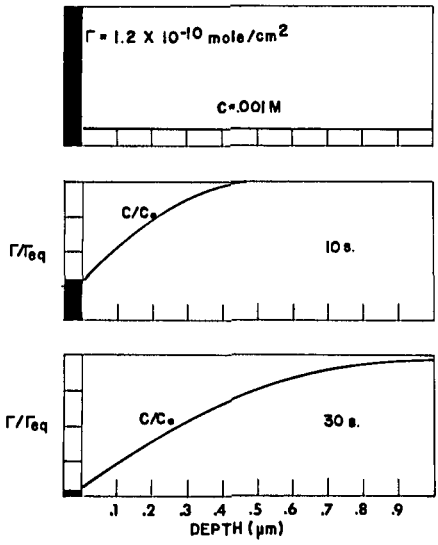

Figure 1. Concentration vs depth at different times under 1 $\mu A/cm^2$ primary ion current density.

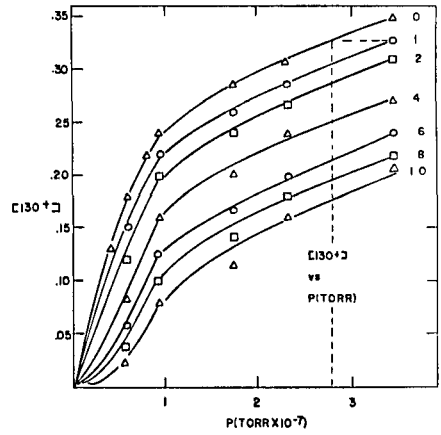

Figure 2. Fractional ion current carried by protonated octylamine as a function of octylamine pressure.

Research sponsored by the U. S. Department of Energy, Office of Basic Energy Sciences, under Contract DE-AC05-84OR21400 with Martin Marietta Energy Systems, Inc.

Literature Cited

1. J. D.Crank, The Mathematics of Diffusion, Clarendon Press, Oxford(1979)

"The submitted manuscript has been authored by a contractor of the U S Government under contract No DE-AC05-84OR21400 Accordingly, the U S Government retains a nonexclusive, royalty-free license to publish or reproduce the published form of this contribution, or allow others to do so, for U S Government purposes "

Presented at the 36th ASMS Conference on Mass Spectrometry and Allied Topics
June 5-10, 1988, San Francisco, CA

APPLICATIONS OF ELECTROPHORESIS COUPLED WITH SECONDARY ION MASS SPECTROMETRY

M.S. Stanley and K.L. Busch
Department of Chemistry, Indiana University, Bloomington, IN 47405

A custom-built secondary ion mass spectrometer (SIMS), originally used in the direct analysis on thin layer chromatograms [1], has now been used in the analysis of compound mixtures separated with paper and slab gel electrophoresis [2].

Paper electrophoresis is a technique that is frequently used in the separation of small charged molecules. For example, in a clinical setting, determination of the chemical composition of a kidney stone has been accomplished through paper electrophoresis [3]. The kidney stone was composed mostly of xanthine and hypoxanthine. The SIMS analysis of xanthine shown in Figure 1, using glycerol acidified with p-toluenesulfonic acid (ptsa), contains a fairly intense ion corresponding to the protonated molecule at m/z 153. Xanthine undergoes little fragmentation under SIMS conditions; the intense ion at m/z 147 appears to be contamination within the instrument (probably a silane-related compound). Hypoxanthine behaves similarly, giving an intense ion corresponding to the protonated molecule and no apparent fragmentation. Xanthine and hypoxanthine can be cleanly separated by paper electrophoresis. The SIMS spectra of the paper electropherogram give spectra of xanthine and hypoxanthine that are qualitatively similar to the spectra acquired from the neat compounds. The SIMS spectrum of xanthine acquired out of a Whatman 3MM paper electropherogram is shown in Figure 1. Glycerol doped with ptsa was used to extract the analyte out of the 3MM paper. The protonated molecule at m/z 153 is still quite intense, and there is a low level of signal corresponding to the glycerol and ptsa matrix as well as the contaminant peak at m/z 147.

For polyacrylamide gel electrophoresis (PAGE), the high water content of the gel (80-90%) precludes the direct analysis of the electropherogram by SIMS. In gel electrophoresis, however, blotting techniques are frequently used to transfer separated mixture components qualitatively and quantitatively from the gel matrix onto a membrane. This renders the components more accessible to reagents. In addition, nitrocellulose, frequently used in the transfer of proteins, is vacuum compatible and can be directly analyzed by mass spectrometry. Small peptides, such as angiotensin I, neoendorphin, and bradykinin, and larger peptides, such as insulin, myoglobin and cytochrome c, as well as the antibiotic bacitracin, are being used to explore the possibilities of mass spectral analysis of gel electropherograms. The secondary ion mass spectrum of bradykinin acquired out of nitrocellulose after transfer from a developed electrophoretic gel is shown in Figure 2. The protonated molecule is clearly visible at m/z 1061 and several of the ions, such as those at m/z 905, m/z 568, and m/z 120, are indicative of structure. The protonated molecule can be monitored to obtain an image of the bradykinin band in the nitrocellulose, Figure 3. The image shows a good signal-to-noise ratio between the actual bradykinin band and the surrounding nitrocellulose. The shape of the image is similar to the shape of the image obtained by staining the band with Coomassie Blue R following mass spectral analysis.

Work is also being started in the analysis of gel electropherograms containing peptides with molecular weights above 3,500 daltons. The current mass range of the chromatography/SIMS instrument is approximately 3,500 daltons, which is too low for the analysis of most peptides separated using gel electrophoresis. In order to analyze higher molecular weight peptides with the chromatography/SIMS instrument, the peptides must be broken down into fragments that are lower in mass but which together define the original peptide structure. The use of reagents such as cyanogen bromide and trypsin, to selectively cleave the peptides after transfer into the membrane and before mass spectral analysis has been considered and is shown schematically in Figure 4.

Presented at the 36th ASMS Conference on Mass Spectrometry and Allied Topics
June 5-10, 1988, San Francisco, CA

1. M.S. Stanley, K.L. Duffin, S.J. Doherty, and K.L. Busch, Anal. Chim. Acta, 200 (1987) 447.
2. M.S. Stanley and K.L. Busch, J. Planar Chromatogr., 1 (1988) 000.
3. J.L. Potter and A.A. Silvidi, Clin. Chem., 33 (1987) 2314.

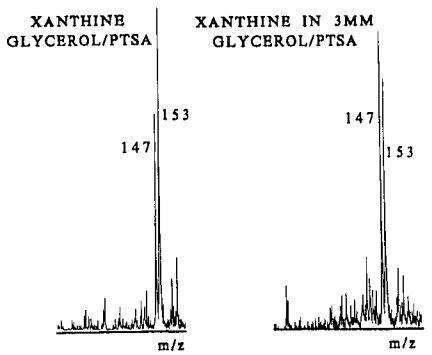

Figure 1

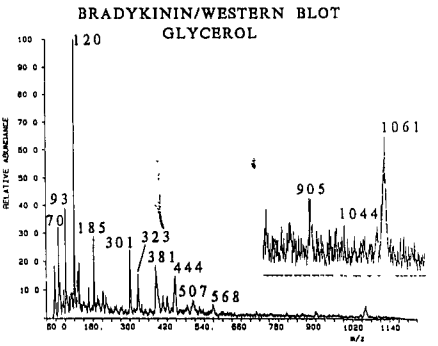

Figure 2

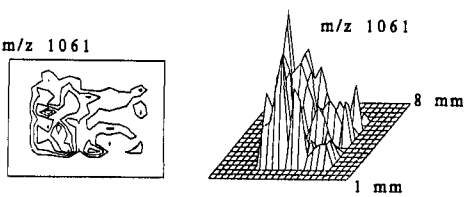

Figure 3

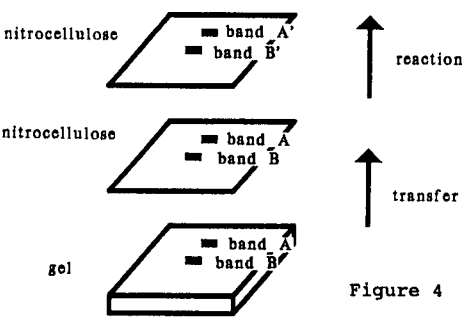

Figure 4

Presented at the 36th ASMS Conference on Mass Spectrometry and Allied Topics
June 5-10, 1988, San Francisco, CA

CAPILLARY ELECTROPHORESIS/FLOW FAB MS

Robert D. Minard, Dean Chin-Fatt, Paul Curry Jr., and Andrew G. Ewing,
Chemistry Dep't., Penn State Univ., University Park, PA 16802 USA.

Capillary electrophoresis (CE) is a new and rapidly advancing separation technique that offers the potential of very efficient separations (> 10^5 theoretical plates with elution times in minutes) with sample mixtures as diverse in nature as simple metal ions and high molecular weight proteins.[1] Resolution improves as the capillary diameter (usually less than 100 μm) and quantities injected (picomoles down to attomoles) decrease. Injection volumes on the order of 10 picoliters to 1 nanoliter and flow rates of less than 100 nanoliters/minute are common. These parameters pose a serious challenge to modern methods of chemical detection. On-column fluorescence detection[2], post column electrochemical detection[3], and electrospray ionization mass spectrometry[4] have shown promise as detection methods with sufficient sensitivity. Of these, mass spectrometry offers the advantages of very nearly universal detection and enhanced molecular characterization. However, detection of higher molecular weight non-volatile compounds requires the use of either spray (thermo-spray, plasma-spray, electro-spray, etc.) or surface (plasma desorption, fast atom bombardment(FAB), liquid SIMS, etc) ionization techniques.

FAB was regarded as a static ionization method until Takeuchi et. al. [5] and Caprioli et. al.[6] demonstrated continuous flow FAB (FFAB). In order to combine capillary electrophoresis and FFAB mass spectrometry, it is necessary to develope an interface which will 1) not degrade the separation efficiency of capillary electrophoresis; 2) allow for completion of the electrophoretic external circuit; and 3) allow different solvent systems to be used in the electrophoresis capillary and the FFAB capillary and 4) supplement the low flow of CE (<100 nL/min).

Based on a previously developed design for coupling post-column detectors with CE , we constructed a flow "make-up" CE-FFAB interface as shown in Fig. 1. Its construction involves the careful alignment of the end of the electrophoresis capillary and the end of the FAB flow capillary with a gap of approximately 20 μm. This open junction is immersed in the FAB matrix solution which was methanol or methanol/acetonitrile with 4 to 20% glycerol. (The glycerol content was varied to control the source pressure and stabilize the ion beam). The electrophoretic circuit was completed as shown with the cathode at the make-up coupling.

Our initial work involved optimizing the transfer in the flow FAB capillary and the CE capillary was not connected. Using the standard KRATOS flow FAB probe tip, we found that sample peak widths (5% above baseline) were greater than one minute using a Rheodyne injector with a 0.5 μL sample loop. Narrower sample peak widths (15 to 30 sec) were obtained when the sample was introduced by dipping the capillary

FIGURE 1:

Capillary Electrophoresis-Flow FAB Interface

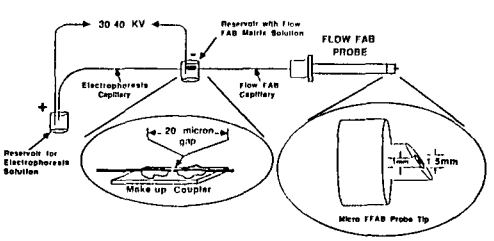

FIGURE 2:

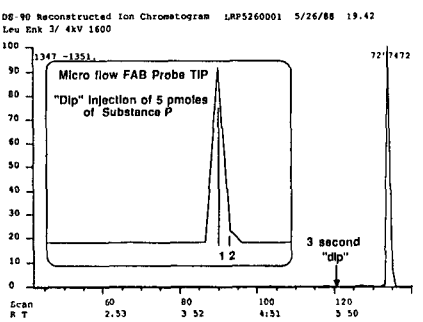

into the sample for one to three seconds but there was still a large amount of tailing. In order to minimize the sample residence time on the flow FAB probe tip, the tip was modified by reducing its size to a 1.5 mm diameter nub on a 1 mm stem. Using this smaller flow FAB probe tip with a 95 cm x 75 μm flow capillary, peak widths of 4 to 6 sec. were obtained when a non-aqueous solvent/matrix was used (4:1 acetonitrile/methanol with 4% glycerol) and samples were introduced using the dipping method. Figure 2 shows the reconstructed ion chromatogram of the molecular ion region (m/z 1347-1352) from a 3 s. "dip" injection injection of about 5 pmole of Substance P. Transit time through the capillary was about 75 s.

Initial results from the use of this CE-FFAB interface are very promising. Figure 3 shows a 3 second, 40 kV electrokinetic injection of a 400 ng/μL solution of leucine enkephalin which is equivalent to 3.6 pmoles of this pentapeptide. The peak width at half height is only 12 seconds. The CE capillary was 60cm by 75μm and the FFAB capillary was 70cm by 50μm. A current of 2.5 uA passed through the 1 mM ammonium formate electrophoresis buffer solution in the CE capillary. The flow FAB make-up matrix consisted of 20% glycerol in 4:1 acetonitrile water. The number of theoretical plates calculated for this separation was 6800 which is a reasonable preliminary result considering the broadening due to the interface, the low buffer concentration, and the fact that the CE capillary was not treated to deactivate its surface. A CE separation is shown in Figure 4. A mixture of approximately 1 ng each of Substance P (MW 1347), leu enkephalin (MW 555) and met enkephalin (MW 573) was injected. Leu and met enkephalin co-elute between scan 150 and 165. Substance P appears earlier (scan 100 to 140) showing that electrophoretic separation has, in fact, occurred.

[1]Mikkers, F.E.P.; Everaerts, F.M.; and Verheggen, Th.P.E.M., J. Chromatogr. *169*, 11-20, (1979); Jorgenson, J.W. and Lukacs, K.D., Science, *222*, 266 (1983)

[2]Gassman, E., Kuo, J.E. and Zare, R.N., Science, *230*, 813 (1985); Burton, D.E.,Sepaniak, M.J. and Maskarinec, M.P., J. Chrom. Sci., *24*, 347 (1986).

[3]Wallingford, R.A.; Ewing, A.G. *Anal. Chem.*, *59*, 1762 (1987)

[4]Olivares, J.A., Nguyen, N.T.,Yonker, C.R., and Smith, R.D., Anal. Chem., *59*, 1230 (1987); Smith, R.D., Olivares, J.A., Nguyen, N.T. and Udseth, H.R., Anal. Chem., *60*, 436 (1988)

[5]Ito, Y.; Takeuchi, T.; Ishi, D.; Goto, M. *J .Chromatogr.* , *346*, 161 (1985).

[6]Caprioli, R.M., Fan, T., *Anal. Chem.*, *58*, 2949 (1986)

FIGURE 3:

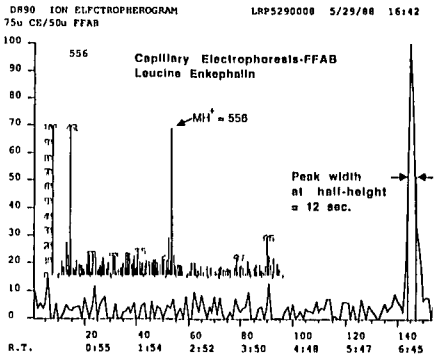

FIGURE 4:

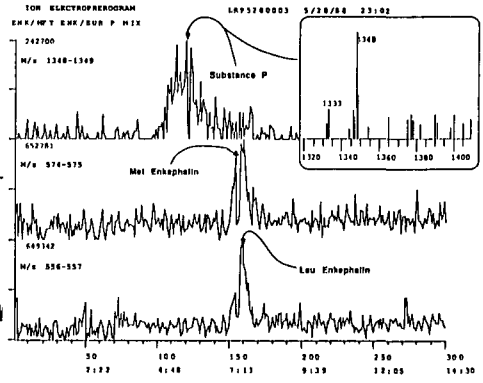

Presented at the 36th ASMS Conference on Mass Spectrometry and Allied Topics
June 5-10, 1988, San Francisco, CA

COMPLETE MS/MS DATA FIELD ACQUISITION ON THE CHROMATOGRAPHIC TIME SCALE BY TIME-RESOLVED ION MOMENTUM SPECTROMETRY (TRIMS) WITH TIME ARRAY DETECTION (TAD)

B.A. Eckenrode, J.T. Watson, J.F. Holland and C.G. Enke
Departments of Chemistry and Biochemistry,
Michigan State University, East Lansing, MI 48824

Mass spectrometry/mass spectrometry, (MS/MS), provides an additional dimension of mass spectral data to aid in mixture analysis or structure elucidation. MS/MS data acquisition consists of detecting daughter ions that arise from dissociation of parent ions produced in the source of a mass spectrometer. The relationships between parent and daughter ions involved in metastable ion decomposition or in collisionally activated dissociation (CAD) can be established by MS/MS analysis. These relationships are often indicative of specific structural characteristics. Acquisition of the **complete** MS/MS map (all daughters of all parents) typically is a relatively lengthy process (requiring up to several minutes) and consequently, much more sample (milligram quantities) is required than for conventional mass spectrometric analysis with electron impact or chemical ionization. Another disadvantage associated with long acquisition time is its incompatibility with sample introduction via a chromatographic inlet.

Time-resolved ion momentum spectrometry (TRIMS) (1,2) in combination with time-array detection (TAD) (3) was developed to remove the limitations described above and to allow for the acquisition of complete MS/MS maps in a single sweep of the magnetic field. A schematic of the instrument is shown in Fig. 1. TRIMS is achieved by determining flight times of ions following momentum analysis. Discrete ion packets are created by post-sector beam deflection and an integrating transient recorder (ITR) records the arrival time transient.

Collecting the full MS/MS data field on the time scale of a chromatographic peak is accomplished by incrementing the magnetic field and summing ion arrival time spectra at each momentum setting (see Fig. 2). To optimize the signal-to-noise ratio, a variable number of transients can be summed at each momentum. Interrogation of the full data field can then be made after the data have been written to disk.

The trade-offs in resolution, sensitivity and acquisition time can be related with the following equations:

(transients/scan)/(transients/sec) = sec/scan (1)

TOF scans/sweep = mass range/mass resolution (2)

mass range/mass resolution x sec/scan = sec/sweep (3)

where scan is defined as the summation of a number of transients, and sweep represents a single magnetic field transit over the desired mass range. Equation (1) is related to the S/N at each momentum setting. Equation (2) is related to the desired mass resolution and is dependent on the nature of the signal and the objectives of the analysis. Equation (3) represents the time for a complete MS/MS map acquisition with TRIMS/TAD and is determined by the temporal characteristics of the sample.

Results for methyl stearate are shown in Fig. 3. This is a GC/MS/MS map acquired in 10 seconds. Unit mass resolution was obtained on both the momentum and time axes.

Presented at the 36th ASMS Conference on Mass Spectrometry and Allied Topics
June 5-10, 1988, San Francisco, CA

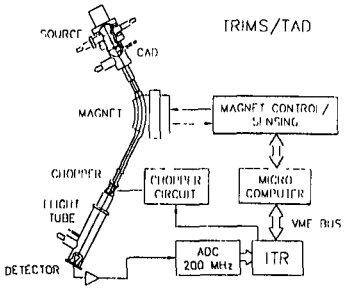

Figure 1. A schematic of the TRIMS/TAD instrument.

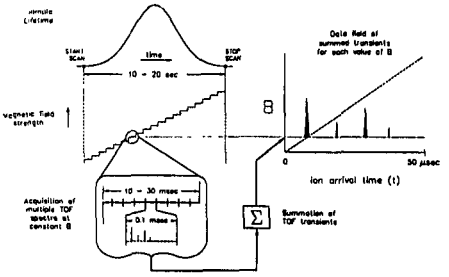

Figure 2. At each momentum increment, multiple TOF transients are summed to produce a scan. The full B-t data field thus consists of several scans for a single sweep of the magnet.

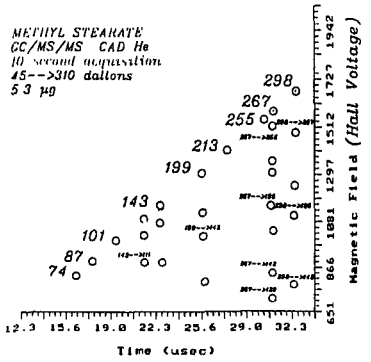

Figure 3. A complete MS/MS map of methyl stearate acquired in 10 seconds. This is a top view of the B-t data field. A wide-bore capillary column was used for the separation.

References:
(1)Stults, J.T.;Enke, C.G. and Holland, J.F. *Anal.Chem., 55, 1983.*
(2)Eckenrode, B.A.;Watson, J.T.;Holland, J.F. and Enke, C.G. *Int. J. Mass Spectrom. Ion Proc., 83(1988)177-187.*
(3)Newcome, B.H.;Erickson,E.;Yefchak,G.;Davenport, M. and Holland, J.F. *ASMS Cincinnatti, June 8-13, 1986.*

Presented at the 36th ASMS Conference on Mass Spectrometry and Allied Topics
June 5-10, 1988, San Francisco, CA

AN IMPROVED INTERFACE FOR CAPILLARY ZONE ELECTROPHORESIS-MASS SPECTROMETRY

R. D. Smith, J. A. Loo, C. J. Barinaga, and H. R. Udseth
Chemical Methods and Separations Group
Chemical Sciences Department
Pacific Northwest Laboratory, Richland, WA 99352

We have recently developed an improved electrospray ionization interface for capillary electrophoresis mass-spectrometry (CZE-MS). Our initial interface employed a vacuum deposited metal film at the exit of the capillary to make an electrical contact with the eluting buffer and establish the electrospray field gradient (1). This interface had several attractive features including negligible dead volume and avoidance of a nebulizing gas with the attendant problems (2). We were able to demonstrate high efficiency separations in excess of 10^5 theoretical plates with detection limits in the attomole range (3) using this interface for selected compounds.

This interface did, however, impose significant limitations on the range of capillary electrophoretic (CE) separations that could be performed. The flow rates typically used were near the minimum at which a stable electrospray could be generated so that separations with low electroosmotic velocity (i.e. CZE with surface modified capillaries, gel filled capillaries, etc.) could not be performed. Since the buffer solution was directly electrosprayed, constraints were placed on its composition. Aqueous solutions cannot be electrosprayed, nor can high ionic strength solutions. Since many separations are optimally performed in aqueous solutions at high ionic strength, it was necessary to compromise the separations by the addition of organic solvents and reduction of ionic strength to utilize the interface. Unfortunately, the use of lower ionic strength buffers also lowers the maximum sample size which can be utilized without degrading separation efficiency. The vacuum deposition of a metal film CZE electrode was also a tedious process. In addition, the vapor deposited metal film had poor adhesion characteristics and a limited lifetime.

To circumvent these limitations an interface that does not require a metalized tip was designed and developed. In the new approach, the electrical contact at the column exit is made through a flowing liquid sheath. Figure 1 shows a schematic illustration of one version of the liquid sheath electrode interface A 1/16" O. D. teflon tube that contains the fused silica capillary and the sheath liquid runs down the center of a polycarbonate holder. The capillary and the sheath liquid are brought together via a teflon tee outside the probe body (not shown). The central teflon tube is slip fit over a 21 gauge stainless steel (ss) needle which is cut flat and electropolished at its tip. The capillary protrudes slightly from the ss tube (approx. 0.3 mm) so that a positive flow of liquid from the sheath is necessary to make electrical contact. The liquid flow is maintained by a small syringe pump (Sage Instruments, Model 341B, Cambridge, MA). The central teflon tube is wedged in place by six concentric teflon tubes. An auxiliary gas flow can be delivered through these tubes to flow over the tip in the direction of the electrospray.

The principal advantage of this interface is that it allows operation with a much broader range of electrophoresis conditions. The sheath flow can be readily varied in both composition and volume. Thus, the composition of the electrosprayed solution, which is the mixture of the sheath and the capillary eluent, can be readily varied independently of the separation buffer. If the buffer is aqueous, an organic solvent such as methanol or acetonitrile can be added in the desired amount at the capillary terminus. If the ionic strength of the buffer is too high, it can be effectively diluted by the sheath liquid at the terminus. Some additional benefits also accrue in this design. The removal of any metal contact eliminates any possibility of electrochemical processes involving the analyte and reduces the likelihood of a corona discharge. (Such discharges are most readily generated from micro protrusions on metal surfaces.) The sheath liquid can also be used for post-column derivitization, to mix reagent ions into the electrospray plume, and to introduce a calibration compound.

Figure 2 shows an example of an ESI spectra for a previously intractable buffer solution. Fig. 2A is the negative ion spectra (the addition of oxygen as done by others (4) is needed to suppress discharges) and 2B is the positive ion spectra from an aqueous solution of 0.05 M sodium dodecylsulfate (SDS). The solution can not be electrosprayed directly, but the addition of 5 μL/min of isopropanol through the sheath produces a stable well behaved electrospray. Details of the interface design and performance will be published elsewhere (5).

We thank the U. S. Department of Energy, Office of Health and Environmental Sciences, for support of this research under Contract DE-AC06-76RLO 1830.

(1) Olivares, J. A.; Nguyen, N. T.; Yonker, C.R.; Smith, R.D. *Anal. Chem.* **1987**, 59, 1230.
(2) Bruins, A. P.; Covey, T. R.; Henion, J. D. *Anal. Chem.* **1987**, 59, 2642.
(3) Smith, R. D.; Olivares, J. A.; Nguyen, N. T.; Udseth, H. R. *Anal. Chem.* **1988**, 60, 436.
(4) Whitehouse, C. M.; Dreyer, R. N.; Yuamashita, M.; Fenn, J. B. *Anal. Chem.* **1985**, 57, 675.
(5) Smith, R. D.; Barinaga, C. J.; Udseth, H. R. *Anal. Chem.* , in press.

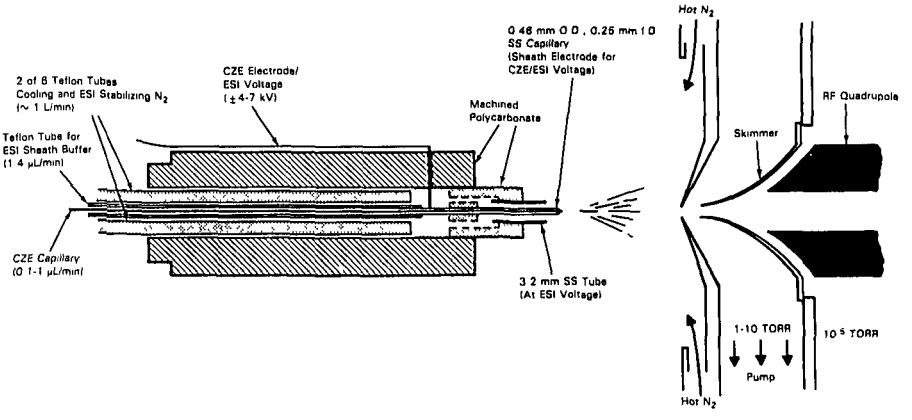

Figure 1. Schematic illustration of the CZE-MS interface utilizing a liquid sheath electrode (not to scale).

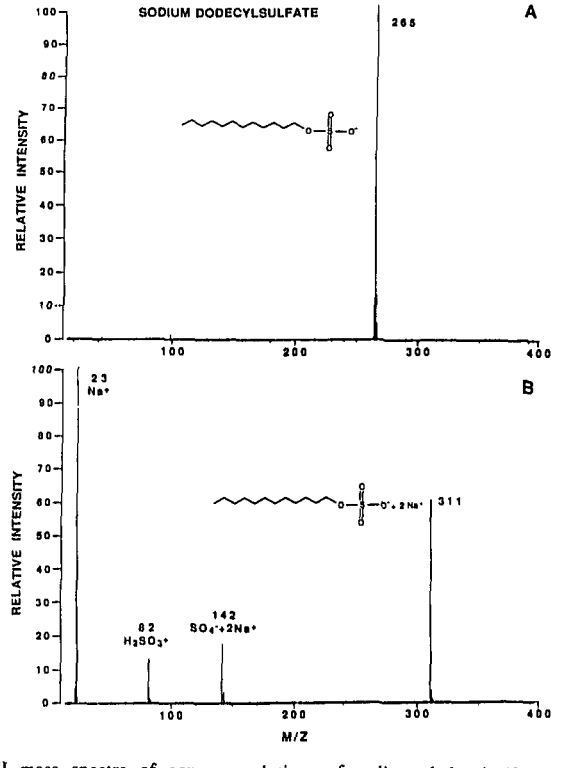

Figure 2. ESI mass spectra of aqueous solutions of sodium dodecylsulfate obtained in the negative (A) and positive (B) ion modes.

Presented at the 36th ASMS Conference on Mass Spectrometry and Allied Topics
June 5-10, 1988, San Francisco, CA

PARTICLE-INDUCED DESORPTION MASS SPECTROMETRY : PRODUCTION, IDENTIFICATION, AND USE OF INCIDENT MEV POLYATOMIC IONS*

D. L. Fishel[a], A. E. Ruthenberg[b], M. Salehpour[c], and J. E. Hunt[c]

[a] Kent State University, Department of Chemistry, Kent, OH 44242
[b] Physics Division, and [c] Chemistry Division, Argonne National Laboratory, 9700 S. Cass Ave., Argonne, IL 60439

The use of accelerators to select incident ion parameters has defined the role of MeV atomic ions in desorption of organic compounds. We have used MeV molecular and polyatomic ions to study desorption. Information about the enhanced energy deposition of polyatomic ions over their constituents atoms[1] has motivated us to investigate the potential of these species as incident particles in desorption ionization mass spectrometry experiments. We have shown that high yields of the secondary molecular ion of interest are observed as a result of incident polyatomic ion impact.[2]

The production and identification of MeV polyatomic ions for use in desorption studies requires an ion source capable of producing such ions coupled to a particle accelerator. The Dynamitron accelerator at Argonne National Laboratory is used to produce MeV polyatomic ions. The useful operating range of the accelerator is from 500keV to approximately 4.5 MeV. An ion source is located at the high-voltage terminal of the accelerator. Polyatomic ions are produced in a modified duoplasmatron ion source. The major alterations to the duoplasmatron ion source are in the electrode structure. A grid covering the electron filament reduces the electron current in the ionization region, thereby preventing the formation of a plasma. In this mode, electrons, which drift into the usual plasma region, are accelerated and impact the gas molecules in the entrance to the extraction region. This modification makes the ion source comparable to a low-current variable-energy electron-impact ion source with a small electron energy spread. As the molecules are ionized they drift through an aperture to an extraction electrode where they are focused and accelerated to an energy determined by the terminal potential of the accelerator. The total output current is typically below 1na. The efficiencies of the ion source and extraction have not been measured, however, for desorption studies reported here the most useful measure of the output is the ion count rate at the target. Depending on the number and type of ions produced in the ion source, the count rate is between 10^2 and 10^4 polyatomic ions/sec. This count rate range is ideal for desorption ionization studies.

The polyatomic ions that have been produced and accelerated are C_2^+, C_3^+, CH^+, CH_3^+, $C_3H_3^+$, $C_4H_9^+$, $C_7H_{15}^+$, CO^+, O_2^+, CO_2^+, CF^+, CF_3^+, $C_3F_5^+$, and $C_4F_7^+$. These ions were produced from allene (C_3H_4), n-decane ($C_{10}H_{22}$), CO_2, and a low-boiling point perflurokerosene mixture (PCR Chemicals, Gainesville, FL, USA). A removable energy detector placed 3 m from the bending magnet was used to identify the polyatomic ions. The collisions with the rest gas in the evacuated beam line (~1 x 10^{-6} torr) fragments a small number of the polyatomic ions, which is useful in identification of the polyatomic ions as follows. Figure 1 shows the energy spectrum of CF_3^+ recorded in a multichannel analyzer. CF_3^+ was produced from perflurokerosene, accelerated to 3.9 MeV with the analyzer tuned to mass 69 and charge state +1. The predominant species observed is CF_3^+. The inset of fig. 1 is an expanded vertical range showing the energy spectrum resulting from the fragmentation of the parent molecule. The mass of the fragments can be deduced from

the fraction of the energy they carry away from the intact polyatomic ion. The analysis of the fragments clearly identifies the accelerated species as CF_3^+. Fig. 2 shows the yield of valine negative molecular ions as a function of the energy of three different incident ion species. For C^+ to CF_3^+, at the same velocity, represents a factor of 40 increase in yield.

The desorption results show that high yields of secondary molecular ions are obtained as a result of polyatomic ion impact. We believe that this polyatomic ion source/accelerator combination should have may applications in the study of the desorption mass spectrometry.

[1] W. Brandt, A. Ratkowski, and R. Ritchie, Phys. Rev. Lett 33 (1974) 1325.
[2] See Salehpour, D.L. Fishel, and J. E. Hunt, "Nonlinear Secondary Ion Yield Enhancement with Fast Incident Molecular Ion", these proceedings.

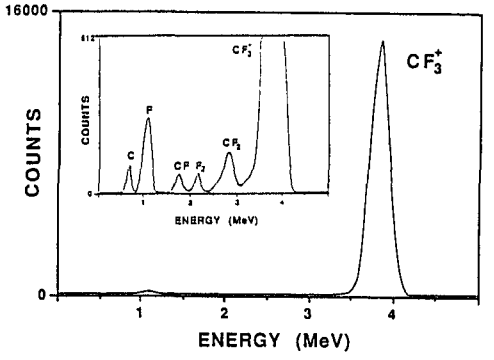

Fig. 1 The energy spectrum of 3.9 MeV CF_3^+ used as a beam diagnostic. The inset, an expanded verticle scale, shows the fragments from the CF_3^+ molecular dissociation.

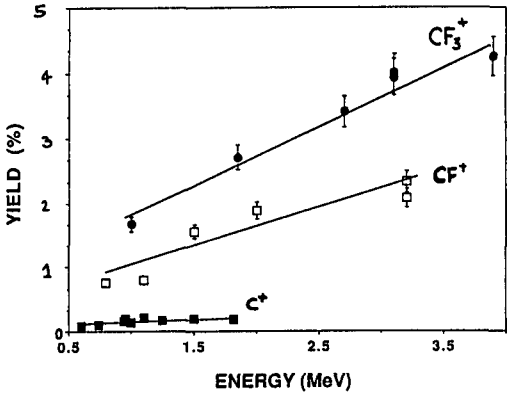

Fig. 2 The yield of valine negative molecular ions, $(M-H)^-$, as a function of the energy of incident C^+, CF^+, and CF_3^+ ions.

Presented at the 36th ASMS Conference on Mass Spectrometry and Allied Topics
June 5-10, 1988, San Francisco, CA

A NEW UHV INSTRUMENT FOR ION/SURFACE COLLISIONS

H-J. Laue, J.W. Amy, B. Winger and R.G. Cooks
Purdue University
Department of Chemistry
West Lafayette, IN 47907, USA

A new ultra high vacuum (UHV) instrument has been designed to allow the study of polyatomic ion/surface collision phenomena as a function of the collision energy, angle of incidence and the nature of the surface. The mass spectrum and translational energies, as well as the angle of scattering of the emerging particles, will be measured. The object is to study collisions over a wide range of collision energies (1 eV to 3000 eV) at surfaces which are well-defined. A significant objective is to study the kinematics and dynamics of surface scattering, both elastic and inelastic, as well as charge changing and reactive collisions. In addition, by using ion beams of higher flux and very low translational energies, chemical modification of the surface will be attempted.

Figure 1 shows the Finnigan MAT 212, the interface chamber and a cross section of the main chamber. The MAT 212 serves as one of two main beam delivery systems for the main chamber. It is capable of delivering a mass analyzed ion beam of up to 3000 eV and, with suitable deceleration, as low as a few eV. The DC-quadrupole doublet, which is located in the interface chamber, is used to focus the ion beam at the target. Depending upon the specific experiment employed, the beam can be focussed, either to a tight spot (most SID experiments), or a high narrow slit (angle resolved experiments). The interface chamber is differentially pumped using a 100 l/s ion pump, therefore allowing for ultra high vacuum conditions to exist in the main chamber. Using the MAT 212 as the main beam delivery system will allow for variations of the collision energy and the mass of the primary ion.

The second main beam delivery system which is incorporated into the design of the instrument is a Riber secondary ion mass spectrometer (SIMS). The SIMS will be used to deliver a low energy, high flux beam to modify the target surface. In one experiment the SIMS-produced beam will be transported into the main chamber. In another experiment the target will be transferred to a satellite preparation chamber for modification. Using the mass analyzing quadrupole, the SIMS will deliver mass selected ions which were previously produced in the desorption ionization process. An overhead view of the entire apparatus, which includes the MAT 212, the main chamber and the Riber SIMS is shown in Figure 2.

The main chamber serves as the scattering and analyzing chamber of the instrument. The sample target, which is mounted on a goniometer, is located in the center of the chamber. The goniometer can be rotated 360°, therefore, the angle of incidence of the primary ion can be varied. As seen in Figure 1, the analyzer system, which consists of an electric sector analyzer (ESA), a quadrupole mass filter and an electron multiplier (not shown), are all mounted on a ring-rail, allowing for rotation of the analyzer system while under UHV. Therefore, the products of an ion/surface collision can be collected and analyzed, independent of the incident angle. To control the selection of the angle and energy of the emerging ions, an externally controllable slit system is located just after the target and after the ESA (Figure 3). The main chamber is pumped by a 270 l/s ion pump supplemented by a 1250 l/s cryopump and is designed to achieve pressures on the order of 10^{-10} torr. An ion pump fitted with a titanium sublimation pump is mounted on the bottom center of the main chamber, allowing for differential pumping of the target region. To maximize the pumping differentially, a tube, which is equipped with an aperture allowing the primary ion beam to enter and a rather long slit on the other side for extracting the secondary ions, encompasses the target. This would enable the target region to attain a pressure in the 10^{-11} torr regime.

Figure 4 is a reproduction of a GIOS [1] calculation which shows the ion beam path from the source of the MAT 212 to D3, the electron multiplier detector located in the main scattering chamber. GIOS and SIMION ion optical programs were used throughout so as to ensure that the instrument was designed with well-defined ion optical characteristics.

References

1. H. Wollnik; Int. J. Mass Spectrom. Ion Phys., 30, 1979, 137.

Presented at the 36th ASMS Conference on Mass Spectrometry and Allied Topics
June 5-10, 1988, San Francisco, CA

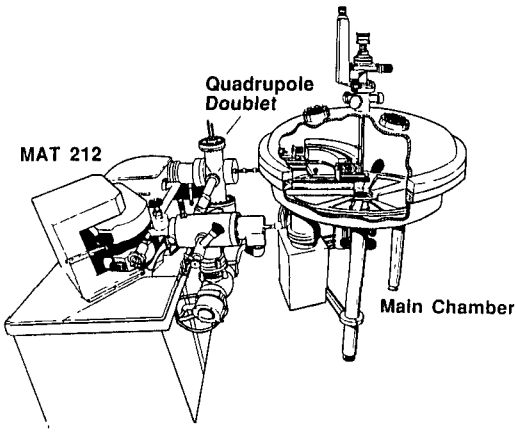

Figure 1. UHV instrument for the study of polyatomic ion/surface collisions.

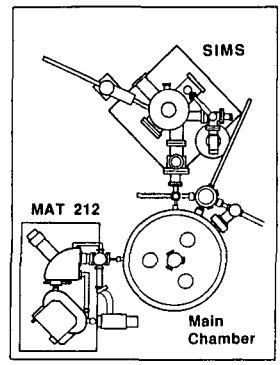

Figure 2. An overhead view of the entire UHV instrument.

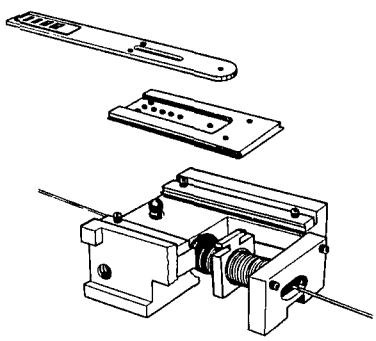

Figure 3. An exploded view of the slit system used to control the selection of the angle and energy of the emerging ions.

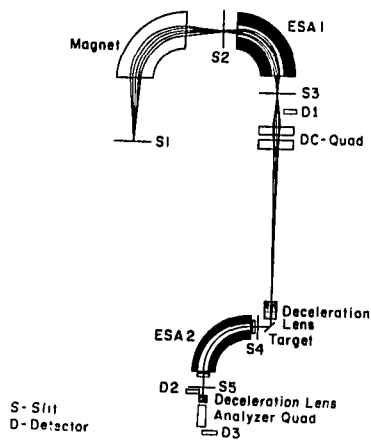

Figure 4. A reproduction of the GIOS calculation displaying the ion optical pathway for the BEEQ geometry.

Presented at the 36th ASMS Conference on Mass Spectrometry and Allied Topics
June 5-10, 1988, San Francisco, CA

QUADRATURE FT/ICR MASS SPECTROMETRY

Francis R. Verdun,§ Steven L. Mullen,# Tom L. Ricca,§ and Alan G. Marshall§

§Dept. of Chemistry (and Dept. of Biochemistry)
The Ohio State University
120 W. 18th Avenue
Columbus, OH 43210

#Dept. of Biohemistry
Michigan State University
East Lansing, MI 48824

A Fourier Transform Ion Cyclotron Resonance (FT/ICR) signal is usually produced by radiofrequency excitation on one pair of opposed pair of plates and subsequent detection on a second pair of opposed plates[1]. However, use of both pairs of plates for excitation effectively reduces the necessary excitation amplitude by a factor of two and, use of both pairs of plates effectively increases the signal-to-noise ratio by a factor of $\sqrt{2}$. Quadrature detection therefore enhances signal-to-noise ratio by the same factor as time-domain two-fold oversampling of the signal, whether done directly or by the interleaving of two spectra (see ref. 2 and paper #TPB3) but requires neither a doubling of the analog-to-digital conversion (ADC) speed nor acquisition of two successive spectra differing by one-half of an ADC dwell period between excitation and reception events.).

In FT/ICR (or any other FT) spectroscopy, the Nyquist limit requires that the time-domain ICR transient signal be sampled at a frequency, 2SW, in which SW is the highest ICR frequency in the detected spectrum. The discrete Fourier transform of such a signal gives a spectrum which correctly represents signals in the frequency range, 0 to 2SW; however signals with frequencies between SW and 2SW violate the Nyquist limit and are "aliased" or "folded over" to appear at mathematically negative frequencies. Stated another way, the signal detected by a **single** pair of opposed receiver plates is linearly polarized and therefore cannot distinguish between positive and negative frequencies (e.g., right- and left-circularly polarized rotations of ions of the same mass but opposite charge). Thus, it is usual to excite (and/or filter out all but) signals in the range only from 0 to BWI (in direct-mode), or from $\nu_{carrier}$ to $\nu_{carrier}$ - SW (in heterodyne mode).

In contrast, detection of signal components from **two** perpendicular pairs of plates makes it possible to discriminate positive and negative frequencies. Advantages of such "quadrature" detection compared to single-channel detection include: (a) for a given ADC rate and number of time-domain data points, the Nyquist frequency is doubled (i.e., the low-mass limit is halved in either direct or heterodyne mode; (b) for a given number of time-domain data points and mass range, the ADC rate is halved; (c) for a given ADC rate and mass range, signal-to-noise ratio is increased by a factor of $\sqrt{2}$.

Experimental

FT/ICR mass spectra were acquired with a modified Nicolet FTMS-1000 instrument. Ions were produced by electron ionization with a standard event sequence.[2] For experimental simplicity, quadrature detection was performed by use of a single ADC operated in either of two possible modes.

Simultaneous sampling, with alternate ADC delay. In this procedure, the signals from both pairs of plates are sampled and held separately and simultaneously. One of the two signals is digitized immediately, and the other is held until the first digitization is complete. Thus, although the signals from the two channels are digitized alternately, they are sampled simultaneously. This process is equivalent to use of two independent

ADC's, each operated at half the sampling rate of the single-ADC experiment. The experimental enhancement of ~30% in signal-to-noise ratio (see Figure 1) is somewhat below the theoretically possible 42%, because the electronic components were not identical for the two detector channels (e.g., a time-shift between the two channels will reduce the orthogonality between the two signals. Improvements are available and are in progress.

Alternate sampling/ADC In this procedure, the signals from the two channels are simply sampled/held/digitized alternately. As a result, it is necessary to phase-correct the data from the second channel for the time-delay between sampling of the two channels. The signal-to-noise improvement (compared to single-channel detection) is again ~30% (see Figure 2) and should again be improveable to the theoretical 42% limit. For strongly damped time-domain ICR signals, simultaneous sample/hold is preferable to avoid change in signal magnitude between alternate-channel readings. A detailed treatment of quadrature and oversampling will be published elsewhere.

This work was supported by grants (to A.G.M.) from the U.S. Public Health Service (N.I.H. GM-31683), the National Science Foundation (8721498), and The Ohio State University. F.R.V. is supported by an Ohio State University Postdoctoral Fellowship.

1. Marshall, A. G., *Acc. Chem. Res.* **1985**, *18*, 316-322.
2. Verdun, F. R.; Ricca, T. L.; Marshall, A. G. *Appl. Spectrosc.* **1988** *42*, 199-203.

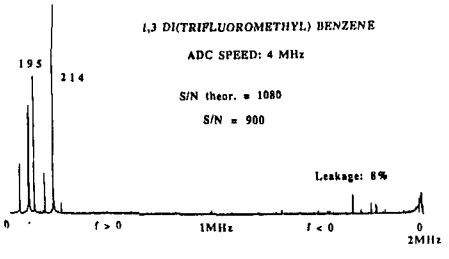

Figure 1

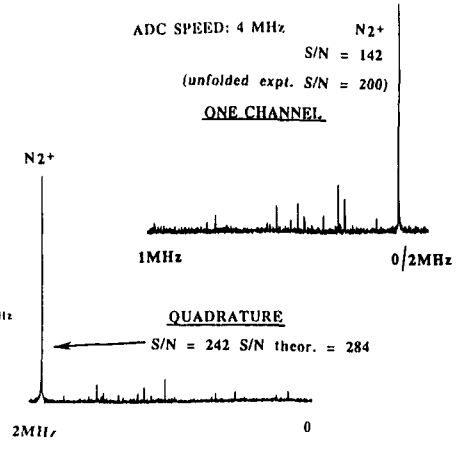

Figure 2

Presented at the 36th ASMS Conference on Mass Spectrometry and Allied Topics
June 5-10, 1988, San Francisco, CA

ICR-TOF. TIME OF FLIGHT MEASUREMENT OF PHOTOFRAGMENT ENERGIES IN THE ICR ION TRAP

R. C. Dunbar, Chemistry Department, Case Western Reserve University, Cleveland, OH 44106.

G. H. Weddle, Chemistry Department, Fairfield University, Fairfield, CT 06430.

A new approach is described which combines the ion-trapping capabilities of the ICR instrument with time-of-flight velocity analysis to observe the kinetic energy of photofragmentation product ions. As indicated in Fig. 1, the experimental sequence is as follows: After electron-impact ionization, the parent ions are thermalized and also relaxed to the center of the cell (along the z axis) by about 30 collisions with parent neutral or other collision gas; Then the laser pulse is fired, and simultaneously the trapping potential is dropped to zero, allowing free flight of all ions along the z axis. After time T the trapping voltage is turned back on, retrapping all those ions which have not yet struck the trapping plate, and an ICR detection sequence is used to measure the fraction of ions remaining in the trap. A plot of fraction of ions retained versus T gives a time-of-flight analysis of the one-dimensional velocity distribution along the z axis. Interpretation of the time-of-flight curves in terms of three-dimensional velocity distributions has been outlined in a forthcoming publication [1]

Figures 2 and 3 show recent results for 2-iodotoluene ions, photodissociated with the 308 nm output of a XeCl excimer laser. Fig. 2 shows the time-of-flight curve for the parent ion, which should reflect a thermalized Maxwell-Boltzmann distribution of velocities: Comparison with the expected 350 K thermal curve shows good agreement with this expectation. Fig 3 shows the m/e 91 photofragment results. The fragment ion has substantial excess kinetic energy: The predicted curve for monoenergetic ions with 75 meV of kinetic energy fits the data moderately well, but the data clearly reflect a spread of kinetic energies. An excellent fit to the data is found for the three-dimensional Maxwell-Boltzmann distribution at a kinetic temperature of 750 K, as shown. This indicates an average kinetic energy of about 98 meV, which can be converted to an average kinetic energy release of about 140 meV for the photofragmentation. This is quite similar to the result quoted earlier for the corresponding photodissociation in 4-iodotoluene ion.[1] The magnitude of kinetic energy release is reasonable for statistical dissociation of a molecule this size excited to 1.8 eV above threshold, as is the case if direct dissociation to the tolyl ion product is assumed. There is no indication of a major extent of rearrangement to benzyl or tropylium product, which would be accompanied by very large kinetic energy release.[2,3]

Valid time-of-flight product-ion analysis depends on the fragmentation being fast compared with flight times, which requires in this case that the dissociation be complete within a few microseconds. PEPICO study[3] has indicated that this is true; Additional confirmation comes from a time-resolved ICR photodissociation experiment, as shown in Fig. 4, showing the amount of m/e 91 formed as a function of delay after the laser pulse. The shortest delay time was 8 μsec, at which time the product signal was already a maximum. Allowing a few additional μsec for cyclotron excitation, this indicates that dissociation is entirely complete within much less than 15 μsec. The ICR-TOF technique is succesful in showing the extent of kinetic energy release for fragmentations of parent ions whose internal excitation (governed by the photon energy) is very well known As in the present case, it is readily discerned whether the kinetic energy release is sharply peaked or is spread out in a more nearly Maxwellian distribution. The technique will be readily applied to a variety of photodissociation systems, and also is promising for similar kinetic energy studies of the fragment ions from dissociative multiphoton ionization, which we intend to carry out soon.

[1]Dunbar, R. C and Weddle, G. H., J. Phys. Chem., In Press.
[2]Holmes, J. L., Blair, A. S., Weese, G. M., Osborne, A. D. and Terlouw, J. K., Adv. Mass Spectrom. 6, 1227 (1978).
[3]Olesik, S., Baer, T., Ridal, J. I., Buschek, J. M., Holmes, J. L. and Morrow, J. C., J. Am. Chem. Soc., In Press.

Presented at the 36th ASMS Conference on Mass Spectrometry and Allied Topics
June 5-10, 1988, San Francisco, CA

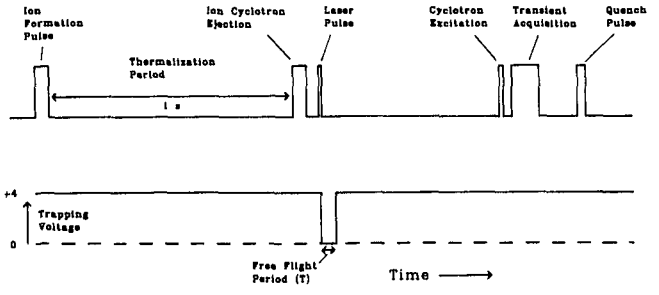

Figure 1. ICR-TOF pulse sequence.

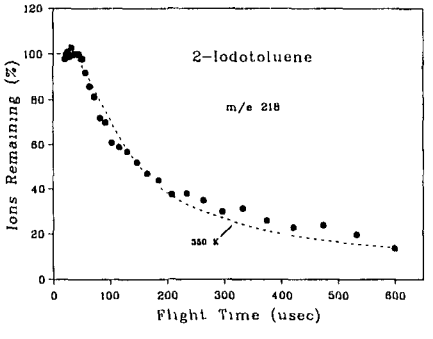

Figure 2. Parent-ion time-of-flight curve for 2-iodotoluene.

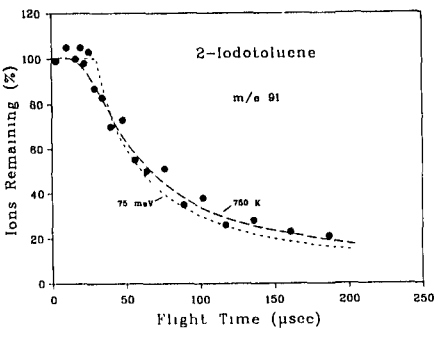

Figure 3. Mass 91 daughter-ion time of flight curve from photodissociation of 2-iodotoluene parent ion at 308 nm.

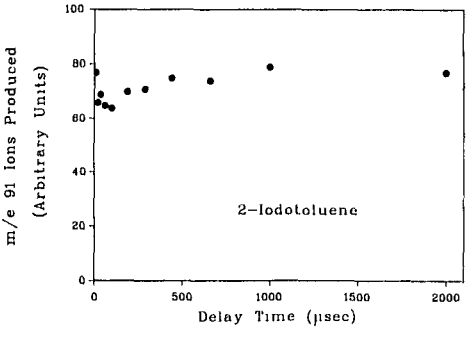

Figure 4. Time-resolved photodissociation curve for the reaction 218 → 91 in 2-iodotoluene at 308 nm.

Presented at the 36th ASMS Conference on Mass Spectrometry and Allied Topics
June 5-10, 1988, San Francisco, CA

The External Ion Source for High Magnetic Field ICR Spectrometry
Experiment and Theory

P. Kofel*, M. Bamberg, I. Pezsa, H. Knoll and K. P. Wanczek,
Inorganic Chemistry, NW 2, University of Bremen, D-28 Bremen 33,
West Germany

External ion sources (1) for ICR can easily be incorporated in instruments with high magnetic field superconducting magnets which have solenoidal fields. The external source has several advantages. Because it can be pumped differentially, ions can be generated at high pressure, the external source is easily accessible. The very elaborated ion sources already available for mass spectrometry can be employed. However, the incorporation of such a source leads to a greatly increased complexity of the instrument, especially of the mechanical structure.

Three important factors have to be considered for an external ion source: ion generation, injection of the ions through the magnetic fringing field, and trapping of the ions.

Two types of external ion sources can be distinguished (2): pulsed and continous sources, while the first allows mass selection according to the different flight times of ions of different masses, the second method is employed for broad band spectroscopy. In axial beam ion sources no disturbance of the site of ion generation by the stray magnetic field is observed. The disturbance of the electron beam by the stray magnetic field can cause severe problems even in magnetically shielded sources.

From the Lagrange-Helmholtz equation criteria for the ion injection can be derived. The focus of the injection lens has to be such that the ions are injected parallel to the magnetic field lines. The properties of electrical lens systems are changed in the magnetic field if the relevant time is not much smaller than the time for one cyclotron gyration.

The axial kinetic energy of the ions does not influence the transfer. For narrow beams of low energy the influence of space charge is high and limits the ion current and the number of ions, which can be transferred. Defocusing of the beam is observed. If the radius of the ion beam is not enlarged and the beam is only focused, a large spread of the axial energies occurs, which can be as great as 1 eV.

Fig. 1 shows the relevant parameters for ions trapping. The spread of the axial energies is $q\Delta V$. Assumig equipartition of the axial translational energies of the ions, the number of ions N which can be trapped is

for $\Delta V \geq V_t$

$$N = \frac{1}{q}\int_{U=0}^{V_t} dQ(U) = \frac{2cI}{q\Delta V}\left(\frac{2mV_t}{q}\right)^{1/2}$$

and for $\Delta V \leq V_t$

Presented at the 36th ASMS Conference on Mass Spectrometry and Allied Topics
June 5-10, 1988, San Francisco, CA

$$N = \frac{1}{q}\int_{U=0}^{\Delta V} dQ(U) = \frac{2cI}{q}\left(\frac{2m}{q\Delta V}\right)^{1/2}$$

where $dQ(U)$ is the charge of the ions with mass m with energies between U and $(U + \Delta U)$, I is the ion current, and V_t is the trapping potential.

The equations show that the trapping of externally generated ions depends in a crucial manner from the energy spread of the ions. With fixed ΔV the maximum of trapping efficiency is reached if $\Delta V \leq V_t$. For fixed V_t, ΔV has to be as small as possible. For high resolution spectra, trapping potentials of approximately 1 V are employed, therefore $\Delta V \leq 1$ V.

The external source can be used to trap the ions in the residual magnetic field. The trapped ions can then be transferred to the ICR cell (3). *This can lead to a great improvement in sensitivity. For a comparable set of spectrum parameters and the same spectrum recording* time of a GC ICR instrument the relative signal-to-noise ratios of a spectrometer with a single cell, a double cell, an external ion source, and an external trapped ion source have been calculated to be 1:70:15:2500. Also the use of a radiofrequency ion trap as external source should be studied.

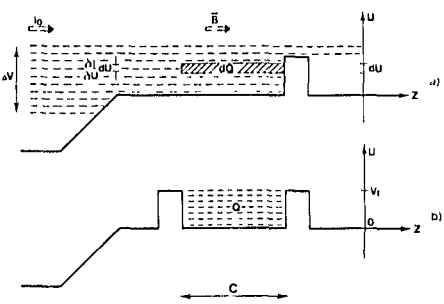

Fig.1. Potentials of the ICR cell (c) during trapping of externally generated ions, (a) ICR cell open, (b) ICR cell closed.

References

1. P. Kofel, M. Allemann, Hp. Kellerhals and K. P. Wanczek, Int. J. Mass Spectrom. Ion Processes, 65 (1985) 97.
2. P. Kofel, M. Allemann, Hp. Kellerhals and K. P. Wanczek, Int. J. Mass Spectrom. Ion Processes, 72 (1986) 53.
3. P. Kofel, M. Allemann, Hp. Kellerhals and K. P. Wanczek, Int. J. Mass Spectrom. Ion Processes, submitted.

*Present address: Department of Chemistry and Guelph-Waterloo Research Centre for Graduate Work in Chemistry, University of Waterloo, Waterloo, Ontario, N2L 3G1, Canada

Presented at the 36th ASMS Conference on Mass Spectrometry and Allied Topics
June 5-10, 1988, San Francisco, CA

NEW FTMS METHOD FOR TRAPPING IONS THAT ARE INJECTED FROM AN EXTERNAL ION SOURCE INTO AN ICR CELL

Carlito B. Lebrilla, I.Jonathan Amster, and Robert T. McIver, Jr.
Dept. of Chemistry, University of California, Irvine, CA 92717

After nearly three years of effort, the new external ion source FTMS instrument at U.C. Irvine is operational. In this paper the features of the spectrometer are described and some of the first mass spectra are presented.

The basic concept of the instrument is the same as the tandem quadrupole-Fourier transform mass spectrometer that was described previously [1-4]. In order to operate at elevated ion source pressures, the instrument has three differentially pumped regions: an external ion source, an ion transport region, and an ion detection region with an ICR cell. The ion source region consists of a 6" stainless steel cube which has mounted on it an ion source (either EI or FAB), a direct insertion probe, a batch sample inlet port for gases, an ionization gauge tube, and a 6" gate valve attached to a Balzers TPU 170 turbomolecular pump. Ions are extracted from the source through a 0.063" diameter hole and accelerated into a RF quadrupole lens assembly which guides them to the ICR cell. The quadrupole lens assembly, which is 46" long, is mounted in a 6" tee along with pumping constrictions, a VAT gate valve, and an Air Products 6" cryopump. A second Air Products 6" cryopump evacuates the ion detection region and the ICR cell. The base pressure in the ICR cell is usually in the 10^{-10} torr range, and a gradient of 40,000:1 can be maintained between the ion source region and the ion detection region. The ICR cell is positioned in the homogeneous region of a 6-T superconducting magnet made by Oxford Instruments, and the FTMS experiments are controlled by an OMEGA data system manufactured by IonSpec Corp.

Much of our effort has been devoted to developing the RF quadrupole lens assembly. It serves two purposes in our experiments. First, it focuses the ions into a tight beam of only a few millimeters diameter and guides them through the fringing fields of the superconducting magnet. When the ion beam is properly focused by the quadrupole lens, very high ion trapping efficiency for injected ions can be achieved. For example, we estimate that from 10% to 20% of the injected ions can be trapped in the cell and that weak ion currents can be accumulated or "integrated" in the cell for 20 seconds. The data in Fig. 1 show that as the injection time period is lengthened, the intensity of the Xe^+ signal increases until the space charge limit is reached. For this particular injection current, the space charge limit is reached after about two seconds. However, a weaker injection current can be accumulated for a much longer time. The second purpose of the quadrupole lens is to select which ions are transported to the cell. Ideally, it should function like a "bandpass filter" so that only ions in a preselected mass range are transmitted to the ICR cell. This is important for the FAB and other experiments we plan to perform because the dynamic range of the ICR cell is limited and the cell can be easily filled to its space charge limit by uninteresting matrix-related ions.

The mass resolution and sensitivity of the new instrument have exceeded our expectations. Figure 2a shows a single narrowband acquisition for m/z 132 formed by EI of xenon gas in the cell. The transient signal extends for more than 6 seconds, and the mass resolution is 2,600,000. Very recently we have begun FAB experiments using a cesium ion beam. Figure 2 (a) shows a single scan, narrowband acquisition for the cluster $(CsI)_9Cs^+$, m/z 2471, at a resolution of 120,000, and Fig. 2c shows a single scan, narrowband acquisition for the cluster $(CsI)_{37}Cs^+$, m/z 9746, at a mass resolution of 53,000. Figure 3 shows a spectrum of Gramacidin S produced by FAB with a glycerol matrix at a resolution of 120,000 for the molecular ions.

---

[1] R. T. McIver, Jr., U.S. Patent 4,535,235, "Apparatus and Method for Injection of Ions into an Ion Cyclotron Resonance Cell", Aug. 13, 1985.
[2] R. T. McIver, Jr., R. L. Hunter, and W. D. Bowers, Int. J. Mass Spectrom. Ion Processes, 64 (1985) 67-77.
[3] D. F. Hunt, J. Shabanowitz, R. T. McIver, Jr., R. L. Hunter, and J.E.P. Syka, Anal. Chem., 57 (1985) 765-768.
[4] D. F. Hunt, J. Shabanowitz, J. R. Yates, III, R. T. McIver, Jr., R. L. Hunter, J.E.P. Syka, and J. Amy, Anal. Chem., 57 (1985) 2728-2733.

Presented at the 36th ASMS Conference on Mass Spectrometry and Allied Topics
June 5-10, 1988, San Francisco, CA

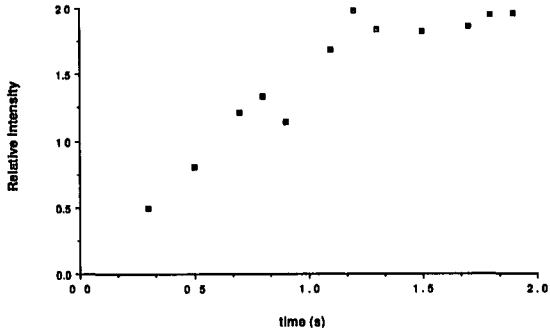

Figure 1. Xe^+ intensity as a function of ion injection time length.

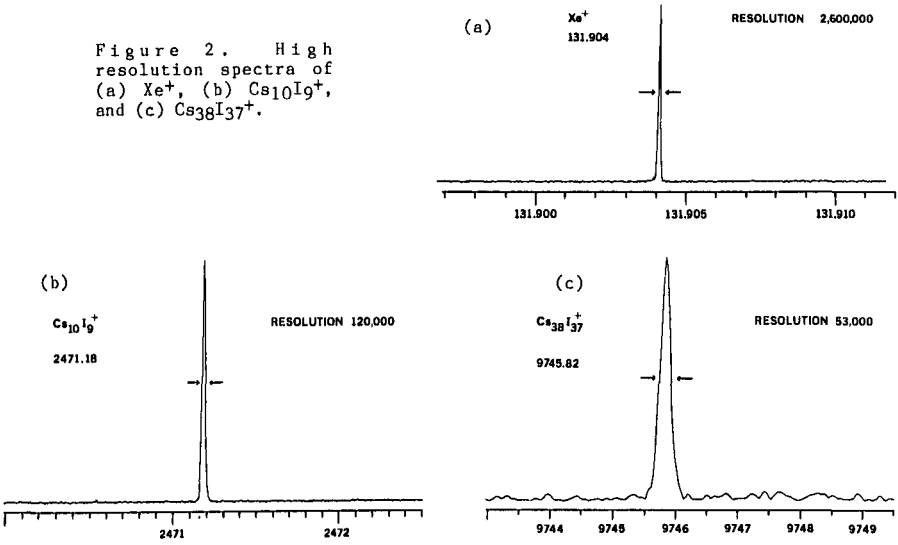

Figure 2. High resolution spectra of (a) Xe^+, (b) $Cs_{10}I_9^+$, and (c) $Cs_{38}I_{37}^+$.

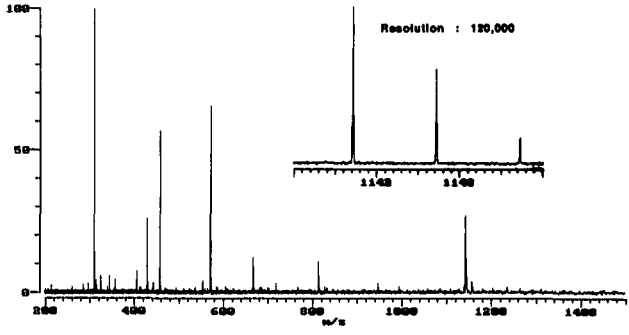

Figure 3. Broad Band and Narrow Band (inset) spectrum of Gramacidin S.

Presented at the 36th ASMS Conference on Mass Spectrometry and Allied Topics
June 5-10, 1988, San Francisco, CA

Desorption Ionization and Ion Injection into a Quadrupole Ion Trap Mass Spectrometer

John N. Louris, Jennifer S. Brodbelt-Lustig, Raymond E. Kaiser, R. Graham Cooks
Purdue University
West Lafayette, IN 47907

The quadrupole ion trap mass spectrometer has become an increasingly important tool for the qualitative and quantitative analysis of relatively volatile organic compounds. Previously, ions were always generated within the cavity of the ion trap rather than being generated outside of the trap and injected into the trap. In theory, ions injected into the trap must eventually strike a wall because of the excess kinetic energy which allowed them to enter the trap from the outside. This requirement severely restricts the use of modern ionization methods such as FAB, SIMS, and laser desorption because of poor access to the cavity of the trap. However, since a relatively high pressure of helium is used in the trap, the possibility exists of trapping injected ions by removing energy through collisions.

We recently reported the construction of an electron impact ion injection source for the trap. Spectra were readily obtained by ion injection. We now report the use of this source for laser desorption ionization. A fiber optic was positioned in an aperture in the side of the ion volume, situated so that the end was 0.2 - 0.4 cm from a metal target within the ion volume. This target was affixed to a removable probe to permit convenient changing of the sample. The fiber optic entered the vacuum manifold through an O-ring seal, and light from a pulsed Nd:YAG laser (532 nm) was focussed 0.1 - 0.3 cm from the end of the fiber optic. Figure 1 shows the arrangement of optics used to separate the harmonics in the laser light and to focus the beam on the fiber optic. Figure 2 shows the external parts of the injection source, including the fiber optic and the probe (which enters the ion volume through a hole in the back of the ion volume). The laser was triggered by the instrument's single board computer when ions were to be admitted into the trap.

A single pulse of the laser was capable of filling the trap to the "space-charge limit". Injected gold ions were used to study the effectiveness of gases other than helium in promoting the trapping of ions; helium, neon, argon, and xenon all promoted the trapping of Au^+. Neon was as effective as helium at promoting trapping, but argon and xenon yielded signals only 10-20% as intense as helium. In addition, xenon produced broad peaks in the mass spectrum (about three mass units wide) whereas the other three gases produced peaks of unit resolution.

Injected metal ions could also be used as CI reagent ions. For example, when gold ions were injected into the trap in the presence of 5×10^{-7} torr benzene vapor, ions were observed corresponding to Au^+, the charge exchange product $C_6H_6^{+\cdot}$ and the condensation products $[Au\text{-}C_6H_6]^+$, $[Au(C_6H_6)_2]^+$ and $[H_2O\text{-}Au\text{-}C_6H_6]^+$. Figure 5 shows the ionization of cyclohexene by injected copper ions. Ions corresponding to the bis-cyclohexene adduct (227/229), the mono adduct (145/147), the mono adduct with water (163/165), and the mono adduct less 28 are observed. This system was studied further by collisionally activated dissociation. The ions of m/z 163 were first isolated using a combination of DC and RF voltage; after excitation, ions of m/z 145 were produced, corresponding to loss of water. After isolation and excitation, ions of m/z 117 and m/z 81, were produced. The ions of m/z 81 probably result from the removal of all substituents on the copper ion, followed by reaction with adventitious water. The use of metal ions for the chemical ionization of organic compounds has been extensively studied using FT-ICR spectrometry (1). The ability to inject metal ions into the quadrupole ion trap provides a practical, alternate method of investigating this chemistry.

Laser desorption and ion injection of organic compounds has also been achieved. Figure 3 shows the spectrum of a quaternary ammonium salt. Amino acids and small peptides gave spectra when mixed with a potassium salt. However, the positioning of the probe proved critical in obtaining strong signals, and the sample was often desorbed before the position could be optimized. A more rigid mechanical arrangement may make the acquisition of such spectra more facile.

The use of a DC component for the isolation of ions (as was done for Figure 6) is explained in Figure 4: the ions of interest are given a q to place them beneath the "upper cusp" of the stability diagram, and DC is applied to bring the ions almost to the cusp itself. Figures 7 and 8 are spectra of xenon (not ion-injection) to help characterize the method. For Figure 8, m/z 132 was given a q beneath the cusp, and the DC component was increased linearly. The ions of other m/z values are excluded from the trap, and m/z 132 is isolated without loss in intensity. In Figure 7, both the RF and the DC are varied (angled axis) such that the DC/RF ratio is constant. This set of spectra is actually a mass analysis using the cusp of the stability diagram, and shows unit resolution in the isolation step.

(1) B.S. Freiser, Talanta, 32 (1985) 697.

Presented at the 36th ASMS Conference on Mass Spectrometry and Allied Topics
June 5-10, 1988, San Francisco, CA

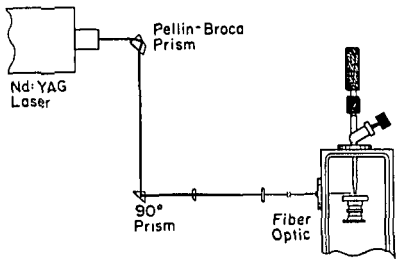

Figure 1

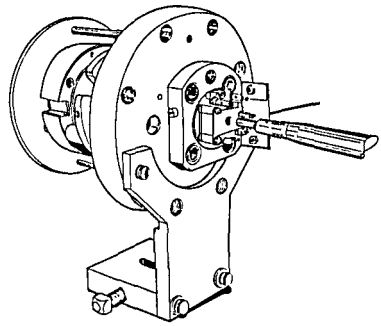

Figure 2

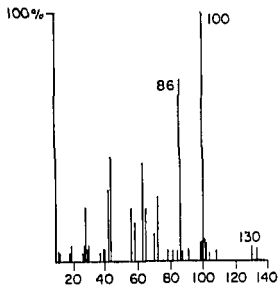

Figure 3

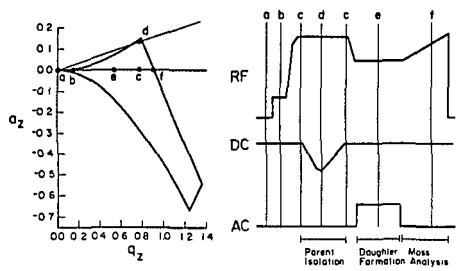

Figure 4

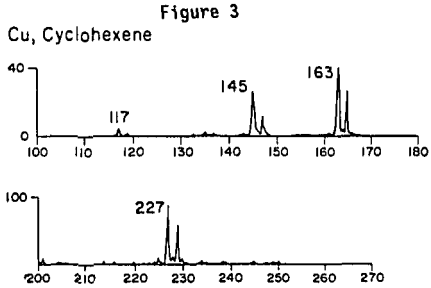

Figure 5

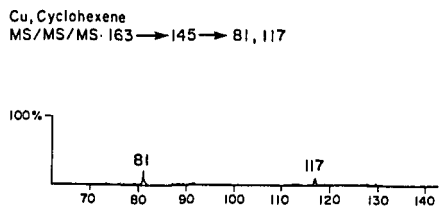

Figure 6

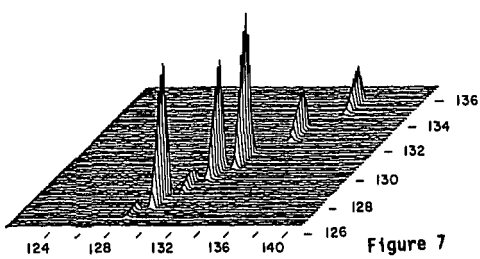

Figure 7

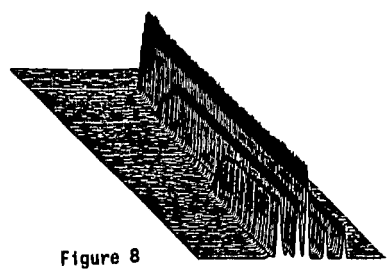

Figure 8

Presented at the 36th ASMS Conference on Mass Spectrometry and Allied Topics
June 5-10, 1988, San Francisco, CA

STEREOCHEMICAL INVERSION OF HALOXYFOP IN THE FISCHER 344 RAT. Michael J. Bartels and Fred A. Smith, Health & Environmental Sciences, Dow Chemical Co., Midland, MI 48674

The compound haloxyfop [2-(4-((3-chloro-5-(trifluoromethyl)-2-pyridinyl)oxy)phenoxy)propionic acid] is currently being evaluated for use as a herbicide. This compound is structurally similar to a group of 2-arylpropionates

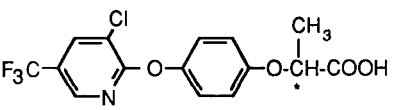

HALOXYFOP

which have been shown previously to undergo stereochemical inversion in a variety of mammalian species. The toxicicity/ oncogenicity studies performed in our laboratory, to support registration of haloxyfop as a herbicide, have been performed with the racemic test material. To support registration of the herbicidally active (R)-enantiomer of haloxyfop, further experiments were carried out to determine if racemic haloxyfop undergoes stereochemical inversion to the (R)-enantiomer in the rat, similar to the related 2-aryl-propionates.

Following administration of racemic test material (11 mg/kg, po) to male and female Fischer 344 rats, urine and feces were collected daily for 10 days. Selected, pooled urine samples were fortified with D_4-haloxyfop (center ring label), acidified, extracted (EtOAc), the haloxyfop enantiomers converted to diastereomeric derivatives ((S)-phenylethylamine) and analyzed by SIM GC/MS. Selected urine samples were also analyzed by HPLC. Selected, pooled fecal samples were fortified with D_4-haloxyfop, base-hydrolyzed (60°C - 30 min), acidified, and extracted with EtOAc. The EtOAc extracts were purified by reverse phase HPLC prior to derivatization and GC/MS analysis.

In the female rat the urinary haloxyfop was found to be nearly all (R)-enantiomer (>98%) and comprised 69.6% of the administered dose. Similar results were obtained for the test material present in all female rat fecal samples analyzed, in which 7.7% of the administered dose was recovered as haloxyfop. In the male rat, 52.2% of the dose was recovered in the day 1-10 urine and feces as haloxyfop. The stereochemistry of the parent compound present in these samples was similar to the results seen in the female rat (>98% (R)). These results show that (S)-haloxyfop undergoes rapid and nearly complete inversion to the (R)-enantiomer in the male and female Fischer 344 rat.

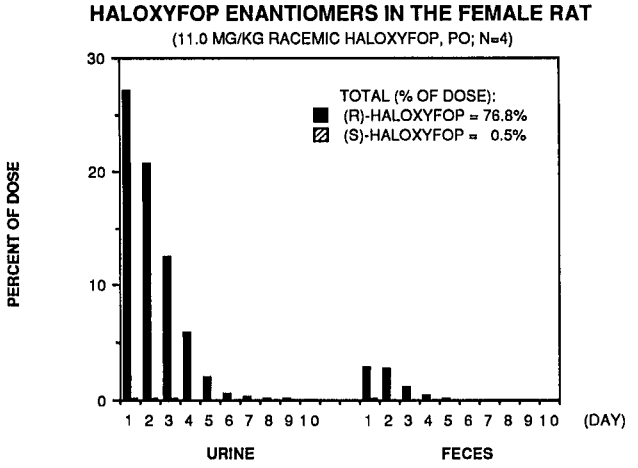
HALOXYFOP ENANTIOMERS IN THE FEMALE RAT
(11.0 MG/KG RACEMIC HALOXYFOP, PO; N=4)
TOTAL (% OF DOSE):
(R)-HALOXYFOP = 76.8%
(S)-HALOXYFOP = 0.5%
PERCENT OF DOSE
30
20
10
0
1 2 3 4 5 6 7 8 9 10
1 2 3 4 5 6 7 8 9 10
(DAY)
URINE
FECES

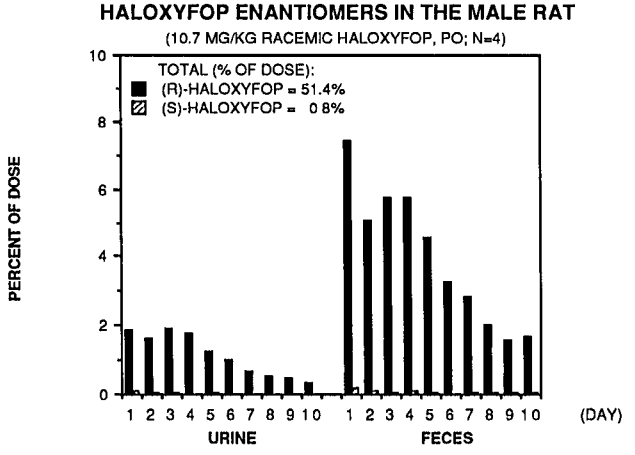
HALOXYFOP ENANTIOMERS IN THE MALE RAT
(10.7 MG/KG RACEMIC HALOXYFOP, PO; N=4)
TOTAL (% OF DOSE):
(R)-HALOXYFOP = 51.4%
(S)-HALOXYFOP = 0 8%
PERCENT OF DOSE
10
8
6
4
2
0
1 2 3 4 5 6 7 8 9 10
1 2 3 4 5 6 7 8 9 10
(DAY)
URINE
FECES

Presented at the 36th ASMS Conference on Mass Spectrometry and Allied Topics
June 5-10, 1988, San Francisco, CA

LY186641 METABOLISM IN HUMANS: DETERMINATION OF HUMAN PLASMA AND URINARY METABOLITE STRUCTURES BY THERMOSPRAY LC/MS AND FAST ATOM BOMBARDMENT MS

Patricia H. Dhahir, Alan Breau, Marta Hamilton,
Richard D. Barton and Winston G. Satterlee
Lilly Research Laboratories, Eli Lilly and Company
Indianapolis, IN 46285

INTRODUCTION:

LY186641, a diarylsulfonylurea derivative (Figure 1), is currently undergoing evaluation for antineoplastic activity against solid tumors. This compound is the first oncolytic application from the diarylsulfonylurea chemical class. During plasma level determinations two putative metabolite peaks were obtained on the HPLC-UV assay for parent. The retention times of the two putative metabolites were identical with two analogs in the LY186641 series. The identification of the two compound related peaks was determined using thermospray LC/MS, fast atom bombardment (FAB) mass spectrometry and chemical derivatization procedures.

MATERIALS AND METHODS:

Isolation and separation of metabolites

Acidified plasma and urine samples were extracted from an Analytichem C-2 cartridge using methanolic HCl. The extracts were reconstituted in mobile phase (25% acetonitrile/75% 0.1 M ammonium acetate) and injected onto a 25 cm x 4.6 mm Supleco LC-18-DB column. A Kratos 400 solvent delivery system pumped mobile phase at 1.0 ml/min through the column into a Waters 441 absorbance detector set at 254 nm. Each metabolite peak fraction was collected, pooled and concentrated under nitrogen.

Identification of metabolites

The concentrates were extracted into 90% hexane/10% ethyl acetate and reinjected onto the HPLC system (vide supra) to compare retention time with the synthetic analogs. Thermospray LC/MS spectra of the concentrates were obtained by analyzing the two concentrates on a Finnigan 3200 mass spectrometer through a Vestec thermospray interface.

The mass spectrometer was scanned from 150-500 amu every 2 seconds. The negative ions were detected at an electronmultiplier setting of 1450 V. The Vestec thermospray interface was operated in the discharge "on" mode with a tip temperature of 150 C, a vapor temperature of 240 C and a source block temperature of 290 C. No molecular ion was observed in thermospray LC/MS analysis, thus the samples were reanalyzed using FAB mass spectrometry. The FAB analyses were performed on a Nermag R30-10 triple stage quadrupole mass spectrometer operated in the single scan mode. The samples were dissolved in "magic bullet" matric on a stainless steel target. The target was bombarded with neutral Xenon gas (7 x 10-5 torr) accelerated to 7 kv using a Wallis M Scan FAB gun. The mass range of 300-800 amu was scanned every 10 seconds. The thermospray and FAB analyses indicated a keto and a hydroxy metabolite were present. The keto group was further confirmed by sodium borohydride reduction to the hydroxy which was monitored using FAB.

RESULTS AND DISCUSSION:

The thermospray LC/MS analyses of LY186641 does not produce a molecular ion but a major fragment at m/z/=180 representing the loss of the HN-(C=O)-NH-ARYL-CL group is observed. Fortuitously the major site of metabolic transformation occurs on the indan ring (Figure 2) which corresponds to the m/z=180 (Figure 3) fragment. The thermospray data indicates that the putative metabolites produce ions at m/z=194 (Figure 4) and m/z=196 (Figure 5) which are consistent with a keto (Figure 6) and hydroxy (Figure 7) indan ring structure. The retention times of synthetic standards of the keto and hydroxy metabolites are identical to the metabolites isolated from biological fluids. Since only one synthetic keto derivative is available, the location of the keto function on the indan ring is accomplished by reducing the keto metabolite with sodium borohydride. The hydroxy derivatrive that is formed can be compared using HPLC retention time data to the known synthetic hydroxy isomers.

Since only the indan ring is monitored using thermospray LC/MS, FAB is used to provide structural information about the total moiety. FAB produces a molecular ion and natriated adducts. The FAB analysis of parent produces a molecular ion at m/z=351 (Figure 8). The keto metabolite produces a molecular ion at m/z=365 (Figure 9) an increase of 14 daltons from the parent drug. The hydroxy metabolite has a molecular ion at m/z=367 (Figure 10) which represents a 16 mass increase over parent. The FAB spectra of the sodium borohydride treated keto metabolite produces a very small hydroxy parent at m/z=367 as well as a series of sodium adducts at m/z+389 and m/z-411 (Figure 11). The FAB spectra are consistent with the parent drug (Figure 1), hydroxy metabolite (Figure 12) and keto metabolite (Figure 13) structural assignments as well as the formation of the hydroxy metabolite following sodium borohydride reduction. The mass range of the FAB acquisitions is sufficient to detect any major conjugates. No major conjugates are observed.

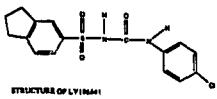

STRUCTURE OF LY186641
FIGURE 1

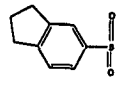

INDAN RING OF LY186641
FIGURE 2

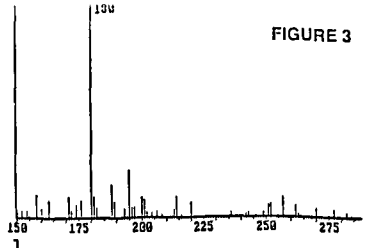

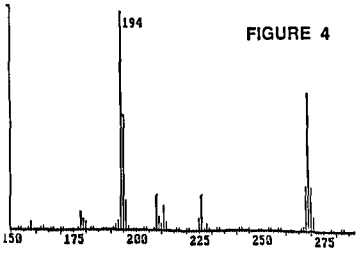

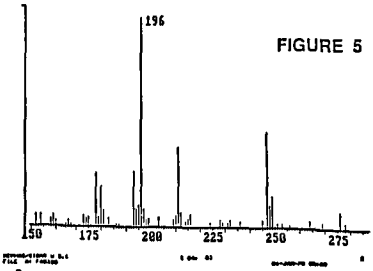

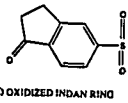

KETO OXIDIZED INDAN RING
FIGURE 6

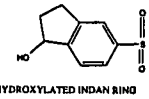

HYDROXYLATED INDAN RING
FIGURE 7

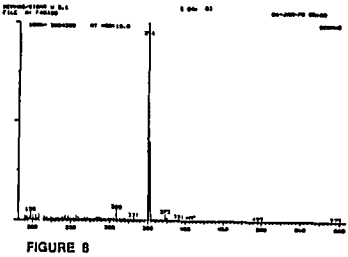

FIGURE 8

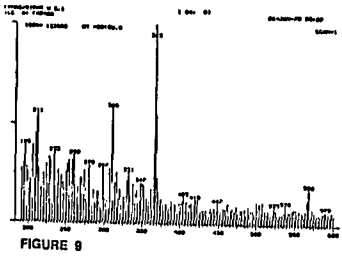

FIGURE 9

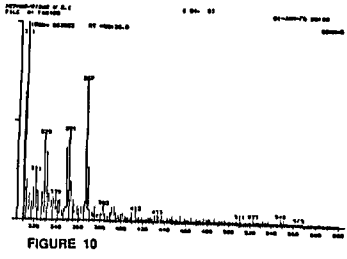

FIGURE 10

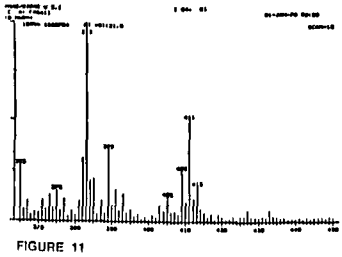

FIGURE 11

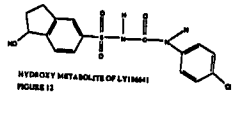

HYDROXY METABOLITE OF LY186641
FIGURE 12

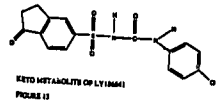

KETO METABOLITE OF LY186641
FIGURE 13

Presented at the 36th ASMS Conference on Mass Spectrometry and Allied Topics
June 5-10, 1988, San Francisco, CA

Characterization of Rat Biliary Metabolites of Daltroban (BM 13.505/SK&F 96148 By Fast Atom Bombardment and Thermospray Liquid Chromatography/Mass Spectrometry.

D. Dulik, G. Kuo, R. Gagnon, M. Davis, and J. Kao, Dept. of Drug Metabolism, SmithKline and French Research Labs, Swedeland, PA 19479

Daltroban (BM 13.505/SK&F 96148, I) is an orally active non-prostanoid thromboxane receptor antagonist currently under development in conjunction with Boehringer Mannheim GmbH for a number of cardiovascular and renal indications. This compound has been shown to be a potent anti-aggregating and antithrombotic agent in vitro and in animal models.

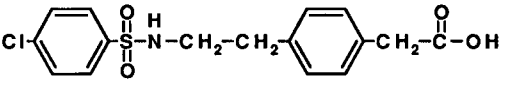

I

The objective of this study was to determine the metabolic profile of I in male and female rat bile and to structurally characterize the metabolites. Early studies by BM indicated that I undergoes extensive first pass metabolism to produce polar conjugates. Male and female Sprague-Dawley rats were bile duct cannulated and exteriorized for collection of samples. ^{14}C-I (171 uCi/mg; 100 mg/kg total dose) was administered as the sodium salt either orally or iv. Bile samples were collected into 10% aqueous glacial acetic acid and frozen immediately at the following time points: 0.5, 1, 2, 4, 6, 8, and 24 hrs. Bile samples were analyzed directly by thermospray LC/MS and LC/MS/MS on a Finnigan TSQ-45. Metabolites were also purified by gradient reversed phase HPLC and characterized by FAB mass spectrometry and proton NMR

Five major drug-related components were found in male rat bile, designated as M1-M5. These components accounted for 14, 20, 49, 14, and 1 percent of the excreted dose in the 2-4 hr collection period. In female bile, no M1 was found; M2 to M5 corresponded to 4, 77, 11, and 6 percent, respectively, for the same collection interval. Time dependent changes in the metabolite profile were evident. In males, the relative percent of M3 decreased from 70% in the 1-2 hr sample to 21% in the 8-24 hr sample. Conversely, the percent of M1 increased from 5 to 34% and M2 increased from 7 to 34% over the same time intervals.

The thermospray LC/MS spectrum of M1 gave a protonated molecular ion at m/z 477, 479 and an ammonium ion at m/z 494, 496. Negative ion FAB analysis produced an $(M-H)^-$ ion at m/z 475, 477. Proton NMR analysis of M1 combined with the mass spectral data was consistent with a taurine conjugate of hydroxylated I. LC/MS/MS analysis of M1 gave diagnostic fragment ions at m/z 126 for the taurine moiety and

m/z 308 for decarboxylated parent, as well as ions corresponding to dehydration products. The thermospray LC/MS spectrum of M2 gave a protonated molecular ion at m/z 461, 463 and ammonium adduct at m/z 478, 480. Negative ion FAB analysis gave an $(M-H)^-$ ion at m/z 459, 461. Proton NMR analysis of M2 was consistent with a taurine conjugate of I. LC/MS/MS analysis of M2 gave a base peak fragment ion at m/z 126 corresponding to loss of the taurine moiety. The thermospray LC/MS spectrum of M3 gave an ammonium adduct ion at m/z 547, 549. Negative ion FAB analysis produced an $(M-H)^-$ ion at m/z 528, 530. Proton NMR showed a strong anomeric proton signal at d 5.5, indicative of a 1-O-acyl glucuronide. LC/MS/MS analysis was also consistent with this proposed structure, with fragments at m/z 371, 373 from loss of glucuronic acid and m/z 194 for glucuronic acid itself. Both thermospray LC/MS and positive ion FAB analysis of M4 gave a protonated molecular ion at m/z 497. Little fragmentation in LC/MS/MS analysis was observed. The proton NMR spectrum combined with mass spectral analysis of M4 was consistent with the carnitine conjugate of I. Several other carnitine conjugates of acidic xenobiotics in animal species and humans have been previously reported. M5 was shown to be parent (I) by coelution in HPLC, thermospray LC/MS and LC/MS/MS, and FAB mass spectra.

The pH stability of M3, the 1-O-acyl glucuronide conjugate, was studied under physiological conditions. Authentic M3 was synthesized using immobilized microsomal UDP-glucuronyltransferases from rabbit liver. The product was purified by HPLC and characterized by mass spectrometry. M3 was stored in aqueous phosphate buffer (0.1 M, pH 7.4) at 37°C overnight. Aliquots were removed at various time points and the incubation mixture was monitored by HPLC. The half-life of M3 was less than 1 hr under these conditions. Stability of M3 was greatly enhanced by decreasing the pH of the incubation mixture to 3.0 and/or decreasing the temperature to -18°C.

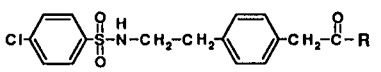

I

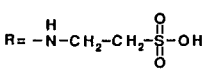

M1 (OH), M2

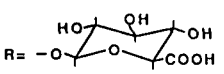

M3

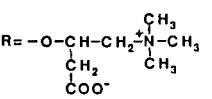

M4

Presented at the 36th ASMS Conference on Mass Spectrometry and Allied Topics
June 5-10, 1988, San Francisco, CA

CHARACTERIZATION OF CONJUGATED BENZAZEPINE METABOLITES IN FEMALE DOGS

M. Davis, K. Straub*, D. Dulik, G. Kuo, B. Hwang, and L. Gutzait
Dept. of Drug Metabolism, Smith Kline & French Laboratories, Swedeland, PA
and *Syntex Research, Palo Alto, CA

SK&F 86466 (6-Chloro-2,3,4,5-tetrahydro-3-methyl-1H-3-benzazepine) is an α_2-adrenoreceptor antagonist which has been shown to be an effective agent for lowering blood pressure in a variety of animal models[1,2]. Female beagle dogs received a 10 mg/kg oral dose of ^{14}C-SK&F 86466. Approximately 75% of the dose was excreted in the urine within 24 hours. Urine was acid stabilized on collection, then subjected to HPLC on a semi-preparative C_{18} column using linear gradients of 0.1% acetic acid (v/v) in water and methanol or 0.1M ammonium acetate and methanol. Fractions of column eluent containing radiolabel were pooled and repurified by isocratic HPLC prior to analysis by mass spectrometry and NMR.

A total of 8 major metabolites were observed, designated as 1-8 on the basis of their relative polarity. Metabolites were analyzed by FABMS, HPLC/MS, HPLC/MS/MS, DEP/EI MS, GCMS, ^{1}H-NMR, and ^{13}C-NMR. FAB mass spectra were obtained on a VG7070-EHF mass spectrometer using glycerol or thioglycerol as the matrix. Accurate mass determinations were made by on-line peak matching using the VG 11-250 data system. HPLC/MS and MS/MS analyses were conducted on a Finnigan TSQ-45 mass spectrometer equipped with a Finnigan Thermospray source and controller. GCMS and DEP/EI mass spectra were recorded on a Finnigan 4535 mass spectrometer. ^{1}H-NMR and ^{13}C-NMR spectra were obtained on a Bruker HX-360 spectrometer.

Metabolites 2 and 3, which account for a total of 22% of the drug-related material present in the urine, correspond, respectively, to the previously identified N-oxide metabolite (SK&F 102102) and the N-desmethyl metabolite (SK&F 101055)[3].

Following repurification by HPLC using the ammonium acetate/methanol mobile phase system, Metabolite 4 was found to be Metabolites 4A-4D, which account for 1%, 2%, 3%, and 10%, respectively, of the total radiolabel in the urine. Analysis of Metabolite 4D by FABMS gave $(M-H)^-$ at m/z 260 in negative ion mode. HPLC/MS gave $(M+NH_4)^+$ at m/z 279. HPLC/MS/MS analysis of m/z 279 yielded m/z 182, which corresponds to a protonated N-desmethyl moiety. The accurate mass of $(M-H)^-$ is 260.0157, which gives an elemental composition match of $C_{10}H_{11}NClSO_3$. The molecular weight information is consistent with an N-sulfonate metabolite of SK&F 101055. Additional evidence for this assignment was obtained by ^{1}H-NMR spectroscopy which showed the three aromatic protons and the eight azepine ring protons to be present. Acid hydrolysis of metabolite 4D resulted in the formation of the N-desmethyl metabolite, SK&F 101055, which was identified by GCMS.

Metabolite 7 accounts for 16% of the drug-related material found in the urine. Analysis by FABMS gave m/z 400 ($(M-H)^-$) in negative ion mode and m/z 402 ($(M+H)^+$) and 424 ($(M+Na)^+$) in positive ion mode. Analysis by HPLC/MS gave m/z 402 ($(M+H)^+$) and m/z 419 ($(M+NH_4)^+$). HPLC/MS/MS analysis of the ion m/z 402 showed fragment ions at m/z 226 (loss of a glucuronic acid moiety) and 182 (protonated SK&F 101055). The accurate mass of $(M-H)^-$ was found to be 400.0789, consistent with the composition $C_{17}H_{19}NClO_8Cl$. A ^{1}H-NMR spectrum of Metabolite 7 revealed three aromatic protons, eight azepine ring protons, and five non-exchangeable glucuronyl protons to be present. When analyzed by ^{13}C-NMR spectroscopy, the carbon resonances of the benzazepine and glucuronide moieties were present with an additional signal corresponding to the carbamate carbonyl. A structure consistent with these data is that of an acyl glucuronide of an intermediate carbamic acid, formed by the addition of CO_2 to the N-desmethyl metabolite.

Metabolite 8 accounts for 14% of the drug-related material in the urine. FABMS in negative ion mode gave $(M-H)^-$ at m/z 372. High resolution FABMS determined the accurate mass of $(M-H)^-$ to be 372.0847, which is consistent with the composition $C_{16}H_{19}NO_7Cl$ and corresponds to the elements of the N-desmethyl metabolite, glucuronic acid, and an additional oxygen. HPLC/MS/MS analysis of $(M+H)^+$ yielded the fragmentation sequence of 374->198->180 which is consistent with an O-glucuronide, but the position of substitution on the benzazepine ring cannot be determined from this data. ^{1}H-NMR analysis of this metabolite showed the three aromatic protons to be present but broadened signals of the azepine ring protons did not allow for accurate integration of their number and subsequent determination of the site of substitution. Following complete exchange in D_2O, Metabolite 8 was analyzed by negative ion FABMS using $^2H_8$-glycerol as the matrix. $(M-D)^-$ was observed at m/z 375 which demonstrated that the structure contains four exchangeble hydrogens. This eliminates all structural possibilities except an N-O-glucuronide, formed from an intermediate hydroxylamine of SK&F 101055.

Metabolite 1 was analyzed by negative ion FABMS with thioglycerol used as the matrix. $(M-H)^-$ was observed at m/z 276. This indicates a shift of 96 amu from the molecular weight of SK&F 101055, which implies the addition of a sulfate group to the N-desmethyl metabolite. High resolution FABMS analysis of m/z 276 determined the accurate mass of $(M-H)^-$ to be 276.0103. The molecular formula, $C_{16}H_{11}O_4NSCl$, is consistent with $(M-H)^-$ of a sulfate ester of SK&F 101055. The DEP/EI mass spectrum of the acid hydrolysis product of Metabolite 1 gave (M^+) of m/z 197, which is consistent with a hydroxylated N-desmethyl metabolite. ^{1}H-NMR analysis of Metabolite 1 showed two doublets in the aromatic region, corresponding to H7 and H8. A singlet, corresponding to H9, present in ^{1}H-NMR spectra of SK&F 101055, is absent in the spectrum of Metabolite 1, indicating C9 as the site of hydroxylation and subsequent sulfation of SK&F 101055.

The limited quantities of other metabolites made full characterization impossible, but molecular weight information was acquired for both Metabolites 4C and 6. FABMS analysis of Metabolite 4C in positive ion mode gave molecular ion species containing a chlorine isotope pattern at m/z 416,418. Fragment ions were observed at m/z 240 (loss of glucuronic acid moiety) and m/z 196 (loss of glucuronic acid moiety and CO_2). HPLC/MS gave a weak signal at m/z 433 and an intense signal at m/z 196 (protonated SK&F 86466). These data are consistent with a quaternary amine carbamate glucuronide of SK&F 86466.

When analyzed by FABMS, Metabolite 6 showed $(M+H)^+$ at m/z 550 and $(M+Na)^+$ at m/z 572 in positive ion mode and $(M-H)^-$ at m/z 548 and $(M+Na-H)^-$ at m/z 570 in negative ion mode. This data is consistent with a diglucuronide of the desmethyl metabolite. ^{1}H-NMR analysis of this metabolite failed to give useful structure elucidation information.

Following oral administration in the dog, SK&F 86466 undergoes N-oxidation to yield the N-oxide and C-oxidation to yield the N-desmethyl metabolite. The N-desmethyl is metabolized further by phenylhydroxylation followed by sulfation, N-sulfation, carbamylation followed by glucuronidation, and oxidation to a hydroxylamine followed by glucuronidation.

1. R.M. DeMarinis, *et. al.*, J. Med. Chem. 26, 1213-1214 (1983).
2. J.P. Hieble, *et. al.*, J. Pharmacol. Exp. Ther. 236, 90-96 (1986).
3. C. Gombar, *et. al.*, Drug Met. Dispos. 14, 540-548 (1986).

Presented at the 36th ASMS Conference on Mass Spectrometry and Allied Topics
June 5-10, 1988, San Francisco, CA

STRUCTURE DETERMINATION OF A54145A. A PEPTOLIPID CONTAINING NON-MAMMALIAN AMINO ACIDS

R. E. Chance, D. S. Fukuda, J. M. Gilliam, A. H. Hunt,
J. S. Mynderse, and J. L. Occolowitz*
Lilly Research Laboratories, Eli Lilly & Co., Indianapolis, IN 46285

The antibiotic A54145A (I) and several related compounds were produced by fermentation. Amino acid analysis showed that approximately 70% of the MW of A54145A, 1643d, was due to known amino acids. I contains one tryptophan residue, and a peak at m/z 341, $C_{21}H_{29}N_2O_2$, in its FABMS suggested that this was due to an N-decanoylated tryptophan moiety. Figs. 1a. and 1b. compare the CID spectra of m/z 341 and m/z 355, an undecanoyltryptophan moiety which occurs in the FABMS of A21978C_1 (II), a known antibiotic. Their similarity confirmed the presence of acyltryptophan in I. Both I and II contain threonine which further suggested that I might bear some structural similarity to II in which a lactone ring is formed by reaction of the C-terminal carboxylic acid with the threonine hydroxyl. This assumption was supported by formation of ring-opened A54145A (III), MW=1661d, by treatment of I with base. Enzymatic deacylation of I resulted in deacyl-A54145A(IV). Subsequently III and IV were used for FABMS, and Edman/FABMS sequencing, respectively.

FABMS of III indicated the partial sequence,
C_9H_{19}CONH-Trp-Glu------Gly-Asn-Glu-Ile-OH.
Fig.2. shows the FABMS evidence for the partial C-terminal sequence.

Edman sequencing of IV indicated the sequence,
H-Trp-Glu-X_1-Thr-Sar-Ala-Asp-Lys-X_2-Gly-Asn-Glu-Ile-OH
where X_1 and X_2 were unknown amino acids. The mass of X_1 was found by subtracting the mass of the residues obtained from the 2nd and 3rd Edman cycles. (Figs. 3a. and 3b.), and its composition determined by subtracting the accurate masses of the b_2 and b_3 sequence ions present in the FABMS. The composition of X_2 was found by subtracting the accurate mass of all of the known moieties from that of III. Thus, X_1 was found to be derived from an amino acid $C_4H_8N_2O_4$ and X_2 from $C_5H_9NO_5$. NMR analysis of IV established that these two amino acids were hydroxyasparagine and methoxyaspartic acid, respectively, and showed that the C-terminal isoleucine was bonded to the threonine hydroxyl in I.

The CID spectrum of the MH^+ from III, Fig. 4., supported its sequence. Sequence ions for the Lys-Asp(OCH_3) cleavage, not present in the CID spectrum, were found in the positive and negative FABMS of III.

The structure of A54145A is shown in Fig. 5.

Captions to Figures

Fig. 1a. CID spectrum of m/z 341 in the FABMS of A54145 (I).
1b. CID spectrum of m/z 355, an undecanoyltryptophan moiety in the FABMS of A21978C_1 (II).
Fig. 2. Part of the FABMS of ring-opened A54145A (III).
Fig. 3a. FABMS of product from 2nd Edman cycle of deacyl A54145A (IV).
3b. FABMS of product from 3rd Edman cycle of deacyl A54145A. NOTE: M_1 arises from the product where Thr has been dehydrated, and M_2 results from dehydration of Thr and addition of PhNCS to Lys.
Fig. 4. CID spectrum of MH^+ from ring-opened A54145A and scheme showing sequence ions
Fig. 5. Structure of A54145A.

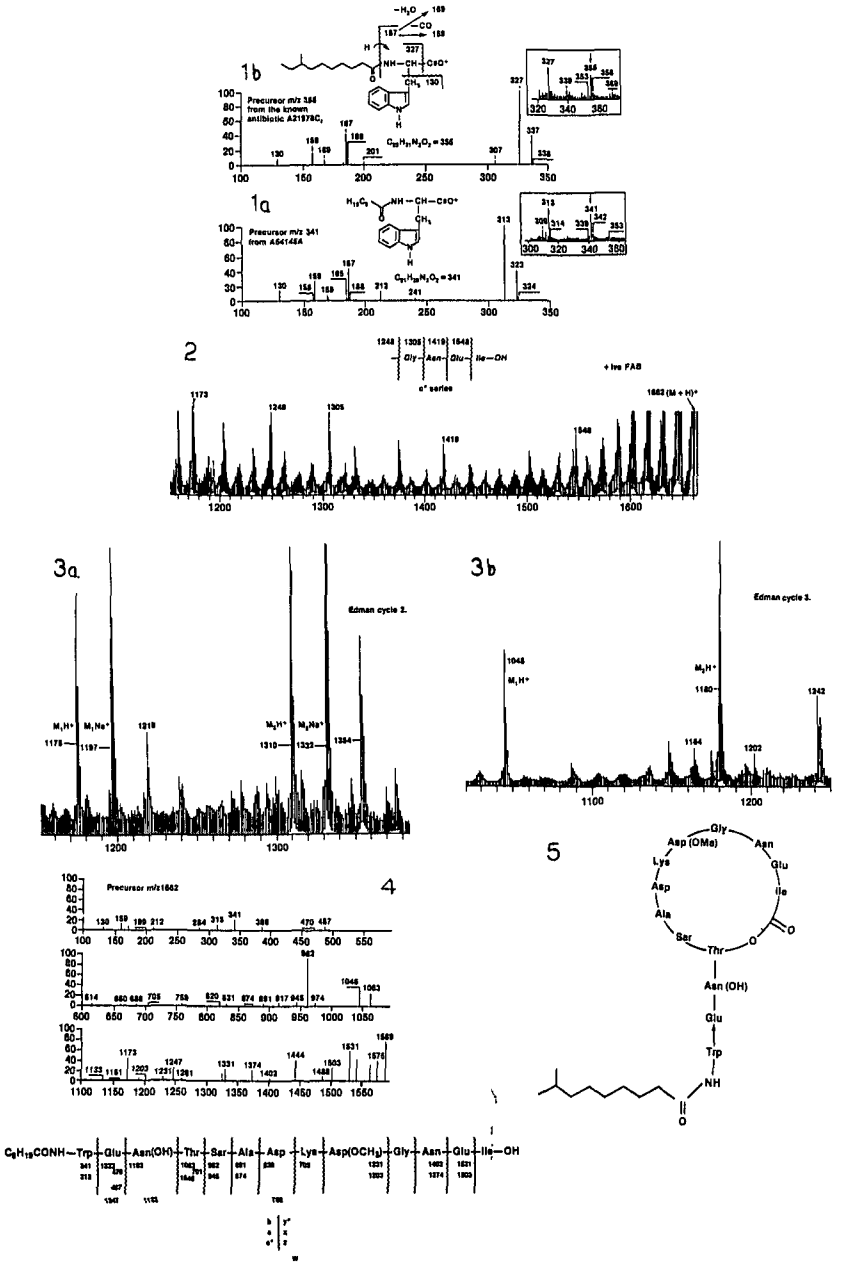
1b
Precursor m/z 356 from the known antibiotic A21978C2
1a
Precursor m/z 341 from A54145A
2
+ve FAB
3a
Edman cycle 2.
3b
Edman cycle 3.
4
Precursor m/z1662
5
Asp (OMe)
Gly
Asn
Glu
Ile
Thr
Ser
Ala
Asp
Lys
Asn (OH)
Glu
Trp
NH
C8H15CONH—Trp—Glu—Asn(OH)—Thr—Ser—Ala—Asp—Lys—Asp(OCH3)—Gly—Asn—Glu—Ile—OH

Presented at the 36th ASMS Conference on Mass Spectrometry and Allied Topics
June 5-10, 1988, San Francisco, CA

THERMOSPRAY LC/MS ANALYSIS OF METABOLITES OF THE CANDIDATE 8-AMINOQUINOLINE ANTILEISHMANIAL DRUG WR 6026 GENERATED IN THE ISOLATED PERFUSED RAT LIVER MODEL (IPRL)

RW Ashmore, LA Shipley, MD Coleman, TG Brewer, and AD Theoharides;
Department of Pharmacology, Walter Reed Army Institute of Research,
Washington, DC 20307-5100

Introduction

Leishmaniases are a widespread group of tropical diseases characterized by protozoal infections of the viscera, skin, and mucous membranes (1). 8-(6-Diethylaminohexylamino)-6-methoxy-4-methyl quinoline dihydrochloride (WR 6026) is a rapidly metabolized candidate antileishmanial drug which is currently in phase I clinical pharmacology studies.

Studies on the disposition of WR 6026 in vivo in the hamster (2) have shown that 48% of the dosed radioactivity was eliminated in the feces with 21% remaining in the liver. It is likely, therefore, that the drug undergoes hepatic uptake and biliary elimination in vivo. Therefore, the Isolated Perfused Rat Liver model (IPRL) would be a useful model to study the metabolism of WR 6026.

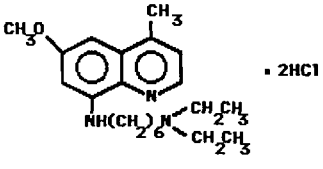

WR 6026.2HCl

Methodology

Rats were anesthetized with sodium pentobarbital and their livers isolated using standard techniques (3). The IPRL preparations were perfused in a circulating system (15 ml/min) at 37 °C as previously described (4). Bile was collected at 30 minute intervals after bolus injection of WR 6026 containing 25 uCi of [14C] labelled drug.

Reverse phase gradient HPLC analyses were performed using a Waters liquid chromatography system equipped with Raytest-Ramona-LS radiodetector. Gradient runs of acetonitrile:0.1 M ammonium acetate (pH 4.5) mixtures from 20:80 v/v to 50:50 v/v, concave curve, 30 minute ramp, at 1.5 ml/min were used. Elution was monitored by UV @ 254 nm and/or radiochemical detection. Radiochemical detection demonstrated the presence of a minimum of 12 more polar metabolites of WR 6026 in bile collected from this perfusion model.

A representative aliquot of total bile production for each half hourly sample was combined for a pooled sample. A subsequent aliquot was removed from this pooled sample for hydrolysis treatment (pH 5.0, 37 °C, 16hr) with b-glucuronidase preparation from bovine liver (1 unit/ml bile) or aryl sulfatase preparation obtained from Helix pomatia (1 unit/ml bile). Bile was injected directly on column for LC/MS analysis with equivalent volumes for hydrolyzed samples. Injection of standard compounds verified retention order and retention times found for some metabolites in the bile samples.

Thermospray LC/MS analyses were performed with identical chromatographic conditions to those described above. The chromatography equipment was interfaced to a NerMag R10-10C quadrupole mass spectrometer with Vestec Thermospray probe and gradient controller. The Finnigan Super INCOS data system was used for data acquisition and manipulation. The thermospray source was operated at 200 °C with probe run with T1 = 105 °C and T2 = 190 °C. No filament, repeller or discharge current was applied.

Results

Biliary excretion of [14C] accounted for 18.20±5.03% of the dose eliminated during the four hour experimental period. Only 2.80±0.68% was identified as WR 6026 and 0.63±0.11% as the desethyl metabolite. The remaining radioactivity was accounted for as highly polar metabolites of WR 6026. Treatment of the bile with hydrolyzing enzymes (B-glucuronidase and aryl sulfatase) facilitated the identification of three glucuronidated and two sulfated metabolites by LC/MS.

LC/MS spectra of all phase I unconjugated metabolites showed a protonated molecular ion as base peak, whereas sulfated and glucuronidated metabolites showed little or no molecular ions in the spectra, however the protonated deconjugated metabolite was base peak in all cases, i.e. $[M-SO3]+$ or $[M-C6H12O7]+$.

The structure of two of the glucuronidated metabolites were assigned as the 6-desmethyl glucuronide and the 6-desmethyl desethyl glucuronide metabolites of WR 6026. The third glucuronidated metabolite, an N-glucuronide of the side chain cleaved 8-amino metabolite could not be assigned exactly as to the position of the glucuronide moiety. The sulfated metabolites were identified as the 6-desmethyl sulfate and the 6-desmethyl desethyl sulfate metabolites.

Unconjugated metabolites identified were the 8-amino (side chain cleaved), desethyl, 6-desmethyl, 6-desmethyl desethyl metabolites. Two unidentified metabolites appeared after hydrolysis, and another metabolite was assigned a dihydroxylated structure, however the exact positions of the hydroxylations are as yet unknown. The HPLC intensity and chromatographic mobility of this metabolite was unaffected by treatment with either enzyme.

Summary

The data show that LC/MS analysis in conjunction with appropriate gradient HPLC conditions and enzyme hydrolysis procedures is a very powerful technique in drug metabolism studies.

References

1. J. D. Chulay and P.E.C. Manson-Bahr. Leishmaniasis-Introduction. In: Hunter's Tropical Medicine Sixth edition (ed. G. T. Strickland), p. 574-578, W.B. Saunder, Philadelphia (1984).
2. A.D. Theoharides, J. Anders, W.E. Ridder, M. Smyth, and H. Chung, Fed. Proc. 43, 959 (1984).
3. I.Bartosek, A. Guaitani, and L.L. Miller, Eds. Isolated Liver Perfusion and Its Application, Raven, New York (1973).
4. G.W. Mihaly, R.A. Smallwood, J.D. Anderson, D.B. Jones, L.K. Webster and F.J. Vajda, Hepatology 2, 828-831 (1982).

Presented at the 36th ASMS Conference on Mass Spectrometry and Allied Topics
June 5-10, 1988, San Francisco, CA

GC/MS CONFIRMATION OF SULFAMETHAZINE AND SULFISOXAZOLE IN MILK.

Agnes Van Langenhove (a) and Elizier Zomer (b); (a) Enseco - Erco Laboratory, 205 Alewife Brook Parkway, Massachusetts, 02138 and (b) Penicillin Assays Inc., 36 Franklin Street, Malden, Massachusetts, 02148.

Sulfamethazine and sulfisoxazole are sulfonamides used in combination with antibiotics as feed supplements to promote growth and retard bacterial infection in cattle. Contamination of milk samples with such sulfonamide residues is now being widely reported across the United States.

We are currently refining the Gas Chromatography/Mass Spectrometry (GC/MS) methodology for the confirmation of sulfonamide residues in milk samples that test positive in a newly developed radio receptor assay for sulfonamides and other antibiotics (1). In this competitive receptor assay, specific binding sites for drug classes are immobilized on microorganisms. For sulfonamide residues, concentrations of 5 ppb can be detected. GC/MS confirmation will only be needed for milk samples that test positive above the action levels set by the Food and Drug Administration. These tolerance limits will range from 10-100 ppb.

Our procedure for confirming the presence of a specific sulfonamide residue currently involves an initial High Performance Liquid Chromatography (HPLC) analysis of the lyophilized milk sample. The sulfonamide is characterized on the basis of its retention time, and quantitative determination is done by linear regression of area calculations of HPLC peaks at 275 nm. Tritium-labeled analogs have been used to validate this methodology. Final confirmation is done by GC/MS/Electron Ionization (EI) in the multiple ion detection mode. For these analyses, the HPLC fractions are collected. After evaporation of the solvent, the residue is methylated with diazomethane and analyzed by GC/MS.

Initial method validation was done for sulfamethazine at low nanogram GC/MS detection levels. Ions at m/z 92, 227, and 228 were monitored. The ions at mz 227/228 are indicative of sulfamethazine and not just of the sulfonamide portion. The methodology was applied to a milk sample that had been found to contain low ng levels of sulfamethazine. The absence of the confirmatory ions in a control blank used in conjunction with the retention time of N^1-methylsulfamethazine in the standard provided conclusive confirmation of sulfamethazine residues in the milk sample.

The methodology was then extended to five other sulfonamides: sulfanilamide, sulfathiazole, sulfapyridine, sulfisoxazole, and sulfadimethoxine. The methylated derivatives of these compounds were well resolved by GC/MS. Representative ions were selected for each individual compound and a combined standard was analyzed by GC/MS/EI in the Multiple Ion Detection (MID) mode. The following ions were selected (m/z values): sulfanilamide (92, 156, 172), sulfisoxazole (281, 156, 92), sulfapyridine (198, 199, 92), sulfathiazole (204, 205, 92), sulfadimethoxine (259, 260, 92). The ions chosen for sulfisoxazole provide less specific information about the compound than the ions selected for the other sulfonamides. The ions at m/z 92 (aniline) and mz 156 are indicative of the sulfonamide class only and are not specific for sulfisoxazole. An attempt to confirm sulfisoxazole at low ng levels in a milk sample by including monitoring of m/z 217 was only partially successful because the abundance of m/z 217 in the mass spectrum of N^1-methylsulfisoxazole is too low.

The GC/MS/EI evaluation studies done so far therefore indicate that selection of confirmatory ions is straightforward if the ions at $(M-SO_2)^+$ and $(M-HSO_2)^+$ can be selected (or for sulfanilamide, the abundant M^+). These ions are of low abundance in the mass spectrum of sulfisoxazole and the mass spectrometric confirmation of sulfisoxazole at low ng levels would therefore be better accomplished by positive chemical ionization mass spectrometry. We are currently awaiting actions levels to be set by the FDA for selection of the final methodology.

References

1. Charm, S.E., and Chi, R., "Microbial Receptor Assay for Rapid Detection and Identification of Seven Families of Antimicrobial Drugs in Milk: Collaborative Study." J.A.O.A.C. 71, 304 (1988).

EI MASS SPECTRA OF THE METHYLATED DERIVATIVES
OF SULFAMETHAZINE AND SULFISOXAZOLE

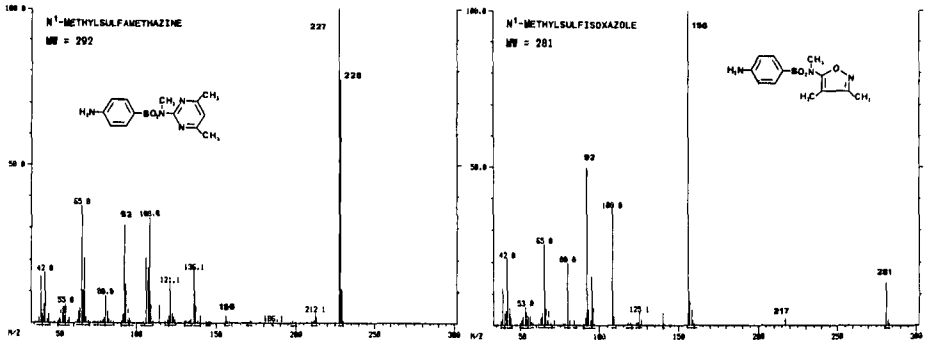

ANALYSIS SULFAMETHAZINE STANDARD

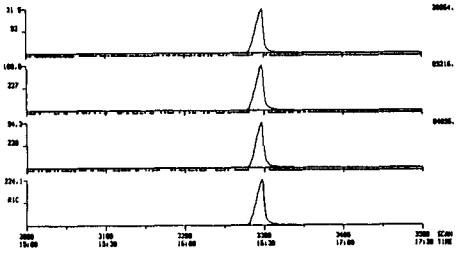

ANALYSIS MILK SAMPLE : confirmation
for sulfamethazine

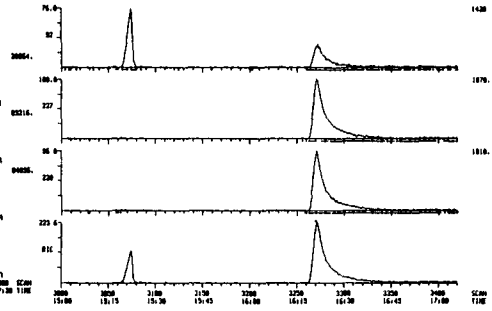

ANALYSIS SULFONAMIDE STANDARD,
20 NG INJECTED
EI/ FULL MASS SCAN
MASS CHROMATOGRAMS OF CONFIRMATORY IONS

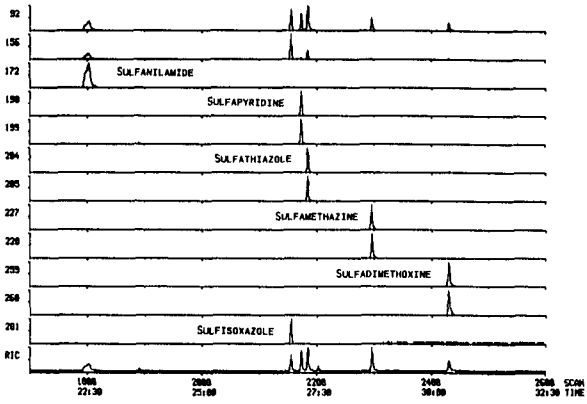

Presented at the 36th ASMS Conference on Mass Spectrometry and Allied Topics
June 5-10, 1988, San Francisco, CA

EXAMINATION OF THE MASS SPECTRA OF AMINOGLYCOSIDE ANTIBIOTICS BY THERMOSPRAY MASS SPECTROMETRY AND FAB MASS SPECTROMETRY

T.A. Getek, W.A. Korfmacher, and J.P. Freeman
National Center for Toxicological Research
Jefferson, AR 72079

ABSTRACT: Aminoglycoside antibiotics represent an important class of broad spectrum antibiotics used in injectables and topical solutions. Thermospray mass spectrometry (TSMS) and fast atom bombardment (FAB) mass spectrometry (MS) are two forms of ionization that are effective for the mass spectral analysis of aminoglcosides and sugars. In the course of investigating the utility of TSMS and FAB MS for the these compounds, it was noted that the aminoglycoside sulfates exhibited unusual behavior in TSMS and FAB MS.

EXPERIMENTAL: The thermospray (TS) mass spectrometer was a DELSI Ribermag R10-10C with a Vestec TS controller capable of discharge assistance at 1 kV. The aminoglycosides and sugars were examined by direct injection from a 20 *u*L loop using 0.1 M ammonium acetate as the liquid carrier at a flow rate of 1.0 mL/min. The FAB MS analyses of the aminoglycosides and sugars were performed on a Finnigan TSQ-70. A thioglycerol matrix and a sample load of 1.5 *u*L was utilized. Concentration of samples was ca. 2 mg/mL in water.

RESULTS AND DISCUSSION: In TSMS, aminoglycoside sulfates fragmented readily yielding only a small percent abundance of $[M+H]^+$ and large peak intensity for the individual sugar fragments formed from the cleavage of the glycosidic bonds (see TABLE I). In the course of maximizing peak intensity with discharge assistance, it was observed that the m/z for the aminoglycoside fragments at high tip temperature increased by one mass unit. One speculation for this one mass unit increase may be proton attachment to a neutral fragment. This neutral fragment may have been formed via a different ionization pathway for the parent molecule due to the discharge being on and higher tip temperature. This anomaly was not observed with the discharge off.

The FAB MS analyses of aminoglycoside sulfates in thioglycerol (TG) showed typical $[M+H]^+$ as well as nH_2SO_4 clusters (see TABLE II). The number (*n*) of clusters observed varied with the aminoglycoside. Confirmation of the effects of sulfate on the FAB mass spectra of aminoglycosides was demonstrated by using tobramycin, a non-sulfate, and adding H_2SO_4 to the matrix. Without H_2SO_4, only the $[M+H]^+$ ion was detected. With H_2SO_4, clusters containing H_2SO_4 were observed in FAB MS.

Several sugars were examined by TSMS and FAB MS including the trisaccharides raffinose and melezitose. In TSMS, behavior of the trisaccharides was simlar to the the aminoglycoside sulfates in that extensive fragmentation occurred with minor ion intensity for $[M+H]^+$. The ions indicative of $[M+NH_4]^+$ and $[M+Na]^+$ were also detected in TSMS. Comparable observations were reported by Hsu and coworkers [1]. The FAB MS analyses gave the expected $[M+H]^+$ ion and a cluster with TG, that is, $[M{\cdot}TG+H]^+$. An undefined ion was also observed at $[M+215]^+$.

In summary, the unique mass spectra of aminoglycoside sulfate antibiotics obtained by TSMS and FAB MS may be a means by which additional structural information may be asecrtained. For TSMS, the observation of fragments due to glycosidic cleavages indicated the overall molecular moiety. The FAB MS analysis suggested that the number of H_2SO_4 clusters observed for aminoglycoside sulfates may be dependent upon the aminoglycoside molecule. At this time, no definitive correlation can be made but is a point for future investigation.

REFERENCES:
[1] Hsu *et al.*, presented at ASMS, 1986, Cincinnati, OH, p.919.

ACKNOWLEDGEMENTS: One of us (TAG) would like to acknowledge the support of the Oak Ridge Associated Universities Postgraduate Research Program. The authors thank Dr. J.O. Lay, Jr. for helpful discussions and C. Hartwick for typing.

Presented at the 36th ASMS Conference on Mass Spectrometry and Allied Topics
June 5-10, 1988, San Francisco, CA

TABLE I
THERMOSPRAY MASS SPECTROMETRY OF AMINOGLYCOSIDES

	$[M+H]^+$	$[F_1]^+$	$[F_2]^+$	$[F_3+3H]^+$	$[F_4+2H]^+$
Gentamicin					
C_1	478	157	160	163	322
C_2	464	143	160	163	322
C_{1a}	450	129	160	163	322
Kanamicin	485	160	162	163	324
Netilmicin	476	127	160	191	350
Sisomicin	448	127	160	163	322

Notes:

1) All aminoglycosides are sulfate form.
2) F_1 and F_2 are indicative of each terminal sugar with glycosidic linkage.
3) F_3 represents the middle sugar of aminoglycoside molecule.
4) F_4 is a disaccharide fragment which contained F_2 and F_3; the fragment for F_1 plus F_3 was not detected in TSMS.

TABLE II
FAB MS OF AMINOGLYCOSIDE SULFATE ANTIBIOTICS

		$[M+H]^+$	$[M \cdot H_2SO_4+H]^+$	$[M \cdot 2H_2SO_4+H]^+$	$[M \cdot 3H_2SO_4+H]^+$
$\underline{n}$[c] detected	Gentamicin				
3	C_1	478	576	674	772[a]
3	C_2	464	562	660	758[a]
3	C_{1a}	450	548	646	744[a]
1	Kanamicin	485	583	b	b
2	Netilmicin	476	574	672	b
3	Sisomicin	448	546	644	742[a]

[a]Less than 0.1% abundance.
[b]Not detected due to background noise.
[c]$\underline{n}$ is number of H_2SO_4 molecules in the cluster.

Presented at the 36th ASMS Conference on Mass Spectrometry and Allied Topics
June 5-10, 1988, San Francisco, CA

CAPILLARY GAS CHROMATOGRAPHY-REACTION INTERFACE/MASS SPECTROMETRY. A HIGHLY SELECTIVE METHOD FOR THE DETECTION OF ^{13}C, ^{15}N, and ^{2}H LABELED DRUGS AND THEIR METABOLITES.

Donald H. Chace and Fred P. Abramson; Department of Pharmacology, The George Washington University Medical Center, Washington, D.C., 20037.

Markey and Abramson (1) developed a microwave-powered reaction interface that converts complex organic molecules in the presence of a reactant gas into small stable molecules which are detected by mass spectrometry (RIMS). These molecules reflect the elemental composition of the original analyte. The combination of a reaction interface and a mass spectrometer produces an element- or nuclide- selective detector for samples which are flowing from a capillary gas chromatograph (GC-RIMS).

In the presence of SO_2, $^{12}CO_2$ at m/z 44 and $^{13}CO_2$ at m/z 45 were produced from carbon atoms contained in the original analyte while ^{14}NO at m/z 30 and ^{15}NO at m/z 31 were produced from nitrogen atoms. These products were detected using a medium resolution Dupont 491 mass spectrometer equipped with a Trek Model 667 power supply. The data were acquired using a Teknivent data system. Using H_2 as the reactant gas rather than SO_2, HD at m/z 3.022 was produced from deuterium atoms which were present in the analyte. This product was detected using a higher resolution Dupont 492 mass spectrometer which was also equipped with the Trek power supply and Teknivent data system. HD was detected at a resolution of 2000.

Following the administration of 50 mg of either 2,4,5-(^{13}C)-, 1,3-(^{15}N)2-(^{13}C)-, or 10(D)-phenytoin (PT) to a male beagle dog, each urine sample was analyzed for its ^{13}C, ^{15}N, or deuterium content by GC-RIMS. The urine was hydrolyzed using enzyme isolated from Helix Pomatia, purified with XAD-2 resin, and derivatized first by extractive ethylation using tetrabutyl ammonium hydroxide and 1:3 ethyl iodide:methylene chloride. This was followed by acylation using trifluroacetylimidazole. The internal standard (I.S.) was either 1,3-(^{15}N)2-(^{13}C)-phenobarbital or 5(D)-primidone which was added to the urine at a concentration between 250 - 500 ng/mL.

M/Z 44, measuring $^{12}CO_2$, is a nonselective detection channel of ^{12}C. The chromatogram for a processed urine sample from a dog administered 2,4,5-(^{13}C)-PT is shown in Figure 1. More than 100 peaks were detected. ^{13}C was detected at M/Z 45 . Because the natural abundance of $^{13}CO_2$ and $^{12}C^{17}O^{16}O$ at M/Z 45 is 0.01182%, the M/Z 45 chromatogram was also nonselective as shown in Figure 2. By subtracting the natural abundance contribution of CO_2 at m/z 45, a net enrichment chromatogram at M/Z 45 is produced. The following equation was used for this computation.

Net M/Z 45 = Gross M/Z 45 - [0.01182% * M/Z 44]

The results are shown in Figure 3. Only ^{13}C-enriched I.S., PT and PT metabolites were detected. The detection limits were in the low nanogram per mL range which represented less than 1% of the metabolites present in the selective chromatogram. Approximately 10 metabolites were detectable. To demonstrate that all the peaks were metabolites of PT, a urine sample which was collected 24 hours prior to drug administration was also processed. The I.S. was added to this urine. The results are shown in Figure 4. No peaks other than the internal standard were detected. (M/Z 44 "Out of Range" indicates that the signal height for this peak at m/z 44 saturated the data system so that the net M/Z 45 equation is not accurate).

In a repeat analysis with the reaction interface turned off, the EI mass spectra of peaks shown by RIMS to be enriched permitted the identification of phenytoin and at least four of the approximately 10 detected metabolites. These have been identified as meta- and para-hydroxyphenytoin, the catechol, and the O-methyl catechol forms of phenytoin.

Similar metabolic profiles for ^{15}N and D-enriched PT were found. The detection of ^{15}N and deuterium by RIMS was as selective and sensitive as for ^{13}C. All three methods were linear and reproducible.

Supported by USPHS Grant NIH-GM36143

[1]Markey, S.P. and Abramson, F.P., Analytical Chemistry, 1982, Vol. 54, 2375.

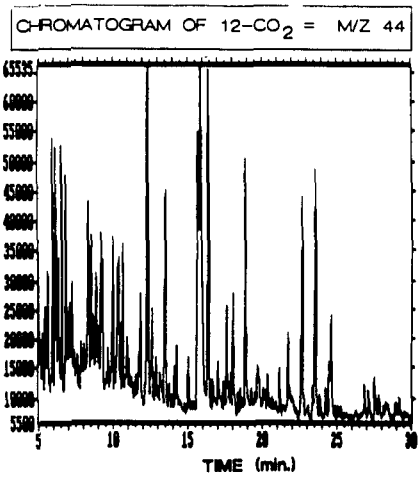

Figure 1: Selected ion chromatogram of 12-CO_2 at M/Z 44. Analysis of 1 µL of processed urine from a dog administered 3(13-C)-phenytoin.

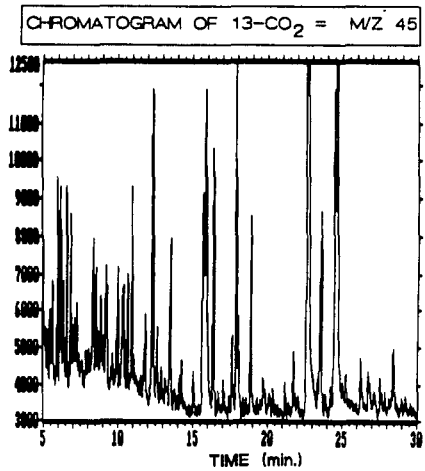

Figure 2: Selected ion chromatogram of 13-CO_2 at M/Z 45. Analysis of 1 µL of processed urine from a dog administered 3(13-C)-phenytoin.

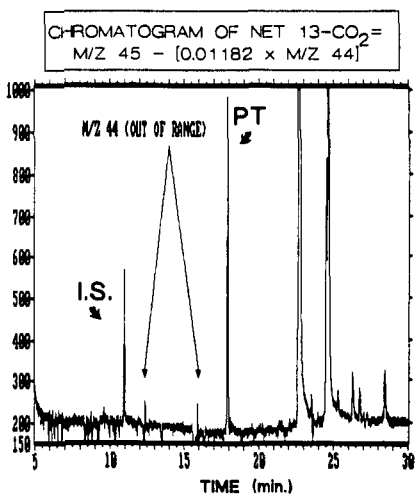

Figure 3: Net selected ion chromatogram of 13-CO_2 obtained by subtracting the natural abundance of 13-C and 17-O from M/Z 45. Analysis of 1 µL of processed urine from a dog administered 3(13-C)-phenytoin.

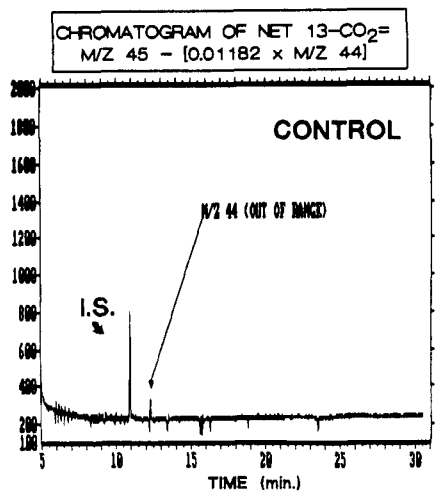

Figure 4: Net selected ion chromatogram of 13-CO_2 obtained by subtracting the natural abundance of 13-C and 17-O from M/Z 45. Analysis of 1 µL of processed urine collected prior to drug administration.

Presented at the 36th ASMS Conference on Mass Spectrometry and Allied Topics
June 5-10, 1988, San Francisco, CA

M.H. Hag Ali, D. Fetterolf[1], F.P. Abramson, and V.H. Cohn

Department of Pharmacology
George Washington University School of Medicine
Washington, DC 20037

[1]Federal Bureau of Investigation
Quantico, VA 22135

Praziquantel (PZQ) is used to treat the parasitic disease schistomiasis. Because schistosomiasis affects the liver, the question being addressed was whether the metabolism of PZQ is altered during this disease. In order to answer this, an assay for PZQ and its metabolites had to be developed. We found that tandem mass spectrometry (MS/MS) was particularly useful in evaluating the structures of PZQ metabolites and changes in their concentration in the urine of the control and infected mice which were the test animals.

EXPERIMENTAL. Groups of control and schistosome-infected CD-1 mice were given 200 mg/kg i.p. injections of PZQ and 24 h urine specimens were collected. Twenty-five ml portions were lyophilized, redissolved in 1 ml of acetate buffer, and enzymatically deconjugated. This mixture was next purified on an Amberlite XAD-4 column which was rinsed with 4 ml of water and eluted with 15 ml of a 1:1 mixture of acetone and methanol. This was dried and reconstituted in 2 ml of the acetone:methanol mixture. The mass spectrometry experiments used a Finnigan Model 3500 triple quadrupole. Two μl of the urine extract was introduced via the direct introduction probe which was heated ballistically from 30 to 450 °C. Positive chemical ionization with methane was used. The collision gas was argon and the collision energy was 20.8 eV.

QUALITATIVE ANALYSIS. The CAD spectrum of the quasimolecular ion of PZQ showed major fragments which represented structurally useful information. One fragment, m/Z 203, represented three of its four rings (the ABC ring fragment), and another, m/Z 83, represented the fourth, a cyclohexyl ring (ring D). We assumed that hydroxylations to any of the four rings would be appropriately recognized by shifts in the masses of these two complementary portions of the molecule. No authentic sample of any metabolite was available so that certain assumptions were made in order to tentatively interpret the spectra. If a hydroxylation occurred on an aromatic ring, it would not dehydrate, while if hydroxylation occurred on an aliphatic carbon it would always dehydrate. Thus, three masses might appear for the ABC ring fragment: m/Z 219 if the OH was in a stable position, m/Z 201 if the OH was unstable and dehydrated, and m/Z 203 if the OH was on the D ring which leaves the ABC group intact. A similar interpretation for dihydroxylated ABC fragments can be developed. By setting the first quadrupole to pass molecular ions of PZQ (m/Z 313), monohydroxyPZQ (m/Z 329), dihydroxyPZQ (m/Z 345), etc., and examining the ABC ring components of the daughter spectra, we were able to tentatively identify 3 monohydroxy- (M1-M3) and 6 dihydroxyPZQ metabolites (D1-D6) from these urine extracts.

QUANTITATIVE. Although the qualitative interpretation scheme was only tentative, the spectra could be quantified in order to examine differences between control and infected mice. To do this, urine samples from 9 groups of control and infected mice were analyzed for intact PZQ, the 3 monohydroxyPZQ metabolites and the 6 dihydroxyPZQ metabolites. PZQ was also analyzed by gas chromatography using nitrogen-selective detection where its area was compared to the total area of the chromatogram. For unchanged PZQ, three different MS/MS quantitation schemes were used: method A used the total ion current from m/Z 313 and its daughter ions compared to the sum of the parent and daughter ions of PZQ metabolites, method B compared only the parent ion intensities, and method C compared only the daughter ion intensities. The results are expressed as the percent of total signal representing PZQ along with the SEM (N = 9). In all cases, there was a significant increase in unmetabolized PZQ in the infected animals.

METHOD	CONTROL MICE	INFECTED MICE
GC	3.9 ± 0.6%	7.8 ± 1.8%
A	1.7 ± 0.2%	2.6 ± 0.2%
B	8.3 ± 0.7%	10.5 ± 0.7%
C	1.0 ± 0.1%	1.7 ± 0.2%

Although the three MS/MS methods gave different values, their precision was comparable to the GC method.

The quantitation of the metabolic pattern of PZQ was accomplished by normalizing each level of hydroxylation to 100% These percentages ± SEM (N = 9) from control mice are reported below.

METABOLITE	RELATIVE AMOUNT	METABOLITE	RELATIVE AMOUNT
M1	1.7 ± 0.1%	D1	8.8 ± 0.7%
M2	16 ± 0.7%	D2	11.3 ± 0.6%
M3	82 ± 0.8%	D3	2.8 ± 0.1%
		D4	6.4 ± 0.2%
		D5	58 ± 1.0%
		D6	13 ± 0.7%

Again, although the accuracy of these data is uncertain, the precision is good implying that MS/MS could be used successfully for quantitative analyses of this type if authentic materials were available as standards.

CONCLUSIONS. The reproducibility of MS/MS for quantitative analysis of metabolic patterns from "real" biological specimens appears good by using structure-defining fragmentations. In this way, an increase in the excretion of PZQ, and alterations in metabolites D2, D3, and D6 were observed in infected animals (data not shown). Thus schistosomiasis affects the metabolism of praziquantel.

Presented at the 36th ASMS Conference on Mass Spectrometry and Allied Topics
June 5-10, 1988, San Francisco, CA

FRAGMENTATION AND TANDEM MASS SPECTROMETRY OF PENICILLINS

SOMCHAI SUWANRUMPHA AND ROYAL B. FREAS
DEPARTMENT OF CHEMISTRY, UNIVERSITY OF HOUSTON, HOUSTON, TEXAS 77204-5641

We have studied ampicillin and its fragment ions using several mass spectrometric techniques. Isobutane chemical ionization (CI) and thermospray ionization (TI) mass spectra of ampicillin (MW 349) exhibit abundant ions at *m/z* 160 and *m/z* 191, and low abundances of the protonated molecule at *m/z* 350 (Figs. 1 & 2). The ions at *m/z* 160 and *m/z* 191 correspond to cleavage of the β-lactam ring. Siegel et al. have reported a similar thermospray mass spectrum.[1] The fragmentation of ampicillin has been discussed.[1] A fast-atom bombardment (FAB) mass spectrum of ampicillin from a glycerol matrix (Fig. 3) shows an abundant protonated molecule at *m/z* 350 and an abundant ion at *m/z* 160. The ion at *m/z* 192 was observed to be more abundant than the ion *m/z* 191. The FAB mass spectrum is similar to that reported in the literature.[2] Collision-induced dissociation (CID) spectra were acquired using a tandem, hybrid (EBQQ) mass spectrometer. Protonated ampicillin (*m/z* 350) fragmented to yield an ion at *m/z* 192, but an ion at *m/z* 191 was not observed (Fig. 4).

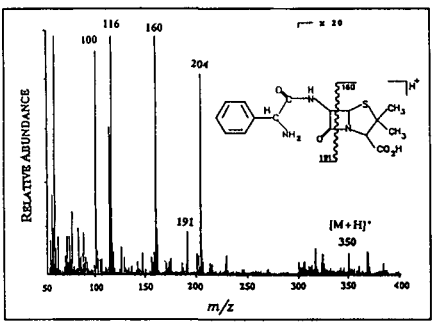

Figure 1. Isobutane CI mass spectrum of ampicillin (MW 349).

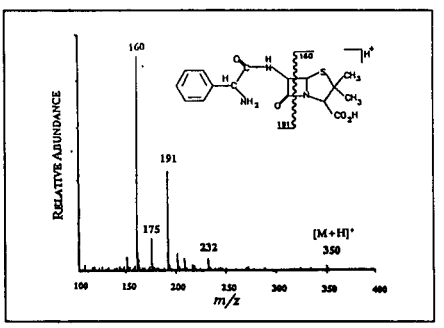

Figure 2. Thermospray ionization mass spectrum of ampicillin (MW 349).

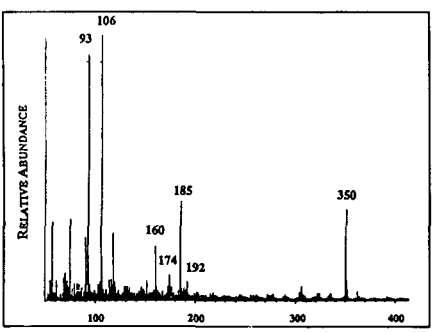

Figure 3. FAB mass spectrum of ampicillin (MW 349).

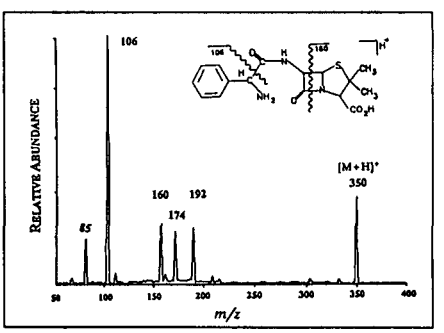

Figure 4. Collision-induced dissociation of protonated ampicillin (*m/z* 350).

The mechanism for forming *m/z* 191 versus *m/z* 192 is elucidated by inspecting the CID spectra of ampicillin, amoxicillin (a substituted analog of ampicillin), ampicillin piperazine-2,5-dione (an ampicillin metabolite), and amoxicillin piperazine-2,5-dione. The CID spectra of *m/z* 192 from ampicillin and of *m/z* 191 from ampicillin piperazine-2,5-dione are comparable except the corresponding fragment ions lie one mass unit apart (Figs 5 & 6). This suggests that the structure of *m/z* 192 from ampicillin is similar to the structure of *m/z* 191 from ampicillin piperazine-2,5-dione. The unit mass difference corresponds to the substitution of an -O- for an -NH- group. A postulated mechanism for forming the ion at *m/z* 192 is

shown in Fig. 7. The mechanism involves losing NH_3 at the amino side chain, an oxygen rearrangement, and a 2+2 cycloreversion to cleave the β-lactam ring. This results in a fragment analogous to the *m/z* 191 fragment from ampicillin piperazine-2,5-dione. The proposed loss of NH_3 in the first step is supported by the CID spectrum of *m/z* 349 from amoxicillin, which corresponds to the loss of NH_3 from protonated amoxicillin (MW 365). The CID spectrum shows the formation of a fragment ion at *m/z* 208 (Fig. 8). The ion at *m/z* 208 from amoxicillin is analogous to ion at *m/z* 192 from ampicillin.

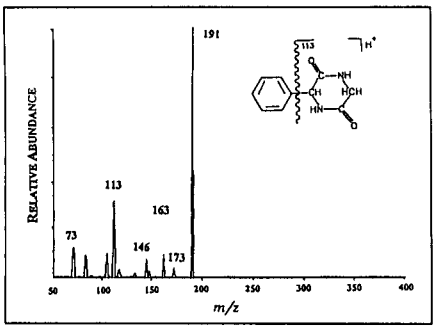

Figure 5. Collision-induced dissociation of *m/z* 192 from ampicillin.

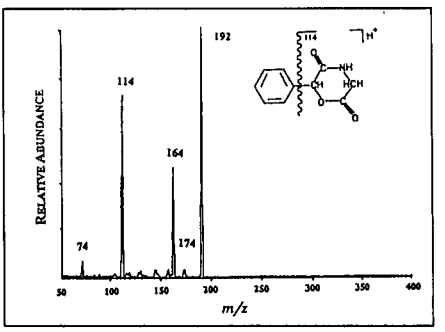

Figure 6. Collision-induced dissociation of *m/z* 191 from ampicillin piperazine-2,5-dione.

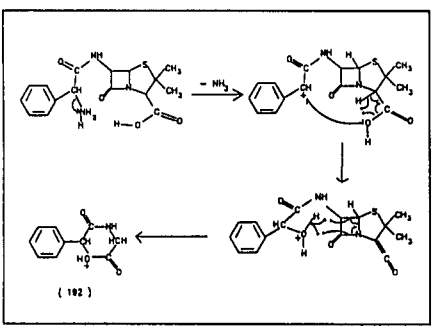

Figure 7. Postulated mechanism to form *m/z* 192 from ampicillin.

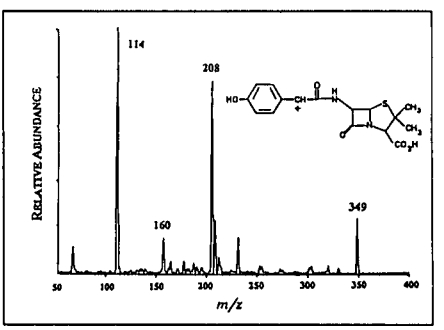

Figure 8. Collision-induced dissociation of *m/z* 349 from amoxicillin.

The formation of *m/z* 191 in the thermospray and CI mass spectra is postulated to arise from a gas-phase protonation of the neutral product (at 190 u) of the β-lactam ring cleavage. The FAB mass spectrum of ampicillin shows substantially less abundant *m/z* 191. This is because gas-phase ion/molecule reactions are less likely occur in the FAB ion source than they are in the CI and TI ion sources due to lower ion source pressures. The importance and usefulness of identifying fragmentations can be used in the determination of penicillins and their metabolites from biological fluids.

ACKNOWLEDGEMENTS

We thank Dr. Marvin Vestal for valuable assistance and the Texas Advanced Technology Research Program for partial support of this work.

REFERENCES

1. Siegel, M.M.; Isensee, R.K.; Beck, D.J. *Anal. Chem.* **1987**, *59*, 989-995.
2. Barber, M.; Bordoli, R.S.; Sedgwick, R.D.; Tyler, A.N., Green, B.N., Parr, V.C.; Gower, J.L. *Biomed. Mass Spectrom.* **1982**, *9*, 11-17.

Presented at the 36th ASMS Conference on Mass Spectrometry and Allied Topics
June 5-10, 1988, San Francisco, CA

DETERMINATION OF DIETHYLSTILBESTROL AND DIENESTROL IN CHICKEN BY GC AND SELECTED ION MONITORING

Yang Yinghua and Liu Li
Jilin Import and Export Commodity Inspection Bureau,
81 Stalin Street, Changchun, China.

Diethylstilbestrol(DES) and dienestrol(DI) are synthetic estrogen,and used as growth promoters in meat-producing animals and fowl. Because of the carcinogenic potential of DES and DI, any residue of it in food is not allowed, and it is necessary to determine DES and DI in chicken for export. DES and DI have been determined by GC and HPLC, but only few reports using MS for the determination. The method described here for the determination of DES and DI is based on the combination of GC and selected ion monitoring technique. This method provides high sensitivity and high specificity.

The recoveries of DES and DI added into chicken samples in different concentration were examined and the detection limits determined. The results obtained from two kinds of derivatives of DES and DI were compared and dicussed

All experiments were carried out on a JMS-D_{300} Mass Spectrometer.
GC: glass column, 2M×2.5mm packed with 3% OV-17, carrier gas, He.
MS: electron impact source; resolution 500; ion source temperature, 220°C;ionization current,300μA; ionization voltage, 70V.

1, Sample treatment: Homogenize 5g chicken sample in 250ml glass stoppered flask, add 3-5ml 10% Na_2CO_3, shake for 2min. add 20ml toluene and shake vigorously for another 5min. 1) TMPH derivative: transfer 2ml clear upper layer toluene into a conical centrifuge tube, add 30μl TMPH shake vigorously by hand for 1min. centrifuge for 2min, and TMPH phase is ready to be determined. 2) TFA derivative: transfer 2ml clear upper layer toluene into a conical centrifuge tube, evaporate it in a gentle N_2 stream at room temperature till it is day. Then add 30μl 1:1 (ethyl acetate:TFA) and TFA phase is ready for determination.

2, Mass spectrum: Mass spectra of DES and DI(two kinds of derivatives) were determined with standard solutions. EI mass spectrum of the derivatives of DES and DI and their structure, major ions, relative intensities are shown in table 1:

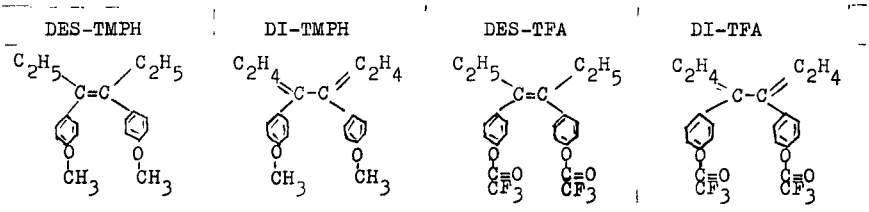

compound	MW.	major ions and relative intensity
DES-TMPH	296	296(1oo),281(18),267(37),159(57),121(84),135(27),91(26).
DI -TMPH	294	294(1oo),279(66),265(31),263(27),241(26),128(3o),115(35).
DES-TFA	46o	46o(1oo),431(43),317(24),241(96),217(23),2o3(71),115(38).
DI -TFA	458	458(1oo),345(64),241(28),217(31),215(31),2o3(27),115(52).

3, According to EI Mass spectra, the base peaks M/Z296,M/Z294,M/Z46o, M/Z458 were chosen as monitoring selected ion respectively. Then recoveries of different spiked chicken samples were determined.Recoveries of the derivatives added into the chicken samples are shown in table 2:

added(ng)	recovery %		added(ng)	recovery %	
	DES-TMPH	DI-TMPH		DES-TFA	DI-TFA
15	85.3	74.9	3o	68.8	9o.4
5	83.2	74.3	15	68.3	88.6

For TMPH derivative the recovery of DES is higher than that of DI; while for TFA derivative the recovery of DES is lower than that of DI.

4, The standard curves obtained are shown in table 3 and figure1-4:

added(ng)	DES-TMPH	DI-TMPH	DES-TFA	DI-TFA
3.75	3.13	o.82	29.74	1o.12
2.5o	2.56	o.56	21.14	6.98
1.25	1.14	o.39	1o.97	3.96
o.5o	o.85	o.29	1.52	o.92

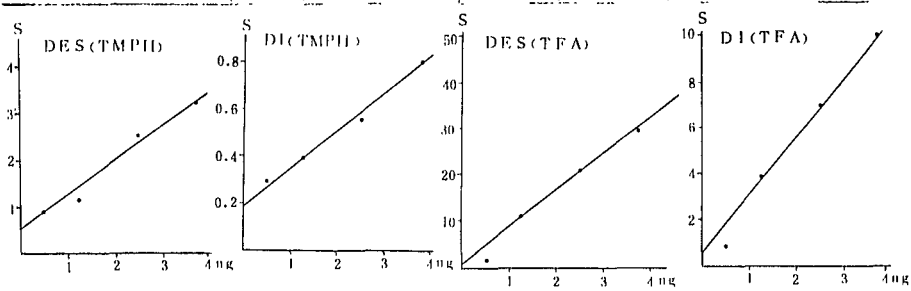

It is shown the standard curve had a good linear relationship from o.5ng-3.75ng of DES-TMPH,DI-TMPH,DES-TFA and DI-TFA. The method has been used to analyse practical samples. Determination of DES and DI residues in actual five chicken samples were all shown a negative result.

Under the experimental conditions above mentioned the detection limit of the method for either species is shown to be o.5ng. It is suitable for determination of trace DES and DI in chicken samples. We have successfully determined trace methyl-alcohol and higher alcohols in beverage by this method.

Presented at the 36th ASMS Conference on Mass Spectrometry and Allied Topics
June 5-10, 1988, San Francisco, CA

The Identification of Products Cosynthesized In the Preparation of Thienylcyclohexylpiperidine (TCP).

Louis A. Jones, M.K. Lee, Department of Chemistry, and
C.A. Haney, GC/MS Facility
North Carolina State University, Raleigh, NC 27695-8204

The thienyl analogue of the Schedule I abused drug Phencyclidine (PCP) is prepared by the addition of 2-thienylmagnesium bromide in ether to 1-piperidylcyclohexyl carbonitrile.[1] Using the reversed-phase ion pair chromatographic system developed for PCP[2], at least 10 other cosynthetic compounds in addition to the major product 1-(2-thienyl-cyclohexyl)-piperidine (TCP) were indicated. In the case of PCP, three of the thirteen PCP cosynthetics have been chromatographically isolated, identified (^{1}H NMR and mass spectrum), and synthesized. They are 1-[1-(phenylethyl)cyclohexyl]piperidine, 1-[1-(1,1'-biphenyl-4-yl)cyclohexyl]piperidine, and 1,1'-(1,4-phenylenedicyclohexylidene)bis[piperidine].[3]

The objective of the research reported herein is to determine if analogous cosynthetics are formed in the TCP preparation. Both TCP[4] and PCP[5] are difficult to analyze by GC/MS because of the numerous thermal decomposition products which occur with injection port temperatures over 180°C. As we had done in our PCP GC/MS investigations,[5] the conditions necessary to reduce this decomposition utilizing capillary column GC/MS were studied. Where cosynthetics from the crude TCP mixture were suggested by GC/MS results, they were synthesized and identified by comparison of GC retention times and mass fragmentation patterns.

Mass chromatograms were obtained with an injection port temperature of 175°C and separation was achieved with a 15m DB-5 column by temperature programming from 50°C (2 minute hold) to 250°C at 5°C/minute with a helium flow of ca. 1 mL/min. Identified in the crude TCP mixture were 1-piperidylcyclohexane, 1-piperidylcyclohexene, 1-piperidyl-1-cyclohexylcarbonitrile (PCC), TCP, 1-(2-thienylmethyl)cyclohexylpiperidine (methyl-TCP),

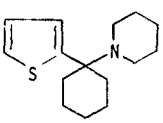

TCP

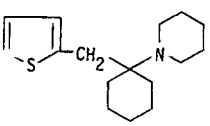

Methyl-TCP

and 1,1'-(2,5-thienylenedecyclohexylidene)bis[piperidine] (bis-TCP). The latter two compounds were confirmed by independent synthesis and GC/MS comparison.

Bis-TCP was found to be thermally stable under direct probe conditions but decomposed under all GC/MS conditions with both processes resulting in characteristic fragmentation patterns suitable for positive identification. Mass spectral evidence suggested that synthetic bis-TCP also contained the compound di-TCP which was not found in the crude TCP mixture. No analogous compound has been found in the PCP preparation.

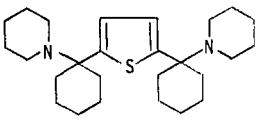

bis-TCP

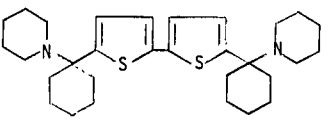

di-TCP

Methyl-TCP decomposes with injection port temperatures in excess of 200°C while 1-piperidylcyclohexene thermally derives from unreacted PCC. This latter decomposition occurs only partially at injection port temperatures of 175°C but increases with increasing injection temperatures.

Interestingly, the 1-piperidylcyclohexane is not observed in the analysis of synthetic bis-TCP, or methyl-TCP or PCC. It is concluded that it is therefore a cosynthetic product of the TCP synthesis but not a PCP cosynthetic. Its synthetic origin is as yet unknown.

1. Kalir, A.; Edery, H.; Pehal, D.; Baldeman, D.; Porath, G. J. Med. Chem., 1969, **12**, 473.
2. Jones, L.A.; Beaver, R.W.; Schmoeger, T.L. Anal. Chem., 1982, **54**, 182.
3. Jones, L.A.; Beaver, R.W.; Schmoeger, T.L.; Ort, J.K.; Leander, J.D. J. Org. Chem., 1981, **70**, 3330.
4. Rao, K.G.; Soni, S.K. JAOAC, 1983, **66**, 1186.
5. Jones, L.A.; Haney, C.A. "Identification of Thermal Degradation Products of Compounds Cosynthesized in The Production of Phencyclidine (PCP)", Poster TPE7, 34th Conference, ASMS, June 10, 1986.

Presented at the 36th ASMS Conference on Mass Spectrometry and Allied Topics
June 5-10, 1988, San Francisco, CA

DIRECT ANALYSIS OF CONTAMINATED PHARMACEUTICAL PREPARATIONS BY LC/MS/MS

IDENTIFICATION OF SUCCINYL CHOLINE IN CONTAMINATED DEXAMETHASONE

Thomas Covey, Sciex Inc., 55 Glencameron Road, Thornhill, Ontario, Canada L3T 1P2

George Maylin, Richard Eckerlin, Edgar Lee, Per Olof Edlund, and Jack Henion, Equine Drug Testing and Toxicology, New York State College of Veterinary Medicine, Cornell University, 925 Warren Drive, Ithaca, NY 14850.

Contaminated pharmaceuticals are encountered in spite of extensive quality control programs at drug manufacturing and packaging facilities. Accidental and malicious contamination of human medicaments have been discovered at the National level over the past few years.

We herein describe a situation where a grossly contaminated vial of dexamethasone, causing the death of three veterinary patients, was rigorously analyzed by many standard methods to no avail. We further describe the methodologies that arrived at the proper diagnosis of the problem. The analytical technique employed was LC/MS and LC/MS/MS using a Sciex TAGA 6000E MS/MS instrument equipped with the standard atmospheric pressure ion source (API) and an ion spray LC/MS interface.

SAMPLE HISTORY

A bottle of generic dexamethasone was used in a clinically acceptable manner by a veterinary practitioner. However, after the loss of three canine patients the formulation became suspect. Within 20 minutes of administration, total physiological collapse and death resulted.

The submitted suspect vial was subjected to extensive chemical analyses including TLC, cyanide testing, inorganic testing with x-ray fluorescence and ICP emission spectroscopy, HPLC with diode array detection, radioimmunoassay for narcotics, endotoxin analysis, and GC/MS. No differences between the toxic suspect vial and a standard vial of injectable dexamethasone could be observed.

METHODS

The injectable material was 50% by weight polypropylene glycol which was used as a carrier. Because no chemical information was available about the toxin no attempt was made to pre-fractionate the sample before HPLC analysis. The viscous sample was injected directly into the LC/MS/MS system.

A 2.1 mm x 10 cm Spherisorb-NH_2 column was used with a 20 minute gradient from 100% methanol to 100% water, simulating normal-phase conditions. A previous analysis utilizing a C_{18} column with a 100% water to 100% methanol reversed-phase gradient system resolved no suspect peaks. The mass spectrometer used was a Sciex TAGA 6000E triple quadrupole mass spectrometer equipped with a standard atmospheric pressure ion source and an ion spray LC/MS interface. The flow rate was 200 uL/min split to introduce 50 uL/minute into the source.

RESULTS

A peak was observed in the chromatogram having only m/z 145 in the mass spectrum. Profiling m/z 145 revealed it to be a doubly charged ion (isotope peaks 0.5 amu spaced) identifying the molecular ion of the suspect compound to be 290 (Figure 1). MS/MS of m/z 290 further verified the doubly charged nature of the compound showing singly charged daughter ions at m/z greater than that of the parent ion at m/z 145 (Figure 2).

Adjustments to the pH of the chromatographic eluant (pH 2-8) produced no shift in the mass spectrum toward the singly charged species (m/z 290). The observation that the functional groups responsible for the positive charges on the molecule could not be titrated suggested that the suspect material was a diquaternary amine having a permanent charge in solution regardless of pH. This hypothesis was derived from knowledge of the mechanism of ion evaporation, which is the means by which the ion spray interface produces gas phase ions (1). Ionic species in solution are directly desorbed to the gas phase as a result of high localized electric fields surrounding the nebulized droplets. Adjustments to the eluent pH will result in changes to the charged state of molecules in solution, and this will be observed in the spectra. Quaternary amines are permanently charged and thus do not respond to pH adjustment. Succinyl choline was the only diquaternary amine compound of molecular weight 290 listed in several molecular weight indices of organic compounds. Analysis of standard succinyl choline gave the same daughter ion spectra and retention time as the suspect compound. Administration of succinyl choline to test animals gave physiological reactions identical to the

contaminated dexamethasone vial.

CONCLUSIONS

Succinyl choline was identified to be the toxic substance in a veterinary formulation of dexamethasone. After employing several analytical methodologies to no avail, ion spray LC/MS/MS finally cracked the case. Investigations are underway to determine the source of the contamination, possibilities being contamination during pharmaceutical preparation, cross contamination by the professionals using the vial, or by sabotage.

REFERENCE

1. Bruins, A.P., Covey, T.R., Henion, J.D. Anal. Chem. 1987, 59, 2642.

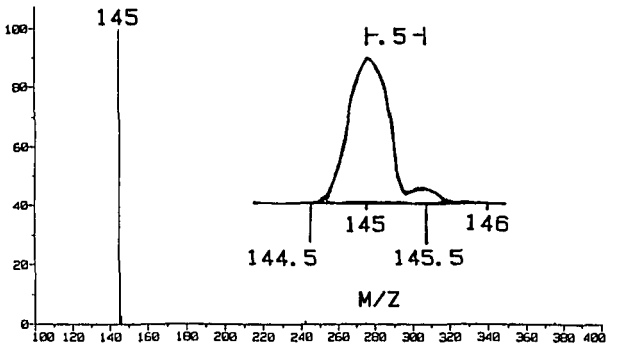

Figure 1. Ion Spray mass spectrum of suspect toxin. Profile of molecular ion verifying doubly charged nature. Isotopes spaced 0.5 daltons.

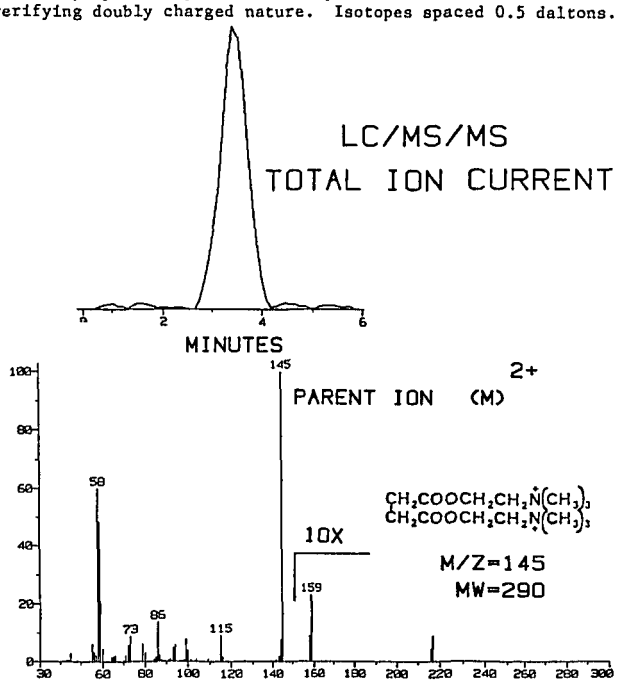

Figure 2. Daughter ion spectrum of suspect toxin. Verified to be succinyl choline.

Presented at the 36th ASMS Conference on Mass Spectrometry and Allied Topics
June 5-10, 1988, San Francisco, CA

STUDIES OF ANABOLIC STEROIDS BY THERMABEAM LC/MS

Matt J. Dilts, Edward W. Sheehan and Ross C. Willoughby
Extrel Corporation, Pittsburgh, PA 15238

INTRODUCTION

Steroids as a class of structurally complex molecules pose a special challenge to the analytical chemist. The mass spectral characterization of free steroids has been dominated by gas chromatography/mass spectroscopy (GC/MS) with both electron (EI) and chemical impact (CI) ionization. Less volatile steroids and steroid conjugates are thermally labile molecules which have been characterized by using other techniques: derivatization to more volatile compounds, DCI, FAB, FD, SIMS and thermospray LC/MS(1,2).

This prompted us to investigate the possibility of using ThermaBeam LC/MS in the analysis of anabolic steroids. Our objectives of this study were to demonstrate (i) the generation of library searchable EI spectra with minimal pyrolysis fragments, (ii) CI spectra, (iii) obviating the derivatization step necessary with GC/MS, (iv) linearity and uniform response over a wide concentration range under SIM (5-50ppm) and full scan conditions (10-50ppm), (v) and the applicability of this technique for clinical and forensic studies by analyzing an injectable form of testosterone propionate.

EXPERIMENTAL

All work described was performed on an EXTREL 400-1 differentially pumped mass spectrometer equipped with EI/CI switchable source interfaced with the liquid chromatography system by means of the ThermaBeam LC/MS interface. The chemical ionization reagent gas was methane. Data was acquired under full scan conditions from 80 to 450 AMU at 100 AMU/sec; or by monitoring the molecular ion of the individual components for the SIM experiments.

The chromatographic system consisted of a Waters Model 600 solvent delivery system equipped with a Model 490 UV detector. The column used was a 2 mm i.d. x 250 mm C-18 reverse phase (Solvent Miser, Alltech) with a precolumn packed with the same material. A gradient elution program using acetonitrile and water as the solvent system was used (Table I) with a flow rate of 0.25ml/min.

Testosterone (TEST), 17-methyltestosterone (METH-TEST), testosterone propionate (TEST-PRO) and testosterone cypionate (TEST-CYP) were chosen as prototypical compounds. Five to fifty ppm solutions were prepared in acetonitrile and analyzed. An injectable form of testosterone propionate (100mg/ml, in sesame oil) was chosen as a real life sample. A working solution of 15ppm was prepared and analyzed the same as the above standards.

RESULTS AND DISCUSSION

The total ion current chromatograph and UV tracing (254nm) of 50ppm each of the above steroids are shown in Figure 1. The peaks eluted in the following order: TEST, METH-TEST, TEST-PRO, and TEST-CYP.

Figure 2A shows the uniform and linear response over the range, 10-50ppm that was obtained. Upon analyzing TEST-PRO in sesame oil, we obtained a reading of 13.8ppm (92%) present in the 15ppm working solution. A comparison plot of sample and TEST-PRO standard is shown in Figure 2B. The EI spectrum shows the presence of the molecular ion (m/z 344) plus the loss of the propionic acid group (M-56, m/z 288) as would be expected.

Presented at the 36th ASMS Conference on Mass Spectrometry and Allied Topics
June 5-10, 1988, San Francisco, CA

CONCLUSION

Using the ThermaBeam LC/MS interface, we did not experience decomposition during the chromatographic separation or the complicated spectra of fragment ions of less volatile steroids upon vaporization. And, in addition, we avoided the need to derivatize nonvolatile steroids to enhance their volatility.

Table I.

Time (min)	Acetonitrile (%)	Water (%)
0	70	30
5	70	30
10	99	1
15	99	1
20	70	30
25	70	30

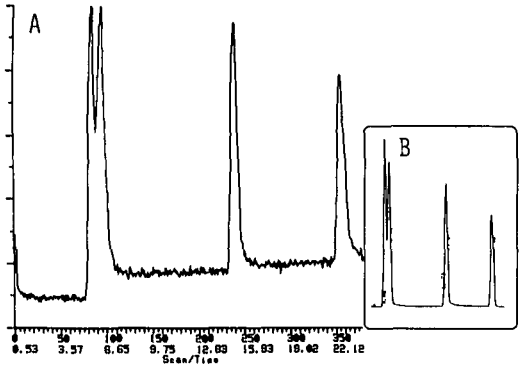

Figure 1. The TIC (A) and UV (B) Trace of 50ppm Levels

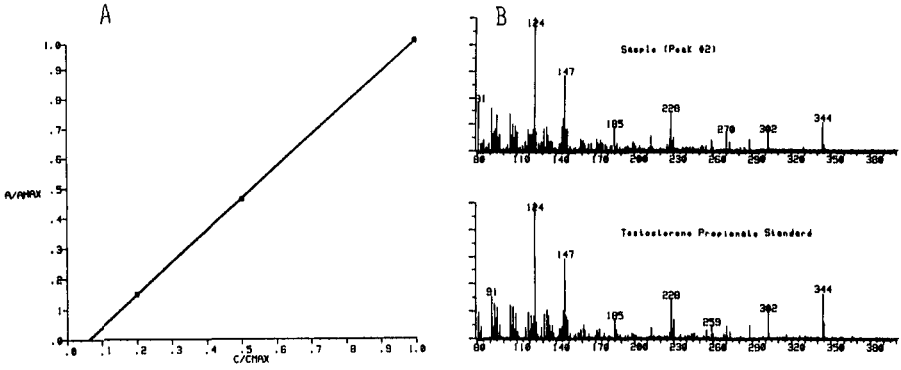

Figure 2. (A) Linear response over the concentration range, 10-50ppm.
(B) Comparison of the sample spectrum and TEST-PRO standard.

---

(1) Lin, Y.Y., Smith, L.L. (1984). Mass Spectrom. Rev. 3, 319-355.
(2) Gaskell, S.J., Rollins, K., Smith, R.W. and Parker, C.E. (1987). Biomed. Environ. Mass. Spectrom., 14, 717-722.

Presented at the 36th ASMS Conference on Mass Spectrometry and Allied Topics
June 5-10, 1988, San Francisco, CA

ON-LINE ANALYSIS OF DRUGS IN LIVE ANIMALS USING CF-FAB AND MICRODIALYSIS

Shen-Nan Lin and Richard M. Caprioli
The University of Texas Medical School
Houston, Texas 77030

An experimental procedure was developed to achieve pharmacokinetic analysis of drugs from single live animals. The schematic diagram of the experimental set-up is shown in Figure 1. The procedure utilizes two new techniques; continuous-flow FABMS (1) and microdialysis (2).

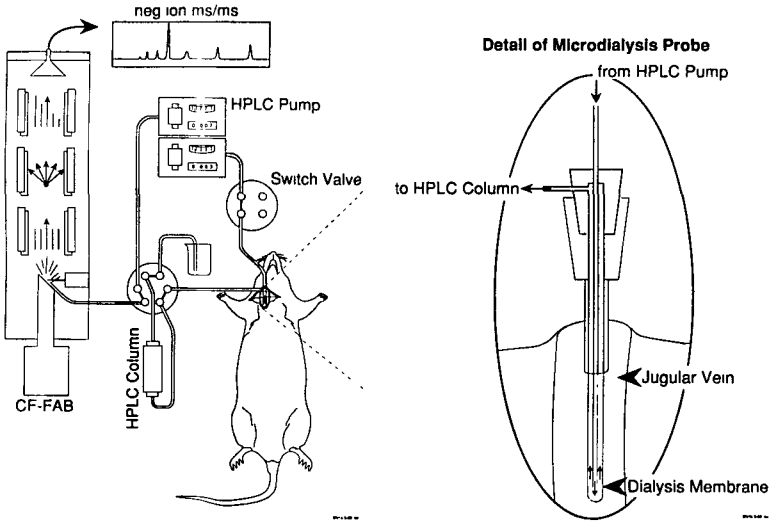

The drug used in this study, penicillin G, was injected intramuscularly. In order to potentiate the drug in the system, the rat was first given an intramuscular injection of probenecid. A microdialysis apparatus (BSA Inc) was inserted through a needle cannula into the jugular vein in the neck of the animal. The drug circulating in the blood dialyzed into the microdialysis probe and was carried to a small HPLC column for concentration. At a proper time interval, the drug was eluted from the column and analyzed on-line by MS/MS via a continuous-flow fast atom bombardment interface fitted to a Finnigan MAT TSQ70. In a typical experiment, the dialysate was allowed to flow through the RP-300 micro HPLC column (2x2 mm) for 5 min, then the column was subjected to a one-step wash with 50% acetonitrile, 5% glycerol, 0.7% TFA in water at a rate of 7 μL/min, and this effluent passed directly into the mass spectrometer. A complete loading and injection cycle took 9 minutes. For penicillin G the $(M-H)^-$ parent negative ion at m/z 333 was analyzed by collision activated decomposition and the daughter ion spectrum obtained by continuously scanning from m/z 100 to 350 in 2 sec.

Figure 2 compares mass spectra obtained 1h and 3.5h after penicillin G administration. The relative intensities between the m/z 192, the major ion fragment of penicillin G, and 149, that of the background at this parent mass, are markedly different. This is the result of the higher concentration of penicillin G in the 1h sample, relative to the 3.5h sample and consequent suppression of background ions to a greater extent. When the relative ratio of ion intensities of 192 and 149 was used to follow the time course of penicillin G in the blood, we found the concentration of the drug peaked at 1.7h. This is in agreement with other work (3) which has

shown that intramuscular administration of penicillin G to a human treated with probenecid was approximately 2h.

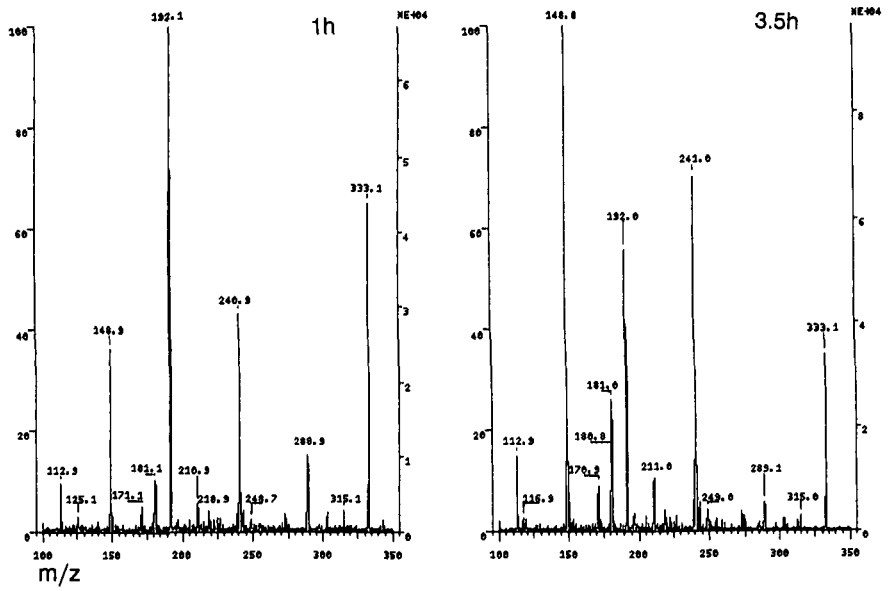

REFERENCES:

1. R.M. Caprioli, T. Fan and J.S. Cottrell, Anal. Chem., 58, 2949 (1986).
2. J.M.R. Delgado, F.M. Defeudis, R.H. Roth, D.K. Ryugo and B.M. Mitruka, Arch. Int. Pharmacodyn. Ther., 9-21 (1971).
3. E.M.C. Dunlop and S.S. Alfgaily, J. Am. Med. Assoc., 241, 2538-2430 (1979).

ACKNOWLEDGEMENT:

The authors wish to thank Ms. Su Chang, Mr. McNamo Shao and Ms. Judy A. Hudson for their excellent technical assistance. We appreciate the useful discussions with Dr. R. L. Reed from the Department of Surgery.

Presented at the 36th ASMS Conference on Mass Spectrometry and Allied Topics
June 5-10, 1988, San Francisco, CA

A SOLID PHASE EXTRACTION METHOD FOR GC/MS ANALYSIS OF COCAINE AND ITS MAJOR METABOLITES IN URINE

R. ESPINOSA-LENIZ, THE AMERICAN UNIVERSITY, WASHINGTON, D.C. 20016, L.R. HILPERT, M.J. WELCH AND E. WHITE V, NATIONAL BUREAU OF STANDARDS, GAITHERSBURG, MD 20899.

The routine testing for drugs of abuse in urine has increased enormously in the last few years. This activity has highlighted the need for certified reference standards for drugs of abuse and their metabolites in urine. The use of Standard Reference Materials (SRMs) improves both the accuracy and reliability of test results and will help insure the compatability of results among laboratories. The National Bureau of Standards (NBS), in cooperation with the College of American Pathologists (CAP), has initiated a program designed to issue SRMs for drugs of abuse in freeze-dried urine. An SRM for THC (marijuana) has already been issued and certification of an SRM for urinary cocaine metabolites is in process.

The present work deals with the certification of an SRM for cocaine and one of its major metabolites, benzoylecgonine, in freeze-dried urine. The development of this SRM has involved developing analytical procedures for the compounds of interest, preparing pools of urine with the compounds present at the desired concentrations, and certifying the concentrations in the SRM by two independent analytical methods: A GC/MS method using the trideuterated analogs (CD3 on the nitrogen) of the analytes as internal standard, and an HPLC method.

We have modified a solid phase extraction method described by Svenson1 for HPLC analysis of benzoylecgonine in urine to make the method suitable for GC/MS. The sample preparation is as follows: 1) spike a 5 mL urine sample with the internal standards; 2) mix the spiked urine with an equal amount of 0.5 M ammonium phosphate buffer at pH 9.3; 3) precondition a Sep-pac C18 solid phase extraction cartridge by rinsing with 3 mL of methanol followed with 5 mL of water; 4) load the cartridge with the buffered urine; 5) wash the cartridge with 10 mL of a 0.01 M NaOH solution in 20% acetonitrile/ water; 6) wash with 15 mL of a 0.01 M NaH_2PO_4 solution in 20% acetonitrile/ water at pH 2.1; 7) elute the analytes with 3 mL acetonitrile; 8) take the eluent to dryness under a gentle flow of N_2; and 9) dissolve the residue in 0.1 mL of bis(trimethylsilyl)acetamide by heating 30 min. at 60 °C.

Gas chromatography is performed on a 30m DB-5 capillary column held at 120 °C for 10 min., then heated at a rate of 30 °C/min to 300 °C which are maintained until the end of the run (25 min. total). The mass spectrometer is a quadropole instrument operated in the electron impact mode(at 70 eV with an ion source temperature of 200 °C).

The mass spectra of cocaine and the TMS derivatives of benzoylecgonine and methylecgonine show intense peaks at m/z 82 (m/z 85 for the internal standards); this means that by single ion monitoring at m/z 82 and 85, it is possible to analyze for all three compounds. The response is not linear and therefore the internal standard is spiked at a level as close as possible to the actual level of the analyte. (For the measurements used for the certification, bracketing at two different concentration levels will be used to improve accuracy).

Mass chromatograms of methylecgonine and its TMS derivative show two (and on occasions three) peaks with almost identical mass spectra, suggesting epimerization occurs under our GC conditions. Since the extent of the epimerization varies from experiment to experiment, methylecgonine will not be certified (although it will be present) in the SRM.

In the manufacturing of the SRM a pool of urine was divided into four equal volumes, one was kept as blank, and the other three were spiked at approximately at 100, 300 and 500 ng/mL each of cocaine, benzoylecgonine and methylecgonine, then freeze-dried in 10 mL aliquots.

A preliminary analysis of four aliquots for each level of cocaine and benzoylecgonine gave the following results:

Target level (ng/mL)	Actual Cocaine (ng/mL)	s.d.	Actual Benzoylecgonine (ng/mL)	s.d.
100	76	9.9%	108	7.1%
300	252	13.0%	292	7.2%
500	473	4.7%	576	2.9%

The precision of these preliminary measurements was unsatisfactory. Since the actual levels of the analytes were different from the target levels, the spiking levels of the internal standard were not as close as intended to the actual level of the analyte. These preliminary results will permit spiking the urine with the correct amount of internal standard. We plan to refine the method further to achieve satisfactory precision for the certification.

1 Svenson, Jan-Olof, J. Anal. Tox., 10, (122-4), 1986.

Presented at the 36th ASMS Conference on Mass Spectrometry and Allied Topics
June 5-10, 1988, San Francisco, CA

STUDIES ON THE STRUCTURE OF DIAMOND PHENOL POLYETHYLENEGLYCOL—LONG LASTING CONTRACEPTIVE BY MASS SPECTRA

YANG KAI -Qun ZHENG HU
Analysis and Testing Center, Chengdu Branch of Chinese Academy of Sciences, Chengdu, CHINA

Diamond phenol(DP) is a very good new contraceptive. But it hasn't long lasting contraception effect. In order to get long lasting contraceptive, we had synthensized diamond phenol polyethyleneglycol (DPPEG) by reaction of DP and polyethyleneglycol (PEG) . DP is a target as low-molecular part connecting PEG. The reasons are as following : 1. A small dosage of DP has been used in the clinic and its weight changes larger. Therefore DP will take obvious proportion of weight in forming new compound when it joins up with polymer. The new compound connected with polymer need not overweight much than the monomer of DP if used in clinic. 2. DPPEG is possible to change its drug metabolism kinetic behavior of DP jointed PEG. The selectivity of the complex with polymer may be increased. 3. DP is insoluble in water. If it attaches to PEG, the product becomes soluble in water.

We have researched the relation between molecular structure and mass spectra peak of the title compound. We separated the synthesis mixture into a series singl chain title compound with thin-layer chromatograph. Then we test average spectra of every component and the synthesis mixture. The quantitative results of every component in the synthesis mixture are computed by matrix method. Therefore we get the molecular weight distribution chart and component quantity of differential chain title compounds.

$DP(PEG)_n$	RELATIVE PEAK HIGH OF AVERAGE SPECTRA (%) (DCI METHOD)	DRUG EFFECT OF EVERY MEMBER
$DP(PEG)_1$	5	-
$DP(PEG)_2$	8	-
$DP(PEG)_3$	12	-
$DP(PEG)_4$	20	*
$DP(PEG)_5$	33	*
$DP(PEG)_6$	42	**
$DP(PEG)_7$	54	**
$DP(PEG)_8$	68	***
$DP(PEG)_9$	71	***
$DP(PEG)_{10}$	69	***
$DP(PEG)_{11}$	58	**
$DP(PEG)_{12}$	40	*
$DP(PEG)_{13}$	28	*
$DP(PEG)_{14}$	24	*
$DP(PEG)_{15}$	10	-

- (representation no effect);
* (representation low effect);
*** (representation high effect);

The method is built by MS which can quickly and reliably test molecular weight distribution chart of long lasting contraceptive. In order to review and control produce of a good DPPEG, we give a good criterid to long lasting contraceptive.

References:

Zheng Hu etc. THE SYNTHESIS OF LONG LASTING CONTRACEPTIVE.
Academia Sinica Reportag 1987,5 P.242

Presented at the 36th ASMS Conference on Mass Spectrometry and Allied Topics
June 5-10, 1988, San Francisco, CA

QUANTIFICATION OF PHYSOSTIGMINE IN PLASMA BY CAPILLARY COLUMN CHROMATOGRAPHY USING CHEMICAL IONIZATION MASS SPECTROMETRY. E.M. Jakubowski, J.R. Smith, US Army Medical Institute of Chemical Defense, Aberdeen Proving Ground, Edgewood, MD 21010-5425; and S.M. Musser, P.S. Callery, Univ of Maryland, Baltimore, MD, 21201.

A novel assay has been proposed to quantify physostigmine, a gem diamine, in human plasma by gas chromatography-mass spectrometry (GC-MS) using isobutane or ammonia chemical ionization. Previous methods ignored the possibility of using direct injection into the GC which would rely on thermal dissociation of the physostigmine salt(1-3). In this study, human plasma (1 mL) was spiked with physostigmine salicylate (0.3 to 12 nanograms free base). To the spiked samples, neostigmine bromide (500 ng/mL) and d_3-(carbamate) physostigmine salicylate (5 ng) were added. Plasma samples were then filtered through CN-solid phase cartridges that were conditioned first with 2x1 mL of methanol and then 2x1 mL of 0.2M phosphate buffer (pH 7.0). The plasma loaded cartridges were washed with 2x1 mL of water and then eluted with 0.4 mL of methanol. Evaporation of the methanol produced a final sample volume of 10 to 20 microliters. One to two microliters were injected into a Finnigan 4500 GC-MS under the following conditions: 250°C injector, 30m DB-1 column, 86°C initial oven temp., 260°C final oven temp., 40°C/min program temp. rate, 1mL/min helium carrier flow rate, and 0.25-1.00 Torr isobutane or ammonia reagent gas pressure. Selected ion monitoring was used to quantify the physostigmine by collecting ion current data on the m/z 276 ion of physostigmine (MH^+) and the m/z 279 ion of the internal standard. In addition, the m/z 219 ion (M-carbamate+H^+) was monitored to ensure correct peak identification. In order to prolong the lifetime of the injector port glass insert a small amount of silanized glass wool was placed into the insert. Figure 1 shows a physostigmine calibration curve generated without the use of an internal standard. Concentrations of methanol solutions ranged from 0.25 to 2 ng of the salicylate salt. Linear regression of this data produced a line with a correlation coefficient of 0.999. Results of the simple methanol matrix confirm the analytical usefulness of thermal dissociation of this amine salt in the injector. Linear calibration curves (r=0.995) were produced by the internal standard method for human plasma spiked in the range of 0.3 to 12ng physostigmine free base (FIG 2). Isobutane was used for the plasma work instead of ammonia. Ammonia provided a factor of 1.5 greater sensitivity, however MS conditions were difficult to control. Methane as a reagent gas caused too much breakdown of the carbamate as compared to isobutane or ammonia. Since the internal standard was located on the carbamate only the ions related to the intact drug could be used for quantification. One of the most important elements of this assay was to control the injector port temperature. Table 1 illustrates the change in signal intensity as the temperature is varied. Besides maximizing the analyte peak area the area of the breakdown product, eseroline, should be considered. Eseroline represents the loss of the carbamate group from physostigmine which can occur in the hot injector. Figure 3 shows a TIC of an injection of physostigmine were the injector temperature was 300°C. The first peak represents eseroline as confirmed by its EI spectrum and the second peak is physostigmine. Figure 3 also shows the spectrum of physostigmine. Above 260°C the efficiency of the thermal dissociation does not increase but degradation to eseroline does increase. Other amine salts demonstrate similar injector port characteristics with respect to thermal dissociation(4). Therefore, the optimum injector temperature was between 260 to 270°C.

References:

1. Whelpton,R.; Moore,T. J.Chromatogr. 341(1985) 361-371.
2. de Wildt,D.J.; Porsius,A.J.; van Rooy,H.H. J.Chromatogr. 225(1981) 381-387.
3. Brodie,R.R.; Chasseaud,L.F.; Robbins,A.D. J.Chromatogr. 415(1987) 423-431.
4. Krikorian,S.E.; Ukpo,G.E.; Force,A.P.; Edwards,C.W. Anal. Chem. 1985, **57**, 312-315

Presented at the 36th ASMS Conference on Mass Spectrometry and Allied Topics
June 5-10, 1988, San Francisco, CA

FIG 2: PHYSOSTIGMINE IN HUMAN PLASMA STD CURVE
USING DEUTERATED INTERNAL STD (ISOBUTANE-CI)

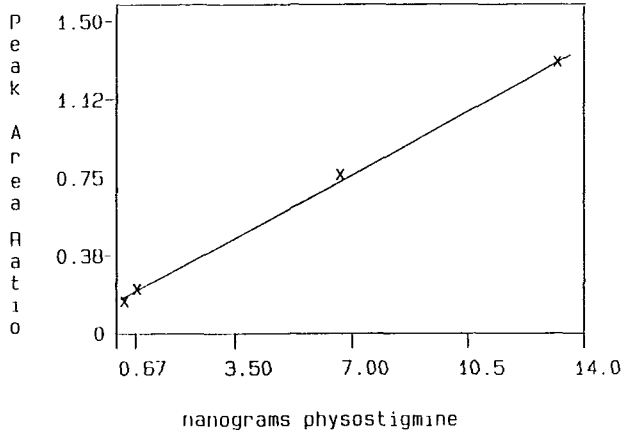

FIG 1: PHYSOSTIGMINE IN METHANOL STD CURVE
USING EXTERNAL CALIBRATION (NH_3-CI MOD

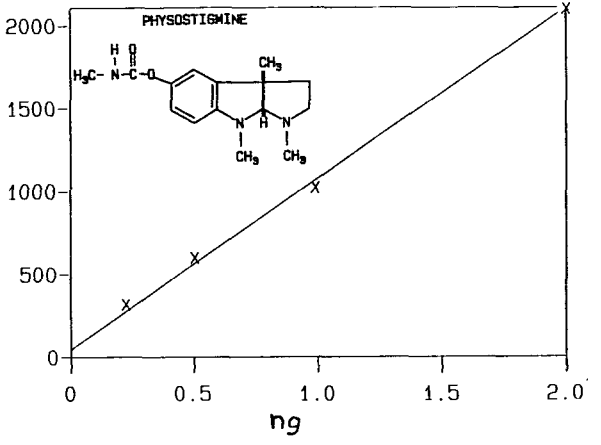

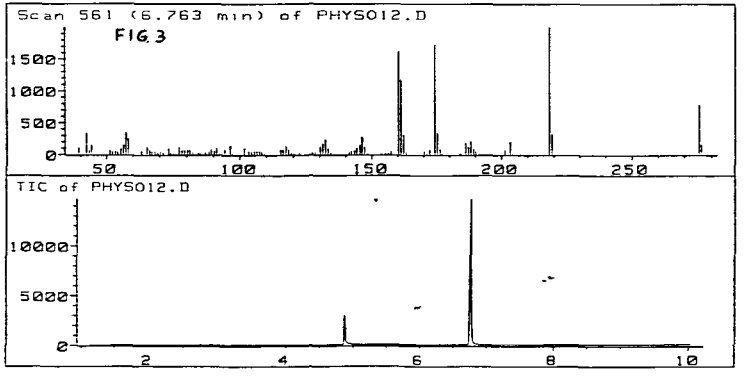

TABLE 1: ANALYTE SIGNAL vs INJECTOR PORT TEMP

INJECTOR PORT TEMP	PHYSO.PEAK AREA	ESEROLINE PEAK AREA	RATIO[b]
220°C	21680[a]	1885[a]	11.5
240	24798	3815	6.5
260	37373	8494	4.4
280	27550	9500	2.9
300	23478	19565	1.2
320	23623	13896	1.7
340	18803	23504	0.8

a) arbitrary units

b) physostigmine/eseroline

Presented at the 36th ASMS Conference on Mass Spectrometry and Allied Topics
June 5-10, 1988, San Francisco, CA

MASS FRAGMENTATION OF ISOQUINOLONES AN UTILITY TO CHARACTERIZE THALICTRUM ALKALOIDS

Ahmed M. Galal, Youssef Aly, Paul L. Schiff, Jr., Lan K. Wong and Emil W. Fu
Dept. of Pharmaceutical Sciences, University of Pittsburgh, School of Pharmacy, Pittsburgh, PA 15261; Sandoz Research Institute, East Hanover, NJ 07936

The mass spectral fragmentation patterns of two synthetic samples of isoquinolones, namely, 1-oxo-2-methyl-5-methoxy-6,7-methylenedioxy-1,2,3,4-tetrahydroisoquinoline (1) and 1-oxo-2-methyl-5,6-methylenedioxy-7-methoxy-1,2,3,4-tetrahydroisoquinoline (2) were elucidated in order to characterize fragment ions which can provide unambiguous assignments of the positions of the methylenedioxy and the methoxy groups. This information is of great utility to clarify the location of the methylenedioxy and the methoxy substituents at the 5, 6 and 7 positions of many Thalictrum alkaloids by oxidizing the alkaloids, such as thalmelatidine (3), to the aforementioned isoquinolones.

The isoquinolone (1) was synthesized according to the scheme shown. The formylation of 1-methoxy-2,3-methylenedioxybenzene by DMF in the third step of the the reaction sequence yielded two isomeric aldehydes, namely, 2-methoxy-3,4-methylenedioxybenzaldehyde indicated in the scheme, and 2,3-methylenedioxy-4-methoxybenzaldehyde (not shown). The two isomeric aldehydes were separated by flash column chromatography. The latter one was used to prepare the isoquinolone (2) by an analogous synthetic sequence. Mass spectra were obtained on a Finnigan-MAT 4600 mass spectrometer with a Superincos data system. The instrument was operated in the electron ionization mode with an electron energy of 70 eV and a source temperature of 110 C.

Both isoquinolones (1) and (2) show prominent M^+ and very intense fragment ions at m/z 192 and 164 in their EI mass spectra. Most spectral features are similar except compound (1) exhibits a significant ion 4 at m/z 134 (about 25%) while the corresponding ions 5 for compound (2) is relatively weak (less than 5%). The higher intensity of 4 is attributed to the greater stability of this ion. Thus by noting the intensity of this ion, it is possible to characterize the isoquinolone products from the oxidation ($KMnO_4$ in acetone) of many Thalictrum alkaloids and definitively assign the methoxy and methylenedioxy substituents at the 5, 6, and 7 position.

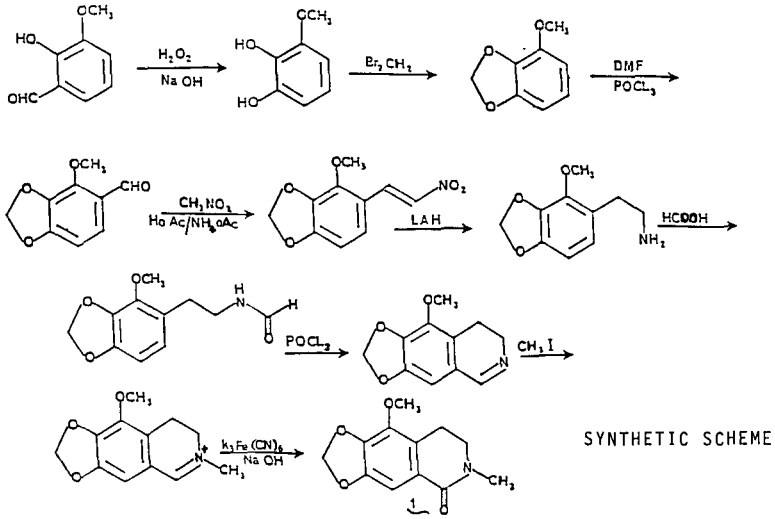

SYNTHETIC SCHEME

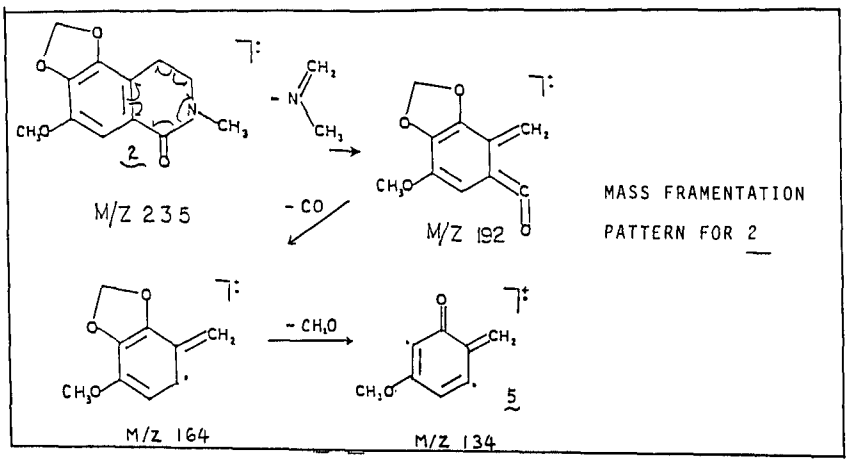

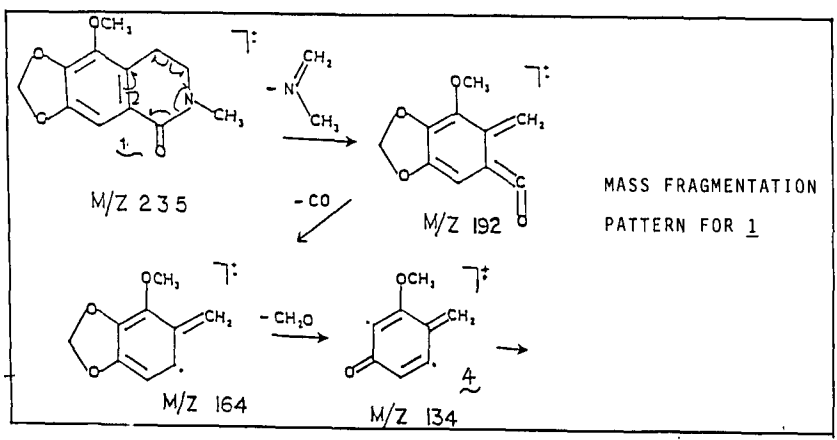

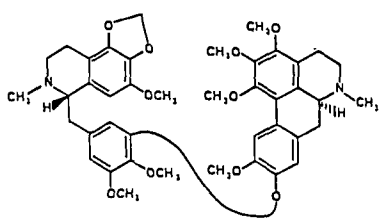

THALMELATIDINE (3)

Presented at the 36th ASMS Conference on Mass Spectrometry and Allied Topics
June 5-10, 1988, San Francisco, CA

IDENTIFICATION OF DECOMPOSITION PRODUCTS OF DELTA-9-TETRAHYDROCANNABINOL BY GC/MS.

D.J. Harvey and N.K. Brown,

University Department of Pharmacology, South Parks Road, Oxford, OX1 3QT, UK.

Delta-9-tetrahydrocannabinol (delta-9-THC, I), the major psychoactive constituent of marihuana, decomposes over a period of several months to cannabinol (CBN, V). Studies, predominantly by Turner et al. using mass spectrometry (1), have resulted in the proposed decomposition pathway shown below.

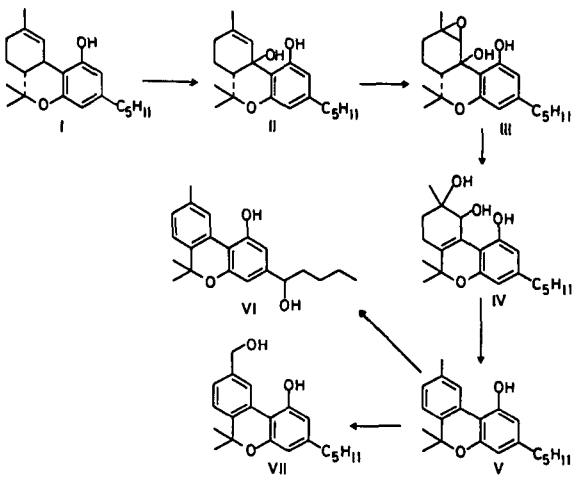

Although the dihydroxy-delta-10a-THCs (cannabitriols) of type IV have been well characterized, the intermediate 10a-hydroxy-THC (II) and its 9,10-epoxide (III) have not been reported. We have investigated several aged samples of cannabis, both dry and ethanolic extracts, and decomposition products resulting from biochemical experiments and have observed several other decomposition products including compounds II and III.

The aged samples were an ethanolic extract dating from about 1840 and three dry samples of plant tops dating from the turn of the century. TMS derivatives were prepared from all three samples. Liver and lung microsomes were obtained from mice, rats and guinea pigs and incubated with delta-9-THC and its [10a-^{2}H]- and [1',1',2',2'-$^2H_4$]-analogues. Products were extracted with ethyl acetate, concentrated by chromatography on Sephadex LH-20 and examined as TMS and [$^2H_9$]TMS derivatives. GC/MS on all of the samples was performed using VG 12B (2m x 2 mm SE-30 packed column) and 70/70F (25 m x 0.2 mm OV-1 fused silica capillary column) mass spectrometers and a VG 11/250 data system.

Details of the analysis of the ethanolic sample have been reported (2). The gas chromatogram (TMS derivative) is shown in Fig. 1. Major constituents were CBN and the cannabitriols of type IV. The dried samples showed a different profile (Fig. 2). CBN was again the major component but the cannabitriols were not observed. However additional oxidation of CBN had occurred to give 1- (VI) and 11-hydroxy-CBN (VII). These compounds have not been observed as decomposition products before although they are known as metabolites. Decomposition products from the microsomal incubations (Fig. 3) contained several novel compounds in addition to CBN and cannabitriol. 10a-Hydroxy-delta-9-THC was identified as a decomposition product by its formation in both normal and boiled microsomal mixtures. Incubations with [1',1',2',2'-$^2H_9$]delta-9-THC and the observation of a 4 mass unit shift in the mass of the molecular ion verified the formation of the compound from THC. Its structure was confirmed by the loss of the deuterium from the 10a-position of [10a-^{2}H]-delta-9-THC. The spectrum of its $^2H_9$TMS derivative indicated formation of the base peak at m/z 459 ([M - CH_3]$^+$ by loss of a gem methyl group following charge localization at the 10a-substituent.

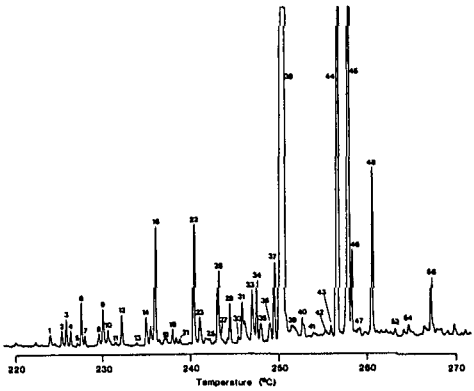

Fig. 1. Gas chromatogram of cannabinoids from a sample of cannabis tincture dating from about 1840. Peak 38 is CBN, peaks 44 and 45 are cannabitriols

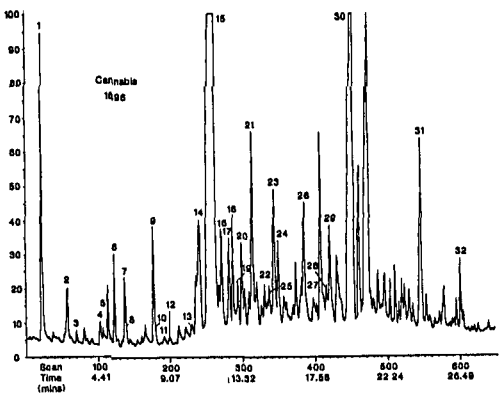

Fig. 2. Gas chromatogram of cannabinoids from a sample of cannabis from 1896. Peak 21 is CBN, peaks 21 and 29 are the 1'- and 11-hydroxy derivatives.

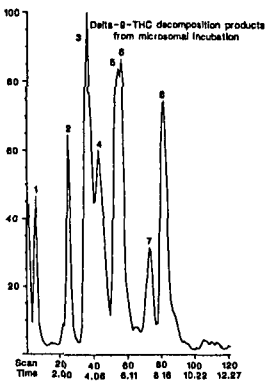

Fig. 3. Ion chromatogram of THC decomposition products from a microsomal incubation. Peak 3 is CBN, peaks 4 and 5 are hydroxyepoxides, peak 8 is 10a-OH-THC.

Several compounds having masses of 490 (TMS derivatives) were present. These compounds all had two TMS groups indicating that hydroxylation of the THC had occurred. The mass increment of mass units indicated the presence of an additional oxygen atom. No reaction with TMS reagents was observed under forcing conditions showing that this was not another hydroxy group and reaction with lithium aluminium deuteride confirmed the presence of an epoxide. This reaction produced cannabitriol demonstrating the presence of a 9,10-epoxide.

These observations confirm the reaction scheme proposed by Turner et al. for CBN formation from delta-9-THC and demonstrate that samples exposed to the air are capable of further hydroxylation CBNs.

This work was supported by the Wellcome Trust and NIDA.

1. C.E. Turner and M.A. ElSohly, J. Heterocyclic Chem., 1979, 16, 1667.
2. D.J. Harvey, In: Marihuana '84: Proceedings of the Oxford Symposium on cannabis, Ed. D.J. Harvey, IRL Press, Oxford, 1985, p. 23.

Presented at the 36th ASMS Conference on Mass Spectrometry and Allied Topics
June 5-10, 1988, San Francisco, CA

Quantification of Pyridostigmine in Plasma by Packed Capillary HPLC/FAB-MS/MS: Preliminary Results

Mark R. Bauer and Mark F. Yancey

Battelle Columbus Division, Columbus, Ohio 43201

Pyridostigmine is a cholinesterase inhibitor used in the treatment of myasthenia gravis, a neuromuscular function disorder. Pretreatment with pyridostigmine, in combination with atropine and an oxime, is also being investigated as an antidote for organophosphorus poisonings. The magnitude of individual differences in absorbtion and disposition of pyridostigmine has not been well defined because of a lack of sensitive analytical methodology for routine quantification in biological fluids.

Pyridostigmine, a quaternary amine, decomposes under normal GC conditions, but is amenable to FAB ionization. Therefore, our proposed approach to quantifying pyridostigmine in plasma at the sub ng/mL level, is to use our recently developed HPLC/FAB interface. Earlier experiments in our laboratory indicated that MS/MS would be necessary because an unidentified species present in the plasma interfered with low level pyridostigmine determinations.

An analog of pyridostigmine, deuterated at the quaternary ammonium methyl group, was prepared for use as an internal standard. Figure 1 shows the low energy CAD daughter ion spectra of pyridostigmine and d_3-pyridostigmine. Both spectra contain daughter ions at m/z 72, indicating that both species could be detected by utilizing parent scans of m/z 72. Figure 2 shows such a parent ion spectrum of a mixture of the two compounds collected using a conventional FAB probe. Using this method we were able to quantitate standards at the 1 pg level. If needed, lower detection limits could be achieved by using reaction monitoring methods.

Figure 3 shows a reconstructed ion chromatogram of the protonated molecular ion of pyridostigmine generated using our HPLC/FAB probe. Chromatography was performed on an HPLC column (1 m x 0.25 mm I.D. packed with 3 μm C-18) contained within a custom continuous flow FAB probe built in-house.(1) The column effluent was transferred to the probe tip via a 2 cm length of 50 μm fused silica capillary tubing. The short interface results in a minimum of peak broadening.

For analysis, plasma samples were first spiked with the d_3-pyridostigmine internal standard and then carried through a simple liquid extraction. The extract was then injected directly onto the HPLC column for quantification by FAB. Figure 4 shows the reconstructed ion chromatogram of a 1/2 μL injection of an extract of plasma which had been spiked with approximately 10 ng of pyridostigmine.

In conclusion, we have found that using d_3-pyridostigmine as an internal standard and m/z 72 parent scans constitutes a viable means of quantifying low levels of pyridostigmine. We have demonstrated that our HPLC/FAB interface works and that plasma extracts containing pyridostigmine can be analyzed by this method. Future work includes testing the method using HPLC/FAB and MS/MS scans, generating standard curves and establishing detection limits, and finalizing extraction conditions.

(1) Bauer, M. R. and Yancey, M. F.; Presented at the 36th ASMS Conference on Mass Spectrometry and Allied Topics, 1988, San Francisco, paper WPB6.

Presented at the 36th ASMS Conference on Mass Spectrometry and Allied Topics
June 5-10, 1988, San Francisco, CA

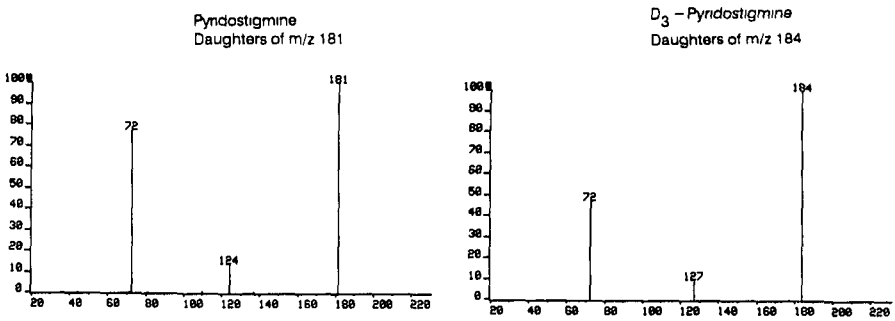

FIGURE 1

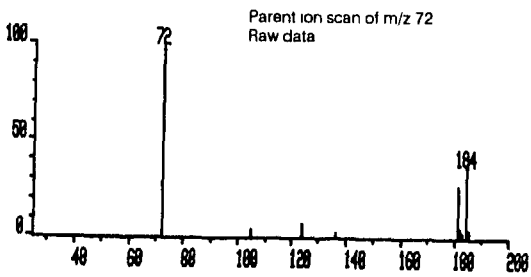

FIGURE 2

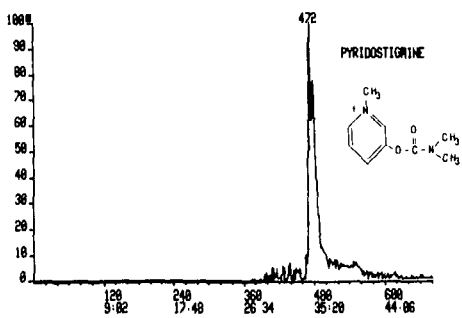

FIGURE 3

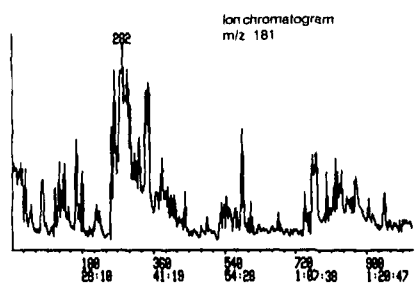

FIGURE 4

Instrument Used: VG70SEQ
FAB Gas: Xe @ 1mA and 8kV
Source Pressure: ~ 4 x 10^{-4} torr
Source Temperature: 100°C

Syringe Pump: Varian 4200
Mobile Phase: Acetonitrile
Flow Rate: 1 μL/min

Presented at the 36th ASMS Conference on Mass Spectrometry and Allied Topics
June 5-10, 1988, San Francisco, CA

Mass Spectral Analysis and Fragmentation of Second Generation ACE-Inhibitors Containing Phosphinic and Phosphorous Acids

Mark S. Bolgar*, G.C. DiDonato, R. Gedamke, T.J. McCormick,
S.E. Unger and B.M. Warrack
The Squibb Institute for Medical Research, Princeton, NJ 08543-4000

INTRODUCTION

Since the introduction of the first angiotensin converting enzyme (ACE) inhibitor for treating hypertension,[1] numerous other drugs of this class have been synthesized[2]. Second generation ACE-inhibitors containing a phosphinic or phosphorous acid moiety are currently under development for NDA filing.

These modified peptides are amenable to characterization using desorption ionization methods such as FD, thermospray and FAB. Facile degradation under thermospray conditons yield ions which are not ascribed to gas-phase unimolecular dissociation but arise as degradants. These species parallel degradation processes seen in long-term stability studies of fosinopril and may be useful for predicting the stability and degradation pathways of certain ACE inhibitors[3].

Accurate mass measurements and MS/MS analysis have been used to define the fragmentation of this class of compounds. Apart from loss of the phosphinic or phoshorous acid and loss of proline derivatives or the sidechain alkane and ester, these compounds exhibit a previously unreported rearrangement. This is the migration of an oxygen atom from the beta-carbonyl to the phosphorus atom, resulting in the phosphorous acid anion.

IONIZATION TECHNIQUES

1) Fast atom bombardment: Due to surface activity of the phosphorus acid group intense molecular or pseudomolecular ions are obtained.
2) Microbore LC/FAB: Molecular ions and fragments obtained. Ion source temperature must be kept below 80°C to avoid thermal decompositon.
3) Field Desorption: Abundant $(M)^+$ ions
4) Electron Ionization/Chemical Ionization: This class of compounds is not amenable to EI/CI due to extreme thermal lability.
5) Thermospray: Weak molecular ions and formation of thermal degradants limits usefulness as an analytical method. Degradation parallels that seen in long term stability studies

FOSINOPRIL
POSITIVE THERMOSPRAY MASS SPECTRUM

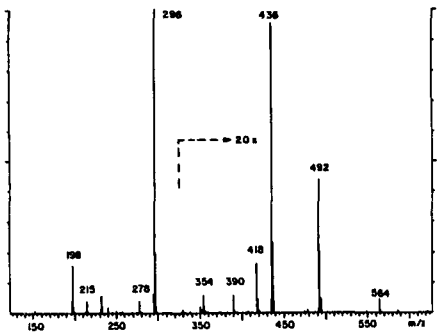

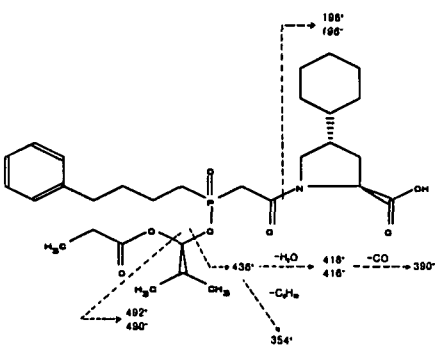

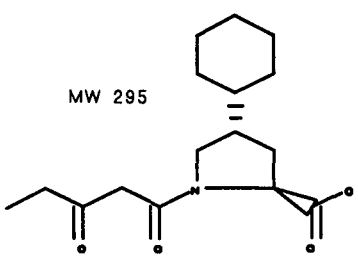

THERMAL DEGRADANT

Presented at the 36th ASMS Conference on Mass Spectrometry and Allied Topics
June 5-10, 1988, San Francisco, CA

DAUGHTER ION MASS SPECTRUM OF (M-H)⁻ ION (m/z 562) FROM FOSINOPRIL

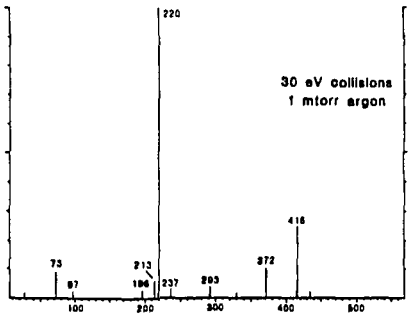

DAUGHTER ION MASS SPECTRUM FROM (M+H)⁺ ION (m/z 441) OF SQ-29852

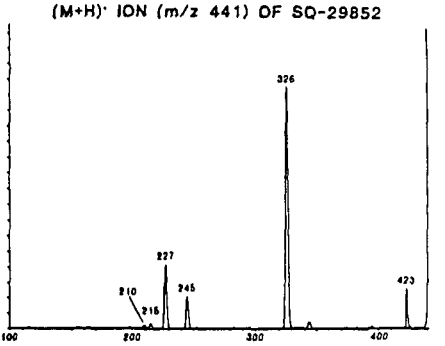

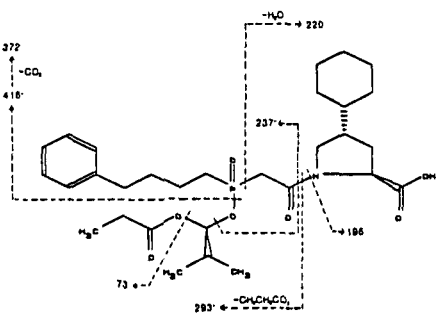

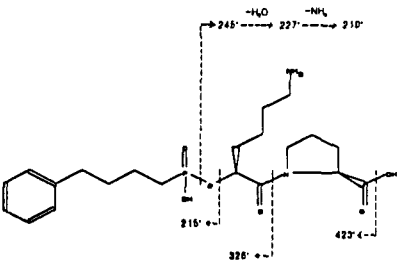

The structure of the 213⁻ ion is assigned as the rearrangement product resulting from the migration of the oxygen atom from the beta-carbonyl to the phosphorus atom.

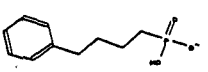

This ion is also present in the negative FAB mass spectrum of fosinopril. The exact mass is m/z 213.0686, which supports the emperical formula $C_{10}H_{14}O_3P$ (calcd. 213.0681). The MS/MS spectrum of the 213⁻ ion and that from authentic material both yield the PO_3 ion as their only daughter.

CONCLUSION

Second-generation ACE-inhibitors containing phosphinic or phosphorous acid moieties are readily characterized using soft ionization techniques such as fast atom bombardment, microbore LC/MS, and field desorption. However, due to the thermal lability of these compounds, techniques such as EI/CI or thermospray produce little or no molecular ions and result in thermal degradants. FAB generated parent ions do yield diagnostic daughter ion spectra upon CID, providing useful structural information. A rearrangement to produce 4-phenyl-n-butyl phosphorous acid is confirmed via MS/MS and accurate mass measurements.

1. Ondetti,M.A.; Rubin,B.,Cushman,D.W. Science 1976, 196,441-44
2. Patchett,A.A.et.al. Nature 1980, 288,280-83
3. Siegel,M.M; Isenaee,R.K.; Beck,D.J. Anal Chem 1987,59, 989-95

Presented at the 36th ASMS Conference on Mass Spectrometry and Allied Topics
June 5-10, 1988, San Francisco, CA

QUANTITATION BY GC/NICI-MS OF TWO ANTI-HYPERCHOLESTEROLEMIC DRUGS IN PLASMA AFTER SOLID PHASE EXTRACTION

D. Wang-Iverson, E. Ivashkiv, P. T. Funke, M. E. Arnold, M. Jemal and A. I. Cohen
The Squibb Institute for Medical Research
New Brunswick, New Jersey 08903.

Pravastatin sodium (P) and lovastatin (L) have been shown to reduce plasma cholesterol in humans. In order to support clinical trials, we developed methods to extract and quantify these compounds.

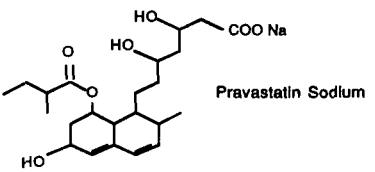

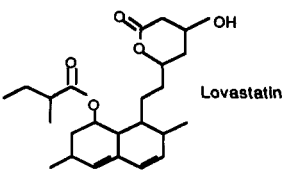

While L is administered as a lactone, it is converted *in vivo* to the free acid which is its active form. Therefore, the methods were devised to take advantage of the now routine technique of esterifying the carboxyl group with pentafluorylbenzyl bromide (PFB). The acid form of compactin was used as an internal standard for the L assays while the tetrahydro form of P was used for the P assays

1.0 ml plasma samples, first spiked with the appropriate internal standards and diluted with phosphate buffer were passed through solid phase extraction columns (C_2 for L and C_{18} for P) The columns were rinsed with 5 ml of buffer, 5 ml of heptane and then the compounds were eluted with 3 ml of methanol for the P extraction or 1.5 ml of acetonitrile for the L extraction. The extracts were first derivatized with pentafluoro-benzyl bromide and then BSTFA. After derivatization, they were diluted with 300 ul of tetradecane and analyzed with an automated quadrupole GC/MS system using ammonia chemical ionization and negative ion detection. Single ions representing the $(M-181)^-$ species for each component were monitored. Typical chromatograms are shown below:

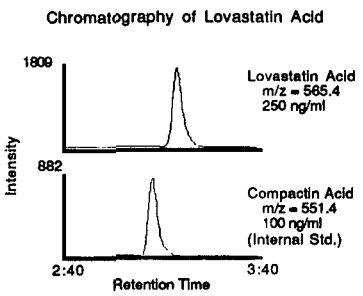

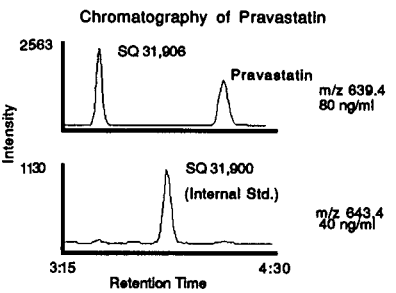

Standard curves for the two compounds were linear over the range of 0-250 ng/ml for L and 0-80 ng/ml for P:

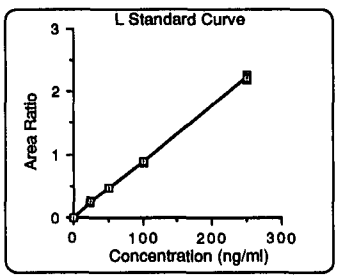

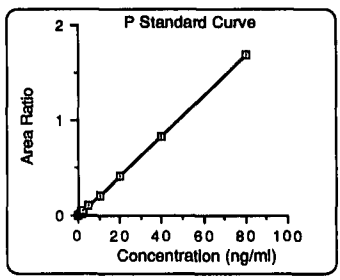

The detection limit for each was approximately 0.5 ng/ml, which represents an injection of 2 pg on column. The table below shows the results of studies performed to determine the accuracy and reproducibility of the assay. Blank plasma samples containing various amounts of the compounds were extracted and analyzed as described above.

Accuracy and Precision of Assay

	Lovastatin			Pravastatin			
Amount Added (ng/ml)	25	50	100	2.5	10	40	80
Amount Determined	26.7	47.9	99.3	2.7	10.5	40.4	80.0
Standard Deviation	2.5	2.6	2.8	0.3	0.3	1.4	2.6
Coefficient of Variation	9.4	5.4	2.8	9.5	2.5	3.5	3.2
No. of Determinations	94	95	96	64	72	72	72

As can be seen, the accuracy and reproducibility of the method are quite good with the amount determined within 10% of theoretical and CVs less than 10%.

We are currently performing this assay on a VG Trio-2 GC/MS/DS which is equipped with a Hewlett-Packard 5890 gas chromatograph and a 7673A autosampler. With this equipment it is possible to analyze upwards of 100 samples per day, usually via unattended overnight runs.

Presented at the 36th ASMS Conference on Mass Spectrometry and Allied Topics
June 5-10, 1988, San Francisco, CA

Mass Spectral Studies of Cholesterol-Lowering Agents

Bethanne M. Warrack*, M.S. Bolgar, G.C. DiDonato, and S.E. Unger
The Squibb Institute for Medical Research, Princeton, NJ 08543-4000

INTRODUCTION

High levels of cholesterol in the blood contribute to the development of *atherosclerosis, a major cause of death in the U.S.* and other countries. Compounds such as mevastatin, pravastatin, lovastatin, and simvastatin have been shown to inhibit cholesterol biosynthesis at its rate-limiting enzyme 3-hydroxy-3-methylglutaryl-coenzyme A (HMG-CoA) reductase. These cholesterol-lowering agents undergo numerous chemical transformations: lactone ring-opening, double bond/hydroxyl migration, hydroxyl epimerization, oxidation, and hydrolytic loss of ester sidechains.

Structural studies of hypocholesterolemic agents and related analogues have been carried out using a variety of techniques, including fast heating *EI and CI, FAB, MS/MS, and TSP LC/MS*, to define characteristic fragmentation for this class of compounds. The use of derivatives, labeled compounds and accurate mass measurement has *assisted in their* characterization.

EXPERIMENTAL

1. Fast heating EI (70 eV) was recorded with a Finnigan TSQ–4600 mass spectrometer equipped with a Finnigan direct exposure probe.
2. Fast heating CI mass and MS/MS spectra were recorded using the instrumentation described above. Reagent gases were NH_3 or a CH_4/N_2O mixture. Collisions were 30 eV with argon.
3. Thermospray spectra were obtained by fitting a Vestec thermospray interface onto the TSQ-4600. The ion source was held at 250°–275°C with the vaporizer adjusted to 160°–240°C. Flow rates of 1.0–1.5 ml/min were used. Mobile phases contained 0.1M NH_4OAc *and* CH_3CN.
4. FAB and MIKES spectra were recorded with a VG-ZAB-HF mass spectrometer using dithiothreitol-dithioerythritol as solvents. Air was used for 8 kV collisions. High resolution was accomplished using poly(*ethylene glycols*) *as internal standard* for peak matching (1:8000).

IONIZATION TECHNIQUES

LACTONES	SODIUM SALTS
1. CI	1. FAB
2. EI	2. TSP
3. TSP	
4. FAB	

The Structures of Pro-Drug Lactones

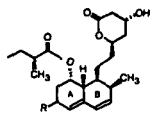

Compound	R	Ring A	Rings A, B
Lovastatin	H_3C		
Mevastatin	H		
RMS–417	HO		
RMS–414	HO		
RCT–186			
RCT–191			
RMS–411			
Simvastatin			

The Structures of Active Acids

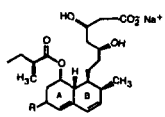

Compound	R	Ring A	Rings A, B
Pravastatin	HO		
RMS–418	HO		
RCT–196	H		
RCT–185			
RCT–190			
RMS–437			
RMS–438			
RMS–416			

Presented at the 36th ASMS Conference on Mass Spectrometry and Allied Topics
June 5-10, 1988, San Francisco, CA

Differentiation of stereoisomers and regioisomers by positive FAB MIKES. Note the difference in 345+: 327+ ratio. These isomers cannot be distinguished using negative ions.

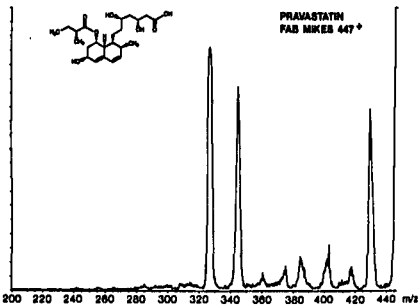

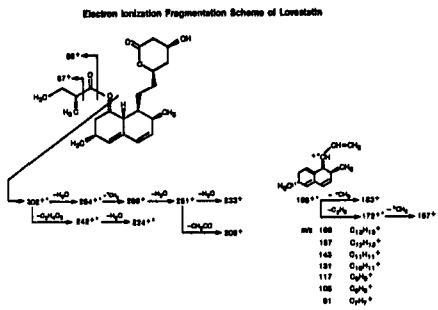

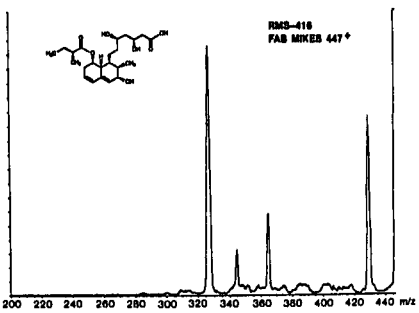

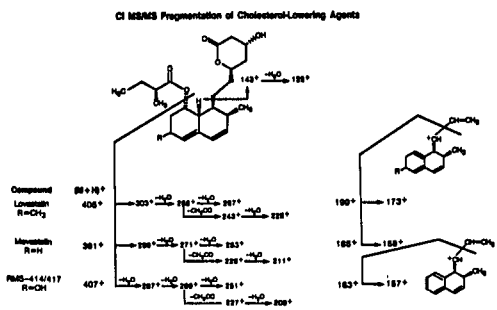

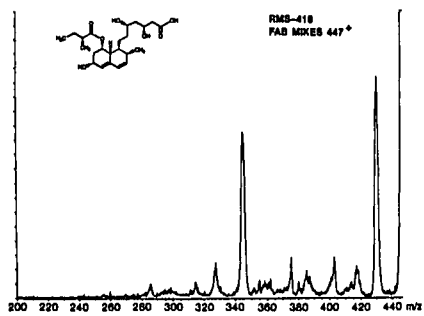

CONCLUSION

Differentiation between the pro-drug lactone and the active acid is possible from their behavior under fast heating CI conditions. Transformations of hypocholesterolemic agents which involve the lactone ring or the ester sidechain are easily determined from their mass and MS/MS spectra. More subtle changes on the fused rings are difficult to characterize and require the use of high energy collision conditions, charge-changing dissociations, and breakdown curves generated from MS/MS data. Positive or negative MIKES is used to differentiate between stereoisomers and regioisomers. Mixtures of such agents are rapidly profiled by monitoring loss of the C_5 and C_6 acids from the ester sidechain in the neutral loss mode.

Presented at the 36th ASMS Conference on Mass Spectrometry and Allied Topics
June 5-10, 1988, San Francisco, CA

FAB-MS OF NOVEL FLUOROGENIC IONOPHORES

D. M. Hindenlang, M. E. Lucas, D. Masilamani, R. D. Sedgwick

Corporate Technology, Allied-Signal Inc., Morristown, NJ 07960

Introduction

FAB-MS has been employed for structural characterization in the development of some novel fluorogenic ionophores for ultimate applications to fiber optic-based clinical analysis of alkali metals in biological fluids. Ionophores are generally cyclic organic structures bearing heteroatoms that ligate ions, and depending on the cavity size may be highly specific for solution binding of a particular ion. The present work involves FAB-MS to guide the development of fluorogenic ionophores which are indicators for alkali ions, with measurable changes in their fluorescence upon binding. Exploratory synthesis has led to an optimal series of coumaro cryptands, highly specific and sensitive for K^+, Na^+, and Li^+. These products are highly selective, sensitive, stable, compatible with aqueous media at neutral pH, and suitable for existing clinical instrumentation or fiber optic-based sensors. The preferential solution binding of these ionophores is reflected in their FAB spectra, which show competitive cationization by the same preferred alkali species. These results indicate FAB ionization by desorption of preformed ionic complexes from solution.

Synthetic Design Guided by FAB-MS

The exploratory development of novel fluorogenic ionophores followed variations of selective ion-recognizing moieties conjugated to diverse aromatic chromophores. The success of these synthetic routes was monitored by FAB-MS analysis of diverse ionophores, intermediates, and side products. Various chromophoric groups were explored incorporating catechol derivatives, dihydroxy-naphthalene units, and a coumarin (1,2-benzopyrone) based moiety. Aryl oxygens from these groups were built into ion-recognizing crown ether and cryptand macrocycles.

The MS instrumentation for this examination of fluorogenic ionophores was a VG Analytical ZAB-HF reverse geometry double focusing mass spectrometer with FAB ion source using 7 keV xenon atom bombardment. Spectra were recorded on the VG 11-250 instrument control and data collection system, with magnetic scanning using field control and an ion energy of 8 keV. Positive ion spectra were more intense and generally of greater analytical value. Negative ion spectra generally provided little information regarding the ionophore, being dominated by halide counter ions remaining from the synthesis.

Positive ion spectra are generally dominated by very intense pseudomolecular ion patterns, MH^+ and alkali cation adducts. The details of the molecular patterns depend on the nature and extent of alkali contamination during the synthesis. The less alkali, the greater is the observed MH^+ intensity, but even minor alkali contamination produces relatively intense cation adducts. Fragmentation information is most useful for open chain intermediates and final products with appended side groups. However, the predominance of molecular weight information facilitates the assignment of even minor side products.

Competitive Binding of Coumaro Cryptands with Alkali Cations

Incorporation of 6,7-dihydroxy-4-methyl coumarin into cryptands provides optimal selectivity and sensitivity for fluorogenic ionophores. Three coumaro cryptands were synthesized and studied: [2.2.2], [2.2.1], and [2.1.1] . With excitation at 330 nm the fluorescence observed at 410 nm is enhanced dramatically by selective alkali binding. This enhancement is quantitative at clinical concentrations, even in the presence of non-target ions. Cationized FAB-MS pseudomolecular ions similarly show selectivity and sensitivity of binding for this series of coumaro cryptands. Competitive alkali binding experiments were conducted in glycerol matrix containing equimolar LiCl, NaCl, and KCl.

The control FAB-MS experiment contained no ionophore, simply glycerol and equimolar concentrations of Li^+, Na^+ and K^+. We observe no specificity of the cations for the glycerol matrix. The spectrum shows nearly equivalent ion intensities for m/z 99^+ (GLi^+); 115^+ (GNa^+); and 131^+ (GK^+) along with considerable m/z 93^+ (GH^+). In experiments with ionophores, this pattern was not reproduced nor were the observed ratios of m/z 7^+ (Li^+), 23^+ (Na^+), and 39^+ (K^+) maintained. The distortions were generally in favor of the alkali ion preferentially bound by the particular ionophore. These results indicate variations in the surface concentration of the alkali cations enhanced by the ion binding and surface activity of the ionophores.

FAB-MS of the coumaro [2.2.2] cryptand (MW506) shows a predominant m/z 545^+ (MK^+) with minor 529^+ (MNa^+) along with weak glycerol matrix adduct ions. No reliable MH^+ or MLi^+ species are observed. These results correlate with solution fluorescence data which show that this system is highly selective and sensitive for K^+. FAB-MS of the coumaro [2.2.1] cryptand (MW462) shows a predominant m/z 485^+ (MNa^+) with minor possible MLi^+ (m/z 469^+) and MK^+ (m/z 501^+) along with glycerol matrix adducts. Fluorescence spectra demonstrate a dramatic enhancement selective for Na^+ as expected. FAB-MS of the coumaro [2.1.1] cryptand (MW418) shows a predominant m/z 425^+ (MLi^+) with weak 419^+ (MH^+), 441^+ (MNa^+), and 457^+ (possible MK^+), along with glycerol matrix adducts. Fluorescence spectra demonstrated a dramatic enhancement with the addition of Li^+.

All three of the above coumaro cryptands were similarly dissolved together in glycerol matrix with equimolar Li^+, Na^+, and K^+ for a competitive binding FAB-MS experiment. The observed three dominant pseudomolecular species (see Figure) are in accord with the solution binding specificity, viz. m/z 425^+ [2.1.1]Li^+; m/z 485^+ [2.2.1]Na^+; and m/z 545^+ [2.2.2]K^+.

Conclusions

FAB-MS of these coumaro cryptands illustrates a clear correlation of cationized pseudomolecular ions with solution binding specificity and fluorogenic sensitivity. The conclusion that the FAB-MS is representative of selective solution binding of alkali cations to these fluorogenic ionophores is particularly emphasized in the final competitive experiment. These data indicate FAB ionization by desorption of specific performed ionophore alkali cation complexes from solution. These results are generally inconsistent with a CI plasma, random cationization model for FAB ionization. A CI model would predict more equivalent intensities for adducts of these equimolar cations, since all alkali pseudomolecular ions appear stable. Alternatively a CI model might favor a modified distribution based on cation gas phase energetics.

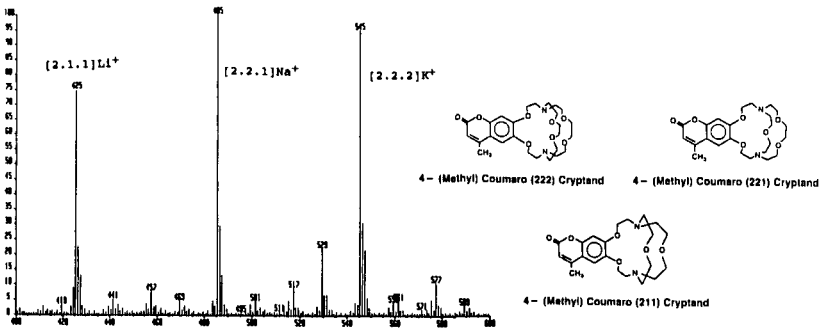

Presented at the 36th ASMS Conference on Mass Spectrometry and Allied Topics
June 5-10, 1988, San Francisco, CA

HRGC-MS MEASUREMENT OF PLASMA NICOTINE LEVELS AFTER SMOKING OR CHEWING NICOTINE GUM.

Enrico Davoli, Giulio Mariani, Emilio Benfenati and Roberto Fanelli; Pharmacological Research Institute "Mario Negri", Milano, Italy, 20157.

INTRODUCTION:
Recently, a new product for the Italian market, nicotine chewing gum (Nicorette) has been released as a therapeutic agent for tobacco addiction.
It is well known that plasma nicotine level is an important factor in physical dependence on cigarette smoking. Smokers can partially regulate their nicotine intake when switching to brand of cigarette with different strength. This indicates the importance of measuring plasma concentrations of the alkaloid during the treatment with a smoking withdrawal aid.
The leading cigarette brand in Italy is MS, a high-tar brand, which represents 32 % of the market. This results in a quite homogeneus population of smokers.
With this in mind it was decided to test in a controlled trial the nicotine plasma levels obtained after smoking MS cigarette or after chewing Nicorette 2 or 4 mg.

EXPERIMENTAL
Human studies
Eight smoker volunteers partecipated to a three day trial, chewing 2 or 4 mg Nicorette tablets or smoking MS cigarettes hourly.
The first day they were asked to smoke a cigarette per hour, the second to chew a 2 mg Nicorette tablet, the third a 4mg tablet. Three 2 ml blood samples were collected after four hours from the beginning of the experiment, 30 min after each treatment. Subjects were asked to chew the tablets for thirty minutes.

Plasma nicotine assay and synthesis of deuterated nicotine
Deuterated nicotine was used as internal standard.
5,5-D2-Nicotine was obtained by reduction of cotinine with LiAlD4 (1).

Instrumental analysis
Experimental conditions for selected ion recording (SIR) were as follows:
Instrument: VG TS-250
Coloumn: CP WAX CB (11m 0.22 ID) Chrompack
Ion recording: m/z 162 (nicotine) and m/z 164 (nicotine-D2).

Extraction from biological samples
Plasma samples were extracted basically as reported (2).

Recovery studies
Recovery studies were performed adding a fixed amount of nicotine-D2 and increasing amounts of nicotine to non smoker plasma samples. Fig.1 shows the calibration curve obtained when spiked plasma samples were prepared and analysed as described above.
The intercept on Y axis corresponds to the sum of signals from background plasma nicotine levels and from contribution of M-2 ions of deuterated nicotine (10 %).

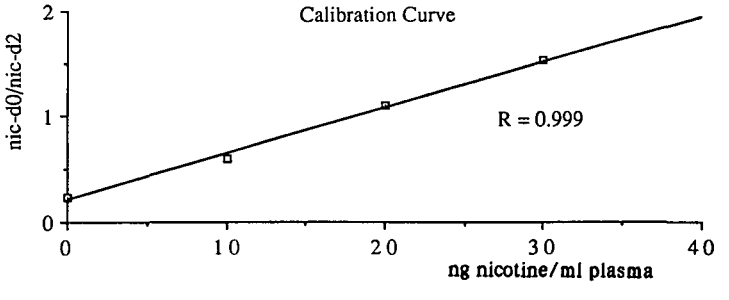

Fig 1: Calibration curve

RESULTS

Results (fig.2) show that the plasma nicotine obtained after cigarette smoking (19.21+1.16 ng/ml) lies between the levels obtained after chewing 2 mg (14.31+0.91 ng/ml) and 4 mg (23.69+1.65 ng/ml) Nicorette.

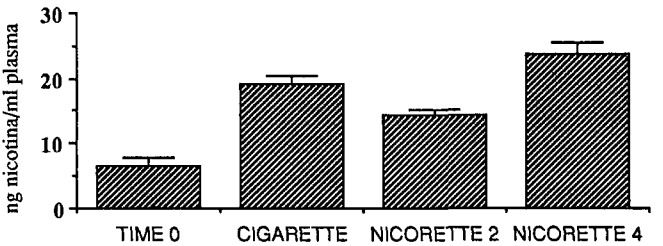

Fig 2: Nicotine plasma levels before the experiment (Time 0) and after smoking or chewing Nicorette (2 or 4 mg).

CONCLUSIONS

These results reflect quite closely data previously obtained by British and American studies (3,4). Our data indicate that nicotine plasma levels obtained after chewing Nicorette gum are comparable with levels obtained smoking the most popular cigarette brand in Italy.

REFERENCES

1. A.M. Duffield, H. Budzikiewicz and C. Djerassi, J. Am. Chem. Soc. 87, 2926, (1965).
2. C. Feyerabend, and M. A. Russel, J. Pharm. Pharmacol. 31, 73, (1978).
3. M. A. H. Russel, S. R. Sutton, C. Feyerabend, P. V. Cole and Y. Salljee, British Medical Jornal, 1, 1060, (1977).
4. M. E. McNabb, R. V. Ebert and K. McCusker, JAMA, 248, 865, (1982).

Presented at the 36th ASMS Conference on Mass Spectrometry and Allied Topics
June 5-10, 1988, San Francisco, CA

PRELIMINARY STUDIES ON THIOTEPA-DNA ADDUCTS USING THERMOSPRAY LC/MS: Steven M. Musser, Patrick S. Callery and Su-Shu Pan, Department of Medicinal Chemistry and Pharmacognosy, Univ. of Maryland, Baltimore, MD. 21201 and Univ. of Maryland Cancer Center, Baltimore, MD. 21201

Thiotepa [tris(1-aziridinyl)phosphine sulfide] is a clinically useful anticancer drug whose proposed mechanism of action is alkylation of DNA bases. Although thiotepa has been used clinically for over 30 years very little is known about its interaction with DNA. Since thermospray LC/MS is an excellent technique for the analysis of nucleosides we proposed that it would also be useful for the identification of unknown modified nucleosides.

Calf thymus DNA and thiotepa were incubated at 37 °C at various pH's ranging from 4.6 to 7.4. The DNA was isolated and digested enzymatically. The enzymatic digest and supernatant remaining after removal of the DNA from the reaction mixture were chromatographed on an HPLC reverse phase C-18 column with the effluent being fed directly into the thermospray ion source of a Hewlett-Packard Mass Selective Detector or a Finnigan 4500 mass spectrometer. The molecular ion of deoxyguanosine was used to optimize thermospray conditions, since the ratio of the molecular ion to the ion corresponding to the purine base without the suger is good measure of the extent of thermal hydrolysis occurring in the ionization process.

The position and bases at which DNA was modified by thiotepa were established using HPLC/thermospray mass spectrometry. The structures of the two adducts have been assigned as 7-(2-aminoethyl)guanine and 7-(2-aminoethyl)adenine. The assignments are based on the observation that N-7 modified purine nucleosides rapidly undergo depurination under neutral or acidic conditions (Hemminki, K., Chem.-Biol. Inter., 48:249-260). Since the adducts were found in the supernatant of the thiotepa-DNA reaction mixture and not in the hydrolyzed DNA fraction and the mass spectra indicate that the deoxyribose is not present on the adducts we conclude that the the N-7 position of guanine and adenine are the sites of alkylation by thiotepa. The ratio of N-7 alkylated guanine to N-7 alkylated adenine is approximately 3:1, making 7-(2-aminoethyl)guanine the principal adduct formed when thiotepa alkylates DNA. Although it is possible for thiotepa to alkylate DNA as the intact molecule the absence of adducts containing a phosphoramide bond indicates that thiotepa may be fuctioning as a prodrug for aziridine.

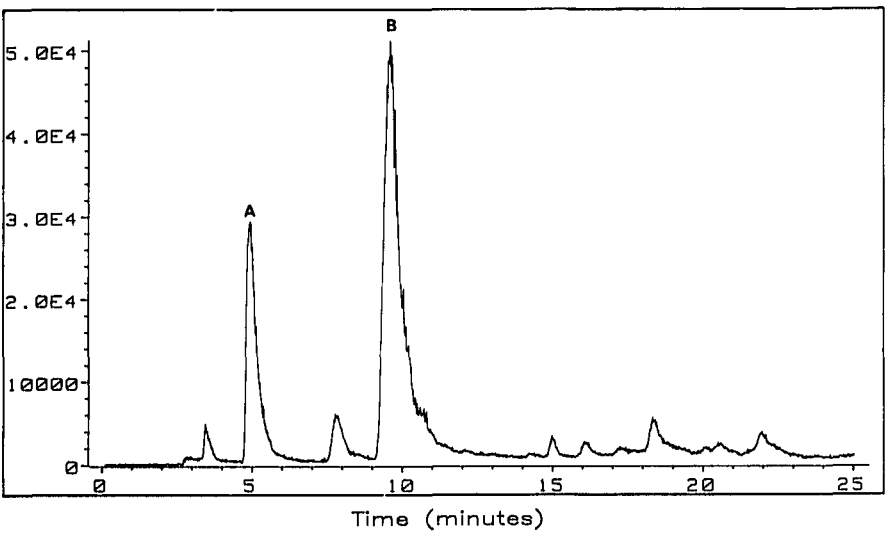

Thermospray total ion chromatogram of the supernatant from the thiotepa/DNA reaction mixture. A. 7-(2-aminoethyl)adenine B. 7-(2-aminoethyl)guanine

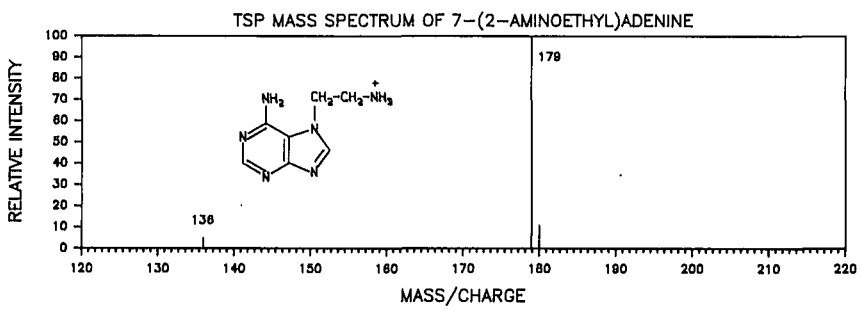

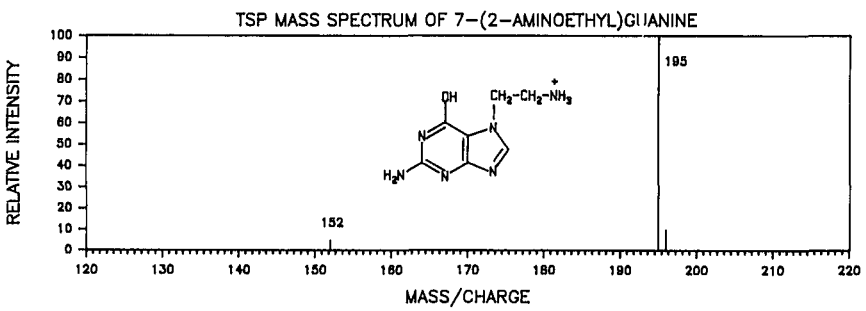

Presented at the 36th ASMS Conference on Mass Spectrometry and Allied Topics
June 5-10, 1988, San Francisco, CA

SIMULTANEOUS QUANTITATION OF CARBAMAZEPINE, CARBAMAZEPINE-10,11-EPOXIDE, AND CARBAMAZEPINE-10,11-DIOL IN PLASMA BY GAS CHROMATOGRAPHY/MASS SPECTROMETRY

D. Alkalay, S. Carlsen, J. Miotto, and D. Gaudry

Development Department, Pharmaceuticals Division,
CIBA-GEIGY Corporation, Ardsley, N.Y. 10502

Carbamazepine (I) is widely used for treating epilepsy and trigeminal neuralgia. The drug is known to undergo extensive biotransformation and to yield many metabolic products. Prominent among these are carbamazepine-10,11-epoxide (II), known to have anticonvulsant activity in animal models, and carbamazepine-10,11-diol (III).

A number of published methods allow the quantitation of I, or I and II. A need existed, however, for a simple procedure permitting the simultaneous determination of all three compounds in biological fluids. The development of such a procedure became the objective of this work.

The method we developed relies on 10-methoxycarbamazepine (IV) as internal standard. It utilizes N-methyl-N-trimethyl-silyltrifluoroacetamide (MSTFA) as derivatizing agent. One-ml plasma samples, containing appropriate amounts of I, II, and III, were spiked with internal standard and extracted with $CHCl_3$. Following treatment with MSTFA, aliquots were injected for GC/MS analysis.

We utilized a Nermag R10-10C mass spectrometer interfaced with a Varian Vista 6000 gas chromatograph. The GC/MS was linked to a PDP 11/73 computer and was equipped with a split/-splitless capillary injector and an Alltech FSOT RSL-150 capillary column (30 m x 0.32 mm). The system was operated under CI conditions with He as carrier and NH_3 as reagent gas. The temperatures were 100 to 250°C for GC programming, 250°C for the injector, and 290°C for the GC/MS interface.

Compounds I, II, III, and IV give the trimethylsilyl (TMS) derivatives V, VI, VIII, and IX, respectively. The epoxide, in addition, undergoes a rearrangement to give 9-acridinecarboxyaldehyde (VII).

Selected ion monitoring was conducted on the M+1 ions of V, VI, VII, VIII, and IX, with respective m/z values of 309, 208, 325, 487, and 339. For determinations of the epoxide, we can use the rearrangement product VI as well as the derivative VII.

All three compounds showed a good linear relationship between the peak area ratio of analyte to internal standard and the concentration of the analyte. The range was tested from 40 ng/ml up to 10 ug/ml.

The method is specific, linear, accurate, and precise. It provides a convenient opportunity to monitor levels of the drug and the two metabolites resulting from single and multiple therapeutic doses. It can be especially useful in pharmacokinetic studies employing cold isotope-labelled carbamazepine.

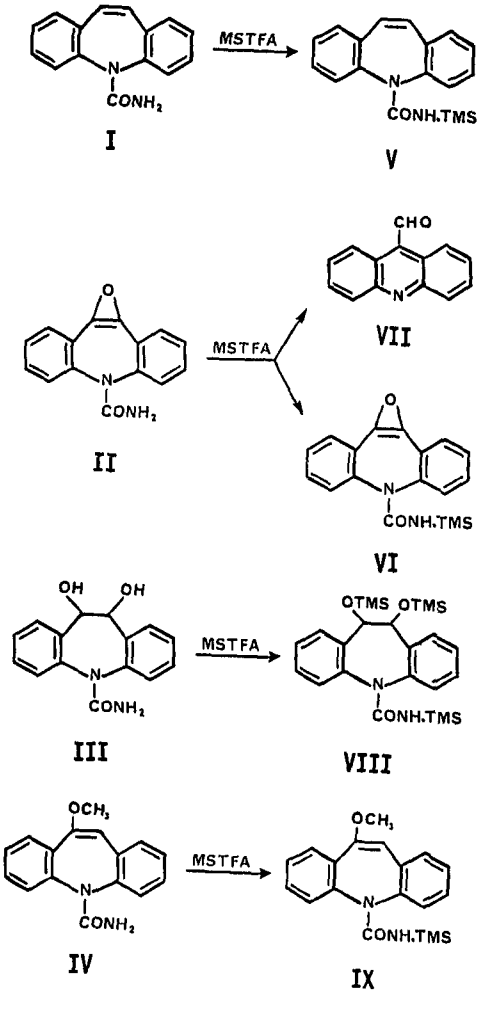
MSTFA
CONH2
I
CONH.TMS
V
CHO
VII
O
MSTFA
CONH2
II
CONH.TMS
VI
OH
OH
MSTFA
OTMS
OTMS
CONH2
III
CONH.TMS
VIII
OCH3
MSTFA
CONH2
IV
OCH3
CONH.TMS
IX

Presented at the 36th ASMS Conference on Mass Spectrometry and Allied Topics
June 5-10, 1988, San Francisco, CA

QUANTITATION OF THE SELECTIVE DOPAMINE AGONIST CGS 15873A IN PLASMA BY GAS CHROMATOGRAPHY/MASS SPECTROMETRY

S. Carlsen, D. Alkalay, D. Gaudry, and J. Miotto

Development Department, Pharmaceuticals Division,
CIBA-GEIGY Corporation, Ardsley, N.Y. 10502

CGS 15873A (I) is a new dopamine autoreceptor agonist currently being evaluated in man. Because of its potency, it is administered at low doses. As a result, the levels attained in plasma are rather low.

In order to investigate the pharmacokinetic behavior of the drug in man, it was necessary to determine the levels it attained in plasma after the administration of a single dose. That need was met by the procedure we describe, which allows the necessary low level drug determinations.

One-ml plasma samples, containing appropriate amounts of I, were spiked with one ng of the analogue CGS 15855A (II), used as an internal standard. They were extracted with a mixture of heptane and ether (7:3) and the extract was evaporated to dryness. The residue was derivatized with a toluene solution saturated with pentafluoropropionic anhydride (PFPA) to yield III and IV. Prior to injection, the excess reagent was destroyed with an aqueous solution of KH_2PO_4.

We utilized a Nermag R10-10C mass spectrometer interfaced with a Varian Vista 6000 gas chromatograph and linked to a PDP 11/73 computer. The system had a split/splitless capillary injector and an Alltech FSOT RSL-150 capillary column (30 m x 0.32 mm). The system was operated under CI conditions with He as carrier and NH_3 as reagent gas. The temperatures were 100 to 300°C for the GC programming, 255°C for the injector, and 290°C for the GC/MS interface.

Selected ion monitoring was conducted at m/z 394, a value common for the M+1 ions of III and IV.

The method is very sensitive and allows dependable analyses down to plasma concentrations as low as 2 pg/ml. We tested the critical range range from 2 to 200 pg/ml. Our results, expressed as % of added drug concentrations, averaged 101.6 + 9.2 (n = 27).

In conclusion, this method is specific, linear, accurate, and precise. It allows dependable low level analyses, which makes it particularly suitable for single dose human pharmacokinetic studies.

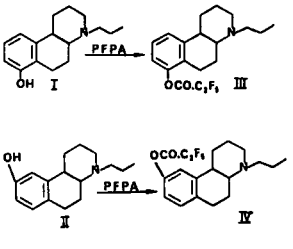

Presented at the 36th ASMS Conference on Mass Spectrometry and Allied Topics
June 5-10, 1988, San Francisco, CA

Determination of Arecoline in Plasma By Selected Ion Monitoring GC/MS

M. J. Hayes, L. Khemani, M. Bax, and D. Alkalay;

Development Department, Pharmaceuticals Division, CIBA-GEIGY Corp.,
Ardsley NY 10502

Arecoline is a natural product of the betel nut. It is known to have parasympathomimetic and cholinergic properties. It is also effective in treating cholinergic brain disfunction.

Previously published analytical methods for arecoline have not had sufficient sensitivity or specificity for use in the determination of arecoline in plasma. Determination of arecoline at levels of clinical interest (1 ng/ml) is made difficult due to its low molecular weight (155) and the many interferences that result from plasma.

The present work describes methodology for the determination of both arecoline (I) and d3-arecoline (II) in human plasma. The quantitation of both unlabeled and labeled arecoline needed for use in conducting comparative bioavailability studies with alternative dosage forms. D6-arecoline was used as the internal standard. The d6-arecoline has 0.03% residual d0 and 0.59% d3 and therefore does not contribute significantly to the blank for either compound.

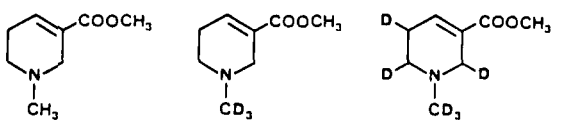

I II III

The removal of drug from plasma was accomplished by a two-step liquid/liquid extraction procedure. The plasma was acidified, then washed with ethyl acetate. Extraction was then done at pH 9 using 5% triethyl amine in ethyl acetate. The wash sequence was critical to achieving the 1 ng/ml quantitation limit.

The mass spectrometer used was a Nermag model R10-10C with a Varian 6000 GC. A 30 m methyl silicone bonded phase capillary column was used for GC. Injections were made in the splitless mode with an injector temperature of 220oC. The temperature program was 60oC for 1 min, then 40oC/min to 220oC, hold for 4 min.

Mass spectrometry was under ammonia CI conditions at a source pressure of 0.2 torr (ammonia flow, 6 ml/min/atm). The [M+H]+ ions were monitored at m/z 156, 159, and 162 for compounds I, II, and III respectively.

Quantitation was done with peak area ratios of drug to internal standard followed by weighted linear least square regression (weighting = 1/x2). Calibration curves were reproducible with regression coefficients of 0.996 or greater. The mean of the absolute deviations of individual standards from the regression line ranged from 4 to 12%. Quality control samples gave a mean recovery of 101.4% with a std. dev. of 7.6% (n = 17).

The application of the method is illustrated with results from a study in dogs. Arecoline was administered to four dogs via the left femoral vein in ascending doses of 0.3, 1.0, 3.0, and 10 ug/kg/min for 30 minutes each. The results of the analysis are plotted in Figure 1. Plasma levels can be seen to rise linearly with increasing dose.

The method described is sensitive, precise, accurate, and selective and has been applied to pharmakokinetic studies in both humans and animals.

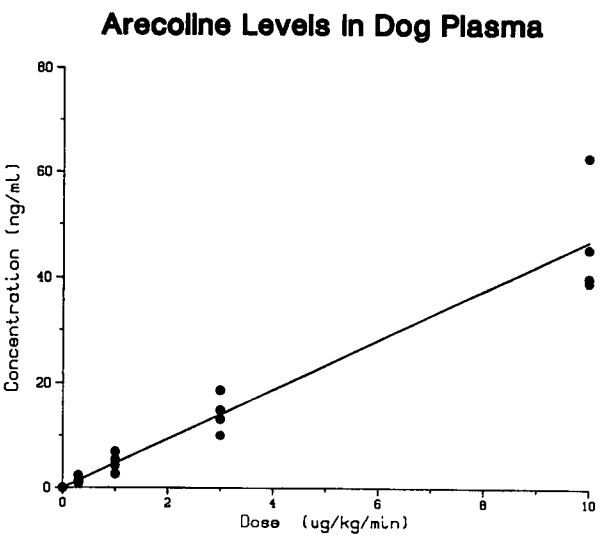

Figure 1. Plasma levels of arecoline following IV infusion in four Beagle dogs.

Presented at the 36th ASMS Conference on Mass Spectrometry and Allied Topics
June 5-10, 1988, San Francisco, CA

Dechlorination Reactions in FAB Mass Spectrometry of Phenothiazine Related Drugs

R.W. Edom, P.W. Brooks and G. McKay
College of Pharmacy, University of Saskatchewan, Saskatoon, Saskatchewan, Canada S7N 0W0

Chlorinated phenothiazine and tricyclic antidepressant drugs appear to undergo extensive dehalogenation reactions in FAB mass spectrometry, resulting in the appearance of characteristic dechlorinated ions in the spectra. This has presented problems in the identification of new metabolites of these drugs using FAB. The presence of artifactual dehalogenated ions can confuse the structure eludication of unknown metabolites. Therefore a study to examine the nature and extent of dechlorination reactions for these two groups of drugs was undertaken using the representative compounds presented below.

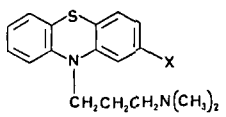

X = H PROMAZINE
X = Cl CHLORPROMAZINE

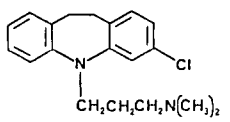

CLOMIPRAMINE

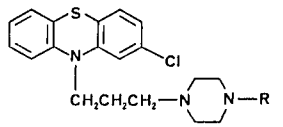

R = CH_3 PROCHLORPERAZINE
R = CH_2CH_2OH PERPHENAZINE

Dechlorination is suspected to result from a reaction in the sample matrix replacing the chlorine atom with a hydrogen, and giving rise to an apparent fragment ion. Presented for example are the positive ion FAB spectra of chlorpromazine and clomipramine. The dechlorinated species in each spectrum is marked with an asterisk. It appears at a mass shift of 34 amu from the MH^+, with no distinictive chlorine isotope. Table 1 summarizes the relative intensity and percent exchange of the dechlorinated species in each compound used for this study. As indicated in the table, dechlorination results in abundant artifactual ions in the FAB mass spectra of these compounds.

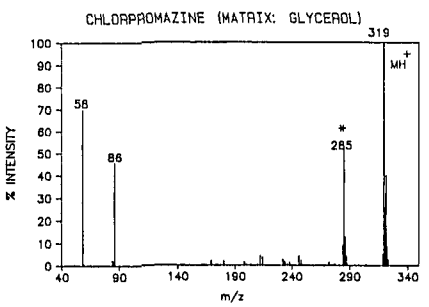

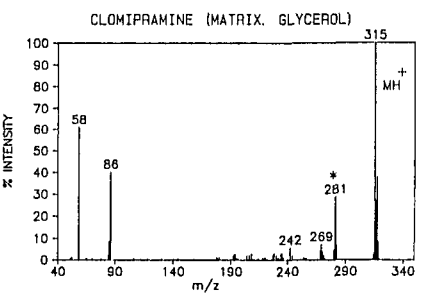

Table 1: Extent of FAB Induced Dechlorination

	Mol. Weight	m/z (% Rel. Intensity) $M_{Cl}H^+$	$M_H H^+$	% Exchange
Chlorpromazine	318	319 (100)	285 (45.7)	26.3
Clomipramine	314	315 (100)	281 (28.7)	17.5
Perphenazine	403	404 (100)	370 (41.9)	23.9
Prochlorperazine	373	374 (100)	340 (31.9)	19.4

Presented at the 36th ASMS Conference on Mass Spectrometry and Allied Topics
June 5-10, 1988, San Francisco, CA

In Table 1 the % Exchange was calculated from the relative intensities of the ions using the equation:

$$\% \text{ Exchange} = M_H H^+ / (M_H H^+ + M_{Cl} H^+)$$

In the equation, $M_{Cl}H^+$ represents the sum of the intensities of the ^{35}Cl and ^{37}Cl isotopes. Where appropriate the intensity of the ^{37}Cl isotope was corrected for the contribution of ^{18}O and ^{34}S from the ^{35}Cl isotopic species.

To confirm the structure of the dechlorinated ion (m/z 285) in chlorpromazine, FAB-MS/MS was conducted on a VG 70SQ mass spectrometer. Promazine (the dechloro-analog of chlorpromazine) was used as an authentic reference. The CAD daughter ion spectrum of m/z 285 from chlorpromazine was identical to the daughter ion spectrum of the MH^+ of promazine, proving the incorporation of hydrogen for chlorine in the process of dechlorination. The spectra are presented below.

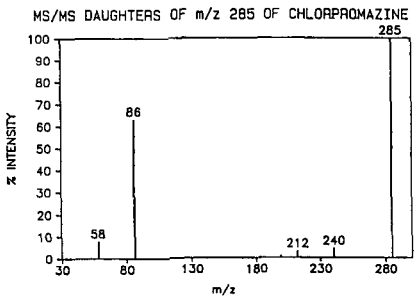

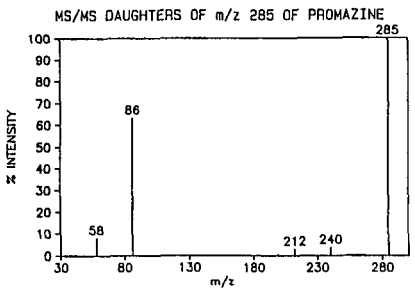

A FAB spectrum of chlorpromazine using d_8-glycerol as the sample matrix is shown below. Here the dechlorinated ion is observed at m/z 287, a shift of 33 amu from the MD^+. This indicates replacement of the chlorine with deuterium. To confirm this observation, a FAB-MS/MS spectrum was determined on m/z 287. Daughter ions were observed at m/z 213 and 241, which proves the incorporation of deuterium for chlorine when compared to the corresponding daughter ions of m/z 285 of chlorpromazine and promazine determined in glycerol.

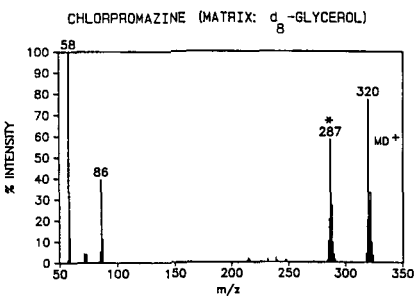

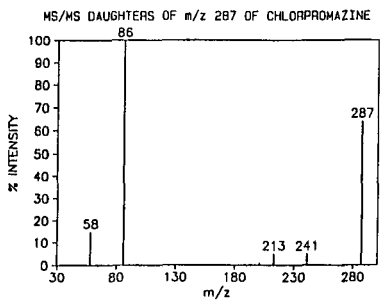

The results of this research have proven that chlorinated phenothiazine and tricyclic antidepressant drugs undergo extensive dechlorination reactions in positive ion FAB mass spectrometry. These reactions produce intense ions in the spectra which account for a range of 17.5% to 26.3% chlorine exchange and appear in the spectra from 28.7% to 45.7% relative abundance. Since metabolic dechlorination is a possiblity, investigators must be alert for the appearance of artifactual dechlorinated ions when attempting to elucidate the structure of unknown metabolites of halogen containing drugs such as those presented in this study.

The authors gratefully acknowledge the financial support of the Medical Research Council of Canada (P.G. 34 and a MRC studentship for R. Edom).

Presented at the 36th ASMS Conference on Mass Spectrometry and Allied Topics
June 5-10, 1988, San Francisco, CA

Quantitation of Dideoxycytidine in Human Plasma by GC/MS. Felix R. Rubio, Theodore Crews, W.A. Garland and Elaine K. Fukuda*, Hoffmann-La Roche Inc., Nutley, NJ 07110.

The 2',3'-dideoxynucleosides are a class of chemicals with potent activity against the human immunodeficiency virus responsible for the AIDS (acquired immunodeficiency syndrome) disease [1,2]. One member of this chemical class, AZT (azidothymidine), has been approved for clinical use [1], and another member, DDC (dideoxycytidine), is undergoing clinical trials [1].

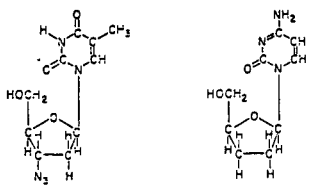

The quantitation by HPLC of these chemicals in the plasma of patients undergoing treatment with the dideoxynucleosides is complicated by interferences due to the intensive concomitant chemotherapy required to treat the effects of the disease. For very potent nucleosides such as DDC, the administered dose also gives plasma concentrations too low to be measured by traditional HPLC [3,4] or LC/MS [3].

This presentation reports a GC/NCIMS assay for DDC in the plasma of AIDS patients undergoing treatment.

The method involves several steps: 1) precipitation of plasma proteins with acetone, 2) ether wash, 3) ethyl acetate:methanol (9:1) extraction reaction with t-butyl dimethyl chlorosilane to silylate the 5'-hydroxyl group, 5) pentafluorobenzoylation of the amino group with pentafluorobenzoyl chloride, 6) methylation of the ring nitrogen adjacent to the amino group with diazomethane. The resulting derivative is quantitated using stable isotope dilution, selective ion monitoring and methane negative chemical ionization mass spectrometry.

Plasma concentrations of DDC were measured over a range of 2 to 200 ng/ml using 1 ml of plasma for extraction.

Plasma concentration-time profile of DDC in the plasma of an AIDS patient given a single oral 5 mg dose of the drug. The continuous line represents the fit of the data (solid circles) to the equation for a one compartment single oral dose [5].

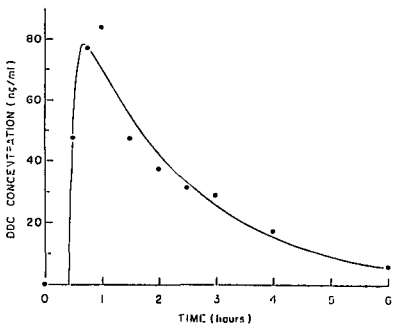

Figure 1

To date, the assay has been used to measure concentrations of DDC in the plasma from AIDS or AIDS related complex patients given 0.5 or 5 mg of either oral or IV doses of DDC. If lower doses are to be used, the sensitivity of the assay will have to be improved.

References

1. R. Yarchoan and S. Broder, N. Eng. J. Med., 9, 557 (1987).
2. V.T. DeVita, S. Broder, A.S. Fauci, J.A. Kovacs and B.A. Chabner, Ann. Intern. Med., 106, 568 (1987).
3. P.A. Blair, J.W. Hines and R.D. Voyksner, J. Chromatog., 420, 1 (1987).
4. J.A. Kelley, C.L. Litterst, J.S. Roth, D.T. Vistica, D.G. Poplack, D.A. Cooney, M. Nadkarni, F.M. Balia, S. Broder and D.G. Johns, Drug Metab. Disp., 15, 595 (1987).
5. P.G. Welling, J. Clin. Pharmacol., 26, 510 (1986).

Presented at the 36th ASMS Conference on Mass Spectrometry and Allied Topics
June 5-10, 1988, San Francisco, CA

APPLICATION OF DICYANDIAMIDE AS A MATRIX ADDITIVE IN FAST ATOM BOMBARDMENT MASS SPECTROMETRY

G. W. Caldwell, A. B. Reitz and J. A. Masucci, Janssen Research Foundation at McNeil Pharmaceutical, Spring House, PA 19477

INTRODUCTION: FAB mass spectra are influenced by various aspects of matrix solution chemistry(1). Chemical reagents are often added to the FAB matrix to confirm the molecular ion and/or improve the sensitivity by enhancing the proton attachment ([M+H]+) or the proton abstraction ([M-H]-) emission(2). The pH of the FAB matrix can be modified with common organic acids or bases with the objective of more fully ionizing the analyte in the solution and thereby increasing its FAB sensitivity(3). Surfactants can be used to enhance the response of an analyte relative to a matrix by enriching the surface composition with analyte(4). In conjunction with the development of the use of chemical additives, a distinct set of derivatization reactions have emerged which endow the analyte with ionic character and/or surface activity(5,6).
This poster describes the properties of dicyandiamide (DCDA) as a chemical additive to the FAB matrices thioglycerol and glycerol for the analysis of organic compounds. We show that DCDA can be used to generate adduct ions for a variety of organic compounds to confirm the protonated molecular ion. It is demonstrated that amines work well with this chemical additive (Table 2).

$$RR'R''NH^+ + N{\equiv}C\text{-}NH\text{-}C(=NH)NH_2 \longrightarrow [RR'R''NH_2..N{\equiv}C\text{-}NHC(=NH)NH_2] \quad (1)$$

Reaction of DCDA with primary and secondary amines produces biguanides (Figures 1-3) (7).

$$RR''NH{\cdot}HCl + N{\equiv}C\text{-}NH\text{-}C(=NH)NH_2 \longrightarrow RR'N\text{-}C(=NH)NHC(=NH)NH_2 \quad (2)$$

The FAB spectra and the high sensitivity of biguanides (nanogram range) are described for the first time (Table 3). The dual role of DCDA makes it an interesting and unique chemical additive.

DISCUSSION: Table 2 demonstrates that DCDA can be used as a chemical additive for a variety of amines to confirm the molecular ion in FAB spectra. Approximately 25 g of amine and 50 g of DCDA were loaded onto the FAB probe tip and analyzed. The protonated amine ion ([M+H]+) and the adduct ion ([M+H+84]+) were observed. The [M+H]+ ion was the base peak in all FAB spectra except compound 11, here, the protonated molecule of DCDA (85 m/z) was the base peak. Relative to the [M+H]+ ion intensity the [M+H+84]+ ion intensity was observed in the range 3-32%. The ratio of the ion intensities [M+H+84]+: [M+H]+ throughout the entire emission period (ca 3 m) changed only slightly (1-2%) with time.
Figure 1 shows the derivatization of compound 15 (267 m/z) with time to its corresponding biguanide (351 m/z). The FAB spectra denotes the reaction initially (time 0) and at 2 h and 7 h. The major matrix background ions for the thioglycerol/DCDA/DMSO mixture were [109 + (108)x]+, [85 + (84)x]+, [79 + (78)x]+, [109 + (84)x]+, and [85 + (78)x]+ where x equals 0-2.
Eight amine hydrochloride salts (1-3, 6, 7, 10, 13 and 15) were derivatized along with three tertiary amine hydrochloride salts (4, 8, 16) used as controls (Table 2). As expected, the ratio of ion intensities [M+H+84]+: [M+H]+ remained constant for tertiary amines and increased for primary and secondary amines. It is clear that primary and secondary amines react via (2) to form biguanides while tertiary amines do not. Compounds 7 and 8 demonstrate that derivatization can distinguish secondary and tertiary amine isomers.
Derivatized amines (biguanides) were readily detected at 200 ng in the full range FAB spectrum (Figure 3). By contrast, underivatized amines 1, 6, 7, 10, 13 and 15 (Table 2) provided no data whatsoever at 200 ng while 3 was detected. Some of the low FAB sensitivity for the underivatized amines may be due to evaporative loss from the FAB probe-tip. The greater enhancement of 3 as compared to the other derivatized (or underivatized) amines appears to be related to the hydrophobic character endowed by the n-hexyl carbon chain(6).
The most abundant ions in the FAB spectra are listed in Table 3 for five commercially available biguanides (17-21). There is little or no fragmentation in these molecules and the base peak is the [M+H]+ ion. The ion abundance is concentrated in the base peak, thereby enhancing its sensitivity. Many biguanides are themselves important medicinal compounds. From the above results, the FAB analyses of biguanides in plasma at the low nanogram range may be possible directly.

Presented at the 36th ASMS Conference on Mass Spectrometry and Allied Topics
June 5-10, 1988, San Francisco, CA

TABLE 2: DICYANDIAMIDE ADDUCT FORMATION FOR A VARIETY OF AMINES.

Amines[a]	$[(M+H)^+/(M+H+84)^+]$ (m/z)	$[(M+H)^+/(M+H)^+]$ [b]	Amines[a]	$[(M+H)^+/(M+H+84)^+]$ (m/z)	$[(M+H+84)^+/(M+H)^+]$ [b]
1	88/172	32	9	190/274	9
2	94/178	12	10	156/240	31
3	102/186	6	11	164/248	20
4	102/186	20	12	198/282	19
5	122/206	~15	13	220/304	15
6	122/206	20	14	246/330	3
7	130/214	16	15	267/351	7
8	130/214	4	16	267/351	3

TABLE 3: BIGUANIDE IONS OBSERVED IN FAB MASS SPECTRA.

	Biguanide	$[M+H]^+$ (Rel Abundance)	$[2M+H]^+$ (Rel Abundance)	$[2M+HCl+H]^+$ (Rel Abundance)	Others (m/z)
17	$(CH_3)_2N\,C(=NH)\,NH\,C(=NH)\,NH_2 \cdot HCl$	130 (100)		295 (10)	
18	$n\text{-}BuNH\,C(=NH)\,NH\,C(=NH)\,NH_2 \cdot HCl$	158 (100)		351 (5)	
19	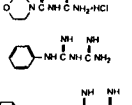 $\cdot HCl$	172 (100)		379 (5)	
20		176 (100)	355 (1)		
21	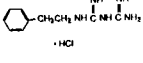 $\cdot HCl$	206 (100)		447 (5)	105 (15)

FIGURE 1: FAB MASS SPECTRUM OF COMPOUND 15

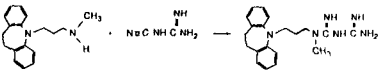

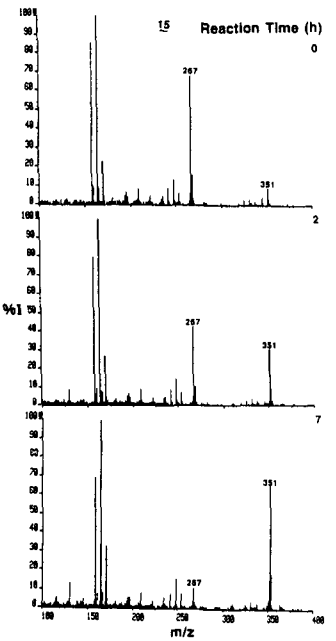

FIGURE 2 REACTION OF AMINES WITH DICYANDIAMIDE.

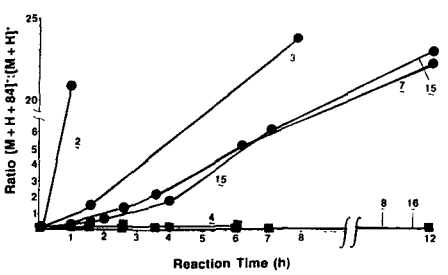

REFERENCES

1 For a review see C Fenselau and R T Cotter, *Chem Rev*, **87**, 501 (1987)

2 G Puzo and J C Promé, *Org Mass Spectrum*, **20**, 288 (1985)

3 S E Unger, T M Ryan and R G Cooks, *Anal Chimica Acta*, **118**, 169 (1980)

4 W V Ligon and S B Dorn, *Int J Mass Spectrom Ion Phys*, **57**, 75 (1984), *ibid*, **61**, 113 (1984)

5 K L Busch, S E Unger, A Vincze, R G Cooks and T Keough, *J Am Chem Soc*, **104**, 1507 (1982)

6 W V Ligon, Jr, *Anal Chem*, **58**, 487 (1986),
W V Ligon, Jr and S B Dorn, *Anal Chem*, **58**, 1892 (1986)

7 R Ray, *Chem Rev*, **61**, 313 (1961)

Presented at the 36th ASMS Conference on Mass Spectrometry and Allied Topics
June 5-10, 1988, San Francisco, CA

LIQUID SIMS OF METALLOPORPHYRINS WITH A STRONG AFFINITY TO TUMOR TISSUE

M. Suzuki, N. Takeda, K. Masuda, K.-I. Harada and A. Tatematsu (Faculty of Pharmacy, Meijo University, Tempaku, Nagoya 468, Japan), I. Sakata (Toyo-Hakka Co. Ltd., Okayama 719-03, Japan) and I. Nakajima (The 1st Department of Surgery, Asahikawa Medical College, Asahikawa 078, Japan)

Introduction

It is well known that porphyrin is apt to extensively accumulate in tumor tissue and yield fluorescence. Investigation of the use of porphyrins and metalloporphyrins for tumor diagnosis and treatment began about half of a century ago[1]. We have also developing a ^{111}In-labeled gallium-containing porphyrin (1), which is semi-synthesized from dimethylester of protoporphyrin, as a new tumor imaging agent[2]. In general structural characterization of porphyrins and related compounds have been performed by UV and NMR spectroscopy, and X-ray analysis. However it is relatively difficult to obtain structural information in the case of **1** which is very complicated because this type compounds become often insoluble and form polymer. In the present study we applied liquid SIMS to structural characterization including determination of molecular weight of metalloporphyrins and further studied the potentiality of the method for the purpose mentioned above.

Material and Methods

About 30 of metalloporphyrins studied were synthetically prepared from dimethylester of protoporphyrin. The detailed synthesis will be reported elsewhere.

SIMS and linked scanning (B/E mode) were performed using a double focusing Hitachi M-80B mass spectrometer fitted with a M-0101 data system. Operating conditions were: primary ion, Xe^+; accelerating voltage, 8 kV (primary) and 3 kV (secondary). Samples were dissolved in a solution of chloroform and methanol (1:4). Each sample solution (1-5 ul) was loaded on a silver target. About 3 ul of matrix material was added to the sample on the target. Glycerol, magic bullet, m-nitrobenzyl alcohol (NOBA) and o-nitrophenyl octylether (NPOE) were used as matrices.

Results and Discussion

ATN-2 (2) is a key intermediate for **1**, in which gallium (III) is coordinated to the porphyrin system through gallium-nitrogen bonds and it has also a hydroxyl group and water as axial ligands. Since **1** and **2** are relatively complex metalloporphyrins, mass spectrometric behavior of such type compound was extensively studied using a simpler model, AT-1-3 (3) which is an important synthetic starting material for **1** and **2**.

When **3** was measured with the four matrices, molecular ion species such as protonated molecule $(M+H)^+$ and cationized molecule $(M+Na \text{ or } K)^+$ were not detected. Instead characteristic ions (**a** and **b**) which were formed by a loss of the axial ligands (H_2O and/or OH) appeared together with their matrix-attached ion (**e**) in molecular ion region. These are corresponding to ions shown in Fig. 1. Additionally their associated ions with Na^+ and K^+ were occasionally found. Other fragmentations such as elimination of carbon monoxide and formic acid mainly occurred in the propionic acid side chains under SIMS conditions.

On the other hand SIMS spectra of an alternative model compound, AT-1-3(OAc) (4), in

which a hydroxyl group and water as axial ligands in **3** are displaced by acetoxyl group and acetic acid, respectively, were measured under same conditions. In this case the $(M+H)^+$ ion clearly appeared at m/z 749 together with **b** type ion. The linked scanning (B/E mode) from the $(M+H)^+$ show that **a** (m/z 689) and **b** (m/z 629) ions are directly derived from the parent ion. These results support that **4** is a six-coordinated metalloporphyrin.

Although the similar results were obtained using the four matrices, a characteristic behavior was observed in the cases of glycerol and magic bullet. That is, these matrices reduced the substrate to give partially reduced product which did not show normally calculated pattern for gallium-containing compound (^{69}Ga:^{71}Ga=6:4), while normal spectra were surely obtained using NOBA and NPOE. However, because NPOE has a drawback that it dissolve poorly this type compound, NOBA proved to be most suitable for our study.

Finally measurements of **1** and **2** were carried out based on the results mentioned above. As expectedly no molecular ion species appeared, but **b**, $(b+Na)^+$ and $(b+K)^+$ ions were observed as the highest ion species. These correctly give molecular weight information apart from axial ligands.

The results accumulated in this study clearly indicate that liquid SIMS with NOBA is promising for structural characterization of metalloporphyrins and would contribute to various studies in this field. Now we are studying metalloporphyrins containing other metals.

References

1. A. Policard, Compt. Rend. Soc. Biol., **91**, 1432 (1924).
2. S. Nakajima et al., Photochem. Photobio., **46**, 783 (1987).

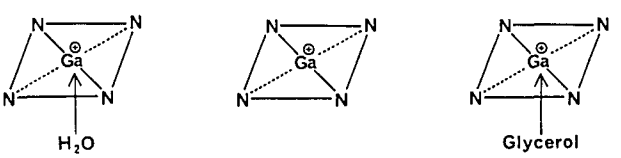

a *b* *e*

Fig. 1

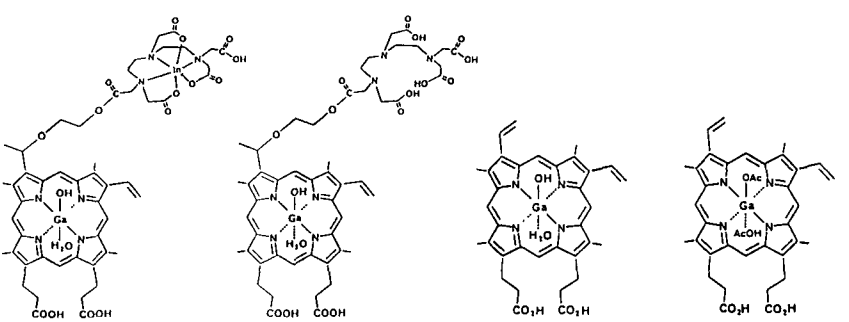

1 **2** **3** **4**

Presented at the 36th ASMS Conference on Mass Spectrometry and Allied Topics
June 5-10, 1988, San Francisco, CA

UTILITY OF LC-MS FOR THE ANALYSIS OF CHLORAMPHENICOL AND SEVERAL OF ITS ANALOGUES

W. A. Korfmacher, T. A. Getek, E. B. Hansen, Jr., C. E. Cerniglia, S. Abou-Khalil[1] and A. A. Yunis[1]

National Center for Toxicological Research, Jefferson AR 72079 and [1]Department of Medicine, University of Miami School of Medicine, Miami, FL 33101

INTRODUCTION

Chloramphenicol (CAP) is a broad spectrum antibiotic. The clinical use of CAP has decreased because CAP is known to be hemotoxic and to cause aplastic anemia in humans (1,2). Therefore, CAP is used in humans only when other less toxic antibiotics have no effect, for example, for treatment of ampicillin resistant H influenza strains. HPLC analysis of CAP in biological fluids is typically performed using ultraviolet detection (3). More recently, electrochemical detection of this compound has been reported (4).

Thermospray (TS) is a recently developed mass spectrometric (MS) ionization technique that is ideal for direct LC-MS analysis of samples (5,6). Thus, it was decided to investigate the utility of TSMS and direct LC-MS for the analysis of CAP and several of its analogues which are potential metabolites of CAP. The TS mass spectrum of CAP has been reported (7), but no information on the LC-MS analysis of this compound or its analogues has been published.

In this report, we describe the LC-TSMS analysis of CAP and 3 of its analogues which are potential metabolites of CAP. The TS mass spectrum of CAP glucuronide is also reported.

EXPERIMENTAL

Chemicals

CAP was purchased from Parke-Davis (Morris Plains, NJ). The dehydrochloramphenicol (DHCAP), the aminodehydrochloramphenicol (ADHCAP), and the *nitrophenylaminopropanediol (NPAPOL) were provided by Zambon Labs (Milan, Italy).* Chloramphenicol glucuronide (CAP-GLU) was purchased from Sigma Chemical Co. (St. Louis, MO).

Thermospray Mass Spectrometry (TSMS)

Thermospray mass spectrometry was performed using a Delsi (Houston, TX) R1010C quadrupole mass spectrometer system equipped with a Vestec (Houston, TX) thermospray source. Twenty microliter volumes of the sample were directly injected into the TSMS system in order to obtain TS mass spectra of the individual samples. Except where indicated, all experiments were performed in the "filament off" and "discharge off" thermospray ionization mode.

Liquid Chromatography-Mass Spectrometry (LC-MS)

LC-MS analyses were performed using the TSMS system described above with a Supelco (Bellefonte, PA) 5 micron diphenyl bonded phase HPLC column (25 cm x 4.6 mm) added in line between the Rheodyne (Cotati, CA) 7125 LC injector and the TS inlet. The mobile phase consisted of 0.05 M ammonium acetate (adjusted to pH 4)/methanol/isopropanol (80/10/10, v/v/v) and was set to 1 ml/min. The source block was set to 286°C, the control temperature was set to 118°C, and the tip temperature was 232°C.

RESULTS AND DISCUSSION

LC-TSMS analysis of a mixture containing CAP, DHCAP, NPAPOL, and ADHCAP was performed using the conditions described above. Baseline separation of the 4 compounds was achieved with an HPLC analysis time of less than 25 min. Figure 1 shows the TS mass spectrum obtained for CAP. Under TSMS conditions, CAP produced $[M+H]^+$ ions at m/z 323 and fragment ions, including a peak at m/z 305 which may be the $[M+H - H_2O]^+$ ion. Similar TSMS results were obtained from the analysis of DHCAP, ADHCAP and NPAPOL.

Using the "discharge on" mode, similar spectra were obtained for these 4 compounds. The main difference was an increase in signal. Using the "discharge on" mode and limited range mass scanning conditions, a detection limit of 10 ng was obtained for CAP when analyzed by direct (flow injection) TSMS.

The results obtained by TSMS analyses of CAP-GLU were found to be particularly dependent upon the TS conditions. In general, a significant peak at m/z 499, corresponding to the $[M+H]^+$ ion, was obtained along with a peak at m/z 516, attributable to the $[M+NH_4]^+$ ion. In addition, fragment ions at m/z 481, m/z 340, m/z 323 and m/z 305 were observed, corresponding to the $[M+H - H_2O]^+$, $[M+NH_4 - 176]^+$, $[M+H - 176]^+$ and $[M+H - H_2O - 176]^+$ ions, respectively. The loss of 176 corresponds to the elimination of dehydroglucuronic acid and is characteristic of glucuronic acid conjugates analyzed by TSMS and FABMS (8,9).

CONCLUSIONS

TSMS has been shown to be a useful method for the analysis of CAP and several of its analogues including CAP-GLU. LC-MS analysis of CAP and 3 of its analogues has also been demonstrated. This methodology should be applicable for the analysis of CAP and its metabolites obtained from *biological* studies.

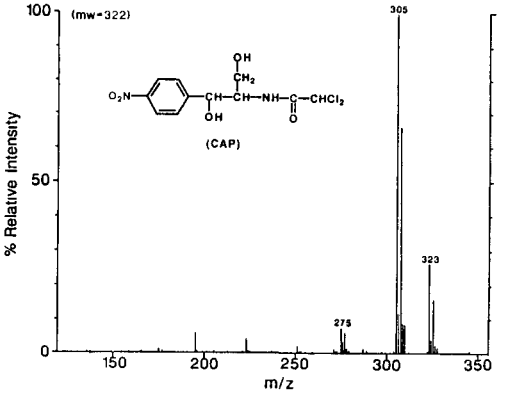

1. Thermospray mass spectrum of CAP.

ACKNOWLEDGEMENTS

One of us (TAG) was supported in part by an appointment to the ORAU Postgraduate Research Program at the National Center for Toxicological Research administered by the Oak Ridge Associated Universities through an interagency agreement between the US Department of Energy and the US Food and Drug Administration. We thank C. Hartwick for typing the manuscript.

REFERENCES

1. U. R. Tjaden, D. S. Stegehuis, B. J. E. A. M. Reeuwijk, H. Lingeman and J. van der Greef, Analyst 113, 171 (1988).
2. E. H. Allen, J. Assoc. Off. Anal. Chem. 68, 990 (1985).
3. D. J. Berry, J. Chromatogr. 385, 337 (1987).
4. S. Abou-Khalil, W. H. Abou-Khalil, A. N. Masoud and A. D. Yunis, J. Chromatogr. 417, 111 (1987).
5. C. R. Blakley and M. L. Vestal, Anal. Chem. 55, 750 (1983).
6. T. R. Covey, E. D. Lee, A. P. Bruins and J. D. Henion, Anal. Chem. 58, 1451A (1986).
7. J. R. Chapman, J. Chromatogr. 323, 153 (1985).
8. C. Fenselau, L. Yelle, M. Stogniew, J. Lehman, P. Teng and M. Colvin, Jr., Int. J. Mass Spectrom. Ion Phys. 46, 411 (1983).
9. W. A. Korfmacher, C. L. Holder, L. D. Betowski and R. K. Mitchum, J. Anal. Toxicol. 11, 182 (1987).

Presented at the 36th ASMS Conference on Mass Spectrometry and Allied Topics
June 5-10, 1988, San Francisco, CA

THERMOSPRAY (TSP) FRAGMENTATIONS OF AMIDINOUREAS AND LC/MS METHOD FOR QUANTIFICATION OF LIDAMIDINE AND ITS N-DESMETHYL METABOLITE

S.-Y. Tang, Rorer Central Research,
800 Business Center Drive, Horsham, PA 19044

Lidamidine, [1-(2,6-dimethylphenyl)-3-methyl amidinourea] hydrochloride (RG W-1142A), has been shown to have potent antimotility, antidiarrheal, and intestinal antisecretory activity in mice, rats, and dogs. It has been tested in man and has demonstrated efficacy as an antidiarrheal drug. Analysis of this drug and its metabolites in biological fluids cannot be obtained by GC/MS techniques because of its thermal lability. GC/MS through chemical derivatization also experienced great difficulty due to low recovery and the formation of secondary reaction products.

TSP is a soft ionization technique which produces predominantly pseudo molecular ions. In most applications fragmentations are minimal, however, for very delicate compounds, fragmentations do occur. Amidinoureas fall into the latter category of compounds which fragment even under pure thermospray ionization. To apply LC/MS as a qualitative and quantitative technique for the analysis of lidamidine and its metabolites, we have studied the thermospray fragmentations of some amidinoureas, lidamidine (RG W-1142A), N-desmethyl lidamidine (RG W-1049), and RG W-1094. Figure 1 shows their structures.

Using 0.1 M ammonium acetate as the buffered solution, amidinoureas gave $M \bullet NH_4^+$ ions at either pH 7 or pH 4, adjusted by either CH_3COOH or CF_3COOH. When an organic modifier (CH_3OH or CH_3CN) was used in the buffer, $M \bullet H^+$ ions started to form. With CH_3OH/0.1 M NH_4OAc (50/50, V/V) adjusted to pH 4.0 with CH_3COOH, lidamidine gives both $M \bullet H^+$ and $M \bullet NH_4^+$ ions. When the pH was adjusted to 4.0 with CF_3COOH, lidamidine forms predominantly the $M \bullet H^+$ ion (Figure 2). The bond cleavages of amidinoureas under thermospray ionization mainly occurred at C-N bond, with hydrogen transfer, and with the formed molecules containing a terminal $-NH_2$ group. Assignments of the TSP ions of the amidinoureas studied are listed in Table 1.

Since RG W-1142, -1049 (Figure 3), and -1094 give predominantly $M \bullet H^+$ ions when a mobile phase of 50/50 (v/v) CH_3OH/0.1 M NH_4OAc (pH adjusted to 4.0 by CF_3OOH) was used, a TSP LC/MS assay for lidamidine (RG W-1142) and its N-desmethylated metabolite (RG W-1049) in rat plasma was developed. The assay involves a solid phase extraction of plasma samples from a C-18 bond-elut column. RG W-1142, -1049, and 1094 (added as internal standard) were eluted from the column with 10% ethylacetate in methanol. Using a Supelco 15 cm x 4.6 mm, 5 μ, LC-8-DB column and the above mentioned mobile phase, the quantities of RG W-1142, -1049, -1094 were determined by selected-ion-monitoring (SIM) of their protonated molecular ions from the TSP mass spectra while they were eluted from the HPLC column.

Linear standard curves were obtained by spiking blank plasma (1 ml) with 100-600 ng of RG W-1142A, 10-100 ng of RG W-1049A, and 300 ng of the internal standard (RG W-1094A). Very good linear (r = 0.99) calibration curves were obtained for RG W-1142A (Figure 4) from 100 to 600 ng/ml and RG W-1049A (Figure 5) from 40 to 100 ng/ml. The results indicate that TSP LC/MS is a suitable quantitation technique for lidamidine in rat plasma.

Presented at the 36th ASMS Conference on Mass Spectrometry and Allied Topics
June 5-10, 1988, San Francisco, CA

Figure 1 - Structure of Amidinoureas

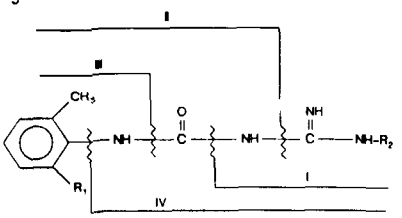

RG W-1142	R_1=CH_3	R_2=CH_3
RG W-1049	R_1=CH_3	R_2=H
RG W-1094	R_1=Cl	R_2=H

TABLE 1 - TSP IONS OF THE AMIDINOUREAS AND THE ASSIGNMENTS**

	RG W-1142A	RG W-1049A	RG W-1094A
MeH^+	221	207	227 *
$MeNH_4^+$	238	224	244 *
$IIMeNH_4^+$	182	182	202 *
$IIMeH^+$	165	165	185 *
$(IIH)_2eH^+$	329	329	369 *
$IIIMeH^+$	122	122	142 *
$IVMeH^+$	117	103	103 *
$(IH)^2eHCLeH^+$ 1-HCL	183 *	155 *	155 *
$(IH)_2eH^+$ 1-CF_3COOH	147	119	119
$(IH)_2eCF_3COOMeH^+$	261	233	233
$MeIMeH^+$	294	266	286 *
$XeCH_3OMeH^+$	132	118	118
XeH^+	100	86	86
$XeIMeCH_3OMeH^+$	205	177	177
$XeIMeH^+$	173	145	145
$IMeCH_3CMeH^+$	115	101	101

X ISOCYANATES
* : ONE-CHLORINE PATTERN
** : ROMAN NUMERALS REFER TO FIGURE 1

Figure 2 - TSP Mass Spectrum of RG W-1142A

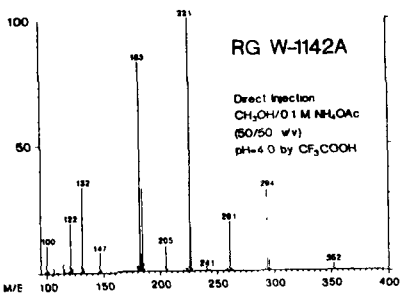

Figure 3 - TSP Mass Spectrum of RG W-1049A

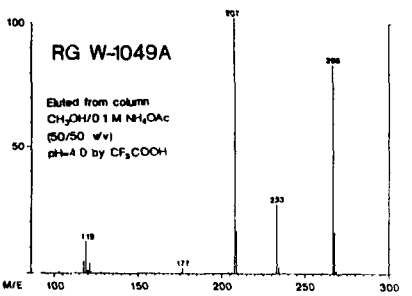

Figure 4 - Calibration Curve and Linear Regression Result

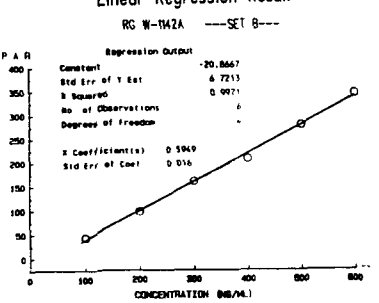

Figure 5 - Calibration Curve and Linear Regression Result

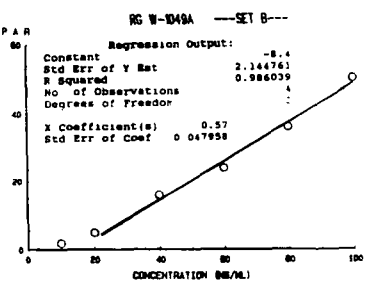

Presented at the 36th ASMS Conference on Mass Spectrometry and Allied Topics
June 5-10, 1988, San Francisco, CA

THE USE OF THERMOSPRAY LC/MS/MS FOR THE CLASS IDENTIFICATION AND STRUCTURAL VERIFICATION OF PHYTOESTROGENS IN SOY PROTEIN PREPARATIONS:

Robert J. Barbuch and John E. Coutant; Merrell Dow Research Institute, Cincinnati, OH 45215; K.D.R. Setchell and Mary Beth Welch; Children's Hospital Medical Center, Cincinnati, OH 45229

The ubiquitous occurrence in plants of compounds possessing estrogenic activity has led to extensive studies of their effects in animals following their ingestion. Deleterious effects upon reproduction have been reported for several animal species including sheep, California quail, rats and exotic cats and attention has recently focussed on the potential role of dietary estrogens in man.

Two main classes of phytoestrogens occur in plants, the isoflavones and coumestans and both groups are heterocyclic phenols having close structural similarity to the naturally occurring mammalian estrogenic steroids.

Suitable methods are therefore required for the detection of this class of compounds and a technique utilizing liquid chromatography with ultraviolet, electrochemical detection and thermospray ionization-mass spectrometry was recently developed (1). The latter procedure, however, yields mass spectra characterized by intense protonated molecular ions with no structural information. We therefore report on the use of a thermospray ionization LC/MS/MS technique for these compounds that affords greatly increased specificity and allows the screening for compounds bearing commonality in structure (see Figure 1). The method has been applied to the detection of phytoestrogens in a variety of diets and biological fluids.

The LC/MS/MS was run with a Vestec LC/MS interface on a Finnigan MAT TSQ-46. The separations were run on a Hypersil ODS (C_{18}) column with a mobile phase of 60/40 methanol/0.1 M ammonium acetate at 1.3 mL/min. Argon was used as the collision gas at an indicated cell pressure of 2 millitorr and a collision energy of -30eV.

The phytoestrogens have intense protonated molecular ions and their daughter ion spectra contain ions unique to the different structural characteristics of each phytoestrogen subclass and can be used both to confirm identification and propose structures for unknowns. In addition to unique ions, phytoestrogens also show a common neutral loss of 56 (due to consecutive losses of CO) that can be used as a class identifier to detect phytoestrogens.

A neutral loss of 18 amu is the subclass identifier for Daidzein, Genistein, and similar compounds. Formononetin, Biochanin A, and similar compounds show neutral losses of 15 and 32 amu. The subclass identifier for Coumestrol is a neutral loss of 44 amu.

In the Old Nebraska Feline Diet, Daidzein and Genistein were detected as well as an unknown phytoestrogen of the Biochanin A subclass. This unknown has been tentatively identified as 6,7-dihydroxy-4'-methoxyisoflavone using its daughter ion spectrum.

These results demonstrate the utility of thermospray LC/MS/MS for the class identification and structural assignments of phytoestrogens in diet preparations.

(1) K.D.R. Setchell and M.B. Welch, J. Chromtogr., 386 (1987) 315.

FIGURE 1

A. LC/MS CHROMATOGRAM OF PHYTOESTROGEN STANDARDS

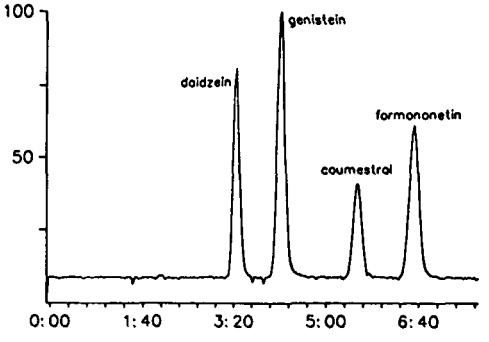

B. MS SPECTRUM OF DAIDZEIN

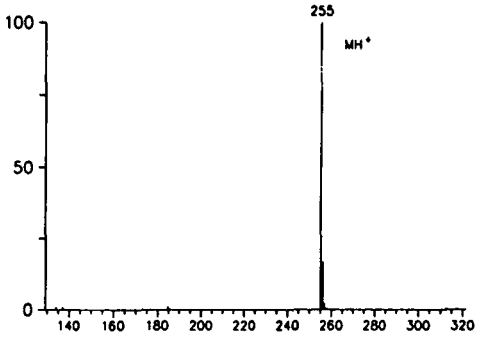

C. MS/MS SPECTRUM OF DAIDZEIN

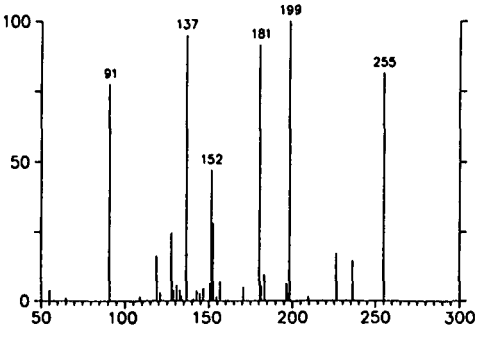

Presented at the 36th ASMS Conference on Mass Spectrometry and Allied Topics
June 5-10, 1988, San Francisco, CA

Thermospray LC/MS and GC/MS analysis of oxygenated metabolites of polyunsaturataed fatty acids

Hee-Yong Kim and Norman Salem Jr.
Laboratory of Clinical Studies, DICBR, NIAAA, ADAMHA, Bldg. 10, Room, 3C-218, 9000 Rockville Pike, Bethesda, MD 20892

Polyunsaturated fatty acids can be oxygenated by lipoxygenase to form hydroperoxy and, subsequently, hydroxy derivatives. It is often suggested that these compounds may possess significant biological activity. Analysis of such compounds produced in biological systems is sometimes quite difficult, since complex mixtures may be formed via several possible enzymatic and non-enzymatic pathways.

Reversed phase liquid chromatography in conjunction with on-line thermospray mass spectrometric and UV detection provides a simple and efficient method for qualitative analyses of eicosanoids or related compounds, since complex mixtures can be separated and analyzed simultaneously. In addition to the molecular weight, the number and type of functional groups can often be deduced from the simple fragmentation pattern found in the thermospray spectra of these oxygenated metabolites (1,2). However, GC/MS analysis after derivatization is usually necessary to confirm the position of oxygenation.

Thermospray LC/MS analysis of the hydroperoxy forms of these polyunsaturates indicates that information concerning the position of this functional group can be readily obtained from the spectra. Using ammonium acetate and methanol as carrier solvent, thermospray ionization resulted in cleavage of the C-C bond adjacent to the hydroperoxy group. Examples are depicted for 15- and 5-hydroperoxyeicosatetraenoic acids (HPETE) in figure 1. The peaks at m/z 336, 320, 319, 318, 303 and 301 represent the $MNH_4^+-H_2O$, $MNH_4^+-H_2O_2$, MH^+-H_2O, $MNH_4^+-2H_2O$, $MH^+-H_2O_2$ and MH^+-2H_2O, respectively. Besides these simple fragments which preserve the intact carbon backbone, additional fragments (F) were observed from the cleavage of $C_{15}-C_{16}$ and C_4-C_5 for 15- and 5-HPETE, respectively. These fragments also produced the cluster of ion peaks including $FNH_4^+-H_2O$, FH^+-H_2O, $FNH_4^+-H_2O$ and FH^+-2H_2O, although the relative intensities of each peak differ between isomers. In order to determine if this fragmentation generally occurs, hydroperoxy derivatives of docosahexaenoic acid (22:6w3) prepared by autooxidation were examined. These derivatives were separated by reversed phase chromatography using an Axxichrom ODS column (5u, 4.6mm x 25cm) and a linear gradient of 0.1M ammonium acetate : methanol ranging from 40:60 to 10:90 in 60 minutes with a flow rate of 0.8 ml/min. Each separated isomer was detected by UV, then analyzed by the thermospray mass spectrometer in a continuous manner. Spectral analysis of the ion chromatogram thus obtained (figure 2) showed that each isomer fragments essentially in the same fashion observed for HPETE's. They all exhibited the same peak clusters of MNH_4^+, MH^+, $MNH_4^+H_2O$, $MNH_4^+-H_2O_2$, MH^+-H_2O, $MNH_4^+-2H_2O$, $MH^=-H_2O_2$ and MH^+-2H_2O at m/z 378, 361, 360, 344, 343, 342, 327 and 325, respectively. However, the fragment ion peaks, $FNH_4^+-H_2O$, FH^+-H_2O, $FNH_4^+-2H_2O$ and FH^+-2H_2O were specific to the corresponding isomers. All of the ten possible isomers could be represented by FH^+-H_2O in this chromatogram except the 8-hydroperoxy derivative which was displayed using $FNH_4^+-H_2O$. From these observations, it is apparent that structure determination based on the fragmentation of the C-C bond adjacent to the hydroperoxy group is generally applicable to isomers of various chain lengths and numbers of double bonds. This procedure can eliminate the need for GC/MS analysis which requires lengthy purification and derivatization steps. This approach is particularly useful for analyzing lipoxygenase reaction mixtures where reductase activity is low or absent, such as in some *in vitro* incubations with pure enzyme preparations.

As an application, 22:6w3 was incubated with soybean lipoxygenase-1 *in vitro*. The spectrum of the primary product showed the peaks at m/z 378, 361, 360, 344, 343, 342, 327 and 325 which were expected for any hydroperoxy 22:6w3. From the fragment ion peaks at m/z 292, 275, 274 and 257 which correspond to $FNH_4^+-H_2O$, FH^+-H_2O, $FNH_4^+-2H_2O$ and FH^+-2H_2O, respectively, the structure was readily deduced to be 17-hydroperoxy 22:6w3.

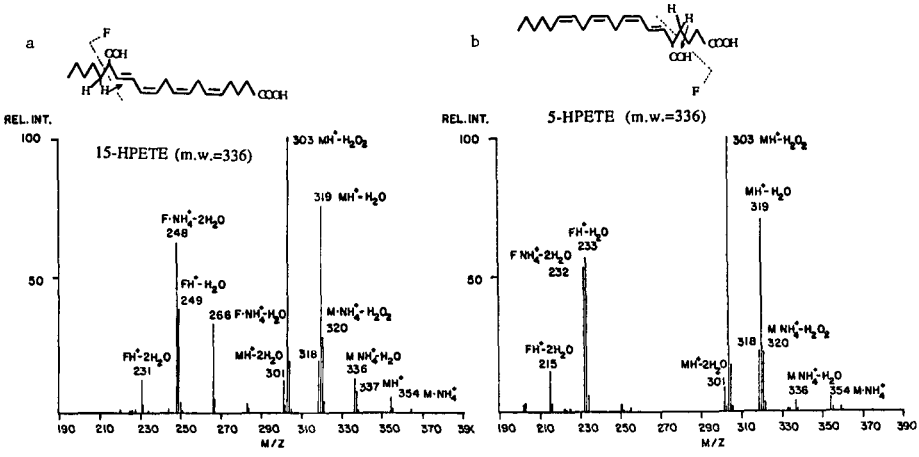

Figure 1. Thermospray mass spectra of 15- (a), and 5-HPETE (b) obtained by injecting lug each through a reversed phase column, as described for the autooxidized 22:6w3 in the text.

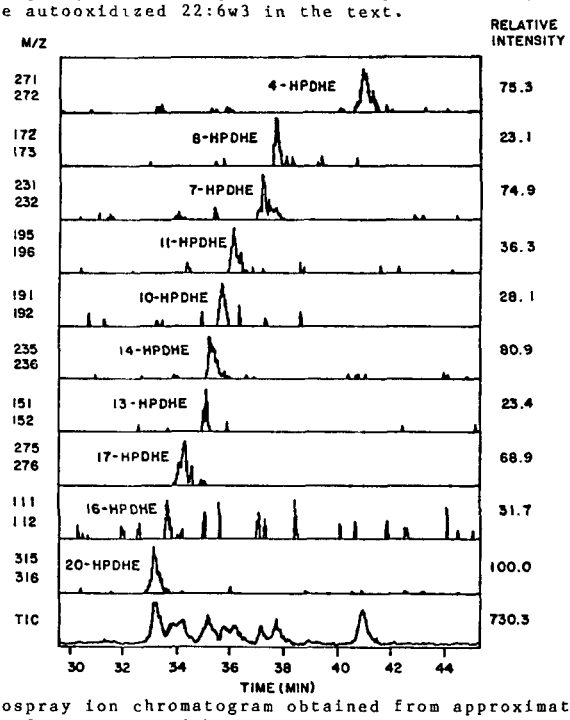

Figure 2. Thermospray ion chromatogram obtained from approximately 10ug total of autooxidized hydroperoxy 22:6w3.

1. J.A. Yergey, H.Y. Kim and N. Salem,Jr., Anal. Chem., 58, 1344-1348, 1987.
2. H.Y. Kim, J.A. Yergey and N. Salem,Jr., J.Chromatogr., 394, 155-170, 1987.

Presented at the 36th ASMS Conference on Mass Spectrometry and Allied Topics
June 5-10, 1988, San Francisco, CA

INVESTIGATION OF FLAVONE-8-ACETIC ACID METABOLITES BY THERMOSPRAY AND GAS CHROMATOGRAPHY MASS SPECTROMETRY

Jan R. Crowley, Robin J. Hood, Department of Chemistry and Guy Chabot, Division of Oncology, Wayne State University, Detroit ,Michigan 48202

Flavone-8-acetic acid (FAA;NSC-347512) is a new anticancer drug with broad solid tumor activity. In preclinical studies it was found to be active against a variety of transplantable solid tumors of mice. Among the tumors studied were some pancreatic ductal adenocarcinomas, colon adenocarcinoma mammary adenocarcinoma and ovarian tumors. It was found to be curative for colon adenocarcinoma #38. Studying the metabolism of a drug can often provide a clearer understanding of how the drug functions. Initial metabolism studies of FAA have been done with the urine of mice injected with the drug using both TSP/MS and GC/MS keeping two questions in mind. Can good TSP spectra be obtained with the drug and if so are there any advantages over GC/MS? And can one use GC/MS and/or TSP/MS to obtain information about the metabolism of the drug.

A Finnigan 4000 GC/MS system equipped with a Vestec Thermospray ionizer was used in the study. Optimum operating parameters for TSP/MS included a reverse phase isocratic solvent system H_2O:CH_3CN:HOAC (65:35:1), a 1.5 ml/min flow rate and a vaporizer temperature of 240-260 degrees. GC conditions included a 15M methyl silicone capillary column with splitless injection. Temperature programming was from 100-280 deg at 20 deg/min. The initial temperature was held at 100 deg for one min. The samples were all heated for 30 min. at 60 deg. with BSA to form a TMS derivative before GC/MS analysis.

Thermospray of FAA and hydroxylated FAA standards gave good spectra. The base peak is M+1 with little other fragmentation observed. An example of this is shown in FIG 1. GC data shown in FIG 2 provided more stuctural information and the M+ was always present. The sensitivity of GC/MS was about 30x greater than TSP/MS.

Ethyl acetate extracts of urine from BGD2F1 mice which had been injected with FAA (180 mg/kg,i.v.) were analyzed. Thermospray data provided supporting evidence, in addition to the H.P.L.C. retention times, that unmetabolized FAA and the glucuronide conjugate of FAA accounted for most of the injected FAA. dose, FIG 3. and FIG 4. Thermospray of the conjugate provided some structural information in addition to the molecular weight data.

Negative ion thermospray gave no additional structural information from that observed with positive ions. However, the molecular ion for the glucuronide was sometimes not observed with positive ions but was always seen with negative ions. If the NH4OAC was not in the solvent the ratio of M+1/fragment ions was improved although the overall sensitivity was down. The glucuronide was not volatile enough for GC analysis. While the FAA conjugate is not important for the function of the drug, if the FAA is metabolized to the antitumor agent this agent could very probably also be conjugated and therefore not found by GC/MS. Therefore TSP/MS will primarily be used for detection in future studies.

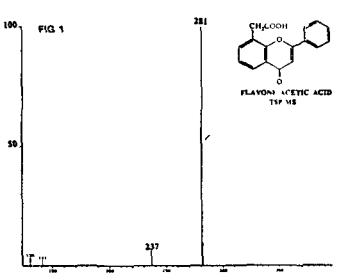

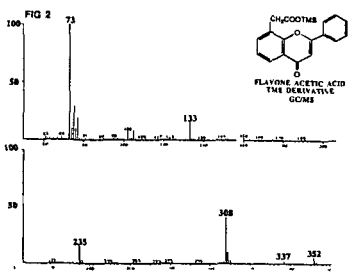

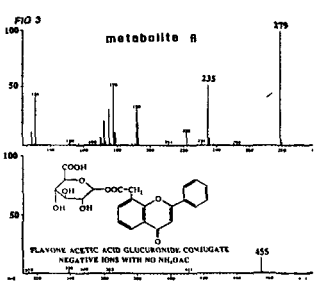

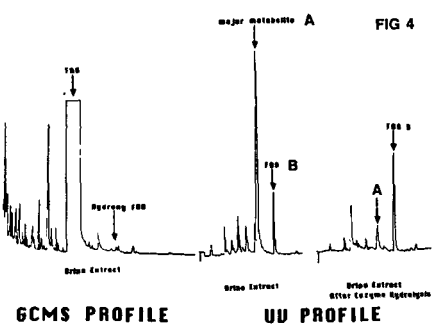

Presented at the 36th ASMS Conference on Mass Spectrometry and Allied Topics
June 5-10, 1988, San Francisco, CA

Analysis of Urinary Organic Acids by LC-MS and LC-MS/MS

G. Mills and V Walker, Dept of Chemical Pathology,
University of Southampton, Southampton General Hospital,
Southampton, UK

M.R. Clench*, R. Owen, V.C. Parr, O. Weir and D. Wood
VG Tritech Ltd, Crewe Road, Wythenshawe, Manchester, UK.

Introduction

Measurement of urinary organic acids can be useful in the diagnosis of a number of inherited metabolic disorders which may be present in infancy. Their usual method of analysis is by capillary gas chromagraphy with or without mass spectrometry after extraction and derivatisation. Recently HPLC using cation exchange columns and ultraviolet (UV) detection at 210nm has been proposed as a rapid alternative technique. To overcome the lack of specificity of ultraviolet detection we have investigated the potential value of combined plasmaspray HPLC-MS for profiling organic acids (1). A problem however was that the detection limits with the initial source design did not allow normal levels of acids to be seen.

We report here experiments with an ion source modified for improved sensitivity, and some preliminary MS/MS experiments.

Experimental

HPLC: Aminex HPX-87W cation exchange column (300 x 7.8mm)
25mmol/litre formic acid at 0.8ml/min 50°C ± 0.1

Mass Spectrometry: VG Tritech TS-250 mass spectrometer with plasmaspray interface
Accelerating Voltage: - 4000V
Resolution: 500 (10% valley)
Source Temperature: 250°C Vapour Temperature: 140°C
Plasma discharge voltage: 500V
CID : 4keV Energy

Results and Discussion

Analytical Results

Under the experimental conditions organic acids exhibit intense (M-H)- ions with little fragmentation. The minimum detection limit of the system in the single ion recording mode (SIR) was 10ng for hipperic acid (Fig 1). This contrasts to a detection limit of 400ng reported with the previous interface and source design (2). The new sensitivity levels allow normal levels of organic acids to be observed.

Daughter ion spectra of the acids (Fig 4 & 5) show characteristic loss of a CO_2 group (M-1-44)-. Multiple reaction monitoring of the transistion 178 -> 134 in hippuric acid gave a detection limit of 50ng. In further work it is hoped to demonstrate the diagnosis by loop only injection of organic aciduras by loop only injection making use of the increased specificity of MRM to eliminate the chromatographic step.

Clinical Results

Figures 2 and 3 show selected ion recording traces for m/z 117 and 115 for two patients diagnosed as suffering from methyl malonicaciduria and fumaric aciduria. The evelated levels of the two acids can be clearly seen.

1) G.A. Mills, V. Walker, M.R. Clench and V.C. Parr. Biomed and Environ Mass spectrom (In press 1988)

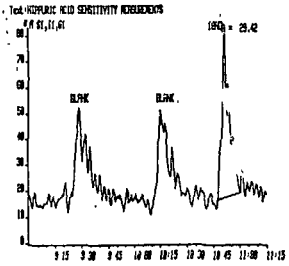

Figure 1.

Limit of Detection for Hippuric Acid = 10ng

Figure 2. SIR trace for m/z 117 from patient exhibiting methyl Malonic Aciduria

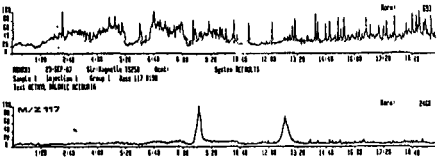

Figure 3. SIR trace for m/z 115 from patient exhibiting Fumaric Aciduria.

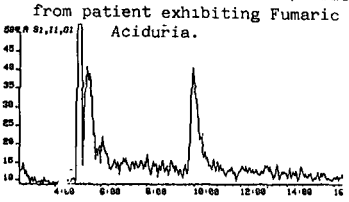

Figure 4. Unimolecular Daughters of 178 Hippuric Acid.

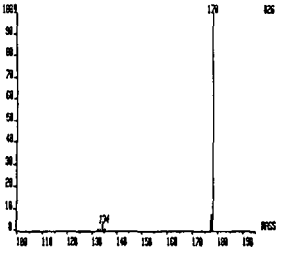

Figure 5. CID Daughters of 178 $4x10^{-7}$ mbar Pressure.

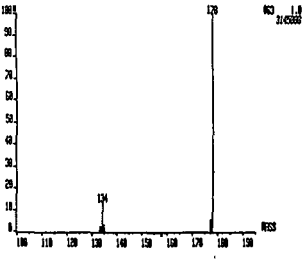

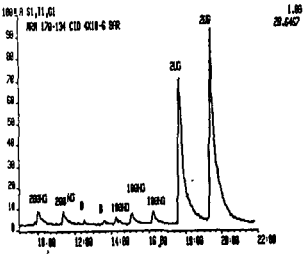

Figure 6. Limit of Detection for Hippuric Acid Monitoring Transistion 178-134 = 50ng.

Presented at the 36th ASMS Conference on Mass Spectrometry and Allied Topics
June 5-10, 1988, San Francisco, CA

Application of Thermospray Liquid Chromatography-Mass Spectrometry to the Analysis of Bile Acids

C. H. Vestal, and K. D. R. Setchell, Vestec Corporation, Houston, TX 77054, and Clinical M.S. Labs., Children's Hospital Res. Found., Cincinnati, OH 45229

Chromatographic techniques are widely used in clinical and clinical-research laboratories for the analysis of bile acids. Most frequently bile acids are analyzed by GC or GC-MS as derivatives of the unconjugated bile acids following isolation and hydrolysis of the conjugate moiety. Direct derivatization of the glycine conjugates without hydrolysis has been applied to serum analysis. Taurine conjugates have not been successfully analyzed by GC without prior hydrolysis. However, major strides have been made in the use of HPLC for bile acid analysis yet the main problems with the technique continue to be the relative lack of specificity and chromatographic resolution. Despite the use of pre- and post-column reactions and more selective detectors, interferences from the biological matrix and difficulties with peak identification remain the main problems to overcome. With the advent of thermospray LC-MS the HPLC eluent may be continuously monitored and mass spectrometer employed as a highly specific and sensitive detector.

A series of glycine and taurine conjugated bile acids were studied using a Vestec Model 201N Dedicated Thermospray LC-MS system. LC separation employed a Beckman Ultrasphere-ODS column (4.6mm x 25cm, 5 micron particle size) with deionized water/methanol (containing 0.1M ammonium acetate), pH = 5.7 (25/75 V/V) as the mobile phase. All of the compounds analyzed elute within 25 minutes at a flow rate of 1.0 mL/min. Figure 1 shows the total ion chromatogram of 8 conjugated bile acids 5 μg each of the standards was injected onto an ODS column while scanning m/z 400-550 in 5.5 seconds and using filament-on ionization. Glycochenodeoxycholic acid (GCDCA) and taurodeoxycholic acid (TDCA) coelute at 11 minutes. Apparently there is partial separation of these two compounds, even though they are not resolved in the TIC. Greater sensitivity is achieved in negative ion detection mode compared with positive ion which tends to give NH_4^+ adducts. The thermospray negative ion spectrum consisted of the base peak at $(M-H)^-$ with some fragmentation corresponding to consecutive losses of water. Typical examples are shown in Figure 2. The most important parameter for the analysis of conjugated bile acids is the thermospray vapor temperature. Increasing either the source temperature or the vaporizer temperature causes an increase in fragmentation, and at vapor temperatures above about 280°C the fragment ion is the base peak. The optimal thermospray conditions are the following: T_1(control temp.) = 126°C, T_2(vaporizer temp.) = 201°C, T_3(source block temp.) = 318°C, T_4(tip heater temp.) = 315°C, T_5(vapor temp.) = 265°C, and T_6(lens heater temp.) = 120°C.

Results for the standards obtained using the thermospray filament-on ionization and negative ion detection are summarized in Table I. The detection limits are in the range of 4 to 10 nanograms (10 to 25 picomoles) using selected ion monitoring (only monitoring the deprotonated molecular ions).

The bile acids and their conjugates from serum were extracted using commercially available reverse-phase octadecylsilane bonded silica cartriges (1). The bile acid concentrations of bile or duodenal aspirate (mmole/L) are much higher than those of serum (μmole/L). Extracts of human bile (patients B1 and B2), pig bile, and serum (patients S1 and S2) were analyzed using thermospray LC-MS. Figure 3 shows the TIC of (a) human bile (patient B1) and (b) pig bile compared with that of the standards under the full scan conditions. Results on the serum extracts using selected ion monitoring are shown in Figure 4 and summarized in Table II. Applications to the analysis of bile acids in biological samples presented in this paper serve to highlight the potential of thermospray LC-MS interface for enhancing the specificity of the HPLC technique.

(1) K.D.R. Setchell and J. Worthington, Clinica Chemica Asta, 125 (1982), 135-144.

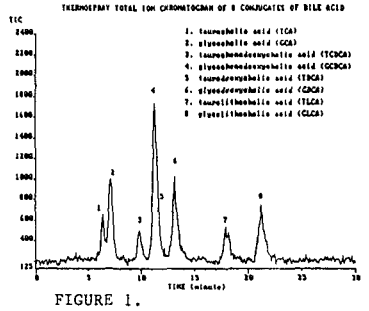

FIGURE 1.

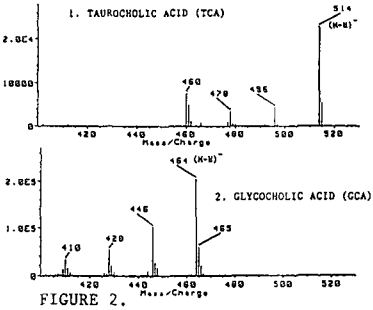

FIGURE 2.

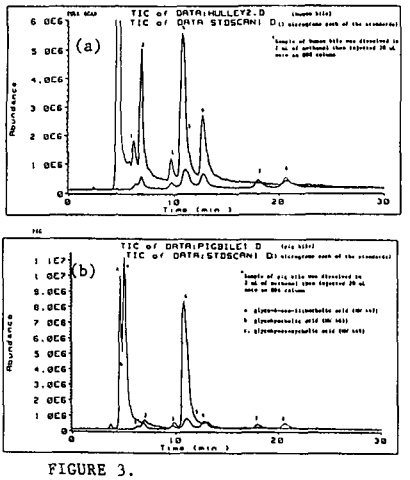

FIGURE 3.

TABLE II. SUMMARY TABLE FOR SERUM EXTRACTS

COMPOUND	AMOUNT FOUND IN (micromoles/L)	
	PATIENT S1	PATIENT S2
TCA	2.76	2.44
GCA	8.21	36.70
TCDCA	1.03	1.06
GCDCA	6.23	9.80
GDCA	0.37	----

PATIENT S1

SERUM EXTRACT #1
THE CONCENTRATION IS 10 micromole/L, AND 0.5 mL OF SERUM WAS EXTRACTED. THE SAMPLE WAS DISSOLVED IN 100 uL OF METHANOL AND 10 uL WAS INJECTED ONTO AN ODS COLUMN.

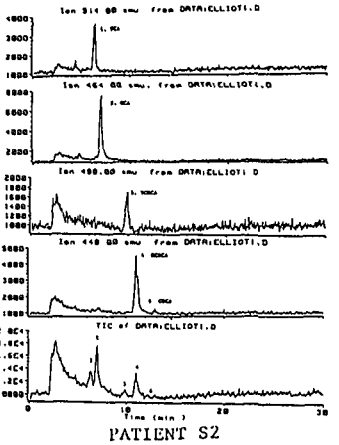

PATIENT S2

SERUM EXTRACT #2
THE CONCENTRATION IS 50 micromole/L, AND 1.0 mL OF SERUM WAS EXTRACTED. THE SAMPLE WAS DISSOLVED IN 100 uL OF METHANOL AND 10 uL WAS INJECTED ONTO AN ODS COLUMN.

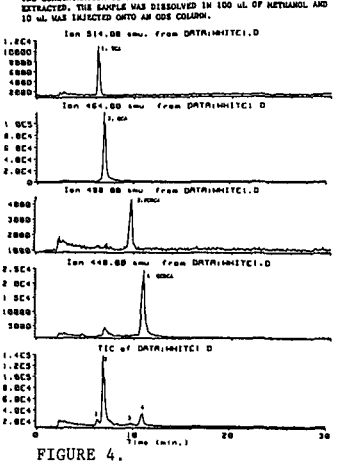

FIGURE 4.

TABLE I.

COMPOUND	M.W.	RETENTION TIME (min.)	*DETECTION LIMITS (ng)
1 Taurocholic Acid (TCA)	515	6.352	4.6
2. Glycocholic Acid (GCA)	465	7.001	6.0
3. Taurochenodeoxycholic Acid (TCDCA)	499	9.816	5.3
4. Glycochenodeoxycholic Acid (GCDCA)	449	11.257	10.0
5. Taurodeoxycholic Acid (TDCA)	499	11.416	6.0
6. Glycodeoxycholic Acid (GDCA)	449	12.856	6.3
7. Taurolithocholic Acid (TLCA)	483	18.151	8.2
8. Glycolithocholic Acid (GLCA)	433	20.808	10.0

*Signal-to-noise ratio was calculated from manually measured peak heights, and the detection limits were estimated by employing the signal-to-noise ratio on the order of 3:1.

Presented at the 36th ASMS Conference on Mass Spectrometry and Allied Topics
June 5-10, 1988, San Francisco, CA

THERMOSPRAY LC/MS STUDIES WITH INOSITOL PHOSPHATES

Fong-Fu Hsu, H. Duane Goldman and William R. Sherman

**Washington University School of Medicine, Department of Psychiatry,
St. Louis, MO, 63110.**

D-myo-Inositol-1,4,5-trisphosphate (IP_3)is an intracellular "second messenger" that is produced from phosphatidylinositol-4,5-bisphosphate following receptor stimulation. The production of this trisphosphate is one of the early steps in a series of metabolic events that lead to the functional result called for by the stimulation. Thus the appearance of the trisphosphate is evidence for the participation of specific receptor-linked events, information that is often difficult to obtain by other means. Recent advances in this area have revealed the presence of a large number of metabolites of IP_3 including mono-through pentakis-inositols as well as isomers of many. Even hexakis-inositol phosphate (phytic acid), previously thought to be only a plant product, has been found as a metabolite in mammalian cells.

The analysis of IP_3 most often used is radiometric, following experiments in which the establishment of labeling equilibrium is usually an uncertainty. Information about minor components is often lost because of the necessity for incremental collection of eluates. Because of the increasing involatility and adsorption losses of inositol phosphates, as the number of PO_4 moieties increase, gas-phase methods have thus far been unusable for biologically-relevant amounts of material (low picomolar amounts per analysis) except in the case of the inositol monophosphates which can be analyzed readily by GC/MS (1). Thus there is a need for a sensitive mass-based and general analytical method that has not yet been met.

When we examined the (+)ive ion thermospray LC/MS of inositol mono- to hexakis-phosphates, using ammonium formate as the eluting buffer, in no case did we find surviving phosphorylated inositols; only the total hydrolysis product is seen as the ion m/z 198, i.e., $[NH_4 \cdot Inositol]^+$. This was the case even with inositol hexaphosphate where all phosphates were removed and no trace of the parent species was seen. Hoping to find that we were only seeing trace amounts of hydrolysis products because the phosphates did not form (+)ive ions we looked to the (-)ive ion spectra and found there only ($[Inositol \cdot HCOOH\text{-}H]^-$) with smaller amounts of $[Inositol\text{-}H]^-$, again, all of the phosphates were removed in every case examined. As a result information regarding the phosphate content of each species is lost and is revealed only by elution order necessitating the establishment of that elution order by other means.

Since it appeared that the loss of phosphate was by hydrolysis as the sample passed through the heated thermospray tip (at a temperature that was determined by the thermospray process) we decided to maximize the hydrolysis by using a heated length of stainless steel or nickel capillary tubing as a reactor prior to thermospray analysis. A cooling section following the reactor was necessary in order to retain thermospray tip temperature regulation by the control thermocouple. By this means the sensitivity was increased over ten-fold (Figure 1), the minimum amount detectable with loop injection being about 50 pmole (s/n 4:1), decreasing, due to adsorptive losses, as the number of phosphate moieties increase.

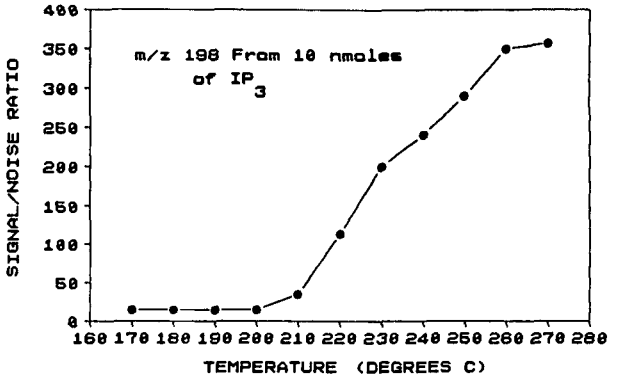

Figure 1

Thermospray ionization is strongly affected by the eluting buffer, and the inositol phosphate separations are brought about by ionic strength gradients. An improvement in the method, which eliminates the effects of the gradient on the thermospray ionization process, is to run a counter-gradient which is mixed with the column effluent to normalize the salt content, thus simplifying the establishment of optimum thermospray ionization conditions. This can be achieved either by using a separate set of gradient-forming HPLC pumps or by using two low-pressure gradient makers each supplying an HPLC pump.

We have also explored the effects of acetylation of inositol phosphates on separations by gradient-elution ion exchange chromatography and the effects of that derivatization on thermospray ionization. The (+)ive ion spectra obtained showed that both thermospray-induced phosphate hydrolysis and acetate hydrolysis took place. Use of the thermal reactor increased the analytical sensitivity of the acetates as it did with the underivatized inositol phosphates. Molecular ions were of low intensity and, surprisingly, the first losses from either MH^+ or $[M{\cdot}NH_4]^+$ is phosphate, not acetate. This is followed by acetate loss (- 42 U, it is not known whether by fragmentation or hydrolysis). No ions corresponding to hydrolytic loss of acetate from either of the parent ions are observed. Because there are high-mass ions that do not lose acetate, information is retained about the degree of phosphorylation of the species eluting from the chromatographic process. Thus an inositol trisphosphate and a tetrakisphosphate will show high mass ions of the triacetate-triol and the diacetate-tetraol respectively. While the total ion current is distributed between a number of ions, the sensitivity, using ion monitoring and a structurally-specific ion, is similar to that obtained with underivatized inositol phosphates. In (-)ive ions the highest mass ion seen, in the case of the acetylated trisphosphate, is the diol-monophosphate, but it is of weaker intensity than the completely dephosphorylated species. This work was supported by NIH grants NS 05159, AM 20579 and RR 00954 as well as a grant from Perstorp Pharma, Perstorp, Sweden.

1. W.R Sherman, K.E. Ackermann, R.A. Berger, B.G. Gish and M. Zinbo, Biomed. Enviorn. Mass Spectrom. 13, 333-341 (1986).

Presented at the 36th ASMS Conference on Mass Spectrometry and Allied Topics
June 5-10, 1988, San Francisco, CA

DEVELOPMENT OF A QUANTITATIVE LCMS ASSAY FOR THE DETERMINATION OF GR 43175 BASE IN PLASMA.

J. Oxford and M.S. Lant.

Department of Biochemical Pharmacology,
Glaxo Group Research Limited, Ware, Hertfordshire, U.K.

INTRODUCTION

GR 43175C is a '5HT$_1$-like' receptor agonist effective in the treatment of migraine (1). During early development of the drug an analytical method was required for the analysis of human plasma samples. The assay requirements were that it should be developed rapidly, have an accuracy and precision of approximately 10% or better and a limit of quantification of 5ng/ml. Thermospray LCMS (TSP LCMS) was selected because it offered the advantages of specificity i.e. minimal sample 'clean-up' would be required and robustness, in that it can be connected on-line to an Advanced Automated Sample Processor (AASP) (2).

METHODS

Compounds: GR 43175C, GR 40370B and [$^2H_3$]GR 43175 base (Figure 1) were supplied by the Chemistry Division, Glaxo Group Research Limited, Ware, Hertfordshire, U.K.

Isolation: 1ml portions of centrifuged plasma samples or standards containing GR 43175 base and either 24ng GR 40370B or 50ng [$^2H_3$]GR 43175 base were applied to conditioned C_2 AASP cartridges. The cartridges were eluted on a Vac-Elut box then washed with 1.8ml water and 1.8ml water : methanol (7 : 3) prior to loading onto the AASP module (Varian) which was connected via a column to the TSP interface (Vestec).

Instrumentation: A 3µm Spherisorb ODS2 column (5cm x 4.6mm i.d.) protected by a Waters C_{18} guard column was eluted with methanol : 0.1M ammonium acetate (60 :40) at a flow rate of 1ml/min. The HPLC pump was an HP 1090. The mass spectrometer (HP 5987A) was operated at a source temperature of 250°C in the positive ion (filament off) mode. The protonated molecular ions m/z 296, 299 and 310 derived from GR 43175 base, [$^2H_3$]GR 43175 base and GR 40370 base respectively were monitored. Data were acquired and processed using the standard HP 1000 software.

RESULTS AND DISCUSSION

The combination of the AASP with TSP LCMS gave the advantage of analysing 100% of a 1ml plasma extract. Although the isolation method was precise (93.9% ± 1.3%, n = 4) an internal standard was needed to compensate for TSP variability. The assay precision using a homologue, GR 40370 base which was partially resolved from GR 43175 base, was too variable, however [$^2H_3$]GR 43175 base gave superior results. Figure 2 shows typical SIR chromatograms obtained from the analysis of plasma standards.

The working range of the assay was 2 - 50ng/ml. The assay was limited to 2ng/ml because a component from the AASP cartridge eluting slowly from the analytical column had an adverse effect on the accuracy and precision of the measurement of lower concentrations. Over the range 5 - 50ng/ml the intra-assay variability was <5%, at 2ng/ml it was 11% (n = 6). Similar results were achieved for the inter-assay variability. In contrast, with GR 40370 base as internal standard, the intra-assay variability was higher (up to 26% at 22ng/ml). The assay has been used for the analysis of human plasma samples following administration of GR 43175C.

Presented at the 36th ASMS Conference on Mass Spectrometry and Allied Topics
June 5-10, 1988, San Francisco, CA

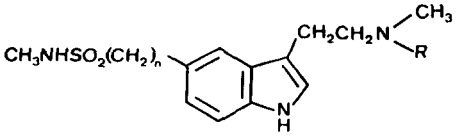

1. GR 43175C n = 1, R = CH_3 monosuccinate.
2. GR 40370B n = 2, R = CH_3 hydrochloride.
3. [$^2H_3$]GR 43175 n = 1, R = C^2H_3 (<0.1% unlabelled GR 43175).

Figure 1. Chemical Structures.

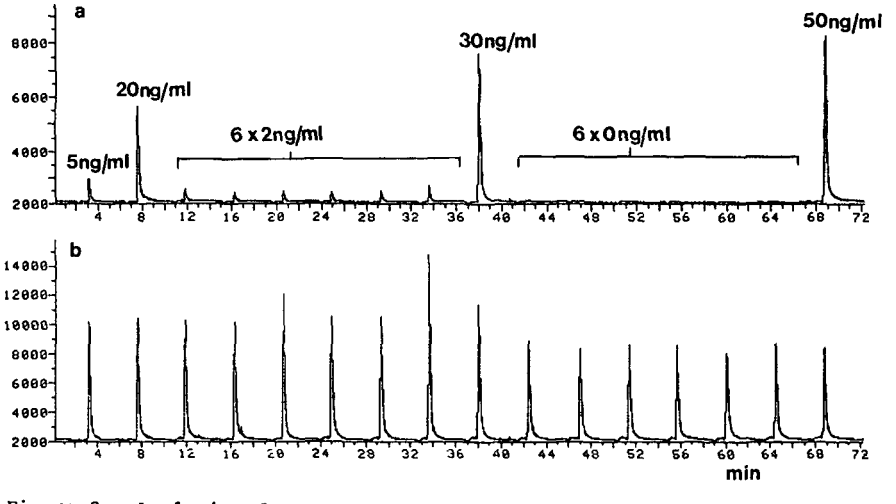

Figure 2. Analysis of 16 prepared AASP cartridges (a) m/z 296-GR 43175 base, (b) m/z 299-50ng, internal standard, [$^2H_3$]GR 43175 base/ml plasma.

CONCLUSIONS

A reliable, accurate and precise LCMS assay was developed for the analysis of GR 43175 base in plasma, meeting specified criteria. Since selective and specific AASP-TSP LCMS assays can be developed relatively quickly, this technique is used in our laboratory to provide an important preliminary assay for drug absorption studies prior to longer term development of a cheaper assay for routine analyses.

Acknowledgement
We thank Mr. I. Fellows, Chemistry Division, Glaxo Group Research Limited for synthesizing [$^2H_3$]GR 43175 base.

References

1. A. Doenicke, J. Brand and V.L. Perrin. Lancet 1988 in press.
2. M.S. Lant, J. Oxford and L.E. Martin. J. Chromatogr. 394,223 (1987).

Presented at the 36th ASMS Conference on Mass Spectrometry and Allied Topics
June 5-10, 1988, San Francisco, CA

pH-related changes in relative ion intensities of fragments of LY170680;

*Breau, A., P. and Goodwin, R. M., Lilly Research Laboratories, Eli Lilly and Company, Indianapolis, IN 46285.

OBJECTIVE: The principal objective of this study has been to evaluate the thermospray LC/MS technique for the detection of LY170680, a leukotriene antagonist in plasma. Since the acid group and tetrazole moiety of the molecule can be ionized in solution it was postulated that pre-formed ions could be generated more easily at low pH, thus enhancing the thermospray ionization efficiency and increasing the sensitivity of the assay. In fact, altering mobile phase pH did not dramatically increase the total ionization of LY170680, but pH dependent relative fragment intensity differences were observed. Previous thermospray studies have noted that source temperature, tip temperature and mobile phase composition influence LC/MS thermospray fragmentation patterns. In this study, ion source temperature, tip temperature and mobile phase composition were held constant and the mobile phase pH altered.

MATERIALS AND METHODS: Investigations of the pH effect were performed using a direct loop mode in order to perform the comparative analyses without having to re-equilibrate the column. This allowed rapid analysis, minimizing any changes in instrument parameters that could influence the fragmentation patterns. Loop injections of 2 ug were made in 20 ul . Mobile phase (60% methanol/ 40% water) was pumped through the Vestec Thermospray interface at 1 ml/minute into a Finnigan 4500 mass spectrometer. The chromatography was monitored in-line with an absorbance detector set at 237nm. The interface was operated in the "discharge on" mode with a tip temperature of 208 C and a source block temperature of 300 C. The mass range was 200-500 amu at 2 seconds/scan. The electron multiplier setting was 1350 v in negative ion detection. The pH of the aqueous component of the mobile phase was varied using acetic acid(pH 4.0) or ammonium hydroxide (pH 8.0 and 10.0).

RESULTS: Mass spectrometric analysis of LY170680 using thermospay "discharge on" ionization did not reveal a prominent molecular ion, but two prominent fragments occured at m/z=366 and m/z=350 in negative ion detection. Using a mobile phase at pH 4.0 the major fragment observed was at m/z=366 with a minor fragment at m/z=350. With a pH 8.0 mobile phase a much more intense ion at m/z=350 was observed. At pH 10.0 the major fragment was at m/z=350.

DISCUSSION: Both the acid and tetrazole moieties of LY170680 (Figure 1) have pka's of approximately 4.5. The negative ion fragment at m/z=366 is due to the loss of S-(CH2)2-COOH (figure 2). A plausible mechanism for the formation of this fragment is through attack of the S by the oxygen through a 5-membered ring mechanism (figure 3). The fragment at m/z=350 occurs through the loss of an additional OH group from the fragment at m/z=366 (figure 4) with proton transfer. Since the acid moiety is protonated at pH 4.0 the ionic state of the acid group may affect the 5-membered cyclic rearrangement mechanism and force an alternative mode of fragmentation leading to the formation of the m/z=350 ion.

CONCLUSIONS: LY170680 is structurally similar to such biologically important molecules as leukotrienes and prostaglandins. In the future, it is likely that thermospray LC/MS will be used for the detection of these types of compounds from biological fluids. Thus in some cases it will be necessary to monitor the pH of plasma extracts in order to assure accuracy in quantitation using LC/MS thermospray ionization especially in conjunction with single ion monitoring detection.(The authors thank Mr. John Occolowitz, Dr. William J. Wheeler and Prof. Klaus Biemann for their helpful discussions.)

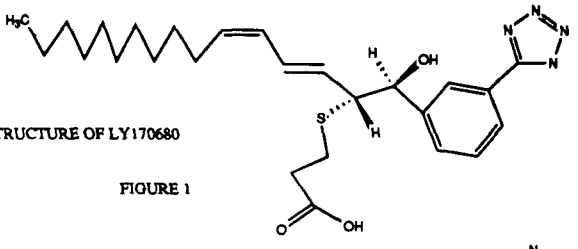

STRUCTURE OF LY170680

FIGURE 1

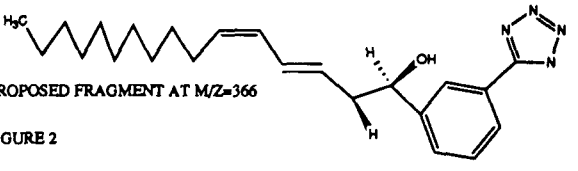

PROPOSED FRAGMENT AT M/Z=366

FIGURE 2

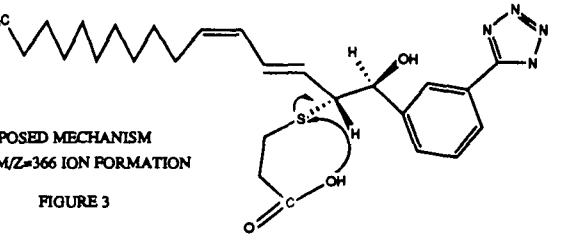

PROPOSED MECHANISM
FOR M/Z=366 ION FORMATION

FIGURE 3

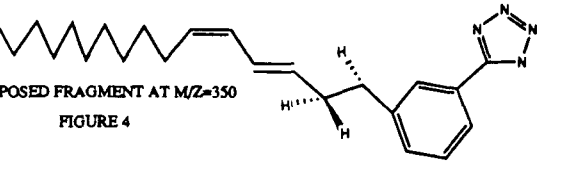

PROPOSED FRAGMENT AT M/Z=350

FIGURE 4

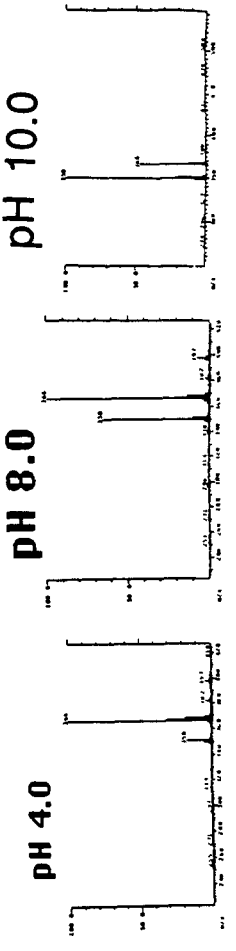

Presented at the 36th ASMS Conference on Mass Spectrometry and Allied Topics
June 5-10, 1988, San Francisco, CA

DEVELOPING ANALYTICAL METHODS FOR DETERMINATION AND CONFIRMATION OF β-LACTAM ANTIBIOTICS IN MILK AND TISSUE USING HPLC/UV AND HPLC/MS.

Robert D. Voyksner and James Raymer, Analytical and Chemical Sciences, Research Triangle Park, NC 27709; Krystyna Tyczkowska, School of Veterinary Medicine, North Carolina State University, 4700 Hillsborough Street, Raleigh, NC 27666.

Maintaining a record for human food safety requires constant efforts in developing and improving analytical methods for animal drug residues in milk or tissue. β-Lactam antibiotics are one class of drugs commonly used in animals destined for human consumption. β-Lactams antibiotics are very polar, non-volatile, and thermally unstable compounds which have few chromophores, preventing sensitive detection. Current research focuses on developing new analytical strategies for the extraction, determination, and confirmation of five β-lactam antibiotics (ampicillin, amoxicillin, hetacillin, cloxacillin, and penicillin G) in tissue and milk by HPLC/UV and thermospray HPLC/MS.

The extraction of the β-lactam antibiotics from a matrix such as milk was performed in one step using a micro separation system. A 0.5 mL milk sample and 0.5 mL of a protein-binding releasing solvent (i.e., acetonitrile:methanol:water 20:40:40) were sonicated then centrifuged through a 10,000 molecular weight cut-off filter. The filtrate can be concentrated or directly analyzed by HPLC/UV or HPLC/MS. The extraction method results in sample recoveries from 68% to 82% for the five β-lactam antibiotics.

HPLC/UV methods were developed for the determination of the five β-lactam antibiotics in milk matrices. The HPLC conditions employed a Brownlee Phenyl-Spheri-5 2.1 mm x 22 cm column using an isocratic mobile phase containing acetonitrile, ion pair reagents S-8 and S-12 and water, (percentages of each solvent were dependent on the particular β-lactam antibiotics analyzed) at a flow of 0.2-0.4 mL/min. The retention time for the target β-lactam antibiotics ranged from 6-13 min. The various β-lactam antibiotics were detected by UV absorbance at 215-225 nm. The HPLC/UV method was very sensitive (detection limit 10-50 ppb) and capable of quantitating each β-lactam antibiotic in milk.

Thermospray HPLC/MS was very specific and sensitive for the detection and confirmation of the β-lactam antibiotics in food matrices. The thermospray spectra of the β-lactam antibiotics exhibited $[M+H]^+$, $[M+NH_4]^+$ and $[M+Na]^+$ ions along with several fragment ions (Table I). The fragment ions detected were postulated to be thermal degradation products. One represented a loss of 26 from the molecular ion due to ring opening followed by hydration and loss of CO_2. The others were from ring opening and cleavage resulting in a common ion for all β-lactam antibiotics at m/z 160 and a specific ion related to the R group of each β-lactam antibiotics. The analysis of hetacillin was also complicated by its conversion to ampicillin in solution (in less than 4 hours).

Thermospray HPLC/MS proved useful for confirming the HPLC/UV assay as well as for quantitation of β-lactam antibiotics in milk. For example, the detection of penicillin G by monitoring the $[M+H]^+$ ion (m/z 335) and $[M+H+H_2O-CO_2]^+$ ion (m/z 309) enabled detection of 10 ng of the β-lactam antibiotic and could be used to generate a linear calibration curve (correlation coefficient 0.9982) from 10-1000 ng. The detection of penicillin G in dosed bovine milk samples showed minimal interference from the milk matrix. The HPLC/MS chromatograms showed a peak at the proper retention time as well as the simultaneous maximization of the ions at m/z 309 and m/z 335 confirming the presence of penicillin G in milk. The comparison of the measured quantity for penicillin G in milk by HPLC/UV and HPLC/MS (Table II) indicates agreement between the two different methods. The mean difference in measured values between HPLC/MS and HPLC/UV was 32%, with the highest errors observed at the lower concentrations. HPLC/UV and HPLC/MS was also useful in showing the difference in the excretion rates of penicillin G in bovine milk. Clearly, penicillin G residue was found in milk 48 hours after bovine dosing at the ppm or high ppb level.

ACKNOWLEDGEMENTS

This research was supported by the Health and Human Services of the Food and Drug Administration under cooperative agreement No. FD-U-000244-01.

Presented at the 36th ASMS Conference on Mass Spectrometry and Allied Topics
June 5-10, 1988, San Francisco, CA

TABLE I

CHARACTERISTIC THERMOSPRAY HPLC/MS ION FOR VARIOUS β-LACTAMS

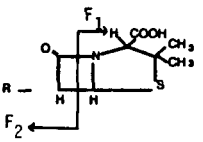

R'		$[F1+H]^+$	$[F2+H]^+$	$[M+H+H_2O-CO_2]^+$	$[M+H]^+$
Ampicillin	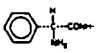	160	191	324	350
Amoxicillin	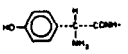	160	207	340	366
Hetacillin(1)	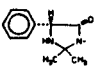	160	246	362	388
			191	324	350
Cloxacillin	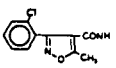	160	277	410	436
Penicillin G		160	176	309	335

(1)Hetacillin converts to Ampicillin.

Table II. COMPARISON OF HPLC/UV AND HPLC/MS MEASURED VALUE OF PENICILLIN G IN MILK.

Sample	LC/UV (ppm)	LC/MS (ppm)
24 hours after 1st dose	0.6	0.3
36 hours after 1st dose, 12 hrs. after 2nd dose	10.4	12.3
12 hours after 1st dose	12.0	14.8
24 hours after 1st dose	0.7	0.4
36 hours after 1st dose, 12 hrs. after 2nd dose	10.0	12.5

Presented at the 36th ASMS Conference on Mass Spectrometry and Allied Topics
June 5-10, 1988, San Francisco, CA

MASS SPECTROMETRIC STUDIES OF NEUROMUSCULAR BLOCKING AGENTS USING CI AND FAB/MS

Timothy R. Baker and Paul Vouros
Northeastern University and Barnett Institute, Boston, MA 02115

J. A. J. Martyn
Harvard Medical School and Massachusetts General Hospital, Boston, MA 02114

Since the introduction in 1942 of curare as an anesthetic, there has been great interest in the chemistry, pharmacology, and clinical uses of a class of compounds known as neuromuscular blocking agents. Among them is Pancuronium, which is a member of a series of bis-quaternary ammonium steroids. Previously reported assays for Pancuronium involved the use of fluorescence, TLC, and direct probe mass spectrometry. There are drawbacks in each one of these methods in terms of specificity and sensitivity.

PANCURONIUM BROMIDE

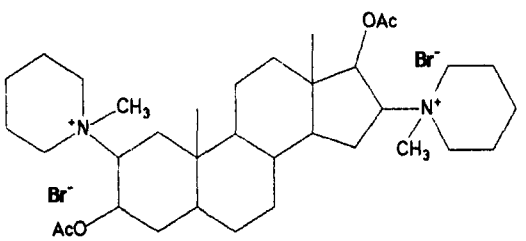

The purpose of this work is the development of mass spectrometric procedures for the analysis of these bromide salts, based on HPLC coupled to

MS. Of particular interest is the differentiation of the drug Pancuronium from a suspected metabolite, the mono-quaternary analog Vecuronium. As these two compounds are thought to be hydrolysed *in vivo*, analysis of the deacetylated analogs was also a focus of this work. Spectra of the compounds were acquired via the moving belt LC/MS interface in the CI and FAB/MS mode.

In the CI analysis the analytes undergo thermal demethylation upon flash vaporization from the moving belt surface. Spectral patterns can be interpreted on the basis of fragmentation derived from protonated demethylation products. Pancuronium and Vecuronium have identical thermal demethylation products resulting in indistinguishable CI spectra. The sensitivity of this technique has been demonstrated by the detection of three nanograms of Pancuronium with single ion monitoring.

Spectra can be obtained by Fast Atom Bombardment of xenon gas applied directly to the moving belt surface. In all cases fragmentation is initiated by loss of bromide followed by a series of eliminations of piperidine, water, and acetyl groups, in various combinations. An obvious advantage of the FAB technique for analysis of these compounds is the ability to differentiate Pancuronium from Vecuronium. The matrix free environment provided by the moving belt has advantages over the more traditional FAB experiment, in terms of spectral purity.

A normal phase HPLC separation on silica has been developed for Pancuronium and Vecuronium. The adsorption of these charged compounds onto any available metal site necessitated the use of non-metallic tubing and a glass column for this LC/CI-MS assay. The spray device, previously reported by us, for deposition of eluent on the moving belt was modified to incorporate a fused silica insert.The possibility for capillary LC coupled to flowing FAB-MS has also been demonstrated.

The work described here illustrates the applicability of the moving belt introduction system for the mass spectrometric analysis of Pancuronium, Vecuronium, and their deacetylated analogs. Identification of these drugs and their suspected metabolites is possible with CI or FAB/MS.

Presented at the 36th ASMS Conference on Mass Spectrometry and Allied Topics
June 5-10, 1988, San Francisco, CA

THERMOSPRAY MS OF MUSTARD GAS AND SELECTED METABOLITES.

E.M. Jakubowski and S. Munavalli
U.S. Army Medical Research Institute of Chemical Defense,
Aberdeen Proving Ground, MD 21010-5425.

Analysis of bis(2-chloroethyl) sulfide, commonly known as mustard gas, has always been difficult due to the reactive nature of the molecule. The ability to analyze for the presence of both mustard gas (actually a liquid, boiling pt 217°C) and its metabolites or degradation products can be of considerable help in their detection and identification as well as in understanding the mechanism of their biological activity. Gas chromatography has been the method of choice for quantification of mustard while mass spectrometry being used for confirmation.[1] The object of this paper was to illustrate the unique capabilities of thermospray LC-MS in the analysis of the warfare agent mustard and its metabolites. Six oxidation and hydrolysis metabolites of mustard have been studied. The mustard was provided by the U.S. Army Medical Research Institute of Chemical Defense in methanol with a concentration of 0.005M. Mustard sulfone, mustard sulfoxide, half mustard, thiodiglycol sulfone, and thiodiglycol sulfoxide were synthesized using known methods from either mustard or thiodiglycol, and their identity and purity were confirmed by GC/MS and NMR. Thiodiglycol was procured from Aldrich Chemical Company, Inc. All analytes were first dissolved in anhydrous methanol and directly injected into the thermospray source using the discharge mode. Characteristic positive and negative ion mass spectra were recorded for all of the compounds listed above except for the negative ion spectrum of mustard due to a low concentration of available mustard solutions. Analytes other than mustard were analyzed at a concentration of 0.01M in methanol. Methanol was glass distilled from EM Science and filtered through a 0.45 micrometer membrane (Millipore, Inc) before being used for TSP LC/MS.

All studies were accomplished on a Finnigan 4500 MS modified with a Vestec interface. A Waters model 510 LC pump was used with a pulse dampener, model LP21 LoPulse, and a Rheodyne injector model 7125. The conditions were as follows: LC flow rate=1.2mL/min, mobile phase=100% methanol, injection volume=20 microliters, TSP control temp.=100°C, TSP tip temp.=150°C, TSP source temp.=300°C.

Direct injection TSP LC/MS of mustard and its metabolites yielded mass spectra dominated by nucleophilic substitution reactions. Representative spectra are shown in Figures 1-4. Ions representative of both condensed phase reaction intermediates and products were observed in the TSP degradation of all analytes. Of particular interest is the appearance of ions that would demonstrate the presence of the postulated three membered cyclic sulfonium ion intermediate or its equivalent. In the condensed phase at ambient temperatures, loss of chloride from mustard has been reported to occur readily to yield a highly reactive positively charged intermediate. Thiodiglycol is stable at room temperature but can under TSP conditions form the thiiranium intermediate or its equivalent (Fig.4 , m/z=105). All of the analytes produced spectra showing the substitution of a methoxy group for either the terminal hydroxy or chloro groups. Mass spectra of the chloro- and hydroxy-congeners differed qualitatively in the methanol matrix. One major difference was the tendency of the hydroxy- compounds to form dimers, trimers, and other polymers. For example, thiodiglycol exhibited an ion at m/z=245 which represents the product of two molecules of the substrate. This ion had a relative abundance of 45%. Polymers were also very characteristic of the negative ion spectra of the thiodiglycol congeners. Another important difference between chloro- and hydroxy-congeners is the appearance of the distinctive chlorine isotopic abundance patterns. For example, mustard has ions at m/z=123 and 125. In general, TSP MS analysis of mustard and its metabolites yielded structural information able to confirm the presence of mustard derivatives.

Reference:

Wils,E.R.J. et al., J.Anal.Toxicol., vol 9 (1985), 254-257.

Presented at the 36th ASMS Conference on Mass Spectrometry and Allied Topics
June 5-10, 1988, San Francisco, CA

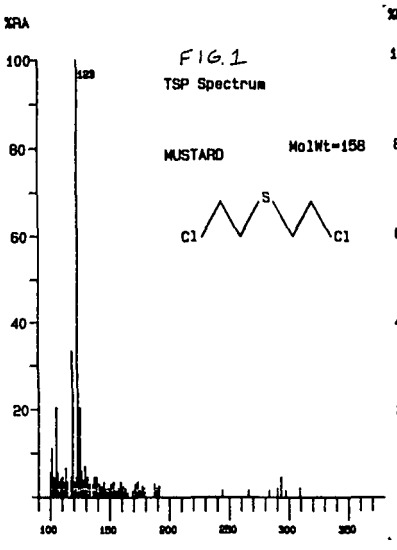

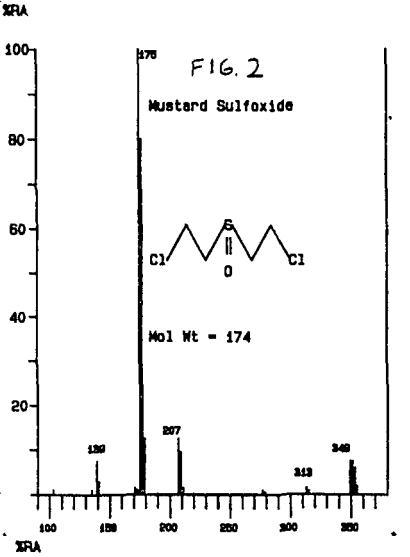

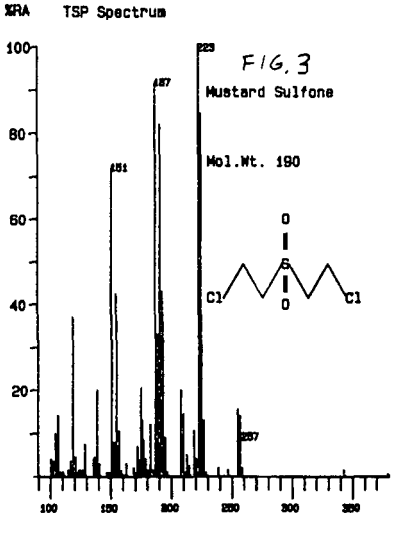

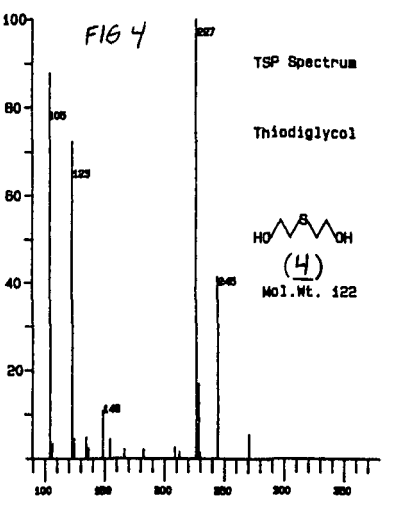

Presented at the 36th ASMS Conference on Mass Spectrometry and Allied Topics
June 5-10, 1988, San Francisco, CA

APPLICATION OF QUANTITATIVE THERMOSPRAY LC/MS TO PULSE DOSE PHARMACOKINETIC STUDIES OF CARBAMAZEPINE IN HUMANS:

M. J. Moor, R. H. Levy, M. S. Rashed* and W. N. Howald*;

Departments of Pharmaceutics and *Medicinal Chemistry, University of Washington, Seattle, WA 98195

Introduction

Thermally labile carbamazepine-10,11-epoxide (CBZ-E), Figure 1, is one of the principal metabolites of the anticonvulsant carbamazepine (CBZ). The majority of CBZ-E formed is ultimately converted to carbamazepine-10,11-transdihydrodiol (CBZ-D) by the enzyme system epoxide hydrolase (EH). Since CBZ-E/CBZ ratios are reportedly higher in children than in adults[1,2], this implies that there may be age-related changes in EH activity. To investigate this possible relationship between age and EH activity in humans, tracer quantities of isotopically-labelled 1-^{15}N, 2-^{13}C-CBZ-E were orally administered to children on CBZ monotherapy.

The analytical objective of the work presented here was to develop and evaluate a thermospray (TSP) liquid chromatographic/mass spectrometric (LC/MS) method enabling the quantitative determination of the thermally labile CBZ-E and the parent compound in blood utilizing stable isotope-labelled internal standards.

Experimental

Carbamazepine was obtained from CIBA Pharmaceutical Co. (Summit, N.J.). Authenticated [$^2H_4$]-CBZ, [$^2H_4$]-CBZ-E and [^{13}C, ^{15}N]-CBZ-E were prepared in-house, the procedure to be published elsewhere. [$^2H_4$]-CBZ and [$^2H_4$]-CBZ-E were employed as internal standards. All solvents used were analytical grade obtained from commercial sources.

Sample Preparation - An aliquot of blood (250µl) was transferred to a screw-capped glass tube and distilled water added to yield a final volume of 500µl. The two internal standards were then added with thorough mixing. After the addition of 5ml of dichloromethane and vortexing, the sample was shaken for 20 min. in a horizontal shaker and centrifuged at 2000 rpm for 5 min. The organic layer was first transferred to a disposable tube and finally to a glass storage tube using a pasteur-pipet. The solvent evaporated under nitrogen , the tube was capped and stored at -20°C prior to LC/MS analysis. Calibration and control samples were prepared in conjunction with each set of patient samples. Calibration samples were prepared by the admixture of appropriate amounts of analytes and the two internal standards to blank human blood, while the two controls, Table 1, were prepared from stocks of spiked human blood utilized throughout the entire study.

Instrumental - The samples were analyzed by thermospray LC/MS/SIM using a LKB 2150 pump and LKB 2152 controller HPLC solvent delivery system (LKB, Bromma, Sweden) interfaced to a Vestec Model 201 Thermospray MS (Vestec Corp., Houston, TX). Sample injection was via a Valco C6W injector (Valco Instruments Houston, TX) fitted with a 100µl sample loop. Separations were performed using a Spherisorb C8 octyl, 25cm x 4.6mm i.d., 5µm analytical column (Phase Separation Inc., Norwalk, CN) and a Brownlee RP-18, 1.5cm x 3.2mm i.d., 7µm guard column (Brownlee Labs, Santa Clara, CA). The mobile phase was acetonitrile: 0.1M ammonium acetate (40:60), at a flow rate of 1.0 ml min^{-1}. Retention times for CBZ-E and CBZ were 5 and 7.5min, respectively. Control and probe tip temperatures were 120°C & 180°C, respectively, and adjusted to maintain a source vapor temperature of 250°C. Selected ion analysis was performed using an HP 59979C ChemStation computer system to monitor and record ion intensities at m/z 253.1, 255.1 and 257.1 corresponding to the [MH]+ of the CBZ-E analytes and deuterated internal standard with a dwell time of 350ms/ion, and m/z 237.1 and 241.1 corresponding to the [MH]+ of CBZ and its deuterated analog with a dwell time of 750ms/ion.

All samples were reconstituted in 100µl of mobile phase prior to analysis. Aliquots of 25µl were taken for TSP LC/MS/SIM analysis.

Figure 1 - Structures

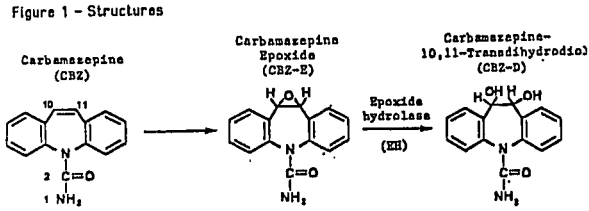

Results and Discussion

As shown in Figure 2, the peak area ratios of 253/257, 255/257 and 237/241 were used to quantify CBZ-E, [^{13}C, ^{15}N]-CBZ-E and CBZ over the concentration ranges of 0.250 - 5μg ml^{-1}, 0.050 - 1μg ml^{-1} and 0.50 - 10μg ml^{-1}, respectively. The areas observed for m/z 255 were corrected for the isotopic contribution of CBZ-E. The method demonstrated excellent linearity with correlation coefficients >0.999 for all analytes.

As shown in Table 1, the method exhibited good precision, with intra- and inter-day coefficients of variation of 5.74 and 6.24, respectively, for [^{13}C, ^{15}N]-CBZ-E at the 100ng ml^{-1} level.

The limit of detection for CBZ-E was found to be 16ng ml^{-1} (S/N = 10:1) or 1ng injected.

Conclusion

The stability, sensitivity and specificity of TSP MS detection combined with the separation and simple sample workup associated HPLC analysis make the method most useful in continued pulse dose pharmacokinetic studies of carbamazepine metabolism.

Acknowledgments

Supported by NIH Grant GM37752. All labelled compounds prepared by Thomas Kalhorn of the Department of Pharmaceutics.

1. McKauge, L. et al., Ther. Drug Monit., 3,63 (1981).
2. Pynnonen, S. et al , Env. J. Clin Pharmacol., 11,129 (1977).

Figure 2 - Standard Curves

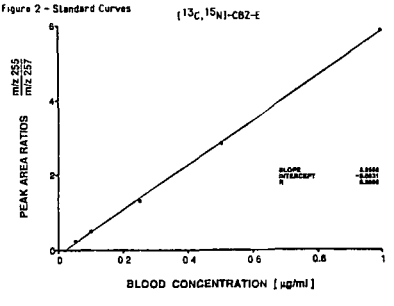

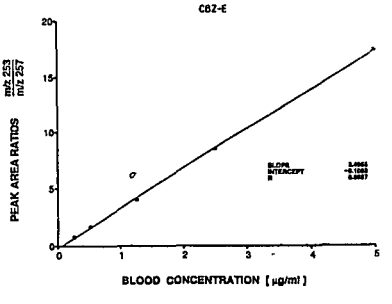

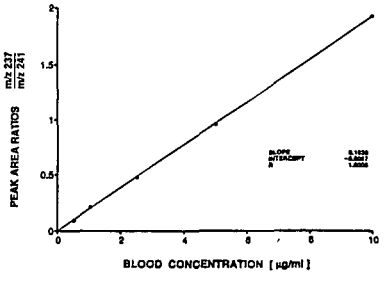

Table 1

INTRA- AND INTER-DAY VARIATIONS FOR 15N-13C-CBZ-E, CBZ-E AND CBZ IN HUMAN BLOOD CONTROL SAMPLES

COMPOUND	NOMINAL CONCENTRATION	INTRA-DAY VARIATION (n=3)		INTER-DAY VARIATION (n=3)	
	[μg/ml]	MEAN [μg/ml]	C.V. [%]	MEAN [μg/ml]	C.V. [%]
15N-13C-CBZ-E	0.100	0.106	5.74	0.107	6.24
	0.750	0.759	2.87	0.723	7.26
CBZ-E	0.500	0.577	0.98	0.543	6.63
	2.000	2.051	0.87	1.975	7.73
CBZ	5.000	5.059	0.39	5.125	1.29
	10.000	10.943	0.14	10.656	0.38

Presented at the 36th ASMS Conference on Mass Spectrometry and Allied Topics
June 5-10, 1988, San Francisco, CA

THERMOSPRAY LC/MS - A VERSATILE TECHNIQUE FOR DETERMINATION OF DRUGS IN PLASMA

Claes Lindberg and Jan Paulson

Bioanalysis, AB Draco (Astra), P.O.Box 34, S-22100 Lund, Sweden

During the last few years thermospray (TSP) LC/MS has been extensively used for the identification of polar and thermally labile compounds of biomedical interest. The technique has been less widely used for quantitative analysis, possibly because careful optimization of TSP conditions is necessary to obtain high sensitivity and reproducibility (1). There is, however, a great potential for the TSP mass spectrometer as a selective and universal LC detector. We have previously applied TSP LC/MS to the determination of terbutaline enantiomers after separation on a chiral column (2) In the present work we have studied a wider range of compounds and implemented automated procedures, which are desirable for routine quantitative analysis.

Fig. 1
Compounds measured by TSP LC/MS

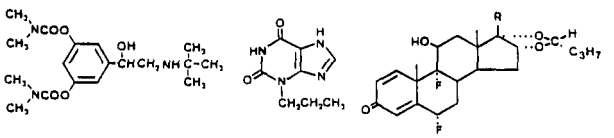

Bambuterol Enprofylline D5116

Methods based on TSP LC/MS were developed for three anti-asthmatic drugs (Fig. 1) Bambuterol and D5116 were isolated from the plasma matrix (2 mL) by solid phase extraction (BondElut C18) Enprofylline could be measured directly in plasma (0.1 mL) after protein precipitation. Deuterium labeled analogues were used as internal standards in all cases. The instrumentation and the LC conditions are shown in Figs. 2 and 3, respectively.

Fig. 2
Instrumentation

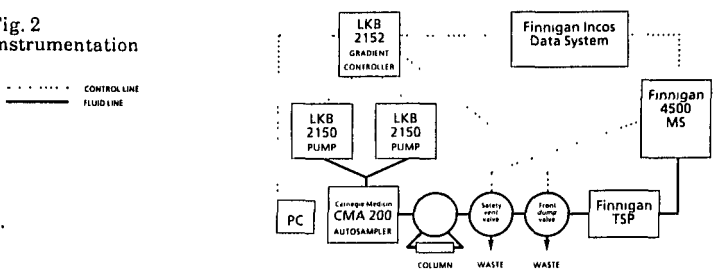

Fig. 3
LC conditions

Column: 33x4 6 mm C18, 3um
Mobile phase: 0 1 M ammonium acetate, pH 5, containing X % methanol

	ENPROFYLLINE	D5116	BAMBUTEROL
Methanol	14%	65%	6.3% for 3 min, linear program to 40% during 12 min
Flow rate	1 60 mL/min	1 50 mL/min	1 40 mL/min

Enprofylline was measured in the range 0.88-22 mg/L (Fig. 4). TSP LC/MS was used as a reference method to check some unexpectedly high plasma concentration measured by LC/UV. No significant difference between the methods was found To check if an artifact was caused by the sample work-up, some samples were reanalyzed by direct injection of 5 uL of plasma (diluted with buffer). The results were the same.

Fig. 4
Determination of **enprofylline** in plasma (standard 0.88 mg/L).

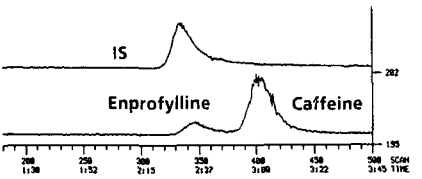

After careful optimization of the TSP conditions D5116 could be measured in plasma down to 0.2 nmol/L (Fig 5) TSP LC/MS increased sample throughput three times compared with a method based on LC with chemiluminescence detection, used for similar corticosteroids. Method development was accomplished in less than a month.

Fig. 5
Determination of **D5116** in plasma (standard 0.2 nmol/L).

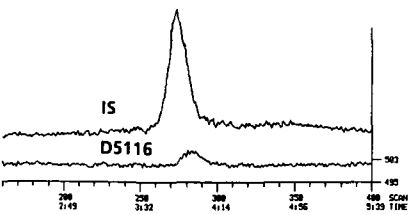

A method based on TSP LC/MS was developed for the simultaneous determination of bambuterol and its metabolite, terbutaline, in dog plasma (Fig 6). The precision of the method was 4.0% (CV) at a bambuterol plasma concentration of 4 nmol/L. The results show that gradient elution is compatible with quantitative TSP LC/MS.

Fig. 6
Determination of **bambuterol** in plasma (standard 2 nmol/L).

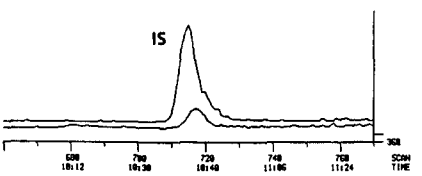

Conclusions

TSP LC/MS can normally be used for measuring drugs in plasma at the nmol/L level, and in favourable cases at the pmol/L level. Minimal sample pretreatment is required and short retention times can be allowed. The mild sample handling and high selectivity makes TSP LC/MS a suitable reference for the validation of other methods. It can also be utilized for quick development of an urgently needed assay. Sample injection and data acquisition can be automated, allowing unattended operation overnight.

References

1. C. Lindberg and J Paulson, J Chromatogr. **394**, 117 (1987).
2. L.-E. Edholm, C. Lindberg, J Paulson and A. Walhagen, J. Chromatogr. **424**, 61 (1988).

Presented at the 36th ASMS Conference on Mass Spectrometry and Allied Topics
June 5-10, 1988, San Francisco, CA

MAGIC-LC/MS ANALYSIS OF ALKALOIDS

W. Eric Harris and Richard F. Browner
School of Chemistry, Georgia Institute of Technology, Atlanta, Georgia 30332-0400

The ability of MAGIC-LC/MS to generate searchable EI spectra for a wide range of compounds is by now well established. This is a result of the interface's highly efficient solvent removal capability. As a consequence, both normal phase and reversed phase LC separations may be carried out with few restrictions on the separation conditions. Gradient elution separations, including those with aqueous buffers, may also be readily used with relatively minor signal loss. As a consequence of these properties, the MAGIC-LC/MS interface is uniquely suited to provide structural information on various classes of compounds of biochemical interest.

This paper will discuss the performance of MAGIC-LC/MS for the separation and identification of a series of alkaloids of the pyrrolizidine group. Pyrrolizidine alkaloids are found in approximately three percent of plant life, and are known to be fatal to humans and animals if ingested. Their prime importance in current biochemical research is as anticancer agents. For instance, indicine-N-oxide has proved effective against advanced gastrointestinal cancer, melanomas and leukemia. The need for reliable mass spectral identification of these compounds is most important to further synthetic and clinical research in this area, but alkaloids of this type are not amenable to GC/MS analysis because of their high thermal lability.

Experimental issues of interest included species detection limits, chromatographic performance and mass spectral fragmentation patterns observed. The alkaloids studied had been either isolated from plant materials or prepared synthetically. Figure 1 shows the single ion monitoring response at m/z 155 for indicine-N-oxide, with 100 ng and 10 ng injections. Signal-to-noise ratios were quite satisfactory, and showed the possibility to obtain low detection limits for this representative compound. Separations were carried out with gradient elution conditions, using an aqueous buffer of 0.05 M NH_4OAc at proportions ranging from 0 - 70 %. Over this range, there was approximately a 3x signal loss. However, the mass spectra obtained under all conditions were quite reproducible, and compared well with the anticipated loss of fragments predicted from the literature (Figures 2 and 3).

From these studies, the feasibility of using MAGIC-LC/MS to provide valuable structural information, not otherwise readily obtainable, has been demonstrated on both natural plant pyrrolizidine alkaloids and on some semi-synthetic analogues.

Presented at the 36th ASMS Conference on Mass Spectrometry and Allied Topics
June 5-10, 1988, San Francisco, CA

FIGURE 1

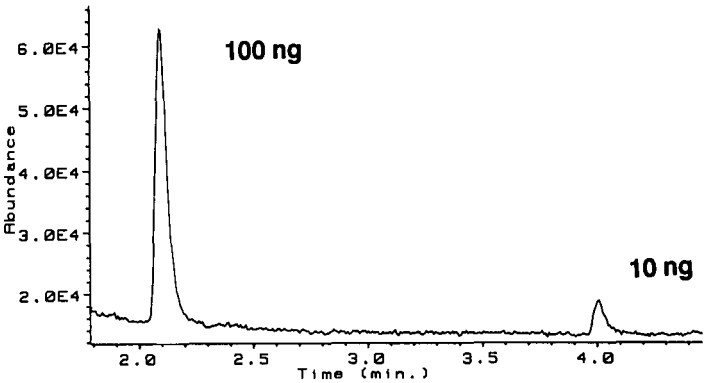

FIGURE 2

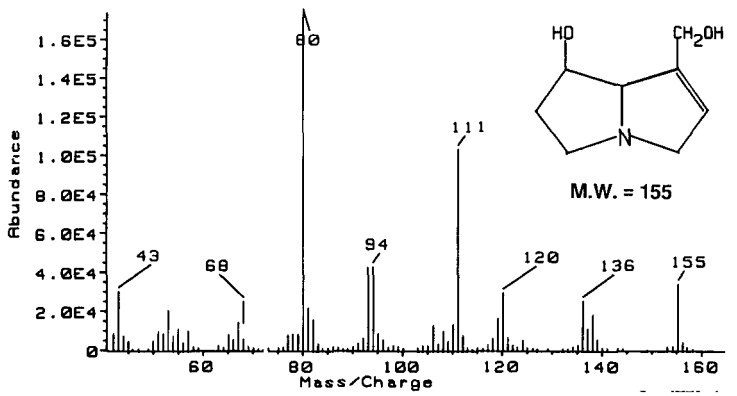

FIGURE 3

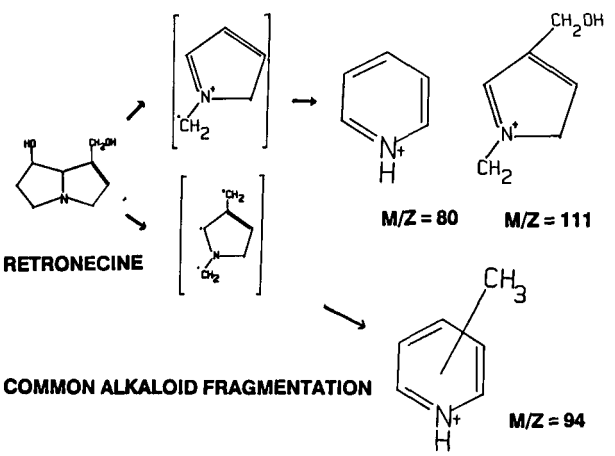

Presented at the 36th ASMS Conference on Mass Spectrometry and Allied Topics
June 5-10, 1988, San Francisco, CA

THERMOSPRAY LC/MS OF PYROLLIZIDINE ALKALOIDS AND METABOLITES

C.E. Parker, S. Verma, and K.B. Tomer

Laboratory of Molecular Biophysics, N.I.E.H.S., P.O. Box 12233, Research Triangle Park, NC 27709

R.L. Reed, B. Kedierski, and D.R. Buhler

Department of Agricultural Chemistry, Oregon State University, Corvallis, OR 97331

Pyrrolizidine alkaloids (PAs), found in a large number of plant species, are important because of their carcinogenic and hepatotoxic properties. They have been responsible for the poisoning of livestock through the direct consumption of PA-containing plants, and may enter the human food chain through the consumption of grain contaminated with PA-containing seeds, or through the drinking of "herbal teas" or milk from exposed animals (1).

The objective of this study was to evaluate thermospray LC/MS for the analysis of pyrrolizidine alkaloids, their metabolites and conjugates. The mass spectrometer used was a VG 12-250 quadrupole mass spectrometer and data system. The thermospray interface was a Vestec model 701 source and controller. Operating conditions for the alkaloid standards in the positive ion mode were: discharge off, block 275°, vaporizer 268°, control (T1) 151°, tip (T2) 295o, tip heater 429°, lens 35°, and repeller 28V. Operating conditions in the negative ion mode were: discharge on, block 275°, vaporizer 271°, control (T1) 146°, tip(T2) 295°, tip heater 429°, lens 35°, and repeller -11V.

Under these conditions, thermospray MS gives very simple spectra for the pyrrolizidine alkaloids studied, containing mainly $(M+1)^+$ ions in the positive ion mode, and $(M-1)^-$ ions in the negative ion mode. Sensitivities are lower for the PA metabolites studied, and the spectra show mainly $(M+1-H_2O)^+$ ions in the positive ion mode.

Thermospray mass spectra obtained from a synthetic cysteine conjugate are consistent with the replacement of one of the DHR hydroxyl groups with a cysteine moiety. No evidence was found of a proposed conjugate with cysteines replacing both DHR hydroxyl groups.

No ions corresponding in mass to either of these cysteine conjugates were found in an incubation of rat hepatic cell microsomes with senecionine and cysteine. Instead, TSP analysis of the reaction mixture shows ions corresponding in mass to a conjugate formed by the addition of cysteine across the DHR double bond.

---

1. Mattocks, A.R., "Chemistry and Toxicity of Pyrrolizidine Alkaloids", Academic Press, London, 1986.

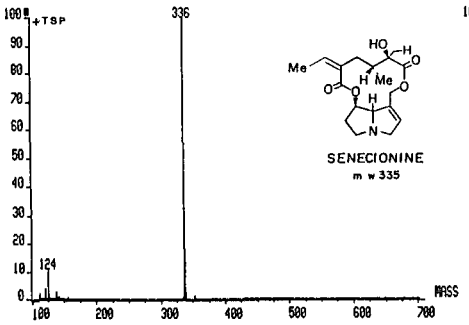

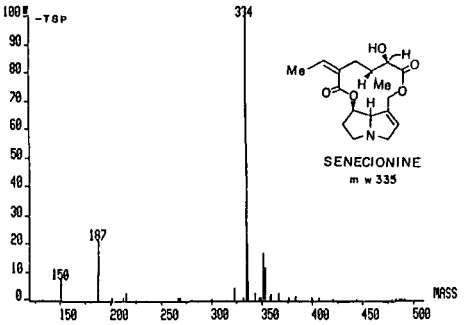

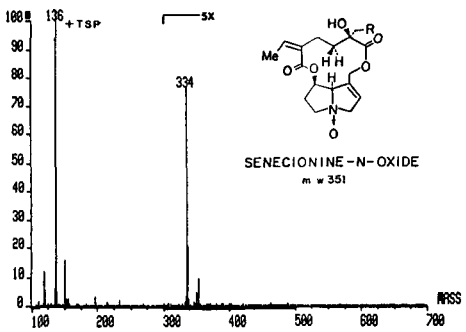

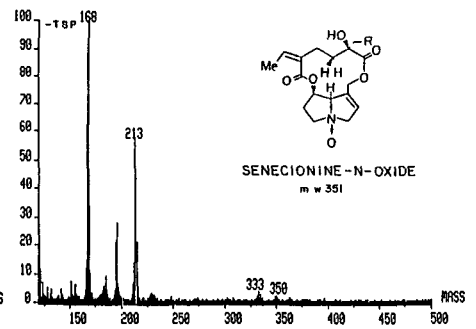

SYNTHETIC DHR-CYS CONJUGATE

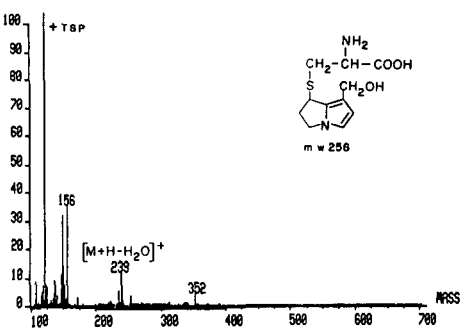

POSSIBLE CONJUGATE FROM MICROSOMAL INCUBATION

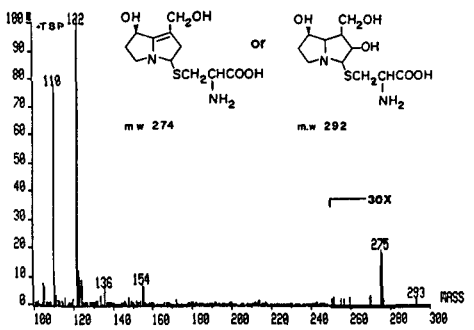

Presented at the 36th ASMS Conference on Mass Spectrometry and Allied Topics
June 5-10, 1988, San Francisco, CA

ANALYSIS OF ACYLCARNITINE BY HPLC AND LC/MS

Toshihiro Shinka, Tokuo Mizuno* and Isamu Matsumoto
Department of Biochemistry, Institute of Human Genetics, Kanazawa Medical University, Uchinada, Ishikawa 920-02, *JEOL, Akishima, Tokyo 196, Japan

L-Carnitine is an essential mediator for the ß-oxidation of fat. Hereditary disorders of fats and amino acids metabolism are often associated with abnormally high ratios of acylated carnitines to free carnitine in the urine and blood. The analysis of acylcarnitine profiles in these parients is very useful for the understanding of the clinical conditions and metabolic abnormalities, and for deciding treatment. We have developed a simple derivatization and determination method of acylcarnitines by HPLC and LC/MS using a disposable/double moving belt interface[1].

The standard acylcarnitine-HCl salts were a generous gift of Dr. D.S.Millington (Duke University). 9-Anthryldiazomethane (ADAM) was purchased from Funacoshi Co. Ltd. (Tokyo, Japan).

Standard acylcarnitines were dissolved in water at concentrations of 1-10µmole/ml. Acylcarnitine solution (100µl) was added to 1 ml urine. The mixture was vortexed and applied to a 0.9 x 4 cm glass column of Bio Rad AG-1X8 (200-400 mesh, Cl- form) anion exchange resin. Excluded species were eluted from the column with 6 ml deionized water. The effluent was collected in a glass test tube and the content was lyophilized. ADAM reagent was dissolved in ethylacetate at a concentrations of 0.2 %. To the dry residue from the isolation procedure was added 200 µl of 0.2 % ADAM solution and allowed to stand for more than 5 hours at 40°C. Sample aliquots(5 µl) were injected diectly into chromatograph.

The liquid chromatograph consisted of Waters Model M 45 pump, UK 6 syringe loading sample injection valve, Soma S-310A UV detector, and Waters 730 data module. Chromatographic separation was carried out on a 3.9 mm x 30 cm column containing µBondapak C_{18} (Waters) or 4.6 mm x 25 cm column containing Chemcosorb SCX cation exchange resin (Chemco, Osaka, Japan). For the reversed phase column, the mobile phase was 0.05 M triethylamine-HCl and acetonitrile (5 : 95, v/v) and the eluent was pumped at 1.5 ml/min. For the cation exchange column, the mobile phase was 0.05 M triethylamine-HCl and acetonitrile (85 : 15, v/v) and the eluent was pumped at 0.8 ml/min. UV spectrum was obtained using Shimadzu SPD-M1A diod-array detector. Absorbance of the effluent stream was monitored at 254 nm.

FABMS at low resolution was performed using a JMS-DX303 mass spectrometer (JEOL) and JMA-DA5000 data acquisition system (JEOL). LC/MS consisted of FAMILIC-300S HPLC (JASCO), JMS-DX303 and JMA-DA5000. µs-Finepak SIL C_{18} (1.5 mm x 25 cm) was used for the separation of acylcarnitines. In LC/MS, the eluent was pumped at 100 µl/min.

Fig. 1 shows the HPLC chromatogram and UV spectrum of propionylcarnitine anthrylmethyl ester. There are two major peaks (P1 and P2) on the chromatogram. The UV spectrum shows that peak 2 was propionylcarnitine. The derivative has the max at 254 nm and the other small peaks at 350, 370 and 385 nm.

The samples were also analyzed by LC/MS equipped with a disposable/double moving belt interface. The block diagram of this interface is shown in Fig. 2. In the conventional

LC/MS, it is hard to use the inorganic salt solvent, and the endless belt type interface has a memory trouble. With the new interface, the sample is covered with the other belt.

Thus, the memory trouble at ion source is completely avoided, and an inorganic solvent system can be used.

Fig. 3 shows the HPLC chromatogram and FAB mass spectrum for octanoylcarnitine anthrylmethyl ester. The difference of the retention time between UV detection and mass chromatogram is coursed by the interface lag time. Octanoylcarnitine anthrylmethyl ester has molecular ion at m/z 478, and a fragment ion at m/z 288 is due to [M-190] (free octanoylcarnitine).

The ion at m/z 191 is assigned to 9-methyleneanthracene.

Eighty percent derivatization of acylcarnitine was accomplished within 1 hour, and the derivatives were stable at room temperature for several weeks.

The sensitivity of HPLC-UV detection method was similar to that of the direct FABMS detection method. The calibration curve for octanoylcarnitine was linear over a sample concentration range of 10 - 150 nmole/ml. More efficient separation of acylcarnitines was achieved by cation exchange resin HPLC. It is possible to detect the acetyl-, propionyl-, butyryl-, isovaleryl-, and hexanoylcarnitine using an isocratic solvent. Using the gradient solvent method, it is possible to separate acylcarnitine more efficiently and obtained longer acylcarnitines.

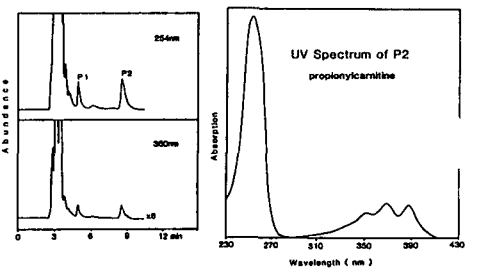

Fig. 1 HPLC chromatograms and UV spectrum of propionylcarnitine anthrylmethyl ester; Column μBondapakC18 (3.9x300mm)

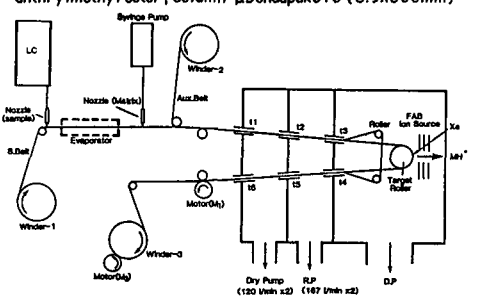

Fig. 2. Block diagram of disposable/double belt LC/MS interface

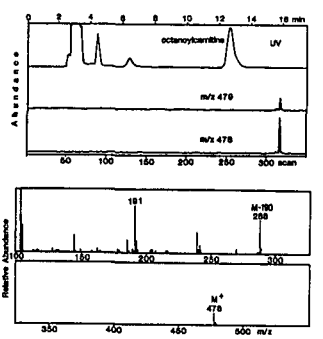

Fig. 3. FAB LC/MS Analysis of octanoylcarnitine anthrylmethyl ester

1) T. Mizuno, K. Azuma and K. Ootsuka
Analytical Science, submitted for publication

Presented at the 36th ASMS Conference on Mass Spectrometry and Allied Topics
June 5-10, 1988, San Francisco, CA

STUDY ON THE DECOMPOSITION OF QUATERNARY AMMONIUM SALTS BY THERMOSPRAY LC/MS.

Domenick Vicchio and Alfred L. Yergey, National Institute of Child Health and Human Development, NIH, Bethesda, MD 20892.

INTRODUCTION:

The biologically active quaternary ammonium compounds, carnitine, choline and their acylated derivatives have been analyzed with both good sensitivity and reproducibility by thermospray LC/MS (1,2). Although the parent ion is usually a prominent peak in the mass spectra of these compounds, there appears to be, especially for the carnitines, a great deal of thermal degradation to tertiary amines and what are believed to be alkenes. Since the mass spectra of these compounds vary considerably with vaporizer and block temperatures, the nature of the degradation was investigated to better understand and predict the thermospray behavior. The mass spectra of substituted and labeled carnitine chlorides, dodecylpyridinium chloride, tetrabutylammonium hydroxide, and benzyldimethyldodecylammonium chloride were recorded at various vaporizer temperatures, and for select compounds at various pH values. The results indicate that there is temperature dependent degradation that varies depending on the structure of the quaternary compound. A pH dependence was also observed. Structures are proposed for the characteristic fragments observed in the mass spectrum of the carnitines.

EXPERIMENTAL:

Twenty nmoles of various carnitines were introduced into the source either directly, i.e. without a column, or through a 15 cm x 4.6 mm ID Ultrasphere ODS column. The mobile phase varied depending on the compound being analyzed; carnitine and acetylcarnitine were eluted from the column with 1.0 ml/min of 1% methanol in 0.1 M ammonium acetate (pH 6.7). Propionylcarnitine was eluted with 5% methanol in the same buffer.

The effect of pH on the mass spectrum of the quaternary compounds was investigated by changing the pH of the effluent with the post column addition of 0.5 ml/min of a basic (NH_4OH) or acidic (CH_3COOH) solution.

Dodecylpyridinium, benzyldimethyldodecyl and tetrabutylammonium salts were eluted from a 15 cm x 2.1 mm ID ODS column with 0.25 ml/min of 90% methanol, and 1 mM pyridine in 0.1 M ammonium acetate. The relative amount of methanol reaching the source was reduced with post column addition 1.0 ml/min of 0.1 M ammonium acetate.

The effluent from the LC column was introduced into a Vestec Thermospray source coupled to a Hewlett-Packard Mass Selective Detector. The block temperature was maintained at 350 ± 20 °C, while the vapor temperature was varied from 250-360 °C. The mass spectrometer was operated in either SIM or scanning mode. In the SIM mode each mass was monitored for 500 msec for direct injections, and 1000 msec for on column injections. When scanning the range was varied from 100-350 amu depending on the mass of the analyte.

Presented at the 36th ASMS Conference on Mass Spectrometry and Allied Topics
June 5-10, 1988, San Francisco, CA

RESULTS:

The data figures 1 and 2 indicate that quaternary ammonium salts undergo thermal degradations when subjected to thermospray mass spectrometry, and that this fragmentation is not the same for all the compounds investigated. For example, at high vapor temperatures, the carnitines degrade completely. Whereas, dodecylpyridinium and tetrabutylammonium salts reach a temperature maximum for fragmentation, and beyond this temperature the parent ion predominates. Further, based on the presence of both a tertiary amine and alkenes in the mass spectra of carnitines, it was concluded that the mechanism of fragmentation is analogous to the Hoffman degradation. Although tertiary amines were also observed in the mass spectra of both tetrabutylammonium hydroxide and dodecylpyridinium chloride, no alkenes was observed for the tetrabutyl salt, while the alkene from the pyridinium salt gave a weak signal, this is likely due to the poor sensitivity of the unsubstituted alkenes by thermospray. Finally based on the order of elimination from benzyldimethyldodecylammmoium chloride it was concluded that the order of elimination from ammonium salts is benzyl>methyl>longer chain alkyls.

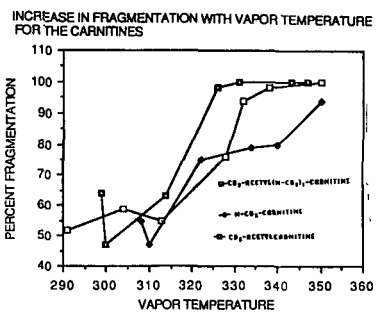

figure 1

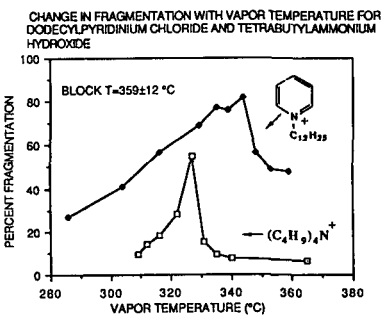

figure 2

References:

1. Yergey, A.L., Liberato, D.J., and Millington, D.S., Anal. Biochem., **139**, 278-283 (1984)
2. Liberato, D.J., Yergey, A.L., and Weintraub, S.T., Biomed. Environ. Mass Spectrom., 13, 171-174 (1986).

We thank Dr. D. S. Millington, Duke University Medical Center, for the gift of labeled and substituted carnitines

Presented at the 36th ASMS Conference on Mass Spectrometry and Allied Topics
June 5-10, 1988, San Francisco, CA

THERMOSPRAY LC/MS OF α-CARBOXYAMIDO AMINO ACIDS AND PEPTIDES

Anthony M. Treston, Alfred L. Yergey, Frank Cuttitta and James L. Mulshine.
SMAMS, LTPB, NICHD, and NCI-Navy MOB, COP, DCT, NCI, NIH, Bethesda, MD 20814.

The most common amino acid modification present in hormonally active peptides is amidation of the α-carboxyl terminus of the peptide. To identify novel or unrecognized peptide hormones involved with lung cancer biology, we are using detection of posttranslational chemical modifications of amino acids (such as amidation) signifying biological activity. Enzymatic cleavage of α-carboxyamidated peptides using the peptidyl amino acid amide hydrolase (PAAAH) activity of selected carboxypeptidases releases α-carboxyamido amino acids which can be separated from non-α-amidated amino acids and identified using thermospray LC/MS.

HPLC of pure amino acids and amino acid amides was carried out on reversed phase (C_{18}) columns with 0.1% trifluoroacetic acid/ammonia, pH 7.0, with a step gradient from water to 20% methanol in water. Alternatively, a cation exchange column was used with a three-stage step gradient from pH 3.5, 10 mM formic acid/ammonia; to pH 7.0, 0.2 M ammonium formate; to pH 7.5, 0.5 M ammonium formate. Post-column addition of ammonium acetate or ammonium formate to a final concentration of at least 0.1M provides the necessary solvent ions for direct (filament-off) thermospray ionization. The mass spectrometer used was a Hewlett-Packard MSD equipped with a Vestec Thermospray source operating in positive ion mode. Moderate vaporization (230°C) and block temperatures (380°C) give the most reproducible mass spectral characteristics. For equimolar mixtures of amino acids and amino acid amides, SIM provides ready quantification (S/N 25-100:1) of 200 pmol on column.

Analysis of serial samples of enzymatic digests was carried out using the C18 column method described above. Rates of release of amino acids and α-carboxyamido amino acids provide sequence information on peptides. Further information can be obtained from mass spectral identification of the series of truncated peptides produced by the enzyme/s. For example, using CCK 30-33 amide (F-G-L-M amide) as a model, digestion with malt carboxypeptidase II or carboxypeptidase Y sequentially liberates the amino acids M amide, L, and G and F. The truncated peptides F-G-L and F-G could also be identified.

A number of model peptides were hydrolyzed using both Malt Carboxypeptidase II and Carboxypeptidase Y, and the released amino acids and amino acid derivatives were resolved using the cation exchange column method described above. Peptides studied include F-G-L-M amide, W-M-D-F amide, Y-F-M-R-F amide, Y-24-R amide (terminating in .....Q-I-R amide), Y-G-G-F-L amide, acetylD-Y-M-G amide, Y-dA-F-G-Y-P-S amide, and Y-P-V-P amide. The spectrum of activity of the enzymes was shown to be dependant on assay pH, peptide sequence, and identity of the C-terminal α-carboxyamido amino acid.

Presented at the 36th ASMS Conference on Mass Spectrometry and Allied Topics
June 5-10, 1988, San Francisco, CA

THERMOSPRAY LC/MS OF α-CARBOXYAMIDO AMINO ACIDS AND PEPTIDES

Anthony M. Treston, Alfred L. Yergey, Frank Cuttitta and James L. Mulshine.
SMAMS, LTPB, NICHD, and NCI-Navy MOB, COP, DCT, NCI, NIH, Bethesda, MD 20814.

RATES OF RELEASE OF AMINO ACID AMIDES AND AMINO ACIDS BY CARBOXYPEPTIDASE HYDROLYSIS OF MODEL PEPTIDES

Carboxypeptidase Y (50 ug/mL)
Hydrolysis of F-G-L-M amide at pH 6.0

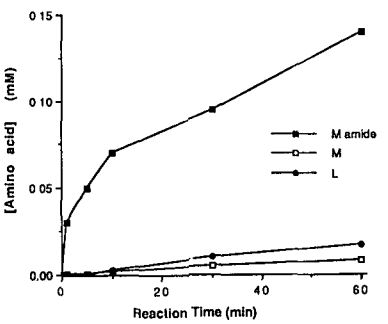

Malt Carboxypeptidase II (200 ug/mL)
Hydrolysis of F-G-L-M amide at pH 6.0

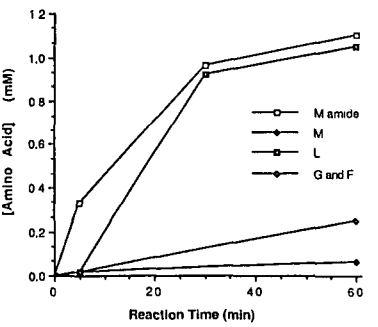

ENZYMATIC HYDROLYSIS OF MODEL PEPTIDES

PEPTIDE SEQUENCE	α-CARBOXYAMIDO AMINO ACID QUANTIFIED	α-CARBOXYAMIDO AMINO ACID DETECTED	OTHER AMINO ACIDS	TRUNCATED PEPTIDES
F-G-L-M amide	M amide		M, L, G, F	+
W-M-D-F amide	F amide		F, M, D, (W)[a]	+[b]
Y-F-M-R-F amide		F amide	(F, R)	-
Y.....Q-I-R amide		-	-	-
Y-G-G-F-L amide	L amide		L, F, G, (Y)	+
acD-Y-M-G amide	G amide		M, Y, (acD, G)	+
Y-dA-F-G-Y-P-S amide		S amide	-	-
Y-P-V-P amide		-	-	-

a: The amino acids shown () were present in concentrations too small to allow quantification
b: W-M-D-F amide-related peptides were detected in a direct injection of the c'ase hydrolysis mix only. The estimated retention volumes were >50 mLs on C18 columns.

Presented at the 36th ASMS Conference on Mass Spectrometry and Allied Topics
June 5-10, 1988, San Francisco, CA

IDENTIFICATION OF PHENYLTHIOCARBAMYL AMINO ACIDS BY THERMOSPRAY LC/MS FOR AMINO ACID COMPOSITION ANALYSIS OF PROTEINS AND PEPTIDES.

Bikash C. Pramanik, Carolyn R. Moomaw and Clive A. Slaughter; Howard Hughes Medical Institute, Dallas, Texas 75235. Claudia Evans; VA Medical Center and University of Texas Southwestern Medical Center, Dallas, Texas 75216. Steven A. Cohen; Waters Chromatography Division of Millipore, Milford, Massachusetts 01757

Amino acid composition analysis of peptides and proteins is commonly accomplished by reverse-phase high performance liquid chromatography (HPLC) of the phenylthiocarbamyl derivatives of amino acids. These derivatives are formed by reaction of the free amino acid residues which phenylisothiocyanate:

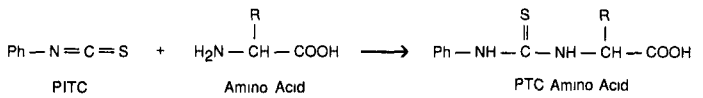

PTC amino acids are readily detected by UV absorption and are normally identified solely by comparing chromatographic retention times with those of synthetic external standards.

The aim of the present study was to establish a method of employing thermospray liquid chromatography/mass spectrometry (LC/MS) for confirming identifications made in this way and acquiring information useful for identifiying non-standard components of amino acid mixtures.

Chromatographic conditions which are compatible with thermospray LC/MS were identified for use in separating PTC amino acids derived from protein and peptide hydrolysates. Fig. 1 shows a typical analysis of a standard PTC amino acid mixture containing 1 nmole per component.

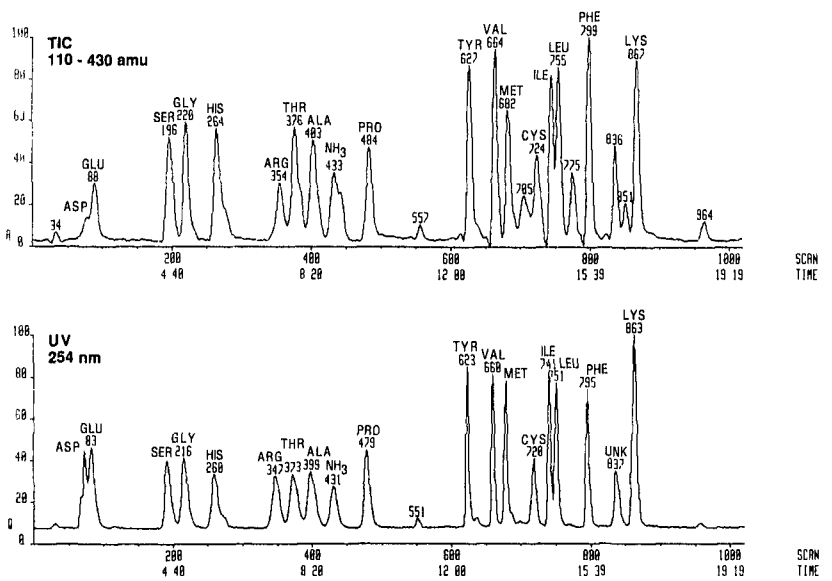

Figure 1

Presented at the 36th ASMS Conference on Mass Spectrometry and Allied Topics
June 5-10, 1988, San Francisco, CA

The protonated molecular ions for all standard and modified PTC amino acids so far tested, except PTC-cys, have been observed in on-column mass spectra. However, fragmentation and pyrolytic cleavages affecting the PTC skeleton, as well as special fragmentation pathways affecting the more reactive amino acid side chains have also been identified. Examples are shown in Fig. 2.

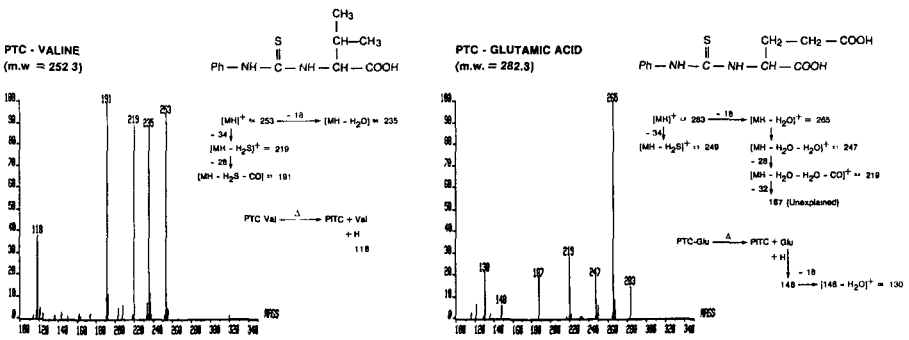

Figure 2

Each amino acid could be identified on the basis of the protonated molecular ion or a characteristic fragment ion with signal-to-noise ratios of 80:1 or better at the 250 pmole level.

The method was used to assist with the identification of two UV absorbing by-products of the coupling reaction: phenylthiourea, which represents the addition of PITC to ammonia, and dimethylphenylthiourea which represents the addition of PITC to ethylamine, a possible breakdown product of the triethylamine coupling buffer.

The procedure was tested on several proteins, including examples containing amino acids which have been covalently modified in vitro (eg. pyridylethylated cysteine) and in vivo (eg. hydroxyproline and hydroxylysine in collagen).

The method was applied to a study in which citrate synthase isolated from porcine heart was compared to the protein expressed by a recombinant porcine gene in E. coli. The data, acquired using a modified gradient method, showed that the recombinant protein lacked a covalently modified residue, trimethylysine, which is characteristically present in the catalytic site of the enzyme expressed in mammalian tissues. Since the recombinant protein was nonetheless catalytically active, the study indicated that this modification is not required for the expression of enzymatic activity.

Presented at the 36th ASMS Conference on Mass Spectrometry and Allied Topics
June 5-10, 1988, San Francisco, CA

REACTION MONITORING USING MICROBORE AND FRONTAL LIQUID CHROMATOGRAPHY WITH CF-FAB

William T. Moore, Beverly DaGue, Millie Martin, and Richard M. Caprioli

Department of Biochemistry and Molecular Biology and the
Analytical Chemistry Center
The University of Texas Medical School at Houston
Houston, Texas 77225

The application of LC/MS techniques is currently of great interest for the analysis of enzymic digests of proteins, particularly those produced by recombinant DNA methods and for the characterization of products from automated synthesis (1). We have previously shown that aqueous samples can be directly analyzed by FAB-MS using the continuous-flow (CF) probe (2). Since glycerol (5%) is miscible with a solution of 60% acetonitrile and 0.1% TFA in water and is an effective sample matrix for the analysis of peptides by CF-FABMS (3), we have in this study used the CF-FAB probe to directly introduce the effluent of a microbore LC column into the source of a mass spectrometer. Representative data in the form of LC/FAB-MS peptide maps obtained from the tryptic digestion of two proteins, apolipoprotein A-I (Fig. 1A) and recombinant human growth hormone (Fig.2A) are presented for evaluation and indicate the augmented analytical resolving power offered by coupled microbore LC/FAB-MS. Molecular ions were observed for all the numbered fragments indicated at the different scan positions of the reconstructed ion chromatograms in the figures. In Figure 1A the numbers of the peaks indicate that 26 out of 27 possible tryptic peptides were detected. Also in Figure 1, a "frontal chromatography" generated specific ion chromatogram profile (Fig. 1C) is compared to a longer (30-min gradient 5-100% B) conventional gradient elution specific ion chromatogram profile (Fig. 1B). Frontal chromatography is the elution of peptides in a solvent front created by performing a steep gradient elution (2.4-min gradient, 5-40%B). This comparison is made to demonstrate that a mass spectrometer detector with its mass resolution capability makes the chemical resolution of peptides on a column a less critical factor in the analysis of protease digests thereby permitting shorter LC run times for analytical purposes. The individual mass chromatograms effectively distinguish between several peptides eluting at the same retention time as indicated by the shapes of the selected ion chromatograms in Fig. 1C.

Microbore HPLC was performed using an Applied Biosystems Inc. Model 130A Separation System and a 1 X 50 mm Aquapore RP-300 (7-um) C8 bonded reverse phase microbore column. Pre- and post-column solvent flow splitters (Waters stainless steel compression screw tees fitted with 0.006-in. Teflon tubing crimped manually by screw clamps for flow rate control) were used to control gradient development times and effluent flow rates. An optimal flow rate for CF-FAB sample introduction into the source of the mass spectrometer is 5 μL/min. Mobile phases consisted of acetonitrile/ /glycerol/water/TFA in the following proportions: Solvent A - 0/5/95/0.1 (v/v); Solvent B - 60/5/35/0.1.

FAB mass spectrometry was performed with a Finnigan MAT 90 equipped with an Ion Tech b11NF saddle field ion gun using Xe to create energetic atoms. The continuous-flow probe used was the Finnigan-MAT Bioprobe. The spectrometer was generally operated at a resolving power of 1500 and an accelerating voltage of 4.8 KV. The magnet was scanned at approximately 10 sec/decade. Data were collected with multichannel analyzer programs available on the data systems. CsI was used to calibrate the instrument.

Another example of the clear advantage of coupling microbore HPLC with FAB-MS via a continuous-flow probe interface is evident from the mass spectral data presented in Figure 2C and 2D derived from scan positions along the RIC representing the LC/FAB-MS tryptic peptide map of a 1% deliberately contaminated recombinant human growth hormone. In this example we were able to detect a modified recombinant human growth hormone fragment (a monosulfoxide derivative) derived from the 1% "contaminant"

eluting at a position indicative of its more hydrophilic character (compare peptide structure inserts in the mass spectra Figure 2 B & C). The tryptic digest of native rhGH + 1% monosulfoxide derivative mixture was provided by Dr. Gerald Becker of Lilly Research Laboratories and was created by a trypsin treatment of a mixture of 10 mg of native rhGH and 100 ug of monosulfoxide derivative for the purpose of this study. Since 240 pmoles of native recombinant human growth hormone had been delivered to the source for FAB analysis, the spectrum for the monosulfoxide derivative is that derived from 2.4 pmole. The signal intensities indicated on the right hand ordinates support this contention.

We conclude that LC/FAB-MS coupling through the CF-FAB probe is a powerful, high resolution, and sensitive tool that can be exploited by the protein chemist to assess protein/peptide structure and the purity of protein preparations.

REFERENCES:

1. Covey, T., Lee, E., Bruin, A. and Henion, J., Anal. Chem., 1986, 58, 1451A.
2. Caprioli, R.M., Fan, T. and Cottrell, J., Anal. Chem., 1986, 58, 2949.
3. Caprioli, R.M., DaGue, B., Fan, T. and Moore, W.T. BBRC 1987, 146, 291.

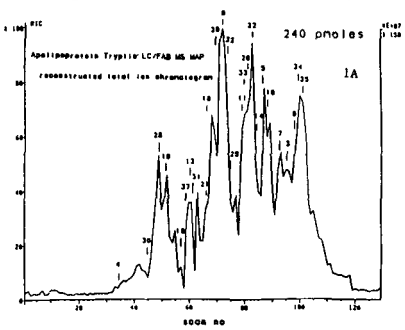

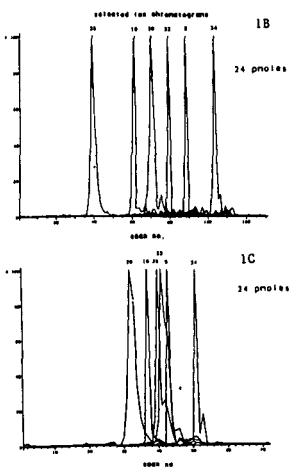

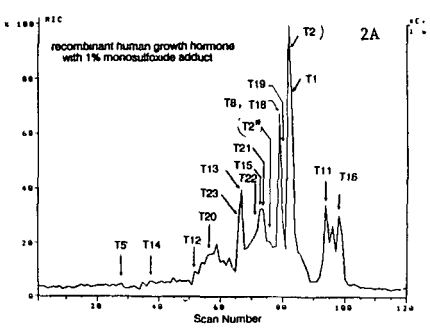

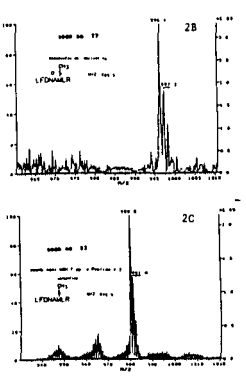

Presented at the 36th ASMS Conference on Mass Spectrometry and Allied Topics
June 5-10, 1988, San Francisco, CA

ANALYSES OF HIGH MOLECULAR WEIGHT POLAR COMPOUNDS BY THERMOSPRAY

R.H. Bateman, S. Hibbert, D.S. Jones & S.T. Krolik.

VG Analytical Ltd., Floats Road, Wythenshawe, Manchester. M23 9LE.

With the possibility to analyse high molecular weight polar molecules[1] by thermospray, there exists a lack of calibrant materials suitable for mass measurement of signals obtained at masses in excess of 3000 daltons.

Indeed, the whole question of calibration to quite moderate mass has been the subject of vigorous debate[2,3]. Currently, calibration of mass spectrometers is routinely possible using polyethylene glycols to mass 1500. For calibration to mass 3000, a suitable mixture of polypropylene glycols is appropriate.

However, obtaining signals of sufficient intensity and simplicity for calibration is far from trivial. Typically the calibration process will involve the following:

1) Choosing a mobile phase suitable for obtaining calibrant signals. Frequently, this is quite different from the mobile phase used for the main investigation.
2) Optimisation of the calibrant signal often involves careful consideration of such parameters as:
   a. source temperature[3]
   b. calibrant concentration[3]
   c. mobile phase
   d. probe tip temperature
3) Preparation of calibrant mixtures at appropriate concentration levels to give ions of balanced intensity over the entire calibration range.

A typical problem for calibration algorithms is that the software choose the most intense mass within a specified mass window. At high mass, the molecular ion (as defined by the ^{12}C isotope) is often not the most abundant as shown by spectra of polypropylene glycol at mass 2000 and 3000 obtained by plasmaspray (Figs. 1 and 2).

A solution to these various problems is to use fast atom bombardment for calibration. The obvious advantage of using caesium iodide as calibrant, is that both component atoms are monoisotopic, effectively avoiding the problem of isotope clusters.

To incorporate the feature of the ease of FAB calibration with the usefulness of thermospray and plasmaspray, we have designed a combined source enabling the user to perform all these functions without removal of the source.

This is achieved by focusing a FAB beam onto a removable target located above the thermospray ion block. This is shown diagramatically as Fig. 3. To illustrate the usefulness at both high and low mass, we show:

1) the molecular ion of bovine insulin (M.W. 5734) mass-measured against caesium iodide (Fig. 4).
2) a mixture of polyethylene glycols (M.W. 200-1000) mass-measured against caesium iodide from m/z 100-1000 with associated mass measurement errors (Fig. 5).

References

1. D.S Jones & S.T Krolik, Rapid Comm. in Mass Spec. 1,67,(1987).
2. M.A Baldwin & G.J Langley, Org. Mass Spec. 22,561,(1987).
3. F. DeMaack, D. Wang-Iverson & J. Ashraf, Vestec News Letter, April 1986.

Presented at the 36th ASMS Conference on Mass Spectrometry and Allied Topics
June 5-10, 1988, San Francisco, CA

PROBLEMS OF THERMOSPRAY CALIBRATION

1 No high mass calibrants

2 Isotope clustering at medium mass

3 Balanced spectral intensities at low mass

4 Parameter dependent

Source and probe temperature
Mobile phase
Concentration

5 Memory effects

THERMOSPRAY SPECTRUM OF MOLECULAR ION REGION OF TENDAMISTAT M.W 7956

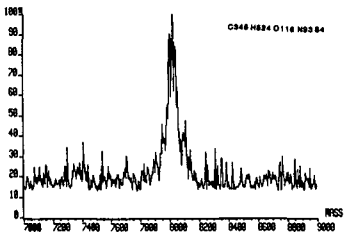

Fig. 1

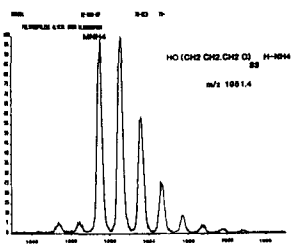

Fig. 2

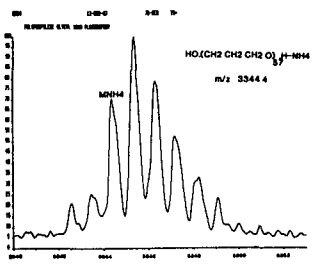

Fig. 4

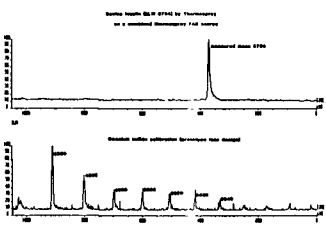

Fig. 5

Calibration Using Combined Thermospray/FAB Source

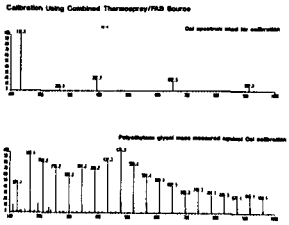

Presented at the 36th ASMS Conference on Mass Spectrometry and Allied Topics
June 5-10, 1988, San Francisco, CA

ON-LINE CAPILLARY ZONE ELECTROPHORESIS/ION SPRAY TANDEM MASS SPECTROMETRY DETERMINATION OF SMALL PEPTIDES

Edgar D. Lee, Jack Henion and Wolfgang Muck, Equine Drug Testing and Toxicology New York State College of Veterinary Medicine, Cornell University, 925 Warren Drive, Ithaca, NY 14850.

Thomas Covey, Sciex, 55 Glencameron Road, Thornhill, Ontario, Canada L3T 1P2

Capillary zone electrophoresis (CZE) has been used primarily to separate species which have a permanent charge in solution such as amino acids, peptides, and salts (1). Typically, CZE is performed in a small diameter capillary of 100 um i.d or less. The capillary is filled with buffer and each end is placed in a separate reservoir containing buffer. A high potential field is then applied across the capillary to accomplish the electrophoretic separation. Samples are introduced at the anode end of the capillary and on-line ultraviolet or fluorescence detection is accomplished a few centimeters before the cathode. Olivares and co-workers (3) have demonstrated with mass spectrometric detection that the cathode need not be in a buffer but requires only an electrical connection at a negative potential relative to the anode.

The Ion Spray interface for combined liquid chromatography/mass spectrometry (LC/MS) produces a mild form of ionization at atmospheric pressure and ambient temperature, and is particularly well-suited for the determination of species which exist as ions in solution (2). Ion spray appears to be ideally suited for interfacing CZE with a mass spectrometer equipped with an API ion source.

A Sciex TAGA 6000E mass spectrometer equipped with an API source was used to sample ions generated from the ion spray LC/MS interface. The electrophoresis system consisted of a Spellman 0-60 kV power supply and a 100 um i.d. x 100 cm fused-silica capillary. High voltage was applied to the anode end of the capillary via a carbon vessel containing a acetonitrile/NH_4OAC buffer. Injections were made by the hydrostatic technique.

The peptide dynorphins 1-6,1-7,1-8,1-9 and leucine enkephalin were separated with a CZE voltage of 27 kV and 50/50 acetonitrile/30 mM ammonium acetate/acidic acid buffer at pH 4.8 (Figure 1). The last eluting peak, leucine enkephalin, exhibited an excess of 200,000 theretical plates, demonstrating the high separation efficiency obtainable by CZE.

Ion spray mass spectra of the peptides studied contained primarily the $[M+H]^+$ and $[M+2H]^{2+}$ ions. The degree of protonation corresponded to the number of terminal basic functionalities. For example, the mass spectrum of leucine enkephalin contained only the $[M+H]^+$ molecular ion and the mass spectra of dynorphin 1-6,1-7,1-8 and 1-9 contained both the $[M+H]^+$ and $[M+H]^{2+}$ ions with the diprotonated species being the base peak. The ratio of the $[M+2H]^{2+}$ ion to the $[M+H]^+$ ion increased with increasing acidity of the eluent. CZE/MS/MS of the $[M+H]^+$ or $[M+2H]^{2+}$ ion contained daughter ions which were consistent with the sequence of the peptide (Figure 2). The limit of detection for this system is in the low fmole range for the compounds investigated.

Reference

1. Jorgenson, J.W.; Lukacs, K.D. Science, 1983, 222, 266-272.
2. Bruins, A.P.; Covey, T.R.; Henion, J.D. Anal. Chem. 1987, 59, 2642-2646.
3. Olivares, J.A.; Nguyen, N.T.; Yonker, C.R.; Smith, R.D. Anal. Chem., 1987, 59, 1230-1233.

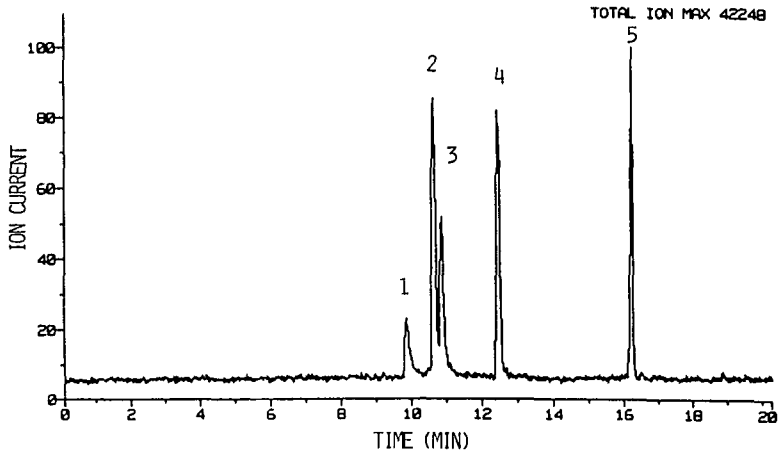

Figure 1. Capillary zone electrophoresis/mass spectrometry total selected ion electropherogram for 5 pmols each of (1) Dynorphin 1-9, (2) Dynorphin 1-7, (3) Dynorphin 1-8, (4) Dynorphin 1-6, and (5) Leucine Enkephalin. Conditions: CZE voltage 27 kV, 50/50 acetonitrile/30 mM NH_4OAc/HOAc,pH = 4.8, 100 um i.d. x 100 cm fused-silica capillary

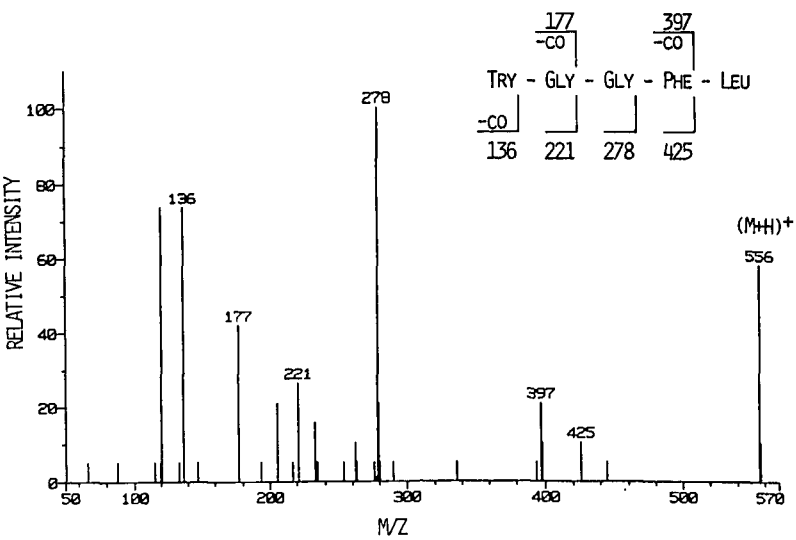

Figure 2. Capillary zone electrophoresis/mass spectrometry/mass spectrometry daughter ion spectrum for 5 pmols of leucine enkephalin. Same conditions used as Figure 1.

Presented at the 36th ASMS Conference on Mass Spectrometry and Allied Topics
June 5-10, 1988, San Francisco, CA

QUANTITATION OF ENDOGENOUS SUBSTANCE P BY COMBINED MICROCOLUMN-LC/DYNAMIC FAB-MS

C.A. Lisek, J. Bailey, L.D. Aimone, L. Benson, T.L. Yaksh and I. Jardine

Depts. of Pharmacology and Neurologic Surgery
Mayo Clinic, Rochester, MN 55905

Substance P (Figure 1), a putative pain transmitter found in the spinal cord, is one of an increasing number of peptides which function as intracellular messengers, i.e. neurotransmitters, in the nervous system. Neurotransmitters are usually quantitated by radioimmunoassay (RIA), an immunological method which affords high sensitivity (fmol range) of analysis but lacks complete specificity. We have developed a strategy (Figure 2) for the quantitative analysis of substance P which combines immunological methods with the sensitivity and specificity of microcolumn LC/dynamic FAB selected ion monitoring (SIM) mass spectrometry. This strategy is detailed below.

Cat spinal cords were boiled in 0.1 N HCl, homogenized, concentrated in vacuo, then dissolved in phosphate-buffered saline (PBS) solution (0.5 M KH_2PO_4, 0.9% NaCl, pH 6.5). An aliquot of the PBS solution of the extract was assayed for substance P (SP) activity by RIA using I^{125}-SP (yield: 252 pmol). To the rest of the extract was added a 10-fold molar excess (2520 pmol) of deuterated (d_8-Phe^8) substance P as an internal standard. One half (26 ml) of this solution was then applied in 2 mL aliquots to an immunoaffinity column containing rabbit polyclonal antibodies (IgG fraction) immobilized on cyanogen bromide-activated Sepharose 4B. Substance P was eluted with 20% aqueous formic acid. The formic acid fractions from all 2 mL aliquots were pooled and lyophilized, and a small aliquot was assayed by RIA for SP activity (yield: 40.7 pmol). The remaining half (26 mL) of the PBS solution of the extract was lyophilized.

Both the immunoaffinity purified and non-immunoaffinity purified samples were desalted on a C4 wide pore (40 μm) disposable filtration column, then quantitated by microcolumn LC/dynamic FAB SIM MS. An aliquot (0.1 or 0.5 μL) of sample was injected onto a C18 packed fused silica microcolumn (0.32 mm ID) fitted to a VG 30-253 quadrupole mass spectrometer dynamic FAB-MS inlet. The mobile phase was 0.1% TFA and 5% glycerol in 75:25 MeOH:H_2O and the flow rate was 5 μL/min. After ionization by FAB-MS, the protonated molecular ions of d_0- and d_8-substance P were selectively monitored.

In Figure 3 is a comparison of the results obtained upon analysis of immunoaffinity purified and non-immunoaffinity purified endogenous substance P. Deuterated internal standard (5 pmol) was injected before and after each endogenous sample. These results strongly suggest that immunoaffinity chromatography is a necessary purification step prior to MS analysis. A comparison of the results from the analysis of the immunoaffinity purified endogenous sample with those results from standard solutions of (d_0 + d_8)-SP is depicted in Figure 4. From the d_0/d_8 ratios obtained from the standard solutions, a response curve (Figure 5) was generated. The d_0/d_8 ratio for the endogenous sample was 0.2585. Since the amount of d_8-SP in the standard solutions was 400 pmol, and the endogenous sample contained 1260 pmol d_8-SP, the corrected d_0/d_8 ratio for the endogenous sample was 0.2585 x 400/1260 or 0.0821. This ratio corresponds to 39.0 pmol of d_0-substance P, which is in agreement with that value (40.7 pmol) determined by RIA.

In conclusion, (1) endogenous substance P was quantitated by combined microcolumn LC/dynamic FAB SIM MS; (2) the dynamic FAB SIM MS results for substance P were in agreement with those determined by RIA; and (3) the combination of immunoaffinity chromatography with both RIA and microcolumn LC/dynamic FAB SIM MS detection provides an optimal analytical methodology for endogenous neuropeptides.

Presented at the 36th ASMS Conference on Mass Spectrometry and Allied Topics
June 5-10, 1988, San Francisco, CA

FIG. 1

SUBSTANCE P

ARG-PRO-LYS-PRO-GLN-GLN-PHE-PHE-GLY-LEU-MET-amide

MW 1347.6

FIG. 2

STRATEGY FOR ANALYSIS OF ENDOGENOUS NEUROPEPTIDES

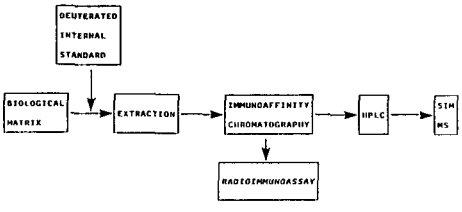

FIG. 3

MICROCOLUMN LC/DYNAMIC FAB SIM MS ANALYSIS OF ENDOGENOUS SUBSTANCE P

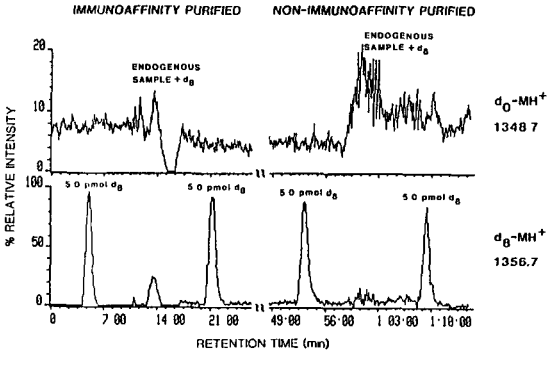

FIG. 4

MICROCOLUMN LC/DYNAMIC FAB SIM MS ANALYSIS OF ENDOGENOUS SUBSTANCE P

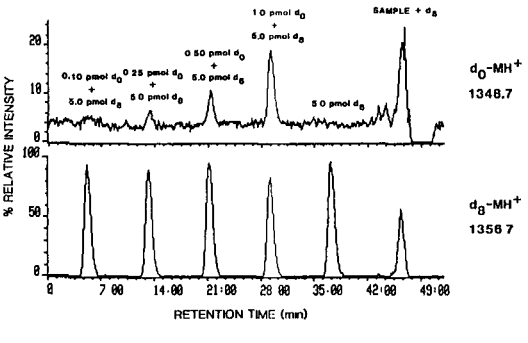

FIG. 5

QUANTITATION OF ENDOGENOUS SUBSTANCE P - RESPONSE CURVE

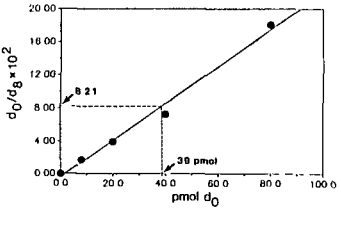

Presented at the 36th ASMS Conference on Mass Spectrometry and Allied Topics
June 5-10, 1988, San Francisco, CA

MIXTURE ANALYSIS BY COMBINED CAPILLARY COLUMN LIQUID CHROMATOGRAPHY - DYNAMIC FAB MASS SPECTROMETRY

R.H. Bateman & D.S. Jones.

VG Analytical Ltd., Floats Road, Wythenshawe, Manchester. M23 9LE.

Fast atom bombardment is now a well established ionisation technique, extremely useful for producing both molecular weight and structural information from a wide variety of compounds. This is especially true in the field of biochemistry where many species of interest are of high molecular weight and thermally labile in nature. The versatility of the technique, however, has been severely limited by the inability to combine the ionisation technique with any method of on-line separation.

However, with the recent development of packed capillary column liquid chromatography, previous incompatibility with liquid chromatography can be largely overcome. In particular, the low solvent flow rates (3-10µl/min) are well-suited to the limited pumping capacity of mass spectrometers. The additional benefit of high chromatographic resolution (up to 100,000 theoretical plates per metre) offers the potential for separation of complex mixtures prior to ionisation.

For this study, a mixture of four enkephalins have been separated by liquid chromatography.

Materials

Samples of leu enkephalin, met enkephalin, leu enkephalinamide and d-ala d-leu enkephalin were obtained from the Sigma Chemical Co.

Mass Spectrometer

Analyses were performed using a VG 70-250S mass spectrometer operated at 8000V accelerating voltage.

Liquid Chromatography

The column used for separation was a home-made packed fused silica column 0.32mm x 10cm packed with ODS2 3 micron particles.

A gradient separation was achieved using:

Solvent A	Solvent B
20% acetonitrile	45% acetonitrile
75% water	50% water
5% glycerol	5% glycerol
0.1% TFA	0.1% TFA

100% solvent A to 100% solvent B in 15 minutes, 100 nanolitres of the mixture of enkephalins was injected onto the column. The injected amount corresponds to 100ng per component.
Flow through the column was 5 microlitres per minute.

Results

Single ion chromatograms are shown as Fig. 1. Figs. 2-5 show corresponding mass spectra for each of the four components. Fig. 6 demonstrates both the capillary column resolution and chromatographic profile of the eluting peak.

Presented at the 36th ASMS Conference on Mass Spectrometry and Allied Topics
June 5-10, 1988, San Francisco, CA

Fig. 1

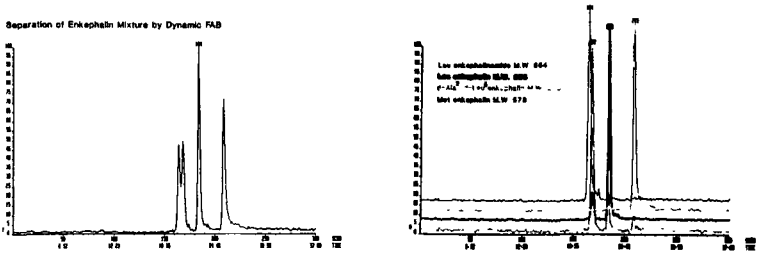

Fig. 2

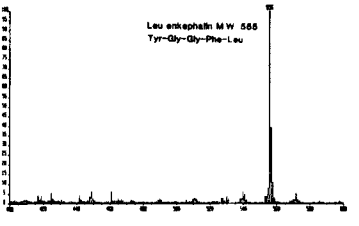

Fig. 3

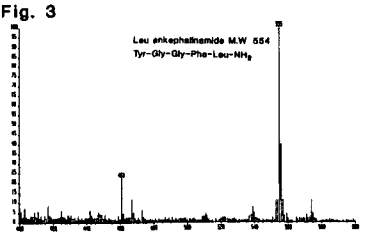

Fig. 4

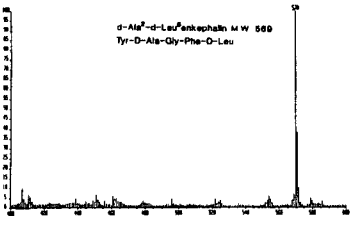

Fig. 5

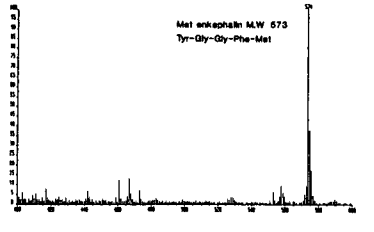

Fig. 6

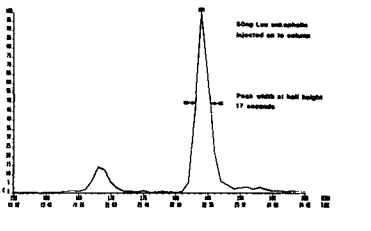

Presented at the 36th ASMS Conference on Mass Spectrometry and Allied Topics
June 5-10, 1988, San Francisco, CA

THERMOSPRAY LC-MS/MS STUDIES ON THE ANTIANXIETY DRUG BUSPIRONE AND ITS METABOLITES

Daniel A. Garteiz, TEXms Inc., Houston, TX.,
Ian A. Blair, Dept. Pharmacology, Vanderbilt Univ., Nashville, TN and R.F. Mayol, H.K. Jajoo, Bristol-Myers Co., Wallingfort, CT.

Buspirone, a potent anti-anxiety drug, has been recently introduced into clinical practice. Due to the polar nature of its metabolites, extensive preparation is required prior to GC/MS analysis. In order to facilitate metabolite identification from different patient populations, an LC/MS/MS study was initiated using a Nermag R3010 triple quadrupole mass spectrometer. Buspirone has excellent thermospray characteristics. Its TSP mass spectrum yields a very intense protonated parent at m/z 386. Using collisional induced dissociation (CAD) with Argon as collision gas, it was possible to fragment the parent ion to yield structural revealing daughter ions.

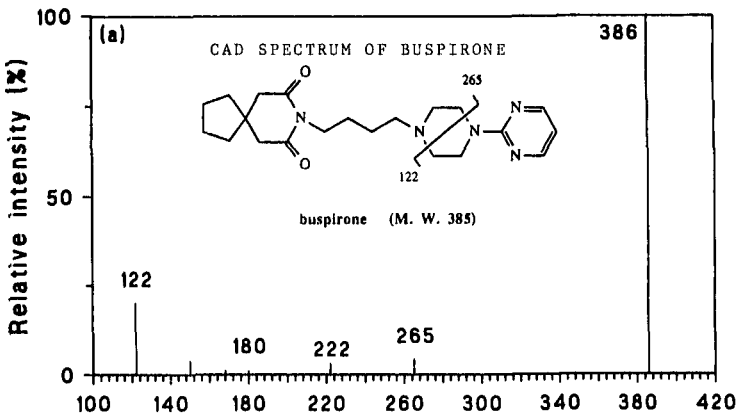

The daughter ion at m/z 122 is thought to arise from cleavage across the piperazine ring. This daughter, as well as the one at m/z 265 are useful for identifying sites of hydroxylation.

Buspirone undergoes a complex series of biotransformations to give a series of hydroxylated products. These products generate protonated molecular ions 16 daltons higher tha buspirone (See figure below.)

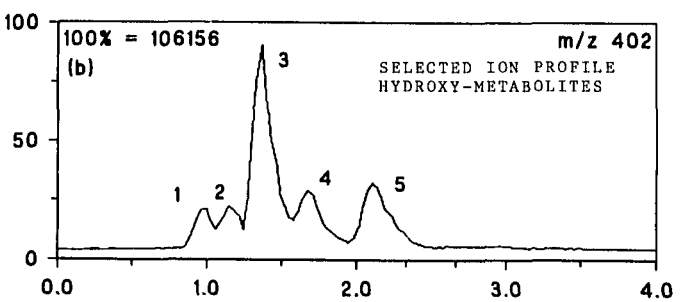

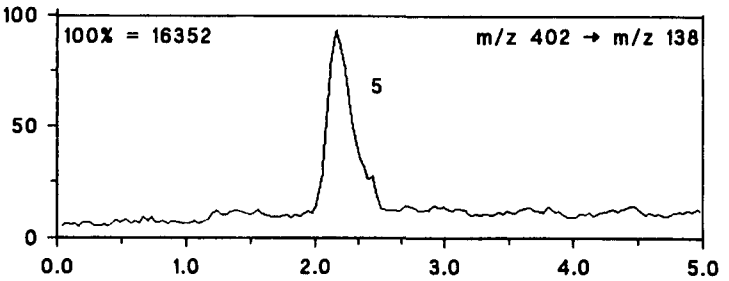

Out of the five hydroxylated metabolites detected, only one was found to contain the transition m/z 402 to m/z 138. This fact immediately identified the metabolite as having undergone pyrimidinyl hydroxylation (See above).

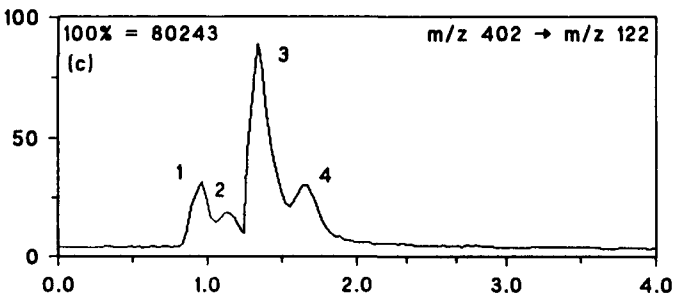

Four other metabolites were found to yield the m/z 402 to m/z 122 transition. Three of these metabolites were tentatively identified as 3-hydroxy, 6'-hydroxy and oxa-buspirone. Their identity was later confirmed by comparison of their CAD spectra and their retention times to the auththentic compounds.

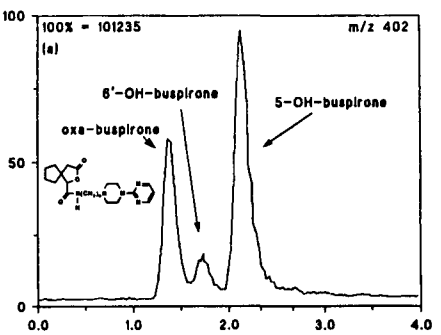

In summary, the combination of hepatocyte incubations followed by TSP-LC/MS/MS analysis provides a powerful tool for the characterization of buspirone metabolites. In addition, TSP-LC/MS/MS greatly reduces the analysis time, which will allow the study of larger patient populations.

Presented at the 36th ASMS Conference on Mass Spectrometry and Allied Topics
June 5-10, 1988, San Francisco, CA

RAPID ANALYSIS OF IFOSFAMIDE IN HUMAN PLASMA BY THERMOSPRAY LC/MS/MS

Daniel A. Garteiz, TEXms Inc., Houston, TX
and Robert A. Newman, Dept. Medical Oncology
Univ. Texas M.D. Anderson Cancer Center

Ifosfamide is an alkylating oxazaphosphorine used in a wide variety of tumors including soft cell lung cancer, soft tissue carcinoma and ovarian cancer. Recently, our laboratories have developed an HPLC assay using cyclophosphamide as an internal standard. Although the HPLC assay reduces sample preparation significantly, the chromatographic separation of ifosfamide from the internal standard requires c.a. 16 minutes. For this reason, the laboratory can only process 3-4 samples per hour.

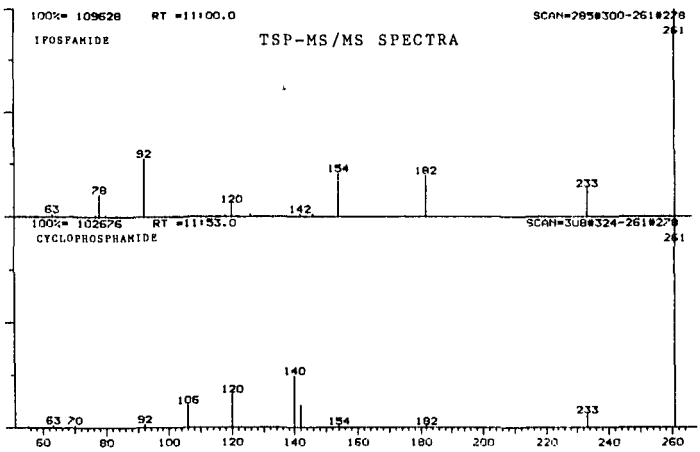

We now wish to report on a rapid analysis method for ifosfamide based on thermospray followed by tandem mass spectrometric analysis. The TSP-MS/MS spectrum of cyclophosphamide displays a daughter ion at m/z 140 which arises from the dichloro substituent on the phosphoramido nitrogen. This daughter is not present in the spectrum of ifosfamide. Ifosfamide displays a daughter at m/z 154 which is absent in the cyclophosphamide spectrum. These daughters were used to quantitate ifosfamide in human plasma.

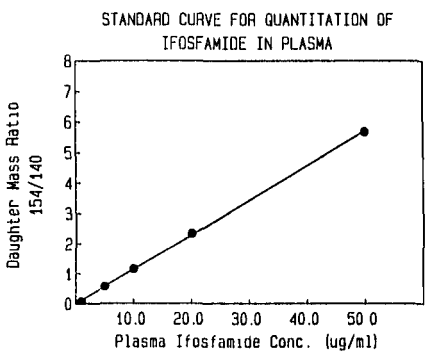

Presented at the 36th ASMS Conference on Mass Spectrometry and Allied Topics
June 5-10, 1988, San Francisco, CA

EXPERIMENTAL: A Nermag R3010 Triple Quadrupole System was used for this work. The TSP-LC/MS/MS conditions were as follows: Collision Gas: Argon Collision Energy: -16ev; Collision Pressure: 50 MilliTorr; LC Flow: 1.5 ml/min.; Mobile Phase: 27/73 Acetonitrile/$NH_4^+Ac^-$ Buffer; RP column

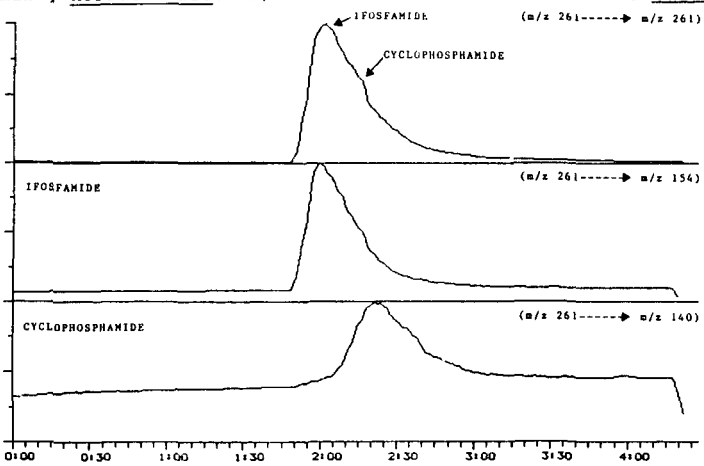

FIGURE 1: SRM TRACE AT 30 MINUTES POST-DOSE

SAMPLE PREPARATION: An aliquot of human plasma is spiked withcyclophosphamide, made basic and extracted with chloroform. After evaporation, the residue is dissolved in mobile phase (200ul) and 20ul are analyzed.

RESULTS: The use of a fast column and the fact that chromatographic resolution was not needed, allowed for analyses every four minutes. Ifosfamide levels were measured in a patient given an IV infusion of the drug. Levels were easily detected 24 hours post dose. The TSP-LC/MS/MS measurements were found to be within 3% of those obtained by HPLC/UV.

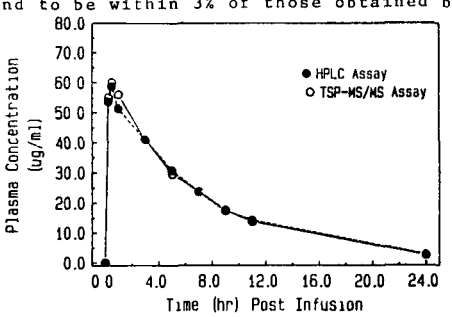

CONCLUSIONS: This work clearly reveals that TSP-LC/MS/MS analyses can be used to carry out quantitative measurements as are required in bioavailability/pharmacokinetic studies. Furthermore, in our study, the speed of analysis resulted in a 500% increase in sample throughput.

Presented at the 36th ASMS Conference on Mass Spectrometry and Allied Topics
June 5-10, 1988, San Francisco, CA

DETERMINATION OF DIANABOL AND ITS METABOLITES BY COUPLED-COLUMN LC/TANDEM MASS SPECTROMETRY, Per Olof Edlund and Jack Henion, Equine Drug Testing and Toxicology, New York State College of Veterinary Medicine, Cornell University, 925 Warren Drive, Ithaca, NY 14850.

Monitoring steroid use requires an understanding of steroid metabolism in the species in question and development of sensitive methods for screening of the steroid or its metabolites in urine. In the present work Dianabol and its metabolites were extracted from equine urine by liquid-liquid extraction and separated from remaining urine components by coupled-column chromatography on two reversed phase columns with different selectivity. The sample was first separated on a phenyl-silica column. The fraction containing the steroid of interest was collected onto a short ODS-column for enrichment (peak compression) and then eluted with reversed flow direction onto an octyl-silica column for the final separation.

Two complimentary LC/MS interfaces were used for on-line LC/MS and MS/MS to confirm the identity of Dianabol and to identify metabolites in equine urine. An atmospheric pressure ion source (API) equipped with a heated pneumatic nebulizer and a corona discharge needle was used for neutral steroids. The corona discharge initiated the ionization of solvent ions which were used for chemical ionization at atmospheric pressure. The ions formed were focussed and declustered through a dry nitrogen curtain and then through a 100 um orifice into the vacuum region for mass analysis.

The ion spray interface which combines some of the characteristics of electrospray and ion evaporation was used for confirmation of Dianabol-sulfate. Both ionization techniques gave little or no fragmentation and collision induced dissociation (CID) was used to obtain fragmentation for structural confirmation. Dianabol was excreted to the urine as an unstable conjugate of sulfuric acid. Nucleophilic attack by water in urine gave 17-epi-Dianabol. Elimination of the sulfate group gave a tertiary carbonium ion at the 17-position that rearranged and eliminated water to form 18-nor-17,17-dimethyl-1,4,13(14)androstatrien-3-one. Mono- and di-hydroxylated metabolites were also identified. LC/LC/MS of Dianabol and 17-epi-Dianabol gave simple positive ion mass spectra showing the $[M+H]^+$ at m/z 301 and a fragment for loss of water. Their MS/MS mass spectra were identical with several characteristic daughter ions presumably corresponding to: loss of water to give m/z 283, a fragment involving the C and D-ring at m/z 149, A-ring and part of B-ring at m/z 173 and A-ring at m/z 135 and 121. The fragment involving the C and D-ring was verified by MS/MS spectrum of 17-deuteromethyl-Dianabol which gave a labeled fragment at m/z 152. Ion spray coupled-column LC/MS of Dianabol-sulfate gave the molecular ion $[M-H]^-$ at m/z 378. CID of this ion gave the parent ion and a fragment corresponding to HSO_4^- at m/z 97. 17-epi-Dianabol was detected in urine by UV up to 6 days after a 250 mg i.m. dose to a horse. The half life of the elimination phase was 78 h.

Presented at the 36th ASMS Conference on Mass Spectrometry and Allied Topics
June 5-10, 1988, San Francisco, CA

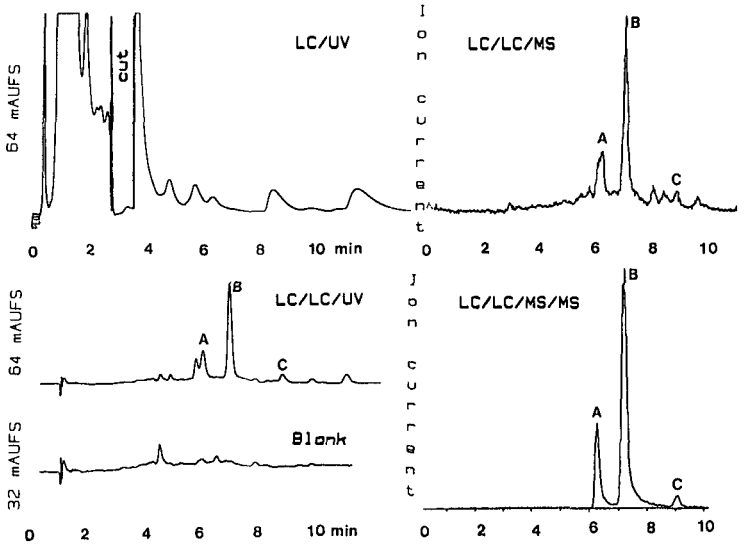

Figure 1. Comparison of LC/UV and LC/MS chromatograms obtained from an extract of a 8 h urine sample containing 46 ng/mL of Dianabol (peak B). The other peaks were identified as 13-hydroxy-17,17-dimethyl-1,4-androstadien-3-one (A) and 17-epi-Dianabol (C) incompletely resolved from Dianabol on the first column. The cut from the phenyl-column (LC/UV) was collected by column switching and separated on the octyl-column with UV detection (LC/LC/UV), detection by mass spectrometry (LC/LC/MS) and tandem mass spectrometry (LC/LC/MS/MS).

Presented at the 36th ASMS Conference on Mass Spectrometry and Allied Topics
June 5-10, 1988, San Francisco, CA

Thermospray LC/MS of the LL-F28249 Macrocyclic Lactones

*Kenion, G.B., Carter, G.T. and Borders, D.B.
American Cyanamid, Pearl River, NY

The macrocyclic lactones **1-4** (LL-F28249 alpa, beta, gamma, and lamda) are highly potent antiparasitic agents effective against many endo- and ectoparisites of mammals[1]. The mass spectra of **1-4** were obtained in the positive and negative ion modes. Since chromatographic considerations precluded the use of ammonium acetate buffer, our study relied upon the discharge electrode and filament modes of ionization.

All spectra were obtained using a Finnigan TSP-46 dedicated thermospray LC/MS system. A 75% MEOH/ 25% H_2O solvent system at 1.2 mL/min was used throughout the study. The optimum vaporizer temperature was 95°C, while the optimum jet temperature was 220°C.

Positive ion spectra generated using filament ionization are characterized by an M+1 ion with a relative abundance of 10-20%. The most abundant fragment ions (including the base peak) correspond to losses of methanol or water. Compounds 1 and 2, with a hydroxy rather than a methoxy substituent at C-5, have a characteristic ion corresponding to a loss of 110 amu from the parent M+1 ion.

Positive ion spectra obtained via discharge electrode ionization exhibited enhanced fragmentation, although essentially the same ions were produced. An M+23 sodium adduct, formed in aproximately equal abundance to the M+1 ion, is unique to the discharge electrode ionization mode. Full spectra (scanning 400-650 amu) are obtainable via loop injection from as little as 265 ng of sample.

Negative ion spectra obtained using the filament ionization mode are dominated by M- peaks produced by electron capture. Gartiez[2] reported a similar M- ion at m/z 874 for a related compound, 22,23 dihydroavermectin B_{1a}, using a solvent system of 80/20 acetonitrile/water with a Vestec Thermospray LC/MS interface. Introduction of acetonitrile and/or ammonium acetate buffer to our solvent system shifted the base peak from the M- ion resulting from electron capture to an M-1 ion characteristic of a deprotonated alchohol. Fragmentation is limited to loss of methanol or water and fairly abundant ions due to loss of 110 amu for the compounds with a hydroxy substituent at C-5. Full spectra (scanning 400-650 amu) are obtainable via loop injection from as little as 212 ng of sample.

Negative ion spectra generated using discharge electrode ionization are

similar to those obtained with filament ionization, although filament ionization produces less background noise and higher sensitivity for LL F28249 alpha,beta,gamma and lambda.

1. G.T. Carter, J.A. Nietsche, M. R. Hertz, D. R. Williams, M.M. Siegel, G.O. Morton, J.C. James and D.B. Borders *J. Antibiotics* **41**,4,512-528 (1988).

2. D.A. Gartiez *LC* **3**,4,334 (1985).

Figure 1 LLF28249 macrocyclic lactones

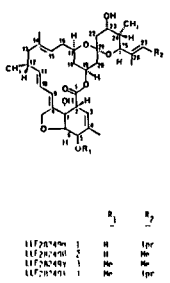

Figure 2. Positive ion spectrum of LLF28249 alpha, discharge electrode ionization

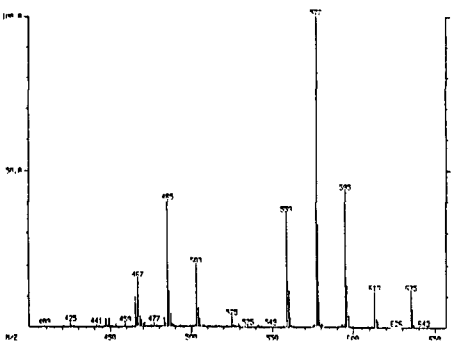

Figure 3 Negative ion spectrum of LLF28249 alpha, filament ionization

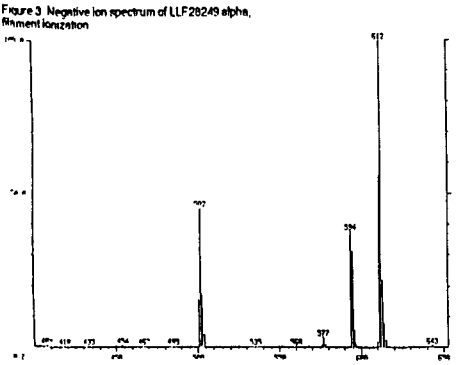

Presented at the 36th ASMS Conference on Mass Spectrometry and Allied Topics
June 5-10, 1988, San Francisco, CA

Thermospray LC/MS of LL-F42248 alpha

*Kenion, G.B., Carter, G.T. and Borders, D.B.
American Cyanamid, Pearl River, NY

The tetrachlorinated, nitropyrrole antibiotic LL-F42248 alpha is the first tricyclic member of the pyrrolomycin family to be reported[1]. Thermospray LC/MS spectra have been obtained in both positive and negative ion modes using buffer only, discharge electrode, and filament ionization. Corresponding spectra have also been obtained for labelled LL-F42248 alphas. Compound **1a** contains >95% ^{15}N enrichment at both nitrogen atoms. Compound **1b** is similarly >95% ^{15}N enriched and also contains 60% ^{18}O enrichment in the two oxygens of the nitro group. Comparison of these spectra allows determination of the fragmentation patterns.

All spectra were obtained from a Finnigan TSP-46 dedicated Thermospray LC/MS. A solvent system of 60% methanol, 40% 0.1 M ammonium acetate at 1.2 mL/min was used throughout the study. The optimum vaporizer temperature was 95°C, while the optimum jet temperature was 230°C. The ^{15}N and ^{18}O labelled LL-F42248 alpha was derived from fermentations of Streptomyces fumanus supplemented with ^{15}N and ^{18}O enriched precursors.

The positive ion fragmentation pattern is outlined in Scheme 1. The number of nitrogens assigned to each struture was based on a corresponding peak two mass units higher for the ^{15}N labelled analogue, while the assignment of nitro group oxygens is based on comparison with the ^{15}N,^{18}O labelled analogue. The discharge electrode and filament enhanced fragmentation. The fragments at m/z 339 and m/z 325 are unique to these ionization modes. It appears that the nitro group is reduced via the oxime to the amine, whereas in the buffer only ionization mode the nitro group is probably lost through protonation and subsequent SN2 dislpacement by the carbonyl oxygen. The filament provides the most efficient means for ionization in the positive mode for LL-F42248 alpha, with a full spectrum (scanning 250-450 amu) obtainable from 1ug of sample.

The negative ion spectra, as outlined in Scheme 2, are dominated by the facile loss of CO corresponding to the base peak fragment at m/z 354 for filament and discharge electrode ionization and m/z 353 for buffer only ionization. The negative ion, filament ionization mode provides optimal sensitivity for LC/MS analysis of LL-F42248 alpha, with a full spectrum obtainable from 42 ng of sample.

Presented at the 36th ASMS Conference on Mass Spectrometry and Allied Topics
June 5-10, 1988, San Francisco, CA

1. Carter, G.T.; Nietsche, J.A.; Goodman, J.J.; Torrey, M.J.; Dunne, T.S.; Borders, D B., Testa, R.T. *J. Antibiotics* **40**, 233, (1987).

Scheme 1 F42248 alpha positive ion fragmentation pathway

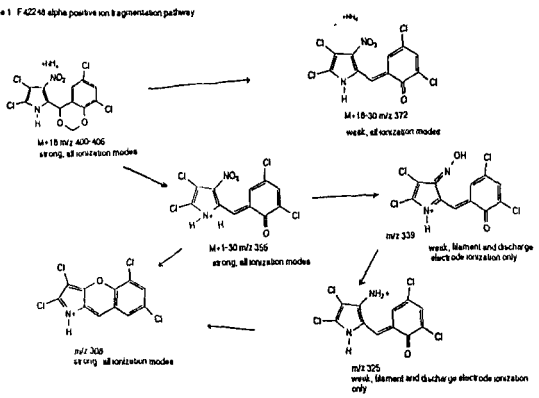

Scheme 2 F42248 alpha negative ion fragmentation pathway

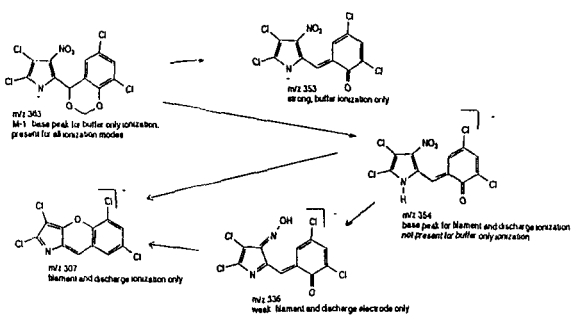

Presented at the 36th ASMS Conference on Mass Spectrometry and Allied Topics
June 5-10, 1988, San Francisco, CA

MASS SPECTRAL INVESTIGATIONS OF BORON NEUTRON CAPTURE THERAPY (BNCT) AGENTS

By

D. L. Miller and L. J. Peterson-Wright
Idaho National Engineering Laboratory
EG&G Idaho, Inc.
P.O. Box 1625
Idaho Falls, ID 83415-2208

Boron neutron capture therapy (BNCT) is a promising technique for the treatment of selected types of brain tumor and potentially for other tumor types. In this therapy, a ^{10}B-enriched species is administered to the bloodstream and selectively deposited in the tumor. The selective deposition in the tumor is due to either the breakdown of the blood-brain barrier or to the chemical nature of the boron-containing compounds. Once a sufficient concentration of boron is attained in the tumor (approximately 25 ppm), the tumor is irradiated with a controlled energy neutron beam (preferably epithermal, 1 eV to 10 keV), at which time neutrons are captured by the incorporated boron atoms. The capture results in the reaction, $^{10}B(n,)^{7}Li$, which produces a localized nuclear reaction capable of destroying the tumor cell containing the boron.

A variety of boron containing compounds have been evaluated for use in BNCT. One of the most promising of the compounds is the disodium salt of mercaptoundecahydrododecaborate ($Na_2B_{12}H_{11}SH$), commonly referred to as BSH. This particular compound has been used in Japan in treatment of more than 90 patients over the last 20 years with good results. Even though good success with this compound has been achieved in Japan, its use has come into question in the United States due to an incomplete characterization of the chemical constituents present in the administered drug. BSH is known to be an unstable compound when exposed to air and moisture. The BSH compound is also known to dimerize and the dimer is known to undergo further oxidation to produce a thiosulfinate species. Both of these secondary products have been demonstrated to have considerably higher toxicity than the parent compound. This high degree of toxicity requires that stringent quality control examination be performed on every lot of BSH prior to use to ensure safety. The analytical procedures utilized to examine the species of interest have consisted primarily of chromatographic procedures (TLC, HPLC, IC, and isotachophoresis) and occassionally nuclear magnetic resonance (NMR). These procedures have proven to be inadequate by themselves due to incomplete chromatographic resolution, lack of sensitivity, and inability to identify unknown peaks arising from manufacture or packaging. Given the nature of the species of interest, it was decided to examine the use of mass spectrometry incorporating fast atom bombardment ionization to determine if the potential existed for the development of a HPLC FAB/MS analytical procedure utilizing the new continuous-flow FAB inlet.

All experiments were conducted on a KRATOS MS890 equipped with an 8 kV MS50-type FAB source. The MS890 was equippped with an Ion Tech (11NF) saddle field ion gun and xenon was used as the FAB gas. Initial experiments using BSH were conducted in both positive and negative ion modes using a variety of FAB matrices. Positive ion experiments were discontinued

when no peaks indicative of the compound of interest were observed. The positive ion spectra were dominated by peaks arising from sodium reacting with the various matrices used.

Experiments conducted in the negative ion mode proved to be much more productive. A variety of matrices were tested with BSH. These matrices included glycerol, thioglycerol, 3-nitrobenzyl alcohol, triethanolamine, and PEG-600. No peaks indicative of the BSH compound were observed when glycerol was used as the matrix, even though the BSH was readily soluble. For the remainder of the matrices tested, good solubility of the BSH was also observed as well as peaks using BSH containing the natural isotopic abundance of boron (approximately 20% ^{10}B and 80% ^{11}B). When examined using thioglycerol as the matrix, a cluster of peaks indicative of boron was observed with the most intense peak occurring at M/Z 197. This cluster arises from the loss of a sodium from the parent compound. The distribution of peaks obtained from the FAB/MS experiment was compared to the expected theoretical distribution for the elemental composition $NaB_{12}H_{11}SH$ and found to closely match. Additional clusters of peaks were observed indicative of $B_{12}H_{11}$ and $B_{12}H_{11}SH$. However, the spectra were complicated and of low intensity due to the distribution of ion current arising from the large numbers of boron atoms and its multi-isotopic nature. To overcome this problem, BSH enriched to 95% ^{10}B (Callery Chemical, Pittsburgh, PA) was used in the remainder of the experiments. Upon reanalysis, using thioglycerol as the matrix, the cluster around M/Z 197 was observed to have collapsed to a single peak at M/Z 187. Similar results were observed for the lower molecular weight fragments. By utilizing the ^{10}B-enriched material, the ion current was concentrated into fewer peaks permitting a more detailed examination of the spectra to be performed. It was observed that, although the majority of the signal from the BSH was arising from the peak at M/Z 187, a minor amount of reaction was occurring between the BSH and the thioglycerol producing clusters of higher molecular weight. Similar results were obtained with 3-nitrobenzyl alcohol and triethanolamine. However, when PEG-600 was used as the matrix, no reaction of the BSH with the matrix was observed. Additional matrices are being examined to find other nonreacting matrices.

Aqueous solutions of the BSH compound, as well as other boron species of interest, were combined with the FAB matrices mentioned above to determine if the presence of water would prevent the detection of the compounds of interest. These experiments were conducted to determine if currently existing HPLC techniques which use paired-ion chromatography with 1:1 water methanol as eluant could be adapted for use in a continuous-flow FAB application. It was determined that the presence of the water did not have an adverse effect of the analysis, thus allowing the use of continuous-flow FAB inlet. Additional work is currently underway to examine the dimer and thiosulfinate form of the dimer which show limited solubility in the matrices examined to date and to convert the existing HPLC technique to a microbore column for use with continuous-flow FAB.

This paper has been authorized by a contract of the U.S. Government under DOE Contract No. DE-AC07-76ID0157. Accordingly, the U.S. Government retains a nonexclusive, royalty-free license to publish or reproduce the published form of this contribution, or allow others to do so for U. S. Government purposes.

Presented at the 36th ASMS Conference on Mass Spectrometry and Allied Topics
June 5-10, 1988, San Francisco, CA

SIMULTANEOUS IDENTIFICATION AND QUANTITATION OF MORPHINE AND CODEINE IN URINE BY GAS CHROMATOGRAPHY/MASS SPECTROMETRY

Wen-neui Lin, Jau-Wen Chu
and Craig C. Foreback

Division of Chemistry, Dept. of Pathology
Henry Ford Hospital, Detroit, MI 48202

A Gas Chromatography/Mass Spectrometry (GC/MS) method has been developed for the simultaneous identification and quantitation of morphine (M) and codeine (C) in urine. Urine (5.0 ml), spiked with internal standards (5 μL of 100 ng/mL morphine-D^3 and codeine-D^3 each) was autoclaved with 0.5 mL of concentrated HCl at 121°C for 20 minutes. After cooling the tube, 0.8 mL of 10 N NaOH and 100 μL of glacial acetic acid were added to each tube. The pH of the sample was adjusted to 4.4-4.6. The CLEAN-SCREEN® DAU column (130 mg, Worldwide Monitoring, Horsham, PA 19044), attached with a stopper, was placed in the Adsorbex system and washed twice with methanol and twice with distilled water. An 8 mL fritted reservoir was attached to the top of the column. Sample was added to the reservoir and pulled through the column at a flow rate of 1.0 mL/min. The column was washed twice with 1.0 mL of distilled water, once with 1.0 mL of 0.1 M acetate buffer (pH 4.0) and twice with 1.0 mL of methanol. The opiates were eluted twice with 1.0 mL of elution solvent (methylene chloride: isopropanol 8:2 with 2% NH_4OH). The eluents were evaporated to dryness under nitrogen and derivatized with 50 μL of N.O-bis(trimethylsilyl)-trifluoroacetamide (BSTFA) at 70°C for 20 minutes. Identification and quantitation of drugs were accomplished by using HP 5970A Mass Selective Detector (MSD), coupled with HP 5890 Gas Chromatograph (HP Ultra-2 capillary column 12m x 0.2mm x 0.33 um) and the HP 59970 ChemStation analytical workstation. All data were acquired by using Hewlett-Packard's GC with the following parameters: injection port temperature, 260°C; transfer line temperature, 290°C; temperature equilibration time, 0.5 min; purge time, 0.8 min; oven initial temperature, 80°C; initial time, 1.0 min; program rate, 20°C/min; final temperature, 280°C; and final time, 2 min. Helium was used as carrier gas at flow rate of 30 mL/min with head pressure of 2.5 psi. Splitless mode was used. For quantitation, the MSD was operated in the Selective Ion Monitoring (SIM) mode. Morphine, morphine-D^3, codeine and codeine-D^3 were monitored at 429, 287, 196 amu; 432, 290, 199 amu; 371, 234, 178 amu and 374, 237, 181 amu respectively. Calibration curves, when plotted as peak area ratios of analyte to internal standard versus the concentrations of analyte, are linear from 5 to 1200 ng/mL for both morphine and codeine. Detection limits are 5 ng/mL for both compounds. Absolute recoveries range from 85% to 95% for both morphine and codeine. Day-to-day variations (N=8) are 4.5% for codeine and 5.3% for morphine. Within-day variations (N=10) are 1.4% for codeine and 1.9% for morphine. The method of sample preparation we have developed using CLEAN-SCREEN® DAU column has resulted in high recoveries with excellent reproducibility for the analysis of morphine and codeine in urine. We conclude that this procedure is simple, rapid, specific and cost-effective and is suitable for the routine confirmation of opiates in clinical laboratories.

Presented at the 36th ASMS Conference on Mass Spectrometry and Allied Topics
June 5-10, 1988, San Francisco, CA

ANALYSIS OF PIPECOLIC ACID IN PEROXISOMAL DISEASES BY GCMS WITH SELECTED ION MONITORING

Yong Y. Lin

N.Y.S. Institute for Basic Research in Developmental Disabilities
Staten Island, New York 10314

OBJECTIVE

Excessive excretion of pipecolic acid(PA) has been used as a biochemical marker for the neurogenetic disorder of peroxisomal diseases, such as Zellweger syndrome(ZS) and neonatal adrenoleukodystrophy(NALD).

However, the analysis of pipecolic acid(PA) by conventional amino acid analysis has been hampered by the lackings of both sensitivity and specificity. The GCMS method with selected ion monitoring is developed for the analysis of PA in plasma and urine. The analytical method is highly sensitive and specific, and accurately determines the levels of PA in different types of peroxisomal diseases.

PEROXISOMAL DISORDERS

1. Zellweger Cerebrohepatorenal Syndrome (ZS):
   * hepatomegaly, renal cortical cyst, hypotonia, do not thrive, usually die in 6 months
   * absence of morphologically detectable peroxisomes in liver and kidney
   * accumulation of very long chain fatty acids ($>C_{24}$)
   * elevation of pipecolic acid

2. Neonatal Adrenoleukodystrophy:
   * progressive destruction of cerebral white matter and adrenal cortex
   * absence or enzyme defects in peroxisomes
   * accumuration of very long chain fatty acids ($>C_{24}$)
   * elevation of pipecolic acid

GCMS ANALYSIS OF PIPECOLIC ACID

1. Sample Preparation:

Plasma or Urine (0.1-0.5ml)

↓ add 50 nmol DL-pipecolic acid-d_{11} as I.S.
adjust to PH 2

AG50W-X8 (H^+)

↓ wash with H_2O, 1N HCOOH
elute with 1N NH_4OH

AG1-X8 (OH^-)

↓ wash with H_2O
elute with 1N HCOOH

Dried Sample

↓ add 100ul HCl/butanol
heat 90 C for 30 min

Butyl Esters

↓ add 100ul 25% trifluoroacetic anhydride in EtOAc
heat 90 C for 30 min

Trifluroacetyl Butyl Ester

2. GCMS
   * DB-17(fused silica column), 0.55u x 15 ft
   80 - 280 C at 15 C/min
   * NH_3CI
   * SIM
      pipecolic acid: m/z 180, 208, 282, 299
      pipecolic acid-d_{11} m/z 189, 217, 291, 308

RESULTS

Patients	Age(yr)	PA in Urine (nmol/mg creat.)	PA in Plasma (nmol/ml)	Diagnosis
1	23 days	539.1	4.7	ZS
2	1/12	111.7	8.6	ZS
3	2/12	541.7	4.7	ZS
4	1/12	1,412.6	*	ZS
5	2/12	13.0	*	Pseudo ZS
6	3/12	*	4.7	Pseudo ZS
7	2/12	11.3	108.7	NALD
8	1	44.4	181.0	NALD
9	1	24.5	208.6	NALD
10	1	19.1	*	NALD
11	5	16.8	*	NALD
12	2	*	261.1	NALD
13	5/12	*	196.0	NALD
14	15	2.3	1.5	NALD variant
15	11	3.6	8.1	NALD variant
16	4	34.7	170.0	NALD or Refsum
17	4	71.2	128.8	Refsum
18	3days	23.6	6.9	Unknown hypotonia
Controls (8)	1 to 15	0.9 to 3.3	0.6 to 3.4	Healthy controls

*) Not measured

CONCLUSION

GCMS with selected ion monitoring technique offers a highly sensitive and specific analysis of PA contents in plasma and urine. The analysis of PA contents in urine and plasma from patients of peroxisomal diseases shows ZS patients are characterized by a large elevation in urinary PA, >100 nmol/mg creatinine, with little elevation in plasma PA levels. On the other hand, NALD patients show a moderate urinary PA level, <50 nmol/mg creatinine, but their plasma PA are largely elevated, >100nmol/ml; thus, differentiation between ZS and NALD may be simply made by the PA analysis. Several variants of ZS and NALD and other non-peroxisomal neurogenetic diseases show no elevation in PA levels. The results further confirm the disorders of lysine metabolism in peroxisomes.

(AKNOWLEDGEMENT) We thank Dr.A. Moser of the Kennedy Institute for Handicapped Childreen, Baltimore for providing us parts of samples and their clinical informations.

Presented at the 36th ASMS Conference on Mass Spectrometry and Allied Topics
June 5-10, 1988, San Francisco, CA

ADVANCES IN MS/MS ANALYSIS WITH THE ION TRAP MASS SPECTROMETER

M. Weber-Grabau, P.E. Kelley, S.C. Bradshaw, D.J. Hoekman
Finnigan MAT, San Jose, California 95134

In a conventional beam mass spectrometer, the steps of ionization, parent ion selection, collison-induced dissociation (CID), and daughter mass analysis are separated in space; in particular, multiple analyzers are required for an MS/MS experiment. In the quadrupole ion trap, the analysis steps are separated in time and all occur inside the ion trap electrode assembly. Since both parent and daughter ions are trapped simultaneously, daughter ion yields are 30-100%. With recently developed electronics and software, it is possible to take full advantage of the inherent multichannel/multianalyzer capability of the ion trap mass spectrometer (ITMS) and conduct novel experiments not possible before.

After creation by EI or CI, parent ions of a single m/z value are isolated by the application of both RF and DC voltages to the ring electrode, i.e., temporary operation of the ion trap near the apex of the stability diagram (1). This single-mass isolation step also eliminates space charge due to other analyte ions or background ions, allowing longer ionization times and resulting in an increase in sensitivity by several orders of magnitude. The selected parent ion is dissociated and the daughter spectrum is acquired in the mass-selective instability mode.

MS^n is easily achieved by adding more mass isolation/dissociation steps to the computer-controlled scan program. An EI/MS/MS/MS scan function is shown in Fig. 1. Fig. 2 gives an example for the application of this scan function; the parent ion chosen is m/z 503 from perfluorotributylamine (FC-43). m/z 503 is the carbon-13 isotope peak of the fragment ion with the elemental composition $C_9F_{20}N$; its abundance, relative to the base peak at m/z 69 in the original EI spectrum, is 0.8% (Fig. 2a). With an efficiency of about 60%, m/z 503 is dissociated into daughter ions at m/z 219, 220, 264, and 265 (Fig. 2b). The ratio of the two intense daughter ions at m/z 264 and 265 (4:5) reflects that the number of carbon atoms in the parent and daughter ions are 9 and 5, respectively. Then, the daughter ion at m/z 265 is isolated (Fig. 2c) and dissociated, and the full granddaughter spectrum is recorded (Fig. 2d). The efficiency of this step is 30%. This experiment also illustrates the sensitivity and internal dynamic range of the instrument; the granddaughter ion at m/z 69 is at a relative abundance level of only 1/10,000 of the intensity of the same mass ion in the original EI spectrum. Fig. 3 shows picogram sensitivity in the isobutane CI/MS/MS analysis of DIMP, a chemical warfare simulant. The daughter ion at m/z 163 is due to an interference; single-stage MS analysis or selected ion monitoring would not allow differentiation between sample and background at m/z 181.

The full-scan sensitivity of the ITMS is increased by more than one order of magnitude with the introduction of axial modulation. For low sample detection limits and high signal-to-noise ratios, it is desirable to build up a large ion population prior to mass analysis. While the maximum ion storage capacity of the ion trap is around 10^6 to 10^7 ions, only 10^4 to 10^5 ions can be stored for mass analysis with unit mass resolution in an RF-only scan. With this limitation, sample ion intensities may be weak compared to ion signals from the chemical background. A similar situation exists when an analyte ion of interest is present only at a very low abundance level. Overloading the trap to increase the number of sample ions leads to resolution loss due to space charge interactions (Fig. 4a). Ions of higher mass, still stored in the trap when a mass is near instability, reduce the effective trapping field; thus, the ion ejection is delayed, and mass peaks show tailing. This effect can be overcome by the application of an axial modulation voltage between the endcaps of the ion trap as Fig. 4b shows.

The modulation is applied at a fixed frequency and amplitude during the mass analysis RF ramp. The frequency is close to 1/2 of the fundamental RF frequency. Unlike the quadrupole field, which is zero in the center of the trap, the field generated by the modulation frequency is nearly homogeneous in the axial direction. Ions that are just about to be ejected from the trap (near q=0.91 and beta=1) are in resonance with this field, and their ejection is facilitated, leading to the improved mass resolution. High-sensitivity EI/GC/MS results with axial modulation are described in (2), but improved resolution at higher sample ion intensities is also observed in CI and MS/MS analyses.

References:

(1) Improved Ion Trap Performance with New CI and MS/MS Scan Functions; M. Weber-Grabau, P.E. Kelley, J.E.P. Syka, S.C. Bradshaw, J.S. Brodbelt. Presented at the 35th ASMS Conference, Denver 1987.

(2) The Application of Novel Ion Trap Scan Modes for High Sensitivity GC/MS; D.B. Tucker, C.R. Hameister, S.C. Bradshaw, D.J. Hoekman, M. Weber-Grabau. Presented at the 36th ASMS Conference, San Francisco 1988.

Presented at the 36th ASMS Conference on Mass Spectrometry and Allied Topics
June 5-10, 1988, San Francisco, CA

Figure 1

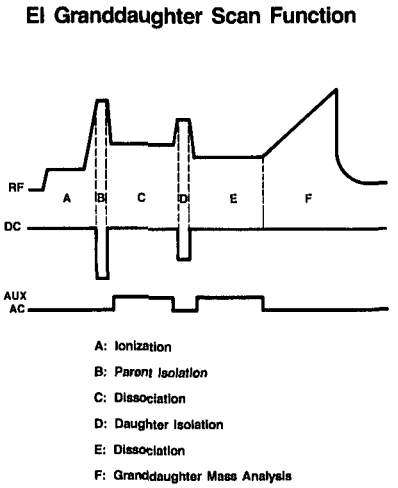

Figure 2

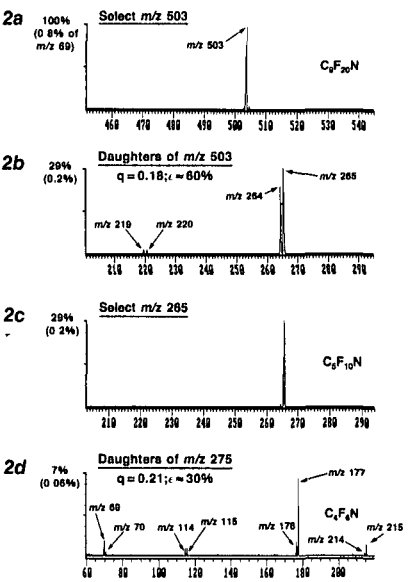

Figure 3

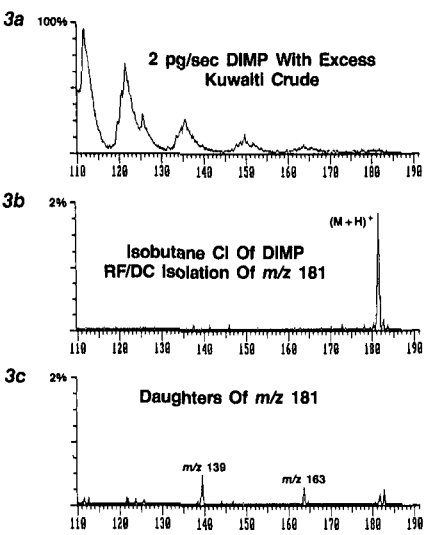

Figure 4

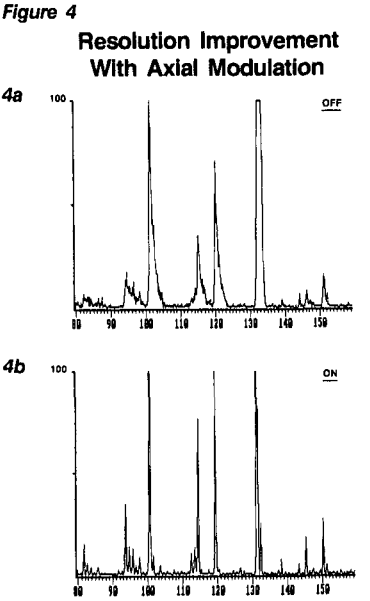

Presented at the 36th ASMS Conference on Mass Spectrometry and Allied Topics
June 5-10, 1988, San Francisco, CA

NEGATIVE ION CHEMICAL IONIZATION AND MS/MS OF NEGATIVE IONS IN AN ION TRAP MASS SPECTROMETER

Scott A. McLuckey, Keiji G. Asano, and Gary L. Glish
Analytical Chemistry Division, Oak Ridge National Laboratory
Oak Ridge, TN

At the 1987 ASMS meeting in Denver we described experiments in which MS and MS/MS analyses were performed on negative ions formed from polyatomic molecules in an Ion Trap Mass Spectrometer.[1] We found that negative ions could be readily formed and that MS/MS efficiencies varied widely depending upon the anion. Since then, we have continued with experiments involving the use of the ITMS for the study of polyatomic anions. These experiments have involved both the formation of anions within the trap, as described in Denver, and the formation of anions in a high pressure ion source followed by injection into the ion trap for analysis. Results from both experiments are described here.

We have found that, in general, it is highly desirable to avoid the build up of positive ions in the trap while forming anions in order to avoid neutralization. This can be done in several ways by using either a DC voltage on the ring electrode, a tickle voltage on the end caps, or a combination of both. In any case, however, we find that the signals obtained for the negative reagent ions are roughly 10^3 lower than those for the positive ions derived from the same reagent gas. This may well be due to the fact that electrons are not stored in the trap under conditions for ion storage. The number density of thermal electrons in the trap is therefore always relatively low resulting in poor conditions for electron capture.

We have studied in greater detail the reagent ions derived from water, i.e. $O^{-\cdot}$ and OH^-. The hydroxide anion is formed form the reaction of the oxide anion with water. We have measured the rate for this reaction to be 2×10^{-10} cm^3/molecule-s under the normal ion trap operating conditions. The hydroxide anion can be selected as the only reagent ion either by mass selecting OH^- using the proper combination of rf and DC voltages, tickling out $O^{-\cdot}$, or simply by allowing all of the $O^{-\cdot}$ to react with water to give OH^-. The ion/molecule reaction chemistry of OH^- can then be studied in a straightforward manner. For example, Figure 1 summarizes the results of the reaction

$$OH^- + CH_3CH_2COOH \longrightarrow H_2O + CH_3CH_2COO^-$$

studied as a function of time. The rate constant derived from these experiments is $k = 3 \times 10^{-9}$ cm^3/molecule-s. Ionization by $O^{-\cdot}$ is less readily studied using water as the reagent gas, on the other hand, due to its reactivity with the parent molecule. Short ionization and reaction times must be used to avoid the conversion of $O^{-\cdot}$ to OH^- which limits the reactions that can be studied to those with rate constants much greater than 2×10^{-10} cm^3/molecule-s and requires sample pressures on the order of the pressure of water. Other reagent gases are therefore likely to be more appropriate for ionization by $O^{-\cdot}$.

For analytical purposes, it is perhaps preferable to form negative ions in an external ion source with high thermal electron concentrations and to inject the anions into the ion trap for analysis. We have recently succeeded in injecting anions into an ITMS from an atmospheric sampling glow discharge ion source and have observed much larger signals than are obtained from forming anions within the trap itself. Although it is possible to avoid injecting positive ions into the trap while anions are injected, care must nevertheless be taken to avoid build-up of positive ions resulting from electron impact ionization by the electrons that are injected with the anions. Most of the positive ions are m/z 32 or less so that recombination is largely avoided by setting the rf voltage on the ring electrode to reject

these low mass ions. Figure 2 shows the mass spectrum and MS/MS spectrum of 2,4,6-trinitrotoluene (TNT) present at a concentration of a few ppb in the air sample drawn into the atmospheric sampling glow discharge ion source. An MS/MS spectrum of sufficient S/N for identification can be obtained for TNT in 0.35 s. These preliminary results are promising for the combination of a high pressure external ion source with the ITMS.

We have obtained MS/MS spectra from a variety of organic acids and nitro compounds during the injection experiments. As a rule, the $(M-H^+)^-$ derived from alkylcarboxylic acids show very poor fragmentation efficiencies (< 1%) in the MS/MS spectra whereas the $M^{-\cdot}$ anions of organic nitro compounds tend to give efficiencies > 10%. These studies have reinforced earlier findings that the competition between electron detachment and fragmentation with charge retention is highly compound dependent.

1. S.A. McLuckey, G.L. Glish, and P.E. Kelley, Anal. Chem., 59, 1670 (1987).

This work was supported by the U.S. Department of Energy, Office of Basic Energy Sciences, through Contract DE-AC05-840R21400 with Martin Marietta Energy Systems, Inc.

Figure 1

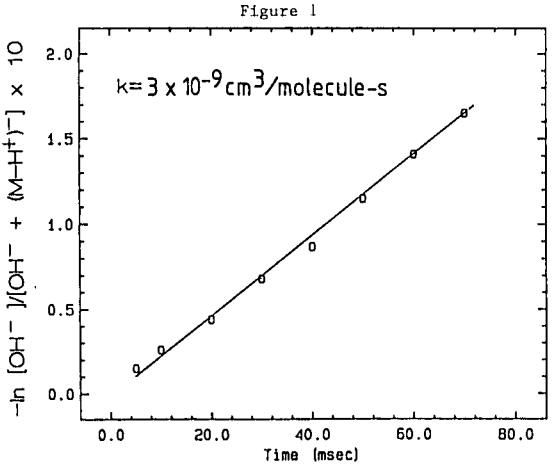

"The submitted manuscript has been authored by a contractor of the U.S. Government under contract No. DE-AC05-84OR21400. Accordingly, the U.S. Government retains a nonexclusive, royalty-free license to publish or reproduce the published form of this contribution, or allow others to do so, for U.S. Government purposes."

Figure 2

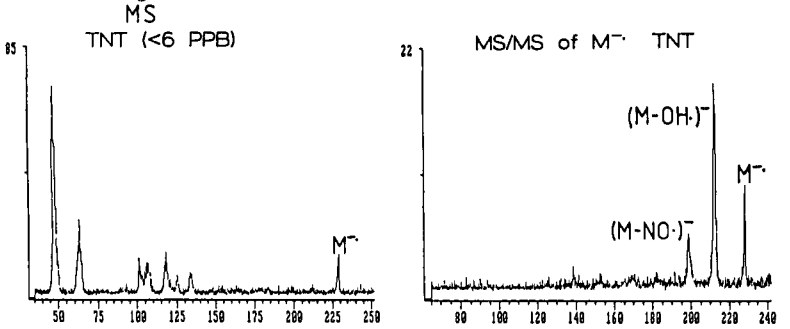

Presented at the 36th ASMS Conference on Mass Spectrometry and Allied Topics
June 5-10, 1988, San Francisco, CA

COMPARISON OF CHARGE EXCHANGE AND ELECTRON IONIZATION IN QUADRUPOLE ION TRAP AND TRIPLE QUADRUPOLE MASS SPECTROMETERS

D.W. Berberich, M.E. Hail, R.A. Yost, University of Florida, Department of Chemistry, Gainesville, FL 32611.

Interest in the quadrupole ion trap has recently undergone a resurgence, due in part to the commercialization of the ion trap detector and the ion trap mass spectrometer (Finnigan MAT ITMS). In traditional quadrupole mass spectrometers, electron ionization (EI) is performed in a low pressure (~ 10^{-6} torr) continuous ionization source located before the mass analyzer. In the ITMS, EI occurs in the same region as mass analysis, in the presence of ~ 10^{-3} torr of helium buffer gas, and with ions stored for several milliseconds. A significant question concerning ionization in the ITMS is what type of ionization, EI or charge exchange (CE), predominates under standard EI operating conditions.

Charge exchange on traditional mass spectrometers is usually performed in ionization sources using reactant gas pressures of 0.3 - 1.5 torr (1,2). The limitation of this approach is that the spectra may be the result of CE of the desired reactant ion and sample molecule, as well as both CE with undesired reactant ions in the source and EI. Alternatively, CE spectra may be obtained with a triple quadrupole (QQQ) instrument (Finnigan MAT TSQ-70) by allowing CE reactions to occur in the collision cell (Q2). A schematic representation of the Q2 CE scan is shown in Figure 1. The reactant gas is introduced into the ion source and ionized with 70 eV electrons. Q1 is used to mass select the desired CE reactant ion and pass it into Q2. Samples are introduced into Q2 via a direct leak from a fine metering valve. The sample molecules and the reactant ions react in Q2 to produce the charge exchange product ions that are mass analyzed by Q3. This approach eliminates spectral interferences produced by EI and CE with undesired reactant ions. Figure 2A shows a normal (Q1) mass spectrum of n-butyl-benzene obtained on QQQ instrument with He reactant gas present in the ion source. The spectrum shows ions produced by various CE processes, as well as by EI. In contrast, Figure 2B shows a CE spectrum of n-butylbenzene obtained with the Q2 CE scan in the collison cell of the QQQ instrument. Note the very low intensity of the molecular ion (m/z 134) and the increased intensity of the fragment ions m/z 39 and m/z 65 in Figure 2B resulting from the energetic He CE.

In the ITMS, CE occurs in the same region as mass analysis, and is achieved by trapping ions for milliseconds at a much lower pressure ($<10^{-3}$ torr). The ITMS is normally operated in a RF-only mode. Operation of the ITMS with both RF and DC voltages (i.e selective mass storage) allows for the storage of a single m/z. Thus, unambiguous CE reactions can be obtained by mass selecting a single reactant ion, and allowing the CE reaction to occur over a specified period of time. The resulting CE spectrum is obtained by ramping the RF voltage and causing the ions to be ejected from the quadrupole ion trap.

Helium, nitrogen, argon, and carbon dioxide were examined as reactant gases, since it was anticipated that these gases would produce markedly different CE spectra. This is due to the fact that the amount of internal energy deposited into a molecule ionized by CE is dependent upon the difference between the recombination energy of the reactant ion and the ionization potential of the molecule (Table 1). The N_2, Ar, and CO_2 CE mass spectra of phenylacetonitrile and n-butylbenzene obtained on the respective instruments are very similar. Figure 3 shows a comparison of N_2 CE on the ITMS (RF-DC mode of operation) and N_2 Q2 CE on a QQQ for n-butylbenzene. The ratio of m/z 91 to m/z 92 ions differ by only 2% on the respective instruments, which is well within the limits of experimental error.

The experiments with helium as a reactant gas indicate that He CE does not contribute significantly to the EI spectra obtained in the ITMS. This may be due to the fact that although helium ions are formed in the ITMS,

they are not stored long enough to allow CE to occur. The experiments on the QQQ indicate that "true" CE can not be effectively performed in the ionization source, while selective CE can be performed using the Q2 CE scan. By means of the Q2 CE scan, it is possible to select a variety of reactant ions from the same reactant gas. For example, argon produces three different reactant ions Ar^{+} , Ar^{+2} , and Ar_2^{+}, which can be used as reactant ions in the Q2 CE scan. This is useful since one may be able to obtain both structural and molecular weight information by simply selecting different reactant ions which have different recombination energies. Similar capabilities exist in the ITMS, although potential interferences may arise from other reactant ions being produced with long reaction times.

References

1) J.S. Brodbelt, J.N. Louris, R.G. Cooks, Analytical Chemistry, 1987, 59(9), 1278-1285.
2) Y.H. Li, J.A. Herman, A.G. Harrison, Canadian Journal of Chemistry, 1981, 59, 1753-1759.

Figure 1. Q2 CE Scan

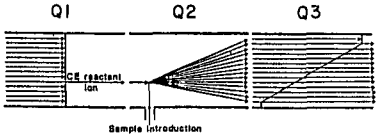

Figure 2. A) Helium and n-butylbenzene in ion source.
B) He Q2 CE spectrum of n-butylbenzene.

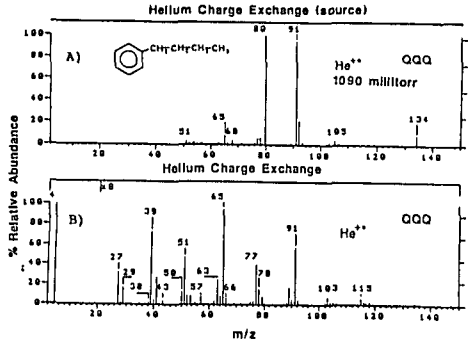

Figure 3. N_2 CE spectra of n-butylbenzene.

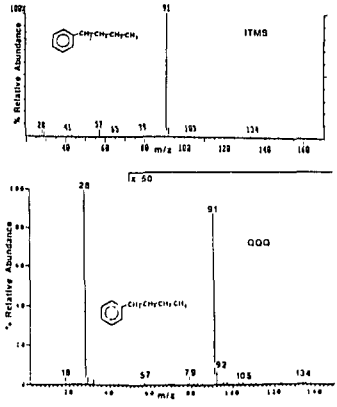

Table 1. Recombination Energies

Species	RE (eV)
$Ar^{+\cdot}$	15.9
Ar^{+2}	24 0
$C_2H_4^{+\cdot}$	11.4
$C_8H_7N^{+\cdot}$	9.4
$C_{10}H_{14}^{+\cdot}$	8 6
$CO^{+\cdot}$	14.0
$CO_2^{+\cdot}$	13.8
$H_2O^{+\cdot}$	12.6
$He^{+\cdot}$	24.6
$N^{+\cdot}$	24.3
$N_2^{+\cdot}$	15.3

"The submitted manuscript has been authored by a contractor of the U.S. Government under contract No. DE-AC05-84OR21400. Accordingly, the U.S. Government retains a nonexclusive, royalty-free license to publish or reproduce the published form of this contribution, or allow others to do so, for U.S. Government purposes."

Presented at the 36th ASMS Conference on Mass Spectrometry and Allied Topics
June 5-10, 1988, San Francisco, CA

MS^n EXPERIMENTS WITH AN ION TRAP MASS SPECTROMETER:

Gary L. Glish, Gary J. Van Berkel, Keiji G. Asano, Scott A. McLuckey
Analytical Chemistry Division, Oak Ridge National Laboratory
Oak Ridge, TN 37831

MS/MS has become a fairly routine analytical technique. Addition of another stage of mass spectrometry or MS/MS/MS (MS^n, n=3) can provide added specificity in an experiment. For beam type instruments in which the ions pass sequential analyzers, each additional stage of MS/MS requires an additional analyzer. However, with trapping type mass spectrometers, the ions are manipulated in time using a sequence of rf (and sometimes DC) voltages. Thus, multiple stages of mass spectrometry can be performed with one analyzer. The experiments discussed in this paper were done with a Finnigan MAT Ion Trap Mass Spectrometer (ITMS), which is a three dimensional quadrupole.

A very simple but potentially very useful MS^n experiment that can be done with the ITMS is selected reagent ion chemical ionization (SRICI). In this experiment the MS/MS capability of the ITMS is used to select one specific reagent ion from the suite of ions usually formed. This ion is then allowed to react with the analyte. A mass spectrum obtained in this way is an MS^n experiment where n=2. Doing MS/MS on an analyte ion makes n=3 and futher stages of MS/MS can also be performed. The SRICI experiment can not be performed on beam instruments unless the analyte has a high vapor pressure under the operating conditions of the reaction region. An example of the effect of the SRICI experiment is shown in Figure 1 where three mass spectra are shown for the compound promethazine, one obtained with all the methane reagent ions present, one in which m/z 17 was selected as the reagent ion, and one in which m/z 29 was selected. As can be seen, the spectra are quite different, especially when using m/z 17 as the reagent ion. The SRICI experiment allows the differentiation of ionization and fragmentation mechanisms. When using ammonia as a reagent gas, only the proton donating species m/z 18 is present so it might be assumed that the SRICI experiment is unnecessary. However, the base peak in the mass spectrum without reagent ion selection is m/z 72, which is completely absent in the spectrum in which m/z 18 was selected as the reagent ion. The ion at m/z 72 is assumed to arrise from residual EI of a thermal decomposition product of the promethazine, which must be in much greater abundance than the promethazine. It should be noted that the mass spectra without reagent ion selection are the same as those observed with conventional CI sources on beam instruments.

One of the characteristics of the ITMS that makes it possible to do MS^n experiments is its high MS/MS efficiency. A series of experiments with 2,5 dimethylpyrrole showed overall ion trapping efficiencies of greater than 50% for MS^n experiments with n=5. Conversion efficiencies of the parent ion to the great,great granddaughter ion of several percent have been obtained with the ITMS.

Another feature of the MS^n experiment is that not all the stages have to be CID. Ion/molecule reactions can be performed at any time during the course of an experiment. Figure 2 shows an example of this in which the structure of the $(M+H-17)^+$ daughter ion from 2,5-dimethylpyrrole was determined by reacting it with methane and then doing two more stages of MS/MS (CID), making the total experiment MS^5. These spectra along with confirming spectra from standards (benzene and toluene) indicate that this $(M+H-17)^+$ ion has the same structure as protonated benzene.

MS^n experiments have been performed with octaethylporphyrin where n is as large as 8. In these experiments the alkyl substituents are sequentially cleaved off of the porphyrin ring. Other MS^n experiments with porphyinogens have demonstrated the utility of the experiment for obtaining pyrrole sequences. This type of experiment should be a powerful tool for structure analysis of these and and many other types of compounds.

Presented at the 36th ASMS Conference on Mass Spectrometry and Allied Topics
June 5-10, 1988, San Francisco, CA

Methane SRICI experiments

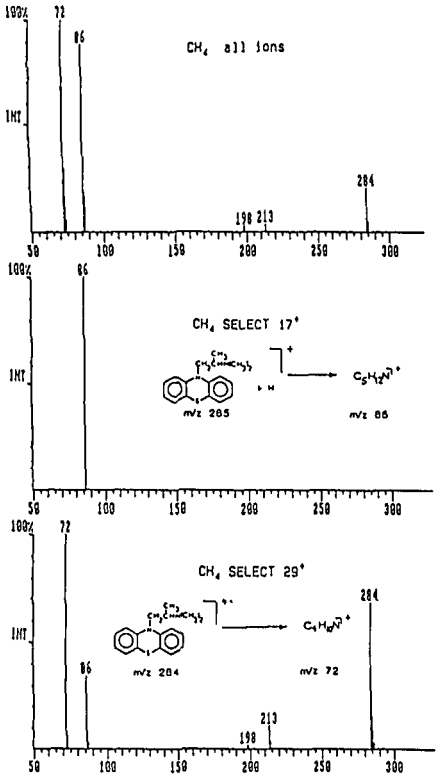

Figure 1

MS5 of 2,5-dimethylpyrrole

96 → 79 → 91 → 65 → 39

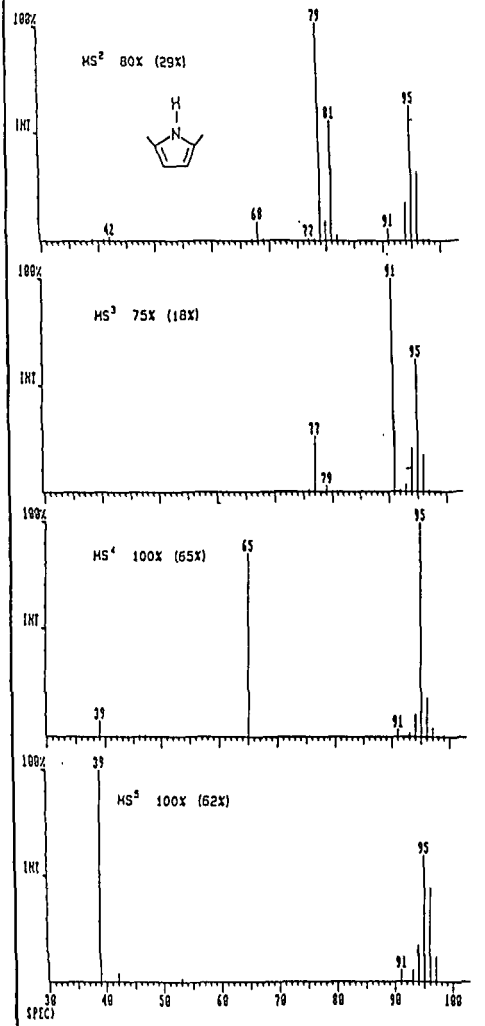

Figure 2

*Research sponsored by the U.S. Department of Energy, Office of Basic Energy Sciences, under contract DE-AC05-84OR21400 with Martin Marietta Energy Systems, Inc.

Presented at the 36th ASMS Conference on Mass Spectrometry and Allied Topics
June 5-10, 1988, San Francisco, CA

ION TRAP MS/MS ASSAYS OF BIOLOGICAL EXTRACTS USING rf/DC

Robert J. Strife and John R. Simms
The Procter and Gamble Co.
Miami Valley Laboratories
P.O. Box 398707
Cincinnati, OH 45239-8707

INTRODUCTION -- The Ion Trap Mass Spectrometer (ITMS) offers the potential for very selective and sensitive GC/MS/MS assays. This is because: 1) it is an ion storage device and 2) using MS/MS scan functions (tandem in time) very high CAD efficiencies are observed, even 100% in some cases.

One objective of MS/MS is to simplify sample preparation prior to analysis. This is especially helpful in studies dealing with fundamental pharmacology or drug disposition. In this study we wanted to examine quantitative GC/isotope-dilution-MS/MS of a known biological system, using the ITMS, before moving on to problem solving of unknowns. The model chosen was tryptamine in rat brain tissue, reported by two separate groups at levels from 100-500 pg/g using GC/MS(SIR) of the bis-pentafluoropropionamide derivative[1,2].

The full scan mass spectrum of the derivative at the 25 pg level is shown in Figure 1 with the reconstructed mass chromatogram (m/z 289) in the inset. It matched the spectrum at the 2.5 ng level fairly well and demonstrates the full scan sensitivity of the ITMS in the rf-only mode. The most obvious choice of a parent ion for sensitive MS/MS is m/z 289. Its structure, based on classical rules of fragmentation, is shown in Figure 1.

rf/DC Scan For MS/MS on the ITMS -- Use of an rf/DC scan function, recently described for prostaglandin analysis[3], allows storage of ions of only one m/z value in the trap. All other ions created by the initial electron pulse go into unstable trajectories and leave the trap. The selected ion, m/z 289 in this case, is then subjected to CAD by the normally used methods. Using rf/DC has important consequences for biological sample analysis (vide infra).

Daughter Ion Spectra -- The GC/MS/MS analysis of a 50 pg standard, using the rf/DC scan function, is shown in Figure 2 with the total daughter ion current trace inset. Two derivative-specific cleavages are seen (m/z 170, loss of C_2F_5, and m/z 142, loss of C_2F_5CO). Based on our previous work, monitoring these reactions may hold marginal benefit for improving the selectivity observed in GC/MS. Finally loss of C_2F_5CO + HCN, from the indole backbone, is observed and would be predicted to give more enhanced selectivity than the other reactions. The loss of HCN vs C_2H_3 (both 27 u) is supported by studying the spectrum of 3-(1,1,2,2-[^{2}H]$_4$-ethylamino)-indole, e.g. deuterated tryptamine. All daughter ions of m/z 292 (corresponding to m/z 289) are shifted by 3 u.

GC/Isotope Dilution MS/MS -- To perform isotope-dilution-MS/MS experiments, rf/DC MS/MS scan functions for the native and deuterated compound are loaded into the firmware and performed alternately. This is accomplished with a FORTH language programming editor. This process is only about half as fast as a normal single-function MS/MS experiment. Two scans are averaged per second for the labelled and unlabelled compound each, giving a data point (averaged spectrum) per second for the d_0- and d_4 chromatograms. Initial results were encouraging. For 100 pg - 2.5 ng tryptamine and about 10 ng of deuterated material on column (5% of the derivatized sample), the equation $y = .00668x - .003$ ($r=.9986$) was found for the reaction ($289^+ \rightarrow 115^+$)/($292^+ \rightarrow 118^+$) vs. ng d_0-tryptamine (Figure 3).

Crude Biological Extract Analysis -- Because sample preparation schemes are shortened for MS/MS analyses, the extracts are of a more-crude nature than

might be prepared for a typical GC/MS assay. Since the trap has a finite storage capacity for ions, it is necessary to eliminate matrix-related ions as efficiently as possible. This is the critical advantage of the rf/DC scan function.

Figure 4a shows an attempted analysis of a crude brain extract spiked with 500 pg derivatized d_4-tryptamine. Using an rf-only MS/MS scan function, the analysis is a failure. Other experiments indicate this is due to an excessive ion population in this mode, since only a high-pass mass filtering is achieved after ionization (e.g. all ions above m/z 289 are stored prior to MS/MS). Using an rf/DC scan function, and analyzing the same sample, the peak is clearly detected (Fig. 4B) and the daughter-ion spectrum is correct. This is a direct result of the selective-mass-storage condition achieved through the use of rf and DC voltages. The initial space-charge is eliminated and spatial focussing may be occurring also[4]. Further work is aimed at understanding these and other factors necessitating rf/DC scan functions for crude extract analysis, and optimizing the extraction scheme for tryptamine.

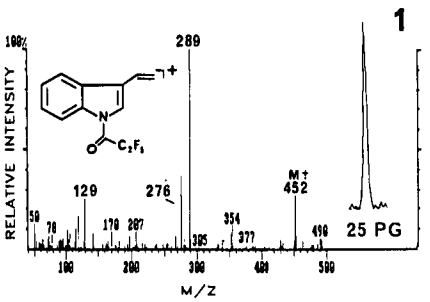

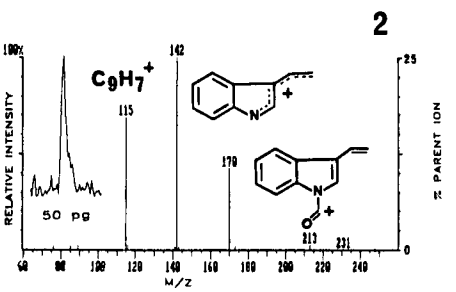

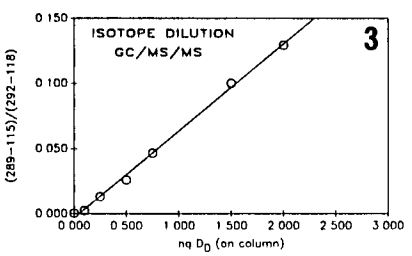

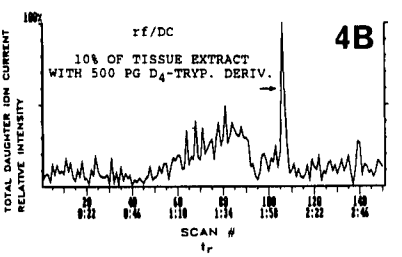

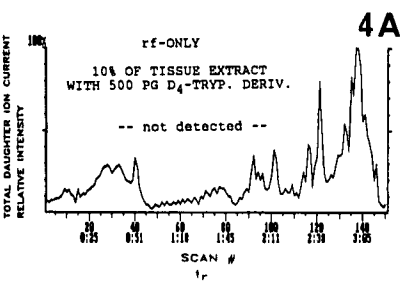

ABBREVIATED REFERENCES

1. Artigas, F. et. al. Biomed. Mass Spectrom. 1984, 11, 142-144.

2. Beck, Olof; Flodberg, Goran Biomed. Mass Spectrom. 1984, 11, 155-158.

3. Strife, Robert J.; Kelley, P.E., Weber-Grabau, M. Rapid Commun. In Mass Spectrom., in press, 6, 1988.

4. Weber-Grabau, M.; Kelley, P.E.; Syka, J. E. P.; Bradshaw, S. C.; Brodbelt, J. S. "Improved Ion Trap Performance With New CI and MS/MS Scan Functions"; 35th ASMS Conference, Denver, CO, May 24-29, 1987.

Presented at the 36th ASMS Conference on Mass Spectrometry and Allied Topics
June 5-10, 1988, San Francisco, CA

SIMULTANEOUS MS-II MEASUREMENTS USING HADAMARD TRANSFORM FOURIER TRANSFORM MASS SPECTROMETRY

S. Y. Loh, E. R. Williams, F. W. McLafferty and R. B. Cody[1]
Chemistry Department, Cornell University, Ithaca, NY 14853-1301
(1) Nicolet Analytical Instruments, 5225-1 Verona Road, Madison, WI 53711

The ideal instrument for MS/MS would have multichannel detection capabilities for both MS-I and MS-II, to be able to dissociate many precursor ions and to collect their daughter spectra simultaneously. Fourier transform mass spectrometry (FTMS) measures all ions of a spectrum simultaneously; in addition, any number of precursor ions can be selected and dissociated simultaneously. We recently proposed [1] a Hadamard method for combining these two features of FTMS for simultaneous recording of multiple MS-II spectra. Using Hadamard masks, different combinations of half of n precursors are selected for dissociation. From the resulting n spectra, individual daughter spectra are obtained by solving n simultaneous equations.

This method has been applied to a synthetic mixture of 11 compounds using a Nicolet FTMS-2000. A SWIFT waveform [2] is used for high resolution selection of the precursor ions formed by 14 eV electrons (figure 1). Different combinations of 6 of these are subsequently excited and allowed to undergo collisionally activated dissociation. After the Hadamard transform, daughter ion spectra for each of the precursors are obtained (figure 2a,b) A signal-to-noise enhancement of 2.4 is achieved over spectra measured individually under identical conditions (figure 3). Spectra collected using both high and low energy collisions makes possible complementary high and low energy fragmentation, respectively. The Hadamard method of multiplexing yields the greatest advantage with large numbers of precursor ions. Thus, daughter ion spectra of 100 precursors can be collected in 1/25 the time.

For MS/MS/MS, Hadamard masks can be applied to n MS-I and i MS-II ions to produce i MS-III spectra. Again, the individual MS-III spectra can be extracted from the different combination of Hadamard masks and will result in a $(n \cdot i)^{0.5}/4$ enhancement in signal-to-noise. The Hadamard method is compatible with alternate methods of ion dissociation, including photodissociation and EIEIO, and can also be used for studying numerous ion-molecule reactions simultaneously. For the latter purpose, the Hadamard method has advantages over the 2D ICR technique of Bodenhausen and Gaumann [3], including a greater S/N advantage and higher MS-I selectivity.

[1] McLafferty, F. W.; Stauffer, D. B.; Loh, S. Y.; Williams, E. R. Anal. Chem. 1987, 59, 2213-2216.
[2] Chen, L.; Wang, T-C. L.; Ricca, T. L.; Marshall, A. G. Anal. Chem. 1987, 59, 449-454.
[3] Pfandler, P.; Bodenhausen, G.; Rapin, J.; Houriet, R.; Gaumann, T. Chem. Phys. Lett. 1987, 138, 195-200.

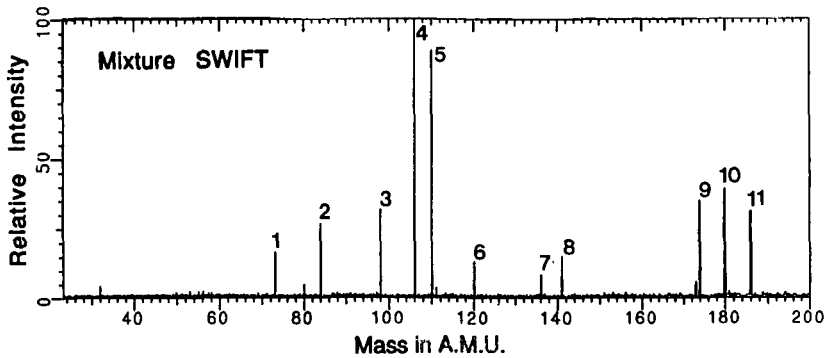

Figure 1: 14 eV EI spectrum of mixture of 1) diethylamine 2) cyclohexane 3) cyclohexanone 4) p-xylene 5) p-fluorotoluene 6) acetophenone 7) alpha-pinene 8) 1-fluoro-4-nitrobenzene 9) 1-bromo-4-fluorobenzene 10) 1,2,4-trichlorobenzene 11) p-bromoanisole, after SWIFT ejection.

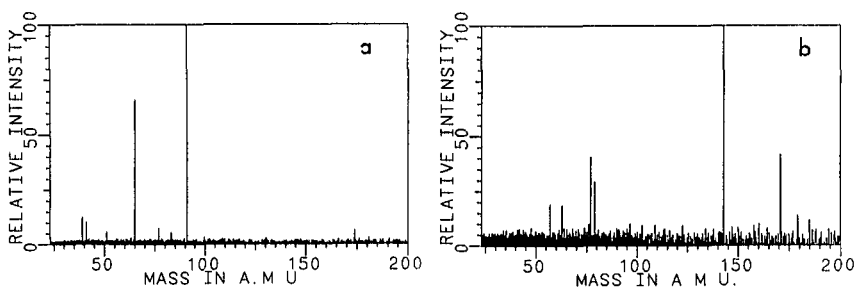

Figure 2: Example of Hadamard transformed MS-II spectra of a) p-xylene (4) and b) p-bromoanisole (11).

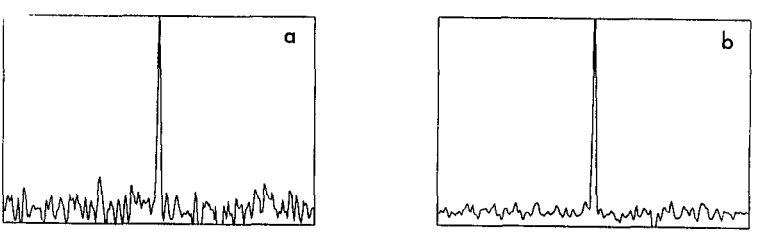

Figure 3: MS-II spectra of $(M - CH_3)^+$ at m/z 171 from p-bromoanisole (11) a) measured individually and b) after Hadamard transform showing 2.4 increase in S/N.

Presented at the 36th ASMS Conference on Mass Spectrometry and Allied Topics
June 5-10, 1988, San Francisco, CA

FOURIER TRANSFORM TANDEM MASS SPECTROMETRY FOR THE QUALITATIVE ANALYSIS OF COMPLEX MIXTURES

Marcus B. Wise and Michelle V. Buchanan
Organic Spectroscopy Group, Analytical Chemistry Division
Oak Ridge National Laboratory, Oak Ridge TN 37831-6120

Tandem mass spectrometry (MS/MS) is a technique of growing importance in the field of analytical chemistry. In particular, the ability to qualitatively analyze complex mixtures without prior chromatographic separation of the constituents often results in faster sample turn-around than a corresponding GC/MS analysis. Further, by having a wide range of parent ion excitation energies available such as is the case with Fourier transform mass spectrometry (FTMS), the fragmentation of an ion is more easily controlled than is the case with electron impact ionization. This in itself can be an important tool for structure determination.

Although FTMS is capable of being operated as a high performance tandem mass spectrometer often with very efficient parent-daughter ion conversion, application of this technique to complicated direct probe or batch inlet samples is very labor intensive. As a result, we have developed software for the Nicolet FTMS-2000 that significantly increases the analytical utility of the MS/MS mode of operation for complex mixture analysis. This software consists of a Fortran program and several command files which operate together as a "batch" data acquisition and processing scheme for automated parent ion MS/MS scans. Since a complete daughter ion spectrum is obtained for each parent ion, a real-time peak extraction routine is used to monitor specific neutral losses and constant daughter ions. Program options allow the storage of the complete daughter ion and extracted ion spectra and at the end of a parent ion scan, hard copies of spectra are output on the plotter.

For a typical direct probe sample, low energy electron impact or chemical ionization is used to minimize fragmentation of constituents in the mixture. Prior to the start of an experiment, several parameters must be entered by the user including the parent ion scan limits, the parent ion excitation energy, the relative threshold below which a parent ion will be ignored, the neutral loss masses to be monitored (up to 5), the constant daughter ions to be monitored (up to 5), and the filenames for data storage. The program then collects a complete mass spectrum of the sample (no MS/MS) in order to determine the maximum peak intensity for the parent ion relative threshold calculations. Once this is accomplished, the parent ions are sequentially dissociated starting at the low mass of the scan limits. Prior to the dissociation step, all ions within 12 amu of the low mass side of the parent ion are ejected from the cell using the double resonance pulses. The parent ion excitation time is then calculated for the specific parent ion mass in order to produce the requested kinetic energy level. Following application of the excitation pulse and a 50 msec collision period, the daughter ion mass spectrum is collected and the specific ions (neutral losses and constant daughters) are extracted. Corresponding mass and intensity information is then directed to the printer and the spectra are stored if desired. This process is then automatically repeated until all parent ions above the relative threshold (an within the scan range) have been dissociated. An option also exists for background subtraction in which a spectrum with no dissociation is collected immediately prior to each MS/MS spectrum and subtracted from the extracted ion results. This is particularly useful for reducing false contributions to the daughter ion spectrum which may result from the incomplete ejection of the low mass ions prior to dissociation.

As an example of the utility of this software, a fuel oil (API Home Heating Oil #975) was run using batch inlet sample introduction. Low energy electron impact ionization was used and 8K data points were collected to produce the spectrum shown in Figure 1. Since this sample contains numerous alkyl-substituted benzenes, one of the neutral losses

"The submitted manuscript has been authored by a contractor of the U S Government under contract No DE-AC05-84OR21400 Accordingly the U S Government retains a nonexclusive, royalty-free license to publish or reproduce the published form of this contribution, or allow others to do so for U S Government purposes."

that was monitored was the loss of 15 (CH_3). A parent ion excitation energy of 175 eV was used and parent ions above a 2% relative threshold were dissociated between 75 and 250 amu. For each daughter ion spectrum, a total of 25 spectra were averaged (8K points, 1 MHz bandwidth) and the background subtraction routine was employed. The corresponding neutral loss spectrum shown in Figure 2 clearly indicates which parent ions undergo loss of CH_3. Combined with MS/MS information, the alkyl aromatics are readily identified and consistent with GC analysis of the same sample. The complete run-time for this spectrum was approximately 30 minutes compared with approximately 2 hours for a corresponding capillary GC run. Other applications of this MS/MS software will be for the qualitative analysis of tobacco smoke tars and biological samples.

*Research sponsored by the National Cancer Institute under Interagency Agreement No. 0485-0485-A1 under Martin Marietta Energy Systems, Inc., contract DE-AC05-840R21400 with the U.S. Department of Energy.

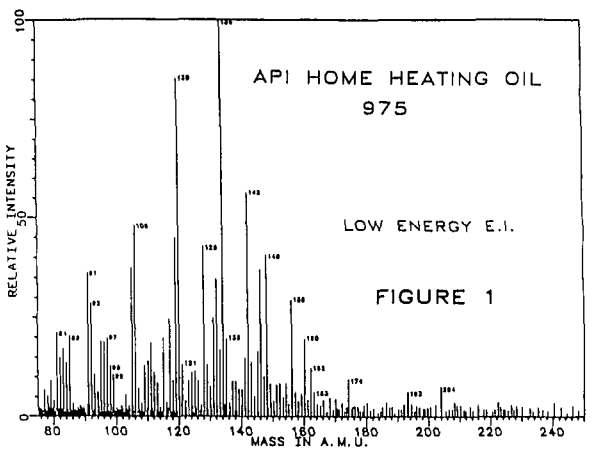

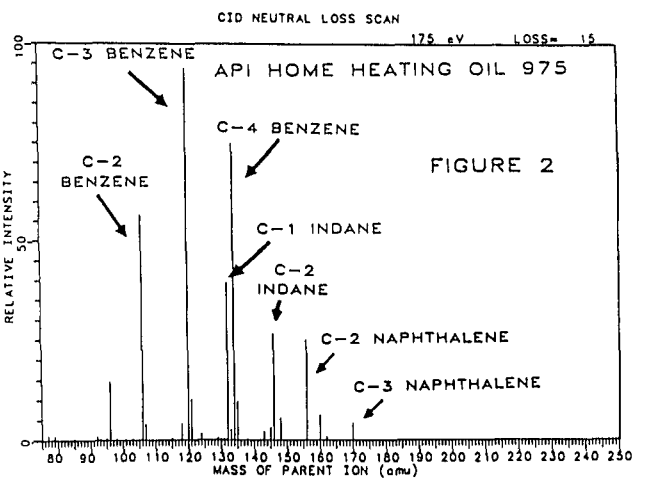

"The submitted manuscript has been authored by a contractor of the U S Government under contract No DE-AC05-840R21400 Accordingly, the U S Government retains a nonexclusive royalty-free license to publish or reproduce the published form of this contribution, or allow others to do so, for U S Government purposes."

Presented at the 36th ASMS Conference on Mass Spectrometry and Allied Topics
June 5-10, 1988, San Francisco, CA

IR LASER DESORPTION FOURIER TRANSFORM ION CYCLOTRON RESONANCE MASS SPECTROMETRY OF NUCLEOSIDES AND NUCLEOTIDES

J.L. Williams, J.A. Mayernik, M.K. Conner, R.R. Weller, and C.S. Giam
Department of Industrial Environmental Health Sciences
Graduate School of Public Health
University of Pittsburgh
Pittsburgh, PA 15261

The ability to evaluate the biological damage produced in the tissues and cells of organisms exposed to chemical carcinogens may facilitate understanding of the role that these agents have in the occurrence of selected cancers. A promising method for assessing such damage is the determination of the covalent interaction of chemical carcinogens with DNA. The methodology currently used to identify and quantitate DNA adducts in organisms exposed to carcinogenic agents consists of chromatographic separation of the components in DNA hydrolyzates followed by fluorescence, ^{14}C radioactivity, or ^{32}P-postlabeling detection. These detection methods, however, yield little structural information and characterization of DNA adducts must be accomplished using some other technique.

In this research, normal and modified nucleosides and nucleotides have been characterized using IR laser desorption Fourier transform ion cyclotron resonance mass spectrometry. The LD-FT-ICR-MS system used coupled a pulsed, TEA CO_2 laser, operating at 10.6 um, with a Nicolet FTMS-1000 spectrometer. Compounds studied were adenosine, guanosine, cytidine, uridine, thymidine, deoxyguanosine, deoxycytidine, 3,N^4-ethenocytidine, adenosine triphosphate, and 1,N^6-ethenoadenosine triphosphate.

All of the nucleosides studies produced positive ion mass spectra dominated by alkali cation attachment (Na^+, K^+) molecular ions (Figures 1 and 2) Similarly, prominent in the negative ion spectra of the nucleosides was the $(M - H)^-$ ion. Use of broadband, medium resolution conditions yielded mass errors of less than 30 mAMU for most of these pseudomolecular ions.

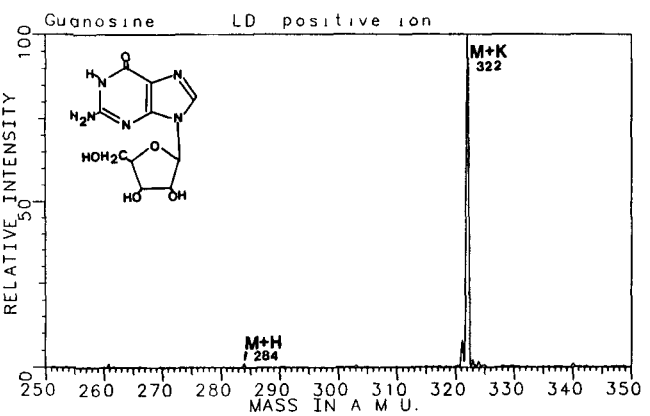

Figure 1.

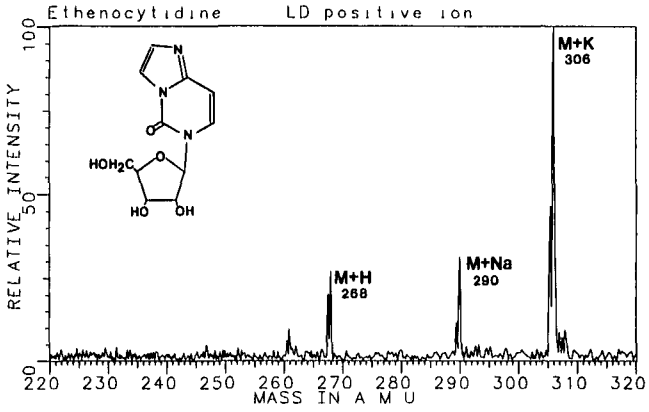

Figure 2.

In contrast, ionization of the nucleotides using the IR laser produced extensive fragmentation; molecular ions were absent in both the positive and negative ion mass spectra. The base peak in the negative ion spectra was the phosphate fragment, PO_3^-. At a lower abundance are the fragment ions corresponding to the nucleobase portion of the molecules. Using negative ion LD-FT-ICR-MS the detection limit of 1,N^6-ethenoadenosine triphosphate was estimated below 100 ng.

The positive ion spectra of the nucleotides were of lower quality than the negative ion spectra. Peaks corresponding to the nucleic base fragment ions, $(B + H)^+$ and $(B + \text{cation})^+$ were present in these spectra. The relative abundance of these ions was quite low, however, and reproducibility of the spectra was poor.

These results demonstrate the ability of LD-FT-ICR-MS to identify modified and unmodified nucleosides and nucleotides present in low levels. This technique combined with other separation methods provides an excellent tool for the study of an important class of compounds.

Presented at the 36th ASMS Conference on Mass Spectrometry and Allied Topics
June 5-10, 1988, San Francisco, CA

LASER IONIZATION FOURIER TRANSFORM MASS SPECTROMETRY FOR THE DIFFERENTIATION OF METHYL GUANOSINE ISOMERS*

R.L. Hettich
Analytical Chemistry Division
Oak Ridge National Laboratory
Oak Ridge, TN 37831-6120

Methylation of deoxyribonucleic acid (DNA) is known to be one form of DNA modification induced by simple alkylating agents. In order to probe the nature of DNA alkylation, it is necessary to identify the structures of the modified species at the isomeric level. This report illustrates the application of laser ionization Fourier transform mass spectrometry (FTMS) for the ionization and structural characterization of five methyl guanosine isomers. Specific emphasis was placed on the identification and differentiation of guanosines containing methyl substitutions on the nucleic base (guanine).

Laser ionization of guanosines containing methyl substitutions in the 1-, N^2-, 3'-O-, O^6-, and 7- positions generated negative ions corresponding to loss of hydrogen to form $(M-H)^-$, and elimination of the sugar ring to generate the negatively charged nucleic base. This fragmentation is shown in Figure 1 for 1-methyl guanosine. All isomers with methyl substitution on the nucleic base fragmented to give negative ions at m/z 164 whereas the 3'-O-methyl guanosine (methyl substitution on the sugar ring) yielded a negative ion at m/z 150, corresponding to the normal guanine nucleic base.

Collisional dissociation was used to differentiate the isomers with methyl substitution on the nucleic bases. Isolation and collisional dissociation of the negative ions at m/z 164 for each isomer gave unique daughter ions. The collisional dissociation spectrum of m/z 164 from 1-methyl guanosine is shown in Figure 2. Loss of CH_3NH_2 from m/z 164 was indicative of methyl substitution in the 1 or N^2 positions, whereas HNCO loss was observed for ions with methyl substitution in the 7 or N^2 positions. Loss of CH_3 from m/z 164 was characteristic for methyl substitution in either the 7 or O^6 positions while CH_3OH elimination was specific to methyl substitution in the O^6 position. Combining these results gave the information necessary to differentiate each of the isomers. These daughter ions could be transferred to the analyzer cell of the FTMS-2000 for accurate mass measurement. By using heterodyne detection, high resolution measurements could be obtained for the daughter ions (a resolution of 298,000 [FWHM] for the m/z 133 negative ion from 1-methyl guanosine is shown in Figure 3).

In order to probe the fragmentation pathways, the daughter ions of m/z 164 were isolated and collisionally dissociated. Figure 4 shows the collisional dissociation spectrum of m/z 133, which has been isolated from Figure 2. This ion at m/z 133 fragments to give daughter ions at m/z 66 $(C_2N_3)^-$ and m/z 26 $(CN)^-$. The ions at m/z 35 and 37 are due to Cl^- which was not completely eliminated during the isolation pulse. Figure 4 verifies that the ions of m/z 106 and m/z 42 observed in Figure 2 are not generated by fragmentation of the m/z 133 ion.

The combination of laser ionization and collisional dissociation with FTMS provides a useful method for the structural characterization of nucleosides and can be used in some cases for isomeric differentiation. High resolution and accurate mass measurements combined with sequential collisional dissociation experiments provided the information necessary to examine the fragmentation mechanisms of ions from these nucleosides.

*Research sponsored by the Office of Health and Environmental Research, U.S. Department of Energy under contract DE-AC05-84OR21400 with Martin Marietta Energy Systems, Inc.

"The submitted manuscript has been authored by a contractor of the U.S. Government under contract No. DE-AC05-84OR21400. Accordingly, the U.S. Government retains a nonexclusive, royalty-free license to publish or reproduce the published form of this contribution, or allow others to do so, for U.S. Government purposes."

Presented at the 36th ASMS Conference on Mass Spectrometry and Allied Topics
June 5-10, 1988, San Francisco, CA

Figure 1

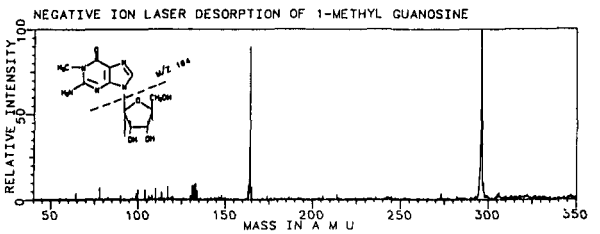

Figure 2

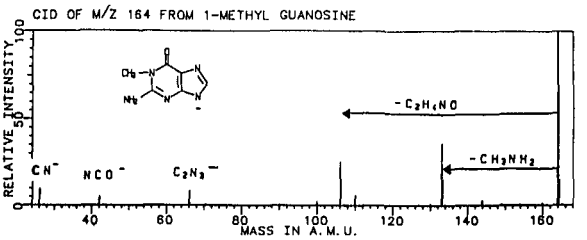

Figure 3

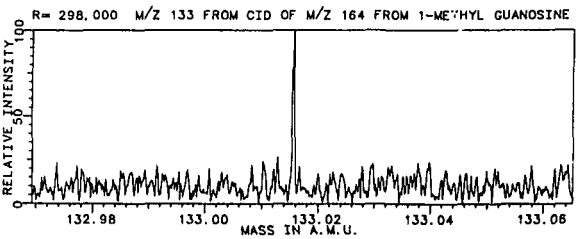

Figure 4

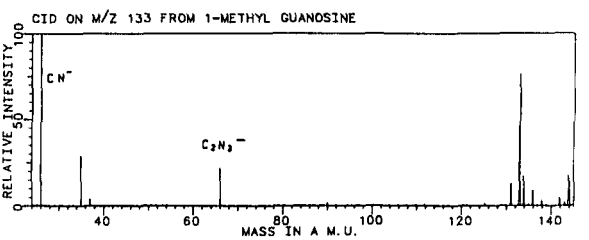

"The submitted manuscript has been authored by a contractor of the U S Government under contract No DE-AC05-84OR21400 Accordingly, the U S Government retains a nonexclusive, royalty-free license to publish or reproduce the published form of this contribution, or allow others to do so, for U S Government purposes "

Presented at the 36th ASMS Conference on Mass Spectrometry and Allied Topics
June 5-10, 1988, San Francisco, CA

SYSTEM FOR LASER MICROPROBE FOURIER TRANSFORM MASS SPECTROMETRY

J. T. Brenna, W. R. Creasy, W. McBain*, and C. Soria*
IBM Corporation, D-T43
1701 North Street
Endicott, New York 13760

*Pacific Precision Labs
21018 Osborne St, Unit 4
Canoga Park, California 91304

We report here a system for laser microprobe Fourier transform mass spectrometry. The system is based on a commercial spectrometer (Nicolet FTMS-2000) and a frequency-doubled or quadrupled Nd:YAG laser (Quantel Int'l). The system consists of three distinct subsystems: optical, electronic interface, and specimen motion. Each is described separately.

A schematic of the optical system is shown in Figure 1. Light emitted from the laser travels through a attenuator (s) which allows continuous ajustment of beam intensity, a telescope system (R) which allows online focussing, into the vacuum system, through a 75 mm objective lens (K), reflects off a UV-protected mirror (L), and is focussed on the specimen surface (E). Light for illumination of the specimen is generated by a high intensity lamp, passes through a fiber optic (A), into vacuum through a viewport, into a high vacuum compatable fiber optic (D), is reflected off a parabolic mirror (F) which gently focusses it onto the specimen. Viewing light is reflected by the same mirror (L) using for the laser, is collected by the 75 mm objective lens (K), passes out of vacuum, is intercepted by a mirror (Q) on a slidong stage placed in the light path, and is directed to a TV Camera or instant photographic camera.

An exploded schematic of the specimen motion stage is shown in Figure 2. A vacuum linear-motion feedthrough mounted on a flange (A) is connected to a plunger (C) mounted on rods holding cell. The plunger is connected to a cable-in-a-tube system (E,F), connected to a second plunger (H) insulated at its tip by a ceramic piece (I). A specially designed spring-loaded, dovetailed, sliding specimen stage fits on the standard solids probe tip. The ceramic piece contacts the pad section of the stage. When the low mass, magnetic cable is placed in the magnetic field, the second plunger is drawn in and slides the stage down. Retraction of the feedthrough allows the stage to return to its normal position. Coupling of this motion with the rotary motion of the probe allows access to an area of about 1 cm^2.

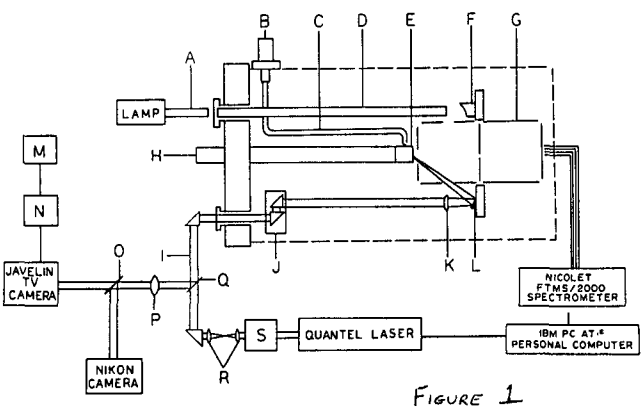

FIGURE 1

A block diagram of the electronic interface is shown if Figure 3. An IBM PC-AT equipped with a Labmaster interface board serves as negotiator between the Nicolet 1280 instrument control computer and the laser electronics. The Labmaster counters are programmed to put out three pulses used to trigger the laser. In "background" mode, only the "charge capacitors" and "fire capacitor" pulses are outputted. This mode allows the YAG rods to attain steady-state temperature without lasing. When a laser pulse is required, the 1280 puts out a pulse which causes the third "Q-switch" pulse to fire, and a laser pulse is obtained. This systems allows optimal laser operation while providing for the use of single or multiple laser pulses for experiment sequences.

The ability of the system to perform local analyses was tested using a 1000 mesh Cu electron microscopy grid silver painted onto a substrate. This specimen presents a surface of copper with interspersed square holes 12 µm on a side. The laser was first directed onto a Cu line. The two Cu isotopes, m/e 63 and 65, are the only ions observed in this spectrum. Next, the beam is directed to ablate material from within in the grid holes. The Ag isotopes, 107 and 109, are observed as the largest peaks in the spectrum. Cu is also present at a level <10%. We conclude from this that the spot size is of the order of 10 µm diameter.

As an additional test of spot size, craters were ablated in a smooth silicon wafer. Minimum crater diameters were shown by electron and reflected light microscopy to be on the order of 3 µm.

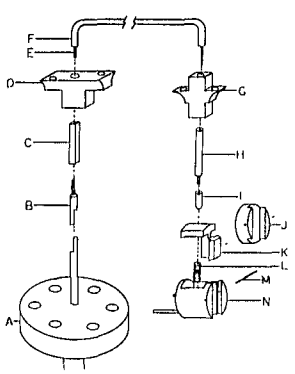

FIGURE 2

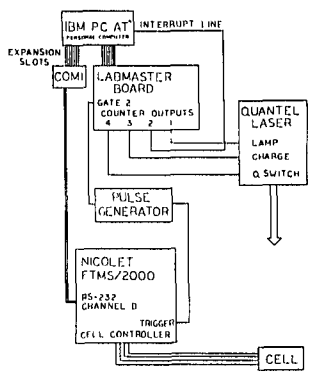

FIGURE 3

Presented at the 36th ASMS Conference on Mass Spectrometry and Allied Topics
June 5-10, 1988, San Francisco, CA

APPLICATIONS OF LASER MICROPROBE USING FOURIER TRANSFORM MASS SPECTROMETRY

Sahba Ghaderi; IBM, General Products Division, San Jose, CA 95193

Laser microprobe mass spectrometry is a proven technique in the area of surface analysis. Several different types of mass spectrometers equipped with laser microprobe are commercially available. The Fourier transform mass spectrometer (FTMS), however, with its pulsed operation, high mass, and high resolution capability is the best suited technique for pulsed laser applications. The limitations, until recently, has been the lack of proper laser delivery system and the means for viewing the the image of the sample with a reasonable magnification.

A Nicolt FTMS-2000 instrument has been modified for the first time in our laboratory to perform laser microprobe experiments. The goal in this implementation to our instrument has been to perform mass analysis of large and small organic and inorganic molecules on different surfaces. It was also important to us to achieve that goal without major hardware changes and without any sacrifice of instrument performance.

In our design a new laser interface has been substituted for the original one, the cell assembly has been rotated by 180 degrees and modified for a larger laser port flange. A focusing lens and flat mirror are also substituted for the parabolic mirror.

In this set up a focused beam of CO2 laser is used for ablation and ionization of samples. Viewing of the magnified image of the sample is accomplished with a video camera through the same optical path as for the laser. A fiber optic bundle and an external light source provide sample illumination. Laser spot size is 30-50u and magnification is in the order of 60 (Fig. 1).

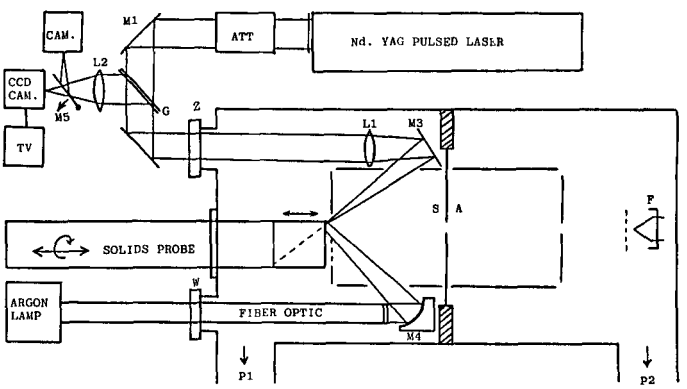

LASER MICROPROBE FTMS AT IBM SAN JOSE

The majority of samples examined by our instrument are related to magnetic storage disk technology. The complex surface of these thin film, multi-layer, ultra high capacity disks provide a very challenging task for the analytical methods used to identify microscopic contaminations.

Other applications of such system include identification of organic and inorganic contaminant on various electronic components, mass analysis of polymers and ceramics, characterization of perfluoriated polyether lubricants on surfaces, as well as general use of the laser in desorption and ionization of different compounds of interest. (Fig. 2 & 3).

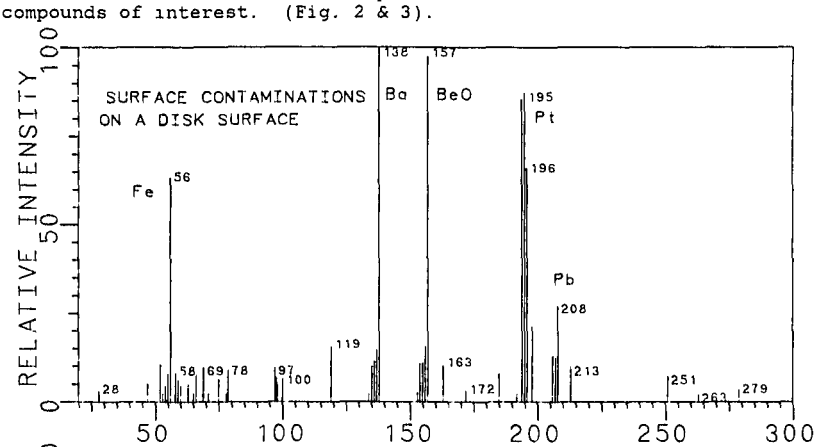

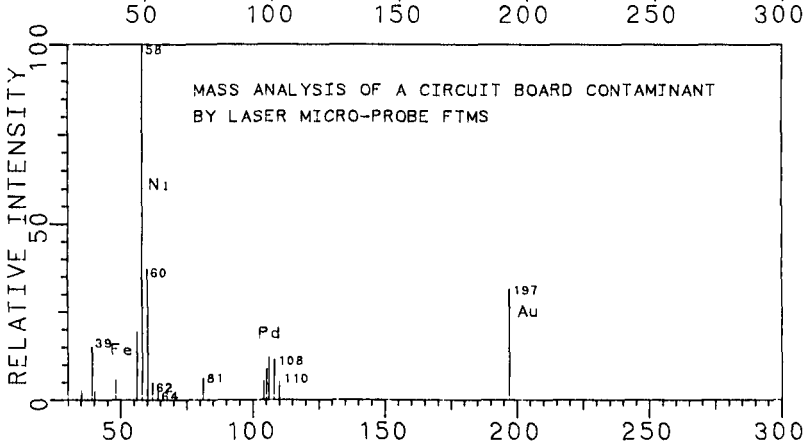

Further improvements in our instrument's capability are underway. They include the use of a Nd/YAG laser and modifications in our laser delivery and optical imaging system. These changes are for reducing the laser spot size to below 10u and to improve signal reproducibility. Design and interfacing of an external ion source is also underway in order to improve sample handling and analysis of larger specimens.

Presented at the 36th ASMS Conference on Mass Spectrometry and Allied Topics
June 5-10, 1988, San Francisco, CA

THE EFFECT OF ION VELOCITY AND PHASE ANGLE γ ON THE COHERENT ION PACKET

C.D. Hanson, E.L. Kerley, M.E. Castro, and D.H. Russell
Department of Chemistry, Texas A & M University
College Station, Texas 77843.

The analytical capabilities and intrinsic versatility of FT-ICR was recognised early.[1] Although there has been great success in the area of ion-molecule studies, many problems in high mass analysis remain unanswered. The problems incurred in FT-ICR are commonly attributed to the loss of a coherent ion packet. Therefore, in order to achieve the theoretical potential of FT-ICR, the dynamics of a coherent ion packet must be understood. The effect of translational energy on the creation of a coherent ion packet is difficult to study in simple cubic ICR cells. The complicated issue of ion motion and ion kinetic energy can be modeled in a two-section cell. By giving ions translational energy prior to the partitioning event, the effect of translational energy on the creation of a coherent ion packet can be systematically studied.

A coherent ion packet is an ensemble of ions which can be approximated by a single ion. To meet these requirements the ion packet must be both spatially and phase defined. Because ions are initially formed in the ICR cell over several milliseconds (*i.e.*, many cyclotron periods) and with initially random motions, there is a random distribution of phases. The mechanism for the production of a coherent ion packet is ion acceleration by a resonant oscillating electric field. An ion which is initially out-of-phase with respect to the rf excitation must change the period of its synchronous orbit (ω_{eff}) to become phase coherent (see figure 1). The required frequency shift can only occur in ion motion which is dominated by an electric field.

Ions whose frequencies are governed by the Lorentz force of a dominant magnetic field ($\omega_{eff}=\omega_c$) are restricted from undergoing a frequency shift and are therefore locked out-of-phase. Owing to the velocity dependence of the Lorentz force ($F=qv_{xy}B$), the effect of the magnetic field increases with translational energy. Thus, an ion formed with significant translational energies will be held out of phase with respect to the excitation field.

It has been demonstrated that an ion which is translationally excited to a larger cyclotron radius by a resonant oscillating electric field can be de-excited by inverting the phase of the applied rf field with respect to the phase of the cyclotron orbit.[2,3] In this manner the translational energy of selected ions can be systematically regulated by an excitation/de-excitation technique.[4] Ions which are originally excited to radii which exceed the dimensions of the conductance limit orifice can be de-excited to radii acceptable for partitioning. Contained in figure 2 is a schematic of the procedure for investigating the effect of translational energy and relative phase angle in a two-section cell. Following ion production in the source region (A), all ions are excited to larger cyclotron radii by an rf excitation sweep (B). Selected ions are de-excited to the original radii by applying a second rf sweep which is 180° out of phase with respect to the cyclotron motion of the selected ions (C). The phase of the second pulse is selected by a variable delay between the first and second excite pulses. If the delay between the pulses corresponds to an odd integral of $\pi r/2$ (where r is the period of the cyclotron orbit) the second excite pulse will be phase inverted. The radius of the de-excited ion can be analyzed by utilizing the orifice of the conductance limit. Only ions de-excited to energies corresponding to the dimensions of the orifice of the conductance limit will be partitioned into the analyzer region of the two-section cell (D).

An ion which is held out-of-phase with respect to the applied oscillating electric field will be de-excited and lose translational energy. As the ion loses translational energy, the effect of the magnetic field will decrease with respect to the applied electric field. At a point at which the force applied by the electric field is greater than the force applied by the magnetic field, phase shifting can occur by frequency advance. An ion which is initially out-of-phase will become phase coherent with the dominant electric field. As the ion gains energy by the rf field, force of the magnetic field increases and the frequency is determined by the m/z ratio.

Contained in figure 3 is the schematic used to probe the energy of phase advancement. Ions are formed with thermal energies by electron impact and accelerated to larger radii by rf excitation (S1). After a delay of $r/2$ ($\gamma=180°$), a second rf excitation is applied. Because the second excitation is out-of-phase with respect to the ion motion, the ions are de-excited and lose translational energy. If the second rf excitation is allowed to de-excite the ions to a point at

which the electric field becomes dominant, the ions will become phase coherent and gain energy. Contained in figure 4 is a plot of signal intensity in the analyzer region of the two-section ion cell vs. the length of the second rf excitation (S2). Only ions which have been de-excited to smaller radii are allowed to partition due to the conductance limit. The centroid of the peak corresponds to the energy at which the ion phase advances. Ions that become phase coherent with the applied field are accelerated to larger radii and not partitioned.

External ion sources produce ions having random phases and significant translational energies. Because of the strong Lorentz force caused by the translationally hot ions, de-excitation followed by phase advancement results in a broad energy distribution. Owing to the extreme significance of the definition of the ion packet on ion detection, initial translational energy of ions trapped in an ICR cell is of profound importance.

References Cited:

1. C.L. Wilkins and M.L. Gross Anal. Chem. 1981,53,1661A.

2. Marshall, A.G.; Wang, T.L.; and Ricca, T.L. Chem. Phys. Lett., 1984,105,233

3. Pfandler, P.; Bodenhausen, G.; Rapin, J.; Houriet, R.; and Gaumann, T. Chem. Phys. Lett., 1987,138,195

4. Hanson,C.D.; Kerley,E.L.; and Russell,D.H. submitted for publication to *Anal. Chem.*

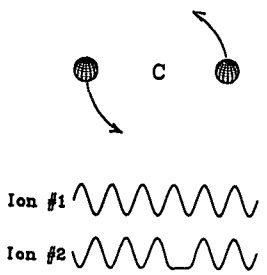

Figure 1.

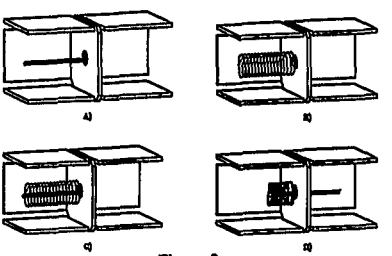

Figure 2.

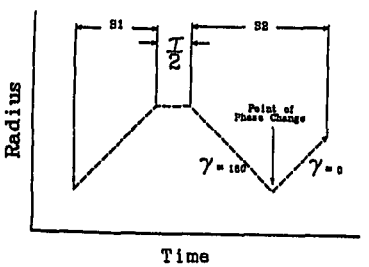

Figure 3.

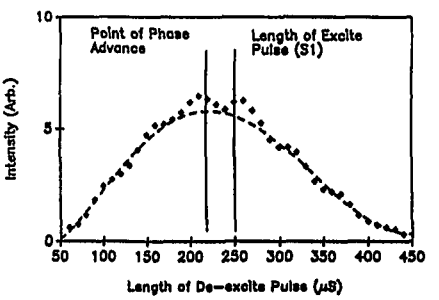

Figure 4.

Presented at the 36th ASMS Conference on Mass Spectrometry and Allied Topics
June 5-10, 1988, San Francisco, CA

PRIMARY STRUCTURE OF PAIM I, AN α-AMYLASE INHIBITOR FROM *Streptomyces corchorushii*, DETERMINED BY THE COMBINATION OF EDMAN DEGRADATION AND FAST ATOM BOMBARDMENT MASS SPECTROMETRY

Kazuo Hirayama
Central Research Laboratories, Ajinomoto Co., Inc.,
1-1 Suzuki-cho, Kawasaki-ku, Kawasaki, 210 Japan

Paim I and II, protein α-amylase inhibitors, inhibit animal α-amylases from pig, dog, cow, horse, *etc.*, but have no activity against human salivary and pancreatic α-amylases. Paim means pig pancreatic α-amylase inhibitor from microbes. The primary structure of Paim I has been determined by Edman degradation and FABMS 1),2). The primary structures of Paim II have been determined by high-performance tandem mass spectrometry.

Positive-ion FAB mass spectra were recorded with a JEOL JMS-HX110 double-focusing mass spectrometer fitted with a 23-kG high-field magnet and operating at accelerating voltages 10 kV. Tandem mass spectra were recorded with a JEOL JMS-HX110/HX110 tandem mass spectrometer.

Figure 1 shows the primary structures and positions of disulphide bridges of Paim I and Paim II determined by this investigation. Figure 2 shows the positive-ion FAB mass spectrum of RCM-Paim I (reduced and carboxymethylated Paim I) and those of subpeptides generated by *Staphylococcus aureus* V8 protease digestion. RCM-Paim I gave a protonated average molecular ion of m/z 7657.0. The caluculated monoisotopic molecular weight of RCM-Paim I from S1, S2, and S3 agreed well with the estimated monoisotopic molecular weight of RCM-Paim I by FABMS(7652.0). Peptides S1, S2, and S3 were chosen for sequencing by an automated Edman degradation.

Automated Edman degradation of RCM-Paim I revealed the sequence up to the 28th cycle ending with valine(28). The amino acid sequence in this region is

```
 1                                   10
Ala-Ser-Glu-Pro-Ala-Pro-Ala-CmCys-Val-Val-Met-Tyr-Glu-Ser-
                                20                      28
Trp-Arg-Tyr-Thr-Thr-Ala-Ala-Asn-Asn-CmCys-Ala-Asp-Thr-Val-
```

N-terminal amino acids of S1, S2 and S3 were determined as glycine, alanine and serine, respectively by dansyl method. Peptide S2 corresponds to Ala(1)-Glu(13) in this sequence on the basis of its molecular weight, N-terminal amino acid and *S. aureus* V8 protease specificity.

The Edman degradation of peptide S3 revealed the sequence up to the 25th cycle:

```
 14                    20
Ser-Trp-Arg-Tyr-Thr-Thr-Ala-Ala-Asn-Asn-CmCys-Ala-Asp-
                30                          38
Thr-Val-Ser-Val-Ser-Val-Ala-Tyr-Gln-Asp-Gly-Ala-
```

After further digestion by *S. aureus* V8 protease, the COOH-terminal peptide S3-2 from S3 was purified by HPLC. Automated Edman degradation of this peptide revealed the sequence up to the 18th cycle, ending at Gly(54). The sequence of the peptide is

```
 37        40                                    50          55
Gly-Ala-Thr-Gly-Pro-CmCys-Ala-Thr-Leu-Pro-Pro-Gly-Ala-Val-X-Y-Val-Gly-Z
```

Three amino acids, X, Y and Z could not be determined by the Edman degradation method. After treatment with carboxypeptidase Y, peptide S3-2 gave mass peaks at m/z 1627.8, 1471.7, 1370.5, 1269.5, 1170.4, 1099.6, and 1042.6 on the FAB mass spectra. The results indicated that the C-terminal sequence of S3-2 is -Gly-Ala-Val-Thr-Thr-(Val,Gly)-Glu.

Automated Edman degradation of the fragment S1 established the sequence of all 18 amino acids shown below.

```
 56          60                                  70
Gly-Tyr-Leu-Gly-Glu-His-Gly-His-Pro-Asp-His-Leu-Ala-Leu-CmCys-Pro-Ser-Ser
```

The positions of disulphide bonds in Paim I were determined as follows.
The *S. aureus* V8 protease digests of Paim I gave a protonated molecular ion at m/z 2523.2 on the FAB mass spectrum. This ion can be assigned to disulphide bridged peptide Gly(37)-Glu(55)+His(66)-Ser(73). This suggests that Cys(42) must be linked with Cys(70).

Fractionated peptide (f) gave a protonated molecular ion at m/z 2836.2 on the FAB mass spectrum. This ion can be assigned to the disulphide bridged peptide Ala(1)-Glu(13)+Ser(14)-Asp(26).

In conclusion, Paim I has two disulphide bonds, Cys(8)-Cys(24) and Cys(42)-Cys(70).

Figure 3 shows protonated molecular ions of RCM-Paim II. Paim II gave a single-band on the SDS gel electrophoresis, but two peaks were observed in this spectrum. One was m/z 7772.2, the other was 7860.6. This means Paim II consists of two proteins, Paim IIa and Paim IIb. The mass difference between the protonated molecular ion of RCM-Paim I and RCM-Paim IIa corresponds to the molecular weight of an aspartic acid residue. The mass difference of these two peaks corresponds to the molecular weight of a serine residue. Therefore, Paim IIa is larger than Paim I by an aspartic acid residue, and Paim IIb is larger than Paim I by aspatric acid and serine residues. If this homology results from N-terminual varietiy of proteins, it is expected that the peptides having molecular weight 1625.7 and 1538.6 will be produced by S. aureusV8 protease digestion. If this homology results from C-terminal variety of proteins, it is expected that the peptides having molecular weight 1629.7 and 1542.6 will be produced by S. aureus V8 protease digestion. The two N-terminal peptides gave peaks at m/z 1626.8 and m/z 1539.7 on the FAB mass spectrum of S. aureus V8 protease digests of RCM-Paim II. Figure 4 shows the tandem mass spectrum from m/z 1626.8. The primary structures of N-terminal peptides of Paim II were determined by b and x series ions as shown below.

Paim IIb	Ser-Asp-Ala-Ser-Glu-Pro-Ala-Pro-Ala-Cys-Val-Val-Met-Tyr-Glu
Paim IIa	(Asp,Ala)-Ser-Glu-Pro-Ala-Pro-Ala-Cys-Val-Val-Met-Tyr-Glu

1) K. Hirayama et al., Biochemistry, 26, 6483 (1987).
2) S. Akashi et al., Biomed. Environ. Mass Spectrom., 15, 541 (1988).

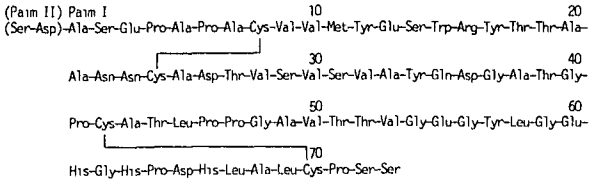

Figure 1

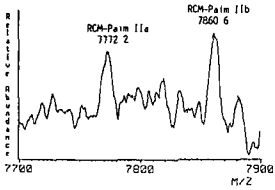

Figure 3

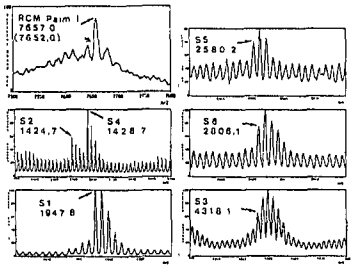

Figure 2

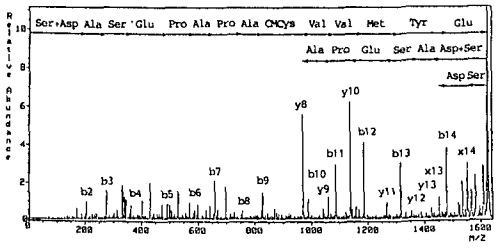

Figure 4

Presented at the 36th ASMS Conference on Mass Spectrometry and Allied Topics
June 5-10, 1988, San Francisco, CA

STRUCTURE ELUCIDATION OF MERREMOSIDES BY LIQUID SECONDARY ION MASS SPECTROMETRY

Yuzo Nakagawa, Yuji Ikenishi, Minoru Uchida*, and Isao Kitagawa**
Shionogi Research Laboratories, Fukushima-ku, Osaka 553, Japan
*Hitachi Naka Works, Katsuta 312, Japan
**Osaka University, Yamada-oka, Suita 565, Japan

INTRODUCTION

Structures of nine merremosides isolated from the Indonesian folk medicine "Bidara upas", which is known as a drug for diabetes and respiratory system disease, were elucidated mainly by mass spectrometric investigations using positive and negative ion liquid secondary ion mass spectrometry (liq.SIMS) and liq.SIMS-metastable ion (MI) spectrum to be resin glycosides.

EXPERIMENTAL

A Hitachi M-90 mass spectrometer, of which ion optics had an additional second electric field to Hitachi M-4000 mass spectrometer was used for measurement of liq. SIMS and liq. SIMS-MI spectrum by using B/E-linked scanning.

RESULTS AND DISCUSSION

1. Structure of merremoside-d (M-d)

The structure elucidation of **M-d** was described as an example of a series of resin glycosides.

1.1 Structure information on M-d (before investigation by mass spectrometry)

a) Methanolysis of **M-d** gave methyl jalapinolate (methyl 11R-hydroxypalmitate), and methyl rhamnoside. This result indicated that the structure of **M-d** was including jalapinolic acid and rhamnose moieties.

b) Alkaline hydrolysis gave a glycosidic acid which is called merremoside-i (M-i) as well as isobutyric acid.

c) ^{1}H-NMR indicated that three kinds of acyl groups were bonding at 3, 3 and 4 position of rhamnose, respectively.

Consequently, **M-d** was assumed to be glycoside composed of a number of rhamnose partially acylated. Then, in order to determine the structure, number and sequences of rhamnoses, and number and substituted position of acyl moieties were required to be elucidated.

1.2 Me M-i derived from M-d

Me **M-i** which was derived from **M-d** by treating with NaOMe/MeOH gave a prominent ion peak at m/z 893 in its positive ion SIMS (PISIMS). This ion could be sodium adduct ion of summation of four rhamnoses and a methyl jalapinolate group. In the SIMS of Me **M-i**, peaks at m/z 585, 439, 293 and 147 were corresponding to the fragment ions composed of four, three two and one rhamnoses, respectively, which are also observed in the MI spectra. The spectral pattern of Me **M-i** suggested that the four rhamnose sequence was in a straight chain, indeed methanolysis of permethylated **M-i** afforded methyl 2,3,4-tri-O-methyl-L-rhamnopyranoside and methyl 2,3-di-O-methyl-rhamnopyranoside in 1:3 ratio. Thus the structure of Me **M-i** should be jalapinolic acid substituted at 11 with 1,4 linked four rhamnoses as shown in Fig. 1. The aglycone group was remained as methyl ester after NaOMe treating of **M-d** suggested **M-d** had a lactone ring.

1.3 Desacyl M-d

PISIMS and negative ion SIMS (NISIMS) of desacyl **M-d** which was given by mild hydrolysis of **M-d** indicated the molecular weight was 838. Since this number was 32 less than the molecular weight of Me **M-i**, desacyl **M-d** still had a lactone ring. The PISIMS of desacyl **M-d** gave ion peaks $[a + H]^+$, $[b + H]^+$, **i** and **ii** which were corresponding to fragment ions as shown in the Fig. 2, but the ions **iii** and **iv**, which appeared in the spectrum of Me **M-i**, were not found. Then, we could assume lactone ring should be linked with the 2nd rhamnose moiety. Although the NISIMS of desacyl **M-d** did not provide any fragment ion which consist of only sugar moieties, successive loss (146, 146, 128 and 146) from end rhamnose showed the sequence (Fig. 2). This behavior indicated the lactone bond at the 2nd rhamnose cleaved and abstracted one hydrogen from the rhamnose to give a carboxylic acid, and a cleavage occurred at a bond between the 1st and 2nd rhamnose. Consequently, it is assumed that the carboxyl group of jalapinolic acid is formed lactone ring with 3-OH of the 2nd rhamnose.

1.4 Liq. SIMS of M-d

Concerning number and substituted position of isobutyryl group, positive and negative ion SIMS of **M-d** were examined. Since the molecular weight was 978

which was 140 larger than desacyl M-d, two isobutyryl groups were substituted. Fragment ions $[a + H]^+$ and $[b + H]^+$ indicated that each isobutyryl group was substituted in the 3rd and 4th rhamnose, respectively, and MI spectra were also compatible with above informations(Fig. 3). NISIMS and NISIMS-MI spectra confirmed the structural information.

Consequently, it was assumed that isobutyryl groups were substituted at 3-OH of the 3rd rhamnose and 4-OH of the 4th rhamnose, respectively.

2. Structure of merremoside-b (M-b) and merremoside-g (M-g)

Studying PISIMS and NISIMS of M-b and M-g with comparing those of M-d clarified the structures of them. M-b is the isomer of M-d and the isobutyryl group is substituted at 2-OH instead of 3-OH of the 3rd rhamnose. M-g is a glucoside of M-b, the glucose moiety is linked with 3-OH at the 3rd rhamnose

CONCLUSION

Investigation of liq. PISIMS and NISIMS and MI spectrum of nine resin glycosides (merremosides-b, -d, -g, and others) isolated from Bidara upas revealed each structure.

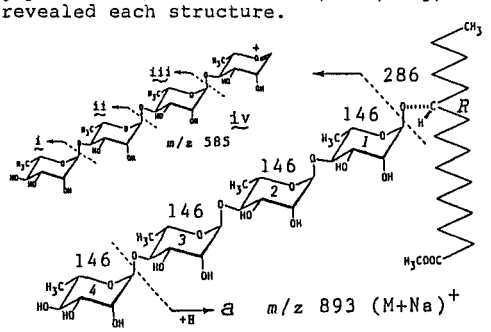

Fig. 1. Merremoside-i

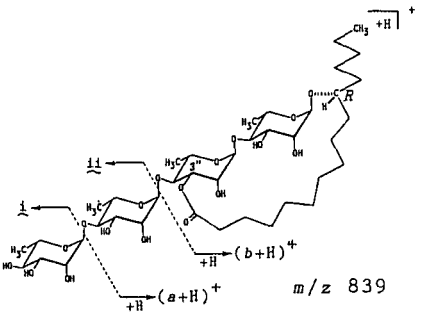

Fig. 2. Desacyl Merremoside

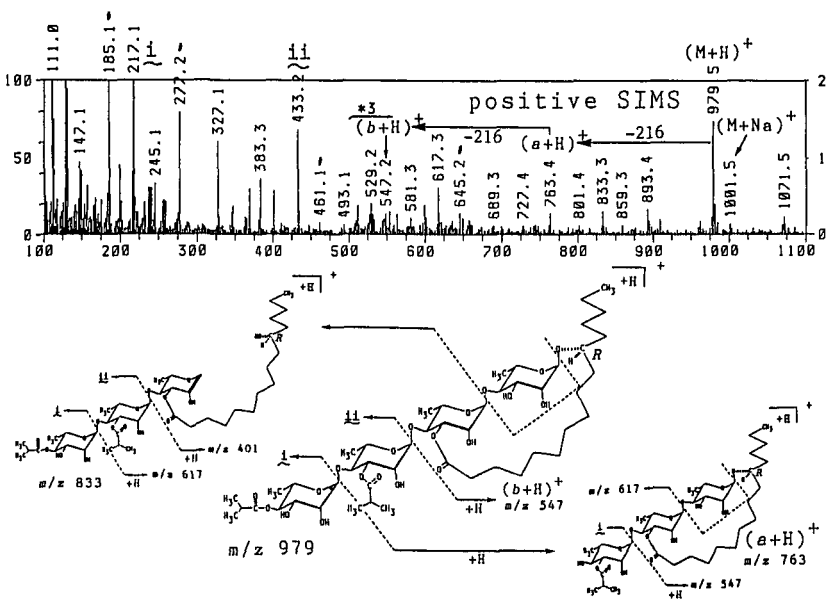

Fig. 3. PISIMS of merremoside-d and its fragmentation

Presented at the 36th ASMS Conference on Mass Spectrometry and Allied Topics
June 5-10, 1988, San Francisco, CA

SEX AND AGE DEPENDENT SULFOCONJUGATION AND IDENTIFICATION OF N-SULFONATE WITH NEGATIVE SECONDARY ION MASS SPECTROMETRY

Kazuhide Iwasaki, Mamoru Fujioka* and Hideyo Noguchi

Product Development Laboratories and *Analytical Research Laboratories
Fujisawa Pharmaceutical Co., Ltd.
1-6, 2-Chome, Kashima, Osaka 532, Japan

Sulfoconjugation is one of the important metabolic pathways of drugs, and other endogenous and exogenous compounds for human and animals. Compounds which contain phenolic and alcoholic hydroxyl group, and arylamine are metabolized to O-sulfate ester and N-sulfonate, respectively. Recently, we reported nobel N-sulfonate of alicyclic amine and alcoholic O-sulfate ester of tiaramide, an anti-inflammatory agent (1). Moreover, a number of compounds containing alicyclic amine, alkylamine and arylamine are also metabolized to respective N-sulfonate of the amines (2).

Sulfoconjugates are highly polar in biological fluid, and structural information of intact sulfoconjugates is hardly obtained by mass spectrometry with conventional ionization devices. Recent development of soft ionization technique in mass spectrometry makes it possible to analyze directly such highly polar compounds. Throughout the study for identification of N- and O-sulfoconjugates, we found many advantages of negative secondary ion mass spectrometry for getting direct information of their intact structures. We analyzed nine sulfoconjugates by secondary ion mass spectrometry (SIMS). By SIMS in negative mode, molecular ion peak $(M-H)^-$ of all sulfoconjugates was observed as shown in Table. The molecular ion peak was more prominent in the spectra of amine N-sulfonates with low molecular weight. By SIMS in positive mode, molecular ion peak $(M+H)^+$ of the sulfoconjugates was seldom observed. Adduct ion peak with potassium was observed in the spectra of some sulfoconjugates. These results strongly suggest that SIMS in negative mode offers direct information of the intact structure of highly polar sulfoconjugates.

Enzymic characteristics of sulfoconjugations were studied. Sulfoconjugations of amines and alcoholic and phenolic compounds were observed in liver 105,000 g supernatants. The activities depended on biologically active sulfate, 3'-phosphoadenosine 5'-phosphosulfate.

Sulfoconjugating activities of amines and alcoholic compound were very low in neonates of rats and increased gradually until the ages of 3-week-old. There were no sex-dependent differences of the activities before puberty of rats. The activities of female rats exhibited constant high levels throughout the ages from 3-week-old to 2-year-old. The activities of male rats decreased after puberty, and the activities of 7-week-old males were about one third of the levels of 7-weel-old females. The low activities were also observed in 1-year-old males, but the activities of 2-year-old males increased to about half of the levels of 2-year-old females.

On the other hand, sulfoconjugating activities of phenolic compound in male and female neonates of rats were half of the levels of 7-week-old females. The activities of 7-week-old rats were nearly 2-fold higher in males than females. The activities of 2-year-old rats were the intermediate levels between the activities of 7-week-old males and females and there were no sex-dependent differences in the activities of 2-year-old rats.

Species differences of sulfoconjugations were studied. Hepatic 105,000 g supernatants of mice, rats, guinea pigs, rabbits, dogs and monkeys exhibited sulfoconjugating activities of amines and hydroxyl compounds. In general, the supernatants of all species studied, exhibited higher sulfoconjugating activities for phenolic compunds than other substrates. On the other hand, the sulfoconjugation of alkylamine was very low or inert by the supernatants of all species examined. There were great variations in the levels of sulfoconjugating activities for other amines and alcoholic compound by the supernatants.

Thus, the results about age- and sex-dependent changes of sulfoconjugations in rats and about species differences of sulfoconjugations indicate that the substrate for sulfoconjugation could be divided into at least two groups; an amine and alcohol type and a phenol type.

Presented at the 36th ASMS Conference on Mass Spectrometry and Allied Topics
June 5-10, 1988, San Francisco, CA

References
(1) Xenobiotica, 13, 565-574 (1984).
(2) Xenobiotica, 16, 651-659 (1986).

Table Mass Spectra of Sulfoconjugate in Secodary Ion Mass Spectrometry

Compound	Negative	Positive		
	$(M-H)^-$	$(M+H)^+$	$(M+K)^+$	$(M-H+2K)^+$
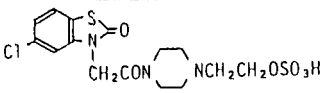	++	+	-	-
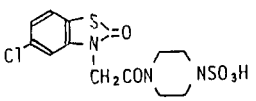	+++	-	+	++
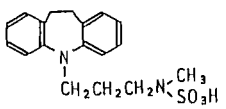	++	-	-	+++
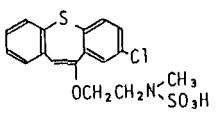	+	-	-	+++
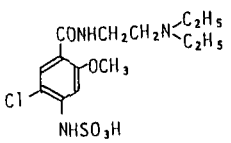	++++	-	+	+++
	++++	-	-	+
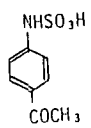	++++	-	+	++
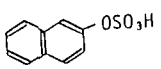	+++	-	-	++
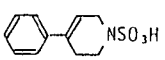	++	-	+	+

Presented at the 36th ASMS Conference on Mass Spectrometry and Allied Topics
June 5-10, 1988, San Francisco, CA

AMINO ACID MIXTURE ANALYSIS BY LASER DESORPTION FOURIER TRANSFORM MASS SPECTROMETRY. M.P. Chiarelli[1], E. Davoli[2], and M.L. Gross[1]. 1. Department of Chemistry, University of Nebraska-Lincoln, Lincoln, NE 68588. 2. Mario Negri Pharmalogical Research Institute, Via Eritrea 62, Milano, Italy.

This investigation is intended to be a pilot project for the analysis of larger peptides and particularly their mixtures. A mixture of 15 amino acids was determined at power density of 2 x 10^6 W/cm^2 and a wavelength of 1064 nm with only 3 ng of each applied to the probe. A FAB/MS comparison was made to assess the generality and detection limits of LD/FTMS. Several matrices and cationizing agents were tried and the best results were obtained in a glycerol matrix, giving 11 components at 350 ng each. Sample-specific ions observed in LD/FTMS were of the $(M - H + 2Na)^+$ type, whereas FAB in glycerol yielded $(M + H)^+$ ions.

It can be seen in the LD/FTMS spectrum that ion abundances seem to increase with mass; which is poopsite of what might be expected due to the fact that equal weights were deposited on the copper probe. Simple binary mixtures of the amino acids in excess NaCl were laser desorbed in order to understand the mechanism of discrimination.

The first mixtures investigated were those of Glycine and the alkyl amino acids at 2 x 10^6 W/cm^2. All alkyl amino acids have similar pka's and hydrophobic R groups, only their masses are different. The laser desorption of these mixtures show that the Gly/AA abundance ratios decrease with the increasing mass of the alkyl amino acid. (Table I).

In the next sequence we decided to evaluate binary mixtures of amino acids with similar masses and widely different pka's (Table II). Mixtures of systiene, valine, and threonine were evaluated under the same experimental conditions described above. The tendency to form $(M - H + 2Na)^+$ ions should be controled in part by the pka's of the amino acid in question and therefore cystiene should be the largest component of either binary mixture. This is not the case, and trend seen is just the opposite. Threonine has the largest pka's and is always the major component when assessed agianst cystiene or valine. The ratios in Table IIB suggest that the mechanism of amino acid desorption is controled by intrinsic properties of the amino acids.

The next property investigated was that of sublimation enthalphy. Sabbah and coworkers have studied the temperature dependence of glycine, alanine, and proline sublimation. The maximum temperature of our copper probe can be estimated to be ca. 800 k (3). Sublimation enthalphies at this temperature were estimated from the data cited above and are given in Table IIIA. The enthalphies extrapolated suggest that proline should dominate the spectra of the binary mixtures and indeed it does. The Ala/Pro ratio is closer to 1 than what is suggested by the Gly/Pro ratio but in this study we are assuming a parralel between the thermodynamic properties of the amino acids and the kinetics of desorption and parralel might not followed strictly. Attempt sublimation enthalphy determination of cystiene failed due to its thermal decomposition (4), and this may very well explain its reduced abundance but the kinetics of the desorption process must be the reason why any $(M - H + 2Na)^+$ is seen from the LD of cystiene at all.

Sublimation enthalphies determined by Knudsen Cell Calorimetry at 455 k indicate that the larger amino acids have larger enthalphies than glycine at this temperature (5). This means that the Gly/AA ratios should get larger as the laser power density is reduced and indeed they do as is indicated by the plot given.

1. Sabbah et al., Thermo Chimica Acta, 20, 371, 1977.

2. Sabbah et al., Bull. Soc. Chim., 1-2, 50, 1978.

3. J.F. Ready in "Effects of High-Powered Laser Radiation", Academic Press, New York, 1970, p. 142.

4. Sabbah, et al., Thermochimica Acta, 43, 269, 1981.

5. H.J. Svec and D.D. Clyde, J. Chem. Ref. Data, 10, 151, 1965.

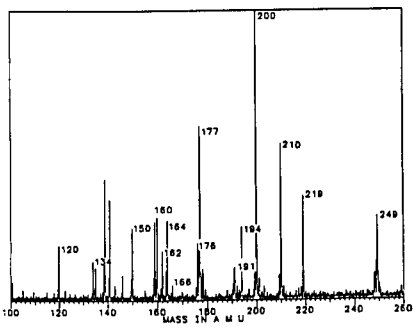

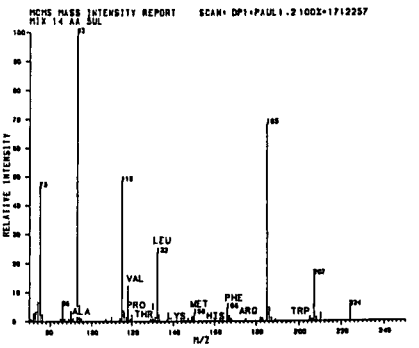

TABLE I: Ion abundance ratios from the Laser Desorption of glycine and other alkyl amino acids in binary mixtures in an NaCl matrix at a wavelenth of 1064 nm. and a power density of 2 x 10^{8} W/cm^{2}.

AMINO ACID	R GROUP	RATIO ON PROBE	ION ABUNDANCE RATIO*
ALANINE	CH_3	1.2	0.37 +/- .07
VALINE	$CH(CH_3)_2$	1.5	0.24 +/- .07
LEUCINE	$CHCH_2(CH_3)_2$	1.6	0.29 - .05

*N = 8 determinations

TABLE IIA: pK values for the amino acids Cys, Val, and Thr.

AMINO ACID	pK COOH	pK NH_3^+	pK side chain
Cysteine	1.71	8.18	10.28
Valine	2.32	9.62	-----
Threonine	2.71	9.62	———

TABLE IIB: Ion abundance ratios of (M - H + 2Na)$^+$ ions desorbed from binary mixtures of Cys, Val, and Thr in a NaCl matrix.

AMINO ACIDS	IONS RATIORD	ABUNDANCE RATIOS*
Val/Thr	(m/z 162)/(m/z 164)	0.24 +/- .06
Cys/Val	(m/z 166)/(m/z 164)	0.21 +/- .02
Cys/Val	(m/z 166)/(m/z 162)	0.77 +/- .05

*N = 8 determinations

TABLE IIIA: Enthalphies of sublimation estimated for Gly, Ala, and Pro at 800K.

AMINO ACIDS	ENTHALPHY	REFERENCE
GLYCINE	108.9 kJ/m	1
Alanine	91.0 kJ/m	1
Proline	22.1 kJ/m	2

TABLE IIIB: Ion abundance ratios of Gly, Ala, and Pro desorbed from binary mixtures in an NaCl matrix.

AMINO ACIDS	ION ABUNDANCE RATIOS	N
Gly/Ala	0.37 +/- 07	8
Gly/Pro	0.08 +/- 01	12
Ala/Pro	0.45 +/ 09	10

1. Sabbah et al., Thermochimica Acta, 20(1977) 171.
2. Sabbah et al., Bull. Soc. Chim., 1-2(1978) 50.

TABLE IV: Enthalpies of sublimation for alkyl amino acids determined at 455K by Knudsen Cell Effusion Method *

AMINO ACID	ENTHALPHY
Glycine	136.5 kJ/m
Alanine	138.1 kJ/m
Valine	162.8 kJ/m
Leucine	150.7 kJ/m

1. H.J. Svec and D.D. Clyde, J. Chem. Eng. Data, 10(1965) 151

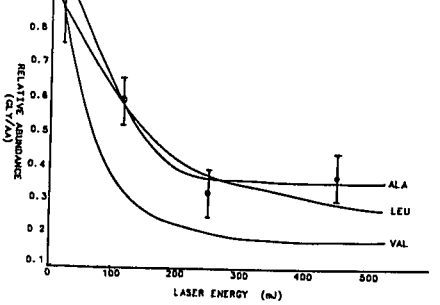

Presented at the 36th ASMS Conference on Mass Spectrometry and Allied Topics
June 5-10, 1988, San Francisco, CA

ON-LINE ENZYMATIC HYDROLYSIS - THERMOSPRAY HPLC/MS DETERMINATION OF ENDORPHINS.

R. D. Voyksner and T. Pack, Analytical and Chemical Sciences, Research Triangle Institute, P. O. Box 12194, Research Triangle Park, NC 27709. H. Swaisgood and D. Chen, Department of Food Science, North Carolina State University, Box 7624, Raleigh, NC 27695.

Progress in neuropeptide research will rely on the existence of specific, sensitive, and accurate methods for identification and quantitation of peptides in various biological matrices. The fact that neuropeptides are active in the picomolar (pM) to femtomolar (fM) range, coupled with the existence of many different individual peptides, places an enormous burden on the analytical methodology. Mass Spectrometry (MS) techniques such as fast atom bombardment (FAB) and thermospray have been used for the detection of peptides in biological matrices. However, both FAB and thermospray are limited in the number of confirming ions (i.e. amino acid sequence ions) for peptides above mw 2000 and lack the sensitivity for low pM analysis. These limitations can be partially overcome by the combination of enzymatic hydrolysis with HPLC/MS.

The two main parameters for enzymatic hydrolysis of peptides are selectivity and activity. Selectivity controls what amino acid bond(s) are hydrolyzed. Selectivity is determined by the particular immobilized enzyme chosen, as shown in Table 1. For example, the analysis of ß-endorphin, a 31 amino acid neuropeptide, by thermospray or FAB/MS results in only the $[M+H]^+$ and multiple charged ions. However, the use of enzymatic hydrolysis with thermospray MS detection enables the detection of specific enzymatic hydrolysis fragments ions related to the amino acid sequence of the peptide. The observed hydrolysis sites for trypsin, chymotrypsin, V8 protease, and thermolysine of ß-endorphin are shown in Figure 1. The extent of hydrolysis (activity) is the other important factor which influences the spectra. Activity of an immobilized enzyme column can be controlled by varying the concentration of the enzyme, recycling the effluent, or altering temperature, pH, and solvent. In most cases immobilized enzyme columns (10cm x 2.1 mm) containing 0.15-0.20g of packing, exhibited activity of 100-200 units/g of packing and were capable of hydrolyzing the endorphins analyzed (Figure 1) Typically, the enzyme activity was greatest at 35-45°C, pH 7.5-8.5, and at low organic HPLC mobile phase concentrations. However, suitable activity (with 30-40% loss in activity) could be achieved at up to 50% organic in the HPLC system.

The combination of thermospray HPLC/MS and immobilized enzyme hydrolysis can be very useful in peptide identification and sequencing. There are a number of ways of combining the enzyme hydrolysis and HPLC with MS detection for peptide analysis. The use of an immobilized enzyme column prior to HPLC/MS will enable the separation of each hydrolysis fragment, permitting acquisition of "clean" mass spectra. The detection of the hydrolysis products aids in specific detection or confirmation of the presence of an endorphin.

The reversal of the column order (i.e., HPLC followed by trypsin hydrolysis) can prove useful in gaining specificity for the detection of individual peptides in a complex matrix. Thermospray mass spectra containing structural information from the tryptic hydrolysis can be acquired from each peptide in a mixture. The increase in organic solvent, necessary for the HPLC separation of the endorphins, lowered the activity of the trypsin column permitting the detection of molecular ions as well as the tryptic fragment ions.

The combination of two or more immobilized enzyme columns with HPLC/MS can prove useful in peptide identification and amino acid sequencing. For example, the tryptic hydrolysis of γ-endorphin results in two peptides. These fragment peptides, separated by HPLC, can undergo further hydrolysis with another immobilized enzyme column (e.g. carboxypeptidase A,B, and Y) for further specificity and to gain amino acid sequence information. Carboxypeptidase hydrolysis enables determination of the amino acid sequence (up to 5 amino acids) on the C-terminus side of each tryptic fragment. The combination of tryptic hydrolysis with aminopeptidase M would enable the determination of the amino acid sequence from the N-terminus of each fragment. Together the trypsin and carboxy and amino peptidases could be used for a complete amino acid sequence for γ-endorphin.

The second advantage of combined immobilized hydrolysis HPLC/MS is sensitivity. The hydrolysis of a peptide with enzymes such as trypsin or chymotrypsin, can drastically lower the molecular weight of the peptide. The lower molecular weight peptide is subject to higher ionization, transmission or detection efficiency over the non-hydrolyzed peptide. For example, the detection of the tryptic hydrolysis fragment T_3 (mw 558) of ß-endorphin resulted in a gain of 30 in sensitivity over the detection of the $[M+2H]^{+2}$ ion of ß-endorphin (mw 3463).

Presented at the 36th ASMS Conference on Mass Spectrometry and Allied Topics
June 5-10, 1988, San Francisco, CA

Clearly the combination of the increased sensitivity and additional structural information obtained through the use of on-line enzymatic hydrolysis-HPLC/MS can prove vital in the identification and detection of neuropeptides.

Acknowledgement

This work was supported in part by the National Institute of Drug Abuse, Grant No. 5 R01 DA 04202-02.

Table 1. SPECIFICITY OF VARIOUS ENZYMES FOR PEPTIDE HYDROLYSIS

Enzyme	Amino Acids Hydrolyzed
Trypsin	Lys,Arg
Chymotrypsin	Phy,Tyr,Try (Leu,Met,Asn)[1]
V8 Protease	Glu,Asp
Thermolysine	Leu,Ile,Phe,Met,Ala,Val
Carboxypeptidase A,B,Y	C-Terminus Cleavage
Aminopeptidase M	N-Terminum Cleavage

[1] secondary amino acid

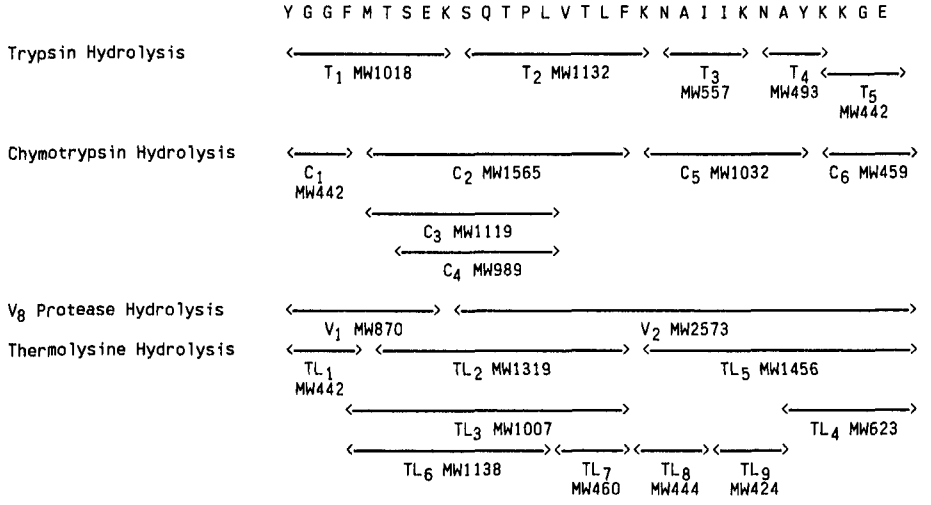

Figure 1. Enzymatic hydrolysis fragments from β-endorphin (mw 3463) detected by thermospray HPLC/MS. Conditions for hydrolysis were: 2 mg of enzyme immobilized on 2000 Å porous glass beads packed in a 10 cm x 2.1 mm column, mobile phase of 20% isopropanol in water, 0.1 M ammonium acetate, pH 7.5, Temp 25°C, flow rate of 1 mL/min.

Presented at the 36th ASMS Conference on Mass Spectrometry and Allied Topics
June 5-10, 1988, San Francisco, CA

DETERMINATION OF PREFERRED GLYCOSYLATION SITES IN A LYSOZYME - GLUCOSE MODEL SYSTEM USING FAB PEPTIDE MAPPING TECHNIQUES;

Hartman, T. G.[1], Rosen, R.T.[1], Ho, C-T.[2], Wu, V.[2], Govindarajan, S.[2] and Rosen, J. D.[2]; Center for Advanced Food Technology[1] and Food Science Dept.[2], Cook College, Rutgers University, New Brunswick, N.J.

The site specificity of glycosylation in a lysozyme-glucose model system was determined using FAB-MS, MS-MS and reverse phase HPLC peptide mapping techniques. The effects of time, temperature and water activity on the glycosylation reaction were measured. Lysozyme (M.W. 14,305) was chosen as a model protein for this investigation since its primary, secondary and tertiary structure has been well characterized (1,2). Native lysozyme and lysozyme glycosylated by reactions with glucose for various times, temperatures and water activities were subjected to tryptic and chymotryptic hydrolysis. The resulting digests were then analyzed by a combination of the previously mentioned techniques to provide peptide maps which are correlated back to the original intact protein. Specific glycosylation sites were determined by observing 162 mass unit differences in peptides from native and reacted lysozyme. These correspond to the presence of glucose derived Schiff bases or Amadori adducts which are formed on the free amino groups of lysines, arginines and the N-terminal of the protein. Preliminary data on the complete tryptic and partial chymotryptic peptide maps of native and glycosylated lysozyme has been presented previously (3). We have now defined the complete chymotryptic peptide map of lysozyme. At several sites chymotrypsin was found to cleave lysozyme at asparagine residues when next to acidic or basic amino acid residues. Since literature reports of such cleavage are rare the identity of the resulting peptide was confirmed by MS-MS. At low moisture content and at two temperatures (25 & 50°C) no glycosylation products were observed in mixtures of lysozyme and glucose. However, when incubated for 3 days in a 65% relative humidity environment glycosylation products began to appear. At 25°C the N and C terminal amino acid region was found to react. At the higher temperature of 50°C the reaction progressed to include 6 sites clustered in the same terminal region of the protein (the N and C terminal regions of lysozyme are linked by a disulfide bridge). We postulate that the observed site specificity of lysozyme glycosylation is directed by the microenvironment created as water is sorbed onto preferred regions of the protein. Figure 1 shows the structure of lysozyme and the observed glycosylation sites. The asterisks (*) indicate potential sites for glucose attack which have not been observed.

References:

1. "The Amino Acid Sequence of Egg White Lysozyme." Canfield, R.E., J. Biol. Chem. 238 (8), 2698-2707, 1963.
2. "The Three-dimensional Structure of an Enzyme Molecule." Phillips, D.C., Sci. Amer. 215, 78-90, 1966.
3. "Analysis of Lysozyme Tryptic Peptides by Fast Atom Bombardment and Tandem Mass Spectrometry." Hartman, T.G. et al., ASMS 34th Annual Conference on Mass Spectrometry., Cincinnatti, OH June 9-13, 1986.

This is a N.J. Agricultural Experiment Station Publication # K-10535-6-88. Also acknowledged is CAFT, an initiative of the New Jersey Commission on Science and Technology.

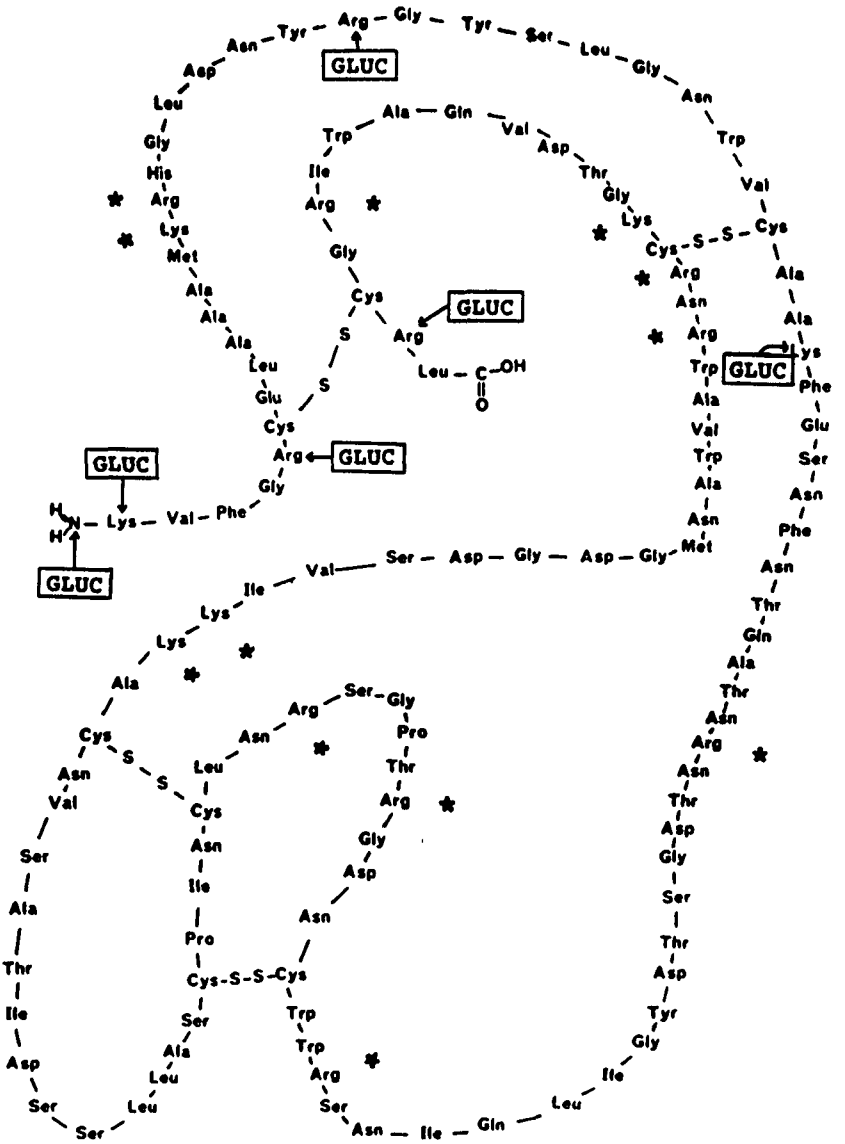
GLUC
GLUC
GLUC
GLUC
GLUC
GLUC
Arg - Gly - Tyr - Ser - Leu - Gly - Asn - Trp - Val - Cys - Ala - Ala - Lys - Phe - Glu - Ser - Asn - Phe - Asn - Thr - Gln - Ala - Thr - Asn - Arg - Asn - Thr - Asp - Gly - Ser - Thr - Asp - Tyr - Gly - Ile - Leu - Gln - Ile - Asn - Ser - Ser - Leu - Leu - Ala - Ser - Pro - Ile - Asn - Leu - Cys - Asn - Val - Cys - Ala - Lys - Lys - Ile - Val - Ser - Asp - Gly - Asp - Gly - Met - Asn - Ala - Val - Trp - Ala - Arg - Asn - Arg - Trp - Cys - Cys - Lys - Gly - Thr - Asp - Val - Gln - Ala - Trp - Ile - Arg - Gly - Cys - Arg - Leu - Glu - Leu - Ala - Ala - Ala - Met - Lys - His - Gly - Leu - Asp - Asn - Tyr - Arg - Gly - Asn - Ser - Gly - Pro - Thr - Arg - Gly - Asp - Asn - Trp - Trp - Arg - Ser - Cys - Cys - Cys

Presented at the 36th ASMS Conference on Mass Spectrometry and Allied Topics
June 5-10, 1988, San Francisco, CA

MS/MS METHODS FOR PEPTIDE SEQUENCING: SUCCESS AND FAILURE.

Lester C. E. Taylor
Wellcome Research Laboratories, RTP, NC. 27709
Linda Poulter
School of Pharmacy, UCSF, San Francisco, CA. 94143

As pointed out by Biemann and others, collision induced decomposition MS/MS often aids in the sequencing of a peptide because the resulting spectrum contains a more complete series of sequence ion types. In addition there is an increase in the number and intensity of fragment ions and the elimination of chemical background.

The analysis of synthetic peptides is usually straightforward because the synthetic route is known and one is looking for problems which may have arisen during the sequential coupling of residues. More challenging however, is the analysis of endogenous peptide material isolated from biological origin where nothing may be known about a particular peptide other than the molecular weight. We have carried out a series of experiments aimed at identifying peptides isolated from bovine adrenal medulla tissue. FABMS analysis of an HPLC fraction from total tissue extract (where standard Leu Enk elutes) shows molecular ion species at 556, 684, 781 and 895 Da, however it would be impossible to conclude that the signal at m/z 556 was due to the MH^+ of Leu Enk. The MS/MS spectrum of the 556 peak gives an intense spectrum which is identical to that observed for standard compound (using ~2 n mol). An estimate for the amount of Leu Enk present in this sample is 50-100 p mol. The presence of Met Enk (MH^+ 574) in another fraction was directly established in the same way. The CID MS/MS spectrum of the m/z 684 peak shows a number of relatively intense daughter ion signals. Interpretation of the spectrum allows the following tentative sequence to be assigned (assuming the molecule is a peptide): V P K/Q L/I D L/I , however there are several daughter ions which are not immediately assignable to this structure and it is possible to assign the peaks to alternative sequences.The degeneracy between K and Q, and L and I cannot be resolved from this spectrum.

Approximately 500 pmol of sample allowed two further experiments to be carried out i) amino acid analysis and ii) manual Edman followed by FABMS. The Edman cycle confirmed the amino terminal V and the presence of one K residue (+135 mass shift from the PTC derivative - valine = MH^+ at 720 Da) which resolves the K/Q assignment. The amino acid analysis confirmed the molar ratios of the amino acids and the presence of L (no isoleucine) and so the sequence is VPKLDL (novel).

The 895 Da peptide gave an MS/MS spectrum from which it was difficult to assign much sequence, however one manual Edman cycle established an amino terminal N and one K residue. It was noticed that an extended form of the 684 Da peptide i.e. the sequence NPVPKLDL is consistent with the 895 Da molecular weight. The amino acid analysis supports the correct molar ratios. Returning to the MS/MS data it now becomes easier to rationalise and explain some of the peaks in the daughter ion spectrum of both the 684 and 895 Da peptides. The peaks at m/z 226,339 and 454 are a series of acylium ions generated from the common ammonium ion PKLDL (585 Da) to give:

P K 226 Da ; P K L 339 Da ; P K L D 454 Da

Unfortunately the occurrence of these ions in the spectrum of an unknown peptide complicates sequence assignment.

Empirically there is a highly variable degree of daughter ion information generated in MS/MS experiments using a hybrid instrument (EBQQ geometry) and we have conducted experiments with several standard peptides and a series of derivatised glucose oligomers.

1. The TRH related peptides <EHPG and <EHPGK give intense fragment ions in their low energy CID spectra. As expected several of the ions arising from the N terminus of the molecule are common to both spectra, e.g. the A and B ions at 221 and 249 Da respectively, as well as the imidazole ion at m/z 110. The <EHPGKR peptide gives a significantly weaker MS/MS

spectrum with little fragmentation.

2. A series of experiments were carried out using Bradykinin (RPPGFSPFR) and des Arg^9 Bradykinin (RPPGFSPF),i.e. one peptide with a basic Arginine on both the N and C terminii and the other with an N terminal Arginine. The low energy CID MS/MS spectrum of the MH^+ using the hybrid instrument was disappointing, with Bradykinin giving only a 904 Da ammonium fragment ion, (also present in the unimolecular spectrum), and some low mass fragments, but nc significant sequence information. The daughter ion spectrum of des Arg^9 Bradykinin also shows a lack of high mass fragmentation over a range of collision energies and gas pressures. One cyle of manual Edman degradation was performed on each of these peptides giving two peptides with an N terminal proline residue. The Bradykinin derived peptide PPGFSPFR exhibits a poor MS/MS spectrum, showing only the ammonium fragment ion at 747 Da and the low mass fragment ions at 155 etc. In contrast however the MS/MS spectrum of the peptide PPGFSPF generated from one Edman cycle on des Arg^9 Bradykinin, gives a high degree of N terminal fragmentation (A and B ions). The presence of a terminal R residue significantly suppresses the intensity and degree of fragmentation observed in the MS/MS spectrum of both the Bradykinin and TRH related peptides.

3. MS/MS experiments were carried out on a series of G_n - ABEE derivatized glucose oligomers. We have studied the CID spectra of compounds with G=3 to 10 to gain some idea of how the MS/MS spectrum changes as a function of mass, by minimising the degree of structural complexity (c.f. peptides). In positive ion mode these compounds give an MH^+ signal but little fragmentation, whereas the negative ion FABMS spectrum shows a series of fragment ions corresponding to cleavage at the glycosidic linkages and charge retention on the derviatized terminus. The positive ion MS/MS spectra of the MH^+ gives a series of product ions also formed by cleavage at the glycosidic linkages as observed in the negative ion MS spectrum, although in this case mass fragment ions were predominant. The unimolecular (i.e. no collision gas) spectra of these sugars show no fragmentation. All the polymers (G3 to G7) gave the same form of MS/MS spectra, although there is a decrease in signal intensity as the molecular weight increases. The experimental upper mass limit was found to be ~1300 Da for the G7 polymer, despite an instrumental limit of ~2000 Da for the second stage MS quadrupole, Fig 1. These sugars give a more consistent series of fragment ions than are observed for peptides of comparable molecular weight, presumably because of the uniformity of structure and the relatively weak hemi-acetal linkage between the glucose units.

The low energy CID MS/MS spectrum of an unknown peptide may contain a variable degree of fragmentation (c.f. the normal FABMS) , albeit A, B" and/or Y" ions, but there may be fragments arising from rearrangement processes. The energies available in the low energy CID experiment give significantly different results from those observed in high energy MS/MS studies where a much greater degree of useful fragmentation is consistently generated at higher mass than in the hybrid instrument.

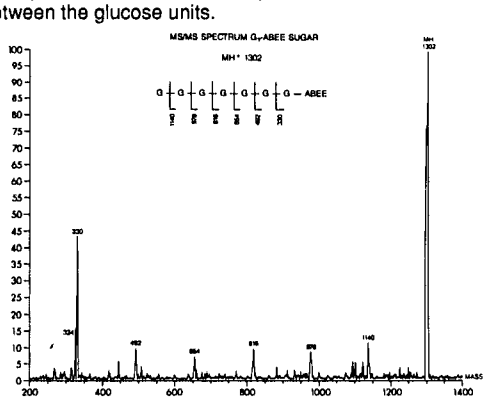

Presented at the 36th ASMS Conference on Mass Spectrometry and Allied Topics
June 5-10, 1988, San Francisco, CA

Characterization of *E. coli* Expressed Human Interleukin-3 by High Performance Tandem Mass Spectrometry, Hubert A. Scoble, Marcia L. Bologna and W. Barry Foster, Genetics Institute, 87 CambridgePark Drive, Cambridge, MA 02140-2387

Interleukin 3 (IL-3) is a multilineage colony stimulating factor capable of supporting *in vitro* the proliferation of human bone marrow hematopoietic progenitors to form granulocytes, erythrocytes, macrophages and megakaryocytes. Due to scarcity of the natural protein, efforts have focussed on the development of bacterial and mammalian expression systems and purification protocols which allow for the isolation of larger quantities of human IL-3. With larger quantities of the protein available, detailed *in vitro* and *in vivo* biochemical studies can begin in order to assess the biological and pharmacologic properties of this important lymphokine. We have extensively characterized *E. coli* expressed human IL-3 using two- and four-sector mass spectrometry. Mass spectrometry offers unique advantages, and in other respects, complements conventional methods of protein structural characterization. One major advantage of mass spectrometric approaches is the ability to rapidly identify posttranslational modifications or posttranslational processing events. This is especially important in the case of a recombinant protein where it is necessary to demonstrate that a natural posttranslational event has occurred, or of equal importance, demonstrate that posttranslational processing has not occurred. Those natural events which one is likely to encounter include: (1) N- and C-terminal processing to the mature protein; (2) N- and O-glycosylation of non-bacterially expressed proteins; (3) phosphorylation; (4) sulphation; (5) acylation; or (6) other natural covalent modification of the protein. Potentially undesirable posttranslational events include: (1) N- and C-terminal processing due to the action of endo- or exoproteases during expression or purification; (2) deamidation; (3) oxidation; (4) inappropriate processing or attachment of N- and O-linked carbohydrate; or (5) undesired covalent modification of the protein. In general, modifications of any amino acid in the protein manifest themselves through a change in mass of the modified amino acid, and thus are detectable mass spectrometrically.

The generalized mass spectrometric strategy which we have employed in the characterization of IL-3 involves specific proteolytic digestion of both native and reduced and alkylated protein, usually with trypsin. Following reversed-phase separation of the digest, the collected fractions are analyzed by FAB/MS. In total, tryptic peptides which have been detected mass spectrometrically account for 98% of the recombinant protein. The small tryptic tripeptide not detected mass spectrometrically is probably not retained under the conditions of the chromatographic separation. The N-terminus of the expressed protein is heterogeneous with 80% of molecules retaining the initiating methionine (Met^1-Ala^2-Pro^3-...) and 20% having the mature sequence (Ala^2-Pro^3-...). Total amino acid compositional analysis yields the expected number of amino acid residues as predicted from the cDNA sequence with the above noted exception of methionine. Conventional carboxy terminal analysis using carboxypeptidase P shows kinetic release of the expected C-terminal amino acids. Mass spectrometrically, however, minor C-terminal species have been detected in which from one to three C-terminal amino acids have been removed, probably due the action of an exoprotease during fermentation or purification. Proteolytic cleavage of recombinant proteins, especially when the N-terminus remains intact, is a difficult problem to assess. The success or failure of conventional carboxy terminal sequencing often depends on the extent of proteolysis. In addition, since most primary protein structural studies involve proteolytic degradation prior to sequencing, it is difficult to ascertain whether cleavage at an unexpected site is due to a nonspecific cut by the enzyme, or is due to proteolysis during expression or fermentation. To answer these questions, tryptic digestion experiments were repeated in $H_2{}^{18}O$ in a procedure similar to that reported by Rose *et al.*. Peptides previously thought to have resulted from nonspecific cleavage during tryptic digestion, had mass shifts indicating incorporation the ^{18}O label. Since, incorporation of the label would not be expected if the peptides were at the carboxy terminus of the protein, the peptides resulted from nonspecific cleavge during digestion. The minor C-terminal peptides previously detected mass spectrometrically had not incorporated the ^{18}O indicating that this cleavge occurred prior to tryptic

digestion. In total, these shortened forms of the C-terminus probably represent less than 1% of the full length C-terminal tryptic peptide. Several peptides incoporated twice as much of the label as expected. Figure 1 shows the MS/MS spectrum of the peptide His-Ile-Pro-His-Ile-Lys which results from tryptic digestion with and without $H_2{}^{18}O$. N-terminal a and b series ions in each spectrum occur at the same mass. The y series ions in panel A ($H_2{}^{18}O$ digestion) occur 4 amu higher than those in panel B.

REFERENCE

K. Rose *et al.*, Biochem. J. (1988) 250, 253-259.

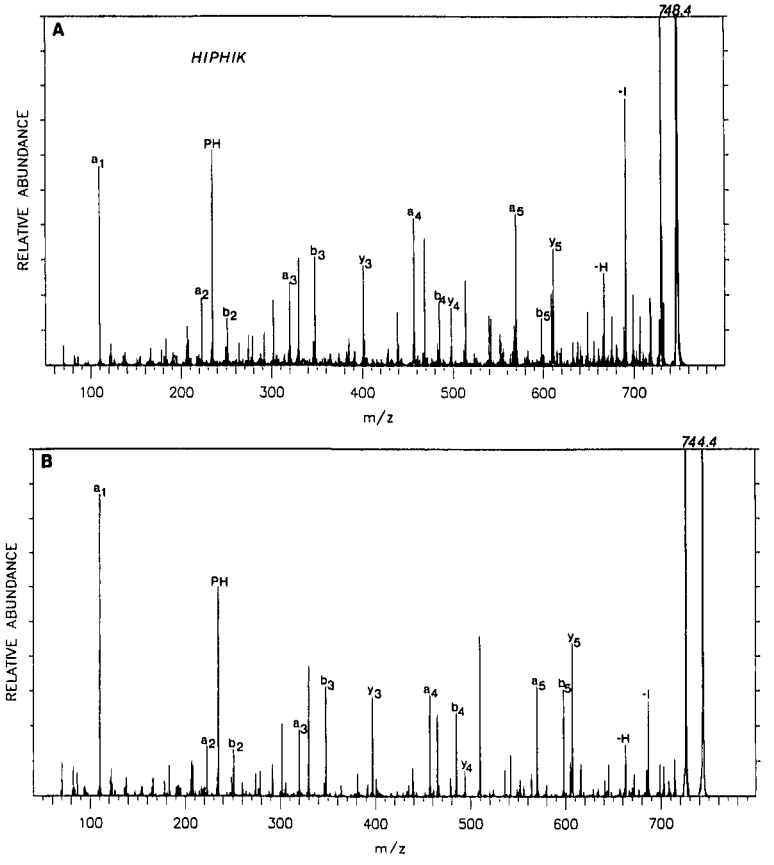

Figure 1. MS/MS spectrum of a tryptic peptide from *E. coli* expressed IL-3. The peptide in panel A, $(M+H)^+$=748.4, results from tryptic digestion in $H_2{}^{18}O$. The peptide in panel B, $(M+H)^+$=744.4, results from normal tryptic digestion. Each spectrum (about 1 nanomole) was recorded by transmission of the ^{12}C ion of the $(M+H)^+$ to MS-2. Precursor ion attenuation was 50% with He at ground potential.

Presented at the 36th ASMS Conference on Mass Spectrometry and Allied Topics
June 5-10, 1988, San Francisco, CA

STRUCTURAL CHARACTERIZATION OF THE IMMUNOACTIVE ENZYMATIC DEGRADATION PRODUCTS OF THE C3 COMPLEMENT PROTEIN BY FAST ATOM BOMBARDMENT AND PLASMA DESORPTION MASS SPECTROMETRY

K. Schneider[1], I. Manz[1], R. Gerardi[2], D. Bitter-Suermann[2] and M. Przybylski[1]

[1]Fakultat fur Chemie der Universitat Konstanz, Postfach 5560, D-7750 Konstanz;
[2]Institut fur Mikrobiologie der Medizin. Hochschule, D-3000 Hannover, FRG.

The third component of serum complement, C3, a 180 000 d glycoprotein plays an important role in the modulation of cellular immune functions such as macro phage activation, antibody formation and lymphocyte proliferation. A fragment preparation of C3 containing primarily the anaphylatoxin polypeptide C3a, formed by specific proteolysis, has been shown to exert potent suppression of mixed lymphocyte proliferation. The mechanism(s) and pathways for this activation have been as yet undefined, but have been assigned to enzymatic degradation products of C3 and/or C3a; of particular interest has been recently a low molecular weight (ca. 4000 d) polypeptide with high activity, C3x.

In a study aimed at defining the immune activation cascade and relating the genesis of biologically active fragments on a molecular level to the intact C3 protein structure, endoprotease digestion combined with fast atom bombardment (FAB) and plasma desorption (PD) mass spectrometry (peptide mapping) methods have been applied to isolated C3 fragments. C3, purified from guinea pig serum was cleaved with the cobra venum factor-dependant C3 convertase yielding the N-terminal polypeptide C3a, and C3a and other low molecular weight fragments isolated by sephadex G-100 chromatography and subsequent FPLC. The molecular weight of intact C3a was determined by PDMS (Figure 1; 9278 d). Detailed structural data and correlation of the guinea pig C3a sequence, by using the known mouse C3a sequence as a guiding structure, was obtained from peptide mapping methods with both FABMS and PDMS. Thus, FABMS analysis after trypsin digestion led to the direct identification of the N- and C-terminal peptides among the series of approx. 10 low molecular weight fragments (Figure 2; T1, SVQLMER; T2, EQLNGLAR). The structures of the terminal and of other parts of the C3a sequence were ascertained by the mass shifts of tryptic fragments after carboxypeptidase B digestion, trypsin digestion after reduction and S-carboxymethylation, and peptide mapping analysis after staph. aureus V8 protease digestion. Approximately 50 % of the guinea pig sequence was found homologous to the mouse C3a (Figure 3). The comparison of the molecular weight of the guinea pig with that of the mouse polypeptide (9214 d) indicates an identical number of amino acids (78) to $\pm$ 1 residue.

The application of peptide mapping methods to the highly active fragment C3x, initially believed to be a cleavage product of C3a, did not show any correlation to the C3a structure. Further studies are therefore directed to relate the genesis of this peptide to the large (170 000 d) protein fragment of C3, C3b. C3b and two further degradation products, C3c (150 000 d) and C3d have been characterized, by using a combination of peptide mapping methods. These results form the basis for the identification, and differentiation of immune activation reactions from the intact protein structure to specific polypeptides.

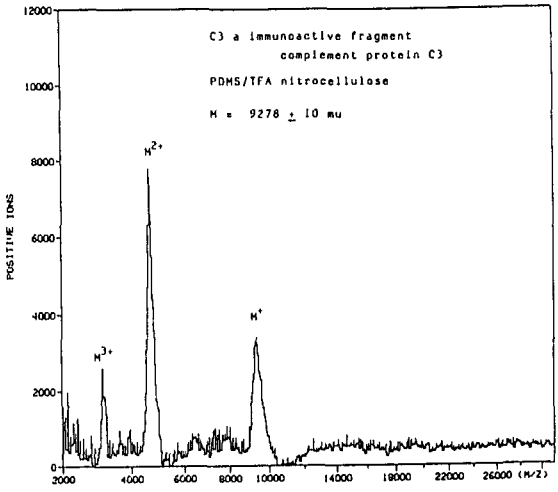

Figure 1
^{252}Cf-PD mass spectrum of polypeptide fragment C3a from guinea pig C3 complement protein. A sample of ca. 300 pmol in 0.2 % trifluoroacetic acid was applied to a nitrocellulose foil; molecular weight determination yielded 9.278 d as an average value.

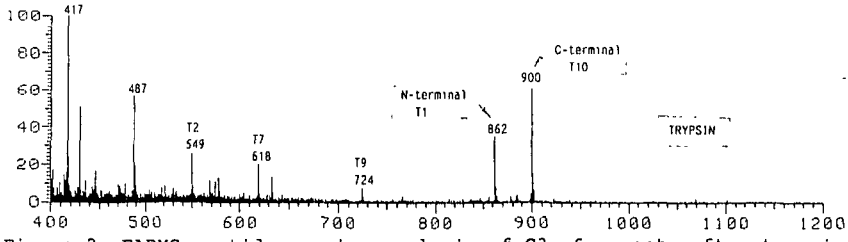

Figure 2. FABMS peptide mapping analysis of C3a fragments after trypsin digestion (ca. 2 nmol; 16 hrs.; 40 mmol NH_4HCO_3). T1 and T10 refer to the N- and C-terminal peptide fragments (S-V-Q-L-M-E-R, T1; E-Q-L-N-G-L-A-R, T10).

```
                1                   10                  20
mouse           H2N-S-V-Q-L-M-E-R-R-M-D-K-A-G-K-Y-D-T-K-G-L-R-R-C-C-E-H-G-M-R-
                └──────T1──────┘└─T2─┘└T3┘└ T4 ┘└────┘└──────T6──────┘
guinea pig      ├──────────────────────────────────────┤

                30                  40                  50                  60
mouse           -Q-V-P-M-K-Y-S-C-Q-R-R-A-Q-L-I-T-Q-G-N-N-C-I-L-A-F-I-N-C-C-E-H-
                └─ T7 ─┘└─ T8 ─┘
guinea pig      ├──────┤

                                    70                  78
mouse           -M-A-Q-L-R-Q-Q-H-R-R-E-Q-L-N-G-L-A-R-COOH          mol. weight   9214
                            └─T9 ─┘└──────T10──────┘
guinea pig                  ├──────────────────────┤               mol. weight   9278  (PDMS)
```

Figure 3. Primary structure of mouse C3a and structural correlation with guinea pig C3a from peptide mapping data. Homologous sequence positions identified in the guinea pig polypeptide are underlined.

Presented at the 36th ASMS Conference on Mass Spectrometry and Allied Topics
June 5-10, 1988, San Francisco, CA

A COMPREHENSIVE SUMMARY OF THE FRAGMENTION OF PEPTIDE IONS UNDER CID CONDITIONS AND THEIR IMPLICATION FOR PEPTIDE SEQUENCING

R. S. Johnson, S. A. Martin, J. E. Vath and K. Biemann
Dept. of Chemistry, Massachusetts Institute of Technology, Cambridge MA 02139

In the course of extensive use of tandem mass spectra for the determination of the amino acid sequence of peptides and proteins of previously unknown structure (among them four different thioredoxins, proteins 100-110 amino acids in length), we were often faced with complex CID mass spectra containing many peaks which did not belong to the familiar a_n, b_n, c_n, x_n, y_n and z_n series (Scheme I). However, in order to be certain that the interpretation is correct all significant peaks in the spectra have to be accounted for.

This led to the discovery of three additional ion types, denoted d_n, v_n and w_n (Scheme II). Because of the mechanism of the formation of these ions, their appearance depends on the structure of the amino acid at the point of backbone cleavage. Two of them (d_n and w_n) permit differentiation of leucine and isoleucine, a long standing problem in mass spectrometry.

In the course of these studies we have measured the CID spectra of peptide derivatives which contain a fixed positive charge in the form of a quaternary ammonium ion. These turned out to be particularly rich in a_n and d_n ions when the charge was localized at the N-terminus while localization at the C-terminus favored v_n, w_n, and y_n ions. We found that there exists a gradual transition in the fragmentation of peptides from those containing no basic group where protonation indeed occurs at the nitrogen of the peptide bond leading to b_n and y_n ions, through peptides with weaker and stronger basic sites which bear the proton more and more exclusively and finally to derivatives with a fixed charge (Scheme III). Our observations also indicate that many of these fragmentations occur remote from the charge.

Figure 1 demonstrates the overriding effect of a fixed positive charge at the N-terminus, which leads exclusively to N-terminal ions, over the strongly basic arginine at the C-terminus. Thus, well planned derivatization, particularly of the N-terminus, can be used to resolve ambiguities in the spectrum of an underivatized peptide.

Scheme I

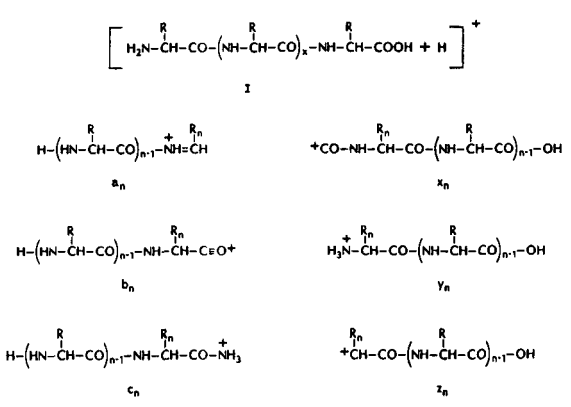

Scheme II

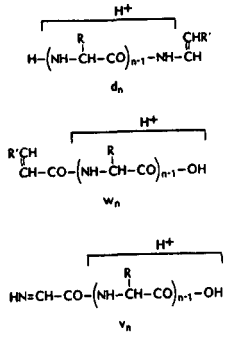

Presented at the 36th ASMS Conference on Mass Spectrometry and Allied Topics
June 5-10, 1988, San Francisco, CA

Scheme III

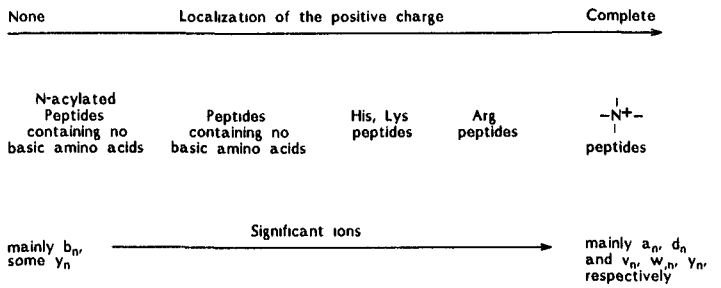

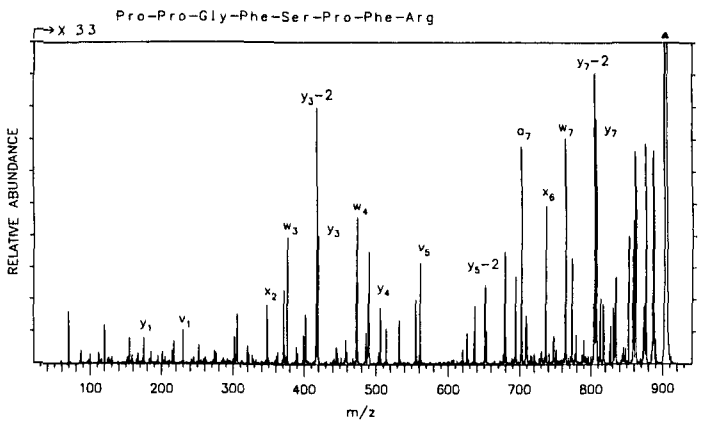

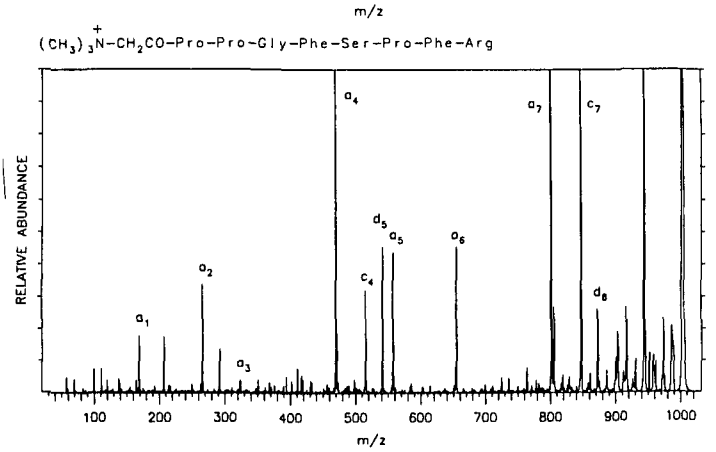

Figure 1. CID mass spectrum of des-Arg[1] bradykinin (top) and its quaternary trimethyl ammonium acetyl derivative (bottom).

Presented at the 36th ASMS Conference on Mass Spectrometry and Allied Topics
June 5-10, 1988, San Francisco, CA

CHARACTERIZATION OF IMPURITIES IN SYNTHETIC PEPTIDES BY FAB MASS SPECTROMETRY

W. Rodney Mathews
Biopolymer Chemistry
The Upjohn Company, Kalamazoo, MI, 49001.

Peter E. Haroldsen and Simon J. Gaskell
Center for Experimental Therapeutics
Baylor College of Medicine, Houston, TX, 77030.

Renin is an enzyme that catalyses the production of Angiotensin I from Angiotensinogen which subsequently produces an increase in blood pressure. This pathway is being explored for the development of new therapeutic agents for hypertension. The synthetic peptide shown in figure 1, U74760, is a specific substrate for Renin and is used in an assay for renin actitity. Renin inhibitory peptides have also been synthesized. While characterizing these peptides, we observed that although amino acid analysis and Edman sequencing results were normal, FAB MS revealed the presence of significant impurities The characterization of the impurities in U74760 is described

FAB MS was carried out on a VG 70SE mass spectrometer. The FAB spectrum of U74760 indicated the presence of several impurities. In addition to the observed MH+ at 1224 (100%), ions at 1236 (P+12, 44%),1238 (P+14; 43%), 1248 (P+24, 19%), 1250 (P+26; 15%) and 1344 (P+120, 15%) were observed. The impurities in the U74760 sample were further characterized by subjecting the sample to 6 cycles of manual Edman degradation followed by FAB MS after each cycle (1) The parent ion at 1224 was observed to shift to 1262, 1125, 1028, 881, 744 and 631 after successive cycles corresponding to the addition of 1 PITC group to the E-amino group of K10 followed by loss of P1,H2,P3,F4,H5,and L6 respectively. After each cycle an additional peak was observed in the FAB spectrum that was 14 mass units larger than the base peak. This corresponded to the loss of the same amino acids from P+14, suggesting that the modification in P+14 was located in the C-terminal portion. The P+12 peptide however did not decrease in mass but shifted from 1236 to 1371 corresponding to the addition of 1 PITC group and no amino acid loss. This suggested that the P+12 peptide was blocked at the N-terminal

Additional information was obtained using tandem mass spectrometry carried out on a VG ZAB SEQ instrument of BEqQ geometry (2). The MS/MS spectrum of U74760 (m/z 1224) is shown in figure 2A. Fragment ions are assigned using the nomenclature of Roepstorff and Fohlman (3). The spectrum shows a nearly complete series of B ions providing sequence information from the N-terminal end. A single C-terminal ion (Y8, m/z 990) is seen. The daughter ion spectrum of the contaiminant P+12 (m/z 1236) is shown in figure 2B. The nomenclature used is the same as in figure 2A *i.e.*, based on the expected fragment ions for U74760. N-terminal ions also dominate this spectrum. The B series is seen to be shifted +12 mass units relative to what was observed with U74760 (2A). A smaller ion series corresponding to the expected B series is also observed The Y8 ion is seen as a doublet at 990 and 1002 (shifted 12 mass units). The assignment of these fragment ions was confirmed by repeating the tandem MS experiment after chemical derivatization of the sample. For example after formation of the methyl ester of the C-terminal -COOH, the C-terminal ions were observed to shift 14 mass units while the N-terminal ions did not change.

These FAB MS results suggest the following interpretation: 1 The P+120 contaiminant is the expected peptide with one benzyloxymethyl (BOM) His protecting group remaining. The P+14 peak is due to a mixture of peptides containing methyl-His. The majority of the methyl His is at position 9 based on the FAB/Edman data. The P+12 impurity is also a mixture consisting primarily of a N-terminal P1- H2 methylene bridge. A second component is probably a methylene bridge between H9 and K10. The P+24 and P+26 are due to combinations of the P+12 and P+14 modifications These byproducts likely result from the reaction of formaldehyde generated during the removal of the BOM protecting group with the peptide. Based on these predictions the synthesis of U74760 was carried out using a different H protecting group and pure U74760 was obtained

REFERENCES

1. G. E. Tarr, in Methods of Protein Microcharacterization, J. E Shively, Ed , Humana Press, 1986
2. P. E. Haroldsen and S. J. Gaskell, Biomed Mass Spectrom. (in Press)
3. P. Roepstorff and J. Fohlman, Biomed Mass Spectrom **11**, 601, 1984.

Presented at the 36th ASMS Conference on Mass Spectrometry and Allied Topics
June 5-10, 1988, San Francisco, CA

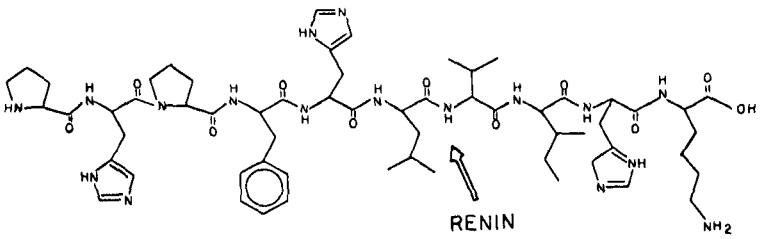

Figure 1. Structure of the Renin substrate peptide U74760. The single letter amino acid code for the sequence is PHPFHLVIHK.

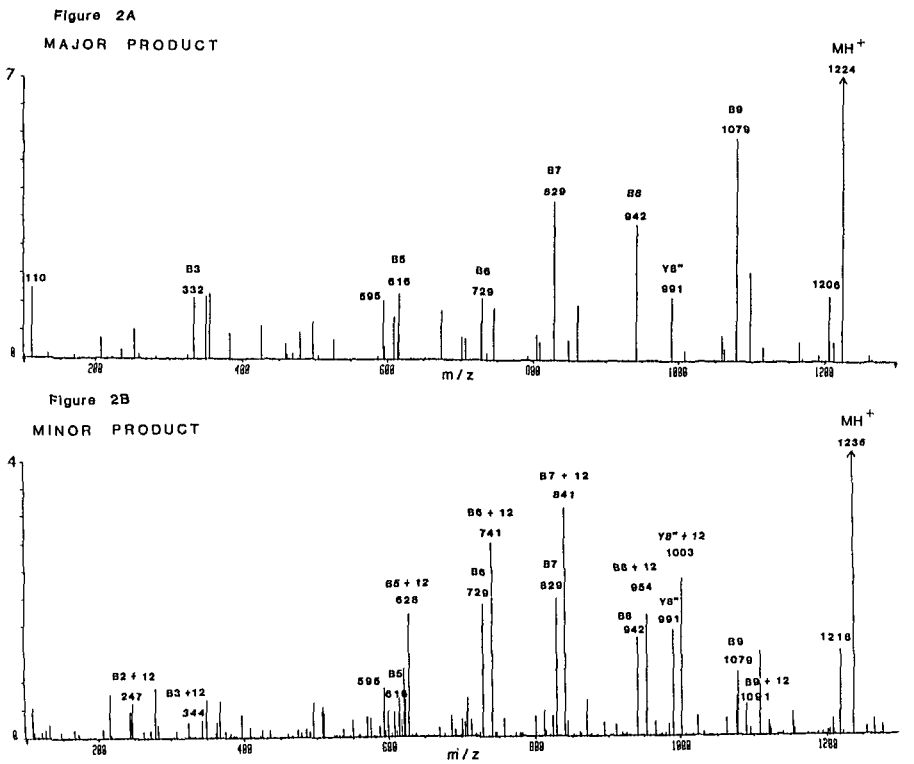

Figure 2. Daughter ion spectrum of U74760 (A) and the P + 12 contaiminant (B).

Presented at the 36th ASMS Conference on Mass Spectrometry and Allied Topics
June 5-10, 1988, San Francisco, CA

FAST ATOM BOMBARDMENT MASS SPECTROMETRY OF RECOMBINANT HUMAN α-2 INTERFERON

T. L. Nagabhushan, James E. Labdon, Birendra Pramanik, Anthony Tsarbopoulos, Pradip Das, Paul Reichert, Thomas C. Hassell, Peter L. Bartner and Paul P. Trotta.
Schering-Plough Corp., Bloomfield, NJ 07003 USA

Interferons (IFNs) are proteins which exhibit a variety of biological effects including antiviral, antiproliferative and antitumor activity. Three classes have been identified: α (from leukocytes), β (fibroblast) and γ (from lymphocytes). The α-IFNs represent at least 13 distinct proteins which display immunomodulatory and antitumor effects. Recombinant α-2 IFN (MW=19,269) has been cloned and expressed in E. coli.[1] It has recently been approved as a treatment for hairy cell leukemia.

We have used fast atom bombardment (FAB) mass spectrometry to confirm the sequence and assign the disulfide bonds of α-2 IFN. The purified protein was digested with trypsin in the presence of 0.5% (w/v) ammonium bicarbonate for 24 hours at 37° and the digest was concentrated and analyzed by FABMS without further purification. The mass spectral data of the digest allowed us to confirm the molecular ions of all of the predicted peptides within the mass range scanned (Table 1). The ions corresponding to the cysteine-containing peptides T1, T5, T10 and T17 were very weak (Figs. 1, 2). The intensities of these ions increased dramatically after reduction of the digest with dithiothreitol (25-fold molar excess over protein, 100° for 2 minutes). Assignment of cysteine-containing peptides was also confirmed by FABMS of a tryptic digest of α-2 IFN in which the cystine residues of the native protein were S-alkylated with 4-vinylpyridine in the presence of tri-N-butyl-phosphine[2]. The resulting pyridylethyl cysteine (PEC) tryptic peptides were observed as strong ions with masses 106 units higher than the unmodified peptides (PEC-T1,PEC-T5 and PEC -T17 , Table 1).

Disulfide pairing was established by the observation of ions at m/z 4616 and 2118 in the high-mass region of the unreduced digest (Fig. 2+). These ions correspond to disulfide bonds between peptides T1 and T10 and between T5 and T17 respectively. These ions disappeared upon DTT reduction or PEC derivatization. The FABMS mapping results allowed us to assign disulfide bonds between Cys-1 and Cys-98 and between Cys-29 and Cys-138 in α-2 IFN.

In another experiment, α-2 IFN was cleaved with cyanogen bromide . The 4 fragments were isolated by HPLC and studied by FAB/MS. Mass spectral data provided sequence information for some of the purified fragments.

1. Streuli, M., Nagata, S. and Weissman, C. *Science* , 209, 1343-1347 (1980)
2. Andrews, P. C. and Dixon, J. E. *Anal. Biochem* . , 161, 524-528 (1987)

Presented at the 36th ASMS Conference on Mass Spectrometry and Allied Topics
June 5-10, 1988, San Francisco, CA

Table 1. FAB/MS ANALYSIS OF α-2 INTERFERON TRYPTIC PEPTIDES

Code	Sequence	Molecular Weight	Ions Observed as $(M+H)^+$ Untreated	PE-Cys Derivative
T1	CDLPQTHSLGSR	1313.61	+	+[1]
T2	R	174.2		
T3	TLMLLAQMR	1076.49	+	
T4	R	174.2		
T5	ISLFSCLK	910.23	+	+[1]
T6	DR	289.3		
T7	HDRGFPQEERGNQFQK	1955.31	+	
T8	AETIPVLHEMIQQIFNLFSTK	2460.17	+	
T9	DSSAAWDETLLDK	1450.68	+	
T10	FYTELYQQLNDLEACVIQGVGVTETPLMK	3304.21	+	ND
T11	EDSILAVR	902.1	+	
T12	K	146.19		
T13	YFQR	612.73	+	
T14	ITLYLK	750.01	+	
T15	EK	275.32		
T16	K	146.19		
T17	YSPCAWEVVR	1209.53	+	+[1]
T18	AEIMR	618.8	+	
T19	SFSLSTNLQESLR	1481.78	+	
T20	SK	233.28	+	
T21	E	147.13		

+ Observed at expected molecular weight

[1] as PE-Cys adduct

ND Not determined. Outside of mass range scanned.

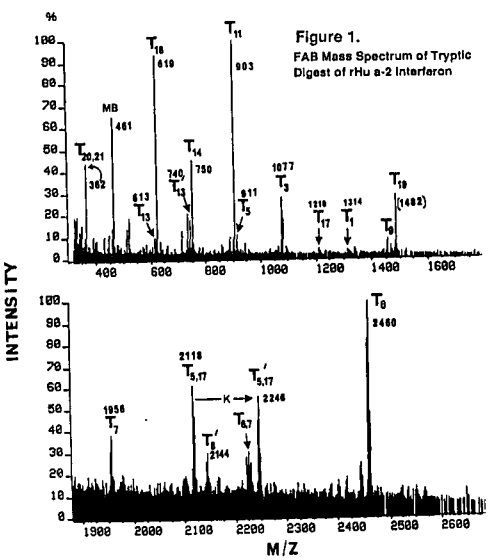

Figure 1.
FAB Mass Spectrum of Tryptic Digest of rHu a-2 Interferon

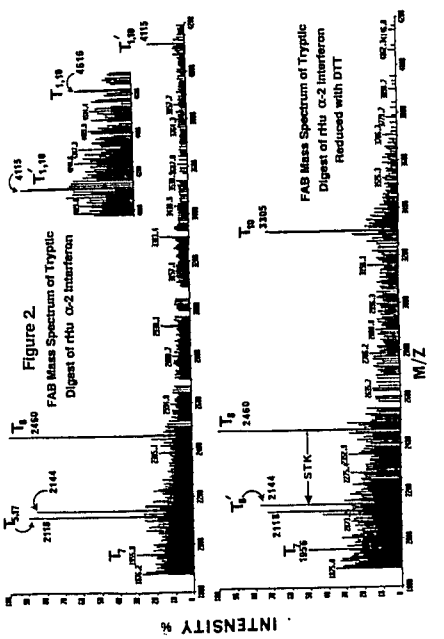

Figure 2.
FAB Mass Spectrum of Tryptic Digest of rHu α-2 Interferon

FAB Mass Spectrum of Tryptic Digest of rHu α-2 Interferon Reduced with DTT

Presented at the 36th ASMS Conference on Mass Spectrometry and Allied Topics
June 5-10, 1988, San Francisco, CA

INACTIVATION OF DOPAMINE β-HYDROXYLASE BY *P*-CRESOL: CHARACTERIZATION OF COVALENTLY MODIFIED ACTIVE SITE PEPTIDES BY MS AND TANDEM MS, S.A. Carr, W. E. DeWolf,Jr., M. Mentzer, G. D. Roberts, P.J. Goodhart, and Lawrence I. Kruse, Smith Kline and French Laboratories, King of Prussia, PA 19406

Dopamine β-hydroxylase (DBH) is a tetrameric glycoprotein complex (ca. 280 kDa) which catalyzes the conversion of dopamine to norepinephrine and thus plays a key role in the biosynthesis of neurotransmitters. *P*-cresol has recently been shown to be an excellent inactivator of DBH, despite the absence of a latent electrophile (1). In order to understand the molecular basis of enzyme inactivation by this new class of inhibitor it was necessary to determine the structure of the inactivated enzyme-suicide substrate complex.

Using a combination of conventional chemical and biochemical strategies in conjunction with MS and tandem MS we have identified the attachment site of the suicide substrate inhibitor *p*-cresol in the sequence of DBH, partially defined the chemical nature of the adduct formed and have determined the sequence of the putative active-site tryptic peptide (2) DBH labeled with tritiated *p*-cresol was digested with trypsin, and a few nanomoles of two labeled peptides, designated hereafter as the early and late eluting peptides, were isolated by RP-HPLC. These peptides were subsequently studied by automated Edman degradation and a variety of biochemical MS techniques. Sequence information obtained by automated Edman degradation on the early and late eluting peptides yielded two virtually identical 24 amino acid long sequences with the exception of residue 13 where a Lys was identified at this position in the former peptide and nothing was detected in the latter peptide. FABMS of 150 pmol of both the early and late eluting peptides yielded chemical average molecular weights of 3131.2. These data clearly indicated that the peptides were substantially larger than suggested by Edman. Furthermore, the difference in mass could not be accounted for by simple addition of one to three residues of *p*-cresol to the obtained sequence suggesting that either the modification involved extensive alteration of the *p*-cresol upon addition or that the amino acid sequence was wrong or terminating prematurely.

In an effort to verify the Edman derived sequence and establish the location within that sequence of the modified residue, ca. 450 pmol of both the late and early eluting tryptic peptides were digested briefly (3h, 37°C, E:S = 1:25) with chymotrypsin and the resulting digests analyzed directly by FABMS. The choice of enzyme was dictated by the Edman sequence data that indicated two prime chymotryptic sites at residues 14 (Trp) and 16 (Tyr). Both the early and late peptides yielded identical spectra exhibiting four peptide signals with $(M+H)^+_{ave}$ of 1131 3, 1455.6, 1695 8, and 2019.8, respectively. None of these peptides could be accounted for simply based on the Edman data. Each of these peptides was analyzed by tandem MS directly from the mixture without isolation or purification. The tandem mass spectrum of the 1695 peptide (Fig. 1) is dominated by amino-terminal sequence ions that define the sequence (Ala,Pro,Asp)-Val-Leu-Ile-Pro-Gly-Gln-Gln-Thr-Thr-Tyc-Trp where Tyc is apparently a modified amino acid residue with an in-chain mass equivalent to the sum of the incremental masses of a Tyr plus cresol (each having lost a H to form a covalent bond), i.e., 163+108−2 = 269; the mass of Tyc is defined by the mass difference from sequence ions C_{13} to C_{12} and B_{13} to B_{12} (Fig. 1). The tandem mass spectrum of this peptide could not be used to independently establish the sequence of the first three residues because amino-terminal sequence ions for the first two residues were not observed. Of course this was not a problem since the Edman data is most reliable at the amino-terminus of a peptide or protein. In a similar fashion we have sequenced the two COOH-terminal peptides in the chymotryptic digest with $(M+H)^+$ of 1131 and 1454. A summary of the sequence information provided in the various chemical and MS experiments on DBH is shown in Figure 2

The linkage of cresol to Tyr was examined by N^2H_3-DCI MS of the PTH-amino acids (ca. 0.5 nmol of each cycle which had not been injected onto the HPLC) from the Edman degradations of the early and late eluting tryptic peptides To achieve subnanomole sensitivity it was necessary to clean up each PTH-amino acid from the large amounts of diphenylurea and diphenylthiourea produced as byproducts of the Edman chemistry by RP-HPLC on C18 in a $H_2O/CH_3CN/TFA$ system prior to analysis by MS. The "core" of a PTH amino acid exhibits two exchangeable protons in the N^2H_3-DCI mass spectra: a rapidly exchanging secondary amine proton and a slowly exchanging methine proton on the α-carbon. Exchangeable protons in the side-chain of the amino acid residue are added to the number of core exchangeables. In the discussion that follows the "H" of the $(M+H)^+$ will be ignored although this clearly increases the apparent number of exchangeable protons by 1 The corresponding DCI mass spectra of cycle 13 from the Edman degradation analyses of the early and late eluting peptides indicated the following numbers of exchangeable protons: 3 rapid, 1 slow vs. 2 rapid, 1 slow, respectively. From this we conclude that the *p*-cresol is C-C linked in the early eluting peptide (i.e., the R group has two free OH groups) while the cresol is C-O linked to Tyr in the late eluting peptide (one free OH in R group). These data are consistent with the elution order from RP-HPLC, as the more hydrophilic derivative should elute earlier

These results provide direct evidence that inactivation of DBH by *p*-cresol is the result of covalent attachment of cresol to the active site Tyr residue presumably by insertion of a benzylic radical or phenolic radical. Tandem MS also provided the sequence of the four amino acids at the C-terminus of the peptide that were not accessible by Edman degradation. All of the studies described here were performed with a total of only 2-3 nanomoles of peptide which highlights the sensitivity of the FABMS and tandem MS methodology employed. Establishing the sequence of this modified peptide and the nature of the linkage by other spectroscopic techniques with such small amounts of material would have been extremely difficult.

1. P.J. Goodhart, W.E. DeWolf, Jr., and L.I Kruse, Biochemistry 26: 2576-2583 (1986).
2 W.E DeWolf, Jr , S.A Carr, L I. Kruse, A. Varrichio, P J. Goodhart, M.A. Mentzer, and G.D. Roberts, Biochemistry, in press (1988).

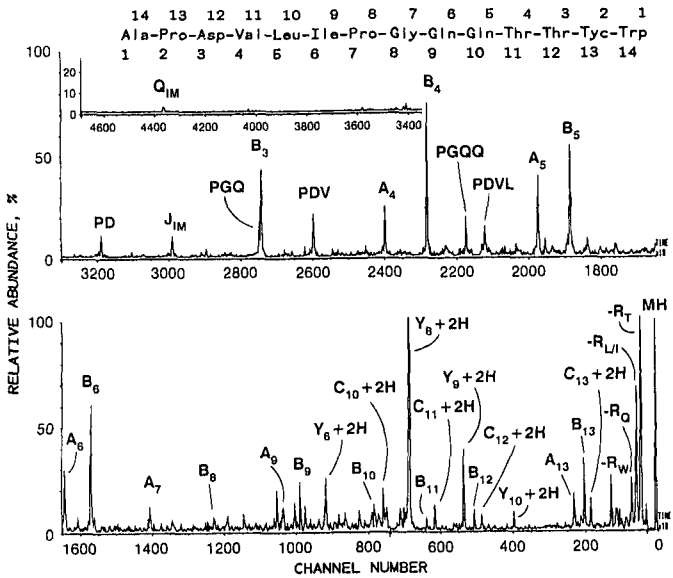

Figure 1. Tandem mass spectrum of the chymotryptic peptide of $(M+H)^+_{ave}$ = 1695.9. FABMS in MS-1 of the VG ZAB SE-4F tandem mass spectrometer was used to identify this parent ion in a mixture of peptides (see text) and to select it for collision with He at 10 keV (atten. = 75%) and mass analysis of the resulting product ions in MS-2. Numbering above the printed single letter code sequence refers to C-terminal ions (V to Z) while that below the printed sequence refers to N-terminal ions (A to C). Low mass fragments with a subscript IM are immonium ions with the general structure $H_2N{=}CHR$, where R is the amino acid side-chain. J = single letter representation of tyrosine with p-cresol covalently attached. PGQ, PDV, PGQQ and PDVL are internal fragments.

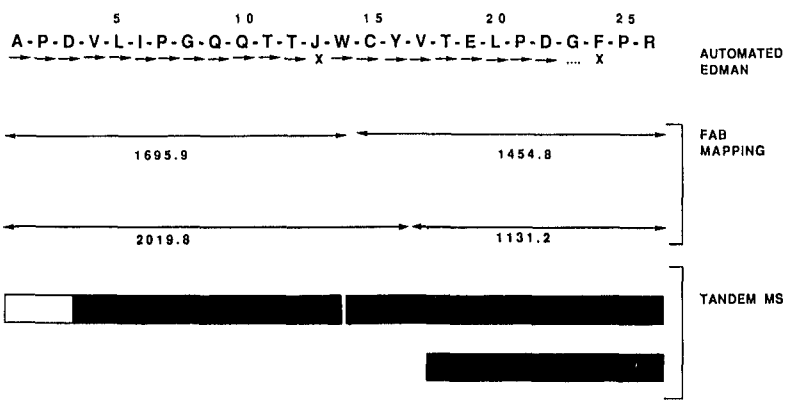

Figure 2. Summary of the sequence information obtained. Single-headed arrows represent cycles of automated Edman degradation, X signifies a residue not identified by Edman and ... corresponds to a weak Edman assignment. Double headed arrows indicate the sequence origins of the signals observed in chymotryptic digests of labeled peptides by FABMS. Rectangles refer to peptides analyzed by tandem MS; blackened regions signify sequences established by tandem MS.

Presented at the 36th ASMS Conference on Mass Spectrometry and Allied Topics
June 5-10, 1988, San Francisco, CA

Recent Developments in High Mass Ionization and Detection Systems

A.E. Ashcroft, R.A.C. Buchanan, G.J. Elliott, S. Evans, D.J. Milton, B. Wright,
Kratos Analytical, Barton Dock Road, Urmston, Manchester, M31 2LD, UK
F.C. Walls,
Mass Spectrometry Facility, Department of Pharmaceutical Chemistry, University of California, San Francisco, CA 94143-0446, USA

Introduction

Two complementary techniques have been developed to facilitate the analysis of higher mass samples on magnetic sector mass spectrometers by enhancing sensitivity: a cesium ion (LSIMS) source to increase ionization efficiency and an electro-optical array detector for simultaneous ion detection over a 4% mass window.

Cesium Ion Source

A cesium ion gun has been incorporated into an LSIMS source to allow cesium ions of high bombarding energy to be used as the primary beam.

The cesium ions, after evaporation from an indirectly heated anode, are accelerated to a few hundred volts, focussed and finally accelerated out of the gun. This ion beam is directed onto the probe tip by a series of deflector plates, and is protected from stray source fields by an aperture plate situated in front of the probe tip.

The impact energy of the cesium ion beam when it reaches the target is variable up to 35keV with respect to ground potential. Using a high energy cesium ion beam provides increeased sensitivity. For example, an increase of a factor of 10 in sensitivity can be expected for a sample of 10,000 daltons.

Electro-optical Array Detector

Parallel detection of a significant portion of the mass range provides an increase in sensitivity as a greater fraction of the ion current leaving the source is being detected at any given time compared to conventional, single ion detection, and an electro-optical array detector has been developed for this purpose[1]. The array data presented here have been obtained from either a two sector EB instrument (MS50RF or Concept II H), or with the array as the final detector on a four sector EBEB instrument (Concept II HH). Data were acquired by a DS90 data system, and the following types of acquisition are possible:-

1) Survey scanning on a two sector (EB) mass spectrometer.

   Data are collected from the 1024 array channels covering a 4% mass window centered on a specific mass, or over a specified mass range. For the latter case, the number of 4% mass windows required to cover this range is calculated, and data are acquired by stepping the DAC controlled magnet to the central point of each of the mass windows sequentially. Once the specified mass range has been covered, the mass windows are "butted" together to produce a complete spectrum. To achieve a high degree of accuracy for this process, the mass spectrometer focal plane dispersion coefficient for the array detector is calculated and stored by the data system.

   The dispersion of the array is given by the equation:-

   $$\frac{\Delta M}{Mc} = an - bn^2 + \text{higher order terms}$$

   where Mc is the mass in the centre of the array, n is the channel number relative to the centre, and a and b are related to the angle of the array with respect to the focal plane, and to the constants for dispersion along the focal plane.

   This calculation enables mass/channel pairs to be used as a calibration file to mass assign acquired spectra.

The spectrum of bovine trypsin (mw 23,290) in figure 1 illustrates an array acquisition. The data system was used to acquire data from 25 consecutive 4% mass windows by stepping the magnet through a cycle of 25 mass positions covering a mass range from 26,000 to 10,000 daltons. A 5 second exposure was taken at each position. One full cycle corresponds to one exposure at each of the 25 magnet positions, and five cycles were accumulated to produce the spectrum illustrated.

2) Peak Matching on a two sector (EB) mass spectrometer.

Mass Measurements to an accuracy of 20 ppm are obtained by a peak matching procedure where the sample ion of interest is located in an array mass window, centroided and mass converted by the mass/channel pairs stored as a result of the array dispersion calculations.

3) Fragment Ion Scanning on a four sector (EBEB) mass spectrometer.

To achieve a fragment ion scan, the sample is ionized in the first ion source, and the first magnet is set by DAC control to select the precursor ion. The second electrostatic analyser and magnet are stepped simultaneously through a specified mass range to produce a cycle of mass windows which are "butted" together, as for a survey scan.

The fragment ion spectrum from the protonated molecular ion (m/z 1348) of 100 pmole of Substance P using array detection is shown in figure 2.

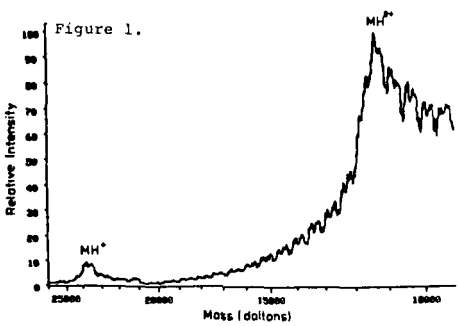

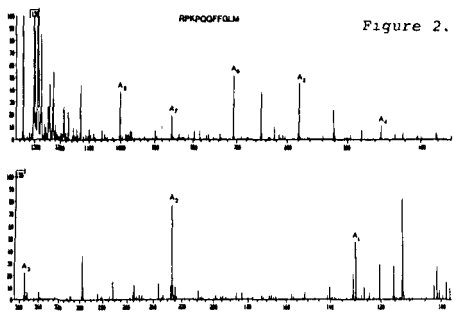

Figure 1 Bovine trypsin (mw 23,290) spectrum acquired from 26,000 to 10,000 daltons over 25 consecutive array detector mass windows.

Figure 2. Substance P (100 pmole) fragment ion scan from m/z 1348 using an EBEB mass spectrometer with array detection.

Conclusion

Ionization and detection efficiencies have been enhanced by the development of a cesium ion source and an electro-optical array detector. A range of software controlled array acquisitions are available for both two and four sector instrumentation.

Reference

1. J.S. Cottrell, S. Evans, Anal. Chem., 59, 1990 (1987)

Presented at the 36th ASMS Conference on Mass Spectrometry and Allied Topics
June 5-10, 1988, San Francisco, CA

LIQUID SIMS OF SYNTHETIC PEPTIDES

P.T.M.Kenny, W.-H.Xu, K.Tachibana and H.Naoki

Suntory Institute for Bioorganic Research,
Shimamoto-cho, Mishima-gun, Osaka 618, Japan.

Liquid SIMS has been extensively used for molecular weight determination of thermolabile and non volatile compounds. Peptides have been subjected to numerous investigations and sequence analysis can be accomplished using liquid SIMS. Recently a bioactive peptide named pardaxin P-1 consisting of 33 amino acids was isolated from the defense secretion of a pacific sole[1]. As this peptide displays shark repellent activity we are currently synthesizing it for biological studies. Thus solid phase synthesis of four fragments and subsequent coupling should furnish the entire peptide. Liquid SIMS was the method chosen for analysis of the solid phase synthetic fragments. Thus crude reaction mixtures could be analysed directly to determine the presence of the required peptides. Also liquid SIMS analysis could I. confirm the synthesis II. determine the presence of the protecting groups and III. determine the status of the carboxyl termini. There are a few reports on liquid SIMS of protected peptides[2-4]. Protonated molecular ion species together with fragments due to loss of the protecting groups were observed. Consequently there is less sequence information than in the case of deprotected peptides. In the present study this was not important as we are primarily interested in obtaining molecular weight information. As some of the peptides we wished to measure had molecular weights in the 1000 to 2000 mass range the initial problem was selection of a suitable matrix. The normal glycerol matrix was found to be totally unsuitable for analysis of the protected peptides presumably due to solubility problems. Consequently several other matrices were evaluated. Thioglycerol, diethanolamine, 'magic bullet' and 2-hydroxyethyldisulphide were employed in analysis of the protected peptides. Initially the following protected peptide was chosen as a model compound. Boc-S(Bzl)ALS(Bzl)S(Bzl)G-OH. All of the above matrices furnished molecular ion species aswell as the classic fragments due to loss of the protecting groups. However the most suitable matrix was 2-hydroxyethyldisulphide[5]. This matrix was up to ten times more sensitive than the other matrices used. On the other hand using glycerol as the matrix the deprotected peptides were analysed. Fragment ions corresponding to cleavage along the backbone of the peptide can

be used to confirm the sequence of the peptide. Therefore with a suitable matrix liquid SIMS was used to characterize synthetic peptides in the 1000 to 2000 mass range.

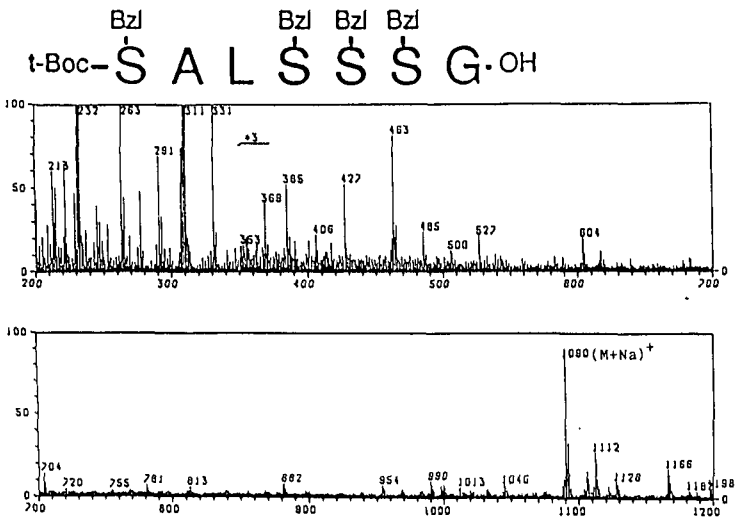

Fig.1. Liquid SIMS of the model compound. Matrix: 2-Hydroxyethyldisulphide.

1. S.A.Thompson, K.Tachibana, K.Nakanishi and I.Kubota, Science 233, 341 (1986)
2. G.V.Garner, D.B.Gordon, L.W.Tetler and R.D.Sedgwick, Org. Mass Spectrom. 18 , 486 (1983)
3. E.R.Bathelt and W.Heerma, Biomed. Environ. Mass Spectrom. 14 , 53 (1987)
4. M.He, Z.Yu, Y.Ye and A.Ji, Org. Mass Spectrom. 23 , 288 (1988)
5. L.Baczynskyj, in "Advances in Mass Spectrometry 1985", J.F.J.Todd, Ed., Wiley, Great Britain, pp. 1611 (1985)

Presented at the 36th ASMS Conference on Mass Spectrometry and Allied Topics
June 5-10, 1988, San Francisco, CA

FAST ATOM BOMBARDMENT, THERMOSPRAY AND DESORPTION CHEMICAL IONIZATION MASS SPECTROMETRY OF DIHYDROPYRIDINE ⇌ PYRIDINIUM SALT-TYPE REDOX SYSTEMS

Laszlo Prokai, B.-H. Hsu and N. Bodor; Center for Drug Design and Delivery, University of Florida, College of Pharmacy, JHMHC Box J-497, Gainesville, FL 32601.

Quaternary pyridinium salts and the corresponding (1,4-)dihydropyridine analogs are involved in redox equilibria (Scheme I) in numerous cases where the chemical/biochemical application, or even the mass spectrometric analysis of these compounds are concerned [1]. Improved transport through biological membranes and/or site-specific delivery were reported for a variety of drugs using a dihydropyridine ⇌ pyridinium salt type redox chemical delivery system [2].

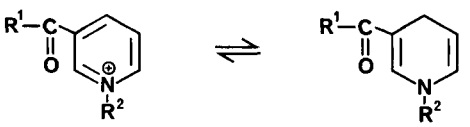

Scheme I

A dihydropyridine carrier is attached to the drug via a suitable functional group (usually ester or amide), and undergoes enzymatic oxidation and hydrolysis in vivo providing sustained release and/or site specific release of the drug. The aim of the present study was to examine the capabilities of some common desorption ionization methods in the characterization of these compounds. Because of the limited knowledge on the processes taking place during the production of gaseous ions from condensed-phase samples using different ionization/desorption techniques, and the possible chemical changes of reactive compounds under the conditions applied, investigation of model compounds are not only justified but necessary. These studies appears to be prerequisite for reliable interpretation of data obtained from biological media in order to identify/determine the compounds concerned.

A KRATOS MS80RFA mass spectrometer with a DS90 data system was used throughout the study. Fast-heating desorption chemical ionization (DCI) mass spectra were recorded using a resistively heated platinum-iridium coil and isobutane or ammonia reagent gas. Thermospray ionization (TSP) mass spectra were obtained by vaporizing the sample in aqueous ammonium acetate/organic solvent (acetonitrile) mixture. The organic phase was adjusted according to the solubility of the compounds. Fast atom bombardment (FAB) mass spectrometry was performed using a source operated with xenon at 6 keV beam energy. The samples were dissolved in a suitable liquid matrix

Our observations are as follows:

Fast-heating DCI results in the intact cation of the pyridinium salts with low to just detectable intensity. Thermal dealkylation was found to be favored over the desorption of intact ions from the condensed phase. Although the 1,4-dihydropyridine analogs exhibit low volatility, they mostly produce sufficient vapor pressure under DCI conditions to allow gas-phase ionication. The typical DCI mass spectrum shows a number of structure-related fragment ions.

TSP ionization is characterized by the lack of the intact pyridinium cation from the spectra. The principal route of decomposition is, however, not purely thermal. The hydrolytically most sensitive bonds (i.e., ester or amide bonds at the quaternary substituent) tend to cleave preferentially during TSP ionization. The reaction most probably takes place within the liquid jet droplets indicating the stress exerted by the elevated temperature or the pH and the ion concentration of the liquid medium to the analyte during thermospray formation. Intact cations from solvent-depleted particles may provide dequaternarized (neutral) products by thermal degradation - identical with those observed in DCI. Furthermore, they can be reduced to the dihydropyridine analogs by thermal electrons present in the jet plasma. The neutral dihydropyridine compounds themselves give spectra similar to those obtained with DCI, but "softer" ionization is achieved with TSP wich results in the preferential formation of quasi-molecular ions and limited fragmentation.
FAB is the only technique studied wich is able to provide intact cations of high intensity from these pyridinium salts. The only major fragment ion is originated from the quaternary substituent. The only major fragment ion is originated from the quaternary subsituent. In addition to the expected MH quasi-molecular ions, species of even higher intensity corresponding to the quaternary ion are detected in the FAB spectra of dihydropyridine analogs. The presence of an intense fragment ion characteristic of the quaternary substituent also reveals a matrix-induced oxidation process. The driving force of the reaction may be attributed to the more favorable desorption ability of the ionic species obtained from the process, in comparison with the competitive acid-base reaction (protonation) products. The process appears to occur at the liquid matrix/gas phase interface region via mechanisms involving either hydride abstraction or two-electron oxidation and deprotonation.

To avoid the appearance of "artifacts" in the mass spectra, FAB is the suggested method for the analysis of these types of pyridinium salts, and DCI and TSP are the preferable ionization methods for the corresponding dihydropyridine analogs.

This work was supported by NIH Grant GM26167 (to N. Bodor).

REFERENCES

[1] Veith, H.J.; Mass Spectrom. Rev., 2, 419 (1983).
[2] Bodor, N.; Ann. N. Y. Acad. Sci., 289 (1988).

Presented at the 36th ASMS Conference on Mass Spectrometry and Allied Topics
June 5-10, 1988, San Francisco, CA

COMPARISON OF LSIMS (FAB) AND DCI MASS SPECTRA OF COBALT CARBONYL COMPLEXES OF PROSTAGLANDIN ANALOGS BY LINKED SCAN TECHNIQUES

K.Chan, A.Spilkin, H.Carpio, J.Mendez, K.Straub
Syntex Research
Palo Alto, California 94304

Numerous studies have revealed similarities between the LSIMS (or FAB) and chemical ionization mass spectra of low molecular weight, moderately polar compounds (1,2). However, compared to CI, LSIMS is more often used to characterize compounds of high molecular weight. Even with the use of rapid heating techniques (eg., 'desorption' CI or DCI), the CI mass spectra of compounds with molecular weights greater than 1500 d. cannot be easily obtained. A direct comparison of the two ionization techniques with respect to the analysis of high molecular weight compounds is therefore not possible. Nevertheless, compounds in the molecular weight range of 800-1200 d. are usually accessible by both DCI and LSIMS, allowing a direct comparison of the two ionization processes to be made. We have observed numerous instances where the mass spectra obtained by LSIMS and DCI differ significantly, particularly in their fragmentation. For example, organometallic compounds such as the neutral prostaglandin cobalt π-complex shown for structure 1 can be analyzed by either DCI or LSIMS, but yield strikingly different spectra. These observations prompted us to explore the possible reasons for these differences.

Mass spectra were recorded on a Finnigan-MAT 8230 double focussing mass spectrometer, operating at Vacc= 3kV. LSIMS spectra were obtained with a Cs+ primary beam of nominal energy 3-5 keV. A liquid matrix consisting of either nitrophenyl octyl ether (NPOE) or triethanolamine (TEA) was used. DCI spectra were obtained using a rapidly heated rhenium wire. Positive ion DCI spectra were obtained using either ammonia or methane as the reagent gas, and negative ion DCI spectra were obtained using hydroxide ion (OH^-, obtained by electron bombardment of a methane-N_2O mixture).

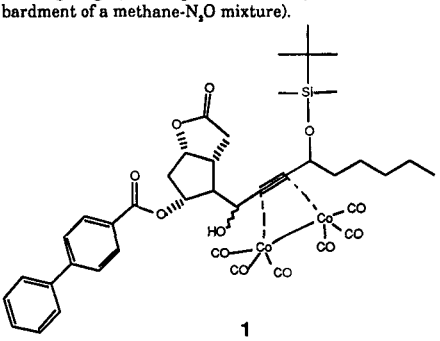

1

Figure 1 shows the negative ion LSIMS spectrum of 1, desorbed from a NPOE matrix. The [M-H] molecular ion species is observed at m/z 875. However, the spectrum is dominated by successive losses of CO or HCO from the parent molecule (m/z 848, 820, 791, etc.). Similar ligand displacement reactions have been attributed to condensed phase chemistry (3). To determine if the detected fragment ions are gas phase unimolecular decomposition products or reaction products in the condensed phase, linked scan MS/MS techniques were employed to characterize the metastable decomposition in the first FFR of the instrument. Figure 2 shows the daughter ion spectrum (B/E scan) of the molecular ion species. The lose of one, two, and three CO ligands is observed. Another decomposition product is the ion of m/z 497. This ion may be rationalized as the loss of *t*-butyldimethylsilanol, water, $Co(CO)_3$, $C_3H_3O_2$, and one additional CO from the parent molecule. The base peak (m/z 469) in the full scan spectrum is therefore a loss of CO from the ion of m/z 497. Other linked scan experiments demonstrate that most of the fragment ions observed in Figure 1 can be formed via gas phase unimolecular processes. These results indicate that the energy imparted to the analyte molecules during LSIMS ionization is large enough to break a number of covalent bonds in the molecule.

In comparison, significantly less fragmentation is observed in the DCI mass spectrum of 1. The negative ion DCI spectrum of 1 obtained with OH^- is shown in figure 3. Only a trace amount of $[M-H]^-$ is detected; the predominant species being the $[M-CO]^-$ ion (m/z 848). Subsequent loss of CO from this ion is small. Other ions detected in the OH- DCI spectrum of 1 may be attributed to the loss of the dicobalt hexacarbonyl group (m/z 590) and an additional loss of the *t*-butyldimethylsiloxy group accompanied by a hydrogen transfer(m/z 460). Linked scan experiments could not confirm the origin of these ions, suggesting that they are not formed via gas phase unimolecular decomposition. Therefore, both of these ions may arise as thermal degradation products formed during the desorption process.

Since the energy imparted to the analyte in the CI process is determined by the difference in proton affinity between the analyte and reagent ions, one may enhance the molecular ion species by selecting an appropriate reagent gas. Figure 4 shows the positive ion DCI mass spectrum of 1 using NH_3 as the reagent gas. The intact molecular ion species $[M+NH_4]^+$ is detected at m/z 894. No loss of CO from the quasimolecular ion is observed. Similar to the OH^- DCI spectrum, other ions detected may be thermal degradation products (*eg.*, m/z 608 as $[590+NH_4]^+$; m/z 478 as $[460+NH_4]^+$) Daughter ion spectra obtained on m/z 894 are characterized by fragments derived from the loss of *t*-butyldimethylsilanol with NH_3 or OH (m/z 745) and a subsequent loss of CO (m/z 717).

In conclusion, both LSIMS and DCI are useful techniques for the characterization of cobaltcarbonyl complexes of prostaglandins analogs such as 1. However, one has to be careful about matrix effects in LSIMS and thermal decomposition in DCI. Our results suggest that, if one can volatilize a compound without degradation into a CI plasma, the energy imparted to the analyte in the CI process can be less than that of the LSIMS process. These results suggest that it may also be possible to control the amount of energy (and therefore the amount of fragmentation) imparted to an analyte during LSIMS ionization by varying the gas phase proton affinity of the liquid matrix.

REFERENCES:
1. J.Sunner, A.Morales, and P.Kebarle, presented at the 35th ASMS Conference. Proceedings 300 (1987).
2. H.Budzikiewicz, H.Munster, and F. Theobald, presented at the 35 th ASMS Conference. Proceedings 749 (1987).
3. R.L.Cerny, B.P.Sullivan, M.M.Bursey, and T.J.Meyer, Anal. Chem. 55, 1954 (1983).

Figure 1
Negative ion LSIMS

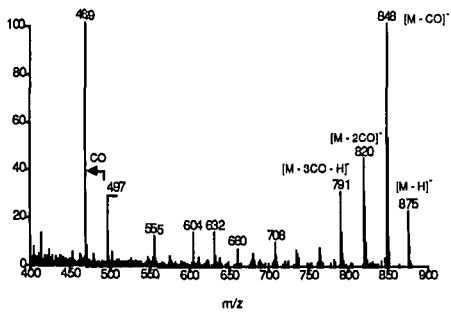

Figure 2
Daughter ions of 875 (LSIMS)

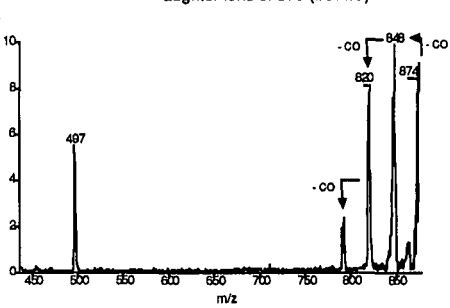

Figure 3
Negative ion DCI (OH⁻)

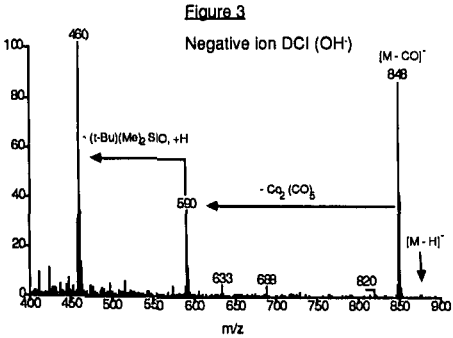

Figure 4
Positive ion DCI (NH_4^+)

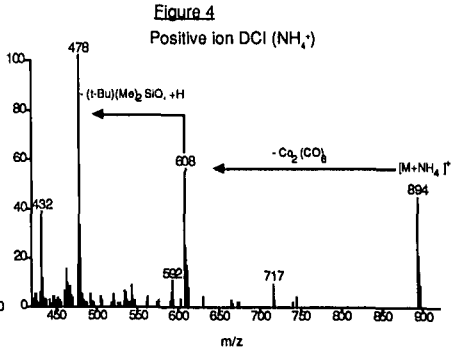

Presented at the 36th ASMS Conference on Mass Spectrometry and Allied Topics
June 5-10, 1988, San Francisco, CA

BEHAVIOR OF FATTY ACID MIXTURES IN VARIOUS FAB MATRICES

K. Caldwell and M.L. Gross, Midwest Center for Mass Spectrometry, Department of Chemistry, University of Nebraska, Lincoln, NE 68588.

FAB has established itself as a useful means for obtaining molecular ions of nonvolatile and/or thermally sensitive compounds The technique has enjoyed the most success with qualitative analysis. Quantitative analysis requires an internal standard which may not always be commercially available or easily made.

If quantitative or at least semiquantitative mixture analysis is to be done by FAB, the problems need to be outlined and understanding of the behavior of simple analyte mixtures in typical FAB matrices is needed.

Some problems associated with quantitative mixture analysis by FAB are: (1) Normal surface activity discrimination resulting in underrepresentation of less surface active species[1]. This is evident in spectra of equimolar mixtures of saturated fatty acids of different chain length and occurs at lower total fatty acid concentrations in the matrix (Fig. 1B and 1C). (2) Formation of micelles leading to underrepresentation of fatty acids with a lower critical micelle concentration in the matrix - typically the longer chain length fatty acids[2]. This is an example of reverse surface activity discrimination and occurs at higher total fatty acid concentrations in the matrix (Fig. 1B and 1C). (3) A change in the relative ratios of a mixture composed of both hydrophilic and hydrophobic fatty acids with time in the atom beam. The early scans are dominated by ions from the most hydrophobic fatty acids and the hydrophilic fatty acids are underrepresented until the hydrophobic fatty acids are sputtered away.

These problems are a manifestation of matrix analyte interactions. Fatty acids greater than about C12 behave much like hydrocarbons. They tend to cluster and even form micelles in polar solvents so that the hydrocarbon tails are closer, thus reducing their energy by the attractive Van der Waals forces. This is evident in the spectrum of the three saturated fatty acids in glycerol/KOH. The KOH was added to the matrix because the fatty acids were not very soluble in glycerol alone. The high ionic strength of a .5M KOH solution also lowers the critical micelle concentration[3].

A means of reducing discrimination effects is to turn to a matrix that shows little differential surface activity effects and minimizes micelle formation. The matrix should have the property of solubilizing the mixture components and so it should resemble the analyte themselves. Dodecanol has been used in this study and Fig. 2 shows an equimolar mixture of 3 saturated fatty acids in the new matrix. Notice that the bulk relative ratios are represented and compare Fig. 1A with 1B and 1C.

The graphs in Fig. 1 were generated by taking the $[M + H]^+$ intensity, in the case of 1A, and the $[M - H]^-$ intensity in the case of 1B, 1C and divided by the actual relative abundances C10:C16:C18 = 1.10:1.00:1.04. If the uncompensated intensities are plotted versus the concentration of each fatty acid in the new matrix, a linear relationship is observed (Fig. 3). The possibility of quantitative analysis by FAB without the use of an internal standard is being explored.

EXPERIMENTAL - The C10, C16, and C18 fatty acids were weighed and dissolved in CCl4. The actual relative molar ratios were: C10:C16:C18 = 1.10:1.00: 1.04. A 33% solution of the matrices in ethanol was mixed with an appropriate amount of the fatty acid stock solution and the volatile solvents allowed to evaporate. The total fatty acid concentrations used in Fig. 1 is assuming 100% evaporation of the volatile solvents. Since dodecanol melts above room temperature, all the solutions just before analysis were brought to 35 °C. Several microliters of these solutions were applied to the probe tip and spectra obtained using an Ion-Tech FAB Gun and a Kratos MS50 TA.

Presented at the 36th ASMS Conference on Mass Spectrometry and Allied Topics
June 5-10, 1988, San Francisco, CA

DISCRIMINATION OF ALKYL FATTY ACIDS IN DODECANOL

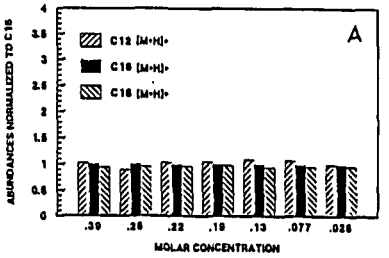

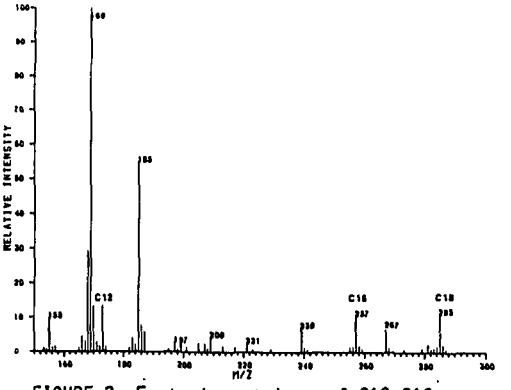

FIGURE 2. Equimolar mixture of C10,C16, and C18 fatty acids desorbed from dodecanol as positive ions. The individual fatty acids are seen as [M+H]+ and [M+H - H2O]+.

DISCRIMINATION OF ALKYL FATTY ACIDS IN TRIETHANOLAMINE

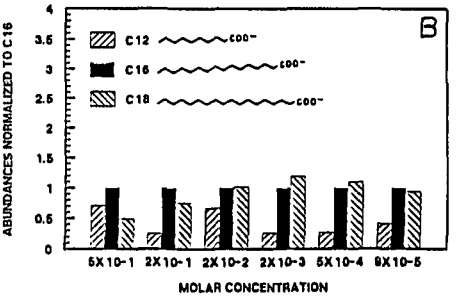

RESPONSE vs. CONCENTRATION OF THREE ALIPHATIC FATTY ACIDS IN DODECANOL

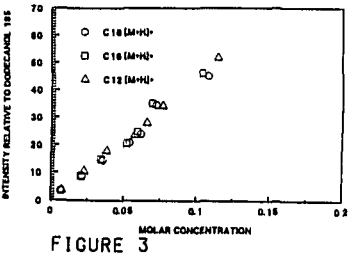

FIGURE 3

DISCRIMINATION OF ALKYL FATTY ACIDS IN GLYCEROL .5M KOH

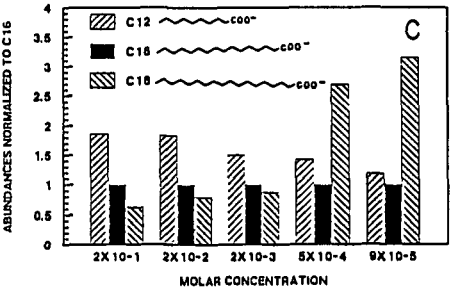

REFERENCES

(1) W.V. Ligon and S.B. Dorn. Int. J. Mass Spectrom. Ion Proc., 661, (1984) 113-122.

(2) M. Barber et al., J. Chem. Soc. Faraday Trans., 79, (1983) 1249-55.

(3) James F. Mead,Roslyn B. Alfin-Slater, David R. Howton, and George Popjak, Lipids Chemistry, Biochemistry, and Nutrition, Plenum Press, 1986 p. 65.

Presented at the 36th ASMS Conference on Mass Spectrometry and Allied Topics
June 5-10, 1988, San Francisco, CA

Matrix Effects and Ion Formation in Fast Atom Bombardment Mass Spectrometry of Cyclic Dithia-Diaza Compounds

B.H. Hsu, Department of Medicinal Chemistry, J-485 JHMHC,
University of Florida, Gainesville, Fl 32610

INTRODUCTION

Cyclic dithia-diaza compounds including monocyclo and bicyclo have been designed as the delivery system for technetinium in brain scanning. Fast atom bombardment (FAB) has been proved to be the only ionization vehicle by the mass spectrometric methods to characterize these substances thus far.

The technique of FAB is limited by the contribution of matrix background and the requirement of a soluble sample in the matrix solution. Furthermore, solute /solvent interactions can play a significant role in desorption ionization mass spectrometry (1.2). This work has been in an effort to provide analytical support to the determination of these cyclic dithia-diaza compounds and to explore the ion formation in connection with matrix and mechanistic aspects of particle-induced desorption. Linked scans (B field/E field, is constant) which produce daughter spectra of selected parent ions was used to study fragmentation mechanism.

EXPERIMENTAL

The FAB/MS data were obtained using a Kratos MS80RFA spectrometer utilizing an Ion Tech Saddefield gun which generate a primary beam of xenon atoms at 7KV and 1.5 mA. FAB/MS/MS data were collected with linked scans (B/E). Collision gas (Ar) was introduced into first field-free region at the indication of source pressure at 2×10^{-3} torr.

DISCUSSION

The structure of cyclic dithia-diaza analogues are shown in Fig. 1. A representative FAB spectrum of an analogue (Compound 2) is given in Figure 2. The spectrum contains hydrated molecular ion along with a few fragment ions and one fragment reminiscent of the $(M-H)^+$. The ratio of the relative intensity of $(M-H)^+$ ions can be varied by the amount of added glycerol matrix from 2:1 without any matrix to 1:2 with 100 fold of glycerol. FAB spectra of compound 3 and 4 show no evidence of $(M-H)^+$ and the loss of sulfur. The instability of the charge delocalization on the imidazole moiety for these two compounds might be responsible for that observation.

Table I summarizes the FAB matrix effects for cyclic dithia-diaza compounds. Glycerol adducts of protonated molecular ions were not found if glycerol was used as the only matrix. However, a series of adducts were detected, which include $[M + H + H_2O]^+$, $[M + H + G]^+$, and $[M + H + G + H_2O]^+$ (where M represents intact molecule and G represents glycerol molecule), if p-toluene sulfonic acid (p-TSA) was added to the glycerol and bombarded by the Xe neutral beam. No adducts were present in the FAB spectra of compounds 3 and 4 even p-TSA was added. This accounts for the fact that the formation of adduct ions are involved in the chemical structures with bicyclic or monocyclic analogues with C=N bond.

Solvation of organic cations in desorption ionization experiment involving formation of strong new bonds have been exclusively studied (1,3). Table II lists the fragmentation behavior of adduct ions of compound 1 and 5. The ions selected for examination are all formally glycerol and/or water adducts of protonated molecular ions generated under conventional FAB conditions. Losses of glycerol or water are commonly found in the MS/MS spectra of $[M + H + H_2O]^+$ and $[M + H + G + H_2O]^+$ ions. Nevertheless, loss of water following the loss of glycerol was not detected for the adduct ion of $[M + H + G + H_2O]^+$. In contrast, glycerated form of $[M + H + G]^+$ ion show markedly different behavior, which displays no loss of glycerol; instead it loose 113 daltons. These observations can be recognized as the strong interactions involving covalently bond formation between analytes and solvation solvents.

Presented at the 36th ASMS Conference on Mass Spectrometry and Allied Topics
June 5-10, 1988, San Francisco, CA

REFERENCES

1. Emary, W.B.; Cooks, R.G. Anal. Chem., 1986, 58, 1218.
2. Tondeur, Y.; Clifford, A.J.; DeLuca, L.M. Org Mass Spectrom., 1985, 20, 159.
3. Glish, G.L.; Todd, P.J.; Busch, K.L.; Cooks, R.G. Int. J. Mass Spectrom. Ion Phys.,1984, 56, 177.

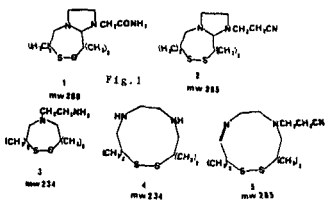

Fig. 1

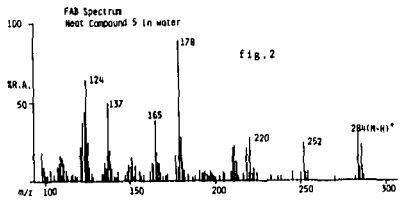

fig. 2

Table I. Matrix Effects on Ion Formation* in FAB/MS for Cyclic Dithio-Diaza Compounds

Compd	Matrix	Ions Formed (%rel abund)
1	neat	$(M-H)^+$(40),$(M+H)^+$(36)
	Glycerol	$(M-H)^+$(36),$(M+H)^+$(100)
	Glycerol+p-TSA	$(M+H)^+$(13),$(M+H+H_2O)^+$(100),$(M+H+G)^+$(10) $(M+H+H_2O+G)^+$(27)
2	neat	$(M-H)^+$(93),$(M+H)^+$(55)
	Glycerol(1-fold)	$(M-H)^+$(75),$(M+H)^+$(30)
	Glycerol(100-fold)	$(M-H)^+$(43),$(M+H)^+$(69)
	n-TSA	$(M-H)^+$(72),$(M+H)^+$(22)
	Glycerol+p-TSA	$(M+H)^+$(100),$(M+H+H_2O)^+$(35),$(M+H+H_2O+G)^+$(15)
3@	neat	$(M+H)^+$(100)
4@	neat	$(M-H)^+$(37),$(M+H)^+$(100)
	Glycerol(3-fold)	$(M-H)^+$(25),$(M+H)^+$(60)
	Glycerol+p-TSA	$(M-H)^+$(6),$(M+H)^+$(100)
5	neat	$(M-H)^+$(32),$(M+H)^+$(23)
	Glycerol(1-fold)	$(M-H)^+$(32),$(M+H)^+$(66)
	Glycerol+p-TSA	$(M+H)^+$(11),$(M+H+H_2O)^+$(100),$(M+H+G)^+$(20) $(M+H+H_2O+G)^+$(27)

*Only ions in the region of molecular ion and adducts are reported.
@No $(M-H)^+$ and adduct ions were detected
#No adduct ions were found.

Table II. Summary of MS/MS data of adduct ions of Compound 1 and 5 admixed with Glycerol and p-Toluenesulfonic acid

Compound	Parent Ion	Fragment Ions (% rel abund)
1	$(M+H-H_2O\ G)^+$	92(70),164(100) with Coll Gas
		92(100),164(80) without Coll Gas
	$(M+H-H_2O)^+$	18(60),71(100) with Coll. Gas
		18(75),71(100) without Coll Gas
5*	$(M+H-H_2O\ G)^+$	92(100),164(75)
	$(M+H-G)^+$	113(100),146(15)
	$(M+H-H_2O)^+$	18(100),71(80)

*No collision gas was introduced in this experiment

Presented at the 36th ASMS Conference on Mass Spectrometry and Allied Topics
June 5-10, 1988, San Francisco, CA

QUANTITATIVE FAB: IS WHAT YOU SEE WHAT YOU'VE GOT ?

S. L. Hunt and P. A. Lyon
3M, St. Paul, MN. 55144.

Fast atom bombardment mass spectrometry has given us a simple and rapid method for the direct analysis of ionic mixtures. Characterization of ionic mixtures often requires both qualitative and quantitative data. The performance of surfactants, for example, depends upon both the type and concentration of each component. Our work focuses upon the largest class of surfactants, the anionics. Conflicting data exists about the reliability of FAB for quantitation. This study explores the factors influencing the relative abundance of anions generated by FAB and evaluates the quantitative capabilities of the technique for analyses where isotopically labeled internal standards are not readily available or easily synthesized.

The compounds and mixtures included in this study were evaluated by full scan FAB mass spectrometry on a Kratos MS50 RFTA. We examined parameters like desorption time, molecular structure and weight, the matrix, polarity of the experiment, and the counterion. Our results suggest that time averaged FAB data reflect the true composition of sulfonate mixtures (Table I). Time averaging was required because the ion relative abundances change with desorption time (fig. I). Molecular weight and/or structure, possibly as they relate to surface activity, play an important role in desorption preference.

The ability of FAB to perform semiquantitative analyses was tested on synthetic mixtures and an industrial sulfonate sample. Based on FAB results, the industrial sample contained C_1 through C_8 perfluoroalkane sulfonates. The same sample was derivatized with diazomethane and analyzed by GC using microwave plasma detection. Fluorinated impurities interfered with quantitation using the microwave fluorine channel. However, the results obtained from the sulfur channel were in excellent with the FAB data (Table II).

The industrial perflurosulfonate sample was analyzed using three different FAB matrices (glycerol, dithioerythreitol/dithiothreitol and triethanolamine). We measured the abundance of FAB-generated positive and negative ions. These experiments suggest that quantitation of perfluoroalkanesulfonates is relatively insensitive to acquisition polarity or type of matrix.

Most of these surfactants are produced as salts. Therefore it seemed necessary to investigate the effect of various counter ions. Decanoic acid was converted into the following salts: Li, Na, K, Mg, Ca and Ba. The relative abundance of significant ions are summarized in Table 3. It appears that the salts are more amenable to FAB than the free carboxylic acids, lithium salts provide the least information and divalent cations produce usable but complex spectra.

We have found that in many FAB analyses "what you see is what you've got". However, since exceptions exist it is hazardous to generalize about the applicability of FAB for semiquantitation of components without internal standards.

Acknowledgements: We gratefully acknowledge assistance from the following individuals: J. Miller (GC-Microwave); R. Farm (salt preparation); G. Lillquist, J. Westberg and W. Peters (IR salt confirmation).

Presented at the 36th ASMS Conference on Mass Spectrometry and Allied Topics
June 5-10, 1988, San Francisco, CA

Table I

FAB IONIZATION

Compound	Actual %	Equimolar Mixture Initial Observed %	% Error	Average Observed %	% Error
$C_2F_5SO_3K$	20.1	0.9	-96	15.5	-22.5
$C_4F_9SO_3K$	20.0	15.1	-24.5	20.5	+2.5
$C_6F_{13}SO_3K$	20.0	37.8	+89.0	20.2	+1.0
$C_8F_{17}SO_3K$	20.0	28.8	+44.0	20.8	+4.0
$C_{10}F_{21}SO_3K$	19.9	17.4	-12.6	23.0	+15.6

Table II

COMPARISON OF FAB/MS AND GC-MICROWAVE

Compound	FAB-MS	GC-Microwave Fluorine channel	Sulfur channel
CF_3SO_3	0.8%	nd	nd
$C_2F_5SO_3$	8.3%	9.6%	12.1%
$C_3F_7SO_3$	34.0%	29.9%	28.6%
$C_4F_9SO_3$	50.0%	53.1%	50.7%
$C_5F_{11}SO_3$	3.0%	4.2%	6.2%
$C_6F_{13}SO_3$	2.7%	3.2%	2.3%

Figure I

Perfluoroalkanesulfonates Equimolar mixture

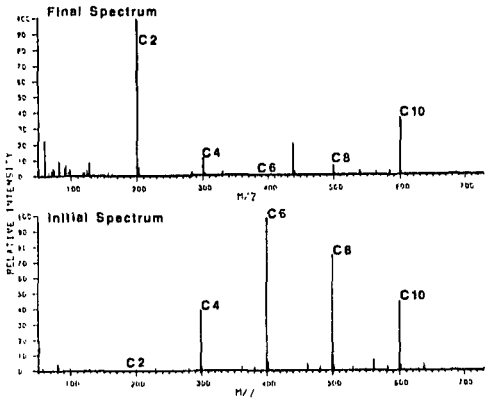

Presented at the 36th ASMS Conference on Mass Spectrometry and Allied Topics
June 5-10, 1988, San Francisco, CA

THE BEHAVIOR OF MIXTURES OF PHOSPHOLIPIDS IN THE FAB MATRIX

D N. Heller, R.J. Cotter, C M Murphy, Johns Hopkins University, Baltimore, MD 21205
O M. Uy, Johns Hopkins Applied Physics Laboratory, Laurel, MD 20707
C. Fenselau, University of Maryland Baltimore County, Catonsville, MD 21228

Lipid analyses of bacteria cells over the past 25 years have revealed that phospholipid and glycolipid distributions occur in patterns that are related to taxonomic grouping[1]. We have used negative ion FAB mass spectrometry to generate "lipid profiles"--mass spectra of complex lipid mixtures--to differentiate or identify bacteria[2,3].

Experiments conducted in our laboratory have shown that lipid signals obtained from lysed cells yield reproducible mass/intensity patterns[2], and also combine linearly when various ratios of cells from two different bacteria are mixed in the FAB matrix[3]. Linear regression analysis, the technique used to demonstrate the latter point, depends on the assumption that individual mixture components--the polar lipids themselves--behave independently of one another during the analysis. In other words, the system requires linear addition of signals but not necessarily quantitative response during FAB desorption

While evidence to date suggests that polar lipids are desorbed and ionized independently under the conditions of our previous experiments, the behavior of phospholipids mixtures has not yet been studied through direct analysis of measured mixtures. Our goal is to define conditions under which linear behavior of phospholipids in mixtures is observed in negative ion FAB-MS.

Previous studies have shown that competition for surface sites has a great influence on FAB spectra: relative surface activity accounts for the suppression of matrix ions by analyte, the preferred desorption of one peptide or tetraalkylammonium ion in a mixture, as well as the efficient desorption of highly surface-active analytes[4]. Formation of a surface monolayer of analyte, determined by surface tension measurements, has been correlated with the onset of altered desorption characteristics[5,6,7,8].

Phosphatidylethanolamine (PE) and phosphatidylglycerol (PG) are two of the most common phospholipids occuring in bacteria; these compounds differ only in their polar head group. Dipalmitoyl PE (ave. MW = 691.5) and dipalmitoyl PG (ave. MW = 722.5) were combined at various concentrations and ratios in $CHCl_3$/MeOH 1:2 before being mixed with diethanolamine (DEA) and placed on the FAB probe. Spectra were acquired with the Kratos MS-50RF operated in negative ion mode and scanned at 30 s/dec from m/z 1500-350 (23 s/scan). The Ion-Tek FAB gun used Xe gas and was operated at 7.5 kV and 40uA discharge current. Found desorption ratios were calculated from the intensity of the [M-H]- monoisotopic mass peak in each scan.

During the first two minutes of particle bombardment the found PE:PG ratio remains relatively constant; consequently all measurements are based on average ratios obtained from the first two minutes of each run.

At or below a combined concentration of about 10^{-4} M (Figure 1) the relative response of PE and PG is close to the ratio of their concentrations in the matrix, but at total concentrations above this range the PE:PG desorption ratio steadily decreases.

At [PE]+[PG] ~ 10^{-4} M, linear desorption response is observed for PE and PG over the range 10:1 to 1:10 (Figure 2). Non-linearity at more extreme ratios can be attributed to the relatively large contribution of chemical noise to the smaller of the two lipid signals (signal-to-noise about 5), and could be improved by chemical baseline subtraction. The relative error in found PE:PG ratios increases as concentration decreases (Figure 1) due to the variation in absolute signal intensity.

Linear and nearly quantitative desorption ratios are obtained from dipalmitoyl PE and PG at total probe concentrations ~ 10^{-4} M. Non-quantitative desorption ratios are obtained at total concentrations > 10^{-4} M. Interpretation of this data in light of previous studies with surface-active analytes suggests that complete surface coverage of DEA is achieved at about 10^{-4} M, while at higher concentrations

PG excludes PE from the surface layers.

Linear behavior for a mixture of two common phospholipids has been demonstrated at a total concentration of the same order of magnitude as polar lipids from 30 ug lysed bacterial cells in 2 ul matrix[2,3]. The results of these experiments suggest that the required linear desorption behavior of phospholipid mixtures can be obtained if sample concentration is low enough that surface saturation by polar lipids does not take place.

REFERENCES

1. Goldfine, H. in "Membrane Lipids of Prokaryotes," Razin, S., Rottem, S., Eds.; Academic: New York, 1982, 1-43.
2. Heller, D.N.; Cotter, R.J.; Fenselau, C.; Uy, O.M. Anal. Chem. 1987, 59, 2806-2809.
3. Platt, J.A.; Uy, O.M.; Heller, D.N.; Cotter, R.J.; Fenselau, C. Anal. Chem. in press.
4. Fenselau, C; Cotter, R.J. Chem. Rev. 1987, 87, 510-512.
5. Allmaier, G. M. Rapid Commun. Mass Spectrom. 1988, 2, 74-76.
6. Heller, D.N.; Fenselau, C.; Yergey, J.A.; Cotter, R.J.; Larkin, D. Anal. Chem. 1984, 56, 2274-2277.
7. Beckner, C.F., Caprioli, R M. Biomed. Mass Spectrom. 1984, 11, 60-62.
8. Ligon, W.V.; Dorn, S.B. Int. J. Mass Spectrom. Ion Proc. 1984, 57, 75-90.

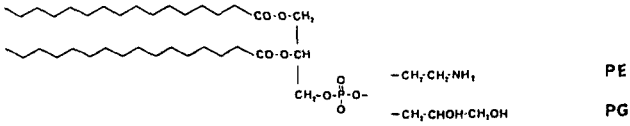

Figure 1

Figure 2

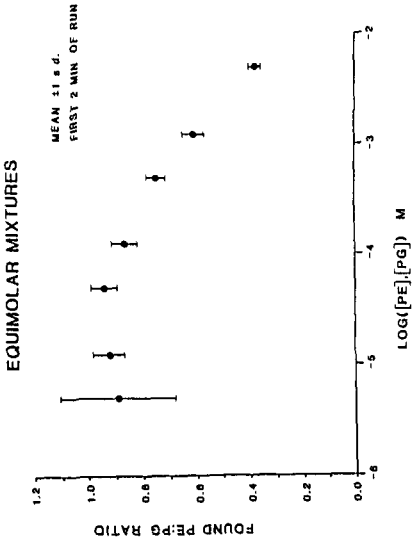

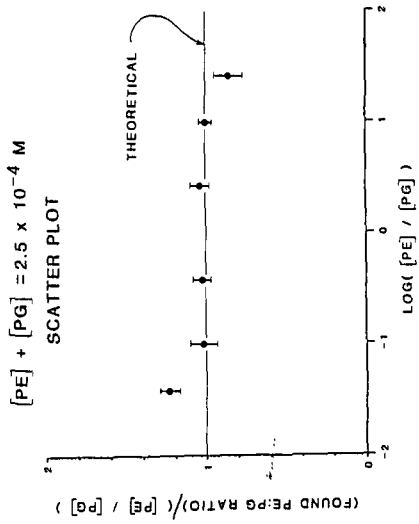

Presented at the 36th ASMS Conference on Mass Spectrometry and Allied Topics
June 5-10, 1988, San Francisco, CA

3-NITROBENZYL ALCOHOL - A VERSATILE MATRIX COMPOUND FOR FAB/MS

B.J. Sweetman and I.A. Blair, Department of Pharmacology
Vanderbilt University, Nashville, Tennessee 37232

Fast atom bombardment (FAB) mass spectrometry was introduced originally by Barber et al. (1,2) in 1981 as a means for the mass spectral analysis of previously intractable polar and/or thermally-labile compounds. To obtain FAB spectra, a compound is usually dissolved in a viscous liquid-matrix and bombarded with fast atoms. The resultant ions arising from the sputtering process are mass-analyzed by the use of the focussing devices of the particular mass spectrometer. Glycerol was the initial matrix suggested for FAB-MS (1,2) and has seen extensive use. A large number of alternative matrix compounds have been suggested to accomplish analyses of specific compounds or specific compound types (3). One of these matrix compounds which has been mentioned occasionally in the literature is 3-nitrobenzyl alcohol (3-NBA). The use of 3-NBA was suggested originally by Meili and Seibl (4) for the analysis of porphyrins and cyclic peptides. Adams and Gross (5) have described recently its use for the structural determination of cationized fatty acids. Miller et al. (6) demonstrated recently that abundant intact doubly-charged cations of certain ruthenium-bidentate ligand complexes could be detected when using 3-NBA as matrix but not with other matrices. They postulated that 3-NBA served as an oxidative quencher for the excited state of the ruthenium complex.

With the availability of a large number of different types of matrix compounds for FAB-MS, the task of the analyst in choosing the optimum matrix compound for a particular analysis is often quite arbitrary and time-consuming. During the past two years we have had the need to characterize a diverse variety of compounds using FAB-MS. Our growing experience has been that 3-NBA comes closer to being a universal FAB matrix compound than any other matrix we have used. This appears to be related to the apparently unique physico-chemical properties of 3-NBA. We have employed 3-NBA to obtain intense, high quality positive and negative ion spectra of a diverse variety of compound types giving, in most instances, results superior to those obtained using glycerol or thiol based matrices. Spectra obtained show little or no interference from matrix or alkali metal cations. Compound types generating excellent results with 3-NBA include peracetylated oligosaccharides, quaternary amine salts, spin labelled nitroxide free radicals, nucleosides, peptides, aryl sulfonates, phosphatidic acids, cephalosporin antibiotics, glutathione and cysteine conjugates of prostaglandins, phosphonium salts, apolar organosulfur and organoselenium compounds. The use of 3-NBA yields particularly useful structural information about phosphonium and quaternary ammonium salts. Alkyl phosphonium bromides are used in the important Wittig reaction in synthetic organic chemistry. Their positive ion spectra show the intact phosphonium cation as base peak and fragment ions corresponding to fission of each C-C bond in the molecule. Primary and secondary phosphonium salts can be differentiated. Negative ion spectra all show $RPBr.Br^-$ attachment ions. The bis-quaternary ammonium salts are representative of compounds such as succinyl choline di-chloride (SC) which are used widely in medicine. The positive ion spectrum of SC shows a peak due to SC.Na-Cl together with a number of structurally significant ions containing a single quaternary ammonium group. Little or no structural information could be obtained from the corresponding spectrum in glycerol.

The spectrum obtained for SC using 3-NBA as a matrix provides a definitive fingerprint for SC. Despite the presence of NaCl, the spectrum is totally free from peaks due to matrix, cationized matrix or cationized SC (Figure). Loss of one chloride from SC gives the doublet at m/z 325/7 and the further loss of the elements of CH_3Cl yields the base peak at m/z 275. Alternatively, loss of the elements of trimethylamine gives m/z 266/8. The spectrum obtained for the same quantity of SC using glycerol (G) as matrix is in striking contrast to the spectrum in 3-NBA. The spectrum is complicated greatly by peaks due to G and G_2 and sodium attachment ions of G and G_2-H. Peaks are also present at m/z 173 and 265, attributed to [GNa.NaCl] and [G_2Na-H.NaCl], respectively. The spectrum obtained using G, by contrast to the spectrum in 3-NBA shows intense peaks at m/z 104 and 204, possibly arising by saponification of SC in G. Abundance of the mono-quaternary ammonium ion at m/z 275 is dramatically reduced. A doublet at m/z 383/5 is attributed to [M-Cl.NaCl] and is not present in the 3-NBA spectrum. 3-NBA failed as a matrix compound for underivatized sugars and the vancomycins because of low solubility of these compounds in 3-NBA. Negative ion spectra obtained using 3-NBA in the presence of halide ions can be complicated by the reaction of matrix with halide ions.

Spectra obtained using 3-NBA are usually prolonged and intense - apparently associated with the unique physical properties of this matrix - low volatility, medium viscosity liquid at room temperature, high dielectric constant and very high dipole moment. 3-NBA has surprisingly good solvent properties for a diverse variety of compound classes and can be used for obtaining either positive or negative ion spectra. 3-NBA is chemically quite inert and we have encountered no instances of reactivity between 3-NBA and solutes during the acquisition of FAB spectra, unlike the use of thiol matrices where reaction of matrix and solute is relatively common. Spectra obtained using 3-NBA almost invariably show molecular ion information (M^+, MH^+, MH_2^+, etc. depending on compound type) and abundant fragment ion information. Spectra of polar molecules such as quaternary ammonium salts, phosphonium salts and phospholipids obtained using 3-NBA are much more resistant to interferences and suppression from alkali metal cations, than are the corresponding spectra obtained using glycerol or thiol matrices. This effect apparently does not extrapolate to acidic peptides, in our limited experiences of these compounds.

On the basis of the results presented here and our experiences with a large variety of compound types, 3-NBA rather than glycerol or thiol matrices should be used as the first-choice matrix compound for the structural analysis of compounds by FAB-MS, where no existing precedent for their analysis exists.

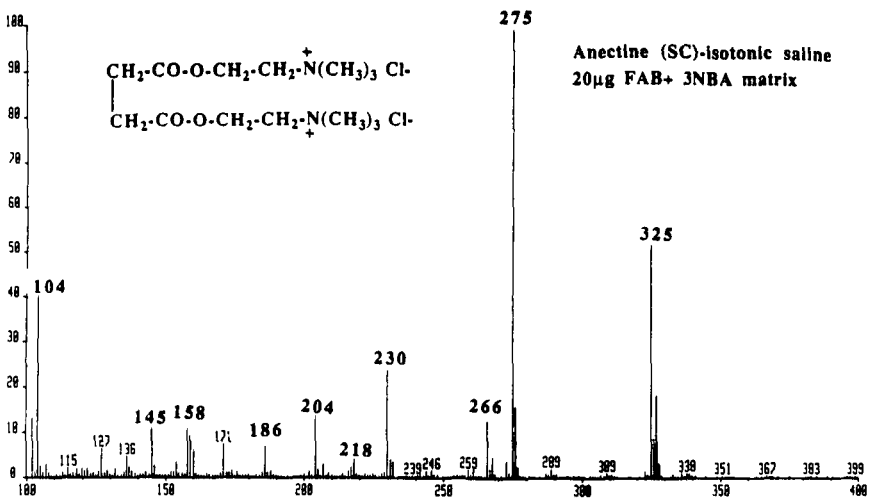

Figure: Positive FAB mass spectrum of anectine (succinyl choline) in 3NBA matrix.

ACKNOWLEDGEMENT

We acknowledge the support of GM-15431, GM-31304, ES-00267 and RR-01688.

REFERENCES

1. Barber M, Bordoli RS, Sedgwick RD and Tyler AN. Nature, 293:270, 1981.
2. Barber M, Bordoli RS, Sedgwick RD and Tyler AN. J. Chem. Soc. Chem. Commun., 7: 325, 1981.
3. Gower JL. Biomed. Mass. Spect., 12:191, 1985.
4. Meili J and Seibl J. Org. Mass. Spect., 19:581, 1984.
5. Adams J and Gross ML. Anal. Chem., 59:1576, 1987.
6. Miller JM, Balasanmugam K, Nye J, Deacon GB and Thomas NC. Inorg. Chem., 26:560, 1987.

Presented at the 36th ASMS Conference on Mass Spectrometry and Allied Topics
June 5-10, 1988, San Francisco, CA

Observation of Surfactant Clusters by Liquid SIMS

E.L. Dorwin, P.W. Bethel and P. Fitch
University of California, San Francisco

The sputtering and ionization of hydrophobic salts at the liquid-vacuum interface is related to the surface activity of the salt. Ion intensities are maximized when surfactant solutions are presented to the bombarding particles at or above the critical micelle concentration. This desorption may involve Marangoni effects or a sputtering of micellar clusters which may decompose before reaching the collector of the mass spectrometer.

Three compounds which are known to form micelles or sub-micellar aggregates in aqueous solutions were studied [1,2]:

$(C_8H_{17})_3N^+CH_2CH_2OH$ mesylate salt

$C_{16}H_{33}N^+(CH_3)_2CH_2CH_2OH$ bromide, chloride salt

In order to characterize the state of aggregation of these hydrophobic salts both before and after ionization, the samples were sputtered from an LSIMS source by bombardment with a cesium ion beam. Clusters were observed at nominal masses corresponding to the aggregate forms (+), (++-), and (+++--) for the mesylate salt sputtered from a tetraglyme matrix. The bromide salt of the cholinate functionalized micelle when sputtered from a glycerol/water matrix (92:8) produced peaks at nominal masses corresponding to (+) and (++-) ions.

Critical micelle concentrations were determined for the cholinate functionalized micelle in the solvent system glycerol/water (92:8). The critical micelle concentration of the bromide salt of the cholinate functionalized micelle was 1.3×10^{-3} M determined by the Wilhelmy Plate method using a Cahn electrobalance. The cmc of the chloride salt of the cholinate functionalized micelle was 3.5×10^{-3} M determined by differential absorption spectrophotometry using phenol as an optical probe of micelle structure [3].

Since the sample of the cholinate functionalized micelle was applied to the probe tip and introduced into the source of the Kratos MS-50 at a concentration of .026 M in glycerol, surface tension measurements indicate that micellar clusters were present in the solution. Whether the aggregates observed at the detector of the mass spectrometer arose from a desorption of pre-formed ion aggregates or a gas phase 'micellization' of surfactant monomers cannot be determined from these preliminary experiments.

Micelle formation in both water and glycerol has been attributed to a combination of hydrophobic and dispersive attractions. The high vacuum of the mass spectrometer would seem to preclude a solvophobic force for cluster formation. The driving force allowing a gas phase micelle to exist may arise from a surface tension difference between the hydrocarbon tails of the surfactants and the vacuum which is even greater than the interfacial tension between hydrocarbons and the glycerol/water matix.

Aside from their theoretical interest for both solution and gas phase aggregate chemistry, functionalized micelles and phase transfer catalysts may have future applications as derivatization reagents in enhancing the surface activity of biopolymers for quantitative Fast Atom Bombardment mass spectrometry.

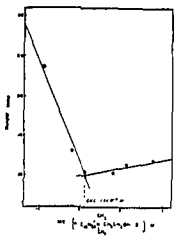

Figure 1. CMC of the cholinate micelle determined by the Wilhelmy Plate method. CMC = 1.3 x 10^{-3} M.

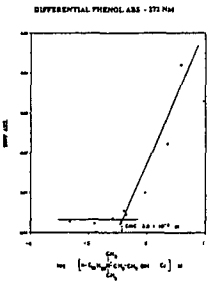

Figure 2. CMC of the cholinate micelle determined by difference absorption spectrophotometry. CMC = 3.5 x 10^{-3} M.

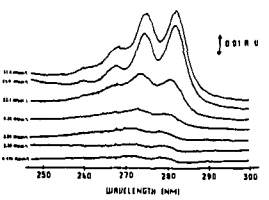

Figure 3. Effect of surfactant concentration on the differential absorbance of phenol.

References:

[1] C.A. Bunton; E.L. Dorwin, J. Org. Chem.51, 1986, 4093.

[2] C.A. Bunton; C.H. Paik, J. Org. Chem. 40, 1976, 41.

[3] L.G. Ionescu; D.S. Fung, Bull. Chem. Soc. Jpn., 54, 1981, 2503.

Presented at the 36th ASMS Conference on Mass Spectrometry and Allied Topics
June 5-10, 1988, San Francisco, CA

ENHANCEMENT OF PEPTIDE IONIZATION IN FAST ATOM BOMBARDMENT MASS SPECTROMETRY USING A NITROCELLULOSE MATRIX

Richard B. van Breemen and John C. Le
Department of Chemistry, North Carolina State University
Raleigh, NC 27695-8304

Nitrocellulose has been shown to improve molecular ion yields when used as a solid matrix for plasma desorption (1) and secondary ion mass spectrometry using a time-of-flight analyzer (2). A solid instead of a liquid matrix was used in these studies for greater compatibility with a time-of-flight mass spectrometer. In the present investigation, nitrocellulose was evaluated as a fast atom bombardment (FAB) matrix either by itself or with the addition of the liquid, thioglycerol. Nitrocellulose was used in the analysis of peptides and proteins weighing 3,000 to 8,000 mass units with a double-focussing mass spectrometer.

A JEOL HX110 double-focussing mass spectrometer, equipped with a high field magnet, FAB gun, and DA5000 data system was operated at an accelerating voltage of 10 KeV for all measurements. Xenon gas at 3 KV was used for FAB. Each spectrum represents the sum of five scans which were accumulated by signal-averaging. For optimum results, nitrocellulose (3.5 µg) was applied to the stainless steel probe tip in an acetone solution to form a 0.6 $\mu g/mm^2$ layer. Thioglycerol (1 µg), if used, was then added to the probe tip followed by the sample, which was dissolved in dimethylsulfoxide or water.

Without the addition of thioglycerol, a solid matrix of nitrocellulose could not sustain sample ionization, probably because of damage to the sample surface by the high flux fast atom beam or depletion of sample at the point of impact. However, nitrocellulose plus thioglycerol appeared to enhance the intensity of the signal for peptide samples. An optimum amount of nitrocellulose on the surface of the probe tip was determined to be between 3 and 6 µg. Too much nitrocellulose produced a strong signal (as measured by ion counts at the detector) but also considerable chemical noise so that the signal-to-noise ratio was low (Figure 1).

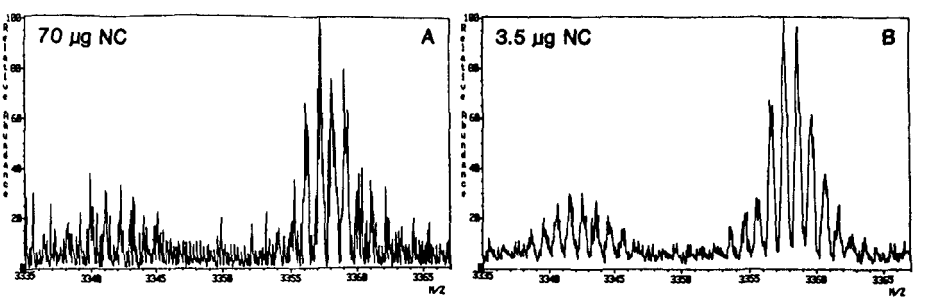

Figure 1. Effect of quantity of nitrocellulose (NC) added to the probe tip along with 1.0 µg thioglycerol. Positive ion FAB mass spectra at a resolving power of 5,000 showing the molecular ion region of human growth hormone releasing factor peptide (amino acids 1-19, 5 µg).

The addition of a layer of nitrocellulose (0.6 µg/mm^2) to the FAB probe tip followed by thioglycerol resulted in a two-fold increase in sensitivity for FAB mass spectrometric analyses of peptides and proteins compared to the use of thioglycerol by itself (Figures 2 and 3). Furthermore, the nitrocellulose/ thioglycerol matrix prolonged sample ionization by reducing the loss of signal associated with redissolving the sample in additional aliquots of thioglycerol after the evaporation of the previous thioglycerol matrix. Nitrocellulose probably reduced the adsorption of peptide and protein molecules to the stainless steel probe tip thereby preventing the effective loss of sample from the liquid matrix solution.

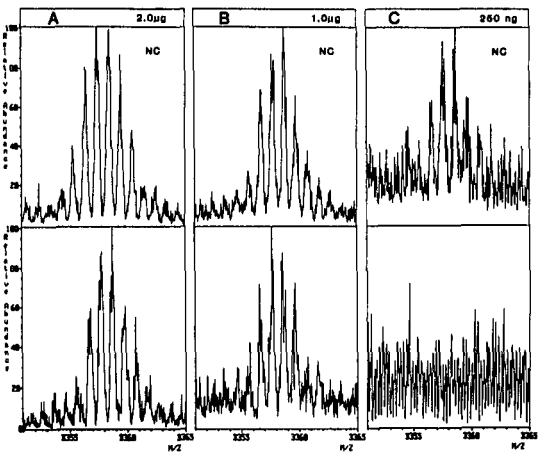

Figure 2. Comparison of sensitivity (detection limit) with or without nitrocellulose (NC) as a function of sample size. The molecular ion region of human growth hormone releasing factor peptide (MW 3357) is shown, obtained by positive ion FAB mass spectrometry at 5,000 resolution.

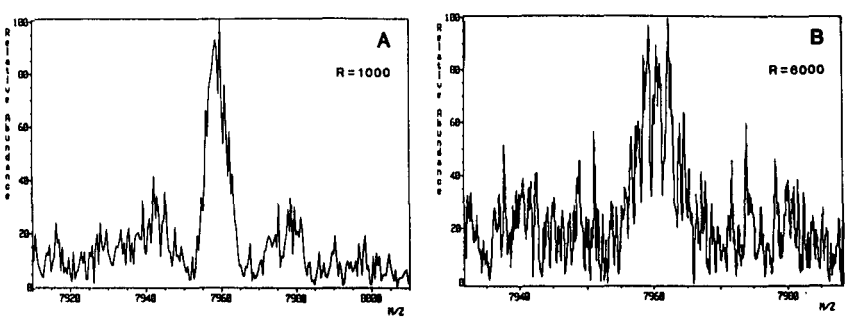

Figure 3. Positive ion FAB mass spectra of α-amylase inhibitor (MW 7958; 100 µg) at 1,000 and 6,000 resolution using nitrocellulose. Without nitrocellulose, twice as much sample was required for similar results.

(1) G. P. Jonsson, A. B. Hedin, P. L. Hakansson, B. U. R. Sundquist, and B. G. S. Save, *Anal. Chem.* 58, 1084 (1986).

(2) F. Lafortune, R. Beavis, X. Tang, K. G. Standing, and B. T. Chait, *Rap. Commun. Mass Spectrom.* 1, 114 (1987).

Presented at the 36th ASMS Conference on Mass Spectrometry and Allied Topics
June 5-10, 1988, San Francisco, CA

Characterization of Tetrakis(benzamidinato)dirhodium(II) by Field Desorption and Fast Atom Bombardment Mass Spectrometry.

John C. Le and Richard B. van Breemen
Department of Chemistry, North Carolina State University
Raleigh, North Carolina 27695-8204

In recent years the structure and chemical reactivity of dirhodium(II) complexes have been investigated extensively, but mass spectrometry has only been used to confirm the molecular weights of these compounds. We recently reported the synthesis of a new dirhodium(II) complex, in which the dirhodium center was coordinated to eight nitrogen atoms (1). Here, we report the first extensive mass spectrometric investigation of this novel dimeric rhodium(II,II) compound and its oxygen adducts using field desorption (FD) and fast atom bombardment (FAB).

The tetrakis(benzamidinato)dirhodium(II) complex was the major product obtained from the reaction of $Rh_2(O_2CCH_3)_4$ with excess N,N -diphenylbenzamidine as previously reported (1). In agreement with literature predictions (2), X-ray crystallography showed that this complex, $Rh_2(N_2R_2CR)_4$ (where R = phenyl), possessed no axial coordination. In an attempt to form axially coordinated oxygen adducts, 50 mg of crystalline $Rh_2(N_2R_2CR)_4$ was exposed to sunlight for 2 months in the presence of atmospheric oxygen. The sample was then dissolved in CH_2Cl_2 (3 g/L), and 1.0 µL aliquots were analyzed by FD, FAB, DCI, or EI mass spectrometry.

All mass spectra were obtained using a JEOL HX110 double-focussing mass spectrometer equipped with a high field magnet and DA5000 data system. The FAB matrix was 3-nitrobenzyl alcohol. The resolving power was 3000 for FAB and DCI and 1000 for FD and EI. A silicon emitter was used for FD measurements.

The molecular weight of the tetrakis(benzamidinato)dirhodium complex was confirmed by FD mass spectrometry, which produced molecular ions at m/z 1290.8 and m/z 430.2 corresponding to the singly charged and triply charged molecular ion radicals. No fragmentation was observed.

FAB formed molecular ion radicals, but also fragment ions corresponding to the sequential loss of the bidentate ligands ($[Rh_2(N_2R_2CR)_n]^{+\cdot}$, n = 1-3) (Figure 1). These types of fragment ions have not been observed in previously reported mass spectra of related dirhodium complexes. It is noteworthy that the intensities of these fragment ions increased or decreased depending upon the energy of the xenon fast atoms. The oxygen adducts, $Rh_2(N_2R_2CR)_4 \cdot O^{+\cdot}$ and $Rh_2(N_2R_2CR)_4 \cdot O_2^{+\cdot}$, were also measured by FAB. Coordination of oxygen to only one axial binding site of the complex occurred during exposure to the sunlight. Fragmentation of these complexes in FAB is summarized in Table 1. Electron impact (EI) and desorption chemical ionization (DCI) mass spectra were also obtained. Molecular ion radicals, $M^{+\cdot}$, as well as the doubly charged molecular ions were observed without fragmentation using these ionization methods.

All four ionization methods, FD, FAB, DCI, and EI produced molecular ions, but FD formed them exclusively. FAB provided the most extensive fragmentation and structural information for this new rhodium complex and its oxygenated adducts. These studies should be applicable to many other organometallic compounds such as Pd or Pt complexes.

Presented at the 36th ASMS Conference on Mass Spectrometry and Allied Topics
June 5-10, 1988, San Francisco, CA

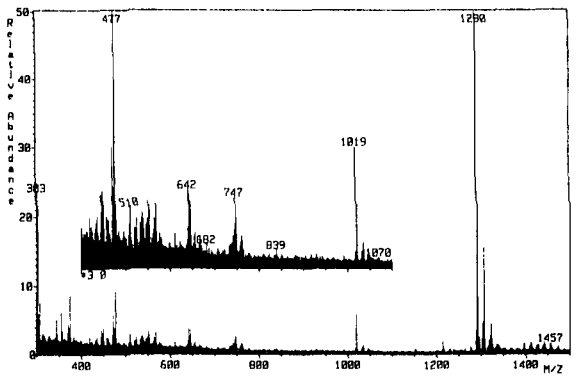

Figure 1. Positive ion fast atom bombardment mass spectrum of tetrakis(benzamidinato)dirhodium(II). (Base peak = m/z 180.)

Table 1. Analysis of $Rh_2(N_2R_2CR)_n \cdot XX$ complexes by positive ion FAB Mass Spectrometry.

(n = 1-4, L = (N_2R_2CR), X = O^-, X = O_2^-)

Fragment	Theoretical M	Measured M
$Rh_2(L)_4$	1290.31	1290.30 ±.3
$Rh_2(L)_3$	1019.30	1019 20 ±.3
$Rh_2(L)_2$	748.25	747.80 ±.5
$Rh_2(L)$	477 26	476.80 ±5
$Rh_2(L)_4 \cdot X$	1306.31	1306 50 ±.3
$Rh_2(L)_4 \cdot X'$	1322 31	1322.50 ±.3
	M^{2+}	M^{3+}
$Rh_2(L)_4$	645.15	645 10 ±.5
$Rh_2(L)_4$	430.11	430.20 ±.3

(1) J.C. Le, M.Y. Chavan, L.D. Chau, J.L. Bear and K.M.Kadish, *J. Am. Chem. Soc.* 107, 7195 (1985)

(2) J.A. Bertrand, F.A. Cotton and W.A. Dollase, *J. Am. Chem. Soc.* 85, 1349 (1973).

(3) "Mass Spectrometry and Crystal Structures Investigation of the Tetrakis(benzamidinato)dirhodium (II) and its Monocarbonmonoxide Adduct complexes " J.C. Le, J.L. Bear and R.B. van Breemen, in preparation.

Presented at the 36th ASMS Conference on Mass Spectrometry and Allied Topics
June 5-10, 1988, San Francisco, CA

FORMATION OF MOLECULAR IONS OF MONOSUBSTITUTED GROUP VI PENTACARBONYLS BY NEGATIVE ION FAB MASS SPECTROMETRY

R. B. van Breemen, L. B. Martin, and A. F. Schreiner
Department of Chemistry, North Carolina State University
Raleigh, N. C. 27695-8204

The first negative ion Fast Atom Bombardment mass spectra of a series of monosubstituted group VIB transition metal pentacarbonyls of the general formula Met(CO)5L (where Met= Cr, Mo, or W, and L = $P(C_6H_5)_3$, $As(C_6H_5)_3$, $Sb(C_6H_5)_3$) were obtained. The positive ion FAB mass spectra, which previously have been reported (1), contained molecular ion radicals as well as fragment ions due to the elimination of neutral ligands. Previous studies have shown that electron impact and electron capture negative ion chemical ionization produced negative ion fragments but no molecular ions (2). In the present investigation, the first molecular negative ions of these compounds formed by any ionization method have been obtained. Molecular ions consisting of $[M-H]^-$, $M^{\bullet -}$, $[M+H]^-$, and $[M+CH_3]^-$ were detected using FAB in an aprotic matrix of 18-crown-6 ether in tetraglyme (3). Fragmentation consisted primarily of elimination of neutral ligands such as $[MH-CO]^-$ and $[MH-2CO]^-$ with evidence shown of loss of cationic species such as protons and phenyl groups from the triphenylphosphine, arsine, or stibine. B/E and constant neutral loss linked scanning with collisional activation and high resolution measurements were carried out on a JEOL HX110 double-focussing mass spectrometer. These techniques were used to confirm fragmentation pathways and determine the site of hydride attachment on the transition metal complex.

The observation of a variety of molecular ions complicates the characterization of the ionization mechanisms involved in FAB of neutral complexes. While some compounds such as $Cr(CO)_5Sb(C_6H_5)_3$ exhibited electron capture as an ionization pathway contributing to the molecular ion, most other compounds formed molecular ions primarily through either hydride addition or proton elimination. Modeling experiments using theoretical isotope patterns show that the molecular ion isotope pattern of $W(CO)_5P(C_6H_5)_3$ is a combination of ions from both the hydride addition and the loss of a proton (Figure 1). High resolution measurements of $Cr(CO)_5P(C_6H_5)_3$ after loss of triphenylphosphine ($[Cr(CO)_5]^-$), separated the ions $[^{53}Cr(CO)_5]^-$ from $[^{52}Cr(CO)_5+H]^-$, with R = 30,000. The presence of both these ions is further evidence of the ionization pathways. Electron capture ionization was more prominent for fragment ions that had already undergone neutral loss.

Figure 1 Tungsten Pentacarbonyl Triphenylphosphine

Negative Ion Fast Atom Bombardment

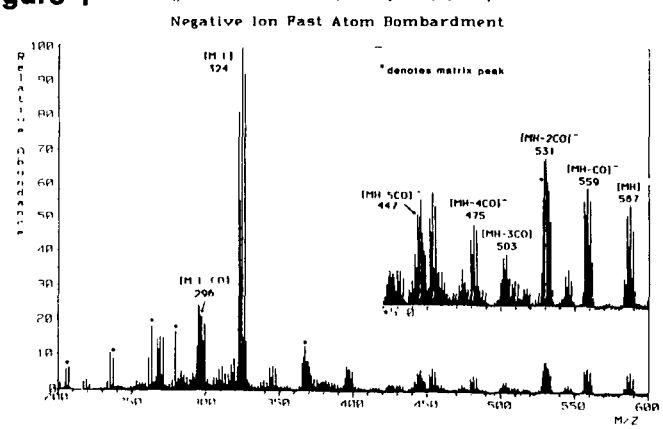

(1). van Breemen, R.B.; Martin, L.B.; Schreiner, A.F.; Anal. Chem., *in press*.
(2). Gregor, I.K.; Guilhaus, *Mass Spectrom. Rev., 1984*, 3, 39-84.
(3). Minard, R.D.; Geoffroy, G.L. paper presented at *the 30th Annual Conference on Mass Spectrometry and Allied Topics*, Honolulu, June 6-11, 1982.

The daughter ion spectrum (Figure 2) of the $[W(CO)_5P(C_6H_5)_3+H]^-$ ion shows ions that have lost a carbonyl neutral but retain the hydride. The constant neutral loss spectrum of $[W(CO)_5P(C_6H_5)_3+H]^-$ (Figure 3) shows ions which have eliminated neutral triphenylphosphine. Each of these ions shows contains a hydride adduct. Because ions that have lost either the triphenylphosphine ligand or all five carbonyls still contain the hydride adduct, this suggests that initial hydride and methide attachment occurs on the metal center. Hydride or methide addition to a six-coordinate complex will most likely result in a seven-coordinate capped octahedral structure, according to LFSE and AO overlap approximations. These experiments highlight the complex nature of FAB ionization, which includes a variety of gas phase ionization mechanisms. The information gathered here will be useful for the further characterization of these compounds as catalytic agents and synthetic intermediates.

Figure 2

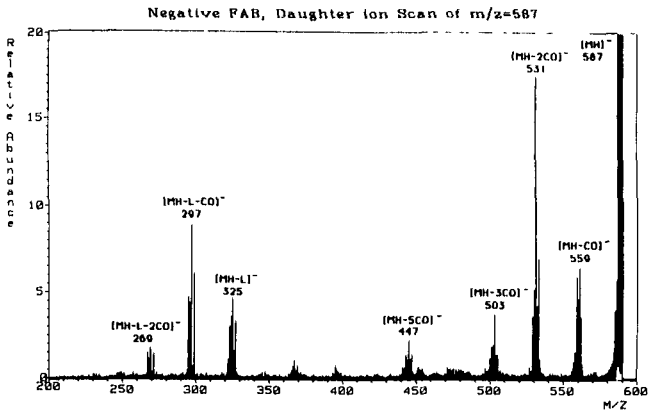

Figure 3

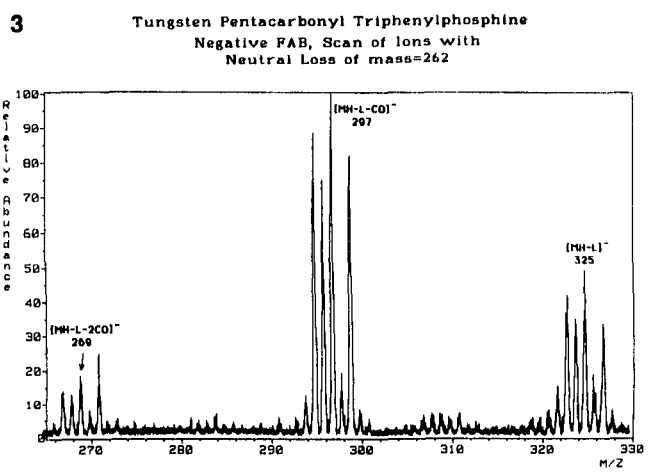

Presented at the 36th ASMS Conference on Mass Spectrometry and Allied Topics
June 5-10, 1988, San Francisco, CA

VARIATIONS IN ANALYTE/MATRIX ION ABUNDANCES IN HIGH-PRESSURE/ FAST-ATOM BOMBARDMENT MASS SPECTROMETRY

John H. Callahan and Mark M. Ross
Code 6112, Chemistry Division
Naval Research Laboratory
Washington, DC 20375-5000

High-pressure/fast-atom bombardment mass spectrometry (also known as chemical ionization/fast-atom bombardment, CI/FAB [1]) is a technique in which ions and neutrals are sputtered into a relatively high pressure (0.05 to 1.0 Torr) of a buffer/reagent gas. Four types of processes have been shown to occur: collisional stabilization, post-desorption ionization (e.g. proton transfer), charge exchange, and adduct formation [2]. In the studies described here, we have investigated the effect of buffer/reagent gases on relative abundances of analyte and matrix ions.

Two types of ion sources and instruments were used in these studies. A modified chemical ionization source with a 0.050-in hole drilled to admit the fast-atom beam was used with a VG ZAB-2F double-focusing reverse-geometry mass spectrometer. Additionally, a modified chemical ionization ion volume with a 0.025-in hole drilled to admit the fast-atom beam was used with a Finnigan TSQ-70 triple quadrupole mass spectrometer. Source pressures were controlled over a range of 0.05 to 1.0 Torr.

Collisional stabilization was found to affect analyte parent ion/fragment ion abundances in high-pressure/FAB. When methadone was sputtered from glycerol, the ratio for the parent ion (protonated methadone, m/z 310) to the major fragment (loss of dimethylamine, m/z 265) increased as the buffer gas pressure was increased. This apparently results from a decrease in the internal energy of the sputtered ions, which was confirmed by the observation of a five-fold decrease in the $[M+H-45]^+/[M+H]^+$ ratio in mass-analyzed ion kinetic energy spectra (MIKES) of methadone sputtered in 0.1 Torr SF_6. These collisional stabilization effects can be reversed by the application of a sample repeller voltage, probably as a result of increases in the energy of collisions with the buffer gas, essentially producing in-source collision-induced dissociation (CID).

Introduction of a buffer/reagent gas also has significant effects on analyte/matrix ion abundances. For example, figure 1 shows the effect of 0.1 Torr of SF_6 on the mass spectrum of 11 mol% m-nitrobenzylalcohol (mNOBA) sputtered from triethanolamine (TEA). In the absence of a gas, the ratio of $[M+H]^+$ from TEA to that from mNOBA is approximately 1000:1. In the presence of SF_6, the ratio is reduced to 10:1 ($M^{+\cdot}$ is also enhanced). Moreover, significant abundances of $[mNOBA + SF_6]^+$ and $[mNOBA + SF_3]^+$ are observed. When all analyte-containing ions are taken into account, there is a 600-fold enhancement of mNOBA species relative to TEA species.

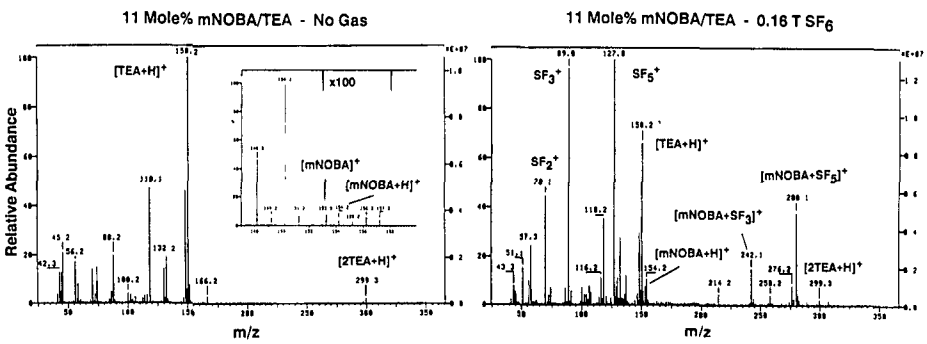

Figure 1. High-pressure/FAB spectra of 11 mol% mNOBA in TEA in the absence and presence of SF_6.

Similar effects have been observed for glycerol (GLY) sputtered from TEA (significant increases in $[GLY + H]^+$ and $[GLY_2 + H]^+$ are observed) and to a lesser extent mNOBA sputtered from glycerol.

Several aspects of the variations of analyte/matrix ion abundances when gases

are present may have implications for models of sputtering processes in FAB. For example, the enhancements in signal intensities due to adduct formation and protonation may result from the significant numbers of neutrals that are sputtered into the gas phase. The results suggest that the neutral/ion ratio in the sputtering process may be on the order of 100:1 - 1000:1. This is similar in magnitude to estimates forwarded by Rollgen and co-workers [3].

A less understood aspect of the sputtering process in high-pressure/FAB is the observation of the enhancement, by non-protonating gases, of protonated species for analytes having gas phase basicities lower than the matrix (e.g. mNOBA in TEA). There are at least two possible explanations for this effect. The first is that $[M+H]^+$ ions that would normally undergo rapid unimolecular decomposition (due to the internal energy obtained from bombardment or from the protonation process) are cooled by collisional stabilization. Alternatively, the buffer gas may affect the kinetics of proton transfer in the selvedge region. For example, if relative analyte/matrix ion abundances are controlled by gas-phase acid-base equilibria (e.g. Kebarle's model [4]) in the selvedge region, then the ion abundances should reflect relative gas-phase basicities. In these experiments, non-protonating buffer gases shift analyte/matrix ion abundance ratios for protonated molecules away from ratios expected based on equilibrium chemistry. This suggests the possibility of kinetic control of ion abundances. In such a model, the initial sputtering event could result in significant numbers of analyte and matrix ions being protonated by fragments and beam damage products. Subsequent collisions between analyte and matrix ions would then begin to establish normally observed equilibria. The presence of a buffer gas could reduce ion and neutral internal and kinetic energies and therefore reduce rate constants for proton transfer. This would in turn prevent establishment of equilibria before the ions were extracted from the source.

In addition to possible implications for models of sputtering mechanisms, high-pressure/FAB may have some important analytical applications. Adduct formation with sputtered neutrals may prove important in structural studies. In one example, low energy CID studies of $[mNOBA + H]^+$ and $[mNOBA + SF_5]^+$ (figure 2) show different fragmentation pathways.

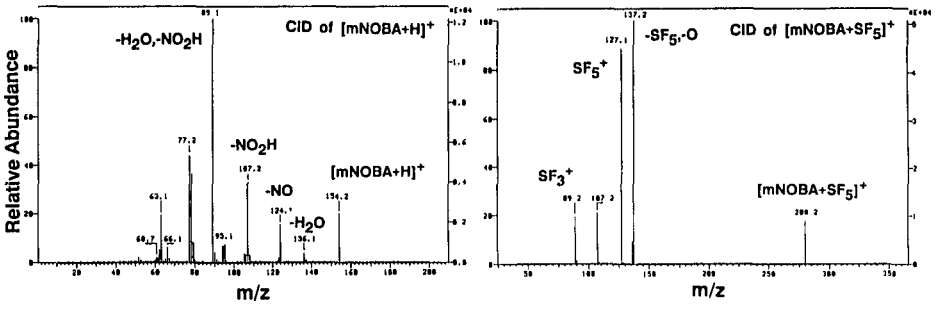

Figure 2. Low-energy CID spectra (10 eV, 1.0 mTorr Ar) of $[M+H]^+$ and $[M+SF_5]^+$ for 11 mol% mNOBA in TEA in the presence of 0.13 Torr SF_6.

The results suggested that while protonation may occur on both the nitro and alcohol groups, adduct formation appears to occur only at the nitro group. High-pressure/FAB may also prove important in improving the sensitivity for sputtered analytes such as peptides, as suggested by the effects noted above. We are currently attempting to gain a better understanding of the structural and thermochemical factors that control such variations in analyte and matrix abundances.

References

1. J.E. Campana and R.B. Freas J. Chem. Soc; Chem. Commun., 1984, 1414.
2. R.B. Freas, M.M. Ross and J.E. Campana J. Am. Chem. Soc., 1985, 107, 6195.
3. S.S. Wong and F.W. Rollgen Nucl. Inst. Methods Phys. Res. Sect. B, 1986, 14, 436.
4. J. Sunner, A. Morales and P. Kebarle Anal. Chem., 1987, 59, 1378.

Presented at the 36th ASMS Conference on Mass Spectrometry and Allied Topics
June 5-10, 1988, San Francisco, CA

THE INFLUENCE OF SURFACE EXCESS CONCENTRATION IN FAB - MS OF PEPTIDES

G. M Allmaier

Institute for Analytical Chemistry, University of Vienna,
Waehringer Str. 38, A-1090 Vienna, Austria

Over the past several years, FAB-MS has revolutionized the analysis of molecules of biological interest that are highly polar and involatile. For the analysis of peptides and tryptic peptide mixtures at first sight this method turned out to be very straightforward. But soon it became clear that matrix effects as well as suppression phenomena were of considerable importance [1,2,3,4] to obtain optimal results, because the solute is dissolved in a liquid sample support material e.g. glycerol. Therefore the physico-chemical interactions between the liquid matrix, the gas-phase and the peptide must be understood [5,6]. Especially in case of quantification of a single component and in multicomponent analysis, e.g. an unseparated enzymatic digest of a protein, are adsorption as well as competitive adsorption at the glycerol/vacuum interface important factor influencing the mass spectrometric response. The related physico-chemical parameters surface tension, surface excess concentration and critical micelle concentration of peptides in the glycerol matrix are of particular interest [7]

The surface tension of four peptides with a molecular weight range of 200 - 1400 dalton was measured at various concentrations (10^{-4}-10^{-1} moles/L) in glycerol. The model peptides showed sufficient varying hydrophobicity indices (derived from the data of J.M.R. Parker et al. [8], including increments for the free α-amino group at the N-terminus and the free α-carboxyl group at the C-terminus) within the hydrophobic range (see Figure 1.). Then the appropriate Gibbs adsorption equation [9] was used to calculate the surface excess concentration. The different surface activities of the peptides have resulted in surface excess concentrations different from the bulk peptide concentrations (as an example see Figure 2.). The differences between both concentration values were characteristic for each measured peptide, reflecting their different hydrophobicity and solubility in glycerol. The distribution of the sputtered ions has therefore reflected the nature of the glycerol matrix surface that means the three-dimensional order and its chemical composition. The mass spectrometric response of the protonated molecular ion followed the changes in surface peptide concentration. As can be seen in Figure 2., there is a straightforward correlation between the sputtering of protonated molecular ions of hydrophobic as well as hydrophilic peptides and surface excess concentration as a function of bulk peptide concentration. From these results it can be expected that the surface excess concentration of each peptide will be different in glycerol solutions of identical bulk concentration and as a consequence any differences in protonated molecular ion yields will reflect differences in surface activity of the peptides. Minor changes in the primary structure of peptides can induce large changes in surface activity and this also explains the fact besides solubility differences that some peptides exhibit extremely good mass spectrometric response, whereas other very similar peptides are hardly detected at all by FAB-MS.

This finding is in good agreement in terms of the principles of surface chemistry. The treatment is applicable, however, to single peptide/glycerol systems, because of the limitations of the Gibbs adsoprtion equation.

Acknowledgment

This work was supported by the Austrian "Fonds zur Förderung der Wissenschaftlichen Forschung" (J0055).

Presented at the 36th ASMS Conference on Mass Spectrometry and Allied Topics
June 5-10, 1988, San Francisco, CA

References

1. K.Biemann, Int. J. Mass Spectrom. Ion Phys. 45 , 183(1982).
2. M.R Clench, G V. Garner, D.B. Gordon and M. Barber, Biomed. Mass Spectrom. 12 , 355(1985).
3. G.M. Allmaier and E.R Schmid, Spectros. Int. J. 4 , 297 (1985).
4. S. Naylor, A.F. Findeis, B.W. Gibson and D.H. Williams, J. Am. Chem. Soc. 108 , 6359 (1986)
5. W.V. Ligon and S.B. Dorn, Int. J. Mass Spectrom. Ion Phys. 78 , 99 (1986).
6. C. Fenselau and R.J. Cotter, Chem. Rev. 87 , 501 (1987).
7. G.M. Allmaier, Rapid Commun. Mass Spectrom. 2 , 74 (1988).
8. J.M.R. Parker, D. Guo and R.S. Hodges, Biochemistry 25 , 5425 (1986).
9. M.J. Rosen, in "Surfactants and Interfacial Phenomena", Wiley, New York (1978).

	MWt	Hydrophobicity index
Arg Val Tyr Ile His Pro Phe Angiotensin III	930 5	1.07
Arg Pro Lys Pro Gln Gln Phe Phe Gly Leu Met-NH_2 Sub. P	1346 7	1.62
Leu Gly Gly	245.1	5.24
Gly Gly Ala	203.1	7.50 ↓ "hydrophil"

Figure 1. Amino acid sequence, molecular weight and hydrophobicity of the model peptides

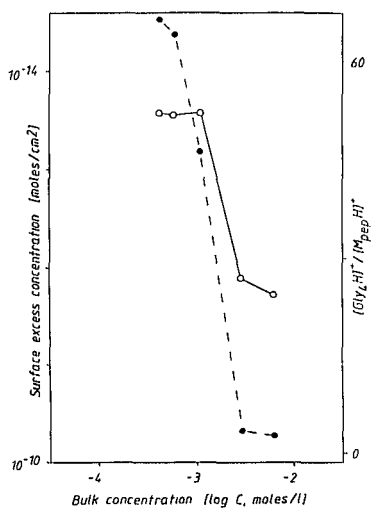

Figure 2 Surface excess concentration (o) and FAB-MS ($[MH]^+$) response (●) of substance P plotted against bulk concentration.

Presented at the 36th ASMS Conference on Mass Spectrometry and Allied Topics
June 5-10, 1988, San Francisco, CA

AN INVESTIGATION OF TETRABUTYLAMMONIUM SALTS UNDER +/- FABMS

Maya B. Kempff and Robin J. Hood
Central Instrumentation Facility
Chemistry Department
Wayne State University
Detroit, MI 48202

Alkylammonium salts are an important class of surfactants in commercial applications. More recently, they have been found[1] to be useful as liquid phases in gas chromatograph because of their low melting points and chemical stability. Various sulfonates are used as ion pairing agents in ion chromatography. In chemical synthesis, novel anions are often isolated and purified as their tetra-n-butyl ammonium salts. The mass spectral identification of this group of compounds is both interesting and challenging. This study looks at a large number of tetra-n-butyl ammonium salts to determine the best methods of analysis and to establish general rules for the interpretation of their mass spectra.

Despite their low melting points, tetra-n-butyl ammonium salts do not yield molecular ion or fragmentation information under electron impact or chemical ionization because of their lack of volatility. It has been shown[2] that fast atom bombardment mass spectrometry in both the positive ion mode and the negative ion mode are useful for obtaining information on the composition of these compounds. It has also been shown[3] that these compounds can be run successfully without a matrix. In order to better understand the conditions and results for analyzing these compounds, twenty-eight tetra-n-butyl ammonium salts were analyzed under positive and negative FAB MS with and without a glycerol matrix.

The positive ion FAB spectrum of these compounds is dominated by the tetra-n-butyl cation (242) and its fragments due to the loss of butane at mass 184 and the loss of C_3H_6 from this ion to give a peak at 142. Samples deposited directly on the probe from aqueous solution and run after evaporation of the water gave low ion intensities and only cation information. Samples run from a glycerol matrix generally showed some cluster ion of the form $[(ML)_n+M]^+$. These cluster ions were most intense in those compounds with very stable anions. For most of the compounds studied the clusters with n=1 represented one to ten percent of the base peak. This often was not sufficient for positive identification of the compound.

The Negative ion FAB spectrum of these compounds were also obtained under similar conditions. In this case, samples run without a matrix usually gave only weak base peak for the anion. The spectra obtained from glycerol was richer, with the anion as the base peak, strong cluster ion of the form $[(ML)_n+L]^-$ and usually an $[L_2+H]^-$ ion peak. Little fragment information of the anion was observed. CAD spectra using tandem mass spectrometry is necessary[4] to obtain structural information on the anion. The following mass spectra are representative of the data one obtains.

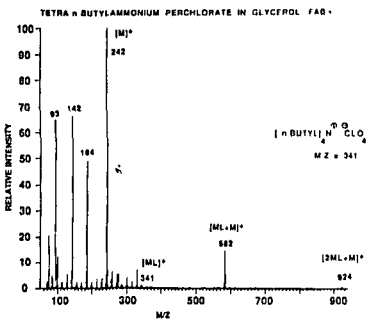

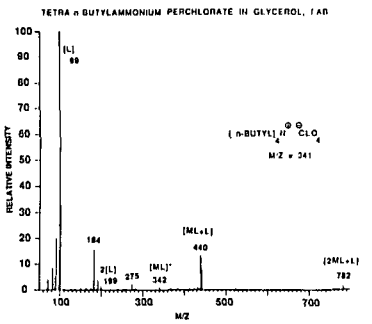

The combination of the positive and negative FAB mass spectra of the alkylammonium salts from a glycerol matrix provide a good method of identification of these compounds.

Acknowledgment

The authors wish to thank Kenneth Furton and Rena Pomaville of WSU, and Marshal Logue of Michigan Technological University for supplying the samples used in this study.

1. C.F. Poole, H.T. Butler, M.E. Coddens, S.C. Dhanesar and F. Pacholec, J. Chromatogr. 289, 299 (1984).

2. P.A. Lyon, W.L. Stebbings, F.W. Crown, K.B. Tomer, D.A. Lippstreu and M.L. Gross, Anal. Chem. 56, 8, (1984).

3. S.S.J. Ho, M.E. Coddens and C.F. Poole, Org. Mass Spectrom. 20 377 (1985).

4. S.L. Hunt, F.E. Behr, L.D. Winter, P.A. Lyon, R.L. Cerny, K.B. Tomer and M.L. Gross, Anal. Chem. 59 2653 (1987).

Presented at the 36th ASMS Conference on Mass Spectrometry and Allied Topics
June 5-10, 1988, San Francisco, CA

Molecular Ion Enhancement of Natural Products Using Salts in FAB Matrices

Pradip R. Das, Birendra N. Pramanik and Peter L. Bartner
Research Division, Schering-Plough Corp., Bloomfield, NJ 07003

The use of Fast Atom Bombardment mass spectrometry technique for the characterization of polar, non-volatile molecules has been well established. The use of matrices is an important aspect of FAB mass spectrometry [1,2] and their selection [3] can influence the intensities of the molecular and fragment ions. We have demonstrated significant enhancement of the molecular ions of various natural products with the use of KCl, NaCl or NH_4Cl in the liquid matrix. These include Everninomicin-D (an oligosaccharide antibiotic), Kijanimicin (a macrotetronolid sugar antibiotic), lactoses, phospholipids, macrocyclic and polyether antibiotics. The use of ammonium chloride in mass spectrometry to enhance ionization was originally demonstrated in these laboratories[4,5]. This report describes the use of salts in FAB MS studies.

All studies were carried out on a VG-ZAB-SE double focussing, reverse geometry instrument with a VG 11-250 data system. Xe gas at a source pressure of $2x10^{-6}$ mbar was used to produce fast atoms. Samples were dissolved in DMSO (2-5 μg/μl) to which the salt was added such that sample to salt ratio was approximately 1:4. A thin layer of glycerol/thioglycerol matrix (50:50) was applied on the copper probe tip to which the sample solution was added and thoroughly mixed. The probe was then inserted into the ion source operating at 8 kV.

Our experiences in FAB mass spectrometry have shown that some natural products produce poor mass spectral data. This could be due to the chemical nature of the compound or presence of impurities or both. We have analysed these compounds without and with salt (KCl, NaCl, NH_4Cl) addition and found a remarkable improvement in ionization with salt addition.
The addition of these salts to the FAB matrix containing the sample produced $[M+K]^+$, $[M+Na]^+$ or $[M+NH_4]^+$ ions as the base peak for compounds which otherwise displayed little or no molecular ions in their mass spectra.
Phosphatidylethanol, molecular weight 702 a.m.u., produced <1% relatively abundant molecular ion, $[M+H]^+$, under FAB condition using glycerol/thioglycerol matrix; however, with KCl addition, $[M+K]^+$ was the base peak in the mass spectrum with all characteristic fragment ions present (Figure 1).
Everninomicin-D, an oligosaccharide antibiotic, is non-volatile and difficult to ionize by MS methods[6]. Figure 2 displays the FAB mass spectra without and with NaCl addition to the matrix. $[M+Na]^+$ at m/z 1558 was the base peak whereas $[M+H]^+$ from the non-treated matrix is <20% relatively abundant.
In the analysis of Nigericin, a polyether antibiotic, the usefulness of adding various salts (KCl, NaCl and NH_4Cl) to FAB matrices in determining the molecular weight is illustrated (Figure 3). Initially, a complex spectra, difficult to interpret, was generated. Addition of salts produced very intense ions (all base peaks) which corresponded to the specific cationization of the molecule.

Our results amply demonstrate that for a variety of complex natural products, which are very difficult to ionize by the ususal glycerol/thioglycerol matrix, addition of salts enhance ionization significantly. The formation of the cationized species depends on the nature of the sample, the salt and their relative concentrations and fragmentation of an alkali metal adduct ion is sometimes different from that of a protonated ion. Based on a limited study, there was a tendency of the potassium/sodium adduct ion of some molecules to produce less fragmentation than the corresponding ammoniated ion.

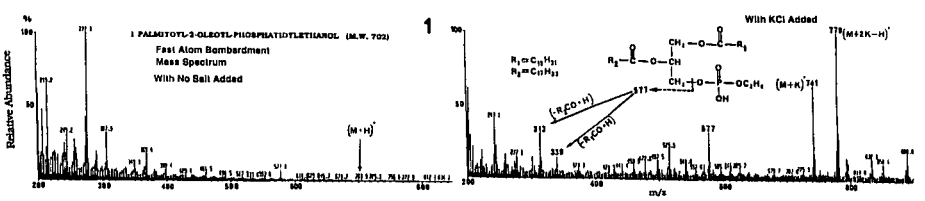

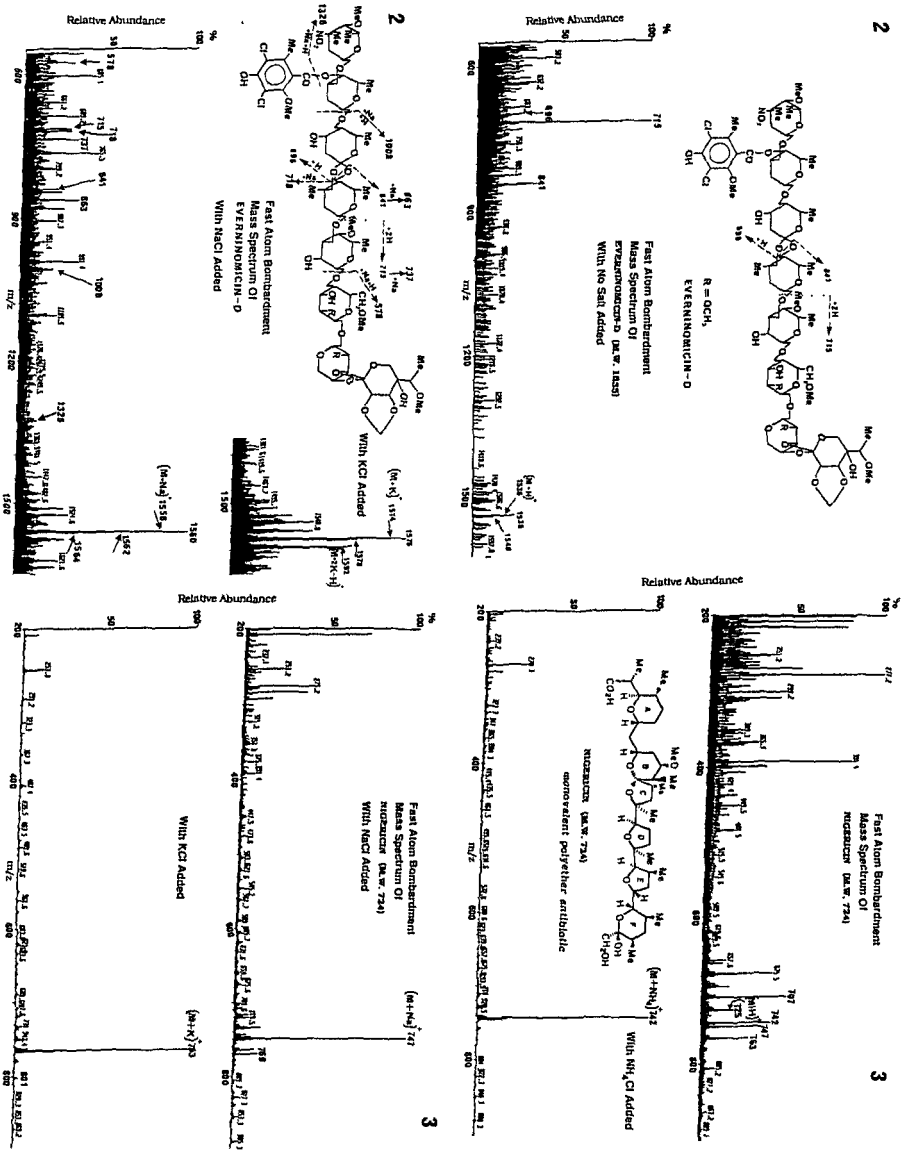

References:
1. E. DePauw, Mass Spectrom. Rev. 5, 191 (1986).
2. C. Fenselau, J. Nat. Prod. 47, 215 (1984).
3. J.L. Gower, Biomed. Mass Spectrom. 12, 191 (1985).
4. A.K. Bose, B.N. Pramanik and P.L. Bartner, J. Org. Chem. 47, 4008 (1982).
5. A.K. Bose, H. Fujiwara, B. Pramanik, E. Lazaro and C. Spillert, Anal. Biochem. 89, 284 (1978).
6. A.K. Ganguly, B. Pramanik, V. Girijavallabhan, O. Sarre and P. Bartner, J. Antibiotics 38, 808 (1985).

Presented at the 36th ASMS Conference on Mass Spectrometry and Allied Topics
June 5-10, 1988, San Francisco, CA

GLUTATHIONE AND NITROCELLULOSE: SOME OBSERVATIONS ON THE DEPENDENCE OF PEAK WIDTHS AND INTENSITIES IN PDMS SPECTRA UPON pH AND pI

L. Silly, R.J Cotter, Johns Hopkins University, Baltimore, MD 21205
C Fenselau, University of Maryland Baltimore County, Catonsville, MD 21228

Plasma desorption mass spectrometry has been used successfully to determine the molecular weights of peptides and small proteins. The recent introduction of two matrices, glutathione (1) and nitrocellulose (2), provide the advantages of improved molecular ion yield, decreased widths of peaks from which isotopically-averaged mass measurements are made and increased relative intensities of peaks from multiply charged ions.

In the present study, we have compared plasma desorption mass spectra of two proteins: bovine milk α-lactalbumin and chicken egg white lysozyme; proteins of similar tertiary structures, approximately the same molecular weights (14,176 and 14,308 amu respectively) but very different isoelectric points (pI=5 and pI=11 respectively). Two experiments are described

- In the first experiment, we have examined the pH dependence of peak width in relation to their isoelectric points. Peptide samples are dissolved in water or in aqueous solutions of glacial acetic acid and ammonium hydroxide at different concentration to achieve a range of pH 1 to 11, then deposited on nitrocellulose foils.
- In the second experiment, the two peptides are "titrated" with glutathione and electrosprayed on the sample foil.

In both cases, the peak widths of singly-, doubly-, triply-charged molecular ions form the major probe for monitoring the formation of ions with low internal and kinetic energy.

In general, for the nitrocellulose matrice, desorption appears to be more facile when solutions of peptides are prepared at pH's close to the isoelectric point. This is translated into spectra with narrow peaks and high intensities (Fig. 1,2). In fact, protein interactions with nitrocellulose are reported to involve mainly hydrophobic interactions (3,4) which are located inside the native proteins (5). This explains why the interactions between nitrocellulose and proteins will be weakest near the isoelectric point where the protein is in a native state. However at acidic pH, broader peak widths observed are due to the unfolded proteins. For these two proteins, the isoelectric point can be correlated with biological activity and stable conformation (6,7,8).

A similar observation has been made when peptides are prepared in a solution containing glutathione. The peak widths are plotted as a function of added glutathione (Fig. 3,4) and reach a minimum at a molar ratio of [30:1] for the lysozyme and of [20:1] for the lactalbumin The reduced form of glutathione has been reported to promote the refolding of peptide (9) and this suggests a relation between protein folding and binding to the sample foil.

In conclusion:

- There is a thereshold of glutathione necessary to get a good spectrum.
- The narrow peak widths are located close to the isoelectric point of proteins.
- Spectra obtained seem sensitive to the conformational structure.
- Molecular ion measurements by PDMS may become an important tool for following conformational changes in peptides.

REFERENCES

1. M.Alai, P. Demirev, C.Fenselau, R.J.Cotter; Anal. Chem. 58, 1303 (1986).
2. G.P.Jonsson, A.Hedin, P.Hakansson, B.U.R.Sundqvist, G.Save, P.F.Nielsen, P.Roepstorff, K.E.Johansson, I.Kamensky, and M.Lindberg; Anal. Chem. 58, 1084 (1986).
3. W.Lin and H Kasamatsu; Anal. Chem. 128, 302 (1983).
4. J.M.Gershoni and G.E.Palade; Anal. Chem. 131, 1 (1983).
5. C.Clothia and G.E.Palade; Anal. Rev. Biochem. 53, 537 (1987).
6. R.C.Davies, A.Neuberger and B.M.Wilson; Biochim. Biophys.Acta. 178, 294 (1969).
7. J.Saint-Blanchard, P.Chuzel, Y.Mathieu, J.Perrot,P.Jolles; Biochim.Biophys. Acta. 220, 300 (1970).
8. I.Hanssens, H.Pottel, W.Herreman and F.Van-Cauverlaert; Biochem. Biophy. Res. Commun. 119, 509 (1984).
9. P.Savena and D B.Wetlaufer; Biochem. 9, 5015 (1970).

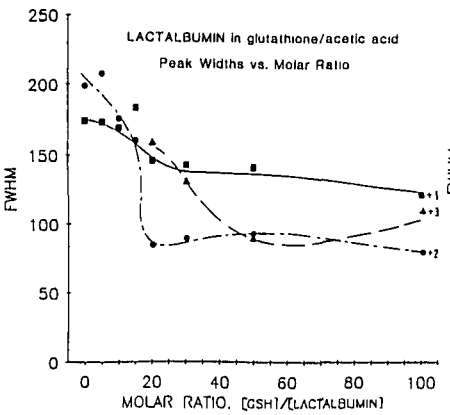

Figure 3

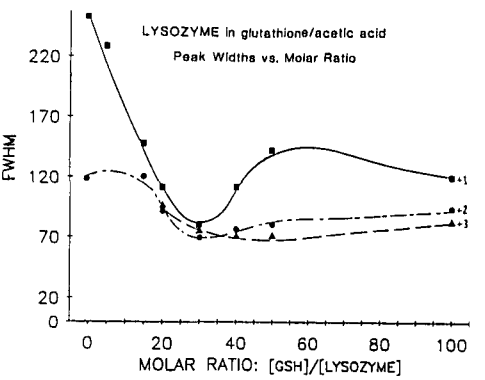

Figure 4

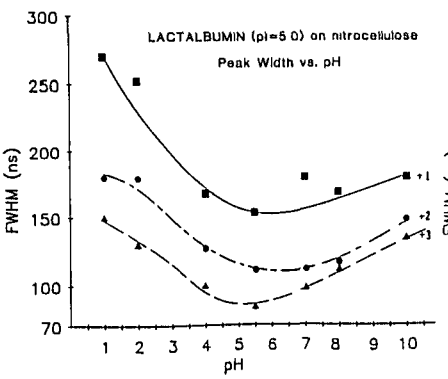

Figure 1

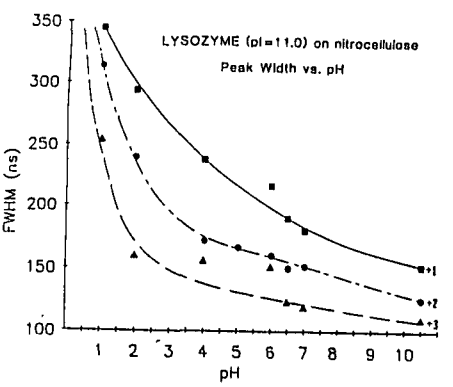

Figure 2

Presented at the 36th ASMS Conference on Mass Spectrometry and Allied Topics
June 5-10, 1988, San Francisco, CA

COMPARISON OF FAB AND Cf-252-PD MASS SPECTROMETRY FOR THE ANALYSIS OF POLAR PESTICIDE METABOLITES

G.M.Allmaier*, E.R.Schmid and P.Roepstorff+

Institute for Analytical Chemistry, University of Vienna, Waehringer Str. 38, A-1090 Vienna, Austria
+Institute for Molecular Biology, University of Odense, Campusvej 55, DK-5230 Odense, Denmark

Highly polar, water-soluble compounds are major metabolites of pesticides in various ecological systems. They are present only in low concentrations either as free acids, glycosides or mainly as alkali salts. After isolation of these polar metabolites from biological matrices (apple peels, Beta vulgaris leaves or soil) and various purification steps as solid phase extraction, TLC, reversed phase HPLC they were characterized by mass spectrometry. Until recently FD or CI mass spectrometry has been used mainly for the analysis of these metabolites, but both techniques showed severe limitations. FAB [1,2] and Cf-252-PD [3] mass spectrometry have been evaluated for the characterization of five polar metabolites of organophosphorus pesticides (Figure 1).

FAB mass spectra in the positive and negative ion mode were obtained with glycerol, triethanolamine and m-nitrobenzyl alcohol as matrix. Quasi molecular ions - $[MH]^+$, $[M-H]^-$ as well as $[MNa]^+$ and $[M-Na]^-$ - were found as dominating ions (see as an example Figure 2). In the negative ion mode the metabolites, which were preformed ions, could be detected in the ng-range. On the other hand the detection limits in the positive mode were in the µg-range. The problem of sample purification prior to MS analysis was critical especially in FAB-MS, because of suppression phenomena in the FAB matrices induced by biological matrix components. The best result for isolated metabolites in terms of S/N-ratio were obtained with m-nitrobenzyl alcohol as FAB matrix.

Positive and negative ion PD mass spectra were recorded from different sample backings. The metabolites were deposited by electrospraying on top of aluminium backing as well as by spin drying on nitrocellulose (NC) backing (with and without rinsing). The positive PD mass spectra were dominated by the cationized molecular ions on both backing materials in contrast to FAB-MS. Cluster ions as $[2MNa]^+$ or $[3MNa]^+$ can be seen with significant intensity (Figure 3). After sample adsorption on NC and subsequent rinsing all sample related ions disappeared except in case of the glycoside (III). The negative PD mass spectra exhibited as dominating ions $[M-Na]^-$. For III the PD technique failed to give an useful negative spectrum. The overall detection limit in the positive as well as negative ion mode was in the µg-range. In contrast to FAB-MS were the negative ion mode was significant more sensitive.

PD- as well as FAB-MS showed no characteristic structural fragments. In summary, both ionization techniques have great potential for the fast identification of highly polar metabolites, especially FAB-MS in the negative ion mode because of the good sensitivity.

References

1. E.R.Schmid, H.Stipsits, K.Wagner and G.M.Allmaier, Adv.Mass Spectrom., ed. J.F.J.Todd (Wiley, Chichester 1986) 1515.

2. G.M.Allmaier and E.R.Schmid, Rapid Commun.Mass Spectrom. 1, 42 (1987).

3. G.M.Allmaier, E.R.Schmid and P.Roepstorff, manuscript in preparation.

Presented at the 36th ASMS Conference on Mass Spectrometry and Allied Topics
June 5-10, 1988, San Francisco, CA

		MWt.
(I)	$R_1\text{-}S\text{-}P(=O)(SCH_3)(ONa)$	325
(II)	$R_1\text{-}SO_3Na$	263
(III)	$R_1\text{-}S\text{-}R_2$	355
(IV)	$C_2H_5\text{-}S(=O)_2\text{-}C_2H_4\text{-}S\text{-}P(=O)(OCH_3)(ONa)$	270
(V)	$C_2H_5\text{-}S\text{-}C_2H_4\text{-}S\text{-}P(=O)(OCH_3)(ONa)$	238

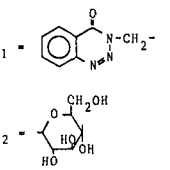

Figure 1. Structure of pesticide metabolites

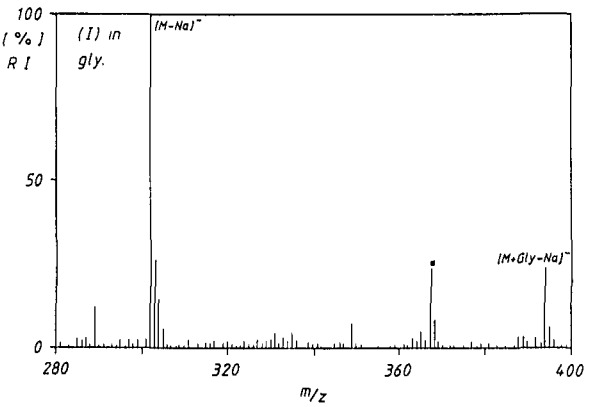

Figure 2. Negative ion FAB mass spectrum of I in glycerol

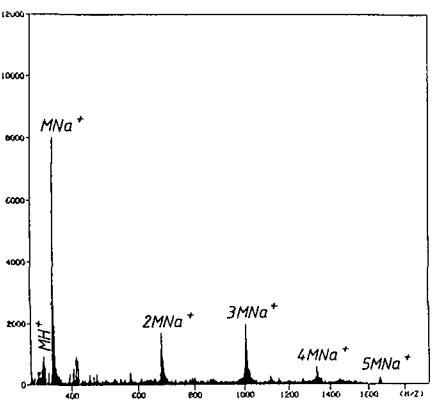

Figure 3. Positive ion PD mass spectrum of I adsorbed to nitrocellulose

Presented at the 36th ASMS Conference on Mass Spectrometry and Allied Topics
June 5-10, 1988, San Francisco, CA

ENHANCED PERFORMANCE OF A VOLCANO-FI SOURCE IN PULSED MODE

Steve Young and Michael J. Coggiola
SRI International, Menlo Park, CA 94025

A new mode of operation is described for the volcano-style field ionization source developed at SRI. Normally, gas molecules are ionized continuously in the intense electric field produced between the 25 μm diameter volcano throat and the concentric 100 μm diameter counter electrode. When used with a quadrupole mass spectrometer, the source is typically operated in a cw mode with the volcano biased at +15 volts and the counter electrode and ion extraction elements maintained at -1.2 to -1.5 kV. In the present experiments, the source was operated in a pulsed mode by reducing the bias on the counter electrode to -800 volts (below the threshold for efficient FI), and then pulsing it to -1.8 kV. The pulse width could be varied between 1 and 10 μs with the repetition rate variable between 100 Hz and 2 kHz. Mass analysis was performed either by scanning the quadrupole in the normal fashion, or by operating the mass filter in the RF-only mode, and using TOF methods in conjunction with a microchannel plate detector.

In addition to mass analysis of the ions produced by the volcano-FI source in pulsed mode, a number of other characteristics were determined. The relative ionization efficiency in pulsed mode as compared with the cw mode was assessed by alternately measuring the ion signal (using pulse counting) with a dc potential and the pulsed voltage, and correcting the latter for the duty cycle of the driving voltage. Both measurements were made with the quadrupole tuned to pass only a single ion species, typically the molecular ion of the gas sample. The temporal evolution of the field ionization signal was measured by accumulating ion counts as a function of time following the pulse using a multichannel analyzer. The MCA was gated on at the end of the counter electrode pulse, and acquired counts in 10 μs time intervals for the full 2 ms duration of the voltage pulse.

Although the absolute signal levels produced in the pulsed mode were less than the cw mode, when the signal levels were corrected for the duty factor of the counter electrode pulsing, the effective ion currents were found to increase in most cases by as much as an order of magnitude. Moreover, as the time between pulses was decreased (higher repetition rate for fixed pulse width of 10 μs), this signal enhancement also decreased, falling smoothly toward the dc level. Interestingly, the pulsed mode of operation also produced significant ion currents of many species not normally observed in the cw mode. For example, a number of water-containing molecular ions were readily observed including, H_3O^+, $H_2O{\cdot}H_3O^+$, and $(H_2O)_2^+$. The former two ions showed the same ionization enhancement observed for the organic compounds, while the latter ion was unique in that the effective signal level dropped as the time between pulses was increased. Under typical cw conditions, none of these molecular ions is observable, except at the highest counter electrode voltages.

Typical results of the signal enhancement measured in the pulsed mode are shown in Figure 1 for benzene, n-propylbenzene, and pyridine. For these three compounds, the degree of ionization enhancement varies between 2 and 25 as the time between 10 μs wide pulses increases from 0 to 10 ms. Other organic compounds investigated showed qualitatively similar behavior. Based on the apparent enhancement of ionization efficiency in the pulsed mode, it is reasonable to assume that as the time between pulses is increased, additional neutral sample molecules become adsorbed onto the active ionization sites of the volcano source. During the "on" period of the counter electrode pulse, these neutrals are desorbed either directly as ions, or as neutrals that are rapidly ionized in the strong local fields. In addition, because the rate of change of the local electric field with time is very fast (> 10^{12} V/cm/sec), it may be possible to ionize

species that would otherwise not undergo efficient FI. It is also possible that because of the long residence time of the neutrals on the active emitter sites, surface mediated reactions may occur, leading to species such as $H_2O{\cdot}H_3O^+$, and $(H_2O)_2^+$.

This simple picture of the pulsed volcano FI source would predict that the ion signal as a function of time should show an initial rapid rise as the local electric field is established in the vicinity of the field ionization sites, and the supply of adsorbed neutrals is the greatest. As the sample supply becomes depleted due to field ionization/desorption, the signal level would be expected to decay . Using the MCA as described above, the parent ion signal of pyridine (m/z 79) was measured as a function of time for a 2 ms wide ionization pulse at 10 Hz repetition rate. The arrival time spectrum is shown in Figure 2. As expected, the measured ion signal was sharply peaked at the beginning of the pulse, decaying rapidly toward the nominal dc level. This type of behavior was observed for a number of other compounds as well.

In addition to the operational characteristics described above, the relative signal enhancement factor was also found to vary with the pulse width in an unexpected manner. If the time between pulses was fixed at 2 ms, and the pulse duration was varied, the ion signal exhibited the anticipated enhancement for pulse widths greater than 4 μs. For pulse widths of less than 4 μs, the signal enhancement dropped rapidly, so that for pulse durations of 3 μs or less, the effective signal level actually fell below the cw level. This characteristic minimum width of 4 μs was found to be independent of the dc bias level applied to the volcano prior to pulsing, and does not appear to be related to the rate at which the local electric field is established. At present, the origin of this behavior is not known.

Using acetone, mass spectra were recorded in both the cw and pulsed mode for comparison with the previously reported pulsed FI results of Rollgen and Beckey [Surface Science, 23 69 (1970)]. The normal cw spectra produced using the volcano source consisted primarily of the M^+ and $(M+1)^+$ ions in a ratio of 10:1, similar to the results of Rollgen and Beckey. In the pulsed mode, this ratio was found to be approximately 1:1. The previous work also showed this ratio to change in the favor of the $(M+1)^+$ ion in accordance with the proposed mechanism of field induced proton transfer from a physically adsorbed layer of acetone molecules.

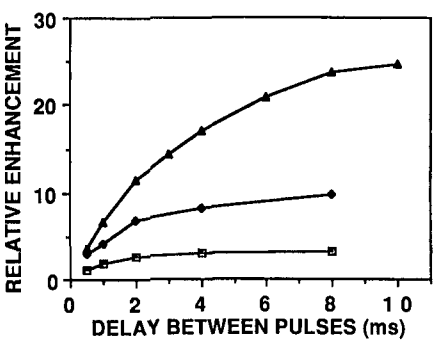

Figure 1. Variation of the ionization efficiency for benzene (—◆—), n-propyl benzene(—▲—), and pyridine (—■—) as a function of the time between 10 μs pulses.

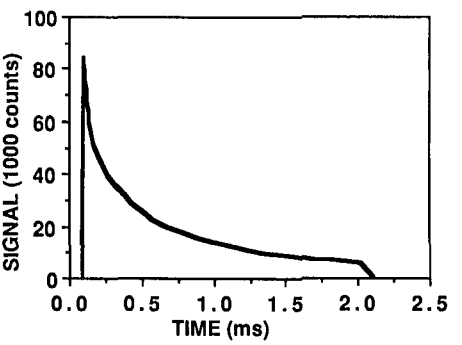

Figure 2. Temporal behavior of the parent ion (m/z 79) from pyridine ionization in the pulsed volcano-FI mode. The pulse duration was 2 ms, and the time between pulses 100 ms.

Presented at the 36th ASMS Conference on Mass Spectrometry and Allied Topics
June 5-10, 1988, San Francisco, CA

AN EHD SOURCE FOR THE MASS SPECTRAL ANALYSIS OF PEPTIDES

Terry D. Lee and Kassu Legesse
Beckman Research Institute of the City of Hope
Duarte, CA 91010

John F. Mahoney and Julius Perel
Phrasor Scientific, Inc.
Duarte, CA 91010

Electrohydrodynamic (EHD) emission is a technique in which gas phase ions are generated from a solution by a strong electrical field. As a gentle ionization process that rarely causes fragmentation, it holds great promise for the molecular weight determination of large biomolecules. The ultimate goal of the project is to develop an ion source capable of producing molecular ions for proteins and other macromolecules which are difficult or impossible to analyze by particle desorption methods. Efforts thus far have been concentrated on understanding the mechanism of ion formation, particularly from volatile solvent solutions.

Previous source designs have suffered from a number of problems including unstable emission, sample amount requirements which greatly exceeded reasonable levels for precious compounds, and cumbersome operation which hindered research efforts. A new source (Fig. 1) has been constructed that largely overcomes these limitations. Sample solutions are transported directly from sample vessels at atmospheric pressure to the end of the emitter needle using a 155 μm fused silica tube with an internal diameter of 50 μm. With a length of 30-40 cm, flow is sufficiently restricted that even with 100% methanol, pressure within the ion source housing of a JEOL HX100HF mass spectrometer is $<5\times10^{-5}$ Torr. Total volume of the feed tube is <1μℓ. The use of a continuous glass surface has largely eliminated bubbles that often form when fluid under vacuum encounters junctions and metal surfaces.

Stable emission from the source has been demonstrated for a number of ammonium acetate solutions with different methanol:water ratios. As water content approaches 75%, emission instability is observed that is likely due to ice formation caused by evaporative cooling. At the other extreme, methanol concentrations approaching 90% result in unstable emission, perhaps due to precipitation of the ammonium acetate.

The EHD emitter needle is constructed from a 1.6 mm stainless steel tube with a 175 μm hole through which the fused silica tube is inserted. Two modes of emission have been observed, depending on the location of emission sites relative to the end of the fused silica capillary. With the capillary flush with the end of the stainless steel nozzle (Fig. 2a), emission is from sites on the stainless steel nozzle somewhat remote from the capillary opening. The spectrum of a 1 M ammonium acetate solution (Fig. 3a) is dominated by acetic acid clusters, the more volatile methanol and water having largely evaporated. With the fused silica protruding ~50 μm beyond the nozzle (Fig. 2b), emission is directly from the rim of the capillary and the spectrum is dominated by water clusters (Fig. 3b).

Metastable spectra for small peptides can be obtained from 0-50% energy loss provided sufficient sample is used (>10 mg/ml). Only protonated and doubly protonated species have been observed with no fragmentation. At these sample levels, operation of the ion source is compromised by sample deposits on the tip. At lower sample levels (<1 mg/ml) source operation is stable for hours but molecular ions are often lost in the spectral background. Sample molecular ions are most prominent under conditions approaching "full energy" spectra.

Presented at the 36th ASMS Conference on Mass Spectrometry and Allied Topics
June 5-10, 1988, San Francisco, CA

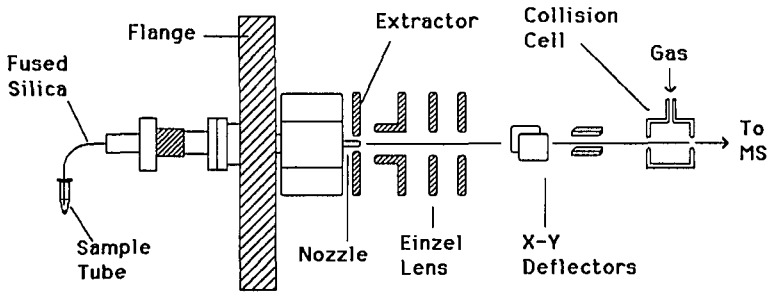

Fig. 1

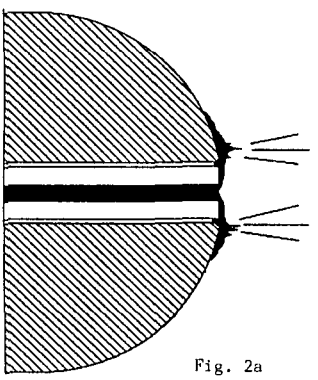

Fig. 2a

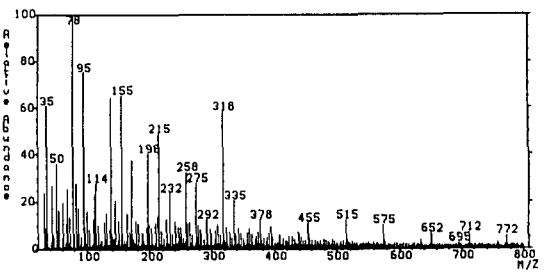

Fig. 3a

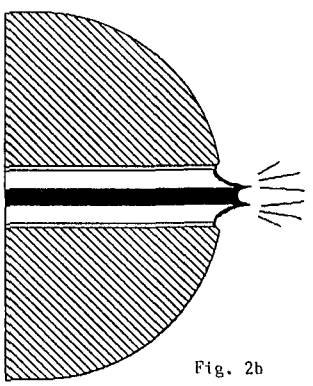

Fig. 2b

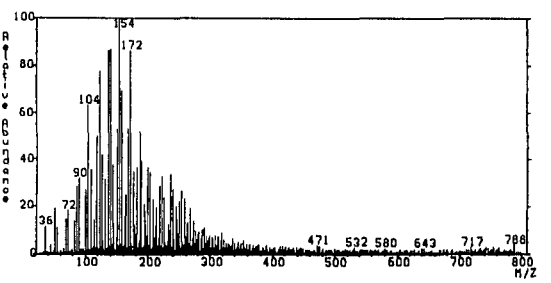

Fig. 3b

EHD spectrum of 1 M ammonium acetate in methanol:water (50:50). ESA=5KV, Source=7KV, Extractor=-2KV. Upper spectrum obtained with capillary flush with the nozzle. Lower spectrum taken with capillary extending approximately 50 μm beyond the nozzle.

Presented at the 36th ASMS Conference on Mass Spectrometry and Allied Topics
June 5-10, 1988, San Francisco, CA

RECENT DEVELOPMENTS IN ELECTROCHEMICALLY ASSISTED FAST ATOM BOMBARDMENT

John E. Bartmess, Department of Chemistry, University of Tennessee, Knoxville TN 37996-1600, and Larry Phillips, Office of Biologics Research and Review, Food and Drug Administration, Bethesda MD 20892.

Electrolysis directly in a thin glycerol drop inside the MS source creates ions, from species which are not ionic to start with, and are normally poorly responsive to FAB MS. We have placed a cage of wires over the top of the "cell", to reduce source detuning effects due to varying the internal disk electrode by up to ±12 V; the outer ring electrode and cage float at the source voltage. The ions sampled are mostly due to processes at the ring electrode, nearest the surface of the matrix.

Since FAB is a surface phenomenon, and ionic surfactants are among the most sensitive compounds to conventional FAB, we have examined <u>non-ionic surfactants</u> for their response to EFAB. Vitamin K1 is chosen as a typical case, due to its long phytyl tail and easily reduced quinone head. As models for the reducible head group, 1,4-benzoquinone (BQ) and 2-methyl-1,4-naphthoquinone (MeNQ) yield negative ion FAB mass spectra whereas 9,10-anthraquinone (AQ) and vitamin K_1 do not. The negative FAB mass spectra of BQ and MeNQ show abundant M^- but with substantial "chemical noise" throughout each spectrum. Reduction processes, giving $(M+H)^-$ corresponding to p-hydroxyphenoxides, also occur. No $(M+2H)^-$ ions are observed; these are not expected to be bound anions. Ions due to simple fragmentations are not observed in either case.

Under EFAB conditions in glycerol, reducing at the ring electrode, BQ and MeNQ still show abundant M^- ions, but with less $(M+H)^-$ and significantly less "chemical noise" in the mass spectrum. In fact, M^- increases considerably, while $(M+H)^-$ and chemical noise remain nearly constant. Ions due to simple fragmentations are not observed in either case. 9,10-Anthraquinone remains resistant to analysis under EFAB conditions.

Vitamin K_1 in glycerol gives only ions due to the matrix in normal negative FAB. Under reducing EFAB conditions, the matrix ions are almost completely suppressed; the predominant ions are m/z 450 (M^-) and m/z 185, from cleavage of the phytyl tail at the benzylic site. Oxidizing EFAB conditions gives more low weight (m/z <100) ions. At V_e = -7.2 V, the intensity of the $[2G-H]^-$ ion at m/z 183 is comparable to that of the m/z 185 fragment. For V_e <-7.2 V, m/z 185 increases in intensity, but not m/z 183.

There is a mass spectral response time to changes in the EFAB voltage. For BQ, both rise and fall of M^- intensity, on application and removal of the reducing potential, has a half-life of ca. 20 sec. The process appears to be reversible over many cycles. For Vitamin K_1, however, the response time is on the order of minutes, presumably due to its reduced diffusion rate. With K_1 in glycerol on a conventional FAB probe, a 9 V battery was connected to two wires, then the wires were placed in either side of the FAB droplet on the probe for a few seconds. Insertion of the FAB probe into the instrument immediately, followed by signal acquisition, resulted in a spectrum typical of the EFAB ones, decaying to a glycerol-like spectrum over several minutes.

We have noticed gradual changes in the electrochemical current drawn by the EFAB probe as pure glycerol ages in the vacuum system. We observe an increase in the conductivity of the glycerol at V_e=-2 V as the probe is warmed in an oven. After FAB bombardment, a similar increase with temperature is observed but at about half the conductivity pre-bombardment. This difference appears to be due to surface aging; if the glycerol drop is stirred after bombardment, and then warmed again, data very close to the pre-bombardment values are obtained. The time response of the current when the probe is bombarded indicates about 1 minute of apparent <u>cooling</u> occurs before the current levels off. After this, a small long-term rise occurs over 10-15 minutes. The change amounts to less than 1°C increase in glycerol temperature.

Presented at the 36th ASMS Conference on Mass Spectrometry and Allied Topics
June 5-10, 1988, San Francisco, CA

OPTIMIZING THE IR-LASER DESORPTION OF NEUTRAL MOLECULES.

R. C. Beavis, J. Lindner, J. Grotemeyer and E. W. Schlag

Institut für Physikalische und Theoretische Chemie, TU München
Lichtenbergstr. 4, D-8046 Garching, Germany.

In order to use Infra-Red (IR) laser desorption of intact neutral molecules (LEIM) coupled with multiphoton ionization (MUPI) as an analytical technique, it is necessary to develop a standard, reliable method of preparing thermolabile organic samples for desorption. Simply applying a powdered sample to a probe will produce a spectrum, but only from relatively large amounts of sample. The goal of the research described here was to understand the parameters that affect IR desorption and with this knowledge, develop an "optimized" sample preparation technique.

The approach taken to examine these parameters was to modify the physical properties of the sample by the addition of a "matrix" substance. For the IR laser used (10.6 μm, CO_2 multimode, 25 μs pulse width and about 10^4 W/cm^2), most organic compounds are relatively transparent. Therefore, the first experiments were done to determine the effect of adding an IR absorbing material to the sample. The absorbers used were inorganic salts (e.g. $Na_{3-x}H_xPO_3$, x=0-2) and some organic materials (e.g. ribose). The results demonstrated that adding IR absorbing materials decreases the yield of neutral molecules and completely extinguishes the yield at high concentration. This effect is probably caused by the high temperatures produced at the surface of an absorber.

The opposite was found for IR transparent materials. Inorganic transparent matrices (e.g. KBr, NH_4NO_3) were found to increase the total yield of neutral molecules by up to 100x. Also the stability of the signal was increased, i.e. the IR laser could shoot on one spot of the sample (about 10 μm thick) for many more shots before the yield per shot decreased. For a dipeptide, the increase in the number of shots possible on one spot was approximately 50x. The increase in yield and sample stability can be explained by the increased mechanical stability of the sample when bound to the surface by a transparent matrix. Rapid heating of powdered samples leads to rapid expansion and expulsion of large diameter (about 1 μm) particles of intact sample. This loss of sample by purely mechanical removal is minimized by binding the sample to the probe with a matrix that is unaffected by the IR laser.

The results using IR transparent inorganic matrices led to using organic IR transparent materials, specifically polyethylene, which has a transmission window in the 940 cm^{-1} region. Polyethylene powder can be pressed into thin, strong sheets by applying a moderate pressure (100 MPa). Mixing the sample of interest with the polyethylene powder and pressing the mixture produced uniform small sheets that were stable under IR desorption conditions. The addition of small amounts of metal powder (1 μm diameter Au or Ag) to these sheets increased the yield and reliability of these sheets. Very thermolabile organo-metallic compounds that produced no intact molecules by IR desorption from powders produced strong signals from these polyethylene sheets. Also, a sheet pressed from polyethylene and metal powder could be used as a desorption substrate, i.e. a small amount of sample could be applied to the sheet from solution. This technique made it possible to decrease the amount of sample necessary to produce a good mass spectrum to 1 ug of total sample applied to the probe.

The improvement in total yield and reliability of samples prepared using powder empregnated polyethylene sheets can be explained using a "mechanical" model of the desorption mechanism. Current ideas on fast particle and UV desorption of ions from surfaces point towards the strong mechanical disruption of a surface, by either a shock wave [1] or a phase explosion [2]. Such an idea can also be applied to low power IR desorption of neutrals and particularly to the case of polyethylene/metal powder sheets with a very thin sample overlayer. Without the metal powder, the yield of neutrals from the surface is very low. When the metal powder is added, the individual metal particles heat very rapidly in the IR laser focus because of currents induced by the laser electric field. The particles become incandecent and cause rapid local expan-

sion of both the polyethylene host matrix and nearby soluted gas in the sheet. This expansion leads to a miniature explosion that expells the hot metal particle from the sheet. These glowing particles can be seen as a plume leaving the sheet during IR irradiation. The explosion disrupts the surface and expells part of the surface layer into the gas phase. Therefore, the IR energy is being absorbed a site remote from the sample molecules of interest. During the desorption process for such a composite material, the molecules only recieve translational energy from the shock of the explosion and not directly from the laser. Producing desorption in such an indirect manner means that changes in the physical properties of the sample molecules are of decreased importance because the desorption mechanism is largely independant of the sample molecule involved. This method of producing gas phase molecules is particularly applicable to the use of MUPI, because the matrix has been chosen so as not to appear in the mass spectrum, i.e. the MUPI process is such that polyethylene produces no interference peaks.

ACKNOWLEDGEMENTS.

The authors would like to thank dem Bundesministerium für Forschung und Technologie, der Deutschen Forschungsgemeinschaft and Bruker Franzen, Analytik (Bremen) for supporting this work. R.C.B. was supported by a NATO PDF Research Grant.

REFERENCES.

[1] I.S. Bitensky and E.S. Parilis; Nucl. Instrum. Meth.; B21, 26 (1987).

[2] J. Sunner, M.G. Ikonomou and P. Kebarle; Int. J. Mass Spectrom. Ion Processes; 82, 221 (1988).

Presented at the 36th ASMS Conference on Mass Spectrometry and Allied Topics
June 5-10, 1988, San Francisco, CA

Resonance Enhanced Multiphoton Ionization of Nucleosides and Oligonucleotides

David M. Lubman and Liang Li
Department of Chemistry
The University of Michigan
Ann Arbor, MI 48109-1055

The study of nucleosides has presented a great challenge to mass spectrometry due to the polarity and thermal lability of these molecules. In this work we use a pulsed laser desorption/volatilization technique as a means of vaporizing neutral nucleosides (1,2). The resulting plume is then entrained in a pulsed supersonic jet expansion of Ar or CO_2 and swept into a TOFMS for detection by resonance enhanced multiphoton ionization (REMPI). This method allows the separation of the vaporization from the desorption step so that REMPI of neutrals can be performed. The REMPI method has several distinct advantages including: (a) an efficient means of softly ionizing molecules to produce $M^{+\cdot}$; (b) a means of producing controllable fragmentation based upon either laser intensity or frequency; and (c) a wavelength selective means of ionization in combination with the supersonic jet technique (2).

The experimental apparatus consists of a standard supersonic beam/time-of-flight mass spectrometer (1). The desorption is produced using a pulsed CO_2 laser (7×10^6 W/cm^2) which impinges upon a Macor™ probe surface. Typically ~ 10-100 ug of the nucleoside is placed on the surface or may be dissolved in a glycerol matrix which provides a more even pulse-to-pulse desorption stability. The desorbed material is entrained in a jet of CO_2 as shown in Figure 1 and carried into a linear TOFMS. Laser induced REMPI is then produced using the 4th harmonic of a Nd:YAG laser (266 nm) and the ions detected in the mass spectrometer.

The laser desorption/laser REMPI method was used to study adenosine, guanosine and cytosine as well as their various modified nucleosides as shown in Table I for the adenosine analogs. These results were obtained at λ = 266 nm and a $P = 8 \times 10^6$ W/cm^2. The salient feature of the mass spectra observed under these conditions is an intense molecular ion peak without the presence of cationization. In addition, there is generally one principal fragment observed due to bond cleavage at the sugar moiety. This fragment denoted BH^+ corresponds to an ion formed from the base portion of the nucleoside with transfer of one hydrogen atom from the sugar moiety. This process is also observed in EI mass spectra of these compounds. The molecular ion peak, along with the characteristic BH^+ peak, can be used to distinguish between ribose and deoxyribose sugars in the nucleoside.

In addition, two characteristic fragments due to cleavage of the sugar moiety are observed which are denoted as S_1 and S_2 respectively as shown in Figure 2. These fragment ions are particularly useful for structural analysis and easily allow the ability to pinpoint whether there is modification on the 2'-oxygen of a nucleoside. As Table 1 indicates, the mass spectrum of 2'-deoxyadenosine shows a strong molecular ion peak m/z 251 and a fragment BH^+, m/z 135. The mass difference between $M^{+\cdot}$ and BH^+ suggests that it is a deoxyribose. Two fragments, m/z 162 and m/z 164, corresponding to S_1 and S_2 notation, respectively, can be used to locate the deoxy position, i.e. the 2'-position in this case. Or for example, in 3'-o-methyladenosine, S_1 and S_2 fragments indicate that there is no methyl substitution on the 2'-oxygen. Consequently, the methyl group must be in either the 3'-oxygen or 5'-oxygen. The formation of S_1 and S_2 in REMPI appears to be similar to EI in which an intramolecular rearrangement of the H from the sugar to the base occurs during fragmentation. These S_1 and S_2 fragments are easy to detect using REMPI as opposed to FAB where their presence may be obscured due to matrix background. In these experiments the glycerol matrix is transparent to the UV laser light and is not observed in the TOFMS.

(1) Tembreull, R.; Lubman, D. M. Anal. Chem. 1987, 59, 1082.
(2) Li, L.; Lubman, D.M. Appl. Spec. 1988, 42, 418.

Presented at the 36th ASMS Conference on Mass Spectrometry and Allied Topics
June 5-10, 1988, San Francisco, CA

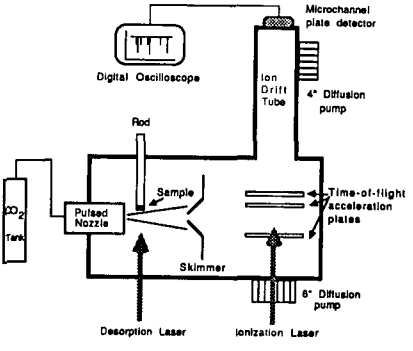

Figure 1. Schematic of the experimental apparatus.

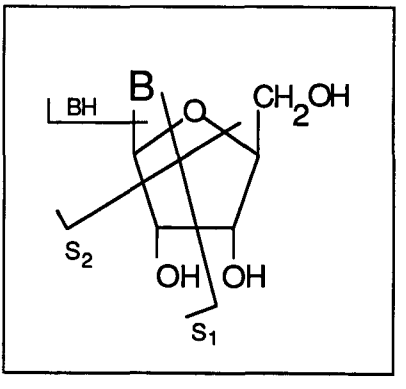

Figure 2. Major ions observed for the nucleosides using laser desorption/ laser ionization technique at 266 nm.

Table I Mass Spectral Fragmentation Patterns of Adenosine analogs

	Compound	M/Z (rel int %)						
		M	S_1	S_2	BH	119	108	others
1	Adenosine	267(43)	178(19)	164(33)	135(100)	119(29)	108(38)	
2	2-Deoxyadenosine	251(42)	162(15)	164(23)	135(100)	119(17)	108(45)	
3	N^6-Methyladenosine	281(51)	192(17)	178(24)	149(100)	119(40)	108(24)	
4	N^6-Methyldeoxyadenosine	265(40)	176(17)	178(18)	149(100)	119(30)	108(23)	
5	1-Methyladenosine	281(42)	192(16)	178(18)	149(100)			
6	N^6,N^6-Dimethyladenosine	295(100)	206(7)	192(14)	163(50)	119(16)	108(5)	148(38),134(69),121(20)
7	3-o-Methyladenosine	281(50)	178(5)	164(32)	135(100)	119(16)	108(19)	147(11)
8	$1,N^6$-Ethenoadenosine	291(99)			159(100)			132(21),105(39)
9	2,6-Diaminopurine-2'-deoxyribosine	266(61)	177(7)		150(100)		108(18)	134(10)
10	N^6-Furfuryladenosine	347(88)			215(100)	119(62)	108(50)	
11	N^6-(2-Isopentenyl)adenosine	335(100)			203(47)	119(73)	108(39)	188(43), 160(34), 135(46)
12	Puromycin Aminonucleoside	294(77)	206(9)	192(35)	163(100)	119(23)	108(77)	222(9), 148(38), 134(47), 121(18), 114(6)

Presented at the 36th ASMS Conference on Mass Spectrometry and Allied Topics
June 5-10, 1988, San Francisco, CA

Analysis of Organic Solids by Combined Stimulated Desorption and Single-Photon Ionization

J. B. Pallix, U. Schühle and C. H. Becker
Chemical Physics Laboratory
SRI International
Menlo Park, California 94025

Secondary ion mass spectroscopy (SIMS) has long been recognized as a highly sensitive surface analytical tool. SIMS spectra from the surfaces of bulk polymers generally contain useful ion peaks but strong structurally important peaks such as the monomer are frequently lacking. Observation of monomer peaks of significant intensity is extremely useful for easy and unambiguous interpretation of mass spectra especially in investigations of unknown materials. Also for SIMS, both positive and negative spectra are sometimes required for successful analyses, and the desorption is limited to sputtering. An obvious solution to these problems is to detect secondary neutrals because neutral species comprise more than 90% of the material removed from a surface by ion beam sputtering, electron beam desorption or laser desorption. This way the various desorption processes can be studied or chosen from.

A technique recently developed at SRI called surface analysis by laser ionization (SALI), has successfully provided both high sensitivity and reliable quantitation in analyses of a wide variety of inorganic materials [1]. With this method neutral species removed from surfaces by the various desorption methods are typically ionized by an intense untuned uv laser and the photoions are then analyzed by reflecting time-of-flight mass spectrometry. A high power excimer laser is typically used which permits nonselective ionization of all two-photon ionizable neutral species within the laser focal volume, greatly reducing matrix effects.

The use of a high power untuned uv laser is essential to obtain the desired sensitivity and quantitation attainable for inorganic samples. However, when using nonresonant multiphoton ionization (MPI) for studies of surfaces of organic materials (which required high sensitivity) excessive fragmentation can occur resulting in mass spectra containing only small fragments giving no useful information. An experimentally simple alternative to MPI is to use vacuum uv wavelengths for single-photon ionization with photon energies not far above the molecular ionization potential. A number of bulk organic polymers and biochemicals have been studied by this method resulting in fragment mass spectra which are highly characteristic of the parent molecular structure [2-3].

The spectra to be presented are obtained using coherent 118 nm (10.5 eV) radiation for ionization of desorbed neutrals. The VUV photons were generated by tripling the third harmonic from a 10 Hz Nd:YAG laser (355 nm) in a Xe tripling cell. The frequency conversion process is enhanced by phase matching with a Xe/Ar gas mixture.

Some fragmentation may still be observed with the single photon ionization method although this is significantly less than when using MPI. This is due largely to the ion bombardment process rather than the ionization step. Less fragmentation has been observed when using electron stimulated desorption (ESD). SALI spectra of a sample containing a blend of poly(isopropene) (PI rubber), and poly(phenylcarbonate) (PPC) obtained by single-photon ionization following ion beam sputtering and ESD are shown in Figures 2a and b, respectively. A large reduction in fragmentation is seen by comparison of the ion beam

sputtering and ESD spectra which shows that the latter results in greater signal in the higher mass region. Note, for example, the dramatic change in intensity of the CH_3 peak at 15 amu. This lower fragmentation desorption process when combined with single-photon post-ionization is clearly valuable for studies of organic materials. Using the relatively soft VUV photoionization provides insight into the nature of bond-breaking for different desorption processes.

The peak at largest mass in the ion beam sputtering mass spectrum of the polymer blend sample (Figure 1a) is that of the PPC monomer at 254 amu. While this and other high mass peaks are weak relative to the low mass fragments they are still quite useful for determining molecular structure. A more extensive analysis was easier using ESD (Figure 1b). The peaks at high mass in the spectrum correspond to the PPC monomer (±2 hydrogen atoms) at 252 and 256 amu and the PPC monomer + CO + 2 hydrogen atoms at 284 amu. Two progressions are observed (labeled with solid circles) which correspond to the addition of $(CH_n + (CH_2)_m)$ fragments to CO_2 and CO_3. The series of peaks labeled with arrows beginning at m/z = 77 correspond to fragments containing phenyl. The progression represented by ▼ is that originating from the PI polymer (protonated monomer observed at 69 amu) showing the loss or addition of CH_2.

References

1. Pallix, J. B.; Becker, C. H.; Newman, N. Materials Research Society Bulletin, 1987, Vol. XII, No. 6, 52.
2. Pallix, J. B.; Schühle, U.; Becker, C. H., Anal. Chem., submitted.
3. Schühle, U.; Pallix, J. B.; Becker, C. H. J. Am. Chem. Soc. 110, 1988, 2323.

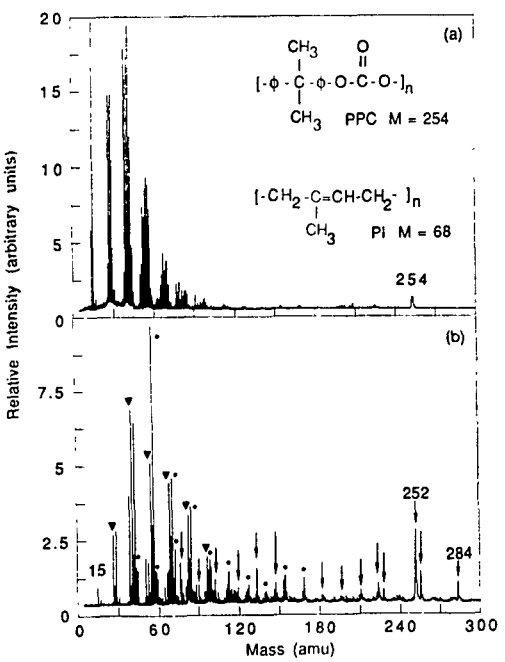

Fig 1. SALI spectra of a combined poly(phenyl-carbonate) (PPC) and poly(isopropene) (PI) sample obtained by single-photon ionization of ion beam sputtered neutrals (a) and neutrals removed by electron stimulated desorption. ↓, •, and ▼ represent fragment peaks originating from PPC and PI, respectively.

Presented at the 36th ASMS Conference on Mass Spectrometry and Allied Topics
June 5-10, 1988, San Francisco, CA

INITIAL KINETIC ENERGY OF LARGE MOLECULES DESORBED BY Cf-252 FISSION FRAGMENTS

D. L. Jacobs and R. D. Macfarlane, Department of Chemistry
Texas A&M University, College Station, Texas 77843

A time-of-flight mass spectrum contains information relating to the initial kinetic energy that an ion receives in the desorption process. Every ion peak is shifted to slightly lower TOF due to this initial energy. If the TOF spectrum is obtained at a very low acceleration voltage, the resulting TOF distribution for each ion peak is dominated by the initial kinetic energy, which can then be calculated for each peak in the spectrum. For this TOF distribution to be usable, it must be well resolved from peaks in the spectrum due to other ions of similar mass and the detection efficiency must be great enough to produce a peak for the ion of interest. These two requirements limit the practical application to small mass ions, i.e. < 500 amu, even though the use of Cf-252 fission fragments is primarily used for the desorption of very large molecules.

However, it is possible to indirectly calculate the initial kinetic energy of ions with a mass > 500 amu. The normal method used to calibrate a TOF spectrum is to take two or more peaks in the spectrum with accurately known masses and use them to generate a calibration curve of TOF vs. $m^{1/2}$ using the method of least squares. This does have the flaw of assuming that all of the ions have the same kinetic energy. An attempt was made to improve the calibration curve for a peptide sample by correcting for the initial kinetic energy. The initial energy for a series of calibration ions (Fig. 1) from the same target as the peptide is measured directly at low acceleration voltages (+800 V). The same target is then run at an acceleration voltage (+17 kV) that is sufficiently high enough to give a strong peak and good TOF value for the molecule of interest (Fig. 2). The initial KE values for the calibration ions are then used to calculate the TOF shift expected due to the initial energy for these ions at high voltage. The TOF values corresponding to E=0 are then used to generate a new calibration curve for any ion in the spectrum with E=0 as shown in table 1. This new calibration curve is then used to a TOF for the molecule of interest at E=0. The difference between this calculated TOF and the experimental TOF should be due solely to the initial kinetic energy of the molecule. This change in TOF can be used to calculate a KE value for the molecule as shown in table 2.

Two peptides, bradykinin (1060.23 amu) and bovine insulin (5733.61 amu), have been examined. These two peptides have been adsorbed onto nitrocellulose. The effect of the conductivity of the substrate has been examined by sputter coating the targets with Au. The results are summarized in table 3.

All of the calculations for the initial kinetic energy were made using absolute tiem-of-flight. A schematic of the the mass spectrometer used is shown in Fig. 3 and the fixed mass spectrometer parameters are shown in table 4. The TOF equation that describes the flight path is shown below.

$$TOF = K\sqrt{\frac{m}{|q|}}\,\frac{a_1\left(\sqrt{|E_0| + sign(q)(U_0 - U_1)} - \sqrt{|E_0|}\right)}{sign(q)(U_0 - U_1)} + K\sqrt{\frac{m}{|q|}}\,\frac{d}{2\sqrt{|E_0| + sign(q)(U_0 - U_1)}} + K\sqrt{\frac{m}{|q|}}\,\frac{a_3\left(\sqrt{|E_0| + sign(q)(U_0 - U_4)} - \sqrt{|E_0| + sign(q)(U_0 - U_3)}\right)}{sign(q)(U_3 - U_4)}$$

The schematic shows that the stop detector is on a movable mount that allows the length of the field free region to be varied. By measuring the TOF of various calibration ions at two different lengths of the field free region, it is possible to reduce the TOF equation to a form that allows calculation of the effective acceleration voltage at the target face, no matter what the magnitude is. This is shown below.

$$U_0 = \left(\frac{1}{2}K\sqrt{\frac{m}{|q|}}\,\frac{\Delta x}{\Delta t}\right)^2$$

Presented at the 36th ASMS Conference on Mass Spectrometry and Allied Topics
June 5-10, 1988, San Francisco, CA

Fig 1 CALIBRATION IONS

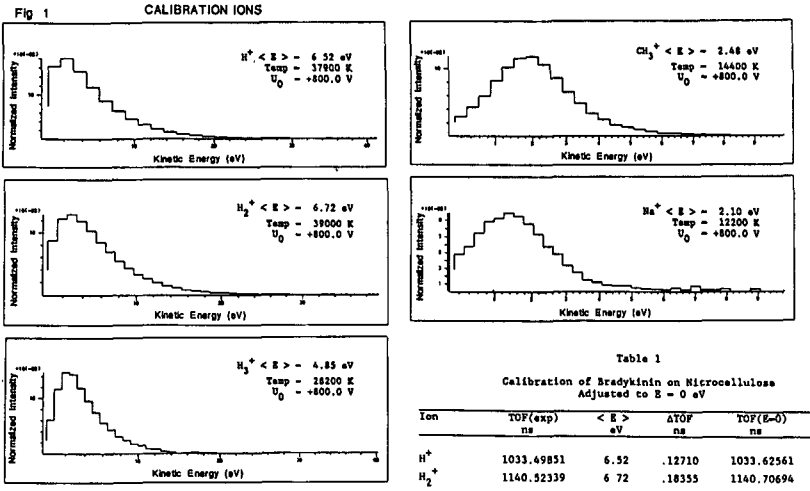

Table 1

Calibration of Bradykinin on Nitrocellulose
Adjusted to E = 0 eV

Ion	TOF(exp) ns	< E > eV	ΔTOF ns	TOF(E=0) ns	σ ns
H^+	1033.49851	6.52	.12710	1033.62561	.00013
H_2^+	1140.52339	6 72	.18355	1140.70694	.00037
H_3^+	1222 60732	4.85	.18010	1222 78742	00103
CH_3^+	1772.65836	2.48	.25917	1772.91753	.00045
Na^+	2009.12991	2.10	.28864	2009.41855	00027

Calculation	Slope	Y-intercept
normal calibration no weighting	257.35094 ±.00728	775 19328 ±.02162
adjusted calibration statistical weighting	257.39066 ±.00382	775.30241 ± 00890

Fig 2

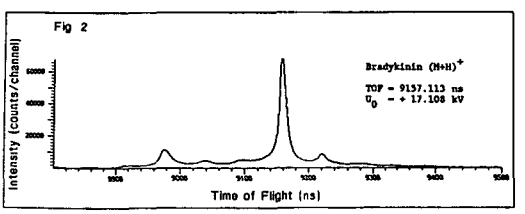

Table 2

Kinetic Energy of Bradykinin
on Nitrocellulose

Compound	Bradykinin
Ion	$(M+H)^+$
Mass	1061.24049 amu
Substrate	Nitrocellulose
TOF (E=0)	9160.237 ns
TOF (exp)	9157.113 ns
ΔTOF	3.124 ns
< E >	4.32 ±0.26 eV

Table 3

Initial Kinetic Energy of Desorbed Proteins

Substrate	Bradykinin	Bovine Insulin
Nitrocellulose	4.32 ±0.26 eV	5.86 ±0.44 eV
Au/Nitrocellulose	3.68 ±0.62 eV	4.55 ±0 93 eV

Fig. 3 SCHEMATIC OF TIME OF FLIGHT MASS SPECTROMETER

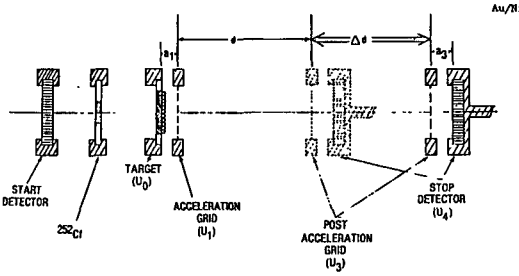

Table 4

Parameters for Kinetic Energy
Analysis of Large Molecules

Parameter	Value
T_{offset}	775 3284 ns
a_1	3 68 mm
U_0	+800.0 V or +17.108 kV
d	450 89 mm
a_3	11 10 mm
U_4	-2.200 kV

Presented at the 36th ASMS Conference on Mass Spectrometry and Allied Topics
June 5-10, 1988, San Francisco, CA

Parent Mass Information From Sequences of Peaks of Multiply Charged Ions

Matthias Mann, Chin Kai Meng and John B. Fenn

Department of Chemical Engineering
Yale University, New Haven, CT 06520-2159

As reported in our companion paper Electrospray (ES) ionization can produce intact ions from large biomolecules in solution and deliver them to a mass analyzer in vacuo. Moreover, these ions are characterized by a high degree of multiple charging so their spectra can be obtained with a quadrupole analyzer whose nominal upper limit for m/z is 1500. Such spectra comprise a series of peaks each of which differs from its neighbor by a single unit charge (see fig. 1). We report here on two different algorithms that we have developed and incorporated into our data acquisition program in order to recover as much information as possible from these spectra.

Algorithm I. For any value of parent mass M the measured peak location (m/z values) A_i and the corresponding number of charges n_i must satisfy: $A_i / A_k = n_k / n_i$. If A_i and A_k are adjacent (i.e. $n_k = n_i + 1$) we immediately obtain for the number of charges: $n_i = A_k / (A_i - A_k)$. From this expression we can assign preliminary values of n_i to each peak and then plot A_k / A_i versus n_i . Any systematic deviation from the correct value given by the first relation indicates a "bad" peak due to background noise or another species or to an incorrectly assigned value of n_i . Figure 2 shows such a plot for the spectrum of myoglobin (fig. 1). With this procedure we can quickly and unambiguously determine the number of charges corresponding to each peak and whether a given peak belongs in the series. The individual peak locations can then be used to determine the parent mass M by means of: $M=(1/n)\,(\Sigma_i A_i * n_i)$. It follows that this procedure reduces the uncertainty in M by a factor $\sqrt{n}$. For example, in the hypothetical case of M= 30kD, n=9 and individual peak errors of 0.1D at m/z=1000, the error would be 10D or 0.03%. It should be pointed out, however, that, because of the limited resolution of the quadrupole we used,we can not yet be certain that we are observing purely protonated peaks.

Algorithm II. We make use of the fact that the function

$$F(M^*) = \sum_i f\left(\frac{M^*}{i}\right) \quad i \in N$$

where f is the measured spectrum, has a maximum at $M^* = M$. At that point all the contributions from measured peaks in the sequence are summed up to produce a quasi molecular mass peak. At ideal resolution, the "deconvoluted" spectrum would have small "side peaks" close to M and oscillate with a period of M/2. With finite resolution these side peaks become enhanced and a non-zero background induces a slope into F because the measured spectrum is sampled more often at higher M^* . As long as the shapes of the peaks in the series are similar (i.e. the same shape and same full width at half maximum (FWHM)), the transformed "molecular peak" can be shown to retain this shape.

Figure 3 and 4 show the transformed myoglobin spectrum (fig.1). The FWHM of 1.6% is about what would be expected on the basis of the FWHM of the measured multiplet peaks (1.7%). The value of the algorithm is particularly apparent in figure 6 where it easily resolves two components (myoglogin and cytochrome C) of a mixture which are not easily separated in the original spectrum (fig.5).

Presented at the 36th ASMS Conference on Mass Spectrometry and Allied Topics
June 5-10, 1988, San Francisco, CA

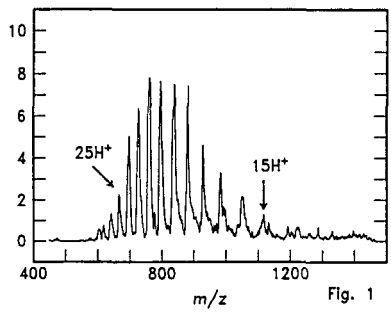

Fig. 1

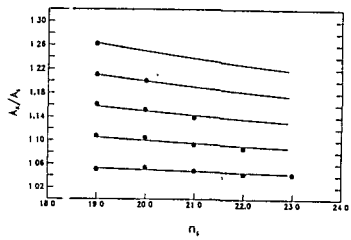

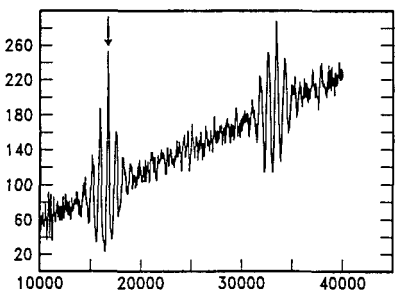
Fig. 3

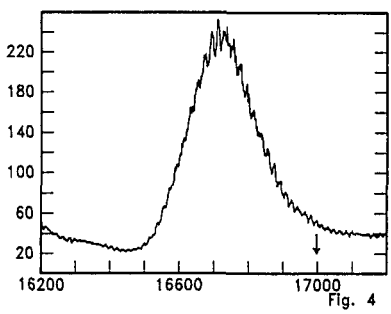
Fig. 4

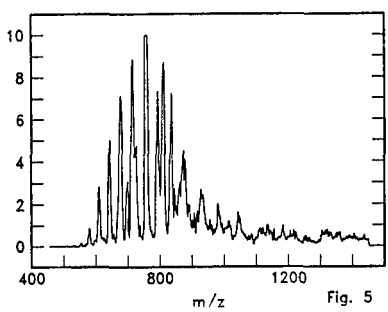

Fig. 5

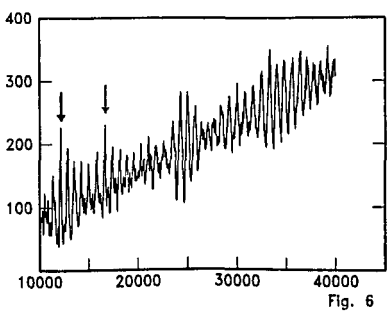
Fig. 6

Presented at the 36th ASMS Conference on Mass Spectrometry and Allied Topics
June 5-10, 1988, San Francisco, CA

SPUTTERING YIELDS FROM GLYCEROL BOMBARDED WITH IONS FROM A FOCUSED LIQUID METAL ION COLUMN

L.F. Jiang, E. Barofsky, and D.F. Barofsky
Department of Agricultural Chemistry
Oregon State University, Corvallis, Oregon 97331

We have previously reported on measuring total yields of secondary particles from liquid, organic substrates by a direct gravimetric method in which the irradiation dose was maintained constant [1] and by a differential gravimetric approach in which the irradiation dose was varied [2]. Our estimates of total particle yields from pure glycerol, bombarded by 3-5 keV indium ions, were determined by the direct gravimetric technique to be in the range of 1,000-3,000 [1]; these yields are two to three orders of magnitude higher than those generally observed from metals in the same energy range. At least one other laboratory has since reported results, which were obtained by an in situ optical method, that are comparable to ours [3-5].

Determinations of total yields based on gravimetric measurements are subject to gross, systematic errors due to evaporation losses, exchanges of volatile materials (e.g. H_2O and MeOH) with the atmosphere, ill-defined or misjudged equilibrium states used as standard states for taking readings, and inaccuracies in calibration. Although a variable-dose or differential method for determining total particle yields reduces the uncertainties due to systematic errors, random sample losses still result from bumping when the sample is exposed to vacuum. Gravimetric techniques are also very time consuming and labor intensive. Indirect in situ methods, such as that of Wong et al. [3-5], incur inaccuracies in estimating and using average evaporation losses and in calibration.

In this study we have taken advantage of the microscopic imaging capability of a finely focusing liquid metal ion column to make direct in situ measurements of mass-losses due to evaporation and sputtering and thereby improve the accuracy of total yield measurements from glycerol. The experimental arrangement consists of a commercial (FEI Corporation), focusing liquid metal ion (LMI) column attached to the FAB-port of a single focusing magnetic sector instrument (Hitachi RMU-6E). Positive ion beams of Ga, In, Sn, Au, and Bi were delivered into 10-25 μm diameter spots on glycerol targets (~40 nL balls) at current densities ranging from 0.1-1.0 mA cm^{-2} and at energies ranging from 10-28 keV. Using an octupole/stigmator (incorporated into the LMI column) to raster the beam over the target, a small electron multiplier located in the vicinity of the sample, and a Tektronix Model 606A display monitor, the apparatus was made to function as a scanning ion microscope and micrographs of the sample probe and its surroundings were recorded at 1-500X. The method used to perform total particle yield measurements is illustrated in Fig. 1.

The total secondary particle yield in a given sputtering experiment is simply the ratio of the number of sputtered molecules (sputtering loss) to the number of primary particles that strike the sample (dose). Doses were determined from measurements of the primary beam current, the bombardment time, and the system's geometry. Sputtering losses were determined from measurement of ball diameters directly off scanning ion micrographs recorded at regular intervals during the course of a sputtering run. The micrographs were accurately calibrated at a given magnification from images of a wire mesh placed exactly in the same position as the sample balls. The second ball permits control for evaporation and other extraneous factors that can affect the yield calculations. This procedure is operationally simpler and more accurate ($\lesssim$ 25%) than previous methods for sample loss determination.

We have determined total particle yields for glycerol as a function of mass (Fig. 2) and energy (Fig. 3). Fig. 4 shows this data combined into a single plot of total particle yield versus momentum. The linear character of the data may be accidental due to the limited energy range; nonetheless, the advantage of using primary ions of the highest combined mass and energy

possible (within the range studied) is obviously increased sputtering yields. Single ion monitoring of secondary ions (glycerol and selected oligopeptides) indicates that ion yields follow, though not linearly, the same trend as do the neutral yields.

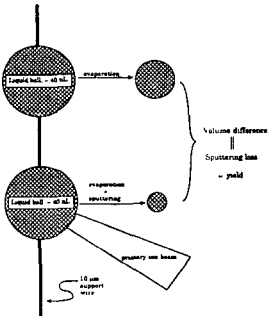

Figure 1.

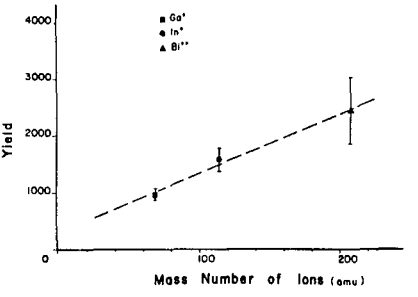

Figure 2.

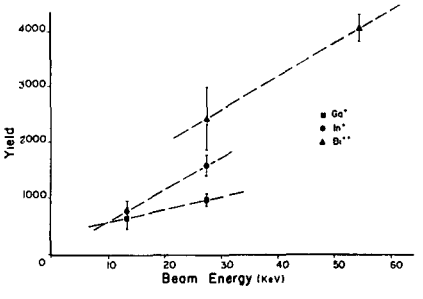

Figure 3.

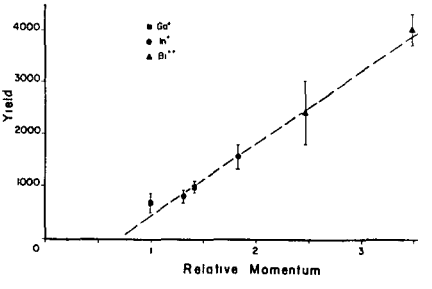

Figure 4.

Acknowledgement. Support for this work was provided by NIADDK Grant AM36050.

References.

1. D.F. Barofsky, A.M. Ilias, E. Barofsky, and J.H. Murphy, 32nd Annual Conference on Mass Spectrometry and Allied Topics (San Antonio, 1984), Bound Volume, p. 182.
2. D.F. Barofsky and E. Barofsky, in Ion Formation from Organic Solids IFOS III; A. Benninghoven, Ed.; Springer-Verlag: Berlin, 1986; p. 86.
3. S.S. Wong, F.W. Röllgen, I. Manz, and M. Przybylski, Biomed. Mass Spectrom. 12, 43 (1985).
4. S.S. Wong, K.P. Wirth, and F.W. Röllgen, in Ion Formation from Organic Solids IFOS III; A. Benninghoven, Ed.; Springer-Verlag: Berlin, 1986; p. 91.
5. S.S. Wong and F.W. Röllgen, Nucl. Instrum. Methods Phys. Res. B14, 436 (1986).

Presented at the 36th ASMS Conference on Mass Spectrometry and Allied Topics
June 5-10, 1988, San Francisco, CA

ALKALINE EARTH SALTS AS CATIONIZATION AGENTS IN LASER DESORPTION FOURIER TRANSFORM ION CYCLOTRON RESONANCE MASS SPECTROMETRY

Donald E. Bracken and Thomas J. Nizolek

New Jersey State Department of Health, Trenton, New Jersey 08625

The exposure of humans to toxic chemicals in the environment and the workplace may cause the formation of metabolites and adducts of DNA, RNA, and Proteins which can lead to undesirable health effects and genetic mutations. A laser desorption mass spectrometric (LDMS) technique, that is being applied to the analysis of these thermally labile and polar xenobiotics, uses metal ions generated from metal foils or directly from salts. These metal ions, which attach to the analyte to form cations, include elements from Groups 1 [1] and 3 [2] and some transition metals [3]. Studies of the Group 2 elements (alkaline earth metals) for their potential as "cationization" agents appear not to have been made.

Presented here are some of the preliminary results of an investigation of the salts of Mg, Ca, Sr, and Ba for their potential as cationization agents in LDMS. Using a Tachisto Model 216 pulsed CO_2 laser (10.6 um) interfaced to a Nicolet FTMS-2000 Fourier transform mass spectrometer, mass spectra were obtained for the individual hydrated chloride salts and several organic compounds. The laser desorption mass spectrum of barium chloride, Figure 1, is qualitatively representative of the chlorides of calcium and strontium also. In addition to the interesting singly-charged metal ions, the formation of the hydroxo- and chloro- metal ions appears to be characteristic of the elements. Magnesium, however, gave no evidence for the formation of AOH^+ or ACl^+ (where A is an alkaline earth element) but did "form" the mono- and diaquo- singly-charged metal ions. These observations are summarized in Table 1. The ability of magnesium to retain at least a partial hydration sphere may be due to its high charge density.

Data that illustrate cationization of an organic compound by an alkaline earth ion are presented in in Figure 2. The major peak at m/z 302 is the pseudomolecular ion resulting from the attachment of a barium ion to a molecule of 7-methylguanine, a component of a DNA adduct. Apparently, the loss of a hydrogen (proton?) accompanies the metal ion attachment. A striking aspect of the spectrum is the pseudomolecular ion cluster with additional peaks at m/z 301,300,and 299. These clusters can aid in the location and identification of the peudomolecuar ion.

Glucose, although not shown here, similarly not only produces a cluster of attachment ions with barium at m/z 317 but also undergoes a hydrogen loss. Insufficient data for a variety of compounds presently precludes any generalization on the hydrogen loss.

At this point it is clear that the alkaline earth chlorides can act as cationization agents in LDMS. Also, the particular suitability of barium chloride arises because it can provide the following features:

(1) a large mass separation of the pseudomolecular ion from fragment and barium background species
(2) pseudomolecular ion clusters
(3) internal calibrants
(4) the least deliquescence of the alkaline earth chlorides.

1. Shomo, R. E., II; Verdun F. R.; Marshall,A. G; Proceedings of the 35th ASMS Conference on Mass Spectrometry and Allied Topics, 1987, p. 938.
2. Chowdhury, A. K.; Wilkins, C. L.; Int. J. Mass Spectrom. Ion Proc. 82 (1988) 163.
3. Forbes, R. A.; Lech, L. M.; Freiser, B. S. Int. J. Mass Spectrom. Ion Proc. 77 (1987) 107.

Presented at the 36th ASMS Conference on Mass Spectrometry and Allied Topics
June 5-10, 1988, San Francisco, CA

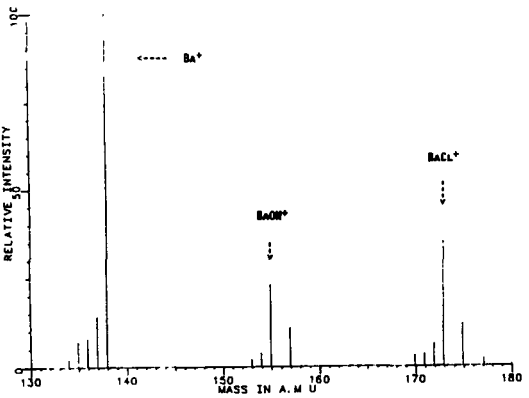

FIGURE 1. LASER DESORPTION MASS SPECTRUM (LDMS) OF BARIUM CHLORIDE

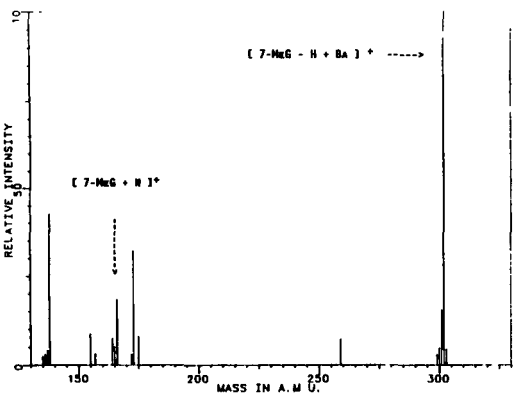

FIGURE 2. LDMS OF 7-METHYLGUANINE (7-MeG) + BARIUM CHLORIDE

TABLE 1. PRINCIPAL SPECIES OBSERVED IN THE LASER DESORPTION MASS SPECTRA OF THE ALKALINE EARTH CHLORIDES

A	A^+	$[A + OH]^+$	$[A + Cl]^+$	$[A + n\ H_2O]^+$
Mg	x			x (n = 1 and 2)
Ca	x	x	x	
Sr	x	x	x	
Ba	x	x	x	

Presented at the 36th ASMS Conference on Mass Spectrometry and Allied Topics
June 5-10, 1988, San Francisco, CA

WHAT HEATING RATES AND FINAL TEMPERATURES ARE REQUIRED FOR DESORPTION OF THERMALLY LABILE MOLECULES? INSIGHTS FROM THE DESORPTION/IONIZATION TECHNIQUE, K^+IDS (K^+ IONIZATION OF DESORBED SPECIES); Karen J. Light, Daniel B. Kassel, John Allison, Department of Chemistry, Michigan State University, East Lansing, MI 48824

The K^+ Ionization of Desorbed Species (K^+IDS) is a desorption/ionization technique that has been presented for the analysis of thermally labile compounds.[1,2] A thermionic emitter (K^+ aluminosilicate composition) is built onto the end of a modified direct insertion probe. This emitter is then positioned inside the ion source of a mass spectrometer such that, when the emitter is resistively heated, a large flux of K^+ ions is formed in the ion source. To produce a K^+IDS mass spectrum, a thermally labile compound is placed on top of this emitter. A rapid increase in temperature causes the analyte to desorb into the gas phase. When K^+ ions and neutral species are present in the gas phase concurrently, K^+ adducts form which produce the K^+IDS mass spectrum.

With the original probe design, described previously[1], sample was placed directly onto the emitter, which led to a poor temporal overlap of sample desorption and K^+ emission. There exists a time lag for K^+ ion production. During this lag time, the analyte was experiencing sufficient heating that most of it desorbed before K^+ emission commenced, and thus was undetected. A new probe design was developed to improve this overlap[3]. This design added a second sample support filament, spatially separated from the emitter, that was only radiatively heated. This produced a slower heating of the surface on which the sample was placed and thus delayed sample desorption to provide a better overlap with K^+ emission. This new probe design did not change the resultant K^+IDS mass spectra significantly and therefore was implemented.

Recently, temperature studies have been performed to determine the conditions, i.e. heating rates and final surface temperatures, necessary for desorption of thermally labile compounds, and subsequent production of K^+IDS mass spectra. A typical plot of how the temperature of the emitter and sample wire surface changes as a function of time once current is applied to the emitter is shown in Figure 1. Combining this temperature/time data with mass spectral data, the temperature of the metal wire surface at the time of sample desorption can be determined. The thermally labile compounds we are currently interested in have molecular weights below 1000 amu. Three such compounds were chosen for this study: tristearin, sucrose and hexaglycine. For these "fragile" compounds the temperatures required for desorption were between 150-170°C. This can be seen in Figure 2 for tristearin, where the onset of sample desorption (scan 16) corresponds to a sample wire temperature of 165°C. The rate of heating of the support filament surface was much lower than originally anticipated when compared to most other D/I techniques that truly utilize rapid heating (e.g., laser desorption). Typical heating rates of the second filament wire were on the order of 15°C/s.

---

1. D.B. Bombick, J.D. Pinkston and J. Allison, Anal. Chem., 56, (1984) 396.

2. D. Bombick and J. Allison, Anal. Chem., 59, (1987) 458.

3. D.B. Kassel and J. Allison, Biomed. Env. Mass Spectrom., in press.

Presented at the 36th ASMS Conference on Mass Spectrometry and Allied Topics
June 5-10, 1988, San Francisco, CA

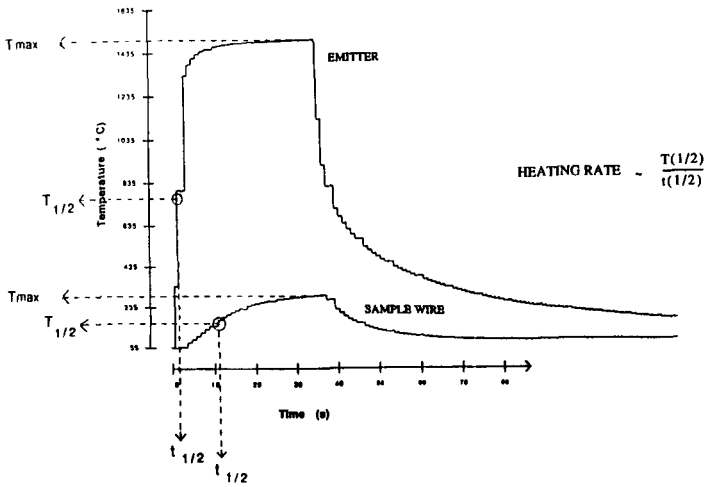

Figure 1. Emitter and Sample Wire Temperatures vs. time
Current applied = 3.0 A

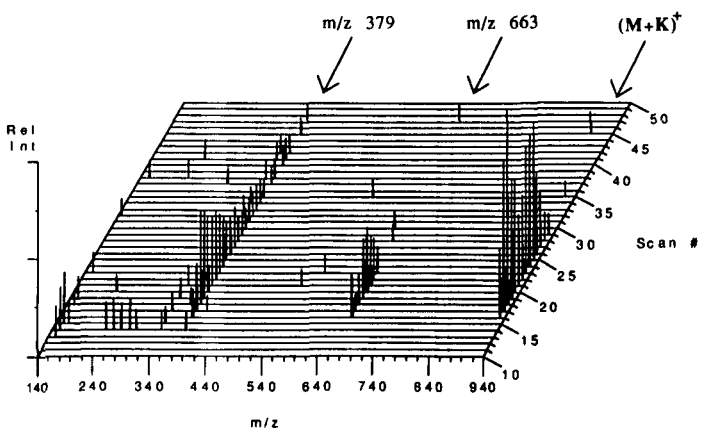

Figure 2. Tristearin on sample support wire. At scan #10, 3.0 A is applied to the emitter. K^+ emission begins at scan #12 [T(emitter) = 800°C]. Sample desorption is first observed at scan #16, as indicated by the $(M+K)^+$ ion at m/z 939. At scan #16, T(emitter) = 1500°C, and T(sample support) = 165°C.

Presented at the 36th ASMS Conference on Mass Spectrometry and Allied Topics
June 5-10, 1988, San Francisco, CA

EFFECTS OF ION PAIRING ON DESORPTION IONIZATION SAMPLING EFFICIENCIES

Johnny D. Reynolds and Kelsey D. Cook, Department of Chemistry, University of Tennessee, Knoxville, TN 37996-1600.

To the extent that preformed ions play an important role in matrix assisted desorption mass spectrometry, ion pairing in solution could be expected to reduce sampling efficiencies for singly charged ions via neutralization. For multiply charged ions, charge reduction (not neutralization) may actually increase the sampling efficiencies by decreasing solvation interactions, thereby decreasing the potential barrier for the removal of the ion from its matrix. In electrohydrodynamic mass spectrometry (EHMS), this effect could be offset to some extent by a corresponding reduction in interactions with the applied extracting field due to the net charge reduction.

As a test for assessing the balance between these effects, a diquat, $[(CH_3)_3\text{-}N\text{-}(CH_2)_5\text{-}N\text{-}(CH_3)_3]^{2+}$ $2I^-$, was used to measure the dependence of ion paring (P) and sampling efficiency (S) on counterion identity for a series of counterions (Table 1). P and S are defined in Equations 1 and 2:

$$(1) \quad P = I_{AX}1+ \; / \; I_A2+$$

$$(2) \quad S = \frac{(I_A \; / \; C_A)}{(I_R \; / \; C_R)}$$

where I = intensity and C = concentration for A (analyte), R (reference), or AX (ion pair). P and S follow the same trend, suggesting that reductions in S due to ion pairing are more than offset by the effects of reduced solvation.

Table 1

Counter Ion	P	S
acetate	0.13	39.8
nitrite	0.75	49.6
perchlorate	0.87	75.6
chloride	4.28	84.3
nitrate	5.44	116.8

These results are pertinent for resolution of a question remaining from an earlier study of sampling efficiency in a homologous series of quats, $[H(CH_2)_n]_4\text{-}N^+$ for n = 1-5. In that study, S increased up to Q4 (n = 4) because of expected decreases in ion-solvent interactions with increasing quat size. However, the intensity of Q5 was anomalously low. The suppression of Q5 was attributed to mass transport effects, but could also be expected if the intensity of Q5 was reduced due to ion pairing. In light of the data in Table 1, the choice of the chloride counterion in the earlier study may have been a poor one since chloride pairs extensively. We have now repeated that study with the acetate counterion, anticipating that any ion pairing induced suppression would be reduced. Instead, even more severe suppression occurred; now both Q4 and Q5 were suppressed (Table 2).

Table 2: S for Quat Series.

	Chloride	Acetate	Nitrite
Q1	0.36	0.45	0.34
Q2	0.84	0.98	0.84
Q3	0.99	1.21	0.96
Q4	1.00	1.00	1.00
Q5	0.67	0.70	0.72

Measurement of the solution viscosities (Table 3) provided an explanation for the results obtained with acetate counterion. As was the case with Li^+ in the earlier study, the acetate ion induces increased solvent structure, thereby increasing the solution viscosity and increasing the mass transport bias that arises from the relatively slow diffusion of the bulkier quats. When the experiment was repeated using the (low-pairing) nitrite ion, results similar to those for chloride ion were obtained (Table 2). Although ion pairing effects can be substantial, in this case each quat seems to be affected in the same manner.

Table 3

Counterion	Viscosity (Glycerol = 1)
Acetate	1.25
Nitrite	1.10
Perchlorate	1.01
Chloride	1.12
Nitrate	1.05

Presented at the 36th ASMS Conference on Mass Spectrometry and Allied Topics
June 5-10, 1988, San Francisco, CA

AUTONEUTRALIZED SF_6^- FOR FAST NEUTRAL BEAM FT/ICR MASS SPECTROMETRY

Ronald E. Shomo, II,# James E. Delmore,@ Anthony D. Appelhans,@, David A. Dahl,@, and Alan G. Marshall#

#Dept. of Chemistry (and Dept. of Biochemistry)
The Ohio State University
120 W. 18th Avenue
Columbus, OH 43210

@Idado Nat'l Engineering Laboratory
EG&G
P.O. Box 1625
Idaho Falls, ID 83415

SF_6^- can be formed in high abundance by attachment of low-energy electrons in the presence of crossed **E** and **B** fields. Acceleration of SF_6^- through a potential of 2.5–28 kV produces a tightly focused ion beam (~0.5 mm circular cross-section). During their ~1 m transit toward a target, about 1/3 of the SF_6^- ions autoneutralize (~10 μs average lifetime[1]) back to neutral SF_6 and an electron:

$$SF_6^- \rightarrow SF_6^- + e^-$$

Because the electron mass is so small, the SF_6 fast neutral beam (FNB) remains tightly focused, and any undissociated SF_6^- and electrons can be removed by passage between charged deflector plates positioned in front of the target.[2]

We have constructed an SF_6 fast neutral beam external ionization source and interfaced it to a Nicolet FTMS-1000 Fourier transform ion cyclotron resonance mass spectrometer, as shown schematically in Figure 1. The beam current is ~5×10^{-12} A, with a circular cross-section of ~0.5 mm diameter. A homebuilt orthorhombic trapped-ion cell was constructed from 400 mesh, with 2" transverse plate separation and 3" separation between the two (end) trapping plates. An electron filament was attached to the cell to confirm its satisfactory conventional FT/ICR performance, and the filament was then removed to permit passage of the fast neutral beam.

FT/ICR - NEUTRAL BEAM SCHEMATIC

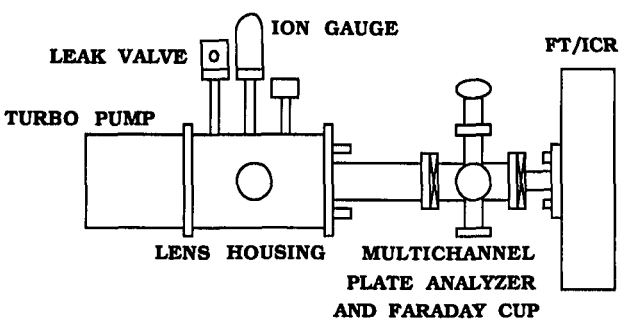

Figure 1. Schematic diagram of fast neutral beam ion source and interface to the ion trap of a Nicolet FTMS-1000 FT/ICR mass spectrometer.

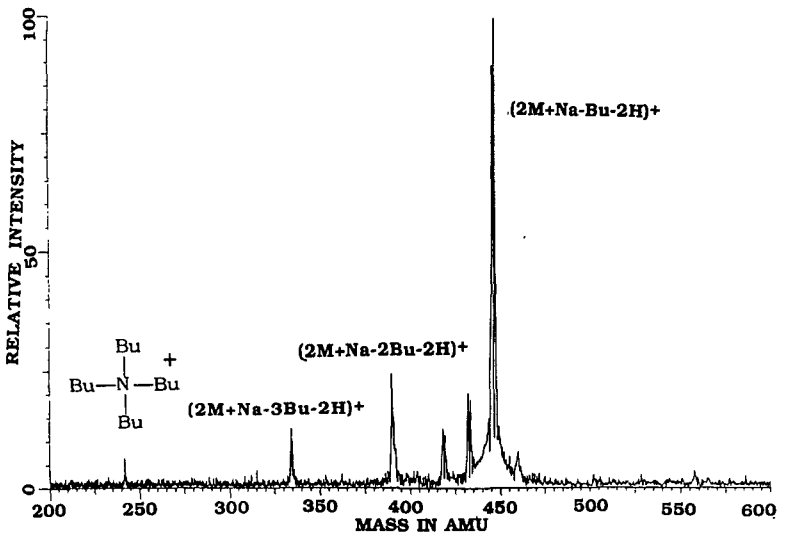

Figure 2. Single-scan FT/ICR spectrum produced by SF_6 fast neutral beam bombardment of evaporated tetrabutylammonium bromide. The molecular ion is at m/z 242, and cluster ions are evident at higher m/z.In contrast to normal pulsed-source operation, in which the signals from many separate pulsed-source experiments are added together, the neutral beam source (10 keV accelerating voltage) was left on continuously for 600 s, and then turned off so that the accumulated ion population could be excited and detected once by FT/ICR. Thus, signal-averaging is effectively continuous rather than discrete.

We are currently engaged in two kinds of systematic comparisons: (a) between FT/ICR and quadrupole mass analyzers for the FNB source; and (b) between FNB and fast atom bombardment as a means for ionizing involatile species. Compared to FAB, the FNB source offers the obvious advantage (in the ICR case) that the neutral beam can be focused and aimed from 2 m away. Moreover, since no liquid matrix is needed for the FNB experiment, FNB should offer an advantage similar to laser desorption for analysis of mixtures of chemically dissimilar species.

This work was supported by grants (to A.G.M.) from the U.S. Public Health Service (N.I.H. GM-31683), the National Science Foundation (8721498), and The Ohio State University. J.E.D. was supported by DOE Office of Health and Environmental Research (#4AA901).

1. Delmore, J. E.; Appelhans, A. D. *J. Chem. Phys.* **1986**, *84*, 6238-6246.
2. Appelhans, A. D.; Delmore, J. E.; Dahl, D. A. *Anal. Chem.* **1987**, *59*, 1685-1691.
3. Delmore, J. E.; Appelhans, D. A.; Shomo, R. E., II,; Dahl, D. A. Biomed. Environ. Mass Spectrom., in press.

Presented at the 36th ASMS Conference on Mass Spectrometry and Allied Topics
June 5-10, 1988, San Francisco, CA

CHEMICAL IONIZATION MASS SPECTROMETRY WITH USE OF LITHIUM ION ATTACHMENT TO MOLECULE

Toshihiro Fujii, Miyoshi Ogura and Hitoshi Jimba

National Institute for Environmental Studies
Tsukuba, Ibaraki 305, JAPAN

Recently a large number of literature have appeared concerning the gas phase chemistry of alkali ions with organic molecules which has been often observed in low energy ionization process. Alkali ions such as Na^+ form adduct ions (also refered to as cationized molecular ions) of the type $(M+Na)^+$.

In general, cationized molecules are more stable than radical molecular ions or protonated molecules. The fragmentation of the polar molecules resulting from a cationization by alkali ions, has a higher activation energy than splitting off functional groups after a protonation. Cationization is therefore an interesting tool for the determination of molecular weights. The important question is the feasibility of using the advantages of cationization for the CIMS as a new ionization method.

The purpose of this study is to construct an optimized Li^+ ion source (LIS), to report response and performance characteristics of acetone and to demonstrate the LIS as a new sensitive ionization source for CIMS. The present system employs the thermionic alkali ion emitter in flow of nitrogen buffer gas and high pressure mass spectrometry with ion counting.

EXPERIMENTAL The developed CIMS is shown in Fig. 1, which is the modification of the apparatus originally prepared by Shimazdu corporation for an atmospheric pressure ionization/ mass spectrometry combination study in our laboratory. The components are lithium ion source sampling interface, vacuum system, electrostatic ion lens system, quadrupole mass spectrometer (QMS), and ion detection system.

Lithium Ion Source (LIS). Shown in Fig.2 is a schematic diagram of the LIS and ion optics. The LIS consists of a lithium ion emitter, reaction chamber, and repeller. Lithium ions are emitted from the lithium ion emitter which is a small mineral bead fused to 0.1 mm diameter Pt filament wire. The bead is prepared with a thoroughly grounded mixture of Li_2O: Al_2O_3 : Si_2O in a 1 : 1 : 1 molar ratio for Li^+ alkali ions.

Sampling Interface. The sample gas from the aperture of cone impinges on the skimmer in the tip of which a 1 mm diameter orifice was drilled.

Vacuum System. The system is evacuated differentially by three pumps. The reaction chamber into which the sample gas was introduced through the carrier gas flow line is maintained at 1 to 760 torr.

Electrostatic Lens. The lens system consisted of an extractor (E), deflector (D) and 4 sets of coaxial, sequential cylinders, each biased at a particular dc valtage.

Mass Analyzer. The QMS was used without the electron impact ionizer. The rods were biased below grounded by connecting separate dc supplies into the dc rod driven circuit. The channel electron multiplier detector was operated both in the pulse mode and in analog mode.

Operational Procedures. The characterization study of the present source was carried out with reference compounds through standard gas generator. By employing a permeation tube, acetone was diluted in pure nitrogen gas to produce standard gas. The acetone was used to characterize the LIS response and performance. The formulated gas sample analysis was done as the example of the analytical applications. The analysis was accomplished by introducing the gas sample directly to the LIS.

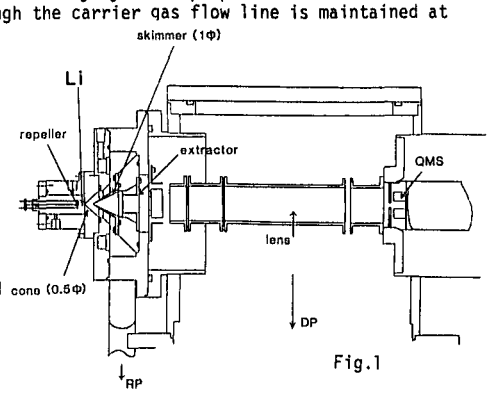

Fig.1

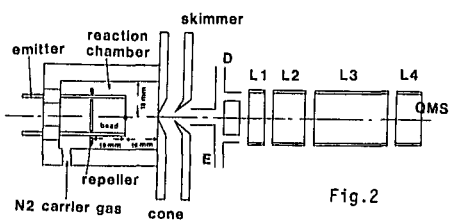

Fig.2

Presented at the 36th ASMS Conference on Mass Spectrometry and Allied Topics
June 5-10, 1988, San Francisco, CA

RESULTS AND DISCUSSION

1. Lithium ion intensity We have tested the lithium alkali ion emitter for different temperatures. A simple diode arrangement was used to measure the total lithium emission current; the maximum emission current of Li^+ ions is more than 6 x 10^{-7} A. The Li^+ ion current through the skimmer was determined by using an ion collector electrode which was positioned at the extractor in the vacuum. The measuremnt yielded a value of 7.2 x 10^{-9} A (4.5 x 10^{10} ions/sec).

2. Reactions in source
Ionization in the present source is initiated by formation of alkali ions on the emitter. Under the appropriate operating conditions, chemical and thermal equilibrium occurs before the ions are sampled and positive ion products results mainly from the attachment reactions. A successful method for obtaining lithium ion cationization mass spctra must provide a means for binding lithium ion to the sample molecules.
The intensity of attachment products was greatly influenced by the voltage applied to the repeller, which provides the reactant ion with the kinetic energy. The relationship of $I(M+Li)^+/[I(Li)^+ + I(M+Li)^+]$ to the repeller voltage was examined under the various ion source pressures, using acetone. As can be seen from Fig.3, the portion of Li^+ ion attachment decreases with increasing repeller voltage and finally no product was observed.

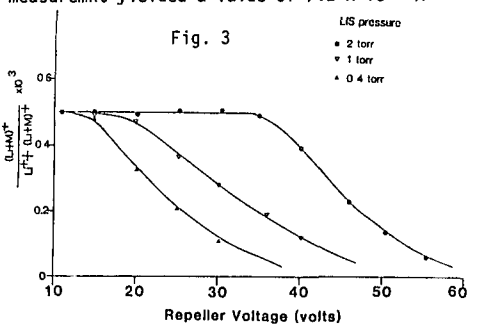

3. Sensitivity Considerations
Fig.4 shows three mass spectra around m/e 7, 23 and 65 respectively in which the primary ion Li^+, Na^+, and the Li^+ adduct ion $(CH_3)_2COLi^+$ are monitored. The sampling conditions are as follows; acetone sample is introduced at the rate of 2.6 x 10^{-10} g/sec from the permeation tube at 25°C. The measurement of the adduct ion yielded a value of 2.9 x 10^{-10} A which is output of the ion multiplier with the gain at 2 x 10^3; this current corresponds to 1.5 x 10^{-13} A.Thus, the sensitivity is 5.8 x 10^{-4} A/g/sec.
The minimum detectable amount (m.d.a.) can be estimated. The background rate of our ion counting system is typically 10 counts/sec with all component operating. As a practical and conservative lower limit of quantitative detectability, a signal to background ratio of 10 may be required. Then for a continuous sample, we required 100 counts/sec. Taking the sensitivity for acetone which was determined to be 5.8 x 10^{-4} A/g/sec experimentally, we estimated that m.d.a. is around 2.8 x 10^{-14} g/sec.

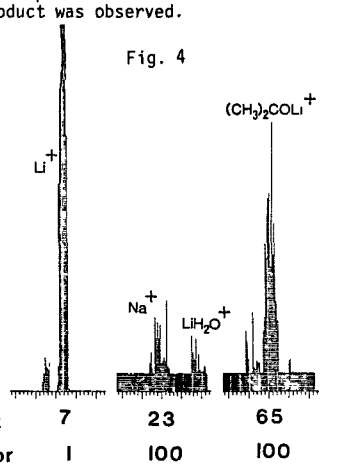

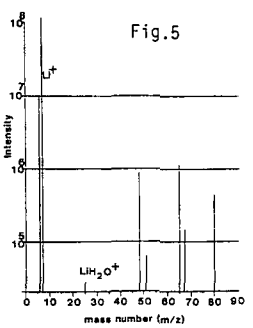

4. Analysis of gas sample
Fig.5 shows the Li^+ CI mass spectrum of a formulated mixture of six compounds in N_2 gas in the single scan mode. The scan time was 10 sec. Presumably the peaks at m/z 48, 51, 65, 67, 80, 85 are due to CH_3CN, CH_3CHO, $(CH_3)_2CO$, C_3H_7OH, $(C_2H_5)_2NH$, C_6H_6. Only the quasimolecular species, Li^+ complexes, are present, demonstrating that Li^+ ion chemical ionization mass spectrometry will find numerous applications in the analysis of mixtures. The alkali ion CI appears to have advantages over the conventional CI of CH_4. Since more than one reactive species are generated in the $CI(CH_4)$ source, it does not always provide the single ion species. Furthermore small pressure change can make the mass spectral interpretation difficult because of pressure effects in many ways.

Presented at the 36th ASMS Conference on Mass Spectrometry and Allied Topics
June 5-10, 1988, San Francisco, CA

TUNING AND CALIBRATION IN THERMOSPRAY MASS SPECTROMETRY:

Joseph F. Greer and Louis L. Martin
Drug Discovery Dept., Pharmaceuticals Div., CIBA-GEIGY Corp.,
556 Morris Ave., Summit, NJ 07901

Most manufacturers of thermospray interfaces recommend the use of either PEG 1000 or a mixture of adenosine and erythromycin for tuning the low mass range. We have found that PEG 1000 is unsatisfactory for thermospray tuning since it decomposes at high thermospray source temperatures, resulting in contamination of the source, and it condenses at cooler temperatures, resulting in contamination of other areas of the mass spectrometer. Adenosine and erythromycin produce strong positive ions between m/z 136 and 734, but are not suitable for negative ion tuning. In this paper, compound mixtures which are suitable for tuning and calibration in both positive and negative ion thermospray mass spectrometry are described.

Samples were analyzed on a Finnigan MAT TSQ-70 triple quadrupole mass spectrometer equipped with a Finnigan MAT thermospray interface. A Waters model 510 pump was used with a Scientific Systems model LP-21 pulse dampener. The mobile phase consisted of 60% acetonitrile in water.

In the first experiment, adenosine, erythromycin and trifluoroacetic acid (TFA) were added to the mobile phase at a concentration of 0.1 mg/ml. The following conditions were used: vaporizer temperature, 125°C; aerosol temperature, 240°C; repeller, -50 V (negative ion), +50 V (positive ion); flow rate, 1.1 ml/min. In the positive ion mode (data not shown), abundant ions appeared at m/z 136 (adenine), 268 (adenosine) and 558,756 and 716 (fragments of erythromycin). In the negative ion mode (fig. 1), abundant ions appeared at m/z 113 (TFA), and 227, 248, 380, 688 and 828 (adducts of TFA with itself, adenine, adenosine and two fragments of erythromycin, respectively).

In the second experiment, GC/MS markers 1329 and 1772 (Regis Chemical Co., Morton Grove, Ill.) were added to the mobile phase at a concentration of 0.1 mg/ml together with 0.1% trifluoroacetic acid (TFA). The thermospray spectra were obtained under the under the following conditions: vaporizer temperature, 90°C; aerosol temperature, 300°C; repeller, -125 V (negative ion), +125 V (positive ion); and a flow rate of 1.9 ml/min. In the positive ion mode (fig 2),

Figure 1. Negative ion mass spectrum of trifluoroacetic acid, adenosine and erythromycin.

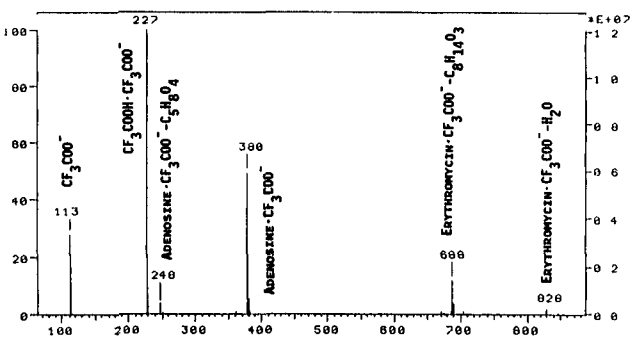

abundant ions appeared at m/z 1330 ($M+H^+$) and 1773 ($M+H^+$). In the negative ion mode, abundant ions appeared at 1442 and 1885 (TFA adducts of markers 1329 and 1772, respectively). By turning the filament on (fig. 3), ions at m/z 1146 and 1589 were seen. These ions correspond to a loss of $C_3F_7CH_2$ from markers 1329 and 1772 respectively.

Figure 2. Positive ion mass spectrum of Regis markers 1329 and 1772.

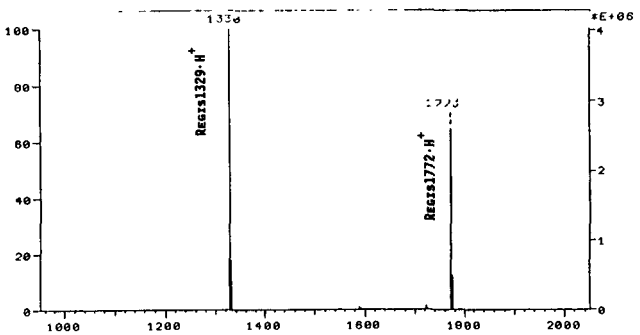

Figure 3. Filament-on negative ion mass spectrum of Regis marker 1329 and 1772 in the presence of TFA.

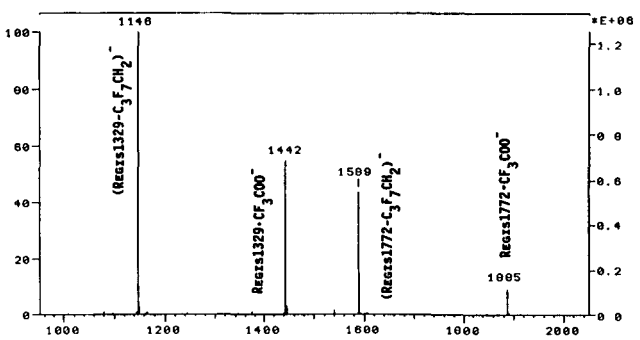

In conclusion, adenosine, erythromycin and mass markers 1329 and 1772 from Regis provide suitable ions in the presence of TFA for tuning in both positive and negative ion thermospray modes. The density of ions is sufficient for low resolution mass spectrometry but may not be adequate for high resolution work. Furthermore, the compounds used in this study produce significantly less contamination of the mass spectrometer than either polyethylene or polypropylene glycol.

Presented at the 36th ASMS Conference on Mass Spectrometry and Allied Topics
June 5-10, 1988, San Francisco, CA

OPTIMIZATION OF THERMOSPRAY VAPORIZER AND ION SOURCE.

C. H. Vestal, J. G. Wilkes, G. J. Fergusson, and M. L. Vestal, Vestec Corporation, Houston, TX 77054

The objectives of this work are to obtain experimental data on the effect of key ion source and vaporizer operating parameters on thermospray ionization efficiency; to achieve a better understanding of the processes occurring in the thermospray ion source; and to provide the information needed to routinely optimize thermospray for difficult nonvolatile samples.

Thermospray is now widely recognized as a practical LC-MS interface, but some problems persist particularly for applications to difficult ionic samples such as peptides and polysulfonated azo dyes. This paper presents initial results from an ongoing study of the important parameters affecting efficiency of the overall ionization and detection process. A key component for these studies is a new thermospray vaporizer with an easily replaceable, yet durable, exit nozzle. This allows the diameter of the nozzle to be varied in a precise, known manner. Other parameters varied include power imput to the vaporizer, distance between vaporizer nozzle and ion exit aperture, and repeller potential.

A Vestec Model 201A Dedicated Thermospray LC-MS System was used for these studies. The standard ion source equipped with a repeller was employed without modification. In place of the standard capillary vaporizer, a new vaporizer with replaceable sapphire nozzles was used. A cross sectional diagram of the tip portion of this new vaporizer is shown in Figure 1. The present work employed vaporizer nozzle diameters of 50, 75, and 100 microns, but additional sizes are available as indicated on the figure.

Test solutions used in this work typically consisted of 10 ppm of sample in 0.1 M aqueous ammonium acetate and these were introduced continuously at a flow rate of 1 mL/min to the thermospray vaporizer. Adenosine and arginine were used as test samples in this initial work. Intensities of the major sample ions (e.g. m/z 136 and 268 from adenosine) and a major solvent ion (e.g. m/z 36) were determined as functions of nozzle diameter, vaporizer control temperature, nozzle to sampling aperture distance, and repeller voltage at fixed ion source temperature (ca. 240 C) and tip heater temperature (ca. 280 C).

Additional work will be required before all of the objectives can be accomplished; nevertheless a model which appears to at least partially account for the observations has been constructed. It appears that ions may be produced by direct ion evaporation from charged droplets in two distinct regions of the ion source; initially as the superheated droplets exit the vaporizer, and further downstream due to heat transfer from the ion source. Buffer ions may be converted to sample ions anywhere within the ion source where collisions between the ions and neutral sample should occur. The ion sampling efficiency depends strongly on the position of ion formation. Ions formed near the vaporizer may be sampled less efficiently because of diffusion loss to the walls, and ions formed further downstream may be swept on past the sampling orifice by the high speed vapor flow. The repeller potential may affect both the ion sampling distribution and the ion formation rate.

The primary effect of applying a high positive potential to the repeller is to decelerate and deflect away from the repeller positive ions and droplets while accelerating negatively charged ions, electrons (if any) and droplets to the repeller. Under some conditions the repeller can cause additional fragmentation of sample ions, but this appears to require the presence of free electrons which was not the case here. Under the conditions used in these studies it appears that the major effects due to the repeller can be described as follows. As the repeller is biased more positively the collection efficiency for positive ions formed near the sampling orifice is increased, while ions formed further upstream are collected less

efficiently. Furthermore, if charged droplets or particles reach the vicinity of the repeller, reducing their velocity increases the probability that ions will be produced in the region of high collection efficiency. Also, increasing (or decreasing) the velocity of the charged droplets relative to the surrounding vapor can cause additional vaporization and ionization due to frictional heating.

In summary the new vaporizer with replaceable nozzle allows meaningful studies of nozzle diameter and other important parameters on thermospray performance. The model outlined above accounts qualitatively for the results obtained, but much work remains before a definitive picture may emerge. From studies of a limited number of samples the 75 micron nozzle generally gives the best results and highest sensitivities with mostly aqueous mobile phases at ca. 1 mL/min. The smaller diameter nozzles should, in principle, give better results at lower flow rates, but this has not yet been established experimentally.

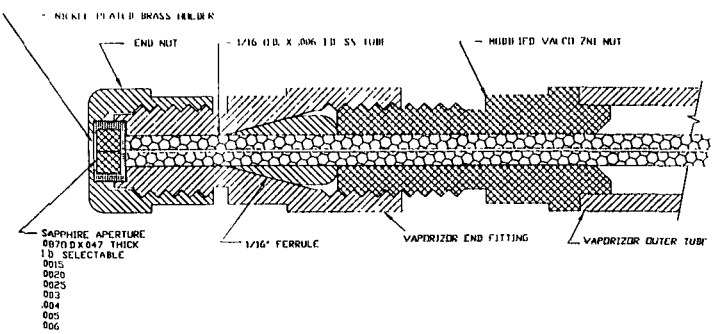

FIGURE 1. Cross sectional view of the new thermospray vaporizer with replaceable sapphire nozzle.

Presented at the 36th ASMS Conference on Mass Spectrometry and Allied Topics
June 5-10, 1988, San Francisco, CA

The Dependence of Ion Formation on Thermospray Plume Characteristics

Mike S. Lee and Richard A. Yost; Department of Chemistry, University of Florida, Gainesville, FL 32611.

Previous studies performed in our laboratory using a specially designed vacuum chamber which permitted sampling of the thermospray plume under vacuum conditions have shown that droplet-rich and vapor-rich regions exist within a thermospray plume and that several instrumental parameters may affect these regions. We now describe the results of our studies of tip temperature, source temperature, flow rate, source pressure, and probe position, obtained on a Vestec thermospray liquid chromatograph/mass spectrometry (LC/MS) interface, which show the dependence of fragment ion and pseudo-molecular ion formation on thermospray plume characteristics. These studies were performed with a pure 0.1 M ammonium acetate buffer and with a 100 ppm (4×10^{-4} M) ribavirin standard prepared in 0.1 M ammonium acetate.

In these studies, the desired solution was filled into an ISCO LC-5000 syringe pump and continuously pumped into a Finnigan triple stage quadrupole (TSQ45) mass spectrometer. The scanning parameters were the same for each experiment (15 to 500 amu in 0.40 seconds). When the desired instrumental parameter was adjusted, a full scan mass spectrum was initiated and allowed to run for 20 seconds to several minutes. At the end of the acquisition, the parameter under investigation was adjusted again and another full scan mass spectrum acquisition was initiated. Since no injections were made, the resulting ion intensity trace contained no peaks. Ion intensity traces were characterized by constant, relatively non-fluctuating ion currents observed above baseline. Areas were obtained by quantitating over a specified scan range, usually five scans (2 seconds) wide which corresponds to 77 µg of ammonium acetate and 1 µg of ribavirin exiting the probe for a flow rate of 1.5 mL/min. Repetitive measurements were obtained by quantitating a series of five scan "peaks" within a single acquisition.

Results of the tip temperature, source temperature, and probe position studies indicate that the formation fragment ions are favored by larger droplets at regions (droplet-rich) close (<1 cm) to the probe tip, while pseudo-molecular ion formation is favored by smaller droplets at regions (vapor-rich) further away (>1 cm) from the probe tip. Figure 1a shows the effects of tip temperature on the ion intensities of pure ammonium acetate. Ion intensities of both the positive and negative ions of ammonium acetate maximize at 208 C. The effects of tip temperature on the ion intensities of ammonium acetate with 100 ppm ribavirin present are shown in Figure 1b. Ion intensities of both the positive and negative ions of ammonium acetate maximize at 194 C and decrease rapidly with increasing tip temperatures. The effects of tip temperature on the positive ion intensities of ribavirin are shown in Figure 2a. The ion intensities of the positive fragment ions at m/z 113 and 130 are optimum at higher tip temperatures. The ion intensity of the $(M+NH_4)^+$ adduct is maximum at 204 C while the $(M+H)^+$ and $(2M+H)^+$ ions are maximum at 208 C. The negative ions of ribavirin showed similar behavior as the positive ions (Figure 2b). Here, the ion intensity of the pseudo-molecular ions $(M-H)^-$, $(M+CH_3COO)^-$, $(M+111)^-$, and $(2M-H)^-$ ions are optimum at 208 C while the negative fragment ions at m/z 111 and 171 are optimum at 200 C. Source temperature studies showed similar behavior of fragment and pseudo-molecular ion formation with temperature; however, excessive temperatures (>300 C) were shown to increase the ion intensities of the fragment ions of ribavirin which may be due to thermal decomposition of the pseudo-molecular ions. The results of the flow rate experiments were rather difficult to interpret since this parameter affected many of the other parameters and the magnitude of the contributions of these other parameters may change with flow rate. However, it is evident that the ion intensities do increase with increasing flow rates (up to 2.0 mL/min). The studies dealing with source pressure indicate that there exist optimum source pressures for both fragment ion and pseudo-molecular ion formation. The ion intensities of the respective positive and negative fragment ions of ribavirin at m/z 113 and 111 increased with increasing source pressures. The corresponding ammonia and acetate adducts of these fragment ions, m/z 130 and 171, showed two maxima at 3.5 and 6 Torr. The presence of two maxima may suggest the occurrence of two competing processes in the ionization mechanism, for example, direct ion evaporation of the adduct of the fragment versus chemical ionization (CI) of the fragment with the corresponding reagent ion (NH_4^+ or CH_3COO^-). The positive and negative pseudo-molecular ions of ribavirin were optimum at intermediate source pressures (4-6 Torr) except for the $(M-H)^-$ ion which was optimum at 8 Torr. The

results of the probe position studies showed that distances less than 1.1 cm (from the probe tip to ion sampling cone) favor the production of fragment ions while distances greater than 1.1 cm favor the production of most of the pseudo-molecular ions at a flow rate of 1.5 mL/min.

These results indicate that vaporization conditions which produce larger and, perhaps, more slowly evaporating droplets at or near the ion sampling cone favor the production of fragment ions, while vaporization conditions which produce smaller and rapidly evaporating droplets favor the production of pseudo-molecular ions. However, many of these large droplets are able to come in contact with the heated source walls and evaporate sample molecules. These sample molecules can become pyrolyzed and produce a molecule (molecular weight 112 corresponding to the triazole ring structure) where it can undergo CI with ammonium acetate reagent ions. This possibility would account for the maximum ion intensity of fragment ions at low tip temperatures. Likewise, the vapor-rich plumes do not contain an abundance of large droplets but rather an abundance of smaller droplets (≤1 μm) and vapor. This condition may be more favorable for the direct ion evaporation of pseudo-molecular ions of ribavirin and/or the evaporation of a neutral ribavirin molecule which can become ionized by CI with the ammonium acetate reagent ions. This possibility would account for the increase in ion intensity of the pseudo-molecular ions with higher tip and source temperatures.

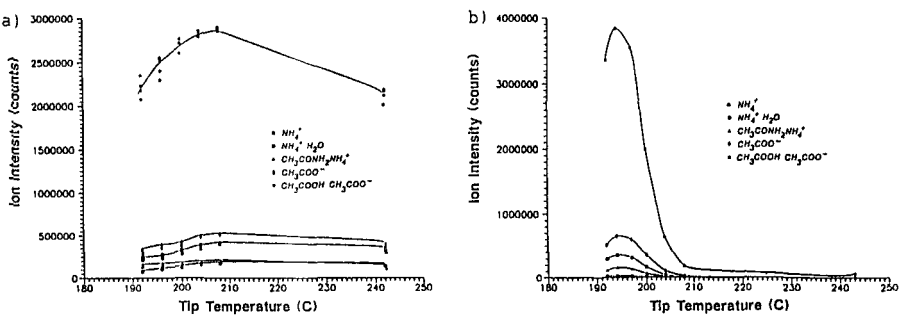

Figure 1. Plots showing the effects of tip temperature on the ion intensities of ammonium acetate. (a) Pure ammonium acetate with 4 replicate measurements shown. (b) Ammonium acetate with 100 ppm ribavirin present (average of 4 replicate measurements).

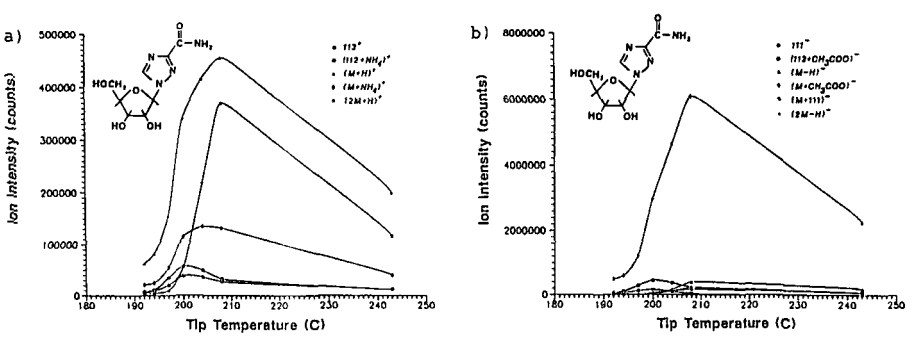

Figure 2. Plots showing the effects of tip temperature on the (a) positive and (b) negative ion intensitites of 100 ppm ribavirin (average of 4 replicate measurements).

Presented at the 36th ASMS Conference on Mass Spectrometry and Allied Topics
June 5-10, 1988, San Francisco, CA

EFFECTS OF REPELLER GEOMETRIES ON THERMOSPRAY MASS SPECTRA

SAUL W. FINK AND ROYAL B. FREAS
DEPARTMENT OF CHEMISTRY, UNIVERSITY OF HOUSTON, HOUSTON, TEXAS 77204-5641

INTRODUCTION: Thermospray ionization is a versatile interface for liquid chromatography/mass spectrometry (LC/MS). Thermospray mass spectra are produced with abundant molecular ions and little or no fragmentation. Therefore, molecular weight information of a sample is obtained, but limited structural information is available. The addition of a repeller in the thermospray ion source has increased the usefulness of this technique. We have studied the placement and geometry of the repeller in the ion source and the effects on the mass spectra. Two basic geometries for the repeller were used: a blunt tip and a needle tip.

EXPERIMENTAL: A quadrupole mass spectrometer (HP Model 5988A) fitted with a Vestec Thermospray™ interface (Model 721A) and a gradient HPLC system (SSI Model 230) was used for these studies. The blunt tip was designed by Vestec Corp. The face of the repeller was placed 4 mm from the ion exit aperture. The mobile phase was 0.1 M ammonium acetate dissolved in HPLC water. The samples were introduced into the mass spectrometer by direct flow. Discharge ionization provided a supplemental source of ions as the repeller potentials were applied. The needle tip consisted of a 1-1/2" 0-80 threaded rod machined to a fine point. The tip of the repeller was placed 2 mm from the ion exit aperture. The polyethylene glycol (PEG) sample was prepared by mixing PEG of average molecular weights 300 u, 600 u, 1000 u, and 1450 u. A vaporizer probe tip was constructed using fused silica capillary tubing (100 μm ID).

RESULTS: The blunt-tip repeller has previously been used to study samples. Fragmentation occurs when a filament or discharge electrode produces ions when large potentials are applied to the repeller.[1-3] Reactions that explain this induced fragmentation are collision-induced dissociation (CID), electron-ionization-induced dissociation (EIID), and electron-induced dissociation (EID). Anthracene and acridine are examples of molecules that undergo fragmentation when repeller potentials are applied.

A needle-tip repeller was employed in our laboratory to study the effect it has on ions from PEG (m/z 300 to m/z 1900). Robbins and Crow had previously found that a needle type of repeller electrode improves high mass sensitivity, but that it has no effect in the low-mass region (m/z < 1000).[4] In contrast to previous work,[4] we observed a significant increase in low mass ion current (m/z 300-1000) as well as for high mass ions (m/z 1000-1900). The effects of applying potentials to the needle repeller are displayed in Figs. 1 & 2. The low mass ions increased more rapidly for lower potentials than did the high mass ions, suggesting that the effect was due to increased ion diffusion, enhancing ion extraction from the ion source.

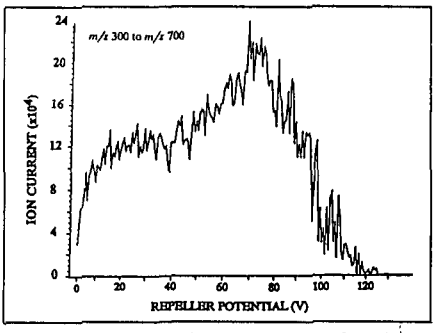

Figure 1. Repeller potential versus ion current for m/z 300-700 of PEG

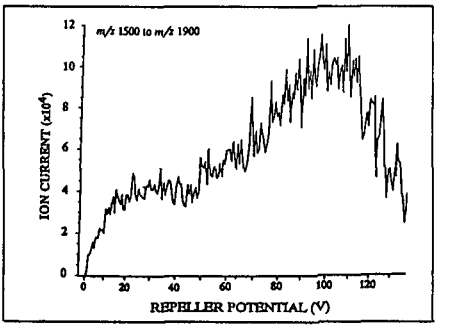

Figure 2. Repeller potential versus ion current for m/z 1500-1900 of PEG

The needle-tip repeller is useful for the study of peptides and proteins. Thermospray LC/MS can be a powerful tool for peptide sequencing. Peptide samples studied with the needle-tip repeller include 20 picomoles of angiotensin I and 10 picomoles of bradykinin (Fig. 3 and 4). The samples were introduced by direct injection using a Rheodyne injection system (Model 7125) fitted with a 20 μL loop.

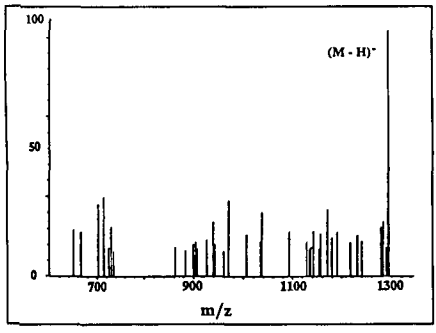

Figure 3. Full-scan mass spectrum of 20 picomoles of angiotensin I (MW 1296).

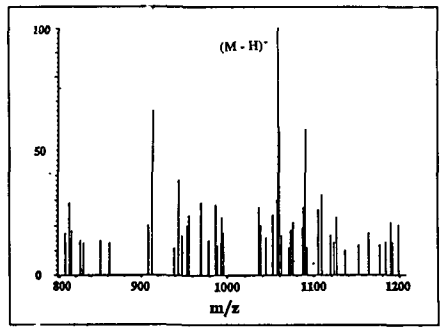

Figure 4. Full-scan mass spectrum of 10 picomoles of bradykinin (MW 1060).

Figure 5 is a chromatogram of hemoglobin W alpha chain. The alpha and beta chains of hemoglobin variants were studied with the previous ion source and have been reproduced using the ion source with the needle-tip repeller.[5] Eight nanomoles of sample were digested in a trypsin column followed by a reverse-phase HPLC column which was connected to the mass spectrometer.

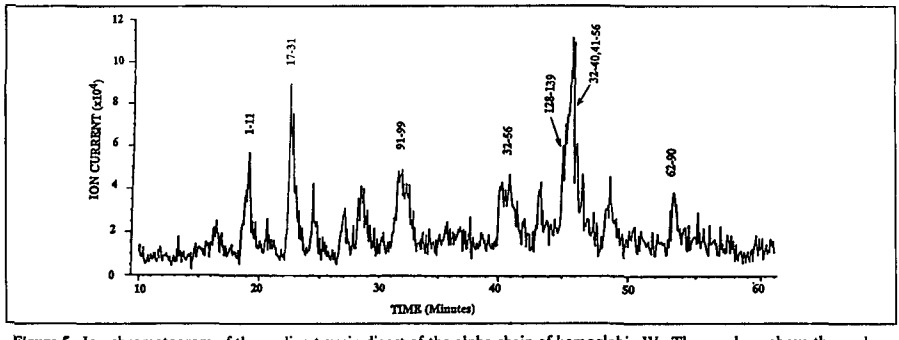

Figure 5. Ion chromatogram of the on-line trypsin digest of the alpha chain of hemoglobin W. The numbers above the peaks correspond to the amino acid sequences in the peptide.

CONCLUSIONS: A blunt-tip repeller electrode has been used to induce fragmentation when repeller potentials are applied in the presence of a supplemental source of ionization. A needle-tip repeller electrode has been used to increase ion currents of low mass ($m/z < 500$) and high mass ($m/z > 1000$). The increase in ion currents is due to increased ion evaporation from the smaller droplets produced by the new vaporizer probe tip and from the influence of an electrostatic field. The increase is also due to the increase in diffusion rates of molecules as the repeller potentials increase.

ACKNOWLEDGEMENTS: We thank Dr. Marvin L. Vestal and Dr. Douglas F. Dyckes for helpful discussions. We acknowledge the EPA and NIH for support of this research.

REFERENCES

1. Zakett, D.; Kallos, G.J.; Savickas, P.J. presented at the 34th Annual conference on Mass Spectrometry and Allied Topics, Cincinnati, OH, 1986.
2. McFadden, W.F.; Lammert, S. *J. Chromatogr.* **1987**, *385*, 201-211.
3. Coutant, J.E.; Ackerman, B.L., Vestal, M.L. presented at the 35th Annual conference on Mass Spectrometry and Allied Topics, Denver, CO, 1987.
4. Robbins, R.H.; Crow, F.W.; *Rapid Comm. Mass Spectrom.* **1988**, *2*, 30-34
5. Stachowiak, K.; Wilder, C.; Vestal, M.L.; Dyckes, D.F. *J. Am. Chem. Soc.* **1988**, *110*, 1758-1765.

Presented at the 36th ASMS Conference on Mass Spectrometry and Allied Topics
June 5-10, 1988, San Francisco, CA

ENHANCED DETECTION OF SULFONATED AZO DYES USING THERMOSPRAY MS

MATTHEW A. MCLEAN[1], DONALD A. FLORY[1], MARVIN L. VESTAL[2], ROYAL B. FREAS[1]
[1] DEPARTMENT OF CHEMISTRY, UNIVERSITY OF HOUSTON, TEXAS 77204-5641
[2] VESTEC CORPORATION, 9299 KIRBY DR., HOUSTON, TEXAS 77054

INTRODUCTION: A better understanding of critical parameters that affect ion evaporation from thermospray droplets has lead us to modify our thermospray ion source and vaporizer to increase sensitivity for sulfonated azo dye detection. Instrument modifications include decreasing the exit aperture of the thermospray vaporizer and the addition of a needle-tip repeller in the thermospray ion source. Restriction of the vaporizer tip decreases the average droplet size of the spray entering the ion source. The field strength on the droplets increases and the field-assisted ion-evaporation process is enhanced. An increase in field strength created by smaller droplet size results in an increase in dye evaporation and consequently an increase in signal. However, only decreasing the thermospray vaporizer tip does not allow for the desired sensitivity to be obtained due to poor ion extraction efficiency from the ion source. For this reason, a repeller opposite the ion exit aperture was added to increase the ion sampling yield.

EXPERIMENTAL: All experiments were performed using a Hewlett Packard Model 5988A mass spectrometer operated in the negative-ion mode. The mass spectrometer was coupled to a Scientific Services Inc. gradient high performance liquid chromatography system via a Vestec thermospray liquid chromatography/mass spectrometry (LC/MS) interface. The Vestec ion source was modified by machining away the step restriction in the ion volume, thus making a more open region around the sampling cone. A needle-tip repeller was added opposite the sampling cone to enhance ion extraction efficiency from the ion source (see Fig. 1). The thermospray vaporizer was modified so the orifice size could be varied by using different sizes of fused silica tubing held in place by a graphite/vespel ferrule and a screw-on cap (see Fig 2). Results for flow rate versus ion abundance and optimum repeller voltage versus ion abundance were obtained by pumping an aqueous solution of 10-5 M Direct Red 81 directly into the mass spectrometer at various flow rates while stepping the repeller voltage through a region of maximum ion current. This was done for the 100 micron and 50 micron tip sizes.

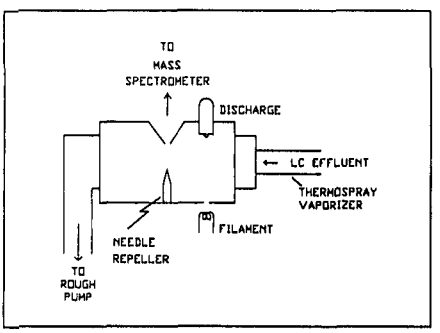

Figure 1. A schematic of the modified thermospray ion source.

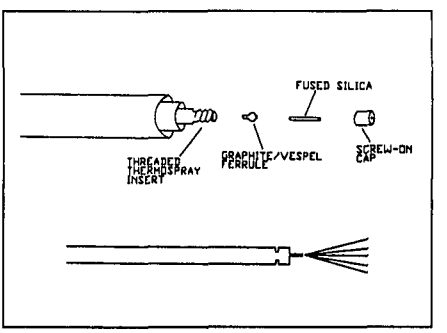

Figure 2. A schematic of the modified thermospray vaporizer probe.

RESULTS: The smaller the thermospray vaporizer tip can be made, the better the sensitivity one can obtain. Reduction of the vaporizer tip decreases the size of the thermospray droplets, which increases the charge per unit area on the surface of the droplets entering the ion source. As a result, field-assisted ion-evaporation is enhanced. Compounds that undergo ionization via chemical ionization (i.e. evaporated as neutrals followed by ionization in the gas phase) should not be affected to a great extent by decreasing the exit orifice of the vaporizer probe and indeed we have found this to be the case. Compounds such as sulfonated azo dyes and peptides, which are ionized in solution and evaporate via field-assisted ion-evaporation, show enhanced sensitivity when the vaporizer tip is restricted.

Figure 3 shows a graph of ion intensity for Direct Red 81 versus repeller voltage for a thermospray probe exit orifice of 100 microns and flow rates of 0.4, 0.6, 0.8 and 1.0 mL/min. Figure 4 shows data for the 100

micron tip at higher flow rates. A summary of the optimum repeller voltage as a function of flow rate for the 100 micron tip is given in Fig. 5.

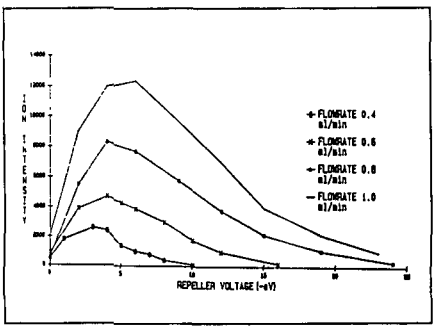

Figure 3. Ion intensity versus repeller voltage at flow rates of 0.4, 0.6, 0.8, and 1.0 mL/min.

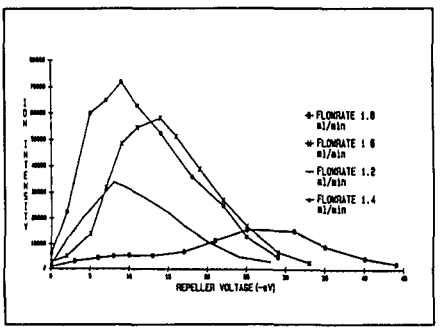

Figure 4. Ion intensity versus repeller voltage at flow rates of 1.2, 1.4, 1.6, and 1.8 mL/min.

Ion source pressure and repeller voltage affect ion extraction efficiency from the thermospray ion source. Both the proper flow rate and repeller voltage are extremely important in optimizing the response for a given vaporizer tip size. The optimum flow rate for a 100 micron tip size was found to be 1.4 mL/min. At this flow rate, a high pressure is achieved in the ion source which allows for high sampling yields while minimizing ion/neutral collisions. At higher flow rates, the greater frequency of collisions within the ion source causes a decrease in ion current due to neutralization reactions between solvent molecules and the dye anion. Similar results were obtained for other tip sizes investigated.

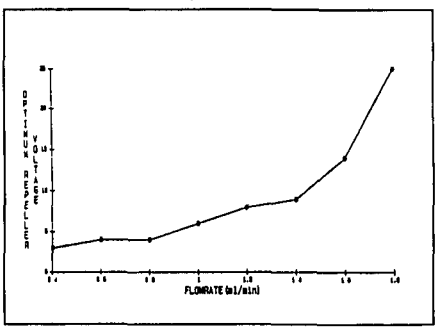

Figure 5. Optimum repeller voltage versus flow rate for a 100 micron vaporizer tip size.

The optimum repeller voltage is also dependent on flow rate. At higher flow rates, higher pressures in the ion source result. The repeller voltage required to influence ion trajectories is then increased. This trend is reflected in Fig. 5.

CONCLUSIONS: Two critical parameters responsible for enhancing thermospray LC/MS sensitivity for sulfonated azo dyes include vaporizer exit orifice size and repeller voltage. Restriction of the thermospray probe exit orifice is needed to enhance field-assisted ion-evaporation and therefore increase the population of dye ions in the gas phase. The ion extraction efficiency of the dyes from the ion source is increased by applying a voltage to a needle-tip repeller located opposite the ion sampling cone. Without these instrument modifications, reproducible thermospray mass spectra of sulfonated azo dyes could not be obtained. For each thermospray probe tip size, an optimum flow rate exists where the total ion current is maximized. For a unique combination of flow rate and tip size, a corresponding optimum repeller voltage also exists.

ACKNOWLDGEMENTS: We acknowledge the Environmental Protection Agency for support of this research.

Presented at the 36th ASMS Conference on Mass Spectrometry and Allied Topics
June 5-10, 1988, San Francisco, CA

Methods to Produce Less Active Probe Surfaces to Minimize the Adsorption and Catalysis of Thermospray Probes.

Philip C. Smith[1] and Alfred L. Yergey, Section on Metabolic Analysis and Mass Spectrometry, National Institute for Child Health and Human Development, NIH, Bethesda, MD 20892.

The analysis of very labile compounds by thermospray LC/MS is not routine and often requires much different probe and source conditions than would be employed for stable polar compounds. With compounds such as peptides, fragmentation products are often dominant in the mass spectra, especially when using the near complete vaporization conditions which produce optimal total ion current. The spectra obtained across a chromatographic peak generally vary for these labile compounds with the molecular ion being more prominant at the beginning of the peak evolution. Tailing of ion chromatograms is common, especially when operating near complete vaporization. We have investigated methods to minimize this undesirable apparent adsorption and catalysis. A more inert surface for the Vetec style probe was developed by modifying the stainless steel (SS) vaporizer capillary. The two approaches attempted are the use of gold plating of the SS capillary and insertion of a fused silica lining within the SS capillary.

Methods

Gold plating. Plating of gold to SS was done using electroless processes as have been applied previously for transfer lines for GC/MS. After some experimentation, the final procedure employed sequential electroless plating with copper, nickel then gold after a complex sequence of activation steps with acids and proprietary products (2). Solutions were pumped through the 0.005 inch ID capillary SS tubing at flow rates of 0.5-1.0 ml/min using HPLC pumps. Preliminary experiments using 0.020 inch ID tubing established that the plating process did occur in the interior bore of the tubing. When plating the narrower ID vaporization probe, plating of the exterior surface was used as an indication of successful plating of the interior bore.

Fused silica lined probes. Commercially available glass lined SS tubing cannot be obtained with ID's compatible with the presently employed thermospray process ($\leq$ 150 μm). Therefore, fused silica capillary cladded with polyimide was employed. The fused silica, 100 μm ID, 200 μm OD, was threaded though the capillary of a modified Vestec thermospray probe where the SS capillary had been removed and replaced with one which had an ID of about 250 μm (0.010"). The fused silica was extended past the inlet end of the vaporizer capillary and held in place with vespel ferulles. The fused silica was allowed to extend a few mm beyond the SS capillary at the source end of the vaporization probe during these investigations.

The probes prepared by the above methods were tested using a Biospect quadrupole mass spectrometer retrofitted with a Vestec thermospray source and controller. Source block and vaporizer tip heater temperatures are controlled independently in this configuration. Test solutes included arginine, tripeptides, and enkephalins. Eluent was 0.1 M ammonium acetate at 1 ml/min. Standard testing of the probes for flow cut off and vaporizer control vs. tip temperature was conducted without vacuum with a flow of 1 ml/min 0.1 M ammonium acetate. Parameters of interest when comparing probes were: i. presense of molecular ion relative to fragmentation ions, ii. tailing of the ions produced from sample introduced by direct injection, and iii. reproducibility of spectra across a sample peak.

Results

Plating of gold to the SS capillary necessitated prior application of copper and then nickel plate. When complete, gold plated vaporization probes had similar heating profile and pressure drop as did unplated probes. The flow cut off, normally used as an indirect measure of the capillary ID, decreased from 1.6-1.7 ml/min to about 0.9-1.1 ml/min when gold plating was done. This is likely due to changes is the surface wetting properties of the gold, since the pressure drop of the probe did not change appreciably upon gold plating. The performance of gold plated probes was not improved relative to SS when measured qualitatively for tailing of fragment ions or presence of molecular ion.

The fused silica lined probes behaved much differently than the metal probes. A plot of control vs. tip temperature shown in Figure 1 exhibited no run away vaporization even when the full current available from a Vestec thermospray controller was used. This was not unexpected, as the polyimide cladded fused silica probably limits heat transfer to the eluent. Also noted was that during operation at high probe temperatures the response of fused silica lined probes changed, presumably due to "burn off" of the polyimide and this was confirmed when

the probe was disassembled. Life time of the fused silica lined probe was limited to several days before plugging occurred. The polyimide burnoff may be the source of probe plugging. Because of the poorer heat transfer of the fused silica lined probes, the rate of response and equilibration to changes in applied current to the probe were much slower than for metal probes. However, when inserted into the tip heater within the mass spectrometer, an apparent "run away" temperature was observed when current applied to the probe capillary was increased.

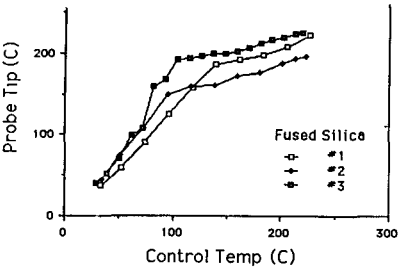

Figure 1. Plot of the vaporization temperature profile conducted without vacuum for 3 fused silica lined vaporizer probes. Flow was 1 ml/min 0.1M ammonium acetate. Highest temperature reflects full applied current of a Vestec thermospray controller.

Compared to the SS probes, the fused silica lined probes gave better thermospray mass spectral performance. Using moderate source block and tip heater temperatures of 300 °C, optimal ion intensities for solvent ions of ammonium acetate were comparable to that obtained with a SS probe. Significant molecular ion was observed for arginine and all the peptides tested and tailing of the total ion current and the fragment ions was significantly reduced (Figure 2). Unlike the SS probe, optimal response for molecular ion and total ion current were correlated and maximal just below the apparent "run away" temperature. Reproducibility of mass spectra across a total ion chromatogram were still not completely satisfactory, but were improved due the reduction in tailing and apparent adsorption of the probe.

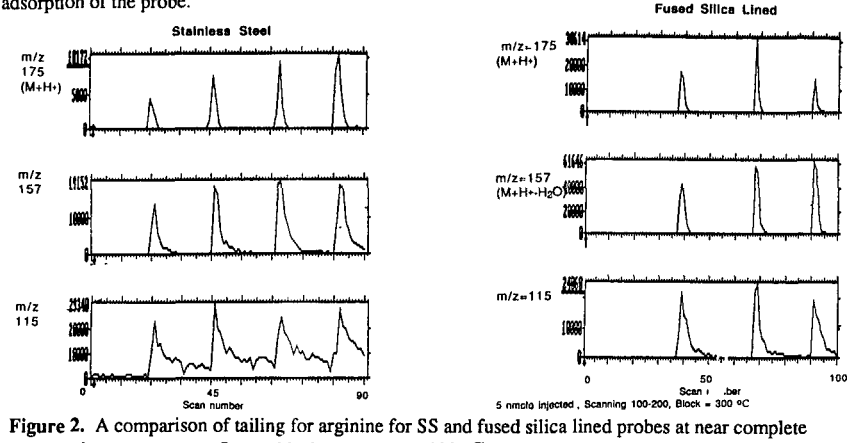

Figure 2. A comparison of tailing for arginine for SS and fused silica lined probes at near complete vaporization temperature. Source block temperature, 300 °C.

Conclusions

The results indicate that the surface of SS probes may be responsible for some of the adsorption and apparent catalysis seen with thermospray LC/MS of labile compounds. Improvements were obtained for the small peptides examined with the polyimide fused silica lined SS probes, but the instability of the polyimide cladding needs to overcome. Presently, we are investigating the use of aluminum cladded fused silica which should have greater temperature stability as well as improved heat transfer properties. The use of fused silica may also have potential application for use with lower flow rates as it is available with ID's as small as 5 μm with precisely controlled tolerances.

1. Present address: College of Pharmacy, UT, Austin, TX 78712.
2. Plating was performed with the technical advice of Mr. Robert Durshlag of Fidelity Chemical Products Corp., Newark, NJ.

Presented at the 36th ASMS Conference on Mass Spectrometry and Allied Topics
June 5-10, 1988, San Francisco, CA

ALTERNATIVE IONIZATION PATHS FOR MAGIC-LC/MS

J. Daniel Kirk and Richard F. Browner
School of Chemistry, Georgia Institute of Technology, Atlanta, Georgia 30332-0400

The advent of MAGIC-LC/MS has created the opportunity to generate reference quality electron impact (EI) and chemical ionization (CI) mass spectra for a wide range of compounds present in liquid chromatographic eluents. The generation of such mass spectra is possible because of the highly efficient manner in which the interface removes solvent from the analyte before it reaches the mass spectrometer. Analyte leaves the interface as a stream of small, desolvated particles which then flash vaporize in the heated ion source area, and may be subsequently ionized using EI or CI processes. These modes of operation are, however, limited to compounds which generate an adequate vapor pressure of analyte at the temperature of the ion source to result in a detectable population of ions.

This paper addresses additional options available for the ionization of samples introduced with the MAGIC-LC/MS interface. The two new modes of ionization discussed are: (1) fast atom bombardment (FAB) ionization and (2) small particle enhanced vaporization (SPEV) ionization. The theoretical and experimental bases for both experiments are described in some detail. The FAB approach involves a crossed-beam experiment, in which the desolvated particle beam leaving the interface is intercepted by a stream of fast atoms from a conventional FAB source. The interaction is capable of producing FAB spectra, which are applicable to molecules with inadequate vapor pressures to generate EI or CI spectra under normal operating conditions. A second FAB experiment involves the deposition of the MAGIC particle beam onto a probe tip, which may then be ionized by a FAB source in a more conventional manner.

The SPEV approach involves the production of particles significantly smaller than those normally produced by the MAGIC interface. The smaller diameter particles should result in an enhanced vapor pressure of analyte species, due to the high curvature of the particle surface. This should result in a significantly higher population of vapor phase species than would be predicted for vaporization from bulk material, such as that generated from a probe.

Thus far we have been unable to observe the SPEV effect with the current particle sizes that we are producing. Laser diffraction studies of aerosol droplet formation has shown us that the production of droplets small enough to produce particles with enhanced vaporization may not be possible with an ordinary pneumatic nebulizer. It may be necessary to find some other means of producing extremely small aerosol droplets.

FAB will certainly give us the means to produce spectra of extremely non-volatile compounds and compounds with high molecular weights. Deposition of the particle beam from MAGIC onto a probe tip has been done. FAB spectra are then obtained in the usual manner with or without a matrix. Further research is necessary to produce FAB spectra from the crossed-beam mode shown in figure 1.

Fig. 1

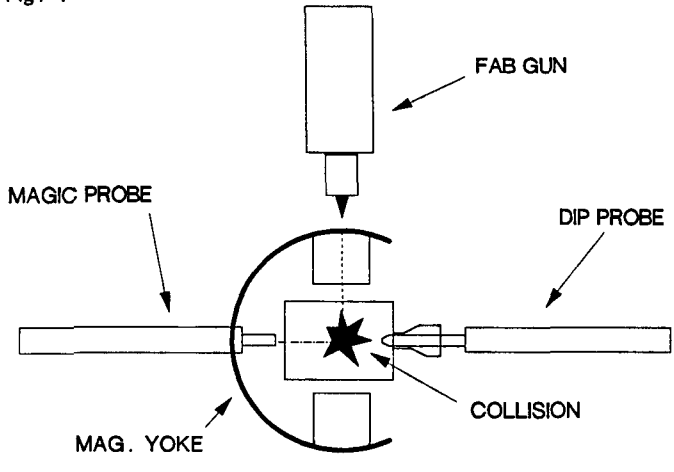

Presented at the 36th ASMS Conference on Mass Spectrometry and Allied Topics
June 5-10, 1988, San Francisco, CA

ON-LINE HPLC WITH A CONTINUOUS FLOW FAB INTERFACE

M.A. McDowall, V. Gould, *C. Slaughter, *B. Pramanik and **T Dourdeville.
VG MassLab Ltd., 3 Tudor Road, Altrincham, WA14 5RZ. *Howard Hughes Medical Institute, Dallas, Texas 75235, USA. **Waters Division of Millipore, Milford, Mass 01757, USA.

Continuous flow (or dynamic) FAB mass spectrometry permits the continuous sampling of a liquid stream into a Fast Atom Bombardment (FAB) ionization source (Figure 1). In such a system a solvent containing a small proportion of glycerol (2-10%) is continuously introduced into a mass spectrometer through a length of fused silica capillary.

In this study we have sought to explore the potential of Dynamic-FAB for on-line LC-MS analysis. Dynamic-FAB systems typically accept liquid flow rates of only a few microlitres per minute. Thus there are two options available for combining HPLC and Dynamic-FAB. Capillary HPLC columns (<0.5mm id.) can be used without the need to "split" the column eluent prior to mass spectral analysis. Alternatively conventional (4.6mm id.) or microbore (2.0 - 0.5mm id.) columns can be used at their optimum flow rates providing that the eluent is "split". Both chromatographic approaches have their merits. Splitless capillary LC-MS systems yield optimum on-column sensitivity. However the loading capacity of capillary HPLC columns is significantly less than their larger counterparts.

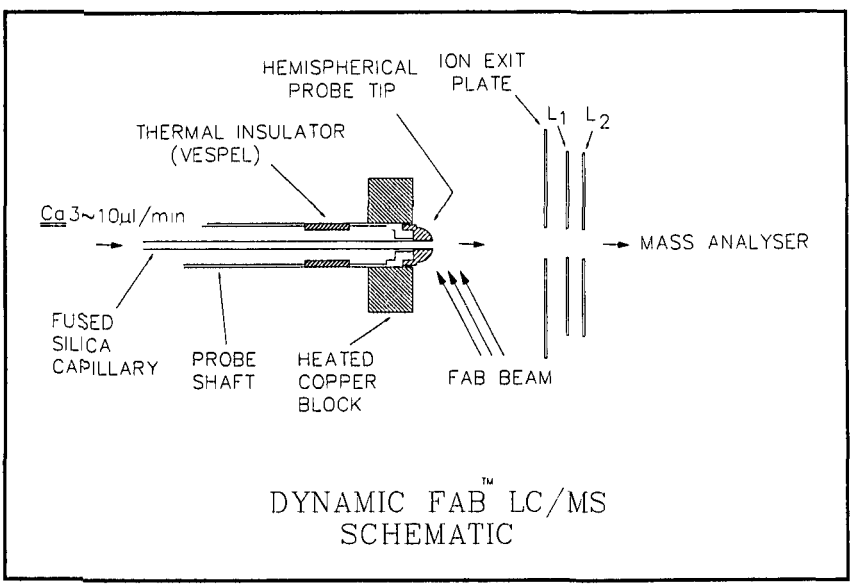

Figure.1. Schematic diagram of the Dynamic-FAB LC/MS ion source used in this study.

In many biomedical applications, sample quantity is severely limited. It is thus desirable to: A) Maximize that portion of the sample which contributes directly to overall signal response. B) Maximize the rate at which individual analytes are delivered to the FAB target to enhance signal-to-noise ratio. C) Minimize the volume in which the analytes are eluted to keep the concentration high at the FAB target. Where on-line flow rates of 10ul/min or less are required, these conditions are best achieved by microbore HPLC.

In transposing a separation method from the conventional to the microbore scale, an HPLC column is chosen with an I.D. appropriate for:
A) Achieving a solvent flow rate compatible with dynamic-FAB.
B) Maintaining the linear solvent velocity constant to minimize alterations in peak retention times.

For example, to sustain a linear velocity of 6.0 cm/min requires in conventional scale HPLC; a flow rate of 1ml/min through a column of 4.6mm I.D. In microbore scale HPLC; a flow rate of 10ul/min through a column of 460mm I.D. would be required.

Experimental

Mass spectra were obtained with a TRIO-3 triple quadrupole mass spectrometer equipped with a Dynamic-FAB LC/MS probe (all from VG MassLab, Altrincham, UK). Conventional (4.6mm I.D.) bore LC-MS was performed using apparatus previously described[1]. Microbore LC-MS was performed using an prototype HPLC system consisting of a pair of syringe pumps (Waters Chromatography, Milford MA. USA) which supply fluid of a programmed composition via a Rheodyne model 7520 microbore injection valve. A microbore reversed-phase column (0.5mm I.D. x 250; C-18) packed in a PTFE capillary was inserted directly into the outlet port of the injection valve. The eluent was conveyed from the column outlet to the FAB target via a fused silica capillary.

Results

Whilst studying small peptides (Met-Arg-Phe-Ala, bradykinin, leu-enkephalin and gramicidin-s) we have found that on-column detection limits (for full scan mass spectra) are improved by circa 100 fold when analyses are transposed to the microbore scale. Of the various stationary phases tested, the large-pore C8 packings such as Brownlee Aquapora RP300 have been found to be the most generally suitable for peptide separations.

Reference

1. D. Games, S. Pleasance, E. Ramsey and M. McDowall. Biomed Environ. Mass Spectrom., 15, 179-182 (1988).

Presented at the 36th ASMS Conference on Mass Spectrometry and Allied Topics
June 5-10, 1988, San Francisco, CA

ACCURATE MASS MEASUREMENT IN CONTINUOUS FLOW FAST ATOM BOMBARDMENT QUADRUPOLE MASS SPECTROMETRY

M.A. McDowall and J. Roboz*. VG MassLab Ltd., Tudor Road, Altrincham, WA14 5RZ, UK. *Department of Neoplastic Diseases, Mount Sinai School of Medicine, New York, NY10029, USA.

This paper presents a new application, the determination of accurate masses by quadrupole mass spectrometry using continuous flow FAB as the method of sample introduction.

Introduction

Continuous flow fast atom bombardment (dynamic-FAB) mass spectrometry permits a significant extension of the ability of FAB to provide mass spectral data from a wide range of involatile and/or polar labile compounds. Because FAB often produces highly abundant pseudomolecular ions, knowledge of the accurate masses of these ions is of considerable help in identification and molecular structure studies. Hitherto accurate mass determination has been performed by magnetic sector mass spectrometry. The ability to obtain accurate mass data (at unit mass resolution) from single quadrupole mass spectrometers extends the utility of such systems and complements structural information obtained from triple quadrupole instruments.

Experimental

The technique is based on computer-controlled internal mass calibration utilizing known non-interfering masses of a calibration standard, selected to bracket, as closely as possible, the peak of interest from the analyte. Mass spectra were obtained with a TRIO-3 triple quadrupole mass spectrometer equipped with a dynamic-FAB LC/MS probe that incorporated a valve loop (100nl) injector (all from VG MassLab, Altrincham, UK). Samples were analysed by injecting directly into a carrier solvent (methanol/water/glycerol/TFA, 45:45:10:0.1 v/v) via the valve loop injector. Inside the ion source the probe tip was maintained at a temperature of 40-45°C and bombarded with a beam of fast (gun voltage 9keV) Xenon atoms. A 1:1:1 molar mixture of cesium, rubidium and sodium iodides was used as a calibration standard for mass measurement.

Results

In preliminary studies we have analysed vinca alkaloids (vinblastin and vincristin)[1] and small peptides (Met-Arg-Phe-Ala and gramicidin-s). The exact mass of protonated vincristin is 825.4075u. In six repeated determinations the mean value was 825.4025±0.0105; 5.0mmu (6ppm) lower than the theoretical value. Comparable data was obtained for vinblastin. The exact mass of protonated gramicidin-s is 1141.7138 u. In a single determination (Fig.1) the calculated mass was 1141.7057 u; 8.1 mmu (7ppm) lower than the theoretical value. Comparable data was obtained for Met-Arg-Phe-Ala.

Presented at the 36th ASMS Conference on Mass Spectrometry and Allied Topics
June 5-10, 1988, San Francisco, CA

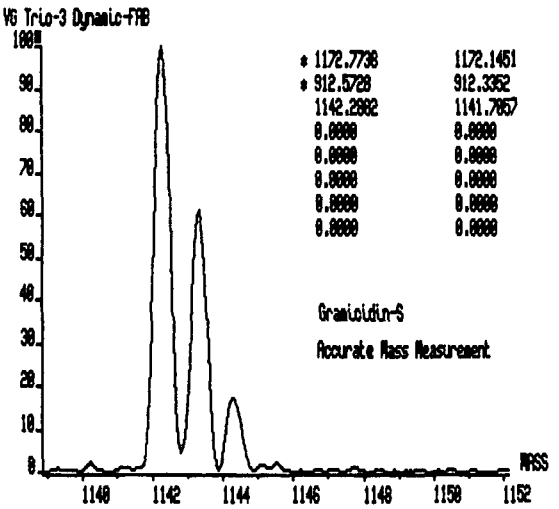

Figure.1. Mass spectrum of the protonated molecular ion region of gramicidin-s, (mass measured against cesium iodide; m/z 1172 and m/z 912). The experimentally determined mass was 1141.7057u; 8.1mmu (7ppm) lower than the theoretical value.

Discussion

The mass measuring accuracy and reproducibility obtained for the compounds studied was, as expected, comparable to that reported by using the same general approach with other types of ionisation [2,3]. Once the exact mass of an ion is obtained, algorithms are available to calculate possible molecular compositions. Although the correct composition may not be immediately obvious from the list of possibilities, identification is usually possible after employing the rules of spectral interpretation (eg. nitrogen rule, DBE) and judiciously considering additional chemical, chromatographic and spectral data.

References

1. J. Roboz, J.F. Holland, M.A. McDowall and M.J. Hillmer, Rapid Comm. in Mass Spectrom. 2,64, (1988).
2. P. Powers, P, D'Arcy, J. Bill and M. Wallington, Proc. 26th ASMS, St. Louis, MO., p480 (1978).
3. J. Welby and P. Watkins, TSP report (Finnigan Corp.) 1(3) (1987).

Presented at the 36th ASMS Conference on Mass Spectrometry and Allied Topics
June 5-10, 1988, San Francisco, CA

ANALYSIS OF DATEM EMULSIFIERS USED IN BREAD PRODUCTION BY CAPILLARY SUPERCRITICAL FLUID CHROMATOGRAPHY/MASS SPECTROMETRY

D.E. Games[1], E. Lewis[2], A. Tomlinson[2] and S. Pleasance[1]
1. Department of Chemistry, University College, P.O. Box 78, Cardiff CF1 1XL, Wales.
2. Dalgetty UK Ltd., Station Road, Cambridge CB1 2JN, England.

The inclusion of emulsifiers in the breadmaking process is well established in the baking industry[1]. One of the most important classes of permitted emulsifiers for use in U.K. bread production is E472(e), diacetyltartaric acid esters of mono- and di-glycerides (DATEM (1)), which are used primarily as dough strengtheners in products where fine texture and volume are important. Its manufacture involves the addition of melted monoglycerides to a reaction mixture of tartaric acid and acetic anhydride in the presence of a trace of acid. The product contains varying amounts of free glycerol, fatty acids, acids, monoglycerides and their combinations. It is also known that DATEM is diluted with triglycerides.

Recently the composition and precise nature of the active species of this additive has generated much interest and a variety of methods for its analysis are being studied. Capillary supercritical fluid chromatography (SFC) has been used for the analysis of lipids and related materials[2,3]. We have used capillary SFC both with FID and mass spectral detection to study mixtures of model glycerides and fatty acids and then applied these techniques to study DATEM emulsifiers with varying degrees of functional properties.

Experimental

Capillary SFC/FID was performed on a 501 Lee Scientific system using an integral frit restrictor (50μm i.d.) with CO_2 as the mobile phase. Samples dissolved in chloroform, were introduced via a 100nl Valco injector and chromatographed on a SB methyl 8m x 100μm column at 150°C with a linear density gradient of 0.2 to 0.6 g/ml at 0.02g/ml/min. preceded by an initial isoconfertic period.

SFC/MS was effected using the pump and data system of the above system and combining to a Finnigan MAT 4500 quadrupole mass spectrometer using our recently described interface[4] which allows heating of the tip of the frit restrictor. Ammonia was used as the reagent gas for CI studies.

Results and Discussion

SFC studies of mixtures of mono-, di- and triglycerides gave good FID traces and DATEM samples gave complex chromatograms indicating the presence of many components. SFC/MS was next performed under CI and EI type conditions on both standard and DATEM samples. The TIC trace obtained under EI conditions for a DATEM sample is shown in fig. 1. This compares favourably with that obtained with FID and both good EI type and CI mass spectra were obtained. The ammonia CI mass spectra gave abundant $[M + 18]^+$ ions together with some structurally useful fragment ions, the spectrum for dipalmitin is shown in fig. 2. Use of this data, together with the EI spectra, enabled ready characterisation of the various standards.

Bases on these observations, we have identified a large number of compounds in the emulsifiers. The main components were found to be mono- and diacetylated esters of palmitate and stearate mono- and diglycerides. In addition, free fatty acids and small quantities of the proposed active stearinoyl and palmitoyl DATEM species were found. The ammonia CI TIC trace of a DATEM sample is shown in fig. 3 together with selected mass chromatograms of ammoniated molecular species.

References

1 J.M.V. Blanshard, P.J. Frazier and T. Galliard (Eds.) 'Chemistry and Physics of Baking', RSC Special Publications No. 56 (1986).

2 R.K. Houch and C.M. White, J. High Resolut. Chromatogr., Chromatogr. Commun., 9, 4, (1986).

3 S.B. Hawthorne and D.J. Miller, J. Chromatogr., 388, 397, (1987).

4 A.J. Berry, D.E. Games, I.C. Mylchreest, J.R. Perkins and S. Pleasance, J. High Resolut. Chromatogr., Chromatogr. Commun., 11, 61, (1988).

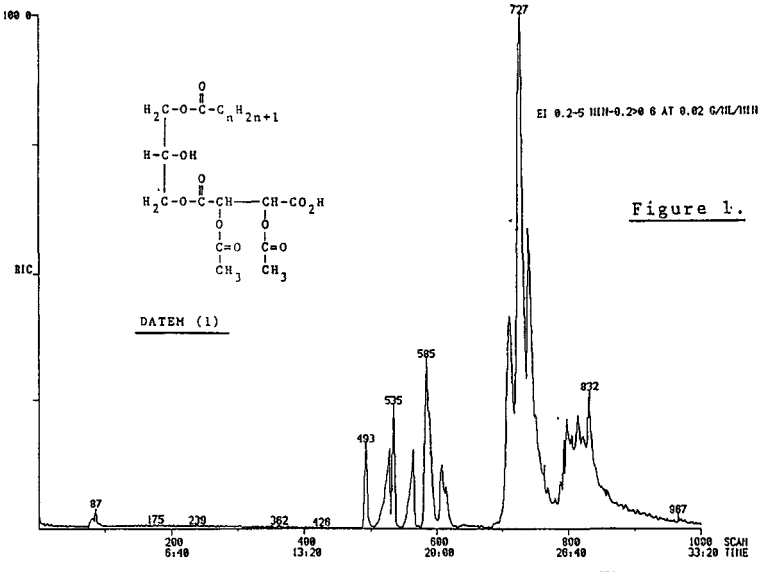

Figure 1.

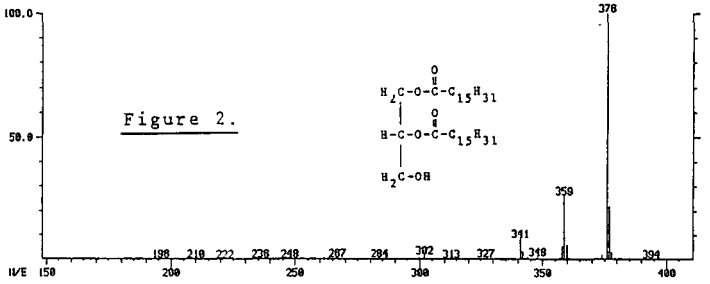

Figure 2.

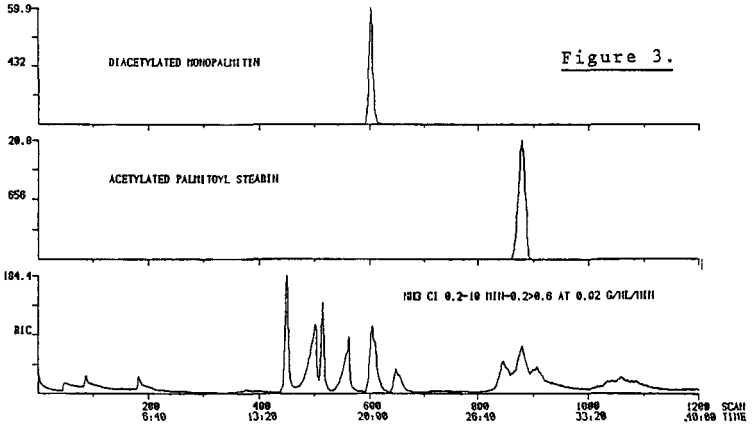

Figure 3.

Presented at the 36th ASMS Conference on Mass Spectrometry and Allied Topics
June 5-10, 1988, San Francisco, CA

LC/MS with atmospheric pressure ionization using the NERMAG R 30-10 triple quadrupole mass spectrometer

A.P. Bruins
State University, Dept. of Pharmacy, 9713 AW Groningen, The Netherlands
C. Beaugrand
S.N. Nermag, 92500 Rueil Malmaison, France

One of the first publications on combined LC/MS described the use of an atmospheric pressure ion source (1). During the following ten years however, developments in API were mainly directed to air sampling.

Ion evaporation, electrospray, and ion spray are API techniques for mass spectrometric observation of ions already present in solutions. Coupled with liquid chromatography and capillary zone electrophoresis, these ionization methods working at room temperature are ideally suited for solving problems in the biomedical field, where most sample molecules are polar, ionic or thermolabile.

We have modified an existing commercially available NERMAG triple quadrupole mass spectrometer for LC/API-MS. Ions are drawn from the atmospheric pressure source through a nozzle into an intermediate pressure region, pumped by a 35 m^3/h rotary pump. A portion of the beam of ions plus neutrals is sampled through a conical skimmer into the original ion source housing pumped by the standard oil diffusion pump. The ions are

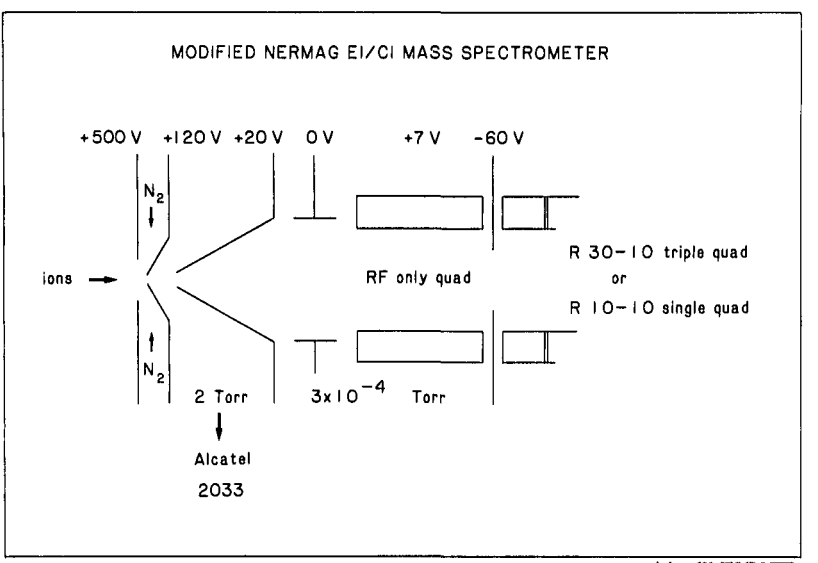

guided into the original analyzing quadrupole system by means of an additional RF only quadrupole assembly and associated focusing elements.

Ions are generated using the electrospray technique (2). A solution of 10 ng/ul of Safranin O was pumped at 5 ul/min (800 pg/sec) by a Jasco Familic 100N micro LC pump via a 50 um i.d. fused silica capillary into a 0.5 mm o.d. x 0.25 mm i.d. stainless steel capillary held at +4.5 kV. The ion sampling nozzle is protected against water vapor by a dry nitrogen gas curtain. Strong signals, adequate for source tuning an recording full scan spectra were observed in our first prototype when we used the aforementioned sample introduction rate of 800 pg/sec. No fragment ions are observed, as was the case in ion spray LC/API-MS (3). A 100 V difference in nozzle and skimmer voltage gave the best sensitivity. At 250 V and above we observed strong fragmentation by CID in the intermediate pressure region. An increased sensitivity should be feasible after optimization of the nozzle and skimmer diameters, their shape, their distance and the ion optics.

1. E.C. Horning et al. J. Chromatogr. 99 (1974) 13-21
2. C.M. Whitehouse et al., Anal. Chem. 57 (1985) 675-679
3. T.R. Covey et al., Org. Mass Spectrom. 23 (1988) 178-186

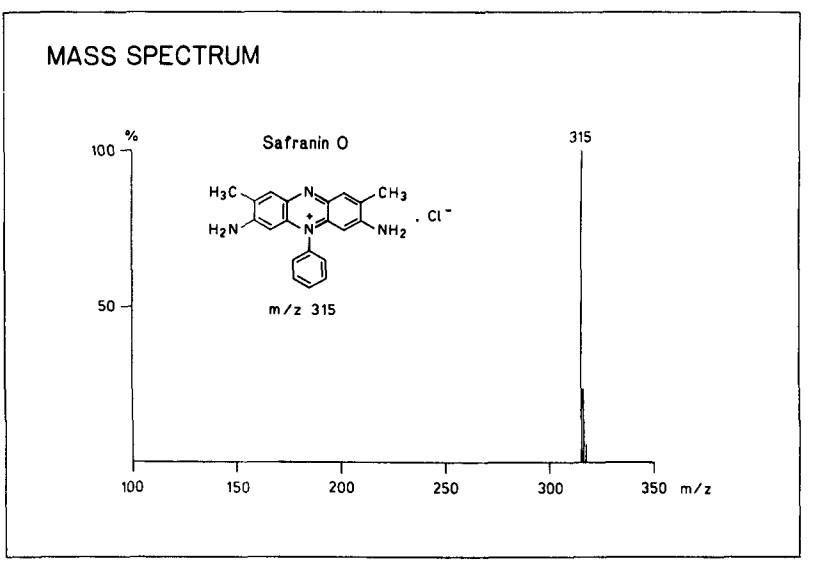

Presented at the 36th ASMS Conference on Mass Spectrometry and Allied Topics
June 5-10, 1988, San Francisco, CA

MASS SPECTROMETRY AS AN ONLINE ANALYSIS TECHNIQUE FOR COUNTER CURRENT CHROMATOGRAPHY.

L.K. Pannell, Lab. of Bioorganic Chemistry, NIDDK, NIH, Bethesda, MD 20892; T.Y. Zhang, Y. Ito, Lab. of Technical Development, NHLBI, NIH, Bethesda, MD 20892; and F.E. Chou, Pharma-Tech Research Corporation, Baltimore, MD 21212.

AIM: Gas and liquid chromatographs are both being routinely used as preseparative devices in conjunction with mass spectrometers. However, Countercurrent Chromatography (CCC) had not previously been interfaced to a mass spectrometer. The aim of this work was to perform this coupling and to present the initial results.

COUNTERCURRENT CHROMATOGRAPHY: During the past few years, CCC has become a more widely used separative technique and there are now at least two manufacturers. Excellent reveiws exist.

EQUIPMENT:

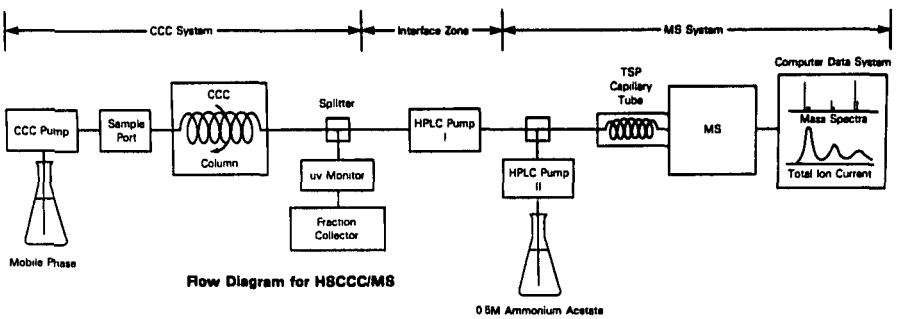

Flow Diagram for HSCCC/MS

A standard Finnigan TSP46 mass spectrometer equiped with a thermospray source was connected to a prototype "small-scale" countercurrent chromatograph developed by one of us (Chou). The CCC used a multilayer coil prepared from heavy wall #20 (0.85mm i.d.) PTFE tubing. The coil had a 2.5" revolutional radius operated at 1820 rpm and a solvent flow rate of 1.0 ml/min.

Countercurrent chromatography is a relatively low pressure technique and operates typically at 100 psi. Conversly, thermospray requires inlet pressures of 500-1000 psi and, at these pressures, the typical PTFE tubing used in CCC instruments would not survive. To surmount this problem, an open split interface was used consisting of a low volume HPLC "tee" joint in which 0.2 ml/min was run to waste (or an auxiliary detector) and the bulk used as the inlet for a first HPLC pump. A length of tubing was attached to the waste end of the "tee" to allow for the inlet piston volume of the HPLC pump. This pump could then send the liquid directly into the mass spectrometer through the thermospray interface or it could be "tee'd" with a second HPLC pump if a makeup or buffer solution was needed as was the case with most of the samples so far run. This is especially relevant where a buffer may effect the partition ratio of a compound in the two immiscible phases. With this post addition, we were able to take separations developed in the analytical laboratory and repeat them with the mass spectrometer as the detector. The advantage of obtaining real-time mass spectra over only spectrophotometry data need not be elaborated!

In the examples reported here, the solvent consisted of a hexane/ethyl acetate/methanol/water mixture and the lower (water/methanol) phase was used as the mobile phase; a buffer of 0.05% ammonium acetate (0.4 ml/min) was added by the second pump and "true" thermospray ionization used.

EXAMPLE 1: INDOLE DERIVATIVES

A mixture of indole-3-acetamide (mwt 174), indole-3-acetic acid (mwt 175) and indole-3-butyric acid were separated on a CCC instrument. When a similar separation was performed on the CCC-MS system, the total ion current (RIC) closely followed the UV profile and the compounds were easily identified by the protonated parent ions in their individual mass spectra.

EXAMPLE 2: ALKALOIDS FROM STEPHANIA TETRANDRA S. MOORE

This plant material was previously found to contain the two major alkaloids tetrandrine and fangchinoline with molecular weights 622 and 608 respectively. On countercurrent chromatography a separation was obtained and the two compounds were independently identified. An almost equivalent chromatogram was obtained on the CCC-MS system and clear protonated parent ions were observed in the spectra.

EXAMPLE 3: SYNTHETIC MIXTURE ANALYSIS

A post-doctorate fellow at NIH performed a reaction with possible products at masses 363,459 and 461: From an initial injection into the LCMS (no column), the ions of interest were determined and a dual positive/negative ion mass chromatogram obtained on the CCC-MS. As can be seen in the traces below, we were able not only to detect the compounds but to also show the resolution of the diasterioisomers on the CCC. These compounds had a weak UV absorption but from these results, a large scale purification of the useful product was possible.

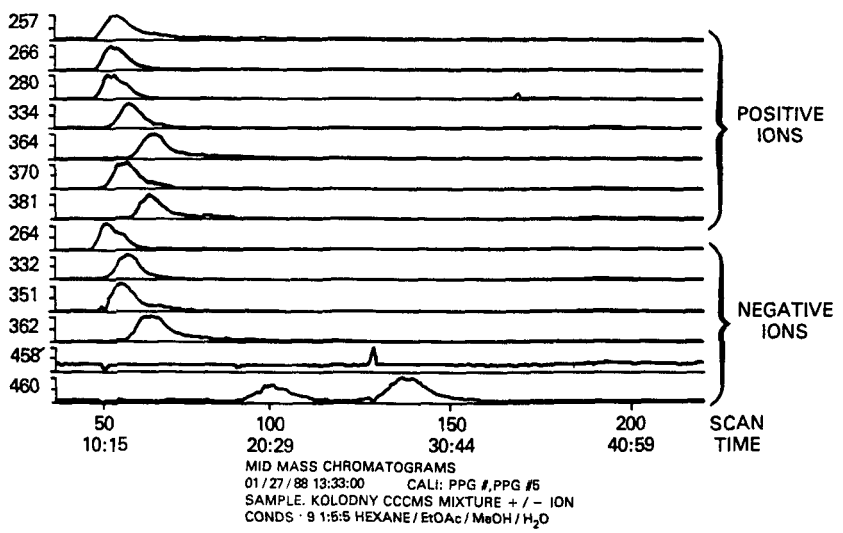

SUMMARY:

A standard countercurrent chromatograph and thermospray mass spectrometer were easily connected to provide on-line mass spectrometry data from a countercurrent separation. Only simple hardware modifications were necessary from routine LCMS and these counld be performed in a matter of minutes.

Presented at the 36th ASMS Conference on Mass Spectrometry and Allied Topics
June 5-10, 1988, San Francisco, CA

PRELIMINARY STUDIES WITH AN ION CHROMATOGRAPHY MASS SPECTROMETRY SYSTEM

A.S. Al-Omair and J.F.J. Todd, Chemical Laboratory,
University of Kent, Canterbury, Kent, CT2 7NH, U.K.

Ion Chromatography (IC), is a novel analytical technique which permits the separation and determination of ionic compounds. The separation of ions is accomplished by utilizing ion exchange chromatography (IEC), ion pair chromatography (IPC) and ion chromatography exclusion (ICE). A major defect in IC is the lack of a universal detector; on the other hand mass spectrometry provides good detection and structural information for many classes of ions, organic and inorganic compounds.

In this study, the possibility of combining IC with fast atom bombardment mass spectrometry (FABMS) using a continuous flow probe has been investigated. The capacity of the system to handle certain modifiers, such as acids, bases and ion pair reagents, which improve the resolution of the IC, has been examined. The effect of such modifiers on the formation of the protonated molecular ion $[M+H]^+$, fragments and cluster ions has been studied.

A home-made IC has been used, and this consisted of a Waters 6000A pump, a Rheodyne injector model 7125 with 20µl sample loop, Hamilton ion separator columns, a Pye Unicam LC3 UV-detector and a pen recorder. The eluent of the IC was admitted to the FAB source through an SGE splitter (model MCVT-1/50) connected at the end of the flow cell fo the UV detector, and a home-made continuous flow probe fitted with a 0.075 mm vitreous silica capillary column. Positive ion FABMS spectra were obtained on an AEI MS9 double focusing mas spectrometer updated by VG analytical Ltd, using fast xenon atoms (2mA at 8KV).

Three groups of samples have been selected for this study. Inorganic anions (chloride and bromide), water soluble vitamins (ascorbic acid, thiamine hydrochloride, pyridoxine and riboflavin), and glucose derivatives (gluconic acid, glucose, and gluconolactone). In all experiments the eluent of the IC contained 5% glycerol.

1. Analysis of Inorganic Anions Utilizing IEC/FABMS.

A mixture containing fluoride, chloride, nitrite, bromide, nitrate and sulphate in aqueous solution was separated on a Hamilton PRP-X100 column of 4.1 mm I.D. x 250 mm, using 1 x 10^{-4} M potassium hydrogen phthalate as eluent at a flow rate of 1.5 ml/min, Fig. 1. Chloride and bromide have been selected for this study and were admitted to the FABMS. The mass spectra of these two ions showed some cluster ions in the form $[K_{n+1}X_n]^+$ up to n = 3, where X is the inorganic anion.

The formation of high molecular weight cluster ions ($n \geq 4$) could be observed for chloride if the concentration of the chloride was increased. High concentrations of sample require a higher column exchange capacity. However high exchange capacity resins require a highly concentrated eluent to maintain the high resolution of the IC. The disadvantage of increasing the concentration of the eluent, is that the mass spectra obtained contain high intensity background peaks.

2. Analysis of Water Soluble Vitamins by IPC/FABMS

The separation of ascorbic acid, thiamine hydrochloride, pyridoxine and riboflavin was performed using a 4.1 mm I.D. x 150 mm PRP-1 column, and 2 x 10^{-5} M hexane sulphonic acid in 50% V/V aqueous methanol containing 1% acetic acid as eluent, and was pumped through the system with a flow rate of 0.7 ml/min, Fig. 1. The mass spectra of riboflavin and thiamine showed that the molecular ion is more stable in it's protonated form, and that no peak was observed in the $[M+H+Na]^+$ region, Fig. 2. However, the molecular ions of pyridoxine and ascorbic acid showed stable molecular ions in the $[M+H+Na]^+$ form of about 20% and 10% relative intensity respectively of the protonated molecular ion $[M+H]^+$. This is may be related to their acidic property, and the existence of the Na^+ ion in the eluent.

Presented at the 36th ASMS Conference on Mass Spectrometry and Allied Topics
June 5-10, 1988, San Francisco, CA

3. Analysis of Glucose Derivatives by ICE/FABMS

The analysis of gluconic acid, glucose and gluconolactone was performed using a 4.2 mm I.D. x 150 mm PRP-X300 IC column. The eluent was 1 x 10^{-4} M Na_2HPO_4 in water, and the flow rate was 0.3 ml/min. The mass spectra of gluconic acid showed no significant peak in the molecular ion region. Other sugars were found to be present in the two molecular ion forms $[M+H]^+$ and $[M+H+Na]^+$. Glucose was found to be more stable in the $[M+Na]^+$ form, and gluconolactone was found to have a considerable stability in the $[M+H+Na]^+$ form. This is may be related to the concentration of Na in the eluent, and also to the acidic properties of these two sugars.

IC/FABMS in it's three separation modes has proved to be a reliable technique for the analysis of three classes of ionic compounds although for successful results the chromatographic conditions have to be optimized.

In this study the conditions were optimized for the study of various known compounds, and more study is needed to evaluate the sensitivity and the reliability of the system to analyze unknown compounds.

For inorganic anions the formation of the cluster ions (e.g. $[K_{n+1}X_n]^+$) is observed, and thought to be governed by the sample concentration, column efficiency and eluent concentration. In the analysis of organic ions, the molecular ion in the form $[M+H+Na]^+$ may be governed by the existence of Na ions in the eluent, and the acidity of the compound itself.

Reference

J.S. Fritz, D.T. Gjerde and C. Pohland, Ion Chromatography, Huthig, New York, 1982.

Acknowledgement

One of the authors (A.S.A.) thanks the Kuwait Institute for Scientific Research for a scholarship.

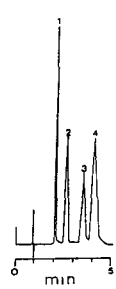

Fig 1 Separation of Ascorbic acid(1), pyridoxine(2), thiamine hydrochloride(3), riboflavin(4) on PRP-1 column using IPC technique

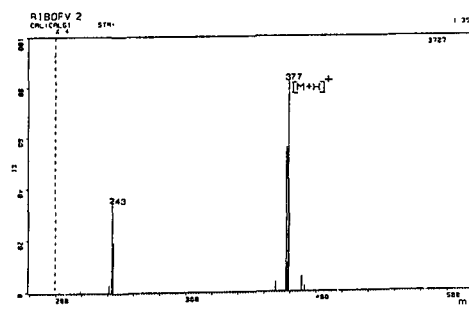

Fig 2. Mass spectrum of Riboflavin eluted from IC system

Presented at the 36th ASMS Conference on Mass Spectrometry and Allied Topics
June 5-10, 1988, San Francisco, CA

DEVELOPMENT OF A THERMOSPRAY HPLC INTERFACE FOR FTICR

W.G. Millen, J.T. Meek, G.W. Stockton, M.L. Thomson and R.S. Wayne,
American Cyanamid Agricultural Research Division, Princeton, New Jersey, 08540

Summary - A thermospray LCMS interface was installed on an FTICR with an external ion source design. The thermospray source was capable of accepting a 2 cc/min flow from an HPLC column while maintaining a $7x10^{-8}$ torr pressure in the ICR cell. At this pressure a FWHM resolution of 47,000 was obtained at m/z = 289. Accurate mass measurements made with errors <2 ppm demonstrated that this instrument combination was successful.

Instrumental - The FTICR used for this work incorporates an external source, three cryopumps and a 7 Tesla magnet. The three cryopumps are mounted on 10 inch flanges and provide a high pumping speed (4000 l/sec H_2O, 1500 l/sec air) to each of the three differentially pumped chambers. The external ion source was built from an Extrel model C-50 ion source and quadrupole with the quadrupole operated in an RF-only mode to eliminate low mass reagent ions which would saturate the ICR cell. A standard thermospray LCMS interface, made by Vestec to connect to Extrel's electrical contacts, was modified by Vestec only to the extent necessary to be compatible with the 10 inch cross used for the source vacuum manifold.

Experimental - The system was tested using a conventional HPLC pump, column and solvents used in analytical separations work. The only concessions made in the operation of the LCMS system are that a high pressure detector cell is used for the in-line uv detector and that analyses are performed at the 1 cc/min optimum flow rate suggested for the thermospray ion source.

The FTICR's vacuum manifold was removed from the magnet and pressure measurements made in each of the vacuum regions while operating the thermospray system. Analyzer pressures of 3.6×10^{-8} and 6.9×10^{-8} torr were obtained at 1 and 2 cc/min solvent flow rates and demonstrated the basic capability of the system for producing high resolution mass spectra.

Sample Analyses - Samples of imazamethabenz (CAS 81405-85-8(mx)) and hydramethylnon (CAS 67485-29-4) were injected onto the thermospray LCMS/FTICR system and data acquired during the elution of each peak. Hexaethylene glycol was added to the solvent to provide a lock mass for monitoring space-charge-induced frequency shifts[1]. The spectra produced (Figures 1 & 2) show that high resolution has been maintained and that accurate mass analysis with errors less than 2 ppm are achieved on this LCMS/FTICR system.

A sample of Gramicidin S also was injected into the system and a FWHM resolution of 11,000 was obtained for its protonated molecular ion. An average error less than 2 ppm was obtained for the elemental composition of its protonated molecular ion; however, a standard deviation of 8 ppm may reflect the absence of a lock mass during the analysis of this sample.

Conclusions - A thermospray LCMS interface can be installed on an FTICR mass spectrometer with an external ion source design. The enhanced vacuum obtained from this design extends the usefulness of the FTICR for making accurate mass measurements to thermally labile compounds or to complex samples for which chromatographic separations are required.

1/ J.T. Meek, W.G. Millen, T.J. Francl, G.W. Stockton, M.L. Thomson and R.S. Wayne, 35th ASMS Conference on Mass Spectrometry and Allied Topics, Denver CO, May 1987

Presented at the 36th ASMS Conference on Mass Spectrometry and Allied Topics
June 5-10, 1988, San Francisco, CA

FIGURE 1

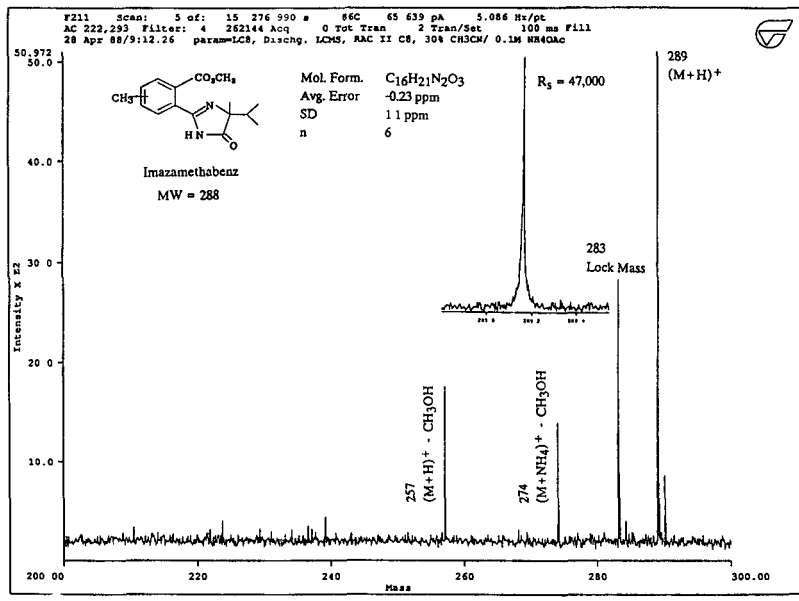

FIGURE 2

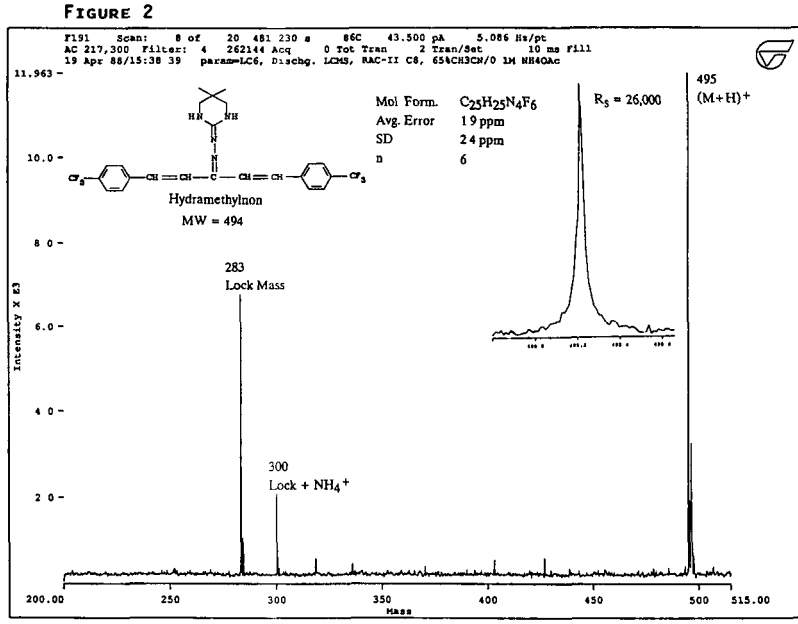

Presented at the 36th ASMS Conference on Mass Spectrometry and Allied Topics
June 5-10, 1988, San Francisco, CA

NEW DESIGN OF A SPLITTER FOR FRIT-FAB LC/MS AND BATCH LIQUID INLET SYSTEM

T.Kobayashi, K.Matsuura, K.Otsuka, E.Kubota
Y.Itagaki, B.D.Musselman, and T.Higuchi
MSG JEOL LTD, 3-1-2 Musashino Akishima Tokyo 196 Japan

Introduction

FRIT-FAB LC/MS interface is a suitable analytical tool for mass spectral determination of thermolabile or nonvolatile compounds (1). In order to connect its interface to a conventional HPLC column, a new splitter has been developed. The performance of the splitter can control the effluent from the column at several micro liter per minute. Using this splitter the reproducibility and sensitivity of FRIT-FAB LC/MS is evaluated.

Principle and characteristics of the new splitter

Fig.1 shows an outline of the splitter and the interface. The splitter is installed at the column outlet. A pressure of several kg/cm^2 is applied to the column outlet by nitrogen gas. A part of effluent flows in a frit although most is exhausted to a drain through a needle valve. The frit flow introduced to the frit depends on the viscosity of the mobile phase and the resistance of the fused silica capillary tube to the frit, and can be controlled by V1. Fig.2 shows the relationship to the split pressure(p), column flow rate and the frit flow. The frit flow is constant over a column flow rate of 50 μl/min to 0.9 ml/min, and proportional to p. The minimum frit flow can be controlled to less than 1 μl/min.

Experimental

The equipment used was the JMS-DX303 mass spectrometer with a JMA-DA5000 data processing system(JEOL). The LC pump used was the TRI ROTAR-V(JASCO). Glycerol was used as the matrix for FAB ionization. LC/MS conditions were as follows ; the column was SFPAK ODS-5S25 1.7mm x 25cm(JEOL), the column flow rate was 150 μl/min and the frit flow was 5 μl/min(split ratio 1/30). The ionization chamber temperature was set at 50 ℃, and Xe gas of a primary beam energy of 4 Kev was selected.

Results and Discussion

Fig.3 shows the selected ion monitoring profile of m/z 363 M+H peak for hydrocortisol, replicated 300 ng(100ng × 3μl) injections to column for an hour. The chromatogram peak's shape was sharp and symmetrical. This indicates that there is no dead volume in the interface with the splitter. The reproducibility of the chromatogram peak intensity was 4.8% (n=19) as a coefficient of variation. Fig.4 shows the detection sensitivity was as high as S/N 10 with the selected ion monitoring profile of m/z 363 for 33 pg of hydrocortisol.

Reference

(1) Y.Ito, T.Takeuchi, D.Ishii, M.Goto and T.Mizuno, J.Chromatogr., 358, 201 (1986)

Presented at the 36th ASMS Conference on Mass Spectrometry and Allied Topics
June 5-10, 1988, San Francisco, CA

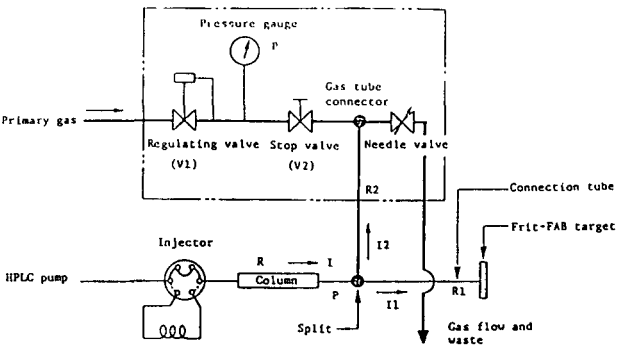

Fig.1 Schematic diagram of a new splitter and FRIT-FAB LC/MS interface

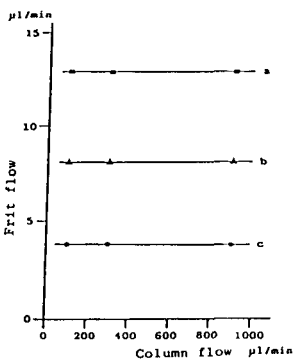

Fig.2 Relationship of frit flow, column flow and split pressure (a:3kg/cm², b:2kg/cm², c:1kg/cm²)

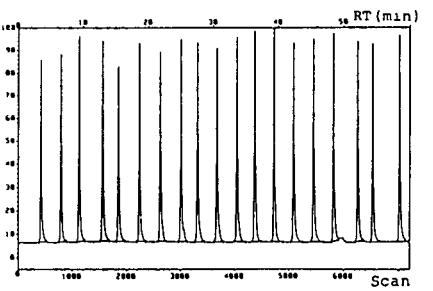

Fig.3 Selected ion monitoring profile of m/z 363 for hydrocortisol replicated 300 ng injections $\sigma/\bar{x}$ = 4.8 % n = 19

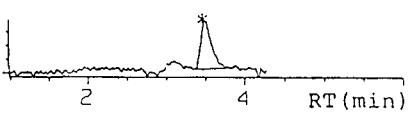

Fig.4 Selected ion monitoring profile for 33 pg hydrocortisol(m/z 363)

Presented at the 36th ASMS Conference on Mass Spectrometry and Allied Topics
June 5-10, 1988, San Francisco, CA

A DIRECT LIQUID INLET FOR TIME-OF-FLIGHT MASS SPECTROMETRY USING RESONANCE ENHANCED MULTIPHOTON IONIZATION

G.R. Kinsel, K.R. Segar, M.V. Johnston
Department of Chemistry, University of Colorado, Boulder, CO 80309

We have developed a direct liquid inlet suitable for use in a time-of-flight mass spectrometer with resonance enhanced multiphoton ionization (REMPI). REMPI offers several advantages for LC-MS:

1. Efficient generation of either soft or hard ionization.
2. Wavelength selective ionization based upon ultraviolet absorption properties. No solvent background will appear in the mass spectrum.
3. The potential for enhanced isomer distinction by selecting the optimum laser wavelength for ionization.

The liquid is pumped through a 45 um diameter fused silica restricting capillary and vaporized in a concentric flow of helium gas. The resulting mixture is then expanded through a 350 um diameter nozzle into the source region of the mass spectrometer. A pressure of 2 to 5 x 10^{-5} torr (depending upon the helium backing pressure in the nozzle) is maintained in the source region by a cryotrapped 6 inch diffusion pump. Further details concerning the inlet design can be found in the 1987 ASMS Conference Proceedings, pp. 405-406.

Figures 1-2 illustrate the inlet operation for a relatively nonvolatile compound, tryptophan. The spectrum in Figure 1 was taken using a glass nozzle heated to a nominal temperature of 165°C. This temperature is too low to thermally desorb tryptophan from a heated probe. (In fact, thermally desorbed tryptophan exhibits extensive sample decomposition.) The inlet can be operated for several hours at this temperature without clogging. There is no evidence of tryptophan precipitation in the restricting capillary, on the inner walls of the nozzle assembly, or at the nozzle orifice even after many hours of operation. In an effort to improve heat conduction to the liquid/gas mixture in the nozzle assembly, the glass nozzle was replaced by a brass nozzle. With the brass nozzle, tryptophan could be observed by heating to a nominal temperature of 135°C (Figure 2). These results suggest that the gas nebulized approach to liquid vaporization has great potential as a liquid inlet for mass spectrometry.

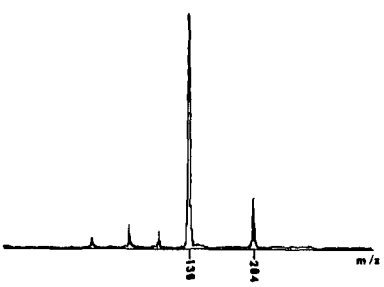

Figure 1

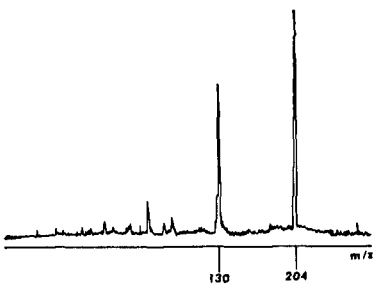

Figure 2

Presented at the 36th ASMS Conference on Mass Spectrometry and Allied Topics
June 5-10, 1988, San Francisco, CA

THERMOSPRAY AND NEGATIVE IONS.

PURE ELECTRON CAPTURE PROCESS BY DISCHARGE IONIZATION.

F. de Maack, G. Devant, M. Lesieur, C. Beaugrand.

SN NERMAG 49, quai du Halage 92500 RUEIL-MALMAISON (France).

The predictability of Thermospray (TSP) spectra is limited by several factors: among them, ionization process, source temperature, flow rate, repeller voltage, electrolyte and sample concentration.

In negative ion mode this situation is complicated by the additional possible occurence of two competitive ionization processes : deprotonation and electron capture, leading to two different molecular ions $(M-H)^-$ and M^- respectively.

Usually it is not possible to obtain pure electron capture process in presence of ammonium acetate at 1 mL/mn flow rate even with a 1000 eV Rhenium filament.

In this paper we report unambiguous spectra in negative ion mode on the antibiotic Chloramphenicol. This non-volatile and thermolabile compound has been studied in LC-MS successively with TSP ionization only and discharge ionization.

A pure TSP ionization is easily observed at a 1mL/mn flow rate of 0.1 M acetate ammonium and leads to M-1 species without fragmentation (Figure 1).

The TSP source is also equipped with a repeller and we demonstrated that this additional electrode at 400 Volts acts as a discharge and leads to the observation of "mixed" spectrum resulting from both competitive ionization processes.

In discharge-on mode, opposite to filament-on mode, a pure electron capture ionization leading to M^- species with extensive fragmentation can be obtained in presence of ammonium acetate (Figure 2).

These two resident ionization capabilities have been complementary used for molecular weight assessment of a potent antiparasitic agent namely AVERMECTIN B1a (Figure 3).

In some cases, e.g. Vitamin B_2 namely, Riboflavin, the discharge is the only ionization mode providing a valuable spectrum in LC/MS with the resulting fragmentation (Figure 4).

Thus we demonstrate that Electron Capture and Proton Abstraction, two competitive ionization processes in a classical TSP Source can be clearly separated.

The Electron Capture is the predominant ionization mode during the DISCHARGE operations even in presence of ammonium acetate.

The major effect of Repeller is an increase of signal intensity and at higher potentials, it is a key parameter for extensive fragmentation.

Presented at the 36th ASMS Conference on Mass Spectrometry and Allied Topics
June 5-10, 1988, San Francisco, CA

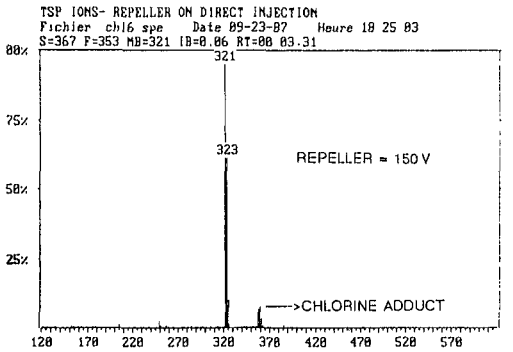

Figure 1 :

CHLORAMPHENICOL

Pure TSP ionization (repeller 150 V)

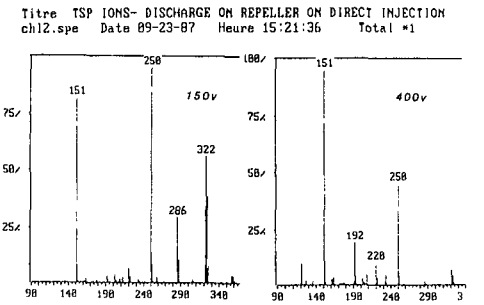

Figure 2 :

CHLORAMPHENICOL

DISCHARGE ionization (repeller 150 V and 400 V)

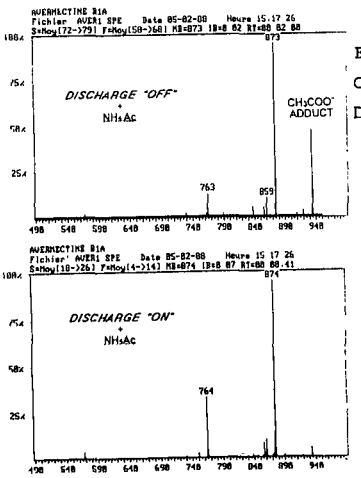

Figure 3 :

AVERMECTIN B1 a

WITH and WITHOUT DISCHARGE

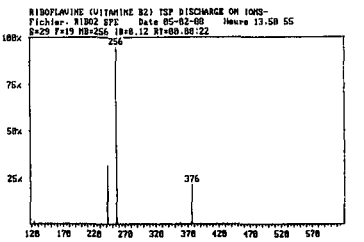

Figure 4 :

VITAMIN B2 DISCHARGE ON

Presented at the 36th ASMS Conference on Mass Spectrometry and Allied Topics
June 5-10, 1988, San Francisco, CA

OTLC/MS Comparison of Quadrupole, Ion Trap, and Magnetic Sector Instruments

M.A. Moseley[1,2], S.R. McGown[1], B.H. Escoffier[1], J.S.M. de Wit[1,2], K.B. Tomer[1], and J.W. Jorgenson[2]

1) Laboratory for Molecular Biophysics, National Institute for Environmental Health Sciences, RTP, NC 27709
2) Kenan Laboratories of Chemistry, University of North Carolina at Chapel Hill, Chapel Hill, NC 27514

The combination of liquid chromatography with mass spectrometry (LC/MS) is one of the most useful analytical methods currently available. Unfortunately, these two techniques are difficult to couple together in a manner where the full power of both LC and MS can be simultaneously utilized. This problem has stimulated the development of a variety of different LC/MS interfaces. The ideal LC/MS interface will allow the use of optimum LC conditions (flow rate and mobile phase composition) while still permitting the acquisition of the most useful classes of mass spectra [electron impact (EI), positive ion chemical ionization (PICI), and negative ion chemical ionization (NICI)].

Most LC/MS interfaces have difficulty in eliminating the large amount of vapor generated by the mobile phase which can result in high source pressures which, in turn, leads to chemical ionization of the analytes. While CI mass spectra give molecular weight information, the minimal amount of fragmentation that is found in CI spectra precludes obtaining structural information without resorting to MS/MS methodology. Only if the source pressure is sufficiently low will EI mass spectra be obtained. Towards this end many LC/MS interfaces resort to elaborate (and expensive) pumping/skimming and/or moving belt techniques to remove the mobile phase vapor. A very attractive alternative is to utilize an inexpensive LC method which not only has <u>very</u> low mobile phase flow rates (nl/min) but offers superior chromatographic separation efficiency - Open Tubular Liquid Chromatography (OTLC).

OTLC utilizes glass or fused silica capillary columns with an i.d. of from 2 to 20 microns and with lengths of from 1 to 10 meters. These columns have stationary phase coated/bonded on the capillary wall similar to capillary open tubular GC columns. Separation efficiencies of greater than 1,000,000 plates can be obtained with mobile phase flow rates of from 1 to 100 nl/min ([1]). This low flow rate permits direct introduction of the entire OTLC effluent into the MS source without significantly increasing the pressure of the source, and thus EI mass spectra can be directly obtained from the OTLC system.

OTLC columns have been successfully interfaced with MS using a probe which is introduced into the mass spectrometer via the direct insertion probe inlet ([2]). Tapering and heating the end of the OTLC column allows for the detection of compounds of low volatility and/or thermal stability while maintaining good chromatographic peak shape.

Presented at the 36th ASMS Conference on Mass Spectrometry and Allied Topics
June 5-10, 1988, San Francisco, CA

The utility of the OTLC/MS interface with quadrupole, ion trap, and magnetic sector instruments has been investigated. Both quadrupole and magnetic sector instruments were found to work well with the OTLC interface with a variety of different analytes and mobile phases (Figures 1 & 2). The magnetic sector instrument generally gave better results. It was able to successfully analyze several compounds which were not detected on the quadrupole instrument, such as adenine and iso-leucine, and also gave better S/N ratios for equivalent amounts of analytes. While a modified version of the OLTC/MS probe was successfully used with the ion trap instrument with non-polar compounds, the ion trap's intolerance for mobile phases containing methanol and/or water severely restricted the utility of the OTLC interface with the ion trap.

REFERENCES

1. J.W. Jorgenson and E.J. Guthrie, J. Chromatog., 1983, 268, 369.

2. J.S.M. de Wit, C.E. Parker, K.B. Tomer, and J.W. Jorgenson, Anal. Chem., 1987, 59, 2400.

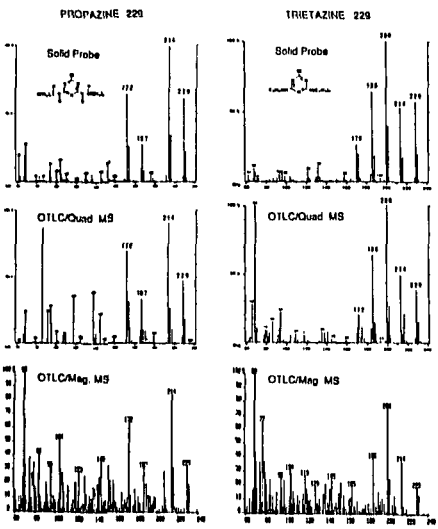

Fig. 1

Comparison of the EI mass spectra of the herbicides propazine and trietazine acquired with direct solid probe, OTLC/quadrupole, and OTLC/magnetic sector methods.

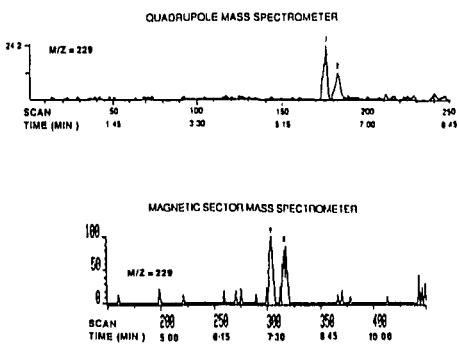

Fig. 2

Single ion chromatograms of the OTLC separation of propazine and trietazine on quadrupole and magnetic sector instruments.

Presented at the 36th ASMS Conference on Mass Spectrometry and Allied Topics
June 5-10, 1988, San Francisco, CA

DEUTERIUM EXCHANGE AND ACTIVE HYDROGEN DETERMINATION IN MULTICOMPONENT ANALYSIS BY COMBINED LIQUID CHROMATOGRAPHY/THERMOSPRAY MASS SPECTROMETRY

Charles G. Edmonds, Steven C. Pomerantz, Fong Fu Hsu and James A. McCloskey
Department of Medicinal Chemistry, University of Utah, Salt Lake City, Utah 84112

Deuterium labeling of organic compounds plays an important role in mass spectrometry in studies of ionic reaction mechanisms, and in applications involving structural characterization. The on-line exchange of deuterium for protium during combined chromatography-mass spectrometry is advantageous because of its direct applicability to mixtures and because high exchange levels with minimum back exchange can be obtained. Directly combined LC/MS provides particular advantages in the analysis of polar compounds for which GC/MS is less well suited. Deuterium-protium exchange using DLI LC/MS was first reported by Henion (1). We report experimental details of thermospray LC/MS carried out in buffered D_2O, useful for studies of reactions associated with thermospray ionization and for structural characterization of constituents of multicomponent mixtures. Exchange levels of heteroatom-bound hydrogen at levels greater than 96% can be routinely achieved. H/D exchange using thermospray LC/MS, with $CH_3CO_2ND_4$-D_2O mobile phase and conventional flow reversed-phase HPLC has been used in this laboratory for several years (2), and the application of this method to the structure elucidation of new nucleosides from RNA has been previously reported (3). Experimental details will be published elsewhere (4). The maximum extent of exchange, measured using the disaccharide trehalose, is 97±1%D (n = 3). This is approximately the same as can be obtained with FAB from deuterated glycerol (5), although the FAB method requires care to avoid back-exchange during sample handling. Exchange levels using the LC/MS method are probably equivalent to the best levels obtained from chemical ionization with labeled reagent gases (6).

Deuterium exchange from a variety of substances is shown in Table 1, emphasizing cases in which some slightly acidic hydrogens nominally bound to carbon have undergone partial exchange. For example, exchange of enolizable hydrogen (22%) is observed in prostaglandin E_1. Additionally, exchange in the tripeptide leu-trp-met is observed and may arise from the imidazole portion of the molecule, mirroring similar exchange of aromatic hydrogens during chemical ionization with labeled reagent gases (6,7). Significant exchange of slightly acidic hydrogen was observed in the purine nucleosides, and is attributed to H-8, which can be quantitatively exchanged in solution by heating for several hours at neutral pH (pD). Partial exchange of H-8 (e.g., adenosine) was found to be generally reproducible from run to run, and relatively insensitive to changes of pD (over a range suitable for reversed-phase HPLC) and vaporizer operating temperatures (vaporizer tip 255-296°C, vapor 280-302°C). Some partial exchange of one hydrogen in cytidine takes place, as anticipated from the slightly acidic character of H-5 in solution.

The D_2O thermospray exchange method may be applied in studies of reactions associated with thermospray ionization, and as an element of structural characterization. An example was given by the differentiation of the isomers N^4,2'-O-dimethylcytidine (1) and 5,2'-O-dimethylcytidine (2), possible constituents of transfer RNA of thermophilic bacteria (3). LC/MS in D_2O of an enzymatic digest of nucleic acids revealed the unknown to contain four active hydrogens in the neutral molecule, in favor of 2.

Experience in applying this method to LC/MS analyses similar to those demonstrated above, involving 20- to 40-component mixtures, with many constituents chromatographically unresolved and in the nanogram range, has provided numerous examples of the utility of the exchange method in confirming and correcting assignments made on the basis of (protium) LC/MS data, and in providing useful deuterium shift data on new or unexpected components.

References

(1) Henion, J.D. J. Chromatogr. Sci. 1981, 19, 57-64.
(2) Hsu, F.F. Ph.D. Dissertation, University of Utah, 1986.
(3) Edmonds, C.G.; Crain, P.F.; Hashizume, T.; Gupta, R.; Stetter, K.O.; McCloskey, J.A. J. Chem. Soc., Chem. Commun. 1987, 909-910.
(4) Edmonds, C.G.; Pomerantz, S.C.; Hsu, F.F.; McCloskey, J.A. Anal. Chem., in press. 1988.
(5) Verma, S.; Pomerantz, S.C.; Sethi, S.K.; McCloskey, J.A. Anal. Chem. 1986, 58, 2898-2902.

(6) Harrison, A.G. Chemical Ionization Mass Spectrometry; CRC Press: Boca Raton, FL, 1983, pp. 129-131.
(7) Hunt, D.F.; Sethi, S.K. J. Am. Chem. Soc. 1980, 102, 6953-6963.

Acknowledgements

We gratefully acknowledge Dr. R. Gupta for isolation of nucleic acid from cells provided by Prof. K. O. Stetter; Drs. T. Hashizume and R. J. Goebel for preparation of synthetic nucleosides; Dr. P. F. Crain for helpful suggestions; specially prepared D_2O by Dr. Suraj Manrau, Merck Frosst, Canada. This work was supported by the Institute of General Medical Sciences through grant GM 21584.

Table 1. Extent of deuterium exchange from thermospray LC/MS in deuterated mobile phase.

	MD^{+a}			
Compound (molecular weight)	m/z	Active Hydrogens	%D[b]	Additional Exchange, %D[c]
16-alphahydroxytestosterone (304)	308	3	99	--
1-O-methylgalactopyranoside (194)	220[d]	8[d]	99	--
prostaglandin E_1 (354)	379[d]	7[d]	(100)	22
threonine (119)	125	5	98	--
leu-trp-met (448)	456	7	(100)	20
cytidine (243)	250	6	(100)	17
5-methylcytidine (257)	264	6	99	--
uridine (244)	250	5	97	--
pseudouridine (244)	251	6	99	--
adenosine (267)	274	6	(100)	59
1-methyladenosine (281)	287	5	(100)	58
N^6-methyladenosine (281)	287	5	(100)	45
guanosine (283)	157[e]	5[e]	(100)	99
7-methylguanosine (297)	170[e]	4[e]	(100)	99
1-methylguanosine (297)	170[e]	4[e]	(100)	99

[a] Exchange of protium bound to O or N in the principal tautomeric form.

[b] Calculated as percent of maximum exchange of active hydrogen, ±3% estimated error. When exchange of non-active H occurs, values in this column cannot be accurately calculated; values in parentheses therefore refer to assumed levels of 100%.

[c] For exchange of one additional protium bound to C in the principal tautomeric form. Calculated assuming 100% exchange of heteroatom-bound hydrogen (values in parentheses); corrected for natural isotopes.

[d] Values given refer to $M{\cdot}ND_4^+$ ion.

[e] Base fragment ion, BD_2^+; MD^+ ion not observed (ref. 5).

Presented at the 36th ASMS Conference on Mass Spectrometry and Allied Topics
June 5-10, 1988, San Francisco, CA

HYDROGEN-DEUTERIUM EXCHANGE STUDIES UTILIZING A THERMOSPRAY MASS SPECTROMETER INTERFACE

Marshall M. Siegel

American Cyanamid Company, Medical Research Division
Lederle Laboratories, Pearl River, NY 10965

SUMMARY

A routine and efficient technique.refered to as the "sandwiched slug injection technique", was developed for exchanging acidic hydrogen for deuterium, utilizing a thermospray mass spectrometer interface, to produce deuterium enriched deuteron-adduct molecular and fragment ions. Samples dissolved in solvents containing acidic deuterium atoms (D_2O/trifluoroacetic acid-d_1 or ammonium acetate-d_4) were introduced via slug injection into the thermospray interface sandwiched between slugs of the deuterated solvent. At all other times, the carrier solvent system introduced into the mass spectrometer consisted of a non-deuterium enriched mixture. Deuterium enrichments achieved were greater than 95%. Deuterium enriched deuteron-adduct molecular and fragment ions enabled the determination of the number of acidic hydrogens and aided in structural elucidation of model compounds of pharmaceutical interest.

EXPERIMENTAL

The spectra were obtained on a Vestec thermospray interface (Model 101) coupled to a Hewlett-Packard mass selective detector (Model 5970) and data system (Series 200 computer with ChemStation software). The interface temperatures were: control ~135 °C, tip 160-170 °C, block 280-285 °C and auxilary tip ~295 °C. These moderately high temperatures were chosen to induce thermal degradation and fragmentation [1]. For most of the experiments, the interface operated in the discharge ionization mode where a discharge electrode, maintained at 1 kV, was used to ionize the vapor exiting the vaporizer nozzle.

Two deuterated solvent systems were used in these studies. One consisted of D_2O/trifluoroacetic acid-d_1 (TFA-d_1) [1mL/3µL, pD ~ 1.3] where the TFA-d_1 served as an acid catalyst to enhance the exchange rate The second solvent system consisted of ammonium acetate (NH_4Ac) dissolved in the D_2O/TFA-d_1 solution to effectively produce 0.1 M ND_4Ac, a nearly neutral [pD ~ 5.8] buffered solution. (Similar experimental results were obtained when using 0.1 M ND_4Ac prepared by titrating ND_4OD with acetic acid-d_1.) To fully dissolve samples which were only partially soluble in these solvent systems, small amounts of acetonitrile methanol-d_1 and/or chloroform-d_1 were added until solubility was achieved. Solutions of the pure compounds were prepared in the deuterated solvents (~5mg/mL), thereby, exchanging the acidic hydrogen atoms in the compounds for deuterium.

A sample loop of 200 or 500 µL was used in which a sample volume of 2 - 15 µL was injected, preceded and followed by 50-200 µL and 100-200 µL, respectively, of deuterated solvent. At all other times, the carrier solvent system introduced into the mass spectrometer was a non-deuterium enriched mixture consisting of methanol/methylene chloride/water (48/48/4 v/v/v) flowing at 1.0 mL/min. This carrier solvent system was chosen since it behaves as a "universal solvent", thereby, minimizing the likelihood for blockage of the vaporizer probe. The mole fraction deuterium enrichments were computed using the "Average Mass Approach" developed by Blom and co-workers [2] for nominal mass data or by dividing the difference in average mass between the enriched and unenriched samples by the number of labile hydrogen atoms in the molecule.

RESULTS AND DISCUSSION

A variety of pharmaceutically important compounds were studied utilizing the sandwiched slug injection technique These compounds contained from 4 to 11 labile hydrogen atoms. As noted in Table I, the percent mole fraction enrichment of deuterium for the compounds ranged from 97.6% to 109.8%. A comparison of the unenriched and deuterium enriched discharge ionization spectra for VAAF and VAAF-d_6 are illustrated in Figure 1. The mass shift between the corresponding ions in the unenriched and enriched spectra correlate with the fragmentations illustrated with the structure in the figure. The key in getting these high deuterium enrichments is the sandwich of solvent around the sample The sandwiched slug injection technique optimizes the hydrogen-deuterium exchange process in both the condensed and gaseous phases. In the condensed phase, excess deuterium containing solvents and catalysts drive the exchange process to completion,

while, in the gaseous phase, the slugs of deuterium containing solvents, introduced before and after the sample, deuterate substances adsorbed on to the surface of the source thereby minimizing back exchange of deuterium for hydrogen. The net result is that the thermospray plasma remains rich in deuterium and more than 95% of the labile hydrogen atoms are exchanged with deuterium utilizing this technique.

If only a slug of the deuterium enriched sample is injected into the TSP system without the sandwich of deuterium enriched solvents, deuterium enrichment is only 40% to 50%. This is insufficient for structural elucidation because the ion distribution is very broad, making it virtually impossible to determine accurately the number of labile hydrogens. Although deuterium enrichment of the sample in the condensed phase is very high, the deuterium atoms back exchange in the gas phase with the hydrogen atoms present in the unenriched carrier solvent.

An interesting feature appearing in the spectra of ampicillin is the pair of abundant ions at m/z 195 and 196. The structures of these ions correspond to substituted ketenes generated from the [2 + 2] retro-cycloaddition (decomposition) of the β-lactam ring. Scheme I illustrates a possible gas phase mechanism for rationalizing the formation of the pair of ions. The hydrogen atom on the deuteron-adduct ketene group, readily undergoes exchange for deuterium via a neutral substituted alkynol, to produce the deuterium enriched ketene. This exchange mechanism is due to resonance stabilization of the delocalized charge associated with the deuteron-adduct ketene molecule.

REFERENCES

1. Siegel, M. M.; Isensee, R. K.; Beck, D. J. Anal. Chem. 1987, 59, 989 - 995.
2. Blom, K.; Dybowski, C.; Munson, B.; Gates, B.; Hasselbring, L. Anal. Chem. 1987, 59, 1372 - 1374.

Table I

DEUTERIUM ENRICHMENT IN THE DEUTERON-ADDUCT MOLECULAR ION REGION

Compound	Deuteron-Adduct Molecular Ion Region[a]	% Deuterium Enrichment
Minocycline-d6	463(5), 464(2), 465(100.100), 466(32:28), 467(7:5), 468(1·1)	98 9
Methotrexate dihydrazide-d11	495(100:100), 496(51:28), 497(6 4)	101 0
Adenosine-d5	272(1),273(10),274(100.100),275(22:13),276(4 2)	99.5
Ampicillin-d4	352(1), 353(2), 354(9), 355(100:100), 356(23 20), 357(8:7), 358(1:1)	98 9
Mitoxantrone-d8	451(3), 452(6), 453(3), 454(100.100),455(30·27), 456(15.5), 457(3:1)	99.8
Leucine-Enkephalin-d8	563(2), 564(18), 565(100 100), 566(57·34), 567(30.7), 568(11:1), 569(6)	103 5
Erythromycin-d5	737(1), 738(4), 739(6), 740(100.100), 741(44·44), 742(12·12), 743(2.2)	97 6

[a]) Nomenclature used. X(Y), X(Y:Z) where X is the mass-to-charge ratio (m/z), Y is the observed relative intensity and Z is the predicted relative intensity based upon the elemental composition of the deuteron-adduct molecular ion

Scheme I

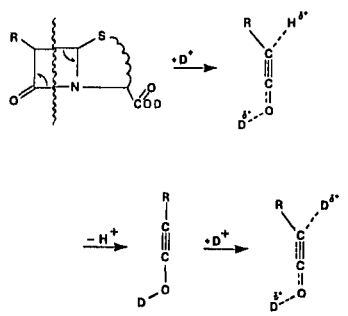

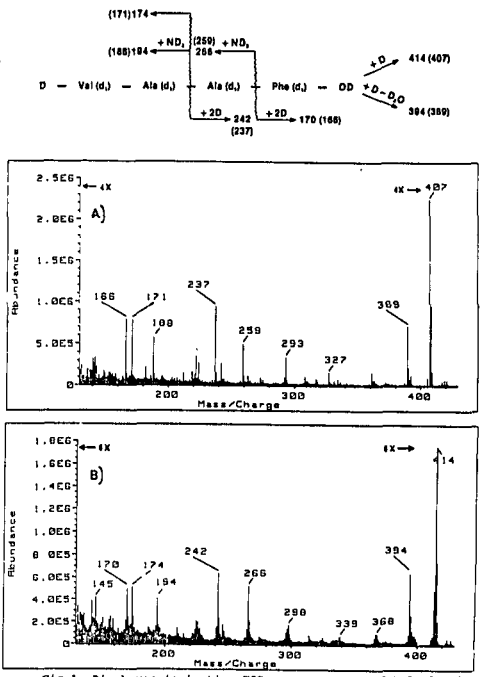

Fig 1. Discharge ionization-TSP mass spectrum of Val-Ala-Ala-Phe, 1, obtained using the sandwiched slug injection technique (150 μL D_2O//50 μL CH_3CN//30 μL sample//50 μL CH_3CN//150 μL D_2O). A. Sample dissolved in H_2O/TFA-d_0/CH_3CN. B. Sample dissolved in D_2O/TFA-d_1/CH_3CN. For the structure, the masses in parenthesis correspond to the unenriched sample.

Presented at the 36th ASMS Conference on Mass Spectrometry and Allied Topics
June 5-10, 1988, San Francisco, CA

SFC/MS ANALYSIS OF BIOLOGICAL SAMPLES WITH ELECTRON IONIZATION, Jack Henion, Per Olof Edlund, Edgar Lee, and Lee McLaughlin, Equine Drug Testing and Toxicology, Cornell University, 925 Warren Drive, Ithaca, NY 14850

The general acceptance of supercritical fluid chromatography (SFC) by analytical chemists appears to be dependent upon its successful combination with mass spectrometry (MS). The combination of these two analytical techniques (SFC/MS) could offer some of the following benefits over GC/MS and LC/MS: faster separations and better chromatographic efficiency then LC/MS, the ability to handle higher molecular weight and more thermally labile compounds than GC/MS, and more facile electron ionization then LC/MS. The latter feature is of particular interest to those who need appropriate structural information for the identification of unknown compounds.

There are two approaches to SFC/MS which parallel modern GC/MS and LC/MS. The first utilizes open tubular columns of somewhat smaller internal diameters than capillary GC/MS. The other uses packed columns of the same type used in modern LC/MS. Although we have evaluated both of these approaches, this paper will present data obtained from packed-column SFC/MS using supercritical carbon dioxide doped with methanol. The novel aspect of this work is the use of a heated, pneumatic nozzle and a two-stage momentum separator for enrichment of the expanded mobile phase prior to transfer of the analyte to the mass spectrometer electron ionization (EI) source. This approach provides full-scan (m/z 50-MW) EI mass spectra from an unmodified conventional EI mass spectrometer.

EXPERIMENTAL

A Hewlett-Packard Model 1084B HPLC system modified for SFC was connected to a homemade heated pneumatic nozzle "probe" which was positioned inside a homemade ambient temperature desolvation chamber. The latter was connected directly to a two-stage momentum separator which was pumped in the first stage by a 400 L/min rotary pump while the second stage was pumped by a 300 L/min rotary pump. The two-stage momentum separator was attached directly to a half-inch o.d. by three-eights inch i.d. tube which was inserted through the standard direct insertion probe vacuum lock of an unmodified Hewlett-Packard Model 5985B GC/MS system. The heated pneumatic nozzle was a modified homemade thermospray probe which accommodated a 50 micron i.d. x 40 cm fused-silica capillary housed in the central 0.010 in i.d. x 0.062 in o.d. stainless steel capillary tube. The central fused-silica capillary acted as a linear restrictor for transport of the carbon dioxide/methanol mobile phase mixed post-column with a make up liquid consisting of methanol, ethanol, or isopropyl alcohol. The flow of the supercritical fluid mixture was maintained at 0.8 mL/min while the make up flow liquid was maintained at 0.3 mL/min. A co-axial flow of helium nebulizing gas was maintained at 0.5 L/min in the annular space between the inside of the stainless steel central capillary tube in the probe and the outside of the central fused-silica capillary. The heated copper probe tip was maintained at 60 degrees during the course of this work. No additional heating was supplied to the desolvation chamber or the two-stage momentum separator. The EI ion source was maintained at 250 degrees.

RESULTS AND DISCUSSION

The packed-column SFC/MS system described in this work was used to obtain full-scan and SIM EI mass spectral data on a variety of compounds. These included coenzyme Q-10, stanozolol, several corticosteroids, 2,4-D and its methyl ester, in addition to several Irganox polymer additives and xanthine-related drugs. In addition, the identification of prednisolone and several of its metabolites were identified in a biological extract of equine urine.

Figure 1 shows, for example the EI packed-column SFC/MS TIC and mass spectrum for prednisolone identified in an ethyl acetate extract of an equine urine collected 2 hours post-administration of prednisolone to a horse. The extracted ion current profile for the base peak of this drug is observed at 5 min retention time and the EI mass spectrum is shown in the lower panel of Figure 1.

CONCLUSIONS

The packed-column SFC/MS system described provides access to EI mass spectra for moderately polar, thermally labile and relatively involatile organic compounds which may be isolated from biological samples. The system has operated for several months on a daily basis with no unusual adverse effects on the mass spectrometer. Conventional tuning procedures are used while ion source cleaning is no more frequent than with GC/MS techniques.

The most serious shortcoming of the present results is the low sensitivity obtained with compounds studied to date (1-5 micrograms on-column for good quality, full-scan SFC/MS EI mass spectra). There appear to be significant transmission losses within the two-stage momentum separator as evidenced by visible build-up of sample around the first skimmer of this device. This may result from inadequate pumping at the two stages of the separator and/or the formation of very small particles which lack the necessary momentum to be efficiently transferred through the separator under the SFC conditions used in this work. Work continues to significantly improve the sensitivity of this system. If the full-scan detection limits could be improved to the 20 ng level we believe this approach would be a very useful and rugged analytical technique.

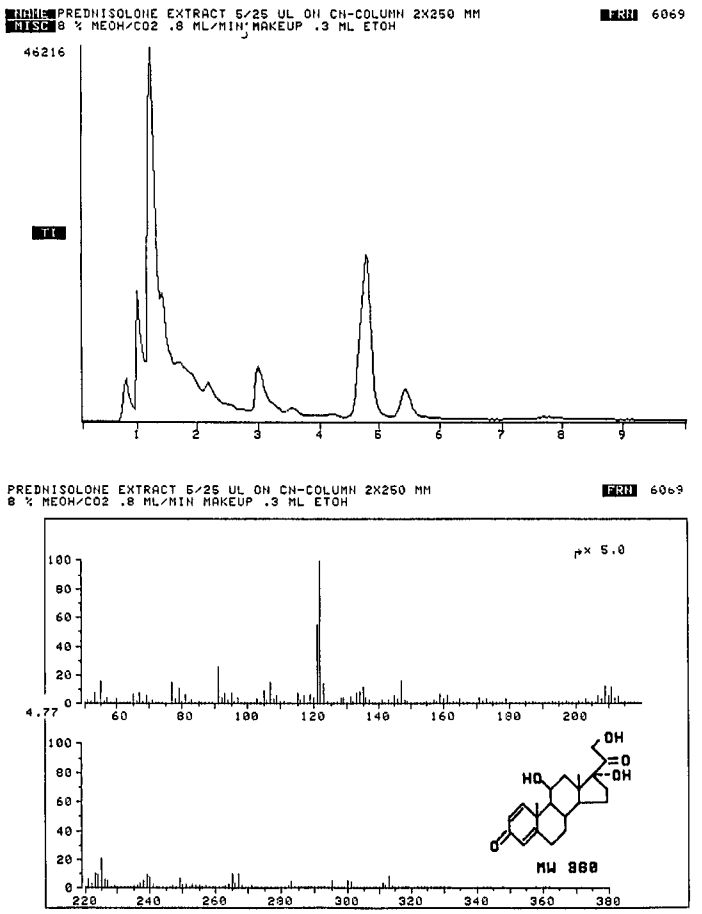

Figure 1. Packed-column SFC/MS full-scan EI mass spectrum of prednisolone (retention time 4.8 min) detected in the extract of an equine urine collected 2 hours after the administration of prednisolone. The peak at 5.4 min retention time is a metabolite, 20-hydroxy prednisolone.

Presented at the 36th ASMS Conference on Mass Spectrometry and Allied Topics
June 5-10, 1988, San Francisco, CA

APPLICATIONS OF SFC-MS TO TOXINS AND COMPOUNDS OF BIOLOGICAL INTEREST

H. R Udseth, H. T. Kalinoski, and R. D. Smith
Chemical Methods and Separations Group
Chemical Sciences Department
Pacific Northwest Laboratory, Richland, WA 99352

The principal applications of supercritical fluid chromatography (SFC) are for compounds that are thermally labile, of low volatility, and of low to moderate polarity. Many compounds of biological and pharmaceutical interest are defined by these criteria. Recently, applications of SFC and SFC-MS to the determination of lower molecular weight compounds of interest due to their biological activity were described (1,2).

As the technique of SFC has developed, CO_2 has become the most widely used mobile phase. Its low critical temperature, 32 °C, makes it an attractive choice for separation of thermally labile compounds. Unfortunately the solubility of many thermally labile compounds with biological activity in CO_2 is insufficient. Experience has shown that the addition of a small amount of modifier, usually 1 to 10% methanol or isopropanol, can dramatically increase the solubility of selected compounds.

The use of both packed and open tubular capillary columns in SFC has become an established as useful compliments. Most initial SFC work was done with packed columns. The initial development of SFC-MS, however involved the use of open tubular fused silica capillary columns due to their more easily addressed flow rates. These columns usually provide greater efficiency than packed columns, but when the efficiency needed for a given analysis is less demanding the speed and sample capacity of packed columns becomes advantageous. Techniques for using both types of column are now sufficiently well established that the optimum type of column for a given separation can be used.

For interfacing to mass spectrometry this desired flexibility in column choice is more difficult to accommodate due to the much higher flow rates typically used in packed columns. We have previously developed a High Flow Rate (HFR) interface that accommodates the higher flow rates of microbore packed columns which can also be used with larger diameter capillary columns at high flow rates and with splitless injection (3).

In this work we have examined selected compounds of moderate to high molecular weight with biological activity. We have used the HFR interface with CO_2 as the mobile phase with from 2 to 5% modifier. A standard gas chromatography (GC) oven was used to contain the capillary column. Both 20 m and 30 m X 100 µm i.d. capillary columns were used. They were coated with a 0.5 µm thick bonded and crosslinked stationary phase of 5% phenyl methylphenylpolysiloxane stationary phase. The 1 mm X 10 cm C-18 (5 µm particles Alltech Associates) microbore column was contained in the inlet probe so as to minimize the length of the transfer line.

One class of compounds potentially addressable by SFC-MS are cyclic peptides (4). These polar compounds require the use of polar fluid modifiers with CO_2 as the mobile phase. The ionic nature of the more hydrophilic portions of such polypeptides can sometimes be shielded, allowing solvation in supercritical fluid solvents. We used cyclosporin A as an example of such a compound. It is a cyclic undecapeptide which exhibits strong immunosuppressive properties.

The compound was successfully separated by SFC-MS using a microbore column using a 2% methanol modifier The compound was also successfully separated with a capillary column. With the capillary column 2% 2-propanol was adequate, whereas with the microbore column more polar methanol was needed. The mass spectra were identical in both cases. The protonated molecular ion (m/z 1203) dominates the spectra and the only other significant peak corresponded to the loss of the largest side chain.

Care must be taken in generalizing these results. Our attempts to chromatograph the cyclic heptapeptide microcystin-LR were unsuccessful even when the modifier content was increased to 5% and the temperature raised to 100 °C. Microcystin-LR is markedly more polar than cyclosporin A (having an amine residue on one of its side chains) which probably accounts for the difference in fluid phase solubility.

Polyethers constitute another class of high molecular weight biologically active compounds of moderate polarity which may be amenable to analysis by SFC-MS. We analyzed the sodium salt of two ionic polyethers, maduramicin a (mol. wt. 938) and a related compound of mol. wt. 996 (5). These compounds are commonly referred to as ionophores. They are potent antibiotics that chelate with ions and transport them across cell membranes. We were not successful in using the microbore column, but 2% isopropanol in CO_2 at 60 °C allowed separation with the capillary column. The peaks showed substantial tailing and this coupled with the low transmission of the quadrupole at high m/z forced operation with reduced resolution (~ 500). The results nonetheless show the mass spectra are dominated by the protonated molecular ion. These results show that the salt is dissolved as an intact ion pair. Small salts are very insoluble in supercritical fluids, but when the hydrophobic region of the molecule becomes large enough the intact compound will often dissolve in fluids such as CO_2.

These compounds are generally thermally labile (~100 °C). This can be used to advantage by controlling fragmentation through changes in the tip heater. The result of raising the indicted temperature from 145 °C to 300 °C is to increase the fragmentation. This increase in fragmentation is potentially useful for compound identification. By raising the modifier content to 5% and the oven temperature to 100 °C the efficiency of the separation was substantially improved. This increase in signal allowed us to increase the resolution to unit mass. The nominal mass was set to 939. The isotopic pattern was clearly seen as was the lack of fragmentation. No decomposition was observed at these temperatures.

Our attempts to work with another polyether, brevetoxin (PbTx2, mol. wt. 894) were only partially successful. A spectra containing the molecular ion and a characteristic fragment loss was obtained, but at low resolution with low sensitivity.

Another class of compounds that is potentially addressable with modified supercritical fluids is unsaturated ring systems of moderate polarity. As an example we took a look at a series of cardio and vascular stimulants of decreasing solubility: khellin (mol. wt. 260), digitoxigenin (mol. wt. 374), digoxigenin (mol. wt. 390) and cymarin (mol. wt. 548). These separations used a 30 m capillary column with 5% isopropanol at 100 °C. Khellin was detected with excellent sensitivity and gave a spectrum that was dominated by the protonated molecular ion. The sensitivity for digitoxigenin was also good, but less than that for khellin. The eluting peak was symmetric with little tailing and the spectrum showed a small amount of fragmentation and adduct ion in addition to the protonated molecular ion. Digoxigenin had a sensitivity comparable to that of digitoxigenin and the eluting peak was similar in shape. The spectrum was still dominated by the $(M+H)^+$ ion, but showed much more fragmentation. Cymarin, which contains a sugar unit, is a more interesting case. Our previous experience with SFC of sugar containing compounds suggested that they would have very low solubility in these supercritical fluids. Cymarin, however was found to elute quite nicely. The spectrum showed considerable fragmentation and while the molecular ion was not the base peak, it was still prominent and the fragmentation gave useful information.

Although supercritical CO_2 has limited solvating powers, the addition of modifiers can extend its useful range substantially. Success with highly polar compounds is still problematical. However, if the polar regions can be successfully shielded by low polarity hydrophobic regions, then the possibility exists of solvation in modified fluids. This is clearly seen for the examples of the ionophores, where a large polyether ion pair has been successfully analyzed by SFC-MS. The stimulant cymarin is another clear example. It is difficult to generalize from these examples but it is safe to say that the application of SFC-MS will continue to grow on a case by case basis. Additional considerations relevant to direct injection SFC-MS are related to compound vapor pressure and to the particular interface design in regards to the flow restrictor region and effectiveness of heat transfer during the fluid expansion (decompression).

We thank the U. S. Army Medical Research Institute of Infectious Diseases for support of this work.

(1) Smith, R. D.; Udseth, H. R.; Kalinoski, H. T. *Mass Spec. Reviews* **1987**, 6, 445.
(2) Crowther, J. B.; Henion, J. D. *Anal. Chem.* **1985**, 57,2711.
(3) Smith, R.D.; Udseth, H. R. *Anal. Chem.* **1987**, 59,13.
(4) White, C. M.; Gere, D. R.; Boyer, D.; Pacholec, F.; Wong, L. K. *Eighth International Symposium on Capillary Chromatography, Volume II*, P. Sandra, Ed., **1987**, 1027.
(5) Siegel, M. M.; McGahren, W. J.; Tomer, D. B.; Chang, T. T. *Biomed. Environ. Mass Spectrom.* **1987**,14, 29.

Presented at the 36th ASMS Conference on Mass Spectrometry and Allied Topics
June 5-10, 1988, San Francisco, CA

SUPERCRITICAL FLUID CHROMATOGRAPHY-MASS SPECTROMETRY (SFC/MS) USING A SIMPLE CAPILLARY-DIRECT INTERFACE

Steven B. Hawthorne and David J. Miller
University of North Dakota
Energy and Mineral Research Center
Grand Forks, North Dakota, 58202

The combination of supercritical fluid chromatography with mass spectrometry (SFC/MS) provides a powerful new approach to the separation and identification of non-volatile and thermally-labile compounds. In general, methods that have been used for interfacing SFC with MS require modifications of existing mass spectrometer interfaces and/or of the ion source which require dedication of the mass spectrometer to SFC/MS. We have developed a simple and effective SFC/MS interfacing method that requires no modification of a commercially-available quadrapole MS, and allows the mass spectrometer to be used for both capillary SFC/MS and GC/MS with a minimal conversion time.

SFC separations were performed using a Lee Scientific Model 501 supercritical fluid pump and split injections (split ratio ca. 1:20). All separations were performed using CO_2 as the carrier fluid at a temperature of 125 ^{o}C and a 10 meter J & W DB-5 or a Lee Scientific SB-phenyl-5 (50 µm i.d.) capillary column. Column pressure was maintained using an integral "Guthrie" restrictor. The restrictor was constructed to yield a gas flow rate of approximately 3 mL/min at 200 atm CO_2 resulting in a source pressure of approximately 5×10^{-5} torr. The physical strength of this restrictor allows the column to be installed and removed without breakage.

A Hewlett-Packard model 5988 GC/MS was modified for SFC/MS by simply installing the SFC injection valve on the outside of the chromatographic oven. The SFC column was then inserted through the interface transfer line until the column restrictor end just entered the ion source. After initial installation of the SFC injector, converting the instrument from GC/MS to SFC/MS and back is achieved simply by installing the appropriate chromatographic column. Since the 5988 allows columns to be changed without venting the source, the conversion can be accomplished in less than 20 minutes. Mass spectrometry was performed in the chemical ionization mode (CI) using methane as the reagent gas at a source pressure of approximately 0.3 torr with polydimethylsiloxane as the CI tuning compound.

The ability of the capillary-direct interface to yield good chromatographic peak shapes is demonstrated in Figure 1 by the SFC/MS total ion current chromatogram of PEG 600 (no background subtraction has been used for either Figure 1 or 2). Figure 2 shows that good sensitivity is achieved and that full scan (160-500 amu) spectra can be obtained at the low ng level. Selected ion monitoring (SIM) detection limits have also been determined for PAHs and oxy-PAHs, and are typically at the low pg level.

Several samples including natural and synthetic waxes, polycyclic aromatic hydrocarbons, triazine herbicide metabolites, polymers, and pine tree resins have been analyzed and these results demonstrate the usefulness of the capillary-direct interface method for SFC/MS analysis. Besides its simplicity, the interfacing method has an additional advantage in that a single instrument can rapidly be converted for either GC/MS or SFC/MS.

CREDIT

Partial financial support from the United States Environmental Protection Agency, Office of Exploratory Research (grant number R-812229-01-0) and the Department of Energy (Cooperative Agreement number DE-FC21-86MC10637) is gratefully acknowledged.

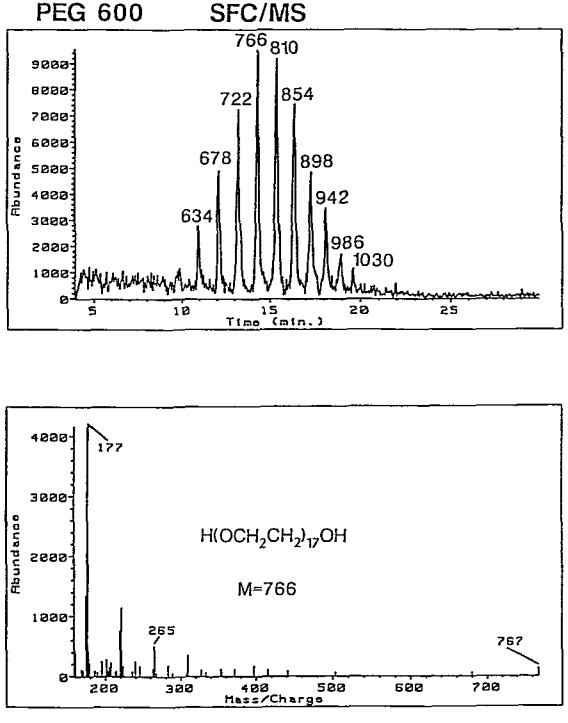

Figure 1: SFC/MS analysis of polyethylene glycol (PEG) 600. The molecular weights are given on each peak. The methane CI spectra is also shown for the M=766 species.

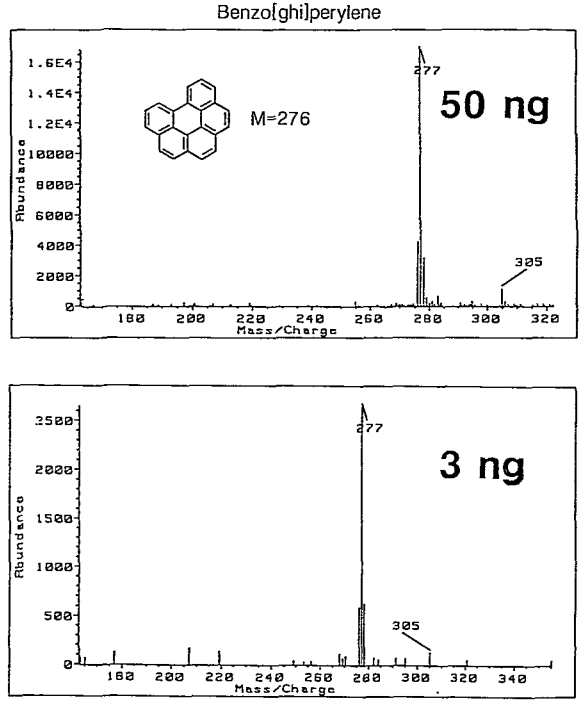

Figure 2: Comparison of the SFC/MS methane CI full scan (160-500 amu) mass spectra for 50 ng and 3 ng of a PAH.

Presented at the 36th ASMS Conference on Mass Spectrometry and Allied Topics
June 5-10, 1988, San Francisco, CA

ANALYSIS OF HIGH MOLECULAR WEIGHT CARBOHYDRATES BY SFC-MS

D. M. Sheeley, J. C. Kuei, G. R. Her, & V. N. Reinhold
Harvard School of Public Health
Boston, MA 02115

Introduction

The application of FAB-MS and comparable soft ionization techniques (e.g. DCI and LD) has introduced the first hope of a sensitive method for studying carbohydrate structures. Unfortunately, for those techniques requiring a desorption matrix (FAB), a problem arises in the biased presentation of sample components, and it is not uncommon for selected samples to exhibit very poor sensitivity or not work at all. For DCI-MS, samples are always detected, but heat initiated desorption leads to pyrolysis of high molecular weight and nonvolatile materials, seriously limiting high mass analysis. An alternative technique not requiring an applied matrix or exhibiting sample suppression has been FAB desorption from a polyimide belt. However, this HPLC-belt interface device is expensive, appears to have high mass limitations, and is technically demanding.

The analysis of nonvolatile compounds by SFC presents an attractive alternative to existing LC-MS configurations. Although as yet unrealized, most significant is the flexibility provided to chromatographic and chemical ionization parameters by simple variations in the mobile phase. These factors, combined with reduced gas loads, ease of solvent elimination, and potential for encompassing greater sensitivity, will certainly make MS detection a major consideration in molecular characterization. This report describes a simple and direct SFC-CIMS interface applicable to derivatized oligosaccharides.

Experimental

SFC separations were performed on a model 501B supercritical fluid chromatograph (Lee Scientific, Inc.) equipped with a flame ionization detector, and a pneumatically actuated submicroliter (0.2 ul) injection valve (Valco Instrument Co. Inc.). Pump cylinder and injection valve temperatures were held at 0 deg C. Capillary columns had inner and outer diameters of 50 and 375 microns, respectively. The column was coated with DB-5, 0.2 um film thickness (J & W Scientific, Inc.). Mobile phase pressure and flow were maintained by fabrication of the integral restrictor described by Guthrie and Schwartz.

Chemical ionization MS was performed on a VG ZAB-SE instrument, operating at 8 kV using ammonia as the reagent gas. The ion source was modified for dedicated CI operation by removal of the columnating magnets, blocking all inlet ports, and use of narrower exit slits. The SFC column tip was introduced through the single DCI inlet and heated at the very tip (1 mm) by a resistance wire connected to and controlled by the DCI unit. With the exception of restrictor tip heating, all temperatures were maintained equal to that of the SFC oven.

Results and Discussion

In previous work, interface temperatures up to 250 degrees higher than that required for SFC separations have been reported. From these reports, usually involving low voltage quadrapole instruments, it was not always clear if there were high-mass limitations. In this application, we have attempted to address the question of heating requirements, analyte desolvation and ionization, sensitivity, and high mass limitations. To approach the latter concern, a comparison between FID signal (mass detection) and TIP plots (molar detection) obtained for permethylated glucose homopolymers suggests that the

ionization efficiency between low and high mass remains relatively constant. Under these SFC-CIMS conditions, each oligomer provided single molecular weight-related ions only, $(M+NH_4)^+$, with little indication of fragmentation. Investigation of a comparable glucose homopolymer, derivatized with trimethylchlorosilane to enhance chromatographic efficiency and increase the molecular weight, demonstrates that chromatographic fidelity is preserved in the interface with anomer separation still apparent at DP15. Moreover, the mass spectra of the latter eluting peaks again indicates that the molecular ion is the major contributor to the total ion current, Fig. 2. To examine the limits of sensitivity samples of permethylated cyclodextrin were studied at varying concentrations. A signal to noise ratio of 10:1 is obtained in the selected ion chromatogram of a 2 picomoles injection. These preliminary studies have provided an understanding of this application to high molecular weight biopolymer problems. Modifications are in progress to improve SFC coupling, higher mass analysis, and sensitivity.

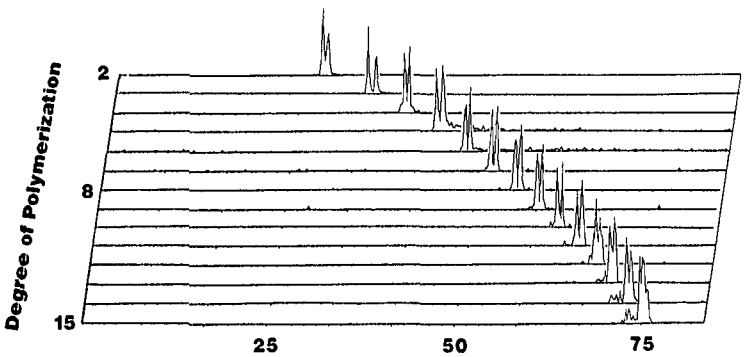

Figure 1

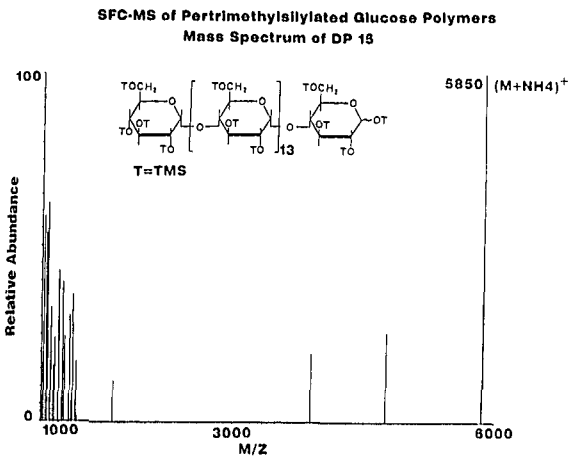

Figure 2

Presented at the 36th ASMS Conference on Mass Spectrometry and Allied Topics
June 5-10, 1988, San Francisco, CA

STUDIES WITH PACKED AND CAPILLARY COLUMN SFC/MS

I.C. Mylchreest and D.E. Games
Department of Chemistry, University College,
P.O. Box 78, Cardiff CF1 1XL, U.K.

Packed and capillary column supercritical fluid chromatography (SFC) are complementary to both gas chromatography (GC) and high-performance liquid chromatography (LC) for the analysis of organic compounds. The former approach offers speed of analysis and method development, together with preparative capability. Whereas the latter provides better chromatographic efficiencies than LC and ease of interfacing to gas chromatographic detectors such as flame ionization.

We have effected packed column SFC/MS using a modified spray deposition device and moving belt LC/MS interfaces[1]. This approach provides both EI and conventional CI mass spectra and good retention of chromatographic efficiency. Packed column SFC/MS has also been developed using a modified Finnigan MAT thermospray source in the filament-on or discharge mode[2]. If only carbon dioxide is used as the mobile phase, charge exchange EI type spectra are obtained, whereas with modified CO_2 (e.g. methanol) solvent moderated CI mass spectra are obtained. For capillary SFC/MS, an interface was constructed which enables direct heating of a frit restrictor[3]. In this mode, charge exchange EI type spectra or conventional CI mass spectra are obtained.

Experimental

Packed column SFC was effected using a modified Hewlett Packard 1084B liquid chromatograph and capillary column SFC using a Lee Scientific 501 supercritical fluid chromatograph. Moving belt SFC/MS was performed on either a VG 70/70 E magnetic mass spectrometer or a Finnigan 4000. Thermospray filament-on or discharge SFC/MS was effected with a Finnigan 4000 or Finnigan MAT TSQ 70. For capillary SFC/MS, a Finnigan MAT ITD700[4], Finnigan 4000 and a Finnigan MAT TSQ 70 were used.

Results and Discussion

In capillary SFC/MS we have recently effected interfacing using an ion trap detector[4]. A directly heated frit restrictor was used for the interface and it was found that addition of helium gave good quality spectra with an increase in detection limits. Mixtures of polynuclear aromatic hydrocarbons were studied and good total ion current traces were obtained, together with library searchable spectra. In addition, collision induced dissociation experiments were successfully undertaken. Most of our studies in this area have been conducted with quadrupole mass spectrometers and studies of a dimethyl polysiloxane with a Finnigan MAT TSQ 70 have shown that informative mass spectra can be obtained to masses just in excess of 4000u. In addition, sensitivity studies of pyrene showed that EI type full scan spectra are obtainable at the 200pg injected level with 50pg being obtainable in the CI mode with methane.

Packed column SFC/MS using a moving belt interface has been used to study indole alkaloids in extracts from Catharanthus roseus and fermentation extracts containing milbemycin antibiotics. In both cases EI mass spectra provided molecular weight information and structurally useful fragment ions, enabling mono- and dimeric indole alkaloids and a range of milbemycins to be readily identified and new compounds located. SFC/MS studies of the indole alkaloids have also been undertaken using a thermospray source in the filament-on or discharge mode. Here spectra consisted mainly of $[M + 1]^+$ ions with few fragment ions. A mixture of isomeric alkaloids, tabersonine, catharanthine, vindoline and epivindolinine were studied and gave very similar mass spectra. Use of a TSQ 70 in the collisional activation mode, however, provided more informative spectra which readily enabled the compounds to be differentiated.

In an alternative approach to obtaining more structurally informative mass spectra from SFC/MS using the thermospray system, we have investigated the effects of variation of repeller voltages, discharge voltages and jet block temperature. Both variation of repeller voltage in the filament-on mode and increasing jet block temperature in the discharge mode yielded more fragmentation.

SFC/MS of ecdysteroids has also been studied. Here, best data was obtained using the thermospray system. The technique has been applied to the identification of these compounds in silene otites.

Acknowledgements

I.C.M. thanks Glaxo Group Research and Finnigan MAT, U.K. for financial support. The indole alkaloid studies are being conducted in collaboration with L.R. Hogge of the Plant Biotechnology Institute, Saskatoon. Studies of the ecdysteroids are a collaboration with D. Morgan, University of Keele. We thank J. Hurst, Finnigan MAT, San Jose, for his assistance with the TSQ 70.

References

1 A.J. Berry, D.E. Games and J.R. Perkins, J. Chromatogr., 1986, 363, 147.

2 A.J. Berry, D.E. Games, I.C. Mylchreest, J.R. Perkins and S. Pleasance, Biomed. Environ. Mass Spectrom., 1988, 15, 105.

3 A.J. Berry, D.E. Games, I.C. Mylchreest, J.R. Perkins and S. Pleasance, J. High Res. Chromatogr. Chromatogr. Commun., 1988, 11, 61.

4 J.F.J. Todd, I.C. Mylchreest, A.J. Berry, D.E. Games and R.D. Smith, Rapid Commun. Mass Spectrom., 1988, 2, 55.

Presented at the 36th ASMS Conference on Mass Spectrometry and Allied Topics
June 5-10, 1988, San Francisco, CA

Analysis of Indole Alkaloids from Leaves of Catharanthus roseus by Means of Supercritical Fluid Chromatography/Mass Spectrometry

J. Balsevich*, A.J. Berry**, D.E. Games**, L.R. Hogge* and I.C. Mylchreest***, National Research Council of Canada, Plant Biotechnology Institute, Saskatoon, Saskatchewan,** Dept. of Chemistry University College, P.O. Box 78

Introduction: Separation and characterization of indole alkaloids in plant extracts can be a very difficult analytical problem because of the wide range of solubilities, molecular weights, and polarities of the components. Thin layer chromatography (TLC) has proven to be a useful method for their separation, while use of spray reagents in conjunction with TLC has proven a sensitive method for their detection. Reversed phase high pressure liquid chromatography (LC) using gradient elution has also been used with some success. Unfortunately both of these techniques have shortcomings. TLC spots obtained from polar compounds sometimes overlap. Furthermore, identification of unknown alkaloids separated by TLC is not possible using spray detection. Co-elution of components is also common when using LC for the separation of these compounds. Recently, supercritical fluid chromatography (SFC), a technology which is well suited to interfacing with a mass spectrometer, has been shown to be more efficient than LC and has proven effective in analyses of various polar compounds, including mixtures of ergot alkaloids (1). Accordingly, as a potentially useful means of directly obtaining pertinent information on the number and type of monoterpene indole alkaloids in a relatively small amount of complex sample, we sought to evaluate the use of a supercritical fluid chromatography/mass spectrometry system (SFC/MS) for the analysis of an alkaloid mixture obtained from the leaves of the medicinal plant Catharanthus roseus (Apocyn).

Experimental: SFC analyses were performed with a Hewlett Packard Model 1084B liquid chromatograph modified for SFC (2). An amino bonded 5 micron Spherisorb 100 x 4.5 mm column was used with CO_2 and a 5-15% gradient of methanol polar modifier as the mobile phase. Eluting peaks were detected at a wavelength of 290 nm. The column temperature was 65°C. Electron impact SFC/MS was performed by coupling the chromatograph to a VG model 70/70 mass spectrometer equipped with a moving belt LC/MS interface. The effluent was deposited on the moving belt by using a Finnigan MAT spray deposition device connected in-line via a "T" piece between the UV detector exit and the back-pressure regulator of the chromatograph (1). The belt speed was 3 cm/sec; the nosetip heater temperature was 250°C. The mass spectrometer was scanned from mass 850 to 85 every 2 sec. Thermospray SFC/MS was performed by coupling the chromatograph to a Finnigan MAT model 4000 GC/MS equipped with a modified Finnigan MAT thermospray LC/MS interface operated in the filament-on mode (3). The thermospray tip temperature was 160°C. The mass spectrometer was scanned from mass 150 to 850 every 2 sec.

Results and Discussion: The results of the SFC analysis of the leaf alkaloids of C. roseus were highly satisfactory both from the points of view of resolution and run time (ca. 8 min). The separations obtained on the amino bonded Spherisorb column (Fig. 1) yielded qualitative information comparable to that obtained via two dimensional TLC on silica gel. Compounds having very similar structures were well spaced. Desacetoxyvindoline (3), vindorosine (5), vindoline (6), and deacetylvindoline (10), complex Aspidosperma alkaloids differing only slightly from each other in their functional groups, were separated by a minimum 0.3 min (between 3 and 5) and a maximum of 1.9 min (between 3 and 10). Similarly, the pharmaceutically important bisindoles leurosine (11), 3', 4'-anhydrovinblastine (12), and vinblastine (14) were easily resolved and well separated from each other, even though they chromatographed as a group away from the majority of the "monomers".

One of the attractive features of SFC is the use of a large proportion of a highly volatile phase (CO_2 in our case) which makes interfacing the chromatograph to a mass spectrometer much less problematic than is the case with HPLC. Both EI and filament-on thermospray ionization were successfully employed in the SFC/MS system. Fig. 2 illustrates four representative EI mass spectra obtained via SFC/MS. With the exception of lochnerinine (1), whose spectrum contained some anomalous peaks (due to the presence of unknown alkaloid having M^+ 338) the spectra were of quality comparable to those obtained from the pure compounds.

The use of thermospray ionization in the SFC/MS system effectively enhanced the sensitivity for detection of the alkaloids. Since in the case of monoterpene indole alkaloids the ionization technique affords predominantly $(M + 1)^+$ ions with little fragmentation, a scan giving rise to a spectrum containing several significant peaks would

be indicative of the presence of several compounds of appropriate molecular weights. The spectrum (Fig. 3) obtained from the eluent proximate to peak 3 (Fig. 1) indicated the presence of components having molecular weights of 350 and 352 in addition to desacetoxyvindoline (M^+ 398).

Conclusion: SFC/MS is a very effective technique for obtaining useful information regarding the numbers and types of monoterpene indole alkaloids present in a complex mixture of plant leaf extracts such as those found in *Catharanthus roseus*. In principle, this system should prove equally effective in the analysis of indole alkaloids from other species of plants and/or plant cell cultures. Among the benefits noted were high resolution, short run times, and the production of high quality mass spectra.

References:

1. A.J. Berry, D.E. Games, and J.R. Perkins, J. Chromatogr. 363, 147 (1986).
2. D.R. Gere, R. Board, and D. McManigill, Anal. Chem. 54 736 (1982).
3. A.J. Berry, D.E. Games, I.C. Mychreet, J.R. Perkins and S. Pleasance, Biomed. Envion. Mass Spectrom. 1987 (in press).

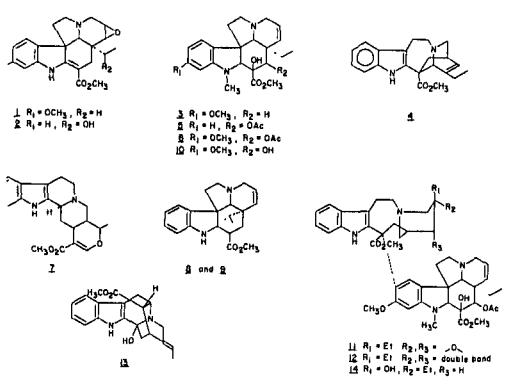

Structures of alkaloids found in this investigation

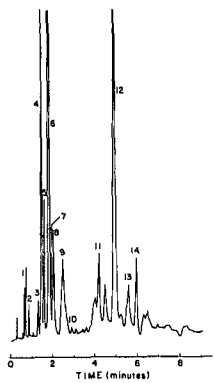

Figure 1

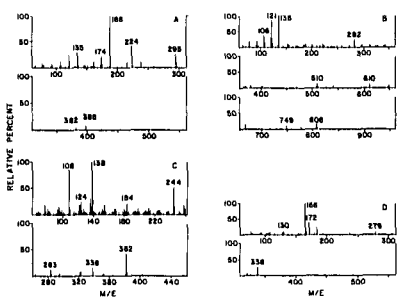

Figure 2
A: desacetoxyvindoline
B: leurosine
C: lochnerinine
D: perivine

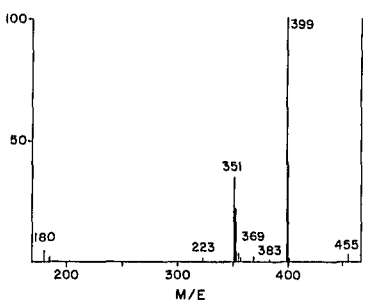

Figure 3

Presented at the 36th ASMS Conference on Mass Spectrometry and Allied Topics
June 5-10, 1988, San Francisco, CA

PDMS OF ALPHA$_1$-PROTEASE INHIBITOR GLYCOPEPTIDES

M Alai, R Townsend, M. Hardy, Y C. Lee
Department of Pharmacology and Biology, Johns Hopkins University, Baltimore, Maryland 21205
C. Fenselau, Department of Chemistry, University of Maryland Baltimore County, Baltimore, MD 21228

Human α_1-protease inhibitor controls proteolytic processes in various tissue fluids by inactivating a number of serine proteases and its low plasma levels has been associated with the development of familial emphysema . This glycoportein is made of 394 amino acids in a single chain with no internal disulfide bridges and an approximate molecular weight of 53,000. One characteristic of α_1-protease inhibitor (α_1-PI) is production of multiple bands on acid (pH 4.9) electrophoresis or electrofocusing. This multiplicity has been attributed to a great extent to microheterogeneity in the carbohydrates attached. Consequently, the structure of the oligosaccharide chains in human α_1-PI has been the subject of numerous studies. Preliminary investigations revealed that this glycoportein contains two types of complex, N-linked oligosaccharides, bi- and tri-antennary, at the ratio of 3:1; bi:tri. The amino acid sequence of human α_1-PI indicated that there are only three putative sites for N-linked glycosylation, asparagine residues 46, 83 and 247; therefore, some varients must differ only in the arrays of bi- and tri-antennary oligosaccharides attached to each site. In this study it was our objective to characterize glycosylation site microheterogeneity by assessing mass heterogeneity at the three glycosylation sites of human α_1-PI. Asialoglycopeptides from human α_1-protease inhibitor were prepared by digestion with pronase, desialylation with Arthrobacter neuraminidase and chromatography on a Bio-Gel P-4 column. Two partially resolved peaks containing carbohydrates were obtained from this column, FP and BP. Both fractions FP and BP were derivatized using t-BOC-Tyr-2,4,5 trichlorophenyl ester and the resulting t-BOC-Tyr-asialoglycopeptides were purified by RP-HPLC and desalted on a Bio-Gel P-6 column, using 0.1 M ammonium acetate, prior to mass spectral analysis (1-5ug was used for PDMS analysis). Most of molecular ions were consistent with previously reported bi- and tri-antennary oligosaccharides. Fraction BP was found to contain mainly biantennary glycopeptides. The biantennary oligosaccharide structure on Asn-247 was identified in one of the RP-HPLC purified peaks of fraction BP. Our assignment of the structures to the ions was made by a combination of amino acid analysis, amino acid sequence around the glycosylation site and the proposed carbohydrate structures. Asparagine-247 seems to contain only biantennary oligosaccharides; whereas, in physiological variants of α_1-PI the usual biantennary oligsaccharides may be replaced in position 83, and to a lesser extent 46, by triantennary oligosaccharides. The triantennary oligosaccharides of sites 83 and 46 were identified in peaks F2 and F6, eluted from RP-HPLC purification of fraction FP. Two molecualr ions were observed from RP-HPLC purified fraction FP, that suggested the addition of another lactosamine unit to a triantennary oligosaccharide. Preliminary amino acid analysis as well as ^{1}H-NMR data support the presence of tetrantennary oligosaccharides in human α_1-protease inhibitor.

REFERENCES

1) R.W.Carrell, J.-O.Jeppsson, C.-B.Laurell, S.O.Brennan, M.C.Owen, L.Vaughan and D.R.Boswell, Nature, 298: 329 (1982).

2) J.Travis and G.S.Salvesen, Ann. Rev. Biochem., 52: 655 (1983).

3) L.Vaughan and R.W.Carrell, Biochem. Int., 2: 461 (1981).

4) T.Mega, E.Lujan and A.Yoshida, J. Biol. Chem., 255: 4057 (1980).

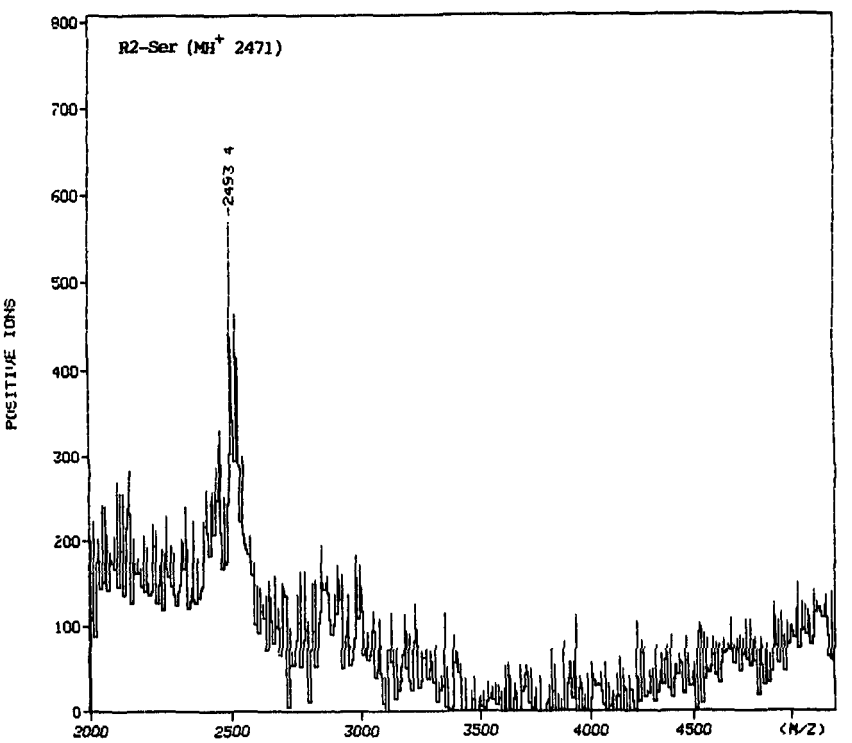

Example of asialoglycopeptides of human α_1-protease inhibitor analyzed by plasma desorption mass spectrometry. By a combination of amino acid sequence, amino acid composition and the proposed structure of oligosaccharides the molecular ion was assigned to R2-Ser (R2= t-BOC-Tyr-Asn-triantennary) and the site was found to be Asn-46.

Presented at the 36th ASMS Conference on Mass Spectrometry and Allied Topics
June 5-10, 1988, San Francisco, CA

ANALYSIS OF DERIVATISED AND UNDERIVATISED OLIGOSACCHARIDES BY LC-MS AND LC-MS-MS

G. Lappin, V. Gould and *M. Rogers.

VG MassLab Ltd., Tudor Road, Altrincha, WA14 5RZ, UK. Phone 061 941 3552. Tlx 669964. *St Mary's Hospital Medical School, Paddington, London, W2 1PG, UK. Phone 01 725 1138.

There has recently developed a growing demand for the rapid analysis of biologically-active oligosaccharides. For example, they are known to be important in cell-cell interactions, antibody recognition and phytoalexin elicitation. Analysis of oligosaccharides by NMR methods are generally too insensitive. GC and GC-MS of derivatised oligosaccharides has molecular weight limitations. HPLC affords good separation at high molecular weight, for derivatised and underivatised oligosaccharides but collected fractions must be analysed separately. The coupling of HPLC and mass spectrometry provides all the advantages of HPLC, plus the on-line analysis of the oligosaccharides. Here we describe the positive ion thermospray spectra of peracetylated, permethylated and underivatised oligosaccharides. In addition, daughter ion data was obtained which provided further structural information.

Permethylated oligosaccharides (maltohexose, raffinose and stachyose) formed strong $[M+NH_4]^+$ ions. Peracetylated oligosaccharides (stachyose, melezituse, melibiose and raffinose) also produced strong $[M+NH_4]^+$ ions.

Daughter ion spectra were obtained from $[M+NH_4]^+$ parent of peracetylated melibiose and peracetylated melezituse. These spectra exhibited some characteristic ions eg. 331 (peracetylated GLU). Underivatised raffinose exhibited weak $[M+H]^+$ and $[M+NH_4]^+$ ions and several other fragment ions. The source temperature had to be increased from 230° to 280°C to obtain good sensitivity.

Using Selective Ion Recording (SIR), on the $[M+NH_4]^+$ ion, derivatised oligosaccharides were detected down to the 500pg level.

The antibiotic kanamycin was also studied (underivatised). This produced a strong 485 $[M+H]^+$ ion. Daughter ion spectra were obtained on this parent which produced further structural information.

Presented at the 36th ASMS Conference on Mass Spectrometry and Allied Topics
June 5-10, 1988, San Francisco, CA

POLYSACCHARIDE STRUCTURAL STUDIES USING LASER DESORPTION/ FOURIER TRANSFORM MASS SPECTROMETRY

Mildred L. Coates and Charles L. Wilkins
Department of Chemistry
University of California
Riverside, CA 92521

Earlier laser desorption/Fourier transform(LD/FT) mass spectra of polyhexoses(1) contained series of fragment ions whose masses corresponded to $[n(162)+X+K]^+$. Since 162 is the mass of the hexose repeating unit, we postulated that X corresponds to the mass of a sugar fragment resulting from a ring cleavage, with the ions in each series corresponding to a particular cleavage. The purpose of this study is to correlate these series with structural features and recently-proposed fragment ion structures(2-4).

The polysaccharides examined are cellulose, guar gum, locust bean gum, lichenan, laminarin, amylose, amylopectin, nigeran, dextran, chitin, and pectin. Spectra were obtained using a pulsed CO2 laser interfaced to a Nicolet FT-2000 mass spectrometer. Powdered polysaccharide samples were attached to the probe tip with double-sided adhesive tape. KCl was added to the samples by depositing a water/methanol solution onto the prepared tip and allowing the solvent to evaporate.

As in the previous study, the masses of the ions observed correspond to $[n(\text{repeating group})+X+\text{cation}]^+$. The mass of the repeating group is 162 for the polyhexoses, 203 for chitin, and 190 for pectin. For all compounds except pectin, the cation is K^+. The pectin sample is contaminated with sodium salts, so its spectrum is dominated by Na^+-attached ions, although K^+-attached ions are also present.

The relative importance of the ion series in a compound's spectrum seems to be more related to the linkages between the monosaccharides than to their identities. For example, LD/FT mass spectra are virtually identical for cellulose, guar gum, and locust bean gum, whose constituent monosaccharides, although different, are linked the same way. This correlates with the earlier observation(1) that LD spectra are not similar for cellulose, starch, and dextran, whose constituent monsaccharides (glucoses in each case) are linked differently.

It has been postulated that many ion series result from a ring or glycosidic cleavage in combination with one or more dehydration reactions(4). In accordance with this, some of the ions series discussed here are grouped into families consisting of the series believed to result from a particular cleavage alone and in combination with dehydration reactions.

B Family of Ion Series-B, A, Q, P

The B series(X=18) seems to arise from cleavage at the glycosidic linkage with proton transfer, to yield a saccharide and a dehydrosaccharide, with charge retention on the saccharide. The A series(X=0) might result from charge retention on the dehydrosaccharide or from B series ions which have undergone a single dehydration. A ions are abundant in the spectra of all the polysaccharides examined, while B ions are of low abundance, if discernable. This may reflect the favorability of dehydration reactions for saccharides. Q ions(X=144 for polyhexoses, 185 for chitin, and 172 for pectin) are usually present, though in low abundance. These may correspond to B ions which have undergone two dehydrations or A ions that have undergone one dehydration. P ions(X=126 for polyhexoses), corresponding to one more dehydration than Q ions, are

Presented at the 36th ASMS Conference on Mass Spectrometry and Allied Topics
June 5-10, 1988, San Francisco, CA

only present in the spectrum of laminarin.

F Family of Ion Series-F, D, N, L

The F(X=60) and N(X=120 for polyhexoses and 161 for chitin) series seem to be complementary, resulting from the same cleavage, but with charge retention on opposite ends of the molecule. D(X=42) and L(X=102 for polyhexoses, 143 for chitin, and 146 for pectin) series ions could result from the combination of F/N cleavages with dehydrations. Chitin has an acetylated amino group on C2. The masses of the F, D, N, and L ions in its spectrum indicate that the F and D ions do not contain C2, while the N and L ions do.

Other Ion Series-G, K

Observation of the G series ions(X=74 for polyhexoses and 120 for pectin) seems to be related to the (1-4) linkage, although they are not observed in the spectrum of chitin. Two G series ions are observed in the spectrum of pectin, a poly(methyl galacturonate). The masses of these ions suggest they contain C5 and C6. K series ions(X=90) seem to be related to the presence of the (1-3) linkage, although there is no evidence for any particular cleavage.

(1) Coates, M. L.; Wilkins, C. L. Anal. Chem. 1987, 59, 197-200.

(2) Takayama, K.; Qureshi, N.; Honovich, J.; Cotter, R. J.; Mascagni, P.; Schneider, H. J. Biol. Chem. 1986, 261, 10624-10631.

(3) Lam, Z.; Comisarow, M. B.; Dutton, G. G. S.; Weil, D. A.; Bjarnason, A. Rapid Commun. Mass Spectrom. 1987, 1, 83-86.

(4) Lam, Z.; Comisarow, M. B.; Dutton, G. G. S. Anal. Chem. 1988, in press.

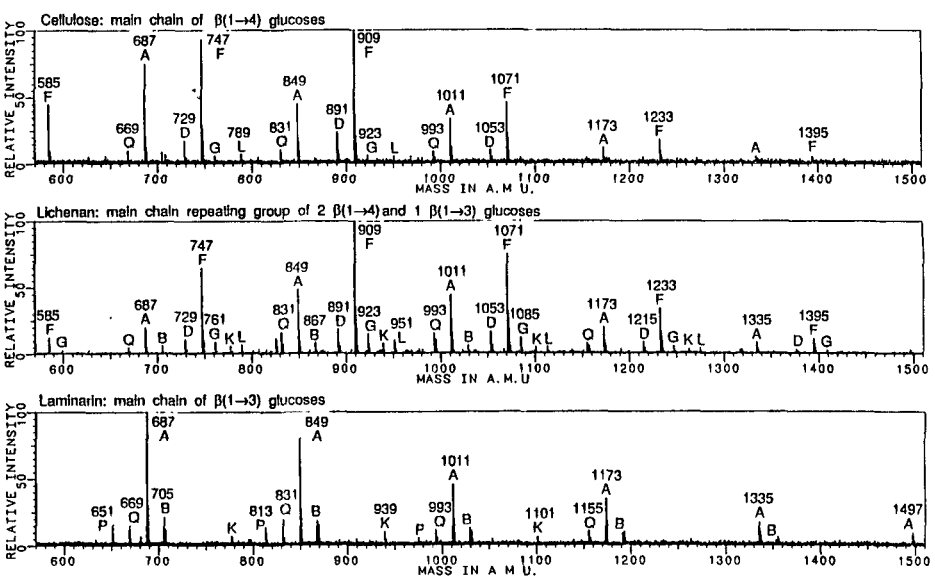

Presented at the 36th ASMS Conference on Mass Spectrometry and Allied Topics
June 5-10, 1988, San Francisco, CA

NOVEL O-LINKED OLIGOSACCHARIDES ISOLATED FROM HUMAN GASTROINTESTINAL MUCINS

A.M. Lawson, E.F. Hounsell*, S.B. Wilson, G. Cashmore, M. Stoll* and T. Feizi*;
Section of Clinical Mass Spectrometry and Section for Glycoconjugate Research, MRC Clinical Research Centre, Watford Road, Harrow, Middlesex. HA1 3UJ, UK.

Introduction: Human gastrointestinal mucins are glycoproteins (1-50 x 10^6 daltons) containing large numbers of heterogeneous oligosaccharides (~ 200 per subunit) each consisting of between 1 and 20 monosaccharides. These are O-linked to serine or threonine in the protein and during synthesis monosaccharides are added to step-wise by specific glycosyltransferases.

The function of mucins, and of the pronounced oligosaccharide heterogeneity, remains obscure although their potential capacity to interact with lectins on the surface of bacteria suggests an important protective mechanism of the mucosal epithelium.

The aim of the present study was to extend earlier work (1), on the major core-region oligosaccharides from gastrointestinal mucus of the human neonate (meconium) by characterising novel backbone sequences which are oligosaccharide antigens of onco-developmental type i.e. antigens of foetal origin which are expressed in adult neoplasia.

Experimental: Carbohydrates were liberated by mild alkali and sodium borohydride from glycopeptides produced by pronase digestion of glycoproteins. Following separation by Biogel P4 chromatography, fractions were individually chromatographed by HPLC on a ODS-Hypersil column and sub-fractions re-chromatographed on a APS-Hypersil column. Methylation analysis was carried out and positive ion FAB-MS (glycerol/thioglycerol) on approximately 0.5nM of permethylated purified oligosaccharides. Native oligosaccharides were analysed by negative ion FAB-MS (glycerol/thioglycerol). NMR ^{1}H spectra were obtained with a 500 MHz Bruker AM500 Spectrometer.

Results: Six of the oligosaccharide structures identified in meconium are listed in the Table. Molecular mass information was obtained from the -ve FAB spectra. The mass spectrum of oligosaccharide K2(4), for example, is shown in Figure 1 with its $[M-1]^-$ ion at m/z 1114 while ions at m/z 1098 and 952 indicate the presence of minor impurities. As little or no fragmentation of these compounds takes place in -ve FAB this is a useful means of detecting multiple components which cannot always be distinguished in the +ve FAB spectra of permethylated derivatives. Figure 2 shows the spectrum of the permethylated derivative of K2(4) which in addition to the $[M+1]^+$ ion at m/z 1410.7 has an intense fragment at m/z 464 (and m/z 432 from 464-MeoH) arising from the two possible cleavages of amino glycosidic bonds. GC-MS of the products of methylation analysis confirmed the monosaccharide composition and gave the linkages for each structure. Further characterisation including anomeric configuration was obtained by NMR.

Conclusion: As part of a continuing study the structure of a number of oligosaccharide moieties from gastrointestinal mucins have been determined. Several of these are of novel structure (e.g. K2(3), K2(4) and K6(3)) while some have been identified previously from other sources (e.g. K3(4), K4(3) and K5(3)2). K2(4) is particularly interesting having an unbranched GlcNAcβ1-6Gal backbone sequence in the absence of a GlcNAcβ1-3 substituent. This may represent a new biosynthetic step and questions the accepted specificity of GlcNAcl-6 transferases.

Presented at the 36th ASMS Conference on Mass Spectrometry and Allied Topics
June 5-10, 1988, San Francisco, CA

Carbohydrate chains in mucins are highly heterogeneous and only by a combination of chromatography, ±FAB-MS, GC-MS and NMR can their structures be fully elucidated. Some of these structures are differentation and tumour associated antigens of monoclonal antibodies and are crucially important to immuno-chemical investigations.

Reference

(1) Hounsell, E.F., Lawson, A.M., Feeney, J., Gooi, H.C., Pickering, N.J., Stoll, M.S., Lui, S.C. and Feizi, T. Eur. J. Biochem., 148 (1985) 367-377.

Table 1. Oligosaccharide structures in meconium glycoproteins.

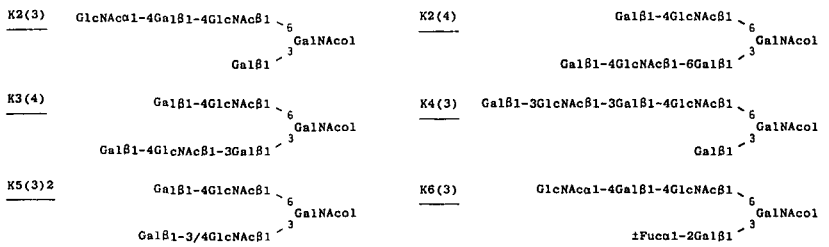

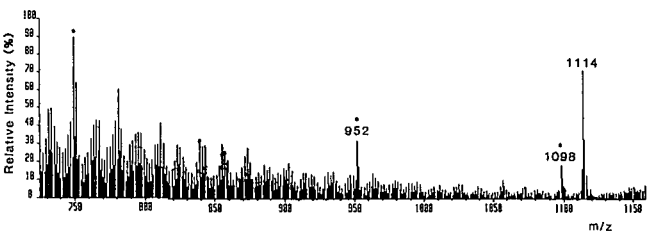

Figure 1.

Negative ion FAB spectrum of oligosaccharide K2(4) (asteriscs indicate ions from minor components)

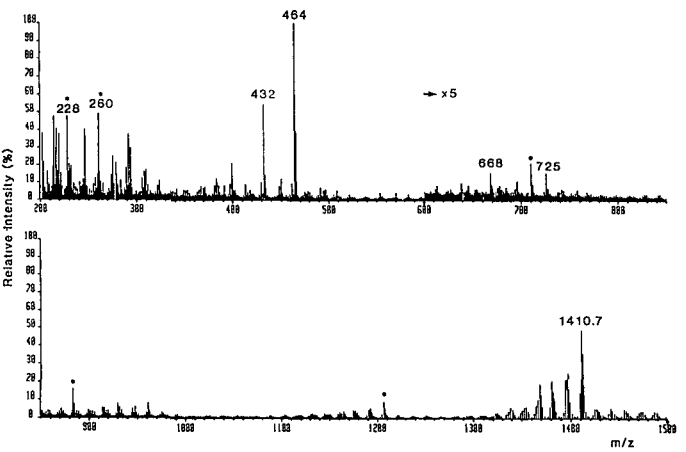

Figure 2.

Positive ion FAB spectrum of the permethylated derivative of K2(4)

Presented at the 36th ASMS Conference on Mass Spectrometry and Allied Topics
June 5-10, 1988, San Francisco, CA

EFFECTS OF CHEMICAL DERIVATIZATION OF OLIGOSACCHARIDES ON FRAGMENTATION IN LASER DESORPTION, PLASMA DESORPTION AND FAST ATOM BOMBARDMENT MASS SPECTROMETRY

M.F. Bean, W.B. Martin, T.J. Raley, Jr., C.M. Murphy and R.J. Cotter,
Department of Pharmacology, The Johns Hopkins University, Baltimore, MD 21205
C. Fenselau, Department of Chemistry, University of Maryland Baltimore County, Baltimore, MD 21225

Derivatization of oligosaccharides has been reported to enhance fragmentation in FAB-MS to provide more reliable data for sequence assignment, [1]. However, the utility of derivatization for other ionization techniques is not clear. This study was undertaken to compare the fragmentation using laser desorption, (LD), plasma desorption, (PD), and fast atom bombardment, (FAB) ionization methods of a variety of glucose and glucosamine oligosaccharides and to determine the effects of chemical derivatization on the two-bond ring cleavages that are characteristically observed in LD spectra of sugars.

The LD spectrum of N,N'-diacetylchitobiose is shown in Figure 1. MK^+ ions are observed at 463 amu and simultaneous cleavage of the O-C_1 and the C_2-C_3 bonds (type IV) and of the C_1-C_2 and C_3-C_4 bonds (type V) in the reducing sugar yield ions at 362 amu. Additionally, simultaneous cleavage of the C_2-C_3 and C_4-C_5 bonds (type VII) occurs to yield an ion at 302 amu. N,N',N"-triacetylchitotriose was studied to determine whether analagous LD type VII fragmentation would occur in the central sugar, however, no corresponding peaks were observed.

The PD spectrum of N,N',N"-triacetylchitotriose is shown in Figure 2, which shows that fragmentation arises chiefly from cleavage of the glycosidic linkage. A molecular ion is observed and oxonium ions are observed at 407 and 204 amu. The ion at 551 amu originates from a type IV or a type V cleavage of the reducing sugar.

The LD spectrum of maltotetraose is shown in Figure 3. The molecular ion, MK^+ is not observed, and unlike the triglucosamine above, two-bond ring cleavages occur throughout the molecule. Type IV cleavage in the reducing sugar and analogous ones in the next two sugars give peaks at 645, 483 and 321 amu (i.e., at 162 amu intervals). Since charge retention is on the distal portion, this series can be used to determine the sequence from the reducing end. Similarly, type VII cleavages result in the series at 585, 423, 261 and 99 amu. A third series at 627, 465 and 303 amu occurs 18 amu below the first. A fourth series was noted at 525, 363 and 201. Laser desorption of the peracetylated derivative, shown in Figure 4, illustrates that essentially all fragmentation is suppressed and only cationized molecular ions are observed. This was observed for LD of all the compounds studied, and was observed for LD of the permethylated derivative of stachyose as well.

The corresponding FAB spectrum is shown in Figure 5. MNH_4^+ molecular ions were observed at 1272 amu (PD produced MNa^+ ions at 1278 amu). Both FAB and PD of exhibit oxonium ions at 1195, 907, 619 and 331 amu. FAB and PD of the native sugar, however, produced little useful structural information. Thus, the sequence can be obtained by FAB and/or PD from the fully derivatized sample.

The LD spectrum of trehalose, a 1'-1 linked disaccharide, Figure 6, was studied to examine the behavior of a sugar with no reducing terminus. None of the characteristic two-bond LD fragmentations are observed; ionization is chiefly cationized molecular ions. LD of the peracetyled sugar showed the same results. However, both the FAB and PD spectra were simplified by peracetylation techniques - molecular ion species and oxonium ions were the major ions observed in contrast to complicated fragmentation in the corresponding spectra of the native sugar.

Thus, LD, FAB and PD provide complimentary fragmentation information useful for structurally elucidation of oligosaccharides. Derivatization improves sensitivity and fragmentation in PD and FAB, but suppresses fragmentation in LD. Clearly, LD is a viable alternative to derivatization to determine sequence information due to the extensive, more complex fragmentation observed.

1 Egge, H.; Dell, A.; von Nicolai, H.; Arch. Biochem. Biophys., 1983 (224), 235.

Presented at the 36th ASMS Conference on Mass Spectrometry and Allied Topics
June 5-10, 1988, San Francisco, CA

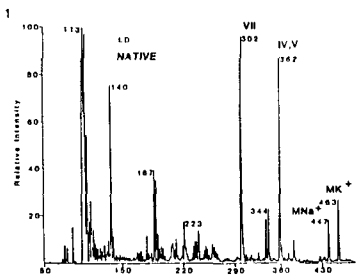

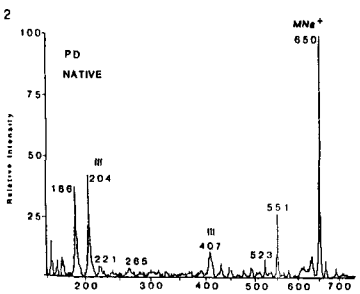

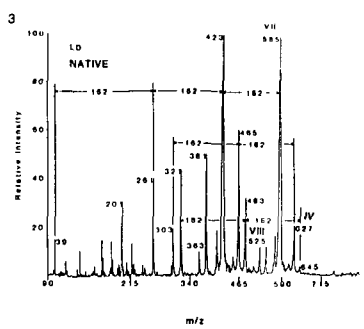

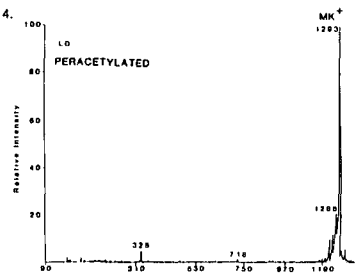

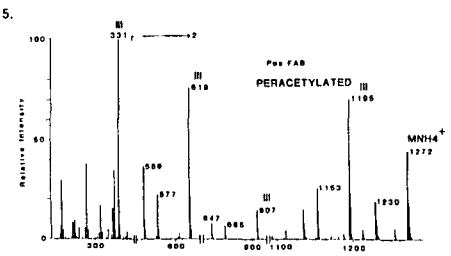

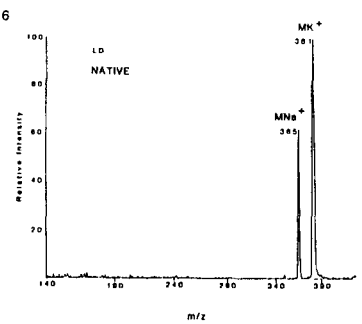

Presented at the 36th ASMS Conference on Mass Spectrometry and Allied Topics
June 5-10, 1988, San Francisco, CA

FRAGMENTATION OF LIPOPOLYSACCHARIDE ANCHORS IN PLASMA DESORPTION MASS SPECTRA: THE LIPID A STRUCTURES FROM E. COLI, R. SPHAEROIDES, AND B. ABORTUS

R. Wang, L. Chen, R.J. Cotter; The Johns Hopkins University, Baltimore, MD 21205
N. Qureshi, K. Takayama; Veterans Administration Hospital, Madison, WI 53705

Lipid A (1) is a lipid component of lipopolysaccharides (LPS) which are amphipathic macromolecules found on the outer surface of the outer membrane of gram-negative bacteria. Lipid A has a basic structure (see Fig. 1) consisting of a mono- or diphosphorylated ß-1,6-linked D-glucosamine disaccharide, with four to seven fatty acids forming amide linkage (at 2 and 2' position of sugar) and acyl linkage (at 3 and 3' position of sugar). The different fatty acid composition appear to be related to toxicity.

Plasma desorption mass spectrometry has been used to elucidate the fine structure of lipid A's from various bacteria (Escherichia coli, Rhodopseudomonas sphaeroides (2), and Bacillus abortus). In the present study, the general fragmentation behavior of lipid A is reported.

Lipid A from E. coli and R. sphaeroids (only E. coli is shown)
MOLECULAR IONS (Fig. 2A) In positive spectra, both free acid and methylated lipid A yield intensive pseudomolecular ion $[M+Na]^+$. The free acid can catch two sodium ions from matrix to form $[M+2Na-H]^+$ ion while the methylated derivative can form $[M-CH_3+Na]^+$ ion.
MAJOR FRAGMENTS (Fig. 2B) The loss of ester-linked fatty acid forms the $[M-R_n]^+$, $[M-R_n+Na]^+$, $[M-R_n]^-$ ions. The oxonium ion is formed by cleavage of the bond between the distal and reducing sugar. These major fragments are very useful to determine the fatty acid composition and substitution positions.
FATTY ACIDS AND PHOSPHATE NEGATIVE IONS (Fig. 2C) The low mass region of PD negative spectra can be used to confirm phosphate and fatty acid compositions. All ester-bonds are cleaved to give free fatty acid negative ions ($R_1'^-$, $R_2'^-$, R_3^-). Note that background peaks are shaded.
ALKYL FRAGMENTATION (Fig. 2D) The low mass regions of positive spectra of all lipid A's exhibit a distinct fragmentation pattern which is characteristic to alkyl groups. These type of fragmentation may be the cause of peak broadening at high mass region.

Lipid A from B. abortus
The fragmentation pattern of tetra-amide-linked lipid A is distinct from previously mentioned lipid A with two ester linkages at 3- and 3'-positions. Instead of the normal cleavage at the ester bonds, cleavage of the C_1-O bond and the C_2-C_3 bond of the reducing sugar results in the loss of a portion of the molecule which includes the amide-linked fatty acid. The other fragmentation involves simultaneous cleavage of the C_4-C_5 and C_1-O bonds. The resultant ions can be used to establish the identity of R_1 and R_2.

Concluding Remarks
1. Plasma desorption mass spectrometry gives important information about the fine structure of lipid A. Negative spectra reveal the phosphate and O-linked fatty acid composition, while the major fragments in positive spectra provide direct information on the positions of the fatty acid chains.
2. Study of lipid A from E. coli and R. sphaeroides shows that major fragmentation in PD mass spectra involves only the cleavage of ester-linked fatty acyl groups, but not the amide-linked fatty acyl groups. Cleavage within the sugar ring is rarely observed. On the contrary, tetra-amide-linked lipid A from B. abortus shows specific fragmentations of the reducing end sugar.

REFERENCES
1. Rietschel,E.Th., Galanos,C., Lüderitz,O. & Westphal,O. (1982) Immunopharmacology and the Regulation of Leukocyte Function (Webb,D.D., Ed) Marcel Dekker, N.Y. pp183-229
2. Qureshi,N., Honovich,J.P., Hara,H., Cotter,R.J. & Takayama,K. (1988) J. Biol. Chem. 263, 5502

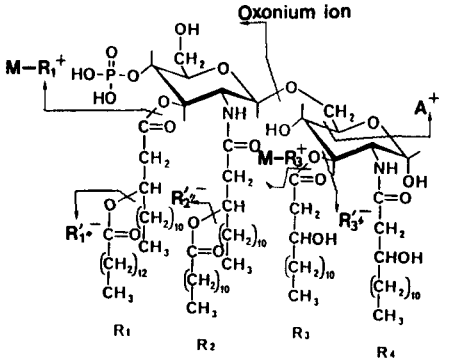

Fig 1. Structrue and fragmentation of monophosphoryl lipid A from E coli (free acid).

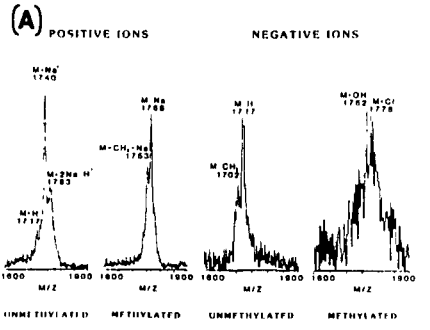

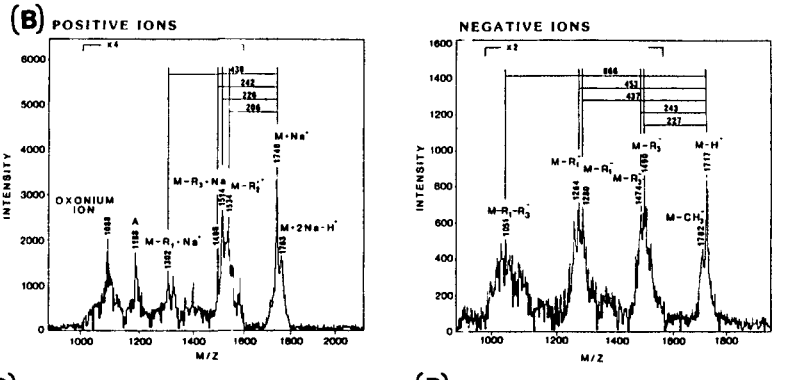

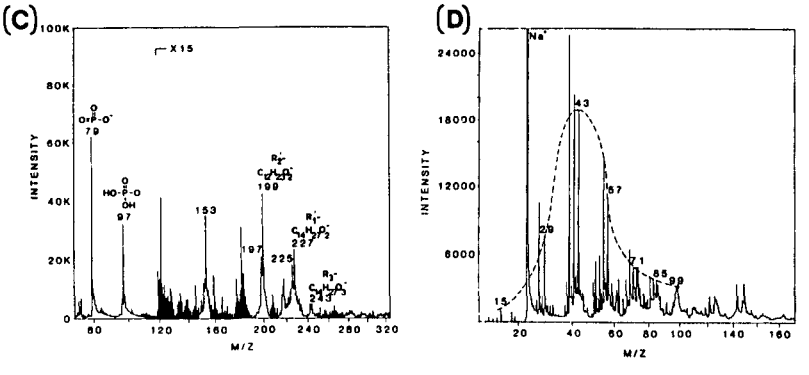

Fig 2. Plasma desorption mass spectra of lipid A (E coli). [A] molecular ion region; [B] major fragments, [C] fatty acid and phosphate negative ions, [D] alkyl fragmentation

Presented at the 36th ASMS Conference on Mass Spectrometry and Allied Topics
June 5-10, 1988, San Francisco, CA

CARBOHYDRATE ANALYSIS OF THE PRE-S(2) REGION OF HEPATITIS B SURFACE ANTIGEN

Mark E. Hemling[1], Steven A. Carr[1], Carine Capiau[2], and Jean Petre[2]
[1]Physical and Structural Chemistry L-940,
Smith Kline & French Laboratories, King of Prussia, PA 19406
and [2]Biological Division, SmithKline-RIT, B-1330 Rixensart, Belgium

The 226 amino acid long S protein of hepatitis B virus is the major surface glycoprotein of the infective agent. The development of vaccines against hepatitis B virus has focused on the immunogenic properties of the S protein, and two recombinant versions of this protein are currently available for use as vaccines. Using FABMS and selective chemical procedures we previously confirmed 85% of the sequence of the protein and identified the presence of an N-acetyl moiety on ca. 70% of the amino-terminal Met residues. Recently, an amino-terminally extended form of the S protein, designated pre-S(2), with 55 additional amino acid residues has been found in minor amounts in infectious particles and has been shown to be significantly more immunogenic in terms of antibody production in vivo than the S region alone. The gene for pre-S(2)-S HBsAg was cloned and expressed in yeast at SmithKline-RIT, and two major protein bands with molecular masses of 30 kDa (p30) and 33 kDa (gp33) were isolated by polyacrylamide gel electrophoresis (SDS-PAGE). The observed molecular mass of gp33 on SDS-PAGE was several kDa higher than expected based on the theoretical amino acid composition of the pre-S(2) protein. Treatment of the gp33 protein with endo-β-acetylglucosaminidase H resulted in a decrease in the apparent mass of the protein by SDS-PAGE suggesting that the mass difference was at least in part due to covalently bound oligosaccharide, probably of the oligomannose family.

Mass spectrometry was enlisted in this study to define the site(s) of attachment of carbohydrate and to determine the compositions and molecular heterogeneity of the carbohydrate at the various attachment sites. In order to study the structure of the pre-S(2) region separate from the rest of the S antigen molecule that we had previously characterized, we took advantage of the fact that the S antigen is refractory to tryptic digestion in the native state whereas the N-terminal pre-S(2) region is readily cleaved. Digestion of native pre-S(2)-S protein with trypsin in the absence of reducing agents should produce three tryptic peptides from the 55 amino acid long pre-S(2) region of the protein, consisting of 16, 2, and 30 amino acids. The 16 amino acid peptide Met_{-55}-Arg_{-40} contains the putative Asn-linked glycosylation site and two potential O-linked sites, while the 30 residue fragment Gly_{-37}-Arg_{-8} contains nine possible O-linked sites. FABMS of the tryptic digest of p30 yielded signals for the two larger peptides. Associated with each of these signals were peaks corresponding to glycosylated peptides containing one or two units of hexose, presumably O-linked.

FABMS of the tryptic digest of gp33 (ca. 40 nanomoles digested) yielded signals for the third tryptic peptide at m/z 2891 [$(M+H)^+$, average mass] with from one to six hexoses (incremental mass = 162) attached to Ser or Thr residues, but only weak signals which might correspond to the amino-terminal tryptic peptide could be detected (Fig. 1, top). Glycosylated peptides containing the Asn-linked glycosylation site were detected by analysis of HPLC fractions of trypsinized gp33. The RP-HPLC chromatogram of the tryptic digest was complicated due to the extensive heterogeneity of the carbohydrate components of the two glycopeptides and the similar retention behavior of the various glycopeptides. It should be noted that, unlike proteins, heterogeneity in the structures of carbohydrates attached to proteins is the rule rather than the exception. Peaks were observed at m/z 3634, 3796, 3958, and 4120 corresponding to peptide Met_{-55}-Arg_{-40} with two N-acetylhexosamine (HexNAc) and from eight to eleven hexose units. Of course, the exact distribution of these sugars among the three potential glycosylation sites present in this peptide (i.e., Asn_{-52}, Ser_{-51}, and Thr_{-50}) cannot be determined from this data. Similarly, signals were observed at m/z 4350, 4512, 4674, and 4835 corresponding to the peptide Gly_{-37}-Arg_{-8} with nine to twelve units of hexose attached From analysis of the fractions we concluded that Met_{-55}-Arg_{-40} has a total carbohydrate composition varying from $HexNAc_2Hex_7$ to $HexNAc_2Hex_{12}$ and that Gly_{-37}-Arg_{-8} is present with zero to thirteen hexose units attached at O-linked sites.

In order to unambiguously define the attachment site of Asn-linked carbohydrate we used the FABMS carbohydrate "mapping" strategy (1). Peptides containing Asn-linked carbohydrate are detected in this strategy by comparing the FABMS-derived peptide maps obtained before and after treatment of the glycoprotein with an endoglycosidase. The most generally useful enzyme for this purpose is peptide:N-glycosidase F (PNGase F) which cleaves the β-aspartylglycosylamine linkage of all known types of Asn-linked sugars and converts the attachment site Asn to Asp which weighs one dalton more. New peaks appearing in the mass spectra after treatment with the glycosidase correspond to formerly glycosylated peptides. Following digestion of trypsinized

gp33 with PNGase F strong peaks were observed at m/z 2255, 2417 and 2579 (Fig. 1, bottom) indicating that carbohydrate is N-linked to Asn_{-52} and that from two to four hexoses are attached via oxygen to Ser_{-51} or Thr_{-50}

The composition and molecular heterogeneity of the carbohydrate in peptide Met_{-55}-Arg_{-40} was examined by peracetylating a portion of the trypsin/PNGase F digest of gp33 which is a mixture of peptides and released carbohydrates. The peracetylated oligosaccharides were extracted from the acetylated peptides into an organic solvent and analyzed by FABMS These data establish that the Asn-linked site in peptide Met_{-55}-Arg_{-40} has a composition of $HexNAc_2Hex_n$ where n = six to nine. A working hypothesis for the structure of the glycopeptide Met_{-55}-Arg_{-40} based on these experiments is shown in Fig. 2. Work is progressing on defining the specific locations of the O-linked sugars in both of the tryptic peptides.

1 S. A. Carr and G. D Roberts (1986) *Anal. Biochem.* **157**, 396-406.

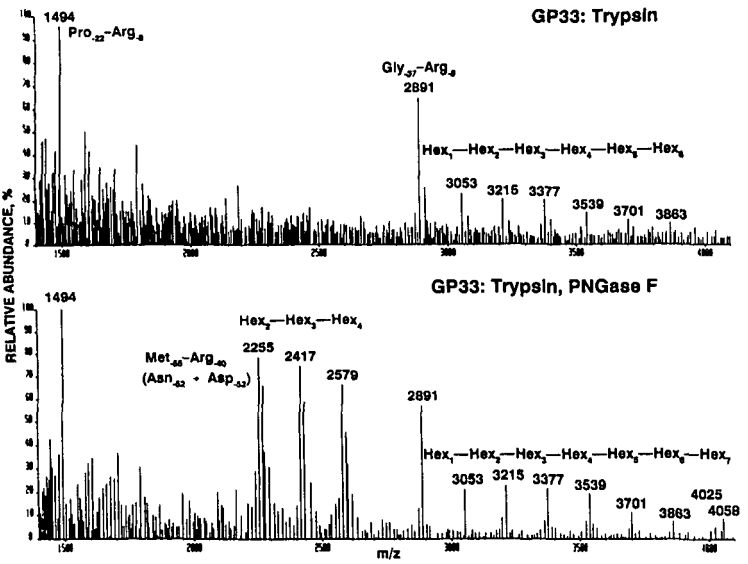

Figure 1. *FAB mass spectrum of the tryptic digest of the 33 kDa pre-S(2)-S glycoprotein (gp33) from HBsAg* (upper) and following treatment with peptide:N-glycosidase F (lower). Weak signals at m/z 3795 and m/z 3957 (upper) can be assigned as Met_{-55}-Arg_{-40} with $HexNAc_2Hex_{9\text{-}10}$.

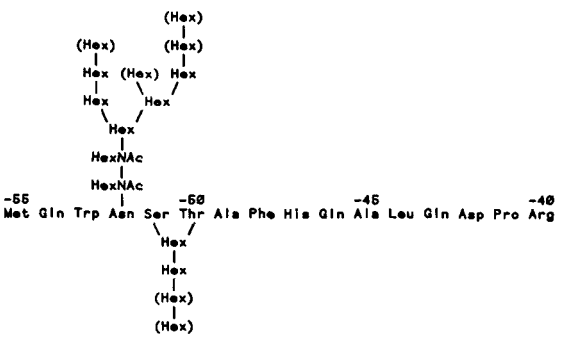

Figure 2. Proposed structure of the N,O-linked glycopeptide Met_{-55}-Arg_{-40}. Position(s) of O-linked glycosylation has not been determined.

Presented at the 36th ASMS Conference on Mass Spectrometry and Allied Topics
June 5-10, 1988, San Francisco, CA

FAB MS/MS FOR ANALYSIS OF A COMPLEX MIXTURE OF LIPO-OLIGOPEPTIDES FROM NOCARDIA RUBRA CELL WALL SKELETON

M. Fujioka, F. Sentoh, S. Koda and Y. Morimoto
Analytical Research Laboratories, Fujisawa Pharmaceutical Co., Ltd.
2-1-6 Kashima, Yodogawa-ku, Osaka 532, Japan

Introduction: Lipopeptide(Peptidolipid or Lipoprotein) is one of the components of bacterial cell wall skeletons, but little is known about its biological function and structure, mainly due to its poor solubility and intrinsic complexities. The lipid moiety consists of a mixture of fatty acid homologues, and it blocks the N-terminus of the peptide moiety. Moreover the peptide moiety contains both D- and L- amino acids, and significant changes both in the fatty acid and amino acid compositions are often observed. We have isolated a lipopeptide fraction(ca. 5,000 daltons by GPC) from Nocardia rubra AN-115 cell wall skeleton(N-CWS) and initiated structure elucidation. Here we report the optimal FAB MS/MS conditions for the analysis of synthesized lipo-oligopeptides and application in determining of N-terminal sequences of the N-CWS lipopeptide.

Results and Discussion: A Finnigan MAT TSQ70(triple quadrupole mass spectrometer) equipped with an Ion Tech FAB11NF saddle field fast atom gun was used for this study. Since the N-CWS lipopeptide has been found to be rich in behenic acid as the lipid moiety, and Gly, Phe, Ala, Ile, and Val in the peptide moiety, behenylglycine(Beh-Gly), Beh-Gly-Phe, Beh-Gly-Phe-Ala were synthesized and used for optimizing FAB MS/MS conditions.

Among the eight matrix compounds examined in this study, 3-Nitrobenzyl alcohol provide the highest secondary molecular ion yield of the synthesized lipo-oligopeptides both in positive ion(+) and negative ion(-) modes except the case of Beh-Gly in the negative mode as shown in Table 1. No significant difference of secondary molecular ion signal duration, which is shown by lifetime of the secondary molecular ions in Table 1, was observed among the three matrix compounds which were chosen since they were superior to the others in respect to an ability of yielding higher signal abundance. It is definitely important for MS/MS experiments to have higher ion intensities, therefore 3-nitrobenzyl alcohol was recommended as the most suitable matrix compound for analysis of the lipo-oligopeptides

Nature of xenon and argon as a collision gas were studied to improve daughter ions yield and sequence imformation. There was no significant difference in the quality of the FAB MS/MS daughter ions spectra between by use of xenon and argon, however, higher collision energy of about 5eV was required in the case of argon compared with xenon.

The (-)FAB was found to yield higher secondary molecular ion abundance than the (+)FAB. Abundance and quality of sequence informative daughter ions generated by collisionally induced dissociation were compared between positive and negative ion modes. The (-)MS/MS is found to be superior to the (+)MS/MS. A plateau of ion intensities was observed in higher collision energy region when collision gas pressure was too low, therefore, higher colligion gas pressure was recommended as far as a sufficient abundance of parent ion intensity was maintained. The (-)FAB MS/MS daughter ions spectrum of Beh-Gly-Phe-Ala recorded at the condition optimized was shown in Figure 1.

A chloroform extractable materials from partial acid hydrolyzate of the N-CWS lipopeptide (in 6N-HCl at 110 ℃ for 30 min) was chromatographed on a silica gel thin layer plate (E. Merck; silica gel 60) using a mixture of petrorum ether, ether, and formic acid (40:30:3, by vol) as a developing solvent to revealed four fractions (Fraction 1 - 4). These fractions were lipids mixture or lipo-oligopeptides mixture, and subjected to the (-)FAB MS/MS analysis. The (-)FAB mass spectrum of the Fraction 4 from the N-CWS lipopeptide showed that this fraction might consist of a mixture of homologous lipo-oligopeptides. The (-)FAB MS/MS daughter and parent ions experiments of the Fraction 4 at the optimal condtions could establish Lipid-Gly-Phe sequence as shown in Figure 2.

Presented at the 36th ASMS Conference on Mass Spectrometry and Allied Topics
June 5-10, 1988, San Francisco, CA

Table 1. Molecular ion yield(arb. unit) and lifetime(T_{50}:min) of molecular ion of the Lipo-oligopeptide at a fixed sample concentration

Matrix	Beh-Gly pos.	Beh-Gly neg.(T_{50})	Beh-Gly-Phe pos.	Beh-Gly-Phe neg.	Beh-Gly-Phe-Ala pos.	Beh-Gly-Phe-Ala neg.(T_{50})
Glycerol	-	0.2	-	0.5	1.0	1.2
Thioglycerol	-	3.0	1.3	4.0	3.8	13.2
Glycerol-Thio-glycerol(1:1)	-	1.2	-	3.2	1.1	8.0
DTT-DTE*(3:1)	3.2	3.7(0.35)	2.8	5.2	4.0	10.1(0.35)
Triton X	-	-	-	-	-	-
PEG 400	-	0.4	-	0.4	-	1.7
Diethanolamine	-	30.0(0.30)	-	13.8	-	11.7(0.31)
3-Nitrobenzyl alcohol	7.4	24.5(0.32)	8.1	30.4	10.2	89.7(0.29)

SEM: 1.2KV, IC: 0.028mA, IC(limit): 1.6-1.8mA, HV: 7.5-8.5KV, Gas: Xe
- : S/N=1
Sample concentration: 10nmol/μl,
*: DTT, Dithiothreitol, DTE: Dithioerythritol

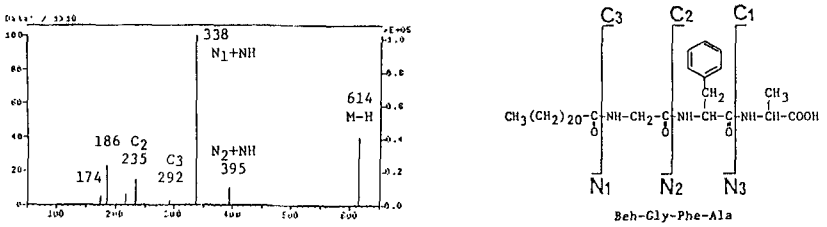

Figure 1. (-)FAB MS/MS Daughter Ions Spectrum of Beh-Gly-Phe-Ala: Collision energy; 15eV(COFF), Xe; 1.0×10^{-5} Torr in manifold, Matrix; 3-nitrobenzyl alcohol.

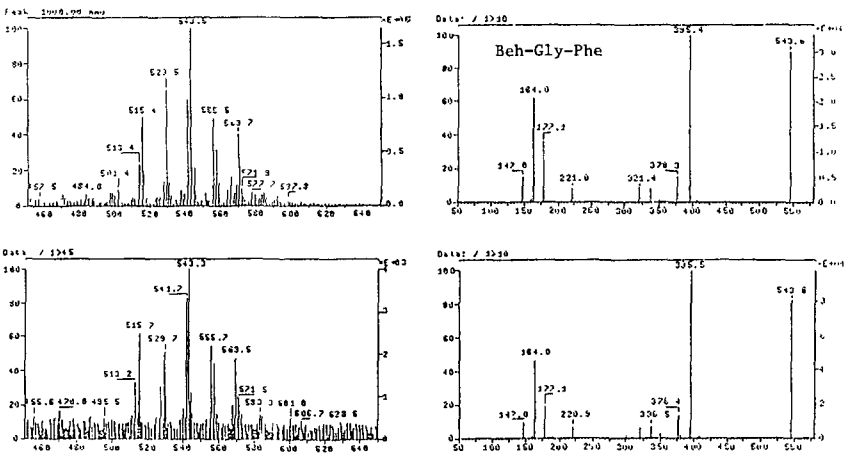

Figure 2. Top left: (-)FAB mass spectrum of the Fraction 4, Bottom left: (-)FAB MS/MS parent ion spectrum of the Fraction 4; daughter ion m/z 221(Gly-Phe residue), Top right: (-)FAB MS/MS daughter ions spectrum of Beh-Gly-Phe, Bottom right: (-)FAB MS/MS daughter ions spectrum of the Fraction 4; parent ion m/z 396.
Condition: Collision energy; 15eV(COFF), Xe; 1.0×10^{-5}Torr in manufold, Matrix; 3-nitrobenzyl alcohol.

Presented at the 36th ASMS Conference on Mass Spectrometry and Allied Topics
June 5-10, 1988, San Francisco, CA

CHARACTERIZATION OF AN ACIDIC EXOPOLYSACCHARIDE ISOLATED FROM AN *R. MELIOTI* MUTANT:

G.R. Her, S.Y. Chan, V.N. Reinhold, J. Glazebrook*, G. Walker*.
Harvard School of Public Health, Boston, MA 02115, and
*Massachusetts Institute of Technology, Cambridge, MA 02139.

Introduction

Our laboratory has recently provided unambiguous evidence that complex exopolysaccharides play crucial roles in the nodulation of alfalfa root hairs by the nitrogen-fixing bacterium *Rhizobium meliloti*. Briefly, we found that colonies of *R. meliloti* fluoresce under UV light when grown on medium containing calcofluor (exo^+). We isolated a large set of mutants generated by the insertion of the transposon tn^5 and showed that all of them failed to synthesize a complex acidic exopolysaccharide previously characterized by Aman, et al., (1). When alfalfa seedlings were inoculated with these exo^- mutants, nodules developed but no nitrogen fixation occurred. Thus, the presence of the exopolysaccharide appears to be required for successful invasion of developing nodules and for establishing an effective symbiotic relationship. A new mutant of *Rhizobium meliloti* isolated in this laboratory fails to synthesize the expected exopolysaccharide but does synthesize a modified structure which is effective in nodulation. Since this new exopolysaccharide can substitute for the previously known material in nodule invasion and symbiosis, the determination of its structure is a matter of extreme interest.

To approach this problem, sample composition, sequence, linkage, and substituent groups were determined. Glycosidic and substituent linkages were determined on the isolated polysaccharide and fractions of an enzymatic digest using both Hakomori (2) and Prehm (3) permethylation procedures. The sequence was established by a combination of FAB-MS (Fig. 1) and DCI-MS (Fig. 2) and NMR was used to determine all anomeric configurations. From these studies it can be concluded that this second exopolysaccharide has a very different structure compared to the wild type 1021 polysaccharide. The determined structure is a linear disaccharide repeating unit with an acetate group attached to glucose and a pyruate group attached to galactose as shown in Fig. 3.

References

1.) Aman, P.M.; Mcneil, L.; Franzen, L.M.; Darvill, A.G. and Albersheim, P. Carbohydr. Res., 95:263-274(1981).
2.) Hakomori, S.I., J. Biochem. (Japan), 55:205-208(1964).
3.) Prehm, P. Carbohydr. Res., 78:372-374(1980).

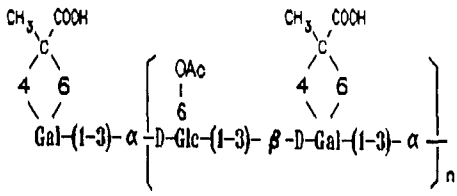

Figure 3. Complete structure of HJ1

Presented at the 36th ASMS Conference on Mass Spectrometry and Allied Topics
June 5-10, 1988, San Francisco, CA

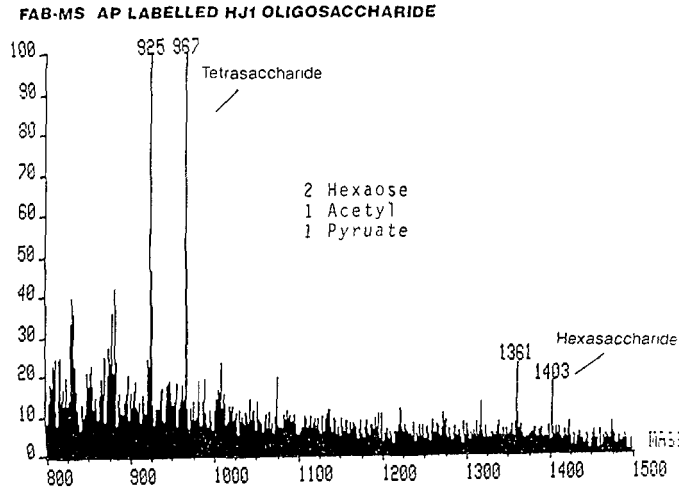

Figure 1. FAB mass spectrum of AP labelled HJ1 oligosaccharide

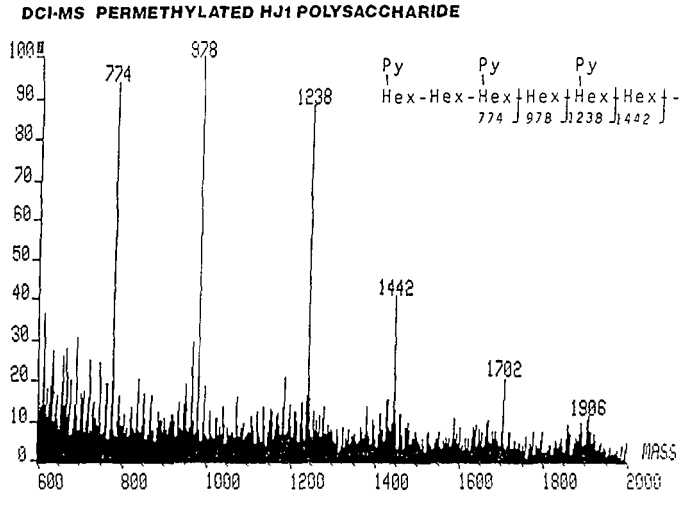

Figure 2. NH_3 DCI mass spectrum of permethylated HJ1 Polysaccharide

Presented at the 36th ASMS Conference on Mass Spectrometry and Allied Topics
June 5-10, 1988, San Francisco, CA

PDMS ANALYSIS OF PEPTIDES, OLIGOSACCHARIDES AND GLYCOPEPTIDES

G. Scanlan, L. Benson, A. Tsarbopoulos, and I. Jardine

Mayo Clinic, Rochester, Mn.

The mass spectrometric analysis of INTACT complex glycopeptides, even to simply obtain unambiguous molecular weight information, but especially to obtain sequence and structural information, still presents a formidable challenge. In this poster is reported progress toward MS analysis of complex glycopeptides using 252-Cf-PDMS.

The model peptide substance P was used to optimize conditions for the routine, reproducible, and reliable PDMS analysis of peptides at the low picomole level. The amount of MNa^+ ions present using normal distilled water to apply the sample to the foil is dependent on the time the foil is allowed to stand before spin-drying. The salt-adduct ions can usually be washed from the NC using water or 0.1% TFA but losses of small peptides inevitably occur. The salt adduct problem can be alleviated by not only desalting the peptide, but also by using highly deionized water. Oxidation occurs more readily in smaller samples, i.e. 2 picomoles, but can be decreased by preparing foils under nitrogen or inserting them immediately into the vacuum system. Figure 1 demonstrates the usefulness of these techniques when looking at small quantities of Substance P. Figure 2 demonstrates the increased resolution and mass accuracy of Substance P using a PDMS-Time-of-Flight-Ion Reflectoer system.

Oligosaccharides can only be desorbed from NC coated PDMS foils with difficulty. The spectra usually consist of the MNa^+ ion even after sample cleanup or washing, but a few hundred picomoles of material are required. A dramatic change occurs when the oligosaccharide is permethylated and/or peracetylated. Sensitivity is increased to the sub-100 pmole level and fragmentation ions resulting from simple cleavages along the sugar chain become evident. Using the short fight path (15 cm) TOF system, the mass accuracy of the MNa^+ ion is fairly reliable , but the accuracy of the fragment ions is poor. The PDMS-TOF-ion reflector system solves this problem.

Analysis of the underivatized species (Tetra-antennary dodecasaccharide; Fig.3) required 5 nanomoles of material and gives a moderate MNa^+ ion signal (Insert in Fig. 3). In contrast, picomole amounts of the peracetylated analog provides an intense MNa^+ ion, accompanied by intense sugar fragment ions.

Prothrombin contains three asparagine-linked sugar chains per molecule. The complete structures of these sugars were previously determined as complex sialic acid containing isomeric oligosaccharides. To determine the precise location of these sugars on the prothrombin chain, the three complex glycopeptides were isolated after tryptic digestion of the molecule. Attempts to analyze these intact sialic acid containing glycopeptides by PDMS were initially unsuccessful. The oligosaccharide portion of the glycopeptides were then shortened using an endoglycosidase to leave only a GlcNAc-GlcNAc residue. Analysis of such molecules by PDMS produces an intense MH^+ ion similar to normal peptides (Fig. 4). When a standard sialic acid containing glycopeptide containing two terminal sialic acid residues and one amino acid (asparagine) was analysed no spectrum resulted. The molecule was derivatized using methylation (HCl/MeOH) then peracetylation, but still no spectrum was obtained using standard PDMS techniques. However, washing these derivatized samples with water and then CHLOROFORM resulted in spectra (Fig. 5). A complex prothrombin tryptic glycopeptide was then methylated, peracetylated, applied to a PDMS foil and washed in the above manner using water and CHLOROFORM (Fig. 6).

Presented at the 36th ASMS Conference on Mass Spectrometry and Allied Topics
June 5-10, 1988, San Francisco, CA

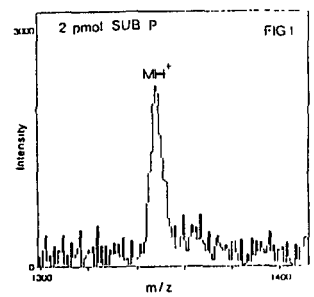

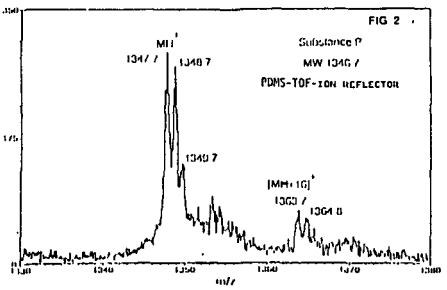

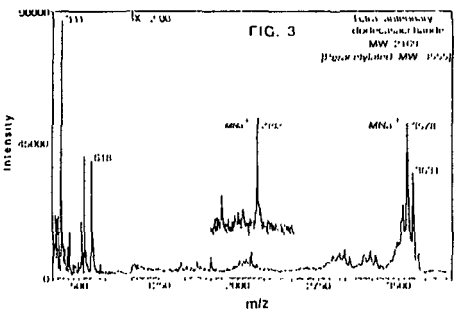

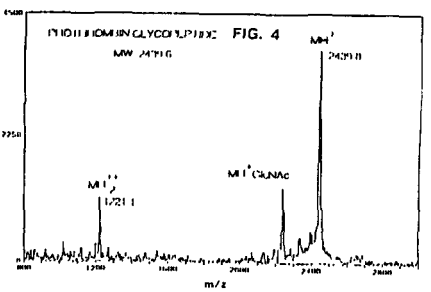

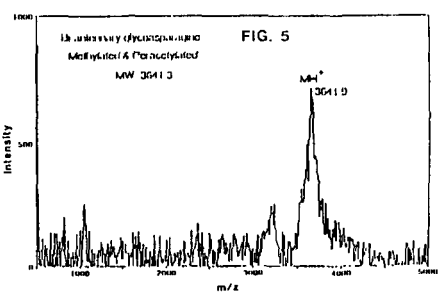

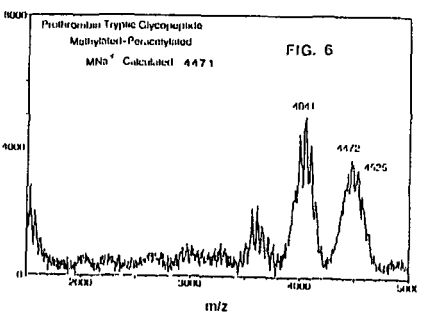

Presented at the 36th ASMS Conference on Mass Spectrometry and Allied Topics
June 5-10, 1988, San Francisco, CA

FAST ATOM BOMBARDMENT MASS SPECTROMETRY OF HEPARIN-DERIVED, HIGHLY SULFATED OLIGOSACCHARIDES

Larry M. Mallis

High Resolution Mass Spectrometry Facility
The University of Iowa
Iowa City, Iowa 52242

H. M. Wang and R. J. Linhardt

Department of Medicinal and Natural Products Chemistry
The University of Iowa
Iowa City, Iowa 52242

Heparin, a polydisperse sulfated copolymer of 1->4 linked glucosamine and uronic acid residues, has been used clinically as an anticoagulant for half a century. Despite a yearly use of over 50 million doses in the U. S. alone, heparin's exact chemical structure remains unclear. Heparin is depolymerized with heparin lyase and fractionated by HPLC into a small number of oligosaccharides. Five of these comprise approximately 86% of the mass. They are:

F1 : ΔIdoAp2S (1->4) -α- D-GlcNp2S6S

F2 : ΔIdoAp2S (1->4) -α- D-GlcNp2S (1->4) -α- L-IdoAp2S (1->4) -α- D-GlcNp2S6S

F3 : ΔIdoAp2S (1->4) -α- D-GlcNp2S6S (1->4) -β- D-GlcAp (1->4) -α- D-GlcNp2S6S

F4 : ΔIdoAp2S (1->4) -α- D-GlcNp2S6S (1->4) -α- L-IdoAp2S (1->4) -α- D-GlcNp2S6S

F5 : ΔIdoAp2S (1->4) -α- D-GlcNp2S6S (1->4) -α- L-IdoAp (1->4) -α- D-GlcNAcp6S (1->4) -β- D-GlcAp (1->4) -α- D-GlcNp2S3S6S

where ΔIdoA is 4-deoxy-α-L-threo-hex-4-enopyronosyluronic acid, GlcA is glucuronic acid and IdoA is iduronic acid (see Figure 1).

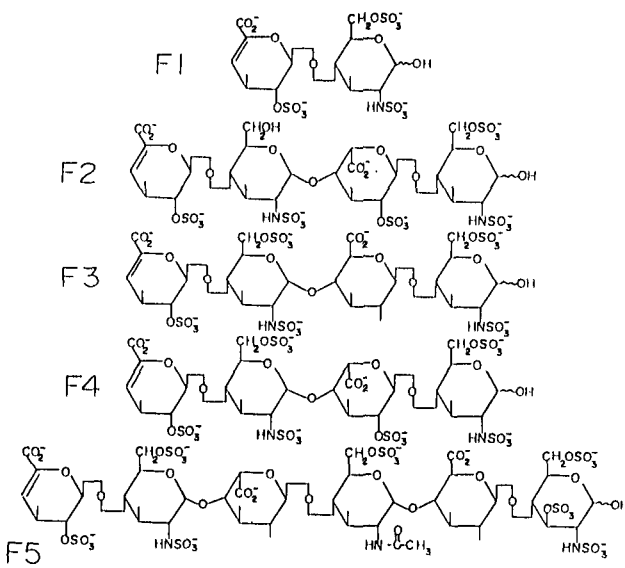

Figure 1

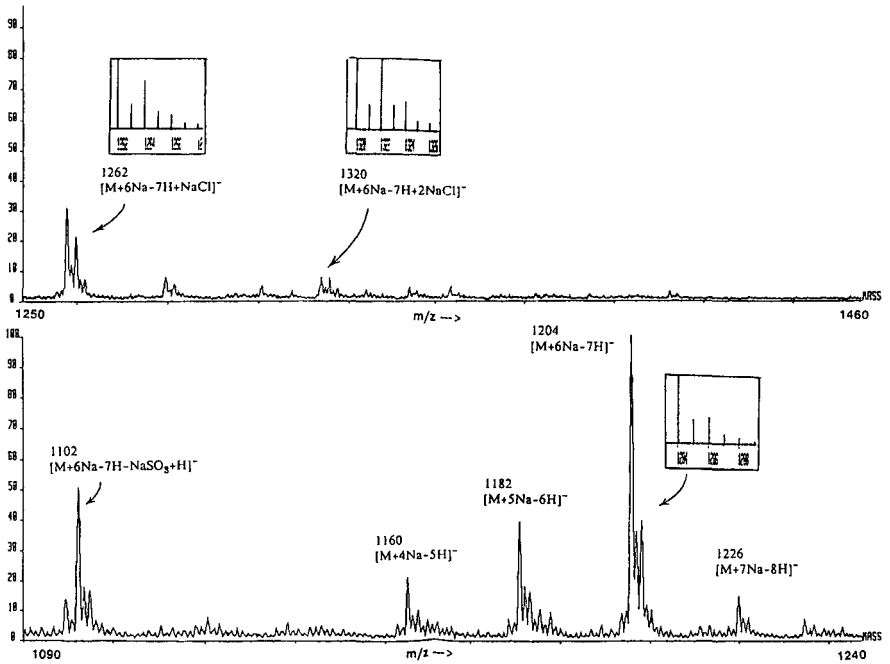

Figure 2

FAB-MS spectra have been reported for disaccharide F1[1] but not for higher oligosaccharides F2-5. In the case of polysaccharides, protonation often leads to cleavage of the glycosidic bond, thus the protonated molecular ion is not observed. In solution, the highly sulfated heparin derived polysaccharides contain up to ten negative charge sites. Clearly, analysis of these compounds should be performed in the negative ion mode. Owing to the potential (in solution) for formation of a molecule with several negative charges, a method for creating a species with a single negative charge without altering the character of the molecule is important.

Owing to the potential for multiple negative charge sites in solution (and gas phase), dodecylmethyl ammonium (DDMA) salts of F1-5 were made and successfully analyzed using plasma desorption (PD) MS (± 6 daltons).[2] Although analysis of these compounds by PDMS is feasible, oligosaccharide F5 (1603 daltons) as a DDMA salt has a molecular mass of 7510 daltons making analysis of even larger polysaccharides impractical.

Recently it has been reported that sodiated molecular ions can provide fragment ions for structural elucidation not obtained for the $[M+H]^+$ or $[M-H]^-$ molecular ions.[3] In addition, formation of sodiated molecular ions of sugars is commonly observed as the prominent molecular ion species, i.e., protonated molecular ions (or deprotonated in the negative ion mode) are often not observed.[4] Therefore negative ion FAB analysis was performed to detect ions of the type $[M+Na_x-H_{x+1}]^-$ (x = 1-10). These analyses were performed using a VG ZAB-HF with triethanolamine as the negative ion FAB matrix. Owing to the abundance of salts in the analyzed samples, sodium salts were not added to facilitate sodium adduct ion formation. As an example, the heparin compound F3 formed a $[M + 6Na - 7H]^-$ type molecular ion (see Figure 2). It is interesting to note that although the samples were considered pure, a considerable amount of NaCl was observed as $[M + 6Na - 7H + xNaCl]^-$ (x = 1-3) adduct ions.

[1]Merchant, Z. M., Kim, Y. S., Rice, K. G. and Linhardt, R. J. *Biochem. J.* **1985**, *229*, 369.
[2]Linhardt, R. J., Rice, K. G., Merchant, Z. M., Kim, Y. S. and Lohse, D. L. *J. Biol. Chem.* **1986**, *261*, 14448.
[3]Mallis, L. M. and Russell, D. H. *Anal. Chem.* **1986**, *58*, 1076; *Anal. Chem.* **1987**, *59*, 980; *Proceedings of the 35th ASMS Conference on Mass Spectrometry and Allied Topics*, May 24-29, 1987, Denver, CO, p 265.
[4]Castro, M. E., Mallis, L. M. and Russell, D. H. *J. Am. Chem. Soc.* **1985**, *107*, 5652.

Presented at the 36th ASMS Conference on Mass Spectrometry and Allied Topics
June 5-10, 1988, San Francisco, CA

Enhanced Separation and LSIMS Fragmentation of Chemical Derivatives of Oligosaccharides Containing 3-Deoxy-2-Keto-Octulosonic Acid (KDO)

Constance M. John and Bradford W. Gibson

Department of Pharmaceutical Chemistry, School of Pharmacy, University of California, San Francisco, CA., 94143-0446

The purification and structural determination of the oligosaccharide (OS) portion of the lipidoligosaccharide (LOS) of gram-negative bacteria, *e.g. Neisseria gonorrhoeae*, is complicated by heterogeneity and the presence of ionic components such as 3-deoxy-2-keto-D-*manno*-octulosonic acid (KDO) and phosphoethanolamine (PEA). Previously, we reported the primary structure determination of the OS of JW31R, a pyocin-resistant gonococcus strain, using a combination of liquid secondary ion mass spectrometry (LSIMS), GC-MS, and MS/MS techniques [1,2]. In order to improve the separation, sensitivity, and obtain more structural information, we prepared several chemical derivatives of OS containing KDO and investigated their MS and HPLC properties [3].

The OS portions of the LOS from *N. gonorrhoeae* JW31R were first released by acid hydrolysis (1% acetic acid, 2 hours, 100°C) and the water-soluble OS was separated on a Sephadex G-50 and Bio-Gel P-4 columns. Fractions from the P-4 column of the OS from JW31R were found to be heterogenous on the basis of refractive index detection and LSIMS analysis. Fraction 53, which contained at least 3 different OS components, was derivatized with p-amino-benzoic acid ethyl ester (ABEE) and reduced to the corresponding amine with $NaCNBH_3$ [3]. Reverse phase HPLC (Vydac C_{18} with H_2O/CH_3CN gradient) was used to purify the derivatized OS components and baseline separation was observed for most components. Analysis by negative ion LSIMS on a Kratos MS50 produced abundant deprotonated molecular ions with extensive fragmentation. Decarboxylation of KDO had also occurred in some of the derivatized OS during the reaction which improved the $(M-H)^-$ abundance by increasing the hydrophobicity of the OS (and presumably its surface activity).

To the contrary, the OS purified from the LOS of *S. typhimurium* TV 119 Ra reacted only slightly with ABEE. After extensive studies, we concluded that the reaction of the sterically hindered reducing terminus (KDO) with ABEE was not quantitative and that the yield was considerably lower with OS containing phosphate and PEA. After treatment of the *S. typhimurium* OS with HF to remove both phosphate and PEA, a much better yield of the derivatized OS was obtained. In addition, a number of well separated fragments of this OS were also present, presumably originating from partial acid cleavage during the HF treatment. Although this limited hydrolysis could be viewed as an unwanted side reaction of the HF cleavage, these smaller OS components gave abundant molecular ions by LSIMS and, therefore, became useful structural elements in determining the structure of the parent OS.

Nonetheless, the reaction of ABEE with KDO was still not quantitative and a more nucleophilic reagent was sought to derivatize these OS. For this purpose, *p*-hydrazino-benzoic acid ethyl ester, a stronger nucleophile, was synthesized and used to produce the corresponding hydrazones. Preliminary results indicated that the yield improved 3-5 fold and the resulting ABEE-hydrazones could be easily separated by HPLC in an identical fashion as for the ABEE derivatives. The LSIMS spectra of these hydrazone derivatives were equal to the best quality spectra of the corresponding ABEE derivatives.

Overall, the addition of hydrophobic UV chromophores to these OS provided excellent HPLC detection efficiency, separation, and LSIMS performance. The ABEE and ABEE-hydrazone OS produced fragmentation almost completely directed towards the reducing terminus. The ABEE-hydrazine reagent was found to be more nucleophilic and, therefore, more reactive with the reducing terminal KDO. It could be argued that the hydrazine-amino benzoates are preferable derivatizing agents to the amino benzoates for all types of oligosaccharides, since they are more reactive and no extraction steps are required prior to HPLC separation.

1. B.W. Gibson, et al. (1987) Abs, 35th ASMS Conf. Mass Spectrom., pp. 876-877
2. B.W, Gibson, et al. (1988), manuscript submitted for publication.
3. C.M. John and B.W. Gibson. (manuscript in preparation).
4. W.T. Wang, et al. (1984) *Anal. Biochem.* 141, 366-381.

This work was supported by grants from NIH (AI 21620, J.McL. Griffiss and RR 01614, A.L. Burlingame) and the Cancer Research Coordinating Committee (B.W. Gibson)

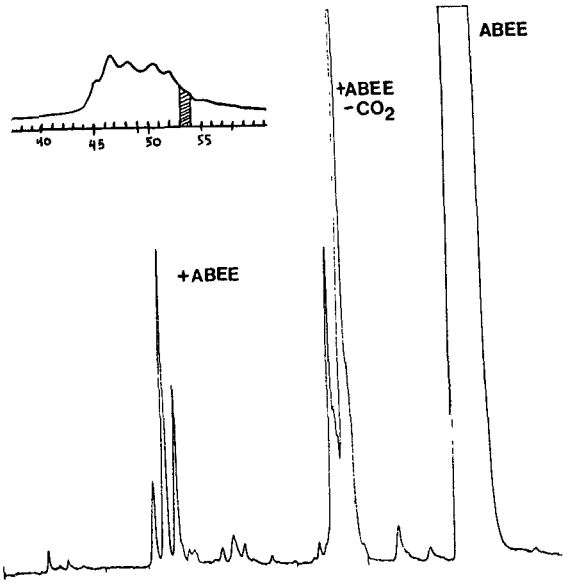

Figure 1. HPLC separation of ABEE-OS from Bio-Gel P-4 fraction 53 (JW31R).

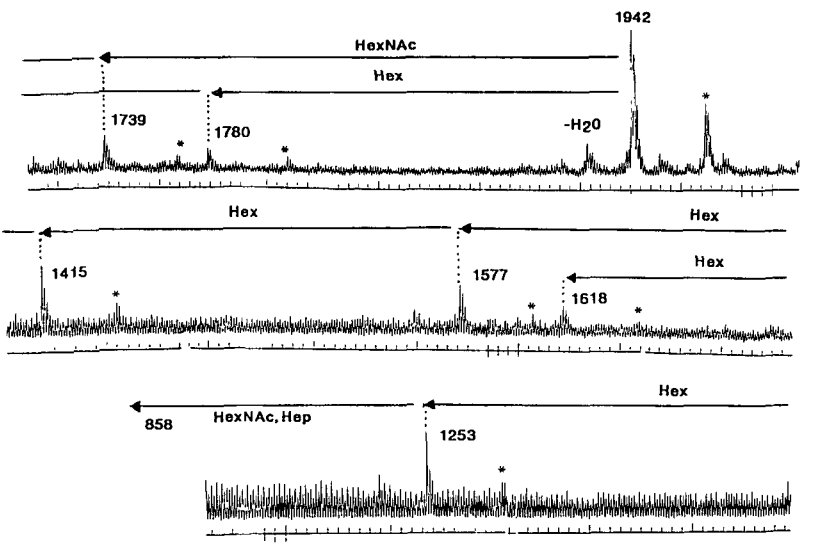

Figure 2. Negative ion LSIMS of decarboxylated ABEE-OS component (JW31R).

Presented at the 36th ASMS Conference on Mass Spectrometry and Allied Topics
June 5-10, 1988, San Francisco, CA

Applications and Further Developments of Liquid Chromatography - Fast Atom Bombardment - Mass Spectrometry (LC-FAB-MS) using a Continuous Flow Probe.

Alison E. Ashcroft, Kratos Analytical, Barton Dock Road, Urmston, Manchester, M31 2LD, UK
Alan A. Herod, British Coal, Coal Research Establishment, Stoke Orchard, Cheltenham, Glos. GL52 4RZ, UK
Gary Manton, ICI Wilton Materials Research Centre, PO Box 90, Middlesbrough, Cleveland, TS6 8JE, UK.

Introduction

The development of Continuous Flow FAB[1] has resulted in a technique well-suited for on-line reaction monitoring[2] and LC-MS using both microbore and micro-LC columns[3]. The Continuous Flow FAB probe also provides for a rapid throughput of routine samples and facilitates the addition of salts and other additives to samples in order to establish the molecular weight by production of quasi-molecular ions.

Experimental

A Kratos Analytical Concept IS equipped with a Continuous Flow FAB probe and an Ion Tech FAB gun was used for this work. A Brownlee MPLC pump was employed to deliver solvents at the rates specified in the text. The LC columns and mobile phases used are discussed below.

Results and Discussion

Relatively polar materials such as peptides are amenable to reversed phase liquid chromatography. These types of samples are readily ionized by Fast Atom Bombardment, and an example of an on-line LC-FAB-MS analysis is shown in figure 1. The chromatogram shows the separation of three closely related neuropeptide derivatives achieved with a Brownlee RP-18, Spheri-5 column (1mm x 25cm) packed with 5µm particles using a gradient elution of 0 to 56% aqueous acetonitrile with a constant 0.1% trifluoroacetic acid and 5% glycerol. The flow rate of 40µl per minute through the column was split 1:8 to direct 5µl per minute to the ion source. A spectrum from the minor component, Kpc.Leu.Pro.NH_2, is shown in figure 2.

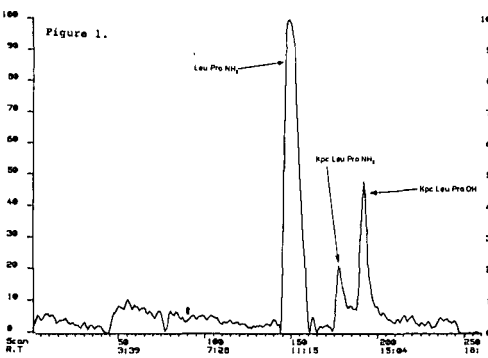

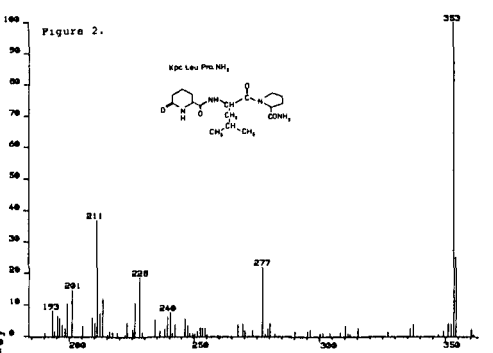

Figure 1. LC-FAB-MS: Neuropeptide mixture separated by reversed phase LC using a gradient of 0-56% aqueous acetonitrile with 0.1% trifluoroacetic acid and 5% glycerol.

Figure 2. LC-FAB-MS: Spectrum of Kpc.Leu.Pro.NH_2 (mw 352)

Complementary types of LC have also been studied. Gel Permeation Chromatography (GPC) has a mechanism based on size exclusion whereby molecules are separated on passage through a porous phase by differences in their effective size ie. smaller solutes have access to a greater proportion of the total pore volume, and are retained for a longer time than larger solutes.

GPC has been used to separate mixtures of asphaltenes, lipids, phthalates etc. In this study, a PLgel GPC column (2mmx 30cm) of 100A pore size packed with 5µm particles was used to separate a mixture of three Irganox samples using FAB-MS as the detection system. Commonly used solvents for this type of column include tetrahydrofuran, toluene and chloroform. Initial studies with the continuous flow FAB probe indicated that both toluene and chloroform were suitable solvents to be used in conjunction with FAB-MS as they evaporated steadily into the ion source and produced few background ions in the mass spectrum. In comparison, tetrahydrofuran produced a high level of background ions and generally caused suppression of sample ions. Using toluene at a flow rate of 400µl per minute through the column with a split of 1:80 to direct 5µl per minute to the ion source, a separation of Irganox 1010, Irganox 1076, and Irganox 1330 was achieved (figure 3). A spectrum from Irganox 1076 is shown in figure 4.

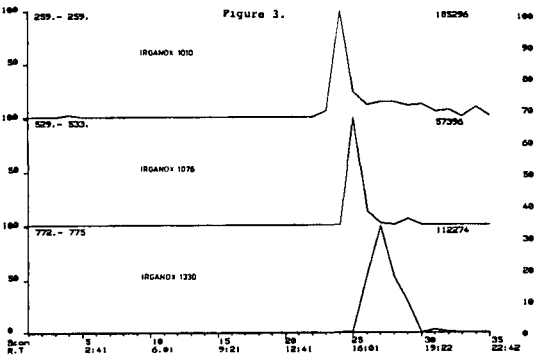

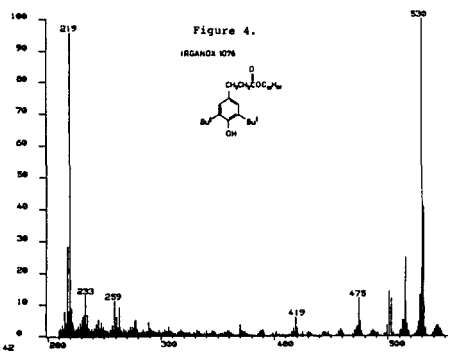

Figure 3. GPC-FAB-MS: Irganox mixture separated by GPC using toluene with 5% m-nitrobenzyl alcohol added.

Figure 4. GPC-FAB-MS: Spectrum of Irganox 1076.

Conclusion

The Continuous Flow FAB probe has been used as an LC-MS interface with both aqueous and organic solvent mixtures using both GPC and reversed phase HPLC columns.

References

1. R.M. Caprioli, T. Fan, J.S. Cottrell, Anal. Chem., 58, 2949 (1986)
2. A.E. Ashcroft, J.R. Chapman, J.S. Cottrell, J. Chromatogr., 394, 15 (1987)
3. A.E. Ashcroft, Org. Mass Spectrom., 22, 734 (1987)

Presented at the 36th ASMS Conference on Mass Spectrometry and Allied Topics
June 5-10, 1988, San Francisco, CA

SECONDARY ION MASS SPECTROMETRY OF SOLUTE PARTICLE BEAMS BY THERMABEAM LC/MS.

Ross C. Willoughby, James D. Buchner, andEdward W. Sheehan;
EXTREL Corporation, Pittsburgh, Pa. 15238.

Continuous introduction of sample into the ion source of the mass spectrometer with subsequent ionization using secondary ion mass spectrometry or fast atom bombardment ; namely, continuous flow FAB (1), has demonstrated several advantages over conventional FAB analysis. Among the advantages are: direct coupling to HPLC systems; enhanced sensitivity, reduced matrix requirements, and decreased background interferences. Unfortunately, present continuous flow FAB devices are limited to microbore flow rates; possibly requiring nonstandard LC hardware and columns; smaller column capacity; and injection volumes.

Introduction of solute in the form of a solvent-depleted solute particle beam intercepting a primary ion beam may result in an alternative approach to continuous sample introduction with secondary ion mass analysis. ThermaBeam LC/MS is a high enrichment particle beam introduction device that has show applications in both EI and CI modes. The objective of the present studies were intended to demonstrate the feasibility of producing FAB spectra by intercepting a primary ion beam (Xe) with a solute particle beam generated with ThermaBeam. The effects of matrix, temperature, and source geometry were studied.

Two experimental configurations were evaluated; a cross-beam and a target intercept (Figure 1). A Xenon saddle field source at 8 KV was used as the primary ion source. The targeted configuration yielded one to two orders of magnitude greater sensitivity than the cross beam experiments. Sample response was highly dependent upon the matrix additives. Most samples were analyzed with a thioglycerol matrix. Peak profiles were symetrical and tailing was not a problem unless the thioglycerol content in the effluent was significantly higher than ten percent. Sodium and potassium cation adducts were observed for many compounds presumably from impurities in the water.

The targeted configuration yielded FAB spectra that were comparable to those obtained under conventional FAB conditions. These experiments demonstrated that a high flow rate (to 2 ml/min) LC/MS interface is feasible for ionization with FAB. Matrix concentration in the effluent is extremely important for sensitive analysis and will probably require post column addition. Spectra were obtained for Substance P and a series of fragments, stachyose, vitamin B12, cobalamide, and PPG 600.

(1) Caprioli, R.M.; Fan, T., Cottrell, J.S.; Anal. Chem. (1986) **58**, 2949.

Presented at the 36th ASMS Conference on Mass Spectrometry and Allied Topics
June 5-10, 1988, San Francisco, CA

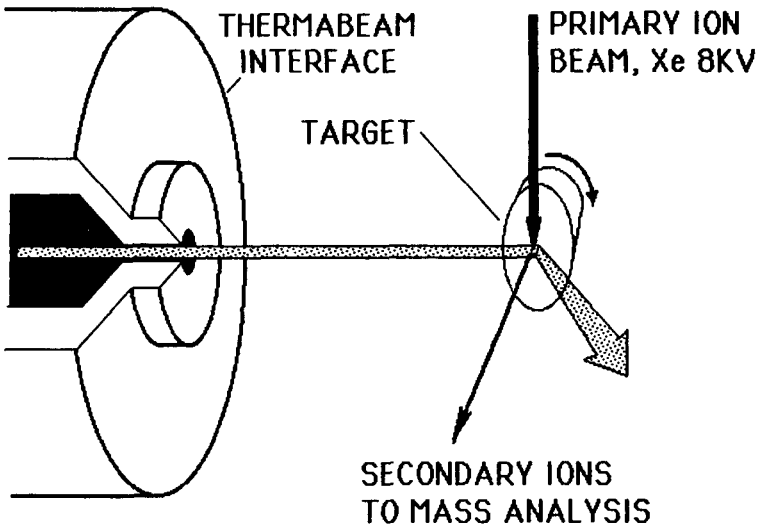

Figure 1. A targeted configuration for particle beam FAB experiemnts with ThermaBeam LC/MS.

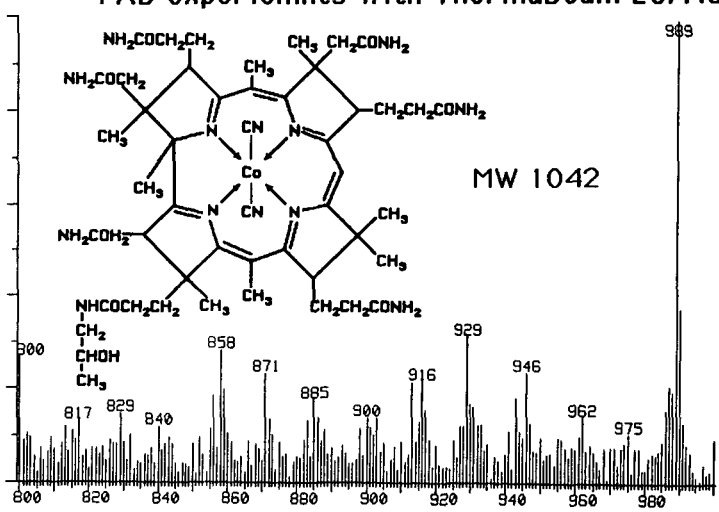

Figure 2. FABTAB spectra of cobalamide dicyanide (MW 1042).

Presented at the 36th ASMS Conference on Mass Spectrometry and Allied Topics
June 5-10, 1988, San Francisco, CA

The Future of Mass Spectrometry: Part I

R. Graham Cooks
Purdue University
West Lafayette, IN 47907

This paper is prepared from the vantage point of the end of a six-year term of office in ASMS and is titled Part I in the hope that later parts will be contributed as the valedictions of future society Presidents. Having missed almost all technical presentations in the service of the society for a long period, one can at least claim a certain uniqueness of perspective in discussing the future of our subject. Here, this future is seen as dependent upon the strengths of both this Society and of the discipline which it represents. Continued interest in mass spectrometry and its wide use seem assured. Indeed, it is not unreasonable to expect ASMS membership to reach 9000 by 1998, the centennial year of mass spectrometry.[1]

Such growth calls for carefully considered changes in our meetings. We will not continue to be the intimate group that some of us persist in imagining us still to be. Smaller meetings, like the Asilomar conference, will surely play a more important role as primary research conferences. I look forward to the annual conference including an instrument exhibit, instrumentation being one of the common denominators of mass spectrometry. A delicate balance is necessary between fundamentals, instrumentation and applications for a discipline like mass spectrometry to thrive. The burgeoning use of mass spectrometry makes the task of education in the subject immensely important. The impact of mass spectrometry on the biological sciences can only be facilitated by a combination of education in mass spectrometry and carefully targeted research. Two areas in which mass spectrometry has a disappointing record are organic analysis and surface science. In both cases this is because only a fraction of available capabilities are employed. With the dissemination of ion traps of several types, one can see the prospect of organic chemistry done in the mass spectrometer, at last coming into its own. Recent developments in quadrupole ion trap instrumentation[2] are occurring at a particularly rapid rate. This year alone has seen ion injection from external sources, high order MS^n experiments, rate constant and thermochemical measurements, and combinations of MS/MS with photoionization and photodissociation.

Areas of greatest future research opportunity seem to lie at the interface with surface science on the one hand and the biological sciences on the other. For example, there is much to be done in developing techniques and elucidating phenomena associated with collisions of polyatomic ions at surfaces. Such efforts offer improved capabilities in tandem mass spectrometry through high internal energy transfer to the projectile ion, as well as opportunity to develop new methods of characterizing molecular adsorbates on surfaces. (Through reactive collisions in which the projectile ion reacts with groups on the surface and so allows their characterization by mass spectrometry). The use of ion beams for tailoring the chemistry of surfaces through soft-landing experiments[3] also stands ready for exploitation. Figure 1 shows a new UHV instrument[4] designed to characterize the scattering of organic ions at well characterized surfaces through angle, mass and velocity measurements on the projectile and emerging particles. The device is also designed to permit modification of surfaces through soft-landing of mass-selected molecular ions.

At the other extreme in instrumental complexity, a simple means has been developed for performing ion/surface collisions in standard quadrupole, sector or hybrid MS/MS instruments. This instrument modification calls for a device with an in-line geometry even though large scattering angles are employed in the ion/surface collisions themselves. Figure 2 shows a version of this device[5] incorporated into a hybrid instrument and Figure 3 shows the result of dissociating the protonated form of the peptide angiotensin in a double quadrupole SID instrument. Even at low collision energy (30 eV) extensive fragmentation of the peptide occurs.

The above examples provide clues to the future of mass spectrometry, there are many others which have been presented at this conference. At the beginning of the week, the very idea of producing organic molecules with 40 or 50 charges might have been thought bizarre, at next year's meeting half a dozen labs might report similar work. This time last year the coupling of mass spectrometry to one of the most widely used and promising separation methods - electrophoresis including capillary gas electrophoresis - was in the future. This week we heard several presentations on these already successful experiments. This week Martin Jarrold reported the deposition of mass-selected Si-clusters on surfaces, and then photographed them with scanning tunnelling microscopy. A year ago an elegant - if poorly named - SIMS method (flow FAB) was barely invented. Now it is being practised in dozens of laboratories. The first paper on MS/MS in the ion quadrupole ion trap appeared two years ago and already the field is exploding with activity. In several presentations at this meeting people treated pg amounts of samples and ppt detection as routine. These capabilities were in the distant future ten years ago. Thirteen years ago MS/MS - for mixture analysis - did not exist. Desorption ionization methods - SIMS and FAB - had not been applied to organic compounds and there was no way to couple LC and MS.

While it is not inevitable that mass spectrometry will thrive, I believe it is within our power to ensure that it does. For this to occur, we must do more than participate in and apply the types of developments just discussed. In addition,

- Individuals of the highest caliber must be willing to serve in the society.
- The effort on education of all mass spectrometry users must be maintained and strengthened.
- The balance between fundamentals/instrumentation/applications - this difficult balance - must be preserved.
- Finally, we need to improve the quality of our competitive interactions we need to be advocates of mass spectrometry, supportive of each other in the larger arena.

Common characteristics unite these developments:

- very rapid progress from concept to widely applied methodology
- ingenuity in implementation e.g. we have half a dozen ingenious methods for crossing the solution vacuum interface.
- daring: mass spectroscopists will tackle anything!

Whatever the exact form of the future in mass spectrometry surely these qualities will be carried forward - energy, ingenuity and daring. With human qualities like this the problems mass spectroscopists' tackle can be large indeed. Alessandro Manzoni suggested:

Truth as subject
Beauty as means
Utility as purpose

There could hardly be a more suitable motto for our science.

Exciting developments are occurring throughout mass spectrometry and we are fortunate that we can be counted amongst its practitioners. As we continue to practice our science, lets lend strength to each others efforts, a strong science can that way only become stronger to the advantage of all.

Given these attitudes we can hardly fail to succeed as we more to really high masses, really small instruments, really wide use of sensitive, mobile, on-line, instruments, and deeper insigts into chemical reactions, physical phenomena and biological structure and function.

Presented at the 36th ASMS Conference on Mass Spectrometry and Allied Topics
June 5-10, 1988, San Francisco, CA

References

1. W. Wien, Berh. d. phys. Gesell, 17 (1898).
2. J.N. Louris, R.G. Cooks, J.E.P. Syka, P.E. Kelley, G.C. Stafford and J.F.J. Todd, Anal. Chem., 59 1677 (1987).
3. V. Franchetti, B.H. Solka, W.E. Baitinger, J.W. Amy and R.G. Cooks, Int. J. Mass Spectrom. Ion Phys., 23 29 (1977).
4. H.-J. Laue, B. Winger, J.W. Amy and R.G. Cooks, unpublished work.
5. M.E. Bier, R.G. Cooks and G.C. Stafford, patent applied for.

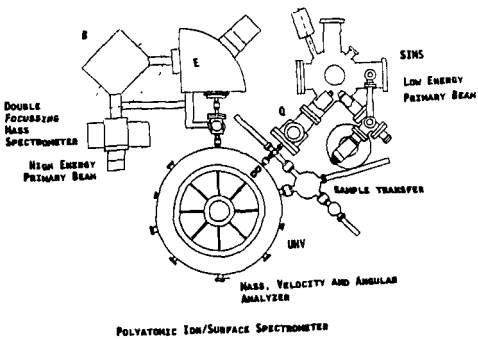

Figure 1. Schematic view of UHV system for studying surface-induced dissociation and other ion/surface collision phenomena as a function of angle and energy. The double focussing mass spectrometer seems as the source of the projectile beam while the SIMS spectrometer provides a beam for surface modification.

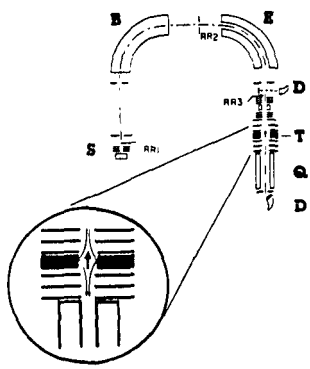

Figure 2. Hybrid MS/MS instrument, modified for ion/surface collisions by addition of the in-line device shown in the inset.

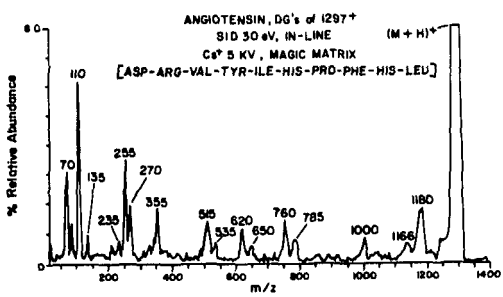

Figure 3. Daughter spectrum (30 eV) of protonated angiotensin produced by surface induced dissociation.

Presented at the 36th ASMS Conference on Mass Spectrometry and Allied Topics
June 5-10, 1988, San Francisco, CA

ANALYTICAL CAPABILITIES AND APPLICATIONS OF FT/ICR MASS SPECTROMETRY

Alan G. Marshall

Dept. of Chemistry (and Dept. of Biochemistry)
The Ohio State University
120 W. 18th Avenue
Columbus, OH 43210

The analytical advantages and disadvantages of FT/ICR mass spectrometry[1] are considered briefly here. Because the device acts to convert mass into frequency, and because frequency is the most accurately measurable physical parameter, the ultrahigh mass resolution (~1,000,000 at m/z 200 at 3.0 tesla) of FT/ICR is limited only by pressure (since FT/ICR line width varies directly with ion-molecule collision frequency) and by the uniformity and magnitude of the electric field in the ion trap (see Grosshans et al. in this volume). Because ions can be trapped for prolonged periods (s or min or longer), ions can be characterized by their reactions with neutrals: the neutrals may be provided by the parent molecules themselves (self chemical ionization without the need (or complications from) an external reagent gas) or by pulsed introduction of collision or reagent gases (MS/MS). Moreover, because successive stages in an FT/ICR experiment are separated in time rather than (as in beam instruments) separated in space, the FT/ICR mass spectrometer is compact and can perform multistage experiments (e.g., MS/MS/MS···) without additional hardware (or cost!). A major advantage is that ion selection can be achieved essentially by means of *software* (e.g., stored waveform inverse Fourier transform techniques)[2] rather than by the *hardware* methods associated with conventional ion focusing and slits. Similarly, a variety of different ion-forming means (E.I., C.I., laser desorption, photodissociation, S.I.M.S., etc.) can all be adapted to the same detector without sacrificing performance of any one of the ionization methods. In particular, laser desorption FT/ICR is uniquely suited for analysis of mixtures of chemically dissimilar species,[3] because most organics desorb under the same experimental conditions. Since ICR excitation and trapping potentials are low (<100 V or so), and since there is no need to direct ions through a narrow slit, the ion source/detector can be operated for extended periods (several months) without the need for disassembly and cleaning. Because ICR experiments can be conducted at pressures ~1000 times lower than those of most other mass spectrometer ion sources, ICR is inherently more sensitive (in the sense of lower sample vapor pressure) for observation of low-volatility heat-labile species. Positive and negative ions may be detected in successive scans, simply by changing the sign of the trapping voltage. Detection is fast--data are generally acquired in 1 sec or less, even for very wide mass range and/or very high mass resolution.

A disadvantage of FT/ICR is its limited dynamic range. Because the detected signal is an image current induced by a coherently orbiting ion packet, the minimum number of ions that can be detected in a single scan is ~100. However, the presence of more than ~100,000 ions in the trap leads to Coulomb broadening and ion ejection. Therefore, the FT/ICR dynamic range is inherently limited to a factor of about 1,000 in a single experiment. However, selective ejection of abundant ions can improve that factor significantly, if two or more scans can be acquired.[4] A disadvantage of any computer-based mass spectrometer is that precision in determining mass (or ion abundance or peak width) is directly related not only to signal-to-noise ratio, but also to the number of data points per peak width. Thus, in order to realize the ultrahigh mass resolution available from FT/ICR, very large data sets (>256K) may be needed.

Accurate measurement of relative ion abundances by FT/ICR, although highly reproducible for a single set of conditions, can be sensitive to various experimental parameters--thus, it is important to compare relative peak areas under identical operating conditions. The low-pressure (~10^{-8} torr or less) requirement of FT/ICR requires differential pumping between the ion source (whether external or dual-cell) and the ion analyzer; as a result, FT/ICR has been interfaced satisfactorily to GC and FAB sources, but with less success for supercritical fluid or liquid chromatography effluents. As for all types of Fourier transform spectrometry, FT/ICR has the problem of foldover--i.e., signals whose frequency exceeds the Nyquist limit of the analog-to-digital converter will appear "aliased" or "folded-over" to incorrect frequencies. Foldover may generally be eliminated by appropriate (computer-selected) bandpass filtering. FT/ICR mass resolution decreases with increasing mass (as for any magnetic field based mass analyzer operated at its magnetic field imposed limit). Moreover, although experimental FT/ICR mass resolution closely approaches its theoretical limit[5] below about m/z 2000, experimental performance (particularly for F.A.B.-generated organic ions) drops well below that limit for ions of higher mass--causes and solutions are addressed in the paper by Grosshans et al. in this volume.

Several exciting new developments in FT/ICR are discussed in our own and other papers at this meeting. For example, our understanding of the origin of the upper mass limit for FT/ICR is improving, and there is reason to believe that new ion trap designs will lead to significantly improved performance at m/z > 2,000. Several research groups are developing new and/or better ways to adapt existing ion sources (e.g., F.A.B., S.I.M.S., plasma desorption, fast neutral beam) to FT/ICR instruments. The best evidence for the analytical advantages of FT/ICR is the good agreement between a best-fit exponential curve and the number of FT/ICR spectrometers shown below. The number of FT/ICR instruments worldwide is already double the number of continuous-wave ICR instruments (which were used mainly by academics for ion-molecule chemistry), due mainly to the analytical and industrial applications to polymers[3] and other areas.

This work was supported by grants (to A.G.M.) from N.I.H. (GM-31683), N.S.F. CHE-8721498 and The Ohio State University.

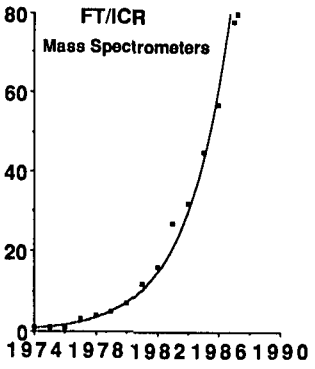

1. Marshall, A. G. *Acc. Chem. Res.* **1985**, *18*, 316-322.
2. Marshall, A. G.; Wang, T.-C. L.; Chen. L.; Ricca. T. L. *A.C.S. Symp. Ser.*, ed. M. L. Buchanan**1987**, *359*, 21-33.
3. Hsu, A. T.; Marshall, A. G. *Anal. Chem.* **1988**, *60*, 932-937.
4. Wang, T.-C. L.; Ricca, T. L.; Marshall, A. G. *Anal. Chem.* **1986**, *58*, 2935-2938.
5. Marshall, A. G.; Comisarow, M. B.; Parisod, G. *J. Chem. Phys.* **1979**, *71*, 4434-4444.

Presented at the 36th ASMS Conference on Mass Spectrometry and Allied Topics
June 5-10, 1988, San Francisco, CA

ENERGY- AND TIME-RESOLVED MEASUREMENTS IN MASS SPECTROMETRY

Chava Lifshitz
Department of Physical Chemistry and
The Fritz Haber Center for Molecular Dynamics
The Hebrew University of Jerusalem, Jerusalem 91904, Israel

Two techniques for ion trapping have been employed by us in recent years: (1) Ion trapping in the space charge of an electron beam; (2) Ion trapping by RF voltages in a Cylindrical Ion Trap (CIT). These techniques allow time-resolved measurements to be made in the range of ion lifetimes from microseconds to milliseconds. They have been combined with energy resolved electroionization and photoionization measurements, respectively. These combinations have been applied to measurements of time-resolved appearance energies, ionization efficiency curves and kinetic shifts. Space charge trapping has also been combined with an MS/MS method called TRIMS (Time-Resolved Ion Momentum Spectrometry) and has been applied to determinations of time-resolved kinetic energy releases.

Figure 1 is a schematic drawing of the photoionization mass spectrometer and Figure 2 is a schematic drawing of the experimental setup which combines TRIMS with ion trapping in the ion-source by an electron space charge.

The primary reaction of the anisole cation-radical – elimination of formaldehyde has been studied by both techniques[1,2] in detail recently. The experimental time-resolved photoionization efficiency curves and kinetic energy releases (KERs) have been modelled by RRKM-QET calculations. An accurate long-time limiting threshold energy was determined for the reaction. The KERs were observed to be time-dependent due to varying contributions of two competitive mechanisms to the reaction.

[1] J.P. Ziesel and C. Lifshitz, Chem. Phys. 117 (1987) 227.
[2] V. Aviente, M. Elam, N. Ohmichi and C. Lifshitz, "Time Dependent Mass Spectra and Breakdown Graphs. II. TRIMS of Anisole", J. Phys. Chem., submitted.

Presented at the 36th ASMS Conference on Mass Spectrometry and Allied Topics
June 5-10, 1988, San Francisco, CA

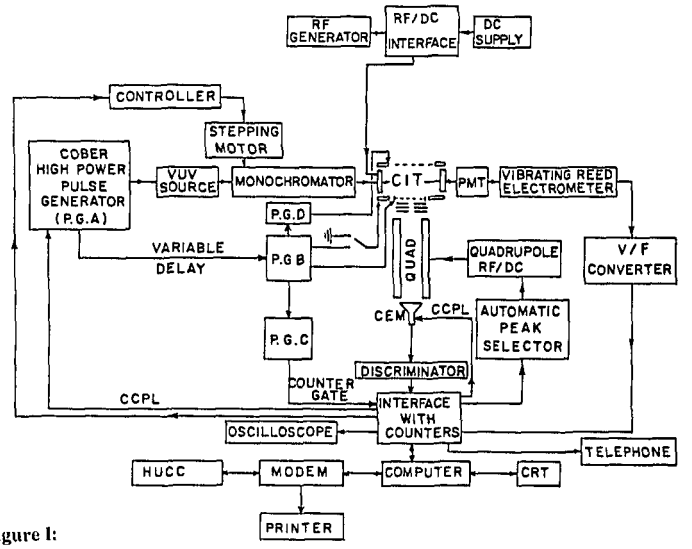

Figure 1:

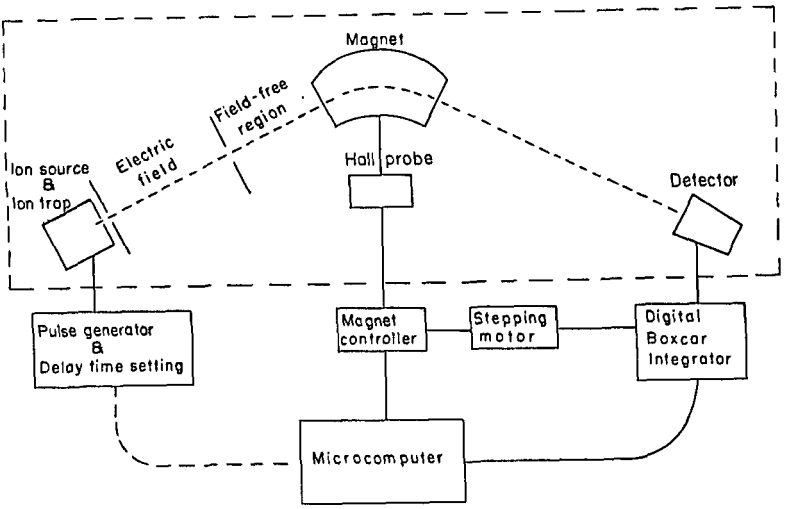

Figure 2:

Presented at the 36th ASMS Conference on Mass Spectrometry and Allied Topics
June 5-10, 1988, San Francisco, CA

RF QUADRUPOLE ION TRAPS - PAST, PRESENT AND FUTURE (?)

J.F.J. Todd, Chemical Laboratory, University of Kent,
Canterbury, Kent, CT2 7NH, U.K.

Although the rf quadrupole ion trap has its origins in the same patent as that which first described the quadrupole mass filter[1] its emergence as a viable commercial mass spectrometer has been only a recent event.

The history of the ion trap (see Table 1) has followed two essential parallel paths. On the one hand successive groups of physicists, originating with Dehmelt [2,3], have utilised the device in systems for studying the spectroscopy of trapped atomic ions and there is now an abundant literature involving this area of application[4]. At the same time the development of ion trap mass spectrometers has passed through three distinct periods: mass selective detection, mass selective storage and, latterly, mass selective ejection.

Table 1. The Ages of the Ion Trap

1953:-	First disclosure (Paul & Steinwedel)	Mass-selective Detection
1959:-	Storage of microparticles (Wuerker et al)	
1959:-	Use as a mass spectrometer by Fischer	
1962:-	Storage of ions for rf Spectroscopy (Dehmelt et al)	
1968:-	Ejection of ions into an external detector (Dawson & Whetten): use as a mass spectrometer	Mass-selective Storage
1972:-	Combination of 'Quistor' with quadrupole for analysis of ejected ions (Todd et al): Characterisation of the trap, CI, ion-molecule kinetics, etc.	
1980:-	Resonant ejection of ions (March et al)	
1984:-	Disclosure of 'Ion Trap Detector' (Stafford, Kelley, Syka, Reynolds & Todd)	Mass-selective Ejection
1987:-	MS/MS, CI, photo-dissociation, injection of ions, mass-range extension, etc.	

The earliest phase saw the ion trap acting as a combined source, analyser and detector, in which the presence of ions was characterised by sensing the motion characteristic of species with particular m/z values, in a manner not dissimilar to ICR. With mass selective storage, ions of specific m/z value were created and stored in the trap prior to ejection into an external detector[5]; a development of this system was the QUISTOR/Quadrupole tandem system for studying the physical and chemical behaviour of trapped ions. Each of these earlier systems contained drawbacks which gave the ion trap few apparent advantages over existing forms of analytical mass spectrometer. These problems have largely been overcome with 'mass selective ejection' [7]. Here ions are first created within the trap and then ejected by increasing the amplitude of the RF drive potential applied to the ring electrode such that the axial component of the motion of the ions becomes unstable. This occurs with increasing value of m/z, so that the detected ion signal corre-

sponds to a mass spectrum. It has been shown that the resolution and sensitivity of the device may be improved considerably by maintaining a background of helium buffer gas present in the trap at a pressure of ca. 10^{-3} Torr.

Using this basic technology a number of improvements and further developments have been possible, including the control of adverse space charge effects through 'automatic gain control' [8], MS/MS studies through the application of supplementary rf fields to excite the secular motion of mass selected ions [9], chemical ionization [10] and photodissociation [11]. At this point in time, therefore, it is of some interest to trace the manner in which the ion trap mass spectrometer has evolved, highlighting the landmarks, and to consider possible directions for the future.

References

1. W. Paul and H. Steinwedel, U.S. Patent 2,939,952 (1960).
2. H.G. Dehmelt, Advan. At. Mol. Phys. 3 (1967) 53,
3. H.G. Dehmelt, Advan. At. Mol. Phys. 5 (1969) 109.
4. H.G. Dehmelt, in 'Advances in Laser Spectroscopy', ed. F.T. Arecchi et al, Plenum (1983), p. 153.
5. P.H. Dawson and N.R. Whetten, J. Vac. Sci. Technol. 5 (1967) 11.
6. J.F.J. Todd, in 'Dynamic Mass Spectrometry, Vol. 6', ed. D. Price and J.F.J. Todd, Heyden (1981), p. 44.
7. G.C. Stafford, Jr, P.E.Kelley, J.E.P. Syka, W.E. Reynolds and J.F.J. Todd, Int. J. Mass Spectrom. Ion Proc. 60 (1984) 85.
8. G.C. Stafford, Jr, D.M. Taylor, S.C. Bradshaw, J.E.P. Syka and M. Uhrich, Proc. 35th ASMS Conference, Denver, CO (1987), p. 775.
9. J.N. Louris, R.G. Cooks, J.E.P. Syka, P.E. Kelley, G.C. Stafford, Jr. and J.F.J. Todd, Anal. Chem. 59 (1987) 1677.
10. J.S. Brodbelt, J.N. Louris and R.G. Cooks, Anal. Chem. 59 (1987) 1278.
11. J.N. Louris, J.S. Brodbelt and R.G. Cooks, Int. J. Mass Spectrom. Proc. 75 (1987) 345.

Presented at the 36th ASMS Conference on Mass Spectrometry and Allied Topics
June 5-10, 1988, San Francisco, CA

COMPARISON OF THERMAL-ASSISTED AND PNEUMATIC-ASSISTED NEBULIZATION FOR ELECTROSPRAY LC/MS

Edgar D. Lee and Jack Henion, Equine Drug Testing and Toxicology, New York State College of Veterinary Medicine, Cornell University, 925 Warren Drive, Ithaca, NY 14850.

Thomas Covey, Sciex, 55 Glencameron Road, Thornhill, Ontario, Canada L3T 1P2.

Electrospray has been demonstrated as a feasible LC/MS interface at eluent flowrates of 5 to 10 uL/min. These low flowrates are compatible with capillary columns or require splitting the majority of the chromatographic effluent from the mass spectrometer. The use of pneumatic-and/or thermal-assistance with electrospray has been investigated in our laboratory to increase the eluent flowrate to be compatible with larger bore HPLC columns.

The mass spectrometer used for these experiments was a Sciex TAGA 6000E triple quadrupole equipped with an atmospheric pressure ion source. The pneumatic-assisted electrospray interface used was the ion spray LC/MS interface (1). This interface was constructed of two concentric stainless steel capillaries held at a potential of ±3 kV. The applied potential and the assistance of nitrogen nebulizing gas which flows through the annular space between the two capillaries forms charged droplets from which the ions are emitted. The inner capillary, through which the chromatographic eluent flows was 100 um i.d. x 225 um o.d. and the outer capillary, with an inside diameter of 500 um, was tapered at the end to a diameter of 300 um. The linear velocity of the nebulizing gas was measured to be 216 m/sec at the exit of the co-axial capillaries. The thermal-assisted electrospray interface was constructed from a homemade thermospray probe. The central tubing in the probe was replaced with a 250 um i.d. tube through which a 100 um i.d. x 200 um o.d. stainless steel capillary was fed. The end of the capillary extended 3 mm beyond the end of the thermospray probe for the electrospray needle necessary to create a high electric field for nebulization. The thermospray probe and power supply were floated at a ±3 kV electrospray potential.

The ion spray LC/MS interface has increased the eluent flowrate of electrospray from 10 uL to 100 uL/min with a small loss in sensitivity. Operation at eluent flowrates compatible with standard bore columns (500 to 750 uL/min) can be used. However, the loss in sensitivity is greater than if a portion of the eluent is split off. The ion spray mass spectrum of 100 ng of the hexa-sulfonated azo dye, direct Red 80 (MW 1240), was obtained at a flow rate of 50 uL/min (Figure 1). The base peak at m/z 205 is the $[M-6H]^{6-}$ molecular ion. The other major ions are m/z 247, 309, 412, which correspond to the $[M-5H]^{5-}$, $[M-4H]^{4-}$ and $[M-3H]^{3-}$ molecular ions.

The thermal-assisted electrospray interface complements ion spray at flowrates greater than 100 uL/min. The thermal-assisted electrospray mass spectrum from 1 ug of the hexa-sulfonated azo dye, direct Red 80, (Figure 2) exhibited comparable total ion intensity to the ion spray spectrum for 100 ng (Figure 1). The thermal-assisted electrospray mass spectrum was obtained at a flowrate of 500 uL/min and probe temperature of 165°C. The same multiply-charged ions are present in the thermal-assisted electrospray mass spectrum as in the ion spray mass spectrum with the exception that in the thermal-assisted mass spectrum m/z 619, corresponding to the doubly deprotonated doubly charged negative molecular ion, is also present. The heat appears to drive the ionization to the lower charged species. This effect can also be seen with other analytes we have studied.

References

1. Bruins, A.P.; Covey, T.R.; Henion, J.D. Anal. Chem., 1987, 59, 2642-2646.

Presented at the 36th ASMS Conference on Mass Spectrometry and Allied Topics
June 5-10, 1988, San Francisco, CA

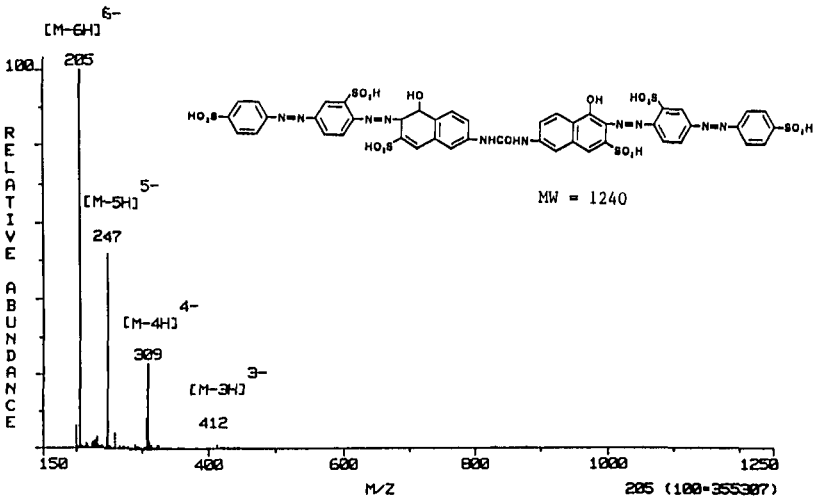

Figure 1. Negative ion spray mass spectrum for 100 ng of the hexa-sulfonated azo dye, direct Red 80. Conditions: 80/20 acetonitrile/1mM NH_4OAC, 50 uL/min. Shandon 1 mm i.d. x 10 cm C-18 column.

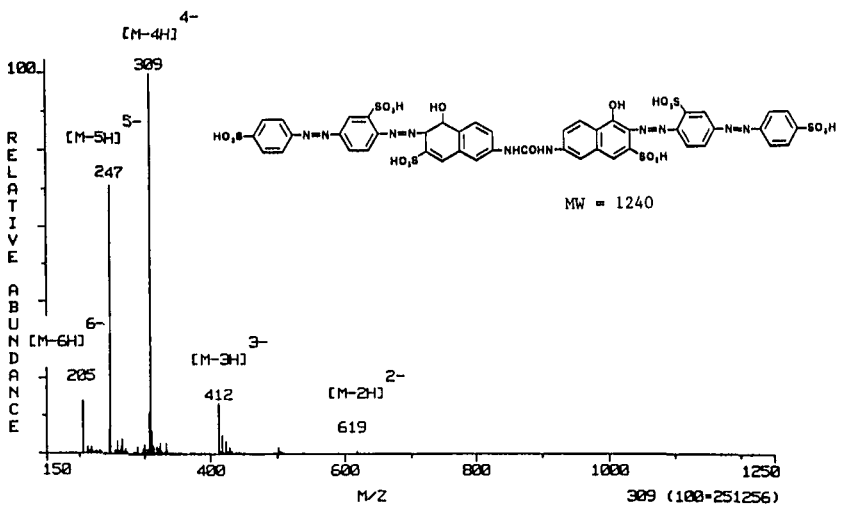

Figure 2. Negative ion thermal-assisted electrospray mass spectrum for 1 ug of the hexa-sulfonated azo dye direct red 80. Condition: 80/20 acetonitrile/1mM NH_4OAC, 500 uL/min, Perkin-Elmer 4.6 mm i.d. x 3 cm C-18 column, probe temperature 165°C.

Presented at the 36th ASMS Conference on Mass Spectrometry and Allied Topics
June 5-10, 1988, San Francisco, CA

Evaluation and Optimization of Continuous Flow Fast Atom Bombardment Interface Between Open Tubular Liquid Chromatography and Mass Spectrometry

M.A. Moseley[1,2], J.S.M. de Wit[1,2], L.J. Deterding[1], K.B. Tomer[1] and J.W. Jorgenson[2]

1) Laboratory for Molecular Biophysics, National Institute of Enviromental Health Sciences, RTP, NC 27709

2) Kenan Laboratories of Chemistry, University of North Carolina at Chapel Hill, Chapel Hill, NC 27514

The combination of liquid chromatography (LC) and continuous flow fast atom bombardment mass spectrometry (CF-FAB/MS) has recently become the topic of active research (1-5) since both LC and CF-FAB/MS are very useful for the analysis of polar, nonvolatile and/or thermally labile compounds.

In the CF-FAB interfaces thus far demonstrated the matrix required for the FAB process is introduced either in the mobile phase and analyte solutions, or is added to the LC effluent post column. Introduction of the matrix into the mobile phase can compromise the chromatography and changing the matrix type or concentration may require reevaluation of the chromatographic conditions. Post column addition of the matrix may lead to significant chromatographic peak broadening, particularly with microbore or open tubular LC.

Therefore, an interface which circumvents both of these problems was designed (5) which uses coaxial flow of the LC and matrix in two separate fused silica capillary columns. In this "column-within-a-column" interface the LC capillary column (150 um o.d.) is inserted into a sheath capillary column (200 um i.d.). A 1/16" stainless steel "tee" (Fig. 1) is used to interface the sheath and LC capillaries. A syringe pump is used to flow the matrix solution coaxially in the sheath column around the capillary LC column, and mixing of the matrix and the LC effluent takes place only at the FAB probe tip. The matrix flow, and the LC flow are regulated separately, which allows for independent optimization of the operating conditions (composition and flow rate) for both the chromatographic and FAB processes. The matrix solution used in this work was 25/75 glycerol/water at a flow rate of 1.2 ul/min. The LC flow was approximately 100 nl/min, an order of magnitude less than the matrix flow, and the combined flows resulted in a source pressure of
2×10^{-5} torr.

The performance of the interface has been evaluated for a range of compounds in terms of chromatographic fidelity, reproducibility, and detection limits. This interface design was found to be suitable for use with open tubular LC columns and with ultra-microbore packed LC columns (50 um i.d.) (Fig. 2). We observed a detection limit of 8 pg (S/N ~ 4/1) (Fig. 3) for the (M+H)+ ion, and a MS/MS full scan detection limit of 640 pg (Fig. 4) for the tripeptide Met-Leu-Phe.

Presented at the 36th ASMS Conference on Mass Spectrometry and Allied Topics
June 5-10, 1988, San Francisco, CA

REFERENCES

1) Caprioli, R.M.; Fan, T.; Cottrell, J.S., **Anal. Chem.**, 1986,58,2949.
2) Games, D.E.; Pleasance, S.; Ramsey, E.D.; McDowell, M.A.; **Biomed. Environ. Mass. Spectrom.**, 1988, 15, 179.
3) Boulengeur, P.; Leroy, Y.; Alonso, J.M.; Montreuil, G.R.; Colbert, C.; Duquet, D.; Dewaele, C., **Anal. Biochem.**, 1988, 168, 164.
4) Takeuchi, T.; Watanabe, S.; Kondo, N.; Ishii, D.; Goto, M., **J. Chromatog.**, 1988, 435, 482.
5) de Wit, J.S.M.; Deterding, L.J.; Moseley, M.A.; Tomer, K.B.; Jorgenson, J.W., **Rapid Comm. Mass Spectrom.**, 1988, 2, 100.

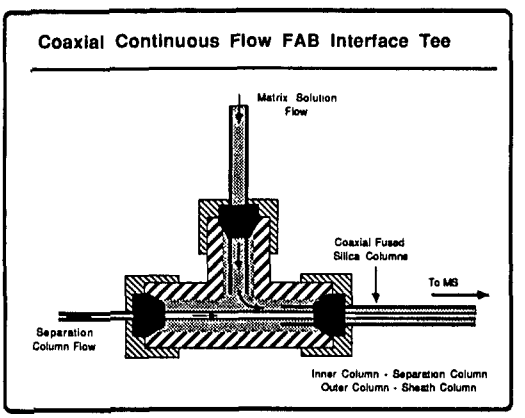

Figure 1

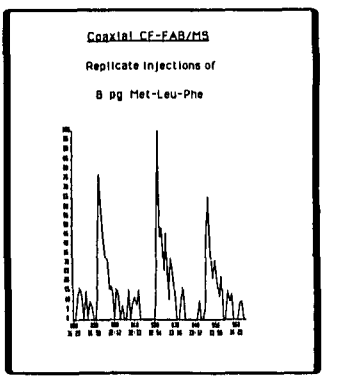

Figure 3

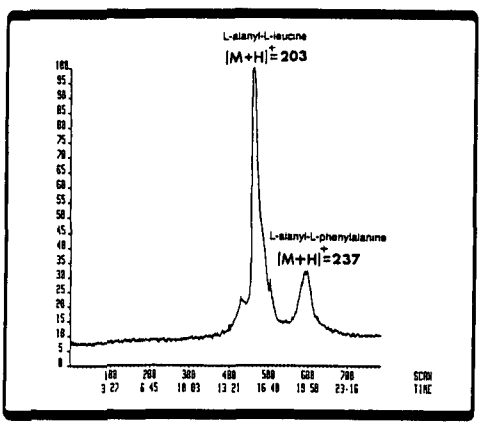

Figure 2

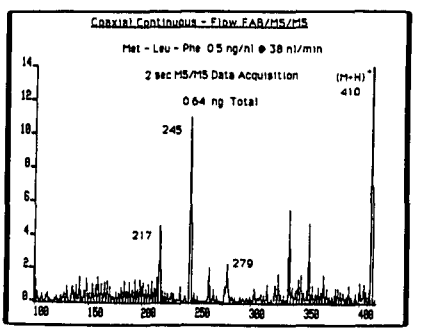

Figure 4

Presented at the 36th ASMS Conference on Mass Spectrometry and Allied Topics
June 5-10, 1988, San Francisco, CA

MS/MS AND CF-FAB FOR THE ANALYSIS OF DRUGS

William E. Seifert, Jr., Shen-Nan Lin, William T. Moore,
Annie Ballatore, and Richard M. Caprioli

The Analytical Chemistry Center and
Department of Biochemistry and Molecular Biology
The University of Texas Medical School at Houston
Houston, Texas 77225

Michael Story and Donald Bradford

Finnigan MAT Corporation
San Jose, California 95134

Continuous-flow fast atom bombardment mass spectrometry (CF-FAB) has been shown to have significant advantages in the direct analysis of aqueous solutions.[1] Our laboratory has previously shown that CF-FAB can be successfully applied to the analysis of peptides and peptide mixtures and can be utilized to obtain on-line kinetic measurements of enzyme reaction mixtures.[2] We have also combined microbore HPLC techniques to provide LC/MS capabilities for the analysis of peptides and small proteins.3 One area in which CF-FAB has not been applied to a significant extent is in the structural analysis of small molecules. Due to the nature of the low energy desorption process, FABMS normally yields spectra with very little fragmentation, and hence, very little structural information other than the molecular weight of the compound. In addition, the chemical noise due to the ions desorbed from the sample matrix is especially high in the low mass range, and complicates spectral interpretation of low molecular weight compounds.

The purpose of this study was to determine if CF-FAB could be successfully applied to the analysis of solutions of small molecular weight drugs (MW < 500) to yield both qualitative and quantitative information. The approach used was to combine CF-FAB with MS/MS techniques using a triple-stage quadrupole mass spectrometer. This combination allowed us to obtain collision-activated decomposition (CAD) mass spectra of the drugs after initial ionization by CF-FAB.

Samples were introduced into a Finnigan MAT TSQ 70 MS/MS system using a continuous-flow introduction inlet which was comprised of a 0.075 mm i.d. capillary and a Rheodyne Model 4010 injector fitted with a 0.5 μL loop. A Waters Model 590 pump was used to pump the carrier solution at a flow rate of 7 μL/min. The carrier solution was comprised of an aqueous mixture of 5% glycerol:15% acetonitrile:0.1% TFA. The sample and carrier solution was deposited on the normal FAB probe tip (Fig. 1), which is kept at 40°C. To aid flow from the probe tip, and maintain a stable surface, an absorbent pad of compressed cellulose is fitted to the probe tip adjacent to the sample surface. Collision-activated decomposition was effected using Ar as the collision gas at a pressure of 0.6-0.8 mTorr and a collision energy of 25-35 V. Mass spectral data was collected in the profile mode. Quantitative estimates were made using the integrated areas of selected ion chromatograms of significant daughter ions or the sum of significant daughter and surviving parent ions.

CF-FAB MS/MS was successfully used to obtain mass spectra from the following drugs or drug metabolites: benzoylecgonine, cocaine, codeine, morphine, penicillin G, pentobarbital, phenobarbital, phentolamine, and THC. Sensitivity and linearity studies were performed for benzoylecgonine, cocaine, penicillin G, and phentolamine. The minimum detection limits were determined to be 500 pg for benzoylecgonine, 250 pg for penicillin G, 50 pg for cocaine, and 50 pg for phentolamine. The range of reproducibility for repetitive injections of the different compounds was 5 - 15%, depending on the amount injected. Areas of selected ion chromatograms were linear for phentolamine and penicillin G for amounts injected from 250 pg to 50 ng (Fig. 2).

Experiments were also performed to determine if the CF-FAB MS/MS technique could be used to determine the presence of drugs in urine without prior sample clean-up procedures. Urine samples were spiked with either cocaine or benzoylecgonine (the primary cocaine metabolite) at concentrations of 0.1 - 10 μg/mL and injected directly into the mass spectrometer via the CF-FAB inlet. Both yielded the characteristic MS/MS spectrum at the 5 - 10 μg/mL level, and could be observed by selected ion chromatograms of the primary daughter ion down to 0.2 μg/mL and 1.0 μg/mL (100 pg and 500 pg injected), for cocaine and benzoylecgonine, respectively. Direct analysis of urine, however, resulted in poor reproducibility for repetitive injections which is attributed to the precipitation of salts and/or proteins in the capillary tubing of the CF-FAB inlet.

These experiments demonstrate that the combination of CF-FAB and MS/MS is useful for the structural identification of small molecular weight compounds such as drugs. The technique was demonstrated to be quantitative with standard errors of determination ranging from 5 - 15%. Sensitivity of the technique varied with the type of compound analyzed, but was in the picogram range for all compounds tested.

References:

1. R. M. Caprioli, T. Fan, and J. S. Cottrell, Anal. Chem., 58, 2949-2954 (1986).

2. R. M. Caprioli, Biochemistry, 27, 513-521 (1988).

3. R. M. Caprioli, B. DaGue, T. Fan, and W. T. Moore, Biochem. Biophys. Res. Comm., 146, 291-299 (1987).

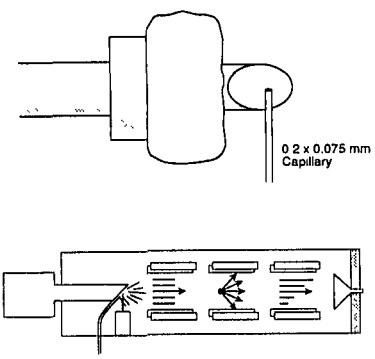

Fig. 1 Schematic diagram of the continuous-flow FAB inlet system showing placement of the capillary on the FAB probe tip.

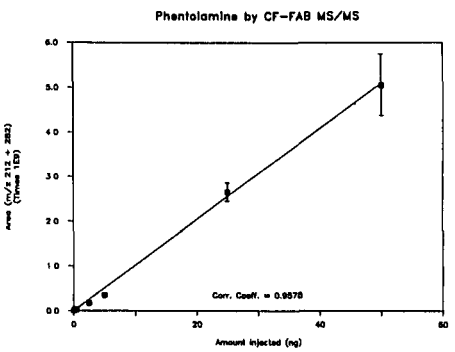

Fig. 2 Integrated area of the sum of surviving parent and major daughter ions vs. amount of phentolamine.

...ted at the 36th ASMS Conference on Mass Spectrometry and Allied Topics
June 5-10, 1988, San Francisco, CA

CONTINUOUS-FLOW FAB LC/MS ANALYSIS OF ACYLCARNITINES AND ACYL-COA COMPOUNDS USING MICROBORE HPLC COLUMNS

David S. Millington and Daniel L. Norwood
Division of Pediatric Genetics and Metabolism, Duke University Medical Center, Box 3028, Durham, NC 27710.

FAB-MS is a sensitive method for the analysis of acylcarnitines and acyl-coA thioesters (1). The recently developed continuous-flow FAB-MS interface is being applied in our research with three major objectives: 1. The analysis of acylcarnitine and acyl-coA mixtures from biological fluids by LC/MS. 2. The rapid, sequential analysis of urine samples for unusual acylcarnitines as a screening technique for metabolic disorders. 3. The development of in vitro enzyme assays by direct monitoring of substrate/product concentration.

Methods A standard pulse-damped HPLC pump (Waters 600-MS) was interfaced to a Valco CWI4 microinjector (100 nL loop) via a splitting 'T' (SGE MCVT 1:50), adjusted to provide a flow-rate of 5-10 µL/min. For direct injection of urine samples (25 µL, dried and methylated with 25 µL 3M MeOH/HCl at 65 °C for 10 min), the effluent was connected directly to the ion source of a VG Trio-3 triple quadrupole mass spectrometer by a length of fused-silica capillary. The manufacturer's interface probe and FAB/MS ion source (maintained at 50 °C) were employed. Acyl-coA thioesters were analyzed in the same manner, and MS/MS spectra were recorded using air as collision gas and with about 5 eV energy. For analysis of acylcarnitine standard mixtures, a "micro-LC" column (150 mm x 0.3 mm) packed with 5 µm C18 stationary phase (Alltech, Carnforth, UK) was employed and a non-linear gradient was used to effect the separation (Fig. 1).

Results The separation and analysis of free carnitine and its C2-C6 esters is shown by the TIC chromatogram in Figure 1. The high stability and sensitivity of the system were maintained despite the severe solvent gradient employed. The mass spectra of the individual components are dominated by (M+H)+ ions, enabling their detection at low pmol levels. For rapid screening of urine samples, it is sufficient to identify putative acylcarnitine signals without chromatographic separation. This was accomplished by analysis of 100 nL eqivalents of urine specimens after methylation (above) with an estimated detection limit for each acylcarnitine of 5 pmol (50 nmol/mL). The analysis cycle time, including syringe and injector flushing, was about 1.3 min. Since there was no evidence of memory effects, the method is apparently suitable for automation using an autosampler or laboratory robot.

The analysis of 0.8 nmol of propionyl-coA (MW = 823) is shown in Fig.2. In 2(a) and 2(b), the RIC profile and full scan mass spectrum at unit mass resolution are shown; and in 2(c), the CID mass spectrum from m/z 824 at reduced resolution (increased transmission) shows fragments at m/z 317 and 215 that contain the acyl group and is qualitatively similar to that previously reported by a metastable (B/E linked) scan on a magnetic sector instrument (1). The direct monitoring of these metabolites in mixtures at sub-nmolar concentration seems feasible.

Reference 1. D. S. Millington, in Mass Spectrometry in Biomed. Research, ed by S. G. Gaskell, Wiley & Sons, Chichester, 1986, pp 97-114.

Presented at the 36th ASMS Conference on Mass Spectrometry and Allied Topics
June 5-10, 1988, San Francisco, CA

FIGURE 1 ⟶

SEPARATION OF CARNITINE AND ITS C2 - C6 ACYL DERIVATIVES BY LC/MS USING CONTINUOUS FLOW (DYNAMIC) FAB

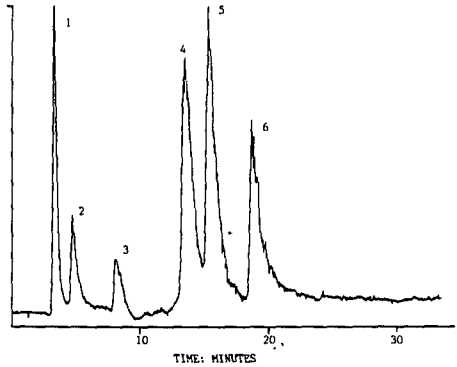

LC CONDITIONS: SOLVENT GRADIENT (NON-LINEAR) FROM 100% A (1 min) TO 50% A + 50% B (5 min) THEN HOLD

SOLVENT A: 95% MeOH : 0.5 M NH_4OAc (5.95)
5% GLYCEROL
pH 5.0 (TFA)

SOLVENT B. 95% MeOH
5% GLYCEROL

FIGURE 2. ANALYSIS OF PROPIONYL-COA

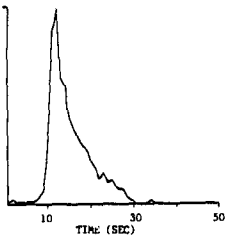

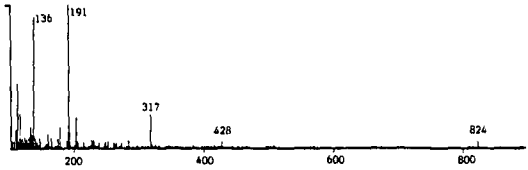

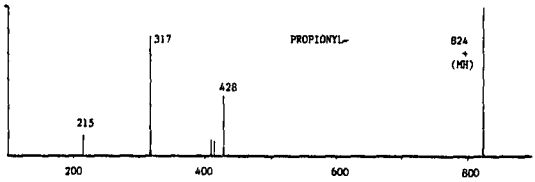

Presented at the 36th ASMS Conference on Mass Spectrometry and Allied Topics
June 5-10, 1988, San Francisco, CA

On line monitoring of nonvolatile products of biocatalytic reactions by mass spectrometric detection.

A.P. Bruins and N. Pras
State University, Dept. of Pharmacy, 9713 AW Groningen, The Netherlands

Mass spectrometers are used for process control and monitoring fermentations by measurement of volatile products .A sample from the head space inside the fermentor or a sample of volatile products that permeate through a membrane is introduced into the mass spectrometer.

On a laboratory scale, the quantitative and qualitative measurement of nonvolatile products of biocatalytic reactions is done by HPLC. Developments in LC/MS interfacing make mass spectrometric detection of such nonvolatile products feasible, by the direct introduction of a portion from the liquid phase of a biocatalytic reaction system into the LC/MS.

In our laboratory, an enzyme present in plant cells is used for the biocatalytic oxidation of substituted phenols to the corresponding catechols (1). Enzyme formulations employed for the oxidation of phenols are: a purified enzyme suspension; a plant cell suspension; plant cells entrapped in calcium alginate. In each system there are high molecular weight materials and particulate matter that cannot be introduced into the LC column and thermospray LC/MS interface.

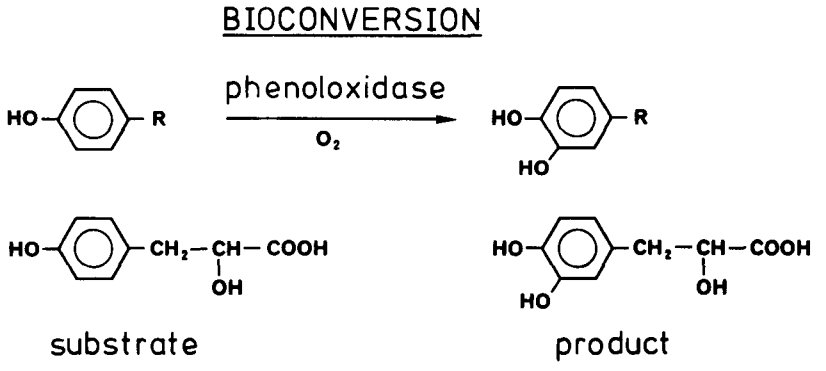

To investigate the feasibility of on line LC/MS monitoring of fermentations a purified enzyme suspension was enclosed in a piece of dialysis tubing. A number of such "sausages" was immersed in an aqueous solution of a phenol, TRIS HCl buffer, and sodium ascorbate. Air was bubbled through. The substituted phenol migrates through the membrane, is oxidised, and the product migrates back into the bulk solution. We have in

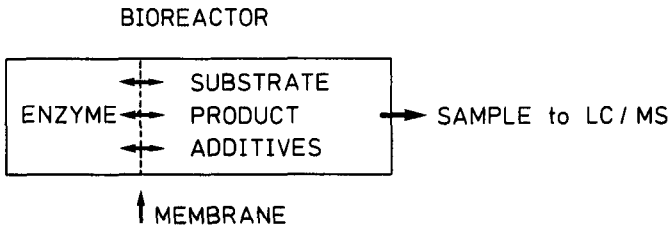

fact created a two compartment system, where particulate matter (the enzyme suspension) is separated from a "clean" solution. A sample from the "clean" solution was injected into the LC/MS. The identity of substrate and product was readily confirmed from negative ion spectra and from daughter ion scans of $(M-H)^-$ ions.

The mass spectrometer was a Nermag R 30-10 triple quadrupole equipped with a Nermag thermospray source, a Vestec probe and controller. A Kratos Spectroflow 400 pump and Spectroflow 757 UV detector (high pressure cell) were used for HPLC.

1. N. Pras, H.J. Wichers, A.P. Bruins and Th.M. Malingre: Bioconversion of para substituted phenols into corresponding catechols by alginate entrapped cells of Mucuna pruriens, Plant cell, tissue and organ culture, in press.

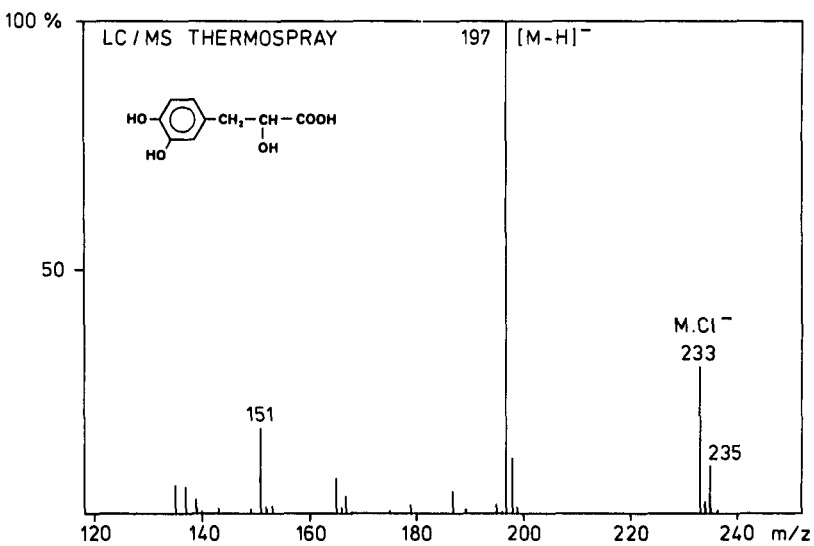

Presented at the 36th ASMS Conference on Mass Spectrometry and Allied Topics
June 5-10, 1988, San Francisco, CA

IMPROVEMENTS IN A PARTICLE BEAM LC/MS INTERFACE

A. Apffel and R. Nordman; Hewlett-Packard Company, Palo Alto, California 94304

During the last several years, experiments using particle beam based interfacing techniques between High Performance Liquid Chromatography and Mass Spectrometry have excited attention because of their potential advantages with respect to existing interface techniques, such as the generation of library searchable electron impact spectra, excellent sensitivity, reproducibility and ease of use.

The Particle Beam LC/MS system consists of three basic components; an aerosol generator, a desolvation region and a momentum separator. Following initial feasibility studies (reported last year), an in-depth investigation into the performance characteristics of each of these subsystems has lead to a redesign of the system resulting in significant improvements in the instrumentation, particularly in the quantitative performance and the ease of use. The purpose of this paper is to summarize these improvements

PB LC/MS is based on earlier work on "MAGIC" (Monodispersed Aerosol Generation Interface Combining LC and MS) done at Georgia Institute of Technology[1]. The development of MAGIC LC/MS utilized a cross-flow pneumatic nebulizer and emphasized the requirements for narrow droplet size dispersion. The current system utilizes a co-axial pneumatic nebulizer which results in a major improvement in sensitivity, nebulization gas consumption and ease of use.

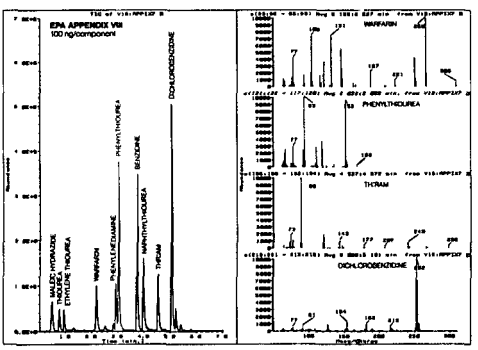

Figure 1. Analysis of 10 EPA Appendix VIII compounds at the 100 nanogram level

In our earlier prototype temperature stability of the desolvation chamber had adverse effects on reproducibility. Optimization of the dimensions and thermal characteristics in the current system has lead to excellent reproducibility (<3% rsd) under a wide range of conditions Finally, modeling of the fluid dynamics of the momentum separator has lead to increased sensitivity.

The Particle Beam LC/MS system can operate with all commonly used HPLC mobile phases (with the exception of non-volatile buffer systems) at flow rates between (0.1 and 1 ml/min. Both electron impact and chemical ionization modes can be used, resulting in typical detection limits of 10-100ng for full scan acquisition. The system shows applicability to a wide range of problems not amenable to GC/MS analysis.

---

[1] Willoughby, R C and Browner, R F, Analytical Chemistry 1984 (56) 2623 - 2631.

Presented at the 36th ASMS Conference on Mass Spectrometry and Allied Topics
June 5-10, 1988, San Francisco, CA

CHARGE EXCHANGE REACTIONS WITH WATER IN THE DETECTION OF PERFLUOROCARBONS BY THERMOSPRAY LIQUID CHROMATOGRAPHY/MASS SPECTROMETRY

S. K. Huang, M. McLoughlin and D. H. Klein
Adamantech inc., 1501 Blueball Ave., Linwood, PA 19061-0895

Perfluorocarbons (PFC's) are thermally and chemically stable materials. They are resistant to microbiological or chemical oxidations. In 1966, Clark et. al. (1) found that perfluoro- tetrahydrofuran equilibrated with oxygen at atmospheric pressure could support the respiration of a mouse. Since then, applications of perfluorochemical emulsions for human therapeutics have been explored.

Valuable information about PFC mixtures could be obtained by an analytical method which determines the composition of the mixture in terms of molecular weight groups, rather than in terms of individual isomers(2). Several packed GC columns were tried but found not useful in achieving the separation of PFC's into different molecular weight groups clearly. Therefore a procedure for liquid chromatographically separating these PFC's clearly into different molecular weight peaks, each of which consists of isomers of a single molecular weight has been developed. This was achieved by using a 4.6mm x 25 cm column with a Fluorodecyl bonded stationary phase and 100% THF as a mobile phase. A Hewlett-Packard Model 5988 LC/MS system equipped with a Vestec thermospray interface was used for this work. Table 1 is a compilation of experimental results for the detection of PFC's. It can be seen that LC/MS detection of PFC's requires the presence of water with filament turned on in the negative ion mode. The best condition in terms of sensitivity and resolution was obtained by the postcolumn addition of 0.1 N ammonium acetate (NH_4OAc) aqueous buffer, or of water only, through a low dead volume tee; addition of water or aqueous buffer directly to the mobile phase resulted in degradation of the separation. The mobile phase was pumped at 1 ml/min, and buffer or water was added to the column effluent at 0.5 ml/min with the stem temperature was taken at 25% less than the vaporizer exit temperature, and at a source temperature of 280° C. Figure 1a shows the total ion chromatogram (m/e 17-600) resulting from injection of a mixture of 60ug each of perfluoro-cyclohexane, perfluoro-methyl cyclohexane, perfluoro- 1,3-Dimethyl cyclohexane, perfluoro decalin and perfluoro-1-methyl decalin, with thermospray LC/MS detection and Figure 1b is the chromatogram of the same mixture using a refractive index(RI) detector. The ions detected are $M^{-\bullet}$ and $(M-F)^-$. It has been reported that proton transfer, anion attachment, and electron capture are responsible for the negative ion thermospray detection(3). Since there was almost no signal detected when THF alone was used as the mobile phase (Table 1), the contribution of the direct electron attachment process to the detection of PFC's is minor. Furthermore, the observations that when water is added to the system the detection of PFC's becomes sensitive, and that the background of the total ion chromatograph shows abundant mass peaks representing $(H_2O)_m(OH)_n^-$ (m=0-4, n=4-6) suggest the charge exchange mechanism. To test this hypothesis, an experiment was performed on perfluoro-toluene. Because the electron affinities of $\bullet OH$ and $C_6F_5CF_3$ are 43.6 ± 2.7 kcal/mole and 39.2 ± 6.9 kcal/mole respectively, $\bullet OH$ should not transfer charge to perfluoro-toluene. This was shown to be the case. Thermospray LC/MS of perfluoro-toluene gave a negligible peak at the same retention time at which the RI detector gave a large peak.

In the experiments reported here, there is no preionization of PFC's as described by Dodd and no chemical ionization of PFC's by the primary reagent ions (here NH_4^+) through gas phase ion/molecule reaction in direct thermospray ionization. This can be ascribed to the inertness and stability of the PFC's. The detection limit of PFC's in thermospray LC/MS can be improved by a factor of 10 when single ion

monitoring (SIM) technique is employed. This is much less effective than in the case of GC/NICI/MS, where the improvement of sensitivity can be as high as 500. Because PFC's appear to be shielded from electron attack by the surrounding THF molecules (The THF molecules are effective shields because they are electrophobic, as shown by the low baseline signal obtained when THF alone is entering the ion source), and because water has no affinity for the PFC's, the intensity of the detected negative ion PFC is limited by the surrounding THF molecules. Therefore greatly increasing the water content in the inlet system does not result in more sensitive detection of the PFC's.

Table 1

LC/MS DETECTION OF PERFLUOROCARBONS

Mode	TSP	Filament	Additives	Results
Negative ion	off	on	none	-
Negative ion	on	on	none	-
Negative ion	on	on	0.002N NH4OAc in THF	-
Negative ion	on	on	1.0N aq. NH4OAc in THF	+
Negative ion	on	on	H2O in THF	+
Negative ion	on	on	post column add. 1.0N aq.NH4OAc	+
Negative ion	on	on	post column add. of H2O	+
Negative ion	on	off	post column add. of H2O	-
Positive ion	on	on	post column add. of H2O	-
Positive ion	on	off	post column add. of H2O	-

Figure 1

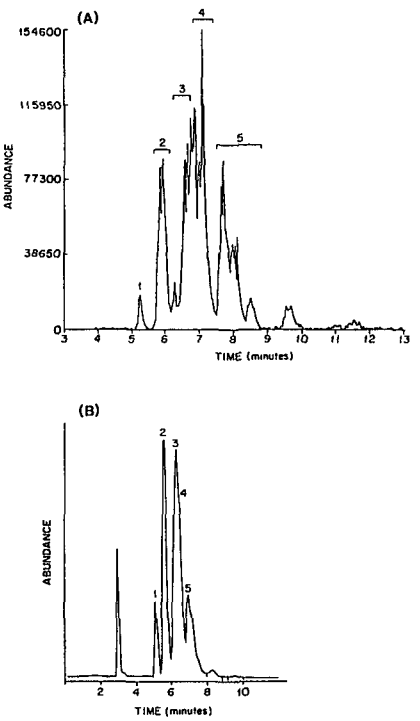

References:

1. L. C. Clark Jr. and F. Gollan, Science, 152, 1755 (1966).

2. R. E. Moore and L. C. Clark Jr. in Perfluorochemical Oxygen Transport, ed. by K. K. Tremper, Little, Brown, Boston (1985).

3. C. E. Parker, R. W. Smith, S. J. Gaskell and M. M. Bursey, Anal. Chem., 58, 1661 (1986).

Presented at the 36th ASMS Conference on Mass Spectrometry and Allied Topics
June 5-10, 1988, San Francisco, CA

Analysis of Middle Mass Peptides by Thermospray LC-MS and LC-MS/MS

Patrick J. Rudewicz, Finnigan MAT, 355 River Oaks Parkway, San Jose, CA 95134

Introduction Since most thermospray (TSP) LC-MS analyses have been done on quadrupole mass spectrometers having mass ranges less than 1800 u, there have been a limited number of applications using TSP for peptide and protein structure determination. Previously, the molecular weights of middle mass (2000 to 4000 u) peptides ionized by TSP had to be determined using multiply charged ions. However, with the latest generation of quadrupole mass spectrometers having extended mass ranges of 4000 u, middle mass peptides can now be analyzed directly by TSP LC-MS.

Experimental These experiments were done using a Finnigan MAT TSQ 70® triple quadrupole mass spectrometer equipped with a Finnigan MAT TSP LC-MS ion source. The HPLC system consisted of two Waters (Milford, MA) 510 HPLC pumps and a Waters 680 gradient controller. The TSP conditions were: source block 190°C; vaporizer 85°C; aerosol 155°C. The mobile phase was 80% methanol/20% 0.1 M ammonium acetate at a flow rate of 1.2 ml/min. For the LC-MS/MS experiments, the collision gas was xenon at 1.5 milliTorr and the collision energy was 25 eV. The sample was introduced continuously into the ion source at a rate of 0.5 nmole/sec, and the parent ion beam was transmitted with a 5 u window. The scan time was 30 sec. The tryptic digest of bovine lactoglobulin A was purchased from Applied Biosystems (Foster City, CA).

Results and Discussion Previous work in our laboratory has demonstrated the potential of TSP LC-MS for the analysis of peptides with molecular weights between 2000 and 4000 u (1,2). Full scan centroid data have been shown for low nanomolar amounts of peptides such as melittin (M_r 2844) and glucagon (M_r 3480). The spectra contained abundant singly protonated molecular ions and the doubly charged species, MH_2^{+2} and $(M+H+Na)^{+2}$. Centroids of molecular ion clusters, recorded at reduced resolution to enhance sensitivity, provided average molecular weight data.

TSP LC-MS As a preliminary evaluation of this methodology for the on-line LC-MS analysis of peptide mixtures, a tryptic digest of bovine lactoglobulin A (MW 18,367) was analyzed. The mixture was eluted from a 3 cm C-8 column using isocratic conditions of 80% methanol/20% 0.1 M ammonium acetate. A mass spectrum displaying the total ion current summed across the entire elution volume is shown in Figure 1. Abundant molecular ions are present for most of the expected tryptic fragments. In the 2000 to 3000 u range, a singly protonated molecular ion for tryptic fragment, T_4, a 20 residue peptide, is present at m/z 2313. The doubly charged ion at m/z 1157 corroborates the molecular weight of this fragment. The presence of a disulfide linkage connecting T_5 and T_{18} is indicated by the ion at m/z 2777.

TSP LC-MS/MS To produce structural information, daughter ion spectra can be obtained on either the singly or doubly protonated molecular ions of peptides (2). As an example, the CID spectrum of the protonated molecular ion of substance P is shown in Figure 2. The principal fragmentation pathways involve cleavage of the -CHR-CO- bonds and the -CO-NH- bonds with charge retention by the N-terminal fragments, A and B type ions, respectively. It has been our experience that CID spectra of peptides up to mass 600 ionized by TSP can be recorded at unit resolution within the time frame of a chromatographic peak. Higher mass peptides, especially above mass 1000, however, require continuous introduction into the TSP source and transmission of the entire molecular ion cluster through the first quadrupole.

Literature Cited

1. Rudewicz P. J. Biomed. and Environ. Mass Spectrom. 1988, 15, 461-463.

2. Rudewicz, P. J. In Analysis of Peptides and Proteins: Proceedings of the Fourth Texas Symposium on Mass Spectrometry. C.J. McNeal, Ed.; John Wiley and Sons, Chichester, England, in press.

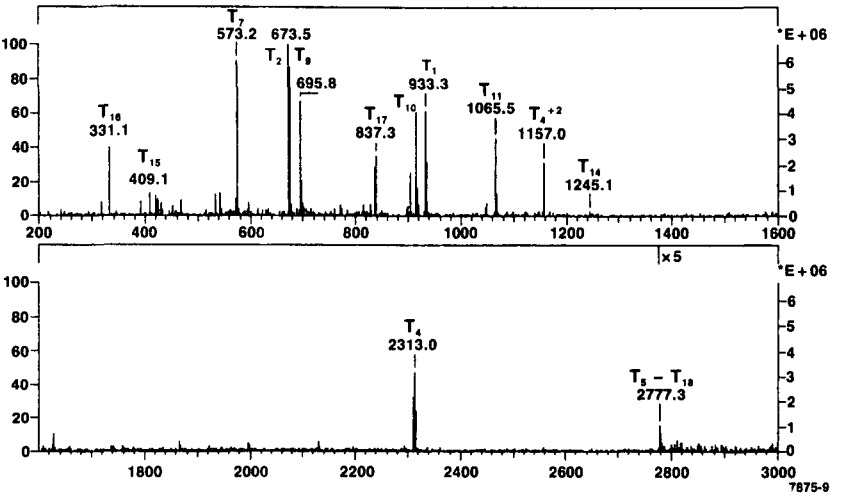

Figure 1. Mass spectrum (sum of 14 scans) of a tryptic digest of bovine lactoglobulin A (10 nanomoles).

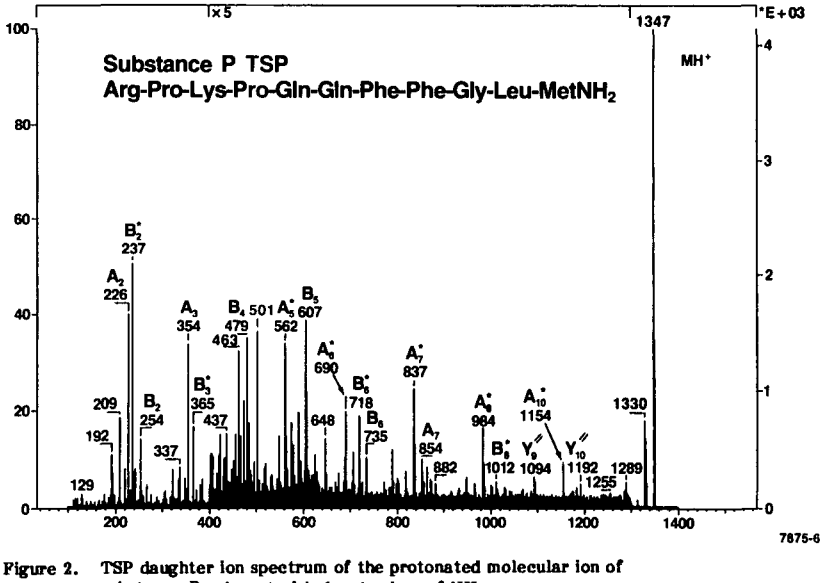

Figure 2. TSP daughter ion spectrum of the protonated molecular ion of substance P. An asterisk denotes loss of NH_3.

Presented at the 36th ASMS Conference on Mass Spectrometry and Allied Topics
June 5-10, 1988, San Francisco, CA

FUNDAMENTAL STUDIES OF SOLUTION-PHASE AND GAS-PHASE REACTIONS IN ELECTROCHEMISTRY/THERMOSPRAY/TANDEM MASS SPECTROMETRY

Kevin J. Volk, Anna Brajter-Toth, and Richard A. Yost
University of Florida, Gainesville, FL 32611

The on-line coupling of an electrochemical cell with thermospray/tandem mass spectrometry (EC/TSP/MS/MS) can provide valuable redox information on a variety of compounds because it is capable of providing molecular weight and structural information of intermediates and products formed in redox processes. After the initial redox reaction has taken place, the intermediates produced during the electrooxidation of uric acid and 6-thiopurine can undergo a variety of chemical reactions (Figs. 1,2) such as hydrolysis, ammonolysis, methanolysis, and other substitution reactions depending on the composition of the mobile phase and the thermospray operating parameters. Here we report the results of our work to determine if such reactions occur in the thermospray probe, source or both.

Our studies were divided into the following categories:

Gas-Phase Studies

Reagent Gas Added	Mobile Phase
1) none	0.1M NH_4OAC
NH_3	0.1M HOAC
2) none	0.1M NH_4OAC/CH_3NH_2
CH_3NH_2	0.1M NH_4OAC
3) none	0.1M NH_4OAC/CH_3OH
CH_3OH	0.1M NH_4OAC

Solution Phase Studies

1) Tip temperature studies
2) Source temperature studies
3) Mobile phase composition

The effect of tip temperature on intermediate formation (mobile phase consists of 0.1M NH_4OAC) can be seen in Figures 3 and 4. These plots indicate that ammonolysis reactions are related to processes which occur inside the vaporizer probe. Unlike the tip temperature studies, source temperature studies did not indicate the presence of temperature dependent chemical reactions. When 0.1M acetic acid is used as the mobile phase and NH_3 is added to the source, only hydrolysis reactions are detected (i.e. no ammonolysis reactions occur for either compound studied). Similar reactions occur inside the vaporizer probe when methylamine and methanol are present in the mobile phase; but do not occur when the these same gases are introduced in the TSP source.

The electrooxidation of 6-thiopurine is thought to be very similar to the chemical oxidation (Figure 5). The inability to detect the dimer by EC/TSP/MS at pH ~7 is consistent with the disproportionation process. Although the sulfinic acid is not detected by EC/TSP/MS, we believe that once formed, it undergoes reactions inside the probe (hydrolysis, ammonolysis, etc.) to

form the observed products, purine, adenine, and hypoxanthine (Figure 2). Gas-phase studies also support the dimer disproportionation process because the dimer can be detected using a mobile phase consisting of 0.1M HOAC with ammonia added to the TSP source. Under the conditions which allow the detection of this dimer, neither hypoxanthine nor adenine are formed. These studies indicate that many of the observed reactions do not occur in the TSP source, but occur inside the vaporizer probe.

Figure 1.

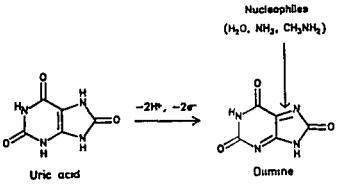

Figure 2.

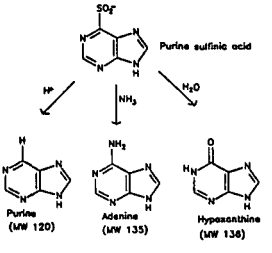

Figure 3.

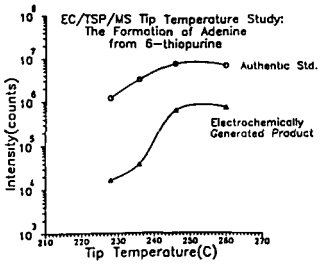

Figure 4.

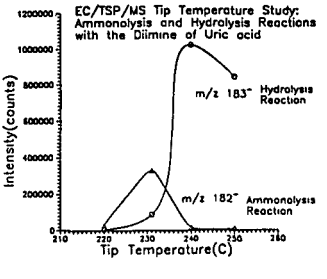

Figure 5.

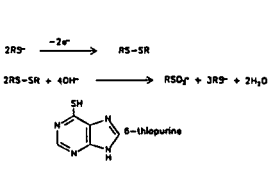

Presented at the 36th ASMS Conference on Mass Spectrometry and Allied Topics
June 5-10, 1988, San Francisco, CA

DEVELOPMENT OF NEW SOFT IONIZATION TECHNIQUES BASED ON PROPERTIES OF SUPERCRITICAL FLUIDS

S. V. Olesik, L. A. Pekay, Department of Chemistry, The Ohio State University, 120 West 18th Ave., Columbus, OH. 43210

The ideal "hyphenated" technique of chromatography - mass spectrometry for high molecular weight, highly polar compounds has the following properties:

1) The separation process is highly efficient.
2) The interface between the chromatography and mass spectrometer is easily made.
3) The ionization process is capable of ultra-soft ionization, as well as, highly controlled energetic ionization.
4) The interface and the ionization process is well suited for use with high-performance mass spectrometers such as magnetic sector instruments and FT-ICR.

None of the present soft ionization techniques share all these attributes. Fast atom bombardment (FAB) is plagued by high background signal and the inability to interface easily to highly efficient separation techniques. In FAB, liquid electrospray, and thermospray the monovalent ions produced are present as solvated ions in solution. High molecular weight nonpolar compounds are very difficult to analyze by any of these techniques.

We are developing a new ionization technique that should have many of the properties desired of an ideal ionization technique. Supercritical Fluid Assisted Ionization depends, as the name implies, on the properties of the supercritical fluid controlling the ionization process.

The fundamental gas-phase chemistry that forms the basis of supercritical fluid assisted ionization will be described. In addition, a detailed description of the new instrument will be included. Finally, preliminary results will be presented.

Presented at the 36th ASMS Conference on Mass Spectrometry and Allied Topics
June 5-10, 1988, San Francisco, CA

Pyrolysis-GC-MS and Fast Atom Bombardment Mass Spectrometry : a useful tool for structure elucidation of complex organic molecules.

Vangaever F., Hendrickx A., Decuyper M., Hancke N.

R&D Analytical Laboratory Agfa-Gevaert,
Septestraat 27, B-2510 Mortsel, Belgium

Mass spectrometry is well suited for structure determination of submilligram amount of pure material. Electron impact ionization was used as such in our laboratory for many years for probing a variety of chemicals used in the photographic industry.

The advent of a simple desorption-based ionization method like Fast Atom Bombardmen mass spectrometry makes nowadays possible the study of, mass-spectrometrically speaking difficult molecules (highly polar and even charged samples most often in a mass range above 500 dalton). Although tremendous achievements have been realized, a major drawback of FAB is the nearly abscence of abundant fragment ions. The occurrence of some minor fragmentation is further compromised by the fact that more often the fragment-ion signals are buried into the matrix background, which cannot be subtracted properly or reliably. Of course, running electron impact mass spectra on the same compound is the solution of this problem, at least for those samples which sustain the evaporation step. In the absence of MS-MS facilities, an alternative approach was used to complement FAB and EIMS data for cyanine dyes (I,II), color-forming compounds (III), and polyethylene oxide surfactants (IV,V). From extensive applications with cyanine dyes some useful fragmentation rules have been derived. These fragmentation reactions are a dealkylation, a retroreaction, a hydrolysis sequence, and the formation of small stable molecules. Basically, PY-GC-MS helps in determining the structure of unknowns b converting intractable parent molecules to many simple daughter molecules (see Fig. 1 for compound II). These daughter molecules reveal substructural features which enable the formulation of plausible candidate structures. Those candidates can be validated b referring to easily accessible reference compounds, commonly used in the synthesis of cyanine dyes. Extension to the structure determination of chromogenic compounds (coupling agents) and to oligomeric monoalkylated polyethylene oxide surfactants shows that PY-GC-MS is useful complementary technique for FAB and EI mass spectrometry.

FIG.1: **PY-GC-MS: SYSTEM B**

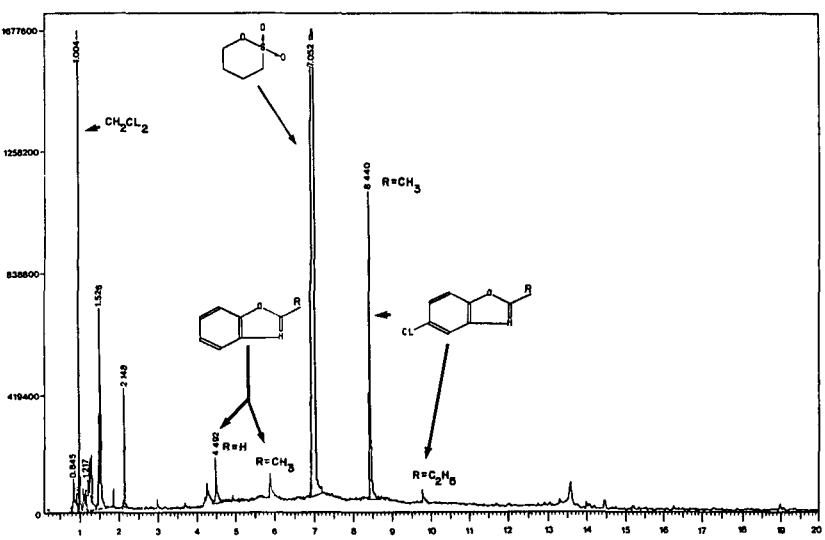

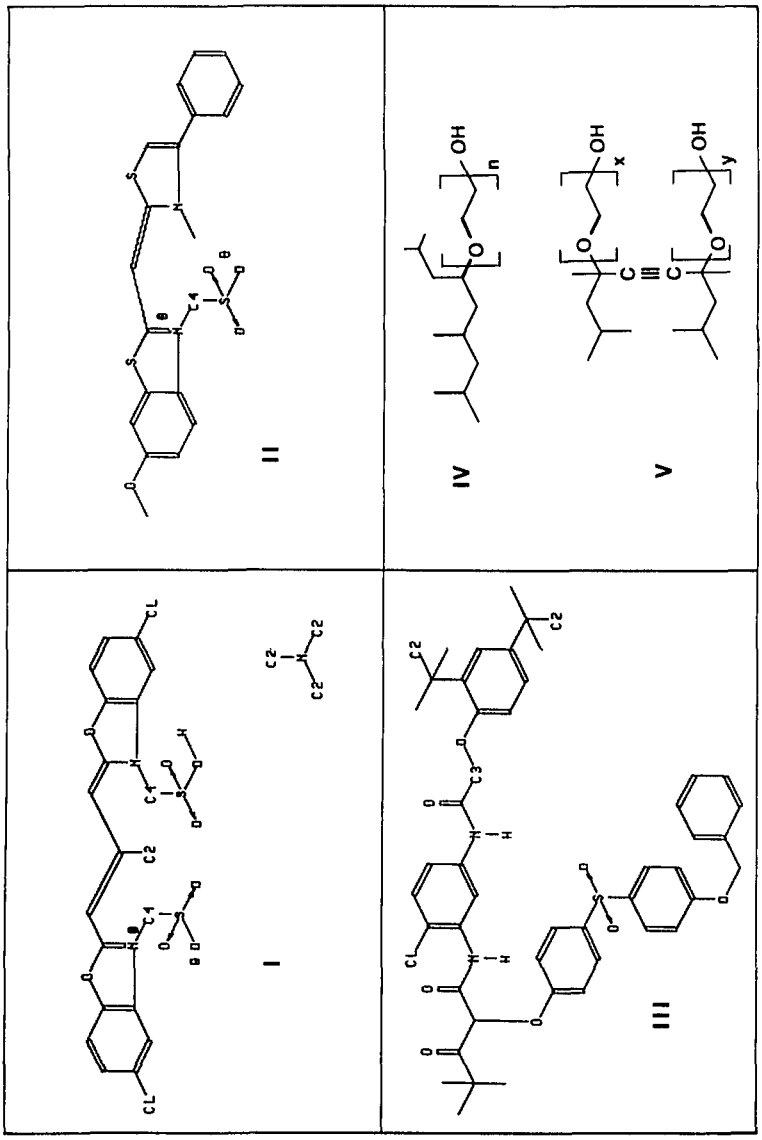
I
II
III
IV
V

Presented at the 36th ASMS Conference on Mass Spectrometry and Allied Topics
June 5-10, 1988, San Francisco, CA

CHARACTERISTICS OF MULTIPOLE COLLISION CELLS

J.E.P. Syka, Finnigan MAT, San Jose, California, 95134; I. Szabo, University of Lund, Lund, Sweden.

Tandem quadrupole mass spectrometers and hybrid sector quadrupole instruments generally use RF-only quadrupole collision cells, which are simple to construct and provide efficient collection of daughter ions. However, the ion transmission through RF-only quadrupoles is strongly dependent on operating parameters such as the applied RF voltage and the axial component of ion kinetic energy (collision energy), requiring the instrument operator to control these parameters carefully if reproducible results are to be obtained. Extensive theoretical calculations (1) suggest that collision cells constructed from higher order multipole fields (hexapole, octopole, etc.) might not exhibit such dependence on operating parameters. Calculations indicate that higher order multipoles have wider stability regions than the quadrupole and, thus, should allow observation of a wider mass range of daughter ions generated from a given parent-ion. Higher order RF-only multipole collision cells have already found use in studies of ion fragmentation energetics, where kinetically correct results are critical (2,3,4). The flat-bottomed, pseudo potential trough generated by the higher order multipole fields adds precision to the determiniation of parent-ion kinetic energy. This paper describes a study undertaken to determine the suitability of higher order RF-only multipoles (hexapoles, octopoles) for incorporation in MS/MS instruments designed for general analytical use.

A study was conducted in which linear quadrupole, hexapole, and octopole RF-only collision cells of identical length and field radius, r_o, were successively installed in a suitably modified TSQ^R 70 tandem quadrupole mass spectrometer. The ion q value (Mathieu stability parameter) corresponding to the stability limit, q_{max}, for the RF-only hexapole and octopole were measured. A measured stability limit for the RF-only quadrupole of q_{max}=0.908 was used as a reference. The measured q_{max} for the RF-only hexapole was ca. 1.5, which compared well to the predicted value of 1.7 (5). However, the measured q_{max} for the RF-only octopole was ca. 1.4, which does not agree with the predicted value of 7.7 (6). This deviation is probably due to the very restricted range of initial radial displacements and velocities of the ions used in the calculations. This extension of the stability limit translates into about a 10% increase in the observable daughter ion mass range and about a 30% reduction in the region at the low end of the daughter mass range that is not observable. Figures 1, 2, and 3 show the effect of ion axial kinetic energy on the transmission of uncollided ions for the RF-only quadrupole, hexapole, and octopole collision cells. The local maxima and minima observed in the intensity vs. kinetic energy characteristics for the RF-only quadrupole are absent from the intensity vs. kinetic energy characteristics of the RF-only hexapole and octopole. However, the RF-only hexapole and octopole have somewhat lower relative transmission at elevated ion kinetic energies. At low kinetic energies, there was no measurable difference in absolute transmission between the three collision cell designs.

Determination of the variation in the intensity of m/z 231, 181, 131, and 69 daughter ions of a m/z 231 parent-ion for a changing parent-ion q show that local maxima and minima are absent from the intensity vs. parent-ion q characteristics of true daughter (fragment) ions for the RF-only quadrupole as well as the RF-only hexapole and octopole collision cells.

The combination of somewhat extended stability regions and more uniform transmission characteristics for unreacted ions makes using RF-only hexapole or octopole collision cells modestly advantageous in comparison to using the conventional RF-only quadrupole collision cells.

References:

(1) C. Hagg and I. Szabo, Int. J. Mass Spectrom. Ion Processes, 73 (1986) 295.

(2) J.D. Morrison, K.A. Stanney and J. Tedder, Design and Development of a Quinquequadrupole Mass Spectrometer, presented at 34th Annual Conf. on Mass Spectrom. and Allied Topics, Cincinnati, OH, June 8-13, 1986.

(3) E. Teloy and D. Gerlich, Chem. Phys., 4 (1974) 417.

(4) P.N. Armentrout, Guided Ion Beam Mass Spectrometry: Kinetic Energy Dependence of Ion-molecule Reactions, presented at 34th Annual Conf. on Mass Spectrom. and Allied Topics, Cincinnati, OH, June 8-13, 1986.

(5) C. Hagg and I. Szabo, Int. J. Mass Spectrom. Ion Processes, 73 (1986) 237.

(6) C. Hagg and I. Szabo, Int. J. Mass Spectrom. Ion Processes, 73 (1986) 237.

Presented at the 36th ASMS Conference on Mass Spectrometry and Allied Topics
June 5-10, 1988, San Francisco, CA

Figure 1

RF-Only Quadrupole Collision Cell
Effect of Ion Axial Kinetic Energy on Ion Transmission

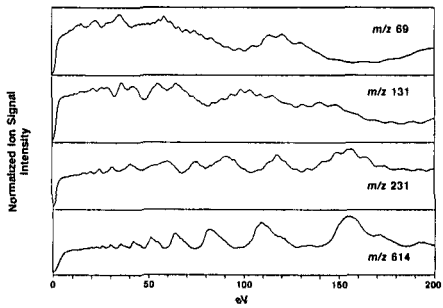

Ion Axial Kinetic Energy in Collision Cell
Conditions No Collision Gas, Ion q Fixed at 0 20, Neutral Loss of 0 0

Figure 2

RF-Only Hexapole Collision Cell
Effect of Ion Axial Kinetic Energy on Ion Transmission

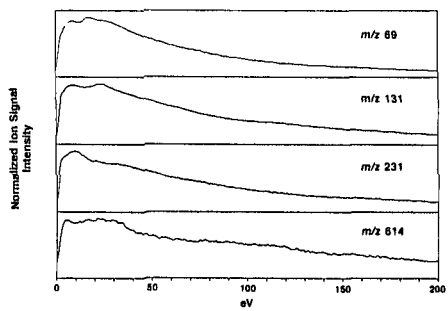

Ion Axial Kinetic Energy in Collision Cell
Conditions: No Collision Gas, Ion q Fixed at 0 20, Neutral Loss of 0.0

Figure 3

RF-Only Octopole Collision Cell
Effect of Ion Axial Kinetic Energy on Ion Transmission

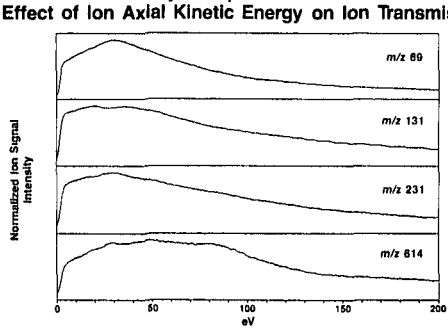

Ion Axial Kinetic Energy in Collision Cell
Conditions. No Collision Gas, Ion q Fixed at 0.20, Neutral Loss of 0.0

Presented at the 36th ASMS Conference on Mass Spectrometry and Allied Topics
June 5-10, 1988, San Francisco, CA

OBTAINING MOLECULAR ION AND STRUCTURAL INFORMATION OF PERFLUOROCARBONS BY MASS SPECTROMETRY

Sunkwei Huang
Adamantech, Inc., 1501 Blueball Ave., Linwood PA 19061

Identification of perfluorocarbons (PFC's) can be achieved in several ways: electron attachment (EA) at near zero electron energy, negative ion chemical ionization (NICI) and electron ionization (EI). EA may provide both molecular weight and structural information. However, as the molecular size of PFC's is increased, the dissociative electron attachment process becomes insignificant and thermal electron attachment becomes the major pathway, possibly due to the rapid distribution of excess energy among the many vibrational degrees of freedom of the molecule. CH_4-NICI in general gives only molecular ion information. On the other hand, EI of perfluoroalkanes yields little or no molecular ion and very abundant low mass fragment ions such as CF_3^+ (m/z 69), $C_3F_5^+$ (m/z 131) and $C_4F_7^+$ (m/z 181), which are not structurally characteristic. EI on perfluoroalkenes very often gives more high mass fragments, but it still yields little or no molecular ion information. An exception was observed for perfluoro-cyclopentene, which gives a sizeable molecular ion upon EI. Typical examples are illustrated in Figure 1. Decreasing the electron energy and lowering the ion source temperature do not increase the abundance of the molecular ion, but instead degrade the sensitivity of detection.

Structural information may be obtained by CAD experiments on the molecular ion generated by EI of the sample. Figure 2 illustrates the CAD result of perfluoro-1,3-dimethyl adamantane (F-DMA) from high energy collisions. Low energy CAD below 30 eV gave the same result. However, negative ion mode CAD did not yield structural information and the result is similar to of NICI. Experimentally, CF_3^+ is found to be the most abundant peak between 5 and 70 eV of electron energy in EI. Therefore, it appears that most of the molecular ion and $(M-CF_3)^+$ ions are formed with large amounts of internal excitation, even at the low electron energies, and undergo further fragmentations to produce low mass fragments such as CF_3^+. In CAD, collision energy is added to the relatively stable molecular ion. In this case, the effective energy transfer during the high energy collisions must be small so that $(M-CF_3)^+$ and other high mass ions are more stable relative to CF_3^+.

It is therefore likely that the CAD technique can be employed to acquire the structural information of PFC's. However, most PFC's give little or no molecular ion upon EI. If the formation of abundant CF_3^+ in EI indeed results from the bombardment of energetic electrons, then the energy deposition distribution can be modified by thermalizing the electrons by letting electrons collide with reagent gases. It was found that the employment of helium provided spectra similar to EI but with more high mass fragment and some molecular ion formation. The employment of methane as the reagent gas resulted in a great formation of $(M-F)^+$. On the other hand, when nitrogen or air was used, abundant molecular ions as well as structural information were obtained (Figure 3). The mass spectrum of a given PFC can be easily changed by mixing different proportion of regent gases. The mass spectra obtained this way did not change between the electron energy of 55 eV and 230 eV, except that at higher electron energies, lower mass fragments are favored and high mass fragments and the molecular ion were formed with one a.m.u higher than in the case of low energies. This could be ascribed to the radical reactions with residual hydrogen on the wall of the ion source. It appears that there are at least three mechanisms operative in producing the above results. They are electron thermalization (He case), high pressure charge exchange (air or N_2 case) and ion molecule reactions (CH_4 case).

Presented at the 36th ASMS Conference on Mass Spectrometry and Allied Topics
June 5-10, 1988, San Francisco, CA

Figure 1

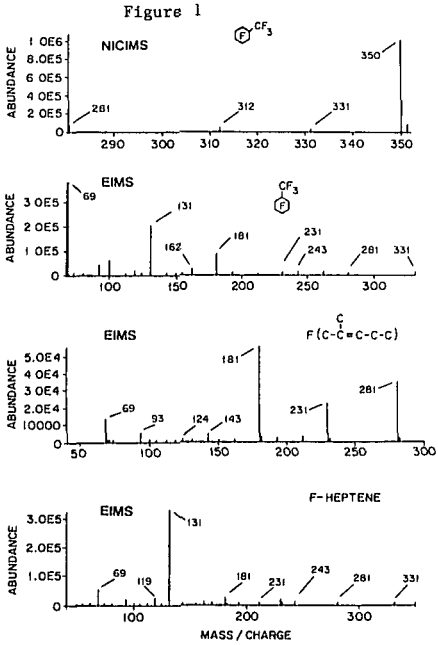

Figure 3 AIR / HPCEMS

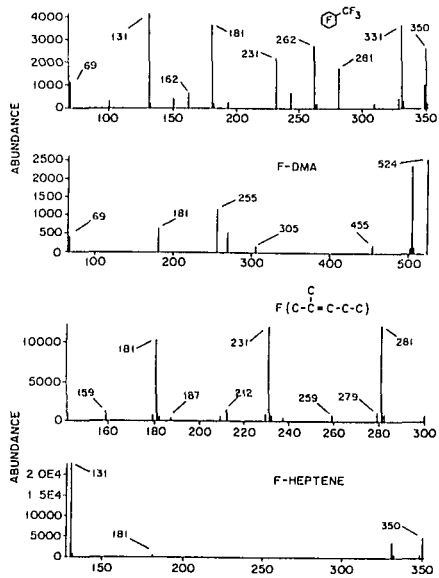

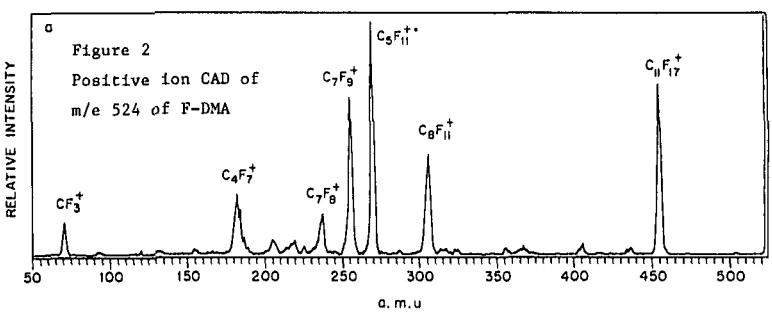

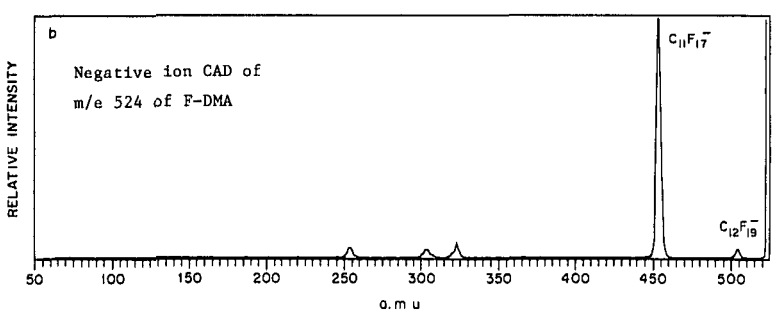

Presented at the 36th ASMS Conference on Mass Spectrometry and Allied Topics
June 5-10, 1988, San Francisco, CA

INTERNAL ENERGY DEPOSITION BY COLLISIONAL ACTIVATION IN FOURIER TRANSFORM MASS SPECTROMETRY

R. B. Cody*, D. A. Weil
Nicolet Analytical Instrument
5225 Verona Rd. Madison, WI 53711

Parent ion kinetic energy is a dominant factor in determining the nature of collisional activation spectra in Fourier transform mass spectrometry (FTMS) [1]. In order to best use FTMS for collisionally activated dissociation (CAD) it is important to understand how parent ion internal energies are affected by collision energies, pressures, collision times, etc. Breakdown curves (i.e. plots of fragment ion abundance vs. collision energy) provide a great deal of information about how such factors affect ion fragmentation.

FTMS breakdown curves have been reported for several compounds, by observing the variation of fragment abundance with collision energy [1]. While informative, these early studies were limited to low kinetic energies by cell size and magnetic field strength; maximum energies were 40 to 60 eV. Further, these studies employed a static collision gas and a single-cell geometry. Under these conditions, ions may collide with the target gas during excitation, or may undergo ion-molecule reactions with sample neutrals following activation.

More modern FTMS instruments are free of these limitations. Higher magnetic field strengths and larger cells provide access to much larger kinetic energies (in the low keV range). Pulsed valve introduction of the collision gas coupled with a differentially-pumped dual-cell geometry avoids problems with collisions during excitation, or subsequent ion-molecule reactions. Therefore, it is of interest to reexamine energy deposition by collisional activation with a state-of-the-art Fourier transform mass spectrometer.

We report here breakdown curves for n-butylbenzene, iron pentacarbonyl, tetraethylsilane, and anthracene. Collision energies employed range from less than 1 eV to greater than 1 keV. Comparisons with previous data and data collected with other types of mass analyzers show many similarities. Internal energy distributions estimated by the method of Wysocki, Kenttamaa and Cooks show reasonable agreement with those reported for hybrid instruments under multicollision conditions [2].

However, some striking differences are also observed. For example, in the previous study [1] the ratio of abundances for m/z 91/92 in the CAD spectrum of n-butylbenzene reached a maximum at 2.5:1 for both the FTMS and hybrid (BQQ) instruments. This contrasted with a the much higher ratio (7:1) observed for photoexcitation studies. In the present study, the ratio of m/z 91/92 is very high. To our knowledge, our present observed ratio of 25:1 is the highest value reported for any activation method.

For collisional activation of the molecular ion of tetraethylsilane, the breakdown curves obtained for FTMS agree at low energies with those obtained using other instruments. However, we observe Si+ at higher collision energies above 100 eV; also, the EtSi+ fragment is not present in the FTMS spectra.

At high energies, collisional activation spectra of anthracene show extensive fragmentation, characteristic of high internal energy deposition. The chief difference between the FTMS spectrum and previously reported spectra is the absence of fragments due to CHn losses, and in the relatively smaller abundance of the doubly charged ion in the FTMS spectrum.

Presented at the 36th ASMS Conference on Mass Spectrometry and Allied Topics
June 5-10, 1988, San Francisco, CA

High energy collisional activation spectra of iron pentacarbonyl show very high internal energy deposition; the spectra are dominated by Fe+ rather than Fe(CO)4+, as in previously reported spectra.

These differences between FTMS CAD and spectra reported for other analyzers may be attributed to several factors. FTMS CAD operates under multicollision conditions. This increases both internal energy deposition and fragmentation efficiency, but makes it more difficult to determine the exact collision energy. FTMS CAD is associated with long ion lifetimes, and is less sensitive to scattering angle.

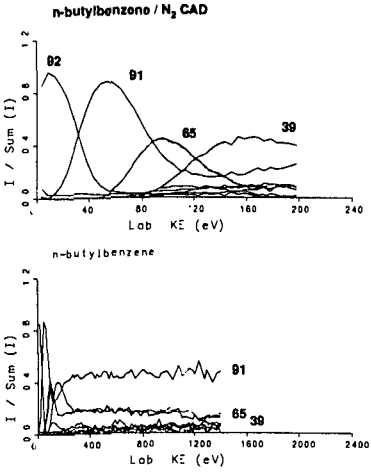

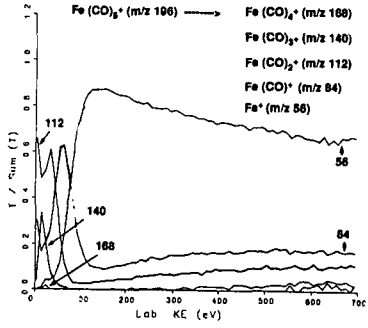

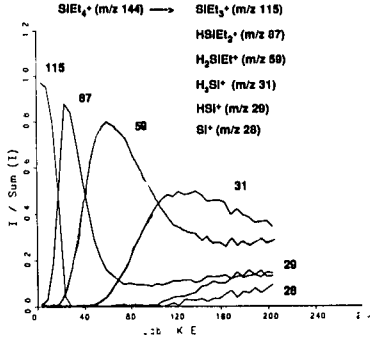

1. McLuckey, S. A. ; Sallans, R.; Cody, R. B.; Burnier, R. C; Verma, S.; Freiser, B. S.; Cooks, R. G. IJMSIP 1982, 44, 215-229.
2. Wysocki, V.; Kenttamaa, H.; Cooks, R. G. IJMSIP 1987,75,181-208.
3. Bier, M. E.; Amy, J. W.; Cooks, R. G.; Syka, J. E. P.; Ceja, P.; Stafford, G. IJMSIP 1987,77,31-47.
4. Pachuta, S. J.; Kenttamaa, H.; Sack, T. M.; Cerny, R.; Tomer, K. B.; Gross, M. L.; Pachuta, R. R.; Cooks, R. G. JACS 1988, 110, 657-665.

Presented at the 36th ASMS Conference on Mass Spectrometry and Allied Topics
June 5-10, 1988, San Francisco, CA

CHEMICAL IONIZATION AS A POST-IONIZATION METHOD FOR LASER-DESORBED NEUTRALS.

I. Jonathan Amster, Donald P. Land, John C. Hemminger, and Robert T.McIver, Jr.; Chemistry Department, University of California, Irvine, CA 92717.

Introduction. Laser desorption is a popular desorption-ionization method for the analysis of nonvolatile compounds. Typically, these experiments are performed in a direct ionization mode in which the laser is used to desorb and ionize the sample in one step. However, laser desorption produces far more neutrals than ions. Post-ionization of these neutrals (that is, ionization as a subsequent step to laser desorption) offers the possibility of enhancing sensitivity and allows the choice of a variety of ionization methods. Multiphoton ionization has been used recently as a post-ionization method for laser-desorbed neutrals of high molecular weight species. Electron post-ionization has been used in our laboratory for the analysis of molecular adsorbates on surfaces present at submonolayer concentration. Chemical ionization has also been reported as a post-ionization method (LD/CI) [1]. However, this early experiment lacked sensitivity as a result of combining a pulsed ionization technique of low duty cycle with the scanning mass analyzer of a sector mass spectrometer. A considerable sensitivity enhancement should be possible by adapting this post-ionization method to a simultaneous mass analyzer, such as a Fourier transform mass spectrometer (FTMS).

Experimental. The results are obtained using an FTMS instrument with a 12" electromagnet (B = 1 Tesla). An excimer laser (Lambda Physik EMG 103 MSC) is used for desorption at wavelengths of 193 nm, 248 nm, and 350 nm. Typical desorption conditions use a laser pulse of 0.3 mJ focused to a 0.25 mm^2 spot size, giving a power density of 1 MW/cm^2. These low power conditions cause desorption of neutrals, without direct formation of ions or cations. All spectra are recorded from a single laser shot at the sample. The sample substrate is platinum for most experiments. Macor with a 100 nm overcoat of gold is used for the peptide and thymidine experiment. The samples are applied to the substrate by evaporation of dilute solutions (thymidine, tetrapeptide), vacuum sublimation (acridine), or by condensation onto a liquid nitrogen cooled sample holder while in the FTMS vacuum system (acetophenone). A 30-ms burst of methane admitted with a pulsed valve creates reagent ions at 10^{-3} torr peak pressures. Ion detection occurs 1 second later when the pressure has dropped to about 10^{-8} torr.

Results. Laser desorbed neutrals from a 30 monolayer thick sample of acetophenone frozen onto a Pt substrate are protonated by methane reagent ions made and stored in a Fourier transform mass spectrometer. The FTMS instrument is used to select CH_5^+ or $C_2H_5^+$ from the reagent ions generated from methane, allowing control of the amount of fragmentation observed in the spectrum. Acetophenone protonated by CH_5^+ produces a mass spectrum in which the molecular ion has a relative abundance of 50%, whereas ionization with $C_2H_5^+$ gives the molecular ion as the base peak of the spectrum. Laser desorption of 9-pentadecylacridine followed by methane chemical ionization produces a strong protonated molecular ion (Fig. 1b), whereas electron ionization produces only fragment ions (Fig. 1a). The first reported attempt to combine chemical ionization with laser desorption in a FTMS instrument [2] was unsuccessful, using thymidine as a test compound. However, we are able to produce an LD/CI spectrum of thymidine, in which the molecular ion has a 10% relative abundance. This method demonstrates exceptionally good sensitivity for a laser desorption method. Ten monolayers of the tetrapeptide Val-Ala-Ala-Phe produce the LD/CI mass spectrum shown in Figure 2 from a single laser shot, and the amount of material desorbed from the 0.25 mm^2 spot is 4 pmol. Since the signal-to-noise ratio in Fig. 2 is approximately 130:1, the detection limit for LD/CI in an FTMS instrument should be in the submonolayer regime, suggesting applicability to surface analysis problems.

---

[1] Cotter, R. J. Anal. Chem. **1980**, 52, 1767-1770.
[2] McCrery, D. A.; Gross, M. L. Anal. Chim. Acta **1985**, 178, 91-103.

Presented at the 36th ASMS Conference on Mass Spectrometry and Allied Topics
June 5-10, 1988, San Francisco, CA

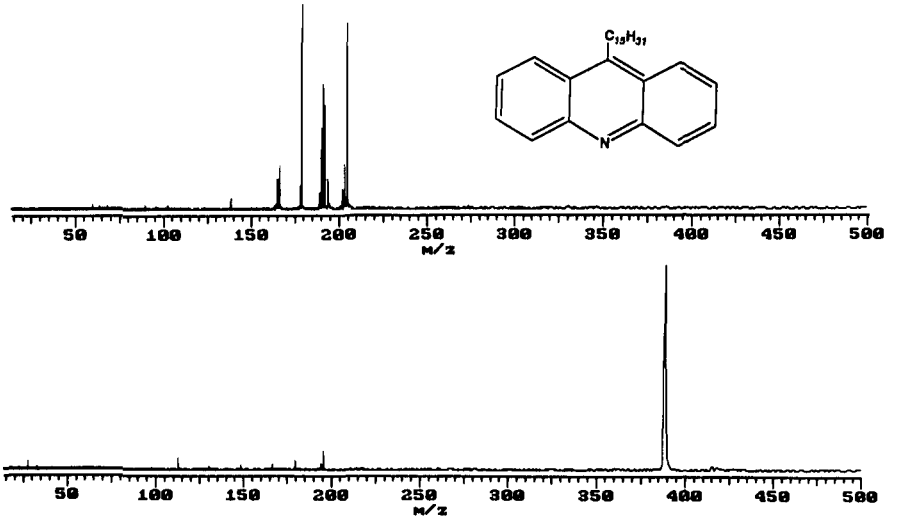

Figure 1. Low power laser desorption spectra of 9-pentadecylacridine, MW 389 amu. a) 70 eV electron ionization of the desorbed neutrals. b)Chemical post-ionization using methane generated reagent ions.

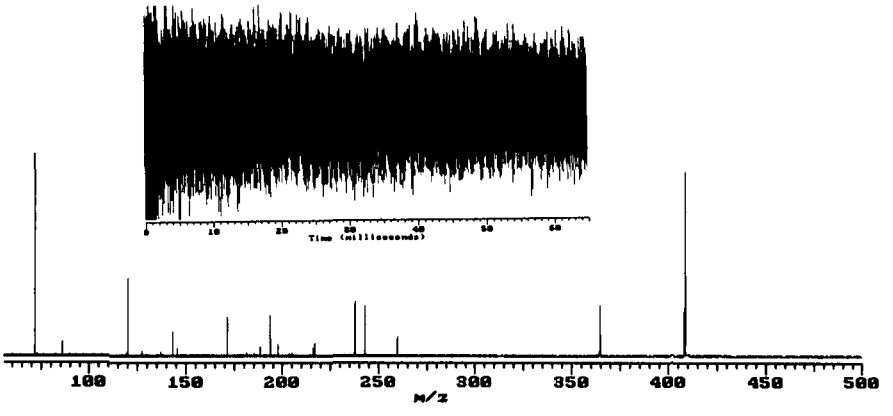

Figure 2. LD/CI spectrum of the tetrapeptide, Val-Ala-Ala-Phe, MW 406 amu, using methane as the reagent gas. This spectrum is produced by a single laser shot at a ten monolayer thick sample, corresponding to 4 pmol of compound (see text). Inset shows the digitized transient, with very little damping after 64 ms of acquisition.

Presented at the 36th ASMS Conference on Mass Spectrometry and Allied Topics
June 5-10, 1988, San Francisco, CA

BUTYLBENZENE RADICAL CATION THERMOCHEMISTRY FROM PEPICO EXPERIMENT USING SYNCHROTRON RADIATION; COMPARISON WITH ION ENERGY MEASUREMENT IN LOW ENERGY CAD

Tomas Baer, University of North Carolina, Chapel Hill, NC 27599, USA
Odile Dutuit, Université Paris-Sud, 91400 Orsay, France
Hélène Mestdagh and Christian Rolando,
Ecole Normale Supérieure, 24 rue Lhomond, 75231 Paris Cedex 05, France

As pointed out by many workers butylbenzene radical cation is ideally suited for experiments on dependence of fragment distribution with ion internal energy. Butylbenzene ion (m/z 134) has indeed two major decomposition pathways leading respectively to m/z 91 and m/z 92 ion; the former arises from a simple bond cleavage, the latter from a rearrangement. Fragment distribution is strongly dependent on the internal energy of the parent ion. Providing this dependence is reliably known, measurement of the 91/92 ratio gives access to the internal energy of the fragmenting ion under any given conditions.

Considering the dispersion of the literature data, it appeared interesting to study the fragmentation of butylbenzene by the PEPICO method, using synchrotron radiation as light source. The abundance curves obtained for parent and fragment ions (Figure 1) allowed to get reliable values of the 91/92 ratio on a wide internal energy range, and to compare the results with literature data (Figure 2). In addition, the measured 92/134 ratio gave access to the absolute dissociation rate to m/z 92 ion as a function of parent ion internal energy. This dependence was fitted using a RRKM-QET model (Figure 3). Extrapolation of the corresponding curve to high internal energy range, combined with the experimental 91/92 ratios, allowed to obtain m/z 91 ion production rate (Figure 4). The best fit of this rate corresponds to a high activation energy (1.6 eV) and a positive activation entropy (+14.6 J/K), as expected for a simple bond cleavage; on the contrary, a lower activation energy (0.99 eV) and an important negative activation entropy (-29 J/K) were found for the formation of m/z 92 ion, involving a rearrangement.

These data were compared to those obtained by the measurement of parent and daughter ion kinetic energy in low energy CAD using the modified "double" RF-only collision cell of a tandem quadrupole mass spectrometer. The dependence of fragment ion kinetic energy with parent ion kinetic energy allows to estimate the average internal energy transfer, Q, from Ar collision gas to the parent ion, for each type of fragmentation separately. Whereas the kinetic energy of m/z 92 ion is close to the maximum value allowed by momentum conservation, corresponding to a low Q value, the average kinetic energy of m/z 91 fragment is close to the minimum value allowed, corresponding to a high Q value (Figure 5). This is in agreement with increasing 91/92 ratio with internal energy of parent ions, as well as with the higher activation energy of m/z 91 ion production.

Presented at the 36th ASMS Conference on Mass Spectrometry and Allied Topics
June 5-10, 1988, San Francisco, CA

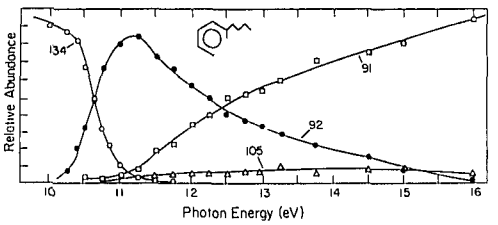

Figure 1 : The breakdown diagram for n-butylbenzene.

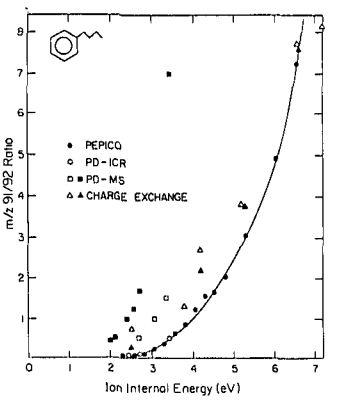

Figure 2 : The m/z 91/92 ratio as a function of the n-butylbenzene ion internal energy.

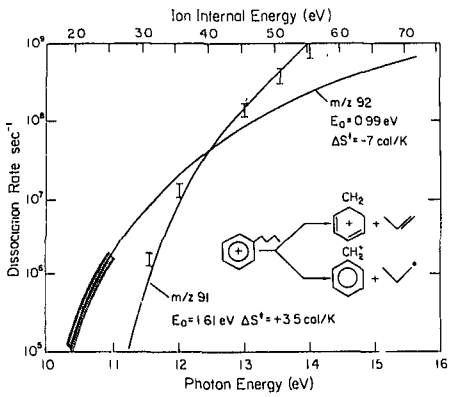

Figure 4 : The rate of m/z 92 production (hatched region) , extrapolated to 16 eV with the RRKM-QET model.

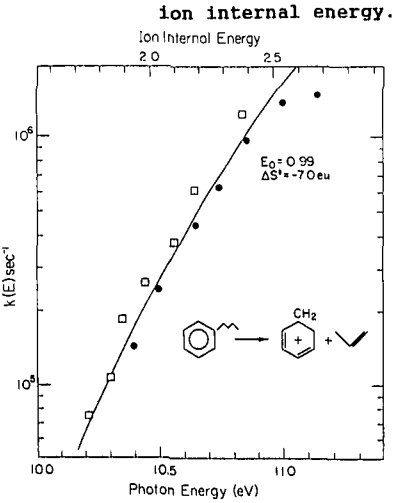

Figure 3 : The derived dissociation rates to the m/z 92 fragment ion.

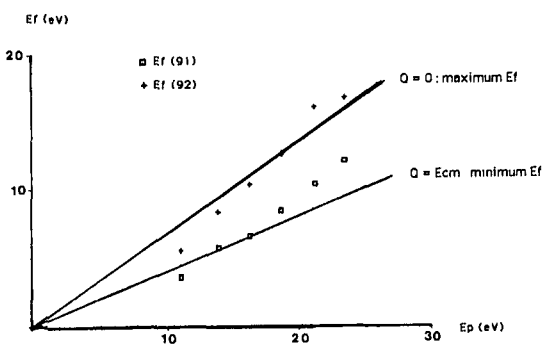

Figure 5 : Dependence of measured fragment ion energy with parent ion energy

Presented at the 36th ASMS Conference on Mass Spectrometry and Allied Topics
June 5-10, 1988, San Francisco, CA

HIGH RESOLUTION LDI-FT-ICR MASS SPECTROMETRY OF UNDERIVATIZED OLIGOSACCHARIDES OBTAINED FROM BIOPOLYMERS

Asgeir Bjarnason[1], Melvin B. Comisarow[2], Guy G. S. Dutton[2], Zamas Lam[2] and David A. Weil[3]

[1]Science Institute, University of Iceland, Dunhaga 3, 107 Reykjavik, Iceland.
[2]Department of Chemistry, University of British Columbia, Vancouver, B.C., Canada V6T 1Y6.
[3]Nicolet Analytical Instruments, 5225-1 Verona Road, Madison, WI 53711-0508, USA.

Carbohydrate-containing macromolecules are found in abundance in all living organisms. These include: a) exclusively carbohydrate polysaccharide polymers, b) glycoproteins, proteoglycans and peptidoglycans, c) glycolipids and lipopolysaccharides, d) teichoic acids, and e) nucleic acids. It is now well established that complex carbohydrates are essential in biological recognition, as hormones, as structural polymers and as energy reserves. The use of desorption mass spectrometric approaches, such as FAB and DCI, to sequence oligosaccharides derived from these biopolymers is well documented[1]. FAB spectra usually show only glycosidic bond cleavages, and the oligosaccharide has to be reduced prior to mass spectrometric analysis for sequencing to be unambiguous[1]. Furthermore, derivatization (permethylation or peracetylation) is normally required. Unfortunately, both methods may remove base- or acid-labile substituents that may be present.

Our laboratory has a long standing interest in bacterial capsular polysaccharides (CPS) which are antigenic. They can be considered in terms of repeating units and consist of simple monosaccharide residues and labile substituents. CPS biopolymers are often of high molecular weight (>40,000 daltons) and therefore generally are not sufficiently volatile for study directly by mass spectrometry. By the use of specific bacteriophage-borne enzymes the CPS can be degraded to oligosaccharides corresponding to the repeating units[2]. Such oligomers are commonly tri- to hepta-saccharides and consequently have molecular weights which are well within the mass range of modern ionization techniques.

The following example illustrates the use of positive and negative ion LDI-FT-ICR mass spectrometry for the complete sequencing of an *underivatized* pentasaccharide. This oligosaccharide is derived from bacteriophage degradation of *Klebsiella* serotype K44 bacterial CPS. The complete sequence can be deduced from each of the positive ion and negative ion spectra. LDI-FT-ICR spectra of the *underivatized* pentasaccharide showed intense fragmentation resulting from glycosidic bond cleavage and ring rupture. The presence of both ring cleavage ions and glycosidic bond cleavage ions allows, without the necessity of a prior reduction step, unambiguous sequencing of oligosaccharides.

From the positive ion spectrum two ring cleavage routes were observed; a) the M-series fragments with cationic attachment to the reducing end[3], and b) the N-series fragments with cationic attachment to the non-reducing end[3]. Two types of M-series fragments were observed. The non-reducing end terminal glucuronic acid, gave a $C_2H_3O_2$ ring fragment, while the adjacent 2-linked rhamnose gave a C_2H_3O ring fragment. As M-series fragments only contain C-1 and C-2 from the ring cleaved residue, the oxygen difference is likely to be the glycosidic oxygen of a 2-linked residue. Two N-series fragments were also observed. The reducing end 4-linked terminal glucose gave a $C_4H_7O_2$ ring fragment, while the adjacent 3-linked glucose gave a $C_4H_9O_3$ ring

fragment. This may indicate that 3-linked residues give a $C_4H_9O_3$ fragment whereas 4-linked residues give a $C_4H_7O_2$ fragment. Dehydration of high molecular weight oligosaccharides is, however, very facile and further work is required to confirm these observations.

Four distinct ring cleavage fragmentation pathways were observed in the negative ion spectrum which we label Q_α, Q_β, R_α and R_β. The Q_α and Q_β-series fragments have the negative charge residing on the reducing end[4]. The R_α and R_β-series fragments have the negative charge residing on the non-reducing end[4]. For the Q_α and Q_β-series, the sub-monosaccharide unit correlated with the anomeric configuration of the ring cleaved residue, i.e. the α anomers gave a C_2H_2O fragment while the β anomers gave a $C_2H_2O_2$ fragment. For the R_α and R_β-series, the sub-monosaccharide unit correlated with the anomeric configuration of the monosaccharide residue adjacent to the ring cleaved residue. In this case, the α anomers gave a $C_2H_4O_2$ fragment while the β anomers gave a $C_2H_2O_2$ fragment.

It could also be argued that the two carbon fragments arising for both Q and R fragment series may indicate the configuration of the highest-numbered chiral carbon, i.e. a D- or L-series sugar, rather than the configuration of the anomeric carbon. The fragmentation of a monosaccharide ring, however, is more likely to manifest itself as either a neighbouring-group effect or as a representation of the stereochemistry of the fragment centre, rather than a reflection of the stereochemistry of a relatively distant group, i.e. C-5 in this case.

In conclusion, high resolution LDI-FT-ICR mass spectrometry can unambiguously sequence *underivatized* oligosaccharides. Tentative additional information on the linkage positions can be obtained from the positive ion spectra, while the anomeric configuration of the individual monosaccharide residues can be deduced from the negative ion spectra.

1 Dell, A.; Tiller, P. R. *Biochem. Biophys. Res. Comm.* 1986, 135, 3, 1126.
2 Rieger-Hug, D.; Stirm, S. *Virology* 1981, 113, 363.
3 Lam, Z.; Comisarow, M. B.; Dutton, G. G. S.; Weil, D. A.; Bjarnason, A. *Rap. Commun. Mass Spectrom.* 1987, 1, 5, 83.
4 Lam, Z.; Comisarow, M. B.; Dutton, G. G. S.; Weil, D. A.; Bjarnason, A. *Carbohydr. Res.* 1988, in press.

Structure of *Klebsiella* serotype K44 oligosaccharide repeating unit.

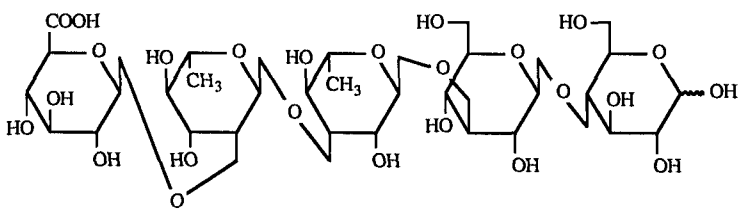

β-D-glucuronic acid[1]---[2]α-L-rhamnose[1]---[3]α-L-rhamnose[1]---[3]β-D-glucose[1]---[4]β-D-glucose

Presented at the 36th ASMS Conference on Mass Spectrometry and Allied Topics
June 5-10, 1988, San Francisco, CA

THE USE OF ^{252}Cf PLASMA DESORPTION MASS SPECTROMETRY FOR THE ANALYSIS OF SYNTHETIC PEPTIDES AND PROTEINS

Brian T. Chait
The Rockefeller University
New York, N.Y. 10021

Over the past several years there has been a dramatic increase of interest in the area of synthetically produced peptides and proteins. These materials find widespread utility in areas as diverse as the raising of antipeptide sera of predetermined specificity against a receptor protein, the development of synthetic peptide based vaccines, and the development of a fundamental understanding of the relationship of protein structure to function. At the Rockefeller University, we have found through the detailed examination of about 800 synthetic proteins and peptides originating from 15 different laboratories in the U.S.A. that plasma desorption mass spectrometry (PDMS) provides an enormously useful, easy, and definitive method for assessing the accuracy of peptide synthesis [1].

The most useful and most easily obtained single piece of information from the PD mass spectrum is the molecular weight (MW) of the compound. In a stepwise peptide synthesis, the identity of each added amino acid is known and so a measured MW which is found to agree with the MW calculated for the desired synthetic product provides a relatively good verification that the material has been correctly assembled. Conversely any disagreement which is observed between the measured and calculated MW's of the synthetic product immediately indicates that an error or undesired modification has occurred. PDMS is also a powerful tool for determining the homogeneity of the desired synthetic product. The strength of the method resides in its high resolving power compared with more commonly employed techniques like HPLC and its ability to provide masses of undesired side products. Fig. 1A shows the results of an HPLC analysis of a purified 39 residue cytochrome-C fragment synthesized by Kent and Selk at the California Institute of Technology where the analysis was made using a C4 reverse-phase column. The dominant chromatographic peak looks quite symmetrical and sharp and one might predict that the synthetic product is homogeneous. Inspection of the mass spectrum obtained from the material (Fig. 1B) shows that this is not the case. The desired material is present - its experimentally determined MW agrees with the predicted MW to within 0.3 u - but so is a substantial amount of a second compound having a MW 114.0 u lower which suggests that a deletion or deletions involving asparagine occurred during the synthesis. The peptide was thus carefully resynthesized and the mass spectrum from this second synthesis is shown in Fig. 1C. The peak corresponding to the deletion peptide is now no longer present in the spectrum demonstrating that this second synthesis yielded a pure product. A great many other errors can and do occur during solid phase synthesis. These errors range from operator or machine related errors to relatively subtle chemical modifications of the peptide during and after synthesis. We have found that the majority of these can be detected by PDMS [1]. The importance of the use of this technique can be gauged from our rather staggering finding that almost half of the 800 purified synthetic peptides and proteins that we examined were found to have a MW different from that calculated for the desired target material or to contain significant amounts of unwanted peptide side products.

We also found PDMS to be very useful for the analysis of fully protected synthetic peptides containing as many as 50 amino acid residues; for the analysis of unusual peptide containing molecules which cannot readily be analyzed by techniques such as Edman sequencing or nuclear magnetic resonance; for studying the folding and thiol oxidation of synthesized proteins; and for evaluating and optomizing details of the synthetic chemistry [2].

1. B.T. Chait in Analysis of Peptides and Proteins ed. by C.J. McNeal, Academic Press, In Press.
2. R.B. Merrifield, J. Singer, and B.T. Chait, Anal. Biochem., In Press.

Presented at the 36th ASMS Conference on Mass Spectrometry and Allied Topics
June 5-10, 1988, San Francisco, CA

Fig. 1 (A) Reverse-phase HPLC of synthetic cytochrome C (66-104). Top trace obtained with 214nm irradiation. Bottom trace obtained with 254nm irradiation.
(B) Partial ^{252}Cf plasma desorption mass spectrum of synthetic spectrum of synthetic cytochrome C (66-104). First synthesis.
(C) Partial ^{252}Cf plasma desorption mass spectrum of synthetic C (66-104). Second synthesis.

(A)

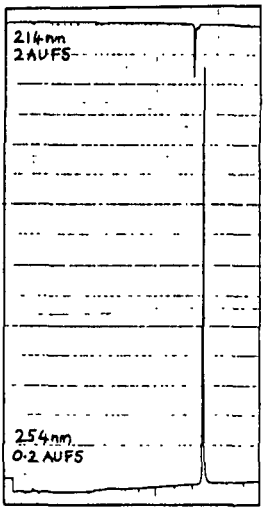

1	2	3	4	5	6	7	8	9	10
Glu -	Tyr -	Leu -	Glu -	Asn -	Pro -	Lys -	Lys -	Tyr -	Ile -
11	12	13	14	15	16	17	18	19	20
Pro -	Gly -	Asn -	Lys -	Met -	Ile -	Phe -	Ala -	Gly -	Ile -
21	22	23	24	25	26	27	28	29	30
Lys -	Lys -	Lys -	Thr -	Glu -	Arg -	Glu -	Asp -	Leu -	Ile -
31	32	33	34	35	36	37	38	39	
Ala -	Tyr -	Leu -	Lys -	Lys -	Ala -	Thr -	Asn -	Glu -	OH

(B)

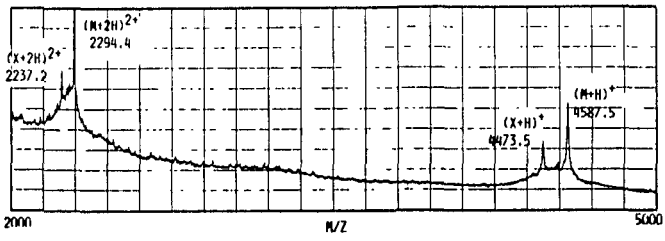

ION SPECIES	MEASURED MW	CALCULATED MW	Δ
$(M+H)^+$	4586.5	4586.4	+0.1
$(X+H)^+$	4472.5	4586.4	-113.9
$(M+2H)^{2+}$	4586.8	4586.4	+0.4
$(X+2H)^{2+}$	4472.3	4586.4	-114.1

(C)

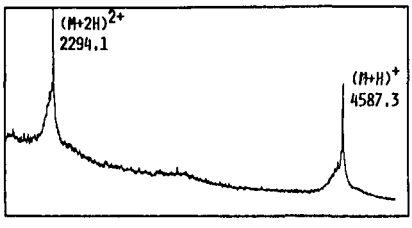

ION SPECIES	MEASURED MW	CALCULATED MW	Δ
$(M+H)^+$	4586.2	4586.4	-0.2
$(M+2H)^{2+}$	4586.3	4586.4	-0.1

Presented at the 36th ASMS Conference on Mass Spectrometry and Allied Topics
June 5-10, 1988, San Francisco, CA

TAGA 6000E QA/QC ANALYSIS PROCEDURES AND THE ASSOCIATED DATA GATHERED DURING FOUR, TWO WEEK BLOCKS OF INDOOR AIR ANALYSES AT THE LOVE CANAL EMERGENCY DECLARATION AREA (EDA)

Thomas H. Pritchett, U.S. EPA Environmental Response Team
Edison, NJ 08837

David Mickunas & Mark Bernick, Roy F. Weston, Inc. (REAC)
Edison, NJ 08837

INTRODUCTION

The U.S. EPA Environmental Response Team was tasked to perform indoor air analyses in the Love Canal Emergency Declaration Area as part of the overall EDA habitability study. The analytical results, in conjunction with results from concurrent soil and dioxin sampling programs, will be used by the New York State Department of Health to determine the overall habitability of the EDA. The sampling took place over four, two week phases which represented the various meteorological seasons. During each phase different sampling shifts were utilized to spread the analyses over the full 24 hours of a day. Each first floor and basement room for every structurally sound residential building in the EDA was sampled whenever possible. The air habitability decision will to be based upon the presence or absence of two sets of indicator compounds (LCICs): chlorobenzene and chlorotoluenes. From the results o a previous pilot study, only a very small percentage of the houses were expected to contain any LCICs. Because of the political nature of the final habitability decision, it was determined that the TAGA data would have to stand up to severe technical reviews by multiple parties.

DATA QUALITY OBJECTIVES

The QA plan which was developed for this program had several goals. The plan had to ensure 1) that the TAGA would have sufficient sensitivity throughout the whole program; 2) that the generated data would be reliable and defensible; 3) that the instrument was performing within defined specifications; 4) that any quantitation errors due to calibration drifts were known and defined; and that the accompanying documentation was 100% complete and consistent.

Eight data quality objectives (DQOs), five of which were directly relate to the instrument's performance, were defined. The instrument related DQOs were 1) accuracy of $\leq$ 25% error, 2) precision of $\leq$ 25% relative standard deviation, 3) LCIC detection limits of $\leq$ 4 ppb, 4) response factor decay between consecutive calibrations of $\leq$ 15%, and sampling lin transport efficiencies of $\geq$ 85%.

PROCEDURES, RESULTS AND DISCUSSION

The TAGA's accuracy was measured by using 6 Liter Summa canister externa performance evaluation samples (daily starting in phase 3), by 16 Liter precision canisters (on alternate days starting in phase 2), by 16 Liter external audit canisters (once per phase), and by internal control standard gas cylinders (daily for all phases). All Summa canisters were provided by Northrop Services, Inc. and the standard gas cylinders were obtained from Scott Specialty Gases. In addition, at the end of each analytical day the TAGA was challenged with a spike of the LCICs at a concentration within 2 ppb of the reported quantitation limits.

The samples, which contained the LCICs at concentrations ranging from 10 - 35 ppm, were analyzed by diluting the sample to 5 - 15 ppb through a mass flow controller into an ambient air sample stream flowing past the TAGA inlet at approximately 1500 ml/sec.

For chlorobenzene the reported errors from these analyses had average absolute percent errors of 5.6%, 5.9%, 14.9%, 6.6%, 9.5%, 10.0%, 3.6%, 13.5%, and 4.4% for the internal control analyses in phases 1-4, for the 6 Liter Summa canister P.E. sample in phases 3 & 4, and for the 16 Liter Summa canister precision samples in phases 2-4, respectively. For chlorotoluene these average absolute percent errors were 4.9%, 5.4%, 13.7%, 8.4%, 10.4%, 13.4%, 3.4%, 16.6%, and 10.6%. Only once did a percent error exceed the 25% (-26.4%) and on that day the two other measurements were within the required 25%. The percent error from the quantitation limit verifications never exceeded 25%.

To minimize the effect that the TAGA's calibration drifts had on the analysis accuracies, new calibrations were performed prior to entering each house. Whenever an investigation was initiated because of the presence of an LCIC in the house, a new calibration was performed immediately after existing. An intermediate set of response factors, which yielded symmetrical error bars, were then calculated from the two sets of response factors (RF_1 & RF_2). This intermediate response factor (RF_i) was calculated as follows:

$$RF_i = 2 * (RF_1 * RF_2) / (RF_1 + RF_2)$$

The TAGA's precision was measured using the results from the 16 Liter Summa precision canister analyses and from the internal control standard analyses. The highest RSD measured for any set of samples during the program was 17.9%.

The TAGA detection limits through the program ranged from 0.4 to 3.7 ppb for chlorobenzene and from 0.4 to 4.2 ppb for chlorotoluene. The detection limit averages for all four phases were 0.8 and 1.0 ppb for chlorobenzene and chlorotoluene, respectively. Only once did a detectio limit exceed 4.0 ppb and the house for which it applied was sampled four additional times during the study.

Although the TAGA response factors did vary throughout each day (typically increasing as the day progressed), the response factor decay (or decrease) only exceeded 15% twelve times during the study. In every case appropriate corrective actions were taken and the decay was either stabilized or reversed.

The sampling line transport efficiencies were measured twice daily. Thi measurement was made by diluting the LCIC standard downstream of the sampling lines, the bulk of which were outside the bus exposed to ambien temperature, at a concentration of 3 - 6 ppb and then averaging the signal for over thirty measurements. The standard gas was delivered through a mass flow controller to a three-way valve and then to the ambient air stream. Once the downstream average was obtained, the three way valve was reset to deliver the standard gas upstream of the sampling lines and the signal was then averaged for another thirty measurements. The ratio of the upstream signal average versus the downstream average defined the transport efficiencies. For the full study the measured transport efficiencies ranged from 88.6% to 122% for chlorotoluene and from 90.7% to 120% for chlorobenzene. During phase 1 a heated 200' sampling line, which was maintained at 70°F, was used while in phases three through four unheated sampling lines were used. The transport efficiencies with the heated lines averaged 100.2 $\pm$8.5% and 100.8 $\pm$5.8% for chlorotoluene and chlorobenzene, respectively. With the unheated lines the transport efficiencies averaged 97.7 $\pm$5.3% and 98.5 $\pm$4.2%. When the unheated lines were used, the outside ambient temperatures were recorded but no correlations were found between the transport efficiencies and ambient temperature.

Presented at the 36th ASMS Conference on Mass Spectrometry and Allied Topics
June 5-10, 1988, San Francisco, CA

OPTIMIZATION OF THE GCMS METHODOLOGY TO MONITOR MULTIPLE LABELED ANALOGS OF ARGININE AND ORNITHINE.

Van Langenhove, A; ENSECO/Erco Laboratory, 205 Alewife Brook Pkwy, Cambridge, MA 02138. Marks, L M, Lin, V K, Hoerr, R A, and Young, V R; MIT Clinical Research Center, 40 Ames Street, Cambridge, MA 02139.

The most straightforward method to evaluate whole body amino acid kinetics in men is to measure the isotopic enrichment of plasma amino acids following a single dose or continious infusion of a stable isotope labeled amino acid tracer. The stable isotope enrichment of plasma amino acids can then be determined with a high degree of sensitivity and accuracy by GCMS analysis.

We are proposing a new and elegant stable isotope tracer approach for the study of arginine metabolism and nutrition in healthy adult humans. Our approach is based on an intravenous infusion of ^{15}N-guanidino-5,5-$^{2}H_2$-arginine together with 13C-ornithine and the monitoring of the stable isotope label in plasma for both amino acids (Fig. 1).

We have been evaluating different derivatization methods and mass spectrometric ionization techniques for the analysis of arginine and ornithine. The conventional amino acid derivatization methods (N-perfluoroacyl, alkyl esters) work well for ornithine. For arginine, however, these methods do not give satisfactory results. We have found two major problems associated with the derivatization of arginine: (i) either incomplete derivatization, or (ii) breakdown of arginine into ornithine. These two problems become intertwined when one tries to derivatize arginine because the guanidino group from arginine can only be acetylated under vigorous reaction conditions.

We also evaluated the procedure described by Nissim et al. (1). The authors' report reproducible formation of N-tetra-TFA arginine in studies with guanidino-^{15}N-arginine in plasma. Our attempts to duplicate this procedure were only partially successful. We were able to form a TFA derivative (presumably the tetra-TFA-arginine) and the EI mass spectrum showed ions that were appropriate for our purpose (i.e. ions that retain the stable isotope label and are not involved in C-5 hydrogen rearrangement processes). For ornithine, a di-TFA derivative was obtained (Fig. 2). Repeated attempts to form a TFA derivative for arginine were, however, unsuccessful.

Another approach to make a GC-amenable derivative for arginine would be conversion of arginine into delta-N-(2-pyrimidinyl) ornithine by condensation with malonaldehyde or acetylacetone (2,3). This ornithine derivative could then be further esterified and trifluoroacetylated to permit its analysis by GCMS. Data obtained so far using this technique are quite encouraging. The reproducibility of the technique is superior to the previously investigated methods. The EI mass spectra of delta-N-(2-pyrimidinyl)-n-propyl di-TFA ornithine and n-propyl-di-TFA ornithine are presented in Fig. 3. Selection of appropriate ions that retain the stable isotope label is not so straightforward as for the TFA derivatives. For the arginine derivative most of the ion current is carried by ions that contain the pyrimidinyl moiety (e.g. m/z 192). Formation of these ions can involve hydrogen rearrangements and involvement of the C-5 deuterium atoms in this rearrangement process. The ion at m/z 347 is a likely candidate. We could monitor m/z 347/348 for the enrichment of 13C in the C-5 position of arginine, m/z 347/349 for the enrichment of 15N2 in the guanidino moiety and m/z 351/347 to follow the course of the proposed arginine tracer of $^{2}H_2$-$^{15}N_2$ arginine. For the ornithine derivative we could monitor the m/z 127/126 for enrichment of ^{13}C at the C-5 position and m/z 128/126 for the $^{2}H_2$ at the C-5 position. The abundances of these ions are low and, also, the ion cluster around m/z 126 could be subject to interferences from plasma because of its low m/z value.

Further chemical ion work will be necessary to deliver the most appropriate ions to monitor for the stable isotope labeled analogs we have available for these studies. Our previous experience with both positive and negative CI analysis of other amino acids suggests that fewer hydrogen rearrangements occur and that there are ions present at high m/z values in

abundance. Mass spectrometric analysis of deuterated ornithine and arginine should actually provide us with information about such fragmentation processes.

Although the formation of delta-N-(2-pyrimidinyl)-n-propyl di TFA ornithine is a reproducible process, we still observe to a small extent the breakdown of arginine into ornithine. Therefore, we are now focusing our efforts on reducing the harshness of the derivatization procedure in particular, the steps where acid and elevated temperatures are involved. We are at the same time looking into the incorporation of a preparative HPLC step which would separate arginine from ornithine and at the same time provide an initial clean-up of the plasma sample. Arginine and ornithine could then be analyzed separately by GCMS and if any breakdown of arginine into ornithine occurred, appropriate corrections could be made.

(1) Nissim I., Yudkoff M., Terwilliger T. and Segal S., Rapid Determination of (guanidino-15N) Arginine in Plasma with Gas Chromatography-Mass Spectrometry: Application to Human Metabolic Studies. Anal. Biochem. 131: 75-82 (1983).

(2) King T.P., Selective Chemical Modification of Arginyl Residues. Biochemistry 5(11): 3454-3459 (1966).

(3) Vetter-Diechtl H., Vetter W., Richter W. and Biemann K., Ein fur Massenspektrometrie und Gaschromatographie geeignetes Argininderivat. Experientia 24: 340-341 (1968).

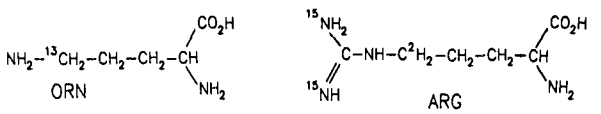

Fig. 1

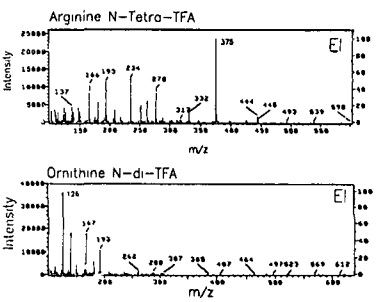

Fig. 2

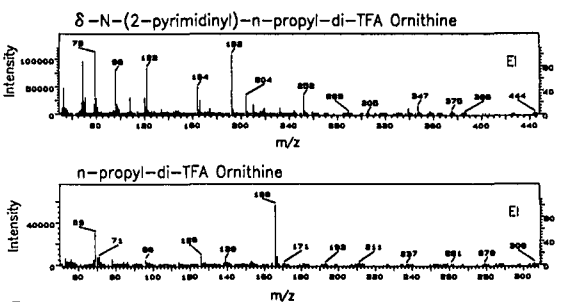

Fig. 3

Presented at the 36th ASMS Conference on Mass Spectrometry and Allied Topics
June 5-10, 1988, San Francisco, CA

QUALITATIVE AND QUANTITATIVE ANALYSIS OF ACYLCARNITINES IN HUMAN PLASMA AND TISSUES BY FAB-MS

Fumio Inoue, Diane Gale and David S. Millington
Duke University Medical Center, Division of Pediatric Genetics and Metabolism, Box 3028, Durham, NC 27710.

A number of inherited metabolic disorders can present with Reye-like or sudden infant death (SIDS) syndromes. The most striking example is the medium-chain acyl-coA dehydrogenase deficiency (MCAD), in which the toxic metabolite octanoic acid accumulates during catabolic episodes and can result in rapid deterioration and death. The retrospective identification of MCAD and related disorders of fat catabolism in a substantial population of SIDS cases has been undertaken with the objectives of defining the incidence of these disorders and identifying families "at risk" for affected siblings. The diagnostic value of urinary acylcarnitine profiling by FAB-MS has been demonstrated. Here we describe methods for the analysis of acylcarnitines in post-mortem tissue and plasma and their applicability to screening for inherited metabolic disease.

Methods Blood plasma (0.2 ml) or frozen tissue (0.2-0.4 g) containing 3-30 nmol total acylcarnitine was homogenized with MeOH (2.0 mL). Deuterium-labeled internal standards were added for quantification when appropriate. After centrifugation, the supernatents were applied to cartridges containing 0.6 g C-18 reverse-phase packing, prewashed with MeOH. The cartridges were eluted with 80% MeOH (4 ml), then with pure MeOH (4 ml). After concentration to 1 ml (N_2) and washing with hexane (3 x 2 ml), the eluate was evaporated and the residue methylated with 50 µl MeOH-HCl (3 N) at 65 °C for 10 minutes. After a further wash with hexane (3 x 1 ml) an aliquot of the residue (2 µl) was analyzed by FAB/MS in a glycerol matrix using a VG 70S mass spectrometer. Signals corresponding to putative acylcarnitine methyl ester cations were further analyzed by HRMS and MS/MS as described previously.

Results Acylcarnitine profiles of a normal plasma control, and of blood samples obtained post-mortem from children with propionic acidemia and with MCAD deficiency (diagnosed retrospectively) are shown in figure 1 a, b and c respectively. In figure 2a the diagnostic "MCAD" metabolite octanoylcarnitine (M^+ = 302) was detected in a post-mortem liver specimen from another child dying of SIDS but not in a normal control liver (2b). Subsequently, MCAD deficiency was also diagnosed in a surviving sibling before symptoms developed, enabling preventive therapeutic intervention. By spiking with known amounts of internal standards, e.g. octanoyl-d_9-carnitine, M^+ = 311 (methylester), it was possible to quantify individual acylcarnitines by HRSIM to levels as low as 5 nmol/g.

The results suggest that blood and tissue obtained at autopsy can be successfully analyzed for disease-specific aclycarnitines by FAB-MS. Routine screening for inherited diseases presenting as SIDS is now possible, and can be improved by use of the continuous-flow FAB-MS device as a rapid sample introduction system.

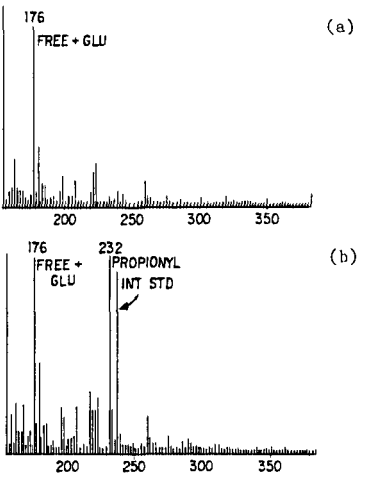

Figure 1. FAB-MS analysis of post-mortem plasma extracts.
(a) Normal control
(b) Propionic acidemia
(c) SIDS case, retrospectively diagnosed as MCAD def.

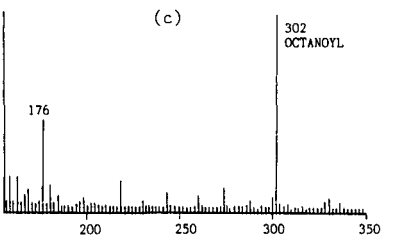

Figure 2. FAB-MS analysis of post-mortem liver extracts.
(a) SIDS case (MCAD)
(b) Normal liver

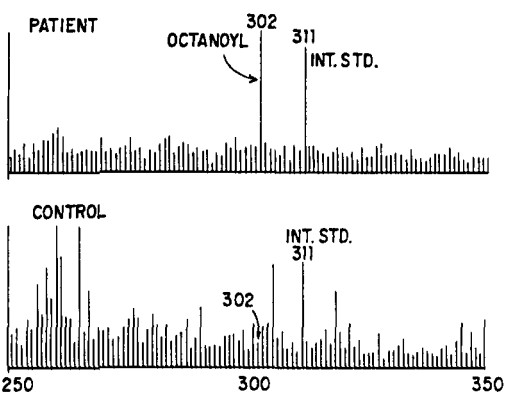

Presented at the 36th ASMS Conference on Mass Spectrometry and Allied Topics
June 5-10, 1988, San Francisco, CA

IDENTIFICATION AND QUANTITATION OF URINARY ADIPIC ACID METABOLITES BY GC/MS

Shiow-Jen Jin and Kou-Yi Tserng
VA Medical Center and Dept. of Pharmacology, Case Western Reserve Univ., Cleveland, OH 44106

Dicarboxylic aciduria, an increased urinary excretion of adipic (DC6), suberic (DC8), and sebacic (DC10) acids, is often resulted from enhanced fatty acid oxidation or inhibited fatty acid metabolism. These acids are produced from medium chain monocarboxylic acids, most likely dodecanoic (MC12) or decanoic (MC10) acids through microsomal omega-hydroxylation and cytosol oxidation. The dicarboxylic acids (DC10 or DC12) are then activated to CoA derivatives, which are then transported to mitochondria or peroxisomes for further beta-oxidation to DC8 and DC6. It is not known whether DC6 can be metabolized further to DC4 (succinic acid) to provide a gluconeogenic pathway from fatty acids, since the direct product-precusor relationship have never been demonstrated. Through the use of gas chromatograph-mass spectrometry, we have identified 3-hydroxyadipic acid 3,6-lactone and trans-2-hexenedioic acid, two intermediates produced in the further beta-oxidation of adipic acid in human urine.

METHODS

URINARY ORGANIC ACID ANALYSIS WITH DUAL COLUMN GC AND GC/MS - Urine sample was spiked with pentadecanoic acid as internal standard, acidified and extracted with solvent mixture of ethyl acetate and diethyl ether. The combined extract was dried and derivatized with BSTFA/TMCS or BSA/d_9. This trimethylsilyl derivative was analyzed with a dual capillary column gas chromatography and a gas chromatography-mass spectrometer. The column temperature was maintained initially at 60 °C and programmed to increase at a rate of 4 °C/min to a final temperature of 250 °C. A repetitive scanning mode was used for compound identification. The eluent from the capillary column was repetitively scanned from m/z 49 to 550.

SYNTHESIS OF AUTHENTIC SAMPLES - 3-Hydroxyadipic acid 3,6-lactone was synthesized from the reduction of 3-oxoadipic acid with sodium borohydride. The resulting 3-hydroxyadipic acid was cyclized to the lactone upon acidification. Trans-2-hexenedioic acid was synthesized from oxidation of 1,3-cyclohexadiene.

RESULTS

In SPB-1 capillary column, a major peak eluted before and another eluted after adipic acid when the urine sample was derivatized as trimethylsilyl derivatives(Fig. 1). The former unknown(Fig. 2b) had highest mass at m/z 201, suggesting a molecular weight of 216. Other diagnostic ions at m/z 188, 157, and 85 and the shifting of masses obtained from its TMS-d_9 derivative suggested the possible structure of this compound as 3-hydroxyadipic acid- 3,6-lactone. The latter eluted unknown(Fig. 2a) had highest mass at m/z 273, suggesting a molecular weight of 288. Other mass fragments occurred at m/z 198, 183, 170, 155, and 139. This compound was identified as 2-hexenedioic acid. The trans configuration was suggested since its eluting sequence came after adipic acid. All structural assignments have been confirmed by comparison with synthetic authentic samples(Table 1).

CONCLUSION

(1) From the correlation between the excretion of lactone and adipic acid(Fig. 3), as well as the knowledge of the degradative pathway of dicarboxylic acid, it appears that 3-hydroxyadipic acid 3,6-lactone is derived from adipic acid through beta-oxidation(Fig. 4).
(2) The obligatory intermediate, t-2-hexenedioic acid, in this pathway was also identified and no other hexenedioic acids could be detected in human urines.

Presented at the 36th ASMS Conference on Mass Spectrometry and Allied Topics
June 5-10, 1988, San Francisco, CA

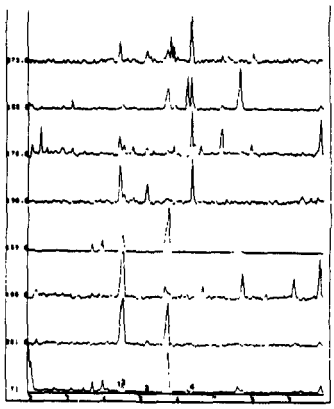

Fig. 1

Fig. 2

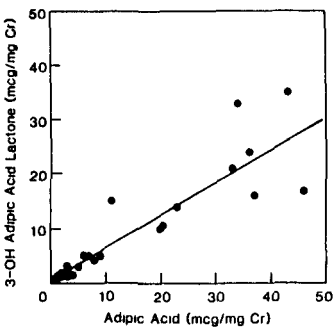

Fig. 3

Table 1

GAS CHROMATOGRAPHY RETENTION TIMES OF URINE UNKNOWNS AND SYNTHETIC AUTHENTIC SAMPLES

COMPOUNDS	METHYLENE UNIT	
	SPB-1	SPB-35
URINE UNKNOWN 2	14.36	17.02
URINE UNKNOWN 4	15.39	16.48
3-OH-ADIPIC ACID-LACTONE	14.36	17.02
CIS-2-HEXENEDIOIC	14.90	15.94
TRANS-2-HEXENE-DIOIC	15.39	16.48
CIS-3-HEXENEDIOIC	15.00	15.97
TRANS-3-HEXENE-DIOIC	15.10	16.17

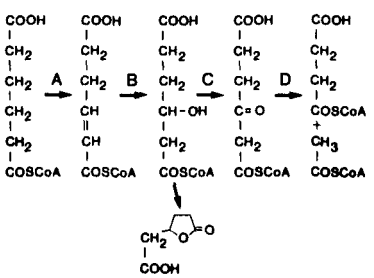

Fig. 4

THE ENZYMES INVOLVED ARE:

A. ACYL-CoA DEHYDROGENASE;
B. ENOYL-CoA HYDRATASE;
C. BETA-HYDROXYACYL-CoA DEHYDROGENASE;
D. BETA-KETOTHIOLASE.

Presented at the 36th ASMS Conference on Mass Spectrometry and Allied Topics
June 5-10, 1988, San Francisco, CA

A GC/MS INVESTIGATION OF IN VITRO METABOLITES OF CANNABICHROMENE AND CANNABIGEROL IN SEVERAL SPECIES.

D.J. Harvey and N.K. Brown,

University Department of Pharmacology, South Parks Road, Oxford, OX1 3QT, UK.

Although metabolism of the major cannabinoids from marihuana, delta-9-tetrahydrocannabinol, cannabidiol and cannabinol, has been well studied, metabolism of some less abundant constituents such as cannabichromene (CBC, I) and cannabigerol (CBG, II) has received little or no attention.

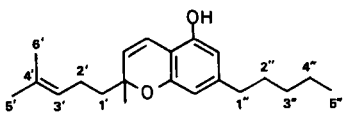

I

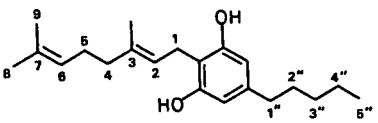

II

CBC, although of low relative concentration it is, nevertheless, the second most abundant cannabinoid in some high delta-9-THC marihuana originating from the USA. CBG has been used to treat glaucoma. This paper reports the in vitro metabolism of these cannabinoids.

Liver microsomes were prepared from mice, rats, rabbits, cats, guinea pigs, gerbils and hamsters and incubated with the two cannabinoids for 1 hr at 37°C. Metabolites were extracted with ethyl acetate, concentrated by chromatography on Sephadex LH-20 and converted into TMS and [$^2H_9$]TMS derivatives for examination by GLC and GC/MS. For GLC, a Hewlett-Packard 5890A gas chromatograph fitted with a 50 m x 0.3 mm OV-1 fused silica capillary column was used with peak integration employing a Hewlett-Packard 3390A recording integrator. GC/MS data were recorded using a VG 70/70F mass spectrometer (70 eV) fitted with a 25 m x 0.2 mm OV-1 fused silica capillary column terminating inside the ion source.

Metabolites from CBC were mainly monohydroxy compounds. Their mass spectra were all similar because of ready formation of the chromenyl ion following loss of the methylpentenyl chain. However, the mass of this ion differentiated metabolites hydroxylated in the pentyl chain (m/z 391) from those hydroxylated in the methylpentenyl chain (m/z 303). Metabolites hydroxylated in all positions of the pentyl chain were detected and were identified by retention time and by the presence of weak diagnostic fragments (1,2) in the spectra of the 1"- and 3"-hydroxy compounds. Metabolites hydroxylated at the terminal methyl groups of the methylpentenyl chain were identified by NMR. Other metabolites were the 3',4'-epoxide and its derived diol. Most of the species gave similar metabolites but in different proportions.

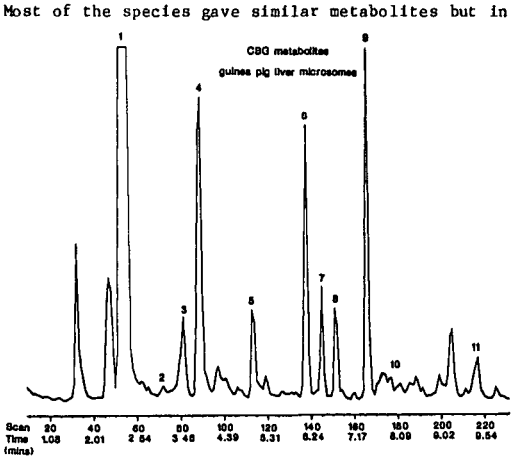

Fig. 1. Limited ion chromatogram (m/z 300-700) of metabolites of CBG isolated from guinea pig liver microsomes.

Metabolism of CBG was similar and consisted mainly of hydroxylation. Fig. 1 shows a limited ion chromatogram (m/z 300-700) of the metabolites from the guinea pig. The mass spectrum of unmetabolized CBG TMS ether (Fig. 2) gave prominent ions at m/z 337 (tropylium ion from cleavage of the C-1 - C-2 bond), 377 (cleavage at C-3 - C-4), 391 (cleavage at C-5 - C-6) and 403 (cleavage at C-5 - C-6). In the mass spectra of the TMS derivatives of metabolites hydroxylated in the pentyl side-chain, all of these ions shifted by 88 mass units. In addition, these metabolites gave rise to prominent diagnostic fragment ions allowing the metabolites to be identified as 1"-OH-CBG [peak 2, diagnostic ion, m/z 417 (100%)], 2"-OH-CBG [peak 5, m/z 14[illegible] (100%)], 3"-OH-CBG, [peak 6, m/z 404 (100%), see Fig. 3], 4-OH-CBG [peak 7, m/z 117, (21%)] and 5"-OH-CBG (peak 10, identified by retention time).

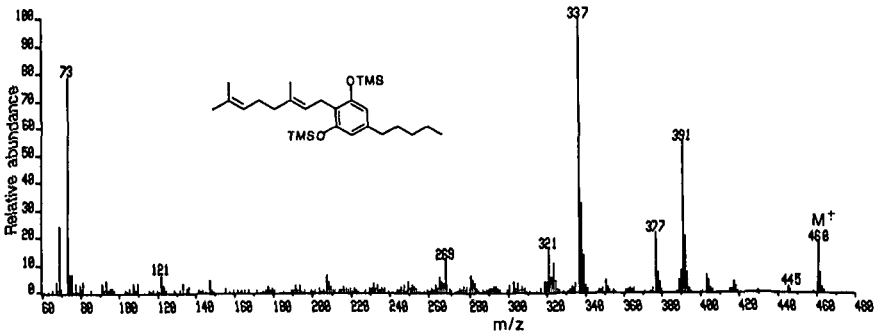

Fig. 2. 70 eV Mass spectrum of the TMS derivative of CBG.

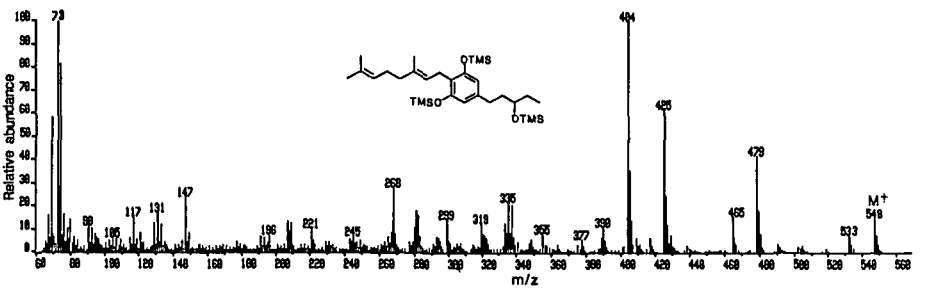

Fig. 3. 70eV Mass spectrum of the TMS derivative of 3"-hydroxy-CBG.

Metabolites hydroxylated in the other chain (carbons 1'-10'), peaks 8 and 9, had similar spectra in which the fragment ions present in the spectrum of CBG-TMS ether had not shifted in mass. This indicated hydroxylation at C-8 and C-9 with the trans-hydroxy metabolite, 8-OH-CBG, being the major metabolite (peak 9). Ions containing the terminal carbon atoms of the chain and the OTMS group were present at m/z 156, 157, and 169. Peak 4 was produced by CBG-6,7-epoxide (M^+, m/z 476) and its derived diol was was also identified (peak 11). The mass spectrum of the latter compound was dominated by the ion at m/z 131 produced by cleavage of the C-6 - C-7 bond. Peak 1 in Fig. 1 is CBG. Most of the species produced these metabolites although in different relative proportions. The cat produced a considerable concentration of a hydroxylated dihydro-CBG (M^+ m/z 550) identified as the 6,7-dihydro analogue of the 8- and 9-hydroxy metabolites (both give the same dihydro compound). The presence of the hydroxy-methyl group was confirmed by the ion at m/z 103.

This work was supported by the Wellcome Trust and NIDA.

1) M. Binder, S. Agurell, K. Leander and J.-E. Lindgren, Helv. Chim. Acta, 1974, 57, 1626.
2) D.J. Harvey, Mass Spectrom. Rev., 1987, 6, 135.

Presented at the 36th ASMS Conference on Mass Spectrometry and Allied Topics
June 5-10, 1988, San Francisco, CA

METABOLISM STUDY OF ETHYLCYCLOHEXANE IN MALE FISCHER RATS BY GC/MS

Kyung O. Yu[a], M. Paul Serve[b], Jacqueline Roberts[b], and Gayle A. McDonald[c]

[a] Toxic Hazards Division, Harry G. Armstrong Aerospace Medical Research Laboratory, Wright-Patterson Air Force Base, OH 45433.
[b] Department of Chemistry, Wright State University, Dayton, OH 45431.
[c] Northrop Services, 101 Woodman Drive, Dayton, OH 45431.

Petroleum products are widely used in our society and hydrocarbons are the principal class of components in petroleum products (gasoline, cleaning solvents and lubricants). The relationship between exposure to petroleum-derived hydrocarbons and renal toxicity in male rats is a fairly recent finding (1,2). Exposure of unleaded gasoline in rats and mice showed the occurance of the dose-related degree of kidney damage in male rats. This kidney insult appeared to be sex and species-specific. Since unleaded gasoline is composed of many hydrocarbons, studies to correlate specific chemical structure with the nephropathy are underway.

Cyclic compounds such as cyclohexane and methylcyclohexane do not appear to produce hyaline droplet nephropathy in proximal tubular epithelium of male rats while a branched chain hydrocarbon substituent (e.g. isopropyl or t-butyl group) attached to the cyclohexane ring produces the nephrotoxicity. The objective of this study is to determine how the ethyl group moity in cyclohexane ring would affect the oxidative metabolic pathway and cause the renal damage in the male rats.

Eight male Fischer 344 rats (283 $\pm$ 10g) were dosed by gavage with 1.0 mL/kg ethylcyclohexane every other day for 14 days. Rats were placed in metabolism cages for the first 48 hours following initial dosing for urine collection. Urine was also collected from water-treated rats (N = 4). Food and water were freely available. Aliquots of urine were ajdusted to a pH of 4.4 and hydrolyzed by β-glucuronidase/aryl sulfatase at 37°C overnight. The samples were filtered through Clin-Elut using methylene chloride as the eluent. Concentrated methylene chloride extracts were analyzed by GC and GC/MS. TMS-derivatives were made by reaction of urine extracts and BSTFA (Pierce chemical Co). Mass spectra and GC retention time of the urinary metabolites were compared with those of synthesized or purchased compounds. All spectra were obtained on HP 5985 quadrupole mass spectrometer equipped with capillary columns (Carbowax 20M 25 meter or DB-1 30 meter for TMS-derivatives). Heluim gas was used as carrier gas ($\bar{\mu}$ = 25 cm/sec), and both injection port and ion source were 200°C. The column temperature was programmed from an initial oven temperature of 100°C held for 1 min, with the program rate of 5°/min, to the final temperature of 180°C held for 1 min.

Urinary metabolites identified by GC/MS are 4-ethyl cyclohexanol, 2-hydroxy-4-ethyl cyclohexanone, cis-diols (2^c-hydroxy-4^c-ethyl cyclohexanol, 2^c-hydroxy-4^t-ethyl cyclohexanol) and trans diols (2^t-hydroxy-4^t-ethyl cyclohexanol, 2^t-hydroxy-4^c-ethyl cyclohexanol). GC trace of the urinary metabolites showed that thermally stable trans-diols are the major metabolites. No attempts were made to assign which diol eluted first in cis-diols or trans-diols.

Monohydroxylation, oxidation to keto alcohol and dihydroxylation were the metabolic pathways for ethylcyclohexane in male rats exposed by gavage. Histopathology showed the mild hyaline droplet formations which were not detected in the proximal tubule of the rats exposed to cyclohexane or methylcyclohexane.

REFERENCES

1. Ridder, G., 1986 Summer Toxicology Forum, given by Institute of Pathology, Aspen, CO, July 1986.

2. MacFarland, H.N., Renal Effects of Petroleum Hydrocarbons, Princeton

Presented at the 36th ASMS Conference on Mass Spectrometry and Allied Topics
June 5-10, 1988, San Francisco, CA

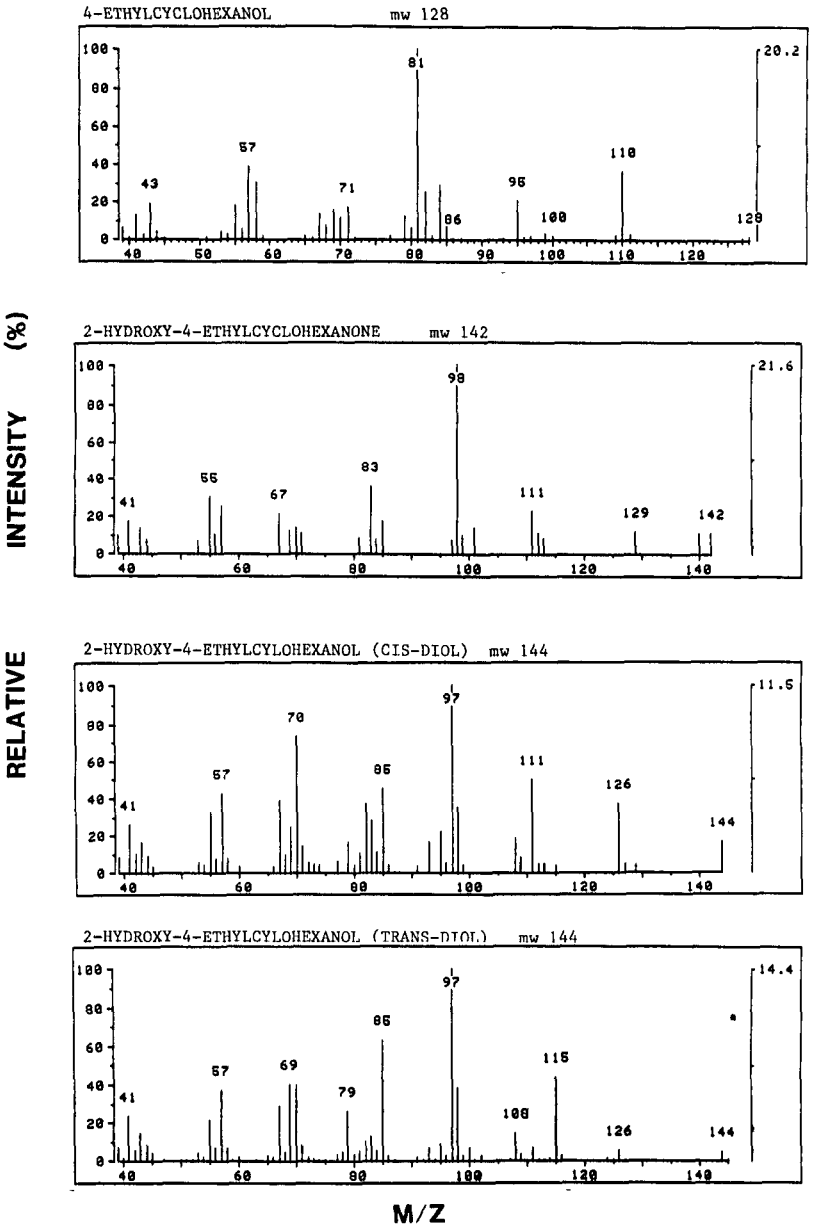

Presented at the 36th ASMS Conference on Mass Spectrometry and Allied Topics
June 5-10, 1988, San Francisco, CA

IDENTIFICATION OF URINARY ARGININOSUCCINIC ACID IN ADULT TYPE CITRULLINEMIA BY FAB MS/MS

Masahiro Matsumoto, Yoshito Inoue, Takashi Ohkura,
*Kimio Isa and Isamu Matsumoto
Department of Biochemistry, Institute of Human Genetics,
Kanazawa Medical University, Uchinada, Ishikawa 920-02, Japan,
*Faculty of Education, Fukui University, Fukui 910, Japan

Citrullinemia or citrullinuria is caused by a hereditary deficiency of argininosuccinic acid (ASA) synthetase. ASA synthetase is located in the liver, brain, and kidney of mammals, and its precursors are citrulline and aspartic acid. Adult type citrullinemia patients are deficient in ASA synthetase in the liver, but not in the kidney.

The quantification of citrulline is done routinely using an amino acid analyzer. ASA is undetectable in healthy normal urine and serum, and can only be detected in urine, blood, and cerebrospinal fluid of patients with argininosuccinase deficiency, argininosuccinic aciduria.

Recently, we detected moderatory intense peaks having the same retention time as ASA by amino acid analysis of urine of a patient with citrullinemia, and analyzed the component by FABMS and/or FAB MS/MS.

Urine specimens were dried under reduced pressure and derivatized to butyl esters by 15%-boron trifluoride n-butanol solution, and applied to FABMS and/or FAB MS/MS.

Quasi-molecular ions ($M+H)^+$ of ASA butyl ester (m/z 459) were detected in the urine from the patient with adult type citrullinemia, but the peak was less intense than that in argininosuccinic aciduria. This was further confirmed by E-B-E type FAB MS/MS. The collision induced decomposition spectra obtained by focussing the ion beam of m/z 459 showed major peaks of m/z 442 in both samples from patients with argininosuccinic aciduria and citrullinemia.

A possible explanation for this contradictory finding is that the ASA synthetase deficiency in the liver caused the accumulation of excess amounts of citrulline, which was then circulated into the kidney and utilized for the synthesis of ASA as ASA synthetase in the kidney has normal activity, which results in the accumulation of ASA.

The FAB mass spectrum of urine from a citrullinemic patient.

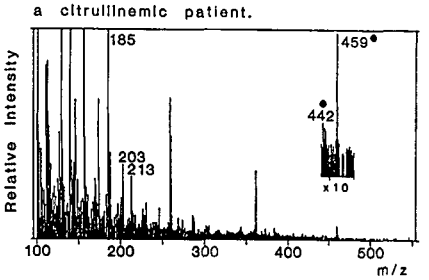

The ions of 459 and 442 are derived from ASA tri-butylester. Other numbers are derived from citrulline butylester.

Presented at the 36th ASMS Conference on Mass Spectrometry and Allied Topics
June 5-10, 1988, San Francisco, CA

The CID spectrum of urine from a patient with argininosuccinic aciduria.

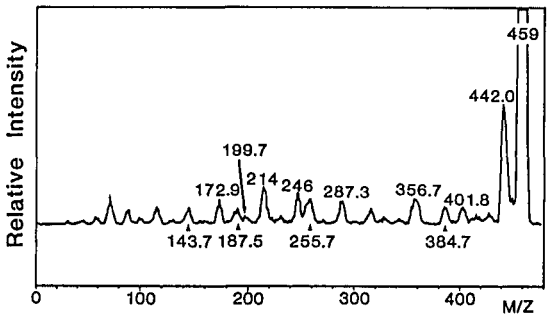

The CID spectrum of urine from a patient with citrullinemia.

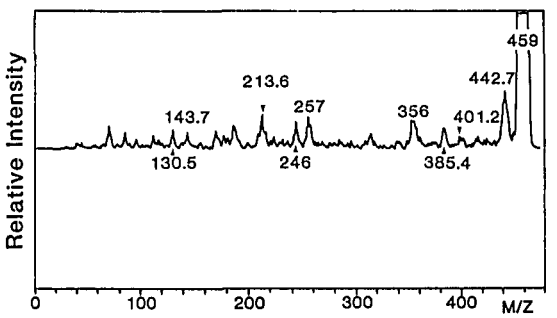

The FAB MS/MS (E-B-E) spectra of the urine from patients with argininosuccinic aciduria and citrullinemia. The collision induced spectra was obtained by focussing the ion beam of m/z 459. The ion of m/z 459 corresponds to $(M+H)^+$ ion of argininosuccinic acid tri-butyl ester.

Presented at the 36th ASMS Conference on Mass Spectrometry and Allied Topics
June 5-10, 1988, San Francisco, CA

ASSESSMENT OF HEXOSE MONOPHOSPHATE SHUNT ACTIVITY IN NEOPLASTIC CELLS

[1]T.P. Krick, [2,3]S.L. Mitchell, [1,3]B.D. Ross and [2,3]M. Garwood
[1]Department of Biochemistry, University of Minnesota, St. Paul, MN
[2]Department of Radiology, University of Minnesota, Minneapolis, MN
[3]Gray Freshwater Biological Institute, University of Minnesota, Navarre, MN

Introduction

The hexose monophosphate shunt (HMPS) provides pentose sugars and NADPH for the synthesis of nucleic acids and lipids, respectively. Since malignant cells of the central nervous system have been shown to have increased HMPS activity relative to normal cerebral tissue [1] and some chemotherapeutic agents affect nucleic acids and the HMPS [2], it is important to be able to gain a better understanding of the activity of this pathway. We present a mass spectrometric method for sequential measurements of the relative contribution of the HMPS to glucose metabolism.

Materials and Methods

C6 glioma cells were grown to confluence in sterile flasks in supplemented Ham's F-10 medium. Prior to the test, the flasks were rinsed with Krebs-Ringer Bicarbonate buffer (KRB) and allowed to metabolize endogenous carbon sources for one hour. Prior to the addition of the test media, the flasks were again rinsed. The test media were KRB with 5.5 mM 1-^{13}C-glucose (KRB-Glu) for control or KRB-Glu with either 0.001 mM phenazine methosulfate (PMS) or 1.0 mM KCN. Eight ml of media was added to the flasks and changed at time points of 1, 2, 3, 5, 7, 9 and 12 hours.

One half ml of each sample with 0.05 ml of U-^{13}C-lactate at a concentration of 0.2384 mg/ml added to some samples was used for mass spectrometric analysis. The U-^{13}C-lactate was added as an internal standard for total lactate determination in samples involving PMS since PMS oxidizes the NADH used in the enzymatic measurement of lactate [3]. The samples were converted to trimethylsilyl (TMS) derivatives in a solution of 25 µl pyridine and 40 µl bis (trimethylsilyl)-trifluoroacetamide with 1% trimethylchlorosilane which was heated to 50° C for 15 minutes prior to injection [4,5]. Seven and a half ml of each aliquot were lyophilized and reconstituted in 0.5 ml deuterium oxide for NMR analysis.

Determination of the HMPS activity depends on the determination of the [3-^{13}C-lactate]/[3-^{12}C-lactate] ratio due to 1-^{13}C-lactate metabolism. The fraction of glucose metabolized to lactate which was metabolized by the HMPS (X) was calculated by the equation, $X = (3-3R)/(3+2R)$, where R is the [3-13C-lactate]/[3-12C-lactate] ratio [6-8].

Mass spectrometric analyses were done on a KRATOS MS-25 gas chromatograph-mass spectrometer coupled to a DS-55 data system. A DB-5 fused silica column (30 m x 0.32 mm) with a 0.25 µm film thickness was used with helium as the carrier gas.. Selected ion monitoring was performed on the m/z 219 through m/z 222 ions which correspond to the molecular ions of the TMS derivatives minus a methyl group. Each sample took approximately 15 to 20 minutes to run.

NMR analyses were done on a Nicolet Magnetics NT-300 (7.05T) spectrometer. The [3-13C-lactate]/[3-12C-lactate] ratios were determined by quantitating the areas of the resonances of the lactate methyl proton satellites due to carbon-13/proton interaction and the resonances of the methyl protons on carbon-12 by spectral

deconvolution using the Nicolet "NMCCAP" routine. Each sample took up to 5 hours to run.

Lactate determinations were done by two methods. An enzymatic method utilizing lactate dehydrogenase for the oxidation of lactate and the concomitant reduction of NAD^+ to NADH. The increase in NADH concentration was determined by a spectrophotometer at 340 nm [3]. Since PMS oxidizes the NADH which is produced in this reaction, this method was not suitable for samples with PMS. U-13C-lactate in a known concentration was added to these samples prior to derivatization and total lactate was determined by the ratio of the m/z 219 and 220 peaks to the m/z 222 peak (as corrected for natural abundance) which correspond to U-^{12}C-lactate and 3-^{13}C-lactate from the metabolism of the 1-^{13}C-glucose and the U-^{13}C-lactate.

Results and Discussion

The HMPS activity was determined for control cells as well as cells treated with PMS or KCN for 12 hours. Individual measurements were made at 1, 2, 3, 5, 7, 9 and 12 hours with a curve being formed of varying activities (fig. 1). After 12 hours of incubation with PMS the HMPS activity was increased to 350% of control activity. Cells cultured with KCN had an activity decreased to only 41% of control after 12 hours. A comparison of the activities as derived from the mass spectrometric and NMR data (fig. 2) revealed no significant difference by Student's t-test.

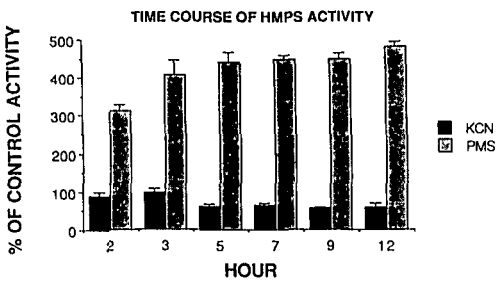

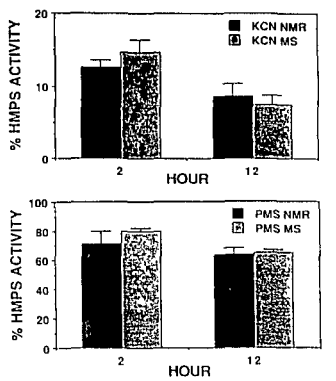

These results demonstrate that this mass spectrometric method correlates well with the previously reported NMR method for sequential monitoring of HMPS activity in cultured cells but takes less sample (0.5 ml vs 7.5 ml) and less time per sample (15-20 minutes vs 5 hours) for analysis than the NMR method.

References

[1] Loreck, D.J., Galarraga, J., Van der Feen, J., Phang, J.M., Smith, B.H. and Cummins, C.J. (1987) Metabol. Brain Dis. 2, 31-46.
[2] Yeh, G.C., Occhipinti, S.J., Cowan, K.H., Chabner, B.A. and Myers, C.E. (1987) Cancer Res. 47, 5994-5999.
[3] Bergmeyer, H.U. (1974) Methods of Enzymatic Analysis, Vol. 3, p. 1468, Verlag Chemie, Weinheim.
[4] Tserng, K-Y., Gilfillan, C.A. and Kalhan, S.C. (1984) Anal. Chem. 56, 517-523.
[5] Mamer, O.A., (1988) Biomed. Env. Mass Spec. 15, 57-62.
[6] Ogino, T., Arata, Y. and Fujiwara, S. (1984) Biochemistry 19, 3684-3691.
[7] Oxley, S.T., Porteous, R., Brindle, K.M., Boyd, J. and Campbell, I.D. (1984) Biochim. Biophys. Acta 805, 19-24.
[8] Willis, J.A., Williams, W.F. and Schleich, T. (1986) BBRC 138, 1068-1073.

Presented at the 36th ASMS Conference on Mass Spectrometry and Allied Topics
June 5-10, 1988, San Francisco, CA

SIMULTANEOUS QUANTITATION OF GEPIRONE AND 1-PP IN HUMAN PLASMA BY CAPILLARY GAS CHROMATOGRAPHY-MASS SPECTROMETRY:

M.A. Sciacca, J.P. Shea, G.F. Duncan, H.C. Faulkner, III, R.H. Farmen and K.A. Pittman, Department of Metabolism and Pharmacokinetics, Bristol-Myers Company, Pharmaceutical Research and Development Division, Syracuse, N.Y. 13221.

Gepirone (I), 4,4-dimethyl-1-[4-[4-(2-pyrimidinyl)-1-piperazinyl]butyl]-2,6-piperidinedione, is a potential anxiolytic and antidepressant agent currently undergoing Phase III clinical trials. 1-PP (II), 1-(2-pyrimidinyl)-piperazine, is a major metabolite of gepirone.

(I)

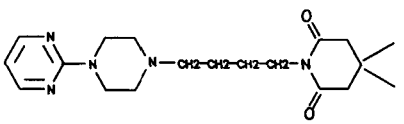

(II)

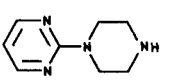

A GC-MS assay was developed and validated to simultaneously quantitate gepirone and 1-PP from human plasma. Analytes were extracted from plasma using C-18 extraction columns. The columns were conditioned with methanol and tris buffer (20 mM, pH 7.3), followed by addition of a 1 ml plasma sample. Columns were then successively washed with buffer and 1 ml of a methanol:water (2:3) mixture followed by analyte elution with 2 ml of 1% triethylamine in acetonitrile (1). After extraction the metabolite and its deuterated internal standard were derivatized with pentafluorobenzoyl chloride to their corresponding amides. The 1-PP derivatives, gepirone and the gepirone internal standard, 5-fluorobuspirone, were then reconstituted in 0.11% triethylamine in toluene (v/v) and injected. Samples were analyzed by capillary GC with automated splitless injection. The HP 5970 MSD was set to monitor the molecular ions of 1-PP and d4-1-PP, M/Z 358 and M/Z 362, followed by the gepirone common ion at M/Z 251 and then the 5-fluorobuspirone common ion at M/Z 277. The lower limit of quantitation, 0.1 ng/ml for both compounds, was determined on 1 ml plasma samples from ten different sources.

Standard curves were linear from 0.1-25 ng/ml when relating the ratio of gepirone and 1-PP to their respective internal standards with the concentration of analyte added to human plasma.

Figure 1 is a selected ion chromatogram of a processed 1 ml plasma standard spiked with 25 ng of gepirone and 1-PP and about 5 ng of the internal standards. The GC conditions employed helium as the carrier gas, with a 10m DB-5 column, 0.18 mm ID, 0.4 um film thickness, (J&W Scientific). The GC oven temperature was held at 150°C for 1 min, increased to 315°C at 25°C/min, and was held at final temperature for 5 min. Interface and injector temperatures were 270°C.

Figure 2 shows gepirone and 1-PP kinetics in a fasted subject given a 20 mg gepirone tablet.

The main advantage of this assay over previous methods (2,3) was the simultaneous quantitation of gepirone and 1-PP, saving both analyst and GC-MS time, with no loss in assay performance. The solid-phase extraction was efficient and simple. Plasma sample volume requirements were also reduced from 4 mls to 1 ml. This assay is currently being used to generate pharmacokinetic data for gepirone and 1-PP in humans.

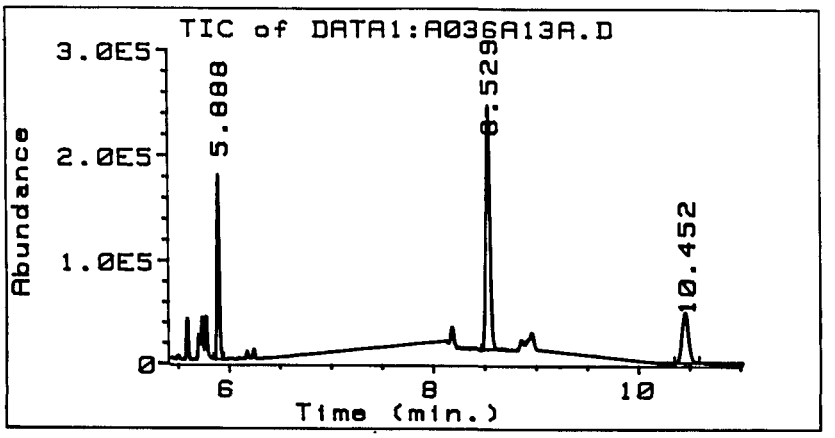

Figure 1. Peaks: 5.8 min. = 1-PP and d_4-1-PP; 8.5 min. = gepirone; 10.4 min. = 5-fluorobuspirone.

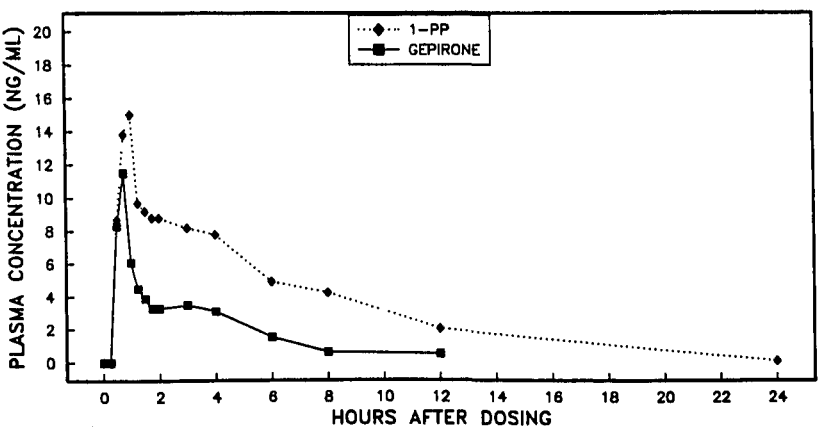

Figure 2.

References:

1. M.A. Sciacca, G.F. Duncan, J.P. Shea, H.F. Faulkner, III, R.H. Farmen and K.A. Pittman. Simultaneous Quantitation of Buspirone and 1-(2-Pyrimidinyl)-Piperazine in Human Plasma and Urine by Capillary Gas Chromatograpy-Mass Spectrometry. In press. J. Chromatogr.

2. R.E. Gammans, E.H. Kerns and W.W. Bullen. Capillary Gas Chromatographic-Mass Spectrometric Determination of Buspirone in Plasma. J. Chromatogr. 345:285-97 (1985).

3. E.H. Kerns, W.W. Bullen and R.E. Gammans. Quantitative Analysis of 1-(2-Pyrimidinyl)-Piperazine in Plasma by Capillary Gas Chromatography-Mass Spectrometry. J. Chromatogr. 377:195-203 (1986)

Presented at the 36th ASMS Conference on Mass Spectrometry and Allied Topics
June 5-10, 1988, San Francisco, CA

METABOLIC PROFILING OF VALPROIC ACID IN PATIENTS USING NEGATIVE ION CHEMICAL IONIZATION GCMS. Frank S. Abbott, Kelem Kassahun, Roland Burton and Kevin Farrell. Faculties of Pharmaceutical Sciences and Medicine, University of British Columbia, Vancouver, Canada, V6T 1W5.

Valproic acid (VPA) is a major antiepileptic drug widely used in the treatment of a variety of seizure types. VPA is metabolized in the body by a combination of mitochondrial, microsomal and cytosolic enzymes to produce at least 16 known metabolites. It is believed that several of the metabolites contribute to both the therapeutic and toxic effects of the drug. Partly because of their large number and the wide concentration range at which they are found in biological fluids, quantitation of VPA metabolites represents a significant analytical challenge. Published methods[1-3] for the assay of VPA metabolites either do not have the necessary sensitivity to quantitate the trace unsaturated metabolites or are not complete in terms of including important metabolites. Here, we report the development of a negative ion chemical ionization (NICI) GCMS method for the simultaneous quantitation of VPA and 14 of its metabolites in one chromatographic run. The assay was employed for metabolic profiling of VPA in pediatric patients on VPA monotherapy and combined therapy with other antiepileptic drugs.

Serum (trough) and overnight urine samples were obtained from 26 patients receiving VPA only and 33 receiving VPA in combination with carbamazepine and/or clobazam. Four internal standards were employed in the assay; di-([3,3,3-^{2}H]propyl)acetic acid ([$^2H_6$]VPA), [3,5,5-^{2}H]3-heptene-4-carboxylic acid ([$^2H_3$]2-ene VPA), [3',3',3'-^{2}H]2-propyl-3-oxopentanoic acid ([$^2H_3$]3-keto VPA) and 2-methylglutaric acid. Serum (100-250 uL) or urine (250 uL) to which internal standards had been added was acidified (pH 1.5-2.0) and extracted with 2x500 mL ethyl acetate. The concentrated extract (200 uL) was derivatized to give the pentafluorobenzyl (PFB) esters. The PFB derivatives were then treated with N-methyl-N-trimethylsilyl-trifluoroacetamide to silylate metabolites containing hydroxyl groups and the 3-oxo moiety. Finally a 1 uL aliquot of the derivatized sample was injected into the GCMS in the splitless mode. The instrument used was a Hewlett-Packard 5987A GCMS fitted with a DB-1 column, 30 m x 0.32 mm (I.D) with a film thickness of 0.25 uM. Operating conditions in the negative ion mode were: ionization energy, 200 eV; source prssure, 1 torr; source temperature, 200°; reagent gas, methane.

The NICI GCMS properties of the PFB esters and O-TMS-PFB derivatives of hydroxy and 3-oxo metabolites proved to be suitable for the simultaneous analysis of VPA and 14 of its metabolites. The PFB derivatives of the hydroxyl metabolites chromatographed poorly on the DB-1 column and sensitivity was poor. Trimethylsilylation of the hydroxyl groups after PFB derivatization, however, greatly improved both peak shape and sensitivity of detection. The use of the DB-1 column enabled the complete resolution of 4-ene VPA from VPA as well as the separation of the monounsaturated metabolites as seen in Fig. 1A. PFB derivatization also resulted in baseline separation of the geometric and/or positional isomers of the diunsaturated metabolites (Fig. 1B).

Quantitation was performed by monitoring the intense $[M-181]^-$ ions. Correlation coefficients were typically greater than 0.99 for all standard curves. The method showed good precision with a day to day variation of less than 15% for all 15 analytes. Trace metabolites, including 4-ene VPA, (E)-2,4-diene VPA and (E,Z)-2,3'-diene VPA were readily quantitated from 100 uL of serum. The major metabolites in serum were found to be (E)-2-ene VPA, (E,E)-2,3'-diene VPA and 3-keto VPA (Table 1). The putative toxic metabolite, 4-ene VPA, was present at low levels (mean = 0.20 ug/mL).

The serum concentrations of 4-keto VPA and 5-OH VPA were significantly higher ($p<0.05$) in the VPA + carbamazepine group compared to the monotherapy group. There was no significant difference in metabolite profile between monotherapy and combined therapy with clobazam. In urine, the unsaturated metabolites were excreted mainly as conjugates, while the oxo metabolites were predominantly excreted in the free form. The hydroxy metabolites and 2-PGA were found in urine in both the conjugated and free forms.

The serum levels of the the unsaturated metabolites including the putative toxic metabolites, 4-ene VPA and (E)-2,4-diene VPA, were higher relative to that of VPA in a single case of VPA-induced liver toxicity. This, however, reflects the elimination characteristics of these metabolites since the sample was taken three days after the withdrawal of therapy. Thus it does not appear that the concentrations of the toxic metabolites were abnormal in this case of VPA-induced liver toxicity.

In summary, a NICI GCMS method has been developed for the simultaneous quantitation of 14 VPA metabolites. The assay demonstrated good reproducibility and sensitivity enabling the accurate determination of trace metabolites in small serum samples. The ω and ω-1 pathways of VPA appeared to be induced when VPA was given in combination with carbamazepine while clobazam apparently had no effect on the VPA metabolite profile.

Supported by the Medical Research Council of Canada

References

1. H. Nau, W. Wittfoht, H. Schafer, C. Jakobs, D. Rating and H. Helge, J.Chromatogr., 226, 69 (1981).
2. F. S. Abbott, J. Kassam, A. Acheampong, S. Ferguson, S. Panesar, R. Burton, K. Farrell and J. Orr, J. Chromatogr., 375, 285 (1986).
3. T. Tatsuhara, H. Muro, Y. Matsuda and Y. Imai, J. Chromatogr., 399, 183 (1987).

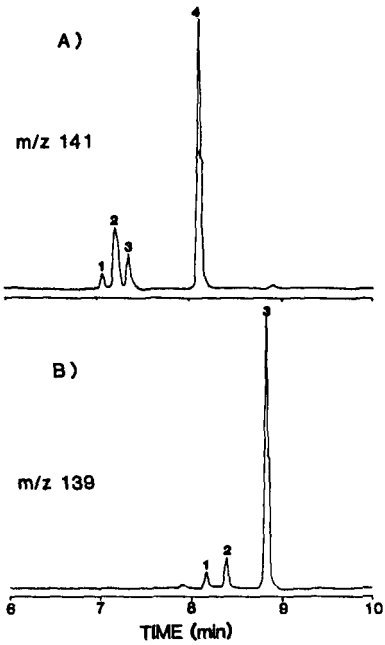

Figure 1. Selected ion current ([M-181]⁻) chromatograms of the PFB derivatives of the unsaturated metabolites of VPA in a patient serum extract. A) Peaks: 1 = 4-ene VPA, 2 = 3-ene VPA, 3 = (Z)-2-ene VPA, and 4 = (E)-2-ene VPA; B) Peaks: 1 = (E,Z)-2,3'-diene VPA, 2 = (E)-2,4-diene VPA and 3 = (E,E)-2,3'-diene VPA.

Table 1. Serum concentrations (ug/mL) of VPA metabolites in 26 pediatric patients on VPA monotherapy.

Compound	Mean	Range	% of VPA
4-Ene VPA	0.20	0.04-0.40	0.2
3-Ene VPA	1.80	0.72-3.30	2.0
(Z)-2-Ene VPA	0.11	0.05-0.18	0.1
(E)-2-Ene VPA	6.44	2.51-10.30	7.2
(E,E)-2,3'-Diene VPA	6.31	2.47-13.50	7.1
(E,Z)-2,3'-Diene VPA	0.28	0.06-0.38	0.3
(E)-2,4-Diene VPA	0.65	0.15-1.16	0.7
VPA	89.2	39.8-134.0	100
4-OH VPA	0.71	0.14-1.64	0.8
3-OH VPA	0.97	0.10-2.27	1.1
5-OH VPA	0.45	0.13-0.96	0.5
4-Keto VPA	0.60	0.16-1.27	0.7
3-Keto VPA	3.63	0.78-8.24	4.1
2-PSA	0.02	Tr.-0.15	0.02
2-PGA	0.16	0.02-0.30	0.2

Presented at the 36th ASMS Conference on Mass Spectrometry and Allied Topics
June 5-10, 1988, San Francisco, CA

MASS SPECTROMETRIC ANALYSIS OF IN VITRO METABOLITES OF ALACHLOR PRODUCED BY RAT, MOUSE, AND MONKEY LIVER AND KIDNEY HOMOGENATES

Hideji Fujiwara, R. Thomas Solsten, James E. Patanella,
Paul Feng, and Eugene W. Logusch

Monsanto Company Life Sciences Research Center
700 Chesterfield Village Parkway
St. Louis, Missouri 63198

Alachlor [2-chloro-N-(2,6-diethylphenyl)-N-(methoxymethyl)acetanilide] **1** is the active ingredient in LASSO ® herbicide, which is manufactured and sold worldwide by Monsanto Company.

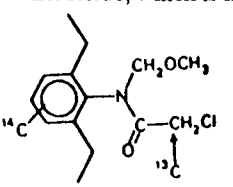

1

Alachlor metabolism was studied in cell-free kidney and liver enzyme preparations from rats, mice, and monkeys. Such *in vitro* studies were useful in elucidating the initial and intermediary pathways of alachlor metabolism (Scheme 1), and in determining species and gender differences in the metabolites produced.

Dual ^{13}C/ ^{14}C-labeled alachlor was used as a substrate in order to monitor metabolic transformations by HPLC/RAD and mass spectrometry. Metabolites were normally produced in the range 1 μg to 5 μg, and mass spectral techniques were essential for structure elucidation. Relatively volatile products were analyzed by GC/MS and by direct probe MS. Nonvolatile metabolites such as sugar and peptide conjugates were analyzed by FD/MS and HPLC/MS.

Two primary routes of alachlor metabolism were found in liver and kidney microsomal preparations from rats, mice, and monkeys: 1) alachlor was conjugated with glutathione by nucleophilic displacement of chlorine. and subsequently transformed via the mercapturic acid pathway; 2) alachlor was oxidized to alcohol derivatives which were subsequently converted to glucuronides. Further enzymatic conversions of initial metabolites produced 2.6-diethylaniline, which underwent aryl hydroxylation followed by sulfation to form 4-amino-3,5-diphenylsulfate.

In summary, the same products of alachlor metabolism were produced by liver and kidney microsomal enzymes from rats, mice, and monkeys. However, there were significant differences between species in the rates of metabolism, which may correlate with differences observed in the distribution and ultimate disposition of alachlor *in vivo*.

Presented at the 36th ASMS Conference on Mass Spectrometry and Allied Topics
June 5-10, 1988, San Francisco, CA

Scheme 1. Metabolic transformations of Alachlor by rat liver and kidney enzymes

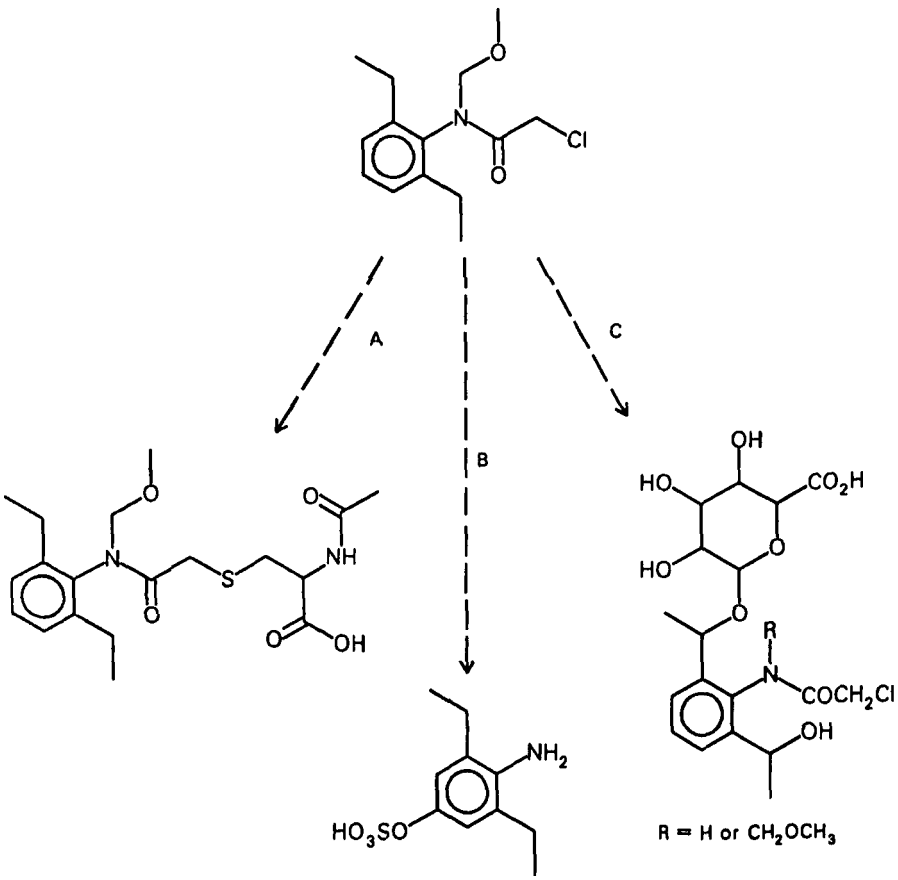

A: Mercapturic acid pathway
B: Deacylation, oxidation, sulfation
C: Oxidation, glucuronidation

Presented at the 36th ASMS Conference on Mass Spectrometry and Allied Topics
June 5-10, 1988, San Francisco, CA

Analysis of Drugs of Abuse in Hair by Tandem Mass Spectrometry

David A. Kidwell, Chemistry Division
Naval Research Laboratory, Washington, DC 20375

Introduction

Analysis of hair for drugs of abuse has several advantages over urinalysis. Drugs have been shown to be stable in hair and non-leaching for long periods of time whereas they are rapidly cleared from urine. Unlike urinalysis, hair analysis can be repeated with many samples at various times if the analytical results are questioned. Hair analysis also provides a long-term profile of drug use to aid as an independent check on an individuals veracity.

Most hair analysis has been by extraction of the drug and its detection in the extract by radioimmunoassay or GC/MS.[1-4] Extraction is time consuming and requires 30-40 pieces of hair. A more rapid and sensitive analytical procedure based on pyrolysis CI/MS/MS has been developed. Tandem mass spectrometry eliminates the tedious washing and extraction steps, can be preformed on single hairs, and can examine metabolites as well as the parent drug. To demonstrate this technique, cocaine and its metabolites and PCP were examined in human hair.

Methodology

Several hairs were weighed. One or two hairs were cut into 0.5 cm pieces, the sections placed in a solids probe cup, and the cup heated at 110°C for 1 minute in air to dry prior to analysis. For longitudinal sectional analysis, five strands of hair were cut at 1 cm points. Instrumental conditions for the Finnigan TSQ 70 were:

Isobutane CI gas at 1.6 torr
Argon collision gas at 1 mtorr
Collisional energy -20V (cocaine)
-18V (PCP)
Probe Heating: Initial at 50°C; 0.5 minute
Ramp to 250°C; 0.5 minute
Hold at 250°C; 2 minutes

Parent spectra of m/z 182 (cocaine), m/z 168 (benzoylecgonine) and m/z 82 (ecgonine) were taken in SIM mode. Cocaine was quantitated with external standards. Daughter spectra of m/z 244 (PCP) and m/z 258 (p-methyl PCP, the internal standard) were taken in SIM mode. Sensitivity for all materials was less than 50 pg.

Results

Typical desorption profiles for cocaine and its metabolites and blank hair are shown in Figure 1. Levels of cocaine and metabolites from different users are given in Figure 2. Hair from only one PCP user was available. Only PCP was found (at 16 ng/mg hair); no metabolites of PCP were detected. The desorption profile was very similar to that for cocaine, shown in Figure 1.

Figure 1 - Typical Desorption Profile for Cocaine Containing and Blank Hair

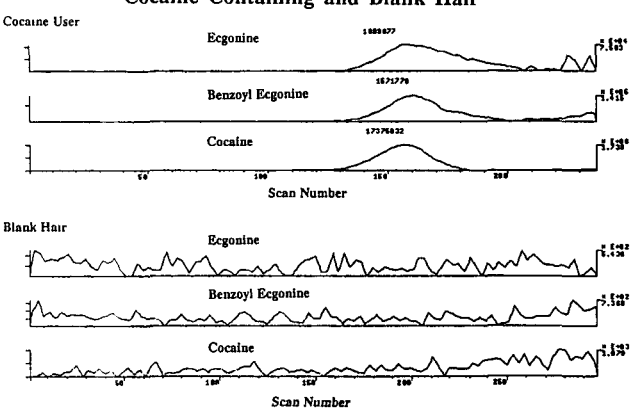

Precautions

Although an excellent filter, a tandem mass spectrometer can be overwhelmed in certain cases. In early work the hair was heated to 350°C. Interferences in some blank hair were observed. When two ions were monitored, as in PCP, high heating temperature produced both ions in approximately the correct ratio. A lower heating temperature resulted in much improved signal/noise ratios. In addition, cleaning of the ion source must be performed frequently when the hair is heated too hot.

Mechanism of Drug Incorporation

Once drugs are incorporated into hair they are not removed under normal cleaning conditions. Drugs may be bound to hair by covalent binding, ionic binding, or Van der Waals forces. Covalent binding cannot be considered for cocaine or PCP since no parts of the molecule are available for binding. Binding through Van der Waals forces also is unlikely since cocaine and its metabolites are highly water soluble and neither water nor organic solvents remove the cocaine.

To test an ionic binding mechanism, hair was soaked in solutions of PCP and washed in various solvents. As shown in Figure 3, the PCP is tightly held in the hair and only removed with acid or base. PCP is rapidly taken-up by hair and only slowly released. Hair soaked in drugs mimics hair from drug users. However, the metabolites are not present. Preliminary experiments indicate that cocaine is not degraded in hair to the metabolites in the presence of base. Thus, the presence of metabolites is an indication of drug use.

Conclusions

Analysis of cocaine and PCP in the hair of drug users is rapid and easy by tandem mass spectrometry. Metabolites of cocaine are readily observed and are in lower concentrations than cocaine. Hydroxy metabolites of PCP were not observed. Since drugs may be tightly bound to hair by exposure in solution, hair analysis must be approached with caution. Analysis for metabolites may be one means of confirming drug use.

References

1. W.A. Baungartner, C.T. Black, P.F. Jones, and W.H. Blahd, J. Nuc. Med. 23 790 (1982).
2. F.P. Smith and R.H. Liu, J. For. Sci., 31 1269(1986).
3. S. Balabanova and J. Homoki, Z. Rechtsmed, 98 235(1987).
4. A.M. Baumgartner, P.F. Jones, and C.T. Black, J. For. Sci., 26 576(1981).

Figure 2 - Levels of Cocaine and Metabolites for Different Users

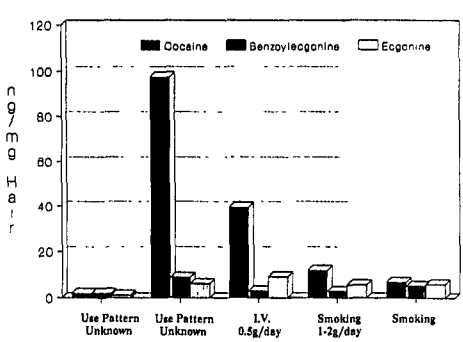

Figure 3 - PCP Remaining Relative to Water After Washing With Solutions

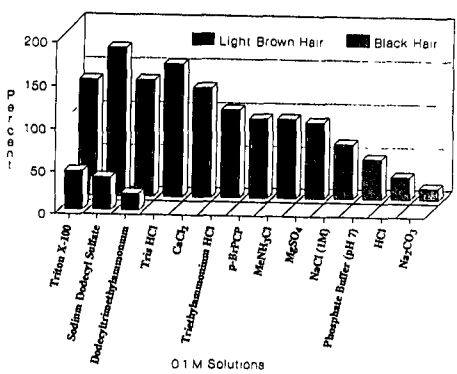

Presented at the 36th ASMS Conference on Mass Spectrometry and Allied Topics
June 5-10, 1988, San Francisco, CA

Determination of Volatile Organic Compounds in Human Blood By Purge and Trap Combined with Gas Chromatography/Mass Spectrometry

F.L. Cardinali, J.M. McCraw, and J.S. Holler

Center for Environmental Health and Injury Control, Centers for Disease Control, Public Health Service, U.S. Department of Health and Human Services, Atlanta, GA 30333

A number of recent findings suggest continuous, low-level human exposure to many volatile organic compounds (VOCs). The main concern of many health scientists is the adverse health effects that may be associated with such exposure. Several of these compounds are known human carcinogens. Others are suspected human carcinogens, that is they have been shown to cause cancer in animal testing programs. Individual VOCs have been associated with neurological and immunological health problems along with adverse reproductive outcomes. Many VOCs are thought to be associated with a new occupational health problem, associated with energy-efficient buildings, known as "sick-building syndrome."

The objective of our program is to measure the extent of exposure in the general population. In this program we will examine blood samples from over 1,000 individuals in conjunction with the third National Health and Examination Survey (NHANES III). By doing this, we will establish reference values that may be used in evaluating the degree of exposure to VOCs.

The analytical approach is purge and trap sample desorption combined with gas chromatography/mass spectrometry(GC/MS). The purge apparatus is a Tekmar LSC 3 with a 25 mL sample vessel operated in the needle sparging mode. Sample vessels are treated with Antifoam B to minimize foaming problems associated with this type of sample. A 10-mL blood sample is purged for 15 minutes by using the helium carrier gas, followed by a 4-minute heating cycle to desorb from the Tenax trap. A Tekmar Model 1000 capillary interface is used to cryofocus the volatiles before they are introducted onto the capillary column, a Vocol column (Supelco, Inc.; Bellefonte, PA) 60M x 0.75mm with a 1.5um film thickness. The capillary column is maintained at 40 ^{o}C for 5 minutes, then increased at 8°C per minute to 170°C and held at the final temperature for 10 minutes. The instrument used for detection is a Finnigan 1050 GC/MS system operating in the full scan mode scanning from 40u to 200u at 0.5 second per scan. Quantifcation is accomplished by using a group of isotopically labeled internal standards which are added to the sample before it is analyzed.

A typical chromatogram is depicted in Figure 1. Detection limits for most compounds are in the range of 100-500 ppt. Preliminary results suggest that the compounds observed depend on recent individual exposure. Use of home deodorizers, wearing clothing that has been dry cleaned, and use of laboratory solvents results in characteristic compounds being observed in the profile of volatiles in the blood.

Use of trade names is for identification only and does not constitute endorsement by the Public Health Service or the Department of Health and Human Services. This research is supported by funds from the Comprehensive Environmental Response, Compensation and Liability Act trust fund.

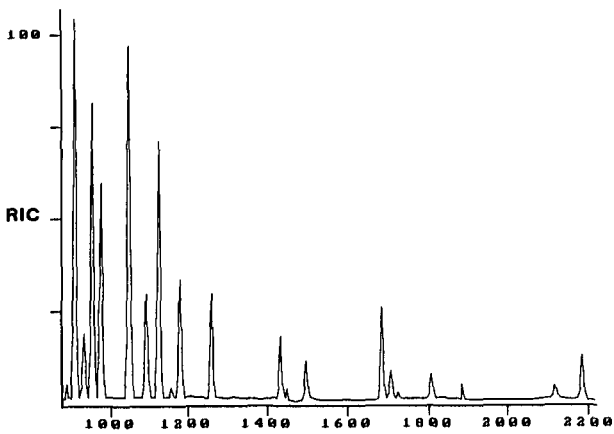

Figure 1. Typical reconstructed ion chromatogram obtained in purging human whole blood. Compounds observed include internal standard mixture spiked at the 3 ppb level.

Presented at the 36th ASMS Conference on Mass Spectrometry and Allied Topics
June 5-10, 1988, San Francisco, CA

DETERMINATION OF MUTAGENIC HETEROCYCLIC AMINES BY ON-COLUMN INJECTION GC/MS,

Lise H. Rovin*[1], Robert T. Rosen[2], Thomas G. Hartman[2], Joseph Ziv[1], and Joseph D. Rosen[1], Food Science Department[1] and Center for Advanced Food Technology[2], Cook College, New Jersey Agricultural Experiment Station, Rutgers University, New Brunswick, New Jersey 08903

The mutagenic activity detected in basic extracts of cooked muscle meats and several model systems involving amino acids, reducing sugars, and water has been attributed to a relatively small number of highly active structurally related heterocyclic amines[1]. The compound 2-amino-3-methylimidazo-[4,5-f]quinoline (IQ) and its analogues 2-amino-3,4-dimethylimidazo[4,5-f]quinoline (MeIQ), 2-amino-3,8-dimethylimidazo[4,5-f]quinoxaline (MeIQx), 2-amino-3,4,8-trimethylimidazo[4,5-f]quinoxaline (4,8-DiMeIQx), and 2-amino-1-methyl-6-phenylimidazo[4,5-b]pyridine (PhIP) have been shown to be potent mutagens which are formed at trace levels (ppb) in some cooked foods via a Maillard reaction. Another analog, 2-amino-3,7,8-trimethylimidazo[4,5-f]quinoxaline (7,8-DiMeIQx) has also been detected in model systems.

The method most frequently used for their determination is HPLC with mass spectrometric single ion detection. The HPLC mass spectral data was difficult to confirm due to lack of significant fragmentation and the presence of high levels of coextracted interfering compounds[2]. In our investigation, on-column injection capillary GC/MS analysis was used to detect and quantify trace levels of IQ formed in a model system and in commercial beef extract. This is the first time GC or GC/MS has been successfully utilized for the determination of these non-derivatized mutagens in beef and model systems. Murray et al[3] successfully used bistrifluoromethylbenzyl derivatives in the electron capture negative ion chemical ionization mode.

With proper cleanup procedures, the reproducibility of this technique is high due to lack of interfering coextracted compounds. By use of mass chromatography, the molecular weights of the mutagens of interest can easily be detected. We have demonstrated that IQ can be detected in model systems as well as in beef extract using GC/MS following efficient extraction and purification procedures. This procedure can be used for analyses of mutagenic and carcinogenic heterocyclic amines in other systems that are of interest and help in assessing the public health risk associated with various methods of cooking meats.

References

1. B.Commoner Science 201 913-916 (1978)
2. C.G. Edmonds, S.K. Sethi, Z.Yamaizumi, H.Kasai, S.Nishimura, and J.A. McCloskey Environmental Health Perspectives 67,35-40 (1986).
3. S.Murray, N.J.Gooderham, A.R.Boobis, and D.S.Davies Carcinogenesis 9,321-325 (1988).

New Jersey Agricultural Experiment Station Publication No.J-10543-2-88. The Center for Advanced Food Technology is an initiative of the New Jersey Commission on Science and Technology.

Presented at the 36th ASMS Conference on Mass Spectrometry and Allied Topics
June 5-10, 1988, San Francisco, CA

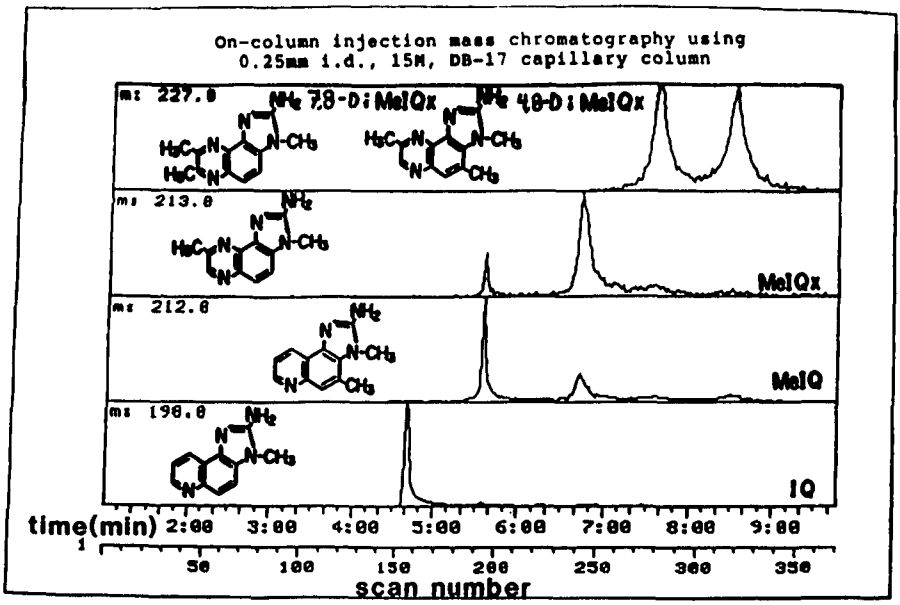

Presented at the 36th ASMS Conference on Mass Spectrometry and Allied Topics
June 5-10, 1988, San Francisco, CA

THE DETERMINATION OF CHLORDIAZEPOXIDE AND ITS MAJOR METABOLITES IN URINE AND POSTMORTEM TISSUES BY CAPILLARY COLUMN GC/MS

Li Yulan Yao Xi Gao Lisheng He Yi Xu Wan

Institute of Forensic Science, Ministry of Public Security,
P. R. CHINA.

Chlordiazepoxide is one of the benzodiazepine hypnotics. Since it is rapidly effective with fewer side effects, it has been used very extensively as hypnotic and anxiolytic agent. However it is potentially toxic. Abuse and misuse may give rise to considerable societal problem.

Chlordiazepoxide is metabolized to biologically active tranquilizer.

This paper describes an analytical method that can be used to identify chlordiazepoxide and its major metabolites, N-desoxydemoxepam and 2-amino-5-chlorobenzophenone, in the decomposed postmortem tissues and urine.

5g postmortem tissues (or 40ml urine) was extracted with 50ml diethyl ether at pH. 9 for three times. The collected organic phase was dried by a anhydrous sodium sulfate and evaporated by K-D evaporator. The residue was dissolved in ethanol (0.2ml). It was purified and separated by using TLC on the silica gel GF with a solvent mixture of cyclohexane-ethyl acetate-isopropyl alcohol (14:2:2) as developer. The eluates from this initial treatment were subjected to futher purification by running them in methanol respectively. They were analyzed by inserting them on the direct probe of mass spectrometer or by GC/MS on the Finnigan Mat 1020 GC/MS in the EI mode. SE-54 column (30m x 0.25mm) was used with column temperature programming from 180°C (for 1 min) at 25°C/min to 270°C (for 20 min).

Organism sample can be easily analyzed using this method for the qualitative identification of chlordiazepoxide and its metabolites. Fig.1 shows a RIC of purification sample from the decomposed postmortem tissues. The mass spectrums of scanning number 343,551 speaks are shown in Fig.2.3. They are 2-amino-5-chlorobenzophenone and N-desoxydemoxepam in accordance with forward library search. They have characteristic peaks which are formed by lossing H and CO from molecular ion and giving the fragment ion at m/e 230

,269 and 202,242 respectively. Under electron impact base peak of N-desoxydemoxepam can be decomposed further by loss of CH≡N group, and then it gives fragment ion at m/e 215.

Chlordiazepoxide is an unstable drug. Under the GC/MS analytical conditions thermolysis has been observed. Since oxygen was lost by heating, deoxychlordiazepoxide was detected(Fig.4). When injection port temperature decreased to 200°C, thermolysis disappeared.

This method has the main merit of overcoming the difficulty in lack of standard sample. It has been successfully used in identification of the chlordiazepoxide and its metabolites from decomposed postmortem tissues and urine. The detection limit is 15ng for chlordiazepoxide.

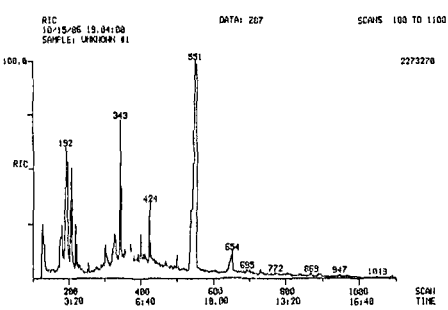

Fig.1. RIC of purification sample from decomposed postmortem tissues

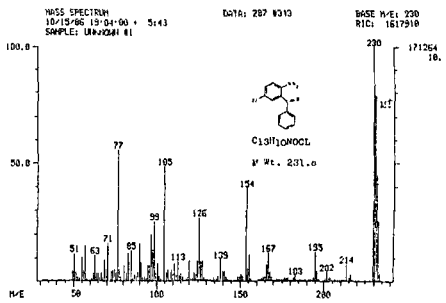

Fig.2. Mass spectrum of 2-amino-5-chlorobenzophenone

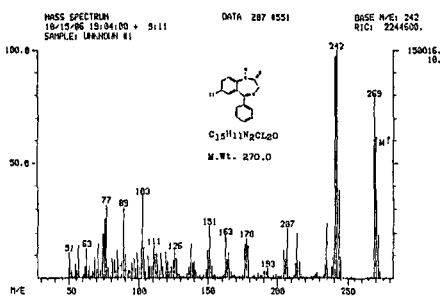

Fig.3. Mass spectrum of N-desoxydemoxepam

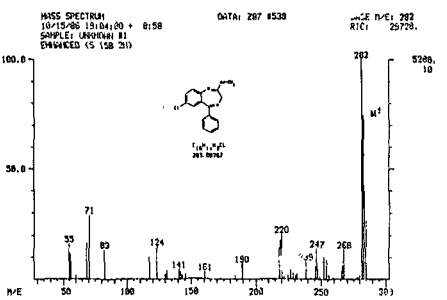

Fig.4. Mass spectrum of deoxychlordiazepoxide

Presented at the 36th ASMS Conference on Mass Spectrometry and Allied Topics
June 5-10, 1988, San Francisco, CA

DETERMINATION OF TRACE VOLATILE N-NITROSOCOMPOUNDS IN FRESH MEAT, FROZEN MEAT AND PUTRID MINCE BY GC AND MATCHING TECHNIQUE

*Yang Yinghua, Ding Jahua, Song Jehuai, Jiang Yunfei,
Shu Lizong, Liu Guixin, Wang Ping, Wu Xia
(Sanitation and Antiepidemic Station of Jilin Province, China)
(*Jilin Import and Export Commodity Inspection Bureau, China)

It has been known that N-nitrosocompound is a kind of strong carcinogens, and it is very important to study its aetiology of carcinogenesis.[1,2] Interational Agency for Research on Cancer (I.A.R.C.) has paid attention to the research since 1969, but there is a few of reports in china.

Because foods to be analysed contain trace of N-nitrosocompounds, high selectivity is required. In 1973, Fine et al.,[3] introduced Thermal Energy Analyser which greatly increased reliability of screening method and became an effective routine technique for analysis of N-nitrosocompounds, but dinitrocompound and something else shall interfere with the determination, so it can not meet the need of the identification. A combined GC/MS technique for the detection of N-nitrosocompounds opens up the wide way. Only retention time of GC,is not enough to determine N-nitrosocompound qualitively and quantitatively, and the results must be confirmed by MS, which was suggested in the conferences of 1973, 1977 IARC.

We studied and compared four kinds of MS methods for the determination of them in 1981:[4] (1) low resolution EI SIM (2) high resolution EI peak matching (3) low resolution CI SIM (4) high resolution peak matching. Results showed that low resolution CI SIM method is also reliable. The method described here is based on above method using to high resolution peak matching technique which can be used to determine N-nitrosocompounds in food.

All experiments were carried out on a JMS-D_{300} Mass spectrometer. Experimental conditions are as follows: glass column, 2M×1.8mm packed with 15% PEG-20M+1% KOH, Chromosorb W, AW DMCS(80-100Mesh); Helium as a carrier gas; Electron impact source (EI); Resolution 7000;ionization voltage 70V; ionization current 300μA; ion source temperature 180°C. When the instrument became stabe, 1μl of N-nitrosodimethylamine (NDMA) standard solution was injected and retention time were determined, then PFK (68.9952) and NDMA base peak (74.0480) was matched, the matching value was 1.07323. The peak height was read out from the oscilloscope at NDMA retention time, in order to avoid error from instrument, a calibration was made using a standard solution. Finally calculate the content of N-nitrosamine in samples according to peak height of

standard and samples from the oscilloscope, the equation is $C_1 = H_1/H_2 \times C_2 \times 1000/N$ where H_1: sample peak height(mm); H_2: standard N-nitrosamine peak height(mm); C_2: standard N-nitrosamine concentration (μg/ml); N: concentration factor; C_1: sample concentration (ng/ml).

table 1: The contents of four volatile N-nitrosamines in fresh meat and over frozen meat

Sample	No	NDMA	NDEA	NDPA	NPYR
fresh meat	1	-	-	-	-
	2	-	-	-	-
	3	-	-	-	-
	4	0.5	-	-	-
	5	-	-	-	-
	6	0.5	-	-	-
	7	0.8	-	-	-
	8	0.6	-	-	-
	9	0.5	-	-	-
	10	-	-	-	-
frozen meat	1	0.8	-	-	-
	2	-	-	-	-
	3	1.4	-	-	-
	4	1.4	-	-	-
	5	0.7	-	-	-
	6	-	-	-	-
	7	1.2	-	-	-
	8	0.8	-	-	-
	9	0.8	-	-	-
	10	-	-	-	-

table 2: The content of NDMA, NDEA, NDPA, NPYR and (TVB-N) formed during putridity of mince

storage time (day)	storage tem. (°C)	NDMA (ppb)	NDEA (ppb)	NDPA (ppb)	NPYR (ppb)	TVB-N (mg/100g)
1	room tem.	0.6	-	-	-	2.410
3	"	0.8	-	-	-	5.455
4	"	0.8	-	-	-	6.330
5	"	7.7	-	-	-	9.745
6	"	8.6	0.6	-	-	15.895
8	"	18.1	0.7	-	-	30.770

NDMA were detected in both fresh meat and over-stored frozen meat, the ratio of detection are 50%, 70% and X are 0.3ppb, 0.7ppb,respectively. The ratio and X in over-stored frozen meat is higher than in fresh meat. This is probably due to nitrosation of over-stored frozen meat. The content of NDMA in pork mince had only a little change within the first 4 days. After 5 days, the amount of NDMA suddenly increased to 7.7ppb (TVB-N 9.7mg/100g) from 0.8ppb (TVB-N 6.3mg/100g), after 8 days, the the amount of NDMA reached 18.1ppb (TVB-N 30.8mg/100g). It was shown the amount of NDMA increased along with the putridity degree of meat.

Reference

1, Freund,H.A.Ann. intern. Med., 10, 1144-1155 (1973)
2, Maggee,P.N.and Barnes,J.M. Ade. Cancer Res.,10, 163-246 (1967)
3, Fine,D.H.and Rufeh,F. IARC Scientific Publication.,40-44 (1974)
4, Yang,Yinghua.et al.,Chinese Society for MS 2nd manual conference(1981)

Presented at the 36th ASMS Conference on Mass Spectrometry and Allied Topics
June 5-10, 1988, San Francisco, CA

QUANTITATION OF TRICHOTHECENE MYCOTOXINS BY MS/MS: A COMPARISON OF ISOTOPICALLY LABELED INTERNAL STANDARDS WITH AN EXTERNAL STANDARD PROCEDURE.

Pawlosky R.J., Wen Y., Abbas H.K., and Mirocha C.J.
The University of Minnesota, Dept. of Plant Pathology
St. Paul, MN 55108

An advantage of tandem mass spectrometry over that of single stage instrumentation is in the analysis of trace substances occurring in complex backgrounds. Trichothecene mycotoxins, are known to be produced by various species of Fusarium inhabiting stored grain. The quantities of the mycotoxins are small compared to the backgrounds in which they are found thus are suitable candidates for trace analysis by MS/MS. Sampling biological fluids of humans or animals for trichothecenes T-2 or the metabolite HT-2 establishes the link in alledged mycotoxicoses.

Multiple Reaction Monitoring (MRM) relies on the collision activated decomposition (CAD) processes of tandem MS/MS. Thus specific sets of reactions are followed by the selection of parent ions with MS I and sequential jumping of daughter ions by MS II. In the analysis of T-2 and HT-2 toxin and their deuterated counterparts three specific reactions were monitored with MRM (figure 1). These reactions produced a high degree of specificity and sensitivity owing to the efficient conversion of the parent ions to the various daughters.

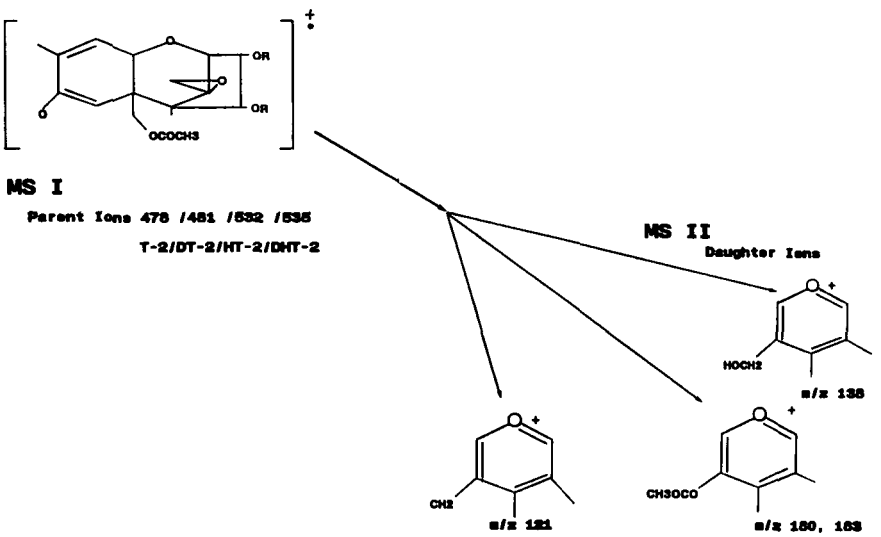

figure 1.

The results of the T-2 and HT-2 analyses are presented in figure 2. The four graphs represent quantitation of the mycotoxins with an external standard procedure as well as using a deuterated internal standard. Blood was amended with the toxins at levels of 20, 10 and 1 ppb and triplicate injections were made of each sample. When using the external standard for quantitation the results were consistantly lower than those obtained using the ISTD. The scatter for both sets of experiments based on standard deviation and coefficient of variance were about the same suggesting reproducibilty of sample handling in the entire series of experiments. Deuterated internal standards are the best choice in the analytical procedure because they provide a means of quantitation based on the dynamic state of the CAD process and duplicate the reactions of the analytes.

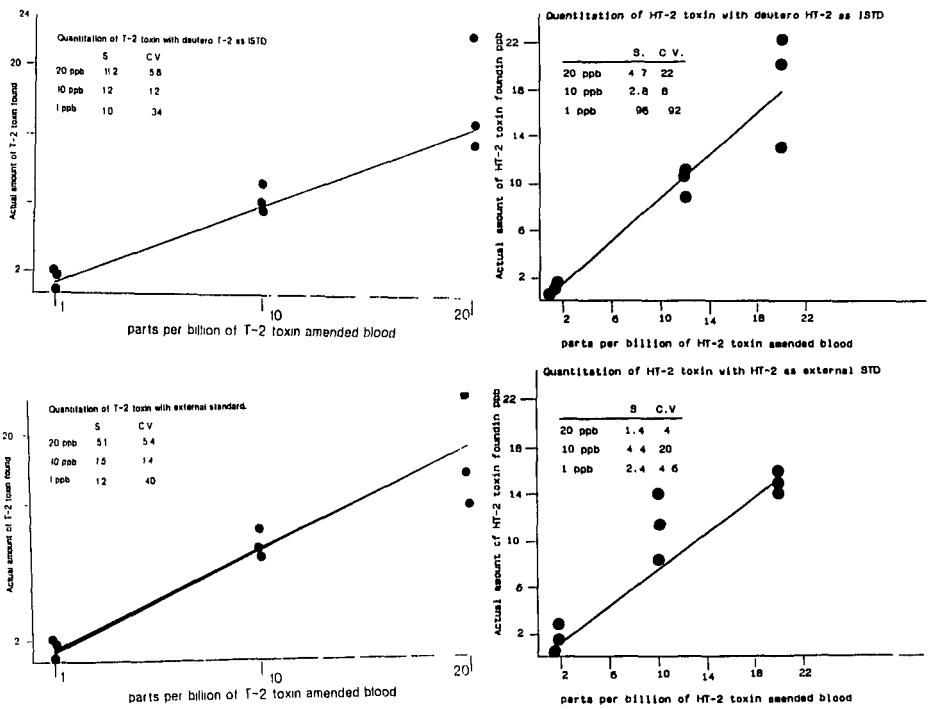

figure 2.

Presented at the 36th ASMS Conference on Mass Spectrometry and Allied Topics
June 5-10, 1988, San Francisco, CA

METABOLISM OF 3,4-METHYLENEDIOXYMETHAMPHETAMINE (MDMA) IN THE RAT: IDENTIFICATION OF METABOLITES WITH AN ION TRAP DETECTOR.

H.K. Lim and R.L.Foltz; Center for Human Toxicology, University of Utah, Salt Lake City, Utah 84112

MDMA has recently been shown to cause selective degeneration of serotonergic neurons in the brains of rats and monkeys, as indicated by the alteration of neurochemical and histological parameters (1). In an effort to understand the mechanism of MDMA-induced neurotoxicity, we have investigated the metabolism of MDMA in the rat, using mass spectrometry with ion trap detection to identify metabolites in vivo and in vitro.

The methanol positive ion chemical ionization (PCI) total ion current chromatogram of TFA-derivatized urine from dosed rats contained eight peaks that were absent in control urine (Fig. 1). Only peaks A, C, D, and E were present in sufficient quantity to permit the acquisition of EI mass spectra, although PCI mass spectra were obtained for all eight peaks. The major metabolite in rat urine, peak C, was identified as 4-hydroxy-3-methoxymethamphetamine from its EI (Fig. 2) and PCI mass spectra (Fig. 3). The identities of all the chromatographic peaks are shown in Table 1. MDMA, MDA, and the 3-O-methyl phenolic amine metabolites were consistently detected in all the specimens examined. The EI mass spectrum of a new metabolite produced in liver and brain tissues in vitro (Fig 4) identified it as 3,4-dihydroxymethamphetamine Other metabolites present in the 10,000 x g liver incubate included 4-hydroxy-3-methoxymethamphetamine, MDA, and 3,4 methylenedioxyphenylacetone ; the major liver metabolite was MDA. In the 10,000 x g brain incubate, the major metabolite was the 3,4-dihydroxymethamphetamine, but MDA, 4-hydroxy-3-methoxymethamphetamine and 4-hydroxy-3-methoxyamphetamine were also found. The structures tentatively assigned to MDMA metabolites were confirmed by comparison of their EI and PCI mass spectra and relative retention times with those of synthetic reference compounds.

The biotransformation pathways for MDMA that we have identified in the rat include O-dealkylation, N-demethylation, deamination, O-methylation, and O-conjugation (Fig. 5). The demonstration that the brain can biotransform MDMA , the neurotoxic MDA being one of the metabolites, provides presumptive evidence for the involvement of metabolites in MDMA-induced neurotoxicity.

References

1. D.M. Barnes, Science 239, 864 (1988).

Fig. 1. Distribution of MDMA and its metabolites

Compounds	Relative Retention Time	PCI MH+ m/z (%)	Urine	Feces	Blood	Liver	Brain
3,4-Methylenedioxymethamphetamine (A)	0.947	290 (10)	+	+	+	+	+
3-Hydroxy-4-methoxymethamphetamine (B)	0.933	388 (100)	+			+	
4-Hydroxy-3-methoxymethamphetamine (C)	0.918	388 (100)	++	+	+	++	+
4-Hydroxy-3-methoxyamphetamine (D)	0.825	374 (100)	+	+	+	+	+
3,4-Methylenedioxyamphetamine (E)	0.813	276 (76)	+	++	++	+	++
4-Hydroxy-3-methoxyphenylacetone (F)	0.629	277 (100)	+		+	+	
3,4-Methylenedioxyphenylacetone (G)	0.602	179 (100)	+		+	+	+
3,4-Dihydroxyphenylacetone (H)	0.552	359 (100)	+				
3,4-Dihydroxymethamphetamine (I)	0.824	470 (100)					+

+ = identified; ++ = major metabolite.

Presented at the 36th ASMS Conference on Mass Spectrometry and Allied Topics
June 5-10, 1988, San Francisco, CA

FIGURE 1. TOTAL ION CHROMATOGRAM OF TFA DERIVATIVE OF URINARY METABOLITES OF A RAT DOSED WITH 5 mg/kg MDMA.

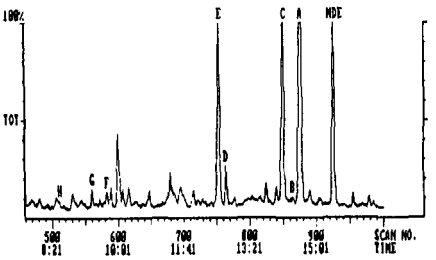

FIGURE 2. EI MASS SPECTRUM OF TFA DERIVATIVE OF COMPOUND C.

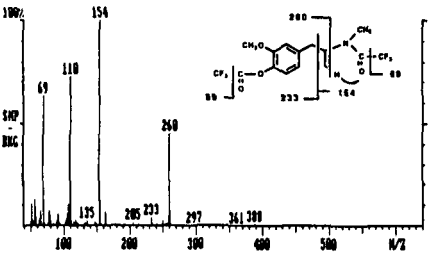

FIGURE 3. PCI MASS SPECTRUM OF TFA DERIVATIVE OF COMPOUND C.

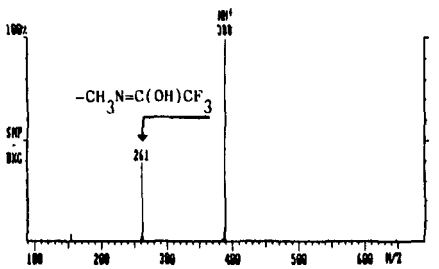

FIGURE 4. EI MASS SPECTRUM OF TFA DERIVATIVE OF COMPOUND I.

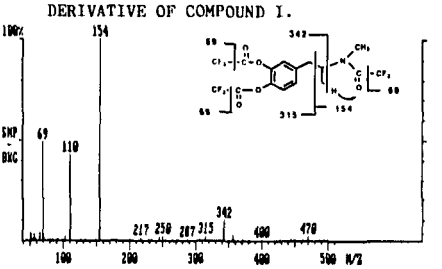

FIGURE 5. BIOTRANSFORMATION PATHWAYS ESTABLISHED FOR MDMA IN RAT.

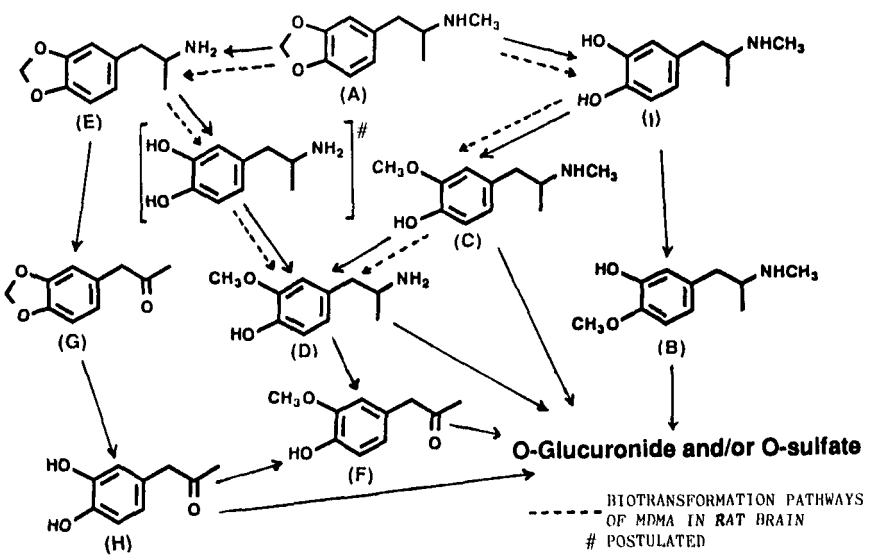

Presented at the 36th ASMS Conference on Mass Spectrometry and Allied Topics
June 5-10, 1988, San Francisco, CA

IDENTIFICATION OF THE METABOLITES OF 4'-METHYLTHIOPROPRANOLOL IN THE DOG BY GC/MS AND HPLC/MS

Carol A. Haney GC/MS Lab N.C. State University, Raleigh, NC and
Stephen A. Bai, College of Veterinary Medicine, N.C. State University
Robert D. Voyksner, Research Triangle Institute, RTP,NC
Thomas Walle, Michael Wilson, U.Kristina Walle, David Easterling and
Norton P. Peet, Department of Cell and Molecular Pharmacology and
and Experimental Theraputics, Medical University of South Carolina,
Charleston, SC.

Structural modifications of a drug molecule can result in important alterations of its metabolism, especially if the modification is at a metabolically important site. Propranolol, the most commonly used beta receptor block, is extensively metabolized in dog and man (1,2). Its metabolism follows three major pathways: ring oxidation, predominently at the 4'-position, N-dealkylation, and glucuronic acid conjugation. Of these pathways, ring oxidation is quantitatively the most important. This study evaluated the effects a methylthio substitution has on the metabolism of this drug when placed in the metabolically active 4' position of propranolol. Liquid scintillation spectrometry allowed for quantitation and mass spectrometry was used for the identification of Phase I and Phase II metabolites.

4'-Methylthiopropranolol (MTP), 10 mg/kg, was given together with 14C-MTP orally to dogs. The 0-48 hr urine, which contained 50% of the total dose, was extracted with ethyl acetate first at pH 9.8 to yield basic, possible phenolic and neutral metabolites, then at pH 2 for acidic metabolites. Based on the total radioactivity in urine, the basic and acidic fractions contained 48.6 $\pm$ 2.8% and 21.6 $\pm$ 3.7%, respectively (mean $\pm$ S.D.;N=3). The pH 9.8 and pH 2 extracts were each separated into their respective components by HPLC/UV. Structure identification of these metabolites was accomplished by GC/MS (positive CI) after derivativization with N,O-bis(trimethylsilyl)trifluoroacetamide with 1% trimethlychlorosilane in pyridine (basic metabolites) and N,O-bis(trimethylsilyl)trifluoroacetamide with 1% trimethylchlorosilane in pyridine following methylation with diazomethane (acidic metabolites). The third fraction, containing non-extractable metabolites, was analyzed directly by HPLC/MS.

The base extractable metabolites were identified as MTP, MTP-glycol, deisopropyl-MTP, and the sulfoxide (-SO) and sulfone ($-SO_2$) metabolites of these metabolites (Table 1). Identification of these metabolites was confirmed by GC/MS of synthetic standards. In the acidic fraction, over 75% of the radioactivity was related to the naphthoxylactic acid metabolites of MTP, and its sulfoxide and sulfone metabolites (Table 1). Three additional acid metabolites, representing less than three percent of the total urine radioactivity, were not identified.

Using DEAE-Sephadex anion-exchange and reverse-phase HPLC/UV chromatography, the major metabolites contained in the nonextractable fraction (30.0 $\pm$ 6.5% of the total urine radioactivity) were separated and purified. These metabolites were identified by HPLC/MS and enzymatic hydrolysis (β-glucuronidase) as consisting of the glucuronic acid conjugates of MTP, MTP-SO, MTP-SO_2, and MTP-glycol-SO_2. The results of this study showed that methylthio substitution at the 4'-position dramatically alters its metabolic profile, shifting the primary route of metabolism from ring oxidation to that of sulfur oxidation.

Presented at the 36th ASMS Conference on Mass Spectrometry and Allied Topics
June 5-10, 1988, San Francisco, CA

[1]Barger E.M.; Walle U.K.; Bai S.A.; and Walle T Drug Metab. Disp. 11 p266-272 1983.

[2]Walle T.; Wilson M.J.; Walle U.K.; Bai S.A. Drug Metab. Disp. 11 p544-549 1983.

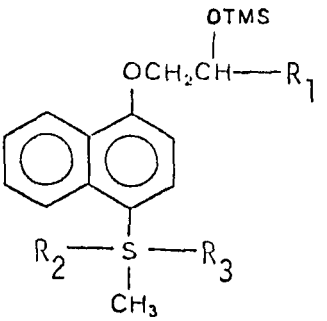

Base Extractable Metabolites

Name	MW	R_1	R_2	R_3
MTP-Sulfoxide[1]	393	$-CH_2NHCH(CH_3)_2$	..	-O
MTP-sulfone[1]	409	$-CH_2NHCH(CH_3)_2$	=O	=O
1° Amine[1]	407	$-CH_2N(TMS)_2$	..	..
1° Amine-Sulfoxide[1]	423	$-CH_2N(TMS)_2$	..	-O
1° Amine-sulfone[1]	439	$-CH_2N(TMS)_2$	=O	=O
MTP-glycol[1]	408	$-CH_2OTMS$	..	..

Acid Extractable Metabolites

Name	MW	R_1	R_2	R_3
MTP-lactic acid[2]	364	$-COOCH_3$	..	..
Acid-sulfoxide[2]	380	$-COOCH_3$	..	-O
Acid-sulfone[2]	396	$-COOCH_3$	-O	=O

[1]TMS derivative

[2]methylester/TMS derivatives

Presented at the 36th ASMS Conference on Mass Spectrometry and Allied Topics
June 5-10, 1988, San Francisco, CA

STRUCTURE ELUCIDATION OF A SERIES OF ACETOGENINS BY MASS SPECTROMETRY

David L. Smith, Ya-mei Liu, Yu-hua Hui, J. Kent Rupprecht, Ahmad Alkofahi, Ching-jer Chang, and Jerry L. Mclaughlin
Department of Medicinal Chemistry and Pharmacognosy
Purdue University, W. Lafayette IN 47907

Tetrahydrofuranoid acetogenins are a new class of higher plant compounds that are characteristic of the plant family Annonaceae. Because these long-chain polyketide derivatives are showing a number of promising biological activities, there is considerable interest in isolating and characterizing acetogenins. Although proton and carbon magnetic resonance spectroscopy has been used to identify the presence of selected functional groups, mass spectrometry has been used to determine the connectivities of these functional groups. This is because the functional groups are joined by saturated hydrocarbon chains which are indistinguishable by NMR, and because the amount of material is often limited.

Although the methane and isobutane CI mass spectra of acetogenins usually have prominent MH^+ ions from which the molecular weights can be determined, the EI spectra have few high mass ions, and are of limited use for structure elucidation. In addition, the relative abundances of many peaks in the EI spectra are not highly reproducible, and often depend on the sample size and rate of heating. Since a probe temperature of approximately 300 °C is required for vaporization, thermal degradation, including intramolecular rearrangement, is likely. The EI spectrum of the trimethylsilyl (TMS) derivative has a good balance of low and high mass peaks from which major features of the structure can be determined.

The usefulness of the EI spectra of the TMS derivative is illustrated below for a new acetogenin, gigantecin, which was isolated from the stem bark of Goniothalamus giganteus. It is important to note that this investigation has made extensive use of the biological activity of crude and fractionated extracts to lead us to the pure bioligically active components, such as gigantecin. The scheme summarizing the proposed fragmentation of this derivative is given in Figure 1. The mass shift for the deuterated derivative is used with exact mass information to determine the elemental compositons of the fragments. The mass shifts found upon hydrogenating the double bond in the γ lactone, 0 or 2, differentiate ions which contain the γ lactone. The molecular ion (926), as well as fragments corresponding to the loss of CH_3 (911) and TMSOH (836), confirm that the gigantecin has a molecular weight of 638.

The elemental composition of all fragments indicated in Figure 1 have been determined from their exact masses. Fragment ions with TMS groups frequently undergo loss of TMSOH, forming new ions which undergo further fragmentation. This has been verified from the daughter ion spectra (E/B linked scans) of

several structurally diagnostic fragments, as indicated by the arrows in Figure 1. For example, the daughter ion spectrum of the fragment at m/z 573 shows two consecutive losses of TMSOH to give the ion at m/z 393, as well as further losses to give ions at m/z 367, 297, and 271. The structures of the ions at m/z 585 and 655 were also confirmed from their daughter ion spectra.

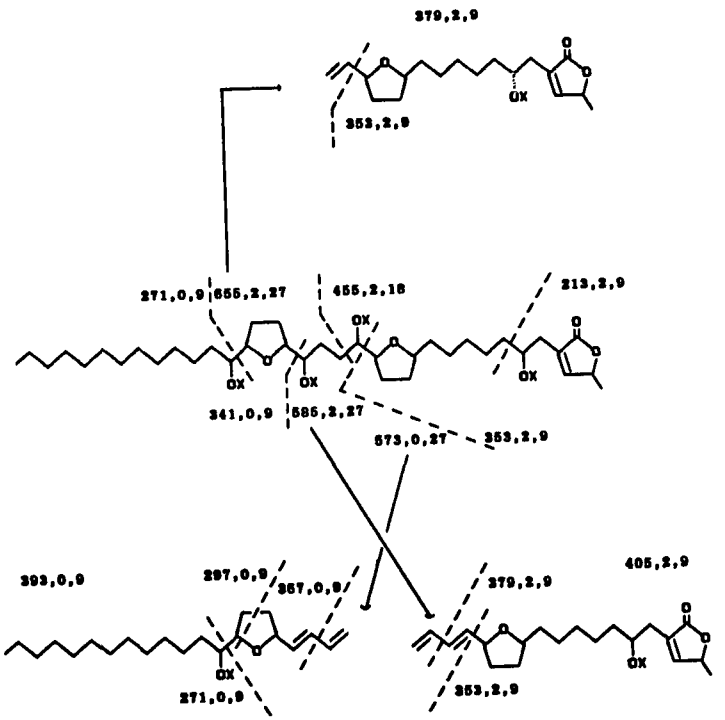

Figure 1 The fragmentation scheme of the TMS derivative of gigantecin. The mass shifts for the hydrogenated and TMS d_9 derivatives are also given.

Presented at the 36th ASMS Conference on Mass Spectrometry and Allied Topics
June 5-10, 1988, San Francisco, CA

DIRECT DETERMINATION OF TNT METABOLITES IN ANIMAL AND HUMAN BODY FLUIDS BY MS/MS

Li Zhong-Min, and Deng Lin
Beijing Institute of Technology
Beijing, P.R. China

A rapid method for characterizing TNT metabolites in human body fluids is needed in research on occupational disease such as hepatitis and cataract caused by TNT dust and vapor. We have studied, by the MS/MS technique, numerous samples such as rabbit urine, rat serum, urine of several workers who are working in TNT related factories, and some urine samples of patients who are in the hospital. A series of CI mass spectra and daughter ion spectra for real samples have been obtained and identified by comparison to authentic compounds. All data were obtained on a Finnigan MAT TSQ 45B triple stage quadruple tandem mass spectrometer with a direct inlet probe.

The results show that 2,4-diamino-6-nitrotoluene (2,4-DA), 2,6-diamino-4-nitrotoluene (2,6-DA), 4-amino-2,6-dinitrotoluene (4-A), and 2-amino-4,6-dinitrotoluene (2-A) are present in rabbit urine. The 2,4-DA, 2,6-DA, 4-A, 2-A, and parent TNT are present in rat serum. The 2-A, 4-A, 2,2', 6,6'-tetranitro-4,4'-azotoluene (4,4'-AZ), 2,4-DA, 2,6-DA, and 4-hydroxyamino-2,6-dinitrotoluene (4-HA) are present in the urine of workers. And 4-A, 2-A, 2,4-DA, 2,6-DA, and original 2,4,6-TNT have been identified in patient urine.

The secondary reduction metabolite of TNT is 4-HA which can not be treated by acidification because of the tendency to form 4,4'-AZ. It also can not be analyzed by GC because of the thermal instability. Fortunately, it can be analyzed very well by MS/MS methodology.

Figure 1a shows the positive ion chemical ionization CAD MS/MS spectrum obtained for the MH^+ from authentic compound 4-HA. Figures 1b, 1c, 1d show the CAD MS/MS spectra of parent ion M/Z 214 from the urine samples of worker B, C, and D who are working in TNT related factories.

The results indicate that the 4-HA is present in the urine of the three workers. And the CAD spectra show that M/Z 197 and M/Z 196 results from loss of $OH^{\cdot}$ and H_2O causing by ortho-effect. The M/Z 168 and 167 are formed by loss of NO_2 and NO_2H from the parent ion M/Z 214. The fragments M/Z 121, 122 are formed from loss of NO_2 and NO_2H and two molecular NO_2 respectively.

The results also show that 4,4'-AZ and parent TNT are present in the urine of the workers. The fragments can be observed in Figure 2 and 3.

The conclusion is that the TSQ MS/MS technique is a rapid, specific, and sensitive method for characterizing TNT metabolites in human body fluids. The urine samples were presented by professor Xian Yin-Lin and Mr. Yao Ming.

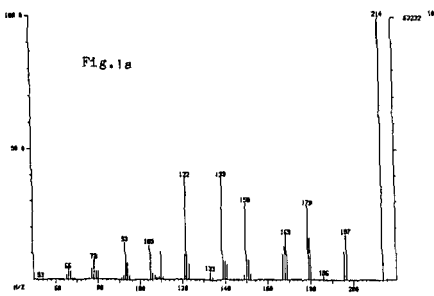

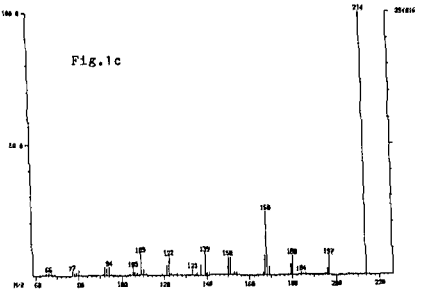

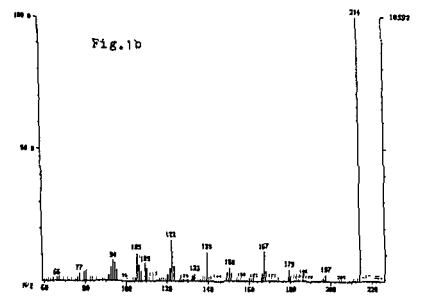

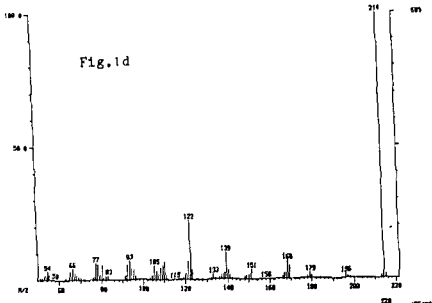

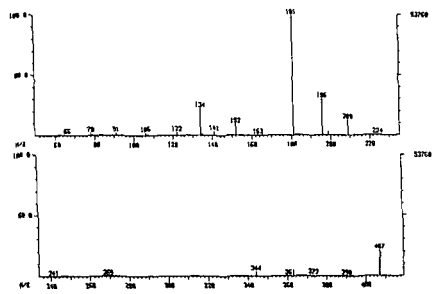

Fig.2a) +/CI/MS/MS of 4,4'-AZ

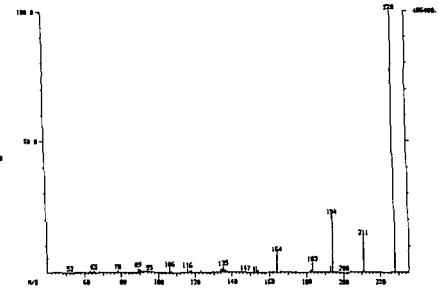

Fig.3a) +/CI/MS/MS of 2,4,6-TNT

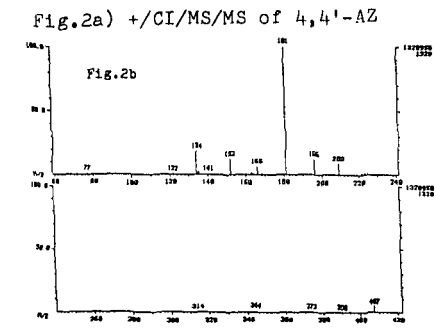

Fig.2b) +/CI/MS/MS of m/z407
from urine of worker B

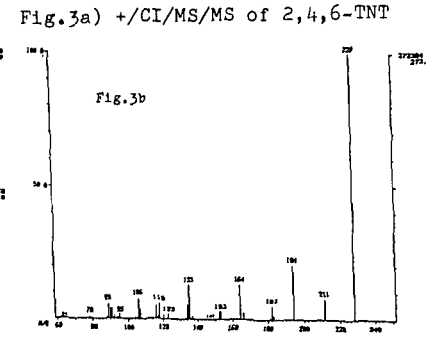

Fig.3b) +/CI/MS/MS of m/z 228
from urine of worker B

Presented at the 36th ASMS Conference on Mass Spectrometry and Allied Topics
June 5-10, 1988, San Francisco, CA

COMPUTERIZED INTERPRETATION OF THE MASS SPECTRA OF ACYCLIC ORGANIC COMPOUNDS

M.J. Bertrand and D. Zidarov
Regional Center for Mass Spectrometry, Department of Chemistry
University of Montreal, P.O. Box 6128, Station A,
Montreal, Quebec, Canada H3C 3J7

The application of computer science to the problem of molecular structure elucidation is an active area of research and new approaches are continuously proposed in the literature. Presently, the computer assisted identification of organic compounds is achieved by i) spectral comparison using a library of reference spectra, ii) use of an expert system including information from one or several analytical techniques or iii) using a combination of the above approaches. This work describes an algorithm that has been developed in order to study the feasibility of synthetizing and ranking the most probable structures of acyclic organic compounds corresponding to experimental mass spectral data.

The approach that is presented essentially involves the construction of a close system of rules and chemical constraints and is based on the hypotheses that i) all or almost all simple cleavages occur in the fragmentation of the molecule, ii) there is at least one sequence of fragment ions that corresponds to one or several acyclic structures for which the sum of the ion intensities in the mass spectrum ΣI is maximized and iii) to each candidate structure can be assigned a probability of coincidence that is not strictly proportional to ΣI. The algorithm using mass spectral data such as exact mass, isotopic peak ratios (if available) and a list of mass-intensity obtained from the high energy collision activated spectrum produces a list of the most probable acyclic structures that correspond to the data.

The generation of the most probable structures from the experimental data proceeds in four steps that are the i) generation of empirical formulae, ii) decomposition of the empirical formulae in sets of superatoms, iii) synthesis of chemical structures from the superatoms and iv) the scoring and ranking of the most probable structures. The generation of empirical formulae is done using the exact mass and isotopic peak ratios (if available) and the empirical formulae obtained are in agreement with the nitrogen rule, an integer number of insaturated sites, and several other chemical composition constraints. The empirical formulae that are retained are then decomposed into sets of saturated and unsaturated superatoms using a base of 74 functional groups that are linearly independant. This process is done by solving equation [1] in which X_i and Y_j refer to the frequency of occurence of the unsaturated and saturated superatoms i and j.

$$C_xH_yO_zN_t \equiv \Sigma X_iS_i + \Sigma Y_iS_j \qquad [1]$$

The sets of superatoms that have been obtained in the proceeding step are used to construct acyclic structures using the molecular topology of pseudo-alkanes where the nodes represent superatoms. At each stage of the construction of the structures, which is done using a backtrack algorithm, predictable ions from the substructures are matched with ions present in the spectrum. Substructures with bad correlations are terminated and the others are scored. The 20 highest scores are retained and ranked in order of probability by considering ion intensities and the presence of consecutive predicted fragments in the spectrum.

The basic functionning of the algorithm can be understood by considering the example shown in figure 1. In the example, the collison activated spectrum of decyaldehyde $CH_3(CH_2)_8CHO$ and the exact measured

mass were given to the program as input. The algorithm found one empirical formula $C_{10}H_{20}O$ which was consistant with the constraints given. In the second step, it is seen that this formula can be decomposed in 72 sets of superatoms of which only a few are shown (the number in parantheses are the frequencies of appearance of each superatom). Then, using the sets of superatoms, the algorithm generates 250 structures that fit the data and on the figure the structures with the five highest scores are shown. The actual structure of decyaldehyde is ranked as first candidate indicating the potential of the approach.

In view of these encouraging results, several refinements are being added to the program with the aim that it will be useful in the interpretation of MS/MS spectra with or without the use of a search data base.

-PROGRAM INPUT

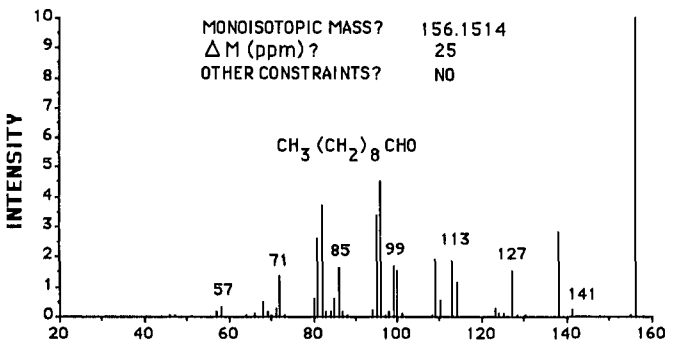

-PROGRAM OUTPUT

NUMBER OF EMPIRICAL FORMULAE FOUND = 1

C	H	N	O	EXACT MASS	ΔM	UNSAT. SITES
10	20	0	1	156.15141	.09	1

NUMBER OF LINEAR COMBINATIONS = 72
PARTIAL LIST OF COMBINATIONS

>C=C< (1)	-CH3 (3)	-OH (1)	-CH2- (5)	
-CH=C< (1)	-CH3 (3)	-CH2- (5)	-O- (1)	
O=C< (1)	-CH3 (3)	-CH2- (5)	-CH< (1)	
-CH=CH- (1)	-CH3 (1)	-OH (1)	-CH2- (7)	
O=CH- (1)	-CH3 (1)	-CH2- (8)		
CH2=CH- (1)	-OH (1)	-CH2- (8)		
-CH=C< (1)	-CH3 (6)	-O- (1)	-CH< (1)	>C< (1)

PROBABLE STRUCTURES GENERATED (250)	SCORE
CH3-CH2-CH2-CH2-CH2-CH2-CH2-CH2-CH2-CHO	1222
CH3-CH2-CH2-CH2-CH2-CH(CH3)-CH2-CH2-CHO	1142
CH3-CH2-CH2-CH2-O-CH=CH-CH2-CH2-CH2-CH3	1083
CH3-CH2-CH2-CH2-CH2-CH2-CH2-CH2-CO-CH3	1072
CH3-CH(CH3)-CH2-CH2-CH2-CH2-CH2-CH2-CHO	1072

Figure 1: Program input and output for the analysis of decaldehyde

Presented at the 36th ASMS Conference on Mass Spectrometry and Allied Topics
June 5-10, 1988, San Francisco, CA

SPECTRAL EXAMINATION TOOLS: IDENTIFICATION OF LOW MASS ION SERIES AND STABLE NEUTRAL LOSSES USING ACCURATE MASS INFORMATION

R. B. Cody
Nicolet Analytical Instruments
5225 Verona Rd., Madison, WI 53711

When interpreting electron ionization mass spectra, mass spectrometrists use various kinds of information. Low mass ion series are a valuable indicator of general compound classes or functional groups. High mass fragments resulting from stable neutral losses provide information about specific structural features.

Identification of such characteristic ions can be automated. For example, low resolution information about ion series and neutral losses are used by McLafferty's STIRS program [1] in comparing an unknown spectrum with library spectra to identify substructures present in the compound.

Through high resolution measurements the reliability of an interpretation algorithm can be greatly improved. We report here the use of two computer programs based upon accurate mass information: one program identifies functional groups based upon low mass ion series, and the other identifies neutral loss fragments and relates them to specific substructures. These "spectral examination tools" are not intended as a comprehensive methodology for interpreting spectra, but are useful aids for identifying features of the mass spectrum and can supplement other interpretive methods.

The basis for these programs is found in the appendices to McLafferty's "Interpretation of Mass Spectra"[2]. We extended the information to include accurate mass information, additional ion series, and constraints on the number of peaks that must be identified for a given series. The programs were tested on electron ionization spectra of pure compounds, a synthetic mixture, and a complex hydrocarbon oil.

The low mass series program searches the spectrum for alkyl series (peaks differing by methylene groups), peak lists (peaks that do not differ by a fixed mass), or user-defined series. To be recognized, ions in the series must meet criteria for accurate mass measurements, minimum number of peaks that constitute a given series, and consecutiveness (e.g. two nonconsecutive peaks are not recognized as a series).

Low mass series analysis of 18 pure compounds showed characteristic functional groups for each compound. Analysis using accurate masses was found to be much more reliable than analysis using nominal mass data. Analysis of a synthetic eight component mixture showed at least one characteristic functional groups for each component. A hydrocarbon oil was found to contain alkanes, alkenes, cyclic hydrocarbons, and also terpenes and alkylbenzenes. The presence of the latter was not reported by the manufacturer, but was confirmed by FTIR analysis. Ion series analysis was also performed on a laser desorption spectrum of a hydrocarbon wax, with electron postionization of desorbed neutrals. Molecular weight distributions were determined from molecular ions of alkenes and dienes.

Neutral loss analysis was found to complement series analysis for all compounds where a molecular wight was known or suspected. However, interpretation of these results requires more skill on the part of the operator, and is slightly less reliable than series analysis, since identifications were based on individual peaks, rather than groups of peaks.

Presented at the 36th ASMS Conference on Mass Spectrometry and Allied Topics
June 5-10, 1988, San Francisco, CA

Partial Output of Low Mass Series Analysis
of A Synthetic Eight Component Mixture

Series Formula: Cn H2n-5
Compound class:
Terpenes and derivatives (rearrangement; other m/z also common)

Meas. Peak:	Series Peak:	Rel. Height:	Dev. (ppm)	
79.054175	79.054226	2.0596293	.64539973	
93.070287	93.069876	2.1008371	-4.4138364	Limonene
107.08558	107.08553	.64101096	-.47422989	
121.10218	121.10118	.39986875	-8.2904284	

Series Formula: Cn H2n Br
Compound class:
Bromoalkyl; m/z 135 largest for R(CH2)5Br

Meas. Peak:	Series Peak:	Rel. Height:	Dev. (ppm)	
92.933378	92.933437	.36858131	.64136920	
106.94888	106.94909	.52654472	1.9082566	Bromohexane
134.98031	134.98039	5.2517113	.59348357	

Hard Wax

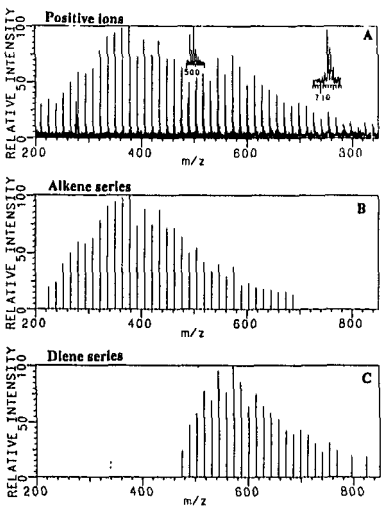

References:

(1) McLafferty, F. W.; Atwater, B. L.; Haraki, K. S.; Hosakawa, K.; Mun, I. K.; Venkataraghavan, R. ; Adv. Mass. Spectrom. 1980b, 8, 1564.

(2) McLafferty, F. W. "Interpretation of Mass Spectra", 3rd edition, University Science Books (Mill Valley, CA) 1980.

Presented at the 36th ASMS Conference on Mass Spectrometry and Allied Topics
June 5-10, 1988, San Francisco, CA

STRUCTURE ELUCIDATION USING SUBSTRUCTURE IDENTIFICATION RULES ON MS/MS DATA

K.J. Hart, P.T. Palmer and C.G. Enke
Department of Chemistry, Michigan State University
East Lansing, Michigan 48824

The development of ACES (Automated Chemical structure Elucidation System) represents the first attempt to fully exploit the huge data space available from MS/MS instrumentation (i.e. triple quadrupole mass spectrometer). Substructure information is obtained by a pattern recognition/ artificial intelligence program called MAPS (Method for Analyzing Patterns in Spectra). The program has two functions. The first function is to generate substructure interpretation rules and the second function is to apply the rules obtained to MS/MS data of an unknown compound. This software was recently modified to produce two types of rules which can be used to predict the presence and absence of substructures in an unknown. The rules are referred to as inclusion (presence) and exclusion (absence) rules.

Both types of substructure identification rules were generated with and without intensity data. There has been some debate as to the reliability of intensity data in daughter spectra due to instrumental variations. Additionally, the environment of a substructure plays a role in the relative intensity of the corresponding fragment ions (i.e. the influence of a heteroatom). Since the MAPS rules are generated from a training set containing substructures in a variety of environments, it was decided to classify the intensity of an ion as strong, medium or weak. This type of classification is often referred to as a "fuzzy set".

The recall and reliability of the MAPS rules was evaluated by applying each rule to the MS/MS data of each training set compound. It was found that the intensity data improved MAPS inclusion rule performance while exclusion rules performed better without intensity data. The exclusion rules performed better without intensity information because it is the absence of highly diagnostic features which are characteristic of the absence of a particular substructure. The uniqueness of the features found in the inclusion rules with an associated intensity were higher than those without an associated intensity leading to better performance.

Sixteen compounds not found in the training set were analyzed using the MAPS inclusion rules. No false positives (incorrect inclusions) occurred in eight of the sixteen compounds. Of the false positives in the other eight compounds, six involved the benzyl and/or the phenol substructure. One reason for these false positives may be the composition of the training set which contains alarge numer of phenols and few benzyl containig compounds. Also, the rule generation process remains under development. Current work is aimed at determining the most reliable combinations of features found in a rule in an

attempt to reduce false positives. The exclusion rules were applied to data for the same compounds. No false positives (incorrect inclusions) were observed using these rules. Exclusion rule results can be used to eliminate specified substructures from consideration before or after structure generation.

Recently, ACES has been modified to include automated structure generation and substructure searching of training set structures. GENOA, a structure generation program originally developed at Stanford University has been updated to include a file interface with MAPS and a molecular formula generation program (MFG). The MAPS and MFG software provide the information (i.e. substructural constraints and molecular formula(e)) required by GENOA. The updated GENOA software runs a structure generation session for each molecular formula found to be consistent with MS/MS data of an unknown. The resulting candidate structures are stored in files with a specified analysis reference name.

The results are then summarized with the use of a structure checking program (STRCHK) included with GENOA. The STRCHK program has been modified to sum the substructure search results for more than one molecular formula. The STRCHK program was also modified to perform automated substructure searching of a library of training set structures. The substructures found in the training set structures are passed to the MAPS software for use in developing spectral feature / substructure correlations. These correlations eventually become the MAPS rules.

The tabulated results from STRCHK will be used by a program under development that will correlate the substructures in the results file with MAPS rules taken under different experimental conditions (i.e. chemical ionization and multiple collision CAD). If a rule exists that will confirm or eliminate the presence of a substructure, the system will recommend to the user that the experiment be run. These experiments are referred to as ancillary experiments. Reduction of the number of possible molecular formulae is another area where the system could recommend an ancillary experiment. Measurement of isotopic ratios in the daughter spectrum of the M+1 ion has been shown value in characterizing the elemental composition of 13C containing compounds. Soft ionization of the compound of interest is often required to obtain a reasonably intense M+1 ion.

The development of the ACES software will continue with the addition of a greater variety of training set compounds. The software itself will be updated to optimize the reliability and recall of the rules generated by MAPS and to provide suggestions for ancillary experiments.

Presented at the 36th ASMS Conference on Mass Spectrometry and Allied Topics
June 5-10, 1988, San Francisco, CA

Improved selectivity in selected ion monitoring by using multiple magnet positions.

Coles, A, Moncur, J and Moore, C.
Kratos Analytical, Barton Dock Road, Urmston, Manchester M31 2LD,

PCDDs and PCDFs unfortunately tend to occur in complex matrices containing many other chlorinated species, therefore SIM at a resolving power of 10,000 (10% valley definition) or greater is generally recommended in the analysis of these compounds[1].

In order to ensure that the correct mass is accurately centred onto the collector, the magnetic field is kept static and the ESA voltage (E) and accelerating voltage (V) are altered so as to focus the desired m/z value ion beam through the analyser. For all polychlorinated dioxins and furans to be monitored E and V must be reduced by at least the fraction of the two extreme masses, in this case m/z 303.90162 from TCDF and m/z 471.77501 from the internal standard ^{13}C-OCDD. As a reduction in V results in a corresponding reduction in sensitivity, the relative intensities of the higher mass ions (for example from HeCDD and HeCDF) will be significantly lower than those for the low mass ions. This is illustrated in Figure 1 which shows the total (summed) response obtained from the analysis of a fly-ash sample[2]. This drop in sensitivity is reduced if the ions to be monitored are divided into groups, and the magnetic field strength optimised at the start of each group.

The individual ions within each group are still monitored by V and E adjustment (the most accurate method) but now the mass range required within each group is much less, for example only m/z 407.78176 to m/z 437.81399 for the hepta series. An experiment of the type shown in figure 1 can be used to select the required start and stop times for each group, and a lock mass is used to ensure that peak tops are monitored.

The results shown in Figure 2 have been obtained in the analysis of the same fly-ash sample shown in Figure 1. In this case, using separate ion groups, the relative intensities of each group of PCCDs and PCDFs are more accurately represented. In this experiment 8 ions have been monitored in each group, two from dioxin, two from furan and two each from the fully ^{13}C labelled internal standards. Figure 3 shows the results of one of the 5 groups monitored - the pentachloro series - expanded in full.

Quantitation of the unlabelled isomers was performed using the ^{13}C labelled standards, and the quantitation report for the PeCDD and PeCDF isomers is shown in table I.

These data were acquired on a CONCEPT IS mass spectrometer operated at 10,000 R.P. (10% valley definition) with a 1 second cycle time. This short cycle time ensures chromatographic resolution is maintained.

With longer cycle times, ultimate sensitivity is increased and a detection limit of 10 fg of TCDD has been achieved (figure 4)

References

1. Protocol for the analysis of 2, 3, 6, 8-tetrachloro-p-dioxin by High Resolution Gas Chromatography - High Resolution Mass Spectrometry. US EPA publication EPA 600/486-004.

2. Standard sample of fly-ash kindly supplied by Cerchar, France.

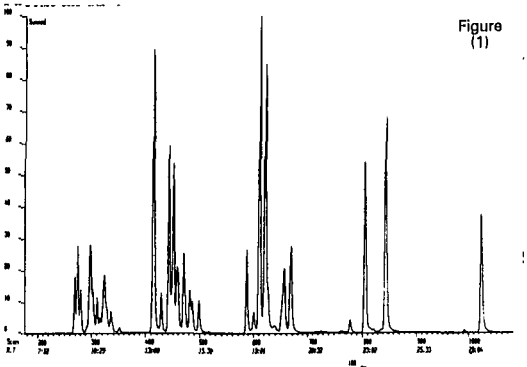

Figure (1)

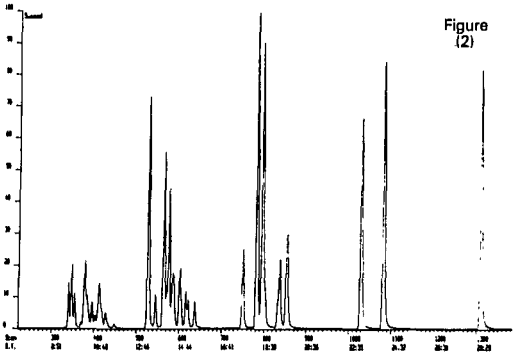

Figure (2)

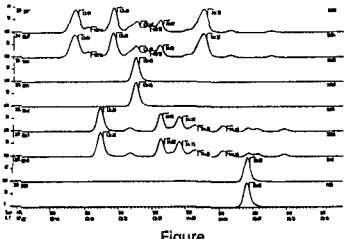

Figure (3)

CONCENTRATION REPORT

CALIBRATION FILE:CALIB
TYPE: QUADRATIC

DATE: 08/26/88 14:37
METHOD: EXTERNAL STANDARD

COMP #	NAME	EXP.RT	ACT RT	MEAN CONC.pg
1	PeCDD	14:00	13:30	461.89
1	PeCDD	14:00	14:01	453.43
1	PeCDD	14:00	14:15	268.00
1	PeCDD	14:00	14:26	314.46
1	PeCDD	14:00	14:46	180.18
3	13C PeCDF	14:00	13:45	100.03
3	13C PeCDD	14:00	15:03	100.01
4	PeCDF	14:00	13:01	633.03
4	PeCDF	14:00	13:11	33.46
4	PeCDF	14:00	13:38	406.95
4	PeCDF	14:00	13:48	206.51
4	PeCDF	14:00	13:52	42.40
4	PeCDF	14:00	14:01	204.41
4	PeCDF	14:00	14:33	703.42

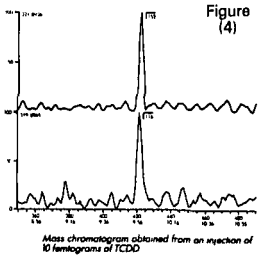

Figure (4)

Mass chromatogram obtained from an injection of 10 femtograms of TCDD

Presented at the 36th ASMS Conference on Mass Spectrometry and Allied Topics
June 5-10, 1988, San Francisco, CA

IMPROVED PEAK DETECTION SYSTEM FOR GC-MS ANALYSES WHICH INCORPORATES THE KRATOS DS-90 STANDARD PEAK DETECTION ALGORITHMS:

J. H. Garrett, J. G. Solch, L. A. Harden, and T. O. Tiernan;
Department of Chemistry and Toxic Contaminant Research Program,
Wright State University, Dayton, Ohio 45435.

The peak detection routines supplied with most GC/MS data systems are generally adequate for delineating isolated ion peaks but are less successful as the peaks broaden or overlap with other peaks. When Selected-Ion-Monitoring of many masses is used as the basis for the identification and quantitation of an analyte in an unknown, the ratios of the intensities of these ions must be within a specified range, consistent with that observed for the pure analyte standard. Frequently, the delineation of one ion to another does not match precisely enough and degrades the quantitation of an analyte or fails to identify the analyte because the ratio is out of the specified range. The peak detection algorithm used in Kratos DS-90 was chosen to be modified because it contained a very good kernel from which to create a more powerful routine that would improve the identification and quantitation of wide-spread analytes in a normal GC/MS run.

The most important item in improving the general peak detection routines is in incorporating the normal peak width of an analyte into the algorithm. From the peak width, one can determine the background noise of each particular ion in the window in which an analyte or its isomer components elute. The background noise is found by segmenting the above window into increments of the normal peak width and finding the increment in which the ion intensity of an ion changes the least. The background noise is then the difference of the highest ion intensity in the increment minus the lowest ion intensity in the increment. Once the background noise is found for each ion, a value for the minimum peak area of each ion is determined and also a fairly reliable S/N value is given for each peak of an ion. An accurate baseline value (the difference between two scans that signifies noise) is also determined for each ion from the background noise of that ion. This baseline value significantly improves the ratio of isolated low S/N peaks. Peak width is also invaluable in determining the leading and trailing edges of a peak when convoluted with other peaks.

Many other rules were also implemented that dealt with the following items. The trailing edge of a peak is terminated when the height drops below a certain level and its slope essentially becomes horizontal. The baseline cannot be drawn at an extreme angle or found at too high of an ion intensity above a previous baseline point. Slight irregularities in a peak's shape are ignored so as not to delineate a peak at an incorrect position. In the presence of changing chemical noise background, baseline values were changed to reflect the change in chemical noise.

The delineations with the improved peak detection algorithm shown in Figure 1 are markedly better than with the DS-90 peak detection algorithm shown in Figure 2. Table 1 shows the results from a GC/MS run that involved looking for the chlorinated dibenzofurans and dibenzodioxins. The ratios and identification of isomers identified in this run that involved very low levels of the analytes showed a marked improvement over the DS-90 implementation.

The above results have shown that additions to an existing peak detection algorithm can significantly improve the identification and quantitation process. Refinements to the routine will proceed as the need arises, e.g. the presence of incorrectly delineated or unidentified peaks.

Presented at the 36th ASMS Conference on Mass Spectrometry and Allied Topics
June 5-10, 1988, San Francisco, CA

FIGURE 1: IMPROVED PEAK DETECTION

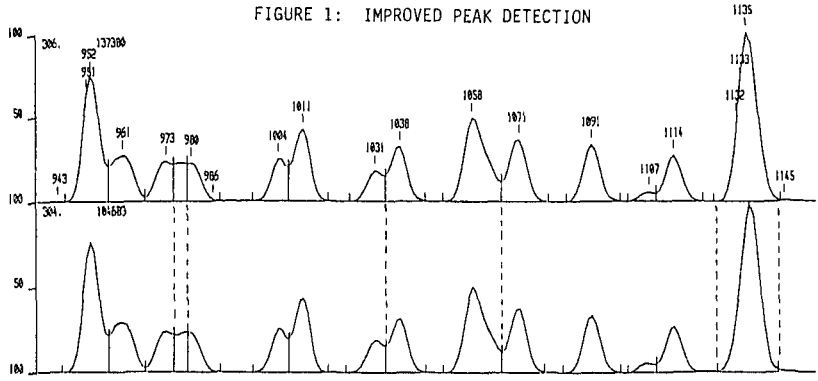

FIGURE 2: DS-90 PEAK DETECTION

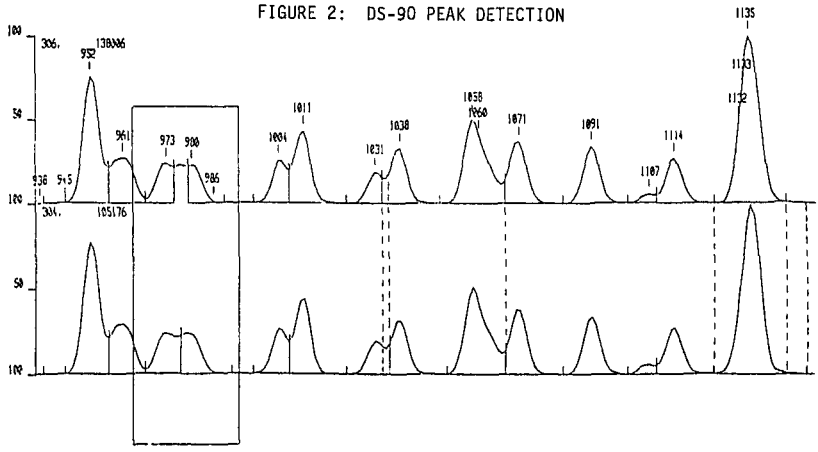

TABLE 1: DS-90 PEAK DETECTION VS IMPROVED ALGORITHM

Region	Theoretical Ratio	DS-90 Peak Detection Number of Peaks	DS-90 Peak Detection Calculated Ratio	Improved Peak Detection Number of Peaks	Improved Peak Detection Calculated Ratio
TCDF	0.77	15	0.81 ± 0.06	17	0.78 ± 0.03
TCDD	0.77	12	0.72 ± 0.10	12	0.77 ± 0.11
PCDF	0.61	13	0.65 ± 0.04	14	0.61 ± 0.05
PCDD	0.61	5	0.49 ± 0.07	5	0.59 ± 0.09
HxCDF	0.81	5	0.93 ± 0.11	6	0.79 ± 0.05
HxCDD	0.81	4	0.91 ± 0.09	5	0.81 ± 0.09
HpCDF	0.98	--	-- --	1	1.10 --
HpCDD	0.98	1	0.93 --	2	1.08 ± 0.10
OCDF	0.89	0	-- --	0	-- --
OCDD	0.89	1	1.11 --	1	1.20 --

Presented at the 36th ASMS Conference on Mass Spectrometry and Allied Topics
June 5-10, 1988, San Francisco, CA

HIGH VOLTAGE AND MAGNETIC SCANNING FOR MIXTURE AND TYPE ANALYSIS USING A PERSONAL COMPUTER

T.A. Wittstruck and T.J. Eskew
Measurement and Analysis Systems, Inc.
Bellefonte, Pa 16823

OBJECTIVE

In the course of upgrading magnetic mass spectrometer systems used in petrochemical laboratories, we sought to develop an automation system to completely control data acquisition, in either magnetic or high voltage scanning modes. Data analysis would then be performed by operator specified Mixture or ASTM Type Analysis methods. To achieve this, a highly-prompted program was written in IBM/Microsoft BASICA to acquire and store data on disk, followed by the appropriate analysis. This program was compiled and linked to increase its speed of operation.

THE PROGRAM

After a brief "setup" during which the operator specifies whether the operation is for Magnetic or High-Voltage scanning, and whether Mixture or Type analysis is to be performed upon the data, the program is menu-driven. From the Main menu, various routines may be accessed that, for example, allow changing scanning parameters, storing the changed values in a disk-file, scanning by one of several modes, listing out the acquired data, re-analyzing old data, etc.

Each of the scanning modes utilize a variable-time-constant filter and peak-detection algorithm. With Faraday-cup collectors, the minimum practical electrometer time constant is about 20 ms, and the digital volt meter (DVM) integration time for each "raw" data point is also typically set at 20 ms (or at 16 2/3 ms if a significant 60-Hz modulation is present). As many as possible of the required computer operations (data storage, digital filtering, peak detection, exponential-scan generation, graphic presentation) are completed within this 20-ms interval. The operations which must take place outside this interval (data transfer and DVM triggering) require about 5 ms. Thus, the data rate is 40 readings/second, with 80% of the time given to actual integration of the ion-beam signal.

The optimum digital filter for a rectangular peak is simply the moving average of N consecutive readings, where N matches the width of the peak. We have found that this filter also gives good results for trapezoidal or Gaussian peaks with random noise in the peak amplitude (1). Since the scan is precisely exponential, the required value of N is independent of mass, and is computed as a function of operator-specified scan half-life and slit-widths.

Presented at the 36th ASMS Conference on Mass Spectrometry and Allied Topics
June 5-10, 1988, San Francisco, CA

Peak detection is based on the digital-filter output. The algorithm searches for the following three events, in sequence:

(1) The first derivative of the filter output must rise above a threshold;
(2) The output must pass through a maximum which exceeds an operator-specified threshold; and
(3) The output must fall below a certain fraction of its maximum.

If these events occur within a certain maximum-expected peak width, a peak is reported. If the first event has not occurred, the baseline is updated by a weighted factor.

The scanning modes available from the Main menu are Peak Profile, Scan for Background, Scan for Sensitivity, Scan for Analysis, Iterative Scanning, and Manual Scan. When using any of the first six modes, the spectrum is displayed on the CRT, in real time. At the conclusion of the scan the display may be graphically printed before proceeding. In the Manual-scanning mode, only the real-time mass and intensity are digitally displayed. However, in this mode, scanning direction can be reversed and/or the scan-rate changed at any time.

Using the Iterative Scanning routine to acquire 10 consecutive scans of the spectrum of n-Butane, we found that the scanning algorithm gave reproducibility for the intensity of m/z 43 that varied by +/- 0.38% over a 20 minute duration (after accounting for the expected intensity decrease arising from sample pressure drop during this time).

For Mixture Analysis of the mass spectral data, a list of 29 components has been specified. For each component, a characteristic mass is specified. A 29x29 matrix is then constructed, consisting of the intensities at each of the masses for each of the components (some will obviously be zero), normalized to that at m/z 43 for n-Butane. The routine Scan for Sensitivity is used for this purpose. A separate sensitivity matrix is required for High-voltage or Magnetic scanning. This matrix is used, with the Gauss-Seidell method, to determine the composition of a mixture using the routine Scan for Analysis. Prior to data analysis, an optional background subtraction may be performed, using spectra acquired and stored by the routine Scan for Background. A typical mixture analysis of the acquired data requires about 5 seconds, after which a report of the analysis is printed.

Type analyses may be performed, based on published ASTM methods, for (1) Low-Olefin gasoline, (2) Middle Distillates, (3) Gas-Oil Saturates, or (4) Gas-Oil Aromatics.

(1) T. J. Eskew, "Minimum-noise data collection with variable scan rate, using a digital filter." Presented at the 29th Annual Conference on Mass Spectrometery and Allied Topics, Minneapolis, MN, May, 1981.

Presented at the 36th ASMS Conference on Mass Spectrometry and Allied Topics
June 5-10, 1988, San Francisco, CA

A GENERAL METHOD FOR ACCURATE MASS MEASUREMENT OF AMMONIA CI SPECTRA USING PFK INTERNAL REFERENCE.

William F. Haddon, D. S. Millington, R. E. England, C.A Elliger and G. D. Manners.

Western Regional Research Center, USDA, 800 Buchanan St., Albany, CA. and Dept of Pediatrics, Duke University, Box 3028, Durham, NC 27710 (DSM).

Introduction. Ammonia is often the reagent gas of choice for structural analysis of newly isolated compounds by mass spectrometry becuase its use uniquely provides molecular weight values in many cases. This report describes the use of PFK to record high resolution positive NH_3CI spectra by a method that avoids the use of non- standard CI conditions[1] or specially tailored reference compounds.[2]

High resolution NH_3 CI measurements have provided essential data for identification or confirmation of over 20 unusual ergostane-type steroids from insect -resistant petunia plants[3] and from series of macrocyclic jatrophane diterpenes isolated from the noxious weed *Euphorbia esula* (leafy spurge).[4] Among the common reagent gasses, only NH_3 gave molecular weight information consistently for about 50 compounds and synthetic analogs in these series of samples.

Experimental. Spectra were recorded at 5-7000 mass resolution using a VG 70/70-HS mass spectrometer scanned at 5 sec./decade or faster for full- scan spectra in CI mode at 1000 µA. total ionizing current and 100 eV. Adjustment of NH_3 pressure is critical. After admitting PFK via the batch inlet, we increase the NH_3 pressure until the intensity ratio for m/z 331:329 is about 1, making certain the direct probe is in the position to be used for subsequent introduction of samples. Under these conditions, the reagent gas spectrum has intensity values NH_3^+, 10%; NH_4^+, 100%; $NH_3NH_4^+$, 1%. It may be necesarry to increase the pressure in the inlet system with N_2 or Argon.

Results and Discussion. Significant changes occur in the PFK spectrum as NH_3 pressure increases to a value appropriate for CI measurements, as shown in Fig. 1. The more saturated PFK ions, including m/z 369,343 and 331 (C_7F_{15}, C_8F_{13} and C_7F_{13}) rapidly decrease with increasing NH_3 pressure, with concomitant increases in m/z 386,360 and 348; in contrast, less saturated ions, for example those at m/z 341 or 329 ($C_{11}F_{11}$, $C_{10}F_{11}$) are unreactive toward NH_3 and display no measureable change in absolute abundance. The increased abundance of m/z 348, 360 and 386 arises from the presence of nitrogen-containing ions from reaction of PFK ions and neutral ammonia. Such peaks are unsuitable reference points for mass assignments because they are doublets with unreactive PFK ions. Ions at m/z 329,331,341,434,355 and 367 remain single peaks in the presence of NH_3. The optimum pressure is that at which these ions retain measureable abundance.

Surprisingly the quality of CI spectra obtained in the presence of PFK is excellent. Figure 2 illustrates this fact by comparison of a spectrum of petuniasterone A recorded with PFK in the ion source and under the usual CI conditions. Major PFK ions are subtracted in the high resolution spectrum in the lower part of the figure.

Mass measurement accuracy below 3 ppm (1 std. dev.) was obtained for peak matching of jatrophane samples above m/z 700, as shown in the Table. For full scan spectra, the error has been 3.8 ppm based on measurements on about fifty samples.

Conclusions. The method described has the advantages of convenience, accuracy and integrity of spectra . As such, it routinely provides compositional identification for both molecular and *fragment* ions in CI spectra. Such measurements have often been inconvenient previously.

Presented at the 36th ASMS Conference on Mass Spectrometry and Allied Topics
June 5-10, 1988, San Francisco, CA

References.

1. G.W. Caldwell, J.A. Masucci and R.R. Inners, Organic. Mass Spectrom., 1988, 23, 86-90.
2. J.A. Ballantine, et. al. Organic Mass Spectrometry Letters, 1987,22,316-318.
3. C.A.Elliger, M.E. Benson, W. F. Haddon, R.E.Lundin, A.C.Waiss,Jr. and R.Y. Wong, J.Chem.Soc. Perkin Trans. I, 1988, 711-717.
4. G. D. Manners and R.Y. Wong, J.Chem.Soc. Perkin Trans., 1985, 2075-79.

FIGURE 1.

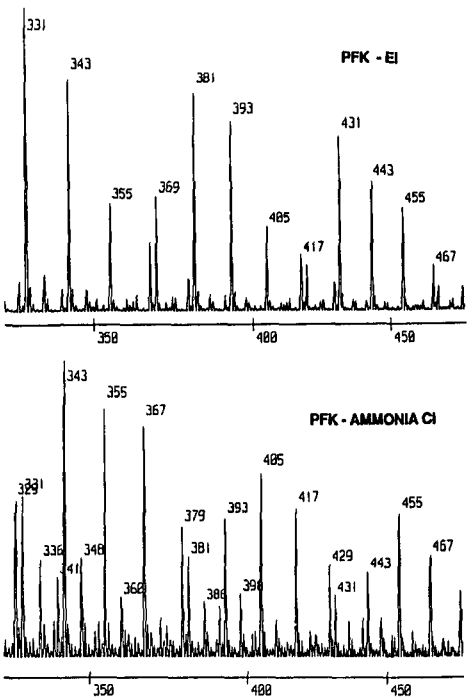

FIGURE 2.

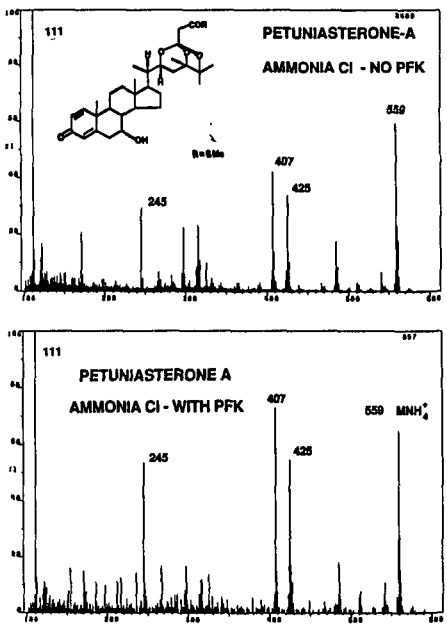

TABLE

PEAK MATCHING RESULTS - JATROPHANE DITERPENES

COMPOUND	R-1	R-4	R-3	R-2	R-6	R-5	MEAS. MASS. ERROR	
ESULONE A	OH	OH	=CH2	OAC	=O		708.2983	+5.2 PPM
ESU. A ACETATE	OAC	OAC	"	"	"		775.2943 (1)	-2.8
ESULONE B	OH	OAC	"	"	"		750.3121	-0.5
ESULONE C	OH	=O	"	"	OH		708.3033	+1.7
ESULONE E	OH	=O	"	"	=O		706.2878	+2.1
ESULONE F	OH	OH	CH3	"	"		710.3180	+0.4

(1) MH+ , ISOBUTANE AS REAGENT GAS.

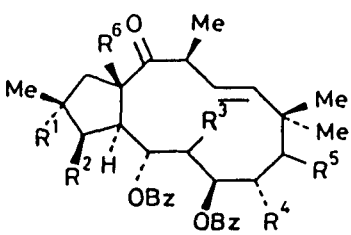

Presented at the 36th ASMS Conference on Mass Spectrometry and Allied Topics
June 5-10, 1988, San Francisco, CA

Computer Program for the Interpretation of CID Mass Spectra Obtained from Peptides of Unknown Sequence

R.S. Johnson and K. Biemann
Department of Chemistry, Massachusetts Institute of Technology
Cambridge, MA 02139

In order to efficiently use CID mass spectral data of peptides, automated methods of interpretation are needed that can be carried out on a time scale similar to that required for the actual experiment. In addition to keeping up with the rate at which data is generated, such automation ought to increase the likelihood of arriving at all sequences that account for most of the ions found in a spectrum (and possibly indicate ambiguities in the CID data).

Past efforts at such programs were directed mostly towards the interpretation of FABMS spectra of single component samples, but, nevertheless, could be used for interpreting CID mass spectral data. One approach (1,2) has been to identify small portions of a peptide sequence (usually referred to as subsequences). Those subsequences that account for the greatest numbers of observed fragment ions are then extended by at least two amino acids at a time to form new sets of subsequences. Eventually subsequences reach a point where they may account for the mass of the peptide, whereupon they are stored as possible sequences of the peptide. A second approach (3-5) involves the generation of all permutations of all amino acid combinations that account for the molecular weight of the peptide. For each of these permutations, scores are assigned based on matches between the calculated m/z values of the expected fragments and those appearing in the spectrum of the unknown. All of these programs, however, have been too slow to use routinely, unless amino acid compositions (3,4) or exact mass measurements (5) were used to limit the CPU time. Acquiring such information both adds to the analytical effort, and eliminates one of the major advantages of tandem mass spectrometry, namely, the ability to work with mixtures. For one of these algorithms (2), the CPU time could be shortened by limiting the number of fragment ions used as input (an input of < 20 fragment ions required 1-3 hours), which is clearly not satisfactory for the large number of fragment ions found in CID mass spectra.

The algorithm described here most closely resembles the subseqencing approach described by Ishikawa and Niwa (1), except that in this program the initial set of subsequences encompasses the C-terminus and are extended one amino acid at a time towards the N-terminus. Furthermore, additional ion types (and differences between FAB and CID fragmentations) not known to these authors were incorporated into the algorithm. Ions of type a_n, b_n, c_n, d_n, v_n, w_n, x_n, y_n, z_n, and z_n+1 are identified in the subsequencing routine, and up to 300 subsequences can be accomodated before eliminating the least likely candidates. The only required input is a list of the mass and relative abundance values from the CID spectrum, the mass of the $(M+H)^+$ ion, and the mass of the C-terminal modification (e.g., amide), if present; amino acid compositions or exact mass measurements of the $(M+H)^+$ ion are not necessary. The program accomodates modified amino acids and N-terminal blocking groups. Unlike most of the other programs, the mass of the N-terminal blocking group is not required as input. Once the subsequencing routine is finished, the list of completed sequences are subjected to a final scoring procedure (a further difference between this program and that of reference 1). In this last step, scores are assigned based on the ions found in the subsequencing routine, plus the nonsequence-specific immonium and acyl internal fragment ions, "secondary" d_n and w_n ions, R-group losses, as well as those ions resulting from loss of H_2O from product ions containing Ser or Thr. The scores are equal to the sum of intensities of ions identified divided by the sum of all intensities in the input data.

The entire procedure requires only 1-5 minutes of CPU time on a VAX 11/750 computer. The program has been used on hundreds of peptides of known and unknown sequences; the results from twenty such peptides are shown in Table I.

Table I: Results obtained on twelve peptides of known sequence and eight of previously unknown sequence. <E indicates pyroglutamic acid; C* indicates carboxymethylated cysteine.

	Sequence	Number of Fragment Ions	CPU Time	Score	Rank[1]
1.	<ELYENK (neurotensin 1-6)	54	2:32	0.92	1(1)
2.	<EHWSYALRPG-NH_2 (D-Ala^6-Luteinizing Hormone Releasing Hormone)	89	4:26	0.94	1(1)
3.	ELAGAPPEPA (β-lipotropin 1-10)	41	2:27	0.95	1(1)
4.	PHPFHFFVYK	60	2:44	0.88	1(1)
5.	RPKPQQFFGLM-NH_2 (substance P)	43	2:23	0.80	2(4)
6.	VHLTPVEK	59	2:04	0.86	1(1)
7.	<EADPNKFYGLM-NH_2 (physalaemin)	58	3:30	0.82	2(2)
8.	RPPGFSPFR (bradykinin)	72	2:17	0.61	1(1)
9.	KRPPGFSPFR (Lys-bradykinin)	65	2:53	0.68	11(11)
10.	TTLSQTLEK	79	3:23	0.92	1(1)
11.	VDMVVGAVPK	53	2:26	0.92	1(1)
12.	GIPTLLLFK	57	2:02	0.95	1(1)
13.	KKGQKVGEF	68	2:41	0.84	3(11)
14.	FHALSEKF	68	1:54	0.89	1(1)
15.	VLDSAGDKLVVVD[2]	83	4:34	----	-
16.	KFNNVVFIE	70	2:55	0.75	1(1)
17.	VDVDDC*KDIAAECE	94	4:21	0.80	6(7)
18.	NFQTEILDSDK	55	2:25	0.79	5(6)
19.	SIPTMLIXK	68	2:58	0.91	1(1)
20.	KIDEHIG	40	2:11	0.91	1(3)

[1] The number in parenthesis indicates the total number of sequences of equal or greater scores than the correct sequence.
[2] No cleavages between Ala and Gly, so the highest scoring sequence was found to be VLDSQDKLVVVD.

References

1. Ishikawa, K. and Niwa, Y. (1986) *Biomed. Mass Spect.* 13, 373
2. Siegel, M.M. and Bauman, N. (1988) *Biomed. and Environ. Mass Spect.* 15, 333
3. Sakurai, T., Matsuo, T., Matsuda, H. and Katakuse, I. (1984) *Biomed. Mass Spect.* 11, 396
4. Hamm, C.W., Wilson, W.E. and Harvan, D.J. (1986) *Comput. Appl. Bioscl.* 2, 115
5. Bertrand, M.J., Thibault, P., Evans, M.J. and Zidarov, D. 35th ASMS Conference on Mass Spectrometry and Allied Topics, Denver, CO, May 24-29, 1987, p. 399

Presented at the 36th ASMS Conference on Mass Spectrometry and Allied Topics
June 5-10, 1988, San Francisco, CA

COMPUTER AIDED PEPTIDE SEQUENCING (CAPS) BY FAB MASS SPECTROMETRY

K. Ishikawa and Y. Niwa
National Chemical Laboratory for Industry, Tsukuba, Ibaraki 305, Japan

It is generally difficult to predict amino acid sequences of unknown peptides from their FAB or FAB MS/MS spectra. We proposed a method CAPS (Computer Aided Peptide Sequencing) (1) which allows us to analyse peptides much larger than 1000 u within a reasonable cpu time and to have a set of probable amino acid sequences which are consistent with observed FAB spectra to varying degrees. Another feature of CAPS is that there is no need to pick sequence ion peaks out of the spectrum; all the ions observed are equally taken into account in the analysis so that one can exhaust the possibilies expected from the whole spectrum.

The method has been applied to 22 known linear peptides composed of 5 to 13 amino acid residues The correct sequences were always found at the top of the candidate sequences with prior knowledge of amino acid composition (Table 1(a)) Without prior knowledge of amino acid composition, the correct sequences were still found among the candidates at high rank (Table 1(b)). α-Mating factor (MW=1682.8) was the peptide whose correct sequence was missing in 100 candidates (designated by "101-" in the table). A part of the correct sequence "WLKLK" was, however, included in all the candidates of high rank (Table 2). In general, candidates at high rank partly reproduced the correct sequence. As was the case for α-mating factor, sequences near peptide terminals were sometimes ambiguous. This is because ions in the higher mass region are often low in intensity and spectra in the lower mass region are crowded with background ions. As a whole, the degree of success in the sequence elucidation strongly depends on the quality of the spectrum used in the analysis.

The difficulty will be further complicated in the case of cyclic peptides since they have much more possible fragmentation pathways than linear peptides (2, 3). Fig. 1 shows the FAB CID spectrum of $[M+H]^+$ (m/z=1043.6) of an unknown cyclic peptide isolated from the substances produced by a strain of *Bacillus subtilis* which inhibits the hypal growth of rice blast fungus, *Pyricularia oryzae* (4, 5). The CAPS analyses of the spectrum were made with prior knowledge of its amino acid composition; it was a octapeptide composed of each one mole of Pro, Ser, Tyr, Gln, 3-amino-tetradecanoic acid (Ata) and 3 moles of Asn. Daughter ions were assumed to be formed by successive and/or competitive losses of amino acid residues from the C-terminal of the linear acylium $[M+H]^+$ resulting from a cleavage of a certain peptide bond. There are 8 cases as to which peptide bond will be ruptured; Scheme 1 illustrates the case where the bond cleavage has taken place between A_1 and A_8. Thus the CID spectrum may be a superposition of, at the maximum, 8 different daughter ion spectra. The CAPS analysis will pick the amino acid sequence of predominant acylium $[M+H]^+$ out of 6720 (8!/3!) possible sequences. The sequence of the most predominant acylium $[M+H]^+$ was deduced to be

H_2N-(Pro, Asn)-Ser-Ata-Asn-Tyr-Asn-Gln-CO^+ (A)

where the order of Pro and Asn was uncertain since the observed CID spectrum gave no daughter ions formed by the bond cleavage between them. Although most ions observed were interpreted in terms of this structure, there still remain several ions of considerable abundance as marked in Fig. 1. The spectrum was again analyzed by CAPS after eliminating the ions related to the amino acid sequence (A). The sequence of the second most predominant acylium $[M+H]^+$ was deduced to be

H_2N-Asn-Tyr-Asn-Gln-Pro-Asn-(Ser, Ata)-CO^+ (B).

On the basis of the structures (A) and (B), the amino acid sequence of the peptide can be represented by

Pro-Asn-Ser-Ata-Asn-Tyr-Asn-Gln (C).

The FAB mass spectrum of the acid hydrolysate of the peptide confirmed this conclusion. The amino acid sequence (C) and the origin of the peptide strongly suggest that it is Iturine A-2 (6, 7).

Presented at the 36th ASMS Conference on Mass Spectrometry and Allied Topics
June 5-10, 1988, San Francisco, CA

References
1. K. Ishikawa and Y. Niwa, *Biomed. Environm. Mass Spectrom.*, **13**, 373 (1986).
2. K. Eckart, H. Schwarz, K. B. Tomer and M. L. Gross, *J. Am. Chem. Soc.*, 107, 6765 (1985).
3. T. Nakamura, H. Nagai and T. Kinoshita, *Mass Spectrosc.*, **34**, 307 (1986).
4. T. Namai, K. Hatakeda and T. Asano, *Tohoku J. Agric. Res.*, **36**, 1 (1985).
5. K. Ishikawa, Y. Niwa, K. Hatakeda and T. Gotoh, *Org. Mass Spectrom.*, **23**, 290 (1988).
6. A. Isogai, S. Takayama, S. Murakoshi and A. Suzuki, *Tetrahedron Lett.*, 23, 3065 (1982).
7. F. Peypoux, M. Guinand, G. Michel, L. Delcambe, B. C. Das and E. Lederer, *Biochemistry*, 17, 3992 (1978).

Table 1 Order at which the correct sequence was found among the candidate sequences

Order	No. of samples* (a)	(b)
1	22	14
2-20	0	6
21-100	0	1
101-	0	1

* With (a) and without (b) prior knowledge of amino acid composition.

Table 2 Candidates for α-mating factor (WHWLQLKPGQPMY)

Order	Sequence*	Score
1	(H, S)VWLKLKPGKPMY	719
3	(H, S)VWLKLKPGLWGY	715
5	(H, S)VWLKLKGPKPMY	710
7	(H, S)VWLKLKPGLCRF	706
9	(H, S)VWLKLKPGLCFR	705

* A common letter K was used for lysine (K) and glutamine (Q), as they have an identical integral molecular weight.

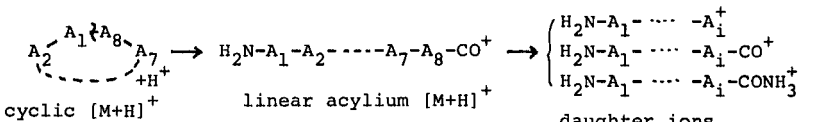

Scheme 1

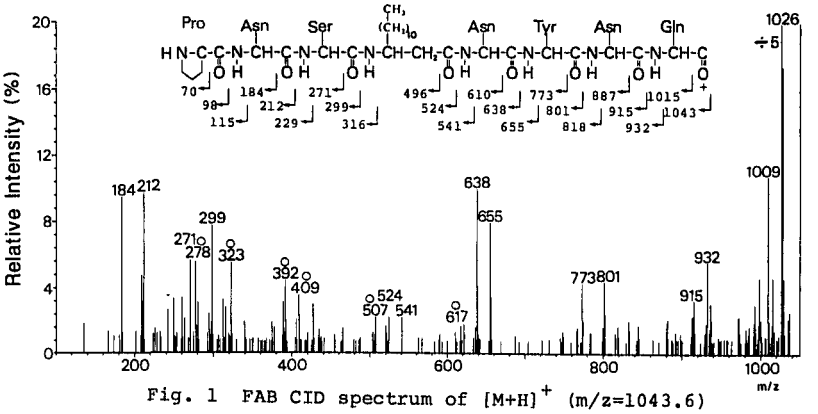

Fig. 1 FAB CID spectrum of $[M+H]^+$ (m/z=1043.6)

Presented at the 36th ASMS Conference on Mass Spectrometry and Allied Topics
June 5-10, 1988, San Francisco, CA

COMPUTER IDENTIFICATION OF BACTERIA VIA MS WITH CI

D.C. Conway and Humberto Lopez, Department of Chemistry, and
J.M. Quarles, Jr., Department of Medical Microbiology and Immunology,
Texas A&M University, College Station, TX., 77843

The object of this research is to develop a rapid method for the identification of bacteria by MS using CI to reduce fragmentation. Time consuming steps such as solvent extraction or making derivatives are to be avoided. The analysis of the bacteria growth medium was complicated by the formation of ion clusters in the low temperature ion source [1]. Therefore, it was decided to pyrolyze the bacteria, but at lower temperatures than is the case with the well-known Curie point method. At lower temperatures pyrolyzates produced by higher activation energy reactions are strongly hindered, and spectra can be taken over several temperature ranges for one sample. The bacteria pyrolysis spectra are more complex than those obtained from the growth media, but this permits the use of more sophisticated data analysis techniques.

The bacteria were grown for 16–18 hrs, killed in 70% ethanol solution, separated by centrifugation, and stored in 70% methanol. A small aliquot of this mixture containing 1 mg of bacteria was placed in a 0.04 ml stainless steel cup and dried in an unheated vacuum oven. Then 0.03 ml of H_2O was added, the mixture stirred, and dried again. The cup was heated in a direct inlet probe, and the pyrolyzates were carried by a gas stream in 0.1 sec through a heated inlet tube at 170–180°C to the MS. (High tube temperatures reduce the formation of ion clusters.) Ions were produced by a 1 kHz pulsed electrical discharge ion source, which was mounted downstream of the MS inlet. The CI gas was CH_4 at 0.56 Torr pressure with a small amount of added H_2O, so the CI reagent ions were mainly $H_3O^{+\cdot}$. The mass spectra were taken for 2 min from 330–390°C. The data were digitized on a microcomputer (Zenith–158 PC) to produce mass intensities as a percentage of the total ion intensity. The data were then analyzed on an IBM 3090 computer.

Four types of bacteria were studied, Escherichia coli, Staphyloccus aureus, Listeria monocytogenes 1706, and Listeria monocytogenes ATCC 9115. Data were taken for 3 batches of the first two bacteria. All the mass spectral data were divided into 7 classes, 4 groups that are standards (knowns) and 3 groups from the last batches that are unknowns. The 4 groups of standard spectra, one for each type of bacteria, were analyzed by stepwise discriminant analysis. By this process 56 mass lines were chosen to give the largest differences between the 4 types of bacteria.

Canonical discriminant analysis yields linear combinations of the mass intensities, the canonical variables, which emphasize the differences between the classes. When canonical discriminant analysis was performed for the 4 classes of knowns, the first and second canonical variables were the same (to 0.002%) for the

members of each class. When the 7 classes of data were analyzed the same way with the 56 masses, the first and second canonical variables shown in the figure below were obtained. The unknowns (squares) are from the last batches grown. In order to keep the intragroup variances of the canonical variables for the unknowns reasonably small, the intragroup variances for the knowns are forced to be larger than when only the knowns were analyzed.

It is encouraging that knowns from 1–3 batches of bacteria and the corresponding unknowns for the last batch cluster together. However, the unknowns and knowns must come from different batches to prove the procedure viable, work presently in progress.

Acknowledgement: We wish to thank the TAMU Honors Program for providing the funds to purchase the microcomputer with a Teacher/Scholar Grant.

Reference: 1. D.C. Conway, Humberto Lopez, and J.M. Quarles, Jr., 35th ASMS Conference on Mass Spectrometry and Allied Topics, pp. 965–966 (1987).

6B. FIRST & SECOND CANONICAL VARIABLES
SAMPLE RANGE 92.21–94.58

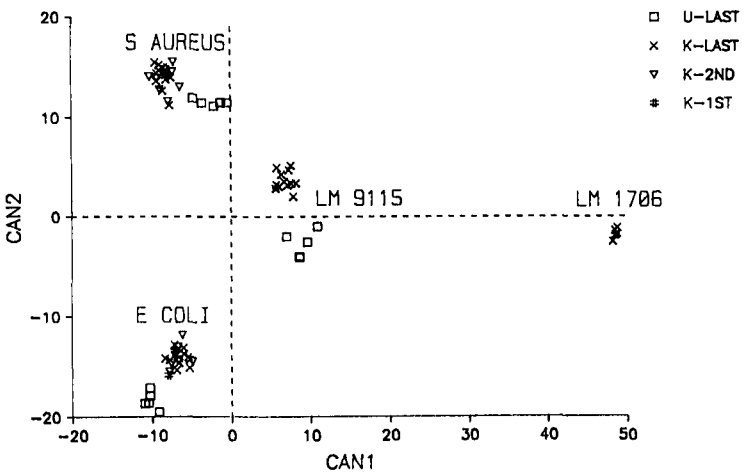

Presented at the 36th ASMS Conference on Mass Spectrometry and Allied Topics
June 5-10, 1988, San Francisco, CA

TOF-SIMS DATA SYSTEM

Jeffrey R. Wyatt, Richard J. Colton, and Steve M. Hues
Naval Research Laboratory, Code 6110, Washington, DC 20375-5000.

Time-of-flight Secondary Ion Mass Spectrometers require high speed digital data acquisition and processing capabilities. During the last few years several groups have constructed specially designed data acquisition systems for this purpose.[1-5] We have recently constructed such a data system solely with commercially available components. It is based upon off-the-shelf CAMAC modules that are controlled by a MicroVAX-II computer.

The mass spectrometer is a reflection time-of-flight instrument. The primary ion pulse is 2-5 nsec long and mass resolution is greater than 2000. Depending on the mass range, secondary mass spectra are 50-200 μsec long. Currently the only multihit time-to-digital (TDC) converter comparable with our system is the LeCroy Model 4208. It can measure up to eight events (ions of different flight time per spectrum) with a time resolution of one nsec. Our system cannot distinguish more than one ion simultaneously (within 3 nsec) striking the detector.

Since it is possible to measure flight times to one nsec, a mass spectrum could contain up to 200,000 points. Due to the small number of events per spectrum, it is desirable to operate the mass spectrometer at as high a repetition rate as possible. These requirements meant that we chose a computer more powerful than an IBM-PC AT. In particular we needed a computer capable of handling efficiently data arrays having greater than 64,000 elements. We wanted a computer with a well-established software base. Thus we selected a MicroVAX-II computer.

The data system is depicted in Figure 1. The computer is interfaced to the CAMAC crate using a Kinetic Systems Model 3920 crate controller and Q-bus interface. Timing pulses are generated using a Kinetic Systems Model 3655 timing generator. Pulses from the timing generator are used to pulse the primary ion gun, clear the TDC, start the TDC, and stop the TDC. Secondary pulses are amplified with a Phillips model 774 amplifier and detected with a Phillips 704 discriminator. The output from the discriminator is used as input for the LeCroy Model 4208 multihit TDC. The sequence of timing pulses is shown in Figure 2.

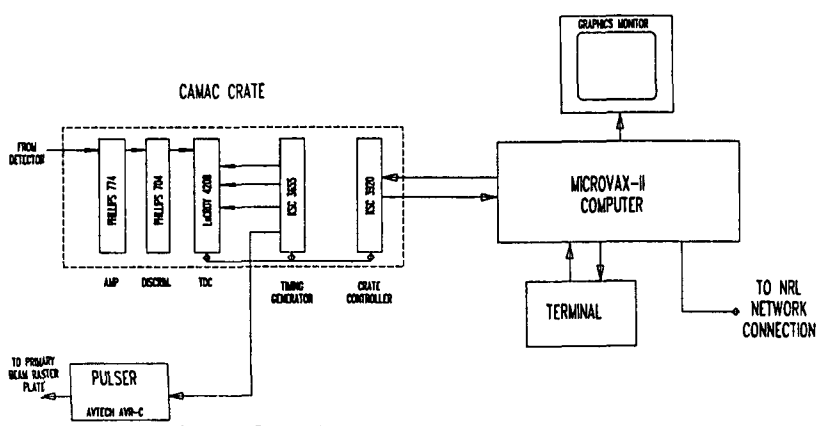

Figure 1. Schematic of the data acquisition system.

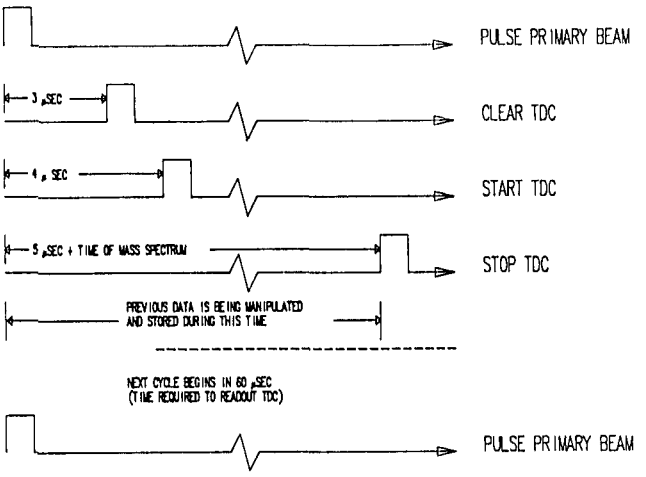

Figure 2. Diagram of the pulse timing.

The principal timing limitation of the system is the time required to readout the TDC. Nine μsec are require to read each channel; thus 72 μsec are required for all eight channels. Approximately 50 μsec are required to manipulate and store the data; this operation is performed while the next spectrum is being acquired. Therefore spectra 100 μsec long can be acquired a rate of 6 kHz. The data acquisition program pauses about 20% of the time to permit a lower priority plotting program to run.

Data are continuously plotted using a DEC VSV21 graphics board driving a color CRT. Plots of the data update several times a second. The rate of plotting depends upon how many points of data need to be reduced to the 500 points shown on the screen. Other information displayed on the screen includes the mass of the ten most intense peaks, low, middle, and high masses, total spectra acquired, and total ions detected. The data can be displayed logarithmically if desired. Hard copies of the data are plotted on the Chemistry Division computer which is connected to the Microvax by a network. A third program is used to control the other programs and interface to the operator. All of the other computer operations can be performed while data is being acquired. All of the software is written in FORTRAN; and thus is easily modified for unique experiments.

References

[1]L. I. Grace, B. T. Chait, and F. H. Field, Biomed. Environ. Mass Spectrom., 14, 295 (1987).

[2]K. G. Standing, R. Beavis, G. Bolbach, W. Ens, F. LaFortune, D. Main, B. Schueler, X. Tang, and J. B Westmore, Anal. Instrum. (N.Y.) 16(1), 173 (1987)

[3]E. Niehuis, T. Heller, H. Field, and A. Benninghoven, J. Vac. Sci. Technol. A 5(4), 1243 (1987).

[4]S. Della Negra and Y LeBeyec, Int. J. Mass Spectrom. Ion Process., 61, 21 (1984).

[5]R. D. Macfarlane, Anal. Chem., 55, 1247A (1983).

Presented at the 36th ASMS Conference on Mass Spectrometry and Allied Topics
June 5-10, 1988, San Francisco, CA

USE OF AN HP-1000 GC/MS DATA REDUCTION ENVIRONMENT AND LOTUS/1-2-3 FOR THE RAPID EVALUATION OF LOW-LEVEL PCB ANALYSIS DATA

by
D. E. McKenzie and B. Mason Hughes
Environmental Sciences Center
Monsanto Company
St. Louis, Missouri 63167

ABSTRACT

Two important considerations in the analysis of complex mixtures are accuracy of the reported results and data reduction costs. The present poster describes a significant step in completely automating the data reduction for the analysis of samples containing polychlorinated biphenyl (PCB) congeners which greatly impacts both of these areas Specific analysis windows are determined from the analysis of a commercially available PCB window standard. Selected Ion Monitoring (SIM) data for each homologous class of PCB isomers is used for the low-level analysis of these congeners. This approach is both rapid, and can be easily modified to expand the analytes beyond the specific PCB congeners of interest It also allows for the inclusion of quality control steps, such as the use of ^{13}C-containing surrogate compounds, with little additional time required for extensive reporting of these results.

Background

Polychlorinated biphenyls are defined as a class of compounds which have from one to ten chlorine atoms attached to a biphenyl moiety. A total of 209 congeners with empirical formula $C_{12}H_{10-X}Cl_X$ comprise the PCB family. These compounds have been analyzed by a number of methods. The two most common analysis approaches for low level PCB analyses use GC/EC (gas chromatography with an electron capture detector) or GC/SIM-MS (gas chromatography with selected ion monitoring mass spectrometry). GC/SIM-MS is the more specific analysis method of the two. However, at least one order of magnitude more data is generated using this analysis technique. Therefore rapid, accurate, cost effective data analysis methods are needed in order to make full use of this more specific information. This paper deals with the instrumental and data analysis methods which have been developed for rapid, cost effective analysis of low-level PCB concentrations using capillary GC/SIM-MS.

Instrumental Analysis

The instrumentation used for this type of analysis, along with operating parameters, is listed in the following table.

Instrumentation	Operating System	Instrument Parameters	
HP-5985/5987	*RTE-VI*	*Run Time:*	*15 - 40 min.*
		Multiplier Voltage:	*1800 - 2800 eV*
Column and Chromatographic Conditions		*Dwell Times:*	*100 - 500 msec/mass*
30-meter (0.32 mm) f.s. J&W DB-5 (0 25 uM)		*Electron Energy:*	*70 eV*
Column Temperature Program: 50(4)/8/300		*Scanning Mode:*	*Selected Ion Monitoring*
Injection Type Splitless			

Analysis Approach

Prior to analysis, appropriate retention time windows for each PCB isomer class must be determined since all masses are not monitored during the total analysis. This is accomplished by the analysis of a commercially available standard which contains the first and last eluting PCB isomer in each chlorine class. This window standard contains: 3- and 4-Cl-biphenyl, 2,6- and 4,4'-Cl_2-biphenyl, 2,4,6- and 3,4,4'-Cl_3-biphenyl, 2,2',6,6'- and 3,3',4,4'-Cl_4-biphenyl, 2,2',4,6,6'- and 3,3',4,4',5-Cl_5-biphenyl, 2,2',4,4',6,6'- and 3,3',4,4',5,5'-Cl_6-biphenyl, 2,2',3,4',5,6,6'- and 2,3,3',4,4',5,5'-Cl_7-biphenyl, 2,2',3,3',5,5',6,6'- and 2,3,3',4,4',5,5',6-Cl_8-biphenyl, 2,2',3,3',4,5,5',6,6'- and 2,2',3,3',4,4',5,5',6-Cl_9-biphenyl, and Cl_{10}-biphenyl.

Once the selected ion monitoring data is collected using the proper retention time windows, the HP-1000/RTE-VI operating system "organizes" the data by producing a graphical output which shows peak integration areas (by solid fill), reduced chromatograms of the M^+ and $(M+2)^+$ chromatograms, and tabular information which is stored in an ASCII file. Graphic outputs similar to those shown in Figure 1, are visually scanned by a trained mass spectroscopist for integration errors, and the ASCII file is corrected using EDIT/1000, when required. The ASCII file for each sample is then transferred to a personal computer by the use of the AdvanceLink program.

A Lotus/1-2-3 template file with "user defined" menu items is then used for further calculations. Menu items allow for the importing of the ASCII files for each sample and standard. From the standard file, the template calculates average response factors for each PCB isomer class. From each sample file, the template calculates the concentration for each set of geometric isomers and sums each isomer class to calculate total PCB concentrations for each sample. The user is prompted to input sample identifications, extract volumes, and sample weight information from which the total PCB concentrations are automatically calculated

Figure 1. Example of Graphic Outputs Produced from the Analysis of Cl_5- and Cl_6-biphenyl Congeners.

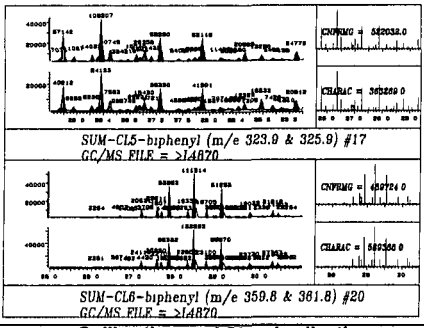

Calibration and Standardization

Quantitative: An internal standard quantitation technique is used to calculate analyte concentrations. Average relative response factors are determined for each chlorine class from the analysis of standard solutions containing various PCB congeners. The calculations, using internal standard methodology, are given by the formula:

$$AC = (AA)/[(ARRF)(ISA)]$$

where:

AC = *analyte concentration*
AA = *analyte characteristic mass area*
ARRF = *analyte relative response factor*
ISA = *internal standard area.*

Total PCB concentrations can be calculated in two ways:
1) If a PCB formulation can be identified from the patterns of PCB congeners, then selected PCB isomers or classes of isomers (i e. all Cl_4-biphenyl isomers) are used to quantify the formulation concentration. Relative Response Factors are calculated using the concentration of the total formulation in the above equation.
2) If no unique PCB formulation is present, then the total PCB concentration is calculated by using standard solutions containing known amounts of monochlorobiphenyl through decachlorobiphenyl congeners. Relative Response Factors for each chlorine class are calculated using the above equation. The RRFs for the corresponding PCB isomer classes are used to calculate total PCB isomer concentrations of each class in unknown samples.

Qualitative: The ratio of characteristic mass response to confirming mass response must be within 20% of those measured for the authentic standard. For PCB congeners between Cl_1-biphenyl and Cl_5-biphenyl, the characteristic and confirming masses are the molecular ions containing all ^{35}Cl isotopes and one ^{37}Cl isotope. For PCB congeners between Cl_6-biphenyl and Cl_9-biphenyl, these masses are the molecular ions containing one ^{37}Cl and two ^{37}Cl isotopes. For Cl_{10}-biphenyl, these masses are the molecular ions containing two ^{37}Cl and three ^{37}Cl isotopes. The following table summarizes the masses monitored for the analysis of internal standard, surrogate standards, and monochlorobiphenyl through decachlorobiphenylphenyl congeners.

Table 1. Summary of Characteristic and Confirming Masses Used for Low-Level PCB Analyses.

Analyte	Characteristic $(M)^+$	Confirming $(M+2)^+$
anthracene-d_{10}	188	190
Cl_1-biphenyls	188	190
4-Cl-biphenyl-$^{13}C_6$	194	196
Cl_2-biphenyls	222	224
Cl_3-biphenyls	255.9	257.9
Cl_4-biphenyls	289.8	291.8
3,4,3',4'-Cl_4-biphenyl-$^{13}C_{12}$	301.8	303.8
Cl_5-biphenyls	323.9	325.9
Cl_6-biphenyls	359.8	361.8
Cl_7-biphenyls	393.8	395.8
Cl_8-biphenyls	427.7	429.7
2,2',3,3',5,5',6,6-Cl_8-biphenyl-$^{13}C_{12}$	439.7	441.7
Cl_9-biphenyls	461.6	463.6
Cl_{10}-biphenyl	497.6	499 6
Cl_{10}-biphenyl-$^{13}C_{12}$	509.6	511.6

Conclusion

Lotus/1-2-3 can be a very effective means of simplifying data reduction of complex mixtures. In the present example, each menu item is actually macro driven and contains 25-100 individual Lotus/1-2-3 commands. While this type of data manipulation could be accomplished manually, the data analysis time would be increased dramatically. However, in order to use this approach for data analysis, one must:

1) Plan carefully in order to anticipate the major properties of the template file,
2) Break down the data analysis steps into specific analysis steps so that one can maximize the amount of information in a minimum amount of time and steps, and
3) Incorporate error detection with the inclusion of graphic outputs which show peak areas and ratios of characteristic to confirming ion intensities for the rapid detection and correction of errors when they occur.

Presented at the 36th ASMS Conference on Mass Spectrometry and Allied Topics
June 5-10, 1988, San Francisco, CA

Networking Mass Spectrometer Data Systems

Robert Johnson, Lester Taylor, James Jackson, Johnny Hewitt,
Burroughs Wellcome Co.
Research Triangle Park, North Carolina 27709

The mass spectrometry facility at Burroughs Wellcome Co. decided to implement a local area network (LAN) for its data systems for three reasons:

1. The amount of data generated by three mass spectrometers can easily exceed the storage capacity of the dedicated instrument data systems within a few working days. With a need to access this data over a period of several weeks, access to large central disk storage was desired.
2. The computer facility at Burroughs Wellcome Co. is much better equipped to handle the long term storage of data generated by our group that falls under the Good Laboratory Practices (GLP) of the FDA and EPA. Therefore efficient transfer of this data to their storage media was desired.
3. The use of remote terminals and personal computers for analyzing data has become essential for report writing and for efficient use of mass spectrometer data system CPU time. Networking was the method that allowed much wider access to the mass spectrometer data systems.

The Automation Group at BW has in place a network system that meets these needs. The system is an ethernet system using DECNET® as the local area network protocol. This system also has in place a DECserver® 200 system that allows for remote terminal access to any DECNET® system computer via RS232 lines at 19200 baud. In order to connect our computers to this network, each mass spectrometer data system was supplied with a DECQNA® interface board and a copy of the DECNET® software. A PDP 11/70 is used for extra disk space and as a host for the archiving and auxiliary storage of mass spectral data upon request. A VAX can also be used for extra disk storage space when the need arises. The transfer of data from one computer to another is conducted via the Network File Transfer (NFT) program of DECNET®. The archival storage of data on the PDP 11/70 is accomplished under a program entitled ARCHIVE which resides on the PDP 11/70 system. This program is called when the user wishes to archive data for future reference under GLP guidelines. The program copies the file to a special disk area from which tape back-up of the file is accomplished. This program was written in-house by the automation group to archive data acquired by chromatography and scintillation counter microcomputer data systems. Other vendor-written archiving software is available for VAX computer systems. This program allows the archiving of any data in the users storage area of the PDP 11/70. The command ARCH is used to call the program. Under program control the user can archive data, review the list of files awaiting archiving, and delete files from the archive list. Archiving of files is accomplished with the full range of wildcard options available under RSX 11M. Alternately the system operator for the PDP 11/70 can request ARCHIVE to automatically archive any file residing in the users storage area once a week. To retrieve archived files, the user simply requests that the operator copy the desired file to his work area from tape storage. A master list of file names stored on tape is kept by the operator under system control and can be searched to give the tape location of any file. The use of remote terminals within the LAN of BW has provided access to mass spectrometry data from virtually any type of microcomputer or terminal available. With the use of office Macintosh computers to cut and paste graphical data into reports, there is faster turn-around time in report and manuscript writing.

Presented at the 36th ASMS Conference on Mass Spectrometry and Allied Topics
June 5-10, 1988, San Francisco, CA

UTILITY PROGRAMS FOR FACILITATING CONTRACT LABORATORY PROGRAM DATA PACKAGE PREPARATION*

E. Y. HWANG AND R. J. WINGENDER

To participate in GC/MS analysis of environmental pollutants for the Contract Laboratory Program (CLP), laboratories are required to maintain an intense quality control (QC) program. Several companies supplying GC/MS equipment have developed specialized software that presents sample results and quality control data in a specific format required by the EPA. We are using the Formaster II software in conjunction with our Finnigan 4021 GC/MS system for the analysis of semivolatile target compounds and have found that, in day-to-day operations, the exclusive use of the Formaster software is not cost effective. To sustain productivity without compromising QC, we developed utility programs to supplement the Formaster software.

1. Initial Calibration (IC) and Continued Calibration (CC)

After the instrument has been tuned to DFTPP specifications as required by the EPA, calibration standards are injected to check system performance. The minimum average relative response factors for the four semivolatile System Performance Check Compounds (SPCC) (N-nitroso-di-n-propylamine, hexachlorocyclopentadiene, 2,4-dinitrophenol, and 4-nitrophenol) must be greater than 0.05. Thirteen other compounds are referred to as the Continued Calibration Check Compounds (CCC):

Acenaphthene	4-chloro-3-methylphenol
1,4-dichlorobenzene	2,4-dichlorophenol
Hexachlorobutadiene	2-nitrophenol
N-nitroso-di-n-phenylamine	Phenol
Di-n-octylphthalate	Pentachlorophenol
Fluoranthene	2,4,6-trichlorophenol
Benzo(a)pyrene	

Analysis of these compounds must have a relative standard deviation (RSD) of less than 30% in the initial calibration and a percent difference of less than 25% in the continued calibration. The actual sample analysis cannot commence until these criteria have been met. Formaster is capable of doing both the initial and continued calibration checks. However, the processes involved to produce calculated results are extremely time consuming because the quantitation list for all 67 target compounds must be edited and updated, and because ASCII files must be created before the data can be transferred to the personal computer on which the Formaster is resident, and then read into the Formaster program after proper headings are typed in.

The IC and CC program has been written as an alternative way to check the initial and continued calibration data. The printed results, formated similarly to the EPA Form VI and Form VII, can be produced within five minutes of the termination of the last standard run. The program is capable of calculating the response factor, average response factor, standard deviation, percent RSD, and percent difference of all compounds of interest or just the SPCC and CCC compounds. It is also flexible enough to be used in different aspects of organic analysis (volatile, semivolatile, and/or PCB/pesticide) through input format modification.

In addition, we have established the capability of transferring all the quantitation data from the personal computer to a VAX, where additional manipulation of data or calculations can be performed.

2. Limit of Detection of Individual Target Compounds

Limits of detection (LOD) are calculated by assuming that a minimum of 1000 counts is needed for the primary ion of any compound to satisfy the requirements for qualitative verification. All but nine compounds on the semivolatile list require a 20 ng calibration standard for the LOD calculation. (The LOD for the nine compounds that require a four-point calibration is computed from the 50 ng calibration standard.) Our utility program reads in data from both the 20 ng and 50 ng standard runs, isolates the nine compounds (marked with an asterisk), and does appropriate calculations. The LOD is presented in three ways in the output: as the minimum quantifiable amount in ng of the specified compound, in μg/L (assuming a one liter water sample was analyzed following the CLP procedure), and in μg/kg [assuming a 30 g (dry) soil sample was analyzed following the CLP procedure].

3. Elution Order of the Semivolatile Compounds

CLP protocol requires that every single peak on the chromatogram from the daily standard be identified and labeled. Our utility program sorts the compounds according to their respective order of elution (in ascending order of scan number) and prints out compound names (including internal standards and surrogate standards), target ions, scan number, and elution time.

This listing eliminates the laborious task of hand-labeling every single chromatographic peak on the reconstructed ion chromatogram.

4. Tentatively Identified Compounds (TICs)

Compounds not on the target compound list are quantitated by using the nearest internal standard free of interference. Area counts from the total ion chromatogram are used for both the compound to be quantitated and the internal standard. A relative response factor (RRF) of 1.0 is assumed. Because the Finnigan IDOS software does not reference the correct internal standard for the TICs and does not give the RRF a default value of 1.0, all TIC quantitative calculations are incorrect. Our utility program corrects this problem and outputs two files. One file lists the internal standards as in the regular quantitation report; this list is included in the data package with the results of a library search. The other file has the internal standards deleted and read into the Formaster program in order to generate Form I TICs.

*Work supported by the U.S. Department of Energy under Contract W-31-109-Eng-38.

Presented at the 36th ASMS Conference on Mass Spectrometry and Allied Topics
June 5-10, 1988, San Francisco, CA

OPTIMIZATION OF GC/MS DATA ANALYSIS USING HEWLETT PACKARD MACRO PROGRAM ENHANCEMENTS

John T. Cody and Dragoslav T. Marcovich
Air Force Drug Testing Laboratory, Brooks AFB TX 78235-5000

The ability of GC/MS data systems to manipulate raw data to produce sophisticated detailed reports has reached impressive proportions even with relatively small bench top computer systems. The need to process data accurately, reliably and rapidly is of paramount importance in a laboratory environment where large numbers of samples are processed. This is of particular significance when the data produced by the laboratory is routinely used in the legal environment.

The ability to generate files containing user defined variables which can then be used for further processing and evaluation of subsequent samples is realized using options found in version 3.2 of the HP ChemStation software. This allows for generation of truly customized reports which can ultimately save not only time in data reduction and analysis but storage space in an archival system. Program load time is substantially reduced by the ability to "compile" macro programs allowing for rapid loading into memory thus reducing system overhead time.

Custom annotation of chromatographic data allows for a data report which is easily understood by individuals not familiar with the data system being used. This is of critical importance for data which is reviewed and presented in legal proceedings to individuals who are generally not intimately familiar with looking at GC/MS data. These capabilities allow for the generation of a complete report which contains all pertinent data from a sample in as compact and easy to read a format as possible (See Figure 1).

The ability to create files which contain calibration and ion ratio data makes it possible to quantitate unknown samples in the Data Editor program, thus eliminating the need to use the Report program. This capability also allows the quantitation portion of the sample data output to indicate only what is deemed by the user as important rather than being forced to work around the manufacturer's standard format. Ion ratio comparison with the standard can also be accomplished within the Data Editor.

Creation of files also gives the user the ability to capture only the data which is critically important for archival purposes. In addition, summary files can be created to hold results for an entire analytical run in a format which can be sent to another computer system (i.e., a laboratory information management system).

In earlier versions of the ChemStation software, the ability of the system to generate a customized report was available, but required a cumbersome and complex sequencing macro as well as numerous internal checks to ensure the proper data was being evaluated at each step along the process. This, with the advent of version 3.2, is not only easier but allows for more customization. The potential for bar code reading and numeric variable input of data by the user makes the potential power of this release even more powerful.

Data file DATA:ASMSSTND.D
File type: GC / MS DATA FILE

Sample Name. 15 ng/ml STANDARD — THC ANALYSIS
Misc Info: AIR FORCE DRUG TESTING LAB — GC/MS # 3
Operator : MARCOVICH / CODY

Date : 2 Jun 88 5:31 pm
Instrument: MS_5970
Inlet : GC

Sequence index . 0
Als bottle num : 0
Replicate num . 0

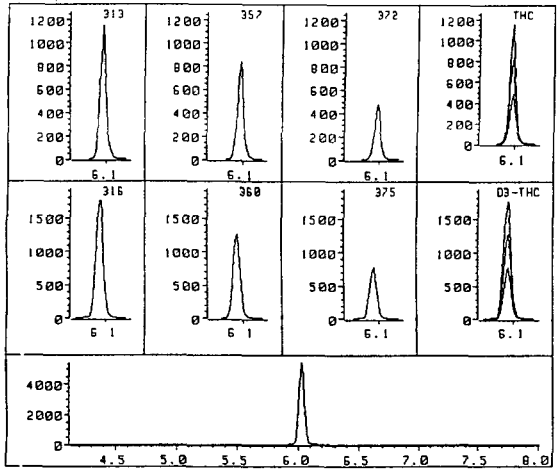

THC RETENTION TIME: 6.04
RELATIVE RETENTION TIME 313/316: 1.00

RETENTION TIME WINDOW: 5.98 - 6.10

ION RETENTION TIMES
Mass 313 = 6.04
Mass 357 = 6.04
Mass 372 = 6.04
Mass 316 = 6.02
Mass 360 = 6.03
Mass 375 = 6 03

MASS ION RATIOS		ACCEPTABLE RANGE	MASS ION ABUNDANCES	
Mass 357/313 :	0.74	0.59 - 0.89	Mass 313:	27331.95
Mass 372/313 :	0.43	0.34 - 0.52	Mass 357:	20294.99
Mass 375/316 :	0.42	0.34 - 0.51	Mass 372:	11759.29
Mass 360/316 :	0 69	0 56 - 0.83	Mass 316:	54097.26
			Mass 360:	37590.19
			Mass 375:	22824.38

Mass 316 amu	Deuterated Internal Standard	30.00 ng/ml
Mass 313 amu	THC-COOH Metabolite	15.00 ng/ml

Data file: DATA:DEMOASMS.D
File type: GC / MS DATA FILE

Sample Name: ASMS DEMO SAMPLE #2 — THC ANALYSIS
Misc Info: AIR FORCE DRUG TESTING LAB — GC/MS # 3
Operator : MARCOVICH / CODY

Date : 3 Jun 88 12:30 pm
Instrument: MS_5970
Inlet : GC

Sequence index 0
Als bottle num : 0
Replicate num : 0

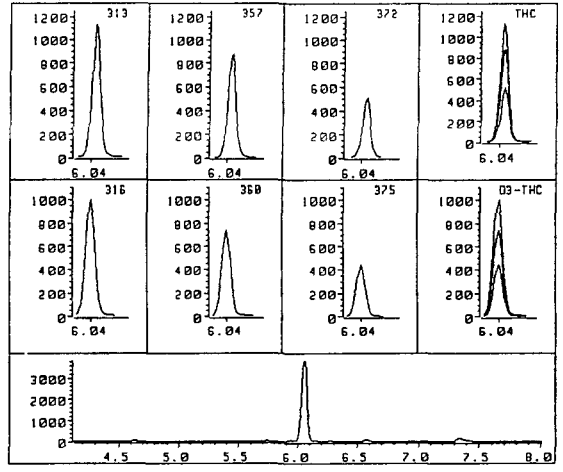

THC RETENTION TIME: 6.06
RELATIVE RETENTION TIME 313/316: 1.00

The Retention Time of THC is acceptable.

ION RETENTION TIMES
Mass 313 = 6.06
Mass 357 = 6.07
Mass 372 = 6.07
Mass 316 = 6.04
Mass 360 = 6.04
Mass 375 = 6.04

MASS ION RATIOS		ION RATIO STATUS	MASS ION ABUNDANCES	
Mass 357/313 :	0.79	OK	Mass 313:	27499.52
Mass 372/313 :	0.44	OK	Mass 357:	21647.61
Mass 375/316 :	0.44	OK	Mass 372:	11979.67
Mass 360/316 :	0.74	OK	Mass 316:	25978.13
			Mass 360:	19289.50
			Mass 375:	11450 17

QUANTITATION BASED ON CALIBRATION STANDARD INJECTED 30 May 88 1:47 pm
BY CODY / MARCOVICH

Mass 316 amu	Deuterated Internal Standard	30.00	ng/ml
Mass 313 amu	THC-COOH Metabolite	31.43	ng/ml

Presented at the 36th ASMS Conference on Mass Spectrometry and Allied Topics
June 5-10, 1988, San Francisco, CA

Presented at the 36th ASMS Conference on Mass Spectrometry and Allied Topics
June 5-10, 1988, San Francisco, CA

DEVELOPMENT OF NOVEL ON-LINE TECHNIQUES FOR GC/MS AUTOMATION IN ENVIRONMENTAL LABORATORIES

G. E. Prill and J. V. Headley
Research & Methods Development Group, Chemistry Wing
Alberta Environmental Centre,
Bag 4000, Vegreville, Alberta, Canada T0B 4L0

The diversity of samples, the large number of analytical services required and the urgency with which information is demanded, have focused the attention of environmental laboratories on automation. The complexity of GC/MS analyses has presented an obstacle to on-line laboratory information management and most laboratories generate GC/MS reports manually. Automatic data input necessitates a communication software package or suitable on-line GC/MS software. This paper reports the development and application of the latter.

The software consists of a series of executable procedure files, developed for Hewlett Packard RTE GC/MS instrumentation equipped with 'AQUARIUS' software (1).

The novel feature of the software is the utilization of on-line sample 'log-in' information to facilitate:

(a) the analysis of outstanding samples
(b) computer assisted data reduction and data validation
(c) the generation of customized analytical client reports and
(d) the generation of an on-line sample 'log-in' data base.

The software is softkey driven and makes extensive use of Edit 1000, RPN and system level commands. Sample 'log-in' information is stored in user designed globals utilizing a 'running' log-template. The latter saves the 'log-in' information of the last sample, a useful feature for batch analyses and multiple 'log-in' entries. Procedure files format the 'log-in' information using a naming convention to automatically append work files, edit text files and update the sample information data base. The sample data base supports up to three linked pattern searches.

An example of a worklist for outstanding samples is illustrated in Figure 1. This worklist contains the information required to assist with the set up of a batch data acquisition file linking the sample to the appropriate laboratory naming convention.

Figure 1. OUTSTANDING SAMPLES

```
T812-1264 Loc:CALGARY BEARSPAW                    =E1264

T812-1265 Loc:CALGARY GLENMORE                    =E1265

T812-1268 Loc:EDMONTON E.L.SMITH                  =E1268

T812-1270 Loc:DRUMHELLER                          =E1270

T812-1284 Loc:1 KM D/S FT.MCMURRAY STP EFFLUENT   =E1284

T812-1285 Loc:LAKE ATHABASCA OFF FT.CHIP          =E1285

T812-1286 Loc:ARS @ JACKFISH VILLAGE              =E1286
```

Figure 2 is a graphical presentation of the integration profile summary workfile. The autogenerated workfile displays quantitation ion profiles, which allow the user to quickly interpret the accuracy of the integration.

Figure 2. INTEGRATION ION PROFILES

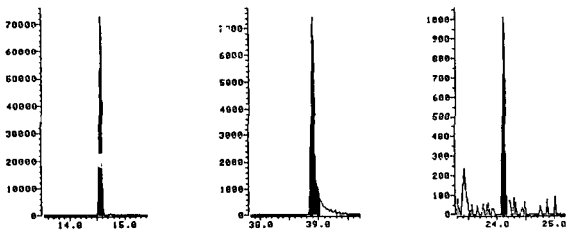

An excerpt from a customized client report is displayed in Figure 3. The procedure files which prepare the report retrieves 'log-in' information as well as other available system information to prepare and assemble the client report.

Figure 3. AUTOGENERATED CLIENT REPORT

```
                                        ALBERTA ENVIRONMENTAL CENTRE
                                        ****************************
File No   :  >E1419                     ORGANICS ANALYSIS DATA SHEET
QT FILE   :  ^E1419
ANALYZED  :  03/21/88 19:23              -------------------------
             MM/DD/YY                    | SEMIVOLATILE COMPOUNDS |
                                         -------------------------

Group_User    :  WQ-LIVINGSTONE            AEC Proj #: BE8
Date Sampled  :  03/15/88                 User Proj #: WQ-B20
Time Sampled  :  09:30     By: SLD
Sample Locat  :  RISSON DRAINAGE DITCH
User Comments:   UNKNOWN SUBSTANCE-100 FT WEST OF POND #3

NAQUADAT                                   ug/L        NAQUADAT
Number                                                 Number
......                                  ............   ... ..

95000    BENZOIC ACID                        0.X       95028    PHENA
95001    4-CHLORO-3-METHYLPHENOL             1.U       95029    PYREN
95002    2-CHLOROPHENOL                     12.        95031    BENZO
95003    2,4-DICHLOROPHENOL                125.        95032    2-CHL
95004    2,4-DIMETHYL PHENOL                 2.U       95033    HEXAC
95005    2-METHYL-4,6-DINITROPHENOL          1.U       95034    HEXAC
```

Examples of autogenerated quality control charts for monitoring sample extractions and instrumental performance are described elsewhere (2). The work files and listings described are automatically appended and scheduled during the 'log-in' process.

Application of the software described provides high volume GC/MS laboratories with automated generation of workfiles and on-line information management. This software is used routinely in our laboratory for the analyses of extractable and volatile priority pollutants, PCB's and hydrocarbons.

References:

(1) A. G. Dexter, E.T.C. Aquarius Reference Manual (1986).
(2) G. E. Prill and J. V. Headley, 35th ASMS conf. proceedings (1987).

Presented at the 36th ASMS Conference on Mass Spectrometry and Allied Topics
June 5-10, 1988, San Francisco, CA

A STRUCTURED MACRO LANGUAGE FOR CONTROLLING GC/MS DATA REDUCTIONS

B.N.Colby and P.W.Ryan
Pacific Analytical, Inc.
1989 B Palomar Oaks Way
Carlsbad, CA 92009

and

P.H.D'Arcy and I.Buttler
VG Masslab Ltd.
Tudor Road, Altrincham
Cheshire WA14 5RZ

Procedure languages have become critical to GC/MS users over the past ten years for efficiently linking software modules into semi-intelligent data reduction processes and for generating customized report formats. As our level of reliance on these user generated procedures has increased, the need for software maintenance and quality assurance (QA) has become critical. In the software industry QA is been addressed through adherence to documented coding protocols and source code review, and software maintenance is dealt with through the use of structured programming languages, named variables, and through extensive use of "commenting" in the source code.

To the end described above, a structured macro programming language has been developed for controlling GC/MS data reduction. It includes:

- Arithmetic and Logical operators,
- User assigned numeric and string variables,
- Structured program control constructs,
- Numeric and string handling functions,
- File, system global and keyboard input functions,
- Printer, screen and file output functions,
- Source code comment delimiters, and
- Single step and error code logging for debugging.

A full set of arithmetic and logical operators for use with user assigned variables. These variables are assigned using the assignment operator, "=". Control structures include IF, IF ELSE, CASE and DO WHILE statements. Program control is achieved using the CALL, EXIT, RETURN and CANCEL commands. Functions are provided for numeric manipulation, string handling and cross conversion between string and numeric. Additional functions provide for formatted writing to the screen, creating windows and accepting formatted input from the keyboard with a prompt on the screen. Disk files can be created, read from, written to and modified in both ASCII and dBase III formats. Full access is provided to the GC/MS system globals as a mechanism to pass information between applications program modules.

Each line of a macro is parsed in turn, The first check is for keywords. These are acted on immediately and the results passed to the applications programs as if it were interactive keyboard input. The parsing sequence is as follows:

1. Find the first non-whitespace character in the macro.

2. If it is a double quote, pass all following characters up to the next double quote. Proceed with step 1.

3. If it is a "(", ignore it and all following characters up to and including the following ")". Proceed with step 1.

4. Temporally store this and all character up to the next whitespace character.

5. If the stored character sequence evaluates to a keyword or an arithmetic expression, process it and subsequent characters as required by the command, Proceed with step 1.

6. Pass the first character of the sequence, then proceed with step 1.

An example of a macro written in this macro language is provided below.

```
(
                                REV_QUAN.MAC

BNC - 5 May 88
)

DISABLE MACRO_FINISHED
ESCAPE ESCAPE ESCAPE ESCAPE ESCAPE                (got to top line
of CLI  )

entry = 1                                         (set  QUAN DB
pointer    )
last_entry = QUAN,L                               (last QUAN DB
entry      )
Chro Para Get "REV_QUAN" CR                       (load parameters
for Chro)
DO WHILE entry <= last_entry                      (loop through QUAN
DB    )
   Edit Quan Get entry CR                         (get & display
peak data )
   Other Write Quan Name 2 TAB 28 CR              (write QUAN DB cpd
name  )
   instr = INPUT('Next, Previous or Edit $','N') (select an
instruction   )
   DO CASE
      CASE (instr = 'N') OR (instr = 'n')         (go to next entry
)
         entry = entry + 1
      CASE (instr = 'P') OR (instr = 'p')         (go to previous
entry    )
         entry = entry - 1
      CASE (instr = 'E') OR (instr = 'e')
         Edit Quan Response Manual PAUSE          (manually edit
response  )
         Write Replace CR                         (replace old data
w/new  )
   ENDCASE
ENDDO
```

THE PC AS A VIABLE ALTERNATIVE TERMINAL FOR THE INCOS DATA SYSTEM

Frank M. Benoit, Health and Welfare Canada, Ottawa, Ontario Canada K1A 0L2.

The Incos data system is based on custom software which is not very flexible, particularly in the preparation of comprehensive quantitative analytical reports. For example, standard INCOS cannot calculate directly the concentration of analytes in the original sample nor combine the results from a batch of samples into one report. Since the inception of INCOS, tremendous advances in computing power have been made, particularly in the area of personal computers. PC systems have available an extensive software library from which many programs can be used to enhance the output from INCOS.

In order to exploit the wealth of PC software, communication between the INCOS and PC systems must be established. In our laboratory we linked the "second terminal" port of INCOS to the serial port of a PC and used a 4010 Tektronix emulator program called PCPLOT to communicate to INCOS. Other terminal emulation programs can be used provided that 4010 graphics are supported. If only ASCII text is transferred, then any terminal program can be used. Crosstalk XVI and Procomm were used successfully to capture text but were incapable of displaying graphics. With the PCPLOT link all the features of the original Tektronix terminal were available with a few exceptions :

1. The PC monitor displayed 22 lines whereas INCOS transmitted 40 lines of text per page. The additional information caused the page to scroll off the top of the screen; the scroll was halted with "control s" and restarted with "control q".
2. A mouse and second PC serial port are recommended for control of the 4010 crosshairs; the "arrow keys" were very slow.

Hence, the PC is a less expensive, viable alternative for the replacement of a Tektronix 4010 terminal. However, the major benefit from this arrangement is the capability to transfer data from INCOS to the PC which is warranted when:

1. It is possible to transfer the data. Not all data accessible to INCOS can be transferred. As a rule the PC can capture any data that INCOS can transmit to the screen. Data that is directed from within an INCOS program to other peripherals such as the printer cannot be diverted to the monitor and hence cannot be captured by the PC.
2. The PC software can import INCOS data for manipulation. For example, the transfer of graphics such as mass spectra to the PC is possible but of limited value unless there is access to software that can import and manipulate INCOS graphics.
3. The manipulation of data using the PC software improves upon the treatment available under INCOS. The quality of INCOS graphics produced by the PC printer is lower than the INCOS printout and hence of little benefit.

Data management and reporting are two of the main weaknesses of INCOS. The quantitative output from INCOS requires additional manipulation to produce the final result. On the other hand, spreadsheet programs such as LOTUS 1-2-3 can import raw data from INCOS and perform a wide variety of calculations to produce quantitative results in a form that can be inserted easily into a final report. We have used two approaches in transferring quantitative data from INCOS. In one approach, the quan list, generated by quantitation of all the peaks in the appropriate regiona of the RIC, is edited in EDQL to exclude all but the relevant data; an entry must exist for each analyte which is identified subsequently by its position in the data list. In the second approach, the quan list is generated by a reverse library search and each entry is labelled with the library name and entry number. This label is used during data manipulation to direct the data to the appropriate location in the worksheet. In this way, target compound analysis, where the target compound may be absent, can be managed.

INCOS data were imported as ASCII files into Lotus 1-2-3 by combining the /File Import Text and /Data Parse commands. The /FIT command imported data as lines of text which were stored in discrete cells. The /DP command converted the data into discrete columns from which the relevant data was extracted. A macro was designed in a Lotus 1-2-3 worksheet to import the raw data from multiple files, calculate the concentrations of each target analyte identified in the sample, normalize multicomponent analytes and prepare the results in tables suitable for insertion in the analytical report.

In our laboratory we analyze routinely indoor air samples in batches of 5 to 15 samples per batch. These samples are screened for 30 target compounds, as well as photocopier fluid residues which consist of a complex collection of aliphatic hydrocarbons in the C_{10} to C_{12} range. The 22 major components in the photocopier fluid mixture provide a characteristic pattern of peaks in the RIC. It is not possible to use quantitative pattern recognition within INCOS because INCOS cannot compare quantitative RIC data from separate datafiles. However, Lotus 1-2-3 can manipulate imported INCOS data from multiple datafiles within one worksheet. Furthermore, statistical operations such as average concentrations in standard solutions, range of concentrations in field samples, differences in the patterns of photocopier residues, correction for incomplete sample recovery, and standard deviations etc. which are not available within INCOS can be carried out easily within Lotus 1-2-3. Of greatest importance is the capability to design and modify the quantitative operations within Lotus 1-2-3 to suit the needs of the analyst.

Using a Lotus macro, the import and data manipulation processes described above took 6.3 s per datafile with an Epson Equity III+ operating at 12 MHz or 26 s per file with an Epson Equity II operating at 7.2 MHz.

The use of the PC as a terminal for the INCOS data system allows access to the raw quantitative data which enables the application of more powerful computational operations than are available under INCOS. The flexibility available with the PC overcomes many of the restrictions and limitations imposed by INCOS.

Presented at the 36th ASMS Conference on Mass Spectrometry and Allied Topics
June 5-10, 1988, San Francisco, CA

THE USE OF PC-COMPATIBLE COMPUTERS TO PULL AND FURTHER REDUCE DATA FROM A SCIEX TAGA 6000E MASS SPECTROMETER/MASS SPECTROMETER

Thomas H. Prichett, U.S. EPA Environmental Response Team,
Gmae Loy and Steve Bottemley, Response Engineering and Analytical Contract.

The U.S. EPA Environmental Response Team (ERT) decided to develop PC-based software to perform the additional data reduction required by the developing Quality Assurance/Quality Control (QA/QC) protocols because of the limitations of the current Sciex software and computer hardware. By replacing one of the Sciex 6000E's terminals with a PC-compatible computer, this PC-compatible computer was used as a smart terminal. Data was captured off the PC-compatible's screen as ASCHII files in MS-DOS with a communication package, XTALK MK4. The ASCHII files were later imported into LOTUS 1-2-3 and parsed into a suitable LOTUS data format. Depending on the LOTUS spreadsheet, data was used for either calibration calculations or QA/QC calculations.

Figure 1 illustrates a sequence of events in capturing flag and intensity data for calibrating the instrument. At event 1, both systems (the TAGA's 6000E Plessey minicomputer and the PC-compatible computer) started at their respective operating systems. At event 2, the TAGA program called Airmon was loaded and several cylinders of different standards were run for intensity and flag data. Event 3 shows a LOTUS spreadsheet, Flags.wk1, making the request for a flag table by writing to an ASCHII file called Filename.dat. Once XTALK is loaded, Filename.dat is read and XTALK dumps the flags and operating parameters into a Plessey file called Mixdat.dmp. The LOTUS spreadsheet, Flags.wk1, remains in resident memory while XTALK is active. Event 4 shows XTALK capturing the Mixdat.dmp file from the Plessey system to a MS-DOS file called MD.dat. Event 5 shows Flags.wk1 importing MD.dat and parsing the sequence numbers of the flag table into LOTUS data format. Another request is made for intensity data of TS ion pair tables. Event 6 shows XTALK being loaded and TS tables being downloaded from the Plessey to the PC-compatible computer. Event 3 through Event 6 is repeated until all of the TS files for each cylinders has been downloaded. Event 7 shows another Lotus file being loaded to do calibration calculations.

These software and hardware techniques became necessary because Airmon, a TAGA program, was unable to calculate the RFs of ion pairs. Airmon had the advantages of monitoring 128 ion pairs and, once the RFs were loaded back into the program, it was able to calculate ion pair concentrations in real time. Similar software techniques were used to calculate the RFs and load RFs data back into Airmon.

By extending the capabilities of the TAGA with a PC-compatible computer, it can be noted that :

1. The tedious operation of data manipulation is removed from human intervention.

2. More time is spent sampling, which allows the TAGA to be more productive.

3. Most of the data can be reduced before leaving the field.

4. Rapid data manipulations provides the project manager with essential information for decision making processes.

5. Modification of spreadsheet macros and communication package macros is possible in the field without long development time.

In conclusion, using a PC-compatible computer to access and reduce data could be a powerful method for extending as well as being cost effective.

Sequence of Events to Capture Flag and TS Table

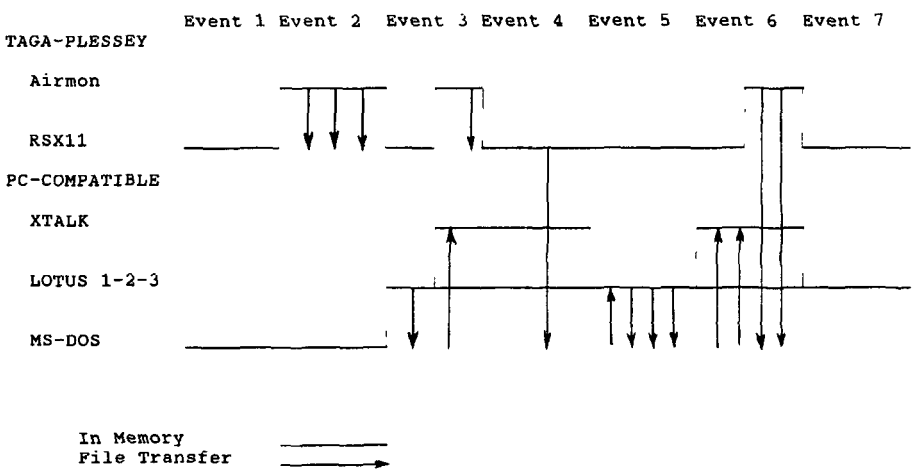

FIGURE 1

Presented at the 36th ASMS Conference on Mass Spectrometry and Allied Topics
June 5-10, 1988, San Francisco, CA

AN IMPROVED VERSION OF THE NBS/EPA/MSDC MASS SPECTRAL DATA BASE, EVALUATION OF THE QUALITY INDEX, AND DATA BASE SOFTWARE FOR AN MS-DOS PERSONAL COMPUTER

Stephen E. Stein and Sharon G. Lias, National Bureau of Standards, Office of Standard Reference Data, Gaithersburg, MD 20899

William L. Budde, U. S. Environmental Protection Agency, Office of Research and Development, 26 W. Martin Luther King Drive, Cincinnati, OH 45268

D. Thomas Terwilliger and Ann L. Behbehani, Computer Sciences Corp., 26 W. Martin Luther King Drive, Cincinnati, OH 45268.

The purpose of this work was to evaluate the 43,005 spectra electron impact (EI) data base and the efficacy of the quality index (QI) which is used to select, from multiple spectra of the same compound, a single spectrum for the data base; and, to implement the data base on an MS-DOS personal computer with software to retrieve and display spectra.

In a previous report of the status of the data base (1), eleven quality factors (QFs) which are used in the QI calculation were evaluated, and new definitions established for some of them. The QI was used to select a 43,005 spectra data base from the archive collection, and a number of the selected spectra were compared with alternative spectra of the same compound in the archive file. As a result of this analysis, several additional QF definition changes were made.

An additional quality factor, QF12, was added to the QI definition to assess the high mass limit of spectra. The quality factor for illogical losses (QF3) was revised to not penalize spectra of low molecular weight hydrocarbons which show losses of multiple hydrogens. The quality factor for detection of spectra with a high air background (QF10) was modified to require the presence of both masses 28 and 32. Quality factors for electron energy (QF1) number of ions (QF5), low mass limit (QF6), calibration date (QF8), and saturation (QF11) were modified slightly. The mean values and standard deviations of the newly defined QFs for the 43,005 spectra data base are as follows:

Quality Factor	QF	Mean	S
Electron energy	QF1	0.9614	0.0733
Ions above M+	QF2	0.987	0.0918
Illogical losses	QF3	0.9824	0.0925
Isotope abundance	QF4	0.9628	0.0819
Number of ions	QF5	0.8953	0.1406
Low mass limit	QF6	0.9572	0.0879
Sample purity	QF7	0.9109	0.0302
Calibration	QF8	0.9536	0.0129
DFTPP refernnce	QF9	0.9017	0.0095
Presence of air	QF10	0.9887	0.0487
Saturation	QF11	0.9769	0.0647
High mass limit	QF12	0.98	0.0634

The most recent changes in the QI algorithm caused the selection of 636 alternative spectra from the archive collection. A careful manual inspection of the 636 pairs of spectra revealed that the alternative spectrum was of better overall quality in only about half of the cases. In the remaining cases, the best spectrum probably was not selected by the revised algorithm.

For example, the spectrum (QI = 589) of hydrazinecarboximidamide with a major ion at mass 46 was selected over an otherwise identical spectrum (QI = 576) of the compound without an ion at mass 46. This ion could only be formed in fragmentation processes which, considering thermochemistry and ion structure, are unlikely. But the atoms present in the parent compound can be combined on paper to form an ion of mass 46. The spectrum with the mass 46 ion is favored by QF5 which penalizes spectra with a smaller number of ions. A very much more sophisticated QI algorithm would be required to rationally distinguish spectra of this type.

Similarly, two spectra of dichloroacetyl chloride were assigned QIs within two points of one another. The spectrum with the higher QI value contained ions at masses 41 and 44, which can only originate from an impurity. We conclude that the QI, at the present level of sophistication, is useful in the automated selection of one EI spectrum when several of the same substance are available. But, the QI must be used with caution, and when the QIs of spectra are within about 10%, the final selection should include the judgement of an expert mass spectroscopist. An effort, based on this approach, is currently underway to improve the overall quality of the data base.

The 43,005 spectra data base was installed on a MS-DOS compatible personal computer (PC), and software developed to retrieve and display spectra. The data base may be searched by Chemical Abstracts Service (CAS) Registry Number, CAS name or other names, internal spectrum identification number, molecular formula, molecular weight, and by the abundances of major ions. More sophisticated searches detailing the presence (or absence) of selected ions may be designed using various options and constraints provided in the search software, including limiting the peak search by molecular weight or elemental composition. Typical searches are completed in 5-15 seconds.

Several thousand spectra are being evaluated for use in the next data base release. Donations of spectra are solicited from laboratories. Computer programs are available, or under development, to assist laboratories in the submission of spectra in machine readable form in a standard format.

(1) D. Thomas Terwilliger, A. L. Behbehani, J. C. Ireland, and William L. Budde, "The Status and Evaluation of a Mass Spectral Data Base", Biomed. and Environ. Mass Spectrom. 1987, 14, 263-270.

Presented at the 36th ASMS Conference on Mass Spectrometry and Allied Topics
June 5-10, 1988, San Francisco, CA

DEVELOPMENT OF A PROPOSED NATIONAL REFERENCE SET OF ELECTRON IMPACT GC/MS RELATIVE RESPONSE FACTORS FOR THE U.S. ENVIRONMENTAL PROTECTION AGENCY'S CONTRACT LABORATORY PROGRAM

by
A. D. Sauter and J. J. Downs, A. D. Sauter Consulting, Henderson, NV 89014; P. Isaacson, Viar and Co., Inc., Alexandria, VA 22314; D. Bottrell, U.S. EPA, EMSL/LV, Las Vegas, NV 89114; D. Youngman, Lockheed Engineering Management Science Corp., Las Vegas, NV 89114; and J. Fisk, C. Dempsey, and A. Carasea, U.S. EPA OERR, Washington, D.C. 20460.

Relatively recent efforts of Mitchum, Tondeur, Fisk, Telliard (1, 2, 3, 4) and others have called to question qualitative and quantitative aspects of the DFTPP criteria published in 1975 (5). Despite the widespread use of these criteria in environmental applications of GC/MS, the impact of these criteria has **never** been definitively tested to establish the qualitative and quantitative consequences of being "in" or "out" of tune. Various tune requirements can add cost to environmental analysis and prohibit the utilization of various types of mass spectrometers in environmental applications of GC/MS. In addition, DFTPP provides limited information for the analysis of higher molecular weight environmental compounds of developing interest. In this regard, a reference set of electron impact GC/MS response factors has merit. Because of these considerations, an interlaboratory study was designed and testing has begun to definitively establish the quantitative and qualitative effects of the old DFTPP criteria on the ability of various GC/MS <u>systems</u> to perform quantitative and qualitative analysis, while developing a reference set of EI GC/MS response factors for the U.S. EPA's Contract Laboratory Program.

Elements of the study include common analytical standards, floppy disc data submission, and an explicit set of directions for the participants. GC/MS data is acquired for 93 organic compounds for seven separate injections, under five different sets of "warped" tunes. Output from the study yields 3255 response factors and 6510 qualitative factors <u>per laboratory</u>. Hence, informative (2-D and 3-D) ways to display the data are useful in understanding the technical consequences of tune (see Figures 1 and 2).

To date, three sets of data have been produced and are currently undergoing study. **Preliminary** indications are:

* Acceptable GC/MS data quality as measured by response and qualitative factors can be achieved outside traditional tune boundaries.

* Suppression of "low" mass sensitivity can greatly increase quantitative uncertainty, as many GC/MS RF values go non-linear.

* For the analytes studied, qualitative library matching and ranking output is largely tune independent except at tune extremes (i.e., when "low" or "high" mass sensitivity are greatly suppressed compared to the old tune).

<u>References</u>:

1. R. K. Mitchum, et al., J. Assn. Off. Anal. Chem., in press 1987.
2. Y. Tondeur, et al., Ion Chemistry of GC/MS Ion Abundance Criteria, BEMS accepted 8/87.
3. J. Fisk, Proceedings from GC/MS Tuning Conference, Alexandria, Virginia, April, 1987.
4. USEPA Method 1625, rev. B, Industrial Technology Division (1985).
5. Budde, et al., Anal. Chem. 47, 995 (1975).

Presented at the 36th ASMS Conference on Mass Spectrometry and Allied Topics
June 5-10, 1988, San Francisco, CA

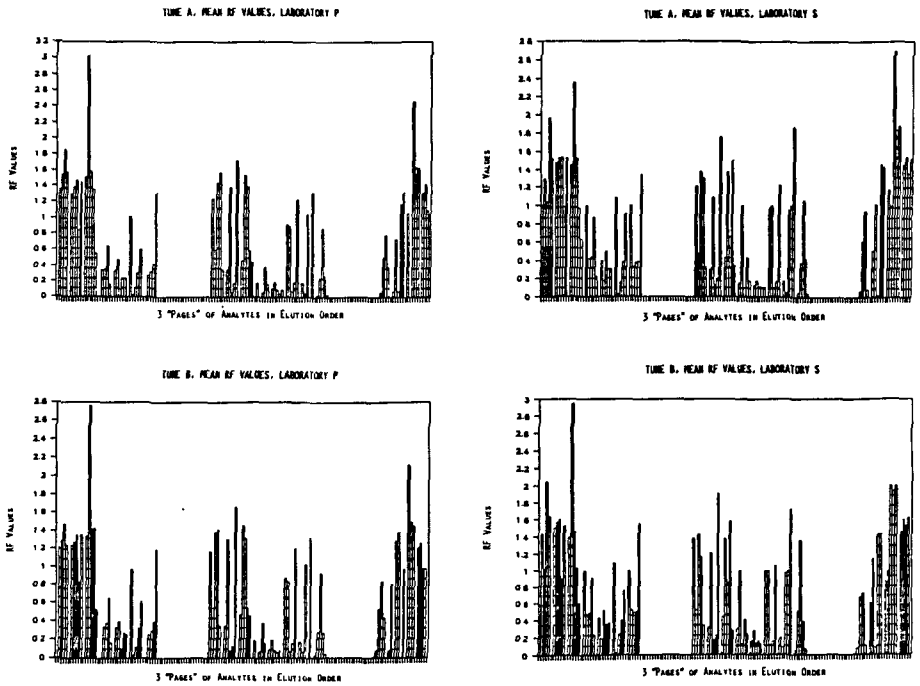

Figure 1. Mean GC/MS response factors versus elution order for laboratory 1 and laboratory 2 for tune A, traditional tune, and tune B, "high" mass enhanced tune.

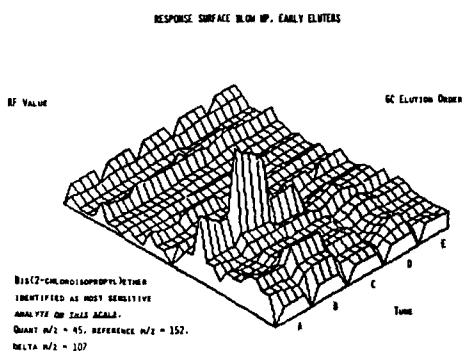

Figure 2. GC/MS RF values for early eluting analytes versus elution order vs. tune.

Presented at the 36th ASMS Conference on Mass Spectrometry and Allied Topics
June 5-10, 1988, San Francisco, CA

AN ELECTRONIC MASS SPECTRAL DATA BOOK

Kogoro MAEDA and Hirotaka ROKUSHA
Electrotechnical Laboratory, 1-1-4 Umezono, Tsukuba, JAPAN

We have noticed for a long time a new trend in the future usage of computer system and emphasized an importance of personal use mode in a small system by microcomputers equipped with large scale storage peripherals. As one of the examples on this theses, we have presented here a new system on mass spectral data base of about 40,000 compounds in a 16 bit microcomputer system with a 20 M bytes hard disk system. Several series of tests have proved so far that the new system is certainly quite good enough for handling a large amount of the data base in a small system and effective as a desk top system for personal use, and further as an electronic data book.

The mass spectral data used are NBS/NIH/EPA/MSDC MSDB edited in 1983, and numerical and character string data in MT were extracted and compiled in FD's in total 17.8 M bytes in a microcomputer system. The terms selected from the MT are: Spectrum number, CAS number, Molecular weight, Chemical formula, Compound name, and a group of Peak heights for all M/Z values.

The computer system used is a combination of PC-9801-UX41 of NEC, Japan, a 4 M bytes RAM disk and a CRT, minimum constituents, but quite an ordinary combination.

Many programs and indices have been developed and compiled for handling the extracted data, and arranged finally into one total system for effective handling of the data base. The whole software systems are written in BASIC compiler language and they run all on MS-DOS Ver.3.1. Searches are available so far for CAS number, Molecular weight, Chemical formula, Base peak and all M/Z values with Peak heights. Any arbitrary combinations are also possible between the two units from the above five operations.

All of the searches can be performed in very short times. For example, only one compound can be picked up from about 40,000 candidates by key-ining a CAS number almost in less than one second, quite a short time. Results of the searching operations can be displayed as tables or mass spectral charts. Mass range for the charts is from m/z 1 to m/z 1800 in six diagrams with unit mass range 300. Two scenes on the same CRT are used for the display, and the two displays on the screen can be changed very quickly from one to the other by pushing the "TAB" key. Table displays also can be changed quickly in the unit of 20 lines by "ROLL UP" and "ROLL DOWN" keys. These efficient replacements on the CRT are quite effective for looking through the candidates found by the searching operations. All the results of the searching operations performed and searching conditions are always displayed as a total list on the CRT. This list is quite effective for following the logics of the searching operations performed.

The present system can be used for many purposes, not only for simple candidate searchings but also for finding rules between compound structures and the mass spectra. In a previous report, we revealed that a clear correlation does exist for the structures and the base peak m/z values for hydrocarbons: that is, when the hydrocarbons are represented as C_nH_{2n-m}, all the base peaks apear for a group of compounds having special m-values always greater than a specific m-value. For example, base peaks m/z 67, 81 and 95 are always found for hydrocarbons C_nH_{2n-m} having the m-values greater than 2. For the case of m/z 79, the base peak is found only for the compounds C_nH_{2n-4}. These rules were revealed for 1813 hydrocarbons extracted from EPA/NIH Mass Spectral Data Book in 4 volumes published in 1978.

The MSDB used here contains 3086 hydrocarbons and the present system has been used in order to confirm whether or not the correlations found previously are still right for more number of the hydrocarbons. To confirm this, we can use the operation No. 8 in the present MENU, AND operation between base peak (BP) and chemical formula (CF). By simple operations, we can find quite instantly the total number is 332 for the compounds having m/z 79 as base peak. Then the system goes to the next stage. By keying "C/H", we obtain the results in 2 - 3 seconds and find the total number of hydrocarbons is 3086, then we can proceed the final stage, AND operation between these two results. The AND operation takes 2 - 3 seconds between the numbers 332 and 3086, and finally we are tought from the system that the number of the candidates required is 123. From the first operation to the final, the total operation takes only 15 - 25 seconds including the key-in operations. Time for display of the results as a list is about 20 seconds, and we take in all about one minute to find all the hydrocarbons having m/z 79 as the base peak. By looking though the list, we could confirm the correlation is still right. All the procedures took several minutes only in all, quite a short time. If we have to do the above procedures by using 6 volumes of MSDB, we will have to consume several hours or more. This is the reason why we call the present system as an "Electronic" Data Book.

As for the compound name search, we sorted all the CAS names by the first capital letters in 26 groups from A- to Z-group, and we can pick up all the compounds having a same first capital letter arbitrarily, then we can see instantly a list of strings of the common first parts of the names with the selected capital letter in next scene on the CRT. If we can find there a string of the same first part as that of compound name required, we have the third list on molecular weight, chemical formula and molecular name for all the compounds having the same first part. By picking up one from the list, we finally obtain all the information on the compound required. The present scheme is quite useful for finding other groups of names together similar to the candidates. Some more experiences, however, are necessary for more convenience. Updates are now in progress.

Author	Page No.
ABBAS, H K	1374
ABBOTT, F S	1360
ABERNATHEY, R M	204
ABERTH, W	73
ABOU-KHALIL, S	1039
ABRAMSON, F P	986
ABRAMSON, F P	988
ACKERMANN, B L	421
ACZEL, T	326
ADAMS, J	379
ADAMS, W J	288
AGGARWAL, S K	510
AHMED, M S	87
AIMONE, L D	1087
AISSA, M	518
AL-OMAIR, A S	1245
ALAI, M	1272
ALAI, M	423
ALDOUS, K M	234
ALEXANDER, A J	831
ALEXANDER, A J	717
ALEXANDER, A J	429
ALEXANDER, L R	36
ALI, M H	988
ALKALAY, D	1029
ALKALAY, D	1026
ALKALAY, D	1028
ALKOFAHI, A	1380
ALLEMAND, P	141
ALLEMANN, M	616
ALLEY, C A	252
ALLEY, C C	246
ALLGOOD, C	669
ALLISON, C E	663
ALLISON, J	711
ALLISON, J	709
ALLISON, J	1213
ALLMAIER, G M	1184
ALLMAIER, G M	1192
ALY, Y	1008
AMSTER, I J	966
AMSTER, I J	1334
AMY, J W	958
ANDERSON, G	429
ANDERSON, M D	1092
ANDREWS, J S	36
ANDREWS, P C	423
ANDRZEJEWSKI, D	807
ANNAN, R	244
ANNAN, R S	490
ANTKOWIAK, J G	492
APFFEL, A	920
APFFEL, A	1318
APPELHANS, A D	1217
ARAKAWA, R	713
ARBOGAST, B	482
ARBOGAST, B	933
ARMENTROUT, P B	226
ARNOLD, M E	1016
ASANO, K G	1112
ASANO, K G	47
ASANO, K G	1108
ASANO, K G	636
ASHCROFT, A E	1156
ASHCROFT, A E	1295
ASHE, T R	328
ASHE, T R	326
ASHLEY, D L	252
ASHMORE, R W	980
AULD, J	274
AZUMA, M	827
BAER, T	563
BAER, T	1336
BAER, T	101
BAHNICK, D	290
BAI, S A	1378
BAILLIE, T A	458
BAKER, T R	1061
BAKTHAVACHALAM, J	244
BALASANMUGAM, K	689
BALAZY, M	875
BALDWIN, M A	839
BALL, L M	931
BALSEVICH, J	1270
BAMBERG, M	964
BAR, I	107
BARBER, M	821
BARBER, M	545
BARBER, M	115
BARBER, M	191
BARBUCH, R J	1043
BARCELO, D	910
BARINAGA, C J	941
BARINAGA, C J	954
BARNES, I L	7
BAROFSKY, D	445
BAROFSKY, D F	753
BAROFSKY, D F	1209
BAROFSKY, D F	482
BAROFSKY, E	1209
BARONAVSKI, A P	228
BARRETT, P	514
BARRETT, P	202
BARSHICK, C M	214
BARTELS, M J	789
BARTELS, M J	970
BARTMESS, J	1198
BARTNER, P L	1188
BARTNER, P L	1152
BARTON, E C	462
BARTON, R D	972
BASS, L M	17
BATEMAN, R H	1089
BATEMAN, R H	715
BATEMAN, R H	1083
BAUER, M R	793
BAUER, M R	1012
BAX, M	1029
BAYER, C W	270
BAYKUT, G	604
BEAN, M F	1279
BEAN, R M	333
BEATO, B D	304
BEAUGRAND, C	707
BEAUGRAND, C	811
BEAVIS, R C	530
BEAVIS, R C	129
BEAVIS, R C	1199
BECKER, C H	1203
BECKER, C H	3
BECKER, H	198
BEHBEHANI, A L	1421
BEHYMER, T D	266
BEIER, R C	189
BELL, D	821
BELL, D J	191
BELL, D J	545
BELL, D J	115
BENCSATH, F A	113
BENFENATI, E	871
BENFENATI, E	417
BENFENATI, E	873
BENFENATI, E	1022
BENNINGHOVEN, A	918
BENOIT, F M	1417
BENSON, L	1289
BENTZ, B L	478
BENTZ, B L	347
BERBERICH, D W	1110
BERMAN, J M	421
BERNICK, M	1342
BERRY, A J	1270
BERTRAM, L K	835
BERTRAND, M	429
BERTRAND, M J	1384
BERTRAND, M J	61
BETHEL, P W	179
BETHEL, P W	1174
BETOWSKI, L D	916
BETOWSKI, L D	32
BETTAZZOLI, L	873
BETTAZZOLI, L	871
BEUHLER, R J	367
BHARGAVA, A K	492
BHARGAVA, A K	494
BIANCHINI-AKBEG, M A	288
BIEMANN, K	849
BIEMANN, K	167
BIEMANN, K	1398
BIEMANN, K	795
BIEMANN, K	1148
BIGGERSTAFF, J	371
BIRKINSHAW, K	649
BITTER-SUERMANN, D	1146
BJARNASON, A	13
BJARNASON, A	1338
BLACK, M S	270
BLAIR, I A	439
BLAIR, I A	1172
BLAIR, I A	1091

Author	Page No.
BLAIR, I A	883
BLAIS, J C	123
BLEASE, T G	685
BLEASE, T G	721
BLEASE, T G	357
BLEASE, T G	443
BOBBIE, B A	238
BODELL, W	496
BODOR, N	1160
BOLGAR, M S	1018
BOLGAR, M S	1014
BOLOGNA, M L	1144
BONI, R	739
BORDERS, D B	1099
BORDERS, D B	1097
BORGERDING, M F	29
BORGERDING, M F	905
BORYSKO, C	498
BOTTOMLEY, S	1419
BOTTRELL, D	1423
BOUCHARD, F	705
BOULAY, W	797
BOULTON, A A	165
BOWERS, M T	17
BOYD, R K	99
BOYD, R K	429
BOYD, R K	831
BOYD, R K	912
BRACKEN, D E	1211
BRADFORD, D	1312
BRADSHAW, S C	628
BRADSHAW, S C	1106
BRAIN, D K	282
BRAJTER-TOTH, A	1323
BRASCH, R C	179
BRASSELL, S	298
BRAUER, F P	208
BREAU, A	972
BREAU, A P	1057
BREEN, J J	242
BRENNA, J T	212
BRENNA, J T	51
BRENNA, J T	1124
BRENNAN, T F	161
BREWER, T G	980
BRINKMAN, D W	310
BRODBELT-LUSTIG, J S	383
BROOKS, P W	534
BROOKS, P W	1031
BROWN, N K	1010
BROWN, N K	1350
BROWN, S M	183
BROWNER, R F	1069
BROWNER, R F	1233
BROWNER, R F	943
BRUINS, A P	1241
BRUINS, A P	1316
BRUMLEY, W C	149
BRUNETON, J	121
BUCHANAN, M V	1118
BUCHANAN, M V	767
BUCHANAN, M V	769
BUCHNER, J D	1297
BUCKNER, S W	703
BUDDE, W L	266
BUDDE, W L	1421
BUHLER, D R	1071
BUNGER, J A	547
BUONARATI, M H	460
BURLINGAME, A L	179
BURLINGAME, A L	925
BURLINGAME, A L	923
BURLINGAME, A L	727
BURLINGAME, A L	496
BURLINGAME, A L	921
BURLINGAME, A L	411
BURSEY, J T	262
BURTON, R	1360
BUSCH, K L	948
BUSCH, K L	765
BUSCH, K L	183
BUSCH, K L	391
BUSCH, K L	339
BUSCH, K L	335
BUSCH, K L	761
BUSH, E D	867
BUTTERWORTH, B C	290
BUTTLER, I	1415
BYCROFT, B W	191
CALDWELL, G W	1035
CALDWELL, K	103
CALDWELL, K	1164
CALLAHAN, J H	1182
CALLERY, P S	1024
CALLERY, P S	1006
CALLIS, E L	204
CAMPBELL, J A	333
CANTLE, J E	202
CANTLE, J E	514
CAO, Z M	59
CAPDEVILA, J	883
CAPIAU, C	1283
CAPRIOLI, R M	549
CAPRIOLI, R M	1081
CAPRIOLI, R M	729
CAPRIOLI, R M	1312
CAPRIOLI, R M	1000
CARASEA, A	1423
CARAVATTI, P	616
CARDIN, D B	331
CARDINALI, F L	1366
CARLSEN, S	1028
CARPIO, H	1162
CARR, S A	425
CARR, S A	1283
CARR, S A	427
CARR, S A	1154
CARR, S A	111
CARRASQUILLO, A	272
CARTER, G T	1097
CARTER, G T	1099
CASHMORE, G	1277
CASTLE, L W	671
CERNIGLIA, C E	1039
CERNY, R L	177
CERNY, R L	393
CERNY, R L	737
CHABOT, G	1047
CHACE, D H	986
CHAIT, B T	413
CHAIT, B T	1340
CHAKEL, J A	837
CHAKEL, J A	405
CHAN, K	1162
CHAN, S Y	1287
CHANCE, R E	978
CHANG, C J	1380
CHANG, V	567
CHARLES, B	121
CHAUDHARY, T	413
CHEN, D	1138
CHEN, K-H	809
CHEN, L	415
CHEN, L	1281
CHEN, S	417
CHEN, S	873
CHEN, T M	419
CHEN, T M	421
CHEN, Y-Z	163
CHENG, M T	571
CHHEDA, G B	492
CHHEDA, G B	494
CHIARELLI, M P	177
CHIARELLI, M P	620
CHIARELLI, M P	1136
CHINN, J W	175
CHINN, J W	173
CHOU, F E	1243
CHOU, P	667
CHOWDHURY, A K	679
CHOWDHURY, A K	693
CHOWDHURY, S	69
CHRIST, JR, C S	699
CHU, J-W	1103
CHUNG, H L	905
CLANDININ, M T	937
CLARK, J	220
CLARK, W D	65
CLAY, K L	893
CLENCH, M	821
CLENCH, M R	1049
CLENCH, M R	719
CLINE, R E	252
COATES, M L	1275
CODY, J T	1411
CODY, R B	1386
CODY, R B	624
CODY, R B	1332
CODY, R B	1116
COGGIOLA, M J	1194

Author	Page No.
COGGIOLA, M J	799
COHEN, A	865
COHEN, A I	1016
COHEN, S A	1079
COHN, V H	988
COLBY, B N	1415
COLE, G T	175
COLE, R	121
COLE, R B	123
COLE, R B	683
COLE, S K	224
COLEMAN, M D	980
COLES, A	1390
COLES, A D	1156
COLTHUP, N B	723
COLTON, R J	1404
COMISAROW, M B	1338
CONCHA, M A	304
CONNER, M K	1120
CONNOR, S	234
CONWAY, D C	1402
CONZEMIUS, R J	218
COOK, K	77
COOK, K D	1215
COOK, K D	939
COOKS, R G	749
COOKS, R G	67
COOKS, R G	958
COOKS, R G	381
COOKS, R G	383
COOKS, R G	968
COOKS, R G	645
COOKS, R G	89
COOKS, R G	1299
COOKS, R G	634
COSTELLO, C E	143
COSTELLO, C E	385
COTTER, R J	423
COTTER, R J	809
COTTER, R J	1281
COTTER, R J	1170
COTTER, R J	415
COTTER, R J	1279
COTTER, R J	1190
COTTRELL, J S	1328
COUTANT, J E	419
COUTANT, J E	1043
COUTANT, J E	421
COVEY, J	1308
COVEY, T	1085
COVEY, T	996
COVEY, T	901
CREASY, W R	51
CREASY, W R	1124
CREASY, W R	212
CREECH, J	407
CREWS, D	173
CREWS, T	1033
CROWLEY, J R	1047
CURRY, P	950
CURTIS, J M	147
CURTIS, J M	715
CUTTITTA, F	1077
D'AGOSTINO, P A	30
D'ARCY, P H	1415
DACUNHA, A R	935
DAGUE, B	1081
DAHL, D A	1217
DALE, F	651
DALE, F	653
DAMHA, M J	488
DAS, B C	119
DAS, P	1152
DAS, P R	117
DAS, P R	1188
DASS, C	551
DASS, C	569
DAVIDSON, T A	516
DAVIS, B A	165
DAVIS, B H	329
DAVIS, D V	331
DAVIS, M	974
DAVIS, M R	976
DAVISON, A	143
DAVOLI, E	1136
DAVOLI, E	103
DAVOLI, E	871
DAVOLI, E	1022
DAVOLI, E	177
DAWSON, P H	355
DAWSON, P H	815
DAYTON, D P	262
DE BELLIS, G	873
DE MAACK, F	1252
DE MAACK, F	817
DE MAACK, F	119
DEAN, L K L	335
DEAN, T A	274
DECKER, K	929
DEINZER, M L	933
DELBERT, S-S	813
DELMORE, J E	1217
DEMPSEY, C	1423
DENG, L	1382
DEPAUW, E	193
DESIDERIO, D M	551
DESIDERIO, D M	569
DETERDING, L J	133
DETERDING, L J	1310
DEVANT, G	817
DEVANT, G	1252
DEVANT, G	119
DEVANT, G	811
DEVANT, G	1241
DEVRIES, N H	143
DEWIT, J S M	906
DEWIT, J S M	1310
DEWIT, J S M	1254
DEWOLF, W E	1154
DHAHIR, P H	972
DIDONATO, G C	1018
DIDONATO, G C	1014
DIETRICH, A M	931
DILTS, M J	998
DING, W H	234
DOHERTY, S J	339
DOMON, B	385
DONG, Z W	59
DONIKE, M	397
DORWIN, E L	1174
DOURDEVILLE, T	1235
DOWNS, J J	1423
DOYLE, R J	573
DRINKWATER, D E	839
DUBAY, G R	567
DUCKWORTH, D	540
DUDEK, G	829
DUFFIN, K L	765
DULIK, D	974
DUNBAR, R C	962
DUNBAR, R C	85
DUNBAR, R C	87
DUNCAN, G F	1358
DUNCAN, M	739
DUNN, R S	905
DUNPHY, J C	391
DURDEN, D A	859
DURDEN, D A	165
DUTTA, S P	492
DUTTA, S P	494
DUTTON, G G S	1338
DUTUIT, O	1336
DWORZANSKI, J	401
DZIDIC, I	322
EASTERLING, D	1378
EBLE, J E	914
ECKENRODE, B A	952
ECKERLIN, R	996
EDLUND, P O	1095
EDLUND, P O	996
EDMONDS, C G	1256
EDOM, R W	1031
EICH, A	855
EICHELBERGER, J W	266
EINHORN, J	27
ELLIGER, C A	1396
ELLIOTT, J	449
ELLS, D R	853
ELSON, C M	276
ELY, T L	466
EMERSON, D E	516
ENGLAND, R E	1396
ENKE, C G	363
ENKE, C G	833
ENKE, C G	1388
ENKE, C G	813
ENKE, C G	952
ENS, W	337
ENS, W	488
ENS, W	63

Author	Page No.
ESCOFFIER, B	906
ESKEW, T J	1394
ESPINOSA-LENIZ, R	1002
ETZEL, R A	252
EVANS, B A	395
EVANS, C J	445
EVANS, J E	395
EVANS, S	1156
EWING, A	950
EYLER, J R	91
EYLER, J R	681
EYLER, J R	699
EYLER, J R	604
EYLER, J R	600
EYLER, J R	125
FACCHETTI, S	193
FALICK, A M	411
FANELLI, R	873
FANELLI, R	1022
FANELLI, R	417
FARMEN, R H	1358
FARRELL, K	1360
FARROW, P E	829
FAULK, J	85
FAULKNER III, H C	1358
FAULL, K F	445
FAULL, K R	435
FEDORA, J W	326
FEISTNER, G J	445
FEISTNER, G J	435
FEIZI, T	1277
FENG, P	1362
FENG, R	839
FENG, R	375
FENN, J B	1207
FENN, J B	771
FENNESSEY, P V	155
FENSELAU, C	1272
FENSELAU, C	1279
FENSELAU, C C	1190
FENSELAU, C C	1170
FERGUSON, A	278
FERGUSSON, G J	1223
FERRIERI, R A	759
FETTEROLF, D	988
FETTEROLF, D D	805
FILBY, R H	304
FINK, S W	1227
FISHEL, D	781
FISHEL, D L	956
FISHER, J J	19
FISK, J	1423
FITE, W L	359
FLORY, D A	903
FLORY, D A	1229
FLORY, D A	1227
FLURER, R A	761
FOLTZ, D J	643
FOLTZ, R L	1376
FOO, L Y	482
FOREBACK, C C	1103
FOSTER, W B	1144
FOURNET, B	735
FRADIN, A	897
FRANCL, T J	935
FRANKEL, A D	415
FRANZEN, J	185
FRANZINI, S	206
FREAS, R B	903
FREAS, R B	1227
FREAS, R B	55
FREAS, R B	990
FREAS, R B	1229
FREDERICK, B	425
FREEMAN, J P	984
FREISER, B S	703
FREISER, B S	614
FREISER, B S	701
FRENCH, M A	937
FREY, R	185
FRIEDMAN, L	367
FU, E W	1008
FUJII, T	1219
FUJII, Y	512
FUJIOKA, M	1134
FUJIOKA, M	1285
FUJIWARA, H	1362
FUKUDA, D S	978
FUKUDA, E K	433
FUKUDA, E K	1033
FUNKE, P T	1016
FUTRELL, J	371
FUTRELL, J	649
FUTRELL, J H	81
GABRIEL, M K	437
GAGE, D	198
GAGE, D A	877
GAGNON, R	974
GALAL, A M	1008
GALE, D	1346
GALE, P J	478
GALE, P J	347
GALEN, T J	45
GAMES, D E	1239
GAMES, D E	1268
GAMES, D E	1270
GAN, L-S	486
GANGULI, B	109
GARDNER, D	763
GARLAND, W A	433
GARLAND, W A	1033
GARRETT, J G	1392
GARRETT, J H	232
GARRETT, J H	256
GARTEIZ, D	1091
GARTEIZ, D A	1092
GARWOOD, M	1356
GASKELL, S	454
GASKELL, S J	879
GASKELL, S J	137
GASKELL, S J	1150
GASKELL, S J	111
GASKELL, S J	895
GAUDRY, D	1028
GAUDRY, D	1026
GAUMANN, T	602
GAVINELLI, M	871
GE, N-C	268
GEDAMKE, R	1014
GELLENE, G I	773
GELLENE, G I	15
GERARDI, R	1146
GETEK, T A	984
GETEK, T A	452
GETEK, T A	1039
GHADERI, S	614
GHADERI, S	1126
GIAM, C S	1120
GIBLIN, D E	83
GIBSON, B W	1293
GIBSON, B W	555
GIBSON, T M	43
GIESE, R	244
GIESE, R W	490
GILLECE-CASTRO, B L	923
GILLEN, G	343
GILLESPIE, T A	127
GILLESPIE, T A	889
GILLIAM, J M	978
GLEDHILL, W E	280
GLISH, G L	47
GLISH, G L	823
GLISH, G L	1108
GLISH, G L	300
GLISH, G L	302
GLISH, G L	639
GLISH, G L	825
GLISH, G L	636
GLISH, G L	1112
GLOTFELTY, D W	577
GOERINGER, D E	835
GOLDMAN, H D	1053
GOODMAN, S D	624
GOODWIN, R M	1057
GORDON, B M	29
GOTLIN, R W	155
GOTT, G A	545
GOULD, V	1235
GOULD, V	783
GOULD, V	454
GOULD, V	1274
GOVINDARAJAN, S	1140
GRABAREK, J	885
GRABOWSKI, J J	747
GRACE, L I	413
GRADY, M C	468
GRANGE, A H	753
GRANT, B C	47
GRANT, J L	179
GRANT, R A	450

Author	Page No.
GRAUL, S	661
GRAYSON, M A	476
GRAYSON, M A	474
GREAVES, J	38
GREEN, B N	191
GREEN, B N	427
GREEN, B N	715
GREEN, J B	310
GREEN, L W	520
GREENE, F T	314
GREER, J F	447
GREER, J F	1221
GREGORY, J F	387
GRESE, R P	135
GRESE, R P	21
GRIFFIN, L L	741
GRIFFIN, P R	553
GRIGSBY, R D	320
GRIGSBY, R D	310
GRINDSTAFF, O G	264
GRIX, R	67
GROCE, D F	246
GROSS, M L	230
GROSS, M L	379
GROSS, M L	103
GROSS, M L	673
GROSS, M L	1164
GROSS, M L	177
GROSS, M L	393
GROSS, M L	620
GROSS, M L	389
GROSS, M L	21
GROSS, M L	1136
GROSS, M L	745
GROSS, M L	83
GROSS, M L	671
GROSS, M L	557
GROSS, M L	737
GROSS, M L	135
GROSSHANS, P B	592
GROSSMANN, P	616
GROTEMEYER, J	1199
GROTEMEYER, J	129
GROTEMEYER, J	530
GUENAT, C R	931
GUEVREMONT, R	831
GUEVREMONT, R	565
GUIXIN, L	1372
HADDON, W F	1396
HAGENHOFF, B	918
HAGNAUER, G	484
HAIL, M E	889
HAIL, M E	803
HAIL, M E	1110
HAJDASZ, D J	23
HAKANSSON, P	337
HALE, R	38
HALES, D H	226
HALLIDAY, J	472
HAMEISTER, C H	628
HAMILTON, M	972
HAMMARGREN, W M	498
HAMMER, M S	536
HAMMOND, I	43
HAMMOND, M J	783
HANES, M	256
HANEY, C A	1378
HANEY, C A	994
HANKINSON, D J	709
HANNAK, P	534
HANSEN, E B	1039
HANSON, C D	612
HANSON, R L	290
HARADA, K I	1037
HARDEN, L A	256
HARDEN, L A	232
HARDEN, L A	1392
HARDY, M	1272
HAROLDSEN, P	454
HAROLDSEN, P E	1150
HAROLDSEN, P E	879
HARPOLD, D N	345
HARRIS, W E	943
HARRIS, W E	1069
HARRISON, A G	69
HARRISON, L M	155
HARRISON, W W	216
HARRISON, W W	214
HARRISON, W W	5
HART, H V	322
HART, K J	1388
HARTMAN, T G	1140
HARTMAN, T G	1368
HARTMAN, T G	34
HARVEY, D J	891
HARVEY, D J	1010
HARVEY, D J	1350
HARVEY, G J	643
HARVEY, R G	278
HASHIZUME, Y	187
HASSELL, T C	1152
HATCH, G E	518
HAW, J F	316
HAWIGER, J	885
HAWTHORNE, S B	1264
HAYASHI, A	431
HAYES, D A	292
HAYES, M J	1029
HAYES, R N	21
HAYES, R N	737
HAYES, R N	557
HAYES, R N	1164
HAYES, R N	393
HAYES, R N	745
HAYES, R N	389
HEAD, S L	252
HEADLEY, J V	1413
HEADLEY, J V	534
HEARN, B A	604
HEDIN, A	337
HEIKES, D L	260
HEIN, R E	624
HEINRICH, N	743
HELLER, D N	1170
HEMBERGER, P H	638
HEMLING, M E	1283
HEMMINGER, J C	1334
HEMMINGER, J C	349
HENION, J	901
HENION, J	996
HENION, J	1095
HENION, J	1260
HENION, J	1085
HENION, J	1308
HENRY, K D	647
HENZEL, W J	405
HEPBURN, J W	705
HER, G R	887
HER, G R	1287
HER, G R	885
HER, G R	1266
HERCULES, D M	318
HERCULES, D M	526
HEROD, A A	1295
HEROLD, D A	510
HETTICH, R L	1122
HEWITT, J	1408
HEYES, M P	881
HICKS, R D	29
HIGUCHI, T	1249
HIGUCHI, T	841
HIGUCHI, T	899
HILKER, D R	234
HILL, J A	795
HILL, J A	849
HILL, J C	847
HILL, R H	252
HILPERT, L R	1002
HINDENLANG, D M	1020
HINDENLANG, D M	437
HIRAYAMA, K	1130
HITES, R A	41
HITES, R A	579
HO, C T	1140
HO, C T	34
HOEKMAN, D J	1106
HOEKMAN, D J	628
HOERR, R A	1344
HOFFMAN, E DE	399
HOGGE, L R	912
HOGGE, L R	1270
HOLLAND, J F	833
HOLLAND, J F	952
HOLLE, A	185
HOLLER, J S	1366
HOLLY, E	173
HOLMAN, R W	673
HOLST III, W P	466
HONOVICH, J P	606
HOOD, R J	1186

Author	Page No.
HOOD, R J	1047
HOOPER, E	709
HORNING, S R	89
HORUP, P	445
HOSOE, M	512
HOUK, R S	218
HOUNSELL, E F	1277
HOWALD, W N	1065
HOWALD, W N	458
HOWARD, S	371
HOWARD, S	649
HOWELL, S A	863
HSU, B H	1166
HSU, B-H	1160
HSU, C S	326
HSU, F F	1256
HSU, F F	1053
HUA, S	163
HUANG, L Q	218
HUANG, S K	1330
HUANG, S K	1319
HUANG, S L	324
HUANG, Y	703
HUES, S M	1404
HUGHES, B M	1406
HUGHES, B M	288
HUGHES, H	895
HUGHES, R J	79
HUI, Y H	1380
HUNT, A H	978
HUNT, D F	553
HUNT, J	781
HUNT, J E	956
HUNT, S L	1168
HUTCHINSON, D W	733
HUTCHINSON, R M	222
HWANG, E Y	1409
IBRAHIM, S	561
ICARDI, G	417
IINO, T	757
IKENISHI, Y	1132
IKONOMOU, M	25
INFANTE, R	272
INOUE, F	1346
INOUE, M	608
INOUE, M	53
INOUE, M	787
INOUE, Y	1354
ISA, K	139
ISA, K	1354
ISAACSON, P	1423
ISHIDA, T	53
ISHIHARA, M	841
ISHIKAWA, K	1400
ITAGAKI, Y	899
ITAGAKI, Y	841
ITAGAKI, Y	1249
ITO, Y	1243
IVASHKIV, E	1016
IWASAKI, K	1134
IWATANI, K	196
JACKSON, J	1408
JACOBS, D	1205
JACOBS, M L	222
JACOBS, P	151
JAHUA, D	1372
JAJOO, H K	1091
JAKUBOWSKI, E M	1006
JAKUBOWSKI, E M	1063
JAMES, H A	43
JAMIESON, W D	912
JAMIESON, W D	276
JAMIESON, W D	99
JAOUEN, D	811
JAOUEN, D	1336
JARDINE, I	1087
JARDINE, I	1289
JARDINE, I	731
JEHUAI, S	1372
JEMAL, M	1016
JENNINGS, K R	733
JENSEN, N J	318
JENSEN, T E	294
JI, D	655
JIANG, K	921
JIANG, L F	1209
JIMBA, H	1219
JIN, S-J	1348
JOHANSON, K O	427
JOHN, C	1293
JOHNSON, C A	893
JOHNSON, J V	630
JOHNSON, R	1408
JOHNSON, R S	1148
JOHNSON, R S	1398
JOHNSTON, M	626
JOHNSTON, M V	777
JOHNSTON, M V	1251
JOHNSTON, M V	71
JONES, A D	460
JONES, A G	143
JONES, D S	1089
JONES, D S	1083
JONES, G G	464
JONES, L A	994
JONES, T L	916
JONES, T L	32
JONNSON, G	337
JORGENSON, J W	1310
JORGENSON, J W	1254
JUNK, G A	218
JUREWICZ, A	425
KAISER, R E	968
KAKKAD, B	439
KALINOSKI, H T	1262
KAMINSKI, H	185
KAMMEI, Y	841
KAMMEI, Y	827
KANEDA, N	187
KANEKO, T	181
KANTOR, E J	908
KAO, J	974
KARANIAN, J W	881
KARCHESY, J J	482
KARRER, R	921
KASS, S	667
KASSAHUN, K	1360
KASSEL, D B	1213
KATAKUSE, I	431
KATAKUSE, I	827
KATTA, V	413
KAUR, S	496
KAWASAKI, E H	466
KAYE, J H	208
KEBARLE, P	944
KEBARLE, P	25
KEDZIERSKI, B	1071
KELLER, P R	643
KELLERHALS, H P	616
KELLEY, P E	634
KELLEY, P E	1106
KEMPFF, M B	1186
KEMPWERTH, G	918
KENION, G B	1097
KENION, G B	1099
KENNY, P T M	1158
KENTTAMAA, H I	749
KEOUGH, T	763
KEOUGH, T	450
KERLEY, E L	612
KETKAR, S N	359
KHEMANI, L	1029
KIDWELL, D A	1364
KIELO, E	937
KILLMER, L	665
KIM, H-Y	1045
KIMERLE, R A	288
KING, F L	216
KINGHAM, D R	353
KINSEL, G R	1251
KINSEL, G R	71
KINTER, M	510
KIPLINGER, J P	675
KIRBY, D J	220
KIRK, J D	943
KIRK, J D	1233
KITAGAWA, I	1132
KLEIN, D H	1319
KLEINER, A I	935
KNAPP, D R	200
KNAPP, D R	889
KNOLL, H	618
KNOLL, H	964
KOBAYASHI, K	181
KOBAYASHI, T	899
KOBAYASHI, T	1249
KOBAYASHI, T	675
KOCH, D	185
KOCH, L	206
KODA, S	1285

Author	Page No.
KOFEL, P	964
KOFEL, P	610
KOLAR, W	540
KOONS, R D	805
KORFMACHER, W A	452
KORFMACHER, W A	1039
KORFMACHER, W A	984
KOSTIAINEN, R	691
KOYANAGI, G K	105
KOYANAGI, G K	79
KRAFT, A	67
KRESBACH, G M	490
KRICK, T P	1356
KRIER, G	626
KROLIK, S T	1083
KRUSE, D	175
KRUSE, L I	1154
KUBOTA, E	899
KUBOTA, E	827
KUBOTA, E	1249
KUBOTA, E	841
KUEHL, D W	290
KUEI, J C H	1266
KUNIHIRO, F	841
KUO, G	974
KUSMIERZ, J	551
KYRANOS, J N	484
LABDON, J E	1152
LABDON, J E	409
LACEY, M	763
LACEY, M P	450
LADISCH, S	198
LAFORTUNE, E	488
LAGNA, W M	785
LAGOW, R J	65
LAM, Z	1338
LAND, D P	1334
LAND, D P	349
LANGVARDT, P W	789
LANT, M S	1055
LAPPIN, G	1274
LARAMEE, J A	933
LAU, B P-Y	254
LAUE, H-J	958
LAWSON, A M	1277
LE, J C	1178
LE, J C	1176
LEARY, J A	538
LEARY, J A	779
LEBO, J A	240
LEBRILLA, C B	966
LECH, L M	701
LEDFORD, E B	592
LEE, E	1260
LEE, E	996
LEE, E	901
LEE, E D	1085
LEE, E D	1308
LEE, G W T	715
LEE, H	278
LEE, J M	288
LEE, M K	994
LEE, M S	1225
LEE, T D	845
LEE, T D	1196
LEE, Y C	1272
LEGESSE, K	845
LEGESSE, K	1196
LEHR, J L	857
LEIKER, T J	248
LEIKER, T J	296
LEMONS, J	506
LEPETIT, G	817
LEROY, Y	735
LESIEUR, M	1252
LETHBRIDGE, P G	369
LEVY, R H	1065
LEWIS, D K	563
LEWIS, S	1321
LEYH, B	839
LI, H	163
LI, L	1201
LI, L	226
LI, L	775
LI, L	992
LI, X	528
LI, Z-M	1382
LIANG, H-D	1382
LIANG, X-T	195
LIAS, S G	1421
LIBERATO, D J	433
LIBERT, R	399
LIFSHITZ, C	1304
LIFSHITZ, C	743
LIGHT, K J	1213
LIM, H K	1376
LIN, C H	59
LIN, S-N	1312
LIN, S-N	1000
LIN, V K	1344
LIN, W-N	1103
LIN, Y Y	1104
LINDBERG, C	1067
LINDEN, H B	618
LINDNER, J	1199
LINDNER, J	129
LINDNER, J	530
LINDQUIST, J M	349
LINEMAN, D	318
LING, Y C	341
LINHARDT, R J	1291
LINNOILA, M	881
LINSCHEID, M	502
LINSCHEID, M	504
LINXING, H	159
LISEK, C A	1087
LISHEING, G	1370
LISTER, A K	645
LIU, K	224
LIU, S	528
LIU, Y M	1380
LIU, Y M	506
LIZONG, J	1372
LOGUSCH, E W	1362
LOH, S K	226
LOH, S Y	1116
LONG, E	950
LOO, J A	647
LOO, J A	954
LOOYE, K M	30
LOPEZ, H	1402
LOUAGE, F	743
LOURIS, J N	968
LOY, G	1419
LUBMAN, D M	361
LUBMAN, D M	775
LUBMAN, D M	1201
LUCAS, D S	450
LUCAS, M E	1020
LUNG, W	543
LYNN, B C	908
LYON, P A	1168
MACCONI, D	871
MACFARLANE, R D	847
MACFARLANE, R D	1205
MACLAREN, D C	655
MACLOUF, J	897
MACMAHON, T J	703
MACRORY, P P	545
MADHUSUDANAN, K P	117
MAEDA, K	1425
MAGEE, C W	1
MAHAFFY, P R	345
MAHONEY, J F	791
MAHONEY, J F	1196
MAHONEY, J F	845
MAJEWSKI, M S	577
MAJOR, H J	240
MALEKNIA, S	65
MALLET, A I	861
MALLET, A I	863
MALLIS, L M	755
MALLIS, L M	1291
MALLIS, L M	536
MALOSSE, C	27
MANN, M	1207
MANN, M	771
MANNERS, G D	1396
MANTUS, D S	341
MANZ, I	1146
MARBURY, G D	908
MARCH, R E	79
MARCH, R E	105
MARCHETTI, M	375
MARCOVICH, D T	1411
MARCUS, P	107
MARCUS, P	809
MARCUS, R K	540
MARIANI, G	1022
MARINELLI, P J	373

Author	Page No.
MARKEY, S P	739
MARKEY, S P	606
MARKS, L M	1344
MARSH, K N	278
MARSHALL, A G	590
MARSHALL, A G	675
MARSHALL, A G	596
MARSHALL, A G	594
MARSHALL, A G	588
MARSHALL, A G	592
MARSHALL, A G	960
MARSHALL, A G	1217
MARSHALL, A G	1302
MARSHALL, D J	857
MARTIN, D	155
MARTIN, L B	1180
MARTIN, L L	447
MARTIN, L L	1221
MARTIN, M	1081
MARTIN, S A	849
MARTIN, S A	1148
MARTIN, S A	795
MARTIN, W B	1279
MARTINEZ, R I	109
MARTYN, J A A	1061
MASILAMANI, D	1020
MASON, R T	173
MASUCCI, J A	1035
MATHEWS, W R	1150
MATSUDA, H	431
MATSUDA, H	827
MATSUMOTO, I	1073
MATSUMOTO, I	1354
MATSUMOTO, M	1354
MATSUO, T	431
MATSUO, T	827
MATSUURA, K	1249
MATSUURA, K	899
MAYER, F	63
MAYERNIK, J A	1120
MAYLIN, G	996
MAYOL, R F	1091
MCADOO, D J	741
MCALLISTER, R A	262
MCAULIFFE, C A	545
MCBAIN, W	1124
MCCLENNEN, W H	641
MCCLENNEN, W H	547
MCCLENNEN, W H	403
MCCLENNY, W A	584
MCCLOSKEY, J A	1256
MCCLOSKEY, J A	145
MCCLUER, R H	395
MCCLURE, T D	500
MCCLURE, T D	927
MCCORMICK, T J	1014
MCCOY, R W	464
MCCRAW, J M	1366
MCDONALD, G A	1352
MCDOWALL, M A	1237
MCDOWALL, M A	1235
MCELVANY, S W	57
MCEWEN, C N	365
MCGOWN, S R	1254
MCGUIRE, J M	524
MCIVER, R T	1334
MCIVER, R T	966
MCIVER, R T	349
MCKAY, G	1031
MCKENZIE, D E	288
MCKENZIE, D E	1406
MCLAFFERTY, F W	839
MCLAFFERTY, F W	647
MCLAFFERTY, F W	1116
MCLAFFERTY, F W	375
MCLAREN, J W	912
MCLAUGHLIN, J L	1380
MCLAUGHLIN, L	1260
MCLEAN, M A	1229
MCLEAN, M A	903
MCLOUGHLIN, M	1319
MCLUCKEY, S A	823
MCLUCKEY, S A	300
MCLUCKEY, S A	1112
MCLUCKEY, S A	636
MCLUCKEY, S A	302
MCLUCKEY, S A	47
MCLUCKEY, S A	639
MCLUCKEY, S A	1108
MCLUCKEY, S A	825
MCLUCKEY, S A	835
MCMAHON, A W	79
MCMAHON, T B	705
MCMAHON, T B	19
MCMAHON, T B	659
MCMAHON, T B	610
MCMAHON, T B	663
MCMURRAY, W J	449
MCREYNOLDS, J H	236
MEEK, J T	1247
MEISELS, G G	557
MEISELS, G G	751
MEISELS, G G	745
MEL, S	411
MENDEZ, J	1162
MENG, C K	771
MENG, C K	1207
MENTZER, M	1154
MERCER, G E	304
MERTENS, S K	292
MESSERLE, L	536
MESTDAGH, H	811
MESTDAGH, H	707
MESTER, T C	906
MEUZELAAR, H L C	403
MEUZELAAR, H L C	547
MEUZELAAR, H L C	401
MEUZELAAR, H L C	641
MEUZELAAR, H L C	329
MEYERS, C A	427
MICHAUD, D P	1061
MICHAUD, D P	161
MICKUNAS, D	1342
MIDERSKI, C A	15
MILBERG, R M	715
MILBERG, R M	147
MILES, L M	427
MILLEN, W G	1247
MILLER, C	709
MILLER, D J	1264
MILLER, D L	1101
MILLER, D L	284
MILLER, D L	867
MILLER, J M	689
MILLINGTON, D S	1396
MILLINGTON, D S	1314
MILLINGTON, D S	1346
MILLINGTON, D S	157
MILLS, G	1049
MILNES, G J	443
MILTON, D J	1156
MINAMI, K	53
MINARD, R D	950
MINNIKIN, D E	861
MIOTTO, J	1026
MIOTTO, J	1028
MIROCHA, C J	1374
MITCHELL, J R	895
MITCHELL, S	1356
MIZUNO, T	1073
MOINI, M	91
MOLINA, M J	575
MONAGHAN, J J	819
MONAGHAN, J J	115
MONAGHAN, J J	721
MONAGHAN, J J	191
MONCUR, J	1390
MONCUR, J G	466
MONTREUIL, J	735
MOODY, L A	242
MOOMAW, C R	1079
MOOR, M J	1065
MOORE, C	462
MOORE, C	561
MOORE, C	1390
MOORE, W T	1081
MOORE, W T	1312
MORALES, A	944
MORDEN, W E	191
MORDEN, W E	721
MORDEN, W E	115
MORELLI, J J	474
MORIMOTO, Y	1285
MORRIS, M	115
MORRIS, M	545
MORRIS, M	191
MORRIS, M	821
MORRIS, M	827
MORRIS, R A	651
MORRISON, G H	341

Author	Page No.
MORROW, J C	101
MORTON, T H	677
MORTON, T H	377
MORTON, T H	655
MOSELEY, M A	1310
MOSELEY, M A	1254
MUDGETT, P D	847
MUKAI, F	929
MULLEN, S L	960
MULLER, J F	626
MULSHINE, J L	1077
MUNAVALLI, S	1063
MUNSON, B	669
MUNSON, B	687
MURPHY, C	415
MURPHY, C M	1170
MURPHY, C M	1279
MURPHY, R C	897
MURRAY, T M	242
MUSSELMAN, B D	1249
MUSSELMAN, B D	899
MUSSELMAN, B D	841
MUSSER, S M	1006
MUSSER, S M	1024
MYERS, T G	456
MYKYTYN, V	171
MYLCHREEST, I C	1268
MYLCHREEST, I C	1270
MYNDERSE, J S	978
NAGABHUSHAN, T L	1152
NAGABHUSHAN, T L	409
NAGATSU, T	187
NAITO, Y	608
NAKAGAWA, Y	196
NAKAGAWA, Y	1132
NAKAJIMA, S	1037
NAKANO, K	927
NANNI, E J	29
NAOKI, H	1158
NARAYAN, R	324
NASAR, K	193
NEAL, P	506
NEEDHAM, L L	36
NEEDHAM, L L	252
NELSON, C C	145
NELSON, S D	456
NERO, V P	308
NEWMAN, R A	1092
NIEHUIS, E	918
NIEMANN, H B	345
NIEMEYER, I	351
NIES, A S	875
NISHIGAKI, S	787
NISHIGAKI, S	53
NISHIMURA, H	522
NISHIMURA, T	751
NISHIMURA, T	557
NIWA, T	153
NIWA, T	187
NIWA, Y	1400
NIZOLEK, T J	1211
NODA, T	53
NODA, T	787
NOGUCHI, H	1134
NORDMAN, R	1318
NORIS, M	871
NORWOOD, D L	1314
NORWOOD, D L	157
O'BRIEN, R J	753
O'CONNELL, L A	143
O'DONNELL, J E	314
O'MALLEY, R M	559
OCCOLOWITZ, J L	978
ODA, M	869
ODOM, R W	351
ODOM, R W	480
OGILVIE, K K	488
OGURA, M	1219
OHASHI, M	757
OHKURA, T	1354
OKAMOTO, M	512
OKANO, J	532
OLESIK, S V	1325
OLIVER, K D	584
OLSON, J R	236
ONG, D E	439
OPFERMANN, G	397
ORLANDO, R	687
ORTH, R G	280
ORTH, R G	582
OSAWA, Y	415
OTSUKA, K	899
OTSUKA, K	1249
OWEN, R	1049
OWEN, R	821
OWEN, R	719
OXENFORD, J	34
OXFORD, J	1055
OZTURK, F	91
OZTURK, F	681
PACK, T	1138
PACK, T	441
PALACZ, Z	514
PALLIX, J B	3
PALLIX, J B	1203
PALMER, P T	1388
PAN, S-S	1024
PAN, Y	11
PAN, Y	598
PANG, E	855
PANG, H M	361
PANNELL, L K	1243
PAPANASTASSIOU, D A	9
PAQUETTE, L A	675
PARENT, D C	57
PARKER, C E	906
PARKER, C E	1071
PARKS, E K	224
PARR, V	821
PARR, V C	719
PARR, V C	1049
PATANELLA, J E	1362
PATKIN, A J	286
PATRZYC, H B	492
PATRZYC, H B	494
PATTERSON, D G	246
PATTERSON, D G	36
PAULS, R E	464
PAULSON, J	1067
PAULSON, J F	651
PAULSON, J F	653
PAWLOSKY, R J	1374
PEAKE, D A	282
PEAKE, D A	620
PEARLSTEIN, R M	143
PEARSON, P G	458
PEDDER, R E	632
PEET, N P	1378
PEGE, G	873
PEKAY, L A	1325
PELLETIER, M	626
PEREIRA, W E	248
PEREIRA, W E	296
PEREL, J	791
PEREL, J	845
PEREL, J	1196
PERKINS, D D	943
PERREAULT, H	61
PETERMAN, P H	240
PETERSEN, H A	322
PETERSON, D L	923
PETERSON, G S	449
PETERSON-WRIGHT, L J	284
PETERSON-WRIGHT, L J	1101
PETRE, J	1283
PEZSA, I	964
PEZSA, I	618
PFLUG, J L	569
PHARAZYN, S	937
PHILLIPS, L R	1198
PIERSON, D L	45
PING, K Y	543
PING, W	1372
PINOLI, P C	466
PIRKLE, J L	36
PITTMAN, K A	1358
PLATZNER, I	107
PLEASANCE, S	1239
PLEIL, J D	584
POESTHORST, D	206
POHL, L R	415
POMERANTZ, S C	1256
PONGRACZ, K	496
POOLE, C F	274
PORCH, R L	262
PORTER, N A	567
POULTER, L	925
POULTER, L	1142
POULTER, L	921
POWERS, R E	695

Author	Page No.
PRAMANIK, B	1152
PRAMANIK, B	1235
PRAMANIK, B C	1079
PRAMANIK, B N	117
PRAMANIK, B N	1188
PRAMANIK, B N	409
PRAS, N	1316
PRICE, D	443
PRILL, G E	1413
PRITCHETT, T H	1342
PRITCHETT, T H	1419
PROKAI, L	1160
PROVOST, L R	30
PRZYBYLSKI, M	1146
PU, Q-L	159
QIAN, K	371
QIAO, S-J	268
QUARLES, J M	1402
QUILLIAM, M A	912
QUILLIAM, M A	276
QUIRKE, J M E	304
QURESHI, N	1281
RADICATI DI BROZOLO, F	480
RAJOTTE, R	937
RALEY, T J	1279
RAMJIT, H G	695
RAMSEY, E D	1239
RANDT, C	504
RAPIDS, M S	208
RAPIN, J	602
RASHED, M S	1065
RASHED, M S	456
RAYMER, J	1059
REDDY, A M	171
REED, R L	1071
REICHERT, P	409
REICHERT, P	1152
REILLY, M H	137
REILLY, M H	111
REIMER, M	500
REINER, E J	238
REINHOLD, V N	1287
REINHOLD, V N	1266
REINHOLD, V N	885
REINHOLD, V N	887
REITZ, A B	1035
REMPEL, D L	586
RENDELL, N B	861
REYNOLDS, J D	1215
RICART, G	735
RICCA, T L	592
RICCA, T L	590
RICCA, T L	960
RICE, J	262
RICHARDS, J M	547
RICHARDS, J M	403
RICHARDSON, B R	316
RICHARDSON, C H	353
RICHARDSON, D E	699
RICHERT, J F O	294
RIDGE, D P	11
RIDGE, D P	697
RIDGE, D P	598
RILEY, S J	224
RINEHART, K L	147
RINEHART, K L	715
ROACH, J A G	807
ROBAUGH, D	314
ROBERTS, G D	1154
ROBERTS, G D	425
ROBERTS, G D	111
ROBERTS, G D	427
ROBERTS, J	1352
ROBERTS, W J	449
ROBINSON, C N	569
ROBINSON, M J	476
ROBOZ, J	1237
ROCK, C	877
ROCKWOOD, A L	598
ROCZKO, A	526
ROEHL, C	17
ROEPSTORFF, P	445
ROEPSTORFF, P	1192
ROGERS, M	1274
ROHRBAUGH, D K	258
ROKUSHA, H	1425
ROLANDO, C	1336
ROLANDO, C	811
ROLANDO, C	817
ROLANDO, C	707
ROLONDO, C	27
ROMKOWSKI, M	206
RONG, L S	147
RONG, L S	715
ROSEN, J D	34
ROSEN, J D	1140
ROSEN, J D	1368
ROSEN, R T	1140
ROSEN, R T	1368
ROSEN, R T	34
ROSENBERG, I E	801
ROSENWAKS, S	107
ROSS, B D	1356
ROSS, M M	1182
ROSS, M M	381
ROSTAD, C E	248
ROSTAD, C E	296
ROVIN, L H	1368
ROVIN, L H	34
RUBIO, F R	1033
RUDEWICZ, P	1321
RUPPRECHT, J K	1380
RUSSELL, D H	97
RUSSELL, D H	93
RUSSELL, D H	95
RUSSELL, D H	612
RUSTLER, E M	502
RUTHENBERG, A E	956
RYAN, P W	1415
SACK, T M	242
SAHA, M G	490
SAITO, K	869
SAITO, Y	53
SAKATA, I	1037
SAKURAI, T	827
SALEHPOUR, M	956
SALEHPOUR, M	781
SALEM, N	881
SALEM, N	1045
SAMPSON, E J	36
SANDERS, R	763
SANDERSON, N E	220
SANTIAGO, N	272
SASAOKA, T	187
SATOUCHI, K	869
SATTERLEE, W G	972
SATZGER, R D	542
SAUTER, A D	1423
SAVORY, J	510
SCANLAN, G	1289
SCHAEFER, W H	439
SCHANZER, W	397
SCHELLENBERG, D H	238
SCHERZER, J	331
SCHEY, K L	67
SCHIFF, P L	1008
SCHLAG, E W	530
SCHLAG, E W	1199
SCHLAG, E W	129
SCHMID, E R	1192
SCHNEIDER, K	1146
SCHOEN, A E	843
SCHRAM, K H	171
SCHRAM, K H	927
SCHRAM, K H	498
SCHRAM, K H	500
SCHREINER, A F	1180
SCHRODER, E	685
SCHROEDER, E	151
SCHRYNEMEECKERS, P J	292
SCHUBERT, R	151
SCHUELER, B	63
SCHWARTZ, J C	634
SCHWARZ, H	743
SCIACCA, M A	1358
SCOBLE, H A	1144
SCOTT, W J	755
SCRIVENS, J H	357
SCRIVENS, J H	685
SCRIVENS, J H	443
SCRIVENS, J H	721
SEDGWICK, R D	1020
SEDGWICK, R D	437
SEGAL, A	929
SEGALL, H J	460
SEGAR, K R	1251
SEGAR, K R	777
SEIBER, J N	577
SEIFERT, W E	1312
SELGREN, S F	773

Author	Page No.
SELLERS-HANN, L	97
SEN, N P	254
SENTOH, F	1285
SERVE, M P	1352
SETCHELL, K D R	1043
SETCHELL, K D R	1051
SHABANOWITZ, J	553
SHALABY, L M	914
SHALER, T A	677
SHAMO, R E	1217
SHAO, J D	101
SHAO, J-D	563
SHARKEY, A G	318
SHARKEY, A G	526
SHARP, T R	278
SHARP, T R	49
SHARP, T R	316
SHAW, R W	210
SHEA, J P	1358
SHEEHA, E W	1297
SHEEHAN, E W	998
SHEELEY, D M	1266
SHEPHERD, M C	292
SHERMAN, W R	1053
SHIEA, J	298
SHIH, M	739
SHIMA, M	522
SHINKA, T	1073
SHIPLEY, L A	980
SHORE, F L	292
SHUKLA, A	81
SHUKLA, A	371
SHUKLA, A	649
SIEGEL, M M	797
SIEGEL, M M	1258
SIEGEL, M M	723
SILLY, L	1190
SIM, P G	276
SIM, P G	99
SIM, P G	912
SIMONS, D S	343
SIMONSICK, W J	468
SIMONSICK, W J	470
SIMPSON, B J	288
SLAGLE, R E	264
SLAUGHTER, C	1235
SLAUGHTER, C A	1079
SMITH, D C	783
SMITH, D H	210
SMITH, D L	1380
SMITH, D L	506
SMITH, E G	476
SMITH, F A	970
SMITH, J R	1006
SMITH, P C	1231
SMITH, R D	1262
SMITH, R D	954
SMITH, R D	941
SMITH, R W	689
SNOW, K B	75
SNYDER, A P	851
SNYDER, A P	641
SO, H Y	39
SOHLBERG, K	81
SOLCH, J G	256
SOLCH, J G	232
SOLCH, J G	1392
SOLOMON, J J	929
SOLSTEN, R T	1362
SOPCHYSHYN, F C	520
SORIA, C	1124
SPALL, W D	638
SPATOLA, A F	133
SPHON, J A	807
SPILKIN, A	1162
SQUIRES, R R	657
SQUIRES, R R	661
SQUIRES, R R	23
SQUIRES, R R	373
STACE, A J	369
STAFFORD, C J	250
STAMS, D A	655
STANDING, K G	63
STANDING, K G	488
STANDLEY, L J	41
STANLEY, M S	948
STEELE, D H	242
STEIN, S E	1421
STEINER, D F	423
STEMMLER, E A	769
STEMMLER, E A	767
STEPNOWSKI, R	711
STEVENS, D L	867
STILLWELL, W G	486
STIPANOVIC, R D	189
STIRCHAK, G	933
STOCKTON, G W	1247
STOFFELS, J J	853
STOFFELS, J J	208
STOLL, M	1277
STORY, M	1312
STOUT, S J	935
STRAUB, K	1162
STRAUB, K M	976
STREBIN, R S	208
STRIFE, R J	1114
STRINGHAM, K R	169
STRINGHAM, K R	324
STROBEL, F	697
STROUD, R M	411
STULTS, J T	837
STULTS, J T	405
STURM, G P	310
SUGIYAMA, Y	787
SULLIVAN, J F	450
SUN, Z L	59
SUNDQVIST, B U R	337
SUNNER, J	944
SUNNER, J	25
SUWANRUMPHA, S	990
SUZUKI, M	1037
SWAISGOOD, H	1138
SWEELEY, C C	198
SWEETMAN, B J	1172
SWERDLOFF, M D	437
SWINEFORD, D M	250
SYKA, J E P	843
SYKA, J E P	1328
SZABO, I	1328
SZULEJKO, J E	659
TABACCHI, R	141
TABET, J C	683
TABET, J C	121
TABET, J C	123
TACHIBANA, K	1158
TAGHIZADEH, K	329
TAGUCHI, V Y	238
TAI, T-L	349
TAKAYAMA, K	1281
TAKEDA, N	1037
TAKEDA, N	187
TAKEDA, N	153
TAN, J-X	1382
TANG, S Y	1041
TANG, X	63
TANI, T	757
TANNENBAUM, S	486
TATEMATSU, A	1037
TATEMATSU, A	153
TATEMATSU, A	187
TAYLER, P J	443
TAYLOR, J W	13
TAYLOR, L	1408
TAYLOR, L C E	1142
TECKLENBURG, R E	97
TECKLENBURG, R E	95
TECKLENBURG, R E	93
TERAI, Y	139
TERNES, T N	264
TERWILLIGER, D T	1421
TETLER, L	821
TETLER, L W	545
TETLER, L W	115
TETLER, L W	191
THEOHARIDES, A D	980
THIBAULT, P	717
THIBAULT, P	429
THIBAULT, P	912
THIBAULT, P	831
THOMAS, T D	655
THOMAS, T F	75
THOMAS, T F	653
THOMSON, A B R	937
THOMSON, M L	1247
THREADGILL, M D	458
TIERNAN, T O	1392
TIERNAN, T O	232
TIERNAN, T O	256
TING, C	536
TODD, D E	783

Author	Page No.
TODD, J F J	1245
TODD, J F J	1306
TODD, P J	946
TOLLITTE, F	626
TOLUN, E	779
TOLUN, E	538
TOMER, K B	131
TOMER, K B	1254
TOMER, K B	133
TOMER, K B	1071
TOMER, K B	931
TOMER, K B	1310
TOMER, K B	906
TONG, H Y	230
TORIGOYE, N	522
TOTH, J P	387
TOWNSEND, L B	498
TOWNSEND, R	1272
TREHY, M L	280
TRESTON, A M	1077
TROTTA, P P	1152
TROTTA, P P	409
TRUMBO, P R	387
TSAO, R	797
TSARBOPOULOS, A	1152
TSARBOPOULOS, A	1289
TSARBOPOULOS, A	709
TSERNG, K-Y	1348
TSOUPRAS, G	141
TSUCHIYA, M	181
TUCKER, D B	628
TUINMAN, A	77
TURNER, L K	341
TURNER, P J	202
TURNER, P J	514
TURNER, W E	36
TUSCHALL, J R	908
TUTTAS, D	206
TWOREK, H A	492
TWOREK, H A	494
UCHIDA, M	1132
UDSETH, H R	954
UDSETH, H R	1262
UDSETH, H R	941
UHRIG, M S	29
UNGARELLI, R	857
UNGER, S E	1018
UNGER, S E	1014
UY, O M	1170
UYEDA, C	532
VAN BERKEL, G J	302
VAN BERKEL, G J	300
VAN BERKEL, G J	1112
VAN BERKEL, G J	639
VAN BERKEL, G J	335
VAN BERKEL, G J	304
VAN BREEMEN, R B	1178
VAN BREEMEN, R B	1176
VAN BREEMEN, R B	407
VAN BREEMEN, R B	1180
VAN EMON, J M	916
VAN LANGENHOVE, A	982
VAN LANGENHOVE, A	1344
VAN LEYEN, D	918
VANCE, J C	264
VANGAEVER, F	1326
VANHOOF, F	399
VANNESS, G F	256
VATH, J E	1148
VATH, J E	385
VATH, J E	167
VERDUN, F R	960
VERDUN, F R	590
VERGES, F M	1239
VERMA, S	1071
VERMA, S	131
VESTAL, C H	1051
VESTAL, C H	1223
VESTAL, M L	903
VESTAL, M L	1229
VESTAL, M L	1223
VICCHIO, D	1075
VICKERS, R	111
VIEIRA, N E	508
VIGGIANO, A A	651
VIGGIANO, A A	653
VINCENTI, M	89
VINEBERG, K A	355
VISWANADHAM, S K	318
VISWANADHAM, S K	526
VOLK, K J	1323
VOLPE, T P	470
VORBURGER, O	614
VOUROS, P	161
VOUROS, P	490
VOUROS, P	1061
VOUROS, P	484
VOUROS, P	244
VOYKSNER, R D	1138
VOYKSNER, R D	1059
VOYKSNER, R D	1378
VOYKSNER, R D	441
VRBANAC, J J	200
VRBANAC, J J	889
WADA, Y	431
WAGEL, D J	256
WAGNER, G	206
WAGONER, D E	262
WALKER, G	1287
WALKER, V	1049
WALLE, T	1378
WALLE, U K	1378
WALSER, M-E	602
WAN, X	1370
WANCZEK, K P	618
WANCZEK, K P	964
WANG, B H	647
WANG, H M	1291
WANG, J	649
WANG, J-S	801
WANG, L	937
WANG, M	588
WANG, M	592
WANG, M	596
WANG, P-R	1382
WANG, R	1281
WANG, T C-L	739
WANG, T H	312
WANG-IVERSON, D	1016
WARD, D M	298
WARD, J R	258
WARNER, C D	673
WARNER, C D	389
WARRACK, B M	1014
WARRACK, B M	1018
WATSON, C H	600
WATSON, C H	604
WATSON, C H	125
WATSON, J T	952
WATSON, J T	877
WAUGH, A R	353
WAYNE, R S	1247
WEBER, D	254
WEBER-GRABAU, M	634
WEBER-GRABAU, M	628
WEBER-GRABAU, M	1106
WEDDLE, G H	962
WEIL, D	626
WEIL, D	357
WEIL, D A	1338
WEIL, D A	624
WEIL, D A	1332
WEIR, O	821
WEIR, O	1049
WEISS, G	185
WEITZ, C J	435
WELCH, M B	1043
WELCH, M J	865
WELCH, M J	1002
WELLER, D	933
WELLER, R R	614
WELLER, R R	1120
WEN, Y	1374
WENCLAWIAK, B	294
WENG, Q	498
WERNERY, J D	282
WESDEMIOTIS, C	839
WESDEMIOTIS, C	375
WESTMORE, J B	488
WESTMORE, J B	63
WHITE, D L	179
WHITE, E	1002
WHITE, E	865
WHITE, E L	29
WILKES, J G	1223
WILKINS, C L	622
WILKINS, C L	39
WILKINS, C L	693
WILKINS, C L	1275
WILKINS, C L	679

Author	Page No.
WILLIAMS, C P	594
WILLIAMS, E R	647
WILLIAMS, E R	1116
WILLIAMS, F	441
WILLIAMS, J I	437
WILLIAMS, J L	1120
WILLIAMS, K	449
WILLOUGHBY, R C	464
WILLOUGHBY, R C	908
WILLOUGHBY, R C	998
WILLOUGHBY, R C	1297
WILLS, M R	510
WILSON, C R	222
WILSON, J M	561
WILSON, L A	935
WILSON, M	1378
WILSON, S B	1277
WINDIG, W	851
WINGENDER, R J	1409
WINGER, B	958
WINTER, C K	460
WISE, M B	1118
WISHNOK, J S	486
WITTSTRUCK, T A	1394
WOLF, A P	759
WOLF, C J	474
WOLLNIK, H	67
WOLSTENHOLME, J	353
WONG, L K	1008
WOOD, D	719
WOOD, D	1049
WOOD, D	821
WOOD, K V	324
WOOD, K V	169
WOODS, M	115
WOODS, M	545
WOODS, M	191
WOOLFITT, A R	733
WORKMAN, D B	657
WOTRING, L	498
WRIGHT, B	819
WRIGHT, B	1156
WRIGHT, J L C	565
WRIGHT, J L C	912
WU, R-M	268
WU, V	1140
WYATT, J R	1404
WYSOCKI, V H	381
XI, Y	1370
XIA, W	1372
XU, H-X	486
XU, L	306
XU, W H	1158
YAKSH, T L	1087
YAMAMOTO, H	0
YAMASHITA, K	883
YANCEY, M F	1012
YANCEY, M F	793
YANG, H-J	163
YANG, K Q	1004
YANG, L C	622
YANG, S S	586
YANG, S-C	739
YANG, Y-C	258
YASAKA, T	927
YATES, J R	553
YEFCHAK, G E	833
YELLE, L M	829
YERGEY, A L	508
YERGEY, A L	1075
YERGEY, A L	1077
YERGEY, A L	1231
YERGEY, J A	881
YI, H	1370
YINGHUA, Y	1372
YINGHUA, Y	992
YOSHIZUMI, H	153
YOST, R A	1110
YOST, R A	632
YOST, R A	1225
YOST, R A	127
YOST, R A	304
YOST, R A	630
YOST, R A	803
YOST, R A	1323
YOST, R A	889
YOUNG, J P	210
YOUNG, S	799
YOUNG, S	1194
YOUNG, V R	1344
YOUNGMAN, D	1423
YU, K O	1352
YU, P H	165
YU, W	55
YUAN, M	528
YULAN, L	1370
YUNFEI, J	1372
YUNIS, A A	1039
ZEEVAART, J A D	877
ZENG, C-H	143
ZHA, Q	745
ZHA, Q	751
ZHA, Q	557
ZHANG, J	159
ZHANG, L	747
ZHANG, M-Y	839
ZHANG, M-Y	375
ZHANG, T Y	1243
ZHAO, H	1382
ZHE, H	543
ZHU, N Z	553
ZHU, Y	528
ZIDAROV, D	1384
ZIMMERMAN, J A	559
ZIRROLLI, J A	897
ZIV, J	1368
ZOMER, E	982
ZUKAS, W	484

Presented at the 36th ASMS Conference on Mass Spectrometry and Allied Topics
June 5-10, 1988, San Francisco, CA

AMERICAN SOCIETY FOR MASS SPECTROMETRY
BUSINESS MEETING

San Francisco Hilton
San Francisco, California
June 8, 1988

President Gerry Meisels called the meeting to order at 11:35 a.m. He announced that the first item of business was the 1988 Research Awards. The representatives of the two participating companies and the grant recipients were asked to come forward. Dr. Denley B. Jacobson of North Dakota State received his award from Dr. Michael Harvey of VG Instruments, and Dr. Mark A. Smith of the University of Arizona was given his award by Dr. Robert Finnigan of Finnigan-MAT.

Susan Weintraub presented the Secretary's report. She asked for any additions or corrections to the 1987 Business Meeting minutes which were printed in the Bound Volume of the 35th Annual Conference. There were no recommended changes to the minutes, and it was moved, seconded and unanimously passed that the minutes be accepted.

The results of the 1988 ASMS elections were then displayed. The new Board Members will be: Vice President for Programs, Robert Murphy; Treasurer, Michelle Buchanan; Member-at-Large (Education), Michael Story; Member-at-Large (Measurements and Standards), Rodger Foltz. Thanks were also expressed to the candidates who were not elected - Tom Cairns, Alan Marshall, Robert Dunbar and Kenneth Standing.

Next, the list of winners of the 1988 Student Travel Awards was shown. The recipients were: Charles S. Christ, Jr., University of Florida; Rick A. Flurer, Indiana University; Mark E. Hail, University of Florida; Peter Haroldsen, Baylor College of Medicine; Kathleen A. Kayganich, Michigan State University; Gary R. Kinsel, University of Colorado; James N. Kyranos, Northeastern University; Leo M. Lech, Purdue University; Matthias Mann, Yale University; Chad C. Nelson, University of Utah; Ron Orlando, University of Delaware; Jian-Dong Shao, University of North Carolina; Elizabeth A. Stemmler, Oak Ridge National Laboratory; and James E. Vath, Massachusetts Institute of Technology. Weintraub explained to the audience that according to current policy regarding the stipends, only one student per advisor is eligible for an award.

In concluding the Secretary's report, it was announced with regret that two members had passed away during the past year - Terry E. Sharp and John D. Connell.

The Treasurer's report was presented by Kelsey Cook. He explained that the society's financial health is excellent and that we have an amount sufficient for 1 year's expenses maintained in reserve. In addition, our expenses for the past year were somewhat less than our total income, allowing our reserves to increase by approximately $36,000. Cook continued by showing a slide which compared assets, expenses, income and reserves for 1985 through 1987. He concluded with an illustration of conference expenses and showed that these expenses have increased each year. Cook explained that in recent times more emphasis has been placed on the scientific program, with the result that expenses for speakers have increased while expenditures for catering have decreased. There were no questions from the audience.

Gary Glish, the Vice President for Arrangements, was next to report. He announced that to this point, there were 1796 registrants for the 36th Annual Conference. In response to earlier questions about the current situation with the ACS meeting being held at the same time as the ASMS Conference, Glish explained that the ACS selected their dates after we had already made our final arrangements.

Details about the upcoming social event were presented, and Glish gratefully acknowledged the efforts of Julie Leary. He also requested suggestions for future social activities. Glish continued by saying that the spouses's program had been very successful this year, and he thanked Lou Story for her assistance.

Glish next explained that the site for the 1989 Conference had been changed from Toronto to Miami Beach, because the hotel in Toronto was planning to initiate major renovations of the meeting space. He added that the facilities at the Fontainbleau in Miami Beach were exceptionally good.

Plans for the 1990 Conference in Tucson were covered next. Glish indicated that there would be 2 main hotels, with shuttle buses operating between them. Tentative arrangements for 1991 have also been made; it is likely that the meeting will be held at Opryland in Nashville on May 19 - 24. There were no questions about Conference arrangements.

Ron Hites, the Vice President for Programs, spoke next. He acknowledged the assistance of the Program Review Committee (T. Cairns, R. Caprioli, G. Glish, P. Hemberger, G. Meisels, R. Murphy, M. Ross and S. Weintraub, with Judith Watson as an ex officio member) and explained that the interests of these people covered a wide range of disciplines in mass spectrometry. In the initial review process about 60 abstracts were rejected, of which approximately 40 were later accepted after revision. He then showed an overview of submitted papers and compared the statistics for 1988 with those of 1987. The popularity of posters was evidenced by an increased number of abstracts requesting the poster format in contrast to a decline in oral presentations. In conclusion, Hites showed that there has been approximately an 8% per year increase in the number of papers presented. No questions were raised.

Willard Harrison serves as the ASMS Board Member-at-Large who is responsible for the Bound Volume. He reported that he anticipates that there will be about 1400 pages in the volume for this year and added that the cost to the society for each volume has decreased from 1987; this is due in great part to the work of Judith Watson.

Harrison then announced that the Board of Directors of ASMS had voted to change the title of what has been informally known as the "Bound Volume" to include the word "Proceedings". This year's issue will be called "Proceedings of the 36th ASMS Conference on Mass Spectrometry and Allied Topics". He continued by saying that growth of the Proceedings at the current rate might necessitate a change to a more convenient format.

The Member-at-Large with the responsibility for Education, Chris Enke, gave his report next. He described the results of a questionnaire about educational resources in mass spectrometry at academic institutions. From the responses it was evident that not only would additional material be beneficial, but also, implementation of some form of clearinghouse for instructional items would be of great value. Enke next explained about the Education Committee's current efforts to prepare a brochure on mass spectrometry; the brochure is designed to help people who are not in the field and will present information about various techniques and applications of mass spectrometry.

Enke then discussed a change in the organization of the Education Committee, saying that the new ASMS Board Member-at-Large with responsibility for Education, Mike Story, will be the chairman of the Education Committee. Enke then gave special thanks to Harry Hertz for his hard work in past years as the chairman of this committee.

Enke next listed the short courses which were offered immediately prior to the 1988 Conference. He explained that there were 120 attendees at the courses and that there had been a waiting list for places in these courses. In conclusion, he announced that the Fall Workshop would be entitled "Environmental Applications of Mass Spectrometry". It will be organized by Ron Hites and Ron Haas and is scheduled to be given during the week of October 17, 1988.

Paul Goodley, the Member-at-Large responsible for Measurements and Standards, reported on that committee's activities and described their upcoming workshop on quality criteria for mass spectral databases. He also said that efforts were currently underway to compile a glossary of terms used in mass spectrometry. He then mentioned that a modification of the JCAMP-DX data format for mass spectral data transfer between PC's was under consideration. Goodley completed his report by explaining that the Measurements and Standards Committee was being reorganized in a manner similar to the Education Committee, and that the new ASMS Board Member-at-Large, Rodger Foltz, would be the Measurements and Standards Committee chairman.

President Gerry Meisels gave his report next. He related his views on the exciting and interesting years he has spent with the ASMS Board, and he predicted a great future for mass spectrometry in response to the challenge of rapid changes in science and technology. He described various growth areas of the society and explained that eventually the annual ASMS Conference will have so many attendees that a convention center will have to be used for the scientific sessions. Meisels reviewed several changes that have taken place over the past few years - for example, affiliation with the Asilomar Conference and removal of the last formal ties with ASTM E-14 - all as evidence of the broadening of ASMS, which must continue to examine how to provide services which will meet the needs of the members. Meisels said that many of the society's activities are directly dependent on action of the ASMS Board of Directors, and he thanked them all collectively. He expressed particular gratitude to Judith Watson and said that the society couldn't function effectively without her. Meisels then thanked the representatives from Japan and China for their participation in making the 36th Conference a special Pacific Rim international meeting. In recognition of the Board members who were leaving office, he asked Graham Cooks, Kelsey Cook, Chris Enke and Paul Goodley to come forward. Meisels presented plaques to each person and thanked them individually for their efforts.

Meisels next asked for comments from the floor. Anne Giordani brought up two issues. She expressed interest in having a salary survey conducted and related her feelings on the need for child care arrangements at the annual conference. Meisels responded by saying that the Board will look into these matters. William Sherman then announced that he unfortunately had to report that another member, David Carroll, had passed away during the year.

In conclusion, Meisels urged the society members to speak with people on the ASMS Board concerning any other questions that may arise. There being no further business, the meeting was adjourned at 12:30 p.m.

Respectfully submitted,

Susan T. Weintraub

Susan T. Weintraub
Secretary

Presented at the 36th ASMS Conference on Mass Spectrometry and Allied Topics
June 5-10, 1988, San Francisco, CA

IN MEMORY OF

Terry E. Sharp

and

John D. Connell

Presented at the 36th ASMS Conference on Mass Spectrometry and Allied Topics
June 5-10, 1988, San Francisco, CA

TERMS TO USE IN YOUR RESEARCH PRESENTATIONS

The following terms occur in ASMS presentations frequently. The translation, given in *italics*, tells what the speaker really means.

It has long been known that.... *I haven't bothered to look up the the original reference.*

...of great theoretical and practical importance *...interesting to me*

While it has not been possible to provide definite answers to these questions... *The experiments didn't work out, but I figured I could at least get a publication out of it.*

The XYZ system was chosen as especially suitable to show the predicted behavior. *The fellow in the next lab had some already made up.*

Three of the samples were chosen for detailed study. *The results on the others didn't make sense and were ignored.*

High-purity... *Composition unknown except for the exaggerated claims of the supplier.*

...handled with extreme care throughout the experiments. *...not dropped on the floor.*

Typical results are shown. *The best results are shown.*

Although some detail has been lost in reproduction, it is clear from the original spectrum that... *It is impossible to tell from the spectrum.*

The agreement with the predicted curve is excellent. *...fair* ...good *...poor* ...satisfactory *...doubtful* ...fair *...imaginary* ...as good as could be expected *...non-existent*

The most reliable values are those of Jones. *Jones was a student of mine.*

It is generally believed that... *A couple of other guys think so too.*

It might be argued that... *I have such a good answer to this objection that I shall now raise it.*

Much additional work will be required before a complete understanding... *I don't understand it...*

Correct within an order of magnitude *Wrong*

It is to be hoped that this work will stimulate further work in the field. *This paper isn't very good, but neither are any of the others on this miserable subject.*

Thanks are due to Joe Hoe for assistance with the experiments and to John Doe for valuable discussions. *Hoe did the work and Doe explained what it meant.*

Preliminary experiments have shown that... *We did it once but couldn't repeat it.*

A survey of the earlier literature.. *I even read through some of last year's journals.*

Careful statistical analysis... *After going though a dozen books, we finally found one obscure test that we could apply.*

We are excited by this finding. *It looks publishable.*

We have a tentative explanation. *I picked this up in a hospitality suite last night.*

We didn't carry out the long-term study. *We like to go home at 5 P.M. What do you think we are, slaves?*

We say this with trepidation. *I don't know anything about this.*

We have repeated So-and-so's experiments in our lab. *Brother, were we surprised!*

Presented at the 36th ASMS Conference on Mass Spectrometry and Allied Topics
June 5-10, 1988, San Francisco, CA

Academic Lab Managers Interest Group Report

Richard W. Kondrat
Department of Chemistry
University of California, Riverside
Riverside, CA 92521

The group held a workshop in order to inform the mass spectrometry community about the academic resources available to researchers. A summary of the capabilities of NIH and NSF funded facilities was prepared prior to the workshop. Each attendee received a copy of the results which were then summarized by Dr. Tom Sharp. Additional information was given to each attendee concerning Biomedical Research Technology Resources (booklet provided by Dr. C. Halloway of NIH). Sufficient copies were available such that extras were left for general distribution following the workshop. Representatives from many of the facilities were introduced and spoke about their facilities. A distinction became evident concerning what types of analytical problems are dealt with at the various facilities. At the end of the workshop, Dr. Cotter from MAMS, suggested we publish our survey of capabilities in Rapid Communications in Mass Spectrometry. Also, Dr. G. Eigendorf (University of British Columbia) informed us that our list of Canadian facilities was far from complete and pointed out several such facilities. It was concluded that our interest group should disseminate and update the information presented at the workshop on an ongoing basis via the SPECNET electronic bulletin board.

Following the workshop, an interest group meeting was held. The decision was made to follow up on Dr. Cotter's suggestion, as well as to update our listing of Canadian facilities. Members were encouraged to use SPECNET and examples were provided as to its utility. A new interest group coordinator was elected - Dr. Tom Sharp of Texas A&M University. Suggestions on future symposia, workshops, etc., were solicited.

Presented at the 36th ASMS Conference on Mass Spectrometry and Allied Topics
June 5-10, 1988, San Francisco, CA

Report of the Biomedical Interest Group

This report is based on comments of members at the Interest Group Meeting on Monday, June 6 and those made throughout the meeting to the coordinator.

Generally, it was felt that the meeting was well organized and ran smoothly. The schedule of events was quite full and in a few instances where workshops and interest group meetings ran over, some minor difficulties were experienced with the set up of the sessions which followed. It was suggested that contributed oral papers be limited in the future to decompress the schedule. Nevertheless, overall, the meeting was reviewed quite positively.

Suggestions for the 1989 meeting for symposia included quantitative analyses using soft ionization methods with emphasis on compounds other than peptides, and coupling of separations techniques to MS other than LC. Workshop suggestions included LC/MS basics using soft ionization methods, and electrophoresis/MS applications. These workshops should cover elementary aspects of theory and practical how-to-do-it tips and procedures for those interested in starting separations and measurements with these techniques.

Members are encouraged to send in additional suggestions for the 1989 meeting, particularly those involving biomedical interest, to the vice president for programs or to the biomedical interest group coordinator. Our group consists of a wide diversity of interests and applications, and our input is vital to the Board in preparing next year's meeting. If you feel there are areas not well represented and which you think are vital to the society, please write and give us your thoughts.

Submitted by
Richard M. Caprioli
Biomedical Interest Group
Coordinator

Presented at the 36th ASMS Conference on Mass Spectrometry and Allied Topics
June 5-10, 1988, San Francisco, CA

"Analysis of Drugs and Drug Metabolites by Tandem MS"

A Workshop Sponsored by the
Biomedical Applications Interest Group

The identification of drug metabolites is in many ways an ideal problem for the application of MS/MS techniques. In part, this is due to the fact that metabolites usually retain structural features of the parent drug, and because most drugs are metabolized by similar biochemical pathways. Recent advances in instrumentation have made sophisticated MS/MS techniques accessible to research groups that are directly concerned with the identification and quantification of drugs and their metabolites within complex biological sample matrices. This workshop was organized to discuss the increasing use of tandem MS by metabolism research groups, and to address the practical aspects of these techniques. Featured speakers included John Coutant (Merrell-Dow Pharmaceuticals), Simon Gaskell (Baylor College of Medicine), Bill Seifert (University of Texas Medical School), Roger Foltz (Center for Human Toxicology, University of Utah), and Bob Strife (Procter & Gamble). Speakers were requested to stress the practical aspects and potential drawbacks of the various techniques in use in their laboratories. The workshop was very well attended, with over 300 participants.

John Coutant outlined the use of the triple quadrupole for rapid identification of metabolites, particularly in combination with thermospray ionization. Issues such as the need for sample clean-up vs. direct mixture analysis, the limitations of thermospray as an ionization technique, and the 'success rate' of MS/MS in solving real problems were addressed in a lengthy question and answer period.

Simon Gaskell discussed the use of MS/MS for metabolite identification and quantification using FAB ionization with a hybrid (BEQQ) instrument. Examples that were discussed included the identification of glutathione conjugates using precursor ion or neutral loss scans, and the quantification of sulfate esters using precursor ion scans. The need for sample cleanup was stressed, and the advantages of immunoaffinity columns for this purpose were demonstrated. The continued need for stable isotope analogues was also stressed, both for quantification purposes (as internal standards) and to assist in distinguishing drug-related materials from endogenous compounds (*eg.*, the use of "isotope twinning" techniques).

Bill Seifert discussed the use of 'flow-FAB' as a means of sample introduction for trace analysis and quantification. Practical advice on operation of this increasingly popular means of sample introduction was provided, and examples of results obtained using a triple quadrupole were shown.

In spite of the obvious suitability of tandem MS for drug and drug metabolite identification, the very high cost of conventional MS/MS instruments continues to inhibit their widespread adoption. This is especially true of applications where large numbers of samples are the norm, such as with clinical and other drug development studies. Accordingly, the last two speakers were invited to discuss the capabilities of potential 'low cost' MS/MS devices.

Roger Foltz gave an introductory talk on the practical aspects of the use of the ion trap mass spectrometer for drug analysis. The capability of this device for high sensitivity, selective chemical ionization was illustrated with a number of examples.

Bob Strife then discussed the concept of doing MS/MS in time rather than in space (as in multiple sector devices) using an ion trap equipped for MS/MS operation. After first presenting a brief introduction into the theory and practical aspects of this device, a number of examples were presented which illustrated the very high intrinsic sensitivity and specificity afforded by MS/MS.

In summary, all of the speakers provided examples which demonstrated that MS/MS offers unique advantages and capabilities for identifying and quantifying drugs and their metabolites. It was stressed, however, that when solving real problems on unknowns, MS/MS should be viewed as an extension of rather than a replacement for existing analytical techniques.

Submitted by Kenneth M. Straub

Presented at the 36th ASMS Conference on Mass Spectrometry and Allied Topics
June 5-10, 1988, San Francisco, CA

ASMS Education Committee Report

ASMS once again sponsored a series of short courses on the weekend preceding the Annual Conference. As in prior years, course evaluations received from the students indicated that the courses were very successful with most students achieving their goals. This year's short courses and organizers were as follows: Interpretation of Mass Spectra - James Kelley; Quantitative Mass Spectrometry - Al Yergey; Intrepid Ion Chasing: SIMION Style - David Dahl; Fast Atom Bombardment Mass Spectrometry - Ken Busch; Practical MS/MS Analysis - Rick Yost.

The Education Committee also sponsored a Symposium and a Workshop at the 36th ASMS Conference. The Symposium, entitled "Mass Education - Introductory Lecturers from ASMS Educational Programs", drew large attendance and provided introductory lectures on Mass Spectrometric Approaches to the Analysis of Biopolymers by Chuck McEwen, Principles of Isotope Dilution Mass Spectrometry for Quantitative Analysis by Al Yergey and Practical MS/MS Analysis by Jodie Johnson and Rick Yost.

The Committee Workshop entitled "Ethics Issues in the Technical Workplace" was organized by Al Yergey. Working on a case study, workshop participants were asked to confront some of the moral and ethical issues which face us as scientists.

As a formal committee of the American Society for Mass Spectrometry, the Education Committee does carry on activities throughout the year. During the past year, members of the committee were Ann Goetz, Paul Goodley, Al Yergey and Harry Hertz. With primary responsibility accepted by Ann Goetz, the committee worked on an introductory brochure for scientists in research areas who could benefit from mass spectrometric measurements. The brochure, to be made available during the coming year, will provide an overview of problem areas where mass spectrometry can provide assistance and an overview of mass spectrometric instrumentation and techniques.

The committee also sent a questionnaire to all members of the Society requesting information on mass spectrometry courses presented at their institutions. Paul Goodley coordinated this activity. He is currently evaluating the many responses received and developing a mechanism for accumulating and organizing the instructional materials offered to ASMS by respondents.

During the coming year, in addition to completing the introductory brochure, the ASMS Education Committee will its attention on preparing a short course package to be made available to local discussion groups. This package will include a complete instructional kit from one of the ASMS basic short courses and will give the instructions needed for local discussion groups to use their own faculty in putting on the short course.

Mike Story will become chairman of the ASMS Education Committee in July. He will welcome suggestions from ASMS members on educational activities which ASMS can provide its members and the scientific community.

Respectfully submitted,

Harry S. Hertz

Presented at the 36th ASMS Conference on Mass Spectrometry and Allied Topics
June 5-10, 1988, San Francisco, CA

Ethics in the Workplace

This workshop was organizes to provide a forum for the discussion of some issues that involve the people of science as well as the science that they do. It was organized around the format of dicussion, in a small group format, of a hypothetical case study concerning a problem that has occurred in laboratories in virtually any setting. Issues addressed were responsible reporting of observations, ability to reproduce work, and some of the personality clashes that occur under those circumstances.

The basis for addressing solutions to the problem were suggested by the very able discussion leaders, Sondra Ford and Carlos Ramos of FMC Corporation, who were kind enough to offer their time to the Society for this purpose. The bases for ethical decisions given were:

When Making an Ethical Decision:

Choose the Alternative That Has:

* Most benefits

*Fewest Harms

*Respects Rights

*Distributes Benfits Fairly

*Distibutes Burdens fairly

Ask:

- Will the Choice Stand Up to Public Scrutiny?

- Will the Choice Stand the Test of Time?

Approximately 30 people participated

Organizer: A.L. Yergey

Presented at the 36th ASMS Conference on Mass Spectrometry and Allied Topics
June 5-10, 1988, San Francisco, CA

ENVIRONMENTAL INTEREST GROUP REPORT
SAN FRANCISCO 1988

The Environmental Interest Group held its annual meeting prior to the workshop on "New Ionization Techniques for Environmental MS". A report on this workshop is included in this volume. The meeting began with approximately 300 attendees, but soon this number swelled to about 700. A number of subjects were suggested for workshops and/or symposia for next year, including:

- Environmental Applications of MS/MS, including water, soils and atmospheric samples. (This was the topic of a workshop sponsored by this group at the Denver meeting in 1987).
- Chemometric Techniques in Conjunction with Environmental Analysis by Mass Spectrometry
- Preparing for the Next Generation of Environmental Contaminants
- QA/QC in Environmental MS
- Air Monitoring by MS

The Group was asked about possible changes they would like to see in the format of the meeting and only one comment was received concerning the overlap of interesting sessions during the week. Otherwise, no complaints or suggestions were offered.

Submitted by:

Michelle V. Buchanan
Environmental Applications Interest Group Chairman
Oak Ridge National Laboratory

Presented at the 36th ASMS Conference on Mass Spectrometry and Allied Topics
June 5-10, 1988, San Francisco, CA

NEW IONIZATION TECHNIQUES FOR ENVIRONMENTAL MS

A Workshop Sponsored by the
Environmental Applications Interest Group

This workshop was organized to examine new ionization techniques which have utility for environmental problems. Featured speakers were Marc Wise (Oak Ridge National Laboratory), Jack Henion (Cornell University), Eric Grimsrud (Montana State University), and Dave Jamieson (National Research Council of Canada). A large audience of about 700 also participated actively in the discussion.

Marc Wise discussed the use of a glow discharge source for the direct analysis of volatiles in soils and water. Analysis is conducted either by monitoring the headspace over the sample or by purging the sample directly into the source, which is operated at 0.2 torr. Potential applications of this source include use as a continuous air monitor, for targeted compound analysis in water and soil (especially as a field instrument) and as a potential CLP equivalence method. The advantages of this technique include rapid sample turnaround (less than 2 minutes), part per billion (ppb) sensitivity, linear response, and good accuracy and precision.

Jack Henion discussed several ionization techniques for the analysis of polar environmental analytes in conjunction with liquid chromatographic separation. Topics discussed included use of an ion spray interface for analysis of low ppb levels of mono- and disulfonated azo dyes and the analysis of higher molecular weight dyes (including Direct Red 80 with a molecular weight of 1240) using thermal assisted electrospray. Phenoxyacetic acids were analyzed using capillary zone electrophoresis (CZE) directly interfaced to the mass spectrometer. The main problem encountered with CZE is the need to balance the sample load of the separation technique with the detection limits of the mass spectrometer. This requires the use of single ion monitoring to avoid overloading the chromatographic column. Using CZE and single ion monitoring, detection limits of less than 1 pmole per component were achieved. CZE with MS/MS was used to analyze waste water extracts for Acid Yellow 49.

Eric Grimsrud discussed the good and bad points of high pressure electron capture mass spectrometry. Besides electron capture reactions, this source can also produce altered neutrals formed by reactions with positive ions, radicals and surfaces, which can then undergo electron capture to produce additional ions. Directions for further research included investigation of buffer gases, ion source materials, ion source volumes and ion/electron density.

Dave Jamieson concluded the workshop by discussing the use of negative ion mass spectrometry for better selectivity and sensitivity. Methane and water have been used as a buffer gas with negative ion chemical ionization (NICI) to analyze polychlorinated biphenyls in marine sediment samples. Oxygen enhanced NICI gives isomeric information on PCBs. Recently carbon dioxide has been used as a buffer gas for the analysis of polycyclic aromatics hydrocarbons in marine sediments and has been shown to differentiate isomers.

Submitted by:

Michelle V. Buchanan, Chairman

Presented at the 36th ASMS Conference on Mass Spectrometry and Allied Topics
June 5-10, 1988, San Francisco, CA

INTEREST GROUP REPORT
FUNDAMENTALS

The symposium on Cluster Ion Mass Spectrometry, sponsored by the Fundamentals Interest Group and organized by Mark Ross, attracted approximately 70-100 delegates over a three hour period during which five interesting and authorative accounts of different aspects of cluster ions were covered. The theme was continued on the following morning when a number of shorter papers on related topics were presented.

The group also sponsored two lunchtime workshops: "Making Metal Ions", organised by Doug Ridge and "Aspects of Photoionisation" organised by David Lubman. In each workshoip, 5-6 "volunters", reviewed appropriate parts of the subject and presented recent data, giving a useful snapshot of some of the themes of current interest in these two topics. Despite a very full program leaving little time for lunch, each workshop attracted over 50 delegates and discussion had to be curtailed to make way for the afternoon sessions.

The Business Meeting was held before the first workshop and continued briefly at the end of the second workshop. Since suggestions for symposia, plenary speakers and workshops form the floor were rather fragmented, delegates were asked to provide suggestions in writing either to Doug Ridge (who will assume responsibility for the group over the next two years) or to myself. For symposia in particular, this produced a gratifying response. Concern was exppressed on several occasions during the conference that the influence of the Fundamentals Interest Group on the meeting is diminishing and there is certainly a need to try to attract back to ASMS meetings those working on fundamental aspects of ion chemistry and physics who no longer see the annual congress as a meeting they wish to attend. Possible topics for symposia which were suggested were (i) Ions and Spectroscopy and/or Lasers and Mass Spectrometry; (ii) Ionisation Processes & Ion Dynamics; (iii) Applications of Mass Spectrometry to Atmospheric Chemistry; (iv) A Comparison of Gas Phase and Condensed Phase Ion Chemistry; and (v) The Interaction between Experimental and Theoretical Gas Phase Ion Chemistry. Other topics, perhaps more suitable for plenary lectures or workshops, include: (i) High Temperature Chemistry and Vaporisation of Species; (ii) Reaction of State Selected Species; (iii) Ion Activation Processes; and (iv) Ionospheric Chemistry relevant to the Space Shuttle. These suggestions, together with names of possible contributors, will be forwarded to the ASMS Board.

Submitted by,
K.R. Jennings

Presented at the 36th ASMS Conference on Mass Spectrometry and Allied Topics
June 5-10, 1988, San Francisco, CA

FUNDAMENTALS WORKSHOP: MAKING METAL IONS

Workshop Coordinator: Douglas P. Ridge

The workshop dealt with techniques for generating gas phase metal ions for chemical studies.

Terry McMahon from the University of Waterloo described the adaptation of an electron impact high pressure source to laser desorptive ionization. A XeCl excimer laser pulsed at 1 Hz was used. There are quartz windows on both the source housing and the source. The source window is a 5 cm lens that focused the laser onto the metal target. Shot to shot reproducibility is good and strong signals are observed. A multichannel analyzer collects the ion intensity as a function of time. Equilibrium constants for solvation of Cu^+ by Xe, N_2 and H_2O have been obtained already. In each case the second ligand is bound more strongly than the first.

John Allison from Michigan State reported evidence concerning the formation of excited states. Ni^+ reacts differently depending on the compound from which it is formed. Reactions with C_6H_5I, $C_6H_5CHOHCH_3$ and $C_6H_5CH_2OH$ were examined. Ni^+ was formed by electron impact on $Ni(CO)_4$, $Ni(PF_3)_4$ and NiCpNO. 70 eV electrons were used. Distinctly different product ratios were observed especially for Ni^+ from NiCpNO.

Steve McElvaney from Naval Research Laboratory described two methods for generating clusters. In one method metal powders are pressed into a pellet with a matrix of boron nitride or graphite. The pellet is then placed in an ICR cell and exposed to a pulsed Nd YAG laser at either the fundamental or the first harmonic. W and Ta in graphite matrices give metal carbide clusters $M_nC_m^+$. In Ta both n and m can be 10 or more. CID on the carbide clusters give a characteristic C_3 loss. A second ionization method also involves laser oblation. In this case the target is a rotating rod in the throat of a pulsed nozzle for a supersonic expansion. Clusters grow from metal atoms ejected from the metal surface into the cooling expansion. Ionic clusters then result from photoionization of the neutral clusters. Bi clusters formed by SIMS and LDI were compared and found to be similar. Ion emission resulting from the first harmonic of the Nd YAG laser and the

fundamental were compared. Recent spectra of ions obtained from Ag in a graphite matrix were shown.

Rob Freas from the University of Houston described results from sputtering metal ions from surfaces. 8 kV Xe atoms bombarded metal foils, metal salts and metal oxides. The yield was 1 to 10^3 particles per Xe atom. Ti foil gives titanium oxide clusters even after several hours of sputtering. This is the result of the reactivity of Ti and contaminants in the vacuum system. When bombarded in the presence of O_2 in a CI source ions of stoichiometry $Ti_nO_{2n-1}^+$ are formed almost exclusively. The distribution of vanadium oxide clusters obtained in a similar experiment agreed with a simple theoretical model. Preliminary spectra resulting from sputtering from a superconducting Ba containing ceramic were shown.

Tim McMahon from Purdue described several experiments with laser oblation of ions into an ICR cell. A Nd YAG laser is focussed on metal targets in the wall of the cell. The targets have holes in them parallel to the laser beam. The beam passes through the holes and the resulting ions emerge into the cell. Glass windows are used. A Nicolet FTMS 2000 has been adapted to bring the laser beam down the axis of the cell so that it impinges vertically on the target ejecting ions into the cell. An external source has also been used to inject metal ions into an ICR cell. The ions formed in the source travel along magnetic field lines into the source. At this point the injection efficiency is low and unreliable. All of the first row transition metal atomic ions and a number of second and third row atomic ions have been formed this way.

Presented at the 36th ASMS Conference on Mass Spectrometry and Allied Topics
June 5-10, 1988, San Francisco, CA

Historical Interest Group Business Meeting - - 6-JUN-88 San Francisco

The meeting was convened at 1:00 PM with 60-70 persons present.

Those in attendance were assured that the outgoing chairman, Bob Kiser, was on his way to good health and was looking forward to joining us again in Miami in 1989.

A sign-up sheet was passed among the attendees soliciting help for the coming year. A group of attendees indicated willingness to provide time and energy to accomplish goals of the historical interest group between now and next year's meeting. Those members are listed below for the benefit of those unable to attend the meeting, and for those interested in knowing more about our activities.

Historical Interest Working Group:

Lyn Bear	NBS	Gaithersburg MD
K. L. Busch	Indiana U	Bloomington IN
P. Chastagner	E I duPont	Aiken SC
R. G. Cooks	Purdue	West Lafayett IN
Fred Elder	Xerox Corp	Webster NY
Jean Futtrell	U of Delaware	Newark DE
Leonard Ingram	Miss. Forest. Lab.	Mississippi State MS
Charles Judson	U of Kansas	Lawrence KS
Bob Kiser	U of Kentucky	Lexington KY
Robert Madden	Extrel Corp	Pittsburgh PA
Fred McLafferty	Cornell U	Ithaca NY
Vince Saltamach	Columbia U	New York NY
Bill Sherman	Washington U	St Louis MO

The ASMS Proceedings has more specific address and phone information if anyone wishes to contact any of these individuals regarding the activities of the historical interest group.

As Chairman for the next two years, I presented to the attendees a plan for historical interest group activities which centered on the collection of information about three specific phases of mass spectrometry:

* Its practitioners
* Its scientific and technological development
* Its instrumentation

The intention is to collect information in these areas since the Society has neither the physical nor financial resources to collect equipment. The group has already embarked on the collection of information on practitioners of mass spectrometry as suggested by Bob Kiser. Small questionnaires were placed in the Spectaker and also provided at the meeting itself, asking individuals to provide the historical interest group with information about how they became involved with mass spectrometry. Approximately 200 responses were collected prior to the meeting and 200 more were collected at the meeting. In addition, a display of photographs of individuals and instrumentation was set up at the meeting on Sunday for the perusal of attendees. Accompanying the display was a request for the loan of photographs of people and/or equipment which would be copied and returned to the contributor. Anyone wishing to loan such material can get more information by contacting me at the phone number listed below.

The collection of information about practitioners will continue throughout the year and efforts to collect information in the other two areas outlined above will be started. In particular, anyone having old advertising literature, manuals or other material on instrumentation from the past is encouraged to contribute such material to the historical interest group for its archives as it becomes obsolete. If you are thinking about pitching it, pitch it to the Historical Interest Group! Based on the response during the coming year, the group will mount a more elaborate display of memorabilia and historical artifacts at the meeting in Miami.

The Workshop consisted of short oral presentations by Charles Judson and Vince Saltamach on some of the history of mass spectrometry which they had witnessed first hand. Charles spoke on the early era of commercial mass spectrometry when Consolidated Engineering Corporation was developing the instrument which eventually became the CEC 103 series of instruments. Vince spoke on the various instruments which were developed at Columbia University in the years before and during the Manhattan project. Pictures and information about each of these topics were posted on poster boards and after the brief oral presentations, the workshop evolved into a miniature poster session with the attendees participating in a lively exchange for the remainder of the time allotted for the workshop.

Respectfully submitted,

Michael A. Grayson
Chairman, Historical Interest Group
McDonnell Douglas Research Laboratories (314) 233-2541

Presented at the 36th ASMS Conference on Mass Spectrometry and Allied Topics
June 5-10, 1988, San Francisco, CA

INSTRUMENTATION AND ION PHYSICS INTEREST GROUP MEETING AND WORKSHOP REPORT

The Instrumentation and Ion Physics Interest Group sponsored the symposium entitled "Ion Trapping: Methods and Applications" held on Friday, June 10 and a workshop entitled "Practical Aspects of Lasers with Mass Spectrometry" held on the evening of Monday, June 6. A short interest group meeting preceded the workshop on Monday where a number of suggestions for topics of future symposia, workshops, and plenary/introductory lectures were offered. Among these were:

- -Formation and analysis of multiply charged ions
- -Ion optics calculations
- -Lasers in mass spectrometry
- -Interfaces in hyphenated techniques
- -Detection systems
- -Molecular beam techniques and sampling ions from high pressures

Other good suggestions were also made that better fit under the purview of other interest groups and have been forwarded to the Board for consideration.

An audience in excess of fifty was present throughout the evening workshop which centered on the types of lasers used today in mass spectrometry and their relative merits. Four speakers gave short presentations with particular emphasis on the important considerations involved in applications with which they were familiar. Each speaker was asked to target the presentation at people relatively unfamiliar with the use of lasers in mass spectrometry experiments. Dr. David Lubman (University of Michigan) led off the workshop with a general discussion of today's commonly used lasers in relation to the photoionization of polyatomic ions. Dr. Douglas Goeringer (Oak Ridge National Laboratory) followed by expanding on some of the previously presented material with emphasis on the photoionization of atomic species for isotope ratio measurements. Dr. Robert Hettich (Oak Ridge National Laboratory) discussed laser desorption of biomolecules in a Fourier Transform mass spectrometer along with photodissociation. Dr. Mark Ross (Naval Research Laboratory) concluded the presentations with a discussion of photodissociation in a beam-type mass spectrometer. The positive feedback from the workshop audience (along with the good attendance) indicates a continued strong interest in lasers among mass spectroscopists. For this reason, another symposium in the rapidly growing area of lasers in mass spectrometry may be appropriate at either next year's meeting (as suggested above) or the following meeting.

Submitted by
Scott A. McLuckey

Presented at the 36th ASMS Conference on Mass Spectrometry and Allied Topics
June 5-10, 1988, San Francisco, CA

ISOTOPE RATIO INTEREST GROUP REPORT

Approximately 50 people attended the business meeting of the Isotope Ratio Interest Group held Tuesday, June 7, 1988.

The group felt that the name Isotope Ratio Interest Group should be changed to Isotopic Applications Interest Group to accommodate a broader range of scientific disciplines. We therefore recommend that the name Isotopic Applications be adopted for next year's meeting.

The Isotopic Applications Group felt that this year's presentation format for inorganic topics (elemental, surface, and isotopic) worked very well. We hope that the format of symposium, regular oral session, and posters can be continued in future meetings. There is strong feeling within our group that oral sessions should be continued at future ASMS meetings, as opposed to an all poster format. Some suggested topics to be included in an isotopic symposium in 1989 include biomedical tracers, geochronology, nuclear materials, environmental analysis, and accelerator mass spectrometry.

A major issue that all isotope ratio mass spectroscopists will soon face is the availability of isotopically enriched materials. The production of enriched isotopes in the U.S. has fallen off in recent years making these materials harder to find for different elements or enrichment levels. This issue might be addressed at a workshop for the 1989 meeting.

The Isotope Applications Group now has a member mailing list that includes about 100 names and addresses. Our group has found this list useful to keep informed about ASMS events; we hope that the mailing list will help to establish stronger communications among us for larger issues, such as the production of enriched isotopes. To receive a copy of or add your name to the mailing list, please send your name and address to:

Dr. Larry Green
Atomic Energy of Canada, Limited
Chalk River Nuclear Laboratories
Chalk River, Ontario
Canada K0J1J0

Submitted by:
P. H. Hemberger
Los Alamos National Laboratory

Presented at the 36th ASMS Conference on Mass Spectrometry and Allied Topics
June 5-10, 1988, San Francisco, CA

ISOTOPE RATIO INTEREST GROUP WORKSHOP
ISOTOPE RATIO MASS SPECTROMETRY--A LOOK TO THE FUTURE

Approximately 50 people attended the workshop for the Isotope Ratio Interest Group held Monday evening, June 6, 1988.

The purpose of the workshop was to address the future of isotope ratio mass spectrometry--what advances in instrumentation are desired and what may be new areas of application. The featured speakers, Linus Barnes (NBS), Guenter Lugmayer (U.C. San Diego/Scripps Institute), and Dick Perrin (Los Alamos), presented an overview of their research to demonstrate the limits of today's instrumentation and isotopic measurements.

Linus Barnes described the development of analytical methods for neodymium and strontium. NBS is obtaining isotopic analysis of picogram samples of neodymium with part-per-million errors. With strontium, the instrumental errors have all but been eliminated, and the remaining problems are related to sample preparation and standards. Some of the drivers behind Linus' work include smaller samples, higher accuracy, faster/automated analyses, and multi-element determinations.

Guenter Lugmayer discussed the applications of isotope ratio mass spectrometry to geochemistry and cosmochemistry. Guenter pointed out that high-purity standards and high-precision thermal ionization mass spectrometers are the important tools of the trade and that the cardinal points in isotope ratio MS are (1) sensitivity, (2) sample/spectral purity, and (3) external precision and accuracy.

Dick Perrin showed applications of isotope ratio mass spectrometry to geochemistry and nuclear chemistry. Dick described some imaginative schemes for incorporation into future instruments. These included an element selective ionization system, an isotope selective detection system, and an automated closed-loop separation system. The concept of the closed-loop separation system interfaced to an automated thermal ionization mass spectrometer invoked the lively, heated, and spontaneous discussion that is the hallmark of the Isotope Ratio Interest Group.

The workshop adjourned into informal discussion groups and enjoyed refreshments graciously provided by Finnigan MAT.

Submitted by:
P. H. Hemberger
Los Alamos National Laboratory

Committee on Measurements and Standards
Meeting on Qualities Desirable in Mass Spectral Data Collections
Organized by: F. McLafferty and S. Lias
Chaired by G. Meisels

The meeting opened with a description of both NBS-EPA and Wiley data collections by S. Lias (NBS). The first contains 43,000 compounds, the second over 130,000 some of which are duplicates. Both are available in hard copy and computer format and they have been combined in a joint publication which will be available about August, 1988. Each is searched by its own system, the PBM-STIRS routines being used in the Wiley collection. These search routines were not discussed further at this meeting, which was concerned with the quality of data collections. Lias discussed certain difficulties in using the various forms of "quality index" to screen spectra. McLafferty agreed that it is a problem. He has each spectrum in the Wiley collection entered in his database by students and then checked by PBM-STIRS. When difficulties are encountered he personally checks the spectrum, changing obviously erroneous peaks McLafferty gave a brief discussion of the history of the Wiley collection and discussed some of its features. It has many more spectra, partly because even highly abbreviated spectra, usually found in papers where mass spectrometry is not the key feature, are included. McLafferty found that such spectra, in spite of their shortcomings, tend to improve the quality of the search which uses only 15-27 of the most important (not necessarily most abundant) peaks.

McLafferty stressed the importance of collections prepared from spectra run by practicing mass spectrometrists since they are likely to be of higher quality and more general interest. He then read the results of a questionnaire he recently sent out to a small number of spectrometrists. As expected, everyone appears to want both quality and quantity but heuristic approaches to providing the former are not sufficiently trustworthy. Discussion of this point led to general agreement that ASMS should convene a committee of referees to inspect new spectra before they are submitted to either data collection. (This has been done; the temporary chairman is Richard W. Crawford). On this same point M. Grayson requested that the committee before a standard form for submission of spectral data. This will be done and Meisels agreed to publish it in a future issue of the Spektaker. Lias stated that NBS would accept data in any ASCII format. McLafferty added that he would accept data in any form, but not from unknown materials. A meeting to discuss the format issue, especially the JCAMP format used for infrared spectra (J.Applied Spec. 1988) was scheduled for Thursday evening (see report of Computer Applications Interest Group).

On the question of subset collections, McLafferty saw no difficulty in such a division provided the subset was sufficiently well defined. He requested the Committee's assistance in this. Discussion followed concerning FAB, EI, and CA collections. These spectra are known to be highly dependent on instrument conditions. Since such spectra are generally used for very specific purposes on well defined samples, it was considered that they would not be included at present. However, about 1000 collision activated spectra are available from McLafferty, provided

the requester will promise to send 50 of his own. He mentioned that these spectra when run through the PBM system required such wide windows that they would be of questionable value.

On the question of sources of new spectra, regional mass spectral facilities were mentioned as one possibility. K. Bieman pointed out that in his experience most of these are other El spectra and he questioned their general quality. Other centers reported more use of El spectra, however.

Some discussion centered on the incorporation of "physics" into the data base, i.e. low electron voltage changes, etc. McLafferty mentioned that his search algorithms already did attempt to take into account such matters as peak skewing due to GC peak elution, etc.

R. Foltz wished to know more characteristics of the users of these collections. What fraction is environmental, drug firms, etc.? It was agreed that this would be of great importance in future considerations of the committee and an effort should be made to determine this point.

Submitted by H.M. Fales

Presented at the 36th ASMS Conference on Mass Spectrometry and Allied Topics
June 5-10, 1988, San Francisco, CA

QUANTITATIVE ANALYSIS OF PEPTIDES

Pharmacology Interest Group Workshop Report
(Formerly Quantitative Organic Analysis)

This workshop considered analytical aspects of the quantitative analysis of peptides by mass spectrometry and was intended to be an extension of the afternoon symposium organized by Dr. Dominic Desiderio titled "Measurement of Peptides". There were approximately 100 in attendance.

The name of the interest group was changed last year from "Quantitative Organic Analysis" to "Pharmacology" with the subject area of the interest group defined as "The structural and quantitative analysis of drugs and their metabolites, and of endogenous bioactive compounds and their metabolites." An unscientific sampling of the membership strongly indicated that the subject area directly overlapped with the "Biomedical Interest Group" and that "Pharmacology" was an inappropriate name. Several suggestions for a more appropriate name were made with "Biochemical Quantitation" having the most support. It is therefore proposed that this new name be adopted for this interest group.

The workshop began with Dr. Dominic Desiderio, University of Tennessee, describing the overall analytical scheme used in his laboratory to discover and quantify biologically active peptides in the mammalian central nervous system. Briefly, the scheme employed solid phase ODS extraction, LC purification, limbic system receptor assay and FAB-MS-MS analysis using a double-focusing MS of reverse geometry. Quantitative analysis of methionine-enkephalin (YGGFM) in cerebospinal fluid was described in detail. Early studies used structural analogue and carboxyl ^{18}O-internal standards. Since exchange of carboxyl ^{18}O is a potential problem, ^{13}C-internal standards (specifically $^{13}C_6$-methionine-enkephaline) are presently being used. Methionine-enkephalin in CSF was quantitated by FAB-MS-MS utilizing the $YGGFM^+ \rightarrow YGGF^+$ parent-daughter pair and monitoring m/z 431 and 425. The CSF sample milieu was described as a simpler matrix than tissue, however, quantitative measurements are complicated by the lower concentration of methionine-enkaphalin present in CSF. The method was described as highly sensitive with calibration data points routinely attainable in the fmole level (standards alone). Addition of HCL and glutathionine to the FAB matrix was observed to increase the molecular ion intensity by a factor of three.

Dr. Carol Lisek of the Mayo Clinic described her work in collaboration with Dr. Ian Jardine on the quantitative analysis of substance P ($PPLPQQFFGLM-NH_2$) in feline spinal cord using continuous flow FAB-MS. The sample preparation consisted of the addition of a deuterated internal standard to the biological matrix, solid phase extraction and immunoaffinity chromatography purification. The immunoaffinity purification was described as critical to successful analysis. LC-MS analysis utilized microcolumn LC/dynamic FAB-SIM-MS, monitoring MH^+ of substance P and MH^+ of $^2H_8$-substance P (1348.7/ 1356.7) using a VG 30-253 quadupole. The limit of detection using this system was observed to be 0.1 pmole (3:1 S:N). A major limitation with this approach is the limited injection volume (0.1μ l injector loop) since a mimimum of 10μl solvent is required to dissolve the purified sample. Members of the audience suggested that it should be possible to use multiple injections and adsorption of the sample at the beginning of the column and then increase the percent organic solvent to chromatograph the sample. It was also suggested that a requirement of 10 l solvent to dissolve the sample could be related to non-specific adsorption at the immunoaffinity purification step and that a more specific elution (e.g. displacement with an analogue) should allow smaller solvent volumes to be used.

Dr. Simon Gaskell of the Baylor College of Medicine presented an overview of some of the general considerations for any quantitative analytical method. The key considerations described were sensitivity, accuracy, precision and intermethod comparability (if possible). Key considerations for accuracy are the degree of selectivity of the method and the demonstration of spiking parallelism. It was noted that both interassay and intra-assay precision should be determined. It was suggested by a member of the audience that a more detailed discussion of quantitative analysis fundamentals would be an appropriate subject for a future workshop. Preliminary studies quantitating leucine-enkephalin and bradykinin using FAB and MS-MS with a hybrid instrument (VG ZAB SEQ) were also described.

Respectfully submitted,

James Vrbanac
Medical University of South Carolina
Charleston, S.C. 29425

Presented at the 36th ASMS Conference on Mass Spectrometry and Allied Topics
June 5-10, 1988, San Francisco, CA

SOLIDS AND SURFACE ANALYSIS INTEREST GROUP REPORT

Approximately twenty-five members of this interest group met Thursday, June 9, from 8:00-10:00 PM to conduct the annual business meeting and participate in the workshop, "Organic Ion Imaging-Problems and Prospects". Members were informed of the decision to divide the present interest group into three new interest groups, namely Inorganic and Elemental Analysis, to be chaired by G. Hieftje, Desorption Processes to be chaired by P. Todd, and Surface Science, with the chair to be named. Volunteers for successor/new chair positions, and recommendations for next years' program were solicited. Recommendations for next year's workshops/symposia included:

Radiation Damage in Organic and Semiorganic Materials
Solutions to Sample Charging Problems
Multichannel detectors and Mass Analyzers
Mass Spectrometry of Laser Ablated Surfaces
Desorption/Ionization of Langmuir-Blodgett Films
Inorganic Elemental Desorption and Surface Science

It is recognized that these topics would fall under the purview of different interest groups that will be formed for next year's meeting. Recommendations for next year's plenary lectures included:

Medical Community Needs That Might Be Met by Imaging Mass Spectrometry
History and Present Capabilities of the Ion Microprobe

The workshop that followed was moderated by P. Todd, and consisted of brief presentations and discussions led by Tom Brenna (IBM), Ken Busch (Indiana), Greg Gillen (NBS), and Robert Odom (Charles Evans and Associates).

Tom Brenna discussed crucial aspects of sample preparation and instrument control for generation of atomic secondary ion images from biological tissue. Many of the lessons learned from determining elemental distributions by using SIMS are directly applicable to organic ion imaging. He pointed out that sample preparation methods that fix spatial distributions best are the most difficult to perform and are the techniques that disrupt physical morphology most. Failure to employ the more demanding preparation techniques has led to misinterpretation of the resulting images. A second point made graphically by Tom was that by changing a single variable in the focusing of a Cameca ion microscope, he was able to create from a single sample, a series of complementary images. That is, a high intensity Ca^+ region appeared in one image where in a subsequent image, that same region yielded a low intensity Ca^+ signal. This led him to state that given the state of the art, secondary ion images would best be presented using single bit picture elements (e.g., white or black) indicating whether a particular ion is detected from that region or not, respectively. Shading and color enhanced imaging can lead to misinterpretation.

In apparent contrast to the results presented by Tom Brenna, Ken Busch discussed the conflicting needs of rigorous sample preparation and high sample throughput. There are many problems to be solved at all levels of sample preparation sophistication and spatial resolution capability. Information generated (and desired) from SIMS of TLC plates, for example, is different from that generated from biological tissue samples. Retention indices and sample identification are the main issues, rather than detailed spatial resolution. Ken also noted that the number of samples he handles regularly precludes extensive sample preparation; nonetheless, very useful information can be obtained from images produced from TLC/SIMS without extensive sample workup. The important issue for the analyst to remember is that the particular information required determines the rigor of the imaging experiment. It was the general consensus that with spatial resolution between 1 μm and 1 mm., sample preparation requirements could be mitigated and still permit a number of important biochemical problems to be addressed.

Greg Gillen discussed his finding that characteristic organic secondary ion mass spectra could still be discerned even after substantial primary ion dose. It is well-known that organic secondary ion emission appears to decay exponentially with time and primary ion dose. At some point before reaching zero characteristic emission, signal decay ceases. Steady-state emission follows. This is because the primary ion beam also sputters damaged material as it erodes the surface of an organic sample, leaving at least some analyte molecules undamaged. The apparent rate of secondary ion decay decreases with decreasing primary ion kinetic energy provides evidence for this hypothesis. This knowledge could be used in conjunction with the known high depth profile resolution of SIMS to produce organic ion images with spatial resolution of 100 Angstroms or so.

Robert Odom addressed the fundamental differences between obtaining organic SIMS images from pure samples dispersed on grids, and from biological samples where analytes exist as trace components of complex mixtures. Even using exceptionally well-characterized experimental conditions, he noted that generation of organic secondary ions from tissue samples can lead to ambiguous interpretation. For example, images of secondary epinephrine-characteristic ions could be generated from grids loaded with epinephrine. The distribution obtained from actual adrenal tissue was inconclusive, even though the image of the tissue sample was clear. He argued that additional information and research on effects of sample thickness and sample charging will be necessary to make micron-level spatial resolution organic SIMS a useful analytical technique.

Submitted,

Peter J. Todd

Presented at the 36th ASMS Conference on Mass Spectrometry and Allied Topics
June 5-10, 1988, San Francisco, CA

WORKSHOP

Use of Mass Spectrometry in Space

Chairman: Carla M. Wong-- NASA Ames Research Center, Moffett Field, CA 94035
Panel: Richard A. Yost-- University of Florida, Gainesville, FL 32611
Steve L. Durfee-- Somatogenetics Instruments, Inc., Broomfield, CO 80020
George Wood-- NASA Langley Research Center, Hampton, VA 23665

(Attendance ~ 100)

The purpose of this workshop was to bring to the attention of the mass spectrometry community some of the very complex analytical problems facing NASA, some of the differences in the working environment that have to be addressed in the solution of these problems and some of the ideas currently being considered. This report is a summary of all information provided in either written or oral form for the workshop.

The most conspicuous use of mass spectrometers in space has been in the analysis of the terrestrial and planetary atmospheres. This activity has spanned more than forty years. It has included rocket-borne experiments with recoverable cryogenic sampling systems to analyze the rare-gas concentrations and atmospheric composition as a function of altitude; Balloon and satellite borne mass spectrometers to determine gas and aerosol composition in the stratosphere and charged particle composition of the ionosphere and magnetosphere; Lunar and Planetary mass spectrometers to analyze the atmospheres of the Moon, Venus, and Mars; and, Energetic ion mass spectrometers to analyze the coma of Halley's Comet. Mass spectrometry will continue to have a predominate role in these applications, both in the forthcoming Galileo mission to Jupiter and in proposed terrestrial studies. An example of the latter is the Downward-deployed Tethered Satellite Program (DOWNTEST), in which instrumented platforms will be deployed downward on long tethers from the Space Shuttle or from expendable launch vehicles in order to obtain atmospheric science and hypersonic aerothermodynamic data at altitudes above 90 km. This will, for the first, time provide a significant quantity of data in the upper half of the region often referred to as the "Ignorosphere". This region, which lies between 55 and 150 km, is too high to be accessed by balloons or research aircraft and too low for orbiting satellites, and has so far been studied only with sounding rockets and to a lesser extent by the re-entering space shuttle. Mass spectrometers will be used on these tethered satellites to measure both the free-stream composition and density, and the composition of the gases in the boundary layer associated with the satellite surface. Both neutral and charged species will be measured over an extended period of time and over dramatically changing experimental conditions as the satellite slowly descends since the orbiting host vehicle will be capable of providing station-keeping, steady state data which will include diurnal variations in composition, density, and solar flux, can be obtained over periods of several orbits.

Of no lower importance are the less conspicuous applications of mass spectrometry in space related activities. Mass spectrometers have been used to monitor gas composition in ground-based research facilities; in studies of spacecraft materials; and, in monitoring the natural atmosphere in the Space Shuttle during fueling operations. They have been used to identify and quantitate outgassing products from materials to be used in the inhabited areas of the spacecraft and will be critical to the development and implementation of life-support systems for long term manned missions on the Space Station and the expedition to Mars. In addition to meeting analytical and control function requirements, while at the same time assuring long term reliability, the instrument system will have to meet the power, weight, and volume constraints imposed by the spacecraft or space station, for which there is a great deal of competition from other on-board systems. These life-support applications will therefore require challenging new developments in instrument configuration and performance, and in automated operation and data reduction methods.

A recent research area has shown that MS/MS capabilities of the ion trap are extremely promising for rapid, sensitive, and selective trace detection for life-support applications. In particular, evaluation of the sensitivity and dynamic range of the ion trap in the MS mode (using automatic control of the ionization time) and of the efficiency of the MS/MS mode suggest that the ion trap may well become the most sensitive MS/MS instrument ever. Another plus for space

applications is that ion trap tandem mass spectrometry offers ease of computer integration for automated control, testing and decision making. Optimization of instrumental sensitivity and resolution involves only electronic, not mechanical, adjustments. Alternating between operational modes (ionization type, ion polarity, MS/MS scan mode) can therefore be accomplished rapidly as the analytical results dictate. Similarly, testing of the instrumental performance (mass calibration, resolution, sensitivity) can be automated. MS/MS with a quadropole ion trap offers an ideal opportunity for instrumental optimization, evolution of analytical protocols, and decision-making by artificial intelligence.

Traditionally, this intelligence and knowledge for decision-making has been provided by highly trained scientists (typically a Ph.D. mass spectrometrist). If such an individual is not to be continually stationed on board the space station, then these requirements will have to be met by telemetry to experts earthside or by artificial intelligence/expert systems on the station.

Artificial intelligence/expert systems have been demonstrated for on-line analysis with real-time optimization (tuning) of instrumental parameters of triple quadropole tandem mass spectrometer; and, recently the first commercial tandem mass spectrometer to implement expert system tuning was introduced. One of the earliest artificial intelligence systems developed, heuristic DENDRAL, was designed to elucidate molecular structure from mass spectrometry; and, recently AI techniques have been expanded to include MS/MS data. The challenge is to extend AI/expert system approaches to the entire analytical process from instrument control to decision-making (screening and confirmation).

Another possible techniques to be considered because of compactness, high speed, and ease of sample preparation is Curie-point pyrolysis for analyzing mixtures and non-volatiles. An added advantage is that computerized methods of pattern recognition may be readily applied to the data, which permits a high level of interpretation by relatively inexperienced interpreters or by artificial intelligence (AI) software. Pattern recognition methods would be necessary to provide data which the AI could then interpret and act upon. The pattern recognition would not make decisions, but would place the data in a state such that a decision could be made.

There is a large body of literature describing the successful analysis and interpretation of highly complex organic mixtures using pyrolysis mass spectrometry (Py/MS) with computerized pattern recognition. Recent work has involved the identification of several species of bacteria which amply illustrates the power of this technique, and, which could be very useful in analysis of manned space environments.

In one experiment, four species of *Mycobacteria* were cultured, applied to Curie point wires, analyzed by Py/MS and interpreted by Principal Component Analysis. Each of the species could be distinguished from the others. In other experiments, two variants of a mycobacterium, which differed with respect to virulence, were distinguished.

In a third set of experiments, forty mixtures were prepared of four species of bacteria (*Proteus vulgaris, Pseudomonas fluorescens, Escherichia coli* and *Enterobacter aerogenes*), pollen and atmospheric particulates. It was possible to determine the relative concentrations of each component in the mixtures, and to identify the species of bacteria in every case despite the varying concentrations of pollen and particulate background. In these experiments, the mass of the bacteria in the mixtures was about one-third of the total mass; by using tandem mass spectrometry this fraction could be significantly lowered.

In summary, recent developments in mass spectrometric instrumentation, analytical methods and data interpretation show great promise for space applications.

Presented at the 36th ASMS Conference on Mass Spectrometry and Allied Topics
June 5-10, 1988, San Francisco, CA

Young Mass Spectrometrists Interest Group Report

The Young Mass Spectrometrists Interest Group held a workshop entitled "Write It Right" at its traditional time of Sunday evening with suitable refreshments (provided by the Group's benefactor, John Wiley & Sons) to kick-off the ASMS Conference in an appropriate manner. The subject of the workshop was proposal writing, and the attendance was approximately 120, demonstrating the importance of this topic. A group of distinguished ASMS members talked about different aspects of obtaining funding based on extensive experiences. First, Graham Cooks and Ken Busch spoke from the vantage points of senior and junior academicians, mainly on NSF proposals. Next, Sue Weintraub explained how NIH shared instrumentation grants can be obtained. Bob Cotter then talked about both NIH and NSF funding procedures. Finally, Paul Goodley offered an alternative funding source through a little-publicized Hewlett-Packard program. The format then became question-and-answer, with great interest displayed especially by the younger members as noted by the copious note-taking. In summary, the key elements to a successful proposal include knowing your funding source desires and requirements, an organized and well-written proposal and learning from rejection. The suggestions for next year's workshop include a follow-up on proposal writing with representatives of the funding agencies, careers for mass spectrometrists and a collaborative workshop with the History Interest Group.

Respectfully submitted,

Mark Ross

Mark Ross

LAWRENCE E ABBEY
VG INSTRUMENTS INC
4026 OAK CREST DRIVE

TUCKER GA 30084

PHONE: 404 934 7131

FRANK S ABBOTT
FAC OF PHARMACEUTICAL SCI
UNIV OF BRITISH COLUMBIA

VANCOUVER, BC V6T 1W5
CANADA
PHONE: 604 228 2566

ROBERT M ABERNATHEY
MS G740
LOS ALAMOS NATIONAL LAB
PO BOX 1663
LOS ALAMOS NM 87545

PHONE: 505 667 9903

WILLIAM H ABERTH
3146 MANCHESTER CT

PALO ALTO CA 94303

PHONE: 415 856 2412

CRAIG ABOLIN
SANDOZ RES INST
ROUTE 10

EAST HANOVER NJ 07936

PHONE: 201 503 8631

LINDA D ABRAMS
ENSECO PHARMACEUTICAL SCI LAB
2240 DABNEY RD

RICHMOND VA 23230

PHONE: 804 359 1900

FRED P ABRAMSON
GEORGE WASHINGTON UNIV
PHARMACOLOGY DEPT
2300 EYE ST NW
WASHINGTON DC 20037

PHONE: 202 994 2946

BRADLEY L ACKERMANN
MERRELL DOW PHARMACEUTICALS
2110 E GALBRAITH RD

CINCINNATI OH 45215

PHONE: 513 948 6081

THOMAS ACZEL
EXXON R/E
ROUTE 22 EAST
CLINTON TOWNSHIP
ANNANDALE NJ 08801

PHONE: 201 730 2231

JEANETTE ADAMS
DEPT OF CHEMISTRY
EMORY UNIVERSITY

ATLANTA GA 30322

PHONE: 404 727 6522

ROBERT A ADAMS
KRATOS ANALYTICAL INC
535 EAST CRESCENT AVE

RAMSEY NJ 07446

PHONE: 201 825 7500

WADE J ADAMS
THE UPJOHN COMPANY
301 HENRIETTA STREET

KALAMAZOO MI 49001

PHONE: 616 385 7642

HOLLY FORTNUM ADAMSONS
3140 COBBLESTONE LN #12

SPRINGFIELD IL 62704

PHONE: 217 788 1265

SOMASUNDARAM SAM ADDANKI
15109 NASHUA LANE

BOWIE MD 20716

PHONE:

JOSEPH B ADDISON
GOVERNORS STATE UNIV
COLL OF ARTS & SCI

UNIVERSITY PARK IL 60466

PHONE: 312 534 5000

S K AGGARWAL
DEPT OF PATHOLOGY
UNIV OF VIRGINIA HOSPITAL
BOX 214
CHARLOTTESVILLE VA 22908

PHONE: 804 924 5691

MOHAMMED S AHMED
DEPT OF CHEMISTRY
CASE WESTERN RESERVE UNIV

CLEVELAND OH 44106

PHONE: 216 368 3599

MOURAD AISSA
NORTHROP SERVICES, INC.
PO BOX 12313

RES TRAINGLE PARK NC 27709

PHONE: 919 541 5005

ALI SALEH AL-OMAIR
CHEM DEPT
UNIV OF KENT
CANTERBURY
KENT CT2 7NH
UK
PHONE:

MEHRSHID ALAI
856 W NELSON ST APT #1607

CHICAGO IL 60657

PHONE:

MARK ALASANDRO
DUPONT
EXPERIMENTAL STATION
BLDG 353/234
WILMINGTON DE 19808

PHONE:

JOHN ALBERG
HONEYWELL
600 2ND ST NE

HOPKINS NJ 55343

PHONE: 612 931 6983

RICHARD ALBERT
ETC CORP
4806 HUNTERS GLEN DR

PLAINSBORO NJ 08536

PHONE: 201 225 6782

KENNETH M ALDOUS
NY STATE HEALTH DEPT
WADSWORTH CENTER
TOWER BLDG
ALBANY NY 12201

PHONE: 518 473 0030

R T ALESSANDRO
ENVIROMENTAL TEST CERT CORP
284 RARITAN CENTER PARKWAY

EDISON NJ 08818

PHONE: 201 225 6725

ANTHONY ALEXANDER
ATLANTIC RESEARCH LAB, NRC
1411 OXFORD ST
HALIFAX
NOVA SCOTIA B3H 3Z1
CANADA
PHONE: 902 426 6357

JERRY W ALEXANDER
CALIF DEPT FOOD & AGRICULTURE
3292 MEADOWVIEW RD

SACRAMENTO CA 95832

PHONE: 916 427 7989

N E ALEXANDER
1201 MOTTER AVE

FREDERICK MD 21701

PHONE: 301 663 9085

E D ALFORD
BROWN & WILLIAMSON
PO BOX 35090

LOUISVILLE KY 40232

PHONE: 502 568 7680

DAVID ALKALAY
CIBA-GEIGY CORP
444 SAWMILL RIVER RD

ARDSLEY NY 10502

PHONE: 914 478 3131

ALEX R ALLAN
MT SINAI HOSPITAL
BOX 156
306 E 96TH STREET
NEW YORK NY 10128

PHONE: 212 241 7729

CYNTHIA C ALLEY
CTRS FOR DIS CONTROL
TOXICOLOGY C17-1814

ATLANTA GA 30333

PHONE: 404 488 4144

CHARLES ALLGOOD
DEPT OF CHEMISTRY
UNIV OF DELAWARE

NEWARK DE 19716

PHONE: 302 451 2917

MAHENDER REDDY ALLIRI
UNIV OF ARIZONA
DEPT OF PHARM SCIENCES
COLLEGE OF PHARMACY
TUCSON AZ 85721

PHONE: 602 626 4072

COLIN ALLISON
UNIV OF WATERLOO
DEPT OF CHEMISTRY

WATERLOO ONTARIO N2L 3G1
CANADA
PHONE: 519 885 1211

JOHN ALLISON
CHEMISTRY DEPARTMENT
MICHIGAN STATE UNIVERSITY

EAST LANSING MI 48824

PHONE: 517 353 4513

LAURA A ALLISON
CONOCO INC
R&D EAST
PO BOX 1267
PONCA CITY OK 74603

PHONE: 405 767 2761

GUNTER ALLMAIER
INST F ANAL CHEMISTRY
UNIV OF VIENNA
WAEHRINGERSTR 38
A-1090 VIENNA
AUSTRIA
PHONE:

NICK ALMASY
MI DEPT OF AGRICULTURE
1615 S HARRISON ROAD

EAST LANSING MI 48823

PHONE: 517 337 5057

MICHAEL F ALMOND
KRATOS ANALYTICAL
535 E CRESENT

RAMSEY NJ 07446

PHONE: 201 825 7500

V O ALTEMOSE
4841 CROSS ST

CAMPBELL NY 14821

PHONE:

ANDREW ALTMAN
VG INSTRUMENTS
10625 TUPPENCE CT

ROCKVILLE MD 20850

PHONE: 301 279 7827

RICH AMANO
ANALYTICAL TECHNOLOGIES INC
5550 MOREHOUSE RD

SAN DIEGO CA 92121

PHONE: 619 458 9141

JON AMSTER
DEPT OF CHEMISTRY
UC IRVINE

IRVINE CA 92717

PHONE: 714 856 6780

M M ANBAR
181 HALWILL DR

SNYDER NY 14226

PHONE: 716 831 2328

ROBERT J ANDEREGG
AUBERT HALL
UNIV OF MAINE

ORONO ME 04469

PHONE: 201 581 1171

BRIAN K ANDERSON
ROSS LABORATORIES
625 CLEVELAND AVE

COLUMBUS OH 43215

PHONE: 614 229 7345

DAVID J ANDERSON
GEOLOGY 541
INDIANA UNIV

BLOOMINGTON IN 47405

PHONE: 812 335 1005

MICHAEL J ANDERSON
MARATHON OIL CO
PO BOX 269

LITTLETON CO 80160

PHONE: 303 794 2601

SCOTT L ANDERSON
CHEMISTRY DEPT
SUNY

STONY BROOK NY 11794-3400

PHONE: 516 632 7915

STEPHEN ANDERSON
367 FLETCHWOOD ROAD APT 37A

ELKTON MD 21921

PHONE: 302 451 1118

SYD ANDERSON
FINNIGAN MAT
355 RIVER OAKS PARKWAY

SAN JOSE CA 95134

PHONE: 408 433 4800

WILLIAM R ANDERSON
LEHIGH UNIV
MUDD BLDG 6

BETHLEHEM PA 18015

PHONE: 215 758 3465

D A ANDRZEJEWSKI
FDA
200 C STREET SW HFF-426
ROOM B821
WASHINGTON DC 20204

PHONE: 202 245 8478

VINCENT ANICICH
JET PROPULSION LABORATORY
M/S 183-601
4800 OAK GROVE DRIVE
PASADENA CA 91109

PHONE:

ROLAND S ANNAN
DEPT OF CHEMISTRY
NORTHEASTERN UNIV
360 HUNTINGTON AVE
BOSTON MA 02115

PHONE: 617 437 2794

CLIFFORD ANNIS
BORG WARNER CHEMICAL CO
TECHNICAL CENTER
PO BOX 68
PARKERSBURG WV 26181

PHONE: 304 863 7652

ALEX APFFEL
HEWLETT-PACKARD
1601 CALIFORNIA AVE

PALO ALTO CA 94304

PHONE: 415 857 1501

R T APLIN
DYSON PERRINS LAB
OXFORD UNIVERSITY
SOUTH PARKS ROAD
OXFORD OX1 3QY
ENGLAND
PHONE:

ANTHONY D APPELHANS
EG&G IDAHO INC
PO BOX 1625
MS 2208
IDAHO FALLS ID 83415

PHONE: 208 526 0862

RYUICHI ARAKAWA
INST OF CHEMISTRY
COLLEGE OF GENERAL EDUCATION
OSAKA UNIV
TOYONAKA 560
JAPAN
PHONE:

RANDALL C ARAMBURU
VG INSTRUMENTS
32 COMMERCE CENTER
CHERRY HILL DRIVE
DANVERS MA 01923

PHONE: 817 430 0033

BRIAN ARBOGAST
ENVIRONMENTAL SCI CTR
WENIGER HALL
OREGON STATE UNIV
CORVALLIS OR 97331

PHONE: 503 754 2906

JANET AREY
AIR POLLUTION RES CTR
UNIV OF CALIFORNIA

RIVERSIDE CA 92521

PHONE: 714 787 3502

SALEH ARGHESTANI
REGION 7 LABORATORY
25 FUNSTON ROAD

KANSAS CITY KS 66115

PHONE: 913 236 3881

EMANUELE ARLANDINI
FARMITALIA-CERBA
VIA GRACCHI, NO 35

MILANO
ITALY
PHONE:

PETER B ARMENTROUT
DEPT OF CHEMISTRY
UNIVERSITY OF UTAH

SALT LAKE CITY UT 84112

PHONE: 801 581 7885

KENNETH ARMOCK
MICH DEPT OF NAT RES
ENVM LAB
315 N CLIPPERT
LANSING MI 48909

PHONE: 517 373 2883

P J ARPINO
LAB DE CHIMIE ANALYTIQUE
INSTITUT NATIONAL AGRONOMIQUE
16 RUE CLAUDE BERNARD
75231 PARIS CED 05
FRANCE
PHONE:

PETER ARROWSMITH
IBM
MS K34/803D
650 HARRY RD
SAN JOSE CA 95120-6099

PHONE: 408 927 2520

GUY P ARSENAULT
RR 2
MIDDLE ROAD

KINGSTON ONT K7L 5H6
CANADA
PHONE: 613 545 7484

BRUCE K ASAMOTO
BP AMERICA RESEARCH
4440 WARRENSVILLE CTR ROAD

CLEVELAND OH 44128

PHONE: 216 581 5776

KEIJI G ASANO
OAK RIDGE NAT'L LAB
PO BOX Y BLDG 9735

OAK RIDGE TN 37831

PHONE: 615 574 2456

TERRENCE ASHE
ESSO PETROLEUM CANADA
PO BOX 3022

SARNIA ONTARIO N7T 7M1
CANADA
PHONE: 519 339 2970

ROBERT W ASHMORE
DEPT OF PHARMACOLOGY
EXPERIMENTAL THERAPEUTICS
WALTER REED AIR
WASHINGTON DC 20307-5100

PHONE: 301 427 5273

JAWEED ASHRAF
AMERICAN CYANAMID
MEDICAL RESEARCH DIVISION

PEARL RIVER NY 10965

PHONE: 914 732 3972

JOHN W AULD
37748 SUNNYDALE

LIVONIA MI 48154

PHONE: 313 897 1395

PIERRE J AUSLOOS
NAT'L BUR OF STAN
CTR FOR CHEM PHYSICS

WASHINGTON DC 20234

PHONE: 301 975 2500

E R AUSTIN
IFDC
PO BOX 2040

MUSCLE SHOALS AL 35660

PHONE: 205 764 8365

MICHAEL J AVERY
IOWA STATE UNIV
113 SPEDDING

AMES IA 50011

PHONE: 515 294 6615

RUSSELL J AYERS
FOOD & DRUG ADMINISTRATION
1560 E JEFFERSON

DETROIT MI 48207

PHONE: 313 226 6260

LUCIA M BABCOCK
CHEMISTRY DEPT
CHOPPIN HALL
LOUISIANA STATE UNIV
BATON ROUGE LA 70803

PHONE: 504 388 3239

STEPHAN BACH
DEPT OF CHEMISTRY
UNIV OF FLORIDA

GAINESVILLE FL 32611

PHONE: 904 392 4892

LUBO BACZYNSKYJ
THE UPJOHN CO
301 HENRIETTA

KALAMAZOO MI 49001

PHONE: 616 385 7401

WILLIAM M BACZYNSKYJ
US FDA
HFF 445, RM 4005
200 C STREET, SW
WASHINGTON DC 20204

PHONE: 202 245 1090

TOMAS BAER
CHEMISTRY DEPARTMENT
UNIV OF NORTH CAROLINA

CHAPEL HILL NC 27514

PHONE: 919 962 1580

THOMAS A BAILLIE
DEPT OF MEDICINAL CHEMISTRY
BLDG 20
UNIV OF WASHINGTON
SEATTLE WA 98195

PHONE: 206 545 2468

E S BAKER
T5-06
WESTINGHUOSE HANFORD CORP
PO BOX 1970
RICHLAND WA 99352

PHONE: 509 373 3872

RANDALL J BAKER
MARION LABS INC
PO BOX 9627

KANSAS CITY MO 64134

PHONE: 816 966 5000

TIMOTHY R BAKER
28 GILBERT STREET

WATERTOWN MA 02172

PHONE: 617 437 4696

MICHAEL BALAZY
UNIV OF COLORADA HSC
DIV OF CLIN PHARM
4200 E 9TH AVE
DENVER CO 80262

PHONE: 303 270 8455

RUSSELL BALDOCK
114 OGONTZ LANE

OAK RIDGE TN 37830

PHONE: 615 483 6779

MICHAEL A BALDWIN
UNIVERSITY OF LONDON
SCHOOL OF PHARMACY
29/39 BRUNSWICK SQUARE
LONDON WC1N 1AX
ENGLAND
PHONE:

JOHN M BALLARD
CELANESE RESEARCH
86 MORRIS AVE

SUMMIT NJ 07901

PHONE: 201 522 7570

N E BALLOU
BATTELLE, PACIFIC NW LABS
PO BOX 999, P7-07

RICHLAND WA 99352

PHONE: 509 376 3061

MICHAEL P BALOGH
MILLIPORE
34 MAPLE STREET

MILFORD MA 01757

PHONE: 617 478 2000

L J BARABAS
MORTON CHEMICAL DIV
PO BOX 2184

GREENVILLE SC 29602

PHONE: 803 244 5351

WAYNE M BARAN
100 E STREAMWOOD BLVD

STREAMWOOD IL 60107

PHONE: 312 391 3378

MICHAEL BARBER
FINNIGAN MAT
1355 REMINGTON RD, SUITE M

SCHAUMBURG IL 60173

PHONE: 312 310 0140

ROBERT J BARBUCH
MERRELL DOW PHARMACEUTICAL
PO BOX 68470

INDIANAPOLIS IN 46268

PHONE: 317 873 4856

DAMIA BARCELO
ENVIRONMENTAL CHEM DEPT
JORGE GIRONA SALGADO 18-26

BARCELONA 08034
SPAIN
PHONE:

CHARLES BARINAGA
BATTELLE PNL
PO BOX 999

RICHLAND WA 99352

PHONE: 509 376 6095

ROBERT M BARKLEY
CIRES
CAMPUS BOX 449
UNIV OF COLORADO
BOULDER CO 80309-0449

PHONE: 303 492 1158

I L BARNES
NBS
A-23 PHYSICS

GAITHERSBURG MD 20899

PHONE: 301 975 4100

RAMON M BARNES
CHEMISTRY DEPT
GRC TOWERS
UNIV OF MASSACHUSETTS
AMHERST MA 01003-0035

PHONE: 413 545 2294

DOUGLAS F BAROFSKY
DEPT OF AGRICULTURAL CHEM
OREGON STATE UNIV

CORVALLIS OR 97331

PHONE: 503 754 2906

ELISABETH BAROFSKY
DEPT OF AG CHEMISTRY
OREGON STATE UNIV

CORVALLIS OR 97331

PHONE: 503 754 2906

ANDREW BARONAVSKI
NAVAL RESEARCH LAB
CODE 6110

WASHINGTON DC 20375

PHONE:

V MICHAEL BARRINGER
CIBA-GEIGY CORP
AG DIVISION
PO BOX 18300
GREENSBORO NC 27419

PHONE: 919 292 7100

ROBERT P BARRON
FDA-CTR DRUGS & BIOLOGICS
HFN-160/DSDDP
5600 FISHERS LANE
ROCKVILLE MD 20857

PHONE: 301 443 3560

MIKE BARRY
2113 S 48TH ST SUITE 107

TEMPE AZ 85282

PHONE: 602 438 1530

REGINA M BARRY
314 S UNION STREET

WILMINGTON DE 19805

PHONE: 302 451 2917

T L BARRY
FDA
850 3RD AVE

BROOKLYN NY 11232

PHONE: 718 965 5722

CHRISTOPHER M BARSHICK
DEPT OF CHEMISTRY
UNIV OF VIRGINIA
MCCORMICK ROAD
CHARLOTTESVILLE VA 22901

PHONE: 804 924 7180

MICHAEL J BARTELS
TOXICOLOGY LAB
1803 BLDG
DOW CHEMICAL CO
MIDLAND MI 48674

PHONE: 517 636 9057

GREG J BARTLING
1014 RIVERVIEW TERRACE

NEW MARTINSVILLE WV 26155

PHONE: 304 455 4400

CANDACE D BARTMAN
EXTREL CORP
PO BOX 11512

PITTSBURGH PA 15238

PHONE: 412 963 7530

JOHN BARTMESS
CHEMISTRY DEPT
UNIV OF TENNESSEE

KNOXVILLE TN 37996

PHONE: 615 974 6578

P L BARTNER
SCHERING CORP
60 ORANGE

BLOOMFIELD NJ 07003

PHONE: 201 429 3989

LOUISETTE J BASA
GENENTECH INC
460 PT SAN BRUNO BLVD

S SAN FRANCISCO CA 94080

PHONE: 415 266 2057

B B BASCHKIN
2 CAPTAINS LANE

RYE NY 10580

PHONE: 914 835 3506

ILORA BASU
INDIANA UNIVERSITY
SPEA, GEOLOGY 541

BLOOMINGTON IN 47405

PHONE: 812 335 6246

THOMAS BAUER
CHEMICAL WASTE MANAGEMENT INC
150 WEST 137TH ST

RIVERDALE IL 60627

PHONE: 312 841 8360

MARK F BEAN
PHYS & STRUCTURAL CHEM L-940
SMITH KLINE & FRENCH LABS
PO BOX 1539
KING OF PRUSSIA PA 19406-0939

PHONE: 215 270 6673

BRIAN DAVID BEATO
3751 SW 20TH AVENUE
APT 132

GAINESVILLE FL 32607

PHONE: 904 335 0631

CLAUDE BEAUGRAND
DELSI NERMAG
49 QUAI DU HALAGE

RUEIL MALMAISON
F 92500 FRANCE
PHONE:

CARL F BECKNER
FINNIGAN MAT
355 RIVER OAKS PKWY

SAN JOSE CA 95134

PHONE: 408 433 4800

CINDY BEGGS
DEPT OF CHEMISTRY
UC SANTA BARBARA

SANTA BARBARA CA 93106

PHONE: 805 961 2673

ROSS C BEIER
USDA
505 GILCHRIST

COLLEGE STATION TX 77840

PHONE: 409 260 9411

JOHN BELAND
EBMUD/LAB SERVICES
PO BOX 24055

OAKLAND CA 94623

PHONE: 415 465 3700

BRENDA P BASILE

18314 ELMDON

HOUSTON TX 77084

PHONE: 713 520 9900

R H BATEMAN
VG ANALYTICAL
FLOATS ROAD
WYTHENSHAWE
MANCHESTER M23 9LE
ENGLAND
PHONE:

CHARLENE W BAYER
GA TECH RESEARCH INSTITUTE
EDL/EHSD/EMRB
EMERSON A112
ATLANTA GA 30332

PHONE: 404 894 3825

JAN M BEANE
CHEMISTRY DEPT
IOWA STATE UNIV

AMES IA 50011

PHONE: 515 294 5958

ALFRED J BEATTIE
E I DUPONT
EXPERIMENTAL STA
PPD BLDG 269
WILMINGTON DE 19898

PHONE: 302 772 2240

DONALD D BECK
GENERAL MOTORS RESEARCH
PHYSICAL CHEMISTRY DEPT

WARREN MI 48098

PHONE: 313 986 1310

RAY G BEDFORD
LLNL
PO BOX 808 MAIL STOP L-357

LIVERMORE CA 94550

PHONE: 415 422 6065

THOMAS D BEHYMER
US EPA
26 W MARTIN LUTHER KING DR

CINCINNATI OH 45268

PHONE:

JON L BEIHOFFER
DENVER FEDERAL CENTER
BOX 25227

DENVER CO 80225

PHONE: 303 236 5132

RONALD L BELANGER
1899 MAPLE HILL ST

YORKTOWN HEIGHTS NY 10598

PHONE: 914 335 6806

LEWIS M BASS
DEPT OF CHEMISTRY
MILLERSVILLE UNIV

MILLERSVILLE PA 17551

PHONE: 717 872 3764

MARK R BAUER
BATTELLE
505 KING AVE

COLUMBUS OH 43201

PHONE: 614 424 3913

M GOKHAN BAYKUT
5051 ALTON PKWY #118

IRVINE CA 92714

PHONE: 714 261 7743

ELLYN S BEARY
NAT'L BUR OF STAN
BLDG 222 RM A 353

GAITHERSBURG MD 20899

PHONE: 301 975 4138

THOMAS C BEATY
KRATOS ANALYTICAL
535 E CRESCENT AVE

RAMSEY NJ 07446

PHONE: 201 825 7500

CHRISTOPHER H BECKER
SRI INTERNATIONAL
M S P8091
CHEMICAL PHYSICS LAB
MENLO PARK CA 94025

PHONE: 415 859 5130

A A BEDNARCZYK
QUEST INTERNATIONAL
10 PAINTERS MILL RD

OWINGS MILLS MD 21117-3686

PHONE: 301 363 2550

WILLIAM R BEHYMER
USI INDUSTRIAL CHEMICAL CO
1275 SECTION ROAD

CINCINNATI OH 45237

PHONE:

ROBERT G BEIMER
S-CUBED
PO BOX 1620

LA JOLLA CA 92038

PHONE:

DAVID BELL
DEPT OF CHEMISTRY
UMIST
PO BOX 88
MANCHESTER M60 1QD
UK
PHONE:

JACKIE BELL
3900 EAST NORTH ST, APT I153

GREENVILLE SC 29615

PHONE: 803 242 9317

MICHAEL G BELL
LOS ALAMOS NATL LAB
PO BOX 1663/E518

LOS ALAMOS NM 87545

PHONE: 505 665 1652

V E BELL
HOFFMANN-LAROCHE INC

NUTLEY NJ 07110

PHONE: 201 235 2852

THOMAS H BELLUS
PUGET SOUND NAVAL SHIPYARD
CODE 134.3

BREMERTON WA 98314

PHONE: 206 476 8092

THEODORE BELSKY
CA DEPT OF HEALTH SERVICES
HAZARDOUS MATERIALS LAB
2151 BERKELEY WAY
BERKELEY CA 94704

PHONE: 415 540 2337

F A BENCSATH
BIOCHEMISTRY USA
MSB 2170

MOBILE AL 36688

PHONE:

J G BENDORAITIS
MOBIL RESEARCH & DEV
BILLINGSPORT RD

PAULSBORO NJ 08066

PHONE: 609 423 1040

EMILIO BENFENATI
INSTITUTE MARIO NEGRI
VIERITREA 62

20157 MILAN
ITALY
PHONE:

BRIAN D BENNETT
CHEMISTRY DEPT
UNIV OF CINCINNATI

CINCINNATI OH 45220

PHONE:

FRANK M BENOIT
HEALTH-WELFARE DEPT
ENVIRONMENTAL HEALTH
TUNNEYS PASTURE
OTTAWA ONTARIO K1A 0L2
CANADA
PHONE:

LINDA BENSON
MAYO CLINIC/FOUNDATION
200 SW 1ST STREET

ROCHESTER MN 55905

PHONE: 507 284 4212

BRYAN L BENTZ
DAVID SARNOFF RES CTR
CN 5300

PRINCETON NJ 08543-5300

PHONE: 609 734 2015

WOLFGANG BENZ
HOFFMANN-LAROCHE INC
KINGSLAND ST

NUTLEY NJ 07110

PHONE: 201 235 3786

DAVID W BERBERICH
1930 SW 14TH TERRACE

GAINESVILLE FL 32608

PHONE: 904 392 0515

PETER J BERG
MAYO ENDOCRINE RES
5-164 W JOSEPH
200 1ST STREET SW
ROCHESTER MN 55905

PHONE: 507 285 5097

PHILIP S BERGER
TEKNIVENT CORP
11684 LILBURN PARK RD

ST LOUIS MO 63146

PHONE: 314 994 0500

JACK BERGES
860 E TWAIN #128-521

LAS VEGAS NV 89109

PHONE: 702 734 3351

ALICE M BERGMANN
SUNY @ BUFFALO
DEPT OF CHEMISTRY
18 ACHESON HALL
BUFFALO NY 14214

PHONE: 716 831 3016

R E BERKLEY
133 MONTCLAIR CIRCLE

DURHAM NC 27713

PHONE: 919 541 2439

JOEL C BERLINGHIERI
THE CITADEL
PHYSICS DEPT

CHARLESTON SC 29409

PHONE: 803 792 6942

MARK BERNICK
287AA MOUNTAIN RD

LEBANON NJ 08833

PHONE:

M J BERTRAND
UNIV OF MONTREAL
CHEMISTRY DEPT
C.P. 6128 STATION A
MONTREAL QUEBEC H3C 3J7
CANADA
PHONE:

PATRICIA BETHEL
1260 HOPKINS APT 40

BERKELEY CA 94702

PHONE: 415 843 0215

ROBERT BETHEM
CAL LABS ENSECO
2544 INDUSTRIAL BLVD

WEST SACRAMENTO CA 95691

PHONE: 916 372 1393

LEON D BETOWSKI
EPA-EMSL
QUAL ASSURANCE DIV
PO BOX 93478
LAS VEGAS NV 89113-3478

PHONE: 702 798 2116

LAURA BETTAZZOLI
U OF COLORADO HEALTH SCI CTR
CAMPUS BOX A072
4200 EAST NINTH AVE
DENVER CO 80220

PHONE:

STEVE BEU
MOTOROLA INC/ UNIV OF TEXAS
3501 ED BLUESTEIN BLVD MD-L12

AUSTIN TX 78721

PHONE: 512 928 6271

ROBERT J BEUHLER
BLDG 555A-CHEMISTRY
BROOKHAVEN NATIONAL LAB

UPTON NY 11973

PHONE: 516 282 4317

J H BEYNON
17 COLTSHILL DRIVE
MUMBLES

SWANSEA SA3 4SN
GREAT BRITAIN
PHONE:

KIRIT H BHATT
PHARMACOLOGY/TOXICOLOGY
UNIV OF KUWAIT
PO BOX 24923
SAFAT
KUWAIT 13110
PHONE:

KLAUS BIEMANN
MIT
CHEMISTRY 56-010

CAMBRIDGE MA 02139

PHONE: 617 253 7221

VERONICA M BIERBAUM
CHEMISTRY DEPT
UNIVERSITY OF COLORADO
CAMPUS BOX 215
BOULDER CO 80309-0215

PHONE: 303 492 7081

NICK BINDER
ISO-MASS CONSULTING LTD
1250 EMERALD CRESCENT

SASKATOON, SASK
CANADA
PHONE:

ASGEIR BJARNASON
SCI INST
UNIV OF ICELAND
DUNHAGA 3
107 REYKJAVIK
ICELAND
PHONE:

WALTER BLACKSTOCK
GLAXO GROUP RESEARCH
GREENFORD ROAD GREENFORD

MIDDLESEX UB6 OHE
ENGLAND
PHONE:

ANTHONY F BLAKE
44 DANBURY

OAKLAND CA 94605

PHONE: 415 562 4074

WILLIAM E BLANTON
2601 WILLIAMS GRANT

SUGAR LAND TX 77479

PHONE: 713 954 6771

LYNN J BLUETT
XEROX CORPORATION
800 PHILLIPS RD 139-64A

WEBSTER NY 14580

PHONE: 716 422 3179

BRIAN BOBBIE
MINISTRY OF THE ENVIRONMENT
PO BOX 213
125 RESOURCES ROAD
REXDALE, ONTARIO M9W 5L1
CANADA
PHONE: 416 235 5890

CORINNE L BOGERT
6707 RALSTON RD

ARVADA CO 80002

PHONE: 303 421 3130

D M BIER
WASHINGTON UNIV
METABOLISM
SCHOOL OF MEDICINE
ST LOUIS MO 63110

PHONE: 314 362 6923

J E BILLER
MIT
CHEMISTRY 56-025
77 MASS AVE
CAMBRIDGE MA 02139

PHONE: 617 253 7232

ROBERT C BINIAKEWITZ
CHAMPION INT'L CORP
WEST NYACK ROAD

WEST NYACK NY 10994

PHONE: 914 578 7208

DAVID L BLACK
VANDERBILT UNIV MED CTR
VCAPH 313
1601 23RD AVENUE, SOUTH
NASHVILLE TN 37212

PHONE: 615 343 5020

MICHAEL BLADES
DEPT OF CHEMISTRY
UNIV OF BRITISH COLUMBIA

VANCOUVER, BC V6T 1Y6
CANADA
PHONE: 604 228 4468

CALVIN R BLAKLEY
2007 WILDERNESS PT DR

KINGWOOD TX 77339

PHONE: 713 796 9677

ERIC BLOCK
CHEMISTRY 56-016
MIT

CAMBRIDGE MA 02139

PHONE: 617 253 7236

DAVID BLYTH
KRATOS ANALYTICAL INC
535 EAST CRESCENT AVE

RAMSEY NJ 07446

PHONE: 201 825 7500

FRANK M BOCKHOFF
BP AMERICA
4440 WARRENSVILLE CTR ROAD

CLEVELAND OH 44128

PHONE: 216 581 5838

VINCE BOJAN
MAAS INC
1155 ZION ROAD

BELLEFONTE PA 16823

PHONE: 814 353 0600

MARK E BIER
FINNIGAN MAT
355 RIVER OAKS PARKWAY

SAN JOSE CA 95134

PHONE: 408 433 4800

STEPHEN S BILLETS
US EPA EMSL-QAD
PO BOX 93478

LAS VEGAS NV 89193-3478

PHONE: 702 798 2232

GEORGE M BIRD
SUN CHEMICAL CORP
631 CENTRAL AVE

CARLSTADT NJ 07072

PHONE: 201 933 4500

SADOR S BLACK
E R SQUIBB & SONS
PO BOX 191

NEW BRUNSWICK NJ 08903

PHONE: 201 519 2800

IAN A BLAIR
PHARMACOLOGY DEPT
VANDERBILT UNIV

NASHVILLE TN 37232

PHONE: 615 322 2094

JULIE A BLANCKAERT
6103 E LONG CIRCLE N

ENGLEWOOD CO 80112

PHONE: 303 796 7504

KARL F BLOM
314 S UNION ST

WILMINGTON DE 19805

PHONE: 302 695 4686

JAMES R BOAL
THE UPJOHN CO
301 HENRIETTA STREET

KALAMAZOO MI 49001

PHONE:

STAN BOEHM
FINNIGAN MAT
355 RIVER OAKS PARKWAY

SAN JOSE CA 95134

PHONE: 408 433 4800

MARK S BOLGAR
SQUIBB INST FOR MED RES
PO BOX 4000

PRINCETON NJ 08540

PHONE: 609 921 5429

KEVIN B BOLGER
10047 LINDA LANE 2N

DES PLAINES IL 60016

PHONE: 312 353 4676

DANIEL D BOMBICK
DEPT OF CHEMISTRY
WRIGHT STATE UNIVERSITY

DAYTON OH 45435

PHONE: 513 873 2340

KRISTI E BONAPARTE
1050 JIMMIE DANIE RD

BOGART GA 30622

PHONE: 404 548 8450

HENRY A BONDAROVICH
IFF
1515 HWY 36

UNION BEACH NJ 07735

PHONE: 201 888 2539

WILLIAM BONE
FINNIGAN MAT
5340 SPECTRUM DRIVE

FREDERICK MD 21701

PHONE: 301 698 9750

ERNIE J BONELLI
HP SCIENTIFIC INSTR
1601 CALIFORNIA AVE

PALO ALTO CA 94304

PHONE: 415 857 6028

RON F BONNER
SCIEX
55 GLENCAMERON RD

THORNHILL ONT L3T 1P2
CANADA
PHONE: 416 881 4646

JEANNE BONURA-MAHONEY
ANALYTICAL TECHNOLOGIES, INC
2113 S 48TH STREET #107

TEMPE AZ 85282

PHONE: 602 438 1530

MATTHEW BOOTH
1355 REMINGTON RD, SUITE M

SCHAUMBURG IL 60173

PHONE:

RICHARD A BORDERS
KIMBERLY-CLARK CORP
1400 HOLCOMB BRIDGE ROAD

ROSWELL GA 30076

PHONE: 404 587 7843

ROBERT S BORDOLI
VG ANALYTICAL LAB
FLOATS ROAD
WYTHENSHAWE
MANCHESTER M239LE
ENGLAND
PHONE:

JULIET H BORTHWICK
2416 RAINTREE COURT

PLANO TX 75074

PHONE: 214 578 8912

DAVID BOSTWICK
CHEMISTRY DEPARTMENT
GEORGIA INST OF TECH

ATLANTA GA 30332

PHONE: 404 894 4061

RENE N BOTTER
CEN SACLAY DPC

91191 GIF SUR YVETTE
CEDEX
FRANCE
PHONE:

FRED BOUCHARD
UNIV OF WATERLOO
DEPT OF CHEMISTRY

WATERLOO, ONT N2V 1L3
CANADA
PHONE:

JAMES H BOURELL
1548 BRENTWOOD CT

WALNUT CREEK CA 94595

PHONE: 415 266 1239

JAMES A BOURG
HEWLETT-PACKARD
4921 JAMES DRIVE

METAIRIE LA 70003

PHONE: 504 467 4100

JOHN P BOWDEN
2428 EL CHICO CIRCLE

RANCHO CORDOVA CA 95670

PHONE: 916/739 5136

D V BOWEN
PFIZER CENTRAL RES
SANDWICH

KENT CT13 9NJ
ENGLAND
PHONE:

LARRY D BOWERS
DEPT OF LAB MED & PATHOLOGY
UNIV OF MINNESOTA
BOX 198 MAYO BLDG
MINNEAPOLIS MN 55455

PHONE: 612 626 3117

MICHAEL T BOWERS
CHEMISTRY DEPARTMENT
UC SANTA BARBARA

SANTA BARBARA CA 93106

PHONE: 805 961 2893

WILLIAM D BOWERS
17 WILD GOOSE CT

NEWPORT BEACH CA 92663

PHONE: 714 856 6780

ROBERT K BOYD
ATLANTIC RES LAB
NATIONAL RES COUNCIL
1411 OXFORD ST
HALIFAX NS B3H 3Z1 CANADA
CANADA
PHONE:

ARTHUR J BOYER
ENVIRONMENTAL RESEARCH CENTER
UNIV OF NEVADA, LAS VEGAS
4505 MARYLAND PARKWAY
LAS VEGAS NV 89154

PHONE:

DONALD E BRACKEN
NJ STATE DEPT OF HEALTH
PUB HEAL & ENVIR LABS
CN 360
TRENTON NJ 08625

PHONE: 609 984 0646

RICHARD T BRACKMANN
EXTREL CORP
PO BOX 11512

PITTSBURGH PA 15238

PHONE: 412 963 7530

ANNE BRADBURN
7901 WEST MORRIS STREET

INDIANAPOLIS IN 46231

PHONE: 317 293 0164

DON BRADFORD
FINNIGAN MAT
355 RIVER OAKS PARKWAY

SAN JOSE CA 95134

PHONE: 408 433 4800

JAMES G BRADLEY
JET PROPULSION LAB
MS 11-116
4800 OAK GROVE DR
PASADENA CA 91109

PHONE: 818 354 4215

JOEL C BRADLEY
CAMBRIDGE ISOTOPE LAB INC
20 COMMERCE WAY

WOBURN MA 01801

PHONE: 617 938 0067

DEVIN K BRAIN
3 WALSH LANE

CINCINNATI OH 45208

PHONE: 513 627 5661

R Y VAN FOSSEN BRAVO
PUC DEPTO QUIMICA
R.M.SAO VICENTE,225
22.453 - GAVEA
RIO DE JANEIRO-RJ
BRAZIL
PHONE:

MIKE BRECHMANN
1414 STANISLAUS STREET

FRESNO CA 93706

PHONE: 209 485 8310

DAVID BRENT
BURROUGHS WELLCOME
3030 CORNWALLIS RD

RESEARCH TRI PARK NC 27709

PHONE: 919 248 4235

ROD A BRITTEN
84 WEST MARIPOSA ST

ALTADENA CA 91001

PHONE: 818 354 2328

VERNON O BRANDT
ETHYL TECHNICAL CENTER
BOX 14799

BATON ROUGE LA 70898

PHONE: 504 768 5837

L L BRAYTON
PO BOX 5075, STN A

CHAMPAIGN IL 61820

PHONE: 217 333 2545

JIM BREECE
PO BOX 92050

ELK GROVE VILLAGE IL 60009-2050

PHONE: 312 694 2700

GARY B BREWSTER
THE COCA-COLA CO
MAIL CODE TEC 6
PO DRAWER 1734
ATLANTA GA 30301

PHONE: 404 676 3668

JENNIFER BRODBELT-LUSTIG
DEPT OF CHEMISTRY
UNIV OF CALIFORNIA

SANTA BARBARA CA 93106

PHONE: 805 961-2673

W E BRASELTON
PHARMACOLOGY DEPARTMENT
MICHIGAN STATE UNIVERSITY

EAST LANSING MI 48824

PHONE: 517 355 7441

ALAN BREAU
DEPT MC909 BLDG 2812
ELI LILLY & COMPANY

INDIANAPOLIS IN 46285

PHONE: 317 276 4382

J THOMAS BRENNA
IBM
DEPT T43-257-2
1701 NORTH STREET
ENDICOTT NY 13760

PHONE: 607 757 1435

FRED W BRILL
105 N MARION DRIVE

GOLDSBORO NC 27530

PHONE: 919 731 5200

CHARLES J W BROOKS
UNIV OF GLASGOW
CHEMISTRY DEPT

GLASGOW G12 8QQ
SCOTLAND
PHONE:

HARRY O BROTHERTON
CHEMISTRY DEPT
NORTHEAST LOUISIANA UNIV

MONROE LA 71209

PHONE: 318 342 4136

COSTELLO L BROWN
CHEMISTRY DEPARTMENT
CALIFORNIA STATE UNIVERSITY

LOS ANGELES CA 90032

PHONE: 213 224 3613

PAT BROWN
MICOLET MASS SPECTROMETRY
5225-1 VERONA ROAD
PO BOX 4508
MADISON WI 53711-4508

PHONE: 608 271 3333

ROBERT S BROWN
CHEMISTRY DEPT
COLORADO STATE UNIV

FORT COLLINS CO 80523

PHONE: 303 491 6485

STEPHEN M BROWN
DEPT OF CHEMISTRY
INDIANA UNIVERSITY

BLOOMINGTON IN 47405

PHONE: 812 335 5705

SUSAN A BROTHERTON
EMS LABORATORIES
7901 W MORRIS

INDIANAPOLIS IN 46231

PHONE: 317 243 8305

JOHNIE C BROWN
CHEMISTRY DEPT
UNIV OF WISCONSIN
1101 UNIVERSITY AVENUE
MADISON WI 53706

PHONE: 608 262 3449

ROBERT BROWN
ELEMENTAL RESEARCH INC
SUITE 309 - 267 WEST ESPLANADE

N VANCOUVER BC V1M 1A5
CANADA
PHONE:

SHARON BROWN
23 NASSAU ROAD

VERONA NJ 07044

PHONE: 201 235 4515

STEVE BROWN
FINNIGAN
355 RIVER OAKS PARKWAY

SAN JOSE CA 95134-1991

PHONE: 408 433 4800

CHARLES E BROWN
DEPT OF BIOCHEMISTRY
MED COLL OF WISCONSIN
8701 WATERTOWN PLANK RD
MILWAUKEE WI 53226

PHONE: 414 257 8436

KEVIN A BROWN
TOXICOLOGY DEPT
INDIANA UNIV MED CTR
1001 WALNUT STREET
INDIANAPOLIS IN 46223

PHONE: 317 274 7824

ROBERT D BROWN
110 WINDBRIDGE DRIVE

WEST CHESTER PA 19380-3940

PHONE: 215 363 0402

SHARON M BROWN
IFF R&D
1515 HWY 36

UNION BEACH NJ 07735

PHONE: 201 264 4500

MARILYN L BROWNAWELL
320 ROBERTS LN

SCOTCH PLAINS NJ 07076

PHONE: 201 463 0003

RICHARD F BROWNER
SCHOOL OF CHEMISTRY
GEORGIA INST OF TECHNOLOGY

ATLANTA GA 30332

PHONE: 404 894 4020

RADICATI DI BROZOLO
C EVANS & ASSOCIATES
301 CHESAPEAKE DR

REDWOOD CITY CA 94063

PHONE: 415 369 4567

PHILIP J BRUCAT
UNIV OF FLORIDA
DEPT OF CHEMISTRY

GAINESVILLE FL 32611

PHONE: 904 392 2006

A P BRUINS
STATE UNIVERSITY
PHARMACY DEPT
A DEUSINGLAAN 2
9713-AW GRONINGEN
NETHERLANDS
PHONE:

DOMINIQUE BRUMENT
DELSI NERMAG
15701 WEST HARDY RD #1

HOUSTON TX 77060

PHONE: 713 847 0811

W C BRUMLEY
US EPA EMSL-LV QMB

LAS VEGAS NV 89193-3478

PHONE:

ROBERT J BRUNFELDT
R J BRUNFELDT CO
PO BOX 2066

BARTLESVILLE OK 74005

PHONE: 918 336 4467

CURT BRUNNEE
FINNIGAN MAT
BARKHAUSENSTR 2
POSTFACH 14 4062
D-2800 BREMEN 10
WEST GERMANY
PHONE:

CARL N BRUNO
NASSAU COUNTY POLICE DEPT
SCI INVESTIGATION BUREAU
1490 FRANKLIN AVE
MINEOLA NY 11501

PHONE: 516 535 7802

MATTHEW S BRYANT
11701 MARA LYNN RD #119

LITTLE ROCK AR 72211

PHONE: 501 225 8299

JOHN MICHAEL BUCHANAN
6922 HIGHLAND STREET

SPRINGFIELD VA 22150

PHONE: 703 642 6823

MICHELLE V BUCHANAN
OAK RIDGE NAT'L LAB
BLDG 4500-S
PO BOX X
OAK RIDGE TN 37831-6120

PHONE: 615 576 6690

JAMES D BUCHNER
EXTREL CORP
PO BOX 11512

PITTSBURGH PA 15238

PHONE: 412 963 7530

JOHN P BUCK
FINNIGAN MAT
900 PARKVIEW LANE

MUKWONAGO WI 53149

PHONE: 312 310 0140

THOMAS J BUCKLEY
NBS
BLDG 222 B-348

GAITHERSBURG MD 20899

PHONE: 301 975 2560

WILLIAM L BUDDE
US EPA
26 W MARTIN LUTHER KING DR

CINCINNATI OH 45268

PHONE: 513 569 7309

PATRICK BUDDRUS
ENSECO CAL LABS
2544 INDUSTRIAL BLVD

W SACRAMENTO CA 95691

PHONE: 916 756 5390

PROF H BUDZIKIEWICZ
INST. ORG. CHEM.
GREINSTR. 4

5000 KOELN 41
WEST GERMANY
PHONE:

JOANNE BUEHLER
SCHOOL OF PHARMACY
UNIV OF CALIFORNIA
513 PARNASSUS
SAN FRANCISCO CA 94143-0446

PHONE: 415 476 5249

VALERIE BUJANOWSKI
DOW CORNING CORP
MAIL STOP 26

MIDLAND MI 48640

PHONE: 517 496 5633

MICHAEL C BULAWA
EXXON RESEARCH & ENGINEERING
PO BOX 4050

BAYTOWN TX 77522

PHONE: 713 425 5417

DAVID A BULPETT
US ARMY METERIALS TECH LAB
ATTN: SLCMT-EMP

WATERTOWN MA 02172

PHONE: 617 923 5649

S S BULUSU
US ARMY ARDEC, BLDG 3028

PICATINNY ARSENAL NJ 07806-5000

PHONE: 201 724 6450

LARRY BURCHFIELD
FINNIGAN MAT
PO BOX 1089

MIDLOTHIAN TX 76065

PHONE: 214 775 3279

MIKE W BURGER
DEPT OF CHEMISTRY
UNIV OF HAWAII AT MANOA
2545 THE MALL
HONOLULU HI 96822

PHONE: 808 948 8184

ROBERT BURGER
UNIROYAL CHEMICAL
ELM STREET, BLDG 81-2

NAUGATUCK CT 06770

PHONE: 203 723 3684

DAVID J BURINSKY
ORTHO PHARMACEUTICAL
RTE 202; PO BOX 300

RARITAN NJ 08869

PHONE: 201 218 6275

A L BURLINGAME
UNIV OF CALIFORNIA
PHARMCEUTICAL CHEM

SAN FRANCISCO CA 94143-0446

PHONE: 415 476 5641

MARK A BURLINGAME
UCSF
521 PARNASSUS
BOX 0446
SAN FRANCISCO CA 94143

PHONE: 415 476 4893

FRANK B BURNS
SANDIA NAT'L LABS
DIV 1821
PO BOX 5800
ALBUQUERQUE NM 87185-5800

PHONE: 505 846 5689

HOLLY BURRIESCI
CHARLES EVANS & ASSOCIATES
301 CHESAPEAKE DRIVE
REDWOOD CITY CA 94063
PHONE: 415 369 4567

D G BURROWS
NORTHWEST & ALASKA
FISHERIES CENTER
2725 MONTLAKE BLVD E
SEATTLE WA 98112
PHONE: 206 442 5660

RICHARD BURROWS
SAN DIEGO STATE UNIV
5300 CAMPANILE DRIVE
SAN DIEGO CA 92109
PHONE: 619 229 2422

JOAN T BURSEY
RADIAN CORPORATION
PO BOX 13000
RES TRI PK NC 27709
PHONE: 919 481 0212

MAURICE M BURSEY
CHEMISTRY DEPT
CB#3290, VENABLE HALL
UNIV NORTH CAROLINA
CHAPEL HILL NC 27599-3290
PHONE: 919 962 4403

PETER C BUSCEMI
ATF-NATL LAB CENTER
1401 RESEARCH BLVD
ROCKVILLE MD 20850
PHONE: 301 294 0410

KENNETH L BUSCH
CHEMISTRY DEPT
INDIANA UNIV
BLOOMINGTON IN 47401
PHONE: 812 335 2081

ERNIE D BUSH
VA MEDICAL CENTER
500 W FORT ST
BOISE ID 83702
PHONE: 208 336 5100

GERRY W BUTTLER
MONSANTO CO
MAIL CODE U4C
800 N LINDBERGH BLVD
ST LOUIS MO 63167
PHONE: 314 694 4213

RONALD BUXTON
ENGINEERING SCIENCE
600 BANCROFT WAY
BERKELEY CA 94710
PHONE: 415 841 7353

JOHN T BYCHOWSKI
WASTE MANAGEMENT INC
3003 BUTTERFIELD RD
OAK BROOK IL 60521
PHONE: 312 572 1066

NEAL D BYINGTON
US CUSTOMS SERVICE LAB
630 SANSOME ST, RM 1429
SAN FRANCISCO CA 94111
PHONE: 415 556 2895

GARY D BYRD
R J REYNOLDS TOBACCO CO
BOWMAN GRAY TECHNICAL CENTER
WINSTON-SALEM NC 27105
PHONE: 919 741 2603

DALE K CABBINESS
CONOCO INC
PO BOX 1267
PONCA CITY OK 74603
PHONE: 405 767 4478

THOMAS CAIRNS
US FDA
1521 W PICO BLVD
LOS ANGELES CA 90015
PHONE: 213 252 7571

GARY CALDWELL
JANSSEN RES FOUNDATION
WELSH & MCKEON RDS
SPRING HOUSE PA 19474
PHONE: 215 628 5537

KENNY CALDWELL
DEPT OF CHEMISTRY
UNIV OF NEBRASKA
LINCOLN NE 68588-0304
PHONE: 402 472 3507

JOHN B CALLAGHAN
680 FRANKLIN STREET
DENVER CO 80218
PHONE: 303 399 3747

JOHN H CALLAHAN
NAVAL RESEARCH LABORATORY
CODE 6112 CHEMISTRY DIV
WASHINGTON DC 20375-5000
PHONE: 202 767 3551

PATRICK S CALLERY
UNIV OF MARYLAND
20 N PINE ST
BALTIMORE MD 21201
PHONE: 301 328 2980

E L CALLIS
LOS ALAMOS NATIONAL LAB
MAIL STOP G740
LOS ALAMOS NM 87545
PHONE: 505 667 9868

DOUGLAS CAMERON
WESTERN RESEARCH CTR
PO BOX 3395
LARAMIE WY 82071
PHONE: 307 721 2365

JOSEPH E CAMPANA
NICOLET INSTRUMENT CORPRY
5225-3 VERONA RD
PO BOX 4451
MADISON WI 53711-4495
PHONE: 608 271 3333

CLAY S CAMPBELL
FINNIGAN MAT
355 RIVER OAKS PKWY
SAN JOSE CA 95134-9990
PHONE: 408 433 4800

JAMES A CAMPBELL
BATTELLE NORTHWEST
329 BLDG/300 AREA
PO BOX 999
RICHLAND WA 99352
PHONE: 509 376 0899

SCOTT CAMPBELL
VG INSTRUMENTS
1008 BRISTOL LANE
MODESTO CA 95350
PHONE: 209 545 8105

THOMAS W CAMPBELL
8009 HILLRISE DRIVE
AUSTIN TX 78759
PHONE: 512 458 7587

DAVID C CANADA
MARTIN MARIETTA CORP
PO BOX P MS 446
OAK RIDGE TN 37831
PHONE: 615 574 9764

DEVON CANCILLA
UCLA
LBES 900 VETERAN AVE
ROOM 2-4-211
LOS ANGELES CA 90024
PHONE: 213 825 3999

RAUL CANEZ
ALCON LABS
6201 S FREEWAY
FORT WORTH TX 76115
PHONE: 817 551 4703

JOHN CANTLE
VG INSTRUMENTS
ROAD 3, WINSFORD

CHESHIRE
UK
PHONE:

ZHONG-MIN CAO
COLLEGE OF CHEMICAL ENGINEERIN
DALIAN INST OF TECHNOLOGY

DALIAN 116024
CHINA
PHONE:

RICHARD J CAPP
108 LAKEVIEW DRIVE

MCKEES ROCKS PA 15136-1233

PHONE: 412 777 8372

ACHILLE CAPPIELLO
DEPT OF CHEMISTRY
56-016
MIT
CAMBRIDGE MA 02139

PHONE: 617 253 7236

JOHN H CAPPIS
C/O IAEA
WAGRAMERSTRASSE 5 BOX 200

A-1400 VIENNA
AUSTRIA
PHONE:

RICHARD M CAPRIOLI
ANALYTICAL CHEM CTR
UNIVERSITY OF TEXAS HSC
PO BOX 20708
HOUSTON TX 77225

PHONE:

H S CARDEN
5361 BIGGER RD

KETTERING OH 45440

PHONE: 513 865 3789

MICHAEL D CARDENAS
T EDISON TECH CENTER
11131 ADAMS RD

FRANKSVILLE WI 53126

PHONE: 414 835 1544

DANIEL B CARDIN
EMSI - R&D GROUP
4765 CALLE QUETZAL

CAMARILLO CA 93010

PHONE: 805 388 5700

FRED CARDINALI
CDC
1600 CLIFTON ROAD MS F17

ATLANTA GA 30333

PHONE: 404 488 4144

JO CARLIN
MERCK SHARP & DOHME
RESEARCH LABORATORY
PO BOX 2000
RAHWAY NJ 07065

PHONE: 201 574 5920

TIMOTHY J CARLIN
CIBA GEIGY CORPORATION
PO BOX 18300

GREENSBORO NC 27419-8300

PHONE:

STEPHEN F CARLSEN
CIBA-GEIGY
444 SAW MILL RIVER ROAD

ARDSLEY NY 10502

PHONE: 914 478 3131

ROBERT F CARNEY
WESTON ANALYTICS
7720 LORRAINE AVE SUITE 102

STOCKTON CA 95210

PHONE: 209 957 3405

STEVEN A CARR
SMITHKLINE & FRENCH
L-940, SWEDELAND RD

KING OF PRUSSIA PA 19406

PHONE: 215 270 6650

BILL CARSON
WATERS CHROMATOGRAPHY
DIVISION OF MILLIPORE
34 MAPLE STREET
MILFORD MA 01757

PHONE: 617 478 2000

DONNA SUE CARTER
DEPT OF CHEMISTRY
INDIANA UNIVERSITY

BLOOMINGTON IN 47405

PHONE: 812 335 5424

JOEL A CARTER
107 WINDSONG RD

CLINTON TN 37716

PHONE: 615 574 2447

ALLEN M CARY
FINNIGAN MAT
355 RIVER OAKS PKWY

SAN JOSE CA 95134

PHONE: 408 483 4800

L F CASABONA
TELEDYNE-ISOTOPES
50 VAN BUREN AVE

WESTWOOD NJ 07675

PHONE: 201 664 7070

HOWARD H CASPER
DEPT OF VETERINARY SCIENCE
NORTH DAKOTA STATE UNIV

FARGO ND 58105

PHONE: 701 237 7529

CAROLYN J CASSADY
12567 BROODMOOR

OVERLAND PARK KS 66209

PHONE: 716 753 7600

EUGENE CASSIS
WATERS ASSOCIATES
34 MAPLE STREET

MILFORD MA 01757

PHONE: 617 478 2000

BILL CASTLE
STATE OF CA DEPT FISH & GAME
WATER POLLUTION CONTROL LAB
2005 NIMBUS RD
RANCHO CORDOVA CA 95670

PHONE: 916 355 0856

LYLE W CASTLE
UNIV OF NEBRASKA-LINCOLN
DEPT OF CHEMISTRY

LINCOLN NE 68588-0304

PHONE: 402 472 3507

P M CASTLE
778 CEDARWOOD DR

PITTSBURGH PA 15235

PHONE: 412 256 7090

ALBERT W CASTLEMAN
CHEMISTRY DEPARTMENT
PENNSYLVANIA STATE UNIV
152 DAVEY LAB
UNIVERSITY PARK PA 16802

PHONE: 814 865 7242

MAURO E CASTRO
DEPT OF CHEMISTRY
TEXAS A&M UNIV

COLLEGE STATION TX 77843

PHONE: 409 845 8839

LARRY C CATTRAN
HEWLETT PACKARD
1601 CALIFORNIA AVE

PALO ALTO CA 94304

PHONE: 415 857 6118

STEVEN P CEPA
ABBOTT LABS
D 417 AP-9

ABBOTT PARK IL 60064

PHONE: 312 937 7534

RONALD L CERNY
CHEMISTRY DEPT
MCMS
UNIV OF NEBRASKA
LINCOLN NE 68588

PHONE: 402 475 8983

JEAN CESARIO
SEA
CEN/FAR BP 6
92265 FRONENAY AUX ROSES
CEDEX
FRANCE
PHONE:

GREGORY CESSNA
EXTREL CORP
PO BOX 11512

PITTSBURGH PA 15238

PHONE: 412 963 7530

DONALD H CHACE
GEORGE WASHINGTON UNIV
MEDICAL CENTER
2300 EYE STREET, NW
WASHINGTON DC 20037

PHONE: 202 994 2947

J W CHAI
DEPT OF CHEMISTRY
HOWARD UNIVERSITY

WASHINGTON DC 20059

PHONE:

BRIAN CHAIT
ROCKEFELLER UNIV
1230 YORK AVE

NEW YORK NY 10021

PHONE: 212 570 8849

JOHN A CHAKEL
GENENTECH INC
460 PT SAN BRUNO

SO SAN FRAN CA 94080

PHONE: 415 266 1246

WALTER S CHAMBERLIN
LOS ALAMOS NATIONAL LAB
BOX 1663 M/S G780

LOS ALAMOS NM 87544

PHONE: 505 667 2054

HANK CHAMBERS
330 ENCINA AVE

DAVIS CA 95616

PHONE: 916 372 1393

C L CHAN
E LOS ANGELES COLLEGE
CHEMISTRY DEPT
1301 E BROOKLYN AVE
MONTEREY PARK CA 91754

PHONE: 213 265 8650

CONNIE K CHAN
40-22 77 STREET

ELMHURST NY 11373

PHONE: 212 367 7879

DANIEL Y K CHAN
BPL TOXICOLOGY
18700 OXNARD ST

TARZANA CA 91356

PHONE: 818 343 8191

KAR WAH CHAN
DOW CHEMICAL CANADA, INC
R&D BLDG 158, PO BAG 16
FORT SASKATCHEWAN
ALBERTA T8L 2P4
CANADA
PHONE:

KELVIN W CHAN
SYNTEX RESEARCH
3401 HILLVIEW AVE

PALO ALTO CA 94304

PHONE: 415 855 5785

HELEN CHANDLER
5101 CUSTIS LN

KNOXVILLE TN 37920

PHONE: 615 690 3211

CHERNG CHANG
MONSANTO RESEARCH CORP
PO BOX 32

MIAMISBURG OH 45342

PHONE: 513 865 4162

JOSEPH SHU-CHENG CHANG
1522 22ND AVE

SAN FRANCISCO CA 94122

PHONE:

RUTH CHANG
CA STATE DEPT OF HEALTH SVCS
HAZARDOUS MATERIALS LAB
2151 BERKELEY WAY
BERKELEY CA 94704

PHONE: 415 540 2651

S Y CHANG
BURROUGHS WELLCOME CO
ORGANIC CHEMISTRY
3030 CORNWALLIS ROAD
RES TRIANGLE PARK NC 27709

PHONE: 919 248 3360

SHAW F CHANG
3M CENTER
BLDG 270-35-05

ST PAUL MN 55144

PHONE: 612 733 7947

TED T CHANG
AMERICAN CYANAMID
1937 W MAIN ST

STAMFORD CT 06904

PHONE: 203 348 7331

PETER J CHANTRY
WESTINGHOUSE
RES & DEV
1310 BEULAH RD
PITTSBURGH PA 15235

PHONE: 412 256 1001

RICHARD CHAPMAN
FINNIGAN MAT
355 RIVER OAKS PKWY

SAN JOSE CA 95134

PHONE: 408 433 4800

DALE L CHAPPELOW
WESTERN ATLAS INTERNATIONAL
PO BOX 2469

HOUSTON TX 77252-2469

PHONE: 713 943 9776

DENNIS M CHARKOWSKI
PHARMACOLOGY DEPT
UNIV OF IOWA
B S B
IOWA CITY IA 52242

PHONE: 319 335 7956

BRIGETTE CHARLES
UNIV PER M CURIE
LAB DE CHIMIE ORGAN STRUCTURE
6 RUE CUVIER, BAR F
PARIS 75 252 CEDEX 05
FRANCE
PHONE:

JUDI CHARLES
DEPT OF ENV SCI & ENGINEERING
CB #7400 ROSENAW HALL
U OF N CAROLINA @ CHAPEL HILL
CHAPEL HILL NC 27599-7400

PHONE: 919 966 3857

BONNIE A CHARPENTIER
PROCTER & GAMBLE CO
6071 CENTER HILL RD
FOODS F1M16
CINCINNATI OH 45224

PHONE: 513 659 7654

PHILIPPE CHASTAGNER
E I DUPONT
SAVANNAH RIVER LAB
MS/735A D106
AIKEN SC 29808-0001

PHONE: 803 725 3293

DALE A CHATFIELD
CHEMISTRY DEPARTMENT
SAN DIEGO STATE UNIV

SAN DIEGO CA 92182

PHONE: 619 265 5806

ENRIQUE CHAVES
DEPT OF NEUROLOGY
EASTERN VIRGINIA MED SCHOOL
825 FAIRFAX AVE
NORFOLK VA 23507

PHONE: 804 446 5940

NANCY WU CHEN
COOK CTY OFF OF THE
MEDICAL EXAMINER
2121 W HARRISON ST
CHICAGO IL 60612

PHONE: 312 666 0500

YAO-ZU CHEN
DEPT OF CHEMISTRY
LANZHOU UNIVERSITY

LANZHOU
P R CHINA
PHONE:

JAY CHEPANONIS
NICOLET MASS SPECTROMETRY
5225-1 VERONA ROAD
PO BOX 4508
MADISON WI 53711

PHONE: 608 271 3333

SHIRLEY CHEW
DEA WESTERN FIELD LAB
PO BOX 36075

SAN FRANCISCO CA 94102-3584

PHONE:

CHIARA CHIABRANDO
MARIO NEGRI INST FOR PHARM RES
VIA ERITREA 62

MILANO 20157
ITALY
PHONE:

H ROGER CHILES
6588 MONTEVISTA DR

CINCINNATI OH 45224

PHONE: 503 522 7053

GARY R CHIPMAN
AMOCO CORP
AMOCO RES CTR
PO BOX 400
NAPERVILLE IL 60566

PHONE: 312 420 5248

YING CHOW
FINNIGAN MAT
355 RIVER OAKS PARKWAY

SAN JOSE CA 95134

PHONE: 408 433 4800

CHUCK CHRIST
DEPT OF CHEMISTRY
UNIV OF FLORIDA

GAINESVILLE FL 32611

PHONE: 904 335 7704

KAI-HSIEN CHEN
PHARMACOLOGY DEPARTMENT
JOHNS HOPKINS UNIV
725 NORTH WOLFE STREET
BALTIMORE MD 21205

PHONE: 301 955 3022

PAUL H CHEN
ENVIRONMENTAL SCI & ENGIN
PO BOX ESE

GAINESVILLE FL 32602

PHONE: 904 332 3318

HAROLD C CHENG
321 KUANG FU ROAD SEC 2

HSINCHU, TAIWAN 30042

P R CHINA
PHONE:

NICHOLAS R CHERICO
SENATE ANALYTICAL SERVICES
545 WILLIAM PITT WAY

PITTSBURGH PA 15238

PHONE: 412 826 3700

SHIRLEY L CHEW
DEA WESTERN LAB
PO BOX 36075
450 GOLDEN GATE AVENUE
SAN FRANCISCO CA 94102

PHONE: 415 556 0951

MICHAEL P CHIARELLI
2205 S 10TH STREET
NO 107

LINCOLN NE 68502

PHONE: 402 475 9423

D M CHINN
FINNIGAN MAT
5088 ESTHER DR

SAN JOSE CA 95124

PHONE: 408 433 4800

DIANE CHO
FINNIGAN MAT
355 RIVER OAKS PKWY

SAN JOSE CA 95134

PHONE: 408 433 4800

ABUL KASEM CHOWDHURY
UNIVERSITY OF CALIFORNIA
DEPT OF CHEMISTRY

RIVERSIDE CA 92521

PHONE: 714 787 4740

ROLANDO CHRISTIAN
ECOLE NORMALE SUPERIEURE
DEPT DE CHIMIE
24 RUE LMOMMOND
75231 PARIS CED 05
FRANCE
PHONE:

LING CHEN
3120 ST PAUL ST. APT 302

BALTIMORE MD 21218

PHONE: 301 889 0012

TENG-MAN CHEN
MERRELL DOW RES INST
2110 E GALBRAITH RD

CINCINNATI OH 45215

PHONE: 513 948 9111

MICHAEL T CHENG
ICI AMERICAS INC
1200 SOUTH 47TH ST

RICHMOND CA 94804

PHONE: 415 527 8998

EDWARD K CHESS
BATTELLE NWST LABS
PO BOX 999

RICHLAND WA 99352

PHONE: 509 376 2234

GIRISH B CHHEDA
ROSWELL PAK MEM INST
666 ELM ST

BUFFALO NY 14263

PHONE: 716 845 2388

TINA M PAWLOWKSI CHICHILA
427 WARREN RD

ITHACA NY 14850

PHONE: 607 255 6555

JOHN W CHINN
CHEMISTRY DEPT
UNIV OF TEXAS

AUSTIN TX 78712

PHONE: 512 471 7344

F E CHOU
334 OVERBROOK RD

BALTIMORE MD 21212

PHONE: 301 391 9116

SWAPAN K CHOWDHURY
DEPT OF CHEMISTRY
UNIV OF TORONTO
80 ST GEORGE STREET
TORONTO, ONTARIO M5S 1A1
CANADA
PHONE: 416 978 3571

W H CHRISTIE
OAK RIDGE NAT'L LAB
PO BOX Y BLDG 9735

OAK RIDGE TN 37831

PHONE: 615 574 2455

RAY CHRISTOPHER
4415 NORWALK DR #18

SAN JOSE CA 95129

PHONE: 408 946 4848

MICHAEL CHU
TRIANGLE LABS
801-10 CAPITOLA DRIVE

RES TRI PARK NC 27713

PHONE: 919 544 5720

T E CHU
FINNIGAN CORP
355 RIVER OAKS PKWY

SAN JOSE CA 95134-9990

PHONE: 408 433 4800

HENRY CHUNG
R J REYNOLDS TOBACCO
BOWMAN GRAY TECH CTR
BLDG 611-13E/002
WINSTON-SALEM NC 27102

PHONE: 919 773 4939

ALLEN CHURCH
4215 E HAMPTON WAY

FRESNO CA 93726

PHONE: 209 638 3544

LILLIAN CHURCHILL
ALLIED-SIGNAL EMRC
50 EAST ALGONQUIN ROAD
BOX 5016
DES PLAINES IL 60017-5016

PHONE: 312 391 3170

JAMES D CIUPEK
MONSANTO CO U1C
800 N LINDBERGH BLVD

ST LOUIS MO 63167

PHONE: 314 694 1678

MAGDA M CLAEYS
UNIV INSTELL ANTWERP
PHARMACY DEPT
UNIVERSITEITSPLEIN 1
B-2610 WILRIJK
BELGIUM
PHONE:

KEITH L CLAY
PHARMACOLOGY DEPT
UNIV OF COLORADO HEALTH SCI
4200 E 9TH AVE
DENVER CO 80262

PHONE: 303 394 8759

MICHAEL P CLAY
CUMMINS ENGINE COMPANY
MAIL CODE 20650
PO BOX 3005
COLUMBUS IN 47202-3005

PHONE: 812 377 8676

S D CLEMANS
STERLING WINTHROP
COLUMBIA TURNPIKE

RENSSELAER NY 12144

PHONE: 518 445 8139

MALCOLM CLENCH
VG TRITECH
CREWE ROAD
WYTHENSHAWE
MANCHESTER
UK
PHONE:

ANDREW J CLIFFORD
DEPT OF NUTRITION
UNIV OF CALIFORNIA

DAVIS CA 95616

PHONE: 916 752 3376

SHARON M CLINE
TENNESSEE EASTMAN CO
PO BOX 511

KINGSPORT TN 37662

PHONE: 615 229 5603

MIDGE COATES
CHEMISTRY DEPT
UNIV OF CALIFORNIA

RIVERSIDE CA 92521

PHONE: 714 787 4740

RONALD L COCHRAN
ASHLAND CHEMICAL CO
PO BOX 2219

COLUMBUS OH 43216

PHONE: 614 889 4642

JOHN T CODY
ANALYTICAL SCIENCES DIVISION
AIR FORCE DRUG TESTING LAB

BROOKS AFB TX 78235-5000

PHONE: 512 536 2961

ROBERT B CODY
NICOLET INST CO
5225-1 VERONA RD
PO BOX 4508
MADISON WI 53711

PHONE: 608 271 3333

PAT COEN
950 PAGE MILL ROAD

PALO ALTO CA 94303

PHONE: 415 494 5125

MICHAEL J COGGIOLA
SRI INTERNATIONAL
333 RAVENSWOOD AVE

MENLO PARK CA 94025

PHONE: 415 859 3045

M J COHEN
PCP INC
2155 INDIAN ROAD

W PALM BEACH FL 33409

PHONE: 305 683 0507

ROY S COHEN
VG INSTRUMENTS
30 COMMERCE CENTER
CHERRY HILL PARK
DANVERS MA 01923

PHONE: 617 777 8034

K H COLBERG
AMERICAN NATIONAL CAN
433 N NORTHWEST HWY

BARRINGTON IL 60010

PHONE: 312 381 1900

BRUCE N COLBY
PACIFIC ANALYTICAL
1989-B PALOMAR OAKS WAY

CARLSBAD CA 92009

PHONE: 619 931 1766

RICHARD B COLE
LAB CHIMIE ORGAN STRUCTURALE
UNIV PIERRE & MARIE CURIE
4 PLACE JUSSIEU, BATIMENT F
75230 PARIS CED 05
FRANCE
PHONE:

STEVEN G COLGROVE
1042 MASTERSON DRIVE

BATON ROUGE LA 70810-4729

PHONE:

GEORGE J COLLINS
FINNIGAN MAT
7 REGENT STREET

LIVINGSTON NJ 07039

PHONE: 201 740 9177

JENNIFER A COLLINS
BIO-ANALYTICAL TECHNOLOGIES
2356 N LINCOLN

CHICAGO IL 60614

PHONE: 312 880 6900

LAWRENCE F COLWELL
RY80L-109, MSDRL
BOX 2000

RAHWAY NJ 07065

PHONE: 201 574 6943

C M COMBS
99 ALEXANDER DR

MERIDEN CT 06450

PHONE: 203 284 6000

KEITH R COMPSON
FAISAN
1 PADDOCK BROW
PRESTBURY
CHESHIRE
U.K.
PHONE:

MARGARET K CONDITT
PROCTER & GAMBLE
5299 SPRING GROVE AVE

CINCINNATI OH 45217

PHONE: 513 627 7841

CONRAD CONE
IFF R&D
1515 HIGHWAY 36

UNION BEACH NJ 07735

PHONE: 204 264 4500

DAN CONN
WITHAM MEMORIAL HOSPITAL
1124 N LEBANON STREET

LEBANON IN 46052

PHONE: 317 482 2700

GERALD R CONNER
LEYBOLD INFICON, INC
6500 FLY ROAD

E SYRACUSE NY 13057

PHONE: 315 437 0377

MICHAEL J CONNOLLY
MDI
900 TECHNOLOGY BLVD

BOZEMAN MT 59715

PHONE: 406 586 4885

VINCENT E CONNOLLY
2156 COUNTRYSIDE CIR
NEW BRUNSWICK LAB, US DOE

NAPERVILLE IL 60565

PHONE: 312 972 2494

VINCENT E CONNOLLY
NEW BRUNSWICK LAB, US DOE
2156 COUNTRYSIDE CIR

NAPERVILLE IL 60565

PHONE: 312 972 2496

VINCENT E CONNOLLY
NEW BRUNSWICK LAB, US DOE
2156 COUNTRYSIDE CIR

NAPERVILLE IL 60565

PHONE: 312 972 2496

MAY JOY CONTADO
CHEMISTRY DEPT
EMORY UNIV

ATLANTA GA 30322

PHONE: 404 727 6625

DENISE A CONTOS
1802 ASHLAND AVE

COLUMBUS OH 43212

PHONE: 614 424 3281

D C CONWAY
CHEMISTRY DEPT
TEXAS A&M UNIV

COLLEGE STATION TX 77843

PHONE: 209 845 4034

ROBERT J CONZEMIUS
1211 GARFIELD AVE

AMES IA 50010

PHONE: 515 294 5822

CHARLES J COOK
8301 DITZLER

RAYTOWN MO 64138

PHONE: 816 997 5541

G L COOK
8220 E GARFIELD M-15

SCOTTSDALE AZ 85257

PHONE: 602 994 3326

J CARTER COOK
VG INSTRUMENTS INC
430 MALL BLVD
SUITE A
SAVANNAH GA 31406

PHONE: 217 333 2545

KELSEY D COOK
CHEMISTRY DEPT
UNIV OF TENNESSEE

KNOXVILLE TN 37996-1600

PHONE: 615 974 8019

TERENCE D COOKE
ANAMETRIX INC
1961 CONCOURSE DRIVE

SAN JOSE CA 95131

PHONE: 408 423 8192

R GRAHAM COOKS
CHEMISTRY DEPT
PURDUE UNIVERSITY

W LAFAYETTE IN 47907

PHONE: 317 494 5262

CHARLES B COOPER
PHYSICS DEPARTMENT
UNIV OF DELAWARE

NEWARK DE 19711

PHONE: 302 451 2666

DON A COOPER
RT 2 BOX 302

PURCEVILLE VA 22132

PHONE: 703 285 2583

W J COOPER
FLORIDA INTERNL UNIV
DRINKING WATER RES CTR

MIAMI FL 33199

PHONE: 305 559 3049

RONALD CORKUM
BARRINGER MAGENTA LTD
304 CARLINGVIEW DR

REXDALE, ONT M9W 5G2
CANADA
PHONE: 416 675 3870

JOHN CORNELIUS
FINNIGAN MAT
355 RIVER OAKS PARKWAY

SAN JOSE CA 95134

PHONE: 408 433 4800

CATHERINE E COSTELLO
MIT
CHEMISTRY 56-029
77 MASS AVE
CAMBRIDGE MA 02139

PHONE: 617 253 7224

DONNA B COSULICH
LEDERLE LABORATORIES
MIDDLETOWN RD

PEARL RIVER NY 10965

PHONE: 914 732 2491

ROBERT J COTTER
JOHNS HOPKINS UNIV
MID ATLANTIC MS LAB
725 N WOLFE ST
BALTIMORE MD 21205

PHONE: 301 955 3431

J E COTTON
2512-102 AVE NE

BELLEVUE WA 98004

PHONE: 237 5399

JOHN S COTTRELL
FINNIGAN MAT LTD
PARADISE
HEMEL HEMPSTEAD
HERTS HP2 4TG
UK
PHONE:

M W COUCH
RESEARCH SERVICES
VA MEDICAL CTR

GAINESVILLE FL 32602

PHONE: 904 374 1611

PIERRE L COULOMBE
ALTERNATIVES
742 MOONEY'S BAY PLACE

OTTAWA ONTARIO K1V 9R2
CANADA
PHONE:

JOHN COUTANT
MERRELL DOW PHARM
2110 E GALBRAITH RD

CINCINNATI OH 45215

PHONE: 513 948 7884

THOMAS COVEY
SCIEX INC
55 GLEN CAMERON ROAD

THORNHILL, ONT
CANADA
PHONE: 607 255 6555

J WAYNE COWENS
GCDC ROOM 371
RPMI
666 ELM STREET
BUFFALO NY 14263

PHONE: 716 845 3563

JOHN COWPAR
VG INSTRUMENTS INC
32 COMMERCE CENTER
CHERRY HILL DRIVE
DANVERS MA 01923

PHONE: 617 777 8034

PAMELA F CRAIN
UNIV OF UTAH
311A SKAGGS HALL

SALT LAKE CTY UT 84112

PHONE: 801 581 5581

A G SKIP CRASKE
240 ALPHA DRIVE
PO BOX 11512

PITTSBURGH PA 15238

PHONE: 412 963 7530

RICHARD W CRAWFORD
LLNL
PO BOX 808
L 310
LIVERMORE CA 94550

PHONE: 415 422 6309

WILLIAM R CREASY
IBM ENDICOTT
1701 NORTH ST D/T43

ENDICOTT NY 13760

PHONE:

IAIN H CROCKER
BOX 496
DEEP RIVER

ONTARIO K0J 1P0
CANADA
PHONE: 613 584 3311

DOUG CROSBY
SHELL CANADA LTD
OAKVILLE RESEARCH CTR
3415 LAKESHORE ROAD W
OAKVILLE ONTARIO L6J 5C7
CANADA
PHONE: 416 827 1141

FRANK W CROW
THE UPJOHN CO
UNIT 7832-259-12
7000 PORTAGE ROAD
KALAMAZOO MI 49001

PHONE: 616 323 4344

JAN R CROWLEY
WAYNE STATE UNIV
435 CHEMISTRY

DETROIT MI 48202

PHONE: 313 577 3073

BO CURRY
HEWLETT-PACKARD CO
PO BOX 10161

PALO ALTO CA 94303-0871

PHONE: 415 857 7660

ZORAH F CURRY
866 BONNIE GLEN DR

MARIETTA GA 30067

PHONE: 404 424 2411

JONATHAN CURTIS
BOX 51, NOYES LABORATORY
SCHOOL OF CHEMICAL SCIENCES
UNIV OF ILLINOIS
URBANA IL 61801

PHONE: 217 333 2545

PAUL A D'AGOSTINO
275 11TH STREET NE
MEDICINE HAT

ALBERTA T1A 6A8
CANADA
PHONE:

DAVID A DAHL
6300 NORTHSIDE CIRCLE

IDAHO FALLS ID 83401

PHONE: 208 526 9915

MARIA-LOURDES DAHL
MONSANTO
800 N LINDBERGH

ST LOUIS MO 63167

PHONE: 314 694 5754

JIM DAHLGRAN
BORG WARNER CHEMICAL
PO BOX 68

WASHINGTON WV 26181

PHONE: 304 863 7325

HOWARD S DANACEU
VG INSTRUMENTS
966 HUNGERFORD DRIVE
UNIT B
ROCKVILLE MD 20850

PHONE: 301 279 2214

PAUL DANIELLO
10911 STATE LINE
APT 4

KANSAS CITY MO 64114

PHONE: 816 756 3162

PAUL O DANIS
ROHM & HAAS
727 NORRISTOWN RD

SPRING HOUSE PA 19477

PHONE: 215 641 2141

ROLF DARSKUS
BIOCONTROL GMBH
PO BOX 16 30

D-6500 MAINZ
W GERMANY
PHONE:

PRADIP R DAS
SCHERING-PLOUGH CORP
60 ORANGE STREET
B-8B
BLOOMFIELD NJ 07003

PHONE: 201 429 3977

CHHABIL DASS
UNIV OF TENNESSEE
MASS SPEC LAB
956 COURT ST
MEMPHIS TN 38163

PHONE: 901 528 5488

G D DAVES
CHEMISTRY DEPT
LEHIGH UNIVERSITY
SEELEY G MUDD BLDG 6
BETHLEHEM PA 18015

PHONE: 215 861 3471

ARTHUR DAVIDSON
DEA WESTERN LAB
PO BOX 36075

SAN FRANCISCO CA 94102

PHONE: 415 556 0951

THOMAS A DAVIDSON
HELIUM OPERATIONS
BUREAU OF MINES
1100 S FILLMORE STREET
AMARILLO TX 79101

PHONE: 806 376 2368

WALTER DAVIDSON
KRATOS
535 E CRESCENT AVE

RAMSEY NJ 07446

PHONE: 201 825 7500

JAC DAVIES
WASHINGTON PUBLIC HEALTH LAB
1610 NE 150TH STREET

SEATTLE WA 98155

PHONE: 206 361 2892

JOHN P DAVIES
217-6 NIMITZ DR

W LAFAYETTE IN 47906

PHONE: 317 494 5474

DEAN V DAVIS
UNOCAL SCIENCE & TECH DIV

BREA CA 92621

PHONE: 714 528 7201

GEOFFREY C DAVIS
TELEDYNE CME
PO BOX 33260

LOS GATOS CA 95031

PHONE: 408 982 1980

IAN M DAVIS
DEPT OF DRUG METABOLISM
GLAXO INC
5 MOORE DR
RES TRI PARK NC 27709

PHONE: 919 941 4184

MARGARET R DAVIS
SK&F LABS
709 SWEDELAND ROAD

KING OF PRUSSIA PA 19406

PHONE: 215 270 6464

W D DAVIS
R D 5
COUNTY FARM ROAD

BALLSTON SPA NY 12020

PHONE:

WILLIAM E DAVIS
NOR-AM CHEMICAL CO
PO BOX 5130
1740 WHITEHALL RD
N MUSKEGON MI 49445

PHONE: 616 744 4711

ENRICO DAVOLI
UNL - DEPT OF CHEMISTRY
HAMILTON HALL RM 29

LINCOLN NE 68588-0304

PHONE: 602 472 3507

PETER H DAWSON
NAT'L RESEARCH COUNCIL
MICROSCTRUCTURAL SCIENCES
MONTREAL ROAD
OTTAWA ONTARIO K1A 0R6
CANADA
PHONE: 613 993 9369

RICHARD A DAY
CHEMISTRY DEPT
UNIV OF CINCINNATI

CINCINNATI OH 45221

PHONE: 513 475 3673

LINDA K DEAN
CHEMISTRY DEPARTMENT
INDIANA UNIVERSITY

BLOOMINGTON IN 47405

PHONE: 812 335 3436

THOMAS A DEAN
175 CHEMISTRY
WAYNE STATE UNIVERSITY

DETROIT MI 48202

PHONE: 313 577 3080

MARK A DEARTH
GEOLOGY 541
INDIANA UNIV

BLOOMINGTON IN 47405

PHONE: 812 335 6246

JAMES J DECORPO
NAVAL SEA SYS COMM
CODE 56YB

WASHINGTON DC 20362

PHONE: 202 692 5307

JOHN A DEFEVER
14469 ELLEN DR

LIVONIA MI 48154

PHONE: 313 554 6824

PAUL DEFUR
MASS SPEC LAB
UNIV OF CALIFORNIA

BERKELEY CA 94720

PHONE: 415 602 0701

JEANNETTE DEGENNARO
KRATOS ANALYTICAL INC
535 EAST CRESCENT AVE

RAMSEY NJ 07446

PHONE: 201 825 7500

F F DEGREVE
CEGEDUR PECHINEY
CENTRE DE RECHERCHES
BP 27
38340 VOREPPE
FRANCE
PHONE:

MAX L DEINZER
OREGON STATE UNIV
AGRICUL CHEM DEPT

CORVALLIS OR 97331

PHONE: 503 754 2906

DAVID A DEIS
2450 DUNSWORTH DR

COLUMBUS OH 43085

PHONE: 614 227 3854

DANA E DEJOHN
WARNER LAMBERT
PO BOX 1047
2800 PLYMOUTH RD
ANN ARBOR MI 48106-1047

PHONE: 313 996 7135

E G DEJONG
NETHERLANDS INST FOR DRUGS &
DOPING RESEARCH
VONDELLAAN 14
3521 GE UTRECHT
THE NETHERLANDS
PHONE:

DON C DEJONGH
FINNIGAN CORP
355 RIVER OAKS PKWY

SAN JOSE CA 95134

PHONE: 408 433 4800

MICHAEL J DEKREY
CONOCO INC RE 228
PO BOX 1267

PONCA CITY OK 74603

PHONE: 405 767 2945

W JOHN DELANEY
39 BITTERWOOD LA

THE WOODLANDS TX 77381

PHONE: 713 367 6201

BROCK DELAPPE
UNIV OF CALIFORNIA SANTA CRUZ
LONG MARINE LAB
100 SHAFFER RD
SANTA CRUZ CA 95060

PHONE: 408 429 3364

SHERRI-SUE DELBERT
CHEMISTRY DEPT
MICHIGAN STATE UNIV

EAST LANSING MI 48824

PHONE: 517 353 5215

JAMES E DELMORE
2245 S 45TH E

IDAHO FALLS ID 83406

PHONE: 208 526 2820

STEPHEN E DELONG
STATE UNIV OF NY @ ALBANY
1400 WASHINGTON AVE

ALBANY NY 12222

PHONE: 518 442 4467

WILLIAM DEMAIO
LEDERLE LABS, 56A-122
1 MIDDLETOWN ROAD

PEARL RIVER NY 10965

PHONE: 914 732 4192

BRUCE R DEMARK
PROCTER & GAMBLE
MIAMI VALLEY LABS
PO BOX 398707
CINCINNATI OH 45239

PHONE: 513 245 2572

PROF G DEMORTIER
DEPT OF PHYSICS
FNDP
61 RUE DE BRUXELLES
B5000 NAMUR
BELGIUM
PHONE:

CHARLES H DEPUY
CHEMISTRY DEPT
UNIVERSITY OF COLORADO
CAMPUS BOX 215
BOULDER CO 80309

PHONE: 303 492 7652

HENRY L DEQUASIE
LABORATORY SERVICES
2120 CRESTMOOR RD #91

NASHVILLE TN 37215

PHONE: 615 292 7667

FRED L DEROOS
TWIN CITY TESTING CORP
662 CROMWELL AVE

ST PAUL MN 55114

PHONE: 612 649 5502

DOMINIC DESIDERIO
UNIV OF TENNESSEE
RM A218 COLEMAN BLDG
956 COURT
MEMPHIS TN 38163

PHONE: 901 528 5488

M M DESPEYROUX
LAB DE CHIMIE ORGANIQUE
STRUCTURE
PLACE JUSSIEU
PARIS 75005
FRANCE
PHONE:

ANTHONY J DESTEFANO
NORWICH EATON PHARM
PO BOX 191

NORWICH NY 13815

PHONE: 607 335 2603

LEESA DETERDING
NIEHS
PO BOX 12233

RES TRIANGLE PARK NC 27709

PHONE: 919 541 2964

J J DEUTSCH
21 HAMASOERERET
RACHEL ST

JERUSALEM 96348
ISRAEL
PHONE:

G L DEVANT
NERMAG
49 QUAI DU HALAGE
RUEIL MALMAISON
F 92500
FRANCE
PHONE:

MATTONJAH S DEVRIES
IBM
K32180
ALMADEN RESEARCH CTR
SAN JOSE CA 95120

PHONE:

JOS SIMON DEWIT
NIEHS
RESEARCH TRIANGLE PARK
PO BOX 12233 MAILDROP 6-01
RES TRI PARK NC 27709

PHONE: 919 541 5709

PATRICIA H DHAHIR
ELI LILLY & CO
WISHARD MEMORIAL HOSPITAL
1001 WEST 10TH STREET
INDIANAPOLIS IN 46202

PHONE: 317 261 4807

SEKSAN DHEANDHANOO
EXTREL CORP
240 ALPHA DR
PO BOX 11512
PITTSBURCH PA 15238

PHONE: 412 963 7530

J R DIAS
CHEMISTRY DEPARTMENT
UNIV OF MISSOURI

KANSAS CITY MO 64110

PHONE: 816 276 2284

V H DIBELER
56 N. PENNA AVE
P O BOX 151

BETHANY BEACH DE 19930

PHONE:

L L DICKERSON
2005 S HIGBEE

IDAHO FALLS ID 83404

PHONE: 208 526 3035

GERALD C DIDONATO
SQUIBB INST FOR MED RES
MS E-2120
PO BOX 4000
PRINCETON NJ 08543-4000

PHONE: 201 921 4987

GERD DIELMANN
FINNIGAN MAT
355 RIVER OAKS PKWY

SAN JOSE CA 95134

PHONE: 408 433 4800

ANDREA M DIETRICH
DEPT CIVIL ENGINEERING
DIV ENVIR ENGR & SCIENCES
VA POLYTECHNIC INST & STATE U
BLACKSBURG VA 24061-0246

PHONE:

DONNA K DIETRICH
2449 HALF MOON DRIVE

ST LOUIS MO 63114

PHONE:

L A DIETZ
1124 MOHEGAN RD

SCHENECTADY NY 12309

PHONE:

GLEN DILLOW
UNIV OF ALBERTA
8515-112 ST #2112

EDMONTON, ALB T6G 1K7
CANADA
PHONE: 403 439 8657

MATTHEW DILTS
EXTREL CORP
PO BOX 11512

PITTSBURGH PA 15238

PHONE: 412 963 7530

JOHN J DINO
5706 LOYAL AVENUE

DURHAM NC 27713

PHONE: 919 541 2963

JIM DISINGER
LEE SCIENTIFIC
4426 SOUTH CENTURY DRIVE

SALT LAKE CITY UT 84123

PHONE: 801 261 2300

ROBERT L DITTRICH
RALSTON PURINA CO
900 CHECKERBOARD SQUARE

ST LOUIS MO 63164

PHONE: 314 982 3416

MARY A DITUSA
1975 NOTTINGHAM LANE

WHEATON IL 60187

PHONE: 312 682 7815

JACK B DIXON
VESTEC
9399 KIRBY DRIVE

HOUSTON TX 77054

PHONE: 713 796 9677

MICHAEL F DIXON
GALILEO ELECTRO-OPTICS
GALILEO PK

STURBRIDGE MA 01518

PHONE: 617 347 9191

A S DOAN
GODDARD SPACE FLIGHT CENTER
CODE 615

GREENBELT MD 20771

PHONE: 301 286 7511

ROY L M DOBSON
PROCTER & GAMBLE CO-MVL
P O BOX 398707

CINCINNATI OH 45239-8707

PHONE: 513 245 2046

DAVID J DOEDENS
INDIANA UNIV MED CTR MF003
1001 WALNUT STREET

INDIANAPOLIS IN 46223

PHONE: 317 274 7824

DENNIS L DOERFLER
422 OAKTREE CROSSING CT

BALLWIN MO 63021-7472

PHONE: 314 537 6756

LINDA DOHERTY
BARNES-HIND INC
895 KIFER RD

SUNNYVALE CA 94402

PHONE: 408 736 5462

PHIL DOHERTY
PO BOX 228

CAMBRIDGE MA 02238

PHONE: 617 666 5500

STEVE DOHERTY
CHEMISTRY DEPT
INDIANA UNIV

BLOOMINGTON IN 47405

PHONE: 812 335 3436

MALCOLM DOLE
110 WOOD ROAD M-1

LOS GATOS CA 95030

PHONE: 408 354 0478

BRUNO M DOMON
CIBA-GEIGY AG
K-127.5.32

CH-4002 BASEL
SWITZERLAND
PHONE:

ZHEN-WEN DONG
DALIAN INST OF TECHNOLOGY

DALIAN
CHINA
PHONE:

JOSEPH R DONNELLY
LOCKHEED
1050 E FLAMINGO
SUITE 120
LAS VEGAS NV 89119

PHONE: 702 798 2299

FRANKLIN G DOOLITTLE
DEPT OF CHEMISTRY
WASHINGTON STATE UNIV

PULLMAN WA 99163

PHONE: 509 335 1707

J WALLACE DOONG
7319 LONGVINE

HOUSTON TX 77072

PHONE: 713 660 0901

R CAMERON DOREY
DEPT OF CHEMISTRY
WICHITA STATE UNIV

WICHITA KS 67208

PHONE: 316 689 3120

STEVEN B DORN
GENERAL ELECTRIC CORP
R&D BLDG K-1 RM2A40
PO BOX 8
SCHENECTADY NY 12301

PHONE: 518 387 6419

MARIE G DORVIL
1085 NW 117TH STREET

MIAMI FL 33168

PHONE: 305 325 2675

ELLEN L DORWIN
LETTERMAN ARMY INST OF RES
SGRD-ULV-T

PRES OF SAN FRAN CA 94129-6800

PHONE: 415 561 3730

B T DOSHI
STEELCAST BHAVANAGAR PVT LTD
220 SAMUEL ST
BOMBAY 400 003

INDIA
PHONE:

RALPH C DOUGHERTY
CHEMISTRY DEPARTMENT
FLORIDA STATE UNIV

TALLAHASSEE FL 32306-3006

PHONE: 904 644 5725

TAD DOURDEVILLE
WATERS CHROMATOGRAPHY
DIV OF MILLIPORE
34 MAPLE ST MAILSTOP RDE
MILFORD MA 01757

PHONE: 617 478 2000

STEPHEN DOWN
MASS SPECTROMETRY DATA CTR
ROYAL SOC OF CHEMISTRY
UNIV OF NOTTINGHAM
NOTTINGHAM NG7 2RD
UNITED KINGDOM
PHONE:

ROBERT J DOYLE
NAVAL RESEARCH LAB
CODE 6110

WASHINGTON DC 20375-5000

PHONE: 202 767 3551

ROBERT C DRAKE
3020 RIMROCK DR

LAWRENCE KS 66046

PHONE: 913 864 3223

PETER A DREIFUSS
W R GRACE CO
WASHINGTON RESEARCH CTR
7379 ROUTE 32
COLUMBIA MD 21044

PHONE: 301 531 4504

DONALD DRINKWATER
BOX 81
BAKER LABORATORY
CORNELL UNIVERSITY
ITHACA NY 14853

PHONE:

D L DROPKIN
3408 MORNINGSIDE DR

RALEIGH NC 27607

PHONE: 919 541 2607

GEORGE R DUBAY
PM GROSS/CHEMICAL LAB
DUKE UNIVERSITY

DURHAM NC 27706

PHONE: 919 684 3549

A M DUFFIELD
UNIV NEW SOUTH WALES
CLINIC PHARMACOLOGY
PO BOX 1
KENSINGTON NSW
AUSTRALIA 2033
PHONE:

KEVIN DUFFIN
CHEMISTRY BLDG
INDIANA UNIV

BLOOMINGTON IN 47405

PHONE: 812 335 3436

MAUREEN DUFFY
CAMBRIDGE ISOTOPE LABS INC
20 COMMERCE WAY

WOBURN MA 01801

PHONE: 617 938 0067

D L DUGGER
114 LEOLBIS DR

MARLBORO MA 01752

PHONE: 617 466 2764

WAYNE K DUHOLKE
THE UPJOHN CO
7171 PORTAGE RD

KALAMAZOO MI 49001

PHONE:

DEANNE M DULIK
L-711 DEPT OF DRUG METABOLISM
SK&F RESEARCH LABS
PO BOX 1539
KING OF PRUSSIA PA 19406-0939

PHONE: 215 270 6163

ROBERT C DUNBAR
CHEMISTRY DEPARTMENT
CASE WESTERN RESERVE

CLEVELAND OH 44118

PHONE: 216 368 3712

CHRIS DUNCAN
CURTIS & TOMPKINS LTD
1250 S BOYLE AVE

LOS ANGELES CA 90023

PHONE: 213 269 7421

MARK DUNCAN
NIH
9000 ROCKVILLE PIKE
BLDG 10 RM 3D40
BETHESDA MD 20814

PHONE: 301 496 2151

MICHAEL A DUNCAN
DEPT OF CHEMISTRY
UNIV OF GEORGIA

ATHENS GA 30602

PHONE: 404 542 1998

LOREN L DUNHAM
2831 MARINA DR

ALAMEDA CA 94501

PHONE: 408 460 1656

JOCELYN C DUNPHY
CHEMISTRY DEPT
INDIANA UNIVERSITY

BLOOMINGTON IN 47405

PHONE: 812 335 3436

RICHARD DUNPHY
ORTHO PHARMACEUTICAL
ROUTE 202 PO BOX 300
RMB139
RARITAN NJ 08869-0602

PHONE: 201 218 6238

R J DUPEYK
LLL
PO BOX 808 L-231

LIVERMORE CA 94550

PHONE: 415 422 6611

DAVID A DURDEN
NEUROPSYCHIATRIC RESEARCH
A114 CMR BLDG
UNIV OF SASKATCHEWAN
SASKATOON SASK S7N 0W0
CANADA
PHONE: 306 966 8824

STEVEN L DURFEE
SOMATOGENETICS INSTRUMENTS
350 INTERLOCKEN PARKWAY
SUITE 100
BROOMFIELD CO 80020

PHONE: 303 460 1585

ANTHONY N DURYEA
PO BOX 111323

PITTSBURGH PA 15238

PHONE: 412 963 7262

ROBERT C DUTKY
SPECTRAL COMPUTING
14112 NEW HAMPSHIRE AVE

COLESVILLE MD 20904

PHONE: 301 384 5305

JACEK P DWORZANSKI
CENTER FOR MICRO-ANALYSIS &
REACTION CHEM, UNIV OF UTAH
EMRL, BLDG 61, ROOM 214
SALT LAKE CITY UT 84112

PHONE:

DANIEL M DYE
ALZA CORP
950 PAGE MILL ROAD
PO BOX 10950
PALO ALTO CA 94303

PHONE: 415 494 5302

JOHN DYKINS
DEPT OF CHEMISTRY
UNIV OF PENNSYLVANIA
231 SOUTH 34TH STREET
PHILADELPHIA PA 19104

PHONE: 215 898 8164

ISMET DZIDIC
1220 BARTLETT
NO 2

HOUSTON TX 77006

PHONE: 713 493 8594

JOSEPH E DZIEDZIC
FRM CORPORATION
PO BOX 8

PRINCETON NJ 08543

PHONE: 609 452 2300

GELPI E
RD GUINARDO 5 7

08024 BARCELONA
SPAIN
PHONE:

DONALD M EADES
WASHINGTON UNIV MED SCHOOL
660 S EUCLID BOX 8118

ST LOUIS MO 63110

PHONE: 314 362 7722

ROSEMARY EARLY
FINNIGAN MAT
355 RIVER OAKS PARKWAY

SAN JOSE CA 95128

PHONE: 408 433 4800

DIANE EASLEY
US EPA
25 FUNSTON RD

KANSAS CITY KS 66115

PHONE: 913 236 3881

JULIE EBLE
DUPONT
E 402/3113

WILMINGTON DE 19898

PHONE:

R E EBY
955 W OUTER DRIVE

OAK RIDGE TN 37830

PHONE: 615 483 1829

M W ECHO
WINCO
PO BOX 536

IDAHO FALLS ID 83405

PHONE: 208 526 2327

BRIAN ECKENRODE
CHEMISTRY DEPT
MICHIGAN STATE UNIV

EAST LANSING MI 48824

PHONE: 517 353 5215

JAMES P EDASERY
17 RAYMOND COURT

GARDEN CITY NY 11530

PHONE: 212 305 1700

MARTHA EIDNES
HENKEL CORP
2330 CIRCADIAN WAY

SANTA ROSA CA 95405

PHONE: 707 575 7155

W NOEL EINOLF
PHILIP MORRIS USA
RESEARCH CENTER
PO BOX 26583
RICHMOND VA 23261

PHONE: 804 274 2530

JAMES F ELDER
R J REYNOLDS TOBACCO
R & D DEPT
BOWMAN GRAY TECHNICAL CTR
WINSTON-SALEM NC 27102

PHONE: 919 741 4941

ROBERT E ELLEFSON
MONSANTO RESEARCH CO
MOUND LAB R171

MIAMISBURG OH 45342

PHONE: 513 865 3791

B JANE ELLIS
ASTER PUBLISHING CORP
PO BOX 10460

EUGENE OR 97401

PHONE: 503 343 1200

CHRISTIE G ENKE
CHEMISTRY DEPARTMENT
MICHIGAN STATE UNIVERSITY

EAST LANSING MI 48824

PHONE: 517 353 4511

PAUL S EPSTEIN
3260 CREEK

ANN ARBOR MI 48104

PHONE: 313/344-1770

JAMES S ERSKINE
DOW CHEMICAL
B-1219

FREEPORT TX 77541

PHONE: 409 238 3244

E L ESMANS
UNIV ANTWERPEN
ORGANISCHE SCHEIKUND
GROENENBORGLN 171
B-2020 ANTWERPEN
BELGIUM
PHONE:

CHARLES G EDMONDS
PACIFIC NW LABS

RICHLAND WA 99352

PHONE:

GUENTER K EIGENDORF
UNIV BRIT COLUMBIA
CHEMISTRY DEPT
2036 MAIN MALL
VANCOUVER BC V6T 1Y6
CANADA
PHONE: 604 228 3235

BRIAN EITZER
541 GEOLOGY BLDG
INDIANA UNIV

BLOOMINGTON IN 47405

PHONE: 812 335 5976

VINCENT A ELDER
FRITO-LAY INC
PO BOX 152231

IRVING TX 75151

PHONE: 214 579 2281

GERRY ELLIOTT
KRATOS ANALYTICAL
BARTON DOCK ROAD
URMSTON
MANCHESTER
ENGLAND
PHONE:

EDGAR M EMERY
ETC CORP
284 RARITAN CTR PARKWAY

EDISON NJ 08818

PHONE: 201 225 6700

WERNER E ENS
UNIV OF MANITOBA
PHYSICS DEPT

WINNIPEG MANITOBA R3T 2N2
CANADA
PHONE:

ERIC ERICKSON
CHEMISTRY DEPT
MICHIGAN STATE UNIV

EAST LANSING MI 48824

PHONE: 517 353 5215

BERNARD ESCOFFIER
NIEHS
PO BOX I2233

RES TRIANGLE PARK NC 27709

PHONE: 919 541 2964

RAMON ESPINO
ALLERGAN INC
2525 DUPONT DR

IRVINE CA 92715

PHONE: 714 354 5954

RICHARD W EDOM
COLL OF PHARMACY
UNIV OF SASKATCHEWAN

SASKATOON SASK S7N 0W0
CANADA
PHONE: 306 966 6370

JACQUE EINHORN
CHEMISTRY DEPT
PURDUE UNIV

W LAFAYETTE IN 47902

PHONE: 317 494 5262

FRED A ELDER
XEROX CORP
800 PHILLIPS RD

WEBSTER NY 14580

PHONE: 716 422 3179

CLAUDIA H ELKINS
AKZO CHEM
EASTERN RESEARCH CENTER

DOBBS FERRY NY 10522

PHONE: 914 693 1200

WILLIAM H ELLIOTT
BIOCHEMISTRY DEPT
ST LOUIS UNIVERSITY
1402 S GRAND BLVD
ST LOUIS MO 63104

PHONE: 314 577 8150

ROGER E ENGLAND
HENKEL RESEARCH CORP
115 DU BOIS STREET

SAN RAFAEL CA 94901

PHONE: 415 485 5510

HANS P EPPLER
BALZERS AG
FL9496 BALZERS

BALZERS
LIECHTENSTEIN
PHONE:

MITCHELL D ERICKSON
ARGONNE NAT'L LAB
9700 S CASS AVENUE

ARGONNE IL 60439

PHONE:

THOMAS J ESKEW
MAAS INC
1155 ZION RD

BELLEFONTE PA 16823

PHONE: 814 353 0600

RAFAEL ESPINOSA-LENIZ
THE AMERICAN U/NBS
BLDG 222, ROOM A-113

GAITHERSBURG MD 20899

PHONE: 301 975 3142

KURT L ETTENHOFER
BENDIX ESD
1400 TAYLOR AVE

BALTIMORE MD 21284-9840

PHONE: 301 321 5330

BARBARA EVANS
23 LLOYD ST

WINCHESTER MA 01890

PHONE: 617 642 0188

C A EVANS
CHARLES EVANS & ASSOC
301 CHESAPEAKE DR

REDWOOD CITY CA 94063

PHONE: 415 369 4567

JAMES E EVANS
E KENNEDY SHRIVER CT
200 TRAPELO RD

WALTHAM MA 02254

PHONE: 617 642 0188

JAMES V EVANS
MILES LABORATORIES
ANALYTICAL RESEARCH CA001
PO BOX 932
ELKHART IN 46515

PHONE: 219 262 7762

M J EVANS
CHEMISTRY DEPT
UNIV OF MONTREAL
C P 6210 SUCCA
MONTREAL QUE H3C 3J7
CANADA
PHONE: 514 343 6884

R F EVANS
QUEENSLAND UNIV
CHEMISTRY DEPT

ST LUCIA QNLAND 40
AUSTRALIA
PHONE:

ROBERT J EVANS
SOLAR ENERGY RES INST
1617 COLE BLVD

GOLDEN CO 80401

PHONE: 303 231 1384

KERRY EVEN
8650 ROSEWOOD LANE

INDIANAPOLIS IN 46250

PHONE: 317 844 4100

J W EWING
1701 LEXINGTON DR

LYNCHBURG VA 24503

PHONE: 804 384 7490

JOHN R EYLER
UNIV OF FLORIDA
CHEMISTRY DEPT

GAINESVILLE FL 32611

PHONE: 904 392 0532

LYN FAAS
METRO WATER QUALITY LAB
322 W EWING

SEATTLE WA 98119

PHONE: 206 684 2306

BARBARA L FABRICANT
OWENS CORNING FIBERGLAS
PO BOX 415

GRANVILLE OH 43023

PHONE: 614 587 7360

SERGIE M FACCHETTI
CCR-EURATOM
RADIOCHEMISTRY DIV

21020 ISPRA-VARESE
ITALY
PHONE:

C DAVID FADA
METRO WATER QUALITY LAB
322 W EWING ST

SEATTLE WA 98119

PHONE: 206 684 2303

I S FAGERSON
51 JEFFREY LANE

AMHERST MA 01002

PHONE:

HENRY M FALES
NAT'L INST OF HEALTH
BLDG 10, ROOM 7N 318

BETHESDA MD 20892

PHONE: 301 496 2135

A M FALICK
SCH OF PHARMACY
PARMACEUTICAL CHEM
UNIV OF CALIFORNIA
SAN FRANCISCO CA 94143-0446

PHONE: 415 476 5160

ROBERTO FANELLI
MARIO NEGRI INST
VIA ERITREA 62

MILANO 20157
ITALY
PHONE:

DUENCHENG FANG
CLEMSON UNIVERSITY
PO BOX 5753 COLLEGE STATION

CLEMSON SC 29632

PHONE:

PENG FANG
CIBA-GEIGY CORP
PO BOX 113

MCINTOSH AL 36553

PHONE: 205 944 2201

JOHN E FARRELL
SIX HASTING ROAD

YARDVILLE NJ 08620

PHONE: 201 225 6792

KAREN FARRELL
NORTH SHORE SANITARY DIST
RUSSELL ROAD
PO BOX 750
GURNEE IL 60031

PHONE: 312 623 6060

PAUL FARROW
ARTHUR D LITTLE INC
15 ACORN PARK

CAMBRIDGE MA 02140

PHONE: 617 864 5770

JACK D FASSETT
NBS
BLDG 221 RM A21

GAITHERSBURG MD 20899

PHONE: 301 975 4109

DOUGLAS FAST
FINNIGAN MAT
1355 M REMINGTON ROAD

SCHAUMBURG IL 60173

PHONE: 312 310 0140

JIM FAULK
CASE WESTERN RESERVE UNIV
CHEMISTRY DEPT

CLEVELAND OH 44106

PHONE: 216 231 2609

KYM F FAULL
PSYCHIATRY DEPARTMENT
STANFORD UNIVERSITY
MEDICAL SCHOOL
STANFORD CA 94305

PHONE: 415 723 7205

JIM FEDORA
ESSO PERTROLEUM CANADA
RESEARCH DIVISION
PO BOX 3022
SARNIA ONT N7T 7M1
CANADA
PHONE: 519 339 4467

VERNON J FEIL
USDA-MRRL
STATE UNIV STATION

FARGO ND 58105

PHONE: 701 239 1236

GOTTFRIED FEISTNER
DEPT OF PSYCHIATRY
STANFORD UNIV MEDICAL CTR

STANFORD CA 94305

PHONE: 415 723 7073

JERRY FELSHER
140 RIDGE ROAD

NEW CITY NY 10956

PHONE: 914 634 8905

RONG FENG
CHEMISTRY DEPT
BAKER LAB
CORNELL UNIV
ITHACA NY 14853

PHONE: 607 256 3731

JOHN B FENN
DEPT CHEMICAL ENG
YALE UNIV
PO BOX 2159 YALE STATION
NEW HAVEN CT 06520-2159

PHONE: 203 432 4379

PAUL V FENNESSEY
UNIV OF COLORADO
MED CTR C232
4200 E 9TH AVE
DENVER CO 80262

PHONE: 303 394 7286

CATHERINE C FENSELAU
CHEMISTRY DEPARTMENT
UNIVERSITY OF MARYLAND
5401 WILKENS AVE
BALTIMORE MD 21228

PHONE: 301 455 2505

ANDREA FENTON
CHEMICAL WASTE MANAGEMENT INC
150 W 137 STREET

RIVERDALE IL 60627

PHONE: 312 841 8360

ANNA M FERGUSON
THERMODYNAMICS RES
ZACHRY BLDG
TEXAS A&M UNIV
COLLEGE STATION TX 77843-3111

PHONE: 409 845 4940

GORDON J FERGUSSON
124 NASSAU PLACE

CLAREMONT CA 91711

PHONE: 714 626 8258

RICHARD A FERRIERI
DEPT OF CHEMISTRY
BLDG 555A
BROOKHAVEN NATIONAL LAB
UPTON NY 11973

PHONE: 516 282 4395

DEAN D FETTEROLF
FED BUREAU OF INVESTIGATION
FORENSIC SCIENCE RESEARCH
FBI ACADEMY
QUANTICO VA 22135

PHONE: 703 640 6131

FRANK H FIELD
ROCKEFELLER UNIV
1230 YORK AVE

NEW YORK NY 10021

PHONE: 212 570 8848

WILLIAM FIES
155 CHEROKEE WAY

PORTOLA VALLEY CA 94025

PHONE: 408 433 4800

RONALD FIETKAU
TEXAS A&M UNIVERSITY
CHEMISTRY DEPT

COLLEGE STATION TX 77843

PHONE:

MICHAEL S FILIGENZI
ENSECO/CAL LABS
2544 INDUSTRIAL BLVD

W SACRAMENTO CA 95616

PHONE: 916 372 1393

H H FINEGOLD
RD 1, BOX 165

DALLASTOWN PA 17313

PHONE:

SAUL W FINK
DEPT OF CHEMISTRY
UNIV OF HOUSTON

HOUSTON TX 77004

PHONE: 713 749 2646

ROBERT E FINNIGAN
FINNIGAN MAT
355 RIVER OAKS PKWY

SAN JOSE CA 95134-9990

PHONE: 408 433 4800

LARRY FINNIN
CA STATE UNIV @ LA
DEPT OF GEOLOGY
5151 STATE UNIVERSITY DR
LOS ANGELES CA 90032

PHONE: 619 224 3388

JOHN W FIOLA
155 MASS AVE #3

ARLINGTON MA 02174

PHONE: 617 275 5444

H PETER FISCHER
PETRO CANADA
RES & DEV DEPT
2489 N SHERIDAN WAY
MISSISSAUGA ONT L5K 1A8
CANADA
PHONE: 416 896 6790

DERRY L FISHEL
CHEMISTRY DEPARTMENT
KENT STATE UNIVERSITY

KENT OH 44242

PHONE: 216 672 2978

DIXIE L FISHER
ALLERGAN INC
ANAL BIOPHARMACEUTICAL RES
2525 DUPONT DRIVE
IRVINE CA 92715

PHONE: 714 752 4500

I P FISHER
PETRO CANADA
RESEARCH & DEVELOP
2489 N SHERIDAN WAY
SHERIDAN PK ONT L5K 1A8
CANADA
PHONE: 403 220 5890

JACOB FISHER
UNIV OF WATERLOO
DEPT OF CHEMISTRY

WATERLOO, ONT N2V 1L3
CANADA
PHONE:

JAMES R FISHER
1000 W AARON DRIVE I-8

STATE COLLEGE PA 16803

PHONE: 814 863 1333

PAMELA FITCH
DEPT OF ENV TOXICOLOGY
UC DAVIS

DAVIS CA 95616

PHONE: 916 752 2409

WILLIAM L FITCH
SOECON RESEARCH INSTITUTE
975 CALIFORNIA AVENUE

PALO ALTO CA 94304

PHONE: 415 354 3458

WADE L FITE
EXTREL CORP
240 ALPHA DR
PO BOX 11512
PITTSBURGH PA 15238

PHONE: 412 963 7530

JOHN FJELDSTED
HEWLETT-PACKARD
1601 CALIFORNIA AVENUE

PALO ALTO CA 94304

PHONE: 415 857 6017

MICHAEL FLANAGAN
ACUREX CORP
405 CLYDE AVE BLDG 12

MOUNTAINVIEW CA 94039

PHONE: 415 964 3200

GERALD D FLESCH
IOWA STATE UNIV
AMES LAB
USDOE
AMES IA 50011

PHONE: 515 294 3887

DENIS L FOERST
HEWLETT-PACKARD S/D
1601 CALIFORNIA AVE

PALO ALTO CA 94304

PHONE: 415 857 6025

JOHN B FOREHAND
A H ROBINS INC
1211 SHERWOOD AVE

RICHMOND VA 23220

PHONE:

G O FOSS
FARRELL ROAD

NEWTOWN CT 06470

PHONE: 203 797 6706

H G FOUDA
PFIZER INC
DRUG METABOLISM

GROTON CT 06340

PHONE: 203 441 4647

BILL FOX
WATERS CHROMATOGRAPHY
MAPLE ST

MILFORD MA 01757

PHONE: 617 478 2000

H G FRANK
UNIV TUEBINGEN
INST TOXIKOLOGIE
WILHELMSTR 56
D 7400 TUEBINGEN
FED REP GERMANY
PHONE:

BLAIR A FRASER
FDA
BOB/DBB/8600
ROCKVILLE PIKE
BETHESDA MD 20892

PHONE: 301 496 1840

ROYAL B FREAS
DEPT OF CHEMISTRY
UNIV OF HOUSTON

HOUSTON TX 77004

PHONE: 713 749 4630

ARTHUR C FLATT
212 CLEARLAKE DR

NASHVILLE TN 37217

PHONE: 615 367 1756

JOHN J FLESCH
215 STERRETT AVENUE

COVINGTON KY 41014

PHONE: 606 261 3865

THEODORE L FOLK
227 WASHINGTON AVE

CUYAHOGA FALL OH 44221

PHONE: 216 796 4217

HANS FORSTER
BOEHRINGER INGELHEIM
6507 INGELHEIM

IRHEIN
FRG
PHONE:

M G FOSTER
ZENON ENVIRONMENTAL
845 HARRINGTON CT

BURLINGTON ONT L7N 3P3
CANADA
PHONE: 416 639 6320

BERNARD FOURNET
LAB DE CHIMIE BIOLOGIQUE
UNIV DES SCI ET TECH DE LILLE
FLANDERS-ARTOIS
VILLENEUVE D'ASCQ 59655
FRANCE
PHONE:

ROBERT E FRAAS
28 FOUNTAIN CIRCLE

RICHMOND KY 40475

PHONE: 606 622 1456

JAMES C FRANKLIN
141 CUMBERLAND VIEW

OAK RIDGE TN 37830

PHONE: 615 574 2284

WILLIAM FRASURE
ANALYTICAL SPECIALTIES
326 MARION AVE

ST LOUIS MO 63119

PHONE: 314 962 8648

J P FREEMAN
1500 ROCK

PINE BLUFF AR 71602

PHONE: 501 541 4369

RONALD H FLEMING
CHARLES EVANS & ASSOCIATES
301 CHESAPEAKE

REDWOOD CITY CA 94063

PHONE: 415 369 4567

RICK A FLURER
DEPT OF CHEMISTRY
INDIANA UNIV

BLOOMINGTON IN 47405

PHONE: 812 335 5705

RODGER L FOLTZ
UNIV OF UTAH
CTR HUMAN TOXICOLOGY
38 SKAGGS HALL
SALT LAKE CTY UT 84112

PHONE: 801 581 5117

CLAUDE J FORTIN
LAB DE POLICE SCIENTIFIQUE
1701 PARTHENAIS, 5TH FL

MONTREAL QUE H2K 3S7
CANADA
PHONE: 514 873 2704

NORMAN G FOSTER
2719 ROBINWOOD LANE

DENTON TX 76201

PHONE: 817 387 4840

FRANCOISE FOURNIER
UNIV PER M CURIE
LAB DE CHIMIE ORG STRUCTURE
8 RUE CUVIER, BAR F
PARIS 75 252 CEDEX 05
FRANCE
PHONE:

DAVID F FRALEY
903 SARBROOK DR

CINCINNATI OH 45231

PHONE: 513 627 6412

JOCHEN FRANZEN
BRUKER INSTRUMENTS INC
MANNING PARK

BILLERICA MA 01821

PHONE: 617 663 7406

LAURA C FRAZIER
HEWLETT-PACKARD
SCIENTIFIC INSTRUMENTS
1601 CALIFORNIA AVE
PALO ALTO CA 94304

PHONE: 415 856 3353

JODY FREEMAN
1700 SW 16TH CT, D-26

GAINESVILLE FL 32608

PHONE: 904 392 0515

LOUIS C FREES
LEYBOLD INFICON INC
6500 FLY ROAD

E SYRACUSE NY 13057

PHONE: 315 437 0377

KELLY D FREGIEN
RTE 2 BOX 88

RUSH CITY MN 55069

PHONE: 612 626 3826

BEN S FREISER
CHEMISTRY DEPT
PURDUE UNIVERSITY

W LAFAYETTE IN 47907

PHONE: 317 494 5270

MARGARET A FRENCH
DEPT OF FOODS & NUTRITION
FACULTY OF HOME ECONOMICS
UNIVERSITY OF ALBERTA
EDMONTON, ALBERTA T6G 2M8
CANADA
PHONE: 403 432 5629

SCOTT B FRENCH
ICI AMERICAS
BIOMED RESEARCH DEPT
CONCORD PIKE
WILMINGTON DE 19897

PHONE: 302 575 2275

ROBERT S FREUND
AT&T BELL LABS
600 MOUNTAIN AVE
ROOM 1D-256
MURRAY HILL NJ 07974

PHONE:

NELSON M FREW
WOODS HOLE OCEAN INS
FYE BUILDING

WOODS HOLE MA 02543

PHONE: 617 548 1400

CARL FREY
DRAGOCO INC
PO BOX 261

TOTOWA NJ 07511

PHONE: 201 256 3850

RUDIGER FREY
BRUKER INSTRUMENTS INC
MANNING PARK

BILLERICA MA 01821

PHONE: 617 663 7406

MARLIN FRIESEN
IARC/CIRC
150 COURS A THOMAS

69372 LYON
FRANCE
PHONE: 72 73 8485

MARGARET A FRISCH
IBM RESEARCH CENTER
PO BOX 218

YORKTOWN HEIGHTS NY 10598

PHONE: 914 945 1037

DAVID FROST
KRATOS ANALYTICAL INC
535 EAST CRESCENT AVE

RAMSEY NJ 07446

PHONE: 201 825 7500

EMIL W FU
SANDOZ INC
59 ROUTE 10
BLDG 404 RM 376
E HANOVER NJ 07936

PHONE: 201 386 8121

ROGER G FUELSTER
US GOV'T DEA
NORTH CENTRAL LAB
RM 500 610 S CANAL
CHICAGO IL 60607

PHONE: 312 353 3640

RALPH W FUHRHOP
HEMAGEN ASSOCIATES
11444 LACKLAND AVE

ST LOUIS MO 63146

PHONE: 314 991 3534

JOHN D FUHRMAN
MONSANTO UEI
800 N LINDBERGH BLVD

ST LOUIS MO 63167

PHONE: 314 694 4238

TOSHIHIRO FUJII
NAT'L INST FOR ENVIRONMENTAL
STUDIES
YATABE-MACHI, TSUKUBA
IBARAKI 305
JAPAN
PHONE:

YASUHIKO FUJII
TOKYO INST OF TECHNOLOGY
RES LAB FOR NUCL REACTORS
O-OKAYAMA, MEGUROKU
TOKYO 152
JAPAN
PHONE:

MAMORU FUJIOKA
FUJISAWA PHARMACEUTICAL CO LTD
KASHIMA 2-1-6
YODOGAWA-KU
OSAKA 532
JAPAN
PHONE:

HIDEJI FUJIWARA
MONSANTO CO
AA1F
700 CHESTERFIELD VILL PWY
CHESTERFIELD MO 63198

PHONE: 314 537 6271

MAKOTO FUJIWARA
UNIV OF ELECTRO-COMMUNICATIONS
CHOFUJAOKA

CHOFU 182
JAPAN
PHONE:

ELAINE K FUKUDA
HOFFMANN LAROCHE
340 KINGSLAND ST

NUTLEY NJ 07110

PHONE: 201 235 4405

ALICE FUKUSHIMA
IBM
5600 COTRE RD E35/013

SAN JOSE CA 95193

PHONE: 408 256 5820

JOHN FULFORD
SCIEX
55 GLENCAMERON ROAD

THORNHILL ONTARIO L3T 1P2
CANADA
PHONE: 416 881 4646

PHILLIP T FUNKE
E R SQUIBB
PO BOX 4000

PRINCETON NJ 08540

PHONE: 609 921 4993

ED FURLONG
US GEOLOGICAL SURVEY
NATL WATER QUALITY LABS
5293 WARD ROAD
ARVADA CO 80002

PHONE: 303 236 9363

JORGE FURLONG
LAB DE QUIMICA-FISICA
UNIV NACIONAL DE SAN LUIS
CHACABUCO Y PEDERNERA
5700 SAN LUIS
ARGENTINA
PHONE:

RAYMOND L FURNER
NEUROPSYCHIATRY
UNIV OF ALABAMA

BIRMINGHAM AL 35294

PHONE: 205 934 2443

JEAN H FUTRELL
DEPT OF CHEMISTRY & BIOCHEM
UNIV OF DELAWARE

NEWARK DE 19716

PHONE: 302 451 1247

STEPHEN GABELER
WATERS
10 WILSHIRE ST

SUDBURY MA 01776

PHONE:

WILLIAM G GABODA
BETZ LABORATORIES
4636 SOMERTON RD

TREVOSE PA 19047

PHONE: 215 355 3300

DOUGLAS A GAGE
MICHIGAN STATE UNIV
MASS SPEC FACILITY
BIOCHEMISTRY BLDG
E LANSING MI 48824

PHONE: 517 353 0612

VILMA E GAINES
BRISTOL-MYERS USPNG
2404 PENNSYLVANIA AVE

EVANSVILLE IN 47721

PHONE: 812 429 7767

JEAN F GAL
UNIV DE NICE
CAMPUS VALROSE
LAB CHIMIE PHYS ORG
NICE 06034 CEDEX
FRANCE
PHONE:

JAMES F GALASYN
EC JORDAN CO
261 COMMERCIAL ST
PO BOX 7050
PORTLAND ME 04112

PHONE: 207 775 5401

DIANE S GALE
PEDIATRIC METABOLISM
BOX 3028
DUKE MEDICAL CENTER
DURHAM NC 27710

PHONE: 919 684 3729

P JANE GALE
DAVID SARNOFF RES CTR
CN-5300

PRINCETON NJ 08543-5300

PHONE: 609 734 3053

THEODORE J GALEN
17625 EL CAMINO REAL

HOUSTON TX 77058

PHONE: 713 483 4641

KENNETH L GALLAHER
BP AMERICA R&D
4440 WARRENSVILLE RD

CLEVELAND OH 44128

PHONE: 216 581 5826

EMILIO J GALLEGOS
CHEVRON
PO BOX 1627

RICHMOND CA 94804

PHONE: 415 620 4113

YAKOV GALPERIN
379 LONGVIEW PLACE

THOUSAND OAKS CA 91360

PHONE: 818 704 0274

DAVID E GAMES
UNIVERSITY COLLEGE
CHEMISTRY DEPT
PO BOX 78
CARDIFF CF1 1XL
WALES
PHONE:

BISHWAJIT GANGULI
NBS
A147 CHEMISTRY

GAITHERSBURG MD 20899

PHONE: 301 975 2517

W A GARLAND
DEPT DRUG METABOLISM
HOFFMANN-LAROCHE

NUTLEY NJ 07110

PHONE: 201 235 2137

ERNEST L GARNER
NAT'L BUR STANDARDS
BLDG 221 ROOM 17363

GAITHERSBURG MD 20899

PHONE: 301 975 2002

JOHN H GARRETT
WRIGHT STATE UNIV
BREHM LAB

DAYTON OH 45435

PHONE:

DANIEL GARTIEZ
TEXMS ANALYTICAL SERVICES
15701 W HARDY ROAD

HOUSTON TX 77060

PHONE: 713 447 2474

JAMES GARVEY
ACHESON HALL
DEPT OF CHEMISTRY
SUNY @ BUFFALO
BUFFALO NY 14214

PHONE: 716 831 3511

SIMON J GASKELL
CENTER FOR EXP THERAPEUTICS
BAYLOR COLLEGE OF MEDICINE
1 BAYLOR PLAZA, ROOM 826E
HOUSTON TX 77030

PHONE: 713 799 4721

TINO GAUMANN
EPFL-ECUBLENS
INST DE CHIMIE PHYS

CH-1015 LAUSANNE
SWITZERLAND
PHONE:

M L GAY
6-H RIDGE RD

GREENBELT MD 20770

PHONE: 301 498 0245

JUANITA N GEARING
MAURICE LAMONTAGNE INST
C P 100
850 ROUTE DE LA MER
MONT-JOLE QUEBEC G5H 3E4
CANADA
PHONE: 418 775 6590

JUDITH E GEBHART
BATTELLE
505 KING AVE

COLUMBUS OH 43201

PHONE: 614 424 4605

RICHARD GEDAMKE
114 N THIRD AVENUE

HIGHLAND PARK NJ 08904

PHONE: 609 921 4990

R A GEHLBACH
5150 EAST 65

INDIANAPOLIS IN 46220

PHONE: 317 849 4990

DAVID L GEIGER
2502 CROSS COUNTRY ROAD

FAIRBORN OH 45324

PHONE: 513 255 2631

PAUL R GEISSLER
EXXON CHEMICAL CO
PO BOX 241

BATON ROUGE LA 70821

PHONE: 504 359 4644

CHRIS F GELIJKENS
PARKLAAN 78

B-2700 ST-NIKLAAS
BELGIUM
PHONE:

GREGORY I GELLENE
DEPT OF CHEMISTRY
UNIV OF NOTRE DAME

NOTRE DAME IN 46556

PHONE: 219 239 7837

EMILIO GELPI
RD GUINARDO 5 7

08024 BARCELONA
SPAIN
PHONE:

MICHAEL GEORGIEFF
3M STEUERGEWANN 2

D-6836 OFTERSHEIM
FED REP GERMANY
PHONE:

SAHBA GHADERI
IBM
5600 COTTLE RD

SAN JOSE CA 95123

PHONE:

BENJAMIN Y GIANG
WESTERN RESEARCH CENTER
ICI AMERICAS
1200 SOUTH 47TH STREET
RICHMOND CA 94804

PHONE: 415 231 1118

BRADFORD W GIBSON
DEPT OF PHARMACEUTICAL CHEM
UNIV OF CALIFORNIA
513 PARNASSUS
SAN FRANCISCO CA 94143-0446

PHONE: 415 476 5320

JEAN LUC GIGUET
DELSI NERMAG
15701 WEST HARDY RD #1

HOUSTON TX 77060

PHONE: 713 847 0811

PHYLLIS W GILBERT
THE CLOROX CO
7200 JOHNSON DRIVE
PO BOX 493
PLEASANTON CA 94566

PHONE: 415 847 6601

BETH GILLECE-CASTRO
2035 9TH AVE
UNIV OF CALIFORNIA

SAN FRANCISCO CA 94116

PHONE: 415 476 5129

P W GILLES
CHEMISTRY DEPT
UNIV OF KANSAS

LAWRENCE KS 66045

PHONE:

BRUNO GIOIA
FARMITALIA CARLO ERBA
VIA DEI GRACCHI 35

MILAN 20146
ITALY
PHONE:

ROBERT M GLIDDEN
US FDA
10 W 35TH STREET

CHICAGO IL 60616

PHONE: 312 886 7074

GARY L GERMANN
1101 CRESCENT DRIVE

SPRINGFIELD IL 62704

PHONE: 217 782 8389

AMIT GHOSH
CHEMISTRY DEPARTMENT
UNIVERSITY OF MAINE

ORONO ME 04469

PHONE: 207 581 1187

SUSAN GIARDINO
INDIANA UNIV
GEOLOGY 541

BLOOMINGTON IN 47405

PHONE: 812 334 6246

GRAHAM GIBSON
4 ELENA COURT M

MEDFORD NJ 08055

PHONE: 609 654 1862

JAMES GILBART
DEPT OF MICROBIOL & IMMUNOLOGY
SCHOOL OF MEDICINE
UNIV OF SOUTH CAROLINA
COLUMBIA SC 29208

PHONE: 803 733 3298

BETSY GILES
44043 SOUTH UMBERLAND

CANTON MI 48187

PHONE: 313 344 1770

GREG GILLEN
CENTER FOR ANALYTICAL CHEM
NATIONAL BUREAU OF STANDARDS
BLDG 222, ROOM A123
GAITHERSBURG MD 20899

PHONE: 602 975 2190

TODD A GILLESPIE
UNIV OF FLORIDA
LEIGH HALL BOX 122

GAINESVILLE FL 32611

PHONE: 904 392 0515

ANNE B GIORDANI
1429 KEARNEY

ANN ARBOR MI 48104

PHONE: 313 996 5017

GARY L GLISH
OAK RIDGE NATIONAL LAB
PO BOX Y
BLDG 9735
OAK RIDGE TN 37831

PHONE: 615 574 2456

TIM GETEK
NCTR, MAIL STOP HFT-233

JEFFERSON AR 72079

PHONE:

C S GIAM
DEPT OF MARINE SCIENCES
TEXAS A&M UNIV
PO BOX 1675
GALVESTON TX 77553

PHONE: 409 740 4486

DARYL GIBLIN
DEPT OF CHEMISTRY
UNIV OF NEBRASKA

LINCOLN NE 68588

PHONE: 402 472 3507

ROGER W GIESE
NORTHEASTERN UNIV 110 MU
360 HUNTINGTON AVE

BOSTON MA 02115

PHONE: 617 437 3227

JEFFREY GILBERT
CHEMISTRY DEPARTMENT
MICHIGAN STATE UNIVERSITY

EAST LANSING MI 48823

PHONE: 517 353 6495

ROBERT A GILL
XEROX CORP
800 PHILLIPS RD
0139-64A
WEBSTER NY 14580

PHONE: 716 422 3571

KEITH T GILLEN
SRI INTERNATIONAL
333 RAVENSWOOD AVE

MENLO PARK CA 94025

PHONE: 415 859 3250

K A GINGERICH
TEXAS A&M UNIVERSITY
CHEMISTRY DEPT

COLLEGE STN TX 77843

PHONE: 409 845 2431

R E GLICK
CHEMISTRY DEPARTMENT
FLORIDA STATE UNIV

TALLAHASSEE FL 32306

PHONE: 904 644 4824

RON GOBLER
NICOLET MASS SPECTROMETRY
5225-1 VERONA ROAD
PO BOX 4508
MADISON WI 53711

PHONE: 608 271 3333

DAVID R GODWIN
NDRC LABORATORIES INC
3553 MILLER PARK DRIVE
GARLAND TX 45042
PHONE: 241 276 2986

DOUGLAS E GOERINGER
OAK RIDGE NAT'L LAB
PO BOX Y BLDG 9735
OAK RIDGE TN 37831
PHONE: 615 574 2452

ANN G GOETZ
HOFFMANN-LAROCHE
BLDG 71
340 KINGSLAND ST
NUTLEY NJ 07110
PHONE: 201 235 2058

MILTON W GOHEEN
1211 KNOLLWOOD CT
RICHLAND WA 99352
PHONE: 509 376 3358

A A GOLDBERG
115 LIVINGSTON AVE
EDISON NJ 08820
PHONE: 201 906 6814

WENDY GOLDBERG
MERCK ISOTOPES
PO BOX 2000
ROOM RY 33-50
RAHWAY NJ 07065
PHONE: 201 574 4207

PAUL C GOODLEY
HEWLETT PACKARD
SCI INST DIV
1601 CALIFORNIA AVE
PALO ALTO CA 94304
PHONE: 415 857 6194

GEORGE W GOODLOE
1359-A HAMPTON DRIVE
AUBURN AL 36830
PHONE: 205 826 5066

SETH GOODMAN
NICOLET MASS SPECTROMETRY
5225-1 VERONA RD
PO BOX 4508
MADISON WI 53711-0508
PHONE: 608 271 3333

GREGORY V GOODRIDGE
NATIONAL MED SVCS INC
2300 STRATFORD AVE
PO BOX 433-A
WILLOW GROVE PA 19090
PHONE: 215 657 4900

S M GORDON
IITRI
CHEMISTRY DIVISION
10 W 35 ST
CHICAGO IL 60616
PHONE: 312 567 4374

GWEN D GORETSAS
HEWLETT-PACKARD
2025 LARPENTEUR
ST PAUL MN 55113
PHONE: 612 641 9500

LEO A GORMAN
VG INSTRUMENTS
32 COMMERCE CENTER
CHERRY HILL DRIVE
DANVERS MA 01932
PHONE: 513 825 1790

JOHN D GORSUCH
GENCORP
RESEARCH DIV
2990 GILCHRIST ROAD
AKRON OH 44305
PHONE: 216 798 4025

VALERIE GOULD
VG MASSLAB
TUDOR ROAD
ALTRINCHAM
CHESHIRE
UK
PHONE:

JOSEPH J GRABOWSKI
DEPT OF CHEMISTRY
HARVARD UNIV
12 OXFORD STREET
CAMBRIDGE MA 02138
PHONE: 617 495 4130

DONALD G GRACZYK
ARGONNE NAT'L LAB
CHEMICAL TECHNOLOGY DIV
9700 S CASS AVENUE
ARGONNE IL 60439
PHONE: 312 972 4460

H H GRADE
GENERAL ELECTRIC CO
R&D CENTER
BLDG K-1 PO BOX 8
SCHENECTADY NY 12301
PHONE: 518 387 6419

WILLIAM L GRADY
114 SPRINGHOUSE ROAD
SAVANNAH GA 31419
PHONE: 912 238 7779

ELIZABETH GRAHAM
FINNIGAN MAT
355 RIVER OAKS PWY
SAN JOSE CA 95134
PHONE: 408 433 4800

ANDREW H GRANGE
LOCKHEED-EMSCO ST
1050 E FLAMINGO DR, SUITE 120
LAS VEGAS NV 89119
PHONE: 503 690 1069

R B GRANT
VG INSTRUMENTS
32 COMMERCE CENTER
CHERRY HILL DRIVE
DANVERS MA 01923
PHONE:

SUSAN T GRAUL
427 S RIVER RD #34
W LAFAYETTE IN 47906
PHONE: 317 743 9690

PETER W GRAVES
DETECTOR TECHNOLOGY
PO BOX K-300
BROOKFIELD MA 01506
PHONE: 617 867 4030

CHARLES L GRAY
RICERCA INC
PO BOX 1000
PAINESVILLE OH 44077
PHONE: 216 357 3343

JOHN W GRAY
GALILEO ELECTRO-OPTICS CORP
GALILEO PARK
STURBRIDGE MA 01518
PHONE: 617 347 9191

MICHAEL GRAYSON
MCDONNELL DOUGLAS RES LAB
PO BOX 516
ST LOUIS MO 63166
PHONE: 314 233 2541

ROGER J GREATHEAD
KRATOS ANALYTICAL
170 WILLIAMS DR
RAMSEY NJ 07466
PHONE:

JOHN GREAVES
SCH OF MARINE SCIENCE
COLLEGE OF WM & MARY
GLOUCESTER PT VA 23062
PHONE: 804 642 7247

BETH L GREEN
1443 GREGORY #20
YIPSILANTI MI 48197
PHONE: 313 484 1416

DAVID T GREEN
QUEST INTERNATIONAL LTD
KENNINGTON ROAD
ASHFORD
KENT TN240LT
UK
PHONE:

LARRY A GREEN
708 UNION ROAD

MICKLETON NJ 08056

PHONE: 609 423 1040

LAWRENCE W GREEN
ATOMIC ENERGY OF CAN
CHALK RIVER NUC LAB

CHALK RIVER ONT K0J 1J0
CANADA
PHONE: 613 584 3311

ROBERT L GREENALL
US EPA
27 TUNSTON ROAD

KANSAS CITY KS 66212

PHONE: 913 236 3881

FRANK T GREENE
MIDWEST RESEARCH INST
425 VOLKER BLVD

KANSAS CITY MO 64110

PHONE: 816 753 7600

WILLIAM GREENE
EXTREL CORP
PO BOX 11512

PITTSBURGH PA 15238

PHONE: 412 963 7530

STEVE H GREENHOUSE
51 SCHUYLER AVE
APT 3 G

STAMFORD CT 06902

PHONE: 203 348 7331

R CLIVE GREENOUGH
29 LYNWOOD DRIVE

MILLDALE CT 06467

PHONE: 203 288 1440

GIL J GREENWOOD
PHILLIPS PETROLEUM
101 94-E

BARTLESVILLE OK 74003

PHONE: 918 661 9586

FIONA GREER
M-SCAN LTD
SILWOOD PARK
SUNNINGHILL
ASCOT
ENGLAND SL5 7P2
PHONE:

GARY GREER
VESTEC CORP
9299 KIRBY DR

HOUSTON TX 77054

PHONE: 713 796 9677

JOSEPH F GREER
CIBA GEIGY
BLDG J RM J210
556 MORRIS AVENUE
SUMMIT NJ 07901

PHONE: 201 277 7948

HUGH GREGG
LLNL
PO BOX 808 L-310

LIVERMORE CA 94550

PHONE: 415 423 7501

I K GREGOR
CHEMISTRY SCHOOL
UNIV OF NSW

KENSINGTON NSW2033
AUSTRALIA
PHONE:

KAY SUE GREGORSKI
USDA, ARS
WESTERN REGIONAL RES CTR
800 BUCHANAN STREET
BERKELEY CA 94710

PHONE:

JOHN M GREGSON
DEPT OF MEDICINAL CHEMISTRY
UNIV OF UTAH

SALT LAKE CITY UT 84112

PHONE: 801 581 5581

RICHARD P GRESE
UNIV OF NEBRASKA LINCOLN
MIDWEST CTR FOR MASS SPEC
DEPT OF CHEMISTRY
LINCOLN NE 68588-0362

PHONE: 402 472 3507

DONALD A GRIFFIN
OREGON STATE UNIV
AGRICULTURAL CHEM

CORVALLIS OR 97331

PHONE: 503 754 2906

LAWRENCE L GRIFFIN
DEPT OF MARINE SCIENCES
TEXAS A&M UNIV AT GALVESTON
PO BOX 1675
GALVESTON TX 77553-1675

PHONE: 409 740 4484

SUSAN J GRIFFIN
ANATEC LABS
445 TESCONI CIRCLE

SANTA ROSA CA 95401

PHONE: 707 526 7200

RONALD D GRIGSBY
NIPER
PO BOX 2128

BARTLESVILLE OK 74005

PHONE: 918 337 4376

CASEY C GRIMM
DEPT OF CHEMISTRY
FLORIDA STATE UNIV

TALLAHASSEE FL 32306

PHONE: 904 644 6484

ERIC P GRIMSRUD
CHEMISTRY DEPT
MONTANA STATE UNIV

BOZEMAN MT 59717

PHONE: 406 994 5418

QUIRINUS G GRINDSTAFF
MARTIN MARIETTA
Y-12 PLANT
PO BOX Y BLDG 9995
OAK RIDGE TN 37831

PHONE: 615 574 0679

GEORGE GRINS
7011 BLACKBERRY DR

ARLINGTON TX 76016

PHONE: 817 467 0211

STEPHEN GRODE
THE UPJOHN CO
1140-230-2

KALAMAZOO MI 49071

PHONE: 616 323 4316

GARY GROENEWOLD
2249 ENELL

IDAHO FALLS ID 83402

PHONE: 208 526 2803

JERRY GROSCHANG
MARION LABS, INC
PO BOX 9627

KANSAS CITY MO 64134

PHONE: 816 966 5000

MICHAEL L GROSS
CHEMISTRY DEPT
UNIV OF NEBRASKA

LINCOLN NE 68588

PHONE: 402 472 2794

PETER GROSSMANN
BRUKER INSTRUMENTS INC
MANNING PARK

BILLERICA MA 08121

PHONE: 617 663 7406

PETER GROSSMANN
SPECTROSPIN AG
INDUSTRIESTRASSE 26

CH-8117 FALLANDEN
SWITZERLAND
PHONE:

MARVIN F GROSTIC
7207 S 27TH

SCOTTS MI 49088

PHONE: 616 323 2804

A A GROTE
NIOSH
4676 COLUMBIA PKWY

CINCINNATI OH 45226

PHONE: 513 841 4308

JUERGEN GROTENEYER
INST F PHYSIKALISCHE CHEMIE
TECHNISCHE UNIV MUNCHEN
LICHENTENBERGSTR 4
8046 GARCHING
WEST GERMANY
PHONE:

IAN GROVE
VG INSTRUMENTS
32 COMMERCE CENTRE
CHERRY HILL DRIVE
DANVERS MA 01932

PHONE: 203 322 4546

LARRY D GRUENKE
DEPT PHARM CHEM
UCSF
BOX 0446
SAN FRANCISCO CA 94143

PHONE: 415 476 2089

ROBERT M GRUVER
PENN STATE UNIV
BORLAND BLDG

UNIVERSITY PARK PA 16802

PHONE: 814 863 2966

SHENHENG GUAN
CHEMISTRY DEPT
UNIV OF THE PACIFIC

STOCKTON CA 95211

PHONE: 209 946 2608

BRIDGET P GUCCIONE
GENERAL TIRE
TIRE TECHNOLOGY - RESEARCH
ONE GENERAL ST PLANT II
AKRON OH 44329

PHONE: 216 798-3371

CHRISTIAN GUENAT
CIBA-GEIGY AG
POSTFACH

4002 BASEL
SWITZERLAND
PHONE:

WOLFGANG GUENTHER
HEWLETT-PACKARD
KARL-LEOPOLD-STR 27

7500 KARLSRUHE 41
GERMANY
PHONE:

J G GUERRERA
27 MIRIAM DRIVE

MATAWAN NJ 07747

PHONE: 201 344 8014

ROGER GUEVREMONT
NRC OF CANADA
1411 OXFORD ST
HALIFAX
NOVA SCOTIA B3H3Z1
CANADA
PHONE: 802 426 6406

DAVID M GUIDO
THE UPJOHN CO
7240-209-0

KALAMAZOO MI 49001

PHONE: 616 385 5461

RICHARD J GUIDOBONI
NORTHERN ANAL LAB
7 TOPSFIELD DR

NASHUA NH 03062

PHONE: 603 673 1420

WILLIAM GUIDOBONI
NORTHERN ANALYTICAL LAB
3 NORTHERN BLVD

AMHERST NH 03031

PHONE: 603 623 1420

STEVE GUPTILL
EMS LABS
7901 WEST MORRIS ST

INDIANAPOLIS IN 46231

PHONE: 317 243 8304

NARINE P GURPRASAD
AGRICULTURE CANADA
LAB SERVICES BLDG 22
CARLING AVENUE
OTTAWA ONT K1A 0C5
CANADA
PHONE:

LUCINDA G GURSKY
NABISCO BRANDS TECHNICAL CTR
200 DEFOREST AVENUE

EAST HANOVER NJ 07936

PHONE: 201 503-3475

JOHN P GUTE
6414 GLENGARRY

WHITTIER CA 90606-1514

PHONE: 613 699 0405

JAMES W GUTHRIE
1119 UPLAND DRIVE NE

ALBUQUERQUE NM 87112

PHONE: 505 298 8388

RAY F HAACK
JET PROPULSION LAB
4800 OAK GROVE DRIVE

PASADENA CA 91109

PHONE: 818 354 6568

KARLEUGEN HABFAST
FINNIGAN MAT
BARKHAUSENSTR.2

2800 BREMEN
W GERMANY
PHONE:

SOHRAB HABIBI-GOUDARZI
P O BOX 2194

WEST LAFAYETTE IN 47906

PHONE: 317 494 9420

DAVID L HACHEY
BAYLOR COLL OF MED
PEDIATRICS DEPT
1200 MOUR SAND
HOUSTON TX 77030

PHONE: 713 799 6002

MURRAY HACKETT
CLSES EPA
6201 CONGDON BLVD

DULUTH MN 55804

PHONE: 208 720 5766

WILLIAM F HADDON
WRRC, USDA
800 BUCHANAN

ALBANY CA 94710

PHONE: 415 486 3693

DON HAEKMAN
FINNIGAN MAT
355 RIVER OAKS PARKWAY

SAN JOSE CA 95134

PHONE: 408 433 4800

LYNN R HAGEMAN
NESTLES FOODS QAL
809 COLLINS ROAD
PO BOX 384
MARYVILLE OH 43040

PHONE: 513 644 8133

ROBERT J HAGEMANN
IRDI/DIR
CEN SALLAY
91191 GIF SUR YVETTE
CEDEX
FRANCE
PHONE:

MARK E HAIL
301 LEIGH HALL
UNIV OF FLORIDA

GAINESVILLE FL 32611

PHONE: 904 392 0515

ROBERT J HALE
TENNESSEE EASTMAN CO
B-150 RESEARCH
PO BOX 1972
KINGSPORT TN 37662

PHONE: 615 229 3066

PATRICIA M HALL
BALL CORP
1509 S MACEDONIA AVE

MUNCIE IN 47302

PHONE: 317 747 6564

JOHN W HALLIDAY
US ARMY NATICK RD&E CENTER
MSB/PSD/SATD BOX 20

NATICK MA 01760

PHONE: 617 651 5531

CHRIS HAMEISTER
FINNIGAN MAT
355 RIVER OAKS FWY

SAN JOSE CA 95134

PHONE: 408 433 4800

THOMAS HAMERLY
DETECTOR TECH INC
PO BOX K300

BROOKFIELD MA 01506

PHONE:

BILL HAMMARGREN
4900 E 5TH ST #1504

TUCSON AZ 85711

PHONE: 602 748 9187

MYNARD C HAMMING
1410 REVEILLE DRIVE

PONCA CITY OK 74604

PHONE: 405 765 4190

OWEN W HAND
DEPT OF CHEMISTRY BOX 473
PURDUE UNIV

W LAFAYETTE IN 47907

PHONE: 317 494 9420

CAROL A HANEY
204 TRAILS END CT

RALEIGH NC 27614

PHONE: 919 737 3746

F J HANKE
T I C
325 N WIGET LN, SUITE 130

WALNUT CREEK CA 94598

PHONE: 415 934 6292

ROBERT E HANNAH
2840 NESTLING RD

PHILADELPHIA PA 19154

PHONE: 215 278 7434

R J HANRAHAN
UNIV OF FLORIDA
NUCLEAR SCIENCE
RM 406
GAINESVILLE FL 32611

PHONE: 904 392 1442

GORDON E HANSEN
BOEHRINGER-INGELHEIM
RES & DEV CTR
175 BRIAR RIDGE RD
RIDGEFIELD CT 06877

PHONE: 203 798 5176

JEFFREY W HANSEN
71 LINCOLN AVE

FAIR LAWN NJ 07410

PHONE: 201 666 6644

STUART HANSEN
HEWLETT-PACKARD CO
1601 CALIFORNIA AVE

PALO ALTO CA 94304

PHONE: 415 857 7271

CURT HANSON
TEXAS A&M UNIVERSITY
DEPT OF CHEMISTRY

COLLEGE STATION TX 77801

PHONE:

JOHN E HANSON
FINNIGAN MAT
355 RIVER OAKS FWY

SAN JOSE CA 95134

PHONE: 408 433 4800

KIMBERLY G HANZELKA
MARTIN MARIETTA ENERGY SYS
PO BOX Y
MSI, BLDG 9769
OAK RIDGE TN 37831

PHONE: 615 576 0736

KEVIN L HARBOL
DEPT OF CHEMISTRY
UNIV OF KENTUCKY

LEXINGTON KY 40506

PHONE: 606 257 6957

LESLIE ALAN HARDEN
WRIGHT STATE UNIV
COL GLENN HIGHWAY

DAYTON OH 45435

PHONE: 513 873 2202

DWAYNE HARDIN
RADIAN CORPORATION
PO BOX 201088

AUSTIN TX 78720-1088

PHONE: 512 454 4797

RITA HARDY
PO BOX 13015

LEXINGTON KY 40512

PHONE: 606 252 5535

R L HARLESS
701 WHITE OAK DR

CARY NC 27513

PHONE: 919 541 2248

ALAN D HARMON
MCCORMICK & CO
RES & DEV LABS
202 WIGHT AVE
HUNT VALLEY MD 21031

PHONE: 301 771 7458

PETER E HAROLDSEN
BAYLOR COLLEGE MEDICINE
ROOM 826E
1 BAYLOR PLAZA
HOUSTON TX 77030

PHONE: 713 799 4728

TERRENCE M HARPER
AMERICAN ANAL LABS, INC
100 LINCOLN ST

AKRON OH 44308

PHONE: 216 535 3232

TIMOTHY W HARPER
17-02 DEER CREEK DRIVE

PLAINIBORO NJ 08536

PHONE: 609 921 5930

D N HARPOLD
GODDARD SPACE FLIGHT CENTER
CODE 615

GREENBELT MD 20771

PHONE: 301 286 8054

WILLIAM L HARRINGTON
EVANS EAST INC
THE OFFICE CENTER
666 PLAINSBORO RD STE #1236
PLAINSBORO NJ 08536

PHONE: 609 799 1904

ROBERT E HARRIS
BOX 41022

BRECKSVILLE OH 44141-0422

PHONE: 216 447 5369

WILLIAM E HARRIS
CHEMISTRY DEPARTMENT
GEORGIA INST OF TECHNOLOGY

ATLANTA GA 30332

PHONE: 404 894 4051

ALEX G HARRISON
UNIV OF TORONTO
CHEMISTRY DEPT

TORONTO ONT M5S 1A1
CANADA
PHONE: 416 978 3577

C BRETT HARRISON
EXTREL CORP
PO BOX 11512

PITTSBURGH PA 15238

PHONE: 412 963 7530

WILLARD W HARRISON
DEPT OF GEOLOGY
STANFORD UNIVERSITY

STANFORD CA 94305

PHONE: 415 723 1716

HASKELL V HART
SHELL DEVELOPMENT CO
PO BOX 1380

HOUSTON TX 77251

PHONE: 713 493 7725

KEVIN J HART
DEPT OF CHEMISTRY
MICHIGAN STATE UNIV

EAST LANSING MI 48824

PHONE: 517 353 5215

RICHARD HARTFORD
FINNIGAN MAT
355 RIVER OAKS PARKWAY

SAN JOSE CA 95134

PHONE: 408 433 4800

THOMAS G HARTMAN
CTR FOR ADVANCED FOOD TECH
COOK COLLEGE
RUTGERS UNIV
NEW BRUNSWICK NJ 08903

PHONE: 201 932 9686

J M HARTWELL
CIL INC
2101 HADWEN RD
SHERIDAN PK RES COMM
MISSISSAUGA ONT L5K 2L3
CANADA
PHONE: 416 823 7160

MARK A HARTWIG
HEWLETT PACKARD
1200 E DIEHL RD

NAPERVILLE IL 60566

PHONE: 312 357 8800

D J HARVAN
RT 1 BOX 171-D
MT. SINAI RD

DURHAM NC 27707

PHONE: 919 544 5729

D J HARVEY
OXFORD UNIVERSITY
PHARMACOLOGY DEPT
SOUTH PARKS RD
OXFORD OX1 3QT
ENGLAND
PHONE:

KEIKO HASE
MEIJO UNIV
15 YAGOTOURAYAMA, TENPAKU-CHO
TENPAKU-KU
NAGOYA-SHI, AICHI 468
JAPAN
PHONE:

YUTAKA HASHIMOTO
NIPPON KAYAKU CO LTD
31-12 SHIMO 3-CHOME
KITA-KU
TOKYO 115
JAPAN
PHONE:

J RONALD HASS
TRIANGLE LABORATORIES
801-10 CAPITOLA DRIVE

RES TRI PARK NC 27709

PHONE: 917 544 5729

FRANK W HATCH
BOEHRINGER INGELHEIM
RESEARCH & DEVELOPMENT CENTER
175 BRIAR RIDGE ROAD
RIDGEFIELD CT 06877

PHONE: 203 798 5177

CAROLINE HATTON
DEPT OF PHARMACOLOGY
UCLA SCH OF MEDICINE
23-278 CHS
LOS ANGELES CA 90024

PHONE: 213 206 6656

RICKY L HATTON
PO BOX 15609

HATTIESBURG MS 39404 5609

PHONE: 601 264 9320

SUSAN HATTOX
BOEHRINGER INGELHEIM
175 BRIAR RIDGE RD

RIDGEFIELD CT 06877

PHONE: 203 748 4200

CHARLES R HAUER
DEPT OF CHEMISTRY
UNIVERSITY OF VIRGINIA

CHARLOTTESVILLE VA 22901

PHONE: 804 924 7994

R L HAWKS
5429 31ST STREET NW

WASHINGTON DC 20015

PHONE: 301 443 5280

RUTH HAWLEY-FEDDER
LLNL
L-310
PO BOX 808
LIVERMORE CA 94550

PHONE: 415 422 6328

STEVEN B HAWTHORNE
UND EMRC
PO BOX 8213 UNIVERSITY STATION

GRAND FORKS ND 58202

PHONE: 701 777 5256

AKIRA HAYASHI
OSAKA MED CTR & RES INST MCH
840 MURODO-CHO
IZUMI
OSAKA 590-02
JAPAN
PHONE:

THOMAS G HAYDEN
VANDERBILT ATHLETIC DRUG TEST
VCAPH SUITE 313
1601 TWENTY-THIRD AVE SOUTH
NASHVILLE TN 37212

PHONE: 315 343 5020

DAVID A HAYES
12400 MOSSY BARK TRAIL

AUSTIN TX 78750

PHONE: 512 454 4797

JOHN M HAYES
INDIANA UNIV
BIOGEOCHEM LABS
GEOLOGY BLDG
BLOOMINGTON IN 47405-5101

PHONE: 812 335 5610

MARION E HAYES
GALILEO ELCTRO-OPTICS
GALILEO PARK

STURBRIDGE MA 01518

PHONE:

MICHAEL J HAYES
CIBA-GEIGY CORP
444 SAW MILL RIVER ROAD

ARDSLEY NY 10502

PHONE: 914 478 3131

ROGER HAYES
MIDWEST CENTER FOR MASS SPEC
DEPT OF CHEMISTRY
UNIV OF NEBRASKA-LINCOLN
LINCOLN NE 68588

PHONE: 402 472 3507

DOUGLAS G HAYWARD
CA STATE DEPT OF HEALTH SVCS
2151 BERKELEY WAY RM 234

BERKELEY CA 94704

PHONE: 415 540 2337

MARK J HAYWARD
255 LINCOLN STREET

WEST LAFAYETTE IN 47906

PHONE: 317 494 6898

JOHN HEADLEY
ALBERTA ENVIRON CTR
CHEMISTRY WING
PO BAG 4000
VEGREVILLE ALBERTA T0B 4L0
CANADA
PHONE: 403 632 6761

BRYAN HEARN
305 LEIGH HALL
DEPT OF CHEMISTRY
UNIV OF FLORIDA
GAINESVILLE FL 32611

PHONE: 904 392 4892

JOHN HEARN
FINNIGAN MAT
355 RIVER OAKS PKWY

SAN JOSE CA 95134-9990

PHONE: 408 433 4800

EUGENE C HEATH
HARRIS LABS
PO BOX 80837

LINCOLN NE 68501

PHONE: 402 476 2811

CHUCK HECHT
CHEMICAL WASTE MANAGEMENT
157 W 137TH ST

RIVERDALE IL 60627

PHONE: 312 841 8360

WILLIAM L HECKLE
2312 FAIRVIEW AVENUE

CINCINNATI OH 45219

PHONE: 513 721 8778

CLYDE HEDIN
1020 WOODBRIDGE DR

LAS VEGAS NV 89108

PHONE: 702 798 2492

DAVID L HEIKES
FDA
1009 CHERRY

KANSAS CITY MO 64106

PHONE: 816 374 5524

LARRY HEIMARK
B-6-139
SCHERING-PLOUGH CO
60 ORANGE ST
BLOOMFIELD NJ 07003

PHONE: 201 429 4211

RICHARD E HEIN
NICOLET INSTRUMENT CORP
5225 VERONA RD
PO BOX 4508
MADISON WI 53711

PHONE: 608 271 3333

THOMAS M HEINZE
1701 EAST 10TH STREET

PAWHUSKA OK 74056

PHONE:

DAVID N HELLER
DEPT OF PHARMACOLOGY
725 N WOLFE ST
JOHNS HOPKINS UNIVERSITY
BALTIMORE MD 21205

PHONE: 301 955 6961

STEPHEN R HELLER
USDA-ARS, ASRI-MDCL
ROOM 56 BLDG 007
BARC-WEST
BELTSVILLE MD 20705

PHONE: 301 344 1709

WILLIAM G HELLIER
2105 SEAGULL CT

PITTSBURGH CA 94565

PHONE: 415 465 3700

ROBERT HELLMANN
WESTINGHOUSE MATERIALS CO
PO BOX 398704

CINCINNATI OH 45239

PHONE: 513 738 6551

PHILIP H HEMBERGER
LOS ALAMOS NAT'L LAB
GROUP CLS-1, MS G740
PO BOX 1663
LOS ALAMOS NM 87545

PHONE: 505 667 7236

MARK E HEMLING
SMITH KLINE & FRENCH L-940
PO BOX 1539

KING OF PRUSSIA PA 19406-0939

PHONE: 215 270 6549

JEFFREY R HENDEL
1170 YARDVILLE-ALLENTOWN RD

ALLENTOWN NJ 08501

PHONE: 201 225 2000

T R HENDERSON
5609 DON FELIPE CT SW

ALBUQUERQUE NM 87105

PHONE: 505 877 4655

JACK D HENION
CORNELL UNIVERSITY
EQUINE DRUG TESTING
925 WARREN ROAD
ITHACA NY 14850

PHONE: 607 256 6556

JOHN HENNINGS
CA DEPT OF HEALTH SERVICES
HAZARDOUS MATERIALS LAB RM 234
2151 BERKELEY WAY
BERKELEY CA 94704

PHONE: 415 540 2988

KENT D HENRY
BAKER LABORATORY BOX 215
CORNELL UNIVERSITY

ITHACA NY 14853-1301

PHONE: 607 255 3726

BILL HENZEL
GENENTECH INC
460 PT SAN BRUNO

SO SAN FRANCISCO CA 94080

PHONE: 415 266 1000

RICHARD A HEPPNER
PERKIN-ELMER CORP
2771 N GAREY AVENUE

POMONA CA 91711

PHONE: 714 593 3581

GUOR-RONG HER
DEPT OF NUTRITION
HARVARD SCHOOL OF PUBLIC HEALT
665 HUNTINGTON AVE
BOSTON MA 02115

PHONE: 617 732 0632

GLEN HERMAN
OCCIDENTAL CHEM CO
LONG RD

GRAND ISLAND NY 14072

PHONE:

JOSEPH HERMAN
STUART PHARMACEUTICALS
202 MURPHY ROAD

WILMINGTON DE 19897

PHONE: 302 575 8219

MARK H HERMANSON
SPEA
INDIANA UNIV

BLOOMINGTON IN 47405

PHONE: 812 335 1005

DAVID A HEROLD
UNIV OF VIRGINIA
PATHOLOGY DEPT
BOX 214; MEDICAL CENTER
CHARLOTTESVILLE VA 22908

PHONE: 804 924 5691

JORG HERRMANN
INST OF ORGANIC CHEMISTRY
UNIV OF BERNE
FREIBSTRASSE 3
3012 BERNE
SWITZERLAND
PHONE:

G R HERTEL
CHEMISTRY DEPT
UNIV CENTRAL FLORIDA
PO BOX 25000
ORLANDO FL 32816

PHONE: 305 275 2246

ROBERT H HERTEL
PERKIN-ELMER CORP
2771 N GAREY AVE

POMONA CA 91767

PHONE: 714 593 3581

HARRY S HERTS
NBS
A309 CHEMISTRY

GAITHERSBURG MD 20899

PHONE: 301 975 3145

L F HERZOG
MAAS/NUCLIDE
1155 ZION ROAD

BELLEFONTE PA 16823

PHONE: 814 353 0600

RICHARD F HERZOG
9221 W BROWARD BLVD
NO 2304

PLANTATION FL 33324

PHONE:

DOUGLAS J HESS
4223 APPIAN WAY W

COHANNA OH 43230

PHONE: 614 476 3101

KENNETH R HESS
DEPT OF CHEMISTRY
FRANKLIN & MARSHALL COLLEGE
PO BOX 3003
LANCASTER PA 17604-3003

PHONE: 717 291 4124

ANTTI HESSO
INST OF OCCUPATIONAL
HEALTH
HAARTMANNINKATU 1
SF-00290 HELSINKI
FINLAND
PHONE:

ROBERT HETTICH
OAK RIDGE NATL LAB
BLDG 4500-S MS-120
PO BOX X
OAK RIDGE TN 37831-1620

PHONE: 615 574 4867

K G HEUMANN
UNIV REGENSBURG
CHEMISCHES INSTITUT
UNIVERSTITAETS STR 31
D-84 REGENSBURG
WEST GERMANY
PHONE:

DENNIS L HEURING
TMS ANAL SERVICES
6376 MORENCI TRAIL

INDIANAPOLIS IN 46268

PHONE: 317 291 5697

DAVID HEWETSON
OHIO STATE RACING COMM LAB
1935 COFFEY RD

COLUMBUS OH 43212

PHONE: 614 292 4299

JOHN A HICKS
AM TEST LABORATORIES
14603 NE 87TH STREET

REDMOND WA 98052

PHONE: 206 885 1664

TONY HICKSON
VG INSTRUMENTS
32 COMMERCE CENTER

DANVERS MA 01923

PHONE:

BRUCE J HIDY
BATTELLE LABS
505 KING AVE

COLUMBUS OH 43201

PHONE: 614 424 4591

GARY M HIEFTJE
DEPARTMENT OF CHEMISTRY
INDIANA UNIVERSITY

BLOOMINGTON IN 47405

PHONE: 812 335 2189

PETER M HIERL
CHEMISTRY DEPT
UNIV OF KANSAS

LAWRENCE KS 66044

PHONE: 913 864 3019

TETSUO HIGUCHI
JEOL
11 DEARBORN ROAD

PEABODY MA 01960

PHONE: 617 535 5900

D L HILDENBRAND
SRI INTERNATIONAL

MENLO PARK CA 94025

PHONE: 415 859 3436

FRED D HILEMAN
MONSANTO UIF
800 N LINDBERGH BLVD
PO BOX 8
ST LOUIS MO 63167

PHONE: 314 694 1275

DAVID R HILKER
NEW YORK STATE HEALTH DEPT
WADSWORTH CTR FOR LAB & RES

ALBANY NY 12201

PHONE: 518 474 1675

JAMES AMHERST HILL
MIT
CHEMISTRY 56-016
77 MASS AVE
CAMBRIDGE MA 02139

PHONE: 617 253 7236

JOSEPH F HILLER
DOW CHEMICAL CO
734 BLDG

MIDLAND MI 48667

PHONE: 517 636 2126

RANDY G HILLIARD
BROWARD SHERIFFS OFFICE
CRIME LABORATORY
201 SE 6TH STREET
FT LAUDERDALE FL 33301

PHONE: 305 357 7320

MARK HILLMER
VG INSTRUMENTS
32 COMMERCE CENTER

DANVERS MA 01923

PHONE: 617 777 8034

LAURENCE R HILPERT
CENTRAL COAST ANALYTICAL SVCS
141 SUBURBAN RD, SUITE C-4

SAN LUIS OBISPO CA 93401

PHONE: 805 543 2553

GEORGE W HIME
15501 SW 106 AVE

MIAMI FL 33157

PHONE: 305 549 7347

DAVID M HINDENLANG
ALLIED CORP
PO BOX 1021R

MORRISTOWN NJ 07960

PHONE: 201 361 5139

HARRY B HINES
1396 HUNTINGTON HORN LANE

FREDERICK MD 21701

PHONE: 301 663 2762

DAVID S HIRANO
ANATEC LAB INC
435 TEBCONI CIRCLE

SANTA ROSA CA 95401

PHONE: 707 526 7200

KAZUO HIRAYAMA
AJINOMOTO CO CENTRAL RESEARCH
1-1 SUZUKI-CHOU
KAWASAKI-KU
KAWASAKI
JAPAN
PHONE:

RONALD A HITES
INDIANA UNIV
SPEA 410 H

BLOOMINGTON IN 47405

PHONE: 812 335 0193

JOSEPH A HNATOW
TMA/ERG
117 N FIRST ST

ANN ARBOR MI 48104

PHONE: 313 662 3104

VEI-SHI HO
MI DEPT OF NAT RESOURCES
ENVIRONMENTAL LAB
31 N CLIPPERT ST
LANSING MI 48912

PHONE: 517 373 2197

J R HOBBS
DOT/TSC
CODE 48
KENDALL SQUARE
CAMBRIDGE MA 02142

PHONE: 617 494 2534

D L HOBROCK
8736 MALTBIE RD

CENTERVILLE OH 45458

PHONE: 513 865 4064

CHARLES H HOCART
UNIVERSITAT BERN
INST FUR ORGANISCHE CHEMIE
FREIESTRASSE 3
CH-3012
SWTIZERLAND
PHONE:

JOSEPH HOCHSTADT
PEPSICO R&TS
100 STEVENS AVENUE

VALHALLA NY 10595

PHONE: 914 742 4552

ALFRED T HODGSON
LAWRENCE BERKELEY LAB
MS 70-110A

BERKELEY CA 94720

PHONE: 415 486 5301

JEFF HOERNING
NICOLET MASS SPECTROMETRY
5225-1 VERONA ROAD
PO BOX 4508
MADISON WI 53711

PHONE: 608 271 3333

HENRY T HOFFMAN
22 VANDER VEER DR

LAWRENCEVILLE NJ 08648

PHONE: 609 292 3950

MICHAEL K HOFFMAN
US DEPT OF AGRICULTURE
300 12TH STREET SW

WASHINGTON DC 20250

PHONE: 202 447 7623

EDMOND DE HOFFMANN
PL PASTEUR 1 BOX 17

LOUVAIN-LA-NEUVE
B-1348 BELGIUM
PHONE:

JERRY HOGAN
CHEMISTRY DEPT
UNIV OF TEXAS

AUSTIN TX 78712

PHONE: 512 471 4992

JERRY D HOGAN
CHEMISTRY DEPT
UNIV OF TEXAS AT AUSTIN

AUSTIN TX 78712

PHONE: 512 471 4992

CARL HOGBERG
6901 BRYN MAWR DR

AUSTIN TX 78723

PHONE: 512 458 7587

ALAN M HOGG
UNIV OF ALBERTA
CHEMISTRY DEPT

EDMONTON ALBERTA T6G 2G2
CANADA
PHONE: 403 432 5577

LAWRENCE R HOGGE
NAT'L RES COUNCIL
110 GYMNASIUM RD

SASKATOON SASK S7N 0W9
CANADA
PHONE: 306 975 4193

DAVID HOLKEBOER
LEYBOLD INFICON INC
6500 FLY RD

E SYRACUSE NY 13057

PHONE: 315 437 0377

J F HOLLAND
MICHIGAN STATE UNIV
BIOCHEMISTRY DEPT

EAST LANSING MI 48824

PHONE:

JAMES S HOLLER
CENTER DISEASE CNTRL
TOXI BRANCH C17-1814

ATLANTA GA 30333

PHONE: 404 452 4144

ANDREW HOLMES
HEALTH & WELFARE
HEALTH PROT BRN
2301 MIDLAND AVE
SCARBOROUGH ONT M1P 4R7
CANADA
PHONE:

JOHN L HOLMES
UNIV OF OTTAWA
CHEMISTRY DEPT

OTTAWA ONTARIO K1N 6N5
CANADA
PHONE: 613 231 2239

WILLIAM F HOLMES
VARIAN INSTRUMENTS
2700 MITCHELL DRIVE

WALNUT CREEK CA 94598

PHONE: 415 945 2168

RICHARD E HONIG
99 DEMPSEY AVE

PRINCETON NJ 08540

PHONE: 609 921 7824

J W HONOUR
MIDDLESEX HOSPITAL
MORTIMER ST

LONDON
ENGLAND
PHONE:

JEFF P HONOVICH
NIMH BLDG 10-3D40

BETHESDA MD 20014

PHONE: 301 496 2151

ROBIN J HOOD
CHEMISTRY DEPT
75 CHEMISTRY
WAYNE STATE UNIV
DETROIT MI 48202

PHONE: 313 577 2046

JOHN J HOPPE
VACUMETRICS INC
2261-#1 PALMA DR

VENTURA CA 93003-5789

PHONE: 805 644 7461

JOSEPH P HOPPESCH
BAXTER HEALTHCARE CORP
6301 LINCOLN AVENUE

MORTON GROVE IL 60053

PHONE: 312 765 3439

EVAN C HORNING
11610 STARWOOD DR

HOUSTON TX 77024

PHONE: 713 799 4721

MARJORIE G HORNING
BAYLOR COLL MEDICINE
RM 826 E
ONE BAYLOR PLAZA
HOUSTON TX 77030

PHONE: 713 799 4721

STEVAN R HORNING
DEPT OF CHEMISTRY BOX 477
PURDUE UNIV

W LAFAYETTE IN 47907

PHONE:

TAKAHITO HOSOKAWA
DEPT OF APPLIED PHYSICS
UNIV OF ELECTRO-COMMUNICATIONS
1-5-1 CHOFUGAOKA, CHOFU-SHI
TOKYO 182
JAPAN
PHONE:

ROBERT S HOUK
CHEMISTRY DEPARTMENT
IOWA STATE UNIV

AMES IA 50011

PHONE: 515 294 9462

M A HOURIEH
PO BOX 686

ALEPPO
SYRIA
PHONE:

K R HOUSTON
413 FOREST OAKS LANE

LAKE JACKSON TX 77556

PHONE: 409 297 5814

WILLIAM N HOWALD
DEPT OF MEDICINAL CHEMISTRY
UNIV OF WASHINGTON

SEATTLE WA 98195

PHONE: 206 543 6439

STEPHEN LEE HOWARD
DEPT OF CHEMISTRY
UNIV OF DELAWARE

NEWARK DE 19716

PHONE: 302 451 1118

J R HOYLAND
QUADRASPEC INC
701 ALPHA DRIVE

PITTSBURGH PA 15238

PHONE: 412 963 9050

DAVID W HOYT
FINNIGAN MAT
355 RIVER OAKS PKWY

SAN JOSE CA 95134

PHONE: 408 433 4800

JERRY D HRIBAR
G D SEARLE & CO P-051
4901 SEARLE PKWY

SKOKIE IL 60077

PHONE: 312 299 5384

WOLFGANG HROSCH
FINNIGAN MAT

2800 BREMEN
GERMANY
PHONE:

TACHENG HSIEH
SANDOZ CROP PROTECTION
ANAL CHEMISTRY
1300 EAST TOUHY AVE
DES PLAINES IL 60018

PHONE: 312 390 3615

THOMAS C HSIEH
DEPT OF FOOD SCIENCE
LOUISIANA STATE UNIV

BATON ROUGE LA 70803-1806

PHONE: 504 388 5193

BIH-HSIUNG HSU
DEPT MEDICINAL CHEMISTRY
COLLEGE OF PHARMACY
PO BOX J485 JHMHC
GAINESVILLE FL 32610

PHONE: 904 392 3421

C SAM HSU
EXXON RES & ENGIN
CLINTON TOWNSHIP

ANNANDALE NJ 08801

PHONE: 201 730 7228

CHIEN-PING HSU
KIMBERLY-CLARK CORP
2100 WINCHESTER ROAD

NEENAH WI 54956

PHONE: 414 721 5360

FONG FU HSU
DEPT OF PSYCHIATRY
WASHINGTON UNIV SCH OF MED
BOX 8134, 4940 AUDUBON AVE
ST LOUIS MO 63110

PHONE: 314 362 7013

FRANCIS S HSU
PHILIP MORRIS USA
PO BOX 26583

RICHMOND VA 23261

PHONE: 804 274 2641

J P HSU
9210 CHADDSFORD

SAN ANTONIO TX 78250

PHONE: 512 522 2228

JOHN S HSU
DEPT OF HEALTH SERVICES
FOOD & DRUG LAB
5705 HOLLIS STREET
EMERYVILLE CA 94608

PHONE: 415 540 2195

YANG YING HUA
JILIN IMPORT & EXPORT COMM
INSPECTION BUREAU
81 STALIN ST, CHANG CHUN
CHANG CHUN
CHINA
PHONE:

C H HUANG
INST MATERIA MEDICA
319 YUE-YANG ROAD
ACADEMIA SINICA
SHANGHAI 200031
CHINA
PHONE:

ERIC HUANG
110 ESC
BRIGHAM YOUNG UNIV

PROVO UT 84602

PHONE: 801 378 4466

LEE Q HUANG
THE CT EXPT STATION
PO BOX 1106

NEW HAVEN CT 06504

PHONE:

SUNKWEI HUANG
ADAMANTECH INC
1501 BLUEBALL AV

LINWOOD PA 19061-0895

PHONE: 215 497 0523

LEE HUBBARD
CIBA-GEIGY CORP AG DIV
PO BOX 18300

GREENSBORO NC 27419

PHONE: 919 292 7100

W C HUBBARD
NIH NCI
DEPT OF HEALTH & HUMAN SVCS
BLDG 560, ROOM 32-60
FREDERICK MD 21701-1013

PHONE: 301 698 1379

W K HUBER
BALZERS AG

FL 9496 BALZERS
LIECHTENSTEIN
PHONE:

TAMMIE R HUCKABY
8 MARK DRIVE

GREENVILLE SC 29611

PHONE: 803 242 9317

F G HUDDA
36 PERRY AVE

LATHAM NY 12110

PHONE: 518 387 6665

JAMES E HUDSON
ALCON LABORATORIES
PO BOX 6600

FORT WORTH TX 76115

PHONE: 817 551 8113

B MASON HUGHES
1065 CAMARGO

BALLWIN MO 63011

PHONE: 314 694 1466

HELEN HUGHES
DEPT OF MED RM 826E
BAYLOR COLL OF MED
1 BAYLOR PLAZA
HOUSTON TX 77030

PHONE: 713 799 4721

JOHN M HUGHES
HEWLETT-PACKARD CO
5725 WEST LAS POSITAS BLVD

PLEASANTON CA 94566

PHONE: 415 460 1666

RICHARD J HUGHES
DEPT OF CHEMISTRY
S C 306A TRENT UNIVERSITY

PETERBOROUGH, ONT K9J 7B8
CANADA
PHONE: 705 748 1361

SUSAN V HUMMEL
US EPA
P O BOX 16602

ARLINGTON VA 22215

PHONE: 703 557 7324

HEINRICH E HUNEIKER
IBM RES DIV
ALMADEN RES CENTER
650 HARRY RD DEPT K34/802
SAN JOSE CA 95120

PHONE: 408 927 2360

JOHN C HUNEKE
CHARLES EVANS & ASSOCIATES
301 CHESAPEAKE DRIVE

REDWOOD CITY CA 94063

PHONE: 415 369 4567

HOYING L HUNG
CHEMISTRY DEPT
NORTHWESTERN UNIV
2145 SHERIDAN RD
EVANSTON IL 60208-2974

PHONE: 312 491 5514

DONALD F HUNT
CHEMISTRY DEPT
UNIV OF VIRGINIA
MCCORMICK ROAD
CHARLOTTESVILLE VA 22901

PHONE: 804 924 3610

JERRY E HUNT
CHEM DIV 200 C173
ARGONNE NATIONAL LAB
9700 S CASS AVE
ARGONNE IL 60439

PHONE: 312 972 3517

SHARON HUNT
3M CENTER
BLDG 201-BW-09

ST PAUL MN 55144

PHONE: 612 733 2533

R L HUNTER
ION SPEC CORP
ONE LONGSTREET

IRVINE CA 92720

PHONE: 714 261 7743

R TRACY HUNTER
DGS/DCLS
1 NORTH 14TH STREET

RICHMOND VA 23219

PHONE: 804 786 4898

W T HUNTRESS
JET PROPULSION LAB
L83-301

PASADENA CA 91109

PHONE: 818 354 8275

H E HURST
DEPT OF PHARMACOLOGY & TOXICOL
MED SCHOOL
UNIV OF LOUISVILLE
LOUISVILLE KY 40292

PHONE: 502 588 5291

JIM HURST
FINNIGAN MAT
355 RIVER OAKS PKWY

SAN JOSE CA 95134

PHONE: 408 433 4800

ELIZABETH Y HWANG
ARGONNE NATL LAB
9700 S CASS AVE

ARGONNE IL 60439

PHONE: 312 972 4557

PAUL M HYDE
BIOCHEMISTRY DEPT
LSUMC
1901 PERDIDO ST
NEW ORLEANS LA 70112-1393

PHONE: 504 568 6585

DONALD IANNELLI
PROCTER & GAMBLE CO
6071 CENTERHILL RD

CINCINNATI OH 45224

PHONE: 513 634 2114

MR A IDELSON
ICON SERVICES
19 OX BOW LANE

SUMMIT NJ 07901

PHONE: 201 273 0449

CHARLES R IDEN
PHARMACOLOGY DEPT
SUNY-STONY BROOK

STONY BROOK NY 11794

PHONE: 516 246 2298

ELAINE C IGO
134 GROVE STREET

MELROSE MA 02176

PHONE: 617 665 8050

CARL F IJAMES
DEPT OF CHEMISTRY
UNIV OF CALIFORNIA

RIVERSIDE CA 92521

PHONE: 714 787 4740

MICHAEL G IKONOMOU
CHEMISTRY DEPT
UNIV OF ALBERTA

EDMONTON ALBERTA T6G 2G2
CANADA
PHONE: 403 432 3502

ANDREAS J ILLIES
CHEMISTRY DEPT
AUBURN UNIV

AUBURN AL 36849

PHONE: 205 826 4043

L L INGRAM
PO DRAWER FP

MISSISSIPPI S MS 39762

PHONE: 601 325 3102

MORRIS M IRWIN
DOW CHEMICAL USA
734 BUILDING

MIDLAND MI 48667

PHONE: 517 636 5622

ILEANA ISERN-FLECHA
PO BOX 3242

BOCA RATON FL 33427

PHONE: 305 998 3058

KEIICHIRO ISHIKAWA
NATL CHEM LAB FOR INDUSTRY
1-1, HIGASHI
TSUKUBA-SHI
IBARAKI 305
JAPAN
PHONE:

YASUHIRO ITAGAKI
JEOL LTD
1-3 MUSASHINO
AKISHIMA
TOKYO 196
JAPAN
PHONE: 0425 43 1111

BRUCE J JACKSON
101 NICB
BRIGHAM YOUNG UNIV

PROVO UT 84602

PHONE: 801 378 5595

THOMAS C JACKSON
EASTMAN KODAK
BUILDING 82, FLOOR 2, RL

ROCHESTER NY 14650

PHONE: 716 477 8515

LEROY JACOBS
WAL INC
6385 W 52ND AVE #5

ARVADA CO 80002

PHONE: 303 278 2506

SOHAIL JAHANI
NANCO LABS, INC
RD 6 ROBINSON LANE

WAPPINGERS FALLS NY 12590

PHONE: 914 221 2485

KEN IMATANI
HEWLETT-PACKARD
1601 CALIFORNIA AVE

PALO ALTO CA 94304

PHONE: 415 857 2021

MASAO INOUE
UNIV OF ELECTRO-COMMUNICATIONS
1-5-1 CHOFUGAOKA, CHOFU-SHI

TOKYO 182
JAPAN
PHONE:

KIMIO ISA
DEPT OF CHEMISTRY
FUKUI UNIVERSITY
BUNKYO 3-9-1
FUKUI 910
JAPAN
PHONE:

MORIO ISHIHARA
JEOL
AKISHIMA MUSASHINO 312

TOKYO
JAPAN
PHONE:

S C ISRAEL
CHEMISTRY DEPT
UNIV OF LOWELL

LOWELL MA 01854

PHONE: 617 452 5000

KAZUHIDE IWASAKI
FUJISAWA PHARMACEUTICAL CO
1-6, 2-CHOME
KASHIMA
OSAKA 532
JAPAN
PHONE:

CARSON JACKSON
R J BRUNFELDT CO
PO BOX 2066

BARTLESVILLE OK 74005

PHONE: 918 336 4467

THOMAS J JACKSON
1614 RICHFOREST

RICHARDSON TX 75081

PHONE: 214 851 8456

DENLEY JACOBSON
NORTH DAKOTA STATE UNIV
DEPT OF CHEMISTRY

FARGO ND 58105

PHONE: 701 237 8811

GEORGE E JAHN
VARIAN ASSOC K407
611 HANSEN WAY

PALO ALTO CA 94303

PHONE: 415 424 5079

RAFAEL N INFANTE
CHEMISTRY DEPT
CATHOLIC UNIV

PONCE PR 00732

PHONE: 809 844 4150

A P IRSA
79 MORTON BLVD

PLAINVIEW NY 11803

PHONE: 516 935 7731

ROBERT K ISENSEE
ONEIDA RES SERVICE
ONE HALSEY ROAD

WHITESBORO NY 13492

PHONE: 315 736 3050

SABURO ISHII
JEOL LTD NPG
3-1-2 MUSASHINO
AKISHIMA-SHI
TOKYO 197
JAPAN
PHONE:

PHILLIP ISSENBERG
UNIV OF NEBRASKA
EPPLEY INST
MEDICAL CENTER
OMAHA NE 68105

PHONE: 402 559 4473

A H JACKSON
UNIVERSITY COLLEGE
CHEMISTRY DEPT

CARDIFF CF1 1XL
WALES
PHONE:

J M JACKSON
MARTIN MARIETTA
ENERGY SYSTEMS INC
PO BOX 1410
PADUCAH KY 42001

PHONE: 502 444 6311

DAVID JACOBS
CHEMISTRY DEPT
TEXAS A&M UNIVERSITY

COLLEGE STATION TX 77843

PHONE: 409 845 1970

NATHAN JACOBSON
NASA LEWIS RES CENTER
MS 106-1
21000 BROOKPARK ROAD
CLEVELAND OH 44135

PHONE: 216 433 5498

EDWARD JAKUBOWSKI
US ARMY
1285 JAMISON CT

BELCAMP MD 21017

PHONE: 301 671 2591

GEORGE M JAKUBOWSKI
BAXTER HEALTHCARE CORP
6301 LINCOLN AVE

MORTON GROVE IL 60053

PHONE: 312 965 4700

J E JALONEN
UNIV OF TURKU
CHEMISTRY DEPT

20500 TURKU 50
FINLAND
PHONE:

ALAN T JAMES
EXXON PRODUCT RESEARCH
PO BOX 2189

HOUSTON TX 77001

PHONE: 713 965 4158

HUW A JAMES
WATER RESEARCH CTR
PO BOX 16 HENLEY RD
MEDMENHAM
MARLOW BUCKS
ENGLAND
PHONE:

W D JAMIESON
NRC
1411 OXFORD ST

HALIFAX NS B3H 3Z1
CANADA
PHONE: 902 426 8279

MARTIN J JANIAK
VG INSTRUMENTS INC
32 COMMERCE CENTER
CHERRY HILL DRIVE
DANVERS MA 01923

PHONE: 617 777 8034

CHARLES H JARBOE
UNIV OF LOUISVILLE
PHAMACOLOGY & TOX

LOUISVILLE KY 40292

PHONE: 502 588 5158

IAN JARDINE
MAYO CLINIC
PHARMACOLOGY DEPT
200 1ST STREET SW
ROCHESTER MN 55905

PHONE: 507 284 4178

J A JARRELL
WATERS, MILLIPORE
34 MAPLE STREET

MILFORD MA 01757

PHONE: 617 478 2000

MARTIN F JARROLD
AT&T BELL LABS
1E313

MURRAY HILL NJ 07974

PHONE: 201 582 6525

KOKA JAYASIMHULU
UNIV OF CINCINNATI
700 MORGAN HALL

CINCINNATI OH 45219

PHONE: 513 872 6349

JIM JEFFERY
CALIF STATE DEPT OF JUSTICE
BUR OF FORENSIC SVC
4949 BROADWAY
SACRAMENTO CA 95820

PHONE: 916 739 5136

DONALD J JENDEN
DEPT OF PHARMACOLOGY
SCHOOL OF MEDICINE, CHS
UNIV OF CALIFORNIA
LOS ANGELES CA 90024-1735

PHONE: 213 825 6694

KEITH R JENNINGS
UNIV OF WARWICK
GIBBET HILL ROAD
CHEMISTRY DEPT
COVENTRY CV4 7AL
ENGLAND
PHONE:

NANCY JEAN JENSEN
PHILIP MORRIS RESEARCH CENTER
PO BOX 26583

RICHMOND VA 23261

PHONE: 804 274 5903

TRESCOTT E JENSEN
FORD MOTOR COMPANY
5574 CASTLETON DRIVE

W BLOOMFIELD MI 48322

PHONE: 313 322 4598

ALFRED H JENSON
662 ARBOR VALLEY

CAMPBELL HALL NY 10916

PHONE: 201 825 7500

JI JIANG
BAYLOR COLLEGE OF MEDICINE
6608 FANNIN, ROOM 514

HOUSTON TX 77030

PHONE: 713 799 6003

LON-FEI JIANG
DEPT OF AGRICULTURAL CHEMISTRY
OREGON STATE UNIV

CORVALLIS OR 97331

PHONE: 503 754 2906

SHIOW-JEN JIN
CASE WESTERN RES UNIV
10701 EAST BLVD
VA MEDICAL CENTER
CLEVELAND OH 44106

PHONE: 216 791 3800

JILL M JOBBINS
1400 MILTON AVE

SOLVAY NY 13209

PHONE: 315 487 4311

JEROME JOHEMKO
FINNIGAN CORP
355 RIVER OAKS PARKWAY

SAN JOSE CA 95134

PHONE:

CAROLYN JOHLMAN
PHILLIPS PETROLEUM CO
RESEARCH & DEVELOPMENT

BARTLESVILLE OK 74004

PHONE: 918 661 4547

CONSTANCE JOHN
SCHOOL OF PHARMACY
DEPT OF PHARM CHEMISTRY
UNIV OF CALIFORNIA
SAN FRANCISCO CA 94143-0446

PHONE: 415 476 5129

BRUCE M JOHNSON
PFIZER INC
CENTRAL RESEARCH

GROTON CT 06340

PHONE: 203 441 3789

CARL G JOHNSON
123 FYE LABORATORY
WOODS HOLE OCEAN INST

WOODS HOLE MA 02543

PHONE: 617 548 1400

ERIC K JOHNSON
1355M REMINGTON ROAD

SCHAUMBURG IL 60173

PHONE: 312 310 0140

JODIE V JOHNSON
UNIV OF FLORIDA
335 LEIGH HALL

GAINESVILLE FL 32611

PHONE: 904 392 0515

JUDITH A JOHNSON
STERLING-WINTHROP RES INST
81 COLUMBIA TURNPIKE

RENSSELAER NY 12144

PHONE: 518 445 8247

KENNETH L JOHNSON
FINNIGAN MAT
355 RIVER OAKS PARKWAY

SAN JOSE CA 95134

PHONE: 408 433 4800

LYLE JOHNSON
SPECTRUM LABS INC
4550 N DIXIE HIGHWAY

FT LAUDERDALE FL 33334

PHONE: 305 491 4691

P E JOHNSON
HUMAN NUTRITION LAB
BOX 7166 UNIV STATN

GRAND FORKS ND 58202

PHONE: 701 795 8416

RICHARD S JOHNSON
MIT
CHEMISTRY 56-016
77 MASS AVENUE
CAMBRIDGE MA 02139

PHONE: 617 253 7236

ROBERT L JOHNSON
BURROUGHS WELCOME CO
3030 CORNWALLIS RD

RES TRI PARK NC 27709

PHONE: 919 248 4353

W H JOHNSON
PHYSICS DEPARTMENT
UNIV OF MINNESOTA
116 CHURCH STREET SE
MINNEAPOLIS MN 55455

PHONE: 612 624 0802

MARK JOHNSTON
NICOLET MASS SPECTROMETRY
5225-1 VERONA ROAD
PO BOX 4508
MADISON WI 53711

PHONE: 608 271 3333

MURRAY V JOHNSTON
DEPT OF CHEMISTRY
CAMPUS BOX 215
UNIV OF COLORADO
BOULDER CO 80309-0215

PHONE: 303 492 5033

A DANIEL JONES
FAC FOR ADVANCED INSTR
9 HUTCHISON HALL
UNIV OF CALIFORNIA
DAVIS CA 95616

PHONE: 916 752 0284

DAVID A JONES
DEPT OF CHEM/BIOCHEM
UNIV OF WINDSOR
SUNSET AVE
WINDSOR, ONTARIO N9A 5T2
CANADA
PHONE: 519 253 4232

DAVID S JONES
VG INSTRUMENTS
FLOATS RD, WYTHENSHAWE

MANCHESTER
ENGLAND
PHONE:

E G JONES
SYSTEMS RESEARCH LAB
RES APPLICATIONS DIV
2800 INDIAN RIPPLE
DAYTON OH 45440

PHONE: 513 426 6000

FRED E JONES
NEW BRUNSWICK LAB
9800 S CASS AVE, BLDG 350

ARGONNE IL 60439

PHONE: 312 972 2467

GILBERT G JONES
AMOCO RESEARCH CTR MSB-5
PO BOX 400

NAPERVILLE IL 60566

PHONE: 312 420 5773

LOUIS A JONES
DEPT OF CHEMISTRY
BOX 8204
NORTH CAROLINA STATE UNIV
RALEIGH NC 27695-8204

PHONE: 919 737 2940

MICHAEL T JONES
AMERICAN CYANAMID
PO BOX 400

PRINCETON NJ 08540

PHONE: 609 799 0400

TAMMY L JONES
5017 WEST GOWAN RD

LAS VEGAS NV 89130

PHONE: 802 798 2144

DANIEL JOULAIN
ROBERTET SA
B.P. 100

06333 GRASSE
FRANCE
PHONE:

GUY GALLELLO, JR
2200 IVY LANE

FINDLAY OH 45840

PHONE: 419 423 3526

CHARLES M JUDSON
CHEMISTRY DEPT
UNIV OF KANSAS

LAWRENCE KS 66044

PHONE: 913 864 3223

ALINE JUERY
CEA-SERVICE RCP
BP 12- BRUYERS LE CHATEL

91680 BRUYERES
FRANCE
PHONE:

GREGORY A JUNGCLAUS
MIDWEST RES INST
425 VOLKER BLVD

KANSAS CITY MO 64110

PHONE: 816 753 7600

GREGOR A JUNK
US DOE
AMES LAB
IOWA STATE UNIV
AMES IA 50011

PHONE: 515 294 9488

JEANETTE JURUSIK
NYS DEPT OF HEALTH
WCL&R
EMPIRE STATE PLAZA
ALBANY NY 12201

PHONE: 518 474 1675

LONNIE G JUSTICE
HEWLETT PACKARD
4501 ERSKINE ROAD

CINCINNATI OH 45242

PHONE: 614 891 3344

MALCOLM KAHN
301 WICHITA TRAIL

FRANKLIN LAKE NJ 07417

PHONE:

ISHENKUMBA A KAHWA
CHEMISTRY DEPT
UNIV OF THE WEST INDIES

MONA, KINGSTON 7
JAMAICA
PHONE:

DAVID G KAISER
THE UPJOHN CO
OU 7256-126-3
301 HENRIETTA STREET
KALAMAZOO MI 49001

PHONE: 616 385 7058

MARY F KAISER
20 N PINE ST
UMAB PHARMACY SCHOOL
DEPT OF MED CHEM/PHARM
BALTIMORE MD 21201

PHONE: 301 328 2982

RAYMOND E KAISER
146-9 ARNOLD DR

W LAFAYETTE IN 47906

PHONE: 317 494 9420

THOMAS KAISER
P O BOX 84

CH-6372
ENNETMOOS NW
SWITZERLAND
PHONE:

JON KAKANOVICH
MESA POLICE DEPT
130 N ROBSON

MESA AZ 85201

PHONE: 602 834 2077

MICHAEL KALBFLEISCH
GOODYEAR T&R CO
142 GOODYEAR BLVD

AKRON OH 44316

PHONE: 216 796 2613

ROBERT G KALEY
MONSANTO
800 N LINDBERGH
MAIL CODE A2 NE
ST LOUIS MO 63167

PHONE: 314 694 8558

HENRY T KALINOSKI
LEVER RESEARCH INC
45 RIVER ROAD

EDGEWATER NJ 07020

PHONE: 201 943 7100

MAUREEN KALLOO
MSD ISOTOPES
3835 BENNER ROAD

MIAMISBURG OH 45432

PHONE: 513 859 1808

GEORGE J KALLOS
DOW CHEMICAL CO
BLDG 574

MIDLAND MI 48640

PHONE: 517 636 5340

IVAN KAMENSKY
BIO-ION
PO BOX 15045

S-75215 UPPSALA
SWEDEN
PHONE:

M S KAMINSKY
SURFACE TREATMENT SCI I
906 SOUTH PARK AVE

HINSDALE IL 60521

PHONE: 312 325 5535

Y Y KAMMEI
JEOL
AKISHIMA

TOKYO
JAPAN
PHONE:

JOHN DE KANEL
TOXICOLOGY TESTING SVC INC
5426 NW 79TH AVENUE

MIAMI FL 33166

PHONE: 305 593 1595

ARTHUR KANT
139 WOODRIDGE RD

WAYLAND MA 01778

PHONE:

IZET M KAPETANOVIC
PRECLIN PHARM SEC EPILEPSY
NINCDS, NIH
BLDG PARK, RM 445
BETHESDA MD 20892

PHONE: 301 496 6777

J J KARLINER
CIBA-GEIGY CORP
ANALYTICAL DEPT

ARDSLEY NY 10502

PHONE: 914 478 3131

TOM KARNS
CHEMISTRY DEPARTMENT
UNIV OF OKLAHOMA
620 PARRINGTON OVAL
NORMAN OK 73019

PHONE: 405 325 2843

ZEEV KARPAS
NRCN
PO BOX 9001

BEER-SHEVA
ISRAEL 84190
PHONE:

RANDOLF KARRER
UNIV OF CALIFORNIA
1980 FELL ST

SAN FRANCISCO CA 94117

PHONE: 415 476 5249

STEVEN KASS
DEPT OF CHEMISTRY
UNIV OF MINNESOTA
207 PLEASANT STREET SE
MINNEAPOLIS MN 55455

PHONE: 612 625 7513

KELEM KASSAHUN
PHARMACEUTICAL SCIENCES
UNIV OF BRITISH COLUMBIA
2146 EAST MALL
VANCOUVER BC V6T 1W5
CANADA
PHONE: 604 228 5946

DANIEL B KASSEL
MIT
BLDG 56-016

CAMBRIDGE MA 02139

PHONE: 617 354 4614

PATRICK E KASTL
DOW CHEMICAL USA
TOXICOLOGY
1803 BLDG
MIDLAND MI 48640

PHONE: 517 636 2060

YOSHIAKI KATO
NAKA WORKS
HITACHI LTD

KATSUTA 312
JAPAN
PHONE:

VISWANATHAM KATTA
MASS SPECTROMETRY GROUP
THE ROCKEFELLER UNIV
1230 YORK AVE
NEW YORK NY 10021

PHONE: 212 570 8852

ROBERT N KATZ
DEPT OF NEOPLASTIC DISEASES
MOUNT SINAI SCHOOL OF MEDICINE
ONE GUSTOVE LEVY PLACE
NEW YORK NY 10029

PHONE: 212 241 7729

SURINDER KAUR
SCHOOL OF PHARMACY
DEPT OF PHARM CHEMISTRY
UNIV OF CALIFORNIA
SAN FRANCISCO CA 94143-0446

PHONE: 415 476 5129

KENJI KAWAOKA
EASTMAN KODAK CO
ATD B-82 KP

ROCHESTER NY 14620

PHONE: 716 477 6733

TOM KAY
HEWLETT-PACKARD
4747 4TH NE

SEATTLE WA 98105

PHONE: 206 643 8859

KATHLEEN A KAYGANICH
DEPT OF CHEMISTRY
MICHIGAN STATE UNIV

EAST LANSING MI 48824

PHONE: 517 353 0612

C W KAZAKOFF
CHEMISTRY DEPT
UNIVERSITY OF OTTAWA

OTTAWA ONTARIO K1N 6N5
CANADA
PHONE: 614 231 4039

CHARLES KAZARIAN
1210 OAK TERRACE

ROUND LAKE BEACH IL 60073

PHONE: 312 937 4469

G L KEARNS
1504 SAN CARLOS BAY DRIVE

SANIBEL ISLAND FL 33957

PHONE:

RONALD KEEFE
INTERNATIONAL PAPER CO
CORPORATE RESEARCH CENTER
LONG MEADOW RD
TUXEDO PARK NY 10987

PHONE: 914 351 2101

JOSEPH B KEENAGHAN
FINNIGAN MAT
5340 SPECTRUM DR

FREDERICK MD 21701

PHONE: 301 698 9750

PETER W KEIDRON
PERKIN-ELMER CORP
2771 NORTH GAREY AVE

POMONA CA 91767

PHONE: 714 593 3581

PAUL R KELLER
PROCTER & GAMBLE
11520 REED HARTMAN

CINCINNATI OH 45241

PHONE: 513 530 3045

DANA E KELLEY
VG INSTRUMENTS INC
13 PEBBLESTONE CIRCLE

SUFFIELD CT 06078

PHONE: 703 668 6270

JAMES A KELLEY
NIH
NCI LAB MED CHEM
BLDG 37 RM 5C02
BETHESDA MD 20892

PHONE: 301 496 3597

MICHAEL A KELLEY
7252 BRUSHWOOD DRIVE

CINCINNATI OH 45069

PHONE: 513 777 5265

PAUL E KELLEY
FINNIGAN MAT
355 RIVER OAKS PKWY

SAN JOSE CA 95134

PHONE: 408 433 4800

RONALD BRUCE KELLEY
CALIF DEPT OF FISH & GAME
2005 NIMBUS RD

RANCHO CORDOVA CA 95670

PHONE: 916 355 0856

SCOTT KELLOGG
SALK INST-BIOTECHNOLOGY
PO BOX 85200

SAN DIEGO CA 92138

PHONE: 619 452 5892

PAMELA KELLY
HEWLETT-PACKARD
8110 RAINBOW RIDGE

FORT WAYNE IN 46825

PHONE: 219 489 6665

SHARON L KELLY
RORER GROUP
800 BUSINESS CENTER DR

HORSHAM PA 19034

PHONE: 215 628 6738

LEONID KELNER
1320 WESTHILLS LN

RESTON VA 22090

PHONE: 703 471 0377

PAUL C KEMPER
DEPT OF CHEMISTRY
UNIV OF CALIFORNIA

SANTA BARBARA CA 93106

PHONE: 805 961 2673

MARIANNE KEMPFF
75 CHEMISTRY BLDG
WAYNE STATE UNIV

DETROIT MI 48202

PHONE: 313 577 3072

ERIC J KEMPSTER
2178 POMPEY-FABIUS ROAD

FABIUS NY 13063

PHONE: 315 463 5297

GRANT B KENION
AMERICAN CYANAMID
LEDERLE LABS

PEARL RIVER NY 10965

PHONE: 914 732 3813

KURT L KENNEDY
PO BOX 43930

TUCSON AZ 85733

PHONE:

DEVON L KENNEY
1111 C DECKER ST

EL CAJON CA 92019

PHONE: 619 588 7792

J M KENNISH
UNIV OF ALASKA
CHEMISTRY DEPT
3211 PROVIDENCE DR
ANCHORAGE AK 99508

PHONE: 907 786 1236

PETER T M KENNY
SUNTORY INST FOR BIORGANIC RES
WAKAYAMADAI, SHIMAMOTO-CHO
MISHIMA-GUN
OSAKA 618
JAPAN
PHONE:

LLOYD KENT
105 RIVERDALE BLVD

POMPTON LAKES NJ 07442

PHONE: 201 867 4100

RICHARD H KENT
REG FORENSIC LAB
27 WOODLAND RD

PAINESVILLE OH 44077

PHONE: 216 325 9517

HILKKA KENTTAMAA
CHEMISTRY DEPT
PURDUE UNIVERSITY

W LAFAYETTE IN 47907

PHONE: 317 494 5265

THOMAS W KEOUGH
9896 BARNSLEY CT

CINCINNATI OH 45242

PHONE: 513 245 2486

EDWARD H KERNS
BRISTOL MYERS CO
5 RESEARCH PARKWAY
PO BOX 5100
WALLINGFORD CT 06492-7660

PHONE: 203 284 6499

SUHAS KETKAR
EXTREL CORP
PO BOX 11512

PITTSBURGH PA 15238

PHONE: 412 963 7530

WILLIAM R KEYES
USDA ARS WHNRC
800 BUCHANAN STREET

ALBANE CA 94710

PHONE: 415 559 5988

ALIREZA KHARRAZI
4541 DA VINCI DRIVE

STOCKTON CA 95207

PHONE: 209 957 3405

DAVID KIDWELL
NAVAL RES LAB
CODE 6170

WASHINGTON DC 20375

PHONE: 202 767 3575

BRET KIEFABER
HEWLETT-PACKARD
PRODUCT SUPPORT
1601 CALIFORNIA AVENUE
PALO ALTO CA 94304

PHONE: 415 857 6146

W E KILLINGER
W R GRACE & CO
RESEARCH DIV
7379 ROUTE 32
COLUMBIA MD 21044

PHONE: 301 531 4479

LEWIS B KILLMER
SK&F R&D LABS MAIL CODE L-940
PO BOX 1539

KING OF PRUSSIA PA 19406-0939

PHONE: 215 270 6656

HEE-YONG KIM
261 CONGRESSIONAL LANE
#308

ROCKVILLE MD 20852

PHONE: 301 496 4900

M S KIM
SEOUL NATIONAL UNIV
CHEMISTRY DEPT
COLL OF NATURAL SCI
SEOUL 151
KOREA
PHONE:

FRED L KING
DEPT OF CHEMISTRY
MCCORMICK ROAD
UNIV OF VIRGINIA
CHARLOTTESVILLE VA 22901

PHONE: 804 924 7180

GRAHAM S KING
ICI PLANT PROTECTION DIV
CDC SECTION
JEALOTTS HILL
BRACKNELL, BERKS
ENGLAND
PHONE:

ROY W KING
CHEMISTRY DEPT
UNIV OF FLORIDA

GAINESVILLE FL 32611

PHONE: 904 392 0592

SHERRILL KING
W R GRACE & CO
CRYOVAC DIV
PO BOX 464
DUNCAN SC 29334

PHONE: 803 433 2559

DONNA J KINNEY-BENSON
RD 1 BOX 309

W SAND LAKE NY 12196

PHONE: 518 474 1675

GARY R KINSEL
CAMPUS BOX 215
UNIV OF COLORADO

BOULDER CO 80309-0215

PHONE: 303 492 6958

ROBIN KINSER
PHILIP MORRIS USA
RESEARCH CENTER
PO BOX 26583
RICHMOND VA 23261

PHONE: 804 274 5905

JAMES A KINSINGER
1680 OAK AVENUE

BOULDER CO 80302-1257

PHONE: 303 447 2291

MICHAEL KINTER
DEPT OF PATHOLOGY
CLINICAL LABS BOX 168
UNIV OF VA MEDICAL CTR
CHARLOTTESVILLE VA 22908

PHONE: 804 924 9204

JEFFREY P KIPLINGER
3039 STADIUM DRIVE #5

COLUMBUS OH 43202

PHONE: 614 292 0480

TADASU KIRIHARA
DEPT OF APPLIED PHYSICS
UNIV OF ELECTRO-COMMUNICATIONS
1-5-1 CHOFUGAOKA, CHOFU-SHI
TOKYO 182
JAPAN
PHONE:

JOHN D KIRK
GEORGIA INST OF TECHNOLOGY
SCHOOL OF CHEMISTRY

ATLANTA GA 30332

PHONE: 404 894 4051

MARION C KIRK
SOUTHERN RES INST
2000-9TH AVE S
BOX 55305
BIRMINGHAM AL 35255

PHONE: 205 323 6592

STEVE KIRKISH
FINNIGAN MAT
355 RIVER OAKS PARKWAY

SAN JOSE CA 95134

PHONE: 408 433 4800

ERNEST KIRKWOOD
JOHN WILEY & SONS
BAFFIN LANE
CHICHESTER
W SUSSEX PO19 1UD
UK
PHONE:

NADIA D KIRZECKY
AMERICAN CYANAMID
PO BOX 400

PRINCETON NJ 08540

PHONE: 609 799 0400

ROBERT W KISER
9-CP BLDG
UNIV OF KENTUCKY

LEXINGTON KY 40506

PHONE: 606 257 4622

HIROSHI KISHI
DEPT OF CHEMISTRY
E3-43 CHEMISTRY BLDG EAST
UNIV OF ALBERTA
EDMONTON ALBERTA T6G 2G2
CANADA
PHONE: 403 432-3254

PETER T KISSINGER
BIOANALYTICAL SYS
2701 KENT AVE

W LAFAYETTE IN 47906

PHONE: 317 463 4527

PIETER KISTEMAKER
FOM INST FOR ATOMIC &
MOLECULAR PHYSICS
KRUISLAAN 407
1098 SJ AMSTERDAM
NETHERLANDS
PHONE:

F G KITSON
3 HARTFORD PLACE

NEWARK DE 19711

PHONE: 302 695 3543

MICHAEL KLANECKY
443 WRIGHT STREET
NO 307

LAKEWOOD CO 80228

PHONE: 303 980 5233

JOSEPH P KLEIMAN
ETHYL CORP
PO BOX 14799

BATON ROUGE LA 70898

PHONE: 504 768 5685

E R KLEIN
6608 FANNIN AVE
SUITE 601

HOUSTON TX 77030

PHONE: 713 799 6183

PETER D KLEIN
6608 FANNIN AVE
RM 601

HOUSTON TX 77030

PHONE: 713 799 6000

J C KLEINGELD
KONINKLIJKE/SHELL-LAB AMSTERDA
DEPT AG
PO BOX 3003
1003AA AMSTERDAM
NETHERLANDS
PHONE:

KEITH S KLINE
8522 SUMMERTREE LANE

INDIANAPOLIS IN 46256

PHONE: 317 848 4990

JEFF KLINGLER
DEPT OF CHEMISTRY
UNIV OF VIRGINIA
MCCORMICK RD
CHARLOTTESVILLE VA 22901

PHONE: 804 924 7180

STEVEN E KLOHR
BRISTOL-MYERS CO
5 RESEARCH PARKWAY, DEPT 902

WALLINGFORD CT 06492

PHONE: 203 284 6410

JAMES KNAK
K&M ELECTRONICS
123 INTERSTATE DRIVE

WEST SPRINGFIELD MA 01089

PHONE: 413 781 1350

DANIEL R KNAPP
MED UNIV S CAROLINA
PHARMACOLOGY DEPT
171 ASHLEY AVE
CHARLESTON SC 29425

PHONE: 803 792 2471

GARY D KNERR
411 N ALMON
NO 523

MOSCOW ID 83843

PHONE: 208 885 6756

T C KNIGHT
2370 S BRENTWOOD ST

LAKEWOOD CO 80227

PHONE: 303 977 4241

W B KNIGHTON
DEPT OF CHEMISTRY
MONTANA STATE UNIV

BOZEMAN MT 59715

PHONE: 406 994 5420

HANS KNOF
AM FORSTTEICH 15/17

D-2000 NORDERSTEDT
WEST GERMANY
PHONE:

KENSEI KOBAYASHI
YOKOHAMA NATL UNIV
156 TOKIWADAI
HODOGAYA-KU
YOKOHAMA 240
JAPAN
PHONE:

CHARLES KOCH
HEWLETT PACKARD
503 LARKSPUR AVE

CORONA DEL MA CA 92625-2317

PHONE: 714 758 5525

H J KOCH
MSD ISOTOPES
TRANSCANADA HWY

KIRKLAND QUEBEC
CANADA
PHONE:

CAROLYN KOESTER
INDIANA UNIVERSITY
GEOLOGY 541

BLOOMINGTON IN 47405

PHONE: 812 335 5424

PETER KOFEL
UNIV OF WATERLOO
DEPT OF CHEMISTRY
WATERLOO N2L3G1 ONTARIO

CANADA
PHONE: 519 888 4591

MINORU KOGA
UCLA SCHOOL OF PUBLIC HEALTH
5531 CORTEEN PL #203

NORTH HOLLYWOOD CA 91607

PHONE:

CATHY J KOLANOWSKI
SPORTS MEDICINE LAB
INDIANA UNIVERSITY
635 BARNHILL DR
INDIANAPOLIS IN 46234

PHONE: 317 274 3220

ERIC W KOLODZIEJ
MONSANTO CO
700 CHESTERFIELD VILLAGE PKWY

CHESTERFIELD MO 63198

PHONE: 314 537 6071

MICHAEL G KOLOR
71 MARGARET KEAHON DRIVE

PEARL RIVER NY 10965

PHONE: 914 735 8622

RICHARD W KONDRAT
CHEMISTRY DEPT
UNIV OF CALIFORNIA

RIVERSIDE CA 92521

PHONE: 714 787 5287

WILFRIED A KONIG
UNIV HAMBURG
INST F ORGAN CHEMIE
M-L-KING-PLATZ6
D-2000 HAMBURG 13
W GERMANY
PHONE:

JOSEPH KONSCHNIK
ANALYTICAL TECHNOLOGIES INC
5550 MOREHOUSE RD

SAN DIEGO CA 92121

PHONE: 619 458 9141

J A KOPRIO
BALZERS AG

FL 9496 BALZERS
LIECHTENSTEIN
PHONE:

WALTER A KORFMACHER
NCTR
BIOCHEM TOX DIV
HFT-154
JEFFERSON AR 72079

PHONE: 501 541 4108

RICHARD A KORNFELD
BATTELLE COLUMBUS DIV
505 KING AVENUE

COLUMBUS OH 43201

PHONE: 614 424 3934

MARK E KOSLIN
PERKIN-ELMER CORP
2771 N GAREY

POMONA CA 91767

PHONE: 714 593 3581

JAMES G KOSTELC
MONSANTO CO
MAIL ZONE BB2I
700 CHESTERFIELD VILL PWY
CHESTERFIELD MO 63198

PHONE: 314 537 6218

RISTO KOSTIAINEN
DEPT OF CHEMISTRY
UNIV OF HELSINKI
VUORIKATU 20
HELSINKI 10
FINLAND
PHONE:

ALVIN N KOTAKE
CIBA-GEIGY PHARMACEUTICAL
556 MORRIS AVE

SUMMIT NJ 07901

PHONE: 201 277 7491

TAPIO KOTIAHO
DEPT OF CHEMISTRY
PURDUE UNIVERSITY

WEST LAFAYETTE IN 47907-3699

PHONE:

GEORGE J KOVES
CTR OF FORENSIC SCIENCE
TOXICOLOGY
25 GROSVENOR STR
TORONTO ONT M7A 2G8
CANADA
PHONE:

JEFFREY A KOWALAK
306 EAST 700 SOUTH #A104
SALT LAKE CITY UT 84111
PHONE: 801 521 8125

GREG KOYANAGI
TRENT UNIVERSITY
DEPT OF CHEMISTRY
PETERBOROUGH
ONTARIO K91 7B8
CANADA
PHONE:

JAROSLAV KRAMAR
HEWLETT-PACKARD
SCIENTIFIC INSTRUMENTS DIV
1601 CALIFORNIA
PALO ALTO CA 94304
PHONE:

STEVEN KRAMER
PEPSICO RES & TECH CTR
100 STEVENS AVENUE
VALHALLA NY 10595
PHONE: 914 742 4813

S W KRASNER
METRO WATER DIST
WATER QUALITY BRANCH
700 NORTH MORENO AVE
LA VERNE CA 91750
PHONE: 714 593 7474

J R KRAUSE
CHEMISTRY DEPT
UNIVERSITY OF OTTAWA
OTTAWA ONTARIO K1N 6N5
CANADA
PHONE: 613 564 4039

MARK KRAUSE
CUBIX CORP
1713 FORTVIEW
AUSTIN TX 78704
PHONE: 512 444 5830

JOHN M KRECISE
SCA CHEMICAL SERVICES
11700 S STONY ISLAND
CHICAGO IL 60617
PHONE: 312 646 5700

MARY J KREEK
ROCKEFELLER UNIV
1230 YORK AVE
NEW YORK NY 10021
PHONE: 212 570 8248

GERHARD M KRESBACH
NORTHEASTERN UNIV
BARNETT INSTITUTE
360 HUNTINGTON AVE
BOSTON MA 02115
PHONE: 617 437 2794

THOMAS KRICK
BIOCHEMISTRY DEPT
UNIV OF MINNESOTA
1479 GORTNER AVE
ST PAUL MN 55108
PHONE: 612 624 7715

THAIYA KRISHNAMURTHY
RES DIRECTORATE
CHEM RES DEV & ENG CTR
APG MD 21010-5423
PHONE: 301 671 2255

MICHAEL J KRISTO
4850 D SUNSET TERRACE
FAIR OAKS CA 95628
PHONE: 916 643 2250

KYLE J KROHA
23 E LAKESHORE DRIVE
No 7
CINCINNATI OH 45237
PHONE: 812 335 3436

JANA L KROTTINGER
CONOCO INC
PO DRAWER 1267
325 R&D
PONCA CITY OK 74603
PHONE: 405 767 2954

FRANCIE M KUBIAK
MILES LABORATORIES
1127 MYRTE ST BOX 932
ELKHART IN 46514
PHONE: 219 262 7979

ALAN J KUBIS
4922 CENTER AVE #4A
PITTSBURGH PA 15213
PHONE: 412 624 8304

EIJI KUBOTA
JEOL LTD
1-2 MUSASHINO 3-CHOME
AKISHIMA
TOKYO 196
JAPAN
PHONE:

LYNN KUBOWICZ
924 ROACH
SALINA KS 67401
PHONE: 913 825 7186

DOUGLAS W KUEHL
EPA
6201 CONGDON BLVD
DULUTH MN 55804
PHONE: 218 720 5558

CHARLES KUHLMAN
PENNWALT CORP
900 FIRST AVE
KING OF PRUSSIA PA 19406-0018
PHONE: 215 337 6549

W F KUHN
PHILIP MORRIS USA
RESEARCH CENTER
PO BOX 26583
RICHMOND VA 23261
PHONE: 804 274 3918

NARAYAN KUMAR
AMERICAN WATER WORKS
1115 S ILLINOIS ST
BELLEVILLE IL 62220
PHONE: 618 235 3600

NANCY KUO
FINNIGAN MAT
355 RIVER OAKS PARKWAY
SAN JOSE CA 95134
PHONE: 408 433 4800

KAREN KUOPPALA
9680 HARISON ST
THORNTON CO 80229
PHONE: 303 659 0497

T JOSEPH KURIAKOSE
HOECHST CELANESE CORP
PO BOX 9077
CORPUS CHRISTI TX 78469
PHONE: 512 993 5873

NICHOLAS J KURLICK
ROY F WESTON, INC
GSA RARITAN DEPOT
WOODBRIDGE AVE BLDG ANNEX
EDISON NJ 08837
PHONE: 201 632 9200

JOZEF KUSMIERZ
UNIV OF TENNESSEE
956 COURT AVE, ROOM A218
MEMPHIS TN 38163
PHONE: 901 528 5488

PHILLIP A KUYKENDALL
FINNIGAN MAT
355 RIVER OAKS PKWY
SAN JOSE CA 95134
PHONE: 408 433 4800

FRANS A KUYPERS
CHILDREN'S HOSPITAL OAKLAND
747 52ND STREET

OAKLAND CA 94609

PHONE: 415 428 3506

JAMES N KYRANOS
191 BILLINGS RD

NORTH QUINCY MA 02171

PHONE: 617 437 3696

KHOSROW LAALI
DEPT OF CHEMISTRY
KENT STATE UNIV

KENT OH 44242

PHONE: 216 672 2988

JAMES E LABDON
SCHERING PLOUGH
60 ORANGE STREET

BLOOMFIELD NJ 07003

PHONE: 201 429 4429

JACQUES L LABROSSE
BALZERS
8 SAGAMORE PARK RD

HUDSON NH 03051

PHONE: 603 889 6888

MARTIN P LACEY
7700 DEARBORN AVENUE

CINCINNATI OH 45236

PHONE: 513 245 2094

IRWIN LADD
UNION CARBIDE CORP
1 SUNSET DR

GROTON/HUDSON NY 10520

PHONE:

A L LAFLEUR
16 WALL STREET

ARLINGTON MA 02174

PHONE: 617 253 3499

LARRY LAFLEUR
NCASI
PO BOX 458

CORVALLIS OR 97339

PHONE: 503 754 2015

PIERRE LAFONTAINE
PLANT RES CTR AGRICULTURE
K W NEATBY BLDG RM 4040
OTTAWA ONTARIO K1A 0C6
CANADA
CANADA
PHONE:

FRANCOIS LAFORTUNE
PHYSICS DEPT
ALLEN BLDG
UNIV OF MANITOBA
WINNIPEG, MANITOBA R3T 2N2
CANADA
PHONE: 204 269 4800

C ROBERT LAGERGREN
2110 HOWELL AVE

RICHLAND WA 99352

PHONE: 509 373 3872

WILLIAM M LAGNA
US ARMY
CRDEC SMCCR-DDT

APG MD 21010-5423

PHONE: 301 671 3729

S T LAI
69 SCANTIC DRIVE

E LONGMEADOW MA 01028

PHONE:

SHIH-TSE JASON LAI
25815 SOUTHBROOK

EL TORO CA 92630

PHONE: 714 770 0039

FRANK LAIB
CHEMISTRY DEPT
UNIV OF WISCONSIN
3210 N CRAMMER
MILWAUKEE WI 53209

PHONE: 414 229 3933

ROGER A LAINE
BIOCHEMISTRY DEPT
LOUISIANA STATE UNIV
322 CHOPPIN HALL
BATON ROUGE LA 70803

PHONE:

ZAMAS LAM
DEPT OF CHEMISTRY
UNIV OF BRITISH COLUMBIA
VANCOUVER BC
V6T 1Y6 CANADA
CANADA
PHONE: 604 228 3266

JOHN G LAMBERTON
REICHHOLD CHEMICALS
PO BOX 1433

PENSACOLA FL 32596

PHONE: 904 433 7621

STEPHEN A LAMMERT
48 KNOLL CREST CT

W LAFAYETTE IN 47906-9990

PHONE: 317 743 9966

CAROLEJEAN H LAMOUREUX
METABOLISM & RADIATION
RESEARCH LABORATORY
STATE UNIV STATION
FARGO ND 58105

PHONE: 701 239 1236

FRED W LAMPE
PENN STATE UNIV
152 DAVEY LAB

UNIVERSITY PARK PA 16802

PHONE: 814 865 6553

DONALD P LAND
CHEMISTRY DEPT
UC IRVINE

IRVINE CA 92717

PHONE: 714 856 6780

HERBERT H LAND
ETTC-TOXICON
3213 MONTERREY BLVD

BATON ROUGE LA 70814

PHONE: 504 925 5012

D A LANE
31 DE VERE GDNS

TORONTO ONTARIO M5M 3E6
CANADA
PHONE: 416 667 4965

DOROTHY C LANE
WESTERN RESEARCH INST
PO BOX 3395

LARAMIE WY 82071

PHONE: 307 821 2267

JACK LANG
MARTIN-MARIETTA ENERGY SYS
DEPT 513 MS 2229
PO BOX 628
PIKETON OH 45661-0628

PHONE: 614 897 5704

RUSSELL F LANG
US DEPT OF COMMERCE
NOAA/AOML
4301 RICKENBACKER CSWY
MIAMI FL 33149

PHONE: 305 361 4387

H G LANGER
28 JOYCE ROAD

WAYLAND MA 01778

PHONE: 617 653 0649

PATRICK LANGVARDT
DOW CHEMICAL CO
1803 BLDG

MIDLAND MI 48640

PHONE: 517 636 1108

VICKI S LANYON
HEWLETT-PACKARD CO
1200 E DIEHL RD

NAPERVILLE IL 60566

PHONE: 312 357 8800

MARK A LAPACK
ANALYTICAL LABS
DOW CHEMICAL CO
574 BUILDING
MIDLAND MI 48640

PHONE: 517 636 6329

JAMES A LARAMEE
AG CHEMISTRY
OREGON STATE UNIV

CORVALLIS OR 97331

PHONE: 503 754 2906

BARBARA LARKA
6818 WOODHILL TRAIL

EDEN PRAIRIE MN 55344

PHONE: 612 641 9485

EDMUND A LARKA
DEPT OF CHEMISTRY
UNIV OF MINNESOTA

MINNEAPOLIS MN 55455

PHONE: 612 625 3053

BARBARA S LARSEN
DUPONT
EXPERIMENTAL STATION E228

WILMINGTON DE 19898

PHONE: 302 772 4876

MICHAEL E LARSON
R D ZANDE & ASSOC
1233 DUBLIN ROAD

COLUMBUS OH 43215

PHONE: 614 486 4383

ROBERT P LATTIMER
B F GOODRICH R & D
9921 BRECKSVILLE RD

BRECKSVILLE OH 44141

PHONE: 216 447 5369

R KAZMER LATVEN
AMERICAN BIOTEST LAB
3350 SCOTT BLVD BLDG 15

SANTA CLARA CA 95054

PHONE: 408 727 5525

JAMES M LAU
HEWLETT-PACKARDRD
122 W CENTURY ROAD

PARAMUS NJ 07653

PHONE:

JOCHEN LAUBER
CIBA-GEIGY
K-127-3 90

BASEL
SWITZERLAND
PHONE:

DAVID LAUDE
DEPT OF CHEMISTRY
UNIV OF TEXAS

AUSTIN TX 78712

PHONE: 512 471 4274

M T LAUG
ARGONNE NATIONAL LAB
PO BOX 2528

IDAHO FALLS ID 83401

PHONE: 208 526 7319

FRANK H LAUKIEN
BRUKER INSTRUMENTS INC
MANNING PARK

BILLERICA MA 01821

PHONE: 617 663 7406

ROY LAUTAMO
J & W SCIENTIFIC
91 BLUE RAVINE RD

FOLSON CA 95630

PHONE: 916 351 0387

WILLIAM LAUWERS
JANSSEN PHARMACEUTIC
TURNHOUTSE BAAN 30

B-2340 BEERSE
BELGIUM
PHONE:

JULIA K LAWRENCE
1320 1/2 W EDWARDS

SPRINGFIELD IL 62704

PHONE: 217 782 7430

A M LAWSON
CLINICAL RES CENTRE
WATFORD ROAD
HARROW
LONDON HA1 3UJ
ENGLAND
PHONE:

DIANE J LAWVER
PO BOX 7877

COLORADO SPRINGS CO 80933

PHONE: 719 598 6777

JACKSON O LAY
NAT'L CTR FOR TOX RESEARCH
HFT-184R

JEFFERSON AR 72079

PHONE: 501 541 4364

JOSEPH LAZAR
1006 N MONROE ST

WILMINGTON DE 19801

PHONE: 302 654 7944

JOHN C LE
3501 HORTON ST #101

RALEIGH NC 27607

PHONE: 919 737 2213

JOHN J LEARY
PFIZER INC
EASTERN POINT RD

GROTON CT 06340

PHONE:

JULIE A LEARY
MASS SPECTROMETRY LAB
COLL OF CHEM
UNIV OF CALIFORNIA
BERKELEY CA 94720

PHONE: 415 642 0701

CARLITO LEBRILLA
DEPT OF CHEMISTRY
UNIV OF CALIFORNIA

IRVINE CA 92717

PHONE:

LEO M LECH
DEPT OF CHEMISTRY
PURDUE UNIV

W LAFAYETTE IN 47907

PHONE: 317 494 5271

PIET A LECLERCQ
EINDHOVEN UNIV TECH
PO BOX 513

5600-MB EINDHOVEN
NETHERLANDS
PHONE:

EDWARD B LEDFORD
624 PEACH ST
PO BOX 80837

LINCOLN NE 68501

PHONE: 402 475 7640

BILL LEE
ENVIRONMENT CANADA
867 LAKESHORE ROAD

BURLINGTON, ONT
CANADA
PHONE: 416 336 4755

EDGAR D LEE
CORNELL UNIV
EQUINE DRUG TESTING
925 WARREN DRIVE
ITHACA NY 14850

PHONE: 607 255 6555

JANET M LEE
3645 HAMBLETONIAN DRIVE

FLORISSANT MO 63033

PHONE: 314 694 1273

ANDRE P DE LEENHEER
STATE UNIV OF GENT
RIJVISSCHEPARK 18

B-9710 GENT
BELGIUM
PHONE:

KASSU LEGESSE
BECKMAN RESEARCH INST
DIV OF IMMUNOLOGY
1450 E DUARTE ROAD
DUARTE CA 91010

PHONE:

JIM LEHMAN
DEPT OF CHEMISTRY
ARIZONA STATE UNIV

TEMPE AZ 85287-1604

PHONE: 602 965 6193

MICHAEL LEHRER
FINNIGAN MAT
7 REGENT ST SUITE #711

LIVINGSTON NJ 07039

PHONE: 201 572 0122

THOMAS LEIKER
US GEOLOGICAL SURVEY
5293 WARD RD
MAIL STOP 408
ARVADA CO 80002

PHONE:

FRANK LEMUNYON
TEKNIVENT CORP
11684 LILBURN PARK RD

ST LOUIS MO 63146

PHONE: 314 994 0500

PAUL GRAHAM LETHBRIDGE
MOLECULAR BEAMS
UNIV OF SUSSEX
FALMER, BRIGHTON
EAST SUSSEX BN1 9QJ
UK
PHONE:

D L LEWIS
DEPT OF AGRICULTURE
TOXICOLOGY LAB
BOX 8070 6909-116TH STREET
EDMONTON ALBERTA T6H 4P2
CANADA
PHONE: 403 436 8410

BERNARD J LEYH
CHEMISTRY DEPT
BAKER LABORATORY
CORNELL UNIVERSITY
ITHACA NY 14853-1301

PHONE: 607 255 3731

MIKE S LEE
BRISTOL MEYERS CO
5 RESEARCH PARKWAY
PO BOX 5100
WALLINGFORD CT 06492-7660

PHONE:

H F LEFEVRE
LEFEVRE ENGINEERING
2945 BURRVILLE RD

FORT RECOVERY OH 45846

PHONE: 419 375 4104

PATRICIA A LEGOTTE
US DOE
ENVIRONMENTAL MEASUREMENTS LAB
376 HUDSON STREET
NEW YORK NY 10014-3621

PHONE:

THOMAS A LEHMAN
PO BOX 435

N NEWTON KS 67117

PHONE: 316 283 2500

CHRIS P LEIBMAN
LOS ALAMOS NATIONAL LAB
256 LOMA ENTRADA

SANTE FE NM 87501

PHONE: 615 574 2455

ROBERT E LEMIEUX
1211 SHERWOOD AVE

RICHMOND VA 23220

PHONE: 804 257 2389

S R LEONE
UNIV OF COLORADO
JILA CAMPUS BOX 440

BOULDER CO 80309-0440

PHONE: 303 492 5128

STEVEN K LEUNG
3401 LA GRANDE BLVD

SACRAMENTO CA 95823

PHONE: 916 428 1193

IVOR LEWIS
DEPT OF CHEMISTRY
KING'S COLLEGE LONDON
STRAND
LONDON WC2R 2LS
ENGLAND
PHONE:

BRIGITTE G LEYH
CHEMISTRY DEPT
BAKER LAB
CORNELL UNIVERSITY
ITHACA NY 14853-1301

PHONE:

TERRY D LEE
BECKMAN RES INST
CITY OF HOPE/DIV OF IMMUNOLOGY
1450 E DUARTE RD
DUARTE CA 91010

PHONE: 818 966 3211

MICHAEL G LEGENDRE
USDA APHIS NMRAL
3505 25TH AVE
PO BOX 3209
GULFPORT MS 39505

PHONE: 601 863 8124

A M LEGRAND
WESTINGHOUSE NFD
PO DRAWER R

COLUMBIA SC 29250

PHONE: 803 776 2610

DENIS C LEHOTAY
HOSPITAL FOR SICK CHILDREN
555 UNIVERSITY AVE

TORONTO, ONT M5G 1X8
CANADA
PHONE: 416 598 5911

ROGER J LEIBRAND
HEWLETT-PACKARD
1601 CALIFORNIA AVE

PALO ALTO CA 94304

PHONE: 415 857 6127

MARK A LEMLEY
ISOTEC INC
3858 BENNER ROAD

MIAMISBURG OH 45342

PHONE: 513 859 1808

KHINGKAN LERTRATANANGKOON
UNIV OF TEXAS MED BRANCH
DEPT OF PHARM & TOXIC J-31

GALVESTON TX 77550

PHONE: 409 761 1561

MILTON I LEVENBERG
ABBOTT LABS
DEPT 418, AP9

ABBOTT PARK IL 60064

PHONE: 312 937 2080

SYDELL LEWIS
FINNIGAN MAT
355 RIVER OAKS PWY

SAN JOSE CA 95134

PHONE: 408 433 4800

YU-LAN LI
INST OF FORENSIC SCIENCE

BEIJING
CHINA
PHONE:

ZHONG-MIN LI
ANALYTICAL DEPT OF CHEM ENGIN
BEIJING INST OF TECH
POB 327
BEIJING
P R CHINA
PHONE:

WEI-SHENG LIANG
DEPT OF SPECTRAL ANALYSIS
BEIJING MEDICAL UNIV

BEIJING
CHINA
PHONE:

XIAO-TIAN LIANG
INST OF MATERIA MEDICA
CHINESE ACADEMY OF MED SCIENCE
1 XIAN NONG TAN STREET
BEIJING
CHINA
PHONE:

WENTA LIAO
STATE OF CALIFORNIA
169 E LIBERTY

ANAHEIM CA 92801

PHONE: 714 680 7901

SHARON G LIAS
NAT'L BUR OF STANDARDS

GAITHERSBURG MD 20899

PHONE: 301 921 2439

L M LIBBEY
DEPT OF FOOD SCIENCE/TECHNOLOG
OREGON STATE UNIV

CORVALLIS OR 97331

PHONE: 503 754 4636

DANIEL J LIBERATO
HOFFMANN-LAROCHE INC
DEPT OF DRUG METABOLISM
BLDG 86 ROOM 742
NUTLEY NJ 07110

PHONE: 201 235 4754

J G LIEHR
UNIV OF TEXAS
MEDICAL BRANCH

GALVESTON TX 77550-2774

PHONE: 409 761 1561

JERROLD M LIESCH
MERCK INSTITUTE
R80 M223
PO BOX 2000
RAHWAY NJ 07065

PHONE: 201 574 5546

CHAVA LIFSHITZ
HEBREW UNIV
PHYSICAL CHEM DEPT
MAIL CODE 91904
JERUSALEM
ISRAEL
PHONE:

KAREN J LIGHT
DEPT OF CHEMISTRY
MICHIGAN STATE UNIVERSITY

E LANSING MI 48824

PHONE: 517 353 6495

W V LIGON
GENERAL ELECTRIC CO
R&D CENTER
BLDG K1 PO BOX 8
SCHENECTADY NY 12301

PHONE: 518 387 6419

HENG-KEANG LIM
CTR FOR HUMAN TOXICOLOGY
38 SKAGGS HALL
UNIV OF UTAH
SALT LAKE CTY UT 84112

PHONE: 801 581 5119

DENIS C K LIN
ENSECO
214 DEEPDALE DR

MIDDLETONN NJ 07748

PHONE: 201 469 5800

DING-PING LIN
3967 IVERNESS LANE

W BLOOMFIELD MI 48033

PHONE: 313 855 6196

ELIZABETH LIN
M&T CHEMICALS
PO BOX 1104

RAHWAY NJ 07065

PHONE: 201 499 2168

SECHOING LIN
WARNER-LAMBERT/PARKE-DAVIS
188 HOWARD AVE

HOLLAND MI 49424

PHONE: 616 392 2375

SHEN NAN LIN
3751 GRENNOCH

HOUSTON TX 77025

PHONE: 713 972 5612

WEN-NUEI LIN
HENRY FORD HOSPITAL
2799 W GRAND BLVD

DETROIT MI 48202

PHONE: 313 876 2324

YONG Y LIN
INST FOR BASIC RESEARCH
1050 FOREST HILL RD

STATEN ISLAND NY 10314

PHONE: 718 494 5242

KENNETH A LINCOLN
2016 STOCKBRIDGE AVE

REDWOOD CITY CA 94061

PHONE: 415 369 7481

CLAES LINDBERG
PHARMACOKINETICS LAB
AB DRACO
BOX 34
LUND S-22100
SWEDEN
PHONE:

H BERNHARD LINDEN
PO BOX 61 03 07
LINDEN-CHROMAS SPEC

D-2800 BREMEN 61
W GERMANY
PHONE:

JAMES L LINDGREN
TEXAS AIR CONTROL BOARD
6330 HWY 290E

AUSTIN TX 78653

PHONE: 512 451 5711

N C LING
THE SALK INSTITUTE
BOX 85800

SAN DIEGO CA 92138

PHONE: 619 453 4100

VICTOR LING
GENENTECH INC
460 PT SAN BRUNO BLVD

S SAN FRANCISCO CA 94080

PHONE: 415 266 2058

MICHAEL W LINSCHEID
SPEKTROCHEM
BUNSEN-KIRCHHOFF
STR 11
D-4600 DORTMUND 1
W GERMANY
PHONE:

RICHARD W LINTON
CHEMISTRY DEPT BOX 3290
UNIV OF N CAROLINA

CHAPEL HILL NC 27599-3290

PHONE: 919 962 0459

ANASTASIA LINVILLE
HOECHST-ROUSSEL
RT 202-206N

SOMERVILLE NJ 08876

PHONE: 201 231 2652

PAUL LIPTON
CHEVRON CHEMICAL CO
PO BOX 4010

RICHMOND CA 94084-0010

PHONE: 415 231 6215

CAROL A LISEK
MAYO CLINIC
PHARMACOLOGY DEPT
200 FIRST STREET SW
ROCHESTER MN 55905

PHONE: 507 284 4213

DAVID LISSY
ACCREDITED LAB
PO BOX 369

CARTERET NJ 07008

PHONE: 201 541 2025

ANITA KAY LISTER
CHEMISTRY DEPT
PURDUE UNIVERSITY
BOX 590
W LAFAYETTE IN 47906

PHONE: 317 494 9420

DOROTHY LITTLE
FRICK CHEMICAL LAB
ROOM 25
PRINCETON UNIV
PRINCETON NJ 08540

PHONE: 609 452 3928

JAMES L LITTLE
TENN EASTMAN (KODAK)
BLDG 150

KINGSPORT TN 37662

PHONE: 615 229 3066

DUANE LITTLEJOHN
LEYBOLD INFICON INC
6500 FLY ROAD

EAST SYRACUSE NY 13057

PHONE: 315 437 0377

JAMES F LITTON
LOCKHEED MISSILES & SPACE
0/48-92 B/195B
1111 LOCKHEED WAY
SUNNYVALE CA 94088-3504

PHONE: 408 756 3646

NORMAN W LIU
SEARLE RES LAB
4901 SEARLE PKWY

SKOKIE IL 60077

PHONE: 312 982 8847

RAY H LIU
CRIMINAL JUSTICE
UNIV OF ALABAMA

BIRMINGHAM AL 35294

PHONE: 205 934 2069

SHU-YING LIU
PO BOX 1022

CHANGCHUN JILIN
CHINA
PHONE:

SHUTING LIU
CHANGCHUN INST OF APPLIED CHEM

CHANGCHUN
CHINA
PHONE:

YA-MEI LIU
MDCH, PHARMACY BLDG
PURDUE UNIVERSITY

W LAFAYETTE IN 47907

PHONE: 317 494 1449

FRANK LIVSEY
LAB INC
PO BOX 130 RR#3

STEWARTSTOWN PA 17363

PHONE: 717 993 2517

H A LLOYD
NIH
BLDG 10 RM 7N312

BETHESDA MD 20892

PHONE: 301 496 3376

JOHN R LLOYD
FINNIGAN MAT
355 RIVER OAKS PKWY

SAN JOSE CA 95134

PHONE: 301 698 9750

HSI HU LO
PO BOS 1207

PLACENTIA CA 92670-1207

PHONE:

JOHN LOGSDON
23566 CURRANT DR

GOLDEN CO 80401-9214

PHONE: 303 421 6611

STANTON LOH
BAKER LAB
CORNELL UNIV

ITHACA NY 14853-1301

PHONE: 607 256 3726

MICHAEL LOMBARSKI
E I DUPONT
POLYMER PRODUCT DEPT
EXP STA 269/214
WILMINGTON DE 19828

PHONE: 302 772 2420

JERRY LOMINAC
TEKNIVENT
RT 1 BOX 1043

HILLSBORO NC 27278

PHONE: 919 732 7385

P A LONGEVIALLE
ICSN CNRS

91190 SIF SUR
YVETTE
FRANCE
PHONE:

JOSEPH A LOO
BATTELLE-PACIFIC NW LABS
PO BOX 999

RICHLAND WA 99352

PHONE: 509 376 1656

JOHN LOPEZ
FINNIGAN MAT
355 RIVER OAKS PARKWAY

SAN JOSE CA 95134

PHONE: 408 433 4800

LAZARO LOPEZ
SUBURBAN LAB, INC
4140 LILT DRIVE

HILLSIDE IL 60162

PHONE: 312 544 3260

VIORICA LOPEZ-AVILA
ACUREX CORP
485 CLYDE AVE

MOUNTAIN VIEW CA 94039

PHONE: 415 961 5700

FREDERICK P LOSSING
CHEMISTRY DEPARTMENT
UNIVERSITY OF OTTAWA

OTTAWA ONTARIO K1N 6N5
CANADA
PHONE: 613 564 4039

KEVIN LOTHRIDGE
260 W ULMERTON RD

LARGO FL 34648

PHONE: 813 584 7345

HARVEY LOUCKS
HEWLETT-PACKARD
SCIENTIFIC INSTRUMENTS
1601 CALIFORNIA AVE
PALO ALTO CA 94304

PHONE: 415 857 6989

EDWARD D LOUGHRAN
LOS ALAMOS NATIONAL LAB
PO BOX 1663
MS C920
LOS ALAMOS NM 87545

PHONE: 505 667 4894

JOHN N LOURIS
CHEMISTRY DEPT
BOX 589
PURDUE UNIV
W LAFAYETTE IN 47907

PHONE: 317 494 6898

JAMES J LOVAS
PO BOX 490

REDONDO BEACH CA 90277-0490

PHONE: 213 974 4647

GMAE LOY
R F WESTON/REAC PROJECT
GSA RARITAN DEPOT
WOODBRIDGE AVE, BLDG ANNEX
EDISON NJ 08837

PHONE: 201 906 3483

ROBERT LUDICKY
MORTON THIOKOL INC
1275 LAKE AVE

WOODSTOCK IL 60098

PHONE: 815 338 1800

WILLIAM S LUM
CA STATE DEPT OF HEALTH SVCS
HAZARDOUS MATERIALS LAB
2151 BERKELEY WAY
BERKELEY CA 94704

PHONE: 415 540 3003

HELMUT LUTSEP
3M
3M CENTER, 209-1S-06

ST PAUL MN 55144

PHONE: 612 733 4022

BERT C LYNN
PO BOX 30851

RALEIGH NC 27622

PHONE: 919 781 7294

F DE MAACK
NERMAG
49 QUAI DU HALAGE
RUEIL MALMAISON
F 92500
FRANCE
PHONE:

ALLAN MACCOLL
UNIVERSITY COLLEGE
CHEMISTRY DEPT
20 GORDON ST
LONDON WC1H 0AJ
ENGLAND
PHONE:

J K MACLEOD
AUSTRALIA NAT UNIV
RES SCHOOL OF CHEM
PO BOX 4
CANBERRA ACT 2600
AUSTRALIA
PHONE:

KOGORO MAEDA
ELECTROTECHNICAL LAB
4-1-1, UMEZONO
TSUKUBA-SHI
IBARAKI 305
JAPAN
PHONE:

ANNETTE M LOVETT
VG INSTRUMENTS CANADA INC
2 SILVER AVENUE

TORONTO ONTARIO M6R 3A2
CANADA
PHONE:

YONG QUAN LU
BIOMEDICAN INSTRUMENT CENTER
ACADEMY OF MILITARY MED SCI

BEIJING
P R CHINA
PHONE:

G W LUGMAIR
UNIV OF CALIFORNIA SAN DIEGO
CODE A-012

LA JOLLA CA 92093

PHONE: 619 534 2746

HENRY E LUMPKIN
1600 DEEP WOOD DR

ROUND ROCK TX 78681

PHONE: 512 255 8386

MICHAEL LUTZ
CHEMISTRY DEPT
UNIV OF CALIFORNIA

IRVINE CA 92717

PHONE: 714 856 5682

PHILIP A LYON
3M COMPANY
CORPORATE RESEARCH
201 BW 09
ST PAUL MN 55144

PHONE: 612 736 3525

ABDUL MABUD
W R GRACE
WASHINGTON RESEARCH CENTER
7379 ROUTE 32
COLUMBIA MD 21044

PHONE: 301 531 4426

RONALD D MACFARLANE
TEXAS A&M UNIVERSITY
CHEMISTRY DEPT

COLLEGE STATION TX 77843

PHONE: 409 845 2021

ROBERT J MADDEN
EXTREL CORP

PITTSBURGH PA 15238

PHONE: 412 963 7530

C W MAGEE
EVANS EAST INC
666 PLAINSBORO RD SUITE 1236

PLAINSBORO NJ 08536

PHONE: 609 799 1904

NORMAN LOW
HEWLETT-PACKARD
1601 CALIFORNIA AVE

PALO ALTO CA 94304

PHONE: 415 857 7381

DAVID M LUBMAN
CHEMISTRY DEPT
UNIV OF MICHIGAN

ANN ARBOR MI 48109

PHONE: 313 764 1669

WILLIAM J LUKSEMBURG
CALIFORNIA ANAL LABS
2544 INDUSTRIAL BLVD

W SACRAMENTO CA 95691

PHONE: 916 372 1393

WILLIAM R LUSBY
USDA
BLDG 467 BARC-EAST

BELTSVILLE MD 20705

PHONE: 301 344 2389

PAUL LYNE
2532 VAN HISE AVENUE

MADISON WI 53705

PHONE: 608 262 1845

LESLIE T LYTLE
4305 MINUTEMAN DR

CINCINNATI OH 45245

PHONE: 606 572 2280

TABER MACCALLUM
PO BOX 689

ORACLE AZ 85623

PHONE: 602 792 2156

D B MACLEAN
MCMASTER UNIVERSITY
CHEMISTRY DEPT

HAMILTON ONTARIO L8S 4M1
CANADA
PHONE: 416 525 9140

JAMES M MADSON
MCDONNELL DOUGLAS
DEPT 223 BLDG 110
PO BOX 516
ST LOUIS MO 63166

PHONE: 314 233 2544

DONALD F MAGIN
PHILIP MORRIS R&D
BOX 26583

RICHMOND VA 23261

PHONE: 804 274 4153

PAUL MAHAFFY
CODE 615-1
GODDARD SPACE FLIGHT CTR

GREENBELT MD 20771

PHONE: 301 286 8184

NELS H MAHLE
DOW CHEMICAL CO
734 BLDG

MIDLAND MI 48667

PHONE: 517 636 9691

KENNETH O MAHLER
SGE INC
2007 KRAMER LANE
SUITE 100
AUSTIN TX 78758

PHONE: 512 837 7190

JOHN MAHONEY
PHRASOR SCIENTIFIC
1536 HIGHLAND AVE

DUARTE CA 91010

PHONE: 213 357 3201

MICHAEL S MAJEWSKI
DEPT OF ENV TOXICOLOGY
UNIV OF CALIFORNIA

DAVIS CA 95616

PHONE: 916 752 2541

HILARY MAJOR
VG ANALYTICAL
FLOATS ROAD
WYTHENSHAWE
MANCHESTER M23 9LE
UK
PHONE:

TAPAN KANTI MAJUMDAR
PURDUE UNIVERSITY
103-16 W STATE STREET

W LAFAYETTE IN 47907

PHONE: 317 494 6898

HAMDY M MAKSOUD
257 E COTTAGE ST

DORCHESTER MA 02125

PHONE: 617 282 1676

SIMIN D MALEKNIA
MASS SPEC LAB
WELCH 1-408C
UNIV OF TEXAS
AUSTIN TX 78712

PHONE: 512 471 7344

A I MALLET
INSTITUTE OF DERMATOLOGY
ST THOMAS HOSPITAL

LONDON SE17EH
ENGLAND
PHONE:

LARRY MALLIS
CHEMISTRY DEPT
UNIV OF IOWA

IOWA CITY IA 52242

PHONE: 319 335 1381

DAVID A MALTBY
DEPT PHARM CHEM
MASS SPEC FACILITY, ROOM C16A
UNIV OF CALIFORNIA
SAN FRANCISCO CA 94143

PHONE:

ORVAL MAMER
MCGILL UNIV
1130 PINE AVE WEST

MONTREAL QUEBEC H3A 1A3
CANADA
PHONE:

RUSH MANBERT
FINNIGAN MAT
355 RIVER OAKS PARKWAY

SAN JOSE CA 95134

PHONE: 408 433 4800

ASHER MANDELBAUM
TECHNION-ISRAEL INST TECHNOLOG
DEPT OF CHEMISTRY

HAIFA 32000
ISRAEL
PHONE:

MATTHIAS MANN
YALE UNIVERSITY
DEPT OF CHEM ENG
PO BOX 2159 YALE STA
NEW HAVEN CT 06520-2159

PHONE: 203 432 4379

SURAJ P MANRAO
MERCK & CO
ISOTOPES R33-50
PO BOX 2000
RAHWAY NJ 07065

PHONE: 201 574 4207

SAMUEL MANUEL
925 ALGONQUIN CT

NASHVILLE TN 37013

PHONE: 615 331 2341

J J MANURA
SCIENTIFIC INSTR SERVICES
ROUTE 179
RD 2, BOX 198
RINGOES NJ 08551-9675

PHONE: 201 788 5550

M F MAQUIN
SOCIETE ROUSSEL UCLAF
SPECTROMETRIE DE MASSE
102 ROUTE DE NOISY
93230 ROMAINVILLE
FRANCE
PHONE:

ROSS MARANO
DELSI/NERMAG
15701 W HARDY RD

HOUSTON TX 77060

PHONE: 713 847 0811

DEAN MARBURY
19 PINNACLE ROAD

DURHAM NC 27705

PHONE: 919 549 0611

ANGELA M MARCELLI
ONE GENERAL STREET
PLANT II

AKRON OH 44329

PHONE: 216 798 3375

RAYMOND E MARCH
TRENT UNIVERSITY
CHEMISTRY DEPT

PETERBOROUGH ONT K9J 7B8
CANADA
PHONE: 705 748 1361

D T MARCOVICH
AFDTL BROOKS AFB
AFDTL (#930)

BROOKS AFB TX 78223-5000

PHONE:

ALVIN B MARCUS
6 BAYARD ROAD
APT 859

PITTSBURGH PA 15213-1946

PHONE: 412 624 8406

PETER MARCUS
28 SIGALON STR
PO BOX 1221

OMER 84965
ISRAEL
PHONE:

RICHARD K MARCUS
CHEMISTRY DEPT
CLEMSON UNIVERSITY

CLEMSON SC 29634-1905

PHONE: 803 656 5011

MARCEL MARGULIES
PERKIN ELMER
761 MAIN STREET

NORWALK CT 06859

PHONE: 203 762 6650

JAY A MARK
HUNTINGTON BCH POLICE
2000 MAIN STREET

HUNTINGTON BEACH CA 92648

PHONE: 714 536 5682

LUCY MK MARK
CA SATE DEPT OF HEALTH SVCS
2151 BERKELEY WAY

BERKELEY CA 94704

PHONE: 415 540 3001

LISA M MARKS
MIT
E18-604 400 MAIN ST

CAMBRIDGE MA 02139

PHONE: 617 253 5183

TERRY D MARRIOTT
CHEMISTRY DEPT
RICE UNIVERSITY
PO BOX 1892
HOUSTON TX 77251

PHONE: 713 527 8101

ALAN G MARSHALL
CHEMISTRY DEPT
120 W 18TH AVE
OHIO STATE UNIV
COLUMBUS OH 43210

PHONE: 614 292 3446

LOUIS MARTIN
CIBA GEIGY
556 MORRIS AVENUE

SUMMIT NJ 07901

PHONE: 201 277 7143

ANDRE MARTINEAU
2485 NAPOLEON

BROSSARD QUEBEC J4Y 1Y5
CANADA
PHONE: 514 253 2832

DAVID MARTINSEN
AMERICAN CHEMICAL SOCIETY
1155 16TH STREET NW

WASHINGTON DC 20036

PHONE: 202 452 2110

ROBERT MASSE
INRS-SANTE
245 BLVD HYMNS

PTE CLAIRE QUEBEC H9R 1G6
CANADA
PHONE: 514 253 2832

MICHAEL MASSIK
BROWN-FORMAN
PO BOX 1080

LOUISVILLE KY 40201

PHONE: 502 774 7299

SHARON MATLOCK
233 NORTH THIRD AVENUE
APT A

MANVILLE NJ 08835

PHONE: 201 906 6878

SANFORD P MARKEY
NIMH NIH
BLDG 10-3D40
9000 ROCKVILLE PIKE
BETHESDA MD 20892

PHONE: 301 496 2151

K M MARNELA
TAMPERE UNIV
PO BOX 607

33101 TAMPERE 10
FINLAND
PHONE:

PHILIP G MARSH
TELEDYNE CME
843 MARIA LANE

SUNNYVALE CA 94084

PHONE:

JERRY D MARTIN
212 FRANK WEST CIRCLE

STOCKTON CA 95206

PHONE: 209 983 1340

STEPHEN A MARTIN
MIT
BLDG 56-035
77 MASSACHUSETTS AVE
CAMBRIDGE MA 02139

PHONE: 617 253 7233

RICHARD I MARTINEZ
A147 CHEMISTRY
NAT'L BUR OF STANDARDS

GAITHERSBURG MD 20899

PHONE: 301 975 2516

ROB MARUYAMA
ADOLPH COORS CO
MAIL #BC600

GOLDEN CO 80401

PHONE:

JERRY MASSETTI
PO BOX 3777

PINEDALE CA 93650

PHONE: 209 294 2982

JOHN A MASUCCI
JANSSEN RES FOUNDATION
WELSH & MCKEAN RDS

SPRINGHOUSE PA 19477

PHONE: 215 628 5539

H H MATSUDA
COLL OF GEN ED, OSAKA UNIV
1-1 MACHIKANEYAMA-CHO
TOYONAKA-SHI
OSAKA 560
JAPAN
PHONE:

JOEL P MARKS
ALLIED-SEGNAL EMRC
50 EAST ALGONQUIN RD
BOX 5016
DES PLAINES IL 60017

PHONE: 312 391 3170

ED MARQUETTE
FINNIGAN MAT
355 RIVER OAKS PARKWAY

SAN JOSE CA 95134

PHONE: 408 433 4800

DANIEL R MARSHAK
COLD SPRING HARBOR LAB
PO BOX 100

COLD SPRING HARBORNY 11724

PHONE: 506 367 8426

LEROY B MARTIN
DEPT OF CHEMISTRY
NCSU
BOX 8204
RALEIGH NC 27695

PHONE: 919 737 2942

WILLIAM B MARTIN
226 STEVENSON LANE

BALTIMORE MD 21212

PHONE: 301 955 3022

KEITH D MARTINKO
TEKNIVENT CORP
11684 LILBURN PARK RD

ST LOUIS MO 63146

PHONE: 314 559 0900

FLOYD C MASELES
CHEMISTRY DEPT
2.204A WELCH HALL
UNIVERSITY OF TEXAS
AUSTIN TX 78712

PHONE: 512 471 5484

IAN J MASSEY
SYNTEX
3401 HILLVIEW AVE

PALO ALTO CA 94304

PHONE: 415 855 6156

W RODNEY MATHEWS
THE UPJOHN CO
BIOPOLYMER CHEM 7240-25-11

KALAMAZOO MI 49001

PHONE: 616 385 7507

HIROSHI MATSUMOTO
FINNIGAN MAT
2-7-1 HIRAGAWACHO CHIYODAKU

TOKYO
JAPAN
PHONE:

ISAMU MATSUMOTO
INST HUMAN GENETICS
KANAZAWA MED UNIV
UCHINADA KAHOKU-GUN
ISHIKAWA 920-02
JAPAN
PHONE:

MASAHIRO MATSUMOTO
DEPT OF BIOCHEMISTRY
KANAZAWA MEDICAL UNIV
UCHINADA, KAHOKU-GUN
ISHIKAWA 920-02
JAPAN
PHONE:

TAKEKIYO MATSUO
INST OF PHYSICS
COLLEGE OF GENERAL EDUCATION
OSAKA UNIVERSITY
TOYONAKA 560
JAPAN
PHONE:

HAJIME MATSUSHIMA
HAMAMATSU UNIV SCH OF MEDICINE
3600 HANDA-CHO
HAMAMATSU 431-31

JAPAN
PHONE:

MICHAEL B MATTAMMAL
111 GRECC
VA MEDICAL CENTER
JEFFERSON BARRACKS
ST LOUIS MO 63125

PHONE: 314 461 0400

DWIGHT E MATTHEWS
CORNELL UNIV MED COLLEGE
DIV ENDOCRIN & METABOLISM
1300 YORK AVE ROOM A150
NEW YORK NY 10021

PHONE: 212 472 4841

MARY JANE I MATTINA
172 HUBBARD STREET

LENOX MA 01240

PHONE: 413 637 2707

JEAN E MATUSIK
FOOD & DRUG ADMN
2 LOPA COURT

GAITHERSBURG MD 20878

PHONE: 202 245 1371

KENNETH MATUSZAK
FINNIGAN MAT
355 RIVER OAKS PWY

SAN JOSE CA 95134

PHONE: 408 433 4800

CRAIG B MAULDIN
GE NEUTRON DEVICES DEPT
BRIAN DAIRY ROAD

LORGO FL 34640

PHONE: 813 541 8811

R K MAULDIN
CELANESE FIBERS
PO BOX 32414

CHARLOTTE NC 28232

PHONE: 704 554 3134

RAYMOND E MAY
7652 COOLFIELDS WAY

SACRAMENTO CA 95828

PHONE: 916 362 5332

TIM MAY
612 MAPLE DRIVE

MOUNT HOREB WI 53572

PHONE: 608 271 3333

FRANZ MAYER
UNIV OF MANITOBA
2-1670 ST MARY'S RD

WINNIPEG, MANITOBA
CANADA
PHONE: 204 476 6184

HOWARD T MAYFIELD
AIR FORCE ENG & SVC CENTER
HQ AFESC/ROVC STOP 21

TYNDALL AFB FL 32403-6001

PHONE: 904 283 4297

SUEANN MAZER
HEWLETT-PACKARD
1601 CALIFORNIA AVE

PALO ALTO CA 95014

PHONE: 415 857 6811

THOMAS MAZER
713 SUEDEN DRIVE

BEAVERCREEK OH 45430

PHONE: 513 252 2989

DAVID J MCADOO
62 LE BRUN COURT W

GALVESTON TX 77551

PHONE: 409 761 2939

L J MCBURNEY
DCIEM
PO BOX 2000

DOWNSVIEW ONT M3M 3B9
CANADA
PHONE: 416 635 2130

JERRY MCCASLIN
CHEMICAL WASTE MANAGEMENT INC
WESTERN PROCESSING LAB
20015 72ND AVE SOUTH
KENT WA 98032

PHONE: 206 395 0415

CRAIG A MCCLELLAND
M&M/MARS, INC
HIGH STREET

HACKETTSTOWN NJ 07840

PHONE: 201 852 1000

WILLIAM MCCLENNEN
BIOMATERIALS PROFILING CTR
391 S CHIPETA WAY SUITE F

SALT LAKE CTY UT 84108

PHONE: 801 581 8431

JAMES A MCCLOSKEY
UNIV OF UTAH
COLLEGE OF PHARMACY
MEDICINAL CHEM DEPT
SALT LAKE CITY UT 84112

PHONE: 801 581 5581

DOUG MCCLURE
RCM POLICE FORENSIC LAB
PO BOX 8885

OTTAWA ONTARIO K1G 3M8
CANADA
PHONE: 613 993 0645

THOMAS D MCCLURE
UNIVERSITY OF ARIZONA
PHARMACEUTICAL SCI

TUCSON AZ 85721

PHONE: 602 626 3434

GARY A MCCLUSKY
PARKE DAVIS
PO BOX 1047

ANN ARBOR MI 48106-1047

PHONE: 313 996 7525

ASHLEY L MCCORMACK
CHEMISTRY DEPARTMENT
UNIV OF VIRGINIA
MCCORMICK RD
CHARLOTTESVILLE VA 22901

PHONE: 904 924 7180

TERRENCE MCCORMICK
LINDEN-CHROMASSPEC
PO BOX 3451

PRINCETON NJ 08540

PHONE: 609 921 5439

J M MCCREA
PO BOX 172

MONROEVILLE PA 15146-0172

PHONE: 412 242 0448

D A MCCRERY
BLDG B1219
DOW CHEMICAL-TX OPERATIONS

FREEPORT TX 77541

PHONE: 409 238 3454

KENNETH E MCCULLOH
10304 ST ALBANS DR

BETHESDA MD 20814

PHONE: 301 530 1617

M A MCDOWALL
VG MASSLAB
3 TUDOR ROAD

ALTRINCHAM
ENGLAND WA14SR2
PHONE:

WILLIAM H MCFADDEN
FINNIGAN MAT
355 RIVER OAKS PKWY

SAN JOSE CA 95134

PHONE: 408 433 4800

STEVEN R MCGOWN
NIEHS
MAIL DROP 601
PO BOX 12233
RES TRI PARK NC 27709

PHONE:

KEVIN MCHUGH
REMSEN HALL
JOHNS HOPKIN UNIVERSITY
N CHARLES & 34TH STREETS
BALTIMORE MD 21218

PHONE: 301 338 4679

ROBERT T MCIVER
CHEMISTRY DEPARTMENT
UNIV OF CALIFORNIA

IRVINE CA 92717

PHONE: 714 856 6085

DAVID MCKENZIE
MONSANTO CO
800 N LINDBERGH BLVD

ST LOUIS MO 63167

PHONE: 314 694 1497

J B MCKINNON
VG ISOTOPES
32 COMMERCE CENTRE
CHERRY HILL DRIVE
DANVERS MA 01923

PHONE:

FRED W MCLAFFERTY
CHEMISTRY DEPARTMENT
CORNELL UNIVERSITY
BAKER LABORATORY
ITHACA NY 14853-1301

PHONE: 607 255 4699

ADAM MCMAHON
UNIV OF TORONTO
DEPT OF CHEMISTRY
80 ST GEORGE ST
TORONTO M551A1 ONT CANADA
CANADA
PHONE: 416 978 3571

R N MCDONALD
KANSAS STATE UNIV
CHEMISTRY DEPT
WILLARD HALL
MANHATTAN KS 66506

PHONE: 913 532 6680

STEPHEN W MCELVANY
CHEMISTRY DIV/CODE 6111
NAVAL RESEARCH LAB

WASHINGTON DC 20375

PHONE: 202 767 2398

DONALD D MCFALL
PPG INDUSTRIES
PO BOX 31

BARBERTON OH 44203

PHONE: 216 848 4161

J M MCGUIRE
ATHENS ENVIRONMENTAL
RESEARCH LABORATORY
COLLEGE STATION RD
ATHENS GA 30613

PHONE: 404 546 3185

D J MCINTOSH
UNIV OF ALASKA
INST MARINE SCIENCE

FAIRBANKS AK 99775-1080

PHONE: 907 474 6731

GORDON MCKAY
COLL OF PHARMACY
UNIV OF SASKATCHEWAN

SASKATOON SASK S7N 0W0
CANADA
PHONE: 306 966 6361

MICHAEL MCKINNEY
CA DEPT OF HEALTH SERVICES
2151 BERKELEY WAY

BERKELEY CA 94704

PHONE: 415 540 3379

W E MCKNIGHT
VG INSTRUMENTS
32 COMMERCE CENTRE
CHERRY HILL
DANVERS MA 01923

PHONE: 617 777 8034

MATTHEW A MCLEAN
UNIV OF HOUSTON
DEPT OF CHEMISTRY
4800 CALHOUN
HOUSTON TX 77004

PHONE: 713 749 2675

T B MCMAHON
DEPT OF CHEMISTRY
UNIV OF WATERLOO

WATERLOO ONT N2L 3G1
CANADA
PHONE: 519 888 4591

RICHARD A MCDONIE
UNION CARBIDE TECH CTR
BLDG 770 ROOM 123A
PO BOX 8361
S CHARLESTON WV 25303

PHONE: 304 747 4591

CHARLES N MCEWEN
DUPONT COMPANY
CENTRAL RES DEPT
EXPER STN 228
WILMINGTON DE 19898

PHONE: 302 695 2952

D L MCGILLIVRAY
UNIV OF VICTORIA
CHEMISTRY DEPT

VICTORIA BC V8W 2Y2
CANADA
PHONE: 604 721 7183

JEFFREY M MCGUIRE
HERCULES INC
RESEARCH CENTER

WILMINGTON DE 19894

PHONE: 302 995 3294

DOUG MCINTYRE
HEWLETT-PACKARD
1601 CALIFORNIA AVE
PO BOX 10161
PALO ALTO CA 94303=0871

PHONE: 415 857 6100

KEITH B MCKELLOP
BOEHRINGER INGELHEIM
RES & DEV
175 BRIAR RIDGE RD
RIDGEFIELD CT 06877

PHONE: 203 798 5176

H S MCKINNON
DEPT OF CHEM & BIOCHEMISTRY
UNIV OF GUELPH
GUELPH, ONTARIO
N1G 2W1
CANADA
PHONE: 519 824 4120

H S MCKOWN
393 EAST DRIVE

OAK RIDGE TN 37830

PHONE: 615 574 2454

SCOTT A MCLUCKEY
OAK RIDGE NATIONAL LABORATORY
BLDG 9735
PO BOX Y
OAK RIDGE TN 37831

PHONE: 615 574 2454

RICHARD A MCMILLIN
US EPA
6608 HORNWOOD DRIVE

HOUSTON TX 77074

PHONE: 713 954 6711

WALTER J MCMURRAY
YALE UNIV SCH OF MEDICINE
333 CEDAR STREET

NEW HAVEN CT 06510

PHONE: 203 785 4525

RUSSELL D MCNIECE
AQUALAB INC
2621-130 RIDGEPOINT DRIVE

AUSTIN TX 78754

PHONE: 512 928 8905

J H MCREYNOLDS
SUNY MEDICAL SCHOOL
BIOPHYSICAL SCIENCE
118 CARY HALL
BUFFALO NY 14214

PHONE: 716 831 3245

GINA M MEAGHER
COMMERCIAL TESTING
490 ORCHARD ST

GOLDEN CO 80401

PHONE: 303 278 9521

J C MEANS
LOUISIANA ST UNIVERSITY
INST FOR ENVIRONMENTAL STUDIES

BATON ROUGE LA 70803

PHONE: 504 388 8521

WILMA K MECKSTROTH
OHIO STATE UNIV
944 BRICE ROAD

REYNOLDSBURG OH 43068

PHONE: 614 366 3321

KATALIN MEDZIHRADSZKY
DEPT OF PHARM, SCHOOL OF PHARM
UNIV OF CALIFORNIA
THIRD AND PARNASSUS
SAN FRANCISCO CA 94143-0446

PHONE: 415 476 4895

JON T MEEK
AMERICAN CYANAMID
PO BOX 400

PRINCETON NJ 08540

PHONE: 609 799 0400

T K MEHRHOFF
14120 82ND AVE N

SEMINOLE FL 34646

PHONE: 813 541 8769

STANLEY MEISELMAN
NAT'L BUR OF STANDARDS
BLDG 222 ROOM A113

GAITHERSBURG MD 20899

PHONE: 301 921 2153

GERRY G MEISELS
UNIV OF NEBRASKA
1223 OLDFATHER HALL

LINCOLN NE 68588-0312

PHONE: 402/472-6262

S J MELFORD
CHEMISTRY DEPT
DEPAUL UNIVERSITY

CHICAGO IL 60614

PHONE: 312 341 8190

KAREN MELIS
EXTREL CORP
PO BOX 11512

PITTSBURGH PA 15238

PHONE: 412 963 7530

G E MELLEN
935 HUGHES DR

ST ALBANS WV 25177

PHONE: 304 727 8126

G G MELLERIO
UNIVERSITY OF PAVIA
C G S LAB MS
VIA TARAMELLI 10
27100 PAVIA
ITALY
PHONE:

DOUGLAS W MENDRALA
ETC FINDLAY
1600 CRYSTAL AVE

FINDLAY OH 45840

PHONE: 415 423 3526

CHIN-KAI MENG
YALE UNIVERSITY
9 HILLHOUSE AVE

NEW HAVEN CT 06520

PHONE: 203 432 4335

ROGER MERCER
80 ST GEORGE STREET

TORONTO ONTARIO M5S 1A1
CANADA
PHONE: 416 978 3571

MARCIA MEREDITH
6858 GOWANDA ST RD

HAMBURG NY 14075

PHONE: 716 631 0360

WILLIAM L MERLING
KRATOS ANALYTICAL INC
535 EAST CRESCENT AVE

RAMSEY NJ 07446

PHONE: 201 825 7500

GUY L MERRILL
GENERAL ELECTRIC CO
KNOLLS ATOMIC POWER LAB
PO BOX 1072
SCHENECTADY NY 12301

PHONE: 518 395 4401

FRANCOIS MESSIER
ENV QUEBEC
850 BOUL VANIER
ST VINCENT DE PAUL (LAVAL)
QUEBEC H7C 2M7
CANADA
PHONE: 514 664 1750

CLIMACO J METRAL
309 BOXFORD COURT

FREDERICK MD 21701

PHONE: 301 698 1226

H L MEUSELAAR
BIOMATERIALS PROFILING CTR
391 S CHIPETA WAY

SALT LAKE CITY UT 84108

PHONE: 801 581 8431

V D MEYER
GTE LIGHTING PRODUCTS
100 ENDICOTT ST

DANVERS MA 01923

PHONE: 617 777 1900

MICHAEL MEYERS
NICOLET INSTRUMENTS
5225-1 VERONA ROAD
PO BOX 4508
MADISON WI 53711

PHONE: 608 271 3333

SEYMOUR MEYERSON
650 N TIPPECANOE ST

GARY IN 46403

PHONE: 219 938 1933

I I MICHAEL
AFGL-PHG

HANSCOM AFB MA 01731

PHONE: 617 277 3102

DENNIS P MICHAUD
BARNETT INST
NORTHEASTERN UNIV
360 HUNTINGTON AVE
BOSTON MA 02115

PHONE: 617 437 5065

JOSEF MICHL
5404 WESTERN HILLS DRIVE

AUSTIN TX 78731-4824

PHONE: 512 471 1782

JOHN A MICHNOWICZ
HEWLETT PACKARD
1601 CALIFORNIA AVE

PALO ALTO CA 94304

PHONE: 415 857 5481

BRIAN S MIDDLEDITCH
BIOCHEMISTRY DEPT
UNIVERSITY OF HOUSTON

HOUSTON TX 77004

PHONE: 713 749 4845

FRANK MIKES
EASTERN LABS INC
3640 MAIN STREET

SPRINGFIELD MA 01107

PHONE: 413 781 2540

BRIAN J MILLARD
KRATOS
BARTON DOCK RD
URMSTON
MANCHESTER M31 2LD
ENGLAND
PHONE:

CHARLES M MILLER
MS J-514
LOS ALAMOS NATL LAB

LOS ALAMOS NM 87545

PHONE: 505 667 8415

DEBORAH MILLER
UNION CARBIDE
BLDG 770-318
PO BOX 8361
S CHARLESTON WV 25303

PHONE: 304 747 4463

LELAND V MILLER
UNIV OF COLORADO
HEALTH SCIENCE CTR C232
4200 E 9TH
DENVER CO 80262

PHONE: 303 394 8126

PAUL MILLS
FIREMAN'S FUND ENV LAB
3700 LAKEVILLE HWY

PETALUMA CA 94952

PHONE: 707 778 4160

PAUL E MILNICOFF
ARGONNE NATL LAB
9700 SOUTH CASS AVE CMT 205

ARGONNE IL 60439-4837

PHONE: 312 972 4411

JAMES MING
NASA/GODDARD SPACE CENTER
CODE 313.2
BLDG 22 ROOM 349
GREENBELT MD 20771

PHONE: 301 286 5289

DUANE L MICKELSON
THE UPJOHN CO
LOC 1140-230-2

KALAMAZOO MI 49001

PHONE: 616 323 4031

CARL H MIDGETT
US TOBACCO CO
800 HARRISON ST

NASHVILLE TN 37202

PHONE: 615 244 5270

RICHARD M MILBERG
UNIV OF ILLINOIS
SCH OF CHEM SCIENCES
505 S MATHEWS
URBANA IL 61801

PHONE: 217 333 2545

JEFFREY ROBERT MILLARD
CHEMISTRY DEPT
INDIANA UNIV

BLOOMINGTON IN 47405

PHONE: 812 335 7723

DAVID J MILLER
UNIV OF NORTH DAKOTA ERC
PO BOX 8213
UNIV STA
GRAND FORKS ND 58202

PHONE: 701 777 5107

DENNIS A MILLER
CHEMISTRY DEPT
BOISE STATE UNIVERSITY

BOISE ID 83725

PHONE: 208 385 3476

MARK MILLER
MONSANTO
260 SPRINGSIDE DR

AKRON OH 44313

PHONE: 216 668 8366

SUSAN K MILLS
KRATOS ANALYTICAL INC
535 EAST CRESCENT AVE

RAMSEY NJ 07446

PHONE: 201 825 7500

DAVID MILTON
KRATOS ANALYTICAL
BARTON DOCK ROAD
URMSTON
MANCHESTER M31 2LD
UK
PHONE:

DONALD M MINTZ
1633 S MARY AVENUE

SUNNYVALE CA 94087

PHONE: 415 493 4000

DAVID MICKUNAS
14-A CEDAR LANE

HIGHLAND PARK NJ 08904

PHONE: 201 632 9200

MICHAEL J MIILE
ENSECO/CAL LABS
2544 INDUSTRIAL BLVD

SACRAMENTO CA 95691

PHONE: 916 372 1393

WALTER F MILES
AGRICULTURE CANADA
LAB SERVICES DIV
BLDG #22 C.E.F.
OTTAWA ONTARIO K1A 0C5
CANADA
PHONE: 613 995 4907

WILLIAM G MILLEN
AMERICAN CYANAMID
PO BOX 400

PRINCETON NJ 08540

PHONE: 609 799 0400

DAVID L MILLER
EG&G IDAHO INC
PO BOX 1625

IDAHO FALLS ID 83415

PHONE: 208 526 9052

JACK M MILLER
BROCK UNIV
CHEMISTRY DEPT

ST CATHERINES ONT L2S 3A1
CANADA
PHONE: 416 688 5550

DAVID S MILLINGTON
DEPT OF PEDIATRICS
BOX 3028
DUKE UNIV MED CTR
DURHAM NC 27710

PHONE: 919 684 2036

TOM A MILNE
SERI
1617 COLE BLVD

GOLDEN CO 80401

PHONE: 303 231 1440

ROBERT D MINARD
PENN STATE UNIV
152 DAVEY LAB

UNIVERSITY PARK PA 16802

PHONE: 814 865 2202

CHESTER J MIROCHA
DEPT PLANT PATHOLOGY
UNIV OF MINNESOTA

ST PAUL MN 55108

PHONE: 612 625 8772

STEPHEN R MISSLER
TEXACO
PO BOX 425

BELLAIRE TX 77401

PHONE: 713 432 2687

LAURA A MITACEK
DU PAGE COUNTY CRIME LAB
501 NORTH COUNTY FARM ROAD

WHEATON IL 60187

PHONE: 312 682 7817

JANET MITCHELL
VG MASSLAB
3 TUDOR ROAD
ALTRINCHAM
CHESHIRE
UK
PHONE:

RONALD K MITCHUM
US EPA
PO BOX 93478

LAS VEGAS NV 89193

PHONE: 702/798-2103

KEI MIYANO
F A I HUTCHINSON HALL
ROOM 9
UNIV OF CALIFORNIA
DAVIS CA 95611

PHONE: 916 752 6272

HIROSHI MIYABAKI
NIPPON KAYAKU CO
1-2-1 MARUNOUCHI
CHIYODA-KU
TOKYO 100
JAPAN
PHONE:

SHARAREH MOADDELI
IT CORPORATION
17605 FABRICA WAY

CERRITOS CA 90701

PHONE: 714 523 9200

STEVE MOCK
MONTANA STATE UNIV
GAINES HALL

BOZEMAN MT 59717

PHONE: 416 994 5419

MEHDI MOINI
DEPT OF PHARMACOLOGY
GEORGE WASHINGTON UNIV
2300 EYE ST., N W
WASHINGTON DC 20037

PHONE: 202 994 2947

MARK TWINING MOJESKY
DEPT OF CHEMISTRY
CHEM/PHYS BLDG ROOM 4
UNIV OF KENTUCKY
LEXINGTON KY 40506

PHONE: 606 257 6957

SERBAN MOLDOVEANU
BROWN & WILLIAMSON TOBACCO CO
1500 BROWN & WILLIAMSON TOWER
PO BOX 35090
LOUISVILLE KY 40232

PHONE: 502 568 7548

MARIO J MOLINA
JET PROPULSION LAB
4900 OAK GROVE DR

PASADENA CA 91109

PHONE: 818 354 5752

J J MONIGNY
UNIV DE LIEGE
INST DE CHIMIE
SART-TILMAN
B-4000 LIEGE
BELGIUM
PHONE:

ALEXANDER A MOMMERS
CHEMISTRY DEPT
UNIV OF OTTAWA
32 GEORGE GLINSKI ST
OTTAWA ONTARIO K1N 6N5
CANADA
PHONE: 613 564 4039

JOHN J MONAGHAN
ICI C&P GROUP
PO BOX 8
THE HEATH RUNCORN
CHESHIRE WA7 4QD
UNITED KINGDOM
PHONE:

JAMES MONCUR
LOCKHEED
3251 HANOVER ST

PALO ALTO CA 94304

PHONE: 415 424 2533

DAVID MONK
KRATOS ANALYTICAL
BARTON DOCK ROAD
URMSTON
MANCHESTER M31 2LD
UK
PHONE:

KARIN MONSON-KIRKLAND
ICI AMERICAS INC
BMRD L-215
CONCORD PK & MURPHY
WILMINGTON DE 19897

PHONE: 302 575 2277

E E MONTER
EEISIGWEG 6

D5653 LEICHLINGEN
WEST GERMANY
PHONE:

FRED MONTGOMERY
DELSI INC NERMAG DIVISION
15701 WEST HARDY RD #1

HOUSTON TX 77060

PHONE: 713 847 0811

RICHARD M MONTGOMERY
243 EAST GLEN AVE

RIDGEWOOD NJ 07450-1709

PHONE: 914 357 2000

KIM M MONTI
CENTER FOR HUMAN TOXICOLOGY
38 SKAGGS HALL
UNIV OF UTAH
SALT LAKE CITY UT 84112

PHONE: 801 581 5117

CATHERINE A MOORE
DEPT OF CHEMISTRY
UNIV OF CALIFORNIA

IRVINE CA 92717

PHONE: 714 856 5682

DENISE S MOORE
R J REYNOLDS TOBACCO
BOWMAN GRAY TECH CTR
PO BOX 2959
WINSTON-SALEM NC 27102

PHONE: 919 773 4938

JOHN A MOORE
MAIL NO 020
DOW CORNING CORP

MIDLAND MI 48646-0995

PHONE: 517 496 5711

WILLIAM T MOORE
ANALYTICAL CHEM CENTER
UT MED SCHOOL
PO BOX 20708
HOUSTON TX 20708

PHONE: 713 792 5612

JOHN MOORMAN
LAB SUPPORT
940 S COAST DRIVE

COSTA MESA CA 92626

PHONE: 714 545-0208

ANGELINA MORALES
DEPT OF CHEMISTRY
UNIV OF ALBERTA

EDMONTON, ALB T6G 2G2
CANADA
PHONE: 403 432 3502

KENNETH L MORAND
BOX 624 CHEMISTRY DEPT
PURDUE UNIV

WEST LAFAYETTE IN 47907

PHONE: 317 494 6898

JOHN J MORELLI
MCDONNELL DOUGLAS RES LABS
DEPT 221 BLDG 110

ST LOUIS MO 63166

PHONE: 314 233 2540

DAVID MORISON
UNIV OF MAINE AT ORONO
473 AUBERT HALL

ORONO ME 04469

PHONE: 207 581 1187

KENT MORRILL
TENN EASTMAN CO
B150
PO BOX 1972
KINGSPORT TN 37662

PHONE: 615 229 4679

FRANK MORRIS
HOLLY OAK TERRACE
301 MAPLE AVE

WILMINGTON DE 19809

PHONE: 302 575 8410

MIKE MORRIS
DEPT OF CHEMISTRY
UMIST
SACKVILLE STREET
MANCHESTER M60 1QD
UK
PHONE:

G H MORRISON
CHEMISTRY DEPT
BAKER LABORATORY
CORNELL UNIVERSITY
ITHACA NY 14853-1301

PHONE: 607 256 3614

JAMES D MORRISON
LA TROBE UNIVERSITY
PHYSICAL CHEMISTRY
BUNDOORA
MELBOURNE VIC 3083
AUSTRALIA
PHONE:

J CHARLES MORROW
UNIV OF NORTH CAROLINA, CH
DEPT OF CHEMISTRY
VENABLE HALL 045A, CB 3290
CHAPEL HILL NC 27599

PHONE: 919 962 1217

SANDRA L MORT
POLLUTION CONTROL SYSTEMS
C R 550 S BOX 17

LA OTTO IN 46763

PHONE: 219 637 3137

THOMAS H MORTON
CHEMISTRY DEPT
UC RIVERSIDE

RIVERSIDE CA 92521

PHONE: 714 787 4735

MARTIN A MOSELEY
1613 VALLEY RUN

DURHAM NC 27707

PHONE: 919 541 5709

NEIL MOSESMAN
SUPELCO INC
SUPELCO PARK

BELLEFONTE PA 16823-0048

PHONE: 814 359 3441

PAUL D MUDGETT
DEPT OF CHEMISTRY
TEXAS A&M UNIV

COLLEGE STATION TX 77843

PHONE: 409 845 1970

MIKE MUEHLEMANN
LEYBOLD INFICON
6500 FLY RD

E SYRACUSE NY 13057

PHONE: 315 437 0377

SANDRA L MUELLER
ABBOTT LABS
D-417 AP9

ABBOTT PARK IL 60064

PHONE: 312 937 2081

THEODORE R MUELLER
OAK RIDGE NAT'L LAB
PO BOX Y

OAK RIDGE TN 37831

PHONE: 615 574 2454

HELMUT MUENSTER
INST OF ORGANIC CHEMISTRY
UNIV OF COLOGNE
GREINSTR 4
5000 COLOGNE 41
WEST GERMANY
PHONE:

M LUIS MUGA
TOFTEC INC
PO BOX 15358

GAINESVILLE FL 32604

PHONE: 904 472 2668

STEVEN L MULLEN
NIH/MSU MASS SPEC FACILITY
BIOCHEMISTRY BLDG
MICHIGAN STATE UNIVERSITY
E LANSING MI 48824

PHONE: 517 353 0612

SIGI MULLER
SPECTRONEV AG
PO BOX 4020

CA 4002 BASEL
SWITZERLAND
PHONE:

MOHAMMAD M MUMTAZ
US EPA
26 W MARTIN LUTHER KING DR

CINCINNATI OH 45268

PHONE: 513 569 7593

IN K MUN
1 APPLE COURT

NANUET NY 10954

PHONE: 212 305 1230

DAVID J MUNCH
US EPA
26 WEST ST CLAIR STREET

CINCINNATI OH 45268

PHONE: 513 569 7945

BURNABY MUNSON
CHEMISTRY DEPARTMENT
UNIVERSITY OF DELAWARE

NEWARK DE 19716

PHONE: 302 451 2340

EDMOND MURAD
AF GEOPHYSICS LAB
PHK

HANSCOM AFB MA 01731

PHONE: 617 377 3176

STANLEY MURAKAMI
SYNTEX CORP
3401 HILLVIEW AVENUE

PALO ALTO CA 94304

PHONE: 415 855 5692

SANDRA MURAWSKI
11781 ROSE LN APT D

CINCINNATI OH 45246

PHONE: 513 530 3749

CONSTANCE M MURPHY
JOHNS HOPKINS UNIV
725 N WOLFE STREET

BALTIMORE MD 21205

PHONE: 301 955 6961

ROBERT C MURPHY
PHARMACOLOGY DEPT
UNIV OF COLORADO
MEDICAL CENTER
DENVER CO 80262

PHONE: 303 394 8962

JOHN S MURRAY
8525 NE 38

KANSAS CITY MO 64161

PHONE: 816 454 0222

TERRY MURRAY
RESEARCH INST
UNIV OF DAYTON

DAYTON OH 45469

PHONE: 513 255 5125

E E MUSCHLITZ
CHEMISTRY DEPT
UNIV OF FLORIDA

GAINESVILLE FL 32611

PHONE: 904 392 9619

BRIAN D MUSSELMAN
JEOL USA INC
11 DEARBORN RD

PEABODY MA 01960

PHONE: 617 665 2170

STEVE MUSSER
DEPT MCPG
UNIV OF MARYLAND
20 N PINE STREET
BALTIMORE MD 21201

PHONE: 301 328 2982

CARL MYERHOLTZ
HEWLETT-PACKARD LABS
1651 PAGE MILL RD 28C

PALO ALTO CA 94304

PHONE: 415 857 3752

JIM MYERS
NICOLET MASS SPECTROMETRY
5225-1 VERONA ROAD
PO BOX 4508
MADISON WI 53711

PHONE: 608 271 3333

LESTER MYERS
MASON & HANGER
PO BOX 30020

AMARILLO TX 79177

PHONE: 806 381 4208

VICTORIA V MYKYTYN
27 CRESTVIEW AVENUE

PEEKSKILL NY 10566

PHONE: 914 739 9243

IAIN C MYLCHREEST
UNIVERSITY COLLEGE CARDIFF
PO BOX 78

CARDIFF CF1 1XL
UK
PHONE:

YASUHIDE NAITO
DEPT OF APPLIED PHYSICS
UNIV OF ELECTRO-COMMUNICATIONS
1-5-1 CHOFUGAOKA, CHOFU-SHI
TOKYO 182
JAPAN
PHONE:

YUZO NAKAGAWA
SHIONOGI RESEARCH LABS
FUKUSHIMA-KU

OSAKA 553
JAPAN
PHONE:

STEPHEN J NANCE
GENERAL ELECTRIC
HIGHWAY 69 SOUTH

MT VERNON IN 47620

PHONE: 812 838 7489

N N NARASIMHACHARI
MEDICAL COL VIRGINIA
PSYCHIATRY DEPT
BOX 710
RICHMOND VA 23298

PHONE: 804 786 5360

HOMER A NAVARRO
KEMRON ENVIRONMENTAL SERVICES
109 STARLITE PARK

MARIETTA OH 45750

PHONE: 614 373 4071

CHAD C NELSON
311A SKAGGS HALL
UNIV OF UTAH

SALT LAKE CITY UT 84112

PHONE: 801 581 5582

HERB NELSON
NAVAL RESEARCH LAB
CODE 6110

WASHINGTON DC 20375

PHONE: 202 767 3686

PAUL R NELSON
R J REYNOLDS TOBACCO CO
BC-TC 611-13/102E

WINSTON-SALEM NC 27102

PHONE: 914 741 4989

ROBERT J NELSON
CHEMISTRY DEPARTMENT
NORTHEASTERN UNIV
360 HUNTINGTON AVE
BOSTON MA 02115

PHONE: 617 437 5069

SIDNEY D NELSON
DEPT OF MEDICINAL CHEMISTRY
BLDG 20
UNIV OF WASHINGTON
SEATTLE WA 98195

PHONE: 206 543 1419

VINCENT P NERO
TEXACO INC
BOX 509

BEACON NY 12508

PHONE: 914 831 3400

ULRICH NEUERT
WERTHERSTR 163

4800 BIELEFELD 1
WEST GERMANY
PHONE:

DONI R NEUFELD
14802 PONT DRIVE

BRIDGETON MO 63044

PHONE: 314 434 6960

RON NEW
CHEMISTRY DEPT
UNIV OF CALIFORNIA

RIVERSIDE CA 92521

PHONE: 714 787 5287

BRUCE NEWCOME
CHARLES EVANS & ASSOC
301 CHESAPEAKE DR

REDWOOD CITY CA 94063

PHONE: 415 369 4567

PAUL NEWHOUSE
FINNIGAN MAT
355 RIVER OAKS PARKWAY

SAN JOSE CA 95134

PHONE: 408 433 4800

A S NEWTON
1665 THOUSAND OAKS

BERKELEY CA 94707

PHONE: 415 486 5040

JOHN C NEWTON
LAW LIV NAT'L LAB
L-310
PO BOX 808
LIVERMORE CA 94550

PHONE: 415 422 6892

ANDY NG
ONTARIO MIN OF ENVIRONMENT
880 BAY STREET

TORONTO, ONT M5S 1Z8
CANADA
PHONE: 416 965 1634

KENNETH T NG
CIBA-GEIGY CORP
444 SAW MILL RIVER ROAD

ARDSLEY NY 10502

PHONE: 914 478 3131

KWOKEI J NG
SCHERING CORP
60 ORANGE STREET B-6-139

BLOOMFIELD NJ 07003

PHONE: 201 429 4213

ANGIE NGO
SCIEX/DIV MDS
55 GLENCAMERON ROAD

THORNHILL, ONT L3T 1P2
CANADA
PHONE: 416 881 4646

HAI NGUYEN
ALLERGAN INC
2525 DUPONT DR

IRVINE CA 92715

PHONE: 714 955 6867

LANCE NICOLAYSEN
VG INSTRUMENTS INC
430 MALL BLVD, SUITE A

SAVANNAH GA 31406

PHONE: 912 351 0000

STUART D NIELSEN
114 SHERWOOD BLVD

LOS ALAMOS NM 87544

PHONE: 505 667 6934

A O NIER
UNIV OF MINNESOTA
PHYSICS/ASTRONOMY

MINNEAPOLIS MN 55455

PHONE: 612 624 6804

MARCIA G NISHIOKA
BATTELLE COL LABS
RM 7248
505 KING AVE
COLUMBUS OH 43201-2693

PHONE: 614 424 4964

MATTHEW W NOALL
BAYLOR COLLEGE OF MEDICINE
ONE BAYLOR PLAZA

HOUSTON TX 77030

PHONE: 713 799 4656

ED NOE
HEWLETT-PACKARD
2000 SOUTH PARK PLACE

ATLANTA GA 30339

PHONE: 404 953 1840

PETER D NORBERG
TEKNIVENT CORP
11684 LILBURN PARK ROAD

ST LOUIS MO 63146

PHONE: 314 994 0500

CURT NORWOOD
EPA ERL
SOUTH FERRY ROAD

NARRAGANSETT RI 02882

PHONE: 401 782 3060

MICHAEL O'CONNOR
VG ANALYTICAL LTD
FLOATS ROAD

MANCHESTER
ENGLAND
PHONE:

N M NIBBERING
JANSHOF 39

1391-XK ABCOUDE
NETHERLANDS
PHONE:

EWALD NIEHUIS
PHYS INST UNIV MUNSTER
DOMAGHSTR 75

4400 MUNSTER
F R GERMANY
PHONE:

HASSO B NIEMANN
NASA GODDARD SPACE
FLIGHT CTR
CODE 615
GREENBELT MD 20771

PHONE: 301 344 8706

JOHN A NIKORA
B F GOODRICH CENTER
CHEMISTRY DIVISION
PO BOX 122
AVON LAKE OH 44012

PHONE: 216 933 0288

ALBERT J NITOWSKI
63 GALPIN STREET

NAUGATUCK CT 06770

PHONE: 203 723 3495

ROY W NOBLE
MONSANTO CO
MAIL CODE U1F
800 N LINDBERGH BLVD
ST LOUIS MO 63167

PHONE: 513 694 1272

KATHLEEN NOON
ELI LILLY & CO
TL 448 T133/3

LAFAYETTE IN 47902

PHONE: 317 477 4300

JAMES D NORMAN
T107 N F D C
TENN VALLEY AUTHORITY

SHEFFIELD AL 35660

PHONE: 205 386 2390

DANIEL L NORWOOD
DUKE UNIV MEDICAL CENTER
BOX 3028

DURHAM NC 27710

PHONE: 919 684 2036

PAUL O'CONNOR
DEPT OF CHEMISTRY
MICHIGAN STATE UNIVERSITY

EAST LANSING MI 48824

PHONE: 517 353 6495

WILLIAM NICHOLS
EASTMAN KODAK
KODAK PARK B339 ATD

ROCHESTER NY 14650

PHONE: 716 722 3241

LAWRENCE NIELSEN
UNION CAMP CORP
PO BOX 3301

PRINCETON NJ 08543-3301

PHONE: 609 896 1200

SIDNEY NIEMEYER
LLNL
PO BOX 808, L-232

LIVERMORE CA 94550

PHONE: 415 422 6672

TOSHIHIDE NISHIMURA
THE UPJOHN COMPANY
122 E CANDLEWYCK #1120

KALAMAZOO MI 49001

PHONE: 616 329 3932

YOSHIO NIWA
NATL CHEM LAB FOR INDUSTRY

YATABE IBARAKE 305
JAPAN
PHONE:

TAMOTSU NODA
TOYOHASHI UNIV OF
TECHNOLOGY
TEMPAKU-CHO
TOYOHASHI 440
JAPAN
PHONE:

JIM NOONAN
OHIO STATE UNIV
1935 COFFEY ROAD

COLUMBUS OH 43210

PHONE: 614 422 4299

D J NORTHINGTON
WEST COAST ANAL SERVICE
9840 ALBURTIS AVE

SANTA FE CA 90670

PHONE: 213 948 2225

LYDIA NUWAYSIR
CHEMISTRY DEPARTMENT
UC RIVERSIDE

RIVERSIDE CA 92507

PHONE: 714 787 4740

ANNE D O'DONNELL
WASTE MANAGEMENT INC
3003 BUTTERFIELD RD

OAK BROOK IL 60521

PHONE: 312 572 1061

J T O'DONOVAN
FINNIGAN INSTRUMENTS
5340 SPECTRUM DRIVE

FREDERICK MD 21701

PHONE: 301 698 9750

JOHN R O'LEAR
PROCTER & GAMBLE
6210 CENTER HILL RD

CINCINNATI OH 45224

PHONE: 513 695 4322

IRVING A O'LEARY
THE UPJOHN CO
UNIT 7256-126-2
301 HENRIETTA
KALAMAZOO MI 49001

PHONE: 616 385 4579

REBECCA M O'MALLEY
CHEMISTRY DEPARTMENT
UNIV OF S FLORIDA

TAMPA FL 33620

PHONE: 813 935 8120

JOHN L OCCOLOWITZ
LILLY CORPORATE CENTER
DEPT MC525

INDIANAPOLIS IN 46285

PHONE: 317 276 4713

R W ODOM
301 CHESAPEAKE DRIVE

REDWOOD CITY CA 94063

PHONE: 415 369 4567

TERESA ODOM
FINNIGAN MAT
355 RIVER OAKS PKWY

SAN JOSE CA 95134

PHONE: 408 433 4800

J J OGDEN
BRIT NUCLEAR FUELS
BLDG 202 MASS SPEC
BNFL CAPENHURST
CHESTER CHIGER
UK
PHONE:

SHERRI OGDEN
CHEMISTRY DEPT
UNIV OF CALIFORNIA

BERKELEY CA 94720

PHONE: 415 642 0701

THOMAS D OGLESBY
CIBA-GEIGY
556 MORRIS AVE

SUMMIT NJ 07840

PHONE: 201 277 5913

MAMORU OHASHI
UNIV OF ELECTRO-COMMUNICATIONS
DEPT OF MATERIALS SCIENCE
CHOFUGAOKA, CHOFU
182 TOKYO
JAPAN
PHONE:

JUN OKANO
COLLEGE OF GENERAL EDUCATION
OSAKA UNIVERSITY
1-1 MACHIKANEYAMA, TOYONAKA
OSAKA 560
JAPAN
PHONE:

ANTHONY OKEEFE
DEACON RESEARCH
900 WELSH RD
STE 203
PALO ALTO CA 94304

PHONE: 415 326 1520

PENTTI OKSMAN
UNIV OF TURKU/CHEM DEPT
VESILINNANTIE 5

TURKU SF-20500
FINLAND
PHONE:

EDWARD L OLBERDING
DOW CHEMICAL CO
NORTH AMERICAN AGRIC PROD DEPT
PO BOX 1706
MIDLAND MI 48640

PHONE: 517 636 8464

RONALD G OLDHAM
3038 ORCHARD HILL

SAN ANTONIO TX 78230

PHONE: 512 494 5213

SUSAN OLESIK
DEPT OF CHEMISTRY
OHIO STATE UNIV
140 W 18TH AVE
COLUMBUS OH 43210-1173

PHONE: 614 292 0733

JOSE A OLIVARES
E I DUPONT
SAVANNAH RIVER LAB

AIKEN SC 29808

PHONE: 803 725 3420

KEITH L OLSON
GM RESEARCH
ANALYTICAL CHEMISTRY
30500 MOUND ROAD
WARREN MI 48090-9055

PHONE: 313 986 0827

BRUCE ONISKO
ICI AMERICAS
1200 S 47TH STREET

RICHMOND CA 94804

PHONE: 415 231 1058

JON D ONSTOT
MIDWEST RES CTR
425 VOLKER BLVD

KANSAS CITY MO 64110

PHONE: 816 753 7600

F I ONUSKA
CCIW-AMRS
PO BOX 5050

BURLINGTON ONT L7R 4A6
CANADA
PHONE: 416 336 4635

RICHARD OPSAL
VESTEC CORP
9299 KIRBY DRIVE

HOUSTON TX 77054

PHONE: 713 796 9677

J DOUGLAS OPTHOFF
CLAYTON ENVIRONMENTAL
CONSULTANTS
22345 ROETHEL DR
NOVI MI 48050

PHONE: 313 344 1770

NICK ORDSMITH
VG ANALYTICAL
FLOATS ROAD, WYTHENSHAW

MANCHESTER
ENGLAND
PHONE:

RON ORLANDO
DEPT OF CHEMISTRY
UNIV OF DELAWARE

NEWARK DE 19716

PHONE: 302 451 2917

CATHERINE ORLEY
IRSC
B P 8

VILLEJUIT 94800
FRANCE
PHONE:

DENNIS J ORR
FINNIGAN MAT
355 RIVER OAKS PKWY

SAN JOSE CA 95134-9990

PHONE: 408 433 4800

ROBERT G ORTH
RT 1 BOX 658A

CEDAR HILL MO 63016

PHONE: 314 694 1271

CHARLES M OSBURN
OSBURN INSTRUMENT SERVICES
THISBE RANCH
RTE 1
SPARKS NV 89431

PHONE: 702 343 1116

REBECCA OSTERMAN
11 ENGLISH VILLAGE

CRANFORD NJ 07016

PHONE:

EDWARD B OVERTON
5536 RIVERBEND BLVD

BATON ROUGE LA 70820

PHONE: 504 388 8521

FEZA OZTURK
CHEMISTRY DEPT
LEIGH HALL
UNIV OF FLORIDA
GAINESVILLE FL 32611

PHONE: 904 392 4892

F G PADRTA
ENGINEERED MATERIAL RES CTR
50 E. ALGONQUIN RD
BOX 5016
DES PLAINES IL 60017-5016

PHONE: 312 391 3175

PIERANGELA PALMA
DEPT OF CHEMISTRY
56-016
MIT
CAMBRIDGE MA 02139

PHONE: 617 253 1816

YING PAN
DEPT OF CHEMISTRY
UNIV OF DELAWARE

NEWARK DE 19711

PHONE: 302 451 1197

EDWARD K PANG
GTE PRODUCTS CORP
100 ENDICOTT STREET

DANVERS MA 01923

PHONE: 617 777 1900

D A PAPANASTASSIOU
CALTECH
MAIL CODE 170-25

PASADENA CA 91125

PHONE: 818 356 6179

J R PARE
1300 GIROUARD EST, STE 6

SAINT HYACINTHE QC J2S 2Y1
CANADA
PHONE: 514 773 6419

CAROL E PARKER
NIEHS
PO BOX 12233

RES TRI PARK NC 27709

PHONE: 919 541 5008

JI OU
XIAMEN UNIVERSITY

XIAMEN FUJIAN
PR OF CHINA
PHONE:

RAY OWEN
VG TRITECH
CREWE ROAD
WYTHENSHAWE
MANCHESTER
ENGLAND M23 9LE
PHONE:

STEVEN J PACHUTA
3M
CORPORATE RESEARCH LABS
201-28-15 3M CENTER
ST PAUL MN 55144

PHONE: 612 736 1922

RODNEY P PAGE
ARCO
388 ULTIMO AVENUE

LONG BEACH CA 90814

PHONE:

CYNTHIA A PALMER
PO BOX 242
UNIVERSITY STATION
SYRACUSE UNIV
SYRACUSE NY 13210-0242

PHONE: 315 423 1008

R J PANCIROV
10 SHADYLAWN DR

MADISON NJ 07940

PHONE: 201 235 4798

LEWIS K PANNELL
NIH
BLDG 8 ROOM B2A-23

BETHESDA MD 20892

PHONE: 301 496 4055

I A PAPAYANNOPOULOS
CHEMISTRY DEPT
RM 56-012
MIT
CAMBRIDGE MA 02139

PHONE: 617 253 7237

DAVID M PAREES
AIR PRODUCTS & CHEM
PO BOX 538

ALLENTOWN PA 18105

PHONE: 215 481 5794

VICTOR C PARR
VG TRITECH
CREWE ROAD
WYTHENSHAW
MANCHESTER
ENGLAND
PHONE:

TODD J OUTHOUSE
871 CHAPIN

BIRMINGHAM MI 48009

PHONE: 313 540 6120

JANET OXFORD
GLAXO RESEARCH LTD
BIOCHEMICAL PHARMACOLOGY
PRIORY STREET
WARE HERTFORDSHIRE
ENGLAND
PHONE:

TERRY W PACK
229 S WOODCREST ST

DURHAM NC 27703

PHONE: 919 541 6678

JOAN PALLIX
SRI INTERNATIONAL
333 RAVENSWOOD AVE

MENLO PARK CA 94025

PHONE: 415 859 4920

PETER T PALMER
CHEMISTRY DEPT
MICHIGAN STATE UNIV

EAST LANSING MI 48824

PHONE: 517 353 5215

R C PANDEY
XECHEM, INC
SUBSIDIARY OF LYPHOMED INC
10401 W TOUHY AVE
ROSEMONT IL 60018

PHONE: 312 390 1626

VINCENT M PAPA
RES RESOURCES CTR M/C 937
835 S WOOD
UNIV OF ILLINOIS AT CHGO
CHICAGO IL 60612

PHONE: 312 996 4853

E R PAQUIN
MINISTERE AGRICULTURE
2700 RUE EINSTEIN
LOCAL C2-105
SAINTE FOY QUE G1P 3W8
CANADA
PHONE: 418 651 2175

DENISE PARENT
NAVAL RESEARCH LAB
CODE 6110

WASHINGTON DC 20375

PHONE: 202 767 0719

N H PARSONS
GENERAL ELECTRIC CO
PO BOX 2908

LARGO FL 34294

PHONE: 813 541 8417

LEE G PARTRIDGE
1529 OAK

SAN FRANCISCO CA 94117

PHONE: 415 235 2633

ROSE PASSARELLA
152 DAVEY LABORATORY
BOX 83
PENN STATE UNIV
UNIV PARK PA 16802

PHONE: 814 863 3583

MICHAEL J PASTEL
LEDERLE LABORATORIES
BLDG 65 ROOM 126

PEARL RIVER NY 10965

PHONE: 914 735 5000

SIDDHARTH M PATEL
GOODYEAR TIRE & RUBBER CO
735 CLIFFSIDE DR

AKRON OH 44313

PHONE: 216 796 5158

SUBHA M PATEL
1573 WASHINGTON VALLEY RD

BRIDGEWATER NJ 08807

PHONE: 201 264 4500

ADAM PATKIN
PERKIN-ELMER
761 MAIN AVENUE

NORWALK CT 06859-0090

PHONE: 203 762 6804

C C PATRIANAKOS
CIBA-GEIGY CORP
444 SAW MILL RIVER ROAD

ARDSLEY NY 10502

PHONE: 914 478 3131

DONALD G PATTERSON
CENTER FOR DISEASE CONTROL
TOXICOLOGY BRANCH

ATLANTA GA 30333

PHONE: 404 488 4176

JOSE A PAULINO
BOX 682 CHEMISTRY DEPT
PURDUE UNIVERSITY

W LAFAYETTE IN 47907

PHONE: 317 494 7539

PAUL J PAULSEN
NBS
BLDG 221 RM A25

WASHINGTON DC 20234

PHONE: 301 921 2781

J F PAULSON
AFGL-LID

HANSCOM AFB MA 01731

PHONE: 617 377 3124

DAVID PAULY
TWIN CITY TESTING CORP
662 CROMWELL AVENUE

ST PAUL MN 55114

PHONE: 612 641 9485

RAPHE PAVLICK
WESTON INC
3360 BETTY LANE

LAFAYETTE CA 94549

PHONE: 209 957 3405

JAMES G PAVLOVICH
DEPT OF CHEMISTRY
OREGON STATE UNIV

CORVALLIS OR 97331

PHONE: 503 754 2081

ROBERT J PAWLOSKY
UNIV OF MINNESOTA
495 BORLAUG HALL
1991 BUFORD CR
ST PAUL MN 55104

PHONE: 612 625 2751

DAVID A PEAKE
PROCTER & GAMBLE
IVORYDALE TECH CTR
5299 SPRING GROVE AVE
CINCINNATI OH 45217

PHONE: 513 627 7584

PAUL G PEARSON
DEPT OF MEDICINAL CHEMISTRY
BG-20
UNIV OF WASHINGTON
SEATTLE WA 98195

PHONE: 206 543 8503

MICHAEL A PEAT
CHEMWEST ANAL LABS
600 W NORTH MARKET BLVD

SACRAMENTO CA 95834

PHONE: 916 923 0840

RANDALL E PEDDER
UNIVERSITY OF FLORIDA
BOX 431 LEIGH HALL

GAINESVILLE FL 32611

PHONE: 904 392 0515

H E PENA
215 RIO VISTA DR

ST CHARLES MO 63303

PHONE: 314 982 5404

M B PENNINGTON
6407 LONGVIEW

SHAWNEE KS 66218-9739

PHONE: 816 997 4187

DANIEL PENTEK
YALE UNIV
CHEMICAL INSTR CTR
225 PROSPECT ST
NEW HAVEN CT 06511

PHONE: 203 432 3935

ROBERT J PERCHALSKI
PHARMATEC INC
PO BOX 730

ALACHUA FL 32615

PHONE: 904 462 1210

JULIUS PEREL
PHRASOR SCIENTIFIC
1536 HIGHLAND AVE

DUARTE CA 91010

PHONE: 818 357 3201

DEBORAH D PERKINS
SCH OF CHEMISTRY
GEORGIA TECH

ATLANTA GA 30332

PHONE: 404 894 4051

PATRICK D PERKINS
HEWLETT-PACKARD
SCIENTIFIC INSTRUMENTS DIV
1601 CALIFORNIA AVE
PALO ALTO CA 94304

PHONE:

HELENE PERREAULT
DEPT OF CHEMISTRY
UNIV OF MONTREAL
CP 6128 SUCC A
MONTREAL, QUEBEC H3C 3J7
CANADA
PHONE:

RICHARD E PERRIN
MOUNTAIN ROUTE 100

JEMEZ SPRINGS NM 87025

PHONE: 501 667 4498

CORTES L PERRY
PO BOX 4325

HUNTSVILLE AL 35815

PHONE: 205 859 7328

DONALD L PERRY
8155 JEFFERSON HWY
APT 703

BATON ROUGE LA 70809

PHONE: 504 928 0232

RICHARD PERRY
MSD/ISOTOPES
P O BOX 899
POINTE CLAIRE, DORVAL
QUEBEC, H9R 4P7
CANADA
PHONE:

REINHOLD PESCH
FINNIGAN MAT
BARKHAUSEN STR 2

2800 BREMEN
W GERMANY
PHONE:

PAUL H PETERMAN
1 ROLLINGWOOD WEST DRIVE
ROUTE 5

COLUMBIA MO 65202-9542

PHONE: 314 875 5399

BRUCE A PETERSEN
ENSECO PHARM SCI LAB
2240 DABNEY RD

RICHMOND VA 23230

PHONE: 804 359 1900

HOWARD A PETERSEN
SHELL DEVELOPMENT
PO BOX 1380

HOUSTON TX 77251-1380

PHONE: 713 493 8070

DAVID W PETERSON
HEWLETT-PACKARD CO
1601 CALIFORNIA AVE

PALO ALTO CA 94304

PHONE:

GLENN S PETERSON
25 BIRCH MEADOW DR

WATERTOWN CT 06795

PHONE: 203 785 6169

R J PETERSON
FIRMENICH INC
PO BOX 5880

PRINCETON NJ 08540

PHONE: 609 452 1000

LAURIE PETERSON-WRIGHT
EG&G IDAHO INC
PO BOX 1625

IDAHO FALLS ID 83415

PHONE: 208 526 9036

ERNIE PETIT
FINNIGAN MAT INST
4450 CARVER WOODS DR

CINCINNATI OH 45242

PHONE: 513 891 2100

G A PETZINGER
9 LAMBERT STREET

WOODBRIDGE NJ 07095

PHONE: 718 965 5722

HANS PFAFF
FINNIGAN MAT
355 RIVER OAKS PARKWAY

SAN JOSE CA 95134

PHONE: 408 433 4800

THOMAS N PHAM
WESTINGHOUSE CNFD
PO DRAWER R

COLUMBIA SC 29250

PHONE: 803 776 2610

DANIEL PHELPS
AMOCO PRODUCTION CO
PO BOX 3385

TULSA OK 74102

PHONE: 918 660 3129

DENNIS R PHILLIPS
UNIVERSITY OF UTAH
311A SKAGGS HALL

SALT LAKE CITY UT 84112

PHONE: 801 581 5581

LAWRENCE R PHILLIPS
19820 COCHRANE WAY

GAITHERSBURG MD 20879-1637

PHONE: 301 496 2542

W C PHILLIPS
1108 FRANK DR

CHAMPAIGN IL 61821

PHONE:

WILLIAM H PHILLIPS
CA DEPT OF JUSTICE, TOXIC UNIT
4649 BROADWAY

SACRAMENTO CA 59820

PHONE: 916 739 5128

MARY JANE PHINNEY
PO BOX 1446

ANGLETON TX 77515

PHONE: 713 796 9677

ADRIAN PIKE
FINNIGAN MAT
2350 S GRAY DRIVE

DENVER CO 80227

PHONE: 303 988 5557

J L PINKUS
75 CLEVELAND ROAD

WELLESLEY MA 02181

PHONE: 617 720 6400

DAVE PINSON
950 PAGE MILL ROAD

PALO ALTO CA 94303

PHONE: 415 494 5125

JAMES W PINSON
AMER LABS & RESEARCH
1008 SOUTHEAST CR

HATTIESBURG MS 39402-1008

PHONE: 601 264 9320

E G PIOTROWSKI
ERRC USDA
600 E MERMAID LN

PHILADELPHIA PA 19118

PHONE: 215 233 6487

ALBERT J PIRONE
ICI AMERICAS INC
ROOM C-120 B

WILMINGTON DE 19808

PHONE: 302 575 8385

MATTHEW V PISERCHIO
3420 PLAZA DRIVE

STATE COLLEGE PA 16801

PHONE: 814 863 1333

H O PITTS
1370 CLAREMONT DR

BOULDER CO 80303

PHONE: 303 966 4106

VINCE PIZZITOLA
EXTREL CORP
PO BOX 11512AITH RD

PITTSBURGH PA 15238

PHONE: 412 963 7530

IRENE PLAKUNOV
BAUSCH & LOMB
1400 N GOODMAN ST
DEPT 70714
ROCHESTER NY 14692

PHONE: 716 338 8594

MARINA PLAT
IBM CORP
RD 52

HOPEWELL JUNCTION NY 12538

PHONE: 914 892 2615

RONALD D PLATTNER
NORTHERN REG LAB
1815 N UNIVERSITY ST

PEORIA IL 61604

PHONE: 309 685 4011

JOACHIM D PLEIL
US EPA
MD-44

RES TRIANGLE PARK NC 27711

PHONE: 919 541 4680

THOMAS R POFAHL
KRAFT INC
801 WAUKEGAN RD

GLENVIEW IL 60025

PHONE: 312 998 3619

LAWRENCE P POLLACK
15321 DELPHINIUM LANE

ROCKVILLE MD 20853

PHONE: 703 750 3000

STEVEN C POMERANTZ
DEPT MEDICINAL CHEMISTRY
311A SKAGGS HALL
UNIV OF UTAH
SALT LAKE CITY UT 84112

PHONE: 801 581 5582

MICHAEL A POQUETTE
UW HOSPITAL TOXICOLOGY LAB
600 HIGHLAND AVE

MADISON WI 53792

PHONE: 608 263 7029

THOMAS POTTER
GC/MS LABORATORY
UNIV OF MASSACHUSETTS

AMHERST MA 01003

PHONE: 413 545 3505

MARGARET A POWERS
FINNIGAN CORP
212 DAVENPORT WAY

PALO ALTO CA 94304

PHONE: 415 856 9444

BIKASH PRAMANIK
HOWARD HUGHES MEDICAL
UT HEALTH SCI CTR
5323 HARRY HINES BLVD
DALLAS TX 75235-9050

PHONE: 214 689 5017

PHILIP C PRICE
UNION CARBIDE
TECH CTR 770-120
PO BOX 8361
S CHARLESTON WV 25303

PHONE: 304 747 5594

T I PLATZNER
NRCN
PO BOX 9001

BEER SHEVA
ISRAEL
PHONE:

CHESTER E PLUCINSKI
10354 W 58TH PLACE #D

GOLDEN CO 80403

PHONE: 303 966 7593

AL POJE
MOBAY CORP
17745 S METRALE

STILWELL KS 66085

PHONE:

CHARLES W POLLEY
ARCO CHEMICAL CO
3801 W CHESTER PIKE

NEWTOWN SQUARE PA 19073

PHONE: 215 359 2440

BING T POON
WALTER REED ARMY INST
DIV OF EXP THERAPEUTICS

WASHINGTON DC 20307-5100

PHONE: 301 427 5426

RANDALL LAMARR PORCH
RADIAN CORP
PO BOX 13000

RES TRI PARK NC 27709

PHONE: 919 481 0212

LINDA POULTER
UCSF
SCHOOL OF PHARMACY S926
3RD & PARNASSUS
SAN FRANCISCO CA 94143

PHONE: 415 476 5249

ROGER E POWERS
MERCK RESEARCH LABS
W28-F1

WEST POINT PA 19486

PHONE: 215 661 7034

JOHN PRATT
KRATOS ANALYTICAL
BARTON DOCK ROAD
URMSTON
MANCHESTER M31 2LD
ENGLAND
PHONE:

DAVID PRIDDLE
UNIV OF TORONTO
CHEMISTRY DEPT

TORONTO ONTARIO M5S 1A1
CANADA
PHONE: 416 978 5088

STEPHEN PLEASANCE
UNIVERSITY COLLEGE CARDIFF
PO BOX 78

CARDIFF CF11XL
UK
PHONE:

FRED O POEPPEL
110 PARKER ROAD

SARVER PA 16055

PHONE: 412 782 3884

S M POLING
263 S CHESTER AVE

PASADENA CA 91106

PHONE: 818 796 0239

JOHN A POLTA
HENKEL RESEARCH CORP
2330 CIRCADIAN WAY

SANTA ROSA CA 95407

PHONE: 707 575 7155

JIM POPPITI
FINNIGAN MAT
5340 SPECTRUM DRIVE

FREDERICK MD 21701

PHONE: 301 698 9750

RICHARD F PORTER
CHEMISTRY DEPARTMENT
CORNELL UNIVERSITY

ITHACA NY 14853

PHONE: 607 256 3483

DAVID H POWELL
ENVIRON SCI & ENGIN
PO BOX ESE

GAINESVILLE FL 32602

PHONE: 904 332 3318

B N PRAMANIK
SCHERING CORP
60 ORANGE ST

BLOOMFIELD NJ 07003

PHONE: 201 429 3993

BILL PRICE
HEWLETT-PACKARD
PO BOX 105005

ATLANTA GA 30339

PHONE: 404 980 7412

GRANT PRILL
ALBERTA ENV CENTER
BAG 4000
VEGREVILLE, ALBERTA
CANADA TOB-4LO
CANADA
PHONE:

R B PRIME
IBM (H20/025)
5600 COTTLE ROAD

SAN JOSE CA 95193

PHONE: 408 256 6167

LASZLO PROKAI
COLL OF PHARMACY
UNIV OF FLORIDA
J H MILLER HLTH CTR, BOX J-497
GAINESVILLE FL 32610

PHONE: 904 392 3415

MICHAEL P PRZYBYLSKI
UNIV KONSTANZ
POSTFACH 5560

D-7750 KONSTANZ 1
WEST GERMANY
PHONE:

HARLAN G PULSIPHER
420 EAST 600 NORTH

BRIGHAM CITY UT 84302

PHONE: 801 863 3303

WU QI-CAN
INST OF JILIN CHEMICAL
INDUSTRY CORPORATION
JILIN CITY
JILIN
CHINA
PHONE:

DIANE QUATTLANDER
THE UPJOHN CO
7171 PORTAGE ROAD

KALAMAZOO MI 49001

PHONE: 616 323 7527

IRV RABINOWITZ
28 PETER ROAD

BREWSTER NY 10509

PHONE: 614 742 4554

ELLIOT M RACHLIN
651 EAST BIRCHFIELD LANE
APT 7U

MURREY UT 84107

PHONE: 801 581 5415

THOMAS P RADUS
BETTIS LABS 14D
PO BOX 79

W MIFFLIN PA 15122

PHONE: 412 476 5824

GREGORY S RAHN
ONEIDA RES SERVICE
ONE HALSEY ROAD

WHITESBORO NY 13492

PHONE: 315 736 3050

D G PRITCHARD
MICROBIOLOGY DEPT
UNIV OF ALABAMA

BIRMINGHAM AL 35294

PHONE: 205 934 6023

LIONEL R PROVOST
DEFENSE RES ESTAB
SUFFIELD
RALSTON
ALBERTA T0J 2N0
CANADA
PHONE:

QUAN-LONG PU
NIH
BLDG 8, RM B2A-23, NIDDK

BETHESDA MD 20892

PHONE: 301 496 4055

JAMES W PYPER
LLNL
PO BOX 808 L-310

LIVERMORE CA 94550

PHONE: 415 422 7311

SHI-JUN QIAO
GANSU PROVINCE INST OF
ENV PROTECTION

LANZHOU
CHINA
PHONE:

M A QUILLIAM
NATL RESEARCH COUNCIL CANAD
ATLANTIC RES LAB
1411 OXFORD ST
HALIFAX NOVA SCOTI B3G 3Z1
CANADA
PHONE: 902 426 9736

B A RABY
1547 ARATA COURT

SAN JOSE CA 95125

PHONE: 408 294 6718

BARBARA D RADECKI
BASF CORPORATION
1419 BIDDLE AVE

WYANDOTTE MI 48192

PHONE: 313 246 6324

FRANK M RAFFO
430 COOPER STREET
APT 2F

WOODBURY NJ 08096

PHONE: 609 853 9053

CARLOS RAJAS
FINNIGAN MAT
355 RIVER OAKS PARKWAY

SAN JOSE CA 95134

PHONE: 408 433 4800

THOMAS H PRITCHETT
US EPA
V8 EPA-ERT
GSA RARITAN DEPOT
EDISON NJ 08837

PHONE: 201 321 6738

JOHN DAVID PRYNE
PROCTER & GAMBLE
6100 CENTER HILL ROAD

CINCINNATI OH 45224

PHONE: 513 659 2543

DAVID C PUDVAH
5010 INDIAN RIVER DR #252

LAS VEGAS NV 89103

PHONE: 702 798 3141

JAN ST PYREK
BIOCHEMISTRY DEPT
RICE UNIVERSITY
PO BOX 1892
HOUSTON TX 77251

PHONE: 713 527 4865

AVELINA Y QUA
CLAIROL INC
2 BLACHLEY ROAD

STAMFORD CT 06902

PHONE: 203 357 5152

CHAD QUINN
ROHM & HAAS CO
727 NORRISTOWN ROAD

SPRINGHOUSE PA 19477

PHONE: 215 641 2090

JOHN A RACE
VG INSTRUMENTS
32 COMMERCE CENTRE
CHERRY HILL DRIVE
DANVERS MA 01923

PHONE: 617 777 8034

GIL RADOLOVICH
MIDWEST RESEARCH INST
425 VOLKER BLVD

KANSAS CITY MO 64110

PHONE: 816 753 7600

LEO RAFTOGIANIS
FINNIGAN MAT
355 RIVER OAKS PKWY

SAN JOSE CA 95134

PHONE: 408 433 4800

KENNETH RAMAGE
NCASI
PO BOX 458
720 SW 4TH STREET
CORVALLI OR 97333

PHONE: 503 752 8801

LOUIS RAMALEY
DALHOUSIE UNIVERSITY
CHEMISTRY DEPT

HALIFAX NS B3H 4J3
CANADA
PHONE: 902 424 3305

HARRI G RAMJIT
MERCK & CO, MSDRL DIVISION
28-1F SUMMNEY TOWN PIKE

WEST POINT PA 19486

PHONE: 215 661 5305

SCOTT W RAMPENTHAL
PB&J ENVIRONMENTAL LABS
6635 EAST COLONIAL DRIVE

ORLANDO FL 32807

PHONE: 407 277 4443

ROWLAND RANDALL
UNIV OF WISCONSIN
BIOCHEMISTRY DEPT
420 HENRY MALL
MADISON WI 53706

PHONE:

SCOTT RANDO
RR 1
BOX 98-31

SHOHOLA PA 18458

PHONE: 717 296 7309

TADIMETI S RAO
NEUROSCIENCE RESEARCH
BLDG J-103
CIBA-GEIGY CORP
SUMMIT NJ 07901

PHONE: 201/277/5506

UWE RAPP
AMD INTECTRA GMBH
KLEIN KOHREN 36

D-2833 BECKELN
WEST GERMANY
PHONE:

MOHAMED S RASHED
DEPT OF MEDICINAL CHEM BG-20
UNIVERSITY OF WASHINGTON

SEATTLE WA 98195

PHONE: 206 543 8503

VITTORIO RAVERDINO
HEWLETT-PACKARD
ROUTE DU MANT D'AVRIL 150

MEYRIN 1228
SWITZERLAND
PHONE:

DAVID B READER
CAMBRIDGE ISOTOPE LABS
20 COMMERCE WAY

WOBURN MA 01801

PHONE: 617 938 0067

CARL E RECHSTEINER
CHEVRON RES CORP
POB 1627 RM 41-3240

RICHMOND CA 94802

PHONE: 415 620 5095

G SUDHAKAR REDDY
SHRADER ANAL LABS
3614 VINEWOOD

DETROIT MI 48208

PHONE: 313 534 4167

DOUGLAS REED
SEARLE R&D
4901 SEARLE PKWY

SKOKIE IL 60077

PHONE: 312 982 4530

DWIGHT REED
FORENSIC SCIENCE SERVICE
PO BOX 449

SANTA ANA CA 92702

PHONE: 714 647 7481

NEIL REID
SCIEX
55 GLENCAMERON RD
THORNHILL, ONTARIO
CANADA L3T 1P2
CANADA
PHONE:

STEVE REID
CHILDREN'S HOSPITAL OF OAKLAND
747 52ND STREET

OAKLAND CA 94609

PHONE: 415 428 3619

JAMES P REILLY
DEPT OF CHEMISTRY
INDIANA UNIV

BLOOMINGTON IN 47405

PHONE: 812 335 1980

MARC H REILLY
VG INSTRUMENTS
6405 HILLCRAFT 238

HOUSTON TX 77081

PHONE:

MARK L J REIMER
DEPT OF PHARMACEUTICAL SCIENCE
UNIV OF ARIZONA

TUCOSN AZ 85721

PHONE:

LORRI G REINDERS
SCHOOL OF PHARMACY
513 PARNASSUS
UNIV OF CALIFORNIA
SAN FRANCISCO CA 94143-0446

PHONE: 415 476 5249

ERIC J REINER
50 CORDOVA AVE
APT 2003

ISLINGTON ONT M9A 4X6
CANADA
PHONE: 416 978 3571

VERNON N REINHOLD
HARVARD SCH OF PUBLIC
HEALTH
665 HUNTINGTON AVE
BOSTON MA 02115

PHONE: 617 732 0631

ROBERT W REISER
E I DUPONT
EXPERIMENTAL STATION
AG DEPT BLDG 402
WILMINGTON DE 19898

PHONE: 302 695 1434

R F REITER
4519 ORR DR

CHANTILLY VA 22021

PHONE: 703 892 6000

DON K REMLING
FINNIGAN MAT
355 RIVER OAKS PARKWAY

SAN JOSE CA 95134

PHONE: 415 484 2408

DON L REMPEL
CHEMISTRY DEPARTMENT
UNIV OF NEBRASKA

LINCOLN NE 68588-0304

PHONE: 402 472 3507

MICHAEL E RENNEKAMP
ONEIDA RESEARCH SERVICES
2756 BELLA VIA AVE

COLUMBUS OH 43229

PHONE: 614 882 8288

CAROL REUTER
SANDOZ CROP PROTECTION
975 CALIFORNIA AVE

PALO ALTO CA 94304

PHONE: 408 255 5160

J A REYNOLDS
SCIEX
55 GLEN CAMERON

THORNHILL, ONT L3T 1P2
CANADA
PHONE: 416 881 4646

JOHNNY D REYNOLDS
3932 PAPERMILL SQUARE
APT H

KNOXVILLE TN 37919

PHONE: 615 974 8679

JOE REZEK
PO BOX 92050

ELK GROVE VILLAGE IL 60009-2050

PHONE: 312 694 2700

LAWRENCE RHODES
NUTRA SWEET R&D
601 E KENSINGTON

MT PROSPECT IL 60056

PHONE: 312 566 9067

GUY RICART
UNIV OF LILLE
UER CHIMIE BAT C4
5G655 VILLENEUVE
D'ASCO CEDEX
FRANCE
PHONE:

W W RICE
121 W MAIDEN LANE

OAK RIDGE TN 37830

PHONE:

JOSEPH RICHARDS
SOMATOGENETICS INSTRUMENTS INC
350 INTERLOCKEN PARKWAY
SUITE 100
BROOMFIELD CO 80020

PHONE: 801 581 8431

CARL H RICHARDSON
VG IONEX LTD
CHARLES AVE, MALTINGS PARK
BURGESS HILL
WEST SUSSEX
UK
PHONE:

WILHELM J RICHTER
CIBA GEIGY
K 127.508

CH-4002 BASEL
SWITZERLAND
PHONE:

DOUGLAS E RICKERT
DEPT DRUG METABOLISM
GLAXO, INC
5 MOORE DR
RESEARCH TRI PARK NC 27709

PHONE: 919 941 4178

DOUGLAS P RIDGE
CHEMISTRY DEPT
UNIV OF DELAWARE

NEWARK DE 19711

PHONE: 302 368 3561

STEPHEN J RILEY
ARGONNE NATL LAB
CHEMISTRY DIVISION
9700 S CASS AVE
ARGONNE IL 60439

PHONE: 312 972 6793

TIM L RILEY
VG INSTRUMENTS
3552 GREENSIDE DR

ANN ARBOR MI 48105

PHONE: 313 996 4046

PIERO RINALDO
YALE UNIV SCH OF MED
NS-393A DEPT HUMAN GEN
333 CEDAR ST PO BOX 3333
NEW HAVEN CT 06510

PHONE: 203 785 5744

KENNETH L RINEHART
CHEM 454 ROGER ADAMS
UNIV OF ILLINOIS
1209 W CALIFORNIA ST
URBANA IL 61801

PHONE: 217 333 0627

RUSSELL D RING
BASF CORP
1419 BIDDLE AVE

WYANDOTTE MI 48192-3736

PHONE: 313 246 6325

NICHOLAS RINGO
EXTREL CORP
PO BOX 11512

PITTSBURGH PA 15238

PHONE: 412 963 7530

NELSON H RISSER
LANCASTER LABORATORIES
2425 NEW HOLLAND PIKE

LANCASTER PA 17601

PHONE: 717 656 2301

JAMES RITTER
ICI AMERICAS INC
400 FARMINGTON AVE

FARMINGTON CT 06032

PHONE: 203 674 6317

ANASTASIA RIZWANIUK
HOECHST-ROUSSEL
ROUTE 202-206 NORTH

SOMERVILLE NJ 08876

PHONE: 201 231 2652

DON J RIZZO
GENERAL FOODS CORP
555 SO BROADWAY

TARRYTOWN NY 10591

PHONE: 914 335 6807

JOHN A G ROACH
FDA
HFF-424
200 C STREET SW
WASHINGTON DC 20204

PHONE: 202 245 1371

EUGENE F ROBBINS
UNIV OF ILLINOIS
RES RESOURCES CTR M/C 937
PO BOX 6998
CHICAGO IL 60680

PHONE: 312 996 7462

RONNY C ROBBINS
2403 ROTH

EDGEWOOD MD 21040

PHONE: 671 4253

DWIGHT F ROBERTS
ENVIR SCI & ENGIN
PO BOX EGE

GAINESVILLE FL 32602

PHONE: 904 332 3318

GERALD D ROBERTS
SMITHKLINE & FRENCH LABS
PO BOX 1539

KING OF PRUSSIA PA 19406

PHONE: 215 270 6660

AL ROBERTSON
CYANAMID OF CANADA
PO BOX 240

NIAGARA FALLS, ONT L2E 6T4
CANADA
PHONE: 416 356 9000

DONALD H ROBERTSON
S.A.T.D.
MATERIALS SCIENCE BRANCH
US ARMY NATICK LABS
NATICK MA 01760-5020

PHONE: 617 651 4675

DENIS ROBILLARD
MINISTERE DE L'ENVIRONMENT
DU QUEBEC
2700 EINSTEIN
ST-FOY, QUEBEC
CANADA
PHONE: 418 643 8225

RUSSELL ROBINS
THE UPJOHN CO
7832-259-12
7000 PORTAGE RD
PORTAGE MI 49008

PHONE:

JAMES ROBINSON
VG INSTRUMENTS CANADA
2 SILVER AVE

TORONTO, ONT M6R 3A2
CANADA
PHONE:

MARGARET ROBINSON
SCHOOL OF CHEMISTRY
GA INST OF TECHNOLOGY

ATLANTA GA 30332

PHONE: 404 894 4070

JOHN ROBOZ
MT SINAI SCH OF MED
1 GUSTAVE LEVY PL

NEW YORK NY 10029

PHONE: 212 650 7382

ALAN L ROCKWOOD
3 CEDAR COURT

NEWARK DE 19702

PHONE:

ALAN ROCZKO
UNIROYAL CO
ELM STREET
BUILDING 81
NAUGATUCK CT 15260

PHONE:

ALLAN W ROCZKO
230 SPRING ST #17

NAGATUCK CT 06770

PHONE: 203 723 3858

RICHARD S RODGERS
158 S MARKET ST

EPHRATA PA 17522

PHONE: 717 656 2301

HENRY RODRIGUEZ
GENENTICH INC
460 PT SAN BRUNO

SO SAN FRANCISCO CA 94080

PHONE: 415 266 1252

COLEEN ROEHL
DEPT OF CHEMISTRY
UNIV OF CALIFORNIA

SANTA BARBARA CA 93106

PHONE: 805 961 2673

PETER ROEPSTORFF
ODENSE UNIVERSITY
DEPT OF MOLECULAR BIOLOGY
CAMPUSVEJ 55
DK 5230 ODENSE M
DENMARK
PHONE:

STEPHEN P ROGERS
1535 N HORNE ROAD
#110

MESA AZ 85203

PHONE: 602 244 3711

PETER F ROGERSON
ANALYTICAL SERVICES BRANCH
US GEOLOGICAL SURVEY
5293 WARD ROAD
ARVADA CO 80002

PHONE: 303 236 5345

DENNIS K ROHRBAUGH
ABERDEEN PROVING GROUND

APG MD 21010

PHONE: 301 671 2366

WILLIAM K ROHWEDDER
USDA
N REGIONAL RESEARCH
3900 N STABLE CT 205
PEORIA IL 61614

PHONE: 309 685 4011

ESTHER ROITMAN
CHILDREN'S HOSPITAL
747 52ND STREET

OAKLAND CA 94609

PHONE: 415 428 3619

DONALD J ROKOP
LANL
BOX 1663

LOS ALAMOS NM 87545

PHONE: 505 667 7796

HIROTAKA ROKUSHA
ELECTROTECHNICAL LAB
4-1-1, UMEZONO
TSUKUBA-SHI
IBARAKI 305
JAPAN
PHONE:

TRACY ROLD
1693 GENEVA CIRCLE

LONGMONT CO 80501

PHONE: 303 924 7437

PETER ROLLER
NIH
NCI
BLDG 37 RM 3C-28
BETHESDA MD 20892

PHONE: 301 496 1323

FRANZ W ROLLGEN
INST PHYSICAL CHEM
UNIV OF BONN
WEGELERSTR. 12
D-5300 BONN
W GERMANY
PHONE:

KEITH ROLLINS
VG INSTRUMENTS
32 COMMERCE CENTRE
CHERRY HILL DRIVE
DANVERS MA 01923

PHONE:

JOHN M ROMAN
NCI-FCRF
PROGRAM RESOURCES
PO BOX B
FREDERICK MD 21701

PHONE: 301 698 1226

MANFRED ROMKOWSKI
KOMM DER EUROPAEISCHEN
GEMEINSCHAFTEN
POSTFACH 2266
7500 KARLSRUHE
FRG
PHONE:

LUSHAN RONG
35 NOYES LABORATORY BOX 51
UNIV OF IL CHEMISTRY DEPT
505 S MATHEWS AVENUE
URBANA IL 61801

PHONE: 217 333 2545

DEBRA J ROSANO
8 JUDITH RD

PEABODY MA 01960

PHONE: 617 561 4496

ANN ROSECRANCE
JTC ENVIRONMENTAL CONSUL
4 RESEARCH PLACE

ROCKVILLE MD 20850

PHONE:

LOUIS ROSEMAN
VESTEC CORP
9299 KIRBY DRIVE

HOUSTON TX 77054

PHONE: 713 796 9677

JOSEPH D ROSEN
DEPT FOOD SCIENCE
COOK COLLEGE
RUTGERS UNIV
NEW BRUNSWICK NJ 08903

PHONE: 201 932 9667

ROBERT T ROSEN
CTR FOR ADVANCED FOOD TECH
COOK COLLEGE
RUTGERS UNIV
NEW BRUNSWICK NJ 08903

PHONE: 201 932 8306

STEPHEN ROSENBLUM
VARIAN
611 HANSEN WAY

PALO ALTO CA 94303

PHONE: 415 424 6738

MARK M ROSS
CODE 6110
NAVAL RESEARCH LAB

WASHINGTON DC 20375-5000

PHONE: 202 767 3148

COLLEEN E ROSTAD
US GEOLOGICAL SURVEY
5293 WARD RD

ARVADA CO 80002

PHONE: 303 236 3616

SUSAN ROTTSCHAEFER
1195 HART LANE

HARTSVILLE PA 18974

PHONE: 215 270 7948

MELVIN D ROZEBOOM
RANDOLPH & ASSOCIATES
8901 N INDUSTRIAL ROAD

PEORIA IL 61615

PHONE: 309 692 5252

PATRICK J RUDEWICZ
FINNIGAN MAT
355 RIVER OAKS PARKWAY

SAN JOSE CA 95134

PHONE: 408 433 4800

MORLEY E RUSSELL
CHEMISTRY DEPARTMENT
NORTHERN ILLINOIS UNIV

DEKALB IL 60115

PHONE: 815 753 6881

PHILIP W RYAN
PACIFIC ANALYTICAL
1989-B PALOMAR OAKS WAY

CARLSBAD CA 92009

PHONE: 619 931 1766

KROLIK S
VG ANALYTICAL
FLOATS RD, WYTHENSHAWE

MANCHESTER
ENGLAND
PHONE:

F E SAALFELD
5510 VENTNOR LANE

SPRINGFIELD VA 22151

PHONE: 202 696 4101

RON SADECKY
COLORADO UNIVERSITY
4142 PIEDRA CT

BOULDER CO 80301

PHONE: 303 443 5246

STEVE SAKALOW
FINNIGAN MAT
355 RIVER OAKS PARKWAY

SAN JOSE CA 95134

PHONE: 408 433 4800

MEHRAN SALEHPOUR
ARGONNE NATL LAB
200 CHM
9700 S CASS AVE
ARGONNE IL 60439

PHONE: 312 963 1973

LISE H ROVIN
RUTGERS UNIV
COOK COLLEGE
COLLEGE FARM ROAD
NEW BRUNSWICK NJ 08901

PHONE: 201 932 9686

ADELE L ROZEK
465 W DOMINION DR
UNIT 306

WOOD DALE IL 60191

PHONE: 312 390 3616

JANE RUDOLPH
RLT-02
BAXTER HEALTH CARE CORP
RTE 120 & WILSON ROAD
ROUND LAKE IL 60073

PHONE: 312 546 6211

JOHN M RUTH
PO BOX 450

COLLEGE PARK MD 20740

PHONE: 301 344 3136

ROBERT J RYBA
STANDARD OIL INDIANA
PO BOX 400

NAPERVILLE IL 60566

PHONE: 312 420 5966

F M SAAD
MICHIGAN PUB HEALTH
3500 N LOGAN ST

LANSING MI 48909

PHONE: 517 335 8076

MARK SABO
DEPT OF CHEMISTRY
MICHIGAN STATE UNIVERSITY

EAST LANSING MI 48824

PHONE: 517 353 6495

ROBERT SADLIER
KRATOS ANALYTICAL CANADA INC
12 BAL HARBOUR DRIVE

GRIMSBY, ONT L3M 4P7
CANADA
PHONE:

MICHAEL W SAKUTA
1750 BRIARWOOD RD, N E
APT AA-5

ATLANTA GA 30329

PHONE: 404 727 2583

LARRY SALLANS
PPG INDUSTRIES INC
PO BOX 31

BARBERTON OH 44203

PHONE: 216 848 4161

TIM ROY
MOBIL OIL
TOXICOLOGY DIV
PO BOX 1029
PRINCETON NJ 08540

PHONE: 609 737 5509

THOMAS P RUANE
BERLEX LABS
110 EAST HANOVER AVE

CEDAR KNOLLS NJ 07927

PHONE: 201 292 8113

JOHN W RUSSELL
BRISTOL MYERS CO
PO BOX 5100

WALLINGFORD CT 06492

PHONE: 203 284 6833

PETER RYAN
KRATOS
BARTON DOCK RD
URMSTON
MANCHESTER M31 2LD
U.K.
PHONE:

R T RYE
CONCORDIA UNIV
CHEMISTRY DEPT
1455 DE MAISONNEUVE
MONTREAL QUEBEC H3G 1M8
CANADA
PHONE: 514 848 3344

JOSEPH J SAADY
MED COLLEGE OF VA
MCV STATION BOX 597

RICHMOND VA 23298-0597

PHONE: 804 786 8165

THOMAS M SACK
MIDWEST RESEARCH INST
425 VOLKER BLVD

KANSAS CITY MO 64110

PHONE: 816 753 7600

KUNIHIKO SAITO
MEDICAL CHEMISTRY
KANSAI MEDICAL SCHOOL
FUMIZONO-CHO MORIGUCHI
OSAKA
JAPAN
PHONE:

ELAINE SALADINO
VARIAN ASSOCIATES
1801 BITTERSWEET LANE

MT PROSPECT IL 60056

PHONE: 312 698 5580

G E SALSER
17 ARTHUR PLACE

YONKERS NY 10701

PHONE: 201 894 6266

VINCENT G SALTAMACH
COLUMBIA UNIV
BOX 555 HAVEMEYER
119TH ST & BROADWAY
NEW YORK NY 10027

PHONE: 212 280 2165

MARY ELLEN K SALYAN
THE BIOMEMBRANE INST
201 ELLIOTT AVE W
SUITE 305
SEATTLE WA 98119

PHONE: 206 285 1309

PAUL C SAMSON
DESOTO INC
1700 SOUTH MOUNT PROSPECT RD

DES PLAINES IL 60017

PHONE: 312 391 9542

PHILLIP E SANDERS
EXTREL CORPORATION
PO BOX 11512

PITTSBURGH PA 15238

PHONE: 412 963 7530

ROBERT A SANDERS
PROCTER & GAMBLE CO
6071 CENTER HILL RD

CINCINNATI OH 45224

PHONE: 513 659 7865

NEIL SANDERSON
VG ELEMENTAL
ION PATH, ROAD 3

WINSFORD CW8 23T
ENGLAND
PHONE:

RONALD E SANDERSON
HEWLETT-PACKARD
1090 SPRINGBORO PIKE

DAYTON OH 45449

PHONE: 513 433 2223

GARY L SANTEE
EASTMAN KODAK
150 BELMEADE ROAD

ROCHESTER NY 14617

PHONE: 716 722 3194

G G SANZONE
CHEMISTRY DEPARTMENT
VIRGINIA POLYTECH

BLACKSBURG VA 24061

PHONE: 703 961 5391

I M SARASOHN
DUPONT
KINSTON PLANT
PO BOX 800
KINSTON NC 28501

PHONE: 919 522 6468

DR SARTHOU
CEA-CESTA
BP NO 2

33830 LE BARP
FRANCE
PHONE:

F G SATKIEWICZ
JOHNS HOPKINS UNIV
APL
JOHNS HOPKINS RD
LAUREL MD 20707

PHONE: 301 953 6247

KIYOSHI SATOUCHI
KANSAI MEDICAL SCHOOL
DEPT OF MEDICAL CHEMISTRY
MORIGUCHI
OSAKA 570
JAPAN
PHONE:

R DUANE SATZGER
USFDA
1141 CENTRAL PARKWAY

CINCINNATI OH 45202

PHONE:

JANICE R SAUCERMAN
BRISTOL-MYERS USPNG
2404 PENNSYLVANIA AVE

EVANSVILLE IN 47721

PHONE: 812 429 7914

ANDREW D SAUTER
2356 AQUA VISTA
A D SAUTER CONSULTING

HENDERSON NV 89015

PHONE: 702 454 7884

MIKE SAVA
EFFECTIVE SOLUTIONS
PO BOX 9879

MARINA DEL RA CA 90295

PHONE:

PHIL SAVICKAS
DOW CHEMICAL CO
BLDG 574

MIDLAND MI 48640

PHONE: 517 636 8728

M D SCAMUFFA
1343 CREEKFORD CIRCLE

SUGARLAND TX 77478-3968

PHONE: 713 776 6038

FRANCIS P SCANLAN
UNIV DE METZ
BP 794
57012 METZ CEDEX 1

FRANCE
PHONE:

GALE F SCANLAN
MAYO CLINIC
738 GUGGENHEIM
200 1ST STREET SW
ROCHESTER MN 55901

PHONE: 507 284 4213

MICHAEL D SCANLON
ECOLOGY & ENVIRONMENT
4285 GENESSEE ST

BUFFALO NY 14220

PHONE: 716 631 0360

G G SCHADEN
FACHBER
PHARMAZIE D UNIV

D-3550 MARBURG
WEST GERMANY
PHONE:

WILLIAM H SCHAEFER
SMITH KLINE & FRENCH LABS
PO BOX 1539 (L711)

KING OF PRUSSIA PA 19046

PHONE: 215 270 4323

RICHARD SCHAEFFER
EXTREL CORP
PO BOX 11512

PITTSBURGH PA 15238

PHONE: 412 963 7530

EGMONT SCHALLER
HOLZWEG 7

D-7803 HEUWEILER
W GERMANY
PHONE:

WILHELM SCHANZER
DEUTSCHE SPORTHOCHSCHULE KOLN
INST FUR BIOCHEMIE
CARL-DIEM-WEG 6
5000 KOLN 41
FRG
PHONE:

MARLENE E SCHAPS
EXXON PRODUCTION RESEARCH
PO BOX 2189
S169A
HOUSTON TX 77252-2189

PHONE: 713 965 7623

RICHARD H SCHEEL
MICH PUBLIC HEALTH
CEHS EPIDEMIOLOGY STUD DIV
3500 N LOGAN ST
LANSING MI 48909

PHONE: 517 335 8349

DALE A SCHEER
4581 LONG ROAD

BRIDGETON MO 63044

PHONE: 314 731 6929

THOMAS A SCHEHL
DE MAO-1
KENNEDY SPACE CENTER

CAPE KENNEDY FL 32899

PHONE: 305 867 3080

KEVIN L SCHEY
BOX 731 CHEMISTRY DEPT
PURDUE UNIVERSITY

WEST LAFAYETTE IN 47907

PHONE: 317 494 5264

ALLEN W SCHINSKY
11326 LOVELAND

LIVONIA MI 48150

PHONE: 313 344 1770

JOHN G SCHMIDT
BRISTOL-MYERS CO
2404 PENNSYLVANIA

EVANSVILLE IN 47721

PHONE: 812 429 8213

H K SCHNOES
BIOCHEMISTRY DEPT
UNIV OF WINSONSIN
420 HENRY MALL
MADISON WI 53706

PHONE: 608 262 0650

DALE A SCHOELLER
UNIV OF CHICAGO
BOX 223
5841 S MARYLAND AVE
CHICAGO IL 60637

PHONE: 312 702 6561

DONALD L SCHOOLEY
MILES INC
1127 MYRTLE ST

ELKHART IN 46515

PHONE: 219 262 7804

E M SCHREIBER
22 FAIRFIELD CT

PITTSBURGH PA 15201

PHONE: 412 624 3113

LEONARD SCHRONK
WYETH LABS
ROOM C084
PO BOX 8299
PHILADELPHIA PA 19101

PHONE: 215 341 2565

JAE C SCHWARTZ
2566 G LEXINGTON CT

LAFAYETTE IN 47905

PHONE: 317 694 5262

STEVEN M SCHEIFERS
31 GOLDEN AVENUE
APT 23B

BATTLE CREEK MI 49015

PHONE: 616 961 2096

S M SCHILDCROUT
CHEMISTRY DEPT
YOUNGSTOWN STATE UNIV

YOUNGSTOWN OH 44555

PHONE: 216 742 7114

U P SCHLUNEGGER
UNIVERSITAT BERN
INSTIT ORGAN CHEMIE
FREIESTRASSE 3
CH-3012 BERN
SWITZERLAND
PHONE:

KEN SCHMIDT
K&M ELECTRONICS
123 INTERSTATE DRIVE

WEST SPRINGFIELD MA 01089

PHONE: 413 781 1350

WILLIAM C SCHNUTE
FINNIGAN CORP
355 RIVER OAKS PKWY

SAN JOSE CA 95134

PHONE: 408 433 4800

ALAN E SCHOEN
FINNIGAN MAT
355 RIVER OAKS PARKWAY

SAN JOSE CA 95134

PHONE: 408 433 4800

DAVID M SCHRADER
CHEMISTRY DEPT
MARQUETTE UNIV

MILWAUKEE WI 53233

PHONE: 414 224 3332

ERNST SCHROEDER
FINNIGAN MAT
BARUHAUSENSTR 138

2800 BREMEN
WEST GERMANY
PHONE:

ADAM J SCHUBERT
ARCO PETROLEUM PRODUCTS
1801 SEPULVEDA

CARSON CA 90745

PHONE: 213 548 8000

MARILYN SCHWARTZ
UC SAN FRANCISCO
S OF PHARMACY, S926

SAN FRANCISCO CA 94143-0446

PHONE: 415 476 2582

STUART E SCHEPPELE
AMOCO CORPORATION
PO BOX 400

NAPERVILLE IL 60540

PHONE: 312 961 7779

J BRUCE SCHILLING
AMOCO CORP
WARRENVILLE & MILL STS

NAPERVILLE IL 60566

PHONE: 312 393 1457

ECKHART SCHMIDT
POSTFACH 2445

7400 TUEBINGEN 1
WEST GERMANY
PHONE:

R J SCHMITT
SRI INTERNATIONAL
333 RAVENWOOD AVE
PS 219
MENLO PARK CA 94025

PHONE: 415 859 5579

ROBERT J SCHOCK
7027 TR 212

FINDLEY OH 45840

PHONE: 419 424 4981

DONALD M SCHOENGOLD
3655 STORRIE CT

LAS VEGAS NV 89103

PHONE: 702 739 3142

KARL H SCHRAM
UNIV OF ARIZONA
COLLEGE OF PHARMACY

TUCSON AZ 85721

PHONE: 602 626 5630

J M SCHROEER
PHYSICS DEPARTMENT
ILLINOIS STATE UNIV

NORMAL IL 61761

PHONE: 309 438 5193

GARY A SCHULTZ
DEPT OF CHEMISTRY
MICHIGAN STATE UNIV

EAST LANSING MI 48823

PHONE: 517 353 0612

KARL E SCHWARZ
HP SCIENTIFIC INSTR
1601 CALIFORNIA AVE

PALO ALTO CA 94304

PHONE: 415 857 6056

ESTON SCHWECKE
HUNTINGTON BCH POLICE
2000 MAIN ST

HUNTINGTON BEACH CA 92648

PHONE: 714 536 5684

R G SCOTT
ARGONNE NATIONAL LAB
D-200
9700 S CASS AVE
ARGONNE IL 60439

PHONE: 312 972 3529

KIM SEGAR
UNIV OF COLORADO
CAMPUS BOX 215

BOULDER CO 80309

PHONE: 303 492 6958

LINDA SELLERS-HANN
DEPT OF CHEMISTRY
TEXAS A&M UNIVERSITY

COLLEGE STATION TX 77843

PHONE: 409 845 0613

ROBERT SERFASS
DEPT OF FOOD & NUTRITION
105 MACKAY HALL
IOWA STATE UNIV
AMES IA 50011

PHONE: 515 294 3570

KENNETH SETCHELL
CHLDN'S HOSPITAL MED CTR
CLINICAL MASS SPECTROMETRY
ELLAND & BETHESDA AVENUES
CINCINNATI OH 45229

PHONE: 513 559 4548

JEFFREY SHABANOWITZ
CHEMISTRY DEPARTMENT
UNIVERSITY OF VIRGINIA

CHARLOTTESVILLE VA 22901

PHONE: 804 924 7994

PARAG K SHAH
NYTEST ENVIRONMENTAL INC
60 SEAVIEW BLVD

PORT WASHINGTON NY 11803

PHONE: 516 625 5500

LARRY SHAMPINE
GLAXO RES LABS
VENABLE HALL 045-A
UNIV OF NC DEPT OF CHEM
CHAPEL HILL NC 27514-7660

PHONE:

A G SHARKEY
321 OLD ENGINEERING HALL
UNIV OF PITTSBURGH

PITTSBURGH PA 15260

PHONE: 412 624 8878

MICHAEL SCIACCA
BRISTOL-MYERS CO
MAP DEPT
PO BOX 4755
SYRACUSE NY 13221-4755

PHONE: 315 432 9508

JOE SEARS
CHEMISTRY DEPT
MONTANA STATE UNIV

BOZEMAN MT 59717

PHONE: 406 994 4801

WILLIAM E SEIFERT
UNIV OF TEXAS MEDICAL SCHOOL
ANALYTICAL CHEMISTRY
PO BOX 20708
HOUSTON TX 77225-0708

PHONE: 713 792 5612

ATISH D SEN
DEPT OF PHYSICS & ASTRONOMY
UNIV OF WYOMING
PO BOX 3905 UNIV STATION
LARAMIE WY 82071

PHONE: 307 766 6150

DAVID B SERGEANT
DEPT FISH & OCEANS
PO BOX 5050
867 LAKESHORE RD
BURLINGTON ONT L7R 4A6
CANADA
PHONE:

SATINDER K SETHI
GLAXCO INC
5 MOORE DRIVE

RES TRI PK NC 27709

PHONE: 919 941 4198

CEDRIC H SHACKLETON
OAKLAND CHILDREN'S HOSPITAL
747 52ND STREET

OAKLAND CA 94609

PHONE: 415 428 3604

LAMAAT M SHALABY
DUPONT EXPER STA
AGRICULTURAL DEPT
E402 3112
WILMINGTON DE 19898

PHONE: 302 772 3481

LIESA A SHANAHAN
PACE LABORATORIES
1710 DOUGLAS DRIVE NORTH

MINNEAPOLIS MN 55422

PHONE:

THOMAS R SHARP
DEPT OF CHEMISTRY
TEXAS A&M UNIVERSITY

COLLEGE STATION TX 77843

PHONE: 409 845 8404

HUBERT A SCOBLE
GENETICS INSTITUTE
87 CAMBRIDGE PARK DRIVE

CAMBRIDGE MA 02140-2387

PHONE: 617 876 1170

DON SEDGWICK
ALLIED CORP
CORPORATE TECHNOLOGY
PO BOX 1021R
MORRISTOWN NJ 07960

PHONE: 201 455 2977

MUSTAFA I SELIM
DEPT OF CHEMISTRY
MURRAY STATE UNIV

MURRAY KY 42071

PHONE: 502 762 3044

DILIP K SENSHARMA
CHEMISTRY DEPT
UCLA
405 HILGARD AVENUE
LOS ANGELES CA 90024

PHONE: 213 825 9810

DR G SEROUSSI
NERMAG
49 QUAI DU HALAGE
RUEIL MALMAISON
F 92500
FRANCE
PHONE:

ULRICH J G SEYDEL
FORSCHUNGSINSTITUT
BIOPHYSICS DIV
PASKALLEE 10
D-2061 BORSTEL
FED REP GERMANY
PHONE:

NIKHIL SHAH
SANDOZ CROP PROTECTION CORP
975 CALIFORNIA AVE

PALO ALTO CA 94304

PHONE: 415 354 3467

TOM SHALER
UC RIVERSIDE
CHEMISTRY DEPT

RIVERSIDE CA 92521

PHONE:

JIAN-DONG SHAO
DEPT OF CHEMISTRY
UNIV OF NORTH CAROLINA

CHAPEL HILL NC 27514

PHONE: 919 962 7577

BRIAN J SHAY
150-1 ARNOLD DRIVE

WEST LAFAYETTE IN 47906

PHONE: 317 799 4917

J PAUL SHEA
BRISTOL MYERS CO
PO BOX 4755

SYRACUSE NY 13221-4755

PHONE: 315 432 2098

EDWARD W SHEEHAN
EXTREL CORPORATION
PO BOX 11512

PITTSBURGH PA 15238

PHONE: 412 963 7530

DOUGLAS MARK SHEELEY
HARVARD SCHOOL PUB HEALTH
DEPT OF NUTRITION
665 HUNTINGTON AVE
BOSTON MA 02115

PHONE: 617/732/0632

MARGARET SHEIL
311 A SKAGGS HALL
UNIVERSITY OF UTAH

SALT LAKE CITY UT 84112

PHONE: 801 581 5581

TRACI SHELL
MONSANTO RESEARCH CORP
PO BOX 32

MIAMISBURG OH 45342

PHONE: 513 865 4752

MICHAEL C SHEPHERD
RADIAN CORP
PO BOX 201088
8501 MO-PAC BLVD
AUSTIN TX 78720-1088

PHONE: 512 454 4797

PETER SHEPHERD
ELSEVIER SCIENCE PUBLISHERS
PO BOX 330

AMSTERDAM 1000 AM
THE NETHERLANDS
PHONE:

DENISE A SHEPPERD
39 BITTERWOOD CIR

WOODLANDS TX 77381

PHONE: 713 292 2431

LAWSON E SHERMAN
TEXACO INC
PO BOX 509

BEACON NY 12508

PHONE: 914 831 3400

PAUL L SHERMAN
MONSANTO - U1F
800 N LINDBERGH BLVD

ST LOUIS MO 63167

PHONE: 314 694 3519

WILLIAM R SHERMAN
WASHINGTON UNIV
SCHOOL OF MEDICINE
PSYCHIATRY DEPT
ST LOUIS MO 63110

PHONE: 314 362 7013

JENTAIE SHIEA
MONTANA STATE UNIV
CHEMISTRY DEPT

BOZEMAN MT 59717

PHONE: 406 994 4801

MING SHIH
US ARMY
SGRD-UV-VA, BLDG E-3100

APG MD 21010-5425

PHONE: 301 671 2591

MING-CHUEN SHIH
NATL INST OF MENTAL HEALTH
BLDG 10, RM 3D-40
9000 ROCKVILLE PIKE
BETHESDA MD 20892

PHONE: 301 496 2151

MASAKO SHIMA
NATL SCIENCE MUSEUM
7-20 UENO-PARK, TAITO-KU

TOKYO 110
JAPAN
PHONE:

CHARLES J SHIMANSKAS
CIBA-GEIGY CORP
444 SAW MILL RIVER ROAD

ARDSLEY NY 10502

PHONE: 914 478 3131

YUKIO SHIMIZU
KOGAI-SHIGEN
KENKYUSHO
YATABE
IBARAKI 305
JAPAN
PHONE:

RONALD SHOMO
CHEMISTRY DEPT BOX 169
OHIO STATE UNIV
140 W 18TH AVENUE
COLUMBUS OH 43210

PHONE: 614 292 0480

STEPHEN SHRADER
SHRADER ANAL LAB
3814 VINEWOOD

DETROIT MI 48208

PHONE: 313 894 4440

ANIL K SHUKLA
DEPT OF CHEMISTRY
UNIV OF DELAWARE

NEWARK DE 19716

PHONE: 302 451 1118

RANDY SHUL
765 EAST MAIN ST

BRIDGEWATER NJ 0880

PHONE: 201 582 2717

BORI I SHUSHAN
SCIEX
55 GLENCAMERON RD

THORNHILL ONT L3T 1P2
CANADA
PHONE: 416 881 4646

GARY D SIDES
1732 TAHITI LANE

ALABASTER AL 35007

PHONE: 205 934 9151

MARSHALL M SIEGEL
LEDERLE LABS
AMERICAN CYANAMID
BLDG 65/ROOM 126
PEARL RIVER NY 10965

PHONE:

MELVIN W SIEGEL
ROBOTICS INSTITUTE
CARNEGIE-MELLON UNIV

PITTSBURGH PA 15213

PHONE: 412 268 8802

EMIL G SIEGMUND
US FDA
1521 W PICO BLVD

LOS ANGELES CA 91042

PHONE: 213 252 7592

JAMES SIGNORELLI
PEPSICO RESEARCH CENTER
100 STEVENS AVE

VALHALLA NY 10595

PHONE: 914 742 4633

MARY LOU SIGSBY
1008 BRAXTON CT

RALEIGH NC 27606

PHONE:

LAURENCE SILLY
JOHNS HOPKINS UNIV
725 N WOLFE ST

BALTIMORE MD 21205

PHONE: 301 955 6961

PEREIRA DA SILVA
AV SUBURBANA 2066

RIO DE JANEIRO
21050 BRAZIL
PHONE:

A H SILVER
1 OVERBROOK PLACE

HILLSDALE NJ 07642

PHONE: 201 943 7100

R W SILVERMAN
PHARMACOLOGY DEPT
UNIVERSITY OF CALIFORNIA
CTR FOR HEALTH SCI
LOS ANGELES CA 90024

PHONE: 213 825 5448

JOHN R SIMMS
PROCTER & GAMBLE CO
MIAMI VALLEY LABS
BOX 398707
CINCINNATI OH 45239-8707

PHONE: 513 245 2366

FRANCOIS Y SIMONDET
L'AIR LIQUIDE CRCD
BP 126

JOUY EN JOSAS
78350 FRANCE
PHONE:

BERND R SIMONEIT
OREGON STATE UNIV
COLL OF OCEANOGRAPHY

CORVALLIS OR 97331

PHONE: 503 754 2155

D S SIMONS
NBS
BLDG 222 RM A121

GAITHERSBURG MD 20899

PHONE: 301 975 3903

WILLIAM J SIMONSICK
DUPONT CO
PO BOX 3886

PHILADELPHIA PA 19146

PHONE: 215 339 6269

KATHLEEN E SINGLETON
BRISTOL MYERS
5 RESEARCH PARKWAY
PO BOX 5100
WALLINGFORD CT 06492-7660

PHONE:

M P SINHA
JET PROPULSION LAB
MS 11-116
4800 OAK GROVE DR
PASADENA CA 91103

PHONE:

CAROLYN A SITES
ANALYTICAL TECHNOLOGIES, INC
5550 MOREHOUSE RD

SAN DIEGO CA 92121

PHONE: 619 458 9141

CARL SITTARD
GALILEO ELECTRO-OPTICS CORP
GALILEO PARK

STURBRIDGE MA 01566

PHONE: 617 347 9191

EVERETTE SIZEMORE
RUSKA LABS
3601 DUNVALE

HOUSTON TX 77063

PHONE: 713 975 0547

RON SKINNER
FINNIGAN MAT
1355 REMINGTON RD SUITE M

SCHAUMBURG IL 60135

PHONE: 815 758 8642

ANTHONY SLAPIKAS
EXTREL CORP
2410 ALPHA DRIVE
BOX 11512
PITTSBURGH PA 15238

PHONE: 412 963 7350

CLIVE A SLAUGHTER
HOWARD HUGHES MED INST
UT SOUTHWESTERN
5323 HARRY HINES BLVD
DALLAS TX 75235

PHONE: 214 689 5051

JOHN SLAYBACK
ONEIDA RESEARCH SERVICES
ONE HALSEY ROAD

WHITESBORO NY 13492

PHONE: 315 736 3050

LAURENCE E SLIVON
BATTELLE LABS
505 KING AVE

COLUMBUS OH 43201

PHONE: 614 424 4274

JAMES SLOVINSKI
12537 W FIRST PLACE

LAKEWOOD CO 80228

PHONE: 303 236 5132

PETE SMIETANA
FINNIGAN CORP
355 RIVER OAKS PARKWAY

SAN JOSE CA 95134

PHONE: 408 433 4800

REIN SMIT
VESTEC CORP
9299 KIRBY DRIVE

HOUSTON TX 77054

PHONE: 713 796 9677

BRIAN SMITH
KRATOS ANALYTICAL INC
535 EAST CRESCENT AVE

RAMSEY NJ 07446

PHONE: 201 825 7500

CHARLES A SMITH
17669 SAN VICENTE

FNTN VALLEY CA 92708

PHONE: 714 896 5280

CHAS SMITH
VG MASSLAB
TUDOR ROAD
ALTRINCHAM
CHESHIRE WA14 5RE
ENGLAND
PHONE:

CHERYL A SMITH
MULTI TECH LABORATORIES
320 TESCONI CIRCLE UNIT R

SANTA ROSA CA 95401

PHONE: 707 544 5570

CYNTHIA SMITH
PO BOX 12194
RESEARCH TRIANGLE INST

RESEARCH TRI PARK NC 27709

PHONE: 919 541 5928

DANNE E SMITH
36 STONE RUN ROAD

BEDMINSTER NJ 07921

PHONE: 201 685 7555

DAVID E SMITH
1230 PATLEN DR

LOS ALTOS CA 94022

PHONE: 408 433 4800

DAVID H SMITH
ORNL MARTIN MARIETTA
PO BOX Y BLDG 9735

OAK RIDGE TN 37831

PHONE: 615 574 2454

DAVID LEE SMITH
MEDICINAL CHEM DEPT
PURDUE UNIV

W LAFAYETTE IN 47907

PHONE: 317 494 6094

EUGENE W SMITH
LOCKHEED-EMSCO
1050 E FLAMINGO RD

LAS VEGAS NV 89119

PHONE: 702 734 3351

GARMON BROOKS SMITH
US EPA
PO BOX 1198

ADA OK 74820

PHONE: 405 332 8800

MARK A SMITH
DEPT OF CHEMISTRY
UNIV OF ARIZONA

TUCSON AZ 85721

PHONE: 602 621 2999

R D SMITH
THE LITTLE HOUSE
BOVINGDON GREEN
BOVINGDON
HERTS HP3 OLD
ENGLAND
PHONE:

ROBERT F SMITH
ROUTE 5
BOX 136

MURPHY NC 28906

PHONE: 704/837-7086

CHARLES R SNELLING
EXXON R&D LABS
PO BOX 2226

BATON ROUGE LA 70821

PHONE: 504 359 8361

A PETER SNYDER
CHEMICAL RES DEV & ENG CTR
SMCCR-RSL

ABERDEEN PRV GRD MD 21010-5423

PHONE: 301 671 2416

JOSEPH G SOLCH
WRIGHT STATE UNIVERSITY
3640 COL GLENN HWY

DAYTON OH 45435

PHONE: 513 845 3889

MALCOLM D SOLOMON
HEWLETT-PACKARD CO
PO BOX 10161

PALO ALTO CA 94303-0871

PHONE: 415 857 7634

NANCY SOMERS
WARNER LAMBERT/PARKE DAVIS
DIVISION PDM
2800 PLYMOUTH ROAD
ANN ARBOR MI

PHONE: 313 996 5178

LUCINDA B SONNENBERG
DEPT ENV SCI & ENGINEERING
ROSENAU HALL CB# 7400
UNIV OF NORTH CAROLINA
CHAPEL HILL NC 27599-7400

PHONE: 919 966 3853

GRANT GILL SMITH
UTAH STATE UNIV
BIOCHEM & CHEM DEPT

LOGAN UT 84322-0300

PHONE:

PAUL V SMITH
FDA LAB
10 WEST 35TH STREET

CHICAGO IL 60616

PHONE: 312 886 7074

RICHARD D SMITH
BATTELLE-NW
BLDG 329 AREA 300

RICHLAND WA 99352

PHONE: 509 376 0723

RONALD G SMITH
MONSANTO AG PRODUCTS
700 CHESTERFLD VILLAGE PKWY

ST. LOUIS MO 63198

PHONE: 314 537 6236

L T SNIEGOSKI
NAT'L BUREAU OF STANDARDS
BLDG 222 RM A361

GAITHERSBURG MD 20899

PHONE: 301 975 3133

JOHN D SNYDER
700 HAWLEY ROAD

MASON MI 48854

PHONE:

BRUCE H SOLKA
7813 W ROSEDALE

CHICAGO IL 60631

PHONE: 312 567 5290

RICHARD T SOLSTEN
MONSANTO CO AA1F
LIFE SCIENCES RES CTR
700 CHESTERFIELD VILL PARK
CHESTERFIELD MO 63198

PHONE: 314 537 6272

PETER F SOMSSICH
36 RAVINE ROAD

AMHERST NH 03031

PHONE: 617 750 2282

JUDY SOPHIANOPOULOS
2994 MCCULLY DR, NE

ATLANTA GA 30345

PHONE: 404 347 7603

JAMES S SMITH
TRILLIUM INC
7A GRACE'S DRIVE

COATESVILLE PA 19320

PHONE: 215 383 6006

PHILIP C SMITH
BLDG 10, ROOM 6C208
NATIONAL INST FOR CHILD HEALTH
NIH
BETHESDA MD 20892

PHONE: 301 496 5531

RICHARD W SMITH
CHEMISTRY DEPT
MCMASTER UNIV
1280 MAIN STREET W
HAMILTON ONTARIO L8S 4M1
CANADA
PHONE: 416 525 9140

T T SMITH
FINNIGAN
355 RIVER OAKS PARKWAY

SAN JOSE CA 95134-1991

PHONE: 408 433 4800

JOSEPH T SNODGRASS
DEPT OF CHEMISTRY
UNIV OF CALIFORNIA

SANTA BARBARA CA 93106

PHONE: 805 961 2673

STEPHEN A SOKOLOW
1901 VALPARAISO

MENLO PARK CA 94025

PHONE: 415 324 2222

JEROME J SOLOMON
NEW YORK UNIV MED CTR
ENVIRONMENTAL MEDICINE
LONG MEADOW ROAD
TUXEDO PARK NY 10987

PHONE: 914 351 4398

B D SOLTMANN
1909 BRIDGEPORT DR

RALEIGH NC 27609

PHONE: 919 847 0744

BAN-HUAT SONG
6810 NEWLIGHT COURT

FT WASHINGTON MD 20744-1036

PHONE: 301 249 4000

G W SOVOCOOL
3155 HIGHVIEW DR

HENDERSON NV 89014

PHONE: 702 798 2212

GLENN E SPANGLER
BENDIX ESD
1400 TAYLOR AVE
PO BOX 9840
BALTIMORE MD 21284-9840

PHONE: 301 321 5261

JAMES SPEAKMAN
VG MASSLAB LTD
3 TUDOR ROAD
ALTRINCHAM
CHESHIRE
ENGLAND
PHONE:

DAVID N SPEIS
ETC CORP
6 CHAMBERLAIN RD

FLEMINGTON NJ 08822

PHONE: 201 225 6759

ROBERT B SPENCER
NICOLET MASS SPECTROMETRY
5225-1 VERONA ROAD
PO BOX 4508
MADISON WI 53711-0508

PHONE: 608 271 3333

JAMES A SPHON
FDA
HFF-426
200 C STREET SW
WASHINGTON DC 20204

PHONE: 202 472 9144

DAVID E SPLICHAL
US ARMY CORPS OF ENG
MRDL
420 SOUTH 18TH STREET
OMAHA NE 68102

PHONE: 402 221 3871

RUSSELL C SPREEN
ICI PHARMACEUTICALS GROUP
RT 202 & MURPHY ROAD

WILMINGTON DE 19897

PHONE: 302 575 3999

G DOUGLAS SPROLES
MERRELL DOW RES INST
9550 ZIONSVILLE RD

INDIANAPOLIS IN 46268

PHONE: 317 873 7149

ROBERT R SQUIRES
CHEMISTRY DEPT
PURDUE UNIVERSITY

W LAFAYETTE IN 47907

PHONE: 317 494 7322

CATHERINE STACEY
WATERS CHROMATOGRAPHY
DIV MILLIPORE
MAPLE STREET
MILFORD MA 01757

PHONE: 617 478 2000

BEN STACKLER
1400 SHATTUCK AVE #7

BERKELEY CA 94709

PHONE: 415 527 9389

JIMMY STACY
HEWLETT-PACKARD
PO BOX 1449

KENNER LA 70063

PHONE: 504 467 4100

ALLAN E STAFFORD
800 BUCHANNAN ST

ALBANY CA 94710

PHONE: 415 486 3657

CHARLES J STAFFORD
PATUXENT WILDLIFE RES CENTER

LAUREL MD 20708

PHONE: 301 498 0287

GEORGE STAFFORD
FINNIGAN MAT
355 RIVER OAKS PKWY

SAN JOSE CA 95134

PHONE: 408 433 4800

C G STANDARD
STERLING CO
PO BOX 1311

TEXAS CITY TX 77592

PHONE: 409 942 3519

KENNETH STANDING
UNIV OF MANITOBA
PHYSICS DEPT

WINNIPEG MANITOBA R3T 2N2
CANADA
PHONE: 204 474 9358

LAUREL J STANDLEY
GEOLOGY 541
INDIANA UNIVERSITY

BLOOMINGTON IN 47405

PHONE: 812/335/6246

MICHELE S STANLEY
CHEMISTRY DEPT
INDIANA UNIV

BLOOMINGTON IN 47405

PHONE: 812 335 3436

DOUGLAS B STAUFFER
2189 ELMIRA RD
PALISADE CORP

NEWFIELD NY 14867

PHONE: 607 564 9993

JAMES L STAUFFER
UNIV OF UTAH
311 A SKAGGS HALL

SALT LAKE CITY UT 84112

PHONE: 801 581 7532

W L STEBBINGS
3M COMPANY
201-BS-05
PO BOX 33221
ST PAUL MN 55144

PHONE: 612 733 4891

JOHN D STEIN
GENERAL ELECTRIC
1334 KATHY CT

LIVERMORE CA 94550

PHONE: 415 862 4317

URS STEINER
FINNIGAN CORP
355 RIVER OAKS PKWY

SAN JOSE CA 95134

PHONE: 408 433 4800

ELIZABETH A STEMMLER
DEPT OF CHEMISTRY
BOWDOIN COLLEGE

BRUNSWICK ME 04011

PHONE:

DANNY O STENE
4200 EAST 9TH
UNIV OF CO HEAL SCI CTR
SCH OF MED BOX 236
DENVER CO 80226

PHONE: 303 270 8961

JAMES L STEPHENSON
13121B SHADYSIDE LN

GERMANTOWN MD 20874

PHONE: 301 698 9750

RICHARD STEPNOWSKI
CHEMISTRY DEPT
MICHIGAN STATE UNIV

EAST LANSING MI 48824

PHONE: 517 353 6495

FRED A STEVIE
AT&T BELL LABS
ROOM 2C-070
555 UNION BLVD
ALLENTOWN PA 18103

PHONE: 215 439 7169

D W STEWART
675 BEACH AVE

ROCHESTER NY 14612

PHONE:

DWIGHT D STIFF
5700 BUNKER HILL STREET
NO 804

PITTSBURGH PA 15206

PHONE: 412 362 2194

R N STILLWELL
10 DANIELS DRIVE

BEDFORD MA 01730

PHONE: 617 275 2964

W SARA STILLWELL
MIT
APPLIED BIOLOGICAL SCIENCE

CAMBRIDGE MA 02139

PHONE: 617 253 3118

B P STIMPSON
AERE HARWELL
INSTR & APPLIED
PHYSICS DIV BD148
OXFORDSHIRE OX11 0
ENGLAND
PHONE:

STEVE STODOLA
20 RIVER STREET

ARLINGTON MA 02714

PHONE: 617 646 6681

JAMES J STOFFELS
BATTELLE-NW
BLDG 320 AREA 300
PO BOX 999
RICHLAND WA 99352

PHONE: 509 376 2142

J A STONE
QUEEN'S UNIVERSITY
CHEMISTRY DEPT

KINGSTON ONTARIO K7L 3N6
CANADA
PHONE: 613 525 2615

HOWARD A STORMS
GENERAL ELECTRIC CO
M/C V08
PO BOX 460
PLEASANTON CA 94566

PHONE: 415 862 4527

MICHAEL STORY
FINNIGAN MAT
355 RIVER OAKS PWY

SAN JOSE CA 95134

PHONE: 408 433 4800

STEVEN J STOUT
AMERICAN CYANIMID
AGRICULTURAL DIV
PO BOX 400
PRINCETON NJ 08540

PHONE: 609 799 0400

JOHN W STRAND
7715 FLANDERS DRIVE
PO BOX 261212

SAN DIEGO CA 92126

PHONE: 213 699 8188

DARYL P STRANDBERGH
8924 PERRIN

LIVONIA MI 48150

PHONE: 313 344 1770

DAVID D STRANZ
HEWLETT-PACKARD
1601 CALIFORNIA AVENUE

PALO ALTO CA 94304

PHONE: 415 857 4657

SCOTT D STRATTON
CURTIS & TOMPKINS LTD
1250 S BOYLE AVE

LOS ANGELES CA 90023

PHONE: 213 269 7421

KENNETH M STRAUB
SYNTEX RESEARCH R6002
3401 HILLVIEW AVE

PALO ALTO CA 94303

PHONE: 415 855 5067

PHILIP STRAUS
HEWLETT-PACKARD
W120 W CENTURY DRIVE

PARAMUS NJ 07652

PHONE: 201 599 5351

ROBERT J STRIFE
MIAMI VALLEY LABS
PROCTER & GAMBLE
PO BOX 39175
CINCINNATI OH 45247

PHONE: 513 245 2655

KELLY STRINGHAM
DEPT OF BIOCHEMISTRY
PURDUE UNIVERSITY

WEST LAFAYETTE IN 47907

PHONE: 317 494 1569

FREDERICK STROBEL
UNIVERSITY OF DELAWARE
DEPARTMENT OF CHEMISTRY

NEWARK DE 19716

PHONE: 302 451 1197

JUSTIN STROH
PFIZER INC

GROTON CT 06340

PHONE: 203 441 4024

J M STRONG
NIH

BETHESDA MD 20906

PHONE: 301 942 4058

SUSAN E STRONG
HEWLETT PACKARD
1601 CALIFORNIA AVE

PALO ALTO CA 94304

PHONE: 415 857 7890

DENNIS L STROTHER
ENV RES INST
UNIV OF CONNECTICUT
190 AUDITORIUM DR
STORRS CT 06268

PHONE: 203 486 5482

JOHN T STULTS
GENENTECH INC
460 POINT SAN BRUNO BLVD

SO SAN FRANCISCO CA 94080

PHONE: 415 266 1203

CATHERINE M STUPAK
VACUMETRICS INC
2261 PALMA DRIVE

VENTURA CA 93003-5789

PHONE: 805 644 7461

G P STURM
NAT'L INST FOR PETRO
AND ENERGY RES
PO BOX 2128
BARTLESVILLE OK 74005

PHONE: 918 337 4314

DEBRA STUTTS
DOW CHEMICAL CO
1803 BLDG, H&ES

MIDLAND MI 48674

PHONE: 517 636 1669

DAVID L STYRIS
205 CRAIGHILL

RICHLAND WA 99352

PHONE: 509 943 9224

T C K SU
SMU
CHEMISTRY DEPT

N DARTMOUTH MA 02747

PHONE: 617 999 8235

BABU SUBRAMANYAM
20 N PINE ST
SCH OF PHARM DEPT OF MED CH
UNIV OF MARYLAND, BALTIMORE
BALTIMORE MD 21201

PHONE: 301 328 2982

CLINT SULFRIDGE
158 WADDELL CIRCLE

OAK RIDGE TN 37830

PHONE: 615 574 2437

JANE SUN
HEWLETT-PACKARD
1601 CALIFORNIA AVE
PO BOX 10161
PALO ALTO CA 94303-0871

PHONE: 415 857 6100

SHUO-LIAN SUN
ANALYTICAL CENTER
CHEMICAL ENGINEERING COLLEGE
DALIAN INST OF TECHNOLOGY
DALIAN
PR OF CHINA
PHONE:

MATTHEW SURICO
PEDNEAULT ASSOCIATES
PO BOX 205

BOHEMIA NY 11716

PHONE: 516 467 8477

CHRIS SUTTON
RUSKA LABS INC
PO BOX 630009

HOUSTON TX 77263-0009

PHONE: 713 975 0547

ROBERT K SUZUKI
SANDOZ PHARMACEUTICALS
RTE 10 404/3

EAST HANOVER NJ 07936

PHONE: 201 503 8520

ROBERT SWAIM
FINNIGAN MAT
PO BOX 5997

KINGWOOD TX 77325

PHONE: 713 360 2740

CHARLES C SWEELEY
MICHIGAN STATE UNIV
BIOCHEMISTRY DEPT

EAST LANSING MI 48824

PHONE: 517 353 3257

JOHN SYKA
FINNIGAN MAT
355 RIVER OAKS PKWY

SAN JOSE CA 95134

PHONE: 408 433 4800

JAN E SZULEJKO
DEPT OF CHEMISTRY
UNIV OF WATERLOO

WATERLOO ONT N2L 3G1
CANADA
PHONE: 519 885 1211

RICHARD E SULLIVAN
26461 MONTECITO LANE

MISSION VIEJO CA 92691-1520

PHONE: 213 933 5991

TUNG SUN
USDA-FSIS
PO BOX 6085

ATHENS GA 30604

PHONE: 404 546 3571

JAN SUNNER
CHEMISTRY DEPARTMENT
MONTANA STATE UNIVERSITY

BOZEMAN MT 59717

PHONE: 406 994 5413

MARC SUTER
INST OF ORGANIC CHEMISTRY
UNIV OF BERNE
FREIESTRASSE 3
3012 BERNE
SWITZERLAND
PHONE:

SOMCHAI SUWANRUMPHA
DEPT OF CHEMISTRY
UNIV OF HOUSTON
UNIVERSITY PARK
HOUSTON TX 77004

PHONE: 713 743 2675

H J SVEC
IOWA STATE UNIV
CHEMISTRY DEPT

AMES IA 50011

PHONE: 515 294 6486

ADRIAN SWANSON
3315 BENJAMIN STREET NE

MINNEAPOLIS MN 55418

PHONE: 612 786 6020

BRIAN J SWEETMAN
VANDERBILT UNIV
PHARMACOLOGY DEPT

NASHVILLE TN 37232

PHONE: 615 322 2094

I I SZABO
UNIVERSITY OF LUND
CHEMICAL CENTER
PO BOX 124
S-22100 LUND
SWEDEN
PHONE:

RAFFAELE TABACCHI
UNIV DE NEUCHATEL
INST DE CHIMIE
AV DE BELLEVAUX 51
CH-2000 NEUCHATEL
SWITZERLAND
PHONE:

RICHARD L SUMMERS
E I DUPONT DE NEMOURS
BOX 347

LA PORTE TX 77571

PHONE: 713 470 3464

YIPING SUN
DEPT MEDICINAL CHEMISTRY
SCH OF PHARMACY
PURDUE UNIV
W LAFAYETTE IN 47907

PHONE: 317 494 1449

PRAKASH SURANA
GENERAL ELECTRIC CO
HWY 69 SOUTH

MT VERNON IN 47620

PHONE: 812 838 7265

TOM SUTLIFF
RLT-02
BAXTER HEALTH CARE CORP
RTE 120 & WILSON ROAD
ROUND LAKE IL 60073

PHONE: 312 546 6311

MAKOTO SUZUKI
MEIJO UNIVERSITY
PHARMACY FACULTY
TEMPAKU
NAGOYA 468
JAPAN
PHONE:

DEBORAH L SWACKHAMER
ENVIRONMENTAL HEALTH
MAYO BLDG BOX 197 U OF MINN
420 DELAWARE STREET SE
MINNEAPOLIS MN 55455

PHONE: 612 626 0435

MIKE SWANSON
NORTHERN STATES POWER CO
1518 CHESTNUT AVE N

MINNEAPOLIS MN 55403

PHONE: 612 347 9400

DENNIS F H SWIJTER
AIR PRODUCTS & CHEMICALS
2085 ASTER RD

MACUNGIE PA 18062

PHONE: 215 481 4629

DEBORAH A SZARO
26 WALNUT STREET

FOXBORO MA 02035

PHONE: 617 860 4312

JEAN-CLAUDE TABET
LAB DE CHIMIE ORGANIQUE STRUCT
UNIV PIERRE ET MARIE CURIE
8 RUE CUVIER
75230 PARIS CED 05
FRANCE
PHONE:

VINCENT TABONE
FINNIGAN CORP
355 RIVER OAKS PKWY

SAN JOSE CA 95134

PHONE: 408 433 4800

M W TABOR
18 JUNEFIELD AVE

CINCINNATI OH 45218

PHONE: 513 872 4830

KOLI TAGHIZADEH
BIOMATERIALS PROFILING CTR
391 S CHIPETA WAY
SUITE F RESEARCH PARK
SALT LAKE CITY UT 84108

PHONE: 801 581 8431

TSONG-LIN TAI
83 JUDITH DRIVE

STORMVILLE NY 12582-9721

PHONE: 914 894 4988

NAOHITO TAKEDA
DEPT OF MEDICINAL CHEMISTRY
311A SKAGGS HALL
UNIV OF UTAH
SALT LAKE CITY UT 84112

PHONE: 801 581 5581

C R PETE TALLEY
E I DUPONT
EXPERIMENTAL STATION
PETRO CHEM BLDG 336
WILMINGTON DE 19898

PHONE: 302 772 2142

DAVID A TAMMARO
CORNING GLASS WORKS
HP-ME-3-070

CORNING NY 14831

PHONE: 617 974 6365

NOBUHIRO TAMURA
ASAHI CHEM IND
SAMEJIMA

FUJI CITY
JAPAN
PHONE:

YULIN TAN
US DOE
ENVIRON MEAS LAB
376 HUDSON ST
NEW YORK NY 10014

PHONE: 212 620 3481

CALVIN K TANAKA
ENSECO-CAL LAB
2544 INDUSTRIAL BLVD

W SACRAMENTO CA 95691

PHONE: 916 372 1393

K K TANAKA
YALE SCHOOL OF MEDICINE
333 CEDAR STREET

NEW HAVEN CT 06510

PHONE: 203 785 2659

JANE TANG
CA STATE DEPT HEALTH SERVICES
2151 BERKELEY WAY

BERKELEY CA 94704

PHONE: 415 540 3060

SHENG-YUH TANG
RORER CENTRAL RESEARCH
BLDG #2
800 BUSSINESS CENTER DR
HORSHAM PA 19044

PHONE: 215 962 3354

AKIRA TATEMATSU
MEIJO UNIVERSITY
PHARMACY FACULTY
TEMPAKU
NAGOYA 468
JAPAN
PHONE:

PAUL J TAYLER
DEPT OF CHEMISTRY
UNIV OF SALFORD

SALFORD M5 4WT
ENGLAND
PHONE:

DAVE TAYLOR
FINNIGAN MAT
355 RIVER OAKS PARKWAY

SAN JOSE CA 95134

PHONE: 408 433 4800

DENNIS TAYLOR
FINNIGAN MAT
355 RIVER OAKS PARKWAY

SAN JOSE CA 95134

PHONE: 408 433 4800

JAMES W TAYLOR
CHEMISTRY DEPARTMENT
UNIVERSITY OF WISCONSIN
1101 UNIVERSITY AVE
MADISON WI 53706

PHONE: 608 262 4561

LESTER TAYLOR
BURROUGHS WELLCOME
3030 CORNWALLIS ROAD

RESEARCH TRI PARK NC 27709

PHONE: 919 248 3218

M L TAYLOR
PEI ASSOCIATES INC
11499 CHESTER ROAD

CINCINNATI OH 45246

PHONE: 513 782 4700

PAUL A TAYLOR
2544 INDUSTRIAL BLVD

W SACRAMENTO CA 95691

PHONE: 916 671 9017

ROBERT J TAYLOR
4154 N 69TH ST

SAN DIEGO CA 92115-6826

PHONE: 619 582 1768

SANDRA M TAYLOR
#10-9201 FOREST GROVE DRIVE

BURNABY, BC V5A 4P8
CANADA
PHONE:

RON TECKLENBURG
TEXAS A&M UNIVERSITY
DEPT OF CHEMISTRY

COLLEGE STATION TX 77843

PHONE: 409 845 0613

ROBERT TEECE
9301 E 33RD STREET

TUCSON AZ 85710

PHONE: 602 744 4236

LYNN TEESCH
CHEMISTRY DEPT
EMORY UNIV
1515 PIERCE DR
ATLANTA GA 30322

PHONE: 404 727 2583

RICHARD M TEETER
203 DEL VALLE CIRCLE

EL SOBRANTE CA 94803

PHONE: 415 222 4860

S S TENG
FINNIGAN
355 RIVER OAKS PARKWAY

SAN JOSE CA 95134-1991

PHONE: 408 433 4800

DAVID TEPLOW
CALTECH
DIV OF BIOLOGY, 147-75

PASADENA CA 91125

PHONE: 818 356 2923

TERRYANN N TERNES
MARTIN MARIETTA ENERGY SYS
BLDG 9995 MS 01
PO BOX Y
OAK RIDGE TN 37831

PHONE: 615 574 2354

JOSEPH TERRELL
CLAYTON ENV CONSULTANTS
22345 ROETHEL DR

NOVI MI 48050

PHONE: 313 344 1770

D THOMAS TERWILLIGER
6350 OAK CREEK DR

CINCINNATI OH 45247

PHONE: 513 385 8825

L W TETLER
DEPT OF CHEMISTRY
UMIST
SAKCVILLE ST
MANCHESTER M60 1QD
UK
PHONE:

EDWARD TEWS
DOW CORNING CORP
MAIL #20

MIDLAND MI 48686-0995

PHONE: 517 496 5003

JAMES THEAN
1624 NW 10TH ST

GAINESVILLE FL 32609

PHONE: 904 332-3318

J P THENOT
LERS
SYNTHELABO
58 RUE DE LA GLACIERE
75013 PARIS
FRANCE
PHONE:

FRANK THEOBALD
INST ORGANIC CHEMISTRY
UNIV OF COLOGNE
GREINSTR 4
5000 COLOGNE 41
WEST GERMANY
PHONE:

TONY THEOHARIDES
WALTER REED ARMY INSTITUTE
DEPT OF PHARMACOLOGY

WASHINGTON DC 20317-5100

PHONE: 301 427 5295

PIERRE THIBAULT
10344 PARTHENAIS

MONTREAL H2B 2L7
CANADA
PHONE: 514 384 6787

DAVID W THOMAS
SRI INTERNATIONAL
ROOM AB-011
333 RAVENSWOOD AVE
MENLO PARK CA 94025

PHONE: 415 859 3787

DEBORAH A THOMAS
3500 SUTHERLAND AVE
H202

KNOXVILLE TN 37919

PHONE: 615 584 4835

FAIRWELL THOMAS
NIH
BLDG 10 RM 7N115

BETHESDA MD 20892

PHONE: 301 496 6508

H R THOMAS
SUBURBAN LABS INC
4140 LITT DT

HILLSIDE IL 60162-1183

PHONE: 312 544 3260

MICHAEL J THOMAS
BIOCHEMISTRY DEPT
BOWMAN GRAY SCH MED
300 S HAWTHORNE RD
WINSTON-SALEM NC 27103

PHONE: 919 748 2313

QUENTIN THOMAS
FINNIGAN MAT
4450 CARVER WOODS ROAD

CINCINNATI OH 45242

PHONE:

TIMOTHY THOMAS
CHEMISTRY DEPT
UNIV OF MISSOURI

KANSAS CITY MO 64110

PHONE: 816 276 2297

DON W THOMPSON
US FDA
60 8TH STREET, NE

ATLANTA GA 30309

PHONE: 404 448 0496

JOHN A THOMPSON
UNIV OF COLORADO
SCHOOL OF PHARMACY

BOULDER CO 80309-0297

PHONE: 303 492 7218

JOHN J THOMPSON
ALLIED SIGNAL
20 PEABODY ST

BUFFALO NY 14210

PHONE: 716 827 6374

RICHARD M THOMPSON
MERRELL DOW RESEARCH INST
PO BOX 68470

INDIANAPOLIS IN 46268-0470

PHONE: 317 877 1508

STEVEN D THOMPSON
USAF

EDWARDS AFB CA 93523

PHONE: 805 275 5651

MICHAEL L THOMSON
AMERICAN CYANAMID
AGRICULTURAL DIV
PO BOX 400
PRINCETON NJ 08540

PHONE: 609 799 0400

KELLY R THORNBURG
MIDWEST RESEARCH INST
425 VOLKER BLVD

KANSAS CITY MO 64110

PHONE: 816 753 7600

JOHN R THORP
HEWLETT-PACKARD
10535 HARWIN

HOUSTON TX 77072

PHONE:

KIM THRESH
MSD/ISOTOPES
P O BOX 899
POINTE CLAIRE, DORVAL
QUEBEC H9R 4P7
CANADA
PHONE:

THOMAS O TIERNAN
WRIGHT STATE UNIV
BREHM LAB

DAYTON OH 45431

PHONE: 513 873 2202

SANDRA J TILLIN
USDA-WRRC
800 BUCHANAN ST

ALBANY CA 94710

PHONE: 415 486 3139

JIM TIMMONS
ARIZONA DEPT OF PUBLIC SAFE
2324 N 20TH AVE

PHOENIX AZ 85009

PHONE: 602 223 2394

UDMUND TING
LA COUNTY SHERIFF
CRIMINALISTICS LAB
2020 W BEVERLY BLVD
LOS ANGELES CA 90057

PHONE: 213 974 4647

PAUL R TITUS
ILLINOIS STATE POLICE
BUREAU OF FORENSIC SCIENCES
515 E WOODRUFF RD
JOLIET IL 60432

PHONE: 815 727 5301

SUSAN S TJOA
UCHSC
4200 E 9TH AVE C232

DENVER CO 80262

PHONE: 303 394 8175

LASZLO TOKES
SYNTEX RESEARCH
3401 HILLVIEW AVE

PALO ALTO CA 94304

PHONE: 415 855 5713

KENNETH B TOMER
NIEHS
PO BOX 12233

RES TRI PARK NC 27709

PHONE: 919 541 1966

FLORENCE E TORBA
P O BOX 32

CLAYTON CA 94517

PHONE: 415 540 2195

JOHN P TOTH
PESTICIDE RESEARCH LAB
UNIV OF FLORIDA

GAINESVILLE FL 32611

PHONE: 904 392 1978

WILLIAM F TRAGER
UNIV OF WASHINGTON
MEDICINAL CHEM
BAGLEY HALL BG-20
SEATTLE WA 98195

PHONE: 206 543 9481

VINH THI TRAN
ROY F WESTON INC
208 WELSH POOL ROAD

LIONVILLE PA 19353

PHONE: 215 524 7360

JOANN TRIMBLE
UNIV OF TENNESSEE
COLEMAN BLDG, RM 2A09
956 COURT ST
MEMPHIS TN 38163

PHONE: 901 528 5488

MICHAEL R TROUTMAN
CHEMISTRY DEPT
INDIANA UNIV

BLOOMINGTON IN 47401

PHONE: 812 335 5976

NANCY L TSAI
5109 GLENBROOK DR

VIENNA WV 26105

PHONE: 304 295 7023

JOHN F J TODD
UNIV CHEM LABORATORY
UNIV OF KENT
CANTERBURY
KENT CT2 7NH
UK
PHONE:

EMIRGUL TOLUN
CHEMISTRY DEPT
MASS SPECTROMETRY LAB
UNIV OF CALIFORNIA-BERKELEY
BERKELEY CA 94720

PHONE: 415 642 0701

HUAYI TONG
MIDWEST CTR FOR MASS SPEC
DEPT OF CHEMISTRY
UNIV OF NEBRASKA
LINCOLN NE 68588

PHONE: 402 472 5554

PAUL C TOREN
MONSANTO CO
800 N LINDBERGH BLVD

ST LOUIS MO 63167

PHONE:

JAMES C TOU
ANALYTICAL SCIENCES, B-1897
DOW CHEMICAL CO

MIDLAND MI 48667

PHONE: 517 636 2551

JOSEPH A TRAINA
BERLEX LABORATORIES
110 E HANOVER AVE

CEDAR KNOLLS NJ 07927

PHONE: 201 292 8084

MICHAEL L TREHY
MONSANTO U4G
800 N LINDBERGH BLVD

ST LOUIS MO 63167

PHONE: 314 694 1515

RAMESH J TRIVEDI
WARNER LAMBERT CO
170 TABOR RD

MORRIS PLAINS NJ 07950

PHONE: 201 540 4706

JEAN-LUC TRUCHE
HEWLETT-PACKARD
SCIENTIFIC INSTRUMENTS DIV
1601 CALIFORNIA AVE
PALO ALTO CA 94304

PHONE: 415 857 1501

C W TSANG
DEPT OF ABCT
HONG KONG POLYTECH, HUNG HOM

KOWLOON
HONG KONG
PHONE:

PETER J TODD
OAK RIDGE NAT'L LAB
PO BOX Y BLDG 9735

OAK RIDGE TN 37831

PHONE: 615 574 2455

ALBERT D TOMASSIAN
PERKIN-ELMER CORP
2771 N GAREY AVENUE

POMONA CA 91767

PHONE: 714 593 3581

STEPHEN S TONG
CORNING GLASS WKS
SULLIVAN PK FR-18

CORNING NY 14831

PHONE: 607 974 3363

ANIBAL TORRES
SK&F LABORATORIES
PO BOX 2700

GUAYAMA PR 00654

PHONE: 809 864 4545

J C TRAEGER
LA TROBE UNIVERSITY
CHEMISTRY

BUNDOORA VIC 3083
AUSTRALIA
PHONE:

THOMAS M TRAINOR
BRUKER INSTRUMENTS, INC
MANNING PARK

BILLERICA MA 01821

PHONE: 617 667 9580

ANTHONY M TRESTON
NIH
LTPB, NICHD, NIH
BLDG. 6 RM. 136
BETHESDA MD 20892

PHONE: 301 496 5531

ROBERT L TROTTIER
LOCTITE CORP
705 N MOUNTAIN RD

NEWINGTON CT 06111

PHONE: 203 278 1280

B P TSAI
19916 SWEETGUM CIRCLE
APT 31

GERMANTOWN MD 20874

PHONE: 301 975 2531

RUSHUNG TSAO
LEDERLE LABORATORIES
RM 126F BLDG 65B

PEARL RIVER NY 10965

PHONE: 914 732 3417

ANTHONY TSARBOPOULOS
SCHERING CORP
86 ORANGE STREET

BLOOMFIELD NJ 07003

PHONE: 201 429 3958

K Y TSERNG
CLINICAL PHARMACOLOGY
VA MEDICAL CTR
10701 EAST BLVD
CLEVELAND OH 44106

PHONE:

YOSHINOBU TSUCHIDA
DEPT OF APPLIED PHYSICS
UNIV OF ELECTRO-COMMUNICATIONS
1-5-1 CHOFUGAOKA, CHOFU-SHI
TOKYO 182
JAPAN
PHONE:

MASAHIKO TSUCHIYA
4 37 27 KUGAYAMA
SUGINAMI KU

TOKYO 168
JAPAN
PHONE:

MASANORI TSUNO
TSUKUBA RES LABS EISAI CO LTD
TOKODAI 5-CHOME TOYOSATO-MACHI
TSUKUBA-GUN
IBARAKI 300-26
JAPAN
PHONE:

DAVID TUCKER
FINNIGAN MAT
355 RIVER OAKS PARKWAY

SAN JOSE CA 95134

PHONE: 408 433 4800

ROBERT L TUCKER
CLOROX CO
7200 JOHNSON DR
PO BOX 493
PLEASANTON CA 94566

PHONE: 415 847 6651

WILLIAM O TUCKER
ROUTE 8
BOX 315

CLINTON TN 37716

PHONE: 615 574 2419

ALBERT TUINMAN
DEPT OF CHEMISTRY
UNIV OF TENNESSEE

KNOXVILLE TN 37996

PHONE: 615 974 0763

ANDERS TUNLID
INST FOR APPLIED MICROBIOL
UNIVERSITY OF TENNESSEE
RESEARCH DR BLDG 1 STE 300
KNOXVILLE TN 37932-2567

PHONE: 615 675 9523

JERRY A TURBETT
TURBETT ASSOC
PO BOX 352

BOULDER CO 80306

PHONE: 303 442 4838

FRANTISEK TURECEK
BAKER LAB
DEPT OF CHEMISTRY
CORNELL UNIV
ITHACA NY 14853-1301

PHONE: 607 255 4096

CRAIG R TURNER
8970 FENNER ROAD

BALDWINSVILLE NY 13027

PHONE: 315 425 5100

LISA V K TURNER
CORNELL UNIV
BOX 421 BAKER LAB

ITHACA NY 14850

PHONE: 607 255 3884

MAX J TURNER
CIIT
PO BOX 12137

RES TRI PK NC 27709

PHONE: 919 541 2070

MONTE D TURNER
USAF ASTRONAUTICS LAB
AFAL/LSX

EDWARDS AFB CA 93523

PHONE: 805 275 5749

P J TURNER
VG MICROMASS LTD
ION PATH
ROAD THREE
WINSFORD CHESHIRE
ENGLAND
PHONE:

JOHN R TUSCHALL
NORTHROP SERVICES
PO BOX 12313

RES TRI PK NC 27709

PHONE: 919 549 0611

W J TUTING
507 SHIRLEEN LANE

MINE HILL NJ 07801

PHONE: 201 328 7529

KRYSTYNA TYCZKOWSKA
SCHOOL OF VET MED, NCSU
4700 HILLSBOROUGH ST

RALEIGH NC 27606

PHONE:

ANDREW N TYLER
METABOLISM DIV
WASHINGTON UNIV MED SCH

ST LOUIS MO 63110

PHONE: 314 302 6929

HAROLD R UDSETH
BATTELLE NORTHWEST
PO BOX 999

RICHLAND WA 99352

PHONE: 509 376 1656

MARK UHRICH
FINNIGAN MAT
355 RIVER OAKS PKWY

SAN JOSE CA 95134

PHONE: 408 433 4828

STANLEY ULICK
VA HOSPITAL
130 W KINGSBRIDGE RD

BRONX NY 10468

PHONE: 212 367 7879

FREDERICK UNG
2002 SCOTT STREET

TORRANCE CA 90503

PHONE: 818 509-6833

STEVE E UNGER
SQUIBB INST FOR MEDICAL
RESEARCH
PO BOX 4000
PRINCETON NJ 08543-4000

PHONE: 609 921 4987

BILLY T UPCHURCH
1213 BLUEBIRD DRIVE

VIRGINA BEACH VA 23451

PHONE: 804 865 2466

ROGER UPHAM
TWIN CITY TESTING CO
662 CROMWELL AVE

ST PAUL MN 55114

PHONE: 612 641 9486

BERNARD L UPSHULTE
DASCOMB RESEARCH PARK
PO BOX 3100

ANDOVER MA 01810

PHONE: 617 475 9030

MICHAEL J URBAN
RD 1 BOX 167-F

JACKSON NJ 08527

PHONE: 201 225 2225

PIRJO VAINIOTALO
UNIV OF JOENSUU
DEPT OF CHEMISTRY
PO BOX 111
SF-80101 JOENSUU
FINLAND
PHONE:

J L VALENTINE
ORAL ROBERTS UNIV
SCHOOL OF MEDICINE
8181 SOUTH LEWIS
TULSA OK 74170

PHONE: 918 493 8134

RICHARD B VANBREEMEN
DEPT OF CHEMISTRY BOX 8204
NORTH CAROLINA STATE UNIV

RALEIGH NC 27695

PHONE: 919 737 2942

ROY W VANDERHAAR
1540 SWALLOW ST.

NAPERVILLE IL 60565

PHONE: 312 357 2777

ALAIN VANDORSSELAER
CNRS INST OF NEUROCHEMISTRY
5,RUE B PASCAL

67084 STRASBOURG
FRANCE
PHONE:

FRANK VANGAEVER
AGFA-GEVAERT NV
SEPTESTRAAT 27

B2510 MORTSEL
BELGIUM
PHONE:

ERIK VANKUIJK
MONTANA STATE UNIV
108 GAINES HALL
CHEMISTRY DEPT
BOZEMAN MT 59717

PHONE: 406 994 5378

JAMES VATH
MIT
RM 56-028

CAMBRIDGE MA 02139

PHONE: 617 253 7229

CAROL VELSKO
LLNL
PO BOX 808, L-232

LIVERMORE CA 94550

PHONE: 415 423 6256

MADAN VERMA
CIBA GEIGY CORPORATION
AG DIVISION
PO BOX 18300
GREENSBORO NC 27419

PHONE: 919 292 7100

SOPHIE VAJTA
1/9 RUE DE GOMETZ

BURES-SUR-YVETTE
91440 FRANCE
PHONE:

LUNN VANATTA
2932 SEYMOUR DR

DALLAS TX 75229

PHONE: 214 579 2331

W J VANDENHEUVEL
MERCK SHARP & DOHME
RESEARCH LABORATORY
PO BOX 2000
RAHWAY NJ 07065

PHONE: 201 574 5443

G J Q VANDERPEIJL
DSM RESEARCH BV
DEPT FA/SO
PO BOX 18
6160 MD GELEEN
THE NETHERLANDS
PHONE:

DONALD L VANDOYNE
LAS INC
PO BOX 130

STEWARTSTOWN PA 17363

PHONE: 717 993 2517

JIM VANIDES
HEWLETT-PACKARD
1601 CALIFORNIA AVENUE

PALO ALTO CA 94304

PHONE: 415 857 3495

AGNES VANLANGENHOVE
ENSECO INC
205 ALEWIFE BROOK PKWY

CAMBRIDGE MA 02138

PHONE: 617 611 3111

RENATA VEDDER
IBM CORP
5600 COTTLE RD

SAN JOSE CA 95193

PHONE: 408 256 3250

FRANCESC VENTURA
INST DE QUIMICA BIO-ORGANICA
J GIRONA SALGADO 18-26

08034 BARCELONA
SPAIN
PHONE:

SUNITA VERMA
DEPT OF HEALTH & HUMAN SERVICE
NATIONAL TOXICOLOGY PROGRAM
PO BOX 12233
RESEARCH TRI PARK NC 27709

PHONE: 919 541 2964

AUSRINE K VALAITIS
AMERICAN INST DRUG DETECT
5515 MILTON PARKWAY

ROSEMONT IL 60018

PHONE: 312 678 2113

GARY J VANBERKEL
OAK RIDGE NATIONAL LAB
PO BOX Y; BLDG 9735

OAK RIDGE TN 37831-6142

PHONE: 615 574 2456

DR J VANDERGREEF
CIVO-TNO
PO BOX 360

3700 AJ ZEIST
NETHERLANDS
PHONE:

G G VANDERVELDE
5715 LAWN DRIVE

WESTERN SPRINGS IL 60558-2226

PHONE: 312 841 8360

SCOTT W VANETTEN
334 WHETHERSFIELD DR

GLASSBORO NJ 08028

PHONE: 201 225 6795

PETRA VANKOPPEN
CHEMISTRY DEPT
UC SANTA BARBARA

SANTA BARBARA CA 93106

PHONE: 805 961 2673

JAMES P VANNOY
9249 DEERCROSS PARKWAY
APT 2D

CINCINNATI OH 45236-4565

PHONE:

KAROLY VEKEY
MERRELL DOW RES INST
VIA R LEPETIT 34

21040 GERENZANO
ITALY
PHONE:

FRANCIS VERDUN
OHIO STATE UNIV
121 JOHNSTON LAB
176 W 19TH AVE
COLUMBUS OH 43210

PHONE: 614 292 0480

WILLIAM J VERRET
6608 HORNWOOD

HOUSTON TX 77074

PHONE: 713 954 6766

CHRISTINA H VESTAL
VESTEC CORP
9299 KIRBY DRIVE

HOUSTON TX 77054

PHONE: 713 796 9677

MARVIN L VESTAL
VESTEC
9299 KIRBY DRIVE

HOUSTON TX 77054

PHONE: 713 749 2675

M M VESTLING
CHEMISTRY DEPT
SUNY COLL @ BROCKPORT

BROCKPORT NY 14420

PHONE: 716 395 5594

STEPHEN W VEYSBY
85A GILMAN HALL
IOWA STATE UNIV

AMES IA 50011

PHONE: 515 294 5958

ALAN VIAU
HEWLETT-PACKARD
6877 GOREWAY DR

MISSISSIGUA, ONT L4V 1M8
CANADA
PHONE: 416 678 9430

DOM VICCHIO
NIH
BLDG 10, ROOM 6C208
9000 ROCKVILLE PIKE
BETHESDA MD 20892

PHONE: 301 496 5531

RICHARD VICKERS
5 GOLFERS WAY SOUTH

THORNDALE PA 19372

PHONE: 617 777 8034

MARK VICTOR
DEPT OF CHEMISTRY
MICHIGAN STATE UNIV

EAST LANSING MI 48824

PHONE: 517 353 5215

NANCY E VIEIRA
NICHD, LTPB
BLDG 10, RM 6C206

BETHESDA MD 20892

PHONE: 301 496 5531

ALBERT VIGGIANO
AIR FORCE GEOPHYSICS LAB
LID

HANSCOM AFB MA 02174

PHONE: 617 377 4028

PAUL VIGNY
INSTITUTE CURIE
11 RUE P ET M CURIE

75231 PARIS CEDEX
FRANCE
PHONE:

RICHARD VILLA
CLOROX TECHNICAL CENTER
PO BOX 493

PLEASANTON CA 94566

PHONE: 415 847 6744

DAN VILLALANTI
SHELL DEVELOPMENT
PO BOX 1380

HOUSTON TX 77001

PHONE:

ADAM VINCZE
ISRAEL INST BIOL RES
PO BOX 19

NESS ZIONA 70450
ISRAEL
PHONE:

JOSIE VISENTINI
DEPT OF CHEMISTRY
UNIV OF MONTREAL
CP 6128 SUCC A
MONTREAL, QUEBEC H3C 3J7
CANADA
PHONE:

S K VISWANADHAM
CHEMISTRY DEPT
BOX 10
UNIV OF PITTSBURGH
PITTSBURGH PA 15260

PHONE: 412 624 8302

T S VISWANATHAN
8409 WEST 90TH ST

OVERLAND PARK KS 66212

PHONE: 913 236 3881

ROBERT D VOCKS
FINNIGAN MAT
355 RIVER OAKS PARKWAY

SAN JOSE CA 95128

PHONE: 408 433 4800

GERARD F VOITY
K&M ELECTRONICS
123 INTERSTATE DRIVE

WEST SPRINGFIELD MA 01089

PHONE: 413 781 1350

KEVIN J VOLK
1676 SW 16TH ST

GAINESVILLE FL 32608

PHONE: 904 376 4559

DAVID W VONENDT
CAL-MSC
SMITHSONIAN INSTITUTE

WASHINGTON DC 20560

PHONE: 202 287 3721

KENT J VOORHEES
COLORADO SCH MINES
CHEMISTRY DEPT

GOLDEN CO 80401

PHONE: 303 273 3616

PAUL VOUROS
NORTHEASTERN UNIV
INST CHEMICAL ANAL

BOSTON MA 02115

PHONE: 617 437 2840

ROBERT D VOYKSNER
RESEARCH TRIANGLE INSTITUTE
PO BOX 12194

RESEARCH TRI PARK NC 27709

PHONE: 919 541 6697

JAMES VRBANAC
PHARMACOLOGY DEPT
MED UNIV OF S CAROLINA

CHARLESTON SC 29425

PHONE: 803 792 2471

DEBRA E WACHEL
KNOLLS ATOMIC POWER LAB
PO BOX 1072

SCHENECTADY NY 12301

PHONE: 518 395 6223

TIMOTHY WACHS
CORNELL UNIVERSITY
CHEMISTRY DEPT
BAKER LAB
ITHACA NY 14853-1301

PHONE: 607 256 4914

KEITH WADDELL
VG ANALYTICAL
FLOATS ROAD
WYTHENSHAWE
MANCHESTER
UK
PHONE:

JOHN I WADDICOR
VG TRITECH
CREWE ROAD
WYTHENSHAWE
MANCHESTER
UK
PHONE:

P A WADSWORTH
814 CHEVY CHASE CIRCLE

SUGAR LAND TX 77478

PHONE: 713 491 4754

BRUCE F WAGNER
IT CORPORATION
312 DIRECTORS DRIVE

KNOXVILLE TN 37923

PHONE: 615 690 3211

DAVID A WAGNER
49 SYMPHONY ROAD
APT 24

BOSTON MA 02115

PHONE: 617 722 3000

GUENTER WAGNER
FINNIGAN MAT
BARKHAUSENSTR 2

BREMEN
GERMANY
PHONE:

L C WAGNER
2030 TOWNGATE DRIVE

GARLAND TX 75041

PHONE: 214 995 2294

AUSTIN L WAHRHAFTIG
CHEMISTRY DEPT
UNIVERSITY OF UTAH

SALT LAKE CITY UT 84112

PHONE: 801 581 6048

MICHAEL R WAKEFIELD
1211 BURNHAM DRIVE

SAN JOSE CA 95132

PHONE: 408 756 3646

LARRY S WAKEMAN
EASTMAN KODAK RESEARCH
BLDG 82

ROCHESTER NY 14650

PHONE: 716 722 4738

FRANCIS J WALCZAK
E I DUPONT
EXP STA, E262/332T

WILMINGTON DE 19898

PHONE: 302 695 3044

KENNETH M WALKER
BROWN & WILLIAMSON TOBACCO
PO BOX 35090

LOUISVILLE KY 40232

PHONE: 502 568 7986

RAYMOND L WALKER
ORNL MARTIN MARIETTA
PO BOX Y BLDG 9735
Y-12 PLANT
OAK RIDGE TN 37831

PHONE: 615 574 2449

KEVIN WALLACE
FINNIGAN
355 RIVER OAKS PARKWAY

SAN JOSE CA 95134-1991

PHONE: 408 732 4266

GEORGE R WALLER
BIOCHEMISTRY DEPT
OKLAHOMA STATE UNIVERSITY

STILLWATER OK 74078

PHONE: 405 624 6199

FRED WALLS
PHARM CHEMISTRY
UNIV OF CALIFORNIA

SAN FRANCISCO CA 94143-0446

PHONE: 415 476 4894

KEN WALSH
SOUTHERN ILLINOIS UNIV
COAL RESEARCH CENTER

CARBONDALE IL 62901

PHONE: 618 536 5526

SHERRIE WALSH
DEPT OF CHEMISTRY
UNIV OF CALIFORNIA

SANTA BARBARA CA 93106

PHONE: 805 961 2673

KARL PETER WANCZEK
PARKALLEE 197

D-2800 BREMEN
WEST GERMANY
PHONE:

BING HUANG WANG
CHEMISTRY DEPT
BAKER LABORATORY
CORNELL UNIV
ITHACA NY 14853

PHONE: 607 255 3731

JEFF S I WANG
ABBOTT LABS
D-418 ABBOTT PARK

N CHICAGO IL 60064

PHONE: 312 937 2082

JIA-SHEN WANG
CLAIROL INC
2 BLACHLEY RD

STAMFORD CT 06922

PHONE: 203 357 5065

RONG WANG
BIOPHYSICS BLDG B-11
725 N WOLFE STREET

BALTIMORE MD 21205

PHONE: 301 955 3022

T HELEN WANG
PENNZOIL PRODUCTS CO
TECHNOLOGY DIV
PO BOX 7569
WOODLANDS TX 77387

PHONE: 713 363 8049

W-T PAUL WANG
CTI CRYOGENICS
266 SECOND AVENUE

WALTHAM MA 02284-9171

PHONE: 617 622-5236

DAVID WANG-IVERSON
SQUIBB INST FOR MEDICAL RES
ROUTE 1 @ COLLEGE FARM ROAD
PO BOX 191
NEW BRUNSWICK NJ 08903

PHONE: 201 519 2190

WAYNE WARGO
2316 SWANSEA RD

COLUMBUS OH 43216

PHONE: 614 227 3456

CHARLES D WARNER
DEPT OF CHEMISTRY
HASTINGS COLLEGE

HASTINGS NE 68901

PHONE: 402 462 2402

BETHANNE WARRACK
E R SQUIBB & SONS
PO BOX 4000

PRINCETON NJ 08543-4000

PHONE: 609 921 5439

PHIL WARREN
FINNIGAN MAT
355 RIVER OAKS PKWY

SAN JOSE CA 95134-9990

PHONE: 408 433 4800

ROBERT W WARREN
SUN REFINING & MFG
ARD
PO BOX 1135
MARCUS HOOK PA 19061

PHONE: 215 447 1814

VIRGIL L WARREN
18534 LIPPITZANER

CYPRESS TX 77433

PHONE:

JAMES R WARRING
NICOLET INSTRUMENTS CORP
5225-1 VERONA RD
PO BOX 4508
MADISON WI 53711

PHONE: 608 271 3333

BRUCE A WASILCHUK
DEPT OF CHEMISTRY
NORTHEASTERN UNIV
360 HUNTINGTON AVE
BOSTON MA 02115

PHONE: 617 437 2794

MARVIN ALAN WATKINS
4917-F DANA DRIVE

RALEIGH NC 17606

PHONE: 919 851 0090

CLIFFORD H WATSON
LEIGH HALL BOX 554

UNIV OF FLORIDA
GAINESVILLE FL 32611

PHONE: 904 376 5816

ERIC WATSON
AMGEN
1900 OAK TERRACE LANE

THOUSAND OAKS CA 91320

PHONE: 805 499 5725

J THROCK WATSON
DEPT BIOCHEMISTRY
MICHIGAN STATE UNIV

EAST LANSING MI 48824

PHONE: 517 353 0855

JAN WATSON
ROCKWELL INTERNATIONAL
ROCKY FLATS PLANT
PO BOX 464, BLDG 559
GOLDEN CO 80401-0464

PHONE: 303 966 4964

DAVID WATT
1044 BELVEDERE LANE

SAN JOSE CA 95129-2901

PHONE:

JAMES G WATT
FINNIGAN CORP
355 RIVER OAKS PKWY

SAN JOSE CA 95134

PHONE: 408 433 4800

GORDON W WEBB
770 STIMSON

IDAHO FALLS ID 83402

PHONE: 208 526 3048

HUGH M WEBB
3746 SAN REMO DR

SANTA BARBARA CA 93105

PHONE: 805 961 4252

LISA SMITH WEBB
ROUTE 6 TOPSIDE ROAD
APT 85-E

LOUISVILLE TN 37777

PHONE: 615 970 3462

MICHAEL R WEBB
USDA
816 CONTRA COSTA

BERKELEY CA 94707

PHONE: 415 527 5186

BILL D WEBER
IBM CORP
D/12W, B/630, E/E70

HOPEWELL JUNCTION NY 12533

PHONE:

DORCAS WEBER
HEALTH & WELFARE CANADA
FOOD RES DIV
TUNNEY'S PASTURE BANTING BLD
OTTAWA, ONTARIO K1A 0L2
CANADA
PHONE: 613 957 0952

MICHAEL WEBER-GRABAU
FINNIGAN MAT
355 RIVER OAKS PWY

SAN JOSE CA 95134

PHONE: 408 433 4800

GARY H WEDDLE
CHEMISTRY DEPT
FAIRFIELD UNIV

FAIRFIELD CT 06430

PHONE: 203 254 4000

C A WEERASINGHE
SMITHKLINE BECKMAN
1600 PAOLI PIKE

WESTCHESTER PA 19380

PHONE: 215 251 7489

ANNEMARIE WEGMANN-SZENTE
CHEMISTRY DEPT
STANFORD UNIV
GC-MS LABS
STANFORD CA 94305

PHONE: 415 723 2859

PATRICK WEHRUNG
UNIV DE STRASBOURG
DEPT DE CHIMIE
1 RUE BLAISE PASCAL
F-67008 STRASBOURG
FRANCE
PHONE:

LEO A WEIBEL
HAELETON LABS
PO BOX 7545

MADISON WI 53707

PHONE: 608 241 7654

JOSEPH M WEIKEL
5027 136TH ST SE

SNOHOMISH WA 98240

PHONE: 206 337 8968

DAVID A WEIL
NICOLET INSTRUMENTS
5225 VERONA ROAD

MADISON WI 53711

PHONE: 608 271 3333

CURT WEILAND
WAYNE ASSOCIATES
2628 BARRETT STREET

VIRGINIA BEACH VA 23452

PHONE: 804 340 0555

ROBERT J WEINKAM
ALLERGAN PHARMACEUTICAL
2525 DUPONT DR

IRVINE CA 92715

PHONE: 714 955 6713

SUSAN T WEINTRAUB
UT HEALTH SCI CTR
7703 FLOYD CURL DR

SAN ANTONIO TX 78284

PHONE: 512 567 4043

ORLA WEIR
VG TRITECH
CREWE ROAD
WYTHENSHAWE
MANCHESTER
UK
PHONE:

CLEMENS R WEISENBERGER
CHEMISTRY DEPARTMENT
OHIO STATE UNIVERSITY
120 W 18TH
COLUMBUS OH 43210

PHONE: 614 292 0488

T J WEISMANN
106 SHORT ST

PITTSBURGH PA 15237

PHONE: 412 434 5824

ADRIAN WEISS
DEPT OF CHEMISTRY
TECHNION-ISRAEL INST OF TECH

32000 HAIFA
ISRAEL
PHONE:

KENNETH J WELCH
SC JOHNSON & SON INC
ANAL R&D STA MS 056
1525 HOWE ST
RACINE WI 53403-5011

PHONE: 414 631 2993

MICHAEL J WELCH
NATIONAL BUREAU OF STANDARDS
RM A-113 BLDG 222

GAITHERSBURG MD 20899

PHONE: 301 975 3100

W DAVID WELDON
DELSI NERMAG
15701 WEST HARDY RD #1

HOUSTON TX 77060

PHONE: 713 847 0811

ROBERT R WELLER
DEPT OF CHEMISTRY
PURDUE UNIVERSITY

W LAFAYETTE IN 47907

PHONE: 312 494 0571

BERND WENCLAWIAK
DEPT OF CHEMISTRY
UNIV OF TOLEDO
2801 W BANCROFT STREET
TOLEDO OH 43606

PHONE: 419 537 2664

QINGMEI WENG
DEPT OF PHARM SCIENCE
COLLEGE OF PHARMACY
UNIV OF ARIZONA
TUCSON AZ 85721

PHONE: 602 626 4072

CURT WENTRUP
DEPT OF CHEMISTRY
UNIV QLD
ST LUCIA
BRISBANE
AUSTRALIA 4067
PHONE:

CHRYS WESDEMIOTIS
BOX 441 BAKER LABORATORY
CORNELL UNIV

ITHACA NY 14853

PHONE: 607 255 3731

DAVID WESLEY
ASHLAND PETROLEUM CO
PO BOX 391

ASHLAND KY 41101

PHONE: 606 327 6457

J B WESTMORE
UNIV OF MANITOBA
CHEMISTRY DEPT

WINNIPEG MAN R3T 2N2
CANADA
PHONE: 204 474 9761

DAVID G WESTMORELAND
ROHM & HAAS CO
727 NORRISTOWN RD

SPRING HOUSE PA 19477

PHONE: 215 641 2033

ALAN F WESTON
OCCIDENTAL CHEMICAL
360 RAINBOW BLVD S BOX 728

NIAGRA FALLS NY 14302

PHONE: 716 286 3607

H R WETHERELL
MICH STATE POLICE LAB
714 SO HARRISON

EAST LANSING MI 48823

PHONE: 517 337 6191

JEFF R WETZLER
WESTINGHOUSE-BETTIS
PO BOX 79

WEST MIFFLIN PA 15122-0079

PHONE: 412 476 5839

CONRAD WHEELER
3235 VICENTE STREET
APT #6

SAN FRANCISCO CA 94116

PHONE: 415 561 2635

HERBERT G WHEELER
SOUTHWEST RESEARCH INST
6220 CULEBRA ROAD

SAN ANTONIO TX 78284

PHONE: 512 522 2119

J W WHEELER
10019 REDDICK DRIVE

SILVER SPRING MD 20901

PHONE: 202 636 6910

SARA WHIPPLE
AMGEN INC
1900 OAK TERRACE LANE

THOUSAND OAKS CA 91320

PHONE:

DAVID C WHITE
INST FOR APP MICROBIOLOGY
10515 RESEARCH DR
SUITE 300
KNOXVILLE TN 37932-2567

PHONE: 615 675 9520

EARL L WHITE
R J REYNOLDS TOBACCO CO
BOWMAN GRAY TECH CTR

WINSTON-SALEM NC 27102

PHONE: 919 741 4015

EDWARD WHITE
NBS
A113 CHEMISTRY

GAITHERSBURG MD 20899

PHONE: 301 921 2153

FREDERICK A WHITE
RENSSELAER POLY INST
NUCLEAR ENG DEPT

TROY NY 12181

PHONE: 518 270 6398

CRAIG M WHITEHOUSE
220 PLEASANT PT RD

BRANFORD CT 06405

PHONE:

ROBERT T WHITT
HEWLETT-PACKARD
930 E CAMPBELL RD

RICHARDSON TX 75081

PHONE: 214 699 4316

N F WHITTAKER
NIH
BLDG 8 RM 62A-21

BETHESDA MD 20892

PHONE: 301 496 4055

JOSEPH K WICHMANN
WALLACE LABS
HALF ACRE ROAD

CRANBURY NJ 08512

PHONE: 609 655 6630

MARGARET E WICKHAM
MIDWEST RESEARCH INST
425 VOLKER BLVD

KANSAS CITY MO 64110

PHONE: 816 753 7600

PALITHA WICKRAMANAYAKE
DEPT OF CHEMISTRY
UNIV OF CINCINNATI

CINCINNATI OH 45221

PHONE:

ROBERT L WIECZOREK
100 DEFOREST AVENUE
TECHNICAL CTR

EAST HANOVER NJ 07936

PHONE: 201 503 4000

RICHARD A WIELESEK
CHEMISTRY DEPT
UNIV OF OREGON

EUGENE OR 97403

PHONE: 503 686 4641

STEVE WILBUR
FIREMAN'S FUND ENV LAB
3700 LAKEVILLE HWY

PETALLUMA CA 94952

PHONE: 707 778 4160

JAMES T WILDER
SIMSPEC
1474 FIELDCREST CIR

PLEASANT HILL CA 94523

PHONE: 415 229 0325

BERNIE WILK
UNOCAL CORP
MAIL STOP M101
376 S VALENCIA AVENUE
BREA CA 92621

PHONE:

BRUCE E WILKES
EAC INC
240 ROCKY STEP RD

SCOTT DEPOT WV 25560-9685

PHONE: 304 757 2499

JON G WILKES
VESTEC CORP
9299 KIRBY DRIVE

HOUSTON TX 77054

PHONE: 713 796 9677

CHARLES L WILKINS
CHEMISTRY DEPARTMENT
U OF C RIVERSIDE

RIVERSIDE CA 92521-0403

PHONE: 714 787 3518

JOANN E WILKINSON
S-CUBED
3398 CARMEL MOUNTAIN ROAD

SAN DIEGO CA 92121

PHONE: 619 453 0060

DALE A WILLCOX
218 W CHESTNUT ST

MACUNGIE PA 18062

PHONE: 215 481 7977

GARY D WILLETT
DEPT OF PHY CHEM
UNIV OF N.S.W.
PO BOX 1 KENSINGTON
N.S.W. 2033
AUSTRALIA
PHONE:

DAVID WILLIAMS
BROWARD-DOBBS, INC
1532 DUNWOODY VILLAGE PKWY
SUITE 200
ATLANTA GA 30338

PHONE: 404 399 0744

EVAN WILLIAMS
BAKER LAB
DEPT OF CHEMISTRY
CORNELL UNIV
ITHACA NY 14853

PHONE: 607 255 3731

FRED P WILLIAMS
RESEARCH TRIANGLE INST
PO BOX 12194

RES TRI PK NC 27709

PHONE: 919 541 6699

NEAL WILLIAMS
DUPONT
331 TREBLE COVE RD

N BILLERICA MA 01862

PHONE: 617 671 8548

TODD D WILLIAMS
MASS SPECTROMETRY LAB
COLLEGE OF CHEMISTRY
UC BERKELEY
BERKELEY CA 94720

PHONE: 415 642 0701

ROSS C WILLOUGHBY
EXTREL
240 ALPHA DRIVE

PITTSBURGH PA 15238

PHONE: 412 963 7530

JOHN M WILSON
DEPT OF PHARMACY
UNIV OF MASS MED CTR
55 LAKE AVENUE
WORCESTER MA 01605

PHONE: 617 856 4926

LOUIS A WILSON
AMERICAN CYANAMID
PO BOX 400

PRINCETON NJ 08540

PHONE: 609 799 0400

MARK WILSON
BALESRS
8 SAGAMORE PARK RD

HUDSON NH 03051

PHONE: 603 880 0213

ROGER T WILSON
USDA FSIS MWL
PO BOX 5080

ST LOUIS MO 63115

PHONE: 314 263 2686

JAMES WINDAK
406 KEECH

ANN ARBOR MI 48103

PHONE: 313 747 2847

RONALD J WINGENDER
ARGONNE NATL LAB
9700 S CASS AVE

ARGONNE IL 60439

PHONE: 312 972 7625

BRIAN WINGER
PURDUE UNIVERSITY
2601 SOLDIERS HM RD#16

W LAFAYETTE IN 47907

PHONE: 317 494 5264

PAUL WINKLER
DOW CHEMICAL USA
PO BOX 1398

PITTSBURG CA 94565

PHONE: 415 432 5403

DAVID L WINMILL
HERCULES INC
RESEARCH CENTER

WILMINGTON DE 19894

PHONE: 302 995 3267

CARL K WINTER
UNIV OF CALIFORNIA
RIVERSIDE CAMPUS

RIVERSIDE CA 92521

PHONE: 714 787 5994

MARCUS B WISE
OAK RIDGE NAT'L LAB
P O BOX X
MS-120 4500-S
OAK RIDGE TN 37831-6120

PHONE: 615 574 4867

JOHN S WISHNOK
MIT
APPLIED BIOLOGICAL SCI
ROOM 56-313
CAMBRIDGE MA 02139

PHONE: 617 253 6795

DENNIS N WITIAK
NEW JERSEY DEPT OF HEALTH
CHEMISTRY LAB 515
JOHN FITCH PLAZA, CN-361
TRENTON NJ 08625

PHONE: 609 984 7255

THOMAS A WITTSTRUCK
NUCLIDE CORP
AGV DIVISION
PO BOX 315
ACTON MA 01720

PHONE: 617 263 2936

RICHARD J WNUK
UPJOHN CO
301 HENRIETTA ST
7255-209-017
KALAMAZOO MI 49001

PHONE: 616 385 7918

MARTA H WOLFE
SHRINERS HOSPITAL
610 TEXAS AVENUE

GALVESTON TX 77550

PHONE: 409 761 6575

ROBERT R WOLFE
SHRINERS HOSPITAL
METABOLISM UNIT
610 TEXAS AVE
GALVESTON TX 77550

PHONE:

HERMANN WOLLNIK
UNIVERSITY GIESSEN
H BUFF RING 16

6300 GIESSEN
WEST GERMANY
PHONE:

W ALAN WOLSTENHOLME
VG INSTRUMENTS
13840 WEST OAK GLEN RD

VALLEY CENTER CA 92082

PHONE: 619 749 9306

CARLA M WONG
NASA M/S 244-18
AMES RESEARCH CENTER

MOFFETT FIELD CA 94035

PHONE: 415 694 4294

JONATHAN WONG
USDA
BOX 4008

ALAMEDA CA 94501

PHONE: 415 273 7753

LAN K WONG
UNIV OF PITTSBURGH
SCHOOL OF PHARMACY
804 SALK HALL
PITTSBURGH PA 15261

PHONE: 412 648 8553

WILLIAM W WONG
MEDICAL TOWERS BLDG
SUITE 601
6608 FANNIN AVENUE
HOUSTON TX 77030

PHONE: 713 799 6000

DAVID WOOD
VG TRITECH
CREWE ROAD
WYTAENSHAWE
MANCHESTER
ENGLAND
PHONE:

GEORGE M WOOD
2 LITTLE BLUFF RD

NEWPORT NEWS VA 23606

PHONE: 804 865 2466

GORDON W WOOD
UNIV OF WINDSOR
VICE PRESIDENT ACADEMIC

WINDSOR ONTARIO N9B 3P4
CANADA
PHONE: 519 253 4232

JOE M WOOD
230 SHEETS ST
APT 7

W LAFAYETTE IN 47906

PHONE: 713 743 8408

KARL V WOOD
PURDUE UNIV
FUELS ANAL LAB
CHEMISTRY BLDG
W LAFAYETTE IN 47907

PHONE: 317 494 7357

NEVILLE WOOD
BASF ARC

RES TRI PK NC 27709

PHONE:

JOHN W WOODS
VG INSTRUMENTS
DOOR #1 LAKESIDE OFFICE PARK

WAKEFIELD MA 01980

PHONE: 617 246 0040

CHRISTOPHER WOODWARD
VG ANALYTICAL
FLOATS RD
WYTHENSHAWE
MANCHESTER
ENGLAND
PHONE:

FRED WOODWARD
830 PINEWOOD AVE

SCHENECTADY NY 12309

PHONE: 518 457 3252

CHARLES J WRIGHT
1210 MAJESTIC WAY

WEBSTER NY 14580

PHONE: 716 477 6733

ELAINE WRIGHT
CLAYTON ENVMNTL CONST, INC
PO BOX 9019

PLEASANTON CA 94566

PHONE: 415 426 2600

LARRY G WRIGHT
DOW CHEMICAL USA
BLDG 1897

MIDLAND MI 48674

PHONE: 517 636 4893

LYNN H WRIGHT
US EPA
EMSL MD-78

RES TRI PARK NC 27711

PHONE: 919 541 2951

JOHN WRONKA
DEPT OF CHEMISTRY
NORTHEASTERN UNIV
360 HUNTINGTON AVE
BOSTON MA 02115

PHONE: 617 437 4513

JI-ZONG WU
1665 KONG-JIANG ROAD

SHANGHAI
CHINA
PHONE:

STEFAN WUDY
CHILDREN'S HOSPITAL OAKLAND
747 52ND STREET

OAKLAND CA 94609

PHONE: 415 428 3619

JEFF R WYATT
NRL
CODE 6110

WASHINGTON DC 20375-5000

PHONE: 202 767 3244

D D WYLIE
FINNIGAN
355 RIVER OAKS PARKWAY

SAN JOSE CA 95134-1991

PHONE: 408 433 4800

VICKI H WYSOCKI
CODE 6112/CHEMISTRY DIVISION
NAVAL RESEARCH LAB

WASHINGTON DC 20375-5000

PHONE: 202 767 3551

WEN-HAO XU
SUNTORY INST FOR BIOORGANIC RE
WAKAYAMADAI SHIMAMOTO-CHO
MISHIMA-GUN
OSAKA 618
JAPAN
PHONE:

ZU-QING XUE
DEPT OF INFORMATION ELECTRONIC
TSING HUA UNIVERSITY

BEIJING
CHINA
PHONE:

L L YAGI
FINNIGAN
355 RIVER OAKS PARKWAY

SAN JOSE CA 95134-1991

PHONE: 408 433 4800

ZIRO YAMAIZUMI
NAT'L CANCER CENTER INST
BIOLOGY DIV
5-1-1 TSUKIJI CHUO-K
TOKYO 104
JAPAN
PHONE:

KOUWA YAMASHITA
PHARMACOLOGY DEPT, SCH OF MED
VANDERBILT UNIV
1161 21ST AVE SOUTH
NASHVILLE TN 37232

PHONE: 615 322 2094

TAKASHI YAMAUCHI
DEPT OF APPLIED PHYSICS
UNIV OF ELECTRO-COMMUNICATIONS
1-5-1 CHOFUGAOKA, CHOFU-SHI
TOKYO 182
JAPAN
PHONE:

RAGHAV YAMDAGNI
UNIV OF CALGARY
CHEMISTRY DEPT

CALGARY ALB T2N 1N4
CANADA
PHONE: 403 220 5890

GEORGE F YAMNITZKY
NORTH CENTRAL LABORATORY
ROOM 500
610 SOUTH CANAL STREET
CHICAGO IL 60607

PHONE: 312 353 3640

MARK YANCEY
BATTELLE
505 KING AVE

COLUMBUS OH 43201

PHONE: 614 424 4654

CATHY L C YANG
INTERNTIONAL PAPER
LONG MEADOW ROAD

TUXEDO PARK NY 07039

PHONE:

KAI-QIONG YANG
CHANGDU BRANCH OF ACADEMIA
SINICA

CHENGDU
CHINA
PHONE:

LILY YANG
12019 PLUM BROOK DR

HOUSTON TX 77099

PHONE:

SYAULAN SOLON YANG
DEPT OF CHEMISTRY
UNIV OF NEBRASKA

LINCOLN NE 68588-0304

PHONE: 402 472 3507

YING-HUA YANG
JILIN IMPORTS & EXPORTS
COMMODITY INSP BUREAU
81 STALIN ROAD
CHANG CHUN
PR CHINA
PHONE:

IKUYA YANO
DEPT OF BACTERIOLOGY
OSAKA CITY UNIV MED SCHOOL
1-4-54, ASAHI-MACHI, ABENO-KU
OSAKA, 454
JAPAN
PHONE:

JOHN R YATES
DEPT OF CHEMISTRY
MCCORMICK RD
UNIV OF VIRGINIA
CHARLOTTESVILLE VA 22901

PHONE: 804 924 7994

RAZIEH YAZDANPARAST
No 1/2, 15TH AVE,
SHAHRARA STREET

TEHRAN
IRAN
PHONE:

SUSAN K YEAGER
ACUREX CORP
405 CLYDE AVENUE

MOUNTAIN VIEW CA 94043

PHONE: 408 756 3236

GEORGE YEFCHAK
CHEMISTRY DEPT
MICHIGAN STATE UNIV

EAST LANSING MI 48824

PHONE: 517 353 5215

LAUREN M YELLE
ARTHUR D LITTLE INC
15 ACORN PARK

CAMBRIDGE MA 02140

PHONE: 617 864 5770

RICHARD O YELTON
FINNIGAN CORP
4450 CARVER WOODS DRIVE

CINCINNATI OH 45242

PHONE: 513 891 2100

ANDREW J YENCHA
SUNY-ALBANY
CHEMISTRY DEPT

ALBANY NY 12222

PHONE: 518 442 4416

KEN S YEOMANS
8405 E HAMPTON AVENUE
APT 3H

DENVER CO 80231

PHONE: 303 745-5756

ALFRED L YERGEY
NIH
BLDG 10, ROOM 6C101

BETHESDA MD 20892

PHONE: 301 496 5531

JAMES A YERGEY
NIAAA/LCS
BLDG 10 RM 3C218

BETHESDA MD 20892

PHONE: 301 496 4900

JEHUDA YINON
WEIZMANN INSTITUTE
ISOTOPE RESEARCH

REHOVOT 76100
ISRAEL
PHONE:

RONALD GLENN YOKUM
RADIAN CORP
8670 FAIR OAKS BLVD

CARMICHAEL CA 95608

PHONE: 916 944 2695

MATTHIAS YOONG
6904 DOVE STREET

VENTURA CA 93003

PHONE: 818 787 7380

DAVID A YORKE
VG INSTRUMENTS GROUP LTD
CREWE ROAD, WYTHENSHAWE

MANCHESTER M23 9BE
UK
PHONE:

GLENN YOSHIMURA
4336 MAIN

SKOKIE IL 60076

PHONE: 312 793 4767

HIDEO YOSHIZUMI
MEIJO UNIV
15 YAGOTOURAYAMA, TENPAKU-CHO
TENPAKU-KU
NAGOYA-SHI, AICHI 468
JAPAN
PHONE:

RICHARD A YOST
CHEMISTRY DEPARTMENT
UNIV OF FLORIDA

GAINESVILLE FL 32611

PHONE: 904 392 0557

ALEX B YOUNG
DEPT OF CHEMISTRY
UNIV OF TORONTO
80 ST GEORGE STREET
TORONTO M5S 1A1
CANADA
PHONE: 416 978 3571

SO HUN YOUNG
UNIV OF CALIFORNIA RIVERSIDE

RIVERSIDE CA 92507

PHONE:

STEVEN E YOUNG
2455 THADDEUS DR

MOUNTAIN VIEW CA 94043

PHONE: 415 859 4806

DAVID R YOUNGMAN
LOCKHEED-EMSCO
1050 E FLAMINGO RD #120

LAS VEGAS NV 89109

PHONE: 702 798 2047

M J YOUSSEFI
UNION CARBIDE
PO BOX 670

BOUND BROOK NJ 08805

PHONE: 201 563 5075

CASEY K YU
RHO-CHEM CORP
425 ISIS

INGLEWOOD CA 90301

PHONE: 213 776 6233

KYUNG YU
AAMRL/THA
WRIGHT-PATTERSON AFB

WRIGHT-PATT AFB OH 45433-6573

PHONE: 513 255 2704

T Y YU
PETROLITE CORP
369 MARSHALL AVE

ST LOUIS MO 63119

PHONE: 314 961 3500

ZHONGHUA YU
DEPT OF PHARM CHEM
S-926
UCSF
SAN FRANCISCO CA 94143

PHONE: 415 476 4893

LI YU-LAN
INST OF FORENSIC SCIENCE
MU XI DI
WEST CITY
BEIJING
PR CHINA
PHONE:

MARC YUDKOFF
CHILDREN'S HOSPITAL OF PHIL
1 CHILDREN'S CTR

PHILADELPHIA PA 19104

PHONE: 215 596 9409

M F ZABIELSKI
UNITED TECH RES CTR
SILVER LANE, MS 30

EAST HARTFORD CT 06108

PHONE: 203 727 7431

DON ZACKETT
DOW CHEMICAL CO
1897 BLDG

MIDLAND MI 48667

PHONE: 517 636 6102

DANIEL W ZAHAREVITZ
4702 SHARON ROAD

CAMP SPRINGS MD 20748

PHONE: 301 496 8315

JULIE A ZALIKOWSKI
JAMES H MONTGOMERY ENG
555 N WALNUT

PASADENA CA 91101

PHONE: 818 796 9141

J J ZAMECNIK
CAMU
HEALTH & WELFARE CAN
BOX 1035 POST STA B
DOWNSVIEW ONT M3H 5V5
CANADA
PHONE: 416 630 8503

A T ZANDER
VARIAN RESEARCH CENTER
611 HANSEN WAY

PALO ALTO CA 95014

PHONE: 415 424 6187

RICHARD G ZAYLSKIE
USDA AG RES SERVICE
STATE UNIV STATION
PO BOX 5674
FARGO ND 58105

PHONE: 701 239 1224

LEAH E ZEBRE
925 CHERRY ST

WHEATON IL 60187

PHONE: 312 260 9883

LOREEN ZELLER-DEAMICIS
8325 TEQUISTA CIRCLE

INDIANAPOLIS IN 46236

PHONE: 317 823 1554

CHENHUI ZENG
DEPT OF CHEMISTRY
ROOM 56-012
MIT
CAMBRIDGE MA 02139

PHONE: 617 253 7237

RENATO ZENOBI
DEPT OF CHEMISTRY
STANFORD UNIVERSITY

STANFORD CA 94305

PHONE: 415 723 4318

L F ZERILLI
MERRELL DOW RES INST
VIA R LEPETIT 34

21040 GERENZANO
ITALY
PHONE:

QINGMEI ZHA
DEPT OF CHEMISTRY
UNIV OF MONTREAL

MONTREAL NE H3C 3J7
CANADA
PHONE:

MEIYI ZHANG
BOX 285
BAKER LABORATORY
CORNELL UNIV
ITHACA NY 14853-1301

PHONE: 607 255 3731

ZHAN-WANG ZHANG
HENAN INST OF CHEMISTRY

ZHANGZHOU
CHINA
PHONE:

HE ZHE
INST OF MARINE GEOLOGY
MINISTRY OF GEOLOGY & MINERAL

QINGDAO
PR CHINA
PHONE:

ZHONGRUI ZHOU
DEPT OF MED CHEM & PHARM
PURDUE UNIVERSITY

W LAFAYETTE IN 47907

PHONE: 317 494 1449

PENGPENG ZHU
DEPT OF CHEMISTRY
UNIV OF CHICAGO
5735 S ELLIS
CHICAGO IL 60637

PHONE: 312 702 8889

ANTHONY K ZIBERNA
FINNIGAN MAT INSTITUTE
4450 CARVER WOODS DR

CINCINNATI OH 45242

PHONE: 513 891 2100

BARBARA ZIELINSKA
STATEWIDE AIR POLLUTION
RESEARCH CTR
UNIV OF CALIFORNIA
RIVERSIDE CA 92521

PHONE: 714 787 3502

DAVID ZIEMBA
FINNIGAN MAT
355 RIVER OAKS PARKWAY

SAN JOSE CA 95134

PHONE: 408 433 4800

LYNN R ZIESKE
APPLIED BIOSYSTEMS INC
850 LINCOLN CENTER DRIVE

FOSTER CITY CA 94404

PHONE: 415 570 6667

JEFFREY ZIMMERMAN
14240 NORTH 42 ST 1003-B

TAMPA FL 33613

PHONE: 813 974 3836

JOSEPH A ZIRROLLI
DEPT OF PHARMACOLOGY C236
UCHSC
4200 E 9TH AVE
DENVER CO 80262

PHONE: 303 394 8961

MARKUS ZOLLINGER
TALSTRASSE 28

CH-8125
ZOLLIKERBERG
SWITZERLAND
PHONE:

DOUGLAS ZOOK
MONTANA STATE UNIV
DEPT OF CHEMISTRY

BOZEMAN MT 59717

PHONE: 406 994 5419

FRANK ZULESKI
STUART PHARMACUETICALS
ICI AMERICAS

WILMINGTON DE 19897

PHONE: 302 575 8219

JOHN E ZUMBERGE
RUSKA LABS INC
3601 DUNVALE

HOUSTON TX 77063

PHONE: 713 975 0547

JERRY ZWEIGENBAUM
EASTMAN KODAK CO
ATD BLDG-318, KODAK PARK

ROCHESTER NY 14650

PHONE: 716 477 4772

PHONE: